

Role of a Disordered Steroid Metabolome in the Elucidation of Sterol and Steroid Biosynthesis

Cedric H. L. Shackleton

Received: 5 May 2011 / Accepted: 19 July 2011 / Published online: 27 August 2011
© AOCs 2011

Abstract In 1937 Butler and Marrian found large amounts of the steroid pregnanetriol in urine from a patient with the adrenogenital syndrome, a virilizing condition known to be caused by compromised adrenal secretion even in this pre-cortisol era. This introduced the concept of the study of altered excretion of metabolites as an *in vivo* tool for understanding sterol and steroid biosynthesis. This approach is still viable and has experienced renewed significance as the field of metabolomics. From the first cyclized sterol lanosterol to the most downstream product estradiol, there are probably greater than 30 steps. Based on a distinctive metabolome clinical disorders have now been attributed to about seven post-squalene cholesterol (C) biosynthetic steps and around 15 en-route to steroid hormones or needed for further metabolism of such hormones. Forty years ago it was widely perceived that the principal steroid biosynthetic defects were known but interest rekindled as novel metabolomes were documented. In his career this investigator has been involved in the study of many steroid disorders, the two most recent being P450 oxidoreductase deficiency and apparent cortisone reductase deficiency. These are of interest as they are due not to mutations in the primary catalytic enzymes of steroidogenesis but in ancillary enzymes needed for co-factor oxido-reduction. A third focus of this researcher is Smith-Lemli-Opitz syndrome (SLOS), a cholesterol synthesis disorder caused by 7-dehydrocholesterol reductase

mutations. The late George Schroepfer, in whose honor this article has been written, contributed greatly to defining the sterol metabolome of this condition. Defining the cause of clinically severe disorders can lead to improved treatment options. We are now involved in murine gene therapy studies for SLOS which, if successful could in the future offer an alternative therapy for this severe condition.

Keywords Cholesterol synthesis · Steroid biosynthesis · Steroid metabolism

Introduction

The class of natural lipids we call steroids all have in common the perhydrocyclopentanophenanthrene structure, the core ring unit produced by the cyclization of oxidosqualene. This structure is used as a backbone of a remarkable suite of essential biochemicals with very diverse tasks, from cholesterol with its global responsibilities (membrane and neuron structure, steroid precursor, etc.), to bile acids with their cell signaling and detergent qualities, to skeletally essential vitamin D, to the gonadal steroids, and to the adrenal hormones that regulate our intermediary metabolism and salt and water balance. While all these vital components are derived from acetate, the first intermediate with the fused ring-structure is the C-30 sterol lanosterol and from that precursor there are likely more than 30 steps leading to the most distal steroid products such as estradiol and the terminal metabolites of cortisol.

Following the confirmation of the structure of cholesterol in 1932, defining the enzymes and other factors that are needed to progress from acetate to the most distal metabolites has taken more than 70 years and remains a work in progress. The study of the hormonal biosynthetic

C. H. L. Shackleton (✉)
Centre for Endocrinology, Diabetes and Metabolism (CEDAM),
The University of Birmingham, Birmingham, UK
e-mail: cshackleton@chori.org

C. H. L. Shackleton
Children's Hospital Oakland Research Institute,
Oakland, CA, USA

process started in the 1940s with the characterization of individual compounds within glandular tissues, mostly obtained from domestic animals. Radioactively labeled versions of these compounds (and their possible precursors) were synthesized and utilized in tissue perfusion studies or incubated with cellular fractions. Step by step a hypothetical biosynthetic scheme for cortisol evolved but its veracity proved difficult to confirm without *in vivo* experimentation.

The field that we now term metabolomics has been key to verifying the biosynthetic pathway leading to cholesterol, the hormonal steroids, and their metabolites. Metabolomics is the systematic study of the unique chemical fingerprints that specific cellular and bodily processes leave behind—specifically the study of small-molecule metabolite profiles. In reality, relatively little information can be obtained solely by studying the blood or excretory metabolic profile of healthy individuals, it is those with biosynthetic disorders (inborn errors) that provide the necessary keys to understanding synthetic sequences as well as defining the biological role and importance of the biosynthetic end product.

In describing the elucidation of the steroid biosynthetic pathway through metabolomics it is useful to focus on cholesterol as the mid-point and discuss the pre-cholesterol (upstream) and post-cholesterol (downstream) processes separately. This author has been involved in research interpreting metabolic profiles of each process and three personal examples will be highlighted, two “Downstream” and one “Upstream”.

Downstream from Cholesterol

Cortisone was the first major adrenal steroid hormone to be identified and as soon as sufficient was synthesized for pharmacological testing it was found to ameliorate the symptoms of arthritis [1]. It was designated the “wonder-drug” of 1949 and for this discovery Kendall, Hench and Reichstein received the 1950 Nobel prize. A little later it was realized that a cortisone precursor, hydrocortisone (or cortisol) was in fact the true adrenally synthesized glucocorticoid. Following the identification of the major glucocorticoids there was a dramatic acceleration of studies of the biosynthesis of these hormones mostly carried out by groups in New York and the Worcester foundation in Massachusetts.

The initial breakthroughs in understanding adrenal steroid biosynthesis were uncovered independently of metabolomics. These studies were conducted *in vitro*, and generally consisted of isolating steroids from bovine adrenal tissues obtained from abattoirs, perfusions of such glands with individual labeled steroids, and finally

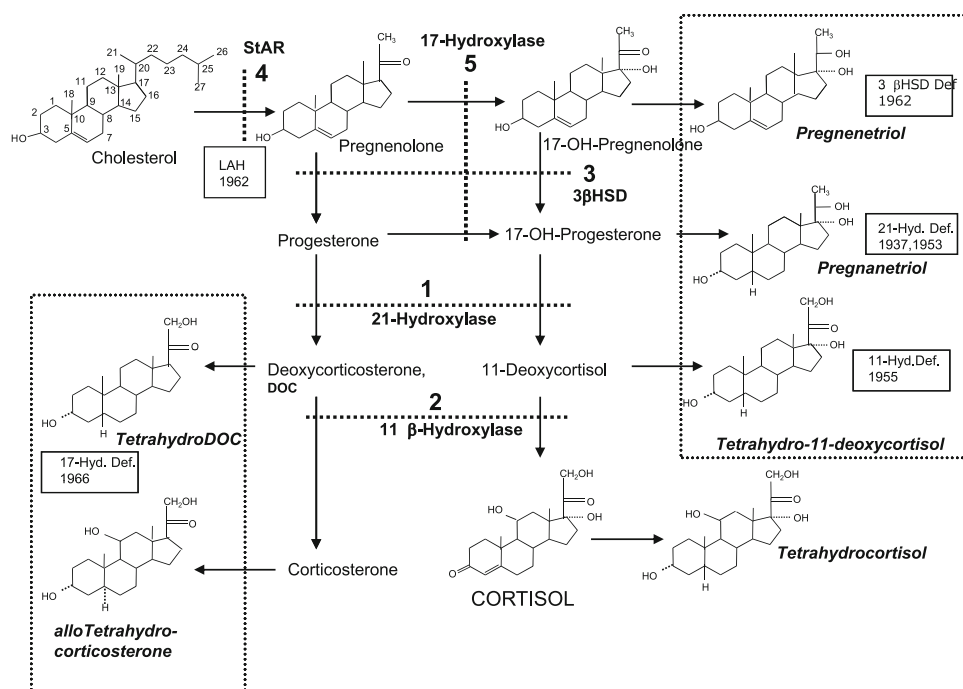
metabolism studies utilizing sub-cellular fractions. By the mid 1950s there was already evidence that the likely synthetic route was pregnenolone oxidation to progesterone, sequential 17-hydroxylation, 21-hydroxylation and 11 β -hydroxylation, finally producing cortisol. It was postulated at the time that cholesterol was the precursor of pregnenolone but there was no direct evidence to prove it. Proposing this biosynthetic pathway was a remarkable achievement based on the methodologies available at that time, and the story is well documented in the 1954 review by Hechter and Pincus [2].

The synthetic scheme, while attractive, still represented a series of deductions based primarily upon the ability of substrates to be converted. What was lacking was information derived from *in vivo* metabolism, and that was soon supplied by what we now refer to as metabolomics. It was the study of the steroidal products produced by patients with inborn errors of steroid biosynthesis that finally verified the postulated biosynthetic sequence. What follows is a brief history of these discoveries which are readily followed by viewing Fig. 1. For the benefit of readers less familiar with the numbering system of steroids, this is detailed in the structure of cholesterol illustrated.

Interestingly, the first metabolomic discovery pre-dated the actual discovery of the primary glucocorticoids (cortisol/cortisone) by a decade. This was the 1937 characterization of pregnanetriol in the urine of patients with the adrenogenital syndrome by Butler and Marrian [3]. The adrenogenital syndrome is a condition in which adrenal insufficiency is associated with masculinization of female fetuses. In their early paper they do not (and cannot) speculate on the reason for this overproduction as the terminal product of the adrenal steroidogenic pathway had yet to be identified. By today’s standards the achievement of metabolite characterization was challenging. A great volume of urine was processed and in these pre-chromatography days identification comprised of nothing more than differential extraction, targeted chemical reactions and crystallization to constant melting point.

It took many more years before a clearer understanding of the significance of the pregnanetriol discovery was obtained. Eberlein and Bongiovanni in 1955 re-identified pregnanetriol as the major urinary metabolite in the adrenogenital syndrome (now referred to as congenital adrenal hyperplasia, CAH), but by then it was possible to connect this to cortisol deficiency [4]. Having deduced that pregnanetriol was a metabolite of 17-hydroxyprogesterone (17OHP) these investigators proposed a block between 17OHP and cortisol and suggested that 21-hydroxylase was deficient. It should be emphasized that in this era only urine analysis was practical, widespread use of sensitive immunoassay procedures that allowed serum hormone measurement were still two decades away.

Fig. 1 Cortisol biosynthesis and the first reported forms of Congenital Adrenal Hyperplasia (CAH). Identifying urinary metabolites and defining these conditions confirmed the postulated adrenal biosynthetic pathway determined by *in vitro* experimentation. The first form of CAH investigated was 21-hydroxylase deficiency [1], followed by 11 β -hydroxylase deficiency [2] and 3 β -hydroxysteroid dehydrogenase deficiency [3]. LAH patients [4] essentially had absence of urinary metabolites, with adrenal cholesterol build-up. 17-Hydroxylase deficiency [5] was the final form defined during the classical era. The major urinary metabolites are shown in italics, steroid hormones and their precursors in conventional script



Following this report on 21-hydroxylase deficiency the same investigators described a hypertensive form of CAH and the metabolic profile was defined by a high excretion of tetrahydro-11-deoxycortisol, pointing to a deficiency of 11 β -hydroxylase [5]. Step by step these metabolite identifications were verifying the biosynthetic pathways proposed by the *in vitro* experimenters. In 1962 Bongoivanni described CAH due to 3 β -hydroxysteroid dehydrogenase deficiency (3 β HSD) hallmarked by high excretion of Δ^5 steroids such as pregnenetriol and DHEA [6]. In 1955, Prader and Gurtner [7] reported on neonates with a fatal condition marked not by the production and excretion of distinctive metabolites, but by the apparent absence of steroid hormone metabolites. At post-mortem examination the adrenal glands of these infants were found to be filled with cholesterol and its esters suggesting a deficiency in the conversion of cholesterol to the first C21 steroid, pregnenolone. This was attributed at the time to cholesterol side-chain cleavage (desmolase) deficiency, but now it is known to be due to a cholesterol transport protein deficiency. This condition was termed lipid adrenal hyperplasia (LAH). The final example of disorders causing cortisol insufficiency was the description in 1966 of a second hypertensive form of CAH, 17-hydroxylase deficiency by Biglieri and co-workers [8]. The metabolome of patients with this disorder was based on the overproduction of 17-deoxycorticoids such as deoxycorticosterone (DOC) and corticosterone.

By the mid 1960s a basic understanding of the biosynthesis of adrenal steroids had pretty much been established, at least from the aspect of defining the primary

transformations and the order in which they occur. These achievements have been summarized in Fig. 1.

Analyzing the Metabolome: The Author's Introduction

In metabolomic studies of urinary steroids the compounds quantified are not secreted hormones or precursors, but rather end products produced by renal or hepatic metabolism. For example, the 3-oxo-4-ene structure of a typical hormone or precursor is reduced to form a 3 α -hydroxysteroid with either a 5 α or 5 β hydrogen. These metabolites are referred to as “tetrahydro-metabolites”, for example tetrahydrocortisol (Fig. 1). A carbonyl group at position 20 may be converted to a hydroxyl and commonly hydroxyl groups at positions 17 β and 11 β are converted to carbonyls. Thus, it seems that whatever functional moiety an active hormone has is to a great extent oxidized or reduced to its “opposite” prior to excretion. Finally, essentially all metabolites with a 3 α -hydroxyl are excreted as glucuronide conjugates and those with 3 β -hydroxy-5-ene groups are excreted as sulfates.

While the earliest characterizations within the urinary steroid metabolome were made without the benefit of chromatography, by the 1950s paper chromatography came into own thanks to the painstaking developments by Ian Bush [9] and Zaffaroni [10]. The former in particular standardized methodologies to the extent that steroid metabolic profiles as we know them could be used clinically [11]. All of the first batch of steroidogenic disorder discoveries were documented by this technique.

My first introduction to the field was my undergraduate thesis entitled “cholesterol and cholesterol esters in the bovine corpus luteum during formation and regression”, a study completed in 1964. My supervisor was the noted cholesterol researcher Robert Cook who published one of the first monographs on the subject [12]. My perseverance in the field was tested severely as I had to spend untold distressing hours at the slaughterhouse in Dundee, Scotland, collecting tissue samples. I started work on steroid metabolomics at the end of the golden age for steroid biochemists when the fundamental biosynthetic route to cortisol had largely been confirmed and primary defects described. I was employed in 1964 in the Dept of Clinical Chemistry, the University of Edinburgh to study the steroid metabolome of newborn infants and determine how it differed qualitatively and quantitatively from later life. My earliest experiments were conducted using paper chromatography for the identification and measurement of the steroids excreted by human newborns but soon realized that the rapidly developing TLC methodologies were much more effective and sensitive. By using this technique with three color reactions we could separate and quantify all the major excreted steroids of humans [13]. Although the methodology was effective it was soon overtaken by gas chromatography and the combined GC/MS technique. In 1966 I was privileged to use the first commercial GC/MS instrument purchased in the UK to identify some of the novel newborn steroids isolated by TLC [14]. This instrument belonged to Professor Charles Brooks of Glasgow University, a seminal steroid researcher of this era.

For post-doc training I went to the Karolinska institute in Stockholm to work with Professor Jan Sjövall, a previous recipient of the Schroepfer medal, to get a thorough education in this new field. Jan was a co-developer with Ragner Ryhage of the first practical GC/MS instrument which was marketed as the LKB 9000. By 1968, GC/MS was truly a metabolomic tool in the steroid field. By use of the combination of methyloxime protection of carbonyl groups and trimethylsilylation of hydroxyls, all neutral human steroids, whatever their origin and complexity could be analyzed in a single chromatogram. In 1970, I returned to the MRC in London and continued my studies on steroid biosynthetic disorders using GC/MS. Our group was at the forefront in introducing capillary column methodology in producing steroid profiles [15], in the use of GC/MS in athletic doping control [16] and in improving steroid recovery techniques by the first use of SPE (solid phase extraction) with cartridges [17].

In 1979 I moved to Berkeley, California to assist Dr Al Burlingame establish a national resource for biomedical mass spectrometry. While there we made the first utilization of the new Fast Atom Bombardment technique to the analysis of steroid of clinical relevance. With my colleague

Ken Straub we showed that single spectrum profiles of urinary steroid conjugates could be used to diagnose five disorders of steroid biosynthesis [18, 19]. This was the first practical analysis of intact conjugates because in previous studies by paper, TLC and GC/MS steroid conjugates had first to be hydrolyzed prior to analysis. This technique was overtaken by development of HPLC/MS, first using the thermospray interface [20] soon followed by electrospray ionization. However, close to 50 years after the introduction of GC/MS for analyzing the steroid metabolome, this technique is still preferred for this role [21]. HPLC/tandem MS now has extreme sensitivity and is ideally suited to the measurement of circulating hormones and precursors but finds challenging the separation and quantitation of the characteristic steroids found in a urinary extracts.

Discovery of the 6th Form of Congenital Adrenal Hyperplasia (CAH)

The description of the five classical forms of CAH seemed to signal an end to the first chapter in the story of steroid biochemistry. As they covered the needed transformations in the ACTH-regulated pathway from cholesterol to cortisol and served to validate the pathway deduced from the original *ex vivo* investigations. In the late 1970s one more unique urinary steroid metabolome was documented by the late Dr Meta Nielsen and myself. Meta from the Glostrup hospital in Copenhagen was second-to-none in her ability to accurately diagnose steroid disorders by TLC of urinary steroids but she still needed a collaborator to confirm steroid identities by GC and GC/MS. A distinctive metabolome was seen in two sisters with masculinized genitalia, one who had been brought up as a boy. The unique feature was that there was elevated excretion of the metabolites of 17 α -hydroxyprogesterone (pregnanetriol and pregnanetriolone, indicative of 21-hydroxylase deficiency) as well as elevated excretion of corticosterone metabolites (tetrahydrocorticosterone and others), a feature suggesting 17-hydroxylase deficiency. We termed the condition “combined 17- and 21-hydroxylase deficiency” but unwisely we did not pursue this to publication.

It was several years before another example of this metabolome was seen and then it was a patient of Dr Ralph Peterson and Julianne Imperato-McGinley at Cornell Medical School in New York. These investigators had an active program studying isolated kindreds in the Dominican Republic with high incidence of ambiguous genitalia and I had a role in diagnosing these individuals by GC/MS analysis. Almost all DSD (Disorders of Sexual Development) individuals had a disorder not directly related to cortisol synthesis called 5 α -reductase deficiency, but one young virilized girl had a steroid profile of combined

17- and 21-hydroxylase deficiency. This patient was studied in detail and a resulting publication became the index case of the disorder [22]. Many years were to pass before the true cause of the disorder was determined but during that period there were isolated reports of other cases where patients were described with features of 17- or 21-hydroxylase deficiency. With my colleague Ewa Malunowicz of Warsaw we reviewed several of these papers and questioned the authors original interpretations as they all seemed to have a metabolome suggesting combined 17- and 21-hydroxylase deficiency [23]. Interestingly, several patients of this type described in the 1990s were not initially investigated because of DSD but because their dominant phenotype was consistent with Antley-Bixler syndrome, a skeletal disorder with features including skull, limb and finger abnormalities.

Enough was known of the genetics of steroidogenesis to render simultaneous errors in both 17- and 21-hydroxylase genes unlikely, so the focus was directed to ancillary factors that are required for the function of both enzymes. The most important co-factor for both 17-hydroxylase and 21-hydroxylase is cytochrome P450 oxidoreductase (OR), the enzyme responsible for regenerating the NADPH required for hydroxylase enzyme function. In 2003 my colleague Prof. Wiebke Arlt at Birmingham started to sequence this enzyme in a few patients (from various clinicians) which we had identified by metabolic profile and a year later several mutations had been found and we published a paper describing the “sixth” form of CAH, a condition caused by deficiency of P450 oxidoreductase [24]. Simultaneous studies on Antley-Bixler syndrome and P450 oxidoreductase deficiency were carried out by Professor Walter Miller’s group in San Francisco and Dr Hisao Hidachi in Japan; these were published the same year [25, 26].

There was one aspect of “combined 17-hydroxylase/21-hydroxylase deficiency” patients which confounded endocrinologists since the first description of the condition. The original forms of CAH (21- and 11 β -hydroxylase deficiencies) were always associated with hyperandrogenism causing masculinization of female fetuses, a hyperandrogenism which persists for life in untreated patients. In this new form caused by oxidoreductase deficiency (ORD) (P450 oxidoreductase deficiency), females were virilized but males had ambiguous genitalia. While it was obvious that females were virilized we found that post-natal androgen levels were low, as one would expect due to the attenuation of 17 α -hydroxylase and 17,20-lyase activity caused by the deficient OR. Hydroxylation of C17 and subsequent lyase activity are carried out by a single enzyme encoded by single mRNA. The OR enzyme is required to facilitate the transfer of electrons from NADPH to CYP17 allowing oxidation. In the presence of co-factor cytochrome b5 the lyase function oxidatively removes the

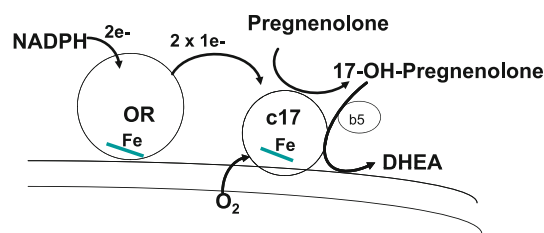


Fig. 2 Oxido-reductase and 17,20-lyase activity. 17-Hydroxylase and C17,20-lyase activities reside in a single protein encoded by a single gene. This enzyme only works effectively in concert with P450 oxido-reductase which is necessary for providing the electrons required for oxidation. The lyase function of the hydroxylase enzyme also needs cytochrome b5

side-chain, the rate-limiting step in the process (Fig. 2). Inactivity of OR attenuates the process and androgen formation is inhibited.

Clearly, the virilization of female fetuses was transient but how could this be explained? We formulated a hypothesis for the transient fetal hyperandrogenism by study of the pregnancy metabolic profile from a mother carrying an OR deficient fetus [27]. We had proof of the presence of ORD in this pregnancy because estriol (a primary product of pregnancy) excretion was almost negligible being replaced in urine by a pregnenolone metabolite. The conversion of pregnenolone to estriol requires active C17,20 lyase activity. In sequential maternal urine steroid assays carried out throughout an affected pregnancy a disproportionate increase in two 5 α -reduced steroids androsterone and 3 α ,17 α -dihydroxy-5 α -pregnan-20-one compared to their 5 β -reduced epimers was also noted [27]. We suggest that the ORD fetus uses a novel pathway where 3 α ,17 α -dihydroxy-5 α -pregnan-20-one is converted to androsterone which in turn is oxidized to the potent androgen 5 α -dehydrotestosterone (DHT). The oxidation of a 3 α -hydroxyl group has always been considered unlikely in human metabolism although this pathway has been shown to be important in the tammar wallaby [28]. The viability of our hypothesis rests on the finding that 3 α ,17 α -dihydroxy-5 α -pregnan-20-one is a much better substrate for residual 17,20-lyase activity than the conventional substrates 17-hydroxypregnenolone or 17-hydroxyprogesterone [29]. We have termed this “the alternative pathway” for fetal androgen synthesis (Fig. 3) and current studies are directed to proving this theory. This is an excellent example of a hypothesis developed by detailed metabolomic studies of urine; it would have been almost impossible to achieve by any form of conventional hormone analysis. The unique metabolic profile of ORD allows for GC/MS to be routinely used for diagnosing this condition both pre- and postnatally [27, 30].

While I have focused on the disorders of cortisol biosynthesis, investigations over the last 30 years have

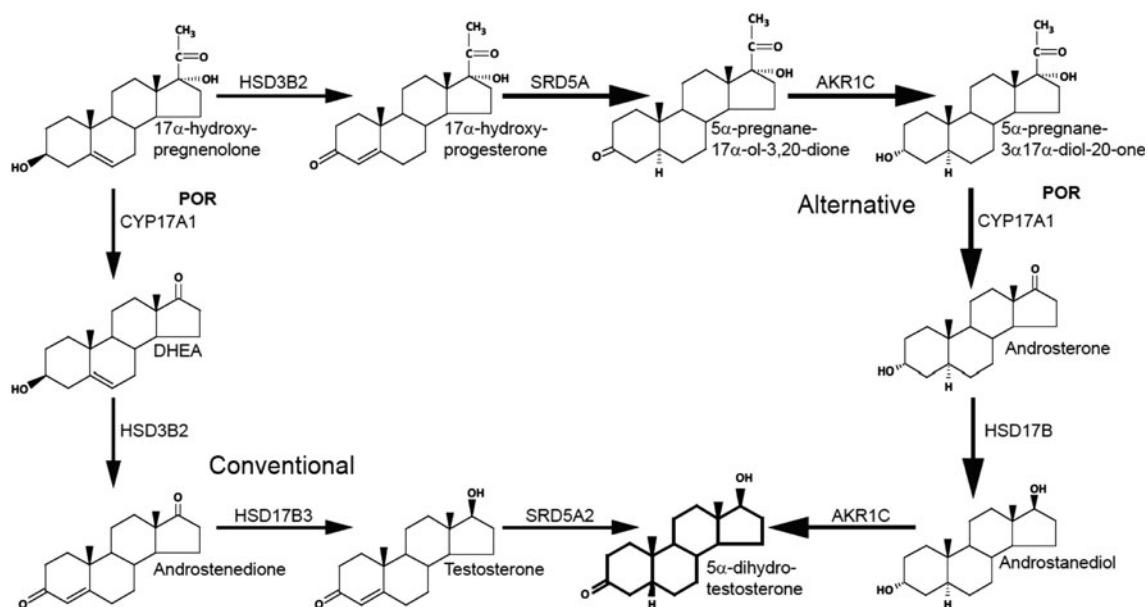


Fig. 3 Proposed alternative pathway of fetoplacental androgen synthesis from 17-hydroxypregnenolone. The *lower-left corner* represents the conventional pathway of androgen synthesis requiring sequential side-chain removal, oxidation by 3β HSD, 17-keto reduction by 17β HSD and finally 5α -reduction terminating in DHT. The

alternative pathway (*upper right corner*) starts with the formation of 17-hydroxyprogesterone and its reduction to 5α -pregnane- $3\alpha,17\alpha$ -diol-20-one. In spite of attenuated 17,20-lyase activity due to POR deficiency this steroid can be converted to androsterone and likely on to DHT

uncovered the causes of many other steroid endocrinopathies. In terms of intersex conditions there have been the description of 5α -reductase [31] and 17β HSD deficiencies [32] causes of incomplete male development and aldosterone (the mineralocorticoid hormone) biosynthetic defects such as aldosterone synthase deficiency and glucocorticoid repressible hyperaldosteronism. The urinary steroid metabolomes of these disorders were first described by the late Dr Stanley Ulick [33, 34].

Studies of the Cortisol-Cortisone Interconversion

Oxidation

Cortisol, with its 11β hydroxy group is the primary glucocorticoid product of the adrenal glands. It can be interconverted with cortisone (which has a carbonyl at position 11) by means of 11β hydroxysteroid dehydrogenase (11β HSD). In the normal human metabolome there are virtually equivalent amounts of metabolites with 11-carbonyl and 11β -hydroxyl functions. The principal cortisone metabolites are tetrahydrocortisone (THE) and the cortolones (20α and 20β); while the principal metabolites of cortisol are tetrahydrocortisols (THF and its 5α -epimer, 5α THF) and the cortols (20α and 20β).

In the late 1970s, GC/MS was used by us and Drs Stanley Ulick and Maria New to study the excretion of

steroids by young patients with an unusual form of hypertension. These patients retained salt which suggested high production of a mineralocorticoid but atypically low aldosterone and low renin, the opposite of what was expected. It was found that the urinary cortisol metabolites essentially only had the 11β -hydroxyl group, the steroids with 11-carbonyl were virtually absent [35, 36]. Further studies showed that the deficient enzyme was a novel renal 11β HSD which was named 11β HSD 2. This enzyme operates exclusively in an oxidative direction and has the function of protecting the renal tubules against cortisol which competes with aldosterone for the mineralocorticoid receptor. In individuals with the deficiency cortisol acts as a potent mineralocorticoid giving rise to sodium retention and hypertension. We termed this interconversion the “cortisol-cortisone” shuttle and demonstrated its importance in blood pressure regulation. In the years following multiple patients with this disorder have been studied and many loss-of-function mutations genetic found. These studies were carried out with my colleagues Chris Edwards, Paul Stewart, Maria New, among others [37].

Reduction

It had long been known that there could be active regeneration of cortisol from cortisone. In fact, for the first years of adrenal hormone discovery it was assumed that cortisone was the glucocorticoid hormone. Kendall and

colleagues received the Nobel prize for their clinical studies with this steroid, as it was successfully used for treatment of rheumatoid arthritis. In the beginning of the 1950s it was finally recognized that cortisol was the true hormone and that the therapeutic efficacy of cortisone was due to its reduction to cortisol. Studies in recent years have shown that regeneration of cortisol is conducted by a long-known liver 11β -hydroxysteroid dehydrogenase, now called 11β HSD 1 after discovery of the kidney enzyme termed 11β HSD 2. It is the concerted action of 11β HSD1 and 11β HSD 2 which gives rise to the quantitative equivalence between the tetrahydrometabolites of cortisol and cortisone in human urine.

In 1996, we did a detailed study of two sisters, patients of Dr George Phillipov in Australia, who had a unique metabolome where essentially only the metabolites of cortisone were present (11-carbonyl containing steroids), i.e., THE and the cortolones. Thus, the metabolome appeared to be exactly the opposite of the aforementioned AME syndrome [38]. Interestingly, these individuals clearly had huge cortisol production but showed no symptoms of hypercortisolism (Cushing's syndrome). This was attributed to the rapid and irreversible metabolism to cortisone, almost certainly catalyzed by hepatic 11β HSD 1. The disorder has been termed Cortisone Reductase Deficiency (CRD) and several more patients with the condition have been described in recent years [39]. The apparent inability of these patients to regenerate cortisol from cortisone causes ACTH-mediated hyperandrogenism which manifests in early pseudopuberty in males and midlife hirsutism and infertility in women.

My colleagues at Birmingham under the direction of Professor Paul Stewart spearheaded studies of the genetics of this disorder. Interestingly, no mutations were found in 11β HSD 1 in affected patients, so analogous to the ORD studies described above, attention was paid to the generation of NADPH, which in the endoplasmic reticulum lumen is carried out by hexose-6-phosphate-dehydrogenase (H6PD). Drs Gareth Lavery and Elizabeth Walker of our department have conducted these studies and have demonstrated loss-of-function mutations in H6PD in four patients with the disorder [39]. The disorder and its affect on the metabolome are summarized in Fig. 4. These studies led to the development of a mouse model for the disorder and study of their steroid metabolome. In contrast to humans the mouse glucocorticoid is the 17-deoxysteroid corticosterone and the metabolic profile was composed of reduced metabolites of this steroid. H6PD knockouts have a high percentage of 11-dehydrocorticosterone metabolites proving the importance of this enzyme co-factor for corticosterone regeneration, strong evidence for the importance of this enzyme in cortisone to cortisol conversion in man.

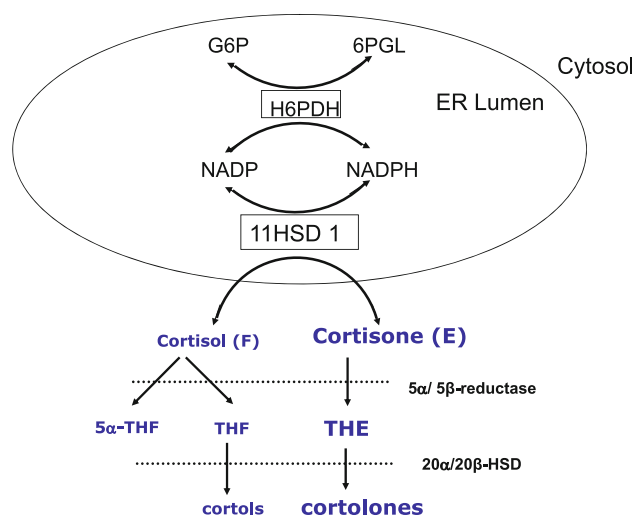


Fig. 4 Cortisone reductase deficiency. This disorder was discovered in affected patients through the domination in urine of THE and the cortolones, corticosteroids with 11-carbonyl function. The analogous steroids with 11β -hydroxyl function, the epimeric tetrahydrocortisols (THFs) and cortols were severely diminished. This reduction was attributed to attenuated 11β HSD1 activity preventing hepatic regeneration of cortisol from cortisone. Reduced activity was shown to be caused by mutations in H6PDH responsible for NADP oxidation

Upstream of Cholesterol

The first product of squalene cyclization is the C-30 sterol lanosterol and conversion of this to the C-27 cholesterol is a multistep process. Disorders of post-squalene cholesterol biosynthesis were unknown prior to 1993 but since then a few have been described in humans, all but one extremely rare. These disorders can be considered more severe than those downstream of cholesterol as they are invariably associated with dysmorphology, mental retardation and are frequently fatal. The original descriptions of the conditions were usually based on increased concentrations of the precursors for enzyme conversion in serum or cellular preparations. Verification of the deficiency has been obtained by detecting mutations in genes for individual proteins and development of transgenic mouse models [40].

In descending order as the disorders appear in the Kandutsch-Russell cholesterol biosynthetic pathway [41] the first is Antley-Bixler syndrome a skeletal dysmorphology syndrome. It was initially proposed that it was caused by lanosterol demethylase (Cyp 51) inactivity although the enzyme itself has been shown to have no mutations in affected individuals [42]. The most likely cause of attenuated Cyp 51 activity is the previously discussed P450 oxidoreductase deficiency since the latter enzyme is required for NADPH regeneration. The second condition is HEM dysplasia initially considered to be

thought due to Δ^{14} reductase deficiency although more likely now a laminopathy [40, 43] and the third desmosterolosis due to inactive Δ^{24} reductase [44]. The fourth condition, is CHILD syndrome probably caused by NHSDHL (4,4-demethylase) deficiency [45] and the fifth, CDPX2 due to deficiency in Δ^7 - Δ^8 isomerase [46]. The sixth post-lanosterol disorder is lathosterolosis caused by deficient 5-desaturase [47] and the seventh and final is Smith-Lemli-Opitz syndrome (SLOS) caused by deficient 3β -hydroxysterol- Δ^7 -reductase (7-dehydrocholesterol reductase DHCR7, EC 1.3.1.21) [48].

SLOS was the first of the cholesterol deficiency syndromes to be reported [48] and has by far the highest incidence. Biochemically, SLOS patients have reduced cholesterol synthesis and elevated levels of 7-dehydrocholesterol (7DHC) and its isomer 8-dehydrocholesterol (8DHC). Phenotypically SLOS presents with a variety of problems such as multiple malformations, delayed development and growth, cognitive deficiency, and autistic-like behavior. Affected individuals have a compromised quality of life and present a lifelong challenge to their families and the medical community. There is no cure for SLOS.

George Schroepfer in whose honor the AOCS medal is awarded, and to whom this paper is dedicated, played a significant role in defining the sterol metabolome of the condition. His studies gave the most comprehensive analysis of circulating steroids as a result of the enzyme deficiency [49]. For the last decade our laboratory in Oakland has focused on the study of this disorder concentrating on three questions: (1) How does the cholesterol deficiency and build-up of 7- and 8-dehydrocholesterol impact the production of hormonal steroids and their metabolites? (2) Does the unique steroid metabolome of the condition offer new diagnostic options, particularly in the form of prenatal diagnosis? and (3) could gene therapy be a treatment option for increasing the deficient cholesterol synthesis?

In studying the steroid metabolome of the disorder, we were indebted to Drs Richard Kelley and Lisa Kratz at the Kennedy Krieger institute for their collaboration, particularly in supplying needed samples from affected individuals they had diagnosed. The other participants were two synthetic chemists Dr William Wilson and Liwei Guo who painstakingly synthesized and authenticated important Δ^7 and Δ^8 reference compounds. These investigators were part of Dr Schroepfer's department at Rice University, which emphasizes how, even after his untimely death, his legacy in SLOS research was cemented through his group's continuing studies on this serious disorder.

In the urine of affected adults and children, we identified multiple steroids with additional 7- or 8-unsaturation indicating that many biosynthetic transformations could take place using the excess 7- and 8-dehydrocholesterol substrates. However, we found little or no formation of

dehydro versions of cortisol metabolites hinting that 21- and 11 β -hydroxylation may not utilize such precursors [50]. We found normal excretions of adrenal hormone metabolites in urine from affected individuals indicating surviving SLOS patients were unlikely to suffer from adrenal insufficiency.

An immediate consideration when we were studying the steroid metabolome in SLOS was the possibility that maternal steroids excreted could include novel components originating in the affected fetuses. Such compounds could provide the basis for developing a non-invasive prenatal test for the disorder. It was predicted that 7- or 8-dehydroversions of estriol (1,3,5(10)-estratrien-3,16 α ,17 β -triol, Fig. 5) in particular would be present since this steroid is almost exclusively of fetal origin. We did indeed find such compounds in urine, also interesting in that they have structures appropriate for the long-known "equine" estrogens, derivatives of equilin and equilenin, prominent estrogens produced by mares [51, 52]. The Rice University researchers chemically synthesized 7- and 8-dehydroestriol and we were able to confirm that the major metabolite in the urine of mothers carrying SLOS fetuses was 8-dehydroestriol (53, Fig. 5). Measurement of this steroid together with a dehydro steroid of the pregnane series has formed the basis of a non-invasive test for this serious disorder. Its efficacy has been evaluated in a large study including a million participants [54]. Not only were we able to validate the test but we were able to provide updated information of the incidence of the disorder in the North American population [54, 55].

At the final analysis, studying the metabolome of specific disorders should lead to new therapeutic options, and we are pursuing this aspect. Current treatment for SLOS is dietary cholesterol supplementation and anecdotal reports show positive, albeit limited, effects of exogenous cholesterol on somatic growth and behavior, but development outcome does not appear to be altered. However, an effect of dietary cholesterol on behavior would be somewhat surprising as the brain is believed to be impervious to external cholesterol, and a recent clinical trial showed no behavioral differences between short-term cholesterol supplementation and placebo. Because both cholesterol deficiency and excess 7-DHC likely contribute to the pathogenesis of SLOS, the therapeutic goal of treatment has been to enhance cholesterol accretion while decreasing accumulation of potentially toxic cholesterol precursors such as 7-DHC. Some studies report a positive effect of combining a high cholesterol diet with administration of a statin inhibitor of sterol biosynthesis.

My institutional colleague Gordon Watson and I considered that the "single enzyme deficiency" nature of SLOS made it an attractive experimental model for gene therapy. We have been conducting experiments on a mouse

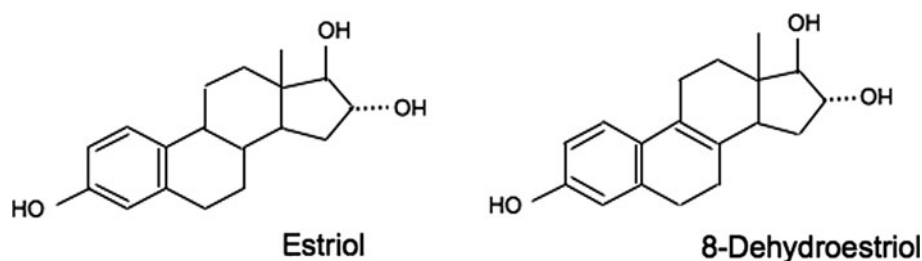


Fig. 5 Structures of Estriol and Dehydroestriol. Estriol together with pregnanediol are the two dominant steroids excreted during pregnancy, products of fetoplacental steroid synthesis. Women with a

SLOS affected steroids excrete dehydroestriols, predominantly Δ^8 . Measurement of 8-dehydroestriol can be used for prenatal diagnosis of the condition

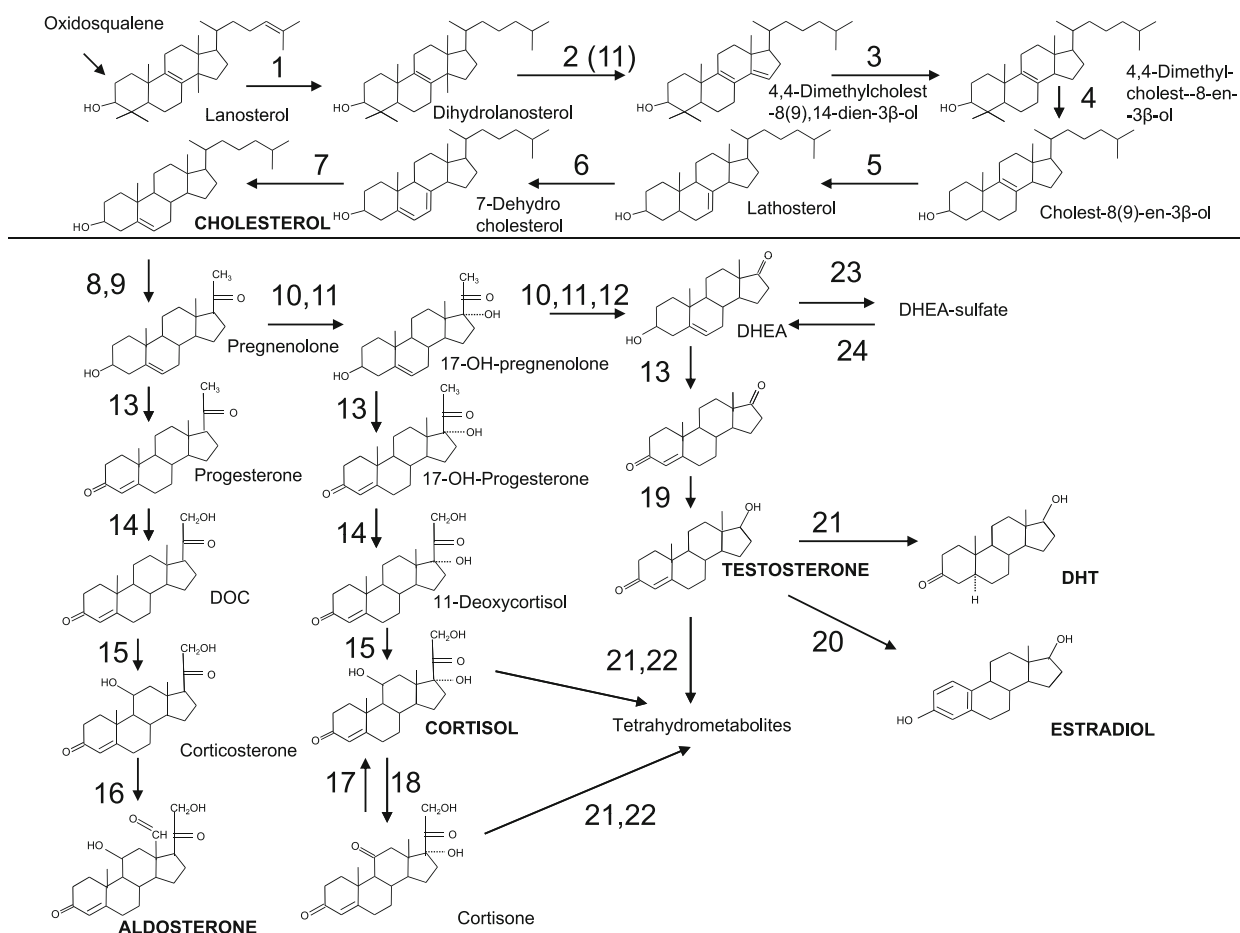


Fig. 6 Sterol and steroid synthesis and metabolism. Simplified scheme showing reported deficiencies in steroid synthesis and metabolism. A list of disorders and the causes attributed are given in Table 1

model of the disorder and have introduced a recombinant adeno-associated virus (AAV) vector containing the human gene to young affected animals and controls. These studies were moderately successful, as we have shown the presence of human DHCR7 DNA and mRNA in liver for several weeks after administration. In addition it was shown that the introduction of a functional gene does increase the amount of cholesterol while simultaneously

decreasing the amount of accumulated 7DHC, i.e., the C/DHC ratio was increased in both liver and serum [56]. While promising, the potential impact of gene therapy must be kept in perspective. Cholesterol synthesis may be stimulated, and potentially toxic precursors limited but the major dysmorphological and developmental outcomes of the disorder cannot be reversed as they result from fetal cholesterol deficiency in the earliest days of pregnancy.

Table 1 Disorders of sterol and steroid synthesis and metabolism

#	Disorder	Attributed to
1	Desmosterolosis	Sterol Δ^{24} reductase (DHCR24) deficiency
2	Antley-Bixler syndrome	CYP51 (sterol C14 demethylase) probably attenuated. Suggested cause P450 oxidoreductase deficiency (#11)
3	Greenberg skeletal dysplasia	Sterol Δ^{14} reductase deficiency
4	CHILD syndrome	4-demethylase (NSDHL) deficiency
5	CDPX2 syndrome	Δ^7 – Δ^8 isomerase (aka. epamomil binding protein, EBP) deficiency
6	Lathosterolosis	Sterol 5-desaturase (Sc5D) deficiency
7	Smith-Lemli-Opitz syndrome (SLOS)	7-dehydrosterol reductase. (DHCR7) deficiency
8	CAH, Lipoid adrenal Hyperplasia (LAH)	Steroid acute regulatory (StAR) protein deficiency
9	CAH, LAH	Cholesterol side-chain cleavage. CYP11A1
10	CAH, 17-hydroxylase deficiency	CYP17A1
11	CAH, oxido-reductase deficiency	P450 Oxidoreductase, POR
13	CAH 3 β -hydroxysteroid dehydrogenase deficiency	HSD3B2
14	CAH, 21-hydroxylase deficiency	CYP21A1
15	CAH, 11 β -hydroxylase deficiency	CYP11B1
16	Hypoadosteronism Aldosterone synthase	CYP11B2
17	Cortisone reductase deficiency (CRD)	Hexose-6-phosphate-dehydrogenase (H6PD)
18	Apparent mineralocorticoid excess (AME) syndrome	11 β -Hydroxysteroid dehydrogenase, HSD11B2
19	17 β -hydroxy-steroid dehydrogenase deficiency	HSD17B3
20	Aromatase deficiency	CYP19A1
21	5 α -Reductase deficiency	SRD5A2
22	5 β -Reductase deficiency	Aldoketoreductase. AKRD1
23	Sulfokinase “deficiency”	SULT2A1 attenuated. Caused by PAPSS2 mutations
24	Steroid Sulfatase deficiency	STS

In Summary

In sense we are closing in on the end of a long and remarkable era in the study of the formation and disposition of cholesterol in mammals. On the basis of study of the circulating and excreted steroid metabolome, as well as tissue conversion experiments, we have now a good understanding of the biosynthesis and further metabolism of cholesterol, the steroid hormones and the genetic errors that cause disease. While the original studies were on the primary enzymes (typically hydroxylases and dehydrogenases) involved in structurally altering a molecule, recent exciting developments have stressed the importance of partner enzymes and other factors that are essential for effecting the transformation. Examples are our own studies on ORD and H6PD without which steroid hydroxylases and 11 β HSD would not function, and the studies by others of StAR transport protein which is essential for enabling cholesterol side-chain cleavage in most steroidogenic tissue, deficiency of which causes LAH [58]. Steroid metabolomics has been a key player in these discoveries.

Table 1 lists most of the known disorders and their proven or putative causes. These are illustrated in the

simplified biosynthetic and metabolic scheme shown in Fig. 6. This scheme pays no attention to the tissue specificity of the many transformations. The known (and in a couple of cases, postulated) errors of transformative proteins (mostly enzymes) are listed in Table 1. Even this scheme is not comprehensive as major pathways have not been included, primarily of those leading to the formation of oxysterols and bile acids. These topics have been discussed by previous recipients of the Schroefer medal such as Professors Björkhem and Sjövall. Unexpected outcomes from detailed study of these metabolic products suggest that not only are they involved in cholesterol disposition but can be important signaling molecules interacting with receptor proteins.

Acknowledgments Firstly, I thank the AOCS for the honor of awarding me the 2010 Schroefer medal. I am most grateful to my Birmingham and Oakland colleagues who made all the recent studies possible, particularly Professors Wiebke Arlt and Paul Stewart and Doctors Nils Krone, Gareth Lavery, Gordon Watson, Josep Marcos, Montserrat Serra and Xavier Matabosch. Ms Beverly Hughes has provided us with an excellent mass spectrometric analytical service. SLOS studies would not have been possible without the collaboration of Drs Lisa Kratz, Richard Kelly, Denny Porter and William Wilson. Final thanks are to Professor Jan Sjövall of the Karolinska Institute

who was fundamental to the early development of GC/MS and steroid metabolomics. My education in this field and continued interest was due to him. Recent grant support comes from the NIH (NICHD 5R01HD053036) and The Wellcome Trust (Grant 082809/Z/07/Z; PI, Prof Paul Stewart).

References

- Hench PS, Kendall EC, Slocum CH, Polley HF (1949) The effect of a hormone of the adrenal cortex (17-hydroxy-11-dehydrocorticosterone; compound E) and of pituitary adrenocorticotrophic hormone on rheumatoid arthritis. *Mayo Clin Proc* 24:181–197
- Hechter O, Pincus G (1954) Genesis of the adrenocortical secretion. *Physiol Rev* 34:459–496
- Butler GC, Marrian GF (1937) The isolation of pregnane-3,17,20-triol from the urine of women showing the adrenogenital syndrome. *J Biol Chem* 119:565–570
- Eberlein WR, Bongiovanni AM (1955) Partial characterization of urinary adrenocortical steroids in adrenal hyperplasia. *J Clin Invest* 34:1337–1343
- Eberlein WR, Bongiovanni AM (1955) Congenital adrenal hyperplasia with hypertension: unusual steroid pattern in blood and urine. *J Clin Endocrinol Metab* 15:1531–1534
- Bongiovanni AM (1962) The adrenogenital syndrome with deficiency of 3 beta-hydroxysteroid dehydrogenase. *J Clin Invest* 41:2086–2092
- Prader A, Gurtner HP (1955) The syndrome of male pseudohermaphroditism in congenital adrenocortical hyperplasia without overproduction of androgens (adrenal male pseudohermaphroditism). *Helv Paediatr Acta* 10:397–412
- Biglieri EG, Herron MA, Brust N (1966) 17-Hydroxylation deficiency in man. *J Clin Invest* 45:1946–1954
- Bush IE (1952) Methods of paper chromatography of steroids applicable to the study of steroids in mammalian blood and tissues. *Biochem J* 50:370–378
- Zaffaroni A, Burton RB, Keutmann EH (1950) Adrenal cortical hormones; analysis by paper partition chromatography and occurrence in the urine of normal persons. *Science* 111:6–8
- Bush IE (1961) *The chromatography of steroids*. Pergamon Press, London
- Cook RP (1958) *Cholesterol: chemistry, biochemistry and pathology*. Academic Press, New York
- Shackleton CH, Charro-Salgado AL, Mitchell FL (1968) Urinary neutral steroid profile analysis in adults and infants. *Clin Chim Acta* 21:105–118
- Shackleton CH, Kelly RW, Adhikary PM, Brooks CJ, Harkness RA, Sykes PJ, Mitchell FL (1968) The identification and measurement of a new steroid 16 beta-hydroxydehydroepiandrosterone in infant urine. *Steroids* 12:705–716
- Shackleton CH, Gustafsson JÅ, Mitchell FL (1973) Steroids in newborns and infants. The changing pattern of urinary steroid excretion during infancy. *Acta Endocrinol (Copenh)* 74:157–167
- Ward RJ, Shackleton CH, Lawson AM (1975) Gas chromatographic: mass spectrometric methods for the detection and identification of anabolic steroid drugs. *Br J Sports Med* 9:93–97
- Shackleton CH, Whitney JO (1980) Use of Sep-pak cartridges for urinary steroid extraction: evaluation of the method for use prior to gas chromatographic analysis. *Clin Chim Acta* 107:231–243
- Shackleton CH, Straub KM (1982) Direct analysis of steroid conjugates: the use of secondary ion mass spectrometry. *Steroids* 40:35–51
- Shackleton CH (1983) Inborn errors of steroid biosynthesis: detection by a new mass-spectrometric method. *Clin Chem* 29:246–249
- Liberato DJ, Yergey AL, Esteban N, Gomez-Sanchez CE, Shackleton CH (1987) Thermospray HPLC/MS: a new mass spectrometric technique for the profiling of steroids. *J Steroid Biochem* 27:61–70
- Krone N, Hughes BA, Lavery GG, Stewart PM, Arlt W, Shackleton CH (2010) Gas chromatography/mass spectrometry (GC/MS) remains a pre-eminent discovery tool in clinical steroid investigations even in the era of fast liquid chromatography tandem mass spectrometry (LC/MS/MS). *J Steroid Biochem Mol Biol* 121:496–504
- Peterson RE, Imperato-McGinley J, Gautier T, Shackleton C (1985) Male pseudohermaphroditism due to multiple defects in steroid-biosynthetic microsomal mixed-function oxidases. A new variant of congenital adrenal hyperplasia. *N Engl J Med* 313:1182–1191
- Shackleton C, Malunowicz E (2003) Apparent pregnene hydroxylation deficiency (APHD): seeking the parentage of an orphan metabolome. *Steroids* 68:707–717
- Flück CE, Tajima T, Pandey AV, Arlt W, Okuhara K, Verge CF, Jabs EW, Mendonça BB, Fujieda K, Miller WL (2004) Mutant P450 oxidoreductase causes disordered steroidogenesis with and without Antley-Bixler syndrome. *Nat Genet* 36:228–230
- Arlt W, Walker EA, Draper N, Ivison HE, Ride JP, Hammer F, Chalder SM, Borucka-Mankiewicz M, Hauffa BP, Malunowicz EM, Stewart PM, Shackleton CHL (2004) Congenital adrenal hyperplasia with apparent combined P450c17 and P450c21 deficiency is caused by mutations in P450 oxidoreductase. *Lancet* 363:2128–2135
- Adachi M, Tachibana K, Asakura Y, Yamamoto T, Hanaki K, Oka A (2004) Compound heterozygous mutations of cytochrome P450 oxidoreductase gene (POR) in two patients with Antley-Bixler syndrome. *Am J Med Genet A* 128A:333–339
- Shackleton C, Marcos J, Arlt W, Hauffa BP (2004) Prenatal diagnosis of P450 oxidoreductase deficiency (ORD): a disorder causing low pregnancy estriol, maternal and fetal virilization, and the Antley-Bixler syndrome phenotype. *Am J Med Genet A* 129A:105–112
- Wilson JD, Auchus RJ, Leihy MW, Guryev OL, Estabrook RW, Osborn SM, Shaw G, Renfree MB (2003) 5alpha-androstane-3alpha, 17beta-diol is formed in tammar wallaby pouch young testes by a pathway involving 5alpha-pregnane-3alpha, 17alpha-diol-20-one as a key intermediate. *Endocrinology* 144:575–580
- Gupta MK, Guryev OL, Auchus RJ (2003) 5alpha-reduced C21 steroids are substrates for human cytochrome P450c17. *Arch Biochem Biophys* 418:151–160
- Shackleton C, Marcos J, Malunowicz EM, Szarras-Czapnik M, Jira P, Taylor NF, Murphy N, Crushell E, Gottschalk M, Hauffa BP, Cragun DL, Hopkin RJ, Adachi M, Arlt W (2004) Biochemical diagnosis of Antley-Bixler syndrome by steroid analysis. *Am J Med Genet A* 128A:333–339
- Imperato-McGinley J, Guerrero L, Gautier T, Peterson RE (1974) Steroid 5alpha-reductase deficiency in man: an inherited form of male pseudohermaphroditism. *Science* 186:1213–1215
- Rösler A, Kohn G (1983) Male pseudohermaphroditism due to 17 beta-hydroxysteroid dehydrogenase deficiency: studies on the natural history of the defect and effect of androgens on gender role. *J Steroid Biochem* 19:663–674
- Ulick S, Gautier E, Vetter KK, Markello JR, Yaffe S, Lowe CU (1964) An aldosterone biosynthetic defect in a salt-losing disorder. *J Clin Endocrinol Metab* 24:669–672
- Ulick S, Chu MD (1982) Hypersecretion of a new corticosteroid, 18-hydroxycortisol in two types of adrenocortical hypertension. *Clin Exp Hypertens A* 4:1771–1777
- Ulick S, Levine LS, Gunczler P, Zanonato G, Ramirez LC, Rauh W, Rösler A, Bradlow HL, New MI (1979) A syndrome of apparent mineralocorticoid excess associated with defects in the

- peripheral metabolism of cortisol. *J Clin Endocrinol Metab* 49:757–764
36. Shackleton CH, Honour JW, Dillon MJ, Chantler C, Jones RW (1980) Hypertension in a four-year-old child: gas chromatographic and mass spectrometric evidence for deficient hepatic metabolism of steroids. *J Clin Endocrinol Metab* 50:786–802
 37. Stewart PM, Corrie JE, Shackleton CH, Edwards CR (1988) Syndrome of apparent mineralocorticoid excess: a defect in the cortisol-cortisone shuttle. *J Clin Invest* 82:340–349
 38. Phillipov G, Palermo M, Shackleton CH (1996) Apparent cortisone reductase deficiency: a unique form of hypercortisolism. *J Clin Endocrinol Metab* 81:3855–3860
 39. Lavery GG, Walker EA, Tiganescu A, Ride JP, Shackleton CH, Tomlinson JW, Connell JM, Ray DW, Biason-Lauber A, Malunowicz EM, Arlt W, Stewart PM (2008) Steroid biomarkers and genetic studies reveal inactivating mutations in hexose-6-phosphate dehydrogenase in patients with cortisone reductase deficiency. *J Clin Endocrinol Metab* 93:3827–3832
 40. Porter FD, Herman GE (2011) Malformation syndromes caused by disorders of cholesterol synthesis. *J Lipid Res* 52:6–34
 41. Kandutsch AA, Russell AE (1960) Preputial gland tumor sterols 3: a metabolic pathway from lanosterol to cholesterol. *J Biol Chem* 235:2256–2261
 42. Kelley RI, Kratz LE, Glaser RL, Netzloff ML, Wolf LM, Jabs EW (2002) Abnormal sterol metabolism in a patient with Antley-Bixler syndrome and ambiguous genitalia. *Am J Med Genet* 110:95–102
 43. Wassif CA, Brownson KE, Sterner AL, Forlino A, Zerfas PM, Wilson WK, Starost MF, Porter FD (2007) HEM dysplasia and ichthyosis are likely laminopathies and not due to 3 β -hydroxysterol Delta14-reductase deficiency. *Hum Mol Genet* 16:1176–1187
 44. Waterham HR, Koster J, Romeijn GJ, Hennekam RC, Vreken P, Andersson HC, FitzPatrick DR, Kelley RI, Wanders RJ (2001) Mutations in the 3 β -hydroxysterol Delta24-reductase gene cause desmosterolosis, an autosomal recessive disorder of cholesterol biosynthesis. *Am J Hum Genet* 69:685–694
 45. König A, Happle R, Bornholdt D, Engel H, Grzeschik KH (2000) Mutations in the NSDHL gene, encoding a 3 β -hydroxysteroid dehydrogenase, cause CHILD syndrome. *Am J Med Genet* 90:339–346
 46. Lindenthal B, Repgen R, Emons D, Lentze MJ, von Bergmann K, Lütjohann D (2004) Serum lipid analysis confirms the diagnosis of X-linked dominant chondrodysplasia punctata: Conradi-Hünermann-Happle syndrome. *Klin Padiatr* 216:67–69
 47. Krakowiak PA, Wassif CA, Kratz L, Cozma D, Kovárová M, Harris G, Grinberg A, Yang Y, Hunter AG, Tsokos M, Kelley RI, Porter FD (2003) Lathosterolosis: an inborn error of human and murine cholesterol synthesis due to lathosterol 5-desaturase deficiency. *Hum Mol Genet* 12:1631–1641
 48. Irons M, Elias ER, Salen G, Tint GS, Batta AK, Irons M, Elias ER, Salen G, Tint GS, Batta AK (1993) Defective cholesterol biosynthesis in Smith-Lemli-Opitz syndrome. *Lancet* 341:1414
 49. Ruan B, Wilson WK, Pang J, Gerst N, Pinkerton FD, Tsai J, Kelley RI, Whitby FG, Milewicz DM, Garbern J, Schroepfer GJ Jr (2001) Sterols in blood of normal and Smith-Lemli-Opitz subjects. *J Lipid Res* 42:799–812
 50. Shackleton C, Roitman E, Guo LW, Wilson WK, Porter FD (2002) Identification of 7(8) and 8(9) unsaturated adrenal steroid metabolites produced by patients with 7-dehydrosterol- Δ^7 -reductase deficiency (Smith-Lemli-Opitz syndrome). *J Steroid Biochem Mol Biol* 82:225–232
 51. Shackleton CH, Roitman E, Kratz LE, Kelley RI (1999) Equine type estrogens produced by a pregnant woman carrying a Smith-Lemli-Opitz syndrome fetus. *J Clin Endocrinol Metab* 84:1157–1159
 52. Shackleton CH, Roitman E, Kratz L, Kelley R (2001) Dehydrooestriol and dehydropregnanetriol are candidate analytes for prenatal diagnosis of Smith-Lemli-Opitz syndrome. *Prenat Diagn* 21:207–212
 53. Guo LW, Shackleton CH, Wilson WK (2001) Synthesis of ring B unsaturated estriols. Confirming the structure of a diagnostic analyte for Smith-Lemli-Opitz syndrome. *Org Lett* 3:2547–2550
 54. Craig WY, Haddow JE, Palomaki GE, Kelley RI, Kratz LE, Shackleton CH, Marcos J, Stephen Tint G, MacRae AR, Nowaczyk MJ, Kloza EM, Irons MB, Roberson M (2006) Identifying Smith-Lemli-Opitz syndrome in conjunction with prenatal screening for down syndrome. *Prenat Diagn* 26:842–849
 55. Shackleton CHL, Marcos J, Palomaki GE, Craig WY, Kelley R, Lisa E, Kratz LE, Haddow JE (2007) Dehydrosteroid measurements in maternal urine or serum for the prenatal diagnosis of Smith-Lemli-Opitz Syndrome (SLOS). *Am J Med Gen A* 143A:2129–2136
 56. Matabosch X, Ying L, Serra M, Wassif CA, Porter FD, Shackleton C, Watson G (2010) Increasing cholesterol synthesis in 7-dehydrosterol reductase (DHCR7) deficient mouse models through gene transfer. *J Steroid Biochem Mol Biol* 122:303–309

Niemann-Pick C2 Protein Expression Regulates Lithogenic Diet-Induced Gallstone Formation and Dietary Cholesterol Metabolism in Mice

Elisa Balboa · Gabriela Morales · Paula Aylwin ·
Gonzalo Carrasco · Ludwig Amigo ·
Juan Castro · Attilio Rigotti · Silvana Zanlungo

Received: 25 January 2011 / Accepted: 11 October 2011 / Published online: 30 October 2011
© AOCs 2011

Abstract Niemann-Pick C2 protein (NPC2) is a lysosomal soluble protein that is highly expressed in the liver; it binds to cholesterol and is involved in intracellular cholesterol trafficking, allowing the exit of lysosomal cholesterol obtained via the lipoprotein endocytic pathway. Thus, this protein may play an important role in controlling hepatic cholesterol transport and metabolism. The aim of this work was to study the relevance of NPC2 protein expression in hepatic cholesterol metabolism, biliary lipid secretion and gallstone formation by comparing NPC2 hypomorph [NPC2 (h/h)] and wild-type mice fed control, 2% cholesterol, and lithogenic diets. NPC2 (h/h) mice exhibited resistance to a diet-induced increase in plasma cholesterol levels. When consuming the chow diet, we observed increased biliary cholesterol and phospholipid secretions in NPC2 (h/h) mice. When fed the 2% cholesterol diet, NPC2 (h/h) mice exhibited low and high

gallbladder bile cholesterol and phospholipid concentrations, respectively. NPC2 (h/h) mice fed with the lithogenic diet showed reduced biliary cholesterol secretion, gallbladder bile cholesterol saturation, and cholesterol crystal and gallstone formation. This work indicates that hepatic NPC2 expression is an important factor in the regulation of diet-derived cholesterol metabolism and disposal as well as in diet-induced cholesterol gallstone formation in mice.

Keywords Niemann-Pick type C2 protein · Cholesterol · Liver · Biliary lipid secretion · Gallstone disease · Gallbladder

Abbreviations

ABC	ATP-binding cassette
HDL	High density lipoproteins
LDL	Low density lipoproteins
LDLR	LDL receptor
NPC	Niemann-Pick type C
NPC1	Niemann-Pick C1 protein
NPC2	Niemann-Pick C2 protein
NPC2 (h/h) mice	NPC2 hypomorph BALB/c mice
SR-BI	Scavenger receptor class B, type I
VLDL	Very low-density lipoproteins
Wild-type mice	Control wild-type BALB/c mice

Electronic supplementary material The online version of this article (doi:10.1007/s11745-011-3625-2) contains supplementary material, which is available to authorized users.

E. Balboa · G. Morales · P. Aylwin · L. Amigo · J. Castro ·
A. Rigotti · S. Zanlungo (✉)
Departamento de Gastroenterología, Escuela de Medicina,
Facultad de Medicina, Pontificia Universidad Católica de Chile,
Marcoleta 367, Casilla 114-D, Santiago, Chile
e-mail: silvana@med.puc.cl

G. Carrasco
Fundación Hospital Parroquial de San Bernardo, Santiago, Chile

A. Rigotti
Departamento de Nutrición, Diabetes y Metabolismo,
Pontificia Universidad Católica de Chile, Santiago, Chile

S. Zanlungo
Fondap-Center of Genome Regulation, Santiago, Chile

Introduction

Niemann-Pick type C (NPC) disease is a fatal hereditary disorder characterized by the accumulation of cholesterol and other lipids in endosomes and lysosomes [1]. There is mounting evidence that the primary cause of this disease is

failure of low-density-lipoprotein (LDL)-derived cholesterol to exit from the lysosomes, which secondarily causes the build-up of other lipids in different tissues [2]. Genetic mutations in either *Npc1* or *Npc2* are responsible for NPC disease. The major disease locus, *Npc1*, is responsible for 95% of NPC cases. *Npc1* encodes a transmembrane protein localized in lysosomes/late endosomes [1, 3]. *Npc2*, the minor disease locus, is responsible for 5% of cases, and encodes a small cholesterol-binding lysosomal soluble protein [1, 4]. Homozygous mutations in either gene in mice essentially produce indistinguishable cellular and biochemical characteristics as well as the same clinical phenotype, providing strong genetic evidence that the two gene products, Niemann-Pick C1 protein (NPC1) and Niemann-Pick C2 protein (NPC2), function in a coordinated manner [5].

NPC2 was previously identified as HE1, one of the major secretion proteins of the human epididymis [6]. NPC2 binds cholesterol specifically with a stoichiometry of 1:1 [6]; its three-dimensional structure is well known [7] with a pocket structure in which cholesterol is bound [8]. Recent studies have shown that NPC2 recognizes the aliphatic cholesterol chain, while NPC1 binds to the cholesterol 3- β hydroxyl group in its soluble amino terminal domain (NTD) [8–11]. On the other hand, it has been demonstrated that NPC2 or the NPC1 NTD can transfer cholesterol to vesicles in vitro and that the speed of cholesterol transfer to membranes by the NPC1 NTD radically increases in the presence of NPC2 [8, 10, 11]. Together, the data suggest a working model in which NPC2 binds the free cholesterol that is generated after hydrolysis of the cholesterol esters that come to the lysosome from LDL-receptor-mediated endocytosis, and delivers it to NPC1, which mediates transfer through the lysosomal membrane [11].

NPC2 expression has been detected in several cellular types, including fibroblasts, hepatocytes, neurons, and astrocytes [4, 12–14]. We have previously reported that NPC2 is expressed in the liver and is secreted into the plasma and bile, suggesting that NPC2 may have a global function in cholesterol homeostasis [15].

In mammals, the liver plays a critical role in lipoprotein cholesterol metabolism and is a key organ for body cholesterol removal into the bile [16–18]. The receptor-mediated endocytic pathway in which the NPC proteins participate is one of the major uptake mechanisms of lipoprotein cholesterol into the liver, including lipoprotein remnant metabolism [17]. Hepatocytes efficiently eliminate sterols through the bile as unesterified cholesterol and bile acids [18]. Biliary cholesterol disposal is critical not only for normal body cholesterol homeostasis, but also for the pathogenesis of cholesterol gallstone, which is a highly prevalent and costly disease condition in Western countries [19, 20].

We have previously shown that NPC1 plays a critical role in controlling the biliary secretion of plasma lipoprotein-derived cholesterol in mice [21, 22]. Hepatic NPC1 overexpression by adenovirus-mediated gene transfer increases biliary cholesterol secretion in wild-type mice and cholesterol-fed NPC1 (–/–) mice [21]. NPC1 (–/–) mice fed a high-cholesterol diet cannot normally process dietary cholesterol, leading to its accumulation in the liver without increasing biliary cholesterol secretion [21, 22]. Furthermore, NPC1-deficient mice are highly resistant to diet-induced cholesterol gallstones due to impaired secretion of excess cholesterol into the bile [22]. In contrast, no information is available on plasma, hepatic, and biliary lipid physiology and pathophysiology in NPC2-deficient mice fed normal chow and high-cholesterol diets.

The present study was undertaken to analyze the physiological relevance of hepatic NPC2-mediated lipoprotein cholesterol trafficking by comparing cholesterol plasma lipoprotein profiles, hepatic cholesterol metabolism, and biliary lipid secretion between NPC2-deficient hypomorph [NPC2 (h/h)] mice expressing 0–4% residual protein in different tissues and wild-type mice. We also analyzed the role of NPC2 in diet-induced cholesterol gallstone formation by studying biliary lipid secretion, gallbladder bile lipid composition, and gallstone formation in NPC2 (h/h) mice fed a lithogenic diet.

The main findings of this study are that reduced NPC2 expression in NPC2 hypomorph mice leads to increased hepatic cholesterol content and reduced biliary cholesterol and bile acid secretion in mice fed with a lithogenic diet (1.5% cholesterol, 0.5% cholic acid). Moreover, NPC2 (h/h) mice fed with this lithogenic diet are protected against cholesterol gallstone formation. Minor effects were observed when NPC2 (h/h) mice were fed a cholesterol alone-enriched diet. The major conclusion of this work is that hepatic NPC2 expression is an important factor in the regulation of diet-derived cholesterol metabolism and disposal as well as in diet-induced cholesterol gallstone formation in mice.

Materials and Methods

Animals and Diet

BALB/c mice carrying a heterozygous genetic mutation in *Npc2* were generously provided by Dr. Peter Lobel (University of Medicine and Dentistry of New Jersey-Robert Wood Johnson Medical School, Piscataway, NJ, USA). As described by Sleat et al. [5], the homozygous mutant animals are hypomorphs (i.e., they express 0–4% of NPC2 protein depending on the tissue analyzed). The heterozygous mice were bred to produce wild-type controls and homozygous

mutant [NPC2 (h/h)] mice, and the offspring was genotyped as described previously [5]. All mice had free access to water and a chow diet (<0.02% cholesterol; Prolab RMH 3000, PMI Feeds, St. Louis, MO, USA) until they were used for the studies. Most measurements were performed on 7 week-old NPC2 (h/h) mice, thus avoiding the detrimental effects observed in older animals with neurodegenerative disease [5]. For the experiments, 5 week-old NPC2 (h/h) and control male mice were fed the chow diet, or either a 2% cholesterol or bile-acid/low-fat lithogenic diet (chow diet supplemented with 1.5% cholesterol and 0.5% cholic acid) for 10 days or 2 weeks. In some experiments, 7 week-old NPC2 (h/h) and control male mice were fed with the lithogenic diet for 14 days. All animals were fasted for 2 h before bile, blood, and liver sampling.

All protocols were approved by our institution's review board for animal studies and were in agreement with the US Public Health Service Policy on Humane Care and Use of Laboratory Animals recommended by the Institute for Laboratory Animal Research in its Guide for Care and Use of Laboratory Animals.

Hepatic and Gallbladder Bile, Blood and Liver Sampling

Mice were anesthetized by intraperitoneal injection of ketamine and xylazine at 80–100 and 5–10 mg/kg, respectively. The abdomen was opened, the cystic duct was ligated, and a common bile duct fistula was performed with a polyethylene catheter. Hepatic bile was collected for 30 min, while mice remained hydrated, warm, and stable [22], and then blood, liver, and gallbladder were removed. The liver was immediately frozen at -80°C . The gallbladder was opened and bile was removed. When present, gallstones were separated from the bile by low-speed centrifugation. Some fresh samples were subjected to biochemical analyses, and the remaining bile was frozen at -20°C until required.

Alanine Aminotransferase Analysis

Serum alanine aminotransferase (ALT) was measured by ALAT kit (Kovalent, Rio de Janeiro, Brazil) following manufacturer's instructions.

Plasma, Hepatic, and Biliary Lipid Analyses

Plasma lipoprotein separation was performed by fast protein liquid chromatography gel filtration using a Superose 6 column [23]. Total plasma and lipoprotein cholesterol were measured as described previously [23]. Hepatic cholesterol content was analyzed after lipid extraction [22]. Hepatic bile and gallbladder bile cholesterol were measured by an

enzymatic method [24], phospholipids were assessed by a colorimetric method [25], and bile acids were determined by an enzymatic method [26]. Hepatic triglyceride content was determined using commercial kits (Sigma Chemicals Co, St. Louis, USA) according to the manufacturer's instructions. Gallbladder bile cholesterol saturation was calculated based on critical tables [27] using biliary lipid measurements performed at 10 days of feeding with the lithogenic diet and before mice developed cholesterol gallstones.

Quantitative Real-Time Reverse Transcriptase-Polymerase Chain Reaction Assay

Total RNA was extracted from liver, pretreated with DNase I (Invitrogen, Carlsbad, CA, USA), and then reverse-transcribed to cDNA using random primers (Invitrogen). The real-time polymerase chain reaction (PCR) was performed by SYBR Green I chemistry (SYBR Green PCR Master Mix, Applied Biosystems, Naerum, Denmark) with 25 ng of template cDNA and each gene-specific primer present at $5\ \mu\text{M}$ using the ABI 7500 sequence detection system (Applied Biosystems). The PCR conditions and gene-specific primer sequences are listed in Table 1. The mRNA levels were quantified using the mathematical model described by Pfaffl et al. [28]. The mRNA levels of different genes were normalized to those of 18S rRNA.

Gallstone Formation

After 2 weeks of consuming the lithogenic diet, fresh gallbladder bile was taken from mice and evaluated for the presence of microscopic and macroscopic features of gallstone formation, according to criteria described by Wang et al. [29].

Statistics

The statistical significance of differences between the means of the experimental groups was evaluated with Student's *t* test and a 95% confidence interval using Prism 5.00 (GraphPad, La Jolla, CA, USA). A difference was considered to be statistically significant at $p < 0.05$.

Results

Analyses of Plasma Lipoprotein Cholesterol, Hepatic Cholesterol and Triglyceride Levels in Wild-Type and NPC2 (h/h) Mice Fed Control, 2% Cholesterol, and Lithogenic Diets

Lipid measurements were performed in 7 week-old NPC2 (h/h) mice since they are at steady state during the first

Table 1 Gene-specific primer sequences for reverse transcription quantitative PCR (RT-QPCR)

Gene	Forward primer	Reverse primer	Accession number
<i>Abca1</i>	CGTTTCCGGGAAGTGTCTTA	GCTAGAGATGACAAGGAGGATGGA	NM_013454.3
<i>Ldlr</i>	TGGCTGTTCCACATCTG	CTCGTCAATATCTTCACACCTG	NM_010700.2
<i>Srbi</i>	CTCCCAGACATGCTTCCCA	CCGTTCCATTTGTCCACCA	NM_016741.1
<i>Npc1</i>	TCTCTGAGACCTCGGCATTT	CAGGATGTCCAGACGGTTTT	NM_008720.2
<i>Mttp</i>	TGACATCCTTTACTCTGGCTCTG	CTTCAATCACCACCTGACTACC	NM_008642.1
<i>Pctp</i>	TGGCATACTGGGAAGTGAAG	GACTTCTCGGGAAACTGAGG	NM_008796.2
<i>Hmgcr</i>	AAGTACATTCTGGGTATTGCTG	AAGCCTGTCAGTTCTTTGTC	NM_008255.2
<i>Cyp7a1</i>	CTTCATCACAAACTCCCTGTC	GTCCAAATGCCTTCGCAG	NM_007824.2
<i>Cyp27</i>	GATCTTCATCGCACAAGGAG	GATAACCTCGTTTAAGGCATCC	NM_024264
<i>Acat2</i>	CTACAAGCAAGACCCAAGAG	CATGTGGTAGATGGTTCCGG	NM_146064.1
<i>Abcb11</i>	AATAGACAGGCAACCCGT	GAGAAGGATAATGGAAGGTCAC	NM_021022.3
<i>Abcb4</i>	GATCAGTGCTCTTAGATGG	ATAGGCGATGTTCTCTG	NM_008830.2
<i>Abcg5</i>	GGAGAACATTGAAAGAGCAC	GTTACTCGCCTCAGCAG	NM_031884.1
<i>Abcg8</i>	GTCTCCAAATGTCACTCGG	GCAAAGAAATAAGGACCAGCA	NM_026180.2
<i>18S</i>	GTAACCCGTTGAACCCCAT	CCATCCAATCGGTAGTAGCG	NR_003278

Thermal cycling involved 35 cycles at 94 °C for 30 s, 55 °C for 30 s, and 72 °C for 30 s. The melting curves were performed according to the manufacturer's procedure

7 weeks of life and before detrimental effects were observed in older animals due to the neurodegenerative disease [5]. The total plasma cholesterol levels in wild-type and NPC2 (h/h) mice in response to these diets are listed in Table 2. The concentrations of total plasma cholesterol were slightly higher in NPC2 (h/h) mice fed the control diet than in wild-type animals. Feeding the mice for 2 weeks with the 2% cholesterol and the lithogenic diets increased the plasma cholesterol concentration in wild-type mice by 14 and 37%, respectively, relative to those fed the control diet. In contrast, no increase in plasma cholesterol was detected in NPC2 (h/h) mice fed with the 2% cholesterol or lithogenic diets (Table 2). We also measured plasma cholesterol levels after 3, 7 and 10 days of feeding with the lithogenic diet (Table 1, Supplementary material). Consistent with our previous results, wild-type mice increased their plasma cholesterol in response to lithogenic diet and days of diet-feeding, whereas this response was not observed in NPC2 (h/h) mice.

The lipoprotein cholesterol profiles of wild-type and NPC2 (h/h) animals fed control, 2% cholesterol, and lithogenic diets are shown in Fig. 1. When consuming the control diet, the amount of cholesterol in the intermediate-density lipoprotein and LDL fractions was slightly increased in NPC2 (h/h) mice compared to wild-type animals (Fig. 1a). Wild-type mice responded as expected to the cholesterol-rich diets [21], exhibiting a greater amount of cholesterol transported in large lipoproteins, presumably in the VLDL fraction, and a slight decrease in cholesterol associated with HDL fractions, which is seen more clearly

after using the lithogenic diet. When consuming the 2% cholesterol diet, the amount of cholesterol present in the VLDL fraction (Fig. 1b) was lower in NPC2 (h/h) mice than in wild-type mice. When consuming the lithogenic diet, NPC2 (h/h) mice exhibited a significant decrease in the amount of cholesterol transported in VLDL and HDL fractions (Fig. 1c).

Hepatic cholesterol concentrations in wild-type and NPC2 (h/h) animals fed the control, 2% cholesterol, and lithogenic diets are listed in Table 2. As expected, when consuming the control diet, the amount of hepatic cholesterol was significantly higher in NPC2 (h/h) mice than in wild-type mice. The difference between the NPC2 (h/h) mice and wild-type mice became even more pronounced when consuming the cholesterol-rich (2% cholesterol and lithogenic) diets. Unlike the wild-type animals, which maintained the liver size within the normal range, NPC2 (h/h) animals developed significant hepatomegaly when fed cholesterol-rich diets (Table 2). Hepatic triglyceride levels showed a decrease under all diets in NPC2 (h/h) mice compared with wild-type mice (Table 2), indicating that NPC2 (h/h) mice specifically accumulate cholesterol rather than triglycerides in the liver.

As expected, liver samples from NPC2 (h/h) animals showed signs of hepatic inflammation and damage as indicated by histological analysis and increased serum ALT levels (Fig. 2; Table 3). Normal portal and lobular architecture was observed in livers of wild-type mice fed the chow-diet, whereas mild lobular inflammatory activity

Table 2 Effect of 2% cholesterol and lithogenic diet feeding on plasma cholesterol, hepatic cholesterol and triglyceride levels and biliary lipid secretion in wild-type and NPC2 (h/h) mice

Strain	Diet	Plasma cholesterol (mg/dL)	Liver weight (g)	Hepatic cholesterol (mg/g liver)		Hepatic triglycerides (mg/g liver)		Biliary lipid secretion (nmol/min/g liver)		Phospholipids
				Unesterified	Esterified	Cholesterol	Triglycerides	Cholesterol	Bile salts	
Wild-type	Chow	98.6 ± 2.9	1.3 ± 0.1	1.5 ± 0.2	1.4 ± 0.1	8.9 ± 0.6	0.7 ± 0.1	47.0 ± 5.4	7.6 ± 0.6	
	2% cholesterol	112.3 ± 5.6 ^a	1.4 ± 0.1	1.8 ± 0.3	5.1 ± 0.6 ^a	17.3 ± 3.9	2.3 ± 0.3 ^a	47.9 ± 8.3	9.7 ± 1.5	
	Lithogenic	135.3 ± 12.3 ^a	1.4 ± 0.1	5.2 ± 0.2 ^a	6.8 ± 0.4 ^a	10.5 ± 1.7	14.4 ± 2.2 ^a	248.7 ± 28.9 ^a	74.9 ± 13.9 ^a	
NPC2 (h/h)	Chow	113.0 ± 2.1 ^a	1.2 ± 0.1	8.3 ± 0.5 ^a	7.9 ± 0.4 ^a	5.7 ± 1.0 ^a	1.2 ± 0.1 ^a	62.6 ± 6.2	11.6 ± 1.0 ^a	
	2% cholesterol	102.6 ± 7.5	1.7 ± 0.1 ^d	20.3 ± 1.6 ^{b,d}	21.9 ± 0.8 ^{b,d}	8.1 ± 1.1	2.2 ± 0.3 ^d	46.4 ± 9.6	17.1 ± 3.3 ^{b,d}	
	Lithogenic	114.2 ± 18.8	1.7 ± 0.1 ^d	26.9 ± 1.2 ^{c,d}	27.0 ± 1.1 ^{c,d}	3.7 ± 1.3 ^c	7.4 ± 1.3 ^{c,d}	215.8 ± 32.6 ^d	82.6 ± 10.6 ^d	

Values are expressed as means ± SEM. Measurements were performed in 5–10 mice per group

^a Significantly different from wild-type mice fed with the control diet

^b Significantly different from wild-type mice fed with the 2% cholesterol diet

^c Significantly different from wild-type mice fed with the lithogenic diet

^d Significantly different from NPC2 (h/h) mice fed with the control diet

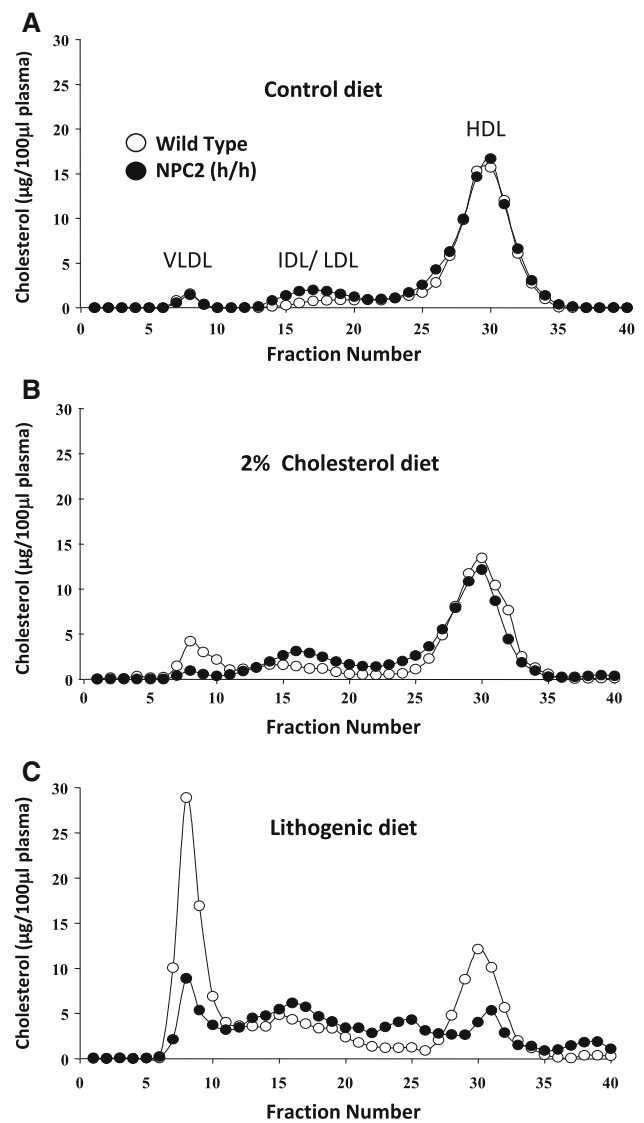


Fig. 1 Plasma lipoprotein cholesterol profile in wild-type and NPC2 (h/h) mice. Plasma lipoproteins were separated by fast protein liquid chromatography and then cholesterol content of each fraction was determined. The lipoprotein profile was analyzed for the following three dietary conditions: control (a), 2% cholesterol (b), and lithogenic (c) in wild-type mice (open circles) and NPC2 (h/h) mice (filled circles)

was observed when they were fed the high-cholesterol diets (Fig. 2, arrowheads). As expected, numerous foamy cells, presumably macrophages, were observed in sinusoids of livers from NPC2 (h/h) mice (arrows in Fig. 2). In addition, an increase of the liver damage-related marker ALT was detected in serum of lithogenic-diet fed-NPC2 (h/h) mice, being more dramatically elevated in older animals (Table 3). Interestingly, 14 days of diet are required to significantly increase ALT levels in both NPC2 (h/h) and wild-type mice, without effect at earlier time points (Table 3).

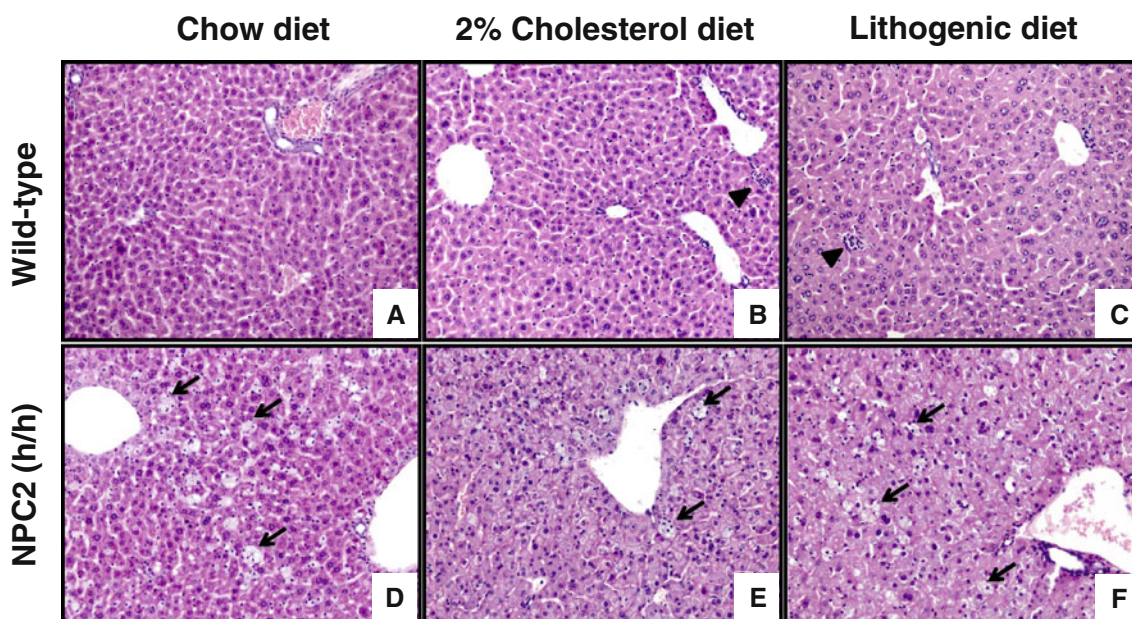


Fig. 2 Hepatic tissue damage in wild-type and NPC2 (h/h) mice. Liver sections were analyzed by hematoxylin and eosin staining. 20× magnifications of livers from wild-type (*upper panel*) and NPC2 (h/h) (*lower panel*) mice fed with chow (**a, d**), 2% cholesterol (**b, e**) and lithogenic diets (**c and f**) are shown. Inflammatory foci (*arrowheads*) and lipid-loaded cells (*arrows*) are indicated

Table 3 Effect of 2% cholesterol and lithogenic diet feeding on serum alanine aminotransferase levels in wild-type and NPC2 (h/h) mice

Strain and age	Diet	Serum ALT (U/L)			
		3 days	7 days	10 days	14 days
Wild-type 5 week-old	Chow	ND	ND	ND	22.7 ± 5.6
	2% cholesterol	ND	ND	ND	30.7 ± 5.7
	Lithogenic	9.4 ± 1.0	16.8 ± 3.2	21.8 ± 2.2	293.7 ± 106 ^a
NPC2 (h/h) 5 week-old	Chow	ND	ND	ND	115.7 ± 28.3 ^a
	2% cholesterol	ND	ND	ND	56.2 ± 15.7
	Lithogenic	11.5 ± 1.6	14.2 ± 4.8	10.9 ± 1.1 ^b	835.2 ± 392 ^c
Wild-type 7 week-old (n: 4)	Lithogenic	ND	ND	ND	258.6 ± 128.0
NPC2 (h/h) 7 week-old (n: 4)	Lithogenic	ND	ND	ND	2781 ± 1,407 ^d

Values are expressed as means ± SEM. Measurements were performed in 5 mice per group, except otherwise indicated. The mice age at onset of treatment with the diets is indicated. 5 week-old wild-type and NPC2 h/h mice were fed with chow and cholesterol diets for 14 days and with the lithogenic diet for 3, 7, 10, and 14 days. 7 week-old wild-type and NPC2 h/h mice were fed with the lithogenic diet for 14 days

ND not determined

^a Significantly different from 5 week-old wild-type mice fed with the control diet

^b Significantly different from 5 week-old wild-type mice fed with the lithogenic diet

^c Significantly different from 5 week-old NPC2 h/h mice fed with the control diet

^d Significantly different from 7 week-old wild-type mice fed with the lithogenic diet

Biliary Lipid Secretion and Gallbladder Bile Lipid Composition in Wild-Type and NPC2 (h/h) Mice Fed the Control, 2% Cholesterol, and Lithogenic Diets

The results for lipid secretion from the liver into bile in wild-type and NPC2 (h/h) mice are shown in Table 2. When consuming the control diet, cholesterol and phospholipid, but not bile salt, secretions were slightly but

significantly higher in NPC2 (h/h) animals than in wild-type animals. No differences in biliary cholesterol and bile salt secretion were found between NPC2 (h/h) and wild-type mice consuming the 2% cholesterol diet; both exhibited similar increases compared to animals fed the control diet. However, NPC2 (h/h) mice exhibited a greater increase in phospholipid secretion. Wild-type animals fed the lithogenic diet exhibited 20-, 10-, and 5-fold increases

in cholesterol, phospholipid, and bile-salt secretion, respectively (Table 2). However, the NPC2 (h/h) mice responded more moderately to the lithogenic diet than did their wild-type counterparts, increasing their cholesterol and phospholipid secretions by six- and seven-folds, respectively, and their bile salt secretion by threefold.

We subsequently analyzed lipid concentrations in the gallbladder bile in wild-type and NPC2 (h/h) mice fed control, 2% cholesterol, and lithogenic diets (Table 4). Cholesterol, phospholipid, and bile salt concentrations in the gallbladder bile did not differ between wild-type and NPC2 (h/h) mice fed the control diet. When consuming the 2% cholesterol diet, the cholesterol concentration was lower and the phospholipid concentration was higher in NPC2 (h/h) mice than in wild-type mice (Table 4). When fed the lithogenic diet, the cholesterol, bile salt, and phospholipid concentrations were 37, 39, and 16%, respectively, lower in NPC2 (h/h) mice than in wild-type mice (Table 4).

Hepatic Gene Expression in Wild-Type and NPC2 (h/h) Mice Fed the Control, 2% Cholesterol and Lithogenic Diets

The differences observed in lipoprotein profiles, biliary lipid secretion, and lipid concentrations in the gallbladder bile of the NPC2 (h/h) mice may be related to changes in the expression of key genes that participate in the hepatic transport and metabolism of lipids. Therefore, we measured the expression of several lipid-related genes in the liver.

The expressions of *Ldlr* and *Srbi* did not differ significantly between wild-type and NPC2 (h/h) mice under any of the dietary conditions (Fig. 3). *Abca1* mRNA levels increased significantly only in NPC2 (h/h) mice fed the lithogenic diet. The hepatic expression of *Npc1* was lower in NPC2 (h/h) mice fed the lithogenic diet compared to their wild-type counterparts (Fig. 3). *Mttp* mRNA levels were not significantly different between wild-type and NPC2 (h/h) mice fed the control and cholesterol-enriched diets. Interestingly, however, the hepatic expression of *Pctp* was dramatically increased in NPC2 (h/h) mice fed the 2% cholesterol and lithogenic diets.

As expected from Lee et al. [30], the expression of *Cyp7a1* was significantly lower in both wild-type and NPC2 (h/h) mice fed the lithogenic diet than in mice fed the control diet (Fig. 3). On the other hand, *Hmgcr* expression decreased under the lithogenic diet condition in both wild-type and NPC2 (h/h) mice, with this change being smaller in the NPC2 (h/h) mice (Fig. 3). *Cyp27* and *Acat2* expression did not vary significantly with the animals' genetic background or dietary manipulation (Fig. 3).

Biliary lipid secretion is mediated by different members of the ABC transporter superfamily. Given that bile salt secretion increases in animals fed the lithogenic diet, it was expected that the expression of the bile-salt transporter *Abcb11* (*Bsep*) would also increase [30]. A small such response was observed in wild-type mice, but was absent in the NPC2 (h/h) mice (Fig. 3). Furthermore, the level of *Abcb11* expression was significantly lower in NPC2 (h/h) animals fed the 2% cholesterol and lithogenic diets than in their wild-type counterparts. An increase in the expression

Table 4 Effect of 2% cholesterol and lithogenic diet feeding on gallbladder bile lipid composition and cholesterol saturation index in wild-type and NPC2 (h/h) mice

Strain and age	Diet	Gallbladder bile lipid composition (mmol/L)			Saturation index ^a (%)
		Cholesterol	Bile salts	Phospholipids	
Wild-type 5 week-old	Chow	2.1 ± 0.3	131.5 ± 11.5	16.4 ± 1.4	28.1 ± 2.1
	2% cholesterol	5.7 ± 0.5 ^b	118.4 ± 16.1	16.5 ± 2.1	83.6 ± 9.7 ^b
	Lithogenic	9.4 ± 0.9 ^b	222.2 ± 26.8 ^b	36.4 ± 3.9 ^b	91.1 ± 1.7 ^b
NPC2 (h/h) 5 week-old	Chow	2.3 ± 0.2	116.4 ± 8.7	16.1 ± 1.1	39.4 ± 4.4 ^b
	2% cholesterol	3.8 ± 0.4 ^{c,e}	106.4 ± 9.7	27.9 ± 3.0 ^{c,e}	52.4 ± 6.0 ^c
	Lithogenic	5.9 ± 0.9 ^{d,e}	136.6 ± 15.7 ^d	30.6 ± 3.1 ^e	51.2 ± 4.3 ^d
NPC2 (h/h) 7 week-old (n:3)	Lithogenic	4.2 ± 0.3	252.6 ± 20.8	25.4 ± 2.2	34.2 ± 2.2

Values are expressed as means ± SEM. Measurements were performed in 5–10 mice per group, except otherwise indicated. The mice age at onset of treatment with the diets is indicated

^a Gallbladder bile cholesterol saturation index

^b Significantly different from wild-type mice fed with the control diet

^c Significantly different from wild-type mice fed with the 2% cholesterol diet

^d Significantly different from wild-type mice fed with the lithogenic diet

^e Significantly different from NPC2 (h/h) mice fed with the control diet

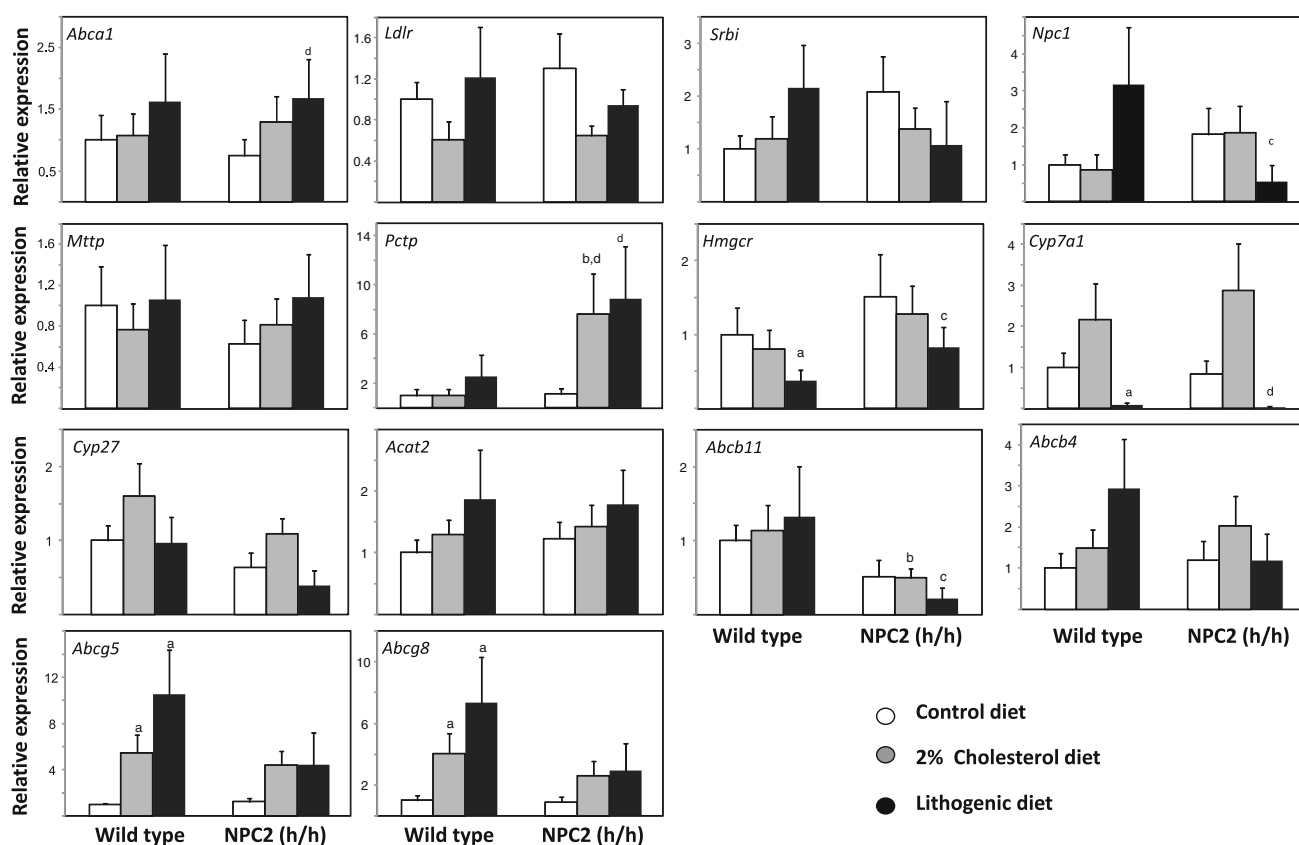


Fig. 3 Hepatic gene expression in wild-type and NPC2 (h/h) mice fed with cholesterol-rich diets. Five wild-type and five NPC2 (h/h) mice were included in each diet group. mRNA levels were normalized to 18S rRNA and expressed as increases relative to the wild-type animals fed with the control diet. The following genes were analyzed: lipoprotein transporters and receptors *Abca1*, *Ldlr*, and *Srbi*; lysosomal cholesterol transport protein *Npc1*; VLDL packing *Mttp* and phospholipid transfer *Pctp* proteins; cholesterol metabolism-related hepatic enzymes *Hmgcr*, *Cyp7a1*, *Cyp27*, *Acat2*, and;

canalicular transporters, *Abcb11*, *Abcb4*, *Abcg5* and *Abcg8*. The statistical analysis of relative expression results in real-time PCR was evaluated using the relative expression software tool (REST, described by Pfaffl et al. [28]). ^aSignificantly different from wild-type mice fed with the control diet; ^bSignificantly different from wild-type mice fed with the 2% cholesterol diet; ^cSignificantly different from wild-type mice fed with the lithogenic diet; ^dSignificantly different from NPC2 (h/h) mice fed with the control diet

of *Abcb4*, which encodes a protein that transports phospholipids into bile, was observed in wild-type mice, but this increase was not significant. Finally, ABCG5/G8 is a heterodimer that transports cholesterol into bile; its expression is expected to be higher when consuming cholesterol-rich diets [31]. This response was observed for the 2% cholesterol and lithogenic diets in wild-type mice but not in NPC2 (h/h) mice (Fig. 3).

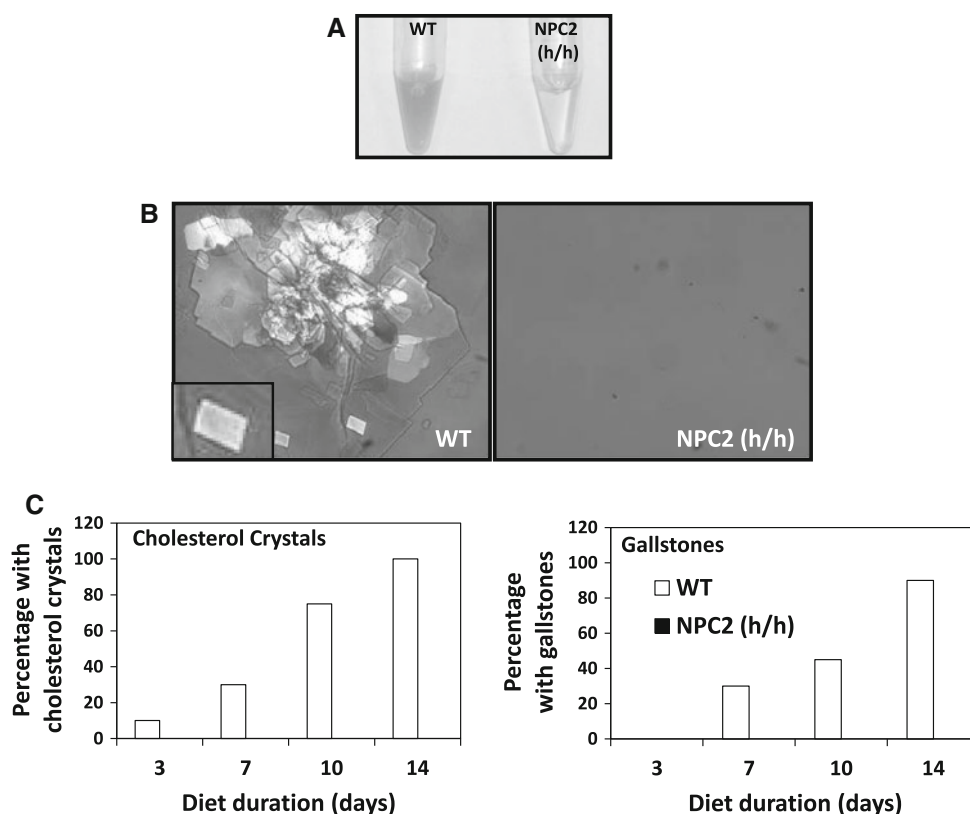
Effect of the Lithogenic Diet on the Formation of Cholesterol Crystals and Gallstones in Wild-Type and NPC2 (h/h) Type Mice

BALB/c mice are gallstone-susceptible when they are subjected to a high-cholesterol and bile acid diet and nearly 100% of them develop cholesterol gallstones after 2 weeks of feeding this diet [22, 32]. We decided to measure gallbladder bile saturation index after 10 days of feeding with

the lithogenic diet before cholesterol crystal or gallstone formation to avoid difficulties in obtaining reliable biliary lipid measurements due to the presence of an excess of cholesterol crystals, which increase at longer dietary intervention (Table 4). The NPC2 (h/h) and wild-type mice exhibited a mean saturation index of 51.2 and 91.1%, respectively (Table 4), indicating that the gallbladder bile of wild-type mice was very close to saturation with cholesterol, while that of the NPC2 (h/h) mice remained unsaturated. When consuming the lithogenic diet, gallbladder bile from NPC2 (h/h) mice after a thaw/freeze cycle was notably translucent, while that from wild-type mice was opalescent (Fig. 4a).

After 14 days on the lithogenic diet, 100 and 90% of wild-type mice exhibited cholesterol crystals and gallstones, respectively (Fig. 4a, b). Furthermore, wild-type animals showed a time-dependent increase in both cholesterol crystals and gallstones between 3 and 14 days of

Fig. 4 Biliary cholesterol crystallization and gallstone formation in wild-type and NPC2 (h/h) mice fed with a lithogenic diet. **a** Macroscopic appearance of gallbladder bile in wild-type and NPC2 (h/h) mice fed the lithogenic diet. The photograph of 0.6 ml tubes containing bile from a single mouse in each group was taken after one freeze/thaw cycle. **b** Polarizing-light microscopy of gallbladder bile from lithogenic diet-fed wild-type and NPC2 (h/h) mice (magnification 20 \times). **c** Prevalence of gallbladder bile cholesterol crystals and gallstones in wild-type and NPC2 (h/h) mice that were fed with the lithogenic diet for 3, 7, 10, and 14 days ($n = 8$ –10 mice in each experimental group)



feeding with this diet (Fig. 4c). On the other hand, NPC2 (h/h) mice did not have either cholesterol crystals or gallstones in the gallbladder after consuming the lithogenic diet (Fig. 4c). This indicates that the NPC2 (h/h) mice were highly resistant to cholesterol cholelithiasis.

Although we decided to perform most of the lipid measurements in 7 week-old NPC2 (h/h) mice before detrimental effects were observed in older animals due to the neurodegenerative disease, we also included a group of older animals (fed for 14 days with the lithogenic diet starting at 7 weeks of age) to analyze gallbladder bile lipid concentrations and gallstone formation. We found that bile in the NPC2 (h/h) mice remained unsaturated (Table 4). Unfortunately, gallbladders of wild-type mice were filled with cholesterol stones, thus we were unable to obtain enough bile for measuring biliary lipid levels. Notably, older NPC2 (h/h) mice showed a higher increase in ALT levels compared to younger animals fed with the same diet (Table 3). Moreover, older NPC2 (h/h) mice did not have cholesterol crystals or gallstones in the gallbladder after consuming the lithogenic diet, whereas all wild-type mice formed cholesterol crystals and gallstones. Our results show that age is not a relevant factor for gallstone formation in these mice and confirm that older NPC2 h/h mice fed with this lithogenic diet remain protected against cholesterol gallstone formation.

Discussion

This study demonstrates that hepatic NPC2 plays important roles in regulating dietary cholesterol transport and biliary lipid secretion. In addition, NPC2 is critical in the pathogenesis of diet-induced gallstone formation in mice, suggesting its potential role during gallstone formation in humans.

Total plasma cholesterol was not different between control and Npc2 (h/h) mice except on the chow diet. Under this latter condition, plasma cholesterol levels were slightly higher in NPC2 (h/h) mice than in wild-type animals, which was not related to changes in the expression of genes associated with lipoprotein cholesterol metabolism, such as *Ldlr*, *Srbi*, or *ApoA1*. Interestingly, NPC2 is found in plasma [15] and may be involved in the transport or metabolism of plasma cholesterol. However, it is not known whether NPC2 present in plasma is functional at neutral pH or whether it is found free or as a component of a plasma lipoprotein complex. Studies in primary astrocytes have shown that most sterols are secreted separately from NPC2 into the surrounding medium, suggesting that secreted NPC2 is not primarily associated with cholesterol-containing particles [13]. Further studies are required to determine how NPC2 deficiency affects cholesterol levels in plasma.

The lower plasma cholesterol detected in NPC2 (h/h) mice fed the 2% cholesterol and lithogenic diets compared to wild-type mice is not attributable to intestinal cholesterol absorption deficiency. Indeed, cholesterol-enriched diets induced a dramatic increase in hepatic cholesterol content in NPC2 (h/h) mice relative to wild-type mice. In accordance with our results, recent studies have established that NPC2 expression is not required for cholesterol absorption in the intestine under a chow diet [33]. The inability of the NPC2 (h/h) mice to increase VLDL cholesterol levels upon receiving a cholesterol-enriched diet suggests that dietary cholesterol is not available for hepatic VLDL packaging and subsequent secretion into the plasma in the NPC2 (h/h) mice. No alterations were found in *Mttp* expression in the NPC2 (h/h) mouse liver, suggesting that a deficiency in cholesterol availability, rather than a global VLDL production defect, is actually limiting cholesterol incorporation in VLDL particles. In addition, our results show that NPC2 (h/h) mice accumulate less triglyceride in livers under all diets, which may also impair VLDL particle assembly. In agreement with our results, it has recently been shown decreased hepatic and serum triglyceride levels in NPC1-deficient mice [34].

The dramatic increase in hepatic unesterified cholesterol content observed in NPC2 (h/h) mice under the 2% cholesterol and lithogenic diets is consistent with the proposed role for NPC2 in cholesterol trafficking from the endosomal endocytic pathway [11]. Although the hepatic cholesterol of wild-type mice also increased with a dietary challenge of cholesterol, changes in free cholesterol were small and a larger contribution was due to the accumulation of hepatic cholesteryl esters.

Biliary lipid concentration and secretion were mainly unaffected under physiological conditions in NPC2 (h/h) mice when compared to wild-type mice. Similar results were obtained with NPC1 (–/–) mice [21]. Additional sources of cholesterol, such hepatic neosynthesis and uptake from HDL, may be compensating for the impaired contribution of lipoprotein endocytosis to the pool of metabolically active cholesterol in livers of NPC2 (h/h) mice. Indeed, rates of cholesterol synthesis are increased in the liver of NPC1 (–/–) mice [35]. Our results show a trend to higher *Hmgcr* mRNA levels in NPC2 (h/h) mice, which suggests that hepatic cholesterol neosynthesis is somewhat increased.

Surprisingly, even though unesterified cholesterol was retained in lysosomes in NPC2 (h/h) mice, no impairments in biliary cholesterol and bile salt secretions were found in NPC2 (h/h) mice after feeding the 2% cholesterol diet. This normal biliary lipid phenotype may be due to the hypomorphic feature of the NPC2-deficient model used in this study, and thus residual NPC2 may be able to export some of the lysosomal cholesterol

obtained from the diet to be secreted into the bile. Support for this hypothesis comes from our observation that NPC2 (h/h) mice are able to convert a fraction of dietary cholesterol into hepatic cholesteryl esters. In contrast, NPC1 (–/–) mice fed a 2% cholesterol diet exhibited a more marked phenotype, with less cholesterol esterification as well as impaired biliary cholesterol and bile salt secretion [21]. Another possibility that cannot be totally excluded is that NPC1 and NPC2 do not have exactly the same function in cholesterol transport from the endocytic pathway, as recently suggested for other lysosomal cargo [36].

Interestingly, we found that biliary phospholipid secretion was greater in NPC2 (h/h) mice fed with normal chow and high-cholesterol diets than in similarly fed wild-type mice. In addition, gallbladder bile phospholipid concentration was increased in NPC2 (h/h) mice fed the 2% cholesterol diet compared to wild-type mice on the same diet. The reasons for these differences are unclear, but it could be related with the increased mRNA levels of the *Pctp* phospholipid transporter observed in livers of NPC2 (h/h) mice that were fed the 2% cholesterol-rich and lithogenic diets, suggesting a facilitated phospholipid delivery to the canalicular pole. However, studies of mice with homozygous disruption of the *Pctp* gene have shown normal phospholipid secretion into bile [37]. Although disruption of the *Pctp* gene did not affect the output of phospholipid, bile salts and cholesterol into bile of *Pctp* lacking mice fed a chow diet, the secretion of these biliary lipids was impaired when these mice were fed a high-fat, high-cholesterol lithogenic diet [38]. This may indicate that under conditions of a dietary challenge phosphatidylcholine transfer protein (PCTP) is critical in the trafficking of the biliary components to the canalicular membrane. PCTP plays a variety of regulatory effects on lipid and glucose metabolism [39–41]. Indeed, its expression is up-regulated by peroxisome proliferator-activated receptor (PPAR) α , a key transcription factor for global metabolism regulation [41]. Further studies are required to determine the consequences of *Pctp* up-regulation in the liver of NPC2 (h/h) mice. No significant difference was found in the mRNA expression levels of *Abcb4* in the livers of NPC2 (h/h) mice.

The decrease detected in cholesterol in the gallbladder bile of NPC2 (h/h) mice consuming the 2% cholesterol diet was not correlated with a decrease in biliary cholesterol secretion from the liver. We cannot rule out that this phenotype is related to a direct function of NPC2 in bile, perhaps as a solubilizing factor or an inhibitor of cholesterol transport from the bile into the gallbladder epithelium. In fact, it is known that active cholesterol transport into the epithelium occurs in the gallbladder by a process that is probably regulated by proteins [42].

The use of a lithogenic diet in mice produces an overload of dietary cholesterol as well as bile salts in the liver. Wild-type animals respond to this diet with an increase in biliary secretion and concentration of cholesterol, bile salts, and phospholipids. These changes are correlated with increased expression of *Abcg5/8* cholesterol transporters and a tendency toward an increase in the expression of *Abcb11* bile salt and *Abcb4* phospholipid transporters (Fig. 3). This response is strongly diminished in NPC2 (h/h) mice, as clearly indicated by the decrease in biliary cholesterol secretion and concentration in NPC2 (h/h) compared with wild-type mice fed the lithogenic diet as well as the lack of regulation in the mRNA levels of *Abcg5/8*. In accordance with our results, it has been shown that NPC1 and NPC2 cells synthesize less oxysterols, the endogenous LXR ligands that induce cholesterol efflux and the expression of cholesterol transporters such as ABCG5/G8 [43, 44].

The expression levels of several additional lipid-related genes were analyzed in the livers of NPC2 (h/h) mice. The mRNA levels of *Acat2*, which encodes an enzyme that converts free cholesterol into cholesterol esters, did not change under any condition. In fact, this gene does not seem to be transcriptionally regulated in the liver of either wild-type or NPC1 mice faced with a dietary cholesterol overload [22]. As expected, *Cyp7A1* mRNA levels decreased in wild-type and NPC2 (h/h) mice fed the bile acid-rich lithogenic diet. *Npc1* levels were decreased in the liver of NPC2 (h/h) mice fed a lithogenic diet. Interestingly, a reciprocal regulation in the levels of NPC1 in the NPC2 (h/h) mice was not found, whereas in various models NPC2 increases in the absence of NPC1 [13, 15]. Further studies are required to elucidate the molecular mechanisms involved in this regulation. Hepatic *Abca1* mRNA levels were increased in NPC2 (h/h) mice fed the lithogenic diet; however, ABCA1 protein regulation in murine liver seems to occur mainly via posttranscriptional mechanisms and has been shown to be increased in NPC1 deficiency [45]. Further studies are required to determine whether hepatic ABCA1 protein levels are regulated in NPC2 (h/h) mice.

Since lithogenic diet-fed NPC2 (h/h) mice exhibited signs of hepatotoxicity as indicated by increased serum alanine aminotransferase and abundance of foamy hepatic cells, it cannot be completely rule out the influence of liver damage in some of the lipid metabolism abnormalities observed in these mice. However, bile flow (data not shown) as well as phospholipid secretion were normal, indicating that some biliary secretory pathways remained functional. Our results differ with those recently published by Yamanashi et al. [46]. They found a decrease in biliary cholesterol secretion in mice fed a control diet with decreased expression of NPC2 mediated by recombinant adenovirus containing a shRNA against NPC2. This discrepancy may be due to differences in the model (transient

decrease in NPC2 expression with adenovirus versus stable manipulation in KO mice) or the mouse strain used.

The dramatic reduction in biliary cholesterol crystallization found in BALB/c NPC2 (h/h) mice fed with a lithogenic diet was correlated with reduced biliary cholesterol secretion in these animals. Our results further show that NPC2 expression regulates cholesterol concentration and saturation index in the gallbladder bile, which are critical factors in initiating the formation of cholesterol crystals. A remarkably finding was that the NPC2 (h/h) mice exhibited a complete resistance to gallstone formation during the 2 week period that they consumed the lithogenic diet, with no cholesterol sludge, crystals, or gallstone formation being observed. Our results suggest a role for the NPC2-dependent endocytic pathway in gallstone formation induced by a lithogenic diet. Consistent with this conclusion, we have shown previously that apolipoprotein E and NPC1, which are cholesterol transport proteins also involved in the hepatic lipoprotein endocytic pathway, play a critical role in regulating biliary secretion of dietary cholesterol and diet-induced cholesterol gallstone formation in mice [22, 23]. Moreover, the findings of this study are very similar with those obtained when studying hepatic cholesterol transport in NPC1 mice, which is not surprising due to the tight functional cooperation of NPC1 and NPC2 [47] allowing cholesterol exit from lysosomes [5]. Our results strongly suggest that NPC1 is incapable of compensating the lack of NPC2 and they agree with previous data showing that NPC gene products participate in the same cholesterol trafficking pathway performing different but complementary functions [5, 11].

On the other hand, it has been demonstrated that NPC2 is found in bile in a pronucleating fraction of glycoproteins that bind to concanavalin A [15]. Therefore, NPC2 may function as a pronucleating factor, favoring cholesterol crystal and gallstone formation in the gallbladder. If so, the deficiency of NPC2 may have protected these mice from gallstone formation. It remains to be determined whether NPC2 has a function in biliary cholesterol solubilization, and further studies such as assays of cholesterol crystallization in vitro in the presence of purified NPC2 are required.

In conclusion, the present study has provided data supporting a role for NPC2 in the regulation of the hepatic availability of lipoprotein cholesterol and its utilization for bile secretion as well as in diet-induced cholesterol gallstone formation in mice. Additional work is required to establish the implications of these findings for human gallstone disease.

Acknowledgments The authors thank Dr. Juan Francisco Miquel for helpful discussions. We also acknowledge the Humboldt Foundation (Germany) for donating the ABI 7500 sequence detection system used for gene expression analysis. Finally, Dr. David Sleat and Dr. Peter Lobel generously provided NPC2 (h/h) mice used in this

study. This work was supported by the Fondo Nacional de Desarrollo Científico y Tecnológico (FONDECYT Grant # 1070622), FONDAP 15090007 and Dirección de Investigación, Facultad de Medicina, UC (Programa Inmersión de Verano, Grant to PA).

References

- Patterson MC, Vanier MT, Suzuki K et al (2001) The metabolic and molecular basis of inherited disease: Niemann-Pick disease type C. A lipid trafficking disorder. In: Valle D, Beaudet AL, Vogelstein B, Kinzler KW, Antonarakis SE, Ballabio A, Scriver CR, Childs B, Sly WS (eds) *The online metabolic & molecular bases of inherited disease*. McGraw-Hill, New York
- Liscum L, Sturley SL (2004) Intracellular trafficking of Niemann-Pick C proteins 1 and 2: obligate components of subcellular lipid transport. *Biochim Biophys Acta* 1685:22–27
- Loftus SK, Morris JA, Carstea ED, Gu JZ, Cummings C, Brown A, Ellison J, Ohno K, Rosenfeld MA, Tagle DA, Pentchev PG, Pavan WJ (1997) Murine model of Niemann-Pick C disease: mutation in a cholesterol homeostasis gene. *Science* 277:232–235
- Naureckiene S, Sleat DE, Lackland H, Fensom A, Vanier MT, Wattiaux R, Jadot M, Lobel P (2000) Identification of HE1 as the second gene of Niemann-Pick C disease. *Science* 290:2298–2301
- Sleat DE, Wiseman JA, El-Banna M, Price SM, Verot L, Shen MM, Tint GS, Vanier MT, Walkley SU, Lobel P (2004) Genetic evidence for nonredundant functional cooperativity between NPC1 and NPC2 in lipid transport. *Proc Natl Acad Sci USA* 101:5886–5891
- Okamura N, Kiuchi S, Tamba M, Kashima T, Hiramoto S, Baba T, Dacheux F, Dacheux JL, Sugita Y, Jin YZ (1999) A porcine homolog of the major secretory protein of human epididymis, HE1, specifically binds cholesterol. *Biochim Biophys Acta* 1438:377–387
- Friedland N, Liou HL, Lobel P, Stock AM (2003) Structure of a cholesterol-binding protein deficient in Niemann-Pick type C2 disease. *Proc Natl Acad Sci USA* 100:2512–2517
- Xu S, Benoff B, Liou HL, Lobel P, Stock AM (2007) Structural basis of sterol binding by NPC2, a lysosomal protein deficient in Niemann-Pick type C2 disease. *J Biol Chem* 282:23525–23531
- Infante RE, Radhakrishnan A, Abi-Mosleh L, Kinch LN, Wang ML, Grishin NV, Goldstein JL, Brown MS (2008) Purified NPC1 protein: II. Localization of sterol binding to a 240-amino acid soluble luminal loop. *J Biol Chem* 283:1064–1075
- Infante RE, Wang ML, Radhakrishnan A, Kwon HJ, Brown MS, Goldstein JL (2008) NPC2 facilitates bidirectional transfer of cholesterol between NPC1 and lipid bilayers, a step in cholesterol egress from lysosomes. *Proc Natl Acad Sci USA* 105:15287–15292
- Kwon HJ, Abi-Mosleh L, Wang ML, Deisenhofer J, Goldstein JL, Brown MS, Infante RE (2009) Structure of N-terminal domain of NPC1 reveals distinct subdomains for binding and transfer of cholesterol. *Cell* 137:1213–1224
- Chikh K, Vey S, Simonot C, Vanier MT, Millat G (2004) Niemann-Pick type C disease: importance of N-glycosylation sites for function and cellular location of the NPC2 protein. *Mol Genet Metab* 83:220–230
- Mutka AL, Lusa S, Linder MD, Jokitalo E, Kopra O, Jauhiainen M, Ikonen E (2004) Secretion of sterols and the NPC2 protein from primary astrocytes. *J Biol Chem* 279:48654–48662
- Ong WY, Sundaram RK, Huang E, Ghoshal S, Kumar U, Pentchev PG, Patel SC (2004) Neuronal localization and association of Niemann Pick C2 protein (HE1/NPC2) with the postsynaptic density. *Neuroscience* 128:561–570
- Klein A, Amigo L, Retamal MJ, Morales MG, Miquel JF, Rigotti A, Zanolungo S (2006) NPC2 is expressed in human and murine liver and secreted into bile: potential implications for body cholesterol homeostasis. *Hepatology* 43:126–133
- Turley SD, Dietschy JM (1988) The metabolism and excretion of cholesterol by the liver. In: Arias IM, Jakoby WB, Popper H, Schachter D, Shafritz DA (eds) *The liver: biology and pathology*. Raven Press, New York
- Dietschy JM, Turley SD, Spady DK (1993) Role of liver in the maintenance of cholesterol and low density lipoprotein homeostasis in different animal species, including humans. *J Lipid Res* 34:1637–1659
- Zanolungo S, Rigotti A (2009) Determinants of transhepatic cholesterol flux and their relevance for gallstone formation. *Liver Int* 29:323–330
- Miquel JF, Covarrubias C, Villaroel L, Mingrone G, Greco AV, Puglielli L, Carvallo P, Marshall G, Del Pino G, Nervi F (1998) Genetic epidemiology of cholesterol cholelithiasis among Chilean Hispanics, Amerindians, and Maoris. *Gastroenterology* 115:937–946
- Lammert F, Miquel JF (2008) Gallstone disease: from genes to evidence-based therapy. *J Hepatol* 48(Suppl 1):S124–S135
- Amigo L, Mendoza H, Castro J, Quinones V, Miquel JF, Zanolungo S (2002) Relevance of Niemann-Pick type C1 protein expression in controlling plasma cholesterol and biliary lipid secretion in mice. *Hepatology* 36:819–828
- Morales MG, Amigo L, Balboa E, Acuna M, Castro J, Molina H, Miquel JF, Nervi F, Rigotti A, Zanolungo S (2010) Deficiency of Niemann-Pick C1 protein protects against diet-induced gallstone formation in mice. *Liver Int* 30:887–897
- Amigo L, Quinones V, Mardones P, Zanolungo S, Miquel JF, Nervi F, Rigotti A (2000) Impaired biliary cholesterol secretion and decreased gallstone formation in apolipoprotein E-deficient mice fed a high-cholesterol diet. *Gastroenterology* 118:772–779
- Allain CC, Poon LS, Chan CS, Richmond W, Fu PC (1974) Enzymatic determination of total serum cholesterol. *Clin Chem* 20:470–475
- Baginski ES, Foa PP, Zak B (1967) Microdetermination of inorganic phosphate, phospholipids, and total phosphate in biologic materials. *Clin Chem* 13:326–332
- Talalay P (1960) Enzymic analysis of steroid hormones. *Methods Biochem Anal* 8:119–143
- Carey MC (1978) Critical tables for calculating the cholesterol saturation of native bile. *J Lipid Res* 19:945–955
- Pfaffl MW, Horgan GW, Dempfle L (2002) Relative expression software tool (REST) for group-wise comparison and statistical analysis of relative expression results in real-time PCR. *Nucleic Acids Res* 30:e36
- Wang DQ, Paigen B, Carey MC (1997) Phenotypic characterization of Lith genes that determine susceptibility to cholesterol cholelithiasis in inbred mice: physical-chemistry of gallbladder bile. *J Lipid Res* 38:1395–1411
- Lee FY, Lee H, Hubbert ML, Edwards PA, Zhang Y (2006) FXR, a multipurpose nuclear receptor. *Trends Biochem Sci* 31:572–580
- Repa JJ, Berge KE, Pomajzl C, Richardson JA, Hobbs H, Mangelsdorf DJ (2002) Regulation of ATP-binding cassette sterol transporters ABCG5 and ABCG8 by the liver \times receptors alpha and beta. *J Biol Chem* 277:18793–18800
- Rege RV, Prystowsky JB (1998) Inflammation and a thickened mucus layer in mice with cholesterol gallstones. *J Surg Res* 74:81–85
- Dixit SS, Sleat DE, Stock AM, Lobel P (2007) Do mammalian NPC1 and NPC2 play a role in intestinal cholesterol absorption? *Biochem J* 408:1–5
- Uronen RL, Lundmark P, Orho-Melander M, Jauhiainen M, Larsson K, Siegbahn A, Wallentin L, Zethelius B, Melander O,

- Syvanen AC, Ikonen E (2010) Niemann-Pick C1 modulates hepatic triglyceride metabolism and its genetic variation contributes to serum triglyceride levels. *Arterioscler Thromb Vasc Biol* 30:1614–1620
35. Xie C, Turley SD, Pentchev PG, Dietschy JM (1999) Cholesterol balance and metabolism in mice with loss of function of Niemann-Pick C protein. *Am J Physiol* 276:E336–E344
36. Goldman SD, Krise JP (2010) Niemann-Pick C1 functions independently of Niemann-Pick C2 in the initial stage of retrograde transport of membrane-impermeable lysosomal cargo. *J Biol Chem* 285:4983–4994
37. van Helvoort A, de Brouwer A, Ottenhoff R, Brouwers JF, Wijnholds J, Beijnen JH, Rijneveld A, van der Poll T, van der Valk MA, Majoer D, Voorhout W, Wirtz KW, Elferink RP, Borst P (1999) Mice without phosphatidylcholine transfer protein have no defects in the secretion of phosphatidylcholine into bile or into lung airspaces. *Proc Natl Acad Sci USA* 96:11501–11506
38. Wu MK, Hyogo H, Yadav SK, Novikoff PM, Cohen DE (2005) Impaired response of biliary lipid secretion to a lithogenic diet in phosphatidylcholine transfer protein-deficient mice. *J Lipid Res* 46:422–431
39. Kanno K, Wu MK, Scapa EF, Roderick SL, Cohen DE (2007) Structure and function of phosphatidylcholine transfer protein (PC-TP)/StarD2. *Biochim Biophys Acta* 1771:654–662
40. Scapa EF, Poci A, Wu MK, Gutierrez-Juarez R, Glenz L, Kanno K, Li H, Biddinger S, Jelicks LA, Rossetti L, Cohen DE (2008) Regulation of energy substrate utilization and hepatic insulin sensitivity by phosphatidylcholine transfer protein/StarD2. *FASEB J* 22:2579–2590
41. Kang HW, Wei J, Cohen DE (2010) PC-TP/StARD2: of membranes and metabolism. *Trends Endocrinol Metab* 21:449–456
42. Ross PE, Butt AN, Gallacher C (1990) Cholesterol absorption by the gall bladder. *J Clin Pathol* 43:572–575
43. Frolov A, Zielinski SE, Crowley JR, Dudley-Rucker N, Schaffer JE, Ory DS (2003) NPC1 and NPC2 regulate cellular cholesterol homeostasis through generation of low density lipoprotein cholesterol-derived oxysterols. *J Biol Chem* 278:25517–25525
44. Zhang JR, Coleman T, Langmade SJ, Scherrer DE, Lane L, Lanier MH, Feng C, Sands MS, Schaffer JE, Semenkovich CF, Ory DS (2008) Niemann-Pick C1 protects against atherosclerosis in mice via regulation of macrophage intracellular cholesterol trafficking. *J Clin Invest* 118:2281–2290
45. Wang MD, Franklin V, Sundaram M, Kiss RS, Ho K, Gallant M, Marcel YL (2007) Differential regulation of ATP binding cassette protein A1 expression and ApoA-I lipidation by Niemann-Pick type C1 in murine hepatocytes and macrophages. *J Biol Chem* 282:22525–22533
46. Yamanashi Y, Takada T, Yoshikado T, Shoda J, Suzuki H (2011) NPC2 regulates biliary cholesterol secretion via stimulation of ABCG5/G8-mediated cholesterol transport. *Gastroenterology* 140:1664–1674
47. Wang ML, Motamed M, Infante RE, Abi-Mosleh L, Kwon HJ, Brown MS, Goldstein JL (2010) Identification of surface residues on Niemann-pick C2 essential for hydrophobic Handoff of cholesterol to NPC1 in lysosomes. *Cell Metab* 12:166–173

Probucol Suppresses Enterocytic Accumulation of Amyloid- β Induced by Saturated Fat and Cholesterol Feeding

Menuka M. Pallegage-Gamarallage ·
Susan Galloway · Ryusuke Takechi ·
Satvinder Dhaliwal · John C. L. Mamo

Received: 7 February 2011 / Accepted: 7 July 2011 / Published online: 31 July 2011
© AOCS 2011

Abstract Amyloid- β ($A\beta$) is secreted from lipogenic organs such as intestine and liver as an apolipoprotein of nascent triacylglycerol rich lipoproteins. Chronically elevated plasma $A\beta$ may compromise cerebrovascular integrity and exacerbate amyloidosis—a hallmark feature of Alzheimer's disease (AD). Probucol is a hypocholesterolemic agent that reduces amyloid burden in transgenic amyloid mice, but the mechanisms for this effect are presently unclear. In this study, the effect of Probucol on intestinal lipoprotein- $A\beta$ homeostasis was explored. Wild-type mice were fed a control low-fat diet and enterocytic $A\beta$ was stimulated by high-fat (HF) diet enriched in 10% (w/w) saturated fat and 1% (w/w) cholesterol for the duration of 1 month. Mice treated with Probucol had the drug incorporated into the chow at 1% (w/w). Quantitative immunofluorescence was utilised to determine intestinal apolipoprotein B (apo B) and $A\beta$ abundance. We found apo B in both the perinuclear region of the enterocytes and the lacteals in all groups. However, HF feeding and Probucol treatment increased secretion of apo B into the lacteals without any change in net villi abundance. On the other hand, HF-induced enterocytic perinuclear $A\beta$ was

significantly attenuated by Probucol. No significant changes in $A\beta$ were observed within the lacteals. The findings of this study support the notion that Probucol suppresses dietary fat induced stimulation of $A\beta$ biosynthesis and attenuate availability of apo B lipoprotein- $A\beta$ for secretion.

Keywords Apolipoprotein B · Amyloid- β · Probucol · Small intestine · Saturated fat · Cholesterol

Abbreviations

AD	Alzheimer's disease
$A\beta$	Amyloid- β
Apo B	Apolipoprotein B
HF	High-fat
LF	Low-fat
TAG	Triacylglycerol(s)

Introduction

Alzheimer's disease (AD) is the most common cause of dementia, characterized by neuronal cell loss and amyloid-beta ($A\beta$) deposition on extracellular matrices and within the cerebrovasculature [1]. Amyloid- β is present at sub-nanomolar levels in most biological fluids, such as cerebrospinal fluid and plasma [2] and, at physiological levels, regulates cell growth [3–5]. A hydrophobic protein, $A\beta$ may undergo oligomerisation when it becomes disassociated from chaperone proteins that ordinarily facilitate kinetics and metabolism. It is the fibrillar form of $A\beta$ that is thought to trigger pro-inflammatory pathways that compromise neuronal integrity [6, 7].

The origin of cerebrovascular $A\beta$ deposits in AD is presently unclear. Amyloid- β may be generated as a

M. M. Pallegage-Gamarallage · S. Galloway · R. Takechi ·
S. Dhaliwal · J. C. L. Mamo
School of Public Health, Curtin University of Technology,
GPO Box U1987, Perth, WA 6845, Australia

M. M. Pallegage-Gamarallage · S. Galloway · R. Takechi ·
J. C. L. Mamo
Australian Technology Network, Centre for Metabolic Fitness,
Perth, Australia

J. C. L. Mamo (✉)
Department of Health Sciences, Curtin University
of Technology, Kent Street, Bentley, WA 6102, Australia
e-mail: J.Mamo@Curtin.edu.au

consequence of proteolytic processing of the amyloid-precursor-protein, which is expressed in significant quantities on the plasma membrane of neuronal cells [8]. However, biogenesis of $A\beta$ is not increased in sporadic and late onset AD—the most common phenotype of AD [9, 10]. Rather, accumulating evidence suggests that enhanced blood-to-brain delivery relative to efflux, or via $A\beta$ degradative pathways within the choroid plexus results in extracellular retention of $A\beta$ and thereafter, inflammatory sequelae [11, 12].

Significant $A\beta$ in blood is associated with apolipoprotein B (apo B) lipoproteins, particularly those enriched in triacylglycerol (TAG). Subjects with AD have greater apo B lipoprotein- $A\beta$ relative to age-matched controls [13], and in transgenic amyloid mice, onset and progression of cerebral amyloidosis is associated strongly with the secretion into and concentration of plasma apo B lipoprotein- $A\beta$ [14]. Apolipoprotein B immunoreactivity is evident in parenchymal amyloid plaque from human cadaver specimens [15]; and in $A\beta$ -transgenic mice, cerebral apo B distribution and abundance strongly colocalise with extracellular deposits of $A\beta$ [16]—observations consistent with a vascular contribution to disease aetiology.

A range of lipoprotein (lipid)-lowering agents are commonly used in clinical practice for the prevention and treatment of cardiovascular disease and may reduce AD risk by reducing cerebrovascular exposure to apo B lipoprotein- $A\beta$. The hydroxy-methyl-glutaryl coenzyme A reductase inhibitors lower plasma cholesterol by enhancing apo B lipoprotein clearance via high affinity receptor pathways and inhibiting apo B lipoprotein biogenesis [17–19]. Similarly, fibrates reduce plasma TAG by suppressing lipogenesis, a driver for the secretion of apo B lipoproteins [20]. Population and clinical studies generally support a risk reduction for all forms of dementia in subjects taking lipid-lowering agents [21, 22], although the mechanisms for this association are not clear.

Probucol is an older generation cholesterol-lowering agent that reduces plasma cholesterol by enhancing uptake via receptor pathways [23, 24]. However, other properties of Probucol make this a particularly interesting lipid-lowering agent relative to the plasma kinetics and metabolism of apo B-lipoprotein- $A\beta$. Probucol is hydrophobic and secreted into blood incorporated within the nascent TAG-rich apo B lipoproteins, a phenomenon that may influence $A\beta$ association with, and secretion of, these macromolecules [23, 25]. In addition, lipoproteins that contain Probucol are cleared from circulation almost exclusively by the liver and consequently vascular retention is substantially reduced [23]. A small clinical study suggested that Probucol reduced cognitive decline in subjects with mild cognitive impairment [26, 27] and, consistent with the human findings, studies in transgenic amyloid mice showed that Probucol reduced the

severity of amyloidosis [26]. In the latter, enhanced $A\beta$ -efflux was put forward as one possible mechanism for the Probucol-induced effects.

The putative effects of Probucol on $A\beta$ biogenesis and lipoprotein synthesis in lipogenic organs have not been reported. This study utilised an *in vivo* high-fat (HF) feeding model previously shown to stimulate enterocytic abundance of $A\beta$, to determine if Probucol modulates the secretion of apo B lipoprotein- $A\beta$ from absorptive epithelial cells of the small intestine—a major site of $A\beta$ biosynthesis [28–30].

Methods and Materials

Animals and Diet Conditions

The Curtin University Animal Experimentation and Ethics Committee approved the animal housing, handling and experimental procedures described. Seven-week-old female wild-type mice (C57BL/6J) were housed in groups and randomised into the diet or drug treatment groups ($n = 8$ mice per group). All mice were maintained on a 12-h light and dark cycle room, at 22°C and with free access to water and food. The low-fat control diet was standard AIN93M rodent chow containing <4% (w/w) fat as polyunsaturates, with <1% total digestible energy as lipids and was free of cholesterol (Glen Forrest Stockfeeders, Perth, Western Australia). To stimulate enterocytic $A\beta$ production, the control feed was replaced with a HF diet enriched in saturated fats 10% (w/w) and 1% (w/w) cholesterol (Glen Forrest Stockfeeders). The principal fatty acid types in the HF treatment group were palmitic (16:0) and stearic (18:0) (total of 13% w/w) and oleic acid (18:1n-9, 6% w/w). Mice treated with Probucol (Sanofi-Aventis, Paris, France) had the drug incorporated into the chow at 1% (w/w) at the time of feed manufacture in order to achieve an estimated dose rate of 30 mg/day [23].

Tissue Collection and Sample Preparation

Mice were maintained for 32 days on the diets indicated and weighed weekly. Thereafter, mice were anaesthetised with pentobarbitone (45 mg/kg *i.p.*) and exsanguinated by cardiac puncture. Blood was collected into heparin tubes and stored in ice. Plasma was separated by short-speed centrifugation at 4°C and stored at –80°C.

A 2 cm segment of the small intestine duodenum at the proximal end was isolated, flushed with chilled phosphate buffer saline (PBS, pH 7.4) and fixed in 10% buffered formal saline for a minimum of 24 h. The tissues were then processed and longitudinal segments embedded in paraffin

wax. Serial sections of 5 μm thick were cut and mounted on silanised slides for histology and immunofluorescence.

Amyloid- β and Apolipoprotein B Immunofluorescence

Intestinal A β and apo B were detected by an immunofluorescent amplification method as previously described [31]. Intestinal tissue sections (5 μm) were deparaffinised, rehydrated and antigen-retrieval was carried out in boiling deionised water for 15 min. Briefly, all sections were permeabilised in PBS and incubated in blocking serum (20% goat serum).

For A β staining, polyclonal rabbit anti-human A $\beta_{1-40/42}$ antiserum (AB5076, Chemicon Temecula, CA), diluted to 1:2,000 in PBS was incubated overnight at 4°C. The specificity of the antibodies was previously established [28]. Sections were washed in PBS and incubated with biotinylated goat anti-rabbit secondary antibody (1:2,000 dilution) (E0432, DAKO, Carpinteria, CA) at room temperature for 1 h, followed by incubation with Streptavidin-Alexa Fluor[®] 546 (1:300 dilution) (S11225, Invitrogen, Victoria, Australia) for another hour in the dark for amplification. The nuclei were counterstained with DAPI (1:1,000 dilution) (Invitrogen, Victoria, Australia) for 5 min. The sections were then mounted with antifade mounting medium.

Enterocytic apo B was determined essentially as described for A β detection. Polyclonal rabbit anti-mouse apo B (ab20737, Abcam, Cambridge, UK) as primary and the biotinylated goat anti-rabbit secondary antibody was used at 1:2,250 dilutions.

Imaging

Digital images for photo microscopy were acquired through AxioCam HRm camera (Zeiss, Jena, Germany) with an AxioVert 200 M inverted microscope by Zeiss at 200 \times magnification (Plan Neofluar \times 20 objective, 1.3 numerical aperture). Excitation and emission were achieved by using filters 43 (Ex BP545/25, beam splitter FT570 and Em BP605/70) and filter 49 (Ex G365, beam splitter FT395 and Em BP445/50) to determine fluorescence of Alexa Fluor[®] 546 and DAPI, respectively. Individual channels are free from fluorescence from other emission sources and are therefore clear of overlap. Each image was captured under identical exposure times utilising AxioVision software (version 4.7.1) to avoid artificial modification in pixel intensity.

Quantitative Immunofluorescent Imaging and Analysis

Images were collected at 200 \times magnification and approximately 30–50 images were captured per group showing at

least four villi in each image (1,388 \times 1,040 pixels per image). Pixel intensity for each fluorescent dye was obtained by calculating the densitometric sum by Automatic Measurement Program in AxioVision (Software version 4.7.1). Densitometric sum was calculated for each image staining intensity of A β , apo B and DAPI (nuclei).

For each image, either apo B or A β pixel intensities were standardised with total DAPI pixel intensity to normalise for cell number in the image, and expressed as per DAPI. Staining intensity in the perinuclear region within the enterocytes was calculated and expressed as perinuclear intensity per total DAPI for the image (perinuclear apo B/total DAPI, perinuclear A β /total DAPI). Lacteal staining intensity was obtained by subtracting perinuclear staining intensity from the whole villi intensity (lacteal apo B/total DAPI, lacteal A β /total DAPI). The data were then collated and final results are expressed as mean intensity \pm standard error of mean per area unit.

Plasma Cholesterol and Triacylglycerol Analysis

Plasma Cholesterol and TAG were determined in duplicate by enzymatic assays (Randox Laboratories, Crumlin, UK) according to the manufacturers' instructions.

Statistical Analysis

All data was analysed by either parametric or non-parametric one-way analysis of variance (ANOVA) to assess the main effects of dietary fat and Probuco treatment and their two-way interactions. Post-hoc comparison of means was done if the associated main effect or interaction was statistically significant within the ANOVA procedure. *P* values < 0.05 were considered to be statistically significant.

Results

The distribution and abundance of immunoreactive apo B, an exclusive marker for nascent chylomicrons, was determined by quantitative immunofluorescent microscopy as previously described. Perinuclear enterocytic and lacteal abundance were utilized as surrogate markers of production and secretion, respectively. In all groups, the majority of immunoreactive apo B (\approx 80%) was located within the lacteals (Fig. 1, 2a), indicative of the efficient packaging and secretory pathway of dietary lipids with chylomicrons. Provision of an HF diet for 32 days resulted in a 60% increase of secreted apo B commensurate with decreased perinuclear apo B (Fig. 1, 2a), but there was no significant change in net villi apo B abundance (perinuclear + lacteal). Incorporation of Probuco in the LF diet, like the HF

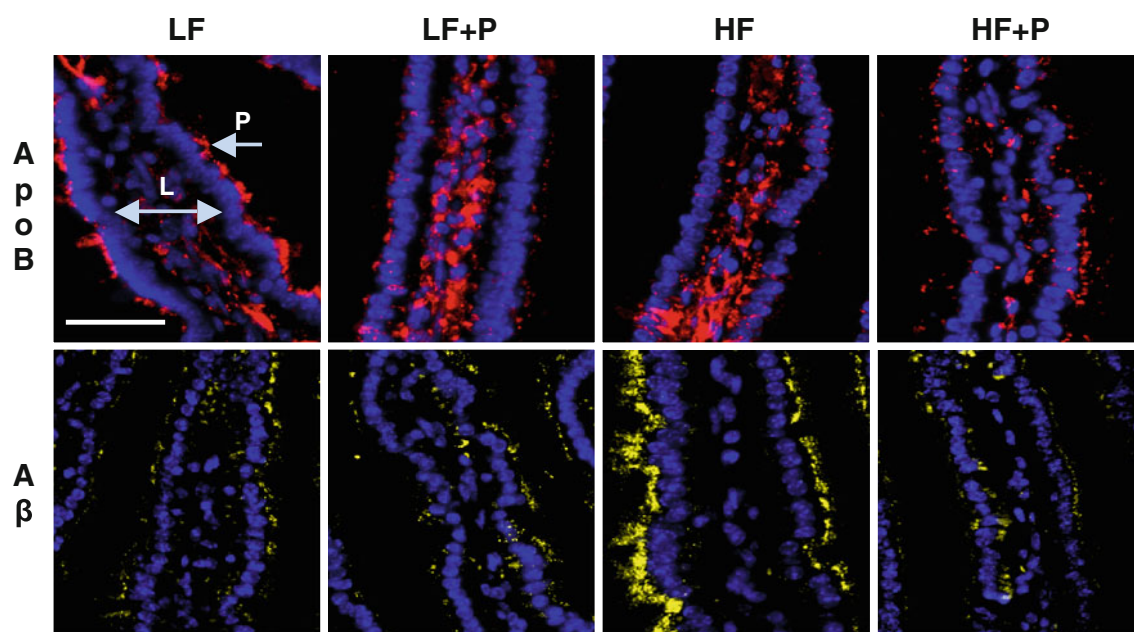


Fig. 1 Images showing apo B (red) and $A\beta$ (yellow) in the intestinal villi. The nuclei are stained blue. The villi are lined with a single layer of absorptive epithelial cells. Amyloid- β staining is concentrated at the perinuclear region of the enterocytes (P arrow) with very little

staining in the lacteals (L arrow). In contrast, a high concentration of the apo B is found within the lacteals of all the groups. Bar 30 μ m, LF low-fat, HF high-fat, P probucol

diet, stimulated secretion of apo B. However, there did not appear to be a synergistic effect of HF + P. The findings of similar net villi abundance of apo B between treatment groups and a strong negative association between the perinuclear- versus lacteal-apo B distribution (Fig. 2c), is consistent with studies suggesting that enterocytic apo B is synthesized constitutively, whereas the secretion of the nascent lipoproteins is modifiable in response to the availability of dietary lipids [32].

The perinuclear and lacteal distribution of $A\beta$ was qualitatively identical to that of apo B. Indeed, co-localisation analysis confirms that $A\beta$ secreted from enterocytes was associated with chylomicrons. However, there were substantial differences in the relative villi abundance of $A\beta$ and apo B and in the pattern of secretion between the two proteins. In contrast to apo B, approximately 70–80% of total intestinal villi $A\beta$ was observed within the baso-lacteal nuclear region of the absorptive epithelial cells, suggesting that only small quantities of the total enterocytic $A\beta$ pool were being secreted (Fig. 1, 2b). The HF-enriched diet doubled intestinal villi $A\beta$ abundance but, in contrast to apo B, this was reflected predominantly in increased enterocytic abundance with virtually no change in the secreted component (Fig. 2b). Incorporation of Probucol in the HF diet normalized enterocytic $A\beta$ to levels that were comparable to the LF control, in the absence of a reduction in lacteal $A\beta$. The latter suggests that Probucol reduced enterocytic $A\beta$ primarily as a consequence of lower rates of biosynthesis. However, correlation analysis of perinuclear versus lacteal

$A\beta$ identified a relatively weak but nonetheless positive association (Fig. 2d), suggesting that increased rates of $A\beta$ production also lead to modest increases in apo B lipoprotein- $A\beta$ secretion.

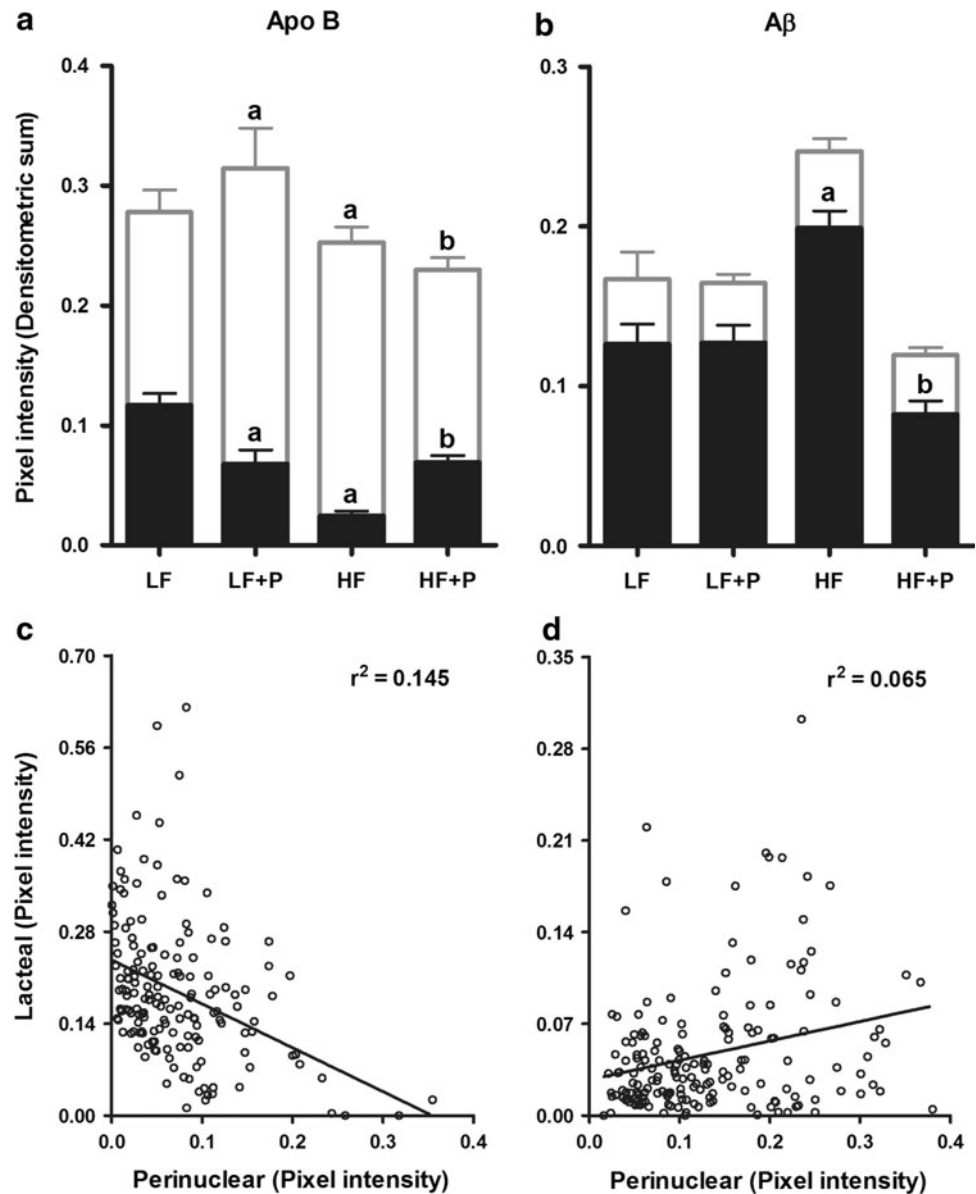
The effects of HF- or Probucol-supplemented diets on plasma cholesterol, plasma TAG and body weight gain for each group of mice is given in Table 1. The mice fed the HF enriched diet had an increase in plasma cholesterol of more than two-fold compared to the LF control; however, the incorporation of Probucol completely abolished this effect. Indeed, the HF + P group had comparable plasma cholesterol to the LF + P treated mice. Probucol also significantly reduced plasma cholesterol in LF mice. In contrast, there was no appreciable effect of HF feeding, or Probucol, on plasma TAG in any treatment group.

Mice maintained on the HF diet were found to have a greater rate of body weight gain compared to mice maintained on the LF diet. Probucol had a synergistic stimulatory effect on body weight gain. Mice on LF + P were similar in weight to mice maintained on the HF diet, and mice on the HF + P were significantly heavier in weight than mice on HF alone.

Discussion

In absorptive epithelial cells of the small intestine, dietary fats regulate enterocytic abundance of $A\beta$ profoundly, reflecting either changes in $A\beta$ biogenesis, or in the

Fig. 2 **a, b** Bar graphs showing quantitative analysis of perinuclear (*filled squares*) and lacteal (*open squares*) apo B and A β staining intensities. Pixel intensity is expressed as densitometric sum as a ratio of nuclei intensity to normalise for nuclei number. **c, d** Scatter plots showing the distribution of apo B and A β between the perinuclear and lacteal regions of all groups. Pearson's correlation analysis (r^2 values) for apo B and A β was 0.145 ($P < 0.0001$) and 0.065 ($P = 0.0006$), respectively. **a** Statistically significant in comparison to the LF group ($P < 0.05$). **b** Statistically significant in comparison to the HF group ($P < 0.05$). LF low-fat, HF high-fat, P probucol



secretion of lipoproteins containing A β [28, 29]. Several lipid-lowering agents, including statins and fibrates, have been shown to suppress apo B secretion [17, 18, 20]; however, ProbucoI may have pleiotropic benefits post-secretion, including enhanced hepatic clearance apo B lipoprotein-A β and anti-oxidant activity.

In this study, an established *in vivo* murine model was used to investigate if ProbucoI modulates the effects of a HF diet on enterocytic A β and its secretion thereafter, with apo B lipoproteins. The study confirms that a HF diet substantially increases enterocytic perinuclear abundance of A β . Apolipoprotein B lipoprotein secretion is enhanced by HF feeding, but without evidence of a concomitant increase in lacteal A β staining. Therefore, the HF-mediated effect on enterocytic A β abundance is likely to be a consequence of greater rates of A β synthesis, rather than

diminished rates of secretion. Previous studies reported that a HF-induced accumulation of enterocytic A β is progressively depleted in the post-absorptive state, or once food is withdrawn [28]. Hence, a dietary fat induced stimulation in A β biogenesis with constitutive rates of secretion as suggested in this study, would result in extended post-prandial amyloidemia. Clinical studies in normal healthy subjects consuming a mixed lipid meal are consistent with a transient single meal effect [34]. A phenomenon of extended exposure may be important in modulation vascular function. Co-administration of ProbucoI with the HF diet completely abolished the HF-induced effect on enterocytic A β abundance in the absence of a significant stimulatory effect on apo B lipoprotein-A β secretion. The findings are consistent with ProbucoI normalising enterocytic A β biogenesis, rather than promoting enterocytic secretion of A β .

Table 1 Effect of various feedings regimes on the average weight and plasma lipids in wild-type mice (C57BL/6J)

Feeding regime ^c	Body weight (g) ^d		Plasma lipids (mM) ^e	
	Final	Weight gain	TC	TAG
LF (<i>n</i> = 8)	20.56 ± 0.27	2.00 ± 0.16	1.86 ± 0.06	0.55 ± 0.05
LF + <i>P</i> (<i>n</i> = 8)	22.23 ± 0.36 ^a	4.55 ± 0.16 ^a	0.83 ± 0.04 ^a	0.65 ± 0.06
HF (<i>n</i> = 8)	22.48 ± 0.33 ^a	4.36 ± 0.19 ^a	2.88 ± 0.17 ^a	0.63 ± 0.10
HF + <i>P</i> (<i>n</i> = 8)	23.58 ± 0.32	5.82 ± 0.19 ^b	0.67 ± 0.05 ^b	0.39 ± 0.04

Data represented as mean ± standard error of the mean (SEM), numbers (*n*) indicate total number of samples used

LF low-fat, HF high-fat, *P* probucol, TC total serum cholesterol, TAG serum triglyceride

Values with lower case ^a and ^b indicate statistical significance in comparison with LF and HF groups, respectively, where *P* < 0.05

^c Wild-type mice (C57BL/6J) were randomised to four different feeding regimens (*n* = 8 mice per group) and were fed their respective diets for 32 days. Weights, total serum cholesterol and triglyceride levels at the end of the experiment were compared between the groups with Post-hoc comparison of means within the ANOVA procedure and *P* < 0.05 was considered significant

^d The average final body weights (per mouse) for LF + *P* and HF groups were significantly greater in comparison to the LF group; however, HF + *P* group final body weight was similar to that of the HF group. There was significant weight gain by all groups (vs LF) and there was also weight gain by the HF + *P* treated mice in comparison to the HF group

^e Total plasma cholesterol level was significantly reduced by probucol treatment alone (vs LF), also by the HF + *P* treated group in comparison to the HF group. Fat feeding significantly have increased the circulating cholesterol level. On the other hand, neither the probucol treatment nor fat feeding did not affect the triglyceride concentration

Indeed, whilst Probucol was found to stimulate apo B lipoprotein secretion in LF-fed mice, there was no evidence that this translated into significantly increased enterocytic release of Aβ.

The HF diet utilized in this study contained both SFA and cholesterol, provided together in a context that it is physiologically relevant in comparison to commonly consumed atherogenic diets. The effects of Probucol on Aβ synthesis and secretion reported in this study must therefore be considered in the context of a mixed dietary lipid setting. Regulation by Probucol may change depending on the interactive effects of dose and duration of dietary lipids.

Several studies have shown synergistic stimulatory effects of fatty acids and cholesterol on apo B lipoprotein secretion [35, 36]. Therefore, the finding of increased apo B lipoprotein secretion shown in this study in HF-fed mice is to be expected. However, previous studies in the same strain of mice fed SFA, or cholesterol, found stimulatory and suppressive effects, respectively, on enterocytic abundance of Aβ [29, 33]. Saturated fatty acids were shown to have a profound stimulatory effect on enterocytic Aβ abundance, whereas dietary cholesterol was inhibitory. The reasons for the paradoxical differences between SFA and cholesterol have not been determined but may include differential regulation of Aβ biogenesis, transfer and association of Aβ with apo B lipoproteins and/or changes in intracellular degradation of Aβ or apo B lipoproteins.

In this study, saturated fats presented at 20% of digestible energy combined with 1% (w/w) cholesterol increased enterocytic abundance by approximately 75% above control mice given the LF diet alone. Hence, it would appear that the effects of SFA on enterocytic Aβ

homeostasis were substantially greater than that of dietary cholesterol. How SFA influence Aβ biogenesis and association with apo B lipoproteins is not known. One possibility is increased lipidation of Aβ, a process found to protect other lipophilic apoproteins from proteolytic degradation.

Several studies suggest that the intracellular distribution between free cholesterol may be important in modulating Aβ homeostasis and intracellular kinetics. Inhibition of cholesterol trafficking in neuronal cells decreased β-secretase but enhanced γ-secretase processing of Aβ precursor protein [37]. The substantial increase in γ-secretase resulted in an increased intracellular concentration of Aβ [37]. Whilst in enterocytes Aβ biogenesis does not appear to occur at the plasma membrane, the subcellular distribution of cholesterol might nonetheless induce critical changes in the cell membranes of intracellular compartments such as within the endoplasmic reticulum and Golgi or re-localise enzymes responsible for Aβ synthesis, or its association with primordial lipoproteins. The notion that Probucol regulates enterocytic biogenesis of Aβ or association with apo B lipoproteins via modulation of intracellular pools of cholesterol is supported by the findings of Tawara et al. [38], who reported that Probucol stimulates cholesterol biosynthesis in absorptive epithelial cells of the small intestine, a process that would suppress Aβ biogenesis.

The HF diet resulted in greater body weight gain compared to LF-fed mice, presumably as a consequence of increased caloric intake and, somewhat surprisingly, Probucol also enhanced body weight gain in LF-fed mice. However, there was no evidence that body weight was associated with perinuclear or lacteal abundance of Aβ, or

of apo B lipoprotein-A β , so it is unlikely there is a causal association.

Clinical and animal studies suggest that ProbucoI may reduce AD risk and attenuate amyloidosis [26, 27, 39]. Suggested mechanisms include enhanced cerebrovascular efflux of soluble A β and neuro-protection as a consequence of suppression of oxidative pathways. Other indirect lines of evidence suggest that ProbucoI could confer AD protection by reducing vascular exposure to cytotoxic compounds including exaggerated plasma cholesterol, fatty acids or a reduction in inflammatory proteins including A β . The findings of this study support the latter notion and show that ProbucoI appears to suppress dietary fat induced stimulation of A β biosynthesis.

The 1 month dietary intervention study described in this study did not identify any significant increase in secretion of apo B lipoprotein-A β per se, and hence may reflect a localised phenomenon that is not particularly relevant to AD risk. Clearly, longer term feeding studies with an emphasis on the effects of ProbucoI on blood–brain barrier integrity and plasma A β homeostasis are warranted.

Acknowledgments The National Health and Medical Research Council of Australia, and the Australian Technology Network Centre supported this research financially.

Conflict of interest The authors have no conflicts of interest to declare in relation to this article.

References

- Pastorino L, Lu KP (2006) Pathogenic mechanisms in Alzheimer's disease. *Eur J Pharmacol* 545:29–38
- Selkoe DJ (1994) Cell biology of the amyloid beta-protein precursor and the mechanism of Alzheimer's disease. *Annu Rev Cell Biol* 10:373–403
- Kapeller R, Cantley L (1994) Phosphatidylinositol 3-kinase. *BioEssays* 16:565–576
- Luo Y, Hirashima N, Li Y, Alkon D, Sunderland T, Etcheberrigaray R, Wolozin B (1995) Physiological levels of β -amyloid increase tyrosine phosphorylation and cytosolic calcium. *Brain Res* 681:65–74
- Luo Y, Sunderland T, Roth GS, Wolozin B (1996) Physiological levels of β -amyloid peptide promote PC12 cell proliferation. *Neurosci Lett* 217:125–128
- Jekabsons A, Mander P, Tickler A, Sharpe M, Brown G (2006) Fibrillar beta-amyloid peptide A β 1–40 activates microglial proliferation via stimulating TNF- α release and H₂O₂ derived from NADPH oxidase: a cell culture study. *J Neuroinflamm* 3:24
- Sondag C, Dhawan G, Combs C (2009) Beta amyloid oligomers and fibrils stimulate differential activation of primary microglia. *J Neuroinflamm* 6:1
- Haass C, Koo EH, Mellon A, Hung AY, Selkoe DJ (1992) Targeting of cell-surface beta-amyloid precursor protein to lysosomes—alternative processing into amyloid-bearing fragments. *Nature* 357:500–503
- Panza F, Solfrizzi V, D'Introno A, Capurso C, Colacicco A, Torres F, Altomare E, Capurso A (2002) Genetics of late-onset Alzheimer's disease: vascular risk and beta-amyloid metabolism. *Recent Prog Med* 93:489–497
- Rocchi A, Orsucci D, Tognoni G, Ceravolo R, Siciliano G (2009) The role of vascular factors in late-onset sporadic Alzheimer's disease. Genetic and molecular aspects. *Curr Alzheimer Res* 6:224–237
- Crossgrove J, Li G, Zheng W (2005) The choroid plexus removes beta-amyloid from brain cerebrospinal fluid. *Exp Biol Med* (Maywood) 230:771–776
- Deane R, Sagare A, Hamm K, Parisi M, LaRue B, Guo H, Wu Z, Holtzman D, Zlokovic B (2005) IgG-assisted age-dependent clearance of Alzheimer's amyloid beta peptide by the blood-brain barrier neonatal Fc receptor. *J Neurosci* 25:11495–11503
- Mamo JCL, Jian L, James AP, Flicker L, Esselmann H, Wiltfang J (2008) Plasma lipoprotein β -amyloid in subjects with Alzheimer's disease or mild cognitive impairment. *Ann Clin Biochem* 45:395–403
- Burges B, McIsaac S, Naus K, Chan J, Tansley G, Yang J, Miao F, Ross C, van Eck M, Hayden M, van Nostrand W, St George-Hyslop P, Westaway D, Wellington C (2006) Elevated plasma triglyceride levels precede amyloid deposition in Alzheimer's disease mouse models with abundant A beta in plasma. *Neurobiol Dis* 24:114–127
- Namba Y, Tsuchiya H, Ikeda K (1992) Apolipoprotein B immunoreactivity in senile plaque and vascular amyloids and neurofibrillary tangles in the brains of patients with Alzheimer's disease. *Neurosci Lett* 134:264–266
- Takechi R, Galloway S, Pallegage-Gamarallage MMS, Wellington CL, Johnsen RD, Dhaliwal SS, Mamo JCL (2010) Differential effects of dietary fatty acids on the cerebral distribution of plasma-derived apo B lipoproteins with amyloid- β . *Br J Nutr* 103:652–662
- Funatsu T, Suzuki K, Goto M, Arai Y, Kakuta H, Tanaka H, Yasuda S, Ida M, Nishijima S, Miyata K (2001) Prolonged inhibition of cholesterol synthesis by atorvastatin inhibits apo B-100 and triglyceride secretion from HepG2 cells. *Atherosclerosis* 157:107–115
- Watts GF, Chan DC, Barrett PHR, O'Neill FH, Thompson GR (2003) Effect of a statin on hepatic apolipoprotein B-100 secretion and plasma campesterol levels in the metabolic syndrome. *Int J Obes Relat Metab Disord* 27:862–865
- Pal S, Allister E, Thomson A, Mamo JCL (2002) Cholesterol esters regulate apoB₄₈ secretion in CaCo₂ cells. *Atherosclerosis* 161:55–63
- Staels B, Dallongeville J, Auwerx J, Schoonjans K, Leitersdorf E, Fruchart J-C (1998) Mechanism of action of fibrates on lipid and lipoprotein metabolism. *Circulation* 98:2088–2093
- Dufouil C, Richard F, Fievet N, Dartigues J, Ritchie K, Tzourio C, Amouyel P, Alperovitch A (2005) APOE genotype, cholesterol level, lipid-lowering treatment, and dementia: the three-city study. *Neurology* 64:1531–1538
- Rockwood K, Kirkland S, Hogan D, MacKnight C, Merry H, Verreault R, Wolfson C, McDowell I (2002) Use of lipid-lowering agents, indication bias, and the risk of dementia in community-dwelling elderly people. *Arch Neurol* 59:223–227
- Mamo J, Elsegood C, Umeda Y, Hirano T, Redgrave T (1993) Effect of probucole on plasma clearance and organ uptake of chylomicrons and VLDLs in normal and diabetic rats. *Arterioscler Thromb* 13:231–239
- Mellies MJ, Gartside PS, Glatfelter L, Vink P, Guy G, Schonfeld G, Glueck CJ (1980) Effects of probucole on plasma cholesterol, high and low density lipoprotein cholesterol, and apolipoproteins A1 and A2 in adults with primary familial hypercholesterolemia. *Metabolism* 29:956–964

25. Gershkovich P, Hoffman A (2005) Uptake of lipophilic drugs by plasma derived isolated chylomicrons: linear correlation with intestinal lymphatic bioavailability. *Eur J Pharm Sci* 26:394–404
26. Poirier J (2003) Apolipoprotein E and cholesterol metabolism in the pathogenesis and treatment of Alzheimer's disease. *Trends Mol Med* 9:94–101
27. Poirier J (2005) Apolipoprotein E, cholesterol transport and synthesis in sporadic Alzheimer's disease. *Neurobiol Aging* 26:355–361
28. Galloway S, Jian L, Johnsen R, Chew S, Mamo JCL (2007) β -Amyloid or its precursor protein is found in epithelial cells of the small intestine and is stimulated by high-fat feeding. *J Nutr Biochem* 18:279–284
29. Pallegage-Gamarallage MM, Galloway S, Johnsen R, Jian L, Dhaliwal S, Mamo JCL (2009) The effect of exogenous cholesterol and lipid-modulating agents on enterocytic amyloid- β abundance. *Br J Nutr* 101:340–347
30. Galloway S, Pallegage-Gamarallage MM, Takechi R, Jian L, Johnsen RD, Dhaliwal SS, Mamo JC (2008) Synergistic effects of high fat feeding and apolipoprotein E deletion on enterocytic amyloid-beta abundance. *Lipids Health Dis* 22:7–15
31. Takechi R, Galloway S, Pallegage-Gamarallage M, Johnsen R, Mamo J (2008) Three-dimensional immunofluorescent double labelling using polyclonal antibodies derived from the same species: enterocytic colocalization of chylomicrons with Golgi apparatus. *Histochem Cell Biol* 129:779–784
32. Lairon D (2008) Macronutrient intake and modulation on chylomicron production and clearance. *Atheroscler Suppl* 9:45–48
33. Galloway S, Takechi R, Pallegage-Gamarallage M, Dhaliwal S, Mamo J (2009) Amyloid-beta colocalizes with apolipoprotein B in absorptive cells of the small intestine. *Lipids Health Dis* 8:46
34. Smith D, Watts GF, Dane-Stewart C, Mamo JC (1999) Post-prandial chylomicron response may be predicted by a single measurement of plasma apolipoprotein B48 in the fasting state. *Eur J Clin Invest* 29:204–209
35. Ohtani H, Hayashi K, Hirata Y, Dojo S, Nakashima K, Nishio E, Kurushima H, Saeki M, Kajiyama G (1990) Effects of dietary cholesterol and fatty acids on plasma cholesterol level and hepatic lipoprotein metabolism. *J Lipid Res* 31:1413–1422
36. Sharon A, Michael IM, Paul ND (2000) The effects of fatty acids on apolipoprotein B secretion by human hepatoma cells (HEP G2). *Atherosclerosis* 150:255–264
37. Runz H, Rietdorf J, Tomic I, de Bernard M, Beyreuther K, Pepperkok R, Hartmann T (2002) Inhibition of intracellular cholesterol transport alters presenilin localisation and amyloid precursor protein processing in neuronal cells. *J Neurosci* 22:1679–1689
38. Tawara K, Tomikawa M, Abiko Y (1986) Mode of action of probucol in reducing serum cholesterol in mice. *Jpn J Pharmacol* 40:123–133
39. Champagne D, Pearson D, Dea D, Rochford J, Poirier J (2003) The cholesterol-lowering drug probucol increases apolipoprotein E production in the hippocampus of aged rats: implications for Alzheimer's disease. *Neuroscience* 121:99–110

Serum 2-Methoxyestradiol, an Estrogen Metabolite, is Positively Associated with Serum HDL-C in a Population-Based Sample

Christopher M. Masi · Louise C. Hawkey ·
John T. Cacioppo

Received: 16 May 2011 / Accepted: 12 July 2011 / Published online: 2 August 2011
© AOCs 2011

Abstract Serum HDL cholesterol (HDL-C) is inversely associated with coronary artery disease, ischemic stroke, and atherosclerosis in men and women. Among postmenopausal women, oral conjugated equine estrogen (CEE) increases serum HDL-C. This is due to activation of hepatic nuclear estrogen receptors, resulting in increased HDL-C expression, as well as modulation of proteins which metabolize HDL-C. 2-methoxyestradiol (2-MeOE2), an estrogen metabolite, has several vasculoprotective effects and may play a role in HDL-C production. 2-MeOE2 inhibits HMG-CoA reductase in vitro but no study has examined the relationship between serum 2-MeOE2 and serum HDL-C. A population-based sample provided information regarding demographic characteristics and use of antihyperlipidemic medications. Serum was analyzed for 17 β -estradiol (E2), estrogen metabolites (EMs), and lipoproteins. Results included serum EM data from 51 men and 47 postmenopausal women. Preliminary analysis revealed no correlation between 2-MeOE2 and serum HDL-C in men so the current analysis includes only women ($N = 40$) with no missing demographic, medication, EM, or lipoprotein data. Linear regression revealed that serum 2-MeOE2 and antihyperlipidemic medications were positively associated with serum HDL-C ($\beta = 0.276$, $P = 0.043$, and $\beta = 0.307$, $P = 0.047$, respectively) when age, race/ethnicity, and body mass index were held constant. Prospective studies are needed to

determine if 2-MeOE2 is causally related to HDL-C in women.

Keywords HDL · Lipoprotein metabolism · Mass spectrometry · Atherosclerosis · Coronary artery disease · HMG-CoA reductase

Abbreviations

Apo A-I	Apolipoprotein A-I
CEE	Conjugated equine estrogen
E2	17 β -Estradiol
EM	Estrogen metabolites
ER	Estrogen receptor
HDL-C	High density lipoprotein cholesterol
HL	Hepatic lipase
HMG-CoA	3-Hydroxy-3methylglutaryl-CoA
HRT	Hormone replacement therapy
LC-MS/MS	Liquid chromatography–tandem mass spectrometry
LDL-C	Low density lipoprotein cholesterol
ln	Natural log
2-MeOE2	2-Methoxyestradiol
MI	Myocardial infarction
SR-BI	Scavenger receptor class B type I
WHI	Women's Health Initiative

Introduction

Serum HDL-C is inversely associated with coronary artery disease [1], ischemic stroke [2], and atherosclerosis in men and women [3]. HDL-C provides atheroprotection by promoting cholesterol efflux from peripheral tissues, transporting cholesterol to the liver for excretion as free

C. M. Masi (✉)
Section of General Internal Medicine, University of Chicago,
5841 S. Maryland Avenue, M/C 2007, Chicago, IL, USA
e-mail: cmasi@medicine.bsd.uchicago.edu

L. C. Hawkey · J. T. Cacioppo
Department of Psychology, University of Chicago,
Chicago, IL, USA

cholesterol or bile acids, serving as an anti-oxidant, and suppressing inflammation [3, 4]. Serum HDL-C levels are higher [5] and cardiovascular disease rates are lower among pre-menopausal women compared to similarly aged men [6]. Recent analysis of WHI data indicate that women in the 50–59 year age group with prior hysterectomy who took CEE without progesterone had a significantly lower risk of MI (HR = 0.54, 95% CI, 0.34–0.86) compared to controls [7]. This effect may have been due to atheroprotection from HDL-C, which is known to increase with oral estrogen supplementation [8].

But how does oral CEE increase serum HDL-C levels? A hepatic first pass effect may be important [9] because transdermal estrogen does not lead to increased serum HDL-C [10]. CEE contains E2 [11] and in the liver, E2 activates nuclear estrogen receptors (ERs) and increases the expression of HDL-C and apo A-I, the major protein component of HDL-C [9, 12]. E2 also modulates the expression of proteins involved in the metabolism of HDL-C, such as HL and SR-BI [13, 14]. Human studies demonstrate a correlation between HL activity and HDL catabolism [15]. Estrogen reduces HL mRNA levels in rats, suggesting transcriptional inhibition of this enzyme [16]. In vitro, E2 increases SR-BI promoter activity via nuclear ERs [13]. SR-BI has several effects, including enhanced HDL cholesterol uptake by the liver (reverse cholesterol transport) [17] and increased efflux to lipoproteins from atheromatous arteries [18].

Increasing evidence suggests that 2-MeOE2, a major endogenous metabolite of E2, also has beneficial effects on serum cholesterol and vascular integrity [19]. In ovariectomized rats, oral administration of 2-MeOE2 reduced total cholesterol levels by 34% compared to controls [20]. Subcutaneous infusion over 24 weeks of 2-hydroxyestradiol, the precursor of 2-MeOE2, into obese ZSF1 rats, a genetic model of obesity and the metabolic syndrome, led to significant reductions in total cholesterol, body weight, fasting plasma glucose, and glycated hemoglobin compared to controls [21]. More recently, subcutaneous infusion of 2-MeOE2 into apolipoprotein E-deficient mice reduced both total serum cholesterol and aortic atherosclerotic plaque size compared to controls [22]. However, the mechanism of these effects is not known [20–22].

A recent study found that 2-MeOE2 inhibits HMG-CoA reductase in vitro [23]. Because HMG-CoA reductase inhibitors reduce LDL-C and raise HDL-C in vivo [24], a mechanism exists by which endogenous 2-MeOE2 may influence circulating cholesterol levels. In addition, the ability of oral CEE to increase serum HDL-C may be augmented by the conversion of E2 in CEE to 2-MeOE2 by hepatic estrogen metabolizing enzymes, such as CYP3A4 [25]. Given its inhibition of HMG-CoA reductase, we hypothesized that serum 2-MeOE2 would be positively

associated with serum HDL-C in a population-based sample of adults.

Materials and Methods

Data for this study were gathered in the fifth year of the Chicago Health, Aging, and Social Relations Study (CHASRS), which is a population-based longitudinal study designed to examine the relationships between psychosocial characteristics and health outcomes among middle-aged and older adults. Written, informed consent was obtained from the subjects prior to their participation in this study (protocol # 11143B), which was approved by the University of Chicago's Institutional Review Board.

Subjects completed surveys regarding their demographic, dietary, and exercise characteristics, as well as their medication usage. Body mass index (BMI) was calculated as weight in kilograms divided by height in meters squared. The following medications were classified as anti-hyperlipidemic agents: HMG-CoA reductase inhibitors (statins), niacin, bile acid sequestrants, and cholesterol absorption inhibitors. Serum was analyzed for E2 and 14 EMs using LC-MS/MS [26]. Mean values for all EMs are reported separately for men and women in Masi et al. [27]. EM values exhibited a positively skewed distribution and were therefore subjected to natural log (ln) transformation. Non-fasting HDL-C, total cholesterol, and triglycerides were measured using the Cholestech LDX kit (Cholestech Corporation, USA), a system that meets CDC reference standards for accuracy and reproducibility. LDL-C was calculated using the Friedewald equation. In year 5, we had serum EM data from 51 men and 51 women; all of the women were postmenopausal. Four women were excluded because they were taking hormone replacement therapy. Preliminary analysis revealed no correlation between 2-MeOE2 and serum HDL-C in men so the current analysis includes only women who had no missing demographic, medication, EM, or cholesterol data ($N = 40$).

Ordinary linear regression analysis was used to evaluate the relationship between serum HDL-C and predictor variables, including age, race/ethnicity, BMI, use of anti-hyperlipidemic medications, and serum 2-MeOE2. Given the directional nature of the hypothesis, a one-tailed t test of the significance of the regression coefficient for 2-MeOE2 was used to evaluate our hypothesis that 2-MeOE2 would be positively associated with HDL-C.

Results and Discussion

Table 1 provides descriptive statistics of the sample of post-menopausal women in the Chicago Health, Aging, and

Table 1 Demographic characteristics, mean 2-MeOE2 concentration, and mean serum lipid profile of study participants

Variable	Women not on HRT (N = 47)
Age (years)	57.3 (3.9) ^a
White (%)	48.9
Black (%)	23.4
Latino (%)	27.7
Body mass index	32.0 (7.3)
Use of antihyperlipidemic medications (%)	32.6
2-Methoxyestradiol (2-MeOE2, pg/ml)	19.0 (17.6)
Serum cholesterol & triglycerides (mg/dl)	
Total cholesterol	205.6 (38.2)
HDL-C	56.2 (18.4)
LDL-C	117.8 (36.9)
Triglycerides	163.0 (84.3)

^a Numbers in parentheses represent standard deviations

Social Relations Study. Correlational analysis revealed a sizeable positive relationship between serum ln 2-MeOE2 and serum HDL-C ($r = 0.31$; $P = 0.05$). Neither serum ln E2 ($r = 0.08$; $P = 0.59$) nor any other serum ln EM was significantly associated with serum HDL-C. Multivariate regression analysis showed that 2-MeOE2 retained a positive association ($\beta = 0.28$, $P < 0.05$) with serum HDL-C when age, BMI, race/ethnicity, and antihyperlipidemic medications were held constant (see Table 2). In the same model, use of antihyperlipidemic medications was also positively associated with serum HDL-C. To test whether the positive relationship between serum ln 2-MeOE2 and serum HDL-C reflected an effect of E2, we added serum ln E2 to the model shown in Table 2. In this ancillary analysis, serum ln E2 was not associated serum HDL-C. In addition, the positive association between serum ln 2-MeOE2 and HDL-C remained unchanged.

Consistent with our hypothesis, we found a positive association between serum 2-MeOE2 and serum HDL-C. This was true among postmenopausal women but not among similarly aged men. Animal studies indicate that 2-MeOE2 lowers serum total cholesterol [20–22] and shrinks atherosclerotic plaque size [22]. A key factor in cholesterol efflux from peripheral tissues, including atherosclerotic plaques, is HDL-C [3]. It is possible, therefore, that the reduction of atherosclerotic plaque size among mice receiving subcutaneous 2-MeOE2 is due to induction of HDL-C by 2-MeOE2. This is plausible given the demonstrated inhibition of HMG-CoA reductase by 2-MeOE2 [23] and that HMG-CoA reductase inhibition increases serum HDL-C in humans [24].

ER-dependent mechanisms of oral E2-induced HDL-C production include increased hepatic expression of HDL-C

Table 2 Model predicting serum HDL-C in postmenopausal women (N = 40)

Predictor	Standardized coefficient (β)	P value
Constant		0.309
Age	0.098	0.289
Black	−0.119	0.250
Latino	−0.258	0.080
Body mass index	−0.121	0.253
Use of antihyperlipidemic medications	0.307	0.047
ln 2-MeOE2	0.276	0.043

and apo A-I [9, 12], as well as modulation of proteins involved in the metabolism of HDL-C [14, 15]. Although the ability of oral E2 to raise serum HDL-C in postmenopausal women is well-recognized [8, 28], research has not established a relationship between endogenous E2 and HDL-C, at least in premenopausal women [8, 29]. The lack of correlation we found between serum E2 and HDL-C is therefore consistent with previous studies. In addition, because E2 was not correlated with HDL-C in univariate or multivariate analysis, we are confident that the association between 2-MeOE2 and HDL-C does not reflect an association between E2 and HDL-C.

The validity of our results is supported by our finding of an expected positive association between use of antihyperlipidemic medications and serum HDL-C. The effect size of these medications ($\beta = 0.31$) is only slightly larger than the effect size of 2-MeOE2 ($\beta = 0.28$), suggesting that 2-MeOE2 may be a potent inducer of HDL-C. However, given the cross-sectional nature of the study design, causal inferences cannot be made. For example, our results are also consistent with induction of 2-MeOE2 by HDL-C or with induction of both by a third variable. Prospective studies are therefore needed to determine the causal direction of this association.

Whereas EMs were once thought to be biologically insignificant, an increasing number of studies have demonstrated the metabolic importance of these molecules [25], particularly with respect to breast cancer risk [30]. We previously demonstrated an inverse relationship between serum 16 α -hydroxyestrone and systolic blood pressure among postmenopausal women [27]. In addition, Dubey et al. have documented several vasculoprotective effects of 2-MeOE2, including inhibition of abnormal growth of vascular smooth muscle cells, cardiac fibroblasts, and glomerular mesangial cells, as well as suppression of inflammation, and enhanced endothelium-dependent arterial relaxation (reviewed in [31]). Despite progress in this area, ours is the first study to document a positive association between serum 2-MeOE2 and serum HDL-C, an

essential component of athero- and cardioprotection. Further studies are needed to determine whether 2-MeOE2 can indeed increase HDL-C and what behavioral and genetic factors lead to higher levels of this EM. If 2-MeOE2 is causally related to HDL-C, this association may point to new strategies for reducing cardiovascular disease risk among postmenopausal women.

Acknowledgments This work was supported by a National Institute on Aging Career Development K08 Award (AG027200, C.M. Masi, PI), a National Institute on Aging R01 Award (AG036433, L.C. Hawley, PI), and a National Institute on Aging R01 Award (AG034052, J.T. Cacioppo, PI).

References

- Ballantyne CM, Herd JA, Ferlic LL, Dunn K, Farmer JA et al (1999) Influence of low HDL on progression of coronary artery disease and response to fluvastatin therapy. *Circulation* 99:736–743
- Sanossian N, Tarlov NE (2008) HDL-C and LDL-C: their role in stroke pathogenesis and implications for treatment. *Curr Treat Options Cardiovasc Med* 10:195–206
- Feig JE, Shamir R, Fisher EA (2008) Atheroprotective effects of HDL: beyond reverse cholesterol transport. *Curr Drug Targets* 9:196–203
- Nofer JR, Walter M, Assmann G (2005) Current understanding of the role of high-density lipoprotein in atherosclerosis and senescence. *Expert Rev Cardiovasc Ther* 3:1071–1086
- Gardner C, Tribble DL, Rohm Young D, Ahn D, Fortmann SP (2000) Population frequency distributions of HDL, HDL₂, and HDL₃ cholesterol and apolipoproteins A-1 and B in healthy men and women and associations with age, gender, hormonal status, and sex hormone use: The Stanford Five City Project. *Prev Med* 31:335–345
- Bello N, Mosca L (2004) Epidemiology of coronary heart disease in women. *Prog Cardiovasc Dis* 46:287–295
- LaCroix AZ, Chlebowski RT, Manson JE, Aragaki AK, Johnson KC et al (2011) Health outcomes after stopping conjugated equine estrogens among postmenopausal women with prior hysterectomy: a randomized controlled trial. *JAMA* 305:1305–1314
- Krauss RM, Lindgren FT, Wingerd J, Bradley DD, Ramcharan S (1979) Effects of estrogens and progestins on high density lipoproteins. *Lipids* 14:113–118
- Lamon-Fava S, Micherone D (2004) Regulation of apoA-1 gene expression: mechanism of action of estrogen and genistein. *J Lipid Res* 45:106–112
- Walsh BW, Li H, Sacks FM (1994) Effects of postmenopausal hormone replacement with oral and transdermal estrogen on high density lipoprotein metabolism. *J Lipid Res* 35:2083–2093
- Bhavnani BR (2003) Estrogens and menopause: pharmacology of conjugated equine estrogens and their potential role in the prevention of neurodegenerative diseases such as Alzheimer's. *J Steroid Biochem Mol Biol* 85:473–482
- Lamon-Fava S, Postfai B, Diffenderfer M, DeLuca C, O'Connor J et al (2006) Role of the estrogen and progestin in hormonal replacement therapy on apolipoprotein A-1 kinetics in postmenopausal women. *Arterioscler Thromb Vasc Biol* 26:385–391
- Lopez D, Sanchez MD, Shea-Eaton W, McLean MP (2002) Estrogen activates the high-density lipoprotein receptor gene via binding to estrogen response elements and interaction with sterol regulatory element binding protein-1A. *Endocrinology* 143:2155–2168
- Jones DR, Schmidt RJ, Pickard RT, Foxworthy PS, Eacho PI (2002) Estrogen receptor-mediated repression of human hepatic lipase gene transcription. *J Lipid Res* 43:383–391
- Brinton EA, Eisenberg S, Breslow JL (1991) Increased apo A-I and apo A-II fractional catabolic rate in patients with low high density lipoprotein-cholesterol levels with or without hypertriglyceridemia. *J Clin Invest* 87:536–544
- Staels B, Jansen H, van Tol A, Stahnke G, Will H et al (1990) Development, food intake, and ethinylestradiol influence hepatic triglyceride lipase and LDL-receptor mRNA levels in rats. *J Lipid Res* 31:1211–1218
- Acton S, Rigotti A, Landshulz KT, Xu S, Hobbs HH et al (1996) Identification of scavenger receptor SR-BI as a high-density lipoprotein receptor. *Science* 271:1518–1520
- Jian B, de la Llera-Moya M, Ji Y, Wang N, Phillips MC et al (1998) Scavenger receptor class B type I as a mediator of cellular cholesterol efflux to lipoproteins and phospholipid acceptors. *J Biol Chem* 271:518–520
- Dubey RK, Tofovic SP, Jackson EK (2004) Cardiovascular pharmacology of estradiol metabolites. *J Pharmacol Exp Ther* 308:403–409
- Liu D, Bachman KA (1998) An investigation of the relationship between estrogen, estrogen metabolites and blood cholesterol levels in ovariectomized rats. *J Pharmacol Exp Ther* 286:561–568
- Tofovic S, Dubey RK, Jackson EK (2001) 2-Hydroxyestradiol attenuates the development of obesity, the metabolic syndrome, and vascular and renal dysfunction in obese ZSF1 rats. *J Pharmacol Exp Ther* 299:973–977
- Bourghart J, Bergstrom G, Krettek A, Sjoberg S, Boren J et al (2007) The endogenous estradiol metabolite 2-methoxyestradiol reduces atherosclerotic lesion formation in female apolipoprotein E-deficient mice. *Endocrinology* 9:4128–4132
- Barchiesi F, Lucchinetti E, Zaugg M, Ogunshola O, Wright M et al (2010) Candidate genes and mechanisms for 2-methoxyestradiol-mediated vasoprotection. *Hypertension* 56:964–972
- Hamilton VH, Racicot FE, Zowall H, Coupal L, Grover SA (1995) The cost-effectiveness of HMG-CoA reductase inhibitors to prevent coronary artery disease: estimating the benefits of increasing HDL-C. *JAMA* 273:1032–1038
- Zhu BT, Conney AH (1998) Functional role of estrogen metabolism in target cells: a review and perspectives. *Carcinogenesis* 19:1–27
- Xu X, Roman JM, Issaq HJ, Keefer LK, Veenstra TD et al (2007) Quantitative measurement of endogenous estrogens and estrogen metabolites in human serum by liquid chromatography–tandem mass spectrometry. *Anal Chem* 79:7813–7821
- Masi CM, Hawley LC, Xu X, Veenstra TD, Cacioppo JT (2009) Serum estrogen metabolites and systolic blood pressure among middle-aged and older women and men. *Am J Hypertens* 22:1148–1153
- Walsh BW, Spiegelman D, Morrissey M, Sacks FM (1999) Relationship between serum estradiol levels and the increases in high-density lipoprotein levels in postmenopausal women treated with oral estradiol. *J Clin Endocrinol Metab* 84:985–989
- Semmens J, Rouse I, Beilin LJ, Masarei JRL (1983) Relationship of plasma HDL-cholesterol to testosterone, estradiol, and sex-hormone-binding globulin levels in men and women. *Metabolism* 32:428–432
- Mueck AO, Seeger H, Lippert TH (2002) Estradiol metabolism and malignant disease. *Maturitas* 43:1–10
- Dubey RK, Jackson EK (2009) Potential vascular actions of 2-methoxyestradiol. *Trends Endocrinol Metab* 20:374–379

High Dose *trans*-10,*cis*-12 CLA Increases Lean Body Mass in Hamsters, but Elevates Levels of Plasma Lipids and Liver Enzyme Biomarkers

Xiaoran Liu · Shama V. Joseph · Andrew P. Wakefield · Harold M. Aukema · Peter J. H. Jones

Received: 30 November 2010 / Accepted: 16 September 2011 / Published online: 1 November 2011
© AOCs 2011

Abstract The current study examined the efficacy of graded doses of *c9,t11* and *t10,c12* CLA isomers on body composition, energy expenditure, hepatic and serum lipid liver biomarkers in hamsters. Animals ($n = 105$) were randomized to seven treatments (control, 1, 2, 3% of *c9,t11*; 1, 2, 3% of *t10,c12*) for 28 days. After 28 days treatment, 1–3% of *t10,c12* lowered ($p < 0.05$) body fat mass compared to the control group. The 1–3% *t10,c12* and 3% *c9,t11* fed groups showed higher ($p < 0.05$) lean mass compared to other groups. We observed unfavorable changes in plasma total cholesterol and non-HDL cholesterol levels in animals fed with 3% *t10,c12* CLA isomers. The 2%, 3% *t10,c12* groups presented elevated ($p < 0.05$) ALT levels. The present data suggest that a diet enriched with more than 2% *t10,c12* led to liver malfunction and poses unfavorable changes on plasma lipid profiles. The 1% *t10,c12* CLA lowered ($p < 0.05$) body fat mass and

increased ($p < 0.05$) lean body mass. The *c9,t11* CLA has less potent actions than *t10,c12* CLA. We conclude that the actions of CLA on energy and lipid metabolism are form and dose dependent in the hamster model.

Keywords *trans*-10,*cis*-12 CLA · *cis*-9,*trans*-11 CLA · Body composition · Lipids · Hamster · Liver biomarker · Safety

Abbreviations

DEXA Dual energy X-ray absorptiometry
AST Aspartate aminotransferase
ALT Alanine aminotransferase
GGT γ -Glutamyltranspeptidase

Introduction

Major isomers of CLA include *cis*-9,*trans*-11 (*c9,t11*) CLA and *trans*-10,*cis*-12 (*t10,c12*) CLA [1]. Over the last decade, health benefits of CLA have received a great deal of attention in various animal models and humans. Results have shown that *c9,t11* and *t10,c12* CLA mixtures possess anticancer effects both in vitro and in vivo [2–5]. Other effects including body composition modulation, atherosclerosis prevention, as well as immune system enhancement, have also been suggested in animal models [6–9]. CLA isomer enriched diets also effectively reduce body fat and increase lean body mass in several species [7, 10, 11]. However, previous studies have mainly focused on the effect of *c9,t11* and *t10,c12* CLA mixtures and conflicting results have been reported in many studies (Supplemental Table 1). Such sizable variation in results may due to the variability in animal model, duration of feeding as well as form, and the dosage of each isomer used. Indeed, the two

Electronic supplementary material The online version of this article (doi:10.1007/s11745-011-3616-3) contains supplementary material, which is available to authorized users.

X. Liu · A. P. Wakefield · P. J. H. Jones (✉)
Richardson Centre for Functional Foods and Nutraceuticals,
University of Manitoba, Winnipeg, MB R3T 2N2, Canada
e-mail: peter_jones@umanitoba.ca

X. Liu · P. J. H. Jones
Department of Food Sciences, University of Manitoba,
Winnipeg, MB R3T 2N2, Canada

S. V. Joseph
Department of Food Science and Nutrition, Laval University,
Quebec, QC G1V 0A6, Canada

H. M. Aukema · P. J. H. Jones
Department of Human Nutritional Sciences,
University of Manitoba, Winnipeg, MB R3T 2N2, Canada

CLA isomers may play different roles in body composition changes as well as lipid metabolism. The favorable modulation of body composition is mainly ascribed to the *t10,c12* CLA isomer [12], while a less potent effect has been reported for the *c9,t11* CLA isomer. Lack of effect on *c9,t11* CLA consumption on body composition modulation may due to the use of mixture of isomers, where the effect of one isomer may overshadow another, or to the relative low dosage used in different trials.

In terms of lipid metabolism and safety, previous investigations have shown that CLA lowers total cholesterol and triglyceride levels in plasma [13, 14]; nevertheless, these appear to be highly species dependent. Less consistent results have been observed in hamster and human studies [13, 15]. Moreover, safety issues have been raised over CLA supplementation since increased spleen and liver weights have been observed in some animal studies [16, 17]. Indeed, a systematic comparison of the two major isomers at graded dosages has not been previously conducted. Very few studies have investigated the effect of highly enriched *c9,t11* and *t10,c12* CLA isomer effect solely (Supplement Table 1). Therefore, the current investigation was aimed to examine both isomer and dosage effect of *c9, t11* and *t10, c12* CLA on body composition changes and serum lipid content modulation in Golden Syrian hamsters. Hamsters are considered to be a suitable model for studying lipid changes due to their similar lipoprotein profile and metabolism compared to humans [18]. Additionally, safety evaluation was also assessed in the present study.

Materials and Methods

Animals and Study Design

One hundred and five male Golden Syrian hamsters (Charles River Laboratories, Montreal, Quebec) weighing between 90 and 100 g were housed individually in plastic cages and subjected to a 12 h light/dark cycle at constant room temperature 25 °C. Upon arrival, the hamsters were provided with free access to rodent chow diet (Nestle, Purina, USA) and water for 3 weeks, and then switched to a semi-purified hypercholesterolemic diet containing 5% fat and 0.25% cholesterol for 3 more weeks. The study used a completely randomized design. Hamsters were randomized into 7 groups of 15 animals. Seven experimental diets were tested, including a control diet with no CLA and treatment diets enriched with 1, 2, 3% of *c9, t11* CLA as well as 1, 2, 3% of *t10,c12* CLA, each provided for 4 weeks. CLA isomers were provided in free fatty acid form and prepared by low temperature crystallization. Both CLA isomers were supplied by Lipid Nutrition

(Wormerveer, Netherlands). Table 1 presents the macronutrient and fatty acid composition of experimental diets. Dietary ingredients were purchased from Harland Laboratories Inc. (Indiana, USA) except cornstarch and sucrose which were purchased locally. Butylated hydroxytoluene (Sigma-Aldrich, Inc. ON, Canada) was added as an antioxidant. Food intake was measured every 2 days and body weight was measured weekly. On day 28, hamsters were anesthetized by isoflurane inhalation. Blood samples were taken by cardiac puncture then transferred into pre-coated heparin tubes. Hamsters were sacrificed followed by evisceration. Organ samples were wrapped and snap frozen by liquid nitrogen then stored at -80 °C until further analysis. The study was approved by the University of Manitoba Animal Care Protocol Review Committee, and carried out in accordance with the guidelines of the Canadian Council on Animal Care [19].

Body Composition Measurement

Body composition was measured by DEXA from Lunar Prodigy Advance. Tissue analyses were conducted by software Encore version 9.30.044. Percentage body fat, body fat mass and lean body mass were assessed using this software.

Lipid Profile and Hepatic Biomarker Measurement

Blood samples were thawed at room temperature then centrifuged at 3,500 rpm for 20 min. Red blood cells (RBC), plasma and serum samples were collected separately. Serum samples were used for lipid profile and liver enzyme assessment. Analyses were conducted by the Vitro Chemistry System 350 (Ortho-Clinical Diagnostics, Inc. Rochester, NY, USA). Triglyceride, total cholesterol and HDL-cholesterol levels were measured directly, whereas non-HDL cholesterol levels were calculated by subtracting HDL-cholesterol from total cholesterol content. Serum concentrations of liver enzymes AST, ALT and GGT were also measured.

Cholesterol Synthesis Measurement

Hamsters received 0.5 ml of deuterium oxide (D_2O , 99.9%, Cambridge Isotope Laboratories, Inc MA, USA) by intraperitoneal injection 2 h prior to sacrifice to assess cholesterol synthesis rate. Deuterium-enriched cholesterol was used as an indication of cholesterol synthesis [20]. Isotope ratios of DH/H_2 of plasma cholesterol were expressed in δ per mil, relative to Vienna Standard Mean Ocean Water. Enrichment of deuterium in both plasma water and RBC cholesterol were measured. Cholesterol samples extracted from RBCs were analyzed by online GC/pyrolysis/isotope

Table 1 Experimental diet composition (% w/w)

	Control	1% <i>c9,t11</i> ^a	2% <i>c9,t11</i> ^a	3% <i>c9,t11</i> ^a	1% <i>t10,c12</i> ^b	2% <i>t10,c12</i> ^b	3% <i>t10,c12</i> ^b
Casein	200	200	200	200	200	200	200
Cornstarch	280	280	280	280	280	280	280
Sucrose	360.3	360.3	360.3	360.3	360.3	360.3	360.3
Cellulose	50	50	50	50	50	50	50
DL-methionine	5	5	5	5	5	5	5
Mineral mix (AIN-93G Hamster)	40	40	40	40	40	40	40
Vitamin (AIN-76A)	10	10	10	10	10	10	10
Choline bitartrate	2	2	2	2	2	2	2
BHT	0.2	0.2	0.2	0.2	0.2	0.2	0.2
Cholesterol	2.5	2.5	2.5	2.5	2.5	2.5	2.5
Lard ^c	25	20	15	10	20	15	10
Safflower oil ^d	25	20	15	10	20	15	10
<i>c9,t11</i> CLA ^a	0	10	20	30	0	0	0
<i>t10,c12</i> CLA ^b	0	0	0	0	10	20	30

^a *c9,t11* CLA:0.2% C14:0, 5.1% C16:0, 0.4% C16:1, 1.6% C18:0, 17.1% C18:1, 3% C18:2, 57.5% *c9,t11*, 10.7% *t10,c12*

^b *t10,c12* CLA:0.2% C14:0, 2.6% C16:0, 0.1% C16:1, 1.6% C18:0, 4.3% C18:1, 0.4% C18:2, 13.2% *c9,t11*, 70.5% *t10,c12*

^c Lard: 2% C14:0, 26% C16:0, 3% C16:1, 14.% C18:0, 44% C18:1, 10% C18:2

^d Safflower oil:7.0% C16:0, 2.0% C18:0, 13% C18:1, 78% C18:2

ratio mass spectrometry (IRMS) equipped with an Agilent 6890N GC and Finnigan Delta V Plus IRMS (Bremen, Germany) through a Finnigan combustion interface (Combustion Interface III, Bremen, Germany). Cholesterol fractional synthesis rates were measured and calculated as previously described [20].

Energy Expenditure Assessment

On day 25, energy expenditure was assessed by the MM100-metabolic monitor system (CWE, Inc Ardmore, USA). Animals were kept in individual air chambers. Oxygen consumption was measured indirectly by monitoring oxygen and carbon dioxide concentrations in the chamber for 2 h per animal.

Hepatic Lipid Content Analysis

Liver lipids were extracted according to the Folch method [21] by chloroform and methanol in a ratio of 2:1 (v/v). Analysis of hepatic triglyceride and cholesterol concentrations was conducted by commercial available enzymatic kits (Roche Diagnostics, QC, Canada).

Statistics Analysis

All statistical analyses were performed by Statistical Analysis System (version 8.1; SAS Institute Inc Cary, NC). Data from different diet groups were analyzed by one-way ANOVA for overall significance then followed by Tukey's

post-hoc tests to identify the significant difference between treatment groups. Results were expressed as means \pm SEM (standard error mean). Regression analysis was also performed. Treatment effects and differences between means were considered significant when $p < 0.05$.

Results

Effects of CLA Consumption on Food Intake, Body Composition and Energy Expenditure

Hamsters fed with *t10,c12* CLA enriched diets showed a lower ($p < 0.05$) food intake in comparison to control and other groups (Table 2). No differences were noted in average daily food intake between the control animals and *c9,t11* treatment groups. Energy expenditure data suggested a strong tendency towards animals on three dosages of *t10,c12* CLA supplementation having greater oxygen consumption rate compared to control group and others ($p = 0.0657$). At the end of the 28-day experimental period, hamsters in all seven treatment groups exhibited similar body weights. Body composition results are presented in Table 2. DEXA analyses data indicate that hamsters fed with 1, 2, and 3% *t10,c12* CLA enriched diets showed 27, 30 and 23% less ($p < 0.0001$) body fat mass compared to control animals, respectively. Additional, higher lean body mass was found in groups fed with all three dosages of *t10,c12* CLA supplemented diets. Such effects were also observed in animals fed with 3% *c9,t11*

CLA compared to control ($p = 0.0002$). Both 1 and 3% *t10,c12* CLA fed animals had a lower body weight gain over 4 weeks, whereas opposite effects were observed in animals on 3% *c9,t11* CLA enriched diet (Fig. 1).

Effect of CLA Consumption on Lipid Profiles

Serum lipid content was affected by *t10,c12* CLA isomer in hamsters (Table 3). Neither the serum HDL-cholesterol concentration nor the triglyceride concentration differed among treatment groups. However, animals consuming 3% *t10,c12* CLA enriched diets displayed the highest total cholesterol and non-HDL cholesterol levels, in contrast to the rest of the treatment groups after 28 days of dietary intervention ($p < 0.05$).

Effect of CLA Consumption on Liver Weight and Hepatic Lipid Content

Data on effects of CLA consumption on liver weight and hepatic lipid content are presented in Table 4. Hamsters in the 2 and 3% *t10,c12* CLA diet groups exhibited higher liver weight ($p = 0.001$). With regard to hepatic lipid content, neither liver cholesterol nor the triglyceride concentration differed between groups after 28 days of consumption of CLA enriched diets. No differences were observed between dosages. Moreover, there was no difference in serum total protein level across the treatment groups (data not shown).

Effect of CLA Consumption on Hamster Liver Enzyme Level

After the 4-week experimental period, elevated ALT levels were observed in hamsters fed 2 and 3% *t10,c12* CLA diets ($p < 0.0001$), however, such results were not noted in any of the other treatment groups. Additionally, ALT levels in animals on 3% *t10,c12* CLA enriched diet were higher ($p = 0.0155$) than those in animals fed with 2% *t10,c12* CLA enriched diet. No differences were noticed in hepatic

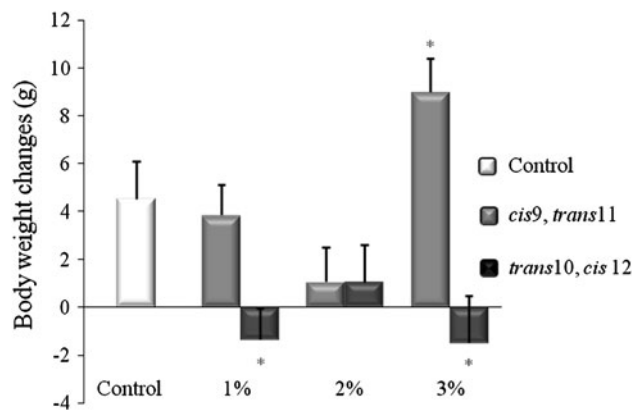


Fig. 1 Body weight changes in hamsters fed diets enriched with 1, 2, 3% *c9,t11* CLA or 1, 2, 3% *t10,c12* CLA for 28 days $n = 15$

AST or GGT levels across the seven experimental diets (Table 5).

Effect of CLA Consumption on Cholesterol Synthesis

Hamsters displayed similar cholesterol synthesis rates regardless of CLA intervention after 28 days (Fig. 2). Regression analysis suggested that the elevated serum cholesterol level of 2 and 3% *t10,c12* CLA treatment groups occurred independently of the individual rates of cholesterol synthesis across animals.

Discussion

The primary finding of the present study was that 1% *t10,c12* CLA effectively altered body composition without exhibiting potential adverse effects on the lipid profile and liver health. Similar body composition changes were also observed at 2 and 3% of *t10,c12* CLA. However, data from both serum lipid profiles and hepatic biomarkers suggest that 3% *t10,c12* CLA led to unfavorable increases in total as well as non-HDL cholesterol levels. Moreover, both 2 and 3% *t10,c12* CLA treatment induced elevated ALT

Table 2 Food intake, body weight and body composition of hamster fed diets enriched with 1, 2, 3% *c9,t11* CLA or 1, 2, 3% *t10,c12* CLA for 28 days

Diets	Food intake (g/day)	Energy expenditure (ml/h)	Final body weight (g)	Fat body mass (g)	Lean body mass (g)
Control	6.5 ± 0.18	0.8 ± 0.1	145.4 ± 3.6	58.2 ± 2.3	65.5 ± 2.8
<i>c9,t11</i> -1%	6.5 ± 0.2	0.8 ± 0.0	144.8 ± 2.6	57.3 ± 2.3	64.9 ± 1.8
<i>c9,t11</i> -2%	6.2 ± 0.1	0.8 ± 0.1	141.9 ± 2.9	51.0 ± 1.7	68.9 ± 1.6
<i>c9,t11</i> -3%	6.3 ± 0.2	0.8 ± 0.1	149.9 ± 3.3	53.4 ± 2.6	73.8 ± 2.8*
<i>t10,c12</i> -1%	5.7 ± 0.1*	0.9 ± 0.1	139.5 ± 3.1	42.5 ± 2.6*	74.8 ± 2.6*
<i>t10,c12</i> -2%	5.9 ± 0.2*	0.9 ± 0.1	141.9 ± 2.7	41.0 ± 1.7*	77.7 ± 1.5*
<i>t10,c12</i> -3%	5.7 ± 0.2*	0.9 ± 0.1	139.5 ± 2.9	44.5 ± 2.1*	71.7 ± 2.0*

Values are expressed as means ± SEM

* $p < 0.05$ vs. control

Table 3 Serum cholesterol, HDL cholesterol and non-HDL cholesterol level of hamster fed with diets enriched with 1, 2, 3% *c9,t11* CLA or 1, 2, 3% *t10,c12* CLA for 28 days

Diets	Cholesterol (mmol/L)	HDL cholesterol (mmol/L)	non-HDL cholesterol (mmol/L)	Triglycerides (mmol/L)
Control	5.9 ± 0.3	3.3 ± 0.1	2.6 ± 0.2	4.4 ± 0.4
<i>c9,t11</i> -1%	6.0 ± 0.3	3.3 ± 0.1	2.6 ± 0.1	4.3 ± 0.3
<i>c9,t11</i> -2%	5.8 ± 0.3	3.2 ± 0.1	2.5 ± 0.1	4.1 ± 0.2
<i>c9,t11</i> -3%	5.9 ± 0.2	3.3 ± 0.1	2.9 ± 0.2	4.4 ± 0.3
<i>t10,c12</i> -1%	5.5 ± 0.2	3.1 ± 0.1	2.3 ± 0.2	4.3 ± 0.4
<i>t10,c12</i> -2%	6.4 ± 0.3	3.2 ± 0.1	3.3 ± 0.2	4.6 ± 0.3
<i>t10,c12</i> -3%	7.5 ± 0.5*	3.4 ± 0.1	3.9 ± 0.2*	4.0 ± 0.3

Values are expressed as means ± SEM

* $p < 0.05$ vs. control

Table 4 Liver cholesterol concentration and triglyceride content fed diets enriched with 1, 2, 3% *c9,t11* CLA or 1, 2, 3% *t10,c12* CLA for 28 days

Diets	Liver weight (g)	Hepatic cholesterol concentration (μmol/g)	Hepatic triglyceride concentration (μmol/g)
Control	7.8 ± 0.2	139.5 ± 26.8	4.8 ± 0.3
<i>c9,t11</i> -1%	8.3 ± 0.2	111.6 ± 10.7	6.0 ± 0.5
<i>c9,t11</i> -2%	8.0 ± 0.2	156.6 ± 22.7	4.9 ± 0.4
<i>c9,t11</i> -3%	8.9 ± 0.3	146.2 ± 30.0	5.8 ± 0.7
<i>t10,c12</i> -1%	8.5 ± 0.3	124.3 ± 19.8	4.7 ± 0.4
<i>t10,c12</i> -2%	9.3 ± 0.4*	105.3 ± 19.0	4.8 ± 0.3
<i>t10,c12</i> -3%	9.4 ± 0.4*	82.3 ± 13.4	5.6 ± 0.5

Values are expressed as means ± SEM

* $p < 0.05$ vs. control

Table 5 Serum concentration of liver enzymes of hamster fed diets enriched with 1, 2, 3% *c9,t11* CLA or 1, 2, 3% *t10,c12* CLA for 28 days

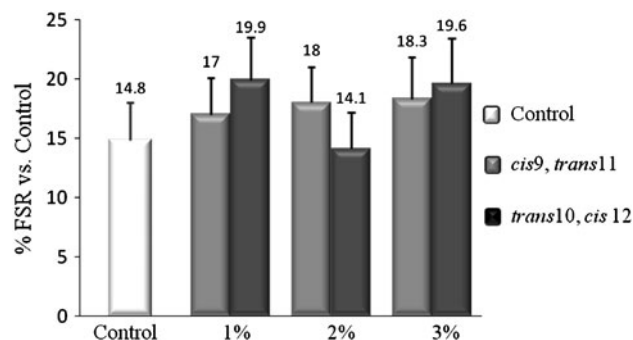
Diets	ALT (U/L)	AST (U/L)	GGT (U/L)
Control	104.8 ± 11.2	151.9 ± 24.5	6.6 ± 0.4
<i>c9,t11</i> -1%	127.7 ± 18.2	131.9 ± 20.4	5.8 ± 0.3
<i>c9,t11</i> -2%	128.6 ± 21.2	148.7 ± 23.5	5.6 ± 0.2
<i>c9,t11</i> -3%	105.0 ± 9.2	123.0 ± 20.5	5.7 ± 0.4
<i>t10,c12</i> -1%	129.3 ± 14.8	126.7 ± 28.9	5.9 ± 0.2
<i>t10,c12</i> -2%	197.8 ± 30.7*	194.9 ± 21.1	6.0 ± 0.3
<i>t10,c12</i> -3%	306.2 ± 50.9**	182.1 ± 35.7	5.4 ± 0.2

Values are expressed as means ± SEM

* $p < 0.05$ vs. control; ** $p < 0.0001$ vs. control

levels. Such changes may suggest health concerns associated with consuming high dosages of *t10,c12* CLA.

As a secondary effect of CLA, data from the current study suggest that *t10,c12* CLA decreases energy intake in hamsters. These data are in line with results reported by others [12, 22, 23]. Data from the present study show that animals on the *t10,c12* CLA treatment had a lower fat body

**Fig. 2** Cholesterol synthesis rate in hamsters fed diets enriched with 1, 2, 3% *c9,t11* CLA or 1, 2, 3% *t10,c12* CLA for 28 days $n = 15$

mass which was in accordance with previous observations [10, 22, 24, 25]. In earlier studies, *t10,c12* CLA isomers were identified as being responsible for biological effects on body composition [13]. Results from the current study also provide evidence supporting a physiological effect of CLA on fat mass in a manner that is isomer dependent. Several possible mechanisms may explain body fat reduction effects in response to CLA supplementation. Much evidence suggests that *t10,c12* CLA may induce fat mass reduction by decreasing energy intake, inhibiting adipogenesis or lipogenesis by suppressing gene expression of sterol regulatory element binding protein (SREBP), liver X-receptor (LXR) α , PPAR- α and PPAR- γ target genes [26–29]. Additional evidence supports a *t10,c12* CLA-induced down regulation of the hypothalamic appetite regulating gene expression which suppresses appetite, leading to reduced energy intakes [30, 31]. Data from current study indicate that reductions in fat mass following the three doses of *t10,c12* CLA were associated with decreased energy intake as well as a tendency towards increased energy expenditure.

Notably, animals fed with 3% *c9,t11* CLA displayed increased lean body mass. The same observation was also noticed in animals fed all three dosages of *t10,c12* CLA. To our knowledge, the current study is the first evidence supporting an effect on hamster body composition by consumption of the *c9,t11* CLA isomer solely. Other work

suggests that a CLA mixture including 25% *c9,t11* CLA induced increased carcass lean tissue in growing pigs [32]. Previous works reported that CLA consumption increases lean body mass in several species (reviewed in [33]). However, the lack of evidence of such an effect on *c9,t11* CLA isomer may be explained by the relative low dose of *c9,t11* CLA isomer or *c9,t11* containing mixture used in previous studies. Recently, Nall et al. [34] demonstrated that CLA and arginine increased lean body mass, due possibly to a depression in muscle protein turnover, however, the mechanism of CLA supplementation increasing lean body mass remains to be fully understood and requires further investigation.

The effects of *c9,t11* and *t10,c12* CLA on serum lipid profiles vary between animals and humans [14, 35]. In the present study, animals fed 3% *t10,c12* enriched diet exhibited the highest total as well as non-HDL cholesterol levels, in comparison with the rest of the groups. These results are in accordance with some studies published by other authors when animals were fed diets with either a CLA mixture or the *t10,c12* CLA isomer. Bissonauth et al. [36] reported an increase in LDL-cholesterol levels induced by 2% highly enriched *t10,c12* CLA. Kritchevsky et al. [9] demonstrated elevated total cholesterol levels induced by CLA mixtures (43:44%, *c9,t11:t10,c12*) in rabbits. In contrast, evidence supports either a positive action or no effects on total cholesterol and non-HDL cholesterol levels by either pure or mixed CLA consumption [37–39]. Current data fail to provide any further positive indication of CLA improving serum lipid profile. Most human studies report no effect of supplementation with CLA mixtures on lipid profiles [35]. Tricon et al. [40] reported that serum concentration of total cholesterol, LDL cholesterol, TG and the ratio of total to HDL cholesterol were elevated after consumption of CLA capsules containing 80% *t10, c12* in healthy subjects. Moloney et al. [41] also demonstrated an increased LDL to HDL ratio in subjects with type II diabetes. Moreover, a recent review has suggested that all fatty acids with a double bond in the *trans*-configuration raise the LDL to HDL ratio [15]. Data from the present work partially reflects this adverse effect of high dose *t10,c12* CLA isomer on serum lipid content. The isotope work indicates that increased total serum cholesterol is not the result of augmented endogenous cholesterol synthesis. Navarro et al. [42] found that *t10,c12* CLA significantly reduced the LDL-receptor number when expressed as an arbitrary value of per mg of protein in hamster liver. One possible theory offered was that *t10,c12* CLA induced an increase in free cholesterol pool size, perhaps related to down regulation of the LDL receptor. In comparison with the aforementioned study, the high dosage of *t10,c12* CLA provided in the current study significantly increased serum total and non-HDL cholesterol levels, with

a lack of change in hepatic lipid content. Taken together, growing evidence suggests that *t10,c12* CLA does not favorably change serum lipid levels.

Recently, the safety of CLA consumption has become a concern. In the present study, the high dosages of *t10,c12* CLA (2 and 3%) increased hamster liver weights compared with control and *c9,t11* CLA treatments. This finding is consistent with those of a number of other studies [13, 21, 43]. Along with this observation, our study has shown that CLA supplementation did not affect lipogenesis in liver since the triglyceride concentrations failed to differ across treatment groups. The increased liver weight in animals fed with *t10,c12* isomer are not necessarily due to liver lipid accumulation but rather from a greater number of hepatocytes [13, 44]. Future histological analysis may provide a better understanding of the underlying cause of elevated liver weight.

It is well known that serum liver enzyme activity exists as an indicator of liver function. In our study, elevated ALT concentrations in liver were observed in animals fed 2 and 3% *t10,c12* CLA. Such results suggest that high doses of *t10,c12* may lead to liver malfunction since ALT serves as a biomarker for hepatocellular necrosis [45]. Elevated ALT level may also indicate increased inflammation and oxidation subsequent to *t10,c12* CLA consumption. In contrast, animal studies conducted by Macarulla et al. [44] reported no changes in hepatic ALT concentration after 6-week consumption of *t10,c12* CLA. The discrepancy could be attributed to the dosage variances between studies (0.5 vs. 2% and higher).

In a recent investigation on the safety of dietary CLA consumption, Iwata et al. [46] reported slight increases in ALT activities in the high dose CLA (6.8/d) group after 12-week intervention in healthy overweight Japanese subjects. Taken together, *c9,t11* CLA and 1% *t10,c12* CLA did not exert any adverse effect on liver health in the hamster model. Present data show clearly that the degree of impact of CLA supplementation on liver health is isomer dependent. Recently, the European Food Safety Authority has issued positive safety opinions about two CLA products as a safe ingredient for food and beverage [47]. In the present study, 1, 2 and 3% CLA-enriched diet correspond to human diet equivalents (2,500 kcal intake daily) of 2, 4 and 6 g/d. These levels of intakes are very similar to what EFSA has recommended. The 3% CLA treatment represented the higher dosages than what has been recommended by EFSA (6 g at 3% vs. 3.5–4.5 g) which provided a better idea for safety evaluation for CLA consumption. Iwata et al. [46] reported mild to moderate adverse effects in overweight male Japanese subjects supplemented with either 3.4 or 6.8 g/d CLA (50:50, *c9,t11:t10,c12*), where slight increases in AST and ALT activity levels were observed at 12 weeks. The author indicated that such elevations were

small and within the normal range. Moreover, one of the most recent reviews conducted by Katan and colleagues [15] has suggested that CLA exerts a negative effect on the circulation lipid profile.

In summary, the present study provided a systematic comparison of two CLA isomers at three different dosages. The most important finding is that low dose intakes of *t10,c12* CLA effectively lower body fat mass and increase lean body mass without posing unfavorable changes in serum lipid profile. Higher dosages (2 and 3%) of *t10,c12* CLA supplementation produce adverse effects in liver function and 3% *t10,c12* CLA has negative effects on serum lipid content. 3% *c9,t11* CLA also increased lean body mass; however, no body fat lowering effects of the *c9,t11* CLA isomers were seen at any of the three dosages. Additionally, *c9,t11* CLA did not have any adverse effect in liver function in the hamster model. Data from the present study suggests that 1% *t10,c12* CLA, which was close to the EFSA recommended level, effectively modulates body composition whereas 2 and 3% cause unfavorable physiological changes.

References

- MacDonald HB (2000) Conjugated linoleic acid and disease prevention: a review of current knowledge. *J Am Coll Nutr* 19(2 Suppl):111S–118S
- Thomas Yeung CH et al (2000) Dietary conjugated linoleic acid mixture affects the activity of intestinal acyl coenzyme A: cholesterol acyltransferase in hamsters. *Br J Nutr* 84(6):935–941
- Durgam VR, Fernandes G (1997) The growth inhibitory effect of conjugated linoleic acid on MCF-7 cells is related to estrogen response system. *Cancer Lett* 116(2):121–130
- Cesano A et al (1998) Opposite effects of linoleic acid and conjugated linoleic acid on human prostatic cancer in SCID mice. *Anticancer Res* 18(3A):1429–1434
- Liew C et al (1995) Protection of conjugated linoleic acids against 2-amino-3-methylimidazo [4,5-f]quinoline-induced colon carcinogenesis in the F344 rat: a study of inhibitory mechanisms. *Carcinogenesis* 16(12):3037–3043
- Drury B et al (2009) Dietary *trans,cis*-12 conjugated linoleic acid reduces early glomerular enlargement and elevated renal cyclooxygenase-2 levels in young obese *fa/fa* Zucker rats. *J Nutr* 139(2):285–290
- Tarling EJ et al (2009) Effect of dietary conjugated linoleic acid isomers on lipid metabolism in hamsters fed high-carbohydrate and high-fat diets. *Br J Nutr* 101(11):1630–1638
- Parra P, Serra F, Palou A (2010) Moderate doses of conjugated linoleic acid isomers mix contribute to lowering body fat content maintaining insulin sensitivity and a noninflammatory pattern in adipose tissue in mice. *J Nutr Biochem* 21:107–115
- Kritchevsky D et al (2000) Influence of conjugated linoleic acid (CLA) on establishment and progression of atherosclerosis in rabbits. *J Am Coll Nutr* 19(4):472S–477S
- West DB et al (2000) Conjugated linoleic acid persistently increases total energy expenditure in AKR/J mice without increasing uncoupling protein gene expression. *J Nutr* 130(10):2471–2477
- Park Y et al (1997) Effect of conjugated linoleic acid on body composition in mice. *Lipids* 32(8):853–858
- Park Y et al (1999) Evidence that the *trans*-10,*cis*-12 isomer of conjugated linoleic acid induces body composition changes in mice. *Lipids* 34(3):235–241
- De Deckere EAM et al (1999) Effects of conjugated linoleic acid (CLA) isomers on lipid levels and peroxisome proliferation in the hamster. *Br J Nutr* 82(4):309–317
- Mitchell PL, McLeod RS (2008) Conjugated linoleic acid and atherosclerosis: studies in animal models. *Biochem Cell Biol* 86(4):293–301
- Brouwer IA, Wanders AJ, Katan MB (2010) Effect of animal and industrial trans-fatty acids on HDL and LDL cholesterol levels in humans—a quantitative review. *PLoS One* 5(3):e9434. doi:10.1371/journal.pone.0009434
- Clement L et al (2002) Dietary *trans*-10,*cis*-12 conjugated linoleic acid induces hyperinsulinemia and fatty liver in the mouse. *J Lipid Res* 43(9):1400–1409
- Perez-Matute P et al (2007) Conjugated linoleic acid inhibits glucose metabolism, leptin and adiponectin secretion in primary cultured rat adipocytes. *Mol Cell Endocrinol* 268(1–2):50–58
- Spady DK, Dietschy JM (1983) Sterol synthesis in vivo in 18 tissues of the squirrel monkey, guinea pig, rabbit, hamster, and rat. *J Lipid Res* 24(3):303–315
- Canadian Council on Animal Care (2006) Guide to the care and use of experimental animals, vol 2, chap XV. Hamsters
- Jones PJ et al (2000) Modulation of plasma lipid levels and cholesterol kinetics by phytosterol versus phytostanol esters. *J Lipid Res* 41(5):697–705
- Folch JM, Lees M, Sloane Stanley GH (1957) A simple method for the isolation and purification of total lipids from animal tissues. *J Biol Chem* 226(1):497–509
- West DB et al (1998) Effects of conjugated linoleic acid on body fat and energy metabolism in the mouse. *Am J Physiol* 275(3 Pt 2):R667–R672
- Takahashi Y et al (2002) Dietary conjugated linoleic acid reduces body fat mass and affects gene expression of proteins regulating energy metabolism in mice. *Comp Biochem Physiol B Biochem Mol Biol* 133:395–404
- DeLany JP, West DB (2000) Changes in body composition with conjugated linoleic acid. *J Am Coll Nutr* 19(4):487S–493S
- Azain MJ et al (2000) Dietary conjugated linoleic acid reduces rat adipose tissue cell size rather than cell number. *J Nutr* 130(6):1548–1554
- Kang K et al (2003) *trans*-10,*cis*-12 CLA inhibits differentiation of 3T3-L1 adipocytes and decreases PPAR gamma expression. *Biochem Biophys Res Commun* 303(3):795–799
- Brown JM et al (2003) Isomer-specific regulation of metabolism and PPARgamma signaling by CLA in human preadipocytes. *J Lipid Res* 44(7):1287–1300
- Granlund L, Pedersen JI, Nebb HI (2005) Impaired lipid accumulation by *trans*10,*cis* CLA during adipocyte differentiation is dependent on timing and length of treatment. *Biochim Biophys Acta* 1687(1–3):11–22
- LaRosa PC et al (2007) *trans*-10,*cis*-12 Conjugated linoleic acid activates the integrated stress response pathway in adipocytes. *Physiol Genomics* 14(31):544–553
- So M, Tse I, Li E (2009) Dietary fat concentration influences the effects of *trans*-10,*cis*-12 conjugated linoleic acid on temporal patterns of energy intake and hypothalamic expression of appetite-controlling genes in mice. *J Nutr* 139:145–151
- Cao Z et al (2007) Intracerebroventricular administration of conjugated linoleic acid (CLA) inhibits food intake by decreasing gene expression of NPY and AgRP. *Neurosci Lett* 418:217–221

32. Ostrowska E et al (1999) Dietary conjugated linoleic acids increase lean tissue and decrease fat deposition in growing pigs. *J Nutr* 129(11):2037–2042
33. Wang YW, Jones PJH (2004) Conjugated linoleic acid and obesity control: efficacy and mechanisms. *Int J Obes Relat Metab Disord* 28(8):941–955
34. Nall JL et al (2009) Dietary supplementation of L-arginine and conjugated linoleic acid reduces retroperitoneal fat mass and increases lean body mass in rats. *J Nutr* 137(7):1279–1285
35. Salas-Salvado J, Marquez-Sandoval F, Bullo M (2006) Conjugated linoleic acid intake in humans: a systematic review focusing on its effect on body composition, Glucose, and lipid metabolism. *Crit Rev Food Sci Nutr* 46(6):479–488
36. Bissonauth V et al (2006) The effect of t10,c12 CLA isomer compared with c9,t11 CLA isomer on lipid metabolism and body composition in hamsters. *J Nutr Biochem* 17:597–603
37. Lee KN, Kritchevsky D, Pariza MW (1994) Conjugated linoleic acid and atherosclerosis in rabbits. *Atherosclerosis* 108(1):19–25
38. Nicolosi RJ et al (1997) Dietary conjugated linoleic acid reduces plasma lipoproteins and early aortic atherosclerosis in hypercholesterolemic hamsters. *Artery* 22(5):266–277
39. LeDoux M et al (2007) Rumenic acid significantly reduces plasma levels of LDL and small dense LDL cholesterol in hamsters fed a cholesterol- and lipid-enriched semi-purified diet. *Lipids* 42(2):135–141
40. Tricon S et al (2004) Opposing effects of *cis-9,trans-11* and *trans-10, cis-12* conjugated linoleic acid on blood lipids in healthy humans. *Am J Clin Nutr* 80(3):614–620
41. Moloney F et al (2004) Conjugated linoleic acid supplementation, insulin sensitivity, and lipoprotein metabolism in patients with type 2 diabetes mellitus. *Am J Clin Nutr* 80(4):887–895
42. Navarro V et al (2007) Effects of *trans-10,cis-12* conjugated linoleic acid on cholesterol metabolism in hypercholesterolaemic hamsters. *Eur J Nutr* 46(4):213–219
43. Navarro V et al (2003) Effects of conjugated linoleic acid on body fat accumulation and serum lipids in hamsters fed an atherogenic diet. *J Physiol Biochem* 59(3):193–199
44. Macarulla MT et al (2005) Effects of conjugated linoleic acid on liver composition and fatty acid oxidation are isomer-dependent in hamster. *Nutrition* 21(4):512–519
45. Meeks RG, Harrison SD, Bull RJ (1991) Liver function tests in the differential diagnosis of hepatotoxicity. In: Meeks RG (ed) *Hepatotoxicology*. CRC Press
46. Iwata T et al (2007) Safety of dietary conjugated linoleic acid (CLA) in a 12-weeks trial in healthy overweight Japanese male volunteers. *J Oleo Sci* 56(10):517–525
47. EFSA, Scientific Opinion on the safety of “conjugated linoleic acid (CLA)-rich oil” (Tonalin® TG 80) as a Novel Food ingredient EFSA Journal, 2010. 8:43.

Dietary CLA Combined with Palm Oil or Ovine Fat Differentially Influences Fatty Acid Deposition in Tissues of Obese Zucker Rats

Susana V. Martins · Paula A. Lopes · Susana P. Alves ·
Cristina M. Alfaia · Matilde F. Castro · Rui J. B. Bessa ·
José A. M. Prates

Received: 28 March 2011 / Accepted: 21 October 2011 / Published online: 17 November 2011
© AOCs 2011

Abstract The effect of dietary conjugated linoleic acid (CLA) supplementation in combination with fat from vegetable versus animal origin on the fatty acid deposition, including that of individual 18:1 and 18:2 (conjugated and non-conjugated) isomers, in the liver and muscle of obese rats was investigated. For this purpose, 32 male Zucker rats were randomly assigned to one of four diets containing palm oil or ovine fat, supplemented or not with 1% of 1:1 *cis(c)9,trans(t)11* and *t10,c12* CLA isomers mixture. Total fatty acid content decreased in the liver and muscle of CLA-fed rats. In the liver, CLA increased saturated fatty acids (SFA) in 11.9% and decreased monounsaturated fatty acids (MUFA) in 6.5%. n-3 Polyunsaturated fatty acids (PUFA) relative proportions were increased in 30.6% by CLA when supplemented to the ovine fat diet. In the

muscle, CLA did not affect SFA but decreased MUFA and PUFA percentages. The estimation of $\Delta 9$ -indices 16 and 18 suggested that CLA inhibited the stearoyl-CoA desaturase activity in the liver (a decrease of 13–38%), in particular when supplemented to the ovine fat diet. Concerning CLA supplementation, the *t10,c12* isomer percentage was 60–80% higher in the muscle than in the liver. It is of relevance that rats fed ovine fat, containing bio-formed CLA, had more *c9,t11* CLA isomer deposited in both tissues than rats fed palm oil plus synthetic CLA. These results highlight the importance to further clarify the biological effects of consuming foods naturally enriched in CLA, alternatively to CLA dietary supplementation.

Keywords Conjugated linoleic acid · Palm oil · Ovine fat · Fatty acid composition · Obese Zucker rat · Liver · Muscle

Abbreviations

Ag ⁺ -HPLC	Silver ion-high pressure liquid chromatography
<i>c9,t11</i>	<i>cis9,trans11</i> CLA isomer
CLA	Conjugated linoleic acid
FAME	Fatty acid methyl esters
GC	Gas chromatography
MUFA	Monounsaturated fatty acids
O	Ovine fat group
OCLA	Ovine fat plus 1% CLA group
P	Palm oil group
PCLA	Palm oil plus 1% CLA group
PUFA	Polyunsaturated fatty acids
SCD	Stearoyl-CoA desaturase
SFA	Saturated fatty acids
<i>t10,c12</i>	<i>trans10,cis12</i> CLA isomer
TFA	<i>trans</i> fatty acids

S. V. Martins · P. A. Lopes · C. M. Alfaia ·
R. J. B. Bessa · J. A. M. Prates (✉)
Secção de Bioquímica, CIISA, Faculdade de Medicina
Veterinária, Universidade Técnica de Lisboa, Av. da
Universidade Técnica, Pólo Universitário do Alto da Ajuda,
1300-477 Lisbon, Portugal
e-mail: japrates@fmv.utl.pt

S. P. Alves · R. J. B. Bessa
Unidade de Produção Animal, L-INIA, INRB I.P.,
2005-048 Vale de Santarém, Portugal

S. P. Alves
REQUIMTE, Instituto de Ciências Biomédicas Abel Salazar,
Universidade do Porto, Rua Padre Armando Quintas,
4485-661 Vairão, VC, Portugal

M. F. Castro
Faculdade de Farmácia, iMed.UL, Av. Professor Gama Pinto,
1649-003 Lisbon, Portugal

Introduction

A huge focus has been attributed to the beneficial properties of conjugated linoleic acid (CLA), which is a group of linoleic acid (*c9,c12-18:2*) isomers with conjugated double bonds in *trans(t)* or *cis(c)* configuration. In particular, the *c9,t11* CLA isomer (*c9,t11-18:2*) has been shown to inhibit carcinogenesis in cell cultures and animal experiments, although studies in humans have revealed inconclusive results [1]. The *t10,c12* CLA isomer has been described as more efficient on lipid metabolism modulation, reducing body fat mass on several models [2].

Ruminant food products are good sources of CLA, predominantly of the *c9,t11* CLA isomer, called rumenic acid, that is produced by bacterial isomerization and hydrogenation of linoleic acid in the rumen. Alternatively, in tissues, the vaccenic acid (*t11-18:1*), also produced in the rumen, is converted to rumenic acid via $\Delta 9$ -desaturation by the action of stearoyl-CoA desaturase (SCD) enzyme [3]. This endogenous synthesis through vaccenic acid is also observed in other animal species, as rodents [4]. Although the majority of dietary CLA isomers in foodstuff is rumenic acid, commercial supplements with synthetic CLA often include the *t10,c12* CLA isomer in equivalent proportions.

Today's unhealthy diet and lifestyles promote excessive intake of saturated fats [5]. High fat diets, which are usually unbalanced in fatty acids, may directly increase the prevalence of obesity worldwide [6]. Concerning different types of dietary fat, Kloss et al. [7] observed that CLA was more beneficial in controlling blood lipids and adiposity when supplemented to a diet rich in saturated (coconut oil) versus unsaturated (corn oil) fat. Butter naturally enriched in CLA had increased serum concentrations of alpha-linolenic acid (18:3n-3), and decreased myristic (14:0) and palmitic (16:0) acids in growing pigs, comparing to animals fed regular butter [8]. This implies a potential benefit of CLA on the serum fatty acid composition [8]. CLA may compete for elongation and desaturation pathways with other unsaturated fatty acids [9], thus modifying the fatty acid profile of different tissues [10]. However, research performed so far has not adequately compared the effects of CLA supplementation on the tissue fatty acid composition facing dietary fats from distinct origins, vegetable and animal. Moreover, the influence of synthetic and bio-formed *c9,t11* CLA isomer on tissues fatty acid profile is not well explored.

Ruminant edible fats are a major contributor to saturated fat intake in human nutrition [11]. Yet, these fats also contain variable amounts of *trans* and *cis* isomers of oleic (*c9-18:1*) and linoleic acids originating from the incomplete biohydrogenation of these fatty acids in the rumen. The production of ruminant edible fats (milk and meat) enriched

in rumenic and vaccenic acids has been extensively exploited [12], as it can be an effective approach to increase human dietary intake of these fatty acids with potential health benefits [13]. The ovine fat used in the present experiment was naturally enriched in rumenic and vaccenic acids, as well as other PUFA and *trans* fatty acids (TFA). The vegetable fat chosen was palm oil as it is the second most consumed edible oil [14], rich in saturated fatty acids (SFA) but having a distinct fatty acid profile comparing to ruminant edible fats. Detailed data on the fatty acid deposition in tissues derived from rumen biohydrogenation intermediates (18:1 and 18:2 fatty acids) ingestion, and possible interactions between them and CLA, are scarce.

In this study, it was hypothesized that *c9,t11* and *t10,c12* CLA isomers supplementation would influence the tissue fatty acid composition of obese Zucker rats according to the type of dietary fat (vegetable vs. animal). In addition, we intended to clarify if *c9,t11* CLA isomer deposition in tissues is dependent on its origin, synthetic (industrially produced) or bio-formed (ruminant fat naturally enriched in CLA).

Materials and Methods

CLA Oil and Experimental Diets

The CLA oil used, from PharmaNutrients Inc. (Gurnee, IL, USA), contained similar proportions of *c9,t11* and *t10,c12* isomers with 80% purity. The remaining ingredients, apart from the ovine fat, were purchased from Provimi Kliba SA (Kaiseraugst, Switzerland) to manufacture the experimental diets. Peritoneal ovine fat was collected from lambs raised with forage enriched in seed oils, as described by Jerónimo et al. [15], thus having high contents of total CLA, other PUFA and TFA. The raw ovine fat was melted, and then filtered to subsequent mixture with the remaining ingredients. Diets were prepared and pelleted by Provimi Kliba following the AIN-93G formulation, with some modifications to obtain high fat diets. The ingredients composition (% feed) was: casein (20.0), dextrose (13.2), sucrose (11.9), corn starch (29.3), cellulose (5.0), vitamin-mixture (0.5), mineral-mixture (2.4), L-cysteine (0.3), cholesterol (2.0), cholic acid sodium salt (0.5) and BHT (0.01). Diets had a dry matter (DM) concentration of 928 g/kg feed and the following crude composition (g/100 g DM): protein (20.0), fat (16.6), ash (3.9), fiber (3.9) and carbohydrate (55.6). The four experimental diets differed in their fat composition. Two groups received fat from vegetable origin: group P—11.25% of palm oil plus 3.75% of sunflower oil; group PCLA—11.25% of palm oil plus 2.53% of sunflower oil and 1.22% of CLA oil. The other two groups (O and OCLA) received ovine fat instead

of palm oil. The fatty acid characterization of the experimental diets is presented in Table 1.

Animals

Thirty-two obese male Zucker rats (*falfa*), a widely used experimental model that develops morbid obesity due to a mutation (*fa*) on the leptin receptor [16], were obtained from Harlan Interfauna Iberia (Barcelona, Spain) at 5 weeks old. Animals were housed individually upon arrival and maintained on a 12 h light:dark cycle at 22 ± 2 °C. After an adaptation period of 1 week, animals were divided into four groups with eight rats each ($n = 8$) and fed the aforementioned semi-purified diets for 13–14 weeks. Animals had free access to water and food. Body weight and feed intake were monitored twice a week. At the end of the animal experiment, rats were killed by decapitation, under light isoflurane anesthesia. Liver and longissimus dorsi muscle were dissected, weighed and stored at -80 °C for further analysis. The experimental protocol of this study was reviewed by the Ethics Commission of CIISA/FMV and approved by the Animal Care Committee of the National Veterinary Authority (Direcção Geral de Veterinária, Portugal), following the appropriated European Union guidelines (N. 86/609/EEC).

Analysis of Fatty Acids

Liver and longissimus dorsi muscle samples were lyophilized (-60 °C and 2.0 hPa) and maintained desiccated at room temperature. Lipids were extracted using the method of Christie et al. [17], slightly modified by Raes et al. [18]. Fatty acids were directly converted to methyl esters by a combined procedure of methylation, base-catalysis followed by acid-catalysis. Briefly, 1 mL of dry toluene was added to 0.25 g of lyophilized samples and fatty acids were methylated, at 50 °C, with sodium methoxide in anhydrous methanol (0.5 mol/L), for 30 min, followed by hydrogen chloride in methanol (1:1 vol/vol), for 10 min. Fatty acid methyl esters (FAME) were extracted twice with 3 mL of *n*-hexane and pooled extracts were evaporated at 35 °C, under a stream of nitrogen, until a final volume of 2 mL was reached. The resulting FAME, including 18:1 and 18:2 non-conjugated, were then analyzed by gas–liquid chromatography (GC) using a fused-silica capillary column (CP-Sil 88; 100 m \times 0.25 mm i.d., 0.20 mm film thickness; Chrompack, Varian Inc., Walnut Creek, CA, USA), equipped with a flame-ionization detector (FID), as described by Bessa et al. [19].

In order to obtain a detailed profile of individual CLA isomers, FAME were injected into a high performance liquid chromatography (HPLC) system (Agilent 1100 Series, Agilent Technologies Inc., Palo Alto, CA, USA), equipped with triple silver-ion columns in series (ChromSpher 5 Lipids,

250 mm \times 4.6 mm i.d., 5 μ m particle size; Chrompack, Bridgewater, NJ, USA), an autosampler and a diode array detector (DAD) adjusted to 233 nm, according to a procedure previously reported [20]. The identification of individual CLA isomers was achieved by comparison of their retention times with commercial and prepared standards, as well as with values published in the literature.

The fatty acid composition was expressed as a percentage, i.e. g/100 g of total fatty acids. The contents of CLA isomers were calculated from their Ag^+ -HPLC peak areas relative to the GC peak area of the main *c9,t11* CLA isomer, which also included *t7,c9* and *t8,c10* CLA isomers, as described by Rego et al. [20]. Diets followed the same analytical procedure described for fatty acid profile in muscle and liver.

Estimation of *c9,t11* CLA Isomer Deposition

An estimate of *c9,t11* CLA isomer deposition in tissues depending on its origin, synthetic or bio-formed, was calculated by comparing two experimental groups PCLA and O. Additionally to the amount of *c9,t11* CLA isomer ingested, the evaluation was also based on its endogenous synthesis. For this purpose, we used the average of 20% for the *t11-18:1* conversion to *c9,t11*, reported for male Wistar rats by Kraft et al. [4]. The deposition values were calculated by dividing the total amount of *c9,t11* quantified in the tissue by the total amount of *c9,t11* ingested (the exogenous contribution) plus 20% of *t11-18:1* derived (the endogenous contribution).

Statistical Analysis

The statistical analysis for fatty acid profiles was performed with the general linear model (GLM) procedure of Statistical Analysis System, version 9.1 (SAS Institute, Cary, NC, USA). Data were reported as means with their standard errors of the mean (SEM). The effects of CLA (with or without 1% of CLA) and dietary fat type (palm oil or ovine fat) were analyzed as a 2×2 factorial arrangement. The model contained the main effects, CLA and fat type, and their interaction (CLA \times fat type). When the interaction effect was significant, differences between experimental groups were analyzed by the Tukey's post hoc test. To test differences on *c9,t11* CLA isomer deposition for each tissue between PCLA and O groups, the ANOVA test was applied. Statistical significance was set up at $P < 0.05$.

Results

Hepatic Fatty Acid Composition

Livers from rats fed CLA had lower total FAME (14.2–14.9 g/100 g organ) than those from rats fed no CLA

Table 1 Fatty acid content (g/100 g diet) and composition (g/100 g total fatty acids) of experimental diets

	P	PCLA	O	OCLA
Total FAME	12.3	10.5	12.0	12.6
Fatty acids				
12:0	0.16	0.18	0.09	0.09
14:0	0.92	1.00	1.35	1.34
15:0	0.05	0.06	0.32	0.32
16:0	35.4	37.5	12.6	12.3
<i>c</i> 7-16:1	0.03	0.03	0.24	0.24
<i>c</i> 9-16:1	0.20	0.14	0.57	0.58
<i>c</i> 9-17:1	0.03	0.02	0.15	0.13
18:0	4.23	4.08	21.0	21.5
<i>c</i> 9-18:1	34.9	32.3	22.3	21.0
18:2n-6	20.0	16.0	15.7	12.2
18:3n-3	0.13	0.11	1.23	1.24
20:0	0.34	0.31	0.22	0.22
20:2n-6	0.01	n.d.	0.02	0.03
22:0	0.22	0.15	0.19	0.15
24:0	0.16	0.12	0.10	0.08
18:1 isomers				
<i>t</i> 6 + <i>t</i> 7 + <i>t</i> 8	0.07	0.07	0.60	0.61
<i>t</i> 9	0.09	0.09	0.51	0.53
<i>t</i> 10	0.09	0.08	0.94	0.83
<i>t</i> 11	0.06	0.06	9.22	9.42
<i>t</i> 12	n.d.	n.d.	1.07	1.13
<i>c</i> 11	1.41	1.11	1.09	1.05
<i>c</i> 12	0.14	0.04	1.13	1.18
<i>c</i> 13	0.02	0.03	0.16	0.14
<i>t</i> 16 + <i>c</i> 14	0.02	0.01	0.44	0.45
<i>c</i> 15	n.d.	n.d.	0.19	0.19
18:2 isomers				
Non-conjugated				
<i>t</i> 9, <i>t</i> 12	n.d.	n.d.	0.44	0.47
<i>t</i> 8, <i>c</i> 12/ <i>c</i> 9, <i>t</i> 12	n.d.	n.d.	0.29	0.41
<i>t</i> 8, <i>c</i> 13/ <i>c</i> 9, <i>t</i> 13	0.38	0.36	0.18	0.18
<i>t</i> 9, <i>c</i> 12	0.36	0.35	0.13	0.14
<i>t</i> 11, <i>c</i> 15	n.d.	n.d.	1.59	1.62
<i>c</i> 9, <i>c</i> 15	n.d.	n.d.	0.18	0.19
<i>c</i> 12, <i>c</i> 15	n.d.	n.d.	0.14	0.14
Conjugated (CLA)				
<i>t</i> 12, <i>t</i> 14	n.d.	n.d.	0.004	0.04
<i>t</i> 11, <i>t</i> 13	n.d.	n.d.	0.11	0.12
<i>t</i> 10, <i>t</i> 12	0.02	0.08	0.03	0.09
<i>t</i> 9, <i>t</i> 11	0.02	0.08	0.07	0.13
<i>t</i> 8, <i>t</i> 10	0.002	0.05	0.01	0.01
<i>t</i> 7, <i>t</i> 9	<0.001	0.001	0.006	0.005
<i>c</i> / <i>t</i> 11,13	0.007	n.d.	0.41	0.46
<i>t</i> 10, <i>c</i> 12	n.d.	2.48	n.d.	2.14
<i>c</i> 9, <i>t</i> 11	0.02	2.55	1.24	3.41

Table 1 continued

	P	PCLA	O	OCLA
<i>t</i> 8, <i>c</i> 10	0.003	0.03	0.03	0.05
<i>t</i> 7, <i>c</i> 9	<0.001	0.002	0.04	0.05

Experimental diets: *P* palm oil, *PCLA* palm oil plus 1% CLA, *O* ovine fat, *OCLA* ovine fat plus 1% CLA, *n.d.* not detected

(16.7–18.1 g/100 g organ) (Table 2). The major fatty acids in the hepatic lipids were 16:0, *c*9-16:1, *c*9-18:1 and 18:2n-6 for all experimental groups. CLA and fat type affected six and 11 of the 20 individual fatty acids depicted in Table 2, respectively. As ovine fat diet contributed with many intermediates of rumen biohydrogenation, the Σ *i*-18:1, Σ *nc*-18:2 and Σ CLA are discriminated below. As expected, the different origins of dietary fat affected all fatty acids identified, excluding the 20:5n-3, according to the fatty acid profile of the diets (Table 1). The percentage (g/100 g total fatty acids) of SFA in hepatic lipids was significantly increased in rats fed CLA. Monounsaturated fatty acids (MUFA) percentage decreased in both PCLA and OCLA groups, although more effectively in the ovine fat group, being the *c*9-16:1, *c*9-18:1 and Σ *i*-18:1 the main fatty acids responsible for these differences. The sum of PUFA was not affected by CLA supplementation in the diet, in contrast to some individual PUFA. The percentages of 18:2n-6, 18:3n-6, 20:5n-3 fatty acids decreased in the liver, whereas 20:4n-6 increased, due to the presence of CLA in the diet. CLA supplementation increased the sum of n-3 PUFA in the liver of animals fed ovine fat, mainly due to the 18:3n-3, 22:5n-3 and 22:6n-3 fatty acids. Contrarily, in the palm oil diets, the percentage of n-3 PUFA did not change. CLA did not affect the sum of n-6 PUFA but palm oil groups were richer in n-6 PUFA than ovine fat groups, mainly due to the linoleic acid. The sum of *trans* fatty acids (TFA; fatty acids with a *trans* double bond, except CLA isomers) was enhanced by CLA supplementation. CLA did not affect the following six fatty acids: 14:0, 15:0, *c*7-16:1, 20:0, 20:3n-6 and 22:5n-6. PUFA/SFA and n-6/n-3 ratios in the liver were decreased by CLA supplementation.

Regarding CLA and fat type interaction, eight of 20 fatty acids were differentially affected by CLA supplementation, depending on the dietary fat origin (Table 2). The *c*9-16:1, 18:3n-3, 20:2n-6, 22:5n-6 and 22:6n-3 fatty acids did not show differences between P and PCLA groups, but were increased in OCLA comparing to O group. The *c*9-17:1 had a decrease in the OCLA group relatively to the O group. CLA increased the 18:0 fatty acid in both fat types but more extensively in the OCLA group. CLA decreased the 22:4n-6 percentage when supplemented

Table 2 Effect of dietary CLA supplementation and fat type on total fatty acid content (g/100 g organ) and composition (g/100 g total fatty acids) in the liver of obese Zucker rats

	P	PCLA	O	OCLA	SEM	Significance level		
						CLA	Fat	CLA × fat
Total FAME	16.7	14.2	18.1	14.9	0.888	**	ns	ns
Fatty acids								
14:0	0.68	0.72	0.86	0.77	0.033	ns	**	ns
15:0	0.17	0.18	0.24	0.24	0.011	ns	***	ns
16:0	18.7	19.9	16.5	18.1	0.334	***	***	ns
<i>c</i> 7-16:1	0.54	0.56	0.61	0.58	0.019	ns	*	ns
<i>c</i> 9-16:1	9.60 ^a	9.24 ^a	9.80 ^a	7.37 ^b	0.306	***	*	**
<i>c</i> 9-17:1	0.27 ^c	0.27 ^c	0.66 ^a	0.60 ^b	0.011	**	***	*
18:0	2.60 ^d	3.56 ^b	3.10 ^c	4.49 ^a	0.100	***	***	*
<i>c</i> 9-18:1	39.2	37.4	36.7	35.4	0.283	***	***	ns
Σ <i>i</i> -18:1 [†]	8.96	8.53	10.5	9.76	0.005	**	***	ns
18:2n-6	9.64	8.36	7.89	7.14	0.219	***	***	ns
Σ <i>nc</i> -18:2 [†]	0.51 ^c	0.49 ^c	1.69 ^a	1.49 ^b	0.028	***	***	**
Σ CLA [†]	0.06 ^d	1.48 ^c	3.07 ^b	4.72 ^a	0.052	***	***	*
18:3n-3	0.09 ^c	0.08 ^c	0.36 ^b	0.61 ^a	0.013	***	***	***
18:3n-6	0.21	0.18	0.15	0.12	0.010	**	***	ns
20:0	0.04	0.04	0.07	0.07	0.003	ns	***	ns
20:2n-6	0.28 ^a	0.29 ^a	0.21 ^b	0.28 ^a	0.012	**	***	**
20:3n-6	0.84	0.71	0.42	0.45	0.044	ns	***	ns
20:4n-6	3.80	4.42	2.85	3.46	0.116	***	***	ns
20:5n-3	0.08	0.06	0.08	0.06	0.005	**	ns	ns
22:4n-6	0.70 ^a	0.52 ^b	0.25 ^c	0.25 ^c	0.029	**	***	*
22:5n-3	0.08 ^c	0.08 ^c	0.19 ^b	0.27 ^a	0.008	***	***	***
22:5n-6	0.55	0.54	0.16	0.19	0.021	ns	***	ns
22:6n-3	0.27 ^c	0.31 ^c	0.58 ^b	0.80 ^a	0.023	***	***	***
Σ Unidentified	2.13	2.10	2.99	2.99	0.064	**	***	ns
Partial sums and ratios								
Σ SFA	22.2	24.4	20.8	23.7	0.344	***	**	ns
Σ MUFA	58.3 ^a	55.5 ^b	55.9 ^b	50.8 ^c	0.343	***	***	**
Σ PUFA	16.6	15.5	13.4	13.8	0.363	ns	***	ns
Σ n-3	0.52 ^c	0.52 ^c	1.21 ^b	1.75 ^a	0.037	***	***	***
Σ n-6	16.0	15.0	11.9	11.9	0.335	ns	***	ns
Σ TFA	0.79	1.01	3.82	4.19	0.069	***	***	ns
PUFA/SFA	0.63	0.58	0.68	0.65	0.024	**	**	ns
n-6/n-3	30.9	29.3	9.92	6.81	0.708	*	***	ns
Desaturation indices								
Δ9-index16	0.66 ^b	0.68 ^{ab}	0.63 ^c	0.71 ^a	0.008	***	ns	**
Δ9-index18	0.06 ^d	0.09 ^b	0.08 ^c	0.11 ^a	0.002	***	***	*

Data are means ± standard error of mean (SEM) for eight rats per group

Σ SFA = 14:0, 15:0, 16:0, 18:0, 20:0; Σ MUFA = *c*7-16:1, *c*9-16:1, *c*9-17:1, *c*9-18:1, *c*11-18:1, *c*12-18:1, *c*13-18:1, *c*15-18:1; Σ PUFA = 18:2n-6, *c*-18:2, 18:3n-6, 18:3n-3, 20:2n-6, 20:3n-6, 20:4n-6, 20:5n-3, 22:4n-6, 22:5n-6, 22:5n-3, 22:6n-3; Σ n-3 = 18:3n-3, 20:5n-3, 22:5n-3, 22:6n-3; Σ n-6 = 18:2n-6, 18:3n-6, 20:2n-6, 20:3n-6, 20:4n-6, 22:4n-6, 22:5n-6; Σ TFA = *t*6, *t*7, *t*8, *t*9, *t*10, *t*11, *t*12, *t*16 + *c*14, *t*9, *t*12, *t*8, *c*12/*c*9, *t*12, *t*8, *c*13/*c*9, *t*13, *t*9, *c*12, *t*11, *c*15 (fatty acids from Table 3); PUFA/SFA = Σ PUFA/Σ SFA; n-6/n-3 = Σ n-6/Σ n-3; Δ9-index16 = 16:0/(16:0 + *c*9-16:1); Δ9-index18 = 18:0/(18:0 + *c*9-18:1)

Experimental diets: *P* palm oil, *PCLA* palm oil plus 1% CLA, *O* ovine fat, *OCLA* ovine fat plus 1% CLA. *nc* non-conjugated, *SFA* saturated fatty acids, *MUFA* monounsaturated fatty acids, *PUFA* polyunsaturated fatty acids, *CLA* conjugated linoleic acid. Significance level: *ns* not significant

[†] These sums are described in Table 3

P > 0.05; * *P* < 0.05; ** *P* < 0.01; *** *P* < 0.001; means in the same row with different superscripts are significantly different (*P* < 0.05)

Table 3 Effect of dietary CLA supplementation and fat type on 18:1 and 18:2 isomeric composition (g/100 g total fatty acids) in the liver of obese Zucker rats

	P	PCLA	O	OCLA	SEM	Significance level		
						CLA	Fat	CLA × fat
18:1 isomers								
<i>t</i> 6 + <i>t</i> 7 + <i>t</i> 8 [†]	0.03	0.03	0.12	0.12	0.003	ns	***	ns
<i>t</i> 9	0.08	0.08	0.25	0.25	0.005	ns	***	ns
<i>t</i> 10	0.05	0.24	0.36	0.52	0.022	***	***	ns
<i>t</i> 11	0.02 ^c	0.04 ^c	1.12 ^b	1.45 ^a	0.027	***	***	***
<i>t</i> 12	0.11	0.13	0.34	0.36	0.009	*	***	ns
<i>c</i> 11	8.45 ^a	7.76 ^b	7.08 ^c	5.78 ^d	0.135	***	***	*
<i>c</i> 12	n.d.	n.d.	0.73 ^a	0.69 ^b	0.007	**	***	**
<i>c</i> 13	0.22	0.26	0.28	0.27	0.018	ns	*	ns
<i>t</i> 16 + <i>c</i> 14	n.d.	n.d.	0.16	0.19	0.011	ns	***	ns
<i>c</i> 15	n.d.	n.d.	0.10 ^b	0.14 ^a	0.008	*	***	*
18:2 isomers								
Non-conjugated								
<i>t</i> 9, <i>t</i> 12	0.02	0.02	0.04	0.04	0.005	ns	**	ns
<i>t</i> 8, <i>c</i> 12/ <i>c</i> 9, <i>t</i> 12 [†]	n.d.	n.d.	0.55 ^a	0.50 ^b	0.010	ns	***	*
<i>t</i> 8, <i>c</i> 13/ <i>c</i> 9, <i>t</i> 13 [†]	0.14 ^b	0.16 ^b	0.29 ^a	0.27 ^a	0.006	ns	***	**
<i>t</i> 9, <i>c</i> 12	0.35	0.32	0.20	0.14	0.011	***	***	ns
<i>t</i> 11, <i>c</i> 15	n.d.	n.d.	0.40 ^a	0.36 ^b	0.008	*	***	*
<i>c</i> 9, <i>c</i> 15	n.d.	n.d.	0.19 ^a	0.15 ^b	0.004	***	***	***
<i>c</i> 12, <i>c</i> 15	n.d.	n.d.	0.04	0.04	0.001	ns	***	ns
Conjugated (CLA)								
<i>t</i> 12, <i>t</i> 14	n.d.	n.d.	0.006 ^b	0.008 ^a	<0.001	**	***	**
<i>t</i> 11, <i>t</i> 13	n.d.	n.d.	0.01 ^b	0.01 ^a	<0.001	*	***	*
<i>t</i> 10, <i>t</i> 12	0.002	0.04	0.006	0.04	0.002	***	*	ns
<i>t</i> 9, <i>t</i> 11	0.005	0.04	0.07	0.09	0.003	***	***	ns
<i>t</i> 8, <i>t</i> 10	0.003 ^b	0.02 ^a	0.006 ^b	0.01 ^a	0.001	***	ns	*
<i>t</i> 7, <i>t</i> 9	0.003 ^c	0.02 ^b	0.02 ^{ab}	0.03 ^a	0.002	***	***	*
<i>c</i> / <i>t</i> 11,13 [†]	<0.001	n.d.	0.04	0.05	0.004	ns	***	ns
<i>t</i> 10, <i>c</i> 12	n.d.	0.21	0.004	0.27	0.008	***	***	ns
<i>c</i> 9, <i>t</i> 11	0.05	1.10	2.81	3.86	0.048	***	***	ns
<i>t</i> 8, <i>c</i> 10	0.003 ^c	0.076 ^b	n.d.	0.11 ^a	0.004	***	***	***
<i>t</i> 7, <i>c</i> 9	n.d.	n.d.	0.07	0.05	0.005	ns	***	ns

Data are means ± standard error of mean (SEM) for eight rats per group

Experimental diets: *P* palm oil, *PCLA* palm oil plus 1% CLA, *O* ovine fat, *OCLA* ovine fat plus 1% CLA. Significance level: *ns* not significant, *n.d.* not detected

[†] These fatty acids co-eluted

P > 0.05; * *P* < 0.05; ** *P* < 0.01; *** *P* < 0.001; means in the same row with different superscripts are significantly different (*P* < 0.05)

to palm oil diets. The Δ9-index16 was higher in the OCLA than in the O group. In addition, CLA increased the Δ9-index18 in both fat types, although more markedly in the OCLA group.

The detailed composition of oleic acid and linoleic acid isomers in the liver, which partial sums were depicted in Table 2 (Σ i-18:1, Σ nc-18:2 and Σ CLA), are presented in

Table 3. CLA and fat type affected 7 and 15 of the 28 fatty acids analyzed, respectively. CLA supplementation increased the percentages of *t*10- and *t*12-, but decreased *c*11-18:1 levels. The *t*11- and *c*15-18:1 isomers only increased in the OCLA group. Among non-conjugated 18:2 isomers, CLA diminished the *t*8,*c*12/*c*9,*t*12-, *t*11,*c*15- and *c*9,*c*15-18:2 isomers. Most of the conjugated 18:2 isomers

increased with CLA supplementation, although *c/t11,13-* and *t7,c9-18:2* levels were not affected. The major CLA isomer found in the liver for all dietary groups, the *c9,t11* isomer, increased ~ 1 g/100 g total fatty acids in the PCLA and OCLA groups. The hepatic level of accumulation was lower for the *t10,c12* than for the *c9,t11* CLA isomer.

Muscle Fatty Acid Composition

Total FAME content in the muscle, which varied from 7.23 to 10.7 g/100 g organ, was significantly lower in CLA-supplemented rats, as well as in the ovine fat, comparing to palm oil fed rats (Table 4). The main fatty acids in the muscle lipids from all dietary groups were 16:0, *c9-16:1*, *c9-18:1* and 18:2n-6. CLA and fat type individually affected nine and 14 of the 20 fatty acids presented in Table 4, respectively. The results of Σ i-18:1, Σ nc-18:2 and Σ CLA are depicted below in further detail. All fatty acids were affected by the type of dietary fat, except for 20:2n-6 and 20:4n-6. Once more, these differences are firstly explained by the dietary fatty acid composition (Table 1). CLA affected the majority of fatty acids, except for 16:0, *c9-16:1*, 18:0, 18:3n-6, 18:3n-3, 20:4n-6, 22:5n-3 and 22:6n-3. The percentage of total SFA in muscle lipids was not affected by CLA, which could be due to the absence of effects on two major SFA, 16:0 and 18:0. CLA decreased the relative proportions of MUFA. Palm oil groups had higher MUFA levels than ovine fat groups. This trend was observed for *c9-18:1*, the main MUFA. PUFA percentages were diminished by dietary CLA. CLA supplementation increased the total CLA level in 1.7 and 1.8 g/100 g of total fatty acids in palm oil and ovine fat diets, respectively. The n-3 PUFA sum was increased in the ovine fat groups and CLA effect was undetected. CLA decreased the n-6 PUFA sum, in particular, 18:2n-6, 20:3n-6, and 22:4n-6 fatty acids. The sum of TFA only increased with CLA supplementation in the palm oil diet. Dietary treatments with CLA decreased PUFA/SFA and n-6/n-3 ratios. The $\Delta 9$ -indices 16 and 18 were not affected by CLA supplementation, while palm oil groups had higher values of $\Delta 9$ -index16, but lower values of $\Delta 9$ -index18, comparing to ovine fat groups.

Some fatty acids displayed significant effects for CLA \times fat interaction (eight of 20 fatty acids). CLA did not change *c9-17:1* and 22:5n-6 fatty acids in the palm oil group but increased their percentages in the ovine fat groups. On the contrary, the 20:2n-6 fatty acid was decreased in the PCLA group. In both dietary fat types, the 15:0 percentage increased but this change was higher in the ovine fat than in the palm oil group. CLA diminished the 22:4n-6 percentage in a higher extent in the palm oil than in the ovine fat group.

Table 5 shows the profile of oleic acid and linoleic acid isomers in the muscle, intermediates of ruminal biohydrogenation of C18 PUFA, for which the partial sums were depicted in Table 4 (Σ i-18:1, Σ nc-18:2 and Σ CLA). CLA and fat type individually affected nine and 15 of the 28 fatty acids presented in the Table 5, respectively. Results showed that *t11-* and *c11-18:1* were the major oleic isomers in muscle lipids. CLA supplemented groups had lower *t9-* and *c11-18:1* percentages but higher *t12-18:1*. The *t10-*, *c12-* and *c15-18:1* were increased by CLA supplementation only in the palm oil groups. Regarding non-conjugated 18:2 isomers, CLA increased the levels of *t8,c13/c9,t13-18:2* but decreased the *t9,c12-18:2*. The *t8,c12/c9,t12-*, *c9,c15-* and *c12,c15-18:2* were not changed. The conjugated 18:2 isomers profile reflected the proportions of the various CLA isomers in the diets. CLA supplementation promoted an increase in most of the isomers percentages, excluding *t12,t14-*, *t11,t13-* and *t7,c9-18:2* isomers. Similarly to the liver, the most prevalent CLA isomer in the muscle from all experimental groups was the *c9,t11* isomer. In contrast, the percentage of the *t10,c12* CLA isomer was much lower, but, nevertheless, the second most prevalent isomer found in diets supplemented with CLA.

Deposition of *c9,t11* CLA Isomer in the Liver and Muscle

The total intake of *c9,t11* CLA isomer during the experiment was 5.57 and 2.88 g, for PCLA and O groups, respectively. Regarding the *t11-18:1* ingestion, values of 0.03 and 4.83 g of *c9,t11* endogenous synthesis were estimated for PCLA and O groups, respectively.

In the liver, the total *c9,t11* CLA isomer deposition was significantly lower ($P < 0.001$) in the PCLA (1.51 g) than in the O group (3.99 g) of *c9,t11*/100 g of exogenous plus endogenous *c9,t11* isomer. In the muscle, the depositions were also significantly different ($P < 0.05$), 0.16 versus 0.25 g of *c9,t11*/100 g of exogenous plus endogenous *c9,t11* CLA isomer for PCLA and O groups, respectively.

Discussion

As expected, obese Zucker rats, a commonly used genetic model for human obesity [16], had relatively high values of total fatty acids in the liver and muscle. This experimental model was selected in order to achieve a better understanding of CLA effects facing an obesity scenario, as this fatty acid has been recognized as an anti-adipogenic agent. Ovine fat contrasts with palm oil because it contains a large number of fatty acids derived from rumen metabolism, which includes *trans* and *cis* isomers of oleic acid and

Table 4 Effect of dietary CLA supplementation and fat type on total fatty acid content (g/100 g organ) and composition (g/100 g total fatty acids) in the muscle of obese Zucker rats

	P	PCLA	O	OCLA	SEM	Significance level		
						CLA	Fat	CLA × fat
Total FAME	10.7	8.80	9.26	7.29	0.639	**	*	ns
Fatty acids								
14:0	1.20	1.34	1.36	1.48	0.040	**	***	ns
15:0	0.10 ^c	0.11 ^{bc}	0.21 ^{ab}	0.24 ^a	0.003	***	***	**
16:0	24.2	24.2	19.2	19.0	0.253	ns	***	ns
<i>c</i> 7-16:1	0.42	0.57	0.47	0.64	0.010	***	***	ns
<i>c</i> 9-16:1	9.57	9.77	8.18	7.77	0.173	ns	***	ns
<i>c</i> 9-17:1	0.12 ^c	0.13 ^c	0.39 ^b	0.42 ^a	0.005	**	***	**
18:0	2.52	2.28	3.95	3.95	0.087	ns	***	ns
<i>c</i> 9-18:1	36.4	35.3	33.6	32.8	0.324	**	***	ns
Σ <i>i</i> -18:1 [†]	5.89 ^b	6.31 ^b	9.21 ^a	9.01 ^a	0.123	ns	***	*
18:2n-6	13.6	12.6	12.4	11.7	0.153	***	***	ns
Σ <i>nc</i> -18:2 [†]	0.46 ^c	0.49 ^c	1.55 ^a	1.49 ^b	0.015	ns	***	**
Σ CLA [†]	0.08 ^d	1.74 ^c	2.52 ^b	4.33 ^a	0.034	***	***	*
18:3n-3	0.14	0.12	0.56	0.54	0.008	***	***	ns
18:3n-6	0.05	0.053	0.04	0.04	0.002	ns	***	ns
20:0	0.04	0.028	0.04	0.04	0.001	***	***	ns
20:2n-6	0.13 ^a	0.11 ^b	0.12 ^b	0.11 ^b	0.003	***	ns	**
20:3n-6	0.34	0.25	0.27	0.23	0.012	***	***	ns
20:4n-6	2.30	2.14	2.07	2.02	0.136	ns	ns	ns
20:5n-3	0.03	0.02	0.04	0.03	0.002	*	***	ns
22:4n-6	0.33 ^a	0.22 ^b	0.18 ^c	0.13 ^d	0.011	***	***	*
22:5n-3	0.12 ^b	0.13 ^b	0.29 ^a	0.38 ^a	0.016	**	***	*
22:5n-6	0.31	0.26	0.13	0.11	0.015	*	***	ns
22:6n-3	0.30	0.33	0.57	0.62	0.030	ns	***	ns
Σ Unidentified	1.43	1.63	2.61	2.94	0.042	***	***	ns
Partial sums and ratios								
Σ SFA	28.0	28.0	24.7	24.7	0.300	ns	***	ns
Σ MUFA	52.1	51.3	48.4	47.1	0.287	***	***	ns
Σ PUFA	17.6	16.3	16.8	16.0	0.253	***	ns	ns
Σ n-3	0.44	0.49	0.90	1.03	0.046	ns	***	ns
Σ n-6	17.0	15.7	15.2	14.3	0.219	***	***	ns
Σ TFA	0.79 ^c	1.04 ^b	4.92 ^a	4.89 ^a	0.046	*	***	**
PUFA/SFA	0.75	0.64	0.64	0.59	0.015	*	***	ns
n-3/n-6	39.9	34.1	17.3	14.1	2.088	*	***	ns
Desaturation indices								
Δ9-index16	0.72	0.71	0.70	0.71	0.004	ns	*	ns
Δ9-index18	0.07	0.06	0.11	0.11	0.003	ns	***	ns

Data are means ± standard error of mean (SEM) for eight rats per group

Σ SFA = 14:0, 15:0, 16:0, 18:0, 20:0; Σ MUFA = *c*7-16:1, *c*9-16:1, *c*9-17:1, *c*9-18:1, *c*11-18:1, *c*12-18:1, *c*13-18:1, *c*15-18:1; Σ PUFA = 18:2n-6, *c*-18:2, 18:3n-6, 18:3n-3, 20:2n-6, 20:3n-6, 20:4n-6, 20:5n-3, 22:4n-6, 22:5n-6, 22:5n-3, 22:6n-3; Σ n-3 = 18:3n-3, 20:5n-3, 22:5n-3, 22:6n-3; Σ n-6 = 18:2n-6, 18:3n-6, 20:2n-6, 20:3n-6, 20:4n-6, 22:4n-6, 22:5n-6; Σ TFA = *t*6, *t*7, *t*8, *t*9, *t*10, *t*11, *t*12, *t*16 + *c*14, *t*9, *t*12, *t*8, *c*12/*c*9, *t*12, *t*8, *c*13/*c*9, *t*13, *t*9, *c*12, *t*11, *c*15 (fatty acids from Table 5); PUFA/SFA = Σ PUFA/Σ SFA; n-6/n-3 = Σ n-6/Σ n-3; Δ9-index16 = 16:0/(16:0 + *c*9-16:1); Δ9-index18 = 18:0/(18:0 + *c*9-18:1)

Experimental diets: *P* palm oil, *PCLA* palm oil plus 1% CLA, *O* ovine fat, *OCLA* ovine fat plus 1% CLA. *nc* non-conjugated, *SFA* saturated fatty acids, *MUFA* monounsaturated fatty acids, *PUFA* polyunsaturated fatty acids, *CLA* conjugated linoleic acid. Significance level: *ns* not significant

[†] These sums are described in Table 5

$P > 0.05$; * $P < 0.05$; ** $P < 0.01$; *** $P < 0.001$; means in the same row with different superscripts are significantly different ($P < 0.05$)

Table 5 Effect of dietary CLA supplementation and fat type on 18:1 and 18:2 isomeric composition (g/100 g total fatty acids) in the muscle of obese Zucker rats

	P	PCLA	O	OCLA	SEM	Significance level		
						CLA	Fat	CLA × fat
18:1 isomers								
<i>t</i> 6 + <i>t</i> 7 + <i>t</i> 8 [†]	0.02	0.03	0.17	0.16	0.005	ns	***	ns
<i>t</i> 9	0.10	0.08	0.31	0.29	0.006	*	***	ns
<i>t</i> 10	0.05 ^c	0.22 ^b	0.44 ^a	0.44 ^a	0.020	***	***	***
<i>t</i> 11	0.04	0.07	2.08	2.10	0.023	ns	***	ns
<i>t</i> 12	0.07	0.09	0.31	0.36	0.010	**	***	ns
<i>c</i> 11	5.39	5.05	4.56	4.34	0.058	***	***	ns
<i>c</i> 12	n.d.	0.30 ^b	0.84 ^a	0.85 ^a	0.027	***	***	***
<i>c</i> 13	0.16	0.15	0.24	0.24	0.009	ns	***	ns
<i>t</i> 16 + <i>c</i> 14	0.05 ^d	0.07 ^c	0.21 ^a	0.18 ^b	0.005	ns	***	***
<i>c</i> 15	0.01 ^c	0.04 ^b	0.07 ^a	0.07 ^a	0.004	*	***	***
18:2 isomers								
Non-conjugated								
<i>t</i> 9, <i>t</i> 12	n.d.	0.02 ^b	0.04 ^a	0.04 ^a	0.002	***	***	***
<i>t</i> 8, <i>c</i> 12/ <i>c</i> 9, <i>t</i> 12 [†]	n.d.	n.d.	0.40	0.40	0.004	ns	***	ns
<i>t</i> 8, <i>c</i> 13/ <i>c</i> 9, <i>t</i> 13 [†]	0.18	0.21	0.26	0.28	0.005	***	***	ns
<i>t</i> 9, <i>c</i> 12	0.28	0.27	0.12	0.11	0.004	**	***	ns
<i>t</i> 11, <i>c</i> 15	n.d.	n.d.	0.60 ^a	0.55 ^b	0.006	***	***	***
<i>c</i> 9, <i>c</i> 15	n.d.	n.d.	0.09	0.08	0.004	ns	***	ns
<i>c</i> 12, <i>c</i> 15	n.d.	n.d.	0.05	0.05	0.001	ns	***	ns
Conjugated (CLA)								
<i>t</i> 12, <i>t</i> 14	n.d.	n.d.	0.007 ^a	0.006 ^b	<0.001	*	***	*
<i>t</i> 11, <i>t</i> 13	n.d.	n.d.	0.02 ^a	0.02 ^b	0.001	***	***	***
<i>t</i> 10, <i>t</i> 12	0.004	0.06	0.01	0.06	0.003	***	ns	ns
<i>t</i> 9, <i>t</i> 11	0.009	0.05	0.08	0.11	0.004	***	***	ns
<i>t</i> 8, <i>t</i> 10	0.004 ^b	0.02 ^a	0.005 ^b	0.01 ^a	0.002	***	ns	*
<i>t</i> 7, <i>t</i> 9	0.002	0.01	0.01	0.02	0.002	***	***	ns
<i>c</i> / <i>t</i> 11, <i>t</i> 13 [†]	0.001	n.d.	0.11	0.10	0.006	ns	***	ns
<i>t</i> 10, <i>c</i> 12	0.004 ^c	0.37 ^b	n.d.	0.43 ^a	0.011	***	**	**
<i>c</i> 9, <i>t</i> 11	0.06	1.18	2.17	3.36	0.032	***	***	ns
<i>t</i> 8, <i>c</i> 10	n.d.	58 ^b	n.d.	0.14 ^a	0.002	***	***	***
<i>t</i> 7, <i>c</i> 9	n.d.	n.d.	0.10 ^a	0.07 ^b	0.007	*	***	*

Data are means ± standard error of mean (SEM) for eight rats per group

Experimental diets: *P* palm oil, *PCLA* palm oil plus 1% CLA, *O* ovine fat, *OCLA* ovine fat plus 1% CLA. Significance level: *ns* not significant, *n.d.* not detected

[†] These fatty acids co-eluted

P > 0.05; * *P* < 0.05; ** *P* < 0.01; *** *P* < 0.001; means in the same row with different superscripts are significantly different (*P* < 0.05)

conjugated and non-conjugated isomers of linoleic acid [19]. Additionally, the ovine fat used in this study derived from animals fed with forage supplemented with seed oils. As a result, this ruminant fat had a more complete fatty acid profile, richer in TFA, PUFA and CLA isomers, than those from animals fed conventional diets [19, 21]. The fatty acid profile of liver and muscle indicates that these isomeric fatty acids were widely deposited in both tissues. Moreover, the high content of palmitic acid provided by

the palm oil diet might constitute an additional factor affecting the results, as well as non-fatty acid components of both fat sources, which were not addressed in this study.

The percentages of SFA and MUFA in the liver and muscle were modulated by the dietary intake of CLA, in particular for 16:0, 18:0, *c*9-16:1 and *c*9-18:1 fatty acids, as seen by others [22, 23]. Therefore, the Δ9-indices were calculated in order to predict the SCD activity. The discussion of these results is limited as SCD activities and

mRNA expression levels were not determined. Nevertheless, the results herein suggest that CLA may have inhibited SCD activity in the liver when supplemented to the ovine fat diet, while in the muscle, CLA had no effect. This tissue discrepancy may derive from the liver's higher sensitivity because it is the key organ in lipid metabolism in rodents [24].

CLA may be incorporated into membrane phospholipids [25] and compete with other PUFA for enzymes that metabolize the conjugated diene metabolites [26]. In particular, dietary CLA may be deposited in the liver at the expenses of linoleic [27] and arachidonic [28] acids. However, in the present study, sunflower oil replaced CLA oil in the experimental diets without CLA supplementation, and a reduction in linoleic acid in CLA supplemented groups was expected. For all dietary groups, similar arachidonic acid percentages were observed in the muscle but, surprisingly, CLA increased the hepatic relative proportions of this fatty acid. The long chain n-3 PUFA, 22:5n-3 and 22:6n-3, prevalent in membrane phospholipids, were higher in the OCLA than in the O livers. This may result from the fact that ovine fat possesses more alpha-linolenic acid, which is the precursor of these fatty acids.

The *trans* and *cis* isomers of oleic acid and conjugated and non-conjugated *trans* isomers of linoleic acid are typical fatty acids of ruminant tissues. Ovine fat diets promoted a deposition of these minor isomers, whose biological effects are not completely understood. In human diets, the most common TFA is the *t*11-18:1 [4], and due to its bioconversion into *c*9,*t*11 CLA isomer by SCD, the *t*11-18:1 has been considered a neutral or beneficial *trans* isomer [13]. Butter naturally enriched in *t*11-18:1 and *c*9,*t*11 CLA isomer reduced lipid deposition in rabbits aorta [29]. As stated in a companion work [30], our rats did not present any morphological alteration in transversal segments of the aorta. CLA supplementation did not change *t*11-18:1 percentages in muscle from animals fed both fat types, but in the liver, CLA supplementation increased its percentages in animals fed the ovine fat. As the OCLA diet provided a higher amount of CLA than any other tested diet, the eventual inhibition of SCD activity could result in a decrease of desaturation *t*11-18:1 leading to higher *t*11-18:1 percentage in tissues. Also in the liver, it was observed an unexpected increase of *t*10-18:1 percentage with CLA supplementation. In the muscle, this augmentation was confined to the PCLA diet. We hypothesized that partial biohydrogenation of dietary *t*10,*c*12 CLA isomer might occur in the rat's intestine and, then, the isomers formed might be absorbed via coprophagy.

The CLA isomeric profile in both tissues reflect, partially, the CLA isomers composition of the diets. However, a differential deposition was observed for some CLA isomers. Interestingly, there was a preferential accumulation

of *t*11,*t*13- and *c*/*t*11,13-18:2 isomers in the muscle comparing to the liver. Concerning the *c*11,*t*13-18:2, Kramer et al. [25] reported a higher percentage of this fatty acid in heart than in liver lipids. Also, the *t*10,*c*12 CLA isomer was higher in the muscle than in the liver. Despite equal amounts of *c*9,*t*11 and *t*10,*c*12 CLA isomers in CLA supplemented animals, their respective depositions in the liver and muscle were quite different. In both tissues, the *c*9,*t*11 CLA isomer was more efficiently deposited than the *t*10,*c*12, as reported by others [23, 30, 31]. Li et al. [32] found more *c*9,*t*11- than *t*10,*c*12-18:2 in the liver, serum, bone and marrow. In contrast, other organs, like spleen, muscle and heart contained more *t*10,*c*12 than *c*9,*t*11 CLA isomer. Tsuzuki and Ikeda [33] observed a similar extent of lymphatic recovery of these two isomers in rats, suggesting that geometrical and positional isomerism of conjugated double bounds had no influence on the absorption by the small intestine. The *t*10,*c*12 CLA isomer has been reported to activate the β -oxidation system more strongly [34, 35] and to be more susceptible to oxidation [36] than the *c*9,*t*11 isomer, which could explain the lower percentage of the *t*10,*c*12 isomer in tissues.

The present experiment allowed the estimation of *c*9,*t*11 CLA isomer deposition from synthetic and bio-formed origins in the liver and muscle from rats fed PCLA and O diets. This estimation had to take into account both exogenous and endogenous sources of CLA. To the best of our knowledge, the conversion of vaccenic to rumenic acid has not been described, yet, for obese Zucker rats. Therefore, calculations were based on a conversion of 20% of vaccenic to rumenic acid described for male Wistar rats [4]. In the liver, the intake of bio-formed *c*9,*t*11 CLA isomer promoted a deposition of this fatty acid two-times higher than the intake of synthetic *c*9,*t*11 CLA. Also in the muscle, the *c*9,*t*11 CLA isomer deposition was higher due to the intake of O diet rather than PCLA diet. Relatively low levels of CLA intake from natural rich sources, as dairy products, can decrease the incidence of cancer [37]. Additionally, other authors reported that dietary beef tallow, itself with negligible contents of CLA, may increase the efficacy of CLA supplementation in reducing mammary and colon carcinogenesis [38, 39].

We report here the fatty acid composition, including the individual 18:1 and 18:2 (conjugated and non-conjugated) isomers in the liver and muscle of obese Zucker rats, as affected by CLA supplementation and type of dietary fat (palm oil or ovine fat). It is a fact that the total CLA contents were different among the various diets. In a future study, this can be easily overcome by equalizing its amount, through the supplementation of a palm oil based diet with the exact CLA content available in the ovine fat. Nevertheless, our data indicate that the effect of dietary CLA supplementation on the fatty acid deposition of liver

and muscle from obese Zucker rats is strongly influenced by the dietary fatty acid composition. The fatty acid profile in both tissues of obese rats fed palm oil and ovine fat displayed many interactions between CLA and fat type. Rats fed diets containing ovine fat and CLA supplementation had increased hepatic percentages of 18:3n-3 and 22:6n-3, although palm oil diets did not change n-3 PUFA. Regarding CLA isomers deposition, muscle had at least 60% higher amounts of *t*10,*c*12 CLA isomer than the liver, contrary to the *c*9,*t*11 isomer that displayed similar values. This finding suggests a differential degree of metabolization of these isomers in both tissues. Furthermore, the high efficiency of the *c*9,*t*11 CLA isomer deposition as a component of the ruminant fat warrants further research. In particular, its aim should focus on the promising health benefits of foods naturally enriched in CLA, such as ovine fat, in comparison to CLA dietary supplements.

Acknowledgments The CLA oil was a generous gift from PharmaNutrients Inc. (Gurnee, IL, USA). This study was supported by the Fundação para a Ciência e a Tecnologia (FCT, Lisbon, Portugal) Grant POCTI/CVT/2002/44750 and individual fellowships to Susana Martins and Susana Alves, SFRH/BD/2005/22566 and SFRH/BD/2007/37793, respectively. Paula A. Lopes is a researcher from the program “Ciência 2008” from FCT.

Conflict of interest None.

References

- Kelley NS, Hubbard NE, Erickson KL (2007) Conjugated linoleic acid isomers and cancer. *J Nutr* 137:2599–2607
- Park Y, Pariza MW (2007) Mechanisms of body fat modulation by conjugated linoleic acid (CLA). *Food Res Int* 40:311–323
- Corl BA, Baumgard LH, Dwyer DA, Griinari JM, Phillips BS, Bauman DE (2001) The role of delta(9)-desaturase in the production of *cis*-9, *trans*-11 CLA. *J Nutr Biochem* 12:622–630
- Kraft J, Hanske L, Möckel P, Zimmermann S, Härtl A, Kramer JK, Jahreis G (2006) The conversion efficiency of *trans*-11 and *trans*-12 18:1 by delta9-desaturation differs in rats. *J Nutr* 136:1209–1214
- World Health Organization (2003) Diet, nutrition and the prevention of chronic diseases—Report of a joint WHO/FAO Expert Consultation, pp 1–55
- Li J-J, Huang CJ, Xie D (2008) Anti-obesity effects of conjugated linoleic acid, docosahexaenoic acid, and eicosapentaenoic acid. *Mol Nutr Food Res* 52:631–645
- Kloss R, Linscheid J, Johnson A, Lawson B, Edwards K, Linder T, Socker K, Petite J, Kern M (2005) Effects of conjugated linoleic acid supplementation on blood lipids and adiposity of rats fed diets rich in saturated versus unsaturated fat. *Pharmacol Res* 51:503–507
- Haug A, Sjogren P, Holland N, Muller H, Kjos NP, Taugol O, Fjerdingby N, Biong AS, Selmer-Olsen E, Harstad OM (2008) Effects of butter naturally enriched with conjugated linoleic acid and vaccenic acid on blood lipids and LDL particle size in growing pigs. *Lipids Health Dis* 7:31–36
- Sébédio JL, Angioni E, Chardigny JM, Grégoire S, Juanéda P, Berdeaux O (2001) The effect of conjugated linoleic acid isomers on fatty acid profiles of liver and adipose tissues and their conversion to isomers of 16:2 and 18:3 conjugated linoleic acids in rat. *Lipids* 36:575–582
- Bretillon L, Chardigny JM, Grégoire S, Berdeaux O, Sébédio JL (1999) Effects of conjugated linoleic acid isomers on the hepatic microsomal desaturation activities in vitro. *Lipids* 34:965–969
- Givens DI (2005) The role of animal nutrition in improving the nutritive value of animal-derived foods in relation to chronic disease. *Proc Nutr Soc* 64:395–402
- Schmid A, Collomb M, Sieber R, Bee G (2006) Conjugated linoleic acid in meat and meat products: a review. *Meat Sci* 73:29–41
- Prates JAM, Bessa RJB (2009) Trans and n-3 fatty acids. In: Nollet LML, Toldrá F (eds) *Handbook of muscle food analysis*, CRC Press, New York, pp 399–417
- Edem DO (2002) Palm oil: biochemical, physiological, nutritional, hematological, and toxicological aspects: a review. *Plant Foods Hum Nutr* 57:319–341
- Jerónimo E, Alves SP, Prates JAM, Santos-Silva J, Bessa RJB (2009) Effect of dietary replacement of sunflower oil with linseed oil on intramuscular fatty acids of lamb meat. *Meat Sci* 83:499–505
- Kurtz TW, Morris RC, Pershadsingh HA (1989) The Zucker fatty rat as a genetic model of obesity and hypertension. *Hypertension* 13:896–901
- Christie WW, Sébédio JL, Juanéda P (2001) A practical guide to the analysis of conjugated linoleic acid (CLA). *Inform* 12:147–152
- Raes K, Smet S, Demeyer D (2001) Effect of double-muscling in Belgian Blue young bulls on the intramuscular fatty acid composition with emphasis on conjugated linoleic acid and polyunsaturated fatty acids. *Animal Sci* 73:253–260
- Bessa RJB, Alves SP, Jerónimo E, Alfaia CM, Prates JAM, Santos-Silva J (2007) Effect of lipid supplements on ruminal biohydrogenation intermediates and muscle fatty acid in lambs. *Eur J Lipid Sci Technol* 109:868–878
- Rego O, Rosa H, Regalo S, Alves S, Alfaia C, Prates J, Vouzela C, Bessa R (2008) Seasonal changes of CLA isomers and other fatty acids of milk fat from grazing dairy herds in the Azores. *J Sci Food Agric* 88:1855–1859
- Bessa RJB, Portugal PV, Mendes IA, Santos-Silva J (2005) Effect of lipid supplementation on growth performance, carcass and meat quality and fatty acid composition of intramuscular lipids of lambs fed dehydrated lucerne or concentrate. *Livest Pro Sci* 96:185–194
- Viswanadha S, McGilliard ML, Herbein JH (2006) Desaturation indices in liver, muscle, and bone of growing male and female mice fed *trans*-10, *cis*-12 conjugated linoleic acid. *Lipids* 41:763–770
- Martin D, Antequera T, Gonzalez E, Lopez-Bote C, Ruiz J (2007) Changes in the fatty acid profile of the subcutaneous fat of swine throughout fattening as affected by dietary conjugated linoleic acid and monounsaturated fatty acids. *J Agric Food Chem* 55:10820–10826
- Chow KC (2000) *Fatty acids in foods and their health implications*. CRC Press, New York, pp 481–516
- Kramer JK, Sehat N, Dugan ME, Mossoba MM, Yurawecz MP, Roach JA, Eulitz K, Aalhus JL, Schaefer AL, Ku Y (1998) Distributions of conjugated linoleic acid (CLA) isomers in tissue lipid classes of pigs fed a commercial CLA mixture determined by gas chromatography and silver ion-high-performance liquid chromatography. *Lipids* 33:549–558
- Park Y, Storkson JM, Albright KJ, Liu W, Pariza MW (2005) Biological activities of conjugated fatty acids: conjugated eicosadienoic (conj. 20:2Δc11, *t*13/*t*12, *c*14), eicosatrienoic (conj. 20:3Δc8, *t*12, *c*14), and heneicosadienoic (conj. 21:2Δc12,

- t14/c13, t15*) acids and other metabolites of conjugated linoleic acid. *Biochim Biophys Acta* 1687:120–129
27. Kelley DS, Bartolini GL, Warren JM, Simon VA, Mackey BE, Erickson KL (2004) Contrasting effects of *t10, c12-* and *c9, t11-* conjugated linoleic acid isomers on the fatty acid profiles of mouse liver lipids. *Lipids* 39:135–141
 28. Sanders AR, Teachey MK, Ptock A, Kraemer K, Hasselwander O, Henriksen EJ, Baumgard LH (2004) Effects of specific conjugated linoleic acid isomers on growth characteristics in obese Zucker rats. *Lipids* 39:537–543
 29. Roy A, Chardigny J-M, Bauchart D, Ferlay A, Lorenz S, Durand D, Gruffat D, Faulconnier Y, Sébédio J-L, Chilliard Y (2007) Butters rich either in *trans*-10–C18:1 or in *trans*-11–C18:1 plus *cis*-9, *trans*-11 CLA differentially affect plasma lipids and aortic fatty streak in experimental atherosclerosis in rabbits. *Animal* 1:467–476
 30. Martins SV, Lopes PA, Alfaia CM, Rodrigues PO, Alves SM, Pinto RA, Castro MF, Bessa RB, Prates JAM (2010) Serum adipokine profile and fatty acid composition of adipose tissues are affected by conjugated linoleic acid and saturated fat diets in obese Zucker rats. *Br J Nutr* 103:869–878
 31. Kelley DS, Bartolini GL, Newman JW, Vemuri M, Mackey BE (2006) Fatty acid composition of liver, adipose tissue, spleen, and heart of mice fed diets containing *t10, c12* and *c9, t11*—conjugated linoleic acid. *Prostag Leukotr Ess* 74:271–282
 32. Li Y, Watkins BA (1998) Conjugated linoleic acids alter bone fatty acid composition and reduce ex vivo prostaglandin E2 biosynthesis in rats fed n-6 or n-3 fatty acids. *Lipids* 33:417–425
 33. Tsuzuki T, Ikeda I (2007) Slow absorption of conjugated linoleic acid in rat intestines, and similar absorption rates of *9c, 11t*-conjugated linoleic acid and *10t, 12c*-conjugated linoleic acid. *Biosci Biotech Biochem* 71:2034–2040
 34. Pariza MW, Park Y, Cook ME (2001) The biologically active isomers of conjugated linoleic acid. *Prog Lipid Res* 40:283–298
 35. Evans ME, Brown JM, McIntosh MK (2002) Isomer-specific effects of conjugated linoleic acid (CLA) on adiposity and lipid metabolism. *J Nutr Biochem* 13:508–516
 36. Tsuzuki T, Igarashi M, Iwata T, Yamauchi-Sato Y, Yamamoto T, Ogita K, Suzuki T, Miyazawa T (2004) Oxidation rate of conjugated linoleic acid and conjugated linolenic acid is slowed by triacylglycerol esterification and alpha-tocopherol. *Lipids* 39:475–480
 37. Knekt P, Jarvinen R, Seppanen R, Pukkala E, Aromaa A (1996) Intake of dairy products and the risk of breast cancer. *Br J Cancer* 73:687–691
 38. Hubbard N, Lim D, Erickson K (2006) Beef tallow increases the potency of conjugated linoleic acid in the reduction of mouse mammary tumor metastasis. *J Nutr* 136:88–93
 39. Shiraishi R, Iwakiri R, Fujise T, Kuroki T, Kakimoto T, Takashima T, Sakata Y, Tsunada S, Nakashima Y, Yanagita T, Fujimoto K (2010) Conjugated linoleic acid suppresses colon carcinogenesis in azoxymethane-pretreated rats with long-term feeding of diet containing beef tallow. *J Gastroenterol* 45: 625–635

Low Levels of Lipogenic Enzymes in Peritumoral Adipose Tissue of Colorectal Cancer Patients

Maria Notarnicola · Angelica Miccolis ·
Valeria Tutino · Dionigi Lorusso · Maria Gabriella Caruso

Received: 25 August 2011 / Accepted: 2 November 2011 / Published online: 17 November 2011
© AOCs 2011

Abstract Lipoprotein lipase (LPL) is the crucial enzyme for intravascular catabolism of triglyceride-rich lipoproteins. Fatty acid synthase (FAS) is a key anabolic enzyme that catalyzes the terminal steps in the *novo* biosynthesis of 18:2n-6. The involvement of both LPL and FAS in tumor biology has been widely demonstrated in different studies and to verify whether there are regional differences in the expression of these enzymes in visceral adipose tissue from patients with colorectal cancer might be representative of events which sustain tumor growth. The objective of this study was to evaluate LPL and FAS activity and expression of their genes in adipose tissue adjacent to neoplasia and distant from it from patients operated for colorectal cancer. LPL enzymatic activity was evaluated by a fluorescent method and FAS activity by a radiometer assay. Reverse-transcription and real-time PCR were used to detect mRNA levels of two enzymes. Our findings show a significant reduction in both LPL and FAS gene expression and activity levels in adipose tissue adjacent to tumor lesion compared to those detected in paired tissue distant from neoplasia. These results underline the influence of tumor microenvironment on lipid metabolism in adipose tissue, demonstrating a tumor-induced impairment in the formation and lipid storing capacity of adipose tissue in patients with colorectal cancer.

Keywords Adipose tissue · Lipoprotein lipase · Fatty acid synthase · Colorectal cancer

Abbreviations

LPL	Lipoprotein lipase
FAS	Fatty acid synthase
PCR	Polymerase chain reaction
CRC	Colorectal cancer
BMI	Body mass index
EDTA	Ethylenediaminetetraacetic acid
DTT	Dithiothreitol
NADPH	Nicotinamide adenine dinucleotide phosphate
CoA	Coenzyme A

Introduction

Adipose tissue is no longer considered to be solely used for energy storage, but exerts important endocrine functions, which are mediated by a complex network of various soluble factors, called adipocytokines [1, 2]. Visceral adipose tissue, in comparison to the subcutaneous depot, is generally accepted to be metabolically more active [3] and it has intrinsic characteristics possibly involved in the pathogenesis of obesity and inflammatory diseases [4, 5].

Adipose tissue synthesizes lipoprotein lipase (LPL), the crucial enzyme for intravascular catabolism of triglyceride-rich lipoproteins [6]. Adipose tissue LPL plays a pivotal role in lipid metabolism and changes in LPL expression could affect both the rate of fat accumulation and the metabolism of triglyceride-rich lipoproteins [3]. In patients with resectable non-small cell lung cancer, higher levels of LPL activity have been detected in cancer tissue than in adjacent non-cancer lung tissue [7]. Moreover, increased LPL activity in non-small cell lung cancer tissue predicts

M. Notarnicola (✉) · A. Miccolis · V. Tutino · M. G. Caruso
Laboratory of Biochemistry, National Institute for Digestive
Diseases “S. de Bellis”, Via Turi, 27, 70013 Castellana Grotte,
Bari, Italy
e-mail: maria.notarnicola@ircsdebellis.it

D. Lorusso
Division of Surgery, National Institute for Digestive Diseases
“S. de Bellis”, Castellana Grotte, Bari, Italy

shorter patient survival, independent of standard prognostic factors [6].

Fatty acid synthase (FAS) is a key anabolic enzyme that catalyzes the terminal steps in the *novo* biosynthesis of 18:2n-6 [8]. Altered expression of FAS appears to be an important process required by many transformed cells for growth and survival in different types of tumor [9–11]. FAS expression appears also to play an important role in the growth and pathogenesis of colon carcinoma [11, 12]. Previously, we demonstrated that FAS activity levels, as well as the expression of its mRNA are up-regulated in colorectal cancer tissues [13].

The involvement of both LPL and FAS in tumor biology has been widely demonstrated in different studies and to find regional differences in the expression of these enzymes in visceral adipose tissue collected from patients with colorectal cancer might be representative of events which sustain tumor growth. Therefore, the aim of this study was to evaluate LPL and FAS activity and expression of their genes in adipose tissue adjacent to neoplasia and distant from it from colorectal cancer patients.

Materials and Methods

Patients

Thirty-two consecutive CRC patients (20 females and 12 males, mean age 65 ± 5.8 years) undergoing surgery of the colon were enrolled in the study. Adipose tissue adjacent to a neoplastic lesion and distant from it (about 10 cm) was obtained from each of them according to a standardized procedure. Specimens were taken within 1 h after the surgical procedure and stored at -80 °C until assayed. All analyses were performed within 3 months.

Anthropometric measurements were obtained by the participants and body mass index (BMI) was calculated as weight in kilograms divided by the square of the height in meters (kg/m^2). The study had institutional approval and all patients gave informed consent to participate in the study.

Adipose Tissue Homogenization

Paired samples of adipose tissue (approximately 50 mg of peritumoral adipose tissue and distant from neoplasia) were homogenized in 20 mM Tris-HCl pH 7.5, 1 mM DTT, 1 mM MgCl_2 , 1 mM EDTA, and centrifuged at $10,000 \times g$ for 10 min at 4 °C. Aliquots of supernatant were used to determine total protein content, LPL and FAS activity.

LPL Activity Assay

LPL enzymatic activity was evaluated on specimens of adipose tissue adjacent to a neoplastic lesion and distant from it by a fluorescent method (LPL activity Kit, Roar Biomedical, New York, NY). An aliquot of supernatant (100 μl) was incubated with 100 μl of pre-diluted substrate emulsion at 37 °C for 1 h, according to the manufacturer's recommendations. The hydrolyzed triglycerides formed were measured at 370 nm excitation and 450 nm emission. The fluorescence intensity values of samples were compared with the fluorescence intensity values of a standard curve applied on the same plate together with samples in each run. LPL activity was expressed as picomoles of hydrolyzed substrate per minute per milligram of total proteins, evaluated using the Lowry method (pmol/min/mg prot). All measurements were made in duplicate and paired samples of the same patient were analyzed in the same batch.

FAS Activity Assay

FAS activity was determined on samples of adipose tissue adjacent to a neoplastic lesion and distant from it. After tissue homogenization and centrifugation, an aliquot of supernatant (50 μl) was pre-incubated with 100 mM potassium phosphate buffer, pH 7 for 15 min at 37 °C. Subsequently, 20 μl of reaction mix (2.5 mM NADPH, 1.25 mM acetyl-CoA, 1.25 mM malonyl-CoA and 0.02 mM 2- ^{14}C -malonyl-CoA (52 mCi/mmol, Amersham Biosciences, UK)) were added and samples were incubated for 10 min at 37 °C. Reactions were stopped by the addition of 500 μl 1N HCl/methanol (6:4, v:v); 18:2n-6 were extracted with 1 ml of petroleum ether and incorporation of 2- ^{14}C -malonyl-CoA was analyzed by scintillation counting. FAS activity was expressed as picomoles of incorporated 2- ^{14}C -malonyl-CoA per minute per milligram of total proteins (pmol/min/mg prot). All measurements were made in duplicate and paired samples of the same patient were analyzed in the same batch.

LPL and FAS Gene Expression Analysis

Total RNA from samples of adipose tissue was isolated with TRI-Reagent (Mol. Res. Center Inc., Cincinnati, OH, USA), following the manufacturer's instruction. Briefly, the tissue was homogenized in 0.25 ml of cold 0.9% NaCl; then, 0.75 ml of TRI-Reagent and 0.2 ml of chloroform were added to the homogenate. The samples were vigorously shaken and centrifuged and the RNA present in the aqueous phase was precipitated with 0.5 ml of isopropanol. The RNA pellet was washed once with 1 ml of 75% eth-

anol, dried, resuspended in sterile water and quantified by UV absorbance. Then 2 µg of total RNA was used for the reverse transcription reaction performed in 20 µl of the final volume at 41 °C for 60 min, using 30 pmol of antisense primer (Table 1) for analyses of the LPL, FAS and the β -actin gene. Human β -actin gene was utilized as the reference gene, selected according to the literature data [14]. Real-time PCRs were performed in 25 µl of the final volume containing 2 µl of cDNA, master mix with SYBR Green (iQ SYBR Green Supermix Bio-Rad, Milan, Italy) and sense and antisense primers for the LPL, FAS and β -actin gene (Table 1).

Real-time PCR was carried out in an iCycler Thermal Cycler System apparatus (Bio-Rad) using the following parameters: one cycle of 95 °C for 1 min and 30 s, followed by 45 cycles at 94 °C for 10 s, 55 °C for 10 s and 72 °C for 30 s and a further melting curve step at 55–95 °C with a heating rate of 0.5 °C per cycle for 80 cycles. The PCR products were quantified by external calibration curves, one for each tested gene, obtained with serial dilutions of known copy number of molecules (10^2 – 10^7 molecules). All expression data were normalized by dividing the target amount by the amount of β -actin used as the internal control for each sample. The specificity of the PCR product was confirmed by gel electrophoresis.

Statistical Analysis

The differences in LPL and FAS activity and their mRNA levels between adipose tissue adjacent to a tumor lesion and distant from it were analysed by the Wilcoxon signed-rank test. Differences were considered significant at a 5% probability level.

Results

The clinical and histopathological features of all patients are shown in Table 2. Considering their histology, all tumors were shown to be adenocarcinomas. They were classified according to their grade of histological differentiation and tumor stage.

There was a significant reduction in both LPL and FAS activity levels in adipose tissue adjacent to a tumor lesion compared to those detected in paired tissue distant from neoplasia (Fig. 1a, b). Median values of LPL and FAS activity between two regions considered were statistically different (63 vs. 115 and 1.45 vs. 3.25 pmol/min/mg prot, $P = 0.031$ and $P = 0.028$, respectively).

According to the findings of enzymatic activity, low levels of LPL and FAS mRNA were observed in peritumoral adipose tissue with respect to mRNA levels detected

in adipose tissue distant from neoplasia (Fig. 2). Median values of LPL and FAS mRNA between two regions considered were statistically different (0.18 vs. 0.78 and 0.04 vs. 0.30 no. molecules of LPL or FAS gene/no. molecules of β -actin, $P = 0.020$ and $P = 0.045$, respectively).

No difference was detected in LPL and FAS activity levels, as well as in mRNA expression in relation to sex, tumor site, stage and histological grading (data no shown).

Table 1 Sequences of amplification primers

Gene	Primer
LPL	
Sense	5'-GAGATTCTCTGTATGGCACC-3'
Antisense	5'-CTGCAAATGAGACACTTTCTC-3'
FAS	
Sense	5'-GCTGCCACACGCTCCTCTAG-3'
Antisense	5'-TATGCTTCTTCGTGCAGCAGTT-3'
β -Actin	
Sense	5'-AAAGACCTGTACGCCAACACAGTGCTGTC TGG-3'
Antisense	5'-CGTCATACTCCTGCTTGCT GATCCACATCTGC-3'

Table 2 Clinico-histopathological features of colorectal cancer patients

	Cases ($n = 32$)
Age (mean \pm SD)	65 \pm 5.8
Sex	
Male	12
Female	20
BMI (kg/m ²) ^a	26.5 \pm 3.2
Tumor side ^b	
Right	9
Left	23
Tumor stage ^c	
Stage I	5
Stage II	8
Stage III	15
Stage IV	4
Histological grading	
Well differentiated (G1)	7
Moderately differentiated (G2)	21
Poorly differentiated (G3)	4

^a Body mass index

^b Right side: hepatic flexure, cecum and ascending colon; Left side: descending colon, sigmoid and rectum

^c Clinical staging performed using UICC System

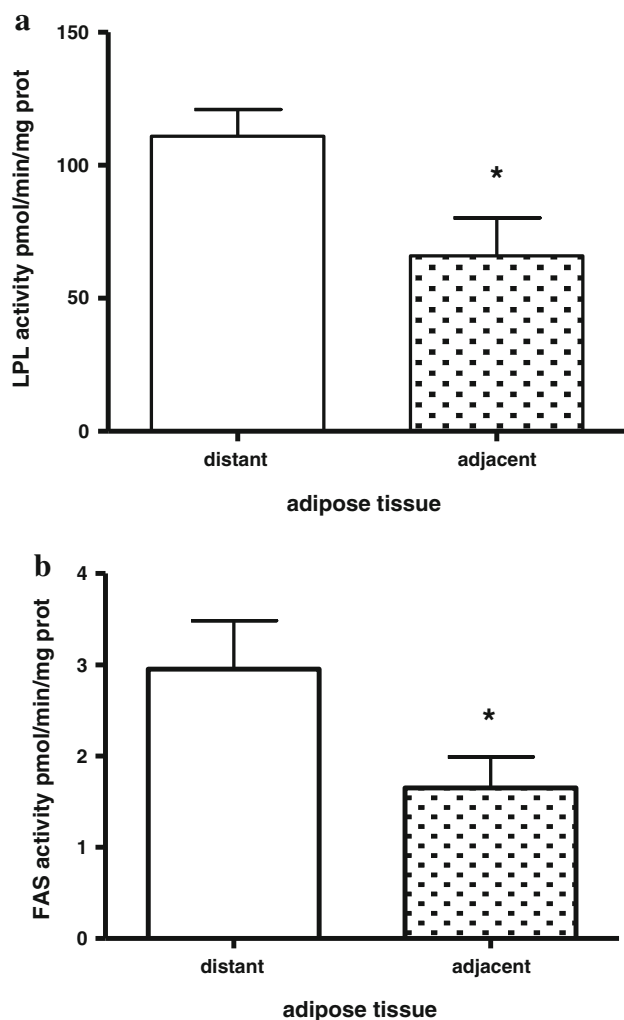


Fig. 1 Levels of LPL (a) and FAS (b) activity in adipose tissue distant from neoplasia and adjacent to tumor lesion from 32 colorectal cancer patients. The bars and whiskers represent the mean value and standard error, respectively. The enzymatic activities are expressed as pmol/min/mg of total proteins. * $P < 0.05$, Wilcoxon signed rank test

Discussion

Tumor growth and abnormal cell proliferation are shown to be associated with a number of cellular metabolic alterations [15]. The present findings seem to indicate changes of metabolic pathways in presence of neoplastic lesion. In contrast to “normal” adipose tissue, adipose cells adjacent to tumor lose the ability to express lipogenic enzymes. In our samples, the significant reduction in both LPL and FAS gene expression and activity levels in adipose tissue adjacent to a tumor lesion compared to those detected in paired tissue distant from neoplasia underlines the influence of tumor microenvironment on lipid metabolism in adipose tissue.

Adipose and colon tissue could interact affecting enzymatic expression of protein involved in cell proliferation.

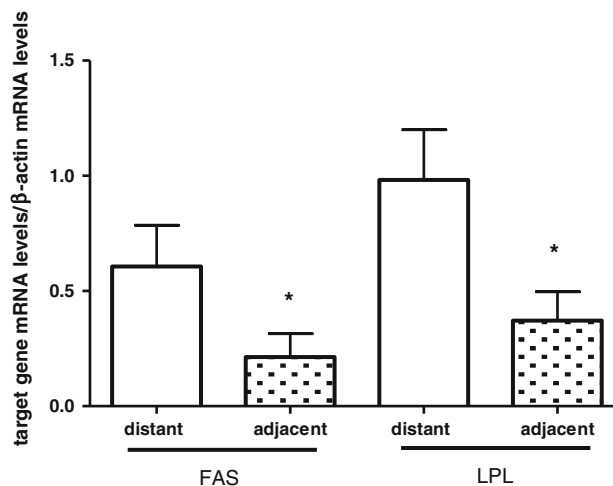


Fig. 2 Levels of FAS and LPL mRNA in adipose tissue distant from neoplasia and adjacent to tumor lesion from 32 colorectal cancer patients. The bars and whiskers represent the mean value and standard error, respectively. The mRNA levels are expressed as no. molecules mRNA FAS or LPL/no. molecules mRNA β -actin. * $P < 0.05$, Wilcoxon signed rank test

The increased demand of long-chain 18:2n-6 by the tumor lead, probably, to adipose atrophy resulting in alterations of lipid metabolism. Adipose atrophy is a hallmark of cancer cachexia, considered a metabolic disorder characterized by progressive loss of body weight with depletion of adipose tissue [16]. Moreover, pronounced morphologic and molecular alterations of adipose tissue have been observed in tumor-bearing mice [17]. The tumor burden seems to alter adipose tissue mass and function by affecting the expression of genes that control lipogenesis and lipid utilization. Several studies have demonstrated a clear association between obesity and the risk of colorectal cancer [18–20]. Mature adipocytes seem to influence colon cancer cell proliferation [21]. This trophic effect of adipose tissue is overall mediated via leptin [21, 22]. Recent experimental studies have shown that leptin stimulates the proliferation and invasiveness of human colon cancer cells [21–23].

The tumor microenvironment is a dynamic network that includes the cancer cells and their neighboring cells. The mechanisms whereby the LPL and FAS expression/activity are decreased in adipose tissue surrounding the tumor are not yet clear. However, it is likely that the tumor secretes humoral factors affecting directly adipose tissue of the host [24]. Moreover, the decreases in the activities of adipose tissue LPL and the lipogenic enzymes during tumor growth in rats are associated with a consistent drop in serum insulin levels, as demonstrated by other authors [25].

There is already evidence suggesting FAS and LPL involvement in tumor progression [7, 9–13]. Our previous study demonstrated that FAS activity levels were significantly higher in cancer than in the corresponding normal

colorectal mucosa [13], demonstrating that FAS is a functionally active enzyme and that the entire fatty acid synthesis pathway is up-regulated in colorectal carcinoma. Moreover, LPL activity has been shown to be highest in areas containing actively proliferating cells in a variety of human sarcomas and carcinomas [16].

The findings of this study demonstrate that a tumor-induced impairment in the formation and lipid storing capacity of adipose tissue occurs in patients with colorectal cancer, underling the influence of tumor microenvironment on lipid metabolism in adipose tissue. Further studies, with a larger number of cases, will be necessary to understand and demonstrate the mechanism underlying malignancy-related lipotrophy and if tumor-associated factors or pro-inflammatory mediators, such as cytokines, can influence lipid metabolism in peritumoral adipose tissue.

Conflict of interest The authors declare that they have no conflict of interest.

References

- Lang K, Ratke J (2009) Leptin and adiponectin: new players in the field of tumor cell and leukocyte migration. *Cell Commun Signaling* 7:27
- Kershaw EE, Flier JS (2004) Adipose tissue as an endocrine organ. *J Clin Endocrinol Metab* 89:2548–2556
- Panarotto D, Poisson J, Devroede G, Maheux P (2000) Lipoprotein lipase steady-state mRNA levels are lower in human omental versus subcutaneous abdominal adipose tissue. *Metabolism* 49:1224–1227
- Peiris AN, Sothmann MS, Hoffmann RG, Hennes MI, Wilson CR, Gustafson AB, Kissebah AH (1989) Adiposity, fat distribution and cardiovascular risk. *Ann Intern Med* 110:867–872
- Kissebah AH, Krakower GR (1994) Regional adiposity and morbidity. *Physiol Res* 74:761–811
- Cerne D, Zitnik IP, Sok M (2010) Increased fatty acid synthase activity in non-small cell lung cancer tissue is a weaker predictor of shorter patient survival than increased lipoprotein lipase activity. *Arch Med Res* 41:405–409
- Trost Z, Sok M, Marc J, Cerne D (2009) Increased lipoprotein lipase activity in non-small cell lung cancer tissue predicts shorter patient survival. *Arch Med Res* 40:364–368
- Kuhajda FP (2000) Fatty-acid synthase and human cancer: new perspectives on its role in tumor biology. *Nutrition* 16:202–208
- Kuhajda FP (2006) Fatty acid synthase and cancer: new application of an old pathway. *Cancer Res* 66:5977–5980
- Van de Sande T, Roskams T, Lerut E, Joniau S, Van Poppel H, Verhoeven G, Swinnen GV (2005) High levels expression of fatty acid synthase in human prostate cancer tissues is linked to activation and nuclear localization of Akt/PKB. *J Pathol* 206:214–219
- Rashid A, Pizer ES, Moga M, Milgraum LZ, Zahurak M, Patermack GR, Kuhajda FP, Hamilton SR (1997) Elevated expression of fatty acid synthase and fatty acid synthetic activity in colorectal neoplasia. *Am J Pathol* 150:201–208
- Visca P, Alo PL, Del Nonno F, Botti C, Trombetta G, Marandino F, Filippi S, Di Tondo U, Perrone Donnorso R (1999) Immunohistochemical expression of fatty acid synthase, apoptotic-regulating genes, proliferating factors, and Ras protein product in nonneoplastic mucosa. *Clin Cancer Res* 5:4111–4118
- Notarnicola M, Altomare DF, Calvani M, Orlando A, Bifulco M, D'Attoma B, Caruso MG (2006) Fatty acid synthase hyperactivation in human colorectal cancer: relationship with tumor side and sex. *Oncology* 71:327–332
- Mori R, Wang Q, Danenberg KD, Pinski JK, Danenberg PV (2008) Both β -actin and GAPDH are useful reference genes for normalization of quantitative RT-PCR in human FFPE tissue samples of prostate cancer. *Prostate* 68:1555–1560
- Farah IO (2007) Differential modulation of intracellular energetics in A549 and MRC-5 cells. *Biomed Sci Instrum* 43:110–115
- Sakayama K, Masuno H, Miyazaki T, Okumura H, Shibata T, Okuda H (1994) Existence of lipoprotein lipase in human sarcomas and carcinomas. *Jpn J Cancer Res* 85:515–521
- Bing C, Russel S, Becket E, Pope M, Tisdale MJ, Trayhurn P, Jenkins JR (2006) Adipose atrophy in cancer cachexia: morphologic and molecular analysis of adipose tissue in tumour-bearing mice. *B J Cancer* 95:1028–1037
- Bianchini F, Kaaks R, Vainio H (2002) Overweight, obesity and cancer risk. *Lancet Oncol* 3:565–574
- Calle EE, Rodriguez C, Walker-Thurmond K, Thun MJ (2003) Overweight, obesity, and mortality from cancer in a prospectively studied cohort of US adults. *N Engl J Med* 348:1625–1638
- Calle EE, Kaaks R (2004) Overweight, obesity and cancer: epidemiological evidence and proposed mechanisms. *Nat Rev Cancer* 4:579–591
- Amemori S, Ootani A, Aoki S, Fujise T, Shimoda R, Kakimoto T, Shiraiishi R, Sakata Y, Tsunada S, Iwakiri R, Fujimoto K (2007) Adipocytes and preadipocytes promote the proliferation of colon cancer cells in vitro. *Am J Physiol Gastrointest Liver Physiol* 292:G923–G929
- Hardwick JC, Van Den Brink GR, Offerhaus GJ, Van Deventer SJ, Peppelenbosch MP (2001) Leptin is a growth factor for colonic epithelial cells. *Gastroenterology* 121:79–90
- Tamakoshi K, Toyoshima H, Wkai K, Kojima M, Suzuki K, Watanabe Y, Hayakawa N, Yatsuya H, Kondo T, Tokudome S, Hashimoto S, Suzuk S, Kawado M, Ozasa K, Ito Y, Tamakoshi A (2005) Leptin is associated with increased female colorectal cancer risk: a nested case-control study in Japan. *Oncology* 68:454–461
- Thompson MP, Koons JE, Tan ETH, Grigor MR (1981) Modified lipoprotein lipase activities, rates of lipogenesis, and lipolysis as factors leading to lipid depletion in C57BL mice bearing the preputial gland tumor, ESR-586. *Cancer Res* 41:3228–3232
- Lanza-Jacoby S, Lansey SC, Miller EE, Cleary MP (1984) Sequential changes in the activities of lipoprotein lipase and lipogenic enzymes during tumor growth in rats. *Cancer Res* 44:5062–5067

Linolenate 9R-Dioxygenase and Allene Oxide Synthase Activities of *Lasiodiplodia theobromae*

Fredrik Jernerén · Felipe Eng · Mats Hamberg · Ernst H. Oliw

Received: 19 August 2011 / Accepted: 15 September 2011 / Published online: 3 November 2011
© AOCs 2011

Abstract Jasmonic acid (JA) is synthesized from linolenic acid (18:3n-3) by sequential action of 13-lipoxygenase, allene oxide synthase (AOS), and allene oxide cyclase. The fungus *Lasiodiplodia theobromae* can produce large amounts of JA and was recently reported to form the JA precursor 12-oxophytodienoic acid. The objective of our study was to characterize the fatty acid dioxygenase activities of this fungus. Two strains of *L. theobromae* with low JA secretion (~0.2 mg/L medium) oxygenated 18:3n-3 to 5,8-dihydroxy-9Z,12Z,15Z-octadecatrienoic acid as well as 9R-hydroperoxy-10E,12Z,15Z-octadecatrienoic acid, which was metabolized by an AOS activity into 9-hydroxy-10-oxo-12Z,15Z-octadecadienoic acid. Analogous conversions were observed with linoleic acid (18:2n-6). Studies using [11S-²H]18:2n-6 revealed that the putative 9R-dioxygenase catalyzed stereospecific removal of the 11R hydrogen followed by suprafacial attack of dioxygen at C-9. Mycelia from these strains of *L. theobromae* contained 18:2n-6 as the major polyunsaturated acid but lacked 18:3n-3. A third strain with a high secretion of JA (~200 mg/L) contained 18:3n-3 as a major fatty acid and produced 5,8-dihydroxy-9Z,12Z,15Z-octadecatrienoic acid

from added 18:3n-3. This strain also lacked the JA biosynthetic enzymes present in higher plants.

Keywords *Botryodiplodia theobromae* · Cytochrome P450 · 9R-HPODE · Heme peroxidase · Jasmonic acid · Oxygenation mechanism

Abbreviations

AOS	Allene oxide synthase
CP	Chiral phase
P450	Cytochrome P450
DiHODE	Dihydroxyoctadecadienoic acid
DOX	Dioxygenase
HHDTrE	Hydroxyhexadecatrienoic acid
HPHDTrE	Hydroperoxyhexadecatrienoic acid
HOME	Hydroxyoctadecenoic acid
HPODE	Hydroperoxyoctadecadienoic acid
HPOTrE	Hydroperoxyoctadecatrienoic acid
JA	(-)-Jasmonic acid
JAs	Jasmonates
(+)-7-iso-JA	3R,7S-JA
LDS	Linoleate diol synthase
LOX	Lipoxygenase
MO	Methyloxime
NP	Normal phase
OPDA	Oxophytodienoic acid
RP	Reversed phase

F. Jernerén · E. H. Oliw (✉)
Department of Pharmaceutical Biosciences,
Uppsala Biomedical Center, Uppsala University,
P.O. Box 591, 751 24 Uppsala, Sweden
e-mail: Ernst.Oliw@farmbio.uu.se

F. Eng
Cuban Research Institute on Sugar Cane Byproducts,
Via Blanca and Carretera Central 804,
P.O. Box 4026, Havana, Cuba

M. Hamberg
Department of Medical Biochemistry and Biophysics,
Karolinska Institutet, 171 77 Stockholm, Sweden

Introduction

Jasmonic acid (JA), an important signal molecule in plant defense and development, is present throughout the plant kingdom as the free acid, the methyl ester, the hydroxyl

derivatives, or amino acid conjugates [1–3]. The tropical and subtropical plant pathogen *Lasiodiplodia theobromae* (synonym *Botryodiplodia theobromae*) secretes JA [4, 5] and some strains could even be used for commercial JA production [5, 6].

JA is formed in plants sequentially from α -linolenic acid (18:3n-3) or hexadecatrienoic acid (16:3n-3) by 13S-lipoxygenase (13S-LOX), allene oxide synthase (AOS), allene oxide cyclase, 12-oxophytodienoate reductase, and three steps of β -oxidation [1–3, 7]. Key intermediates are 12-oxophytodienoic acid (12-OPDA) and dinor-12-OPDA from 18:3n-3 to 16:3n-3, respectively. JAs have a wide array of biological activities in plants (plant defense, stress adaptation and development) and can inhibit aflatoxin production and delay spore germination of *Aspergillus flavus* [8]. A recent report also suggests that JA could be of medical value as a growth suppressor of human cancer cells [9].

A biosynthetic pathway from 18:3 to 16:3 to JAs, essentially as described in plants, seems likely in fungi [6, 10], and plants and fungi form JAs with identical absolute configuration [5, 11]. JAs and the methyl ester of a key intermediate, 12-OPDA, were identified as a metabolite of 18:3n-3 in the culture medium of *L. theobromae* [10]. However, whether JA and 12-OPDA are formed by the same enzymes as in plants is unknown. LOXs are ubiquitous in plants, but only few LOXs of fungi have been identified and characterized. Unfortunately, the genome of *L. theobromae* has not yet been sequenced. Hydroperoxy fatty acids can be formed in fungi also by heme containing dioxygenases, e.g., linoleate diol synthases (LDS) and other oxygenases of the dioxygenase-cytochrome P450 (DOX-CYP) family of fusion proteins [12–16]. For comparison, *Aspergillus terreus* was recently found to express linoleic acid 9R-dioxygenase (9R-DOX) and AOS activities [17]. This 9R-DOX activity could be due to a heme containing dioxygenase, as LOX genes have not been identified in the genome of *A. terreus* [17].

The aim of the present study was to investigate the oxidation and further transformation of polyunsaturated fatty acids by *L. theobromae*. This fungus is a devastating plant pathogen, and its access from many fungal collection centers is restricted for environmental safety reasons. The few strains, which produce JA in large amounts [18], are also guarded by commercial interests. In this study, we used two strains of *L. theobromae* from the CBS Fungal Biodiversity Center, and a non-commercial strain with prominent JA biosynthetic capacity [19].

Materials and Methods

Materials

16:3n-3 (99%), oleic acid (18:1n-9; 99%), 12Z-octadecenoic acid (18:1n-6; 99%), linoleic acid (18:2n-6; 99%),

U[¹³C]18:2n-6 (98%), 18:3n-3 (99%), γ -linolenic acid (18:3n-6; 99%), and 9Z,12Z-eicosadienoic acid (20:2n-6; 99%) were from Lipidox, Sigma and Larodan, and stored as stock solutions (50–100 mM) in ethanol at -20°C . HPLC solvents were from VWR. [11S-²H]18:2n-6 (>95% ²H) was prepared as described [20, 21]. 9-Hydroxy-10-oxo-10,12Z-octadecadienoic acid was from Lipidox (Stockholm, Sweden). 11S- and 11R-hydroperoxy-7Z,9E,13Z-hexadecatrienoic acids (11-HPHDTRE), 9S-hydroperoxy-10E,12Z-octadecadienoic acid (9S-HPODE), 13R-hydroperoxy-9Z,11E-octadecadienoic acid (13R-HPODE), 13R-hydroperoxy-9Z,11E,15Z-octadecatrienoic acid (13R-HPOTRE), and 13S-HPODE were prepared with LOXs (tomato fruit [22], recombinant manganese LOX (Mn-LOX) [23], and soybean LOX-1 (Lipoxidase, Sigma)). 11S- and 11R-HOME(12Z) were prepared with PGH synthase-1 and Mn-LOX [24, 25]. A racemic mixture of HPODE was obtained by photo oxidation with methylene blue [26]. The O-methylxime (MO) derivative of [5,5,7-²H₃](–)-JA used as an internal standard during quantification of JA was synthesized by treatment of (–)-JA with Na₂CO₃ in D₂O followed by preparation and isolation of the MO derivative. Solvents for HPLC and other chemicals were of analytical grade and obtained from VWR and Sigma-Aldrich. *L. theobromae* (CBS 117454; CBS 122127) were from CBS Fungal Biodiversity Center (Baarn, Delft, The Netherlands). The *B. theobromae* strain 2334 was isolated in Cuba, characterized and grown as described [19], and it will be referred to as *L. theobromae* strain 2334.

Fungal Growth

The two CBS strains were grown on agar slants (15 g agar/2 g malt extract/0.75 g NaNO₃/0.35 g MgSO₄·7H₂O/5 g sucrose) at 27 °C for 3–4 days and then stored at +4 °C. For analysis, a piece of the agar slants of *L. theobromae* were grown in a modified Czapek-Dox medium (per liter: 2 g KH₂PO₄, 0.6 g MgSO₄·7H₂O, 0.3 g KCl, 7.5 g NaNO₃, 50 g sucrose, 1 ml trace metals ([27])); pH was adjusted to 5.5 with KOH) at 27 °C without shaking for 10–12 days. The *L. theobromae* strain 2334 was grown in malt extract agar slant at 30 °C for 3 days and then stored at 4 °C; for analysis, a piece of the agar slants of this fungus was grown in a medium previously described [19]. The mycelia of the strains were harvested by filtration. The filtrate was assayed for JAs, whereas the mycelia were washed with saline, blotted dry, weighed, grinded in liquid nitrogen and stored at -80°C until analysis.

Assay of Enzyme Activity

The nitrogen powder was homogenized (glass-Teflon, 10 passes; +4 °C) in 10–20 vols. (w/v) of 0.1 mM KH₂PO₄

buffer (pH 7.4)/2 mM EDTA/0.04% Tween-20, and centrifuged at $15,000\times g$ (10 min, $+4\text{ }^{\circ}\text{C}$). The supernatant was used immediately for studies of enzyme activities. Typically, an aliquot (0.25–0.5 ml) was incubated with 80–100 μM of fatty acids or fatty acid hydroperoxides for 30–40 min on ice. The incubation was terminated with ethanol (4 vols.) and centrifuged. The supernatant was diluted with water and extracted (SepPak/C₁₈; Waters), as described [21, 28]. Triphenylphosphine was used to reduce hydroperoxy fatty acids to alcohols. The subcellular distributions of enzyme activities were determined by differential centrifugations ($15,000\times g$, 10 min; $+4\text{ }^{\circ}\text{C}$; $100,000\times g$; $+4\text{ }^{\circ}\text{C}$; 60 min) and assay of enzyme activities in the high speed supernatant and the microsomal fractions.

LC–MS/MS

Reversed phase-HPLC (RP-HPLC) with MS/MS analysis was performed with a Surveyor MS pump (ThermoFisher), a manual or an automatic injector (Surveyor; ThermoFisher), and with an octadecyl silica column (5 μm ; $150\times 2.1\text{ mm}$; Phenomenex), which was eluted at 0.3 ml/min with methanol/water/acetic acid, 750/250/0.05 or 800/200/0.05. The effluent was subjected to electrospray ionization (ESI) in a linear ion trap mass spectrometer (LTQ, ThermoFisher) with analysis of negative ions. In some experiments, we also analyzed the effluent by UV absorption (photodiode array detector, path length 5 cm; Surveyor PDA plus, ThermoFisher). The heated transfer capillary was set at $315\text{ }^{\circ}\text{C}$ and the ion isolation width usually at 1.5 (and at 5 in the first selection for MS³ analysis of hydroperoxides [26]). The collision energy was set at 35 (arbitrary scale) and the tube lens at 90–120 V. For analysis of products formed from [²H₁]18:2n-6, we used an isolation width of 6 for the carboxylate anion.

Normal phase HPLC (NP-HPLC) and chiral phase-HPLC (CP-HPLC) were performed as described in [17, 28]. Steric analysis of 10-HODE was performed with a Reprosil Chiral-NR column (8 μm ; $250\times 2\text{ mm}$; eluted with isopropanol/hexane/acetic acid, 3/97/0.01). The enantiomers of 9- and 13-HODE, 9-HOTRE, HOME, HHDTRE and α -ketols were resolved with Reprosil Chiral AM (5 μm ; $250\times 2\text{ mm}$; eluted with methanol/hexane/acetic acid or ethanol/hexane/acetic acid, 5/95/0.01, at 0.15–0.2 ml/min) [28]. The effluent was mixed with isopropanol/water, 60/40, from a second pump (Surveyor MS) [28] and subjected to ESI with MS/MS analysis of carboxylate anions.

Quantitative Determination of (–)-JA and (+)-7-iso-JA and Fatty Acid Analysis

The medium (0.05–2 mL) of the growing cultures of *L. theobromae* was diluted with water to make a total volume

of 2 mL and treated with 8 mL of a methanolic solution of 30 mM methoxyamine hydrochloride. The mixture was vortexed and kept at room temperature for 15 h. The *O*-methyloxime (MO) derivative of [5,5,7-²H₃](–)-JA (3 μg) was added as an internal standard, and the material obtained following extraction with diethyl ether was dissolved in chloroform/2-propanol (2:1, v/v) and applied to a Supelclean LC-NH₂ solid phase extraction cartridge (Supelco, Bellefonte, PA). Elution with diethyl ether/acetic acid (98:2, v/v) afforded the JA-MO derivative, which was methyl-esterified by treatment with diazomethane and subjected to GC–MS analysis. For this purpose, a Hewlett-Packard model 5970B mass selective detector connected to a Hewlett-Packard model 5890 gas-chromatograph was used. The instrument was operated in the selected ion monitoring mode using the ions m/z 253 (unlabeled JA-MO methyl ester) and 256 (deuterium-labeled JA-MO methyl ester). Amounts of (–)-JA and (+)-7-iso-JA were calculated from areas of the m/z 253 peaks due to these compounds and from the area of the m/z 256 peak due to the deuterated standard.

The fatty acid composition of *L. theobromae* was determined by GC–MS analysis after hydrolysis as described [29]. The fatty acid methyl esters were separated on a Supelcowax-10 Capillary GC Column (30 m, film thickness 0.25 μm , carrier gas helium), and the column temperature was raised from $150\text{ }^{\circ}\text{C}$ at $5\text{ }^{\circ}\text{C}/\text{min}$.

Results

Fatty Acid Composition

We analyzed the fatty acid composition of *L. theobromae* strains CBS 122127 and 2334.

The four main fatty acids in the mycelium of CBS 122127 were 16:0 (37%), 18:2 (25%), 18:1 (24%), and 18:0 (14%). Traces of 20:0 were detected, but not the two expected precursor fatty acids of JA biosynthesis, 18:3n-3 and 16:3n-3. In contrast, the mycelium of *L. theobromae* strain 2334 contained 18:3n-3 as a major fatty acid, as illustrated in Fig. 1 along with the major fatty acids also found in CBS122127. 16:3n-3 was not detected.

Jasmonic Acid Production

Both commercial strains produced JAs, but (–)-JA and (+)-JA could only be detected in the growth medium in low concentrations [$<0.2\text{ }\mu\text{g}/\text{mL}$; e.g., $57\text{ ng}/\text{mL}$ (–)-JA, $109\text{ ng}/\text{mL}$ (+)-7-iso-JA (3R,7S-JA)]. In contrast, *L. theobromae* strain 2334 formed JAs in large amounts, about $200\text{ }\mu\text{g}/\text{mL}$ (e.g., $196\text{ }\mu\text{g}/\text{mL}$ (–)-JA and $13\text{ }\mu\text{g}/\text{mL}$ (+)-7-iso-JA) in agreement with previous reports [18]. In

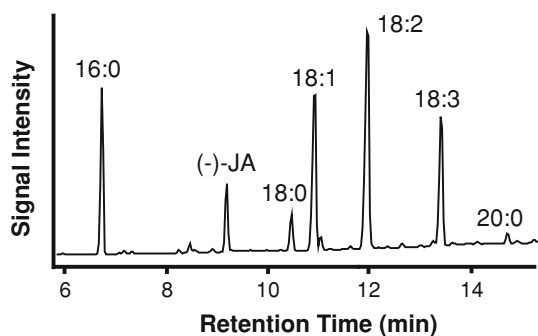


Fig. 1 GC–MS analysis of the fatty acid composition of *L. theobromae* strain 2334 with prominent JA biosynthesis. The fatty acids were analyzed as methyl ester derivatives. The commercial strain CBS 122127 lacked 18:3n-3, contained the other fatty acids of strain 2334, and formed only relatively small amounts of JA (0.2 vs 200 mg/L)

another experiment, media collected after growth of strain 2234 for 10 and 12 days were found to contain 216 $\mu\text{g}/\text{mL}$ and 178 $\mu\text{g}/\text{mL}$, respectively, of (–)-JA plus (+)-7-*iso*-JA.

Oxylin Biosynthesis by Subcellular Fractions

Subcellular fractions (10,000 $\times g$) of all three strains contained 5,8-LDS activity as judged from 8-hydro(per)oxy metabolites and 5,8-diols formed from 18:2n-6, [U- ^{13}C] 18:2n-6, and 18:3n-3. Unexpectedly, subcellular fractions of the strain 2334 with prominent secretion of JA did not produce significant amounts of other oxylin metabolites than 8-hydro(per)oxy metabolites and 5,8-diols, whereas the two commercial strains appeared to oxygenate fatty acids to these and to additional metabolites.

18:3n-3 and 16:3n-3 18:3n-3 was oxidized by nitrogen powder of the two *L. theobromae* CBS strains to 5,8-DiHOTrE and to an α -ketol, 9-hydroxy-10-keto-12Z,15Z-octadecadienoic acid, as shown in Fig. 2a. The ESI–MS/MS spectrum of the α -ketol (m/z 309 \rightarrow full scan) is shown in Fig. 2b. A characteristic ion with mass of even number was noted at m/z 200, likely a radical ion, which is also present in the corresponding spectrum of 9-hydroxy-10-oxo-12Z-octadecenoic acid [17]. Significant amounts of the corresponding γ -ketol could neither be detected by RP-HPLC nor NP-HPLC. The α -ketol was likely formed from an allene oxide, 9,10-epoxy-10,12Z,15Z-octadecatrienoic acid. Hydrolysis of this allene oxide was expected to mainly form the *S* stereoisomer, and this was confirmed (insert in Fig. 2a).

The MS/MS spectrum of 5,8-DiHOTrE was as reported [30]. The less polar metabolites were identified as a mixture of 8-H(P)OTrE, 10-H(P)OTrE, and 9-H(P)OTrE (mainly 9*R*). Although 13-HPOTrE was not detected, we investigated whether 13*S*- or 13*R*-HpOTrE were substrates of the AOS activity, but this was not the case.

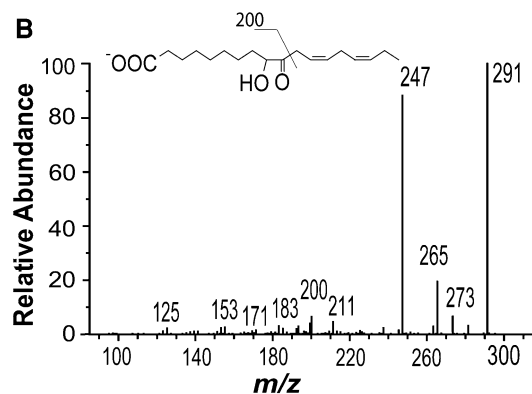
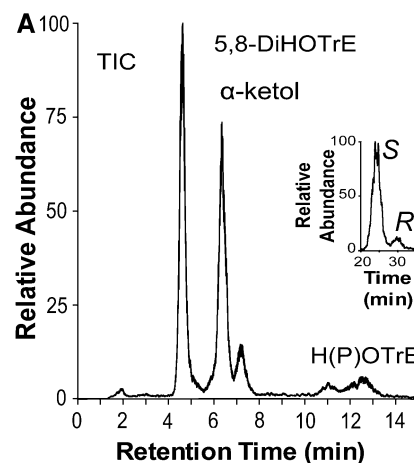


Fig. 2 LC–MS/MS analysis of oxidation of 18:3n-3 by subcellular fractions of *L. theobromae*. **a** RP-HPLC–MS analysis of metabolites formed by CBS 117454. TIC from MS/MS analysis of m/z 309 and 293. The two major peaks contained 5,8-DiHOTrE and an α -ketol, as indicated. Small amounts of H(p)OTrE were also detected. Strain CBS 122127 yielded a similar pattern. The inset chromatogram shows that the *S* and *R* stereoisomers of α -ketols were formed from hydrolysis of the allene oxide in a $\sim 10:1$ ratio (CP-HPLC–MS/MS). **b** MS/MS spectrum (m/z 309 \rightarrow full scan) of the α -ketol derived from hydrolysis of an allene oxide. The insert shows formation of the even numbered signal at m/z 200, which presumably is due to a radical anion [17]

16:3n-3 was oxidized to approximately equal amounts of 10-HHDTrE and 11-HHDTrE (Fig. 3). A steric analysis by CP-HPLC showed that 10*R*-HHDTrE and 11*S*-HHDTrE were mainly formed (Fig. 3b, c). It seems likely that the 10*R*- and 11*S*-DOX activities are due to the linolenate 9*R*-DOX activity. Chain shortening of 18:3n-3 by two carbons thus changed the oxygenation from C-9 to C-10, and led to biosynthesis 11*S*-HPHDTrE after hydrogen abstraction at C-9. 11*S*-HPHDTrE is a precursor of JA in plants [2], but it was not transformed by AOS of *L. theobromae*.

18:2n-6, 18:3n-6, and 20:2n-6 18:2n-6 was transformed to a major polar metabolite, which eluted after 7 min during LC–MS/MS analysis (Fig. 4a). [U- ^{13}C]Linoleic acid was oxidized in the same way. The mass spectrum of the main metabolite was identical with that of an α -ketol, 9-hydroxy-10-oxo-12Z-octadecenoic acid [17]. Small

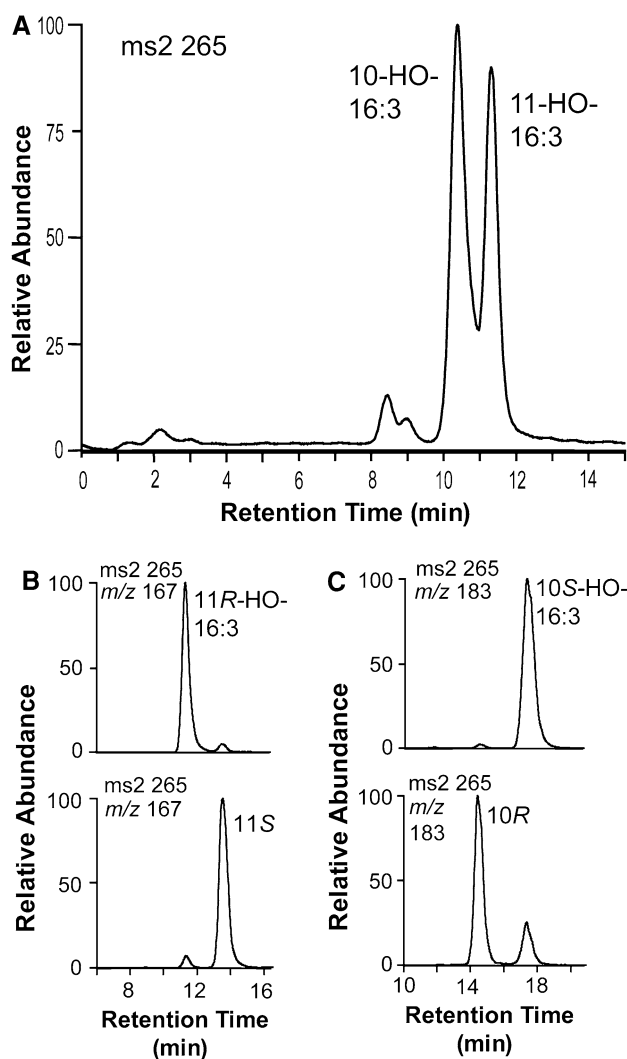


Fig. 3 Analysis of oxidation of 16:3n-3 by subcellular fractions of *L. theobromae*. The products formed by strain CBS 122127 were analyzed by RP- and CP-HPLC with ESI-MS/MS after reduction to alcohols with triphenylphosphine. **a** RP-HPLC. The first eluting major peak contained 10-HHDTRE (marked 10-HO-16:3) and the second peak II 11-HHDTRE (marked 11-HO-16:3). **b** CP-HPLC-MS analysis of 11-HHDTRE (bottom chromatogram) with aid of an 11R-HHDTRE standard (top chromatogram; the 11R stereoisomer was produced with Mn-LOX [32]). **c** CP-HPLC-MS analysis of 10-HHDTRE (bottom chromatogram) with aid of the 10S stereoisomer (prepared with Mn-LOX [32])

amounts of the γ -ketol, 13-hydroxy-10-oxo-11E-octadecenoic acid, was detected after 5 min (Fig. 4a); MS/MS and MS/MS/MS spectra as reported [17]. The two ketols were apparently formed from 9R-HPODE via hydrolysis of an unstable allene oxide, 9,10-epoxy-10,12Z-octadecadienoic acid [17]. Steric analysis of the α -ketol supported this mechanism of biosynthesis from 9R-HPODE, as CP-HPLC showed that it consisted mainly of the 9S stereoisomer (cf. insert in Fig. 2a). The 9R-DOX activity was present in the soluble fraction and the AOS activity in the microsomal

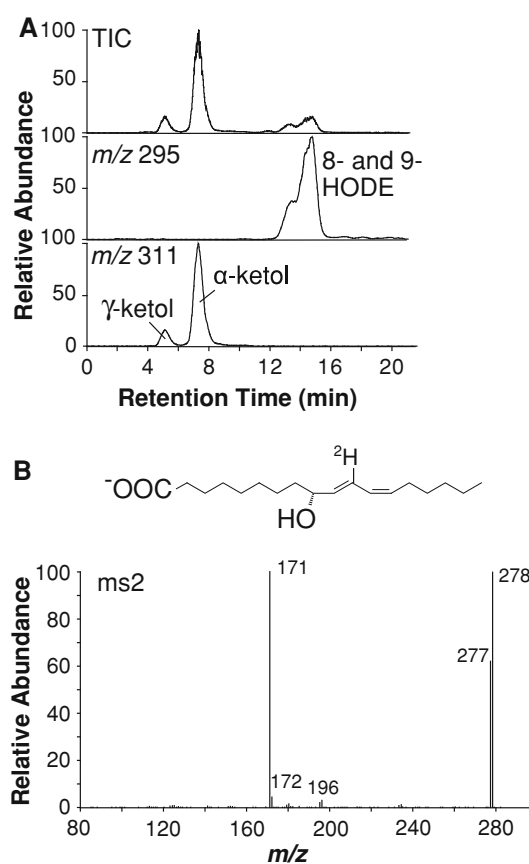


Fig. 4 LC-MS/MS analysis of oxidation of 18:2n-6 by subcellular fractions of *L. theobromae* (CBS 117454). **a** RP-HPLC-MS analysis showed that the major products were α - and γ -ketols and 8- and 9-HODE. **b** MS/MS analysis (m/z 292–298) \rightarrow full scan of 9-HODE from an incubation with [11S- ^2H]18:2n-6 (95% ^2H). The latter was diluted with endogenous 18:2n-6 in the incubation. The signals at m/z 277 and 278 of this mass spectrum, mainly due to loss of water from the carboxyl group, showing that the deuterium label was retained, as m/z 277 and 278 were present in the same relative intensities as in 8-HODE of this experiment

fraction, which are in agreement with the distribution of plant LOX and AOS (CYP74) [2].

Other metabolites were 5,8-DiHODE, 8-H(P)ODE, and small amounts of 10-H(P)ODE and 13-H(P)ODE (\sim 5% of 9-H(P)ODE). Steric analyses showed that 10-HODE was almost racemic (\sim 60% S), whereas 13-HODE was mainly formed with S configuration (data not shown).

The oxidation of 18:2n-6 was investigated with [11S- ^2H]18:2n-6 (95% ^2H). RP-HPLC with MS and MS/MS analysis of 9R-HODE showed that this deuterium label was retained (Fig. 4b), suggesting that the 9R-DOX of *L. theobromae* catalyzes suprafacial hydrogen abstraction at C-11 relative to the oxygenation at C-9. The apparent deuterium content, as judged from the ion intensities at m/z 277 and 288 of both 8- and 9-HODE, was 60%, due to dilution with endogenous 18:2n-6. The deuterium label was also retained in 13S-HODE, a minor metabolite in comparison with 9-HODE.

The 9*R*-DOX activity also transformed 18:3n-6 to 9-HPOTrE(n-6) as the main metabolite, but further transformation to an α -ketol could not be detected. This fatty acid was not oxygenated by 5,8-LDS in agreement with previous reports [31]. Significant formation of 13-HO-TrE(n-6) was also detected, as judged from the signal intensities of characteristic ions [m/z 169 (80%; 9-HO-TrE(n-6)) and m/z 193 (20%, 13-HOTrE(n-6))].

20:2n-6 was oxidized at C-11 and C-15, but these hydroperoxides were not further converted to α -ketols.

18:1n-9 and *18:1n-6* Oleic acid was exclusively oxidized by *L. theobromae* to 5,8-DiHOME and 8-H(P)OME, as shown in Fig. 5a. We could not detect signs of hydrogen abstraction at C-11, as judged from insignificant formation of 9-HOME(10*E*) and 11-HOME(9*Z*). This suggested that 18:1n-9 was not oxidized by the 9*R*-DOX activity.

The 9*R*-DOX activity might conceivably abstract the hydrogen at C-11 of 18:1n-6 with formation of 11*S*-HOME(12*Z*) or 13*S*-HOME(11*E*), whereas LDS enzymes mainly oxidize 18:1 with formation of stereoisomers with *R* configuration [25]. 13*S*-HOME(11*E*) was not detected. As shown in Fig. 5b, the formation of 11*S*-HOME(12*Z*) was only 10–15% of the biosynthesis of 11*R*-HOME(12*Z*) and could be attributed to oxidation by 5,8-LDS [24, 25].

In conclusion, 18:1n-9 and 18:1n-6 did not appear to be oxidized to a significant extent by the 9*R*-DOX activity.

13S-HPHTrE and *11S-HPHDTrE*—these hydroperoxides were not transformed by the AOS activity.

Discussion

Tsukada et al. [10] demonstrated that JA is formed in *L. theobromae* from 18:3n-3 [10]. In these experiments, the fungus was grown for 10 days with ^{13}C -labeled sodium acetate or with $^2\text{H}_6$ 18:3n-3, and found to secrete significant amounts of [^{13}C]JA, [$^2\text{H}_5$]JA, and [$^2\text{H}_5$]-iso-JA, respectively. These authors also isolated 12-OPDA (methyl ester), a key intermediate in the biosynthesis of JA in higher plants. Interestingly, NMR analysis of the deuterated 12-OPDA indicated a stereochemical difference between the fungal and plant cyclopentenone reductase reactions. This result suggested that fungal JA biosynthesis could have evolved independently from plant biosynthesis with both similarities and differences.

We did not find evidence for the presence in *L. theobromae* of the JA biosynthetic enzymes present in higher plants. Instead, we report that mycelia of two commercial strains of *L. theobromae* express prominent linolenate 9*R*-DOX and AOS activities after growth for about 10 days. These strains only secreted small amounts of JA, and we therefore also investigated the strain 2334 with large

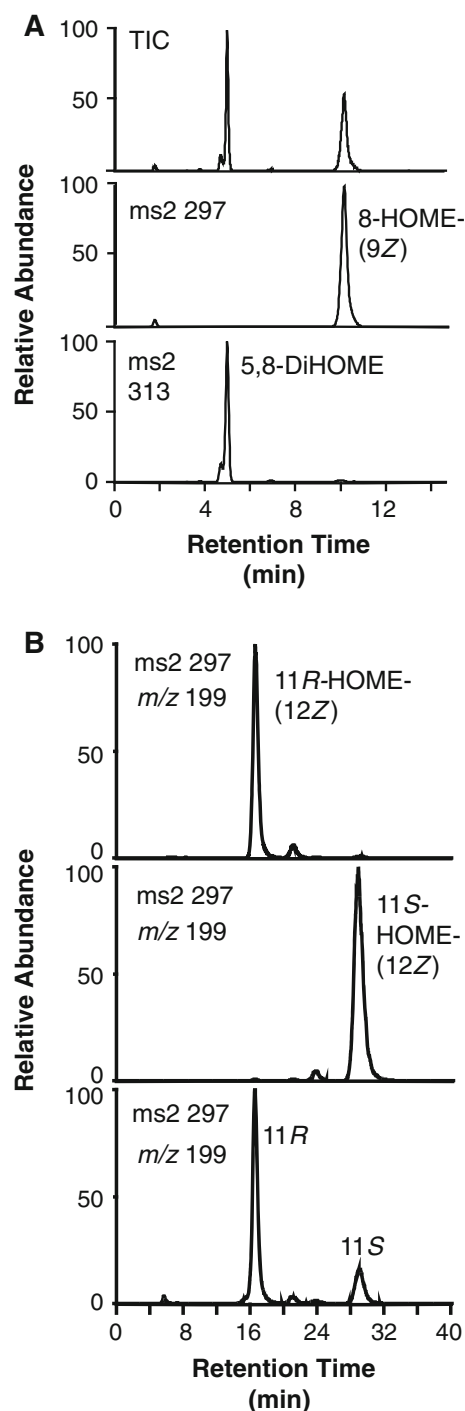


Fig. 5 LC–MS analysis of products formed during oxygenation of 18:1n-9 and 18:1n-6 by subcellular fractions of *L. theobromae*. **a** RP-HPLC analysis of oxidation of 18:1n-9 by strain CBS 122127. The two main products were 5,8-DiHOME and 8-HOME. **b** CP-HPLC analysis of oxidation of 18:1n-6–11-HOME(12*Z*) with aid of standards; the *top chromatogram* showing elution of 11*R*-HOME (prepared with Mn-LOX), the *middle chromatogram* elution of 11*S*-HOME (prepared with COX-1). The *bottom chromatogram* showing separation of products formed by *L. theobromae*. The latter thus mainly formed the 11*R* stereoisomer, and this metabolite can be attributed to the 5,8-LDS activity [25]

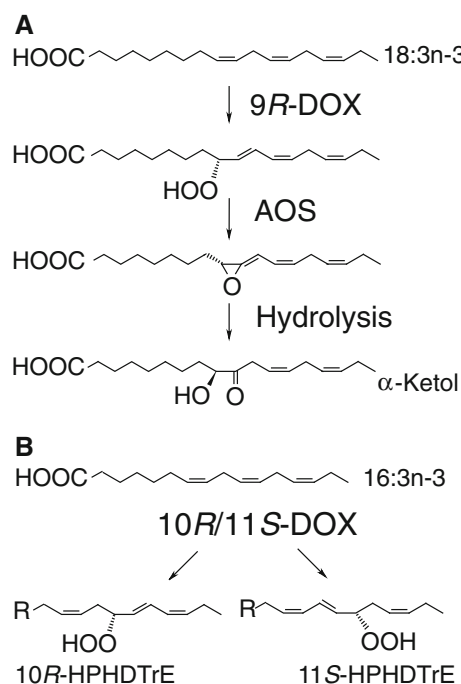


Fig. 6 Overview of the transformation of 18:3n-3 and 16:3n-3 to *cis-trans* conjugated hydroperoxides and an allene oxide by *L. theobromae*. **a** Oxidation of 18:3n-3. The soluble 9R-DOX activities are likely due to a lipoxygenase and the microsomal AOS activities to P450. **b** Oxidation of 16:3n-3. These metabolites are also formed by Mn-LOX but with the opposite chirality, and presumably formed by the same enzyme with oxidizes 18:2n-6 and 18:3n-3 to 9R-hydroperoxy metabolites

capacity to secrete JA. This strain contained 18:3n-3 and secreted large amounts of JA at time points (10 and 12 days).

We found that 18:3n-3 and 18:2n-6 were both oxygenated to 9R-hydroperoxides, which were further transformed to allene oxides. The oxidation of 18:3n-3 by this pathway is summarized in Fig. 6a. The 9R-DOX activity showed broad substrate specificity, and also oxidized 16:3n-3, 18:3n-6, and 20:2n-6.

16:3n-3 can be converted to JA in plants, and the first step is biosynthesis of 11S-HPHDTRE [3]. This metabolite was formed by *L. theobromae*. 16:3n-3 was oxidized to approximately equal amounts of 10R-HHDTRE and 11S-HHDTRE (Fig. 6b), however, since we could not detect formation of α -ketols it is apparent that these hydroperoxides were not substrates of AOS. The oxidation of 16:3n-3 is summarized in Fig. 6b.

9R-DOX and AOS activities have also been reported in *A. terreus* [17]. The genome of *A. terreus* appears to lack LOXs, whereas there is no information of the genome of *L. theobromae*. At first, it seemed likely that these two fungi could form 9R-HPODE and allene oxides by homologous enzymes. The 9R-DOX activity was present in the soluble fraction, whereas the AOS activity was mainly

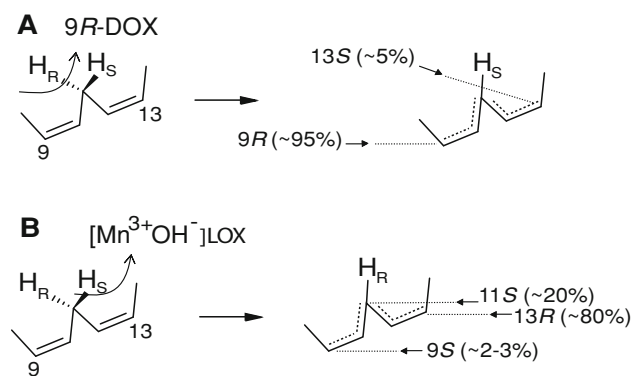


Fig. 7 A schematic presentation of the hydrogen abstraction mechanisms of 9R-DOX and Mn-LOX. **a** Mechanism of hydrogen abstraction of 18:2n-6 and direction of oxygenation by the 9R-DOX activity. **b** Mechanism of hydrogen abstraction of 18:2n-6 and direction of oxygenation by Mn-LOX. If the substrate could be oxidized by Mn-LOX in the reverse orientation, the products and the oxygenation mechanism would be similar to that of the 9R-DOX activity

present in microsomal fraction. Both fungi therefore likely express microsomal AOS of the cytochrome P450 family, but the 9R-DOX activities of *L. theobromae* and *A. terreus* could be due to different classes of dioxygenases, i.e., a heme-containing dioxygenase in case of *A. terreus* and a lipoxygenase in case of *L. theobromae*. The latter hypothesis is based on the following observations.

First, γ -linolenic acid (18:3n-6) was oxidized to 9-HPOTRE(n-6) as a prominent metabolite by *L. theobromae*. This fatty acid is readily oxidized by many plant LOX, but it is not oxidized by a series of fungal DOX-CYP fusion proteins, e.g., 5,8-LDS, 7,8-LDS, and 10R-DOX, and not by the 9R-DOX of *A. terreus* [17]. Second, LOXs oxygenate 18:1 only slowly [24], and we could not attribute the oxidation of 18:1n-6 or 18:1n-9 to the 9R-DOX activity of *L. theobromae*. Thirdly, we were struck by the similarities of Mn-LOX and 9R-DOX.

Both enzymes oxidize 16:3n-3 at the n-7 (C-10) and the n-6 carbons (C-11), albeit with different chirality [32]. The oxidation at the n-7 position is not a common feature of LOXs, but was recently reported by the LOX domain of a fusion protein of a cyanobacterium [33]. Oxygenation by 9R-DOX and Mn-LOX differ with regard to regiochemical and stereochemical specificity, but both enzymes catalyze suprafacial hydrogen abstraction and oxygenation [34], as outlined in Fig. 7. It is tempting to speculate that 9R-DOX activity of *L. theobromae* could be due to a LOX homologue of Mn-LOX with reverse substrate orientation in the active site (cf. Fig. 7). DOX-CYP fusion proteins and PGH synthases catalyze antarafacial hydrogen abstraction [24], whereas the 9R-DOX activity of *A. terreus* also is suprafacial [17]. The main difference between the two fungal 9R-DOX activities resides in the oxidation of 18:3n-3.

The AOS activity of *L. theobromae* appeared to be specific for 9R-HPODE and 9R-HPOTrE, since we could not detect significant formation of α -ketols from 16:3n-3, 18:3n-6, 20:2n-6, 13S- or 13R-HpOTrE. The substrate specificity of AOS of *A. terreus* is restricted to 9R-HPODE. In contrast, AOS (CYP74A) of plants are specific for 9S- or 13S-hydroperoxides [35, 36].

In summary, we report that *L. theobromae* efficiently oxidized 18:2n-6 and 18:3n-3 sequentially to 9R-hydroperoxides and to unstable allene oxides. The AOS activity is microsomal and probably catalyzed by a homologue of CYP74, whereas the soluble 9R-DOX activity might be due to a LOX. It appears that the genome sequence of *L. theobromae* will be needed to elucidate the detailed mechanism of JA formation in this fungus.

Acknowledgments Supported by VR Medicine (03X-06523) and by The Knut and Alice Wallenberg Foundation (KAW 2004.123). F Eng was supported by a project of Dr Mariano Gutierrez-Rojas from UAM Campus Iztapalapa (Mexico). Presented at the Third European Workshop on Lipid Mediators, Pasteur Institute, Paris June 3–4, 2010.

References

- Schaller A, Stintzi A (2009) Enzymes in jasmonate biosynthesis—structure, function, regulation. *Phytochem* 70:1532–1538
- Wasternack C, Kombrink E (2010) Jasmonates: structural requirements for lipid-derived signals active in plant stress responses and development. *ACS Chem Biol* 5:63–77
- Gfeller A, Dubugnon L, Liechti R, Farmer EE (2010) Jasmonate biochemical pathway. *Sci Signal* 3:1–6
- Cross BE, Webster GRB (1970) New metabolites of *Gibberella fujikuroi*. *J Chem Soc C* 1970:1838–1842
- Aldridge D, Galt S, Giles D, Turner W (1971) Metabolites of *Lasiodiplodia theobromae*. *J Chem Soc C* 1971:1623–1627
- Miersch O, Bohlmann H, Wasternack C (1999) Jasmonates and related compounds from *Fusarium oxysporum*. *Phytochem* 50:517–523
- Wasternack C (2007) Jasmonates: an update on biosynthesis, signal transduction and action in plant stress response, growth and development. *Ann Bot* 100:681–697
- Goodrich-Tanrikulu M, Mahoney NE, Rodriguez SB (1995) The plant growth regulator methyl jasmonate inhibits aflatoxin production by *Aspergillus flavus*. *Microbiol* 141:2831–2837
- Cohen S, Flescher E (2009) Methyl jasmonate: a plant stress hormone as an anti-cancer drug. *Phytochem* 70:1600–1609
- Tsukada K, Takahashi K, Nabeta K (2010) Biosynthesis of jasmonic acid in a plant pathogenic fungus, *Lasiodiplodia theobromae*. *Phytochem* 71:2019–2023
- Miersch O, Preiss A, Sembdner G, Schreiber K (1987) (+)-7-iso-jasmonic acid and related compounds from *Botryodiplodia theobromae*. *Phytochem* 26:1037–1039
- Lee DS, Nioche P, Hamberg M, Raman CS (2008) Structural insights into the evolutionary paths of oxylipin biosynthetic enzymes. *Nature* 455:363–368
- Brodowsky ID, Hamberg M, Oliw EH (1992) A linoleic acid (8R)-dioxygenase and hydroperoxide isomerase of the fungus *Gaeumannomyces graminis*. Biosynthesis of (8R)-hydroxylinoic acid and (7S, 8S)-dihydroxylinoic acid from (8R)-hydroperoxylinoic acid. *J Biol Chem* 267:14738–14745
- Brodhun F, Göbel C, Hornung E, Feussner I (2009) Identification of PpoA from *Aspergillus nidulans* as a fusion protein of a fatty acid heme dioxygenase/peroxidase and a cytochrome P450. *J Biol Chem* 284:11792–11805
- Brodhun F, Schneider S, Göbel C, Hornung E, Feussner I (2010) PpoC from *Aspergillus nidulans* is a fusion protein with one active heme. *J Biochem* 425:553–565
- Garscha U, Oliw EH (2009) Leucine/valine residues direct oxygenation of linoleic acid by (10R)- and (8R)-dioxygenases: expression and site-directed mutagenesis of (10R)-dioxygenase with epoxyalcohol synthase activity. *J Biol Chem* 284:13755–13765
- Jernerén F, Hoffmann I, Oliw EH (2010) Linoleate 9R-dioxygenase and allene oxide synthase activities of *Aspergillus terreus*. *Arch Biochem Biophys* 495:67–73 (Erratum 2010; 500; 210)
- Dhandhukia PC, Thakkar VR (2008) Response surface methodology to optimize the nutritional parameters for enhanced production of jasmonic acid by *Lasiodiplodia theobromae*. *J Appl Microbiol* 105:636–643
- Eng F, Gutierrez-Rojas M, Favela-Torres E (1998) Culture conditions for jasmonic acid and biomass production by *Botryodiplodia theobromae* in submerged fermentation. *Process Biochem* 33:715–720
- Hamberg M, Zhang LY, Brodowsky ID, Oliw EH (1994) Sequential oxygenation of linoleic acid in the fungus *Gaeumannomyces graminis*: stereochemistry of dioxygenase and hydroperoxide isomerase reactions. *Arch Biochem Biophys* 309:77–80
- Garscha U, Jernerén F, Chung D, Keller NP, Hamberg M, Oliw EH (2007) Identification of dioxygenases required for *Aspergillus* development. Studies of products, stereochemistry, and the reaction mechanism. *J Biol Chem* 282:34707–34718
- Matthew JA, Chan HW, Galliard T (1977) A simple method for the preparation of pure 9-*n*-hydroperoxide of linoleic acid and methyl linoleate based on the positional specificity of lipoxygenase in tomato fruit. *Lipids* 12:324–326
- Cristea M, Engström A, Su C, Hörnsten L, Oliw EH (2005) Expression of manganese lipoxygenase in *Pichia pastoris* and site-directed mutagenesis of putative metal ligands. *Arch Biochem Biophys* 434:201–211
- Oliw EH, Jernerén F, Hoffmann I, Sahlin M, Garscha U (2011) Manganese lipoxygenase oxidizes bis-allylic hydroperoxides and octadecenoic acids by different mechanisms. *Biochim Biophys Acta* 1811:138–147
- Oliw EH, Wennman A, Hoffmann I, Garscha U, Hamberg M, Jernerén F Stereoselective oxidation of regioisomeric octadecenoic acids by fatty acid dioxygenases. *J Lipid Res* 52:1995–2004
- Garscha U, Nilsson T, Oliw EH (2008) Enantiomeric separation and analysis of unsaturated hydroperoxy fatty acids by chiral column chromatography–mass spectrometry. *J Chromatogr B Analyt Technol Biomed Life Sci* 872:90–98
- Jernerén F, Sesma A, Franceschetti M, Hamberg M, Oliw EH (2010) Gene deletion of 7,8-linoleate diol synthase of the rice blast fungus: studies on pathogenicity, stereochemistry, and oxygenation mechanisms. *J Biol Chem* 285:5308–5316
- Garscha U, Oliw EH (2007) Steric analysis of 8-hydroxy- and 10-hydroxyoctadecadienoic acids and dihydroxyoctadecadienoic acids formed from 8R-hydroperoxylinoic acid by hydroperoxide isomerases. *Anal Biochem* 367:238–246
- Martinez E, Hamberg M, Busquets M, Diaz P, Manresa A, Oliw EH (2010) Biochemical characterization of the oxygenation of unsaturated fatty acids by the dioxygenase and hydroperoxide isomerase of *Pseudomonas aeruginosa* 42A2. *J Biol Chem* 285:9339–9345
- Oliw EH, Su C, Skogström T, Benthin G (1998) Analysis of novel hydroperoxides and other metabolites of oleic, linoleic, and

- linolenic acids by liquid chromatography–mass spectrometry with ion trap MSn. *Lipids* 33:843–852
31. Hoffmann I, Jernerén F, Garscha U, Oliw EH (2011) Expression of 5,8-LDS of *Aspergillus fumigatus* and its dioxygenase domain. A comparison with 7,8-LDS, 10-dioxygenase, and cyclooxygenase. *Arch Biochem Biophys* 506:216–222
 32. Cristea M, Oliw EH (2007) On the singular, dual, and multiple positional specificity of manganese lipoxygenase and its G316A mutant. *J Lipid Res* 48:890–903
 33. Gao B, Boeglin WE, Brash AR (2010) Omega-3 fatty acids are oxygenated at the n-7 carbon by the lipoxygenase domain of a fusion protein in the cyanobacterium *Acaryochloris marina*. *Biochim Biophys Acta* 1801:58–63
 34. Hamberg M, Su C, Oliw E (1998) Manganese lipoxygenase. Discovery of a bis-allylic hydroperoxide as product and intermediate in a lipoxygenase reaction. *J Biol Chem* 273:13080–13088
 35. Hamberg M (2000) New cyclopentenone fatty acids formed from linoleic and linolenic acids in potato. *Lipids* 35:353–363
 36. Grechkin AN, Mukhtarova LS, Latypova LR, Gogolev Y, Toporkova YY, Hamberg M (2008) Tomato CYP74C3 is a multifunctional enzyme not only synthesizing allene oxide but also catalyzing its hydrolysis and cyclization. *Chembiochem* 9:2498–2505

Differences in Lipid Characteristics Among Populations: Low-Temperature Adaptability of Ayu, *Plecoglossus altivelis*

Changhu Xue · Masaya Okabe · Hiroaki Saito

Received: 28 February 2011 / Accepted: 21 October 2011 / Published online: 26 November 2011
© AOCS 2011

Abstract The lipid and fatty acid compositions of the total lipids of three cultured populations (migratory between fresh and salt water, Lake Biwa landlocked, and Setogawa River forms) of ayu, *Plecoglossus altivelis*, were investigated to clarify the difference in lipid characteristics and temperature adaptability among the three groups. Triacylglycerols were the dominant depot lipids of the three populations, while phospholipids, such as phosphatidylcholine and phosphatidylethanolamine, were found to be the major components of the polar lipids, and their lipid classes are similar to each other. The major fatty acids in the triacylglycerols of all specimens were 16:0, 18:0, 16:1n-7, 18:1n-7, 18:1n-9, 18:2n-6 (linoleic acid), 20:5n-3 (EPA, icosapentaenoic acid), and 22:6n-3 (DHA, docosahexaenoic acid), similar to the tissue phospholipids of the three populations, 16:0, 18:0, 16:1n-7, 18:1n-7, 18:1n-9, 18:2n-6, 20:4n-6, EPA, and DHA. All classes had high levels of 18:2n-6, which originates from their dietary lipids. Compared with the lower DHA levels of the triacylglycerols, the higher levels in the phospholipids suggest their selective accumulation or a biosynthetic pathway to DHA as in freshwater fish. Two populations (the migratory

and Setogawa River forms) adapted to lower temperatures with comparatively high levels of polyunsaturated fatty acids (PUFA) for their membrane fluidities. With significantly higher levels of n-3 PUFA and total PUFA, the mean DHA content in the lipids of the Setogawa River form (the population that adapted to lower temperatures) was significantly higher than that of the migratory form. From these results, we concluded that the Setogawa River population actively concentrates long-chain PUFA in its polar lipids and has high adaptability to low temperature.

Keywords Arachidonic acid · Chemoecology · Docosahexaenoic acid · Fish physiology · Freshwater fish · Membrane fluidity · Polyunsaturated fatty acid · Temperature tolerance

Abbreviations

DHA	Docosahexaenoic acid
DMA	Dimethylacetals
DMOX	4,4-Dimethyloxazoline
EPA	Eicosapentaenoic acid
GC/MS	Gas chromatography/mass spectrometry
PtdCho	Phosphatidylcholine
PtdEtn	Phosphatidylethanolamine
PUFA	Polyunsaturated fatty acids
TAG	Triacylglycerols
TFA	Total fatty acids
TL	Total lipids

C. Xue · M. Okabe · H. Saito (✉)
National Research Institute of Fisheries Science,
Fisheries Research Agency, 2-12-4 Fuku-ura,
Kanazawa-ku, Yokohama-shi 236-8648, Japan
e-mail: hiroakis@affrc.go.jp

Present Address:

C. Xue
Ocean University of Qingdao, 5 Yushan, Qingdao, China

Present Address:

M. Okabe
Kochi Prefectural Freshwater Fisheries Center,
687-4 Takagawara, Tosa-Yamada, Kochi 782-0016, Japan

Introduction

It is generally known that all marine animals, not only marine fishes but also invertebrates, characteristically

accumulate various types of n-3 long-chain polyunsaturated fatty acids (PUFA) in their lipids, in particular docosahexaenoic acid (DHA, 22:6n-3) and icosapentaenoic acid (EPA, 20:5n-3), while n-6 PUFA with n-3 PUFA are always observed as major PUFA in terrestrial animal lipids [1–3]. For example, linoleic (18:2n-6) and arachidonic acids (20:4n-6) are simply accumulated in freshwater animals, which take terrestrial prey, while n-3 long-chain PUFA are considered to originate from phytoplankton and to accumulate in marine animals in higher trophic levels through the food web [4–6]. There are many reports about the chemical components of pelagic sea water fish, in particular, on the fatty acids of fish, with growing recognition of the beneficial uses of dietary fish oils for humans [7–9]. As for a detailed determination of the fatty acid in freshwater species, little information has been available except for salmonids, such as rainbow trout *Oncorhynchus mykiss* [10–12].

Ayu, *Plecoglossus altivelis* Temminck et Schlegel (Plecoglossidae, Salmonidae, Salmoniformes), is an osmerid fish with an annual life cycle [13, 14]. The species ranges over the Japanese archipelago and is also found on the Korean Peninsula and some parts of the Chinese continent, migrating amphidromously between rivers and the sea. Commercially, it is the most important and expensive freshwater fish species in Japan because it possesses a characteristic watermelon-like aroma on its skin surface, making it a favorite seafood throughout Japan and Korea. The aroma is due to the dietary freshwater algae by its adult' herbivorous feeding [15, 16]. In general, animals in cold water require low-melting-point membrane lipids to maintain their fluidity [17–19]. Therefore, fishes in cold environments contain high levels of PUFA in their lipids [20–22]. Despite considerable attention paid to the biological and ecological aspects of *P. altivelis* (ecology: 23–25, phylogeny: 26–28), only a few reports on determination of the chemical components have been published [16, 29]. In particular, there has been no report of a detailed analysis of the fatty acid composition of *P. altivelis* [30–32] in different environments.

There are two primary populations of *P. altivelis* in Japan, the migratory and the Lake Biwa landlocked forms. The Lake Biwa is an ancient lake, which was closed 4 million years ago, where more than 50 species live indigenously. The Lake Biwa landlocked form is often cultured in many Japanese farms.

The migratory form ranges over all the rivers in the Japanese archipelago and the Lake Biwa landlocked form spans only the rivers that flow into Lake Biwa (Fig. 1). In 1975, the Sameura dam was built on the Yoshino River in Shikoku Island. The Setogawa River, which is a branch of the Yoshino River, flows into the artificial lake

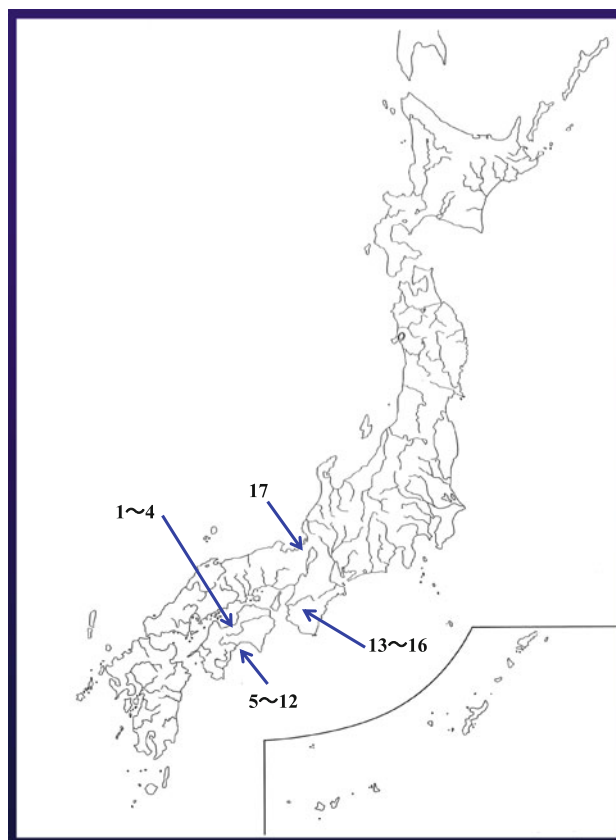


Fig. 1 The sampling site of *P. altivelis*. Parents of the Setogawa River artificially landlocked form (sample no. 1–4) were collected from the Setogawa River on Shikoku Island in spring 1995. Parents of the migratory form (sample no. 5–8) were collected in Tosa Bay in the Pacific Ocean in spring 1996. In 1997, other parents of the migratory form (sample no. 9–12) were collected from Monobe River flowing into Tosa Bay. Clone samples of the migratory form (sample no. 13–16) were continuously produced at Wakayama Prefectural Freshwater Fisheries Center in 1987. Parents of the Lake Biwa landlocked form (sample no. 17) were collected from Lake Biwa in 1996

formed by the Sameura dam, closing the Setogawa River system. The Setogawa River is at a high altitude in Shikoku with severely cold weather in winter. In the 1980s, the migratory form of *P. altivelis* was stocked in the Setogawa River. The form adapted to the low temperature, naturally reproduced, and became known as the Setogawa River form, which is considered tolerant of low temperatures.

In the present study, the lipid class and fatty acid compositions of the three cultured populations of *P. altivelis* (migratory, Setogawa River, and Lake Biwa landlocked forms) were investigated to determine the differences in their lipid characteristics and their lipid physiology. In particular, the differences of their PUFA levels under different water temperatures is discussed to assess the influence of environmental conditions.

Table 1 Biological data of the three populations of *Plecoglossus altivelis*

Sample no.	Population	Date	Temperature (°C)	Length (cm)	Weight (g)
1	<i>n</i> = 10	June 18, 1998	15.0	8.1 ± 0.1	6.4 ± 0.1
2	<i>n</i> = 10	June 18, 1998	18.0	7.6 ± 0.1	5.4 ± 0.2
3	<i>n</i> = 10	June 18, 1998	20.0	7.6 ± 0.0	5.0 ± 0.1
4	<i>n</i> = 10	June 18, 1998	23.0	7.6 ± 0.0	4.9 ± 0.1
Migratory form F2					
5	<i>n</i> = 10	June 18, 1998	15.0	8.4 ± 0.1	6.5 ± 0.2
6	<i>n</i> = 10	June 18, 1998	18.0	8.3 ± 0.1	7.1 ± 0.2
7	<i>n</i> = 10	June 18, 1998	20.0	8.1 ± 0.1	5.8 ± 0.2
8	<i>n</i> = 10	June 18, 1998	23.0	7.8 ± 0.1	5.0 ± 0.1
Migratory form F1					
9	<i>n</i> = 10	August 12, 1998	15.0	8.0 ± 0.1	5.4 ± 0.4
10	<i>n</i> = 10	August 12, 1998	18.0	8.0 ± 0.1	5.7 ± 0.5
11	<i>n</i> = 10	August 12, 1998	20.0	7.9 ± 0.0	5.1 ± 0.4
12	<i>n</i> = 10	August 12, 1998	23.0	7.4 ± 0.1	4.4 ± 0.3
Migratory clone					
13	<i>n</i> = 10	August 12, 1998	15.0	8.9 ± 0.2	7.0 ± 0.8
14	<i>n</i> = 10	August 12, 1998	18.0	9.4 ± 0.3	8.2 ± 1.0
15	<i>n</i> = 10	August 12, 1998	20.0	8.9 ± 0.2	6.8 ± 0.4
16	<i>n</i> = 10	August 12, 1998	23.0	9.0 ± 0.2	7.6 ± 0.6
Lake Biwa landlocked					
17	<i>n</i> = 4	August 12, 1998	18.0	8.8 ± 0.5	8.9 ± 1.7

Results are expressed as means ± standard error (*n* = 4–6) for each sample

Materials and Methods

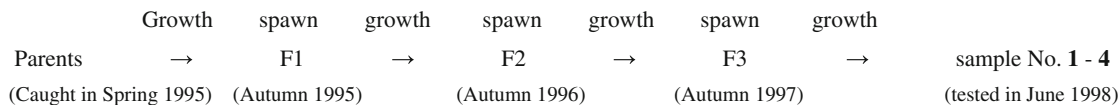
Materials

The biological data of *P. altivelis* are listed in Table 1. In spring 1995, parents of the Setogawa River artificially landlocked form were collected from the Setogawa River (40°50'N and 133°35'E) on Japan's Shikoku Island (samples 1–4; Fig. 2). In the autumns of 1995 and 1996, hundreds of F1 and F2 larvae of the landlocked form were hatched. In autumn 1997, hundreds of F3 (samples 1–4) larvae from the landlocked F2 were obtained and then tested in June 1998. In spring 1996, parents of the migratory form were collected in Tosa Bay in the Pacific Ocean (samples 5–12; Fig. 2). In autumn 1996, hundreds of F1 larvae of the migratory form were also hatched. F2 larvae (samples 5–8) were obtained in autumn 1997 and then tested in June 1998. In 1997, other parents of the migratory form were collected from the Monobe River (33°33'N and 133°43'E) flowing into Tosa Bay. In autumn 1997, hundreds of F1 larvae (samples 9–12) of the migratory form were hatched, cultured, and then tested in August 1998. Clone samples of the migratory form were continuously produced at Wakayama Prefectural

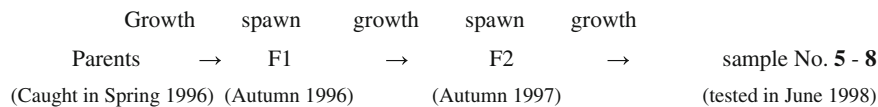
Freshwater Fisheries Center in 1987. In autumn 1997, hundreds of F1 larvae (samples 13–16) of the clone sample were hatched, cultured, and then tested in August 1998 [33]. Parents of the Lake Biwa landlocked form were collected from Lake Biwa (35°19'N and 136°05'E) in 1996. In autumn 1996, hundreds of F1 larvae of the Lake Biwa landlocked form were hatched, and F2 larvae (sample 17) were obtained in autumn 1997 and then tested in August 1998.

All samples were cultured at the Kochi Freshwater Fisheries Center for nine months (from November 1997 to August 1998). The samples were cultured with the same artificial feedstuff (samples 18–19 in Tables 2, 3) in 2-ton FRP aquariums indoors at 19 °C. Before acclimation to different water temperatures (15.0, 18.0, 20.0, and 23.0 °C), all populations were cultured for about 200 days under the same conditions. Samples 1–16 of *P. altivelis* were cultured at four different temperatures for 2 weeks (Table 1). Before starting the experiments, fish were acclimated and starved 2 days. Feed was offered by hand as restricted feeding for 2 weeks; the fish in all groups were fed at 3.0% of their body weight per day (two times daily at 10:00 and 16:00 h). In June 1998, the samples 1–8 were fed by the same feed stuff (sample 18), and the samples

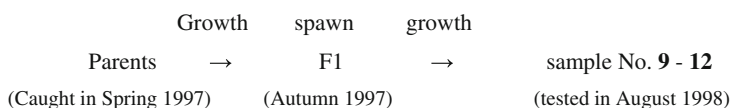
1. The Setogawa River Form



2. The amphidromous Form F2



3. The amphidromous Form F1



4. The amphidromous clone sample



5. The Lake Biwa landlocked Form

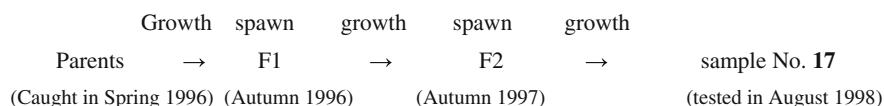


Fig. 2 In spring 1995, parents of the Setogawa River form were collected. In the autumns 1995 and 1996, F1 and F2 larvae of the landlocked form were hatched. In autumn 1997, F3 (samples 1–4) larvae from the landlocked F2 were obtained, cultured, and then tested in June 1998. In spring 1996, parents of the migratory form were collected in Tosa Bay. In autumn 1996, F1 larvae of the migratory form were hatched. F2 larvae (samples 5–8) were obtained in autumn 1997, cultured, and then tested in June 1998. In 1997, other

parents of the migratory form were collected from Monobe River. In autumn 1997, F1 larvae (samples 9–12) of the migratory form were hatched, cultured, and then tested in August 1998. In autumn 1997, F1 larvae (samples 13–16) of the clone sample were hatched, cultured, and then tested in August 1998. Parents of the Lake Biwa landlocked form were collected in 1996. In autumn 1996, F1 larvae of the Lake Biwa landlocked form were hatched, and F2 larvae (sample 17) were obtained in autumn 1997, cultured, and then tested in August 1998

9–17 in August 1998, were fed with another feedstuff (sample 19), respectively. A total of 2,000 individual *P. altivelis* were cultured in an aquarium, from which 10 randomly selected specimens were chosen for lipid analysis. After their biological data were measured, the specimens were immediately frozen at -40°C .

Lipid Extraction and Analysis of Lipid Classes

After 2 months storage in the laboratory at -40°C , each individual *P. altivelis* was dissected into ordinary muscle and other organs, which contained skin, dark muscle, and viscera. Each sample was homogenized in a mixture of chloroform and methanol (2:1, v/v), and a portion of each homogenized sample was extracted according to the Folch procedure [34]. Each crude total lipid was separated into

classes on silicic acid columns (Merck and Co. Ltd., Kieselgel 60, 70–230 mesh). Quantitative analysis of the lipid constituents was performed using gravimetric analysis of fractions collected from column chromatography. The first eluate (dichloromethane/*n*-hexane, 2:3, v/v) was collected as steryl ester, wax ester, and diacylglycerol ether fractions. This was followed by eluting the triacylglycerols (TAG) with dichloromethane and eluting the sterols with dichloromethane/ether (35:1, v/v); eluting the diacylglycerols with dichloromethane/ether (9:1, v/v); eluting the free fatty acids with dichloromethane/methanol (9:1, v/v); eluting the phosphatidylethanolamine (PtdEtn) with dichloromethane/methanol (1:5, v/v); eluting other minor phospholipids with dichloromethane/methanol (1:20, v/v); and eluting phosphatidylcholine (PtdCho) with dichloromethane/methanol (1:50, v/v) [35].

Table 2 The lipid contents and lipid classes of the three populations of *P. altivelis*

Sample no.	Temperature	Lipid contents ^a	Steryl esters ^{b,c,d}	TAG ^{b,c,d}	Sterols ^{b,d}	Diacyl glycerols ^{b,c}	Free fatty acids ^{b,c,d}	PtdEtn ^{b,c}	Phospholipids ^{b,c,d}	PtdCho ^{b,c}
Setogawa river population F3										
1	15	11.1 ± 1.4	1.6 ± 0.3	88.3 ± 1.7	2.2 ± 0.4	2.9 ± 0.3	1.6 ± 0.3	1.9 ± 0.7	0.8 ± 0.1	0.6 ± 0.3
2	18	11.1 ± 0.6	1.3 ± 0.1	79.9 ± 1.2	5.1 ± 0.8	4.5 ± 0.9	4.7 ± 1.0	2.2 ± 0.4	1.7 ± 0.3	0.6 ± 0.2
3	20	10.2 ± 0.9	1.5 ± 0.2	79.9 ± 2.3	5.0 ± 1.3	4.8 ± 0.6	5.2 ± 0.7	2.1 ± 0.3	0.8 ± 0.2	0.8 ± 0.3
4	23	12.0 ± 0.8	2.2 ± 1.1	80.2 ± 2.2	4.5 ± 0.8	5.3 ± 0.8	4.9 ± 0.9	1.7 ± 0.2	0.7 ± 0.3	0.5 ± 0.1
Migratory form F2										
5	15	10.4 ± 0.6	0.8 ± 0.2	91.7 ± 1.2	1.6 ± 0.8	0.2 ± 0.1	1.8 ± 0.3	1.2 ± 0.4	1.8 ± 0.3	0.8 ± 0.2
6	18	10.7 ± 0.6	0.8 ± 0.2	89.8 ± 1.0	3.7 ± 0.9	0.5 ± 0.1	1.8 ± 0.3	1.2 ± 0.1	0.9 ± 0.2	1.2 ± 0.3
7	20	10.6 ± 0.6	0.8 ± 0.2	85.3 ± 2.6	5.8 ± 2.7	1.6 ± 0.7	2.3 ± 0.6	1.4 ± 0.2	1.8 ± 0.3	1.0 ± 0.2
8	23	9.9 ± 0.7	1.5 ± 0.2	80.0 ± 1.8	4.0 ± 0.9	5.1 ± 0.6	6.8 ± 1.3	1.8 ± 0.2	0.4 ± 0.1	0.4 ± 0.2
Migratory form F1										
9	15	7.8 ± 0.8	2.3 ± 0.3	72.1 ± 1.5	5.1 ± 0.3	3.5 ± 0.5	10.7 ± 0.6	2.8 ± 0.3	0.7 ± 0.3	3.0 ± 0.6
10	18	9.3 ± 1.3	1.5 ± 0.1	79.9 ± 2.6	3.7 ± 0.5	3.1 ± 0.6	7.6 ± 1.4	1.6 ± 0.3	0.3 ± 0.1	2.3 ± 0.6
11	20	9.4 ± 1.1	1.3 ± 0.1	74.1 ± 2.8	3.8 ± 0.4	4.6 ± 0.3	11.1 ± 1.4	2.2 ± 0.4	0.3 ± 0.1	2.5 ± 0.3
12	23	7.8 ± 0.9	1.5 ± 0.2	68.5 ± 2.7	5.1 ± 0.3	5.1 ± 0.3	13.0 ± 1.3	3.5 ± 0.6	0.7 ± 0.3	2.6 ± 0.5
Migratory clone										
13	15	4.9 ± 0.7	1.9 ± 0.8	68.6 ± 7.5	5.6 ± 1.5	3.8 ± 1.6	13.2 ± 3.3	3.7 ± 1.8	3.3 ± 1.8	3.3 ± 1.8
14	18	7.0 ± 0.6	1.3 ± 0.3	71.2 ± 9.3	5.4 ± 1.7	4.4 ± 1.1	11.4 ± 4.5	3.5 ± 1.6	2.8 ± 1.1	2.8 ± 1.1
15	20	4.7 ± 0.4	2.4 ± 0.3	65.1 ± 3.8	5.6 ± 0.5	4.7 ± 0.6	13.1 ± 2.1	4.2 ± 0.7	4.9 ± 1.7	4.9 ± 1.7
16	23	7.0 ± 0.7	1.6 ± 0.3	77.3 ± 4.2	3.9 ± 0.4	3.2 ± 0.4	7.2 ± 1.3	2.5 ± 0.7	4.4 ± 1.5	4.4 ± 1.5
Lake Biwa landlocked population										
17	18	9.1 ± 1.0	1.0 ± 0.0	84.9 ± 2.5	5.9 ± 1.8	2.5 ± 0.4	3.8 ± 0.4	1.0 ± 0.1	0.4 ± 0.1	0.6 ± 0.3
Feedstuffs										
18	Feedstuffs 1	10.4 ± 0.4	3.7 ± 0.4	50.5 ± 2.8	5.7 ± 0.5	8.0 ± 0.8	14.6 ± 10.2	6.8 ± 0.2	2.5 ± 1.2	8.0 ± 4.1
19	Feedstuffs 2	5.7 ± 0.0	2.3 ± 0.3	69.8 ± 3.9	5.2 ± 2.0	3.8 ± 1.0	10.7 ± 7.4	4.4 ± 0.6	1.4 ± 0.2	1.8 ± 0.4

Data are means ± standard deviation ($n = 6$ for fish and $n = 2$ for feedstuffs)

^a Results are expressed as weight percent of wet tissues

^b Results are expressed as weight percent of total lipids

^c “TAG”, “PtdEtn”, and “PtdCho” mean triacylglycerols, phosphatidylethanolamine, and phosphatidylcholine, respectively

^d The “steryl esters” fraction contained trace amounts of wax esters and diacylglycerol ethers. The “free fatty acids” fraction contained small levels of monoacylglycerols and diacylglycerols. “TAG” fractions in samples No. **1** and **5** contained small levels of sterols. The “phospholipids” fraction mainly contained other phospholipids, such as phosphatidyl inositol, with a small amount of PtdEtn and PtdCho

Table 3 The fatty acid composition of the lipids in the feedstuffs

	Feedstuffs 1 (June) 18 (TAG)	Feedstuffs 2 (August) 19 (TAG)	Feedstuffs 1 (June) 18 (PtdEtn)	Feedstuffs 2 (August) 19 (PtdEtn)	Feedstuffs 1 (June) 18 (PtdCho)	Feedstuffs 2 (August) 19 (PtdCho)
Total saturated	28.5 ± 0.1	29.2 ± 1.0	26.5 ± 0.2	29.0 ± 0.5	25.6 ± 0.2	23.1 ± 1.3
14:0	5.4 ± 0.0	4.7 ± 0.3	0.6 ± 0.1	2.1 ± 0.0	0.8 ± 0.0	1.1 ± 0.1
15:0	0.3 ± 0.0	0.5 ± 0.0	0.2 ± 0.0	0.6 ± 0.0	0.3 ± 0.1	0.3 ± 0.0
16:0	17.4 ± 0.1	17.7 ± 0.5	20.5 ± 0.2	15.0 ± 0.2	19.0 ± 0.4	15.7 ± 1.6
17:0	0.8 ± 0.0	0.7 ± 0.1	0.3 ± 0.0	0.6 ± 0.0	0.3 ± 0.0	0.7 ± 0.4
18:0	3.5 ± 0.0	4.4 ± 0.1	4.3 ± 0.1	8.0 ± 0.2	3.4 ± 0.0	3.4 ± 0.1
22:0	0.0 ± 0.0	0.0 ± 0.0	0.0 ± 0.0	0.1 ± 0.0	0.2 ± 0.0	0.4 ± 0.1
24:0	0.1 ± 0.0	0.1 ± 0.0	0.0 ± 0.0	0.1 ± 0.1	0.5 ± 0.0	0.2 ± 0.0
Total monoenoic	41.8 ± 0.1	35.9 ± 0.3	13.8 ± 0.2	23.7 ± 0.4	19.1 ± 0.1	20.5 ± 0.6
16:1n-11	0.2 ± 0.1	0.3 ± 0.1	0.3 ± 0.0	1.0 ± 0.0	0.4 ± 0.0	0.9 ± 0.1
16:1n-7	5.9 ± 0.1	5.3 ± 0.3	0.8 ± 0.1	1.9 ± 0.1	1.0 ± 0.0	1.7 ± 0.2
16:1n-5	0.7 ± 0.0	0.3 ± 0.0	0.1 ± 0.0	0.2 ± 0.0	0.2 ± 0.0	0.4 ± 0.2
17:1n-8	0.3 ± 0.0	0.5 ± 0.0	0.1 ± 0.0	0.3 ± 0.0	0.2 ± 0.0	0.3 ± 0.0
18:1n-9	19.6 ± 0.0	18.4 ± 0.2	7.0 ± 0.1	11.0 ± 0.1	9.9 ± 0.1	10.4 ± 0.3
18:1n-7	6.5 ± 0.0	3.8 ± 0.3	3.8 ± 0.0	5.0 ± 0.3	4.5 ± 0.0	2.6 ± 0.1
18:1n-5	0.7 ± 0.1	0.4 ± 0.2	0.4 ± 0.0	0.4 ± 0.1	0.4 ± 0.1	0.2 ± 0.0
20:1n-11	2.4 ± 0.0	1.6 ± 0.1	0.2 ± 0.0	0.7 ± 0.0	0.6 ± 0.0	1.0 ± 0.0
20:1n-9	1.7 ± 0.0	1.9 ± 0.0	0.6 ± 0.0	1.4 ± 0.1	0.9 ± 0.0	1.0 ± 0.0
20:1n-7	0.5 ± 0.0	0.4 ± 0.1	0.1 ± 0.0	0.2 ± 0.0	0.2 ± 0.0	0.2 ± 0.0
22:1n-11	2.2 ± 0.0	2.0 ± 0.1	0.1 ± 0.0	0.7 ± 0.0	0.4 ± 0.0	0.7 ± 0.1
22:1n-9	0.5 ± 0.0	0.5 ± 0.0	0.0 ± 0.0	0.3 ± 0.0	0.1 ± 0.0	0.5 ± 0.0
Total polyenoic	29.9 ± 0.2	33.7 ± 1.2	59.3 ± 0.3	46.1 ± 0.8	54.8 ± 0.3	53.2 ± 1.4
Total n-4 polyenoic	1.3 ± 0.0	1.1 ± 0.1	0.5 ± 0.0	2.4 ± 0.2	0.4 ± 0.0	1.1 ± 0.2
16:2n-4	1.2 ± 0.0	0.6 ± 0.0	0.3 ± 0.0	0.7 ± 0.1	0.4 ± 0.0	0.4 ± 0.0
16:4n-1	0.1 ± 0.0	0.3 ± 0.1	0.2 ± 0.0	0.7 ± 0.1	0.0 ± 0.0	0.0 ± 0.0
Total n-6 polyenoic	11.1 ± 0.1	14.1 ± 0.3	40.7 ± 0.3	13.3 ± 0.1	22.0 ± 0.4	6.9 ± 0.2
18:2n-6	10.2 ± 0.1	12.5 ± 0.2	39.6 ± 0.3	10.1 ± 0.1	20.2 ± 0.5	2.6 ± 0.1
20:2n-6	0.1 ± 0.0	0.3 ± 0.1	0.1 ± 0.0	0.3 ± 0.0	0.1 ± 0.0	0.6 ± 0.2
20:4n-6	0.3 ± 0.0	0.6 ± 0.0	0.9 ± 0.0	1.9 ± 0.0	1.1 ± 0.0	2.0 ± 0.0
22:5n-6	0.0 ± 0.0	0.2 ± 0.0	0.1 ± 0.0	0.5 ± 0.0	0.1 ± 0.0	0.9 ± 0.1
Total n-3 polyenoic	16.2 ± 0.0	17.3 ± 0.7	17.5 ± 0.1	28.0 ± 0.4	31.9 ± 0.6	44.1 ± 0.9
18:3n-3	1.2 ± 0.0	1.6 ± 0.1	5.3 ± 0.1	1.0 ± 0.0	2.0 ± 0.1	0.4 ± 0.0
18:4n-3	1.8 ± 0.0	1.4 ± 0.1	0.1 ± 0.0	0.3 ± 0.0	0.6 ± 0.0	0.3 ± 0.0
20:4n-3	0.3 ± 0.0	0.5 ± 0.0	0.1 ± 0.0	0.3 ± 0.0	0.2 ± 0.0	0.3 ± 0.0
20:5n-3	8.5 ± 0.0	6.4 ± 0.3	4.5 ± 0.0	6.1 ± 0.1	13.1 ± 0.2	11.8 ± 0.3
22:5n-3	0.6 ± 0.0	1.2 ± 0.1	0.4 ± 0.0	1.4 ± 0.0	0.6 ± 0.0	1.7 ± 0.0
22:6n-3	3.8 ± 0.0	6.0 ± 0.1	7.1 ± 0.1	18.9 ± 0.4	15.4 ± 0.6	29.5 ± 1.1
Total fatty acids	98.9 ± 0.1	97.7 ± 0.4	99.1 ± 0.0	96.4 ± 0.3	99.1 ± 0.1	95.7 ± 0.7

Results are expressed as mol% of the total fatty acids. Data are means ± standard error ($n = 5-6$)

In Tables 3, 4, 5, 6, 7, the major fatty acids are selected if at least one mean datum was detected at a level of 0.4% or more of total fatty acids

Individual lipids from each lipid class, such as the phospholipid class, were qualitatively identified with standards by comparing the R_f values using thin-layer chromatography (Merck & Co. Ltd., Kieselgel 60, thickness of 0.25 mm for analysis). All the sample lipids were dried under argon at room temperature and stored at $-40\text{ }^\circ\text{C}$ under argon.

Preparation of Methyl Esters and Gas–Liquid Chromatography (GLC) of Esters

Individual components of TAG, PtdEtn, and PtdCho fractions were converted to fatty acid methyl esters by direct trans-esterification with methanol containing 1% concentrated hydrochloric acid under reflux for 1.5 h, as previously reported [35]. The methyl esters were purified using silica gel column chromatography by elution with dichloromethane/*n*-hexane (2/1, v/v).

Composition of the fatty acid methyl esters was determined by gas–liquid chromatography. Analysis was performed using Shimadzu GC-8A (Shimadzu Seisakusho Co. Ltd., Kyoto, Japan) and HP-5890 (Hewlett Packard Co. Ltd., Yokogawa Electric Corporation, Tokyo, Japan) gas chromatographs equipped with an Omegawax 250 fused silica capillary column (30 m \times 0.25 mm i.d.; 0.25 μm film, Supelco Japan Co. Ltd., Tokyo, Japan). The temperatures of the injector and the column were held at 230 and 215 $^\circ\text{C}$, respectively, and the split ratio was 1:76. Helium was used as the carrier gas at a constant flow rate of 0.7 mL/min. Quantitation of individual components was performed by means of Shimadzu Model C-R3A (Shimadzu Seisakusho Co. Ltd.) and HP ChemStation System (A. 06 revision, Yokogawa HP Co. Ltd., Tokyo, Japan) electronic integrators.

Preparation of 4,4-Dimethyloxazoline Derivatives (DMOX) and Analysis of DMOX by Gas Chromatography—Mass Spectrometry (GC/MS)

The DMOX derivatives were prepared by adding an excess amount of 2-amino-2-methyl propanol to a small amount of fatty acid methyl esters in a test tube under an argon atmosphere. The mixture was heated for 18 h at 180 $^\circ\text{C}$ [35, 36].

Analysis of the DMOX derivatives was performed using a HP G1800C GCD Series II (Hewlett Packard Co., Yokogawa Electric Corporation, Tokyo, Japan) GC/MS equipped with the same capillary used for determining the respective fatty acids with the HP WS (HP Kayak XA, G1701BA version, PC workstations). The temperatures of the injector and the column were held at 230 and 215 $^\circ\text{C}$, respectively. The split ratio was 1:76; the ionization voltage was 70 eV. Helium was used as the carrier gas at a

constant flow rate of 0.7 mL/min. The fatty acid methyl esters were identified by comparing the methyl ester and DMOX derivative mass spectral data obtained by GC/MS. The DMOX derivatives were identified by comparing them with the mass spectral data obtained from authentic samples collected by Christie [37].

Statistical Analyses

The mean DHA, total n-3 PUFA, total PUFA levels in the PtdEtn and PtdCho of sample **1** were compared with those in samples **5** and **9**. Significant mean differences were determined using a one-way analysis of variance (ANOVA) to test the influence of the water temperature. Tukey's multiple procedure was used to compare the differences among mean values. Differences were regarded as significance level of $P < 0.05$.

Results

Lipid Content of the Three Populations of *P. altivelis* Under the Four Different Temperatures

The biological data of *P. altivelis* samples are listed in Table 1 with relevant data. The size and weight of the clone (No. 13–16) and Lake Biwa landlocked (No. 17) samples were slightly larger than were those of the other samples (No. 1–12). The total lipid content of the *P. altivelis* samples is listed in Table 2 with the lipid classes. Lipid levels of the normal samples (Setogawa samples 1–4 and migratory samples 5–8) collected in June 1998 were similar to each other. For example, the growth and lipid content at the lowest temperature condition (15 $^\circ\text{C}$; Setogawa sample 1 and migratory sample 5) were similar to those at higher temperatures (18–23 $^\circ\text{C}$; Setogawa samples 2–4 and migratory samples 6–8). As shown in Table 2, TAG (64.4–92.8% of TL) was the major component in all sample lipids, with small levels of sterols, PtdEtn, and PtdCho.

Fatty Acid Composition in TAG Deposit Lipids of *P. altivelis*: Relationship with Dietary Lipids

The fatty acids in TAG of the feedstuff and all samples under different conditions are listed in Tables 3, 4. Both the diets (samples 18 and 19) have high levels of fat contents (5.7–10.4% in Table 2); therefore, their TAG mainly influence the fatty acid composition of the ayu depot lipids. Nine dominant fatty acids (more than 3% of total fatty acids: TFA) in the dietary lipids (Table 3) were found: 14:0, 16:0, and 18:0 as saturated fatty acids; 16:1n-7, 18:1n-9, and 18:1n-7 as monounsaturated fatty acids (MUFA); 18:2n-6 as n-6 dienoic fatty acid; EPA and DHA

Table 4 The fatty acid composition of the triacylglycerols in the three populations of *P. altivelis*

Sample no.	Setogawa river F3				Migratory form F2			
	1 (15 °C)	2 (18 °C)	3 (20 °C)	4 (23 °C)	5 (15 °C)	6 (18 °C)	7 (20 °C)	8 (23 °C)
Total saturated	36.4 ± 1.0	37.3 ± 0.2	35.7 ± 0.7	37.5 ± 1.1	34.7 ± 0.7	36.8 ± 0.5	34.8 ± 0.5	35.1 ± 0.8
14:0	4.0 ± 0.2	4.4 ± 0.2	4.0 ± 0.3	3.8 ± 0.2	3.7 ± 0.2	3.9 ± 0.4	4.0 ± 0.2	4.1 ± 0.3
15:0	0.3 ± 0.0	0.4 ± 0.0	0.4 ± 0.1	0.4 ± 0.0	0.3 ± 0.0	0.3 ± 0.0	0.3 ± 0.0	0.3 ± 0.0
16:0	26.1 ± 0.9	26.3 ± 0.2	25.3 ± 0.7	26.7 ± 0.9	25.1 ± 0.6	26.4 ± 0.4	24.8 ± 0.4	25.1 ± 0.8
17:0	0.3 ± 0.0	0.4 ± 0.0	0.4 ± 0.0	0.4 ± 0.0	0.3 ± 0.0	0.4 ± 0.0	0.4 ± 0.0	0.3 ± 0.0
18:0	4.4 ± 0.2	4.5 ± 0.1	4.4 ± 0.1	4.9 ± 0.1	4.2 ± 0.1	4.5 ± 0.4	4.2 ± 0.1	4.2 ± 0.1
Total monoenoic	39.2 ± 1.0	37.8 ± 0.3	37.2 ± 0.5	37.8 ± 0.5	38.9 ± 0.7	37.5 ± 1.0	37.0 ± 0.5	37.1 ± 0.5
16:1n-7	8.5 ± 0.4	7.7 ± 0.3	7.7 ± 0.4	7.2 ± 0.2	8.6 ± 0.4	7.9 ± 0.5	7.8 ± 0.2	7.6 ± 0.5
17:1n-8	0.4 ± 0.0	0.4 ± 0.0	0.4 ± 0.0	0.4 ± 0.0	0.4 ± 0.0	0.4 ± 0.0	0.4 ± 0.0	0.4 ± 0.0
18:1n-9	20.8 ± 0.7	20.2 ± 0.4	19.8 ± 0.5	21.0 ± 0.3	21.0 ± 0.5	20.1 ± 0.7	19.9 ± 0.4	19.9 ± 0.6
18:1n-7	3.5 ± 0.1	3.5 ± 0.1	3.7 ± 0.2	3.3 ± 0.2	3.4 ± 0.1	3.4 ± 0.1	3.4 ± 0.1	3.7 ± 0.1
18:1n-5	0.3 ± 0.0	0.3 ± 0.0	0.4 ± 0.1	0.3 ± 0.0	0.3 ± 0.0	0.3 ± 0.0	0.3 ± 0.1	0.2 ± 0.0
20:1n-11	1.3 ± 0.1	1.3 ± 0.1	1.2 ± 0.1	1.4 ± 0.0	1.2 ± 0.0	1.2 ± 0.1	1.2 ± 0.0	1.2 ± 0.1
20:1n-9	1.4 ± 0.1	1.4 ± 0.0	1.4 ± 0.1	1.4 ± 0.1	1.3 ± 0.1	1.2 ± 0.3	1.2 ± 0.0	1.3 ± 0.1
22:1n-11	1.1 ± 0.1	1.0 ± 0.0	1.0 ± 0.1	1.1 ± 0.1	1.0 ± 0.0	1.1 ± 0.2	0.9 ± 0.0	1.0 ± 0.1
22:1n-9	0.3 ± 0.0	0.3 ± 0.0	0.3 ± 0.0	0.3 ± 0.0	0.3 ± 0.0	0.3 ± 0.1	0.3 ± 0.0	0.3 ± 0.0
24:1n-9	0.5 ± 0.0	0.5 ± 0.0	0.5 ± 0.0	0.5 ± 0.0	0.5 ± 0.0	0.5 ± 0.1	0.4 ± 0.0	0.5 ± 0.0
Total polyenoic	24.1 ± 1.8	24.9 ± 0.3	26.9 ± 0.6	24.6 ± 1.1	25.9 ± 1.3	25.2 ± 1.1	28.0 ± 0.6	27.9 ± 0.9
Total n-4 polyenoic	0.7 ± 0.1	0.8 ± 0.0	0.8 ± 0.0	0.8 ± 0.0	0.7 ± 0.1	0.8 ± 0.1	0.8 ± 0.0	0.8 ± 0.0
16:2n-4	0.5 ± 0.0	0.5 ± 0.0	0.5 ± 0.0	0.5 ± 0.0	0.5 ± 0.0	0.4 ± 0.1	0.5 ± 0.0	0.6 ± 0.0
Total n-6 polyenoic	10.9 ± 0.5	11.7 ± 0.3	12.0 ± 0.3	11.3 ± 0.3	11.5 ± 0.6	10.7 ± 0.4	12.5 ± 0.2	12.3 ± 0.6
18:2n-6	9.4 ± 0.4	10.3 ± 0.2	10.5 ± 0.3	9.7 ± 0.3	9.7 ± 0.5	9.2 ± 0.3	10.9 ± 0.2	10.7 ± 0.5
20:2n-6	0.2 ± 0.0	0.3 ± 0.0	0.2 ± 0.0	0.2 ± 0.0	0.3 ± 0.1	0.2 ± 0.0	0.2 ± 0.0	0.2 ± 0.0
20:4n-6	0.5 ± 0.0	0.5 ± 0.0	0.5 ± 0.0	0.5 ± 0.0	0.5 ± 0.0	0.5 ± 0.0	0.5 ± 0.0	0.5 ± 0.0
22:5n-6	0.2 ± 0.0	0.1 ± 0.0	0.2 ± 0.0	0.2 ± 0.0	0.2 ± 0.0	0.2 ± 0.0	0.2 ± 0.0	0.2 ± 0.0
Total n-3 polyenoic	11.8 ± 1.2	11.7 ± 0.4	13.3 ± 0.5	11.8 ± 0.9	12.9 ± 0.7	12.9 ± 0.8	14.0 ± 0.4	13.9 ± 0.7
18:3n-3	1.0 ± 0.1	1.0 ± 0.0	1.1 ± 0.0	1.0 ± 0.1	1.0 ± 0.1	0.9 ± 0.1	1.2 ± 0.0	1.2 ± 0.0
18:4n-3	0.4 ± 0.1	0.4 ± 0.0	0.5 ± 0.0	0.4 ± 0.0	0.4 ± 0.0	0.4 ± 0.1	0.5 ± 0.0	0.5 ± 0.0
20:4n-3	0.4 ± 0.0	0.4 ± 0.0	0.4 ± 0.0	0.4 ± 0.0	0.4 ± 0.0	0.4 ± 0.0	0.4 ± 0.0	0.4 ± 0.0
20:5n-3	3.2 ± 0.4	3.2 ± 0.1	3.6 ± 0.1	3.1 ± 0.3	3.3 ± 0.3	3.4 ± 0.5	3.8 ± 0.1	3.7 ± 0.2
22:5n-3	1.2 ± 0.1	1.2 ± 0.0	1.4 ± 0.0	1.2 ± 0.1	1.3 ± 0.1	1.3 ± 0.1	1.7 ± 0.1	1.7 ± 0.1
22:6n-3	5.6 ± 0.5	5.4 ± 0.3	6.3 ± 0.3	5.6 ± 0.4	6.5 ± 0.2	6.5 ± 0.2	6.2 ± 0.2	6.3 ± 0.4
Total fatty acids	99.1 ± 0.1	99.2 ± 0.1	99.0 ± 0.2	99.1 ± 0.1	98.7 ± 0.2	98.7 ± 0.2	99.0 ± 0.1	99.3 ± 0.0

Sample no.	Migratory form F1				Lake Biwa landlocked
	9 (15 °C)	10 (18 °C)	11 (20 °C)	12 (23 °C)	17 (18 °C)
Total saturated	33.7 ± 0.3	35.5 ± 0.4	36.3 ± 0.6	38.0 ± 0.6	37.1 ± 0.5
14:0	3.8 ± 0.1	3.9 ± 0.0	3.9 ± 0.0	4.6 ± 0.2	4.0 ± 0.2
15:0	0.4 ± 0.0	0.4 ± 0.0	0.4 ± 0.0	0.4 ± 0.0	0.3 ± 0.0
16:0	23.1 ± 0.4	25.0 ± 0.5	25.6 ± 0.7	26.3 ± 0.5	27.4 ± 0.5
17:0	0.4 ± 0.0	0.4 ± 0.0	0.5 ± 0.0	0.5 ± 0.0	0.4 ± 0.0
18:0	4.7 ± 0.1	4.6 ± 0.1	4.7 ± 0.1	4.8 ± 0.1	4.3 ± 0.1
Total monoenoic	37.4 ± 0.4	37.6 ± 0.3	38.4 ± 0.3	37.8 ± 0.6	38.9 ± 0.4
16:1n-7	7.5 ± 0.3	8.0 ± 0.4	8.2 ± 0.3	7.9 ± 0.3	9.3 ± 0.5
17:1n-8	0.5 ± 0.0	0.5 ± 0.0	0.5 ± 0.0	0.4 ± 0.1	0.4 ± 0.0
18:1n-9	19.8 ± 0.2	20.3 ± 0.3	20.6 ± 0.2	20.3 ± 0.4	20.2 ± 0.7

Table 4 continued

Sample no.	Migratory form F1				Lake Biwa landlocked
	9 (15 °C)	10 (18 °C)	11 (20 °C)	12 (23 °C)	17 (18 °C)
18:1n-7	3.6 ± 0.1	3.3 ± 0.1	3.5 ± 0.1	3.5 ± 0.1	3.4 ± 0.2
18:1n-5	0.3 ± 0.0	0.3 ± 0.0	0.3 ± 0.0	0.3 ± 0.0	0.3 ± 0.0
20:1n-11	1.2 ± 0.0	1.1 ± 0.1	1.0 ± 0.1	1.2 ± 0.1	1.0 ± 0.1
20:1n-9	1.6 ± 0.0	1.5 ± 0.1	1.6 ± 0.1	1.6 ± 0.1	1.4 ± 0.0
22:1n-11	1.1 ± 0.0	1.0 ± 0.0	1.0 ± 0.1	1.0 ± 0.0	0.9 ± 0.1
22:1n-9	0.4 ± 0.0	0.3 ± 0.0	0.3 ± 0.0	0.3 ± 0.0	0.3 ± 0.0
24:1n-9	0.6 ± 0.0	0.5 ± 0.0	0.5 ± 0.0	0.5 ± 0.0	0.5 ± 0.0
Total polyenoic	28.9 ± 0.6	26.9 ± 0.5	25.2 ± 0.5	24.2 ± 0.8	23.9 ± 0.5
Total n-4 polyenoic	0.8 ± 0.0	0.8 ± 0.0	0.7 ± 0.0	0.7 ± 0.0	0.7 ± 0.1
16:2n-4	0.6 ± 0.0	0.5 ± 0.0	0.4 ± 0.0	0.4 ± 0.0	0.5 ± 0.0
Total n-6 polyenoic	12.7 ± 0.2	11.6 ± 0.4	11.0 ± 0.4	11.1 ± 0.2	9.9 ± 0.1
18:2n-6	10.8 ± 0.2	9.8 ± 0.4	9.3 ± 0.3	9.6 ± 0.3	8.1 ± 0.1
20:2n-6	0.3 ± 0.0	0.2 ± 0.0	0.3 ± 0.0	0.2 ± 0.0	0.2 ± 0.0
20:4n-6	0.6 ± 0.0	0.6 ± 0.0	0.6 ± 0.0	0.5 ± 0.0	0.6 ± 0.0
22:5n-6	0.3 ± 0.1	0.2 ± 0.0	0.2 ± 0.0	0.2 ± 0.0	0.2 ± 0.0
Total n-3 polyenoic	14.5 ± 0.3	13.7 ± 0.1	12.8 ± 0.3	11.7 ± 0.6	12.6 ± 0.4
18:3n-3	1.1 ± 0.0	1.1 ± 0.0	0.9 ± 0.0	0.9 ± 0.1	0.8 ± 0.0
18:4n-3	0.4 ± 0.0	0.4 ± 0.0	0.4 ± 0.0	0.4 ± 0.0	0.4 ± 0.0
20:4n-3	0.5 ± 0.0	0.4 ± 0.0	0.4 ± 0.0	0.3 ± 0.0	0.4 ± 0.0
20:5n-3	3.5 ± 0.1	3.3 ± 0.1	3.0 ± 0.1	2.6 ± 0.2	2.9 ± 0.2
22:5n-3	1.6 ± 0.0	1.5 ± 0.0	1.4 ± 0.0	1.4 ± 0.1	1.3 ± 0.1
22:6n-3	7.2 ± 0.2	6.9 ± 0.1	6.5 ± 0.1	5.9 ± 0.3	6.8 ± 0.3
Total fatty acids	99.2 ± 0.1	99.2 ± 0.0	99.2 ± 0.1	99.3 ± 0.1	99.2 ± 0.2

Results are expressed as mol% of the total fatty acids. Data are means ± standard error ($n = 4-6$)

In Tables 3, 4, 5, 6, 7, the major fatty acids are selected if at least one mean datum was detected at a level of 0.4% or more of total fatty acids

as n-3 PUFA. In particular, the fatty acid compositions were similar to each other and medium levels (more than about 10% of TFA) of 18:2n-6 (10.3–12.5% of TFA) were found in both the feedstuff lipids.

Similar to the fatty acid compositions of the dietary lipids, the same nine dominant fatty acids in the tissue TAG were also found in all the different areas and conditions: 14:0, 16:0, and 18:0; 16:1n-7, 18:1n-9, and 18:1n-7; 18:2n-6 as n-6 dienoic fatty acid; EPA and DHA as n-3 PUFA, with noticeable levels (more than about 1% of TFA) of five fatty acids: 20:1n-11, 20:1n-9, 22:1n-11, 18:3n-3, and 22:5n-3 (docosapentaenoic acid). This suggests that the depot lipids in all samples (Table 4) are directly influenced by the fatty acid composition of the feedstuff TAG lipids (Table 3).

Fatty Acid Composition in Tissue Phospholipids in *P. altivelis*

Similar to the fatty acid compositions of TAG in the three populations, which were acclimated to different conditions with various temperatures, the major fatty acids of the

phospholipids (PtdEtn and PtdCho) are listed in Tables 5, 6, 7. In the fatty acid composition of PtdEtn (Tables 5, 6), nine similar major fatty acids were consistently found in all samples. The major fatty acids were 16:0 and 18:0; 16:1n-7, 18:1n-9, and 18:1n-7; 18:2n-6 and 20:4n-6; EPA and DHA, with noticeable levels of three fatty acids, 14:0, 24:1n-9, and 22:5n-3. Similarly, in the fatty acid compositions of PtdCho (Tables 5, 7), the same major fatty acids were consistently found in all samples. These were 16:0 and 18:0; 16:1n-7, 18:1n-9, and 18:1n-7; 18:2n-6; EPA and DHA, with noticeable levels of four fatty acids, 14:0, 24:1n-9, 20:4n-6, and 22:5n-3.

Discussion

Lipid Content of the Three Populations of *P. altivelis* Under the Four Different Temperatures

In Table 2, the lipid content of all the samples was higher than that of the wild fish species [32], because they were

Table 5 The fatty acid composition of the in the amphidromous clone lipids of *P. altivelis*

Sample no.	Migratory clone (TAG)				Migratory clone (PtdEtn)			
	13 (15 °C)	14 (18 °C)	15 (20 °C)	16 (23 °C)	13 (15 °C)	14 (18 °C)	15 (20 °C)	16 (23 °C)
Total saturated	33.9 ± 0.6	36.2 ± 0.6	35.2 ± 0.5	34.5 ± 0.6	26.8 ± 2.2	28.2 ± 1.6	28.3 ± 1.7	38.4 ± 4.1
14:0	4.6 ± 0.2	4.9 ± 0.2	5.0 ± 0.0	4.8 ± 0.1	1.6 ± 0.4	1.2 ± 0.3	0.9 ± 0.1	3.2 ± 1.0
15:0	0.5 ± 0.0	0.5 ± 0.0	0.5 ± 0.0	0.5 ± 0.0	0.2 ± 0.0	0.2 ± 0.1	0.1 ± 0.0	0.3 ± 0.1
16:0	22.5 ± 0.7	24.6 ± 0.6	23.2 ± 0.5	23.2 ± 0.6	12.5 ± 2.3	13.9 ± 1.1	15.4 ± 3.0	25.5 ± 4.1
17:0	0.6 ± 0.0	0.6 ± 0.0	0.6 ± 0.0	0.5 ± 0.0	0.6 ± 0.1	0.5 ± 0.0	0.5 ± 0.0	0.6 ± 0.1
18:0	4.7 ± 0.1	4.7 ± 0.1	4.9 ± 0.1	4.5 ± 0.1	10.7 ± 0.8	11.3 ± 0.3	10.7 ± 1.5	7.8 ± 1.8
20:0	0.3 ± 0.0	0.3 ± 0.0	0.3 ± 0.0	0.3 ± 0.0	0.3 ± 0.0	0.5 ± 0.3	0.3 ± 0.0	0.3 ± 0.0
Total monoenoic	36.8 ± 0.3	36.6 ± 0.1	36.6 ± 0.3	34.9 ± 0.2	27.4 ± 1.4	26.1 ± 2.0	24.7 ± 0.8	33.2 ± 2.6
16:1n-7	6.8 ± 0.4	7.3 ± 0.4	6.4 ± 0.1	6.8 ± 0.3	4.5 ± 1.4	3.3 ± 0.6	2.5 ± 0.3	5.5 ± 1.3
16:1n-5	0.2 ± 0.0	0.2 ± 0.0	0.3 ± 0.0	0.3 ± 0.1	0.5 ± 0.3	0.3 ± 0.0	0.2 ± 0.0	0.2 ± 0.0
17:1n-8	0.5 ± 0.0	0.5 ± 0.0	0.5 ± 0.0	0.5 ± 0.0	0.3 ± 0.1	0.6 ± 0.3	0.2 ± 0.1	0.4 ± 0.1
18:1n-9	19.0 ± 0.3	18.7 ± 0.2	18.8 ± 0.1	18.0 ± 0.2	13.5 ± 1.0	13.5 ± 0.8	13.8 ± 0.5	18.3 ± 1.2
18:1n-7	3.7 ± 0.1	3.7 ± 0.1	3.8 ± 0.1	3.5 ± 0.1	3.5 ± 0.2	3.2 ± 0.4	2.9 ± 0.1	3.5 ± 0.3
18:1n-5	0.3 ± 0.0	0.3 ± 0.0	0.4 ± 0.1	0.3 ± 0.0	0.1 ± 0.0	0.1 ± 0.0	0.1 ± 0.0	0.2 ± 0.0
20:1n-11	1.6 ± 0.1	1.5 ± 0.1	1.6 ± 0.1	1.4 ± 0.1	0.6 ± 0.1	0.5 ± 0.1	0.5 ± 0.0	0.8 ± 0.1
20:1n-9	1.6 ± 0.0	1.5 ± 0.1	1.6 ± 0.0	1.4 ± 0.0	0.6 ± 0.1	0.6 ± 0.1	0.6 ± 0.1	0.9 ± 0.2
22:1n-11	1.3 ± 0.0	1.2 ± 0.1	1.3 ± 0.1	1.2 ± 0.1	0.4 ± 0.1	0.4 ± 0.1	0.3 ± 0.0	0.7 ± 0.2
22:1n-9	0.3 ± 0.0	0.3 ± 0.0	0.3 ± 0.0	0.3 ± 0.1	0.1 ± 0.0	0.1 ± 0.0	0.1 ± 0.0	0.2 ± 0.0
24:1n-9	0.6 ± 0.0	0.6 ± 0.0	0.6 ± 0.0	0.5 ± 0.0	1.2 ± 0.1	1.0 ± 0.1	1.1 ± 0.1	0.9 ± 0.3
Total polyenoic	29.2 ± 0.8	27.0 ± 0.6	28.2 ± 0.5	29.9 ± 0.5	39.5 ± 2.7	40.9 ± 3.4	41.0 ± 1.2	24.9 ± 5.6
Total n-4 polyenoic	0.8 ± 0.0	0.8 ± 0.0	0.9 ± 0.0	0.9 ± 0.0	0.8 ± 0.1	0.7 ± 0.1	0.6 ± 0.1	0.4 ± 0.1
16:2n-4	0.5 ± 0.0	0.5 ± 0.0	0.5 ± 0.0	0.5 ± 0.0	0.6 ± 0.0	0.6 ± 0.0	0.6 ± 0.1	0.4 ± 0.1
Total n-6 polyenoic	14.0 ± 0.4	13.0 ± 0.4	13.6 ± 0.3	13.3 ± 0.3	10.4 ± 0.2	10.6 ± 0.4	10.5 ± 0.8	8.5 ± 1.5
18:2n-6	12.1 ± 0.4	11.0 ± 0.4	11.8 ± 0.2	11.5 ± 0.3	5.7 ± 0.4	5.5 ± 0.2	5.6 ± 0.5	5.9 ± 1.2
20:4n-6	0.6 ± 0.0	0.6 ± 0.1	0.6 ± 0.0	0.6 ± 0.0	3.0 ± 0.3	3.5 ± 0.3	3.4 ± 0.3	1.5 ± 0.5
22:5n-6	0.3 ± 0.0	0.2 ± 0.0	0.2 ± 0.0	0.3 ± 0.0	0.5 ± 0.0	0.5 ± 0.1	0.5 ± 0.0	0.2 ± 0.1
Total n-3 polyenoic	13.6 ± 0.5	12.5 ± 0.4	12.8 ± 0.3	14.8 ± 0.2	27.5 ± 2.6	28.9 ± 3.1	29.3 ± 1.7	15.7 ± 4.9
18:3n-3	1.2 ± 0.0	1.1 ± 0.0	1.1 ± 0.0	1.1 ± 0.0	0.4 ± 0.0	0.4 ± 0.0	0.4 ± 0.0	0.4 ± 0.1
18:4n-3	0.4 ± 0.0	0.4 ± 0.0	0.4 ± 0.0	0.4 ± 0.0	0.3 ± 0.0	0.3 ± 0.0	0.4 ± 0.0	0.2 ± 0.1
20:4n-3	0.4 ± 0.0	0.4 ± 0.0	0.4 ± 0.0	0.4 ± 0.0	0.2 ± 0.0	0.2 ± 0.0	0.3 ± 0.1	0.3 ± 0.1
20:5n-3	3.3 ± 0.2	2.9 ± 0.1	3.0 ± 0.1	3.5 ± 0.1	2.0 ± 0.4	2.3 ± 0.2	2.8 ± 0.5	2.2 ± 0.7
22:5n-3	1.4 ± 0.1	1.3 ± 0.0	1.4 ± 0.0	1.6 ± 0.0	1.6 ± 0.2	1.7 ± 0.2	1.5 ± 0.2	1.0 ± 0.2
22:6n-3	6.8 ± 0.3	6.2 ± 0.3	6.4 ± 0.2	7.7 ± 0.1	23.0 ± 2.5	23.8 ± 2.7	23.9 ± 1.3	11.4 ± 4.2
Total fatty acids	99.1 ± 0.1	99.1 ± 0.2	99.1 ± 0.2	98.4 ± 0.0	92.9 ± 0.9	94.6 ± 0.6	93.5 ± 1.4	96.2 ± 1.6

Sample no.	Migratory clone (PtdCho)			
	13 (15 °C)	14 (18 °C)	15 (20 °C)	16 (23 °C)
Total saturated	32.3 ± 0.6	34.8 ± 0.8	33.5 ± 1.0	33.7 ± 2.4
14:0	0.5 ± 0.0	0.6 ± 0.0	0.7 ± 0.1	1.0 ± 0.3
15:0	0.2 ± 0.0	0.3 ± 0.0	0.2 ± 0.0	0.2 ± 0.0
16:0	26.5 ± 0.4	28.9 ± 0.6	25.7 ± 2.8	24.4 ± 3.5
17:0	0.5 ± 0.0	0.4 ± 0.0	0.5 ± 0.0	0.5 ± 0.0
18:0	3.6 ± 0.2	3.5 ± 0.1	4.9 ± 1.4	6.5 ± 1.4
20:0	0.1 ± 0.0	0.2 ± 0.0	0.2 ± 0.0	0.2 ± 0.0
Total monoenoic	22.7 ± 0.5	25.1 ± 0.7	24.4 ± 0.8	27.8 ± 1.1
16:1n-7	1.5 ± 0.1	1.7 ± 0.1	1.8 ± 0.2	2.9 ± 0.5

Table 5 continued

Sample no.	Migratory clone (PtdCho)			
	13 (15 °C)	14 (18 °C)	15 (20 °C)	16 (23 °C)
16:1n-5	0.1 ± 0.0	0.1 ± 0.0	0.1 ± 0.0	0.2 ± 0.0
17:1n-8	0.2 ± 0.0	0.2 ± 0.0	0.2 ± 0.0	0.6 ± 0.4
18:1n-9	15.7 ± 0.3	17.7 ± 0.5	16.7 ± 0.7	17.1 ± 1.1
18:1n-7	2.4 ± 0.1	2.6 ± 0.2	2.6 ± 0.1	3.1 ± 0.3
18:1n-5	0.2 ± 0.0	0.1 ± 0.0	0.2 ± 0.0	0.1 ± 0.0
20:1n-11	0.3 ± 0.0	0.3 ± 0.0	0.3 ± 0.0	0.5 ± 0.1
20:1n-9	0.3 ± 0.0	0.3 ± 0.0	0.4 ± 0.0	0.5 ± 0.1
22:1n-11	0.2 ± 0.0	0.2 ± 0.0	0.2 ± 0.0	0.4 ± 0.1
22:1n-9	0.1 ± 0.0	0.1 ± 0.0	0.1 ± 0.0	0.2 ± 0.1
24:1n-9	1.4 ± 0.1	1.5 ± 0.1	1.6 ± 0.2	1.3 ± 0.1
Total polyenoic	43.7 ± 0.7	39.4 ± 1.5	40.9 ± 1.4	36.2 ± 2.7
Total n-4 polyenoic	0.3 ± 0.0	0.3 ± 0.0	0.4 ± 0.1	0.6 ± 0.1
16:2n-4	0.2 ± 0.0	0.2 ± 0.0	0.3 ± 0.1	0.3 ± 0.1
Total n-6 polyenoic	6.5 ± 0.1	6.8 ± 0.2	7.8 ± 1.1	8.1 ± 1.3
18:2n-6	3.2 ± 0.1	3.4 ± 0.1	3.9 ± 0.5	4.7 ± 0.9
20:4n-6	2.2 ± 0.1	2.2 ± 0.1	2.7 ± 0.5	2.3 ± 0.3
22:5n-6	0.5 ± 0.0	0.5 ± 0.0	0.5 ± 0.0	0.4 ± 0.0
Total n-3 polyenoic	36.7 ± 0.8	32.1 ± 1.5	32.4 ± 1.0	27.0 ± 2.5
18:3n-3	0.2 ± 0.0	0.3 ± 0.0	0.3 ± 0.0	0.3 ± 0.0
18:4n-3	0.1 ± 0.0	0.1 ± 0.0	0.1 ± 0.0	0.2 ± 0.0
20:4n-3	0.2 ± 0.0	0.2 ± 0.0	0.2 ± 0.0	0.2 ± 0.0
20:5n-3	4.4 ± 0.5	4.6 ± 0.3	4.6 ± 0.4	3.4 ± 0.5
22:5n-3	1.6 ± 0.0	1.4 ± 0.1	1.5 ± 0.1	1.4 ± 0.2
22:6n-3	30.1 ± 0.8	25.4 ± 1.2	25.6 ± 0.7	21.5 ± 2.0
Total fatty acids	98.4 ± 0.7	99.0 ± 0.2	98.5 ± 0.5	97.1 ± 1.1

Results are expressed as mol% of the total fatty acids. Data are means ± standard error ($n = 6$)

In Tables 3, 4, 5, 6, 7, the major fatty acids are selected if at least one mean datum was detected at a level of 0.4% or more of total fatty acids

cultured under better nutritional conditions. Although the lengths and weights of clone samples **13–16** were larger than were those of Setogawa and migratory samples **1–12** (Table 1), their lipid content was markedly lower than the normal sexually reproduced samples. This finding suggests that the activity of lipid accumulation in the clone samples may be weaker than those in normal samples. Moreover, lipid levels of the normal samples (Setogawa samples **1–4** and migratory samples **5–8**) collected in June 1998 were similar to each other. Therefore, the nutrient intakes of the samples were similar to each other in spite of various water temperatures and different populations.

Fatty Acid Composition in TAG Deposit Lipids of *P. altivelis*: Relationship with Dietary Lipids

Medium levels of 18:2n-6 were found in the feedstuff lipids, and this finding is characteristic of dietary lipids, which are added with plant lipids.

Although the fatty acid compositions of TAG of the migratory, Lake Biwa and Setogawa River forms varied slightly among the samples (Setogawa and migratory samples **1–12**, Lake-Biwa landlocked sample **17**) under four different conditions (water temperature: 15.0, 18.0, 20.0, and 23.0 °C; Table 4), the major fatty acids in tissue TAG were almost the same in all samples. The levels of the major fatty acids were also similar to each other under all conditions among the different populations. Similarly, the same fatty acids were found as major acids in the TAG of the clone samples, as shown in Table 5.

The depot lipids of *P. altivelis* were probably influenced by dietary lipids, which originated from the same feedstuff [38]. The three populations of *P. altivelis* presumably accumulated intact dietary lipids as their depot lipids. Interestingly, high levels of 18:2n-6 (8.2–11.0% in Table 4 and 11.2–12.1% in Table 5) in the TAG of all populations were observed, suggesting that TAG was influenced by that in the dietary lipids (18.5–19.8%; Table 3), because it is

Table 6 The fatty acid composition of the phosphatidylethanolamines in the three populations of *P. altivelis*

Sample no.	Setogawa River F3				Migratory form F2			
	1 (15 °C)	2 (18 °C)	3 (20 °C)	4 (23 °C)	5 (15 °C)	6 (18 °C)	7 (20 °C)	8 (23 °C)
Total saturated	23.5 ± 1.0	27.6 ± 1.3	31.5 ± 2.2	31.9 ± 1.6	27.4 ± 2.3	24.2 ± 1.4	29.4 ± 2.7	35.4 ± 2.5
14:0	0.7 ± 0.1	1.1 ± 0.3	1.7 ± 0.5	2.4 ± 0.4	1.2 ± 0.2	1.2 ± 0.2	1.7 ± 0.4	2.9 ± 0.5
15:0	0.3 ± 0.1	0.5 ± 0.3	0.2 ± 0.0	0.2 ± 0.0	0.3 ± 0.1	0.2 ± 0.1	0.4 ± 0.2	0.5 ± 0.1
16:0	13.0 ± 2.2	13.5 ± 2.0	19.3 ± 1.4	17.5 ± 1.7	14.8 ± 2.2	11.8 ± 1.0	13.8 ± 1.3	19.8 ± 2.8
16:0i	0.3 ± 0.2	0.2 ± 0.1	0.1 ± 0.0	0.5 ± 0.3	0.4 ± 0.1	0.2 ± 0.2	0.6 ± 0.1	0.6 ± 0.2
17:0	0.4 ± 0.1	0.4 ± 0.1	0.5 ± 0.1	0.4 ± 0.0	0.4 ± 0.1	0.3 ± 0.0	0.5 ± 0.1	0.4 ± 0.1
18:0	7.7 ± 1.2	10.6 ± 0.9	8.1 ± 1.3	9.4 ± 1.1	8.7 ± 1.3	9.2 ± 0.5	10.3 ± 0.5	9.4 ± 1.3
18:0i	0.1 ± 0.0	0.1 ± 0.0	0.2 ± 0.0	0.1 ± 0.0	0.3 ± 0.2	0.2 ± 0.1	0.1 ± 0.0	0.4 ± 0.1
20:0	0.2 ± 0.0	0.2 ± 0.0	0.2 ± 0.0	0.3 ± 0.0	0.2 ± 0.0	0.2 ± 0.0	0.3 ± 0.1	0.2 ± 0.0
24:0	0.1 ± 0.0	0.1 ± 0.0	0.1 ± 0.0	0.1 ± 0.0	0.2 ± 0.1	0.3 ± 0.1	0.1 ± 0.0	0.1 ± 0.1
Total monoenoic	18.5 ± 0.6	21.3 ± 2.0	28.6 ± 2.8	30.0 ± 2.4	22.9 ± 1.3	22.7 ± 1.9	24.8 ± 1.8	29.5 ± 3.5
16:1n-7	1.7 ± 0.1	2.6 ± 0.4	4.5 ± 1.2	5.2 ± 0.8	2.3 ± 0.4	2.9 ± 0.6	3.6 ± 0.4	5.6 ± 1.2
17:1n-8	0.2 ± 0.1	0.2 ± 0.0	0.3 ± 0.1	0.3 ± 0.0	0.5 ± 0.2	0.2 ± 0.0	0.3 ± 0.0	0.4 ± 0.0
18:1n-9	10.8 ± 0.7	12.4 ± 1.1	16.6 ± 0.9	16.4 ± 0.9	12.0 ± 0.9	12.5 ± 0.8	12.6 ± 0.9	15.9 ± 1.6
18:1n-7	3.0 ± 0.4	3.0 ± 0.4	3.4 ± 0.5	3.6 ± 0.3	4.5 ± 0.5	3.7 ± 0.3	3.5 ± 0.2	3.7 ± 0.7
20:1n-11	0.3 ± 0.0	0.4 ± 0.1	0.6 ± 0.1	0.6 ± 0.1	0.3 ± 0.0	0.4 ± 0.0	0.6 ± 0.1	0.7 ± 0.1
20:1n-9	0.5 ± 0.1	0.6 ± 0.1	0.7 ± 0.1	0.9 ± 0.1	0.7 ± 0.1	0.7 ± 0.0	0.8 ± 0.0	0.9 ± 0.1
22:1n-11	0.2 ± 0.0	0.3 ± 0.1	0.4 ± 0.1	0.5 ± 0.1	0.2 ± 0.0	0.3 ± 0.0	0.5 ± 0.1	0.6 ± 0.1
24:1n-9	1.2 ± 0.1	1.0 ± 0.2	1.2 ± 0.2	1.0 ± 0.1	1.2 ± 0.1	1.1 ± 0.1	2.0 ± 0.6	0.7 ± 0.1
Total polyenoic	56.4 ± 1.4	48.8 ± 2.9	39.0 ± 3.6	36.5 ± 3.5	48.6 ± 3.5	52.2 ± 3.0	44.4 ± 4.7	33.9 ± 5.5
Total n-4 polyenoic	1.0 ± 0.3	1.5 ± 0.4	0.7 ± 0.2	1.0 ± 0.1	1.1 ± 0.1	1.1 ± 0.3	1.2 ± 0.1	1.2 ± 0.2
16:2n-4	0.3 ± 0.1	0.5 ± 0.1	0.4 ± 0.1	0.6 ± 0.1	0.5 ± 0.1	0.6 ± 0.0	0.3 ± 0.0	0.5 ± 0.1
16:4n-1	0.7 ± 0.2	1.1 ± 0.4	0.2 ± 0.1	0.3 ± 0.1	0.5 ± 0.2	0.5 ± 0.3	0.8 ± 0.2	0.4 ± 0.2
Total n-6 polyenoic	11.2 ± 1.5	11.5 ± 1.2	10.2 ± 1.6	12.8 ± 0.4	12.3 ± 1.4	13.2 ± 0.3	13.4 ± 1.9	11.5 ± 0.8
18:2n-6	5.8 ± 1.0	6.4 ± 1.0	6.8 ± 1.6	9.0 ± 0.8	7.0 ± 0.9	7.8 ± 0.7	7.9 ± 1.2	7.8 ± 0.6
20:2n-6	0.3 ± 0.0	0.2 ± 0.0	0.2 ± 0.0	0.3 ± 0.0	0.4 ± 0.1	0.3 ± 0.1	0.5 ± 0.1	0.3 ± 0.1
20:3n-6	0.5 ± 0.1	0.4 ± 0.1	0.3 ± 0.0	0.4 ± 0.0	0.5 ± 0.1	0.6 ± 0.0	0.8 ± 0.4	0.3 ± 0.0
20:4n-6	3.5 ± 0.5	3.4 ± 0.4	2.1 ± 0.2	2.3 ± 0.5	3.4 ± 0.3	3.3 ± 0.5	3.2 ± 0.6	2.2 ± 0.7
22:4n-6	0.3 ± 0.0	0.3 ± 0.0	0.2 ± 0.0	0.2 ± 0.0	0.3 ± 0.0	0.3 ± 0.0	0.3 ± 0.0	0.2 ± 0.0
22:5n-6	0.6 ± 0.0	0.5 ± 0.0	0.4 ± 0.1	0.3 ± 0.0	0.5 ± 0.0	0.6 ± 0.1	0.4 ± 0.1	0.3 ± 0.1
Total n-3 polyenoic	43.2 ± 1.2*	34.3 ± 2.4	27.5 ± 5.2	21.8 ± 3.5	34.2 ± 3.2*	36.7 ± 3.1	28.7 ± 2.7	20.1 ± 4.7
18:3n-3	0.6 ± 0.1	0.6 ± 0.1	0.6 ± 0.1	0.8 ± 0.1	0.6 ± 0.1	0.8 ± 0.1	0.7 ± 0.1	0.7 ± 0.1
18:4n-3	0.2 ± 0.0	0.3 ± 0.0	0.2 ± 0.1	0.3 ± 0.0	0.2 ± 0.0	0.4 ± 0.2	0.3 ± 0.1	0.3 ± 0.1
20:4n-3	0.4 ± 0.0	0.3 ± 0.1	0.3 ± 0.1	0.4 ± 0.1	0.4 ± 0.0	0.4 ± 0.0	0.4 ± 0.0	0.3 ± 0.0
20:5n-3	4.5 ± 0.8	3.2 ± 0.3	3.7 ± 1.0	2.3 ± 0.3	3.4 ± 0.5	3.0 ± 0.1	2.8 ± 0.3	2.4 ± 0.4
22:5n-3	3.0 ± 0.1	2.4 ± 0.2	1.7 ± 0.2	1.6 ± 0.2	2.1 ± 0.2	2.8 ± 0.1	2.2 ± 0.3	1.8 ± 0.5
22:6n-3	34.4 ± 0.9	27.5 ± 2.2	20.9 ± 4.3	16.3 ± 3.0	27.5 ± 2.7	29.3 ± 3.1	21.9 ± 2.2	14.6 ± 3.9
Total fatty acids	97.3 ± 0.6	96.3 ± 1.0	98.4 ± 0.3	97.5 ± 0.9	97.9 ± 0.3	97.9 ± 0.7	97.4 ± 0.3	97.7 ± 0.6
Sample no.	Migratory form F1				Lake Biwa landlocked			
	9 (15 °C)	10 (18 °C)	11 (20 °C)	12 (23 °C)	17 (18 °C)			
Total saturated	24.0 ± 0.8	25.9 ± 1.0	30.0 ± 1.2	35.5 ± 1.8	23.3 ± 1.0			
14:0	0.7 ± 0.1	1.1 ± 0.2	1.4 ± 0.2	2.3 ± 0.3	1.0 ± 0.2			
15:0	0.1 ± 0.0	0.2 ± 0.1	0.2 ± 0.0	0.3 ± 0.0	0.2 ± 0.0			
16:0	11.2 ± 0.6	13.1 ± 1.0	15.4 ± 1.0	18.9 ± 1.5	12.2 ± 0.9			
16:0i	0.9 ± 0.4	0.2 ± 0.1	0.3 ± 0.1	0.1 ± 0.0	0.0 ± 0.0			

Table 6 continued

Sample no.	Migratory form F1				Lake Biwa landlocked
	9 (15 °C)	10 (18 °C)	11 (20 °C)	12 (23 °C)	17 (18 °C)
17:0	0.3 ± 0.0	0.3 ± 0.0	0.4 ± 0.0	0.5 ± 0.0	0.3 ± 0.0
18:0	9.3 ± 0.4	9.5 ± 0.5	10.7 ± 0.5	12.0 ± 0.3	8.0 ± 0.5
18:0i	0.2 ± 0.1	0.1 ± 0.0	0.1 ± 0.1	0.1 ± 0.0	0.6 ± 0.1
20:0	0.2 ± 0.0	0.2 ± 0.0	0.4 ± 0.1	0.3 ± 0.0	0.2 ± 0.0
24:0	0.1 ± 0.0	0.1 ± 0.0	0.0 ± 0.0	0.1 ± 0.0	0.1 ± 0.0
Total monoenoic	19.6 ± 0.6	22.4 ± 1.1	25.8 ± 1.5	30.0 ± 2.2	21.9 ± 0.9
16:1n-7	2.1 ± 0.2	3.0 ± 0.4	4.0 ± 0.4	5.0 ± 0.5	2.9 ± 0.2
17:1n-8	0.2 ± 0.0	0.2 ± 0.0	0.3 ± 0.1	0.3 ± 0.1	0.2 ± 0.0
18:1n-9	10.5 ± 0.5	12.9 ± 0.4	14.7 ± 0.7	17.2 ± 1.2	12.4 ± 0.4
18:1n-7	3.3 ± 0.2	2.8 ± 0.1	3.0 ± 0.2	3.1 ± 0.2	2.8 ± 0.2
20:1n-11	0.3 ± 0.0	0.5 ± 0.0	0.5 ± 0.1	0.8 ± 0.1	0.4 ± 0.1
20:1n-9	0.5 ± 0.0	0.7 ± 0.0	0.7 ± 0.1	0.9 ± 0.1	0.6 ± 0.1
22:1n-11	0.2 ± 0.0	0.3 ± 0.0	0.4 ± 0.1	0.8 ± 0.1	0.3 ± 0.0
24:1n-9	1.1 ± 0.1	1.3 ± 0.1	1.2 ± 0.1	0.9 ± 0.2	1.0 ± 0.1
Total polyenoic	54.9 ± 1.5	49.2 ± 2.1	41.7 ± 2.6	31.7 ± 4.0	49.2 ± 1.9
Total n-4 polyenoic	2.4 ± 0.2	1.9 ± 0.2	1.4 ± 0.2	1.7 ± 0.3	1.3 ± 0.7
16:2n-4	0.6 ± 0.0	0.6 ± 0.0	0.6 ± 0.0	0.6 ± 0.0	0.6 ± 0.1
16:4n-1	1.5 ± 0.1	1.2 ± 0.2	0.8 ± 0.2	1.0 ± 0.3	0.7 ± 0.7
Total n-6 polyenoic	10.3 ± 0.4	10.6 ± 0.4	10.3 ± 0.2	9.2 ± 0.8	9.3 ± 0.8
18:2n-6	5.2 ± 0.3	5.5 ± 0.4	5.8 ± 0.2	5.4 ± 0.4	4.0 ± 0.4
20:2n-6	0.3 ± 0.0	0.3 ± 0.1	0.2 ± 0.0	0.2 ± 0.0	0.2 ± 0.0
20:3n-6	0.3 ± 0.0	0.3 ± 0.0	0.3 ± 0.0	0.2 ± 0.0	0.4 ± 0.1
20:4n-6	3.3 ± 0.2	3.3 ± 0.4	3.1 ± 0.3	2.6 ± 0.3	3.1 ± 0.5
22:4n-6	0.4 ± 0.0	0.3 ± 0.0	0.3 ± 0.0	0.2 ± 0.0	0.4 ± 0.0
22:5n-6	0.7 ± 0.0	0.6 ± 0.0	0.5 ± 0.0	0.3 ± 0.0	0.8 ± 0.0
Total n-3 polyenoic	39.9 ± 1.6	34.8 ± 1.9	28.5 ± 2.4	19.1 ± 2.8	37.3 ± 0.9
18:3n-3	0.4 ± 0.0	0.4 ± 0.0	0.5 ± 0.0	0.4 ± 0.0	0.3 ± 0.0
18:4n-3	0.3 ± 0.0	0.3 ± 0.0	0.2 ± 0.0	0.3 ± 0.0	0.3 ± 0.0
20:4n-3	0.3 ± 0.0	0.3 ± 0.0	0.3 ± 0.0	0.2 ± 0.0	0.3 ± 0.0
20:5n-3	3.5 ± 0.0	2.9 ± 0.1	2.7 ± 0.1	1.8 ± 0.2	2.4 ± 0.1
22:5n-3	2.6 ± 0.1	2.3 ± 0.1	1.8 ± 0.2	1.2 ± 0.2	2.3 ± 0.2
22:6n-3	32.7 ± 1.6	28.5 ± 1.8	23.0 ± 2.1	15.3 ± 2.3	31.6 ± 0.7
Total fatty acids	96.2 ± 0.4	95.6 ± 0.6	96.1 ± 0.8	95.4 ± 0.9	93.0 ± 1.2

Results are expressed as mol% of the total fatty acids. Data are means ± standard error ($n = 4-6$)

In Tables 3, 4, 5, 6, 7, the major fatty acids are selected if at least one mean datum was detected at a level of 0.4% or more of total fatty acids. Values in a column with different superscripts (*) are significantly different at the 5% level.

known that artificial feedstuff contains plant seed oils, which have high levels of 18:2n-6 [30–32].

Fatty Acid Composition in Tissue Phospholipids in *P. altivelis*

Although the kinds of fatty acids between the TAG and phospholipids of *P. altivelis* were the same, their levels in the phospholipids of *P. altivelis* significantly differed from

those in TAG. For example, high levels of total n-3 PUFA (21.4–46.7% for PtdEtn and 30.4–50.8% for PtdCho) were found in the polar phospholipids, different from those in TAG (13.2–16.4%). This indicates that n-3 PUFA is specifically transferred from depot lipids to tissue polar lipids in the ayu, similar to the circumstances in other aquatic animals such as fishes [4, 6, 38] and mollusks [39]. In particular, high DHA levels were found in both PtdEtn (38.3–46.76% for samples Setogawa-15 °C sample 1,

Table 7 The fatty acid composition of the phosphatidylcholines in the three populations of *P. altivelis*

Sample no.	Setogawa River form F3				Migratory form F2			
	1 (15 °C)	2 (18 °C)	3 (20 °C)	4 (23 °C)	5 (15 °C)	6 (18 °C)	7 (20 °C)	8 (23 °C)
Total saturated	26.7 ± 0.8	26.9 ± 0.9	31.7 ± 2.7	32.4 ± 1.8	28.2 ± 0.6	26.6 ± 3.6	36.7 ± 4.8	35.7 ± 1.3
14:0	0.7 ± 0.2	0.4 ± 0.1	0.9 ± 0.2	1.7 ± 0.6	0.5 ± 0.0	0.7 ± 0.1	1.3 ± 0.4	1.3 ± 0.3
16:0	17.4 ± 2.0	19.1 ± 1.5	21.8 ± 2.5	18.7 ± 1.3	21.4 ± 0.4	19.1 ± 3.4	23.1 ± 1.8	21.2 ± 2.5
17:0	0.6 ± 0.1	0.5 ± 0.1	0.5 ± 0.1	0.5 ± 0.1	0.3 ± 0.1	0.4 ± 0.1	0.4 ± 0.1	0.5 ± 0.1
18:0	6.1 ± 1.7	4.9 ± 0.6	5.8 ± 0.6	8.8 ± 1.9	3.7 ± 0.1	4.2 ± 0.5	9.1 ± 3.2	9.3 ± 1.7
20:0	0.2 ± 0.1	0.2 ± 0.0	0.2 ± 0.0	0.4 ± 0.1	0.2 ± 0.0	0.2 ± 0.0	0.3 ± 0.0	0.4 ± 0.1
22:0	0.2 ± 0.0	0.3 ± 0.0	0.3 ± 0.0	0.2 ± 0.1	0.3 ± 0.0	0.1 ± 0.1	0.3 ± 0.1	0.5 ± 0.2
24:0	0.1 ± 0.0	0.8 ± 0.5	0.9 ± 0.5	0.1 ± 0.0	1.1 ± 0.3	0.7 ± 0.3	0.0 ± 0.0	0.4 ± 0.3
Total monoenoic	18.8 ± 0.6	19.1 ± 0.6	22.4 ± 2.0	26.4 ± 2.2	20.8 ± 0.6	26.4 ± 2.9	25.2 ± 2.4	26.1 ± 1.0
16:1n-7	1.9 ± 0.2	1.1 ± 0.2	2.0 ± 0.4	3.4 ± 0.9	1.6 ± 0.2	3.2 ± 1.3	2.6 ± 0.7	3.2 ± 0.7
16:1n-5	0.1 ± 0.0	0.1 ± 0.0	0.3 ± 0.2	0.1 ± 0.0	0.1 ± 0.0	0.4 ± 0.3	0.1 ± 0.0	0.2 ± 0.0
17:1n-8	0.2 ± 0.0	0.2 ± 0.0	0.3 ± 0.1	0.3 ± 0.1	0.2 ± 0.0	0.2 ± 0.0	0.4 ± 0.1	0.4 ± 0.1
18:1n-9	11.7 ± 0.5	12.5 ± 0.6	13.8 ± 1.6	15.8 ± 0.8	13.6 ± 0.4	14.6 ± 0.7	14.8 ± 1.3	15.6 ± 0.7
18:1n-7	1.7 ± 0.1	2.1 ± 0.3	2.3 ± 0.2	2.7 ± 0.5	2.0 ± 0.1	3.9 ± 1.5	3.2 ± 0.8	2.3 ± 0.1
18:1n-5	0.1 ± 0.0	0.1 ± 0.0	0.2 ± 0.0	0.2 ± 0.0	0.1 ± 0.0	0.4 ± 0.3	0.1 ± 0.0	0.2 ± 0.0
20:1n-11	0.3 ± 0.0	0.3 ± 0.0	0.4 ± 0.1	0.5 ± 0.1	0.2 ± 0.0	0.3 ± 0.0	0.5 ± 0.1	0.5 ± 0.1
20:1n-9	0.3 ± 0.0	0.4 ± 0.0	0.4 ± 0.1	0.7 ± 0.1	0.4 ± 0.0	0.4 ± 0.0	0.6 ± 0.1	0.6 ± 0.0
22:1n-11	0.2 ± 0.0	0.2 ± 0.0	0.3 ± 0.1	0.3 ± 0.1	0.2 ± 0.0	0.2 ± 0.0	0.4 ± 0.1	0.3 ± 0.0
24:1n-9	1.5 ± 0.2	1.6 ± 0.1	1.7 ± 0.3	1.1 ± 0.3	1.8 ± 0.1	1.7 ± 0.1	1.4 ± 0.3	1.6 ± 0.1
Total polyenoic	53.4 ± 1.2*	53.1 ± 1.4	43.9 ± 3.3	40.4 ± 4.0	50.0 ± 1.2	45.9 ± 1.7	36.8 ± 5.9	36.3 ± 2.3
Total n-4 polyenoic	0.2 ± 0.0	0.3 ± 0.1	0.5 ± 0.1	0.9 ± 0.2	0.5 ± 0.1	0.5 ± 0.1	0.9 ± 0.5	0.6 ± 0.1
16:2n-4	0.2 ± 0.0	0.3 ± 0.1	0.3 ± 0.1	0.5 ± 0.1	0.4 ± 0.1	0.3 ± 0.0	0.3 ± 0.1	0.4 ± 0.1
16:4n-1	0.1 ± 0.0	0.0 ± 0.0	0.1 ± 0.0	0.3 ± 0.1	0.0 ± 0.0	0.1 ± 0.0	0.5 ± 0.4	0.1 ± 0.0
Total n-6 polyenoic	5.9 ± 0.2	6.6 ± 0.3	7.0 ± 1.1	9.7 ± 1.1	6.6 ± 0.1	7.5 ± 0.9	6.7 ± 0.9	8.0 ± 0.6
18:2n-6	2.4 ± 0.1	2.8 ± 0.1	3.5 ± 0.7	5.4 ± 1.0	2.9 ± 0.1	3.6 ± 0.5	3.4 ± 0.8	3.8 ± 0.2
20:2n-6	0.2 ± 0.0	0.4 ± 0.2	0.4 ± 0.2	0.6 ± 0.3	0.3 ± 0.0	0.2 ± 0.0	0.3 ± 0.1	1.4 ± 0.6
20:3n-6	0.3 ± 0.0	0.3 ± 0.0	0.3 ± 0.0	0.4 ± 0.1	0.3 ± 0.0	0.3 ± 0.0	0.4 ± 0.1	0.3 ± 0.1
20:4n-6	1.9 ± 0.1	2.1 ± 0.1	1.8 ± 0.1	2.4 ± 0.6	1.9 ± 0.0	2.3 ± 0.5	1.7 ± 0.2	1.4 ± 0.2
22:5n-6	0.8 ± 0.0	0.6 ± 0.0	0.6 ± 0.0	0.4 ± 0.1	0.7 ± 0.0	0.6 ± 0.0	0.4 ± 0.1	0.5 ± 0.0
Total n-3 polyenoic	47.0 ± 1.2**	45.9 ± 1.2	36.0 ± 3.1	28.8 ± 4.9	42.4 ± 1.3	37.4 ± 1.7	28.4 ± 6.4	27.2 ± 2.7
18:3n-3	0.3 ± 0.0	0.3 ± 0.0	0.3 ± 0.1	0.5 ± 0.1	0.3 ± 0.0	0.3 ± 0.0	0.3 ± 0.0	0.3 ± 0.0
18:4n-3	0.1 ± 0.1	0.2 ± 0.1	0.1 ± 0.0	0.2 ± 0.1	0.1 ± 0.0	0.2 ± 0.0	0.3 ± 0.1	0.3 ± 0.1
20:4n-3	0.3 ± 0.0	0.5 ± 0.1	0.3 ± 0.1	0.3 ± 0.1	0.3 ± 0.0	0.3 ± 0.0	0.3 ± 0.0	0.2 ± 0.0
20:5n-3	5.5 ± 0.6	6.3 ± 0.3	4.6 ± 0.6	3.4 ± 0.9	5.9 ± 0.2	5.0 ± 0.6	3.9 ± 1.2	2.7 ± 0.7
22:5n-3	2.5 ± 0.2	2.5 ± 0.3	2.0 ± 0.3	1.7 ± 0.2	2.2 ± 0.1	2.3 ± 0.3	1.7 ± 0.4	2.0 ± 0.2
22:6n-3	38.3 ± 1.1***	36.0 ± 0.8	28.6 ± 2.5	22.6 ± 4.0	33.6 ± 1.0	29.3 ± 1.1	21.9 ± 5.0	21.5 ± 2.2
Total fatty acids	98.7 ± 0.2	98.7 ± 0.3	97.6 ± 1.1	98.3 ± 0.4	98.5 ± 0.2	98.4 ± 0.2	97.8 ± 0.4	97.5 ± 0.5
Sample no.	Migratory form F1				Lake Biwa landlocked			
	9 (15 °C)	10 (18 °C)	11 (20 °C)	12 (23 °C)	17 (18 °C)			
Total saturated	29.1 ± 1.2	29.7 ± 0.4	32.7 ± 0.7	36.6 ± 1.3	26.4 ± 2.8			
14:0	0.4 ± 0.0	0.4 ± 0.0	0.5 ± 0.0	0.6 ± 0.0	0.7 ± 0.2			
16:0	24.1 ± 1.2	24.9 ± 0.4	27.2 ± 0.6	29.9 ± 1.3	20.4 ± 3.7			
17:0	0.4 ± 0.1	0.3 ± 0.0	0.4 ± 0.0	0.5 ± 0.1	0.3 ± 0.0			
18:0	3.1 ± 0.0	3.1 ± 0.1	3.5 ± 0.2	4.1 ± 0.3	3.2 ± 0.3			
20:0	0.1 ± 0.0	0.1 ± 0.0	0.2 ± 0.0	0.2 ± 0.0	0.2 ± 0.0			

Table 7 continued

Sample no.	Migratory form F1				Lake Biwa landlocked 17 (18 °C)
	9 (15 °C)	10 (18 °C)	11 (20 °C)	12 (23 °C)	
22:0	0.2 ± 0.0	0.2 ± 0.0	0.3 ± 0.0	0.3 ± 0.0	0.2 ± 0.0
24:0	0.1 ± 0.0	0.1 ± 0.0	0.1 ± 0.0	0.3 ± 0.3	0.2 ± 0.1
Total monoenoic	22.1 ± 0.8	23.3 ± 0.6	25.2 ± 0.7	27.2 ± 1.1	22.1 ± 0.9
16:1n-7	1.6 ± 0.1	1.6 ± 0.0	1.8 ± 0.1	2.0 ± 0.1	2.6 ± 0.8
16:1n-5	0.1 ± 0.0	0.1 ± 0.0	0.1 ± 0.0	0.2 ± 0.1	0.1 ± 0.1
17:1n-8	0.2 ± 0.0	0.2 ± 0.0	0.2 ± 0.0	0.2 ± 0.0	0.2 ± 0.0
18:1n-9	14.9 ± 0.7	16.2 ± 0.5	17.7 ± 0.5	19.1 ± 0.8	13.3 ± 1.9
18:1n-7	2.3 ± 0.1	2.2 ± 0.1	2.3 ± 0.1	2.3 ± 0.1	1.9 ± 0.2
18:1n-5	0.2 ± 0.0	0.2 ± 0.0	0.1 ± 0.0	0.2 ± 0.0	0.2 ± 0.0
20:1n-11	0.2 ± 0.0	0.2 ± 0.0	0.3 ± 0.0	0.4 ± 0.0	0.3 ± 0.0
20:1n-9	0.3 ± 0.0	0.3 ± 0.0	0.3 ± 0.0	0.3 ± 0.1	0.4 ± 0.1
22:1n-11	0.1 ± 0.0	0.1 ± 0.0	0.1 ± 0.0	0.2 ± 0.0	0.3 ± 0.1
24:1n-9	1.6 ± 0.1	1.8 ± 0.1	1.8 ± 0.1	1.9 ± 0.2	1.9 ± 0.4
Total polyenoic	47.9 ± 1.9*	46.3 ± 0.9	41.4 ± 1.2	35.7 ± 2.2	49.9 ± 3.0
Total n-4 polyenoic	0.3 ± 0.1	0.4 ± 0.0	0.2 ± 0.0	0.2 ± 0.0	1.1 ± 0.6
16:2n-4	0.2 ± 0.1	0.3 ± 0.0	0.2 ± 0.0	0.2 ± 0.0	0.3 ± 0.0
16:4n-1	0.1 ± 0.0	0.1 ± 0.0	0.1 ± 0.0	0.1 ± 0.0	0.3 ± 0.3
Total n-6 polyenoic	6.7 ± 0.1	6.7 ± 0.1	6.3 ± 0.0	5.7 ± 0.2	8.7 ± 2.0
18:2n-6	2.9 ± 0.1	2.8 ± 0.1	2.9 ± 0.1	2.8 ± 0.1	2.5 ± 0.2
20:2n-6	0.2 ± 0.0	0.2 ± 0.0	0.2 ± 0.0	0.2 ± 0.0	2.6 ± 2.3
20:3n-6	0.3 ± 0.0	0.2 ± 0.0	0.2 ± 0.0	0.2 ± 0.0	0.3 ± 0.0
20:4n-6	2.3 ± 0.0	2.4 ± 0.1	2.2 ± 0.1	1.9 ± 0.1	2.2 ± 0.2
22:5n-6	0.7 ± 0.0	0.6 ± 0.0	0.5 ± 0.0	0.4 ± 0.0	0.7 ± 0.2
Total n-3 polyenoic	40.7 ± 2.0**	38.9 ± 0.9	34.6 ± 1.2	29.5 ± 2.1	39.0 ± 3.5
18:3n-3	0.2 ± 0.0	0.2 ± 0.0	0.2 ± 0.0	0.2 ± 0.0	0.2 ± 0.1
18:4n-3	0.1 ± 0.0	0.1 ± 0.0	0.1 ± 0.0	0.1 ± 0.1	0.5 ± 0.4
20:4n-3	0.2 ± 0.0	0.2 ± 0.0	0.2 ± 0.0	0.1 ± 0.0	0.3 ± 0.1
20:5n-3	6.1 ± 0.2	5.6 ± 0.2	5.3 ± 0.2	4.3 ± 0.3	5.8 ± 0.5
22:5n-3	2.0 ± 0.1	1.9 ± 0.1	1.6 ± 0.1	1.3 ± 0.1	1.9 ± 0.2
22:6n-3	32.0 ± 1.8***	30.8 ± 0.8	27.3 ± 1.0	23.4 ± 1.8	30.2 ± 4.2
Total fatty acids	98.8 ± 0.0	98.9 ± 0.0	99.0 ± 0.1	99.2 ± 0.2	97.4 ± 1.2

Results are expressed as mol% of the total fatty acids. Data are means ± standard error ($n = 3-6$)

In Tables 3, 4, 5, 6, 7, the major fatty acids are selected if at least one mean datum was detected at a level of 0.4% or more of total fatty acids. Values in a column with different superscripts (*, **, ***) are significantly different at the 5% level, respectively

migratory-15 °C sample 5, and migratory-15 °C sample 9 in Table 6) and PtdCho (44.4–50.8% for samples 1, 5, and 9 in Table 7) under low temperature conditions, markedly different from that in TAG. The high n-3 PUFA levels that accumulated in the phospholipids suggest the importance of long-chain n-3 PUFA for *P. altivelis* plasma membrane lipids as a fish species [6]. *P. altivelis* might biosynthesize or actively accumulate n-3 PUFA at the tissue level because of the biosynthetic ability of freshwater fishes to long-chain n-3 PUFA [40, 41].

Accumulation and Biosynthesis of 20:4n-6 at the Tissue Levels of *P. altivelis*

Both TAG and PtdEtn contained similar levels of total n-6 PUFA (11.0–13.0% for TAG and 10.2–13.3% for PtdEtn of normal samples 1–12 and 17), as shown in Tables 4 and 6. With medium levels of 18:2n-6 and trace levels of 20:4n-6 in *P. altivelis* TAG, noticeable 20:4n-6 levels in the polar lipids (PtdEtn and PtdCho in Tables 6, 7) suggest the biosynthesis of long-chain n-6 PUFA in *P. altivelis* PtdEtn.

18:2n-6 is modified to 18:3n-6 by 6-desaturase, and 20:4n-6 is derived from 18:3n-6 by C₂-elongation and Δ⁵-desaturation [8, 42–44]. 18:2n-6 in all polar lipids (4.9–8.8% for PtdEtn and 2.2–5.2% for PtdCho) is thought to be transferred from TAG 18:2n-6 (9.3–11.0%), which is directly influenced by dietary lipids. In particular, the lower levels of PtdCho 18:2n-6 also suggest enzymatic modification to 20:4n-6.

Furthermore, there were tendencies in regard to the variations of n-6 PUFA in PtdEtn influenced by temperature differences. For example, the slightly higher levels of 20:4n-6 (3.6, 3.5, and 3.3% for samples **1**, **5**, and **9** at 15 °C; 3.5, 3.4, and 3.4% for samples **2**, **6**, and **10** at 18 °C; 2.2, 3.3, and 3.2% for samples **3**, **7**, and **11** at 20 °C; 2.5, 2.3, and 2.8% for samples **4**, **8**, and **12** at 23 °C) under lower temperature conditions were found with lower levels of 18:2n-6 (5.5, 4.5, and 4.9% for samples **1**, **5**, and **9** at 15 °C; 6.2, 7.4, and 5.3% for samples **2**, **6**, and **10** at 18 °C; 6.7, 7.6, and 5.6% for samples **3**, **7**, and **11** at 20 °C; 8.8, 7.8, and 5.3% for samples **4**, **8**, and **12** at 23 °C) under all other conditions of higher temperature.

Accumulation and Biosynthesis of DHA in the *P. altivelis*

The high levels of total n-3 PUFA in the phospholipids, markedly different from those in TAG as mentioned above, suggest biosynthesis of long-chain n-3 PUFA in *P. altivelis* tissue lipids, and that freshwater fishes are able to synthesize DHA [40–42]. With low levels of DHA in *P. altivelis* TAG, the high DHA levels in the polar lipids (PtdEtn and PtdCho) of *P. altivelis* suggest the biosynthesis and accumulation of DHA in the *P. altivelis* polar lipids. The levels of 22:5n-3 in the polar lipids were slightly higher than were those in TAG. 22:5n-3, which is an intermediate to DHA, was probably derived from EPA by C₂-elongation [8, 42–44]. Although we did not find 24:5n-3 and 24:6n-3 in the *P. altivelis* phospholipids, DHA can be speculatively considered to be derived from 22:5n-3, similar to biosynthesis in mammal (Sprecher's shunt: 45, 46).

Influence of Different Temperatures on *P. altivelis* Tissue Lipids: Adaptation to Low Temperature by Increase of DHA

Although the fatty acid compositions in the TAG of *P. altivelis* were similar to each other in all specimens (Table 4), and there were no such tendencies of the fatty acids in TAG among the four different-temperature samples, those in PtdEtn and PtdCho show a clear trend (Tables 6, 7). For example, in all samples (Setogawa River form samples: **1–2**, migratory type samples: **5–6** and **9–10**) in PtdEtn (Table 6) and PtdCho (Table 7) under lower

temperature conditions, significantly higher levels of total PUFA, total n-3 PUFA, and DHA were found, compared with those in other samples (**3–4**, **7–8**, and **11–12**) under higher temperature conditions. In particular, under the lowest temperature (15 °C, for samples **1**, **5**, and **9**), the highest levels of these long-chain n-3 PUFA were found. Especially, only DHA varied markedly according to temperature changes. Therefore, DHA is certainly the most important acid for acclimation of the fish plasma membrane to low temperatures. These findings suggest a mechanism for increasing unsaturation to DHA for membrane fluidity under low temperatures [17–19, 47]. A similar trend was found in the clone samples (**13–16** in Table 5). However, the concentration of DHA in the clone samples under low temperatures is not so clear, and this implies the weakness of enzyme activity in the clone samples compared with that in the normal sexually reproduced samples.

Difference of Temperature Adaptability Among Populations of *P. altivelis*

In two populations (Setogawa River and migratory forms), which are acclimatized to various temperature conditions, the major fatty acids of the phospholipids (PtdEtn and PtdCho) are listed in Tables 6, 7. Higher DHA levels in accordance with lower temperature acclimatization were found in both populations. Compared with the levels of the key fatty acids (total PUFA, total n-3 PUFA, and DHA) in the polar lipids at 15 °C in the two populations, many data in PtdEtn and PtdCho show them to have significant differences (Tables 6 and 7) and some data show to have tendencies, which mean higher levels of these PUFA in the Setogawa River form. For example, in PtdCho, the level of DHA in Setogawa samples **1** ($41.8 \pm 1.2\%$) was significantly (ANOVA with a Tukey's test) higher than were those in migratory samples **5** and **9** (36.9 ± 1.2 and $35.4 \pm 1.8\%$). The biosynthetic and accumulative abilities of the Setogawa River form in regard to DHA are probably higher than are those in the migratory form. Although we investigated only one temperature condition (18 °C) in the case of the Lake Biwa landlocked form (sample: **17**), the levels of n-3 PUFA, such as DHA in PtdEtn and PtdCho (Tables 6, 7), were similar to those in the migratory form (samples **6** and **10**).

The increase of DHA in the tissue levels of freshwater fishes is important for supplying a healthful diet [8, 9]. As for the level of DHA, which was accumulated or biosynthesized in *P. altivelis* tissues, the Setogawa River form is superior among the three populations, and are thus a useful food source rich in long-chain n-3 PUFA. The Setogawa River form has adaptability to high temperature and is a novel and valuable ayu population as a healthful food rich in DHA.

Acknowledgments The authors thank Ms. Mikiko Tanaka and Mr. Kojiro Ogomori for their skilled technical assistance. H. Saito performed all aspects of the study including the designing the experiments, analyzing the data, and writing the manuscript. C. Xue assisted in data collection and analysis. M. Okabe assisted in culturing the fish and collecting samples.

References

- Ackman RG (1989) Fatty Acids. In: Ackman RG (ed) Marine biogenic lipids, fats, and oils, vol I. CRC Press, Boca Raton, pp 103–137
- Morris RJ, Culkin F (1989) Fish. In: Ackman RG (ed) Marine biogenic lipids, fats, and oils, vol II. CRC Press, Boca Raton, pp 145–178
- Joseph JD (1989) Invertebrates. In: Ackman RG (ed) Marine biogenic lipids, fats, and oils, vol II. CRC Press, Boca Raton, pp 145–178
- Saito H, Yamashiro R, Ishihara K, Xue C (1999) The lipids of three highly migratory fishes: *Euthynnus affinis*, *Sarda orientalis* and *Elagatis bipinnulata*. *Biosci Biotech Biochem* 63:2028–2030
- Budge SM, Iverson SJ, Bowen WD, Ackman RG (2002) Among- and within-species variability in fatty acid signatures of marine fish and invertebrates on the Scotian Shelf, Georges Bank, and southern Gulf of St Lawrence. *Can J Fish Aquat Sci* 59:886–898
- Saito H, Seike Y, Ioka H, Osako K, Tanaka M, Takashima A, Keriko JM, Kose S, Souza JCR (2005) High docosahexaenoic acid levels in both neutral and polar lipids of a highly migratory fish: *Thunnus tonggol* Bleeker. *Lipids* 40:941–953
- Ackman RG (2000) Fatty acids in fish and shellfish. In: Chow CK (ed) Fatty acids in food and their health implications, 2nd edn. Marcel Dekker, New York, pp 47–65
- Arts MT, Ackman RG, Holub BJ (2001) “Essential fatty acids” in aquatic ecosystems: a crucial link between diet and human health and evolution. *Can J Fish Aquat Sci* 58:122–137
- Lands WEM (2009) Human life: caught in the food web. In: Arts MT, Brett MT, Kainz MJ (eds) *Lipids in aquatic ecosystem*. Springer, Berlin, pp 327–354
- Aslan SS, Guven KC, Gezgin T, Alpaslan M, Tekinay A (2007) Comparison of fatty contents of wild and cultured rainbow trout *Oncorhynchus mykiss* in Turkey. *Fisheries Sci* 73:1195–1198
- Naylor RL, Williams SL, Strong DR (2009) Aquaculture: a gateway for exotic species. *Science* 294:1655–1656
- Megdal PA, Craft NA, Handelman GJ (2009) A simplified method to distinguish farmed (*Salmo salar*) from wild salmon: fatty acid ratios versus astaxanthin chiral isomers. *Lipids* 44:569–576
- Nishida M (1985) Substantial genetic differentiation in Ayu *Plecoglossus altivelis* of the Japan and Ryukyu Islands. *Bull Jpn Soc Fish* 51:1269–1274
- Takahashi I, Azuma K, Fujita S, Kinoshita I, Hiraga H (2003) Annual changes in the hatching period of the dominant cohort of larval and juvenile ayu *Plecoglossus altivelis altivelis* in the Shimanto Estuary and adjacent coastal waters during 1986–2001. *Fisheries Sci* 69:438–444
- Iguchi K, Hino T (1996) Effect of competitor abundance on feeding territoriality in a grazing fish, the ayu *Plecoglossus altivelis*. *Ecol Res* 11:165–173
- Moon S-K, Jeong W-G, Jeong B-Y, Maita M (2002) Effect of perilla oil and *Enteromorpha compressa* meal on biological and biochemical properties in cultured sweet smelt. *Fisheries Sci* 68:993–994
- Farkas T, Roy R (1989) Temperature mediated restructuring of phosphatidylethanolamines in livers of freshwater fishes. *Comp Biochem Physiol* 93:217–222
- Buda C, Dey I, Balogh N, Horvath LI, Maderspach K, Juhasz M, Yeo YK, Farkas T (1994) Structural order of membranes and composition of phospholipids in fish brain cells during thermal acclimation. *Proc Natl Acad Sci USA* 91:8234–8238
- Tiku PE, Gracey AY, Macartney AI, Beynon RJ, Cossins AR (1996) Cold-induced expression of Δ^9 -desaturase in carp by transcriptional and posttranslational mechanisms. *Science* 271:815–818
- Hazel JR, Landrey SR (1988) Time-course of thermal adaptation in plasma membranes of trout kidney I.: headgroup composition. *Am J Physiol* 255:622–627
- Gillis TE, Ballantyne JS (1999) Mitochondrial membrane composition of two Arctic marine bivalve molluscs, *Serripes groenlandicus* and *Mya truncat*. *Lipids* 34:53–58
- Gillis TE, Ballantyne JS (1999) Influences of subzero thermal acclimation on mitochondrial membrane composition of temperate zone marine bivalve molluscs. *Lipids* 34:59–66
- Iguchi K, Nishida M (2000) Genetic biogeography among insular populations of the amphidromous fish *Plecoglossus altivelis* assessed from mitochondrial DNA analysis. *Conserv Genet* 1:147–156
- Otake T, Yamada C, Uchida K (2002) Contribution of stocked ayu (*Plecoglossus altivelis altivelis*) to reproduction in the Nagara River, Japan. *Fisheries Sci* 68:948–950
- Kawakami T, Tachihara K (2005) Diet shift of larval and juvenile landlocked Rhukyu-ayu *Plecoglossus altivelis ryukyensis* in the Fukuji Reservoir, Okinawa Island, Japan. *Fisheries Sci* 71:1003–1009
- Iguchi K, Watanabe K, Nishida M (1999) Reduced mitochondrial DNA variation in hatchery populations of ayu (*Plecoglossus altivelis*) cultured for multiple generations. *Aquaculture* 178:235–243
- Seki S, Agresti JJ, Gall GAE, Taniguchi N, May B (1999) AFLP analysis of genetic diversity in three populations of Ayu *Plecoglossus altivelis*. *Fisheries Sci* 65:888–892
- Azuma K, Takahashi I, Fujita S, Kinoshita I (2003) Recruitment and movement of larval ayu occurring in the surf zone of a sandy beach facing Tosa Bay. *Fisheries Sci* 69:355–360
- Yamaguchi T, Miyamoto K, Yagi S, Horigane A, Sato M, Takeuchi M (2001) Identification of tetradecanal, tetradecenal and hexadecenal from plasmalogen in ayu *Plecoglossus altivelis* plasma lipoprotein. *Fisheries Sci* 67:200–202
- Ohshima T, Widjaja HD, Wada S, Koizumi C (1982) A comparison between cultured and wild Ayu lipids. *Bull Jpn Soc Fish* 48:1795–1801
- Yao S-J, Umino T, Nakagawa H (1994) Effect of feeding frequency on lipid accumulation in ayu. *Fisheries Sci* 60:667–671
- Jeong B-Y, Moon S-K, Jeong W-G, Ohshima T (2000) Lipid classes and fatty acid compositions of wild and cultured sweet smelt *Plecoglossus altivelis* muscles and eggs in Korea. *Fisheries Sci* 66:716–724
- Taniguchi N, Seki S, Fukai J, Kijima A (1988) Induction of two types of gynogenetic diploids by hydrostatic pressure shock and verification by genetic marker in Ayu. *Nippon Suisan Gakkaishi* 54:1483–1491
- Folch J, Lees M, Stanley GH (1957) A simple method for the isolation and purification of total lipids from animal tissues. *J Biol Chem* 226:497–509
- Saito H (2011) Characteristics of fatty acid composition of the deep-sea vent crab, *Shinkaia crosnieri* Baba and Williams. *Lipids* 46:723–740
- Yu QT, Liu BN, Zhang JY, Huang ZH (1989) Location of double bonds in fatty acids of fish oil and rat testis lipids: gas chromatography-mass spectrometry of the oxazolone derivatives. *Lipids* 24:79–83
- Christie WW (2010) Dimethylloxazoline (DMOX) derivatives of fatty acids in Mass Spectra. The lipid library, <http://www.lipidlibrary.co.uk/>

38. Osako K, Saito H, Kuwahara K, Okamoto A (2006) Year-round high arachidonic acid levels in *Siganus fuscescens* tissues. *Lipids* 41:473–489
39. Saito H, Hashimoto J (2010) Characteristics of the fatty acid composition of a deep-sea vent gastropod, *Ifremeria nautilei*. *Lipids* 45:537–548
40. Owen JM, Adron JW, Middleton C, Cowey CB (1975) Elongation and desaturation of dietary fatty acids in turbot *Scophthalmus maximus* L., and rainbow trout *Salmo gairdnerii* Rich. *Lipids* 10:528–531
41. Yamada K, Kobayashi K, Yone Y (1980) Conversion of linolenic acid to ω 3-highly unsaturated fatty acids in marine fishes and rainbow trout. *Bull Jpn Soc Sci Fish* 46:1231–1233
42. Zhukova NV (1991) The pathway of the biosynthesis of non-methylene-interrupted dienoic fatty acids in molluscs. *Comp Biochem Physiol* 100B:801–804
43. Seiliez I, Panserat S, Corraze G, Kaushik S, Bergot P (2003) Cloning and nutritional regulation of a Δ^6 -desaturase-like enzyme in the marine teleost gilthead seabream (*Sparus aurata*). *Comp Biochem Physiol* 135B:449–460
44. Francis DS, Peters DJ, Turchini GM (2009) Apparent in vivo Δ^6 -desaturase activity, efficiency, and affinity are affected by total dietary C₁₈ PUFA in the freshwater fish Murray cod. *J Agric Food Chem* 57:4381–4390
45. Sprecher H (2000) Metabolism of highly unsaturated n-3 and n-6 fatty acids. *Biochim Biophys Acta* 1486:219–231
46. Leonard AE, Pereira SL, Sprecher H, Huang Y-S (2004) Elongation of long-chain fatty acids. *Prog Lipid Res* 43:36–54
47. Singer SJ, Nicolson GL (1972) The fluid mosaic model of the structure of cell membranes. *Science* 175:720–731

Separation of Lipid Classes by HPLC on a Cyanopropyl Column

Petter Olsson · Jan Holmbäck · Bengt Herslöf

Received: 1 September 2011 / Accepted: 20 October 2011 / Published online: 20 November 2011
© AOCS 2011

Abstract A new method for the separation and identification of lipid classes by normal-phase HPLC on a cyanopropyl column is described. The use of a simple binary gradient, with toluene as a component, provided a rapid separation of non-polar as well as phospholipid classes. The inherent small differences in performances between possible non-polar eluent components of the gradient, such as hexane, heptane, and iso-octane, had a pronounced impact on retention times for individual phospholipid classes. Separation of molecular species within a lipid class could also be observed.

Keywords Cyanopropyl column · Normal-phase HPLC · Lipid classes · Phospholipids · Toluene · Hexane · Heptane · Iso-octane

Abbreviations

ELSD	Evaporative light scattering detector
PVA	Polyvinyl alcohol
TAG	Triacylglycerols
DAG	Diacylglycerols
MAG	Monoacylglycerols
PC	Phosphatidylcholine
PE	Phosphatidylethanolamine
PG	Phosphatidylglycerol
PI	Phosphatidylinositol
PS	Phosphatidylserine
SM	Sphingomyelin

Introduction

For more than three decades HPLC has been the method of choice for the separation and quantification of lipid classes. During this period of time, several technical advancements have been introduced, such as new detection systems (evaporative light scattering detectors) [1] and various types of interfaces to the mass spectrometer [2, pp. 279–303]. However, none of the numerous methods that have been reported has become widely adopted or found to be generally useful for the many applications and lipid sources that need to be analyzed. In contrast to the analysis of fatty acid methyl esters by gas chromatography, which is more or less a standard procedure, it seems that most laboratories have to work out their own procedures for the analysis of lipid class composition. There are several reasons for this, the most important being that lipid classes are, with respect to their respective structures, a very heterogeneous group of compounds which require a broad composition of the eluent system ranging from very unpolar to strong polar conditions. Another important factor is related to the many different applications that require lipid class analysis, where the specific case can vary very much in terms of number and proportions of the classes involved. It is very unusual that all types of lipid classes are represented in one sample, which means that methods are often optimized for a certain source or type of application which might be less useful in the analysis of other types of lipid samples.

Since the advent of HPLC, silica has been the most favored stationary phase for the separation of lipid classes [3]. The introduction of the evaporative light scattering detectors (ELSD) in the 1980s made gradient elution of lipids possible and the first lipid class separation was performed on a silica column in 1985 [4]. The wide differences in polarities between the classes often led to that the

P. Olsson · J. Holmbäck · B. Herslöf (✉)
Department of Analytical Chemistry, Stockholm University,
Svante Arrhenius väg 16, 10691 Stockholm, Sweden
e-mail: bengt.herslof@anchem.su.se

silica columns slowly changed performances due to their actual water content, which resulted in poor reproducibilities and variabilities between column manufacturers and laboratories. The use of bonded phases was a possible way to avoid such problems. Lipid class separations had earlier been performed with UV-detection on amino [5, 6], cyanopropyl [7, 8], and diol [9] columns. The ELSD gave the possibility to use complex gradient systems which greatly increased the separation opportunities. This area has been extensively described and reviewed by Christie [2, pp. 73–76, 103–116].

Christie et al. [10] published excellent separations of plant lipids on cyanopropyl and polymerized vinyl alcohol (PVA) columns in 1995. Some difficulties were observed with phosphatidylserine on the cyanopropyl column in the rather complex elution system, which was a combination of a solvent gradient and a flow rate gradient. The PVA column performed slightly better, and the separation is described in detail by Christie [2, pp. 113–115] also in 2010. In the last few years, PVA columns [11, 12], diol columns [13, 14], and amino columns [15, 16] have been used by other groups in the separation of polar lipid classes. Cyanopropyl columns have been employed in the separation of non-polar lipid classes, mainly in applications related to transesterification reaction products [17–19].

After Christie's work on plant lipids [10] there have not been any reports in the literature related to the separation of phospholipids or polar lipid classes on the cyanopropyl column. This work was undertaken because we the authors believe that there is an undisclosed potential for lipid separations on the cyanopropyl phase. The aim of this initial study was to reinvestigate the use of cyanopropyl columns for the simultaneous separation of non-polar as well as polar lipid classes, primarily phospholipids. Alkanes such as hexane, heptane, or iso-octane were used as the non-polar eluent component and a toluene/methanol mixture was used as the polar eluent component. It was found that the choice of alkane had a pronounced impact on the retention pattern of phospholipid classes, and that separation of molecular species within a class could also be observed.

Experimental

Materials

All solvents were HPLC grades (Rathburn Chemicals Ltd, Walkerburn, Scotland. Lipid class standards 1,3-dioleoylglycerol 99% (DAG), 1-monooleoylglycerol 99% (MAG), phosphatidylserine from bovine spinal cord >98% (PS), phosphatidylinositol from soybean >98% (PI), and sphingomyelin from chicken egg yolk >98% (SM) were purchased

from Larodan Fine Chemicals AB (Malmö, Sweden). 1,2-dioleoyl-*sn*-glycero-3-phosphatidylcholine >98% (dioleoyl-PC) and 1,2-dimyristoyl-*sn*-glycero-3-phosphatidylcholine >99% (dimyristoyl-PC), 1,2-dipalmitoyl-*sn*-glycero-3-phosphatidylglycerol >98.5% (dipalmitoyl-PG) and 1,2-dioleoyl-*sn*-glycero-3-phosphatidylethanolamine >98% (dioleoyl-PE), was obtained from Lipoid GmbH (Ludwigshafen, Germany). Samples of palm oil triglycerides (TAG), sunflower lecithin, and egg-PC were kindly donated by Lipid Systems Sweden AB (Norberg, Sweden). A mixture of the lipids in chloroform/methanol 1:2 was prepared containing TAG 0.142 mg/ml, DAG 0.142 mg/ml, MAG 0.163 mg/ml, PE 0.142 mg/ml, PG 0.060 mg/ml, PC 0.142 mg/ml, PS 0.177 mg/ml, SM 0.071 mg/ml and PI 0.177 mg/ml (Standard mixture).

HPLC

Chromatography was performed on a Reprosil-Pur 120 CN column 250 × 4.6 mm i.d. with 5 μm particles with a 10 × 4.6 mm guard column of the same material (Dr. Maisch GmbH, Ammerbuch, Germany). The gradient system shown in Table 1 was used at a flow rate of 1.0 ml/min and a column temperature of 22 °C. A YL9110 pump was used connected to a YL9181 evaporative light scattering detector (Young Lin Instruments Co. Ltd, Korea) with the spray chamber at 40 °C, the drift tube at 80 °C, and the exhaust tube at 70 °C. The gas pressure was 49.7 psi (nitrogen). The samples were dissolved in chloroform/methanol 1:2 and the injection volume was 5 μl.

Results and Discussion

Several solvents were investigated to constitute the strong eluent, i.e. solvent B in the binary gradient system. In order to avoid chloroform (safety regulations) a number of solvents were tested, including 2-propanol, tetrahydrofuran, acetone, methanol, acetonitrile, ethyl acetate, methyl *tert*-butyl ether, dichloromethane, and toluene. Although rarely

Table 1 Binary gradient elution scheme used for lipid class separation on the Reprosil-Pur 120 CN column

Time (min)	Solvent A (%)	Solvent B (%)
0	90	10
3	90	10
20	60	40
21–24	50	50

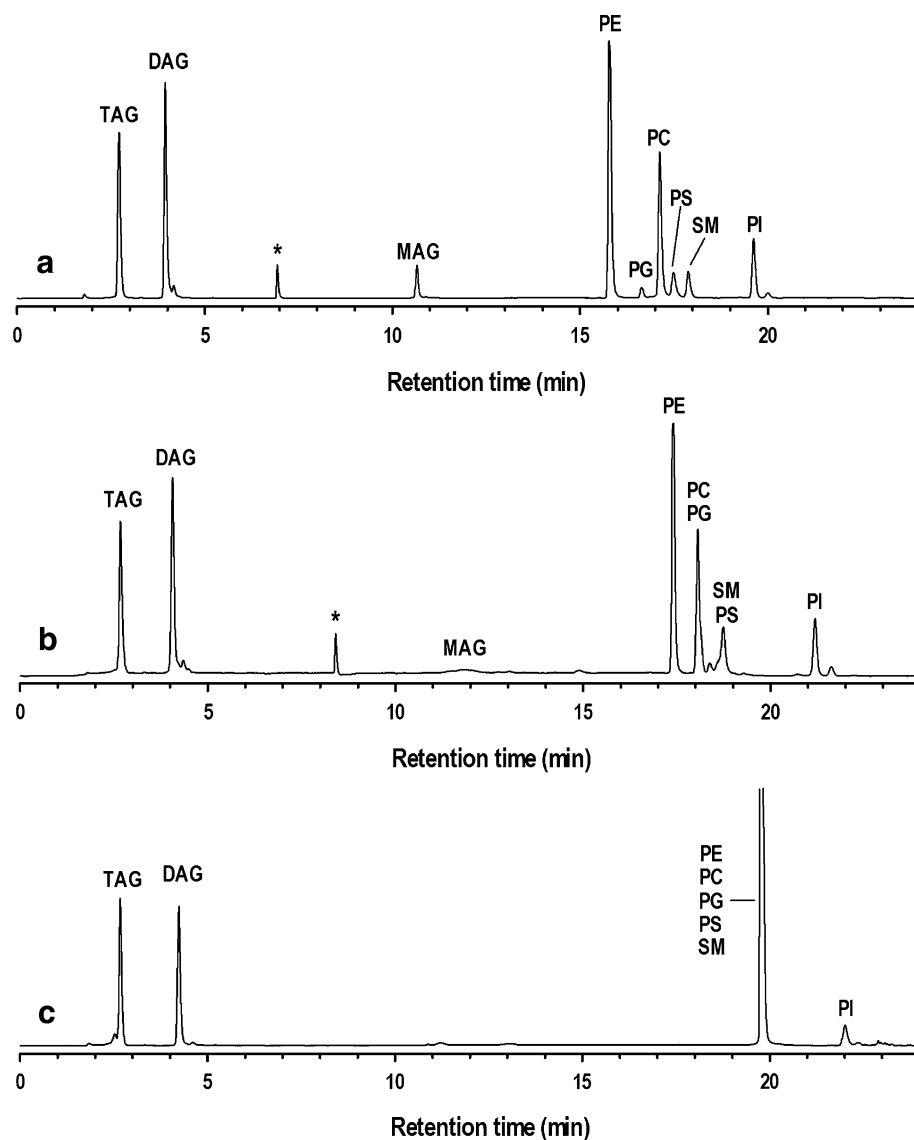
Solvent A was a hydrocarbon (specified in each case) and solvent B was a mixture of toluene/methanol with the addition of acetic acid and triethylamine (60:40:0.2:0.1 by wt). A linear gradient was applied at a flow rate of 1.0 ml/min

used in the chromatography of lipids, toluene proved to be an effective component due to its compatibility with non-polar hydrocarbon components as well as polar solvents, such as methanol. By applying a fractional factorial design, the effect of different parameters was studied. For example, an increase in the toluene concentration affects

Table 2 Retention times (min) for standard lipid classes run according to the gradient scheme in Table 1 with identical solvent B (toluene-methanol-acetic acid-triethylamine 60:40:0.2:0.1 w/w/w/w)

Lipid class solvent A	TAG	DAG	MAG	PE	PG	PC	PS	SPH	PI
n-Hexane	2.86	4.28	10.80	15.81	16.70	17.16	17.57	17.88	19.77
Pentane	2.90	4.10	8.87	13.19	13.85	15.30	14.88	15.75	16.72
iso-Hexane	2.73	3.96	10.47	16.54	17.27	<---18.18--->		18.77	20.12
Cyclohexane	2.56	4.03	12.63	<---18.48--->		<-----19.02----->			19.96
iso-Octane	2.67	4.06	12.30	17.41	<---18.06--->		<---18.74--->		21.18
Heptane	2.66	4.12	10.60		<-----19.21----->				21.82

Fig. 1 Separation of standard lipid classes with *n*-hexane (a), iso-octane (b), and heptane (c) as solvent A respectively. An asterisk denotes an unidentified compound



phosphatidylglycerol to a higher extent than phosphatidylcholine and accordingly the elution order can be reversed for these two components. The gradient profile was also studied in order to find a good compromise between peak shape, resolution and analysis time. A mixture of toluene and methanol 60:40 modified with small amounts of acetic acid and triethylamine turned out to be an excellent solvent B capable of separating and eluting all the investigated lipid classes with acceptable peak shapes in a linear gradient in less than 20 min.

A range of hydrocarbon solvents was investigated for the weak eluent, i.e. solvent A. Pentane, *n*-hexane, iso-hexane, cyclohexane, heptane, and iso-octane were evaluated. Surprisingly it was found that the elution pattern of the polar lipid classes could vary quite dramatically due to the hydrocarbon composition of solvent A which is shown in Table 2.

n-Hexane as solvent A gave the best overall resolution of the standard compounds (Fig. 1). All phospholipid classes were clearly separated including PG, PS and PI. Pentane gave also a reasonably good resolution, with shorter retention times and PS appeared before PC in contrast to the order in *n*-hexane. Iso-hexane gave a somewhat poorer resolution with PC and PS co-eluting.

Cyclohexane gave a poor resolution with the co-elution of PE/PG and PC/PS/SM respectively. Iso-Octane co-eluted PG/PC and PS/SM. However the most pronounced differences was observed with heptane, in which solvent all phospholipid classes except PI eluted in one peak. These observations indicate the subtle and delicate interactions between the analyte and the mobile and stationary phases.

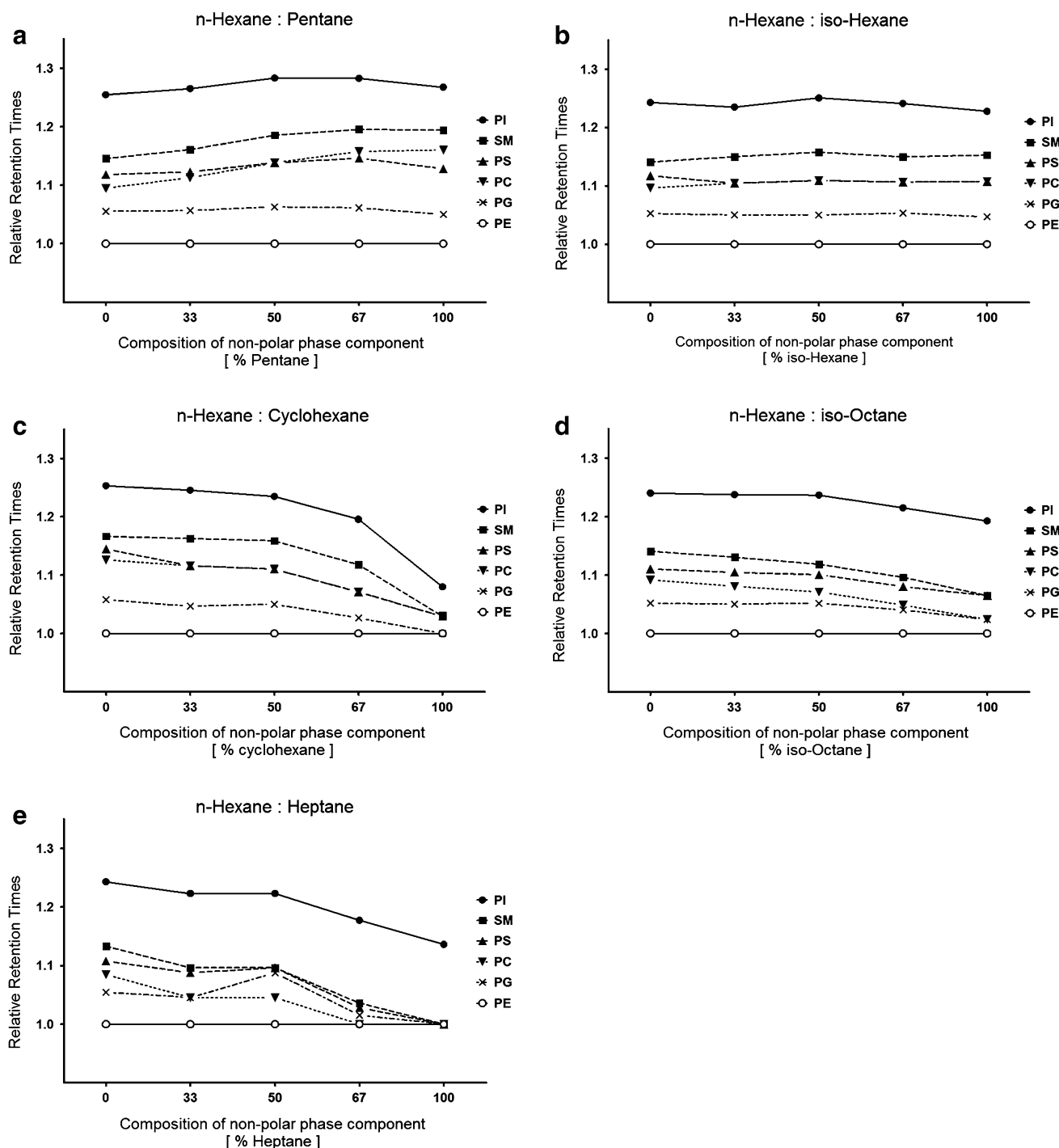


Fig. 2 Changes in relative retention times (PE = 1) of phospholipid classes in *n*-hexane/pentane mixtures (a) *n*-hexane/iso-hexane mixtures (b), *n*-hexane/cyclohexane mixtures (c), *n*-hexane/iso-octane mixtures (d), and in *n*-hexane/heptane mixtures (e) respectively

To verify these observations solvent mixtures from *n*-hexane with increasing proportions of the five other investigated hydrocarbon solvents were prepared and used as solvent A. The observed retention times of the investigated lipid classes in each of the five solvent pairs are shown in Fig. 2.

The separation behavior of the cyanopropyl column used was confirmed by testing two columns from other suppliers: Nucleosil CN column 250 × 4.6 mm i.d. with 5- μ m particles and Hypersil GOLD CN column 150 × 4.6 mm i.d. with 3- μ m particles.

The observed differences in retention behavior were obvious in the analysis of a sunflower lecithin sample. Figure 3 shows two separate runs of sunflower lecithin with *n*-hexane and heptane as solvent A respectively. The observed patterns indicate the presence of a fair amount of PI in the sample.

The sunflower lecithin was further fractionated by a semi-preparative cyanopropyl column (250 × 10 mm version of the analytical cyanopropyl column used; to be published). The collected fractions were investigated by NMR which indicated that two peaks (1 and 2 in Fig. 3) relate to PE and three peaks (3, 4, and 5 in Fig. 3) relate to PC. These indications mean that the separation capabilities of the cyanopropyl phase also could distinguish between certain molecular species within a class. Standard PC-species were analyzed in order to find out if this type of separation is possible. Figure 4 shows the baseline

separation of dioleoyl-PC from dimyristoyl-PC. Further evidence was found in the separation of PC from egg yolk (Fig. 4) which gave four peaks, which tentatively correspond well to the molecular species distribution reported by Holub and Kuksis [20], who report the four most abundant species (>60%) to be 16:0,18:1-PC, 18:0,18:1-PC, 18:0,18:2-PC, and 18:0,20:4-PC.

The separation of molecular species is a complicating factor since late eluting peaks from one class might overlap with early eluting peaks from another class. This phenomenon needs to be taken into account in the interpretation of the lipid class chromatograms in general since it is probably not limited to the elution system used in this work.

Hydrocarbons have previously been used as non-polar components in the analysis of lipids by LC-MS and LC-MS/MS [21], but according to the authors' judgment this field has not been sufficiently investigated, and the use of the cyanopropyl column as described in this article may be a useful tool in further development of such applications.

Conclusions

From the present work it can be concluded that the cyanopropyl phase has the potential to be used in advanced separations of lipid classes. As could be expected, the composition of the mobile phase is crucial and minor changes can have a great impact on the separations.

Fig. 3 Sunflower lecithin with *n*-hexane (a) and with heptane (b) as solvent A respectively. NMR assigned peaks 1 and 2 as PE species and peaks 3–5 as PC species (a)

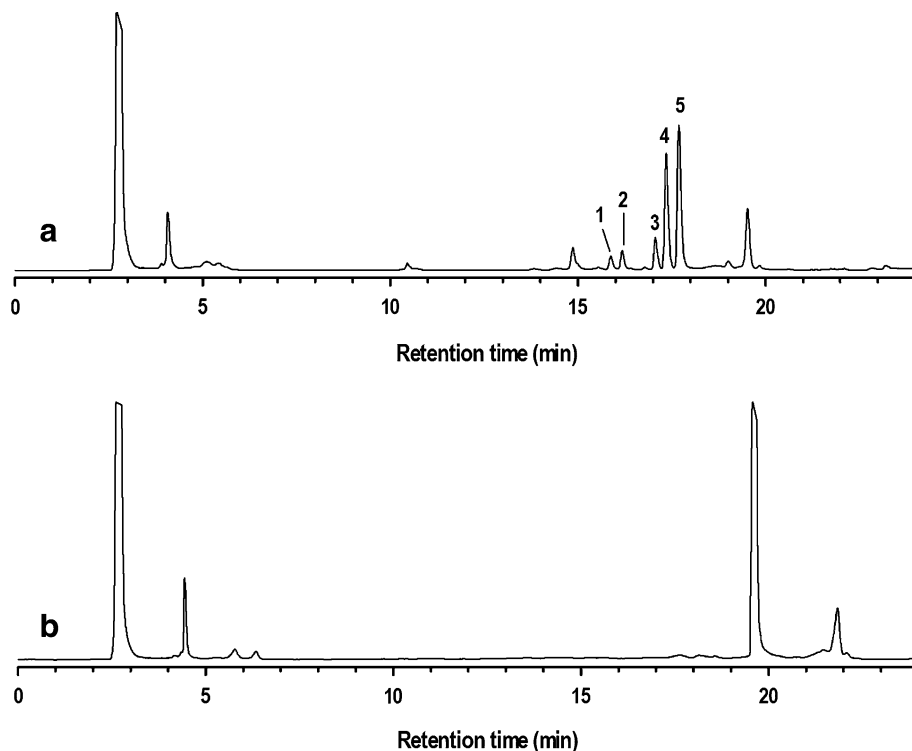
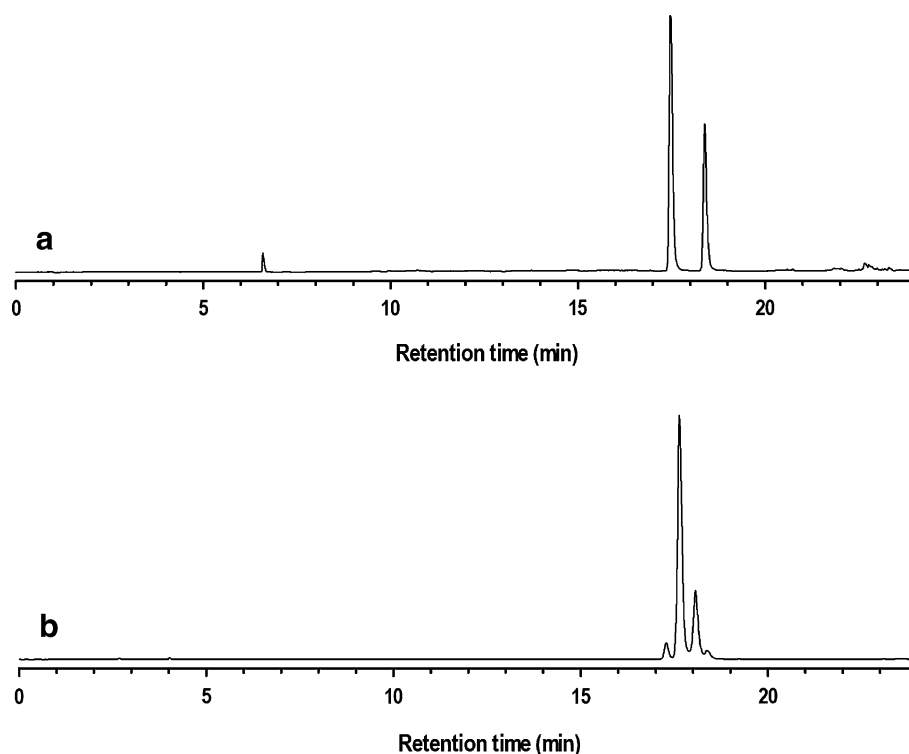


Fig. 4 Separation of molecular species in standard PC samples (dioleoyl-PC/dimyristoyl-PC; **a**) and egg-PC (**b**). Hexane was used as solvent A and toluene/methanol/acetic acid/triethylamine 60:40:0.2:0.1 by wt as solvent B



Toluene as a component seems to be a good alternative to chloroform. However, the importance of the hydrocarbon component which was clearly demonstrated in this work, has to the authors' knowledge not been reported before, and adds to the tools which can be utilized to tailor make a method for the analysis of specific lipid samples, for example in LC–MS or LC–MS/MS applications

Acknowledgments The authors gratefully acknowledge financial support from Lipidor AB, Sweden.

References

- Charlesworth JM (1978) Evaporative analyzer as a mass detector for liquid chromatography. *Anal Chem* 50:1414–1420
- Christie WW, Han X (2010) *Lipid analysis*, 4th edn. The Oily Press, Calgary
- Patton GM, Fasulo JM, Robins SJ (1982) Separation of phospholipids and individual molecular species of phospholipids by high-performance liquid chromatography. *J Lipid Res* 23:190–196
- Christie WW (1985) Rapid separation and quantification of lipid classes by high performance liquid chromatography and mass (light-scattering) detection. *J Lipid Res* 26:507–512
- Chen SSH, Kou AY (1982) High-performance liquid chromatography of methylated phospholipids. *J Chromatogr Biomed Appl* 232:237–249
- Hanson VL, Park JY, Osborn TW, Kiral RM (1981) High-performance liquid chromatographic analysis of egg yolk phospholipids. *J Chromatogr* 205:393–400
- Palmer DN, Anderson MA, Jolly RD (1984) Separation of some neutral lipids by normal-phase high-performance liquid chromatography on a cyanopropyl column: ubiquinone, dolichol, and cholesterol levels in sheep liver. *Anal Biochem* 140:315–319
- Andrews AG (1984) Estimation of amniotic fluid phospholipids by high-performance liquid chromatography. *J Chromatogr B Biomed Sci Appl* 336:139–150
- Briand RL, Harold S, Blass KG (1981) High-performance liquid chromatographic determination of the lecithin/sphingomyelin ratio in amniotic fluid. *J Chromatogr Biomed Appl* 223:277–284
- Christie WW, Urwin RA (1995) Separation of lipid classes from plant tissues by high performance liquid chromatography on chemically bonded stationary phases 18:97–100
- Ramos RG, Libong D, Rakotomanga M, Gaudin K, Loiseau PM, Chaminade P (2008) Comparison between charged aerosol detection and light scattering detection for the analysis of Leishmania membrane phospholipids. *J Chromatogr A* 1209:88–94
- Merle C, Laugel C, Chaminade P, Baillet-Guffroy A (2010) Quantitative study of the stratum corneum lipid classes by normal phase liquid chromatography: comparison between two universal detectors. *J Liq Chromatogr Relat Technol* 33:629–644
- Doehlert DC, Moreau RA, Welti R, Roth MR, McMullen MS (2010) Polar lipids from oat kernels. *Cereal Chem* 87:467–474
- Korzhenevskiy DA, Selischeva AA (2009) Evaluation of phospholipid composition of erythrocytes from healthy volunteers by the method of high-performance liquid chromatography with a light scattering detector. *Bull Exp Biol Med* 147:489–492
- Pelillo M, Ferioli F, Iafelice G, Marconi E, Caboni MF (2010) Characterisation of the phospholipid fraction of hulled and naked tetraploid and hexaploid wheats. *J Cereal Sci* 51:120–126
- Xie J, Liu W-y, Zhou J-p (2010) Determination of lysophosphatidyl choline in soybean phospholipid by HPLC-ELSD assay. *Zhongguo Xinyao Zazhi* 19:243–245
- Foglia TA, Jones KC (1997) Quantitation of neutral lipid mixtures using high performance liquid chromatography with light scattering detection. *J Liq Chromatogr Relat Technol* 20:1829–1838

18. Foglia TA, Jones KC, Nunez A, Phillips JG, Mittelbach M (2004) Comparison of chromatographic methods for the determination of bound glycerol in biodiesel. *Chromatographia* 60:305–311
19. Mangos TJ, Jones KC (1999) Normal-phase high performance liquid chromatographic separation and characterization of short- and long-chain triacylglycerols. *Chromatographia* 49:363–368
20. Holub BJ, Kuksis A (1969) Molecular species of phosphatidylethanolamine from egg yolk. *Lipids* 4:466–472
21. Holmbäck J, Karlsson AA, Arnoldsson KC (2001) Characterization of *N*-acylphosphatidylethanolamine and acylphosphatidylglycerol in oats. *Lipids* 36:153–165

Applications of Stereospecifically-Labeled Fatty Acids in Oxygenase and Desaturase Biochemistry

Alan R. Brash · Claus Schneider · Mats Hamberg

Received: 6 June 2011 / Accepted: 30 August 2011 / Published online: 5 October 2011
© AOCS 2011

Abstract Oxygenation and desaturation reactions are inherently associated with the abstraction of a hydrogen from the fatty acid substrate. Since the first published application in 1965, stereospecific placement of a labeled hydrogen isotope (deuterium or tritium) at the reacting carbons has proven a highly effective strategy for investigating the chemical mechanisms catalyzed by lipoxygenases, hemoprotein fatty acid dioxygenases including cyclooxygenases, cytochromes P450, and also the desaturases and isomerases. This review presents a synopsis of all published studies through 2010 on the synthesis and use of stereospecifically labeled fatty acids (71 references), and highlights some of the mechanistic insights gained by application of stereospecifically labeled fatty acids.

Keywords Lipid biochemistry · Lipoxygenase · Cyclooxygenase · Cytochrome P450 · Desaturase · Eicosanoids · Oxylipins

Introduction

In 1965, Schroepfer and Bloch reported the preparation of four different stearic acids containing a single stereospecific D or L tritium label on either the 9- or 10-carbon and

their use in analyzing the mechanism of desaturation to oleic acid [1]. Other applications in unraveling mechanisms of fatty acid transformation soon followed, and many of the fundamental concepts in fatty acid, eicosanoid or oxylipin biosynthesis rest squarely on the results of this type of experiment. The heart of this review is a chronological list of all the primary literature we could find that used stereospecifically labeled substrates to study mechanisms of fatty acid oxygenation, desaturation, or double bond isomerization (Refs. 1–71, Tables 1, 2). The approach was recognized as a powerful tool back in the 1960s and it continues to be fruitfully applied, with about one third of our list of citations being published from the year 2000 onwards. Although there are numerous additional applications in which stereoselective hydrogen abstraction is measured from other types of substrate, for example in the cytochrome P450 field, this review is limited to fatty acid-related biochemistry. We also do not include purely regiospecific labeling experiments (e.g. using [11,11-²H₂] linoleic acid).

Mechanistic Insights in Oxygenase and Desaturase Reactions: General “Rules”

Insights gained from an understanding of the stereoselectivity of hydrogen abstraction are a spatial understanding of the biochemical transformation, and from isotope effects, the order of events. Among the fundamental mechanisms established using this methodology is the almost universal “rule” in cyclooxygenase and lipoxygenase catalysis that reaction is initiated by a stereospecific hydrogen removal from the CH₂ between two *cis* double bonds, and that molecular oxygen is covalently coupled on the opposite face of the reacting fatty acid—the so-called antarafacial

A. R. Brash (✉) · C. Schneider
Department of Pharmacology and the Vanderbilt Institute
of Chemical Biology, Vanderbilt University School of Medicine,
Nashville, TN 37232, USA
e-mail: alan.brash@vanderbilt.edu

M. Hamberg
Division of Chemistry II, Department of Medical Biochemistry
and Biophysics, Karolinska Institutet, 17177 Stockholm, Sweden

Table 1 Use of stereospecifically-labeled fatty acids in mechanistic studies on oxygenases

Author(s)	Year	Fatty acid	Label	Reaction (Enzyme)	Reference	Reaction, or synthetic product
Hamberg & Samuelsson	1967	20:3 ω 3	13- 3 H	Soybean L-1 (15-LOX)	[2]	
Hamberg & Samuelsson	1967	20:3 ω 3	13- 3 H	COX-1 (RSVM)	[3]	
Hamberg & Samuelsson	1967	20:3 ω 3	13- 3 H	COX-1 (RSVM)	[4]	
Morris & Hitchcock	1968	16:0	2- 3 H	α -hydroxylation, pea leaves	[5]	
Jones	1968	18:0	17- 3 H	ω -1 hydroxylation, yeast	[6]	
Heinz et al.	1969	18:0	17- 3 H	ω -1 hydroxylation, yeast	[7]	
Hamberg & Björkhem	1971	10:0	9- 2 H	ω -1 hydroxylation, rat liver	[8]	
Egmond et al.	1972	18:2 ω 6	11- 3 H	Soybean 13-LOX, corn 9-LOX	[9]	
Egmond et al.	1973	18:2 ω 6	11- 3 H	Synthesis of label	[10]	
Hamberg & Samuelsson	1980	18:2 ω 6	11- 3 H	COX-1 (RSVM)	[11]	
Hamberg & Hamberg	1980	20:4 ω 6	10- 3 H	Platelet 12-LOX	[12]	
Panossian et al.	1982	20:4 ω 6	10- 3 H	PMN 5-LOX	[13]	
Maas et al.	1982	20:4 ω 6	10- 3 H	PMN 5-LOX, platelet 12-LOX	[14]	
Hammarstrom	1983	20:5 ω 3	10- 3 H	Mastocytoma cells, 5-LOX	[15]	
Maas & Brash	1983	20:4 ω 6, 15-HPETE	10- 3 H	Platelet, leukocyte 12-LOX	[16]	
Corey & Lansbury	1983	20:4 ω 6	7- 2 H	Rat 5-LOX, potato 5-LOX	[17]	
Maas et al.	1985	20:3/20.4 15-HPETE	10- 3 H	Synthesis of label, soybean L-1	[18]	
Brash et al.	1985	20:4 ω 6, 15-HPETE	10- 3 H	Autoxidation of 20.4 ω 6, 15-HPETE	[19]	
Brash et al.	1986	20:4 ω 6	10- 3 H	Platelet 12-LOX	[20]	
Shimizu et al.	1986	5-HPETE	10- 3 H	Murine mast cell 5-LOX	[21]	
Ueda et al.	1986	20:4 ω 6	10- 3 H	Porcine 5-LOX	[22]	
Hawkins & Brash	1987	20:5 ω 6	10- 3 H	Sea urchin 12R-LOX	[23]	
Brash et al.	1989	20:4/15-HPETE	10- 3 H	Porcine leukocyte 12-LOX	[24]	

Table 1 continued

Author(s)	Year	Fatty acid	Label	Reaction (Enzyme)	Reference	Reaction, or synthetic product
Fahlstadius et al.	1990	9-HPODE	8- ² H	Potato divinyl ether synthase	[25]	
Hughes & Brash	1991	20:4ω6	10- ³ H	Coral 8R-LOX, mouse 8S-LOX	[26]	
Hamberg	1992	18:3ω6	8- ² H, 11- ² H	Alga 18.4ω6 & 11-OH-C18.3ω6 syn.	[27]	
Hamberg	1993	18:3ω3, 18.3ω6	8- ² H, 11- ² H	Alga 18.3ω6/ω3 oxygenation	[28]	
Hamberg & Gerwick	1993	10-HPOTrE (ω6)	8- ² H, 11- ² H	Alga fatty acid hydroperoxide isomerase	[29]	
Oliw et al.	1993	18:2ω6	11- ² H	HODE syn., rat liver microsomes	[30]	
Hamberg et al.	1994	18:2ω6	7- ² H, 8- ² H	Linoleate 8-dioxygenase/isomerase	[31]	
Rao et al.	1994	18:2ω6	11- ² H	“LOX” activity of myoglobin	[32]	
Hamberg	1997	18:2ω6	11- ² H	C18.2 oxygenation by myoglobin	[33]	
Boeglin et al.	1998	20:4ω6	10- ³ H	Human epidermis 12R-LOX	[34]	
Hamberg	1998	18:2ω6	11- ² H	COX-2	[35]	
Hamberg et al.	1998	18:2ω6	11- ² H	Manganese LOX	[36]	
Hombeck et al.	1999	9S-HPETE	16- ² H	Diatom dictyopterene A synthesis	[37]	
Rickert & Klinman	1999	18:2ω6	11- ² H	Soybean LOX-1 [+ label synthesis]	[38]	
Schneider & Brash	2000	20:4ω6	13- ³ H	Acetylated COX-2, 15R-HPETE syn.	[39]	
Schneider et al.	2000	20:4ω6	10- ³ H, 13- ³ H	Synthesis of label, LOX, COX	[40]	
Schneider et al.	2001	20:4ω6	10- ³ H	12S-LOX, 12R-LOX	[41]	
Peng et al.	2002	20:4ω6	13- ² H	Synthesis of label	[42]	
Hamberg et al.	2002	18:3	2- ² H	α-Dioxygenase	[43]	
Coffa et al.	2005	18:2ω6	11- ³ H	Soybean LOX-1 mutants	[44]	
Hamberg	2005	9S- & 13S-HPODE	8- ² H, 14- ² H	Plant divinyl ether synthase	[45]	
Garscha et al.	2007	18:2ω6, 8R-HPODE	5- ² H, 8- ² H, 11- ² H	Aspergillus dioxygenases	[46]	

Table 1 continued

Author(s)	Year	Fatty acid	Label	Reaction (Enzyme)	Reference	Reaction, or synthetic product
Andreou et al.	2010	18:2 ω 6	11- 2 H	Cyanobacterial linoleate 11-LOX	[47]	
Jernerén et al.	2010	18:2 ω 6	11- 2 H	<i>Aspergillus terreus</i> dioxygenase	[48]	
Jernerén et al.	2010	18:2 ω 6	5- 2 H, 8- 2 H, 11- 2 H	<i>Aspergillus clavatus</i> dioxygenase	[49]	
Jernerén et al.	2010	18:2 ω 6	7- 2 H, 8- 2 H, 11- 2 H	<i>Magnaporthe oryzae</i> dioxygenase	[50]	
Martinez et al.	2010	18:2 ω 6	7- 2 H, 8- 2 H	<i>P. aeruginosa</i> dioxygenase	[51]	
Hamberg	2010	18:2 ω 6	11- 2 H	Singlet oxygen	[52]	

relationship of hydrogen abstraction and oxygen insertion (Fig. 1a) [2, 3, 9, 72].

The antarafacial relationship in dioxygenase reactions contrasts with the predominantly suprafacial character of cytochrome P450 monooxygenation first observed already in the late 1950s ([73]; for review, see Ref. [74, 75]) (Fig. 1b). In the case of cytochrome P450, the oxygen rebound mechanism is sufficiently fast to secure hydroxylation of the substrate mainly on the face suprafacial to the initial hydrogen abstraction. There is, however, sufficient time-lapse (on the order of picoseconds) to allow some rotation of substrate prior to oxygen rebound, thus giving partial racemization to the process, observed as less than “pure” suprafacial oxygenation (e.g. Refs. [30, 76, 77]).

The fundamentals of desaturase mechanism were also revealed using stereospecifically labeled substrates (included in the following reviews, Refs. [78–81]). Invariably the initial and rate-limiting hydrogen abstraction occurs on the carbon nearest the fatty acid carboxyl (or polar head-group, e.g. in ceramides, the amide linkage to sphingosine), followed by the second hydrogen removal, and depending on the conformation of the carbon chain, forming either a *cis* or *trans* double bond (Fig. 1c).

Applications related to desaturases are summarized in Table 2 and the order of the stereospecific hydrogen abstractions in Fig. 1c, and otherwise desaturase biochemistry is not discussed further in our review. For insightful analysis of the mechanism of desaturases as it relates to stereospecific hydrogen abstractions, we particularly recommend the excellent review by Buist [81], also Shanklin and Cahoon’s review of desaturase biochemistry

[82], and the earlier classic on stereospecific hydrogen abstractions by Morris [78].

Insights from Kinetic Isotope Effects

Experiments with stereospecifically-labeled substrates provide not only an understanding of the reaction stereochemistry but also further insights into the enzymatic mechanism. As outlined by Fersht [83], it is easier to break a C–H bond compared to a C–D bond by a factor of 7 at 25 °C. Because of the greater mass of tritium, C–T bonds are broken even more slowly (by a factor of ~ 16.5 over C–H). These differences translate into kinetic isotope effects (KIE) in enzymatic reactions involving abstraction of a deuterium or tritium label. If abstraction is the rate-limiting step, as commonly occurs, then the heavy atom-labeled molecules will react at a slower rate, giving one measure of the KIE. Furthermore, in competitive reactions involving both labeled and unlabeled substrate molecules, during the course of the reaction there will be a gradual enrichment of the heavy atom-labeled molecules in the pool of unreacted substrate, providing a second parameter for quantitative analysis. Alternatively, if the H-abstraction is stereo-random and occurs after the commitment to reaction, the isotope effect can result in an enrichment of heavy atom label in the product: with the option of losing a hydrogen or deuterium/tritium from the same carbon, the KIE will lead to selective retention of the heavy atom (e.g. Ref. [18]).

Quantitative differences in reaction rate reflect the enzymatic mechanism involved in bond breaking. Purely

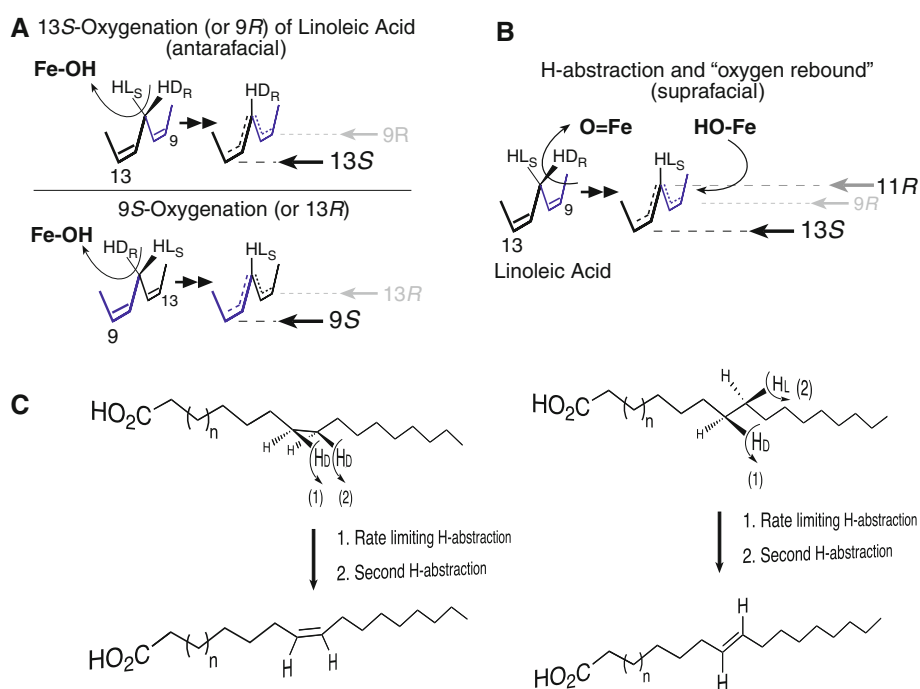
Table 2 Use of stereospecifically-labeled fatty acids in mechanistic studies on desaturases and isomerases

Author(s)	Year	Fatty acid	Label	Reaction (Enzyme)	Reference	Structure
Schroepfer & Bloch	1965	18:0	9- ³ H, 10- ³ H	Desaturation, <i>C. diphtheria</i>	[1]	
Morris et al.	1967	18:0	9- ³ H, 12- ³ H	Desaturation, <i>Chlorella</i>	[53]	
White	1980	16:0	10- ² H	<i>E. coli</i> desaturase	[54]	
Rawlings et al.	1989	18:0	[2- ² H]C9-diCOOH	<i>C. cladosporioides</i> Δ9-desaturase	[55]	
Boland et al.	1993	16:0	11- ² H, 12- ² H	moth Δ11-desaturase	[56]	
Frössl & Boland	1993	16:0	11- ² H, 12- ² H	Synthesis of label	[57]	
Wise et al.	1994	18:3ω6	8- ² H, 11- ² H	Alga, conjugated triene FA syn.	[58]	
Navarro et al.	1997	14:0	<i>Spodoptera littoralis</i> desaturase	[59]		
Svatos et al.	1999	16:0	11- ² H, 12- ² H	Moth acyl-CoA Δ11-desaturase	[60]	
Abad et al.	2000	13:0	9- ² H, 10- ² H	Synthesis of label	[61]	
Abad et al.	2001	13:0	9- ² H, 10- ² H	Moth Δ9-desaturase of 11E–14:1	[62]	
Behrouzian et al.	2002	18:0	9- ² H	Castor stearyl-ACP Δ9-desaturase	[63]	
Beckmann et al.	2002	16:0	6R- ² H, 7R- ² H	Sunflower Δ8-sphingolipid desaturase	[64]	
Hoskovec et al.	2002	16:1-ol	1- ² H	Moth fatty alcohol oxidation	[65]	
Beckmann et al.	2003	16:0	2R- ² H, 3S- ² H	<i>C. albicans</i> Δ4-sphingolipid desaturase	[66]	
Abad et al.	2004	16:0	12- ² H	Synthesis of label; moth desaturase	[67]	
Carlsson et al.	2004	18:1ω9	12- ² H, 13- ² H	Moss and dicot plant desaturase	[68]	
Abad et al.	2007	(11Z)-16:1	13- ² H, 14- ² H	Moth Δ13-desaturase	[69]	
Tremblay et al.	2007	16:0	4- ² H	<i>H. helix</i> , Δ4 dehydrogenation	[70]	
Liavonchanka et al.	2009	18:2ω6	11- ² H	<i>Propionibact. acnes</i> FA isomerase	[71]	

based on bond energies, one might expect a relative rate for k_H/k_D of ~ 7 , yet distinctly different numbers are observed with specific enzymes. The exceedingly high deuterium KIE of ~ 80 associated with hydrogen abstraction in LOX catalysis is used to infer a lower energy transition pathway available only for the H-labeled species, a phenomenon known as hydrogen tunneling [38]. By contrast, a recent

estimate for the deuterium KIE in COX catalysis is only 1.6–2.3 [84], clear evidence for the different mechanisms employed by LOX and COX for hydrogen removal. Those mechanisms center around a proton-coupled electron transfer to non-heme iron in LOX enzymes [85, 86], compared to abstraction of a hydrogen atom by a tyrosyl radical in COX [87, 88]. Further distinctions are observed

Fig. 1 Stereospecific hydrogen abstractions in fatty acid biochemistry. **a** The antarafacial relationship of the initial hydrogen abstraction and oxygen insertion, a characteristic feature of cyclooxygenase and lipoxygenase catalysis, here illustrated on linoleic acid in either of two head-to-tail orientations in the active site. **b** Suprafacial hydrogen abstraction and oxygenation as typified in cytochrome P450 catalysis, and illustrated here on linoleic acid in one of the two possible head-to-tail orientations. **c** Stereospecific hydrogen abstractions associated with desaturation to produce a *cis* double bond (*left side*), or *trans* (*right side*)



in association with hydrogen abstraction by cytochromes P450, which exhibit deuterium KIE values more reflective of relative bond energies, ~ 9 in aliphatic hydroxylations [89]; these P450 data are interpreted as consistent with the abstraction–recombination mechanism for aliphatic hydroxylation [90].

C18:3 ω 6, yet pro-*R* in C18:3 ω 3. For the same reason, the pro-*R* and pro-*S* hydrogens at C-10 in arachidonate (designated using both systems as D_R and L_S, respectively), remain as D or L in 15-hydroperoxy-eicosatetraenoic acid (15-HPETE), but the pro-*R*, pro-*S* designations reverse. To get around this potentially confusing issue with the *R/S* system, sometimes there is a cautionary note to the

Stereochemistry of the Hydrogens in Fatty Acids

Many of the older papers assign chirality and prochiral hydrogens using the Fischer (D/L) system, which is less commonly used nowadays, although it does have an advantage in some situations. Because the Fischer system is based solely on the left or right orientation of the hydrogen in space, changing the nearby substituents has no effect on the D/L designation, whereas it might or might not change the *R/S* assignment based on Cahn-Ingold-Prelog. For substituents on fatty acids, making the D or L assignment is easy. Imagine the molecule hanging down with the carboxyl group on top. The chiral or prochiral carbon is then pointed towards the viewer (as in Fig. 2) and from there the hydrogen, hydroxyl, or other substituent on the chain is either on the right side (D), or the left (L).

A couple of specific examples illustrate the useful features of the Fischer nomenclature. The prochiral 11L-hydrogen in linoleic acid is also 11L in γ -linolenate or α -linolenic acid because it occupies the same position in space (on the left, when observed as in Fig. 2). However, adding the 15,16 double bond in α -linolenate changes the priority order at C-11 such that 11L is pro-*S* in C18:2 ω 6 or

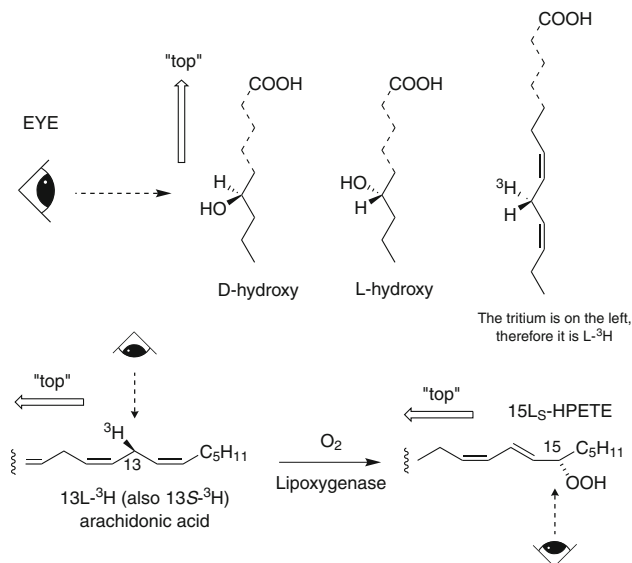


Fig. 2 Prochiral hydrogens in fatty acids, D/L assignment. With the fatty acid carboxyl on top and the carbon bearing the substituent aligned towards the viewer, the assignment is D (on the *right*) or L (*left*). The figure is a slight modification of an earlier version, reproduced with permission from Academic Press [137]

effect that chirality assignments throughout a report refer to the assignment in the parent fatty acid.

Synthesis of Stereospecifically Labeled Fatty Acids

Numerous fatty acids stereospecifically labeled with deuterium or tritium have been prepared by total organic synthesis, starting either with chiral natural products or by sequences involving chemical or enzymatic resolution of intermediates [17, 37, 42, 62, 64–67, 69, 70]. For example, a potentially general approach involving resolution of terminal epoxides was reported for synthesis of both enantiomers of palmitic acid stereospecifically deuterated at C-4 or C-5 [70]; the method offers flexibility and generality for synthesis of various saturated deuterated acyl chains simply by selection of the desired chain lengths of the building blocks. An interesting extension of such syntheses is to generate an isotopically labeled non-chiral compound into which chiral center(s) are introduced by an enzymatic method. Thus, [2*R*,3*R*-²H₂]heptanoic acid was generated by exposing [2,3-²H₂]2*E*-heptenoic acid to the enoate reductase of *Clostridium tyrobutyricum* [56, 60]. Alternatively, the unlabeled 2*E*-heptenoic acid was incubated with the reductase in ²H₂O to afford [2*S*,3*S*-²H₂]heptanoic acid. In another study, soybean lipoxygenase-1 was used to prepare [11*S*-²H]linoleic acid from synthetically prepared [11*RS*-²H₁]linoleic acid (i.e. singly deuterated linoleate, racemic at C-11), a process which is based upon the strong kinetic deuterium isotope effect accompanying the lipoxygenase-catalyzed conversion. As a consequence of this isotope effect, molecules containing a C-11 pro-*S* deuterium are almost unreactive and accumulate as [11*S*-²H₁]linoleic acid, while the molecules unlabeled in the pro-*S* position (which are deuterated at pro-*R*) are removed by enzymatic transformation to hydroperoxide [38, 52].

A common strategy for stereospecific introduction of isotope into acyl chains, used already in the first study in this area [1], is based on the availability of enantiomerically pure long-chain hydroxy derivatives, most often hydroxystearates, as starting materials. These are converted into the corresponding *p*-toluenesulfonate derivatives which are treated with lithium aluminum deuteride/tritide for introduction of isotope. It has been clearly shown that substitution of the *p*-toluenesulfonyloxy group by deuteride takes place as an S_N2 reaction resulting in inversion of the absolute configuration of the carbon attacked [91]. The required chiral hydroxy fatty acids can in many cases be isolated in optically pure form from natural sources; examples are ricinoleic acid, β-dimorphelic acid and 2*R*-hydroxylinolenic acid (for review, see Ref. [92]). Furthermore, certain optically active

hydroxy acids such as 9*R*- and 13*S*-hydroxyoctadecanoates can easily be prepared by catalytic hydrogenation of lipoxygenase-generated fatty acid hydroperoxides. Stereospecifically labeled stearates may also be prepared by chemical synthesis [4, 14, 18, 45]. This may involve an optically active short-chain hydroxy acid as starting material, obtained from commercial sources, as a natural product or prepared by resolution of an alkaloid salt of the racemic compound. Additionally, enantiomerically pure 3*R*-hydroxy acids can be obtained from polyhydroxyalkanoates [93] or prepared by enzymatic reduction of the corresponding β-keto acid using baker's yeast [46]. Subsequent elongation to the required chain-length can conveniently be performed using anodic coupling (the so-called Kolbe synthesis; see Ref. [94]). Chiral HPLC separation of racemic *p*-toluenesulfonate derivatives of hydroxystearates labeled with tritium at the chiral carbon followed by elimination of the tosylate by LiAlH₄ reduction offers an additional possibility to generate stereospecifically labeled stearates [40].

In the vast majority of papers given in Table 1, the above-mentioned procedures end up with stereospecifically labeled stearic acids. For studies of dioxygenases, which most often operate on mono- or polyunsaturated fatty acids of 18 or 20 carbon chain lengths, the labeled stearates have to be desaturated. Four organisms have found use for such conversions, i.e. *Tetrahymena pyriformis*, *Saprolegnia parasitica*, *Chlorella vulgaris*, and a readily available mutant of *Saccharomyces cerevisiae*. *Tetrahymena* is a ciliated protozoan which efficiently takes up exogenous stearate converting it mainly to γ-linolenate without noticeable scrambling of the isotope label [4]. Also labeled oleate and linoleate can be prepared using this organism. The proportion of unsaturated fatty acids in *Tetrahymena* is temperature-dependent; lower temperatures (20–25 °C) favor formation of γ-linolenate. *Saprolegnia parasitica* converts added stearate mainly to linoleate, arachidonate, and 5,8,11,14,17-eicosapentaenoate [95]; a reversed-phase HPLC chromatogram of the profile of fatty acids is illustrated in Schneider et al. [40]. The green alga *Chlorella vulgaris* has been used to prepare linoleate from stearate [10]. A practical disadvantage associated with these bio-desaturations is dilution of the specific activity of the labeled material with endogenous unlabeled fatty acid. The extent of dilution can be severe, perhaps in the order of ten- to 100-fold, and particularly confounds the analysis of protium/deuterium ratios by mass spectrometry. A mutant of *S. cerevisiae* constructed by Reed et al. [96] converts labeled stearates to oleates and linoleates with very little isotopic dilution. This methodology, which was used by the original authors to prepare [12-²H]-, [13-²H]- and [18,18,18-²H₃]-linoleic acids, is readily adaptable for production of stereospecifically labeled oleates and linoleates.

A new approach to the generation of stereospecifically-labeled unsaturated fatty acids involves chemical rearrangements of a specific fatty acid hydroperoxide via a chiral epoxyalcohol, with dehydroxylation-desaturation leading to a primary alcohol that is oxidized back to the original (now stereospecifically ^2H -labeled) polyunsaturated fatty acid (Fig. 3). Potentially the method is generally applicable to any polyunsaturated fatty acid, if sufficient chiral fatty acid hydroperoxide is available. A very active lipoxygenase such as soybean LOX-1 can be used to prepare 100+ milligrams of $\omega 6$ hydroperoxides as starting material, and the use of other natural or recombinant enzymes could broaden the scope of this method.

Lipoxygenase Mechanism, Stereospecific Hydrogen Abstraction, in Historical Context

The stereochemical features of lipoxygenase-catalyzed oxygenation as we understand them today were first described by Hamberg and Samuelsson [2, 97]. They established both the stereochemistry of oxygenation of

polyunsaturated fatty acids and the stereospecificity of the associated hydrogen abstraction. Prior to their reports, there was some indication that lipoxygenase reactions differ from autoxidation in producing chiral product(s) with optical rotation [98], but the precise structure(s) were unknown. Hamberg and Samuelsson showed that the soybean lipoxygenase oxygenates C18 and C20 polyunsaturated substrates mainly in the $\omega 6$ position, i.e. producing the 13-hydroperoxide product of linoleic or linolenic acids and the 15-hydroperoxide of the C20 substrates [97]. The *S* stereochemistry of these products was established, both by hydrogenation of 13-hydroxylinoleate and comparison of its optical rotation with known derivatives such as ricinoleic acid, and by oxidative ozonolysis and optical rotation of the resulting α -hydroxy-heptanoate fragment [97]. Using stereospecifically labeled [13D- ^3H]- and [13L- ^3H]20:3 $\omega 6$, the specific removal of the 13L (pro-*S*) hydrogen was demonstrated in forming the 15L₅-hydroperoxide. A strong kinetic isotope effect associated with this transformation proved that H-abstraction is, or coincides with, the rate-limiting step of lipoxygenase catalysis [2].

Further analysis of lipoxygenase stereochemistry over the next twenty years established the existence of other *S*-specific lipoxygenases, which in all cases were found to operate with an antarafacial relationship of hydrogen abstraction and oxygenation. These enzymes included the plant 9*S*-LOX [9, 99], and the mammalian leukocyte 5*S*-LOX [17, 100], platelet 12*S*-LOX [12, 101, 102], and reticulocyte and leukocyte 15*S*-LOX (and its rodent and porcine homologue 12/15-LOX) [24, 103, 104].

In plants, linoleic acid is commonly oxygenated by either 9*S*-LOX or 13*S*-LOX. Both exhibit the antarafacial relationship, but the reactions are initiated on opposite faces of the substrate and their product hydroperoxides are also on opposite sides. Indeed, the results of experiments with stereospecifically-labeled linoleic acids indicated that 9*S*-oxygenation is associated with removal of the 11D hydrogen whereas 13*S* oxygenation is associated with removal of the 11L hydrogen [2, 9]. One explanation is that the oxygenation machinery in the enzyme active site of these two types of lipoxygenase are spatially reversed, although this is highly unlikely in view of their close structural homology [105]. Far more credibly, the linoleate aligns in opposite head-to-tail orientation in 9*S*-LOX and 13*S*-LOX, thus presenting either the 11D or 11L hydrogen for abstraction (Fig. 2a), a concept that was deduced by Egmond, Vliegthart and Boldingh who first made the observation on the opposite hydrogen abstractions [9].

In the early 1980s, the recent discovery of the leukotrienes prompted many studies on their cellular biosynthesis, and the search was on for the leukotriene A (LTA) synthase that catalyzes the committed step into the LT

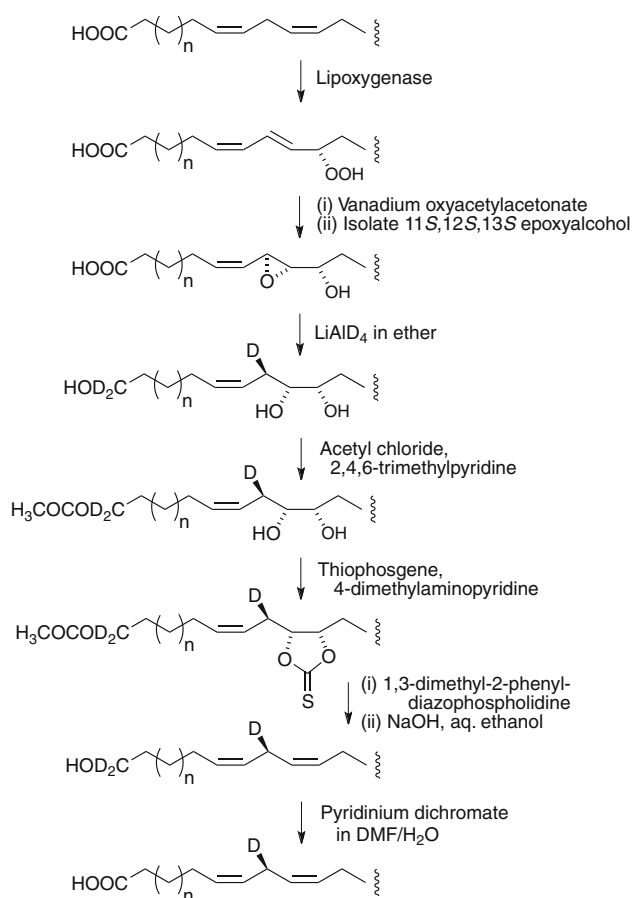
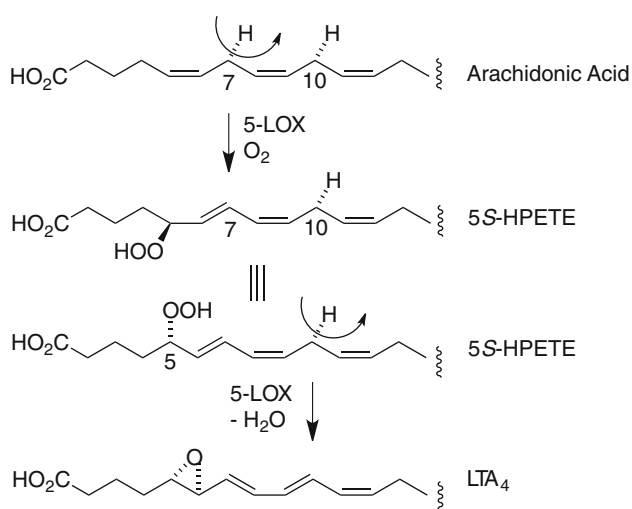


Fig. 3 Synthesis of stereospecifically labeled polyunsaturated fatty acid via a chiral fatty acid hydroperoxide and epoxyalcohol [52]



Scheme 1

pathway. The discovery that the LTA synthase is none other than the lipoxygenase that produces the HPETE substrate was quite unexpected at the time. It was surprising because there was no such precedent from analysis of the soybean lipoxygenase, upon which almost all LOX biochemistry was founded. Initially, one of the main lines of evidence making the connection between LOX and LTA synthase—even before purification of the enzyme—was the demonstration that LTA epoxide synthesis proceeds with an initial stereospecific hydrogen abstraction, the well-established feature of lipoxygenase catalysis [13–17]. Taking leukocyte 5-LOX as the prototypical example, in forming 5S-HPETE the enzyme catalyzes a stereospecific hydrogen abstraction from C-7, then in a simple “frame-shift” along the carbon chain to the next available pentadiene, hydrogen abstraction from C-10 initiates the synthesis of LTA₄ (Scheme 1). As suggested in Scheme 1, to form LTA₄ as the correct *trans* epoxide requires positioning of the hydroperoxide such that it is suprafacial to the C-10 hydrogen abstraction, as the lipoxygenase iron participates in both the H-abstraction and cleavage of the hydroperoxide (cf. Refs. [106–108]). Ultimately several lipoxygenases were purified and shown to catalyze the conversion of HPETE to an LTA-type epoxide [21, 104, 109, 110].

The apparent occurrence of exclusively *S* lipoxygenases in Nature was first contradicted by the report of Gordon Bundy and colleagues of the Upjohn Company that arachidonic acid is converted to its 8*R*-hydroperoxide (8*R*-HPETE) by extracts of the Caribbean coral *Plexaura porosa* [111]. It was soon found that other corals and marine invertebrates also produce 8*R*-HPETE or other *R*-configuration hydroperoxides (e.g. Refs. [23, 112–117]), although at first there was no indication whether this new type of enzyme was structurally related to the

lipoxygenases of plants and higher animals. That 12*R*-HPETE is produced in sea urchin eggs via an antarafacial relationship of H-abstraction and oxygenation was reported by Hawkins and Brash [118], and later the same relationship was shown for 8*R*-HPETE in coral extracts by Hughes and Brash [26]. A decade later, a search for the enzyme responsible for biosynthesis of 12*R*-HETE in human skin led to the cloning and expression of mammalian 12*R*-lipoxygenase; the report demonstrated the now universally observed antarafacial relationship of H-abstraction and oxygenation in lipoxygenase catalysis, in this case the formation of 12*R*-H(P)ETE by recombinant human 12*R*-LOX and in samples of human skin containing the enzyme activity [34].

Purification and molecular cloning of an enzyme producing 8*R*-HPETE from the coral *Plexaura homomalla* proved that the 8*R*-lipoxygenase belongs to the same enzyme superfamily as the *S*-LOX already characterized [119]. More recent X-ray crystallographic analysis of a *P. homomalla* 8*R*-LOX [120] demonstrated that the coral 8*R*-LOX protein has a very similar overall topology to the plant and mammalian *S*-specific LOX [121–123]. Meanwhile, a search for active site residues that might influence *R* or *S* oxygenation specificity in lipoxygenases resulted in the discovery of a critical residue, conserved as Gly in *R*-LOX and Ala in *S*-LOX [124]. This provided evidence that rationalized the difference between *R* and *S* LOX enzymes. Oxygenation can occur at either end of the reacting pentadiene, at one end giving the *S* configuration, at the other *R* (Fig. 1a). Switching the Ala-to-Gly residue or vice versa by site directed mutagenesis induces this transformation between *R* and *S* oxygenation. Following up on this finding, it was shown using stereospecifically 11-³H-labeled linoleic acids and soybean lipoxygenase with mutated active site Ala-to-Gly that, as had been predicted, 9*R* and 13*S* oxygenation of linoleic acid involve the same initial hydrogen abstraction with oxygenation occurring at opposite ends of the same face of the reacting pentadiene (Fig. 1a) [44]. Similarly, the equivalent Ala-to-Gly mutation in 9*S*-LOX induces the formation of 13*R*-product [125].

The effects of this Ala-to-Gly interconversion are now substantiated with several other LOX enzymes [126]. Occasionally there is a twist to the “rule” such as the natural occurrence of the larger Ala in association with *R*-LOX activity, with site-directed mutagenesis to Val or Ile inducing formation of *S*-configuration products [127, 128]. Interestingly, there is a naturally occurring Ala-to-Gly “mutant” lipoxygenase in the olive plant (GenBank accession no. EU678670) encoding Gly568 rather than the expected Ala. In accord with the above concepts, the enzyme produces 13*R*-HPODE in addition to 9*S*-HPODE [129], as predicted from the results of site-directed mutagenesis experiments with recombinant LOX enzymes.

Cyclooxygenase Mechanism, Stereospecific Hydrogen Abstraction, in Historical Context

Fundamental insights into the cyclooxygenase reaction of prostaglandin biosynthesis were reported by Hamberg and Samuelsson in two papers published side-by-side with their soybean lipoxygenase studies [2, 4]. At the time (1967) it was recognized that prostaglandins are formed from a linear C₂₀ polyunsaturated fatty acid via a putative endoperoxide intermediate in which a cyclopentane ring is comprised of carbons 8–12, with the two atoms of a molecule of molecular oxygen bridging C-9 and C-11, and another oxygen molecule reacting at C-15. Using two labeled eicosatrienoic acids (20:3 ω 6) with stereospecific tritium at the 13-carbon, the authors demonstrated that the 13L_S hydrogen is selectively removed in the transformation of 20:3 ω 6 to prostaglandin E₁ [4]. A strong associated kinetic isotope effect, which resulted in the gradual enrichment of the specific activity of the unreacted substrate during the course of the transformation, indicated that 13L_S hydrogen abstraction is, or coincides with, the initial and rate-limiting step of prostaglandin biosynthesis. This alone provided circumstantial evidence that the initial oxygenation of the fatty acid occurs at C-11 and that the resulting 11-peroxyl radical goes on to form the peroxide bridge spanning C-11 to C-9 in the endoperoxide intermediate.

Additional studies on the formation of cyclooxygenase side products also made use of the labeled [13-³H]20:3 ω 6 substrates [2]. The 12-hydroxy-C_{17:2} fatty acid side-product (the 20:3 equivalent of 12-hydroxyheptadecatrienoic acid (HHT) from arachidonic acid) was shown to exhibit a similar stereospecific loss of the 13L_S hydrogen and retention of the 13D_R hydrogen as occurs in biosynthesis of PGE₁. Use of other 20:3 ω 6 substrates with tritium labels at either C-9, C-10, C-11 or C-15, provided the proof that this 12-hydroxy-C_{17:2} side product is formed with loss of three carbons from the cyclopentane ring. Furthermore it was noted that cyclooxygenase substrates that gave rise to the C₁₇-OH by-product also formed significant thiobarbituric acid reactive substances (indicative of an aldehyde), and indeed, the radioactive 3-carbon fragment formed from [11-³H]20:3 ω 6 was isolated and identified as malondialdehyde [2]. This line of evidence provided additional support for the formation of a cyclic endoperoxide as an intermediate in the formation of the stable prostaglandins.

In these early papers it was noted that C₁₈ polyunsaturated fatty acids are also metabolized by the preparation of COX-1 (sheep seminal vesicle microsomes) and the products from linoleic acid were identified as the 9- and 13-hydroxy derivatives [3]. In 1980, Hamberg and Samuelsson reported on the stereochemistry associated with transformation of [11-³H]linoleic acid [11]. The 9-hydroxy

product was mainly of the 9L_R configuration (equivalent to the 11R-HETE by-product from arachidonic acid) and the other was mainly 13L_S-hydroxy. These were each formed with ~80% removal of the 11L (pro-S) hydrogen from the substrate. The stereo fidelity was not so high as found using the 20:3 ω 6 substrate, apparently reflecting less than perfect control of oxygenation of linoleic acid by COX-1. Later studies by Hamberg gave similar results using COX-2 [35]. The subsequent description of COX-1 crystal structures with bound substrate indicated that, similar to 20:3 ω 6 and arachidonic acid, linoleic acid lies in the cyclooxygenase active site with the appropriate bis-allylic hydrogen (the 13L_S of the C₂₀ substrates and 11L_S of linoleic acid) poised for reaction with an incipient radical on Tyr-385 [130, 131]. By contrast to the better COX substrates, oxygenation of linoleic acid (and EPA) were much more severely compromised by active site mutations that modified the positioning of the α or ω ends of the fatty acid carbon chain [131]. Linoleic acid in particular has to assume a more stretched out α chain in order for the carboxyl to make contact and be stabilized by interaction with the Arg-120 and Tyr-355 at the entrance to the oxygenase substrate-binding channel, making the interactions more easily disturbed by mutagenesis within the COX active site.

In the early 1990s an interesting and unexpected arachidonic acid metabolite was detected upon reaction with aspirin-acetylated COX-2. Whereas aspirin inhibition completely blocks all oxygenase activity in COX-1, aspirin treatment of COX-2 blocks prostaglandin biosynthesis, but switches the oxygenation specificity to produce 15R-HETE as the only enzymatic product [132–134]. This 15R specificity is opposite to the usual 15S oxygenation associated with the final steps of prostaglandin endoperoxide biosynthesis. Accordingly, Schneider and Brash questioned the specificity of the hydrogen abstraction associated with this 15R-HETE production. The result that might have been anticipated, based on parallels to R and S oxygenation in lipoxygenase catalysis, is that the substrate would assume a reversed orientation and that the H-abstraction would also be the reverse of normal. Using 13R-³H and 13S-³H arachidonic acids, however, it was found that the specificity matches that in normal prostaglandin production, i.e. specifically the pro-S hydrogen at C-13 is removed in formation of PG endoperoxide with normal COX-2 and in 15R-HETE synthesis in the aspirin-treated enzyme. This formation of 15R-HETE appears, therefore, to be the one known example in which the relationship of stereospecific hydrogen abstraction to oxygenation is suprafacial, rather than antarafacial. The authors rationalized this result by proposing that the main body of the substrate (including the 13-carbon) lies in the usual orientation, but the tail carbons are twisted over to expose the 15R position to attack by O₂ (Fig. 4). In discussion, it was further proposed that the

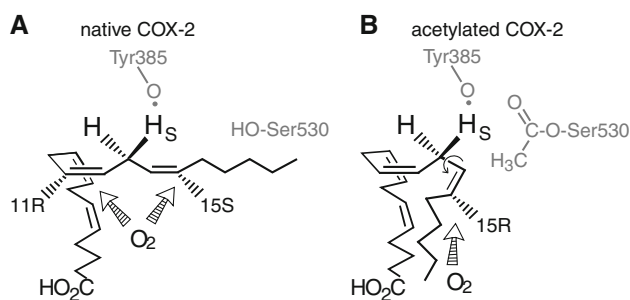


Fig. 4 Synthesis of 15*R*-HETE by aspirin-acetylated COX-2. Unlike all specific oxygenations by COX and LOX enzymes, this reaction exhibits suprafacial relationship of hydrogen abstraction and the 15*R* oxygenation. The figure is reproduced from Ref. [39] with permission

terms suprafacial and antarafacial begin to lose their utility under these circumstances [39].

Fatty Acid Monooxygenation and Stereospecific Hydrogen Abstraction

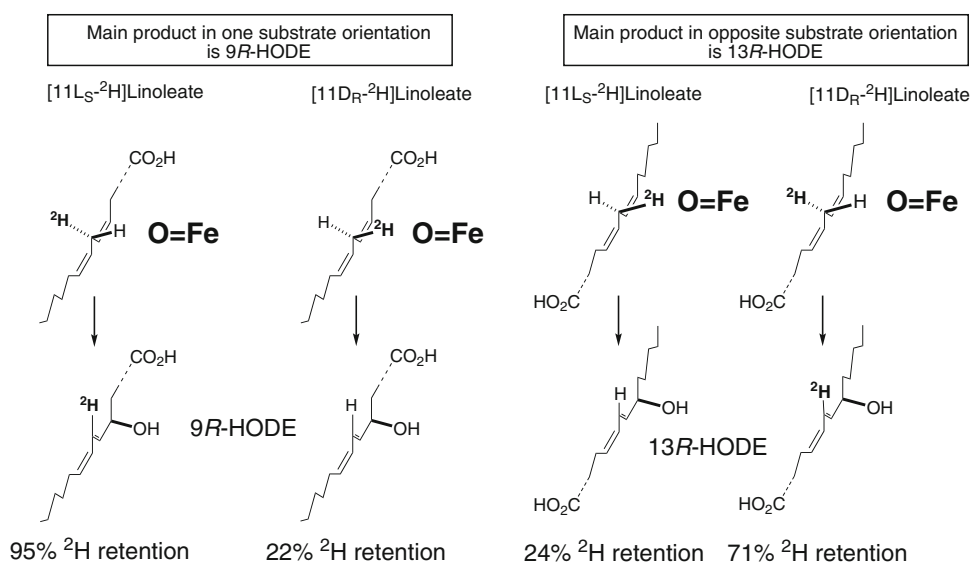
Cytochrome P450 is the prototypical fatty acid monooxygenase (hydroxylase and epoxidogenase). The principles related to hydrogen abstraction in P450 reactions were mainly worked out using other substrates, and the “rules” subsequently shown to apply to fatty acid monooxygenation (reviewed in Refs. [74, 75] and in earlier editions of the book). Typically, the relationship of the hydrogen abstraction and oxygenation (“oxygen rebound”) in P450 catalysis is suprafacial (Figs. 1b, 5). Unlike in LOX and COX reactions the activated oxygen in P450s is covalently bound to the reactive heme iron. Also, it is this very same ferryl species which catalyzes the H-abstraction.

Depending on the substrate, there may be sufficient mobility within the active site so that it can spin around prior to oxygen rebound, in which case the relationship between H-abstraction and oxygenation appears to be antarafacial.

Therefore for the reasons cited, with many substrates there is an element of apparently stereorandom oxygenation following hydrogen abstraction in P450 catalysis. There may be some evidence of this in the results of linoleic acid oxygenation as reported by Oliw and co-workers in rat liver microsomes [30], yet mainly the results hold to the suprafacial relationship of H-abstraction and oxygenation. The major products detected were 9*R*-HODE (formed with 95% retention of deuterium from [11*L*_S-²H]linoleic acid and 22% retention from [11*D*_R-²H]linoleic acid), and 13*R*-HODE (24% retention from [11*L*_S-²H]linoleic acid and 71% retention from the 11*D*_R-²H). What may not have been discussed before is the concept that formation of these two products and their associated hydrogen abstractions can be accounted for by a change in the head-to-tail orientation of the substrate in the P450 active site (Fig. 5). This is akin to the concepts of reversal of substrate binding orientation that is well established in the lipxygenase literature.

Formation of the minor hydroxy products in the same study (9*S*-HODE and 13*S*-HODE) can be rationalized similarly. The 9*S* position on linoleate is on the same face of the substrate as 13*R*, and by-and-large the results of Oliw et al show qualitatively similar deuterium retentions in the 9*S*-HODE and 13*R*-HODE products [30]. Based on these results, it can be inferred that the substrate is mainly in the same head-to-tail orientation in forming 9*S*- and 13*R*-HODE. A similar match applies for the major 9*R*-HODE and the minor 13*S*-HODE, which assume the

Fig. 5 Suprafacial H-abstraction and oxygenation in cytochrome P450 mediated oxidation of linoleic acid in rat liver microsomes [30]. The reported retentions of deuterium in the major products from [11*D*_R-²H]- and [11*L*_S-²H]linoleic acids are rationalized here in terms of two possible head-to-tail orientations of the substrate, thus accounting for formation of 9*R*-HODE and 13*R*-HODE with predominantly suprafacial hydrogen abstraction and oxygenation. A similar analysis can rationalize formation of the two minor products reported, 9*S*-HODE and 13*S*-HODE (not shown)



opposite orientation. It also follows from this line of thinking that each major product is formed by oxygenation at the “top” end of the pentadiene as cartooned in Fig. 5, while the minor products are each formed at the lower end.

Finally, the other significant mono-hydroxylated product in this study is 11-HODE, which showed 38% retention of the $11D_R$ - 2H label and 69% retention of the $11L_S$ - 2H . Because the $11D_R$ deuterium label is largely retained, and assuming a suprafacial relationship of H-abstraction and oxygenation, these data suggest that 11-HODE is mainly formed in the head-to-tail orientation on the right side of Fig. 5.

Future Prospects/Open Issues

The fundamentals of the catalytic mechanisms of lipoxygenases, cyclooxygenases, cytochromes P450, desaturases, and isomerases have long been established, yet new enzymes and reactions continue to arise. Quite recently, stereospecifically labeled fatty acids were applied in exploring the reaction mechanism of novel dioxygenases in fungal pathogens of the *Aspergillus* species and a similar type of enzyme in the bacterium *Pseudomonas aeruginosa* [48–51]; these enzymes have both dioxygenases and peroxidase (P450-related) domains which this mechanistic approach can help unravel. The discovery of a catalase-related hemoprotein from *Anabaena* PCC 7120 that converts 9*R*-hydroperoxylinolenic acid into a leukotriene A-type epoxide together with a highly unusual bicyclobutane fatty acid presents another opportunity to glean insights using this methodology [135]; the proposed intermediates in the transformation are carbocations, and an enzyme-catalyzed hydrogen abstraction is required in the course of the transformation. Equivalent reactions initiated on linoleic acid produce a conjugated diene analog of LTA [136]. Among other issues, comparison with the mechanism of the lipoxygenase-catalyzed route to LTA epoxides should be of interest.

Acknowledgments This study was supported by NIH grants GM-015431, GM-074888 and GM-076592, and by a grant from the Swedish Research Council (project 2009-5078).

References

- Schroepfer GJ Jr, Bloch K (1965) The stereospecific conversion of stearic acid to oleic acid. *J Biol Chem* 240:54–63
- Hamberg M, Samuelsson B (1967) On the specificity of the oxygenation of unsaturated fatty acids catalyzed by soybean lipoxygenase. *J Biol Chem* 242:5329–5335
- Hamberg M, Samuelsson B (1967) Oxygenation of unsaturated fatty acids by the vesicular gland of sheep. *J Biol Chem* 242:5344–5354
- Hamberg M, Samuelsson B (1967) On the mechanism of biosynthesis of prostaglandins E_1 and $F_{1\alpha}$. *J Biol Chem* 242:5336–5343
- Morris LJ, Hitchcock C (1968) The stereochemistry of α -oxidation of fatty acids in plants. The stereochemistry of biosynthesis of long-chain 2-hydroxyacids. *Eur J Biochem* 4:146–148
- Jones DF (1968) Microbiological oxidation of long-chain aliphatic compounds. Part V. Mechanism of hydroxylation. *J Chem Soc C*:2827–2833
- Heinz E, Tulloch AP, Spencer JFT (1969) Stereospecific hydroxylation of long chain compounds by a species of *Torulopsis*. *J Biol Chem* 244:882–888
- Hamberg M, Björkhem I (1971) ω -Oxidation of fatty acids: mechanism of microsomal ω_1 - and ω_2 -hydroxylation. *J Biol Chem* 246:7411–7416
- Egmond MR, Vliegthart JFG, Boldingh J (1972) Stereospecificity of the hydrogen abstraction at carbon atom n-8 in the oxygenation of linoleic acid by lipoxygenases from corn germs and soya beans. *Biochem Biophys Res Commun* 48:1055–1060
- Egmond MR, Vliegthart JFG, Boldingh J (1973) Synthesis of 11(n-8) L_S tritium-labelled linoleic acid. *Biochim Biophys Acta* 316:1–7
- Hamberg M, Samuelsson B (1980) Stereochemistry in the formation of 9-hydroxy-10,12-octadecadienoic acid and 13-hydroxy-9,11-octadecadienoic acid from linoleic acid by fatty acid cyclooxygenase. *Biochim Biophys Acta* 617:545–547
- Hamberg M, Hamberg G (1980) On the mechanism of oxygenation of arachidonic acid by the human platelet lipoxygenase. *Biochem Biophys Res Commun* 95:1090–1097
- Panossian A, Hamberg M, Samuelsson B (1982) On the mechanism of biosynthesis of leukotrienes and related compounds. *FEBS Lett* 150:511–513
- Maas RL, Ingram CD, Taber DF, Oates JA, Brash AR (1982) Stereospecific removal of the D_R hydrogen atom at carbon 10 of arachidonic acid in the biosynthesis of leukotriene A_4 by human leukocytes. *J Biol Chem* 257:13515–13519
- Hammarström S (1983) Stereospecific elimination of hydrogen at C-10 in eicosapentaenoic acid during the conversion to leukotriene C_5 . *J Biol Chem* 258:1427–1430
- Maas RL, Brash AR (1983) Evidence for a lipoxygenase mechanism in the biosynthesis of epoxide and dihydroxy leukotrienes from 15(S)-hydroperoxyicosatetraenoic acid by human platelets and porcine leukocytes. *Proc Natl Acad Sci USA* 80:2884–2888
- Corey EJ, Lansbury PT Jr (1983) Stereochemical course of 5-lipoxygenation of arachidonate by rat basophil leukemic cell (RBL-1) and potato enzymes. *J Am Chem Soc* 105:4093–4094
- Maas RL, Ingram CD, Porter AT, Oates JA, Taber DF, Brash AR (1985) Investigation of the chemical conversion of hydroperoxy-eicosatetraenoate to leukotriene epoxide using stereospecifically labeled arachidonic acid. *J Biol Chem* 260:4217–4228
- Brash AR, Porter AT, Maas RL (1985) Investigation of the selectivity of hydrogen abstraction in the non-enzymatic formation of hydroxyeicosatetraenoic acids and leukotrienes by autoxidation. *J Biol Chem* 260:4210–4216
- Brash AR, Ingram CD, Maas RL (1986) A secondary isotope effect in the lipoxygenase reaction. *Biochim Biophys Acta* 875:256–261
- Shimizu T, Izumi T, Seyama Y, Tadokoro K, Rådmark O, Samuelsson B (1986) Characterization of leukotriene A_4 synthase from murine mast cells: evidence for its identity to arachidonate 5-lipoxygenase. *Proc Natl Acad Sci USA* 83:4175–4179
- Ueda N, Yamamoto S, Oates JA, Brash AR (1986) Stereoselective hydrogen abstraction in leukotriene A_4 synthesis by

- purified 5-lipoxygenase of porcine leukocytes. Prostaglandins 32:43–48
23. Hawkins DJ, Brash AR (1987) Eggs of the sea urchin, *Strongylocentrotus purpuratus*, contain a prominent (11*R*) and (12*R*) lipoxygenase activity. J Biol Chem 262:7629–7634
 24. Brash AR, Yokoyama C, Oates JA, Yamamoto S (1989) Mechanistic studies of the dioxygenase and leukotriene synthase activities of the porcine leukocyte 12*S*-lipoxygenase. Arch Biochem Biophys 273:414–422
 25. Fahlstadius P, Hamberg M (1990) Stereospecific removal of the *pro-R* hydrogen at C-8 of (9*S*)-hydroperoxyoctadecadienoic Acid in the biosynthesis of colneleic acid. J Chem Soc Perkin Trans 1:2027–2030
 26. Hughes MA, Brash AR (1991) Investigation of the mechanism of biosynthesis of 8-hydroxyeicosatetraenoic acid in mouse skin. Biochim Biophys Acta 1081:347–354
 27. Hamberg M (1992) Metabolism of 6, 9, 12-octadecatrienoic acid in the red alga *Lithothamnion corallioides*: mechanism of formation of a conjugated tetraene fatty acid. Biochem Biophys Res Commun 188:1220–1227
 28. Hamberg M (1993) Oxidation of octadecatrienoic acids in the red alga *Lithothamnion corallioides*—structural and stereochemical studies of conjugated tetraene fatty-acids and bis allylic hydroxy-acids. J Chem Soc Perkin Trans 1:3065–3072
 29. Hamberg M, Gerwick WH (1993) Biosynthesis of vicinal dihydroxy fatty acids in the red alga *Gracilariopsis lemaneiformis*: identification of a sodium-dependent 12-lipoxygenase and a hydroperoxide isomerase. Arch Biochem Biophys 305:115–122
 30. Oliw EH, Brodowsky D, Hörnsten L, Hamberg M (1993) bis-Allylic hydroxylation of polyunsaturated fatty acids by hepatic monooxygenases and its relation to the enzymatic and nonenzymatic formation of conjugated hydroxy fatty acids. Arch Biochem Biophys 300:434–439
 31. Hamberg M, Zhang LY, Brodowsky ID, Oliw EH (1994) Sequential oxygenation of linoleic acid in the fungus *Gaeumannomyces graminis*: stereochemistry of dioxygenase and hydroperoxide isomerase reactions. Arch Biochem Biophys 309:77–80
 32. Rao SI, Wilks A, Hamberg M, Ortiz de Montellano PR (1994) The lipoxygenase activity of myoglobin. Oxidation of linoleic acid by the ferryl oxygen rather than protein radical. J Biol Chem 269:7210–7216
 33. Hamberg M (1997) Myoglobin-catalyzed bis-allylic hydroxylation and epoxidation of linoleic acid. Arch Biochem Biophys 344:194–199
 34. Boeglin WE, Kim RB, Brash AR (1998) A 12*R*-lipoxygenase in human skin: mechanistic evidence, molecular cloning and expression. Proc Natl Acad Sci USA 95:6744–6749
 35. Hamberg M (1998) Stereochemistry of oxygenation of linoleic acid catalyzed by prostaglandin-endoperoxide H synthase-2. Arch Biochem Biophys 349:376–380
 36. Hamberg M, Su C, Oliw E (1998) Manganese lipoxygenase. Discovery of a bis-allylic hydroperoxide as product and intermediate in a lipoxygenase reaction. J Biol Chem 273:13080–13088
 37. Hombeck M, Pohnert G, Boland W (1999) Biosynthesis of dictyopterene A: stereoselectivity of a lipoxygenase/hydroperoxide lyase from *Gomphonema parvulum* (Bacillariophyceae). Chem Commun 3:243–244
 38. Rickert KW, Klinman JP (1999) Nature of hydrogen transfer in soybean lipoxygenase 1: separation of primary and secondary isotope effects. Biochemistry 38:12218–12228
 39. Schneider C, Brash AR (2000) Stereospecificity of hydrogen abstraction in the conversion of arachidonic acid to 15*R*-HETE by aspirin-treated cyclooxygenase-2. J Biol Chem 275:4743–4746
 40. Schneider C, Boeglin WE, Lai S, Cha JK, Brash AR (2000) Synthesis and applications of stereospecifically ³H-labeled arachidonic acids as mechanistic probes for lipoxygenase and cyclooxygenase catalysis. Anal Biochem 284:125–135
 41. Schneider C, Keeney DS, Boeglin WE, Brash AR (2001) Detection and cellular localization of 12*R*-lipoxygenase in human tonsils. Arch Biochem Biophys 386:268–274
 42. Peng S, Okeley NM, Tsai AL, Wu G, Kulmacz RJ, van der Donk WA (2002) Synthesis of isotopically labeled arachidonic acids to probe the reaction mechanism of prostaglandin H synthase. J Am Chem Soc 124:10785–10796
 43. Hamberg M, Sanz A, Castresana C (2002) α -Dioxygenase, a new enzyme in fatty acid metabolism. In: Ishimura Y, Nozaki M, Yamamoto S, Shimizu T, Narumiya S, Mitani F (eds) Oxygen and life—oxygenases, oxidases and lipid mediators. Elsevier, Amsterdam, pp 307–317
 44. Coffa G, Imber AN, Maguire BC, Laxmikanthan G, Schneider C, Gaffney BJ, Brash AR (2005) On the relationships of substrate orientation, hydrogen abstraction and product stereochemistry in single and double dioxygenations by soybean lipoxygenase-1 and its Ala542Gly mutant. J Biol Chem 280:38756–38766
 45. Hamberg M (2005) Hidden stereospecificity in the biosynthesis of divinyl ether fatty acids. FEBS J 272:736–743
 46. Garscha U, Jermerén F, Chung D, Keller NP, Hamberg M, Oliw EH (2007) Identification of dioxygenases required for *Aspergillus* development. Studies of products, stereochemistry, and the reaction mechanism. J Biol Chem 282:34707–34718
 47. Andreou A, Goebel C, Hamberg M, Feussner I (2010) A bis-allylic mini-lipoxygenase from cyanobacterium *Cyanothece* sp. that has an iron as cofactor. J Biol Chem 285:14178–14186
 48. Jermerén F, Hoffmann I, Oliw EH (2010) Linoleate 9*R*-dioxygenase and allene oxide synthase activities of *Aspergillus terreus*. Arch Biochem Biophys 495:67–73. (Erratum in: Arch Biochem Biophys. (2010) 500:210)
 49. Jermerén F, Garscha U, Hoffmann I, Hamberg M, Oliw EH (2010) Reaction mechanism of 5,8-linoleate diol synthase, 10*R*-dioxygenase, and 8,11-hydroperoxide isomerase of *Aspergillus clavatus*. Biochim Biophys Acta 1801:503–507
 50. Jermerén F, Sesma A, Francheschetti M, Hamberg M, Oliw EH (2010) Gene deletion of 7,8-linoleate diol synthase of the rice blast fungus. Studies on pathogenicity, stereochemistry, and oxygenation mechanisms. J Biol Chem 285:5308–5316
 51. Martinez E, Hamberg M, Busquets M, Diaz P, Manresa A, Oliw EH (2010) Biochemical characterization of the oxygenation of unsaturated fatty acids by the dioxygenase and hydroperoxide isomerase of *Pseudomonas aeruginosa* 42A2. J Biol Chem 285:9339–9345
 52. Hamberg M (2010) Stereochemistry of hydrogen removal during oxygenation of linoleic acid by singlet oxygen and synthesis of 11(*S*)-deuterium-labeled linoleic acid. Lipids 46:201–206
 53. Morris LJ, Harris RV, Kelly W, James AT (1967) The stereospecificity of desaturations of long-chain fatty acids in *Chlorella vulgaris*. Biochem Biophys Res Commun 28:904–908
 54. White RH (1980) Stoichiometry and stereochemistry of deuterium incorporated into fatty acids by cells of *Escherichia coli* grown on [methyl-²H₃]acetate. Biochemistry 19:9–15
 55. Rawlings BJ, Reese PB, Ramer SE, Vederas JC (1989) Comparison of fatty acid and polyketide biosynthesis—stereochemistry of cladosporin and oleic acid formation in *Cladosporium cladosporioides*. J Am Chem Soc 111:3382–3390
 56. Boland W, Frössl C, Schöttler M, Toth M (1993) Sex-pheromone biosynthesis in *Mamestra brassicae* L. (Lepidoptera,

- Noctuidae)—stereochemistry of the Δ^{11} desaturation. *J Chem Soc Chem Commun*:1155–1157
57. Frössl C, Boland W (1993) Synthesis of deuterium-labelled (11*S*,12*R*)- and (11*R*,12*S*)-[$^2\text{H}_{14}$]-palmitic acids; a facile route to highly labelled fatty acids. *Tetrahedron* 49:6613–6618
 58. Wise ML, Hamberg M, Gerwick WH (1994) Biosynthesis of conjugated triene-containing fatty acids by a novel isomerase from the red marine alga *Prilota filicina*. *Biochemistry* 33:15223–15232
 59. Navarro I, Font I, Fabrias G, Camps F (1997) Stereospecificity of the (*E*)- and (*Z*)-11 myristoyl CoA desaturases in the biosynthesis of *Spodoptera littoralis* sex pheromone. *J Am Chem Soc* 119:11335–11336
 60. Svatos A, Kalinova B, Boland W (1999) Stereochemistry of lepidopteran sex pheromone biosynthesis: a comparison of fatty acid-CoA Δ^{11} -(*Z*)-desaturases in *Bombyx mori* and *Manduca sexta* female moths. *Insect Biochem Mol Biol* 29:225–232
 61. Abad JL, Fabrias G, Camps F (2000) Synthesis of dideuterated and enantiomers of monodeuterated tridecanoic acids at C-9 and C-10 positions. *J Org Chem* 65:8582–8588
 62. Abad JL, Camps F, Fabrias G (2001) Stereospecificity of the (*Z*)-9 desaturase that converts (*E*)-11-tetradecenoic acid into (*Z,E*)-9,11-tetradecadienoic acid in the biosynthesis of *Spodoptera littoralis* sex pheromone. *Insect Biochem Mol Biol* 31:799–803
 63. Behrouzian B, Savile CK, Dawson B, Buist PH, Shanklin J (2002) Exploring the hydroxylation-dehydrogenation connection: novel catalytic activity of castor stearoyl-ACP Δ^9 desaturase. *J Am Chem Soc* 124:3277–3783
 64. Beckmann C, Rattke J, Oldham NJ, Sperling P, Heinz E, Boland W (2002) Characterization of a Δ^8 -sphingolipid desaturase from higher plants: a stereochemical and mechanistic study on the origin of *E*, *Z* isomers. *Angew Chem Int Ed* 41:2298–2300
 65. Hoskovec M, Luxova A, Svatos A, Boland W (2002) Biosynthesis of sex pheromones in moths: stereochemistry of fatty alcohol oxidation in *Manduca sexta*. *Tetrahedron* 58:9193–9201
 66. Beckmann C, Rattke J, Sperling P, Heinz E, Boland W (2003) Stereochemistry of a bifunctional dihydroceramide Δ^4 -desaturase/hydroxylase from *Candida albicans*; a key enzyme of sphingolipid metabolism. *Org Biomol Chem* 1:2448–2454
 67. Abad JL, Villorbina G, Fabrias G, Camps F (2004) Synthesis and use of stereospecifically deuterated analogues of palmitic acid to investigate the stereochemical course of the Δ^{11} desaturase of the processionary moth. *J Org Chem* 69:7108–7113
 68. Carlsson AS, Thomaes S, Hamberg M, Szymne S (2004) Properties of two multifunctional plant fatty acid acetylenase/desaturase enzymes. *Eur J Biochem* 271:2991–2997
 69. Abad JL, Camps F, Fabrias G (2007) Substrate-dependent stereochemical course of the (*Z*)-13-desaturation catalyzed by the processionary moth multifunctional desaturase. *J Am Chem Soc* 129:15007–15012
 70. Tremblay AE, Whittle E, Buist PH, Shanklin J (2007) Stereochemistry of Δ^4 dehydrogenation catalyzed by an ivy (*Hedera helix*) Δ^9 desaturase homolog. *Org Biomol Chem* 5:1270–1275
 71. Liavonchanka A, Rudolph MG, Tittmann K, Hamberg M, Feussner I (2009) On the mechanism of a polyunsaturated fatty acid double bond isomerase from *Propionibacterium acnes*. *J Biol Chem* 284:8005–8012
 72. McGinley CM, van der Donk WA (2003) Enzymatic hydrogen atom abstraction from polyunsaturated fatty acids. *Chem Commun (Camb)*:2843–2846
 73. Corey EJ, Gregoriou GA (1959) Stereospecific syntheses of the 7-deuterio- and 7-tritiocholesterols. The mechanism of enzyme-catalyzed hydroxylation at a saturated carbon atom. *J Am Chem Soc* 81:3127–3133
 74. Groves JT (2005) Models and mechanisms of cytochrome P450 action. In: de Ortiz Montellano PR (ed) *Cytochrome P450: structure, mechanisms, and biochemistry*. Kluwer Academic/Plenum Publishers, New York, pp 1–44
 75. Ortiz de Montellano PR (2010) Hydrocarbon hydroxylation by cytochrome P450 enzymes. *Chem Rev* 110:932–948
 76. White RE, Miller JP, Favreau LV, Bhattacharyya A (1986) Stereochemical dynamics of aliphatic hydroxylation by cytochrome P450. *J Am Chem Soc* 108:6024–6031
 77. Oliw EH (1993) bis-Allylic hydroxylation of linoleic acid and arachidonic acid by human hepatic monooxygenases. *Biochim Biophys Acta* 1166:258–263
 78. Morris LJ (1970) Mechanisms and stereochemistry in fatty acid metabolism. The Fifth Colworth Medal Lecture. *Biochem J* 118:681–693
 79. Diekmann S, Weston J, Anders E, Boland W, Schonecker B, Hettmann T, von Langen J, Erhardt S, Mauksch M, Brauer M, Beckmann C, Rost M, Sperling P, Heinz E (2002) Metal-mediated reactions modeled after nature. *J Biotechnol* 90:73–94
 80. Sperling P, Ternes P, Zank TK, Heinz E (2003) The evolution of desaturases. *Prostaglandins Leukot Essent Fatty Acids* 68:73–95
 81. Buist PH (2004) Fatty acid desaturases: selecting the dehydrogenation channel. *Nat Prod Rep* 21:249–262
 82. Shanklin J, Cahoon EB (1998) Desaturation and related modifications of fatty acids. *Annu Rev Plant Physiol Plant Mol Biol* 49:611–641
 83. Fersht A (1999) Structure and mechanism in protein science: a guide to enzyme catalysis and protein folding. W. H. Freeman, New York, pp 96–97
 84. Wu G, Lu JM, van der Donk WA, Kulmacz RJ, Tsai AL (2011) Cyclooxygenase reaction mechanism of prostaglandin H synthase from deuterium kinetic isotope effects. *J Inorg Biochem* 105:382–390
 85. Fukuzumi S (2006) Proton-coupled electron transfer of unsaturated fatty acids and mechanistic insight into lipoxygenase. *Helv Chim Acta* 89:2425–2440
 86. Klinman JP (2007) How do enzymes activate oxygen without inactivating themselves? *Acc Chem Res* 40:325–333
 87. Smith WL, DeWitt DL, Garavito RM (2000) Cyclooxygenases: structural, cellular, and molecular biology. *Annu Rev Biochem* 69:145–182
 88. Rouzer CA, Marnett LJ (2003) Mechanism of free radical oxygenation of polyunsaturated fatty acids by cyclooxygenases. *Chem Rev* 103:2239–2304
 89. Nelson SD, Trager WF (2003) The use of deuterium isotope effects to probe the active site properties, mechanism of cytochrome P450-catalyzed reactions, and mechanisms of metabolically dependent toxicity. *Drug Metab Dispos* 31:1481–1498
 90. Groves JT, McClusky GA, White RE, Coon MJ (1978) Aliphatic hydroxylation by highly purified liver microsomal cytochrome P-450. Evidence for a carbon radical intermediate. *Biochem Biophys Res Commun* 81:154–160
 91. Helmkamp GK, Rickborn BF (1957) Stereochemistry of some lithium aluminium deuteride reductions. *J Org Chem* 22:479–482
 92. Badami RC, Patil KB (1981) Structure and occurrence of unusual fatty acids in minor seeds oils. *Prog Lipid Res* 19:119–153
 93. Ren Q, Ruth K, Thony-Meyer L, Zinn M (2010) Enantiomerically pure hydroxycarboxylic acids: current approaches and future perspectives. *Appl Microbiol Biotechnol* 87:41–52
 94. Serck-Hanssen K (1978) Optically active higher aliphatic hydroxy compounds synthesized from chiral precursors by chain extension. *Prog Lipid Res* 16:179–193
 95. Gellerman JL, Schlenk H (1979) Methyl-directed desaturation of arachidonic to eicosapentaenoic acid in the fungus, *Saprolegnia parasitica*. *Biochim Biophys Acta* 573:23–30
 96. Reed DW, Polichuk DR, Buist PH, Ambrose SJ, Sasata RJ, Savile CK, Ross AR, Covello PS (2003) Mechanistic study of an

- improbable reaction: alkene dehydrogenation by the $\Delta 12$ acetylenase of *Crepis alpina*. *J Am Chem Soc* 125:10635–10640
97. Hamberg M, Samuelsson B (1965) On the specificity of the lipoxidase catalyzed oxygenation of unsaturated fatty acids. *Biochem Biophys Res Commun* 21:531–536
 98. Privett OS, Nickell C, Lundberg WO, Boyer PD (1955) Products of the lipoxidase-catalyzed oxidation of sodium linoleate. *J Am Oil Chem Soc* 32:505–511
 99. Hamberg M (1971) Steric analysis of hydroperoxides formed by lipoygenase oxygenation of linoleic acid. *Anal Biochem* 43:515–526
 100. Borgeat P, Hamberg M, Samuelsson B (1976) Transformation of arachidonic acid and homo- γ -linolenic acid by rabbit polymorphonuclear leukocytes. Monohydroxy acids from novel lipoygenases. *J Biol Chem* 251:7816–7820
 101. Hamberg M, Samuelsson B (1974) Prostaglandin endoperoxides. Novel transformations of arachidonic acid in human platelets. *Proc Natl Acad Sci USA* 71:3400–3404
 102. Nugteren DH (1975) Arachidonate lipoygenase in blood platelets. *Biochim Biophys Acta* 380:299–307
 103. Schewe T, Halangk W, Hiebsch C, Rapoport SM (1975) A lipoygenase in rabbit reticulocytes which attacks phospholipids and intact mitochondria. *FEBS Lett* 60:149–153
 104. Yokoyama C, Shinjo F, Yoshimoto T, Yamamoto S, Oates JA, Brash AR (1986) Arachidonate 12-lipoygenase purified from porcine leukocytes by immunoaffinity chromatography and its reactivity with hydroperoxyeicosatetraenoic acids. *J Biol Chem* 261:16714–16721
 105. Feussner I, Wasternack C (2002) The lipoygenase pathway. *Annu Rev Plant Biol* 53:275–297
 106. Bryant RW, Schewe T, Rapoport SM, Bailey JM (1985) Leukotriene formation by a purified reticulocyte lipoygenase enzyme. Conversion of arachidonic acid and 15-hydroperoxyeicosatetraenoic acid to 14,15-leukotriene A₄. *J Biol Chem* 260:3548–3555
 107. Corey EJ, Wright SW, Matsuda SPT (1989) Stereochemistry and mechanism of the biosynthesis of Leukotriene A₄ from 5(S)-hydroperoxy-6(E),8,11,14(Z)-eicosatetraenoic acid. Evidence for an organoiron intermediate. *J Am Chem Soc* 111:1452–1455
 108. Zheng Y, Brash AR (2010) Formation of a cyclopropyl epoxide via a leukotriene A synthase-related pathway in an anaerobic reaction of soybean lipoygenase-1 with 15S-hydroperoxyeicosatetraenoic acid. Evidence that oxygen access is a determinant of secondary reactions with fatty acid hydroperoxides. *J Biol Chem* 285:13427–13436
 109. Shimizu T, Rådmark O, Samuelsson B (1984) Enzyme with dual lipoygenase activities catalyzes leukotriene A₄ synthesis from arachidonic acid. *Proc Natl Acad Sci USA* 81:689–693
 110. Ueda N, Kaneko S, Yoshimoto T, Yamamoto S (1986) Purification of arachidonate 5-lipoygenase from porcine leukocytes and its reactivity with hydroperoxyeicosatetraenoic acids. *J Biol Chem* 261:7982–7988
 111. Bundy GL, Nidy EG, Epps DE, Mizesak SA, Wnuk RJ (1986) Discovery of an arachidonic acid C-8 lipoygenase in the gorgonian coral *Pseudoplexaura porosa*. *J Biol Chem* 261:747–751
 112. Brash AR, Baertschi SW, Ingram CD, Harris TM (1987) On non-cyclooxygenase prostaglandin synthesis in the sea whip coral *Plexaura homomalla*: an 8(R)-lipoygenase pathway leads to formation of an α -ketol and a racemic prostanoid. *J Biol Chem* 262:15829–15839
 113. Corey EJ, Matsuda SPT, Nagata R, Cleaver MB (1988) Biosynthesis of 8-R-HPETE and preclavulone A from arachidonate in several species of Caribbean coral. A widespread route to marine prostanoids. *Tetrahedron Lett* 29:2555–2558
 114. Meijer L, Brash AR, Bryant RW, Ng K, Maclouf J, Sprecher H (1986) Stereospecific induction of starfish oocyte maturation by (8R)-hydroxyeicosatetraenoic acid. *J Biol Chem* 261:17040–17047
 115. Brash AR, Hughes MA, Hawkins DJ, Boeglin WE, Song W-C, Meijer L (1991) Allene oxide and aldehyde biosynthesis in starfish oocytes. *J Biol Chem* 266:22926–22931
 116. Hampson AJ, Rowley AF, Barrow SE, Steadman R (1992) Biosynthesis of eicosanoids by blood cells of the crab, *Carcinus maenas*. *Biochim Biophys Acta* 1124:143–150
 117. Hada T, Swift LL, Brash AR (1997) Discovery of 5R-lipoygenase activity in oocytes of the surf clam, *Spisula solidissima*. *Biochim Biophys Acta* 1346:109–119
 118. Hawkins DJ, Brash AR (1989) Mechanism of biosynthesis of 11R- and 12R-hydroxyeicosatetraenoic acids by eggs of the sea urchin *Strongylocentrotus purpuratus*. *FEBS Lett* 247:9–12
 119. Brash AR, Boeglin WE, Chang MS, Shieh B-H (1996) Purification and molecular cloning of an 8R-lipoygenase from the coral *Plexaura homomalla* reveal the related primary structures of R- and S-lipoygenases. *J Biol Chem* 271:20949–20957
 120. Oldham ML, Brash AR, Newcomer ME (2005) Insights from the X-ray crystal structure of coral 8R-lipoygenase: Calcium activation via a C2-like domain and a structural basis of product chirality. *J Biol Chem* 280:39545–39552
 121. Boyington JC, Gaffney BJ, Amzel LM (1993) The three-dimensional structure of an arachidonic acid 15-lipoygenase. *Science* 260:1482–1486
 122. Minor W, Steczko J, Stec B, Otwinowski Z, Bolin JT, Walter R, Axelrod B (1996) Crystal structure of the soybean lipoygenase L-1 at 1.4 Å resolution. *Biochemistry* 35:10687–10701
 123. Gillmor SA, Villaseñor A, Fletterick R, Sigal E, Browner MF (1997) The structure of mammalian 15-lipoygenase reveals similarity to the lipases and the determinants of substrate specificity. *Nat Struct Biol* 4:1003–1009
 124. Coffa G, Brash AR (2004) A single active site residue directs oxygenation stereospecificity in lipoygenases: stereocontrol is linked to the position of oxygenation. *Proc Natl Acad Sci USA* 101:15579–15584
 125. Boeglin WE, Itoh A, Zheng Y, Coffa G, Howe GA, Brash AR (2008) Investigation of substrate binding and product stereochemistry issues in two linoleate 9-lipoygenases. *Lipids* 43:979–987
 126. Ivanov I, Heydeck D, Hofheinz K, Roffeis J, O'Donnell VB, Kuhn H, Walther M (2010) Molecular enzymology of lipoygenases. *Arch Biochem Biophys* 503:161–174
 127. Zheng Y, Boeglin WE, Schneider C, Brash AR (2008) A 49-kDa mini-lipoygenase from *Anabaena* sp. PCC 7120 retains catalytically complete functionality. *J Biol Chem* 283:5138–5147
 128. Andreou AZ, Vanko M, Bezakova L, Feussner I (2008) Properties of a mini 9R-lipoygenase from *Nostoc* sp. PCC 7120 and its mutant forms. *Phytochemistry* 69:1832–1837
 129. Palmieri-Thiers C, Cnaan S, Brunini V, Lorenzi V, Tomi F, Desseyn JL, Garscha U, Oliw EH, Berti L, Maury J (2009) A lipoygenase with dual positional specificity is expressed in olives (*Olea europaea* L.) during ripening. *Biochim Biophys Acta* 1791:339–346
 130. Malkowski MG, Ginell SL, Smith WL, Garavito RM (2000) The productive conformation of arachidonic acid bound to prostaglandin synthase. *Science* 289:1933–1937
 131. Malkowski MG, Thuresson ED, Lakkides KM, Rieke CJ, Micielli R, Smith WL, Garavito RM (2001) Structure of eicosapentaenoic and linoleic acids in the cyclooxygenase site of prostaglandin endoperoxide H synthase-1. *J Biol Chem* 276:37547–37555
 132. Holtzman MJ, Turk J, Shornick LP (1992) Identification of a pharmacologically distinct prostaglandin H synthase in cultured epithelial cells. *J Biol Chem* 267:21438–21445

133. Lecomte M, Laneuville O, Ji C, DeWitt DL, Smith WL (1994) Acetylation of human prostaglandin endoperoxide synthase-2 (cyclooxygenase-2) by aspirin. *J Biol Chem* 269:13207–13215
134. Mancini JA, O'Neill GP, Bayly C, Vickers PJ (1994) Mutation of serine-516 in human prostaglandin G/H synthase-2 to methionine or aspirin acetylation of this residue stimulates 15-*R*-HETE synthesis. *FEBS Lett* 342:33–37
135. Schneider C, Niisuke K, Boeglin WE, Voehler M, Stec DF, Porter NA, Brash AR (2007) Enzymatic synthesis of a bicyclobutane fatty acid by a hemoprotein-lipoxygenase fusion protein from the cyanobacterium *Anabaena* PCC 7120. *Proc Natl Acad Sci USA* 104:18941–18945
136. Niisuke K, Boeglin WE, Murray JJ, Schneider C, Brash AR (2009) Biosynthesis of a linoleic acid allylic epoxide: mechanistic comparison with its chemical synthesis and leukotriene A biosynthesis. *J Lipid Res* 50:1448–1455
137. Brash AR, Hawkins DJ (1990) High performance liquid chromatography for chiral analysis of eicosanoids. *Methods Enzymol* 187:187–195

Myristic Acid Increases Dihydroceramide Δ 4-Desaturase 1 (DES1) Activity in Cultured Rat Hepatocytes

Hélène Ezanno · Jérôme le Bloc'h ·
Erwan Beauchamp · Dominique Lagadic-Gossmann ·
Philippe Legrand · Vincent Rioux

Received: 21 July 2011 / Accepted: 17 November 2011 / Published online: 3 December 2011
© AOCs 2011

Abstract Dihydroceramide Δ 4-desaturase 1 (DES1) catalyzes the last step of the de novo ceramide biosynthesis, which consists of the introduction of a *trans* Δ 4-double bond in the carbon chain of the dihydroceramide. It was previously observed that myristic acid binds DES1 through N-myristoylation. This N-terminal modification significantly increased the activity of the recombinant DES1 in COS-7 cells and targeted part of the enzyme initially present in the endoplasmic reticulum to the mitochondrial outer membrane, leading to an increase in ceramide levels. Since these results were obtained in a recombinant COS-7 cell model with high expression of rat DES1, the purpose of the present study was to investigate if the native DES1 enzyme was really upregulated by its N-myristoylation in cultured rat hepatocytes. We first showed that DES1 was the main dihydroceramide desaturase isoform expressed in rat hepatocytes. In this model, the wild-type myristoylable recombinant form of rat DES1 was found in both the endoplasmic reticulum and the mitochondria whereas the mutated non-myristoylable recombinant form (N-terminal glycine replaced by an alanine) was almost exclusively localized in the endoplasmic reticulum, which evidenced the importance of the myristoylation. Then, we showed that compared to other fatty acids, myristic acid was the only one to increase native DES1 activity, in both total cell

lysates and mitochondrial fractions. The myristic acid-associated increase in DES1 activity was not linked to elevated mRNA or protein expression but more likely to its N-terminal myristoylation. Finally, the myristic acid-associated increase in DES1 activity slightly enhanced the number of apoptotic cells.

Keywords Myristic acid · N-myristoylation · Rat · Sphingolipid · Dihydroceramide desaturase · Lipoapoptosis

Abbreviations

ALA	α -Linolenic acid
DES	Dihydroceramide Δ 4-desaturase
LAU	Lauric acid
LNA	Linoleic acid
MYR	Myristic acid
NMT	Myristoyl-CoA: protein N-myristoyltransferase
OLA	Oleic acid
PAM	Palmitic acid
SFA	Saturated fatty acid(s)
VDAC	Voltage dependant anion channel

Introduction

Saturated fatty acids (SFA) are usually associated with negative consequences for human health, but recent evidence highlighted that they also carry out important and specific biological roles at the molecular level in the cells [1]. Among the SFA, myristic acid (14:0) displays a unique function in the cells, through its ability to acylate proteins [2]. This reaction is called N-terminal myristoylation and consists of the linkage, via an irreversible amide bond, between myristoyl-CoA and the NH_2 -terminal glycine

H. Ezanno · J. le Bloc'h · E. Beauchamp · P. Legrand ·
V. Rioux (✉)
Laboratoire de Biochimie-Nutrition Humaine,
Agrocampus Ouest, INRA USC 2012, 65 rue de Saint-Brieuc,
CS 84215, 35042 Rennes cedex, France
e-mail: Vincent.Rioux@agrocampus-ouest.fr

D. Lagadic-Gossmann
EA 4427 SeRAIC/IRSET, Université Rennes 1, IFR 140,
Rennes, France

residue of eukaryotic and viral proteins, as described in increasing numbers of reports regarding myristoylated proteins [3]. Myristoylation is catalyzed by the Myristoyl-CoA: protein *N*-myristoyltransferases (NMT) and has been shown to mediate protein subcellular localization, protein–protein interaction or protein–membrane interaction of the myristoylated proteins [2, 3]. Therefore, through this covalent modification of proteins, myristic acid exhibits a specific and important role in modulating protein functions [4].

The family of myristoylated proteins includes not only key components in intracellular signaling pathways [5], oncogenes [6], structural viral proteins [7], caspase-cleaved proteins which are post-translationally myristoylated [8], but also common constitutive eukaryotic proteins [2, 9]. Among this last group, the dihydroceramide $\Delta 4$ -desaturases type 1 (DES1) and 2 (DES2) have recently been identified as new members of the myristoylated protein family [10]. These enzymes are involved in the *de novo* ceramide biosynthesis pathway, which requires four successive steps starting with the condensation of palmitoyl-CoA with serine and ending with the introduction of a *trans* $\Delta 4$ -double bond in the carbon chain of the dihydroceramide leading to the production of ceramide [11, 12]. This last step is specifically catalyzed by DES1, whereas the DES2 isoform has been shown to possess a bifunctional $\Delta 4$ -desaturase/C4-hydroxylase activity in the intestine [13]. The introduction of the *trans* $\Delta 4$ -double bond in the sphingoid base is necessary for the acquisition of the biological activities of ceramide. Indeed ceramide but not dihydroceramide [14, 15] is involved in cell growth [16], stress response and apoptosis [17, 18]. DES activity depends on the tissue considered [19], on the chain length of the sphingoid base and on the length of the *N*-acyl chain [12], but its regulation is still poorly understood. Recently, we showed that myristoylation increases recombinant DES1 activity when expressed in COS-7 cells [10]. We also showed that the myristoylation of recombinant DES1 can target part of the enzyme pool from the endoplasmic reticulum to the mitochondrial outer membrane, leading to an increase in ceramide levels which in turn leads to increased apoptosis in the COS-7 cell model [20].

The purpose of the present study was therefore to increase our knowledge of the regulation of DES1 by different fatty acids. We first demonstrated that cultured rat hepatocytes are a suitable model to study native DES1 regulation, because this DES isoform is highly expressed and active. As already shown in COS-7 cells, the subcellular localization of the recombinant DES1 is governed by its myristoylated status in cultured rat hepatocytes. Then, we compared the effect of myristic acid with other saturated and unsaturated fatty acids on native DES1 enzymatic activity, protein expression and mRNA level, and showed that myristic acid only increased DES1 activity. Finally,

we evaluated the effect of each saturated fatty acid on apoptosis induction.

Materials and Methods

Chemicals

[9,10-³H]-Myristic acid was purchased from American Radiolabeled Chemicals (Isobio, Fleurus, Belgium). [1-¹⁴C]-*N*-octanoyldihydroceramide was chemically synthesized in our laboratory, as previously described [21]. Reagents for electrophoretical application were from GE Healthcare (Orsay, France) and BioRad (Marnes-la-Coquette, France). Solvents (HPLC grade) came from Thermo Scientific (Elancourt, France). Other chemicals were obtained from VWR (Fontenay-sous-Bois, France) or from Sigma (Saint-Quentin-Fallavier, France).

Animals and Cultured Rat Hepatocytes

The experimental procedure was in compliance with recommendations of the 2003/65/CEE European directive for animal experimentation. The agreement reference to carry out experiments with living vertebrate animals is #A35-238-38 and the experimental authorization number is #35-83. Hepatocytes were obtained from rats after *in situ* collagenase perfusion of liver, as previously described [22]. The culture medium (Williams' E) was supplemented with 26 mmol L⁻¹ NaHCO₃, 12.5 mmol L⁻¹ HEPES, 15 μ mol L⁻¹ BSA, antibiotic mixture (50,000 IU L⁻¹ penicillin, 50 mg L⁻¹ streptomycin, 10 mg L⁻¹ gentamycin), 1 μ mol L⁻¹ insulin, 1 μ mol L⁻¹ dexamethasone and 7% (vol/vol) FBS for plating only (1.6×10^6 cells/dish of 60 mm diameter and 4.8×10^6 cells/dish of 100 mm diameter). After plating, the cells were maintained in a humidified incubator at 37 °C under 5% CO₂ in air. The plating medium was changed after 4 h with a serum-free culture medium.

Incubation with Fatty Acid Albuminic Complexes

The incubation media containing the fatty acid albuminic complexes were prepared as previously described [22]. Briefly, each fatty acid (lauric acid 12:0, LAU; myristic acid 14:0, MYR; palmitic acid 16:0, PAM; oleic acid 18:1n-9, OLA; linolenic acid 18:2n-6, LNA; α -linolenic acid 18:3n-3, ALA) was incubated for 30 min at 70 °C with 1 mL NaOH 0.5 mol L⁻¹ in methanol. The fatty acid salts obtained were dissolved at a molar concentration of 0.5 mM at pH 10 in Williams' E medium containing 0.15 mmol/L BSA. The fatty acid:albumin molar ratio was 3.3:1. After 24 h of shaking, the incubation media were

obtained by adjusting pH to 7.35 and adding antibiotic mixture (50,000 IU L⁻¹ penicillin, 50 mg L⁻¹ streptomycin, 10 mg L⁻¹ gentamycin), 1 μmol L⁻¹ insulin, and 1 μmol L⁻¹ dexamethasone. At 4 h of culture, incubation was initiated by replacing the culture medium with 2 mL of the medium with each fatty acid albuminic complex. The medium was renewed at 26 h of culture. Incubation with fatty acids was carried out for 40 h at 37 °C in 5% CO₂ atmosphere. At the end of the incubation, the medium was taken-off and cells were washed and harvested in PBS (phosphate buffer saline: NaH₂PO₄ 4 mM, Na₂HPO₄ 0.94 mM, NaCl 150 mM, pH 7.4). The protein content of the cell lysates was determined by a modified Lowry procedure [23].

Transfection and Purification of Recombinant DES1

The plasmids coding for the wild-type myristoylable form of rat DES1 (referred to as pcDNA3.1/V5/His/DES1-Gly) and its mutant non-myristoylable form (pcDNA3.1/V5/His/DES1-Ala) have already been described [10]. At 24 h of culture, cultured rat hepatocytes were transfected with 10 μg of plasmid/1.6 × 10⁶ cells by using the jetPEITM-Hepatocyte kit (Polyplus-transfection, France). Histidine-tagged recombinant wild-type and mutated DES1 were then immunopurified using HisTrap column (GE Healthcare).

Subcellular Fractionation

After having been washed in ice-cold PBS (phosphate buffer saline: NaH₂PO₄ 4 mM, Na₂HPO₄ 0.94 mM, NaCl 150 mM, pH 7.4), rat hepatocytes were incubated on ice for 10 min in a lysis buffer (Nuclei EZ prep nuclei isolation kit, Sigma). The suspension was homogenized using a Dounce homogenizer (40 strokes) and the mixture was centrifuged for 5 min at 500g to remove unbroken cells and nuclei. The supernatant was centrifuged at 11,000g for 30 min to isolate the mitochondria. The mitochondrial pellet was washed by PBS and resuspended in a sucrose buffer (0.25 M). The supernatant containing the microsomes and the cytosol was conserved.

Immunoblot and Characterization of Subcellular Fractions

Reduced protein samples were separated by SDS-PAGE and blotted onto nitrocellulose. To detect the native DES, membranes were probed with an anti-DES polyclonal antibody raised against the peptide 153-CTTLRKLWVVI LQPL-167 and purified on HiTrap NHS-activated HP column (GE Healthcare). Recombinant DES1 expressed in hepatocytes was detected using an anti-V5 antibody

(Invitrogen, France). Antibodies against VDAC (voltage dependent anion channel), calreticulin and GAPDH were used to characterize the mitochondria, endoplasmic reticulum and cytosol, respectively. Primary antibodies were then coupled to HRP conjugated anti-IgG antibodies and peroxidase activity was determined by chemiluminescent detection using Immobilon reagents (Millipore, Guyancourt, France). The protein level was estimated using anti-actin antibody for total cell lysates and anti-VDAC antibody for mitochondrial fractions.

Dihydroceramide Δ4-Desaturase Activity Assay

Dihydroceramide desaturase assay was performed as previously described [10]. After incubation of the cells with each fatty acid (0.5 mM), 50 μL of hepatocyte homogenate or mitochondrial fraction were incubated in a reaction mixture containing 110 μL of 150 mM phosphate buffer (pH 7.2), NADH and NADPH 2 mM and 40 μL of radio-labeled [1-¹⁴C]-*N*-octanoyldihydroceramide (30 μM in octylglucoside 1.5%; 5 mCi/mmol) as the starter of the reaction. After 2 h of incubation at 37 °C, the reaction was stopped by adding 1,520 μL of chloroform, 1,520 μL of methanol and 800 μL of water. Sphingolipids were extracted twice in chloroform and separated by HPLC (Alliance Integrated System, Waters, France) [10]. *N*-octanoylceramide was separated from *N*-octanoyldihydroceramide by elution (1 mL/min) with a mixture of methanol/H₂O (90:10) during 10 min increasing to 100% methanol in 15 min, and quantified by liquid scintillation counting (Perkin Elmer Life Science, France).

Quantification of the *des1* and *des2* mRNA Level by Real-Time PCR

RNA was isolated from the hepatocytes by Extract-All[®] reagent (Eurobio, France). Retrotranscription was performed from 2 μg of total RNA in duplicates using SuperScriptTM II reverse transcriptase (Invitrogen, France) according to the supplier's instructions. Real-time PCR was performed in duplicate with the TaqMan Universal PCR Master Mix (Applied Biosystems, France) containing 40 ng of retrotranscribed RNA, 0.5 μM of forward and reverse primers, and 0.25 μM of TaqMan probe (Table 1) in a total volume of 40 μL. PCR was run using ABI Prism 7000 sequence detection system (Applied Biosystems, France) as follow: 2 min at 50 °C, 5 min at 95 °C, 40 cycles of 10 s at 95 °C and 1 min at 60 °C. Normalization was realized using the Yakima Yellow[®]-Eclipse[®] Dark Quentcher 18S rRNA control kit (Eurogentec, France). The relative expression was evaluated as: $2^{(-\Delta Ct_{des1})/2^{(-\Delta Ct_{18S})}}$.

Table 1 Primers and TaqMan probes designed for quantitative RT-PCR analysis of rat DES genes

	Forward primer (5'-3')	Reverse primer (5'-3')	TaqMan probe (5'-Fam/TAMRA-3')
<i>des1</i>	gatcatgttgagcagcctcct	aatgttcggctatgaaatgccc	tggcctgggcttgaccc
<i>des2</i>	cggatgattgacccgaata	ccagagcacttcaccagg	tacgaccatctgccgacaccac

Apoptosis Assays

Microscopic detection of apoptosis was carried out with adherent cells after treatment using nuclear chromatin staining with 10 $\mu\text{g/mL}$ Hoechst 33342 in 1 mL of culture medium for 30 min at 37 °C. Cells with apoptotic nuclei (condensed or fragmented) were directly counted in dishes in comparison with total population ($n \geq 200$ cells) using a fluorescence Olympus BX60 microscope. Caspase activity assays were realized as previously described [24]. Briefly, both floating and adherent hepatocytes were lysed in the caspase activity buffer (20 mM PIPES, 100 mM NaCl, 1 mM EDTA, 0.1% CHAPS, 10% sucrose and 10 mM DTT, pH 7.2) and 40 μg of crude cell lysates were incubated with 80 μM DEVD-AMC (Asp-Glu-Val-Asp-7-amido-4-methylcoumarin) for 2 h at 37 °C. Caspase-mediated cleavage of DEVD-AMC was measured by spectrofluorimetry (Spectramax Gemini, Molecular Devices) at an excitation/emission wavelength pair of 380/440 nm at different times ($t = 0, 60$ and 120 min). The caspase activity was expressed as the % of fluorescence arbitrary units compared with control.

Statistical Analysis

Results are expressed as the mean \pm SD or SEM. Data were analyzed by analysis of variance with the R statistical software, followed by Student t test for two-group comparison. The level of significance was $P < 0.05$.

Results

DES1 is the Main Native DES Isoform in Cultured Rat Hepatocytes

In the first part of this study, we wanted to investigate if cultured rat hepatocytes are a suitable model to study the regulation of DES1. In order to discriminate between the *des1* and *des2* genes, the levels of *des1* and *des2* mRNAs were measured by real-time quantitative PCR in cultured rat hepatocytes. Figure 1 shows that the expression of *des1* mRNA was five times higher than that of *des2* mRNA. Therefore, these results show that DES1 is the main DES isoform expressed in cultured rat hepatocytes.

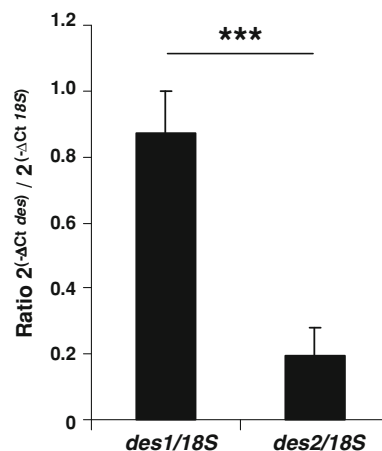


Fig. 1 Comparison of mRNA expression of the two isoforms of dihydroceramide $\Delta 4$ -desaturase in rat hepatocytes. Expression of *des1* and *des2* mRNA measured by real-time quantitative PCR in rat hepatocytes. Values are means \pm SD, $n = 7$ (** $P < 0.001$)

Cultured rat hepatocytes exhibited functional DES1 activity (Fig. 2). Radiolabeled dihydroceramide incubated with hepatocyte homogenate was converted into ceramide and no C4-hydroxylation activity (corresponding to the bifunctional DES2) was detected (data not shown). When measured in vitro, the activity was linear up to 2 h of incubation time (Fig. 2a). DES1 activity increased linearly with protein amount (Fig. 2b) in the 0–700 μg range. The activity showed a plateau with dihydroceramide concentrations higher than 20 μM (Fig. 2c). By using Lineweaver–Burk representation, the obtained apparent K_m value was 1.48 μM and the maximal velocity (V_{max}) was 12.5 pmol/min/mg protein. In addition, hepatocytes exhibited dihydroceramide $\Delta 4$ -desaturase activity at up to 72 h of culture (Fig. 2d).

The Subcellular Localization of the Recombinant DES1 is Governed by its Myristoylated Status

We have already shown in the recombinant COS-7 cell model that DES1 myristoylation can modify its subcellular localization [20]. We therefore wanted to know if myristoylation of DES1 also occurs in cultured rat hepatocytes. Hepatocytes were transiently transfected with plasmids encoding the wild-type myristoylable form of rat DES1 and its mutated non-myristoylable form (N-terminal glycine

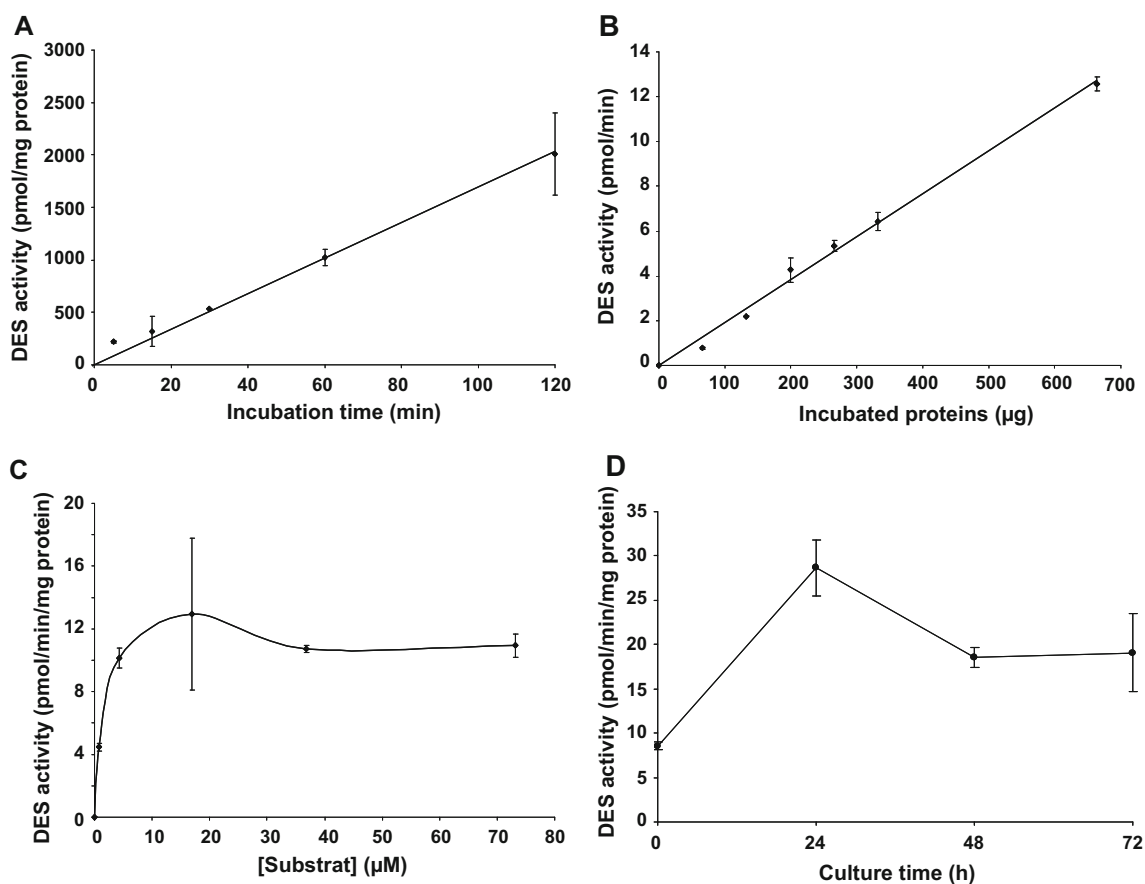


Fig. 2 Dihydroceramide $\Delta 4$ -desaturase 1 (DES1) activity in the cell homogenates of rat hepatocytes. DES1 activities are expressed as a function of incubation time (a), incubated proteins (b), substrate

concentration (c) and culture time of hepatocytes (d). Results were calculated from the amount of radiolabeled ceramide produced. Values are means \pm SD ($n = 3$)

replaced by an alanine), followed by subcellular fractionation. In this model, the wild-type myristoylable rat DES1 was found in both the endoplasmic reticulum and the mitochondria (Fig. 3) whereas the mutated non-myristoylable recombinant form was almost exclusively localized in the endoplasmic reticulum. This result evidenced the importance of the myristoylation of DES1 in this cellular model.

Myristic Acid Increases DES1 Activity in Cultured Rat Hepatocytes

The above results suggested that cultured rat hepatocytes are a suitable model to further study the regulation of native DES1 activity, especially through its N-terminal myristoylation. Therefore, we subsequently measured the effect of several fatty acids on DES1 activity in this model. We were especially interested in studying the effect of myristic acid on DES1 activity. Lauric and palmitic acids were also used because they flanked myristic acid by their carbon chain length. As shown in Fig. 4a, myristic acid added at 0.5 mM in the culture medium for 40 h

significantly increased DES1 activity compared to control cells incubated without fatty acids. On the contrary, palmitic acid induced a significant decrease in DES1 activity, compared with both myristic acid-treated cells and control cells. Lauric acid had no effect on DES1 activity.

We also investigated the effects of several unsaturated fatty acids on DES1 activity by incubating cultured rat hepatocytes with 0.5 mM oleic, linoleic and α -linolenic acids. Figure 5 shows that oleic acid did not modify DES1 activity compared to control cells whereas the 2 polyunsaturated fatty acids inhibited DES1 activity significantly.

Myristic Acid also Significantly Increases DES1 Activity in the Mitochondria of Cultured Rat Hepatocytes

Having previously shown that myristoylation can target recombinant DES1 from the endoplasmic reticulum to the mitochondria (Fig. 3), we also measured native DES1 activity in the mitochondrial fraction of rat hepatocytes, after incubation with the saturated fatty acids. Figure 6a once more shows a significant activation of DES1 activity

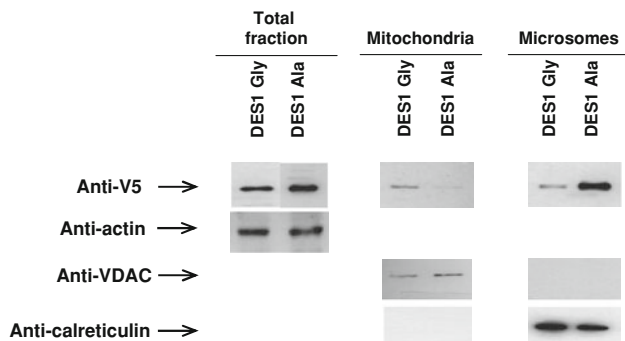


Fig. 3 Effect of recombinant dihydroceramide Δ 4-desaturase 1 (DES1) expression and myristic incubation on the subcellular distribution of the protein in rat hepatocytes. Immunoblot was performed to control the protein expression in the different fractions of hepatocytes after immunopurification of recombinant DES1. V5 epitope was detected to analyze the expression of recombinant DES1 Gly (*wild-type*) or DES1 Ala (*mutant*) proteins fused to V5 epitope. The fractions were characterized with actin, VDAC and calreticulin which are the markers of total cells, mitochondria and endoplasmic reticulum, respectively

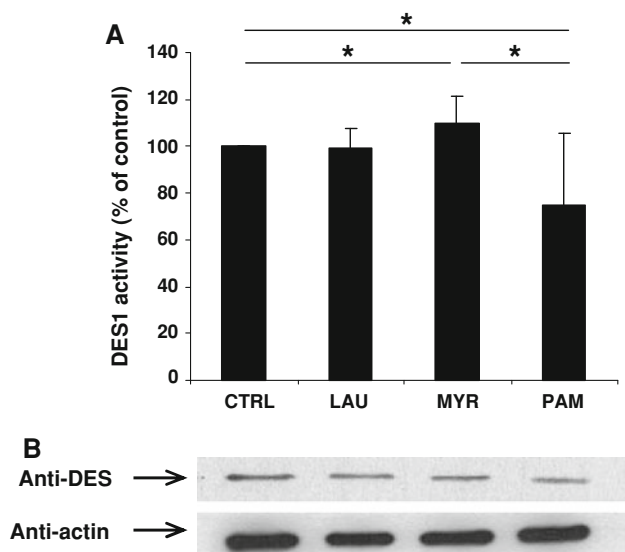


Fig. 4 Effect of saturated fatty acids on dihydroceramide Δ 4-desaturase 1 (DES1) activity and expression in rat hepatocytes. **a** DES1 activity measured in rat hepatocytes after an incubation of 40 h with 0.5 mM of lauric (LAU), myristic (MYR) or palmitic acids (PAM). Control cells (CTRL) were incubated without fatty acids. The results are expressed as a percentage of the activity obtained with control cells. Values are mean \pm SD ($n = 7$; $*P < 0.05$). **b** DES1 was detected by immunoblot with the anti-DES antibody. Actin is a control of similar protein loading

after incubation with myristic acid (increase of 60% compared to control cells) and a significant inhibition after incubation with palmitic acid. A smaller but significant increase of DES1 activity was also observed after incubation with lauric acid.

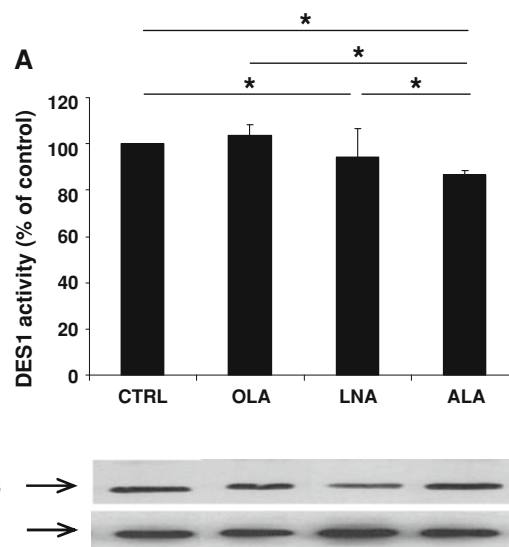


Fig. 5 Effect of unsaturated fatty acids on dihydroceramide Δ 4-desaturase 1 (DES1) activity in rat hepatocytes. **a** DES1 activity measured in rat hepatocytes after an incubation of 40 h with 0.5 mM of oleic (OLA), linoleic (LNA) and α -linolenic acids (ALA). Control cells (CTRL) were incubated without fatty acids. The results are expressed as a percentage of the activity obtained with control cells. Values are means \pm SD ($n = 5$; $*P < 0.05$). **b** DES1 was detected by immunoblot with the anti-DES antibody. Actin is a control of similar protein loading

The Myristic Acid-Associated Increase of DES1 Activity is not Linked to mRNA or Protein Expression

In order to determine why myristic acid is the single fatty acid that increases DES1 activity, we measured *des1* mRNA transcript levels after incubation of the cells with the same fatty acids. As shown in Fig. 7, saturated and unsaturated fatty acids did not significantly modify the *des1* mRNA level in rat hepatocytes. Moreover, when analyzing the DES1 protein expression, we showed that saturated fatty acids did not modify the DES1 protein level in the whole or mitochondrial fractions of rat hepatocytes (data not shown).

The Increase in Native DES1 Activity Has Small Effects on Apoptosis

To go further, we wanted to know whether the myristic acid-associated increase in DES1 activity could induce apoptosis in the cells, via the production of ceramide. Therefore, we measured the effect of myristic acid and other SFA on apoptosis in cultured rat hepatocytes. The potential pro-apoptotic effect of these fatty acids was measured by counting apoptotic cells (Fig. 8a) and measuring caspase 3 activity (Fig. 8b). Figure 8a showed that the three SFA, and especially palmitic acid, increased slightly but significantly the number of apoptotic cells,

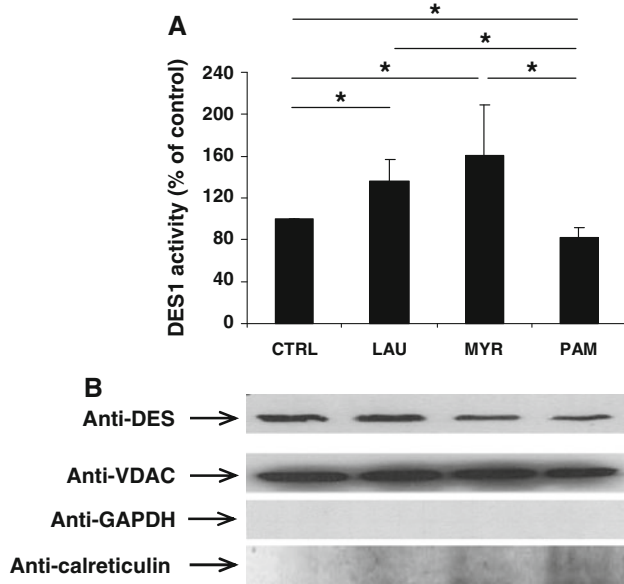


Fig. 6 Effect of saturated fatty acids on dihydroceramide $\Delta 4$ -desaturase 1 (DES1) activity and expression in the mitochondrial fraction of rat hepatocytes. **a** DES1 activity measured in the mitochondrial fraction of rat hepatocytes after an incubation of 40 h with 0.5 mM of lauric (LAU), myristic (MYR) or palmitic acids (PAM). Control cells (CTRL) were incubated without fatty acids. The results are expressed as a percentage of the activity obtained with control cells. Values are means \pm SD ($n = 5$; $*P < 0.05$). **b** DES1 was detected by immunoblot with the anti-DES antibody; anti-VDAC, anti-GAPDH and anti-calreticulin level assessed by immunoblot are the markers of mitochondrial fraction purity

compared to control cells. However, none of these SFA increased caspase 3 activity (Fig. 8b).

Discussion

Dihydroceramide $\Delta 4$ -desaturase (DES) is responsible for introducing a *trans* 4,5-double bond in the sphingoid

backbone of dihydroceramide, leading to the biosynthesis of ceramide [11]. Because this double bond is critical for the acquisition of the biological activities of ceramide, and because the enzyme modulates the dihydroceramide/ceramide ratio in the cells, the regulation of DES isoforms has become a focus of interest [12, 19, 25–27]. It has been shown for instance that dihydroceramide $\Delta 4$ -desaturase activity is modulated by oxidative stress in several cell lines [26]. In C2C12 myotubes, with a view to study the sphingolipid-mediated insulin resistance, physiologically relevant concentrations of palmitate increased *des1* mRNA and DES1 activity and this effect was attenuated by oleate co-treatment [28]. We have also contributed to decrypt the mechanistic insights as to how DES1 is regulated. Recently, we showed that both rat DES isoforms are myristoylated and that N-myristoylation increased the recombinant DES1 activity in COS-7 cells [10]. We also showed that the myristoylation of recombinant DES1 can target part of the enzyme from the endoplasmic reticulum to the mitochondrial outer membrane, leading to an increase in ceramide levels which in turn leads to apoptosis in the COS-7 cell model [20]. Therefore, we then focused our attention on studying the effect of myristic acid and other saturated or unsaturated fatty acids on the native DES1 in cultured rat hepatocytes.

Rat hepatocytes were chosen as a useful physiological model of cultured cells because, in the rat, a tissue distribution study has shown that the liver contains the highest DES activity [19]. Ceramide de novo biosynthesis was also shown to occur in cultured rat hepatocytes incubated with radiolabeled serine [12, 29]. In addition, DES activity was detected in permeabilized rat hepatocytes incubated with radiolabeled dihydroceramide [11] and in microsomes from rat liver [19]. However, all these studies were carried out before the identification of the two mammalian *des1* and *des2* genes encoding for the two protein isoforms of

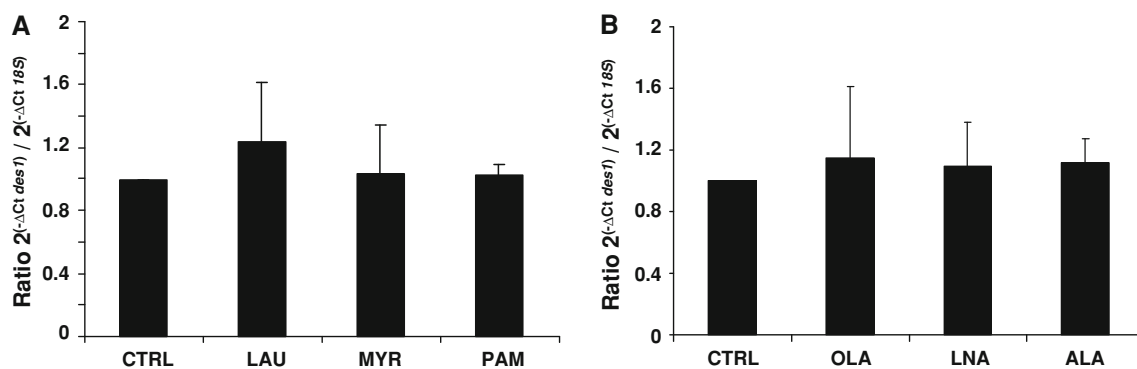


Fig. 7 Effect of saturated and unsaturated fatty acids on dihydroceramide $\Delta 4$ -desaturase 1 (*des1*) mRNA expression in rat hepatocytes. *des1* mRNA expression in rat hepatocytes after an incubation of 40 h with 0.5 mM of saturated fatty acids **a** lauric (LAU), myristic (MYR) or

palmitic acids (PAM); or **b** with unsaturated fatty acids: oleic (OLA), linoleic (LNA) and α -linolenic acids (ALA). Control cells (CTRL) were incubated without fatty acids. Values are mean \pm SD ($n = 3$). No significant difference was observed ($P < 0.05$)

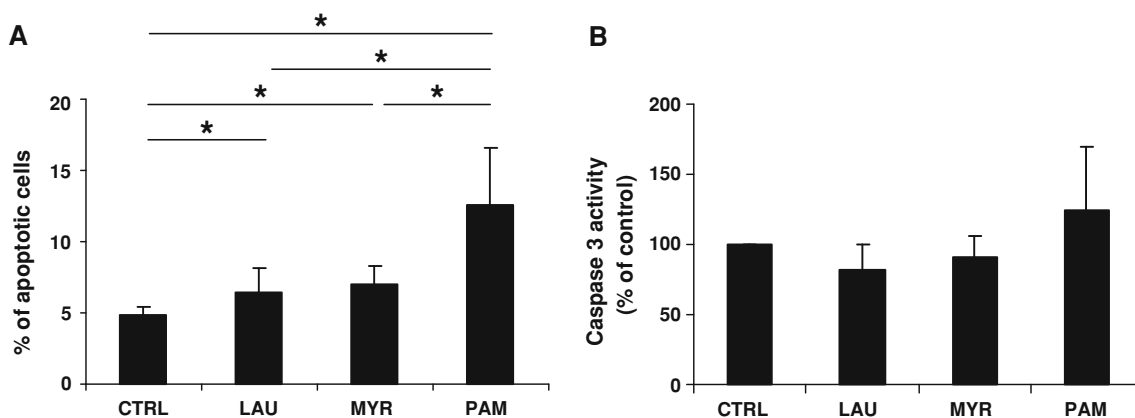


Fig. 8 Effect of saturated fatty acids on apoptosis induction in rat hepatocytes. **a** Number of apoptotic nuclei (fragmented or condensed) after staining by Hoechst and, **b** caspase 3 activity (% of control) in cultured rat hepatocytes incubated for 40 h with 0.5 mM of lauric

(LAU), myristic (MYR) or palmitic acids (PAM). Control cells (CTRL) were incubated without fatty acids. The results are expressed as a percentage of the activity obtained with control cells. Values are means \pm SD ($n = 4$; $*P < 0.05$)

DES [13, 25]. Although it has been suggested that the bifunctional Δ^4 -desaturase/C4-hydroxylase DES2 is mainly expressed in the small intestine in mice, with preferential phytoceramide production [13], we first characterized the relative expression level of DES1 and DES2 isoforms in cultured rat hepatocytes. By analyzing mRNA levels (Fig. 1), our results demonstrated that DES1 is the main dihydroceramide desaturase isoform expressed in hepatocytes.

The present study also shows that rat hepatocytes in culture exhibited DES1 activity at up to 72 h of culture (Fig. 2d). In order to measure the dihydroceramide desaturase activity in vitro, we used N -[1- 14 C]octanoyldihydroceramide as substrate. We chose this substrate with a short 14 C-labeled fatty acyl chain engaged in the amide bond because Michel et al. [12] have shown that optimal in vitro activity of the desaturase is obtained with substrates with N -acyl chain length of 8 carbon atoms compared to 12 or 18 carbons. In another study by Causeret et al. [19], the chain length of the N -linked fatty acid hardly affected the activity of the desaturase from rat liver microsomes. However, little is known about the chain length that is actually optimal in cells and it is very difficult to determine if this substrate is a good one for all DES isoforms, which could explain why no hydroxylase activity corresponding to the potential DES2 isoform was detected. Other studies have been carried out by using an in situ dihydroceramide desaturase assay (C12-dhCCPS converted to C12-CCPS) [26, 27]. DES1 activity presented a typical Michaelis–Menten kinetic (Fig. 2c). The level of activity reported here was between 10 and 25 pmol/min/mg protein when considering the whole cell homogenate, which is consistent with the values reported in the tissues (2–3 pmol/min/mg protein in fresh rat liver) [19]. The kinetic parameters (K_m , V_{max}) that we obtained are also consistent with the

values very recently described in rat liver microsomes [30]. Altogether, the optimization of the conditions for the DES1 activity assay (Fig. 2) provides a reliable tool for investigating the effect of individual parameters on its regulation.

Since we had previously demonstrated that myristoylation can target part of the DES1 from the endoplasmic reticulum to the mitochondria in the COS-7 cell model [20], we wanted to know if myristoylation of DES1 also occurs in cultured rat hepatocytes. Hepatocytes were transfected with plasmids coding for the wild-type myristoylable (DES1 Gly) or mutant unmyristoylable (DES1 Ala) forms of DES1, followed by incubation with myristic acid. We showed that the wild-type of DES1 was present in the microsomes and mitochondria, whereas the mutant was mainly in the microsomes (Fig. 3). This result provides indirect proof that myristoylation of native DES1 occurs in rat hepatocytes, consistent with previous results showing that native dihydroceramide Δ^4 -desaturase activity was found in both the endoplasmic reticulum and the mitochondria in isolated hepatocytes [20]. This result is also consistent with a previous study showing that Myristoyl-CoA: protein N -myristoyltransferase (NMT) is active in cultured rat hepatocytes and can use exogenous myristic acid added to the culture medium to acylate proteins [31]. Altogether, these results suggest that cultured rat hepatocytes are a suitable model to study further the regulation of DES1 activity, especially through its N -terminal myristoylation.

Cultured rat hepatocytes were then incubated with different saturated and unsaturated fatty acids, solubilized in the culture medium at the physiological range of 0.5 mM. Fatty acids were supplied to the cells after complexation with albumin, with a fatty acid:albumin molar ratio equal to 3.3:1. Among these fatty acids (Figs. 4a, 5a), myristic acid was the single one able to upregulate DES1 activity compared to control cells. Lauric and oleic acids had no

effect on the activity whereas palmitic, linoleic and α -linolenic acids inhibited DES1 activity measured in the whole cell homogenate. The activation of DES1 by myristic acid was slight (about 10%) but significant and reproducible compared not only to control cells but also to palmitic acid-treated cells (Fig. 4a). This myristic acid-associated increase in DES1 activity was more significant in the mitochondrial fraction compared to both control cells (about 60%) and palmitic acid-incubated cells (Fig. 6a). No significant effect was shown upon incubation with the different fatty acids on *des1* mRNA (Fig. 7) and DES1 protein levels (data not shown). Although the mechanism is not fully demonstrated, all these results argue for a regulation of DES1 through its N-terminal myristoylation. First, the specific effect of myristic acid on native DES1 activity (Fig. 4a), with no effect at the transcriptional and translational levels, is in accordance with the increased activity shown in COS-7 cells expressing the recombinant wild-type DES1-Gly and incubated with myristic acid, compared to cells expressing the myristoylation-site-deficient mutant DES1-Ala [10]. In cultured rat hepatocytes, the effect on native DES1 is not that high, probably because myristic acid is not the rate-limiting molecule for myristoylating DES1, as it becomes in transfected cells expressing high level of recombinant DES1 protein [10]. We had previously carried out extensive studies on the metabolic fate of lauric, myristic and palmitic acids in cultured rat hepatocytes [22, 31, 32]. Based on these previous studies, we placed emphasis on several major differences between saturated fatty acid utilization by liver cells in terms of both lipid metabolism (including incorporation into cellular and secreted lipids, β -oxidation, conversion to other fatty acids by elongation and desaturation) and fatty acid acylation of proteins (N-terminal myristoylation and lateral acylation). In addition, depending on the fatty acid used, it is also possible that some fatty acids were not bound to albumin but rather present in free form. In a previous work [22], we measured the level of unbound myristate and palmitate at different fatty acid:albumin molar ratios in the incubation medium and shown that albumin binding capacity for myristic acid was always smaller than for palmitic acid. Consequently, myristic acid was more rapidly taken up by the cells than was palmitic acid. However, this higher uptake rate of myristic acid did not exceed the esterification ability of the cells, and we did not find any differences when we measured the incorporation of myristic acid and palmitic acid into the cellular non-esterified fatty acids in this previous work. Secondly, the effect of myristic acid on native DES1 activity was significantly higher in the mitochondrial fraction than in the whole cell homogenate (Fig. 4). This last result can be related to the subcellular targeting of part of DES1 from the endoplasmic reticulum to the

mitochondrial outer membrane when the protein is myristoylated, as already shown with the recombinant protein in the COS-7 cell model [20], and in rat hepatocytes in the present study (Fig. 3). This result also suggests a decrease in the cellular pool of native non-myristoylated DES1 proteins and a concomitant increase in the level of myristoylated DES1 upon incubation with myristic acid for 40 h. Another interesting result of the present study was that, although lauric acid had no effect on DES1 activity in the whole cell homogenate, a significant positive effect appeared in the mitochondria (Fig. 6a). This result can be explained by the elongation of lauric acid to myristic acid, as previously described in rat hepatocytes [33], which therefore supplies a higher amount of endogenous myristic acid available for the myristoylation of DES1. The presence of myristoyl-CoA in the cells is indeed required for myristoylating DES1.

Therefore, the myristic acid-associated increase in DES1 activity shown in the present study was possibly the consequence of its N-terminal myristoylation. In addition, DES proteins are believed, like other mammalian desaturases and especially fatty acid desaturases, to cooperate with NADH-cytochrome b5 reductase (NCb5R) in the endoplasmic reticulum [34]. Since NCb5R is also known to be myristoylated [35–37], both the myristoylation of DES and NCb5R could account for the increased activity of the whole complex of desaturation, as recently suggested for the $\Delta 6$ -desaturase (FADS2) involved in polyunsaturated fatty acid biosynthesis [38].

Now, we can also put forward several hypotheses concerning the negative effect of palmitic acid on DES1 activity. Palmitic acid is the preferred substrate of the first step of ceramide biosynthesis (condensation with a serine). Incubation with palmitic acid, but not with stearic or oleic acid, has been shown to increase sphingolipid de novo synthesis in rat liver cells [29, 39]. In our study, the high concentration of palmitic acid brought by the medium could therefore stimulate the whole metabolic pathway leading to ceramide biosynthesis. The higher level of cellular ceramide could inhibit the last step catalyzed by DES1, as a negative feed-back. In addition, although NMT displays a high affinity for myristoyl-CoA [40], the high level of cellular palmitoyl-CoA could compete with myristoyl-CoA for the N-myristoylation of DES1 [41], leading to a decrease of its myristoylated status and a subsequent decrease of its enzymatic activity. In C2C12 mouse myotubes, palmitate markedly increased *des1* mRNA and DES1 activity, suggesting that the effect of individual saturated fatty acid on DES1 could vary with the tissue considered [28].

Because ceramide is involved in apoptosis [18], we finally wanted to measure the effect of the myristic acid-associated increase in DES1 activity on apoptosis induction

in cultured rat hepatocytes incubated with myristic acid and other saturated fatty acids. Moreover, it is well known that ceramide induces apoptosis via mitochondrial dysfunction [42, 43]. Indeed, chemically-modified ceramide analogs that target mitochondria promote autophagy, retard cell growth and induce apoptosis [44]. We hypothesized that the level of synthesized ceramides could increase in cells incubated with myristic acid, due to the higher rate of conversion of dihydroceramide to ceramide by DES1. Indeed, our results demonstrate that apoptosis measured by counting apoptotic cells was weakly, but significantly, increased in cultured rat hepatocytes incubated with myristic acid, compared to control cells (Fig. 8a). Lauric acid and especially palmitic acid also increased the number of apoptotic cells. In COS-7 cells expressing recombinant DES1, we showed that myristic acid highly increased both the number of apoptotic cells and caspase 3 activity [20]. Interestingly, the modest increase of DES1 activity when cultured hepatocytes were incubated with myristic acid (Fig. 4a) is correlated with the weak effect on apoptosis (Fig. 8a). In contrast, the induction of apoptosis by palmitic acid is higher than that induced by myristic acid (Fig. 8a), whereas palmitic acid inhibited DES1 activity (Fig. 4a). It is actually well known that a high concentration of free saturated fatty acids (C16:0 and C18:0) incubated with various type of cells induce apoptosis, a mechanism that has therefore been called lipoapoptosis. Two complementary type of mediation have been explored to explain this lipotoxicity, involving or not ceramide. First, palmitic and stearic acids are also both able to induce partial mitochondria uncoupling [47], endoplasmic reticulum stress [48] and to generate reactive oxygen species [49] and nitric oxide [50]. Second, apoptosis induced by these saturated free fatty acids is correlated with de novo synthesis of ceramide. In the present study, we focused on the pathway leading to the de novo synthesis of ceramide and especially on the last step catalyzed by DES1. As discussed above, since palmitic acid is the preferred substrate of the first step of ceramide biosynthesis, we suggest that incubation with palmitic acid could therefore stimulate the whole metabolic pathway leading to ceramide biosynthesis (and therefore to apoptosis induction), even if the last desaturation step catalyzed by DES1 is less active compared to control cells or to cells incubated with myristic acid. In addition it is possible that the higher effect shown on the induction of apoptosis with palmitic acid could be the consequence of the other pathway (mitochondria uncoupling, endoplasmic reticulum stress and generation of reactive oxygen species and nitric oxide) since myristic acid has not been described as having these effects.

However, none of the 3 saturated fatty acids significantly increased caspase 3 activity, which is an important

marker of apoptosis (Fig. 8b). Therefore, although cultured rat hepatocytes are a suitable model for studying DES1 regulation, they would not be a good model to study apoptosis induction under these conditions because primary cells are more resistant to apoptosis induced by free fatty acids than other cellular models [45] and because insulin added to the culture medium is known to protect liver cells from saturated fatty acid-induced apoptosis [46].

In summary, our data demonstrate that myristic acid is the single fatty acid able to increase enzymatic DES1 activity, possibly through its myristoylation, in the suitable physiological model of cultured rat hepatocytes.

Acknowledgments We are indebted to the Centre National Interprofessionnel de l'Economie Laitière (CNIEL, France) for its financial support and constructive discussions. We thank N. Monthéan, F. Boissel and R. Marion for able technical assistance and animal care. We thank Béatrice Dendele and Fatiha Djoudi for technical assistance concerning apoptosis assays. We thank Jane Wilson-Giron for her English revision of the manuscript.

References

1. Legrand P, Beauchamp E, Catheline D, Pedrono F, Rioux V (2010) Short chain saturated fatty acids decrease circulating cholesterol and increase tissue PUFA content in the rat. *Lipids* 45:975–986
2. Beauchamp E, Rioux V, Legrand P (2009) New regulatory and signal functions for myristic acid. *Med Sci (Paris)* 25:57–63
3. Johnson DR, Bhatnagar RS, Knoll LJ, Gordon JI (1994) Genetic and biochemical studies of protein N-myristoylation. *Annu Rev Biochem* 63:869–914
4. Rioux V, Pedrono F, Legrand P (2011) Regulation of mammalian desaturases by myristic acid: N-terminal myristoylation and other modulations. *Biochim Biophys Acta* 1811:1–8
5. Aderem AA, Albert KA, Keum MM, Wang JK, Greengard P, Cohn ZA (1988) Stimulus-dependent myristoylation of a major substrate for protein kinase C. *Nature* 332:362–364
6. Shoji S, Kurosawa T, Inoue H, Funakoshi T, Kubota Y (1990) Human cellular src gene product: identification of the myristoylated pp60c-src and blockage of its myristoyl acylation with N-fatty acyl compounds resulted in the suppression of colony formation. *Biochem Biophys Res Commun* 173:894–901
7. Schultz AM, Oroszlan S (1983) In vivo modification of retroviral gag gene-encoded polyproteins by myristic acid. *J Virol* 46:355–361
8. Martin DD, Beauchamp E, Berthiaume LG (2011) Post-translational myristoylation: fat matters in cellular life and death. *Biochimie* 93:18–31
9. Maurer-Stroh S, Gouda M, Novatchkova M, Schleiffer A, Schneider G, Sirota FL, Wildpaner M, Hayashi N, Eisenhaber F (2004) MYRbase: analysis of genome-wide glycine myristoylation enlarges the functional spectrum of eukaryotic myristoylated proteins. *Genome Biol* 5:R21
10. Beauchamp E, Goenaga D, Le Bloc'h J, Catheline D, Legrand P, Rioux V (2007) Myristic acid increases the activity of dihydroceramide Delta4-desaturase 1 through its N-terminal myristoylation. *Biochimie* 89:1553–1561
11. Geeraert L, Mannaerts GP, van Veldhoven PP (1997) Conversion of dihydroceramide into ceramide: involvement of a desaturase. *Biochem J* 327(Pt 1):125–132

12. Michel C, van Echten-Deckert G, Rother J, Sandhoff K, Wang E, Merrill AH Jr (1997) Characterization of ceramide synthesis. A dihydroceramide desaturase introduces the 4,5-*trans*-double bond of sphingosine at the level of dihydroceramide. *J Biol Chem* 272:22432–22437
13. Omae F, Miyazaki M, Enomoto A, Suzuki M, Suzuki Y, Suzuki A (2004) DES2 protein is responsible for phytoceramide biosynthesis in the mouse small intestine. *Biochem J* 379:687–695
14. Bielawska A, Crane HM, Liotta D, Obeid LM, Hannun YA (1993) Selectivity of ceramide-mediated biology. Lack of activity of erythro-dihydroceramide. *J Biol Chem* 268:26226–26232
15. Obeid LM, Linardic CM, Karolak LA, Hannun YA (1993) Programmed cell death induced by ceramide. *Science* 259:1769–1771
16. Yang J, Yu Y, Sun S, Duerksen-Hughes PJ (2004) Ceramide and other sphingolipids in cellular responses. *Cell Biochem Biophys* 40:323–350
17. Hannun YA, Luberto C (2000) Ceramide in the eukaryotic stress response. *Trends Cell Biol* 10:73–80
18. Andrieu-Abadie N, Gouaze V, Salvayre R, Levade T (2001) Ceramide in apoptosis signaling: relationship with oxidative stress. *Free Radic Biol Med* 31:717–728
19. Causeret C, Geeraert L, Van der Hoeven G, Mannaerts GP, Van Veldhoven PP (2000) Further characterization of rat dihydroceramide desaturase: tissue distribution, subcellular localization, and substrate specificity. *Lipids* 35:1117–1125
20. Beauchamp E, Tekpli X, Marteil G, Lagadic-Gossmann D, Legrand P, Rioux V (2009) N-Myristoylation targets dihydroceramide Delta4-desaturase 1 to mitochondria: partial involvement in the apoptotic effect of myristic acid. *Biochimie* 91:1411–1419
21. Schwarzmann G, Sandhoff K (1987) Lysogangliosides: synthesis and use in preparing labeled gangliosides. *Methods Enzymol* 138:319–341
22. Rioux V, Lemarchal P, Legrand P (2000) Myristic acid, unlike palmitic acid, is rapidly metabolized in cultured rat hepatocytes. *J Nutr Biochem* 11:198–207
23. Bensadoun A, Weinstein D (1976) Assay of proteins in the presence of interfering materials. *Anal Biochem* 70:241–250
24. Huc L, Sparfel L, Rissel M, Dimanche-Boitrel MT, Guillouzo A, Fardel O, Lagadic-Gossmann D (2004) Identification of Na⁺/H⁺ exchange as a new target for toxic polycyclic aromatic hydrocarbons. *Faseb J* 18:344–346
25. Ternes P, Franke S, Zahringer U, Sperling P, Heinz E (2002) Identification and characterization of a sphingolipid delta 4-desaturase family. *J Biol Chem* 277:25512–25518
26. Idkowiak-Baldys J, Apraiz A, Li L, Rahmaniyan M, Clarke CJ, Kravka JM, Asumendi A, Hannun YA (2010) Dihydroceramide desaturase activity is modulated by oxidative stress. *Biochem J* 427:265–274
27. Kravka JM, Li L, Szulc ZM, Bielawski J, Ogretmen B, Hannun YA, Obeid LM, Bielawska A (2007) Involvement of dihydroceramide desaturase in cell cycle progression in human neuroblastoma cells. *J Biol Chem* 282:16718–16728
28. Hu W, Ross JS, Geng T, Brice SE, Cowart LA (2011) Differential regulation of dihydroceramide desaturase by palmitate vs. monounsaturated fatty acids: implications to insulin resistance. *J Biol Chem* 286:16596–16605
29. Merrill AH Jr, Lingrell S, Wang E, Nikolova-Karakashian M, Vales TR, Vance DE (1995) Sphingolipid biosynthesis de novo by rat hepatocytes in culture. Ceramide and sphingomyelin are associated with, but not required for, very low density lipoprotein secretion. *J Biol Chem* 270:13834–13841
30. Rahmaniyan M, Curley RW Jr, Obeid LM, Hannun YA, Kravka JM (2011) Identification of dihydroceramide desaturase as a direct in vitro target for fenretinide. *J Biol Chem* 286:24754–24764
31. Rioux V, Galat A, Jan G, Vinci F, D'Andrea S, Legrand P (2002) Exogenous myristic acid acylates proteins in cultured rat hepatocytes. *J Nutr Biochem* 13:66–74
32. Rioux V, Daval S, Guillou H, Jan S, Legrand P (2003) Although it is rapidly metabolized in cultured rat hepatocytes, lauric acid is used for protein acylation. *Reprod Nutr Dev* 43:419–430
33. Rioux V, Catheline D, Legrand P (2007) In rat hepatocytes, myristic acid occurs through lipogenesis, palmitic shortening and lauric acid elongation. *Animal* 1:820–826
34. Enomoto A, Omae F, Miyazaki M, Kozutsumi Y, Yubisui T, Suzuki A (2006) Dihydroceramide:sphinganine C-4-hydroxylation requires Des2 hydroxylase and the membrane form of cytochrome b5. *Biochem J* 397:289–295
35. Ozols J, Carr SA, Strittmatter P (1984) Identification of the NH₂-terminal blocking group of NADH-cytochrome b5 reductase as myristic acid and the complete amino acid sequence of the membrane-binding domain. *J Biol Chem* 259:13349–13354
36. Borgese N, Aggujaro D, Carrera P, Pietrini G, Bassetti M (1996) A role for N-myristoylation in protein targeting: NADH-cytochrome b5 reductase requires myristic acid for association with outer mitochondrial but not ER membranes. *J Cell Biol* 135:1501–1513
37. Colombo S, Longhi R, Alcaro S, Ortuso F, Sprocati T, Flora A, Borgese N (2005) N-myristoylation determines dual targeting of mammalian NADH-cytochrome b5 reductase to ER and mitochondrial outer membranes by a mechanism of kinetic partitioning. *J Cell Biol* 168:735–745
38. Jan S, Guillou H, D'Andrea S, Daval S, Bouriel M, Rioux V, Legrand P (2004) Myristic acid increases delta6-desaturase activity in cultured rat hepatocytes. *Reprod Nutr Dev* 44:131–140
39. Messmer TO, Wang E, Stevens VL, Merrill AH Jr (1989) Sphingolipid biosynthesis by rat liver cells: effects of serine, fatty acids and lipoproteins. *J Nutr* 119:534–538
40. Kishore NS, Lu TB, Knoll LJ, Katoh A, Rudnick DA, Mehta PP, Devadas B, Huhn M, Atwood JL, Adams SP et al (1991) The substrate specificity of *Saccharomyces cerevisiae* myristoyl-CoA:protein N-myristoyltransferase. Analysis of myristic acid analogs containing oxygen, sulfur, double bonds, triple bonds, and/or an aromatic residue. *J Biol Chem* 266:8835–8855
41. Rudnick DA, Lu T, Jackson-Machelski E, Hernandez JC, Li Q, Gokel GW, Gordon JI (1992) Analogs of palmitoyl-CoA that are substrates for myristoyl-CoA:protein N-myristoyltransferase. *Proc Natl Acad Sci USA* 89:10507–10511
42. Siskind LJ (2005) Mitochondrial ceramide and the induction of apoptosis. *J Bioenerg Biomembr* 37:143–153
43. Garcia-Ruiz C, Colell A, Mari M, Morales A, Fernandez-Checa JC (1997) Direct effect of ceramide on the mitochondrial electron transport chain leads to generation of reactive oxygen species. Role of mitochondrial glutathione. *J Biol Chem* 272:11369–11377
44. Hou Q, Jin J, Zhou H, Novgorodov SA, Bielawska A, Szulc ZM, Hannun YA, Obeid LM, Hsu YT (2011) Mitochondrially targeted ceramides preferentially promote autophagy, retard cell growth, and induce apoptosis. *J Lipid Res* 52:278–288
45. Malhi H, Barreyro FJ, Isomoto H, Bronk SF, Gores GJ (2007) Free fatty acids sensitise hepatocytes to TRAIL mediated cytotoxicity. *Gut* 56:1124–1131
46. Pagliassotti MJ, Wei Y, Wang D (2007) Insulin protects liver cells from saturated fatty acid-induced apoptosis via inhibition of c-Jun NH₂ terminal kinase activity. *Endocrinology* 148:3338–3345
47. Carlsson C, Borg LA, Welsh N (1999) Sodium palmitate induces partial mitochondrial uncoupling and reactive oxygen species in rat pancreatic islets in vitro. *Endocrinology* 140:3422–3428
48. Wei Y, Wang D, Topczewski F, Pagliassotti MJ (2006) Saturated fatty acids induce endoplasmic reticulum stress and apoptosis

- independently of ceramide in liver cells. *Am J Physiol Endocrinol Metab* 291:E275–E281
49. Listenberger LL, Ory DS, Schaffer JE (2001) Palmitate-induced apoptosis can occur through a ceramide-independent pathway. *J Biol Chem* 276:14890–14895
50. Shimabukuro M, Ohneda M, Lee Y, Unger RH (1997) Role of nitric oxide in obesity-induced beta cell disease. *J Clin Invest* 100:290–295

Tissue Distribution of α - and γ -Tocotrienol and γ -Tocopherol in Rats and Interference with Their Accumulation by α -Tocopherol

Tomono Uchida · Chisato Abe · Saki Nomura ·
Tomio Ichikawa · Saiko Ikeda

Received: 12 July 2011 / Accepted: 23 September 2011 / Published online: 1 November 2011
© AOCS 2011

Abstract The aim of this study was to evaluate tissue distribution of vitamin E isoforms such as α - and γ -tocotrienol and γ -tocopherol and interference with their tissue accumulation by α -tocopherol. Rats were fed a diet containing a tocotrienol mixture or γ -tocopherol with or without α -tocopherol, or were administered by gavage an emulsion containing tocotrienol mixture or γ -tocopherol with or without α -tocopherol. There were high levels of α -tocotrienol in the adipose tissue and adrenal gland, γ -tocotrienol in the adipose tissue, and γ -tocopherol in the adrenal gland of rats fed tocotrienol mixture or γ -tocopherol for 7 weeks. Dietary α -tocopherol decreased the α -tocotrienol and γ -tocopherol but not γ -tocotrienol concentrations in tissues. In the oral administration study, both tocopherol and tocotrienol quickly accumulated in the adrenal gland; however, their accumulation in adipose tissue was slow. In contrast to the dietary intake, α -tocopherol, which has the highest affinity for α -tocopherol transfer protein (α TTP), inhibited uptake of γ -tocotrienol to tissues including adipose tissue after oral administration, suggesting that the affinities of tocopherol and tocotrienol for α TTP in the liver were the critical determinants of their uptake to peripheral tissues. Vitamin E deficiency for 4 weeks depleted tocopherol and tocotrienol stores in the

liver but not in adipose tissue. These results indicate that dietary vitamin E slowly accumulates in adipose tissue but the levels are kept without degradation. The property of adipose tissue as vitamin E store causes adipose tissue-specific accumulation of dietary tocotrienol.

Keywords Adipose tissue · Distribution · Rat · Tocopherol · Tocotrienol · Vitamin E

Abbreviations

CEHC	Carboxyethyl-hydroxychroman
α -CEHC	2,5,7,8-Tetramethyl-2(2'-carboxyethyl)-6-hydroxychroman
γ -CEHC	2,7,8-Trimethyl-2(2'-carboxyethyl)-6-hydroxychroman
CYP	Cytochrome P450
SR-BI	Scavenger receptor class B type I
α TTP	α -Tocopherol transfer protein

Introduction

Vitamin E is a fat-soluble antioxidant that inhibits lipid peroxidation in biological membranes. In nature, compounds with vitamin E activity are α -, β -, γ -, and δ -tocopherol and α -, β -, γ -, and δ -tocotrienol. α - and γ -tocopherol are abundant in dietary vitamin E whereas tocotrienol is only present in some plant sources such as palm oil and rice bran; dairy foods contain low levels of tocotrienol. Although tocotrienol has been suggested to have some beneficial biological effects including antioxidative [1, 2], anticancer [3, 4], antiatherosclerotic [5, 6], and neuroprotective [7, 8] effects, its concentration in various tissues is extremely low compared with α -tocopherol.

T. Uchida · S. Nomura · T. Ichikawa · S. Ikeda (✉)
Department of Nutritional Sciences,
Nagoya University of Arts and Sciences,
57 Takenoyama, Iwasaki, Nisshin 470-0196, Japan
e-mail: saiko@nuas.ac.jp

C. Abe
Department of Life and Environmental Science,
Tsu City College, Tsu 514-0112, Japan

Dietary tocopherol and tocotrienol are absorbed in the small intestine and secreted with triacylglycerol-rich chylomicrons into the lymph and blood [9, 10]. After lipolysis of the triacylglycerol-rich chylomicrons in the circulation, the dietary tocopherol and tocotrienol are transported to the liver [11]. α -Tocopherol is preferentially incorporated into VLDL and transported to various tissues by lipoprotein [12, 13] because of its high affinity for α -tocopherol transfer protein (α TTP) [14]. In contrast, the other vitamin E isoforms, γ -tocopherol and tocotrienol, are catabolized and excreted. Therefore, α -tocopherol has the highest biological activity among vitamin E isoforms. Levels of α - and γ -tocotrienol fell below measurable limits in plasma and major tissues of rats fed a diet containing α -tocopherol and α - and γ -tocotrienol for 8 weeks, in contrast to the high levels of α -tocopherol [15].

Some reports showed peripheral tissue-specific accumulation of tocotrienol in animals. Hayes et al. [16] observed significant amounts of α - and γ -tocotrienol in adipose tissue of hamsters fed a diet containing α - and γ -tocotrienol. Podda et al. [17] showed that α - and γ -tocotrienol were present in the skin of hairless mice fed a commercial diet containing small amounts of tocotrienol with a high amount of α -tocopherol. We also observed α - and γ -tocotrienol accumulation in adipose tissue and skin of rats fed a diet containing α -tocopherol and α - and γ -tocotrienol [15, 18]. Thus, tocotrienol accumulates in some peripheral tissues including adipose tissue and skin of rats fed not only tocotrienol but also tocotrienol with α -tocopherol as vitamin E. The tocotrienol accumulation in the peripheral tissues is not explained by its low affinity for α TTP.

We previously found that dietary α -tocopherol decreases α -tocotrienol but not γ -tocotrienol concentration in some tissues including adipose tissue and skin of rats fed tocotrienol for 8 weeks [19]. To obtain more information on tocotrienol metabolism we examined in this study the effect of α -tocopherol supplementation on α - and γ -tocotrienol and γ -tocopherol concentrations in various tissues of rats by both dietary intake and oral administration by gavage of vitamin E isoforms. To detect γ -tocotrienol, which is quickly catabolized, the rats used for the dietary study had free access to food until killed in contrast to food deprivation for 24 h until killed in our previous reports [15, 19]. We also determined the effect of vitamin E on tocopherol and tocotrienol stores in adipose tissue.

Materials and Methods

Materials and Animals

RRR- α -tocopherol, *RRR*- γ -tocopherol, and a tocotrienol mixture extracted from palm oil and purified by HPLC

were used for experimental diets and emulsified solutions for gavage administration. The tocotrienol mixture comprised α -tocotrienol (339 mg/g), β -tocotrienol (40 mg/g), γ -tocotrienol (471 mg/g), δ -tocotrienol (110 mg/g), and *RRR*- δ -tocopherol (1 mg/g); α -, β - and γ -tocopherol were undetectable in the mixture. *RRR*- α -tocopherol, *RRR*- γ -tocopherol, and the tocotrienol mixture were generously donated by Eisai Food and Chemical (Tokyo, Japan).

Male Wistar rats aged 6 weeks were purchased from Japan SLC (Shizuoka, Japan) and maintained at 24 °C with a 12 h light cycle (lights on from 0800 to 2000 hours). This study was approved by the Laboratory Animal Care Committee of Nagoya University of Arts and Sciences; all procedures were performed in accordance with the Animal Experimentation Guidelines of Nagoya University of Arts and Sciences.

Experiment 1

Rats were fed a diet containing 147.5 mg tocotrienol mixture/kg (T3 group), 147.5 mg tocotrienol mixture/kg with 50 mg α -tocopherol/kg (T3 + α T group), 50 mg γ -tocopherol/kg (gT group) or 50 mg γ -tocopherol/kg with 50 mg α -tocopherol/kg (gT + α T group) for 7 weeks. The tocotrienol mixture (147.5 mg) contained 50 mg of α -tocotrienol and 69 mg of γ -tocotrienol. The composition of the diets is shown in Table 1. The diets were freshly prepared, stored at -30 °C, and used within 1 week. The rats had free access to food until sacrifice and were killed by decapitation. The perirenal adipose tissue, epididymal fat, skin, serum, liver, lung, thymus, heart, testis, kidney, adrenal gland, spleen, muscle, and aorta were taken and stored at -30 °C until use for the determination of vitamin E concentration.

Experiment 2

Rats were fed a vitamin E-free diet (Table 1) for 1 month to deplete tissue stores of α -tocopherol. Then, they were administered by gavage 1 mL of an emulsion containing 10 mg of α -tocopherol, 10 mg of γ -tocopherol, or 29.5 mg of tocotrienol mixture. All three emulsions contained 200 mg of sodium taurocholate, 200 mg of triolein, and 50 mg of albumin. The tocotrienol mixture (29.5 mg) contained 10 mg of α -tocotrienol and 14 mg of γ -tocotrienol. The rats had free access to food until vitamin E administration and were deprived of food thereafter. Eight or 24 h after administration, the rats were killed by decapitation and the perirenal adipose tissue, epididymal fat, skin, serum, liver, lung, heart, kidney, adrenal gland, muscle, aorta, and brain were taken and stored at -30 °C until use for the determination of vitamin E concentration. Rats without vitamin E administration were used as the group at 0 h.

Table 1 Composition of experimental diets

	Experiment 1				Experiment 4	Experiments 2, 3, 4
	T3	T3 + aT	gT	gT + aT	aT + T3	E free
g/kg diet						
Casein	200.0	200.0	200.0	200.0	200.0	200.0
L-Cystine	3.0	3.0	3.0	3.0	3.0	3.0
Mineral mixture ^a	35.0	35.0	35.0	35.0	35.0	35.0
Vitamin mixture ^b	10.0	10.0	10.0	10.0	10.0	10.0
Choline	2.5	2.5	2.5	2.5	2.5	2.5
Corn oil ^c	70.0	70.0	70.0	70.0	70.0	70.0
Cellulose powder	50.0	50.0	50.0	50.0	50.0	50.0
Sucrose	100.0	100.0	100.0	100.0	100.0	100.0
Cornstarch	529.4	529.3	529.5	529.4	529.3	529.5
mg/kg diet						
<i>RRR</i> - α -Tocopherol	–	50.0	–	50.0	40.0	–
<i>RRR</i> - γ -Tocopherol	–	–	50.0	50.0	–	–
Tocotrienol mixture ^d	147.5	147.5	–	–	147.5	–

^a AIN93-MX [20]

^b Vitamin E-free AIN93-VX [20]

^c Vitamin E-stripped corn oil (Funabashi Farm, Chiba, Japan)

^d Tocotrienol mixture (147.5 mg) contained 50 mg α -tocotrienol and 69 mg γ -tocotrienol

Experiment 3

Rats were fed a vitamin E-free diet (Table 1) for 1 month to deplete tissue stores of α -tocopherol. Then, they were administered by gavage 1 mL of an emulsion containing 29.5 mg of tocotrienol mixture (T3 group), 29.5 mg of tocotrienol mixture with 1 mg of α -tocopherol (T3 + aT1 group), 29.5 mg of tocotrienol mixture with 10 mg of α -tocopherol (T3 + aT10 group), 10 mg of γ -tocopherol (gT group), 10 mg of γ -tocopherol with 1 mg of α -tocopherol (gT + aT1 group), or 10 mg of γ -tocopherol with 10 mg of α -tocopherol (gT + aT10 group). All six emulsions contained 200 mg of sodium taurocholate, 200 mg of triolein, and 50 mg of albumin. The tocotrienol mixture (29.5 mg) contained 10 mg of α -tocotrienol and 14 mg of γ -tocotrienol. The rats had free access to food until vitamin E administration and were deprived of food thereafter. Eight hours after administration, the rats were killed by decapitation and the perirenal adipose tissue, epididymal fat, skin, serum, liver, lung, heart, kidney, adrenal gland, muscle, aorta, and brain were taken and stored at -30°C until use for the determination of vitamin E concentration.

Experiment 4

Rats were fed a diet containing 40 mg α -tocopherol/kg and 147.5 mg tocotrienol mixture/kg for 6 weeks. The tocotrienol mixture (147.5 mg) contained 50 mg of

α -tocotrienol and 69 mg of γ -tocotrienol. Then, the rats were fed a vitamin E-free diet for 0, 1, 2, 3, or 4 weeks. The composition of the diets is shown in Table 1. The diets were freshly prepared, stored at -30°C , and used within 1 week. After food deprivation overnight, the rats were killed by decapitation and the liver and perirenal adipose tissue taken and stored at -30°C until use for the determination of vitamin E concentration.

Measurement of vitamin E and lipid concentrations

Vitamin E concentration was determined by HPLC with a fluorescence detector, as described previously [11]. Serum cholesterol and triacylglycerol concentrations were measured by commercial kits (Wako Pure Chemical Industries, Osaka, Japan).

Statistical analysis

Data are presented as means \pm SEM for six (experiment 1), five (experiments 2 and 3), or eight rats (experiment 4) per group. Data were analyzed by 1-way ANOVA followed by Tukey's post hoc test. In experiment 1, vitamin E concentration (Figs. 1, 2) were analyzed by Student's *t* test for parameters with equal variance or by Welch's test for parameters with unequal variance. Differences were regarded as significant at $P < 0.05$. All data were analyzed using GraphPad Prism 5 for Windows (GraphPad Software, La Jolla, CA, USA).

Results

Experiment 1

The dietary vitamin E isoforms did not affect growth, organ weights, and serum lipid concentrations (data not shown). Both α - and γ -tocotrienol were present in the perirenal adipose tissue, epididymal fat, skin, serum, liver, lung, thymus, heart, testis, kidney, adrenal gland, spleen, muscle, and aorta in the rats fed the diet containing the tocotrienol mixture (Fig. 1). In the T3 group the α -tocotrienol concentration in adrenal gland was highest among those in all tissues and serum, and the α -tocotrienol concentration in the tissues and serum was lower in the T3 + aT group than in the T3 group. In contrast, the γ -tocotrienol concentration was higher in the adipose tissues than in the other tissues and serum in the T3 group whereas the γ -tocotrienol concentration in almost all tissues of the T3 and T3 + aT groups was similar.

γ -Tocopherol was also present in all tissues and serum of the gT group, and the γ -tocopherol concentration in the

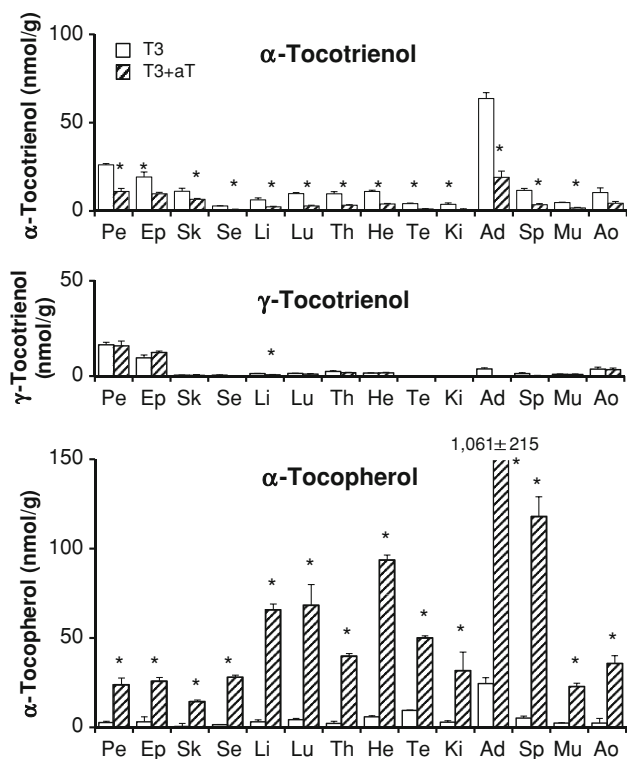


Fig. 1 Tissue distribution of α - and γ -tocotrienol and α -tocopherol in rats fed a diet containing a tocotrienol mixture (T3) or a tocotrienol mixture with α -tocopherol (T3 + aT) in experiment 1. γ -Tocotrienol was undetectable in adrenal gland of the T3 + aT group. Values are means \pm SEM; $n = 6$. * $P < 0.05$ vs. T3 group. *Pe* perirenal adipose tissue, *Ep* epididymal fat, *Sk* skin, *Se* serum, *Li* liver, *Lu* lung, *Th* thymus, *He* heart, *Te* testis, *Ki* kidney, *Ad* adrenal gland, *Sp* spleen, *Mu* muscle, *Ao* aorta

adrenal gland was higher than those that in the other tissues (Fig. 2). The γ -tocopherol concentration in all tissues except for liver and aorta was lower in the gT + aT group than in the gT group. In the T3 + aT (Fig. 1) and gT + aT (Fig. 2) groups fed a diet containing α -tocopherol, α -tocopherol concentration in the adrenal gland was extremely high ($>1 \mu\text{mol/g}$) compared with in other tissues and serum.

Experiment 2

The α -tocopherol concentration in serum, liver, kidney, adrenal gland, heart, lung, and skin was higher at 8 and 24 h than that at 0 h, however, the concentrations in the aorta, perirenal adipose tissue, epididymal fat, and brain at 24 h were not different from that at 0 h (Fig. 3). At 8 and 24 h, the α -tocopherol concentration was highest among four isomers in serum, liver, kidney, adrenal gland, aorta, muscle, perirenal adipose tissue, epididymal fat, and brain. γ -Tocopherol and α - and γ -tocotrienol were present in serum and tissues except for epididymal fat and brain at 8 and 24 h, although they were undetectable at 0 h. The γ -tocotrienol concentration was lower than those of γ -tocopherol and α -tocotrienol in serum, liver, kidney, adrenal gland, and lung at 8 h.

Experiment 3

The α -tocopherol in serum, liver, kidney, and adrenal gland was higher in the T3 + aT1 group than in the T3 group, and

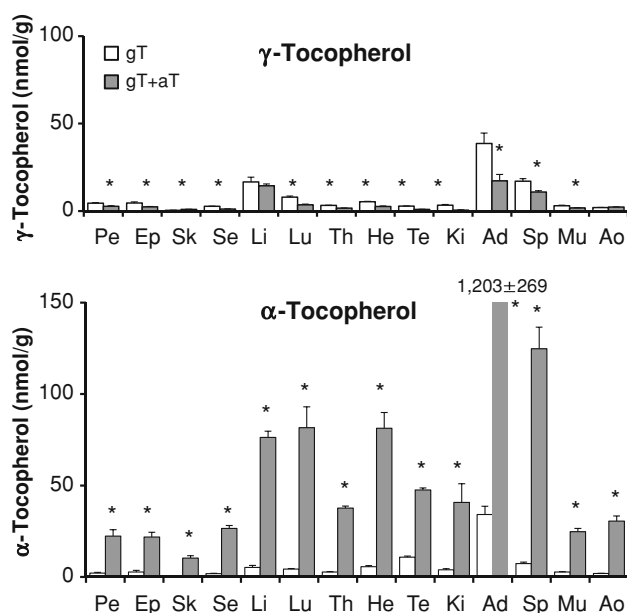


Fig. 2 Tissue distribution of γ - and α -tocopherol in rats fed a diet containing γ -tocopherol (gT) or γ -tocopherol with α -tocopherol (gT + aT) in experiment 1. Values are means \pm SEM; $n = 6$. * $P < 0.05$ vs. gT group. *Pe* perirenal adipose tissue, *Ep* epididymal fat, *Sk* skin, *Se* serum, *Li* liver, *Lu* lung, *Th* thymus, *He* heart, *Te* testis, *Ki* kidney, *Ad* adrenal gland, *Sp* spleen, *Mu* muscle, *Ao* aorta

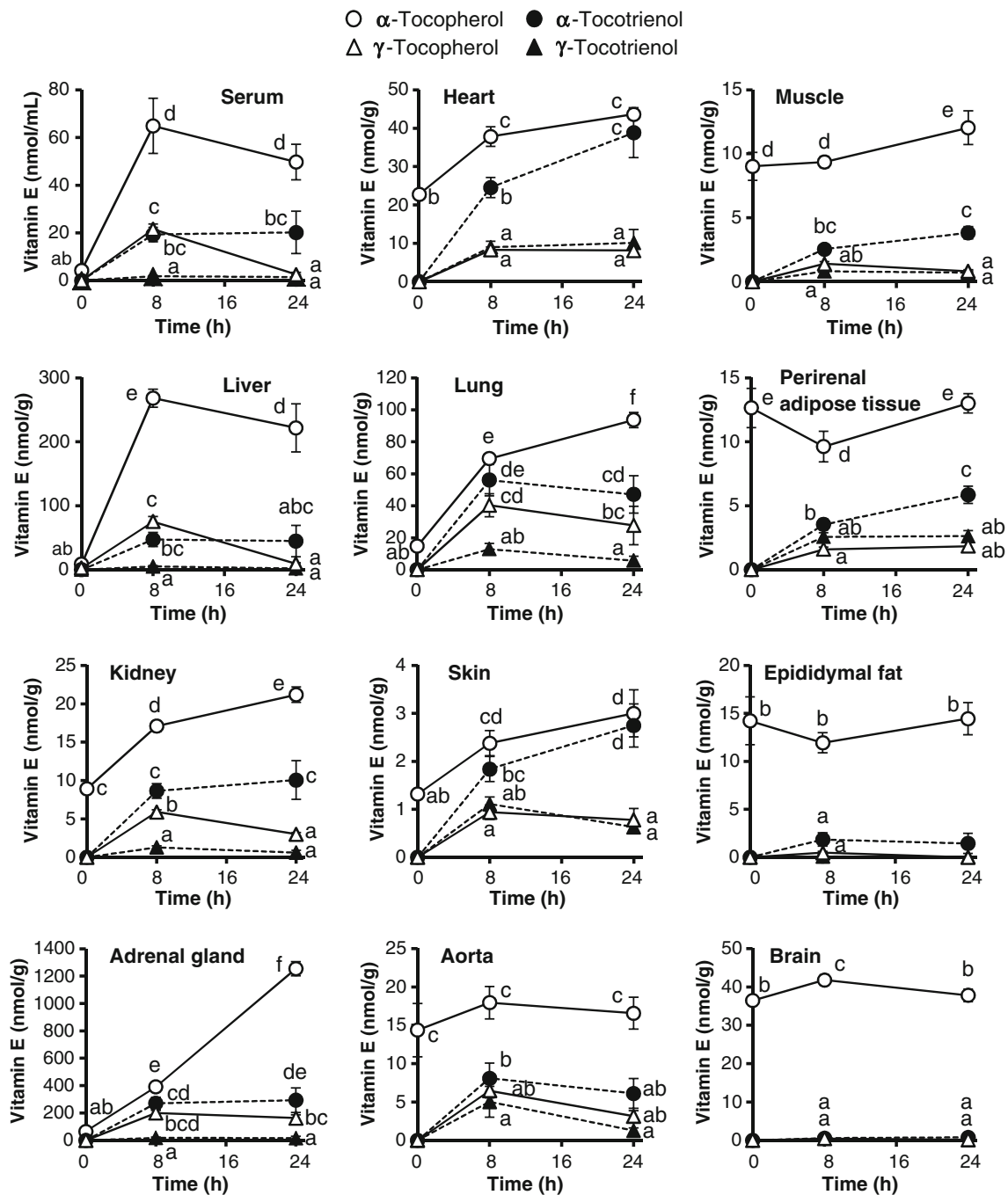


Fig. 3 Time-course changes of α - and γ -tocopherol and α - and γ -tocotrienol concentrations in tissues and serum after oral administration of α - or γ -tocopherol or a tocotrienol mixture in experiment 2. Values are means \pm SEM; $n = 5$. Means not sharing a letter differ at

a significance of $P < 0.05$; symbols without letters are below the detection limits. Only α -tocopherol was detected in serum and tissues at 0 h. γ -Tocopherol was undetectable in epididymal fat and γ -tocotrienol was undetectable in epididymal fat and brain at 24 h

the concentrations in serum, liver, kidney, adrenal gland, heart, lung, skin, and aorta were higher in the T3 + aT10 group than in the T3 group (Fig. 4). In contrast, α -tocotrienol concentrations in serum, kidney, adrenal gland, heart, lung, skin, aorta, muscle, and perirenal adipose tissue were lower in the T3 + aT1 and T3 + aT10 groups than in the T3 group. In heart, skin, aorta, and perirenal adipose tissues the

γ -tocotrienol concentrations were also lower in the T3 + aT1 and T3 + aT10 groups than in the T3 group.

In addition, the α -tocopherol concentration in the kidney was higher in the gT + aT1 group than in the gT group, and α -tocopherol concentrations in serum, liver, kidney, adrenal gland, heart, lung, skin, and aorta were higher in the gT + aT10 group than in the gT group (Fig. 5). In

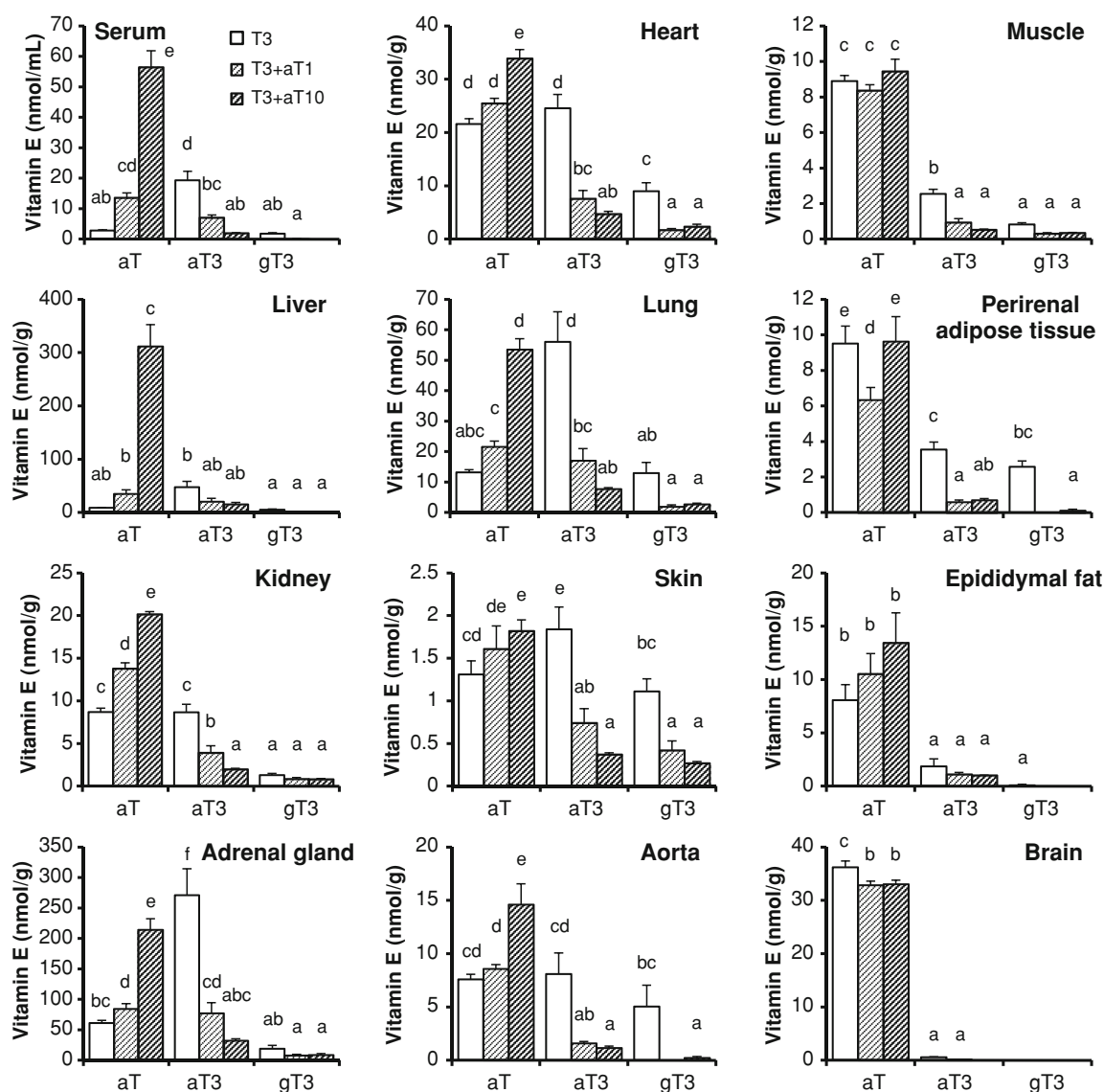


Fig. 4 Concentrations of α -tocopherol (aT), α -tocotrienol (aT3), and γ -tocotrienol (gT3) in tissues and serum 8 h after oral administration of 29.5 mg of tocotrienol mixture (T3), 29.5 mg of tocotrienol mixture with 1 mg of α -tocopherol (T3 + aT1), or 29.5 mg of

tocotrienol mixture with 10 mg of α -tocopherol (T3 + aT10), in experiment 3. The tocotrienol mixture (29.5 mg) contained 10 mg of α -tocotrienol and 14 mg of γ -tocotrienol. Values are mean + SEM; $n = 5$. Means not sharing a letter differ at $P < 0.05$

contrast, γ -tocopherol concentration in adrenal gland, lung, and aorta was lower in the gT + aT1 group than in the gT group, and γ -tocopherol concentrations in serum, kidney, adrenal gland, heart, lung, and skin were lower in the gT + aT10 group than in the gT group.

Experiment 4

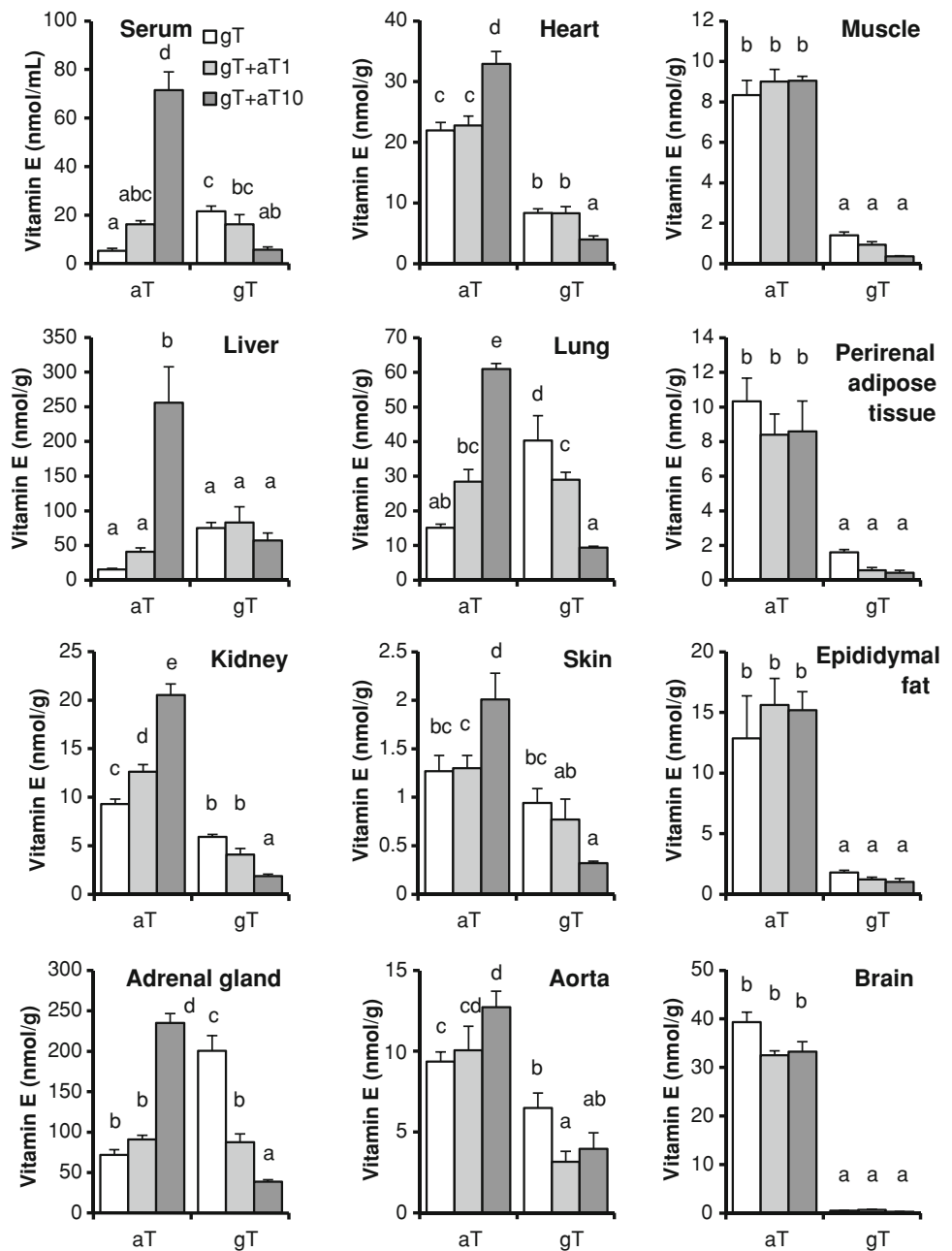
The body weight of rats after feeding on a diet containing α -tocopherol and α - and γ -tocotrienol for 6 weeks was 234.6 ± 4.6 g, and those at 0, 1, 2, 3, and 4 weeks after intake of vitamin E-free diet were 221.9 ± 4.7 , 242.8 ± 4.8 , 256.8 ± 4.6 , 272.5 ± 7.1 , and 291.2 ± 3.5 g, respectively.

The vitamin E-deficient periods did not affect liver and spleen weights (data not shown). α -Tocopherol and α - and γ -tocotrienol concentrations in perirenal adipose tissue were unchanged for 4 weeks, although α -tocopherol and α -tocotrienol concentrations in liver decreased over a period of 1–4 weeks (Fig. 6). γ -Tocotrienol was undetectable in liver at 4 weeks.

Discussion

We had previously found that dietary intake of tocotrienol for 8 weeks caused accumulation of a significant amount of

Fig. 5 Concentrations of α -tocopherol (aT) and γ -tocopherol (gT) in tissues and serum at 8 h after oral administration of 10 mg of γ -tocopherol (gT), 10 mg of γ -tocopherol with 1 mg of α -tocopherol (gT + aT1), or 10 mg of γ -tocopherol with 10 mg of α -tocopherol (gT + aT10), in experiment 3. Values are means + SEM; $n = 5$. Means not sharing a letter differ at $P < 0.05$

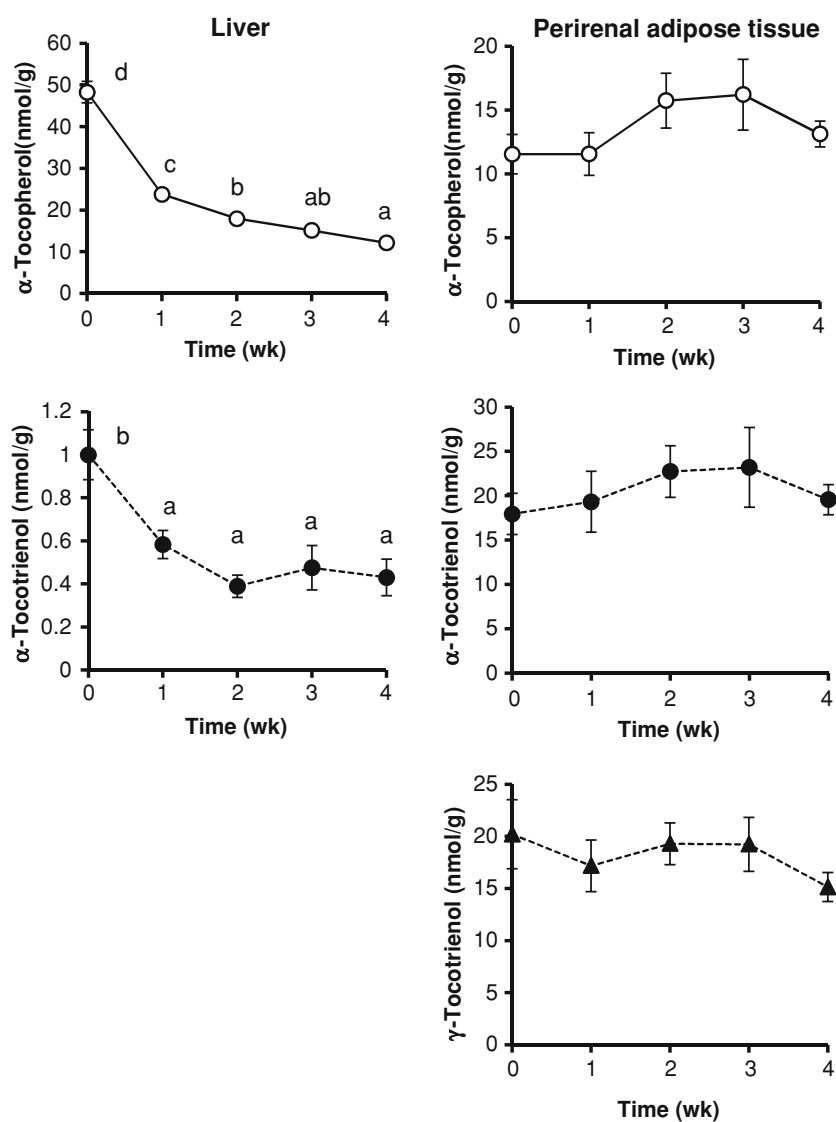


tocotrienol in adipose tissue [15, 19]. Dietary α -tocopherol decreased α -tocotrienol but not γ -tocotrienol concentration in liver, kidney, heart, lung, brain, muscle, perirenal adipose tissue, epididymal fat, skin, and plasma [19]. In the present study, we examined the effect of dietary α -tocopherol on α - and γ -tocotrienol and γ -tocopherol concentrations in the same tissues along with the thymus, testis, adrenal gland, spleen, and aorta of rats killed without food deprivation.

A considerable amount of α - and γ -tocotrienol accumulated in the perirenal adipose tissues and epididymal fat of rats fed a tocotrienol mixture (Fig. 1), as seen in the

previous study [19], whereas the γ -tocopherol concentrations were lower in the adipose tissues than in some tissues including adrenal gland, liver, and spleen of rats fed γ -tocopherol (Fig. 2). The α -tocopherol concentration was also lower in adipose tissue than those in the adrenal gland, liver, and spleen of rats fed α -tocopherol (Figs. 1, 2). The tissue-specific accumulation of tocotrienol is not explained by its affinity for α TTP because the affinity of α -tocotrienol for α TTP is nearly identical to that of γ -tocopherol—12.4 and 8.9% of the affinity of α -tocopherol, respectively [14]. Moreover, the α - and γ -tocotrienol concentrations were 9.4- and 36.4-fold higher, respectively, in the perirenal adipose

Fig. 6 Time-course changes of α -tocopherol and α - and γ -tocotrienol concentrations in liver and perirenal adipose tissue of rats fed vitamin E-free diet for 4 weeks in experiment 4. Rats were fed diet containing α -tocopherol and tocotrienol mixture for 6 weeks before intake of a vitamin E-free diet. γ -Tocotrienol was undetectable in the liver at 4 weeks. Values are means \pm SEM; $n = 8$. Means not sharing a letter differ at $P < 0.05$



tissue than in serum whereas the α - and γ -tocopherol concentrations were 0.9- and 1.7-fold higher. The data suggest that adipose tissue preferentially uptakes or stores tocotrienol compared with tocopherol.

To confirm the preferential uptake of tocotrienol into adipose tissue, the time-course change of the tocotrienol concentration for 24 h after tocotrienol administration by gavage was determined in experiment 2 (Fig. 3). Both tocopherol and tocotrienol quickly accumulated in the adrenal gland. However, tocopherol and tocotrienol slowly accumulated in skin, muscle, adipose tissues, and brain. α -Tocotrienol concentrations in these tissues at 8 h were <5 nmol/g. Moreover, γ -tocotrienol was undetectable in epididymal fat at 24 h after administration of the tocotrienol mixture. This suggests that tocotrienol accumulation in the adrenal gland in experiment 1 was caused by preferential uptake of tocotrienol, but that in adipose tissue was not.

Dietary α -tocopherol lowered α -tocotrienol and γ -tocopherol concentrations in the tissues of rats fed the tocotrienol mixture or γ -tocopherol (Figs. 1, 2). However, dietary α -tocopherol did not lower γ -tocotrienol concentrations in the tissues of rats fed the tocotrienol mixture (Fig. 1). Since the affinities of tocopherol and tocotrienol for α TTP in the liver are critical for their discrimination [14], the data indicate a possibility of liver-independent transport of dietary γ -tocotrienol into the various tissues. In experiment 3, the effect of α -tocopherol supplementation on the other tocopherol and tocotrienol concentrations at 8 h after oral administration of the isoforms to vitamin E-deficient rats were determined. α -Tocopherol supplementation inhibited α -tocotrienol and γ -tocopherol uptake to the various tissues (Figs. 4, 5). Both α -tocotrienol and γ -tocopherol concentrations in the adrenal gland and α -tocotrienol concentration in the perirenal adipose tissue were clearly lowered by simultaneous administration of

α -tocopherol. Surprisingly, α -tocopherol supplementation also inhibited γ -tocotrienol uptake to some peripheral tissues such as heart, skin, aorta, and perirenal adipose tissue, although those concentrations were low. Thus α -tocopherol inhibits uptake of not only α -tocotrienol and γ -tocopherol but also γ -tocotrienol to the peripheral tissues after their oral administration. The interference with the tissue accumulation of the other isoforms by α -tocopherol does not suggest a liver-independent transport of dietary γ -tocotrienol to the tissues but a similar transport mechanism to that of α -tocotrienol. It is likely that both α - and γ -tocotrienol along with tocopherol are transported to the tissues by liver-dependent transport mechanism.

Tissue accumulation of vitamin E results from flux, balance of its uptake, and efflux. We compared vitamin E decreases in liver and adipose tissue by vitamin E deficiency in experiment 4. Machlin et al. [21] reported that α -tocopherol depletion from adipose tissue was extremely slow in vitamin E-deficient guinea pigs, whereas α -tocopherol concentration in the liver decreased within 1 week. In the present study, α -tocopherol and α - and γ -tocotrienol concentrations in adipose tissue were unchanged at 4 weeks after the change from diet containing α -tocopherol and α - and γ -tocotrienol to vitamin E-free diet. In contrast, both α -tocopherol and α -tocotrienol concentrations in the liver decreased after 1 week. Therefore, adipose tissue is a unique site for body storage of not only tocopherol but also tocotrienol. These data indicate that vitamin E uptake to adipose tissue is slow (Fig. 3) but the vitamin E levels in adipose tissue are maintained without degradation for several weeks. We believe that maintenance of the vitamin E level without degradation causes adipose tissue-specific accumulation of dietary tocotrienol (Fig. 1). However, the reason for γ -tocotrienol accumulation without interference by α -tocopherol (Fig. 1), unlike in the study of oral administration of γ -tocotrienol (Fig. 4), remains unclear.

It was revealed that a significant amount of α -tocopherol accumulated in the adrenal gland. The adrenal α -tocopherol concentration was $>1 \mu\text{mol/g}$ in rats fed a diet containing 50 mg/kg of α -tocopherol for 7 weeks (Figs. 1, 2). Moreover, α -tocopherol quickly accumulated in the adrenal gland, and the concentration reached $>1 \mu\text{mol/g}$ at 24 h after α -tocopherol administration by gavage (Fig. 3). The adrenal gland has high steroidogenic activity, and the steroidogenesis involves cytochrome P450 (CYP)-dependent reactions, which are major sources of free radical formation. The tissue has high levels of not only α -tocopherol but also other antioxidants, ascorbic acid, and reduced glutathione and is resistant to prooxidant-induced damage [22]. Additionally, vitamin E deficiency reduces synthesis and secretion of corticosterone in rats [23]. These data suggest that antioxidants protect the adrenal gland from oxidative stress associated with steroidogenesis.

Rats have high levels of HDL, a major lipoprotein associated with α -tocopherol in the circulation. Recent studies suggest that the scavenger receptor class B type I (SR-BI), which mediates cellular uptake of cholesteryl ester from HDL, is also involved in α -tocopherol uptake in the brain [24, 25], lung [26], and its intestinal absorption [27]. In SR-BI-deficient mice, the α -tocopherol concentrations in some tissues including ovary, testis, lung, and brain decrease in contrast to increasing in plasma [28]. SR-BI might be involved in the preferential uptake of α -tocopherol in adipose tissue because SR-BI is highly expressed in the adrenal gland [29] and contributes to steroidogenesis.

Vitamin E catabolism is another important factor for its bioavailability. Tocopherol and tocotrienol undergo catabolism to phytyl short-chain carboxyethyl-hydroxychromans (CEHCs) such as 2,5,7,8-tetramethyl-2(2'-carboxyethyl)-6-hydroxychroman (α -CEHC), a metabolite of α -tocopherol and α -tocotrienol, and 2,7,8-trimethyl-2(2'-carboxyethyl)-6-hydroxychroman (γ -CEHC), a metabolite of γ -tocopherol and γ -tocotrienol [30–32]. The catabolic pathway involves ω -hydroxylation of the phytyl chain and subsequent β -oxidation [33]. The rate-limiting step is ω -hydroxylation of tocopherol and tocotrienol by CYP4F2 in humans [34, 35]. CEHC is then conjugated with glucuronate in humans or with sulfate in rats and subsequently excreted in the urine. Vitamin E metabolites are found in the liver, kidneys, small intestine, and serum of rats after oral administration of tocopherol or tocotrienol [36].

After oral administration of α - and γ -tocopherol, γ -tocopherol is rapidly catabolized to γ -CEHC whereas α -tocopherol is maintained in the plasma and little is metabolized to α -CEHC in humans [37]. In addition, tocotrienol is rapidly catabolized compared with tocopherol in human liver microsomes [35]. We found that ketoconazole, a potent CYP inhibitor, decreased urinary excretion of α - and γ -CEHC, and increased α - and γ -tocotrienol concentrations in various tissues of rats after oral administration of α - and γ -tocotrienol [38]. Ketoconazole also increased γ -tocopherol concentrations in rat tissues by inhibiting its catabolism to γ -CEHC, suggesting that CYP-dependent catabolism of vitamin E is a critical determinant of its bioavailability. Some reports indicate that α -tocopherol enhances γ -tocopherol catabolism to γ -CEHC [35, 36, 39]. In contrast, dietary α -tocopherol does not affect urinary excretion of γ -CEHC in rats fed a diet containing γ -tocotrienol for 8 weeks [19]. The minor effect of α -tocopherol on γ -tocotrienol catabolism might contribute towards γ -tocotrienol accumulation without interference by α -tocopherol (Fig. 1).

In the present study, we found high levels of α -tocotrienol in adipose tissue and adrenal gland, γ -tocotrienol in adipose tissue but not in the adrenal gland, and

γ -tocopherol not in adipose tissue but in adrenal gland of rats fed diet containing α - and γ -tocotrienol and γ -tocopherol. After oral administration, tocotrienol slowly accumulated in adipose tissue compared with in other tissues including adrenal gland. The α - and γ -tocotrienol uptake to some peripheral tissues including adipose tissue was clearly inhibited by α -tocopherol. Moreover, adipose tissue kept high vitamin E levels without degradation for several weeks in vitamin E-free rats, suggesting that the property of the adipose tissue as a vitamin E store causes adipose tissue-specific accumulation of dietary tocotrienol.

Acknowledgments This work was supported by KAKENHI (21700771, 22500782). We acknowledge generous donation of vitamin E isoforms and CEHC from Eisai Food & Chemical.

References

- Schaffer S, Müller WE, Eckert GP (2005) Tocotrienols: constitutional effects in aging and disease. *J Nutr* 135:151–154
- Serbinova EA, Packer L (1994) Antioxidant properties of α -tocopherol and α -tocotrienol. *Methods Enzymol* 234:354–366
- Miyazawa T, Shibata A, Sookwong P, Kawakami Y, Eitsuka T, Asai A, Oikawa S, Nakagawa K (2009) Antiangiogenic and anticancer potential of unsaturated vitamin E (tocotrienol). *J Nutr Biochem* 20:79–86
- Nesaretnam K (2008) Multitargeted therapy of cancer by tocotrienols. *Cancer Lett* 269:388–395
- Qureshi AA, Salser WA, Parmar R, Emeson EE (2001) Novel tocotrienols of rice bran inhibit atherosclerotic lesions in C57BL/6 ApoE-deficient mice. *J Nutr* 131:2606–2618
- Parker RA, Pearce BC, Clark RW, Gordon DA, Wright JJ (1993) Tocotrienols regulate cholesterol production in mammalian cells by post-transcriptional suppression of 3-hydroxy-3-methylglutaryl-coenzyme A reductase. *J Biol Chem* 268:11230–11238
- Khanna S, Parinandi NL, Kotha SR, Roy S, Rink C, Bibus D, Sen CK (2010) Nanomolar vitamin E α -tocotrienol inhibits glutamate-induced activation of phospholipase A2 and causes neuroprotection. *J Neurochem* 112:1249–1260
- Sen CK, Khanna S, Roy S (2004) Tocotrienol: the natural vitamin E to defend the nervous system? *Ann NY Acad Sci* 1031:127–142
- Kayden HJ, Traber MG (1993) Absorption, lipoprotein transport, and regulation of plasma concentrations of vitamin E in humans. *J Lipid Res* 34:343–358
- Traber MG, Sies H (1996) Vitamin E in humans: demand and delivery. *Annu Rev Nutr* 16:321–347
- Abe C, Ikeda S, Uchida T, Yamashita K, Ichikawa T (2007) Triton WR1339, an inhibitor of lipoprotein lipase, decreases vitamin E concentration in some tissues of rats by inhibiting its transport to liver. *J Nutr* 137:345–350
- Traber MG, Arai H (1999) Molecular mechanisms of vitamin E transport. *Annu Rev Nutr* 19:343–355
- Traber MG, Burton GW, Hamilton RL (2004) Vitamin E trafficking. *Ann NY Acad Sci* 1031:1–12
- Hosomi A, Arita M, Sato Y, Kiyose C, Ueda T, Igarashi O, Arai H, Inoue K (1997) Affinity for α -tocopherol transfer protein as a determinant of the biological activities of vitamin E analogs. *FEBS Lett* 409:105–108
- Ikeda S, Toyoshima K, Yamashita K (2001) Dietary sesame seeds elevate α - and γ -tocotrienol concentrations in skin and adipose tissue of rats fed the tocotrienol-rich fraction extracted from palm oil. *J Nutr* 131:2892–2897
- Hayes KC, Pronczuk A, Liang JS (1993) Differences in the plasma transport and tissue concentrations of tocopherols and tocotrienols: observations in humans and hamsters. *Proc Soc Exp Biol Med* 202:353–359
- Podda M, Weber C, Traber MG, Packer L (1996) Simultaneous determination of tissue tocopherols, tocotrienols, ubiquinol, and ubiquinones. *J Lipid Res* 37:893–901
- Ikeda S, Niwa T, Yamashita K (2000) Selective uptake of dietary tocotrienols into rat skin. *J Nutr Sci Vitaminol* 46:141–143
- Ikeda S, Tohyama T, Yoshimura H, Hamamura K, Abe K, Yamashita K (2003) Dietary α -tocopherol decrease α -tocotrienol but not γ -tocotrienol concentration in rats. *J Nutr* 133:428–434
- American Institute of Nutrition (1993) AIN-93 purified diets for laboratory rodents: final report of the American Institute of Nutrition ad hoc writing committee on the reformulation of the AIN-76A rodent diet. *J Nutr* 123:1939–1951
- Machlin LJ, Keating J, Nelson J, Brin M, Filipinski R, Miller ON (1979) Availability of adipose tissue tocopherol in the guinea pig. *J Nutr* 109:105–109
- Azhar S, Cao L, Reaven E (1995) Alteration of the adrenal antioxidant defense system during aging in rats. *J Clin Invest* 96:1414–1424
- Abidi P, Leers-Sucheta S, Azhar S (2004) Suppression of steroidogenesis and activator protein-1 transcription factor activity in rat adrenals by vitamin E deficiency-induced chronic oxidative stress. *J Nutr Biochem* 15:210–219
- Goti D, Hrzenjak A, Levak-Frank S, Frank S, van der Westhuyzen DR, Malle E, Sattler W (2001) Scavenger receptor class B, type I is expressed in porcine brain capillary endothelial cells and contributes to selective uptake of HDL-associated vitamin E. *J Neurochem* 76:498–508
- Balazs Z, Panzenboeck U, Hammer A, Sovic A, Quehenberger O, Malle E, Sattler W (2004) Uptake and transport of high-density lipoprotein (HDL) and HDL-associated α -tocopherol by an in vitro blood-brain barrier model. *J Neurochem* 89:939–950
- Kolleck I, Schlame M, Fechner H, Looman AC, Wissel H, Rüstow B (1999) HDL is the major source of vitamin E for type II pneumocytes. *Free Radic Biol Med* 27:882–890
- Reboul E, Klein A, Bietrix F, Gleize B, Malezet-Desmoulins C, Schneider M, Margotat A, Lagrost L, Collet X, Borel P (2006) Scavenger receptor class B type I (SR-BI) is involved in vitamin E transport across the enterocyte. *J Biol Chem* 281:4739–4745
- Mardones P, Strobel P, Miranda S, Leighton F, Quiñones V, Amigo L, Rozowski J, Krieger M, Rigotti A (2002) α -Tocopherol metabolism is abnormal in scavenger receptor class B type I (SR-BI)-deficient mice. *J Nutr* 132:443–449
- Landschulz KT, Pathak RK, Rigotti A, Krieger M, Hobbs HH (1996) Regulation of scavenger receptor, class B, type I, a high density lipoprotein receptor, in liver and steroidogenic tissues of the rat. *J Clin Invest* 98:984–995
- Schultz M, Leist M, Petrzika M, Gassmann B, Brigelius-Flohé R (1995) Novel urinary metabolite of α -tocopherol, 2,5,7,8-tetramethyl-2(2'-carboxyethyl)-6-hydroxychroman, as an indicator of an adequate vitamin E supply? *Am J Clin Nutr* 62:1527S–1534S
- Swanson JE, Ben RN, Burton GW, Parker RS (1999) Urinary excretion of 2,7,8-trimethyl-2-(β -carboxyethyl)-6-hydroxychroman is a major route of elimination of γ -tocopherol in humans. *J Lipid Res* 40:665–671
- Lodge JK, Ridlington J, Leonard S, Vaule H, Traber MG (2001) α - and γ -Tocotrienols are metabolized to carboxyethyl-hydroxychroman derivatives and excreted in human urine. *Lipids* 36:43–48

33. Birringer M, Pfluger P, Kluth D, Landes N, Brigelius-Flohé R (2002) Identities and differences in the metabolism of tocotrienols and tocopherols in HepG2 cells. *J Nutr* 132:3113–3118
34. Sontag TJ, Parker RS (2002) Cytochrome P450 ω -hydroxylase pathway of tocopherol catabolism: novel mechanism of regulation of vitamin E status. *J Biol Chem* 277:25290–25296
35. Sontag TJ, Parker RS (2007) Influence of major structural features of tocopherols and tocotrienols on their ω -oxidation by tocopherol- ω -hydroxylase. *J Lipid Res* 48:1090–1098
36. Uchida T, Nomura S, Ichikawa T, Abe C, Ikeda S (2011) Tissue distribution of vitamin E metabolites in rats after oral administration of tocopherol or tocotrienol. *J Nutr Sci Vitaminol* 57:326–332
37. Leonard SW, Paterson E, Atkinson JK, Ramakrishnan R, Cross CE, Traber MG (2005) Studies in humans using deuterium-labeled α - and γ -tocopherols demonstrate faster plasma γ -tocopherol disappearance and greater γ -metabolite production. *Free Radic Biol Med* 38:857–866
38. Abe C, Uchida T, Ohta M, Ichikawa T, Yamashita K, Ikeda S (2007) Cytochrome P450-dependent metabolism of vitamin E isoforms is a critical determinant of their tissue concentrations in rats. *Lipids* 42:637–645
39. Kiyose C, Saito H, Kaneko K, Hamamura K, Tomioka M, Ueda T, Igarashi O (2001) α -Tocopherol affects the urinary and biliary excretion of 2, 7, 8-trimethyl-2(2'-carboxyethyl)-6-hydroxychroman, γ -tocopherol metabolite, in rats. *Lipids* 36:467–472

Fish Oil Normalizes Plasma Glucose Levels and Improves Liver Carbohydrate Metabolism in Rats Fed a Sucrose-Rich Diet

Gustavo J. Hein · Adriana Chicco ·
Yolanda B. Lombardo

Received: 27 April 2011 / Accepted: 4 October 2011 / Published online: 2 November 2011
© AOCs 2011

Abstract A sucrose-rich diet (SRD) induces insulin resistance and dyslipidemia with impaired hepatic glucose production and gluconeogenesis, accompanied by altered post-receptor insulin signaling steps. The aim of this study was to examine the effectiveness of fish oil (FO) to reverse or improve the impaired hepatic glucose metabolism once installed in rats fed 8 months a SRD. In the liver of rats fed SRD in which FO replaced corn-oil during the last 2 months, as dietary fat, several key enzyme activities and metabolites involved in glucose metabolisms (phosphorylation, glycolysis, gluconeogenesis and oxidative and non oxidative glucose pathway) were measured. The protein mass levels of IRS-1 and α p85 PI-3K at basal conditions were also analyzed. FO improved the altered activities of some enzymes involved in the glycolytic and oxidative pathways observed in the liver of SRD fed rats but was unable to restore the impaired capacity of glucose phosphorylation. Moreover, FO reversed the increase in PEPCK and G-6-Pase and reduced the G-6-Pase/GK ratio. Glycogen concentration and GSa activity returned to levels similar to those observed in the liver of the control-fed rats. Besides, FO did not modify the altered protein mass levels of IRS-1 and α p85 PI-3K. Finally, dietary FO was effective in reversing or improving the impaired activities of several key enzymes of hepatic carbohydrate metabolism contributing, at least in part, to the normalization of plasma glucose levels in the SRD-fed rats. However, these positive effects of FO were not observed under basal conditions in the early steps of insulin signaling transduction.

Keywords Sucrose-rich diet · n-3 Polyunsaturated fatty acids · Hepatic glucose metabolism · IRS-1 · α p85 PI-3K · Insulin resistance

Abbreviations

AKt	Serine/threonine protein kinase
AMPK α 2	AMP activated kinase isoform
C	Cholesterol
CD	High starch diet
ChREBP	Carbohydrate response element binding protein
CO	Corn oil
DAGT	Diacylglycerol acyltransferase
FFA	Unesterified fatty acids
FO	Fish oil
G-6-Pase	Glucose-6-phosphate phosphatase
GK	Glucokinase
Glucose-6-P	Glucose-6-phosphate
Glut2 and Glut4	Glucose transporters 2 and 4
GSa	Glycogen synthase a
HK	Hexokinase
IRS	Insulin receptor substrate
JNK	c-jun N terminal kinase
LXR	Liver X receptor
PDHa	Pyruvate dehydrogenase active form
PDHc	PDH complex
PEPCK	Phosphoenolpyruvate carboxykinase
PI-3K	Phosphoinositide-3 kinase
PK	Pyruvate kinase
PPAR α	Peroxisome proliferators activated receptor α
PUFA	Polyunsaturated fatty acid(s)
SRD	Sucrose rich diet
TAG	Triacylglycerol(s)

G. J. Hein · A. Chicco · Y. B. Lombardo (✉)
Department of Biochemistry, School of Biochemistry,
University of Litoral, Ciudad Universitaria Paraje El Pozo,
CC 242 (3000), Santa Fe, Argentina
e-mail: ylombard@fbc.unl.edu.ar

Introduction

The liver plays a central role in the regulation of glucose metabolism and maintenance of blood glucose homeostasis by regulating glycogen storage and breakdown and gluconeogenesis. It is well known that alterations in the composition of dietary macronutrients (e.g. carbohydrates, lipids, etc.) could deeply and rapidly modify the hepatic glucose metabolism in rats and humans [1–4]. In this regard, several studies have observed reduced insulin suppression of glucose production and hepatic gluconeogenesis, increased capacity for gluconeogenesis, reduced protein mass levels of Glut2 (isolated hepatocytes) and high TAG contents in the liver of rats fed a high sucrose/fructose diet for 1–8 weeks [1, 5–7]. Moreover, sucrose induced the impairment of hepatic insulin action involving multiple post-receptor insulin signaling steps such as tyrosine phosphorylation of insulin receptor substrate proteins-1 and 2 (IRS-1, IRS-2), interaction of phosphoinositide kinase (PI-3K) with IRS protein and phosphorylation of AKt [8]. Recent studies have suggested that the c-jun N terminal kinase (JNK) may also contribute to fructose induced antagonist of insulin signaling in liver [9].

On the other hand, animal studies have demonstrated that the quality of dietary fat is as important as its quantity to induce or prevent insulin resistance [10]. There is accumulated evidence of the beneficial role of n-3 long chain fatty acids (20:5 n-3, 22:6 n-3 PUFA) contained in dietary fish oil on animal and human health, especially concerning their protecting role against the adverse symptoms of the metabolic syndrome [11–13]. It has been shown that dietary fish oil prevents the onset of insulin resistance and dyslipidemia, hepatic steatosis as well as impaired glucose tolerance in rats fed a high-fat or high-sucrose diet [13–15]. However, few studies have analyzed the capacity of dietary fish oil to reverse insulin resistance once installed in rats after a long-term (6 months) feeding of a sucrose-rich diet (SRD). Using this experimental model we have previously demonstrated that partial changes in the dietary fat composition—from corn oil (18% total energy) to fish oil (cod liver oil 16% plus corn oil 2% of total energy)—lead to a normalization of the preexisting state of dyslipidemia, altered glucose homeostasis, whole body peripheral insulin insensitivity and visceral adiposity without detectable changes in plasma insulin levels [11, 16, 17]. However, a study by Podolin et al. [18] found that when the sucrose-rich diet containing a lower amount of menhaden oil (6% total energy) was given to insulin-resistant rats, the insulin action on the glucose metabolism remained impaired. The amount, duration and fatty acid composition of supplemented n-3 PUFA could also contribute to this discrepancy.

N-3 PUFA regulate the expression of a number of genes involved in lipid and carbohydrate metabolism by modulating the activity or expression of several transcription factors [19]. In the liver of rats fed a SRD during 8 months, Hein et al. [20] have recently demonstrated a decrease in the protein mass expression of liver X receptor α (LXR α) while enhancing peroxisome proliferators activated receptor α (PPAR α) after shifting the source of dietary fat from corn oil to fish oil during the last 2 months of the experimental period. This was accompanied by a decrease in the activities of hepatic enzymes involved in “de novo” lipogenesis, stimulating fatty acid oxidation and therefore decreasing liver steatosis, hyperlipidemia and normalizing the whole body peripheral insulin resistance produced by the SRD. Among the effects of n-3 PUFA on liver carbohydrate metabolism, Liimatta et al. [21] demonstrated that n-3 PUFA decrease liver pyruvate kinase activity while Jump et al. [22] showed that they suppress mRNA encoding glucokinase. Recently, it was shown that a carbohydrate response element binding protein (ChREBP) is a pivotal transcription factor implicated in the reciprocal regulation of lipogenesis and glycolysis by glucose and n-3 PUFA [23].

To our knowledge, no studies have been reported focusing on the possible beneficial effect of dietary n-3 PUFA to improve/reverse the impaired hepatic glucose metabolism and insulin insensitivity in rats fed a SRD for a long time in which a well-established dyslipidemia and insulin resistance was present at 6 months of diet before the source of dietary fat was partially replaced by fish oil during the following 2 months (6–8 months). Therefore, the aim of this study was to analyze the effect of fish oil on: (i) the enzyme activities and metabolites involved in glucose metabolisms (phosphorylation, glycolysis, gluconeogenesis and oxidative and non oxidative glucose disposal pathways); and (ii) the protein mass levels on the early proximal insulin signaling steps: insulin receptor substrate-1 (IRS-1) and the subunit α p85 of phosphoinositol-3 kinase (PI-3K) in the liver of rats chronically fed a SRD under the experimental conditions described above.

Materials and Methods

Animals and Diets

Male Wistar rats initially weighing 180–190 g and purchased from the National Institute of Pharmacology (Buenos Aires, Argentina) were maintained under controlled environmental conditions (temperature 22 ± 1 °C; humidity and air flow condition; 12-h light/dark cycle, light-on 0700 to 1900). After 1-week period of acclimation, the rats were randomly divided into two groups (control

and experimental). The sucrose-rich diet (SRD) group ($n = 72$) received a purified high-sucrose diet containing by weight, 62.5% sucrose, and 8% corn oil (CO). The control group ($n = 36$) received the same semisynthetic diet, but sucrose was replaced by cornstarch (62.5%) [high starch diet (CD)]. The SRD group was fed the diet for 6 months, after which the rats were randomly subdivided into two subgroups. The rats of the first subgroup continued on the SRD up to month 8 of feeding. The second subgroup (SRD + FO) received the SRD in which the source of fat (CO 8 g/100 g) had been replaced by FO (7 g/100 g of cod liver oil, ICN Biomedical, Costa Mesa, CA, plus 1 g/100 g of CO) from month 6 to 8 (Table 1). The control group received the CD during 8 months. The SRD without the addition of FO used for the 2 last months and the CD were balanced for cholesterol and vitamins D and A, present in the FO. Dietary fats were analyzed by capillary GC as previously described [24]. The fatty acid composition of the different fat sources is shown in Table 2. Diets were isoenergetic, providing approximately 16.3 kJ/g of food and were available ad libitum as previously described [20]. The weight of each rat was recorded twice each week over 8 months. In a separate experiment, the individual energy intakes and weight gains of eight rats in each group and subgroup were assessed twice each week. At the end of the 8-month dietary period, experiments were performed before 10:00 h. Rats were anesthetized with intraperitoneal pentobarbital sodium (60 mg/kg of body weight). Blood and liver samples were obtained as previously described [20]. The experimental protocol was approved by the

Human and Animal Research Committee of the School of Biochemistry, University of Litoral, Santa Fe, Argentina.

Analytical Methods

Plasma triacylglycerols (TAG), cholesterol (C) free fatty acids (FFA) and glucose levels were measured by spectrophotometric methods as previously described [25, 26]. The immunoreactive insulin assays were calibrated against a rat insulin standard (Novo Nordisk, Copenhagen, Denmark) as previously described [25, 26]. Homogenates of frozen liver powder were used for the determination of TAG, glycogen, glucose-6-P and fructose-2,6-bisphosphate by standard spectrophotometric methods as previously described [25]. Fructose-1-P was assayed by the method of Eggleston L [27].

Enzymes Activity Assays

Hepatic glucokinase (GK) (EC 2.7.1.2) and hexokinase (HK) (EC 2.7.1.1) activities were assayed in homogenates of frozen liver by the spectrophotometric method described by Barzilai and Rossetti [28]. Glucose-6-Phosphate phosphatase (G-6-Pase) (EC 3.1.3.9) activity was assayed by the method described by Harper [29]. The rate of reaction was measured by the increase in inorganic phosphate with time according to the method of Fiske and Subbarow [30]. The extraction of phosphoenolpyruvate carboxykinase (PEPCK) (EC 4.1.1.32) was performed according to Blakely et al. [31], and the determination of PEPCK

Table 1 Composition of control (CD), sucrose-rich (SRD) or SRD + fish oil (FO) experimental diets fed to male Wistar rats

Ingredients	CD (%)		SRD (%)		SRD + FO (%)	
	Weight	Calories	Weight	Calories	Weight	Calories
Casein free vitamin	17.0	17.5	17.0	17.5	17.0	17.5
Salt mix ^a	3.5		3.5		3.5	
Vitamin mix ^b	1.0		1.0		1.0	
Choline chloride	0.2		0.2		0.2	
Methionine	0.3		0.3		0.3	
Cellulose	7.5		7.5		7.5	
Corn-starch	62.5	64.0				
Sucrose			62.5	64.0	62.5	64.0
Corn oil	8.0	18.5	8.0	18.5	1.0	2.3
Fish oil					7.0	16.2

Diets were based on the AIN-93M diet

^a Salt mix is based on salt mix AIN-93MX (in g/Kg of diet): calcium carbonate, 37.0; potassium phosphate (monobasic) 250.0; sodium chloride, 74.0; potassium sulfate, 46.6; potassium citrate, tri-potassium (monohydrate) 28.0; magnesium oxide, 34.0; ferric citrate, 6.06; zinc carbonate, 1.65; manganese carbonate, 0.63; cupric carbonate, 0.30; potassium iodate, 0.01; sodium selenate, 0.01025; ammonium paramolybdate, 0.00795; chromium potassium sulfate, 0.2174

^b Vitamin mix is based on vitamin mix AIN-93VX (in g/Kg of diet): niacin 3.00; calcium pantothenate, 1.60; pyridoxine HCl, 0.70; thiamin HCl, 0.60; riboflavin, 0.60; folic acid, 0.20; d-biotin, 0.02; vitamin B-12 (0.1% triturated in mannitol) 2.5; vitamin E (500 IU/g), 15.00; vitamin A (500,000 IU/g) 0.80; vitamin D3 (400,000 IU), 0.25; vitamin K, 0.075

Table 2 Fatty acid composition of the fat source included in each experimental diet

Fatty acids	CO ^a g/100 g total fatty acids	CO + FO ^b	FO ^c
14:0	Tr	4.1	4.7
16:0	10.4	12.8	12.8
16:1 n-7		9.5	10.8
18:0	2.6	2.8	3.0
18:1 n-9	32.1	26.0	25.0
18:2 n-6	51.5	9.0	2.6
18:3 n-3	0.4		Tr
20:0	0.4	0.9	0.9
20:1 n-9	1.6	12.0	13.7
20:4 n-3		3.1	3.5
20:5 n-3		9.0	10.3
22:5 n-3		0.5	0.6
22:6 n-3		8.1	9.3
Total			
Saturated	13.4	20.6	21.4
Monounsaturated	33.7	47.5	49.5
Polyunsaturated			
n-6	51.50	9.00	2.60
n-3	0.40	20.70	23.70
P/S	3.87	1.44	1.23
n-3/n-6	0.008	2.30	9.11

Other minor fatty acids have been excluded

^a Corn Oil (CO), Mazola (Best Foods Canada Starch, Montreal, Quebec, Canada)

^b Includes 1% CO plus 7% FO

^c FO: cod liver oil (ICN Biomedical, Costa Mesa, CA)

activity according to Petrescu et al. [32]. Pyruvate kinase (PK) (EC 2.7.1.40) activity was assayed in homogenates of fresh liver according to Osterman et al. [33]. Glycogen synthase (GSa) (EC 2.4.1.11) activity was determined and the fractional velocity of GSa was calculated as previously described in detail [9]. The extraction and determination of pyruvate dehydrogenase (PDHc) (EC 1.2.4.1) activity from liver tissue has been previously described in detail [34].

Western Blot Analysis of Liver Protein Mass Levels of Insulin Receptor Substrate-1 (IRS-1), α p85 Subunit of Phosphoinositide-3 kinase (PI-3K), Glucokinase (GK) and Hexokinase (HK)

Animals were killed before 10:00 h. To minimize differences in time being euthanized between treatments, three rats were chosen randomly in the three different dietary groups and were killed simultaneously. Frozen liver powder (100 mg) was homogenized and centrifuged at 16,000g for 20 min to remove insoluble materials [2] for IRS-1 and α p85

PI-3K. Liver homogenates were prepared as described by Zhang et al. [35] for GK and HK protein mass levels analysis. Total protein samples were resolved on SDS-PAGE and transferred to PVDF membranes. For immunoblotting, the membranes were probed with specified antibodies (rabbit polyclonal antibody anti-IRS-1, anti- α p85, anti-GK or polyclonal goat antibody anti-HK, from Santa Cruz Biotechnology, Inc., Santa Cruz, CA). The blots were then incubated with horseradish peroxidase-linked secondary antibody followed by chemiluminescence detection according to the manufacturer's instructions (Super Signal West Pico chemiluminescence detection, Pierce Biotechnology, Rockford, IL). The protein levels were normalized to β actin. The intensity of the bands was quantified by NIH imaging software. The relationship between the amount of sample subjected to immunoblotting and the signal intensity observed was linear under the conditions described above.

Statistical Analysis

Sample sizes were calculated on the basis of measurements previously made in our laboratory with rats fed either a CD or a SRD [16, 20, 34], considering an 80% power. Results were expressed as means \pm SEM. Statistical comparisons were done transversely between different dietary groups. The statistical significance between groups was determined by one-way ANOVA, with one factor (diet) followed by the inspection of all differences between pairs of means by the Newman-Keuls test [36]. Differences having *p* values lower than 0.05 were considered to be statistically significant. In all cases the interclass correlation coefficients were at least 0.73.

Results

Body-Weight Gain, Energy Intake, Plasma Metabolites and Insulin Levels

Energy intake and body weight were carefully monitored in all groups of rats throughout the experimental period. As we have previously shown [17, 20] a significant increase ($p < 0.05$) in body weight and energy intake occurred in rats fed a SRD for 6 months compared with rats fed a CD (Table 3). These differences in body weight and energy intake were still present in the SRD group when the diet was extended till month 8 of feeding. The presence of FO did not modify the body weight of the SRD-fed rats. However, in spite of a similar energy intake between the SRD and SRD + FO fed rats at month 8, the weight gain was moderately decreased in the latter group (Table 3). The daily individual intake of fatty acids in the three dietary groups was as follows (mean \pm SEM, $n = 8$): monounsaturated: CD:

0.455 ± 0.016 g; SRD: 0.565 ± 0.028 g and SRD + FO: 0.743 ± 0.024 g; polyunsaturated: CD: 0.700 ± 0.024 g (0.77% of n-3); SRD: 0.869 ± 0.043 g (0.77% of n-3) and SRD + FO: 0.0466 ± 0.150 g (69.6% of n-3).

In agreement with previous publications [17, 20] plasma levels of TAG, FFA, C and glucose were higher in rats fed the SRD for 8 months compared with the age-matched controls fed a CD (Table 3). Similar values were obtained in rats fed a SRD for 6 months (data not shown). All the variables returned to control values in the SRD-fed rats in which FO replaced corn oil for the last 2 months of feeding. No statistically significant differences in plasma insulin levels were observed at the end of the experimental period among the three dietary groups. Under these experimental conditions, plasma insulin/glucose ratio showed a significant decrease $p < 0.05$ in the SRD fed group compared with both CD and SRD + FO (Table 3). Furthermore, the enhanced liver TAG

content in the SRD-fed rats decreased when the diet was switched to SRD + FO (Table 3).

Liver Enzymes Activities and Metabolites Concentration

Table 4 depicts the activities of GK and HK (enzymes involved in glucose phosphorylation); PK (glycolytic pathway); the active form of PDHc (PDHa)—as an estimation of glucose oxidation—the protein mass levels of GK and HK and the concentration of fructose-1-P and fructose-2,6-bisphosphate in the liver of the three dietary groups at the end of the experimental period.

SRD-fed rats showed a significant decrease ($p < 0.05$) of GK without changes in HK activities and their protein mass levels compared to the CD-fed rats. However, PK and the PDHa activities increased approximately 4 and

Table 3 Body weight, energy intake, plasma metabolites, insulin levels, insulin/glucose ratio and liver TAG content of rats fed a control (CD), sucrose-rich (SRD) or SRD + fish oil (FO)

	CD	SRD	SRD + FO
Body weight at 6 months (g)	403.4 ± 19.8 ^b	467.4 ± 11.3 ^a	461.7 ± 10.9 ^a
Energy intake (initial to month 6) (kJ/d)	272.0 ± 12.5 ^b	340.0 ± 12.8 ^a	338.7 ± 11.9 ^a
Body weight at 8 months (g)	438.5 ± 11.1 ^b	506.3 ± 18.8 ^a	479.6 ± 6.9 ^a
Energy intake (months 6–8) (kJ/d)	275.0 ± 9.4 ^b	341.2 ± 17.0 ^a	318.8 ± 10.5 ^a
Weight gain (g) (months 6–8)	34.6 ± 4.9 ^a	33.6 ± 5.1 ^a	17.2 ± 6.1 ^b
Plasma			
TAG (mM)	0.61 ± 0.06 ^b	2.04 ± 0.10 ^a	0.78 ± 0.06 ^b
FFA (μM)	304.4 ± 17.5 ^b	805.5 ± 42.0 ^a	328.0 ± 39.6 ^b
C (mM)	2.19 ± 0.06 ^b	3.30 ± 0.15 ^a	2.06 ± 0.11 ^b
Glucose (mM)	6.37 ± 0.13 ^b	8.24 ± 0.13 ^a	6.55 ± 0.19 ^b
Insulin (μU/ml)	58.30 ± 4.03	60.10 ± 5.37	52.60 ± 3.26
Insulin/Glucose ratio (μU/μmol)	9.30 ± 0.56 ^a	7.03 ± 0.54 ^b	8.43 ± 0.30 ^a
Liver			
TAG (μmol/g wet weight)	12.60 ± 0.64 ^b	22.70 ± 2.00 ^a	11.10 ± 0.43 ^b

Values are expressed as means ± SEM; $n = 8$. Values in each lane that do not share the same superscript letter are significantly different ($p < 0.05$) when one variable at a time was compared by the Newman–Keuls test

Table 4 Glucokinase, hexokinase, pyruvate kinase and pyruvate dehydrogenase activities, glucokinase and hexokinase protein mass levels and metabolites concentration in the liver of rats fed a control (CD), sucrose-rich (SRD) or SRD + fish oil (FO)

	CD	SRD	SRD + FO
Enzyme activities			
Glucokinase (mU/mg protein)	7.24 ± 0.42 ^a	5.14 ± 0.38 ^b	5.15 ± 0.41 ^b
Hexokinase (mU/mg protein)	2.09 ± 0.08	1.82 ± 0.12	1.97 ± 0.07
Pyruvate Kinase (mU/mg protein)	69.63 ± 3.41 ^c	305.25 ± 4.15 ^a	153.42 ± 8.81 ^b
Pyruvate Dehydrogenase active form (% of total PDH complex)	35.02 ± 1.61 ^b	50.55 ± 3.04 ^a	36.33 ± 1.54 ^b
Protein mass levels			
Glucokinase (% of control)	100.0 ± 2.8	103.0 ± 7.1	98.6 ± 6.1
Hexokinase (% of control)	100.0 ± 3.1	91.3 ± 5.7	90.3 ± 11.6
Metabolites			
Fructose-1-P (μmol/g wet tissue)	0.27 ± 0.02 ^b	0.53 ± 0.07 ^a	0.33 ± 0.03 ^b
Fructose-2,6-bisphosphate (μmol/g wet tissue)	10.66 ± 0.26	9.40 ± 0.57	10.57 ± 0.62

Values are expressed as means ± SEM; $n = 6$. Values in each lane that do not share the same superscript letter are significantly different ($p < 0.05$) when one variable at a time was compared by the Newman–Keuls test

1.4-fold, respectively compared to those fed a CD. Besides, a twofold increase in fructose-1-P without changes in fructose-2,6-bisphosphate concentration was recorded in the SRD fed rats. Dietary fish oil did not modify the behavior of both HK and GK activities. The latter stayed similarly lower than those observed in the SRD fed rats. Interestingly, no statistically significant differences in the protein mass levels of GK and HK were observed in the liver of SRD + FO rats (Table 4).

On the other hand, under FO administration, the PK activity significantly decreased ($p < 0.05$) while both the activity of PDHa and fructose-1-P contents reached values similar to those recorded in the CD group. FO did not induce changes in fructose-2,6-bisphosphate levels.

Table 5 shows the activities of key enzymes related to glycogen synthesis, gluconeogenesis and glucose homeostasis and the concentration of glycogen and glucose-6-P in the liver of the three dietary groups. Glycogen synthase (GSa)—expressed as a percentage of the fractional activity—as well as glycogen levels were significantly increased in the SRD-fed rats. A reduction in both GSa activity and glycogen content was observed when the source of fat in the SRD (corn oil) was partially replaced by FO. However, while the glycogen content returned to values similar to those recorded in the CD group, the GSa activity was still significantly higher than that in the CD-fed rats. No changes in liver glucose-6-P concentration were observed among all dietary groups.

In addition, Table 5 depicts that the liver of the SRD-fed rats showed a significant increase in the activities of two enzymes involved in the gluconeogenesis pathway: PEPCK and G-6-Pase. Both enzyme activities reached values similar to those observed in the CD-fed rats in the group of rats fed a SRD + FO.

On the other hand, the terminal step of glucose release from the liver is a function of the activities of G-6-Pase and GK. The addition of FO that normalizes G-6-Pase activity was able to significantly decrease G-6-Pase/GK ratio. Values were as follows (means \pm SEM, $n = 6$) 13.45 \pm 2.1 for CD, 27.24 \pm 3.2 for SRD and 19.81 \pm 2.3 for

SRD + FO; $p < 0.05$ CD vs SRD and SRD + FO; $p < 0.05$ SRD vs SRD + FO.

Protein Mass Levels of IRS-1 and α p85 PI-3K

The immunoblotting of liver tissue revealed a single 175 kDa band consistent with IRS-1 and 85 kDa bands for α p85 PI-3K. Each gel contained an equal number of samples from the CD, SRD and SRD + FO groups (Fig. 1a). After densitometry of immunoblots, both the IRS-1 and α p85 PI-3K of the CD group were normalized to 100% and the levels of IRS-1 and α p85 PI-3K from SRD and SRD + FO were expressed relative to this. The qualitative and quantitative analysis of the Western blot showed that the relative abundance of IRS-1 and α p85 PI-3K were significantly decreased ($p < 0.05$) in the liver of the SRD group when compared with rats fed a CD (Fig. 1b). The addition of FO to the diet of the SRD-fed rats did not induce any changes in either IRS-1 or α p85 PI-3K; values were similar to those recorded in the SRD-fed rats.

Discussion

The main purpose of this work was to explore whether dietary FO can improve or reverse the altered hepatic glucose metabolism and insulin resistance induced in rats by the chronic administration of a sucrose-rich diet, to investigate the key enzymatic steps and early proximal insulin signaling responsible for these changes. The new major findings in the present study are as follows: (i) The significant increase in PK and PDHa activities, key enzymes of the glycolytic and oxidative glucose pathways, as well as fructose-1-P level observed in the liver of the SRD-fed rats were significantly improved or normalized, reaching values similar to those of the CD-fed group in which FO replaced corn oil as a dietary fat during the last 2 months of the experimental period (8 months). However, FO was unable to restore the altered capacity of glucose phosphorylation (decreased GK activity) present in the

Table 5 Glycogen and glucose-6-phosphate concentration and glycogen synthase, glucose-6-phosphate phosphatase and phosphoenolpyruvate carboxykinase activities in the liver of rats fed a control (CD), sucrose-rich (SRD) or SRD + fish oil (FO)

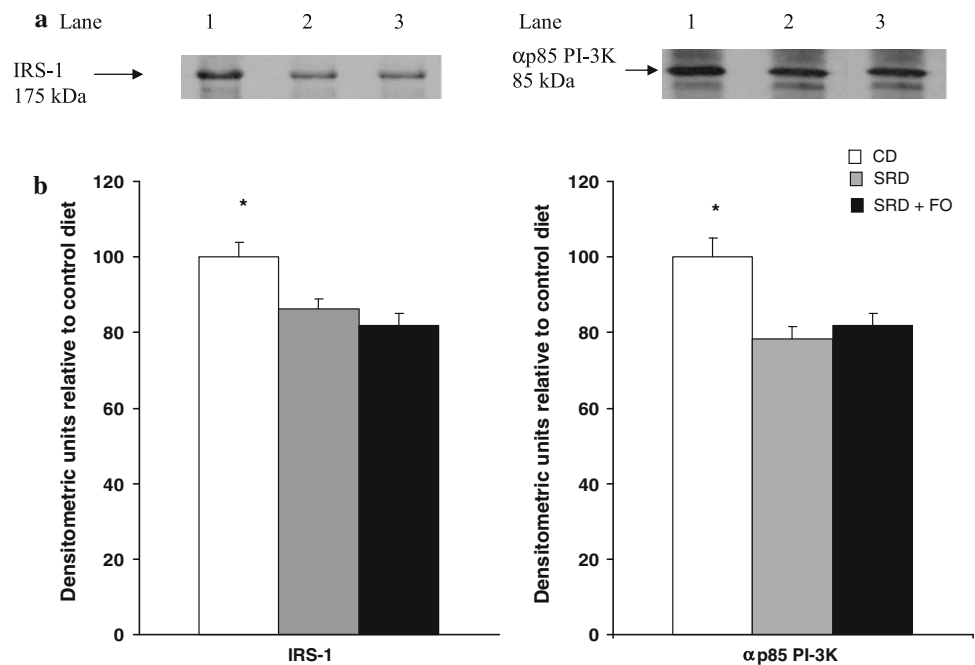
	CD	SRD	SRD + FO
Metabolites and enzyme activities			
Glycogen (μ mol/g wet tissue)	239.3 \pm 22.3 ^b	390.4 \pm 25.0 ^a	292.0 \pm 30.8 ^b
Glucose-6-phosphate μ mol/g wet tissue)	0.23 \pm 0.02	0.20 \pm 0.01	0.22 \pm 0.02
Glycogen Synthase (% of fractional activity)	13.16 \pm 1.16 ^b	18.50 \pm 0.50 ^a	15.70 \pm 1.55 ^{ab}
Glucose-6-P-phosphatase (mU/mg protein)	97.4 \pm 15.4 ^b	140.0 \pm 6.1 ^a	102.0 \pm 11.5 ^b
Phosphoenolpyruvate Carboxykinase (mU/mg protein)	2.29 \pm 0.17 ^b	3.21 \pm 0.20 ^a	2.49 \pm 0.17 ^b

Values are expressed as means \pm SEM; $n = 6$. Values in each lane that do not share the same superscript letter are significantly different ($p < 0.05$) when one variable at a time was compared by the Newman–Keuls test

Fig. 1 Liver protein mass levels of IRS-1 and α p85 PI-3K of rats fed a control (CD), sucrose-rich (SRD) or a SRD + fish oil (FO).

a Immunoblots of liver IRS-1 and α p85 PI-3K from CD, SRD and SRD + FO. Molecular marker is shown on the right. Lane 1 CD, lane 2 SRD and lane 3 SRD + FO.

b Densitometric immunoblot analysis of IRS-1 and α p85 PI-3K protein mass in liver tissue of rats fed a CD, SRD or SRD + FO. Values are expressed as means \pm SEM ($n = 6$) and expressed as percentage relative to control diet in both IRS-1 and α p85 PI-3K. * $p < 0.05$ CD versus SRD and SRD + FO



liver of the SRD-fed rats. (ii) FO was able to reverse the increased activities of PEPCK and G-6-Pase, enzymes involved in the gluconeogenesis pathway. FO significantly reduced the G-6-Pase/GK ratio, which led to decreased hepatic glucose output. In addition, increased glycogen concentration and GSa activity returned to levels similar to those recorded in the CD-fed rats. (iii) Dietary FO did not modify the altered protein mass levels of IRS-1 and the subunit of α p85 PI-3K.

Glucose release from hepatocytes is a function of the enzymatic activities of GK and G-6-Pase. The present work shows a decrease in GK and conversely, an increase in G-6-Pase activities in the SRD-fed rats. This could in part contribute to losing control of the hepatic glucose output. Interestingly, at that time, the reduction in the hepatic GK activity was not accompanied by changes in their protein mass level. Although we did not evaluate the GK translocation in the present study, Shin et al. [37] in ZDF-rats recently demonstrated a lack of GK translocation from the nucleus to the cytoplasm altered expression of the enzyme leading to an inadequate endogenous glucose production and glucose uptake. When FO replaced corn oil as a source of fat in the SRD, no further changes in the already decreased GK activity and protein mass level were observed. However, in mice fed 2–5% of n-3 PUFA in vivo and in vitro Dentin et al. [23] showed that hepatic GK gene expression is inhibited decreasing the amount of total GK protein content and activity. They observed that the suppressive effect of n-3 PUFA on the gene expression of GK and liver PK is caused by an alteration of ChREBP nuclear translocation. On the other hand, FO decreases the activity

and mRNA of G-6-Pase in rats fed a high-fat diet [38]. The present data shows that the increase in G-6-Pase activity in the liver of rats fed a SRD was significantly decreased when FO replaced corn oil in this diet. Therefore, although glucose phosphorylation is still impaired in the SRD + FO group, an inhibiting effect of FO on the G-6-Pase activity leading to a decreased G-6-Pase/GK ratio could improve the altered hepatic glucose homeostasis present in the SRD-fed rats.

Several studies showed that the hepatic disposal of a large amount of fructose increased the liver PK and PEPCK activities and expression as well as the PDHc activity [31, 39–41]. The current study in which rats were fed a SRD for an extended period (8 months) shows a substantial increase in PK, PEPCK and G-6-Pase activities that leads to an elevated hepatic glucose production. Moreover, the glucose oxidation estimated by PDHc activity as well as fructose-1-P concentration was also increased without changes in the fructose-2,6-bisphosphate level. No change in the latter metabolite was observed in sucrose-fed rats by Sommercorn et al. [42]. The present data shows that FO oil was able to normalize the hepatic fructose-1-P level, and decrease the PK activity thus decreasing the flux through pyruvate and in turn diminishing the PDHc activity that reached values similar to those of the CD-fed group. A decrease in both hepatic PK activity and gene expression was observed by Higuchi et al. [43] in mice fed dietary fish oil compared to those fed a lard diet. Dietary fish oil significantly decreased the PEPCK activity reaching values similar to those recorded in the CD fed group. Neschen et al. [44] showed that FO decreased PEPCK mRNA when

compared with safflower oil. On the other hand, FO significantly reduced the high plasma FFA levels measured in the SRD-fed rats, since fatty acids provide fuel for gluconeogenesis, thus a reduction in the hepatic availability of these metabolites could contribute, at least in part, to the normalization of this metabolic pathway.

On the other hand, we recently demonstrated [20] that under the same experimental conditions, FO was able to inhibit hepatic lipogenesis through the up regulation of PPAR α and down regulation of LXR α and normalized liver TAG content.

Gergely et al. [45] showed that fructose-1-P stimulates glycogen synthesis in normal rats intravenously injected with fructose. Moreover, fructose-1-P concentration inhibited glycogen phosphorylase and regulated glycogen accumulation when fructose delivery was increased [5]. Similarly, our results show an increase in glycogen synthase activity, and both glycogen and fructose-1-P contents in the liver of the SRD-fed rats. Dietary FO decreased all

these parameters which reached values similar to those of the CD group.

Hepatic changes in the early steps of insulin signaling transduction may play a role in the insulin resistance induced by high sucrose or fructose diet. Under basal conditions Bezerra et al. [2] reported no differences in IR and IRS-1 protein levels in both liver and muscle of rats fed a high fructose diet for a short time (4 weeks). However, after insulin stimulation, they demonstrated a significant reduction in tyrosine phosphorylation of IR and IRS-1 phosphorylation levels in both tissues. A reduction in IRS-1/PI-3kinase association was also observed in liver and muscle. Besides, in rats fed a high sucrose diet for 5 weeks, Wei et al. [9] showed that hepatic insulin resistance was mediated in part via activation of the JNK activity through changes in serine phosphorylation of IRS-1. Our present results extend those described by Bezerra et al. [2] since when the SRD was administered for 8 months instead of 4 weeks, a reduction in liver protein mass levels of IRS-1

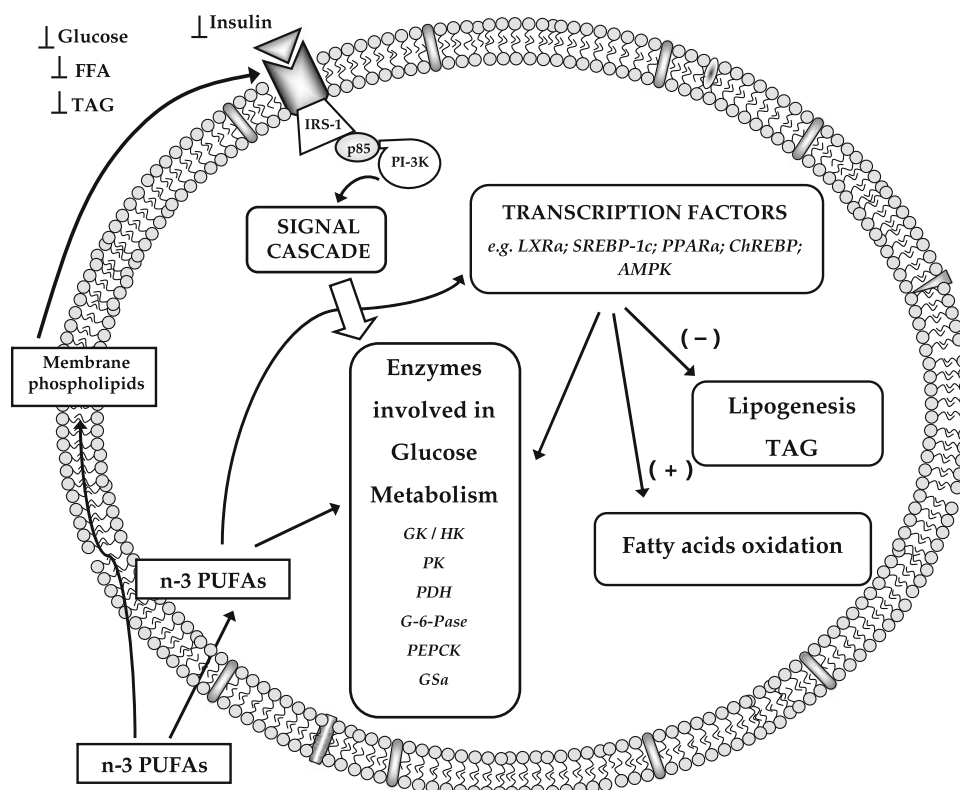


Fig. 2 Integrated effect of fish oil (FO) on liver glucose and lipid metabolism in the SRD-fed rats. FO regulates glucose and lipid metabolism through changes in the activity or abundance of different transcription factors families (e.g. PPARs, SREBPs, LXRs, ChREBP). In the SRD-fed rats FO enhanced hepatic fatty acid oxidation and decreased lipogenesis, leading to normalization of liver and plasma TAG levels, thus contributing to its hypolipemic effects. Several liver key enzymes activities and metabolites involved in

hepatic glucose metabolism were improved. FO reversed the increased activities of PEPCK and G-6-Pase and reduced the G-6-Pase/GK ratio which leads to reduce hepatic glucose output but was unable to restore the impaired capacity of glucose phosphorylation. FO restored glucose oxidation and GSa activity. Besides, FO did not modify protein mass levels of IRS-1 and α p85 PI-3K involved on the early steps of insulin signaling transduction. FO normalized glucose homeostasis without changes in circulating insulin levels

and α p85 PI-3K was observed just under basal conditions, without the stimulus of insulin. The replacement of corn oil by FO did not improve the decreased protein mass levels of IRS-1 and α p85 PI-3K. This was a particularly unexpected result, since FO normalizes both the altered plasma basal insulin/glucose ratio and hyperglycemia without changes in insulinemia. Moreover, as previously demonstrated [11], it reverts the low plasma adiponectin levels and insulin resistance (euglycemic–hyperinsulinemic clamp), thus normalizing whole body peripheral insulin sensitivity. Klimes et al. [46] showed no changes in insulin binding and autophosphorylation of the insulin receptor beta subunit under basal conditions and/or after insulin stimulation from the liver of rats fed a SRD or SRD plus FO diet for 3 weeks. However, FO improved insulin-stimulated tyrosine kinase activity and insulin action. On the other hand, a decrease in PI-3K activity in the liver and muscle with an increase in adipose tissue was observed by Corporeau et al. [47] in rats fed a low amount of FO into a normolipidic diet. Taouis et al. [14] showed that a high fat diet enriched in n-3 PUFA in rats maintained IR, IRS-1 tyrosine phosphorylation, PI-3K activity and total Glut4 in muscle but not in liver. Figure 2 depicts the effect of n-3 PUFA on liver glucose metabolism in the SRD fed rats.

Finally, dietary FO was effective in reversing or improving the impaired activities of several key enzymes of hepatic carbohydrate metabolism contributing at least in part to the normalization of plasma glucose levels in the experimental model of dyslipidemia and insulin resistance. FO reversed liver steatosis and dyslipidemia. However, these positive effects of FO were not observed under basal conditions in the early steps of insulin signaling transduction. Further studies are needed in order to clarify this matter.

Acknowledgments This study was supported by Grants PICT 05-38157 BID 1728 OC/AR and PIP # 11220090100105, 2010 from the Agencia Nacional de Promoción Científica y Tecnológica and CONICET.

References

- Wei Y, Wang D, Topczewski F, Pagliassotti MJ (2007) Fructose-mediated stress signaling in the liver: implication for hepatic insulin resistance. *J Nutr Biochem* 18:1–9
- Bezerra RMN, Ueno M, Silva MS, Tavares DQ, Carvalho CRO, Saad MJA (2000) A high fructose diet affects the early steps of insulin action in muscle and liver of rats. *J Nutr* 130:1531–1535
- Bisschop PH, de Metz J, Ackermans MT, Endert E, Pijl H, Kuipers F, Meijer AJ, Sauerwein HP, Romijn J (2001) Dietary fat content alters insulin-mediated glucose metabolism in healthy men. *Am J Clin Nutr* 73:554–559
- Anai M, Funuaki M, Ogihara T, Kanda A, Onishi Y, Sakoda H, Inukai K, Nawano M, Fukushima Y, Yazaki Y, Kikuchi M, Oka Y, Asano T (1999) Enhanced insulin stimulated activation of phosphatidylinositol 3 kinase in the liver of high-fat fed rats. *Diabetes* 48:158–169
- Bizeau ME, Pagliassotti MJ (2005) Hepatic adaptation to sucrose and fructose. *Metabolism Clin Exp* 54:1189–1201
- Bizeau ME, Thresher JS, Pagliassotti M (2001) Sucrose diets increase glucose-6-phosphatase and glucose release and decrease glucokinase in hepatocytes. *J Appl Physiol* 91:2041–2046
- Libal-Weksler Y, Gotlibovitz O, Stark AH, Madar A (2001) Diet and diabetic state modify glycogen synthase activity and expression in rat hepatocytes. *J Nutr Biochem* 12:455–464
- Pagliassotti MJ, Kang J, Thresher JS, Sung CK, Bizeau ME (2002) Elevated basal PI-3kinase activity and reduced insulin signaling in sucrose-induced hepatic insulin resistance. *Am J Physiol Endocrinol Metab* 282:E170–E176
- Wei Y, Pagliassotti MJ (2004) Hepatospecific effects of fructose on c-junc NH₂-terminal kinase: implications for hepatic insulin resistance. *Am J Physiol Endocrinol Metab* 287:E926–E933
- Storlien LH, Jenkins S, Chisholm DJ, Pascoe WS, Khouri S, Kraegen EW (1991) Influence of dietary fat composition on development of insulin resistance in rats. Relationship to muscle triglyceride and omega-3-fatty acids in muscle phospholipids. *Diabetes* 40:280–289
- Lombardo YB, Chicco A (2006) Effect of dietary polyunsaturated fatty acids on dyslipidemia and insulin resistance in rodents. *J Nutr Biochem* 17:1–13
- Carpentier YA, Portois L, Malaisse WJ (2006) N-3 fatty acids and the metabolic syndrome. *Am J Clin Nutr* 83(suppl):1499S–1540S
- Fedor D, Kelley DS (2009) Prevention oil insulin resistance by n-3 polyunsaturated fatty acids. *Curr Opin Clin Nutr Metab Care* 12:138–146
- Taouis M, Dagou C, Ster C, Durand G, Pinault M, Delarue J (2002) N-3 polyunsaturated fatty acids prevent the defect of insulin receptor signaling in muscle. *Am J Physiol Endocrinol Metab* 282:E664–E671
- Ghafoorunissa, Ibrahim A, Rajkumar L, Acharya V (2005) Dietary (n-3) long-chain polyunsaturated fatty acids prevent sucrose-induced insulin resistance in rats. *J Nutr* 135:2634–2638
- Lombardo YB, Chicco A, D'Alessandro ME, Martinelli M, Soria A, Gutman R et al (1996) Dietary fish oil normalizes dyslipidemia and glucose intolerance with unchanged insulin levels in rats fed a high sucrose diet. *Biochim Biophys Acta* 1299:175–182
- Rossi A, Lombardo YB, Chicco A (2010) Lipogenic enzyme activities and glucose uptake in fat tissue of dyslipemic, insulin-resistant rats. Effects of fish oil. *Nutrition* 26:209–217
- Podolin DA, Gayles EC, Wei Y, Thresher JS, Pagliassotti J (1998) Menhaden oil prevents but does not reverse sucrose-induced insulin resistance in rats. *Am J Physiol Regulatory Integ Comp Physiol* 274:R840–R848
- Jump DB, Botolin D, Wang Y, Xu J, Christian B, Demeure O (2005) Fatty acid regulation of hepatic gene transcription. *J Nutr* 135:2503–2506
- Hein G, Bernasconi AM, Montanaro MA, Pellon-Maison M, Finarelli G, Chicco A, Lombardo YB, Brenner RR (2010) Nuclear receptors and hepatic lipogenic enzyme response to a dyslipidemic sucrose-rich diet and its reversal by fish oil n-3 polyunsaturated fatty acids. *Am J Physiol Endocrinol Metab* 298:E429–E439
- Liimatta M, Towle HC, Clare S, Jump DB (1994) Dietary polyunsaturated fatty acids interfere with the insulin/glucose activation of L-type pyruvate kinase gene transcription. *Mol Endocrinol* 8:1147–1153
- Jump DB, Clarke SD, Thelen A, Liimatta M (1994) Coordinate regulation of glycolytic and lipogenic gene expression by polyunsaturated fatty acids. *J Lip Res* 35:1076–1084
- Dentin R, Benhamed F, Pegorier JP, Fougelle F, Viollet B, Vaulont S, Girard J, Postic C (2005) Polyunsaturated fatty acids

- suppress glycolytic and lipogenic genes through the inhibition of ChREBP nuclear protein translocation. *J Clin Invest* 115:2843–2854
24. Lombardo YB, Chicco A, D'Alessandro ME, Martinelli M, Soria A, Gutman R et al (1996) Dietary fish oil normalize dyslipidemia and glucose intolerance with unchanged insulin levels in rats fed a high sucrose diet. *Biochim Biophys Acta* 1299:175–182
 25. Chicco A, Soria A, Fainstein-Day P, Gutman R, Lombardo YB et al (1994) Multiphasic metabolic changes in the heart of rats fed a sucrose-rich diet. *Horm Metab Res* 26:397–403
 26. Herbert V, Lau KS, Gottlieb CH, Bleicher S et al (1995) Coated charcoal immunoassay of insulin. *J Clin Endocrinol Metab* 25:1375–1384
 27. Eggleston LV (1974) D-fructose-1-phosphate. In: Bergmeyer HU (ed) *Methods of enzymatic analysis*, 2^o English edition. New York Academic Press, pp 1308–1313
 28. Barzilai N, Rossetti L (1993) Role of glucokinase and glucose-6-phosphatase in the acute and chronic regulation of hepatic glucose fluxes by insulin. *J Biol Chem* 268:25019–25025
 29. Harper AE (1963) Glucose-6-phosphatase. In: Bergmeyer HU (ed) (1974) *Methods of enzymatic analysis*. New York Academic Press, pp 788–792
 30. Fiske CH, Subbarow P (1925) The colorimetric determination of phosphorus. *J Biol Chem* 66:375–400
 31. Blakely SR, Hallfrisch J, Reiser S, Prather ES (1981) Long-Term effects of moderate fructose feeding on glucose tolerance parameters in rats. *J Nutr* 111:307–314
 32. Petrescu I, Bojan O, Saied M, Barzu O, Schmidt F, Kühnle HF (1979) Determination of phosphoenolpyruvate carboxykinase activity with deoxyguanosine-5'-diphosphate as nucleotide substrate. *Anal Biochemistry* 96:279–281
 33. Osterman J, Fritz PJ, Wuntch T (1973) Pyruvate kinase isozymes from rat tissues. *J Biol Chem* 248:1011–1018
 34. D'Alessandro ME, Chicco A, Karabatas L, Lombardo YB et al (2000) Role of skeletal muscle on impaired insulin sensitivity in rats fed a sucrose rich diet. Effect of moderate levels of dietary fish oil. *J Nutr Biochem* 11:273–280
 35. Zhang X, Liang W, Mao Y, Li H, Yang Y, Tan H (2009) Hepatic glucokinase activity is the primary defect in alloxan-induced diabetes of mice. *Biomed Pharmacother* 63:180–186
 36. Snedecor GWP, Cochran WG (1967) *Statistical methods applied to experimental in agriculture and biology*. (Ames, IA). University Press Iowa State, USA
 37. Shin JS, Torres TP, Catlin RL, Donahue EP, Masakazui S (2007) A defect in glucose-induced dissociation of glucokinase from the regulatory protein in Zucker diabetic fatty rats in the early stage of diabetes. *Am J Physiol Regulatory Integrative Comp Physiol* 292:1381–1390
 38. Delarue J, LeFoll C, Corporeau C, Lucas D (2004) N-3 long chain polyunsaturated fatty acids: a nutritional tool to prevent insulin resistance associated to type 2 diabetes and obesity? *Reprod Nutr Dev* 44:289–299
 39. Lemaigre FP, Rosseau GG (1994) Transcriptional control of genes that regulate glycolysis and gluconeogenesis in adult liver. *Biochem J* 303:1–14
 40. Munnich A, Lyonnet S, Chauvet D, Van Scaftingen E, Kahn A (1987) Differential effects of glucose and fructose on liver L-type pyruvate kinase gene expression in vivo. *J Biol Chem* 262:17065–17071
 41. Da Silva LA, De Marucci OL, Kuhnle ZR (1993) Dietary polyunsaturated fats suppress the high-sucrose-induced increase of rat liver pyruvate dehydrogenase levels. *Biochim Biophys Acta* 1169:126–134
 42. Sommercorn J, Freedland RA (1984) Effects of diets on concentrations of 6-phosphogluconate and fructose 2,6-bisphosphate in rat livers and an assay of fructose 2,6-bisphosphate with an improved method. *J Nutr* 114:1462–1469
 43. Higuchi T, Shirai N, Saito M, Suzuki H, Kagawa Y (2008) Levels of plasma insulin, leptin and adiponectin, and activities of key enzymes in carbohydrate metabolism in skeletal muscle and liver in fasted ICR mice fed dietary n-3 polyunsaturated fatty acids. *J Nutr Biochem* 19:577–586
 44. Neschen S, Morino K, Dong J, Wang-Fisher Y, Cline GW, Romanelli AJ, Rossbacher JC, Moore IK, Regittnig W, Munoz DS, Kim JH, Shulman GI (2007) N-3 fatty acids preserve insulin sensitivity in vivo in a peroxisome proliferators-activated receptor- α -dependent manner. *Diabetes* 56:1034–1047
 45. Gerfely P, Toth B, Farkas I (1985) Bot G (1985) Effect of fructose 1-phosphate on the activation of liver glycogen synthase. *Biochem J* 232:133–137
 46. Klimes I, Sebkova E, Vrana A, Kazdova L (1993) Raised dietary intake of N-3 polyunsaturated fatty acids in high sucrose-induced insulin resistance: animal studies. *Ann N Y Acad Sci* 683:69–81
 47. Corporeau C, Le Foll C, Taouis M, Gouygou JP, Bergé JP, Delarue J (2006) Adipose tissue compensates for defect of phosphatidylinositol-3'-kinase induced in liver and muscle by dietary fish oil in fed rats. *Am J Physiol Endocrinol Metab* 290:E78–E86

Daily Intake of Cod or Salmon for 2 Weeks Decreases the 18:1n-9/18:0 Ratio and Serum Triacylglycerols in Healthy Subjects

Vibeke H. Telle-Hansen · Laila N. Larsen ·
Arne T. Høstmark · Marianne Molin ·
Lisbeth Dahl · Kari Almendingen · Stine M. Ulven

Received: 19 August 2011 / Accepted: 16 November 2011 / Published online: 4 December 2011
© AOCS 2011

Abstract Intake of fish and omega-3 (n-3) fatty acids is associated with a reduced concentration of plasma triacylglycerols (TAG) but the mechanisms are not fully clarified. Stearoyl-CoA desaturase-1 (SCD1) activity, governing TAG synthesis, is affected by n-3 fatty acids. Peripheral blood mononuclear cells (PBMC) display expression of genes involved in lipid metabolism. The aim of the present study was to estimate whether intake of lean

and fatty fish would influence n-3 fatty acids composition in plasma phospholipids (PL), serum TAG, 18:1n-9/18:0 ratio in plasma PL, as well as PBMC gene expression of SCD1 and fatty acid synthase (FAS). Healthy males and females ($n = 30$), aged 20–40, consumed either 150 g of cod, salmon, or potato (control) daily for 15 days. During intervention docosahexaenoic acid (DHA, 22:6n-3) increased in the cod group ($P < 0.05$), while TAG concentration decreased ($P < 0.05$). In the salmon group both eicosapentaenoic acid (EPA, 20:5n-3) and DHA increased ($P < 0.05$) whereas TAG concentration and the 18:1n-9/18:0 ratio decreased ($P < 0.05$). Reduction of the 18:1n-9/18:0 ratio was associated with a corresponding lowering of TAG ($P < 0.05$) and an increase in EPA and DHA ($P < 0.05$). The mRNA levels of SCD1 and FAS in PBMC were not significantly altered after intake of cod or salmon when compared with the control group. In conclusion, both lean and fatty fish may lower TAG, possibly by reducing the 18:1n-9/18:0 ratio related to allosteric inhibition of SCD1 activity, rather than by influencing the synthesis of enzyme protein.

V. H. Telle-Hansen · M. Molin · K. Almendingen ·
S. M. Ulven (✉)
Department of Health, Nutrition and Management,
Faculty of Health Sciences, Oslo and Akershus University
College of Applied Sciences, Postbox 4, St. Olavsplass,
0130 Oslo, Norway
e-mail: StineMarie.Ulven@hioa.no

V. H. Telle-Hansen
Department of Nutrition, Institute of Basic Medical Sciences,
Faculty of Medicine, University of Oslo, Postbox 1046,
Blindern, 0316 Oslo, Norway

L. N. Larsen
EpiGen Institute, Research Centre, Akershus University
Hospital, Postbox 26, 1478 Lørenskog, Norway

A. T. Høstmark
Section of Preventive Medicine and Epidemiology,
University of Oslo, Postbox 1130, Blindern, 0318 Oslo, Norway

M. Molin
Institute of Basic Medical Sciences, Faculty of Medicine,
University of Oslo, Postbox 1110, Blindern, 0317 Oslo, Norway

L. Dahl
National Institute of Nutrition and Seafood Research (NIFES),
Postbox 2029, Nordnes, 5817 Bergen, Norway

K. Almendingen
Unit of Clinical Research, Research Centre, Akershus University
Hospital, Postbox 26, 1478 Lørenskog, Norway

Keywords Fish · 18:1n-9/18:0 ratio · Omega 3 ·
Triacylglycerols · Gene expression · PBMC · Humans

Abbreviations

CE	Cholesterol ester
CVD	Cardiovascular disease
DHA	Docosahexaenoic acid
EPA	Eicosapentaenoic acid
FAS	Fatty acid synthase
GUS β	Glucuronidase-beta
HDL-C	High density lipoprotein cholesterol
LA	Linoleic acid
LDL-C	Low density lipoprotein cholesterol

n-3	Omega-3
PBMC	Peripheral blood mononuclear cell
PL	Phospholipid
PPAR α	Peroxisome-proliferator activated receptor alpha
PUFA	Polyunsaturated fatty acid
SCD1	Stearoyl-CoA desaturase-1
SREBP1	Sterol regulatory element-binding protein 1
TBP	TATA binding protein
TAG	Triacylglycerol
VLDL	Very low density lipoprotein

Introduction

Numerous epidemiological studies have demonstrated a reduced risk of cardiovascular diseases (CVD) in response to an increased intake of fish or fish oils [1–3]. Especially fatty fish is a major source of long chain omega-3 polyunsaturated fatty acids (n-3 PUFA), such as eicosapentaenoic acid (EPA, 20:5n-3) and docosahexaenoic acid (DHA, 22:6n-3). Many of the beneficial health effects of fish and fish oils have been linked to intake of these fatty acids [4–10]. Serum triacylglycerols (TAG) is recognized as an independent risk factor of CVD [11] and marine n-3 fatty acids in high doses (>3 g/day) have been shown to reduce serum TAG by 25–30% [12–15]. The magnitude of the TAG reducing effect seems to be dependent on n-3 fatty acid dose and baseline TAG concentrations [14, 16]. The American heart association (AHA) recommend the consumption of a variety of fish (preferably fatty fish) at least twice a week as guidance for healthy people [17]. However, intake of lean fish is also known to provide health benefits [18–20] in which one effect is reduced serum TAG [20]. Whether the health beneficial effects of lean fish are related to the n-3 fatty acids content, or to other bioactive components, is not known.

The molecular mechanisms involved in the hypotriglyceridemic effect of marine n-3 fatty acids have not been clarified. In general, the effects could be due to reduced production, and/or to increased elimination of TAG [2]. In the present work we have focused upon some aspects of the synthesis of TAG. In the fasted state serum TAG is mainly carried in very low density lipoproteins (VLDL), which are synthesized and secreted in the liver. TAG, cholesterol esters (CE) and phospholipids (PL) in VLDL preferably contain monounsaturated fatty acids, i.e., palmitoleic (16:1n-7) and oleic (18:1n-9) acid. The rate limiting enzyme for the synthesis of these fatty acids is stearoyl-CoA desaturase-1 (SCD1 or $\Delta 9$ desaturase). Mice lacking SCD1 have reduced hepatic lipogenesis and lower plasma TAG concentration [21, 22]. Accordingly, one mechanism

by which fish intake decreases serum TAG could be inhibition of desaturase activities in the liver, caused directly or indirectly by some of the constituents in fish. In general, the rate of an enzyme catalyzed reaction may be influenced by the amount of enzyme protein, by phosphorylation and dephosphorylation of the enzyme, or by allosteric regulation [23]. Oleic acid is a major constituent of TAG produced by de novo lipogenesis, and therefore the 18:1n-9/18:0 ratio, i.e., a product/precursor ratio, in plasma may be used to estimate SCD1 activity [22, 24–26]. Animal studies have demonstrated that marine n-3 fatty acids can suppress hepatic lipogenesis [4], and one regulatory mechanism may be inhibition of SCD1 activity [27] or by transcriptional regulation of sterol regulatory element-binding protein 1 (SREBP1) [28]. SREBP1 is regulating the expression of lipogenic genes such as SCD1 and fatty acid synthase (FAS) [28], and an inhibition of SREBP1 by n-3 fatty acids will cause a down-regulation of these genes [29]. To study whether n-3 fatty acids might influence human hepatic gene expression in vivo is challenging. However, since human PBMC can display the expression of genes involved in lipid metabolism [30–35] we have chosen PBMC as a test system.

The aim of the present exploratory study was accordingly to investigate whether daily intake of lean and fatty fish for 2 weeks would influence n-3 fatty acids composition in plasma PL, serum TAG levels, 18:1n-9/18:0 ratio in plasma PL (an estimated indication of SCD1 activity), and to assess SCD1 and FAS by their mRNA levels in PBMC, in healthy subjects.

Subjects and Methods

This study is an extension of a previous study involving 38 healthy subjects randomized to four different intervention groups consuming either salmon ($n = 11$), cod ($n = 9$), blue mussel ($n = 8$) or potato (control) ($n = 10$) in order to study arsenic metabolism (Molin et al., manuscript in preparation). The opportunity was taken to investigate lean versus fatty fish in this exploratory study ($n = 30$).

Subjects

Thirty subjects (7 men and 23 women) aged 20–40 were recruited from Akershus University College, Lillestrøm, Norway. Healthy subjects with C-reactive protein (CRP) <10 mg/L using no medication, except for oral contraceptives (female subjects ($n = 11$)), all subjects maintained the use throughout the study, except for one subject in the control group, were included in this study. Smoking, pregnancy and lactation were exclusion criteria. Additionally, subjects who had a habitual seafood consumption

of more than three servings per week were excluded. All subjects were compliant with the protocol throughout the study. Compliance was assessed based on observations of the participants during the test meals, served at the University College and the amount of leftovers after the experimental period. Compliance was estimated to be 95–100% in all three groups. The study protocol was approved by Regional Committee of Medical Ethics in Norway. Written informed consent for participation was obtained from each subject and it complied with the Declaration of Helsinki.

Study Design

A 15 days randomized controlled parallel-group study was conducted. The participants were randomized but not stratified by gender, and therefore by chance all the subjects in the salmon group were females. The subjects received a daily test meal of 150 g of either farmed salmon (*Salmo salar*) ($n = 11$), cod (*Gadus morhua*) ($n = 9$) or potato (control) ($n = 10$) for 15 consecutive days. The subjects were carefully instructed not to eat any seafood except the seafood provided in the study, and not to take any dietary supplements during the intervention period. Marine n-3 supplements (including cod liver oil) were prohibited 5 weeks prior to and during the study. Each subject was requested not to change dietary and exercise habits during the study.

Test Meals

A homogenous mixture of cod or salmon fillets was prepared as fish puddings and cut into cubes. Potatoes were cooked and cut into cubes. The test meal menu was a 7-day menu which was served hot and repeated twice and all the dishes were similar for all intervention groups except for the fish/potato. The test meal was served at Akershus University College Monday–Friday, and lunch boxes to bring home were provided for the weekend.

Blood Sampling and Biochemical Analysis

Blood samples were collected from fasting subjects (minimum 12 h) at the same time (between 8 a.m. and 10 a.m.) at baseline and at the end of the study. PBMC were isolated using cell preparation tubes (CPT) according to the manufacturer's instructions (Becton, Dickinson and Company, NJ 07417, USA). Determination of serum total cholesterol (total-C), HDL cholesterol (HDL-C), LDL cholesterol (LDL-C), TAG and CRP was performed using routine laboratory methods (Først Medical laboratory, Norway). Plasma was obtained from EDTA tubes and kept frozen ($-70\text{ }^{\circ}\text{C}$) until analysis.

Fatty Acid Composition in Fish

Homogenous mixture of cod or salmon fillets were kept frozen ($-20\text{ }^{\circ}\text{C}$) until analysis and total lipids were extracted by adding chloroform/methanol (2:1, vol/vol), and non-adeyclic acid (19:0) was added as internal standard. The samples were filtered, saponified, and methylated using 12% BF_3 in methanol. Fatty acid composition of total lipids was analyzed using methods as described earlier [36, 37].

Fatty Acid Composition in Plasma PL

Fatty acid composition in plasma PL was determined as previously reported [38]. The 18:1n-9/18:0 ratio was calculated from the fatty acid composition in plasma PL and used as an estimate of desaturase activity.

RNA Isolation and Quantitative Real-Time Polymerase Chain Reaction (Q-RT-PCR)

Total RNA was extracted from PBMC using a combination of TRIzol Reagent (Invitrogen, Carlsbad, CA, USA) and RNeasy mini kit (Qiagen, Hilden, Germany) purified with RNase-free DNase (Invitrogen). Subsequently the samples were stored in RNase-free water at $-80\text{ }^{\circ}\text{C}$. RNA quality was measured on an Agilent Bioanalyser 2100 system (Agilent Technologies, Santa Clara, CA, USA) and showed RNA integrity numbers (RIN) between 8.7 and 9.8. Total RNA yield was measured on a Nanodrop ND-1000 Spectrophotometer (NanoDrop Technologies, Wilmington, DE, USA). For cDNA synthesis, 500 ng RNA of each total RNA sample was reverse-transcribed by Super Script (Invitrogen) according to the manufacturer's protocol, using oligo dT as primers. The Taqman real-time polymerase chain reaction (RT-PCR) technique was used to quantify the mRNA expression of each gene. cDNA corresponding to 15 ng RNA was applied to each well and each sample was run in triplets. Quantification was performed using the relative standard curve method. A combination of aliquots from all cDNA samples was made and diluted in order to make a dilution curve that was included on each plate. The points on the standard curve corresponded to 50, 25, 12.5 and 6.25 ng RNA. The average of the three values measured per gene per sample were divided by the average of the corresponding combined Glucuronidase-beta ($\text{GUS}\beta$) and TATA binding protein (TBP) values, generating a normalized value used to compare the relative amount for each gene in the different samples. $\text{GUS}\beta$ and TBP were chosen as endogenous genes due to the results from running a TaqMan Human Endogenous Control Plate-test from Applied Biosystems (data not shown). The primers and probes for $\text{GUS}\beta$ and TBP were initially designed as three assays per gene, and validated for efficiency and specificity. The best of the three was then

chosen. The primers and probe for the GUS β assay were: forward primer: 5'-GAAAATATGTGGTTGGAGAGCTCATT-3', probe: 5'-CCAGCACTCTCGTCCGGTGACTGTTCA-3' and reverse primer: 5'-CCGAGTGAAGATCCCCTTTTTA-3'. TBP forward primer: 5'-CTGGAAAAGTTGTATTAACAGGTGC-3', probe: 5'-AGCAGAAATTTATGAAGCATTGAAAACATCTACCCTATT-3' and reverse primer: 5'-CATTACGTCGTCTTCTGAATC-3'. All other genes were measured by "single tube" assays, which are a premade combination of primers and probe, specific for the gene to be determined (Applied Biosystems, Foster City, CA) and utilized according to the manufacturer's protocol. SCD1 (Δ -9 desaturase): no. Hs01682761_m1 and FAS: no. Hs00188012_m1. RT-PCR was carried out on a 7900HT real time PCR machine from Applied Biosystems (Applied Biosystems, Foster City, CA, USA).

Statistical Analysis

Probability values (asymptotic) were considered statistically significant at a value of $P \leq 0.05$. Non-parametric tests were used due to the small sample size and values are given as median (25–75 percentile). Percent change is calculated from median values. Differences between the randomization groups were analysed at end of study (baseline adjusted values). Delta values refer to values at end of study minus baseline values for the plasma parameters, while gene expression delta values refer to values at end of study divided with baseline values (fold change). The present study is considered an exploratory study and therefore no adjustment for multiple testing was performed. Mann–Whitney U test and Wilcoxon matched-pair signed-rank test were used to either compare changes between groups or within-groups, respectively. Coefficients of correlation were calculated by the Spearman's rho test. The SPSS for Windows (version 18.0) was used for all statistical analyses.

Results

Baseline Characteristics

There were no significant differences in baseline characteristics between the study groups (Table 1).

Intake of n-3 Fatty Acids from the Intervention Meals

Daily intake of EPA and DHA provided from the seafood lunch meal were 1.4 and 1.7 g/day in the salmon group while the total daily n-3 fatty acids intake was 5.4 g (Table 2). Corresponding intake were 0.048 and 0.086 g/day in the cod group with a total n-3 intake of 0.15 g/day. The potatoes did not contain any marine n-3 fatty acids, but

total intake of n-3 fatty acids (α -linolenic acid, 18:3n-3) was 0.14 g/day (Table 2).

Fatty Acid Profile in Plasma PL

Daily intake of 150 g fish for 15 days significantly increased the amount of total n-3 fatty acids (EPA and DHA) in plasma PL in both the cod ($P = 0.008$) and the salmon ($P < 0.001$) groups, compared to the control group (Table 3). DHA increased in the cod group ($P = 0.003$) while both EPA and DHA increased in the salmon group ($P < 0.001$ and $P = 0.001$, respectively), compared to the control group. The baseline values of EPA and DHA were not different between the groups, nor were any of the other fatty acids in the plasma PL.

Serum Concentration of TAG, Total-C, HDL-C and LDL-C

As shown in Table 4, the serum concentration of TAG was significantly decreased both in the cod group ($P = 0.02$) and in the salmon group ($P = 0.003$) as compared with the control group. The reduction was significant within the cod ($P = 0.05$) and the salmon ($P = 0.008$) groups, corresponding to a reduction of 11 and 22%, respectively. No significant alteration in the TAG concentration was seen within the control group. Serum HDL-C was significantly increased after intake of salmon compared with the control group ($P = 0.009$), and the within-group increase was 5% ($P = 0.02$). Serum total-C and serum LDL-C was not changed between or within any of the groups (Table 4).

The change in both EPA and DHA in plasma PL correlated negatively with the change in TAG ($n = 30$) ($r = -0.5$, $P = 0.007$ and $r = -0.4$, $P = 0.04$, respectively) (Data not shown).

Effects on the 18:1n-9/18:0 Ratio in Plasma PL

As shown in Fig. 1, there was a significant reduction in the 18:1n-9/18:0 ratio in plasma PL in the salmon group compared with the control group ($P = 0.004$), and a significant within-group reduction after intake of cod ($P = 0.04$) and salmon ($P = 0.003$) for 2 weeks. In contrast, there was no significant within-group change in the control group during the experiment (Fig. 1).

Relationship Between Serum TAG, Marine n-3 Fatty Acids and the 18:1n-9/18:0 Ratio in Plasma PL

As illustrated in Fig. 2, there was a positive correlation ($r = 0.5$, $P = 0.01$) between change in the 18:1n-9/18:0 ratio and change in serum TAG ($n = 30$) (Fig. 2). Since previous studies suggest that SCD1 might be regulated by

Table 1 Baseline characteristics [median (25–75 percentile)]

Parameter	Study groups		
	Control (<i>n</i> = 10)	Cod (<i>n</i> = 9)	Salmon (<i>n</i> = 11)
Gender			
Female (<i>n</i>)	6	6	11 ^a
Male (<i>n</i>)	4	3	0
Age (years)	25 (21–29)	22 (21–25)	25 (23–27)
BMI (kg/m ²)	24 (23–27)	23 (22–24)	23 (21–24)
CRP (mg/L)	1 (1–2)	1 (1–2)	1 (1–2)
TAG (mmol/L)	1.2 (0.5–1.3)	0.9 (0.7–1.3)	0.9 (0.6–1.6)
Total-C (mmol/L)	4.3 (3.8–4.7)	4.2 (4.2–5.1)	4.1 (3.9–5.3)
LDL-C (mmol/L)	2.4 (1.8–3.0)	2.3 (2.2–3.2)	2.4 (2.0–3.1)
HDL-C (mmol/L)	1.7 (1.4–1.9)	1.8 (1.5–2.0)	1.9 (1.5–2.2)

^a The groups were randomized, but not stratified, and therefore by chance all the participants in the salmon group were females

Table 2 The composition of n-3 fatty acid in the served seafood (fish puddings) and potato (raw)

Fatty acids	Control ^a (mg/day)	Cod (mg/day)	Salmon (mg/day)
Hexadecatrienoic acid (16:3)	–	0.0	82.9
Hexadecatetraenoic acid (16:4)	–	0.0	122.9
α -Linolenic acid (18:3)	144.0	8.4	906.3
Stearidonic acid (18:4)	0.0	2.5	220.1
Eicosatrienoic acid (20:3)	–	0.0	0.0
Eicosatetraenoic acid (20:4)	0.0	2.1	225.9
EPA (20:5)	0.0	47.7	1398.1
Heneicosapentaenoic acid (21:5)	–	2.1	171.5
Docosapentaenoic acid (22:5)	0.0	5.3	574.7
DHA (22:6)	0.0	86.1	1709.7
Sum n-3	144.0	154.3	5412.1

^a The n-3 fatty acids content of the potatoes [old, raw (February–June)] are calculated from the Danish food composition databank, version 7.01 March 2009, National Food Institute, Technical University of Denmark. http://www.foodcomp.dk/v7/fcdb_default.asp

EPA and DHA, we investigated whether the 18:1n-9/18:0 ratio was related to n-3 fatty acids in plasma PL. Indeed, as shown in Fig. 3, there was a highly significant negative correlation between the increase in marine n-3 fatty acids in plasma PL and reduction in the 18:1n-9/18:0 ratio (*n* = 30) ($r = -0.7$, $P < 0.001$).

Effects on mRNA Expression in PBMC

There was no significant change in mRNA level of the two selected lipogenesis related genes in the two intervention groups when compared to the control group (Fig. 4). However, mRNA level of FAS was significantly increased within the salmon group ($P = 0.008$) (Fig. 4).

Discussion

In this exploratory study in healthy subjects we found that a short term intake of both lean and fatty fish decreased serum TAG levels (Table 4) and the 18:1n-9/18:0 ratio in plasma PL (an estimated indication of SCD1 activity) (Fig. 1). The marine n-3 fatty acid DHA in plasma PL

increased significantly after intake of lean and fatty fish, while EPA increased only after fatty fish intake (Table 3).

Most studies have investigated health effects after intake of relatively high doses of n-3 fatty acids, often administered as supplements. In the present study n-3 fatty acids were provided as regular fish meals. The hypotriglyceridemic effect of fatty fish has been largely attributed to n-3 fatty acids, and our finding of a decrease in serum TAG in the salmon group is consistent with previous reports [12]. However, as shown in the present study also cod significantly reduced serum TAG. The main carriers of TAG in fasting plasma are VLDL, and in general the hypotriglyceridemic effect of fish could be related to reduced production, and/or to increased elimination of these lipoproteins. The present work focused only upon some aspects of TAG synthesis. TAG, CE and PL in VLDL preferably contain monounsaturated fatty acids, i.e., palmitoleic and oleic acid. Since SCD1 is the rate limiting enzyme for the synthesis of these fatty acids, one mechanism by which fish intake decreases serum TAG could be a reduced hepatic desaturase activity, caused directly or indirectly by some of the constituents in fish. Fish intake might influence the amount of SCD1 enzyme protein and

Table 3 Fatty acids in plasma phospholipids at baseline and at end of study [median (25–75 percentile)]

Parameter (mg/ml)	Treatment	<i>n</i>	Baseline	End of study	<i>P</i> value ^a	<i>P</i> value ^b
Palmitic acid (16:0)	Control	10	0.282 (0.231–0.323)	0.281 (0.255–0.327)	0.05	
	Cod	9	0.276 (0.245–0.323)	0.281 (0.255–0.327)	NS	NS
	Salmon	11	0.267 (0.221–0.401)	0.295 (0.228–0.345)	NS	0.04
Stearic acid (18:0)	Control	10	0.115 (0.099–0.138)	0.129 (0.120–0.141)	NS	
	Cod	9	0.125 (0.112–0.145)	0.129 (0.120–0.141)	NS	NS
	Salmon	11	0.132 (0.107–0.149)	0.144 (0.118–0.153)	NS	NS
Sum SFA	Control	10	0.409 (0.327–0.459)	0.409 (0.379–0.468)	0.05	
	Cod	9	0.404 (0.366–0.461)	0.412 (0.397–0.445)	NS	NS
	Salmon	11	0.393 (0.334–0.575)	0.418 (0.354–0.498)	NS	NS
Oleic acid (18:1n9)	Control	10	0.079 (0.068–0.094)	0.086 (0.071–0.096)	NS	
	Cod	9	0.087 (0.079–0.102)	0.086 (0.071–0.096)	NS	0.03
	Salmon	11	0.095 (0.059–0.116)	0.063 (0.052–0.075)	0.005	0.001
Linoleic acid (18:2n6)	Control	10	0.215 (0.181–0.227)	0.254 (0.202–0.265)	0.05	
	Cod	9	0.205 (0.182–0.236)	0.254 (0.202–0.265)	NS	NS
	Salmon	11	0.243 (0.200–0.295)	0.189 (0.164–0.221)	0.004	0.001
Arachidonic acid (20:4n6)	Control	10	0.074 (0.062–0.089)	0.081 (0.066–0.087)	NS	
	Cod	9	0.080 (0.075–0.103)	0.081 (0.066–0.087)	NS	NS
	Salmon	11	0.077 (0.056–0.099)	0.078 (0.059–0.083)	NS	0.04
Sum n-6	Control	10	0.285 (0.253–0.313)	0.319 (0.294–0.338)	0.05	
	Cod	9	0.291 (0.268–0.331)	0.306 (0.299–0.330)	NS	NS
	Salmon	11	0.297 (0.268–0.386)	0.262 (0.221–0.308)	0.06	0.001
EPA (20:5n3)	Control	10	0.006 (0.000–0.009)	0.008 (0.007–0.009)	NS	
	Cod	9	0.007 (0.003–0.009)	0.008 (0.007–0.009)	0.03	NS
	Salmon	11	0.009 (0.006–0.010)	0.057 (0.043–0.073)	0.003	<0.001
DHA (22:6n3)	Control	10	0.052 (0.046–0.063)	0.053 (0.050–0.058)	NS	
	Cod	9	0.052 (0.042–0.066)	0.066 (0.061–0.070)	0.01	0.003
	Salmon	11	0.078 (0.054–0.089)	0.092 (0.078–0.108)	0.003	0.001
Sum n-3	Control	10	0.054 (0.052–0.065)	0.061 (0.058–0.066)	NS	
	Cod	9	0.056 (0.0495–0.072)	0.077 (0.074–0.082)	0.01	0.008
	Salmon	11	0.088 (0.054–0.099)	0.141 (0.123–0.181)	0.003	<0.001

^a Wilcoxon test for within-group changes from baseline to end of study

^b Mann–Whitney *U* test for between-group changes (the cod and salmon groups compared to control group) (baseline adjusted values)

during the past decade, several human intervention studies have focused on diet-induced gene interactions using PBMC as a model system [33, 34, 39, 40]. From the present work it would appear that fish intake might not affect the amount of enzyme protein in PBMC, since there was no alteration in mRNA levels of SCD1 in response to fish intake. Even so, this observation does not rule out the possibility that fish/n-3 fatty acids intake affect the hepatic SCD1 mRNA levels, which have been reported by others [25, 41–45]. Human PBMC display the expression of genes involved in lipid metabolism [30–35, 46, 47] and recently we showed that n-3 fatty acids regulate lipid gene expression in ex vivo PBMC [48]. Human research has limitations in tissue availability except for blood samples which is readily and easily obtained. It has been shown that the expression of genes involved in lipid metabolism are

regulated in PBMC in a similar pattern as in liver upon fasting [33] and several dietary intervention studies have shown that expression of genes involved in lipid metabolism is altered in PBMC after intervention [34, 35, 46, 47]. This indicates that PBMC is a potentially good model system in dietary intervention studies to study genes related to lipid metabolism. However, liver cells and PBMC do have different biochemical properties and the use of PBMC as a model system of hepatic activity is at its very beginning and weaknesses with this model system may exist. It is also likely that due to the small sample size in the present study, type 2 errors are liable to occur and a false effect on gene expression cannot be ruled out. The increase in FAS mRNA in PBMC after intake of salmon in the present work (Fig. 4) is in contrast to previous observations from in vitro and mice studies where it has been shown that PUFA

Table 4 Serum lipids at baseline and at end of study [median (25–75 percentile)]

Parameter	Treatment	<i>n</i>	Baseline	End of study	<i>P</i> value ^a	<i>P</i> value ^b
TAG (mmol/L)	Control	10	1.2 (0.5–1.3)	1.2 (0.6–1.8)	NS	
	Cod	9	0.9 (0.7–1.3)	0.8 (0.6–0.9)	0.05	0.02
	Salmon	11	0.9 (0.6–1.6)	0.7 (0.5–0.8)	0.008	0.003
Total-C (mmol/L)	Control	10	4.3 (3.8–4.7)	4.4 (3.7–5.0)	NS	
	Cod	9	4.2 (4.2–5.1)	4.7 (4.3–5.1)	NS	NS
	Salmon	11	4.1 (3.9–5.3)	4.0 (3.8–5.8)	NS	NS
LDL-C (mmol/L)	Control	10	2.4 (1.8–3.0)	2.5 (1.8–3.2)	NS	
	Cod	9	2.3 (2.2–3.2)	2.5 (2.0–3.4)	NS	NS
	Salmon	11	2.4 (2.0–3.1)	2.3 (1.9–2.9)	NS	NS
HDL-C (mmol/L)	Control	10	1.7 (1.4–1.9)	1.6 (1.4–1.8)	NS	
	Cod	9	1.8 (1.5–2.0)	1.8 (1.6–2.1)	NS	NS
	Salmon	11	1.9 (1.5–2.2)	2.0 (1.6–2.6)	0.02	0.009

^a Wilcoxon test for within-group changes from baseline to end of study

^b Mann-Whitney *U* test for between-group changes (the cod and salmon groups compared to control group) (Baseline adjusted values)

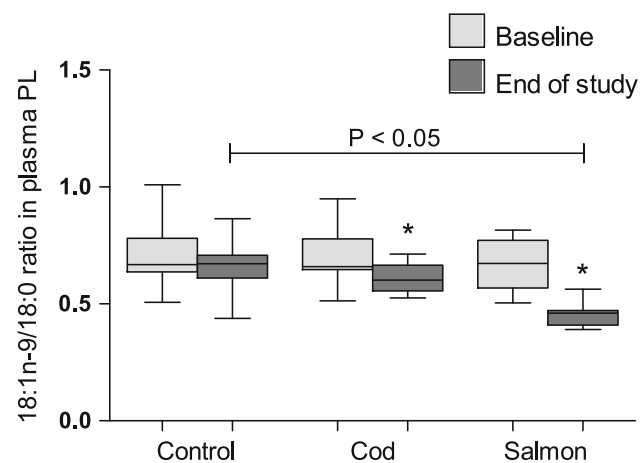


Fig. 1 18:1n-9/18:0 ratio in plasma phospholipids in the three intervention groups. Values are given as median with 25–75 percentiles. **P* < 0.05 within-groups

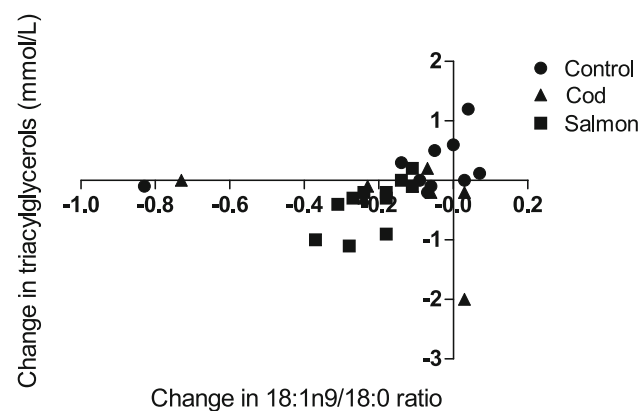


Fig. 2 Relationship between the change in serum triacylglycerols concentration and corresponding change in the 18:1n9/18:0 ratio in plasma phospholipids in response to the intervention (*n* = 30). *r* = 0.453, *P* = 0.001

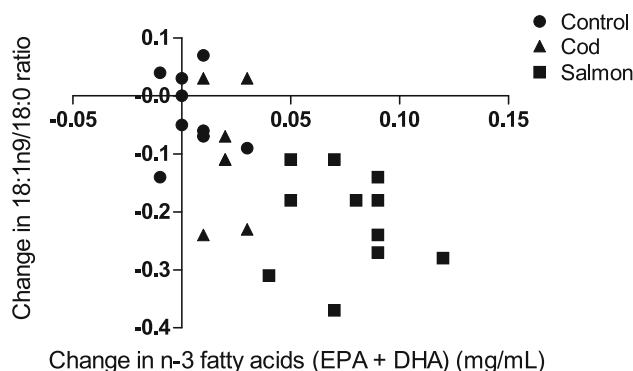


Fig. 3 Relationship between the increase in omega-3 fatty acids in plasma phospholipids and reduction in 18:1n-9/18:0 ratio (*n* = 30). *r* = −0.7, *P* < 0.001

suppress the hepatic expression of FAS [25, 28, 29, 49–51]. Even though the present mRNA level of FAS in the salmon group has two outliers, the within-group change is still significant (*P* = 0.02) when these are removed from the analysis. However, Knight et al. [52] showed that the gene expression of FAS and SCD1 was increased in mice liver injected with a synthetic activator of β -oxidation (a peroxisome-proliferator activated receptor alpha (PPAR α) agonist). Thus, discrepancy exists regarding the effect of PUFA in the hepatic regulation of lipogenesis.

Even though fish intake did not influence mRNA levels involved in synthesis of SCD1, the data seem to fit the hypothesis that n-3 fatty acids can reduce the activity of SCD1, indirectly estimated in the present study by the 18:1n-9/18:0 ratio, as has been previously reported by others [27]. However, this “desaturase index” approach is an indirect method to assess whether desaturases are inhibited, in lack of a more direct biochemical measure which is required to demonstrate an inhibiting effect.

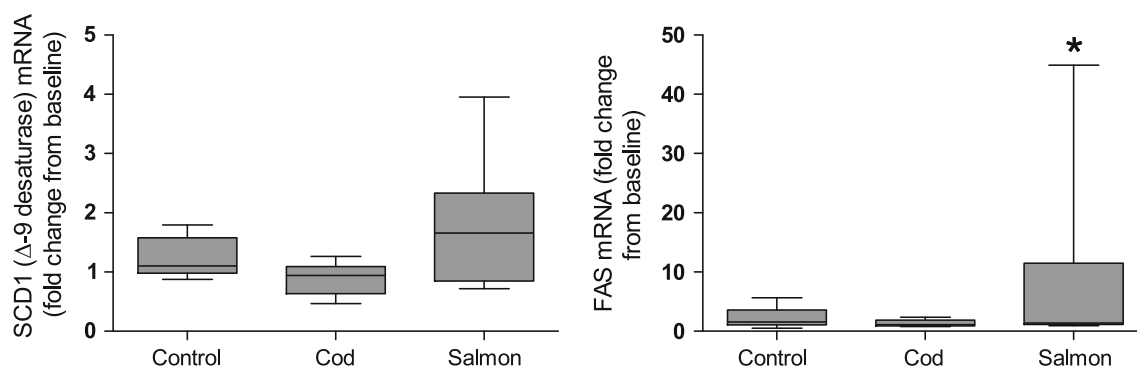


Fig. 4 The fold change PBMC mRNA levels of lipogenic enzymes in the three intervention groups (control ($n = 10$), cod ($n = 9$), or salmon ($n = 11$)). Target genes are related to the mean value of the endogenous controls TBP and GUS β . Values are given as median

with 25–75 percentiles. * $P < 0.05$ within-groups. FAS Fatty acid synthase, GUS β Glucuronidase β , PBMC peripheral blood mononuclear cell, SCD1 Stearoyl-CoA desaturase-1, TBP TATA binding protein

Nevertheless, we suggest that fatty acids like EPA and DHA might serve as allosteric inhibitors. In support of this suggestion are the lowered 18:1n-9/18:0 ratio after intake of fatty fish (Fig. 1), the positive correlation between the 18:1n-9/18:0 ratio and serum TAG (Fig. 2), as well as the inverse relationship between the 18:1n-9/18:0 ratio and EPA and DHA (Fig. 3). It would appear that various fatty acids compete for being incorporated into PL. Although monounsaturated fatty acids seem to be the preferred ones for PL formation [53], both EPA and DHA can be incorporated into the same position in plasma PL. By mass action it is assumed that the level of plasma PL 18:1n-9 should decrease as the levels of EPA and DHA increase. Hence, other unsaturated fatty acids in plasma PL, in addition to EPA and DHA, should be inversely associated with the 18:1n-9/18:0 ratio. This is not the case in the present study. The change in linoleic acid (18:2n-6) is in fact positively associated with the change in the 18:1n-9/18:0 ratio ($r = 0.5$, $P = 0.003$), while the change in arachidonic acid (20:4n-6) shows no association at all. It is however hard to appreciate the magnitude of this possible mass effect, as compared with the other suggested explanations for obtaining reduced desaturase indexes after fish intake. Even though the intake of cod contributed to only 0.13 g of marine n-3 fatty acids per day, the level of DHA (but not EPA) in plasma PL in this group increased significantly compared to the control group (Table 3), and both the level of DHA and EPA in plasma PL correlated positively with the treatment effect on TAG ($n = 30$) (data not shown). The n-3 fatty acids in cod are largely incorporated into PL, in contrast to fatty fish which mainly have the fatty acids incorporated in TAG in adipose tissue. We recently demonstrated that the bio-availability of n-3 fatty acids from krill oil (also mainly incorporated into PL [54]) is more efficient than n-3 fatty acids from fish oil (TAG) [55]. This may partly be the reason why we find positive health effects (reduced TAG

concentration) also after cod intake, despite low levels of n-3 in cod. Previously, DHA has been demonstrated to have similar TAG-lowering effects as EPA [56–58] and the increase in DHA observed in the cod group in the present study may at least partly explain the reduction in serum TAG.

Also other bioactive molecules in fish, like taurine, have been suggested to have TAG reducing effects [59]. Yanagita et al. [59] found that when HepG2 cells were stimulated with taurine, there was a reduction in TAG in both cells and medium. They also found that taurine reduced the incorporation of [14 C]-labelled oleic acid into cellular TAG, suggesting the inhibition of TAG synthesis. Or there may be a synergistic effect of taurine and marine n-3 fatty acids which have the reducing effect on TAG [18]. Since our data suggest that also lean fish may reduce serum TAG, it would appear that the TAG lowering effect of lean fish is relevant to reduce CVD risk, thus supporting a previous study by Leaf and Hatcher [20]. In addition to increased TAG levels being a risk factor of CVD, HDL-C levels correlate inversely with cardiovascular risk [60]. In the present study HDL-C levels are increased after intervention with fatty fish (Table 4), which is in line with a previous report [61]. There is a well-known inverse relationship between plasma TAG levels and HDL-C [62], and this may be the reason why salmon intake might increase HDL-C. However, there is a discrepancy in the n-3 fatty acids effect on HDL-C as reviewed by Harris [13].

In conclusion, both lean and fatty fish can increase the level of marine n-3 fatty acids in plasma PL, and reduce the serum TAG levels in healthy subjects after short term intervention. The hypotriglyceridemic action of dietary marine n-3 fatty acids can be related to a reduced 18:1n-9/18:0 ratio in plasma PL, but whether gene expression in PBMC is influenced is not clarified. Our results would seem to fit the hypothesis that components in both lean and

fatty fish may lower serum TAG possibly by reducing the 18:1n-9/18:0 ratio related to allosteric inhibition of SCD1 activity, rather than by influencing the synthesis of enzyme protein.

Acknowledgments We are grateful to all the participants who made this work possible. We are also grateful to researcher Mari C.W. Myhrstad for critically reading the manuscript. The study was supported by Akershus University College, Norwegian Research Council (grant number 176619/V00 and grant number 142468/140), The Norwegian Cancer Society (grant number 88309/010) and Eastern Norway Regional Health Authority RHF (grant number 2006094 and grant number 2007021). Akershus University College is Member of SYSDIET, a Nordic Centre of excellence financed by Nordforsk (project number 070014).

Conflict of interest There is no conflict of interest among the authors and financial supporters.

References

- Holub DJ, Holub BJ (2004) Omega-3 fatty acids from fish oils and cardiovascular disease. *Mol Cell Biochem* 263:217–225
- Harris WS, Miller M, Tighe AP, Davidson MH, Schaefer EJ (2008) Omega-3 fatty acids and coronary heart disease risk: clinical and mechanistic perspectives. *Atherosclerosis* 197:12–24
- Balk EM, Lichtenstein AH, Chung M, Kupelnick B, Chew P, Lau J (2006) Effects of omega-3 fatty acids on serum markers of cardiovascular disease risk: a systematic review. *Atherosclerosis* 189:19–30
- Harris WS, Bulchandani D (2006) Why do omega-3 fatty acids lower serum triglycerides? *Curr Opin Lipidol* 17:387–393
- von Schacky C, Harris WS (2007) Cardiovascular benefits of omega-3 fatty acids. *Cardiovasc Res* 73:310–315
- Burr ML, Fehily AM, Gilbert JF, Rogers S, Holliday RM, Sweetnam PM, Elwood PC, Deadman NM (1989) Effects of changes in fat, fish, and fibre intakes on death and myocardial reinfarction: diet and reinfarction trial (DART). *Lancet* 2:757–761
- (1999) Dietary supplementation with n-3 polyunsaturated fatty acids and vitamin E after myocardial infarction: results of the GISSI-Prevenzione trial. Gruppo Italiano per lo Studio della Sopravvivenza nell'Infarto miocardico. *Lancet* 354:447–455
- Marchioli R, Barzi F, Bomba E, Chieffo C, Di Gregorio D, Di Mascio R, Franzosi MG, Geraci E, Levantesi G, Maggioni AP, Mantini L, Marfisi RM, Mastrogiuseppe G, Mininni N, Nicolosi GL, Santini M, Schweiger C, Tavazzi L, Tognoni G, Tucci C, Valagussa F (2002) Early protection against sudden death by n-3 polyunsaturated fatty acids after myocardial infarction: time-course analysis of the results of the Gruppo Italiano per lo Studio della Sopravvivenza nell'Infarto Miocardico (GISSI)-Prevenzione. *Circulation* 105:1897–1903
- Yokoyama M, Origasa H (2003) Effects of eicosapentaenoic acid on cardiovascular events in Japanese patients with hypercholesterolemia: rationale, design, and baseline characteristics of the Japan EPA Lipid Intervention Study (JELIS). *Am Heart J* 146:613–620
- Bang HO, Dyerberg J, Sinclair HM (1980) The composition of the Eskimo food in north western Greenland. *Am J Clin Nutr* 33:2657–2661
- Cullen P (2000) Evidence that triglycerides are an independent coronary heart disease risk factor. *Am J Cardiol* 86:943–949
- Harris WS (1997) n-3 Fatty acids and serum lipoproteins: human studies. *Am J Clin Nutr* 65:1645S–1654S
- Harris WS (1989) Fish oils and plasma lipid and lipoprotein metabolism in humans: a critical review. *J Lipid Res* 30:785–807
- Skulas-Ray AC, West SG, Davidson MH, Kris-Etherton PM (2008) Omega-3 fatty acid concentrates in the treatment of moderate hypertriglyceridemia. *Expert Opin Pharmacother* 9:1237–1248
- Davidson MH (2006) Mechanisms for the hypotriglyceridemic effect of marine omega-3 fatty acids. *Am J Cardiol* 98:27i–33i
- Skulas-Ray AC, Kris-Etherton PM, Harris WS, Vanden Heuvel JP, Wagner PR, West SG (2011) Dose-response effects of omega-3 fatty acids on triglycerides, inflammation, and endothelial function in healthy persons with moderate hypertriglyceridemia. *Am J Clin Nutr* 93:243–252
- Kris-Etherton PM, Harris WS, Appel LJ (2002) Fish consumption, fish oil, omega-3 fatty acids, and cardiovascular disease. *Circulation* 106:2747–2757
- Elvevoll EO, Eilertsen KE, Brox J, Dragnes BT, Falkenberg P, Olsen JO, Kirkhus B, Lamglait A, Osterud B (2008) Seafood diets: hypolipidemic and antiatherogenic effects of taurine and n-3 fatty acids. *Atherosclerosis* 200:396–402
- Tidwell DK, McNaughton JP, Pellum LK, McLaurin BP, Chen SC (1993) Comparison of the effects of adding fish high or low in n-3 fatty acids to a diet conforming to the Dietary Guidelines for Americans. *J Am Diet Assoc* 93:1124–1128
- Leaf DA, Hatcher L (2009) The effect of lean fish consumption on triglyceride levels. *Phys Sportsmed* 37:37–43
- Miyazaki M, Kim YC, Gray-Keller MP, Attie AD, Ntambi JM (2000) The biosynthesis of hepatic cholesterol esters and triglycerides is impaired in mice with a disruption of the gene for stearoyl-CoA desaturase 1. *J Biol Chem* 275:30132–30138
- Attie AD, Krauss RM, Gray-Keller MP, Brownlie A, Miyazaki M, Kastelein JJ, Lusis AJ, Stalenhoef AF, Stoehr JP, Hayden MR, Ntambi JM (2002) Relationship between stearoyl-CoA desaturase activity and plasma triglycerides in human and mouse hypertriglyceridemia. *J Lipid Res* 43:1899–1907
- Murray RM, Granner DK, Mayes PA, and Rodwell VW 2000. Harper's biochemistry. Appleton & Lange, New York. 927 pp
- Warenso E, Riserus U, Gustafsson IB, Mohsen R, Cederholm T, Vessby B (2008) Effects of saturated and unsaturated fatty acids on estimated desaturase activities during a controlled dietary intervention. *Nutr Metab Cardiovasc Dis* 18:683–690
- Vellicette RA, Gillies PJ, Kris-Etherton PM, Green JW, Zhao G, Vanden Heuvel JP (2009) Regulation of human stearoyl-CoA desaturase by omega-3 and omega-6 fatty acids: implications for the dietary management of elevated serum triglycerides. *J Clin Lipidol* 3:281–288
- Shiwaku K, Hashimoto M, Kitajima K, Nogi A, Anuurad E, Enkhmaa B, Kim JM, Kim IS, Lee SK, Oyunsuren T, Shido O, Yamane Y (2004) Triglyceride levels are ethnic-specifically associated with an index of stearoyl-CoA desaturase activity and n-3 PUFA levels in Asians. *J Lipid Res* 45:914–922
- Christiansen EN, Lund JS, Rortveit T, Rustan AC (1991) Effect of dietary n-3 and n-6 fatty acids on fatty acid desaturation in rat liver. *Biochim Biophys Acta* 1082:57–62
- Guillou H, Martin PG, Pineau T (2008) Transcriptional regulation of hepatic fatty acid metabolism. *Subcell Biochem* 49:3–47
- Kim HJ, Takahashi M, Ezaki O (1999) Fish oil feeding decreases mature sterol regulatory element-binding protein 1 (SREBP-1) by down-regulation of SREBP-1c mRNA in mouse liver. A possible mechanism for down-regulation of lipogenic enzyme mRNAs. *J Biol Chem* 274:25892–25898
- Chinetti G, Griglio S, Antonucci M, Torra IP, Delerive P, Majd Z, Fruchart JC, Chapman J, Najib J, Staels B (1998) Activation of proliferator-activated receptors alpha and gamma induces

- apoptosis of human monocyte-derived macrophages. *J Biol Chem* 273:25573–25580
31. Marx N, Kehrle B, Kohlhammer K, Grub M, Koenig W, Hombach V, Libby P, Plutzky J (2002) PPAR activators as antiinflammatory mediators in human T lymphocytes: implications for atherosclerosis and transplantation-associated arteriosclerosis. *Circ Res* 90:703–710
 32. Marx N, Mackman N, Schonbeck U, Yilmaz N, Hombach V, Libby P, Plutzky J (2001) PPARalpha activators inhibit tissue factor expression and activity in human monocytes. *Circulation* 103:213–219
 33. Bouwens M, Afman LA, Muller M (2007) Fasting induces changes in peripheral blood mononuclear cell gene expression profiles related to increases in fatty acid beta-oxidation: functional role of peroxisome proliferator activated receptor alpha in human peripheral blood mononuclear cells. *Am J Clin Nutr* 86:1515–1523
 34. Bouwens M, Afman LA, Muller M (2008) Activation of peroxisome proliferator-activated receptor alpha in human peripheral blood mononuclear cells reveals an individual gene expression profile response. *BMC Genomics* 9:262
 35. Bouwens M, Grootte Bromhaar M, Jansen J, Muller M, Afman LA (2010) Postprandial dietary lipid-specific effects on human peripheral blood mononuclear cell gene expression profiles. *Am J Clin Nutr* 91:208–217
 36. Lie O, Lambertsen G (1991) Fatty acid composition of glycerophospholipids in seven tissues of cod (*Gadus morhua*), determined by combined high-performance liquid chromatography and gas chromatography. *J Chromatogr* 565:119–129
 37. Torstensen BE, Lie O, Froyland L (2000) Lipid metabolism and tissue composition in Atlantic salmon (*Salmo salar* L.)—effects of capelin oil, palm oil, and oleic acid-enriched sunflower oil as dietary lipid sources. *Lipids* 35:653–664
 38. Almendingen K, Hostmark AT, Fausa O, Mosdol A, Aabakken L, Vatn MH (2007) Familial adenomatous polyposis patients have high levels of arachidonic acid and docosahexaenoic acid and low levels of linoleic acid and alpha-linolenic acid in serum phospholipids. *Int J Cancer* 120:632–637
 39. Zhao G, Etherton TD, Martin KR, Gillies PJ, West SG, Kris-Etherton PM (2007) Dietary alpha-linolenic acid inhibits proinflammatory cytokine production by peripheral blood mononuclear cells in hypercholesterolemic subjects. *Am J Clin Nutr* 85:385–391
 40. de Mello VD, Erkkila AT, Schwab US, Pulkkinen L, Kolehmainen M, Atalay M, Mussalo H, Lankinen M, Oresic M, Lehto S, Uusitupa M (2009) The effect of fatty or lean fish intake on inflammatory gene expression in peripheral blood mononuclear cells of patients with coronary heart disease. *Eur J Nutr* 48:447–455
 41. Jeffcoat R, James AT (1977) Interrelationship between the dietary regulation of fatty acid synthesis and the fatty acyl-CoA desaturases. *Lipids* 12:469–474
 42. Mauvoisin D, Mounier C (2011) Hormonal and nutritional regulation of SCD1 gene expression. *Biochimie* 93:78–86
 43. Ntambi JM (1999) Regulation of stearoyl-CoA desaturase by polyunsaturated fatty acids and cholesterol. *J Lipid Res* 40:1549–1558
 44. Kajikawa S, Harada T, Kawashima A, Imada K, Mizuguchi K (2009) Highly purified eicosapentaenoic acid prevents the progression of hepatic steatosis by repressing monounsaturated fatty acid synthesis in high-fat/high-sucrose diet-fed mice. *Prostaglandins Leukot Essent Fat Acids* 80:229–238
 45. Bellenger J, Bellenger S, Clement L, Mandard S, Diot C, Poisson JP, Narce M (2004) A new hypotensive polyunsaturated fatty acid dietary combination regulates oleic acid accumulation by suppression of stearoyl CoA desaturase 1 gene expression in the SHR model of genetic hypertension. *FASEB J* 18:773–775
 46. Mutungi G, Torres-Gonzalez M, McGrane MM, Volek JS, Fernandez ML (2007) Carbohydrate restriction and dietary cholesterol modulate the expression of HMG-CoA reductase and the LDL receptor in mononuclear cells from adult men. *Lipids Health Dis* 6:34
 47. Patalay M, Lofgren IE, Freake HC, Koo SI, Fernandez ML (2005) The lowering of plasma lipids following a weight reduction program is related to increased expression of the LDL receptor and lipoprotein lipase. *J Nutr* 135:735–739
 48. Myhrstad MC, Narverud I, Telle-Hansen VH, Karhu T, Bodtker Lund D, Herzig KH, Makinen M, Halvorsen B, Retterstol K, Kirkhus B, Granlund L, Holven KB, and Ulven SM (2011) Effect of the fat composition of a single high-fat meal on inflammatory markers in healthy young women. *Br J Nutr* 106:1826–1835
 49. Hagen RM, Rodriguez-Cuenca S, Vidal-Puig A (2010) An allostatic control of membrane lipid composition by SREBP1. *FEBS Lett* 584:2689–2698
 50. Jump DB (2008) N-3 polyunsaturated fatty acid regulation of hepatic gene transcription. *Curr Opin Lipidol* 19:242–247
 51. Ou J, Tu H, Shan B, Luk A, DeBose-Boyd RA, Bashmakov Y, Goldstein JL, Brown MS (2001) Unsaturated fatty acids inhibit transcription of the sterol regulatory element-binding protein-1c (SREBP-1c) gene by antagonizing ligand-dependent activation of the LXR. *Proc Natl Acad Sci USA* 98:6027–6032
 52. Knight BL, Hebbachi A, Hauton D, Brown AM, Wiggins D, Patel DD, Gibbons GF (2005) A role for PPARalpha in the control of SREBP activity and lipid synthesis in the liver. *Biochem J* 389:413–421
 53. Flowers MT, Ntambi JM (2008) Role of stearoyl-coenzyme A desaturase in regulating lipid metabolism. *Curr Opin Lipidol* 19:248–256
 54. Tou JC, Jaczynski J, Chen YC (2007) Krill for human consumption: nutritional value and potential health benefits. *Nutr Rev* 65:63–77
 55. Ulven SM, Kirkhus B, Lamglait A, Basu S, Elind E, Haider T, Berge K, Vik H, Pedersen JI (2011) Metabolic effects of krill oil are essentially similar to those of fish oil but at lower dose of EPA and DHA, in healthy volunteers. *Lipids* 46:37–46
 56. Grimsgaard S, Bonna KH, Hansen JB, Nordoy A (1997) Highly purified eicosapentaenoic acid and docosahexaenoic acid in humans have similar triacylglycerol-lowering effects but divergent effects on serum fatty acids. *Am J Clin Nutr* 66:649–659
 57. Schwellenbach LJ, Olson KL, McConnell KJ, Stolcpar RS, Nash JD, Merenich JA (2006) The triglyceride-lowering effects of a modest dose of docosahexaenoic acid alone versus in combination with low dose eicosapentaenoic acid in patients with coronary artery disease and elevated triglycerides. *J Am Coll Nutr* 25:480–485
 58. Park Y, Harris WS (2003) Omega-3 fatty acid supplementation accelerates chylomicron triglyceride clearance. *J Lipid Res* 44:455–463
 59. Yanagita T, Han SY, Hu Y, Nagao K, Kitajima H, Murakami S (2008) Taurine reduces the secretion of apolipoprotein B100 and lipids in HepG2 cells. *Lipids Health Dis* 7:38
 60. Libby P, Ridker PM, Hansson GK (2011) Progress and challenges in translating the biology of atherosclerosis. *Nature* 473:317–325
 61. Lara JJ, Economou M, Wallace AM, Rumley A, Lowe G, Slater C, Caslake M, Sattar N, Lean ME (2007) Benefits of salmon eating on traditional and novel vascular risk factors in young, non-obese healthy subjects. *Atherosclerosis* 193:213–221
 62. Gordon T, Castelli WP, Hjortland MC, Kannel WB, Dawber TR (1977) High density lipoprotein as a protective factor against coronary heart disease. The Framingham Study. *Am J Med* 62:707–714

Stable Carbon Isotope Composition of *c9,t11*-Conjugated Linoleic Acid in Cow's Milk as Related to Dietary Fatty Acids

Eva Katharina Richter · Jorge E. Spangenberg ·
Fenja Klevenhusen · Carla R. Soliva ·
Michael Kreuzer · Florian Leiber

Received: 4 February 2011 / Accepted: 12 July 2011 / Published online: 12 August 2011
© AOCS 2011

Abstract This study explores the potential use of stable carbon isotope ratios ($\delta^{13}\text{C}$) of single fatty acids (FA) as tracers for the transformation of FA from diet to milk, with focus on the metabolic origin of *c9,t11*-18:2. For this purpose, dairy cows were fed diets based exclusively on C_3 and C_4 plants. The FA in milk and feed were fractionated by silver-ion thin-layer chromatography and analyzed for their $\delta^{13}\text{C}$ values. Mean $\delta^{13}\text{C}$ values of FA from C_3 milk were lower compared to those from C_4 milk (-30.1% vs. -24.9% , respectively). In both groups the most negative $\delta^{13}\text{C}$ values of all FA analyzed were measured for *c9,t11*-18:2 (C_3 milk = $-37.0 \pm 2.7\%$; C_4 milk $-31.4 \pm 1.4\%$). Compared to the dietary precursors 18:2n-6 and 18:3n-3, no significant ^{13}C -depletion was measured in *t11*-18:1. This suggests that the $\delta^{13}\text{C}$ -change in *c9,t11*-18:2 did not originate from the microbial biohydrogenation in the rumen, but most probably from endogenous desaturation of *t11*-18:1. It appears that the natural $\delta^{13}\text{C}$ differences in some dietary FA are at least partly preserved in milk FA. Therefore, carbon isotope analyses of individual FA could

be useful for studying metabolic transformation processes in ruminants.

Keywords $\delta^{13}\text{C}$ values · Vaccenic acid · Milk · α -linolenic acid · C_3 plants · C_4 plants

Abbreviations

Ag^+ -TLC	Silver-ion thin-layer chromatography
CLA	Conjugated linoleic acid
CSIA	Compound-specific isotope analysis
$\delta^{13}\text{C}$ values	Stable carbon isotope composition
FA	Fatty acid(s)
FAME	Fatty acid methyl ester(s)
GC/C/IRMS	Gas chromatography-combustion-stable isotope ratio mass spectrometry
MUFA	Monounsaturated fatty acid(s)
PUFA	Polyunsaturated fatty acid(s)
VPDB	Vienna Pee Dee Belemnite standard

E. K. Richter · F. Klevenhusen · C. R. Soliva · M. Kreuzer ·
F. Leiber

Institute of Agricultural Sciences, ETH Zurich,
Universitaetstrasse 2, 8092 Zurich, Switzerland

J. E. Spangenberg (✉)

Institute of Mineralogy and Geochemistry,
University of Lausanne, Building Anthropole,
1015 Lausanne, Switzerland
e-mail: Jorge.Spangenberg@unil.ch

Present Address:

F. Klevenhusen
Department of Veterinary Public Health and Food Science,
Institute of Nutrition, University of Veterinary Medicine,
1210 Vienna, Austria

Introduction

Diet formulation for dairy cows is the most efficient tool to enhance milk quality strategically in terms of lipid composition. However, a substantial amount of FA not present in the diet is formed by microbial activity in the rumen during passage of the lipids through the digestive tract. Maintaining the delicate balance of intact transfer of desired FA to the milk and its enrichment with favorable primary or secondary products of ruminal biohydrogenation is an important issue of research in ruminant nutrition [1]. For humans ruminant-derived foods are the major source of conjugated linoleic acids (CLA) [2, 3], a group of

positional and geometric isomers of octadecadienoic acid with conjugated double bonds [4]. *Cis*-9, *trans*-11 octadecadienoic acid (*c9,t11*-18:2; ruminic acid) is the main isomer in ruminants and represents up to 90% of total CLA in cow's milk [5] but its concentration depends on the diet. Especially this isomer is supposed to have anti-carcinogenic [6, 7], anti-atherogenic [8, 9], and anti-diabetic effects [10]. It therefore gained attention both in human [11] and animal nutrition research [12, 13].

The concentration of *c9,t11*-18:2 depends on the dietary proportions of linoleic acid (18:2n-6) and α -linolenic acid (18:3n-3) [14] as it occurs as an intermediate in the rumen during microbial biohydrogenation of these polyunsaturated FA (PUFA). During this process 18:2n-6 originating from the diet is first isomerized at the *cis*-12 double bond, producing *c9,t11*-18:2, which is then converted to vaccenic acid (*t11*-18:1) [4, 15]. Similarly, 18:3n-3 first undergoes an isomerization step to *c9,t11,c15*-18:3, which is followed by a hydrogenation of the *cis*-double bonds to *t11*-18:1 [4]. This intermediate of 18:3n-3 and 18:2n-6 biohydrogenation can endogenously be desaturated to *c9,t11*-18:2 by Δ^9 -desaturase in the tissue. It has been estimated that >60% of *c9,t11*-18:2 in milk fat originate from desaturation and the remaining <40% directly from microbial isomerization [4, 16]. Thus, the metabolic availability of *c9,t11*-18:2 in ruminants depends on (i) the extent of ruminal production of *c9,t11*-18:2 and *t11*-18:1, determined by nutritional factors and ruminal biohydrogenation processes [12, 14, 17], and (ii) the extent of endogenous desaturation of *t11*-18:1 to *c9,t11*-18:2 [16].

To be able to influence concentrations of *c9,t11*-18:2 strategically in ruminant-source foods it is necessary to know the proportions of this FA which originate from 18:2n-6 or 18:3n-3. This can be accomplished by using specifically labeled FA as metabolic tracers. DeNiro and Epstein [18] showed that the isotopic composition ($\delta^{13}\text{C}$ values in ‰ vs. Vienna Pee Dee Belemnite standard, VPDB) of the body of animals is determined by their diet, with a ^{13}C enrichment (trophic shift) of about 1‰. Therefore, stable isotope ratios of FA have been used before in animals when dealing with ecological [19–21], traceability [21–23], and metabolic research questions [24–26]. Using specifically labeled FA for oral administration in large animals is a very expensive approach, and artificial diet components may have to be used. Alternatively, the natural difference between feeds from C_3 and C_4 plants, differing in their stable carbon isotope composition might be utilized. This approach has been successfully applied in transfer studies in ruminants [27]. Molkentin et al. [27] reported ^{13}C -depleted organic milk as compared to conventional milk as a consequence of a wide exclusion of maize as a forage plant in this production system. The metabolism of C_4 plants like maize using the Hatch-Slack

cycle discriminates less against ^{13}C during photosynthetic fixation of atmospheric CO_2 ($\delta^{13}\text{C}$ of -16 to -9‰), while C_3 plants such as temperate climate grasses and cereals follow the Calvin-Benson cycle ($\delta^{13}\text{C}$ of -34 to -22‰) [28]. Since various feeds from C_3 and C_4 plants are available, a less expensive approach to evaluate the metabolic origin of FA in ruminant products could be developed on this basis. Indeed, differences in $\delta^{13}\text{C}$ values have been found between individual FA of various plant species [29–36]. For methyl branched FA, de novo synthesized by microorganisms, clear differences in the $\delta^{13}\text{C}$ values from those of straight-chain FA have been shown [26]. However, the rumen microbial influence on the isotopic composition of FA, which are only hydrogenated and isomerized in the rumen, is not yet documented.

In the present study we explore the possible use of naturally occurring differences in the C isotope composition of individual long-chain FA between C_3 and C_4 plant species to trace the digestive and metabolic fate of these FA in ruminants. This would offer an approach to quantify the relative contribution of diet components to the pools of long-chain FA used for tissue (meat) and milk synthesis. In particular, this study aims at evaluating changes in the $\delta^{13}\text{C}$ values between dietary 18:2n-6 or 18:3n-3 and *c9,t11*-18:2 in milk fat, which may originate from endogenous desaturation in the tissues and/or from microbial isomerization in the rumen. This should elucidate whether such an approach can give useful information for the description of *c9,t11*-18:2 synthesis pathways. The separation of FA groups by silver-ion thin-layer chromatography (Ag^+ -TLC) prior to compound-specific isotope analysis (CSIA) of individual FA with gas chromatography-combustion-stable isotope ratio mass spectrometry (GC/C/IRMS) could be a useful approach to trace transformations of dietary FA in ruminants digestion (biohydrogenation of PUFA) and endogenous processes (chain-elongation of dietary PUFA). Here we compare the stable C isotope composition of individual FA from two experimental diets based on C_3 and C_4 plants with those extracted from the milk of cows consuming these diets.

Materials and Methods

Animals and Diets

Two isoenergetic and isonitrogenous diets were designed and fed to dairy cows that were in mid to end of lactation and having a limited milk yield of on average 15 kg/day. In this stage of lactation cows were assumed to be in a steady or anabolic phase and to be not mobilizing body lipids. Six cows received a diet composed of feeds obtained only from C_3 plants. These included [g/kg dry matter (DM)] barley

straw (459 g/kg dry matter, DM), barley grain (266 g/kg DM), soybean meal (238 g/kg DM) and sugar beet molasses (21 g/kg DM). Another five animals received a diet composed exclusively of C₄ plant feeds, namely maize straw (444 g/kg DM), maize pellets (368 g/kg DM), maize gluten (151 g/kg DM) and sugar cane molasses (22 g/kg DM). Both diets were supplemented by minerals, vitamins and some urea. The C₃ and C₄ diets contained 18.6 and 36.0 g/kg DM total fat and were balanced in net energy for lactation (5.46 MJ/kg DM) and protein (217 and 211 g/kg DM, respectively). At the start of the experiment, the diet was changed stepwise within 6 days from hay ad libitum and 3 kg/day of barley grain to the experimental diets. Data and sample collection did not start before a further 14 days had passed, thus minimizing carry-over effects in C-isotope composition from the previous diet. Then feed intake and milk yield were measured daily, and milk samples were collected every morning and evening for another 8 days. These samples were pooled per cow. Feed samples were collected two times. The feed samples were homogenized and pulverized and stored in 150 mL PET flasks at room temperature until analysis. Milk fat was obtained by centrifugation of milk samples and stored in the dark at –20 °C. For analysis, milk fat samples were thawed at room temperature. The governmental veterinary authority for animal welfare approved the animal experiment. Further information about diets and other experimental details are given elsewhere [14, 24].

Lipid Extraction from Feed Samples

Aliquots of 2–3 g of each compound of the powdered feed samples (except molasses), were weighed in metallic extraction thimbles (Dionex Corporation, Sunnyvale, CA, USA). Lipids were extracted with hexane/isopropanol (3:2, v/v) over night by accelerated solvent extraction (ASE 200, Dionex Corporation, Sunnyvale, CA, USA) [37]. The solvent was then evaporated under a N₂ stream and residues were dissolved in dichloromethane. Evaporation under N₂-atmosphere was repeated and the lipid extract was saponified as described below.

Saponification of Lipid Extracts and Milk Fat, and FA Derivatization

The lipids in the samples were saponified with methanolic sodium hydroxide. For FA conversion, methanolic boron trifluoride was used according to IUPAC method 2.301 [38]. After boiling, approximately 100 mg of pure fat with 2 mL NaOH (0.5 M) for 3 min, 3 mL methanolic boron trifluoride (1.3 M) was added and the mixture was heated again for 4 min. The reaction was stopped by adding 7 mL NaCl (0.34 M) and 2 mL hexane. Subsequently, tubes were

shaken for 30 s and centrifuged at 1,100×g for 1 min. A 1 mL aliquot of the upper layer, containing the FA methyl esters (FAME), was cleaned (e.g., removal of dyes) in a solid phase extraction column filled with silica gel (Isolute, Biotage, Cardiff, UK). The FAME were eluted with 6 mL dichloromethane and stored in three 2-mL vials with a final total FA concentration of approximately 20 mg/mL.

Silver-Ion Thin-Layer Chromatography

The Ag⁺-TLC was used to separate saturated from mono- and from polyunsaturated FAME. This step was necessary to improve C18 FA (e.g., *cis*-18:1 and *trans*-18:1) separation in compound-specific C-isotope analysis. The Ag⁺-TLC was applied for all samples as described by Richter et al. [39]. The TLC silica gel glass plates (60F-254 glass plates, 20 × 20 cm, MERCK, Darmstadt Germany) were first conditioned in TLC tanks filled with chloroform/methanol (1:1, v/v). After impregnation with 10% AgNO₃ in acetonitrile, plates were dried at 110 °C and 500 μg FAME were applied as a narrow linear band in the lower part of the plate. The mobile phase contained toluene/hexane (1:1, v/v). After the mobile phase reached the area between the borders of silver-ion and stationary phase, plates were dried at room temperature for 1 h. Four FAME bands, representing PUFA, monounsaturated FA (MUFA), *trans* FA (TFA) and saturated FA (SFA) were visualized by spraying with 2,7-dichlorofluorescein in ethanol. Each band was detached by scraping and washed with 4 mL chloroform/methanol (9:1, v/v) into filtration tubes filled with sodium sulfate and fiberglass. Eluents were dried under nitrogen and residues were dissolved in 200 μL hexane and stored at +4 °C for further analyses.

FA Analysis by GC/MS and GC/FID

In advance of CSIA, GC/MS and GC/FID analyses were performed in order to identify and quantify the individual FA. The analysis of FA in feed and milk fat was performed in duplicate on a gas chromatograph (GC; Agilent 6890 Series GC-Systems, Wilmington, DE, USA) equipped with a 30 m × 320 μm × 0.25 μm Supelcowax-10 column (Sigma Aldrich, Bellefonte, PA, USA) and a flame ionization detector. Helium was used as carrier gas with a constant flow of 1.1 mL/min. Samples were injected at a temperature of 200 °C and a split of 10:1. The oven temperature program was 2 min at 150 °C, +5 °C/min up to 160 °C for 5 min, +10 °C/min up to 190 °C for 5 min and +3 °C/min up to 250 °C for 5 min and the total time was 42 min. Individual FAME were identified by comparison of retention times with those of a standard FAME mixture (Supelco 37 component FAME Mix, Inc., Bellefonte, PA,

USA), after characterization of the single FA by gas chromatograph–mass spectrometry (Thermo Fisher, Argenteuil, France) equipped with a Supelcowax-10 column (see above). Chromatograms were evaluated by using the HP ChemStation software (Hewlett Packard, Palo Alto, CA, USA).

Carbon Isotope Analyses of FA Using a Gas Chromatography-Combustion-Isotope Ratio Mass Spectrometer

The $\delta^{13}\text{C}$ values of individual FA were obtained by using an Agilent 6890 GC coupled to a Thermo Fisher (Bremen, Germany) Delta V isotope ratio mass spectrometer (IRMS) by a combustion (C) interface III (GC/C/IRMS) under a constant helium flow of 1.1 mL/min. The combustion interface consists of two ceramic furnaces: an oxidation reactor with CuO/NiO/Pt wires at 940 °C and a reduction reactor with Cu wires at 600 °C. Water was removed from the effluent gas by passing it through a Nafion tube (Perma Pure, Toms River, NJ, USA) with an annular back-flow of helium. The GC was operated with the same type of column (Supelco-Wax 10 column) and temperature program used for GC/FID analyses. The background subtraction and $\delta^{13}\text{C}$ values calculation were performed using the Thermo Fisher ISODAT 2.5 software. The standard deviations for repeatability ranged between 0.03 and 1.0‰ for the main FAME. The accuracy of the GC/C/IRMS analyses was checked every 10 analyses by injection of a 20:0 methyl ester isotope standard prepared by A. Schimmelman from the Biogeochemical Laboratories at Indiana University, USA. The isotopic shift due to the carbon introduced in the FA methylation was corrected by a mass balance equation [33]: $\delta^{13}\text{C}_{\text{FAME}} = f_{\text{FA}}\delta^{13}\text{C}_{\text{FA}} + f_{\text{MeOH}}\delta^{13}\text{C}_{\text{MeOH}}$ where $\delta^{13}\text{C}_{\text{FAME}}$, $\delta^{13}\text{C}_{\text{FA}}$ and $\delta^{13}\text{C}_{\text{MeOH}}$ are the C-isotope compositions of the FAME, the FA, and the methanol used for methylation of the FA, respectively, and f_{FA} and f_{MeOH} are the C-fractions in the FAME due to the alkanolic chain and methanol, respectively. Since *trans* 18:1 isomers elute close to each other, the $\delta^{13}\text{C}$ value reported as *t*11-18:1* include isomers *t*9, *t*10, *t*11 with *t*11 being by far the most abundant (e.g., in the milk from C₃ fed cows *t*11-18:1 ~ 71.3%; in the milk from C₄ fed cows *t*11-18:1 ~ 81.2%) [14].

Statistical Evaluation

Isotopic values for total diets were calculated based on proportionate intakes of individual FA from the individual feeds [14]. To compare the stable C isotope composition of the diets at two different sample collection dates, a *t*-test was carried out on the individual FA of the diet components, but no significant differences (data not shown) between the sampling dates were found. The isotopic

values of the individual FA in the three C₃ feeds and the three C₄ feeds, as well as of the six and five milk samples were subjected to analysis of variance using the general linear model (GLM procedure; SAS software, version 9.1, SAS Institute Inc., Cary NC, USA), considering as effects individual FA and diet type and the interaction. Multiple comparisons among FA means in the feeds were performed using Tukey's method. Mean values of individual milk FA within one diet group were compared by the least significant difference test ($p < 0.05$).

Results

Carbon Isotopic Composition of the FA in the C₃ and C₄ Feeds

The carbon isotope composition measured in the FA of individual feeds and calculated for the total C₃ and C₄ diets are given in Table 1. All the FA $\delta^{13}\text{C}$ values in C₃ feeds (mean value: -32.3‰) were more negative ($p < 0.001$) than those in C₄ feeds (mean value: -23.4‰). In both diet types, the lower $\delta^{13}\text{C}$ values were measured in 18:0 and FA with <18 C-atoms compared to the unsaturated C18 fatty acids (Table 1). Within the groups of isotopically light FA, there was a further differentiation for 18:0, which had a more negative $\delta^{13}\text{C}$ than 16:0 and 16:1. No significant interaction between feed type and FA occurred for $\delta^{13}\text{C}$ values.

Carbon Isotopic Composition of FA in Cow's Milk

The mean $\delta^{13}\text{C}$ values of the main FA of milk samples from animals fed with C₃ or C₄ diets were lower compared to those of C₄ milk (-30.1 ± 4.4‰ and -24.9 ± 3.8‰, respectively; Table 2). Significant differences in $\delta^{13}\text{C}$ of most FA (except 14:1, 16:1, 17:1 and 18:3n-3) were observed between milk samples from C₃ and C₄ diets. Within a diet group, differences ($p < 0.001$) in $\delta^{13}\text{C}$ values between the main FA were found. In both groups the lowest $\delta^{13}\text{C}$ values were measured for *c*9,*t*11-18:2 (C₃ milk = -37.0 ± 2.7‰; C₄ milk = -31.4 ± 2.6‰; Table 2). A trend was identified in the $\delta^{13}\text{C}$ values of C18 FA in C₃ milk. They were enriched in ¹³C with increasing degree of desaturation (18:0 < 18:1n-9 and *t*11-18:1 < 18:2n-6 < 18:3n-3), with the exception of *c*9,*t*11-18:2 (Table 1). In C₄ milk, such enrichment was only observed for *t*11-18:1 and 18:2n-6. The $\delta^{13}\text{C}$ values of 18:1n-9 and *t*11-18:1 were not significantly different in both groups (C₃ milk: -31.8 ± 1.4 and -30.6 ± 2.6‰, C₄ milk: -26.5 ± 2.1 and -23.4 ± 1.4‰). Different results between groups were observed for 18:3n-3, which had lower $\delta^{13}\text{C}$ values than *t*11-18:1 in C₄ milk but higher $\delta^{13}\text{C}$

Table 1 Means for stable carbon isotope composition in individual fatty acids from the diet ($\delta^{13}\text{C}$, ‰ VPDB)

	C ₃ diet				C ₄ diet				Average $\delta^{13}\text{C}$ values		
	Total diet ⁺	Barley straw	Barley grain	Soybean meal	Total diet ⁺	Maize straw	Maize pellets	Maize gluten	C ₃ feeds	C ₄ feeds	<i>p</i> -value C ₃ versus C ₄
16:0	-34.0	-35.2	-34.3	-32.1	-23.9	-26.3	-23.6	-22.8	-33.9 ^c	-24.2 ^b	<0.001
16:1	-33.2	-33.1	-33.9	-32.0	-24.7	-24.5	-26.0	-23.6	-33.0 ^{bc}	-24.7 ^b	<0.001
18:0	-36.8	-40.3	-37.3	-34.3	-26.3	-28.2	-25.8	-25.3	-37.3 ^d	-26.4 ^b	<0.001
18:1n-9	-30.0	-31.5	-30.9	-28.2	-21.0	-20.4	-21.2	-20.6	-30.2 ^{ab}	-20.7 ^a	<0.001
18:2n-6	-29.4	-30.2	-30.2	-27.8	-19.9	-18.6	-19.8	-20.5	-29.4 ^a	-19.6 ^a	<0.001
18:3n-3	-30.5	-31.4	-31.6	-27.8	-17.2	-22.7	-16.8	-15.0	-30.3 ^{ab}	-18.1 ^a	<0.001
<i>p</i> -value fatty acids									<0.001	<0.001	

⁺ Total C₃ and C₄ diets were determined by mass balance calculations from the proportion of fatty acid intake from the three dietary components a,b,c,d Fatty acid means within a column with different superscript letters are significantly different ($p < 0.05$)

Table 2 Means and ranges for stable carbon isotope composition in individual milk fatty acids ($\delta^{13}\text{C}$, ‰ VPDB)

Milk origin	From cows fed the C ₃ diet (n = 6)	From cows fed the C ₄ diet (n = 5)	<i>p</i> -value diet
12:0	-28.8 (-31.5 to -25.9)	-22.6 (-24.9 to -20.7)	<0.001
14:0	-32.3 (-32.8 to -31.5)	-23.2 (-24.6 to -21.5)	<0.001
14:1	-27.0 (-29.0 to -22.4)	-22.9 (-27.1 to -19.9)	0.044
15:0	-35.0 (-37.5 to -34.2)	-27.0 (-29.0 to -25.3)	<0.001
16:0	-29.6 (-31.0 to -28.4)	-22.3 (-23.8 to -21.0)	<0.001
16:1	-26.8 (-29.8 to -22.6)	-24.4 (-29.6 to -20.2)	0.274
17:1	-26.3 (-29.2 to -21.2)	-24.4 (-29.6 to -20.2)	0.352
18:0	-34.6 (-36.5 to -32.6)	-26.6 (-29.3 to -23.5)	<0.001
18:1n-9	-31.8 (-34.0 to -29.8)	-26.5 (-29.1 to -23.6)	<0.001
<i>t</i> 11-18:1*	-30.6 (-33.2 to -25.6)	-23.4 (-25.2 to -21.2)	<0.001
18:2n-6	-29.3 (-36.7 to -26.8)	-22.4 (-25.9 to -20.2)	<0.005
18:3n-3	-26.5 (-29.0 to -24.5)	-26.0 (-33.8 to -19.4)	0.818
<i>c</i> 9, <i>t</i> 11-18:2	-37.0 (-40.4 to -32.5)	-31.4 (-35.3 to -29.1)	0.007
Least significant difference	2.73	3.41	
<i>p</i> -value fatty acids	<0.001	<0.001	

* Proportions of the *trans* 18:1 isomers in %: milk from the C₃ diet: *t*9 = 14.9%, *t*10 = 13.8%, *t*11 = 71.3%; milk from the C₄ diet: *t*9 = 10.2%, *t*10 = 8.5%, *t*11 = 81.2% [14]

values in C₃ milk. There was an interaction between milk samples from different diet types and individual FA in $\delta^{13}\text{C}$ ($p = 0.002$).

Relationships of $\delta^{13}\text{C}$ Values of Individual FA Between Feed and Milk

The 16:0 was ^{13}C enriched in milk fat by 4.4‰ when fed the C₃ diet and by 1.6‰ with the C₄ diet relative to the plant 16:0 (Tables 1, 2; Fig. 1). Mean $\delta^{13}\text{C}$ values of milk 16:1 were similar to those of the C₄ diet, and 6‰ higher for the C₃ diet. The $\delta^{13}\text{C}$ values of 18:3n-3 and 18:0 in milk from C₃ fed cows were higher (-26.5 ± 1.5 and -34.6 ± 1.4 ‰, respectively) than for the FA of the calculated total C₃ diet (-30.5 and -36.8 ‰ respectively; Fig. 1). The $\delta^{13}\text{C}$ value of 18:2n-6 from C₃ diet and milk

samples were similar (-29.3 ± 3.7 ‰ and -29.4 ‰, respectively). For *c*9,*t*11-18:2 the value was much lower (-37.0 ± 2.7 ‰) than for its precursors 18:2n-6 (-29.4 ‰) and 18:3n-3 (-30.5 ‰) in the C₃ diet.

The $\delta^{13}\text{C}$ values for 18:3n-3 in the C₄ milk samples were up to 9‰ lower than those calculated by mass balance from the total C₄ diet (milk = -26.0 ± 5.5 ‰, diet = -17.2 ‰; Fig. 1). The isotopic composition of 18:0 in the milk (-26.6 ± 3.7 ‰) was similar to the calculated total C₄ diet (-26.3 ‰, Fig. 1), and for 18:2n-6 the $\delta^{13}\text{C}$ values of the milk samples (-22.4 ± 2.2 ‰) were always lower. The highest intake of 18:3n-3 and 18:2n-6 was from maize pellets, due to the comparatively higher total fat content. The isotopic value of *c*9,*t*11-18:2 (-31.4 ± 2.6 ‰) was much lower than for its precursors 18:2n-6 (-19.9 ‰) and 18:3n-3 (-17.2 ‰) in the C₄ diet.

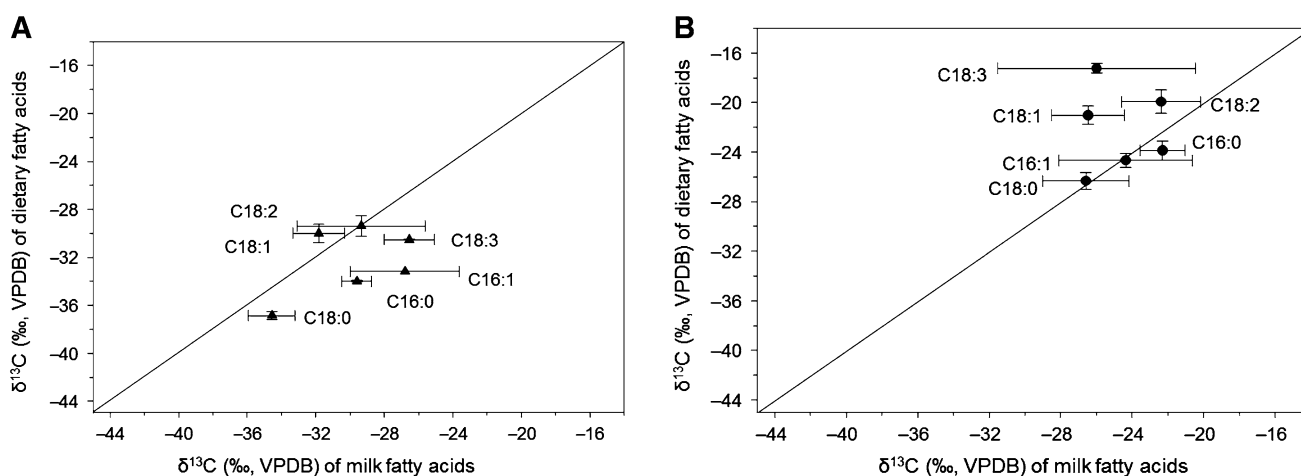


Fig. 1 Mean and standard deviation of $\delta^{13}\text{C}$ values (‰, VPDB) of individual fatty acids in the milk samples as opposed to those of the C_3 (a) and the C_4 diet (b). The isotopic composition of the total C_3 and C_4 diets were determined by mass balance calculations

Discussion

$\delta^{13}\text{C}$ Values of Individual FA in Feeds and Diets Derived from C_3 and C_4 Plants

Significant isotopic differences between (1) a specific FA in different plant species (e.g., C_3 versus C_4 plants), or (2) between FA of the same plant or (3) both are required to be able to trace transformations of FA in digestion and metabolism through natural stable C isotope compositions. A C isotope discrimination between C_3 and C_4 plants is well documented for total biomass [28] and for individual FA [29–31, 33–36, 40]. The $\delta^{13}\text{C}$ values measured in the experimental feeds for individual FA were in good agreement with these published values. The isotopic difference between 16:0 and 18:0 in the C_3 and C_4 feeds was 3.4 and 2.2‰, respectively. In both C_3 and C_4 feeds the unsaturated C18 fatty acids were depleted in ^{13}C on average by about 8‰ compared to 18:0. These differences are higher than those reported for pure vegetable oils [29–36].

Differentiation was not significant between 18:3n-3 and its precursor FA 18:1n-9 and 18:2n-6 with feeds from both C_3 and C_4 plants. In plants, 18:0 is used for the production of 18:1n-9, which is synthesized by Δ^9 -desaturase. The 18:1n-9 can then be desaturated to 18:2n-6 (via Δ^{12} -desaturase) at a different site of the plant cell and a further desaturation step produces 18:3n-3 (via Δ^{15} -desaturase). These biosynthetic pathways may explain the small variations found in the $\delta^{13}\text{C}$ values. However, the highest $\delta^{13}\text{C}$ values compared to the other C18 FA were observed in the 18:3n-3 extracted from maize gluten and pellets (made from maize grains), but not in the maize straw composed mainly of leaves and stem. This ^{13}C enrichment might have resulted from the preferential cleavage of ^{12}C – ^{12}C bonds over ^{12}C – ^{13}C bonds during oxidation [33] of 18:3n-3

triggered by the separation of gluten from corn, pellet preparation, and their storage. Such ^{13}C enrichment of 18:3n-3 compared to 18:0, 18:1n-9 and 18:2n-6 was recently reported for poppy oil [31].

$\delta^{13}\text{C}$ Values of Individual FA in Milk from Cows Fed C_3 and C_4 Diets

In the present study, the mobilization of adipose lipids for milk synthesis was considered to be negligible. Cows were in a stage of lactation and had a milk yield where energy intake can be easily covered by intake and cows typically even deposit FA in their adipose tissues. The differences measured in the isotopic composition between individual milk FA within diet groups therefore reflect initial differences in the diets, the isotopic fractionation during biosynthesis, and differences in rates of their metabolic turnover. FA in milk from ruminants originate either directly from the diet (plant FA such as 18:2n-6 or 18:3n-3), from microbial modification in the rumen (such as *trans* 18:1 isomers), from microbial synthesis in the rumen (odd- and branched-chain FA) or from de novo synthesis within the mammary gland (short-chain and medium-chain FA with 4–14 C atoms). The C16 FA can originate from both sources [41, 42], where the endogenous synthesis of 16:0 uses acetate from ruminal fermentation of carbohydrates as precursor. Even though the fat content of the C_3 total diet was lower than of the C_4 diet, in both groups of cows the 16:0 intake was similar [14]. However, the 16:0 concentration in the C_3 milk was higher [14], which suggests a higher endogenous synthesis. This is additionally supported by the ^{13}C enrichment, found in the C_3 milk fat for 16:0 and 16:1 relative to the dietary C16, which most probably reflects the isotopic composition of acetate, originating from ruminal degradation of the heavier

carbohydrates and being the endogenous precursor of C16. The bulk feed samples mainly consisted of carbohydrates and were isotopically heavier [24] than the individual fatty acids. Lipids are ^{13}C depleted relative to carbohydrates as a result of isotopic fractionation during biosynthesis [43]. The difference between the $\delta^{13}\text{C}$ values of 16:0 and 18:0 for C₃ and C₄ milk was $+5.0 \pm 1.4$ and $+4.3 \pm 1.6\text{‰}$, respectively. Apart from dietary origin, 18:0 may be produced by microbial biohydrogenation of unsaturated C18 FA being the terminal product of ruminal biohydrogenation [41]. The $\delta^{13}\text{C}$ values of 18:0 in milk from C₃- and C₄-fed cows were different by $+2.2$ and -0.3‰ , respectively, compared with those of the dietary 18:0. This may be explained by the trophic enrichment of ^{13}C and probably microbial activity. The 18:1n-9 in milk is derived to a large proportion from desaturation of 18:0 in the mammary gland. However, 18:1n-9 in milk of cows fed the C₃ diet was enriched in ^{13}C relative to 18:0 in the milk, as it was also observed in the diets, whereas no effect was found with the C₄ diet. With the C₃ diet, the isotopic difference between 18:0 and 18:1n-9 in milk was -2.7‰ compared to -6.8‰ in the diet. These observations suggest that feeding the C₃ diet (20% 18:1n-9) [14] either caused quantitatively more 18:1n-9 to be transferred directly from the feed or that an isotopic fractionation during the endogenous synthesis of 18:1n-9 with 18:0 as a precursor took place or both. Since no such fractionation took place with the C₄ diet (15% 18:1n-9) [14], the latter seems less likely.

Dietary polyunsaturated C18 FA undergo intensive modification during ruminal digestion [12, 15]. Important intermediates and end products of these processes are *c9,t11-18:2*, *t11-18:1* and 18:0 [4, 16]. Being essential, 18:2n-6 and 18:3n-3 may occur in the endogenous metabolism only as primary dietary FA. However, their $\delta^{13}\text{C}$ was not the same in feed and milk. In C₃ milk, 18:3n-3 was 4‰ enriched in ^{13}C compared to the total diet. This suggests a preferential biohydrogenation of the isotopically light 18:3n-3 molecules in the rumen followed by a transfer of the residual 18:3n-3, which is more enriched in ^{13}C to the milk. By contrast, the $\delta^{13}\text{C}$ value of 18:3n-3 in C₄-plant derived milk was much lower (about -9‰) compared to the corresponding diet. Further work is in progress to confirm these results and explain these apparently opposite isotopic trends of 18:3n-3 in milk from animals feed with C₃ or C₄ diets.

The *c9,t11-18:2* was depleted in ^{13}C in milk from both diet types, compared to all other milk FA. This would suggest an isotope fractionation occurring during the isomerization step in ruminal biohydrogenation. Microbial C isotope fractionation has been observed previously for the conversion of *cis-16:1* to *trans-16:1* by the bacterium *Pseudomonas putida*, with the *trans*-molecule being

depleted in ^{13}C by up to 2.1‰ [44]. However, in the milk of the present study, *t11-18:1* (with minor proportions of other 18:1 *trans* isomers) did not show a comparably large deviation in $\delta^{13}\text{C}$ values from the precursors 18:2n-6 and 18:3n-3 as that found with *c9,t11-18:2*. Since *t11-18:1* occurs after *c9,t11-18:2* in the biohydrogenation pathway, it seems unlikely that the isotopic difference measured for *c9,t11-18:2* was a consequence of the rumen microbial activity. Therefore, as *c9,t11-18:2* can also be produced in the body tissue from *t11-18:1* by Δ^9 -desaturase [4, 16], the enzyme catalyzing the endogenous desaturation might discriminate against ^{13}C . This could be explained by stronger chemical bonds of the heavier isotopologues ($^{12}\text{C}-^{13}\text{C}$, $^{13}\text{C}-^{13}\text{C}$) compared to $^{12}\text{C}-^{12}\text{C}$ followed by lower enzymatic rate constants [33]. Accordingly, Gilmore et al. [45] suggested that the variations in $\delta^{13}\text{C}$ values of individual FA in Arctic foxes could be attributed to isotopically distinct dietary sources and isotopic fractionation during desaturation and chain elongation. Also Fang et al. [46] assumed that a kinetic isotope effect, resulting in intermolecular isotope fractionation during desaturation and chain elongation, could be responsible for $\delta^{13}\text{C}$ differences in FA in seep organisms.

The significant interaction found between diet type and FA suggests that the differentiation in $\delta^{13}\text{C}$ values of individual FA in milk might depend on both, the diet type and the precursor FA. That implies that measurements of stable C-isotope ratios may be a useful approach to differentiate metabolic pathways of FA in ruminants if the dietary conditions are controlled.

Conclusion

By using GC/C/IRMS combined with Ag⁺-TLC we were able to demonstrate natural differences between $\delta^{13}\text{C}$ values of dietary FA and milk FA. The differences in the C₃ and C₄ diets were partly preserved in the cows' milk. In particular, *c9,t11-18:2* was depleted in ^{13}C compared to its dietary precursors. The study provided evidence that this was a result of the endogenous desaturation of *t11-18:1* to *c9,t11-18:2* in the body tissue rather than from rumen microbial biohydrogenation. These findings could be the basis for initiating more detailed stable isotope-based research in ruminant FA metabolism. Especially studies on various ruminant species and with different diet types are required to quantify by observing such fractionations the relative importance (species specificity, frequency, persistence) of precursors of milk FA.

Acknowledgments This work was financially supported by the Vontobel foundation, Switzerland.

References

- Lourenço M, Van Ranst G, Vlaeminck B, De Smet S, Fievez V (2008) Influence of different dietary forages on the fatty acid composition of rumen digesta as well as ruminant meat and milk. *Anim Feed Sci Technol* 145:418–437
- Dannenberger D, Nuernberg G, Scollan N, Schabbel W, Steinhart H, Ender K, Nuernberg K (2004) Effect of diet on the deposition of n-3 fatty acids, conjugated linoleic and C18:1 *trans* fatty acid isomers in muscle lipids of German Holstein bulls. *J Agric Food Chem* 52:6607–6615
- Martins SV, Lopes PA, Alfaia CM, Ribeiro VS, Guerreiro TV, Fontes CMGA, Castro MF, Soveral G, Prates JAM (2007) Contents of conjugated linoleic acid isomers in ruminant-derived foods and estimation of their contribution to daily intake in Portugal. *Br J Nutr* 98:1206–1213
- Bauman DE, Baumgard LH, Corl BA, Griinari JM (2000) Biosynthesis of conjugated linoleic acid in ruminants. *J Anim Sci* 77:1–15
- Parodi P (1976) Distribution of isomeric octadecenoic fatty acids in milk fat. *J Dairy Sci* 59:1870–1873
- Ip C, Banni S, Angioni E, Carta G, McGinley J, Thompson HJ, Barbano D, Bauman D (1999) Conjugated linoleic acid-enriched butter fat alters mammary gland morphogenesis and reduces cancer risk in rats. *J Nutr* 129:2135–2142
- Belury MA (2002) Inhibition of carcinogenesis by conjugated linoleic acid: potential mechanisms of action. *J Nutr* 132:2995–2998
- Khosla P, Fungwe TV (2001) Conjugated linoleic acid: effects on plasma lipids and cardiovascular function. *Curr Opin Lipidol* 12:31–34
- Lee JH, Cho KH, Lee K-T, Kim MR (2005) Antiatherogenic effects of structured lipid containing conjugated linoleic acid in C57BL/6 J mice. *J Agric Food Chem* 53:7295–7301
- Moloney F, Toomey S, Noone E, Nugent A, Allan B, Loscher CE, Roche HM (2007) Antidiabetic effects of cis-9, trans-11-conjugated linoleic acid may be mediated via anti-inflammatory effects in white adipose tissue. *Diabetes* 56:574–582
- Benjamin S, Spener F (2009) Conjugated linoleic acids as functional food: an insight into their health benefits. *Nutr Metab* 6:36
- Chilliard Y, Glasser F, Ferlay A, Bernard L, Rouel J, Doreau M (2007) Diet, rumen biohydrogenation and nutritional quality of cow and goat milk fat. *Eur J Lipid Sci Technol* 109:828–855
- Kraft J, Collomb C, Möckel P, Sieber R, Jahreis G (2003) Differences in CLA isomer distribution of cow's milk lipids. *Lipids* 38:657–664
- Khiaosa-Ard R, Klevenhusen F, Soliva CR, Kreuzer M, Leiber F (2010) Transfer of linoleic and linolenic acid from feed to milk in cows fed isoenergetic diets differing in proportion and origin of concentrates and roughages. *J Dairy Res* 77:331–336
- Jenkins TC, Wallace RJ, Moate PJ, Mosley EE (2008) Board-invited review: recent advances in biohydrogenation of unsaturated fatty acids within the rumen microbial ecosystem. *J Anim Sci* 86:397–412
- Griinari JM, Corl BA, Lacy SH, Chouinard PH, Nurmela KVV, Bauman DE (2000) Conjugated linoleic acid is synthesized endogenously in lactating dairy cows by delta-9-desaturase. *J Nutr* 130:2285–2291
- Khiaosa-Ard R, Bryner SF, Scheeder MRL, Wettstein HR, Leiber F, Kreuzer M, Soliva CR (2009) Evidence for the inhibition of the terminal step of ruminal alpha-linolenic acid biohydrogenation by condensed tannins. *J Dairy Sci* 92:177–188
- DeNiro MJ, Epstein S (1978) Influence of diet on the distribution of carbon isotopes in animals. *Geochim Cosmochim Acta* 42:495–506
- Hobson KA (1987) Use of stable-carbon isotope analysis to estimate marine and terrestrial protein content in gull diets. *Can J Zool* 65:1210–1213
- Pond CM, Gilmour I (1997) Stable isotopes in adipose tissue fatty acids as indicators of diet in arctic foxes (*Alopex lagopus*). *Proc Nutr Soc* 56:1067–1081
- Trust Hammer B, Fogel ML, Hoering TC (1998) Stable carbon isotope ratios of fatty acids in seagrass and redhead ducks. *Chem Geol* 152:29–41
- Stott AW, Davies E, Evershed RP (1997) Monitoring the routing of dietary and biosynthesised lipids through compound-specific stable isotope ($\delta^{13}\text{C}$) measurements at natural abundance. *Naturwissenschaften* 84:82–86
- Camin F, Perini M, Colombari G, Bontempo L, Versini G (2008) Influence of dietary composition on the carbon, nitrogen, oxygen and hydrogen stable isotope ratios of milk. *Rapid Comm Mass Spectrom* 22:1690–1696
- Klevenhusen F, Bernasconi SM, Kreuzer M, Soliva CR (2010) Experimental validation of the intergovernmental panel on climate change default values for ruminant-derived methane and its carbon-isotope signature. *Anim Prod Sci* 50:159–167
- Metges C, Kempe K, Schmidt HL (1990) Dependence of the carbon-isotope contents of breath carbon dioxide, milk, serum and rumen fermentation products on the $\delta^{13}\text{C}$ value of food in dairy cows. *Br J Nutr* 63:187–196
- Vetter W, Gaul S, Thurnhofer S, Mayer K (2007) Stable carbon isotope ratios of methyl-branched fatty acids are different to those of straight-chain fatty acids in dairy products. *Anal Bioanal Chem* 389:597–604
- Molkentin J (2009) Authentication of organic milk using $\delta^{13}\text{C}$ and the α -linolenic acid content of milk fat. *J Agric Food Chem* 57:785–790
- O'Leary M (1981) Carbon isotope fractionation in plants. *Phytochem* 20:553–567
- Angerosa F, Breas O, Contento S, Guillou C, Reniero F, Sada E (1999) Application of stable isotope ratio analysis to the characterization of the geographical origin of olive oils. *J Agric Food Chem* 47:1013–1017
- Kelly S, Parker M, Sharman M, Dennis J, Goodall I (1997) Assessing the authenticity of single oils using fatty acid stable carbon ($^{13}\text{C}/^{12}\text{C}$) seed vegetable isotope ratios. *Food Chem* 59:181–186
- Richter EK, Spangenberg JE, Kreuzer M, Leiber F (2010) Characterization of rapeseed (*Brassica napus*) oils by bulk C, O, H, and fatty acid C stable isotope analyses. *J Agric Food Chem* 58:8048–8055
- Royer A, Gerard C, Nault N, Lees M, Martin GJ (1999) Stable isotope characterization of olive oils. I-Compositional and carbon-13 profiles of fatty acids. *Am Oil Chem Soc* 76:357–363
- Spangenberg JE, Macko SA, Hunziker J (1998) Characterization of olive oil by carbon isotope analysis of individual fatty acids: Implications for authentication. *J Agric Food Chem* 46:4179–4184
- Spangenberg JE, Ogrinc N (2001) Authentication of vegetable oils by bulk and molecular carbon isotope analyses with emphasis on olive oil and pumpkin seed oil. *J Agric Food Chem* 49:1534–1540
- Spangenberg JE, Dionisi F (2001) Characterization of cocoa butter and cocoa butter equivalents by bulk and molecular carbon isotope analyses: Implications for vegetable fat quantification in chocolate. *J Agric Food Chem* 49:4271–4277
- Woodbury SE, Evershed RP, Rossell JB (1998) Purity assessments of major vegetable oils based on $\delta^{13}\text{C}$ values of individual fatty acids. *J Am Oil Chem Soc* 75:371–379
- Wettstein HR, Scheeder MRL, Sutter F, Kreuzer M (2001) Effect of lecithins partly replacing rumen-protected fat on fatty acid

- digestion and composition of cow milk. *Eur J Lipid Sci Technol* 103:12–22
38. International Union of Pure and Applied Chemistry (IUPAC) (1992) Standard methods for the analysis of oils, fats and derivatives, 1st supplement to the 7th edition. In: Dieffenbacher A, Pocklington WD (eds) Applied chemistry division, commission on oils, fats and derivatives. Blackwell Scientific, Oxford
 39. Richter EK, Albash Shawish K, Scheeder MRL, Colombani PC (2009) Trans fatty acid content of selected Swiss foods: the TransSwissPilot study. *J Food Compos Anal* 22:479–484
 40. Camin F, Larcher R, Perini M, Bontempo L, Bertoldi D, Gagliano G, Nicolini G, Versini G (2010) Characterisation of authentic Italian extra-virgin olive oils by stable isotope ratios of C, O and H and mineral composition. *Food Chem* 118:901–909
 41. Bauman DE, Griinari JM (2003) Nutritional regulation of milk fat synthesis. *Annu Rev Nutr* 23:203–227
 42. Iverson SJ, Oftedal TO (1995) Phylogenetic and ecological variation in the fatty acid composition of milks. In: Jensen RG (ed) Handbook of Milk Composition. Academic Press, San Diego, pp 798–834
 43. Park R, Epstein S (1961) Metabolic fractionation of ^{13}C and ^{12}C in plants. *Plant Physiol* 36:133–138
 44. Heipieper HJ, Neumann G, Kabelitz N, Kastner M, Richnow HH (2004) Carbon isotope fractionation during cis-trans isomerization of unsaturated fatty acids in *Pseudomonas putida*. *Appl Microbiol Biotechnol* 66:285–290
 45. Gilmour I, Johnston MA, Pillinger CT, Pond CM, Mattacks CA, Prestrud P (1995) The carbon isotopic composition of individual fatty acids as indicators of dietary history in Arctic foxes on Svalbard. *Phil Trans R Soc Lond B Biol Sci* 349:135–142
 46. Fang J, Abrajano TA, Comet PA, Brooks JM, Sassen R, MacDonald IR (1993) Gulf of Mexico hydrocarbon seep communities. XI. Carbon isotopic fractionation during fatty acid biosynthesis of seep organisms and its implication for chemosynthetic processes. *Isot Geosci* 109:271–279

Identification of C18 Intermediates Formed During Stearidonic Acid Biohydrogenation by Rumen Microorganisms In Vitro

S. P. Alves · M. R. G. Maia · R. J. B. Bessa ·
A. J. M. Fonseca · A. R. J. Cabrita

Received: 1 August 2011 / Accepted: 23 September 2011 / Published online: 30 October 2011
© AOCS 2011

Abstract In vitro batch incubations were used to study the rumen biohydrogenation of unsaturated fatty acids. An earlier study using increasing supplementation levels of stearidonic acid (18:4n-3), revealed that the rumen microbial population extensively biohydrogenates 18:4n-3 after 72 h of in vitro incubation, though several intermediates formed were not completely characterized. Therefore, in the present study, samples were reanalyzed in order to identify the 18:2, 18:3 and 18:4 biohydrogenation intermediates of 18:4n-3. Gas–liquid chromatography coupled to mass spectrometry was used to characterize these intermediates. The acetonitrile chemical ionization mass spectrometry of the fatty acid methyl esters derivatives enabled the discrimination of fatty acids as non-conjugated or conjugated biohydrogenation intermediates. In addition, the acetonitrile covalent adduct chemical ionization

tandem mass spectrometry yielded prominent ions indicative of the double bond position of the major 18:3 isomers, i.e. $\Delta 5,11,15$ 18:3. Furthermore, the 4,4-dimethyloxazoline derivatives prepared from the fatty acid methyl esters enabled the structure of novel 18:2, 18:3 and 18:4 biohydrogenation intermediates to be elucidated. The intermediates accumulated in the fermentation media after 72 h of incubation of 18:4n-3 suggest that similar to the biohydrogenation pathways of linoleic (18:2n-6) and α -linolenic (18:3n-3) acids, the pathway of the 18:4n-3 also proceeds with the formation of conjugated fatty acids followed by hydrogenation, although no conjugated dienes were found. The formation of the novel biohydrogenation intermediates of 18:4n-3 seems to follow an uncommon isomerization pattern with distinct double bond migrations.

Keywords Biohydrogenation intermediates · Stearidonic acid · Gas–liquid chromatography · Mass spectrometry · 4,4-Dimethyloxazoline · Covalent adduct chemical ionization

Abbreviations

CACI	Covalent adduct chemical ionization
CACIMS/MS	Covalent adduct chemical ionization tandem mass spectrometry
CI	Chemical ionization
DHA	Docosahexaenoic acid
DM	Dry matter
DMOX	4,4-Dimethyloxazoline
EI	Electron impact
EPA	Eicosapentaenoic acid
FAME	Fatty acid methyl ester(s)
GLC	Gas–liquid chromatography
MS	Mass spectrometry
PFI	Polyenoic fatty acid isomerase

S. P. Alves (✉) · R. J. B. Bessa
INRB, Instituto Nacional dos Recursos Biológicos,
Unidade de Produção Animal, 2005-048 Fonte-Boa,
Vale de Santarém, Portugal
e-mail: susana_alves@sapo.pt

S. P. Alves · M. R. G. Maia · A. J. M. Fonseca
REQUIMTE, ICBAS, Instituto de Ciências Biomédicas de Abel
Salazar, Universidade do Porto, Rua Padre Armando Quintas,
4485-661 Vairão, Portugal

R. J. B. Bessa
Faculdade de Medicina Veterinária, Universidade Técnica de
Lisboa, CIISA, Pólo Universitário do Alto da Ajuda, Av. da
Universidade Técnica, 1300-477 Lisbon, Portugal

A. R. J. Cabrita
REQUIMTE, Departamento de Geociências, Ambiente e
Ordenamento do Território, Faculdade de Ciências,
Universidade do Porto, Rua Padre Armando Quintas,
4485-661 Vairão, Portugal

PUFA	Polyunsaturated fatty acid methyl ester(s)
SDA	Stearidonic acid
Ag ⁺ -SPE	Silver ion solid-phase extraction

Introduction

Stearidonic acid (SDA; 18:4n-3) is a polyunsaturated fatty acid (PUFA) that constitutes the first metabolite of α -linolenic acid (18:3n-3) in the metabolic pathway leading to the endogenous production of eicosapentaenoic acid (EPA; 20:5n-3) and docosahexaenoic acid (DHA; 22:6n-3) [1]. An increased interest has emerged in the last few years on these long chain n-3 PUFA due to their benefits to human health [2, 3]. Recently it was suggested that 18:4n-3 itself may be a surrogate for 20:5n-3 for health promotion and disease prevention [4]. In dairy products, the potential of 18:4n-3 enriched soybean oil to increase the n-3 fatty acid content was demonstrated by Bernal-Santos et al. in rumen fistulated cows [5].

In ruminants, PUFA are biohydrogenated in the rumen, often resulting in the formation of *cis* and *trans* isomers, including conjugated isomers, *trans* monoenes or others intermediates. The biohydrogenation of PUFA by the rumen microbial population has been widely studied in vitro, mostly by using linoleic acid (18:2n-6), 18:3n-3, 20:5n-3, and 22:6n-3 as fatty acids or oil sources [6–11]. Recently, in vitro batch incubations were conducted to evaluate the biohydrogenation of 18:4n-3 by the rumen microbial population with increasing supplementation levels [12]. These in vitro incubations showed an extensive biohydrogenation of 18:4n-3. However, at high 18:4n-3 supplementation levels several 18:2, 18:3 and 18:4 biohydrogenation intermediates accumulated after 72 h of incubation. As far as we know, there are no reports on the characterization of the intermediates formed during the biohydrogenation of 18:4n-3. A more complete characterization of these intermediates is important to understand the overall biohydrogenation process and underlying mechanisms for their formation. The importance of disclosure all the detailed information on isomeric profile is linked to the current knowledge that slight structural differences can profoundly modify the biological action of these fatty acids [13].

Gas–liquid chromatography coupled to mass spectrometry (GLC–MS) has been widely used for the characterization of fatty acids, despite the location of the double bonds being particularly difficult. For this, several methods have been used, including covalent adduct chemical ionization tandem mass spectrometry (CACIMS/MS) of fatty acid methyl esters (FAME) derivatives [14, 15], and the

mass spectrometry analysis of others derivatives, such as 4,4-dimethyloxazoline (DMOX), picolinyl, and pyrrolidides [16–20]. The objective of this study was to determine the structure and composition of the novel biohydrogenation intermediates formed during in vitro incubations with 18:4n-3, and the effect of increasing supplementation levels on the pattern of biohydrogenation intermediates formed.

Materials and Methods

Chemicals

All reagents and solvents were analytical and chromatographic grade, and were obtained from Sigma-Aldrich (St. Louis, MO, USA). Ag⁺-ion SPE cartridges (750 mg/6 mL) and a mixture of FAME standards were purchased from Supelco Inc. (Bellefonte, PA, USA). A bacterial acid methyl esters mix was purchased from Matreya LLC (Pleasant Gap, PA, USA).

In Vitro Incubations

Samples from batch incubations were obtained from an experiment described elsewhere [12]. Briefly, Hungate tubes containing 4.5 mL buffered ruminal fluid, obtained from 3 adult cows, were supplemented with increasing levels of 18:4n-3 (pure free fatty acid from Sigma-Aldrich, St. Louis, MO, USA) and incubated at 39 °C for 72 h. Stearidonic acid was supplemented at 0 (control), 0.25, 0.50, 0.75, 1.00, 1.25, and 1.50 mg per 33 mg total mixed ration (TMR, dry matter (DM) basis). Each treatment was replicated in triplicate within the incubation. Reactions were stopped after 72 h by cooling in an ice-slurry, and tubes stored at –20 °C until analysis.

Preparation of Fatty Acid Methyl Esters

Lipids from in vitro incubations were extracted from freeze-dried whole fermentation media using a mixture of dichloromethane and methanol (2:1, by vol.) and FAME were prepared by a combined transesterification method, as described by Maia et al. [12]. In order to detect FAME co-elutions during GLC analysis, selected samples were fractionated into saturated, *trans*-18:1, *cis*-18:1, 18:2, 18:3 and 18:4 isomers by Ag⁺-SPE using hexane with increasing amounts of acetone, according to Kramer et al. [21].

Preparation of 4,4-Dimethyloxazoline Derivatives

4,4-Dimethyloxazoline derivatives were prepared from FAME by adding 0.5 μ L of 2-amino-2-methyl-1-propanol,

and left at 170 °C for 16 h under nitrogen. Once cooled, DMOX derivatives were extracted twice with a mixture of diethyl ether and hexane (1:1, by vol.) and rinsed with water. After drying over anhydrous sodium sulphate the solvent was evaporated under nitrogen at 34 °C and the residue dissolved in 1 mL of hexane (GC-grade).

Instrumentation

Quantification of FAME was determined using a gas chromatograph HP6890A (Hewlett-Packard, Avondale, PA, USA), equipped with a flame-ionization detector (GLC-FID) and a CP-Sil 88 capillary column (100 m; 0.25 mm i.d.; 0.20 µm film thickness; Chrompack, Varian Inc., Walnut Creek, CA, USA). The injector and detector temperatures were 250 and 280 °C, respectively. Initial oven temperature of 100 °C was held for 1 min, increased at 50 °C/min to 150 °C and held for 20 min, increased at 1 °C/min to 190 °C and held for 5 min, and then increased at 1 °C/min to 200 °C and held for 35 min. Helium was used as carrier gas at a flow rate of 1 mL/min, the split ratio was 1:10 and 1 µL of sample was injected.

Identification of C18 biohydrogenation intermediates of FAME and DMOX derivatives was achieved by GLC–MS analysis using an ion trap Varian Saturn 2200 system (Varian Inc., Walnut Creek, CA, USA) and the same capillary column and oven temperatures used in GLC-FID analysis. The ion trap parameters used in the present analyses are similar to those described in Alves and Bessa [22]. Identification of fatty acids was achieved by electron impact (EI) and chemical ionization (CI) mass

spectrometry, using acetonitrile as the reagent of CI. Additionally, the acetonitrile CACIMS/MS technique was used for location of the double bond position in some biohydrogenation intermediates.

Statistical Analysis

The effect of increasing 18:4n-3 supplementation levels on the concentration of the novel biohydrogenation intermediates after 72 h of incubation was analyzed by a single effect model using the GLM procedure of SAS (SAS Inst. Inc., 2002, Cary, NC). When a significant effect was observed the means were compared using the least square difference method.

Results

Identification of C18 FAME Derivatives by EI and CI Mass Spectrometry

Two partial GLC chromatograms of the C18 FAME region from ruminal in vitro incubations supplemented with 0 and 1.5 mg of 18:4n-3 per 33 mg of TMR DM are presented in Figs. 1 and 2. Both figures show that several 18:2, 18:3 and 18:4 fatty acids were produced during the incubation of 1.5 mg of 18:4n-3. The mass spectrometry analysis under EI or CI, of the C18 FAME intermediates allowed the recognition of the carbon chain length and number of double bonds in incubation samples. Electron impact mass spectra of homoallylic (methylene-interrupted) 18:3n-3,

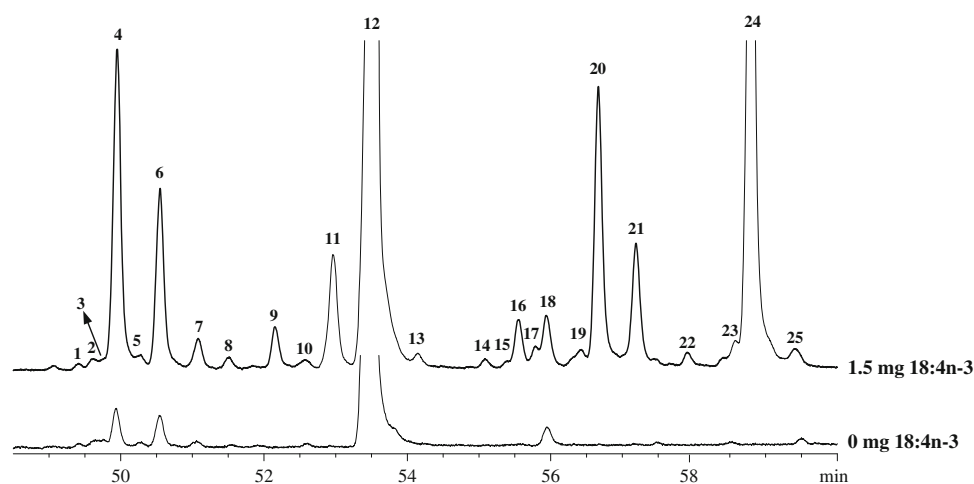


Fig. 1 Partial GLC-FID chromatograms using a CP-Sil 88 capillary column, showing the 18:1, 18:2 and 18:3 FAME region from ruminal in vitro incubation samples supplemented with 0 (control) and 1.5 mg of 18:4n-3 per 33 mg total mixed ration (DM basis). Peak identification: 1 unresolved *trans*-6 to *trans*-8 18:1; 2 *trans*-9 18:1; 3 *trans*-10 18:1; 4 *trans*-11 18:1; 5 *trans*-12 18:1; 6 *cis*-9 + *trans*-13 + *trans*-14 18:1; 7 *cis*-11 + *trans*-15 18:1; 8 *cis*-12 18:1; 9

trans-5,*trans*-10 18:2; 10 unresolved *trans*-16 and *cis*-14 18:1; 11 unresolved *cis*-15 18:1 and *trans*-5,*trans*-11 18:2; 12 internal standard-19:0; 13 18:2 unidentified; 14 *cis*-16 18:1; 15 *trans*-9,*cis*-12 18:2; 16 *trans*-11,*cis*-15 18:2; 17 unidentified peak; 18 18:2n-6; 19 unidentified peak; 20 Δ 5,11,15 18:3; 21 Δ 5,11,14 18:3; 22 Δ 5,10,15 18:3; 23 unidentified peak; 24 Δ 5,11,15 18:3; 25 20:0

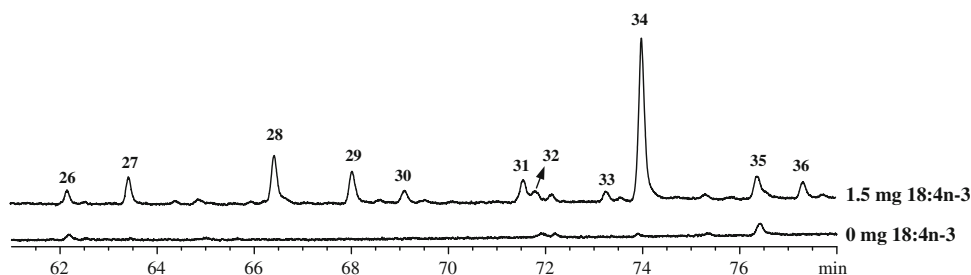
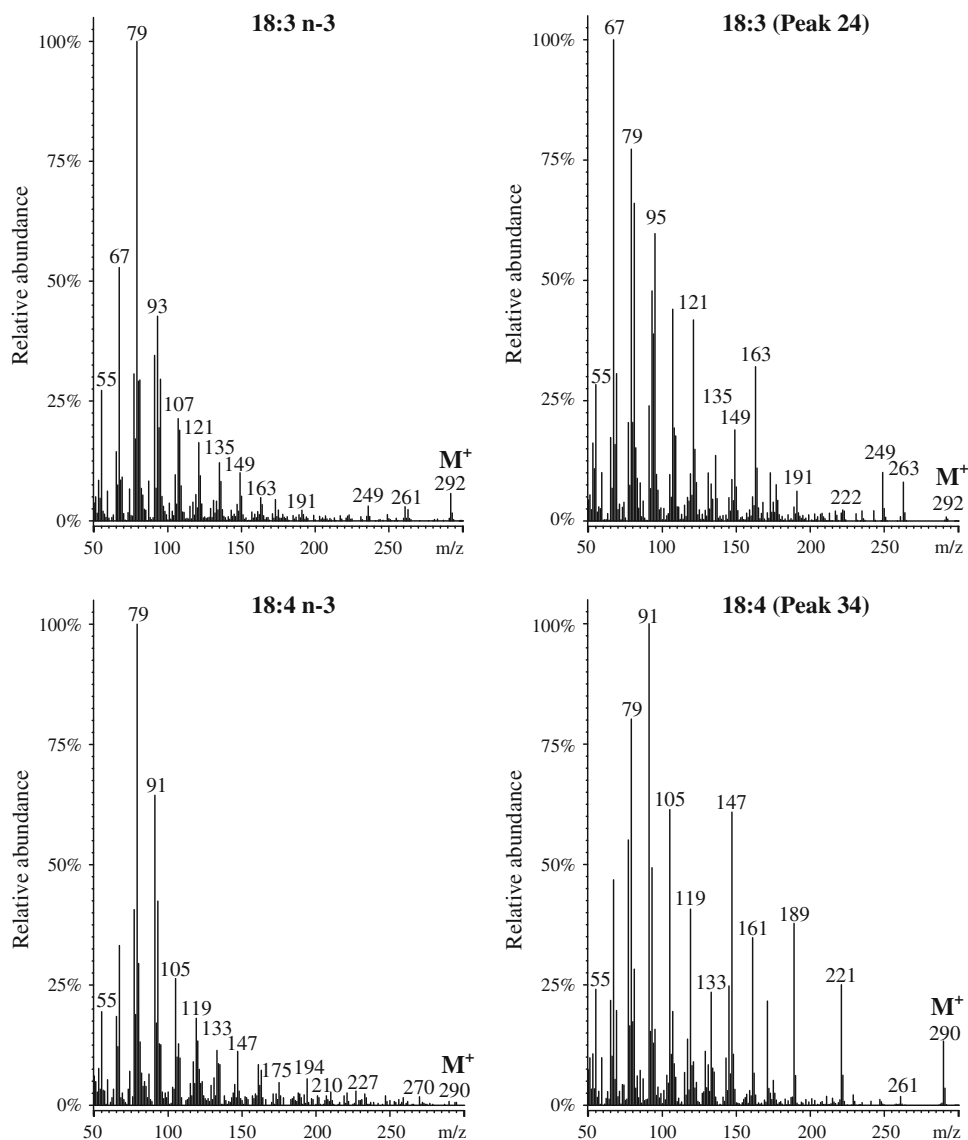


Fig. 2 Partial GLC-FID chromatograms using a CP-Sil 88 capillary column, showing the 18:4 FAME region from ruminal in vitro incubation samples supplemented with 0 (control) and 1.5 mg of 18:4n-3 per 33 mg total mixed ration (DM basis). Peak identification:

26 18:3n-3; 27 CLA *cis-9,trans-11*; 28 18:4n-3; 29 18:3 unidentified; 30 18:3 unidentified; 31 Δ 5,7,11,15 18:4; 32 22:0; 33 Δ 5,8,10,15 18:4; 34 Δ 5,8,10,15 18:4; 35 unidentified peak; 36 Δ 5,8,10,15 18:4

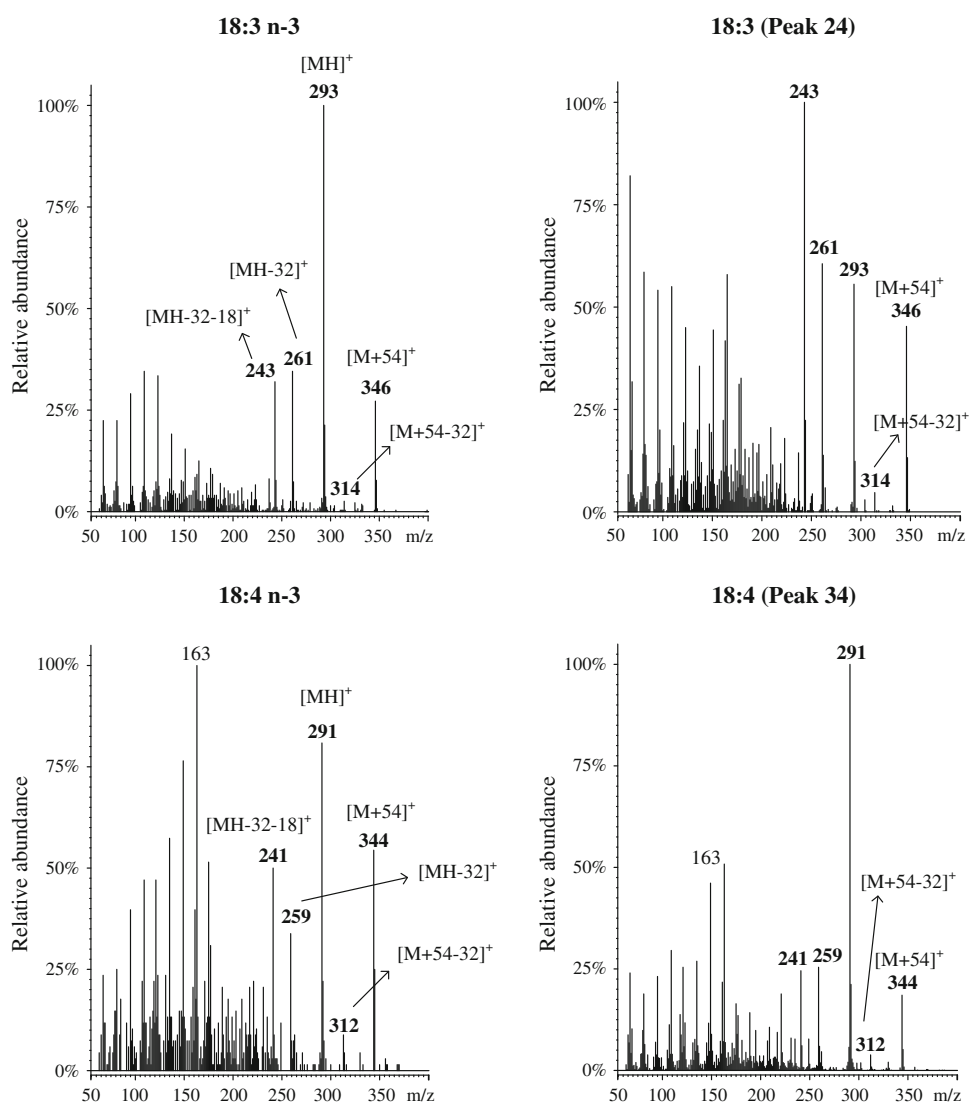
Fig. 3 EI mass spectra of 18:3 and 18:4 isomers. Peak numbers correspond to peaks in Figs. 1 and 2



18:4n-3 and of two novel biohydrogenation intermediates formed are presented in Fig. 3. There are small differences between 18:3 mass spectra, however no diagnostic ions were produced to clarify the position of the double bonds.

Similarly, there are no diagnostic ions in the EI mass spectrum of the novel 18:4 isomer (peak 34), although its mass spectrum is quite different from the mass spectrum of 18:4n-3. The ion at m/z 91 is presumably formed from the

Fig. 4 CACIMS spectrum of 18:3 and 18:4 isomers showing the base peak $[M + 54]^+$ and the common ions $[MH]^+$, $[MH - 32]^+$ and $[M + 54 - 32]^+$. Peak numbers correspond to peaks in Figs. 1 and 2



tropylium ion. The homologous series m/z 105, 119, 133, 147 are also probably tropylium ions with alkyl substituent [23].

The acetonitrile CI mass spectra also allowed the identification of the number of double bonds in C18 fatty acid intermediates. The product of acetonitrile self-reaction, generated under CACIMS conditions, reacts with the fatty acid double bond to yield molecular ions with 54 atomic mass units above the parent analyte. The $[M + 54]^+$ ions at m/z 346 and 344 for the 18:3 and 18:4 isomers, respectively, are shown in Fig. 4. The CACIMS also produce other ions, corresponding to the protonated molecule ($[MH]^+$), and losses of methanol from the protonated molecule ($[MH - 32]^+$) and from adduct ($[M + 54 - 32]^+$), at m/z 293, 261 and 314 for the 18:3 isomers and at m/z 291, 259 and 312 for the 18:4 isomers. The intensity ratios of $[M + 54]^+ / [M + 54 - 32]^+$ have previously been shown to be related to double bond geometry [14, 24, 25]. Table 1 shows the

CACIMS $[M + 54]^+ / [M + 54 - 32]^+$ ratios for the 18:2, 18:3 and 18:4 isomers. The non-conjugated 18:2 isomers showed ratios around 4.33 whereas the conjugated linoleic acid isomer (CLA) *cis*-9,*trans*-11 18:2 showed a ratio of 0.35. Similarly, the 18:3n-3 and others four isomers eluting before the 18:3n-3 showed ratios between 22.1 and 61.3, and other two 18:3 isomers eluting after 18:3n-3 showed ratios lower than 3. The 18:4n-3 showed a ratio of 61, whereas its isomers showed ratios between 3.25 and 4.79.

Identification of C18 DMOX Derivatives by EI Mass Spectrometry

The DMOX derivatives were prepared from FAME incubation samples in order to characterize the novel C18 biohydrogenation intermediates formed. Table 2 presents the characteristic ion fragments of DMOX derivatives of C18 biohydrogenation intermediates. The base peak in all

Table 1 CACIMS $[M + 54]^+/[M + 54 - 32]^+$ ratios for non-conjugated, partially conjugated and conjugated 18:2, 18:3 and 18:4 isomers identified in samples from ruminal in vitro incubation of 1.5 mg of 18:4n-3 per 33 mg total mixed ration (DM basis)

Peak ^a	FAME	$[M + 54]^+/[M + 54 - 32]^+$
	18:2 isomers	
	Non-conjugated	
9	<i>trans</i> -5, <i>trans</i> -10	4.76
11	<i>trans</i> -5, <i>trans</i> -11	5.47
16	<i>trans</i> -11, <i>cis</i> -15	3.85
18	18:2n-6	3.86
	Conjugated	
27	<i>cis</i> -9, <i>trans</i> -11	0.35
	18:3 isomers	
	Non-conjugated	
20	Δ 5,11,15	55.2
21	Δ 5,11,14	61.3
22	Δ 5,10,15	41.0
24	Δ 5,11,15	22.1
26	18:3n-3	30.3
	Partially conjugated	
29	18:3*	2.54
30	18:3*	1.82
	18:4 isomers	
	Non-conjugated	
28	18:4n-3	61.0
	Partially conjugated	
31	Δ 5,7,11,15	3.33
33	Δ 5,8,10,15	3.67
34	Δ 5,8,10,15	4.79
36	Δ 5,8,10,15	3.25

^a Peak numbers correspond to peaks in Figs. 1 and 2

* Unidentified 18:3 isomers

fatty acids was observed at m/z 126 formed by cyclization-displacement reaction. The abundant ion at m/z 113 is also a characteristic ion in DMOX derivatives and is produced by a McLafferty rearrangement.

Two of the five 18:2 biohydrogenation intermediates identified in incubation samples at high supplementation levels are novel intermediates and their EI mass spectra of DMOX derivatives (Fig. 5) showed the molecular ion at m/z 333. The even mass homologous series at m/z 126 + 14 amu is interrupted in the region of the double bond, with a gap of 12 amu. Although the mass spectra of both 18:2 peaks, showed a gap of 13 amu at m/z 140/153 and a gap of 12 amu at m/z 208/220 and 222/234, for peaks 9 and 11, respectively. The presence of odd-numbered ion at m/z 153 accompanied by the m/z 152, are diagnostic ions in the mass spectra of DMOX derivatives of fatty acids with their first double bond at carbon-5 [26, 27]. The published rules

for unsaturated fatty acids reveal the presence of intense peaks containing $n - 2$ and $n + 2$ carbon atoms, therefore the presence of the intense ion at m/z 208 in spectrum of peak 9 presumed a double bond at carbon-11. However, the 12 amu gap was observed between m/z 208 and 220, locating the double bond at carbon-10. The order of elution of either peaks 9 and 11 in GLC-FID presumed a *trans*,-*trans* configuration system.

Four novel 18:3 non-conjugated fatty acids were putatively identified by their DMOX mass spectra, showing all the molecular ion at m/z 331 (Fig. 6). Peaks 20 and 24 showed identical mass spectra, both having a prominent ion at m/z 262 (Fig. 6), which is characteristic of a *bis*-methylene interrupted double bond system, resulting in the formation of stabilized allylic radical fragments, and confirming the location of double bonds at carbons-11, 15 in either peaks 20 and 24. The third double bond was putatively identified at carbon-5 because a gap of 12 amu was observed between m/z 140 and 152. However, this does not match with the published rules for the presence of a double bond at carbon-5 and what was observed for the Δ 5,10 and Δ 5,11 dienes. The published rules for the DMOX derivatives with double bonds at C-4, C-5 and C-6, presume that the ions (i.e., m/z 138, 152 and 166, respectively) derived from cleavage at the double bond are accompanied by intense odd-numbered ions (i.e., m/z 139, 153 and 167, respectively). Nevertheless, as none of these intense odd ions were observed, peaks 20 and 24 were putatively characterized as Δ 5,11,15 18:3 having different *cis/trans* configurations. Seeing that peak 20 elutes before peak 24 in the CP-Sil88 capillary column, and taking in account the order of elution of geometric 18:3 isomers [28, 29], we assume that peak 20 might contain three *trans* double bonds and peak 24 might contain at least one *trans* double bond.

The mass spectrum of the DMOX derivatives of peaks 21 and 22 (Fig. 6) showed a gap of 12 amu between ions at m/z 140 and 152, similarly to what was observed for the Δ 5,11,15 18:3 isomers, suggesting that both peaks might have a double bond at carbon-5. Moreover, peak 21 contained ion fragments with mass interval of 12 amu at m/z 222/234 and 262/274 that were separated by gaps of 14 amu, which enabled the characterization of peak 21 as Δ 5,11,14 18:3. Additionally, the mass spectrum of peak 22 showed ion fragments with gaps of 12 amu at m/z 220/234 and 276/288, allowing the Δ 5,10,15 18:3 structure to be elucidated. On the other hand, the geometry of the double bonds of both Δ 5,11,14 and Δ 5,10,15 18:3 isomers could not be determined.

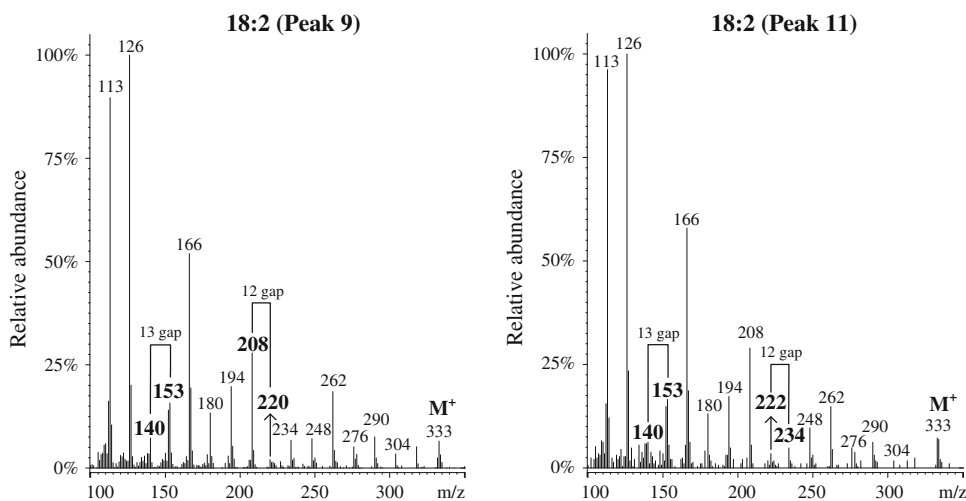
Four partially conjugated 18:4 isomers were identified in incubation samples at high supplementation levels of 18:4n-3. The mass spectra of DMOX derivatives of 18:4n-3 and peaks 28, 31 and 34 are presented in Fig. 6. The mass

Table 2 Characteristic ion fragments recorded during GLC–MS analysis of DMOX derivatives of novel C18 biohydrogenation intermediates in samples from ruminal in vitro incubation of 1.5 mg of 18:4n-3 per 33 mg total mixed ration (DM basis)

Peak ^a	Fatty acid	Characteristic ion fragments (m/z, relative intensity)
9	<i>trans</i> -5, <i>trans</i> -10 18:2	113(90), 126(100), 140(7) , 152(14) , 153(16), 166(52), 180(13), 194(20), 208(28) , 220(2) , 234(7), 248(7), 262(19), 276(5), 290(8), 304(3), 318(5), 333(M ⁺ , 7)
11	<i>trans</i> -5, <i>trans</i> -11 18:2	113(96), 126(100), 140(6) , 152(15) , 153(17), 166(58), 180(13), 194(17), 208(29), 222(3) , 234(5) , 248(10), 262(15), 276(5), 290(6), 304(2), 318(2), 333(M ⁺ , 7)
20	Δ 5,11,15 18:3	113(35); 126(100), 140(8) , 152(10) , 166(40), 180(9), 194(21), 208(28), 222(4) , 234(4) , 248(4), 262(77), 276(3) , 288(5) , 302(4), 316(5), 331(M ⁺ , 4)
21	Δ 5,11,14 18:3	113(41), 126(100), 140(7) , 152(10) , 166(37), 180(8), 194(16), 208(21), 222(2) , 234(5) , 248(11), 262(16) , 274(1) , 288(4), 302(5), 316(2), 331(M ⁺ , 1)
22	Δ 5,10,15 18:3	112(18), 126(100), 140(8) , 152(10) , 166(38), 180(13), 194(21), 208(21) , 220(4) , 234(6), 248(16), 262(16), 276(3) , 288(5) , 302(8), 316(2), 331(M ⁺ , 1)
24	Δ 5,11,15 18:3	113(53), 126(100), 140(8) , 152(10) , 166(41), 180(8), 194(23), 208(28), 222(2) , 234(5) , 248(4), 262(81), 276(3) , 288(4) , 302(4), 316(5), 331(M ⁺ , 4)
31	Δ 5,7,11,15 18:3	113(28), 126(100), 140(3) , 152(5) , 166(44) , 178(4) , 192(11), 206(28), 220(3) , 232(5) , 246(3), 260(94), 274(2) , 286(2) , 300(1), 314(5), 329(M ⁺ , 22)
33	Δ 5,8,10,15 18:4	113(48), 126(100), 140(5) , 152(12) , 166(22), 167(19), 180(16) , 192(14) , 206(4) , 218(22) , 232(12), 246(41), 260(9), 274(1) , 286(2) , 300(8), 314(7), 329(M ⁺ , 16)
34	Δ 5,8,10,15 18:4	113(48), 126(100), 140(7) , 152(10) , 166(22), 167(15), 180(13) , 192(16) , 206(7) , 218(18) , 232(13), 246(38), 260(21), 274(1) , 286(4) , 300(8), 314(6), 329(M ⁺ , 17)
36	Δ 5,8,10,15 18:4	113(45), 126(100), 140(6) , 152(10) , 153(4), 166(19), 167(13), 180(13) , 192(8) , 206(5) , 218(17) , 232(11), 246(38), 260(19), 274(2) , 286(2) , 300(7), 314(5), 329(M ⁺ , 14)

Bold numbers indicate ions fragments used for the location of the double bonds

^a Peak numbers correspond to peaks in Figs. 1 and 2

Fig. 5 GLC–MS mass spectra of DMOX derivatives of 18:2 isomers

spectra of 18:4n-3 (peak 28) clearly shows the 12 amu gaps at *m/z* 194/206, 234/246 and 274/286 enabling the three end double bonds to be located at carbons-9, 12, 15. The first double bond was identified at carbon-6 by the presence of an intense odd ion at *m/z* 167 and the even ion at *m/z* 166, confirming the presence of the Δ 6,9,12,15 18:4 (18:4n-3).

In the mass spectrum of peak 31, an intense peak at *m/z* 260 characteristic of an ethylene interrupted double bond system together with gaps of 12 amu at *m/z* 220/232 and 274/286 enabled the location of two double bonds at

carbons-11, 15. The conjugated double bond was putatively identified at carbons-5, 7 by the gap of 12 amu at *m/z* 140/152 and 166/178. Thus, peak 31 was tentatively identified as Δ 5,7,11,15 18:4.

Three 18:4 peaks (33, 34 and 36) showing identical DMOX mass spectra were identified in the incubation samples, their mass spectra containing ion fragments with a mass interval of 12 amu at *m/z* 180/192, 206/218 and 274/286, which enabled the conjugated double bond to be located at carbons-8, 10 and a terminal double bond at carbon-15. The first double bond was putatively identified

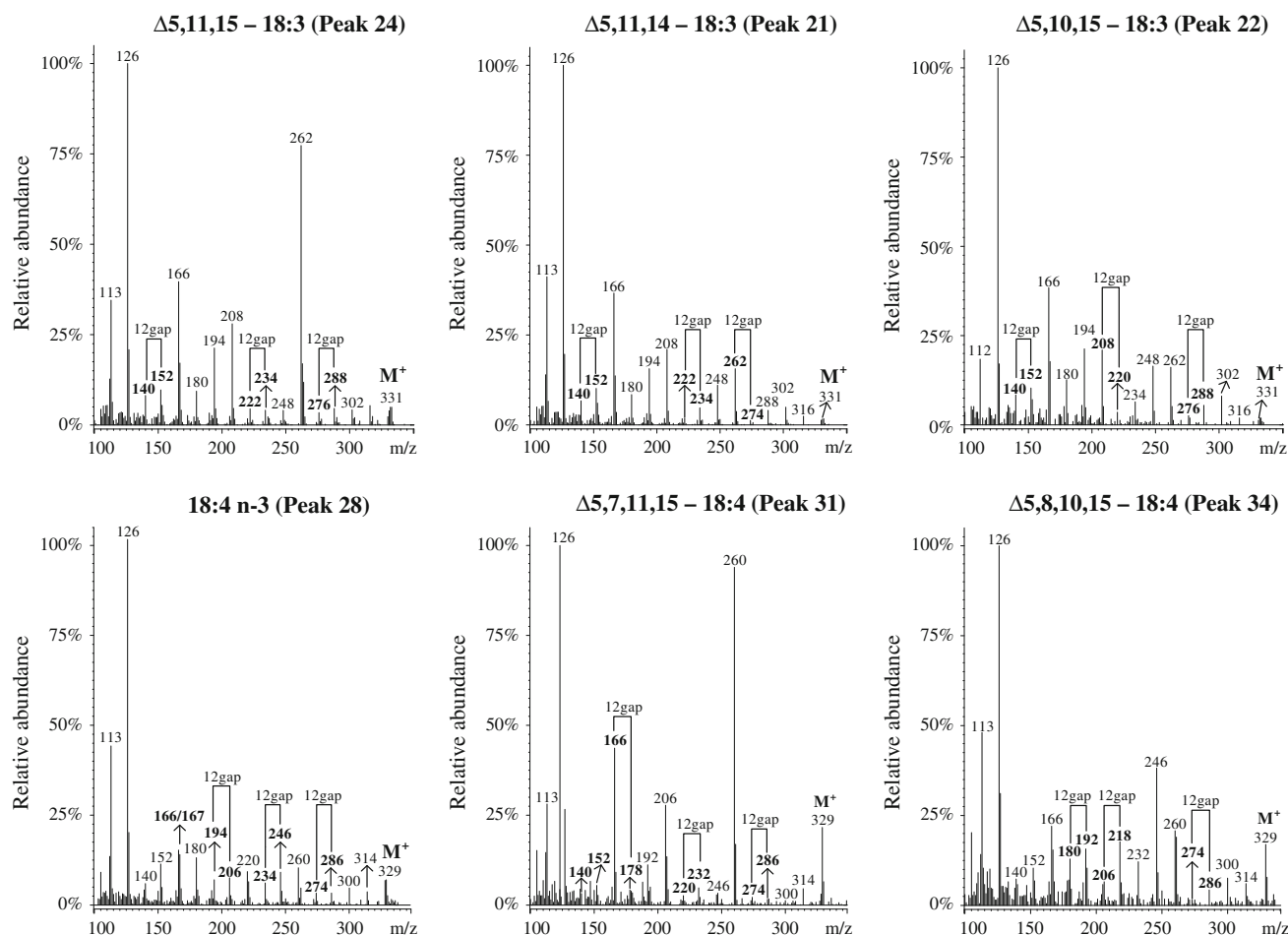


Fig. 6 GLC–MS mass spectra of DMOX derivatives of 18:3 and 18:4 isomers

at carbon-5 (Fig. 6) by the gap of 12 amu between ion fragments at m/z 140 and 152. Once more, no intense odd ions were observed accompanying the even ion at m/z 152 and 166.

Identification C18 FAME Derivatives by CACIMS/MS Mass Spectrometry

The CACIMS/MS technique was applied for the identification of the major 18:3 biohydrogenation intermediates. Peaks 20 and 24 showed identical CACIMS/MS mass spectra, peak 24 being obtained by collisionally activated dissociation of the $[M + 54]^+$ ion at m/z 346 (Fig. 7). The ion at m/z 318 corresponds to a cleavage between C16 and C17, indicating a double bond at carbon-15. The series of ions containing the carboxyl group at m/z 264, 276 and 290, and the end of the molecule at m/z 162, 176 and 190, indicates a double bond at carbon-11. Finally, the fragment at m/z 246 corresponds to a cleavage vinylic to the double bond between C4 and C5. These fragmentations allowed to establish the structures as $\Delta 5,11,15$ 18:3, however the

geometry could not be determined. The identification of the others minor 18:3 and 18:4 intermediates by CACIMS/MS was not successfully achieved, due to the low amount of these intermediates in samples or because mass spectra did not show prominent ions useful to establish the double bond.

Effect of 18:4n-3 Supplementation on C18 Biohydrogenation Intermediates

Table 3 shows the effect of increasing 18:4n-3 supplementation levels on 18:2, 18:3 and 18:4 biohydrogenation intermediates accumulated after 72 h of ruminal incubations. Supplementations at 0 and 0.25 mg of 18:4n-3 per 33 mg of TMR DM were not included because almost no novel biohydrogenation intermediates were detected at these levels. Increasing the 18:4n-3 supplementation level, increased the number of novel biohydrogenation intermediates formed. Indeed, the *trans*-5,*trans*-10 18:2, $\Delta 5,11,15$ 18:3, $\Delta 5,11,14$ 18:3, $\Delta 5,12,15$ 18:3 and $\Delta 5,7,11,15$ 18:4 accumulate from supplementation level of 1.0 mg onwards.

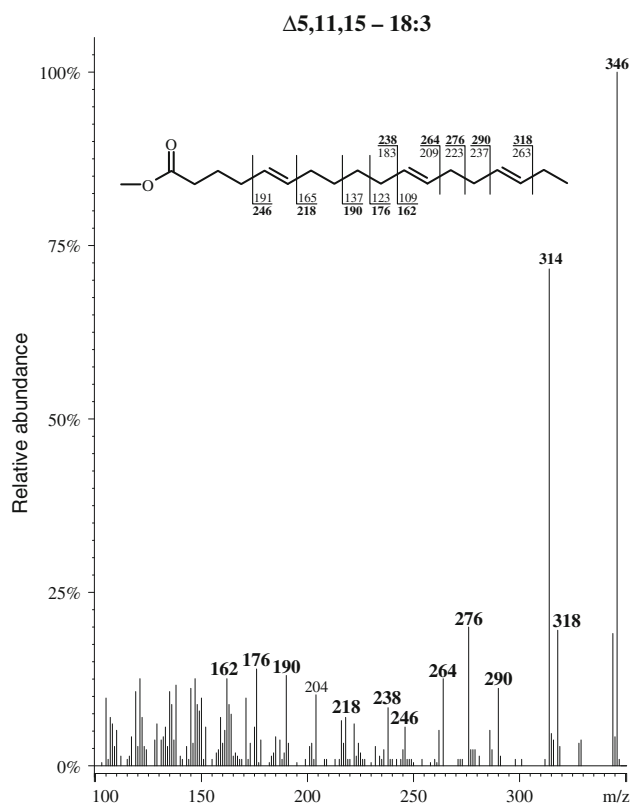


Fig. 7 CACIMS/MS spectra obtained upon collisionally deactivated dissociation of $[M + 54]^+$ ion for $\Delta 5,11,15$ 18:3 isomer

The 18:3 and 18:4 biohydrogenation intermediates that occurred at greater percentages were the $\Delta 5,11,15$ 18:3 (peak 24) and the $\Delta 5,8,10,15$ 18:4 (peak 34), reaching 64.4 and 66.9% of the total 18:3 and 18:4 fatty acids identified in 1.50 mg supplementation level, respectively.

Discussion

Recently, we reported that the supplementation of 18:4n-3 by the rumen microbial population in vitro promoted an accumulation of several unknown octadecapolyenoic biohydrogenation intermediates, though not completely characterized [12]. The present work reports the characterization of those C18 biohydrogenation intermediates.

The octadecapolyenoic intermediates comprised five 18:2, four 18:3, and four 18:4 fatty acids, which were almost undetected at supplementation level of 0.25 mg of 18:4n-3 per 33 mg of TMR DM. The electron impact and chemical ionization GLC–MS analysis of FAME were used for the identification of carbon chain length and number of double bonds. According to the literature, the location and geometry of double bonds in EI mass spectra of FAME cannot be accurately determined because positional and geometrical isomers show almost identical mass spectra.

Indeed, the double bond becomes mobile and moves up and down the chain under EI ionization, hence its original position cannot be reliably determined. This is mainly due to the high sensitivity of the carboxyl group to fragmentation and to double bond migration [30, 31]. Isomerization of double bonds during DMOX preparation was reported by some authors [32], therefore the identification of double bond position using DMOX derivatives should be used carefully. Thus, complementary methods that do not use chemical treatment of the sample such as CACIMS are preferred.

The acetonitrile CI mass spectra of FAME derivatives, apart from the recognition of carbon chain length and number of double bonds, allows a rapid recognition of the non-conjugated, partially conjugated and fully conjugated structure. The CACIMS $[M + 54]^+/[M + 54 - 32]^+$ ratios of non-conjugated fatty acids are substantially higher than the partially conjugated and fully conjugated ratios [14, 24, 25]. Lawrence and Brenna [24] reported that partially conjugated 18:3 isomers showed ratios around 2 whereas fully conjugated 18:2 and 18:3 isomers showed ratios lower than 1. Based on these rules, we could discriminate the novel 18:3 and 18:4 fatty acids as non-conjugated or partially conjugated structures. The GLC retention time in the cyanopropylpolysiloxane stationary phase can also be used to predict the conjugated structure seeing that FAME with conjugate double bonds have higher retention times compared with homologous non-conjugated FAME [33]. Indeed, the partially conjugated 18:4 isomers showed higher retention times than the homoallylic 18:4n-3. Conversely, the novel non-conjugated 18:3 isomers identified in incubated samples showed much lower retention times compared with the 18:3n-3.

The single stage MS analysis of FAME does not give information about the location of the double bond position. Although the MS/MS using acetonitrile, i.e., CACIMS/MS, has been successfully used for the identification of double bond position in a variety of fatty acids including methylene-interrupted [15, 34], conjugated and partially conjugated [14, 24], and long chain non-methylene interrupted highly unsaturated FAME [25]. Therefore, the CACIMS/MS technique was used to clarify the position of the double bonds of 18:3 and 18:4 isomers. However, only the major 18:3 biohydrogenation intermediates were successfully identified by CACIMS/MS. Nitrogen containing derivatives, like DMOX derivatives, have also been used for the location of double bond in a variety of fatty acids [16, 20, 35], these derivatives being only slightly less volatile than FAME and with comparable resolution. Indeed, during EI mass spectrometry the amide moiety carries the charge when the molecule is ionized preventing the double bond to become mobile and move up and down through the chain [23]. In the mass spectra of DMOX derivatives, a saturated

Table 3 Effect of increasing 18:4n-3 supplementation levels on the 18:2 (% total 18:2), 18:3 (% total 18:3) and 18:4 (% total 18:4) biohydrogenation intermediates, total fatty acid concentration (mg/g DM) and total 18:2, 18:3 and 18:4 (g/100 g total fatty acids)

Peak ^B	Fatty acid	Supplementation level ^A					SEM	P
		0.50	0.75	1.00	1.25	1.50		
	Total fatty acid (mg/g DM)	14.1c	15.6c	16.3bc	20.1ab	20.8a	1.28	0.016
	18:2 isomers (% of total 18:2)							
18	18:2n-6	45.3a	39.0a	27.1b	16.6b	20.7b	3.76	0.001
9	<i>trans</i> -5, <i>trans</i> -10	n.d. ⁴	n.d.	9.16b	15.4a	11.6b	0.83	0.012
11	<i>trans</i> -5, <i>trans</i> -11 ^C	9.75b	14.7b	18.2b	43.1a	35.7a	2.73	<0.001
13	18:2 unidentified	13.6a	16.2a	14.2a	6.40b	6.87b	1.465	0.002
15	<i>trans</i> -9, <i>cis</i> -12	7.46b	8.99ab	9.35a	1.84c	1.48c	0.564	<0.001
16	<i>trans</i> -11, <i>cis</i> -15	17.9ab	16.1bc	19.3a	14.7c	17.7ab	0.85	0.026
27	<i>cis</i> -9, <i>trans</i> -11	6.04	5.09	5.82	2.01	5.97	1.412	0.286
	Total 18:2 (g/100 g total FA)	3.89c	3.81c	7.32b	11.5a	8.16b	0.941	<0.001
	18:3 isomers (% of total 18:3)							
26	18:3n-3	100a	100a	26.2b	1.15c	0.76c	6.04	<0.001
20	Δ 5,11,15	n.d.	n.d.	35.1a	29.9b	21.4c	0.95	0.006
21	Δ 5,11,14	n.d.	n.d.	11.2b	14.7a	9.79b	0.642	0.008
22	Δ 5,10,15	n.d.	n.d.	15.0a	1.31b	1.37b	3.782	0.067
24	Δ 5,11,15	n.d.	n.d.	27.9c	50.4b	64.4a	3.17	<0.001
	Total 18:3 (g/100 g total FA)	0.45c	0.40c	2.61c	30.5b	39.1a	1.22	<0.001
	18:4 isomers (% of total 18:4)							
28	18:4n-3	100a	66.2b	66.8b	18.7c	11.3c	8.97	<0.001
31	Δ 5,7,11,15	n.d.	n.d.	8.24	12.7	8.61	2.425	0.411
33	Δ 5,8,10,15	n.d.	n.d.	n.d.	5.04	4.60	0.365	0.439
34	Δ 5,8,10,15	n.d.	33.8c	37.5bc	54.4ab	66.9a	5.61	0.016
36	Δ 5,8,10,15	n.d.	n.d.	n.d.	9.21	8.56	1.172	0.714
	Total 18:4 (g/100 g total FA)	0.26d	0.81cd	1.03c	2.60b	5.43a	0.203	<0.001

Within a row, means with different letters are significantly different, $P < 0.05$

n.d. Not detected

^A Supplementation level: supplementation with 0.50, 0.75, 1.00, 1.25, and 1.50 mg of 18:4n-3 per 33 mg of a commercial total mixed ration per dry matter

^B Peak numbers correspond to peaks in Figs. 1 and 2

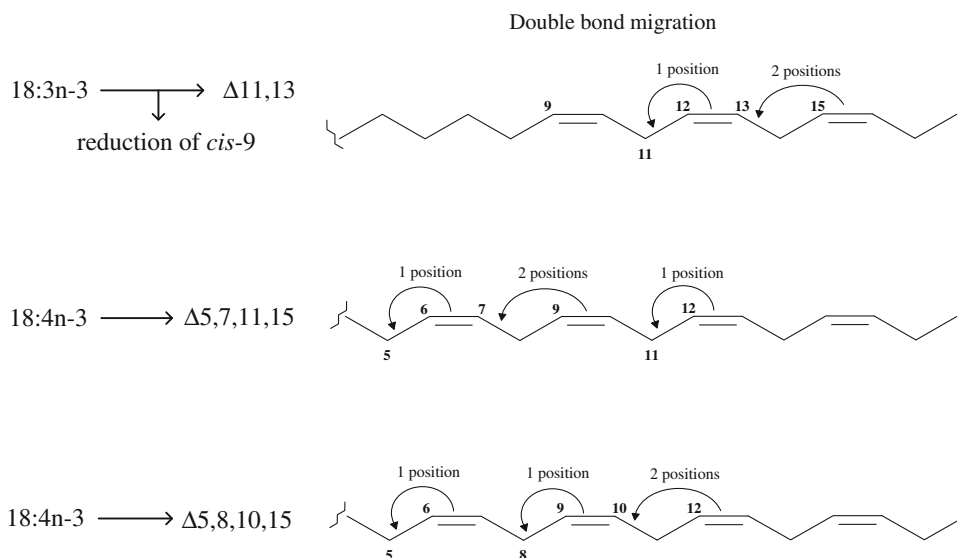
^C This peak co-elutes with *cis*-15 18:1

chain is indicated by regular gaps of 14 amu between ions, in unsaturated derivatives an interval of 12 amu between ions, corresponding to fragments containing $n - 1$ and n , identifies a double bond positioned between carbons n and $n + 1$ [27]. In addition, some exceptions can be found for double bonds closer to the carbonyl group. Several authors reported that odd numbered fragments at m/z 139, 153 and 167 accompanied by even mass ions at m/z 138, 152, and 166 are used to locate double bonds at C-4, C-5 and C-6, respectively [26, 27]. This rule was used for the identification of peaks 9 and 11 (Δ 5,10 and Δ 5,11, showing intense ions at m/z 152 and 153) and 18:4n-3 peak (*cis*-6,9,12,15, showing intense ions at m/z 166 and 167). However, it could not be applied for the identification of the others 18:3 and 18:4 biohydrogenation intermediates. The intense ion at m/z 180 in the DMOX mass spectra of peaks 20, 21, 22, 24, 31, 33, 34 and 36, suggests that a double bond exists at carbon-4, -5 or -6. However, a double bond at carbon-4 implies a reduction in the intensity of the ion at m/z 126, which was not observed. Therefore, as no odd ions at m/z 153 and 167 were observed, the gap of 12 amu rule was used to infer the double bond position at carbon-5 for the 18:3 isomers (Δ 5,11,15, Δ 5,11,14 and Δ 5,10,15) and 18:4 isomers (Δ 5,7,11,15 and Δ 5,8,10,15).

Although geometry of the double bonds could not be determined, at least one *trans* double bond should be present in the novel biohydrogenation intermediates, as two Δ 5,11,15-18:3 isomers and three Δ 5,8,10,15-18:4 isomers were identified from 1.00 mg 18:4n-3 level onwards. Considering the order of elution in the cyanopropylpolysiloxane stationary phase, we can expect that the two Δ 5,11,15-18:3 isomers might be the *trans*-5,*trans*-11,*trans*-15 and the *trans*-5,*trans*-11,*cis*-15. The tentative allocation of *cis* double bond position at carbon-15 was achieved by biological plausibility given that this isomer was the highest biohydrogenation intermediate accumulated in samples and because the *trans*-11,*cis*-15 double bond system is commonly found in ruminal C18 intermediates.

The biohydrogenation intermediates formed in 1.00, 1.25, and 1.50 mg supplementation levels, suggest that different patterns of isomerizations and hydrogenations had occurred. The 18:4n-3 biohydrogenation pathway in the rumen is still unknown, however, taking into account the recognized biohydrogenation pathways of 18:2n-6 and 18:3n-3 [36, 37], the results herein obtained suggest that the 18:4n-3 pathway also involves the formation of conjugated fatty acids and hydrogenation of double bonds. The

Fig. 8 Schematic representation of the double bonds migration from 18:3n-3 and 18:4n-3 into conjugated dienoic derivatives. The arrows do not imply proven biochemical conversions



main biohydrogenation pathway of 18:2n-6 in the rumen involves the formation of the conjugated diene *cis*-9,*trans*-11, followed by reductions to *trans*-11 18:1 and to 18:0. However, others pathways have been hypothesized because new intermediates have been reported to be formed during the 18:2n-6 metabolism in the rumen, like the CLA isomers Δ 10,12, Δ 11,13 and others Δ 9,12 isomers with different *cis/trans* configurations [38, 39]. The main biohydrogenation pathway of 18:3n-3 in the rumen involves the formation of the partially conjugated *cis*-9,*trans*-11,*cis*-15 18:3, which is subsequently hydrogenated to the non-conjugated *trans*-11,*cis*-15 18:2 and further hydrogenated to 18:1 isomers and 18:0 [36]. However, several new 18:3 biohydrogenation intermediates have been identified [37, 40–43]. Very recently, rumen incubation of ^{13}C labelled 18:3n-3 was described to produce fourteen 18:3 isomers, 5 non-conjugated 18:2 isomers and 8 CLA isomers, indicating that 18:3n-3 biohydrogenation pathways are more complex than those previously reported [42]. Similarly, rumen biohydrogenation of 18:4n-3 might also produce 18:4 conjugated isomers, which is supported by the tentative identification of several partially conjugated 18:4 isomers after 72 h of rumen incubations.

The formation of the partially conjugated 18:4 isomers may involve multiple *cis/trans* and carbon–carbon isomerizations, including shifts of the double bonds two-carbons away, and isomerizations close to the carboxyl group. Indeed, three double bonds in the novel 18:4 isomers moved position, despite not being clear if these multiple migrations occurred sequentially or simultaneously. A sequential migration of the double bonds implies the formation of intermediate isomers between 18:4n-3 and the conjugated 18:4 isomers identified. We could not detect these intermediates, but it is not clear if they were not formed, which would exclude the sequential double bond

migration, or if they were transient and were not present after the 72 h of incubation.

The 18:4 biohydrogenation intermediates identified showed isomerizations of double bonds to two-carbons away from the initial position, i.e., the double bonds at carbons-9 and -12 in 18:4n-3 were converted into double bonds at carbons -7 and -10 in the conjugated Δ 5,7,11,15 and Δ 5,8,10,15, respectively (Fig. 8). A migration of double bonds two-carbons away might also occur during the biohydrogenation of 18:3n-3 because *trans*-11,*cis*-13 and *trans*-11,*trans*-13 have been proposed as intermediates of 18:3n-3 [42, 44–46], suggesting a shift of double bonds at carbons-12, 15. A polyenoic fatty acid isomerase (PFI) found in *Ptilota filicina* marine algae was described to perform a single enzymatic isomerization of two double bonds, one allylically and one homoallylically [47, 48]. These authors reported the conversion of *cis*-6,9,12 18:3 (γ -linolenic) into a conjugated triene by the PFI, in which double isomerization in that the double bond at carbon-9 is transferred to the carbon-8 and the double bond at carbon-12 migrates two-carbons away to form the double bond at carbon-10, producing the conjugated triene *cis*-6,*trans*-8,*trans*-10. Although not yet described in the rumen ecosystem, a similar unusual enzymatic mechanism might occur in microbial isomerases. However, further work is necessary to evaluate the occurrence of this feature in the rumen microbial ecosystem. Hypothetical migrations of the double bonds from both 18:3n-3 and 18:4n-3 into conjugated derivatives are presented in Fig. 8.

Although isomerization from carbon-6 to carbon-5 have not been reported, Kairenius et al. [16] recently suggested that hydrogenation of long chain polyenoic fatty acids in the rumen may proceed via two distinct mechanisms that involve sequential reduction and/or isomerization of *cis* double bonds closest to the carboxyl group.

The three 18:3 non-conjugated isomers putatively identified are probably formed by hydrogenation of the second double bond (closest to the carbonyl group) in the partially conjugated 18:4 isomers. The double bond at carbon-15 may be further hydrogenated to produce the novel 18:2 biohydrogenation intermediates identified in samples. However, the double bond at carbon-15 is considered less likely to be hydrogenated in the first steps of biohydrogenation as demonstrated through the known pathways of 18:3n-3, in which its biohydrogenation leads to the formation of the triene *cis*-9,*trans*-11,*cis*-15 and the dienes *trans*-11,*cis*-15 [36]. Nevertheless, recent results showed that the biohydrogenation of 18:3n-3 can produce the conjugated diene *cis*-9,*trans*-11. Lee and Jenkins [42] found an enrichment of about 40% of *cis*-9,*trans*-11 with labeled ^{13}C from 18:3n-3, implying a reduction of the double bond at carbon-15. The same authors also detected enrichments in others CLA isomers, including *trans*-9,*cis*-11, *cis*-9,*cis*-11, *trans*-11,*trans*-13, *trans*-8,*trans*-10 and *cis*-10,*cis*-12 at 3–48 h of incubation. In the present study, no increase of conjugated dienes was found during the biohydrogenation of 18:4n-3. This suggests that either the 18:4n-3 biohydrogenation pathway does not involve the formation of CLA isomers or that after 72 h of incubation they could have been reduced to monoenoic acids.

A putative metabolic pathway for the formation of the novel 18:2, 18:3 and 18:4 biohydrogenation intermediates identified in incubation samples at the 1.00 mg supplementation level and greater is presented in Fig. 9. The intermediates accumulated after 72 h of incubation are probably the main intermediates formed in the 18:4n-3 biohydrogenation pathway and are not end products

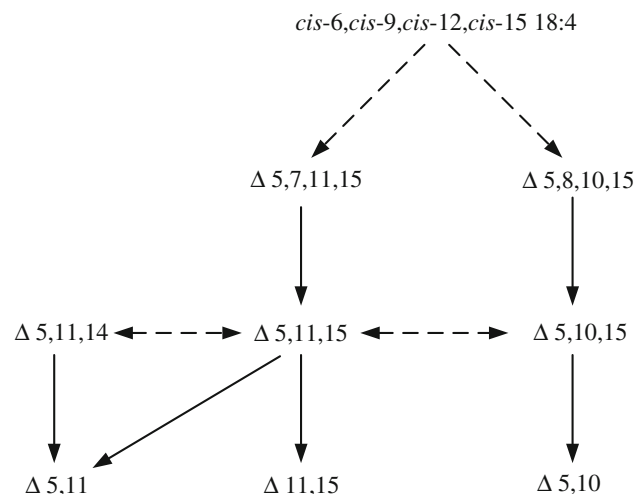


Fig. 9 Putative metabolic pathway for the formation of the novel 18:2, 18:3 and 18:4 biohydrogenation intermediates from 18:4n-3 by rumen microbes. Dotted arrows represent suggested carbon-carbon isomerization and solid arrows represent proposed hydrogenations, based on the identified biohydrogenation intermediates

because in the incubations at lower supplementation levels of 18:4n-3, none of these novel intermediates were found.

In vitro incubation of rumen fluid with increasing supplementation levels of 18:4n-3 produced several novel biohydrogenation intermediates comprising non-conjugated 18:2 and 18:3, and partially conjugated 18:4 isomers, particularly at greater levels (1.0–1.5 mg 18:4n-3 per 33 mg TMR DM). The identification of these intermediates was achieved by gas-liquid chromatography coupled to mass spectrometry analysis of fatty acid methyl esters and DMOX derivatives. However, the *cis* and *trans* geometry of the novel intermediates was not determined.

Acknowledgments An individual Ph.D. Grant (SFRH/BD/37793/2007) to S.P. Alves, and a Pos-Doc Grant (SFRH/BPD/70176/2010) to M.R.G. Maia from Fundação para a Ciência e Tecnologia (FCT), Ministério da Ciência, Tecnologia e Ensino Superior, Portugal, are gratefully acknowledge. This work has been supported by Fundação para a Ciência e a Tecnologia through grant PEst-C/EQB/LA0006/2011.

References

1. Yamazaki K, Fujikawa M, Hamazaki T, Yano S, Shono T (1992) Comparison of the conversion rates of [α]-linolenic acid (18:3n-3) and stearidonic acid (18:4n-3) to longer polyunsaturated fatty acids in rats. *Biochim Biophys Acta* 1123:18–26
2. Guil-Guerrero JL (2007) Stearidonic acid (18:4n-3): metabolism, nutritional importance, medical uses and natural sources. *Eur J Lipid Sci Technol* 109:1226–1236
3. Horrocks LA, Yeo YK (1999) Health benefits of docosahexaenoic acid (DHA). *Pharmacol Res* 40:211–225
4. Whelan J (2009) Dietary stearidonic acid is a long chain (n-3) polyunsaturated fatty acid with potential health benefits. *J Nutr* 139:5–10
5. Bernal-Santos G, O'Donnell AM, Vicini JL, Hartnell GF, Bauman DE (2010) Hot topic: enhancing omega-3 fatty acids in milk fat of dairy cows by using stearidonic acid-enriched soybean oil from genetically modified soybeans. *J Dairy Sci* 93:32–37
6. Fowad A, Marie-Claude N, Pierre W, Francis E (2006) Effects of preconditioning and extrusion of linseed on the ruminal biohydrogenation of fatty acids. 2. In vitro and in situ studies. *Anim Res* 55:261–271
7. Troegeler-Meynadier A, Nicot MC, Bayourthe C, Moncoulon R, Enjalbert F (2003) Effects of pH and concentrations of linoleic and linolenic acids on extent and intermediates of ruminal biohydrogenation in vitro. *J Dairy Sci* 86:4054–4063
8. Boeckert C, Vlaeminck B, Mestdagh J, Fievez V (2007) In vitro examination of DHA-edible micro algae: 1. effect on rumen lipolysis and biohydrogenation of linoleic and linolenic acids. *Anim Feed Sci Technol* 136:63–79
9. AbuGhazaleh AA, Jenkins TC (2004) Disappearance of docosahexaenoic and eicosapentaenoic acids from cultures of mixed ruminal microorganisms. *J Dairy Sci* 87:645–651
10. AbuGhazaleh AA, Holmes LD, Jacobson BN, Kalscheur KF (2006) Short communication: eicosatrienoic acid and docosatrienoic acid do not promote vaccenic acid accumulation in mixed ruminal cultures. *J Dairy Sci* 89:4336–4339
11. AbuGhazaleh AA, Jenkins TC (2004) Short communication: docosahexaenoic acid promotes vaccenic acid accumulation in mixed ruminal cultures when incubated with linoleic acid. *J Dairy Sci* 87:1047–1050

12. Maia MRG, Correia CAS, Alves SP, Fonseca AJM, Cabrita ARJ (2011) Technical note: stearidonic acid metabolism by mixed ruminal microorganisms. *J Anim Sci*. doi:10.2527/jas.2011-4118
13. Pariza MW (2004) Perspective on the safety and effectiveness of conjugated linoleic acid. *Am J Clin Nutr* 79:1132S–1136S
14. Michaud AL, Yurawecz MP, Delmonte P, Corl BA, Bauman DE, Brenna JT (2003) Identification and characterization of conjugated fatty acid methyl esters of mixed double bond geometry by acetonitrile chemical ionization tandem mass spectrometry. *Anal Chem* 75:4925–4930
15. Michaud AL, Diau GY, Abril R, Brenna JT (2002) Double bond localization in minor homoallylic fatty acid methyl esters using acetonitrile chemical ionization tandem mass spectrometry. *Anal Biochem* 307:348–360
16. Kairenius P, Toivonen V, Shingfield K (2011) Identification and ruminal outflow of long-chain fatty acid biohydrogenation intermediates in cows fed diets containing fish oil. *Lipids* 46:587–606
17. Christie W, Brechany E, Holman R (1987) Mass spectra of the picolinyl esters of isomeric mono- and dienoic fatty acids. *Lipids* 22:224–228
18. Christie WW, Robertson GW, McRoberts WC, Hamilton JTG (2000) Mass spectrometry of the 4,4-dimethylloxazoline derivatives of isomeric octadecenoates (monoenes). *Eur J Lipid Sci Technol* 102:23–29
19. Christie WW, Brechany EY, Johnson SB, Holman RT (1986) A Comparison of pyrrolidide and picolinyl ester derivatives for the identification of fatty-acids in natural samples by gas chromatography–mass spectrometry. *Lipids* 21:657–661
20. Destailats F, Sebedio JL, Berdeaux O, Juaneda P, Angers P (2005) Gas chromatography-mass spectrometry determination of metabolites of conjugated *cis*-9,*trans*-11,*cis*-15 18: 3 fatty acid. *J Chromatogr B: Biomed Sci Appl* 820:15–22
21. Kramer JKG, Hernandez M, Cruz-Hernandez C, Kraft J, Dugan MER (2008) Combining results of two GC separations partly achieves determination of all *cis* and *trans* 16: 1, 18: 1, 18: 2 and 18: 3 except CLA isomers of milk fat as demonstrated using Ag-ion SPE fractionation. *Lipids* 43:259–273
22. Alves SP, Bessa RJB (2007) Identification of *cis*-12,*cis*-15 octadecadienoic acid and other minor polyenoic fatty acids in ruminant fat. *Eur J Lipid Sci Technol* 109:879–883
23. Dobson G, Christie WW (2002) Mass spectrometry of fatty acid derivatives. *Eur J Lipid Sci Technol* 104:36–43
24. Lawrence P, Brenna JT (2006) Acetonitrile covalent adduct chemical ionization mass spectrometry for double bond localization in non-methylene-interrupted polyene fatty acid methyl esters. *Anal Chem* 78:1312–1317
25. Alves SP, Tyburczy C, Lawrence P, Bessa RJB, Thomas Brenna J (2011) Acetonitrile covalent adduct chemical ionization tandem mass spectrometry of non-methylene-interrupted pentaene fatty acid methyl esters. *Rapid Commun Mass Spectrom* 25:1933–1941
26. Luthria DL, Sprecher H (1993) 2-Alkenyl-4,4-dimethylloxazolines as derivatives for the structural elucidation of isomeric unsaturated fatty-acids. *Lipids* 28:561–564
27. Spitzer V (1996) Structure analysis of fatty acids by gas chromatography low resolution electron impact mass spectrometry of their 4,4-dimethylloxazoline derivatives: a review. *Prog Lipid Res* 35:387–408
28. Kramer JKG, Blackadar CB, Zhou J (2002) Evaluation of two GC columns (60-m SUPELCOWAX 10 and 100-m CP Sil 88) for analysis of milkfat with emphasis on CLA, 18:1, 18:2 and 18:3 isomers, and short- and long-chain FA. *Lipids* 37:823–835
29. Alves SP, Bessa RJB (2009) Comparison of two gas-liquid chromatograph columns for the analysis of fatty acids in ruminant meat. *J Chromatogr A* 1216:5130–5139
30. Christie WW (1998) Gas chromatography–mass spectrometry methods for the structural analysis of fatty acids. *Lipids* 33:343–353
31. Murphy RC (1993) Mass spectrometry of lipids. Plenum Press, New York
32. Lamberto M, Ackman RG (1995) Positional isomerization of *trans*-3-hexadecenoic acid employing 2-amino-2-methyl-propanol as a derivatizing agent for ethylenic bond location by gas-chromatography/mass spectrometry. *Anal Biochem* 230:224–228
33. Kramer JKG, Cruz-Hernandez C, Zhou JQ (2001) Conjugated linoleic acids and octadecenoic acids: analysis by GC. *Eur J Lipid Sci Technol* 103:600–609
34. Van Pelt CK, Brenna JT (1999) Acetonitrile chemical ionization tandem mass spectrometry to locate double bonds in polyunsaturated fatty acid methyl esters. *Anal Chem* 71:1981–1989
35. Wasowska I, Maia MRG, Niedzwiedzka KM, Czauderna M, Ribeiro JMCR, Devillard E, Shingfield KJ, Wallace RJ (2006) Influence of fish oil on ruminal biohydrogenation of C18 unsaturated fatty acids. *Br J Nutr* 95:1199–1211
36. Harfoot CG, Hazlewood GP (1997) Lipid metabolism in the rumen. In: Hobson PN (ed) *The rumen microbial ecosystem*. Elsevier, London, pp 382–426
37. Jenkins TC, Wallace RJ, Moate PJ, Mosley EE (2008) Board-invited review: recent advances in biohydrogenation of unsaturated fatty acids within the rumen microbial ecosystem. *J Anim Sci* 86:397–412
38. Shingfield K, Bernard L, Leroux C, Chilliard Y (2010) Role of *trans* fatty acids in the nutritional regulation of mammary lipogenesis in ruminants. *Animal* 4:1140–1166
39. Or-Rashid MM, AlZahal O, McBride BW (2011) Comparative studies on the metabolism of linoleic acid by rumen bacteria, protozoa, and their mixture in vitro. *Appl Microbiol Biotechnol* 89:387–395
40. Bessa RJB, Alves SP, Jeronimo E, Alfaia CM, Prates JAM, Santos-Silva J (2007) Effect of lipid supplements on ruminal biohydrogenation intermediates and muscle fatty acids in lambs. *Eur J Lipid Sci Technol* 109:868–878
41. Gomez-Cortes P, Tyburczy C, Brenna JT, Juarez M, de la Fuente MA (2009) Characterization of *cis*-9 *trans*-11 *trans*-15 C18:3 in milk fat by GC and covalent adduct chemical ionization tandem MS. *J Lipid Res* 50:2412–2420
42. Lee YJ, Jenkins TC (2011) Biohydrogenation of linolenic acid to stearic acid by the rumen microbial population yields multiple intermediate conjugated diene isomers. *J Nutr* 141:1445–1450
43. Destailats F, Trotter JP, Galvez JMG, Angers P (2005) Analysis of alpha-linolenic acid biohydrogenation intermediates in milk fat with emphasis on conjugated linolenic acids. *J Dairy Sci* 88:3231–3239
44. Jouany JP, Lassalas B, Doreau M, Glasser F (2007) Dynamic features of the rumen metabolism of linoleic acid, linolenic acid and linseed oil measured in vitro. *Lipids* 42:351–360
45. Dannenberger D, Nuernberg K, Nuernberg G (2009) Diet-dependent occurrence of CLA isomers in rumen and duodenal digesta of slaughtered bulls. *Eur J Lipid Sci Technol* 111: 553–562
46. Fukuda S, Nakanishi Y, Chikayama E, Ohno H, Hino T, Kikuchi J (2009) Evaluation and characterization of bacterial metabolic dynamics with a novel profiling technique, real-time metabolotyping. *PLoS One* 4:e4893
47. Wise ML, Hamberg M, Gerwick WH (1994) Biosynthesis of conjugated triene-containing fatty acids by a novel isomerase from the red marine alga *Ptilota filicina*. *Biochem* 33:15223–15232
48. Wise ML, Rossi J, Gerwick WH (1997) Characterization of the substrate binding site of polyenoic fatty acid isomerase, a novel enzyme from the marine alga *Ptilota filicina*. *Biochem* 36: 2985–2992

Steryl Glucoside and Acyl Steryl Glucoside Analysis of *Arabidopsis* Seeds by Electrospray Ionization Tandem Mass Spectrometry

Kathrin Schrick · Sunitha Shiva · James C. Arpin ·
Nicole Delimont · Giorgis Isaac · Pamela Tamura ·
Ruth Welti

Received: 17 December 2010 / Accepted: 22 July 2011 / Published online: 10 August 2011
© AOCs 2011

Abstract Establishment of sensitive methods for the detection of cellular sterols and their derivatives is a critical step in developing comprehensive lipidomics technology. We demonstrate that electrospray ionization tandem (triple quadrupole) mass spectrometry (ESI-MS/MS) is an efficient method for monitoring steryl glucosides (SG) and acyl steryl glucosides (ASG). Comparison of analysis of SG and ASG by ESI-MS/MS with analysis by gas chromatography with flame ionization detection (GC–FID) shows that the two methods yield similar molar compositions. These data demonstrate that ESI-MS/MS response per molar amount of sterol conjugate is similar among various molecular species of SG and ASG. Application of ESI-MS/MS to seed samples from wild-type *Arabidopsis* and a mutant deficient in two UDP-glucose:sterol glucosyltransferases, UGT80A2 and UGT80B1, revealed new details on the composition of sitosteryl, campesteryl and stigmasteryl glucosides and ASG. SG were decreased by 86% in the *ugt80A2, B1* double mutant, compared to the wild-type, while ASG were reduced 96%. The results indicate that these glucosyltransferases account for much of the accumulation of the sterol conjugates in wild-type *Arabidopsis* seeds.

Keywords Steryl glucosides · Acyl steryl glucosides · Sterols · Electrospray ionization tandem mass spectrometry ·

Electronic supplementary material The online version of this article (doi:10.1007/s11745-011-3602-9) contains supplementary material, which is available to authorized users.

K. Schrick (✉) · S. Shiva · J. C. Arpin · N. Delimont ·
G. Isaac · P. Tamura · R. Welti
Division of Biology, 116 Ackert Hall, Kansas State University,
Manhattan, KS 66506-4901, USA
e-mail: kschrack@ksu.edu

Gas chromatography · *Arabidopsis thaliana* ·
UDP-glucose:sterol glucosyltransferase · *ugt80A2, B1*,
UGT80A2, *UGT80B1*

Abbreviations

SG	Steryl glucosides
ASG	Acyl steryl glucosides
ESI-MS/MS	Electrospray ionization tandem (triple quadrupole) mass spectrometry
GC	Gas chromatography
FID	Flame ionization detection

Introduction

Sterols are ubiquitous constituents of eukaryotic cells. In contrast to animals and fungi, which contain primarily cholesterol and ergosterol, respectively, plants synthesize a complex mixture of sterols comprised of sitosterol, campesterol, stigmasterol and additional minor sterols that include cholesterol [1]. While sitosterol and stigmasterol are implicated in membrane functions [2, 3], campesterol is the precursor to the brassinosteroids, which are plant steroid hormones required for cell division and cell expansion [4, 5]. In plants, steryl glycosides (SG) and acyl steryl glycosides (ASG) are major derivatives of sterols [6–9]. Variation in SG originates from differences in the type of sterol, the sugar, the configuration of the linkage, number of sugar groups, and acylation of the sugar(s). In the most common form of SG, a sugar monomer, usually the pyranose form of D-glucose, is attached to the 3 β -hydroxy group on the C3 of the sterol (Fig. 1a). Acylation may occur at the C6 of the sugar moiety with fatty acids (Fig. 1b), palmitic (16:0) being most common.

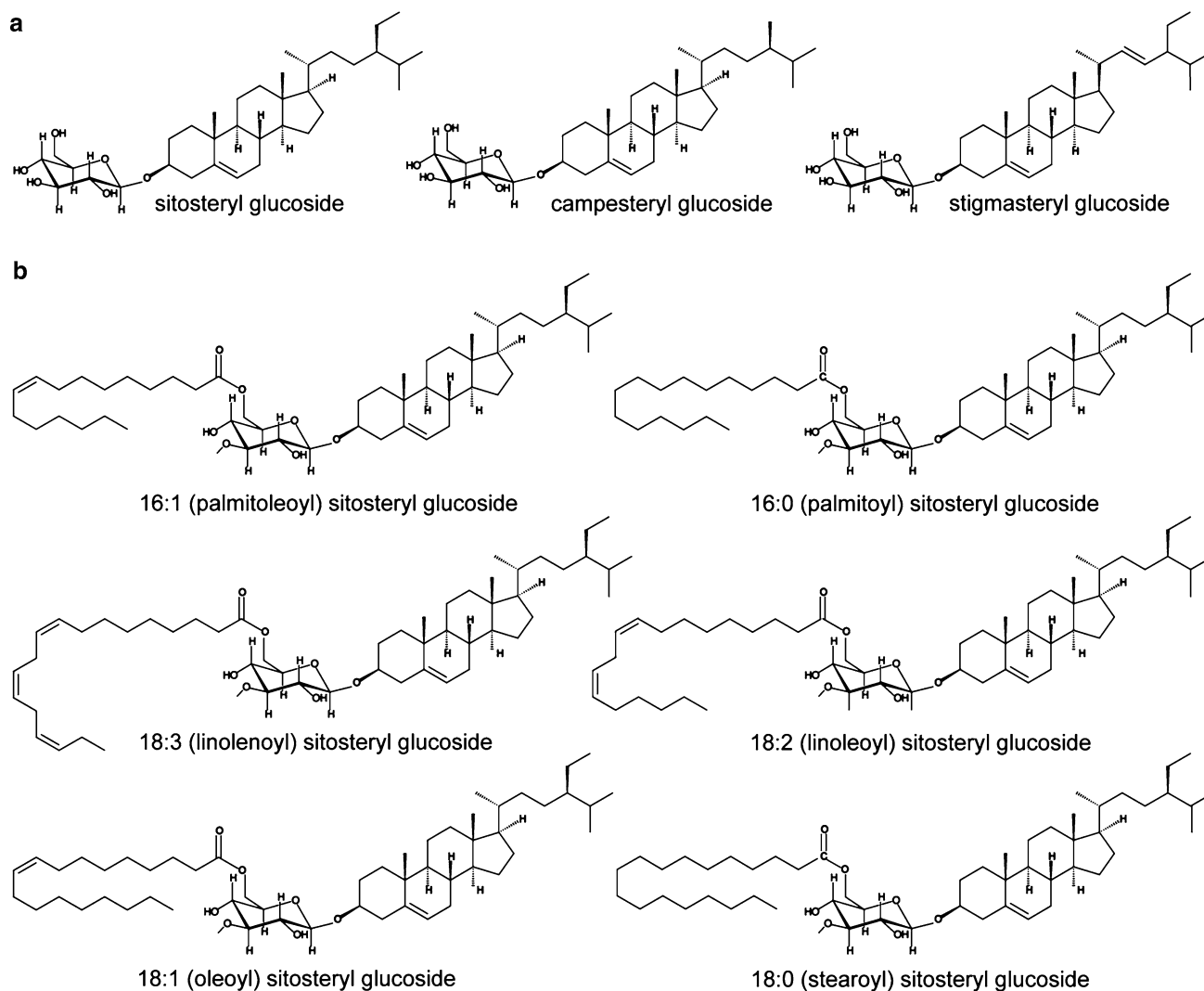


Fig. 1 Molecular structures for SG and ASG. **a** SG structures are shown for sitosteryl, campesteryl, and stigmasteryl glucosides. The pyranose form of D-glucose is covalently attached to the 3 β -hydroxy group on C3 of the A ring of the sterol. **b** ASG structures are shown

for sitosteryl glucosides with various acyl chain modifications: 16:1 (palmitoleic), 16:0 (palmitic), 18:3 (linolenic), 18:2 (linoleic), 18:1 (oleic) and 18:0 (stearic) acids. The acyl modification occurs on C6 of the D-glucose monomer that is attached to the sterol

As sterol conjugates, SG and ASG, which are biosynthetically interconvertible, serve as membrane components, storage forms of sterols, transporters, and/or signaling molecules in plants [6], and one report has suggested the role of SG as primers in the synthesis of cellulose [10]. SG are synthesized by UDP-glucose:sterol glucosyltransferases (UGTs) which catalyze the glucosylation of the 3 β -hydroxy group of sterols to produce 3- β -D-glucosides [11, 12]. *Arabidopsis ugt80A2,B1*, double mutant for *UGT80A2* and *UGT80B1*, was shown to have a significant reduction in SG and ASG levels in several plant tissues [13]. These mutants display an array of phenotypes in the seed, including small embryo size, transparent testa, defects in flavonoid deposition, loss of the cuticle layer, and a decrease in aliphatic suberin and cutin-like polymers.

Characterization of the *ugt80A2,B1* mutants has indicated a role for SG and ASG in trafficking of lipid polyester precursors in seeds [13].

After isolation of SG and ASG from tissues, gas chromatography (GC) can be used to quantify these lipids. To perform the analysis, the SG and ASG are each hydrolyzed to yield sterols and trans-esterified to yield fatty acid methyl esters. Gas chromatography with flame ionization (GC-FID) is quantitative, but the classes need to be isolated and hydrolyzed/transesterified. In this report we demonstrate the detection of underivatized SG and ASG conjugates of sitosterol, campesterol, and stigmasterol from seed samples using electrospray ionization tandem (triple quadrupole) mass spectrometry (ESI-MS/MS). Mass spectrometry methods, exemplified by ESI-MS/MS, have

enabled high sensitivity and high mass resolution specificity for the identification and quantification of lipids from diverse biological samples [14]. Previously it was shown that ESI-MS/MS can be utilized to efficiently quantify phospholipids and polar glycerolipids from *Arabidopsis* [15, 16].

In the present study we show that ESI-MS/MS is a simple and rapid detection method that is advantageous over GC methods for the analysis of steryl glycolipids, since there is no need for derivatization, and quantitative information about the specific SG and ASG molecular species is readily obtained. Using seed samples from *ugt80A2, B1* mutants and wild-type, ESI-MS/MS analysis has revealed new details about SG and ASG molecular species, adding to our understanding of the roles of the UGT80 glucosyltransferases in *Arabidopsis* seeds.

Experimental Procedure

Plant Materials and Growth Conditions

Wild-type and mutant *Arabidopsis thaliana* lines were in the Wassilewskija (WS)-O background. *ugt80A2, B1*, double mutant for *UGT80A2* (At3g07020) and *UGT80B1* (At1g43620), was previously described [13]. Plants were grown on soil comprised of 7:3:4 Metro-Mix 380:Vermiculite (Therm-O-Rock #10-2200):Perlite (Therm-O-Rock #10-1123) (Hummert International, Topeka, KS, USA) under continuous light at 23 °C and 70% humidity in a standard growth chamber. Dry seeds were harvested at 8 weeks. For the comparison of ESI-MS/MS to GC-FID analysis, mixtures of isolated soybean-derived SG (catalog #1117: 54% sitosteryl glucoside, 27% campesteryl glucoside, 17% stigmasteryl glucoside, 1% Δ^5 -avenasteryl glucoside) and ASG (catalog #1118: esterified steryl glucosides, fatty acid composition: 34% 16:0, 8% 18:0, 8% 18:1, 36% 18:2, 4% 18:3, 1% 20:0, 4% 22:0, 2% 23:0, 2% 24:0 and 1% others; According to the Matreya LLC 2011–2012 catalog, “actual composition may vary according to dietary history and condition of the source”) were purchased from Matreya LLC, Pleasant Gap, PA, USA.

Lipid Extraction from Seeds

Seeds were extracted by a modification of the method of Bligh and Dyer [17]. 100 *Arabidopsis* seeds were added to 2.0 ml isopropanol with 0.01% butylated hydroxytoluene at 75 °C; the heating at 75 °C was continued for 15 min, before cooling to room temperature. To the seed–solvent mixture precise amounts of internal standards: 10 nmol of di12:0 PtdGro and 10 nmol of di20:0 (diphtanoyl) PtdGro

(Avanti Polar Lipids, Alabaster, AL) were added. The mixture was then transferred to a Dounce homogenizer, homogenized to allow for complete and consistent extraction of lipids, and transferred to a glass tube. The homogenizer was rinsed with 2.0 ml each of chloroform and methanol to recover the sample fully, and the rinse was combined with the isopropanol–seed mixture. 1.6 ml water was added and the one-phase mixture was shaken. An additional 1.0 ml each of chloroform and water were added, followed by shaking and centrifugation to form two phases. The lower layer was removed. 2.0 ml of chloroform were added, the tube was shaken and centrifuged, and the lower layer was removed. This was repeated and the three lower layers were combined. 1.0 ml of 1 M KCl was added, the mixture shaken and centrifuged for 10 min, and the upper layer was removed and discarded. A second wash was performed with 1.0 ml water, followed by evaporation of the solvent. Samples were dissolved in 1 ml chloroform and 5–15 μ l of each of these samples were added to 1.2 ml chloroform/methanol/300 mM ammonium acetate in water (300/665/35) for ESI-MS/MS analysis.

Gas Chromatography

The SG mixture (#1117, Matreya LLC, Pleasant Gap, PA, USA) and the ASG mixture (#1118, Matreya LLC, Pleasant Gap, PA, USA), both isolated from soybean by the commercial provider, were prepared for sterol analysis according to Rintoul et al. [18]. SG (40–100 μ g) were hydrolyzed by heating at 70 °C for 1 h in 2.5 ml 2 M sodium hydroxide in methanol/water (5:1). 2.0 ml water was added and the sample was extracted twice with pentane. Combined pentane extracts were dried with sodium sulfate. The pentane was evaporated, and the samples were redissolved in 100 μ l pentane, of which 1 μ l was analyzed. Sterols were analyzed on a Hewlett Packard 5890A gas chromatograph on a 15-m, 0.25 mm inner diameter, Rtx-65TG column (#17005 Restek; distributed by Alltech, State College, PA). Injection was in the splitless mode, with helium as the carrier gas with a head pressure of 125 kPa and a flow of 54 ml/min. The oven temperature was maintained isothermally at 240 °C and the injector and detector temperatures were at 300 °C. Total analysis time was 12 min with the major plant sterols eluting between 8 and 11 min. Detection was by flame ionization. Peak areas were integrated with a Beckmann 427 integrator. The areas were divided by the molecular weights before determining the mole percentage of each sterol.

The ASG mixture (#1118, Matreya LLC, Pleasant Gap, PA, USA) was prepared for analysis of fatty acid composition by converting the acyl groups to fatty acid methyl esters. ASG (~200 μ g) in 1.0 ml 3 M methanolic HCl was heated under nitrogen at 78 °C for 1 h. Then 2.0 ml water

was added, followed by two extractions with pentane. Water was removed from the combined extracts with sodium sulfate, pentane was evaporated, and the sample was dissolved in ~30 μl of carbon disulfide, of which 1 μl was analyzed. Fatty acid methyl esters were analyzed on a Hewlett Packard 5890A gas chromatograph, on a 30-m SP2380 column with a 0.32 mm inner diameter (#2-4115, Supelco, Bellefonte, PA, USA). Injection was in the splitless mode with helium as the carrier gas with a head pressure of 50 kPa and a flow of 52 ml/min. The oven temperature was maintained isothermally at 160 °C, and the injector and detector temperatures were 220 °C. Detection was by flame ionization. Total analysis time was 25 min with the fatty acid methyl esters of interest eluting between 13 and 21 min. Peak areas were integrated with a Beckmann 427 integrator. The areas were divided by the molecular weights before determining the mole percentage of each fatty acid methyl ester. To calculate the mol% of SG and ASG for the spike-in experiment, the signals (in weight %) were adjusted for the molecular weights of the free sterols and fatty acid methyl esters, and a random distribution of fatty acids on the various sterols in ASG was assumed.

Electrospray Ionization Tandem Mass Spectrometry

Purified SG or ASG (Matreya LLC, Pleasant Gap, PA, USA) or unfractionated lipid extracts were introduced by continuous infusion into the ESI source on a triple quadrupole MS/MS (4000 QTrap, Applied Biosystems, Foster City, CA, USA). Subsequently, 5–15 μl of *Arabidopsis* extracts or 1–20 nmol of purified SG or ASG in 1.2 ml of chloroform/methanol/300 mM ammonium acetate in water (300/665/35) were introduced by an autosampler (LC Mini PAL, CTC Analytics AG, Zwingen, Switzerland) fitted with the required injection loop for the acquisition time and presented to the ESI needle at 30 $\mu\text{l}/\text{min}$. Targeted methods for analysis of internal standards, SG and ASG lipid species were employed. In the *Arabidopsis* samples, the internal standards (di12:0 PtdGro and di20:0 PtdGro) were detected with a scan for neutral loss of the head group moiety, NL 189.04 ($\text{C}_3\text{H}_9\text{O}_6\text{P} + \text{NH}_3$) in positive mode. In all samples, SG were revealed with a scan for neutral loss of the hexose moiety, NL 197.09 ($\text{C}_6\text{H}_{12}\text{O}_6 + \text{NH}_3$) in the positive mode, and ASG lipid species were detected with the following neutral loss scans for the hexose moiety acylated with a particular fatty acid: 16:1, NL 433.30 ($\text{C}_{22}\text{H}_{40}\text{O}_7 + \text{NH}_3$); 16:0, NL 435.32 ($\text{C}_{22}\text{H}_{42}\text{O}_7 + \text{NH}_3$); 18:3, NL 457.30 ($\text{C}_{24}\text{H}_{40}\text{O}_7 + \text{NH}_3$); 18:2, NL 459.32 ($\text{C}_{24}\text{H}_{42}\text{O}_7 + \text{NH}_3$); 18:1, NL 461.34 ($\text{C}_{24}\text{H}_{44}\text{O}_7 + \text{NH}_3$); and 18:0, NL 463.35 ($\text{C}_{24}\text{H}_{46}\text{O}_7 + \text{NH}_3$). While adducts other than the $[\text{M} + \text{NH}_4]^+$ can be formed by ESI, the addition of ammonium acetate to the lipid mixture

enhances the formation of $[\text{M} + \text{NH}_4]^+$, and scanning for NL of the ammonia-containing hexose or acylated hexose fragments is critical to assure that $[\text{M} + \text{NH}_4]^+$ adducts are the detected precursors.

The collision gas pressure was set at 2 (arbitrary units). Collision energies, with nitrogen in the collision cell, were +21 V for SG and +30 V for ASG. Declustering potentials were +65 V for SG and +100 V for ASG. Entrance potentials were +10 V for SG and +14 V for ASG. Exit potentials were +10 V for SG and +14 V for ASG. The mass analyzers were adjusted to a resolution of 0.7 u full width at half height. For each spectrum, 400 continuum scans were averaged in multiple channel analyzer (MCA) mode. The source temperature (heated nebulizer) was 100 °C, the interface heater was on, +5.5 kV was applied to the electrospray capillary, the curtain gas was set at 20 (arbitrary units), and the ion source gases were set at 45 (GS1) and 45 (GS2) (arbitrary units). Mass spectra were detected by fragment ion counting.

For each spectrum, background subtraction, data smoothing and peak area integration were performed using a custom script and Applied Biosystems Analyst software. Within each spectra, the data were isotopically deconvoluted based on the sterol portion of SG and ASG. For purified SG and ASG samples, the signals for containing each indicated sterol or fatty acid group were summed and divided by the total signal to obtain mol fractions. For *Arabidopsis* samples, the sterol derivatives in each class were quantified in comparison to the two internal standards (di12:0 PtdGro and di20:0 PtdGro) using LipidomeDB Data Calculation Environment at the website <http://lipidome.bcf.ku.edu:9000/Lipidomics/> [19]. The SG and ASG signals were normalized such that a signal of 1.0 represents a signal equal to the average signal of 1.0 nmol of di12:0 PtdGro and di20:0 PtdGro, and were additionally corrected for isotopic overlap between head groups (NL fragments).

Total phosphatidylcholine (PtdCho) and phosphatidylethanolamine (PtdEtn) of the wild-type and *ugt80A2,B1* seed extracts were analyzed using 10 μl of extract and the mass spectral conditions described in Devaiah et al. [16], considering the amounts for all the PtdCho species in that publication except minor species PtdCho(36:1) and all the PtdEtns, except minor species PtdEtn(34:1), PtdEtn(36:1), PtdEtn(38:6), and PtdEtn(42:4). The PtdCho and PtdEtn mass spectral signals were quantified in relation to the same PtdGro internal standards used for the SG and ASG analysis.

Spike-in Experiment

Varying quantities of soybean SG containing various known amounts of each glucoside (as determined by GC

analysis of derived sterols) in varying quantities were spiked into 5 μ l from 1 ml of extract from 100 wild-type seeds and into 5 μ l of 1 ml of extract from 100 mutant seeds (each containing 50 pmol di12:0 and di20:0 PtdGro internal standards). ASG containing known concentrations of 18:2 and 16:0 ASG (as determined by GC analysis of fatty acids and sterols and assuming random combinations into ASG) in varying quantities were spiked into 15 μ l of 1 ml of extract from 100 wild-type seeds and 15 μ l of 1 ml extract from 100 mutant seeds (each containing 150 pmol di12:0 and di20:0 PtdGro internal standards). The samples were analyzed by ESI-MS/MS and the data processed as described above, except 939–1,000 continuum scans for each analysis were averaged in multiple channel analyzer (MCA) mode. Five biological replicate analyses were performed for SG and each ASG. Signals for SG and ASG analytes, normalized to the average signal for the internal standards in the analyzed sample, are shown.

Results

A direct infusion ESI-MS/MS approach was used to detect and quantify SG and ASG containing sitosterol, campesterol

and stigmasterol (Fig. 1). A major advantage of this approach is that it is not necessary to separate SG and ASG from other compounds prior to analysis. Both SG and ASG can be analyzed as $[M + NH_4]^+$ ions, and detected in positive mode by a series of neutral loss scans specific for the hexose or acyl hexose moieties. SG and ASG with greater than one sugar are very rare [7] and we did not target these compounds in our analysis. Table 1 shows the mass spectral scan values that were used to detect SG and ASG molecules. A previous report on analysis of cholesteryl esters using ESI-MS/MS indicated that mass spectral response varied considerably among sterol esters with different acyl groups [20]. To determine whether various SG and ASG molecular species have variable mass spectral responses, isolated soybean-derived SG and ASG mixtures from a commercial source were separately analyzed by GC-FID and the results were compared with those obtained by ESI-MS/MS. The data indicate that, although there was a slight tendency of the mass spectrometer to be more sensitive to SG and ASG containing campesterol relative to those containing the sitosterol and stigmasterol, the mole fractions of each sterol in the SG and ASG mixtures detected by the two methods were very similar (Fig. 2). Sitosterol was the most prominent sterol found in both commercially-obtained

Table 1 Mass spectral scan values for sterol glucosides and acyl sterol glucosides

Class	Formula [M]	Scan mode	Mass of intact ion analyzed $[M + NH_4]^+$ (<i>m/z</i>)
Steryl glucoside (SG)			
Campesterol	C ₃₄ H ₅₈ O ₆	+NL 197.09	580.46
Stigmasterol	C ₃₅ H ₅₈ O ₆	+NL 197.09	592.46
Sitosterol	C ₃₅ H ₆₀ O ₆	+NL 197.09	594.47
Acyl sterol glucoside (ASG)			
16:1 campesterol	C ₅₀ H ₈₆ O ₇	+NL 433.30	816.67
16:1 stigmasterol	C ₅₁ H ₈₆ O ₇	+NL 433.30	828.67
16:1 sitosterol	C ₅₁ H ₈₈ O ₇	+NL 433.30	830.69
16:0 campesterol	C ₅₀ H ₈₈ O ₇	+NL 435.32	818.69
16:0 stigmasterol	C ₅₁ H ₈₈ O ₇	+NL 435.32	830.69
16:0 sitosterol	C ₅₁ H ₉₀ O ₇	+NL 435.32	832.70
18:3 campesterol	C ₅₂ H ₈₆ O ₇	+NL 457.30	840.67
18:3 stigmasterol	C ₅₃ H ₈₆ O ₇	+NL 457.30	852.67
18:3 sitosterol	C ₅₃ H ₈₈ O ₇	+NL 457.30	854.69
18:2 campesterol	C ₅₂ H ₈₈ O ₇	+NL 459.32	842.69
18:2 stigmasterol	C ₅₃ H ₈₈ O ₇	+NL 459.32	854.69
18:2 sitosterol	C ₅₃ H ₉₀ O ₇	+NL 459.32	856.70
18:1 campesterol	C ₅₂ H ₉₀ O ₇	+NL 461.34	844.70
18:1 stigmasterol	C ₅₃ H ₉₀ O ₇	+NL 461.34	856.70
18:1 sitosterol	C ₅₃ H ₉₂ O ₇	+NL 461.34	858.72
18:0 campesterol	C ₅₂ H ₉₂ O ₇	+NL 463.35	846.72
18:0 stigmasterol	C ₅₃ H ₉₂ O ₇	+NL 463.35	858.72
18:0 sitosterol	C ₅₃ H ₉₄ O ₇	+NL 463.35	860.73



Fig. 2 Sterols from purified soybean SG and ASG as a mole fraction of the total detected sterol compounds. After hydrolysis of the SG or ASG, sterols were determined by GC-FID, or the SG and ASG were analyzed intact by ESI-MS/MS. In the ESI-MS/MS data, the signals for various ASG molecular species with each sterol component were summed. **a** SG. **b** ASG. Error bars represent standard deviations (SD) for GC ($n = 3$ for the number of independent samples) and ESI-MS/MS ($n = 12$ for the number of independent samples)

soybean SG and ASG. Campesterol and stigmasterol were the other major sterols, while minor sterols comprised $\sim 2\%$ or less.

Analysis of the purified ASG mixture by GC-FID and ESI-MS/MS showed a tendency of the mass spectrometer to be less sensitive to 18:2 (linoleic acid)-containing ASG than to other fatty-acyl SG, but the fatty acid compositions of the purified ASG determined by the two methods were similar overall (Fig. 3). The major fatty acid found in purified commercially-obtained soybean ASG was 16:0 (palmitic acid), comprising greater than 50% of the total, followed by 18:2 (linoleic), 18:0 (stearic), 18:1 (oleic), 18:3 (linolenic) and 16:1 (palmitoleic) acids. Taken together, the data indicate that the composition of SG and ASG determined by ESI-MS/MS of the isolated compounds is very close to that determined by GC-FID, indicating that various SG and ASG molecular species have similar molar mass spectral responses. In addition, our data are comparable to the percentile compositions provided by Matreya LLC, the commercial source of the SG and ASG mixtures (see “Experimental Procedure”).

We next applied ESI-MS/MS to seed samples from wild-type *Arabidopsis* and the *ugt80A2, B1* mutant using a spike-in experiment to verify linearity of response of the normalized mass spectral signals. SG and ASG were analyzed by direct infusion of unseparated seed extracts, and known amounts of soybean SG and ASG were spiked-in to wild-type and mutant samples to determine the linearity of their ESI-MS/MS response in the presence of other seed lipids. The linearity of SG and ASG response was good

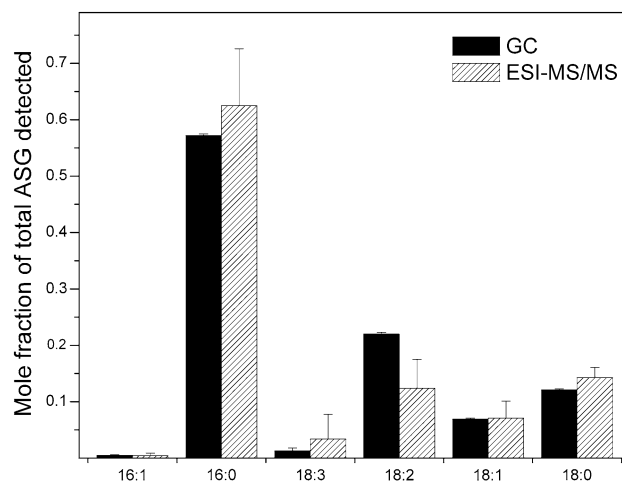
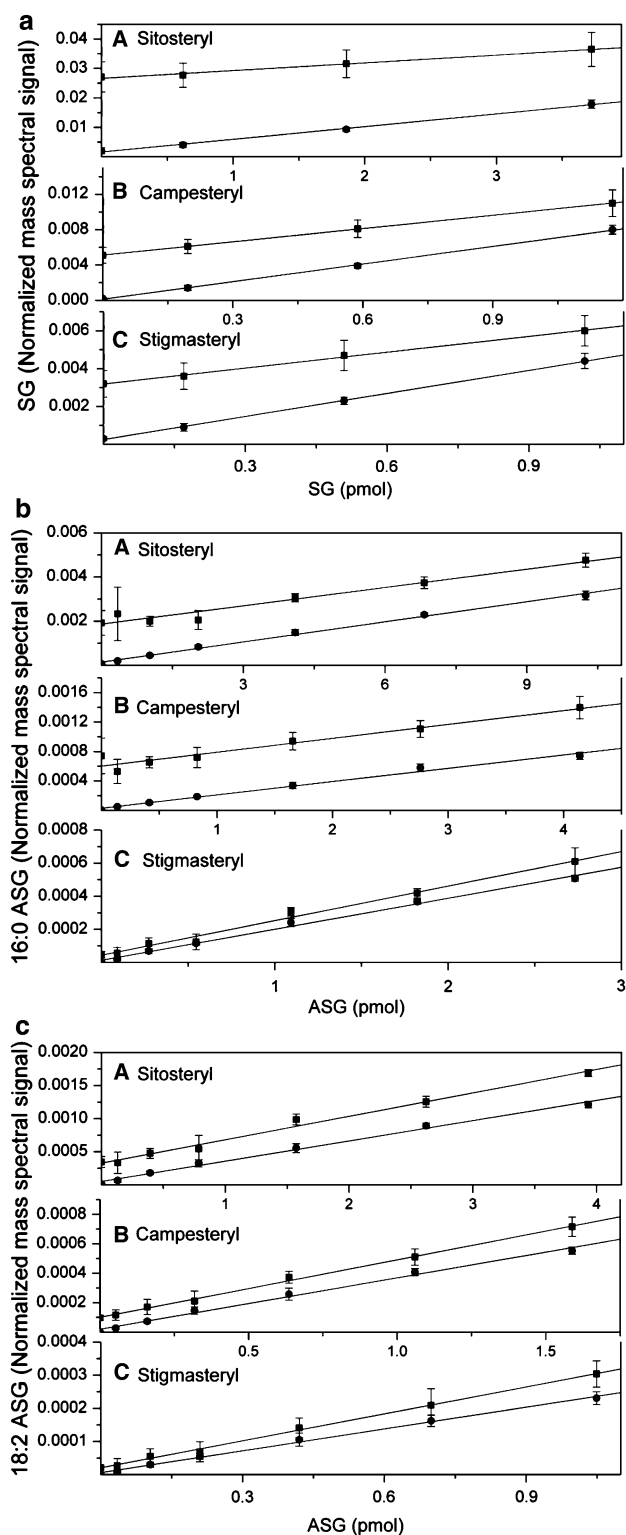


Fig. 3 Fatty acids of purified soybean ASG as a mole fraction of the total detected fatty acids. Fatty acids were determined by GC-FID after formation of methyl esters, or the ASG were analyzed intact by ESI-MS/MS. In the ESI-MS/MS data, the signals for various ASG molecular species with each fatty acid component were summed. Error bars represent standard deviations (SD) for GC ($n = 3$ for the number of independent samples) and ESI-MS/MS ($n = 12$ for the number of independent samples)

over the range in which the mutant and wild-type are compared, and the mutant and wild-type spike-in data form parallel lines (Fig. 4). The data show that wild-type values fall within the linear range of the spike-in to the mutant samples, indicating that the amounts of SG and ASG in the wild-type samples are linearly related to the amounts in the mutant samples. These data indicate that the ESI-MS/MS method is useful for comparison of biological samples.

Levels of SG and ASG in *Arabidopsis* seeds of *ugt80A2, B1* mutants and wild-type are shown in Fig. 5 (Table S1) with individual molecular species of SG and ASG indicated. The masses detected were consistent with identification of sitosterol, campesterol, and stigmasterol as the three major sterols in *Arabidopsis* seed SG and ASG. Minor sterols, with masses consistent with identifications of cholesterol and brassicasterol, were also detected by ESI-MS/MS as $\sim 2\%$ or less of the total SG (data not shown). The data show that sitosteryl, campesteryl, and stigmasteryl glucosides were significantly reduced by 85, 92, and 82% (7-, 13- and 6-fold), respectively, in *ugt80A2, B1* in comparison to wild-type seeds, and total SG were reduced by 86% (sevenfold) (Fig. 5; Table S1). Although SG levels were reduced in *ugt80A2, B1*, the relative proportions of SG that contained sitosterol, campesterol and stigmasterol were similar to those in wild-type. In addition, we observed that the levels of phospholipids PtdCho and PtdEtn were very similar in the mutant and wild-type (Table S2), indicating that the *ugt80A2, B1* mutant is specifically deficient in SG and ASG.



The major ASG molecular species, 16:0 (palmitic), 18:1 (oleic), 18:2 (linoleic), and 18:3 (linolenic) acids were reduced to a slightly greater extent than SG in *ugt80A2,B1* compared to wild-type seeds. Total ASG levels were reduced 96% (23-fold) in the double mutant (Fig. 5; Table

Fig. 4 Spike-in experiments indicate linear responses in mass spectral signals from ESI-MS/MS analysis of SG and ASG. Normalized mass spectral signals are shown for compounds from *Arabidopsis* seeds of wild-type (squares) and the *ugt80A2,B1* mutant (circles) for **a** SG, **b** 16:0 ASG, and **c** 18:2 ASG in three panels from top to bottom. Each panel is further sub-divided to indicate quantification of (A) sitosteryl, (B) campesteryl, and (C) stigmasteryl SG, 16:0 ASG or 18:2 ASG, respectively. A normalized signal of 1.0 for SG and ASG is the same amount of signal as the average signal produced by 1.0 nmol of the internal standards, di12:0 and di20:0 PtdGro. Error bars represent standard deviations (SD) for $n = 5$ biological replicates

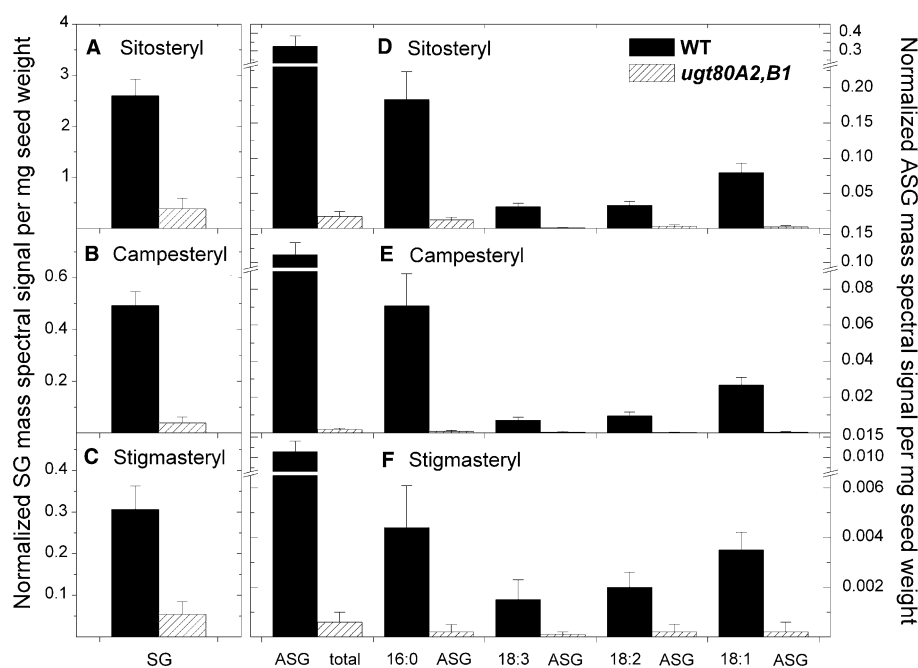
S1). Among the ASG detected in seeds, 16:0 (palmitic acid) was the predominant acyl group accounting for 57 and 66% of the total ASG signal in wild-type and mutant, respectively. Strikingly, campesterol-containing ASG were reduced 98% (61-fold), while decreases in sitosterol- and stigmasterol-containing ASG were reduced to a lesser extent. Campesterol-containing ASG accounted for only 10% of the ASG in *ugt80A2,B1* in comparison to 25% in wild-type. In wild-type, the signal from SG accounted for 88% of the total glucosylated sterol signal (SG + ASG), and in the *ugt80A2,B1* mutant the signal from SG accounted for 96% of the total glucosylated sterols. Overall, there was a reduction of 87% (eightfold) in SG + ASG content in the mutant in comparison to wild-type.

Discussion

The development of a high throughput platform for the detection of sterol conjugates will enhance our ability to characterize mutations that affect the levels of these compounds. Here we present a first step towards including SG and ASG analysis in a comprehensive lipidomics platform. We show that ESI-MS/MS, with a direct injection non-chromatographic approach, allows us to analyze seed extracts directly without purification of the SG and ASG classes from the lipid extract. This approach is simple compared to the traditional GC-FID method since derivatization and chromatographic separation of products is not required. Our spike-in data reveal the mass spectral signals behave linearly to spiked-in standards for a given matrix (Fig. 4). The levels of SG and ASG were comparable to those reported for tobacco seeds [21] and various *Arabidopsis* tissues [13, 22].

While this article was in review and revision, another article describing the mass spectral analysis of SG and ASG was published [22]. Wewer et al. analyzed SG and ASG by direct infusion, but used quadrupole time-of-flight mass spectrometry in contrast to the triple quadrupole method that was applied in our work. In agreement with our data, these authors determined that naturally-occurring

Fig. 5 SG and ASG levels are reduced in seeds from *ugt80A2,B1* mutants of *Arabidopsis*. ESI-MS/MS was applied to analyze SG and ASG from seeds of wild-type (WT) (solid bars) and *ugt80A2,B1* (stippled bars). Normalized mass spectral signals per mg seed weight are indicated for each compound: **a–c** SG and **d–f** 16:0, 18:3, 18:2, and 18:1 ASG. **a** SG and **d** ASG containing sitosterol. **b** SG and **e** ASG containing campesterol. **c** SG and **f** ASG containing stigmasteryl. The total ASG amount was calculated by adding the normalized mass spectral signal of molecular lipid species of that group. Error bars represent standard deviations (SD) for $n = 5$ biological replicates



sterol derivatives had similar response factors in ESI-MS/MS analysis. Sample preparation by Wewer et al. [22] included a solid phase extraction step followed by direct infusion of samples to the mass spectrometer. Addition of this step yielded increased sensitivity and reduced matrix effects during ionization, which the authors deemed critical for the development of a comprehensive lipidomics platform encompassing linear responses of mass spectral signals from multiple lipid classes. In the current work, care was taken to keep the matrix relatively constant during analysis. Our results, like those of Wewer et al. [22], indicate that ESI mass spectrometry methods are very sensitive for SG and ASG from biological samples. In particular, the use of the triple quadrupole mass spectrometer in our work allowed detection of changes in SG and ASG at sub-picomole levels.

Application of ESI-MS/MS to seed samples from wild-type *Arabidopsis* and a mutant in two UGT enzymes (UGT80A2 and UGT80B1) has revealed new details on the composition of SG and ASG in the *ugt80A2,B1* mutant. A previous study, using GC-FID analysis, showed that combined SG + ASG content was decreased 5-, 21-, and 22-fold in leaf, stem, and inflorescence + silique tissues of *ugt80A2,B1* mutants in comparison to wild-type [13]. In our work, analyses of dry seeds from *ugt80A2,B1* and wild-type indicate that total SG + ASG levels were reduced similarly, 87% or about 8-fold, in *ugt80A2,B1* seeds. The ESI-MS/MS analysis revealed that the reduction is slightly greater in ASG than in SG levels. In addition, the lower levels of acyl campesteryl glucosides in the mutant, compared to other ASG, may reflect a preference of the

acylating enzymes for sitosteryl and stigmasteryl glucosides, or possibly a different subcellular localization of the various SG and/or acylating enzymes. Our results demonstrate that mass spectrometry methods such as ESI-MS/MS are poised to accelerate research in the detection of SG and ASG lipids whose biological roles are just beginning to be uncovered.

Acknowledgments K.S. was supported by National Research Initiative Competitive Grants Program grant no. 2007-35304-18453 from the United States Department of Agriculture National Institute of Food and Agriculture and by the National Science Foundation (MCB 0517758). Equipment acquisition and method development at the Kansas Lipidomics Research Center were funded by the National Science Foundation (EPS 0236913, MCB 0455318 and 0920663, DBI 0521587), Kansas Technology Enterprise Corporation, Kansas IDeA Network of Biomedical Research Excellence (K-INBRE) of National Institutes of Health (P20RR16475), and Kansas State University. This is contribution no. 11-374-J from the Kansas Agricultural Experiment Station.

References

1. Benveniste P (2004) Biosynthesis and accumulation of sterols. *Annu Rev Plant Biol* 55:429–457
2. Grandmougin-Ferjani A, Schuler-Muller I, Hartmann MA (1997) Sterol modulation of the plasma membrane H^+ -ATPase activity from corn roots reconstituted into soybean lipids. *Plant Physiol* 113:163–174
3. Schuler I, Milon A, Nakatani Y, Ourisson G, Albrecht AM, Benveniste P, Hartmann MA (1991) Differential effects of plant sterols on water permeability and on acyl chain ordering of soybean phosphatidylcholine bilayers. *Proc Natl Acad Sci USA* 88:6926–6930

4. Asami T, Nakano T, Fujioka S (2005) Plant brassinosteroid hormones. *Plant Horm* 72:479–504
5. Kim TW, Wang ZY (2010) Brassinosteroid signal transduction from receptor kinases to transcription factors. *Annu Rev Plant Biol* 61:681–704
6. Grille S, Zaslowski A, Thiele S, Plat J, Warnecke D (2010) The functions of sterol glycosides come to those who wait: Recent advances in plants, fungi, bacteria and animals. *Prog Lipid Res* 49:262–288
7. Kovganko NV, Kashkan ZN (1999) Sterol glycosides and acylglycosides. *Chem Nat Compd* 35:479–497
8. Heinz E (1996) Plant glycolipids: structure, isolation and analysis. In: Christie WW (ed) *Advances in lipid methodology—3*. The Oily Press, Dundee, pp 211–332
9. Wojciechowski ZA (1991) Biochemistry of phytosterol conjugates. In: Patterson GW, Nes WD (eds) *Physiology and biochemistry of sterols*. American Oil Chemists Society, Champaign, pp 361–395
10. Peng L, Kawagoe Y, Hogan P, Delmer D (2002) Sitosterol-beta-glucoside as a primer for cellulose synthesis in plants. *Science* 295:147–150
11. Ury A, Benveniste P, Bouvier-Navé P (1989) Phospholipid-dependence of plant UDP-glucose sterol beta-d-glucosyl transferase: IV. Reconstitution into small unilamellar vesicles. *Plant Physiol* 91:567–573
12. Warnecke DC, Baltrusch M, Buck F, Wolter FP, Heinz E (1997) UDP-glucose:sterol glucosyltransferase: cloning and functional expression in *Escherichia coli*. *Plant Mol Biol* 35:597–603
13. DeBolt S, Scheible WR, Schrick K, Auer M, Beisson F, Bischoff V, Bouvier-Navé P, Carroll A, Hematy K, Li Y, Milne J, Nair M, Schaller H, Zemla M, Somerville C (2009) Mutations in UDP-glucose:sterol glucosyltransferase in *Arabidopsis* cause transparent testa phenotype and suberization defect in seeds. *Plant Physiol* 151:78–87
14. Wenk MR (2010) Lipidomics: new tools and applications. *Cell* 143:888–895
15. Welti R, Li W, Li M, Sang Y, Biesiada H, Zhou HE, Rajashekar CB, Williams TD, Wang X (2002) Profiling membrane lipids in plant stress response: role of phospholipase D alpha in freezing-induced lipid changes in *Arabidopsis*. *J Biol Chem* 277:31994–32002
16. Devaiah SP, Roth MR, Baughman E, Li M, Tamura P, Jeannotte R, Welti R, Wang X (2006) Quantitative profiling of polar glycerolipid species from organs of wild-type *Arabidopsis* and a phospholipase D alpha1 knockout mutant. *Phytochemistry* 67:1907–1924
17. Bligh EG, Dyer WJ (1959) A rapid method of total lipid extraction and purification. *Can J Biochem Physiol* 37:911–917
18. Rintoul DA, Chou SM, Silbert DF (1979) Physical characterization of sterol-depleted LM-cell plasma membranes. *J Biol Chem* 254:10070–10077
19. Zhou Z, Marepally SR, Nune DS, Pallakollu P, Ragan G, Roth MR, Wang L, Lushington GH, Visvanathan M, Welti R (2011) LipidomeDB data calculation environment: online processing of direct-infusion mass spectral data for lipid profiles. *Lipids* 46:879–884
20. Liebisch G, Binder M, Shifferer R, Langmann T, Schulz B, Schmitz G (2006) High throughput quantification of cholesterol and cholesteryl ester by electrospray ionization tandem mass spectrometry (ESI-MS/MS). *Biochim Biophys Acta* 1761:121–128
21. Bush PB, Grunwald C (1972) Sterol changes during germination of *Nicotiana tabacum* seeds. *Plant Physiol* 50:69–72
22. Wewer V, Dombrink I, Vom Dorp K, Dörmann P (2011) Quantification of sterol lipids in plants by quadrupole time-of-flight mass spectrometry. *J Lipids Res* 52:1039–1054

Suitability of Soxhlet Extraction to Quantify Microalgal Fatty Acids as Determined by Comparison with In Situ Transesterification

Jesse McNichol · Karen M. MacDougall ·
Jeremy E. Melanson · Patrick J. McGinn

Received: 24 May 2011 / Accepted: 3 October 2011 / Published online: 6 November 2011
© AOCS 2011

Abstract To assess Soxhlet extraction as a method for quantifying fatty acids (FA) of microalgae, crude lipid, FA content from Soxhlet extracts and FA content from in situ transesterification (ISTE) were compared. In most cases, gravimetric lipid content was considerably greater (up to sevenfold) than the FA content of the crude lipid extract. FA content from Soxhlet lipid extraction and ISTE were similar in 12/18 samples, whereas in 6/18 samples, total FA content from Soxhlet extraction was less than the ISTE procedure. Re-extraction of residual biomass from Soxhlet extraction with ISTE liberated a quantity of FA equivalent to this discrepancy. Employing acid hydrolysis before Soxhlet extraction yielded FA content roughly equivalent to ISTE, indicating that acidic conditions of ISTE are responsible for this observed greater recovery of FA. While crude lipid derived from Soxhlet extraction was not a useful proxy for FA content for the species tested, it is effective in most strains at extracting total saponifiable lipid. Lipid class analysis showed the source of FA was primarily polar lipids in most samples (12/18 lipid extracts contained <5% TAG), even in cases where total FA content was high (>15%). This investigation confirms the usefulness of ISTE, reveals limitations of gravimetric methods for projecting biodiesel potential of microalgae,

and reinforces the need for intelligent screening using both FA and lipid class analysis.

Keywords In situ transesterification · Soxhlet · Microalgae · Biodiesel

Abbreviations

FA	Fatty acid
FAME	Fatty acid methyl ester
TE	Transesterification
ISTE	In-situ transesterification
R-ISTE	Residual ISTE
TE-AH	TE preceded by acid hydrolysis
PUFA	Polyunsaturated fatty acid
GC	Gas chromatography
TAG	Triacylglycerol
HPLC-CAD	High performance liquid chromatography-charged aerosol detection
LC-MS	Liquid chromatography/mass spectrometry

Introduction

Microalgae have been suggested as a sustainable source of biodiesel based on a number of perceived advantages. Many species grow quickly, have the ability to accumulate a large proportion of triacylglycerols (TAG) as biomass under certain conditions, and can use waste sources of CO₂ and nutrients such as flue gas and municipal wastewater to support growth. The application of microalgae to economical production of biodiesel requires that a high percentage of microalgal biomass be composed of fatty acid containing compounds that can be converted to fatty acid

J. McNichol · K. M. MacDougall · J. E. Melanson ·
P. J. McGinn
Institute for Marine Biosciences, National Research
Council of Canada, Halifax, NS B3H 3Z1, Canada

Present Address:

J. McNichol (✉)
MIT/Woods Hole Oceanographic Institution Joint Program
in Biological Oceanography, 266 Woods Hole Rd,
MS# 52, Woods Hole, MA 02543-1050, USA
e-mail: McNichol@mit.edu

methyl esters (FAME). This fraction, otherwise known as ‘saponifiable lipid’ includes neutral lipid such as TAG, but may also derive from other cellular components such as membrane lipids.

Considerable uncertainty remains as to whether it is possible to satisfy this requirement with scaled-up cultivation efforts. One of the challenges in resolving this question is the unclear meaning of various lipid content values reported in the scientific literature [19], generally referred to as ‘oil content’ or ‘lipid content’, with wide-ranging [25], and even unreferenced estimates commonly cited to make the case for microalgal biofuels [7]. In addition, there are researchers growing microbial heterotrophs [4] or algae heterotrophically [30], who consistently report higher lipid content values that may be included when modeling phototrophic biodiesel production as a sustainable fuel source. For example, the heterotrophic thraustochytrid *Schizochytrium* sp. and heterotrophic microalgae *Cryptothecodinium cohnii* were both included in a table that was labeled “Oil content of some microalgae” in a well-cited paper on microalgal biodiesel [7].

Contributing to this uncertainty, a number of different techniques are currently in use to evaluate crude lipid content, many based on the classic methods of Folch [14] and Bligh and Dyer [3]. Other examples include spectrofluorometric determinations where lipid bodies are directly stained and quantified [6], supercritical CO₂ extraction [13] and Soxhlet extraction [30, 17, 22]. It is clear that whichever method is chosen, careful attention is required to optimize the extraction conditions—pre-processing is in some cases essential [27], as is reaction time and reagent concentration [12, 40].

Even assuming optimized pre-treatment and extraction conditions, a key limitation of the above techniques is that they are unable to resolve lipid classes, as in liquid chromatography or thin layer chromatography. Although it is apparent to experienced lipid chemists that lipid extracts may contain polar lipids, sterols, pigments, waxes, and oxidatively-altered fats in addition to TAG [37], many biofuel studies still rely on simple gravimetric estimations (hereafter referred to as ‘crude lipid’) to assess biodiesel yields [31, 39], despite the fact that including non-saponifiable lipid overestimates the suitability of a feedstock for biodiesel fuel. In contrast, other publications report crude lipid and FAME profiles [18], while others studies rigorously combine crude lipid, FAME profiles and quantification of FAME/TAG [42]. Also confounding simple comparison between studies is the polarity of the solvent used, which has a significant impact on the yield and composition of extracts from microalgae [22].

The use of gas-chromatography (GC) techniques, which yield accurate quantification and identification of FAME, is a simple procedure to resolve this uncertainty. FAME

quantification gives information on the amount of biomass that is potentially convertible to biodiesel and also indirectly quantifies the amount of additional material extracted as crude lipid which has no value as a fuel.

The most commonly applied procedure for preparing FAME is an initial solvent extraction followed by transesterification (TE) of the resulting lipid with an alcohol, typically methanol [9]. To reduce the time required for this process, other authors [21] have suggested a single-step method where biomass is simultaneously extracted and transesterified, known variously as *in situ* transesterification (ISTE), direct transesterification, or one-step transesterification. Omitting the initial extraction step offers a significant savings in time and energy, results in increased precision [28], and a more complete extraction of fatty acids compared to conventional extraction (i.e. Folch, Bligh and Dyer) followed by transesterification [21, 29]. The various applications of ISTE have been thoroughly reviewed by Carrapiso and García [5].

In addition to requiring less time and potentially resulting in more complete extraction of fatty acids [21, 29], a key advantage of ISTE is that since the entire extraction/transesterification is carried out in a single vessel and quantified by GC, this procedure can be easily applied to small quantities (<10 mg) of biomass without concerns for either loss of sample or analytical precision that would be expected using traditional extraction methods [5]. With these advantages in mind, a standardized ISTE protocol was developed in this laboratory, which was based on previously published standard transesterification procedures [8] as well as information from several recent investigations into ISTE of microalgal lipids [12, 40].

The goal of this investigation was to use ISTE to assess the relevance of gravimetric lipid data from Soxhlet solvent extraction to making projections about biodiesel productivity from microalgae. By comparing these two methods, it was also possible to investigate the factors responsible for the increased efficiency of ISTE procedures versus solvent extraction that have been previously reported [21]. Across 18 samples representing 16 species of microalgae, gravimetric lipid data was found to be an inconsistent metric for measuring total fatty acid content when compared with ISTE. This result confirms the effectiveness of ISTE for measuring total fatty acids in microalgae, and argues for caution in interpreting gravimetric lipid data from microalgae.

Experimental Procedure

Microalgal Culture

A list of the microalgae species cultivated to provide biomass for this study is listed in Table 1. All cultures were

Table 1 Microalgae species used in the study, their taxonomic grouping and media requirements

Species	Taxonomy	Media
<i>Scenedesmus dimorphus</i>	Freshwater chlorophyte	Freshwater with F/2 [24]
<i>Porphyridium aeruginum</i> UTEX 755	Brackish rhodophyte	10% v/v seawater/ freshwater with F/2 media
<i>Nannochloropsis granulata</i> CCMP 529	Marine eustigmatophyte	Seawater with F/2
<i>Nannochloropsis granulata</i> CCMP 535	Marine eustigmatophyte	Seawater with F/2
<i>Phaeodactylum tricornutum</i> CCMP 1327	Marine bacillariophyte	Seawater with F/2
<i>Neochloris oleoabundans</i> UTEX 1185	Freshwater chlorophyte	Bold's 3 N [38]
<i>Botryococcus braunii</i> Race B UTEX 572	Freshwater chlorophyte	Freshwater with F/2
<i>Emiliana huxleyi</i> CCMP 1324	Marine pyrmnesiophyte	Seawater with F/2
<i>Tetraselmis chuii</i> PLY429	Marine chlorophyte	Seawater with F/2
<i>Glossomastix chrysolasta</i> CCMP 1537	Marine pinguiophyte	Seawater with F/2
<i>Chlamydomonas</i> sp. CCMP 2095	Marine chlorophyte	Prov 50 Medium [1]
CCMP 2321	Marine bacillariophyte	Seawater with F/2
CCMP 1142	Marine chlorophyte	Seawater with F/2
<i>Chlorella vulgaris</i>	Freshwater chlorophyte	Freshwater with F/2
CCMP 2327	Marine bacillariophyte	Seawater with F/2
<i>Eutreptiella pomquetensis</i> CCMP 1491	Marine euglenophyte	L1 Medium [23]

grown under continuous illumination, and all diatom cultures were supplemented with 100 μM silicate. Cultures were harvested by centrifugation with the exception of CCMP 1142, which was harvested by sieving. Photosynthetic batch cultivation was conducted in either enclosed 'Brite-Box' photobioreactors ranging in capacity from 200–1,000 L [10] or in 18-L plastic carboys. All batch cultures were harvested at a stationary phase of growth. One strain, *Isochrysis galbana*, was cultivated in an N-limited chemostat and harvested at steady-state at a dilution rate of 0.5 day^{-1} . All cultures were lyophilized after harvest and stored at $-20\text{ }^{\circ}\text{C}$ prior to analysis. Three separate biomass samples of *Botryococcus braunii* Race B were analyzed, indicated by the numbers 1, 2 and 3.

Soxhlet Lipid Extraction

Freeze-dried biomass (0.5 g) was homogenized with a mortar and pestle and extracted using the Soxtec 2050 automated solvent extraction system (FOSS North America, Eden Prairie MN) with the following program: boiling 25 min, rinsing 40 min, solvent recovery 15 min and pre-drying 2 min. Extraction temperatures for different solvents were as follows: chloroform/methanol (2:1)— $150\text{ }^{\circ}\text{C}$, acetone— $150\text{ }^{\circ}\text{C}$, hexane— $155\text{ }^{\circ}\text{C}$, ethanol— $250\text{ }^{\circ}\text{C}$.

The solvents used in all Soxhlet extractions for two-step FAME analyses (TE) were chloroform/methanol (2:1). All solvents were HPLC grade or better (Fisher Optima). After extraction with the Soxtec 2050, lipids were dried at

$105\text{ }^{\circ}\text{C}$ for 1 h, placed in a desiccator for 1 h, and weighed to determine gravimetric lipid yield. All values were standardized to ash-free dry weight of algal biomass unless otherwise indicated. Ash-free dry weights were determined by baking biomass overnight at $550\text{ }^{\circ}\text{C}$ and reweighing the combusted residue [43].

Lipids were resolubilized in chloroform/methanol (2:1) and stored under nitrogen at $-20\text{ }^{\circ}\text{C}$ until further analysis. Some extractions were done on residual 'defatted' biomass previously extracted in the Soxhlet apparatus (Fig. 1). Defatted biomass was kept in a fume hood to evaporate solvent, and stored at $-20\text{ }^{\circ}\text{C}$ before re-analysis.

For acid hydrolysis pre-treatment, samples were processed with the Soxcap 2047 acid hydrolysis kit, according to application note 3907 (FOSS North America, Eden Prairie, MN). Briefly, the samples were boiled for 1 h in 3 M HCl, rinsed with tap water until neutralized, dried at $60\text{ }^{\circ}\text{C}$ overnight and extracted in the Soxtec 2050 as previously described above.

Lipid Derivatization and In Situ Derivatization

Standard transesterification procedures [8] and recent investigations into ISTE of microalgal biomass [12, 40] were used to develop lipid derivatization protocols. For two-step lipid derivatization (TE), a maximum of 20 mg of lipids extracted with the Soxtec apparatus were dried under nitrogen at room temperature to constant weight in pre-weighed Pyrex tubes (previously baked at $450\text{ }^{\circ}\text{C}$ overnight to minimize lipid contamination). For in situ

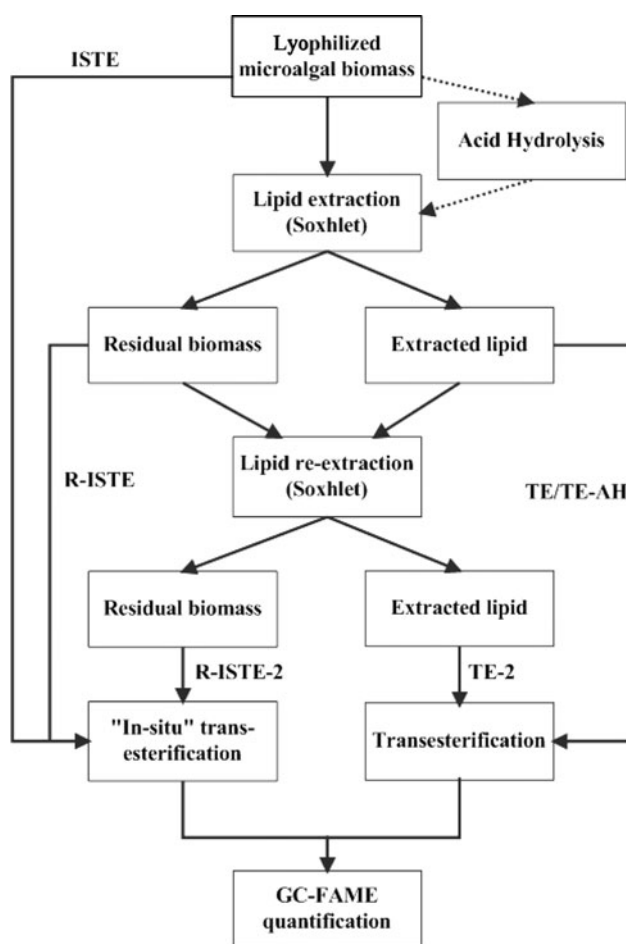


Fig. 1 Flow chart describing lipid analysis as presented in Table 1, as well as Figs. 2, 3, 4 and 5. The lipid re-extraction steps designated TE-2 and R-ISTE-2 are presented solely in Fig. 5. Acid hydrolysis pre-treatment followed by transesterification (TE-AH) was performed only for data presented in Fig. 6

derivatization, a maximum of 20 mg of biomass was weighed directly into clean Pyrex tubes. For both treatments, 1 mL of anhydrous toluene (Sigma-Aldrich) was added, followed by 2 mL of 5% acetyl chloride (Fluka)/anhydrous methanol (99.8% Sigma-Aldrich), prepared fresh for each reaction. Tubes were purged with nitrogen, capped, mixed gently, and kept at 105 °C in a heating block for 1 h. Derivatized lipids were cooled to room temperature, washed with 5 mL of 18.2 MΩ H₂O with 5% NaCl (w/v), 4 mL of 18.2 MΩ H₂O with 2% NaHCO₃ (w/v), dried over anhydrous sodium sulfate and filtered through glass wool to exclude residual sodium sulfate.

Total derivatized lipid was then dried under nitrogen, weighed, diluted to 5 mg/mL with hexane and analyzed using gas chromatography. All reactions included a reagent blank to confirm clean solvents and glassware. Lipid and FAME yields were standardized to the ash-free dry weight of the biomass, with the FAME yield from the re-extracted

defatted biomass represented as a percentage of the original biomass. Readers may refer to Fig. 1 for a schematic description of these steps.

GC Quantification and Identification

All samples were analyzed on an Omegawax 250 column with an Agilent 7890 gas chromatograph equipped with a FID. Samples were run in constant flow mode (3 mL/min) and temperature programmed as follows: 110 °C for 1 min, then 5 °C/min to 250 °C where the program was held for 20 min (total run time 49 min). Inlet temperature was set at 250 °C, and detector temperature to 300 °C. The carrier gas was helium. Peaks were automatically integrated by Chemstation software (Agilent).

A known quantity of internal standard (nonadecanoic acid, Sigma-Aldrich) was added to each tube before adding sample. The concentration of all other integrated peaks was calculated by calibrating to the area of the internal standard peak as per Tran et al. [40] and Griffiths et al. [21]. Individual fatty acids were provisionally identified by comparing retention times to two standard mixtures (Supelco 37 and PUFA No. 3, Sigma-Aldrich). Long-chain fatty acids (C28:1 and C28:2) in *B. braunii* were provisionally identified from previous LC-MS analysis of Soxhlet lipid extracts (data not shown). For the comparison of individual FA, only components that comprised >2% of the total fatty acid pool by area % in the ISTE extracts were considered.

TAG Quantification by HPLC-CAD

Lipid profiling of the Soxhlet extracts of 18 different algal strains was carried out using HPLC with Charged Aerosol Detection (CAD). An Agilent 1100 HPLC binary pump was used with a Halo C8 50 × 3.0 mm column held at 40 °C. The detector was an ESA Biosciences Corona-Plus CAD detector operated with a N₂ gas pressure of 37 psi and the range was set to 100 pA. The mobile phase was delivered at 0.4 mL/min and consisted of (A) 20% water/80% methanol and (B) 70% isopropanol/30% methanol. The gradient was held at 50% B from 0 to 5 min, then increased from 50 to 100% B from 5 to 8 min, and held at 100% B from 8 to 15 min. The column was then equilibrated back to starting conditions for an 8 min period. Liquid chromatography solvents methanol and isopropanol were HPLC-grade and purchased from Caledon (Georgetown, ON, Canada). Samples were diluted to 0.1 mg/mL in methanol and filtered in 0.22 μm centrifugal tubes before analysis. Triolein (18:1/18:1/18:1) was purchased from Nu-Chek Prep (Elysian, MN, USA) and calibration standards ranged from 0.1 to 100 μg/mL. The injection volume in all cases was 10 μL.

Results

Figure 1 shows a flow diagram of the analyses that were performed for this investigation and the acronyms used to refer to them in the text. All microalgal biomass samples were initially extracted by both one-step ISTE and Soxhlet methods as described in “Experimental Procedure”. For the Soxhlet extractions, lipid extracts were subsequently transesterified to FAME in a second step (TE). A number of additional processing reactions were then carried out on some of the ‘defatted’ biomass residues recovered from the Soxhlet apparatus to assess its effectiveness for determining saponifiable fatty acid content. Several residual biomass samples were subjected to re-extraction by the ISTE method (designated R-ISTE) in addition to back extraction by Soxhlet and transesterification (TE-2) in identical fashion to TE extractions. The residues from the TE-2 analysis were again subjected to ISTE analysis (designated R-ISTE-2). In other experiments, biomass samples were pre-treated with acid hydrolysis, subjected to Soxhlet extraction and transesterification (designated TE-AH).

The Effect of Extraction Solvent on Gravimetric Lipid Content

Initial experiments on Soxhlet extraction for three microalgal species (Fig. 2) demonstrated a clear effect of solvent polarity on crude lipid yield. Polar solvents (chloroform/methanol (2:1), ethanol and acetone) yielded higher lipid content, while the non-polar solvent hexane gave a lower yield. With the exception of *B. braunii*, which is known to contain a high proportion of neutral lipids such as TAG [2], hexane extracted little lipid (~4%) relative to more polar

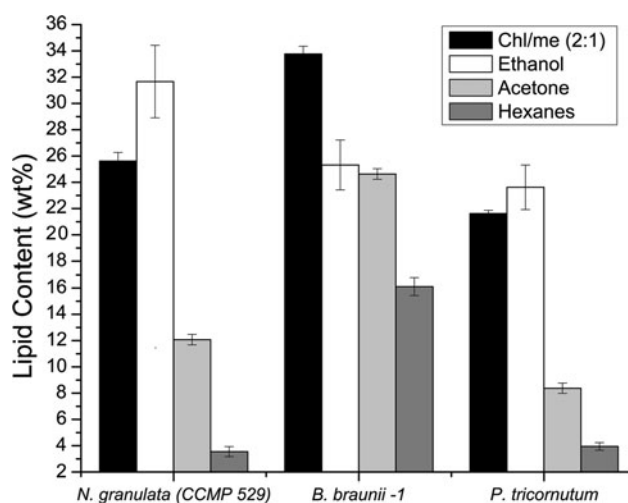


Fig. 2 Lipid content using different solvent matrices for three microalgal species, as determined by Soxhlet extraction. Bars indicate standard deviation of the mean ($n = 6$). Values are not standardized for ash or dry weight content of individual samples

solvents such as ethanol or chloroform/methanol (2:1). Ethanol showed a higher variability in lipid content relative to the other solvent matrices.

Comparison of Fatty Acid Content from Soxhlet and In Situ Transesterification (ISTE) Methods

Figure 3a shows that for 12 samples, TE and ISTE methods yielded a similar amount of FAME, with little or no FAME detected in R-ISTE extracts. In contrast, Fig. 3b shows that six samples yielded additional FAME with re-extraction of residual biomass from Soxhlet extraction (R-ISTE), indicating an incomplete extraction of fatty acids with the Soxhlet procedure. For *B. braunii*, the marine chlorophyte designated CCMP 1142 and *Tetraselmis chuii*, FAME yield derived from Soxhlet extraction-TE was not similar to ISTE. In two cases (CCMP 1142 and *B. braunii*-3), >50% of the total FAME extracted with the ISTE method was not detected with the TE method, but subsequently recovered with R-ISTE treatment.

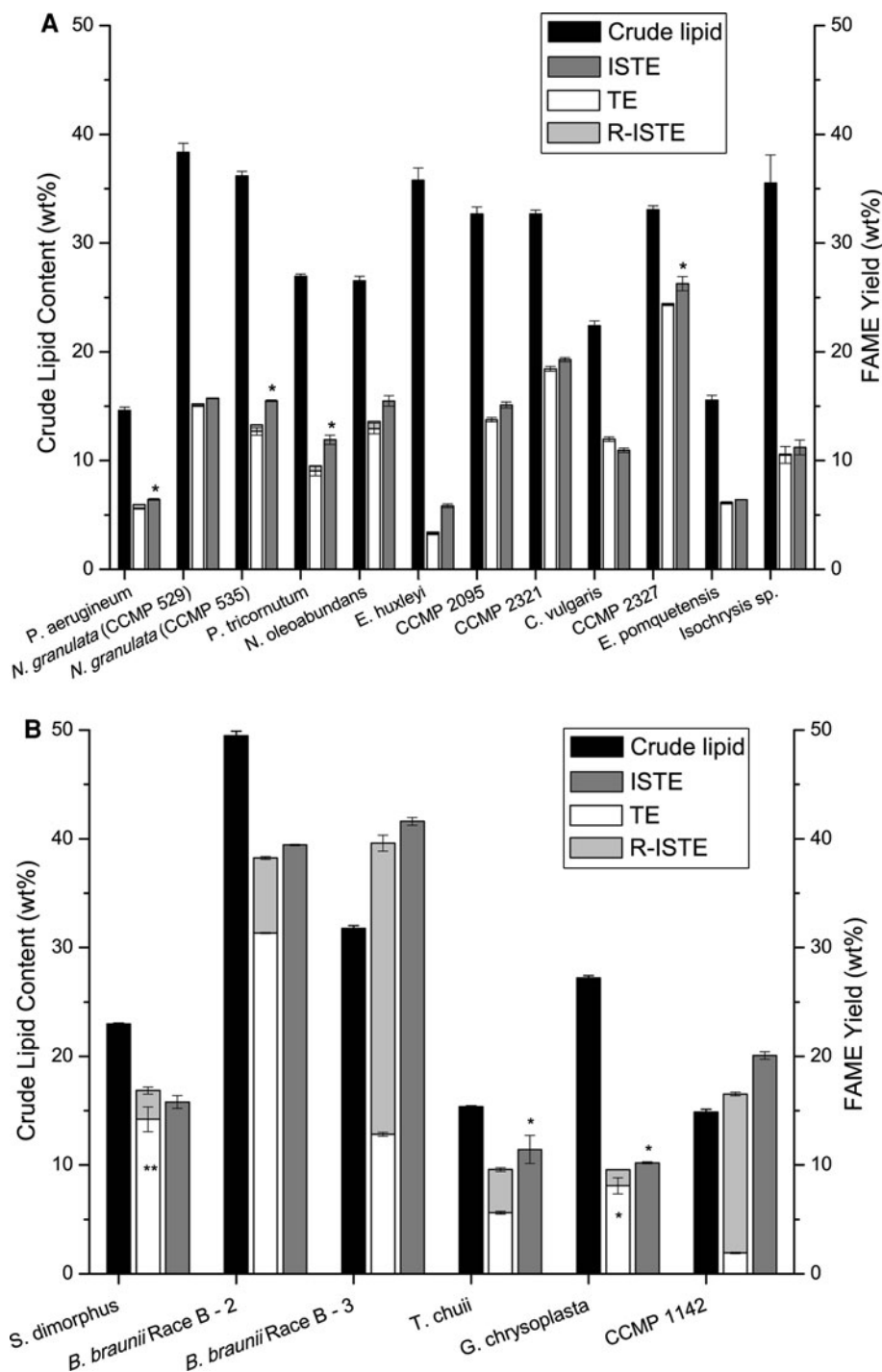
Gravimetric Lipid Yield Compared with Total Fatty Acid Content

In 16 of 18 samples (Fig. 3a, b), gravimetric lipid content as determined by solvent extraction was, as expected, greater than the weight of fatty acids determined by quantification of FAME using both methods (TE, ISTE). In *Emiliania huxleyi* extracts, the lipid content was $\sim 7\times$ greater than the fatty acid content as determined by TE or ISTE, but for most species the lipid content was between 2 and $3\times$ greater than the total FAME content. In two cases where Soxhlet extraction was not effective at liberating all extractable fatty acids (Fig. 3b: CCMP 1142, *B. braunii*-3), gravimetric lipid content was less than the fatty acid content of the biomass as determined by ISTE.

Intact Lipid Analysis by High Performance Liquid Chromatography

To gain an understanding of these apparent discrepancies between the gravimetric lipid content and the lipid content determined by GC-FAME analysis, 18 algal strains were also analyzed by HPLC-CAD to obtain profiles of intact lipids. CAD was chosen over the more commonly used evaporative light scattering detector (ELSD), as it offers higher sensitivity, wider dynamic range, and more consistent response factors [41]. The HPLC method was developed to rapidly resolve TAGs from other major lipid classes to allow for total TAG quantification, as shown in Fig. 4a. Moderately polar lipids, such as free fatty acids, phospholipids, and chlorophylls eluted early in the chromatogram between 1 and 5 min, while TAGs eluted

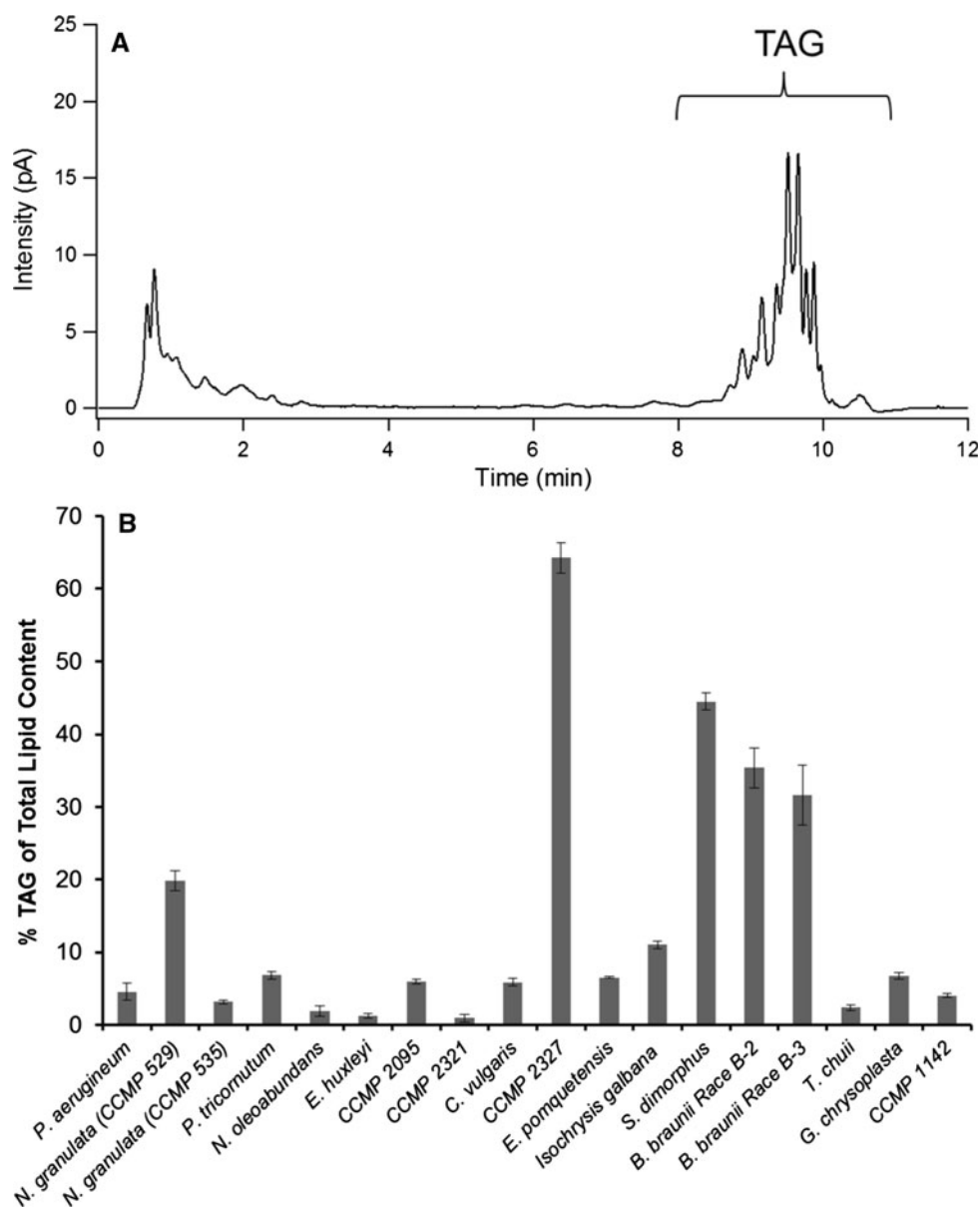
Fig. 3 Comparison of gravimetric crude lipid content to FAME yield for microalgal biomass. Methods to determine yield of FAME include Soxhlet extraction followed by transesterification (TE), in situ transesterification (ISTE) and in situ transesterification of residual biomass from Soxhlet extraction (R-ISTE). Bars represent mean values with error plotted as range ($n = 2$) except where otherwise indicated. Single asterisks (*) represent triplicates, and double asterisks (**) indicate $n = 4$. In these cases, the error is plotted as the standard deviation of the mean. Values are standardized to AFDW



between 8 and 12 min. TAGs were eluted over a narrow region of the chromatogram to minimize variation in response caused by the gradient [32]. Quantification of TAGs was achieved by summing the total peak area of the TAG region of the chromatogram and calibrating with triolein (C18:1), previously demonstrated as an effective calibrant for a wide range of TAGs [32]. Shown in Fig. 4b are the TAG levels measured across

the 18 algal strains, calculated as the percentage of the total lipid content measured gravimetrically. As anticipated, TAG content varied between species, ranging from roughly 1% of lipid content for CCMP 2321 and *E. huxleyi* to as high as 64% for the Antarctic marine bacillariophyte CCMP 2327. Furthermore, the strains with low TAG content exhibited high levels of the moderately polar lipids in the chromatograms, while those with high

Fig. 4 a HPLC-CAD chromatogram of the Antarctic marine bacillariophyte CCMP 2337 and **b** comparison of TAG content across the 18 algal strains, calculated as the percentage of the total lipid content measured gravimetrically using HPLC-CAD with triolein (C18:1) for calibration



TAG levels yielded proportionally lower levels of the polar lipid classes.

Effect of Extractions on Recovery of Individual Fatty Acids

Table 2 shows that for all species tested, the sum of FAME from re-extraction of the residual biomass (R-ISTE) and Soxhlet extraction (TE) closely approximated the values for the initial in situ procedure (ISTE), indicating that individual fatty acids were recovered effectively from residual biomass by the R-ISTE procedure. Table 2 also compares the amount of major fatty acids (>2% by weight) extracted with different procedures, standardized to original ash-free dry weight. For *B. braunii*-3 (Table 2), Soxhlet

solvent extraction was selective in its effect, with C16:0/C18:3n3 being preferentially extracted with respect to other fatty acids. The marine chlorophyte CCMP 1142 showed a slight extraction bias for some fatty acids (e.g. C16:0 vs. C17:1), but *T. chuii* did not follow a similar trend—all fatty acids were extracted with similar effectiveness.

Effect of Soxhlet Re-Extraction of Residual Biomass on the Extraction of Fatty Acids

In order to test whether or not the lower yield of fatty acids with Soxhlet extraction was due to non-optimized extraction conditions, pre-extracted ('defatted') biomass was subjected to an additional Soxhlet extraction step. Figure 5

Table 2 Extraction of specific fatty acids of using different techniques for three microalgal species

		mg FA/g AFDW				
Fatty acid	TE	R-ISTE	ISTE	Sum of R-ISTE and TE	% Sum represented by R-ISTE	
a		<i>Botryococcus braunii</i> Race B				
	*	*	*			
C16:0	7.5 ± 0.0	3.9 ± 0.1	11.1 ± 0.1	11.3	34	
C18:1n9	68.8 ± 0.5	193.9 ± 4.8	275.2 ± 3.3	262.7	74	
C18:3n3	12.9 ± 0.0	5.8 ± 0.1	18.7 ± 0.1	18.6	31	
C28:1	4.2 ± 0.0	21.9 ± 0.6	28.1 ± 0.4	26.1	84	
C28:2	5.1 ± 0.0	29.7 ± 0.6	37.5 ± 0.3	34.8	85	
Total FA	98.4 ± 0.6	255.1 ± 6.0	370.5 ± 4.1	353.5	72	
b		<i>Tetraselmis chuii</i>				
	*	*	†			
C16:0	8.9 ± 0.1	7.8 ± 0.2	18.4 ± 0.4	16.7	46	
C18:1n9	3.3 ± 0.0	2.9 ± 0.1	6.8 ± 0.2	6.1	47	
C18:1n7	1.7 ± 0.0	1.4 ± 0.0	3.4 ± 0.1	3.1	46	
C18:2n6c	2.7 ± 0.0	2.4 ± 0.1	5.7 ± 0.1	5.1	46	
C18:3n3	7.7 ± 0.1	6.7 ± 0.2	16.1 ± 0.4	14.3	47	
C18:4n3	7.6 ± 0.1	6.7 ± 0.2	16.1 ± 0.4	14.3	47	
C20:5n3	3.2 ± 0.1	2.8 ± 0.1	6.8 ± 0.2	6.0	47	
Total FA	35.0 ± 0.5	30.6 ± 0.8	73.3 ± 1.7	65.7	47	
c		CCMP 1142				
	*	*	†			
C16:0	6.2 ± 0.0	28.4 ± 2.8	34.1 ± 0.3	34.6	82	
C17:1	0.6 ± 0.0	5.0 ± 0.5	6.1 ± 0.1	5.6	90	
C18:1n9	5.5 ± 0.1	30.1 ± 2.9	36.1 ± 0.4	35.6	85	
C18:1n7	1.5 ± 0.0	7.6 ± 0.7	9.2 ± 0.1	9.2	83	
C18:2n6c	3.9 ± 0.1	28.9 ± 2.9	34.8 ± 0.2	32.7	88	
C18:3n3	2.9 ± 0.2	26.8 ± 2.6	32.4 ± 0.4	29.7	90	
C18:4n3	0.7 ± 0.1	7.8 ± 0.7	9.6 ± 0.3	8.5	92	
C20:1n9	0.6 ± 0.0	3.4 ± 0.3	4.0 ± 0.0	4.0	85	
C22:6n3	0.8 ± 0.1	5.8 ± 0.5	6.7 ± 0.2	6.6	88	
Total FA	22.6 ± 0.4	143.9 ± 13.8	173.1 ± 2.0	166.5	86	

Values given as averages with ranges* ($n = 2$) or averages with standard deviation† ($n = 3$). Only individual FA comprising >2% of the area of total integrated peaks were used for this comparison. The values in column four are derived as indicated by the title. The percentages in column five are calculated as follows: $[R-ISTE / (R-ISTE + TE)] \times 100\%$
 TE 2-step transesterification (solvent extraction followed by acidic transesterification), R-ISTE 1-step transesterification of residual biomass from Soxhlet solvent extraction, ISTE 1-step extraction-transesterification, FA fatty acid, AFDW ash-free dry weight

shows that while additional extractions increased the FAME recovery in all species (TE-2), residual biomass from the second extraction still contained FAME recoverable by the ISTE method (R-ISTE-2). These results indicated that low fatty acid yields obtained in the initial Soxhlet extractions (TE) could not have been significantly improved by doubling the extraction time.

The Effect of Acid Hydrolysis on Soxhlet Extraction of Fatty Acids

A major difference between Soxhlet extraction and the ISTE procedure is the absence of an acidic catalyst with Soxhlet extraction. To test the importance of an acidic reagent for complete extraction of fatty acids, biomass was

treated with an acid hydrolysis step prior to Soxhlet extraction and the results for four biomass samples are shown in Fig. 6. Acid treatment increased FAME yields in all strains tested, and in the case of *B. braunii*, fatty acid content with acid hydrolysis pre-treatment (TE-AH) closely matched ISTE values, in contrast to untreated biomass where there was a large discrepancy (Fig. 3b).

Discussion

This paper investigated the effectiveness of using automated Soxhlet extraction to assess biodiesel potential of microalgal biomass. Soxhlet solvent extraction is a commonly used lipid extraction technique, and has the potential

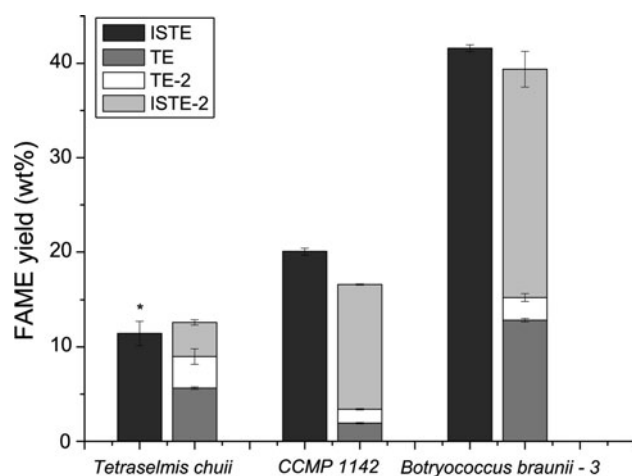


Fig. 5 The effect of increased extraction steps on FAME yield for three species. Values obtained from in situ transesterification (ISTE) are plotted against the sum of transesterification of solvent-extracted lipid (TE), the subsequent re-extraction of ‘defatted’ biomass and transesterification (TE-2), and the in situ transesterification of the resultant biomass (ISTE-2). Bars represent mean values with error plotted as range ($n = 2$) except where otherwise indicated. Single asterisks (*) represent triplicates, and in these cases, error is plotted as standard deviation of the mean. Values are standardized to AFDW

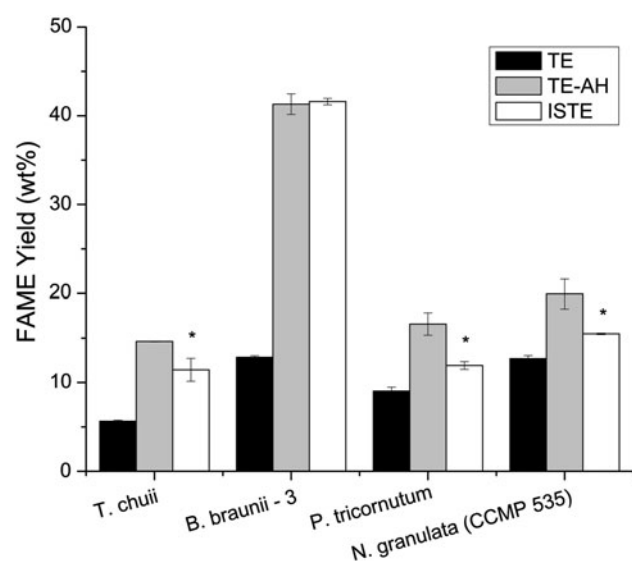


Fig. 6 The effect of acid hydrolysis on FAME content of biomass. Solvent-extracted and transesterified lipid (TE) was compared to an identical extraction with acid hydrolysis pre-treatment (TE-AH) and in situ transesterification (ISTE). Bars represent mean values with error plotted as range ($n = 2$) except where otherwise indicated. Single asterisks (*) represent triplicates, and in these cases, error is plotted as standard deviation of the mean. Values are standardized to AFDW

to be automated for high sample throughput. However, initial data generated in this lab from Soxhlet extraction of microalgal biomass showed that the choice of solvent had a large effect on gravimetric lipid content (Fig. 2), which

was anticipated and agrees with data from previous investigations [22]. For example, in the case of biomass from *Nannochloropsis granulata* (Fig. 2, CCMP 529) hexane extracted ~3% lipid, while ethanol and chloroform/methanol (2:1) extracted >25% lipid on a dry weight basis.

Based on these higher yields with polar solvents, and observation of significant pigmentation in polar solvent extracts, it was hypothesized that polar solvents are able to extract additional polar lipids, as well as a significant quantity of non-esterifiable matter [37]. Any non-saponifiable lipid co-extracted with fatty acid-containing lipid will invalidate the use of gravimetric determinations from Soxhlet systems to estimate total fatty acid content.

In order to assess whether or not this was the case for several species, 18 samples of microalgal biomass were processed by Soxhlet extraction with chloroform/methanol (2:1), and subsequently transesterified with methanol to quantify FAME (Fig. 3). In the “Results” section, the terms “FAME yield/FAME content” are used interchangeably as a proxy for total fatty acid content of biomass as determined by transesterification. Chloroform/methanol (2:1) was chosen for all analyses because of its ability to liberate polar and non-polar lipids, as well as its wide application as a standard lipid extraction solvent in methods such as Folch and Bligh and Dyer.

In situ transesterification was used as a comparative method to assess the efficacy of Soxhlet extraction based on previous reports indicating that ISTE is more effective than standard solvent extraction methods at liberating fatty acids from biomass [21], as well as experiments in our lab that revealed the identical phenomenon. Initial experiments with *B. braunii* biomass showed a discrepancy in the yield of FAMES between the TE and ISTE methods, with TE giving considerably lower yields. Based on this data, residual biomass from Soxhlet extractions was analyzed with the ISTE method (R-ISTE) to attempt to explain this difference. These data, summarized in Fig. 3, show that ISTE yielded comparable or higher values than extraction–transesterification in all but one case (*C. vulgaris*). While it appears that Soxhlet extraction was effective at liberating all fatty acid-containing lipid for the majority of species tested (Fig. 3a), ISTE was reliable even in cases where the Soxhlet system did not extract all saponifiable lipid, showing a similar result to a recent investigation [21] which compared ISTE to the lipid extraction techniques of Folch, Bligh and Dyer, and Smedes and Askland.

A key finding of this study is that gravimetric yields were not a reliable estimate of total fatty acid content. While this result is not unexpected, we were able to show that the magnitude of this difference was highly variable between samples. Data presented in Fig. 3a, b shows that in most cases gravimetric lipid content does not correlate well

with total fatty acid content, with gravimetric lipid content being several-fold greater in many cases (Fig. 3a, b), and in certain samples (Fig. 3b) actually underestimating total fatty acid content of the biomass due to incomplete Soxhlet extractions. Thus, Soxhlet methods used alone can significantly overestimate or underestimate the potential of specific microalgal strains for biodiesel production, resulting in projected values several times larger than those determined by quantification of FAME. In addition, variations in the percent of FAME in gravimetric extracts between samples (Fig. 3a, b), precludes the use of gravimetric values as an estimate of fatty acid content across diverse strains.

The technique of ISTE proved to be a useful tool that did not share this weakness, and data on individual fatty acids extracted (Table 2) show that re-extraction of residual biomass (R-ISTE) accounted for the balance of individual fatty acids. This confirms that the ISTE procedure is extracting the balance of FAME that were not liberated by Soxhlet extraction rather than extracting additional lipid. Interestingly, values for polyunsaturated fatty acids corresponded well between the two treatments, indicating minimal oxidative damage from Soxhlet extraction, despite exposing extracted lipids to a drying step at 105 °C for 1 h without protection from oxygen.

By comparing the ratio of fatty acids extracted in the TE and R-ISTE treatments to the total for these two treatments, it could be determined that for *B. braunii* (Table 2), Soxhlet extraction was selective in its effect, with C16:0/C18:3n3 being preferentially extracted with respect to other fatty acids, indicating that certain FAME-convertible lipids are more ‘recalcitrant’, notably C28:1, C28:2 and C18:1n9. Data from CCMP 1142 and *T. chuii* did not follow a similar trend (Table 2)—all fatty acids were extracted with identical effectiveness. It should be noted that the results obtained from the *B. braunii* analysis indicate that either technique used in isolation (TE, ISTE) will produce a different FA profile. This argues for caution when interpreting fatty acid data for microalgae, as the extraction technique chosen may bias the profile obtained [22].

In order to test the possibility that the lower FAME yields from TE were due to inadequate and therefore incomplete Soxhlet extractions, residual biomass from ‘recalcitrant’ strains was subjected to an additional, identical solvent extraction treatment, followed by TE of the lipid generated (TE-2) and ISTE of the resulting residual biomass (R-ISTE-2). The results (Fig. 5) show that this additional treatment did not extract all of the remaining fatty acids, indicating that manipulating Soxhlet extraction conditions will not likely result in the maximum yield of fatty acids in this case. It should be noted that these ‘recalcitrant’ fatty acids in *B. braunii* have been shown to

be present at high abundance as C28:1/C18:1/C18:1 and C28:2/C18:1/C18:1 TAGs by previous liquid chromatography-mass spectrometry (LC-MS) studies [33]. These TAG may be difficult to extract due to their large molecular weight, though further analysis of intact TAG would be required to confirm this. Alternatively, *B. braunii* is known to produce degradation-resistant biopolymers that include the identified C28:1/C28:2 fatty acids [26], which may also explain this phenomenon.

In order to understand why ISTE was able to extract total fatty acids more effectively, several experiments were conducted. The use of an identical solvent matrix as the ISTE procedure with the Soxhlet system did not result in an increase in total FA content (data not shown), so it was hypothesized that the acidic nature of the transesterification catalyst was responsible for this pattern. Acidic treatments have been demonstrated to increase the extraction of fatty acids from microalgae [11], presumably due to the hydrolytic release of lipid from other macromolecules as in conventional acid extraction [5].

To demonstrate that acidic treatment was necessary for maximal FAME yields in certain samples, an acid-hydrolysis pre-treatment step was employed for four species (Fig. 6). There was a clear effect of acid hydrolysis, with total fatty acid yield being increased in all cases, although TE-AH approximated the ISTE procedure only in the case of *B. braunii*. This is likely due to the cumbersome nature of this procedure—the extracted lipid from this procedure is not easily re-solubilized in the extraction solvent, and sample loss during boiling steps is possible. In addition, a disadvantage of this procedure is that it yields a gravimetric lipid percentage that is in some cases up to twice that from non-hydrolyzed biomass (data not shown). In the case of *Botryococcus braunii*, this resulted in yields of >70% lipid, which is unlikely to accurately reflect ‘oil’ or biofuel potential, unless other hydrocarbons known to accumulate in *B. braunii* under certain conditions [35, 36] are present in large quantities (not measured in this study).

In addition to offering more rigorous extraction conditions, acidic catalysts have the additional advantage of being able to transesterify all classes of saponifiable lipids [8], which will undoubtedly include compounds other than neutral lipids, such as phospholipids and sphingolipids. In this manner, this technique will likely give an upper limit for the maximum amount of biodiesel that can be produced from microalgal biomass, neither underestimating (Fig. 3b) nor overestimating in the case of crude lipid determinations (Fig. 3a, [13, 34]).

While ISTE analysis is a useful tool, it gives no information on lipid class, a critical consideration for biodiesel where TAG is the preferred feedstock. Thus, while ISTE can give information about esterifiable lipid content, one cannot determine the original source of the FAME. We

therefore decided to use HPLC-CAD to quantify TAG and polar lipids as a percentage of the gravimetric extract. For several samples, the overestimations of fatty acid content by gravimetric yields inversely correlate with TAG levels as measured by HPLC. For instance, *E. huxleyi* exhibited the largest discrepancy between gravimetric lipid content and FAME content (Fig. 3a), while TAG levels were measured at just greater than 1% of overall lipid content (Fig. 4b). In contrast, the Antarctic marine bacillariophyte CCMP 2337, *Scenedesmus dimorphus* and *B. braunii* Race B-2, which showed the smallest discrepancies between gravimetric lipid content and FAME content by ISTE, yielded the highest relative TAG contents of the lipid extract at 64, 45, and 35%, respectively (Fig. 4b). On the other hand, the samples CCMP 2321 and *T. chuii* which also showed a low discrepancy between ISTE and gravimetric yield, had very low TAG content (<5%, Fig. 4b), showing that while the extract had a high fraction of esterifiable matter, TAG was not the main source of the FAME detected. For samples CCMP 1142 and *B. braunii* Race B-3, Soxhlet extraction did not effectively extract total esterifiable lipid, so comparisons could not be confidently made.

Most of the remaining extracts examined that showed larger discrepancies between gravimetric lipid yield and FAME yield by ISTE had correspondingly lower TAG content, with the exception of *N. granulata* CCMP 529 which showed 20% TAG content of the lipid extract. Therefore, the presence of various moderately polar lipid classes and other co-extracted compounds that do not generate FAME upon esterification contribute significantly to the overestimations of gravimetric yields for total fatty acid content. Also, these data show that higher FAME content derived from ISTE does not necessarily suggest TAG accumulation (e.g. CCMP 2321, Figs. 3a, 4b).

In this investigation, the majority of microalgal strains analyzed do not contain greater than ~15% esterifiable lipid with low TAG content, a yield that is likely to decline in an industrial-scale extraction scenario. It is important to point out however, that with the exception of the single N-limited *Botryococcus braunii* culture (Fig. 3b, *B. braunii* Race B-2), and the *I. galbana* chemostat culture (Fig. 3a), none of the microalgae used in this study were cultivated under conditions designed to induce lipid accumulation. Under conditions of nutrient stress, many species of microalgae respond by accumulating lipid, particularly TAG, in storage bodies, presumably as a mechanism to dissipate excess energy capture and/or as a readily available source of energy to mobilize when favorable conditions return [19, 25]. The comparatively low FAME yields presented here may be due to the cultivation conditions employed, which were designed to maximize growth rate and biomass productivity, rather than lipid content.

This investigation has confirmed the potential of strains such as *B. braunii* for biodiesel production, but has also shown that under conditions of fast growth, other purportedly oleaginous strains have low FAME yields, suggesting minimal triacylglycerol accumulation. Lipid content values obtained from hexane extractions strongly suggested minimum neutral lipid content, a conclusion supported by LC-MS analysis [33]. In the future, our lab will be following the lead of other investigators [15, 42] to directly quantify TAG accumulation to support these analyses.

This study confirms the main advantages for using ISTE which include increased precision and accuracy, reduced time and labor costs, elimination of time-consuming pretreatment [27] and easy applicability for routine screening of new microbial isolates [4]. In this lab, replicable FAME data from small scale algal physiological experiments is routinely generated from biomass samples of ~1 mg, something not easily achievable to the authors' knowledge with two-step extraction–transesterification procedures. In addition, the previously mentioned strategies for increasing algal lipid productivity are poorly understood from a physiological perspective [25], and ISTE will be useful in determining whether or not increases in neutral lipid content represent an increase of the total cellular lipid content, rather than a reallocation of FA from one pool to another [16].

Results obtained here argue for caution in projecting oil productivities of microalgal culture using solely gravimetric analyses. The crude lipid values obtained in this study correspond well with the values cited by Chisti [7] for the 'oil content' of selected species of microalgae, including many of the species studied in this paper. Such gravimetric data might lead an inexperienced analyst to conclude a strain has a high potential for biodiesel production, despite the fact that gravimetric data alone cannot give an accurate measure of biodiesel potential.

While Soxhlet extraction of microalgae does not yield crude lipid values useful for judging biodiesel potential, it appears that it is an effective method for extracting total lipids for class analysis, based on the similar FAME yields between TE and ISTE procedures for 12/18 samples investigated here. Based on this data, we suggest the use of quick and accurate GC-FAME analyses such as ISTE, combined with lipid class analysis by GC-TAG or HPLC-CAD to generate an accurate value for 'biodiesel potential' of microalgae. When standardized to daily productivity [20], this offers a robust technique to evaluate microalgal strains for the production of biodiesel.

Acknowledgments Many people contributed to this project, either by providing biomass or assisting with lipid analysis. We would like to thank (in alphabetical order): Mather Carscallen, Katie Dickinson,

Laura Garrison, Jenny MacPherson, Scott MacQuarrie, Ron Melanson, Stephen O'Leary, Kyoung Park and Crystal Whitney. This work was funded by the National Bioproducts Program in Microalgal Biofuels. This is NRC Publication No. 54055.

References

- Andersen RA, Jacobson DM, Sexton JP (1991) Provasoli-Guillard center for culture of marine phytoplankton, catalog of strains. Provasoli-Guillard Center for Culture of Marine Phytoplankton, West Boothbay Harbor
- Banerjee A, Sharma R, Chisti Y, Banerjee UC (2002) *Botryococcus braunii*: a renewable source of hydrocarbons and other chemicals. *Crit Rev Biotechnol* 22:245–279
- Bligh EG, Dyer WJ (1959) A rapid method of total lipid extraction and purification. *Can J Biochem Physiol* 37:911–917
- Burja A, Radianingtyas H, Windust A, Barrow C (2006) Isolation and characterization of polyunsaturated fatty acid producing *Thraustochytrium* species: screening of strains and optimization of omega-3 production. *Appl Microbiol Biotechnol* 72:1161–1169. doi:10.1007/s00253-006-0419-1
- Carrapiso AI, García C (2000) Development in lipid analysis: some new extraction techniques and in situ transesterification. *Lipids* 35:1167–1177. doi:10.1007/s11745-000-0633-8
- Chen W, Zhang C, Song L, Sommerfeld M, Hu Q (2009) A high throughput Nile red method for quantitative measurement of neutral lipids in microalgae. *J Microbiol Methods* 77:41–47
- Chisti Y (2007) Biodiesel from microalgae. *Biotechnol Adv* 25:294–306. doi:10.1016/j.biotechadv.2007.02.001
- Christie WW (1989) Gas chromatography and lipids: a practical guide. Dundee, The Oily Press
- Christie WW (1993) Advances in lipid methodology—two. The Oily Press, Dundee
- Craigie JS, Armstrong SM, Staples LS, Bauder AG (2003) Photobioreactor. United States patent application publication. US 2003/0059932 A1
- Dubinsky Z, Aaronson S (1979) Increase of lipid yields from some algae by acid extraction. *Phytochem* 18:51–52. doi:10.1016/S0031-9422(00)90914-2
- Ehimen EA, Sun ZF, Carrington CG (2010) Variables affecting the in situ transesterification of microalgae lipids. *Fuel* 89:677–684. doi:10.1016/j.fuel.2009.10.011
- Eller FJ, King JW (1998) Supercritical CO₂ extraction of fat: comparison of gravimetric and GC-FAME methods. *J Agric Food Chem* 46:3657–3661. doi:10.1021/jf980236a
- Folch J, Lees M, Sloane-Stanley GH, others (1957) A simple method for the isolation and purification of total lipids from animal tissues. *J Biol Chem* 226:497–509
- Gardner R, Peters P, Peyton B, Cooksey KE (2010) Medium pH and nitrate concentration effects on accumulation of triacylglycerol in two members of the Chlorophyta. *J Appl Phycol* 1–12. doi:10.1007/s10811-010-9633-4
- Gordillo FJL, Goutx M, Figueroa FL, Niell FX (1998) Effects of light intensity, CO₂ and nitrogen supply on lipid class composition of *Dunaliella viridis*. *J Appl Phycol* 10:135–144
- Gouveia L, Oliveira A (2009) Microalgae as a raw material for biofuels production. *J Ind Microbiol Biotechnol* 36:269–274. doi:10.1007/s10295-008-0495-6
- Gouveia L, Marques AE, da Silva TL, Reis A (2009) *Neochloris oleoabundans* UTEX #1185: a suitable renewable lipid source for biofuel production. *J Ind Microbiol Biotechnol* 36:821–826. doi:10.1007/s10295-009-0559-2
- Greenwell HC, Laurens LML, Shields RJ, Lovitt RW, Flynn KJ (2009) Placing microalgae on the biofuels priority list: a review of the technological challenges. *J R Soc Interface* 7:703–726. doi:10.1098/rsif.2009.0322
- Griffiths MJ, Harrison STL (2009) Lipid productivity as a key characteristic for choosing algal species for biodiesel production. *J Appl Phycol* 21:493–507. doi:10.1007/s10811-008-9392-7
- Griffiths MJ, Hille RP, Harrison STL (2010) Selection of direct transesterification as the preferred method for assay of fatty acid content of microalgae. *Lipids* 45:1053–1060. doi:10.1007/s11745-010-3468-2
- Guckert JB, Cooksey KE, Jackson LL (1988) Lipid solvent systems are not equivalent for analysis of lipid classes in the microeukaryotic green alga, *Chlorella*. *J Microbiol Methods* 8:139–149. doi:10.1016/0167-7012(88)90015-2
- Guillard RRL, Hargraves PE (1993) *Stichochrysis immobilis* is a diatom, not a chrysophyte. *Phycologia* 32:234–236
- Guillard RRL, Ryther JH (1962) Studies of marine planktonic diatoms. I. *Cyclotella nana* Hustedt and *Detonula confervacea* Cleve. *Can J Microbiol* 8:229–239
- Hu Q, Sommerfeld M, Jarvis E, Ghirardi M, Posewitz M, Seibert M, Darzins A (2008) Microalgal triacylglycerols as feedstocks for biofuel production: perspectives and advances. *Plant J* 54:621–639
- Laureillard J, Largeau C, Waeghemaeker F, Casadevall E (1986) Biosynthesis of the resistant polymer in the alga *Botryococcus braunii*. Studies on the possible direct precursors. *J Nat Prod* 49:794–799
- Lee J-Y, Yoo C, Jun S-Y, Ahn C-Y, Oh H-M (2010) Comparison of several methods for effective lipid extraction from microalgae. *Bioresour Technol* 101:S75–S77. doi:10.1016/j.biortech.2009.03.058
- Lepage G, Roy CC (1986) Direct transesterification of all classes of lipids in a one-step reaction. *J Lipid Res* 27:114
- Lewis T, Nichols PD, McMeekin TA (2000) Evaluation of extraction methods for recovery of fatty acids from lipid-producing microheterotrophs. *J Microbiol Methods* 43:107–116. doi:10.1016/S0167-7012(00)00217-7
- Li X, Xu H, Wu Q (2007) Large-scale biodiesel production from microalga *Chlorella protothecoides* through heterotrophic cultivation in bioreactors. *Biotechnol Bioeng* 98:764–771. doi:10.1002/bit.21489
- Liang Y, Sarkany N, Cui Y (2009) Biomass and lipid productivities of *Chlorella vulgaris* under autotrophic, heterotrophic and mixotrophic growth conditions. *Biotechnol Lett* 31:1043–1049. doi:10.1007/s10529-009-9975-7
- Lisa M, Lynen F, Holcapek M, Sandra P (2007) Quantitation of triacylglycerols from plant oils using charged aerosol detection with gradient compensation. *J Chromatogr A* 1176(1–2):135–142
- MacDougall KM, McNichol J, McGinn PJ, O'Leary SJB, Melanson JE (2011) Triacylglycerol profiling of microalgae strains for biofuel feedstock by liquid chromatography—high resolution mass spectrometry. *Anal Bioanal Chem* 401(8):2609–2616. doi:10.1007/s00216-011-5376-6
- Matsunaga T, Matsumoto M, Maeda Y, Sugiyama H, Sato R, Tanaka T (2009) Characterization of marine microalga, *Scenedesmus* sp. strain JPCC GA0024 toward biofuel production. *Biotechnol Lett* 31:1367–1372. doi:10.1007/s10529-009-0029-y
- Metzger P (1994) Phenolic ether lipids with an n-alkenylresorcinol moiety from a Bolivian strain of *Botryococcus braunii* (A race). *Phytochem* 36:195–212. doi:10.1016/S0031-9422(00)97038-9
- Metzger P, Largeau C (2004) *Botryococcus braunii*: a rich source for hydrocarbons and related ether lipids. *Appl Microbiol Biotechnol* 66:486–496. doi:10.1007/s00253-004-1779-z
- Palmquist DL, Jenkins TC (2003) Challenges with fats and fatty acid methods. *J Anim Sci* 81:3250–3254
- Provasoli L, Pintner IJ (1959) Artificial media for fresh-water algae: problems and suggestions. In: Tryon CA Jr, Hartmann RT

- (eds) The ecology of algae. Spec. Pub. No. 2, Pymatuning Laboratory of Field Biology. University of Pittsburgh, Pittsburgh, pp 84–96
39. Pruvost J, Van Vooren G, Cogne G, Legrand J (2009) Investigation of biomass and lipids production with *Neochloris oleoabundans* in photobioreactor. *Bioresour Technol* 100:5988–5995
 40. Tran H-L, Hong S-J, Lee C-G (2009) Evaluation of extraction methods for recovery of fatty acids from *Botryococcus braunii* LB 572 and *Synechocystis* sp. PCC 6803. *Biotechnol Bioprocess Eng* 14:187–192. doi:[10.1007/s12257-008-0171-8](https://doi.org/10.1007/s12257-008-0171-8)
 41. Vehovec T, Obreza A (2010) Review of operating principle and applications of the charged aerosol detector. *J Chromatogr A* 1217(10):1549–1556
 42. Wahlen BD, Willis RM, Seefeldt LC (2011) Biodiesel production by simultaneous extraction and conversion of total lipids from microalgae, cyanobacteria, and wild mixed-cultures. *Bioresour Technol* 102:2724–2730. doi:[10.1016/j.biortech.2010.11.026](https://doi.org/10.1016/j.biortech.2010.11.026)
 43. Woyewoda AD, Shaw SJ, Ke PJ, Burns BG (1986) Recommended laboratory methods for assessment of fish quality. Canadian Tech Report of Fisheries and Aquatic Sciences No. 1448, Fisheries and Oceans Canada ISSN 0706-6473

Quantitation of Multiple Sphingolipid Classes Using Normal and Reversed-Phase LC–ESI–MS/MS: Comparative Profiling of Two Cell Lines

M. Athar Masood · Raghavendra P. Rao ·
Jairaj K. Acharya · Josip Blonder ·
Timothy D. Veenstra

Received: 14 September 2011 / Accepted: 4 November 2011 / Published online: 29 November 2011
© AOCS (outside the USA) 2011

Abstract Sphingolipids are an important class of compounds that regulate signal transduction and other vital cellular processes. Herein, we report sensitive normal and reversed phase LC–MS/MS methods for quantitation of multiple sphingolipid classes. In the normal-phase ESI/MS/MS method, a high content of organic solvents was utilized, which, although it included hexane, ethyl acetate, acetonitrile containing 2% methanol, 1–2% acetic acid, and 5 mM ammonium acetate, resulted in a very efficient electrospray ionization of the ceramides (Cers) and hexosylceramides (MHCers). Three normal-phase LC–MS/MS methods using segmented phases were developed to specifically target Cers, MHCers, or sphingomyelins (SMs). This segmentation scheme increases the number of data points acquired for a given analyte and enhances the sensitivity and specificity of the measurements. Nine separate reversed phase chromatography methods were developed for the three classes of compounds. These assays were used for comparing the levels of Cers, SMs, and MHCers from mouse embryonic fibroblast (pMEF) and human embryonic kidney (HEK293) cells. These findings were then compared with the reported data from RAW264.7 mouse macrophage cells, BHK21 hamster cells, and human plasma and serum samples. The analysis of cell lines, using both normal and reversed phase chromatography, revealed discrimination based on the type of

chromatography chosen, while sphingolipid assays of samples containing different amounts of protein showed different results, even after normalizing for protein content. Also, LC/MS/MS profiles were provided for the classes and individual compounds so that they could be used as “molecular profiles” for class or individual sample analysis.

Keywords Ceramides · Hexosylceramides · Sphingomyelins · Normal-phase and reversed-phase LC–MS/MS · Quantitation · Mouse embryonic fibroblast · Human embryonic kidney cells

Abbreviations

Cers	Ceramides
MHCers	Hexosylceramides or monohexosylceramides
SMs	Sphingomyelins
LC–MS/MS	Liquid chromatography–tandem mass spectrometry
Rt	Retention time
MA and AA	Manually and automatic integrated areas
MRM	Multiple reaction monitoring
d-saturated	The sphingoid base core without any double bonds
d-unsaturated	Sphingoid base core containing double bonds
Notation d18:1 ^{Δ4} c16:0	A dihydroxy 18 carbon sphingoid base core structure with a double bond on the fourth carbon atom starting from the hydroxyl terminus of the core chain, and the c16:0 represents the number of carbon atoms linked to the amino side chain

M. A. Masood (✉) · J. Blonder · T. D. Veenstra
Laboratory of Proteomics and Analytical Technologies,
SAIC-Frederick, Inc., National Cancer Institute at Frederick,
Frederick, MD 21702-1201, USA
e-mail: masoodaa@mail.nih.gov

R. P. Rao · J. K. Acharya
Laboratory of Cell and Developmental Signaling,
National Cancer Institute at Frederick, Frederick,
MD 21702-1201, USA

Introduction

Sphingolipids, such as ceramides (Cers), hexosylceramides (MHCers), and sphingomyelins (SMs), are an important class of compounds that play vital roles in cell architecture and function [1, 2]. They are highly conserved and are involved in a number of metabolic functions and signal transduction cascades [3–9]. Abnormalities in these compounds are associated with a variety of human diseases, including inborn errors of metabolism, diabetes, atherosclerosis, arrhythmias, myocardial infarction, Alzheimer's, and other neurodegenerative diseases [4, 10–24]. Importantly, certain types of human malignancies, including breast, prostate, colon, ovary, and endometrium cancers, exhibit high levels of fatty acid synthase expression and activity, implicating a role for these compounds in the biology of cancer [25–29]. Considering their role in diseases, these Cers, MHCers, and SMs may represent reasonable biomarkers for providing diagnostic or prognostic information [17, 21, 30–33]. For example, sphingolipids can be potentially used as biomarkers for Alzheimer's disease or other neurodegenerative disorders, disease progression, and therapeutic intervention [30].

Owing to their chemical diversity, no single analytical method is sufficient for studying all the analytes of each of the sub-classes/classes of the lipids. Liquid chromatography–tandem mass spectrometry (LC–MS/MS) methods for sphingolipid analysis, utilizing both electrospray (ESI) and atmospheric pressure chemical ionization (APCI) [34–44], have been reported. It is well established that each class of sphingolipids (i.e., Cers, SMs, and MHCers; the representative compounds with their product ions are shown in Fig. 1), does not separate into individual components by normal-phase chromatography. Instead, all components from a distinct class (e.g., Cers) will move as a single head-group when normal phase chromatography is used. In reversed-phase chromatography, however, each group of compounds (e.g., Cers) tends to separate into individual components [34–39].

Herein we report specific normal-phase and reversed-phase LC–MS/MS methods, where the individual component of analytes from each class of sphingolipids is found to exhibit high sensitivity and good individual peak separations. The sensitivity and specificity of these assays were enhanced because in each method only a few analyte transitions were incorporated that allowed sufficient time to collect more data points on each analyte, and all individual components of analytes exhibited good selectivity. For analysis of analytes by normal-phase ESI/MS utilizing non-polar solvents such as hexane, the organic phase is mixed with 5% isopropanol and ≥ 50 mM buffer salt [43, 44]. In the present context of normal phase chromatography, a high content of organic solvents that includes hexane, ethyl acetate, acetonitrile containing 2%

methanol, 1% acetic acid, and 5 mM ammonium acetate was utilized, yet this method resulted in a very efficient electrospray ionization of the ceramides and hexosylceramides. For normal phase assay, three MS/MS methods were developed, and each of these methods was segmented to include only specifically targeted analytes from each sphingolipid class according to their chromatographic retention times. These three methods were sufficient to incorporate the entire range of analytes from the Cers, SMs, and MHCers. Due to the wider chromatographic selectivity of reversed-phase chromatography, a total of nine methods, three for each individual class of compounds, was developed. Subsequently, these optimized analytical methods were applied to quantitate and compare cellular sphingolipid contents from mouse embryonic fibroblasts (pMEF) and human embryonic kidney (HEK293) cells. We also show the evidence of quantitative discrimination related to the type of chromatography used, and the amount of protein present in compared samples.

Experimental Section

Materials

The following were purchased from Avanti Polar Lipids, Inc., Alabaster, AL. *N*-arachidonoyl-*D*-erythro-sphingosine (Cer d18:1^{Δ4} c20:0); *N*-nervonoyl-*D*-erythro-sphingosine (Cer d18:1^{Δ4} c24:1), *N*-palmitoyl-*D*-erythro-sphingosylphosphorylcholine (SM d18:1^{Δ4} c16:0); *N*-stearoyl-*D*-erythro-sphingosylphosphorylcholine (SM d18:1^{Δ4} c18:0); and LM 6002 internal standard, which is a 25- μ M mixture of 10 different sphingolipids; Sphingosine (C17:1 base); Sphinganine (C17:0 base); Sphingosine-1-PO₄ (C17:1 base); Sphinganine-1-PO₄ (C17:0 base); Lactosyl(β) C12 Ceramide; 12:0 Sphingomyelin; Glucosyl(β) C12 Ceramide; 12:0 Ceramide; 12:0 Ceramide-1-PO₄; and 25:0 Ceramide. Reagents and all HPLC-grade solvents were purchased from either Fisher Scientific (Pittsburgh, PA) or Sigma-Aldrich (St. Louis, MO). The HEK293 cell line was obtained from the American Type Culture Collection (ATCC; [#CRL-10892]), designation 293 C18.

HEK293 Cell Growth and Lysis

HEK293 cells were grown in suspension, using serum-free medium. After harvesting, the cells were washed three times in PBS buffer and the cell pellets were stored at -80 °C. To obtain the lysate, cells were resuspended in 50 mM NH₄HCO₃ (pH 7.9), placed in a Dounce homogenizer, and homogenized by 10 gentle strokes. The supernatant was collected after centrifugation at low speed (500 \times g) for 15 min, and assayed for protein content using a BCA assay.

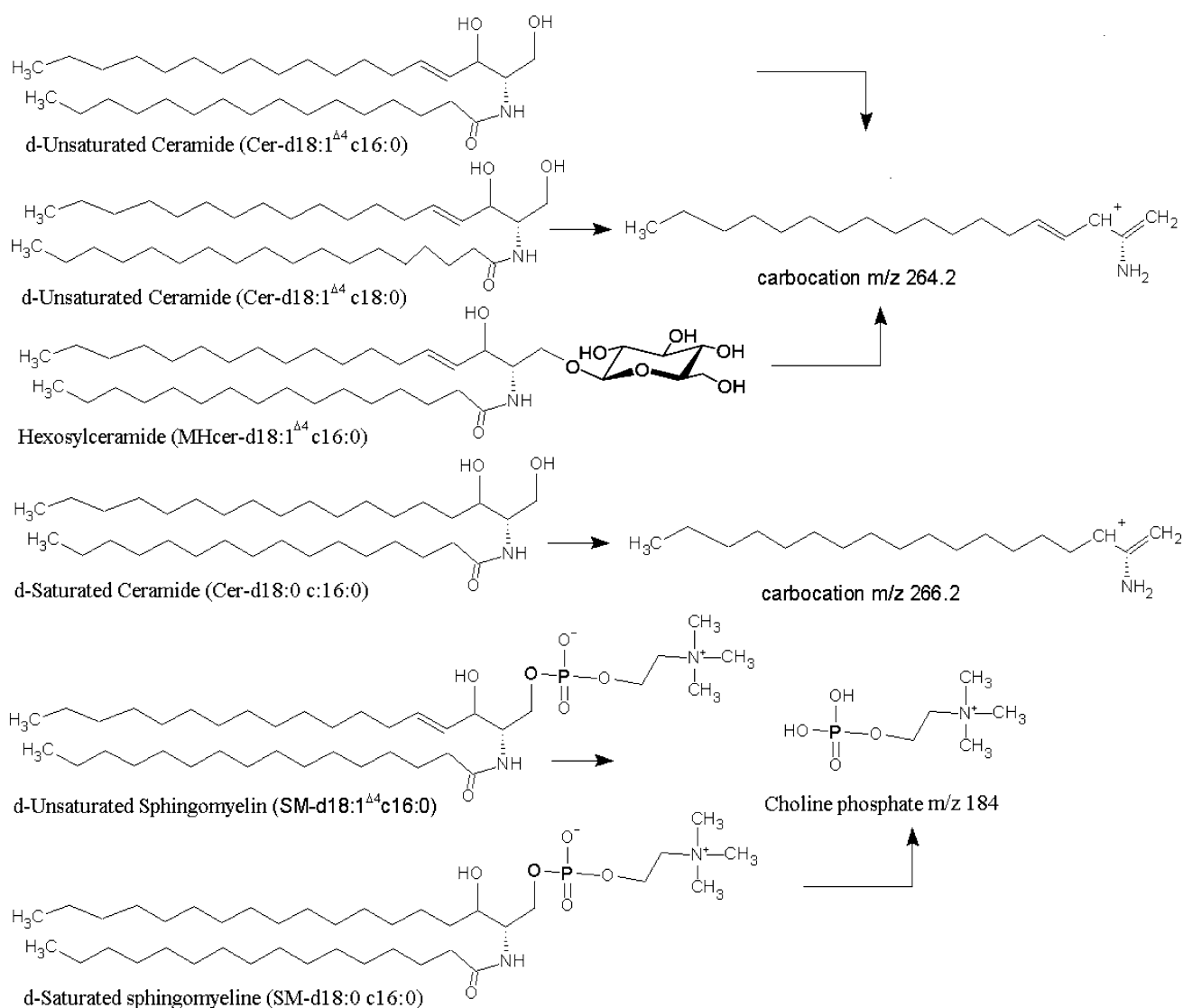


Fig. 1 Structures for some of the representative ceramides, hexosylceramides, and sphingomyelins and their associated specific product ions that were monitored. A core chain for a sphingoid base can be saturated or unsaturated and contains a 2-amino-1,3-dihydroxy moiety, and a notation d18:1^{Δ4}; for example, a dihydroxy 18 carbon core chain with a double bond on the fourth carbon atom starting from

the hydroxyl terminus of the core chain. The notation c18:0 is for the number of carbon atoms on the *N*-acyl side chain. All d18:1^{Δ4} and d18:0 ceramides, hexosylceramides, and sphingomyelins can form specific carbocation product ion fragments of *m/z* 264 and 266, respectively. Sphingomyelins will form a highly sensitive product ion choline phosphate of *m/z* 184

Isolation of Primary Mouse Embryonic Fibroblasts (pMEF)

The cells were isolated from pregnant mice as follows. E 10.5 dpc (day post-coitum) embryos were separated from the yolk sac, washed twice with PBS buffer (pH 7.2), and trypsinized for 10 min. The cells were disaggregated by pipetting several times and suspended in 1 mL of pre-warmed (37 °C) DMEM supplemented with 10% FBS. The suspension was allowed to stand for 2–3 min at room temperature, and the visible clumps were removed. The suspension was centrifuged at 500×*g* for 3 min, and the

cell pellet was collected, resuspended in MEF media (DMEM + 10% FBS), and plated on a 6-well plate. The plates were incubated at 37 °C with 3% O₂ and 5% CO₂ [45]. The medium was replaced the next day, and the cells cultured for 4–5 days. Forty-eight hours before extracting the lipids, the cells were shifted to serum-free DMEM medium. Total cell lysate was prepared by homogenizing the cells by applying 20 strokes using a Dounce homogenizer and homogenization buffer (50 mM tris, pH 7.4, 1 mM EDTA, 50 mM NaCl). Cell debris was removed using low-speed centrifugation (500×*g* for 15 min) and the sample assayed for protein content using BCA assay.

Preparation of Sphingolipid Extracts

Lipid extracts were prepared according to the method described by Merrill et al. [37–39]. In brief, to 50 μL of pMEF cell extract containing ~ 250 μg of protein, or 1×10^7 of HEK293 cell lysate taken in a 4-mL Teflon-capped glass vial (Fisher scientific, cat # W 224582) were added 0.5 mL of methanol (CH_3OH), 0.250 mL of chloroform (CHCl_3), 50 μL of water (H_2O), and 30 μL of 25 μM solution of LM-6002, providing 750 pmol of each of its individual constituent internal standards. The lipid aggregates were dispersed by sonicating 6 times, using a Branson tip sonicator at an amplitude setting of 21% for 10 s each, with a resting interval of 5 s between pulses. The samples were further sonicated for 1 h, using a bench top sonicator, and incubated overnight at 48 $^\circ\text{C}$ with shaking. After cooling the sample to ambient temperature, 75 μL of 1 M methanolic potassium hydroxide (KOH) was added, followed by incubation at 37 $^\circ\text{C}$ for 2 h with shaking to hydrolyze glycerophospholipids. The sample solution was divided into two equal aliquots. One aliquot was neutralized by the addition of 7 μL of glacial acetic acid (CH_3COOH) and 2 mL of water. The mixture was extracted twice, using two 1.2-mL volumes of CHCl_3 . The lower organic portions were collected, combined, and evaporated to dryness using a Savant Speed Vac Concentrator (GMI, Ramsey, MN). The dried sample was re-suspended in 300–400 μL of 1:3 (v/v) CHCl_3 and normal-phase A (5 mM $\text{CH}_3\text{COONH}_4$ dissolved in 20 mL CH_3OH , 15 mL CH_3COOH , 270 mL CH_3CN , 300 mL $\text{CH}_3\text{COOCH}_2\text{CH}_3$, and 400 mL hexanes). The other half of the sample was evaporated to approximately 25 μL , using a Speed Vac Concentrator, and reconstituted by adding 300–400 μL of 1:1 (v/v) reversed mobile phase A (74/25/1 [v/v/v] $\text{H}_2\text{O}:\text{CH}_3\text{OH}:\text{HCOOH}$ containing a final concentration of 5 mM HCOONH_4) and reversed mobile phase B (99:1 [v/v] $\text{CH}_3\text{OH}:\text{HCOOH}$ containing a final concentration of 5 mM HCOONH_4). The sample was vortexed for 1 min, followed by centrifugation at 13,200 $\times g$ (Eppendorf Centrifuge 5415 D) for 2 min, and the supernatant was transferred to a fresh Eppendorf tube.

Liquid Chromatography–Tandem Mass Spectrometry

Liquid chromatography–tandem mass spectrometry (LC–MS/MS) analysis was performed using a TSQ Discovery triple quadrupole mass spectrometer (Thermo Electron Corp., San Jose, CA, USA) equipped with an electrospray ionization (ESI) source. The mass spectrometer was coupled to an Agilent 1100 series HPLC system fitted with a 100- μL /min max flow controller and a 40- μL sample injection loop.

Normal-phase chromatography was performed using a binary system and a 7.5 cm \times 3.0 mm \times 3 μm Supelcosil

LC-NH₂ column operating at a flow rate of 100 $\mu\text{L}/\text{min}$ and maintained at 37 $^\circ\text{C}$. Initially, a high flow rate method was tried using this column; however, at the slow flow rate of 100 $\mu\text{L}/\text{min}$, good optimal results were observed. The mobile phase buffer A consisted of 5 mM $\text{CH}_3\text{COONH}_4$ dissolved in 20 mL CH_3OH , 10 mL CH_3COOH , 270 mL CH_3CN , 300 mL $\text{CH}_3\text{COOCH}_2\text{CH}_3$, and 400 mL hexanes. Mobile phase buffer B consisted of 5 mM $\text{CH}_3\text{COONH}_4$ in 99:1 (v/v) $\text{CH}_3\text{OH}:\text{CH}_3\text{COOH}$. Approximately 10 μL of sample was injected onto the column and the following gradient conditions were applied: 0% B was held for 5 min, increased to 18% mobile phase B over 1.5 min and held there for 2.5 min; increased to 65% B over 0.5 min and held there for 3.5 min; increased to 98% B over 5 min and held there for 3.5 min; and decreased to 0% B over 0.5 min. The column was re-equilibrated for 8 min prior to the next injection.

Reversed-phase chromatography was performed using a 5 cm \times 1 mm i. d. \times 5 μm Discovery C18 column (Supelco, Bellefonte, PA), operating at a flow rate of 100 $\mu\text{L}/\text{min}$ and maintained at 37 $^\circ\text{C}$. Mobile phase A consisted of 5 mM HCOONH_4 in 74/25/1 (v/v/v) $\text{H}_2\text{O}:\text{CH}_3\text{OH}:\text{HCOOH}$, while mobile phase B consisted of 5 mM HCOONH_4 in 99:1 (v/v) $\text{CH}_3\text{OH}:\text{HCOOH}$. For each LC–MS/MS experiment, ca. 10 μL of sample was injected onto the column and was fractionated using the following gradient conditions: 10% B was held for 4 min; increased to 95% B over 3 min and held there for 4 min; increased to 99% B buffer over 6 min and held there for 6 min; decreased to 10% B over 0.5 min. The column was re-equilibrated for 6.5 min prior to the next injection. Both normal-phase and reversed-phase chromatography were performed in main-pass flow in a normal mode on a 40- μL injection volume and without any post-time column flow.

The ESI source conditions were optimized at a LC flow rate of 100 $\mu\text{L}/\text{min}$, using a mixture of LM 6002, brain porcine, and other Cer and SMs, including Cer d18:1 $^{\Delta 4}$ c12:0, Cer d18:1 $^{\Delta 4}$ c18:1, Cer d18:1 $^{\Delta 4}$ c18:0, Cer d18:1 $^{\Delta 4}$ c20:0, Cer d18:1 $^{\Delta 4}$ c24:1, Cer d18:1 $^{\Delta 4}$ c24:0, SM d18:1 $^{\Delta 4}$ c12:0, SM d18:1 $^{\Delta 4}$ c16:0, and SM d18:1 $^{\Delta 4}$ c18:0. The optimized source parameters were as follows: ionization mode, positive; sheath gas pressure, 7 psi; auxiliary gas pressure, 3 (arbitrary units); electrospray needle voltage, 4,500 V; capillary temperature, 300 $^\circ\text{C}$; skimmer offset, –5 V. No in-source fragmentation was observed when the reference compounds were analyzed using direct infusion with skimmer offset values of –7 and less. However, at higher skimmer offset values of 15, ceramides seemed to undergo some water loss to form $[\text{M}+\text{H}-\text{H}_2\text{O}]^+$ ions.

Collision energies between 23 and 31 V provided optimal fragmentation of $[\text{M}+\text{H}]^+$ ions to product ions at m/z 264.2 and 266.2, corresponding to doubly dehydrated product ion fragments for unsaturated and saturated d18:1 $^{\Delta 4}$ or d18:0 sphingoid base backbones, respectively, from Cer

and MHCer, and m/z 184.1, corresponding to the choline phosphate moiety of sphingomyelin. Collision-induced dissociation was performed using nitrogen gas within Q2, which was offset from Q1 by 10 V. Prior to running SRM experiments, precursor ion scans were performed for m/z 184, 264, and 266 to detect choline containing analytes or sphingolipid constituents with d18:1 or d18:0 sphingolipid base backbone. For experiments conducted using normal-phase chromatography, a total of three single-reaction monitoring (SRM) methods were constructed, each partitioned into 5 segments. Between six and eight analyte transitions from a specific sphingolipid class, along with the corresponding internal standard, were included in each segment to maximize the number of data points and attain maximum sensitivity. The first (3 min) and fifth segments (6 min) of each method contain fictional analyte transitions. In the second segment (3 min), transitions targeting Cer were included, while the third (10.5 min) and fourth segments (7.5 min) contain transitions to measure MHCers and

SMS, respectively. Because no analytes were monitored in the fifth segment, a dummy transition was incorporated in this segment. For reversed-phase chromatography experiments, three individual SRM methods comprised of three segments were constructed for each class of compounds; therefore, for three classes of compounds Cers, MHCers, and SMS, nine individual methods were constructed as analytes from each sub-class, spanning a much wider zone. The first and the last segments, spanning 6 and 3 min, respectively, contain the fictional transition, as no analytes were eluted during these time spans, while the second segment (21 min) contains 6–7 analytes and their internal standard transitions.

The acquisition parameters common to all analytes were: scan width (m/z) 0.10; scan time, 0.20 s for each transition; peak width (FWHM) 0.70 for both Q1 and Q3; collision pressure 1.5 mTorr; and skimmer offset at -5 V. Other acquisition parameters and chromatographic retention times are listed in Tables 1, 2, and 3. Data acquisition

Table 1 Retention times and compound-specific SRM parameters for ceramides (Cer), hexosylceramides (MHCer), and sphingomyelins (SM) transitions that are included in the 2nd, 3rd, and 4th segments of the five-segmented normal-phase HPLC–ESI–MS/MS method 1

Analyte	Segment duration (min)	Precursor $[M+H]^+$ → product ion (m/z)	Retention time		Collision energy (V)	Tube lens (V)
			NP (min)	RP (min)		
Segment 1	3.00 (To waste)	999.00 → 950.00 (dummy transition)				
Cer in Segment 2	3.00					
Cer d18:1 ^{Δ4} c12:0 (ISTD)		482.43 → 264.14	4.45	13.75	23	64
Cer d18:1 ^{Δ4} c16:0		538.62 → 264.16	4.36	16.64	24	65
Cer d18:0 c16:0		540.67 → 266.16	4.34	17.22	25	67
Cer d18:1 ^{Δ4} c18:1		564.52 → 264.16	4.32	13.23	24	69
Cer d18:1 ^{Δ4} c18:0		566.52 → 264.17	4.30	18.30	26	74
Cer d18:0 c18:0		568.63 → 266.16	NO	18.81	26	73
MHCer in Segment 3	10.50					
MHCer d18:1 ^{Δ4} c12:0 (ISTD)		644.51 → 264.08	11.36	13.18	29	74
MHCer d18:1 ^{Δ4} c16:0		700.54 → 264.11	9.96	16.46	28	73
MHCer d18:0 c16:0		702.50 → 266.11	NO	17.08	28	73
MHCer d18:1 ^{Δ4} c18:0		728.51 → 264.09	9.38	18.15	29	72
MHCer d18:0 c18:0		730.51 → 266.11	NO	NO	29	71
MHCer d18:1 ^{Δ4} c20:0		756.52 → 264.10	8.94	19.81	29	70
MHCer d18:0 c20		758.53 → 266.12	NO	NO	29	73
SM in Segment 4	7.50					
SM d18:1 ^{Δ4} c12:0 (ISTD)		647.49 → 184.01	17.76	13.51	23	79
SM d18:1 ^{Δ4} c16:0		703.58 → 184.01	17.59	16.41	27	57
SM d18:0 c16:0		705.56 → 183.97	17.26	17.09	37	71
SM d18:1 ^{Δ4} c18:0		731.58 → 183.95	17.52	18.07	31	73
SM d18:0 c18:0		733.59 → 183.95	17.19	18.81	26	53
SM d18:1 ^{Δ4} c20:0		759.61 → 183.91	17.44	19.79	27	72
SM d18:0 c20:0		761.62 → 183.98	NO	20.50	28	71
Segment 5	6.00	999.00 → 950.00 (dummy transition)				

Table 2 Retention times and compound-specific SRM parameters for ceramides (Cer), hexosylceramides (MHCer), and sphingomyelins (SM) transitions that are included in the 2nd, 3rd, and 4th segments of the five-segmented normal-phase HPLC–ESI–MS/MS method 2

Analyte	Segment Duration (min)	Precursor [M+H] ⁺ → product ion (m/z)	Retention time		Collision energy (V)	Tube lens (V)
			NP (min)	RP (min)		
Segment 1	3.00 (To waste)	999.00 → 950.00 (dummy transition)				
Cer in Segment 2	3.00					
Cer d18:1 ^{Δ4} c12:0 (ISTD)		482.43 → 264.14	4.45	13.76	23	64
Cer d18:1 ^{Δ4} c20:0		594.55 → 264.16	4.25	20.02	24	74
Cer d18:0 c20:0		596.64 → 266.19	NI	20.67	25	75
Cer d18:1 ^{Δ4} c22:0		622.71 → 264.17	4.21	21.88	26	73
Cer d18:0 c22:0		624.61 → 266.18	NI	22.63	27	74
Cer d18:1 ^{Δ4} c24:1		648.59 → 264.19	4.19	21.92	28	71
MHCer in Segment 3	10.50					
MHCer d18:1 ^{Δ4} c12:0 (ISTD)		644.51 → 264.08	11.36	13.48	29	74
MHCer d18:1 ^{Δ4} c22:0		784.53 → 264.12	8.49	21.07	29	68
MHCer d18:0 c22:0		786.59 → 266.11	NO	21.85	29	70
MHCer d18:1 ^{Δ4} c24:1		810.59 → 264.12	8.45	21.11	29	73
MHCer d18:0 c24:1		812.64 → 266.11	8.12	NO	29	75
MHCer d18:1 ^{Δ4} c24:0		812.65 → 264.11	8.35	23.05	29	72
SM in Segment 4	7.50					
SM d18:1 ^{Δ4} c12:0 (ISTD)		647.49 → 184.01	17.76	13.38	23	79
SM d18:1 ^{Δ4} c22:0		787.64 → 184.01	17.38	21.43	26	72
SM d18:0 c22:0		789.65 → 183.97	16.85	22.34	27	71
SM d18:1 ^{Δ4} c23:0*		801.65 → 183.92	17.33	22.48	27	73
SM d18:1 ^{Δ4} c24:1		813.66 → 183.95	17.34	21.48	28	75
SM d18:1 ^{Δ4} c24:0 or SM d18:0 c24:1		815.68 → 183.98	17.29	23.58	28	74
SM d18:0 c24:0		817.68 → 184.07	16.28	24.76	29	73
Segment 5	6.00	999.00 → 950.00 (dummy transition)				

and analysis were accomplished using Xcalibur software v.2.0.5 (Thermo Electron Corp.). Quantitation data was not corrected for the double bond differences since the degree of unsaturation is limited, due to the existence of up to only two double bonds. However data was corrected for the carbon number difference between a given molecular species and the selected internal standard (i.e., to include the difference in degrees of freedom due to varying carbon chain lengths, which results in different ionization efficiencies) according to the following formula: $z_1 = (1 + 0.011n + 0.011^2 n(n - 1)/2)/(1 + 0.011s + 0.011^2 s(s - 1)/2)$ [42].

The internal standard LM 6002 was added to each sample at the beginning of sample preparation, and the ratio of peak areas of an analyte versus internal standard was calculated. An advantage of this quantitative technique is that ionization suppression effects of the matrix, and the variation in ionization efficiency between standards and analytes are compensated.

Results and Discussion

Normal-Phase Liquid Chromatography–Tandem Mass Spectrometry

Ceramides, SMs, and MHCers can be resolved and quantitated using normal-phase liquid chromatography, since the separation is based on head group characteristics rather than on the presence of different lengths of fatty-*N*-acyl side chains [46, 47]. Therefore, the components of an individual sphingolipid class elute together when separated by normal-phase liquid chromatography, and a single peak, primarily due to lipophilic (hydrophobic) interaction, is displayed. Thus, all Cers elute with similar retention times, as do MHCers and SMs, etc., which are displayed as single peaks but at different retention times. Accordingly, the quantitative analysis of the head group classes by normal-phase chromatography is not capable of distinguishing the isotopic ¹³C contributions from [M+H+1]⁺ and

Table 3 Retention times and compound-specific SRM parameters for ceramides (Cer), hexosylceramides (MHCer), and sphingomyelins (SM) transitions that are included in the 2nd, 3rd, and 4th segments of the five-segmented normal-phase HPLC–ESI–MS/MS method 3

Analyte	Segment duration (min)	Precursor [M+H] ⁺ → product ion (<i>m/z</i>)	Retention time		Collision energy (V)	Tube lens (V)
			NP (min)	RP (min)		
Segment 1	3.00 (To waste)	999.00 → 950.00 (dummy transition)				
Cer in Segment 2	3.00					
Cer d18:1 ^{Δ4} c12:0 (ISTD)		482.43 → 264.14	4.45	13.80	23	64
Cer d18:1 ^{Δ4} c24:0		650.61 → 264.15	4.16	24.15	28	79
Cer d18:0 c24:1		650.61 → 266.17	NI	22.01	28	73
Cer d18:0 c24:0		652.81 → 266.18	4.17	25.19	28	74
Cer d18:1 ^{Δ4} c26:1		676.83 → 264.18	4.15	24.19	27	75
Cer d18:0 c26:1		678.82 → 266.19	NI	NI	29	75
Cer d18:0 c26:0		680.78 → 266.18	NI	NI	29	78
MHCer in Segment 3	10.50					
MHCer d18:1 ^{Δ4} c12:0 (ISTD)		644.51 → 264.08	11.36	13.25	29	74
MHCer d18:0 c24:0		814.63 → 266.11	8.12	22.96	29	70
MHCer d18:1 ^{Δ4} c26:1		838.63 → 264.12	8.15	22.94	30	73
MHCer d18:0 c26:1		840.64 → 266.11	7.79	NI	30	70
MHCer d18:1 ^{Δ4} c26:0		840.63 → 264.12	NI	25.48	30	69
MHCer d18:0 c26:0		842.63 → 266.11	NI	NI	31	72
SM in Segment 4	7.50					
SM d18:1 ^{Δ4} c12:0 (ISTD)		647.49 → 184.00	17.76	13.46	23	79
SM d18:1 ^{Δ4} c25:1*		827.68 → 184.07	17.37	22.50	29	74
SM d18:0 c25:0		829.68 → 183.94	17.34	24.77	29	75
SM d18:1 ^{Δ4} c26:1		841.69 → 183.93	17.28	23.55	28	77
SM d18:1 ^{Δ4} c26:0 or SM d18:0 c26:1		843.69 → 183.97	17.25	26.18	28	76
SM d18:0 c26:0		845.70 → 184.12	17.35		29	75
Segment 5	6.00	999.00 → 950.00 (dummy transition)				

NP Normal phase; RP reversed phase; NO not observed; NI not identified; V Volts; min minutes; *m/z* mass to charge ratio

[M+H+2]⁺ and other isomeric species, since it does not provide a distinction between the compounds containing an unsaturated (sphingosine) and/or saturated (sphinganine) base structures, as all the components are displayed at a single retention time. The MS/MS mass filters that are used to identify these analytes cannot differentiate between co-eluting compounds with overlapping *m/z* values, unless the transition ions used for SRM are widely different for each analyte that was monitored. Therefore, normal-phase chromatography is typically employed to quantitate total Cers or SMs inclusive of all low- and high-abundant species, rather than individual components of Cers and SMs. In normal-phase chromatography, although all lipid classes are separated, components of the same lipid class elute together; thus, there exists the possibility of inter-molecular interactions from individual components within the lipid class that may lead to some ion suppression. In comparative analysis, when performed, for example, between wild and mutant species, such effects during analysis do cancel each other out.

In the present non-polar LC–MS/MS method presented here, many of the components from each class of compounds (e.g., MHCer d18:1^{Δ4}c16:0 [retention time, 9.96 min, Fig. 2, panel j], MHCer d18:1^{Δ4}c18:0 [rt: 9.41 min, Fig. 2, panel l], MHCer d18:1^{Δ4}c20:0 [rt: 8.91 min, Fig. 2, panel n] or between cer d18:1^{Δ4}c16:0 [rt: 4.33 min, Fig. 2, panel c] and cer d18:1^{Δ4}c18:0 [rt: 4.30, Fig. 2, panel f]) were well resolved. This method is also capable of differentiating between saturated (sphinganine-containing) and unsaturated (sphingosine-containing) isomorphous components that differ only by two hydrogen atoms (e.g., SM d18:1^{Δ4}c18:0 [rt: 17.52 min, Fig. 2, panel t], and SM d18:0 c18:0 [rt: 17.16 min, Fig. 2, panel u]). The present method exhibits picogram-level sensitivity for each lipid class.

Three SRM–MS assays that rely on normal-phase separation to analyze Cers, SMs, and MHCers from mammalian cells, as described in the Experimental Section, were developed. Using these methods, as shown in Figs. 2, 3, and 4 and Tables 1, 2, and 3, Cers appear at retention times between 4.1 and 4.5 min, while MHCers and SMs

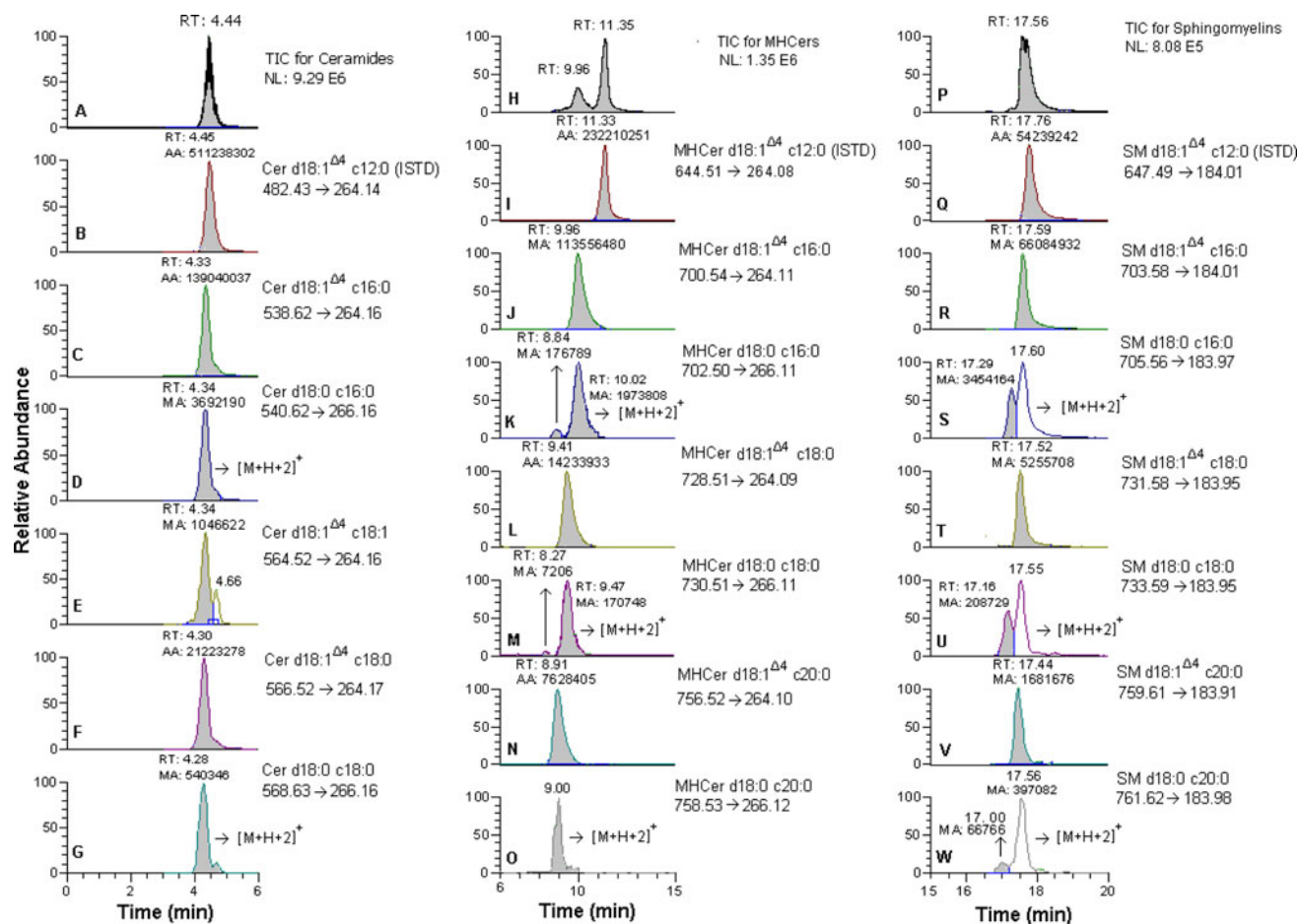


Fig. 2 Extracted ion chromatogram from SRM scans of precursor \rightarrow double-dehydrated carbocation product fragment for the ceramides (transitions from molecular ions of 482–568), hexosylceramides (transitions from molecular ions of 644–758), and sphingomyelins

(transitions from molecular ions of 644–758), including the respective internal standards by method 1 of the normal-phase liquid chromatography–tandem mass spectrometry

elute over wider retention time ranges, (7.7–11.5 and 16.2–17.8 min, respectively). Compounds containing the sphingoid base backbone that differ by two hydrogen atoms, but contain equivalent numbers of all other atoms, are fully resolved for MHCers and reasonably well to partially resolved for SMs by using this method. A few trends are clearly discernable within the data. As the number of methylene groups within the Cers, MHCers, and SMs increase, the retention times decrease. For example, Cer d18:1 Δ^4 c16:0 appears at a retention time of 4.33 min (Fig. 2, panel C), while Cer d18:1 Δ^4 c18:0 appears at a retention time of 4.30 min (Fig. 2, panel f). Compounds with unsaturated sphingoid base backbones and their saturated counterparts containing the same number of non-hydrogen atoms but differing by only two hydrogen atoms, always appear as pairs, with the saturated compound eluting first. For example, SM d18:1 Δ^4 c22:0 (Fig. 3, panel Q) and SM d18:0 c22:0 (Fig. 3, panel r) appears at a retention time of 17.38 and 16.85 min, respectively. For compounds with an equivalent number of non-hydrogen

atoms, the saturated compound elutes fastest, followed by the one in which the double bond is present on the sphingoid base backbone. When double bonds are present both on the sphingoid base and the fatty-*N*-acyl moiety, then such a compound elutes last. This is illustrated in the example for the following series of compounds with 18 carbon atoms on the sphingoid chain and 24 carbon atoms in the *N*-acyl fatty acid side chain, where the order of elution is: d18:0 c24:0 < d18:1 Δ^4 c24:0 < d18:0 c24:1 < d18:1 Δ^4 c24:1. Finally, the retention times shown for compounds possessing an unsaturation in both their sphingoid base backbone and side chain are similar to the compound that contains the same sphingoid base backbone but with two fewer methylene groups and does not possess any unsaturation in its *N*-acyl side chain. For example, the retention time exhibited for MHCer d18:1 Δ^4 c24:1 (Rt: 8.45 min, Fig. 3, panel l) is similar to that of MHCer d18:1 Δ^4 c22:0 (Rt: 8.49 min, Fig. 3, panel j), or SM d18:1 Δ^4 c24:1 (Rt: 17.34 min, Fig. 3, panel t) is similar to that of SM d18:1 Δ^4 c22:0 (Rt: 17.38 min, Fig. 3, panel q).

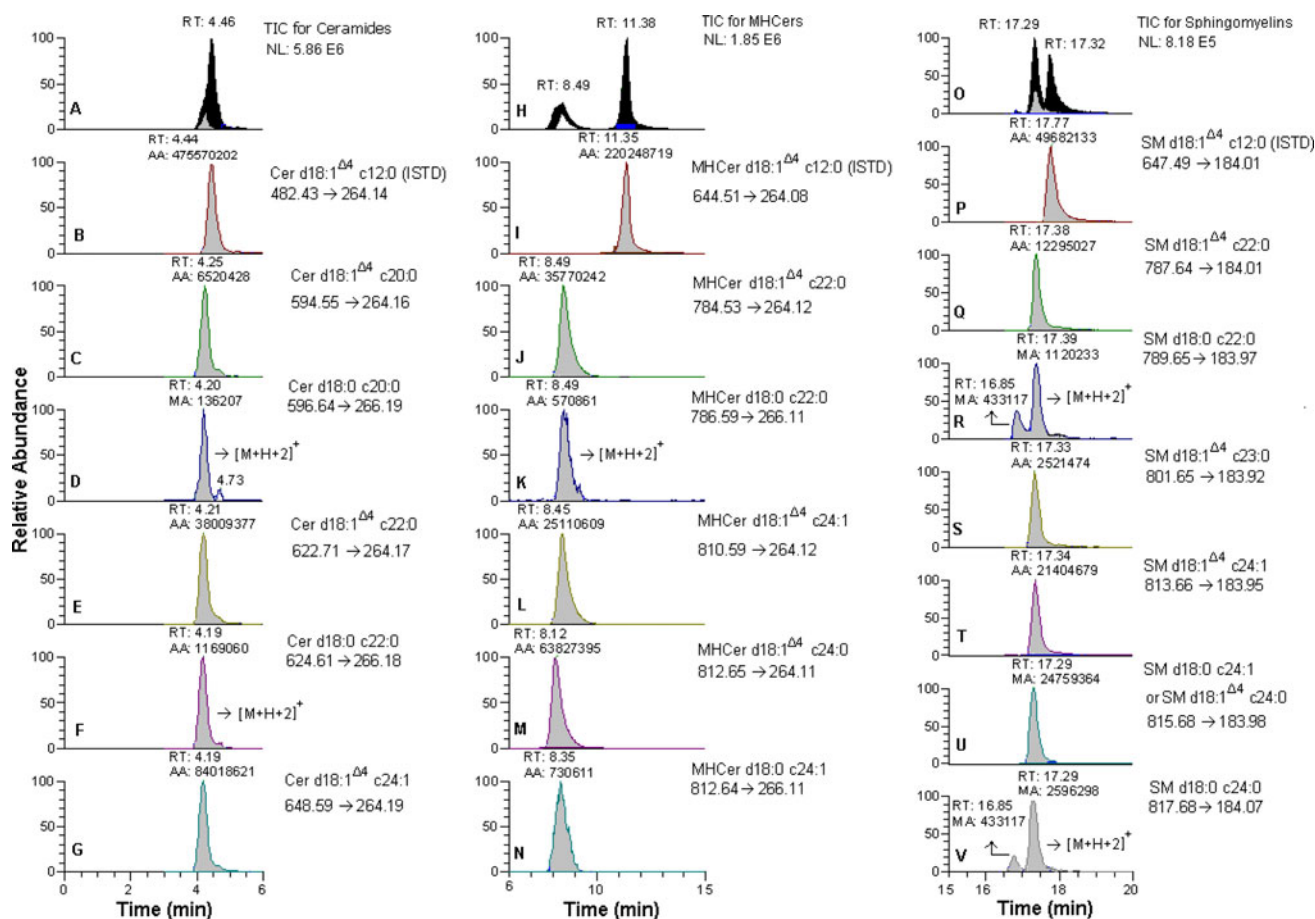


Fig. 3 Extracted ion chromatogram from SRM scans of precursor \rightarrow double-dehydrated carbocation product fragment for the ceramides (transitions from molecular ions of 594–648), hexosylceramides (transitions from molecular weight of 784–812), and sphingomyelins

(transitions from molecular ions of 787–817), including the respective internal standards by method 2 of the normal-phase liquid chromatography–tandem mass spectrometry

Sphingolipid analysis of RAW264.7 cells using normal-phase LC–MS/MS has been reported previously by Shaner et al. [35]; however, individual analytes from each sphingolipid class were not chromatographically resolved. In their study, ceramides and hexosylceramides eluted as single peaks, as did SMs and lactosylceramides. If the components from each class of analytes are not resolved, there will be considerable overlap of not only the compounds with the same nominal masses such as isomeric and isobaric species, but also, due to the $[M+H+1]^+$ and $[M+H+2]^+$ carbon ^{13}C isotopic contributions from 2 Da lower sphingoid core unsaturated compounds to a 2 Da higher sphingoid base saturated molecular species. This problem is compounded when the unsaturated analogue is more abundant than its corresponding saturated sphingoid base analogue. Theoretically, the isotopic contribution from $[M+H+1]^+$ and $[M+H+2]^+$ can be calculated based on the number and kind of atoms present or the intensity of the peak observed, and for the $[M+H+2]^+$, should be in the theoretical range ca. 6–10%, depending upon the number of

atoms present; in addition, the double ^{13}C isotope must be contained in both the precursor and product ion. In the present experiments, the isotopic contributions to the saturated sphingoid base dihydro species due to $[M+H+2]^+$ from the corresponding sphingoid base dehydro species (e.g., un-saturated d-18 sphingoid base with product ion of m/z 264.2), are found to be 6–10% of the amount of the unsaturated species, even if for example m/z 266.2 of the saturated d-18 sphingoid base product ion transition is monitored by SRM. Thus, the dehydro species almost always seems to exhibit a lingering (residual) small d-saturated product ion transition coming from the sphingoid base skeleton, similar to that arising from the dihydro species, or could as well be due to some isobaric contribution. Hence, unless the d-unsaturated and d-saturated analogues are chromatographically resolved, or if the retention times for both species are the same, the existence of the dihydro-saturated species can only be considered if the peak area of the saturated dihydro compound is more than 5–10% of the corresponding dehydro-unsaturated species.

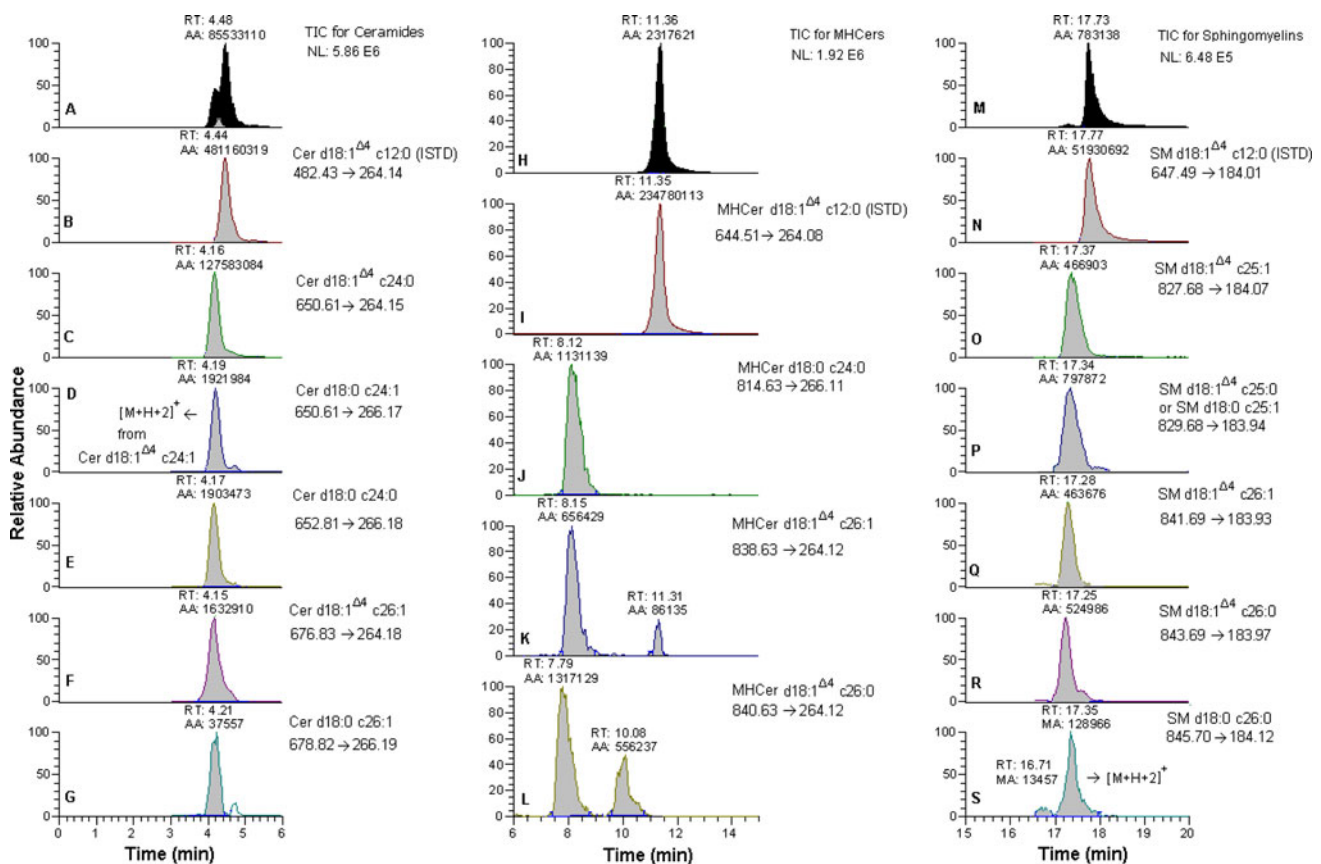


Fig. 4 Extracted ion chromatogram from SRM scans of precursor \rightarrow double-dehydrated carbocation product fragment for the ceramides (transitions from molecular ions of 650–679), hexosylceramides (transitions from molecular weight of 814–840), and spingomyelins

(transitions from molecular ions of 827–845), including the respective internal standards by method 3 of the normal-phase liquid chromatography–tandem mass spectrometry

The LC–MS/MS data for sphingolipids obtained from the analysis of HEK293 and MEF cells are presented in Tables 4 and 5, respectively. Table 4 presents the data obtained using normal-phase chromatography to analyze the HEK293E cells, while Table 5 provides comparative data obtained by both normal-phase and reversed-phase chromatography to analyze MEF cells. The quantitative data indicates that the ceramide levels in HEK293E cell present are ca. 10 nmol, while the levels for MHCers and SMs are <50 nmol each. Therefore, the fatty acid contribution from these sphingolipid classes is <200 nmol in this cell analysis.

Comparative Sphingolipid Measurements

Normal-phase LC–MS/MS methods were developed to quantify and compare the levels of SMs, Cers, and M in HEK293 and MEF cells (Tables 4, 5). In both cell types, d18:1 Δ^4 c16:0 represents ~45–55% of the total amount of SM, followed by d18:1 Δ^4 c24:1 (~20%) and d18:1 Δ^4 c24:0 (~17.5 and 10% in HEK293 and MEF cells, respectively). The major Cer present in HEK293 cells is d18:1 Δ^4 c24:0

(~32% of total), followed by d18:1 Δ^4 c16:0 (25%), d18:1 Δ^4 c24:1 (25%), and d18:1 Δ^4 c22:0 (17%). In MEF cells, a similar pattern was observed with d18:1 Δ^4 c16:0, d18:1 Δ^4 c24:1, d18:1 Δ^4 c24:0, and d18:1 Δ^4 c22:0 constituting about 80–90% of the total Cer content.

The measurement of monohexosylceramide, i.e., hexosylceramide (MHCer), levels in HEK293 cells using normal-phase chromatography, shows d18:1 c24:0 as the dominant MHCer (~50% of total), followed by d18:1 Δ^4 c22:0 (~21%), d18:1 Δ^4 c24:1 (~14%), and d18:1 Δ^4 c16:0 (~10%), respectively. In MEFs, d18:1 Δ^4 c16:0 (30%) and d18:1 Δ^4 c24:0 (30%) are the dominant MHCers, followed by d18:1 Δ^4 c24:1 (20%) and d18:1 Δ^4 c22:0 (11%). Overall, the Cer, MHCer, and SM profiles of the two cell types are similar, with the predominant species being the d18:1 Δ^4 c16:0, d18:1 Δ^4 c24:0, d18:1 Δ^4 c24:1, and d18:1 Δ^4 c22:0 molecules. Importantly, the sphingolipids mixture of internal standard containing C17 or C12 bases (LM6002) are unnatural synthetic lipids, and consequently, no endogenous signals of these categories were observed from the cell lines.

In the study by Shaner et al. [35], the most abundant SM in RAW264.7 mouse macrophage cells was d18:1 Δ^4 c16:0,

Table 4 Normal-phase liquid chromatography selected reaction monitoring data obtained for the evaluation of sphingomyelins (SM), ceramides (Cer), and hexosylceramides (MHCer) from HEK293 cells

Analyte	SM			Cer			MHCer		
	Mean \pm SD (pmol/l \times 10 ⁷ cells)	CV (%)	Analyte (%)	Mean \pm SD (pmol/l \times 10 ⁷ cells)	CV (%)	Analyte (%)	Mean \pm SD (pmol/l \times 10 ⁷ cells)	CV (%)	Analyte (%)
d18:1 ^{Δ4} c16:0	14,467.8 \pm 372.1	2.7	44.7	2,220.8 \pm 109.1	4.9	24.6	4,464.1 \pm 102.8	2.3	9.2
d18:0 c16:0	594.6 \pm 17.5	3.1	1.8	NO	–	–	15.2 \pm 0.8	5.2	0.0
d18:1 ^{Δ4} c18:0	2,885.1 \pm 102.4	3.8	8.9	324.3 \pm 16.9	5.2	3.6	772.1 \pm 20.9	2.7	1.6
d18:1 ^{Δ4} c18:1	NO	–	–	20.5 \pm 1.1	5.6	0.1	NO	–	–
d18:0 c18:0	185.5 \pm 5.0	2.9	0.6	NO	–	–	6.6 \pm 0.1	1.6	0.0
d18:1 ^{Δ4} c20:0	505.9 \pm 17.1	3.7	1.6	131.7 \pm 10.1	7.7	1.5	815.2 \pm 32	3.9	1.7
d18:0 c20:0	115.4 \pm 3.4	3.2	0.4	NO	–	–	NO	–	–
d18:1 ^{Δ4} c22:0	2,805.9 \pm 152.7	6.0	8.7	1,053.5 \pm 30.9	2.9	11.7	10,011.5 \pm 283.9	2.8	20.6
d18:0 c22:0	187.7 \pm 10.2	6.1	0.6	NO	–	–	28.6 \pm 0.9	3.1	0.1
d18:1 ^{Δ4} c23:0	50.2 \pm 3.0	6.6	0.2	NO	–	–	NO	–	–
d18:1 ^{Δ4} c24:1	6,445.2 \pm 340.7	5.9	19.9	2,279.2 \pm 42.0	1.8	25.2	6,814.7 \pm 275.5	4.0	14.0
d18:1 c24:0	5,656.5 \pm 257.1	5.1	17.5	2,868.4 \pm 113.9	3.2	31.8	24,291.2 \pm 1,122.6	4.6	49.9
d18:0 c24:0	597.4 \pm 39.0	7.4	1.8	73.0 \pm 5.0	6.8	0.8	NO	–	–
d18:1 ^{Δ4} c26:1	241.1 \pm 23.9	11.5	0.7	51.6 \pm 4.2	8.1	0.6	322.8 \pm 30.4	9.4	0.7
d18:1 ^{Δ4} c26:0	216.8 \pm 19.3	10.3	0.7	4.8 \pm 0.6	12.1	0.1	1,116.5 \pm 97.3	8.7	2.3
d18:0 c26:1	26.9 \pm 1.9	8.2	0.1	NO	–	–	37.8 \pm 3.2	8.4	0.1
Total in the Cells	32,389.6 \pm 1,193.3	3.7		9,027.7 \pm 286.9	3.1		48,696.2 \pm 1,446.3	3.0	

CV is based on triplicate run of samples. *NO* not observed; *NI* not identified

followed by d18:0 c16:0 and d18:1 ^{Δ 4} c24:1. These results are similar to what we observed for HEK293 and MEF cells, except that we found much lower levels of d18:0 c16:0. The levels of Cer d18:1 ^{Δ 4} c24:0, d18:1 ^{Δ 4} c16:0, and d18:1 ^{Δ 4} c24:1 found using our method, are also similar to those reported by Merrill et al. While we and Merrill et al. found that MHCer d18:1 ^{Δ 4} c16:0 was the most abundant MHCer in MEF cells, this lipid was the third most abundant species in HEK293 cells. Previously Koivusalo et al. [47] found only three SMs in the BHK21 hamster cells, SM, d18:1 ^{Δ 4} c16:0 (65% of total sphingolipid content), SM d18:1 ^{Δ 4} c24:1 (20%), and SM d18:1 ^{Δ 4} c24:0 (15%), similar to the top three SMs observed in HEK293 and MEF cells. Other SMs in their studies might not have been observed, perhaps due to the lack of the sensitivity of their assay. Hammad et al. [48] performed the sphingolipidomic analysis of the serum and plasma samples of both healthy human males and females, and these authors reported d18:1 ^{Δ 4} c16:0, and d18:1 ^{Δ 4} c24:1 as the two most abundant sphingomyelins and monohexosylceramides, and d18:1 ^{Δ 4} c24:0, d18:1 ^{Δ 4} c24:1 as the two most abundant ceramide species. Thus, from all these quantitative analyses of different cells and tissues, we can say with some confidence that d18:1 ^{Δ 4} c16:0 and d18:1 ^{Δ 4} c24:1 might be the top sphingomyelin candidates, and Cer d18:1 ^{Δ 4} c24:0, d18:1 ^{Δ 4} c16:0, and d18:1 ^{Δ 4} c24:1 might be the top three ceramide

species present in many types of mammalian cells; and therefore, comparison of these dominant top sphingolipids in healthy and disease cells might provide some insights into the prognosis of health and disease. It should be noted that nerve tissues that are not studied here might have some other Cers and SMs, such as those that contain hydroxyl fatty acids in their chains as the dominating species.

Impact of the Sample Protein Amount on Sphingolipids Quantitation

When different batches of MEF cell samples containing different amounts of protein were collected and processed for NP-LC/MS/MS, the quantitative data was irreproducible, even after normalization based on protein concentration. Initially, it was thought that this discrepancy in data might be due to a subtle variation in the cell preparation and collection technique, and consequently in the sample handling; hence, the samples might have varying matrix type of effects. However, this discrepancy might also be due to the different protein levels that were present in the samples when different amount of samples were taken; and if this is true, then at what range of protein content in the sample will the sample give consistent quantitative estimation of analytes. To test these hypotheses, aliquots of MEF cells containing different amount of proteins

Table 5 Comparative normal-phase and reversed-phase liquid chromatography–tandem mass spectrometric (SRM) data obtained for the evaluation of sphingomyelins (SM), ceramides (Cer), and hexosylceramides (MHCer) from mouse embryonic cells at the 1-mg protein level

Analyte	Normal Phase LC/MS/MS			Reversed Phase LC/MS/MS		
	Mean \pm SD (1 mg Protein Level)	CV (%)	Analyte (%)	Mean \pm SD (1 mg Protein Level)	CV (%)	Analyte (%)
<i>SM</i>						
SM d18:1 ^{Δ4} c16:0	5,732.0 \pm 402.9	7.0	55.1	6,804.4 \pm 245.4	3.6	50.6
SM d18:0 c16:0	208.4 \pm 28.9	13.7	2.0	357.7 \pm 6.7	1.9	2.7
SM d18:1 ^{Δ4} c18:0	534.9 \pm 59.8	11.2	5.1	682.4 \pm 25.1	3.7	5.1
SM d18:0 c18:0	7.0 \pm 0.9	12.4	0.1	14.6 \pm 1.4	9.4	0.1
SM d18:1 ^{Δ4} c20:0	198.2 \pm 13.8	7.0	1.9	230.9 \pm 15.3	6.6	1.7
SM d18:0 c20:0	NI	–	–	5.8 \pm 0.5	8.4	0.1
SM d18:1 ^{Δ4} c22:0	442.0 \pm 37.2	8.4	4.2	618.2 \pm 25.9	4.2	4.6
SM d18:0 c22:0	NI	–	–	12.6 \pm 0.8	6.4	0.1
SM d18:1 ^{Δ4} c23:0	81.8 \pm 4.1	5.0	0.8	111.5 \pm 12.1	10.8	0.8
SM d18:1 ^{Δ4} c24:1	2,166.9 \pm 212.3	9.8	20.8	3,404.2 \pm 156.1	4.6	25.3
SM d18:1 ^{Δ4} c24:0	1,012.9 \pm 102.5	10.1	9.7	1,157.2 \pm 68.8	5.9	8.6
SM d18:1 ^{Δ4} c26:0	19.2 \pm 3.6	14.9	0.2	56.2 \pm 1.8	3.2	0.4
Total in pmol	10,403.3 \pm 705	7.0	–	13,456.6 \pm 402.1	3.0	–
<i>Cer</i>						
d18:1 ^{Δ4} c16:0	62.8 \pm 0.9	1.5	25.3	182.7 \pm 1.6	0.9	48.3
d18:0 c16:0	1.6 \pm 0.1	8	0.6	NI	–	–
d18:1 ^{Δ4} c18:1	1.4 \pm 0.1	6.5	0.6	13.5 \pm 0.8	5.7	3.6
d18:1 ^{Δ4} c18:0	13.5 \pm 0.1	0.5	5.4	20.4 \pm 1.2	5.8	5.4
d18:1 ^{Δ4} c20:0	5.8 \pm 0.11	0.3	2.3	8.5 \pm 0.8	9.6	2.2
d18:1 ^{Δ4} c22:0	26.7 \pm 0.7	2.5	10.7	20.5 \pm 1.3	6.5	5.4
d18:1 ^{Δ4} c24:1	66.2 \pm 0.3	0.5	26.6	68.7 \pm 4.9	6.4	18.2
d18:1 ^{Δ4} c24:0	61.8 \pm 0.9	1.4	25.3	62.1 \pm 4.8	5.1	16.4
d18:1 ^{Δ4} c26:1	7.8 \pm 0.2	2.4	3.1	1.7 \pm 0.1	6.2	0.4
Total in pmol	248.6 \pm 1.4	1.6	–	378.1 \pm 21.8	4.8	–
<i>MHCer</i>						
d18:1 ^{Δ4} c16:0	257.4 \pm 39.9	15.5	30.3	481.2 \pm 5.0	1.0	52.7
d18:0 c16:0	NI	–	–	NI	–	–
d18:1 ^{Δ4} c18:0	39.7 \pm 5.1	12.9	4.7	20.5 \pm 0.4	1.7	2.2
d18:0 c18:0	NI	–	–	NI	–	–
d18:1 ^{Δ4} c20:0	28.0 \pm 3.5	12.5	3.3	16.4 \pm 2.1	12.8	1.8
d18:1 ^{Δ4} c22:0	92.3 \pm 8.6	9.3	10.9	66.6 \pm 7.9	11.9	7.3
d18:0 c22:0	NI	–	–	NI	–	–
d18:1 ^{Δ4} c24:1	165.4 \pm 19.1	11.5	19.5	127.2 \pm 6.4	5.0	13.9
d18:0 c24:1	3.9 \pm 0.5	12.1	0.5	NO	–	–
d18:1 ^{Δ4} c24:0	256.7 \pm 31.3	12.2	30.2	197.2 \pm 11.9	6.0	21.6
d18:1 ^{Δ4} c26:1	5.8 \pm 0.7	11.5	0.7	3.8 \pm 0.2	6.6	0.4
Total in pmol	849.3 \pm 109.2	12.8	–	912.7 \pm 24.4	2.7	–

(i.e., 400, 250, 100, 50, and 25 μ g of total protein levels) were processed for LC–MS analysis. The sphingolipid data for SMs and Cers along with their percentages are presented in Table 6. These samples were prepared identically and then processed at the same time. It is very clear from

Table 6 that as the absolute amount of protein in the samples decreases, the total amount of Cer measured increases. At moderately high protein content (400 μ g), the Cer levels measured were only half as great compared to those found in the sample containing the lowest amount of

Table 6 Comparative liquid chromatography selected reaction monitoring data obtained for the evaluation of sphingomyelin (SM), and ceramides (CER) from mouse embryonic fibroblast cells that contain

different amount of absolute protein. Data is normalized to the 1-mg protein level

	Amount of Protein									
	400 µg		250 µg		100 µg		50 µg		25 µg	
	pmol	%	pmol	%	pmol	%	pmol	%	pmol	%
<i>Ceramides</i>										
Cer d18:1 ^{Δ4} c16:0	108.0	51.6	134.8	48.6	137.3	45.3	145.0	43.8	174.0	41.5
Cer d18:1 ^{Δ4} c18:1	1.5	0.7	1.4	0.5	3.9	1.3	2.5	0.7	2.9	0.7
Cer d18:1 ^{Δ4} c18:0	10.2	4.9	12.2	4.4	14.1	4.7	17.1	5.2	32.6	7.8
Cer d18:1 ^{Δ4} c20:0	3.3	1.6	4.3	1.6	6.0	2.0	9.4	2.8	13.8	3.3
Cer d18:1 ^{Δ4} c22:0	8.8	4.2	12.0	4.3	14.3	4.7	15.7	4.8	15.7	3.7
Cer d18:1 ^{Δ4} c24:1	44.0	21.0	62.5	22.6	74.3	24.5	83.6	25.3	117.2	28.0
Cer d18:1 ^{Δ4} c24:0	32.2	15.4	48.8	17.6	51.4	17.0	54.8	16.6	63.1	15.0
Cer d18:1 ^{Δ4} c26:1	1.0	0.5	1.1	0.4	1.3	0.4	2.5	0.7	NO	–
Total	209.1		277.1		302.7		330.6		419.2	
<i>Sphingomyelins</i>										
SM d18:1 ^{Δ4} c16:0	6,618.0	59.3	6,084.2	55.2	7,123.0	59.9	7,421.4	64.3	8,677.7	64.2
SM d18:0 c16:0	174.8	1.6	199.9	1.8	194.1	1.6	155.9	1.4	206.7	1.5
SM d18:1 ^{Δ4} c18:0	448.3	4.0	569.0	5.2	540.3	4.5	536.0	4.6	622.6	4.6
SM d18:0 c18:0	9.4	0.1	9.0	0.1	8.8	0.1	6.1	0.1	6.4	0.0
SM d18:1 ^{Δ4} c20:0	141.1	1.3	184.7	1.7	172.8	1.5	160.2	1.4	182.0	1.3
SM d18:0 c20:0	45.9	0.4	37.6	0.3	NO	–	NO	–	NO	–
SM d18:1 ^{Δ4} c22:0	411.6	3.7	470.0	4.3	440.1	3.7	403.2	3.5	472.1	3.5
SM d18:1 ^{Δ4} c23:0	80.8	0.7	89.9	0.8	82.6	0.7	69.7	0.6	85.6	0.6
SM d18:1 ^{Δ4} c24:1	2,284.4	20.5	2,410.1	21.8	2,253.3	18.9	2,053.6	17.8	2,376.8	17.6
SM d18:1 ^{Δ4} c24:0	818.9	7.3	861.4	7.8	967.6	8.1	648.1	5.6	828.0	6.1
SM d18:0 c24:0	22.9	0.2	5.1	0.0	5.1	0.0	NO	–	NO	–
SM d18:1 ^{Δ4} c25:1	45.2	0.4	43.6	0.4	45.5	0.4	34.6	0.3	32.8	0.2
SM d18:1 ^{Δ4} c25:0	22.0	0.2	25.2	0.2	22.6	0.2	17.0	0.1	NO	–
SM d18:1 ^{Δ4} c26:1	41.9	0.4	40.7	0.4	35.8	0.3	29.6	0.3	32.9	0.2
Total amount	11,165.2		11,030.5		11,891.7		11,535.3		13,523.6	

protein (25 µg). However, it is apparent that the overall percentages of the individual Cer components remain similar. Ceramide levels in the samples containing 50–250 µg of protein exhibited minimal differences. To measure Cer in cells, the absolute range of protein levels should be between 50 and 300 µg; otherwise, the data will lose quantitative integrity in terms of absolute amounts.

For SM, the data shows consistency between 50 and 400 µg of protein, whereas at 25 µg of protein, the total SM levels appear to be relatively high; however, some of the signals were of low intensity and showed poor peak shape. Therefore, if sphingolipids such as Cers, MHCers, and SMs are being measured in comparative samples, it is important to begin with samples containing similar amounts of total protein. The recommended protein level is between 50 and 300 µg.

It is known that analyzing lipids by direct infusion into the mass spectrometer at high concentrations (i.e.,

10 pmol/µL or ca. 150 pmol/µL of total lipids), the relative response decreases strongly to increasing acyl chain length [47]. At lower concentrations (i.e., 5 or 60 pmol/µL of total lipids), however, the response is essentially linear with the chain length as lipid–lipid interactions and lipids-to-solution droplets crowding at the ESI inter-phase are minimized [42, 47]. It should, however, be noted that use of chromatography will essentially dilute this process because of the separation of analytes, and at a given duration of time not many analytes co-elute. This is particularly true for RP chromatography, where individual analytes from each class are well separated. Even with NP chromatography, all the sphingolipid classes viz. ceramides, hexosylceramides, and sphingomyelins are well separated into bands appearing at vastly different retention times, with many individual analytes from each class partially to fully resolved. Further, the volume of sample solution injected on to a column in this study is ca. 10–20 µL from a total

sample volume of ca. 700–800 μL divided between the NP and RP chromatography; therefore, given the amount of protein assayed in these samples, the lipid contents in this injected volume might not be too high at all.

Sphingolipid Analysis Using Reversed-Phase Liquid Chromatography–Tandem Mass Spectrometry

We also developed reversed-phase LC–MS/MS methods to quantitate Cers, MHCers, and SMs. The SRM profiles are shown in Figs. 5, 6, and 7, respectively. Reversed-phase chromatography has higher selectivity and specificity for these compounds than normal phase chromatography, owing to its superior resolution of these molecules. The separation in reversed-phase chromatography is based on the hydrophobicity of the fatty-*N*-acyl side chains, rather than on head group separation of these molecules. For each class of analytes, three SRM methods were constructed, each employing between 5 and 7 analyte transitions, enabling the analysis of 18–20 molecules within each class. Excellent signals were observed for all SMs (Fig. 7); however, signals for MHCer were very poor for samples

containing low and moderate levels of these compounds (Fig. 6). Some of the elution trends observed when separating the compounds using normal-phase chromatography were reversed in reversed-phase chromatography, e.g., as the number of methylene groups increased in each class of sphingolipids, their retention times increased, while the *d*-unsaturated and *d*-saturated still appeared as pair, the dihydro species appearing at a higher retention time, compared to the corresponding dehydro compound.

Obtaining the necessary sensitivity for some of the low-abundant species, particularly for hexosylceramides in reversed-phase chromatography, may require injecting larger amounts of material onto the column. This need can be a limiting factor when little biological sample is available. Furthermore, the interaction of Cers, MHCers, and SMs with the solvents used in reversed- and normal-phase chromatography differ. Owing to their choline head group, SMs have stronger dipole–dipole and H-bonding type of interactions with reversed-phase solvents, compared to weaker van der Waals, London–London and other dispersion forces with normal-phase solvents. Consequently, SMs resolve better under reversed-phase conditions.

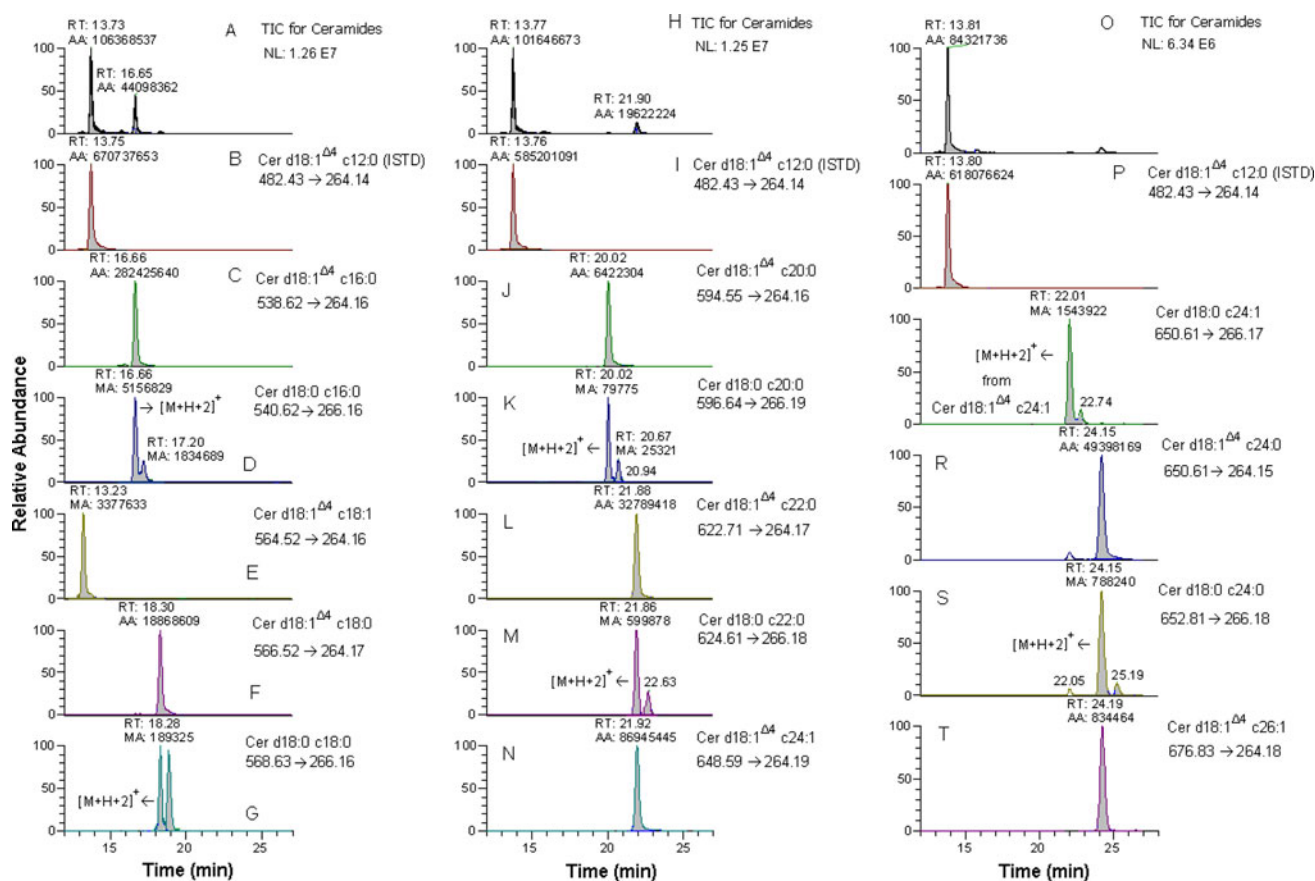


Fig. 5 Extracted ion chromatogram from SRM scans of precursor \rightarrow double-dehydrated carbocation product fragment for all the ceramides, as observed by three reversed-phase methods. All three

reversed-phase methods contain only transitions from ceramides. Each method also comprises a transition from the ceramide internal standard

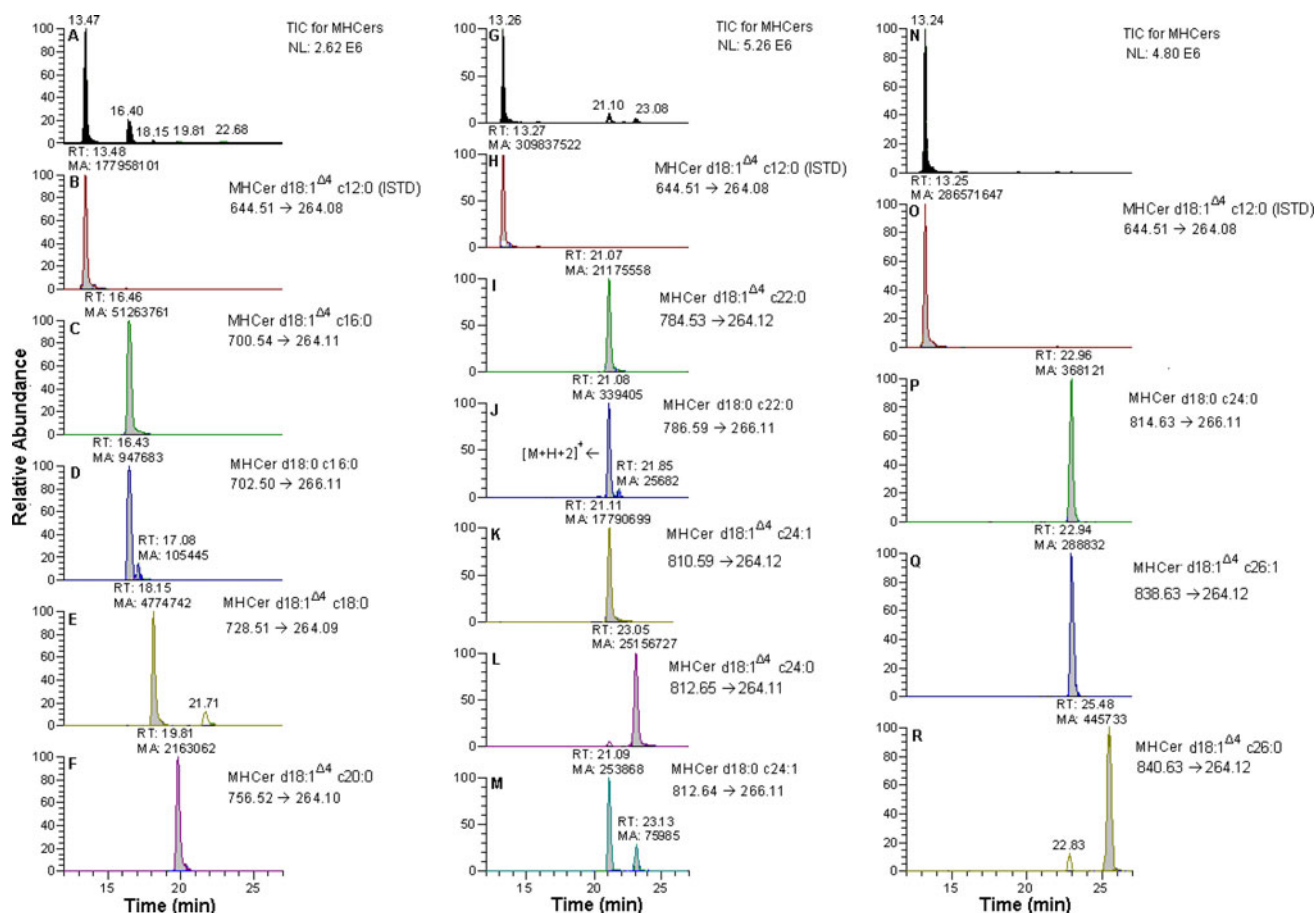


Fig. 6 Extracted ion chromatogram from SRM scans of precursor \rightarrow double-dehydrated carbocation product fragment for all the hexosylceramides (MHCer), as observed using three reversed-phase methods.

Although ESI normally does not ionize efficiently under the high content of non-polar organic solvents, such as hexane, CHCl_3 , ethyl acetate or ether, but in the presence of 5 mM $\text{CH}_3\text{COONH}_4$ dissolved in 20 mL CH_3OH and containing 1–2% CH_3COOH , the ceramides and MHCers seem to exhibit good ionization efficiency and good sensitivity, in comparison to their ionization efficiency with reversed-phase solvents. It should be noted that the run times in both normal- and reversed-phase chromatography are almost identical (ca. 22 min); however, in normal-phase chromatography, each of the three classes of sphingolipids is displayed within a narrow elution time window of its own: Cers elute between 3.7 and 4.5 min, MHCers between 8 and 12 min, and SMs between 16 and 19 min, thus making it possible to combine analytes from each subclass together into different segments to run them concurrently in each method. The individual MRM pair that uniquely identifies each species can then be summed to yield the total class species. In reversed-phase chromatography compounds from each class of sphingolipids are well resolved, with retention time ranging widely between

All three reversed-phase methods contain only transitions from MHCer. Each method also comprises a transition from the MHCer internal standard

12 and 27 min. Further, because of a large elution window between the internal standard that was used and the respective analytes of that class, each sub-class of sphingolipids was run separately, instead of juxtaposing the peaks over each other chromatographically. Because of this larger elution window, as, for example, there is more than 10 min difference between the elution time of Cer d18:1 Δ^4 c12:0 internal standard and the analyte Cer d18:1 Δ^4 c24:1, there remains a strong possibility for ionization differences between earlier and later eluting analytes, in comparison to the use of only one either earlier or later eluting internal standard, which might result in a disparity of data between the normal- and reversed-phase chromatography. However, data from Table 5 shows the calculated amounts of individual Cers, MHCers, and SMs obtained by both reversed- and normal-phase chromatography, indicating the overall bias is less for SMs. For Cers and MHCers, the earlier eluting analytes exhibit higher amounts in comparison to the use of only one earlier eluting internal standard for each. Thus, it seems prudent to use more than two internal standards that span the entire elution window for each class

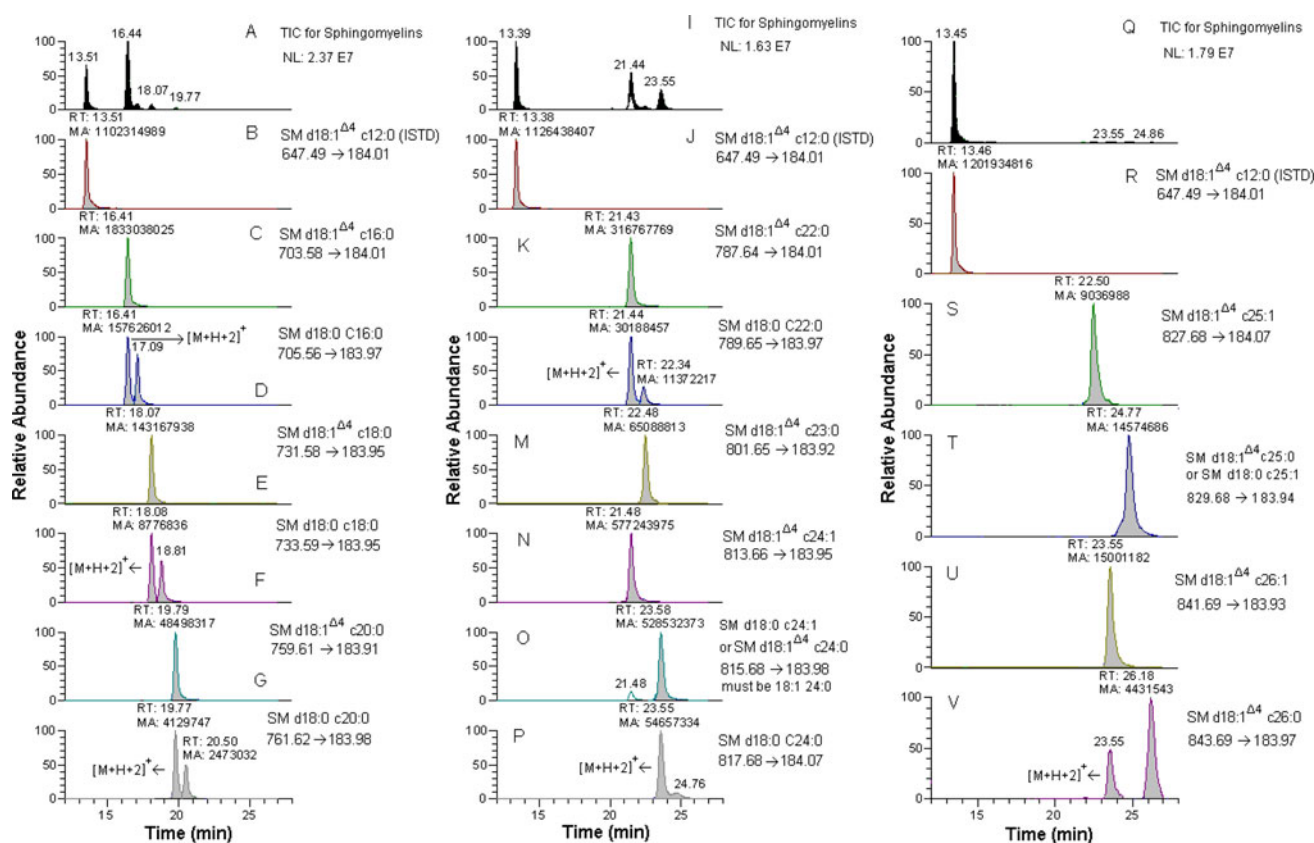


Fig. 7 Extracted ion chromatogram from SRM scans of precursor \rightarrow double-dehydrated carbocation product fragment for all the spingomyelins (SM), as observed by three reversed-phase methods. All three

reversed-phase methods contain only transitions from SM. Each method also comprises a transition from the SM internal standard

of analytes when reversed-phase chromatography is performed.

As the NP and RP-LC/MS/MS quantitation results were inconsistent between the two, a solution containing four reference standards, two each of ceramides and spingomyelins, viz. Cer d18:1 Δ^4 c20:0, Cer d18:1 Δ^4 c24:1, SM d18:1 Δ^4 c16:0, and SM d18:1 Δ^4 c18:0, were prepared at the 1- μ g/mL level and then spiked in equal amounts and studied by both NP and RP-LC/MS/MS. The peak areas obtained by NP chromatography for these reference standards were 2.85×10^7 , 3.19×10^8 , 4.64×10^8 , and 2.41×10^8 , while under reversed-phase conditions, the respective peak areas were 9.63×10^7 , 1.17×10^7 , 2.01×10^9 , 1.04×10^9 ; these results also suggest different ionization efficiencies in NP and RP chromatography. Thus, data obtained with these spiked reference standards also suggested the similar discriminatory results between the NP and RP chromatography. Recovery between 70–80% and 90–95% were observed for samples processed by normal-phase and reversed-phase, respectively, using the comparative calculations of the peak areas of individual components from neat and LM6002 prespiked sample.

A series of reliable, efficient, and highly sensitive LC-MS (SRM) methods using normal-phase and reversed-phase liquid chromatography was developed to quantitate mammalian Cers, MHCers, and SMs containing saturated and unsaturated sphingoid base cores. In the context of normal phase chromatography a high content of organic solvents still provided efficient electrospray ionization of the ceramides and hexosylceramides. Using non-polar solvents in normal phase chromatography, even low abundant Cers having similar retention times were implicitly resolved, while reversed-phase chromatography was used to resolve the Cer compounds explicitly. SMs could be resolved using either type of chromatography, however, reversed-phase chromatography provided better specificity, selectivity, and sensitivity. Hexosylceramides were best resolved and quantitated using normal phase chromatography. Because the interaction of Cers, MHCers, and SMs differs between normal-phase and reversed-phase solvents and there is a possibility of some ion suppression effects, it is essential to link the quantitative results to the type of chromatography utilized. An absolute total amount of protein amounts between 100 and 300 μ g is essential to

get consistent quantitative results for all the sphingolipids. Overall, the quantitative results show that for MEF and HEK293 cells, more than 75% of the Cers, MHCers, and SMs exist as d18:1^{Δ4} c16:0, d18:1^{Δ4} c24:1, and d18:1^{Δ4} c24:0.

Acknowledgments This project has been funded in whole or in part with federal funds from the National Cancer Institute, National Institutes of Health, under contract HHSN261200800001E. The content of this publication does not necessarily reflect the views or policies of the Department of Health and Human Services, nor does mention of trade names, commercial products, or organizations imply endorsement by the US Government.

References

- Eyster KM (2003) The membrane and lipids as integral participants in signal transduction: lipid signal transduction for the non lipid biochemist. *Adv Physiol Edu* 31:5–16
- Merrill AH Jr, Stokes TH, Momin A, Park H, Portz BJ, Kelly S, Wang E, Sullards MC, Wang MD (2009) Sphingolipidomics: a valuable tool for understanding the roles of sphingolipids in biology and disease. *J Lipid Res* 50:S97–S102
- Oskouian B, Saba JD (2004) Death and taxis: what non-mammalian models tell us about sphingosine-1-phosphate. *Semin Cell Dev Biol* 15:529–540
- Acharya U, Acharya JK (2005) Enzymes of sphingolipid metabolism in *Drosophila melanogaster*. *Cell Mol Life Sci* 62:128–142
- Holthius JC, Pomorski T, Raggars RJ, Sprong H, Van Meer G (2001) The organizing potential of sphingolipids in intracellular membrane transport. *Physiol Rev* 81:1689–1723
- Dickson RC (1998) Sphingolipid functions in *Saccharomyces cerevisiae*: comparison to mammals. *Annu Rev Biochem* 67:27–48
- Futerman AH, Hannun YA (2004) The complex life of simple sphingolipids. *EMBO Rep* 5:777–782
- Hla T (2004) Physiological and pathological actions of sphingosine-1-phosphate. *Semin Cell Dev Biol* 15:513–520
- Spiegel S, Milstein S (2003) Exogenous and intracellularly generated sphingosine-1-phosphate can regulate cellular processes by divergent pathways. *Biochem Soc Trans* 31:1216–1219
- Crawford MA, Doyle W, Drury P, Lennon A, Costeloe K, Leighfield M (1989) n-6 and n-3 fatty acids during early human development. *J Intern Med* 225:159–169
- Innis SM (1991) Essential fatty acids in growth and development. *Prog Lipid Res* 1:39–103
- Acharya U, Patel S, Koundakjian E, Nagashima K, Han X, Acharya JK (2003) Modulating sphingolipid biosynthetic pathway rescues photoreceptor degeneration. *Science* 299:1740–1743
- Wang X, Rao RP, Cholady TK, Masood MA, Southon E, Zhang H, Berthet C, Nagashima K, Veenstra TK, Tessarolla L, Acharya U, Acharya JK (2009) Mitochondrial degeneration and not apoptosis is the primary cause of embryonic lethality in ceramide transfer protein mutant mice. *J Cell Biol* 184:143–158
- Rao RP, Yuan C, Allegood JC, Rawat SS, Edwards MB, Wang X, Merrill AH Jr, Acharya U, Acharya JK (2007) Ceramide transfer protein function is essential for normal oxidative stress response and lifespan. *Proc Natl Acad Sci USA* 104:11364–11369
- Acharya JK, Dasgupta U, Rawat SS, Yuan C, Sanxaridis PD, Yonamine I, Karim P, Nagashima K, Brodsky MH, Tsunoda S, Acharya U (2008) Cell non-autonomous function of ceramidase in photoreceptor homeostasis. *Neuron* 57:69–79
- Ma D (2007) Lipid mediators in membrane rafts are important determinants of human health and disease. *Appl Physiol Nutr Metab* 32:341–350
- Ichi I, Nakahara K, Kiso K, Kojo S (2007) Effect of dietary cholesterol and high fat on ceramide concentration in rat tissues. *Nutrition* 23:570–574
- Ozbayraktar FB, Ulgen KO (2009) Molecular facets of sphingolipids: mediators of diseases. *Biotechnol J* 4:1028–1041
- Wymann MP, Schneider R (2008) Lipid signaling in disease. *Nat Rev Mol Cell Biol* 9:162–176
- Cowart L (2009) A bioactive sphingolipids: players in the pathology of metabolic disease. *Trends Endocrinol Metab* 20:34–42
- Katsikas H, Wolf C (1995) Blood sphingomyelin from two European countries. *Biochim Biophys Acta* 1258:95–100
- Lemaitre RN, King IB, Mozaffarian D, Kuller LH, Tracy RP, Siscovick DS (2003) n-3 Polyunsaturated fatty acids, fatal ischemic heart disease, and nonfatal myocardial infarction in older adults: the cardiovascular health study. *Am J Clin Nutr* 77:319–325
- Simon JA, Hodgkins ML, Browner WS, Neuhaus JM, Bernert JT Jr, Hulley SB (1995) Serum fatty acids and the risk of coronary heart disease. *Am J Epidemiol* 142:469–476
- Kang JX, Leaf A (1996) The cardiac antiarrhythmic effects of polyunsaturated fatty acids. *Lipids* 31:S41–S44
- Wang Y, Kuhajda FP, Li JN, Pizer ES, Han WF, Sokoll LJ, Chan DW (2001) Fatty acid synthase (FAS) expression in human breast cancer cell culture supernatants and in breast cancer patients. *Cancer Lett* 167:99–104
- Benedettini E, Nguyen P, Loda M (2008) The pathogenesis of prostate cancer: from molecular to metabolic alterations. *Diagn Histopathol* 14:195–201
- Ogino S, Kawasaki T, Ogawa A, Kirkner CJ, Loda M, Fuchs CS (2007) Fatty acid synthase overexpression in colorectal cancer is associated with microsatellite instability, independent of CpG island methylator phenotype. *Hum Pathol* 38:842–849
- Zhou W, Han WF, Landree LE, Thupari JN, Pinn ML, Bililign T, Kim EK, Vadlamudi A, Medghalchi SM, Meskini RE, Ronnett GV, Townsend CA, Kuhajda FP (2007) Fatty acid synthase inhibition activates AMP-activated protein kinase in SKOV3 human ovarian cancer cells. *Cancer Res* 67:2964–2971
- Pizer ES, Lax SF, Kuhajda FP, Pasternack GR, Kurman RJ (1998) Fatty acid synthase expression in endometrial carcinoma: correlation with cell proliferation and hormone receptors. *Cancer* 83:528–537
- Meilke MM, Lyketsos GG (2010) Alterations of the sphingolipid pathway in Alzheimer disease: New biomarkers and treatment targets. *Neuromolecular Med*. doi:10.1007/s12017-010-8121-y
- Abnet CC, Borkowf CB, Qiao YL, Albert PS, Wang E, Merrill AH Jr, Mark D, Dong WJ, Taylor PR, Dawsey SM (2001) Sphingolipids as biomarkers of fumonisin exposure and risk of esophageal squamous cell carcinoma in China. *Cancer Causes Control* 12:821–828
- Lands B (2009) Measuring blood fatty acids as a surrogate indicator for coronary heart disease risk in population studies. *World Rev Nutr Diet* 100:22–34
- Lands B (2009) Planning primary prevention of coronary disease. *Curr Atheroscler Rep* 11:272–280
- Griell AE, Cao Y, Bagshaw DD, Cifelli AM, Holub B, Etherton PMK (2008) A macadamia nut-rich diet reduces total and LDL cholesterol in mildly hypercholesterolemic men and women. *J Nutr* 138:761–767
- Shaner RL, Allegood JC, Park H, Wang E, Kelly S, Haynes CA, Sullards MC, Merrill AH Jr (2009) Quantitative analysis of sphingolipids for lipidomics using triple quadrupole linear ion trap mass spectrometers. *J Lipid Res* 50:1692–1707
- Haynes CA, Allegood JC, Park H, Sullards MC (2009) Sphingolipidomics: methods for comprehensive analysis of sphingolipids. *J Chromatogr B* 877:2696–2708

37. Sullards MC, Allegood JC, Kelly S, Wang E, Haynes CA, Park H, Chen Y, Merrill AH Jr (2007) Structure-specific, quantitative methods for analysis of sphingolipids by liquid chromatography–tandem mass spectrometry: “Inside-Out” sphingolipidomics. *Methods Enzymol* 432:83–115
38. Sullards MC, Merrill AH Jr (2001) Analysis of sphingosine 1-phosphate, ceramides, and other bioactive sphingolipids by high-performance liquid chromatography–tandem mass spectrometry. *Sci STKE* 67:1–11
39. Merrill AH Jr, Sullards MC, Allegood JC, Kelly S, Wang E (2005) Sphingolipidomics: high-throughput, structure-specific, and quantitative analysis of sphingolipids by liquid chromatography–tandem mass spectrometry. *Methods* 36:207–224
40. Sullards C (2000) Analysis of SM, glucosylceramide, ceramide, sphingosine, and sphingosine 1-phosphate by tandem mass spectrometry. *Methods Enzymol* 312:32–45
41. Han X (2002) Characterization and direct quantitation of ceramide molecular species from lipid extracts of biological samples by electrospray ionization tandem mass spectrometry. *Anal Biochem* 302:199–212
42. Han X, Gross RW (2005) Shotgun lipidomics: electrospray ionization mass spectrometric analysis and quantitation of cellular lipidomes directly from crude extracts of biological samples. *Mass Spectrom Rev* 24:367–412
43. Masukawa Y, Narita H, Shimizu E, Kondo N, Sugai Y, Oba T, Homma R, Ishikawa J, Takagi Y, Kitahara T, Takema Y, Kita K (2008) Characterization of overall ceramide species in human stratum corneum. *J Lipid Res* 49:1466–1476
44. Masukawa Y, Tsujimura H, Narita H (2006) Liquid chromatography–mass spectrometry for comprehensive profiling of ceramide molecules in human hair. *J Lipid Res* 47:1559–1571
45. Parrinello S, Samper E, Krtolica A, Goldstein J, Melov S, Campisi J (2003) Oxygen sensitivity severely limits the replicative lifespan of murine fibroblasts. *Nat Cell Biol* 5:741–747
46. Watson AD (2006) Lipidomics: a global approach to lipid analysis in biological systems. *J Lipid Res* 47:2101–2111
47. Koivusalo M, Haimi P, Heikinheimo L, Kostianen R (2001) Quantitative determination of phospholipid compositions by ESI–MS: effects of acyl chain length, unsaturation, and lipid concentration on instrument response. *J Lipid Res* 42:663–672
48. Hammad SM, Pierce JS, Soodavar F, Smith KJ, Al Gadban MM, Rembiesa B, Klein RL, Hannun YA, Bielawski J, Bielawska A (2010) Blood sphingolipidomics in healthy humans: impact of sample collection methodology. *J Lipid Res* 51:3074–3087

The Front-end Desaturase: Structure, Function, Evolution and Biotechnological Use

Dauenpen Meesapyodsuk · Xiao Qiu

Received: 30 July 2011 / Accepted: 26 August 2011 / Published online: 19 October 2011
© AOCS 2011

Abstract Very long chain polyunsaturated fatty acids such as arachidonic acid (ARA, 20:4n-6), eicosapentaenoic acid (EPA, 20:5n-3), docosapentaenoic acid (DPA, 22:5n-3) and docosahexaenoic acid (DHA, 22:6n-3) are essential components of cell membranes, and are precursors for a group of hormone-like bioactive compounds (eicosanoids and docosanoids) involved in regulation of various physiological activities in animals and humans. The biosynthesis of these fatty acids involves an alternating process of fatty acid desaturation and elongation. The desaturation is catalyzed by a unique class of oxygenases called front-end desaturases that introduce double bonds between the pre-existing double bond and the carboxyl end of polyunsaturated fatty acids. The first gene encoding a front-end desaturase was cloned in 1993 from cyanobacteria. Since then, front-end desaturases have been identified and characterized from a wide range of eukaryotic species including algae, protozoa, fungi, plants and animals including humans. Unlike front-end desaturases from bacteria, those from eukaryotes are structurally characterized by the presence of an N-terminal cytochrome *b₅*-like domain fused to the main desaturation domain. Understanding the structure, function and evolution of front-end desaturases, as well as their roles in the biosynthesis of very long chain polyunsaturated fatty acids offers the opportunity to

engineer production of these fatty acids in transgenic oil-seed plants for nutraceutical markets.

Keywords Desaturases · n-3 fatty acids · n-6 fatty acids · Polyunsaturated fatty acids (PUFA) · Biotechnology · Lipid biochemistry · General area

Introduction

A desaturase is a special type of oxygenase that can remove two hydrogens from a hydrocarbon chain, especially from a fatty acyl chain, catalyzing the formation of a double bond in the substrate [1, 2]. Unlike normal oxygenases which directly transfer molecular oxygen to a substrate; a desaturase uses activated molecular oxygen to abstract hydrogens from the substrate creating a carbon/carbon double bond in a fatty acid and a molecule of water [1, 3].

According to their regioselectivity, desaturases are typically categorized as Δ_x desaturase that introduces a double bond at position *x* referred to from the carboxyl end of a fatty acid; or ω_y desaturase that introduces a double bond at position *y* referred to from the methyl end [4–6]. In addition, desaturases can additionally be labelled as $\nu+z$ or $\nu-z$ desaturases. The $\nu+z$ desaturase introduces a double bond at *z* carbons after the pre-existing double bond ν , [7] i.e. towards the methyl end, while the $\nu-z$ desaturase can introduce a double bond at *z* carbons before the pre-existing double bond ν , i.e. towards the carboxyl end. An example of a Δ_x desaturase is the acyl-ACP Δ_9 desaturase from plants, a soluble enzyme introducing a first Δ_9 double bond into saturated palmitoyl-ACP or stearoyl-ACP [8, 9]. The membrane-bound ω_3 desaturase from nematode *Caenorhabditis elegans* is an example of a ω_y desaturase that inserts an ω_3 double bond into a polyunsaturated fatty acid

D. Meesapyodsuk · X. Qiu
Department of Food and Bioproduct Sciences,
University of Saskatchewan, 51 Campus Drive,
Saskatoon, SK S7N5A8, Canada

D. Meesapyodsuk · X. Qiu (✉)
Plant Biotechnology Institute, National Research
Council of Canada, 110 Gymnasium Place,
Saskatoon, SK S7N0W9, Canada
e-mail: xiao.qiu@usask.ca

[10, 11]. An example of $\nu+3$ desaturase is the *Claviceps purpurea* “ $\Delta 12$ ” desaturase that has a preference for introducing double bonds at the $\Delta 12$ position, three carbons after the pre-existing double bond at the ninth position [7], while the $\Delta 4$ desaturase from *Thraustochytrium* is catalytically a $\nu-3$ desaturase and can only introduce a double bond at position 4 which is three carbons before the pre-existing double bond at the seventh position [12].

Based on the position of the double bond insertion relative to a pre-existing double bond in a fatty acyl chain, desaturases can also be referred to as front-end desaturases or methyl-end desaturases [13]. Unsaturated fatty acids are essential for all living species in which the initial de novo fatty acid synthesis generally results in production of saturated fatty acids with 18 carbons or 16 carbons in length. The first double bond is often inserted at approximately the middle position of a fatty acid chain. Fatty acids with different chain length and double bond position are generated later by various fatty acid modifying enzymes, such as elongases and desaturases. A methyl-end desaturase introduces a double bond between the pre-existing double bond and the methyl-end, while a front-end desaturase inserts a double bond between the pre-existing double bond and the carboxyl end of a fatty acid [14]. Commonly-found membrane-bound ωy and $\nu+z$ desaturases such as “ $\Delta 12$ ”, “ $\Delta 15$ ” and $\omega 3$ desaturases in plants are examples of methyl-end desaturases, while widely spread $\nu-z$ desaturases in microorganisms such as $\Delta 4$, $\Delta 5$, $\Delta 6$ and $\Delta 8$ desaturases belong to front-end desaturases.

Although both methyl-end desaturase and front-end desaturase are involved in the biosynthesis of very long chain polyunsaturated fatty acids, their occurrence in living species is not identical. The former is widely present in plants and microorganisms, while the latter mostly occur in animals and microorganisms, although certain types of front-end desaturases have been identified in a small number of higher plants, such as borage [15], echium [16] and conifers [17]. Higher animals including humans lack the methyl-end desaturase such as “ $\Delta 12$ ”, “ $\Delta 15$ ” and $\omega 3$ desaturase [18]. Consequently, they cannot synthesize linoleic acid (LA, 18:2-9,12) and linolenic acid (ALA, 18:3-9,12,15) from oleic acid (OA, 18:1-9), the two essential fatty acids that have to be acquired from the diet. LA and ALA are precursors for the biosynthesis of very long chain polyunsaturated fatty acids such as arachidonic acid (20:4n-6, ARA), eicosapentaenoic acid (20:5n-3, EPA) and docosahexaenoic acid (22:6n-3, DHA). As shown in Fig. 1, to synthesize these fatty acids, LA and ALA are desaturated by a first front-end desaturase—the $\Delta 6$ desaturase, introducing a $\Delta 6$ double bond into the substrates giving gamma-linolenic acid (GLA, 18:3-6,9,12) in the $\omega 6$ pathway, and stearidonic acid (SDA, 18:4-6,9,12,15) in the $\omega 3$ pathway, respectively. GLA and SDA are elongated by a $\Delta 6$ elongase

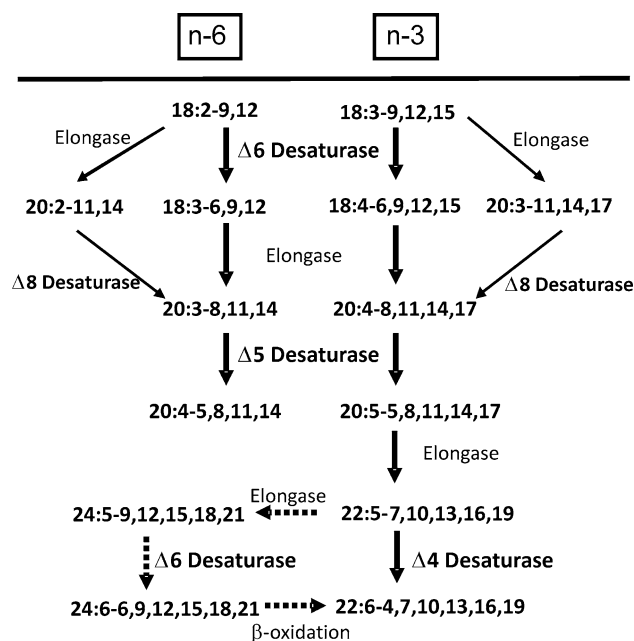


Fig. 1 Front-end desaturases involved in the biosynthesis of very long chain polyunsaturated fatty acids. The dotted arrow indicates Sprecher’s pathway for DHA biosynthesis

to dihomo-gamma-linolenic acid (DGLA, 20:3-8,11,14) and eicosatetraenoic acid (ETA, 20:4-8,11,14,17), which are then desaturated by a second front-end desaturase—the $\Delta 5$ desaturase giving rise to arachidonic acid (ARA, 20:4-5,8,11,14) and eicosapentaenoic acid (EPA, 20:5-5,8,11,14,17), respectively. EPA is elongated to docosapentaenoic acid (DPA, 22:5-7,10,13,16,19) which is then desaturated by a third front-end desaturase—the $\Delta 4$ desaturase, giving docosahexaenoic acid (DHA, 22:6-4,7,10,13,16,19) in the $\omega 3$ pathway. However, mammals including humans lack the $\Delta 4$ desaturase. Biosynthesis of DHA in mammals takes “the retro-conversion pathway” [19] which involves two rounds of chain elongation of EPA and another $\Delta 6$ desaturation on the elongated product, followed by a single 2-carbon chain shortening of the $\Delta 6$ desaturated product in the peroxisome, giving DHA. The $\Delta 8$ desaturase is another front-end desaturase involved in the biosynthesis of very long chain polyunsaturated fatty acids [20–22]. This desaturase works on a branching pathway of the biosynthesis, introducing a $\Delta 8$ double bond into elongated products LA or ALA, i.e. 20:2-11,14 or 20:3-11-14,17, giving rise to DGLA and ETA, respectively, which can then be desaturated by a $\Delta 5$ desaturase, giving ARA and EPA as described above (Fig. 1). The individual front-end desaturases are described below.

$\Delta 6$ Desaturase

The first $\Delta 6$ desaturase gene was cloned in 1993 from the cyanobacterium *Synechocystis* using a gain-of-function

expression approach [23]. The protein sequence of this first front-end desaturase shows a similarity to other acyl-lipid desaturases with different regioselectivity from cyanobacteria [23]. Like its homologous sequences, the $\Delta 6$ desaturase from *Synechocystis* does not contain a cytochrome b_5 -like domain as was later found in eukaryotic $\Delta 6$ desaturases. A similar $\Delta 6$ desaturase was later cloned from another cyanobacterium *Spirulina platensis* [24]. In 1997, the first eukaryotic $\Delta 6$ desaturase gene was cloned from borage plant by two independent groups [15, 25]. Unlike bacterial $\Delta 6$ desaturases, the $\Delta 6$ desaturase encoded by this gene is a modular protein that has a cytochrome b_5 -like domain fused to the N-terminus of the main desaturation domain. This modular structure was later observed to be a feature of all the $\Delta 6$ desaturases isolated from eukaryotes including algae [26–28], moss [29], plants [15, 16], fungi [30–32], animals [33, 34] and humans [35]. The existence of an N-terminal cytochrome b_5 -like domain is not exclusive to this front-end desaturase, a similar motif has been also observed in other front-end desaturases such as $\Delta 5$, $\Delta 8$ and $\Delta 4$ desaturases and some sphingolipid desaturases from eukaryotes [36]. Beside the cytochrome b_5 -like domain at the N-terminus, the rest of the $\Delta 6$ desaturase sequences have sequence similarity to methyl-end desaturases with characteristics of three highly conserved histidine-rich motifs, i.e. H-X_{3,4}-H, H-X_{2,3}-H-H and H/Q-X_{2,3}-H-H. However, the first histidine of the third motif in the front-end desaturase is usually replaced by glutamine [15]. Conversion of this residue back to histidine resulted in loss of the activity, implying this residue might be very important for the structural configuration of this modular type of desaturases for front-end desaturation [37].

The function of $\Delta 6$ desaturases isolated from prokaryotes and eukaryotes was mostly established by their expression either in yeast (*Saccharomyces cerevisiae* or *Pichia pastoris*) or in plants. Functional enzymatic studies have showed that most of $\Delta 6$ desaturases isolated from eukaryotes can use both LA and ALA as substrates effectively at the similar level. However, some $\Delta 6$ desaturases showing a preference for ALA have also been reported [38]. A bifunctional $\Delta 6$ desaturase was identified in *Ceratodon purpureus* that can convert the $\Delta 6$ double bond it creates to a triple bond [39]. A human $\Delta 6$ desaturase was found to have the capability of introducing a $\Delta 6$ double bond into two distinct substrates with different chain lengths, i.e. 18:2-9,12 and 24:5-9,12,15,18,21 [40]. The observation of the $\Delta 6$ desaturation of the latter substrate provides the important evidence supporting the retro-conversion pathway that requires the desaturation step for DHA biosynthesis in humans.

The first published transgenic production of GLA, a $\Delta 6$ desaturated fatty acid in the $\omega 6$ pathway, in plants using a $\Delta 6$ desaturase was reported by Reddy and Thomas (1996)

who expressed the *Synechocystis* $\Delta 6$ desaturase under the control of a constitutive CaMV 35S promoter in tobacco. Transgenic tobacco carrying the gene produced very small amounts of GLA and SDA in leaves, but not in seeds [15, 41]. That the prokaryotic $\Delta 6$ desaturase did not work well in plants might be due to incompatible cofactors required for the desaturation (see below). Production of high levels of GLA and SDA, two $\Delta 6$ desaturated fatty acids, in transgenic oilseeds has since been achieved by several other groups using eukaryotic $\Delta 6$ desaturases [42]. The seed-specific expression of a fungal $\Delta 6$ desaturase and $\Delta 12$ desaturase from *Mortierella alpina* produced up to 43% GLA in seeds of *Brassica napus* [43]. A similar level of GLA was produced in *B. juncea* seeds by expressing a single $\Delta 6$ desaturase from fungus *Pythium irregulare* [32]. Seed expression of a *B. napus* $\Delta 15$ desaturase gene with *M. alpina* $\Delta 6$ and $\Delta 12$ desaturases resulted in production of SDA accounting for 16–23% of the total fatty acids [44]. Co-expression of a borage $\Delta 6$ desaturase and an *Arabidopsis* $\Delta 15$ desaturase in soybean produced up to 30% of SDA [45]. Very recently, a very high level of GLA (more than 60%) in transgenic safflower oilseeds was achieved using a $\Delta 6$ desaturase from *Saprolegnia diclina* [46].

$\Delta 5$ Desaturase

The first $\Delta 5$ desaturase gene was cloned in 1998 from the fungus *M. alpina* by two independent groups almost simultaneously using sequence information of the front-end $\Delta 6$ desaturases from borage for degenerate RT-PCR [47, 48]. Since then, many $\Delta 5$ desaturases have been cloned from diverse species including lower plants [49, 50], animals [51] including human [52], fungi [48, 53], moss [54], protozoa [55] and algae [28, 56]. Like $\Delta 6$ desaturases from eukaryotes, the $\Delta 5$ desaturase comprises a cytochrome b_5 -like domain fused at the N-terminus of the sequence.

The function of the $\Delta 5$ desaturases was mostly established by expressing the genes in yeast. Like the $\Delta 6$ desaturase, $\Delta 5$ desaturase can use two substrates, both $\omega 3$ (ETA) and $\omega 6$ (DGLA) are desaturated almost equally effectively, producing EPA and ARA, respectively. However, besides the two major substrates, some $\Delta 5$ desaturases are active on LA and ALA, producing polymethylene-interrupted $\Delta 5$ desaturated fatty acids such as pinolenic acid (18:3-5,9,12), which was found naturally in seeds of some conifer trees [53]. A $\Delta 5$ desaturase from zebrafish also carries $\Delta 6$ desaturase activity at the similar level, i.e. it is bifunctional [57].

Various $\Delta 5$ desaturase have been used to transform plants for transgenic production of $\Delta 5$ desaturated polyunsaturated fatty acids. Abbadi et al. [58] (2004) introduced a $\Delta 5$ desaturase from *M. alpina* along with a $\Delta 6$ desaturase and $\Delta 6$ elongase from *Physcomitrella patens*

into tobacco and flax, which led to the accumulation of small amounts of ARA and EPA in transgenic seeds. An acyl-CoA $\Delta 5$ desaturase from an alga, along with other genes, was also used to transform *Arabidopsis* resulting in production a small amount of $\Delta 5$ desaturated fatty acids in seeds [27]. Recently a high level of EPA in transgenic *Brassica carinata* was reported using a *Thraustochytrium* $\Delta 5$ desaturase along with a $\Delta 6$ desaturase from *Pythium irregulare* and an elongase from *Thraustochytrium* [59]. It appears that $\Delta 5$ desaturase from fungal species works very effectively when expressed in plants.

$\Delta 4$ Desaturase

The $\Delta 4$ desaturase gene was first cloned in 2001 using the degenerate RT-PCR approach from *Thraustochytrium*, a single cellular Thraustochytrid that can accumulate a high level of DHA [12]. In 1991, 10 years previously, Sprecher and co-workers published their systematic work on the biosynthesis of DHA which suggested that DHA biosynthesis in mammals occurs independently of a $\Delta 4$ desaturase and involves retro-conversion of a 24-carbon $\Delta 6$ fatty acid through a controlled β -oxidation [60]. According to this pathway, the intermediate C24 polyunsaturated fatty acid required for DHA synthesis would be expected to be observed in *Thraustochytrium*. However, when the fatty acid profile of *Thraustochytrium* was examined, no polyunsaturated fatty acids more than 22 carbons in length were found. Therefore, DHA biosynthesis in *Thraustochytrium* was suggested not to follow the Sprecher's pathway, but instead to involve a $\Delta 4$ desaturase that might have a primary structure similar to other eukaryotic front-end desaturases such as the $\Delta 6$ desaturase in borage and the $\Delta 5$ desaturase in *M. alpina*. The $\Delta 4$ desaturase gene was thus isolated from *Thraustochytrium* using the degenerate RT-PCR strategy and it indeed encodes a fusion protein with $\Delta 4$ desaturation activity introducing a $\Delta 4$ double bond in docosapentaenoic acid (22:5n-3) and docosatetraenoic acid (22:4n-6), respectively. Since then, a few other $\Delta 4$ desaturases have been isolated from protists [61, 62] and microalgae [63, 64] using the sequence information of this desaturase. It is noteworthy that the first $\Delta 4$ desaturase of vertebrate animals involved in the DHA biosynthesis was recently identified in teleost fish (*Signus canaliculatus*) [65].

The discovery of the first $\Delta 4$ desaturase in microorganisms provides a simple pathway for DHA biosynthesis and suggests the possibility of producing this important fatty acid in heterologous systems, especially in plants, in a cost-effective way. Indeed, several laboratories worldwide have since actively pursued reconstitution of this simple pathway to produce DHA in plants, such as in soybean [66], *Brassica juncea* [67] and *Arabidopsis thaliana* [68]. However, so far, these efforts to produce DHA in oilseeds

have met with only limited success; a level of DHA in transgenic oilseeds that is commercially viable has not been achieved.

$\Delta 8$ Desaturase

The first $\Delta 8$ desaturase gene was cloned in 1999 using degenerate RT-PCR amplification from the protist *Euglena gracilis* [20]. The deduced protein sequence is highly similar to the $\Delta 6$ desaturase from *Caenorhabditis elegans* with a cytochrome b_5 -like domain at the N-terminus. Functional analysis of this gene in yeast shows the desaturase introduces a $\Delta 8$ double bond in 20:2-11,14 and 20:3-11,14,17 which could be produced by the elongation of LA and ALA [69], giving 20:3-8,11,14 and 20:4-8,11,14,17, respectively. Since the discovery of the $\Delta 8$ desaturases, this branching pathway has drawn much attention because it provides an alternative to the traditional $\Delta 6$ desaturation pathway for the biosynthesis of very long chain polyunsaturated fatty acids. Homologous $\Delta 8$ desaturases have now been isolated from protozoan [20–22], mammals [70] and marine algae [71].

Use of the $\Delta 8$ desaturase was first attempted, along with a $\Delta 9$ elongase from *Isochrysis galbana*, and a $\Delta 5$ desaturase from *M. alpina* for production of $\Delta 5$ desaturated fatty acids in vegetative tissues of *Arabidopsis* [72]. The branching pathway via this front-end desaturase was perceived to be advantageous over the traditional $\Delta 6$ desaturase pathway in overcoming the elongation bottleneck. However, the $\Delta 8$ desaturase from *Euglena* appeared to have low activity in plants. As such, only a very low amount of ARA and EPA was produced in oilseed crops when this desaturase along with other elongases and desaturases was co-expressed (Qiu et al. unpublished data). Recently, a new $\Delta 8$ desaturase from *Pavlova salina*, a $\Delta 9$ elongase from *I. galbana* and a $\Delta 5$ desaturase from *P. salina* were co-expressed in transgenic *Arabidopsis thaliana* and *Brassica napus*, respectively, resulting in production of a relatively high level of ARA (20%) in *Arabidopsis* seeds and a low level of EPA (approximately 3%) in *B. napus* seeds [73].

Acyl Carrier Substrate Specificity of Front-end Desaturases

Desaturases can be classified as acyl-CoA desaturases, acyl-ACP desaturases and acyl-lipid desaturases based on the acyl-carrier they use as substrate. Acyl-ACP desaturases have only been found in the lumen of plastids in plants where de novo biosynthesis of fatty acids occurs. Saturated fatty acids freshly synthesized in the plastids which are still linked to acyl carrier protein are the

substrate for this type of desaturase [74]. Acyl-CoA desaturases are usually membrane-bound and located in the endoplasmic reticulum of eukaryotes using fatty acid linked to Coenzyme A as substrate, while acyl-lipid desaturases introduce double bonds into fatty acids linked to complex lipid molecules such as glycolipid, phosphoglycerolipid and sphingolipids [2]. Depending on the origin, front-end desaturases can be either acyl-CoA desaturases or acyl-lipid desaturases. All known mammalian desaturases are believed to be acyl-CoA desaturases [14], thus front-end desaturases from higher animals would be predicted to use acyl-CoA as substrates. In plants, evidence on the substrate specificity of front-end desaturase was provided by Stymne and colleagues using borage $\Delta 6$ desaturation as an example where [^{14}C]-linoleoyl phosphatidylcholine was desaturated to radioactive γ -linolenoyl phosphatidylcholine in developing seeds, indicating that the substrate for the linoleate $\Delta 6$ -desaturase was phosphatidylcholine. In addition, they also showed that the $\Delta 6$ desaturase was positionally specific to linoleate at the *sn*-2 position of phosphatidylcholine [75, 76]. Recently, the acyl carrier substrate specificity of front-end desaturases was systematically examined in a yeast system using a variety of $\Delta 6$ and $\Delta 5$ desaturases by Heinz and colleagues. Detailed analysis of desaturated products in acyl-CoA, phospholipid and neutral lipid pools during a time course showed that front-end desaturases from lower plants, fungi, worms and algae belong to acyl-lipid desaturases where the desaturation occurs predominately at the *sn*-2 position of phosphatidylcholine. On the other hand, a human $\Delta 6$ desaturase tested uses linoleoyl-CoA as the substrate [26, 77]. Since then, a few acyl-CoA front-end desaturases have been identified from microalgae using the same approach [27, 78]. However, it is worthwhile to point out that all these assignments for acyl carrier specificity are solely based on the *in vivo* experiment where the yeast strain expressing a heterologous front-end desaturase was supplied with substrates and presence of desaturated products in different lipid classes in a time course was used to assign the substrate form. Although this *in vivo* approach can provide useful information on the likely acyl carriers used by front-end desaturases, direct evidence such as that obtained from *in vitro* assays is needed for conclusive determination of the substrate form of the desaturases.

Electron Donors of Front-end Desaturases

The front-end desaturation reaction, like other oxygenation reactions, is an aerobic process requiring molecular oxygen and an electron donor for the oxidation. Like acyl-ACP desaturase and glycolipid desaturases from plastids of plants, front-end desaturases in cyanobacteria are the prokaryotic type of acyl-lipid desaturases that use ferredoxin,

ferredoxin reductase and NADPH as the electron transport system [2]. The front-end desaturases located in endoplasmic reticulum of eukaryotes such as acyl-CoA desaturases from animals and phospholipid desaturases from plants and fungi are the eukaryotic type that utilizes cytochrome *b*₅, cytochrome *b*₅ reductase and NADH as the electron transport system [79]. As mentioned above, most of front-end desaturases, except for the ones from cyanobacteria [23, 24] are fusion proteins with a cytochrome *b*₅-like domain at the N-terminus. This structure suggests that all these front-end desaturase would use cytochrome *b*₅ as electron donor for the desaturation. It is noteworthy that the existence of a cytochrome *b*₅ fusion is also observed in a yeast $\Delta 9$ desaturase where the cytochrome *b*₅-like domain is fused at the C-terminus [80]. Deletion of the C-terminal cytochrome *b*₅ domain of the yeast $\Delta 9$ desaturase resulted in complete loss of enzymatic activity [81]. Similarly, when expressed in the endogenous cytochrome *b*₅-disrupted strain or the wild type yeast strain, the borage $\Delta 6$ desaturase is able to functionally introduce a $\Delta 6$ double bond into the substrate, whereas, deletion of the N-terminal cytochrome *b*₅-like domain of the desaturase resulted in the loss of the function [82], indicating that cytochrome *b*₅-like domain is an essential part of the enzyme such that the free cytochrome *b*₅ could not substitute the electron transport function. *Spirulina platensis* $\Delta 6$ desaturase is a smaller polypeptide which does not contain the cytochrome *b*₅-like domain. When expressed in *Escherichia coli* with supplementation of ferredoxin, the transformant produced GLA from exogenous LA. However, when expressed in yeast, *Spirulina* $\Delta 6$ desaturase N-fused or co-expressed with the cytochrome *b*₅ from *Mucor rouxii* produced GLA from LA [83]. This result indicates that the prokaryotic front-end desaturases may not have a strict requirement for a particular electron transport system. The ferredoxin requirement of the prokaryotic $\Delta 6$ desaturase can be complemented by the corresponding eukaryotic electron donor, cytochrome *b*₅. However, for eukaryotic front-end desaturases, the requirement for electron donor appears to be more stringent that deletion of cytochrome *b*₅ domain or mutation of the heme-binding motif in the cytochrome *b*₅ domain of front-end desaturases totally eliminates the activity [82, 84].

Structural Determinants for Regioselectivity of Front-end Desaturases

The regioselectivity of a desaturase refers to the specific positioning of a double bond in a fatty acyl chain. Generally, front-end desaturases, regardless of their origin, have high regioselectivity and substrate specificity which are determined by the structure of the desaturase proteins. However, due to lack of information of three-dimensional structures of front-end desaturases, there is little

information available on the exact relationship between the structure and function of these enzymes. Nevertheless, a model previously proposed [11] for the methyl-end desaturases can shed some light on the structure–function relationship of the front-end desaturase. In this model, structural determinants for substrate specificity and regioselectivity include a head group binding domain or a methyl group-binding domain, a pre-existing double bond binding domain, and the active site. From this model, we would presume that the substrate specificity and regioselectivity of front-end desaturases might be controlled by more than one domain. Targeted mutagenesis of amino acid residues that are present in close proximity to the histidine boxes of *Mucor rouxii* $\Delta 6$ desaturase revealed that some of these residues are involved in substrate binding [85]. Using domain swapping, Napier and colleagues showed that the regions of first two membrane-spanning helices and carboxyl terminus of borage front-end desaturases are important for the substrate binding and regioselectivity [86]. Despite these studies, our understanding of the individual functional domains of front-end desaturases still remains very limited.

The Catalytic Mechanism of Front-end Desaturases

Like other desaturases, the front-end desaturases belong to a group of metalloenzymes that activate the molecular oxygen using non-heme di-iron active sites to abstract two hydrogens from fatty acids resulting in the introduction of a front-end double bond [87]. Non-heme iron-containing oxygenases have been widely found in nature. They catalyze not only fatty acid desaturation, but also a wide range of other oxygenation reactions [87, 88]. For instance, non-heme iron-containing alkane monooxygenase catalyzes hydroxylation of alkane producing alcohol, which has been the focus of recent research on petroleum contamination remediation [89]. Non-heme iron-containing lipoxygenase that catalyzes the insertion of a molecular oxygen into the (1Z,4Z)-pentadiene of a polyunsaturated fatty acid producing hydroperoxide, a key precursor for a variety of oxylipins involved in the response to biotic and abiotic stresses [90]. Catechol dioxygenase is another non-heme iron-containing enzyme that converts 3,4-dihydroxybenzoate to β -carboxy-*cis,cis*-muconate [91]. Although these oxygenases have distinct primary structure in protein sequences, and catalyze different enzymatic reactions, the catalytic mechanism is found to be similar by using the oxo-ferric intermediate in the catalytic reaction [1, 88]. The di-iron catalytic center is believed to be coordinated by three conserved histidine-rich motifs [92]. Abstraction of two hydrogens by front-end desaturases usually takes place in a stepwise manner as *syn*-elimination with the initial oxidation site close to the carbon at the carboxyl end

according to deuterium kinetic isotope effects associated with the C–H bond cleavages [93]. Actual stereospecific *syn*-dehydrogenation might be controlled by the geometry of the hydrophobic pocket that is in the proximity of the di-iron center of the desaturase [79, 94]. However, the detailed mechanism underlying the front-end desaturation remains to be elucidated.

Evolution of Front-end Desaturases

The evolution of desaturases as a whole has been thoroughly reviewed by Heinz and colleagues [79]. According to the solubility in an aqueous environment, desaturases can be classified into two major groups, soluble desaturases and membrane-bound desaturases. Each group of desaturases possesses characteristic features in their primary structure and is believed to have evolved independently [79]. Front-end desaturases are membrane-bound enzymes with a wide range of substrate selectivity and high regioselectivity and/or stereospecificity. This type of desaturases is recalcitrant to biochemical purification, thus no information is available on the three dimensional structure of the desaturases. In the past decade, the number of front-end desaturase sequences that have been functionally characterized has grown rapidly with the advance of molecular cloning and genome sequencing technologies. This has provided opportunities for an evolutionary analysis of the front-end desaturases to elucidate their phylogenetic origin and catalytic diversity based on amino acid sequence information. As shown in Fig. 2, front-end desaturases in microorganisms, plants and animals are evolutionarily distinct from methyl-end desaturases from cyanobacteria and plants. In another words, the evolution of front-end desaturases has undertaken a path different from that of the methyl-end desaturases. Front-end desaturases selected from a wide range of organisms including cyanobacteria, algae, protozoa, moss, fish, plants and mammals can be phylogenetically grouped into three main clades. The first clade consists of animal front-end desaturases including those from fish and humans. The second clade comprises front-end desaturases mainly from plants, worms and fungi. The third clade contains front-end desaturase mainly from algae, fungi and cyanobacteria. The cyanobacterial front-end desaturases grouped with those of algae and fungi, but not with the methyl end (“ $\Delta 12$ ”) desaturases from their own species, reaffirms that front-end desaturases might take an evolutionary path different from the methyl-end desaturases. The prototype of prokaryotic $\Delta 6$ desaturase might be the progenitor of all the front-end desaturases in eukaryotes, even though their primary structures are quite different. In addition, it could also be seen from the phylogenetic tree that front-end desaturases are not always clustered according to their

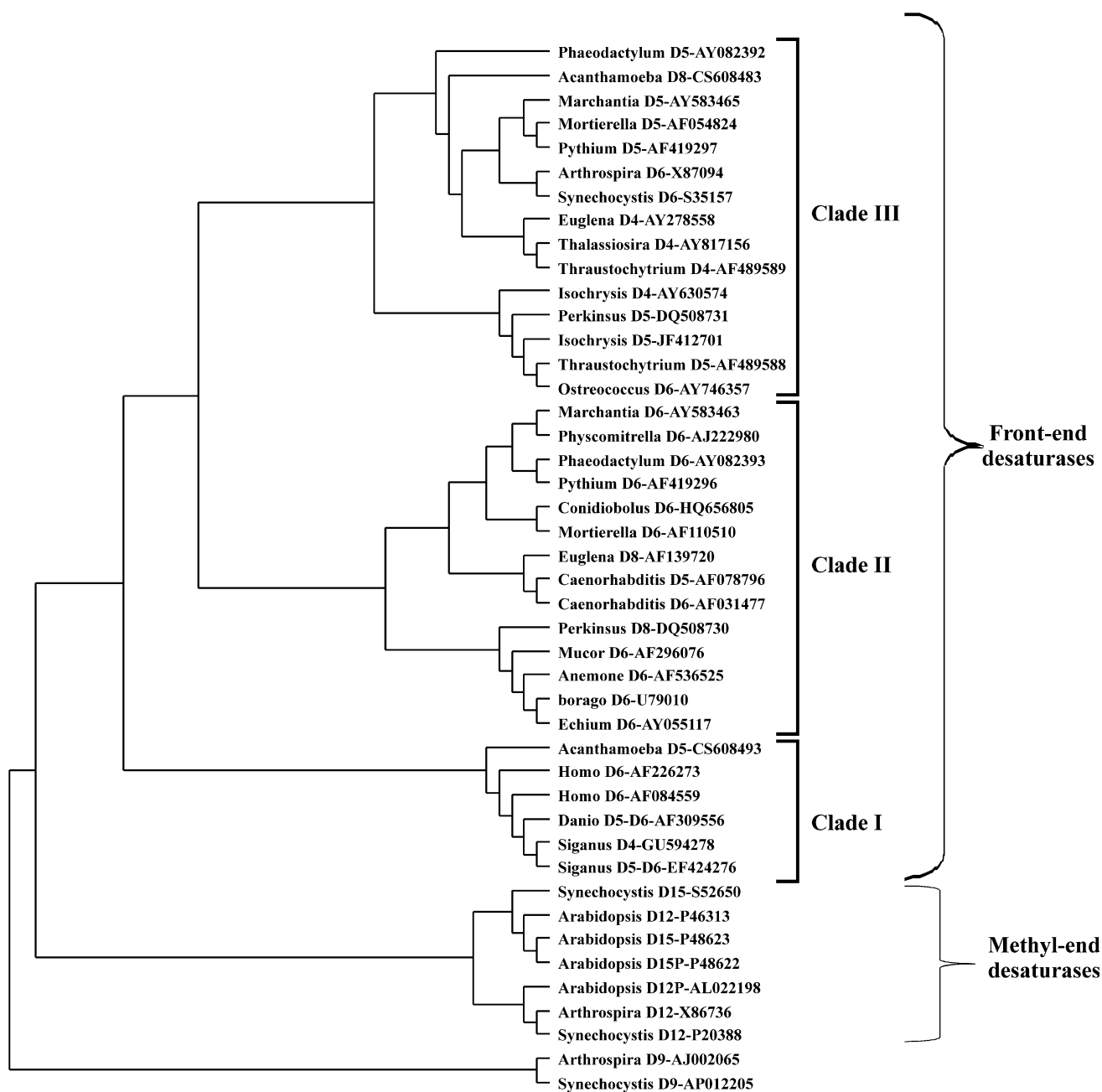


Fig. 2 Phylogenetic analysis of front-end desaturases. Amino acid sequences retrieved from NCBI by their accession number were aligned using ClustalW using default parameters. The resulting

alignment was used to generate a rooted phylogenetic tree using the neighbor joining method and visualized by Treeview

regioselectivity and origin. For instance, $\Delta 5$ and $\Delta 6$ desaturases from *C. elegans* which are tightly grouped together belong to the clade of front-end desaturases including $\Delta 8$ desaturases from protist, $\Delta 6$ desaturases from fungi and plants. On the other hand, the *Mortierella* $\Delta 6$ desaturase forms a clade with other $\Delta 6$ desaturases from algae and plants, while the *Mortierella* $\Delta 5$ desaturase belongs to the clade of front-end desaturases with $\Delta 4$, $\Delta 5$, $\Delta 6$ and $\Delta 8$ regioselectivity from algae and fungi. From an

evolutionary point of view, front-end desaturases with $\Delta 5$, $\Delta 8$ and $\Delta 4$ regioselectivity in eukaryotes might have evolved independently from the progenitor $\Delta 6$ desaturase through multiple independent gene duplication events and diversification. It is noteworthy that we should not rule out the other possibility that eukaryotic front-end desaturases might have evolved from their sphingolipid desaturases as the latter occur more widely and are very closely related to the front-end desaturases. Since sphingolipid desaturases

do not belong to front-end desaturase, they are not described here.

Concluding Remarks

Front end desaturases are remarkable for their structural similarity and functional diversity. Almost all the front-end desaturases except for cyanobacterial ones are modular proteins containing a cytochrome *b₅*-like domain at the N-terminus and a desaturation domain at the C-terminus. Three conserved histidine-rich motifs which are believed to be responsible for di-iron binding at the catalytic center are located at the C-terminal domain. All of front-end desaturases from eukaryotes share a similar hydrophobicity profile, which indicates a common membrane topology [86]. Phylogenetic analysis of front-end desaturases provides very interesting insights into the structure–evolution relationships of these desaturases. Substrate specificity and regioselectivity and catalytic mechanisms of eukaryotic front-end desaturases involve not only the structure feature of the desaturase, but also substrate features such as fatty acid chain length, existing double bonds and acyl carrier [11, 95].

Very long chain polyunsaturated fatty acids are synthesized by a series of front-end desaturases and elongases which play important roles in the integrity and function of biological membranes in eukaryotes. Perceivably, their biosynthesis in the cells should be subjected to the tight control through expression regulation of these enzymes. However, so far, there has been no information available on how the expression of these desaturases and elongases is regulated. There is evidence that the biosynthesis of unsaturated fatty acids in bacteria and human is achieved by the feedback control of transcriptional regulation of fatty acid desaturase genes, mediated through signalling pathways activated by sensors embedded in cellular membranes, in response to environmental factors [96]. The regulation of front-end desaturases is likely to adopt the similar strategy. If so, how is the transcriptional regulatory control achieved for front-end desaturase genes? Answering this question will be an attractive target for the future research of front-end desaturases.

Very long chain ω 3 polyunsaturated fatty acids are essential for human health and well-being. Numerous randomized, placebo-controlled and double blind trials have shown that dietary supplementation of these fatty acids can provide protection against many common chronic diseases such as cardiovascular diseases, diabetics and inflammatory disorders. Moreover, they also play important roles in maintaining the function or enhancing performance of the eyes and brain. Unfortunately, the current dietary source for these fatty acids is limited to oils from

wild fish and oleaginous fungi. Oils from marine fish for these fatty acids are already over-exploited, which results in dramatic reductions of fish populations in ocean. In addition, possible contamination in fish oil with heavy metals and toxins is increasingly becoming a concern. Oil from oleaginous fungi is expensive due to the high cost of fungal culture and oil extraction. Therefore, the scientific community and commercial entities are currently under intensive pressure to explore alternatives to these fatty acids. Transgenic production of very long chain polyunsaturated fatty acids in plants using genes encoding the front-end desaturases and elongases cloned from microalgae and fungi have been viewed as an attractive alternative source for these fatty acids. The biosynthetic pathways of these fatty acids have been successfully reconstituted in plants independently by several groups worldwide [97, 98]. A high level of EPA and ARA has already been achieved in transgenic oilseed crops, which provide great opportunity for nutraceutical markets for these fatty acids as dietary supplements. However, an economically viable level of DHA in transgenic plants has not been realized due to the metabolic bottleneck of acyl trafficking in the complex pathways involving too many genes [58, 67] comprising three to four of those for front-end desaturases. Our further understanding of the mechanism underlying the structure, function and evolution of front-end desaturases is vital for us to reach the goal—production of a high level of very long chain ω 3 fatty acids in transgenic oilseed crops for nutraceutical and functional food markets [99–102].

Acknowledgments We thank Drs. Mark Smith and Patrick Covello for their critical reading of this manuscript. We also wish to thank the authors for their wonderful works referred here. As there are a large number of publications in this field, we apologize to those authors whose works are relevant but might have been overlooked and thus not included in this review.

References

1. Shanklin J, Cahoon EB (1998) Desaturation and related modifications of fatty acids. *Annu Rev Plant Physiol Plant Mol Biol* 49:611–641
2. Los DA, Murata N (1998) Structure and expression of fatty acid desaturases. *Biochim Biophys Acta* 1394:3–15
3. Buist PH (2004) Fatty acid desaturases: selecting the dehydrogenation channel. *Nat Prod Rep* 21:249–262
4. Yadav NS, Wierzbicki A, Aegerter M, Caster CS, Perez-Grau L, Kinney AJ, Hitz WD, Booth JR Jr, Schweiger B, Stecca KL (1993) Cloning of higher plant omega-3 fatty acid desaturases. *Plant Physiol* 103:467–476
5. Hitz WD, Carlson TJ, Booth JR Jr, Kinney AJ, Stecca KL, Yadav NS (1994) Cloning of a higher-plant plastid omega-6 fatty acid desaturase cDNA and its expression in a cyanobacterium. *Plant Physiol* 105:635–641
6. Reed DW, Schafer UA, Covello PS (2000) Characterization of the *Brassica napus* extraplastidial linoleate desaturase by

- expression in *Saccharomyces cerevisiae*. *Plant Physiol* 122:715–720
7. Meesapyodsuk D, Reed DW, Covello PS, Qiu X (2007) Primary structure, regioselectivity, and evolution of the membrane-bound fatty acid desaturases of *Claviceps purpurea*. *J Biol Chem* 282:20191–20199
 8. Fox BG, Shanklin J, Somerville C, Munck E (1993) Stearoyl-acyl carrier protein delta 9 desaturase from *Ricinus communis* is a diiron-oxo protein. *Proc Natl Acad Sci USA* 90:2486–2490
 9. Fox BG, Shanklin J, Ai J, Loehr TM, Sanders-Loehr J (1994) Resonance Raman evidence for an Fe-O-Fe center in stearoyl-ACP desaturase. Primary sequence identity with other diiron-oxo proteins. *Biochemistry* 33:12776–12786
 10. Spychalla JP, Kinney AJ, Browse J (1997) Identification of an animal omega-3 fatty acid desaturase by heterologous expression in *Arabidopsis*. *Proc Natl Acad Sci USA* 94:1142–1147
 11. Meesapyodsuk D, Reed DW, Savile CK, Buist PH, Ambrose SJ, Covello PS (2000) Characterization of the regiochemistry and cryptoregiochemistry of a *Caenorhabditis elegans* fatty acid desaturase (FAT-1) expressed in *Saccharomyces cerevisiae*. *Biochemistry* 39:11948–11954
 12. Qiu X, Hong H, MacKenzie SL (2001) Identification of a Delta 4 fatty acid desaturase from *Thraustochytrium* sp. involved in the biosynthesis of docosahexanoic acid by heterologous expression in *Saccharomyces cerevisiae* and *Brassica juncea*. *J Biol Chem* 276:31561–31566
 13. Aitzetmuller K, Tsevegsuren N (1994) Seed fatty acid “front-end” desaturases and chemotaxonomy—a case study in the Ranunculaceae. *J Plant Physiol* 143:538–543
 14. Nakamura MT, Nara TY (2004) Structure, function, and dietary regulation of delta6, delta5, and delta9 desaturases. *Annu Rev Nutr* 24:345–376
 15. Sayanova O, Smith MA, Lapinskas P, Stobart AK, Dobson G, Christie WW, Shewry PR, Napier JA (1997) Expression of a borage desaturase cDNA containing an N-terminal cytochrome *b*₅ domain results in the accumulation of high levels of delta6-desaturated fatty acids in transgenic tobacco. *Proc Natl Acad Sci USA* 94:4211–4216
 16. Garcia-Maroto F, Garrido-Cardenas JA, Rodriguez-Ruiz J, Vilches-Ferron M, Adam AC, Polaina J, Alonso DL (2002) Cloning and molecular characterization of the delta6-desaturase from two echium plant species: production of GLA by heterologous expression in yeast and tobacco. *Lipids* 37:417–426
 17. Piispanen R, Saranpaa P (2002) Neutral lipids and phospholipids in Scots pine (*Pinus sylvestris*) sapwood and heartwood. *Tree Physiol* 22:661–666
 18. Pereira SL, Leonard AE, Mukerji P (2003) Recent advances in the study of fatty acid desaturases from animals and lower eukaryotes. *Prostaglandins Leukot Essent Fatty Acids* 68:97–106
 19. Sprecher H, Luthria DL, Mohammed BS, Baykousheva SP (1995) Reevaluation of the pathways for the biosynthesis of polyunsaturated fatty acids. *J Lipid Res* 36:2471–2477
 20. Wallis JG, Browse J (1999) The Delta8-desaturase of *Euglena gracilis*: an alternate pathway for synthesis of 20-carbon polyunsaturated fatty acids. *Arch Biochem Biophys* 365:307–316
 21. Sayanova O, Haslam R, Qi B, Lazarus CM, Napier JA (2006) The alternative pathway C20 Delta8-desaturase from the non-photosynthetic organism *Acanthamoeba castellanii* is an atypical cytochrome *b*₅-fusion desaturase. *FEBS Lett* 580:1946–1952
 22. Venegas-Caleron M, Beaudoin F, Sayanova O, Napier JA (2007) Co-transcribed genes for long chain polyunsaturated fatty acid biosynthesis in the protozoan *Perkinsus marinus* include a plant-like FAE1 3-ketoacyl coenzyme A synthase. *J Biol Chem* 282:2996–3003
 23. Reddy AS, Nuccio ML, Gross LM, Thomas TL (1993) Isolation of a delta 6-desaturase gene from the cyanobacterium *Synechocystis* sp. strain PCC 6803 by gain-of-function expression in *Anabaena* sp. strain PCC 7120. *Plant Mol Biol* 22:293–300
 24. Deshniem P, Paithoonrangsarid K, Suphatrakul A, Meesapyodsuk D, Tanticharoen M, Cheevadhanarak S (2000) Temperature-independent and -dependent expression of desaturase genes in filamentous cyanobacterium *Spirulina platensis* strain C1 (*Arthrospira* sp. PCC 9438). *FEMS Microbiol Lett* 184:207–213
 25. Thomas TL, Reddy AS, Nuccio M, Nunberg AN, Freyssinet GL (1997) Production of gamma-linolenic acid by a delta6-desaturase. U.S. Patent 4,736,866
 26. Domergue F, Abbadi A, Zahringer U, Moreau H, Heinz E (2005) In vivo characterization of the first acyl-CoA Delta6-desaturase from a member of the plant kingdom, the microalga *Ostreococcus tauri*. *Biochem J* 389:483–490
 27. Hoffmann M, Wagner M, Abbadi A, Fulda M, Feussner I (2008) Metabolic engineering of omega3-very long chain polyunsaturated fatty acid production by an exclusively acyl-CoA-dependent pathway. *J Biol Chem* 283:22352–22362
 28. Domergue F, Lerchl J, Zahringer U, Heinz E (2002) Cloning and functional characterization of *Phaeodactylum tricorutum* front-end desaturases involved in eicosapentaenoic acid biosynthesis. *Eur J Biochem* 269:4105–4113
 29. Girke T, Schmidt H, Zahringer U, Reski R, Heinz E (1998) Identification of a novel delta 6-acyl-group desaturase by targeted gene disruption in *Physcomitrella patens*. *Plant J* 15:39–48
 30. Laoteng K, Mannontarat R, Tanticharoen M, Cheevadhanarak S (2000) Delta6-desaturase of *Mucor rouxii* with high similarity to plant delta 6-desaturase and its heterologous expression in *Saccharomyces cerevisiae*. *Biochem Biophys Res Commun* 279:17–22
 31. Sakuradani E, Kobayashi M, Shimizu S (1999) Delta6-fatty acid desaturase from an arachidonic acid-producing *Mortierella* fungus. Gene cloning and its heterologous expression in a fungus, *Aspergillus*. *Gene* 238:445–453
 32. Hong H, Datla N, Reed DW, Covello PS, MacKenzie SL, Qiu X (2002) High-level production of gamma-linolenic acid in *Brassica juncea* using a delta6 desaturase from *Pythium irregulare*. *Plant Physiol* 129:354–362
 33. Zheng X, Tocher DR, Dickson CA, Bell JG, Teale AJ (2005) Highly unsaturated fatty acid synthesis in vertebrates: new insights with the cloning and characterization of a delta6 desaturase of Atlantic salmon. *Lipids* 40:13–24
 34. Seilliez I, Panserat S, Kaushik S, Bergot P (2001) Cloning, tissue distribution and nutritional regulation of a Delta6-desaturase-like enzyme in rainbow trout. *Comp Biochem Physiol B Biochem Mol Biol* 130:83–93
 35. Cho HP, Nakamura MT, Clarke SD (1999) Cloning, expression, and nutritional regulation of the mammalian Delta-6 desaturase. *J Biol Chem* 274:471–477
 36. Sperling P, Zahringer U, Heinz E (1998) A sphingolipid desaturase from higher plants. Identification of a new cytochrome *b*₅ fusion protein. *J Biol Chem* 273:28590–28596
 37. Sayanova O, Beaudoin F, Libisch B, Castel A, Shewry PR, Napier JA (2001) Mutagenesis and heterologous expression in yeast of a plant Delta6-fatty acid desaturase. *J Exp Bot* 52:1581–1585
 38. Sayanova OV, Beaudoin F, Michaelson LV, Shewry PR, Napier JA (2003) Identification of primula fatty acid delta 6-desaturases with n-3 substrate preferences. *FEBS Lett* 542:100–104
 39. Sperling P, Lee M, Girke T, Zahringer U, Stymne S, Heinz E (2000) A bifunctional delta-fatty acyl acetylenase/desaturase from the moss *Ceratodon purpureus*. A new member of the cytochrome *b*₅ superfamily. *Eur J Biochem* 267:3801–3811
 40. de Antueno RJ, Knickle LC, Smith H, Elliot ML, Allen SJ, Nwaka S, Winther MD (2001) Activity of human Delta5 and

- Delta6 desaturases on multiple n-3 and n-6 polyunsaturated fatty acids. *FEBS Lett* 509:77–80
41. Reddy AS, Thomas TL (1996) Expression of a cyanobacterial delta 6-desaturase gene results in gamma-linolenic acid production in transgenic plants. *Nat Biotechnol* 14:639–642
 42. Truksa M, Vrinten P, Qiu X (2008) Metabolic engineering of plants for polyunsaturated fatty acid production. *Mol Breed* 23:1–11
 43. Liu JW, Huang YS, DeMichele S, Bergana M, EJR Bobik, Hastilow C, Chuang LT, Mukerji P, Knutzon D (2001) Evaluation of the seed oils from a canola plant genetically transformed to produce high levels of gamma-linolenic acid. In: Huang YS, Ziboh VA (eds) *Gamma-linolenic acid: recent advances in biotechnology and clinical applications*. AOCS Press, Champaign, IL, pp 61–71
 44. Ursin VM (2003) Modification of plant lipids for human health: development of functional land-based omega-3 fatty acids. *J Nutr* 133:4271–4274
 45. Eckert H, La VB, Schweiger BJ, Kinney AJ, Cahoon EB, Clemente T (2006) Co-expression of the borage Delta 6 desaturase and the *Arabidopsis* Delta 15 desaturase results in high accumulation of stearidonic acid in the seeds of transgenic soybean. *Planta* 224:1050–1057
 46. Knauf VC, Shewmaker C, Flider F, Emlay D, Rey E (2011) Safflower with elevated gamma-linolenic acid. U.S. Patent 7,893,321B2
 47. Knutzon DS, Thurmond JM, Huang YS, Chaudhary S, Bobik EG Jr, Chan GM, Kirchner SJ, Mukerji P (1998) Identification of Delta5-desaturase from *Mortierella alpina* by heterologous expression in bakers' yeast and canola. *J Biol Chem* 273:29360–29366
 48. Michaelson LV, Lazarus CM, Griffiths G, Napier JA, Stobart AK (1998) Isolation of a Delta5-fatty acid desaturase gene from *Mortierella alpina*. *J Biol Chem* 273:19055–19059
 49. Kajikawa M, Matsui K, Ochiai M, Tanaka Y, Kita Y, Ishimoto M, Kohzu Y, Shoji S, Yamato KT, Ohshima K, Fukuzawa H, Kohchi T (2008) Production of arachidonic and eicosapentaenoic acids in plants using bryophyte fatty acid Delta6-desaturase, Delta6-elongase, and Delta5-desaturase genes. *Biosci Biotechnol Biochem* 72:435–444
 50. Kajikawa M, Yamato KT, Kohzu Y, Nojiri M, Sakuradani E, Shimizu S, Sakai Y, Fukuzawa H, Ohshima K (2004) Isolation and characterization of delta(6)-desaturase, an ELO-like enzyme and delta(5)-desaturase from the liverwort *Marchantia polymorpha* and production of arachidonic and eicosapentaenoic acids in the methylotrophic yeast *Pichia pastoris*. *Plant Mol Biol* 54:335–352
 51. Saito T, Ochiai H (1999) Identification of Delta5-fatty acid desaturase from the cellular slime mold *Dictyostelium discoideum*. *Eur J Biochem* 265:809–814
 52. Cho HP, Nakamura M, Clarke SD (1999) Cloning, expression, and fatty acid regulation of the human delta-5 desaturase. *J Biol Chem* 274:37335–37339
 53. Hong H, Datla N, MacKenzie SL, Qiu X (2002) Isolation and characterization of a delta5 FA desaturase from *Pythium irregulare* by heterologous expression in *Saccharomyces cerevisiae* and oilseed crops. *Lipids* 37:863–868
 54. Kaewsuwan S, Cahoon EB, Perroud PF, Wiwat C, Panvisavas N, Quatrano RS, Cove DJ, Bunyapraphatsara N (2006) Identification and functional characterization of the moss *Physcomitrella patens* delta5-desaturase gene involved in arachidonic and eicosapentaenoic acid biosynthesis. *J Biol Chem* 281:21988–21997
 55. Tavares S, Grotkjaer T, Obsen T, Haslam RP, Napier JA, Gunnarsson N (2011) Metabolic engineering of *Saccharomyces cerevisiae* for production of eicosapentaenoic acid, using a novel {Delta}5-desaturase from *Paramecium tetraurelia*. *Appl Environ Microbiol* 77:1854–1861
 56. Tonon T, Sayanova O, Michaelson LV, Qing R, Harvey D, Larson TR, Li Y, Napier JA, Graham IA (2005) Fatty acid desaturases from the microalga *Thalassiosira pseudonana*. *FEBS J* 272:3401–3412
 57. Hastings N, Agaba M, Tocher DR, Leaver MJ, Dick JR, Sargent JR, Teale AJ (2001) A vertebrate fatty acid desaturase with Delta 5 and Delta 6 activities. *Proc Natl Acad Sci USA* 98:14304–14309
 58. Abbadi A, Domergue F, Bauer J, Napier JA, Welti R, Zahringer U, Cirpus P, Heinz E (2004) Biosynthesis of very-long-chain polyunsaturated fatty acids in transgenic oilseeds: constraints on their accumulation. *Plant Cell* 16:2734–2748
 59. Cheng B, Wu G, Vrinten P, Falk K, Bauer J, Qiu X (2010) Towards the production of high levels of eicosapentaenoic acid in transgenic plants: the effects of different host species, genes and promoters. *Transgenic Res* 19:221–229
 60. Voss A, Reinhart M, Sankarappa S, Sprecher H (1991) The metabolism of 7,10,13,16,19-docosapentaenoic acid to 4,7,10,13,16,19-docosahexaenoic acid in rat liver is independent of a 4-desaturase *J Biol Chem* 266:19995–20000
 61. Meyer A, Cirpus P, Ott C, Schlecker R, Zahringer U, Heinz E (2003) Biosynthesis of docosahexaenoic acid in *Euglena gracilis*: biochemical and molecular evidence for the involvement of a Delta4-fatty acyl group desaturase. *Biochemistry* 42:9779–9788
 62. Tripodi KE, Buttigliero LV, Altabe SG, Uttaro AD (2006) Functional characterization of front-end desaturases from trypanosomatids depicts the first polyunsaturated fatty acid biosynthetic pathway from a parasitic protozoan. *FEBS J* 273:271–280
 63. Tonon T, Harvey D, Larson TR, Graham IA (2003) Identification of a very long chain polyunsaturated fatty acid Delta4-desaturase from the microalga *Pavlova lutheri*. *FEBS Lett* 553:440–444
 64. Zhou XR, Robert SS, Petrie JR, Frampton DM, Mansour MP, Blackburn SI, Nichols PD, Green AG, Singh SP (2007) Isolation and characterization of genes from the marine microalga *Pavlova salina* encoding three front-end desaturases involved in docosahexaenoic acid biosynthesis. *Phytochemistry* 68:785–796
 65. Li Y, Monroig O, Zhang L, Wang S, Zheng X, Dick JR, You C, Tocher DR (2010) Vertebrate fatty acyl desaturase with Delta4 activity. *Proc Natl Acad Sci USA* 107:16840–16845
 66. Kinney AJ, Cahoon EB, Damude HG, Hitz WD, Kolar CW, Liu ZB (2004) Production of very long chain polyunsaturated fatty acids in oilseed plants. *WO* 2004/071467
 67. Wu G, Truksa M, Datla N, Vrinten P, Bauer J, Zank T, Cirpus P, Heinz E, Qiu X (2005) Stepwise engineering to produce high yields of very long-chain polyunsaturated fatty acids in plants. *Nat Biotechnol* 23:1013–1017
 68. Robert SS, Singh SP, Zhou X, Petrie JR, Blackburn SI, Mansour PM, Nichols PD, Liu Q, Green AG (2005) Metabolic engineering of *Arabidopsis* to produce nutritionally important DHA in seed oil. *Funct Plant Biol* 32:473–479
 69. Qi B, Fraser TC, Bleakley CL, Shaw EM, Stobart AK, Lazarus CM (2003) The variant 'his-box' of the C18-Delta9-PUFA-specific elongase IgASE1 from *Isochrysis galbana* is essential for optimum enzyme activity. *FEBS Lett* 547:137–139
 70. Park WJ, Kothapalli KS, Lawrence P, Tyburczy C, Brenna JT (2009) An alternate pathway to long-chain polyunsaturates: the *FADS2* gene product Delta8-desaturates 20:2n-6 and 20:3n-3. *J Lipid Res* 50:1195–1202
 71. Sayanova O, Haslam RP, Caleron MV, Lopez NR, Worthy C, Rooks P, Allen MJ, Napier JA (2011) Identification and functional characterisation of genes encoding the omega-3

- polyunsaturated fatty acid biosynthetic pathway from the coccolithophore *Emiliania huxleyi*. *Phytochemistry* 72:594–600
72. Qi B, Fraser T, Mugford S, Dobson G, Sayanova O, Butler J, Napier JA, Stobart AK, Lazarus CM (2004) Production of very long chain polyunsaturated omega-3 and omega-6 fatty acids in plants. *Nat Biotechnol* 22:739–745
 73. Petrie JR, Shrestha P, Belide S, Mansour MP, Liu Q, Horne J, Nichols PD, Singh SP (2011) Transgenic production of arachidonic acid in oilseeds. *Transgenic Res*. doi:10.1007/s11248-011-9517-7
 74. Shanklin J, Somerville C (1991) Stearoyl-acyl-carrier-protein desaturase from higher plants is structurally unrelated to the animal and fungal homologs. *Proc Natl Acad Sci USA* 88:2510–2514
 75. Stymne S, Stobart AK (1986) Biosynthesis of gamma-linolenic acid in cotyledons and microsomal preparations of the developing seeds of common borage (*Borago officinalis*). *Biochem J* 240:385–393
 76. Griffiths G, Stobart AK, Stymne S (1988) Delta 6- and delta 12-desaturase activities and phosphatidic acid formation in microsomal preparations from the developing cotyledons of common borage (*Borago officinalis*). *Biochem J* 252:641–647
 77. Domergue F, Abbadi A, Ott C, Zank TK, Zahringer U, Heinz E (2003) Acyl carriers used as substrates by the desaturases and elongases involved in very long-chain polyunsaturated fatty acids biosynthesis reconstituted in yeast. *J Biol Chem* 278:35115–35126
 78. Petrie JR, Shrestha P, Mansour MP, Nichols PD, Liu Q, Singh SP (2010) Metabolic engineering of omega-3 long-chain polyunsaturated fatty acids in plants using an acyl-CoA Delta6-desaturase with omega3-preference from the marine microalga *Micromonas pusilla*. *Metab Eng* 12:233–240
 79. Sperling P, Ternes P, Zank TK, Heinz E (2003) The evolution of desaturases. *Prostaglandins Leukot Essent Fatty Acids* 68:73–95
 80. Stuke JE, McDonough VM, Martin CE (1989) Isolation and characterization of *OLE1*, a gene affecting fatty acid desaturation from *Saccharomyces cerevisiae*. *J Biol Chem* 264:16537–16544
 81. Mitchell AG, Martin CE (1995) A novel cytochrome *b*₅-like domain is linked to the carboxyl terminus of the *Saccharomyces cerevisiae* delta-9 fatty acid desaturase. *J Biol Chem* 270:29766–29772
 82. Qiu X, Hong H, Datla N, MacKenzie SL, Taylor DC, Thomas TL (2002) Expression of borage delta-6 desaturase in *Saccharomyces cerevisiae* and oilseed crops. *Can J Bot* 80:42–49
 83. Hongsthong A, Subudhi S, Sirijuntarut M, Kurdrid P, Cheevadhanarak S, Tanticharoen M (2006) Revealing the complementation of ferredoxin by cytochrome *b* (5) in the Spirulina-(6)-desaturation reaction by N-terminal fusion and co-expression of the fungal-cytochrome *b* (5) domain and Spirulina-(6)-acyl-lipid desaturase. *Appl Microbiol Biotechnol* 72:1192–1201
 84. Sayanova O, Shewry PR, Napier JA (1999) Histidine-41 of the cytochrome *b*₅ domain of the borage delta6 fatty acid desaturase is essential for enzyme activity. *Plant Physiol* 121:641–646
 85. Na-Ranong S, Laoteng K, Kittakoop P, Tanticharoen M, Cheevadhanarak S (2006) Targeted mutagenesis of a fatty acid Delta6-desaturase from *Mucor rouxii*: role of amino acid residues adjacent to histidine-rich motif II. *Biochem Biophys Res Commun* 339:1029–1034
 86. Libisch B, Michaelson LV, Lewis MJ, Shewry PR, Napier JA (2000) Chimeras of Delta6-fatty acid and Delta8-sphingolipid desaturases. *Biochem Biophys Res Commun* 279:779–785
 87. Lange SJ, Que L Jr (1998) Oxygen activating nonheme iron enzymes. *Curr Opin Chem Biol* 2:159–172
 88. Shanklin J, Guy JE, Mishra G, Lindqvist Y (2009) Desaturases: emerging models for understanding functional diversification of diiron-containing enzymes. *J Biol Chem* 284:18559–18563
 89. Whyte LG, Schultz A, Beilen JB, Luz AP, Pellizari V, Labbe D, Greer CW (2002) Prevalence of alkane monooxygenase genes in Arctic and Antarctic hydrocarbon-contaminated and pristine soils. *FEMS Microbiol Ecol* 41:141–150
 90. Feussner C, Wasternack C, Kindl H, Kuhn H (1995) Lipoxygenase-catalyzed oxygenation of storage lipids is implicated in lipid mobilization during germination. *Proc Natl Acad Sci USA* 92:11849–11853
 91. Arciero DM, Orville AM, Lipscomb JD (1985) [17O]Water and nitric oxide binding by protocatechuate 4,5-dioxygenase and catechol 2,3-dioxygenase. Evidence for binding of exogenous ligands to the active site Fe²⁺ of extradiol dioxygenases. *J Biol Chem* 260:14035–14044
 92. Shanklin J, Whittle E, Fox BG (1994) Eight histidine residues are catalytically essential in a membrane-associated iron enzyme, stearoyl-CoA desaturase, and are conserved in alkane hydroxylase and xylene monooxygenase. *Biochemistry* 33:12787–12794
 93. Fauconnot L, Buist PH (2001) Gamma-linolenic acid biosynthesis: cryptoregiochemistry of delta6 desaturation. *J Org Chem* 66:1210–1215
 94. Behrouzian B, Buist PH (2003) Mechanism of fatty acid desaturation: a bioorganic perspective. *Prostaglandins Leukot Essent Fatty Acids* 68:107–112
 95. Meesapyodsuk D, Reed DW, Savile CK, Buist PH, Schafer UA, Ambrose SJ, Covello PS (2000) Substrate specificity, regioselectivity and cryptoregiochemistry of plant and animal omega-3 fatty acid desaturases. *Biochem Soc Trans* 28:632–635
 96. Aguilar PS, de MD (2006) Control of fatty acid desaturation: a mechanism conserved from bacteria to humans. *Mol Microbiol* 62:1507–1514
 97. Napier JA (2007) The production of unusual fatty acids in transgenic plants. *Annu Rev Plant Biol* 58:295–319
 98. Sayanova O, Napier JA (2011) Transgenic oilseed crops as an alternative to fish oils. *Prostaglandins Leukot Essent Fatty Acids* 85:253–260
 99. Singh SP, Zhou XR, Liu Q, Stymne S, Green AG (2005) Metabolic engineering of new fatty acids in plants. *Curr Opin Plant Biol* 8:197–203
 100. Napier JA, Graham IA (2010) Tailoring plant lipid composition: designer oilseeds come of age. *Curr Opin Plant Biol* 13:330–337
 101. Graham IA, Larson T, Napier JA (2007) Rational metabolic engineering of transgenic plants for biosynthesis of omega-3 polyunsaturates. *Curr Opin Biotechnol* 18:142–147
 102. Cahoon EB, Shockey JM, Dietrich CR, Gidda SK, Mullen RT, Dyer JM (2007) Engineering oilseeds for sustainable production of industrial and nutritional feedstocks: solving bottlenecks in fatty acid flux. *Curr Opin Plant Biol* 10:236–244

7-Ketocholesterol is Not Cytotoxic to U937 Cells When Incorporated into Acetylated Low Density Lipoprotein

Lucy D. Rutherford · Steven P. Gieseg

Received: 10 June 2011 / Accepted: 7 November 2011 / Published online: 29 November 2011
© AOCs 2011

Abstract The growth of the necrotic core region within advanced atherosclerotic plaque is thought to be driven by oxidised low density lipoprotein (oxLDL)-induced death of macrophage cells. OxLDL and atherosclerotic plaque are rich in oxysterols, especially 7-ketocholesterol (7KC). As 7KC triggers cell death at physiological concentrations when added directly to the cell culture media, 7KC and other oxysterols have been suggested to be the main cytotoxic agent of oxLDL. We investigated this hypothesis by examining the toxicity of 7KC to monocyte-like U937 cells when incorporated into high-uptake non-toxic acetylated LDL (acLDL). Incorporation of 7KC into acLDL greatly reduced the oxysterol toxicity when compared with an equivalent amount of 7KC added directly to U937 cells. Enrichment of oxLDL with 7KC did not significantly enhance lipoprotein toxicity. OxLDL was highly cytotoxic yet generated only low levels of intracellular 7KC. In comparison, 7KC-acLDL generated high intracellular 7KC concentrations with little loss in cell viability. The data show that when incorporated into lipoprotein, 7KC cytotoxicity is greatly reduced, even though intracellular levels exceed those measured when cells are incubated with oxLDL, which suggests 7KC is not the significant toxic agent within oxLDL.

Keywords Oxidised low density lipoprotein · OxLDL · 7-Ketocholesterol · Oxysterol · Cell death · Toxicity · U937

Abbreviations

acLDL	Acetylated LDL
oxLDL	Oxidised low density lipoprotein
7KC	7-Ketocholesterol
HNE	4-Hydroxynonenal
HPLC	High performance liquid chromatography
MDA	Malondialdehyde
MTT	3-(4,5-dimethylthiazol-2-yl)-2,5-diphenyl tetrazolium bromide
PBS	Phosphate buffered saline

Introduction

The formation of oxidised low density lipoprotein (oxLDL) and the resulting cytotoxicity of oxLDL to macrophage cells is a key driver in the development of the necrotic core of advanced atherosclerotic plaque [1, 2]. OxLDL contains numerous oxidised components that could potentially be cytotoxic. Copper ion-, peroxy radical- and macrophage-oxidised LDL all contain high levels of lipid and protein hydroperoxides, as well as oxidation products of the various antioxidants [3, 4]. The decay of lipid peroxides is a dominant reaction in the later stages of LDL oxidation, resulting in the formation of oxysterols, isoprostanes and reactive short chain aldehydes [5]. The short chain aldehydes, 4-hydroxynonenal (HNE) and malondialdehyde (MDA), derivatise the lysine residues of apolipoprotein B100, destroying the binding site for the LDL receptor but rendering the particle a ligand for the scavenger receptors [6, 7].

Oxysterols, aside from being implicated in the formation of foam cells, have also been cited as a key agent in oxLDL-induced cell death [8–10]. Oxysterols are known to be abundant in atherosclerotic lesions [5, 11] and are produced in significant quantities by various methods of *in vitro* LDL

L. D. Rutherford · S. P. Gieseg (✉)
Free Radical Biochemistry Laboratory, School of Biological
Sciences, University of Canterbury, Private Bag 4800,
Christchurch 8140, New Zealand
e-mail: Steven.Gieseg@canterbury.ac.nz

oxidation [12, 13]. Several of these oxysterols, including 7-ketocholesterol (7KC), 7-hydroxycholesterol, 7 β -hydroxycholesterol and 25-, 26- and 27-hydroxycholesterol have been shown to have potent cytotoxic effects on cell viability when delivered directly to cultures of endothelial cells [14], macrophages [8], monocytes [10] and smooth muscle cells [14]. The suggested mechanisms of 7KC-induced cytotoxicity arise from its disruption of lipid raft micro-domains in the plasma membrane, which allows calcium ion influx and the associated calcium-dependent activation of pro-apoptotic pathways [15]. 7KC incorporation into unoxidised acetylated LDL (acLDL) has also been reported to inhibit sterol export from macrophages, leading to the formation of lipid-laden foam cells [16].

Though these studies have been very informative they assume that free oxysterols, suspended in a tissue culture media, will interact with and be handled by cells in the same way as the oxysterols within oxLDL. Being hydrophobic, oxysterols are normally trapped within the LDL particle and become available to the cell only when the oxLDL particle is taken up by scavenger receptors and degraded in the lysosomes [16]. In vivo, it is highly unlikely that oxysterols could leach from oxLDL particles to become free in the media (as micelles or liposomes), as used in the cited cytotoxicity experiments. Our study examined whether the oxysterol 7KC is still cytotoxic when packaged into unoxidised lipoprotein particles. To achieve the high uptake of particles seen with oxLDL, we used acLDL which has no cytotoxic effect on cells [16] and contains no oxidised components. The 7KC added to the acLDL is therefore the only “oxidised” component of the acLDL particle.

7KC is the major oxysterol present in oxLDL [12], in oxLDL-loaded human monocyte-derived macrophages [17] and advanced atherosclerotic plaque [18]. In human monocyte-like U937 cells, 7KC triggers cell death with oxidative stress and caspase activation [19]. U937 cells are an excellent model system, as oxLDL triggers the same cytotoxic events in U937 cells as those observed in actual human monocyte-derived macrophages (prepared from human blood) [2, 20, 21]. In this study we treated U937 cells with increasing levels of 7KC loaded acLDL and compared the cytotoxicity to oxLDL and 7KC added directly to the cells. We have also examined the effect of adding additional 7KC to already oxidised LDL. The experiments described here directly test the hypothesis that 7KC is the main cytotoxic agent in oxLDL.

Methods

Chemicals

All chemicals and reagents were of analytical grade or better and obtained from the Sigma Chemical Company

(USA), BDH Chemicals New Zealand Ltd., or Merck (Germany). All solutions were prepared using ion-exchanged ultra-filtered water, which was produced using a NANOpure ultrapure water system from Barnstead/Thermolyne (IA/USA). Cell culture plasticware was supplied by Greiner Bio-one through Raylab Ltd. 7KC was obtained from the Sigma-Aldrich Chemical Co. (USA) and 7,8-dihydroneopterin from Schircks Laboratories (Switzerland). Phosphate buffered saline (PBS) consisted of 150 mM sodium chloride and 10 mM sodium phosphate, pH 7.4.

Lipoprotein Isolation

Human plasma (anti-coagulated with EDTA) was isolated by venipuncture from healthy male and female donors following an overnight fast (ethics approval from Upper South A Ethics Committee, CTY/01/04/036). LDL was isolated from human plasma by buoyant density gradient ultracentrifugation using an NVTi 60 rotor (Beckman Coulter, USA) [22]. The LDL concentration was determined by enzymatic cholesterol assay using a CHOL kit (Roche Diagnostic, USA) assuming an LDL molecular weight of 2.5 MDa and a cholesterol content of 31.6% [22]. The KBr and EDTA were removed and the LDL concentrated by ultrafiltration using Amicon® Ultra-15 filter tubes (Millipore, USA). LDL preparations were filter-sterilised (0.22 μ m, Membrane Solutions, USA) and stored in the dark at 4 °C under argon gas.

Incorporation of 7KC into LDL

Human plasma was combined with 7KC dissolved in ethanol, to give a final concentration in plasma of 2.4 mM 7KC with an ethanol concentration less than 2.6% (v/v) and incubated at 37 °C with gentle shaking for 6 h [16]. The 7KC-enriched LDL was isolated by buoyant density gradient ultracentrifugation, then ultra-filtered and concentrated as described for native LDL.

Lipoprotein Modifications

Copper-oxidised LDL was prepared using a method adapted from Gerry et al. [13]. LDL at 10 mg/ml total mass (2 mg/ml apoB protein) was placed in a dialysis bag (12–14 kDa, Medicell International, UK) with the addition of CuCl₂ to give a final concentration of 0.5 mM. The dialysis bag was placed in a solution of PBS (100 ml buffer per 5 mg of LDL total mass) containing 0.5 mM CuCl₂ and incubated at 37 °C for 24 h. Oxidised lipoprotein was dialysed against three changes of Chelex-containing PBS at 4 °C for 24 h.

7KC-oxLDL was prepared by first loading the LDL with 7KC before oxidising 7KC-LDL with copper ions, as described above.

AcLDL and 7KC-acLDL were prepared using an adaptation of the method described by Kritharides et al. [23]. Specifically, the lipoprotein solution (10 mg/ml) was combined, on ice with very gentle stirring, with an equal volume of saturated sodium acetate solution. Acetic anhydride was added to lipoprotein, in 2- μ l aliquots, at 10-min intervals to a final concentration of 6 μ l acetic anhydride per mg LDL protein. The acetylated lipoprotein solution was buffer-exchanged and concentrated by ultra-filtration before filter-sterilisation.

Gel Electrophoresis

Modification of the lipoprotein was confirmed by non-denaturing gel electrophoresis using a Beckman Paragon[®] native gel electrophoresis kit and apparatus in B-2 barbital buffer at 100 V for 30 min. The relative electrophoretic mobility (REM) was calculated as the distance travelled by the oxidised or acetylated LDL relative to the reference native LDL.

Cell Culture

U937 human monocyte-like cells were grown in suspension in culture medium consisting of RPMI-1640 containing penicillin G (100 U/ml) and streptomycin (100 μ g/ml) (Gibco Invitrogen, NZ) supplemented with 5% heat-inactivated foetal bovine serum (Invitrogen, USA). Cells were incubated at 37 °C in a humidified atmosphere containing 5% CO₂ (Sanyo CO₂ Incubator). Cells in serum-free RPMI-1640 at 5×10^5 cells/ml were transferred to non-adherent suspension plates coated with 8 μ l of 50 mg/ml bovine serum albumin per well containing a total of 1 ml of medium, to prevent cells sticking to plastic. Serum is known to inhibit oxLDL toxicity to cell lines, so serum was removed from the cell medium by centrifugation and washing in PBS immediately prior to use in experiments and the serum-free medium was used in all experiments.

A 10 mM 7KC stock solution was prepared in absolute ethanol (Merck, Germany) and diluted to a concentration of 100 μ M with RPMI-1640 before addition to wells, so that the final concentration of ethanol in the culture medium was below 0.5% (v/v). A 2 mM 7,8-dihydroneopterin stock solution was prepared immediately before use in experiments, before dilution with further RPMI-1640 to working concentrations. When cells were treated simultaneously with 7,8-dihydroneopterin and 7KC, the 7,8-dihydroneopterin was introduced into the culture medium 10 min prior to treatment with 7KC.

Cell Viability

Cell viability was determined by 3-(4,5-dimethylthiazol-2-yl)-2,5-diphenyl tetrazolium bromide (MTT) reduction assay using the method of Mosmann [24] but using 10% (w/v) sodium dodecyl sulphate to lyse cells and solubilise the insoluble MTT-formazan salt.

Measurement of 7KC

Measurement of unesterified 7KC was performed by solvent extraction followed by high performance liquid chromatography (HPLC) analysis [25]. Following treatments, cells were washed twice with warm PBS and lysed with 0.2 M NaOH for 15 min before extraction into hexane. Hexane extracts were evaporated under nitrogen gas and re-dissolved in acetonitrile:isopropanol (4:5) before being quantified by isocratic reverse phase HPLC using a Phenosphere C-18 column (4.6 \times 250 mm, 5 μ m particle size, Phenomenex, Auckland, NZ) developed with a mobile phase of acetonitrile/isopropanol/water in a ratio of 44:54:2. The 7KC was detected by absorbance at 234 nm and quantification was by comparison to pure standards.

Cellular GSH

Glutathione (GSH) levels were measured by derivatisation with monobromobimane and reverse phase C-18 HPLC analysis of the fluorescent derivative using monobromobimane-derivatised GSH as a standard [26].

Statistical Analysis

Data shown are the result of single experiments and representative of three separate experiments. The mean and standard error of the mean (SEM) shown within each experiment were calculated from triplicate samples in every case. Data were analysed using the Prism software package (version 4.0, GraphPad Software Inc., USA). Significance was confirmed via one way analysis of variance (ANOVA) followed by Tukey's multiple comparison test. Asterisks indicate significance from the control or initial value (unless otherwise indicated) when * $p \leq 0.05$, ** $p \leq 0.01$ and *** $p \leq 0.001$.

Results

OxLDL-Induced U937 GSH Loss, Cell Viability Loss and 7KC Uptake

OxLDL induced a dramatic loss of U937 cell viability, as measured by the cells' ability to metabolically reduce MTT

(Fig. 1a). With 0.2 mg/ml oxLDL, cell viability after 24 h was only 32% of the control, with the viability loss occurring predominantly between 1.5 and 6 h of incubation (Fig. 1c). Loss of metabolic activity was consistent with changes in cellular morphology (data not shown) such as blebbing, cell swelling and lysis and appearance of cellular debris, consistent with the caspase-independent necrosis previously described in U937 cells [20].

OxLDL triggers reactive oxygen species formation in U937 cells as shown by the rapid and early loss of cellular glutathione [20, 27]. The decrease in cellular glutathione levels closely followed the loss of cell viability (Fig. 1d), showing that the oxidative stress was intense and developed rapidly in response to oxLDL exposure [20]. Increasing concentrations of oxLDL resulted in a concentration-dependent increase in cellular 7KC content, indicating the internalisation of the oxysterol (Fig. 1b).

7KC-Induced U937 GSH Loss, Cell Viability Loss and 7KC Uptake

Treatment of U937 cells with 7KC, added to the culture medium dissolved in ethanol, induced a dramatic and

concentration-dependent loss of cell viability with an estimated LD₅₀ of 18 μ M (Fig. 2a). The concentration of 7KC is reported to be approximately 25 μ M in advanced lesions so this concentration is similar to physiological levels within plaques [11]. The viability loss was not due to the ethanol, as the maximum concentration used caused no significant loss of cell viability (as in the 0 μ M 7KC control). In contrast to oxLDL, the 7KC-induced viability loss occurred only after a 9-h lag period (Fig. 2c). Cell viability loss occurred predominantly between 12 and 28 h, which was also much slower than that observed with oxLDL. This lag phase kinetic followed by a slow decline in viability was mirrored by the loss of cellular glutathione (Fig. 2d) which is consistent with other published reports using U937 cells [28] and suggests a much lower level of reactive oxygen species production with 7KC compared to oxLDL. Examination of cells at 24 h showed that 7KC was absorbed into the cell to a maximum intracellular concentration of 19 nmol 7KC/10⁶ cells (Fig. 2b). As many of the cells were undergoing necrosis above 20 μ M added 7KC, this resulted in an apparent saturation effect in the uptake kinetics and impairment of the cellular uptake mechanisms, due to the cell death process. We have

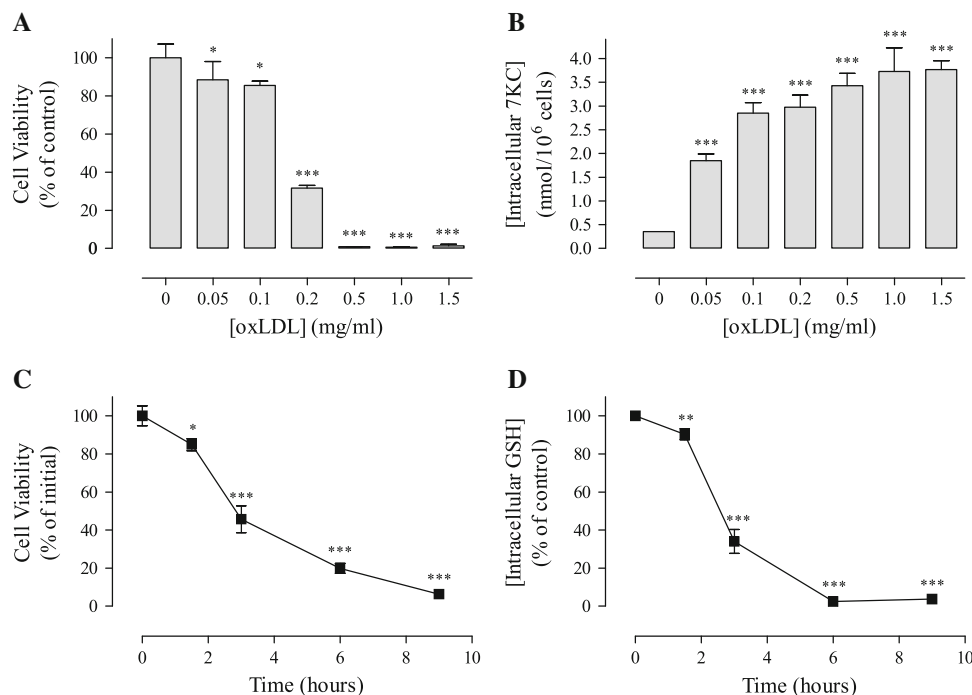


Fig. 1 OxLDL causes U937 cell viability loss, GSH loss and increased 7KC content. U937 cells were incubated with increasing concentrations of oxLDL in RPMI-1640 for 24 h before **a** cell viability was determined by MTT reduction assay and **b** cellular 7KC content was measured by HPLC analysis. Cell viability is expressed as a percentage of the 0 mg/ml oxLDL treatment. U937 cells were incubated with 0.25 mg/ml oxLDL in RPMI-1640 and cell samples

were taken at various time points for measurement of **c** cell viability by MTT reduction assay and **d** intracellular GSH content by HPLC analysis. Cell viability is expressed as a percentage of the initial viability and intracellular GSH is expressed as a percentage of the GSH content at corresponding time points. Untreated U937 cell GSH concentration is 11 nmol/mg protein of cell protein

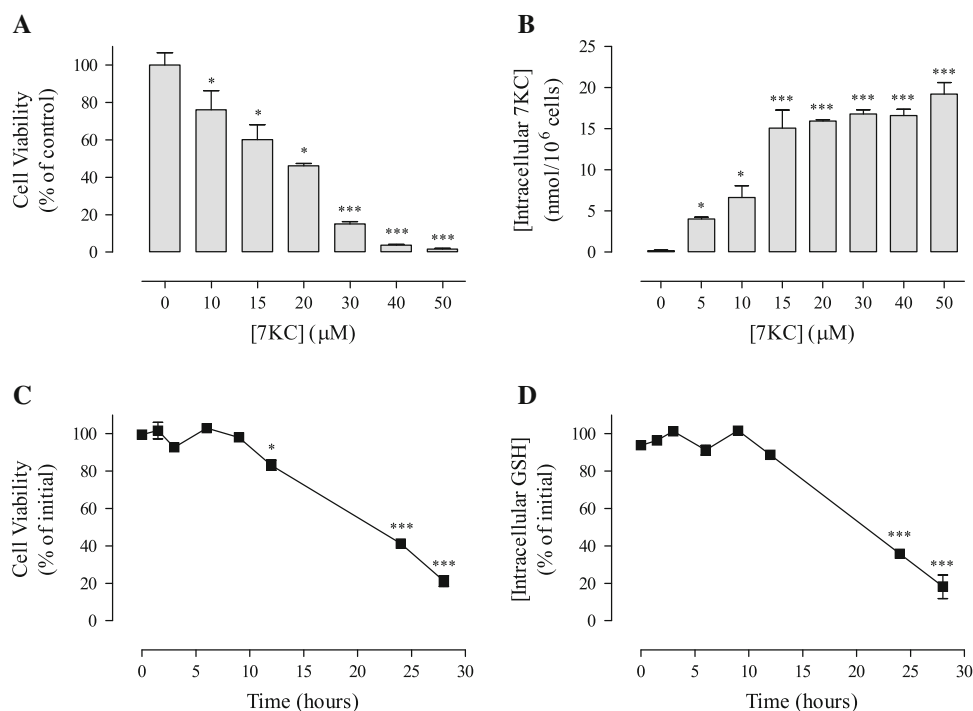


Fig. 2 7KC causes U937 cell viability loss, GSH loss and increased 7KC content. U937 cells were incubated with increasing concentrations of 7KC in RPMI-1640 for 24 h before **a** cell viability was determined by MTT reduction assay and **b** cellular 7KC content was measured by HPLC analysis. Cell viability is expressed as a percentage of the 0 μM 7KC treatment. The 0 μM 7KC control contained 0.5% (v/v) ethanol which was the maximum concentration

of ethanol used as a vehicle for 7KC. U937 cells were incubated with 30 μM 7KC in RPMI-1640 and cell samples were taken at various time points for measurement of **c** cell viability by MTT reduction assay and **d** intracellular GSH content by HPLC analysis. Cell viability and GSH content are each expressed as a percentage of the initial level. Untreated U937 cell GSH concentration is 11 nmol/mg protein of cell protein

measured only unesterified intracellular 7KC levels as esterification has been shown to prevent 7KC cytotoxicity in U937 cells [29].

7,8-Dihydroneopterin Does Not Protect Against 7KC-Induced U937 Cell Viability Loss

We had previously shown that the water soluble antioxidant, 7,8-dihydroneopterin, inhibits oxLDL toxicity by scavenging intracellular oxidants. 7,8-Dihydroneopterin inhibits oxLDL toxicity by scavenging intracellular oxidants independently of other antioxidants such as glutathione or α-tocopherol [30, 31]. Using 7,8-dihydroneopterin as a probe of the toxicity mechanism, we found that it did not protect U937 cells from the cytotoxic effect of 7KC, indicating that oxidative stress was not a key factor in driving the 7KC-induced cell death (Fig. 3). This is in direct contrast to that observed with oxLDL-treated U937 cells [20, 27].

7KC-acLDL Displays High 7KC Uptake and Low Toxicity to U937 Cells

To examine the effect of 7KC on lipoprotein toxicity, LDL was purified from human plasma, which had been enriched

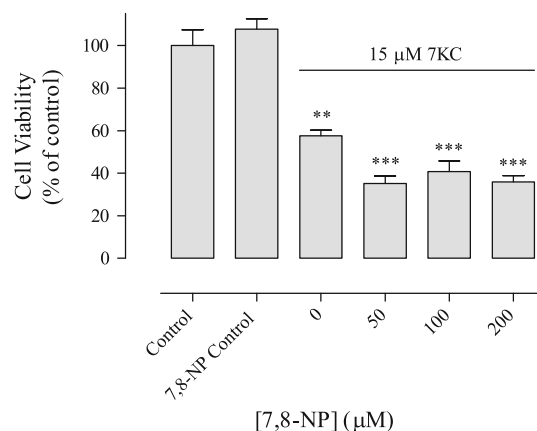


Fig. 3 7,8-Dihydroneopterin (7,8-NP) does not protect against 7KC-induced U937 cell viability loss. U937 cells were treated with increasing concentrations of 7,8-dihydroneopterin for 10 min before incubation with or without (control and 7,8-dihydroneopterin control containing 200 μM 7,8-dihydroneopterin) 15 μM 7KC in RPMI-1640 for 24 h at which point, cell viability was determined by MTT reduction assay. Results are expressed as a percentage of the viability of the control treatment and significance is indicated from the control

with 7KC. The purified lipoprotein was converted to the high-uptake form by acetylation. As expected, acetylation increased the electrophoretic mobility of the LDL 4-fold

over native LDL, while extensive copper oxidation increased the lipoprotein mobility 4.4-fold (Fig. 4a). Importantly, the incorporation of 7KC did not alter the electrophoretic mobility of the acLDL, showing that there were no major changes to the LDL charge/mass ratio. Analysis of the 7KC-acLDL showed a 7KC content of 228 mol/mol LDL while the copper-oxidised LDL used for comparison had a 7KC content of 131 mol/mol LDL (Fig. 4b). Zero or minute quantities of 7KC were measured in native and acLDL, respectively.

The U937 cells rapidly internalised 7KC-acLDL, with the intracellular 7KC concentration reaching 80% of maximum within 6 h (Fig. 5a). The intracellular concentration of 20 nmol 7KC/ 10^6 cells achieved with 1.5 mg/ml 7KC-acLDL after 24 h incubation (Fig. 5b), was 5-fold higher than that measured with oxLDL (Fig. 1b). The increase in intracellular 7KC concentration achieved with 7KC-acLDL did not translate into increased cytotoxicity. Using 0.2 mg/ml 7KC-acLDL, which contains 18 μ M 7KC, there was no viability loss (Fig. 5c), while a similar concentration of

7KC (20 μ M) added as an ethanol solution caused 55% loss in viability (Fig. 2a). If we compare just the intracellular levels of 7KC, there was a 17% loss of viability with 15 nmol 7KC/ 10^6 cells (0.5 mg/ml of 7KC-acLDL, Fig. 5) while with 7KC added in ethanol, an intracellular concentration of 16 nmol 7KC/ 10^6 cells resulted in a 54% decrease in cell viability (Fig. 2). The 7KC toxicity was greatly reduced when incorporated into acLDL. The overall levels of intracellular 7KC achieved with 7KC-acLDL were up to five times higher than that achieved with oxLDL, yet oxLDL was far more cytotoxic.

7KC-oxLDL and OxLDL Display Similar Toxicity to U937 Cells

The higher toxicity of oxLDL compared to 7KC-acLDL is possibly due to different processing of the lipoprotein particle. If 7KC is the toxic agent within oxLDL, the selective enrichment of oxLDL with 7KC should therefore make it more toxic. The 7KC content of oxLDL was increased more than 5-fold (Fig. 5e) yet this did not affect the toxicity with U937 cells, except at concentrations of 1 mg/ml 7KC-oxLDL or above (Fig. 5e). With 0.3 mg/ml of either oxLDL (10 μ M 7KC) or 7KC-oxLDL (60 μ M 7KC) there was only a small viability loss of 10% for each. At 0.5 mg/ml lipoprotein, the 7KC loading appeared to decrease the toxicity by 10%, though this was well beyond the LD₅₀. It was only at extremely toxic concentrations of oxLDL (80% viability loss) and above, that the corresponding 7KC-oxLDL induced further loss of viability. This shows that raising oxLDL 7KC levels without causing further oxidative damage does not increase cytotoxicity.

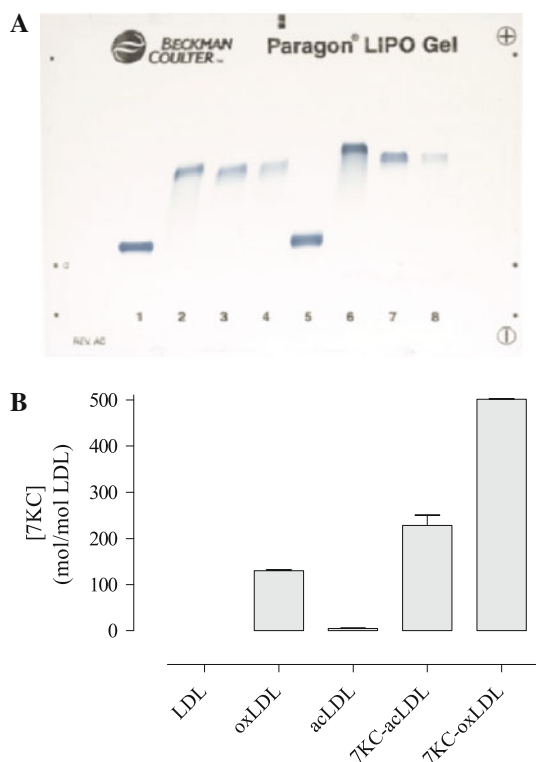


Fig. 4 Relative electrophoretic mobility and 7KC content of native and modified LDL. Native and modified LDL were prepared as described at “Lipoprotein Isolation”, “Incorporation of 7KC into LDL” and “Lipoprotein Modifications”, and **a** relative electrophoretic mobility was examined on a non-denaturing Paragon[®] LIPO gel. Lanes 1 and 5 were loaded with native LDL, lanes 2 and 6 with oxLDL, lanes 3 and 7 with acLDL and lanes 4 and 8 with 7KC-acLDL, at 2.0 mg/ml LDL protein. **b** The non-esterified 7KC content of individual lipoprotein preparations was measured by HPLC analysis and is representative of at least three separate preparations

Discussion

Oxysterol cytotoxicity has been measured in numerous *in vitro* studies by direct addition to the cell culture medium. As oxysterols are normally located within lipoproteins *in vivo*, the findings presented here have been generated using a more physiologically relevant model system where 7KC was incorporated into LDL.

The U937 cell line we used was found to be very sensitive to oxLDL and 7KC toxicity (Figs. 1, 2). Yet when U937 cells were incubated with 7KC incorporated into high-uptake acLDL (7KC-acLDL) the toxicity was greatly reduced (Fig. 5). Across the different methods of 7KC exposure to U937 cells, there was no correlation between intracellular 7KC concentration and cytotoxicity. While relatively low intracellular concentrations of 7KC correlated with very high oxLDL toxicity, comparatively large intracellular 7KC concentrations from the uptake of 7KC-acLDL caused only a small viability loss. Furthermore, the

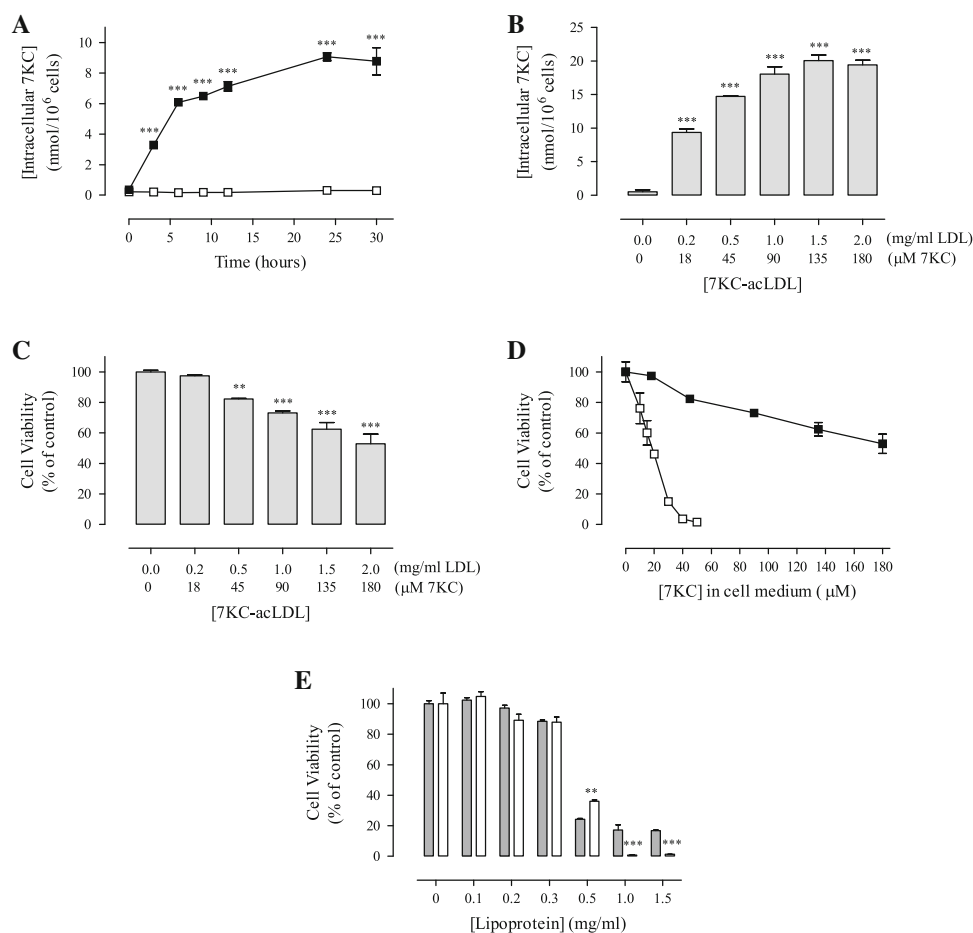


Fig. 5 7KC-acLDL displays high uptake and low toxicity to U937 cells. **a** Intracellular 7KC content was measured at various time points during incubation of U937 cells with (*black squares*) or without (*white squares*) 0.2 mg/ml 7KC-acLDL (equivalent to 18 μM 7KC) in RPMI-1640 over 30 h. Significance is indicated from the control data for each time point. U937 cells were incubated with increasing concentrations of 7KC-acLDL in RPMI-1640 for 24 h before **b** measurement of cellular non-esterified 7KC content by HPLC analysis and **c** determination of cell viability by MTT reduction assay. The X axis values give both the 7KC and total lipoprotein

concentration in the media for each treatment. Cell viability is expressed as a percentage of the 0 mg/ml 7KC-acLDL treatment. **d** Data from Figs. 2a and 5c are represented together, showing the comparison of U937 cell viability with 7KC (*white square*) and 7KC-acLDL (*black squares*). **e** U937 cell viability was measured following a 24 h incubation with oxLDL (*grey bars*) and 7KC-oxLDL (*white bars*). The oxLDL preparation contained 87 mol 7KC/mol LDL and the 7KC-oxLDL preparation contained 501 mol 7KC/mol LDL. Significance is indicated from the respective oxLDL data for each concentration

treatment of cells with 7KC-oxLDL, which contained 6-fold more 7KC than normal oxLDL, did not show an increased level of cell viability loss, except at the very highest 7KC-oxLDL concentrations. Collectively, these findings do not support the hypothesis that 7KC is the main cytotoxic agent in oxLDL.

OxLDL toxicity to U937 cells and human monocyte-derived macrophages is driven by the induction of reactive oxygen species generation, which can be inhibited by antioxidants such as 7,8-dihydroneopterin [2, 21, 27]. Though 7KC cytotoxicity is reportedly inhibited by glutathione in U937 cells [28] and NADPH-oxidase inhibitors in mouse J774A.1 cells [32], 7,8-dihydroneopterin was unable to prevent cell viability loss when 7KC was added directly to cells (Fig. 3). We have previously demonstrated that

7,8-dihydroneopterin is taken up by cells [21] suggesting that in the case of oxLDL, the inhibition of the oxidative stress is most likely to occur intracellularly whereas much of the cytotoxic effect of 7KC may occur on the plasma membrane [33]. This indicates that oxLDL and 7KC exert toxicity via different mechanisms and that oxLDL toxicity is unlikely to be dependent on 7KC toxicity. This is also mirrored in the rate of GSH loss; which was rapid with oxLDL and much slower with the direct addition of 7KC.

The key difference in cytotoxicity between 7KC added directly to the cell media and 7KC in a lipoprotein appears to be how the cell handles the oxysterol. When given directly to cells, 7KC collects on the plasma lipid membrane within the lipid rafts, disrupting calcium control [15]. In contrast, when 7KC enters the cells via a lipoprotein, it

is rapidly rendered non-toxic through esterification after release from the lipoprotein in the lysosomes [29]. The esterified 7KC appears to be unable to concentrate in the plasma membrane and disrupt the lipid rafts.

7KC is not the only oxysterol found within heavily oxidised LDL. 25-Hydroxycholesterol and 7-beta-hydroperoxycholest-5-en-3-beta-ol, to name a few have been shown to be cytotoxic when added directly to the cells [10, 34]. The toxic effects described for this class of compounds appear similar, suggesting that like 7KC they may also have reduced cytotoxicity when incorporated into a lipoprotein. If this is the case, the question remains, what is the main cytotoxic component in copper-oxidised LDL? Lipid oxidation and oxLDL cytotoxicity are strongly linked [8], as are protein oxidation and oxLDL cytotoxicity, where the lipid peroxyl radical attacks the apoB100 protein moiety [4]. HOCl treatment of LDL oxidises predominately the protein moiety with very little oxysterol formation, yet is just as toxic as copper ion-oxidised LDL to U937 cells [35]. This suggests that the toxicity of oxLDL is via advanced protein oxidation products rather than oxysterols. This does not mean that oxLDL oxysterols are irrelevant, since 7KC in 7KC-acLDL has been shown to impair sterol efflux to ApoA-I from mouse peritoneal macrophages [16], implicating oxysterols in actual foam cell formation and fatty streak formation.

Although our results indicate that the toxicity of 7KC (and possibly other oxysterols) is massively diminished when incorporated into high-uptake LDL, they do not preclude the possibility that 7KC is a significant toxin within atherosclerotic plaques. Although we are not aware of any possible mechanism, our research does not rule out the possibility that within the environment of the plaque 7KC and other oxysterols may be removed from the lipoprotein particles and concentrated onto the surface of the macrophage foam cells, so inducing cell death.

Acknowledgments This work was partly funded through a project grant from the National Heart Foundation of New Zealand and Student Research Support from the School of Biological Sciences, University of Canterbury. We would like to thank our blood donors for our source of blood and the Nurses from The Health Centre for carrying out the blood collection.

Conflict of interest The authors have no conflict of interest.

References

- Ball RY, Stowers EC, Burton JH, Cary NRB, Skepper JN, Mitchinson MJ (1995) Evidence that the death of macrophage foam cells contributes to the lipid core of atheroma. *Atherosclerosis* 114:45–54
- Gieseg SP, Leake DS, Flavall EM, Amit Z, Reid L, Yang Y (2009) Macrophage antioxidant protection within atherosclerotic plaques. *Front Biosci* 14:1230–1246
- Esterbauer H, Dieber-Rotheneder M, Waeg G, Striegl G, Jurgens G (1990) Biochemical, structural, and functional properties of oxidized low-density lipoprotein. *Chem Res Toxicol* 3:77–92
- Gieseg SP, Pearson J, Firth CA (2003) Protein hydroperoxides are a major product of low density lipoprotein oxidation during copper, peroxyl radical and macrophage-mediated oxidation. *Free Radic Res* 37:983–991
- Brown AJ, Jessup W (1999) Oxysterols and atherosclerosis. *Atherosclerosis* 142:1–28
- Haberland ME, Olch CL, Fogelman AM (1984) Role of lysines in mediating interaction of modified low density lipoproteins with the scavenger receptor of human monocyte macrophages. *J Biol Chem* 259:11305–11311
- Hoff F, O'Neil J, Chisolm GM, Cole TB, Quehenberger O, Esterbauer H, Jurgens G (1989) Modification of low density lipoproteins with 4-hydroxynonenal induces uptake by macrophages. *Atherosclerosis* 9:538–549
- Clare K, Hardwick S, Carpenter KL, Weeratunge N, Mitchinson MJ (1995) Toxicity of oxysterols to human monocyte-macrophages. *Atherosclerosis* 118:67–75
- Colles SM, Maxson JM, Carlson SG, Chisolm GM (2001) Oxidized LDL-induced injury and apoptosis in atherosclerosis—potential roles for oxysterols. *Trends Cardiovasc Med* 11:131–138
- Larsson DA, Baird S, Nyhalah JD, Yuan XM, Li W (2006) Oxysterol mixtures, in atheroma-relevant proportions, display synergistic and proapoptotic effects. *Free Radic Biol Med* 41:902–910
- Garcia-Cruset S, Carpenter KLH, Guardiola F, Stein BK, Mitchinson MJ (2001) Oxysterol profiles of normal human arteries, fatty streaks and advanced lesions. *Free Radic Res* 35:31–41
- Brown AJ, Dean RT, Jessup W (1996) Free and esterified oxysterol formation during copper-oxidation of low density lipoprotein and uptake by macrophages. *J Lipid Res* 37:320–335
- Gery AB, Satchell L, Leake DS (2007) A novel method for production of lipid hydroperoxide- or oxysterol-rich low-density lipoprotein. *Atherosclerosis* 197:579–587
- Yang L, Sinensky MS (2000) 25-Hydroxycholesterol activates a cytochrome c release-mediated caspase cascade. *Biochem Biophys Res Commun* 278:557–563
- Berthier A, Lemaire-Ewing S, Prunet C, Monier S, Athias A, Bessede G, De Barros JPP, Laubriet A, Gambert P, Lizard G, Neel D (2004) Involvement of a calcium-dependent dephosphorylation of BAD associated with the localization of TRPC-1 within lipid rafts in 7-ketocholesterol-induced THP-1 cell apoptosis. *Cell Death Differ* 11:897–905
- Gelissen IC, Brown AJ, Mander EL, Kritharides L, Dean RT, Jessup W (1996) Sterol efflux is impaired from macrophage foam cells selectively enriched with 7-ketocholesterol. *J Biol Chem* 271:17852–17860
- Jialal I, Freeman DA, Grundy SM (1991) Varying susceptibility of different low-density lipoproteins to oxidative modification. *Arterioscler Thromb* 11:482–488
- Brown AJ, Leong S, Dean RT, Jessup W (1997) 7-Hydroperoxycholesterol and its products in oxidised low density lipoprotein and human atherosclerotic plaque. *J Lipid Res* 38:1730–1745
- Lizard G, Miguet C, Bessede G, Monier S, Gueldry S, Neel D, Gambert P (2000) Impairment with various antioxidants of the loss of mitochondrial transmembrane potential and of the cytosolic release of cytochrome c occurring during 7-ketocholesterol-induced apoptosis. *Free Radic Biol Med* 28:743–753
- Baird SK, Hampton M, Gieseg SP (2004) Oxidised LDL triggers phosphatidylserine exposure in human monocyte cell lines by both caspase-dependent and independent mechanisms. *FEBS Lett* 578:169–174

21. Giese SP, Amit Z, Yang YT, Shchepetkina A, Katouah H (2010) Oxidant production, oxLDL uptake, and CD36 levels in human monocyte derived macrophages are down regulated by the macrophage generated antioxidant 7,8-dihydroneopterin. *Antioxid Redox Signal* 13:1525–1534
22. Giese SP, Esterbauer H (1994) Low density lipoprotein is saturable by pro-oxidant copper. *FEBS Lett* 343:188–194
23. Kritharides L, Jessup W, Mander EL, Dean RT (1995) Apolipoprotein A1 mediated efflux of sterols from oxidised LDL load macrophages. *Atheroscler Thromb Vasc Biol* 15:276–289
24. Mosmann T (1983) Rapid colorimetric assay for cellular growth and survival: application to proliferation and cytotoxicity assays. *J Immunol Methods* 65:55–63
25. Kritharides L, Jessup W, Gifford J, Dean RT (1993) A method for defining the stages of low-density lipoprotein oxidation by the separation of cholesterol and cholesterol ester-oxidation products using HPLC. *Anal Biochem* 213:79–89
26. Cotgreave IA, Moldeus P (1986) Methodologies for the application of monobromobimane to the simultaneous analysis of soluble and protein thiol components of biological systems. *J Biochem Biophys Meth* 13:231–249
27. Baird SK, Reid L, Hampton M, Giese SP (2005) OxLDL induced cell death is inhibited by the macrophage synthesised pterin, 7,8-dihydroneopterin, in U937 cells but not THP-1 cells. *Biochim Biophys Acta* 1745:361–369
28. Lizard G, Gueldry S, Sordet O, Monier S, Athias A, Miguet C, Bessede G, Lemaire S, Solary E, Gambert P (1998) Glutathione is implied in the control of 7-ketocholesterol-induced apoptosis, which is associated with radical oxygen species production. *FASEB J* 12:1651–1663
29. Monier S, Samadi M, Prunet C, Denance M, Laubriet A, Anne AA, Berthier A, Steinmetz E, Jurgens G, Negre-Salvayre A, Bessede G, Lemaire-Ewing S, Neel D, Gambert P, Lizard G (2003) Impairment of the cytotoxic and oxidative activities of 7 beta-hydroxycholesterol and 7-ketocholesterol by esterification with oleate. *Biochem Biophys Res Commun* 303:814–824
30. Giese SP, Reibnegger G, Wachter H, Esterbauer H (1995) 7,8-Dihydroneopterin inhibits low density lipoprotein oxidation in vitro. Evidence that this macrophage secreted pteridine is an antioxidant. *Free Radic Res* 23:123–136
31. Giese SP, Duggan S, Rait C, Platt A (2002) Protein and thiol oxidation in cells exposed to peroxy radicals, is inhibited by the macrophage synthesised pterin 7,8-dihydroneopterin. *Biochim Biophys Acta* 1591:139–145
32. Leonarduzzi G, Vizio B, Sottero B, Verde V, Gamba P, Mascia C, Chiarpotto E, Poli G, Biasi F (2006) Early involvement of ROS overproduction in apoptosis induced by 7-ketocholesterol. *Antioxid Redox Signal* 8:375–380
33. Massey JB (2006) Membrane and protein interactions of oxysterols. *Curr Opin Lipidol* 17:296–301
34. Chisolm GM, Ma GP, Irwin KC, Martin LL, Gunderson KG, Linberg LF, Morel DW, Dicorleto PE (1994) 7-Beta-hydroperoxycholest-5-en-3-beta-ol, a component of human atherosclerotic lesions, is the primary cytotoxin of oxidized human low-density-lipoprotein. *Proc Natl Acad Sci USA* 91:11452–11456
35. Ermak N, Lacour B, Goirand F, Drüeke TB, Vicca S (2010) Differential apoptotic pathways activated in response to Cu-induced or HOCl-induced LDL oxidation in U937 monocytic cell line. *Biochem Biophys Res Commun* 393:783–787

Involvement of Liver X Receptor Alpha in Histone Modifications Across the Target Fatty Acid Synthase Gene

Huihong Yu · Jinfeng Wu · Mei Yang · Jinjun Guo ·
Lili Zheng · Mingli Peng · Qin Zhang · Yingxia Xiang ·
Jie Cao · Wei Shen

Received: 11 June 2011 / Accepted: 7 November 2011 / Published online: 8 December 2011
© AOCs 2011

Abstract The liver X receptor alpha (LXR α), a member of the nuclear receptor superfamily, has been shown to regulate the expression of the fatty acid synthase (FAS) gene through direct interaction with the *FAS* promoter. However, its regulation of gene expression is not completely understood. Histone modifications and chromatin remodeling are closely linked to transcriptional activation of genes. In the present study, we examined the effect of LXR α activation or silencing on histone modifications (i.e., acetylation, methylation, and phosphorylation) across the *FAS* gene, with the aim to investigate whether LXR α could regulate its target gene expression at the epigenetic level.

Electronic supplementary material The online version of this article (doi:10.1007/s11745-011-3635-0) contains supplementary material, which is available to authorized users.

H. Yu · J. Guo · Y. Xiang · J. Cao · W. Shen (✉)
Department of Digestive Diseases, The Second Affiliated Hospital, Chongqing Medical University, Chongqing, China
e-mail: shenwei315@126.com

J. Wu
Department of Digestive Diseases, The Fifth People's Hospital of Shenzhen, Shenzhen, China

M. Yang
The Third People's Hospital of Chengdu, Chengdu, China

L. Zheng
Department of Digestive Diseases, Chongqing General Hospital of Chinese Armed Police, Chongqing, China

M. Peng
Institute for Viral Hepatitis, The Second Affiliated Hospital, Chongqing Medical University, Chongqing, China

Q. Zhang
Department of Digestive Diseases, The First People's Hospital of Liangshan, Liangshan, China

The addition of LXR agonist T0901317 or ectopic expression of LXR α stimulated the *FAS* transcription, which was coupled with increased levels of histones H3 and H4 acetylation and H3 phosphorylation and methylation at the LXR response element (LXRE). LXR ligation or overexpression induced distinct histone modification patterns at the distal region 2,272 bp upstream from the transcription start site (TSS) and TSS of the *FAS* gene. Moreover, RNA interference-mediated downregulation of LXR α impaired the histone acetylation and methylation but not phosphorylation on the *FAS* gene. In conclusion, we provide evidence that LXR α ligation-mediated transcriptional activation of the *FAS* gene is associated with LXR α -dependent histone acetylation and methylation rather than phosphorylation on this target gene.

Keywords FAS · LXR α · Chromatin remodeling · Gene regulation · Lipid metabolism

Abbreviations

ASC-2	Activating signal cointegrator-2
ChIP	Chromatin immunoprecipitation
FAS	Fatty acid synthase
FXR	Farnesoid X-receptor
LXR	Liver X receptor
LXRE	LXR response element
qRT-PCR	Quantitative real-time PCR
TSS	Transcription start site

Introduction

Liver X receptors (LXRs) belong to a class of ligand-dependent nuclear receptors that play an important role in

hepatic bile and fatty acid synthesis, glucose metabolism, as well as sterol efflux [1, 2]. They are known to be activated by oxysterols [3]. Ligand-activated LXRs form obligate heterodimers with retinoid X receptors (RXRs) and regulate the transcription of their target genes by binding to specific LXR response elements (LXREs) [4]. There have been two subtypes of LXRs identified: LXR α and LXR β . The inducible LXR α is abundantly expressed in liver, spleen, kidney, adipose, and small intestine, whereas LXR β is ubiquitously expressed [5]. LXR α plays a critical role in maintaining the homeostasis of cholesterol, which is supported by the finding that LXR α knockout mice, when fed a high-cholesterol diet, develop massive hepatic accumulation of cholesterol [6]. Apart from affecting cholesterol metabolism, LXR α is also involved in the control of lipogenesis. Genetic ablation of LXR α impairs the expression of several lipogenic genes including fatty acid synthase (FAS), acetyl coenzyme A, steroyl-coenzyme A desaturase, and sterol regulatory element binding protein 1 (SREBP-1) [6]. The biosynthetic enzyme FAS is a central enzyme required for the anabolic conversion of dietary carbohydrates to fatty acids [7]. The expression of FAS is controlled primarily at the level of transcription and is tightly regulated by both hormonal and nutritional signals [7, 8]. Previous work has demonstrated that LXRs regulate FAS expression through direct interaction with the *FAS* promoter [1]. Demeure et al. [9] also reported that there is a functional LXRE in the promoter of chicken *FAS* gene, which is responsible for the induction of *FAS* expression by a pharmacological LXR agonist, T0901317.

Eukaryotic chromatin is the complex of DNA and histone proteins that form nucleosomes. It is well known that chromatin remodeling plays a crucial role in gene transcription. The structure of chromatin is altered to allow greater accessibility by transcription factors when a gene is to be activated [10]. Nuclear receptors are involved in the change to a more accessible state by recruiting two classes of chromatin remodelers, histone modifying enzymes and ATP-dependent chromatin remodeling factors [11]. These remodelers modify chromatin structure at target gene promoters by posttranslational modification of histones and by disrupting DNA-histone interactions, respectively. Progesterone and glucocorticoid receptors have been found to recruit different coactivator complexes and promote distinct patterns of histone modification [12]. Ananthanarayanan et al. [13] reported that the nuclear hormone receptor, farnesoid X-receptor (FXR), facilitates arginine methylation of histone H3 by co-activator-associated arginine methyltransferase 1. Considering that LXRs and FXR are structurally and closely related nuclear receptors that play critical roles in lipid metabolism [14], we speculated that LXRs might also have an influence on chromatin modification, providing a novel mechanism for its

regulation of gene transcription. To test this hypothesis, we examined herein the histone modification status of different regions of the *FAS* gene upon the stimulation with LXR agonist T0901317 for varying durations (30–120 min), and investigated the role of the LXR α isoform in the modification of histones using RNA interference (RNAi) and overexpression approaches.

Materials and Methods

Cell Culture and Reagents

Samples of the human hepatocellular carcinoma cell line HepG2 were purchased from the Chinese Academy of Sciences (Shanghai, China) and cultured in Dulbecco's modified Eagle's medium (Hyclone, Logan, UT, USA) with 10% heat-inactivated fetal bovine serum (Hyclone), 100 U/ml penicillin, and 100 μ g/ml streptomycin in a 5% CO₂ incubator at 37 °C. T0901317 was obtained from Cayman Chemical (Ann Arbor, MI, USA) and dissolved in dimethyl sulfoxide (DMSO; Sigma, St. Louis, MO, USA). If not stated otherwise, 1 μ M T0901317 [15] was used to treat cells.

Plasmids, Small Interfering RNA (siRNA), and Transient Transfection

Constructs expressing LXR α -specific siRNA (siLXR α) or nonspecific scrambled siRNA as negative control were purchased from Wuhan GeneSil Biotechnology Co. Ltd. (Wuhan, China). The sense sequence of the siLXR α and control siRNA was 5'-GCAACTCAATGATGCCGAGTT-3' and 5'-GACTTCATAAGGCGCATGC-3', respectively. HepG2 cells at 85–90% confluence were transfected with either siLXR α or control siRNA using PolyJet in vitro DNA transfection reagent (SignaGen Laboratory, Gaithersburg, MD, USA) according to the manufacturer's instructions. To monitor the transfection efficiency, cells were in parallel co-transfected with a plasmid expressing enhanced green fluorescent protein (EGFP). The transfection efficiency, measured by counting EGFP-positive cells using a fluorescence microscope, was about 72%. The siRNA-mediated silencing of LXR α was determined by polymerase chain reaction (PCR) and Western blot analysis as described below.

For overexpression studies, a plasmid expressing human wild-type LXR α (GenBank accession number: NM_001130101) was purchased from Shanghai Genechem (Shanghai, China). HepG2 cells at 85–90% confluence were transfected with the LXR α -expressing plasmid or GV142 empty vector, using PolyJet in vitro DNA transfection reagent. At 0, 12, 24, and 36 h after transfection, cells were

harvested and subjected to chromatin immunoprecipitation (ChIP) assays.

RNA Isolation, PCR, and Quantitative Real-Time PCR (qRT-PCR)

Total RNA was extracted from HepG2 cells using Trizol reagent (Invitrogen, Carlsbad, CA, USA) and was reverse-transcribed with RevertAid First Strand cDNA Synthesis kit (Fermentas, Ontario, Canada) according to the manufacturer's recommendations. PCR amplification of cDNA was conducted using primers specific for LXR α : 5'-TGGGAACA CGATGGGAGAAC-3' (forward) and 5'-CTGCCGTGCC ACCTTG-3' (reverse); and β -actin 5'-TGACGGTCAGG TCATCACTATCGGCAATGA-3' (forward) and 5'-TTG ATCTTCATGGTGATAGGAGCGAGGGCA-3' (reverse). Amplification of β -actin cDNA served as an internal control. Quantitative PCR experiments were carried out on an ABI 7300 real-time PCR system (Applied Biosystems, Foster City, CA, USA) using commercial primers for human FAS and β -actin (Applied Biosystems). All samples were run in triplicate. Gene expression was normalized to β -actin transcripts, and the relative mRNA expression was calculated using the $2^{-\Delta\Delta C_t}$ method (where C_t is the cycle threshold number) [16].

ChIP Coupled to Detection by qRT-PCR

The ChIP assay was performed using the Chromatin Immunoprecipitation Assay Kit (Upstate Biotechnology, Lake Placid, NJ, USA) according to the manufacturer's protocol with minor modifications [17]. Unstimulated or T0901317-treated HepG2 cells ($\sim 2 \times 10^6$) were cross-linked for 10 min at 37 °C using 1% formaldehyde. Cells were resuspended in 400 μ l of ChIP lysis buffer [10 mM EDTA, 50 mM Tris-HCl (pH 8.0), 1% sodium dodecyl sulfate (SDS), and protease inhibitors] on ice for 10 min. The chromatin was sheared by sonication using an ultrasonic processor (VC130P; Sonics & Materials, Newtown, CT, USA) in an ice bath to produce DNA fragments ranging from 200 to 1,000 bp, as determined by agarose gel electrophoresis. After removal of debris by centrifugation, the chromatin solution was diluted 10-fold with ChIP dilution buffer [2 mM EDTA, 16.7 mM Tris-HCl (pH 8.1), 0.01% SDS, 16.7 mM NaCl, and 1.1% Triton X-100] and precleared with Protein A Agarose/Salmon Sperm DNA at 4 °C for 30 min. For immunoprecipitation, the following antibodies were used: anti-histone H3, anti-histone H4, anti-acetyl-histone H3, anti-acetyl-histone H4, anti-phospho-histone H3 (ser10), and anti-trimethyl-histone H3 lysine 4 (H3K4; Upstate Biotechnology). The antibody-chromatin complexes were precipitated by incubation with Protein A Agarose/Salmon Sperm DNA. DNA-protein crosslinks were reversed by incubation at

65 °C for 4 h followed by proteinase K treatment. DNA was recovered by purification with the Qiaquick PCR purification column (Qiagen, Hilden, Germany). Quantification of immunoprecipitated DNA was determined using qRT-PCR with primers listed in Supplementary Table S1. Each assay was performed in triplicate. The relative amount of immunoprecipitated DNA to input DNA was calculated.

Western Blot Analysis

Samples of protein extracts from cells were resolved by sodium dodecyl sulfate polyacrylamide gel electrophoresis and transferred to polyvinylidene fluoride membranes. After blocking with 5% bovine serum albumin (Sigma) for 1 h, the membranes were incubated overnight at 4 °C with mouse anti-human LXR α monoclonal antibodies (ab41902, abcam, Cambridge, UK; 1:1,500 dilution) or β -actin (Sigma), followed by incubation with horseradish peroxidase-linked secondary antibodies (Santa Cruz Biotechnology, Santa Cruz, CA, USA). Bound antibodies were visualized by an enhanced chemiluminescence detection kit (Amersham Biosciences, Piscataway, NJ, USA).

Statistical Analysis

Data are expressed as means \pm standard deviation. All experiments were performed in triplicate. Differences among groups were determined by the Student–Newman–Keuls test. $P < 0.05$ was considered statistically significant.

Results

LXR Activation Affects the Histone Modification Pattern on the FAS Gene

qRT-PCR analysis revealed that HepG2 cells exposed to LXR agonist T0901317 had a rapid increase in the abundance of FAS mRNA (Fig. 1a). The increase began approximately 2 h after the T0901317 treatment and peaked at 16 h, suggesting transcriptional upregulation of FAS by LXR activation. Western blot analysis demonstrated that the LXR α protein level was profoundly elevated 16 h after the T0901317 treatment, and remained elevated for up to 48 h (Fig. 1b).

To get more insight into the mechanism(s) regulating the FAS expression, we used ChIP to measure the effect of LXR activation on histone modifications at different regions of the FAS gene (Fig. 1c), i.e., the distal site 2,272 bp upstream from the transcription start site (TSS; referred to as the distal site), LXRE (−756/−718), TSS (+1), and exon 3 (+2,818/+2,905) used as a negative

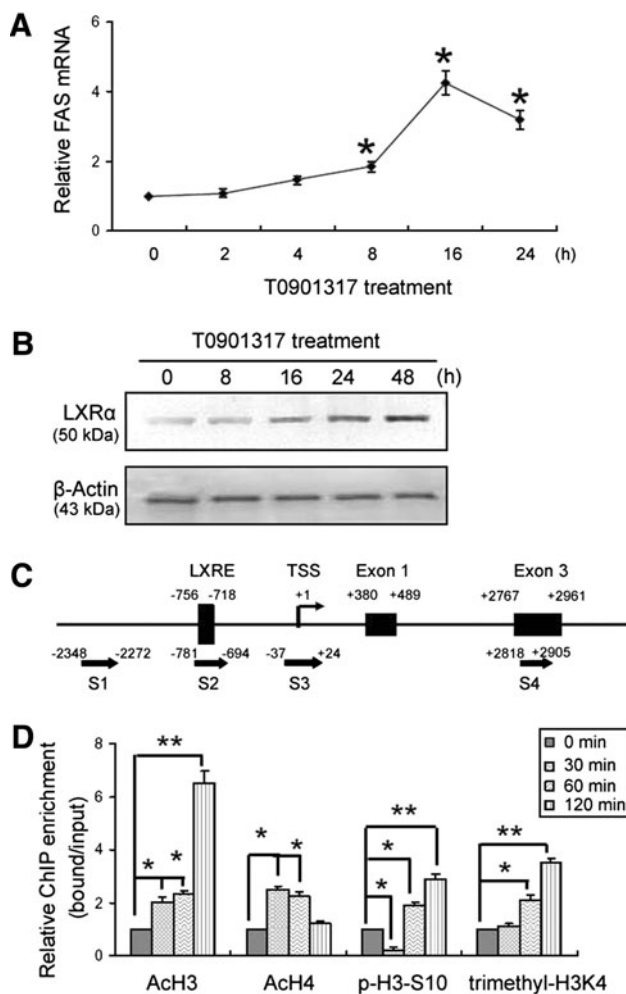


Fig. 1 LXR ligation induces FAS expression and histone modifications at the LXRE of the *FAS* gene. **a** Relative expression of FAS mRNA analyzed by qRT-PCR. HepG2 cells were treated for indicated time with 1 μ M T0901317 and were subjected to real-time PCR assays. The FAS levels were determined relative to that at time 0 and normalized to β -actin levels. * P < 0.05 compared to that at time 0; n = 3. **b** Western blot analysis for LXR α expression in HepG2 cells treated with 1 μ M T0901317 for indicated durations. Representative blots of three independent experiments with similar results are shown. β -Actin was used as loading control. **c** Schematic illustration of the human *FAS* gene. The primers (named S1, S2, S3, and S4) used for quantitative ChIP analysis of histone modifications are indicated by arrows. Numbers represent the nucleotide position relative to the transcription start site (TSS). **d** Histone modifications at the LXRE of the *FAS* gene induced by LXR agonist. HepG2 cells were exposed to T0901317 (1 μ M) for 0, 30, 60, or 120 min, and ChIP assays were conducted with antibodies against acetylated H3 (AcH3), acetylated H4 (AcH4), phosphorylated H3-S10 (p-H3-S10), trimethylated H3K4 (trimethyl-H3K4), as well as H3 and H4. Immunoprecipitated DNA was analyzed by real-time PCR using the S2 primer set indicated in Fig. 1c. The ratio of immunoprecipitated DNA to total input DNA was determined for each antibody. The value for the level of acetylation, phosphorylation, and trimethylation of H3 was divided by H3 occupancy respectively, and that for the level of acetylation of H4 was divided by H4 occupancy. Values at time 0 were set to be 1. * P < 0.05, ** P < 0.01 for indicated comparisons; n = 3

control site. Antibodies specific for acetylated H3 and H4 revealed a prompt acetylation at the LXRE (Fig. 1d). Both revealed a strong increase in histone acetylation at the 30-min time point. H4 acetylation was transient, peaking at 30 min, whereas acetylated H3 remained elevated up to 120 min. The level of H3-S10 phosphorylation increased after a transient reduction, reaching a maximum at 120 min. Additionally, T0901317-treated cells showed a >3-fold increase in the level of trimethylated H3K4 120 min post stimulation.

Notably, there was a divergent pattern of histone modifications on the other regions examined. Acetylation of H4 at both the distal site and the TSS, and H3 phosphorylation at the distal site were potentiated by T0901317 (Fig. 2b, c). However, there was a marked reduction in the acetylation, phosphorylation, and methylation of H3 at the TSS (Fig. 2a, c, d). No evident changes in histone modifications were found at the exon 3 (Fig. 2).

LXR α is Required for Histone Acetylation and Methylation but not Phosphorylation on the *FAS* Gene

Next, we attempted to determine whether LXR α was required for the modifications of histone on the *FAS* gene. We specially knocked down the endogenous expression of LXR α in HepG2 cells using siRNA. Both semiquantitative PCR and Western blotting analysis confirmed the downregulation of LXR α in siLXR α -transfected cells (Fig. 3a). Targeted inhibition of LXR α abrogated the induction of FAS by T0901317 (Fig. 3b).

Of note, the histone modifications on the *FAS* gene were markedly affected by siRNA-mediated targeting of LXR α . As illustrated in Fig. 4, LXR α knockdown impaired T0901317-induced H3 acetylation at the LXRE, H4 acetylation at the distal site, the LXRE, and the TSS, as well as H3 methylation at the LXRE. Conversely, T0901317-mediated reduction of H3 acetylation and methylation at the TSS were reversed by LXR α downregulation (Fig. 4a, d). However, knockdown of LXR α had little influence on H3 phosphorylation (Fig. 4c).

Overexpression of LXR α Modulates Histone Modifications on the *FAS* Gene

We also examined the effects of LXR α overexpression on histone modifications on the *FAS* gene. Western blot analysis revealed an overexpression of LXR α in the cells transfected with LXR α relative to mock transfectants (data not shown). Ectopic expression of LXR α significantly facilitated H3 and H4 acetylation, H3-S10 phosphorylation,

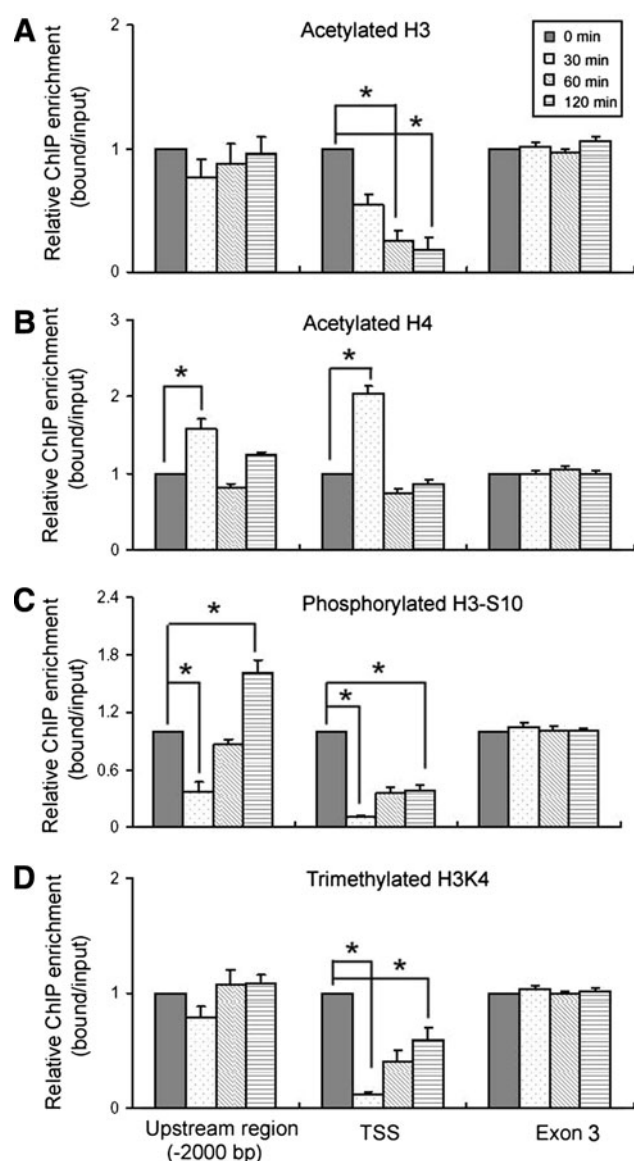


Fig. 2 Histone modifications at the upstream region, TSS, and exon 3 of the *FAS* gene in response to LXR activation. HepG2 cells were exposed to T0901317 (1 μ M) for indicated durations, and ChIP assays were conducted with antibodies against acetylated H3, acetylated H4, phosphorylated H3-S10, trimethylated H3K4, as well as H3 and H4. Immunoprecipitated DNA was analyzed by real-time PCR using S1, S3, or S4 primer sets as indicated in Fig. 1c. The ratio of immunoprecipitated DNA to total input DNA was determined for each antibody. The value for the level of acetylation, phosphorylation, and trimethylation of H3 was divided by H3 occupancy respectively, and that for the level of acetylation of H4 was divided by H4 occupancy. Values at time 0 were set to be 1. * $P < 0.05$, ** $P < 0.01$ for indicated comparisons; $n = 3$

and H3K4 methylation at the LXRE in comparison with mock transfection ($P < 0.01$; Fig. 5a–d). There were lower levels of H3 acetylation, phosphorylation, and methylation and higher levels of H4 acetylation at the TSS in LXR α -overexpressing cells than in mock-transfected cells

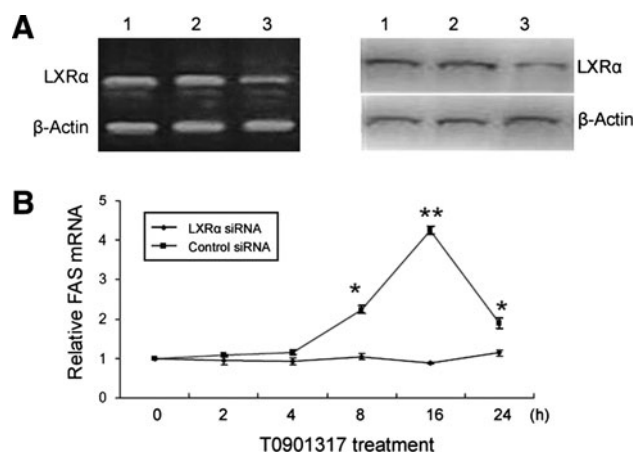


Fig. 3 siRNA-mediated knockdown of LXR α abrogates the induction of FAS by LXR agonist. **a** Downregulation of endogenous LXR α by siRNA delivery. Untransfected HepG2 cells (lane 1) and those transfected with negative control siRNA (lane 2) or specific LXR α siRNA (lane 3) were assessed for the LXR α mRNA (left) and protein (right) expression. Shown are representative images of three independent experiments with similar results. β -Actin was used as loading control. **b** Relative expression of FAS mRNA analyzed by qRT-PCR. HepG2 cells transfected with negative control siRNA or specific LXR α siRNA were treated for indicated time with 1 μ M T0901317 and were subjected to real-time PCR assays. The FAS levels were determined relative to that at time 0 and normalized to β -actin levels. * $P < 0.05$, ** $P < 0.01$ compared to control cells; $n = 3$

(Fig. 5a–d). LXR α overexpression resulted in a transient reduction in H3-S10 phosphorylation at the distal site (Fig. 5c), but did not markedly affect H3 and H4 acetylation or H3K4 methylation at the same site (Fig. 5a, b, d).

Discussion

The present study was undertaken to characterize more definitively the mechanism involved in the regulation of FAS expression by LXR α . We examined the effects of LXR α on histone modifications at 4 different regions of the *FAS* gene. LXRE and the region surrounding the TSS play important roles in the control of gene transcription. In addition to the proximal promoter elements, FAS expression may be regulated by distal transcriptional regulatory elements. The distal site about 2,000 bp upstream of the TSS was used to study epigenetic changes in the distal promoter of *FAS* gene. The exon 3 region was used as a negative control for histone modifications; no apparent epigenetic changes were observed at this region under the experimental conditions of this study. We showed that LXR ligation-mediated transcriptional activation of FAS is associated with the modifications of histones on this gene. The LXR α isoform is implicated in the induction of FAS by LXR agonist T0901317, probably through alteration of histone acetylation and methylation rather than

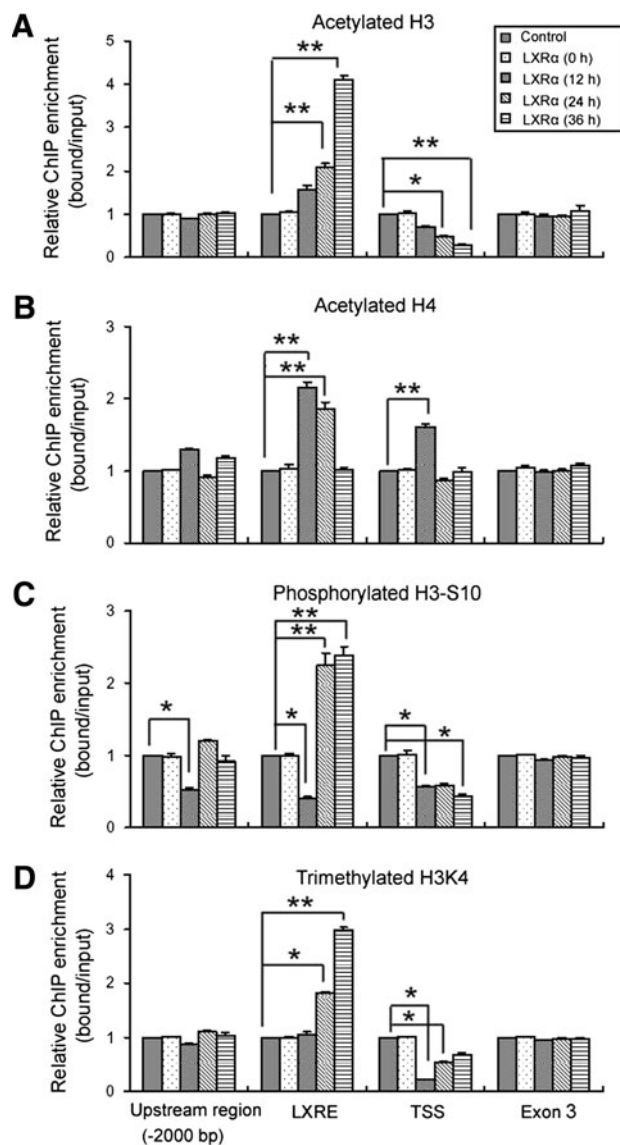
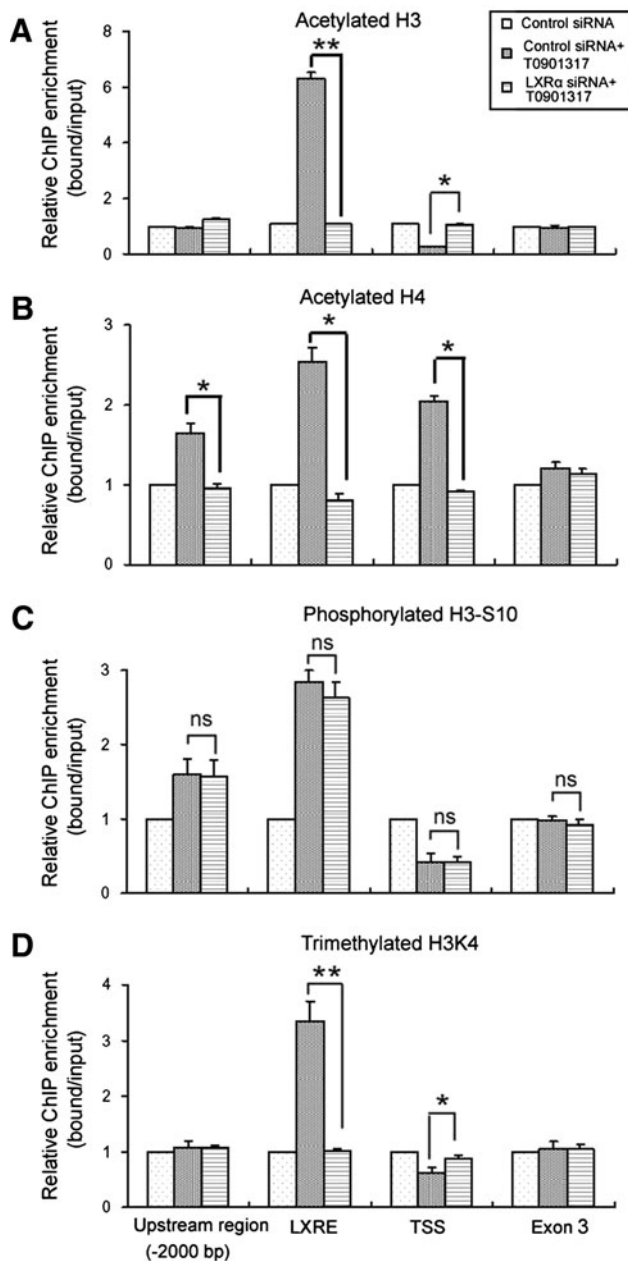


Fig. 5 Ectopic expression of LXR α modulates histone modifications on the *FAS* gene. HepG2 cells were transfected with the LXR α -expressing plasmid or GV142 empty vector. At 0, 12, 24, and 36 h after transfection, LXR α -transfected cells were collected and subjected to ChIP assays that were performed with antibodies against acetylated H3, acetylated H4, phosphorylated H3-S10, trimethylated H3K4, as well as H3 and H4. Empty vector-transfected cells were used as control. Immunoprecipitated DNA was analyzed by real-time PCR using primer sets indicated in Fig. 1c. The ratio of immunoprecipitated DNA to total input DNA was determined for each antibody. The value for the level of acetylation, phosphorylation, and trimethylation of H3 was divided by H3 occupancy respectively, and that for the level of acetylation of H4 was divided by H4 occupancy. The results are expressed relative to the corresponding values for control cells (set to be 1). * P < 0.05, ** P < 0.01 for indicated comparisons; n = 3

phosphorylation. Our data highlight an important role for LXR α in chromatin modification, providing more insight into their regulation of gene expression.

Chromatin structure has been tightly linked to the control of gene expression. Many factors, including histone variants, histone modifications, DNA methylation, and the binding of non-histone architectural proteins regulate the structure of chromatin [18]. LXRs act as ligand-dependent transcription factors to bind to specific DNA elements in the promoters of target genes. Besides of a set of basic transcriptional factors, a number of transcriptional co-regulators are required for ligand-dependent transcriptional controls by nuclear receptors [19, 20]. Histone modifying enzymes and chromatin remodelers are these potential co-regulators that modulate chromatin organization and thereby support transcriptional regulation by nuclear receptors. Kim et al. [21] have revealed that activating signal co-integrator-2 (ASC-2), a coactivator of multiple nuclear receptors and transcription factors, controls FXR transactivation through its associated histone H3K4 methyltransferase activity. Similarly, ASC-2 plays a key role in the transactivation by LXRs by recruiting H3K4 methyltransferases to LXRs [22]. Here, we demonstrate that manipulation of LXR α expression has a profound influence on the histone modifications of the *FAS* gene. Overexpression of LXR α was found to induce acetylation, methylation, and phosphorylation of histones at the LXRE of the *FAS* promoter. Targeted depletion of LXR α using siRNA reversed these histone modifications except phosphorylation. Accumulating evidence indicates that co-regulator complexes that associated with nuclear receptors contribute to histone acetylation and methylation [23–26]. Chen et al. [26] reported that the histone acetyltransferase activity of CREB-binding protein/p300 is responsible for hormone-mediated dramatic hyperacetylation at endogenous target genes. DiRenzo et al. [24] showed that the co-regulator Brahma-related gene one is recruited to estrogen-responsive promoters by estrogen receptor and cooperates with other factors to promote histone acetylation. In light of these findings, we propose that LXR α ligation might recruit several co-regulators and target them to the regulatory regions of *FAS*, facilitating histone modifications and chromatin remodeling. Further studies are needed to define the assumed LXR α -associated co-regulators.

Histone acetylation is believed to increase the accessibility of transcription factors to nucleosomal DNA and correlates with transcriptional activity [27, 28]. The addition of LXR agonist has been found to promote H3 and H4 acetylation at the promoter of the target gene ATP-binding cassette transporter A1 in macrophages from LXR^{+/+} mice, leading to relief of transcriptional repression [29]. Consistent with this study, our data demonstrated that H3 and H4 acetylation was significantly enriched at the LXRE within 30 min of ligand addition. This increased state of H3 acetylation remained for up to 120 min, while H4 acetylation was slowly reduced to the basal level after

120 min. Similarly, LXR α overexpression enhanced H3 and H4 acetylation at the LXRE. In the presence of T0901317, there were increased levels of H4 acetylation at the distal site and the TSS, whereas levels of H3 acetylation were reduced at the TSS and remained unaffected at the distal site. Likewise, elevated H4 acetylation levels and reduced H3 acetylation levels were observed at the TSS region in LXR α -overexpressing cells. These results collectively indicate that LXR α induces a dispersed pattern of histone acetylation on the *FAS* gene. LXR α ligation-mediated transcriptional activation of the *FAS* gene may be linked to enrichment of acetylated histones at the upstream and proximal promoter regions.

The consequences of histone methylation on transcription are dependent on the specific residue and degree of methylation. Trimethylation of H3K4 is associated with active transcription, whereas H3K9 methylation has been shown to correlate with transcriptional repression [30, 31]. H3K4 trimethylation is often enriched near the TSS of actively transcribed genes [32, 33]. However, we found that T0901317 treatment resulted in reduced trimethylation of H3K4 at the TSS region. Conversely, levels of H3K4 trimethylation at the LXRE were significantly increased by T0901317. The unique pattern of histone methylation may reflect the important role of the LXRE in the LXR α -mediated transcriptional activity. Indeed, gain- and loss-of-function studies revealed that the levels of H3K4 trimethylation at the LXRE were positively associated with LXR α -mediated transcriptional activation of the *FAS* gene.

In addition to acetylation and methylation, histone phosphorylation has been shown to regulate gene transcription. The location of the serine 10 residue in close proximity to other modifiable amino acids in the histone H3 tail enables the possibility of an interaction between phosphorylation of serine 10 and methylation and/or acetylation of lysine 9 and lysine 14 [34]. H3-S10 phosphorylation has been reported to be functionally linked to Gcn5-mediated acetylation at lysine 14 [35]. However, we did not observe a parallel increase between H3 acetylation and phosphorylation in T0901317-treated HepG2 cells. Indeed, the level of H3-S10 phosphorylation at the LXRE was unexpectedly decreased within the first 30 min and afterwards increased stably. This finding, combined with the independence of LXR α on H3-S10 phosphorylation on the *FAS* gene, likely reflects the existence of LXR-independent co-receptor complex that were responsible for H3 phosphorylation. H3-S10 phosphorylation was also enriched at the distal region upon LXR α ligation, suggesting a possible transcriptional regulatory element in this region. Unexpectedly, LXR α ligation or overexpression resulted in decreased levels of H3-S10 phosphorylation at the TSS, which coincided with a reduction in H3 methylation and acetylation at this region. It still remains to be determined whether and how, if any, the

inactive histone modifications at the TSS contribute to the LXR α -mediated transcriptional activation of the *FAS* gene.

Gene knockout mouse studies reveal that LXR β does not have a role comparable to that of LXR α in hepatic cholesterol metabolism and exhibits subtle effects on the expression of lipid metabolism-related genes such as *FAS* and *SREBP-1* [36]. Therefore, in this study, we did not examine the role of LXR β in epigenetic regulation of the *FAS* gene. However, we cannot exclude the possibility that LXR β might contribute to the T0901317-induced epigenetic changes across the *FAS* gene in the hum context. Indeed, in the setting of LXR α deficiency, there was still a marked increase in H3 phosphorylation in T0901317-treated HepG2 cells.

In summary, our data demonstrate that histone acetylation and methylation near the promoter of the *FAS* gene are dependent on the expression of LXR α and correlate with active transcription of this gene. However, T0901317-induced H3 phosphorylation across the *FAS* gene is LXR α -independent. Additional studies are required to address to what extent these histone modifications are involved in the liganded LXR α -mediated transcriptional activation of target genes.

Acknowledgments This work was supported by the Natural Science Foundation of China (30871160).

Conflict of interest The authors declare no conflict of interest.

References

- Joseph SB, Laffitte BA, Patel PH, Watson MA, Matsukuma KE, Walczak R, Collins JL, Osborne TF, Tontonoz P (2002) Direct and indirect mechanisms for regulation of fatty acid synthase gene expression by liver X receptors. *J Biol Chem* 277:11019–11025
- Laffitte BA, Chao LC, Li J, Walczak R, Hummasti S, Joseph SB, Castrillo A, Wilpitz DC, Mangelsdorf DJ, Collins JL, Saez E, Tontonoz P (2003) Activation of liver X receptor improves glucose tolerance through coordinate regulation of glucose metabolism in liver and adipose tissue. *Proc Natl Acad Sci USA* 100:5419–5424
- Lehmann JM, Kliewer SA, Moore LB, Smith-Oliver TA, Oliver BB, Su JL, Sundseth SS, Winegar DA, Blanchard DE, Spencer TA, Willson TM (1997) Activation of the nuclear receptor LXR by oxysterols defines a new hormone response pathway. *J Biol Chem* 272:3137–3140
- Korf H, Vander Beken S, Romano M, Steffensen KR, Stijlemans B, Gustafsson JA, Grooten J, Huygen K (2009) Liver X receptors contribute to the protective immune response against *Mycobacterium tuberculosis* in mice. *J Clin Invest* 119:1626–1637
- Zhao C, Dahlgren-Wright K (2010) Liver X receptor in cholesterol metabolism. *J Endocrinol* 204:233–240
- Peet DJ, Turley SD, Ma W, Janowski BA, Lobaccaro JM, Hammer RE, Mangelsdorf DJ (1998) Cholesterol and bile acid metabolism are impaired in mice lacking the nuclear oxysterol receptor LXR α . *Cell* 93:693–704
- Sul HS, Wang D (1998) Nutritional and hormonal regulation of enzymes in fat synthesis: studies of fatty acid synthase and mitochondrial glycerol-3-phosphate acyltransferase gene transcription. *Annu Rev Nutr* 18:331–351
- Soncini M, Yet SF, Moon Y, Chun JY, Sul HS (1995) Hormonal and nutritional control of the fatty acid synthase promoter in transgenic mice. *J Biol Chem* 270:30339–30343
- Demeure O, Duby C, Desert C, Assaf S, Hazard D, Guillou H, Lagarrigue S (2009) Liver X receptor α regulates fatty acid synthase expression in chicken. *Poult Sci* 88:2628–2635
- Mellor J (2006) Dynamic nucleosomes and gene transcription. *Trends Genet* 22:320–329
- Buranaprast M, Chakravarti D (2009) Chromatin remodeling and nuclear receptor signaling. *Prog Mol Biol Transl Sci* 87:193–234
- Li X, Wong J, Tsai SY, Tsai MJ, O'Malley BW (2003) Progesterone and glucocorticoid receptors recruit distinct coactivator complexes and promote distinct patterns of local chromatin modification. *Mol Cell Biol* 23:3763–3773
- Ananthanarayanan M, Li S, Balasubramanian N, Suchy FJ, Walsh MJ (2004) Ligand-dependent activation of the farnesoid X-receptor directs arginine methylation of histone H3 by CARM1. *J Biol Chem* 279:54348–54357
- Kalaany NY, Mangelsdorf DJ (2006) LXRS and FXR: the yin and yang of cholesterol and fat metabolism. *Annu Rev Physiol* 68:159–191
- Staybrook KR, Rogers PM, Savkur RS, Wang Y, Su C, Varga G, Bu X, Wei T, Nagpal S, Liu XS, Burris TP (2008) Regulation of human 3 α -hydroxysteroid dehydrogenase (AKR1C4) expression by the liver X receptor α . *Mol Pharmacol* 73:607–612
- Livak KJ, Schmittgen TD (2001) Analysis of relative gene expression data using real-time quantitative PCR and the 2^{-Delta}Delta C(T) method. *Methods* 25:402–408
- Tong EH, Guo JJ, Xu SX, Mak K, Chung SK, Chung SS, Huang AL, Ko BC (2009) Inducible nucleosome depletion at OREBP-binding-sites by hypertonic stress. *PLoS One* 4:e8435
- Li G, Reinberg D (2011) Chromatin higher-order structures and gene regulation. *Curr Opin Genet Dev* 21:175–186
- Rosenfeld MG, Lunyak VV, Glass CK (2006) Sensors and signals: a coactivator/corepressor/epigenetic code for integrating signal-dependent programs of transcriptional response. *Genes Dev* 20:1405–1428
- Lonard DM, O'Malley BW (2007) Nuclear receptor coregulators: judges, juries, and executioners of cellular regulation. *Mol Cell* 27:691–700
- Kim DH, Lee J, Lee B, Lee JW (2009) ASCOM controls farnesoid X receptor transactivation through its associated histone H3 lysine 4 methyltransferase activity. *Mol Endocrinol* 23:1556–1562
- Lee S, Lee J, Lee SK, Lee JW (2008) Activating signal co-integrator-2 is an essential adaptor to recruit histone H3 lysine 4 methyltransferases MLL3 and MLL4 to the liver X receptors. *Mol Endocrinol* 22:1312–1319
- Kiskinis E, Hallberg M, Christian M, Olofsson M, Dilworth SM, White R, Parker MG (2007) RIP140 directs histone and DNA methylation to silence *Ucp1* expression in white adipocytes. *EMBO J* 26:4831–4840
- DiRenzo J, Shang Y, Phelan M, Sif S, Myers M, Kingston R, Brown M (2000) BRG-1 is recruited to estrogen-responsive promoters and cooperates with factors involved in histone acetylation. *Mol Cell Biol* 20:7541–7549
- Bouliasis K, Talianidis I (2004) Functional role of G9a-induced histone methylation in small heterodimer partner-mediated transcriptional repression. *Nucleic Acids Res* 32:6096–6103
- Chen H, Lin RJ, Xie W, Wilpitz D, Evans RM (1999) Regulation of hormone-induced histone hyperacetylation and gene activation via acetylation of an acetylase. *Cell* 98:675–686

27. Grunstein M (1997) Histone acetylation in chromatin structure and transcription. *Nature* 389:349–352
28. Struhl K (1998) Histone acetylation and transcriptional regulatory mechanisms. *Genes Dev* 12:599–606
29. Wagner BL, Valledor AF, Shao G, Daige CL, Bischoff ED, Petrowski M, Jepsen K, Baek SH, Heyman RA, Rosenfeld MG, Schulman IG, Glass CK (2003) Promoter-specific roles for liver X receptor/corepressor complexes in the regulation of ABCA1 and SREBP1 gene expression. *Mol Cell Biol* 23:5780–5789
30. Esteller M (2007) Cancer epigenomics: DNA methylomes and histone-modification maps. *Nat Rev Genet* 8:286–298
31. Stewart MD, Li J, Wong J (2005) Relationship between histone H3 lysine 9 methylation, transcription repression, and heterochromatin protein 1 recruitment. *Mol Cell Biol* 25:2525–2538
32. Wright JR, Siegel TN, Cross GA (2010) Histone H3 trimethylated at lysine 4 is enriched at probable transcription start sites in *Trypanosoma brucei*. *Mol Biochem Parasitol* 172:141–144
33. Vermeulen M, Mulder KW, Denissov S, Pijnappel WW, van Schaik FM, Varier RA, Baltissen MP, Stunnenberg HG, Mann M, Timmers HT (2007) Selective anchoring of TFIID to nucleosomes by trimethylation of histone H3 lysine 4. *Cell* 131:58–69
34. Nowak SJ, Corces VG (2004) Phosphorylation of histone H3: a balancing act between chromosome condensation and transcriptional activation. *Trends Genet* 20:214–220
35. Lo WS, Trievel RC, Rojas JR, Duggan L, Hsu JY, Allis CD, Marmorstein R, Berger SL (2000) Phosphorylation of serine 10 in histone H3 is functionally linked in vitro and in vivo to Gcn5-mediated acetylation at lysine 14. *Mol Cell* 5:917–926
36. Alberti S, Schuster G, Parini P, Feltkamp D, Diczfalussy U, Rudling M, Angelin B, Björkhem I, Pettersson S, Gustafsson JA (2001) Hepatic cholesterol metabolism and resistance to dietary cholesterol in LXRbeta-deficient mice. *J Clin Invest* 107:565–573

Paraoxonase 1 Activity in Chylomicrons and VLDL: The Effect of Type 2 Diabetes and Meals Rich in Saturated Fat and Oleic Acid

Patrick J. Manning · Sylvia A. de Jong ·
Anne R. Ryalls · Wayne H. F. Sutherland

Received: 26 July 2011 / Accepted: 21 November 2011 / Published online: 10 December 2011
© AOCs 2011

Abstract Paraoxonase 1 (PON 1) has antioxidant and cardioprotective properties and is abnormally low in type 2 diabetic serum. This study aimed to determine the effect of type 2 diabetes and meals rich in saturated fat and oleic acid on PON1 activity in chylomicrons and very low density lipoproteins (VLDL). PON1 arylesterase activity was measured in chylomicrons and VLDL that were isolated in serum from 20 patients with type 2 diabetes and 20 age- and gender-matched, overweight controls 3 h after meals rich in cream or olive oil in a randomized, cross-over study. Chylomicron–PON1 activity (45%, $P = 0.02$), ratio chylomicron–PON1/chylomicron–triacylglycerides (TAG) (42%, $P = 0.03$) and chylomicron–protein content (46%, $P < 0.001$) were significantly lower in patients with type 2 diabetes compared with controls after the olive oil meal with comparable findings after the meal rich in cream. After ingestion of olive oil, chylomicron–PON1 activity was significantly higher in controls ($P = 0.01$) and marginally higher ($P = 0.06$) in diabetic patients and chylomicron–TAG were significantly ($P < 0.05$) higher in both groups of subjects, compared with values after ingestion of cream. VLDL–PON1 increased (two-fold) significantly ($P < 0.003$) during both meals. Chylomicron–PON1 activity was correlated significantly with chylomicron–protein ($P < 0.001$, $n = 40$) and with postprandial serum PON1 activity ($P \leq 0.001$, $n = 40$). Our data suggest that type 2 diabetes is associated with abnormally low chylomicron–PON1 activity after fatty meals and this may be linked to lower chylomicron–protein content and serum PON1

activity. Switching from saturated fat to olive oil in the meal increases PON1 activity in the chylomicron fraction largely due to increased numbers of chylomicron particles.

Keywords Arylesterase · Chylomicrons · Monounsaturated fat · Paraoxonase 1 · Postprandial · Saturated fat · VLDL

Abbreviations

HDL High density lipoproteins
PON1 Paraoxonase 1
TAG Triacylglycerides
VLDL Very low density lipoproteins

Introduction

Human serum paraoxonase 1 (PON1) is an enzyme with esterase and lactonase activities [1, 2]. In vitro, PON1 inhibits the oxidative modification of low density lipoproteins (LDL) [3] that is believed to be a crucial step in the development of atherosclerotic lesions. In animal models of atherosclerosis, genetic deletion of PON1 increases atherosclerotic lesion formation [4, 5] while overexpression of human PON1 transgene attenuates lesion formation [6]. Serum PON1 arylesterase activity is abnormally low in individuals with angiographic evidence of coronary artery disease compared with those who do not have coronary artery disease [7]. Furthermore, low systemic levels of PON1 arylesterase activity is associated with the presence of angiographically determined coronary artery disease and prospectively with increased numbers of major cardiovascular events in subjects with or without pre-existing coronary artery disease [7]. In patients with type 2 diabetes, serum PON1 mass and

P. J. Manning · S. A. de Jong · A. R. Ryalls ·
W. H. F. Sutherland (✉)
Department of Medicine, Dunedin School of Medicine,
University of Otago, PO Box 913, Dunedin 9012, New Zealand
e-mail: wayne.sutherland@otago.ac.nz

arylesterase activity are abnormally low [8–10] and risk of coronary artery disease is high. In addition, increasing expression of PON1 attenuates the development of streptozotocin-induced diabetes in mice [11].

In fasted serum, PON1 is almost entirely associated with high density lipoproteins (HDL) and is thought to contribute to their antioxidative, antiatherogenic properties [12]. Small quantities of PON1 are also present on triacylglyceride (TAG)-rich lipoproteins including chylomicrons and very low density lipoproteins (VLDL) in human serum [13, 14]. There is evidence that this PON1 in chylomicrons and VLDL is partly derived by transfer of PON1 from HDL to these TAG rich lipoproteins [13, 14]. In the postprandial state after a fatty meal, levels of PON1 increase in the serum VLDL fraction [13]. In patients with type 2 diabetes, plasma concentrations of TAG-rich lipoproteins are often abnormally high after an overnight fast and in the postprandial state following a fatty meal [15]. The effect of type 2 diabetes on PON1 activity in fasted and postprandial triglyceride-rich lipoproteins is uncertain.

Lipids play an important role in the maintenance of PON1 in serum. PON1 binds to HDL phospholipids through its N-terminal hydrophobic region [16]. Lipids containing oleic acid, the predominant fatty acid in olive oil, stabilizes PON1 and protect it from oxidative deactivation *in vitro* [17]. Furthermore, intake of oleate elevates serum PON1 activity in rats [18]. Diets rich in saturated fat increase risk of coronary artery disease while adherence to a Mediterranean type of diet that includes olive oil as the major fat component, is thought to attenuate risk of developing coronary artery disease [19, 20]. There is little information on the effect of the type of fat in the meal and the presence of type 2 diabetes on activity of PON1 in serum chylomicron and VLDL fractions. The aim of the present study was to test the effect of type 2 diabetes and meals rich in saturated fat in the form of cream, and olive oil on PON1 activity in chylomicrons and VLDL. These lipoprotein fractions were isolated from serum by ultracentrifugation and their PON 1 arylesterase activity was measured. Our study showed that PON1 arylesterase activity was abnormally low in patients with type 2 diabetes and changing from saturated fat to monounsaturated fat rich meals increases PON1 activity in both chylomicrons and VLDL fractions mainly due to increased postprandial levels of these lipoproteins after ingestion of monounsaturated fat.

Subjects and Methods

Subjects

Twenty patients with type 2 diabetes (10 men and 10 women) and 20 healthy controls who were matched with

the diabetic patients for gender and age within 5 years, were recruited. The diabetic patients were recruited from the Diabetes Clinic at Dunedin hospital and were aged >18 years. Diabetic patients who had a glycated hemoglobin >10% indicating poor diabetic control, were excluded. Seven diabetic patients were receiving diet treatment for their diabetes, five were receiving metformin, four metformin plus gliclazide, two gliclazide alone, one metformin plus gliclazide plus insulin and one metformin plus insulin. Seven patients were receiving statin therapy, five were receiving aspirin and three were treated with cilazapril. Controls were recruited from overweight subjects who had previously participated in a study in our laboratory and from respondents to a newspaper advertisement. Controls were excluded if they had a history of serious illness, smoked cigarettes, or took medications. Written and informed consent was obtained from the participants prior to the study. The study was approved by the Lower South Regional Ethics Committee (protocol number: LRS/07/06/022).

Study Design

The study had a randomized, cross-over design with a 1-week washout period. Participants were randomized to receive either a meal rich in olive oil or cream and then after at least a week, they received the alternate meal. The 1-week period between test meals during which time approximately 21 other free-choice meals would have been consumed, eliminates credible carry-over effects from one test meal to the next. Participants were advised to maintain their usual lifestyle during the study.

Meals

The cream meal contained dairy cream (105 g/m² body surface area, low fat milk (150 ml), tinned apricots without syrup and sugar (50 g), low fat yoghurt (10 g), egg yolk (12 g), egg white (30 g) and sugar-free chocolate flavoring (3 tsp). The olive oil meal contained olive oil (40 g/m² body surface area), low fat milk (200 ml), and the same amounts of the other ingredients that were in the cream meal. The meals were homogenized into a milkshake and contained 44 g fat/m² body surface area, 34 g carbohydrate and 12 g protein.

Methods

Blood was collected in a plain tube. Serum was prepared by low speed centrifugation at 4 °C of blood that had been allowed to clot during 30 min at room temperature. To isolate chylomicrons, 3 ml serum was added to a 6.5-ml ultraclear ultracentrifuge tube that was topped up with a

$d = 1.0063$ solution of sodium chloride containing 1 mmol/l calcium chloride and then spun for 30 min at 22,000 rpm and 4 °C in a 50.3 Ti rotor in a Beckman L8-70 ultracentrifuge. The chylomicrons were harvested from the top 1 ml of the tube and this was made up to 5 ml using the $d = 1.0063$ solution of sodium chloride. The chylomicron fraction was not washed or subjected to dialysis in order to prevent dissociation of PON1 from the lipoproteins. The chylomicron fraction was stored overnight at 4 °C and assayed for PON1 activity the next day. The VLDL fraction was isolated by adding 4 ml of fasted serum or chylomicron depleted postprandial serum to 6.5-ml Ultraclear® ultracentrifuge tubes, filling the tubes with $d = 1.0063$ sodium chloride solution containing 1 mmol/l calcium chloride and ultracentrifuging the tubes for 18 h at 40,000 rpm and 4 °C in a Beckman 50.3 Ti rotor. The upper fraction of the tube containing VLDL was isolated and diluted to 5 ml using the $d = 1.0063$ sodium chloride solution and assayed for PON1 activity. Arylesterase activity was determined in triplicate essentially as was described previously [13, 21]. Aliquots of 40-fold diluted serum (60 μ l), chylomicron fraction (300 μ l) or VLDL fraction (500 μ l) were incubated at 22 °C with 3 ml buffer containing phenyl acetate (1 mmol/l), calcium chloride (0.9 mmol/l) in 20 mmol/l Tris-HCl and pH 8 and absorbance at 270 nm was measured. After subtraction of appropriate blank values to allow for spontaneous hydrolysis of phenyl acetate, the initial rate of phenyl acetate hydrolysis as μ mol/ml/min was determined. Absorbance readings that were taken at minute intervals were linear during the 6-min incubation of the phenyl acetate reagent with chylomicron and VLDL fractions. The rate of phenylacetate hydrolysis during the 6-min period was calculated and arylesterase activity in the chylomicron fraction was calculated as change in absorbance during 6 min (ΔA_6) \times 2.33 μ mol/ml/min. The arylesterase activity in the fasted VLDL fraction was calculated as $\Delta A_6 \times 1.113$ μ mol/ml/min and in the postprandial VLDL fraction as $\Delta A_6 \times 1.854$ μ mol/ml/min. A molar extinction coefficient of 1,310 mol l⁻¹ cm⁻¹ for phenol was used in the calculation of arylesterase activities. The concentration of salt in the assay of PON1 arylesterase activity in chylomicron and VLDL fractions was at a level (≤ 0.02 M) that does not affect arylesterase activity [22]. Furthermore, we showed that serum PON1 arylesterase activity was comparable (113 versus 118 μ mol/ml/min) when 60 μ l of serum diluted 40-fold with saline plus 300 μ l saline or 60 μ l serum diluted 40-fold with 10 mM Tris buffer (pH 7) plus 300 μ l of this Tris buffer were added to the assay buffer (3 ml) containing phenyl acetate. Serum cholesterol, TAG, HDL cholesterol, chylomicron-TAG and VLDL-TAG were measured enzymatically using commercial kits (Roche Diagnostics). Protein in chylomicron and VLDL fractions was measured using a modified Lowry method [23].

Statistics

Values are median (interquartile range) unless stated otherwise. The nonparametric Wilcoxon's tests for paired data were used to test for differences in the postprandial response (3 h change) between the meals. Wilcoxon's test for unpaired data was used to compare values between diabetic patients and controls. Spearman's rank correlation coefficients were used to test for relationships between variables.

Results

The characteristics of the participants at baseline (first visit) are summarized in Table 1. The diabetic patients had significantly lower plasma cholesterol concentrations, serum PON1 activity, and ratio VLDL-protein/VLDL-TAG and significantly higher ratio VLDL-PON1 activity/VLDL protein compared with the age and gender matched controls. Fasted PON1 activity in the serum VLDL fraction

Table 1 Characteristics of the diabetic patients and controls at baseline (first visit)

	Diabetic patients (n = 20)	Controls (n = 20)	P*
Age (years)	63 \pm 7	61 \pm 7	
BMI (kg/m ²)	30.6 \pm 5.1	30.1 \pm 4.4	0.62
HbA1c (%)	7.3 \pm 1.3	–	
TC (mmol/l)	4.56 \pm 1.06	5.84 \pm 0.98	<0.001
HDL-C (mmol/l)	1.32 \pm 0.46	1.48 \pm 0.46	0.30
TAG (mmol/l)	1.56 \pm 0.81	1.42 \pm 0.64	0.72
VLDL-TAG (mmol/l)	0.98 \pm 0.83	0.85 \pm 0.57	0.99
VLDL-PR (mg/l)	2.38 \pm 1.60	3.12 \pm 1.59	0.13
VLDL-PR/TAG (mg/mmol)	2.77 \pm 0.87	4.19 \pm 1.08	<0.001
PON1 (μ mol/ml/min)	80 \pm 22	96 \pm 17	0.02
VLDL-PON1 (μ mol/ml/min)	0.09 (0.03, 0.19)	0.08 (0.04, 0.14)	0.74
VLDL-PON1/TAG (μ mol/min/mmol)	123 (81, 148)	120 (91, 134)	0.93
VLDL-PON1/PR (μ mol/min/mg)	45 (30, 56)	30 (21, 39)	0.02

Values are means \pm SD or median (interquartile range)

BMI body mass index, HbA1c glycated hemoglobin, TC total cholesterol, HDL-C, high density lipoprotein cholesterol, TAG triacylglycerides, VLDL-TAG very low density lipoprotein triacylglycerides, VLDL-PR very low density lipoprotein protein, PON1 paraoxonase 1 arylesterase activity, VLDL-PON1 very low density lipoprotein paraoxonase 1 arylesterase activity

* Significance diabetic patients versus controls using Wilcoxon's rank test for unpaired values

was not significantly different between diabetic patients and controls.

Table 2 shows TAG, protein and PON1 activity in serum chylomicron fractions harvested 3 h after the meals in diabetic patients and controls. Serum chylomicron–TAG concentrations were not significantly different between diabetic patients and healthy controls and were significantly higher after the olive oil meal compared with the cream meal in both diabetic patients and controls. Chylomicron–PON1 activity and chylomicron–protein content were significantly lower in diabetic patients compared with controls after the meals. The ratio chylomicron PON1 activity/chylomicron TAG was significantly lower in diabetic patients compared with controls following the meal rich in olive oil and was lower but not significantly following the meal rich in cream. The ratio chylomicron–PON1 activity/chylomicron–protein was not significantly different between diabetic patients and controls. Chylomicron–PON1 activity was significantly ($P = 0.01$) higher after the olive oil meal compared with the cream meal in control subjects and was higher at a marginal level of

significance ($P = 0.06$) after the meal rich in olive oil compared with the cream meal in diabetic patients.

Table 3 shows baseline and 3 h changes in serum lipids, lipoprotein lipids and protein, PON1 and VLDL–PON1 activities in diabetic patients and controls during the fatty meals. VLDL–PON1 activity increased significantly ($P < 0.003$) by approximately two-fold after both meals in diabetic patients and by 88 and 44% during the olive oil and cream meals respectively in the controls. In control subjects, the 3 h increase in VLDL–PON1 activity was significantly ($P = 0.001$) larger following the olive oil meal compared with the meal rich in cream. The ratios VLDL–PON1/VLDL–TAG and VLDL–PON1/VLDL–protein also increased significantly during the meals in both diabetic patients and controls with significantly larger increases during the olive oil meal compared with the cream meal in controls. The increase in the ratio VLDL–PON1/VLDL–protein during the cream meal was significantly higher in diabetic patients compared with controls. As expected, serum TG, VLDL–TAG and VLDL–protein concentrations increased significantly ($P < 0.003$) 3 h after both meals in the diabetic patients and controls. In the control subjects, the increase in plasma TG ($P = 0.002$) was significantly larger following ingestion of the olive oil meal compared with the cream meal. Serum HDL cholesterol decreased significantly ($P = 0.01$) during the olive oil meal in diabetic patients and this decrease was significantly ($P = 0.004$) different compared with the corresponding change during the cream meal and was significantly ($P = 0.04$) different from the change in HDL cholesterol during the olive oil meal in controls. Serum PON1 activity did not change significantly during the meals.

Figure 1 shows the relationships between serum chylomicron–PON1 activity and serum concentrations of chylomicron–TAG and protein and serum PON1 activity 3 h after the meals in the total study population. Serum chylomicron–PON1 activity was correlated significantly with serum chylomicron–TAG concentrations after the meal rich in olive oil in the total study population. The corresponding correlation during the meal rich in cream did not quite attain statistical significance. This relationship was also marginally significant in diabetic patients after the olive oil meal ($r = 0.443$, $P = 0.05$) and highly significant in the control subjects after both meals (olive oil $r = 0.723$, $P < 0.001$; cream $r = 0.566$, $P = 0.009$). Serum chylomicron–PON1 activity was correlated significantly with serum chylomicron–protein concentrations after both the meals. This relationship was also significant in both diabetic patients (olive oil $r = 0.765$, $P < 0.001$; $r = 0.452$, $P = 0.05$) and controls (olive oil $r = 0.841$, $P < 0.001$; $r = 0.792$, $P < 0.001$) after both meals. During both the meals, chylomicron–PON1 activity was correlated significantly with postprandial PON1 activity in the total study population and

Table 2 Chylomicron triacylglycerides, protein, and paraoxonase 1 arylesterase activity in serum 3 h after ingestion of the meals

Meal	Diabetic patients ($n = 20$)	Controls ($n = 20$)	P^*
CHY–TAG (mmol/l)			
OL	0.64 (0.39, 1.06) [†]	0.78 (0.43, 1.30) [§]	0.53
CR	0.47 (0.15, 0.66) [†]	0.37 (0.15, 0.67) [§]	0.66
CHY–PR (mg/l)			
OL	5.4 (4.1, 8.2)	10.4 (6.9, 18.4)	<0.001
CR	4.9 (4.1, 5.6)	9.0 (5.5, 11.7)	0.002
CHY–PR/TAG (mg/mmol)			
OL	7.1 (6.4, 11.5) [†]	13.7 (9.2, 21.3) [‡]	0.001
CR	10.8 (7.8, 27.5) [†]	21.0 (16.4, 49.9) [‡]	0.02
CHY–PON1 ($\mu\text{mol/ml/min}$)			
OL	0.31 (0.22, 0.44)	0.56 (0.33, 0.91) [‡]	0.02
CR	0.26 (0.17, 0.41)	0.42 (0.25, 0.53) [‡]	0.02
CHY–PON1/TAG ($\mu\text{mol/min/mmol}$)			
OL	441 (393, 555)	755 (472, 1,142) [‡]	0.03
CR	677 (390, 1,101)	1,024 (708, 1,842) [‡]	0.07
CHY–PON1/PR ($\mu\text{mol/min/mg}$)			
OL	58 (49, 70)	47 (40, 61)	0.07
CR	59 (36, 76)	45 (40, 59)	0.36

Values are median (interquartile range)

OL olive oil, CR cream, CHY–TAG chylomicron triacylglycerides, CHY–PR chylomicron protein, CHY–PON1 chylomicron paraoxonase 1 arylesterase activity

* Significance diabetic patients versus controls using Wilcoxon's rank test for unpaired data

[†] $P = 0.02$, [‡] $P \leq 0.01$, [§] $P < 0.001$, OL versus CR meals using Wilcoxon's rank sign test for paired data

Table 3 Baseline and 3-h change in serum lipids, lipoprotein lipids, paraoxonase 1 activity and very low density lipoprotein-paraoxonase 1 activity in diabetic patients and healthy controls during the meals

Meal	Diabetic patients (<i>n</i> = 20)		Controls (<i>n</i> = 20)	
	Baseline	3 h change	Baseline	3 h change
TAG* (nmol/l)				
OL	1.51 (0.95, 1.91)	1.18 (0.73, 1.98)	1.12 (0.91, 1.73)	1.36 (0.71, 2.19) ^b
CR	1.50 (0.91, 1.93)	1.31 (0.55, 1.44)	1.21 (0.98, 1.94)	0.76 (0.40, 1.23) ^b
VLDL-TAG* (mmol/l)				
OL	0.91 (0.32, 1.22)	0.29 (0.16, 0.47)	0.62 (0.35, 1.09)	0.34 (0.14, 0.47)
CR	0.80 (0.40, 1.33)	0.34 (0.23, 0.54)	0.65 (0.45, 1.30)	0.25 (0.11, 0.41)
VLDL-PR* (mg/l)				
OL	2.46 (1.01, 3.53)	0.56 (−0.08, 1.07)	2.61 (1.64, 4.10)	0.66 (0.44, 1.07)
CR	1.81 (1.06, 3.60)	0.46 (0.24, 0.69)	2.59 (1.72, 4.35)	0.52 (0.28, 0.92)
HDL-C [†] (mmol/l)				
OL	1.25 (0.96, 1.67)	−0.04 (−0.09, 0) ^{‡,a}	1.35 (1.18, 1.58)	0.01 (−0.02, 0.07) [‡]
CR	1.28 (0.92, 1.50)	0 (−0.04, 0.03) ^a	1.34 (1.22, 1.67)	0 (−0.04, 0.04)
PON1 (μmol/ml/min)				
OL	79 (62, 97)	−1 (−3, 2)	94 (82, 108)	2 (−4, 7)
CR	82 (57, 101)	0 (−5, 4)	94 (85, 105)	−1 (−4, 3)
VLDL-PON1* (μmol/ml/min)				
OL	0.09 (0.03, 0.22)	0.09 (0.04, 0.14)	0.08 (0.04, 0.14)	0.07 (0.03, 0.10) ^c
CR	0.08 (0.04, 0.16)	0.08 (0.03, 0.13)	0.09 (0.04, 0.14)	0.04 (0.02, 0.06) ^c
VLDL-PON1/TAG* (μmol/min/mmol)				
OL	124 (78, 146)	38 (22, 50)	120 (92, 138)	29 (18, 53) ^a
CR	123 (81, 147)	25 (13, 32)	119 (83, 141)	13 (2, 31) ^a
VLDL-PON1/PR* (μmol/min/mg)				
OL	44 (29, 59)	18 (9, 33)	27 (20, 40)	13 (6, 19) ^a
CR	44 (32, 56)	20 (10, 27) [‡]	30 (24, 38)	7 (2, 14) ^{‡,a}

Values are median (interquartile range)

OL olive oil, CR cream, TAG triacylglycerides, VLDL-TAG very low density lipoprotein-triacylglycerides, TC total cholesterol, HDL-C high density lipoprotein cholesterol, PON1 paraoxonase 1, VLDL-PON1 very low density lipoprotein paraoxonase 1 activity

* All 3 h changes significant at $P \leq 0.003$, [†] 3 h change after OL meal in diabetic patients $P = 0.01$, using Wilcoxon's rank sign test for paired data

[‡] $P < 0.01$, 3 h changes in diabetic patients versus healthy controls using Wilcoxon's rank test for unpaired data

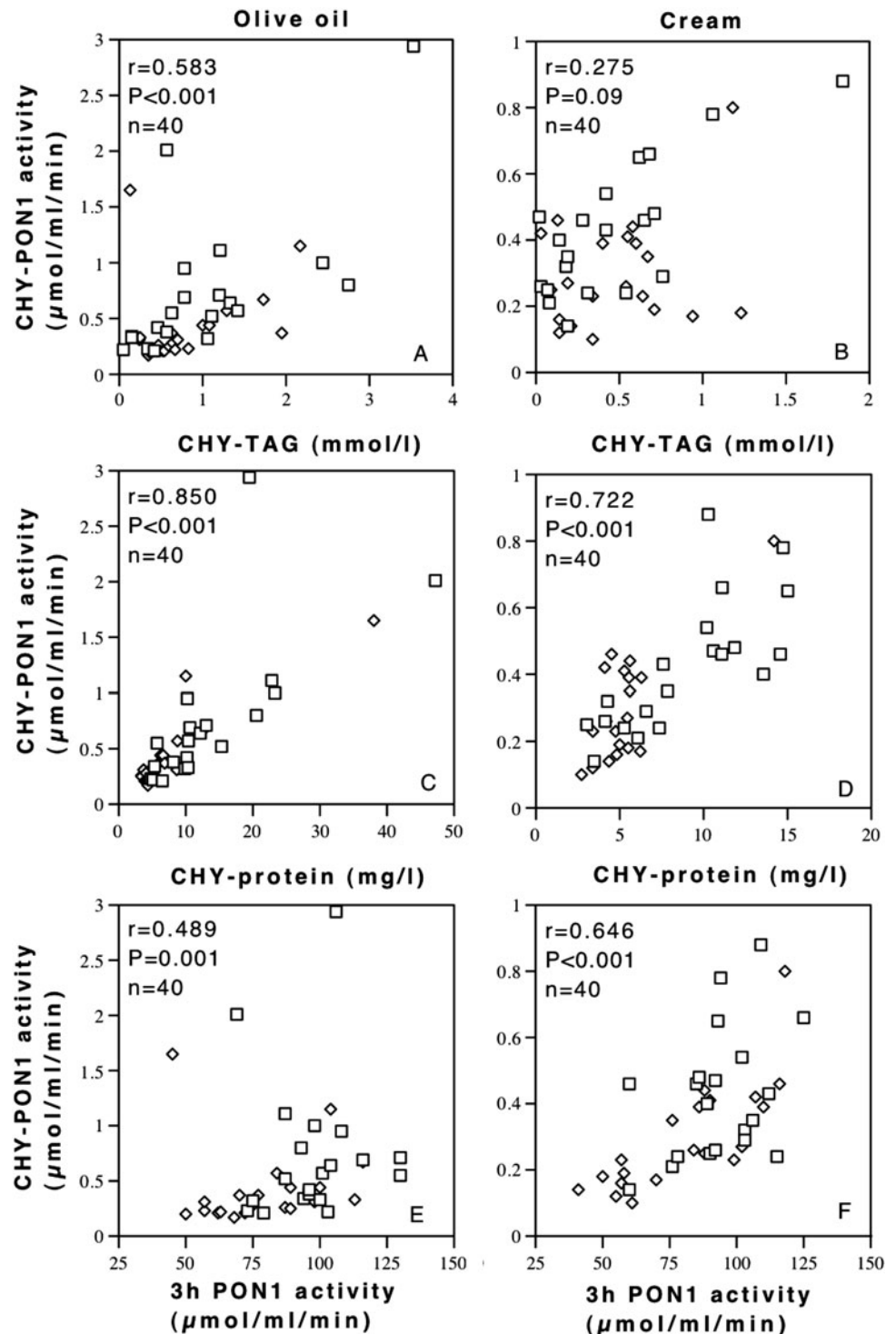
^a $P < 0.05$; ^b $P = 0.002$; ^c $P = 0.001$, OL versus CR meals

in diabetic individuals (olive oil $r = 0.460$, $P = 0.04$; cream 0.832 , $P < 0.001$). The corresponding correlations in the healthy controls did not achieve statistical significance (olive oil $r = 0.257$, $P = 0.27$; cream $r = 0.357$, $P = 0.12$). Chylomicron-PON1 activity was also correlated significantly with fasted serum PON1 activity (olive oil meal $r = 0.461$, $n = 40$, $P = 0.003$; cream meal $r = 0.638$, $n = 40$, $P < 0.001$). The ratio chylomicron-PON1 activity/chylomicron protein was correlated significantly with the 3 h postprandial serum PON1 activity after both meals (olive oil meal $r = 0.454$, $n = 40$, $P = 0.003$; cream meal $r = 0.614$, $n = 40$, $P < 0.001$) in the total study population.

Serum VLDL-PON1 activity was correlated significantly with serum VLDL-TAG and serum VLDL-protein

at first visit baseline and after the meals in the total study population (correlation coefficients between 0.714 and 0.930, all $P < 0.001$). Serum VLDL-PON1 activity was not correlated significantly with serum PON1 activity at first visit baseline ($r = -0.011$) and 3 h after the meals (olive oil $r = 0.168$; cream $r = 0.188$) in the total study population. The increases in serum VLDL-PON1 activity were correlated significantly with the corresponding increases in serum total TAG concentrations (olive oil $r = 0.853$, $P < 0.001$; cream $r = 0.803$, $P < 0.001$) and serum VLDL-TAG concentrations (olive oil $r = 0.782$, $P < 0.001$; cream $r = 0.809$, $P < 0.001$) during the meals in the total study population ($n = 40$) and in diabetic patients and controls separately (data not shown).

Fig. 1 Correlations between serum chylomicron paraoxonase 1 arylesterase activity (CHY-PON1) and serum chylomicron-triacylglyceride (CHY-TAG) concentration, chylomicron-protein (CHY-protein) concentration and PON1 arylesterase activity in patients with type 2 diabetes (*open diamonds*) and healthy controls (*open squares*) 3 h after meals rich in olive oil (**a, c, e**) and cream (**b, d, f**). Spearman's rank correlation coefficients are shown



Discussion

These data suggest that after a meal rich in fat, chylomicron-PON1 activity is lower in patients with type 2 diabetes compared with similarly overweight but otherwise healthy controls.

Chylomicron-PON1 arylesterase activities in ten healthy male controls in the present study (1.20 and 1.88 μmol/

ml/min) were comparable with reported values (1.20 μmol/ml/min) in ten healthy men [13] when data were adjusted to levels of chylomicron-TAG (1.71 mmol/l) similar to those in the previous study [13]. This adjustment gives a comparison of chylomicron-PON1 arylesterase activity between the studies at similar numbers of chylomicron particles. A similar adjustment of fasting, first visit levels of VLDL-PON1 arylesterase activity, gave a mean

VLDL–PON1 activity of 0.18 $\mu\text{mol}/\text{ml}/\text{min}$ in healthy men that was 59% lower than the corresponding reported activity [13]. The factors responsible for the lower fasting VLDL–PON1 activity in the current study are unclear. We cannot exclude the possibility that PON1 was dissociated from or inactivated in VLDL during its isolation. On the other hand, time taken to isolate VLDL was under half the corresponding time in the previous study [13].

In the present study, total PON1 activity in the chylomicron fraction and chylomicron–PON1 arylesterase activity normalized to chylomicron–TAG, were abnormally low in patients with type 2 diabetes. The factors responsible for this low chylomicron–arylesterase activity in diabetic patients are unclear but may include abnormal composition of chylomicron particles, reduced transfer of PON1 from HDL to chylomicrons, inactivation of PON1 by glycation and glycooxidation, and incorporation of less PON1 into chylomicrons during their synthesis in the intestine. The composition of chylomicrons in the diabetic patients appeared to be abnormal including a low protein content as indicated by the abnormally low ratio chylomicron–PR/chylomicron–TAG. Low chylomicron protein content may include low levels of PON1 protein and may account for much of the difference in chylomicron–PON1 activity between diabetic patients and controls. Chylomicron–protein levels were closely correlated with PON1 activity and when chylomicron PON1 activity was expressed in relation to chylomicron–protein content values were no longer appreciably different between diabetic patients and controls. The factors responsible for the abnormally low protein content of diabetic chylomicrons are unclear. Few studies have reported on the total protein content of chylomicrons in patients with type 2 diabetes. A previous study has reported transfer of PON1 from HDL to chylomicrons *in vitro* [13]. It is possible therefore that this process also occurs *in vivo*. In diabetic patients, low levels of HDL and PON1 activity in serum and HDL [24] could potentially limit transfer of PON1 from HDL to chylomicrons during the postprandial period after a fatty meal resulting in lower chylomicron–PON1 content and activity. The correlation between chylomicron–PON1 and serum PON1 activities in the present study appears to be consistent with this mechanism. There is evidence that glycation and glycooxidation inhibit PON1 activity [25, 26]. In patients with type 2 diabetes, the activity and mass of PON1 are abnormally low and amounts of glycated PON1 in serum are high [25]. Lastly, animal studies have detected PON1 mRNA in several tissues including the intestine [27]. Further studies are needed to test the mechanisms we have postulated to account for lower PON1 activity in diabetic chylomicrons.

In this study, the presence of type 2 diabetes did not appear to influence PON1 activity in endogenous TAG-rich lipoproteins. The activity of PON1 in the total VLDL

fraction of fasted serum and PON 1 activity per VLDL particle as indicated by the ratio VLDL–PON1 activity/VLDL–TAG, were not appreciably different between diabetic patients and controls. The higher ratio VLDL–PON1 activity/VLDL–protein may reflect the abnormal composition of VLDL in the diabetic patients as was indicated by a low ratio protein/TAG. A previous study has reported abnormally low protein content of VLDL 2 in patients with type 2 diabetes [28]. We cannot exclude the possibility that treatment of diabetic patients with lipid lowering drugs and hypoglycemic medications may have attenuated the effect of diabetes on serum VLDL concentration and VLDL–PON1 activity. Serum VLDL–TAG concentrations were not clearly different between the diabetic patients and controls. By contrast, previous studies have reported abnormally high concentrations of serum VLDL–TAG in patients with type 2 diabetes [29].

The 25% higher PON 1 arylesterase activity in the serum chylomicron fraction of healthy subjects after a meal rich in olive oil compared with a meal rich in cream in the present study may be due to the formation of a greater number of chylomicrons and delayed clearance of chylomicron remnants after ingestion of olive oil. Chylomicron–TAG concentrations were higher after the meal rich in olive oil and were associated with chylomicron–PON1 activity. The higher levels of chylomicron–PON1 activity normalized to chylomicron–TAG and the higher protein content of chylomicrons after the meal rich in cream may reflect greater enrichment of chylomicrons with proteins including PON1. Enrichment of chylomicrons with PON1 activity appeared to be proportional to enrichment with protein. The ratio chylomicron–PON1 activity/chylomicron–protein was not altered appreciably during the meals. However, any enrichment of chylomicrons with PON 1 activity had minimal effect on PON1 activity in the serum chylomicron fraction after ingestion of cream, as this activity was lower than the corresponding activity after the meal rich in olive oil. Increased numbers of chylomicrons after ingestion of olive oil may have the predominant effect on serum chylomicron–PON1 activity. Previous studies have reported higher levels of postprandial lipemia, greater numbers of chylomicrons and large TAG-rich lipoproteins and higher levels of chylomicron remnants after meals rich in olive oil compared with meals rich in saturated fat [30–32]. Also, there is evidence that oleic acid may increase numbers of chylomicron particles by increasing the expression of apo B mRNA and may be more efficiently incorporated into lipoproteins by microsomal triacylglycerol transfer protein [33].

Meals rich in olive oil and saturated fat may also have differential effects on postprandial HDL–cholesterol levels including a decrease in levels after ingestion of saturated fat and unchanged levels after olive oil meals in healthy

subjects and patients with type 2 diabetes [34, 35]. In the present study, by contrast, there was a small (3%) decrease in HDL cholesterol following the olive oil meal in the patients with type 2 diabetes. However, the magnitude of this decrease was comparable with measurement error. Furthermore, this change in HDL-cholesterol was not accompanied by corresponding changes in PON1 activity in the serum chylomicron and VLDL fractions.

Fuhrman and coworkers reported a nearly two-fold increase in VLDL-PON1 arylesterase activity in healthy men 3 h after a fatty meal [13]. In the present study, there were increases in VLDL-PON1 activity of comparable proportions 3 h after the fatty meals in diabetic patients and controls. These postprandial increases in serum VLDL-PON1 activity were closely linked with the corresponding increases in serum total TAG and VLDL-TAG concentrations suggesting that increased production of VLDL particles contributed to the increase in VLDL-PON1 activity during the meals. However, increased numbers of VLDL particles did not appear to be solely responsible for the increases in VLDL-PON1 activity. The postprandial increases in VLDL-PON1 activity remained when serum VLDL-PON1 activity was normalized to VLDL-TAG and VLDL-protein content. This finding suggests that enrichment of VLDL particles with PON1 activity may also have occurred. PON1 may be incorporated into VLDL in the liver or may be transferred from HDL in the circulation. Both PON1 [36] and VLDL are synthesized in the liver and there is evidence that VLDL can support PON1 secretion from cells [14]. Furthermore, transfer of PON1 from VLDL to HDL occurs *in vitro* [14]. In the present study, the greater increase in serum VLDL PON1 activity may be due to the greater and closely related increase in serum TAG with a similar trend in serum VLDL-TAG, during the meal rich in olive oil compared with the meal rich in cream in the controls. This finding is reminiscent of the pattern for chylomicrons during the meals and may also be at least partly attributable to reported increase in numbers of large TAG-rich lipoproteins formed during meals rich in oleic acid [30–33].

This study has limitations. The PON1 protein content of chylomicrons and VLDL was not measured. Approximately two-thirds of the diabetic patients were receiving drugs including statins, sulphonylureas, and aspirin, which have been reported previously as increasing serum PON 1 activity in some studies [37]. On the other hand, treatment with statins does not appear to affect serum PON 1 activity in patients with type 2 diabetes [38]. Also, the effect of sulphonylurea hypoglycemic agents on serum PON 1 activity has only been tested in animals and the effects of aspirin therapy on serum PON 1 activity are controversial [37]. Furthermore, in the present study, serum PON 1 activity was markedly lower in diabetic patients compared

with controls suggesting that the effect of diabetes on this enzyme activity remained predominant over any effects of drug therapy. Treatment with statins may contribute to the lower plasma TC concentrations in the diabetic patients and may have attenuated the effect of diabetes on serum TG and HDL cholesterol concentrations.

Low PON1 activity in chylomicrons may be relevant to the high risk of coronary artery disease in patients with type 2 diabetes. There is evidence that chylomicron-PON1 activity may participate in the removal of potentially atherogenic, oxidized lipids. *In vitro*, chylomicrons inhibit copper ion-induced oxidation of LDL by a mechanism which relies on the initial hydrolysis of lipid peroxides that may be at least partly mediated by PON1 [13]. Thus, low chylomicron PON1 activity in diabetic patients may potentially attenuate metabolism of atherogenic, oxidized lipids.

In conclusion, our data suggest that the presence of type 2 diabetes is associated with lower PON1 arylesterase activity in chylomicrons. In overweight but otherwise healthy individuals, switching from saturated fat to olive oil in a meal increases PON1 activity in the chylomicron and VLDL fractions largely due to a concomitant increase in numbers of chylomicron and VLDL particles. Whether lower PON1 activity in chylomicrons contributes to the increased risk of coronary artery disease that is associated with type 2 diabetes, remains to be determined.

Acknowledgments This study was funded by a grant from the Otago Medical Research Foundation Laurensen Award. The authors are grateful to the participants in the study. We dedicate this paper to the memory of our colleague and friend Sylvia de Jong who died recently.

References

1. La Du BN (1996) Structural and functional diversity of paraoxonase. *Nat Med* 2:1186–1187
2. Jakubowski H (2000) Calcium-dependent human serum homocysteine-thiolactone hydrolase: a protective mechanism against protein N-homocysteinylolation. *J Biol Chem* 275:3957–3962
3. Mackness MI, Arrol S, Durrington PN (1991) Paraoxonase prevents accumulation of lipoperoxides in low-density lipoproteins. *FEBS Lett* 286:152–154
4. Shih DM, Xia YR, Wang XP, Miller E, Castellani IW, Subbanagounder G, Cheroutre H, Faull KF, Berliner JA, Witztum JL, Lusis AJ (2000) Combined serum paraoxonase/knockout/apolipoprotein E knockout mice exhibit increased lipoprotein oxidation and atherosclerosis. *J Biol Chem* 275:17527–17535
5. Shih DM, Gu L, Xia YR, Navab M, Li WF, Hama S, Castellani IW, Furlong CE, Costa LG, Fogelman AM, Lusis AJ (1998) Mice lacking serum paraoxonase are susceptible to organophosphate toxicity and atherosclerosis. *Nature* 394:284–287
6. Tward A, Xia YR, Wang XP, Shia YS, Park C, Castellani IW, Lusis AJ, Shih DM (2002) Decreased atherosclerotic lesion formation in human serum paraoxonase transgenic mice. *Circulation* 106:484–490

7. Bhattacharyya T, Nicholls SJ, Topol EJ, Zhang R, Yang X, Schmitt D, Fu X, Shao M, Brennan DM, Ellis SG, Brennan M-L, Allayee H, Lusis AJ, Hazen SL (2008) Relationship of paraoxonase 1 (PON1) gene polymorphisms and functional activity with systemic oxidative stress and cardiovascular risk. *JAMA* 299:1265–1276
8. Abbot CA, Mackness MI, Kumar S, Boulton AJ, Durrington PN (1995) Serum paraoxonase activity, concentration, and phenotype distribution in diabetes mellitus and its relationship to serum lipids and lipoproteins. *Arterioscler Thromb Vasc Biol* 15:1812–1818
9. Mackness B, Mackness MI, Arrol S, Turkie W, Julier K, Abuasha B, Miller JE, Boulton AJ, Durrington PN (1998) Serum paraoxonase (PON1) 55 and 192 polymorphism and paraoxonase activity and concentration in non-insulin dependent diabetes mellitus. *Atherosclerosis* 139:341–349
10. Mastorikou M, Mackness M, Mackness B (2006) Defective metabolism of oxidized phospholipid by HDL from people with type 2 diabetes. *Diabetes* 55:3099–3103
11. Rozenberg O, Shiner M, Aviram M, Hayek T (2008) Paraoxonase 1 (PON1) attenuates diabetes development in mice through its antioxidative properties. *Free Radic Biol Med* 44:1951–1959
12. Mackness M, Mackness B (2004) Paraoxonase 1 and atherosclerosis: is the gene or the protein more important? *Free Radic Biol Med* 37:1317–1323
13. Fuhrman B, Volkova N (2005) Aviram M (2005) Paraoxonase 1 (PON1) is present in postprandial chylomicrons. *Atherosclerosis* 180:55–61
14. Deakin S, Moren X, James RW (2005) Very low density lipoproteins provide a vector for secretion of paraoxonase-1 from cells. *Atherosclerosis* 179:17–25
15. Taskinen M-R (2003) Diabetic dyslipidaemia: from basic research to clinical practice. *Diabetologia* 46:733–749
16. Sorenson RC, Bisgaier CL, Aviram M, Hsu C, Billecke S, La Du BN (1999) Human serum paraoxonase/arylesterase's retained hydrophobic N-terminal leader sequence associates with HDLs by binding phospholipids: apolipoprotein A-I stabilizes activity. *Arterioscler Thromb Vasc Biol* 19:2214–2225
17. Nguyen SD, Sok D-E (2003) Beneficial effect of oleoylated lipids on paraoxonase: protection against oxidative inactivation and stabilization. *Biochem J* 375:275–285
18. Kudchodkar BJ, Lacko AG, Dory L, Fungwe TV (2000) Dietary fat modulates serum paraoxonase 1 activity in rats. *J Nutr* 130:2427–2433
19. Buckland G, González CA, Agudo A, Vilardell M, Berenguer A, Amiano P, Ardanaz E, Arriola L, Barricarte A, Basterretxea M, Chirriague MD, Cirera L, Dorronsoro M, Egües N, Huerta JM, Larranaga N, Marin P, Martinez C, Molina E, Navarro C, Quirós JR, Rodriguez L, Sanchez MJ, Tormo MJ, Moreno-Iribas C (2009) Adherence to the Mediterranean diet and risk of coronary heart disease in the Spanish EPIC cohort study. *Am J Epidemiol* 170:1518–1529
20. Sofi F, Cesari F, Abbate R, Gensini GF, Casini A (2008) Adherence to Mediterranean diet and health status: meta-analysis. *BMJ* 337(112):a1344–a1350
21. Sutherland WHF, Walker RJ, de Jong SA, van Rij AM, Phillips V, Walker HL (1999) Reduced postprandial serum paraoxonase activity after a meal rich in used cooking fat. *Arterioscler Thromb Vasc Biol* 19:1340–1347
22. Eckerson HW, Wyte CM, La Du BN (1983) The human serum paraoxonase/arylesterase polymorphism. *Am J Human Genet* 35:1126–1138
23. Markwell MAK, Haas SM, Bieber LL, Tolbert NE (1978) A modification of the Lowry procedure to simplify protein determination in membranes and lipoprotein samples. *Anal Biochem* 87:207–210
24. Ferretti G, Bacchetti T, Busni D, Rabini RA, Curatola G (2004) Protective effect of paraoxonase activity in high-density lipoproteins against erythrocyte membrane peroxidation: a comparison between healthy subjects and type 1 diabetic patients. *J Clin Endocrinol Metab* 89:2957–2962
25. Mastorikou M, Mackness B, Liu Y, Mackness M (2008) Glycation of paraoxonase-1 inhibits its activity and impairs the ability of high-density lipoprotein to metabolize membrane lipid hydroperoxides. *Diabetic Med* 25:1049–1055
26. Heydrick CC, Thorpe SR, Fu M-X, Harper CM, Yoo J, Kim S-M, Wong H, Peters AL (2000) Glycation impairs high-density lipoprotein function. *Diabetologia* 43:312–320
27. Primo-Parma SL, Sorenson RC, Teiber J, La Du BN (1996) The human serum paraoxonase/arylesterase gene (PON1) is one member of a multigene family. *Genomics* 33:498–507
28. Hiukka A, Fruchart-Najib J, Leinonen E, Hilden H, Fruchart J-C, Taskinen M-R (2005) Alterations of lipids and apolipoprotein CIII in very low density lipoprotein subspecies in type 2 diabetes. *Diabetologia* 48:1207–1215
29. Cummings MH, Watts GF, Umpleby AM, Hennessey TR, Naoumova R, Slavin BM, Thompson GR, Sonksen PH (1995) Increased hepatic secretion of very-low density lipoprotein apolipoprotein B-100 in NIDDM. *Diabetologia* 38:959–967
30. Higashi K, Ishikawa T, Shige H, Tomiyasu K, Yoshida H, Ito T, Nakajima K, Yonemura A, Sawada S, Nakamura H (1997) Olive oil increases the magnitude of postprandial chylomicron remnants compared with milk fat and safflower oil. *J Am Coll Nutr* 16:429–434
31. Jackson KG, Robertson MD, Fielding BA, Frayn KN, Williams CM (2002) Olive oil increases the number of triacylglycerol-rich chylomicron particles compared with other oils: and effect retained when a second standard meal is fed. *Am J Clin Nutr* 76:942–949
32. Jackson KG, Wolstencroft EJ, Bateman PA, Yaqoob P, Williams CM (2005) Greater enrichment of triacylglycerol-rich lipoproteins with apolipoprotein E and C-III after meals rich in saturated fatty acids than after meals rich in unsaturated fatty acids. *Am J Clin Nutr* 81:25–34
33. Van Greevenbroek MMJ, Robertus-Teunissen MG, Erkelens DW, de Bruin TWA (1996) Effects of saturated, mono-, and polyunsaturated fatty acids on the secretion of apo B containing lipoproteins by Caco-2 cells. *Atherosclerosis* 121:139–150
34. Thomsen C, Rasmussen O, Lousen T, Holst JJ, Fenselau S, Schrezenmeier J, Hermansen K (1999) Differential effects of saturated and monounsaturated fatty acids on postprandial lipemia and incretin responses in healthy subjects. *Am J Clin Nutr* 69:1135–1143
35. Thomsen C, Storm H, Holst JJ, Hermansen K (2003) Differential effects of saturated and monounsaturated fats on postprandial lipemia and glucagon-like peptide-1 responses in patients with type 2 diabetes. *Am J Clin Nutr* 77:605–611
36. Leviev I, Negro F, James RW (1997) Two alleles of the human paraoxonase gene produce different amounts of mRNA. *Arterioscler Thromb Vasc Biol* 17:2935–2939
37. Costa LG, Giordano G, Furlong CE (2011) Pharmacological and dietary modulators of paraoxonase 1 (PON1) activity and expression: the hunt goes on. *Biochem Pharmacol* 81:337–344
38. Dullaart RPF, de Vries R, Voorbij HAM, Sluiter WJ, van Tol A (2009) Serum paraoxonase-1 activity is unaffected by short term administration of simvastatin, bezafibrate, and their combination in type 2 diabetes mellitus. *Eur J Clin Invest* 39:200–203

An Egg-Enriched Diet Attenuates Plasma Lipids and Mediates Cholesterol Metabolism of High-Cholesterol Fed Rats

Fang Yang · Meihu Ma · Jia Xu · Xiufang Yu ·
Ning Qiu

Received: 5 September 2011 / Accepted: 12 December 2011 / Published online: 11 January 2012
© AOCS 2012

Abstract We investigated the influence of an egg-enriched diet on plasma, hepatic and fecal lipid levels and on gene expression levels of transporters, receptors and enzymes involved in cholesterol metabolism. Sprague–Dawley rats fed an egg-enriched diet had lower plasma triglycerides, total cholesterol, low density lipoprotein (LDL)-cholesterol, hepatic triglyceride, and cholesterol concentrations, and greater plasma high-density lipoprotein cholesterol concentration, fecal neutral sterol and bile acid concentrations than those fed a plain cholesterol diet. Chicken egg yolk had no effect on sterol 12 α -hydroxylase and sterol 27 α -hydroxylase; but upregulated mRNA levels of hepatic LDL-receptor, cholesterol 7 α -hydroxylase (CYP7A1) and lecithin cholesterol acyltransferase, and downregulated hepatic hydroxymethylglutaryl-(HMG)-CoA reductase and acyl-CoA:cholesterol acyltransferase (ACAT) after 90 days. Modification of the lipoprotein profile by an egg-enriched diet was mediated by reducing de novo cholesterol synthesis and enhancing the excretion of fecal cholesterol, via upregulation of CYP7A1 and the LDL receptor, and downregulation of HMG-CoA reductase and ACAT.

Keywords Egg-enriched diet · Cholesterol · Plasma lipids · mRNA expression

Abbreviations

CVD	Cardiovascular disease
PC	Phosphatidylcholine
SM	Sphingomyelin
SHR	Spontaneously hypertensive rats
RT-qPCR	Real time quantitative polymerase chain reaction
OV	Ovomucin
CCG	Common control group
CLG	Cholesterol group
EYG	Egg yolk group
WEG	Whole egg group
HBA	Total bile acid
apoB	Apolipoprotein-B-100
apoA1	Apolipoprotein-A-1
HE	Hematoxylin and eosin
GAPDH	Glyceraldehyde-3-phosphate dehydrogenase
HMG-CoA R	Hydroxymethylglutaryl CoA reductase
LDLr	LDL receptor
CYP7A1	Cholesterol 7 α -hydroxylase
CYP27A1	Sterol 27 α -hydroxylase
CYP8B1	Sterol 12 α -hydroxylase
ACAT	Acyl-CoA:cholesterol acyltransferase
LCAT	Lecithin cholesterol acyltransferase
EWP	Egg white protein

Introduction

Hypercholesterolemia is one of the most prevalent risk factors for arteriosclerosis, which can contribute to many forms of human disease, most notably cardiovascular disease (CVD). A multitude of epidemiological studies has shown a direct link between high plasma cholesterol,

F. Yang · M. Ma (✉) · X. Yu · N. Qiu
National R&D Center for Egg Processing, College of Food
Science and Technology, Huazhong Agricultural University,
Wuhan 430070, Hubei, People's Republic of China
e-mail: mameihuhn@yahoo.com.cn

J. Xu
College of Animal Science and Technology,
Huazhong Agricultural University, Wuhan 430070,
Hubei, People's Republic of China

particularly of low-density lipoprotein (LDL)-cholesterol and the risk of CVD [1]. Coronary dietary guidelines to prevent CVD emphasize the reduction in dietary cholesterol to <300 mg/day. Consequently, eggs, as a food high in dietary cholesterol, have been targeted as a food to limit when advising patients on a diet aimed at lowering serum cholesterol levels [2].

Even though it has been reported that dietary cholesterol increases the concentrations of both LDL-cholesterol and high-density lipoprotein (HDL)-cholesterol, an egg-rich diet is unlikely to have substantial overall impact on the risk of CVD among healthy men and women [3, 4]. Thus, it is thought that some components in the egg might help in controlling serum cholesterol concentrations. Animal experiments confirmed that the egg yolk intakes for *apoE*^{-/-} knockout mice had little effect on plasma cholesterol [5], probably because phosphatidylcholine (PC) and sphingomyelin (SM) present in egg can markedly inhibit the absorption of cholesterol, fat and other lipids. Phospholipids might slow the rate of luminal lipolysis, micellar solubilization and transfer of micellar lipids to the enterocytes [6, 7]. Another possible functional factor that can lower the cholesterol concentration in blood is egg white protein (EWP), which is digested in the stomach and intestines. Animal experiments also indicated that EWP intake for rats could reduce cholesterol concentrations in the blood. Thus, long-term consumption of egg white hydrolyzed with pepsin (hEW) on spontaneously hypertensive rats (SHR) exerted a beneficial effect on the lipid profile, lowering triglycerides and total cholesterol without changing HDL levels [8, 9]. Egg ovomucin (OV) experiments in vitro and in vivo suggested that the suppression of cholesterol absorption might occur by direct interaction between cholesterol mixed micelles, which could also inhibit the reabsorption of bile acids [10]. However, few experiments have been conducted to investigate the roles of egg yolk and whole egg intakes on cholesterol metabolism in healthy rats. Eggs are a central food in human diets that span all socioeconomic classes and come from a unique animal source providing high bioavailability [11]. Moreover, increases in one food type might lead to changes in the consumption of other foods that could modulate disease

risk. Therefore, we have focused on the overall effect of cholesterol in healthy rats fed with whole egg and egg yolk.

We evaluated the effect of the long-term consumption of an egg yolk diet or whole egg diet on plasma, hepatic and fecal lipid levels and on pathological changes in the liver of Sprague–Dawley (SD) rats, using real time quantitative polymerase chain reaction (RT-qPCR) amplification to measure the mRNA expression of enzymes associated with cholesterol metabolism. No association between egg supplementation and blood lipid profile in the rats was found. Moreover, we found an egg-enriched diet could mediate excretion and deposition of cholesterol, which might be indicative of some special functional factors in egg that need to be identified in the future.

Materials and Methods

Animals and Diet

Male SD rats ($n = 70$; aged 8 weeks with a body weight (BW) of 250 ± 15 g) were obtained from the Animal Center of Tongji Medical University, Wuhan, China. Rats were housed in cages each containing five animals in a temperature-controlled room (21 ± 2 °C $60 \pm 5\%$ relative humidity) with a 12/12-h light/dark cycle fed a commercial rodent chow and water ad libitum. After a 7-day wait, the rats were randomly divided into four groups which began to consume the experimental diets (Table 1) for 3 months. In the Common Control Group, CCG ($n = 18$), rats were given commercial chow according to the recommendation of the Chinese Association for Laboratory Animal Sciences [12]; in the Cholesterol Group, CLG ($n = 18$), rats were fed a supplemented cholesterol diet containing 0.75% cholesterol and 17.5% lard; in the Egg Yolk Group, EYG ($n = 18$), rats were fed a supplemented egg yolk diet containing 31.25% vacuum freeze-dried egg yolk powder containing 24 mg/g cholesterol; in the Whole Egg Group, WEG ($n = 16$), rats were fed a whole egg diet containing 55.56% vacuum-freeze-dried whole egg powder containing 13.5 mg/g cholesterol. Except for the CCG rats, the other groups' diets contained 0.75% cholesterol and similar fat. Egg yolk

Table 1 Composition of the diets

Group	Crude protein (%)	Crude fat (%)	Carbohydrate (%)	Crude ash (%)	Moisture (%)	Cholesterol (%)
CCG	19.87	1.55	60.13	8.86	9.58	0.002
CLG	19.81	18.83	41.81	8.81	9.74	0.750
EYG	21.78	20.23	43.03	5.61	8.60	0.750
WEG	36.09	14.72	39.28	3.26	5.90	0.750

CCG ($n = 18$), rats were given standard chow; CLG ($n = 18$), rats were fed a cholesterol diet containing 0.75% cholesterol and 17.5% lard; EYG ($n = 18$), rats were fed a egg yolk diet containing 31.25% vacuum freeze-dried egg yolk powder with 24 mg/g cholesterol; WEG ($n = 16$), rats were fed a whole egg diet containing 55.56% vacuum freeze-dried whole egg powder with 13.5 mg/g cholesterol

powder and whole egg powder were made by vacuum-freeze-drying, then analyzed for cholesterol content [13]. In a previous experiment, we added different cholesterol contents in commercial chow to SD rats and found that a 0.75% cholesterol concentration could increase plasma lipids.

Sample Collection

After consuming the experimental diets for 60 and 90 days, the rats were weighed and deprived of food overnight (~14 h); then they were anesthetized with 1 g/L sodium pentobarbital in a 0.9% sodium chloride solution and killed by exsanguination from the abdominal aorta. Blood was centrifuged at 1,200g for 15 min at 4 °C and the plasma was collected. The livers of rats in all groups were removed. Liver fragments measuring 1 × 0.5 × (0.2–0.3) cm were placed into 4% paraformaldehyde fixative for routine histological examination. Fecal samples of the rats in each group were collected for 3 days at the end of the experimental period. All samples were frozen at –70 °C until analysis. The internal organs were weighed and recorded. The animal protocol was approved by the Institutional Animal Care and Use Committee of Tongji Medical University, Wuhan, People's Republic of China.

Biochemical Analyses

The plasma triglyceride, cholesterol, total bile acid (HBA), HDL-cholesterol, LDL-cholesterol, apolipoprotein-A-1 (apoA1) and apolipoprotein-B-100 (apoB) were determined spectrophotometrically using appropriate kits (Daiichi Pure Chemicals Co., Tokyo, Japan). Total lipids were extracted from the liver [14], and cholesterol and triglyceride contents were measured as above. Because the amount of the fecal sample for individual rats in the same group was insufficient to analyze neutral sterols and bile acids, fecal samples were pooled in the same group, then divided into five equal portions, freeze-dried and ground. Neutral sterols and bile acids were extracted [15] and determined using cholesterol and bile acids kits (Daiichi Pure Chemicals Co., Tokyo, Japan).

Histopathology

The remaining liver samples were fixed in 4% formaldehyde at room temperature and were processed by standard methods. Briefly, tissues were embedded in paraffin wax, sectioned at 5 μm, stained with hematoxylin and eosin, and then picked up on glass slides for light microscopy. An experienced pathologist blinded to the experiment evaluated all samples. All fields in each section were examined for grading of steatosis and necroinflammation according to the criteria described by Brunt [16].

Quantitative RT-qPCR

Total RNA was isolated from rat liver by TRIZOL reagent (Life Technologies Co., Carlsbad, CA, USA) according to the manufacturer's protocol. The RNA concentration was estimated by measurement with a UV spectrophotometer at 260 and 280 nm. Samples of 300 ng of total RNA from eight rats were run in triplicate and subjected to RT-PCR amplification using the One-Step RT-PCR Quick Master Mix (Toyobo Co. Ltd., Tokyo, Japan). The messenger RNA (mRNA) expression of genes was measured by RT-qPCR using Real Time PCR Master Mix (SYBR Green; Toyobo Co. Ltd., Tokyo, Japan) and an iCycler (Bio-Rad, Hercules, CA, USA). For determining mRNA concentration, a threshold cycle was obtained from each amplification curve using iQ5 software (Bio-Rad, Bio-Rad, Hercules, CA, USA). Calculation of the relative mRNA concentration was made using the $2^{-\Delta\Delta C_t}$ threshold cycle method [17]. We used the housekeeping gene for glyceraldehyde-3-phosphate dehydrogenase (GAPDH; EC1.2.1.12) for normalization. The primer sequences used for RT-PCR are described in Table 2. The total reaction volume was adjusted to 25 μl. Five microliters of a 1:100 dilution of each cDNA was used for reactions with primers, which were all used at a final concentration of 100 nM. The annealing temperature used was 60–62 °C and 40 amplification cycles were performed. Melting curves were done after each run and a single distinct peak was obtained for each primer set.

Statistical Analysis

All values are expressed as mean ± SD. Data were analyzed using a one-way analysis of variance and all differences were inspected by Duncan's new multiple-range test using SPSS 18.0 statistical software (SPSS Inc., Chicago, IL, USA); $p < 0.05$ was considered statistically significant.

Results

Weight Gain and Organ Index

Weight gain in the four groups was similar during the first 40 days of the study (data not shown), indicating that all diets met the nutritional requirement of rats in their growing phase, but at the end of the experiment (60 and 90), the CLG rats gained more body and liver weight than rats fed other diets ($p < 0.05$; Table 3); however, the WEG rats gained less weight than those fed other diets ($p < 0.05$). The food intake and food titer during the experimental period did not differ among the groups. Compared with the liver index in the CCG rats, that in the CLG rats was higher than others ($p < 0.05$), while as time

Table 2 Primer sequences used for the RT-qPCR analysis

Gene (accession no)	Primer sequences (5′–3′)	T_m (°C)	Amplicon size (bp)
GAPDH (NM_017008)	F: GCAAGTTCAACGGCACAG R: CGCCAGTAGACTCCACGAC	60	169
HMG-CoA R (NM_013134)	F: TGTGGGAACGGTGACACTTA R: CTTCAAATTTTGGGCACTCA	60	95
LDL-R (NM_175762)	F: AGCCGATGCATTCCTGACTC R: AGTTCATCCGAGCCATTTTCAC	61	89
CYP7A1 (NM_012942)	F: ACGTGGTTGGAAGAAGCG R: GAATGTGGGCAGCGAGAA	60	173
CYP27A1 (NM_178847)	F: GGAAGGTGCCCCAGAACAA R: GCGCAGGGTCTCCTTAATCA	61	113
CYP8B1 (AB 009686)	F: GTACACATGGACCCCGACATC R: GGGTCCATCAGGGTTGAG	60	102
ACAT (NM_017075)	F: GCTGAAGTGAACCTACCCCTT R: GAGCCATGCCTCTAGTACCT	60	200
LCAT (NM_017024)	F: CCAAGGCTGAACCTCAGTAACCA R: CGGTAGCACAGCCAGTTACCA	62	111

increased, that in the EYG rats was lower than in other groups ($p < 0.01$). As to visceral fat index, the WEG rats were also significantly lower than others at the end of 90 days ($p < 0.01$) because of the low levels of epididymal fat and low mesenteric fat index.

Plasma Lipid Levels

After 60 and 90 days of treatment, the triglyceride and cholesterol levels in the plasma of CLG rats were significantly higher than in other groups ($p < 0.05$; Table 4). The triglyceride and total cholesterol levels among the EYG, WEG and CCG rats showed no significant differences, while the triglyceride level in WEG rats was the lowest. The LDL-cholesterol and apoB level in the plasma of CLG rats were significantly greater than others at the end of 90 days ($p < 0.01$) and there was no significant difference between the EYG, WEG and CCG rats. In contrast, the HDL-cholesterol and apoA1 in plasma of CLG were significantly lower than others ($p < 0.01$). The total bile acid (TBA) concentrations of the CLG, EYG and WEG rats were greater than in the CCG rats ($p < 0.05$), especially for WEG ($p < 0.01$). The TBA levels of the four groups were ranked WEG > EYG > CLG > CCG.

Hepatic Triglyceride and Cholesterol Levels

At the end of 60 and 90 days treatment, the total cholesterol level in the liver of EYG and WEG rats were greater than in the CCG rats ($p < 0.05$; Table 4) but the total cholesterol level in the liver of CLG rats was much higher ($p < 0.01$),

showing that dietary egg can partially increase hepatic cholesterol with little effect on overall mechanics. However, at the end of 90 days, triglyceride levels in the liver of CLG rats was significantly higher than in other groups ($p < 0.01$) and there were no significant differences between the CCG, EYG and WEG rats. Interestingly, the triglyceride level in the WEG rats was the lowest, similar to the triglyceride level in plasma.

Neutral Sterol and Bile Acid Levels in Feces

After 90 days of treatment, the dried fecal neutral sterol excretions by the CLG, EYG and WEG rats were 13.92, 23.52 and 27.48 $\mu\text{mol/g}$ greater than in the CCG rats (5.12 $\mu\text{mol/g}$; $p < 0.05$; Table 4), especially in the WEG rats ($p < 0.01$). Fecal bile acid levels excreted by the CCG, CLG, EYG and WEG rats were 17.64, 41.76, 91.73 and 123.66 $\mu\text{mol/g}$ dry feces, respectively.

Pathological Changes in Livers

Before obtaining the histopathology, the rats' livers were observed in each group. The CCG, EYG and WEG rats had normal liver appearance with moderate shape, red color and soft texture, while the CLG rat livers were a little different with larger shape, khaki color, moderate texture and greasy feeling of the cut surface (data not shown). Subsequently, liver sections from rats fed with the regular dry rat chow (CCG) and egg diet (EYG and WEG) had a normal morphological appearance. The hepatocytes were polygonal, clear, with abundant cytoplasm and morphologically

Table 3 Effects of diet consumption for 60 and 90 days on the rats' growth, food intake and organ index

Item	Experimental intervention 60 days				Experimental intervention 90 days			
	CCG	CLG	EYG	WEG	CCG	CLG	EYG	WEG
Body weight gain (g)	183.31 ± 19.21 ^{bc}	257.53 ± 15.53 ^a	203.63 ± 21.64 ^b	166.53 ± 20.41 ^c	216.27 ± 20.34 ^{bc}	287.48 ± 17.82 ^a	232.64 ± 23.56 ^b	200.87 ± 21.14 ^c
Food intake (g)	1,668.00 ± 10.83	1,687.78 ± 9.37	1,686.00 ± 6.78	1,650.00 ± 9.11	2,514.00 ± 10.95	2,572.78 ± 8.94	2,565.00 ± 7.26	2,496.00 ± 9.46
Food titer (%)	0.110 ± 0.013 ^b	0.153 ± 0.015 ^a	0.121 ± 0.011 ^b	0.101 ± 0.008 ^b	0.086 ± 0.014	0.112 ± 0.013	0.091 ± 0.012	0.080 ± 0.009
Liver weight (g)	11.5 ± 1.50 ^b	13.78 ± 1.26 ^a	12.24 ± 0.98 ^{ab}	11.24 ± 1.04 ^b	12.77 ± 0.64 ^b	17.00 ± 1.75 ^a	14.16 ± 1.80 ^b	10.91 ± 1.06 ^c
Liver index (%)	2.61 ± 0.24 ^b	2.83 ± 0.14 ^a	2.63 ± 0.11 ^b	2.61 ± 0.15 ^b	2.69 ± 0.13 ^b	3.07 ± 0.29 ^a	2.85 ± 0.33 ^a	2.32 ± 0.31 ^c
Spleen index (%)	0.27 ± 0.08	0.31 ± 0.09	0.23 ± 0.04	0.21 ± 0.03	0.23 ± 0.04 ^{ab}	0.29 ± 0.09 ^a	0.22 ± 0.04 ^b	0.17 ± 0.04 ^b
Kidney index (%)	0.54 ± 0.03	0.53 ± 0.07	0.53 ± 0.03	0.53 ± 0.05	0.55 ± 0.04	0.57 ± 0.08	0.58 ± 0.06	0.53 ± 0.06
Visceral fat index (%)	3.39 ± 0.32 ^b	3.85 ± 0.33 ^a	3.77 ± 0.40 ^a	3.67 ± 0.47 ^{ab}	3.34 ± 0.18 ^b	3.68 ± 0.45 ^a	3.41 ± 0.52 ^{ab}	3.04 ± 0.30 ^c

Values are mean ± SD. $n = 9$ (except for the WEG rats; $n = 8$). Means in a row with superscripts without a common letter differ significantly ($p < 0.05$). Food titer = body weight gain/food intake. Organ index = organ weight/body weight. Visceral fat index = (perirenal fat + epididymal fat + mesenteric fat)/body weight

Table 4 Effects of diet consumption for 60 and 90 days on the rats' plasma, liver and fecal lipid concentrations and protein content

Item	Experimental intervention 60 days				Experimental intervention 90 days			
	CCG	CLG	EYG	WEG	CCG	CLG	EYG	WEG
Plasma (mmol/L)								
Triglyceride	0.61 ± 0.09 ^b	1.21 ± 0.15 ^a	0.52 ± 0.18 ^b	0.58 ± 0.15 ^b	0.67 ± 0.07 ^{bc}	1.22 ± 0.06 ^a	0.732 ± 0.07 ^b	0.615 ± 0.10 ^c
Total cholesterol	1.05 ± 0.12 ^c	1.75 ± 0.38 ^a	1.38 ± 0.20 ^b	1.21 ± 0.16 ^b	1.42 ± 0.15 ^b	1.77 ± 0.32 ^a	1.55 ± 0.20 ^{ab}	1.47 ± 0.07 ^b
LDL-C	0.27 ± 0.05 ^{ab}	0.39 ± 0.06 ^a	0.29 ± 0.02 ^{ab}	0.24 ± 0.02 ^b	0.23 ± 0.03 ^c	0.42 ± 0.03 ^a	0.29 ± 0.05 ^b	0.24 ± 0.07 ^{bc}
HDL-C	0.84 ± 0.07 ^a	0.70 ± 0.06 ^b	0.79 ± 0.09 ^{ab}	0.82 ± 0.04 ^a	0.85 ± 0.06 ^a	0.49 ± 0.17 ^c	0.76 ± 0.04 ^b	0.89 ± 0.07 ^a
Apo-A1 (g/L)	0.53 ± 0.01 ^a	0.39 ± 0.01 ^b	0.51 ± 0.01 ^{ab}	0.52 ± 0.07 ^a	0.53 ± 0.01 ^a	0.39 ± 0.01 ^b	0.50 ± 0.01 ^{ab}	0.54 ± 0.01 ^a
Apo-B (g/L)	0.32 ± 0.02 ^b	0.52 ± 0.01 ^a	0.36 ± 0.01 ^b	0.30 ± 0.01 ^b	0.31 ± 0.01 ^b	0.61 ± 0.01 ^a	0.35 ± 0.05 ^b	0.32 ± 0.01 ^b
Total bile acid (μmol/L)	107.8 ± 16.4 ^c	133.3 ± 18.0 ^b	149.0 ± 20.8 ^{ab}	166.3 ± 16.0 ^a	112.2 ± 9.7 ^c	141.1 ± 12.7 ^b	163.3 ± 13.2 ^a	172.5 ± 25.5 ^a
Liver lipids (μmol/g, liver)								
Triglyceride	27.11 ± 4.47 ^c	68.56 ± 3.35 ^a	32.89 ± 3.33 ^b	27.39 ± 2.30 ^c	32.61 ± 4.82 ^b	65.28 ± 4.51 ^a	33.00 ± 4.31 ^b	31.00 ± 1.94 ^b
Total cholesterol	5.31 ± 0.69 ^c	9.19 ± 0.60 ^a	7.51 ± 0.55 ^b	6.79 ± 0.39 ^b	5.49 ± 0.64 ^c	11.66 ± 0.50 ^a	6.63 ± 0.41 ^b	6.30 ± 0.62 ^b
Fecal lipids (μmol/g, dry feces)								
Neutral sterol	5.60 ± 0.10 ^d	14.76 ± 0.19 ^c	18.12 ± 0.68 ^{ab}	22.76 ± 1.17 ^a	5.12 ± 0.12 ^c	13.92 ± 0.70 ^b	23.52 ± 1.23 ^a	27.48 ± 0.85 ^a
Total bile acid	16.80 ± 1.59 ^d	41.03 ± 2.30 ^c	68.86 ± 5.32 ^b	93.32 ± 6.75 ^a	17.64 ± 2.15 ^d	41.76 ± 2.64 ^c	91.73 ± 5.98 ^b	123.66 ± 9.53 ^a

Values are mean ± SD. $n = 9$ (except for the WEG group, $n = 8$). Means in a row with superscripts without a common letter differ significantly ($p < 0.05$). Food titer = body weight gain/food intake

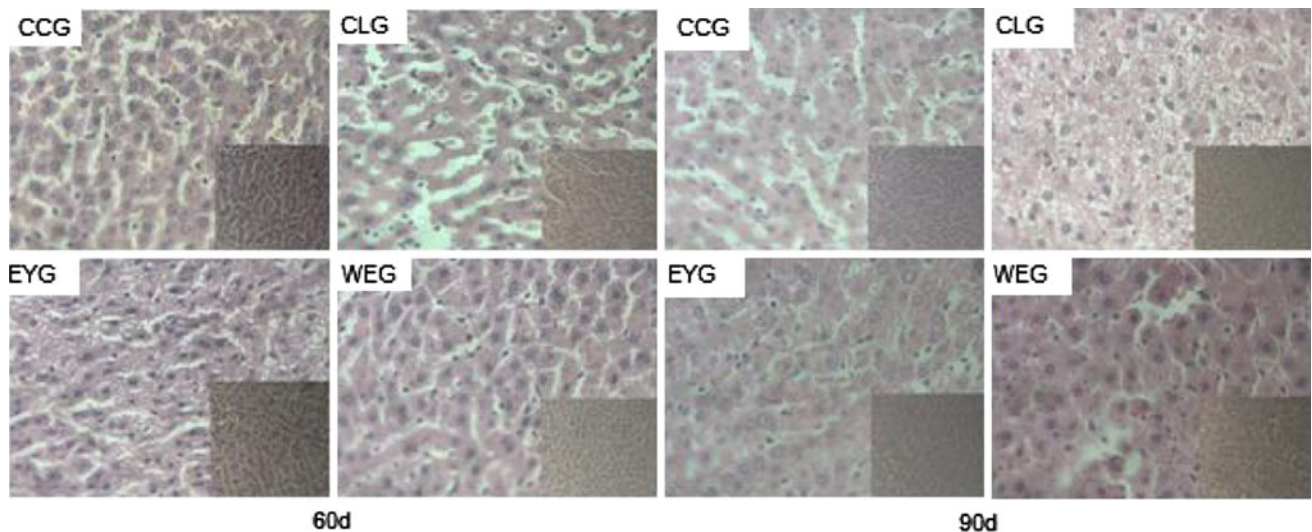


Fig. 1 Effects of the diet consumption for 60 and 90 days on pathological changes in the liver ($\times 400$, $\times 100$)

normal. In the CLG rats, hepatocytes were swollen with loose cytoplasm and many different sizes of fat vacuoles pushing the nucleus to one side (Fig. 1).

mRNA Expression Levels of Hepatic Enzymes Associated with Cholesterol Metabolism

HMG-CoA reductase catalyzes the conversion of HMG-CoA to mevalonic acid and is subject to both short-term and long-term effects on hepatic cholesterol de novo synthesis. Its mRNA expression levels in the CLG, EYG and WEG rats were 13-, 40- and 15-fold lower than in the CCG rats at the end of 90 days, respectively ($p < 0.01$; Fig. 2). LDL receptor is a mosaic protein found in clathrin-coated pits on the cell surface that mediates the endocytosis of LDL-cholesterol. Its mRNA expression levels in the EYG and WEG rats were 6.2- and 8.8-fold higher than in the CCG rats at the end of 90 days, respectively, while they were 1.8- and 2.6-fold higher than in the CLG rats ($p < 0.01$).

Cholesterol 7 α -hydroxylase (CYP7A1) is the rate-limiting enzyme in the synthesis of bile acid from cholesterol, catalyzing the formation of 7 α -hydroxycholesterol. Its mRNA expressions in the EYG and WEG rats were 4.7- and 5.5-fold higher than in the CCG rats at the end of 90 days, respectively, while they were 2.2- and 2.6-fold higher than in the CLG rats ($p < 0.01$; Fig. 2). CYP7A1 mRNA expression level in WEG rats was higher than in the EYG rats at the end of 90 days. Sterol 27 α -hydroxylase (CYP27A1) is the key regulatory enzyme in the alternative pathway and sterol 12 α -hydroxylase (CYP8B1) controls the ratio of cholic acid and chenodeoxycholic acid synthesis in both the neutral and acidic pathways; there were no significant differences in its mRNA expression levels in the four groups.

Acyl-CoA:cholesterol acyltransferase (ACAT) is responsible for esterification of cholesterol absorbed from the intestine, its mRNA expression in the CLG rats was significantly higher than in the other groups ($p < 0.01$; Fig. 2), while the other three groups had no significant difference between them (at the end of 90 days). The lecithin cholesterol acyltransferase (LCAT) mRNA expression in the EYG rats was 2.8-, 2.7- and 1.9-fold higher than in the CCG, CLG and WEG rats, while in the WEG rats it was 1.4-fold higher than in both the CCG and CLG rats ($p < 0.01$; Fig. 2).

Discussion

Because the plasma levels of LDL-cholesterol correlate strongly with the incidence of human coronary heart disease, much effort has been directed at developing and implementing therapies to lower plasma LDL-cholesterol levels. Excessive intake of cholesterol could explain a significant increase in plasma LDL-cholesterol level and decrease in HDL-cholesterol level. However, the same intake of cholesterol among the CLG, EYG and WEG rats in the present study caused different results. Though the fat content among these three groups was not exactly the same and high level of protein in WEG, we focus on the need for adding the whole egg yolk or egg to commercial chow and evaluating the effect of the long-term consumption of egg diet to parameters relative with cholesterol, while not to investigate the specific effect of one factor from egg. Total saturated fatty acids concentration in lard was remarkably higher than egg yolk which was consistent with our diet composition, being that high proportion of saturated fatty acids and cholesterol content in meat may easily result in

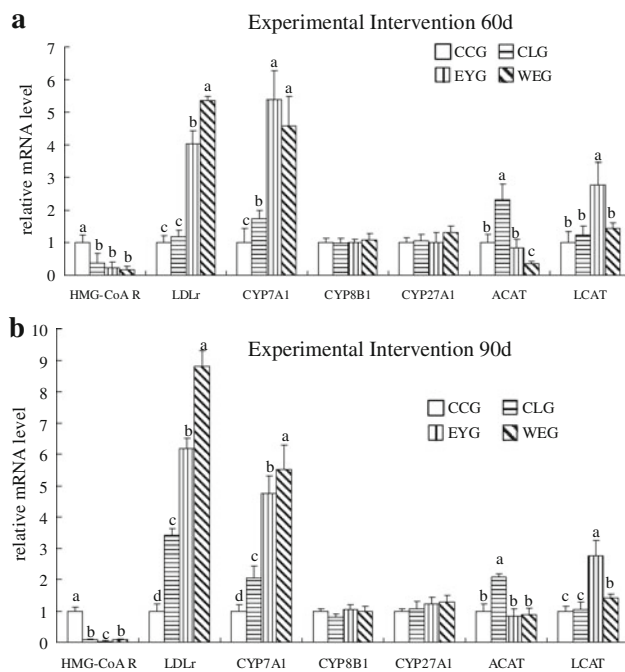


Fig. 2 Effects of diet consumption for 60 days (a) and 90 days (b) on cholesterol-related metabolic enzymes mRNA expressions. The graph represents the mRNA levels from quantitative RT-PCR relative to the control gene, GAPDH. Values are mean \pm SEM; $n = 9$ (except for the WEG rats; $n = 8$). Mean values in a row with different superscript letters differ significantly ($p < 0.05$)

atherosclerosis disease. Particularly as a substitute for dietary saturated fatty acids, the benefit of increasing unsaturated fatty acids intakes deserves considerable attention [18]. Possibly, the egg diet promoted the transformation and excretion of cholesterol by ways other than remaining in the blood and organs and some components repaired the damage to LDL-cholesterol, which was in agreement with previous studies. Bartov et al. studied the hypercholesterolemic effects in the female rats of egg yolk and crystalline cholesterol dissolved in lard. That study demonstrated that serum and liver cholesterol levels were significantly higher in the animals fed cholesterol dissolved in lard than those fed diets containing air-dried or lyophilized egg yolk, apparently from the significantly higher retention of neutral sterols [19]. Patricia et al. [5] investigated the protective effect of lutein and egg yolk supplementation on plasma lipid profile in apolipoprotein E-deficient (*apoE*^{-/-}) mice and showed that egg yolk significantly reduced plasma triglyceride levels without change in total cholesterol, decreased plasma lipid peroxidation and improved the lipid profile. These results are in disagreement with other studies, which seems mainly to arise from differences in the methodology. The earlier studies were carried out on human subjects, the amount of cholesterol fed was extremely high (3–10 g, equivalent to

12–40 eggs per day) and the composition of the experimental diets was not always equalized [20, 21]. Moreover, in the present study the diets contained a more realistic content of cholesterol.

Because of the same cholesterol content in the CLG, EYG and WEG diets, the abundance of cholesterol sources would inhibit rate-limiting enzyme HMG-CoA reductase activity of cholesterol synthesis, but the inhibitory effect of the egg diet seemed more obvious. Furthermore, the synthesis rate of the LDL receptor was negatively correlated with cellular cholesterol content. This is the main receptor on the hepatocyte surface acting to remove LDL from the circulation. The higher LDL receptor expression levels in the EYG and WEG rats were consistent with decreased LDL-cholesterol concentrations in plasma and increased fecal excretion of bile acids and neutral sterols. Spady et al. [22] demonstrated that overexpression of the exogenous CYP7A1 gene effectively reduced the plasma cholesterol level in hamsters fed a low- or high-fat diet. The higher CYP7A1 mRNA expression levels in the EYG and WEG rats showed that the egg diet promoted CYP7A1 enzyme activity and increased bile acid synthesis. This might have accelerated the exclusion of fecal bile acid because it was consistent with a high fecal bile acid level. Moreover, the plasma cholesterol level was negatively correlated with the CYP7A1 mRNA level. In the present study, the liver CYP7A1 mRNA level was upregulated by egg supplementation in the diet. This may be the mechanism by which dietary egg content could reduce plasma cholesterol levels. At the beginning, the EYG rats seemed to excrete more cholesterol through this channel, but after 2 months the WEG rats excreted more. This phenomenon needs further study. We speculate that the egg diet increased hepatic LDL receptor expression, which facilitated the lowering of LDL-cholesterol and increased CYP7A1 expression, which in turn facilitated cholesterol catabolism and upregulation.

The 3-OH group of cholesterol can become fatty-acylated to form cholesterol esters that can be stored in cytoplasmic lipid droplets, which enzyme responsible for this activity is ACAT. To transport excessive amount of cholesterol intake in rats—except to excrete with bile acids—the major route is to generate the conversion of cholesterol esters stored in lipid droplets. Egg yolk and whole egg intake significantly inhibited ACAT activity and decreased cholesterol stored in the body in the form of cholesterol esters. LCAT is responsible for the maturation of the HDL pool and promote the efflux of cholesterol from peripheral tissues. Evidence for this comes from studies of LCAT-deficiency syndromes in which only nascent type HDL accumulates in the plasma [23]. The high LCAT mRNA expressions in the EYG and WEG rats showed that the egg diet promoted LCAT activity and accelerated the removal of cholesterol from the body. This inference was consistent with the low cholesterol and

LDL-cholesterol levels of plasma in the EYG and WEG rats and the high HDL level of plasma in the EYG and WEG rats, compared with the CLG rats. Thus reverse cholesterol transport is one of several proposed mechanisms by which HDL provides protection from CVD. Previous studies have demonstrated that overexpression of LCAT results in an anti-atherogenic lipoprotein profile with reduced apolipoprotein-B-containing lipoproteins in addition to elevated plasma levels of HDL [24]. Currently, ACAT inhibition and overexpression of LCAT are promising avenues of intervention with the development of atherosclerosis and clinical trials in patients are underway [25].

Compare with CLG, egg yolk diet could mediate plasma lipids level in a good way with the similar composition of the diet, while whole egg diet could maintain the same plasma lipids level as CCG and attenuate the damage from excessive intake of cholesterol with higher protein content and lower fat content. Thus, some egg components including phospholipids, active proteins, fatty acids and other trace elements might have cholesterol-lowering activity, were suspected to play regulatory roles in the cholesterol absorption, transportation, metabolism and excretion. This finding agrees with previous *in vivo* studies [6, 7]. *In vitro* studies using intestinal segments [26] or intestinal cell lines [27] showed that egg phospholipids, whether in mixed micelles or in lipid emulsions, interfere with the intestinal uptake of cholesterol by altering the rates of micellar formation and diffusion and/or impeding the hydrolysis of TG and subsequent uptake of cholesterol. Asato et al. [28] have reported that the consumption of EWP reduced the serum total- and LDL-cholesterol concentrations in humans. Nagaoka et al. [10] reported that ovomucin, which is an EWP, inhibited the incorporation of cholesterol into Caco-2 cells by binding to bile acids. However, the ovomucin content of EWP is only 1.5–3.5% [29]. Therefore, it is unlikely that the cholesterol-lowering activity of EWP is due to ovomucin alone. Some have reported that cysteine supplementation or cysteine-enriched protein reduced the total serum cholesterol concentration in rats fed a high-cholesterol diet [30]. Mansoa et al. [8] indicated that hEW played an important role in the antioxidative defense in SHR and exerted a beneficial effect on the lipid profile, lowering triglycerides and total cholesterol without changing HDL levels. Possible regulating roles of these egg active components on cholesterol metabolism still need to be validated. Even though the differences on protein, fat and carbohydrates might be in part responsible for the effects, this difference is the unity of relativity which might help us to find out which active constituents from egg do work.

The conventional approach to weight reduction is a high-carbohydrate, low-fat, energy-deficient diet that reduces total energy intake, increases satiation and is metabolized with less energetic efficiency compared with high-fat diets

[31]. In theory, the egg diet would be more likely to cause obesity. However, the conventional dietary approach has not proven to be very effective for many obese and overweight individuals, so they have turned to the use of other diets approaches to attain healthier weights, such as the Atkins' diet, a low-carbohydrate/high-fat/high-protein diet [32]. Low-carbohydrate diets appear to have beneficial lipoprotein effects in individuals with atherogenic dyslipidemia, which comprises a triad of increased blood concentrations of small, dense low-density lipoprotein particles, decreased high-density lipoprotein particles, and increased triglycerides [33]. The egg diet has its origins in the induction phase of the Atkins Diet, as eggs are one of the healthiest ways to consume a high-protein, low-carbohydrate diet that is also a significant source of vitamins without increasing saturated fats. The difference in weight gain and organ index might be attributed to the low-carbohydrate, high-protein and high-fat in the EYG and WEG diets in comparison with the CCG and CLG groups in the present study.

The present study has demonstrated that an egg-enriched diet could significantly reduce cholesterol absorption, restrain *de novo* cholesterol synthesis and deposits in the form of cholesterol esters, and activate bile acid synthesis and excretion in feces and deposition. However, the mechanisms by which an egg diet lowers plasma cholesterol need to be further characterized and the special functional factors in egg need to be identified.

Acknowledgments We duly acknowledge the financial support received from the earmarked fund for Modern Agro-industry Technology Research System (Project Code No.: nycytx-41-g22).

Conflict of interest All authors declare that there are no conflicts of interest.

References

1. Richard E, Ligthart SA, Moll van Charante EP, van Gool WA (2010) Vascular risk factors and dementia—towards prevention strategies. *Neth J Med* 68(10):284–290
2. Ostör E, Jánosi A, Adám Z, Bárczy G, Borbás S, Dávid B, Gallai I, Podmaniczky M, Ruzsányi T (2003) Secondary prevention of coronary disease—at the turn of the millennium in light of the Hungarian data of the EUROASPIRE I-II. *Studies. Orv Hetil* 144(49):2399–2404
3. Greene CM, Zern TL, Wood RJ, Shrestha S, Aggarwal D, Sharman MJ, Volek JS, Fernandez ML (2005) Maintenance of the LDL cholesterol: HDL cholesterol ratio in an elderly population given a dietary cholesterol challenge. *J Nutr* 135: 2793–2798
4. Mutungi G, Ratliff J, Puglisi M, Torres-Gonzalez M, Vaishnav U, Leite JO, Quann E, Volek JS, Fernandez ML (2008) Dietary cholesterol from eggs increases plasma HDL cholesterol in overweight men consuming a carbohydrate-restricted diet. *J Nutr* 138:272–276

5. Fernández-Robredo P, Rodríguez JA, Sádaba LM, Recalde S, García-Layana A (2008) Egg yolk improves lipid profile, lipid peroxidation and retinal abnormalities in a murine model of genetic hypercholesterolemia. *J Nutr Biochem* 19:40–48
6. Jiang YZ, Noh SK, Koo SI (2001) Egg phosphatidylcholine decreases the lymphatic absorption of cholesterol in rats. *J Nutr* 131:2358–2363
7. Noh SK, Koo SI (2004) Milk sphingomyelin is more effective than egg sphingomyelin in inhibiting intestinal absorption of cholesterol and fat in rats. *J Nutr* 134:2611–2616
8. Mansoa MA, Miguela M, Evena J, Hernández R, Aleixandre A, López-Fandiño R (2008) Effect of the long-term intake of an egg white hydrolysate on the oxidative status and blood lipid profile of spontaneously hypertensive rats. *Food Chem* 109:361–367
9. Yu HL, Li Y, Wang JB, Zheng LP, Yan WX (2005) Chinese soft-shelled turtle egg powder lowers serum cholesterol, increases faecal neutral steroids and bile acid excretion and up-regulates liver cytochrome P450 mRNA level in rats. *Br J Nutr* 94:315–320
10. Nagaoka S, Masaoka M, Zhang Q, Hasegawa M, Watanabe K (2002) Egg ovomucin attenuates hypercholesterolemia in rats and inhibits cholesterol absorption in Caco-2. *Lipids* 37:267–272
11. Applegate E (2000) Introduction: nutritional and functional roles of eggs in the diet. *J Am Coll Nutr* 19:495–498
12. Chinese Association for Laboratory Animal Sciences (2001) GB 14924.3—2001 Laboratory animals—mice and rats formula feeds. Standards Press of China, Beijing
13. Bragagnolo N, Rodríguez-Amay DB (2003) Comparison of the cholesterol content of Brazilian chicken and quail eggs. *J Food Compos Anal* 16:147–153
14. Folch J, Lees M, Sloane-Stanley GH (1957) A simple method for isolation and purification of total lipids from animal tissues. *J Biol Chem* 226:497–509
15. Post SM, de Crom R, van Haperen R, van Tol A, Princen HM (2003) Increased fecal bile acid excretion in transgenic mice with elevated expression of human phospholipid transfer protein. *Arterioscler Thromb Vasc Biol* 23(5):892–897
16. Brunt EM, Janney CG, Di-Bisceglie AM, Neuschwander-Tetri BA, Bacon BR (1999) Nonalcoholic steatohepatitis: a proposal for grading and staging the histological lesions. *Am J Gastroenterol* 94:2467–2474
17. Livak KJ, Schmittgen TD (2001) Analysis of relative gene expression data using real-time quantitative PCR and the $2^{-\Delta\Delta C_t}$ method. *Methods* 25:402–408
18. Gillingham LG, Harris-Jan S, Jones PJH (2011) Dietary monounsaturated fatty acids are protective against metabolic syndrome and cardiovascular disease risk factors. *Lipids* 46(3):209–228
19. Bartov I, Reiser R, Henderson GR (1973) Hypercholesterolemic effect in the female rat of egg yolk versus crystalline cholesterol dissolved in lard. *J Nutr* 103:1400–1405
20. Messinger WL, Porosowska Y, Steele JM (1950) Effect of feeding egg yolk and cholesterol on serum cholesterol levels. *Arch Intern Med* 86:189–195
21. Gordon H, Wilkens J, Brock JF (1958) Serum-cholesterol levels after consuming eggs with increased content of unsaturated lipids. *Lancet* 2:244–245
22. Spady DK, Cuthbert JA, Willard MN, Meidell RS (1995) Adenovirus-mediated transfer of a gene encoding cholesterol 7 α -hydroxylase into hamsters increases hepatic enzyme activity and reduces plasma total and low density lipoprotein (LDL) cholesterol. *J Clin Invest* 96:700–709
23. Glomset JX, Assmann G, Gjone E, Norum KK (1989) Lecithin: cholesterol acyltransferase deficiency and fish eye disease. In the metabolic and molecular bases of inherited disease. McGraw-Hill, New York
24. Hoeg JM, Santamarina-Fojo S, Berard AM (1996) Overexpression of lecithin: cholesterol acyltransferase in transgenic rabbits prevents diet-induced atherosclerosis. *Proc Natl Acad Sci* 93:11448–11453
25. Llaverias G, Laguna JC, Alegret M (2003) Pharmacology of the ACAT inhibitor avasimibe (CI-1011). *Cardiovasc Drug Rev* 21:33–50
26. Homan R, Hamelehle KL (1998) Phospholipase A₂ relieves phosphatidylcholine inhibition of micellar cholesterol absorption and transport by human intestinal cell line Caco-2. *J Lipid Res* 39:1197–1209
27. Eckhardt ER, Wang DQ, Donovan JM, Carey MC (2002) Dietary sphingomyelin suppresses intestinal cholesterol absorption by decreasing thermodynamic activity of cholesterol monomers. *Gastroenterology* 122:948–956
28. Asato L, Wang MF, Chan YC, Yeh SH, Chung HM, Chung SY, Uezato T, Suzuki I, Yamagata N, Kokubu T, Yamamoto S (1996) Effect of egg white on serum cholesterol concentration in young women. *J Nutr Sci Vitaminol* 42:87–96
29. Matsuoka R, Kimura M, Muto A, Masuda Y, Sato M, Imaizumi K (2008) Mechanism for the cholesterol-lowering action of egg white protein in rats. *Biosci Biotechnol Biochem* 72:1506–1512
30. Nakamura R, Takeyama M, Nakamura K, Umemura O (1980) Constituent proteins of globulin fraction obtained from egg white. *Agric Biol Chem* 44:2357–2363
31. Lucas F, Sclafani A (1999) Differential reinforcing and satiating effects of intragastric fat and carbohydrate infusions in rats. *Physiol Behav* 66:381–388
32. Atkins RC (1992) Dr. Atkins' new diet revolution, Revised edition. Avon Books, New York
33. Musunuru K (2010) Atherogenic dyslipidemia: cardiovascular risk and dietary intervention. *Lipids* 45(10):907–914

A Low-Protein, High-Carbohydrate Diet Increases Fatty Acid Uptake and Reduces Norepinephrine-Induced Lipolysis in Rat Retroperitoneal White Adipose Tissue

Maísa P. dos Santos · Suélem A. de França · José Tiago F. dos Santos ·
Samyra L. Buzelle · Gisele L. Bertolini · Maria Antonieta R. Garófalo ·
Isis C. do Kettelhut · Danúbia Frasson · Valéria E. Chaves · Nair H. Kawashita

Received: 17 July 2011 / Accepted: 8 December 2011 / Published online: 8 January 2012
© AOCS 2012

Abstract A low-protein, high-carbohydrate (LPHC) diet for 15 days increased the lipid content in the carcass and adipose tissues of rats. The aim of this work was to investigate the mechanisms of this lipid increase in the retroperitoneal white adipose tissue (RWAT) of these animals. The LPHC diet induced an approximately two- and tenfold increase in serum corticosterone and TNF- α , respectively. The rate of de novo fatty acid (FA) synthesis in vivo was reduced (50%) in LPHC rats, and the lipoprotein lipase activity increased (100%). In addition, glycerokinase activity increased (60%), and the phosphoenolpyruvate carboxykinase content decreased (27%). Basal [U- 14 C]-glucose incorporation into glycerol-triacylglycerol did not differ between the groups; however, in the presence of insulin, [U- 14 C]-glucose incorporation increased by 124% in adipocytes from only control rats. The reductions in IRS1 and AKT content as well as AKT phosphorylation in the RWAT from LPHC rats and the absence of an insulin response suggest that these adipocytes have reduced insulin

sensitivity. The increase in NE turnover by 45% and the lack of a lipolytic response to NE in adipocytes from LPHC rats imply catecholamine resistance. The data reveal that the increase in fat storage in the RWAT of LPHC rats results from an increase in FA uptake from circulating lipoproteins and glycerol phosphorylation, which is accompanied by an impaired lipolysis that is activated by NE.

Keywords Low-protein · High-carbohydrate diet · Lipogenesis · Glycerol-3-phosphate · Retroperitoneal white adipose tissue · Lipolysis · Growing rats

Abbreviations

ACTH	Adrenocorticotrophic hormone
AKT	Serine/threonine protein kinase
ATGL	Adipose triglyceride lipase
cAMP	Cyclic adenosine monophosphate
EAT	Epididymal adipose tissue
EtOH	Ethyl alcohol
FA	Fatty acids
FFA	Free fatty acid
G3P	Glycerol-3-phosphate
GLUT-4	Glucose transporter type 4
GyK	Glycerokinase
HPA	Hypothalamic-pituitary-adrenal axis
HSL	Hormone-sensitive lipase
IR	Insulin receptor
IRS-1	Insulin receptor substrate 1
LPHC	Low-protein, high-carbohydrate diet
LPL	Lipoprotein lipase
NE	Norepinephrine
PDE3B	Phosphodiesterase 3B
PEPCK	Phosphoenolpyruvate carboxykinase
PI3K	Phosphatidylinositol 3-kinase
PKA	Protein kinase A

M. P. dos Santos · S. A. de França · J. T. F. dos Santos ·
S. L. Buzelle · N. H. Kawashita (✉)
Department of Chemistry, Federal University of Mato Grosso,
Cuiabá, MT, Brazil
e-mail: nairhonda@terra.com.br

G. L. Bertolini · V. E. Chaves
Department of Basic Sciences in Health, Federal University
of Mato Grosso, Cuiabá, MT, Brazil

M. A. R. Garófalo
Department of Physiology, University of São Paulo,
Ribeirão Preto, SP, Brazil

I. C. do Kettelhut · D. Frasson
Department of Biochemistry, Immunology,
University of São Paulo, Ribeirão Preto, SP, Brazil

PPAR γ	Peroxisome proliferator-activated receptors γ
RWAT	Retroperitoneal white adipose tissue
SE	Standard error
T3	Triiodothyronine
T4	Thyroxine
TAG	Triacylglycerol
TNF- α	Tumor necrosis factor- α
WAT	White adipose tissue

Introduction

The role of adipose tissue in energy balance was first recognized in energy storage in the form of TAG and its mobilization in energy-demanding situations. It was later demonstrated that white adipose tissue (WAT) also maintains body homeostasis by synthesizing and releasing adipokines [1]. Adipokines bind to receptors in several tissues, including adipocytes, and control many functions of these organs. Leptin, the first adipokine described, contributes to the central control of energy balance by regulating food intake and energy expenditure [1]. The discovery of other adipokines (TNF- α , adiponectin) has renewed interest in understanding both WAT physiology and the role of these adipokines in the control of energy storage in adipose tissue itself.

The TAG content in WAT depends on the balance of lipogenesis and lipolysis, two opposing processes that are controlled by a complex interaction of several factors. Accumulation of lipids within white adipocytes is generally associated with stimulation of lipogenesis by anabolic hormones, such as insulin, and the inhibition of the lipolytic activity of catabolic agents, such as norepinephrine (NE), epinephrine, glucocorticoids and others [1]. Adipokines, such as TNF- α and leptin, have an important lipolytic function in WAT in several metabolic situations, such as stress and obesity, in humans and rodents [1, 2].

Previous studies have shown that a low-protein diet correlates with an increase in absolute and/or relative body lipid content [3, 4]. Data reveal that when the amount of protein in the diet is near the protein requirement [5], the increase in body lipid content is accompanied by an increase in food intake [4, 6]. However, many studies have shown that even with a higher food intake, the amount of protein ingested is lower when compared with the requirement [7], and the increase in food intake can be stimulated by an increase in energy expenditure [3]. Aparecida de França et al. [8] confirmed this theory in rats fed a low-protein, high-carbohydrate diet (LPHC; 6% protein and 74% carbohydrate) for 15 days in the growth stage (when the animal's energy expenditure is high) and also demonstrated that these animals have an increase in lipid content in the whole carcass, epididymal adipose tissue (EAT) and retroperitoneal adipose tissue (RWAT).

Preliminary studies performed in the EAT of LPHC rats showed that glycerol-3-phosphate (G3P) generation (from glucose, by glyceroneogenesis and phosphorylation of glycerol) and de novo fatty acids (FA) in this tissue are not altered by the diet. Moreover, lipoprotein lipase (LPL) activity was reduced, which suggests a decreased utilization of FA from circulating lipoproteins [9]. Thus, available data indicate that lipogenesis is not increased in the EAT of LPHC rats and suggest a reduced sensitivity to the lipolytic action of NE in isolated adipocytes that could account for the higher TAG storage in this depot [9].

The alterations observed in the lipid metabolism of EAT in LPHC rats are not necessarily valid for other adipose tissues because different responses to the same stimulus are fundamental for maintaining body homeostasis in different metabolic situations. Pond et al. [10] showed that dietary manipulations, hormones and cytokines induce distinct metabolic responses at different fat depots. Regional differences in the sensitivity of WAT depots to dietary manipulations have also been described by Belzung et al. [11]. Gaíva et al. [12] observed some differences between retroperitoneal and epididymal WAT metabolic responses to dietary fat. The distinct responses of adipose tissue when submitted to the same stimulus can be attributed to the different roles of these depots in the energy metabolism of the body: while EAT seems to be involved in local metabolic control, RWAT seems to be the main adipose depot responsible for the maintenance of energy homeostasis of the organism as a whole [13, 14]. The RWAT that we studied is different from EAT, but there are no relations of these tissues with human visceral or subcutaneous adipose tissues.

Thus, the aim of this study was to identify the effect of the LPHC diet on lipogenesis, lipolysis and the insulin signaling pathway in RWAT to better understand the mechanisms of lipid accumulation in this tissue and also to understand the adaptive mechanisms of the organism to a diet containing low protein and high carbohydrate. In turn, understanding the mechanisms that lead to lipid accumulation in animals with hyperphagia can provide insights into diet-induced obesity in humans. Furthermore, the consumption of a low-protein diet with a higher intake of carbohydrates (similar to the LPHC diet) after weaning is particularly common in developing countries.

Materials and Methods

Animals and Treatment

Male Wistar rats (7–14 animals) with an initial body weight of approximately 100 g were randomly divided into two groups. The control rats were fed a diet composed of 17% protein, 63% carbohydrate and 7% lipid, whereas the

LPHC rats were fed a diet composed of 6% protein, 74% carbohydrate and 7% lipid for 15 days. The decrease in dietary protein was compensated with an increase in dietary carbohydrates to maintain isocaloric diets (16.3 kJ g⁻¹, Table 1). The rats were maintained in individual metabolic cages at 22 ± 1 °C with a 12-h light:dark cycle. The rats received water and food ad libitum. The body weight and food intake of each rat was recorded daily. All of the experiments were performed between 08:00 and 10:00 a.m., and all of the rats were killed on day 15 of treatment. The rats were housed according to the Brazilian College of Animal Experimentation Rules, and the experiments were approved by the Ethics Committee of the Federal University of Mato Grosso (protocol no. 23108.033936/08-3).

NE Turnover Rates and NE Content in RWAT

NE turnover rates in RWAT (found on the dorsal side of the peritoneum) were estimated from the decline in tissue NE levels after inhibition of catecholamine synthesis with the drug DL- α -methyl-p-tyrosine methyl ester (α -MT, Sigma). This procedure has previously been described in detail [15].

Briefly, tissues were homogenized in 0.2 N perchloric acid with EDTA and sodium metabisulfite as antioxidants. Dihydroxybenzylamine was used as internal standard. After protein removal by centrifugation, catecholamines were adsorbed in alumina, eluted with 0.1 N perchloric acid and isolated by HPLC (LC-7A, Shimadzu Instruments) with a Spherisorb ODS-2 (5 μ m) (Sigma-Aldrich) reversed-phase column. NE and an internal standard were quantitated with an electrochemical detector (LC-ECD-6A, Shimadzu).

Table 1 Compositions (g kg⁻¹) of the control and low-protein, high-carbohydrate diets

Ingredient	Control diet (17%)	Low-protein, high-carbohydrate diet (6%)
Casein (84% protein)	202	71.5
Cornstarch	397	480
Dextrinized cornstarch	130.5	159
Sucrose	100	121
Soybean oil	70	70
Fiber (cellulose)	50	50
Mineral mix (AIN 93 G) ^a	35	35
Vitamin mix (AIN 93 G) ^a	10	10
L-cystine	3	1
Choline bitartrate	2.5	2.5

^a For detailed composition, see Reeves et al. (1993)

In Vivo Rates of Lipogenesis

In vivo rates of FA synthesis were evaluated by the incorporation of tritiated water into RWAT FA. ³H₂O (3 mCi in 0.5 mL saline) was injected intraperitoneally into fed and nonanesthetized animals. After 1 h, they were killed by decapitation, and blood samples were collected for plasma water-specific radioactivity determination. The RWAT was rapidly removed for measurement. The lipids were extracted, TAG-FAs were isolated, and FA radioactivity, as well as plasma water-specific activity, was determined by liquid scintillation counting as previously described [16].

Isolation of Adipocytes

After cervical dislocation, the RWAT from rats was removed and pooled (until ~5 g was collected). According to Rodbell's method [17], the RWAT was disaggregated with collagenase in Krebs-Henseleit buffer (27 mM HEPES, 137 mM NaCl, 4.2 mM NaHCO₃, 0.4 mM Mg SO₄·7H₂O, 0.5 mM MgCl₂·6H₂O, 0.4 mM KH₂PO₄, 5.4 mM KCl, 1.3 mM CaCl₂·2H₂O), pH 7.4, supplemented with 10 g L⁻¹ fatty acid-free albumin and 0.55 mM glucose. After continuous shaking for 40 min at 37°C, the adipocytes were filtered through a 300- μ m nylon mesh and washed three times with the same buffer in the absence of glucose. An aliquot of the isolated adipocytes suspension was diluted five times, and the number of cells was determined in four fields of the Neubauer's chamber in a microscope (Nikon eclipse E200, Melville, NY, USA), using a 10 \times objective. The isolated adipocytes were used in the [U-¹⁴C]-glucose incorporation into TAG-glycerol and lipolysis experiments.

Incorporation of [U-¹⁴C]-glucose into TAG-glycerol

Aliquots of the adipocytes suspension (1 mL) were incubated for 1 h at 37°C in Krebs-Henseleit buffer supplemented with 10 g L⁻¹ fatty acid-free albumin, 5.0 mM glucose and 0.5 μ Ci mL⁻¹ [U-¹⁴C]-glucose. The incorporation of [U-¹⁴C]-glucose into TAG-glycerol was evaluated in the absence or presence of 1 mU mL⁻¹ insulin. Lipids were extracted, saponified and the radioactivity of TAG-glycerol was determined by liquid scintillation counting as previously described [16].

Lipolysis

Aliquots of the adipocyte suspension (1 mL) were incubated for 1 h at 37°C in Krebs-Henseleit buffer supplemented with 10 g L⁻¹ fatty acid-free albumin and 5.0 mM glucose in the absence or presence of various

concentrations of NE (10^{-7} , 10^{-6} or 10^{-5} M). The lipolysis rate was estimated by measuring glycerol release into the buffer and was expressed as $\mu\text{mol} \times 10^6 \text{ cells}^{-1} \text{ h}^{-1}$. The concentration of glycerol was determined enzymatically using a commercial kit (Labtest).

Enzyme Activity Measurement

Following the recommendations of Newsholme et al. [18], glycerokinase (GyK) activity was measured in the supernatants obtained after RWAT homogenization using an Omni mixer in ice-cold 1% KCl with 1 mM EDTA and centrifugation at 2,000g. Aliquots of the 2,000 g supernatant were incubated for 30 min in an assay mixture containing: 0.1 M Tris, pH 7.5, 6 mM ATP, 4 mM MgCl_2 , 1 mM EDTA, 25 mM NaF, 20 mM 2- β -mercaptoethanol, 10 mM phosphocreatine, 26 U mL^{-1} creatine kinase, 1 mM glycerol, 10 $\mu\text{Ci mL}^{-1}$ [^{14}C -glycerol] and 1% albumin. After the incubation period, the reaction was stopped with EtOH. The synthesized [^{14}C]-glycerol p-phosphate was isolated by paper chromatography and quantified using liquid scintillation counting as previously described [16]. The protein concentration of the homogenate for assay was determined by the Lowry [21].

LPL activity was determined in the supernatants obtained after preincubation of RWAT in heparin-containing medium. The supernatant was incubated with tri-[^{14}C]-oleoylglycerol, stabilized by lecithin and prepared in glycerol as previously described [19]. The ^{14}C -FA produced during incubation was isolated using a modification of the liquid-liquid partition system as previously described [20] and quantified by liquid scintillation counting. The enzyme activities were expressed by mg protein of homogenate used in the evaluation.

Western Blot for Protein Analysis

Rats were anesthetized by intramuscular administration of ketamine (0.1 mL) and xylazine (0.05 mL) for each 100 g of body weight. The abdominal cavity was opened, and 0.5 mL of insulin (4 U mL^{-1}) dissolved in saline was administered into the portal vein. RWAT fragments were collected 2 min before and after insulin administration and immediately homogenized in 100 mM Tris-HCl buffer, pH 7.4, containing 1% Triton X-100, 100 mM sodium pyrophosphate, 100 mM sodium fluoride, 10 mM EDTA, 10 mM sodium orthovanadate, 2.0 mM phenylmethylsulfonyl fluoride and 0.1 mg mL^{-1} aprotinin at 4°C. The total protein concentration was determined by the Bradford method [22]. RWAT proteins (100 μg for the detection of PEPCK and α -tubulin, and 125 μg for the detection of insulin signaling intermediates) were separated by 10% SDS-PAGE, transferred to nitrocellulose membranes and blotted with antibodies against PEPCK, IR, IRS-1, PI3-K_(p85), AKT1, α -tubulin and

phospho-AKT1/2/3 (Ser 473). Specific bands were detected with the SuperSignal West Pico chemiluminescent substrate, and the band intensity was quantified using the Scion Image Program (version 4.03, Frederick, MD, USA). The PEPCK band intensity was normalized to the α -tubulin band intensity. There was no difference between α -tubulin band intensities of the different groups. The band intensity of phosphorylated AKT was normalized to the total AKT band intensity. The results are expressed as the relative ratios.

Other Chemical Analyses

The serum concentrations of triiodothyronine (T3), thyroxine (T4), corticosterone, tumor necrosis factor- α (TNF- α) and free fatty acids (FFA) were determined using commercial kits. Only the FFA concentration was determined in rats that had been fasted for 14 h. Total tissue lipids were determined gravimetrically after extraction using the procedure from Folch et al. [23].

Chemicals

The radioisotopes [^{14}C]-glucose, $^3\text{H}_2\text{O}$, glycerol tri[^{14}C]-oleate and [^{14}C]-glycerol were purchased from PerkinElmer Life and Analytical Sciences (MA, USA). SX20-5 scintillation liquid was from Fisher Scientific (ON, Canada). The commercial kits for T3 and T4, TNF- α , corticosterone, FFA and glycerol determination were obtained from Interkit (CA, USA), Thermo Scientific (IL, USA), Assay Designs (MI, USA), Wako Chemicals (VA, USA) and Labtest (MG, Brazil), respectively. Collagenase (type I) and insulin (Humulin Regular human insulin for phosphorylated AKT and insulin from porcine pancreas for lipolysis experiments) were obtained from Worthington Biochemical (NJ, USA), Eli Lilly (SP, Brazil) and Sigma-Aldrich (MO, USA), respectively. Nitrocellulose membranes were purchased from Amersham Bioscience (NJ, USA). Anti-PEPCK, anti-IR β , anti-IRS-1, anti-PI3-K_(p85), anti-AKT1, anti-phospho-AKT1/2/3 (Ser273) and anti- α -tubulin antibodies (all recommended for the detection of rat proteins) were purchased from Santa Cruz Biotechnology (CA, USA), and anti-goat IgG was purchased from Invitrogen (CA, USA). Ketamine hydrochloride and xylazine hydrochloride were obtained from Agribands (SP, Brazil) and Bayer (ON, Canada), respectively. All other chemicals were of analytical grade and were purchased from Sigma-Aldrich (MO, USA).

Statistical Analysis

All data were expressed as the mean \pm standard error (SE) for the number of rats indicated in parentheses. Statistical analysis was performed using the Statistic Software package (Statsoft, Tulsa, OK, USA). Bartlett's test for the

homogeneity of variances was initially used to determine whether the data complied with the assumptions for parametric analysis of variance. When necessary, the data were log-transformed to correct for variance in heterogeneity or non-normality [24]. The incorporation of [U-¹⁴C]-glucose into TAG-glycerol, lipolysis and pSer-AKT levels were tested with two-way variance analysis (effects of diet and stimulus). When necessary, these analyses were complemented by the least significant difference test to determine the significance of individual differences (Tukey HSD test). Except for the calculated rates of turnover, which were compared using 95% confidence intervals as described by Taubin et al. [25], and the analyses cited above (incorporation of [U-¹⁴C]-glucose into TAG-glycerol, lipolysis and pSer-AKT), the statistical significance of all other experiments was analyzed using a Student's *t* test. The criterion of significance was $p < 0.05$.

Results

The total food intake of LPHC rats was approximately 14% higher than that of control rats during the experimental period. However, despite this increase in food intake, the final body weight in the LPHC group was 12% lower than in the control group at the end of the 15th day of treatment. Despite the reduction in body weight, the weight and lipid content of the RWAT increased 29 and 42%, respectively (Table 2), in LPHC rats. These data agree with previously published results by Aparecida de França et al. [8] and Buzelle et al. [9].

Serum corticosterone and TNF- α increased approximately two- and tenfold, respectively, in the LPHC animals as compared with the control group. There was no difference in serum T3, T4 and FFA levels.

The RWAT NE content was similar between the LPHC and control rats. However, the NE turnover rate, an indicator of sympathetic flux, was higher in the RWAT from LPHC rats ($t_{1/2} = 9.5$ h) than in the RWAT from control rats ($t_{1/2} = 14.9$ h, Table 3).

The de novo FA synthesis rate estimated in vivo via ³H₂O was markedly lower by approximately 50% in the RWAT from LPHC rats than in the RWAT from control rats (Fig. 1). This finding is consistent with the low level of postprandial plasma insulin, which had previously been observed [8]. In contrast, the LPHC diet induced an approximate 100% increase in the LPL activity of RWAT (Fig. 2), which suggests an increased uptake of FAs from circulating lipoproteins in this tissue.

Evaluation of the G3P pathways showed that LPHC rats had approximately 27% less PEPCK content (Fig. 3) and approximately 60% higher levels of GyK activity (Fig. 4). These results suggest that glyceroneogenesis is reduced,

Table 2 Final body weight, total food intake, and weight and lipid content of retroperitoneal adipose tissue and the serum concentrations of corticosterone, free fatty acid, thyroxine, triiodothyronine and tumor necrosis factor- α from LPHC and control rats after 15 days of treatment

	Control diet	LPHC diet
Final body weight (g)	190.80 \pm 0.22 (11)	167.80 \pm 0.28* (12)
Total food intake (g)	230.70 \pm 4.60 (11)	263.50 \pm 8.30* (12)
Retroperitoneal adipose tissue (g)	1.70 \pm 0.13 (11)	2.20 \pm 0.13 [†] (12)
Lipid content (mg g tissue ⁻¹)	1.20 \pm 0.12 (6)	1.70 \pm 0.10 [†] (6)
Free fatty acid (mEq L ⁻¹)	0.74 \pm 0.08 (5)	0.61 \pm 0.05 (5)
Corticosterone (pg mL ⁻¹)	147.50 \pm 1.52 (11)	304.10 \pm 1.94 [†] (12)
Thyroxine (ng mL ⁻¹)	3.07 \pm 0.01 (7)	3.09 \pm 0.01 (7)
Triiodothyronine (ng mL ⁻¹)	2.74 \pm 0.07 (7)	2.86 \pm 0.09 (7)
Tumor necrosis factor- α (pg mL ⁻¹)	54.3 \pm 22.6 (4)	588.2 \pm 69.6 [†] (5)

All of the values of the serum concentrations are from fed rats except FFA

The data are represented as the mean \pm SE with the number of rats in parentheses

* $P < 0.05$ versus control diet. [†] $P < 0.01$ versus control diet

Table 3 Norepinephrine content, fractional turnover rate (*k*), turnover rate (TR) and half-life of NE disappearance ($t_{1/2}$) in retroperitoneal adipose tissue

	Control diet	LPHC diet
NE (ng total tissue ⁻¹)	86.0 \pm 4.9	80.5 \pm 5.7
<i>k</i> (% h ⁻¹)	4.6 \pm 3.43	7.3 \pm 3.78
TR (ng tissue ⁻¹ h ⁻¹)	4.0 (3.27–4.70)	5.8 (4.69–6.99)*
$t_{1/2} = 0.693$ (<i>k</i> ⁻¹)	14.9	9.5

Data are expressed as the mean \pm SE. interval. Parentheses contain the 95% confidence interval

There are five rats per diet group at each time interval (0, 6 and 12 h) in the turnover experiments

* $P < 0.05$ versus control diet

and the generation of G3P by direct glycerol phosphorylation is increased in RWAT. G3P generation from glucose, which was evaluated by the incorporation of [U-¹⁴C]-glucose into TAG-glycerol in isolated adipocytes, was similar in the LPHC and control rats in the absence of insulin ($p < 0.10$, Fig. 5). The rate of [U-¹⁴C]-glucose incorporation into TAG-glycerol increased approximately 124% in isolated adipocytes from control rats when incubated with insulin (Fig. 5). However, insulin did not affect the [U-¹⁴C]-glucose incorporation into TAG-glycerol in adipocytes from LPHC rats (Fig. 5).

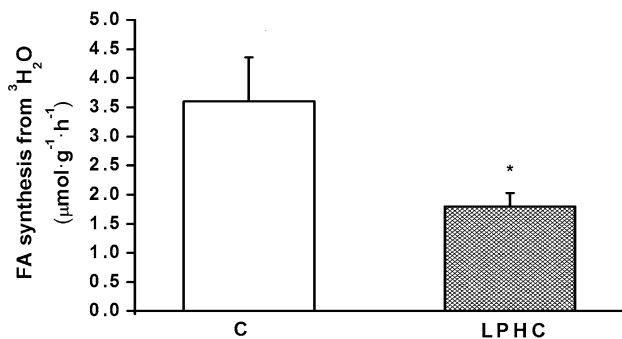


Fig. 1 The effect of the low-protein, high-carbohydrate diet on the in vivo rate of de novo fatty acid synthesis in retroperitoneal adipose tissue. The data are represented as the mean \pm SE of 14 rats per diet group. * $P < 0.05$ versus control (Student's t test). C control diet, LPHC low-protein, high-carbohydrate diet

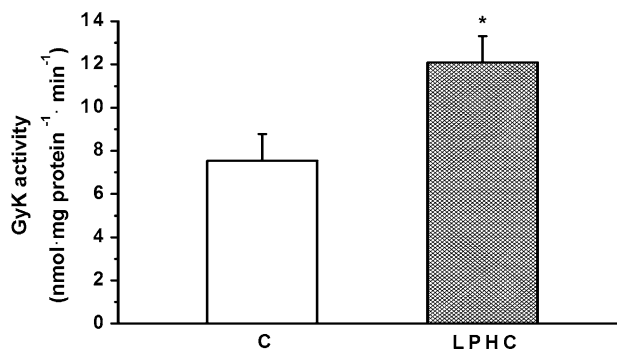


Fig. 4 The effect of the low-protein, high-carbohydrate diet on glycerokinase activity in retroperitoneal adipose tissue. The data are represented as the mean \pm SE of five rats per diet group. * $P < 0.05$ versus control (Student's t test). C control diet, LPHC low-protein, high-carbohydrate diet

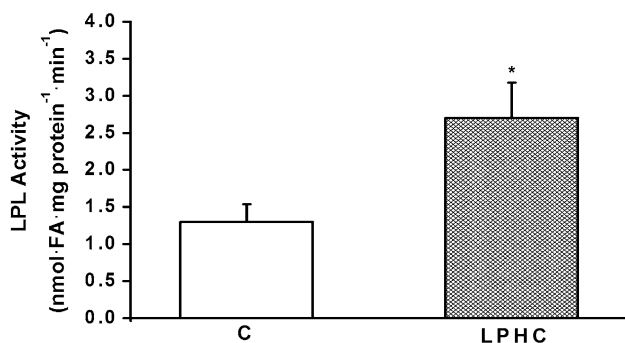


Fig. 2 The effect of the low-protein, high-carbohydrate diet on lipoprotein lipase activity in retroperitoneal adipose tissue. The data are represented as the mean \pm SE of 14 rats per diet group. * $P < 0.05$ versus control (Student's t test). C control diet, LPHC low-protein, high-carbohydrate diet

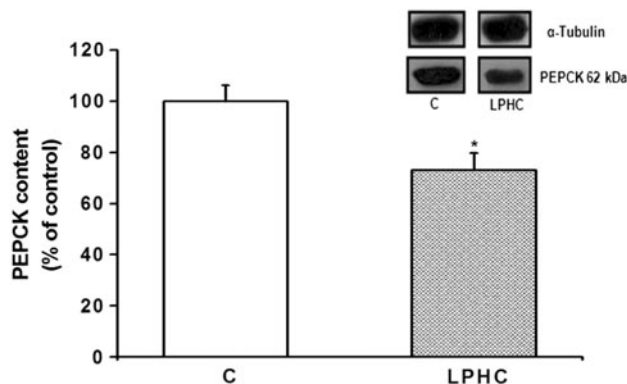


Fig. 3 The effect of the low-protein, high-carbohydrate diet on the phosphoenolpyruvate carboxykinase protein level in retroperitoneal adipose tissue. The data are represented as the mean \pm SE of six rats per diet group. * $P < 0.01$ versus control (Student's t test). C control diet, LPHC low-protein, high-carbohydrate diet

Examination of the insulin signaling pathway showed that the LPHC diet induced a decrease in IRS-1 and AKT content by approximately 40 and 14%, respectively,

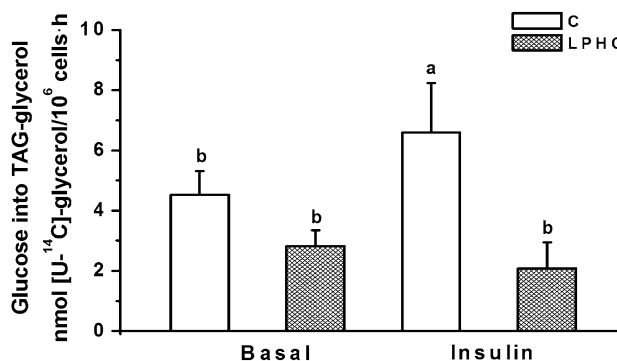


Fig. 5 The effect of the low-protein, high-carbohydrate diet on the rate of [U- 14 C]-glucose incorporation into TAG-glycerol in the absence and presence of insulin. Adipocytes were isolated from the retroperitoneal adipose tissue of LPHC and control rats. The data are represented as the mean \pm SE of six tubes per experimental condition of each diet group. Mean values with different letters are significantly different ($P < 0.05$; two-way ANOVA). C control diet, LPHC low-protein, high-carbohydrate diet

(Fig. 6b and 6d), but did not change IR β and p85-PI3-K content (Fig. 6a and 6c). Basal AKT phosphorylation was also reduced by approximately 48% in the RWAT from LPHC rats when compared to control rats (Fig. 6e). In vivo insulin administration induced an increase in AKT phosphorylation by approximately 70% in the RWAT from control rats, but did not affect AKT phosphorylation in the RWAT from LPHC rats (Fig. 6e).

The rate of basal lipolysis, which was evaluated in isolated adipocytes by glycerol release into the incubation buffer, did not differ between the two groups. There was a significant increase in the lipolysis of adipocytes from control rats, which was proportional to the increase in NE concentration in the incubation buffer. However, the lipolytic response to adrenergic stimulus by noradrenaline was impaired in the LPHC rats when compared with basal lipolysis even under high NE concentrations (Fig. 7).

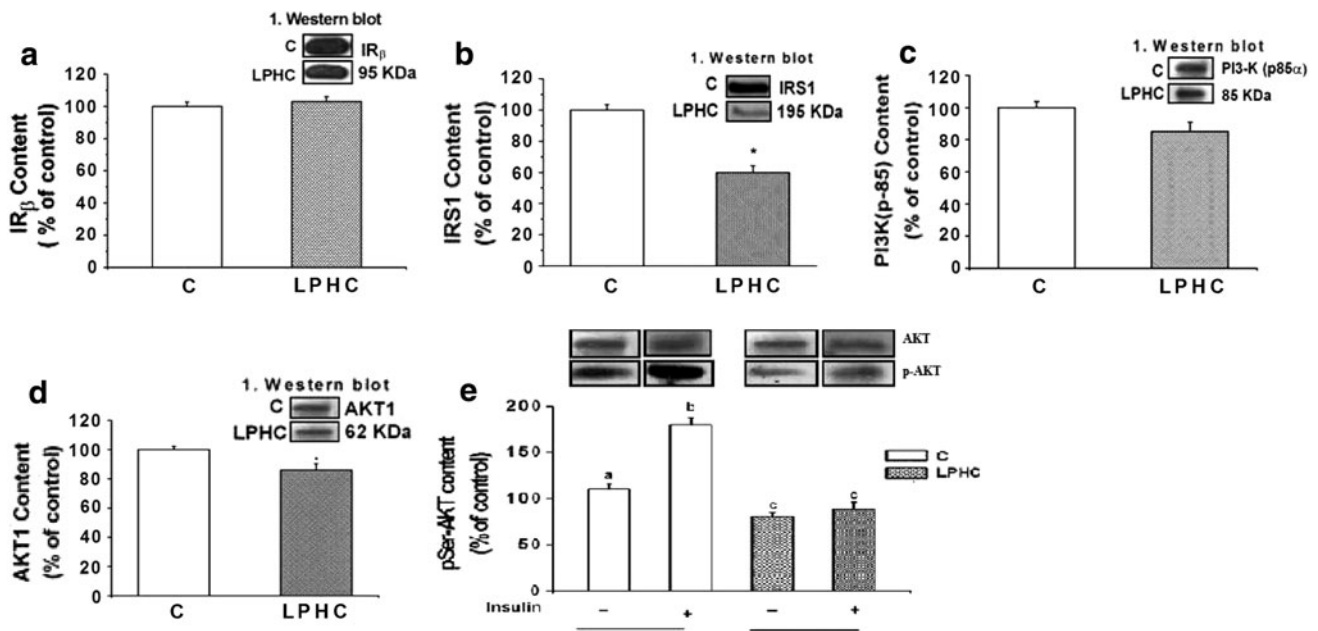


Fig. 6 The effect of the low-protein, high-carbohydrate diet on **a** IR β , **b** IRS-1, **c** PI3-K, **d** AKT protein content and **e** AKT phosphorylation in the retroperitoneal adipose tissue of rats. The data are represented as the mean \pm SE of six rats per diet group. * $P < 0.01$ versus control

(Student's *t* test for protein content). Mean values with different lowercase letters are significantly different ($P < 0.05$; two-way ANOVA for AKT phosphorylation). C control diet, LPHC low-protein, high-carbohydrate diet

Discussion

The TAG content stored in adipose tissue is a balance between esterification of FA with G3P and its mobilization. Thus, we evaluated the biochemical parameters and pathways involved in these two metabolic processes to help clarify the factors responsible for TAG accumulation in the RWAT of rats fed by a LPHC diet for 15 days during the growth stage, as previously observed by Aparecida de França et al. [8].

LPHC rats represent the first physiological situation that decreases insulin plasma levels [8] and increases serum corticosterone, TNF- α (Table 2), norepinephrine [9] and leptin [8]. The increase in serum corticosterone in the LPHC group (100%) agrees with other published data that show hormonal and neuronal changes induced by consuming a protein-restricted diet are similar to those changes induced by chronic stress. This chronic increase in corticosterone is an important and characteristic alteration observed in this condition as a consequence of hypothalamic-pituitary-adrenal axis (HPA) dysfunction [26]. Rats fed a diet consisting of 8% protein for 30 days had higher levels of serum corticosterone as well as an increase in adrenal gland weight and the number of ACTH-secreting cells (63.8%) in the pituitary gland as compared to rats fed a normoproteic diet [27], suggesting activation of the HPA system. Other investigations have shown a direct correlation between malnutrition and elevated blood glucocorticoid levels [28]. There is evidence that TNF- α induces

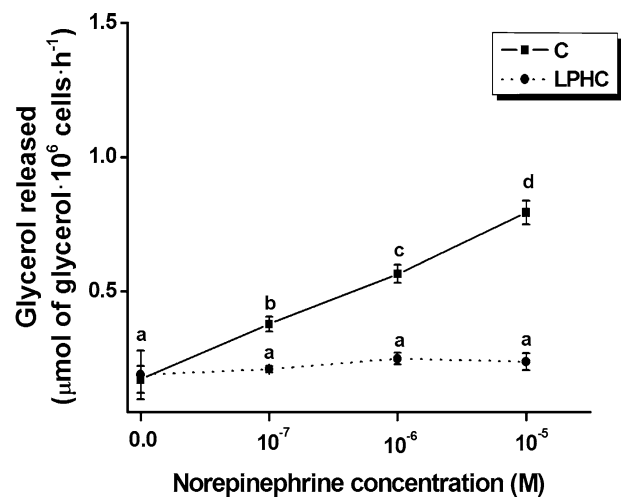


Fig. 7 The effect of different concentrations of norepinephrine on the rate of lipolysis in adipocytes. Adipocytes were isolated from the retroperitoneal adipose tissue of LPHC and control rats. Each point represents the mean \pm SE of six tubes per experimental condition of each diet group. Mean values with different lowercase letters are significantly different ($P < 0.05$; two-way ANOVA). C control diet, LPHC low-protein, high-carbohydrate diet

activation of the HPA system in response to various threats to homeostasis [2]. Thus, it is possible that the high level of TNF- α in LPHC rats can be responsible for the corticosterone release in these animals. In turn, the TNF- α plasma level seems to be controlled by glucocorticoids; this control is exerted through the reduction of TNF- α secretion and half-life [29]. In opposition to glucocorticoid action,

adrenergic stimulation induces an increase in plasma TNF- α levels [30] simultaneously with stimulation of sympathetic activity by high levels of TNF- α and leptin [31]. The high levels of corticosterone may also be associated with the reduced plasma insulin levels of rats fed an LPHC diet [8], and studies have demonstrated that chronic exposure to elevated levels of glucocorticoids severely impairs glucose-stimulated insulin secretion from islets derived from normal rodents [32]. Therefore, the complex interrelation of factors determined by glucocorticoids, TNF- α , insulin, leptin and sympathetic activity in LPHC rats deserves further study. Increase in the sympathetic flux in the RWAT of these animals was also observed in brown adipose tissue [8] and EAT [9], which could simultaneously be related to the high-carbohydrate and low-protein content of the diet. NE turnover rates increased in the RWAT from rats fed on a cafeteria diet supplemented with 20% sucrose in the drinking water [33] and after supplementation of a standard rat diet with glucose or fructose [34]. It has previously been shown that the consumption of a low-protein diet (5% casein) increases the NE turnover in the EAT and brown adipose tissue of rats [35].

The increase in FA uptake from circulating lipoproteins in LPHC rats is essential for the increase in TAG content of the RWAT in these animals (Fig. 2). However, the LPHC diet induced a reduction in de novo FAs synthesis in this tissue (Fig. 1), which may be a consequence of impaired insulin signaling in the RWAT of LPHC rats as evidenced by the reduction in IRS-1 and AKT protein levels as well as AKT phosphorylation (Fig. 6). The reduction in insulin signaling can also impair glucose uptake by adipocytes in the RWAT of LPHC rats. The lack of an insulin response in the incorporation of [U- 14 C]-glucose into glycerol-TAG in vitro by adipocytes from LPHC rats corroborates this hypothesis. Studies have shown that TNF- α and glucocorticoids impair the response to insulin. In vitro, TNF- α reduces the expression and phosphorylation of IR and IRS-1 as well as the synthesis and translocation of GLUT-4 to the membrane of adipocytes, which in turn leads to a decreased glucose uptake mediated by insulin [36, 37]. The effect of TNF- α on insulin resistance correlates to a reduced PPAR γ expression at the pre- and post-translational levels through activation of serine kinases that inhibit transmission of the insulin signal [38]. Dexamethasone also decreases IRS-1 expression and phosphorylation in 3T3-L1 cells, which also diminishes PI3-K activation and GLUT-4 translocation without affecting GLUT-4 expression [39, 40]. In addition, glucocorticoids reduce glucose uptake mainly by completely inhibiting glucose transport, as the normalization of IRS-1 expression and PI3-K activity in adipocytes 3T3-L1 previously treated with dexamethasone did not affect the reduced glucose uptake [39]. Despite reduced plasma insulin levels and impaired insulin signaling, the

increase in LPL activity in the RWAT from LPHC rats can be explained by elevated glucocorticoid levels. Studies have shown that glucocorticoids increase LPL activity in the RWAT of rats [41]. Glucocorticoids increase the activity of LPL either through increases in transcription or posttranscriptional modifications such as increased activation or decreased degradation [42]. However, the effect of glucocorticoids in regulating LPL seems to be fat pad-specific [43] because the LPL activity in the EAT of LPHC rats is not altered when compared with the LPL activity from the EAT of control rats [9].

Regarding the generation of G3P, it seems clear that the route of direct phosphorylation of glycerol by Gyk seems to guarantee the supply of G3P for FA esterification and increases the TAG content in the RWAT of the LPHC rats, since the generation of G3P by other means was not increased (low content of PEPCK and glucose incorporation of insulin-stimulated G3P is impaired).

Under normal conditions, GyK activity is relatively low in WAT; however, our data show that this activity is increased by 60% in LPHC rats (Fig. 4). The literature reports that in various experimental models, Gyk activity is fundamental for obesity manifestation. Experiments performed in genetically obese animals and in knockout animals for GyK have demonstrated an increase in the activity of Gyk and established a positive relationship of its activity and the accumulation of TAG [44–48].

We have previously shown that GyK expression/activity is directly controlled by the sympathetic nervous system in brown adipose tissue and WAT [16, 33, 49]. Other studies have demonstrated that the expression and content of PEPCK in WAT are strongly inhibited by insulin and glucocorticoids [50, 51]. The fact that the LPHC group presented a high level of corticosterone and an impairment of insulin signaling suggests that the effect of glucocorticoids on expression and content of PEPCK outweighs the effect of reduced insulin in the RWAT of these animals (Fig. 3).

Glucocorticoids repress transcription of the PEPCK gene in adipocytes by inhibiting the CCAAT/enhancer-binding protein (C/EBP)-mediated activation. Previous work has demonstrated that glucocorticoid treatment of 3T3-F442A adipocytes reduces nuclear C/EBP α concentration and markedly diminishes the binding of nuclear proteins to the C/EBP recognition sites (but not to the PPAR/RXR recognition sites) in the PEPCK gene promoter [52].

As mentioned earlier, the TAG content depends not only on lipogenesis, but also on lipolysis. The increases in the serum levels of glucocorticoids, TNF- α (Table 2), catecholamines [9] and leptin [8] and the increased NE turnover in RWAT of LPHC rats (Table 3) are associated with high levels of lipolysis. However, these animals did not show a difference in the levels of circulating FFA when

compared with the control animals. Catecholamines, mainly NE, released by sympathetic terminals, induce lipolysis by activating a cAMP-dependent classical signaling pathway that activates PKA, which phosphorylates perilipin A and simultaneously stimulates hormone-sensitive lipase (HSL) and adipose triglyceride lipase (ATGL) to promote FA mobilization from WAT [52, 53]. In addition, studies have recently demonstrated that dexamethasone directly stimulates lipolysis by remodeling the elements of the lipolytic cascade in isolated adipocytes [54]. Dexamethasone downregulates the mRNA and protein levels of PDE3B [51], and directly increases cAMP production by promoting basal and forskolin-stimulated activity of adenylyl cyclase in adipocytes [55]. Dexamethasone also induces the phosphorylation of perilipin and the downregulation of perilipin proteins [54]. In spite of the induction of ATGL and HSL mRNA by glucocorticoids in adipocytes, dexamethasone does not induce HSL translocation to the lipid droplet surface in differentiated adipocytes [55]. The increase in insulin resistance in response to glucocorticoids could also contribute to FA mobilization. Insulin inhibits lipolysis, stimulates cAMP degradation by PDE3B and reduces HSL and perilipin phosphorylation [56]. TNF- α -induced lipolysis also involves remodeling of the elements of the lipolytic cascade in isolated adipocytes by downregulating PDE3B and perilipin expression in adipocytes [57, 58]. However, other studies have shown that TNF- α reduces the HSL and ATGL content [59, 60], impairing the lipolytic activity of adipocytes. Lipolysis suppression in the presence of forskolin and dibutyryl-cAMP in adipocytes previously treated with TNF- α [61] reinforces this hypothesis. Our findings show that the adipocytes of the RWAT from LPHC rats are less responsive to NE *in vitro* (Fig. 7). The impaired response to catecholamines can be related to any of the points in the lipolytic cascade, such as reduction in the adrenoceptor number or in the signaling pathway responsible for lipolysis activation or even in the lipase content. Isolated adipocytes from the EAT of rats submitted to one daily foot-shock session on 3 consecutive days demonstrate elevated corticosterone levels accompanied by a reduction in glucocorticoid receptors and β_1 - and β_3 -adrenoceptors, and an increase in β_2 -adrenoceptors [62]. These *in vitro* experiments demonstrate that a high corticosterone concentration downregulates glucocorticoid receptors [62]. These effects can attenuate the lipolytic actions of catecholamines, glucocorticoids and TNF- α in LPHC rats.

Thus, the results of this study show that the increase in FA uptake from circulating lipoproteins, direct phosphorylation of glycerol by Gyk and a decreased response to catecholamine may contribute to the increase in weight and lipid content in the RWAT of LPHC rats. Moreover, it

seems that the source of glycerol for phosphorylation by Gyk is the diet (fed rats), and although the lipid content in both diets is the same, the animals of the LPHC group ingested more food (14%) than the animals of the control group during the 15 days of treatment. Given the low activity of Gyk in WAT (in spite of a 60% increase in LPHC rats) and because it is probably the only G3P-generating pathway activated in the RWAT of these animals, the impaired stimulation of the tissue by catecholamine may be the main mechanism that preserves the lipid content.

Acknowledgments We thank Air Francisco Costa, Marlene Mariano and Celso Roberto Afonso for their technical assistance. We also thank Renato Hélio Migliorini in memoriam for being an exemplary scientist and professor. This work was supported by grants from Fundação de Amparo à Pesquisa do Estado de Mato Grosso (FAPEMAT) and Coordenação de Aperfeiçoamento de Pessoal de Nível Superior (CAPES).

References

- Vázquez-Vela ME, Torres N, Tovar AR (2008) White adipose tissue as endocrine organ and its role in obesity. *Arch Med Res* 39:715–728
- Turnbull AV, Rivier C (1995) Regulation of the HPA axis by cytokines. *Brain Behav Immun* 9:253–275
- Meyers JH, Hargus WA (1959) Factors influencing food intake of rats fed low-protein rations. *Am J Physiol* 197:1350–1352
- White BD, Porter MH, Martin RJ (2000) Protein selection, food intake, and body composition in response to the amount of dietary protein. *Physiol Behav* 69:383–389
- National Research Council, Subcommittee of Laboratory Animals Nutrition (1995) In: Nutrient requirements of the laboratory animals, 4th Revised edn. National Academy Press, Washington, pp 11–79
- Du F, Higginbotham DA, White BD (2000) Food intake, energy balance and serum leptin concentrations in rats fed low-protein diets. *J Nutr* 130:514–521
- Webster AJ (1993) Energy partitioning, tissue growth and appetite control. *Proc Nutr Soc* 52:69–76
- Aparecida de França S, Dos Santos MP, Garófalo MAR, Navegantes LC, Kettelhut IC, Lopes CF, Kawashita NH (2009) Low protein diet changes the energetic balance and sympathetic activity in brown adipose tissue (BAT) of growing rats. *Nutrition* 25:1186–1192
- Buzelle SL, Santos MP, Baviera AM, Lopes CF, Garófalo MA, Navegantes LC, Kettelhut IC, Chaves VE, Kawashita NH (2010) A low-protein, high-carbohydrate diet increases the adipose lipid content without increasing the glycerol-3-phosphate or fatty acid content in growing rats. *Can J Physiol Pharmacol* 88:1157–1165
- Pond CM (1999) Physiological specialisation of adipose tissue. *Prog Lipid Res* 38:225–248
- Belzung F, Raclot T, Groscolas R (1993) Fish oil n-3 fatty acids selectively limit the hypertrophy of abdominal fat depots in growing rats fed high-fat diets. *Am J Physiol* 264:r1111–r1118
- Gaíva MH, Couto RC, Oyama LM, Couto GE, Silveira VL, Riberio EB, Nascimento CM (2001) Polyunsaturated fatty acid-rich diets: effect on adipose tissue metabolism in rats. *Br J Nutr* 86:371–377

13. Arner P (1997) Regional adiposity in man. *J Endocrinol* 155:191–192
14. Caesar R, Manieri M, Kelder T, Boekschoten M, Evelo C, Müller M, Kooistra T, Cinti S, Kleemann R, Drevon CA (2010) A combined transcriptomics and lipidomics analysis of subcutaneous, epididymal and mesenteric adipose tissue reveals marked functional differences. *PLoS One* 5:e11525
15. Garófalo MAR, Kettelhut IC, Roselino JE, Migliorini RH (1996) Effect of acute cold exposure on norepinephrine turnover rates in rat white adipose tissue. *J Auton Nerv Syst* 60:206–208
16. Kawashita NH, Festuccia WT, Brito MN, Moura MA, Brito SR, Garófalo MA, Kettelhut IC, Migliorini RH (2002) Glycerokinase activity in brown adipose tissue: a sympathetic regulation? *Am J Physiol Regul Integr Comp Physiol* 282:R1185–R1190
17. Rodbell M (1964) Metabolism of isolated fat cells. I— Effects of hormones on glucose metabolism and lipolysis. *J Biol Chem* 239:375–380
18. Newsholme EA, Robinson J, Taylor KA (1967) A radiochemical enzymatic activity assay for glycerol kinase and hexokinase. *Biochim Biophys Acta* 132:338–346
19. Nilsson-Ehle P, Schotz MC (1976) A stable, radioactive substrate emulsion for assay of lipoprotein lipase. *J Lipid Res* 17:536–541
20. Brito SC, Festuccia WL, Kawashita NH, Moura MF, Xavier AR, Garófalo MA, Kettelhut IC, Migliorini RH (2006) Increased glyceroneogenesis in adipose tissue from rats adapted to a high-protein, carbohydrate-free diet: role of dietary fatty acids. *Metabolism* 55:84–89
21. Lowry OH, Rosebrough NJ, Farr AL, Randall RJ (1951) Protein measurement with the Folin phenol reagent. *J Biol Chem* 93:265–275
22. Bradford MM (1976) A rapid and sensitive method for the quantitation of microgram quantities of protein utilizing the principle of protein-dye binding. *Anal Biochem* 72:248–254
23. Folch J, Lees M, Stanley GA (1957) A simple method for the isolation and purification of total lipids from animal tissues. *J Biol Chem* 226:497–509
24. Sokal RR, Rohlf FJ (1995) Assumptions of analysis of variance. In: Sokal RR, Rohlf FJ (eds) *Biometry: the principles and practice of statistics in biological research*. WH Freeman and Co, New York, pp 392–450
25. Taubin HL, Djahanguiri B, Landsberg L (1976) Noradrenaline concentration and turnover in different regions of the gastrointestinal tract of the rat: an approach to the evaluation of sympathetic activity in the gut. *Gut* 13:790–795
26. Kyrou I, Tsigos C (2007) Stress mechanisms and metabolic complications. *Horm Metab Res* 39:430–438
27. Herbert DC, Carrillo AJ (1982) The hypophyseal-adrenal axis in the protein-calorie malnourished rat. *Horm Metab Res* 14:205–207
28. Huang ZL, Fraker PJ (2003) Chronic consumption of a moderately low protein diet does not alter hematopoietic processes in young adult mice. *J Nutr* 133:1403–1408
29. Sherry B, Cerami A (1988) Cachectin/tumor necrosis factor exerts endocrine, paracrine, and autocrine control of inflammatory responses. *J Cell Biol* 107:1269–1277
30. Orban Z, Remaley AT, Sampson M, Trajanoski Z, Chrousos GP (1999) The differential effect of food intake and beta-adrenergic stimulation on adipose-derived hormones and cytokines in man. *J Clin Endocrinol and Metabolism* 84:2126–2133
31. Rayner DV (2001) The sympathetic nervous system in white adipose tissue regulation. *Proc Nutr Soc* 60:357–364
32. Koizumi M, Yada T (2008) Sub-chronic stimulation of glucocorticoid receptor impairs and mineralocorticoid receptor protects cytosolic Ca^{2+} responses to glucose in pancreatic beta-cells. *J Endocrinol* 197:221–229
33. Chaves VE, Frasson D, Martins-Santos ME, Boschini RP, Garófalo MA, Festuccia WT, Kettelhut IC, Migliorini RH (2006) Glyceroneogenesis is reduced and glucose uptake is increase in adipose tissue from cafeteria diet-fed rats independently of tissue sympathetic innervation. *J Nutr* 136:2475–2480
34. Young JB, Weiss J, Boufath N (2004) Effects of dietary monosaccharides on sympathetic nervous system activity in adipose tissues of male rats. *Diabetes* 53:1271–1278
35. Kevonian AV, Tuig JGV, Romsos DR (1984) Consumption of a low protein diet increase norepinephrine turnover in brown adipose tissue of adult rats. *J Nut* 114:543–549
36. Stephens JM, Lee J, Pilch PF (1997) Tumor necrosis factor-alpha-induced insulin resistance in 3T3-L1 adipocytes is accompanied by a loss of insulin receptor substrate-1 and GLUT4 expression without a loss of insulin receptor-mediated signal transduction. *J Biol Chem* 272:971–976
37. Hotamisligil GS (1999) Mechanisms of TNF-alpha-induced insulin resistance. *Exp Clin Endocrinol Diabetes* 107:119–125
38. Ye J (2008) Regulation of PPARgamma function by TNF-alpha. *Biochem Biophys Res Commun* 374:405–408
39. Sakoda H, Ogihara T, Anai M, Funaki M, Inukai K, Katagiri H, Fukushima Y, Onishi Y, Ono H, Fujishiro M, Kikuchi M, Oka Y, Asano T (2000) Dexamethasone-induced insulin resistance in 3T3-L1 adipocytes is due to inhibition of glucose transport rather than insulin signal transduction. *Diabetes* 49:1700–1708
40. Turnbow MA, Keller SR, Rice KM, Garner CW (1994) Dexamethasone down-regulation of insulin receptor substrate-1 in 3T3-L1 adipocytes. *J Biol Chem* 269:2516–2520
41. Berthiaume M, Laplante M, Tchernof A, Deshaies Y (2007) Metabolic action of peroxisome proliferator-activated receptor gamma agonism in rats with exogenous hypercortisolemia. *Int J Obes* 31:1660–1670
42. Peckert AJ, Wright DC, Riddell MC (2011) The effects of glucocorticoids on adipose tissue lipid metabolism. *Metabolism*. doi: [10.1016/j.metabol.2011.06.012](https://doi.org/10.1016/j.metabol.2011.06.012)
43. Lee MJ, Gong DW, Burkey BF, Fried SK (2011) Pathways regulated by glucocorticoids in omental and subcutaneous human adipose tissues: a microarray study. *Am J Physiol Endocrinol Metab* 300:E571–E580
44. Thenen SW, Mayer J (1975) Adipose tissue glycerokinase activity in genetic and acquired obesity in rats and mice. *Proc Soc Exp Biol Med* 148:953–957
45. Martin RJ, Lamprey PM (1975) Early development of adipose cell lipogenesis and glycerol utilization in Zucker obese rats. *Proc Soc Exp Biol Med* 149:35–39
46. Stern JS, Hirsch J, Drewnowski A, Sullivan AC, Johnson PR, Cohn CK (1983) Glycerol kinase activity in adipose tissue of obese rats and mice: effects of diet composition. *J Nutr* 113:714–720
47. Chakrabarty K, Tauber JW, Sigel B, Bombeck CT, Jeffay H (1984) Glycerokinase activity in human adipose tissue as related to obesity. *Int J Obes* 8:609–622
48. Hibuse T, Maeda N, Funahashi T, Yamamoto K, Nagasawa A, Mizunoya W, Kishida K, Inoue K, Kuriyama H, Nakamura T, Fushiki T, Kihara S, Shimomura I (2005) Aquaporin 7 deficiency is associated with development of obesity through activation of adipose glycerol kinase. *Proc Natl Acad Sci* 102:10993–10998
49. Festuccia WT, Guerra-Sá R, Kawashita NH, Garófalo MA, Evangelista EA, Rodrigues V, Kettelhut IC, Migliorini RH (2003) Expression of glycerokinase in brown adipose tissue is stimulated by the sympathetic nervous system. *Am J Physiol Regul Integr Comp Physiol* 284:R1536–R1541
50. Chakravarty K, Hanson RW (2007) Insulin regulation of phosphoenolpyruvate carboxykinase-c gene transcription: the role of sterol regulatory element-binding protein 1c. *Nutr Rev* 65:S47–S56

51. Olswang Y, Blum B, Cassuto H, Cohen H, Biberman Y, Hanson RW, Reshef L (2003) Glucocorticoids repress transcription of phosphoenolpyruvate carboxykinase (GTP) gene in adipocytes by inhibiting its C/EBP-mediated activation. *J Biol Chem* 278:12929–12936
52. Brasaemle DL, Subramanian V, Garcia A, Marcinkiewicz A, Rothenberg A (2009) Perilipin A and the control of triacylglycerol metabolism. *Mol Cell Biochem* 326:15–21
53. Yamaguchi T (2010) Crucial role of CGI-58/alpha/beta hydrolase domain-containing protein 5 in lipid metabolism. *Biol Pharm Bull* 33:342–345
54. Xu C, He J, Jiang H, Zu L, Zhai W, Pu S, Xu G (2009) Direct effect of glucocorticoids on lipolysis in adipocytes. *Mol Endocrinol* 23:1161–1170
55. Lacasa D, Agli B, Giudicelli Y (1988) Permissive action of glucocorticoids on catecholamine-induced lipolysis: direct “in vitro” effects on the fat cell beta-adrenoreceptor-coupled-adenylate cyclase system. *Biochem Biophys Res Commun* 153:489–497
56. Saltiel AR, Pessin JE (2002) Insulin signaling pathways in time and space. *Trends Cell Biol* 12:65–71
57. Rahn Landström T, Mei J, Karlsson M, Manganiello V, Degerman E (2000) Down-regulation of cyclic-nucleotide phosphodiesterase 3B in 3T3–L1 adipocytes induced by tumour necrosis factor alpha and cAMP. *Biochem J* 346:337–343
58. Rydén M, Arvidsson E, Blomqvist L, Perbeck L, Dicker A, Arner P (2004) Targets for TNF-alpha-induced lipolysis in human adipocytes. *Biochem Biophys Res Commun* 318:168–175
59. Laurencikiene J, van Harmelen V, Arvidsson Nordstrom E, Dicker A, Blomqvist L, Näslund E, Langin D, Arner P, Rydén M (2007) NF-kappaB is important for TNF-alpha-induced lipolysis in human adipocytes. *J Lipid Res* 48:1069–1077
60. Kim JY, Tillison K, Lee JH, Rearick DA, Smas CM (2006) The adipose tissue triglyceride lipase ATGL/PNPLA2 is downregulated by insulin and TNF-alpha in 3T3–L1 adipocytes and is a target for transactivation by PPARgamma. *Am J Physiol Endocrinol Metab* 291:E115–E127
61. Bézaire V, Mairal A, Anesia R, Lefort C, Langin D (2009) Chronic TNFalpha and cAMP pre-treatment of human adipocytes alter HSL, ATGL and perilipin to regulate basal and stimulated lipolysis. *FEBS Lett* 583:3045–3049
62. Farias-Silva E, dos Santos IN, Corezola do Amaral ME, Grassi-Kassisse DM, Spadari-Bratfisch RC (2004) Glucocorticoid receptor and Beta-adrenoceptor expression in epididymal adipose tissue from stressed rats. *Ann N Y Acad Sci* 1018:328–332

Interaction Between Marginal Zinc and High Fat Supply on Lipid Metabolism and Growth of Weanling Rats

Edgar Weigand · Christine Boesch-Saadatmandi

Received: 4 August 2011 / Accepted: 3 November 2011 / Published online: 30 November 2011
© The Author(s) 2011. This article is published with open access at Springerlink.com

Abstract The impact of a moderate Zn deficiency on growth and plasma and liver lipids was investigated in two 4-week experiments with male weanling rats fed fat-enriched diets. Semisynthetic, approximately isocaloric diets containing 3% soybean oil were supplemented with either 7 or 100 mg Zn/kg diet and with 22% beef tallow (BT) or sunflower oil (SF). In Experiment 1, which compared the dietary fat level and the fat source in a factorial design of treatments, all diets were fed ad libitum to 6×8 animals, whereas intake of the high-Zn BT and SF diets was restricted in Experiment 2 (5×6 rats) to the level of intake of the respective low-Zn diets. The low-Zn SF diet consistently depressed food intake and final live weights of the animals to a greater extent than the other low-Zn diets, while intake and growth were comparable among the animals fed the high-Zn diets. The marginal Zn deficit per se did not alter plasma triglyceride and cholesterol concentrations nor hepatic concentrations of triglyceride, cholesterol and phospholipids. The fatty acid pattern of liver phospholipids did not indicate that chain elongation and desaturation of fatty acids was impaired by a lack of zinc. It was concluded that dietary energy and fat intake, and fat source have a greater effect on plasma and liver lipids than a moderate Zn deficiency. Marginally Zn-deficient diets enriched with sunflower oil as a major energy source cause a greater growth retardation than diets rich in carbohydrates or beef tallow.

Keywords Zinc deficiency · Growth · Plasma lipids · Liver lipids · Fatty acid metabolism · Rats

Abbreviations

ANOVA	Analysis of variance
AP	Alkaline phosphatase
BT	Beef tallow
CT	Control
DNL	De novo lipogenesis
GE	Gross energy
G6PD	Glucose-6-phosphate dehydrogenase
HDL-C	High density lipoprotein cholesterol
ME	Metabolizable energy
MUFA	Monounsaturated fatty acid(s)
PUFA	Polyunsaturated fatty acid(s)
PL	Phospholipids
SF	Sunflower (seed) oil
SFA	Saturated fatty acid(s)
TAG	Triacylglycerol(s)
TC	Total cholesterol
VLDL	Very low density lipoproteins
Zn	Zinc

Introduction

In young animals, early signs of severe zinc (Zn) deficiency are growth retardation, depressed food intake and a cyclic feeding pattern [1–3]. The dietary fat source and fat level may alter the effects of dietary Zn depletion on growth rate and lipid metabolism. Bettger et al. [4] found that dietary substitution of 5% hydrogenated coconut oil for corn oil as a source of essential fatty acids improved the growth of young rats, suggesting an interaction between these nutrients. In

E. Weigand (✉)
Institute of Animal Nutrition and Nutrition Physiology,
Justus Liebig University, 35396 Giessen, Germany
e-mail: edgar.weigand@ernaehrung.uni-giessen.de

C. Boesch-Saadatmandi
School of Agriculture, Food and Rural Development,
Newcastle University, Newcastle upon Tyne NE1 7RU, UK

similar studies with chicks [5], the effects were the opposite. The addition of corn oil, soybean oil or a mixture of polyunsaturated fatty acids (PUFA) to Zn-deficient diets retarded growth of the animals to a greater extent as compared to hydrogenated coconut oil and exacerbated the symptoms of Zn deficiency. Huang et al. [6] reported that growth retardation of young rats was partially alleviated when the animals were given daily subcutaneous injections of primrose oil, but when safflower oil was injected the effect was minimal. In a recent study [7], fat source in fat-enriched diets markedly affected growth rates of weanling rats when the dietary Zn supply was marginal, i.e. about two-third of the minimum requirement for unlimited growth. Low-Zn diets supplemented with 18% sunflower oil or olive oil depressed final live weights of the animals to a greater extent than diets enriched with beef tallow, whereas no difference was evident among corresponding high-Zn diets.

The objective of the present study was to investigate the impact of highly fat-enriched diets on growth and lipid metabolism of weanling rats when dietary Zn supply is either marginal or adequate for unlimited growth. Semi-synthetic diets were supplemented with 7 or 100 µg Zn/g and were enriched with 22% fat as beef tallow (BT) or as sunflower oil (SF) above a basal fat content of 3% soybean oil in all diets. In a first experiment, which included diets without supplemental fat, all diets were fed ad libitum for 4 weeks, whereas intake of the high-Zn diets was restricted in a second experiment according to the intake of the respective low-Zn BT and SF diets. The low-Zn SF diet consistently reduced food and energy intake and final live weights to a greater extent than the other low-Zn diets. Changes in plasma and liver lipids observed in response to dietary treatments were primarily attributable to differences in energy and fat intake and to fat source rather than to the moderate Zn deficiency. We conclude that dietary energy and fat intake, and fat source have a greater effect on plasma and liver lipids than a moderate Zn deficit, and that Zn-deficient diets enriched with sunflower oil as a major energy source cause a greater growth retardation than diets rich in carbohydrates or beef tallow.

Experimental Procedures

Animals and Diets

In Experiment 1, a total of 48 male weanling Wistar rats (Harlan Winkelmann, Borcheln, Germany) with an initial live weight of 48 ± 2.8 g (mean \pm SD) were randomly assigned to six treatment groups of eight animals each, following a 2×3 factorial design for dietary Zn and fat treatments. Semisynthetic diets for these groups differed in

Zn supplementation (7 vs. 100 µg/g, added as $\text{ZnSO}_4 \cdot 7\text{H}_2\text{O}$), and in fat supplementation: 22% beef tallow (BT) or 22% sunflower oil (SF) versus a low-fat, carbohydrate-rich control diet (CT). All diets contained 3% soybean oil to offer sufficient amounts of essential fatty acids. The major components of the diets are summarized in Table 1. They contributed a basal Zn level of about 0.5 µg/g by analysis. In the high-fat diets parts of cornstarch were replaced by cellulose to compensate for differences in energy. The fatty acid composition of the low- and high-fat diets is shown in Table 2. Diets were stored at 4 °C. Ad libitum feeding was practiced, replacing remainders by fresh portions daily.

In Experiment 2, six male weanling rats each (50 ± 2.8 g initial live weight) were randomly allocated to five dietary treatments: (1) low-Zn BT diet fed ad libitum, (2) high-Zn BT diet fed in restricted amounts according to

Table 1 Composition of the experimental diets (Experiment 1 and 2)

	Low-fat diets	High-fat diets	
	Control (CT)	BT diets	SF diets
Ingredients (g/kg diet)			
Egg albumen	200	200	200
Cornstarch ^a	527	77	77
Sucrose	100	100	100
Cellulose	50	280	280
Vitamin premix ^b	15	15	15
Mineral premix ^b	50	50	50
Zinc premix ^c	25	25	25
L-Lysine + DL-methionine (1:1)	3	3	3
Soybean oil	30	30	30
Beef tallow (BT)	–	220	–
Sunflower oil (SF)	–	–	220
Total	1,000	1,000	1,000
Nutrient composition (by analysis)			
Protein content (g/kg DM)	179	176	177
Fat content (g/kg DM)	36	260	263
NDF content (g/kg DM)	134	276	280
ME content (MJ/kg DM)	16.7	17.0	17.6
Carbohydrate energy (% of ME)	69	22	21
Fat energy (% of ME)	8	55	58

DM dry matter, NDF neutral detergent fiber, ME metabolizable energy

^a Additional cornstarch was contained in the mineral, vitamin and zinc premixes (total of 43.5 g/kg)

^b Details of the vitamin and mineral mixtures have been reported previously [8]

^c Zinc premix provided 7 or 100 µg Zn/g diet as $\text{ZnSO}_4 \cdot 7\text{H}_2\text{O}$ above a basal level of 0.5 µg/g diet

Table 2 Fatty acid composition of experimental diets (mol/100 mol fatty acid)

Fatty acid ^a	CT diets	BT diets	SF diets
Myristic acid	0.21	6.73	0.11
Palmitic acid	16.7	25.5	7.51
Palmitoleic acid	0.0	3.09	0.19
Stearic acid	3.90	15.6	3.43
Oleic acid	21.1	35.1	26.1
Linoleic acid	51.1	11.2	60.5
α -Linolenic acid	5.68	1.44	0.85

Values are means of three independent determinations per diet

^a The concentration of additional fatty acids was less than 1.5 mol/100 mol across diets

average intake of group 1, (3) low-Zn SF diet fed ad libitum, (4) high-Zn SF diet fed in restricted amounts according to average intake of group 3, and (5) high-Zn SF diet fed ad libitum. Diet composition was the same as described in Tables 1 and 2 regarding ingredients, Zn and fat supplementation. Food consumption was determined daily to control intake of the rats in group 2 and 4.

Approval of the experimental protocols for use and care of laboratory animals in research was obtained by the regional Animal Protection Authority (Regierungspräsidium Giessen, II 25.3-19c20/15c GI 19/3). The rats were housed individually in stainless steel metabolic cages in an environmentally controlled room (22 °C, rel. humidity of 55%, 12 h light and dark cycle). They had free access to deionized water. In Experiment 1, feces were collected daily during week 2 and 3, freeze-dried and stored at 4 °C for determination of energy and fat content. After 4 weeks, the animals were fasted overnight and anesthetized with carbon dioxide followed by decapitation. Blood was collected in test tubes containing heparin and centrifuged (3,000g for 10 min at 4 °C), and the resulting plasma was stored at -80 °C. The liver and right femur were excised, weighed and frozen on dry ice for subsequent measurements.

Analytical Procedures

Diets were analyzed for dry matter, crude protein, fat and neutral detergent fiber by official methods [9]. Fecal samples were treated with 4 M HCl before fat extraction using *n*-hexane. Gross energy (GE) in diets and feces was determined by adiabatic bomb calorimetry. The metabolizable energy (ME) of the low- and high-fat diets was calculated as digestible energy (intake minus fecal excretion of GE during week 2 and 3 of Experiment 1) multiplied by 0.96 [10].

Zn concentration in the femur bone and diets was analyzed by ICP-AES (inductively coupled plasma atomic emission spectrometry) after dry-ashing (450 °C) and dissolving in 3 M HNO₃. Plasma Zn concentration was measured directly after dilution with 0.1 M hydrochloric acid by flame atomic absorption spectrometry. The activity of the alkaline phosphatase (AP; EC 3.1.3.1) in plasma was determined photometrically with a standard method [11]. The activity of the glucose-6-phosphate dehydrogenase (G6PD; EC 1.1.1.49) in liver homogenates was assayed with a commercial reagent kit (Boehringer Mannheim GmbH, Germany). The protein content in liver homogenates was determined by the Lowry method [12].

Liver total lipids were extracted with a mixture of hexane:isopropanol (3:2, by vol) according to the method of Hara and Radin [13] with minor modifications. Briefly, frozen liver was weighed and homogenized in 0.15 M NaCl solution. Hexane:isopropanol (3:2, by vol), containing 0.005% (wt/vol) butylhydroxytoluol, was added and the mixture centrifuged for 10 min at 3,000g and 10 °C. The upper organic phase was collected and the solvent evaporated under liquid nitrogen. The resulting residues were quantified gravimetrically as total lipids and resuspended in hexane:isopropanol (3:2, by vol). Aliquots of the liver lipid extracts and plasma samples were analyzed for their content of triglycerides and cholesterol using commercial test kits (Ecoline 25, Merck KGaA, Darmstadt, Germany). The phospholipid (PL) content was quantified by phosphate measurement in aliquots of the liver lipid extracts using a commercial test combination for phosphorus and phospholipids (Boehringer Mannheim GmbH, Germany).

Liver PL were separated from the total lipid extracts for subsequent fatty acid analysis by aminopropyl-bonded phase columns (Bond Elut, Agilent Technologies); this solid phase extraction method has been shown to be superior to other separation techniques [14]. Aliquots of liver lipid extracts were dissolved in chloroform and applied to hexane pre-conditioned columns. After treatment with several other solvents that released neutral lipids and free fatty acids from the column, methanol was added to provoke the elution of the PL fraction. These fractions, to which heptadecanoic acid (17:0) was added as internal standard, were subjected to transmethylation with *N*-trimethyl sulfonium hydroxide. Fatty acid methyl esters (FAME) were separated by gas chromatography. They were identified by comparing retention times of FAME in a standard mix (Supelco 37, Sigma-Aldrich, Inc) that was supplemented with docosapentaenoic acid (D5679, Sigma-Aldrich, Inc). Individual FA were quantified on the basis of area under the curve and internal standard response as molar percentage of the total amount of fatty acids.

Statistical Analyses

Statistical analyses were performed using IBM SPSS Statistics 19 for Windows (IBM Company, Chicago, IL, USA). Data were analyzed by two-way analysis of variance (ANOVA) according to the linear model for a completely randomized design to test for treatment effects of Zn, fat and Zn × fat interaction (2 × 3-factorial in Expt. 1 and 2 × 2-factorial in Expt. 2). Since the factor “fat” included fat level (low vs. high) and fat source (BT vs. SF) in Experiment 1, bifactorial ANOVA was also applied to the high-fat treatments to test for effects of fat source. In addition, univariate analysis was applied to test for differences among groups within each dietary Zn level in Experiment 1 and among the three groups fed the SF diets in Experiment 2. The Tukey test was used as a post hoc test to compare treatment means or, alternatively, the Games–Howell test if homogeneity of variance (Levene test) could not be attained by logarithmic (*ln*) or square root transformation of the data. The significance was set at $p < 0.05$ in post hoc tests.

Table 3 Effect of diets differing in Zn concentration and fat supplementation on food and energy (ME) intake, final live weight, fat and energy digestibility, plasma and femur Zn concentration,

Diet Zn concentration		7 µg/g			100 µg/g			ANOVA: <i>p</i> values		
		CT	BT	SF	CT	BT	SF	Zn	Fat	Zn × Fat
Food intake (g/day)	<i>M</i>	14.4 ^c	11.8 ^b	9.9 ^a	16.6 ^b	15.1 ^a	14.3 ^a	<0.001	<0.001	NS
	<i>SD</i>	1.6	1.8	1.6	0.7	0.8	1.1			
ME intake ^d (kJ/day)	<i>M</i>	216 ^b	189 ^{ab}	166 ^a	250 ^a	242 ^a	238 ^a	<0.001	<0.001	<0.05
	<i>SD</i>	24	28	26	10	13	18			
ME intake (kJ/g wt gain)	<i>M</i>	39.1 ^a	38.2 ^a	40.1 ^a	38.2 ^a	37.1 ^a	37.5 ^a	<0.05	NS	NS
	<i>SD</i>	2.7	1.2	1.9	1.3	3.6	2.1			
Final live weight (g)	<i>M</i>	204 ^b	188 ^b	165 ^a	232 ^a	233 ^a	228 ^a	<0.001	<0.01	<0.05
	<i>SD</i>	17	22	20	8	20	18			
Fat digestibility (%)	<i>M</i>	97.6 ^b	89.7 ^a	98.2 ^b	97.0 ^b	89.1 ^a	98.7 ^b	NS	<0.001	NS
	<i>SD</i>	0.9	1.5	0.3	0.6	0.9	0.4			
GE digestibility (%)	<i>M</i>	93.7 ^c	73.9 ^a	77.6 ^b	93.1 ^c	73.3 ^a	77.9 ^b	NS	<0.001	NS
	<i>SD</i>	0.2	0.5	0.5	0.7	0.7	0.6			
Plasma zinc (µg/mL)	<i>M</i>	1.36 ^b	1.11 ^a	0.90 ^a	2.04 ^c	1.86 ^b	1.65 ^a	<0.001	<0.001	NS
	<i>SD</i>	0.20	0.22	0.25	0.12	0.20	0.14			
Femur zinc ^d (µg/g fresh wt)	<i>M</i>	51.9 ^a	46.9 ^a	48.0 ^a	134 ^b	123 ^a	123 ^a	<0.001	<0.01	NS
	<i>SD</i>	4.5	4.6	4.3	5.9	7.3	11.1			
Plasma AP (mU/mL)	<i>M</i>	378 ^a	383 ^a	415 ^a	445 ^a	529 ^b	543 ^b	<0.001	<0.01	NS
	<i>SD</i>	62	76	62	59	50	44			
Liver G6PD ^d (mU/mg protein)	<i>M</i>	51.9 ^b	12.6 ^a	12.3 ^a	50.6 ^b	13.7 ^a	18.5 ^a	NS	<0.001	NS
	<i>SD</i>	22.4	2.6	2.2	17.0	4.6	7.7			

GE gross energy, *ME* metabolizable energy, *NS* not significant, *SD* standard deviation

^{a, b, c} Group means (*M*) with different superscript letters within rows and within the same zinc level significantly differ ($p < 0.05$; Tukey test; in the case of G6PD Games–Howell test)

^d ANOVA after *ln* transformation of data

Results

Experiment 1

Food and Energy Intake and Final Live Weight

In Experiment 1, in which all diets were offered ad libitum during the 28-days feeding period, the marginal Zn supplementation of the diets markedly ($p < 0.001$) reduced food and energy intake and final live weights (Table 3). ME intake and final live weights significantly differed among the rats fed the low-Zn diets, but not among the animals fed the high-Zn diets. Both level and source of dietary fat contributed to a significant Zn × fat interaction, as the reductions in ME intake and final live weights due to the moderate Zn deficiency differed among the CT, BT and SF groups (about 14, 22 and 30% in ME intake and 12, 19 and 28% in final weights relative to the respective high-Zn groups). ME intake per gram of weight gain was significantly higher for the rats fed the low-Zn diets, but the difference was relatively small (less than 7%), and may be attributed primarily

plasma alkaline phosphatase activity, and liver glucose-6-phosphate dehydrogenase (G6PD) activity in weanling rats (Experiment 1)

to a higher proportion of energy expended for maintenance in the animals fed the low-Zn diets.

Fat and Energy Digestibility

Fat digestibility in the BT groups was approximately 8–9% U lower than in the CT and SF groups independent of the dietary Zn level (Table 3). This difference may be attributed to the high content of saturated fatty acids in beef tallow. Gross energy (GE) digestibility of the BT and SF diets was markedly lower than that of the CT diets (about 20 and 15% U, respectively; $p < 0.001$), reflecting the pronounced difference in dietary cellulose content. GE digestibility also significantly ($p < 0.001$) differed between the BT and SF diets according to the difference in fat digestibility.

Zinc and Metabolic Status

Zn concentrations in plasma and femur and activity of the alkaline phosphatase (AP) in plasma, which were analyzed as indicators of Zn status, were substantially reduced ($p < 0.001$) by the marginal dietary Zn supply in Experiment 1 (Table 3). Dietary fat level and fat source also affected these parameters to different degrees. Plasma Zn concentrations were lower in the rats fed the high-fat diets as compared to those fed the CT diets. This difference was

most marked for the SF-fed animals. The plasma AP activity was enhanced by the high-fat diets.

The activity of glucose-6-phosphate dehydrogenase (G6PD), a member of the lipogenic enzyme family [15], was greatly reduced ($p < 0.001$) in the liver of the rats fed the high-fat diets as compared to those given the low-fat CT diet, regardless of the dietary Zn level (Table 3).

Plasma and Liver Lipids

Plasma concentrations of triglycerides (TAG), total cholesterol (TC) and HDL-C were not significantly altered by the dietary Zn level, but they were by the level and type of fat in the diets in Experiment 1 (Table 4). The SF diets consistently reduced plasma TAG concentrations regardless of the dietary Zn level. TC and HDL-C concentrations in the low-Zn CT group were significantly higher ($p < 0.05$) than in the low-Zn BT and SF groups, but not when the dietary Zn level was high. Fat source did not significantly affect plasma TC and HDL-C concentrations.

Liver concentrations of total lipids, TAG and cholesterol (Table 4) were significantly higher in the rats fed the high-Zn BT and SF diets than in those fed the respective low-Zn diets, while they did not differ between the two CT-fed groups. Concentrations of these lipids were substantially higher for the SF-fed than for the BT-fed animals

Table 4 Effect of diets differing in Zn concentration and fat supplementation on plasma and liver lipid concentrations (Experiment 1)

Diet Zn concentration	7 µg/g			100 µg/g			ANOVA: <i>p</i> values			
	Fat supplement	CT	BT	SF	CT	BT	SF	Zn	Fat	Zn × Fat
Plasma lipids										
Triglycerides ^d (mg/dL plasma)	<i>M</i>	113 ^b	102 ^b	28 ^a	108 ^b	100 ^b	40 ^a	NS	<0.001	NS
	<i>SD</i>	36	20	6	35	42	18			
Total cholesterol (mg/dL plasma)	<i>M</i>	104.3 ^b	67.2 ^a	73.7 ^a	82.5 ^a	73.8 ^a	73.7 ^a	NS	<0.001	<0.01
	<i>SD</i>	14.5	11.0	9.5	17.2	10.5	11.2			
HDL-Cholesterol (mg/dL plasma)	<i>M</i>	83.1 ^b	45.4 ^a	50.5 ^a	61.5 ^a	54.7 ^a	58.6 ^a	NS	<0.001	<0.001
	<i>SD</i>	13.3	7.0	6.2	12.3	10.7	10.4			
Liver lipids										
Total lipids ^d (mg/g fresh wt)	<i>M</i>	39.6 ^a	48.8 ^{ab}	58.7 ^b	42.3 ^a	61.4 ^b	82.2 ^c	<0.001	<0.001	NS
	<i>SD</i>	5.4	10.4	9.0	5.5	10.0	15.3			
Triglycerides ^e (mg/g fresh wt)	<i>M</i>	14.9 ^{ab}	11.7 ^a	25.3 ^b	14.3 ^a	25.1 ^b	46.3 ^c	<0.001	<0.001	<0.01
	<i>SD</i>	5.6	6.3	12.0	5.2	8.7	6.9			
Cholesterol ^d (mg/g fresh wt)	<i>M</i>	2.00 ^a	2.98 ^b	4.74 ^c	2.15 ^a	3.40 ^b	7.24 ^c	<0.001	<0.001	<0.01
	<i>SD</i>	0.22	0.43	0.80	0.25	0.45	1.02			
Phospholipids (mg/g fresh wt)	<i>M</i>	23.0 ^a	25.2 ^a	24.7 ^a	23.5 ^a	25.0 ^a	26.0 ^a	NS	NS	NS
	<i>SD</i>	1.9	2.8	4.1	3.1	2.4	3.5			

NS not significant, SD standard deviation

^{a, b, c} Group means (*M*) with different superscript letters within rows and within the same zinc level significantly differ ($p < 0.05$; Tukey test)

^d ANOVA after \ln transformation of the data

^e ANOVA after $x^{1/2}$ transformation of the data

($p < 0.001$). In contrast, hepatic PL concentrations were not altered by any of the dietary treatments.

Fatty Acid Composition of Liver Phospholipids

Table 5 presents the fatty acid pattern in the PL extracted from the liver in Experiment 1. Total molar proportions of saturated fatty acids (SFA) were comparable across dietary treatments. However, the percentages of 16:0 and 18:0 significantly differed among groups ($p < 0.001$). Palmitic acid (16:0) was the major SFA in the CT groups, whereas 18:0

dominated in the BT and SF groups. Oleic acid (18:1) was the predominant monounsaturated fatty acid (MUFA) in all groups. The highest mean percentage of this fatty acid was recorded in the BT groups. As expected, the SF diets increased the total percentages of n-6 PUFA, especially those of 18:2, 20:4 and 22:4, and depressed the percentages of n-3 PUFA, leading to substantially higher ratios of n-6 PUFA to n-3 PUFA in the SF-fed groups. Significant Zn effects were noted in the case of linoleic (18:2), γ -linolenic (18:3n-6) and docosapentaenoic acid (22:5n-3), which were present in higher proportions when the rats were fed the low-Zn BT and

Table 5 Fatty acid composition of liver phospholipids (mol/100 mol total fatty acids) (Experiment 1)

Diet Zn concentration		Zinc: 7 μ g/g			Zinc: 100 μ g/g			ANOVA: p values		
		CT	BT	SF	CT	BT	SF	Zn	Fat	Zn \times Fat
Sum SFA ^e	<i>M</i>	41.1 ^a	40.0 ^a	38.7 ^a	40.3 ^a	41.6 ^a	39.3 ^a	NS	<0.05	NS
	<i>SD</i>	2.9	1.9	2.0	3.1	1.4	0.7			
16:0	<i>M</i>	21.7 ^b	15.9 ^a	14.0 ^a	22.3 ^c	17.3 ^b	14.2 ^a	NS	<0.001	NS
	<i>SD</i>	2.4	1.1	0.9	2.0	2.0	1.1			
18:0	<i>M</i>	18.0 ^a	22.9 ^b	23.4 ^b	16.8 ^a	23.2 ^b	23.9 ^b	NS	<0.001	NS
	<i>SD</i>	1.4	1.8	1.7	1.5	1.4	1.4			
Sum MUFA ^f	<i>M</i>	5.53 ^b	4.16 ^a	4.72 ^a	5.73 ^b	4.01 ^a	4.20 ^a	NS	<0.001	NS
	<i>SD</i>	0.77	0.64	0.76	1.14	0.56	0.45			
18:1	<i>M</i>	3.51 ^a	4.16 ^a	3.55 ^a	3.61 ^b	4.01 ^b	2.83 ^a	NS	0.001	NS
	<i>SD</i>	0.62	0.64	0.78	0.81	0.56	0.24			
Sum n-6 PUFA	<i>M</i>	40.2 ^a	41.0 ^a	49.8 ^b	40.9 ^b	39.5 ^a	48.0 ^b	NS	<0.001	NS
	<i>SD</i>	2.5	1.2	1.2	2.8	1.3	1.2			
18:2	<i>M</i>	7.14 ^a	5.76 ^a	10.53 ^b	7.26 ^b	4.63 ^a	7.60 ^b	<0.001	<0.001	0.001
	<i>SD</i>	0.81	1.07	1.61	0.99	0.53	1.25			
18:3	<i>M</i>	0.23 ^b	0.10 ^a	0.21 ^b	0.16 ^b	0.07 ^a	0.13 ^b	<0.001	<0.001	NS
	<i>SD</i>	0.06	0.08	0.07	0.05	0.04	0.03			
20:3	<i>M</i>	1.26 ^a	1.37 ^a	1.07 ^a	1.56 ^a	1.60 ^a	1.21 ^a	NS	NS	NS
	<i>SD</i>	0.85	0.75	0.46	0.74	0.97	0.65			
20:4	<i>M</i>	30.8 ^a	33.1 ^b	35.0 ^b	31.2 ^a	32.6 ^a	36.7 ^b	NS	<0.001	NS
	<i>SD</i>	2.4	1.6	1.2	2.8	1.6	0.9			
22:4 ^d	<i>M</i>	0.53 ^a	0.61 ^a	1.85 ^b	0.50 ^a	0.62 ^a	1.74 ^b	NS	<0.001	NS
	<i>SD</i>	0.06	0.12	0.18	0.07	0.11	0.29			
Sum n-3 PUFA	<i>M</i>	13.2 ^b	14.9 ^b	7.1 ^a	13.0 ^b	14.6 ^c	8.5 ^a	NS	<0.001	NS
	<i>SD</i>	1.3	1.7	0.9	1.6	0.9	0.9			
22:5 ^d	<i>M</i>	0.97 ^b	1.53 ^c	0.68 ^a	0.94 ^b	1.18 ^b	0.61 ^a	<0.01	<0.001	NS
	<i>SD</i>	0.15	0.26	0.07	0.15	0.31	0.11			
22:6	<i>M</i>	12.2 ^b	13.3 ^b	6.4 ^a	12.1 ^b	13.4 ^b	7.8 ^a	NS	<0.001	NS
	<i>SD</i>	1.3	1.8	0.9	1.5	0.8	0.9			
Sum n-6/Sum n-3 PUFA ^d	<i>M</i>	3.07 ^a	2.79 ^a	7.02 ^b	3.17 ^a	2.72 ^a	5.74 ^b	<0.05	<0.001	<0.05
	<i>SD</i>	0.25	0.35	0.98	0.32	0.19	0.70			

NS not significant, *SD* standard deviation

^{a, b, c} Group means (*M*) with different superscript letters within rows and within the same zinc level significantly differ (Tukey test, $p < 0.05$)

^d ANOVA after \ln transformation of the data

^e The sum of saturated fatty acids (SFA) includes small amounts of 14:0 (<0.6 mol%) and 21:0 (<0.5 mol%)

^f The sum of monounsaturated fatty acids (MUFA) includes small amounts of 16:1 (about 1.2 mol%), 20:1 (<0.1 mol%) and 22:1 (about 0.8 mol%) in the case of the CT groups, and 20:1 (0.2 mol%) and 22:1 (about 1.0 mol%) in the case of the SF groups

SF diets as compared to the respective high-Zn diets. The highly significant Zn \times fat interaction observed for 18:2 ($p = 0.001$) is basically due to the different direction and height of response to the dietary fat level among the corresponding low- and high-Zn groups. This diet effect on 18:2 is also reflected in a significant Zn \times fat interaction of the n-6 PUFA to n-3 PUFA ratio ($p < 0.05$).

Experiment 2

Energy Intake and Final Live Weight

In Experiment 2, in which food intake of the high-Zn BT and SF diets was restricted to amounts consumed by the animals offered the corresponding low-Zn diets, final live weights were not affected by the difference in Zn supply, whereas the animals allowed to consume the high-Zn SF diet ad libitum reached significantly higher final live weights (Table 6). ME intake and final live weights of the rats fed the low-Zn SF diet were lower (about 13%; $p < 0.01$) than those fed the low-Zn BT diet. As in Experiment 1, ME intake per gram weight gain was reduced by the high-Zn diets, presumably due to a slightly leaner tissue gain.

Zinc Status

Plasma and femur Zn concentrations and plasma activity of the alkaline phosphatase (AP) were markedly reduced

($p < 0.001$) by the marginal dietary Zn supply in Experiment 2 (Table 6). Fat source did not significantly ($p > 0.05$) affect these parameters.

Plasma and Liver Lipids

Plasma concentrations of TAG, TC and HDL-C were not significantly altered by the dietary Zn level in Experiment 2 (Table 7). TAG concentrations in the SF groups were lower than those in the BT groups. But plasma TC and HDL-C concentrations were not significantly affected by fat source. The livers of the rats consuming the corresponding low- and high-Zn BT and SF-diets in equivalent quantities had comparable concentrations of total lipids, cholesterol and PL (Table 7). However, the animals fed the high-Zn SF diet ad libitum showed a significantly ($p < 0.05$) increased hepatic TAG content. PL concentrations were about 10% higher in the SF-fed than in the BT-fed animals.

Discussion

The present experiments were designed to investigate the effect of a moderate Zn deficiency on growth and selected features of lipid metabolism in weanling rats fed diets that greatly differed in fat level and fat source. As expected, the low-Zn diets (7 $\mu\text{g/g}$ supplemental zinc) were associated with notable reductions in food and energy intake and final

Table 6 Effect of high-fat diets differing in Zn concentration and fat source on energy (ME) intake, final live weight, plasma and femur Zn concentration, and plasma alkaline phosphatase activity in weanling rats fed high-fat diets (Experiment 2)

Zinc ($\mu\text{g/g}$ diet)		7	100	7	100	100	ANOVA ^c		
Fat source		BT	BT	SF	SF	SF	<i>p</i> values		
Feeding protocol ^f		AL	RF	AL	RF	AL	Zn	Fat	Zn \times Fat
ME intake ^d (kJ/d)	<i>M</i>	218	208	189 ^a	185 ^a	256 ^b	NS	<0.01	NS
	<i>SD</i>	33.8	3.2	20.3	4.7	8.0			
Final live weight (g)	<i>M</i>	207	202	179 ^a	186 ^a	237 ^b	NS	<0.001	NS
	<i>SD</i>	14.0	5.7	19.4	7.4	9.9			
ME intake/wt gain ^d (kJ/g)	<i>M</i>	38.7	37.8	40.8 ^a	37.8 ^a	38.2 ^a	<0.05	NS	NS
	<i>SD</i>	1.7	0.6	2.4	2.1	1.7			
Plasma zinc ($\mu\text{g/mL}$)	<i>M</i>	0.91	1.33	0.80 ^a	1.38 ^b	1.20 ^b	<0.001	NS	NS
	<i>SD</i>	0.08	0.32	0.12	0.20	0.11			
Femur zinc ($\mu\text{g/g}$ fresh wt)	<i>M</i>	52.6	138.8	51.4 ^a	131.3 ^b	126.5 ^b	<0.001	NS	NS
	<i>SD</i>	6.6	6.4	5.8	10.4	11.0			
Plasma AP activity (mU/mL)	<i>M</i>	505	631	520 ^a	737 ^b	628 ^c	<0.001	NS	NS
	<i>SD</i>	29	83	106	62	65			

NS not significant, *SD* standard deviation

^{a, b, c} Means (*M*) with different superscript letters among SF groups significantly differ ($p < 0.05$; Tukey test)

^d ANOVA after *ln* transformation of the data

^e Bifactorial ANOVA (without group fed SF diet with 100 μg Zn/g ad libitum)

^f Feeding protocol: *AL* ad libitum, *RF* restricted-fed

Table 7 Effect of high-fat diets differing in Zn concentration and fat source on plasma and liver lipid concentrations (Experiment 2)

Zinc ($\mu\text{g/g}$ diet)		7	100	7	100	100	ANOVA ^d		
Fat source		BT	BT	SF	SF	SF	<i>p</i> values		
Feeding protocol ^c		AL	RF	AL	RF	AL	Zn	Fat	Zn \times Fat
Plasma lipids									
Triglycerides (mg/dL plasma)	<i>M</i>	95.6	101.8	48.1 ^a	60.4 ^a	76.4 ^a	NS	<0.001	NS
	<i>SD</i>	15.6	31.5	14.6	33.7	32.3			
Cholesterol (mg/dL plasma)	<i>M</i>	85.5	84.4	72.4 ^a	92.5 ^a	89.6 ^a	NS	NS	NS
	<i>SD</i>	9.4	17.0	13.2	14.3	19.2			
HDL-Cholesterol (mg/dL plasma)	<i>M</i>	44.4	39.6	46.0 ^a	51.1 ^a	58.1 ^a	NS	NS	NS
	<i>SD</i>	8.3	7.7	6.6	11.8	13.8			
Liver lipids									
Total lipids (mg/g fresh wt)	<i>M</i>	51.4	50.9	64.4 ^a	71.0 ^{ab}	82.7 ^b	NS	<0.001	NS
	<i>SD</i>	9.5	5.4	7.7	8.4	12.8			
Triglycerides (mg/g fresh wt)	<i>M</i>	16.2	16.8	19.7 ^a	25.6 ^a	35.0 ^b	NS	<0.05	NS
	<i>SD</i>	6.4	4.7	5.9	6.9	11.7			
Cholesterol ^c (mg/g fresh wt)	<i>M</i>	2.53	2.37	4.67 ^a	4.65 ^a	5.21 ^a	NS	<0.001	NS
	<i>SD</i>	0.47	0.08	0.80	0.53	0.72			
Phospholipids (mg/g fresh wt)	<i>M</i>	25.4	24.4	28.5 ^a	27.3 ^a	26.6 ^a	NS	<0.001	NS
	<i>SD</i>	1.8	2.5	1.3	0.7	1.8			

NS not significant, SD standard deviation

^{a, b} Group means (*M*) with different superscript letters among SF diets significantly differ ($p < 0.05$; Tukey test)

^c ANOVA after \ln transformation of the data

^d Bifactorial ANOVA (without group fed SF diet with 100 μg Zn/g ad libitum)

^e Feeding protocol: AL ad libitum, RF restricted-fed

live weights compared to animals fed the high-Zn diets (100 $\mu\text{g/g}$ supplemental zinc), but without the complications that would arise from feeding severely Zn-deficient diets, i.e. growth arrest, development of a cyclic feeding pattern, conspicuous inanition, and the manifestation of clinical deficiency symptoms [1–3]. The increase in dietary fat level implied a pronounced difference in energy intake as carbohydrate and fat in Experiment 1. Available carbohydrates (cornstarch and sucrose) and fat accounted for about 69 and 8% of ME intake of the rats fed the low-fat diets, respectively, whereas carbohydrates contributed no more than about 22% and fat at least 55% of ME intake in the case of the high-fat diets (Table 1). There was a small difference in ME content between the BT and SF diets due the fact that fat digestibility was significantly lower for the BT diets than for the SF and CT diets (Table 3).

In Experiment 1, in which all diets were fed ad libitum, mean daily ME intake and final live weights were comparable among the rats fed the three high-Zn diets regardless of dietary fat level and fat source. This, however, was not the case among the animals fed the corresponding low-Zn diets. The animals given the low-Zn SF diet displayed the greatest reductions in ME intake (about 30%) and final live weights (about 28%) relative to those consuming the corresponding high-Zn diet

(Table 3). Again in Experiment 2, daily ME intake and final live weights were significantly lower for the rats fed the low-Zn SF diet as compared to the low-Zn BT diet (Table 6). This observation supports a previous study in which marginally Zn-deficient diets enriched with sunflower or olive oil depressed food intake and weight gain of young rats to a greater extent than did low-Zn diets containing equivalent percentages of beef tallow, butterfat or coconut oil [7]. Although it is a common observation that both food intake and growth rate are depressed by dietary Zn deficiency, previous studies have clearly shown that growth retardation cannot be attributed to the lower food or energy intake. Chesters and Quarterman [1] observed that force-feeding Zn-deprived rats a Zn-deficient diet not only failed to alleviate the growth arrest but rapidly induced signs of severe ill-health and morbidity. This finding has been confirmed by later investigators reporting that young rats with an initially normal Zn status cease to tolerate force-feeding of Zn-deficient diets in amounts exceeding voluntary consumption after about 9–11 days [16–18]. These studies demonstrate that a deficit of zinc per se must be responsible for the growth retardation. It is well established that a lack of zinc impairs cell division, differentiation and growth in various species, including microorganisms, plants and vertebrates (see [19] for review).

Zn concentrations in plasma and femur and AP activity in plasma, known to be sensitive indicators of Zn status under experimental conditions, responded markedly to the difference in dietary Zn nutrition in both experiments (Tables 3, 6). In Experiment 1, the rats fed the SF diets had the lowest plasma Zn concentrations at either dietary Zn level. This finding may suggest a decreased intestinal Zn availability as a possible explanation for the lower final live weights of the rats consuming the low-Zn SF diet. In Experiment 2, mean plasma Zn concentration was again lower (12%) in the low-Zn SF than in the low-Zn BT group, but the difference failed to be statistically significant. In addition, femur Zn concentrations and plasma AP activities, which reflect Zn status over a longer period than plasma zinc, were comparable between the low-Zn BT and SF groups in either experiment, and thus argue against the idea that enriching the diets with sunflower oil may have lowered Zn availability and hence growth of the animals.

Regarding the effect of dietary Zn depletion on plasma or serum lipids, the literature data are not uniform. Some authors reported that Zn-deficient rats had decreased triglyceride (TAG) concentrations compared to pair-fed or ad libitum-fed control animals [20, 21], whereas others found that Zn depletion did not significantly alter TAG levels [22–24]. In a series of studies, in which young rats were force-fed Zn-deficient diets containing different fat levels and fat sources, TAG concentrations were increased or remained unaffected relative to values of control rats force-fed equal quantities of the same diets with adequate Zn supply [18, 24, 25]. In our experiments, the difference in dietary Zn supply did not significantly affect plasma TAG concentrations regardless of fat content and fat source (Tables 4, 7). Thus, it does not appear that a moderate Zn deficit plays a primary role in modulating TAG levels in circulating blood. In contrast, fat source significantly influenced plasma TAG concentrations. Proposed mechanisms explaining the lower plasma TAG levels in response to the ingestion of polyunsaturated relative to saturated fats include a decreased rate of lipoprotein secretion [26–29] and an increased lipoprotein clearance from circulation [30, 31]. Gene expression studies provide support for both of these mechanisms (see [32] for a recent review).

The effect of Zn deficiency on plasma or serum cholesterol concentrations has also been found to differ among previous studies. In several investigations, Zn depletion of young rats was associated with lower cholesterol levels [20, 21, 33–35], whereas in others cholesterol values of Zn-depleted rats did not differ from those of pair-fed or ad libitum-fed control animals [22, 23, 36–38]. Young rats force-fed Zn-deficient diets in quantities above those voluntarily consumed by Zn-deprived animals showed rather regularly elevated cholesterol levels compared to animals force-fed equivalent amounts of Zn-adequate diets [19, 25].

In Experiment 1 of our study, plasma total and HDL cholesterol concentrations were also higher in the rats consuming the low-Zn, low-fat diet as compared to the corresponding high-Zn CT diet. In both experiments, however, the rats fed the high-fat diets displayed comparable cholesterol levels regardless of dietary Zn level, fat source and energy intake. This finding agrees with a former study in which serum cholesterol concentrations were comparable among rats fed diets containing 20% fat as beef tallow or sunflower oil [39]. A possible explanation for the lower HDL-cholesterol levels in plasma of the animals given the high-fat diets may be the former observation that activation of the peroxisome proliferator-activated receptor alpha (PPAR α) decreases circulating HDL in rodents [40].

A few former investigations found that dietary Zn depletion did not alter TAG concentrations in the liver of young rats [33, 41], whereas others reported reduced contents compared to animals fed Zn-adequate diets either ad libitum [21, 38] or in restricted amounts [42]. Our experiments indicate that dietary fat content and level of energy intake have a greater impact on liver lipids than a moderate Zn deficit. In Experiment 1, the livers of the animals fed the high-Zn BT and SF diets had significantly higher TAG contents than those given the corresponding low-Zn diets (Table 4), but their energy intake was also significantly higher due to the ad libitum feeding protocol (Table 3). In Experiment 2, in which intake of the high-Zn diets was restricted to the intake of the respective low-Zn diet, the difference in dietary Zn intake did not alter hepatic TAG concentrations. But the rats offered the high-Zn SF diet for ad libitum intake had a markedly higher hepatic TAG content than those consuming the SF diet in lower amounts (about 27%). Data documented by Cunnane [41] also suggest that a difference in food intake of about 20% may be sufficient to affect TAG levels in the liver of growing rats fed diets supplemented with greatly different levels of zinc.

The fat source was a significant factor for hepatic lipid concentrations in both experiments of our study. The SF diet effected substantially higher TAG concentrations in the liver than the BT diet. This agrees with numerous former investigations reporting that diets containing oils rich in unsaturated fatty acids (including sunflower oil among other vegetable oils) increase hepatic TAG concentrations compared to saturated fats [21, 29, 43, 44] or to diets low in fat [45]. Various mechanisms have been proposed for the differences in hepatic TAG concentration. Monsma and Ney [45] reported that the intestinal absorption of the stearate-rich diets was reduced. A reduced fat digestibility was also evident in our study for the BT diet compared to the other diets (as discussed before). The lower digestibility of the beef tallow, however, must be considered insufficient to explain the lower hepatic TAG levels in our experiments for the following reasons. First,

TAG levels of the rats fed the BT diets were comparable to those observed for the rats given the low-fat control diets. Secondly, ME intake per unit weight gain was closely comparable among diets within the same dietary Zn level in both experiments. Finally, other workers demonstrated that PUFA-rich diets reduce the assembly and secretion of VLDL in the liver (see [32, 46] for reviews).

Previous studies, in which low-fat diets were fed to growing rats, showed that dietary Zn depletion of rats does not significantly alter hepatic cholesterol concentrations [21, 33, 47]. The livers of the rats fed the low-fat diets in Experiment 1 of our study also had comparable cholesterol concentrations regardless of the dietary Zn level. This was also true for the high-fat diets in Experiment 2, in which intake of the high-Zn diets was restricted. Therefore, the significant difference in liver cholesterol concentrations between the low-Zn and high-Zn BT and SF groups in Experiment 1 must be attributed to the difference in energy or fat intake. Higher cholesterol concentrations in the liver of young rats in response to an increased dietary fat supply have been observed previously [48, 49]. The rats consuming the SF diets had the highest cholesterol concentrations in both experiments of our study. This effect is consistent with numerous former studies showing higher hepatic cholesterol concentrations in rats fed diets enriched with (15% or more) unsaturated vegetable oils as compared to diets supplemented with saturated fats [44, 48–50]. Increased hepatic cholesterol levels in response to the feeding of diets rich in n-6 PUFA may result from a lower formation and secretion of VLDL as discussed before in the case of hepatic TAG concentrations.

Previous studies with young rats have found that phospholipid (PL) concentrations are barely affected by feeding Zn-deficient diets [18, 41, 47] or by different fat sources [45]. In agreement, the hepatic PL concentrations remained closely comparable in the present study despite substantial differences in zinc, fat and energy intake and dietary fat source. The fatty acid composition of the hepatic PL also reflects a remarkable resistance to the dietary variables, most notable in the similar total percentages of saturated (SFA) across diets. There is no evidence from our data that the conversion of linoleic and α -linolenic acid into longer-chain PUFA might have been impaired by the moderate Zn deficiency, even though linoleic, γ -linolenic (18:3n-6) and docosapentaenoic (20:5n-3) acid were present in significantly higher proportions in the PL of the rats fed the low-Zn diets than in those given the corresponding high-Zn diets. The percentages of arachidonic (20:4n-6) and docosahexaenoic (22:6n-3) acid, the main end products of linoleic and α -linolenic acid, respectively, were closely comparable between the corresponding low- and high-Zn groups. This supports those former studies showing that dietary Zn deficiency per se does not impair the chain

elongation/desaturation pathway of essential fatty acids (see [51] for review).

As expected, the diet enriched with sunflower oil, containing linoleic acid as dominant fatty acid, markedly promoted the incorporation of n-6 PUFA, especially arachidonic acid, into the PL, mostly at the expense of docosahexaenoic acid. A significant effect of the dietary fat level is evident among the SFA. The hepatic PL of the rats fed the low-fat diets contained higher proportions of palmitic than stearic acid. The proportions of these two SFA were reversed in the case of the animals consuming the high-fat diets. Two major reasons may explain this shift. First, hepatic de novo lipogenesis was evidently the major source of palmitic acid in the liver of the CT-fed rats, whereas SFA intake was low. In support, the activity of glucose-6-phosphate dehydrogenase, which belongs to the lipogenic enzyme family and closely correlates with the rate of fatty acid synthesis in the liver [15], was very much higher in the CT groups than in the high-fat groups (Table 3). Secondly, stearic acid was presumably desaturated to oleic acid in the liver of the CT-fed animals to a major extent, since its intake was also low, yet its proportions in the PL fraction approximately as high as those in the high-fat groups, for which oleic acid was available in appreciable amounts from dietary intake.

Conclusion

Taken together, the current study shows that diets highly enriched with either beef tallow or sunflower oil have a quantitatively greater impact on plasma and liver lipid composition than a moderate Zn deficiency. Yet, none of the lipid parameters seems to offer a possible explanation why the marginal Zn supply caused a greater growth retardation when the diet contained sunflower oil instead of beef tallow. Fatty acids certainly were the major energy source in either of these groups. However, in the SF diet over 85% of the fatty acids were unsaturated, mainly linoleic acid, whereas the BT diet contained less unsaturated fatty acids (about 52%). Considering the limited dietary supply of carbohydrates and SFA from the SF diet and the need of SFA in the synthesis of membrane and storage lipids, it is conceivable that the SF-fed rats may have largely relied on PUFA as energy source. Mitochondrial and peroxisomal β -oxidation of unsaturated fatty acids, including linoleic and oleic acid, requires Δ^3, Δ^2 enoyl-CoA isomerase (EC1, EC 5.3.3.8) as key auxiliary enzyme [52, 53]. In the liver of young rats force-fed Zn-deficient diets, mRNA profiling showed that the transcription of genes coding for enzymes of the β -oxidation scheme, including EC1, was markedly reduced compared to Zn-adequate control animals [54, 55]. Further research is needed to

investigate whether and to what extent a moderate Zn deficiency may lead to a reduced ECI activity as a possible explanation of the consistently attenuating effect of diets enriched with sunflower oil on weight gain of weanling rats in the present experiments and in a previous study [7].

Acknowledgments We are grateful for the technical support provided by Dr. Erika Most.

Open Access This article is distributed under the terms of the Creative Commons Attribution Noncommercial License which permits any noncommercial use, distribution, and reproduction in any medium, provided the original author(s) and source are credited.

References

- Chesters JK, Quarterman J (1970) Effects of zinc deficiency on food intake and feeding pattern of rats. *Br J Nutr* 24:1061–1069
- Pallauf J, Kirchgessner M (1971) Experimenteller Zinkmangel bei wachsenden Ratten. *Z Tierphysiol Tierernährg u Futtermittelkde* 28:128–139
- Kramer TR, Priske-Anderson M, Johnson SB, Holman AT (1984) Influence of reduced food intake on polyunsaturated fatty acid metabolism in zinc-deficient rats. *J Nutr* 114:1224–1230
- Bettger WJ, Reeves PG, Moscatelli EA, Reynolds G, O'Dell BL (1979) Interaction of zinc and essential fatty acids in the rat. *J Nutr* 109:480–488
- Bettger WJ, Reeves PG, Moscatelli EA, Savage JE, O'Dell BL (1980) Interaction of zinc and polyunsaturated fatty acids in the chick. *J Nutr* 110:50–58
- Huang YS, Cunnane SC, Horrobin DF, Davignon J (1982) Most biological effects of zinc deficiency corrected by γ -linolenic acid (18:3 ω 6) but not by linoleic acid (18:2 ω 6). *Atherosclerosis* 41:193–207
- Weigand E (2011) Fat source affects growth of weanling rats fed high-fat diets low in zinc. *J Anim Physiol Anim Nutr*. doi:10.1111/j.1439-0396.2010.01114.x
- Boesch-Saadatmandi C, Most E, Weigand E (2007) Influence of dietary fat supplementation on the iron utilization in growing rats. *Ann Nutr Metabol* 51:395–401
- Naumann C, Bassler R (2006) Methodenbuch. Band III: Die chemische Untersuchung von Futtermitteln, 3. Auflage. VDLUFA-Verlag, Darmstadt, Germany
- Blaxter K (1989) Energy metabolism in animals and man. Cambridge University Press, Cambridge, p 34
- Deutsche Gesellschaft für Klinische Chemie (1972) Standardisierung von Methoden zur Bestimmung von Enzymaktivitäten in biologischen Flüssigkeiten. *Z Klin Chem Klin Biochem* 8:658–660
- Lowry OH, Roseborough NJ, Farr AL, Randall RJ (1951) Protein measurements with the Folin phenol reagent. *J Biol Chem* 183:265–273
- Hara A, Radin NS (1978) Lipid extraction of tissues with a low-toxicity solvent. *Anal Biochem* 90:420–426
- Kaluzny MA, Duncan LA, Merrit MV, Epps DE (1985) Rapid separation of lipid classes in high yield and purity using bonded phase columns. *J Lipid Res* 26:135–140
- Salati SM, Amir-Ahmady B (2001) Dietary regulation of expression of glucose-6-phosphate dehydrogenase. *Annu Rev Nutr* 21:121–140
- Flanagan PR (1984) A model to produce pure zinc deficiency in rats and its use to demonstrate that dietary phytate increases the excretion of endogenous zinc. *J Nutr* 114:493–502
- Park JH, Grandjean CJ, Antonson DL, Vanderhoof JA (1986) Effects of isolated zinc deficiency on the composition of skeletal muscle, liver and bone during growth in rats. *J Nutr* 116:610–617
- Eder K, Kirchgessner M (1996) Effects of zinc deficiency on concentrations of lipids in liver and plasma of rats. *Trace Elem Electrolytes* 13:60–65
- Vallee BL, Falchuk KH (1993) The biochemical basis of zinc physiology. *Physiol Rev* 73:79–118
- Koo SI, Williams DA (1981) Relationship between the nutritional status of zinc and cholesterol concentration of serum lipoproteins in adult male rats. *Am J Clin Nutr* 34:2376–2381
- Huang YS, Cunnane SC, Horrobin DF, Davignon J (1982) Most biological effects of zinc deficiency corrected by γ -linolenic acid (18:3 ω 6) but not by linoleic acid (18:2 ω 6). *Atherosclerosis* 41:193–207
- Roth HP, Kirchgessner M (1977) Zum Einfluss von Zinkmangel auf den Fettstoffwechsel. *Int J Vit Nutr Res* 47:277–283
- Schneeman BO, Lacy D, Ney D, Lefevre ML, Keen CL, Lonnerdal B, Hurley LS (1986) Similar effects of zinc deficiency and restricted feeding on plasma lipids and lipoproteins in rats. *J Nutr* 116:1889–1895
- Eder K, Kirchgessner M (1997) Concentrations of lipids in plasma and lipoproteins and oxidative susceptibility of low-density lipoproteins in zinc-deficient rats fed linseed oil or olive oil. *J Nutr Biochem* 8:46–468
- Kettler SI, Eder K, Kirchgessner M (2000) Zinc deficiency and the activities of lipoprotein lipase in plasma and tissues of rats force-fed diets with coconut oil or fish oil. *J Nutr Biochem* 11:132–138
- Engelberg H (1966) Mechanisms involved in the reduction of serum triglycerides in man upon adding unsaturated fats to the normal diet. *Metabolism* 15:796–807
- Chait A, Onitiri A, Nicoll A, Rabaya E, Davies J, Lewis B (1974) Reduction of serum triglyceride levels by polyunsaturated fat. Studies on the mode of action and on very low density lipoprotein composition. *Atherosclerosis* 20:347–364
- Shimomura Y, Tamura T, Suzuki M (1990) Less body fat accumulation in rats fed a safflower oil diet than in rats fed a beef tallow diet. *J Nutr* 120:1291–1296
- Lai HC, Lasekan JB, Yang H, Clayton MK, Ney DM (1991) In vivo determination of triglyceride secretion using radioactive glycerol in rats fed different dietary saturated fats. *Lipids* 26:824–830
- Green MH, Massaro ER, Green JB (1984) Multicompartmental analysis of the effects of dietary fat saturation and cholesterol on absorptive lipoprotein metabolism in the rat. *Am J Clin Nutr* 40:82–94
- Groat PHE, de Boer BCJ, Haddeman E, Houtsmuller UMT, Hülsmann WC (1988) Effect of dietary fat composition on the metabolism of triacylglycerol-rich plasma lipoproteins in the postprandial phase in meal-fed rats. *J Lipid Res* 29:541–551
- Rakhshandehroo M, Knoch B, Müller M, Kersten S (2010) Peroxisome proliferator-activated receptor alpha target genes. *PPAR Res* 2010:1–20. Article ID 612089. doi:10.1155/2010/612089
- Patel PB, Chung RA, Lu JY (1975) Effect of zinc deficiency on serum and liver cholesterol in the female rat. *Nutr Rep Int* 12:205–210
- Frimpong NA, Magee AC (1981) Effects of dietary copper and zinc on serum lipid parameters of young male rats. *Nutr Rep Int* 35:551–559
- Koo SI, Lee CC (1988) Compositional changes in plasma high-density lipoprotein particles in marginally zinc-deficient male rats. *Am J Clin Nutr* 47:909–919
- Quarterman J, Florence E (1972) Observations on glucose tolerance and plasma levels of free fatty acids and insulin in the zinc-deficient rat. *Br J Nutr* 28:75–79

37. Koo SI, Henderson DA, Algilani K, Norvell JE (1985) Effect of marginal zinc deficiency on the morphological characteristics of intestinal nascent chylomicrons and distribution of soluble apoproteins of chylomicrons. *Am J Clin Nutr* 42:671–680
38. Lefevre M, Keen CL, Lönnerdal B, Hurley LS, Schneeman BO (1985) different effects of zinc and copper deficiency on composition of plasma high density lipoproteins in rats. *J Nutr* 115:359–368
39. Portillo MP, Chavarri M, Duran D, Rodriguez VM, Macarulla MT (2001) Differential effects of diets that provide different lipid sources on hepatic lipogenic activities in rats under ad libitum or restricted feeding. *Nutrition* 17:467–473
40. Vu-Dac N, Chopin-Delannoy S, Gervois P et al (1998) The nuclear receptor peroxisome proliferator-activated receptors α and Rev-erb α mediate the species specific regulation of apolipoprotein A-I expression by fibrates. *J Biol Chem* 273:25713–25720
41. Cunnane SC (1988) Evidence that adverse effects of zinc deficiency on essential fatty acid composition in rats are independent of food intake. *Br J Nutr* 59:273–278
42. Fogerty AC, Ford GL, Dreosti IE, Tinsley IJ (1985) Zinc deficiency and fatty acid composition of tissue lipids. *Nutr Rep Int* 32:1009–1019
43. Monsma CC, Ney DM (1993) Interrelationship of stearic acid content and triacylglycerol composition of lard, beef tallow and cocoa butter in rats. *Lipids* 28:539–547
44. Monsma CC, Gallaher DD, Ney DM (1996) Reduced digestibility of beef tallow and cocoa butter affects bile acid excretion and reduces hepatic esterified cholesterol in rats. *J Nutr* 126:2028–2035
45. Rustan AC, Christiansen EN, Drevon CA (1992) Serum lipids, hepatic glycerolipid metabolism and peroxisomal fatty acid oxidation in rats fed omega-3 and omega-6 fatty acids. *Biochem J* 283:333–339
46. Kersten S (2008) Peroxisome proliferator activated receptors and lipoprotein metabolism. *PPAR Res* 2008. Article ID 132960. doi: [10.1155/2008/132960](https://doi.org/10.1155/2008/132960)
47. Clejan S, Maddaiah VT, Castro-Magana M, Collipp PJ (1981) Zinc deficiency induced changes in the composition of microsomal membranes and in the enzymatic regulation of glycerolipid synthesis. *Lipids* 16:454–460
48. Reiser R, Williams MC, Sorrels MF, Murty NL (1963) Biosynthesis of fatty acids and cholesterol as related to diet fat. *Arch Biochem Biophys* 102:276–285
49. Wiggers KD, Richard MJ, Stewart JW, Jacobson NL, Berger PJ (1977) Type and amount of dietary fat affect relative concentration of cholesterol in blood and other tissues of rats. *Atherosclerosis* 27:27–34
50. Kellog TF (1974) Steroid balance and tissue cholesterol accumulation in germfree and conventional rats fed diets containing saturated and polyunsaturated fats. *J Lipid Res* 15:574–579
51. Eder K, Kirchgessner M (1996) Dietary zinc deficiency and fatty acid metabolism in rats. *Nutr Res* 16:1179–1189
52. Gurvitz A, Wabnegger L, Yagi AI, Binder M, Hartig A, Ruis H, Hamilton B, Dawes IW, Hiltunen JK, Rottensteiner H (1999) Function of human mitochondrial 2,4-dienoyl-CoA reductase and rat monofunctional Δ^3 - Δ^2 -enoyl-CoA isomerase in β -oxidation of unsaturated fatty acids. *Biochem J* 344:903–914
53. Janssen U, Stoffel W (2002) Disruption of mitochondrial β -oxidation of unsaturated fatty acids in the 3, 2-trans-enoyl-CoA isomerase-deficient mouse. *J Biol Chem* 277:19579–19584
54. Tom Dieck H, Döring F, Roth HP, Daniel H (2003) Changes in rat hepatic gene expression in response to zinc deficiency as assessed by DNA arrays. *J Nutr* 133:1004–1010
55. Tom Dieck H, Döring F, Fuchs D, Roth HP, Daniel H (2005) Transcriptome and proteome analysis identifies the pathways that increase hepatic lipid accumulation in zinc-deficient rats. *J Nutr* 135:199–205

Characterization of Secretory Phospholipase A₂ with Phospholipase A₁ Activity in Tobacco, *Nicotiana tabacum* (L.)

Yukichi Fujikawa · Ritsuko Fujikawa ·
Noriaki Iijima · Muneharu Esaka

Received: 2 September 2011 / Accepted: 7 November 2011 / Published online: 29 November 2011
© AOCS 2011

Abstract A cDNA encoding protein with homology to plant secretory phospholipase A₂ (sPLA₂), denoted as Nt1 PLA₂, was isolated from tobacco (*Nicotiana tabacum*). The cDNA encodes a mature protein of 118 amino acid residues with a putative signal peptide of 29 residues. The mature form of Nt1 PLA₂ has 12 cysteines, Ca²⁺ binding loop and catalytic site domain that are commonly conserved in plant sPLA₂s. The recombinant Nt1 PLA₂ was expressed as a fusion protein with thioredoxin in *E. coli* BL21 cells and was purified by an ion exchange chromatography after digestion of the fusion proteins by Factor Xa protease to obtain the mature form. Interestingly, Nt1 PLA₂ could hydrolyze the ester bond at the *sn*-1 position of glycerophospholipids as well as at the *sn*-2 position, when the activities were determined using mixed-micellar phospholipids with sodium cholate. Both activities for the *sn*-1 and -2 positions of glycerophospholipids required Ca²⁺ essentially, and maximal activities were found in an alkaline region when phosphatidylcholine, phosphatidylglycerol or phosphatidylethanolamine was used as a substrate. The level of Nt1 PLA₂ mRNA was detected at a higher level in tobacco flowers than stem, leaves and roots, and was induced by salicylic acid.

Keywords cDNA cloning · Phospholipid · *Nicotiana tabacum* · Phospholipase

Abbreviations

AGPC	Acid guanidinium thiocyanate-phenol–chloroform
PLA	Phospholipase A
POPC	1-Palmitoyl-2-oleoyl- <i>sn</i> -glycero-3-phosphocholine
POPE	1-Palmitoyl-2-oleoyl- <i>sn</i> -glycero-3-phosphoethanolamine
POPG	1-Palmitoyl-2-oleoyl- <i>sn</i> -glycero-3-phosphoglycerol
RACE	Rapid amplification of cDNA ends
RT	Reverse-transcription

Introduction

Phospholipase A₂ (phosphatide 2-acylhydrolase, EC 3.1.1.4, PLA₂) catalyzes the hydrolysis of the *sn*-2 fatty acyl ester bond of glycerophospholipids, liberating free fatty acids and lysophospholipids. PLA₂ comprises a large family with multiple isoforms exhibiting different structure and catalytic properties [1]. In plant, PLA₂s have been proposed to involve in seed germination [2], cell division and growth [3], wounding response [4] and auxin signal [5]. One of the plant PLA₂ groups is constituted of secretory enzyme (sPLA₂) with a low molecular mass. The sPLA₂s have been purified from elm (*Ulmus glabra*) [6] and partially purified from rice (*Oryza sativa*) [7]. The cDNA clones of sPLA₂s from rice [7], carnation (*Dianthus caryophyllus* L. cv. *Degio*) [8], *Arabidopsis* (*Arabidopsis thaliana*) [9–11], tobacco (*Nicotiana tabacum*) [12] and citrus (*Citrus sinensis*) [13] are also isolated. Plant sPLA₂s have been classified to two groups, group XIA and XIB,

Y. Fujikawa and R. Fujikawa contributed equally to this work.

Electronic supplementary material The online version of this article (doi:10.1007/s11745-011-3632-3) contains supplementary material, which is available to authorized users.

Y. Fujikawa · R. Fujikawa · N. Iijima · M. Esaka (✉)
Graduate School of Biosphere Science, Hiroshima University,
Higashi-Hiroshima, Hiroshima 739-8528, Japan
e-mail: mesaka@hiroshima-u.ac.jp

based on their primary structures [14]. The gene expression analysis of the plant sPLA₂s has shown that the expression levels of carnation and citrus sPLA₂ mRNAs were induced during flower development [8] and by light [13], respectively. In *Arabidopsis*, four genes of sPLA₂(AtsPLA₂) denoting AtsPLA₂- α , - β , - γ and - δ , exist in its genome and are found to be a functional enzyme [15]. AtsPLA₂- β and - γ transcripts were detected in flower at a higher level than the other tissues [10, 11], and the gene suppression of AtsPLA₂- β , - γ and - δ simultaneously is caused sterility with less pollen germination [16], indicating that AtsPLA₂s play a role in the process of reproduction. From the analysis of the transgenic plants suppressing and overexpressing AtsPLA₂s, AtsPLA₂- β was found to be involved in cell elongation by mediating auxin, shoot gravitropism [10], and stomatal movement [17]. On the other hand, AtsPLA₂- α is negatively regulated during the hypersensitive response of plants resistant to microbial pathogens [18] and is involved in PIN-FORMED protein trafficking [19]. Although the information concerning plant sPLA₂ has now been accumulated, the physiological functions of plant sPLA₂ remain to be elucidated.

In our previous study [12], we found high PLA₂ activities in tobacco flower and cloned a cDNA encoding a sPLA₂ with homology to plant group XIB sPLA₂, denoted Nt PLA₂ (renamed Nt2 PLA₂ in this study). Furthermore, we have reported that another sPLA₂ is expressed in tobacco flower. In this study, we newly isolated a cDNA encoding a sPLA₂ with homology to that of group XIA PLA₂ from tobacco flower, and investigated enzymatic characteristics of recombinant mature enzyme, using mixed-micellar phospholipid substrate with sodium cholate. We also investigated the mRNA expression pattern in tobacco tissues and the influence of plant hormones on the mRNA expression of tobacco sPLA₂s.

Materials and Methods

Materials

1-Palmitoyl-2-oleoyl-*sn*-glycero-3-phosphocholine (POPC), 1-palmitoyl-2-oleoyl-*sn*-glycero-3-phosphoethanolamine (POPE), and 1-palmitoyl-2-oleoyl-*sn*-glycero-3-phosphoglycerol (POPG) were purchased from Avanti Polar Lipids, Inc. (Birmingham, AL, USA). 9-Anthryldiazomethane and sodium cholate were obtained from Funakoshi Co., Ltd. (Tokyo, Japan). POROS HS/M cation-exchange column (4.6 × 100 mm) and cosmosil 5C18 column were obtained from Perseptive Biosystems (Framingham, MA, USA) and Nacalai Tesque (Kyoto, Japan), respectively. The Silver Staining II Kit was purchased from Wako Pure Chemicals (Osaka, Japan), Factor Xa

proteinase was purchased from Promega (Madison WI, USA) and pET32a and *E. coli* BL21 (DE3) were obtained from Novagen (Madison, WI, USA). The DC Protein assay kit was obtained from Bio-Rad Laboratories (Hercules, CA).

Tobacco Culture

Tobacco BY-2 cells (*Nicotiana tabacum* cv. Bright Yellow 2) were cultured on Linsmaier and Skoog's medium containing 2.5 mM KH₂PO₄, 3 mM thiamin-HCl, 3%(w/v) sucrose and 1 μM 2,4-dichlorophenoxyacetic acid (2,4-D) solidified with 0.8% (w/v) agar at 28 °C in the dark for 3 days. To test the effects of plant hormones on PLA activities (PLA₁ and PLA₂ activities) and mRNA expression levels of Nt1 and Nt2 PLA₂s, the BY-2 cells were cultured on the above medium excluding 2,4-D with or without 50 μM salicylic acid, 20 μM 3-indoleacetic acid or 1.8 μM 2,4-D, at 28 °C in the dark for 24 h.

Tobacco Plant

Tobacco (*Nicotiana tabacum* L. cv. SR-1) plants were grown at 28 °C in light/dark (16/8 h) in the green house.

Preparation of Crude Extract from Tobacco Tissues or BY-2 Cells

Tobacco tissues and BY-2 cells were homogenized in the extraction buffer (20 mM Tris-HCl, pH 8.0, 1 M KCl, 2 mM EDTA, and 2 mM PMSF) and centrifuged at 10000×g for 10 min. The resulting supernatant was used as a crude extract for determination of PLA activities (PLA₁ and PLA₂ activities) and protein concentration.

Standard Assay for PLA Activity and Determination of Protein Concentration

PLA activities were assayed as described previously [12]. The standard incubation system (100 μL) for the assay of PLA activities contains 2 mM POPC, 8 mM sodium cholate, 100 mM NaCl, 10 mM CaCl₂, and 50 mM Tris-HCl (pH 8.0). The reaction was carried out at 37 °C for 60 min. Palmitic acid released by PLA₁ and oleic acids released by PLA₂ action were labeled with 9-anthryldiazomethane, and the derivatized fatty acids were detected by a reverse-phase HPLC with a spectrofluorometer. One unit (U) was defined as the liberation of 1 μmol free fatty acid (free palmitic acid released from the *sn*-1 position of glycerophospholipid for PLA₁ activity or free oleic acid released from the *sn*-2 position of glycerophospholipid for PLA₂ activity) per min. Each experiment was performed two times, and the results presented were the means.

Ca²⁺-dependent PLA activities in the tissue and BY-2 extracts, were determined by subtracting the activities assayed with 20 mM EDTA showing Ca²⁺-independent PLA activity, from those with 10 mM CaCl₂ including both Ca²⁺-independent and -dependent PLA activities.

Protein concentration was measured with DC Protein assay kit using bovine serum albumin as a standard.

RT (Reverse-Transcription)-PCR

Total RNA was isolated from tobacco flowers with the acid guanidinium thiocyanate–phenol–chloroform (AGPC) method as described previously [12]. Total RNA (3 µg) was reverse-transcribed by using PowerScript Reverse Transcriptase (BD Biosciences Clontech, Tokyo, Japan) and oligo-dT primer. The primers used in this study are shown in Supplemental Table 1. Primers, T1a and T1b, were designed according to the partial amino acid sequences, Ile62–Gly68 and Gly73–Cys81 of the putative tomato sPLA₂ (GeneBank Accession No. BG127198), respectively. PCR was carried out for 40 cycles of 30 s at 95 °C for denaturation, 30 s at 58 °C for annealing and 60 s at 72 °C for polymerization, with ExTaq DNA polymerase (Takara Bio, Shiga, Japan) using T1a and P1 as forward and reverse primers, respectively. An aliquot of the primary PCR products was used in secondary PCR with T1b and P2 as forward and reverse primers, respectively. The secondary PCR was carried out under the same conditions to the primary PCR. The PCR product was subcloned into the pGEM-T Easy vector (Promega, Madison, WI) and used to transform into *E. coli* XL-1 Blue cells. After selecting positive clones according to the manufacturer's protocol, plasmid DNAs were purified from positive clones with the QIAprep Spin Miniprep Kit (Qiagen, Tokyo, Japan). The nucleotide sequence was determined by the ABI 373A sequencer (Applied Biosystems, USA) using the DYEnamic ET Terminator Cycle Sequencing Kit (Amersham Biosciences Corp, Piscataway, NJ), according to the manufacturer's protocol.

5'-RACE (Rapid Amplification of cDNA Ends)-PCR

5' Rapid amplification of the cDNA ends (5'-RACE) was performed essentially as described previously [12]. An adaptor-ligated double-stranded cDNA was synthesized using the Marathon cDNA Amplification Kit (BD Biosciences Clontech) according to the manufacturer's instruction. From the determined nucleotide sequence of the internal cDNA, new primers, 5T1a and 5T2b (complementary to nt 393–417 and nt 426–450 in GeneBank Accession No. AB190177, respectively), were designed for 5'-RACE. PCR was carried out for 40 cycles of 30 s at 94 °C, 30 s at 58 °C and 60 s at 72 °C with AP1 and 5T1a

as forward and reverse primers, respectively. An aliquot of the primary PCR product was used in secondary PCR with AP2 and 5T1b as forward and reverse primers, respectively. PCR was carried out for 40 cycles of 30 s at 95 °C, 30 s at 63 °C and 60 s at 72 °C. A unique band obtained by the RACE was subcloned into the pGEM-T Easy vector as described above.

Expression and Purification of Recombinant Nt1 PLA₂

A sense primer that contains restriction enzyme sites and nucleotide sequence for a factor Xa cleavage site (Ile-Glu-Gly-Arg) adjacent to the N-terminal residue of mature protein of Nt1 PLA₂, and antisense primer are shown in Supplemental Table 1. A PCR fragment encoding for a factor Xa cleavage site followed by mature Nt1 PLA₂ was prepared with ExTaq DNA polymerase, and subcloned into pGEM-T Easy vector as described above. The insert was subcloned into an expression vector pET32a encoded thioredoxin (Trx), and the resulting plasmid transformed *E. coli* BL21 (DE3). For recombinant protein preparation, 4 mL of overnight culture was inoculated at 30 °C in 400 mL of LB medium containing 1% tryptone peptone, 0.5% yeast extract, 0.5% NaCl and 50 µg/mL ampicillin. When the absorbance at 600 nm of the cultures reached 0.5, the recombinant proteins were expressed by induction with 0.1 mM IPTG for 3 h at 30 °C. Cells were harvested at 3000×g for 5 min and frozen at –20 °C. The cells were resuspended in 15 mL of 20 mM Tris–HCl (pH 8.0) containing 2 mM EDTA. The cells were lysed by adding 6 mL of 1 M NaOH and neutralized with 1 M HCl. The lysate was centrifuged at 8000×g for 30 min at 4 °C, and the resulting cell extract was dialyzed against 2 L of 20 mM Tris–HCl (pH 7.0). The dialysate was digested with Factor Xa proteinase for 90 min at 37 °C (the ratio of Factor Xa to protein was 1:1,000, w/w), and loaded on POROS HS/M column at a flow rate of 2 ml/min, which had been equilibrated with 20 mM MES–NaOH (pH 6.0). The protein was eluted with a linear gradient of NaCl. The active fractions were pooled and stored at –40 °C.

SDS-PAGE

SDS-PAGE was carried out as described previously [12] by using a 16% polyacrylamide gel in the presence of 2-mercaptoethanol, and the proteins were visualized with the Coomassie brilliant blue staining.

RNA Extraction and Quantitative RT-PCR

Total RNA was isolated from the tobacco tissues such as flowers, leaves, stems and roots, and BY-2 cells by the AGPC method as described above and treated with DNase

I (Takara, Tokyo, Japan). 500 ng of total RNA was reverse-transcribed by using PowerScript Reverse Transcriptase and oligo-dT primer. Quantitation of mRNAs for Nt1 and Nt2 PLA₂s and actin as an internal reference gene (GeneBank Accession No. AB190177) was performed using Chromo4 System for Real-Time PCR Detection (Bio-Rad, Hercules, CA) according to the manufacturer's instructions. Forward and reverse primers are shown in Supplemental Table 1, Nt1 PLA₂ (identical to nt 50–67 and complementary to nt 148–160 in GeneBank Accession No. AB190177, respectively); Nt2 PLA₂ (identical to nt 78–95 and complementary to nt 180–190 in GeneBank Accession No. AB190178, respectively); Actin as an internal reference (identical to nt 933–952 and complementary to nt 1100–1119 in GeneBank Accession No. AB158612, respectively). PCR amplification was initiated by denaturation at 95 °C for 15 s and annealing at 55 °C for 30 s, and then by extension at 72 °C for 30 s. Fluorescence was acquired during extension using an excitation wavelength of 470 nm and emission detection at 530 nm. A melting-curve analysis was carried out by continuously monitoring fluorescence between 55 and 95 °C with 0.5 °C increments every 10 s. Threshold values (Ct) were set manually in each experiment to correspond to the early exponential phase of amplification, and Opticon monitor program provided with the system was used to determine the cycle at which the threshold was attained. The level of each transcript levels was determined from standard curves generated using each known concentration of PCR product amplified with each specific primer set. Normalization was done by dividing the transcript levels of Nt1 and Nt2 PLA₂s by those of the actin. The reaction products were electrophoresed on a 1% agarose gel for checking a single amplifying band. All reactions were performed triplicate.

Results

Isolation of cDNA Clone for Nt1 PLA₂

Primers for PCR were designed based on the amino acid sequence of the putative tomato sPLA₂. RT-PCR was performed with total RNA prepared from tobacco flowers. A partial cDNA fragment was isolated, and the nucleotide sequence of the cDNA showed a significant homology to that of tomato sPLA₂. Using a RACE method, the full-length cDNA sequence was determined. The cDNA clone has a 441 bp open reading frame that encodes 147 amino acids. The protein encoded in the cDNA was named Nt1 PLA₂. Therefore, another tobacco PLA₂ encoded in a cDNA isolated previously [12], was named Nt2 PLA₂ in this report. The nucleotide sequence of Nt1 PLA₂ cDNA was registered in GeneBank under an Accession Number

AB190177. The calculated molecular mass and pI value of Nt1 PLA₂ were 16,195 Da and 8.24, respectively. The hydrophathy profile suggests that the N-terminal amino acid sequence of Nt1 PLA₂ includes a signal sequence as well as that of Nt2 PLA₂. From the analysis of the amino acid sequence by Signal P program [20], Nt1 PLA₂ contains 29 residue of a potential signal sequence preceding the mature enzyme. An alignment of the amino acid sequence of Nt1 PLA₂ with the sequences of various plant and animal sPLA₂s is shown in Fig. 1. The amino acid sequence of Nt1 PLA₂ showed 31% homology to that of Nt2 PLA₂ (showed in the lower far right of Fig. 1). The Ca²⁺ binding loop (Tyr84–Gly94) and the catalytic domain (Pro100–Asp112) were highly conserved in Nt1 PLA₂. In addition, Nt1 PLA₂ contains 12 Cys residues in the mature protein. The positions of Cys residues in the mature protein are well conserved among the plant sPLA₂s. Nt1 PLA₂ has the sequences, KLEEL, at the C-terminus, which is similar to the endoplasmic reticulum retention sequence (KDEL) [21]. A phylogenetic tree was derived from an alignment of the amino acid sequences between plant and animal sPLA₂s, using the CLSUTAL W program [22] and Tree view [23] (Supplemental Fig. 1). This tree shows that Nt1 and Nt2 PLA₂s are placed in the branch of the plant sPLA₂s, but are separated into two subgroups, XIA and XIB PLA₂s. The group XIA PLA₂ contains tobacco Nt1 PLA₂, three *Arabidopsis* PLA₂s (AtsPLA₂-β, -γ and -δ) and rice Rice-I PLA₂, while the group XIB PLA₂ contains tobacco Nt2 PLA₂, carnation PLA₂, elm PLA₂, *Arabidopsis* AtsPLA₂-α, and rice Rice-II PLA₂. Therefore, Nt1 PLA₂ was suggested to be group XIA PLA₂, which maybe localized in the endoplasmic reticulum.

Expression, Purification and Characterization of Recombinant Nt1 PLA₂

Nt1 PLA₂ was expressed by *E. coli* BL21 cells using pET32a as a fusion protein with thioredoxin having the factor Xa cleavage site adjacent to the N-terminal residue of mature Nt1 PLA₂. The fusion protein digested with Factor Xa protease was applied to a POROS HS/M column. As the PLA₂ activity was detected only in the peak indicated in supplemental Fig. 2a, the peak was pooled as the purified Nt1 PLA₂ to yield a final enzyme preparation. SDS-PAGE analysis showed that Nt1 PLA₂ could be purified as a single protein band (Supplemental Fig. 2b). The purified recombinant Nt1 PLA₂ was used for analyzing the enzymatic properties. Some studies for enzymatic properties of *Arabidopsis* AtsPLA₂s showed that the premature form containing the signal peptide had lower enzymatic activities than that of the mature form [9–11]. Therefore, the mature form of Nt1 PLA₂ was prepared for enzymatic assay. PLA activity was determined using

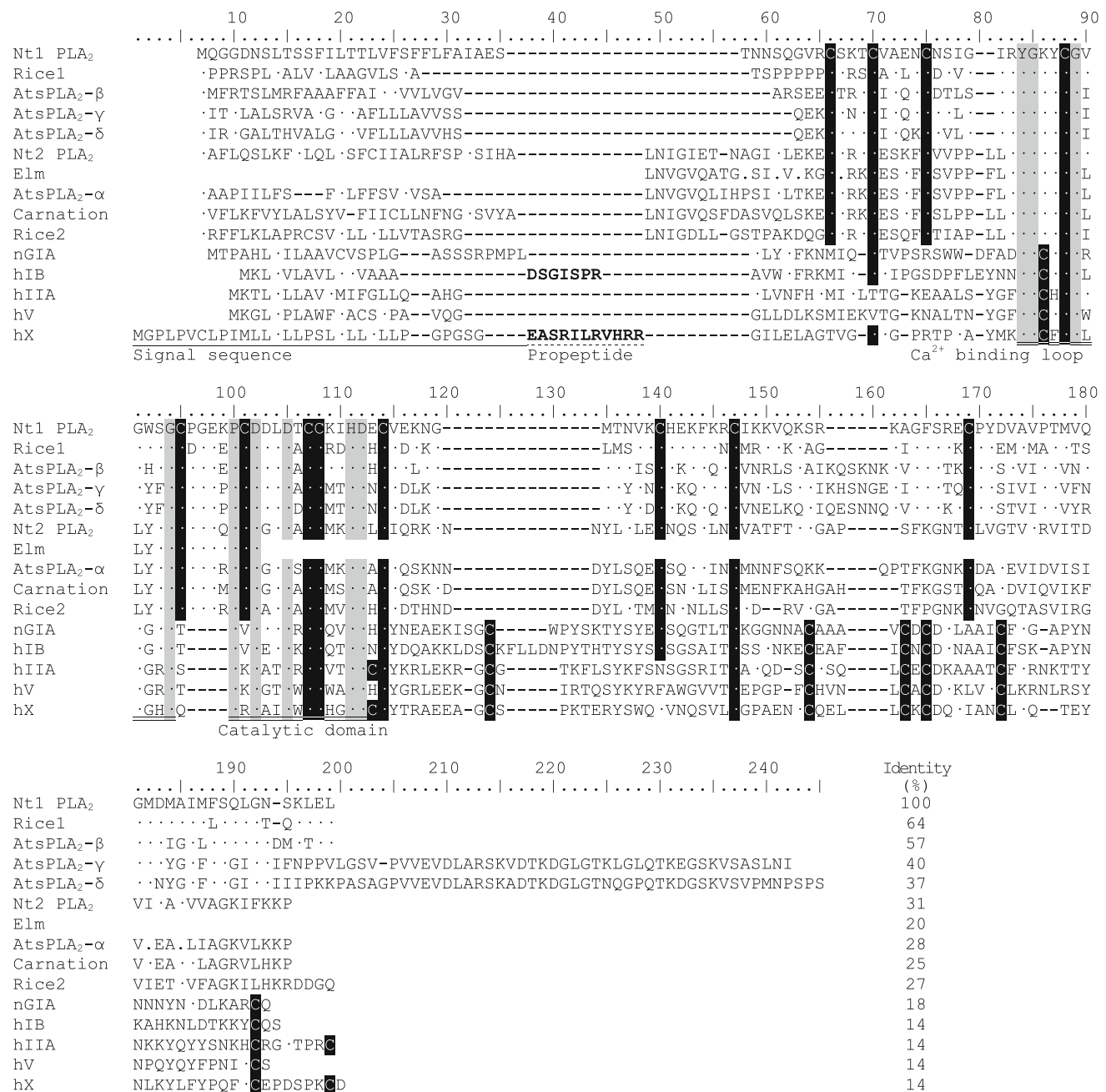


Fig. 1 Alignment of amino acid sequences of tobacco Nt1 PLA₂ with other plant and animal sPLA₂s. The N-terminal signal sequences were predicted by the SignalP program. Propeptide is shown in **bold**. Dots indicate the conserved amino acid residues identical to those of Nt1 PLA₂. Sequence identities (%) of plant and animal sPLA₂ with Nt1 PLA₂ are indicated in the lower far right of the table. Nt1 PLA₂, tobacco Nt1 PLA₂ (this study, Acc. No. AB190177); Rice1, rice Rice-I PLA₂ (Acc. No. AJ238116); AtsPLA₂-β, *Arabidopsis* sPLA₂-β (Acc. No. AF541915); AtsPLA₂-δ, *Arabidopsis* sPLA₂-δ (Acc. No.

AY148347); AtsPLA₂-γ, *Arabidopsis* sPLA₂-γ (Acc. No. AY148346); Nt2 PLA₂, tobacco Nt2 PLA₂ (Acc. No. AB190178); Elm, Elm PLA₂; AtsPLA₂-α, *Arabidopsis* sPLA₂-α (Acc. No. AAC69277); Carnation, Carnation PLA₂ (Acc. No. AF064732); Rice2, rice Rice-II PLA₂ (Acc. No. AJ238117); nGIA, *Naja naja atra* group IA sPLA₂ (Acc. No. CAA54802); hIB, human group IB sPLA₂ (Acc. No. NP_000928); hIIA, human group IIA sPLA₂ (Acc. No. NP_000291); hV, human group V sPLA₂ (Acc. No. NP_000920); hX, human group X sPLA₂ (Acc. No. NP_003552)

mixed-micellar phospholipids with sodium cholate. Nt1 PLA₂ could hydrolyze both palmityl ester bonds at the *sn*-1 and oleoyl-ester bonds at *sn*-2 positions in phosphatidylcholine, respectively, while Nt2 PLA₂ was only at the *sn*-2

position (Fig. 2). Therefore, the PLA₁ activity of Nt1 PLA₂ was determined as the liberation of free palmitic acid, and PLA₂ activity was done as that of free oleic acid in this study. Effects of pH and concentrations of Ca²⁺ and

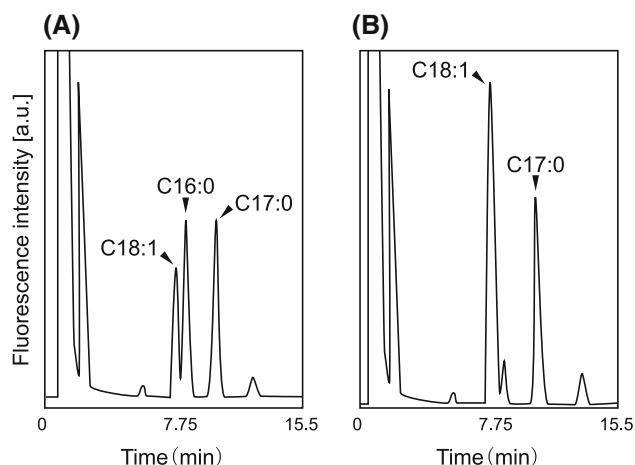


Fig. 2 Elution profile of the derivatized fatty acids on a reverse-phase HPLC. The reaction mixture with Nt1 PLA₂ (a) or Nt2 PLA₂ (b) using POPC as a substrate was applied a Cosmosil 5C18 column, which was pre-equilibrated with acetonitrile. The elution of the fatty acids derivatized with 9-anthryldiazomethane was followed by monitoring with a spectrofluorometer. C18:1; oleic acid, C16:0; palmitic acid, C17:0; *n*-heptadecanoic acid

sodium cholate on the activities of Nt1 PLA₂ toward phospholipids containing three head groups (POPC, POPG and POPE) are shown in Fig. 3. The activities of Nt1 PLA₂ for POPE were increased with increasing pH, while the maximal activities for POPC and POPG were found in pH 8–10 and in pH 8, respectively (Fig. 3a, b, c). The activities of Nt1 PLA₂ toward all three phospholipids were not detected in the presence of 1 mM EDTA (Fig. 3d, e, f). The activities of Nt1 PLA₂ toward the phospholipids were observed in the presence of Ca²⁺, and maximal activities were detected above 1 mM Ca²⁺ (Fig. 3d, e, f). Although the activities of Nt1 PLA₂s toward the phospholipids were not detected in the absence of sodium cholate, it was greatly increased by the addition of sodium cholate. The maximal activities of Nt1 PLA₂ were found at 20 mM sodium cholate (cholate/phospholipids molar ratio of 10) (Fig. 3g, h, i).

Distribution of PLA Activity, and Expression of Nt1 PLA₂ and Nt2PLA₂ mRNA in Tobacco Tissues

The crude extracts and total RNA were prepared from flowers, stems, leaves and roots of tobacco. PLA activities (PLA₁ and PLA₂ activities) in the extract were measured using the mixed-micellar POPC substrate with sodium cholate. As the Nt1 PLA₂ (Fig. 3) as well as Nt2 PLA₂ [12] required essentially millimolar concentration of Ca²⁺ for the optimal enzyme activities (Fig. 3), Ca²⁺ dependent PLA activities in the extract were determined as described in the materials and methods sections. As shown in Fig. 4a, both Ca²⁺ dependent PLA₁ and PLA₂ activities were extremely high in the flowers, followed by the root and

stem, but it was hardly detected in the leaf. To investigate the expression levels of Nt1 and Nt2 PLA₂ mRNAs in tobacco tissues, quantitative RT-PCR using the Chromo4 System (Bio-Rad) was performed with specific primers for Nt1 and Nt2 PLA₂s and actin. The each reaction product amplified with their specific primers was shown as a single band on an agarose gel electrophoresis (data not shown). In addition, each PCR product had a single melting temperature (data not shown). These results showed that all PCR reaction specifically amplified the cDNAs of Nt1 and Nt2 PLA₂s and actin in the PCR conditions. As shown in Fig. 4b, the expression level of Nt1 PLA₂ mRNA was higher in the flower than in the other tissues. Although the expression levels of Nt1 PLA₂ mRNA were 13- to 22-fold lower than those of Nt2 PLA₂ mRNA in tobacco tissues, the patterns of both mRNA expressions in tobacco tissues were similar with each other.

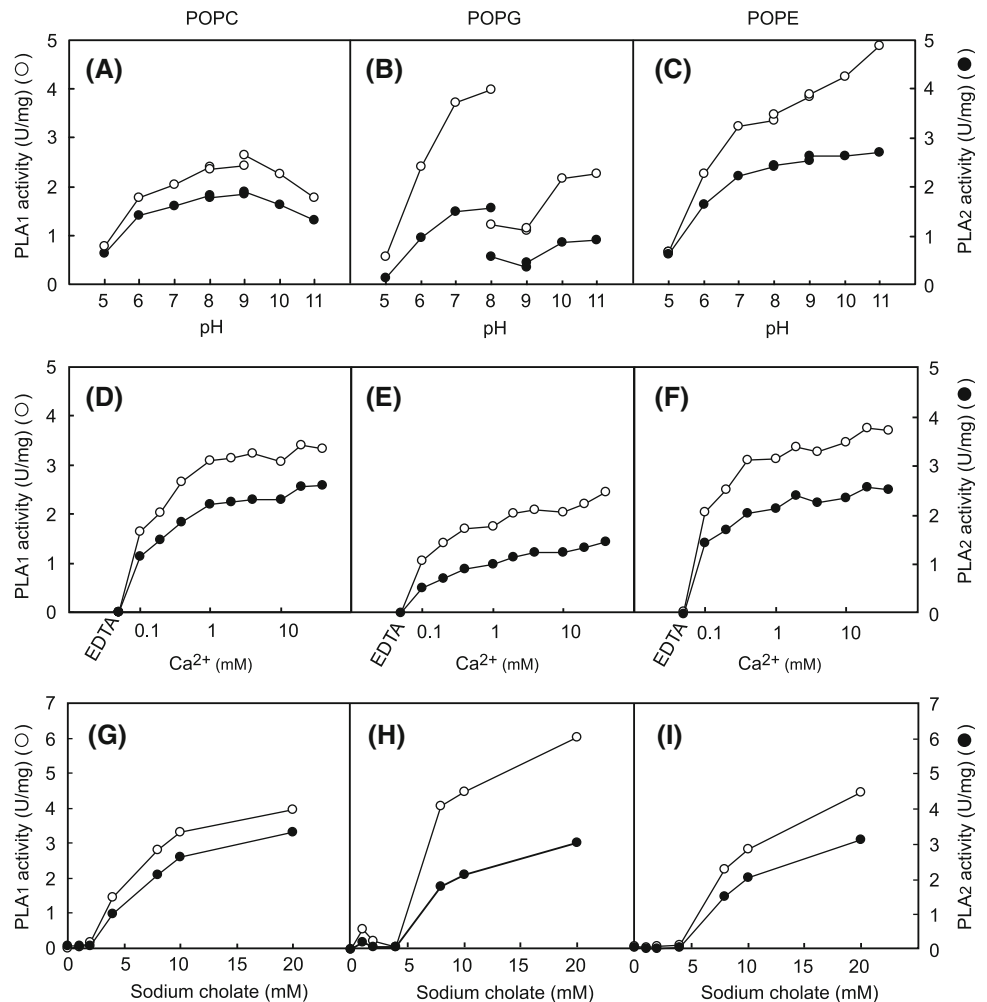
Effect of the Plant Hormones on the PLA Activities and Expression of Nt1 PLA₂ and Nt2 PLA₂ mRNA in Tobacco BY-2 Cells

As shown in Fig. 5a, both Ca²⁺ dependent PLA activities in tobacco BY-2 cells were increased by treatment by plant hormones, salicylic acid (SA), 3-indoleacetic acid (3-IAA) and 2,4-dichlorophenoxyacetic acid (2,4-D). In the meanwhile, the expression level of Nt1 PLA₂ mRNA was higher in BY-2 cells treated by SA, but not by 3-IAA and 2,4-D, than that in the mock-treated cells, whereas Nt2 PLA₂ mRNA levels were decreased in all hormone treated cells (Fig. 5b).

Discussion

We had previously cloned a cDNA for Nt2 PLA₂ named in this report, showing a high homology to plant group XIB sPLA₂s [12]. In this study, we isolated a cDNA encoding a novel sPLA₂, denoted as Nt1 PLA₂. The primary structure of Nt1 PLA₂ revealed that it belongs to group XIA PLA₂ including three *Arabidopsis* (AtsPLA₂-β, -γ, and -δ) and rice (Rice1) sPLA₂s. Similarly to the other plant sPLA₂s, the N-terminus of Nt1 PLA₂ was suggested to have a signal sequence. There are some reports about the subcellular localization of *Arabidopsis* sPLA₂s (AtsPLA₂) with the analysis of fluorescence protein fused to portion of AtsPLA₂s. The N-terminal regions of AtsPLA₂s appear to function as a signal sequence for the secretion of protein [10, 11]. Nt1 PLA₂ is presumably processed between Ser29 and Thr30 by a signal peptidase at the endoplasmic reticulum (ER). However, the existence of an ER retention signal had been predicted at the C-terminus of AtsPLA₂-β, and it was recently reported that AtsPLA₂-β may be

Fig. 3 Effects of pH (a–c), Ca^{2+} (d–f) and sodium cholate (g–i) on the activities of purified recombinant tobacco Nt1 PLA₂ for various phospholipids, POPC (a, d, g), POPG (b, e, h) and POPE (c, f, i). a–c The reaction mixtures containing purified Nt1 PLA₂, 2 mM phospholipid, 6 mM sodium cholate, 100 mM NaCl, and 5 mM CaCl_2 were incubated for 60 min at 37 °C in a total volume of 100 μL . The buffers used were 50 mM Tris-maleate buffer at pH 5, 6, 7 and 8, 50 mM Tris-HCl at pH 8 and 9, and 50 mM glycine-NaOH at pH 9, 10 and 11 d–f The reaction mixtures containing purified Nt1 PLA₂, 2 mM phospholipid, 6 mM sodium cholate, 100 mM NaCl, 50 mM Tris-HCl (pH 8.0), and 1 mM EDTA or 0–40 mM CaCl_2 were incubated. g–i The reaction mixtures containing purified Nt1 PLA₂, 2 mM phospholipid, 100 mM NaCl, 50 mM Tris-HCl (pH 8.0), and various concentrations of sodium cholate. PLA₁ (open circle) and PLA₂ (closed circle) activities were measured as described in “Materials and Methods”



localized to the ER of guard cells [17]. As Nt1 PLA₂ has an ER retention-like sequence (KLELE shown in Fig. 1) at the C-terminus as well as *Arabidopsis* sPLA₂(AtsPLA₂- β), Nt1 PLA₂ is assumed to retain in the ER after processing its signal sequence by signal peptidase at the ER membrane. On the other hand, Nt2 PLA₂ is suggested to secrete into the intercellular space, because it has no ER retention like-sequence at its C-terminus. Thus, it is possible that Nt1 and Nt2 PLA₂s are localized at different subcellular organelles in tobacco tissues. The mature form of Nt1 PLA₂ has structural characteristics similar to those of other plant sPLA₂s, such as 12 Cys residues, the Ca^{2+} binding loop, and the catalytic domain. The gene of Nt1 PLA₂ encodes a functional enzyme in tobacco, because recombinant Nt1 PLA₂ is able to hydrolyze mixed-micellar phospholipid substrates. Although Nt1 PLA₂ requires Ca^{2+} for the enzyme activity as well as the other plant sPLA₂s, it is very interesting to note that Nt1 PLA₂ can hydrolyze the ester bond at the *sn*-1 position of glycerophospholipids, as well as at the *sn*-2 position. The elm and *Arabidopsis* sPLA₂s can hydrolyze only at the *sn*-2 position of

glycerophospholipids. The enzymatic characteristics of rice sPLA₂ (Rice1), which showed the highest similarity (64%) to Nt1 PLA₂, have not been investigated. High molecular mass PLA₂, patatin-like PLA₂, has both PLA₁ and PLA₂ activities [24]. However, there is no report that low molecular mass sPLA₂s have both PLA₁ and PLA₂ activities. From the similarity of the primary structures of plant sPLA₂ in the region involved in catalytic reaction, His110 of Nt1 PLA₂ (Fig. 1) is suggested to be an active site in catalysis [25]. However, because there is little information on the enzymatic characteristics of plant sPLA₂ in contrast to that of animal sPLA₂, it is difficult to explain the detailed mechanism to hydrolyze the ester bonds at both *sn*-1 and *sn*-2 positions of glycerophospholipids by Nt1 PLA₂.

The gene expression analysis of tobacco sPLA₂ to speculate on its physiological functions revealed that both Nt1 and Nt2 PLA₂ mRNAs were highly expressed in the flowers, followed by stems, roots and leaves. In carnation and *Arabidopsis*, the gene expression of sPLA₂ was induced during flower development [8, 16], suggesting that

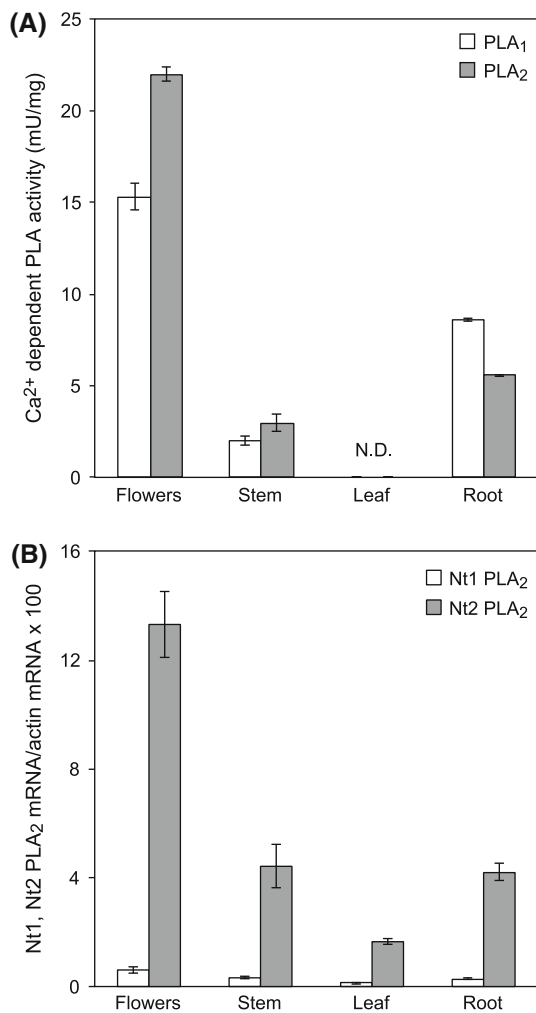


Fig. 4 Distribution of PLA activity (**a**), and expression (**b**) of Nt1 PLA₂ and Nt2 PLA₂ mRNA in the various tissues of tobacco. **a** The reaction mixture consisted of 50 mM Tris-HCl (pH 8.0), 2 mM 1-palmitoyl-2-oleoyl-sn-glycero-3-phosphocholine, 8 mM sodium cholate, 10 mM CaCl₂, 0.1 M NaCl in a final volume of 0.1 mL. Data were obtained in duplicate. Ca²⁺ dependent PLA₁ (open bar) and PLA₂ (closed bar) activities were determined as the activities subtracted from those of the activities from the activity assayed with 20 mM EDTA in place of 10 mM CaCl₂. ND not detected. **b** Quantitative RT-PCR analysis for expression of Nt1 PLA₂ (open bar) and Nt2 PLA₂ (closed bar) mRNA in the tobacco tissue was performed as described in “Materials and Methods”. Data were obtained in triplicate

plant sPLA₂s play important roles in flower tissues. Besides higher gene expression levels of Nt1 PLA₂ in flowers, Nt1 PLA₂ mRNA level in tobacco BY-2 cells was dramatically increased with treatment with salicylic acid (SA) [26] known as a defense signal factor by pathogen attack. Plant phospholipase is suggested to release fatty acid from membrane phospholipids for the biosynthesis of oxylipin in response to environmental stress [3, 27]. Recently, AtsPLA₂- α was demonstrated to interact with the *Arabidopsis* transcription factor, AtMYB-30, in the nucleus of the cells

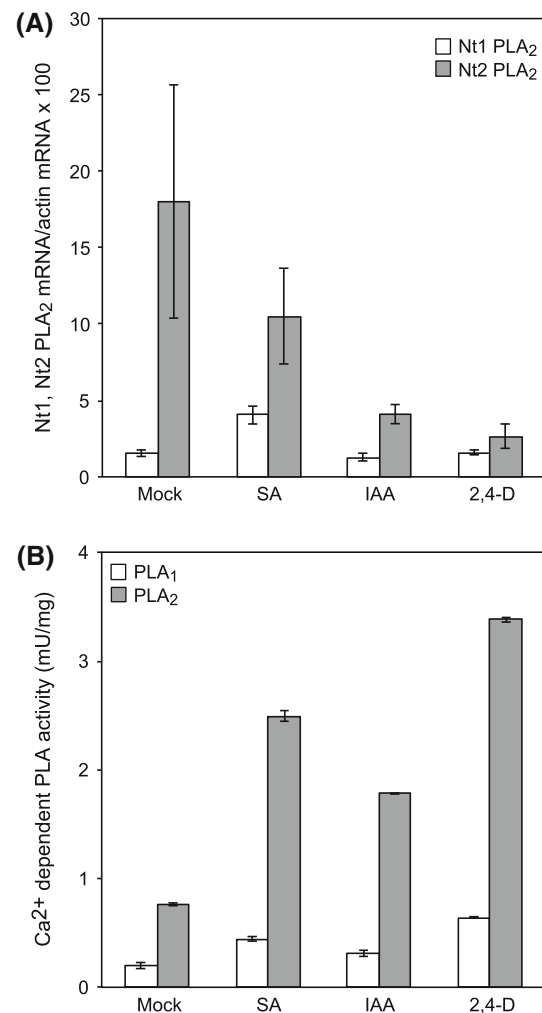


Fig. 5 Effect of various hormones, SA, IAA and 2,4-D, on PLA₁ and PLA₂ activities (**a**) and expression (**b**) of Nt1 PLA₂ and Nt2 PLA₂ mRNA in tobacco BY-2 cells. **a** PLA₁ (open bar) and PLA₂ (closed bar) activities in the crude extract were measured as described in the legend of Fig. 4. **b** Nt1 PLA₂ (open bar) and Nt2 PLA₂ (closed bar) mRNA in tobacco BY-2 cells were analyzed by quantitative RT-PCR as described in the “Materials and methods” section

adjacent to those infected by the pathogen. This indicates that AtsPLA₂- α inhibits the binding of AtMYB-30 to DNA to activate the transcription of the plant defense genes causing programmed cell death (hypersensitive response) [18]. Although the physiological function of plant sPLA₂ remains unclear at present, Nt1 PLA₂ has a possibility to be involved in the SA-related plant defense response. On the other hand, the mRNA expression levels of Nt1 PLA₂ and Nt2 PLA₂ in BY-2 cells were not increased by auxin, but Ca²⁺ dependent PLA₂ activities were increased by auxin. In *Arabidopsis*, gene expression of low molecular mass sPLA₂, AtsPLA₂- β and patatin-related high molecular mass PLA₂, AtPLA IIA, was induced by auxin [10, 28]. In the *Arabidopsis* genome, there are 4 and 10 members of low molecular mass and patatin-related high molecular

mass PLA₂s, respectively [15, 29]. So far, three PLA₂ isozymes with high molecular mass (about 46 kDa) in tobacco leaves have been reported [30]. Therefore, a marked increase in Ca²⁺-dependent PLA₂ activity should be due to the induction of the gene expression of other PLA₂ isozymes, except Nt1 and Nt2 PLA₂s, in auxin-treated tobacco cells.

In this study, a cDNA clone for a novel low molecular mass PLA₂ was isolated from tobacco flowers. The primary structures of Nt1 and Nt2 PLA₂s suggest that they are differentially localized in tobacco cells. Our results hypothesize that Nt1 and Nt2 PLA₂s play some role in flower tissues and multiple PLA₂ isozymes have some role in lipid signaling for SA and auxin responses in the tobacco plant. To resolve the above question, the gene expression in response to plant hormone treatment and pathogen attack will provide valuable information on the cellular function of Nt1 and Nt2 PLA₂s in tobacco tissues. Furthermore, transgenic plants over expressing or suppressing these PLA₂s will also provide powerful tools for investigating physiological roles of Nt1 and Nt2 PLA₂s in tobacco.

References

- Schaloske RH, Dennis EA (2006) The phospholipase A₂ superfamily and its group numbering system. *Biochim Biophys Acta* 1761(11):1246–1259
- May C, Preisig-Muller R, Hohne M, Gnau P, Kindl H (1998) A phospholipase A₂ is transiently synthesized during seed germination and localized to lipid bodies. *Biochim Biophys Acta* 1393(2–3):267–276
- Chapman KD (1998) Phospholipase activity during plant growth and development and in response to environmental stress. *Trends Plant Sci* 3(11):419–426
- Narvaez-Vasquez J, Florin-Christensen J, Ryan CA (1999) Positional specificity of a phospholipase A activity induced by wounding, systemin, and oligosaccharide elicitors in tomato leaves. *Plant Cell* 11(11):2249–2260
- Scherer GF (2002) Secondary messengers and phospholipase A₂ in auxin signal transduction. *Plant Mol Biol* 49(3–4):357–372
- Stahl U, Ek B, Stymne S (1998) Purification and characterization of a low-molecular-weight phospholipase A₂ from developing seeds of elm. *Plant Physiol* 117(1):197–205
- Stahl U, Lee M, Sjobahl S, Archer D, Cellini F, Ek B, Iannaccone R, MacKenzie D, Semeraro L, Tramontano E, Stymne S (1999) Plant low-molecular-weight phospholipase A₂s (PLA₂s) are structurally related to the animal secretory PLA₂s and are present as a family of isoforms in rice (*Oryza sativa*). *Plant Mol Biol* 41(4):481–490
- Kim JY, Chung YS, Ok SH, Lee SG, Chung WI, Kim IY, Shin JS (1999) Characterization of the full-length sequences of phospholipase A₂ induced during flower development. *Biochim Biophys Acta* 1489(2–3):389–392
- Ryu SB, Lee HY, Doelling JH, Palta JP (2005) Characterization of a cDNA encoding *Arabidopsis* secretory phospholipase A₂-alpha, an enzyme that generates bioactive lysophospholipids and free fatty acids. *Biochim Biophys Acta* 1736(2):144–151
- Lee HY, Bahn SC, Kang YM, Lee KH, Kim HJ, Noh EK, Palta JP, Shin JS, Ryu SB (2003) Secretory low molecular weight phospholipase A₂ plays important roles in cell elongation and shoot gravitropism in *Arabidopsis*. *Plant Cell* 15(9):1990–2002
- Bahn SC, Lee HY, Kim HJ, Ryu SB, Shin JS (2003) Characterization of *Arabidopsis* secretory phospholipase A₂-γ cDNA and its enzymatic properties. *FEBS Lett* 553(1–2):113–118
- Fujikawa R, Fujikawa Y, Iijima N, Esaka M (2005) Molecular cloning, expression, and characterization of secretory phospholipase A₂ in tobacco. *Lipids* 40(9):901–908
- Liao HL, Burns JK (2010) Light controls phospholipase A₂ α and β gene expression in *Citrus sinensis*. *J Exp Bot* 61(9):2469–2478
- Six DA, Dennis EA (2000) The expanding superfamily of phospholipase A₂ enzymes: classification and characterization. *Biochim Biophys Acta* 1488(1–2):1–19
- Lee HY, Bahn SC, Shin JS, Hwang I, Back K, Doelling JH, Ryu SB (2005) Multiple forms of secretory phospholipase A₂ in plants. *Prog Lipid Res* 44(1):52–67
- Kim HJ, Ok SH, Bahn SC, Jang J, Oh SA, Park SK, Twell D, Ryu SB, Shin JS (2011) Endoplasmic reticulum- and Golgi-localized phospholipase A₂ plays critical roles in *Arabidopsis* pollen development and germination. *Plant Cell* 23(1):94–110
- Seo J, Lee HY, Choi H, Choi Y, Lee Y, Kim YW, Ryu SB (2008) Phospholipase A₂β mediates light-induced stomatal opening in *Arabidopsis*. *J Exp Bot* 59(13):3587–3594
- Froidure S, Canonne J, Daniel X, Jauneau A, Briere C, Roby D, Rivas S (2010) AtsPLA₂-α nuclear relocalization by the *Arabidopsis* transcription factor AtMYB30 leads to repression of the plant defense response. *Proc Natl Acad Sci USA* 107(34):15281–15286
- Lee OR, Kim SJ, Kim HJ, Hong JK, Ryu SB, Lee SH, Ganguly A, Cho HT (2010) Phospholipase A₂ is required for PIN-FORMED protein trafficking to the plasma membrane in the *Arabidopsis* root. *Plant Cell* 22(6):1812–1825
- Nielsen H, Brunak S, von Heijne G (1999) Machine learning approaches for the prediction of signal peptides and other protein sorting signals. *Protein Eng* 12(1):3–9
- Gomord V, Faye L (1996) Signals and mechanisms involved in intracellular transport of secreted proteins in plants. *Plant Physiol Biochem* 34(2):165–181
- Thompson JD, Higgins DG, Gibson TJ (1994) CLUSTAL W: improving the sensitivity of progressive multiple sequence alignment through sequence weighting, position-specific gap penalties and weight matrix choice. *Nucleic Acids Res* 22(22):4673–4680
- Page RD (1996) TreeView: an application to display phylogenetic trees on personal computers. *Comput Appl Biosci* 12(4):357–358
- Senda K, Yoshioka H, Doke N, Kawakita K (1996) A cytosolic phospholipase A₂ from potato tissues appears to be patatin. *Plant Cell Physiol* 37(3):347–353
- Mansfeld J, Gebauer S, Dathe K, Ulbrich-Hofmann R (2006) Secretory phospholipase A₂ from *Arabidopsis thaliana*: insights into the three-dimensional structure and the amino acids involved in catalysis. *Biochemistry* 45(18):5687–5694
- Klessig DF, Durner J, Noad R, Navarre DA, Wendehenne D, Kumar D, Zhou JM, Shah J, Zhang S, Kachroo P, Trifa Y, Pontier D, Lam E, Silva H (2000) Nitric oxide and salicylic acid signaling in plant defense. *Proc Natl Acad Sci USA* 97(16):8849–8855
- Scherer GF, Ryu SB, Wang X, Matos AR, Heitz T (2010) Patatin-related phospholipase A: nomenclature, subfamilies and functions in plants. *Trends Plant Sci* 15(12):693–700
- Rietz S, Holk A, Scherer GF (2004) Expression of the patatin-related phospholipase A gene AtPLA IIA in *Arabidopsis thaliana*

- is up-regulated by salicylic acid, wounding, ethylene, and iron and phosphate deficiency. *Planta* 219(5):743–753
29. Holk A, Rietz S, Zahn M, Quader H, Scherer GF (2002) Molecular identification of cytosolic, patatin-related phospholipases A from *Arabidopsis* with potential functions in plant signal transduction. *Plant Physiol* 130:90–101
30. Dhondt S, Geoffroy P, Stelmach BA, Legrand M, Heitz T (2000) Soluble phospholipase A₂ activity is induced before oxylipin accumulation in tobacco mosaic virus-infected tobacco leaves and is contributed by patatin-like enzymes. *Plant J* 23(4):431–440

The Production of Conjugated α -Linolenic, γ -Linolenic and Stearidonic Acids by Strains of Bifidobacteria and Propionibacteria

Alan A. Hennessy · Eoin Barrett · R. Paul Ross ·
Gerald F. Fitzgerald · Rosaleen Devery ·
Catherine Stanton

Received: 22 June 2011 / Accepted: 15 November 2011 / Published online: 10 December 2011
© AOCS 2011

Abstract Conjugated fatty acids are regularly found in nature and have a history of biogenic activity in animals and humans. A number of these conjugated fatty acids are microbially produced and have been associated with potent anti-carcinogenic, anti-adipogenic, anti-atherosclerotic and anti-diabetogenic activities. Therefore, the identification of novel conjugated fatty acids is highly desirable. In this study, strains of bifidobacteria and propionibacteria previously shown by us and others to display linoleic acid isomerase activity were assessed for their ability to conjugate a range of other unsaturated fatty acids during fermentation. Only four, linoleic, α -linolenic, γ -linolenic and stearidonic acids, were converted to their respective conjugated isomers, conjugated linoleic acid (CLA), conjugated α -linolenic acid (CLNA), conjugated γ -linolenic acid (CGLA) and conjugated stearidonic acid (CSA), each of which contained a conjugated double bond at the 9,11 position. Of the strains assayed, *Bifidobacterium breve* DPC6330 proved the most effective conjugated fatty acid producer, bio-converting 70% of the linoleic acid to CLA, 90% of the α -linolenic acid to CLNA, 17% of the γ -linolenic acid to CGLA, and 28% of the stearidonic acid to CSA at a substrate concentration of 0.3 mg mL⁻¹. In conclusion, strains of bifidobacteria and propionibacteria can bio-convert linoleic, α -linolenic,

γ -linolenic and stearidonic acids to their conjugated isomers via the activity of the enzyme linoleic acid isomerase. These conjugated fatty acids may offer the combined health promoting properties of conjugated fatty acids such as CLA and CLNA, along with those of the unsaturated fatty acids from which they are formed.

Keywords Bifidobacteria · Propionibacteria · CLA · α -Linolenic acid · γ -Linolenic acid · Stearidonic acid

Abbreviations

CGLA	Conjugated γ -linolenic acid
CLA	Conjugated linoleic acid
CLNA	Conjugated α -linolenic acid
CSA	Conjugated stearidonic acid
DAD	Diode array detector
DMOX	4,4-Dimethyloxazoline
EPA	Eicosapentaenoic acid
FAME	Fatty acid methyl esters
FID	Flame ionization detector
MRS	DeMan-Rogosa-Sharpe
GLC	Gas liquid chromatography
GLC-MS	Gas liquid chromatography mass spectrometry
GIT	Gastrointestinal tract
MTAD	4-Methyl-1,2,4-triazoline-3,5-dione
PUFA	Polyunsaturated fatty acids
RP-HPLC	Reverse phase high performance liquid chromatography

A. A. Hennessy · E. Barrett · R. Paul Ross · C. Stanton (✉)
Teagasc Food Research Centre, Moorepark, Fermoy, Co.,
Cork, Ireland
e-mail: catherine.stanton@teagasc.ie

A. A. Hennessy · R. Devery
National Institute for Cellular Biotechnology,
Dublin City University, Dublin, Ireland

E. Barrett · R. Paul Ross · G. F. Fitzgerald · C. Stanton
Alimentary Pharmabiotic Centre, BSI, University College Cork,
Cork, Ireland

Introduction

Conjugated fatty acids are the positional and geometric isomers of several polyunsaturated fatty acids (PUFA) with

one or more conjugated double bonds. These conjugated isomers are commonly found in nature, being detected in the milkfat and tallow of ruminant animals [1, 2], plant seed oils [3–6] and marine algae [7–10]. In addition, conjugated fatty acids may be formed chemically via the alkaline isomerisation of unsaturated fatty acids [11, 12]. Of these natural and synthetic fatty acids, the conjugated linoleic acid (CLA) isomers are the best characterised. These fatty acids have been demonstrated to exhibit a range of potentially health-promoting properties, including anti-atherosclerotic, anti-obesogenic and anti-diabetogenic activities; however, it is the anti-carcinogenic properties which are most extensively reported [13, 14]. In addition to CLA isomers, other conjugated fatty acids have been shown to exhibit biological activities with relevance to human health. Indeed, naturally occurring CLNA isomers traditionally found in plant seed oils and in ruminant fats have been reported to exhibit anti-carcinogenic and anti-obese activities [15–18]. Other synthetically produced conjugated isomers, such as conjugated eicosadienoic acids (C20:2) and conjugated eicosatrienoic acids (C20:3) have been associated with body fat reduction and increased lean mass [12]. Conjugated eicosapentaenoic acids (C20:5) have been reported to exhibit anti-carcinogenic activity, and conjugated docosahexaenoic acids (C22:6) to exert anti-carcinogenic and anti-adipogenic activity [11, 19–22]. The mechanisms of action of conjugated fatty acids are reported to be either via competitive inhibition during the metabolism of proinflammatory n-6 fatty acids to eicosanoids, via increased cellular lipid peroxidation, or at the genetic level via their impact on the expression of cell cycle arrest regulators, transcription factors, and key metabolic enzymes (for reviews see [13, 14, 17]). Given the extent and significance of the health promoting biological activities associated with conjugated fatty acids, economic strategies for their production are highly desirable.

The potency of conjugated fatty acids has prompted increased research into their identification and economic production [23, 24]. These investigations have highlighted in particular the ability of a range of microbes to produce CLA [25, 26]. Indeed, it has been reported that dairy propionibacteria and intestinally isolated bifidobacteria possess the ability to conjugate the *c*9,*c*12 double bond of linoleic acid (C18:2) yielding the *c*9,*t*11-C18:2 and *t*9,*t*11-C18:2 CLA isomers, via the action of the enzyme linoleic acid isomerase [27–29]. Furthermore, recent *in vitro* evidence has highlighted the ability of strains of bifidobacteria to produce the *c*9,*t*11,*c*15-C18:3 CLNA isomer from free α -linolenic acid, and of *Lactobacillus plantarum* AKU 1009a to produce conjugated γ -linolenic acid (CGLA) from free γ -linolenic acid [16, 30]. These observations demonstrate the potential of CLA producing bacteria to conjugate a range of PUFA. Similar to CLA, the ability of

propionibacteria and bifidobacteria to produce novel conjugated fatty acids may be used to enrich milk and yoghurt with conjugated fatty acids through fermentation, or the establishment of microbiota in the human gastrointestinal tract (GIT) capable of producing these fatty acids *in situ*. Indeed, further credence is given to this theory in light of the recent evidence pertaining to the *ex vivo* production of CLA by intestinally isolated strains of lactobacilli and bifidobacteria reported by Ewaschuk et al. [31] and our studies on *in vivo* production of CLA by bifidobacteria from dietary linoleic acid in mice [32].

The aims of this study were (1) to assess the ability of strains of bifidobacteria and propionibacteria previously shown by us to conjugate linoleic acid to CLA to bioconvert a range of PUFA during fermentation [27–29, 33], and (2) to identify and characterise any novel microbially produced conjugated fatty acids.

Materials and Methods

Bacterial Strains and Fatty Acid Substrates

The strains of *Bifidobacterium* and *Propionibacterium* used in this study are listed in Table 1, and were selected based on their ability to bioconvert linoleic acid (*c*9,*c*12-C18:2) to the *c*9,*t*11 CLA isomer [27–29]. All strains were grown in DeMan-Rogosa-Sharpe (MRS) medium (Difco, Detroit, MI, USA) containing 0.05 mg mL⁻¹ L-cysteine hydrochloride (Sigma Aldrich., St Louis, MO, USA) (cys-MRS) under anaerobic conditions (Anaerocult A Gas Packs (78% N₂, 18% CO₂, 4% Other), Merck, Darmstadt, Germany) at 37 °C for 18 h. Where solid media was required, 1.5% (wt/vol) bacteriological agar (Oxoid, Basingstoke, Hampshire, UK) was added to the cys-MRS medium. Cell counts were determined by serial dilutions and plating using cys-MRS agar.

All fatty acid substrates were of the highest purity (Table 2) and were delivered to the growth medium in the form of a 30 mg mL⁻¹ stock solution containing 2% (wt/vol) Tween 80 (Merck-Schuchardt, Hohenbrunn, Germany). To ensure sterility, all substrates were filter sterilized through a 0.45 μ m Ministart filter (Sartorius AG, Goettingen, Germany).

Microbial Conjugated Fatty Acid Production

A 4% (vol/vol) inoculum of the activated culture was added to 10 mL cys-MRS medium containing 0.45 mg mL⁻¹ [exceptions being 0.15 mg mL⁻¹ for eicosapentaenoic acid (EPA), and stearidonic acid] of the respective unsaturated fatty acid substrates and incubated anaerobically (Anaerocult A, Merck) at 37 °C (bifidobacteria) or 30 °C

Table 1 Strains of *Bifidobacterium* and *Propionibacterium*

Strain	Source	References
<i>Bifidobacterium</i>		
<i>Bifidobacterium breve</i> NCIMB 702258	Infant intestine	[27]
<i>Bifidobacterium breve</i> NCIMB 8807	Nursling stools	[27]
<i>Bifidobacterium breve</i> DPC6330	<i>C. difficile</i> (+) subject	[29]
<i>Bifidobacterium breve</i> DPC6331	<i>C. difficile</i> (+) subject	[29]
<i>Bifidobacterium longum</i> DPC6315	Healthy adult	[29]
<i>Bifidobacterium longum</i> DPC6320	<i>C. difficile</i> (+) subject	[29]
<i>Propionibacterium</i>		
<i>Propionibacterium freudenreichii</i> subsp. <i>shermanii</i> JS	Dairy starter	[28]
<i>Propionibacterium freudenreichii</i> subsp. <i>shermanii</i> 9093	Dairy starter	[28]
<i>Propionibacterium freudenreichii</i> subsp. <i>freudenreichii</i> Propioni-6	Dairy starter	[28]
<i>Propionibacterium freudenreichii</i> subsp. <i>freudenreichii</i> ATCC 6207	Dairy starter	[28]

Table 2 Fatty acid substrates

Name	Chemical formula	Source	Purity (%)
Linoleic acid	(C18:2- <i>c</i> 9, <i>c</i> 12)	Sigma Aldrich, St Louis, MO	99
α -Linolenic acid	(C18:3- <i>c</i> 9, <i>c</i> 12, <i>c</i> 15)	Sigma Aldrich, St Louis, MO	99
γ -Linolenic acid	(C18:3- <i>c</i> 6, <i>c</i> 9, <i>c</i> 12)	Nu-Chek Prep, Elysian, MN	99
Stearidonic acid	(C18:4- <i>c</i> 6, <i>c</i> 9, <i>c</i> 12, <i>c</i> 15)	Cayman Europe, Tallinn, Estonia	98
Nonadecadienoic acid	(C19:2- <i>c</i> 10, <i>c</i> 13)	Nu-Chek Prep, Elysian, MN	99
Eicosadienoic acid	(C20:2- <i>c</i> 11, <i>c</i> 14)	Nu-Chek Prep, Elysian, MN	99
Eicosatrienoic acid	(C20:3- <i>c</i> 11, <i>c</i> 14, <i>c</i> 17)	Nu-Chek Prep, Elysian, MN	99
Homo- γ linolenic	(C20:3- <i>c</i> 8, <i>c</i> 11, <i>c</i> 14)	Nu-Chek Prep, Elysian, MN	99
Arachidonic acid	(C20:4- <i>c</i> 5, <i>c</i> 8, <i>c</i> 11, <i>c</i> 14)	Nu-Chek Prep, Elysian, MN	99
Eicosapentaenoic acid	(C20:5- <i>c</i> 5, <i>c</i> 8, <i>c</i> 11, <i>c</i> 14, <i>c</i> 17)	Nu-Chek Prep, Elysian, MN	99
Heneicosadienoic acid	(C21:2- <i>c</i> 12, <i>c</i> 15)	Nu-Chek Prep, Elysian, MN	99
Docosadienoic acid	(C22:2- <i>c</i> 13, <i>c</i> 16)	Nu-Chek Prep, Elysian, MN	99
Docosatrienoic acid	(C22:3- <i>c</i> 13, <i>c</i> 16, <i>c</i> 19)	Nu-Chek Prep, Elysian, MN	99
Docosatetraenoic acid	(C22:4- <i>c</i> 7, <i>c</i> 10, <i>c</i> 13, <i>c</i> 16)	Nu-Chek Prep, Elysian, MN	99
Docosapentaenoic acid	(C22:5- <i>c</i> 7, <i>c</i> 10, <i>c</i> 13, <i>c</i> 16, <i>c</i> 19)	Nu-Chek Prep, Elysian, MN	99
Docosahexaenoic acid	(C22:6- <i>c</i> 4, <i>c</i> 7, <i>c</i> 10, <i>c</i> 13, <i>c</i> 16, <i>c</i> 19)	Nu-Chek Prep, Elysian, MN	99

(propionibacteria) for 72 h with regular spectrophotometric monitoring of conjugate production (6, 12, 24, 48, and 72 h) [29]. Fatty acids were extracted from 4 mL of the fermentation medium using 2 mL of 2-propanol (Fisher Scientific Ltd, Dublin, Ireland) and 4 mL of *n*-hexane (Fisher Scientific Ltd), as described by Coakley et al. [27]. Following extraction, the *n*-hexane was removed by heating under N₂, and the extracted fatty acids converted to fatty acid methyl esters (FAME) by acid catalyzed methylation with 12 mL of 4% (vol/vol) methanolic-HCl for 10 min under nitrogen at ambient temperature, followed by extraction with 4 mL *n*-hexane. Gas liquid chromatography (GLC) was used to separate FAME using a CP-SELECT CB column (100 m × 0.25 mm id × 0.25 μm film thickness, Varian BV, Middelburgh, The Netherlands) and Varian 3400 Capillary GC (Varian, Walnut Creek, CA, USA) fitted with a flame ionization detector (FID) as described by Coakley

et al. [27]. The presence of a conjugated double bond was confirmed spectrophotometrically, using a modification of the method of Barrett et al. [29] using FAME rather than free fatty acids. Briefly, 200 μl of the methylated sample, prepared as described above, was dispensed into a UV transparent 96 well plate (Costar, Corning NY) and the absorbance of UV light at a wavelength of 234 nm measured using a 96 well plate spectrophotometer (GENios Plus, Medford, MA). All experiments were performed in triplicate. Conjugated fatty acid production was expressed as mg mL⁻¹ and percentage bioconversion, the latter calculated by:

$$Cc/Sc \times 100 = \% \text{ bioconversion}$$

Sc = Substrate concentration prior to fermentation.

Cc = Conjugated fatty acid concentration following fermentation

Purification and Identification of Microbially Produced Conjugated Fatty Acids

Total fatty acids extracted using the method of Coakley et al. [27] were partially concentrated using a rotary evaporator (<50 °C) (Buchi Rotavapor R-210) and washed once with 0.88% (wt/vol) KCl and twice with water/methanol (1:1, vol/vol). The hexane was then evaporated by heating at 45 °C under a steady flow of nitrogen. The remaining lipid was resuspended at a concentration of 100 mg mL⁻¹ in acetonitrile/acetate (100:0.14, vol/vol), and stored at -20 °C under nitrogen until use. The conjugated fatty acids were isolated using RP-HPLC on a Luna 5 μ C18 (2) 100A preparative column (250 mm \times 21.20 mm) (Phenomenex, Macclesfield, Cheshire, UK) and the Varian Prostar HPLC system (Varian). The mobile phase used to obtain optimal separation was acetonitrile/water/acetate (70:30:0.12, vol/vol) at a flow rate of 10 mL min⁻¹. Conjugated fatty acids were detected using a diode array detector (DAD) at an absorbance of 234 nm. Fractions containing the conjugated fatty acids were collected and pooled. Following removal of the acetonitrile from the pooled fractions by rotary evaporation (<50 °C), the conjugated fatty acids were re-extracted as described above. Fatty acid compositions of the pure oils were confirmed by GLC as previously described [27]. Conjugated fatty acids were identified by Mylnefield Lipid Analysis (Dundee, Scotland) by the preparation and analysis of FAME, 4,4-dimethyloxazoline (DMOX), 4-methyl-1,2,4-triazoline-3,5-dione (MTAD) and/or pyrrolidide derivatives by GLC-mass spectrometry (GLC-MS) [34].

Following their identification by GC-MS, samples of the purified oils produced by *B. breve* DPC6330 were used as GLC standards to identify similar conjugated fatty acids produced by the additional strains of bifidobacteria and propionibacteria assayed. The methylation was conducted as described above, while the GLC conditions were as described by Coakley et al. [27].

CLNA, CGLA and CSA Production by *B. breve* DPC6330

During the initial assessment of the strains for conjugated fatty acid production *B. breve* DPC6330 proved most efficient in terms of the bio-production of conjugated fatty acids from linoleic, α -linolenic, γ -linolenic and stearidonic acid. Subsequently, to determine the impact of substrate fatty acid concentration on conjugated fatty acid production, *B. breve* DPC6330 was incubated anaerobically for 72 h at 37 °C in the presence of linoleic acid, α -linolenic acid (Sigma Aldrich), γ -linolenic acid (Nu-Chek Prep, Elysian, MN) or stearidonic acid (Cayman Europe, Akadeemia tee, Tallinn, Estonia) at concentrations of 0.15,

0.3 and 0.45 mg mL⁻¹ ($n = 3$). To determine the time course of CLNA, CGLA and conjugated stearidonic acid (CSA) production by *B. breve* DPC6330, 16 individual fermentations (10 mL volumes) were set up in triplicate for each fatty acid at a substrate fatty acid concentration of 0.3 mg mL⁻¹. At 16 different time points, over the 80-h fermentation period, triplicate aliquots were removed and assessed for bacterial cell numbers by serial dilution and plating using *cys*-MRS agar and for fatty acid composition by GLC following extraction and methylation of lipids.

Results

Conjugated Fatty Acid Production by Bifidobacteria and Propionibacteria

The performance of the intestinally isolated bifidobacteria and dairy propionibacteria when exposed to 0.45 mg mL⁻¹ of the respective PUFA (0.15 mg mL⁻¹ of EPA or stearidonic acid) was visually observed to be strong (Table 3). Using GLC and UV spectrophotometric analysis, it was determined that four of the PUFA substrates were microbially bioconverted to their respective conjugated fatty acid isomers (Table 4). These fatty acid substrates were linoleic, α -linolenic, γ -linolenic and stearidonic acids, all of which contained the *c*9,*c*12 double bond. The production of the *c*9,*t*11 and *t*9,*t*11 CLA isomers from linoleic acid by the strains of bifidobacteria and propionibacteria was confirmed using GLC and a range of commercial CLA standards (Matreya LLC, PA), while the conjugated fatty acids derived from α -linolenic, γ -linolenic and stearidonic acids were identified by GLC-MS.

Identification of Microbially Produced Conjugated Fatty Acids

The predominant conjugated fatty acid isomer produced by the strains of bifidobacteria and propionibacteria from free α -linolenic acid was identified as 9,11,15-C18:3 (CLNA1). The mass spectrum derived from the FAME confirmed the molecular weight as 278 (Fig. 1a), while the mass spectrum of its DMOX derivative identified the molecule as the 9,11,15-C18:3 isomer (Fig. 1b). Further confirmation of the structure was achieved by the comparison of the DMOX spectra of this fatty acid with that of CLNA1 identified by both Destailats et al. [18] and Winkler and Steinhart [35].

The predominant conjugated fatty acid isomer produced by the strains of bifidobacteria and propionibacteria from free γ -linolenic acid was identified as 6,9,11-C18:3 (CGLA1). The mass spectrum of the FAME confirmed the molecular weight as 278 (Fig. 2a). However, due to the

Table 3 Production of conjugated fatty acids by growing cultures of *Bifidobacterium* and *Propionibacterium*

Substrate	Growth	Species			
		<i>B. breve</i> ^a	<i>B. longum</i> ^b	<i>Prop. freudenreichii</i> subsp. <i>shermanii</i> ^c	<i>Prop. freudenreichii</i> subsp. <i>freudenreichii</i> ^d
Linoleic acid	C18:2 (c9,c12)	(+)	(+)	(+)	(+)
α -Linolenic acid	C18:3 (c9,c12,c15)	(+)	(+)	(+)	(+)
γ -Linolenic acid	C18:3 (c6,c9,c12)	(+)	(+)	(+)	(-)
Stearidonic acid ^f	C18:4 (c6,c9,c12,c15)	(+)	(+)	(+)	(+)
Nonadecanoic acid	C19:2 (c10,c13)	(+)	(-)	(-)	(-)
Eicosadienoic acid	C20:2 (c11,c14)	(+)	(-)	(-)	(-)
Homo-gamma linolenic	C20:3 (c8,c11,c14)	(+)	(-)	(-)	(-)
Eicosatrienoic acid	C20:3 (c11,c14, c17)	(+)	(-)	(-)	(-)
Arachidonic acid	C20:4 (c5,c8,c11,c14)	(+)	(-)	(-)	(-)
Eicosapentaenoic acid ^f	C20:5 (c5,c8,c11,c14, c17)	(+)	(-)	(-)	(-)
Heneicosadienoic acid	C21:2 (c12,c15)	(+)	(-)	(-)	(-)
Docosadienoic acid	C22:2 (c13,c16)	(+)	(-)	(-)	(-)
Docosatrienoic acid	C22:3 (c13,c16,c19)	(+)	(-)	(-)	(-)
Docosatetraenoic acid	C22:4 (c7,c10,c13,c16)	(+)	(-)	(-)	(-)
Docosapentaenoic acid	C22:5 (c7,c10,c13,c16,c19)	(+)	(-)	(-)	(-)
Docosahexaenoic acid	C22:6 (c4,c7,c10,c13,c16,c19)	(+)	(-)	(-)	(-)

^a *B. breve* NCIMB 702258, NCIMB 8807, DPC6330, DPC6331

^b *B. longum* DPC6315, DPC6320

^c *Prop. freudenreichii* subsp. *shermanii* JS, 9093

^d *Prop. freudenreichii* subsp. *freudenreichii* Propioni-6, ATCC 6207

^e Only by *Prop. freudenreichii* subsp. *freudenreichii* Propioni-6

^f Strains assayed at a fatty acid concentration of 0.15 mg mL⁻¹

migration of the 9,11-double bond system to the 8,10-position during the DMOX derivatization process (Fig. 2b) MTAD and pyrrolidide derivatizations were also employed in the identification of the molecule. The mass spectrum of the MTAD derivative, with the ion at $m/z = 250$, confirmed that the fatty acid possessed a conjugated double bond in the 9,11-position, with the third double bond located on the carboxyl side of the conjugated double bond (Fig. 2c) [36]. Pyrrolidide derivatization with the fingerprint of ions at $m/z = 140$, $m/z = 154$ and $m/z = 166$ characterised the position of a double bond in position-6 of the carbon chain (Fig. 2d) [37].

The predominant conjugated fatty acid isomer produced by strains of bifidobacteria and propionibacteria from stearidonic acid was identified as 6,9,11,15-C18:4 (CSA1). The mass spectrum of the FAME confirmed the molecular weight as 276 (Fig. 3a). Once again, DMOX derivatization of the fatty acid resulted in the migration of the 9,11-double bond system to the 8,10-position (Fig. 3b). The spectrum produced for the MTAD derivative, with the base ion now at $m/z = 248$, confirmed the presence of a conjugated double bond in the 9,11-position, along with the presence of a double bond on either side of this (Fig. 3c). Although the use of DMOX derivatives did not allow the identification of

the position of the first three double bonds, a double bond at position-15 of the carbon backbone was confirmed by the presence of a gap of 12 amu between $m/z = 274$ and $m/z = 286$ (Fig. 3b). The mass spectrum observed with the pyrrolidide derivative of this fatty acid confirmed the presence of a double bond at position-6 (Fig. 3d).

Using GLC-MS analysis, it was not possible to determine the double bond conformation of CLNA1, CGLA1 and CSA1. However, given the specificity of the enzyme linoleic acid isomerase for the conjugation of c9,c12 double bond to the c9,t11 bond conformation, the most probable bond conformation for CLNA1 is c9,t11,c15-C18:3, while that of CGLA1 and CSA1 are likely to be c6,c9,t11-C18:3 and c6,c9,t11,c15-C18:4, respectively [27, 28]. This prediction is supported by the studies of Ogawa et al. [24] and Kishino et al. [38] who successfully identified the production of c9,t11,c15-C18:3 (CLNA1) and c6,c9,t11-C18:3 (CGLA1) from free α -linolenic acid and γ -linolenic acid, respectively, by strains of lactobacilli exhibiting linoleic acid isomerase activity.

In addition to the production of CLNA1, CGLA1 and CSA1 by the strains of bifidobacteria and propionibacteria, a second conjugated isomer was also produced from α -linolenic acid, γ -linolenic acid and stearidonic acid,

Table 4 Bioconversion of 0.45 mg mL⁻¹ of selected PUFA to CLA, CLNA, CGLA and CSA by strains of *Bifidobacterium* and *Propionibacterium*

Linoleic acid	Concentration mg mL ⁻¹		Percentage bioconversion	
	c9 t11 CLA	t9 t11 CLA	c9 t11 CLA	t9 t11 CLA
<i>Bifidobacterium</i>				
<i>B. breve</i> NCIMB 702258	0.254 ± 0.012	0.005 ± 0.001	58.94	1.08
<i>B. breve</i> NCIMB 8807	0.249 ± 0.019	0.028 ± 0.002	57.92	6.39
<i>B. breve</i> DPC6330	0.291 ± 0.004	0.009 ± 0.000	64.66	2.00
<i>B. breve</i> DPC6331	0.092 ± 0.001	0.004 ± 0.000	20.44	0.89
<i>B. longum</i> DPC6315	0.049 ± 0.002	0.003 ± 0.000	11.02	0.79
<i>B. longum</i> DPC6320	0.198 ± 0.004	0.007 ± 0.000	43.89	1.59
<i>Propionibacterium</i>				
<i>Prop. freudenreichii</i> subsp. <i>shermanii</i> JS ^a	0.044 ± 0.001	0.005 ± 0.000	8.56	1.05
<i>Prop. freudenreichii</i> subsp. <i>shermanii</i> 9093 ^a	0.243 ± 0.000	0.016 ± 0.000	47.37	3.17
<i>Prop. freudenreichii</i> subsp. <i>freudenreichii</i> Propioni-6 ^a	0.214 ± 0.007	0.016 ± 0.003	41.63	3.02
<i>Prop. freudenreichii</i> subsp. <i>freudenreichii</i> ATCC 6207 ^a	0.006 ± 0.000	0.002 ± 0.001	1.07	0.31
α-linolenic acid	Concentration mg mL ⁻¹		Percentage bioconversion	
	CLNA1	CLNA2	CLNA1	CLNA2
<i>Bifidobacterium</i>				
<i>B. breve</i> NCIMB 702258	0.180 ± 0.013	0.019 ± 0.014	45.09	4.65
<i>B. breve</i> NCIMB 8807	0.234 ± 0.002	0.038 ± 0.000	58.85	9.44
<i>B. breve</i> DPC6330	0.282 ± 0.013	0.049 ± 0.002	70.79	12.18
<i>B. breve</i> DPC6331	0.028 ± 0.000	0.003 ± 0.000	6.91	0.79
<i>B. longum</i> DPC6315	0.000 ± 0.000	0.000 ± 0.000	0.10	0.00
<i>B. longum</i> DPC6320	0.000 ± 0.000	0.000 ± 0.000	0.00	0.00
<i>Propionibacterium</i>				
<i>Prop. freudenreichii</i> subsp. <i>shermanii</i> JS	0.018 ± 0.001	0.001 ± 0.000	3.52	0.19
<i>Prop. freudenreichii</i> subsp. <i>shermanii</i> 9093	0.258 ± 0.017	0.017 ± 0.002	50.34	3.23
<i>Prop. freudenreichii</i> subsp. <i>freudenreichii</i> Propioni-6	0.043 ± 0.004	0.003 ± 0.000	8.41	0.53
<i>Prop. freudenreichii</i> subsp. <i>freudenreichii</i> ATCC 6207	0.008 ± 0.000	0.000 ± 0.000	1.65	0.00
γ-linolenic acid	Concentration mg mL ⁻¹		Percentage bioconversion	
	CGLA1	CGLA2	CGLA1	CGLA2
<i>Bifidobacterium</i>				
<i>B. breve</i> NCIMB 702258	0.100 ± 0.010	0.049 ± 0.012	25.13	12.34
<i>B. breve</i> NCIMB 8807	0.004 ± 0.000	0.001 ± 0.001	1.05	0.16
<i>B. breve</i> DPC6330	0.058 ± 0.003	0.023 ± 0.001	14.64	5.71
<i>B. breve</i> DPC6331	0.005 ± 0.001	0.002 ± 0.000	1.24	0.51
<i>B. longum</i> DPC6315	0.004 ± 0.005	0.004 ± 0.004	1.08	0.95
<i>B. longum</i> DPC6320	0.002 ± 0.003	0.000 ± 0.000	0.55	0.00
<i>Propionibacterium</i>				
<i>Prop. freudenreichii</i> subsp. <i>shermanii</i> JS	0.000 ± 0.000	0.000 ± 0.000	0.00	0.00
<i>Prop. freudenreichii</i> subsp. <i>shermanii</i> 9093	0.001 ± 0.000	0.000 ± 0.000	0.13	0.00
<i>Prop. freudenreichii</i> subsp. <i>freudenreichii</i> Propioni-6	0.000 ± 0.000	0.000 ± 0.000	0.00	0.00
<i>Prop. freudenreichii</i> subsp. <i>freudenreichii</i> ATCC 6207	0.000 ± 0.000	0.000 ± 0.000	0.00	0.00

Table 4 continued

Stearidonic acid ^b Strain	Concentration mg mL ⁻¹		Percentage bioconversion	
	CSA1	CSA2	CSA1	CSA2
<i>Bifidobacterium</i>				
<i>B. breve</i> NCIMB 702258	0.030 ± 0.001	0.008 ± 0.000	19.85	5.15
<i>B. breve</i> NCIMB 8807	0.014 ± 0.001	0.002 ± 0.000	9.49	1.46
<i>B. breve</i> DPC6330	0.039 ± 0.001	0.002 ± 0.000	25.81	1.52
<i>B. breve</i> DPC6331	0.022 ± 0.000	0.006 ± 0.000	14.80	3.74
<i>B. longum</i> DPC6315	0.004 ± 0.000	0.001 ± 0.000	3.04	0.87
<i>B. longum</i> DPC6320	0.029 ± 0.000	0.003 ± 0.000	19.25	2.11
<i>Propionibacterium</i>				
<i>Prop. freudenreichii</i> subsp. <i>shermanii</i> JS	0.004 ± 0.000	0.000 ± 0.000	2.66	0.00
<i>Prop. freudenreichii</i> subsp. <i>shermanii</i> 9093	0.005 ± 0.000	0.000 ± 0.000	3.09	0.00
<i>Prop. freudenreichii</i> subsp. <i>freudenreichii</i> Propioni-6	0.005 ± 0.000	0.000 ± 0.000	3.58	0.00
<i>Prop. freudenreichii</i> subsp. <i>freudenreichii</i> ATCC 6207	0.001 ± 0.000	0.000 ± 0.000	0.81	0.00

^a 0.5 mg mL⁻¹

^b 0.15 mg mL⁻¹

Fig. 1 a Mass spectrum of the FAME, **b** Mass spectrum of the DMOX derivative, of 9,11,15-C18:3 (CLNA1)

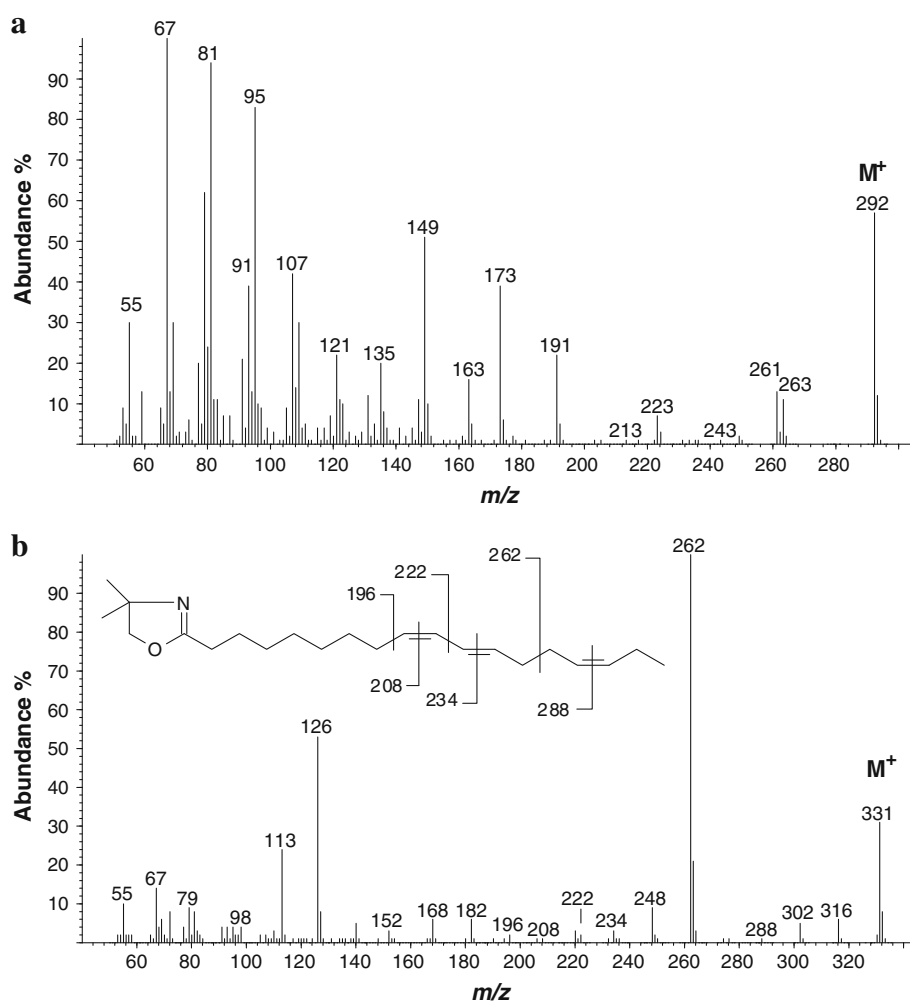
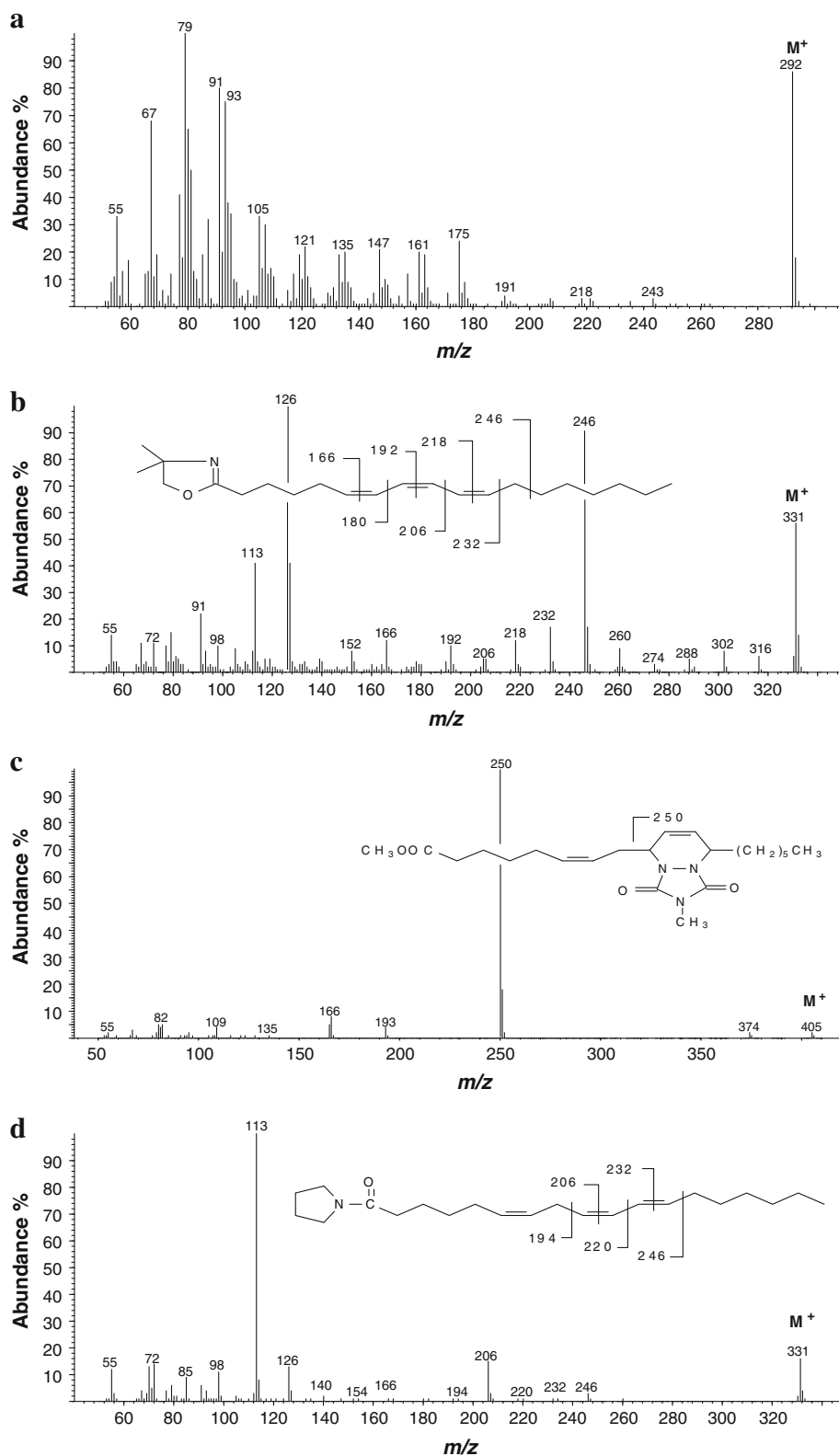


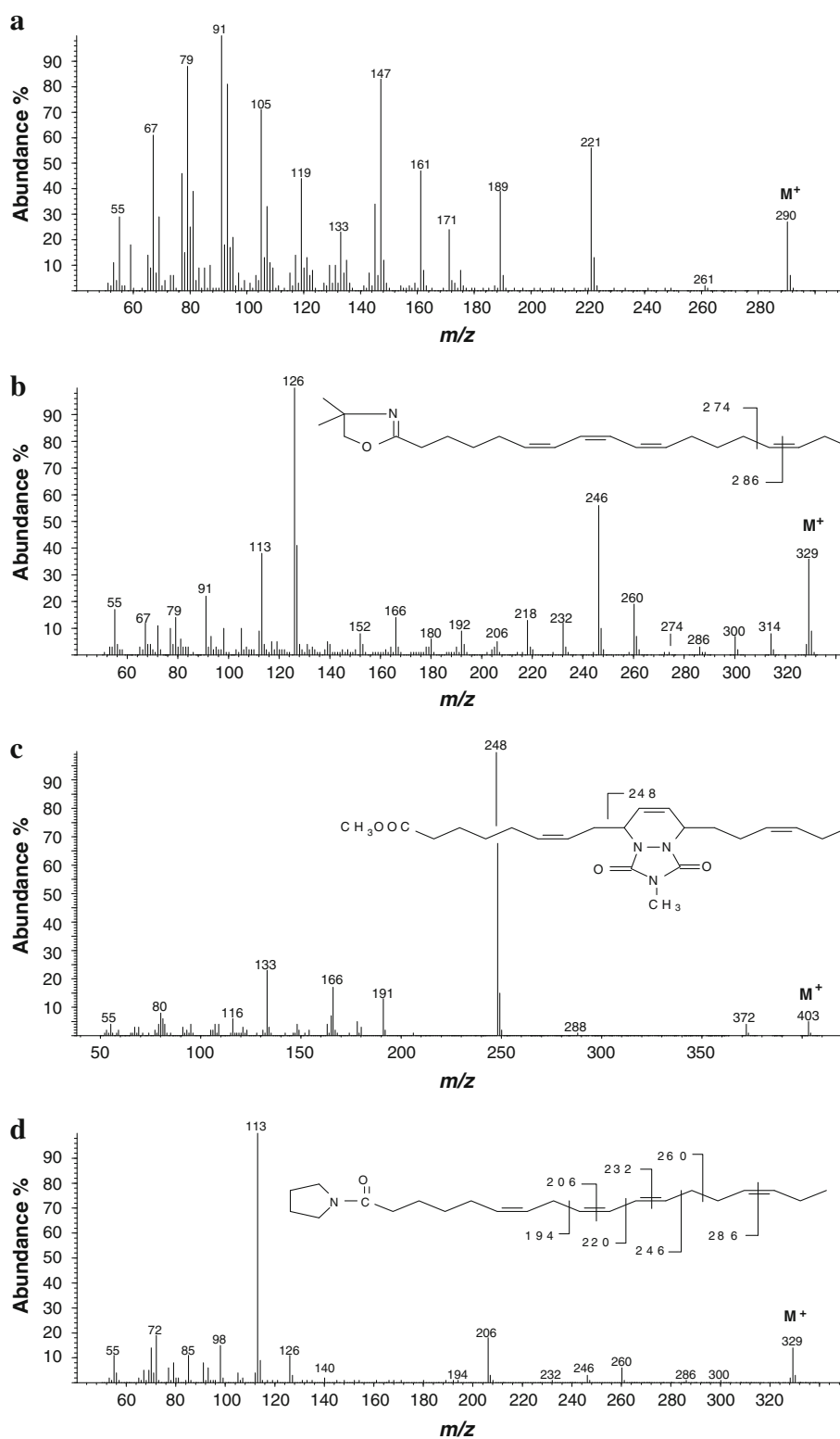
Fig. 2 **a** Mass spectrum of the FAME, **b** Mass spectrum of the DMOX derivative, **c** Mass spectrum of the MTAD adduct, **d** Mass spectrum of the pyrrolidide derivative, of 6,9,11-CLA (CGLA1)



respectively. Comparisons of the GLC retention time of these isomers and RP-HPLC analysis would suggest that these isomers share equivalence with the *t*9,*t*11 CLA isomer, which is found in small quantities along with the

predominant *c*9,*t*11 CLA isomer following conjugation of linoleic acid by strains of bifidobacteria and propionibacteria (this isomer may also be produced as a methylation artefact from *c*9,*t*11 CLA) [23, 27] (Fig. 4).

Fig. 3 **a** Mass spectrum of the FAME, **b** Mass spectrum of the DMOX derivative, **c** Mass spectrum of the MTAD adduct **d** Mass spectrum of the pyrrolidide derivative, of 6,9,11,15-C18:4 (CSA1)

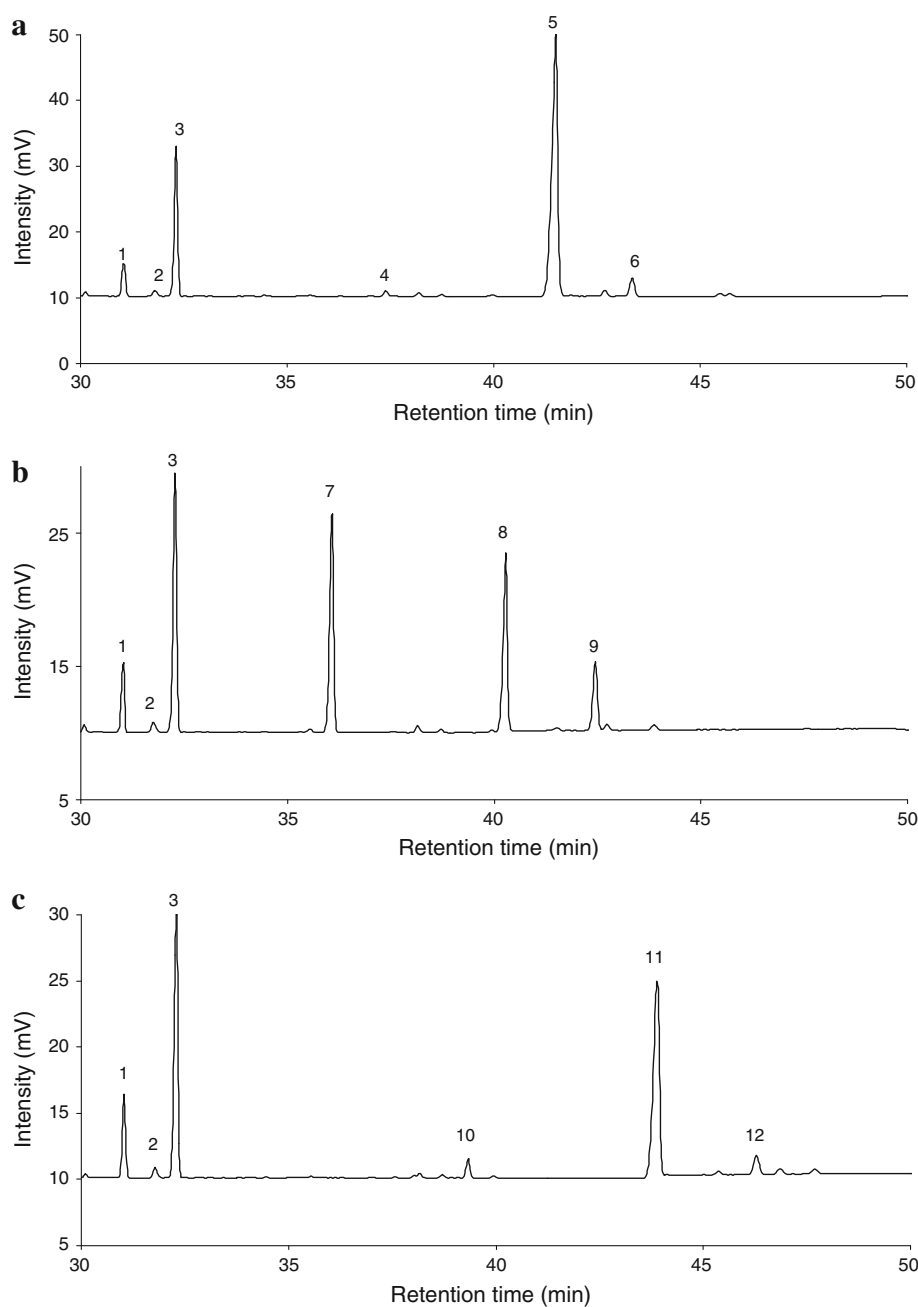


Production of Conjugated Fatty Acids by *B. breve* DPC6330

Of the strains assayed in the present study, *B. breve* DPC6330 was the most effective in terms of ability to

convert linoleic, α -linolenic, γ -linolenic and stearidonic acids to their respective conjugated isomers (Table 4). Consequently, this strain was selected for further studies to assess the impact of incrementally increasing the concentration of substrate fatty acids on the production of the

Fig. 4 GLC profiles of *B. breve* DPC6330 grown in cys-MRS containing 0.3 mg mL^{-1} of the PUFA **a** α -linolenic acid, **b** γ -linolenic acid and **c** stearidonic acid, following 80 h anaerobic incubation. 1 Stearic acid, 2 Vaccenic acid, 3 Oleic acid, 4 α -linolenic acid, 5 CLNA1, 6 CLNA2, 7 γ -linolenic acid, 8 CGLA1, 9 CGLA2, 10 Stearidonic acid, 11 CSA1, 12 CSA2



conjugated fatty acid isomers CLNA, CGLA and CSA, as well as to assess the time-scale of conjugated fatty acid production.

Increasing the concentration of the substrate α -linolenic acid from 0.15 to 0.45 mg mL^{-1} resulted in an increase in the concentration of CLNA1 and the putative CLNA2 isomers following 72 h incubation (Table 5). However, the effect of increasing substrate concentration on the percentage bioconversion of α -linolenic acid to CLNA was less profound (Table 5). In an attempt to elucidate the time-scale for the production of both CLNA1 and the putative CLNA2 isomers by *B. breve* DPC6330, growth and CLNA

production by the strain was monitored over 80 h in cys-MRS containing 0.3 mg mL^{-1} α -linolenic acid ($n = 3$) (Fig. 5). Following the initial inoculation at $8.0 \text{ log cfu mL}^{-1}$, production of both the CLNA1 and putative CLNA2 isomers corresponded with a 16-h period of logarithmic growth by the strain (0 – 0.292 mg mL^{-1} CLNA 1, and 0 – 0.016 mg mL^{-1} CLNA 2, respectively) (Fig. 5).

Increasing the concentration of the substrate γ -linolenic acid from 0.15 to 0.45 mg mL^{-1} resulted in subsequent increases in the total concentration of the CGLA1 isomer produced by *B. breve* DPC6330, but a decrease in the percentage bioconversion of γ -linolenic acid to CGLA1

Table 5 Effect of substrate concentration on the production of conjugated fatty acids CLNA, CGLA and CSA and the concentration of residual substrate following 72 h anaerobic fermentation

Strain	Substrate concentration (mg mL ⁻¹)	Concentration mg mL ⁻¹		Percentage bioconversion	
		<i>c9,t11</i> CLA	<i>t9,t11</i> CLA	<i>c9,t11</i>	<i>t9,t11</i>
<i>B. breve</i> DPC6330	0.15	0.101 ± 0.000	0.003 ± 0.000	67.73	2.00
<i>B. breve</i> DPC6330	0.3	0.209 ± 0.002	0.003 ± 0.000	69.67	1.00
<i>B. breve</i> DPC6330	0.45	0.252 ± 0.004	0.010 ± 0.002	56.00	2.22
		CLNA1	CLNA2	CLNA1	CLNA2
<i>B. breve</i> DPC6330	0.15	0.113 ± 0.001	0.002 ± 0.000	87.80	1.71
<i>B. breve</i> DPC6330	0.3	0.272 ± 0.007	0.004 ± 0.000	89.93	1.34
<i>B. breve</i> DPC6330	0.45	0.282 ± 0.013	0.049 ± 0.002	70.79	12.18
		CGLA1	CGLA2	CGLA1	CGLA2
<i>B. breve</i> DPC6330	0.15	0.026 ± 0.001	0.009 ± 0.000	20.81	6.99
<i>B. breve</i> DPC6330	0.3	0.047 ± 0.011	0.009 ± 0.002	16.63	3.09
<i>B. breve</i> DPC6330	0.45	0.058 ± 0.003	0.023 ± 0.001	13.60	5.30
		CSA1	CSA2	CSA1	CSA2
<i>B. breve</i> DPC6330	0.15	0.039 ± 0.001	0.002 ± 0.000	25.81	1.52
<i>B. breve</i> DPC6330	0.3	0.064 ± 0.005	0.002 ± 0.000	28.45	0.97
<i>B. breve</i> DPC6330	0.45	0.000 ± 0.000	0.000 ± 0.000	0.00	0.00

was obtained (Table 5). Increasing the concentration of the substrate γ -linolenic acid from 0.15 to 0.45 mg mL⁻¹ did not increase the concentration of γ -linolenic acid bioconverted to the putative CGLA2 isomer (Table 5). Growth and CGLA production by *B. breve* DPC6330 was monitored over 80 h in cys-MRS containing 0.3 mg mL⁻¹ γ -linolenic acid ($n = 3$) (Fig. 5). Conjugated fatty acid production occurred during a 16-h period of logarithmic growth by *B. breve* DPC6330 (Fig. 5). This resulted in CGLA1 concentrations increasing from 0 to 0.035 mg mL⁻¹ during this period.

When the concentration of substrate stearidonic acid was increased from 0.15 to 0.3 mg mL⁻¹, a subsequent increase in the concentration of CSA1 produced by *B. breve* DPC6330 was observed along with a small increase in the concentration of the putative CSA2 isomer (Table 5). Increasing the substrate concentration from 0.15 to 0.3 mg mL⁻¹ resulted in a 2.64% increase in the percentage bioconversion of stearidonic acid to CSA1, and a 0.55% decrease in the percentage bioconversion of stearidonic acid to the putative CSA2 isomer (Table 5). At a stearidonic acid concentration of 0.45 mg mL⁻¹, growth of *B. breve* DPC6330 was completely inhibited and neither CSA isomer was produced (Table 5). CSA production by *B. breve* DPC6330 from stearidonic acid was characterised over an 80 h-period in cys-MRS containing 0.3 mg mL⁻¹ of stearidonic acid ($n = 3$) (Fig. 5), and it was observed that following 3 h exposure to stearidonic acid the viability of the strain declined steadily (by 3.83 log cfu mL⁻¹

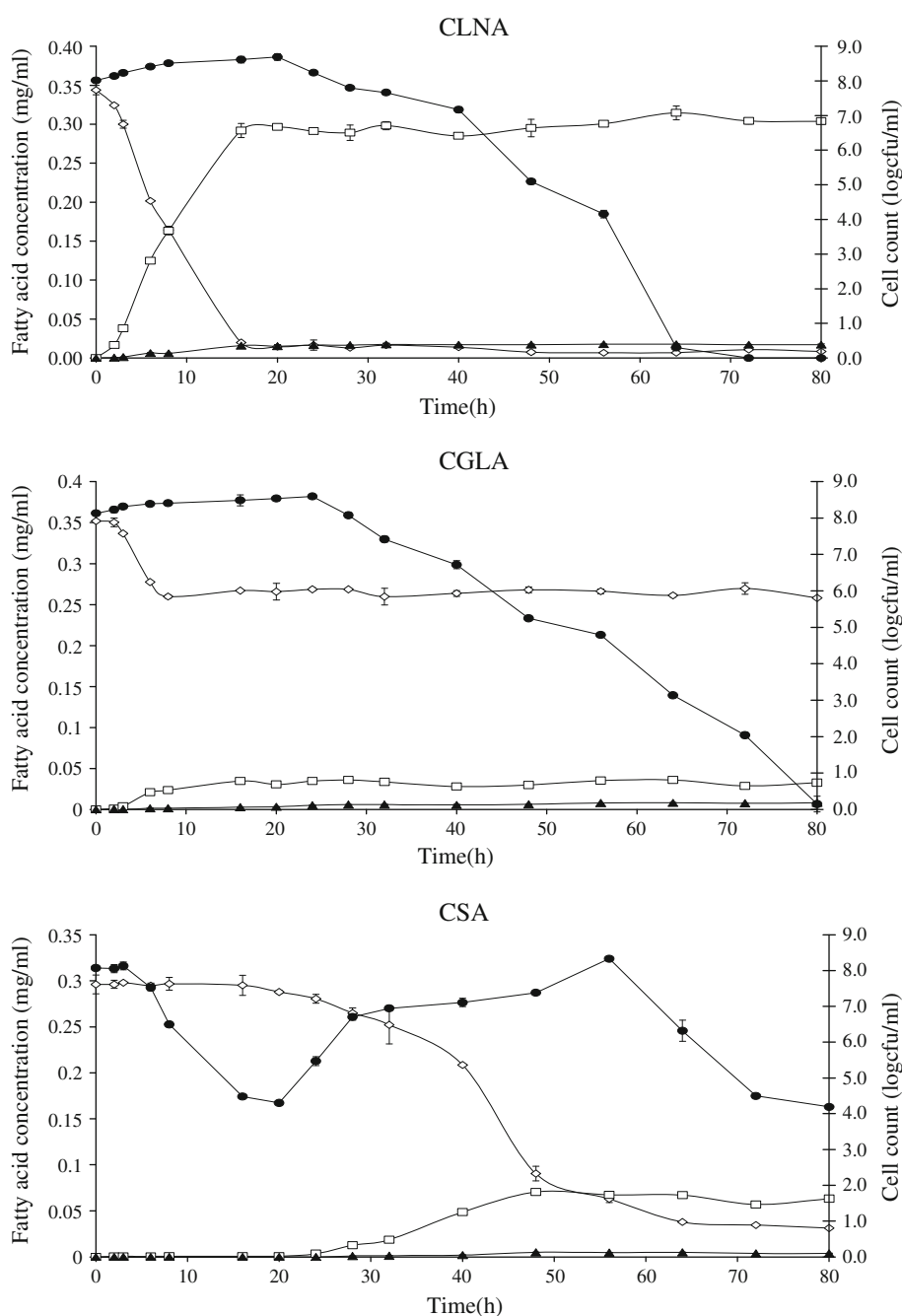
following 20 h) (Fig. 5). Subsequently, following this time an increase in cell numbers was observed from 4.30 to 6.70 log cfu mL⁻¹ during which time the production of both CSA1 and the putative CSA2 isomer was observed (Fig. 5).

We assessed the substrate preference of *B. breve* DPC6330 to isomerise the C18 unsaturated fatty acids linoleic acid, α -linolenic acid, γ -linolenic acid and stearidonic acid (0.3 mg mL⁻¹) to CLA, CLNA1, CGLA1 and CSA1 over an 80-h fermentation period, relative to the percentage bioconversion of linoleic acid to the *c9,t11* CLA isomer which was set at 100% (Table 5). We found that *B. breve* DPC6330 has a preference for the conjugation of C18 fatty acid substrates in the order: α -linolenic acid (130%) > linoleic acid (100%) > stearidonic acid (27%) > γ -linolenic acid (14%).

Discussion

In this study, we report that certain strains of bifidobacteria and propionibacteria possess the ability to bioconvert substrate fatty acids containing a *c9,c12* double bond to their conjugated isomers. Two conjugated fatty acids products were produced by most strains from each unconjugated fatty acid substrate, which were believed to share equivalence with the *c9,t11* CLA and *t9,t11* CLA isomers produced by certain bifidobacteria and propionibacteria from linoleic acid, although the latter isomer has

Fig. 5 Growth and CLNA/ CGLA/CSA production by *B. breve* DPC6330 over 80 h in the presence of 0.3 mg mL^{-1} α -linolenic acid/ γ -linolenic acid/ stearidonic acid. CLNA1/ CGLA1/CSA1 (squares), CLNA2/CGLA/CSA2 (filled triangles), α -linolenic acid/ γ -linolenic acid/stearidonic acid (diamonds) and log cfu/ml (filled circles)



also been known to be produced from $c9,t11$ CLA under methylation conditions [23, 27, 28]. GLC-MS confirmed that the strains used in the present study catalysed the bioconversion of the $c9,c12$ double bond of the substrate fatty acids linoleic, α -linolenic, γ -linolenic and stearidonic acids, to the conjugated 9,11-double bond form via linoleic acid isomerase activity. These observations correspond with the findings of others who identified the production of CLNA1 and CGLA1 by *Lactobacillus* strains via the activity of the enzyme linoleic acid isomerase [24, 38]. In these studies, the bond conformation of CLNA1 was

identified as $c9,t11,c15$ -C18:3, with that of CGLA1 determined to be $c6,c9,t11$ -C18:3 [18, 24, 38].

The extent to which α -linolenic, γ -linolenic and stearidonic acids were bioconverted to their respective conjugated fatty acid isomers differed substantially between the strains and among the fatty acid substrates used in the present study. Differences in the extent to which bacterial strains conjugated linoleic acid to CLA have been reported with some regularity and attributed to variations in the toxicity of the substrate fatty acids to the strains [26–29], but may also be a result of the bond position of the substrate fatty acids [39].

Increasing the concentration of the substrate fatty acid resulted in increased conjugated fatty acid production by *B. breve* DPC6330, but also to increased residual substrate concentrations. These observations may be, respectively, attributed to the increased availability of substrate fatty acid, and to the substrate concentration exceeding the isomerising capacity of the growing culture [28, 40, 41].

Of the strains assayed, *B. breve* DPC6330 was most efficient in terms of the bio-production of conjugated fatty acids from linoleic, α -linolenic, γ -linolenic and stearidonic acid with results suggesting a higher affinity of the strain to conjugate α -linolenic acid than γ -linolenic acid. Although stearidonic acid substantially inhibited the growth of *B. breve* DPC6330, CSA production from stearidonic acid exceeded CGLA production from γ -linolenic acid at a substrate fatty acid concentration of 0.3 mg mL⁻¹. The inhibition of bacterial growth by stearidonic acid is likely related to the ability of certain fatty acids to disrupt cell membrane composition and cell energetics [42–44]. However, when the conjugation of linoleic, α -linolenic, γ -linolenic, and stearidonic acids by the strain were viewed together, it was apparent that the presence of an additional double bond towards the distal end of the fatty acid molecule (e.g. α -linolenic acid) encouraged conjugation by the strain, while the addition of a double bond between the carboxyl group and the c9,c12 double bond (e.g. γ -linolenic acid) discouraged conjugation of the double bond.

In this study, we found that in particular, when γ -linolenic acid and stearidonic acid were provided as fatty acid substrate to *B. breve* DPC6330 the sum of the concentration of conjugated fatty acids produced and residual substrate following fermentation was not equivalent to the quantity of substrate initially provided. Although it would require the use of labelled fatty acids to discern the exact fate of this missing substrate, it is likely that this difference is attributable to bifidobacterial metabolic activity [45–47].

Overall, this study has demonstrated the ability of strains of certain commensal bifidobacteria and dairy propionibacteria to produce a range of novel conjugated fatty acids from PUFA containing the c9,c12 double bond system. If bioactive in vivo, the production of such conjugated fatty acids by commensals and potential probiotics offers a valuable strategy for the production and delivery of these novel conjugated fatty acids to the GIT [25, 48–50]. Furthermore, the production of conjugated fatty acids such as CLNA1, CGLA1 and CSA1 by potentially probiotic bifidobacteria may present a valuable strategy for the in situ production of bioactive molecules in the human GIT. As the substrate fatty acids can be found in the human diet, it is not unreasonable to assume their in vivo production occurs [51–53]. Indeed, further credence is given to this theory in light of the evidence pertaining to the ex vivo and in vivo production of CLA from linoleic acid [31, 32].

Acknowledgments We would like to thank Seamus Aherne and Lina Cordeddu for their technical assistance. The assistance with GLC-MS by Mylnefield Lipid Analysis is gratefully acknowledged. A. A. Hennessy is in receipt of a Teagasc Walsh Fellowship. This research was funded by EU project QLK1-2001-02362 and by Alimentary Pharmabiotic Centre (APC).

References

1. Stanton C, Murphy J, McGrath E, Devery R (2003) Animal feeding strategies for conjugated linoleic acid enrichment of milk. In: Sebedio JL, Christie WW, Adlof R (eds) Advances in conjugated linoleic acid research, vol 2. AOCS Press, Champaign, pp 123–145
2. Dhiman TR, Nam SH, Ure AL (2005) Factors affecting conjugated linoleic acid content in milk and meat. Crit Rev Food Sci Nutr 45(6):463–482
3. Yasui Y, Hosokawa M, Sahara T, Suzuki R, Ohgiya S, Kohno H, Tanaka T, Miyashita K (2005) Bitter melon seed fatty acid rich in 9c,11t,13t-conjugated linolenic acid induces apoptosis and up-regulates the GADD45, p53 and PPARgamma in human colon cancer Caco-2 cells. Prostaglandins Leukot Essent Fatty Acids 73(2):113–119
4. Liu L, Hammond EG, Nikolau BJ (1997) In vivo studies of the biosynthesis of [alpha]-eleostearic acid in the seed of *Momordica charantia* L. Plant Physiol 113(4):1343–1349
5. Kohno H, Yasui Y, Suzuki R, Hosokawa M, Miyashita K, Tanaka T (2004) Dietary seed oil rich in conjugated linolenic acid from bitter melon inhibits azoxymethane-induced rat colon carcinogenesis through elevation of colonic PPARgamma expression and alteration of lipid composition. Int J Cancer 110(6):896–901
6. Chisholm MJ, Hopkins CY (1967) Conjugated fatty acids in some Cucurbitaceae seed oils. Can J Biochem 45(7):1081–1086
7. Wise ML, Hamberg M, Gerwick WH (1994) Biosynthesis of conjugated triene-containing fatty acids by a novel isomerase from the red marine alga *Ptilota filicina*. Biochemistry 33(51):15223–15232
8. Lopez A, Gerwick WH (1987) Two new icosapentaenoic acids from the temperate red seaweed *Ptilota filicina* J Agardh. Lipids 22(3):190–194
9. Burgess JR, de la Rossa RI, Jacobs RS, Butler A (1991) A new eicosapentaenoic acid formed from arachidonic acid in coralline red algae *Bossiella orbigniana*. Lipids 26:162–165
10. Mikhailova MV, Bemis DL, Wise ML, Gerwick WH, Norris JN, Jacobs RS (1995) Structure and biosynthesis of novel conjugated polyene fatty acids from the marine green alga *Anadyomene stellata*. Lipids 30(7):583–589
11. Yonezawa Y, Hada T, Uryu K, Tsuzuki T, Eitsuka T, Miyazawa T, Murakami-Nakai C, Yoshida H, Mizushima Y (2005) Inhibitory effect of conjugated eicosapentaenoic acid on mammalian DNA polymerase and topoisomerase activities and human cancer cell proliferation. Biochem Pharmacol 70(3):453–460
12. Park Y, Storkson JM, Albright KJ, Liu W, Pariza MW (2005) Biological activities of conjugated fatty acids: conjugated eicosadienoic (conj. 20:2delta(c11,t13/t12,c14)), eicosatrienoic (conj. 20:3delta(c8,t12,c14)), and heneicosadienoic (conj. 21:2delta(c12,t14/c13,t15)) acids and other metabolites of conjugated linoleic acid. Biochim Biophys Acta 1687(1–3):120–129
13. Bhattacharya A, Banu J, Rahman M, Causey J, Fernandes G (2006) Biological effects of conjugated linoleic acids in health and disease. J Nutr Biochem 17(12):789–810
14. Wahle KW, Heys SD, Rotondo D (2004) Conjugated linoleic acids: are they beneficial or detrimental to health? Prog Lipid Res 43(6):553–587

15. Igarashi M, Miyazawa T (2000) Newly recognized cytotoxic effect of conjugated trienoic fatty acids on cultured human tumor cells. *Cancer Lett* 148(2):173–179
16. Coakley M, Banni S, Johnson MC, Mills S, Devery R, Fitzgerald G, Ross RP, Stanton C (2009) Inhibitory effect of conjugated α -linolenic acid (CALA) from bifidobacteria of intestinal origin on SW480 cancer cells. *Lipids* 44(3):249–256
17. Hennessy AA, Devery R, Ross RP, Stanton C (2011) The health promoting properties of the conjugated isomers of α -linolenic acid (CALA). *Lipids* 46(2):105–119
18. Destailats F, Trottier JP, Galvez JM, Angers P (2005) Analysis of alpha-linolenic acid biohydrogenation intermediates in milk fat with emphasis on conjugated linolenic acids. *J Dairy Sci* 88(9):3231–3239
19. Tsuzuki T, Tanaka K, Kuwahara S, Miyazawa T (2005) Synthesis of the conjugated trienes 5E,7 E,9E,14Z,17Z-eicosapentaenoic acid and 5Z,7E,9E,14Z,17Z-eicosapentaenoic acid, and their induction of apoptosis in DLD-1 colorectal adenocarcinoma cells. *Lipids* 40(2):147–154
20. Tsujita-Kyutoku M, Yuri T, Danbara N, Senzaki H, Kiyozuka Y, Uehara N, Takada H, Hada T, Miyazawa T, Ogawa Y, Tsubura A (2004) Conjugated docosahexaenoic acid suppresses KPL-1 human breast cancer cell growth in vitro and in vivo: potential mechanisms of action. *Breast Cancer Res* 6(4):R291–R299
21. Tsuzuki T, Kawakami Y, Nakagawa K, Miyazawa T (2005) Conjugated docosahexaenoic acid inhibits lipid accumulation in rats. *J Nutr Biochem* 17(8):518–524
22. Danbara N, Yuri T, Tsujita-Kyutoku M, Sato M, Senzaki H, Takada H, Hada T, Miyazawa T, Okazaki K, Tsubura A (2004) Conjugated docosahexaenoic acid is a potent inducer of cell cycle arrest and apoptosis and inhibits growth of colo 201 human colon cancer cells. *Nutr Cancer* 50(1):71–79
23. Coakley M, Johnson MC, McGrath E, Rahman S, Ross RP, Fitzgerald GF, Devery R, Stanton C (2006) Intestinal bifidobacteria that produce *trans*-9,*trans*-11 conjugated linoleic acid: a fatty acid with antiproliferative activity against human colon SW480 and HT-29 cancer cells. *Nutr Cancer* 56(1):95–102
24. Ogawa J, Kishino S, Ando A, Sugimoto S, Mihara K, Shimizu S (2005) Production of conjugated fatty acids by lactic acid bacteria. *J Biosci Bioeng* 100(4):355–364
25. Sieber R, Collomb M, Aeschlimann A, Jelen P, Eyer H (2004) Impact of microbial cultures on conjugated linoleic acid in dairy products—a review. *Int Dairy J* 14(1):1–15
26. Hennessy AA, Ross RP, Stanton C, Devery R (2007) Development of dairy based functional foods enriched in conjugated linoleic acid with special reference to ruminic acid. In: Saarela M (ed) *Functional dairy products*. Woodhead Publishing Limited, Cambridge, pp 443–495
27. Coakley M, Ross RP, Nordgren M, Fitzgerald G, Devery R, Stanton C (2003) Conjugated linoleic acid biosynthesis by human-derived *Bifidobacterium* species. *J Appl Microbiol* 94(1):138–145
28. Jiang J, Bjorck L, Fonden R (1998) Production of conjugated linoleic acid by dairy starter cultures. *J Appl Microbiol* 85(1):95–102
29. Barrett E, Ross RP, Fitzgerald GF, Stanton C (2007) Rapid screening method for analyzing the conjugated linoleic acid production capabilities of bacterial cultures. *Appl Environ Microbiol* 73(7):2333–2337
30. Kishino S, Ogawa J, Ando A, Yokozeki K, Shimizu S (2009) Microbial production of conjugated gamma-linolenic acid from gamma-linolenic acid by *Lactobacillus plantarum* AKU 1009a. *J Appl Microbiol* 108(6):2012–2018
31. Ewaschuk JB, Walker JW, Diaz H, Madsen KL (2006) Bioproduction of conjugated linoleic acid by probiotic bacteria occurs in vitro and in vivo in mice. *J Nutr* 136(6):1483–1487
32. Wall R, Ross RP, Shanahan F, O'Mahony L, O'Mahony C, Coakley M, Hart O, Lawlor P, Quigley EM, Kiely B, Fitzgerald GF, Stanton C (2009) The metabolic activity of the enteric microbiota influences the fatty acid composition of murine and porcine liver and adipose tissues. *Am J Clin Nutr* 89(5):1393–1401
33. Jiang C, Ting AT, Seed B (1998) PPAR-gamma agonists inhibit production of monocyte inflammatory cytokines. *Nature* 391(6662):82–86
34. Christie WW, Han X (2010) *Lipid analysis— isolation, separation, identification and lipidomic analysis*, 4th edn. Oily Press, Bridgewater
35. Winkler K, Steinhart H (2001) Identification of conjugated isomers of linolenic acid and arachidonic acid in cheese. *J Sep Sci* 24(8):663–668
36. Dobson G (1998) Identification of conjugated fatty acids by gas chromatography mass spectrometry of 4-methyl-1,2,4-triazoline-3,5-dione adducts. *J Am Oil Chem Soc* 75:137–142
37. Andersson BA, Holman RT (1974) Pyrrolidides for mass spectrometric determination of the position of double bonds in monounsaturated fatty acids. *Lipids* 9:185–190
38. Kishino S, Ogawa J, Ando A, Shimizu S (2003) Conjugated alpha-linolenic acid production from alpha-linolenic acid by *Lactobacillus plantarum* AKU 1009a. *Eur J Lipid Sci* 105(10):572–577
39. Kepler CR, Tucker WP, Tove SB (1970) Biohydrogenation of unsaturated fatty acids. IV. Substrate specificity and inhibition of linoleate delta-12-cis, delta-11-trans-isomerase from *Butyrivibrio fibrisolvens*. *J Biol Chem* 245(14):3612–3620
40. Raychowdhury MK, Goswami R, Chakrabarti P (1985) Effect of unsaturated fatty acids in growth inhibition of some penicillin-resistant and sensitive bacteria. *J Appl Bacteriol* 59(2):183–188
41. Maia MR, Chaudhary LC, Figueres L, Wallace RJ (2006) Metabolism of polyunsaturated fatty acids and their toxicity to the microflora of the rumen. *Antonie Van Leeuwenhoek* 91(4):303–314
42. Knapp HR, Melly MA (1986) Bactericidal effects of polyunsaturated fatty acids. *J Infect Dis* 154(1):84–94
43. Greenway DL, Dyke KG (1979) Mechanism of the inhibitory action of linoleic acid on the growth of *Staphylococcus aureus*. *J Gen Microbiol* 115(1):233–245
44. Kenny JG, Ward D, Josefsson E, Jonsson IM, Hinds J, Rees HH, Lindsay JA, Tarkowski A, Horsburgh MJ (2009) The *Staphylococcus aureus* response to unsaturated long chain free fatty acids: survival mechanisms and virulence implications. *PLoS One* 4(2):e4344
45. Kanehisa M, Goto S, KE GG (2000) KEGG: Kyoto encyclopedia of genes and genomes. *Nucleic Acids Res* 28(1):27–30
46. Kanehisa M, Goto S, Hattori M, Aoki-Kinoshita KF, Itoh M, Kawashima S, Katayama T, Araki M, Hirakawa M (2006) From genomics to chemical genomics: new developments in KEGG. *Nucleic Acids Res* 34(Database issue):D354–D357
47. Devillard E, McIntosh FM, Duncan SH, Wallace RJ (2007) Metabolism of linoleic acid by human gut bacteria: different routes for biosynthesis of conjugated linoleic acid. *J Bacteriol* 189(6):2566–2570
48. Xu S, Boylston TD, Glatz BA (2004) Effect of lipid source on probiotic bacteria and conjugated linoleic acid formation in milk model systems. *J Am Oil Chem Soc* 81:589–595
49. Xu S, Boylston TD, Glatz BA (2005) Conjugated linoleic acid content and organoleptic attributes of fermented milk products produced with probiotic bacteria. *J Agric Food Chem* 53(23):9064–9072
50. Florence ACR, da Silva RC, Espírito Santo AP, Gioielli LA, Tamime AY, Oliveira MN (2009) Increased CLA content in

- organic milk fermented by bifidobacteria or yoghurt cultures. *Dairy Sci Technol* 89:541–553
51. Fan YY, Chapkin RS (1998) Importance of dietary gamma-linolenic acid in human health and nutrition. *J Nutr* 128(9): 1411–1414
52. Whelan J (2009) Dietary stearidonic acid is a long chain (n-3) polyunsaturated fatty acid with potential health benefits. *J Nutr* 139(1):5–10
53. Li D, Bode O, Drummond H, Sinclair AJ (2003) Omega-3 (n-3) fatty acids. In: Gunstone FD (ed) *Lipids for functional foods and nutraceuticals*. The Oily Press, Bridgewater, pp 225–262

Comparison of Separations of Fatty Acids from Fish Products Using a 30-m Supelcowax-10 and a 100-m SP-2560 Column

Viviana Santercole · Pierluigi Delmonte ·
John K. G. Kramer

Received: 7 April 2011 / Accepted: 12 December 2011 / Published online: 14 January 2012
© AOCS 2012

Abstract Commercial fish oils and foods containing fish may contain *trans* and/or isomerized fatty acids (FA) produced during processing or as part of prepared foods. The current American Oil Chemists' Society (AOCS) official method for marine oils (method Ce 1i-07) is based on separation by use of poly(ethylene glycol) (PEG) columns, for example Supelcowax-10 or equivalent, which do not resolve most unsaturated FA geometric isomers. Highly polar 100-m cyanopropyl siloxane (CPS) columns, for example SP-2560 and CP Sil 88 are recommended for separation of geometric FA isomers. Complementary separations were achieved by use of two different elution temperature programs with the same CPS column. This study is the first direct comparison of the separations achieved by use of 30-m Supelcowax-10 and 100-m SP-2560 columns for fatty acid methyl esters (FAME) prepared from the same fish oil and fish muscle sample. To simplify the identification of the FA in these fish samples, FA were fractionated on the basis of the number and type of double bonds by silver-ion solid-phase extraction (Ag^+ -SPE) before GC analysis. The results showed that a

combination of the three GC separations was necessary to resolve and identify most of the unsaturated FA, FA isomers, and other components of fish products, for example phytanic and phytenic acids. Equivalent chain length (ECL) values of most FAME in fish were calculated from the separations achieved by use of both GC columns; the values obtained were shown to be consistent with previously reported values for the Supelcowax-10 column. ECL values were also calculated for the FA separated on the SP-2560 column. The calculated ECL values were equally valid under isothermal and temperature-programmed elution GC conditions, and were valuable for confirmation of the identity of several unsaturated FAME in the fish samples. When analyzing commercially prepared fish foods, deodorized marine oils, or foods fortified with marine oils it is strongly recommended that quantitative data acquired by use of PEG columns is complemented with data obtained from separations using highly polar CPS columns.

Keywords Supelcowax-10 · SP-2560 · GC · Fish oil · Fish muscle · Fatty acid determination · Silver-ion SPE columns · Equivalent chain length (ECL)

V. Santercole (✉)
Porto Conte Ricerche Srl, S.P. 55 Porto Conte Capo-Caccia
Km 8.4, Località Tramariglio-Alghero (SS),
07040 Santa Maria La Palma, Italy
e-mail: vivianas@uniss.it

P. Delmonte
US Food and Drug Administration, College Park,
MD 20740, USA
e-mail: Pierluigi.delmonte@fda.hhs.gov

J. K. G. Kramer
Agriculture and Agri-Food Canada, Guelph Food Research
Center, Guelph, ON N1G5C9, Canada
e-mail: jkgkramer@rogers.com

Abbreviations

CLA	Conjugated linoleic acid
CPS	Cyanopropyl siloxane
DHA	Docosahexaenoic acid
ECL	Equivalent chain length
EPA	Eicosapentaenoic acid
FA	Fatty acid
FAME	Fatty acid methyl ester
FT-NIR	Fourier transform near infrared
GC	Gas chromatography
LC	Long-chain
MUFA	Monounsaturated fatty acid

NMI	Non-methylene interrupted
PEG	Poly(ethylene glycol)
pha	Phytanic acid
phe	Phytenic acid
PUFA	Polyunsaturated fatty acid
SPE	Solid-phase extraction

Introduction

The nutritional value of the long-chain n-3 polyunsaturated fatty acids (LC n-3 PUFA) in marine oils and products prepared from fish is well recognized [1], in large part because of humans' low capacity to bioconvert linolenic acid (18:3n-3) into the highly unsaturated n-3 metabolites [2]. For this reason increased consumption of LC n-3 PUFA is recommended to improve the health of infants, nursing mothers [3], and other adults [4]. The fatty acids (FA) in marine oils are usually determined by gas chromatography (GC) after their conversion to fatty acid methyl esters (FAME). The latest official method of analysis of saturated FA, *cis*-monounsaturated fatty acids (MUFA), and *cis*-PUFA in marine and other oils (method Ce 1i-07) was approved by the American Oil Chemists' Society (AOCS) in 2007 [5]. It recommended the use of 30-m fused silica capillary columns coated with poly(ethylene glycol) (PEG) phases [5]. These GC stationary phases separate FAME primarily on the basis of chain length, then on the basis of the number of double bonds and their position [6–9]. However, PEG-coated GC columns are not suitable for separation of the geometric isomers and unsaturated FA commonly occurring in natural products including fish oils [8, 10].

Formation of positional and *trans* isomers from naturally occurring all-*cis* unsaturated FA is difficult to avoid during most domestic or commercial preparation of fish [11, 12], deodorization of fish oils [13–17], preparation and storage of infant formulas supplemented with docosahexaenoic (DHA; 22:6n-3) and arachidonic (20:4n-6) acids [18], or commercial production of enriched n-3 PUFA supplements [19]. Separation and identification of the *trans* isomers of LC n-3 PUFA contained in marine oils or foods, or processed foods containing fish, requires the use of 100-m highly polar 100% cyanopropyl siloxane (CPS) columns [13–16]. Many of the unsaturated FA with one or more *trans* double bonds coelute with their all-*cis* isomers when separated on PEG-coated columns [10], which could lead to overestimation of the all-*cis* LC n-3 PUFA content of fish products. This observation was recently confirmed when Fourier transform near-infrared (FT-NIR) spectroscopy was evaluated as an alternative method for LC n-3

PUFA determination [20]. FT-NIR quantification based on calibrated data acquired with a PEG column overestimated the amount of the all-*cis* LC n-3 PUFA compared with FT-NIR quantification based on calibration data obtained by use of a 100-m highly polar CPS column. In addition, the 30-m PEG column was unable to separate, and enable quantification of, the *trans* 18:1 isomers contained in the fish oil supplements [20].

For this reason there seems to be a need to combine the results obtained by use of a PEG column, that makes identification of PUFA easier [7, 8], and by use of a highly polar CPS column, that is able to resolve, and enable identification of, geometric FA isomers [18, 21–24]. Comparison of the separation of the same fish oil and fish muscle samples on a 30-m PEG column and a 100-m CPS column has not been reported. Mjøs [25] compared separation of the geometric isomers of eicosapentaenoic acid (EPA) and DHA on a 50-m PEG column (BP-20; SGE, Ringwood, Australia) with that on a 60-m BPX-70 column that has only 70% the polarity of a CPS column [26], and he only compared the immediate EPA and DHA chromatographic regions.

Equivalent chain length (ECL) calculations have been used to describe the relative elution of FA on specific columns [7–9, 27, 28]. However, a summary of ECL values for the FA identified in fish oils using the GC columns recommended for marine oil analysis [5] and the CPS GC columns recommended for *trans* FA analysis [29] is not available. A summary of the ECL of many PUFA found in fish oil obtained by use of a BPX-70 column can be found at http://www.chrombox.org/data/class_fame/ECL-kart%20BPX-03.pdf. However, because the polarity of the BPX-70 column is only 70% that of CPS columns (for example SP-2560), this means that, even though the elution sequence within a group of FAME of similar structure will be comparable, because of the higher polarity, the relative elution pattern between the FAME groups will be different. For instance, on a BPX-70 column the saturated FAME 20:0 elutes just before the conjugated linoleic acid (CLA) isomers and most 20:1 isomers coelute among the CLA isomers (same web site); on a CPS column, however, all the 20:1 isomers elute before the CLA isomers [10].

In this study we compared separations of the FAME prepared from menhaden oil and from a fish muscle lipid extract on a 30-m Supelcowax-10 and a 100-m SP-2560 capillary column. Complementary silver-ion solid-phase extraction (Ag⁺-SPE) was conducted as described elsewhere [24] to confirm the identity of unsaturated FA on the basis of their chain length, double bond number and position, and geometric configuration in the fish products. To obtain further support for their identities the ECL values of all separated FAME on both GC columns were calculated from their retention times.

Materials and Methods

All chemicals and solvents (hexane, acetone, methanol, and acetonitrile) were of analytical grade, and all gases used in the GC operations were of the highest purity.

Standards

Pure FAME reference materials and reference mixtures were purchased from Nu-Chek Prep (Elysian, MN, USA). Commercial GC reference mixtures (#463 and #674) were spiked with a mixture of four positional CLA isomers (#UC-59M) and long-chain saturated FAME 21:0 and 23:0. Menhaden fish oil analytical standard (#47116), 0.5 N methanolic base (#33080), and Discovery Ag⁺-Ion SPE tubes (#54225-U, 750 mg/6 ml) were purchased from Supelco (Bellefonte, PA, USA). Several PUFA standards (16:2n-4, 16:3n-3, 18:4n-3, 20:4n-3, 21:5n-3, and 22:5n-6) were purchased from Larodan Fine Chemical (Malmö, Sweden). A sample of fresh gilthead sea bream (*Sparus aurata*) tissue was obtained from a local fish farm and stored frozen at -80°C until analyzed. A sample of the diet fed was also analyzed.

Sample Preparation

The sample of fresh gilthead sea bream (*Sparus aurata*) tissue was divided into five portions of approximately 5 g each and freeze-dried (lyophilized). The lipids were extracted by use of a modification of the Bligh and Dyer procedure as described by Cruz-Hernandez et al. [23]. All extracts from fish samples were methylated by use of 0.5 N methanolic base (#33080; Supelco) as described elsewhere [23]. In addition, the total lipids extracted from fish muscle were fractionated by use of silver-ion solid-phase extraction (Ag⁺-SPE) cartridges as described elsewhere [24] (see below).

Ag⁺-SPE Fractionation

Ag⁺-SPE cartridges (750 mg/6 mL) were conditioned with 4 mL acetone, to remove any moisture, then with 4 mL hexane. One milliliter of total lipid FAME prepared from fish muscle was dissolved in hexane and loaded on to the Ag⁺-SPE tube. The FAME were eluted with consecutive 6 mL volumes of hexane containing increasing amounts of acetone [24]. One percent acetone in hexane eluted saturated FAME (Fraction 1; F1), 4% acetone eluted mono-*trans* FAME plus the *t/t*-CLA (F2), 10% acetone eluted mono-*cis* FAME plus the *c,t/t,c*-CLA (F3), and 100% acetone eluted dienoic FAME (F4). This was followed by 3% acetonitrile in acetone to elute trienoic FAME (F5), 6% acetonitrile in acetone to elute tetraenoic FAME (F6), and 100% methanol to elute most of the remaining unsaturated

FAME (F7). All fractions were evaporated to dryness in a stream of N₂ and reconstituted in appropriate volumes of hexane before GC analysis.

Gas Chromatography

Samples were analyzed by use of an Agilent 7890A gas chromatograph (Agilent Technologies, Wilmington, DE, USA) equipped with two FID detectors, two split/splitless injection ports, and an autosampler. The system was controlled by the Agilent ChemStation (Version B.04.02) chromatography manager. A Supelco SP-2560 GC column (100 m × 0.25 mm internal diameter × 0.20 μm film thickness) was installed on one injection port, and a Supelcowax-10 (30 m × 0.25 mm internal diameter × 0.25 μm film thickness) on the other. The carrier gas was H₂, the injection volume was 1 μL (equivalent to approximately 1–2 μg FAME). The split ratio was set to 100:1 for the GC standards and test samples, and to 20:1 for the Ag⁺-SPE fractions. Further details of the two GC columns and the chromatographic conditions are reported in Table 1. When utilizing the SP-2560 GC column, two different temperature programs denoted 175 and 150 °C (on the basis of their plateau temperatures) were used to separate co-eluting FAME [24, 26]. Monounsaturated FA and non-methylene interrupted (NMI) PUFA were designated by use of the Δ nomenclature, i.e., 9c-18:1. FA with two or more methylene-interrupted double bonds were designated by use of the n-notation, i.e., 18:2n-6.

Results

The GC separations of the FAME prepared from the menhaden oil analytical standard (#47116, Supelco) and from the fish muscle (gilthead sea bream, *Sparus aurata*) by use of the SP-2560 GC and Supelcowax-10 columns are shown in Figs. 1 to 4. In each figure the upper panel (a) shows the separation obtained by use of the SP-2560 column and the elution temperature with plateau at 175 °C, the middle panel (b) shows the separation obtained by use of the SP-2560 column and the plateau at 150 °C, and the lowest panel (c) shows the separation obtained by use of the Supelcowax-10 column. In each panel the chromatograms show separations of menhaden oil (MO) and/or of fish muscle (FM) FAME, followed by the FAME contained in selected Ag⁺-SPE fractions from fish muscle (F1–F7), and, at the bottom, GC reference mixture #463 or #674. The GC separations were divided into Figs. 1 to 4 on the basis of the elution principle of PEG columns in which all unsaturated FA of chain length *x* elute between the retention time of the saturated FAME C_{*x*}:0 and the saturated FAME (C_{*x*+2}):0. Figure 1 shows the separation segment of

Table 1 Details of the GC conditions, GC columns and temperature programs used

Description	SP-2560 ^a	Supelcowax-10 ^b
Column dimensions	100 m × 0.25 mm i.d. × 0.20 μm film thickness	30 m × 0.25 mm i.d. × 0.25 μm film thickness
Injector temperature	250 °C	235 °C
Detector temperature	250 °C	300 °C
H ₂ flow to detector	30 mL/min	30 mL/min
Air flow to detector	300 mL/min	400 mL/min
Makeup gas to detector (N ₂)	20 mL/min	25 mL/min
Carrier flow (H ₂)	1 mL/min	1.2 mL/min
Temperature program	45 °C (4 min)–13 °C/min–175 °C (27 min)–4 °C/min–215 °C (35 min) = 86 min	170 °C (0 min) –1 °C/min–225 °C = 60 min
Temperature program-2	45 °C (4 min)–13 °C/min–150 °C (47 min)–4 °C/min–215 °C (35 min) = 110.3 min	

Both GC columns were purchased from Supelco (Bellefonte, PA, USA)

^a Conditions were essentially the same as described elsewhere [24]

^b Conditions were essentially the same as recommended in the official AOCS method (Ce 1i-07) for marine oil analysis [5]

FAME from 16:0 to 18:0, Fig. 2 from 18:0 to 20:0, Fig. 3 from 20:0 to 22:0, and Fig. 4 from 22:0 to 22:6n-3. Identification of the *cis/trans*-16:1, *cis/trans*-18:1, and *cis/trans*-20:1 isomers was based on the principles of silver-ion separation, direct comparison with selected isomers contained in the GC reference standards, and comparison with previously synthesized compounds and published reports [5, 10, 23, 24, 30–32]. Selected fractions and total menhaden oil were also analyzed by use of a 100-m SLB-1L111 ionic-liquid column [33] to compare their elution times with those of synthetic FAME [32].

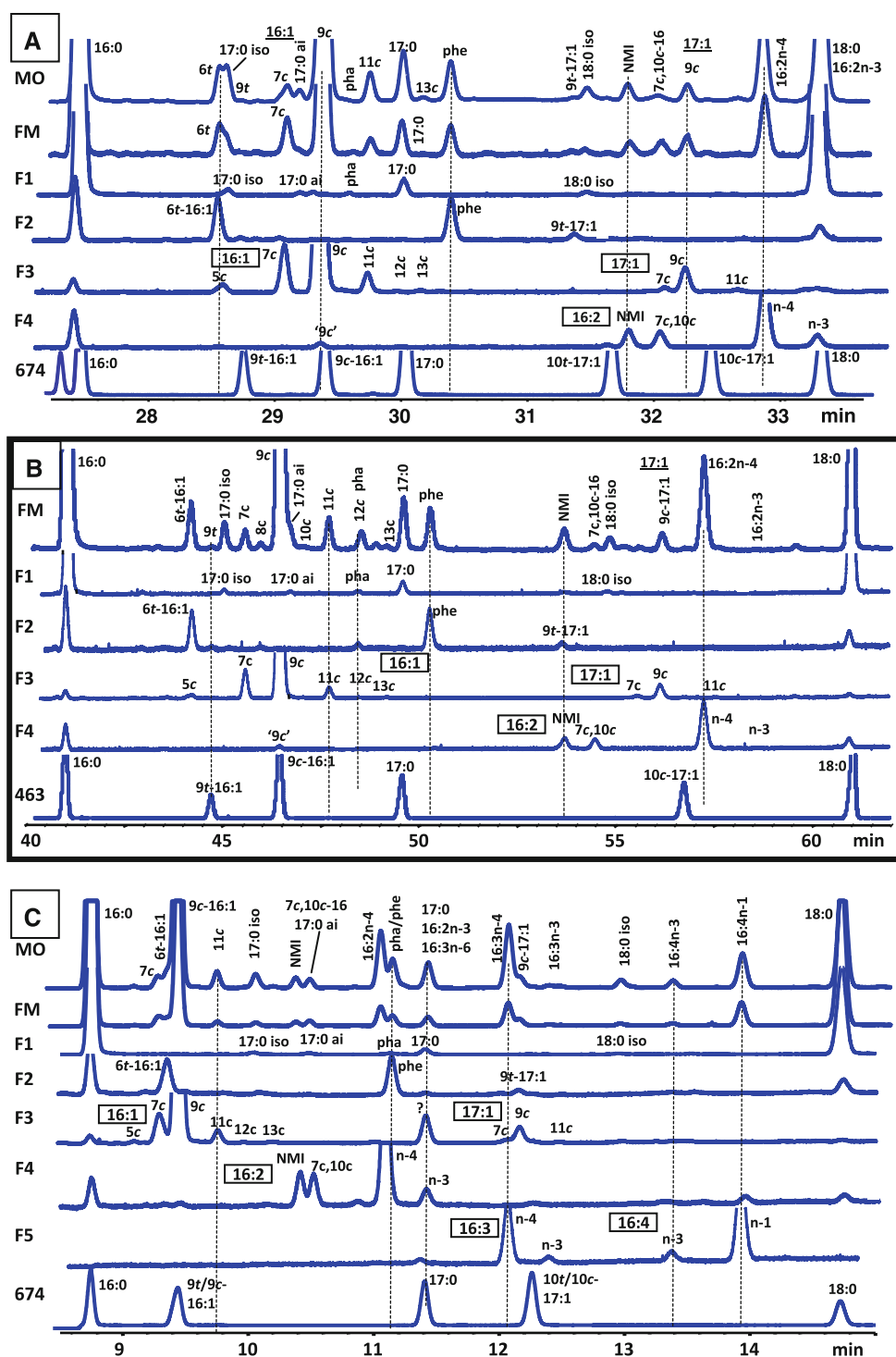
Each panel shows the separation of only the Ag⁺-SPE fractions that provide useful information for identification of the FAME eluting in that region. The GC separation of the Ag⁺-SPE fractions showed there was only minor carryover of the saturated (F1), *trans*-MUFA (F2), *cis*-MUFA (F3), and diunsaturated FA (F4) into subsequent fractions. However, partial overlap of the trienoic and tetraenoic unsaturated FAME was observed for fractions F5 to F7 (e.g. Figs. 3, 4), and some overlap of the tetraenoic and pentaenoic unsaturated FAME was observed for F6 and F7 (e.g. Figs. 3, 4). DHA, and FAME with six double bonds were not recovered even by use of 100% methanol as eluent.

Figure 1 shows the separation of the geometric and positional isomers of 16:1 by use of the SP-2560 column with both the 175 and 150 °C temperature programs (Fig. 1a, b), and by use of the Supelcowax-10 column (Fig. 1c). The Supelcowax-10 column enabled some resolution of the positional isomers of MUFA methyl esters, but it failed to resolve the geometric isomers of 9-16:1 and 10-17:1, which is present in GC #674, and to resolve 6*t*-16:1 from the 6-7-8-9-16:1 cluster (Fig. 1c). In contrast, the unsaturated C16 FA were well resolved from each other by use of this column (Fig. 1c), all eluting before the 18:0 FAME, including four 16:2 (F4; Fig. 1c), two 16:3 (F5;

Fig. 1c), and two 16:4 FAME isomers (F5; Fig. 1c). However, some C16 PUFA overlapped, for example 16:2*n*-4 with methyl phytanate and phytanate, 16:2*n*-3 with 17:0, and 16:3*n*-4 with 9*c*-17:1. The separation of the unsaturated C16 FA on the SP-2560 column was very different, because of the higher polarity of its stationary phase. Considering the C16 PUFA, only the four 16:2 isomers eluted before 18:0 (F4; Fig. 1a), and one of the isomers (16:2*n*-3) overlapped with 18:0 when the 175 °C temperature program was used (F4; Fig. 1a). However, the latter pair was resolved at 150 °C (F4; Fig. 1b). The more unsaturated FA of C16 eluted in the 18:1 FA region on the SP-2560 column, irrespective of the elution temperature plateau used. Branched-chain iso and anteiso-17:0 FA coeluted with other FA on both columns. These branched-chain FA were identified in the SP-2560 separations by comparing the separations obtained in the elution profiles with plateaus at 150 and 175 °C (Fig. 1a, b); 17:0 anteiso coeluted with 7*c*, 10*c*-16:2 on the Supelcowax -10 column (Fig. 1c). Of special interest was the identity of a *trans*-16:1 isomer that coeluted with 17:0 iso at 175 °C, but was resolved at 150 °C. Menhaden oil and fraction F2 were analyzed by use of a 100-m SLB-1L111 column that resolves the 6*t*-, 7*t*-, and 8*t*-16:1 isomers [33] that coelute on a SP-2560 column [32]. This result showed that this peak eluted at the same time as 6*t*-16:1.

Phytanic acid (3,7,11,15-tetramethylhexadecanoic acid) and phytenic acid (3,7,11,15-tetramethylhexadec-2-enoic acid) were generally present in fish muscle, but their identification required Ag⁺-SPE fractionation before GC analysis. As seen in the separations obtained by use of the SP-2560 (Fig. 1a, b) and Supelcowax -10 columns (Fig. 1c), methyl phytanate (pha) eluted in the SPE saturated FA fraction (F1), and methyl phytenate (phe) in the *trans*-MUFA SPE fraction (F2). These results showed that trace amounts of methyl phytanate were present in fish

Fig. 1 Partial GC separation of the FAME that eluted between 16:0 to 18:0 obtained from menhaden oil (MO), a fish muscle (FM) sample, fractions 1–5 from Ag^+ -SPE of FM, and GC standard mixtures #674 and/or #463. The separations presented in panel **a** were obtained by use of a 100-m SP-2560 column operated using a temperature program from 45 to 215 °C with a plateau at 175 °C; those in panel **b** were obtained by use of the same 100-m SP-2560 column operated using a temperature program from 45 to 215 °C with a plateau at 150 °C, and panel **c** was obtained by use of a Supelcowax-10 column operated using a temperature program from 170 to 225 °C. Complete details of the chromatographic conditions are reported in Table 1. Monounsaturated FA were designated by use of the “ Δ ” nomenclature whereas the more unsaturated FA were designated by use of the “n-x” nomenclature. *DMP* dimethyl phthalate, *NMI* non-methylene interrupted, *pha* methyl phytanate, *phe* methyl phytenate, *c cis*, *t trans*, *ai* anteiso. Fatty acids shown in quotation marks are residual fatty acids in the subsequent Ag^+ -SPE fractions; those with a question mark are tentative identifications

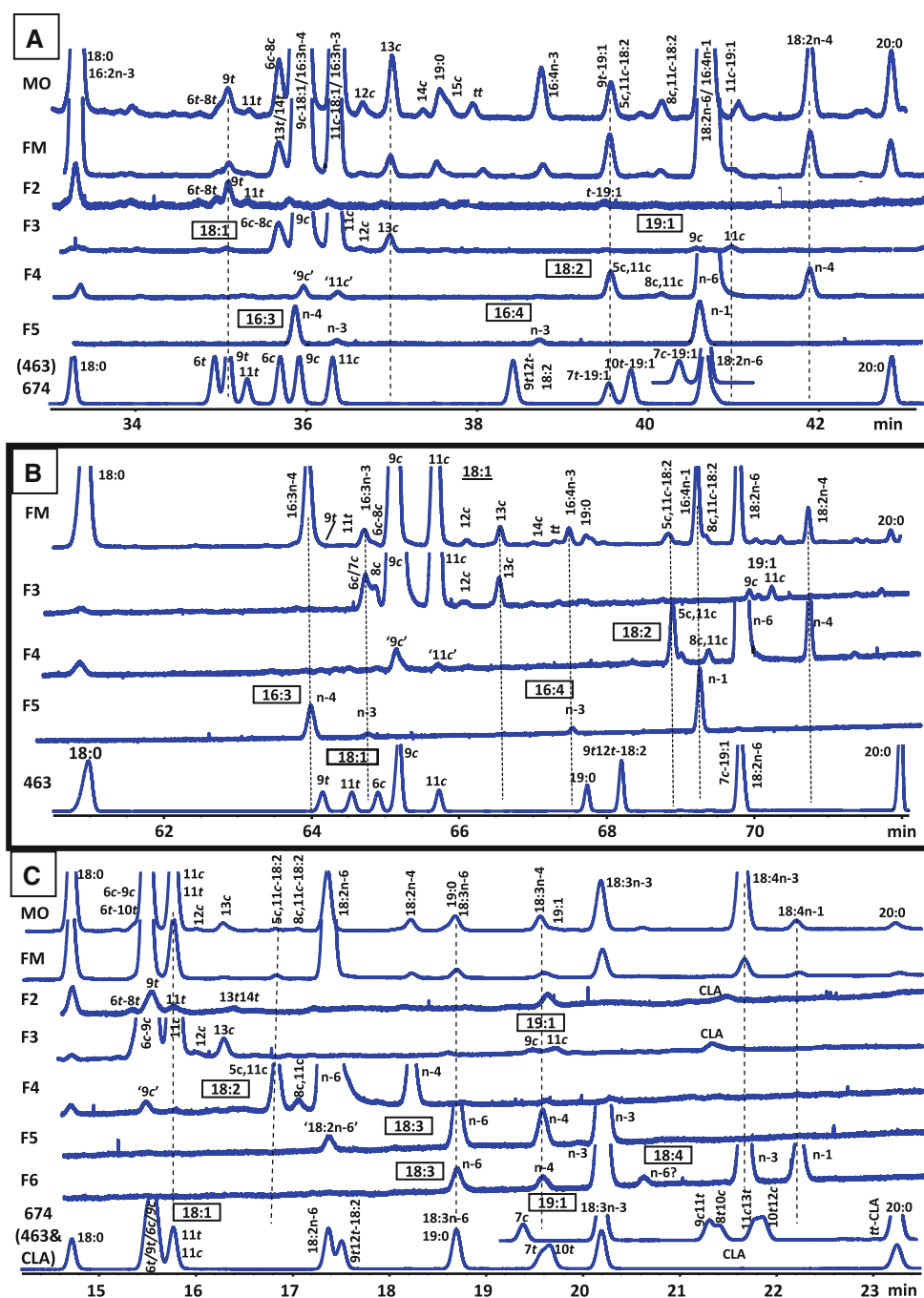


muscle and eluted in the tail of the 9c-16:1 peak on the SP-2560 column with the 175 °C plateau (Fig. 1a) and just ahead of 12c-16:1 with the 150 °C plateau (Fig. 1b). On the other hand, a significant amount of methyl phytenate was present in fish muscle and eluted after 17:0 FA on the SP-2560 column used with either temperature program (Fig. 1a, b). The elution of methyl phytenate and phytenate using the SP-2560 column and both temperature programs

has previously been established by use of authentic standards (Kramer et al., unpublished). Methyl phytenate and phytenate coeluted when using the Supelcowax-10 column, and these two compounds were only partially separated from 16:2n-4 FA (Fig. 1c).

Figure 2 shows the partial GC chromatogram from 18:0 to 20:0 FA using both GC columns. Separations using the SP-2560 column included mainly the 18:1 and 18:2

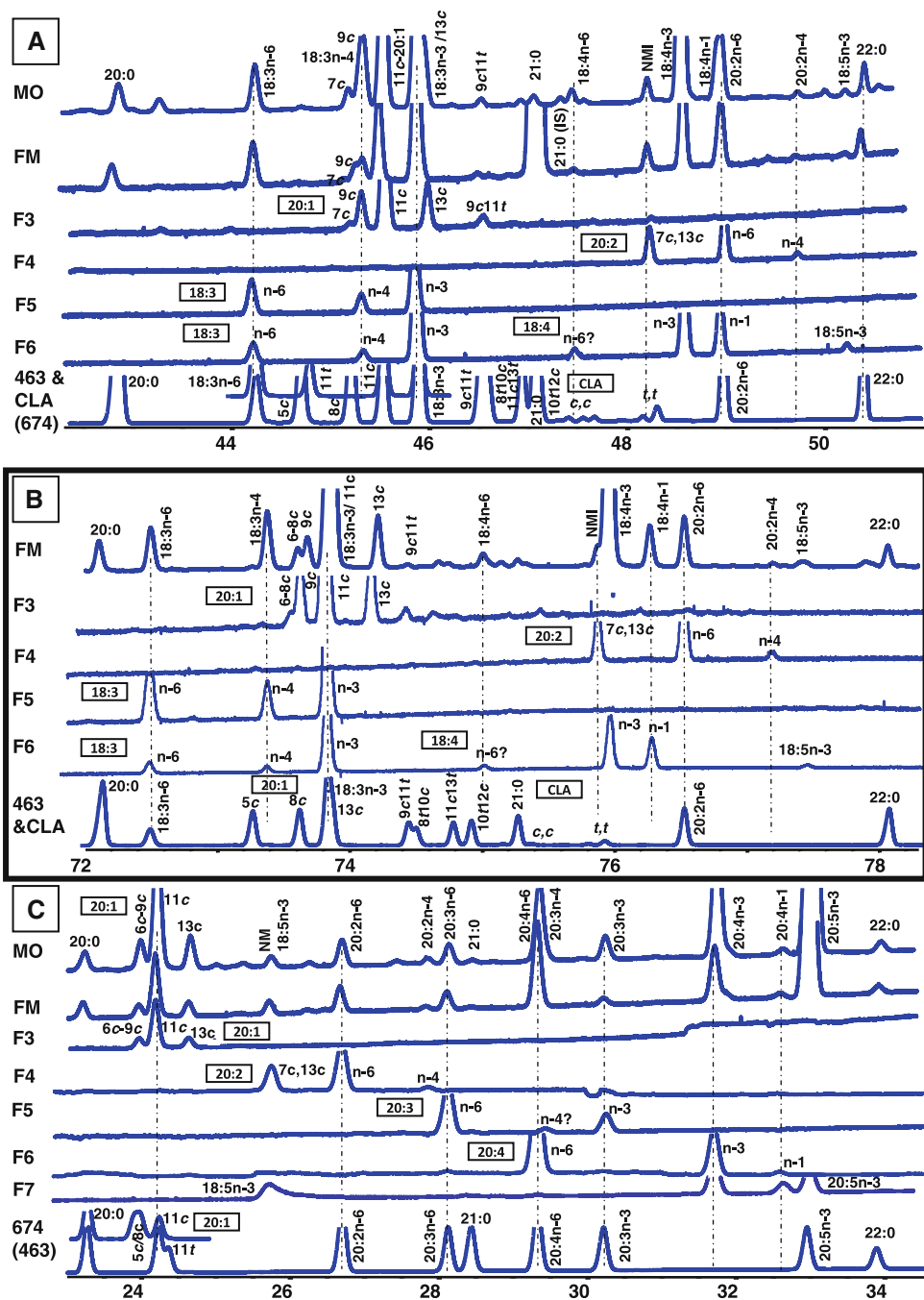
Fig. 2 Partial GC separation of the FAME that eluted between 18:0 to 20:0 obtained from menhaden oil (MO), a fish muscle (FM) sample, fractions 2–6 from Ag⁺-SPE of FM, and GC standard mixtures #674 (with a partial insert from #463). Other details are the same as for Fig. 1



isomers plus the highly unsaturated C16 FA (Fig. 2a, b), whereas this selected portion of the chromatogram using the Supelcowax-10 column included all the 18:1, 18:2, and 18:3 plus CLA isomers (Fig. 2c). Small amounts of several *trans*-18:1 isomers were identified in both the menhaden oil and fish muscle samples, as was evident from the separations achieved by use of the SP-2560 column (F2; Fig. 2a). To see whether the *trans*-18:1 isomers were derived from the diet, the feed was analyzed and found to contain 0.16% FAME; this amount was similar to that found in the fish muscle (0.14%) and the distribution of

trans-18:1 was also similar. In contrast, the commercial menhaden oil contained 0.20 and 0.13% *trans*-18:1 and CLA, respectively. By contrast, when the Supelcowax-10 column was used, these isomers all coeluted with the *cis*-18:1 isomers (Fig. 2c). The SP-2560 column also resulted in improved resolution of the positional isomers of *cis*-18:1 (Fig. 2a, b) compared with that obtained by use of the Supelcowax-10 column (Fig. 2c). GC separation of reference mixture #674 confirmed the lack of resolution of the geometric isomers of 6-18:1, 9-18:1, and 11-18:1, and the positional isomers of 6-18:1 and 9-18:1, and 7*t*-19:1 and

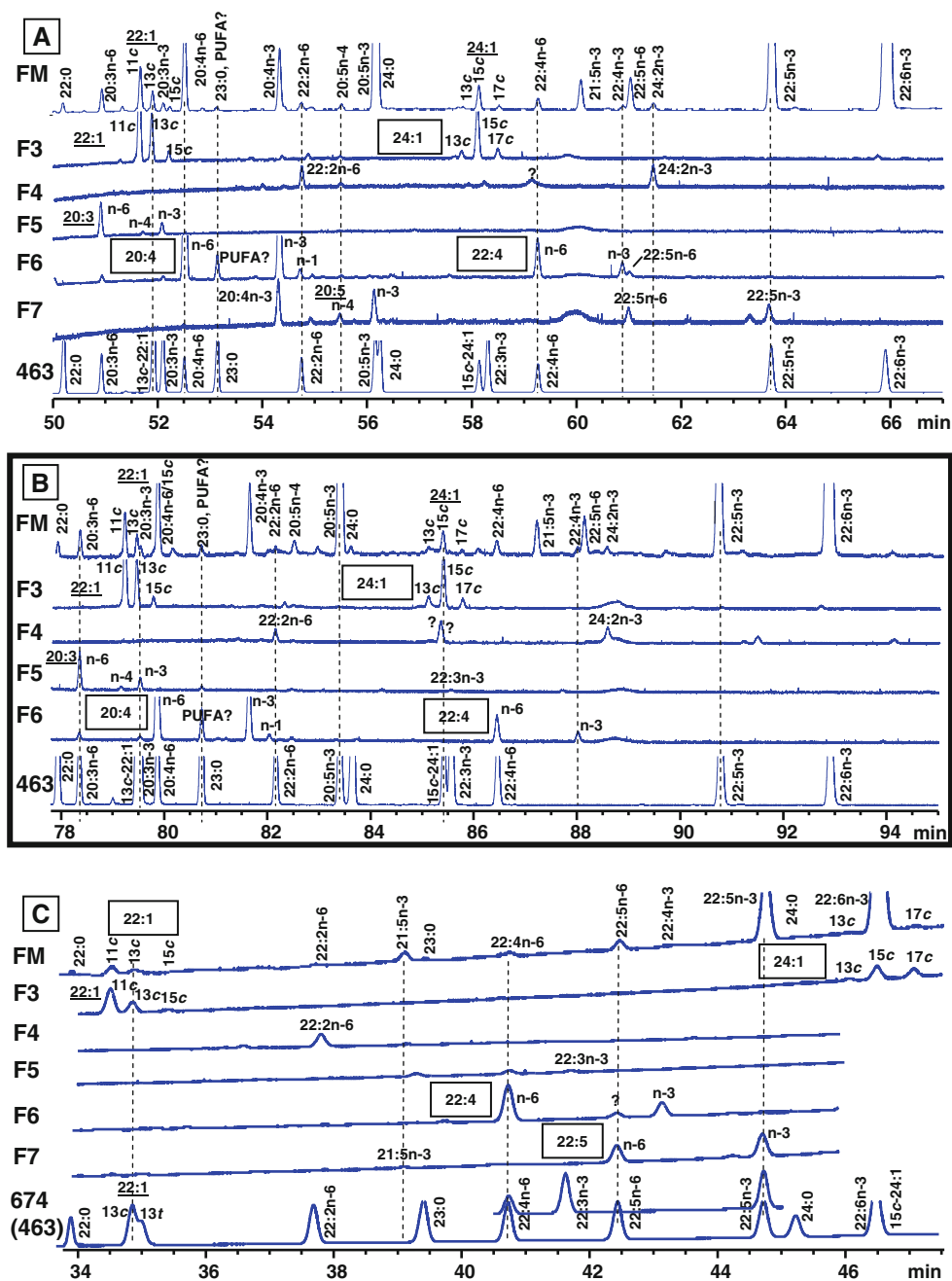
Fig. 3 Partial GC separation of the FAME that eluted between 20:0 to 22:0 obtained from menhaden oil (MO), a fish muscle (FM) sample, fractions 3–7 from Ag⁺-SPE of FM, and GC standard mixture #463 spiked with CLA mixture #UC-59M, and FAME 21:0. Other details are the same as for Fig. 1



10*t*-19:1 (Fig. 2c). However, the Supelcowax-10 column clearly resolved four 18:2 (F4; Fig. 2c), three 18:3 (F5 and F6; Fig. 2c), and possibly three 18:4 (F6; Fig. 2c) isomers with little interference from other FA, except for 18:3*n*-6 with 19:0, 18:3*n*-4 with several 19:1 isomers, and 18:4*n*-3 and 18:4*n*-1 with a number of *c/t* and *c/c* CLA isomers (Fig. 2c). Identification of two 16:3 and two 16:4 isomers in fish products was a challenge when using the SP-2560 column; 16:3*n*-4 and 16:3*n*-3 coeluted with 9*c*-18:1 and 11*c*-18:1, respectively, at 175 °C (Fig. 2a) whereas at 150 °C both of these FA pairs were separated (Fig. 2b).

Identification of 16:3*n*-3 was confirmed by use of an authentic standard. A similar situation occurred with the two 16:4 isomers—16:4*n*-3 was better separated at 175 °C (Fig. 2a) whereas 16:4*n*-1 was better resolved at 150 °C (Fig. 2b). The structure of the two NMI 18:2 isomers was established by comparison with similar peaks in GC chromatograms obtained by use of the official AOCS method (Ce li-07) for marine oils. The 18:0–20:0 region of the chromatogram obtained by use of the SP-2560 column also included the four 18:2 isomers (F4), which were resolved by use of either temperature program (Fig. 2a, b).

Fig. 4 Partial GC separation of the FAME that eluted between 22:0 to 22:6n-3/24:1 obtained from menhaden oil (MO), a fish muscle (FM) sample, fractions 3–7 from Ag^+ -SPE of FM, and GC standard mixtures #463 or #674 (with a partial insert from #463). Other details are the same as for Fig. 1



When the Supelcowax-10 column was used the *c,t/t,c*-LA isomers eluted among the 18:4 FA, and the *t,t*-CLA isomers eluted just before 20:0.

Figure 3 shows the partial GC chromatograms obtained from 20:0 to 22:0 FA. In this region, four *cis*-20:1 isomers isolated in Ag^+ -SPE fraction F3 are eluted from both GC columns. This region on the SP-2560 column also included three 20:2 (F4; Fig. 3a, b), three 18:3 (F5; Fig. 3a, b), three 18:4 (F6; Fig. 3a, b), and the CLA isomers (Fig. 3a, b). This region on the Supelcowax-10 column (Fig. 3c) included three 20:2 (F4), three 20:3 (F5), and three 20:4 (F6) isomers. Trace amounts of *trans*-20:1 isomers were

detected in fish muscle (F2 fraction not included in Fig. 3a). The Supelcowax-10 column only partially separated the *cis/trans* isomers of 11-20:1 FA contained in GC reference standard #674 (Fig. 3c). However, the C20, C21, and C22 unsaturated FA were all well separated, with the exception of 20:3n-4 and 20:4n-6 FA (Fig. 3c). The *cis* and *trans* 20:1 isomers were well resolved by use of the SP-2560 column, but they overlapped with several 18:3 isomers (Fig. 3a, b). Little separation of the geometric and positional isomers of 20:1 was achieved by use of the Supelcowax-10 column, but no other FA interfered with them (Fig. 3c). Use of the SP-2560 column with the 175 °C

temperature program resulted in the coelution of two 18:3 isomers with *cis*-20:1 isomers (18:3n-4 with 9*c*-20:1 and 18:3n-3 with 13*c*-20:1), and of 18:4n-1 with 20:2n-6 (Fig. 3a). Each of these three pairs of FA were separated, or coeluted with different FA, when the 150 °C program was used (Fig. 3b), thus enabling their resolution. The chromatogram obtained from the reference mixture shows that the CLA isomers eluted in a region free of other FA when the SP-2560 column was used, with the exception of 21:0 (Fig. 3a). When the 175 °C program was used 21:0 eluted close to 10*t*,12*c*-CLA (Fig. 3a) whereas at 150 °C 21:0 eluted among the *c,c*-CLA isomers (Fig. 3b). When the Supelcowax-10 column was used the CLA isomers eluted among the 18:4 FA isomers, and well before 20:0 (Fig. 2c). Minor peaks observed in both fish products that eluted in the CLA region were tentatively identified as *c,t*-CLA, *t,c*-CLA, and *t,t*-CLA isomers; the distribution of these CLA isomers seems to be random.

Figure 4 shows the partial GC chromatograms obtained from the remaining FA starting from 22:0 FA. This segment contained the long-chain MUFA (LC-MUFA) 22:1 and 24:1, plus the most unsaturated PUFA present in fish products. Three positional isomers of *cis*-22:1 and *cis*-24:1 were detected, and were well resolved by use of either GC column, as is evident in the separation of fraction F3 from Ag⁺-SPE. Cetoleic acid (11*c*-22:1) was the most abundant 22:1 isomer, and nervonic acid (15*c*-24:1) was the most abundant 24:1 isomer (Fig. 3). When the Supelcowax-10 column was used the two geometric isomers of 22:1 present in GC reference standard #674 were not resolved (Fig. 4c). No *trans* isomers of 22:1 and 24:1 were detected in fish muscle (data for F2 not shown). The SP-2560 column separated three isomers of 20:3 (F5; Fig. 4a, b), three isomers of 20:4 (F6; Fig. 4a, b), two isomers of 22:4 (F6; Fig. 4a, b), two isomers of 20:5 (F7; Fig. 4a), and two isomers of 22:5 (F7; Fig. 4a, b). Fraction F7 was not included in Fig. 3b (150 °C program) because of the weak detector response. The separation of 20:5n-3 and 24:0 by use of the SP-2560 column at 175 °C was partly obscured by the dominant 20:5n-3 peak in these fish products (Fig. 4a). However, these two FA were resolved by use of the 150 °C program (Fig. 4b). The Supelcowax-10 column separated most C22 and C24 unsaturated FA, which included two 22:4 isomers (F6; Fig. 4c), 21:5n-3, and two 22:5 isomers (F7; Fig. 4c), with the exception of 22:6n-3 from 15*c*-24:1 in the reference standard (Fig. 4c). On the other hand, when utilizing the SP-2560 column, two 20:3 isomers coeluted with *cis*-22:1 isomers (20:3n-4 with 11*c*-22:1 at 175 °C (Fig. 4a), and 20:3n-3 with 13*c*-22:1 at 150 °C (Fig. 4b)). Trace amounts of 23:0 were detected in Fraction 1 on both columns (data not shown in Fig. 4); in addition, when the SP-2560 column was used, an unknown PUFA eluted in Fraction 6 with the same retention time as

23:0 both at 175 °C (Fig. 4a) and at 150 °C (Fig. 4b). However, this additional PUFA peak was not clearly evident in Fraction 6 of Figs. 3c or 4c when the Supelcowax-10 column was used.

Discussion

The separations presented here, obtained by use of the 30-m Supelcowax-10 and the 100-m SP-2560 columns, provide complementary results in the analysis of FAME prepared from fish oils or fish tissues. The Supelcowax-10 column was very useful for identifying unsaturated FA by chain-length, and number and position of their double bonds. On the basis of this observation, Ackman [8] first suggested the use of PEG columns as reference in inter-laboratory studies for quantification of FA in marine oils by GC to minimize overlaps of unsaturated FA. Since then, PEG-coated GC columns have been used to confirm the presence of highly unsaturated FA in marine and other oils containing LC PUFA. This type of GC column is currently recommended in the most recent official AOCS method (Ce 1i-07) for quantification of FA in marine oils [5]. However, the limitations of separations achieved by use of PEG-coated columns are equally evident, particularly regarding the coelution of geometric isomers of unsaturated FA. For instance, the Supelcowax-10 column could not separate the geometric isomers of the 16:1, 18:1, 19:1, 20:1, and 22:1 FA contained in reference mixtures #674 and #463, but was able to resolve the positional isomers themselves except the ones with the double bond toward the methyl end of the molecule. On the other hand, the SP-2560 column separated the geometric isomers of all 16:1, 18:1, 19:1, 20:1, and 22:1 FA, and also enabled superior separation of the positional isomers themselves. Selecting a 60-m Supelcowax-10 column, instead of the 30-m version recommended in AOCS official method Ce 1i-07, would result in improved separation of some FAME and in a slight shift of the order of elution of others [10]. For instance, the 60-m Supelcowax-10 column resulted in separation of 22:6n-3 and 15*c*-24:1, but 22:0 and 20:5n-3 overlapped, and the *t,t*-CLA isomers coeluted with the 20:1 FA isomers. However, most importantly, increasing the length of the Supelcowax-10 column did not improve the separation of the geometric isomers of the unsaturated FAME. Mjøs [25] used a 50-m BP-20 (PEG type) column and achieved separation of several mono-*trans* and di-*trans* isomers of EPA and DHA, but did not comment whether this column could resolve other geometric isomers that might be present in fish products.

The lack of separation of geometric isomers of unsaturated FA using the PEG columns is a major concern that has serious implications for the analysis of fish oil and

fish-containing products whenever *trans* FA isomers are suspected to be present. Mjøs [13] isomerized pure EPA and DHA, by use of *p*-toluenesulfonic acid in dioxane, and was able to separate most of their mono and di-*trans* geometric isomers on a 100-m SP-2560 column, after isolating the compounds by silver-ion HPLC chromatography. In a similar study, Fournier et al. [15–17] investigated the geometric isomers of EPA and DHA produced during the deodorization of fish oil, and showed that separation of the geometric isomers required the use of a 100-m CP-Sil 88 column. Mjøs [25] further showed that the geometric isomers of EPA and DHA could be equally well resolved by use of a 50-m BP-20 (PEG) or a 60-m BPX-70 column; Fournier et al. [15–17] did not report the separation of these FA isomers by use of PEG-coated columns. These results are consistent with the observations of Sébédio et al. [11] who found only small quantities of geometric isomers of the LC highly unsaturated PUFA in deep fried mackerel by use of a 30-m Supelcowax-10 column. It would seem from these results that PEG columns, for example the 50-m BP-20 column, are able to resolve many of the geometric isomers of EPA and DHA.

On the basis of our results with the 30-m Supelcowax-10 column, isomers of EPA and DHA were not detected, but the geometric isomers 16:1–22:1 were not separated. This would explain why Sébédio et al. [11] found only geometric isomers of LC highly unsaturated PUFA in deep fried mackerel by use of a 30-m Supelcowax-10 column, the same GC column we used. We recently evaluated FT-NIR for quantification of FA in fish oil preparations enriched with EPA and DHA [20]. We observed that the amount of the all-*cis* highly unsaturated FA contained in these oils was significantly overestimated when a 30-m PEG FAMEWAX column was used for calibration of the FT-NIR spectrometer, rather than when a 100-m CP Sil 88 column was used. Similar results would be expected in analysis of the PUFA and *trans* FA content of foods containing fish or fish oil, infant formulas supplemented with marine or algal oils, or n-3-enriched capsules using any 30-m PEG-coated GC column. The observation of a *trans*-16:1 peak in fish muscle (Fig. 1) was of interest. This FA could not be identified by use of the Supelcowax-10 column, but on the CPS column it had the same elution time as the *6t/7t/8t*-16:1 peak [32]. On further investigation of the fish sample by use of an SLB-1L111 ionic-liquid column [33] it was shown that this isomer had the same elution time as *6t*-16:1 in the synthetic mixture of 16:1 isomers [33]. It is interesting to note that Ackman [34] reported the occurrence of *6t*-16:1 in a number of marine species. A single *trans*-16:1 isomer, *3t*-16:1, was also identified in spinach by use of similar CPS columns [35].

It was tempting to determine the presence of isomerized FA in fish products by using the recommended SP-2560

column for the analysis of *trans* FA [29] in addition to using the Supelcowax-10 column recommended for marine oil analysis [5]. However, such a detailed comparison of elution profiles provided by these two GC columns for the same fish samples is not currently available. Complete analysis of the unsaturated FA in fish muscle and fish oil by use of the highly polar SP-2560 capillary column proved to be a challenge, because of the extensive overlap of unsaturated FA with those of longer chain length, and the presence of *trans* isomers. To confirm the identity of several FA contained in menhaden oil and fish muscle samples, complementary silver-ion separation of the total fish muscle FAME was conducted by use of Ag⁺-SPE cartridges. These Ag⁺-SPE cartridges proved to enable rapid, economical, and effective fractionation of the total FAME of fish muscle on the basis of their number of double bonds and geometric configuration. The success of Ag⁺-SPE fractionation depends on loading the SPE tubes with a moderate amount of FAME; approximately 0.4–1 mg was generally sufficient. Each of the seven fractions obtained from Ag⁺-SPE was then compared with the original fish muscle FAME preparation, utilizing the results from both GC columns. The identities reported in Figs. 1 to 4 were established only when there was agreement between the FA separated using both GC columns, the results obtained by use of both temperature programs with the SP-2560 column, and the fractions obtained by use of the Ag⁺-SPE cartridges. Additional confirmation using GC–mass spectrometry was considered but suitable equipment was not available.

Every effort was made in this study to avoid conditions leading to isomerization of menhaden oil and lipids extracted from the fish muscle sample, and the results indicate no *trans* isomers of 22:6n-3, 22:5n-3, and 20:5n-3 were present. However, trace amounts of *trans* and CLA isomers were observed in the separations using the SP-2560 column. It was suspected that the diet might be the source of the minor *trans*-18:1, *trans*-20:1, and CLA isomers (Figs. 2, 3) as suggested by Ackman [36], because fish from the ocean do not contain these FA [34]. To confirm the presence of the CLA isomers, Fraction 3 could have been analyzed by Ag⁺-HPLC with UV detection at 233 nm [23]. Minor peaks observed in Figs. 3 and 4 were also tentatively identified as geometric and positional isomers of dienoic and trienoic FA. Identification of geometric isomers of PUFA in fish oil and fish muscle was made difficult by the unavailability of reference materials of isomerized C20 and C22 unsaturated FA. To locate the region in the chromatogram where the C18 to C22 unsaturated FA isomers would be expected to elute, separation of the FAME prepared here from the menhaden oil sample was compared with that of fractions obtained from a partially hydrogenated fish oil (PHFO) sample acquired during a previous study (Kraft and Kramer, unpublished data). The

PHFO sample had been fractionated by Ag^+ -SPE, by following the same procedure described here, yielding, among others, fraction F4 that contained non-conjugated dienoic FA and fraction F5 that contained trienoic FA. These fractions were analyzed by GC with an SP-2560 column operated under the same chromatographic conditions described here, and the temperature program with the elution plateau at 175 °C [24]. Figure 5 shows the stacked separations of menhaden oil FAME, fractions F4 and F5 from the PHFO sample, and of GC reference mixture #463 spiked with CLA. Direct comparison of the individual FAME isomers of menhaden oil and fractions F4 and F5 from PHFO is obviously not possible, or intended, because partial hydrogenation and thermal isomerization would produce different sets of FA isomers, but it does provide an indication of where these dienoic and trienoic FA might elute. Minor unidentified peaks were evident in the menhaden oil FAME separation at retention times corresponding to the clusters of *c,t/t,c* and *c,c-18:2*, *c,t/t,c* and *c,c-20:2*, *c,t/t,c* and *c,c-22:2* in F4, and *c,c,t*, *c,t,t*, and *c,c,c-18:3*, *c,c,t*, *c,t,t*, and *c,c,c-20:3*, and *c,c,t*, *c,t,t*, and *c,c,c-22:3* in F5 (Fig. 5), indicating the possible presence of FA with similar chemical structure. The total amounts of all the peaks that were not assigned in the GC chromatogram of menhaden oil and fish muscle were 0.91 and 0.60%, respectively. This value would be the sum of unknown natural PUFA in the fish and possible isomerized FA; the

latter could also originate from the feed that contained 0.71% unassigned peaks.

ECL values are often calculated for FAME separated on different GC columns to provide greater ease of comparison, because the logarithms of the retention times have a characteristic relationship with common FA structures [8, 9, 27, 28, 37]. MUFA and methylene-interrupted PUFA with the same number of double bonds, in the same geometric configuration, and in the same position relative to the terminal carbon have similar ECL values when separated with the same GC column, irrespective of their chain length. The ECL values reported in Table 2 for the FA identified in the separations achieved on both GC columns were calculated by use of the equations described by Bannon et al. [27] for uncorrected FA retention times. Only the ECL values obtained from the uncorrected retention times for most of the FAME of interest in fish oil are presented in Table 2, because differences between ECL values obtained by use of uncorrected and corrected retention time values were minimal. FAME with the same terminal double bond system using the “*n-x*” nomenclature gave similar ECL differences, or fractional chain lengths (FCL), relative to the corresponding saturated FA analogues. The average FCL values of unsaturated FA within each “*n-x*”-FA family is also presented. Although the ECL concept was primarily developed for isothermal GC operations [8], these results suggest the concept applies to ECL

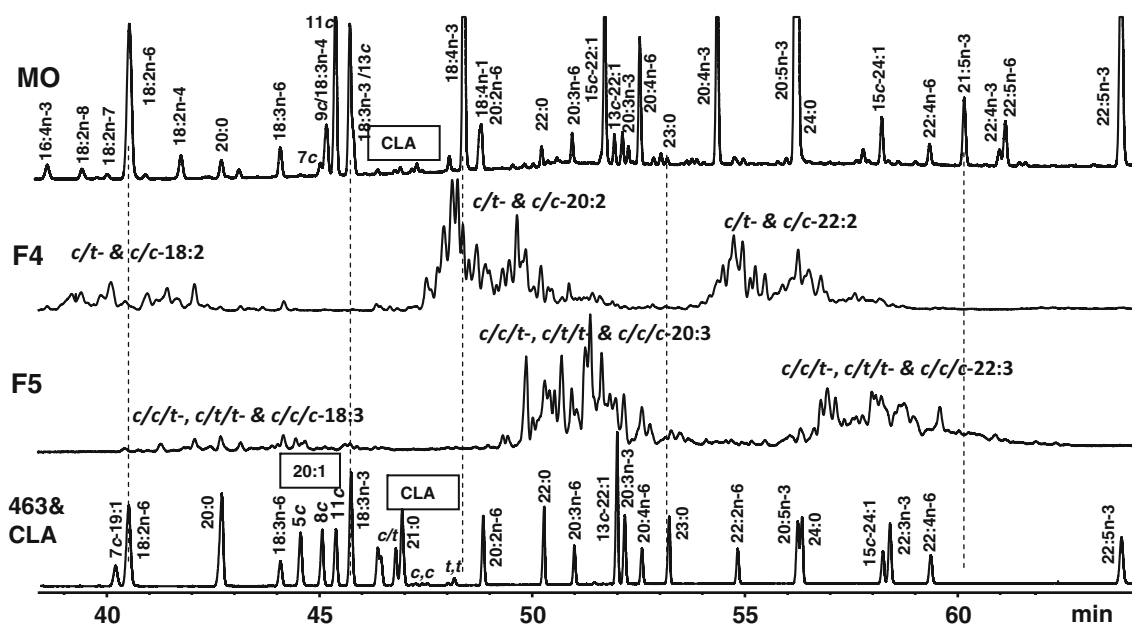


Fig. 5 Partial GC separations of the FAME that eluted between 16:4n-3 and 22:6n-3 from the top: FAME prepared from menhaden oil (MO); Ag^+ -SPE fractions 4 (dienoic FA) and 5 (trienoic FA) obtained from separation of FAME prepared from partially hydrogenated fish oil using the same Ag^+ -SPE technique (Kramer et al. [24]);

GC standard mixtures #463 spiked with CLA mixture #UC-59M, and FAME 21:0 and 23:0. All separations were achieved by use of an SP-2560 capillary column operated using the temperature program with a plateau at 175 °C (Kraft and Kramer, unpublished data), as described in Table 1

Table 2 Equivalent chain length (ECL), determined as described by Bannion et al. [27], of unsaturated fatty acids found in fish products. Also included are differences between ECL values for each fatty acid and for the corresponding saturated fatty acid analogue, i.e., the fractional chain length (FCL), and the average (Avg) within each of the unsaturated “*n-x*”-fatty acid families

FAME	Supelcowax-10 (30 m)			SP-2560 (100 m)		
	ECL	FCL	Avg FCL	ECL	FCL	Avg FCL
15:0 iso	14.514	0.514		14.465	0.465	
16:0 iso	15.515	0.515		15.463	0.463	
17:0 iso	16.518	0.518		16.464	0.464	
18:0 iso	17.499	0.499	0.511	17.452	0.452	0.461
15:0 anteiso	14.672	0.672		14.688	0.688	
17:0 anteiso	16.683	0.683	0.677	16.686	0.686	0.687
Pristanate	14.746	0.746		14.751	0.751	
Phytanate	16.908	0.908		16.782	0.782	
Phytenate	16.908	0.908		17.121	1.121	
16:1n-3 (13c)	16.575	0.575	0.575	17.054	1.054	1.054
14:1n-5 (9c)	14.405	0.405		14.915	0.915	
16:1n-5 (11c)	16.408	0.408		16.905	0.905	
18:1n-5 (13c)	18.429	0.429	0.414	18.878	0.878	0.899
17:1n-6 (11c)	17.383	0.383		17.812	0.812	
18:1n-6 (12c)	18.354	0.354	0.369	18.805	0.805	0.808
16:1n-7 (9c)	16.287	0.287		16.763	0.763	
17:1n-7 (10c)	17.285	0.285		17.716	0.716	
18:1n-7 (11c)	18.291	0.291		18.729	0.729	
20:1n-7 (13c)	20.296	0.296		20.725	0.725	
22:1n-7 (15c)	22.310	0.310	0.294	22.700	0.700	0.727
24:1n-7 (17c)	nd			24.326	0.326	ni
17:1n-8 (9c)	17.254	0.254	0.254	17.699	0.699	0.699
16:1n-9 (7c)	16.225	0.225		16.654	0.654	
18:1n-9 (9c)	18.218	0.218		18.641	0.641	
20:1n-9 (11c)	20.205	0.205		20.642	0.642	
22:1n-9 (13c)	22.209	0.209		22.589	0.589	0.631
24:1n-9 (15c)	24.197	0.197	0.211	24.265	0.265	ni
17:1n-10 (7c)	17.233	0.233		17.629	0.629	
19:1n-10 (9c)	19.272	0.272	0.253	19.672	0.672	0.651
20:1n-11 (9c)	20.158	0.158		20.600	0.600	
22:1n-11 (11c)	22.144	0.144	0.151	22.511	0.511	0.556
24:1n-11 (13c)				24.207	0.207	ni
NMI-16:2?	16.647	0.647		17.557	1.557	
7c,10c-16:2	16.683	0.683		17.629	1.629	
5c,11c-18:2	18.565	0.565		19.396	1.396	
7c,13c-20:2	20.512	0.512		21.347	1.347	
8c,11c-18:2	18.622	0.622		19.507	1.507	
18:2n-6 (9c12c)	18.699	0.699		19.609	1.609	
20:2n-6 (11c14c)	20.692	0.692		21.575	1.575	
22:2n-6 (13c16c)	22.711	0.711	0.696	23.487	1.487	1.575
16:2n-4 (9c12c)	16.887	0.887		17.874	1.874	
18:2n-4 (11c14c)	18.903	0.903		19.831	1.831	
20:2n-4 (13c16c)	20.912	0.912	0.901	21.802	1.802	1.835
16:2n-3 (10c13c)	17.000	1.000	1.000	18.000	2.000	2.000
18:3n-6 (6c9c12c)	19.014	1.014		20.344	2.344	
20:3n-6 (8c11c14c)	20.961	0.961	0.992	22.255	2.255	2.300

Table 2 continued

FAME	Supelcowax-10 (30 m)			SP-2560 (100 m)		
	ECL	FCL	Avg FCL	ECL	FCL	Avg FCL
16:3n-4 (6c9c12c)	17.233	1.233		18.641	2.641	
18:3n-4 (8c11c14c)	19.214	1.214		20.593	2.593	
20:3n-4? (10c13c16c)	21.339	1.339	1.262	22.511	2.511	2.582
16:3n-3 (7c10c13c)	17.339	1.339		18.729	2.729	
18:3n-3 (9c12c15c)	19.356	1.356		20.725	2.725	
20:3n-3 (11c14c17c)	21.369	1.369		22.657	2.657	
22:3n-3? (13c16c19c)	23.394	1.394	1.364	24.291	2.291	2.600
18:4n-6? (3c6c9c12c)	19.449	1.449		21.116	3.116	
20:4n-6 (5c8c11c14c)	21.193	1.193		22.794	2.794	
22:4n-6 (7c10c13c16c)	23.233	1.233	1.291	24.441	2.441	2.784
16:4n-3 (4c7c10c13c)	17.643	1.643		19.243	3.243	
18:4n-3 (6c9c12c15c)	19.670	1.670		21.456	3.456	
20:4n-3 (8c11c14c17c)	21.637	1.637		23.363	3.363	3.354
22:4n-3 (11c13c16c19c)	23.648	1.648	1.650	24.690	2.690	ni
16:4n-1 (6c9c12c15)	17.805	1.805		19.609	3.609	
18:4n-1 (8c11c14c17)	19.785	1.785		21.557	3.557	
20:4n-1 (10c13c16c19)	21.793	1.793	1.794	23.546	3.546	3.571
22:5n-6 (4c7c10c13c16c)	23.528	1.528	1.528	24.711	2.711	2.711
18:5n-3 (4c,7c,10c,13c,16c)	20.512	2.512		21.940	3.940	
20:5n-3 (5c8c11c14c17c)	21.864	1.864		23.909	3.909	
21:5n-3 (6c9c12c15c18c)	22.936	1.936		24.567	3.567	
22:5n-3 (7c10c13c16c19c)	23.907	1.907	1.903	25.109	3.109	3.631
22:6n-3 (4c7c10c13c16c19c)	24.188	2.188	2.188	25.421	3.421	3.421

Fatty acids are presented as A:Bn-x, where A = chain length, B = number of double bonds, n-x = number of carbons (n) from the terminal methyl group (x). The positions of double bonds from the carboxyl end of the fatty acids (Δ values) are given in parentheses

nd not detected; ni not included in average; NM non-methylene interrupted

values of FA determined after use of temperature programs (Table 2). However, the ECL values did decrease somewhat for the very LC PUFA of C22 and C24 (Table 2). The ECL values calculated in this study from the separations achieved by use of the Supelcowax-10 column were consistent with previously published ECL values for the same FA using the same GC column [7, 27, 37, 38]. In this study we include the ECL values of all FA of interest from fish oil using both the Supelcowax-10 and SP-2560 columns (Table 2).

There were some differences in the FCL values within the “n-x”-FA families that were mainly attributed to how the retention times of the FAME were determined. In chromatography, peaks are expected to have a Gaussian shape, and the retention time is the elution time at which the tangent of the chromatographic signal turns from positive to negative. As noted by Delmonte and Rader [39], when separating FAME on a GC capillary column coated with a highly polar stationary phase, the retention time of the FAME is affected by the amount injected on to the

column. FAME, especially those with a long chain and few double bonds, are poorly soluble in the thin coating of the highly polar stationary phase covering the internal wall of the capillary tube. The longer the hydrophobic chain of these FAME, the lower is the solubility of the FAME in the liquid stationary phase. During elution, if the concentration of the FAME reaches the condition of saturation into the liquid stationary phase, it will no longer correctly repartition between the gas carrier and the liquid coating, causing the peak to lose symmetry and resulting in a triangular shape and a progressive increase in retention time. For FAME that will not reach the saturation point in the liquid stationary phase, the top of their chromatographic peak gives a good estimate of the retention time. However, when the peak loses symmetry and acquires the classic triangular shape the beginning of the peak provides a better estimate of the FAME retention time. The ECL values in Table 2 were calculated on the basis of the retention times at maximum peak height. When the beginning of the peak, rather than the maximum peak height, was used to estimate

the FAME retention times of some peaks the ECL values for those FAME proved more consistent.

In this study, ECL values in combination with Ag^+ -SPE fractions were used to assign several FA peaks in the separations achieved by use of the Supelcowax-10 column that were not labeled in the chromatograms presented in the AOCS official method (Ce 1i-07) for analysis of marine oils [5]. This included several FAME tentatively identified as 16:2n-3, 12c-18:1, 18:4n-6, 6c-9c-20:1, 9c-19:1, 20:2n-4, 20:3n-4, 20:4n-1, 11c-22:1(n-11), 15c-22:1(n-7), 22:4n-4, and 24:4n-3. In addition, several coeluting *trans* isomers of 16:1 and 18:1 FA were clearly observed, as well as a 20:2 isomer and 18:5n-3. The 20:2 isomer seems to be 7c,13c-20:2, a chain elongated metabolite of 5c,11c-18:2, because they have a similar ECL (Table 2). Furthermore, some FA in the commercial marine standard seem to be incorrectly labeled (10c-17:1 should be 9c-17:1, 13c-18:1 should be 12c-18:1, 9c-11c-22:1 should be 11c-22:1(n-11), and 13c,16c,19c-22:3(n-3) and 7c,10c,13c,16c-22:4(n-6) should be exchanged). Identification of methyl phytanate and methyl phytenate in fish muscle by use of the Supelcowax-10 column proved particularly difficult, because these two isoprenoid FA coeluted and partially overlapped with 16:2n-4 (Fig. 1c). The major isoprenoid FA in fish muscle seemed to be phytenic acid rather than phytanic acid. These two isoprenoid FA were well separated on the SP-2560 column, and their identity was assigned on the basis of similar retention times from the GC analysis, the Ag^+ -SPE fraction in which they eluted, and consistency in the three separations (Fig. 1a, b, c).

The complementary results obtained by use of these two GC columns suggest that there is a need to use more than the PEG column to evaluate the FA composition of fish products, particularly when fish products are combined with other fats, for example partially hydrogenated vegetable oils or dairy fats. It is becoming evident that even a 100-m CPS by itself is limited in its capacity to resolve these FAME mixtures in a single analysis. Mjøs and Haugsgjerd [40] recently reported extensive overlap of FA common in fish oils with 16:1, 18:1, 18:2, and 18:3 isomers present in other fats. FAME were identified on the basis of the distinct differences in their electron impact mass spectra, but identification of minor and overlapping peaks by mass spectrometry was not possible [40]. There are numerous instances of such limitations in GC separations, indicating that mass spectrometric analysis and silver-ion separations will both be necessary to resolve these mixtures. We have recently evaluated the separation of FAME mixtures achieved by use of new ionic liquid capillary GC columns that are more polar than CPS columns [33]. Compared with CPS columns, the SLB-1L111 ionic liquid capillary column had increased capacity in the separation of unsaturated FAME on the basis of double bond number, position, and

geometric configuration, but also generated a different set of co-elutions. The elution pattern of FAME from ionic-liquid columns is sufficiently different from patterns from CPS columns to become a valuable complementary GC separation for analysis of complex FA mixtures.

Conclusion

The current official capillary GC method for analysis of saturated, *cis*-MUFA, and *cis*-PUFA in marine and other oils containing LC PUFA (AOCS Ce 1i-07) recommends the use of 30-m PEG-coated GC columns, for example Supelcowax-10 [5]. This GC column proved valuable for identifying unsaturated FAME but was ineffective for separation of unsaturated geometric FA isomers that can be present in fish products when subjected to processing or thermal stress or when combined with other foods. Evaluation of the FA composition of the same fish products by use of a 100-m SP-2560 column, a GC column recommended for analysis of *trans* FA contained in other food matrices, enabled enhanced separation of several FA and led to identification of *trans* FA and other components, for example phytanic and phytenic acids, and 6*t*-16:1. When the Supelcowax-10 column was used, many of these compounds were not resolved. Fractionation of the FAME mixture from the original fish sample by Ag^+ -SPE before GC analysis proved valuable in establishing the identity of many unsaturated FA contained in fish products. GC separation of the Ag^+ -SPE fractions resulted in little overlap of unsaturated FA with different numbers of double bonds and geometric configuration, with the exception of very highly unsaturated FA (F5–F7). Several of the pentaenoic and hexaenoic FA were not completely eluted from Ag^+ -SPE cartridges, even by 100% methanol. Calculation ECL values provided valuable assistance in the identification of many unsaturated FA contained in fish products, and the results were in agreement with those obtained by use of Ag^+ -SPE fractionation. Thorough examination of the separations obtained from the Supelcowax-10 and SP-2560 columns (the latter used with two temperature programs), with analysis of the samples before and after Ag^+ -SPE fractionation, provided the information necessary to identify most of the FA in fish oil and fish muscle. The approach described here complements the chromatographic separation recommended by AOCS official method Ce 1i-07 for marine oil analysis [5] with separations on a 100-m CPS column. This will be needed for analysis of commercially prepared fish foods, deodorized marine oils, or foods fortified with marine oils.

Acknowledgments The authors thank Drs Roberto Anedda and Carlo Piga for their encouragement and for assistance with extraction

of lipids from the fish muscles, and the staff at Porto Conte Ricerche Srl for their assistance with these studies.

References

1. Barceló-Coblijn G, Murphy EJ (2009) Alpha-linolenic acid and its conversion to longer chain n-3 fatty acids: benefits for human health and a role in maintaining tissue n-3 fatty acid levels. *Progr Lipid Res* 48:355–374
2. Degirolamo C, Kelley KL, Wilson MD, Rudel LL (2010) Dietary n-3 LCPUFA from fish oil but not α -linolenic acid-derived LCPUFA confers atheroprotection in mice. *J Lipid Res* 51: 1897–1905
3. Koletzko B, Lien E, Agostoni C, Böhles H, Campoy C, Cetin I, Decsi T, Dudenhausen JW, Dupont C, Forsyth S, Hoesli I, Holzgreve W, Lapillonne A, Putet G, Secher NJ, Symonds M, Szajewska H, Willatts P, Uauy R (2008) The roles of long-chain polyunsaturated fatty acids in pregnancy, lactation and infancy: review of current knowledge and consensus recommendations. *J Perinat Med* 36:5–14
4. Kris-Etherton PM, Hill AM (2008) n-3 Fatty Acids: food or supplements? *J Am Diet Assoc* 108:1125–1130
5. AOCS Official Method Ce 1i-07 (2007) Determination of saturated, *cis*-monounsaturated and *cis*-polyunsaturated fatty acids in marine and other oils containing long-chain polyunsaturated fatty acids (PUFA) by capillary GLC. AOCS. Urbana, IL
6. Ackman RG (1967) The chain-length overlap problem in gas-liquid chromatography with polyester liquid phases. *Lipids* 2: 502–505
7. Kramer JKG, Fouchard RC, Jenkins KJ (1985) Differences in chromatographic properties of fused silica capillary columns, coated, crosslinked, bonded, or crosslinked and bonded with poly(ethylene glycol)s (CARBOWAX 20M) using complex fatty acid methyl ester mixtures. *J Chromatogr Sci* 23:54–56
8. Ackman RG (1986) WCOT (capillary) gas-liquid chromatography. In: Hamilton RJ, Rossell JB (eds) *Analysis of oils and fats*. Elsevier Applied Science Publishers, New York, pp 137–206
9. Thompson RH (1996) Simplifying fatty acid analyses in multi-component foods with a standard set of isothermal GLC conditions coupled with ECL determinations. *J Chromatogr Sci* 34: 495–504
10. Kramer JKG, Blackadar CB, Zhou J (2002). Evaluation of two GC columns (60-m Supelcowax-10 and 100-m CP Sil 88) for analysis of milkfat with emphasis on CLA, 18:1, 18:2 and 18:3 isomers, and short- and long-chain FA. *Lipids* 37:823–835
11. Sébédio J-L, Ratanayake WMN, Ackman RG, Prevost J (1993) Stability of polyunsaturated omega-3 fatty acids during deep fat frying of Atlantic mackerel (*Scomber scombrus* L.). *Food Res Int* 26:163–172
12. Kolanowski W, Laufenberg G (2006) Enrichment of food products with polyunsaturated fatty acids by fish oil addition. *Eur Food Res Technol* 222:472–477
13. Mjøs SA (2005) Properties of *trans* isomers of eicosapentaenoic acid and docosahexaenoic acid methyl esters on cyanopropyl stationary phases. *J Chromatogr A* 1100:185–192
14. Mjøs SA, Solvang M (2006) Geometrical isomerisation of eicosapentaenoic acid and docosahexaenoic acid at high temperatures. *Eur J Lipid Sci Technol* 108:589–597
15. Fournier V, Juanéda P, Destailats F, Dionisi F, Lambelet P, Sébédio J-L, Berdeaux O (2006) Analysis of eicosapentaenoic and docosahexaenoic acid geometrical isomers formed during fish oil deodorization. *J Chromatogr A* 1129:21–28
16. Fournier V, Destailats F, Juanéda P, Dionisi F, Lambelet P, Sébédio J-L, Berdeaux O (2006) Thermal degradation of long-chain polyunsaturated fatty acids during deodorization of fish oil. *Eur J Lipid Sci Technol* 108:33–42
17. Fournier V, Destailats F, Hug B, Golay P-A, Joffre F, Juanéda P, Sémon E, Dionisi F, Lambelet P, Sébédio J-L, Berdeaux O (2007) Quantification of eicosapentaenoic and docosahexaenoic acid geometrical isomers formed during fish oil deodorization by gas-liquid chromatography. *J Chromatogr A* 1154:353–359
18. Golay P-A, Giuffrida F, Dionisi F, Destailats F (2009) Streamlined methods for the resolution and quantification of fatty acids including *trans* fatty acid isomers in food products by gas chromatography. *J AOAC Int* 92:1301–1309
19. Curtis JM (2007) Analysis of oils and concentrates. In: Breivik H (ed) *Long-chain omega-3 specialty oils*. The Oily Press, Bridgewater, pp 219–241
20. Azizian H, Kramer JKG, Ehler S, Curtis JM (2010) Rapid quantitation of fish oil fatty acids and their ethyl esters by FT-NIR models. *Eur J Lipid Sci Technol* 112:452–462
21. Precht D, Molkenin J (2003) Overestimation of linoleic acid and *trans*-C18:2 isomers in milk fats with emphasis on *trans* Δ 9, *trans* Δ 12-octadecadienoic acid. *Milchwissenschaft* 58:30–34
22. Ratnayake WMN (2004) Overview of methods for the determination of *trans* fatty acids by gas chromatography, silver-ion thin-layer chromatography, silver-ion liquid chromatography, and gas chromatography/mass spectrometry. *J AOAC Int* 87:523–539
23. Cruz-Hernandez C, Deng Z, Zhou J, Hill AR, Yurawecz MP, Delmonte P, Mossoba MM, Dugan MER, Kramer JKG (2004). Methods for analysis of conjugated linoleic acid and *trans*-18:1 isomers in dairy fats by using a combination of gas chromatography, silver-ion thin-layer chromatography/gas chromatography, and silver-ion liquid chromatography. *J AOAC Int* 87:545–562
24. Kramer JKG, Hernandez M, Cruz-Hernandez C, Kraft J, Dugan MER (2008) Combining results of two GC separations partly achieves determination of all *cis* and *trans* 16:1, 18:1, 18:2 and 18:3 except CLA isomers of milk fat as demonstrated using Ag ion SPE fractionation. *Lipids* 43:259–273
25. Mjøs SA (2008) Retention behavior of *trans* isomers of eicosapentaenoic and docosahexaenoic acid methyl esters on a poly(ethylene glycol) stationary phase. *Eur J Lipid Sci Technol* 110:547–553
26. Mossoba MM, Moss J, Kramer JKG (2009) *Trans* fat labeling and levels in US foods: assessment of gas chromatographic and infrared spectroscopic techniques for regulatory compliance. *J AOAC Int* 92:1284–1300
27. Bannon CD, Craske JD, Norman LM (1988) Effects of overload of capillary gas-chromatographic columns on the equivalent chain lengths of C18 unsaturated fatty acid methyl esters. *J Chromatogr* 447:43–52
28. Christie WW (1988) Equivalent chain-lengths of methyl ester derivatives of fatty acids on gas-liquid chromatography. *J Chromatogr* 447:305–314
29. AOCS Official Method Ce 1h-05 (2005) Determination of *cis*-, *trans*-, saturated, monounsaturated and polyunsaturated fatty acids in vegetable or non-ruminant animal oils and fats by capillary GLC. AOCS, Champaign
30. Precht D, Molketin J (1999) C18:1, C18:2 and C18:3 *trans* and *cis* fatty acid isomers including conjugated *cis* Δ 9, *trans* Δ 11 linoleic acid (CLA) as well as total fat composition of German human milk lipids. *Nahrung* 43:233–244
31. Precht D, Molketin J (2000) Identification and quantitation of *cis/trans* C16:1 and C17:1 fatty acid positional isomers in German human milk lipids by thin-layer chromatography and gas chromatography/mass spectrometry. *Eur J Lipid Sci Technol* 102: 102–113
32. Delmonte P, Fardin Kia A-R, Hu Q, Rader JI (2009) Review of methods for preparation and gas chromatographic separation of *trans* and *cis* reference fatty acids. *J AOAC Int* 92:1310–1326

33. Delmonte P, Fardin Kia A-R, Kramer JKG, Mossoba MM, Sidisky L, Rader JI (2011) Separation characteristics of fatty acid methyl esters using SLB-1L111, a new ionic liquid coated capillary gas chromatographic column. *J Chromatogr* 1218:545–554
34. Ackman RG (1989) Fatty acids. In: Ackman RG (ed) *Marine biogenic lipids, fats, and oils*, vol 1. CRC Press, Boca Raton, pp 103–137
35. Destailats F, Wolff RL, Precht D, Molkentin J (2000) Study of individual *trans*- and *cis*-16:1 isomers in cow, goat, and ewe cheese fats by gas-chromatography with emphasis on the *trans*-3 isomer. *Lipids* 35:1027–1032
36. Ackman RG (1999) Conjugated linoleic acid (CLA) in lipids of fish tissue. In: Yurawecz MP, Mossoba MM, Kramer JKG, Pariza MW, Nelson GJ (eds) *Advances in conjugated linoleic acid research*, vol 1. AOCS Press, Champaign, pp 283–295
37. Jamieson GR (1975) GLC identification techniques for long-chain unsaturated fatty acids. *J Chromatogr Sci* 13:491–497
38. Wijesundera RC, Ackman RG (1989) Evaluation of calculation of ECL values for *cis* and *trans* isomers of some diethylenic C₂₀ fatty acids: mono- and diethylenic capillary GLC data for the liquid phases SP-2340, Supelcowax-10, and SPB-1. *J Chromatogr Sci* 27:399–404
39. Delmonte P, Rader JI (2007) Evaluation of gas chromatographic methods for the determination of *trans* fat. *Anal Bioanal Chem* 389:77–85
40. Mjøs SA, Haugsgjerd BO (2011) *Trans* fatty acid analyses in samples of marine origin: the risk of false positives. *J Agric Food Chem* 59:3520–3531

New 2-Methyl-13-Icosenoic Acid from the Temperate Calcisponge *Leuconia johnstoni*

Elodie Quévrain · Gilles Barnathan ·
Tarik Meziane · Isabelle Domart-Coulon ·
Vony Rabesaotra · Marie-Lise Bourguet-Kondracki

Received: 16 May 2011 / Accepted: 3 November 2011 / Published online: 27 November 2011
© AOCS 2011

Abstract The fatty acid composition of the temperate calcareous marine sponge *Leuconia johnstoni* Carter 1871 (Calcaronea, Calcarea) was characterized for the first time in specimens collected off the Brittany coast of France over four years from October 2005 to September 2008. Forty-one fatty acids (FA) with chain lengths ranging from C₁₄ to C₂₂ were identified as fatty methyl esters (FAME) and *N*-acyl pyrrolidide (NAP) derivatives by gas chromatography–mass spectrometry (GC–MS). Twenty-two saturated fatty acids (SFA) were identified accounting for 52.1–59.0% of the total FA and dimethylacetals (DMA). In addition, among the SFA, we noticed the presence of numerous methyl-branched *iso* and *anteiso* FA, suggesting a large number of associated bacteria within *L. johnstoni*. Thirteen monounsaturated fatty acids (MUFA, 28.0–36.0% of total FA + DMA) were also identified as well as six polyunsaturated fatty acids (PUFA, 4.0–8.2%). A noticeable DMA was detected at a high level, particularly in September 2008 (11.8%), indicating the presence of plasmalogens in this sponge species. This calcareous sponge lacked the non-methylene-interrupted FA (NMI FA) with a $\Delta 5,9$ system typical of siliceous

Demosponges and Hexactinellids. The occurrence of the unusual 8,13-octadecadienoic acid was reported for the first time as a minor PUFA in a calcareous sponge. The major FA, representing 20–25% of this sponge FA, was identified as the new 2-methyl-13-icosenoic acid from mass spectra of its methyl ester and its corresponding *N*-acyl pyrrolidide derivatives as well as a dimethyl disulfide adduct.

Keywords Calcareous sponge · *Leuconia johnstoni* · Fatty acids · 2-Methyl-13-icosenoic acid · 8,13-Octadecadienoic acid · Dimethylacetal

Abbreviations

amu	Atomic mass unit
DMA	Dimethylacetal(s)
DMDS	Dimethyl disulfide
DUFA	Diunsaturated fatty acid(s)
ECL	Equivalent chain length
FA	Fatty acid(s)
FAME	Fatty acid methyl ester(s)
GC–MS	Gas chromatography–mass spectrometry
MS	Mass spectrum (spectra)
MUFA	Monounsaturated fatty acid(s)
NAP	<i>N</i> -Acyl pyrrolidide(s)
NMI FA	Non-methylene-interrupted fatty acid(s)
PUFA	Polyunsaturated fatty acid(s)
SFA	Saturated fatty acid(s)
TLC	Thin layer chromatography

E. Quévrain · M.-L. Bourguet-Kondracki (✉)
Molécules de Communication et Adaptation
des Micro-organismes UMR 7245 MNHN-CNRS,
Muséum National d'Histoire Naturelle, 57 rue Cuvier,
C.P. 54, 75005 Paris, France
e-mail: bourguet@mnhn.fr

G. Barnathan · V. Rabesaotra
Groupe Mer Molécules Santé EA 2160, Equipe Lipides marins à
activité biologique, Faculté de Pharmacie, Université de Nantes,
BP 53508, 44035 Nantes Cedex 1, France

T. Meziane · I. Domart-Coulon
Biologie des Organismes et des Ecosystèmes Aquatiques,
UMR 7208 MNHN-CNRS-UPMC, Muséum National d'Histoire
Naturelle, 57 rue Cuvier, C.P. 26, 75005 Paris, France

Introduction

Sponges are very ancient metazoans, with fossils dating back to the Early Cambrian period about 530 million years

ago. Interestingly these sessile marine invertebrates have the ability to biosynthesize a wide variety of structurally unique secondary metabolites, with no equivalent in terrestrial natural products. Because many of these metabolites display biological and pharmacological activities with potential applications in human health and biotechnological industry, they have become excellent candidates for the discovery of new bioactive natural products [1, 2]. While the siliceous Demospongia and Hexactinellida sponge classes, which represent about 90% of the species in the Porifera phylum, have been extensively studied, the chemistry of the Calcarea sponges was barely investigated. Chemical investigations on Calcispongiae have mostly concerned sponges of the Calcinea subclass and very few studies included representatives of the Calcaronea subclass [3–5].

Marine sponges have also proved to be a major source of unusual fatty acids (FA) including very long-chain (up to 34) non-methylene-interrupted fatty acids (NMI FA) with the particular unsaturation pattern $\Delta 5,9$ [6]. Although numerous usual and original FA have been identified from marine Demosponges [7] and some Hexactinellids [5], to the best of our knowledge, only five studies report on the phospholipid FA composition of a few calcareous sponge species [8–12], two of them revealing antimicrobial activity or protein kinase C inhibition activity [11, 12].

The widespread association of marine sponges with a great variety of microorganisms has generated much recent interest, as in numerous chemical studies associated microorganisms proved to be the true producers of sponge metabolites. Our investigations on the role of sponge associated bacterial communities led us to detect bacterial markers in their calcareous sponge hosts through cellular localization, chemical and microbial approaches [13, 14]. The temperate calcareous sponge *Leuconia johnstoni* Carter 1871 (class Calcispongiae, subclass Calcaronea, order Baerida, family Baeriidae) was selected for investigation of its FA composition which can be linked to the abundance of its resident bacteria. Indeed, previous studies have reported that significant levels of *i/ai* SFA can be assigned to bacterial sponge symbionts [15]. However, due to the low available biomass of this small encrusting calcareous species and the observation by thin layer chromatography (TLC) that phospholipids constituted the major class of this sponge lipids, the study was focused on the characterization of its FA composition. These FA were identified through gas chromatography coupled to mass spectrometry (GC–MS) on their methyl esters (FAME) and *N*-acyl pyrrolidide (NAP) derivatives to determine the chain length, degree and position of unsaturations.

Materials and Methods

Sponge Material

Leuconia johnstoni Carter 1871 [16] is a small-sized calcareous sponge species with an encrusting growth form (compressed lobes fused at the base, with a maximum size of 50 mm in diameter and 15 mm thick) living on sub-vertical rock surfaces in wave exposed sites with a distribution ranging from the British Isles to the French Brittany coasts [17]. Specimens of the intertidal calcareous sponge *L. johnstoni* were collected off the Brittany coast (North–East Atlantic, Finistère, France) near Concarneau (Plage des Dames, 47°52'N and 3°55'W). Four successive collections of specimens pooled from several rock-encrusting colonies were realized on the same site on October 2005, September 2007, March 2008 and September 2008 (through a permit granted to S. Derrien, MNHN-Concarneau). Samples were frozen immediately after collection and stored at -80°C until further investigations. Four voucher specimens are available from the Muséum National d'Histoire Naturelle in Paris as collection number MNHN n°C2009-3, n°C2009-10, n°C2009-15 and n°C2009-12, respectively.

Extraction of Total Lipids and Preparation of Fatty Acid Methyl Esters

The extraction was based on the Bligh and Dyer method [18] as amended by Meziane and Tsuchiya [19] and included four successive steps: extraction of total lipids, saponification, methylation and purification of FA by TLC.

Briefly, frozen sponge samples were lyophilized and extracted twice with water/chloroform/methanol (1:1:2, v/v/v) mixture. The combined chloroform extracts yielded the crude total lipids.

The mixture was heated with 2 mL of methanol and 1 mL of sodium hydroxide (2 M). The saponification reaction was stopped by adding an aliquot of hydrochloric acid (35%). After two successive washes with chloroform, followed by centrifugation at 2,000 rpm for 5 min, the lipid fraction was evaporated under a nitrogen stream.

Methylation of FA was obtained by adding 1 mL of a solution of 10% of boron trifluoride (BF_3) in methanol. After 10 min at 90°C , all FA of the total lipids were converted into the fatty methyl esters (FAME). Samples were then extracted twice by a water/chloroform (1:1, v/v) mixture and centrifuged at 2,000 rpm during 5 min. The chloroform was evaporated under nitrogen and FAME were dissolved in a chloroform/methanol (2:1, v/v) mixture, suitable for their preservation.

The lipids extracts were evaporated to dryness and recovered with three washings of 500 μL of a chloroform/methanol (98:2, v/v) mixture. Neutral and polar lipids were separated by column chromatography on silica gel micro-columns (30 \times 5 mm I.D. Kieselgel 70-230 mesh, Merck) using a chloroform/methanol (98:2, v/v) mixture to elute the neutral lipids, followed by neat methanol to elute the polar lipids. Each fraction was then treated in the same way as the bulk sample.

Preparation of *N*-Acyl Pyrrolidides

N-acyl pyrrolidide derivatives (NAP) were prepared by direct treatment of the FAME with a pyrrolidine/acetic acid (10:1, v/v) mixture under reflux for 2 h [20].

Preparation of the Dimethyl Disulfide Adduct

The dimethyl disulfide (DMDS) adduct was obtained from a FAME mixture (2 mg) in dimethyl disulfide (0.48 mL) by adding a solution (0.1 mL) of iodine in diethyl ether (60 mg mL⁻¹) under agitation for 24 h at room temperature [21]. The reaction was stopped by adding hexane (6 mL), washed with a dilute solution of sodium thiosulfate (1.2 mL of a 7 mg/100 mL solution) and dried over anhydrous sodium sulfate and evaporated to dryness. The product was taken up in fresh hexane for injection onto the GC–MS.

Gas Chromatography–Mass Spectrometry Analyses

Gas chromatography coupled with mass spectrometry (GC–MS) experiments were performed on a Hewlett-Packard HP-6890 chromatograph (Agilent Technologies, Massy, France) linked to a HP-5989 spectrometer (70 eV) equipped with a HP-9000-345 integrator and using a SLB™ 5-ms 60 mm \times 0.25 mm \times 0.25 μm fused silica capillary column (splitless) (Supelco, Bellefonte, PA, USA). The carrier gas was helium (flow rate 1 mL/min). Injector and detector temperatures were used at 250 and 280 °C, respectively. The oven temperature was maintained at 170 °C for 4 min and then programmed from 170 to 310 °C at a rate of 3 °C/min and at 200 °C for 4 min and then programmed from 200 to 310 °C at a rate of 3 °C/min for FAME and NAP derivatives, respectively.

Mass spectral data for the two novel FA structures in the calcareous sponge *L. johnstoni*, identified as their FAME and NAP derivatives or DMDS adduct, are presented below.

2-Methyl-13-icosenoic acid methyl ester MS *m/z* (rel. intensity %) [M^+] 338 (1.3), 307 (4.0), 306 (6.1), 291 (0.7), 278 (1.2), 263 (0.5), 250 (1.2), 242 (0.4), 235 (0.4), 222 (0.3), 208 (1.4), 194 (0.7), 181 (0.5), 167 (0.8), 166 (1.0), 165 (1.1), 157 (2.2), 151 (1.2), 143 (2.3), 125 (3.8), 101

(25.8), 98 (18.1), 88 (100), 83 (22.6), 69 (34.6), 57 (16.5), 55 (46.0), 43 (20.5), 41 (26.5).

2-Methyl-13-icosenoic acid pyrrolidide MS *m/z* (rel. intensity %) [M^+] 377 (8.4), 362 (0.8), 348 (1.5), 334 (1.9), 320 (4.6), 306 (3.1), 292 (1.1), 278 (0.8), 266 (0.8), 252 (2.3), 238 (1.5), 224 (1.5), 210 (2.3), 196 (4.4), 182 (4.6), 168 (2.3), 154 (3.8), 140 (26.7), 127 (100), 113 (15.3), 98 (22.1), 83 (9.2), 70 (19.1), 55 (40.5), 43 (22.1), 41 (18.3).

Dimethyl disulfide adduct of 2-methyl-13-icosenoic acid methyl ester MS *m/z* (rel. intensity %) [M^+] 418 (3.4), 403 (1.3), 386 (2.2), 369 (1.4), 355 (0.8), 339 (1.4), 322 (2.1), 307 (0.7), 291 (2.2), 273 (28.1), 241 (27.3), 255 (2.0), 208 (4.2), 193 (4.5), 177 (3.8), 165 (4.5), 145 (37.9), 125 (16.7), 111 (31.2), 109 (26.5), 97 (50.8), 95 (36.3), 85 (36.4), 83 (50.8), 82 (43.1), 69 (80.3), 55 (100), 43 (84.8), 41 (40.1).

8,13-Octadecadienoic acid methyl ester MS *m/z* (rel. intensity %) [M^+] 294 (5.3), 263 (4.5), 241 (1.4), 222 (2.3), 220 (2.1), 199 (2.3), 180 (2.4), 177 (4.2), 164 (5.1), 150 (10.5), 149 (6.8), 137 (8.9), 135 (10.5), 123 (15.8), 109 (29.3), 95 (60.2), 87 (28.6), 81 (85.7), 74 (44.3), 69 (54.2), 67 (100), 55 (87.2), 43 (54.1), 41 (76.7).

8,13-Octadecadienoic acid pyrrolidide MS *m/z* (rel. intensity %) [M^+] 333 (6.8), 318 (0.4), 304 (0.6), 290 (1.6), 276 (1.3), 262 (1.4), 250 (1.6), 236 (3.0), 222 (6.8), 208 (3.8), 194 (4.6), 182 (7.6), 168 (6.1), 154 (4.5), 140 (7.6), 126 (64.4), 113 (100), 98 (26.5), 85 (16.0), 72 (27.4), 70 (41.7), 67 (20.4), 55 (42.4), 43 (25.8), 41 (25.1).

Results

The fatty acid (FA) composition of *L. johnstoni* was identified for four samples corresponding to four successive collections on the same geographical site, in the period 2005 to 2008 including autumn (3 replicates) and spring (1 replicate) as reported in Table 1. FA were characterized as their methyl esters (FAME) and *N*-acyl pyrrolidide (NAP) derivatives using gas chromatography-mass spectrometry (GC–MS). Identification of FA was confirmed by comparing their equivalent chain length values (ECL) and their mass spectra (MS) with those of known standards.

Forty-one FA with chain lengths between C₁₄ and C₂₂ were identified in the different samples, as illustrated in Table 1.

Saturated Fatty Acids

In all three samples collected in autumn from October 2005 to September 2008, similar SFA were determined whereas in the sample collected in early spring, March 2008,

Table 1 Fatty acid composition of the sponge *Leuconia johnstoni* (4 samples collected off Concarneau, France, each sample pooled from several colonies)

Fatty acids (symbol)	Abundance (wt%)				
	ECL	October 2005	September 2007	March 2008	September 2008
<i>Saturated fatty acids</i>					
Tetradecanoic (14:0)	14.00	0.2	0.8	1.4	1.9
4,8,12-Trimethyltridecanoic (br-13:0)	14.50	0.5	0.8	3.1	1.9
13-Methyltetradecanoic (<i>i</i> -15:0)	14.65	3.1	2.5	2.3	4.1
12-Methyltetradecanoic (<i>ai</i> -15:0)	14.72	3.6	3.6	3.2	6.3
Pentadecanoic (15:0)	15.00	0.2	0.4	0.4	0.4
14-Methylpentadecanoic (<i>i</i> -16:0)	15.63	2.0	1.3	0.7	0.8
13-Methylpentadecanoic (<i>ai</i> -16:0)	15.71	0.7	0.3	–	0.5
Hexadecanoic (16:0)	16.00	20.1	23.5	22.8	16.0
15-Methylhexadecanoic (<i>i</i> -17:0)	16.61	1.9	0.6	0.9	2.2
14-Methylhexadecanoic (<i>ai</i> -17:0)	16.69	0.7	0.3	1.4	1.1
Heptadecanoic (17:0)	17.00	0.6	0.8	0.9	0.6
15-Methylheptadecanoic (<i>ai</i> -18:0)	17.75	0.9	0.4	1.6	1.3
Octadecanoic (18:0)	18.00	9.6	13.8	14.9	10.0
17-Methyloctadecanoic (<i>i</i> -19:0)	18.69	3.4	2.7	2.9	2.1
Nonadecanoic (19:0)	19.00	0.7	0.4	–	0.5
18-Methylnonadecanoic (<i>i</i> -20:0)	19.66	1.5	0.3	1.4	0.9
Icosanoic (20:0)	20.00	1.4	1.8	1.1	1.2
Heneicosanoic (21:0)	21.00	0.6	0.4	–	0.3
Total SFA	–	51.7	54.7	59.0	52.1
<i>Monounsaturated fatty acids</i>					
5-Hexadecenoic (16:1)	15.80	0.5	1.0	0.3	1.4
9-Hexadecenoic (16:1)	15.87	1.8	1.8	0.9	0.7
9-Octadecenoic (18:1)	17.80	2.0	1.4	1.4	0.8
11-Octadecenoic (18:1)	17.90	4.1	3.2	2.0	0.7
13-Icosenoic (20:1)	19.75	1.9	2.5	1.5	–
2-Methyl-13-icosenoic (br-13-20:1) ^a	20.18	24.3	22.4	20.8	25.8
Heneicosenoic (21:1) ^b	20.86	1.4	1.5	1.1	–
Total MUFA	–	36.0	33.8	28.0	29.4
<i>Di- and poly-unsaturated fatty acids</i>					
8,13-Octadecadienoic (18:2) ^c	17.82	0.8	0.6	0.9	0.7
9,12-Octadecadienoic (18:2)	17.85	0.8	0.8	1.1	1.0
11,15-Icosadienoic (20:2)	20.30	3.1	1.9	1.4	0.8
5,8,11,14-Icosatetraenoic (20:4)	18.96	1.7	1.9	1.4	0.8
5,8,11,14,17-Icosapentaenoic (20:5)	19.20	1.8	1.5	0.9	0.7
Total DUFA and PUFA	–	8.2	6.7	5.7	4.0
<i>Dimethylacetal</i>					
DMA (21:2) ^b	20.75	2.9	3.2	5.9	11.8

FA identified as traces: SFA (ECL) 16-Methylheptadecanoic (17.64), 19-Methyl-icosanoic (20.66), 16-Methyloctadecanoic (18.79), Docosanoic (22.00); MUFA 13-Methyl-4-tetradecenoic (14.32), 10-Hexadecenoic (15.90), 15-Methyl-5-hexadecenoic (16.40), 6-Octadecenoic (17.54), 14-Octadecenoic (17.94), 9-Icosenoic (19.30); DUFA 13, x-Docosadienoic (21.80)(not previously characterized in a calcareous sponge)

^a Not previously reported in nature

^b Undetermined unsaturations

^c Not previously characterized in a calcareous sponge

ai-16:0, 19:0 and 21:0 were lacking. The linear SFA hexadecanoic acid (16:0) and octadecanoic acid (18:0) were always determined as dominant. They represented between 16.0 and 23.5% and between 9.6 and 14.9% of the total FA + DMA, respectively. The minor linear SFA (20:0) was observed at similar levels (between 1.1 and 1.8%) in the four samples. In contrast, the shortest length SFA (14:0) was identified between 0.2 and 1.9% depending on sample. Additional linear SFA were also observed at noticeable levels of the total FA and DMA in all samples (less than 0.5% for 15:0 and less than 1% for 17:0).

Furthermore, *L. johnstoni* also contained a high proportion of branched SFA including *iso* (*i*) and *anteiso* (*ai*) FA. The diversity of *iso* FA was similar to those of *anteiso* FA (*ilai*-15:0 to *ilai*-19:0) excepted for *i*-18:0, *ai*-19:0 and *i*-20:0, only identified as traces. The isoprenoid-type 4,8,12-tridecanoic acid (*br*-13:0) was also identified from 0.5 to 3.1% of the FA + DMA (ECL value of the FAME = 14.50).

Monounsaturated Fatty Acids

Monounsaturated FA (MUFA) represented from 28.0 to 36.0% of the total FA + DMA in the sponge. Surprisingly, an unusual MUFA was present in all samples with an aliphatic chain of 20 carbons (ECL value of 20.18). The mass spectrum (MS) of its methyl ester (FAME) revealed a molecular ion $[M]^+$ at m/z 338 corresponding to a $C_{20:1}$ FA structure (Fig. 1).

In the MS of its FAME, the fragment ion at m/z 88 (C_3 fragment + H) as the base peak and the major ion at m/z 101 could remind a McLafferty rearrangement of a FA ethyl ester. But, the presence in the MS of the relatively intense fragment ion at m/z 306 ($[M-31]^+$) indicated that the

compound was obviously a FAME. These key observations allowed to identify this compound as a MUFA with a methyl group at C-2, which was also supported by the MS of its NAP derivative, showing the molecular ion at m/z 377 (Fig. 2).

The MS of its pyrrolidide derivative displayed the expected McLafferty ion at m/z 113, while the base peak was present at m/z 127, confirming the 2-methyl branching nature of this MUFA. This observation was in accordance with the occurrence of an elevated peak at m/z 140, as depicted in the Lipid Library, for a 3-methyl branched NAP. In addition, the gap of 12 amu between fragment ions at m/z 278 and m/z 266 suggested localization of the double bond between carbons C-13 and C-14 of the aliphatic chain. In order to confirm this hypothesis, the dimethyl disulfide (DMDS) adduct of this 2-methyl MUFA was prepared as previously described by Imbs et al. [21]. Analysis of the MS of the corresponding DMDS adduct showed the presence of characteristic fragments at m/z 145, 213, 241 and 273 (Fig. 3), confirming unambiguously the localization of the unsaturation between C-13 and C-14. However its configuration could not be determined.

This MUFA was unequivocally identified as 2-methyl-13-icosenoic acid (2-Me-13-20:1). Its occurrence in all samples of *L. johnstoni* collected at the same geographical site at different seasons is noteworthy. Indeed, this unusual 2-methyl FA represented 22.4% and 24.3% in autumn (September 2007 and October 2005 respectively) and 20.8% of the total FA + DMA of specimens collected in spring (March 2008). However in winter (February 2006 and 2007) the sponge lipid profile was dominated by SFA and the abundance of this unusual 2-Me-13-20:1 dropped to respectively 7.8 and 9.8% of FA + DMA, although it still dominated the sponge MUFA (data not shown, publication in preparation).

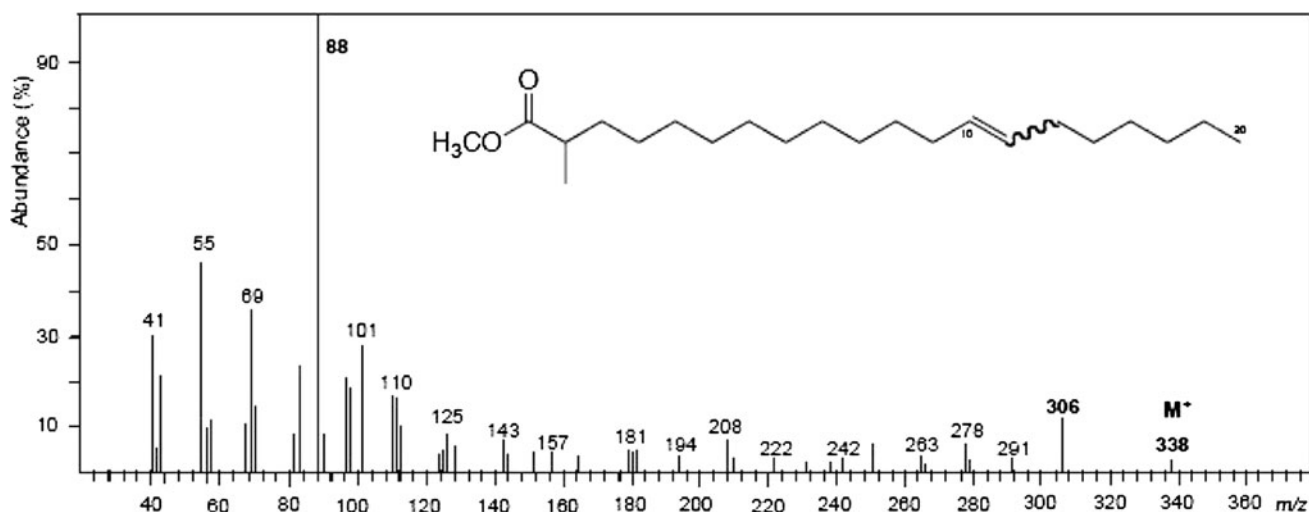


Fig. 1 Mass spectrum of 2-methyl-13-icosenoic acid methyl ester from *L. johnstoni*

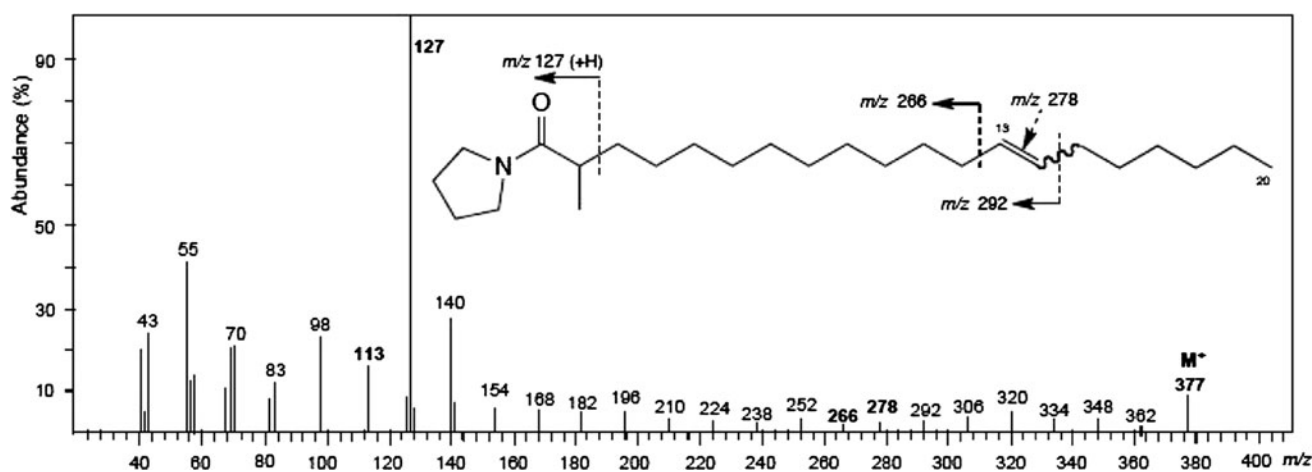


Fig. 2 Mass spectrum of 2-methyl-13-icosenoic acid pyrrolidide derivative from *L. johnstoni*

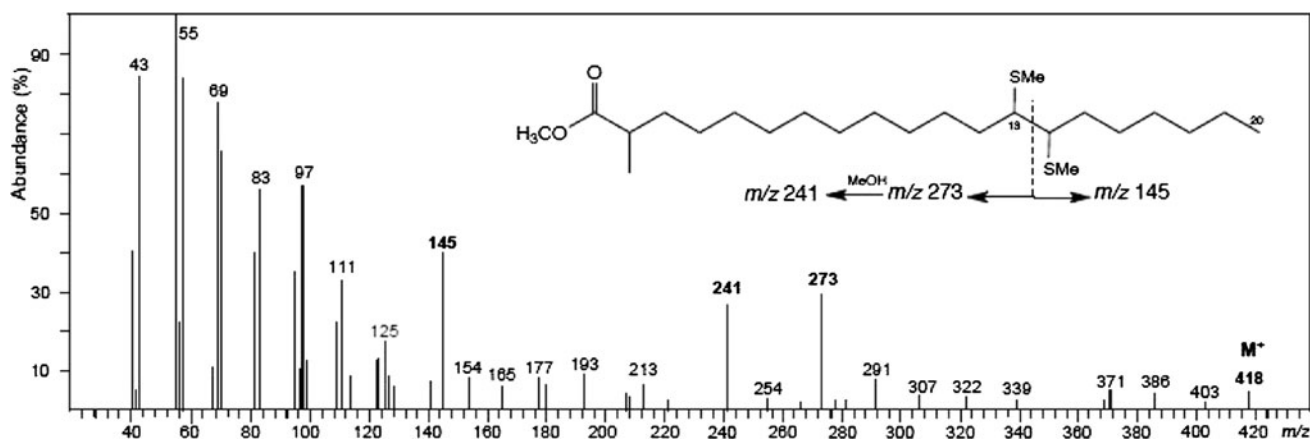


Fig. 3 Mass spectrum of 2-methyl-13-icosenoic acid dimethyl disulfide derivative from *L. johnstoni*

It appeared to us that the peak representing the new 2-methyl-13-icosenoic acid was highly represented in the polar phospholipid fraction.

Two additional hexadecenoic-type MUFA, 5-hexadecenoic and 9-hexadecenoic, were also identified in low amounts (0.3–1.4 and 0.7–1.8%, respectively) as well as two octadecenoic-type MUFA: 9-octadecenoic (0.8–2.0%) and 11-octadecenoic (0.7–4.1%). 13-icosenoic (1.5–2.5%) and heneicosenoic acid (1.1–1.5%) were only identified in three specimens out of four.

In addition, six MUFA were identified as traces: 13-methyl-4-tetradecenoic, 10-hexadecenoic, 15-methyl-5-hexadecenoic, 6-octadecenoic, 14-octadecenoic, 9-icosenoic (Table 1).

The two monomethyl branched MUFA, 13-methyl-4-tetradecenoic and 15-methyl-5-hexadecenoic, were readily identified from their GC mobilities (ECL of 14.32 and 16.40, respectively) and from their corresponding NAP derivatives MS spectra. The MS of the NAP of 13-methyl-4-tetradecenoic displayed the molecular ion at m/z 293

(15:1 FA structure), as well as fragment ions at m/z 139 and 152, and an intense fragment ion at m/z 166 (53%) indicating a double bond between C-4 and C-5, as shown in the Lipid Library [22]. Furthermore, a very weak ion at m/z 264 indicated an *iso*-branched FA. Similarly, the MS of the NAP of 15-methyl-5-hexadecenoic displayed the molecular ion at m/z 321 (17:1 FA structure), and fragment ions at m/z 140 and 153, indicating a double bond between C-5 and C-6. In this case, the *iso*-branched was indicated by a weak peak at m/z 292.

Polyunsaturated Fatty Acids

Four DUFA were observed, in low amounts (<2%).

The DUFA, eluted just before the 9,12-octadecadienoic (0.8–1.1%), had an ECL value of 17.82 as methyl ester and showed in its MS a molecular ion at m/z 294, indicating a 18:2 acid structure. The MS of its NAP showed a molecular ion at m/z 333 (18:2). The two double bonds were located by the 12 amu gaps between the peaks at m/z 182 (C-7) and

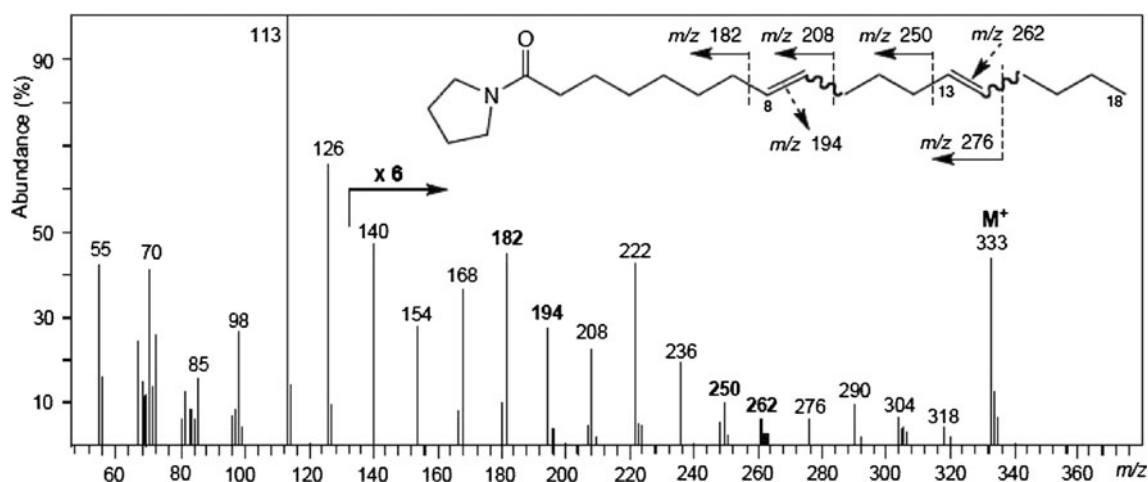


Fig. 4 Mass spectrum of 8,13-octadecadienoic acid pyrrolidide derivative from *L. johnstoni*

m/z 194 (C-8) and between the peaks at m/z 250 (C-12) and m/z 262 (C-13), indicating $\Delta 8$ - $\Delta 13$ unsaturations. Major diagnostic fragmentations of FAME and NAP of 8,13-octadecadienoic acid under electron impact are given in the “Materials and Methods” section. This DUFA 8,13-octadecadienoic acid occurred in low abundance in all samples with values ranging from 0.6 to 0.9% of total FA + DMA (Fig. 4).

The two other detected DUFA are 11,15-icosadienoic acid (0.8–3.1%) and 13, x -docosadienoic acid (traces). Complete identification of the latter failed due to its very small amount.

Two other PUFA 5,8,11,14-icosatetraenoic acid (0.8–1.9%) and 5,8,11,14,17-icosapentaenoic acid (0.7–1.8%) were also observed.

Dimethylacetals

Several DMA were detected at trace levels in the lipid fraction of *L. johnstoni*. However, one of them was detected at a significant amount in all samples, accounting for 11.8% of total FA + DMA in September 2008. MS of this dominant DMA (ECL = 20.75), showed characteristic fragment ions at m/z 75 ($[(\text{CH}_3\text{O})_2\text{-CH}]^+$) [23] and m/z 322 corresponding to $[\text{M}-31]^+$, indicating a C_{21} saturated fatty aldehyde with two unsaturations.

Discussion

By contrast with siliceous Demosponges and Hexactinellids, only a few reports have characterized the lipid composition of Calcisponges [8–10]. To obtain further insight into the FA content of Calcisponges, we selected *Leuconia johnstoni* as a calcareous sponge model belonging to the chemically poorly studied Calcaronea subclass. We investigated its FA

composition comparing four specimens collected at the same site in a time series over 4 years.

Out of the forty-one identified FA, twenty-two were saturated FA (SFA), including eighteen major SFA represented between 52.1 and 59.0% of the total FA + DMA. In addition to the known linear SFA, *ilai* C_{14} – C_{22} , typical FA of bacteria, were observed in all *L. johnstoni* specimens at significant levels ranging from 9 to 16% of total FA + DMA. Previous studies had reported that *ilai* FA were found as minor compounds or traces in terrestrial eukaryotes but in high amounts in some marine eukaryotes such as sponges, nudibranch molluscs, asteroidea and tunicates [9, 24, 25]. These mid-chain-branched *ilai* FA, which are considered as membrane constituent especially in Gram-positive bacteria, have often been assigned to bacterial sponge symbionts [15, 26, 27]. Recently, methyl-branched fatty acids were proposed to be synthesized by Poribacteria [28]. Nevertheless, 16-methyl-octadecanoic acid (*ai*-19:0) which is reported as a major FA in several Calcareous sponge species mostly of the Calcinea subclass [9] was found in low amounts in *L. johnstoni*. Furthermore, although 17-methyl-nonadecanoic acid (*ai*-20:0) was previously reported as a major compound of presumably sponge cell origin in Calcispongiae [9], this FA was lacking in our samples even as traces.

Other branched FA have also been considered as bacterial markers, especially some monounsaturated FA (MUFA). In this study, thirteen MUFA were observed, among which seven had major relative abundance (28.0–36.0%). However, *iso*-15:1 and *iso*-17:1 MUFA with various positions of the double bond, which were previously reported as characteristic of sulfate-reducing bacteria of the genus *Desulfovibrio* [29, 30], were both lacking in all samples of *L. johnstoni*.

As a major result, our study led to the identification for the first time in a calcareous sponge of a new natural

MUFA identified as 2-methyl-13-icosenoic acid as the dominant MUFA. Its high relative abundance, ranging from 20.8 to 25.8% of the total FA + DMA in all four samples of *L. johnstoni*, suggests that it might play a significant role in the biology of this sponge, potentially in the function of its cellular membranes. Unfortunately, despite of its high relative abundance, the purification of this 2-methyl FA remained difficult due to the low available sponge biomass of *L. johnstoni*.

Previously, some 2-methyl branched unsaturated FA have already been isolated but only from siliceous marine sponges. In 1990, the first 2-methyl branched FA, 2-methyloctadecanoic acid was identified from the Demosponge *Plakortis halichondroides* [31]. Later, two additional 2-methyl branched MUFA, 2-Me-24:1n-7 and 2-Me-26:1n-9 were isolated in small amounts (7.1% of sponge total FA) from the Demosponge *Halichondria panicea* [21].

Further chemotaxonomic studies would be necessary to demonstrate the specificity of this new 2-methyl-13-icosenoic acid as potential biomarker for sponges of the genus *Leuconia*.

Six polyunsaturated FA (PUFA) accounting between 4.0 and 8.2% of the total FA + DMA, including the two non-methylene-interrupted FA (NMA) 8,13-18:2 and 11,15-20:2 and one additional diunsaturated FA (DUFA) 9,12-18:2, were also detected. This is the first time that the unusual 8,13-octadecadienoic acid was characterized in a calcareous sponge. Numerous NMI FA, such as 5,11-20:2, 5,13-20:2, 7,13-22:2 and 7,15-22:2 have already been identified from marine sponges [6, 7, 32]. The 11,15-icosadienoic acid NMI observed in this study was previously identified from the Caribbean Demosponge *Amphimedon complanata* and the Axinellida sponge *Pseudaxinella* cf. *lunaecharta* [7, 33, 34]. The origin of the two PUFA 5,8,11,14-icosatetraenoic acid and 5,8,11,14,17-icosapentaenoic acid, which were detected in all samples of *L. johnstoni*, remains unknown [35]. They were observed at a very low level, representing less than 2% of the total FA and DMA content. No other PUFA with 3 or more double bonds were identified.

Furthermore, we noticed that demospongiac acids, defined by Christie for the database Lipid Library as long-chain FA with a Δ 5,9 unsaturation system and recently revisited as NMI FA, were totally absent in *L. johnstoni*. These NMI FA, observed in various marine sources with a large range of chain-lengths (C₁₆–C₃₂) [36] were previously reported in specimens of calcareous sponges in the genera *Clathrina* (Calceinea subclass) and *Sycon* (Calcareo-na subclass) [8].

Finally, some DMA were observed, of which one was abundant, identified as 21:2 and accounting for 2.9–11.8% of the total FA + DMA.

The finding of DMA among FAME in *L. johnstoni* points to the presence of plasmalogens (1-*O*-1'-enyl-2-acyl-glycerophospholipids) in the sponge. The DMA are produced from aldehydes, released from plasmalogens, concomitantly with the FAME during the esterification step [23]. These plasmalogens are widely distributed in the animal kingdom and also occur in some anaerobic microorganisms and marine invertebrates [37]. In mammals, they could have a role in physical properties of cell membranes, storage of arachidonic acid, activation of phospholipase A₂ and cellular signalization. They are also involved in protection against oxidative stress [38]. The presence of plasmalogens was previously reported in the Demosponge *Polymastia penicillus* but their structures could not be determined due to both low amounts and co-elution with other lipids during purification [7]. However, to date, the biological role of plasmalogens in sponges is not clearly determined. We speculate that they may have similar functions as in more complex metazoan organisms including protection against oxidative stress or against attack by microorganisms.

Surprisingly, by contrast with all other FA, which were in constant relative abundance in the four specimens collected during two seasons over 4 years, detection of this DMA was variable and fluctuated between 2.9 and 11.8% without any seasonal corroboration.

In conclusion, this first investigation of the fatty acid composition of the Calcareo-na species *Leuconia johnstoni* Carter 1871 identified the new 2-methyl-13-icosenoic FA in a calcareous sponge. It also revealed the occurrence at low levels of the unexpected PUFA 20:4 and 20:5 and of the DMA 21:2 although in fluctuating ratios. The nearly constant high relative abundance of the new 2-methyl-13-icosenoic FA in *L. johnstoni* suggests that this MUFA might be further explored as a potential biomarker. Further investigations on lipids and FA composition of *Leuconia* species remain to be carried out to substantiate this hypothesis.

Acknowledgments This work is part of Elodie Quévrain's Ph.D. thesis, supported by a grant from the French Ministère de l'Enseignement Supérieur et de la Recherche. The authors also thank the director and staff of the Laboratoire de Biologie Marine du Muséum National d'Histoire Naturelle, Station Marine de Concarneau, France, for providing access to facilities for regular sponge collections.

References

1. Sipkema D, Franssen MCR, Osinga R, Tramper J, Wijffels RH (2005) Marine sponges as pharmacy. *Mar Biotechnol* 7:142–162
2. Blunt JW, Copp BR, Munro MH, Northcote PT, Prinsep MR (2010) *Mar Nat Prod* 27:165–237
3. Ralifo P, Tenney K, Valeriote FA, Crews P (2007) A distinctive structural twist in the imidazole alkaloids from a calcareous

- marine sponge: isolation and characterization of leucosolenamines A and B. *J Nat Prod* 70:33–38
4. Hagemann A, Voigt O, Wörheide G, Thiel V (2008) The sterol of calcareous sponges (Calcarea, Porifera). *Chem Phys Lipids* 156:26–32
 5. Thiel V, Blumenberg M, Hefter J, Pape T, Pomponi S, Reed J, Reitner J, Wörheide G, Michaelis W (2002) A chemical view of the most ancient metazoan—biomarker chemotaxonomy of hexactinellid sponges. *Naturwissenschaften* 89:60–66
 6. Barnathan G (2009) Non-methylene-interrupted fatty acids from marine invertebrates: occurrence, characterization and biological properties. *Biochimie* 91:671–678
 7. Denis C, Wielgosz-Collin G, Bret  ch   A, Ruiz N, Rabesatrova V, Boury-Esnault N, Kornprobst JM, Barnathan G (2009) New 17-methyl-13-octadecenoic acid and 3,16-docosadienoic acids from the sponge *Polymastia penicillus*. *Lipids* 44:655–663
 8. Bergquist PR, Lawson MP, Lavis A, Cambie RC (1984) Fatty acids composition and the classification of Porifera. *Biochem Syst Ecol* 1(2):63–84
 9. Schreiber A, Wörheide G, Thiel V (2006) The fatty acids of calcareous sponges (Calcarea, Porifera). *Chem Phys Lipids* 143:29–37
 10. Carballeira NM, Shalabi F (1995) The rare Caribbean sponge *Leucosolenia canariensis*: phospholipid fatty acids and sterols. *Lipids* 30:467–470
 11. Tianero MD, Hanif N, de Voogd NJ, van Soest RW, Tanaka J (2009) A new antimicrobial fatty acid from the calcareous sponge *Paragrantia cf waguensis*. *Chem Biodivers* 6:1374–1377
 12. Willis RH, de Vries DJ (1997) BRS-1, a C₃₀ bis-amino, bis-hydroxy polyunsaturated lipid from an Australian calcareous sponge that inhibits protein kinase C. *Toxicon* 35:125–1129
 13. Qu  vrain E, Domart-Coulon I, Pernice M, Bourguet-Kondracki ML (2009) Novel natural parabens produced by a *Microbulbifer* bacterium in its calcareous sponge host *Leuconia nivea*. *Environ Microbiol* 11:1527–1539
 14. Rou   M, Domart-Coulon I, Ereskovsky A, Djediat C, Perez T, Bourguet-Kondracki ML (2010) Cellular localization of clathridimine, an antimicrobial 2-aminoimidazole alkaloid produced by the Mediterranean calcareous sponge *Clathrina clathrus*. *J Nat Prod* 73:1277–1282
 15. Gillian FT, Stoilov IL, Tam Ha TB, Raederstorff D, Doss GA, Li HT, Djerassi C (1988) Fatty acids as biological markers for bacterial symbiont in sponges. *Lipids* 23:1139–1145
 16. Carter HJ (1871) A description of two new calcispongiae (*Trichogypisia*, *Leuconia*). *Ann Mag Nat Hist* 8:1–28
 17. Van Soest RWM, Boury-Esnault N, Hooper JNA, R  tzler K, de Voogd NJ, Alvarez B, Hajdu E, Pisera AB, Vacelet J, Manconi R, Sch  nberg C, Janussen D, Tabachnick KR, Klautau M (2008) World Porifera database. Available online at <http://www.marine-species.org/porifera>. Accessed 15 Oct 2010
 18. Bligh EG, Dyer WJ (1959) A rapid method of total lipid extraction and purification. *Can J Biochem Physiol* 37:911–917
 19. Meziane T, Tsuchiya M (2002) Organic matter in a subtropical mangrove-estuary subjected to wastewater discharge: origin and utilization by two macrozoobenthic species. *J Sea Res* 47:1–11
 20. Andersson BA (1978) Mass spectrometry of fatty acid pyrrolidides. *Prog Chem Fats other Lipids* 16:279–308
 21. Imbs AB, Rodkina SA (2004) Isolation of 2-methyl branched unsaturated very long fatty acids from marine sponge *Halichondria panicea* and identification of them by GC–MS and NMR. *Chem Phys Lipids* 129:173–181
 22. Christie WW. AOCs Lipid Library. <http://lipidlibrary.aocs.org/ms/ms03b/index.htm> Accessed 29 Mar 2011
 23. Christiansen K, Mahadevan V, Viswanathan CV, Holman RT (1969) Mass spectrometry of long-chain aldehydes, dimethyl acetals and alk-1-enyl ethers. *Lipids* 4:421–427
 24. Sargent JR, Falk-Petersen IB, Calder AG (1983) Fatty acid compositions of neutral glycerides from the ovaries of the asteroids *Ctenodiscus crispatus*, *Asterias lincki* and *Pteraster militaris* from Balsfjorden, northern Norway. *Mar Biol* 72:257–264
 25. Carballeira NM, Shalabi F, Stefanov K, Dimitrov K, Popov S, Kujumgiev A, Andreev S (1995) Comparison of the fatty acids of the tunicate *Botryllus schlosseri* from the Black Sea with two associated bacterial strains. *Lipids* 30:677–679
 26. Kaneda T (1977) Fatty acids of the genus *Bacillus*: an example of branched-chain preference. *Bacteriol Rev* 41:391–418
 27. Kaneda T (1991) *Iso*- and *anteiso*-fatty acids in bacteria: biosynthesis, function and taxonomic significance. *Microbiol Rev* 55:288–302
 28. Hochmuth T, Niederkr  ger H, Gernert C, Siegl A, Taudien S, Platzer M, Crews P, Hentschel U, Piel J (2010) Linking chemical and microbial diversity in marine sponges: possible role for poribacteria as producers of methyl-branched fatty acids. *Chembiochem* 11:2572–2578
 29. Taylor J, Parkes JR (1983) The cellular fatty acids of the sulfate-reducing bacteria, *Desulfobacter* species, *Desulfobulbus* species and *Desulfovibrio desulfuricans*. *J Gen Microbiol* 129:3303–3309
 30. Boon JJ, de Leeuw JW, Hoek GJ, Vosjan JH (1977) Significance and taxonomic value of *iso* and *anteiso* monoenoic fatty acids and branched hydroxy acids in *Desulfovibrio desulfuricans*. *J Bacteriol* 129:1183–1191
 31. Carballeira NM, Shalabi F (1990) Identification of naturally-occurring *trans,trans* Δ -5,9-fatty acids from the sponge *Plakortia halichondroides*. *Lipids* 25:835–840
 32. Christie WW, Brechany EY, Marekov KL, Stefanov KL, Andreev SN (2004) The fatty acids of the sponge *Hymeniacidon sanguinea* from the Black Sea. *Comp Biochem Physiol A* 109:245–252
 33. Carballeira NM, Restituyo J (1991) Identification of the new 11, 15-icosadienoic acid and related acids in the sponge *Amphimedon complanata*. *J Nat Prod* 54:315–317
 34. Barnathan G, Kornprobst JM, Doumenq P, Mirall  s J (1996) New unsaturated long-chain fatty acids in the phospholipids from the axinellida sponges *Trikentrion loeve* and *Pseudaxinella cf lunaecharta*. *Lipids* 31:193–200
 35. Valentine RC, Valentine DL (2004) Omega-3 fatty acids in cellular membranes: a unified concept. *Lipid Res* 43:383–402
 36. Kornprobst JM, Barnathan G (2010) Demospongiac acids revisited. *Mar Drugs* 8:2569–2577
 37. Kraffe E, Soudant P, Marty Y (2004) Fatty acids of serine, ethanolamine, and choline plasmalogens in some marine bivalves. *Lipids* 39:59–66
 38. Kuczynski B, Reo NV (2006) Evidence that plasmalogens are protective against oxidative stress in the rat brain. *Neurochem Res* 31:639–656

N-Acyl Taurines are Anti-Proliferative in Prostate Cancer Cells

Vicky Chatzakos · Katharina Slätis ·
Tatjana Djureinovic · Thomas Helleday ·
Mary C. Hunt

Received: 23 August 2011 / Accepted: 17 November 2011 / Published online: 11 December 2011
© AOCS 2011

Abstract Endocannabinoids have been implicated in cancer development and cause heterogenous effects in tumor cells, by inducing apoptosis, reducing migration, causing anti-angiogenic activity and alterations in the cell cycle resulting in growth arrest. Recently, several novel amides of fatty acids that are structurally related to endocannabinoids have been isolated from mammalian sources, although the functions of these fatty amides are not well studied. One group of these novel fatty acid amides are the *N*-acyl taurines (fatty acids conjugated to the amino acid taurine). This study examined if *N*-acyl taurines, specifically *N*-arachidonoyl taurine and *N*-oleoyl taurine could function in a similar way to endocannabinoids and result in cell cycle alterations or growth arrest in the human prostate adenocarcinoma cell line PC-3. PC-3 cells were treated with various concentrations of *N*-arachidonoyl taurine and *N*-oleoyl taurine and cell proliferation and viability was measured using resazurin and colony formation assays. Effects of *N*-acyl taurines on the cell cycle was measured using FACS analysis. Treatment with *N*-arachidonoyl taurine and *N*-oleoyl taurine resulted in a significant reduction in proliferation of PC-3 cells, even at concentrations as low

as 1 μ M. Treatment with *N*-oleoyl taurine resulted in an increased number of cells in the subG1 population, suggesting apoptosis, and a lower number of cells in S-phase of the cell cycle. In summary, our results show that novel biologically active lipids, the *N*-acyl taurines, result in reduced proliferation in PC-3 cells.

Keywords *N*-Arachidonoyl taurine · *N*-Oleoyl taurine · Fatty acid amide hydrolase · *N*-Acyl amino acids · PC-3 cells · Cell proliferation

Abbreviations

NAGly *N*-Arachidonoyl glycine
TRPV Transient receptor potential vanilloid type channel

Introduction

The endocannabinoid system is an endogenous signaling system that has pleiotropic effects on metabolism, cell proliferation, appetite, pain sensation and neuromodulatory effects (for review see [1]). Currently, several amides of fatty acids have been isolated from mammalian sources, which are structurally related to endocannabinoids, however, details of how these molecules are synthesized and degraded in vivo are only emerging. One group of these fatty acid amides is the *N*-acyl amino acids present in mammalian species, which have generated renewed research interest in part because of their structural relationship to the endocannabinoids [2, 3]. *N*-Acyl amino acids are fatty acids conjugated to amino acids such as glycine, taurine, alanine, serine etc. and fatty acid conjugates with the common 20 amino acids have now been

V. Chatzakos · K. Slätis · T. Helleday
Department of Genetics, Microbiology and Toxicology,
Stockholm University, Svante Arrhenius väg 20C,
106 91 Stockholm, Sweden

T. Djureinovic
Department of Immunology, Genetics and Pathology,
Rudbeck Laboratory, Uppsala University, 751 85 Uppsala,
Sweden

M. C. Hunt (✉)
School of Biological Sciences, Dublin Institute of Technology,
Kevin Street, Dublin 8, Ireland
e-mail: mary.hunt@dit.ie

identified in mammalian tissues [2]. However, *N*-acyl amino acids are not considered endocannabinoids as they do not activate the cannabinoid receptors. The functions of *N*-acyl amino acids are still not clear but it is emerging that they function as putative signaling molecules with a wide range of biological activities (for review see [4]). The first *N*-acyl amino acid detected in mammalian systems was *N*-arachidonoyl glycine (NAGly-arachidonic acid conjugated to glycine) which was found in rat brain and other tissues [5]. NAGly is synthesized by several pathways, including an enzymatic conjugation of arachidonoyl-CoA with glycine [6], synthesis by cytochrome c in the presence of arachidonoyl-CoA and hydrogen peroxide [7], and finally by oxidation of anandamide (an endocannabinoid) by alcohol and aldehyde dehydrogenases [8].

A further group of *N*-acyl amino acids identified in 2005 are the *N*-acyl taurines (fatty acids conjugated to taurine). *N*-Acyl taurines were first detected by global metabolic profiling in the fatty acid amide hydrolase (FAAH) knockout mouse model in brain, spinal cord, testes and liver [9, 10]. Saturated, monounsaturated and polyunsaturated *N*-acyl taurines of various fatty acid chain-lengths have been identified in vivo in mouse, with the liver and kidney containing higher levels of polyunsaturated *N*-acyl taurines than saturated *N*-acyl taurines, while the brain contains higher levels of saturated rather than polyunsaturated *N*-acyl taurines [11]. It was also shown recently that *N*-arachidonoyl taurine can be oxidized by lipoxygenase enzymes, resulting in oxidative metabolites of *N*-arachidonoyl taurine which may have their own biological function [12]. Interestingly, *N*-arachidonoyl taurine was shown to activate transient receptor potential (TRP) vanilloid type channels, TRPV1 ($EC_{50} \sim 28 \mu\text{M}$) and TRPV4 ($EC_{50} 21 \mu\text{M}$), suggesting a role for taurine conjugated fatty acids in cell signaling via cell surface receptors [11]. The TRPV1 and TRPV4 are cation channels, activated by a number of endogenous substances, resulting in an influx of calcium into cells. They play roles in pain regulation, regulation of blood pressure, osmotic sensation and in respiratory diseases (for review see [13]). Increased expression of TRPV1 has been found to be associated with human prostate carcinoma and cancers associated with colon, pancreas and bladder [14].

It is known that endocannabinoids (e.g. anandamide and 2-arachidonoylglycerol) exert anti-proliferative actions on a wide spectrum of tumor cells in culture [15, 16]. Endocannabinoids cause heterogenous effects in tumor cells, by inducing apoptosis, reducing migration, causing anti-angiogenic activity and cause alterations in the cell cycle resulting in growth arrest. The anti-proliferative effects of endocannabinoids occurs mainly by binding and activating their specific cannabinoid receptors and inhibiting adenylyl cyclase/cyclic AMP resulting in altered downstream

pathways such as mitogen-activated protein kinases, survival pathways and forkhead transcription factors [15, 16]. As endocannabinoids have been shown to have anti-proliferative effects in cancer models, and the *N*-acyl taurines are structurally related to endocannabinoids, we were interested to investigate the anti-proliferative effects of *N*-acyl taurines in two cancer cell lines, PC-3 (human prostate adenocarcinoma cell line) and MCF-7 (human breast adenocarcinoma cell line). Our results show that *N*-arachidonoyl taurine (C20:4 taurine) and *N*-oleoyl taurine (C18:1 taurine) significantly inhibit cell proliferation in PC-3 cells, and were more effective in PC-3 cells than in MCF-7 cells.

Materials and Methods

Chemicals and Reagents

N-Arachidonoyl taurine and *N*-oleoyl taurine were purchased from Cayman Chemical Company (Ann Arbor, MI, USA). A 10 mM stock was prepared in 100% DMSO (Sigma-Aldrich, St. Louis, MO, USA) and stored at -20°C . Propidium iodide (PI) was purchased from Invitrogen (Eugene, OR, USA) and RNase A was purchased from Fermentas (Burlington, Canada). Cell culture medium and supplements were purchased from Gibco (Carlsbad, CA, USA).

Cell Culture

PC-3 human prostate adenocarcinoma cell and MCF-7 human breast adenocarcinoma cell lines were kindly provided by Professor Thomas Helleday. Both cell lines were cultured in Dulbecco's modified Eagle's medium (DMEM) supplemented with 10% foetal bovine serum, penicillin 100 U/ml and streptomycin 100 $\mu\text{g/ml}$ at 37°C in an atmosphere containing 5% CO_2 .

Cell Viability Assay (Proliferation Assay)

20,000 cells/well were plated in six-well plates in 2 ml of complete DMEM medium. The next day the cells were treated with *N*-acyl amino acids or vehicle (DMSO) in delipidated foetal bovine serum in DMEM at concentrations of 10 and 40 μM for 24, 48 and 72 h. Viable cells were collected by trypsinization and counted in Coulter Counter (Coulter Electronics, Bedfordshire, England). Resazurin assay (Sigma-Aldrich, St. Louis, MO, USA) was used to estimate cell numbers in accordance with the manufacturer's instructions. The dehydrogenase activity was fluorometrically determined by measuring the reduction of resazurin (blue, non-fluorescent) to resorufin (pink,

highly fluorescent). Cells were plated in 96-well plates at 5,000 cells/well in 200 μ l of complete DMEM medium. The next day the cells were treated with *N*-acyl amino acids or vehicle in delipidated serum in DMEM at a range of concentrations for 24, 48 and 72 h. After treatment cells were washed with PBS and incubated with 10 μ g/ml resazurin for 1 h at 37 °C in an atmosphere containing 5% CO₂. The cell viability was determined by measuring the fluorescence at 535/590 nm (excitation/emission) using Polar Star Omega multi-plate reader (BMG Labtech, Offenburg, Germany).

Colony Formation Assay (Cytotoxicity Assay)

Cells were plated in 100-mm dishes at a density of 500 cells/dish in complete DMEM medium. The next day the cells were treated with *N*-acyl amino acids or vehicle in delipidated serum in DMEM at concentrations of 10 and 40 μ M and after 48 h the medium was replaced with fresh complete DMEM. After 2 weeks incubation (at 37 °C/5% CO₂), when colonies could be observed, the colonies were fixed and stained with methylene blue in methanol (4 g/l) and counted.

Propidium Iodide Staining and FACS Analysis

0.5×10^6 cells in 75-cm² flasks (Sarstedt, Nümbrecht, Germany) were treated with *N*-acyl amino acids (10 and 40 μ M) or vehicle in delipidated serum in DMEM and collected after 48 h by trypsinization. Cells were fixed in ice-cold 70% ethanol overnight at –20 °C for FACS analysis. The cells were then rehydrated in PBS and stained with 50 μ g/ml propidium iodide (PI) and 10 μ g/ml RNase A in PBS for 30 min at room temperature (in the dark). Samples were further analyzed on a BD Biosciences FACScan. The data was analyzed using the WinMDI software version 2.9.

Statistical Analysis

All data are presented as means \pm SEM. Statistical analysis was performed using two-way ANOVA, except for the resazurin assay which was analyzed using one-way ANOVA.

Results

N-Arachidonoyl Taurine and *N*-Oleoyl Taurine Significantly Reduce Proliferation of PC-3 Cells

Two different human adenocarcinoma cell lines were used as model systems to study the effect of *N*-arachidonoyl taurine and *N*-oleoyl taurine on proliferation of PC-3

cells (prostate) and MCF-7 (breast). The effect of *N*-arachidonoyl taurine and *N*-oleoyl taurine on cell proliferation was analyzed using three different assays. In the first assay, PC-3 and MCF-7 cells were treated with 10 or 40 μ M of either lipid and cells were counted following treatment for 24, 48 and 72 h. These concentrations of 10 or 40 μ M were chosen as previous studies showed that *N*-arachidonoyl taurine activates the TRPV1 and TRPV4 channels; EC₅₀ \sim 28 μ M (11–70 μ M, 95% confidence limits) and EC₅₀ \sim 21 μ M (3–130 μ M, 95% confidence limits) respectively [11]. The number of PC-3 cells treated with vehicle increased over the period of treatment, while treatment with *N*-arachidonoyl taurine had no effect on the cell number after 24 h treatment at 10 and 40 μ M concentrations, but 40 μ M *N*-arachidonoyl taurine resulted in a slower rate of cellular proliferation after 48 and 72 h of treatment (Fig. 1a). However, this effect was not statistically significant.

Treatment with *N*-oleoyl taurine resulted in a slower rate of cellular proliferation than control cells following treatment with 10 and 40 μ M *N*-oleoyl taurine and a significant

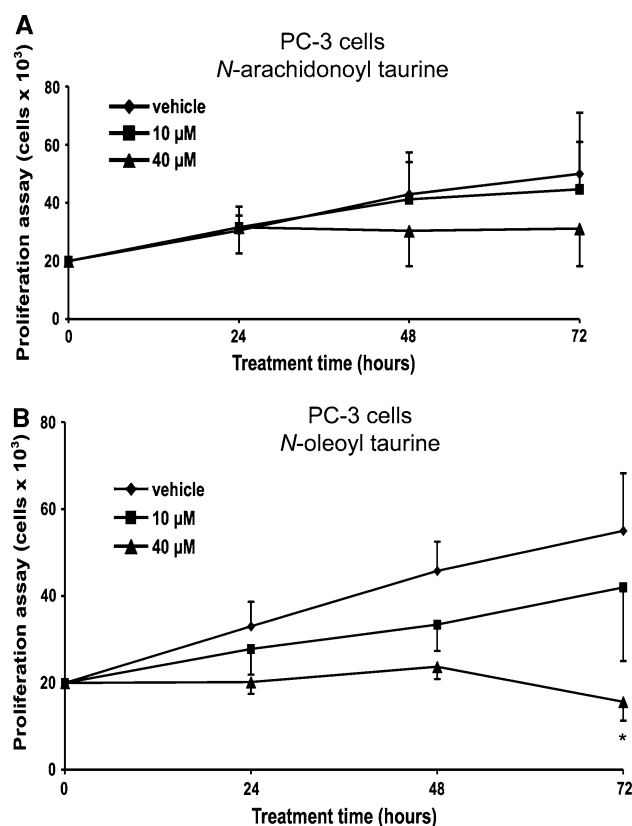


Fig. 1 *N*-Oleoyl taurine inhibits proliferation of PC-3 cells. Cells were seeded in six-well plates with 20,000 cells/well and treated with **a** *N*-arachidonoyl taurine **b** *N*-oleoyl taurine, or vehicle (DMSO) at concentrations of 10 and 40 μ M for 24–72 h. Cell viability was determined by cell counting. Data are presented as means \pm SEM ($n = 3$). *Significantly different from control treatment, $p < 0.05$

decrease in proliferation seen after 72 h of treatment with 40 μM *N*-oleoyl taurine ($p < 0.05$) (Fig. 1b).

A second assay using a resazurin labeling method, which is a more sensitive method to measure cell viability and proliferation, was used. PC-3 cells were treated with 10, 20 and 40 μM *N*-arachidonoyl taurine and *N*-oleoyl taurine and cell viability was examined. *N*-Arachidonoyl taurine resulted in a reduced proliferation of PC-3 cells after 48 and 72 h (after 48 h ($p < 0.001$) and 72 h ($p < 0.001$)) (Fig. 2a). *N*-Oleoyl taurine was particularly potent in reducing cell proliferation even at 10 μM ($p < 0.001$) (Fig. 2b), and therefore similar experiments were carried out with lower concentrations of *N*-oleoyl taurine, using 1 and 5 μM . Following 48 h treatment, a significantly reduced cellular proliferation was evident (Fig. 2c). Interestingly, *N*-oleoyl taurine decreased cellular proliferation significantly after 24 h with 10 μM to 80% ($p < 0.0126$) and to 70% with concentrations as low as 1 μM after 48 and 72 h ($p < 0.0010$ and $p < 0.0001$) (Fig. 2c).

To identify whether the effects of *N*-acyl taurines were specific for PC-3 cells, MCF-7 cells were also treated with *N*-acyl taurines. Treatment with both *N*-arachidonoyl taurine and *N*-oleoyl taurine resulted in a reduced cell proliferation of MCF-7 cells, showing that anti-proliferative effects of *N*-acyl taurines were not specific for prostate cell lines. *N*-Arachidonoyl taurine had a significant effect on cell proliferation of MCF-7 cells at 20 μM after 24/48 h of treatment (Fig. 3a), whereas significant effects were evident in PC-3 cells after 48/72 h treatment (Figs. 2a and 3a). *N*-Oleoyl taurine was more potent at reducing proliferation of MCF-7 cells than *N*-arachidonoyl taurine, with significant effects evident after 24 h and especially after 72 h treatment (Fig. 3b), although *N*-oleoyl taurine was more potent in PC-3 cells than MCF-7 cells (compare Figs. 2b and 3b).

PC-3 cell survival was further investigated following treatment with *N*-arachidonoyl taurine and *N*-oleoyl taurine, using the colony formation assay. Cells were treated for 48 h with *N*-arachidonoyl taurine and *N*-oleoyl taurine (10 or 40 μM) in delipidated serum and allowed to proliferate for 2 weeks in complete medium (medium changed every other day). In this assay treatment of PC-3 cells with 40 μM of *N*-arachidonoyl taurine and *N*-oleoyl taurine reduced the colony number significantly ($p < 0.01$) to 56 and 62% respectively (Fig. 4).

N-Oleoyl Taurine Treatment Increases the Number of Cells in SubG1 Phase in PC-3 Cells

As *N*-arachidonoyl taurine and *N*-oleoyl taurine resulted in reduced cellular proliferation of PC-3 cells, the effect of treatment with these lipids at different stages of the cell cycle was examined by flow-cytometry. No significant effects were seen after treatment with *N*-arachidonoyl

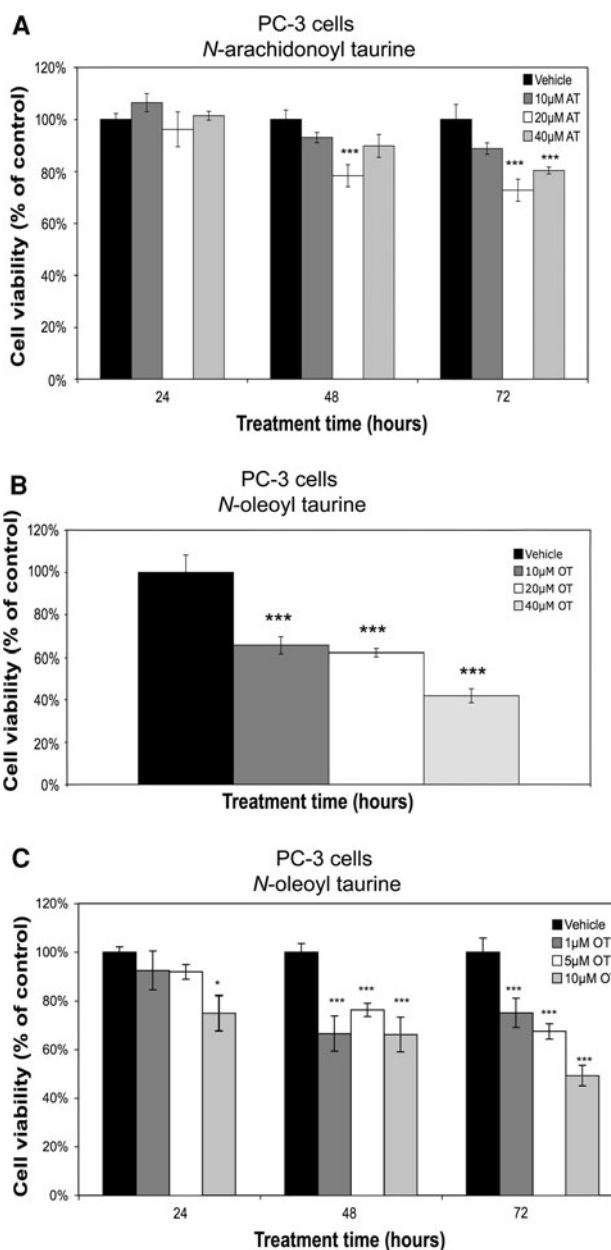


Fig. 2 *N*-Arachidonoyl taurine and *N*-oleoyl taurine inhibit proliferation of PC-3 cells. Cells were seeded in 96-well plates in the amount of 5,000 cells/well and cell viability was determined by a resazurin-based method following 24–72 h treatment with different concentrations of *N*-acyl taurines or vehicle (DMSO). **a** PC-3 cells treated with 10, 20 and 40 μM of *N*-arachidonoyl taurine (AT) after 24, 48 and 72 h. **b** PC-3 cells treated with 10, 20 and 40 μM of *N*-oleoyl taurine (OT) after 72 h. **c** PC-3 cells treated with 1, 5 and 10 μM of *N*-oleoyl taurine after 24, 48 and 72 h. Data are presented as means \pm SEM. * $p < 0.05$, *** $p < 0.001$

taurine in any phases of the cell cycle (Fig. 5a, c). Interestingly, *N*-oleoyl taurine treatment resulted in an increase in the number of cells in the subG1 phase (40 μM *N*-oleoyl taurine ($p < 0.001$)), with a reduction of cell numbers in the S and G2/M phases (Fig. 5b, c).

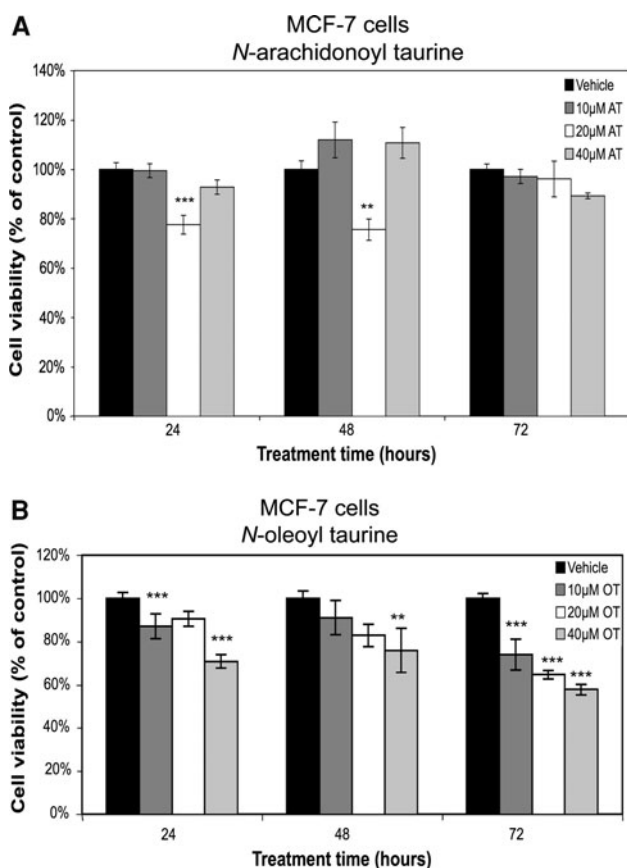


Fig. 3 *N*-Arachidonoyl taurine and *N*-oleoyl taurine inhibit proliferation of MCF-7 cells. Cells were seeded in 96-well plates in the amount of 5,000 cells/well and cell viability was determined by a resazurin-based method following 24–72 h treatment with different concentrations of *N*-acyl taurines or vehicle (DMSO). **a** MCF7 cells treated with 10, 20 and 40 μM of *N*-arachidonoyl taurine (AT) after 24, 48 and 72 h. **b** MCF7 cells treated with 10, 20 and 40 μM of *N*-oleoyl taurine (OT) after 24, 48 and 72 h. Data are presented as means ± SEM. ** $p < 0.01$, *** $p < 0.001$

Discussion

The discovery of novel lipids which are structurally related to endocannabinoids indicates the existence of novel signaling pathways in mammals. Endocannabinoids have been implicated in cancers and cause heterogenous effects in tumor cells by inducing apoptosis, reducing migration, by possessing anti-angiogenic activity and cause alterations in the cell cycle resulting in growth arrest [15–17]. This study aimed to elucidate if *N*-acyl taurines, a recently identified family of novel lipids [10], may have similar effects on pathways controlling cell growth and proliferation.

In this study, the major anti-proliferative effects on PC-3 cells were identified with *N*-oleoyl taurine (C18:1 taurine), even at concentrations as low as 1 μM. The effects on PC-3 cells were also significant with *N*-arachidonoyl taurine (C20:4 taurine) at various concentrations. Various endogenous lipids act as ligands for multiple types of receptors

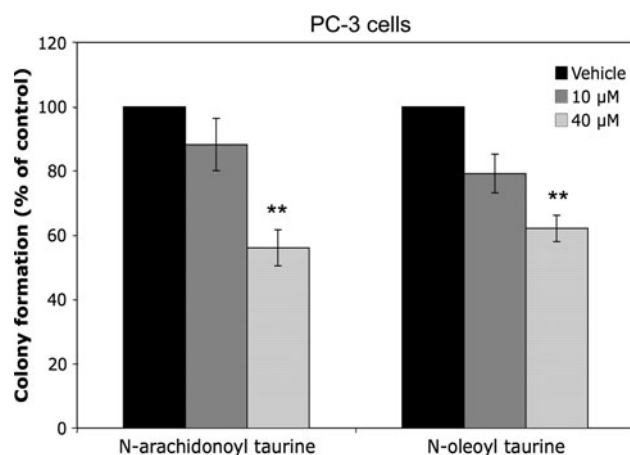
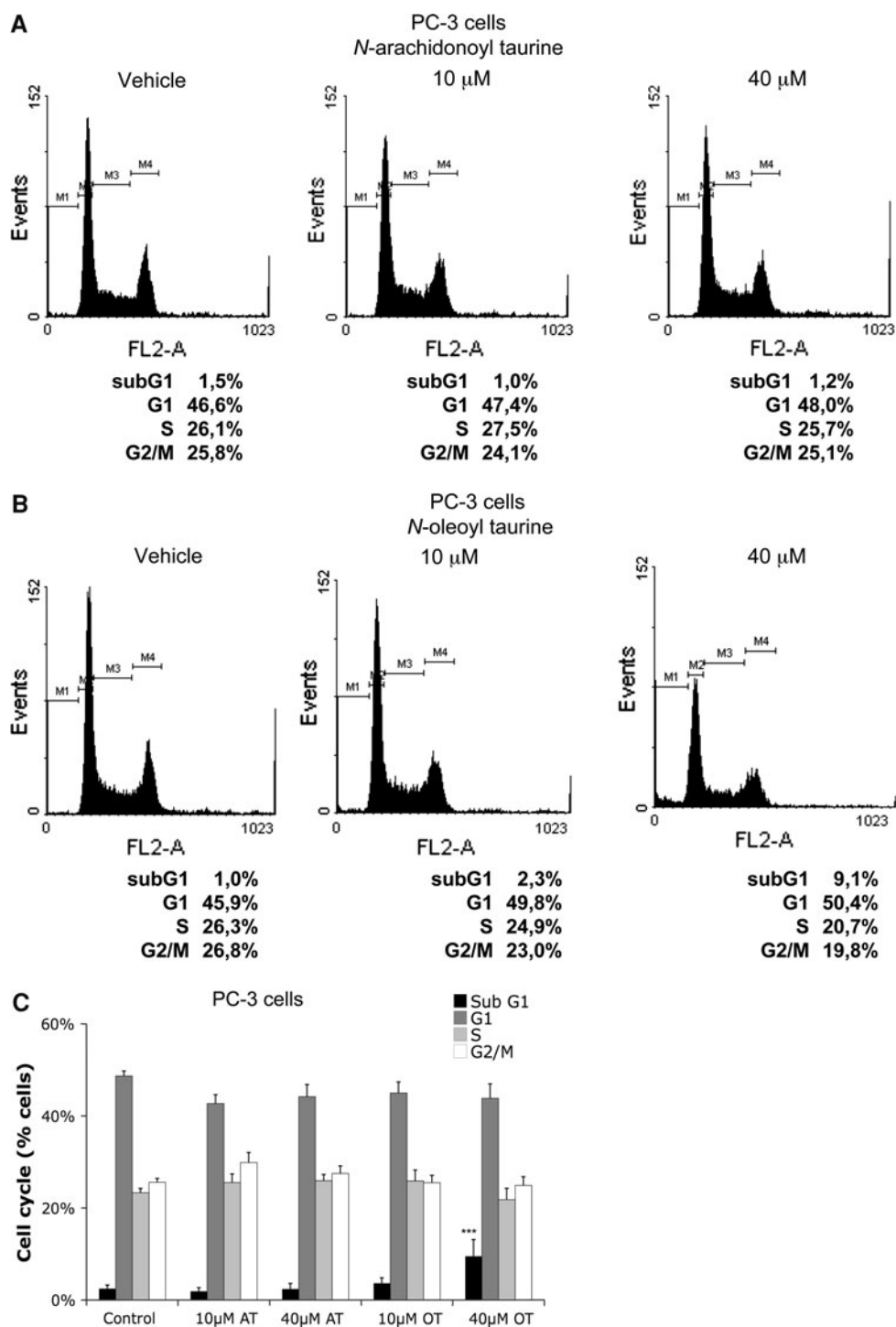


Fig. 4 *N*-Oleoyl taurine and *N*-arachidonoyl taurine reduces the colony-forming abilities of PC-3 cells. Cells were seeded in 100 mm dishes at a density of 500 cells/dish in DMEM with delipidated serum and treated with *N*-arachidonoyl taurine, *N*-oleoyl taurine or vehicle at concentrations of 10 and 40 μM for 48 h. After 48 h, medium was replaced with DMEM + foetal bovine serum (complete medium). Colonies formed were counted after 2 weeks in culture. Data are presented as means ± SEM ($n = 3$). ** $p < 0.01$

and *N*-arachidonoyl taurine activates the TRPV1 and TRPV4 channels; $EC_{50} \sim 28 \mu\text{M}$ (11–70 μM, 95% confidence limits) and $EC_{50} \sim 21 \mu\text{M}$ (3–130 μM, 95% confidence limits) respectively, whereas no activity with *N*-arachidonoyl taurine was identified with the cannabinoid receptors CB1 and CB2 or nuclear receptors such as peroxisome proliferator-activated receptors [11]. In our study concentrations of *N*-acyl taurines in the region of those required to activate the TRPV1 and TRPV4 channels were used, although significant effects on cell proliferation with 1 μM *N*-oleoyl taurine were identified. The anti-proliferative effects of *N*-oleoyl taurine in carcinoma cells were comparable to other fatty acid amides. Anandamide (*N*-arachidonylethanolamide) inhibits the proliferation of MCF-7 and EFM-19 cells at concentrations of between 0.5 and 1.5 μM [17] and also inhibits the proliferation of PC-3 cells at concentrations of 1–10 μM [18].

There are potentially two pathways to regulate the intracellular levels of *N*-acyl taurines: a) hydrolysis by the FAAH (which hydrolyzes *N*-acyl taurines to the free fatty acid and taurine) or b) oxidative metabolism of *N*-acyl taurines, resulting in generation or termination of novel signaling molecules [12]. The FAAH has been shown to hydrolyze both *N*-arachidonoyl taurine and *N*-oleoyl taurine [19]. Inhibition of the FAAH in mice resulted in accumulation of micromolar levels of *N*-acyl taurines in liver, kidney and the CNS, suggesting that micromolar levels can be reached in vivo [11]. An enzymatic pathway for the synthesis of saturated *N*-acyl taurines has been identified in peroxisomes [20], but as yet a pathway for synthesis of unsaturated *N*-acyl taurines is not known.

Fig. 5 *N*-Oleoyl taurine treatment increases the subG1 population of PC-3 cells. Cell cycle analysis was performed on PC-3 cells treated with *N*-acyl taurines or vehicle for 48 h. Cells were stained with propidium iodide and analyzed by FACS and data analyzed using the WinMDI software version 2.9. Representative histograms are shown in **a** *N*-arachidonoyl taurine (AT) and **b** *N*-oleoyl taurine (OT). **c** Data are presented as means \pm SEM
*** $p < 0.001$ = significantly different from SubG1 phase in control cells treated with vehicle ($n = 4$)



Interestingly, the FAAH is not expressed in PC-3 cells [21] and therefore *N*-oleoyl taurine and *N*-arachidonoyl taurine should remain 'active' for a longer period of time as a bioactive lipid signaling molecule as they will not be hydrolyzed by FAAH. It would be of interest to test these bioactive lipids in DU-145 and LNCaP prostate carcinoma cell lines, as LNCaP express high levels of FAAH, whereas DU-145 cells express low levels of FAAH [21], which may

result in different effects on cellular proliferation in different prostate carcinoma cell models. Interestingly, our results identified significant differences in how the two *N*-acyl taurines studied affected the cell cycle with a significant increase in the number of cells in subG1 phase following treatment with *N*-oleoyl taurine, suggesting apoptosis. The different effects may be due to acyl chain composition [*N*-arachidonoyl taurine (polyunsaturated) vs.

N-oleoyl taurine (monounsaturated) and chain length (C20:4 vs. C18:1 respectively)].

The second pathway regulating intracellular levels of *N*-acyl taurines was identified following a study by Turman et al. on the ability of cyclooxygenases (COXs) and lipoxygenases (LOXs) to oxygenate *N*-arachidonoyl taurine [12]. Although *N*-arachidonoyl taurine was a poor substrate for COXs, mammalian 12 S and 15 S-LOXs oxygenated *N*-arachidonoyl taurine very efficiently, generating 12 and 15-hydroxyicosatetraenoyltaurines (HETE-Ts) and dihydroxyicosatetraenoyltaurines (diHETE-Ts). *N*-Arachidonoyl taurine was rapidly taken up and converted primarily to 12-HETE-T in murine resident peritoneal macrophages [12]. Therefore, the oxidative metabolism of polyunsaturated *N*-acyl taurines may represent a pathway for the generation or termination of novel signaling molecules. At present, it is not known if *N*-arachidonoyl taurine or *N*-oleoyl taurine are further oxidized to HETE-Ts in PC-3 cells, but this is likely as LOX is expressed in prostate cancer and PC-3 cells [22].

Conclusions

In summary, our results show that novel biologically active lipids, the *N*-acyl taurines, result in reduced cell proliferation in PC-3 cells, due to an increased number of cells in the subG1 population and fewer cells in the S-phase. Therefore, an increase in intracellular levels of *N*-acyl taurines in vivo may result in effects on cell proliferation and lead to apoptosis in various cells and tissues such as the prostate gland.

Acknowledgments We are indebted to Jan-Olov Persson, Division of Mathematical Statistics, Stockholm University, for statistical analysis. This study is supported by The Swedish Research Council, Carl Tryggers Foundation, Åke Wibergs stiftelse, Ruth och Richard Julins Stiftelse, and Stiftelsen Professor Nanna Svartz fond. The authors have no conflict of interest.

References

- De Petrocellis L, Di Marzo V (2009) An introduction to the endocannabinoid system: from the early to the latest concepts. *Best Pract Res Clin Endocrinol Metab* 23(1):1–15
- Tan B, O'Dell DK, Yu W, Monn MF, Hughes HV, Burstein S, Walker JM (2010) Identification of endogenous acyl amino acids based on a targeted lipidomics approach. *J Lipid Res* 51(1):112–119
- Bradshaw HB, Rimmerman N, Hu SS-J, Burstein S, Walker JM (2009) Novel endogenous *N*-acyl glycines: identification and characterization. *Vitam Horm* 81:191–205
- Bradshaw HB, Walker JM (2005) The expanding field of cannabinimimetic and related lipid mediators. *Br J Pharmacol* 144(4):459–465
- Huang SM, Bisogno T, Petros TJ, Chang SY, Zavitsanos PA, Zipkin RE, Sivakumar R, Coop A, Maeda DY, De Petrocellis L, Burstein S, Di Marzo V, Walker JM (2001) Identification of a new class of molecules, the arachidonoyl amino acids, and characterization of one member that inhibits pain. *J Biol Chem* 276(46):42639–42644
- Waluk D, Schultz N, Hunt MC (2010) Identification of glycine *N*-acyltransferase-like 2 (GLYATL2) as a transferase that produces *N*-acyl glycines in humans. *FASEB J* 24(8):2795–2803
- McCue JM, Driscoll WJ, Mueller GP (2008) Cytochrome c catalyzes the in vitro synthesis of arachidonoyl glycine. *Biochem Biophys Res Commun* 365:322–327
- Burstein SH, Rossetti RG, Yagen B, Zurier RB (2000) Oxidative metabolism of anandamide. *Prostaglandins Other Lipid Mediat* 61(1–2):29–41
- Saghatelian A, Trauger SA, Want EJ, Hawkins EG, Siuzdak G, Cravatt BF (2004) Assignment of endogenous substrates to enzymes by global metabolite profiling. *Biochemistry* 43:14332–14339
- Saghatelian A, Cravatt BF (2005) Discovery metabolite profiling—forging functional connections between the proteome and metabolome. *Life Sci* 77:1759–1766
- Saghatelian A, McKinney MK, Bandell M, Patapoutian A, Cravatt BF (2006) A FAAH-regulated class of *N*-acyl taurines that activates TRP ion channels. *Biochemistry* 45(30):9007–9015
- Turman MV, Kingsley PJ, Rouzer CA, Cravatt BF, Marnett LJ (2008) Oxidative metabolism of a fatty acid amide hydrolase-regulated lipid, arachidonoyltaurine. *Biochemistry* 47(12):3917–3925
- Vriens J, Appendino G, Nilius B (2009) Pharmacology of vanilloid transient receptor potential cation channels. *Mol Pharmacol* 75(6):1262–1269
- Czifra G, Varga A, Nyeste K, Marincsak R, Toth B, Kovacs I, Kovacs L, Biro T (2009) Increased expressions of cannabinoid receptor-1 and transient receptor potential vanilloid-1 in human prostate carcinoma. *J Cancer Res Clin Oncol* 135(4):507–514
- Guzman M (2003) Cannabinoids: potential anticancer agents. *Nat Rev Cancer* 3:745–755
- Flygare J, Sander B (2008) The endocannabinoid system in cancer—potential therapeutic target? *Semin Cancer Biol* 18:176–189
- De Petrocellis L, Melck D, Palmisano A, Bisogno T, Laezza C, Bifulco M, Di Marzo V (1998) The endogenous cannabinoid anandamide inhibits human breast cancer cell proliferation. *Proc Natl Acad Sci USA* 95:8375–8380
- Nithipatikom K, Isbell MA, Endsley MP, Woodliff JE, Campbell WB (2011) Anti-proliferative effect of a putative endocannabinoid, 2-arachidonoylglycerol ether in prostate carcinoma cells. *Prostaglandins Other Lipid Mediat* 94(1–2):34–43
- McKinney MK, Cravatt BF (2005) Structure and function of fatty acid amide hydrolase. *Annu Rev Biochem* 74:411–432
- Reilly S-J, O'Shea EM, Andersson U, O'Byrne J, Alexson SEH, Hunt MC (2007) A peroxisomal acyltransferase in mouse identifies a novel pathway for taurine conjugation of fatty acids. *FASEB J* 21:99–107
- Endsley MP, Thill R, Choudhry I, Williams CL, Kajdacsy-Balla A, Campbell WB, Nithipatikom K (2008) Expression and function of fatty acid amide hydrolase in prostate cancer. *Int J Cancer* 123:1318–1326
- Matsuyama M, Yoshimura R, Mitsuhashi M, Hase T, Tsuchida K, Takemoto Y, Kawahito Y, Sano H, Nakatani T (2004) Expression of lipoxygenase in human prostate cancer and growth reduction by its inhibitors. *Int J Oncol* 24(4):821–827

Aberrations in Plasma Phospholipid Fatty Acids in Lung Cancer Patients

Rachel A. Murphy · Taylor F. Bureyko · Marina Mourtzakis · Quincy S. Chu · M. Thomas Clandinin · Tony Reiman · Vera C. Mazurak

Received: 6 September 2011 / Accepted: 25 November 2011 / Published online: 10 December 2011
© AOCs 2011

Abstract Abnormalities in lipid metabolism have been frequently observed in cancer and are associated with a poor prognosis. However, a detailed, longitudinal characterization of fatty acid status is lacking. This study aimed to assess plasma phospholipid fatty acids before chemotherapy, immediately after and 1 month following chemotherapy in a group of 50 patients newly diagnosed with lung cancer and explore factors which may contribute to aberrations in fatty acids. Their mean \pm SD characteristics: age 64 ± 8.5 years, 75% advanced stage disease, body mass index 27.0 ± 5.4 kg/m², 6 month weight loss $-4.6 \pm 6.1\%$. Compared to patients with early stage disease, patients with advanced disease had

abnormal fatty acid profiles including significantly lower ($P < 0.05$) amounts of total phospholipid fatty acids, saturated, and polyunsaturated fatty acids (linoleic, arachidonic, eicosapentaenoic and docosahexaenoic). Longitudinal analysis revealed that patients with advanced disease who completed chemotherapy had stable fatty acid levels and continued to maintain levels 1 month following completion of chemotherapy. Comparatively, patients who did not complete chemotherapy due to toxicity or disease progression had progressive loss of total phospholipid fatty acids, stearic, linoleic and n-6 fatty acids and a trend towards lower docosahexaenoic, arachidonic, palmitic, n-3 and saturated fatty acids. These results suggest that loss of fatty acids is prevalent, progressive and potentially influenced by advanced disease and chemotherapy treatment.

Electronic supplementary material The online version of this article (doi:10.1007/s11745-011-3641-2) contains supplementary material, which is available to authorized users.

R. A. Murphy · T. F. Bureyko · M. T. Clandinin · V. C. Mazurak (✉)

Department of Agricultural, Food and Nutritional Science, University of Alberta, 4-126A Li Ka Shing Centre, Edmonton, AB T6G 2E1, Canada
e-mail: vera.mazurak@ualberta.ca

M. Mourtzakis
Department of Kinesiology, University of Waterloo, 200 University Avenue W, Waterloo, ON N2L 3G1, Canada

Q. S. Chu
Department of Oncology, University of Alberta, 11560 University Avenue, Edmonton, AB T6G 1Z2, Canada

T. Reiman
Department of Oncology, Dalhousie University, Saint John Regional Hospital, 400 University Avenue, PO Box 2100, Saint John, NB E2L 4L2, Canada

Keywords Eicosapentaenoic fatty acid · Nutrition · n-3 Fatty acids · Lung cancer · Plasma lipids · Phospholipids

Abbreviations

ALA	Alpha-linolenic acid
ARA	Arachidonic acid
AST	Aspartate aminotransferase
BMI	Body mass index
DHA	Docosahexaenoic acid
EPA	Eicosapentaenoic acid
MUFA	Monounsaturated fatty acid(s)
NSCLC	Non-small cell lung cancer
PL	Phospholipid(s)
PUFA	Polyunsaturated fatty acid(s)
n-3	Sum of n-3 fatty acids
n-6	Sum of n-6 fatty acids
SFA	Saturated fatty acid(s)

Introduction

In advanced cancer, metabolism of nutrients may differ from healthy individuals. Abnormalities in lipid metabolism, including increased lipolysis [1] and oxidation of free fatty acids [2] have been observed in advanced cancer. Plasma phospholipids (PL) reflect the metabolism of endogenous and dietary fatty acids and contain the majority of n-6 and n-3 polyunsaturated fatty acids (PUFA) in blood. Thus, the fatty acid composition of plasma PL has been used as a measure of dietary intake and fatty acid status in a variety of conditions [3–5].

Several studies have reported alterations in PL fatty acids in patients with advanced cancer compared to healthy individuals [6–9]. In particular, striking differences in n-6 and n-3 fatty acids have been observed including decreased arachidonic acid (ARA, 20:4n-6), eicosapentaenoic acid (EPA, 20:5n-3) and docosahexaenoic acid (DHA, 22:6n-3) in patients with cancer. These differences were independent of changes in caloric and fat intake [9]. Total PL and phosphatidylcholine which is the main constituent of membrane PL, were also found to be low [10, 11], likely due to elevated phosphatidylcholine turnover by tumor cells [12].

The causes of the aberrations in PL fatty acids are unclear. One study suggested that chemotherapy may contribute to depletion of n-6 and n-3 fatty acids [9], but low n-3 and n-6 fatty acids have also been observed in the absence of chemotherapy [6, 10]. Cvetković et al. [10] showed an association between aggressive and advanced stage non-Hodgkin lymphoma and lower PL EPA and DHA. However, this is the only study to explore the relationship between cancer stage and the composition of PL.

Deficits in plasma fatty acids could be expected to affect the availability of fatty acids to peripheral tissues for tissue repair and other physiological processes. In support of this notion, loss of plasma PL has been observed to occur concurrently with weight loss [11], loss of skeletal muscle and adipose tissue in advanced cancer patients [13]. Thus, identification of potential causes or the point in time during the course of the disease trajectory and treatment that this evolves is important for planning effective and timely intervention. However, a detailed, longitudinal characterization of fatty acid status in patients with cancer is lacking. The objectives of this study were to assess fatty acids before, immediately after chemotherapy and 1 month post chemotherapy in patients with lung cancer and determine factors which may influence amounts of fatty acids.

Methods

Patient Population

This study was approved by the Alberta Cancer Research Ethics board as a minimal risk study (chart review, no intervention). All patients were recruited from the lung cancer new patient clinic at the Cross Cancer Institute (Edmonton, Alberta, Canada) between August 2007 and November 2009 and were followed for >1.5 years. The Cross Cancer Institute is the major cancer center for all of Northern Alberta (population 1.8 million) and sees >95% of referrals for consideration of treatment with chemotherapy or radiation therapy. All newly referred patients with lung cancer attend a medical oncology clinic. At clinic, patients are given a handout that briefly describes available nutritional studies and patients are asked to indicate interest. Patient response informs investigators who to approach regarding participation in research studies. Patients in this study were accrued with the purpose of detailing changes in fatty acids during chemotherapy and the potential impact this has on clinical outcomes. A portion of these patients served as a control group (standard of care, no intervention) for a study which examined the effect of fish oil supplementation on body composition [14] and chemotherapy efficacy [15].

Study Design

Patients with a histologically confirmed diagnosis of non-small cell lung cancer (NSCLC) were included. This patient population was chosen because a high proportion of patients with lung cancer experience malnutrition [16]. Additional inclusion criteria were: >18 years of age, no gastrointestinal tumors, able to maintain oral intake, naive to chemotherapy and able to provide written, informed consent. Since this study was focused on change in fatty acids during chemotherapy, patients were only approached for study participation if they were referred for either adjuvant chemotherapy or first-line palliative chemotherapy for advanced/metastatic disease based on standard practice specifically agreed upon as Clinical Practice Guidelines by the Alberta Provincial Lung Tumor Group.

Stage of disease was based on the American Joint Committee on Cancer stage groupings, I, II, III, and IV [17]. Height was measured by a stadiometer and weight was measured using a medical balance beam scale at baseline and at each time point. Height and weight were used to compute body mass index (BMI) (kg/m^2). World Health Organization [18] categories were used to classify patients as: underweight, BMI <18.5; normal, BMI 18.5–24.9;

overweight BMI 25.0–29.9; or obese BMI \geq 30.0. Self-reported weight loss history in the 6 months preceding referral was obtained from medical records or the Patient Generated Subjective Global Assessment [19] which is completed by patients at their first clinic visit.

Chemotherapy Treatment

All patients were seen in consultation for treatment with standard chemotherapy. At our cancer center, chemotherapy for NSCLC consists of platinum-based doublet chemotherapy. Typically, cisplatin and vinorelbine are used for adjuvant chemotherapy and carboplatin in combination with vinorelbine or gemcitabine is used to treat patients with advanced disease. This chemotherapy regimen is typically administered on a 3-week cycle for 2 cycles, after which response to chemotherapy for those with advanced lung cancer is assessed by imaging. If there is disease response (stable disease or decreased disease burden) chemotherapy is continued for 4 cycles, otherwise chemotherapy is stopped. The end of the study was considered to be akin to completion/the end of chemotherapy as this coincided with the last study blood draw. As per chemotherapy protocol, all patients had an Eastern Cooperative Performance Status [20] between 0 (fully active, no limitations) and 2 (up and about more than 50% of waking hours).

Lipid Extraction and Phospholipid Separation

Blood (12 mL) was drawn into a heparinized tube by a Registered Nurse prior to starting chemotherapy (baseline), prior to each 3 week cycle of chemotherapy and 1 month following chemotherapy if patients continued to be followed at our cancer institute. To minimize patient burden, blood draws were arranged to coincide with routine blood work that was ordered as part of routine clinical protocol. Serum aspartate aminotransferase (AST) levels recorded from complete blood count tests were recorded as an indication of liver dysfunction.

Blood was centrifuged, plasma was isolated and immediately frozen at -80°C until analysis. Fatty acids were extracted from plasma using a modified Folch method [4] and the PL fraction was isolated using thin layer chromatography. The PL band was visualized, scraped and C17:0 (10.1 mg/100 mL; Supelco, Bellefonte, PA, USA; Sigma Chemical, St. Louis, MO, USA) was added as an internal standard followed by methylation at 110°C for 1 h. Plasma PL fatty acid composition was determined using gas liquid chromatography (Varian 3900CX Gas Chromatograph) equipped with a flame ionization detector, autosampler and a 30-meter BP-20 fused capillary column (SGE Instruments Australia). Peaks of saturated (SFA),

monounsaturated (MUFA) and PUFA fatty acids between 6 and 24 carbon chain lengths were identified by comparison with a commercially available standard of known fatty acid composition and quantified using the C17:0 standard peak. Fatty acid content of PL was calculated using the area peak of the internal standard and expressed as $\mu\text{g/mL}$. Mean fatty acid amounts were calculated from duplicates. An acceptable level of variation between duplicates was set at 5%. A random selection of 20 samples were run twice on the gas chromatograph on separate days. The co-efficient of variation between fatty acids amounts from the two runs was $<5\%$.

Statistical Analysis

Data are reported as means \pm standard deviation. Two sample *t* tests or Fischer's exact test were used to compare groups as appropriate. Pearson correlation was used to identify a potential relationship between serum AST and total amounts of PL fatty acids. All tests were two-sided. Repeated measures analysis of variance with Bonferroni post hoc comparisons was used to compare changes in fatty acids from baseline to end of study. Significance was reported at levels of $P < 0.05$ and trends were identified at $P < 0.10$. Statistical analysis was completed using SPSS for Windows (version 18.0, SPSS, Chicago, IL, USA).

Results

Patient Demographics

Overall, 60 patients were accrued, 50 received at least a baseline blood draw and 42 completed the study. The number of patients who consented but were subsequently withdrawn is a reflection of the patient population. The majority of patients had advanced stage disease and many had disease related symptoms which impacted upon performance status and their ability to tolerate chemotherapy. Patients who received at least a baseline blood draw were included in this analysis.

Of the 50 patients with a baseline blood draw, three did not receive any chemotherapy due to rapid decline in performance status, and four patients had baseline blood draws only. Thus, these 7 patients were only included in baseline analyses. Baseline patient demographics and anthropometrics are shown in Table 1. Despite generally advanced disease, patients had heavy body weights and only one patient was underweight (BMI $<18.5\text{ kg/m}^2$). Similar to the general lung cancer population [21], comorbid conditions were common. The most frequently reported conditions were hypertension (44%), chronic obstructive pulmonary disease (20%) and hyperlipidemia/

Table 1 Baseline patient demographics and anthropometrics

	Men (<i>n</i> = 19)	Women (<i>n</i> = 31)	<i>P</i>
Age (years)	67 ± 6.2	61 ± 9.0	0.03
Stage			
I & II, <i>n</i> (%)	4 (21.1)	8 (25.8)	1.00
III & IV, <i>n</i> (%)	15 (78.9)	23 (74.2)	
Body mass index (kg/m ²)	28.7 ± 5.3	26.5 ± 5.4	0.17
Range	18.8–43.3	17.0–39.0	
Weight loss in preceding 6 months (%) ^a	−2.0 ± 3.0	−6.3 ± 6.9	0.02

Mean ± standard deviation, two sample *t* test or Fischer's exact test

^a Data not available for 3 patients

hypercholesterolemia (16%). Median survival was not determined due to the inclusion of patients with early stage disease and insufficient power for survival analyses on the subset of patients with advanced disease.

Plasma Phospholipid Fatty Acids at Baseline

At baseline, total plasma PL ranged widely from a minimum of 94.6 µg/mL to a maximum of 1,284 µg/mL. To examine potential sources of this variation, patients were divided into groups based upon stage of disease (advanced stage; III and IV, *n* = 38 or early stage; I and II, *n* = 12). The patients with advanced stage cancer were further divided into two groups based upon the presence or absence of liver metastases.

Table 2 Baseline plasma PL fatty acids in patients with early versus advanced stage disease

Fatty acid (µg/mL)	Stage I & II (<i>n</i> = 12)	Stage III & IV (<i>n</i> = 38)	<i>P</i>
C16:0	251 ± 49.8	181 ± 67.6	0.002
C18:0	120 ± 21.4	91.0 ± 34.9	0.009
C18:1	95.1 ± 15.7	80.4 ± 32.0	0.13
C18:2n-6	155 ± 38.4	120 ± 44.2	0.02
C18:3n-3	1.6 ± 1.6	1.4 ± 1.1	0.52
C20:4n-6	76.1 ± 23.4	59.4 ± 25.6	0.05
C20:5n-3	10.3 ± 3.7	5.5 ± 4.7	0.002
C22:6n-3	18.1 ± 4.8	13.4 ± 7.0	0.03
n-6	268 ± 63.7	204 ± 71.8	0.008
n-3	29.7 ± 7.6	21.9 ± 12.1	0.04
SFA	385 ± 68.0	282 ± 103	0.002
MUFA	110 ± 19.4	92.7 ± 35.6	0.11
PUFA	299 ± 68.8	227 ± 80.7	0.007
Total	772 ± 166	598 ± 206	0.01

Mean ± standard deviation, two sample *t* test

SFA saturated fatty acids, MUFA monounsaturated fatty acids, PUFA polyunsaturated fatty acids

Patients with advanced stage lung cancer were not different for age, gender, or BMI compared to patients with early stage lung cancer. The presence of hyperlipidemia and hypertension also did not differ between groups (*P* = 0.35). However, compared to early stage patients, patients with advanced disease had lower total PL and alterations in most fatty acids (Table 2). The amount of EPA was particularly disparate between disease stages, and was nearly 50% lower in patients with advanced cancer.

Liver function and liver metastases did not appear to influence fatty acid amounts. There was no relationship between total PL amounts and serum AST levels (Pearson correlation *r* = 0.04; *P* = 0.79). Individual fatty acids, classes of fatty acids and total fatty acid amounts in patients with liver metastases (*n* = 13) were not different from patients without liver metastases (*n* = 25) (Supplementary data).

Plasma Phospholipid Fatty Acids During Chemotherapy

During the course of the study, two clear groups emerged: patients who completed a full course of chemotherapy (≥4 cycles; completers, *n* = 27) and patients who stopped chemotherapy due to either disease progression or toxicity (<4 cycles; non-completers, *n* = 16). The mean duration of chemotherapy was 11.4 ± 2.4 weeks in the completers group and 7.2 ± 2.9 weeks in the non-completers group. The groups were similar in age, gender and BMI, but the proportion of patients with early and advanced stage differed. Only 3 patients (19%) in the non-completers group had early stage disease compared to 9 patients (33%) in the completers group. Patients with early stage disease generally tolerate chemotherapy better, with fewer and milder side effects than patients with advanced disease. In addition, total and individual amounts of fatty acids were influenced by stage of disease (Table 2), and thus the comparison between completers and non-completers was limited to patients with advanced disease (13 in the non-completers group and 18 in the completers group). A comparison between early stage completers and non-completers was not undertaken as there were only 3 patients in the non-completers group with early stage disease.

There were no changes in fatty acids from baseline to end of chemotherapy in advanced stage patients who completed chemotherapy (Table 3). Conversely, advanced stage patients who did not complete chemotherapy had lower linoleic, stearic acid, n-6 fatty acids, PUFA and total PL fatty acids at the end of chemotherapy compared to baseline and a trend towards lower palmitic, ARA, DHA, n-3 and SFA at the end of chemotherapy (Table 3). Comparison of fatty acids at the end of chemotherapy between

Table 3 Change in plasma PL fatty acids from baseline to end of study in advanced stage patients who did not complete chemotherapy due to intolerance or disease progress (<4 cycles) and patients who completed a full course of chemotherapy (≥ 4 cycles)

Fatty acid ($\mu\text{g/mL}$)	Non-completers ($n = 13$)			Completers ($n = 18$)		
	Baseline	End of study	<i>P</i>	Baseline	End of study	<i>P</i>
C16:0	194 \pm 82.9	156 \pm 93.3	0.06	177 \pm 53.8	169 \pm 58.8	0.44
C18:0	95.8 \pm 27.9	76.4 \pm 43.7	0.05	88.8 \pm 27.9	90.7 \pm 30.1	0.74
C18:1	80.2 \pm 43.6	70.8 \pm 47.9	0.17	80.2 \pm 25.4	74.7 \pm 24.0	0.35
C18:2n-6	127 \pm 58.5	102 \pm 63.2	0.04	121 \pm 35.3	118 \pm 46.4	0.71
C18:3n-3	1.0 \pm 0.9	1.3 \pm 1.0	0.31	1.6 \pm 1.1	1.6 \pm 0.9	0.99
C20:4n-6	62.9 \pm 33.0	51.2 \pm 37.2	0.09	57.0 \pm 21.7	54.7 \pm 25.2	0.59
C20:5n-3	5.3 \pm 4.9	4.0 \pm 2.8	0.35	5.9 \pm 5.1	6.3 \pm 4.1	0.65
C22:6n-3	14.4 \pm 9.0	11.5 \pm 10.2	0.11	13.2 \pm 5.9	12.8 \pm 5.9	0.77
n-6	215 \pm 99.4	173 \pm 99.2	0.03	202 \pm 53.4	198 \pm 68.0	0.78
n-3	21.5 \pm 13.1	16.9 \pm 12.5	0.10	23.2 \pm 2.9	22.2 \pm 10.5	0.71
SFA	298 \pm 132	251 \pm 142	0.10	277 \pm 81.7	282 \pm 103	0.79
MUFA	91.8 \pm 48.3	81.5 \pm 53.1	0.16	93.0 \pm 28.2	86.5 \pm 27.3	0.37
PUFA	237 \pm 110	194 \pm 117	0.05	227 \pm 62.3	219 \pm 77.0	0.63
Total	623 \pm 283	513 \pm 285	0.05	593 \pm 156	589 \pm 184	0.88

Mean \pm standard deviation, repeated measures analysis of variance with Bonferroni post hoc comparisons

SFA saturated fatty acids, MUFA monounsaturated fatty acids, PUFA polyunsaturated fatty acids

completers and non-completers revealed no differences except for a trend towards lower EPA in the non-completers group (4.0 ± 2.8 vs. 6.3 ± 4.1 $\mu\text{g/mL}$; $P = 0.09$).

Plasma Phospholipid Fatty Acids Following Chemotherapy

Of the patients who completed chemotherapy, 17 had a follow-up blood draw approximately 1 month following study and chemotherapy completion (mean 38.1 ± 20.2 days). All fatty acid amounts were stable between chemotherapy completion and follow-up (mean increase of total PL fatty acids by 19.9 $\mu\text{g/mL}$, equivalent to approximately a 3% increase). There were also no significant differences in any fatty acid amounts between baseline and follow-up.

Discussion

The fatty acid profile of patients with cancer is not well characterized due to a limited number of studies in patients with heterogeneous tumor types. Here we provide a comprehensive assessment of plasma PL fatty acids in a major tumor group prior to, immediately after chemotherapy and 1 month following the end of chemotherapy. Using this approach, we report that patients with advanced stage lung cancer have alterations in PL fatty acid composition at diagnosis which may be further exacerbated during chemotherapy.

Patients with advanced disease had lower amounts of most fatty acids compared to patients with early stage disease. This is similar to what has been reported in serum PL in non-Hodgkin lymphoma [10]. The significance of

these differences is unclear, but we have previously reported that low PL fatty acids indicate poor prognosis [22] and now suggest that low PL fatty acids may relate to the ability to complete all planned chemotherapy. The differences in PL fatty acids between disease stages may be the culmination of several factors. During periods of tumor growth, there is increased demand for PL by the tumor for cell replication and altered PL membrane metabolism [23, 24]. Proximity to death may have also contributed to the difference in fatty acids between early and advanced stage patients. Although survival was not assessed, it is expected that advanced stage patients have shorter survival compared to patients with early stage disease and declines in fatty acids have been reported near death in advanced cancer patients [13]. Medications such as statins, fibrates and beta blockers for treatment of hypertension and hyperlipidemia may affect lipids levels. Although we were not privy to medication details (brand, dose and frequency), the presence of hypertension and hyperlipidemia was similar between groups. It is also unlikely that differences in PL fatty acids between early and advanced stage patients resulted from differences in diet as fat intake would be expected to alter the composition but not the amount of PL fatty acids. Fatty acid amounts also appeared to be unaffected by the presence of liver metastases.

Loss of fatty acids is progressive, with further decreases from baseline in patients who did not complete chemotherapy. Of interest, change in n-3 fatty acids during chemotherapy appears to be minimal, with only a trend towards lower n-3 fatty acids and DHA and no change in EPA. To provide a frame of reference, PL fatty acids in the non-completers group were compared to the fatty acid profile of advanced cancer patients from the same cancer center that has been previously published [13] (Table 4).

Table 4 Plasma PL fatty acids at the end of study in advanced stage patients receiving <4 cycles of chemotherapy and in a group of advanced cancer patients <8 or >8 months from death

Fatty acid ($\mu\text{g/mL}$)	Non-completers End of study ($n = 13$)	<8 months to death ($n = 36$)	>8 months to death ($n = 36$)
C16:0	156 \pm 93.3	133 \pm 100	212 \pm 112
C18:0	76.4 \pm 43.7	61.9 \pm 46.1	100 \pm 45.5
C18:1	70.8 \pm 47.9	56.8 \pm 38.4	89.2 \pm 48.1
C18:2n-6	102 \pm 63.2	82.0 \pm 58.0	125 \pm 63.0
C18:3n-3	1.3 \pm 1.0	0.7 \pm 0.8	1.6 \pm 2.3
C20:4n-6	51.2 \pm 37.2	43.0 \pm 35.0	60.0 \pm 40.0
C20:5n-3	4.0 \pm 2.8	4.4 \pm 7.8	5.9 \pm 5.2
C22:6n-3	11.5 \pm 10.2	13.0 \pm 12.0	21.0 \pm 15.0
n-6	173 \pm 99.2	142 \pm 107	216 \pm 117
n-3	16.9 \pm 12.5	19.0 \pm 17.0	29.0 \pm 19.0
SFA	251 \pm 142	209 \pm 150	329 \pm 158
MUFA	81.5 \pm 53.1	69.0 \pm 50.0	106 \pm 61.0
PUFA	194 \pm 117	164 \pm 123	249 \pm 134
Total	513 \pm 285	442 \pm 316	686 \pm 336

Mean \pm standard deviation. Data from a previous study of advanced cancer patients [13] is shown for reference and were not statistically compared to patients in this study

SFA saturated fatty acids, MUFA monounsaturated fatty acids, PUFA polyunsaturated fatty acids

Patients who were <8 months from death had similar levels of EPA and DHA as the non-completers at the end of their treatment whereas the amount of all other fatty acids were in the range of or appeared greater than fatty acids reported in patients >8 months from death. This may suggest that loss of n-3 fatty acids precedes depletion of other classes of fatty acids and may serve as a predictive marker for survival and response to chemotherapy, especially in the palliative setting. However, this hypothesis needs to be tested in larger populations.

It seems possible that depletion of fatty acids is related to either indirect or direct effects of chemotherapy treatment. Disturbances in the gastrointestinal tract resulting from chemotherapy may affect the availability, absorption or metabolism of fatty acids [25]. This may explain the decline in fatty acids in the non-completers group which included a number of patients with severe chemotherapy toxicity. Low levels of n-6 and n-3 fatty acids in plasma PL have been observed in advanced breast cancer following induction chemotherapy, with further declines following high dose chemotherapy [9]. However, here we report little variation in amounts of fatty acids throughout chemotherapy in over half of our patients (patients that completed chemotherapy). It appears that change in fatty acids during chemotherapy may be related to disease control as patients with progressive disease (non-completers group) lost fatty

acids. Conversely, patients experiencing a benefit from treatment (reduced tumor burden or stable disease) exhibited stable fatty acids which showed no change even one month following the end of chemotherapy. Given the short disease trajectory of advanced lung cancer, this hypothesis could be tested by following patients with stable disease until the point of disease progression and quantifying fatty acids throughout this time period.

Conclusion

This research shows that loss of fatty acids is prevalent, progressive and possibly influenced by the stage of the disease, chemotherapy treatment and disease control. Larger studies which account for these variables and follow patients over a longer period of time would help to define these relationships further.

Acknowledgments We would like to thank Kelly-Ann Leonard and Lisa Martin for their assistance with the study. This work was supported by Canadian Institutes of Health Research and by Queen Elizabeth II Graduate scholarship (RAM) and TD Interdisciplinary Health Studentship (RAM).

Conflict of interest The authors report no conflicts of interest.

References

- Rydén M, Agustsson T, Laurencikiene J, Britton T, Sjölin E, Isaksson B, Permert J, Arner P (2008) Lipolysis—not inflammation, cell death, or lipogenesis—is involved in adipose tissue loss in cancer cachexia. *Cancer* 113:1695–1704
- Douglas RG, Shaw JH (1997) Metabolic effects of cancer. *Br J Surg* 77:246–543
- Clandinin MT, Van Aerde JE, Parrott A, Field CJ, Euler AR, Lien EL (1997) Assessment of the efficacious dose of arachidonic and docosahexaenoic acids in preterm infant formulas: fatty acid composition of erythrocyte membrane lipids. *Pediatr Res* 42: 819–825
- Pratt VC, Tredget EE, Clandinin MT, Field CJ (2001) Fatty acid content of plasma lipids and erythrocyte phospholipids are altered following burn injury. *Lipids* 36:675–682
- Plourde M, Chouinard-Watkins R, Vandal M, Zhang Y, Lawrence P, Brenna JT, Cunnane SC (2011) Plasma incorporation, apparent retroconversion and β -oxidation of ^{13}C -docosahexaenoic acid in the elderly. *Nutr Metab* 8:5
- McClinton S, Moffat LE, Horrobin DF, Manku MS (1991) Abnormalities of essential fatty acid distribution in the plasma phospholipids of patients with bladder cancer. *Br J Cancer* 63:314–367
- Chaudry A, McClinton S, Moffat LE, Wahle KW (1991) Essential fatty acid distribution in the plasma and tissue phospholipids of patients with benign and malignant prostatic disease. *Br J Cancer* 64:1157–1160
- Zuijgeest-van Leeuwen SD, van der Heijden MS, Rietveld T, van den Berg JW, Tilanus HW, Burgers JA, Wilson JH, Dagnelie

- PC (2002) Fatty acid composition of plasma lipids in patients with pancreatic, lung and oesophageal cancer in comparison with healthy subjects. *Clin Nutr* 21:225–230
9. Pratt VC, Watanabe S, Bruera E, Mackey J, Clandinin MT, Baracos VE, Field CJ (2002) Plasma and neutrophil fatty acid composition in advanced cancer patients and response to fish oil supplementation. *Br J Cancer* 87:1370–1378
 10. Cvetković Z, Vucić V, Cvetković B, Petrović M, Ristić-Medić D, Tepsić J, Glibetić M (2010) Abnormal fatty acid distribution of the serum phospholipids of patients with non-Hodgkin lymphoma. *Ann Hematol* 89:775–782
 11. Taylor LA, Arends J, Hodina AK, Unger C, Massing U (2007) Plasma lyso-phosphatidylcholine concentration is decreased in cancer patients with weight loss and activated inflammatory status. *Lipids Health Dis* 6:17
 12. Baburina I, Jackowski S (1999) Cellular responses to excess phospholipid. *J Biol Chem* 274(14):9400–9408
 13. Murphy RA, Wilke MS, Perrine M, Pawlowicz M, Mourtzakis M, Lieffers JR, Maneshgar M, Bruera E, Clandinin MT, Baracos VE, Mazurak VC (2010) Loss of adipose tissue and plasma phospholipids: relationship to survival in advanced cancer patients. *Clin Nutr* 29:482–487
 14. Murphy RA, Mourtzakis M, Chu QS, Baracos VE, Reiman T, Mazurak VC (2011) Nutritional intervention with fish oil provides a benefit over standard of care for weight and skeletal muscle mass in patients with nonsmall cell lung cancer receiving chemotherapy. *Cancer* 117:1775–1782
 15. Murphy RA, Mourtzakis M, Chu QS, Baracos VE, Reiman T, Mazurak VC (2011) Supplementation with fish oil increases first-line chemotherapy efficacy in patients with advanced nonsmall cell lung cancer. *Cancer* 117:3774–3780
 16. Ross PJ, Ashley S, Norton A, Priest K, Waters JS, Eisen T, Smith IE, O'Brien ME (2004) Do patients with weight loss have a worse outcome when undergoing chemotherapy for lung cancers? *Br J Cancer* 90:1905–1911
 17. Edge SB, Byrd DR, Compton CC, Fritz AG, Greene FL, Trotti A (2009) American joint committee on cancer staging manual, 7th edn. Springer, New York
 18. WHO (2000) Obesity: preventing and managing the global epidemic. World Health Organization, Geneva
 19. Ottery FD (1996) Definition of standardized nutritional assessment and interventional pathways in oncology. *Nutrition* 12:S15–S19
 20. Oken MM, Creech RH, Tormey DC, Horton J, Davis TE, McFadden ET, Carbone PP (1982) Toxicity and response criteria of the Eastern Cooperative Oncology Group. *Am J Clin Oncol* 5:649–655
 21. Janssen-Heijnen ML, Schipper RM, Razenberg PP, Crommelin MA, Coebergh JW (1998) Prevalence of co-morbidity in lung cancer patients and its relationship with treatment: a population-based study. *Lung Cancer* 21:105–113
 22. Murphy RA, Mourtzakis M, Chu QS, Reiman T, Mazurak VC (2010) Skeletal muscle depletion is associated with reduced plasma (n-3) fatty acids in non-small cell lung cancer patients. *J Nutr* 140:1602–1606
 23. Raffelt K, Moka D, Sullentrop F, Dietlein M, Hahn J, Schicha H (2000) Systemic alterations in phospholipid concentrations of blood plasma in patients with thyroid carcinoma: an in vitro (31)P high-resolution NMR study. *NMR Biomed* 13:8–13
 24. Kuliszkievicz-Janus M, Janus W, Baczynski S (1996) Application of ³¹P NMR spectroscopy in clinical analysis of changes of serum phospholipids in leukemia, lymphoma and some other non-haematological cancers. *Anticancer Res* 16:1587–1594
 25. Peters BG (1994) An overview of chemotherapy toxicities. *Top Hosp Pharm Manage* 14:59–88

Multifunctional Acyltransferases from *Tetrahymena thermophila*

Eva-Maria Biester · Janine Hellenbrand ·
Margrit Frentzen

Received: 7 November 2011 / Accepted: 23 November 2011 / Published online: 14 December 2011
© The Author(s) 2011. This article is published with open access at Springerlink.com

Abstract Multifunctional acyltransferases are able to catalyze the esterification of various acyl-acceptors with activated fatty acids. Here we describe the identification of four proteins from *Tetrahymena thermophila* that share certain properties with mammalian acyltransferases regarding their predicted transmembrane structure, their molecular mass and the typical acyltransferase motif. Expression of the *Tetrahymena* sequences results in production of triacylglycerols and wax esters in recombinant yeast when appropriate substrates are provided. The in vitro characterization shows, that these enzymes are capable of esterifying different acyl-acceptors including fatty alcohols, diols, diacylglycerols and isoprenols with acyl-CoA thioesters. Based on these catalytic activities and the sequence similarities of the *Tetrahymena* proteins with acyl-CoA:diacylglycerol acyltransferase 2 (DGAT2) family members, we conclude that we identified a new group of DGAT2-related multifunctional acyltransferases from protozoan organisms.

Keywords Multifunctional acyltransferase · *Tetrahymena* · Wax ester · DGAT · Prenyl ester · Diester

Abbreviations

ASAT Acyl-CoA:sterol acyltransferase, steryl ester synthase

CoA Coenzyme A
DGAT Acyl-CoA:diacylglycerol acyltransferase
DES Diester synthase
PES Prenylester synthase
TAG Triacylglycerol(s)
WE Wax ester(s)
WS Wax synthase

Introduction

Acyltransferases belong to the large group of enzymes, transferring groups other than amino-acyl groups (EC 2.3.1) onto acyl-acceptors like fatty alcohols (EC 2.3.1.75) or diacylglycerols (EC 2.3.1.20). Genes encoding multifunctional acyltransferases catalyzing the esterification of a variety of acyl-acceptor moieties with acyl-CoA thioesters have been characterized from prokaryotic and eukaryotic organisms [1–5].

More recently, genes essential for wax ester synthesis became important tools for developing renewable resources for the technical industry [6–8]. The increasing prices of fossil material make up the market for tailor-made wax esters (WE). These lipids in general are excellent lubricants with good stability under high temperature and pressure and they are very resistant to hydrolysis [6], which makes them attractive as lubricants. While saturated long-chain monoesters have good lubricity but poor low temperature fluidity, unsaturated monoesters or diesters overcome this lack and combine it with good thermal and oxidative stability and high viscosity indices [9]. To achieve the renewable production of WE, experiments are in progress to identify new enzymes catalyzing respective esterification

Electronic supplementary material The online version of this article (doi:10.1007/s11745-011-3642-1) contains supplementary material, which is available to authorized users.

E.-M. Biester (✉) · J. Hellenbrand · M. Frentzen
Institute for Biology I, RWTH Aachen University,
Worringer Weg 1, 52074 Aachen, Germany
e-mail: em.biester@bio1.rwth-aachen.de

reactions [10–13]. Production of high levels of WE in oil crops [6, 7] or microorganisms [8, 12] might be able to replace fossil materials in future.

Tetrahymena is a unicellular protozoan and belongs to the phylum of Ciliophora [14]. It is common in temperate freshwater [15] and can be cultivated in the laboratory. *Tetrahymena* is a model system for eukaryotic cells that provides features of higher eukaryotic organisms which cannot be found in other unicellular model systems like *Saccharomyces cerevisiae* [16]. Studies on lipid components in *Tetrahymena thermophila* (before 1976 *T. thermophila* was referred to as *T. pyriformis* variety or syngen 1 [17]) showed that the cells are able to accumulate large amounts of lipids. During the logarithmic phase, 24% of the cell dry weight is made up by lipids [18], 28% of which are neutral lipids located in lipid droplets [19], mainly triacylglycerols (TAG) esterified with saturated fatty acids of 14–18 carbon atoms [20]. The WE make up a small portion of the total lipid content of only about 0.15% [21]. Unlike TAG they contain branched-chain acyl-groups of 17–21 carbon atoms (76%) and branched-chain alcohols of 17–19 carbon atoms (45%) [21]. In addition to long-chain WE, fatty acid methyl and ethyl esters have also been found in *Tetrahymena*, of which methyl linoleate, ethyl myristate and ethyl linoleate are the most abundant [22]. The physiological function of these esters and WE is not clear because the low amount excludes storage functions [21]. They might be communication scents or simply a way to control the level of free alcohols to prevent toxic effects for the cells [22].

Like other ciliates, *Tetrahymena* has two specialized nuclei: the micronucleus (MIC) is the diploid germline while the haploid macronucleus (MAC), which differentiates from the MIC, is the somatic gene expression machine [15, 23]. The recent whole genome shotgun sequencing and assembly of the *Tetrahymena* MAC genome by the Institute for Genomic Research (TIGR) in 2006 revealed that the genome contains 104 Mb which cluster on 250–300 chromosomes [16, 24]. Computational analyses revealed about 25,000 protein coding reading frames, about 17,000 of which have strong matches to genes in other organisms [16]. Similarity based analyses of the *Tetrahymena* genome database (TGD) [24] with known mammalian wax synthase sequences [1, 3, 13] revealed several proteins, some of which were analyzed in this work.

In this study we identified four sequences related to DGAT2 family members. Heterologous expression studies in a suitable yeast mutant and enzyme assays with transgenic yeast membranes revealed that these sequences encode multifunctional acyltransferases which accept various acyl-acceptors.

Materials and Methods

Identification and Cloning of Putative Wax Synthases

BLASTp [25] studies were undertaken to investigate the predicted *Tetrahymena thermophila* proteome for putative wax synthases using the NCBI server (<http://blast.ncbi.nlm.nih.gov/>). Human wax synthase sequences AWAT1 (NCBI: NP_001013597) and AWAT2 (NCBI: NP_001002254) were used as query sequences. The derived protein sequences (for NCBI accession numbers and nomenclature see below) were used to generate nucleotide sequences adapted to expression in *Brassica* and synthesized by GeneArt. The respective sequences were cloned from GATEWAY® entry vectors (pDONR221) into pYES-DEST52 expression vectors (Invitrogen) and expressed in *S. cerevisiae* BY4741 Δ lro1 Δ dgal [26], a yeast mutant lacking TAG synthesis (MAT α his3 Δ 1 leu2 Δ 0 met15 Δ 0 ura3 Δ 0 lro1- Δ ::kanMX4 dgal- Δ ::natMX4). In the following the *Tetrahymena* proteins are termed as follows: XP_001027910: TtWS1; XP_001026090: TtWS2; XP_001008104: TtWS3; XP_001017939: TtWS4.

Functional Analysis in Yeast

Transgenic yeast strains expressing a *Tetrahymena* sequence in pYES-DEST52 vectors (Invitrogen) were cultivated in SD minimal medium containing 0.17% (w/v) yeast nitrogen base (MP Biomedicals), 0.068% (w/v) complete supplement medium without uracil and leucine (MP Biomedicals), 0.5% NH₄SO₄ (w/v), 0.01% (w/v) leucine and 2% glucose (Roth) for 24 h at 28 °C. The cells of 50 ml cultures were induced with 2% galactose for 48 h and were supplemented with 125 μ M decanol, dodecanol, tetradecanol, hexadecanol and octadecanol (Roth). Cells were harvested, washed and stored at –20 °C until extraction.

Extraction of yeast cells was performed according to the protocol of Bligh and Dyer [27]. The lipid extracts were separated by TLC on preparative TLC plates (Silica Gel 60 plates 0.5 mm thickness, Merck) in heptane/diethyl ether/acetic acid (90/30/1, v/v/v) and visualized under UV light after spraying with dichlorofluorescein (0.3% (w/v) dissolved in isopropanol) [28]. Myristoyl-dodecanoate (Sigma Aldrich) and TAG isolated from sunflower oil were used as standards.

GC Analysis of WE and TAG

Bands co-chromatographing with the WE and TAG standards were transmethylated in 0.5 M sulfuric acid and 3% dimethoxypropane in methanol for 1 h at 80 °C. 250 nmol docosanoic acid was added as an internal standard before

transmethylation. Fatty acid methyl esters (FAME) and fatty alcohols were extracted with heptane, concentrated and analyzed via gas chromatography (GC) with flame ionization detection (FID). For quantification of WE the total amount of fatty alcohols in the fractions was summarized, for quantification of TAG the sum of FAME was divided by 3.

GC-FID analysis was carried out using the HP6890 gas chromatograph equipped with an OPTIMA225 column (Macherey & Nagel) (25 m length, 0.25 mm diameter, 0.25 μ m film thickness). 1 μ l of the extract was analyzed in splitless injection with N₂ as carrier gas (constant flow, 0.9 bar pressure, total column flow 1 ml/min) and inlet and detector temperatures of 260 °C. A temperature program was carried out starting at 120 °C, 8 °C/min to 144 °C, 4 °C/min to 240 °C. Peaks were identified via comparison of the respective retention times with standard substances of different fatty alcohols and FAME (Sigma Aldrich).

Phylogenetic Analysis and Structure Prediction

Sequence analyses were carried out using ClustalX2 [29] and GeneDoc [30] software. Phylograms were computed with MEGA5 [31] and neighbor-joining method [32] with 1,000 bootstrap replicates using *p*-distance method. All gaps were deleted for computation of evolutionary distances.

Molecular mass and isoelectric points were calculated using ProtParam [33] on the ExPASy Server (<http://web.expasy.org/protparam/>). Transmembrane structures of *Tetrahymena* proteins and mammalian wax synthases were predicted using TMHMM software (<http://www.cbs.dtu.dk/services/TMHMM/>) [34–36]. Predictions were compared to Kyte Doolittle plots [37] with window parameters of 19, which revealed similar results. Acyltransferase superfamily motifs and putative acyl-acceptor binding pockets were discovered by NCBI conserved domain search (<http://www.ncbi.nlm.nih.gov/Structure/cdd/>) [38].

Preparation of Yeast Membranes and In Vitro Wax Synthase Assay

Transgenic yeast cells of 200-ml cultures were harvested after 16 h of induction, washed in Tris–H₂SO₄ (50 mM, pH 7.4), frozen for 15 min at –20 °C and disrupted using glass beads (0.75–1 mm diameter, Roth) by vortexing for 5 min in 2 ml Tris–H₂SO₄ buffer. Cell disruption was repeated three times and the supernatants were collected by centrifugation and combined. After sonication (two times for 30 s) the cell debris was sedimented (2,500 \times *g*, 15 min and 4 °C) and the membranes were isolated from the supernatant by high speed centrifugation (1 h, 140,000 \times *g*, 4 °C). The sedimented membranes were resuspended in an

appropriate volume of Tris–H₂SO₄ buffer and stored in aliquots at –80 °C. The protein concentration was determined [39].

WS activity was measured in 10 mM BIS–Tris-propane pH 9, 13 μ M [1-¹⁴C]-labeled acyl-CoA ([1-¹⁴C]-myristoyl-CoA and [1-¹⁴C]-stearoyl-CoA purchased from Biotrend, specific activity 2.03 Bq/pmol, [1-¹⁴C]-palmitoyl-CoA purchased from Perkin Elmer, specific activity 2.22 Bq/pmol, [1-¹⁴C]-oleyl-CoA purchased from Perkin Elmer, specific activity 2.03 Bq/pmol, [1-¹⁴C]-decanoyl-CoA specific activity 0.09 Bq/pmol and [1-¹⁴C]-dodecanoyl-CoA, specific activity 0.7 Bq/pmol and 2-methyl-acyl-CoA (14:0, 16:0 and 18:0) specific activity 0.62 Bq/pmol were prepared by Prof. Sten Stymne and members of his laboratory, SLU Alnarp, Sweden) and 300 μ M acyl-acceptors (Sigma Aldrich) using 1–2 μ g protein from total membrane fractions. Acyl-acceptors were dissolved in heptane and evaporated to dryness in the reaction tubes before addition of further assay components, DGAT activity was measured under standard WS assay conditions with endogenous DAG present in the yeast membranes. Incubation was carried out at 35 °C for 20 min. Lipids were extracted with 250 μ l chloroform:methanol (1:1) and 100 μ l 0.45% NaCl-solution. 80 μ l of chloroform phase was applied to TLC silica gel plates (Merck) and chromatographed in heptane/diethyl ether/acetic acid (90/20/1 v/v/v). The bands were visualized with the FLA-3000 bioimager system (Fujifilm). For quantification, single bands were analyzed in a liquid scintillation counter LS 6500 (Beckman Coulter).

Results

Identification of Putative Wax Synthases from *Tetrahymena thermophila*

Sequence similarity based searches conducted with human AWAT1 and AWAT2 wax synthase sequences as query against the annotated *Tetrahymena thermophila* proteome resulted in several protein sequences with similarities to the human wax synthases. Four sequences (for NCBI accession number see experimental procedures) with the highest identities to human sequences (15–21%) were analyzed. Sequence identity between the *Tetrahymena* proteins varied between 34 and 44%. No sequence similarities could be detected with jojoba type wax synthases from plants [11, 40] or *Euglena* [10] or the bifunctional proteins from petunia [41] or *Acinetobacter* [4, 42]. The *Tetrahymena* sequences share certain identities with DGAT2 related proteins from plants and fungi (13–20%) [43–47]. As shown in Fig. 1, the *Tetrahymena* proteins build a new branch of proteins related to the DGAT2 protein family.

The relation to the mammalian DGAT2 family is supported by some distinct features that can be found in both families. All proteins contain 306–333 amino acids and have a predicted molecular mass between 35 and 38 kDa. The isoelectric point lies between 9.3 and 9.4, which is a typical feature of DGAT2 family members [48]. In addition TtWS1, TtWS2 and TtWS4 contain a predicted transmembrane helix at the N-terminus like AWAT1 (Fig. 2a), while the C-terminal part of the protein is predicted to be exposed to the cytoplasmic phase. TtWS3, like AWAT2, shows a slightly different topology in the models with two to three transmembrane domains at the N-terminal part of the protein, but the C-terminus is also reaching out into the cytosol. Conserved sequence search displayed an acyltransferase superfamily motif (NCBI database c100357) in all sequences in which several conserved amino acids can be found that are predicted to belong to an acyl-acceptor binding pocket (cd07986) (Fig. 2a).

Sequence alignments with human AWAT showed the highest variety in the N-terminal part of the protein, where the transmembrane domains are located. Furthermore the HPHG (amino acids 103–106 in HsAWAT1) motif which

is characteristic for DGAT2 family members [48–50] was found in TtWS1 and TtWS4, while TtWS2 and TtWS3 showed a modified version in which glycine is substituted with asparagine or tyrosine, respectively (Fig. 2b, Supplemental data 1).

Functional Expression in Yeast

To determine the identities of the four *Tetrahymena* proteins, lipid extracts of transgenic yeasts expressing a *Tetrahymena* sequence were analyzed. Thin layer chromatography suggested that TtWS2, TtWS3 and TtWS4 were able to restore triacylglycerol synthesis in yeast, while TtWS1, TtWS2 and TtWS4 appear to cause wax production as well, if they are provided with appropriate alcohols. The identities of the products were verified and the amounts were quantified by GC analysis after transmethylation of the WE and TAG bands scraped off from the TLC plates (Fig. 3).

By GC analysis decanol (10:0-OH), dodecanol (12:0-OH), tetradecanol (14:0-OH) and hexadecanol (16:0-OH) and the FAME corresponding to palmitic (16:0),

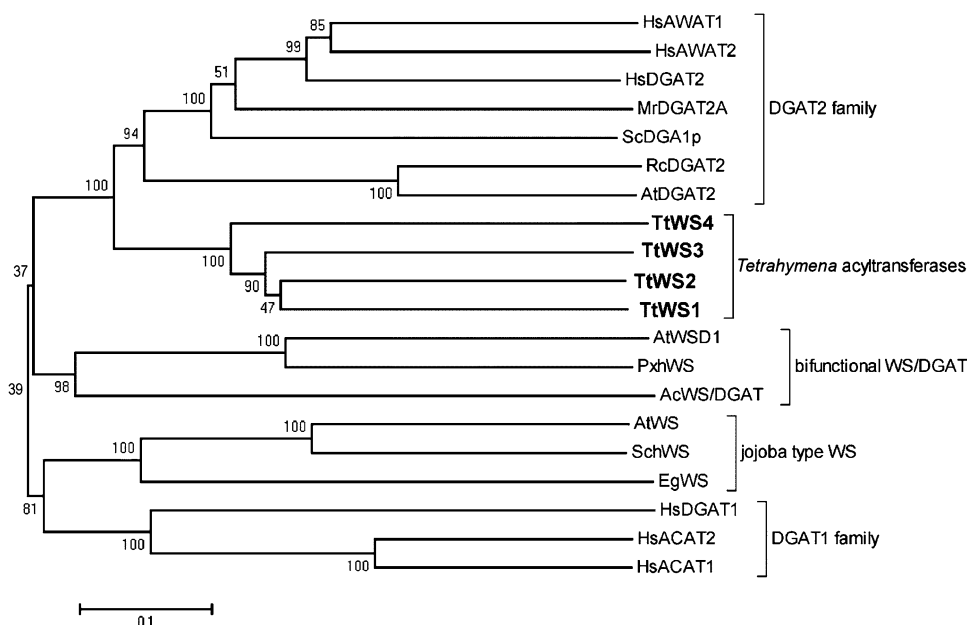


Fig. 1 Phylogram showing the relation of four *Tetrahymena* acyltransferases with selected acyltransferases from human, plant, fungi and bacteria. HsAWAT2 (*Homo sapiens*, NCBI: NP_001013597.1), HsAWAT1 (*H. sapiens*, NCBI: NP_001002254.1), HsDGAT2 (*H. sapiens*, NCBI: NP_115953.2), MrDGAT2A (*Mortierella ramanniana*, NCBI: AF391089_1), ScDGAT1p (*Saccharomyces cerevisiae*, NCBI: NP_014888.1), RcDGAT2 (*Ricinus communis*, NCBI: ABI83668.1), AtDGAT2 (*Arabidopsis thaliana*, NCBI: Q9ASU1.1), TtWS1 (*Tetrahymena thermophila*, NCBI: XP_001027910), TtWS2 (*T. thermophila*, NCBI: XP_001026090), TtWS3 (*T. thermophila*, NCBI: XP_001008104), TtWS4 (*T. thermophila*, NCBI: XP_001017939),

AtWSD1 (*A. thaliana*, NCBI: NP_568547.1), PxlWS (*Petunia x hybrida*, NCBI: AAZ08051.1), AcWS/DGAT (*Acinetobacter calcoaceticus*, NCBI: YP_045555.1), AtWS (*A. thaliana*, NCBI: NP_200345.1), SchWS (*Simmondsia chinensis*, NCBI: AF149919.1), EgWS (*Euglena gracilis*, NCBI: ADI60058.1), HsDGAT1 (*H. sapiens*, NCBI: NP_036211.2), HsACAT2 (*H. sapiens*, NCBI: NP_003569.1), HsACAT1 (*H. sapiens*, NCBI: NP_003092.4). The scale corresponds to amino acid substitutions per site in the given alignment with 237 positions and 20 sequences. Numbers next to the branches are bootstrap values indicating the probability of this relationship in %. The phylogram was created with ClustalX2 and MEGA5 software

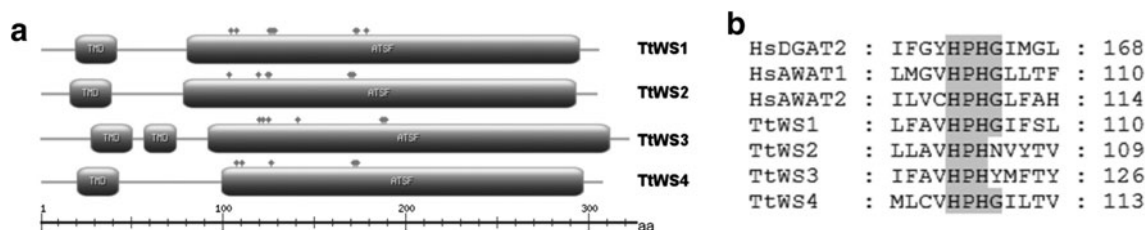


Fig. 2 Predicted domains and motifs of *Tetrahymena* WS proteins. The putative transmembrane domain (TMD) and the acyltransferase superfamily motif (ATSF) are shown by squares, amino acids of the putative acyl-acceptor binding pocket are labeled with pins (a). The

conserved HPHG motif of DGAT2 family members and the substitutions of the glycine residues in TtWS2 and TtWS3 are depicted (b). Figure a was created using ExPASy Prosite Mydomains and the alignment (b) was created with ClustalX2 and GeneDoc

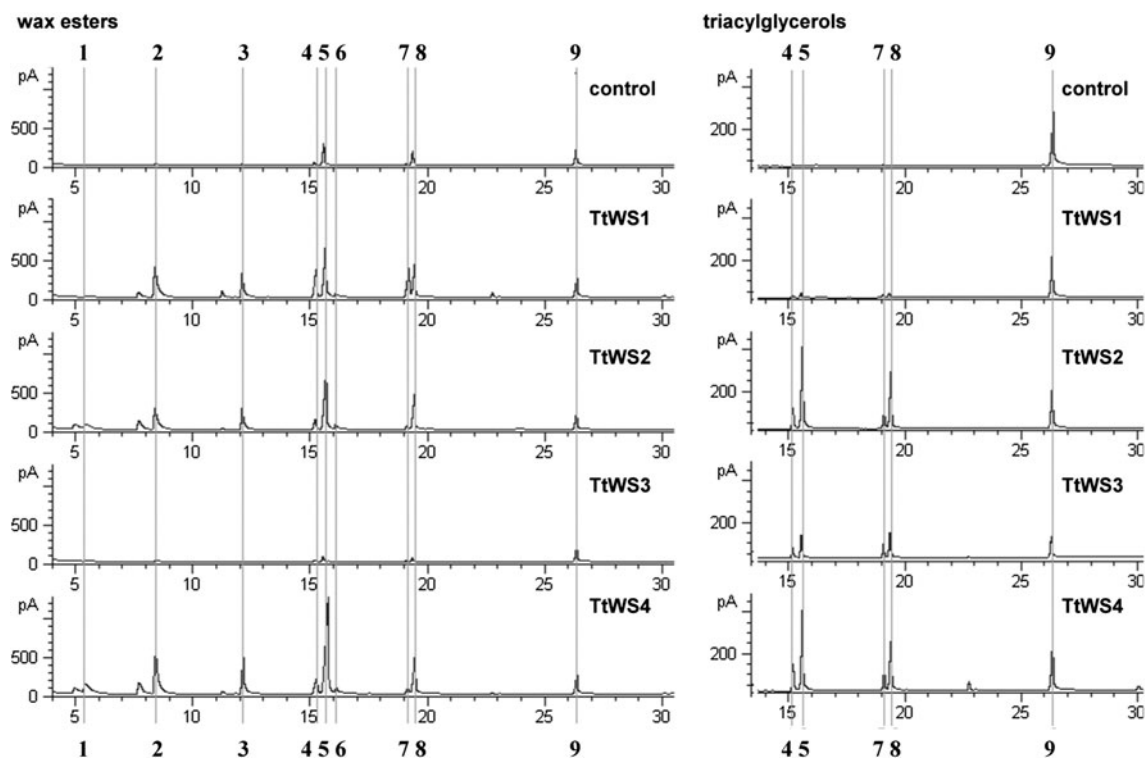


Fig. 3 Functional expression of TtWS sequences in yeast cells. Lipids were extracted from the yeast cells after 48 h cultivation in medium supplemented with 125 μ M 10:0-, 12:0-, 14:0-, 16:- and 18:0-OH, separated by TLC and wax esters and triacylglycerols were quantified by GC using 250 nmol methyl docosanoate as internal

standard. The respective GC chromatograms of transmethylated WE and TAG are depicted, the *x*-axis displays the retention time [min] and the *y*-axis corresponds to the FID signal strength [pA]. 1 10:0-OH, 2 12:0-OH, 3 14:0-OH, 4 methyl-16:0, 5 methyl-16:1, 6 16:0-OH, 7 methyl-18:0, 8 methyl-18:1, 9 methyl-22:0 (internal standard)

palmitoleic (16:1), stearic (18:0) and oleic acid (18:1) were identified. The empty vector control and TtWS3 expressing cells showed very small amounts of alcohols in the WE fractions only, while TtWS1, TtWS2 and TtWS4 expressing cells contained distinctly higher amounts (Fig. 4). 12:0-OH was the most abundant alcohol (50% of alcohol in WE) followed by 14:0-OH (5–30%) then 10:0-OH (10–15%) and 16:0-OH (<10%). Regarding the fatty acids in the WE fraction the biggest portion was made up by mono-unsaturated fatty acids with 16 or 18 carbon atoms (Fig. 3). The fatty acid pattern of the TAG fractions (Fig. 3) of TtWS2, TtWS3 and TtWS4 expressing cells resembled the one

found in the WE fractions, where the 16:1 and 18:1 were most abundant and comprised 80% of the total fatty acid mixture of WE and TAG. GC-analysis of WS and TAG of TtWS3 expressing cells showed almost equal amounts of C₁₆ and C₁₈ fatty acids.

Quantification of the WE and TAG content showed that TtWS4 expressing cells had the highest content of waxes of about 5 μ mol WE per gram cell fresh weight; the TAG production was about 1 μ mol/g. TtWS2 expressing yeasts produced about 4 μ mol/g WE and 1 μ mol/g TAG. In TtWS1 expressing yeast cells, about 2 μ mol/g WE could be detected but no significant amounts of TAG. TtWS3

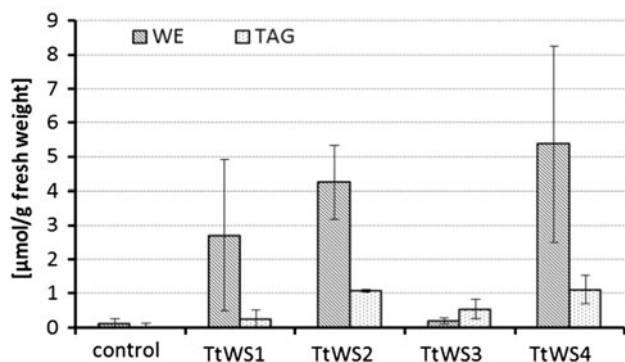


Fig. 4 Production of wax esters (WE) and triacylglycerols (TAG) in transgenic yeast cultures expressing the empty vector (control) or one of the *Tetrahymena* sequences (TtWS1–4). The amount of wax esters and TAG was quantified by GC as shown in Fig. 3. Mean values and standard deviations of three preparations are given

showed low amounts of both WE and TAG, but merely the TAG level was significantly above the background level (Fig. 4).

In summary it can be concluded that all four proteins were functionally expressed in yeast and caused wax ester or TAG production.

Optimizing an In Vitro WS Assay

To analyze the properties of the four *Tetrahymena* enzymes, an in vitro wax synthase assay was optimized, using membranes of TtWS1 expressing yeast cells as the enzyme source. Enzymatic activity was only detectable in the membrane fraction and not in the soluble fraction indicating that the protein is associated with membranes. These results are in line with the predicted protein structure. The highest wax synthase activities were obtained using approximately 13 μ M palmitoyl-CoA (Supplemental data 2a), 300 μ M decanol (Supplemental data 2b) and 10 mM BIS-Tris-propane buffer at pH 9.0 (Supplemental data 2c). Under these conditions the WS activities were linear with at least 2 μ g membrane protein and an incubation time of 20 min at 35 °C.

Substrate Specificities

As wax synthesis was already observed in yeast when cultures were provided with straight-chain alcohols, they were tested as acyl-acceptors in the optimized enzyme assay first. It could be shown that all enzymes had the highest wax synthase activities with medium-chained saturated alcohols of 10–12 carbon atoms (Fig. 5), while all except TtWS3 were inactive with alcohols of <9 carbon atoms. In contrast to TtWS1, which showed a narrow chain-length preference between 10:0-OH and 12:0-OH, TtWS2 and TtWS4 also accepted alcohols with chain-

lengths of 14 or 16 carbon atoms and TtWS3 esterified 16:0-CoA with 8:0-OH (Fig. 5).

In addition to WE, one further product was detected on TLC that co-migrated with TAG. It was clearly detected in all WS assays using membranes from yeasts expressing TtWS2, TtWS3 and TtWS4, but it was barely detected in assays with TtWS1 expressing membranes. These results were in line with the TAG level determined in the yeast cells expressing one of the *Tetrahymena* sequences (Fig. 4). The amount of TAG produced inversely depended on the amount of WE synthesized. When less attractive alcohols were used as acyl-acceptors, more TAG were produced and vice versa, which led to the assumption, that there was a competition reaction for the acyl-acceptor binding site of the enzyme. Since these *Tetrahymena* proteins were at least bifunctional and the fact that several acyltransferases show quite broad substrate acceptances [1, 2, 5], we had a closer look at further substrates.

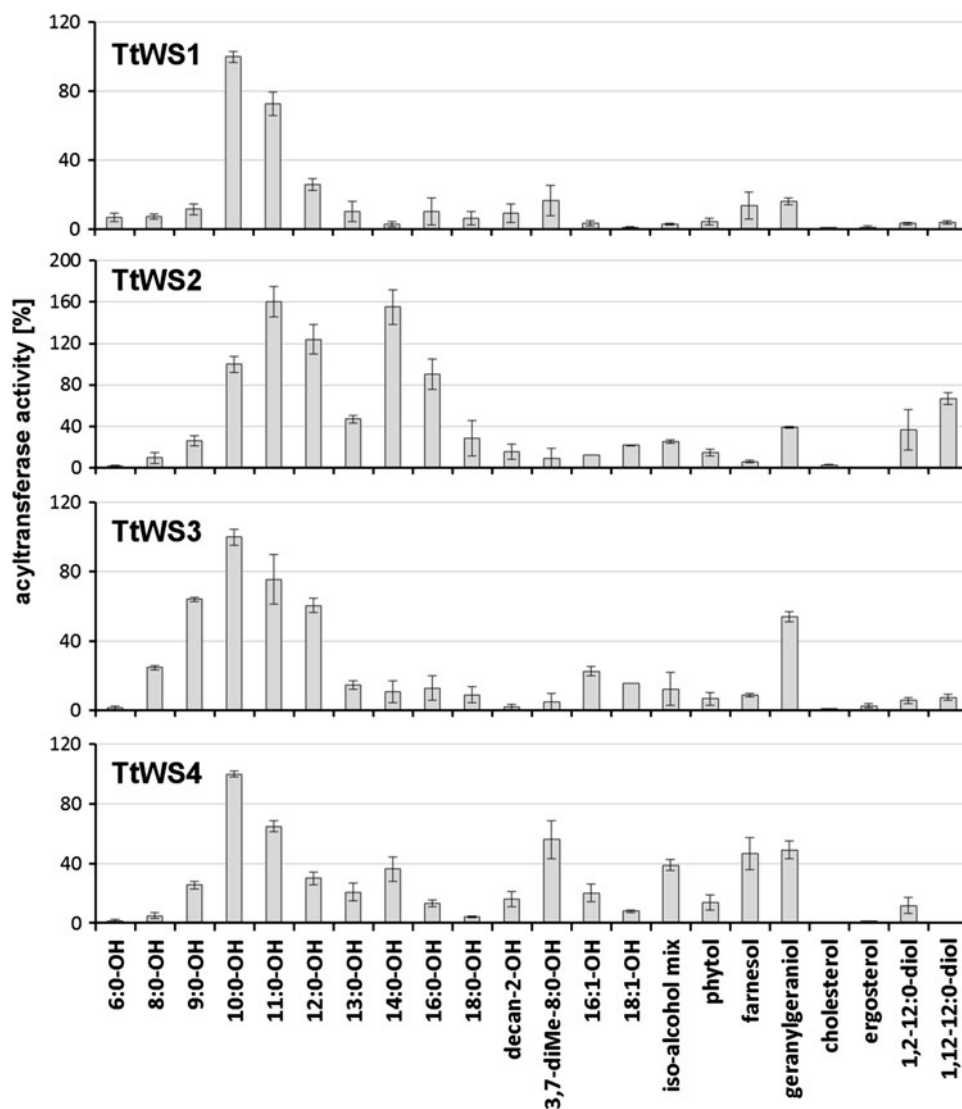
In addition to saturated 1-alcohols, we ran assays with decan-2-ol and mono-unsaturated fatty alcohols. All enzymes had distinctly lower activities with 2-alcohols than with 1-alcohols of the same chain length. With the mono-unsaturated fatty alcohols 16:1-OH and 18:1-OH, TtWS2, TtWS3 and TtWS4 performed higher activities than with the corresponding saturated alcohols, while TtWS1 was inactive with unsaturated alcohols (Fig. 5).

As branched-chain WE are of high interest for the chemical industry, we assayed different kinds of branched-chain alcohols. TtWS4 was found to be active with 3,7-dimethyl-octanol (3,7-diMe-8:0-OH), but transferred the branched alcohols to palmitoyl-CoA at nearly the same rate as 10:0-OH. As some *Tetrahymena* species contain 2-methyl-branched alcohols in their waxes [21], it was interesting to see whether the *Tetrahymena* enzymes were active with a mixture of 2-methyl-branched alcohols of 16–20 carbon atoms. As given in Fig. 5, TtWS2 and TtWS4 performed WS activities with iso-alcohols, while TtWS1 and TtWS3 did not.

Another class of branched alcohols are isoprenols which can be esterified with acyl-CoAs to form prenyl esters. We investigated phytol, farnesol and geranylgeraniol as substrates for prenyl ester synthase (PES) activity. Especially TtWS4 displayed high activities with farnesol and geranylgeraniol, but a lower one with phytol. Unlike TtWS4, TtWS2 and TtWS3 were active with geranylgeraniol (Fig. 5) only.

As *Tetrahymena* also contains sterol esters, we investigated whether these acyltransferases possess sterol ester synthase (ASAT) activity. *Tetrahymena* species contain a special sterol termed tetrahymanol [51], but they are able to utilize both exogenously added cholesterol and ergosterol for ester synthesis [52]. WS assays with those sterols revealed that none of the *Tetrahymena* enzymes was active

Fig. 5 Acyl-acceptor specificities of TtWS enzymes expressed in yeast. Relative formation rates of WE by yeast membranes harboring a TtWS enzyme from 16:0-CoA and the given acyl-acceptors under otherwise standard assay conditions are depicted as mean values of at least four enzyme assays. Before calculating the mean values, the activities of the control membranes (empty vector) of about $18 \text{ pmol mg}^{-1} \text{ min}^{-1}$ were subtracted from the activity of the yeast membranes with the *Tetrahymena* enzymes. 100% correspond to the activity of the respective TtWS enzyme with 10:0-OH and 16:0-CoA, namely TtWS1: $330 \text{ pmol mg}^{-1} \text{ min}^{-1}$, TtWS2: $270 \text{ pmol mg}^{-1} \text{ min}^{-1}$, TtWS3: $114 \text{ pmol mg}^{-1} \text{ min}^{-1}$, TtWS4: $558 \text{ pmol mg}^{-1} \text{ min}^{-1}$



with cholesterol and ergosterol, suggesting that they possess no ASAT activity (Fig. 5).

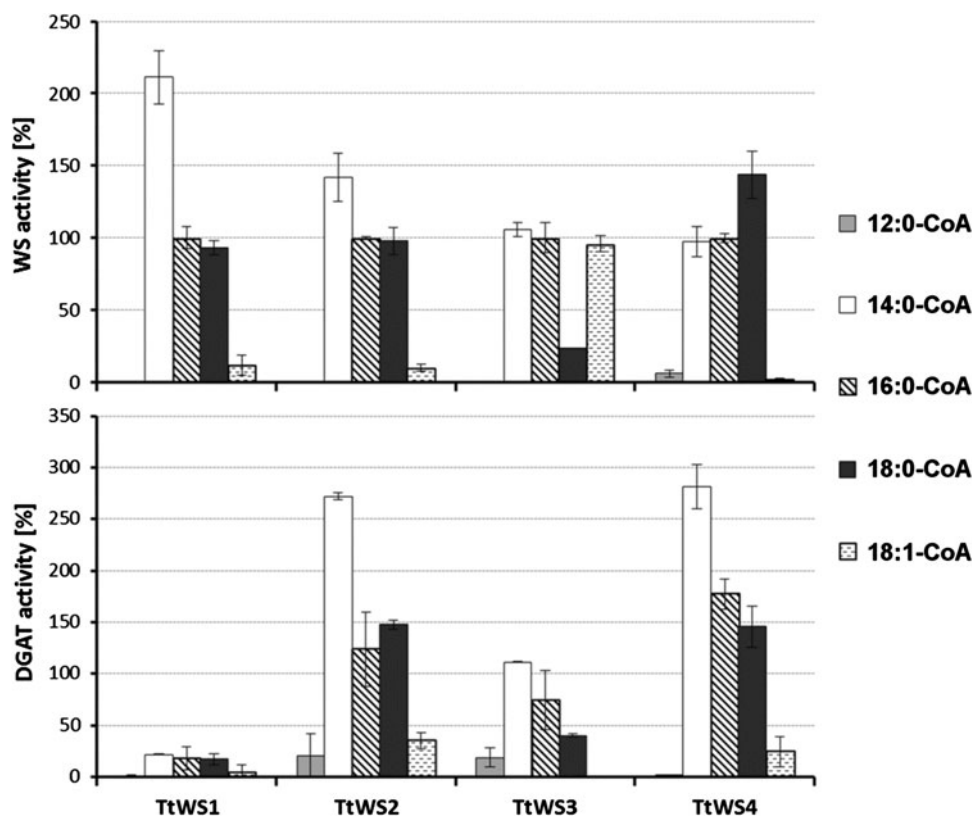
A last group of interesting alcohols are diols. These can be esterified with two acyl-CoAs to form wax diesters, or they are esterified at only one hydroxyl-group to form a hydroxyl-wax monoester. Diester synthase (DES) activity was obtained with TtWS2 and 1,2-dodecanediol (1,2-12:0-diol) and the respective 1,12-isomer (1,12-12:0-diol), while the other enzymes were hardly active with these substrates (Fig. 5).

Analyses of the acyl-CoA specificities of the TtWS enzymes gave the following results (Fig. 6): the highest WE formation rates were obtained with saturated long-chain acyl-CoA thioesters of 14–18 carbon atoms, while activities with 18:1-CoA were detectable with TtWS3 only. Acyl-CoAs with chain-lengths of 10–12 carbon atoms were hardly incorporated into WE or TAG. The thioester specificity of TtWS3 and TtWS4 differed between WS and

acyl-CoA:diacylglycerol acyltransferase (DGAT) activities. While TtWS3 produced high levels of WE with 18:1-CoA, TAG were hardly detectable. TtWS4 performed the highest WS activity with 18:0-CoA and the highest DGAT activity with 14:0-CoA (Fig. 6). In addition to straight-chain acyl-CoAs, we also investigated 2-methyl-branched acyl-CoAs with chain-lengths of 14–18 carbon atoms. The activities with these substrates were distinctly lower than with the non-branched acyl-CoAs and could only be detected when incubation time and protein amount were increased (data not shown).

In summary, we were able to characterize four new acyltransferases with different properties (Fig. 7). TtWS1 synthesized WE as the main product especially with 10:0-OH and 14:0-CoA. DGAT and PES activities of TtWS1 were distinctly lower than WS activities, while DES and ASAT activity were hardly detectable. TtWS2 displayed high WS and DGAT activities with a broad range of

Fig. 6 Acyl-CoA specificities of TtWS enzymes expressed in yeast. Relative formation rates of WE and TAG by yeast membranes harboring a TtWS enzyme from 10:0-OH and the given acyl-CoA thioester under otherwise standard assay conditions are depicted as mean values of at least four enzyme assays. 100% correspond to the activity of the respective TtWS enzyme with 10:0-OH and 16:0-CoA as given in Fig. 5



saturated and mono-unsaturated alcohols ranging from 10 to 18 carbon atoms and saturated acyl-CoAs of 14–18 carbon atoms. In addition, it readily accepted diols as substrates. TtWS3 performed similar DGAT and WS activity, while PES activity was twofold lower. It had the highest activities not only with 10:0-OH and 14:0-CoA, but also with 10:0-OH and 18:1-CoA. In comparison to

TtWS2, TtWS4 had a broad but different substrate specificity. WS activity of TtWS4 was high with straight-chain alcohols from 9 to 14 carbon atoms as well as with methyl-branched alcohols or isoprenols. TtWS4 formed more TAG than WE, but the proportion of the two products varied depending on the acyl-group of the thioester as observed with TtWS3 (Fig. 6).

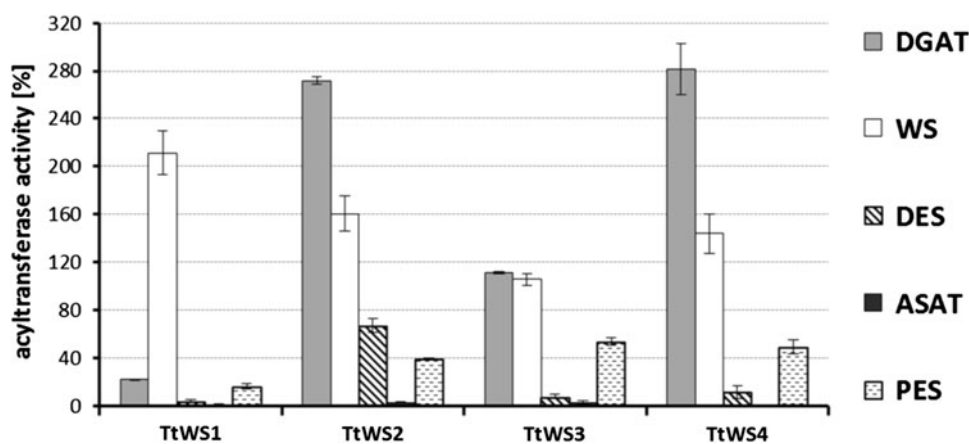


Fig. 7 Comparison of the maximal acyltransferase activities of yeast membranes harboring *Tetrahymena* enzymes with various acyl-acceptors. Data of the highest activities with different substrate groups were taken from Figs. 5 and 6. (DGAT: diacylglycerol acyltransferase activity determined with 10:0-OH and 14:0-CoA, WS:

wax synthase activity with 10:0 or 11:0-OH and 16:0-CoA, DES: diester synthase activity with 12:0-diol and 16:0-CoA, PES: prenyl-ester synthase activity with geranylgeraniol and 16:0-CoA, ASAT: sterol-ester synthase activity with ergosterol and 16:0-CoA)

Discussion

In this study we identified four proteins from *Tetrahymena thermophila* which possess distinct properties of DGAT2 family members including the HPHG motif [49]. This motif is found in vertebrate DGAT2 acyltransferases [48–50] and the histidine and proline residues have been shown to be essential for acyltransferase activity [49]. Mutagenesis experiments will show whether these amino acids conserved in the four *Tetrahymena* proteins are critical for the enzymatic activities as well and whether the glycine group in the motif, which is substituted by arginine or tyrosine in two of the four *Tetrahymena* proteins (Fig. 2b), affects the activity or the properties of the enzymes. Sequence analyses suggest that these TtWS proteins build up a new branch of DGAT2 related multifunctional acyltransferases (Fig. 1), which are perhaps typical for protozoal organisms, as protein sequences similar to those of *Tetrahymena* were identified in other protozoa like *Paramecium tetraurelia* (NCBI: XP_001425482, XP_001451326, XP_001433749).

The identity of the TtWS proteins was further supported by functional expression studies in yeast in combination with in vitro enzyme assays. These experiments clearly demonstrated that the four *Tetrahymena* proteins possess acyltransferase activities but differ in their acyl-acceptor and -donor specificities, as they caused the formation of different patterns of lipophilic reaction products when provided with the respective substrates. TtWS1 was found to have the most pronounced and TtWS2 and TtWS4 the most relaxed acyl-acceptor specificity (Fig. 5). Unlike TtWS1, which largely produces WE when expressed in yeast membranes, expression of the other TtWS proteins caused biosynthesis of TAG, WE, prenyl esters and diesters but in different proportions (Fig. 6).

Multifunctional acyltransferases like the ones described here have been identified in human. AWAT2, for instance, shows equal WS and diacylglycerol synthase activities and lower DGAT and retinyl ester synthase activities [1, 3]. DGAT1, which belongs to a protein family different from that of AWAT2 (Fig. 1) efficiently catalyzes the production of TAG, while production of WE, diesters and retinyl esters was eightfold lower [2]. Hence both mammalian enzymes utilize an acyl-acceptor spectrum different from that of the *Tetrahymena* enzymes. An acyltransferase from *Acinetobacter*, which does not possess sequence similarity to the enzymes from *Tetrahymena* or mammals, was found to be a multifunctional acyltransferase as well [5]. Unlike *Tetrahymena* enzymes it performs not only WS, DGAT and diester, but also steryl ester synthase activity.

The broad acyl-acceptor specificities of most *Tetrahymena* acyltransferases and the observation that the amount of TAG production depended inversely on that of WE, suggests that *Tetrahymena* acyltransferases have flexible hydrophobic binding pockets in which various acyl-acceptors compete for binding. However, we cannot exclude other protein models like different interacting binding sites. Protein structure analyses will show in which way the acyltransferases mediate and regulate the esterification of acyl-acceptors.

In contrast to the broad acyl-acceptor specificities of the *Tetrahymena* proteins, the acyl-donor specificities were more pronounced and higher activities were obtained with saturated than with unsaturated acyl-CoA thioesters (Fig. 6). In that way, the *Tetrahymena* enzymes differ from that of *Acinetobacter*, which was shown to readily accept acyl-CoA thioesters of 8–20 carbon atoms [42]. They also have an acyl-donor specificity different from that of AWAT2, that was highly active with unsaturated long-chain acyl-CoA thioesters [3]. Interestingly, yeast cells expressing a *Tetrahymena* sequence formed WE and TAG mainly esterified with unsaturated acyl-groups (Fig. 3). These results are likely caused by the high level of unsaturated acyl groups in yeast cells [53] so that the introduced acyltransferases are predominantly provided with 16:1- and 18:1-CoA. Such a substrate channeling might allow incorporation of branched-chain acyl-moieties into WE as well.

The application of heterologous expression of genes encoding wax synthesizing enzymes in host systems is well under way. For instance, expression of genes from jojoba in transgenic *Arabidopsis thaliana* seeds led to the accumulation of WE [11, 40]. The protozoan enzymes described here were found to differ not only in their acyl-CoA but also in their acyl-acceptor specificities. Expression of sequences like TtWS2 or TtWS4 in plant systems in combination with suitable fatty acyl-CoA reductases will reveal their suitability for field application and industrial uses.

Acknowledgments We are grateful to Professor Sten Stymne (SLU Alnarp, Sweden) for the coordination of the ICON project and his research group (especially Dr. Jenny Lindberg Yilmaz and Dr. Ida Lager) for providing us with the labeled acyl-CoA thioesters and teaching us acyl-CoA synthesis. Furthermore we would like to thank Professor Mats Hamberg (Karolinska Institute Stockholm, Sweden) for providing us with labeled and unlabeled 2-methyl-branched fatty acids. This work was funded in part by the European Commission through the FP7 ICON project.

Open Access This article is distributed under the terms of the Creative Commons Attribution Noncommercial License which permits any noncommercial use, distribution, and reproduction in any medium, provided the original author(s) and source are credited.

References

- Yen CL, Brown CH 4th, Monetti M, Farese RV Jr (2005) A human skin multifunctional *O*-acyltransferase that catalyzes the synthesis of acylglycerols, waxes, and retinyl esters. *J Lipid Res* 46:2388–2397
- Yen CL, Monetti M, Burri BJ, Farese RV Jr (2005) The triacylglycerol synthesis enzyme DGAT1 also catalyzes the synthesis of diacylglycerols, waxes, and retinyl esters. *J Lipid Res* 46:1502–1511
- Turkish AR, Henneberry AL, Cromley D, Padamsee M, Oelkers P, Bazzi H, Christiano AM, Billheimer JT, Sturley SL (2005) Identification of two novel human acyl-CoA wax alcohol acyltransferases: members of the diacylglycerol acyltransferase 2 (DGAT2) gene superfamily. *J Biol Chem* 280:14755–14764
- Kalscheuer R, Steinbüchel A (2003) A novel bifunctional wax ester synthase/acyl-CoA:diacylglycerol acyltransferase mediates wax ester and triacylglycerol biosynthesis in *Acinetobacter calcoaceticus* ADP1. *J Biol Chem* 278:8075–8082
- Kalscheuer R, Luftmann H, Steinbüchel A (2004) Synthesis of novel lipids in *Saccharomyces cerevisiae* by heterologous expression of an unspecific bacterial acyltransferase. *Appl Environ Microbiol* 70:7119–7125
- Carlsson AS, Lindberg Yilmaz J, Green AG, Stymne S, Hofvander P (2011) Replacing fossil oil with fresh oil—with what and for what? *Eur J Lipid Sci Technol* 113:812–831
- Metzger J, Bornscheuer U (2006) Lipids as renewable resources: current state of chemical and biotechnological conversion and diversification. *Appl Microb Biotechnol* 71:13–22
- Alvarez HM (2010) Biotechnological production and significance of triacylglycerols and wax esters. In: Timmis KN (ed) *Handbook of hydrocarbon and lipid microbiology*. Springer, Berlin, pp 2995–3002
- Kohashi H (1991) Application of fatty acid esters for lubricating oil. In: Applewhite TH (ed) *World conference on oleochemicals into the 21st Century: proceedings*. Instituti Penyelidikan Minyak Kelapa Sawit Malaysia: American Oil Chemists' Society, ASEAN Oleochemical Manufacturers Group, pp 243–255
- Teerawanichpan P, Qiu X (2010) Fatty acyl-CoA reductase and wax synthase from *Euglena gracilis* in the biosynthesis of medium-chain wax esters. *Lipids* 45:263–273
- Lardizabal KD, Metz JG, Sakamoto T, Hutton WC, Pollard MR, Lassner MW (2000) Purification of a jojoba embryo wax synthase, cloning of its cDNA, and production of high levels of wax in seeds of transgenic arabidopsis. *Plant Physiol* 122:645–656
- Kalscheuer R, Stöveken T, Luftmann H, Malkus U, Reichelt R, Steinbüchel A (2006) Neutral lipid biosynthesis in engineered *Escherichia coli*: jojoba oil-like wax esters and fatty acid butyl esters. *Appl Environ Microbiol* 72:1373–1379
- Cheng JB, Russell DW (2004) Mammalian wax biosynthesis. II. Expression cloning of wax synthase cDNAs encoding a member of the acyltransferase enzyme family. *J Biol Chem* 279:37798–37807
- Mehlhorn H, Ruthmann A (1992) *Allgemeine Protozoologie*. Gustav Fischer Verlag, Jena
- Collins K, Gorovsky MA (2005) *Tetrahymena thermophila*. *Curr Biol* 15:R317–R318
- Eisen JA, Coyne RS, Wu M, Wu D, Thiagarajan M, Wortman JR, Badger JH, Ren Q, Amedeo P, Jones KM et al (2006) Macro-nuclear genome sequence of the ciliate *Tetrahymena thermophila*, a model eukaryote. *PLoS Biol* 4:e286
- Nanney DL, McCoy JW (1976) Characterization of the species of the *Tetrahymena pyriformis* complex. *Trans Am Microsc Soc* 95:664–682
- Aaronson S, Baker H (1961) Lipid and sterol content of some protozoa. *J Eukaryot Microbiol* 8:274–277
- Allison BM, Ronkin RR (1967) Lipid cytochemistry and morphologic change in aging populations of *Tetrahymena*. *J Eukaryot Microbiol* 14:313–319
- Erwin J, Bloch K (1963) Lipid metabolism of ciliated protozoa. *J Biol Chem* 238:1618–1624
- Wheeler M, Holmlund C (1975) Identification of wax esters in *Tetrahymena pyriformis*. *Lipids* 10:260–262
- Chu IM, Wheeler MA, Holmlund CE (1972) Fatty acid methyl and ethyl esters in *Tetrahymena pyriformis*. *Biochimica et Biophysica Acta (BBA). Lipids and Lipid Metabolism* 270:18–22
- Gorovsky MA (1980) Genome organization and reorganization in *Tetrahymena*. *Annu Rev Genet* 14:203–239
- Stover NA, Krieger CJ, Binkley G, Dong Q, Fisk DG, Nash R, Sethuraman A, Weng S, Cherry JM (2006) *Tetrahymena* genome database (TGD): a new genomic resource for *Tetrahymena thermophila* research. *Nucleic Acids Res* 34:D500–D503
- Altschul SF, Gish W, Miller W, Myers EW, Lipman DJ (1990) Basic local alignment search tool. *J Mol Biol* 215:403–410
- Wagner M, Hoppe K, Czabany T, Heilmann M, Daum G, Feussner I, Fulda M (2010) Identification and characterization of an acyl-CoA: diacylglycerol acyltransferase 2 (DGAT2) gene from the microalga *O. tauri*. *Plant Physiol Biochem* 48:407–416
- Bligh EG, Dyer WJ (1959) A rapid method of total lipid extraction and purification. *Can J Biochem Physiol* 37:911–917
- Dunphy PJ, Whittle KJ, Pennock JF (1965) On the use of fluorescein and dichlorofluorescein as non-destructive stains for lipids. *Chem Ind* 27:1217–1218
- Larkin MA, Blackshields G, Brown NP, Chenna R, McGettigan PA, McWilliam H, Valentin F, Wallace IM, Wilm A, Lopez R et al (2007) Clustal W and Clustal X version 2.0. *Bioinformatics* 23:2947–2948
- Nicholas KB, Nicholas HB, Deerfield DW (1997) GeneDoc: analysis and visualization of genetic variation. *EMBNEW News* 4:14
- Tamura K, Peterson D, Peterson N, Stecher G, Nei M, Kumar S (2011) MEGA5: molecular evolutionary genetics analysis using maximum likelihood, evolutionary distance, and maximum parsimony methods. *Mol Biol Evol* 28:2731–2739
- Saitou N, Nei M (1987) The neighbor-joining method: a new method for reconstructing phylogenetic trees. *Mol Biol Evol* 4:406–425
- Gasteiger E, Hoogland C, Gattiker A, Duvaud Se, Wilkins MR, Appel RD, Bairoch A (2005) Protein identification and analysis tools on the ExPASy server. In: Walker JM (ed) *The proteomics protocols handbook*. Humana Press, Totowa, pp 571–607
- Sonnhammer EL, von Heijne G, Krogh A (1998) A hidden Markov model for predicting transmembrane helices in protein sequences. In: Glasgow J, Littlejohn T, Major F, Lathrop R, Sankoff D, Sensen C (eds) *Proceedings of the sixth international conference on intelligent systems for molecular biology*. AAAI Press, Menlo Park, pp 175–182
- Krogh A, Larsson B, von Heijne G, Sonnhammer EL (2001) Predicting transmembrane protein topology with a hidden Markov model: application to complete genomes. *J Mol Biol* 305:567–580
- Möller S, Croning MDR, Apweiler R (2001) Evaluation of methods for the prediction of membrane spanning regions. *Bioinformatics* 17:646–653
- Kyte J, Doolittle RF (1982) A simple method for displaying the hydropathic character of a protein. *J Mol Biol* 157:105–132
- Marchler-Bauer A, Lu S, Anderson JB, Chitsaz F, Derbyshire MK, DeWeese-Scott C, Fong JH, Geer LY, Geer RC, Gonzales NR et al (2011) CDD: a conserved domain database for the

- functional annotation of proteins. *Nucleic Acids Res* 39:D225–D229
39. Bradford MM (1976) A rapid and sensitive method for the quantitation of microgram quantities of protein utilizing the principle of protein-dye binding. *Anal Biochem* 72:248–254
 40. Lassner MW, Lardizabal K, Metz JG (1999) Producing wax esters in transgenic plants by expression of genes derived from jojoba. In: Janick J (ed) *Perspectives on new crops and new uses*. ASHS Press, Alexandria, pp 220–224
 41. King A, Nam JW, Han J, Hilliard J, Jaworski JG (2007) Cuticular wax biosynthesis in petunia petals: cloning and characterization of an alcohol-acyltransferase that synthesizes wax-esters. *Planta* 226:381–394
 42. Stöveken T, Kalscheuer R, Malkus U, Reichelt R, Steinbüchel A (2005) The wax ester synthase/acyl coenzyme A:diacylglycerol acyltransferase from *Acinetobacter* sp. strain ADP1: characterization of a novel type of acyltransferase. *J Bacteriol* 187:1369–1376
 43. Kroon JT, Wei W, Simon WJ, Slabas AR (2006) Identification and functional expression of a type 2 acyl-CoA:diacylglycerol acyltransferase (DGAT2) in developing castor bean seeds which has high homology to the major triglyceride biosynthetic enzyme of fungi and animals. *Phytochemistry* 67:2541–2549
 44. Zhang M, Fan J, Taylor DC, Ohlrogge JB (2009) DGAT1 and PDAT1 acyltransferases have overlapping functions in *Arabidopsis* triacylglycerol biosynthesis and are essential for normal pollen and seed development. *Plant Cell Online* 21:3885–3901
 45. Li R, Yu K, Hildebrand D (2010) DGAT1, DGAT2 and PDAT expression in seeds and other tissues of epoxy and hydroxy fatty acid accumulating plants. *Lipids* 45:145–157
 46. Oelkers P, Cromley D, Padamsee M, Billheimer JT, Sturley SL (2002) The DGA1 gene determines a second triglyceride synthetic pathway in yeast. *J Biol Chem* 277:8877–8881
 47. Lardizabal KD, Mai JT, Wagner NW, Wyrick A, Voelker T, Hawkins DJ (2001) DGAT2 is a new diacylglycerol acyltransferase gene family: purification, cloning, and expression in insect cells of two polypeptides from *Mortierella ramanniana* with diacylglycerol acyltransferase activity. *J Biol Chem* 276:38862–38869
 48. Holmes RS (2010) Comparative genomics and proteomics of vertebrate diacylglycerol acyltransferase (DGAT), acyl CoA wax alcohol acyltransferase (AWAT) and monoacylglycerol acyltransferase (MGAT). *Comp Biochem Physiol Part D Genomics Proteomics* 5:45–54
 49. Stone SJ, Levin MC, Farese RV Jr (2006) Membrane topology and identification of key functional amino acid residues of murine acyl-CoA:diacylglycerol acyltransferase-2. *J Biol Chem* 281:40273–40282
 50. Yen CL, Stone SJ, Koliwad S, Harris C, Farese RV Jr (2008) Thematic review series: glycerolipids. DGAT enzymes and triacylglycerol biosynthesis. *J Lipid Res* 49:2283–2301
 51. Thompson GA Jr, Nozawa Y (1972) Lipids of protozoa: phospholipids and neutral lipids. *Annu Rev Microbiol* 26:249–278
 52. Conner RL, Landrey JR, Czarkowski N (1982) The effect of specific sterols on cell size and fatty acid composition of *Tetrahymena pyriformis* W. *J Eukaryot Microbiol* 29:105–109
 53. van der Rest M, Kamminga A, Nakano A, Anraku Y, Poolman B, Konings W (1995) The plasma membrane of *Saccharomyces cerevisiae*: structure, function, and biogenesis. *Microbiol Rev* 59:304–322

Fish Oil Supplementation Improves Neutrophil Function During Cancer Chemotherapy

Sandro J. R. Bonatto · Heloisa H. P. Oliveira · Everson A. Nunes · Daniele Pequito · Fabiola Iagher · Isabela Coelho · Katya Naliwaiko · Marcelo Kryczyk · Gleisson A. P. Brito · João Repka · Luciano V. Sabóia · George Fukujima · Philip C. Calder · Luiz C. Fernandes

Received: 24 November 2010 / Accepted: 21 November 2011 / Published online: 11 December 2011
© AOCs 2011

Abstract Cancer chemotherapy is associated with neutropenia and impaired neutrophil function. This study aimed to investigate whether supplementation with low dose fish oil (FO), providing n-3 polyunsaturated fatty acids, in cancer patients receiving chemotherapy after surgical tumor (mainly gastrointestinal) removal is able to improve the function of blood neutrophils. Patients ($n = 38$) receiving chemotherapy (5-fluorouracil and leucovorin) were randomized into two groups; one group (control) did not receive a supplement, while the other group (FO) received 2 g FO/day for 8 weeks; the FO provided 0.3 g eicosapentaenoic acid plus 0.4 g docosahexaenoic acid per day. Patients in the control group lost an average of 2.5 kg of weight over the 8 weeks of the study. The number of blood polymorphonuclear cells (PMNC), mainly neutrophils, and their functions (phagocytosis and

hydrogen peroxide production) decreased in the control group (average decreases of approximately 30, 45 and 17%, respectively). FO prevented these decreases and actually increased body weight (average of 1.7 kg weight gain; $p < 0.002$ vs. control group), PMNC number (average 29% increase), phagocytosis (average 14% increase) and superoxide production (average 28% increase). FO may be useful in preventing chemotherapy-induced decline in neutrophil number and function.

Keywords Cancer · Fish oil · n-3 · PUFA · Immunology

Abbreviations

EPA	Eicosapentaenoic acid
DHA	Docosahexaenoic acid
FO	Fish oil
PUFA	Polyunsaturated fatty acid
PMNC	Polymorphonuclear cell
T0	Week 0 (study entry)
T8	Week 8

S. J. R. Bonatto (✉) · H. H. P. Oliveira · E. A. Nunes · D. Pequito · F. Iagher · I. Coelho · K. Naliwaiko · M. Kryczyk · G. A. P. Brito · L. C. Fernandes
Department of Physiology, Biological Sciences Building, Federal University of Paraná, Curitiba, PR 81540-990, Brazil
e-mail: sandrobonatto@hotmail.com

S. J. R. Bonatto
Instituto Pelé Pequeno Príncipe, Curitiba, PR, Brazil

J. Repka · L. V. Sabóia · G. Fukujima
Angelina Caron Hospital, Campina Grande do Sul, PR 83430-000, Brazil

P. C. Calder
Institute of Human Nutrition, School of Medicine, University of Southampton, Southampton SO16 6YD, UK

P. C. Calder
College of Applied Medical Sciences, King Saud University, Riyadh 11451, Saudi Arabia

Introduction

Dietary fat may influence a variety of physiological events and cellular functions in the human body and thereby could impact on the pathogenesis of several diseases [1–3]. Changes in dietary fatty acid profile can modify the fatty acid composition of many cell types, including those involved in the development of inflammatory and immunologic diseases [4–6]. There has been a great interest in the immunomodulatory effects of n-3 polyunsaturated fatty

acids (PUFA), particularly those found in fish oil (FO) [7]. These are eicosapentaenoic acid (EPA) and docosahexaenoic acid (DHA). Dietary supplementation with the n-3 PUFA (from FO capsules or FO-supplemented enteral formulas) has been reported to attenuate weight loss in cancer patients [8–12], and improvement in body weight over 14 days in cancer patients receiving oral FO supplements was linearly related to increased EPA content of plasma phospholipids [13]. Neutrophils play a crucial role in the first-line defense against invading microorganisms through phagocytosis, generation of reactive oxygen metabolites and release of microbiocidal substances [14]. Cancer chemotherapy induces neutropenia and impairment of neutrophil function [15–17]. Thus, chemotherapy induces effects that increase the risk of infection, so predisposing to poor patient outcome. Therefore, strategies that maintain neutrophil number and function may be of clinical benefit. Because FO has been shown to influence aspects of human immune cell function [7], including neutrophil responses [18–28], we considered that FO might have a role in improving neutrophil function in patients receiving cancer chemotherapy. Therefore, we have investigated the effect of FO in patients receiving chemotherapy following surgery for removal of a tumor.

Materials and Methods

Materials

Unless otherwise indicated chemicals were purchased from the Sigma Chemical Company (USA). Trypan blue and Ficoll Paque Plus were from GE Healthcare Bio-sciences, Sweden. FO capsules were kindly donated by Herbarium[®], Colombo, PR, Brazil.

Subjects

Procedures involving human subjects were approved by the Angelina Caron Hospital and Local Research Ethics Committee. Patients who had recently undergone surgery for removal of tumors at various sites, predominantly gastrointestinal, and who were about to begin chemotherapy were recruited. All 38 patients recruited gave written informed consent. Patients were randomly allocated to two groups. The control group received standard chemotherapy [5-fluorouracil (425 mg/m²) and leucovorin (20 mg/m²) intravenously] three times a week, and the other group (FO) received 2 g/day FO in addition to the standard chemotherapy. All patients received the same dose of FO which provided approximately 0.3 g EPA plus 0.4 g DHA per day. This dose was determined pragmatically; it was thought to be tolerable by the patients (previous studies of

FO supplements in cancer patients have noted a lack of tolerability [29–31] and a resulting high drop-out rate of patients from the study [29, 30]), it represents a significant increase in anticipated intake of EPA and DHA, and is in line with recommended intakes for the general population and for various patient groups [32]. The study lasted for 8 weeks. At study entry and 8 weeks later patients were weighed and a blood sample taken; the initial blood sample was taken immediately prior to initiating chemotherapy and the 8 week blood sample was taken prior to administration of that days dose of chemotherapy. Characteristics of patients in the two groups are shown in Table 1.

Isolation of Plasma and Polymorphonuclear Cells

Venous blood samples were collected into tubes containing the calcium chelator EDTA as anti-coagulant. Polymorphonuclear cells (PMNC), mainly neutrophils, were isolated by centrifugation on a Ficoll Paque gradient [33]. PMNC isolation was initiated within 15 min of collecting blood samples. PMNC were collected and washed twice with phosphate-buffered saline (PBS). They were placed in RPMI 1640 culture medium and cell viability and number were determined by Trypan Blue dye exclusion (greater than 98% for all samples) in a Neubauer chamber. PMNC purity was typically 90%. A portion of the cells was pelleted and frozen immediately at –80 °C for fatty acid composition analysis. The rest of the cells were used for functional assays. PMNC functions were assessed and cultures initiated within 2 hours of cell isolation.

Fatty Acid Composition of Polymorphonuclear Cells

Total lipids were extracted from PMNC using chloroform–methanol (2:1 vol/vol). The crude lipid extracts were suspended in methanol and the pH adjusted to ≥ 12 with 5 mol/L NaOH. The aqueous solution was acidified

Table 1 Characteristics of subjects in the two groups

	Control group	Fish oil group
<i>n</i>	19	19
Male/female	10/9	12/7
Age (y)	54.9 ± 3.2	53.8 ± 2.4
Cancer site (<i>n</i>)	Gastrointestinal (14)	Gastrointestinal (14)
	Other (5)	Other (5)
Initial body weight (kg)	69.5 ± 3.6	65.8 ± 3.6
Final body weight (kg)	67.1 ± 3.6	67.4 ± 3.5
Change in body weight (kg)	–2.5 ± 0.8	+1.7 ± 0.9*

* $p < 0.002$ versus control group

(pH \leq 2.0) with concentrated hydrochloric acid, followed by solvent extraction of fatty acids with hexane. The extracts were evaporated until dry under a gentle stream of nitrogen (40 °C). Fatty acids were derivatized with 4-bromomethyl-7-coumarin and then separated on a Varian pro-Star high performance liquid chromatograph using an octadecylsilica column (25 cm \times 4.6 mm i.d.; particle size 5 μ m). Fatty acid derivatives were resolved isocratically using a mobile phase of acetonitrile–water (gradient from 77:23 to 90:10 vol/vol) at a flow rate of 1 mL/min. Fatty acid derivatives were detected by fluorescence (325-nm excitation; 395-nm emission) and integration data was acquired by Pro-Star LC 6.0 workstation.

Phagocytosis of Zymosan by Polymorphonuclear Cells

PMNC were seeded in 96-well flat-bottomed tissue culture plates (2×10^5 cells in 0.1 mL). Neutral red stained zymosan (10 μ L containing 10^6 particles) was added and the plates incubated for 30 min. Then, cells were fixed with Baker's formol-calcium solution (4% formaldehyde, 2% sodium chloride, 1% calcium acetate) for 30 min and centrifuged at 453 g for 5 min. The neutral red stain was extracted by 0.1 mL of acidified alcohol (10% acetic acid, 40% ethanol in distilled water) for 30 min. The absorbance was read on a microplate reader at 550 nm. Phagocytosis was calculated from a standard curve of stained zymosan and results expressed as absorbance (Abs)/ 10^6 PMNC/mL.

Polymorphonuclear Cell Lysosomal Volume

The volume of the lysosomal system of PMNC was assessed as described previously [34]. Briefly, 2×10^5 cells (in 0.1 mL) were incubated for 30 min in 20 μ L of neutral red (3% in PBS) and then washed twice with PBS by centrifugation (453 g for 5 min). Neutral red was solubilized in 0.1 mL of ethanol-acetic acid (40:10%, v:v). The absorbance was read at 550 nm and lysosomal volume was expressed as absorbance (Abs)/ 10^6 PMNC/mL.

Superoxide Anion Production by Polymorphonuclear Cells

Superoxide anion production by PMNC was measured by the reduction of nitroblue tetrazolium [35]. PMNC (10^5 in 0.1 mL) suspended in PBS were incubated for 1 h at 37 °C in the presence of 10 μ L of phorbol myristyl acetate (4 μ M final concentration) and 0.1% (wt/v) nitroblue tetrazolium. Then the mixture was centrifuged for 5 min at 453 g and the cells were fixed with 50% methanol for 10 min and then air-dried and centrifuged as before. Reduction of

nitroblue tetrazolium results in the formation of blue formazan which was solubilized by 30 min incubation with 120 μ L of 2 M potassium hydroxide and 140 μ L of dimethyl sulfoxide per well. The absorbance was read at 550 nm. The results are expressed as absorbance (Abs)/ 10^6 PMNC/mL.

H₂O₂ Production by Polymorphonuclear Cells

Hydrogen peroxide production by PMNC was measured as described previously [35]. This assay is based on the horseradish peroxidase (HRPO)-dependent conversion of phenol red into a colored compound by H₂O₂. PMNC (10^5 in 0.1 mL) were incubated in the presence of glucose (5 mM), phenol red solution (0.56 mM), and HRPO (8.5 U/mL) in the dark for 1 h at 37 °C. After this period, the absorbance was measured at 620 nm on a plate reader. The concentration of H₂O₂ was determined from a standard curve prepared in parallel. The results are expressed as μ mol/ 10^6 PMNC/mL.

Statistical Analysis

Data were normally distributed and are presented as means \pm SEM. Statistical analyses using data for both groups and time points were performed by ANOVA followed by a post hoc Tukey test. Changes over time were compared between the groups using independent Student's *t* tests. In all cases differences were considered statistically significant when $p < 0.05$.

Results

Subjects

The two groups did not differ significantly in age or body weight at study entry (Table 1). Body weight did not differ significantly between groups after chemotherapy. However, the patients in the control group lost an average of 2.5 kg while subjects in the FO group gained an average of 1.7 kg. The change in weight over the 8 week period was significantly different ($p < 0.002$) between groups (Table 1).

Fatty Acid Composition of Polymorphonuclear Cells

Fatty acid composition of PMNC did not change significantly over 8 weeks in the control group (Table 2). EPA and DHA in PMNC increased significantly and arachidonic acid (AA) decreased significantly after 8 weeks of FO (Table 2). The ratio of AA to EPA was significantly decreased by FO (Table 2).

Table 2 Content of eicosapentaenoic acid (EPA), docosahexaenoic acid (DHA) and arachidonic acid (AA) in polymorphonuclear cells from Control and Fish oil supplemented patients at study entry (T0) and after 8 weeks (T8)

	Control group			Fish oil group		
	T0	T8	T8–T0	T0	T8	T8–T0
AA	6.70 ± 0.26	7.24 ± 0.16	0.54 ± 0.25	6.43 ± 0.20	5.15 ± 0.30 ^{*, #}	–1.28 ± 0.15 [¶]
EPA	0.48 ± 0.10	0.38 ± 0.90	–0.10 ± 0.01	0.65 ± 0.09	1.07 ± 0.09 ^{*, #}	0.42 ± 0.03 [¶]
DHA	0.26 ± 0.50	0.20 ± 0.05	–0.06 ± 0.05	0.27 ± 0.03	0.52 ± 0.06 ^{*, #}	0.25 ± 0.07 [¶]
AA/EPA	18.03 ± 5.09	21.70 ± 4.43	3.6 ± 1.43	13.64 ± 3.22	5.35 ± 0.69 ^{*, †}	–8.29 ± 0.82 [¶]

Fatty acids are expressed as percentage of total fatty acids in PMNC. Data are mean ± SEM

* $p < 0.05$ versus control group at T8

$p < 0.05$ versus fish oil group at T0

† $p < 0.001$ versus fish oil group at T0

¶ $p < 0.05$ versus control group

Table 3 PMNC number and functions in control and fish oil supplemented patients at study entry (T0) and after 8 weeks (T8)

	Control group			Fish oil group		
	T0	T8	T8–T0	T0	T8	T8–T0
PMNC (10^6 /mL)	8.75 ± 1.18	6.05 ± 0.79	–2.69 ± 0.03	7.46 ± 1.37	9.59 ± 1.36 [*]	2.13 ± 0.05 [§]
Phagocytosis (Abs/ 10^6 PMNC/mL)	0.62 ± 0.05	0.34 ± 0.02 [‡]	–0.28 ± 0.06	0.65 ± 0.03	0.75 ± 0.04 ^{¶, #}	0.09 ± 0.04 [§]
Neutral red uptake (Abs/ 10^6 PMNC/mL)	0.21 ± 0.01	0.13 ± 0.01 [¥]	–0.08 ± 0.01	0.22 ± 0.01	0.23 ± 0.01 [*]	0.01 ± 0.02 [§]
Superoxide anion production (Abs/ 10^6 PMNC/L)	0.45 ± 0.03	0.45 ± 0.03	0.01 ± 0.48	0.46 ± 0.03	0.58 ± 0.03 ^{*, #}	0.13 ± 0.03 [§]
Hydrogen peroxide production (μ M/ 10^6 PMNC/mL)	56.65 ± 2.47	47.01 ± 2.20 [‡]	–9.64 ± 3.38	55.16 ± 1.79	55.82 ± 1.78 [¶]	0.66 ± 2.09 [§]

Data are shown as means ± SEM

Abs absorbance

¥ $p < 0.05$ versus control group at T0

‡ $p < 0.001$ versus control group at T0

* $p < 0.05$ versus control group at T8

¶ $p < 0.001$ versus control group at T8

$p < 0.05$ versus fish oil group at T0

§ $p < 0.05$ versus control group

Polymorphonuclear Cell Number and Function

PMNC number tended to decline in the control group ($p = 0.06$) but not in the FO group, such that after 8 weeks the number of PMNC was higher (by about 30% on average) in the FO group than in the control group (Table 3). The change in PMNC number over the 8 week study period was significantly different between the control and FO groups. Phagocytosis of zymosan by PMNC declined significantly in the control group (Table 3); the average decrease was about 45%. In contrast, in the FO group PMNC phagocytosis did not decline, but increased on average by 15% (Table 3). At the end of the 8 week treatment period phagocytosis by PMNC was greater in the

FO group than in the control group. Uptake of neutral red by PMNC decreased by an average of about 40% in the control group (Table 3). This did not occur in the FO group (Table 3). FO significantly increased superoxide production by PMNC (Table 3). Hydrogen peroxide production by PBMC decreased significantly in the control group (Table 3). This did not occur in the FO group.

Discussion

This was a randomized trial examining the effect of FO, rich in n-3 PUFA, on PMNC number and function in patients receiving chemotherapy post-surgical resection,

mainly of gastrointestinal tumors; neutrophils make up the bulk of PMNC. The dose of FO and of n-3 PUFA used here was lower than that used in a number of previous studies of neutrophil function in healthy humans [18–27] and in previous studies in weight losing cancer patients [8–13, 29–31, 36]. However, it was important to use a tolerable dose of FO in these patients who would be sensitive to possible adverse effects of higher FO doses, such as off flavors. Indeed, previous studies of FO supplements in cancer patients have noted a lack of tolerability, expressed as fishy aftertaste and belching, nausea, and fish smelling breath and perspiration [29–31] and a resulting high drop-out rate of patients from the study [29, 30]. In the control group receiving chemotherapy alone PMNC number declined and PMNC function became impaired. This is entirely consistent with reports in the literature [15–17]. The reduction in PMNC number observed in the current study is consistent with reductions seen previously [15–17] and is considered to be clinically relevant. The combination of reduced PMNC and impaired PMNC function would most likely result in an inability to provide vigorous host defense against pathogens, so increasing the risk of infection.

In contrast to the effects seen in the control group, oral FO supplementation prevented the decline in PMNC number and function, and in some cases improved these measures. As far as we are aware this is the first study to report that oral FO can prevent some of the deleterious effects of chemotherapy on PMNC numbers and function. However, a recent study reported that oral FO improved the response rate to chemotherapy in patients with advanced non-small cell lung cancer and had a clinical benefit [36]. How n-3 PUFA might prevent the loss of neutrophils that accompanies chemotherapy is not clear. However, these fatty acids might affect the concentrations of hematopoietic cytokines active on cells of the leukocyte lineages. The mechanism involved needs further investigation. If the reduction in PMNC numbers and function induced by chemotherapy is of clinical relevance, then preventing those reductions would be of great clinical importance, perhaps lowering the risk of infections. Unfortunately, in the current study we did not evaluate clinical outcomes such as infections and antibiotic use.

The findings of the current study suggest that there may be a role for n-3 PUFA in maintaining innate immune function in patients receiving chemotherapy and this maintenance of function could be important in preventing infections during this sensitive time and may also contribute to prevention of tumor regrowth. PMNC became enriched in EPA and DHA over the 8 week period of supplementation with FO. The level of enrichment in these bioactive n-3 PUFA is likely strongly related to the dose provided [6]. In order to explore this further, data for EPA

enrichment from the current study was compared with data for EPA enrichment in neutrophils reported in other studies in humans [13, 18, 27, 28, 37], irrespective of their duration. Such interrogation showed the findings to be extremely varied. Thus, two studies using high doses of EPA [37] or EPA + DHA [27] for 4 weeks in healthy humans report marked neutrophil enrichment in EPA. In contrast, a third study using high dose EPA + DHA for 6 weeks reported much more modest EPA enrichment in neutrophils of healthy volunteers [18], while high dose EPA + DHA for 2 weeks in advanced cancer patients did not alter neutrophil phosphatidylcholine fatty acid composition [13]. These studies suggest that there may be many exogenous factors that influence the changes in neutrophil fatty acids induced by n-3 PUFA. Healy et al. [28] reported on the dose-dependent incorporation of n-3 PUFA into neutrophils over 12 weeks in healthy humans; the range of doses included the dose used in the current study. Figure 1 shows the mean neutrophil enrichment in EPA as a function of oral EPA dose reported by Healy et al. [28] with the findings of the current study superimposed. It is evident that the incorporation observed in the current study accords well with that reported by Healy et al. [28].

Patients in the control group lost weight during the 8 weeks of the study period. Patients in the FO group did not lose weight and, in fact, on average they gained weight. This observation is surprising given the low dose of n-3 PUFA used. However, it is consistent with some other studies, especially those in pancreatic cancer [8–12]; these

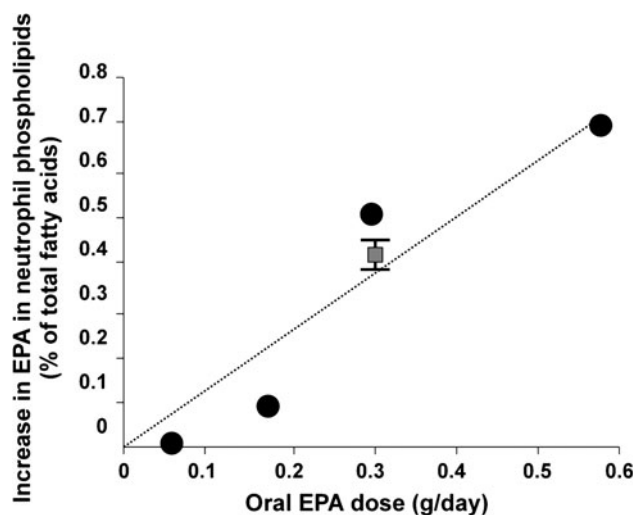


Fig. 1 Comparison of blood neutrophil enrichment with EPA in the current study and in the dose-response study of Healy et al. [28]. Mean enrichment of neutrophil phospholipids with EPA in healthy volunteers consuming one of four doses of fish oil for 12 weeks taken from Healy et al. [28] is shown in the black circles (average of $n = 8$ for each dose); the line of best fit (forced to go through zero) is shown. Mean enrichment of neutrophil lipids with EPA in the current study is shown in the grey squares, with the bars indicating + SEM

studies used higher doses of n-3 PUFA than used here. It is not clear how this benefit on body weight occurs. It may relate to maintained or improved appetite in the FO group, as has been reported in some studies of weight losing cancer patients [11, 31] and in patients with Alzheimer's disease [38]. We did not measure appetite or food intake in the current study, but it will be useful for these to be assessed in follow-up studies.

Many studies show that n-3 PUFA can modify aspects of neutrophil function in healthy humans [18–28]. Neutrophils constitute the first line of host defense against bacterial infection. Three processes are important for the role of neutrophils in host defense: phagocytosis, degranulation, and release of reactive oxygen species (ROS) derived from the superoxide-generating NADPH oxidase. Phagocytosis is the process of recognition and engulfment of microorganisms and tissue debris that accumulate during infection, inflammation and wound repair. Phagocytosis declined over 8 weeks in the group receiving chemotherapy only. Eight weeks of FO prevented this decline and the resulting activity was higher at 8 weeks than in the control group at this time. The mechanism by which FO promotes neutrophil phagocytosis (or prevents its decline) is not clear. Many membrane proteins and lipids are involved in the phagocytic process, as is the formation of membrane microdomains termed rafts [39]. It is known that n-3 PUFA influence the fatty acid composition of neutrophil phospholipids [18, 27, 28, 37]. Thereby they might alter membrane fluidity or the formation of raft regions [4–6]. In a cross-sectional study the content of n-3 PUFA was positively correlated with the ability of human blood neutrophils to phagocytosis *E. coli* [40], suggesting that a higher membrane content of these fatty acids improves phagocytosis.

Lysosomal volume, indicated here by neutral red uptake, indicates the extent of lysosomal swelling as a result of post-phagocytosis processing of engulfed material. Lysosomal volume declined over 8 weeks in the group receiving chemotherapy only. Eight weeks of FO prevented this decline and the resulting volume was higher at 8 weeks than in the control group at this time. This is consistent with the changes seen for phagocytosis according to chemotherapy and FO exposure.

Generation of superoxide anions by the NADPH oxidase complex follows from phagocytosis and is an indispensable component of the host defense response, since it is essential for the killing of invading microorganisms. FO was shown to better maintain or to improve production of superoxide radicals and hydrogen peroxide. Superoxide generation was initiated by exposure to PMA bypassing the need for phagocytosis and early membrane-mediated processes. Thus, n-3 PUFA must have an enhancing effect on protein kinase C activity and/or the events that follow it. In a cross-

sectional study the content of n-3 PUFA was positively correlated with the ability of human blood neutrophils to produce superoxide in response to PMA [40], suggesting that a higher membrane content of these fatty acids improves phagocytosis.

Thus n-3 PUFA in the form of FO improve neutrophil numbers and function in cancer surgery patients undergoing chemotherapy. These data suggest that a higher content of n-3 PUFA improves the functioning of the cells.

In summary FO supplementation (2 g/day) for 8 weeks in chemotherapy patients altered the fatty acid composition and function of blood PMNC, mainly neutrophils. This may represent an improvement in host defense in these patients which would increase the likelihood of a positive clinical outcome.

Acknowledgments The authors would like to thank the nurses and physicians of the Oncology Department of the Angelina Caron Hospital.

References

1. British Nutrition Foundation (1992) Report of the task force on unsaturated fatty acids: nutritional and physiological significance. Chapman and Hall, London
2. Smit LA, Mozaffarian D, Willett W (2009) Review of fat and fatty acid requirements and criteria for developing dietary guidelines. *Ann Nutr Metab* 55:44–55
3. Elmadfa I, Kornsteiner M (2009) Fats and fatty acid requirements for adults. *Ann Nutr Metab* 55:56–75
4. Calder PC (2007) Immunomodulation by omega-3 fatty acids. *Prostaglandins Leukot Essent Fatty Acids* 77:327–335
5. Yaqoob P, Calder PC (2007) Fatty acids and immune function: new insights into mechanisms. *Brit J Nutr* 98:S41–S45
6. Calder PC (2008) The relationship between the fatty acid composition of immune cells and their function. *Prostaglandins Leukot Essent Fatty Acids* 79:101–108
7. Calder PC (2001) N-3 polyunsaturated fatty acids, inflammation and immunity: pouring oil on troubled waters or another fishy tale? *Nutr Res* 21:309–341
8. Wigmore SJ, Ross JA, Falconer JS, Plester CE, Tisdale MJ, Carter DC, Fearon KC (1996) The effect of polyunsaturated fatty acids on the progress of cachexia in patients with pancreatic cancer. *Nutrition* 12(1 Suppl):S27–S30
9. Wigmore SJ, Fearon KC, Maingay JP, Ross JA (1997) Down-regulation of the acute-phase response in patients with pancreatic cancer cachexia receiving oral eicosapentaenoic acid is mediated via suppression of interleukin-6. *Clin Sci* 92:215–221
10. Wigmore SJ, Barber MD, Ross JA, Tisdale MJ, Fearon KC (2000) Effect of oral eicosapentaenoic acid on weight loss in patients with pancreatic cancer. *Nutr Cancer* 36:177–184
11. Barber MD, Ross JA, Voss AC, Tisdale MJ, Fearon KC (1999) The effect of an oral nutritional supplement enriched with fish oil on weight-loss in patients with pancreatic cancer. *Br J Cancer* 81:80–86
12. Barber MD, Ross JA, Preston T, Shenkin A, Fearon KC (1999) Fish oil-enriched nutritional supplement attenuates progression of the acute-phase response in weight-losing patients with advanced pancreatic cancer. *J Nutr* 129:1120–1125

13. Pratt VC, Watanabe S, Bruera E, Mackey J, Clandinin MT, Barracos VE, Field CJ (2002) Plasma and neutrophil fatty acid composition in advanced cancer patients and response to fish oil supplementation. *Br J Cancer* 87:1370–1378
14. Faurschou M, Borregaard N (2003) Neutrophil granules and secretory vesicles in inflammation. *Microbes Infect* 5:1317–1327
15. Kim SK, Demetri GD (1996) Chemotherapy and neutropenia. *Hematol Oncol Clin North Am* 10:377–395
16. Nirenberg A, Bush AP, Davis A, Friese CR, Gillespie TW, Rice RD (2006) Neutropenia: state of the knowledge part I. *Oncol Nurs Forum* 33:1193–1201
17. Zitvogel L, Apetoh L, Ghiringhelli F, Kroemer G (2008) Immunological aspects of cancer chemotherapy. *Nat Rev Immunol* 8:59–73
18. Lee TH, Hoover RL, Williams JD, Sperling RI, Ravalese J, Spur BW, Robinson DR, Corey EJ, Lewis RA, Austen KF (1985) Effects of dietary enrichment with eicosapentaenoic acid and docosahexaenoic acid on in vitro neutrophil and monocyte leukotriene generation and neutrophil function. *N Eng J Med* 312:1217–1224
19. Andres S, Ghorbani R, Kelley VE, Georgilis K, Lonnemann G, van der Meer JMW, Cannon JG, Rogers TS, Klemmner MS, Weber PC, Schaeffer EJ, Wolff SM, Dinarello CA (1989) The effect of dietary supplementation with n-3 polyunsaturated fatty acids on the synthesis of interleukin-1 and tumor necrosis factor by mononuclear cells. *N Eng J Med* 320:265–271
20. Schmidt EB, Pedersen JO, Ekelund S, Grunnet N, Jersild C, Dyerberg J (1989) Cod liver oil inhibits neutrophil and monocyte chemotaxis in healthy males. *Atherosclerosis* 77:53–57
21. Schmidt EB, Varming K, Pedersen JO, Lervang HH, Grunnet N, Jersild C, Dyerberg J (1992) Long-term supplementation with n-3 fatty acids, II: Effect on neutrophil and monocyte chemotaxis. *Scand J Clin Lab Invest* 52:229–236
22. Fisher M, Levine PH, Weiner BH, Johnson MH, Doyle EM, Ellis PA, Hoogasian JJ (1990) Dietary n-3 fatty acid supplementation reduces superoxide production and chemiluminescence in a monocyte-enriched preparation of leukocytes. *Am J Clin Nutr* 51:804–808
23. Thompson PJ, Misso NL, Passarelli M, Phillips MJ (1991) The effect of eicosapentaenoic acid consumption on human neutrophil chemiluminescence. *Lipids* 26:1223–1226
24. Luostarinen R, Siegbahn A, Saldeen T (1992) Effect of dietary fish oil supplemented with different doses of vitamin E on neutrophil chemotaxis in healthy volunteers. *Nutr Res* 12:1419–1430
25. Sperling RI, Benincaso AI, Knoell CT, Larkin JK, Austen KF, Robinson DR (1993) Dietary omega-3 polyunsaturated fatty acids inhibit phosphoinositide formation and chemotaxis in neutrophils. *J Clin Invest* 9:651–660
26. Varming K, Schmidt EB, Svaneborg N, Møller JM, Lervang HH, Grunnet N, Jersild C, Dyerberg J (1995) The effect of n-3 fatty acids on neutrophil chemiluminescence. *Scand J Clin Lab Invest* 55:47–52
27. Luostarinen R, Saldeen T (1996) Dietary fish oil decreases superoxide generation by human neutrophils: relation to cyclooxygenase pathway and lysosomal enzyme release. *Prostaglandins Leukot Essent Fatty Acids* 55:167–172
28. Healy DA, Wallace FA, Miles EA, Calder PC, Newsholme P (2000) Effect of low-to-moderate amounts of dietary fish oil on neutrophil lipid composition and function. *Lipids* 35:763–768
29. Bruera E, Strasser F, Palmer JL, Willey J, Calder K, Amyotte G, Baracos V (2003) Effect of fish oil on appetite and other symptoms in patients with advanced cancer and anorexia/cachexia: a double-blind, placebo-controlled study. *J Clin Oncol* 21:129–134
30. Burns CP, Halabi S, Clamon GH, Hars V, Wagner BA, Hohl RJ, Lester E, Kirshner JJ, Vinciguerra V, Paskett E (1999) Phase I clinical study of fish oil fatty acid capsules for patients with cancer cachexia: cancer and leukemia group B study 9473. *Clin Cancer Res* 5:3942–3947
31. Cerchietti LC, Navigante AH, Castro MA (2007) Effects of eicosapentaenoic and docosahexaenoic n-3 fatty acids from fish oil and preferential Cox-2 inhibition on systemic syndromes in patients with advanced lung cancer. *Nutr Cancer* 59:14–20
32. Calder PC, Yaqoob P (2009) Understanding omega-3 polyunsaturated fatty acids. *Postgrad Med* 121:148–157
33. Boyum A (1976) Isolation of lymphocytes, granulocytes and macrophages. *Scand J Immunol* 5:9–15
34. Bonatto SJR, Folador A, Aikawa J, Yamazaki RK, Pizzato N, Oliveira HHP, Vecchi R, Curi R, Calder PC, Fernandes LC (2004) Lifelong exposure to dietary fish oil alters macrophage responses in Walker 256 tumor-bearing rats. *Cell Immunol* 231:56–62
35. Pick E, Mizel M (1981) Rapid microassays for the measurement of superoxide and hydrogen peroxide production by macrophages in culture using an automatic enzyme immunoassay reader. *J Immunol Meth* 46:211–226
36. Murphy RA, Mourtzakis M, Chu QS, Baracos VE, Reiman T, Mazurak VC (2011) Supplementation with fish oil increases first-line chemotherapy efficacy in patients with advanced nonsmall cell lung cancer. *Cancer*. doi:10.1002/cncr.25933 (in press)
37. Kew S, Mesa MD, Tricon S, Buckley R, Minihane AM, Yaqoob P (2004) Effects of oils rich in eicosapentaenoic and docosahexaenoic acids on immune cell composition and function in healthy humans. *Am J Clin Nutr* 79:674–681
38. Irving GF, Freund-Levi Y, Eriksdotter-Jönhagen M, Basun H, Brismar K, Hjorth E, Palmblad J, Vessby B, Vedin I, Wahlund LO, Cederholm T (2009) Omega-3 fatty acid supplementation effects on weight and appetite in patients with Alzheimer's disease: the omega-3 Alzheimer's disease study. *J Am Geriatr Soc* 57:11–17
39. Yeung T, Ozdamar B, Paroutis P, Grinstein S (2006) Lipid metabolism and dynamics during phagocytosis. *Curr Opin Cell Biol* 18:429–437
40. Kew S, Banerjee T, Minihane AM, Finnegan YE, Williams CM, Calder PC (2003) Relation between the fatty acid composition of peripheral blood mononuclear cells and measures of immune cell function in healthy, free-living subjects aged 25–72 y. *Am J Clin Nutr* 77:1278–1286

Expression of Enzymes and Transcription Factors Involved in n-3 Long Chain PUFA Biosynthesis in Limousin Bull Tissues

Maya Cherfaoui · Denys Durand · Muriel Bonnet ·
Isabelle Cassar-Malek · Dominique Bauchart ·
Agnès Thomas · Dominique Gruffat

Received: 6 July 2011 / Accepted: 6 December 2011 / Published online: 8 January 2012
© AOCS 2012

Abstract The current low consumption of n-3 long chain polyunsaturated fatty acids (n-3 LCPUFA) led scientists to wonder about the possible enrichment of human food, including meats such as beef, with n-3 LCPUFA. However, their biosynthesis from dietary n-3 PUFA seems limited in mammalian tissues implying that a better understanding of the molecular mechanisms responsible for this down regulation is needed. This study aimed at identifying and comparing the limiting steps of n-3 LCPUFA synthesis in liver, intermuscular adipose tissue (IM-AT) and semitendinosus muscle (ST) from six Limousin bulls. Tissue FA composition was analysed by GLC and mRNA abundance of enzymes and transcription factors involved in n-3 LCPUFA synthesis was assessed by RT-qPCR. In liver, mRNA encoding proteins involved in n-3 LCPUFA synthesis were present in agreement with the significant high content of n-3 LCPUFA (8.4 mol% of total FA, 257 mg/100 g of fresh tissue) in this organ. In IM-AT, these mRNA were all present, but at a tenfold lower intensity than in liver in agreement with the low contents of n-3 LCPUFA in this tissue. In ST muscle, these mRNA were all present except elongase 5 mRNA which was only present as trace, the corresponding protein being undetectable, probably inducing a break of n-3 LCPUFA synthesis from 18:4n-3. In conclusion, Limousin bull ST muscle seemed unable to synthesize n-3 LCPUFA. However, the presence of 20:5n-3 (EPA) and 22:5n-3 (DPAn-3) in muscle raised the question of the origin of these n-3 LCPUFA.

Keywords Bovine · n-3 LCPUFA · Synthesis · Liver · Muscle · Adipose tissue · Gene expression

Abbreviations

ALA	Alpha linolenic acid (18:3n-3)
AU	Arbitrary unit
cDNA	Complementary deoxyribonucleic acid
EPA	Eicosapentaenoic acid (20:5n-3)
DHA	Docosahexaenoic acid (22:6n-3)
DPAn-3	Docosapentaenoic acid (22:5n-3)
FA	Fatty acids
GLC	Gas liquid chromatography
IM-AT	Intermuscular adipose tissue
LCPUFA	Long chain polyunsaturated fatty acids
mRNA	Messenger ribonucleic acid
RT-qPCR	Reverse transcription-quantitative polymerase chain reaction
ST	Semitendinosus

Introduction

The long chain polyunsaturated fatty acids of the n-3 family (n-3 LCPUFA), particularly EPA, DPAn-3 and DHA (22:6n-3), have been shown to have many beneficial biological effects [1]. Thus, DHA was shown to be essential for the development and the functioning of retina and brain [2] and in the prevention of various chronic diseases such as cardiovascular and inflammatory disorders, depression, Parkinson's and Alzheimer's diseases and some cancers [1]. Similarly, EPA and DPAn-3 were also recognized to participate to the prevention of cardiovascular diseases [3, 4] and in cell membrane functions via eicosanoid production [5].

M. Cherfaoui · D. Durand · M. Bonnet · I. Cassar-Malek ·
D. Bauchart · A. Thomas · D. Gruffat (✉)
INRA, UR 1213 Herbivore, Site de Theix,
63122 Saint-Genès-Champanelle, France
e-mail: dominique.gruffat@clermont.inra.fr

Currently, seafood products, notably oily fishes and fish oils, are among the most important dietary sources of n-3 LCPUFA for humans. However, their consumption in most western populations is sub-optimal since it corresponds to only 54% of the minimal amount recommended by the European Food Safety Authority [6]. Therefore, the current challenge to ensure an optimal n-3 LCPUFA intake for human is to diversify food sources for humans. An attractive strategy would be the enrichment in n-3 LCPUFA of terrestrial animal products such as beef, as they are largely consumed in industrialized countries.

Several nutritional strategies are proposed to directly increase n-3 LCPUFA content in meat or to increase tissue deposition of linolenic acid (ALA), as a precursor of n-3 LCPUFA in cells of vertebrates. Thus, the addition of fish oil or of marine algae in diets of ruminants significantly increases n-3 LCPUFA content of phospholipids in bovine [7] and lamb [8] muscles. However, the addition of fish oil in terrestrial animal ration is currently excluded in some Western countries, in particular for ruminants because of the animal origin. On the other hand, the use of micro-algae was not recommended because they modify ruminal bacteria, thus altering dietary PUFA biohydrogenation and favoring accumulation of *trans* 18:1 in the rumen contents [9]. Feeding of rations rich or enriched with ALA represents an alternative strategy. Thus, for grazing ruminants [10], ALA content of muscles significantly increases with non negligible increase in n-3 LCPUFA contents. In contrast, although the addition of linseed or rapeseed in diets of ruminant [11, 12] also significantly increase the ALA content of muscles, n-3 LCPUFA levels stay unchanged or increase only modestly. These results suggest a low conversion of ALA to DHA in ruminant as reported in humans [13]. Consequently, the abundance of n-3 LCPUFA in bovine muscles appears to depend not only on dietary n-3 PUFA but also on their endogenous biosynthesis via elongation and desaturation of dietary n-3 PUFA.

Metabolic studies in rodents had identified the various steps involved in the conversion of ALA to DHA. This biosynthesis is performed through alternating steps of desaturation and elongation followed by a final step of peroxisomal β -oxidation. This mainly involves activities of two desaturases ($\Delta 5$ and $\Delta 6$ desaturases), two elongases (elongases 2 and 5) and of enzymes of the peroxisomal β -oxidation [14–16] (Scheme 1). The activity of these enzymes is currently regarded as potential limiting steps in this biosynthesis probably in a tissue and/or species dependent manner. Indeed, $\Delta 6$ desaturase is considered to be the main rate limiting step for the conversion of ALA to DHA in dog liver [17] and in fish muscle [18] whereas elongase 2 is missing in rat heart [19, 20]. Additionally, the low expression of some peroxisomal β oxidation enzymes (L-PBE and ACOX1) could cause a bottle neck in n-3

LCPUFA synthesis for neuroblastoma cells [21]. Moreover, several studies have recently shown in rodents that the main regulators of these enzymes are transcription factors such as SREBP-1c, RXR, LXRs and PPARs [14, 15].

In this context, we hypothesized that one or several enzymes and/or transcription factors were very low in abundance in the bovine muscles leading to the reduced level of n-3 LCPUFA reported in these tissues. To answer this hypothesis, we focused on identifying accurately the possible limiting steps of this synthesis by quantifying the mRNA abundance of known enzymes and transcription factors involved in this pathway in bovine liver that plays a central role of lipid metabolism [22], the inter-muscular adipose tissue that is the major site of lipogenesis in ruminant [23] and the ST muscle as an edible tissue.

Materials and Methods

Animals, Diet and Tissue Sampling

The experiment was conducted according to the national legislation on animal care (Certificate of Authorization for Experimentation on Living Animals n° 7740, Ministry of Agriculture and Fish Products). Six young Limousin bulls (15–18 month old) were given a concentrate/straw based diet (75:25) (representative of a standard diet) for the 100-day finishing period. Fatty acid composition of the diet is given Table 1. Animals were slaughtered at an average body weight of 627 ± 16.3 kg in the INRA experimental abattoir (Saint-Genès Champanelle, France). Representative samples (~ 50 g) of the liver, the inter-muscular adipose tissue (IM-AT, between the thoracic portion of the trapezius muscle and the rhomboideus thoracis muscle) and the semitendinosus muscle (ST) were collected within 30 min and immediately frozen in liquid nitrogen and stored at -80 °C until analysis.

Lipid Analysis

Tissue samples of liver, IM-AT and ST (~ 50 g) were ground into a fine and homogeneous powder in liquid nitrogen with a mixer mill (Retch MM 301, Germany). Total lipids were extracted according to the method of Folch [24] by mixing tissue powder with a mixture chloroform–methanol 2/1 (vol/vol) and determined by gravimetry. Transmethylation into fatty acid methyl esters (FAME) was performed as previously described [11]. FAME analysis was achieved by gas–liquid chromatography (GLC) using the Peri 2100-model chromatograph (Perichrom Society, Saulx-les-Chartreux, France) fitted with the CP-Sil 88 glass capillary column (Varian, USA) (length: 100 m; \varnothing : 0.25 mm) with H_2 as the carrier gas,

Scheme 1 Metabolic pathway of biosynthesis of n-3 LCPUFA in mammals. The conversion of ALA (18:3n-3) occurs in the endoplasmic reticulum to successively produce EPA, DPAn-3 and 24:6n-3. Then, 24:6n-3 is transferred to the peroxisomes to be β -oxidized in DHA involving several specific enzymes

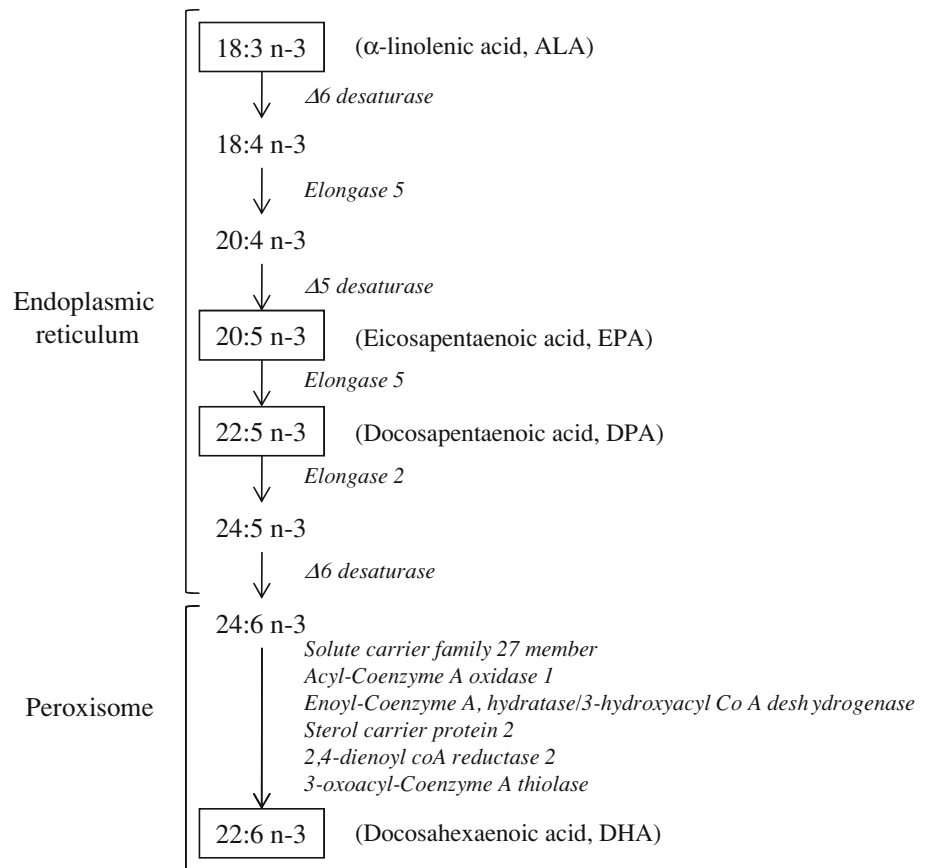


Table 1 Lipid content and fatty acid composition of the concentrate-based diet given to bulls

Dry matter (DM, %)	91.71
Lipids (% DM)	3.5
Fatty acids (% of total fatty acids)	
12:0	0.22
14:0	0.66
15:0	0.17
16:0	17.48
18:0	3.16
18:1n-9	0.06
18:2n-6	42.58
18:3n-6	0.06
20:2n-6	0.11
20:3n-6	0.39
20:4n-6	0.11
18:3n-3	11.96

under temperature conditions described by Scislowski et al. [25]. Total FA were quantified by using C19:0 as the internal standard. Identification and calculation of the response coefficient of each individual FAME was obtained by using the quantitative mix C4–C24 FAME (Supelco, Bellefonte, USA).

RNA Isolation and cDNA Synthesis

Total RNA was extracted from the powder of liver (300 mg), IM-AT (1,000 mg) and ST muscle (500 mg) by using Trizol reagent (Invitrogen, Life Technologies, CA, USA) according to the manufacturer's recommendations. Total RNA was then treated with DNase to remove genomic DNA using NucleoSpin[®] mini kit columns (Machery-Nagel, PA, USA) according to the manufacturer's protocol, except for samples of adipose tissue for which were used RNA mini kit columns (Invitrogen, Life Technologies, CA, USA) as previously described [26]. Tissue RNA was quantified with the Nanodrop ND-1000 Spectrophotometer (Nanodrop Technologies, Wilmington, DE, USA) given RNA concentrations of about 2.19, 0.04 and 0.22 mg/g of fresh tissue for liver, IM-AT- and ST muscle, respectively. The quality and integrity of RNA were examined by the RNA Integrity Number (RIN) determined by using the kit RNA 6000 Nano Assay on the 2100 bio-analyzer (Agilent technologies, Palo Alto, CA, USA). Only samples displaying a RIN \geq 8.0 and an $A_{260/280} > 1.8$ were considered. The corresponding cDNA (about $0.38 \pm 0.01 \mu\text{g}/\mu\text{l}$ for all tissues) was synthesized by reverse transcription from 2.5 μg of total RNA using 100 U of Superscript II reverse transcriptase (Invitrogen,

Life Technologies, CA, USA) and 0.5 μg of oligodT in a final volume of 50 μl . RNA and cDNA samples were stored at $-80\text{ }^{\circ}\text{C}$ until analysis.

Quantitative Real Time PCR

The qPCR was performed by using a StepOne Plus (Applied Biosystems, Foster City, CA, USA) from a dilution of cDNA of 1/50 for the liver and 1/25 for the IM-AT and the ST muscle. A total of 17 genes involved in n-3 LCPUFA biosynthesis were studied and 3 genes were used as reference genes (Table 2). The primers were designed by using The ProbeFinder Software from Roche Applied Science and ordered from Sigma Aldrich. The PCR reaction was performed by using Power Sybergreen PCR master mix (Applied Biosystems, Foster City, CA, USA) in a reaction buffer (cDNA + each of forward and reverse primers + DNase/RNase free water + Sybergreen PCR master mix) in a MicroAmp Optical 96-well reaction plate (Applied Biosystems, Foster City, CA, USA). qPCR conditions were as follows: $95\text{ }^{\circ}\text{C}/10\text{ min}$, 40 cycles of $95\text{ }^{\circ}\text{C}/15\text{ s}$ (denaturation), $60\text{ }^{\circ}\text{C}/45\text{ min}$ (annealing), $95\text{ }^{\circ}\text{C}/15\text{ s}$ (extension). The melting cycle consisted in $60\text{ }^{\circ}\text{C}/1\text{ min}$, increased by $0.6\text{ }^{\circ}\text{C}$ up to $95\text{ }^{\circ}\text{C}$ and held 15 s. The specificity of primers was confirmed by melting curve analysis and by electrophoresis of PCR products on 2% agarose gel stained with ethidium bromide. Samples were run in triplicate and concentration of each mRNA was determined from a calibration curve prepared from a cDNA pool from the three bovine tissues. The qPCR data were expressed in arbitrary units taking into account differences in cDNA dilutions between tissues. Data were normalized using the geometric mean of the three reference genes TOP2B, TBP, RPLPO as previously described by Bonnet et al. (Unpublished data), Goossens et al. [27] and Wang et al. [28].

Protein Extraction and Expression

Liver samples (3 g) were homogenized in 10 ml of Tris-sucrose buffer (250 mM sucrose, 50 mM Tris-base, pH 7.4) supplemented with a mixture of inhibitors of proteolytic enzymes (PMSF 1 mM, benzamidine 1 mM, leupeptine 5 $\mu\text{g}/\text{ml}$). After centrifugation at 10,000g for 30 min at $4\text{ }^{\circ}\text{C}$, the supernatant was collected. For ST muscle and IM-AT, total protein extraction was performed as previously described by Bouley et al. [29] and Taga et al. [30], respectively. Tissue protein concentrations were determined using the Lowry's method [31] with bovine serum albumin as the standard by using the RCDC protein assay kit (Biorad, Marnes-la-Coquette, France).

Elongase 5 protein contents in the liver, the IM-AT and the ST muscle were determined by Western Blot analysis

on 12% polyacrylamide gel slabs in denaturing conditions according to Laemmli [32] from 50 μg of total proteins. Immunoblot analysis was performed by using purified rabbit polyclonal antibody raised against amino acids 211–299 mapping at the C-terminus of ELOVL5 of human origin (1:200 dilution, Santa Cruz Biotechnology Inc., Santa Cruz, CA, USA). Control of loading was assayed by using purified mouse monoclonal Actin α antibody (1:10,000 dilution, IgG2a, Clone AC-40, Sigma-Aldrich, St. Louis, MO, USA) and purified mouse monoclonal Actin β antibody (1:4,000 dilution of IgG1a, Clone AC-74, Sigma-Aldrich, St. Louis, MO, USA). The secondary fluorescent-conjugated IRDye 800CW antibodies (anti-rabbit or anti-mouse IgG) were supplied by LICOR Biosciences (Lincoln, Nebraska, USA). Protein bands were visualized by infrared fluorescence detection using a scanner Odyssey (LI-COR Biosciences) (800 nm laser, 169 μm spatial resolution and fixed gain = 5).

Statistical Analysis

Values are expressed as means \pm SEM of six animals. Comparison of data between the liver, the IM-AT and the ST muscle were analysed according to a split-plot design using the MIXED procedure of SAS (Cary, NC, USA) in which tissues were accepted as constant factors and animals as a random factor. Statistical significance was set at $p < 0.01$.

Results

Fatty Acid Composition

Total PUFA accounted for about 42.9 mol% of total FA in the liver (Table 3), but only for 4.4 and 23.8 mol% of total FA in IM-AT and ST muscle, respectively, the predominate FA in these tissues being SFA (53.3 mol% and 40.2 mol% in IM-AT and ST, respectively) and MUFA (41.8 mol% and 35.6 mol% in IM-AT and ST, respectively) (Table 3). Among PUFA and in all tissues, n-6 PUFA relative amounts were 3- to 8-fold higher than those of n-3 PUFA. However, the part of n-3 PUFA was able to reach 9.4 mol% in the liver while it represented only 0.5 and 4.0 mol% of total FA in IM-AT and ST muscle, respectively. The two predominant n-3 PUFA in the liver were 22:5n-3 and 22:6n-3 that corresponded to about 5.14 and 1.55 mol% of the total FA, respectively. In contrast, the predominant n-3 PUFA in the IM-AT was 18:3n-3 (0.53 mol% of total FA). In the ST muscle, equivalent levels of 18:3n-3 and 22:5n-3 were observed. In the IM-AT and the ST muscle, 22:6n-3 were present as only traces (Table 3).

Table 2 Specifications of oligonucleotides used for RT-qPCR

Gene and accession	Primer sequence (5′–3′)	Location on template	Amplicon length (bp)	Efficiency ^a of primer pair
PUFA biosynthesis				
FADS2	F: AAAGGGTGCCTCTGCCAACT	641–661	101	99.98%
NM_001083444	R: ACACGTGCAGCATGTTTACA	742–722		($R^2 = 0.990$)
ELOVL5	F: CTGAATACCTTCTCCACAGGAGGA	2353–2377	154	93.45%
NM_001046597	R: GCTCCCTGTAATATGAATGTGCAA	2507–2483		($R^2 = 0.995$)
FADS1	F: TTTGTGATCGGTCACCTGAA	1182–1202	65	103.3%
NM_001083517	R: TGGTGTGGAAGTGCAAGT	1247–1228		($R^2 = 0.996$)
ELOVL2	F: CTTCTTACATGATGACGCTGGT	757–779	67	100.2%
NM_001083517	R: GGCTTTTCCGGTATGTCTG	824–804		($R^2 = 0.991$)
Peroxisomal oxidation				
SLC27A2	F: AAGGCCCGCTTTCTAAG	2144–2162	61	97.68%
XM_615837	R: TCGGTGTTTAAAAGTTCAGTG	2205–2183		($R^2 = 0.996$)
SLC27A4	F: CAAGACAGGGACATTCAAGCTA	1900–1922	74	97.84%
NM_001075667	R: GGTCTTTTACAAGTGTGGGTCA	1974–1951		($R^2 = 0.994$)
ACOX1	F: GAGTGAGCTGCCTGAGCTTC	1142–1162	62	100.6%
NM_001035289	R: TTGTCCAGGACGTGAAAGC	1204–1185		($R^2 = 0.996$)
L-PBE	F: GTTGCCCGTGGAAATAAAGA	106–126	231	99.57%
BC102238	R: CTCCAGTCCCCCTCTAAAG	356–336		($R^2 = 0.990$)
SCP2	F: ACGATTGCTTTTCTGCCAAT	982–1002	71	97.22%
NM_001033990	R: TCCACCTTGACCTTCTGGAC	1053–1033		($R^2 = 0.993$)
Thiolase	F: GTTATCACGCTGCTCAACGA	1252–1272	62	97.28%
NM_001034319	R: ATGGACACCACCCCGTAG	1314–1296		($R^2 = 0.992$)
DECR2	F: ACCTTTGCTTGACCGAAATC	1433–1453	60	99.51%
BC103065	R: GGGCAGCTCTCAGACACAC	1494–1474		($R^2 = 0.992$)
Incorporation of PUFA in PL				
GNPAT	F: CAGCATTCTTCTGCATTCA	1050–1070	244	98.95%
NM_001103286	R: GCATAGGAAGCGAAAGCAAC	1259–1239		($R^2 = 0.984$)
Transcription factors				
PPAR α	F: CGCGGAAAAGAGGCTTCTC	1649–1668	101	99.81%
NM_001034036	R: TTCCAAGGTTTCCATGGTGG	1750–1730		($R^2 = 0.991$)
PPAR γ_2	F: GCGTTCCCAAGTTTACTGC	67–87	83	97.82%
NM_181024	R: CACGACTCCCACCGATATTT	156–136		($R^2 = 0.992$)
LXR α	F: AAGACGTCTGCGATTGAGGT	1053–1073	64	101.27%
NM_001014861	R: TCTCACTTCCAGGGTTGTACC	1117–1096		($R^2 = 0.991$)
LXR β	F: CACTGGGGTAGGAAGGGACT	1673–1693	68	97.66%
NM_001014883	R: GCCAAGGCTTTAGCTCCAA	1741–1722		($R^2 = 0.991$)
RXR α	F: ACTCCAAGGGGCTCTCAA	1014–1033	63	100.5%
XM_881943	R: GGGACGCATAGACCTTCTCA	1077–1057		($R^2 = 0.990$)
SREBP-1c	F: CCAGCTGACAGCTCCATTGA	2923–2943	87	101.11%
NM_001113302	R: TGCGCGCCACAAGGA	2990–2975		($R^2 = 0.990$)

F forward primer, R reverse primer

^a Determined by plotting the C_T -values of cDNA pool dilutions from 0.1 to 0.001 ng versus the logarithm of the corresponding cDNA amount

mRNA Expression

In the liver, mRNA encoding for proteins involved in the biosynthesis of n-3 LCPUFA were all present at a

significant level (Fig. 1). In the same way, mRNA of transcription factors involved in the regulation of n-3 LCPUFA biosynthesis were all present (Fig. 2) excepted for the mRNA of PPAR γ_2 that was undetectable.

Table 3 Centesimal distribution (mol% of total FA) and tissue concentration (mg/100 g of fresh tissue) of fatty acids in total lipids of the liver, the inter-muscular adipose tissue (IM-AT) and the semitendinosus muscle (ST) of young Limousin bulls given a concentrate-based diet

	Liver	IM-AT	ST muscle	Anatomic site effect (<i>p</i>)
	mol%			
Total SFA	42.1 ± 1.5 ^a	53.3 ± 1.4 ^b	40.2 ± 0.4 ^a	0.0001
Total MUFA	14.4 ± 1.0 ^a	41.8 ± 0.98 ^b	35.6 ± 1.1 ^c	0.0001
Total PUFA	42.9 ± 0.6 ^a	4.4 ± 0.6 ^b	23.8 ± 1.3 ^c	0.0001
n-6 PUFA	33.5 ± 0.5 ^a	3.9 ± 0.5 ^b	19.8 ± 1.2 ^c	0.0001
n-6 LCPUFA	18.2 ± 1.1 ^a	0.10 ± 0.04 ^b	5.9 ± 0.3 ^c	0.0001
n-3 PUFA	9.4 ± 0.6 ^a	0.50 ± 0.09 ^b	4.0 ± 0.3 ^c	0.0001
n-3 LCPUFA	8.4 ± 0.5 ^a	0.01 ± 0.01 ^b	2.9 ± 0.2 ^c	0.0001
18:3n-3	0.99 ± 0.18 ^a	0.53 ± 0.08 ^b	1.15 ± 0.14 ^a	0.0005
20:4n-3	0.67 ± 0.06 ^a	ND	0.09 ± 0.02 ^b	0.0001
20:5n-3	0.94 ± 0.09	ND	1.02 ± 0.09	NS
22:5n-3	5.14 ± 0.34 ^a	0.01 ± 0.01 ^b	1.56 ± 0.10 ^c	0.0001
22:6n-3	1.55 ± 0.13 ^a	ND	0.19 ± 0.03 ^b	0.0001
	mg/100 g fresh tissue			
Total SFA	1101 ± 85.2 ^a	37147 ± 6994 ^b	364 ± 52.2 ^a	0.0001
Total MUFA	381 ± 82.7 ^a	30130 ± 3197 ^b	339 ± 65.1 ^a	0.0001
Total PUFA	1238 ± 120 ^a	3534 ± 828 ^b	236 ± 17.4 ^c	0.0001
n-6 PUFA	938 ± 68.0 ^a	2806 ± 633 ^b	191 ± 15.8 ^c	0.0001
n-6 LCPUFA	529 ± 12.2 ^a	82.8 ± 14.3 ^b	61.4 ± 1.85 ^b	0.0001
n-3 PUFA	284 ± 59.9 ^a	383 ± 121 ^b	41.2 ± 5.64 ^c	0.0001
n-3 LCPUFA	257 ± 11.4 ^a	5.13 ± 12.6 ^b	30.6 ± 1.03 ^b	0.0001
18:3n-3	26.7 ± 12.9 ^a	378 ± 118 ^b	10.6 ± 2.10 ^a	0.0001
20:4n-3	19.2 ± 4.08 ^a	ND	0.94 ± 0.64 ^b	0.0001
20:5n-3	27.0 ± 7.16 ^a	ND	10.3 ± 1.33 ^b	0.0001
22:5n-3	161 ± 33.6 ^a	5.13 ± 12.6 ^b	17.3 ± 2.88 ^b	0.0001
22:6n-3	47.9 ± 9.57 ^a	ND	2.05 ± 0.49 ^b	0.0001

Data are means ± SE of six animals

FA fatty acids, SFA saturated fatty acids (12:0 + 14:0 + 15:0 + 16:0 + 17:0 + 18:0 + 20:0 + 22:0 + 23:0 + 24:0), MUFA monounsaturated fatty acids (14:1 + 15:1 + 16:1 + 17:1 + 18:1 + 20:1), n-6 PUFA n-6 polyunsaturated fatty acids (18:2n-6 + 18:3n-6 + 20:2n-6 + 20:3n-6 + 20:4n-6 + 22:2n-6 + 22:4n-6 + 22:5n-6), n-6 LCPUFA n-6 long chain polyunsaturated fatty acids (20:2n-6 + 20:3n-6 + 20:4n-6 + 22:2n-6 + 22:4n-6 + 22:5n-6), n-3 PUFA n-3 polyunsaturated fatty acids (18:3n-3 + 20:3n-3 + 20:4n-3 + 20:5n-3 + 22:5n-3 + 22:6n-3), n-3 LCPUFA n-3 long chain polyunsaturated fatty acids (20:3n-3 + 20:4n-3 + 20:5n-3 + 22:5n-3 + 22:6n-3), ND non detectable

a, b, c Significant differences between anatomic sites ($p < 0.01$)

In the IM-AT, mRNA encoding for proteins involved in n-3 LCPUFA biosynthesis (Fig. 1) were also all present, but their abundance was 10-fold lower than that in the liver ($p < 0.02$). In the same manner, abundance of mRNA of all transcription factors involved in the regulation of n-3 LCPUFA biosynthesis were 6-fold lower in the IM-AT than in the liver ($p < 0.003$) (Fig. 2).

In the ST muscle, the level of mRNA encoding for proteins known to be involved in n-3 LCPUFA biosynthesis was about 1.8- to 5.1- fold lower than in the liver excepted for elongase 5, elongase 2 and GNPAT (Fig. 1). The expression of GNPAT gene was similar between ST muscle and liver. The main differences affected the genes of elongases 5 and 2, their mRNA abundance being 100- and 25-fold lower in ST muscle than in liver, respectively

($p < 0.0015$). For transcription factors (Fig. 2), expressions of SREBP-1c, RXR α and LXRs genes were 1.4- to 2.3-fold lower in the ST muscle than in liver ($p \leq 0.0001$) whereas PPAR γ_2 mRNA was undetectable in the both tissues.

Protein Expression

Protein level of elongase 5 in the liver, the IM-AT and the ST muscle were determined by Western blot analysis (Fig. 3). This method revealed a single and intense band with a molecular mass of approximately 35 kDa corresponding to the elongase 5 molecular weight reported in the liver of bulls. In the IM-AT and the ST muscle, this band was undetectable.

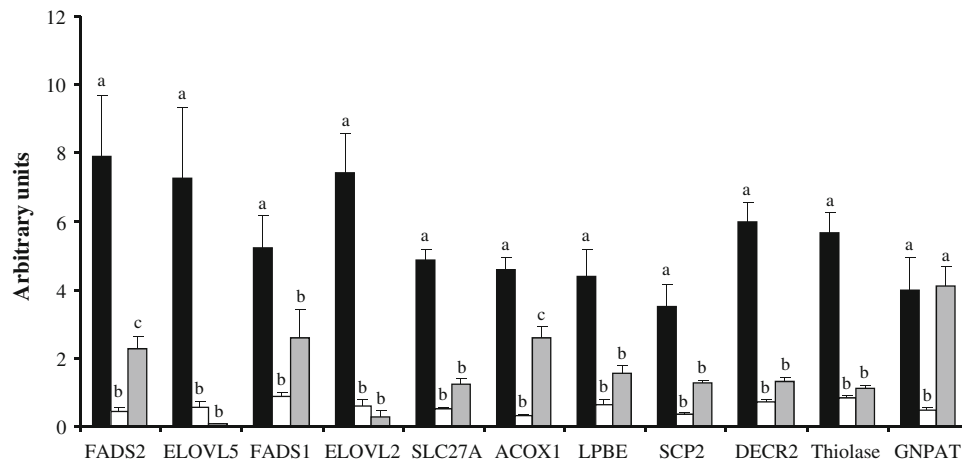


Fig. 1 mRNA expression of various genes involved in the synthesis of n-3 LCPUFA in the liver (*filled squares*), the inter-muscular adipose tissue (*open squares*) and the semitendinosus (ST) muscle (*grey filled squares*) of young Limousin bulls fed a concentrate-based diet. Values are means \pm SE ($n = 6$). ^{a, b, c}Significant differences between anatomic sites ($p < 0.01$). FADS2: fatty acid desaturase 2, ELOVL5: elongation of very long chain fatty acids protein 5, FADS1: fatty acid desaturase 1, ELOVL2: elongation of very long chain fatty

acids protein 2, SLC27A2: solute carrier family 27 member 2 (liver), SLC27A4: solute carrier family 27 member 4 (IMAT and ST), ACOX1: acyl-Coenzyme A oxidase 1, L-PBE: L-bifunctional protein (Enoyl-Coenzyme A, hydratase/3-hydroxyacyl Coenzyme A dehydrogenase), SCP2: sterol carrier protein 2, DECR2: 2,4-dienoyl CoA reductase 2, thiolase: 3-oxoacyl-coenzyme A thiolase, GNPAT: glycerone-phosphate O-acyltransferase

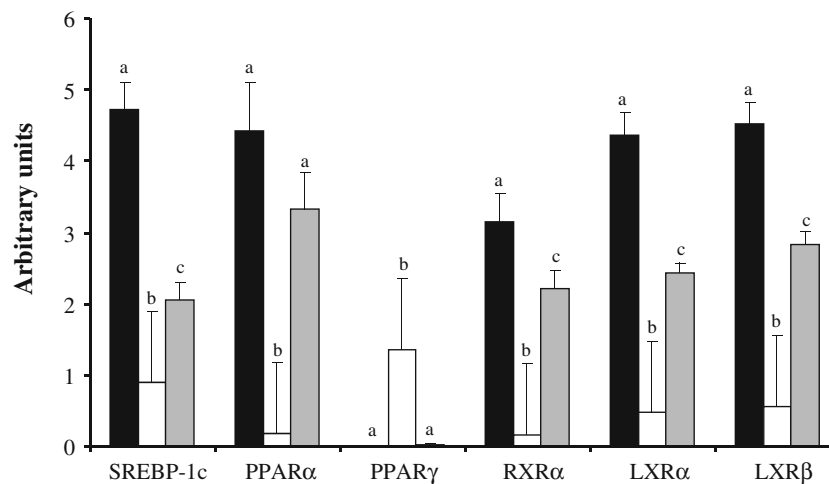


Fig. 2 mRNA expression of various transcription factor genes involved in the regulation of the synthesis of n-3 LCPUFA in the liver (*filled squares*), the inter-muscular adipose tissue (*open squares*) and the semitendinosus (ST) muscle (*grey filled squares*) of young Limousin bulls fed a concentrate-based diet. Values are means \pm SE

($n = 6$). ^{a, b, c}Significant differences between anatomic sites ($p < 0.01$). SREBP-1c: sterol regulatory element binding protein 1c, PPAR α : peroxisome proliferator activated receptor alpha, PPAR γ : peroxisome proliferator activated receptor gamma-2, RXR α : retinoid X receptor alpha, LXR α : liver X receptor alpha, LXR β : liver X receptor beta

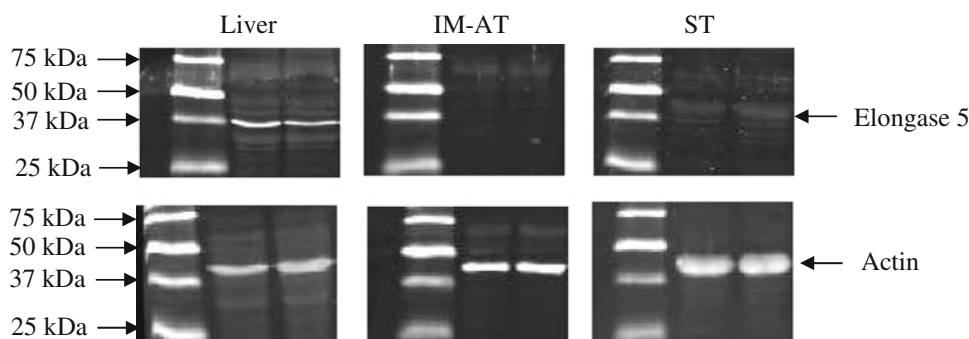
Discussion

To our knowledge, the present study has reported for the first time the identification of the possible limiting steps of the endogenous synthesis of n-3 LCPUFA by using both biochemical (FA composition) and molecular biology (expression of the seventeen proteins and the six nuclear transcriptional factors regulating the transcription of these genes) techniques in various tissues of Limousin bulls such

as the liver, the inter-muscular adipose tissue and the ST muscle.

Several studies had clearly shown that the conversion of ALA to n-3 LCPUFA in mammalian cells involved serial steps of desaturation and elongation reactions with a final peroxisomal chain shortening [13, 33]. Our present study demonstrated that the bovine liver expressed all genes encoding proteins and transcription factors involved in n-3 LCPUFA biosynthesis. This suggests that the bovine liver

Fig. 3 Representative Western blot analysis of elongase 5 from the liver, the intermuscular adipose tissue (IMAT) and the semitendinosus (ST) muscle of Limousin bulls fed a concentrate-based diet. Loading control proteins were β actin for the liver and the IM-AT and α actin for the ST muscle



could efficiently convert dietary ALA to n-3 LCPUFA in agreement with the significant amount of DHA present in this organ (around 47 mg/100 g tissue). Various studies, using radiotracer or heavy isotope labelled ALA infusion, had already suggested the ability of the liver to such metabolic conversion both on models for human research such as the rat liver [34] or the HepG2 cells [35], and on animals of agronomic interest such as swine [36], poultry [37] and fish [38]. However, the study of gene expression of enzymes known to be involved in this biosynthesis has never been reported until now. Moreover, in the current study, bovine liver expressed mRNA of all transcription factors involved in the regulation of n-3 LCPUFA biosynthesis except the peroxisome proliferator activated receptor gene $PPAR\gamma_2$. Distribution of $PPAR$ isoforms is tissue specific [39]. $PPAR\gamma$ was mainly expressed in the adipose tissue [40] to stimulate FA uptake and adipogenesis [41] whereas $PPAR\alpha$ is markedly expressed in the liver [39] where it generally induces expression of FA β -oxidation genes [42] but also of $\Delta 5$ and $\Delta 6$ desaturase genes [43]. Consequently, our results first demonstrate the implication of genes necessary for n-3 LCPUFA biosynthesis in the bovine liver. Thereby, the liver represents an appropriate model to study n-3 LCPUFA biosynthesis in bovine tissues and therefore can be considered as an appropriate positive control.

In the inter-muscular adipose tissue, mRNA encoding the various proteins involved in ALA conversion to n-3 LCPUFA were present but with a 10-fold lower abundance than in the liver, suggesting that IM-AT is less oriented towards the n-3 LCPUFA than liver. These results are in agreement with the very low content of n-3 LCPUFA determined in lipids of IM-AT. The low proportion of phospholipids compared to triacylglycerols in the adipose tissue and the preferential incorporation of n-3 LCPUFA in this polar fraction in ruminant animals could explain this result [44]. Moreover, a recent study using the *in vitro* method of incubated bovine adipose tissue slices in presence of radiolabeled fatty acids showed that only 1.3% of ALA taken up by adipose tissues are converted to 20:5n-3 without any detectable synthesis of DHA [45]. In the same

way, mRNA of all transcription factors were poorly represented in IM-AT. It is well known that the mRNA abundance of these factors is not necessary representative of the activity of their corresponding protein (which could be stimulated by ligand binding, alterations in protein-protein interaction and transcription factor phosphorylation) [46]. However, it can be hypothesized that the low gene expression of these transcription factors would be related to the low mRNA abundance of enzymes involved in n-3 LCPUFA biosynthesis in IM-AT of bovine.

In the ST muscle, mRNA encoding proteins involved in n-3 LCPUFA biosynthesis were less abundant than in liver, particularly for the elongases 5 and 2. The concomitant undetectable elongase 5 protein in ST muscle strongly argued for a lack in elongase activity. This enzyme is predominately involved in the elongation of C_{18} and C_{20} PUFA [47] and is expressed in most human [48] and rat [19] tissues. Little is known about the regulation of elongase family members, both regarding mRNA and protein expression, as well as enzymatic activity. However, available data in the literature would indicate a controlled elongase activity by transcriptional regulation [15]. Two studies suggested a regulatory role of LXR, SREBP-1c and $PPAR$ through transcriptional activation of elongase 5 in human hepatoblastoma Huh7 cells [49] and on mice [50]. In the bovine muscle, SREBP-1c, $PPAR\alpha$ and LXR mRNAs were present but, as discussed above, their mRNA abundance is not necessary representative of their activity. Elongases are condensing enzymes that interact with the 3-keto acyl-CoA reductase, a dehydratase, and *trans*-2, 3 enoyl-CoA reductase to elongate FA [51]. The rate of FA elongation is generally regulated by the activity of the elongase (condensing enzyme) and not by reductase or dehydratase. However, the low elongase 5 gene expression noted in the bovine muscle might be the result of deficient expression of reductase and dehydratase as well as of elongase. Additional studies will be required to examine the expression of these enzymes in bovine muscle. Although elongase 5 mRNA and protein was undetectable in bovine muscle suggesting a limitation of n-3 LCPUFA synthesis from 18:4n-3, this did not explain the low but

significant amount of n-3 LCPUFA determined in muscle lipids, especially EPA and DPAn-3. This result is corroborated by numerous studies on fatty acid composition of bovine muscles [12, 52, 53]. The presence of these FA in muscle could be explained by their essential role in cell function, especially through the regulation of membrane fluidity and eicosanoid production [5]. Two hypotheses can be proposed: (i) ST muscle could take up circulating EPA and DPAn-3 coming from the diet. However, EPA and DPAn-3 contents in the concentrate-based diet were not detected (ii) ST muscle could take up n-3 LCPUFA synthesized in the liver from dietary ALA and subsequently release them into the blood as part of the VLDL particles. Indeed, numerous studies using an isotope tracer technique on rodents reported that the liver plays a major role in supplying n-3 LCPUFA to various organs and tissues especially the brain, retina, heart and kidney [54–57]. Uptake of long chain FA across cell membranes is known to involve two main mechanisms: (i) a passive diffusion through the membrane bilayer [58] and (ii) a protein facilitated transfer [59]. Nowadays, it is generally recognized that membrane-associated FA-binding proteins not only facilitate but also regulate cellular FA uptake through their inducible rapid translocation from intracellular storage pools to the plasma membrane [60, 61]. A number of FA transporters has been identified (CD36/FAT, FABPm, FATP1-6, etc) and it has been recently reported that CD36 downregulation in 3T3-L1 adipocytes decrease n-3 LCPUFA uptake by cells [62]. Consequently, the intensity of gene expression of FA transporters in bovine muscle could explain the presence of n-3 LCPUFA in this tissue. Despite the presence of DHA precursors (namely EPA and DPAn-3) in the bovine ST muscle, DHA deposition was very low and the involved metabolic mechanisms were not elucidated. This could not result from a higher intensity of β -oxidation of DHA than of EPA and DPAn-3 since EPA was reported to be more readily β -oxidized than DHA [63, 64]. One hypothesis is that circulating DHA could be preferentially taken up by tissues other than muscles (e.g. brain, retina) linked to (i) a higher abundance of FA transporters on membranes of these tissues, (ii) an easier diffusion of DHA through the membranes of these tissues. Another hypothesis is that muscle DHA has a greater sensitivity to lipoperoxidation than muscle EPA and DPA. Indeed, it is well known that n-3 PUFA are particularly susceptible to peroxidation due to their high degree of unsaturation. Recently, the sensibility to peroxidation of three n-3 PUFA (ALA, EPA and DHA) was compared in rats [65]. The serum lipid peroxidation index, assessed by the level of TBA-reactive substances, becomes higher and the α -tocopherol levels are inversely lower with an increasing number of double bonds in PUFA. Therefore, further investigations are needed to test this hypothesis.

In conclusion, our present study shows for the first time that the Limousin bull ST muscle may be unable to convert ALA to n-3 LCPUFA because of the undetectable elongase 5 protein and corresponding mRNA. However, additional studies are required to validate these results such as the measurement of elongase 5 activity and the enlargement of experimental conditions (number of animals, other muscles, breed, type of animals). The presence of EPA and DPAn-3 in the ST muscle suggested that these FA, probably synthesized by the liver, could be efficiently taken up by this tissue. In contrast, the low level of DHA in the ST muscle could be the consequence of its preferential peroxidation or of its preferential uptake by other tissues/organs. A better understanding of peroxidation phenomena of n-3 LCPUFA as well as the regulation of DHA uptake by extra-hepatic tissues should provide further insights for future efforts to improve beef nutritional quality taking into accounts the risks that such manipulations could lead to animal health.

Acknowledgments This work was conducted within the framework of European ProSafeBeef Program (Project N° FOOD-CT-2006-36241). We are grateful to the experimental installations and the abattoir of INRA (Clermont-Ferrand/Theix) for animal rearing and slaughtering. We thank Dr. Brigitte Picard for her scientific advice on protein analysis. We also thank Françoise Duboisset and Christiane Legay for her excellent technical support, Geneviève Gentes, Sébastien Bes and Nicole Dunoyer for their technical advice.

References

- Anderson BM, Ma WL (2009) Are all n-3 polyunsaturated fatty acids created equal? *Lipids Health Dis* 8:33. <http://www.lipidworld.com/content/8/1/33>
- Ryan AS, Astwood JD, Gautier S, Kuratko CN, Nelson EB, Salem N Jr (2010) Effects of long-chain polyunsaturated fatty acid supplementation on neurodevelopment in childhood: a review of human studies. *Prostaglandins Leukotrienes Essent Fatty Acids* 82:305–314
- Sun Q, Ma J, Campos H, Rexrode KM, Albert CM, Mozaffarian D, Hu FB (2008) Blood concentrations of individual long-chain n-3 fatty acids and risk of nonfatal myocardial infarction. *Am J Clin Nutr* 88:216–223
- Kaur G, Cameron-Smith D, Garg M, Sinclair AJ (2011) Docosapentaenoic acid (22:5n-3): a review of its biological effects. *Progr Lipid Res* 50:28–34
- Kidd PM (2007) Omega-3 DHA and EPA for cognition, behavior, and mood: clinical findings and structural functional synergies with cell membrane phospholipids. *Altern Med Rev* 12:207–227
- Whelan J, Jahns L, Kavanagh K (2009) Docosahexaenoic acid: measurements in food and dietary exposure. *Prostaglandins Leukot Essent Fat Acids* 81:133–136
- Scollan ND, Choi NJ, Kurt E, Fisher AV, Enser M, Wood JD (2001) Manipulating the fatty acid composition of muscle and adipose tissue in beef cattle. *Br J Nutr* 85:115–124
- Cooper SL, Sinclair LA, Wilkinson RG, Hallett KG, Enser M, Wood JD (2004) Manipulation of the n-3 polyunsaturated fatty acid content of muscle and adipose tissue in lambs. *J Anim Sci* 82:1461–1470

9. Or-Rashid MM, Kramer JKG, Wood MA, McBride BW (2008) Supplemental algal meal alters the ruminal *trans*-18:1 fatty acid and conjugated linoleic acid composition in cattle. *J Anim Sci* 86:187–196
10. Noci F, Monahan FJ, French P, Moloney AP (2005) The fatty acid composition of muscle fat and subcutaneous adipose tissue of pasture-fed beef heifers: influence of the duration of grazing. *J Anim Sci* 83:1167–1178
11. Bauchart D, Durand D, Scislowski V, Chilliard Y, Gruffat D (2005) Effects of diets supplemented with oils on specific fatty acids of rectus abdominis muscle in Charolais fattening bulls. In: Hocquette JF, Gigli S (eds) Indicators of milk and beef quality. EAAP Publ. n°112. Wageningen Acad. Publishers, pp 431–436
12. Raes K, Haak L, Balcaen A, Claeys E, Demeyer D, De Smet S (2004) Effect of linseed feeding at similar linoleic acid levels on the fatty acid composition of double-muscled Belgian Blue young bulls. *Meat Sci* 66:307–315
13. Burdge GC, Calder PC (2005) Conversion of α -linoleic acid to longer-chain polyunsaturated fatty acids in human adults. *Reprod Nutr Dev* 45:581–597
14. Nakamura MT, Nara TY (2004) Structure, function and dietary regulation of $\Delta 6$, $\Delta 5$ and $\Delta 9$ desaturases. *Ann Rev Nutr* 24:345–376
15. Jakobsson A, Westerberg R, Jakobsson A (2006) Fatty acid elongases in mammals: Their regulation and roles in metabolism. *Prog Lipid Res* 45:237–249
16. Ferdinandusse S, Denis S, Mooijer PAW, Zhang Z, Reddy JK, Spector AA, Wanders RJA (2001) Identification of the peroxisomal β -oxidation enzymes involved in the biosynthesis of docosahexaenoic acid. *J Lipid Res* 42:1987–1995
17. Dunbar BL, Bauer JE (2002) Conversion of essential fatty acids by delta 6-desaturase in dog liver microsomes. *J Nutr* 132:1701S–1703S
18. Bharadwaj AS, Hart SD, Brown BJ, Li Y, Watkins BA, Brown PB (2010) Dietary source of stearidonic acid promotes higher muscle DHA concentrations than linolenic acid in hybrid striped bass. *Lipids* 45:21–27
19. Wang Y, Botolin D, Christian B, Busik J, Xu J, Jump DB (2005) Tissue-specific, nutritional, and developmental regulation of rat fatty acid elongases. *J Lipid Res* 46:706–715
20. Igarashi M, Ma K, Chang L, Bell JM, Rapoport SI (2008) Rat heart cannot synthesize docosahexaenoic acid from circulating α -linolenic acid because it lacks elongase-2. *J Lipid Res* 49:1735–1745
21. Langellier B, Alessandri JM, Perruchot MH, Guesnet P, Lavialle M (2005) Changes of the transcriptional and fatty acid profiles in response to n-3 fatty acids in SH-SY5Y neuroblastoma cells. *Lipids* 40:719–723
22. Gruffat D, Durand D, Graulet B, Bauchart D (1996) Regulation of VLDL synthesis and secretion in the liver. *Reprod Nutr Dev* 36:375–389
23. Hanson RW, Ballard FJ (1967) The relative significance of acetate and glucose as precursors for lipid synthesis in liver and adipose tissue from ruminants. *Biochem J* 105:529–536
24. Folch J, Lees M, Sloane-Stanley GH (1957) A simple method for the isolation and purification of total lipids from animal tissues. *J Biol Chem* 226:497–509
25. Scislowski V, Durand D, Gruffat D, Bauchart D (2004) Dietary linoleic acid-induced hypercholesterolemia and accumulation of very light HDL in steers. *Lipids* 39:125–133
26. Bonnet M, Faulconnier Y, Leroux C, Jurie C, Cassar-Malek I, Bauchart D, Boulesteix P, Pethick D, Hocquette JF, Chilliard Y (2007) Glucose-6-phosphate dehydrogenase and leptin are related to marbling differences among Limousin and Angus or Japanese Black x Angus steers. *J Anim Sci* 85:2882–2894
27. Goossens K, Van Poucke M, Van Soom A, Vandesompele J, Van Zeveren A, Peelma LJ (2005) Selection of reference genes for quantitative real-time PCR in bovine preimplantation embryos. *BMC Dev Biol* 5:27
28. Wang YH, Byrne KA, Reverter A, Harper GS, Taniguchi M, McWilliam SM, Mannen H, Oyama K, Lehnert SA (2005) Transcriptional profiling of skeletal muscle tissue from two breeds of cattle. *Mamm Genome* 16:201–210
29. Bouley J, Chambon C, Picard B (2004) Mapping of bovine skeletal muscle proteins using two-dimensional gel electrophoresis and mass spectrometry. *Proteomics* 4:1811–1824
30. Taga H, Chilliard Y, Meunier B, Chambon C, Picard B, Zingarretti MC, Cinti S, Bonnet M Cellular and molecular large-scale features of fetal adipose tissue: is bovine perirenal adipose tissue brown? *J Cell Physiol* (in press) doi:10.1002/jcp.22893
31. Lowry OH, Rosebrough NJ, Farr AL, Randall RJ (1951) Protein measurement with the folin phenol reagent. *J Biol Chem* 193:265–275
32. Laemmli UK (1970) Cleavage of structural proteins during the assembly of the head of bacteriophage T4. *Nature (Lond.)* 227:680–685
33. Sprecher H (2000) Metabolism of highly unsaturated n-3 and n-6 fatty acids. *Biochim Biophys Acta* 1486:219–231
34. Rapoport SI, Igarashi M, Gao F (2010) Quantitative contributions of diet and liver synthesis to docosahexaenoic acid homeostasis. *Prostaglandins Leukot Essent Fat Acids* 82:273–276
35. Harnack K, Andersen G, Somoza V (2009) Quantitation of alpha-linolenic acid elongation to eicosapentaenoic and docosahexaenoic acid as affected by the ratio of n6/n3 fatty acids. *Nutr Metab* 6:1–11
36. Li Z, Kaplan ML, Hachey DL (2000) Hepatic microsomal and peroxisomal docosahexaenoate biosynthesis during piglet development. *Lipids* 35:1325–1333
37. Lopez-Ferrer S, Baucells MD, Barroeta AC, Galobart J, Grashorn MA (2001) N-3 enrichment of chicken meat. 2. Use of precursors of long-chain polyunsaturated fatty acids: linseed oil. *Poult Sci* 80:753–761
38. Buzzi M, Henderson RJ, Sargent JR (1996) The desaturation and elongation of linolenic acid and eicosapentaenoic acid by hepatocytes and liver microsomes from rainbow trout (*Oncorhynchus mykiss*) fed diets containing fish oil or olive oil. *Biochim Biophys Acta* 1299:235–244
39. Auboeuf D, Rieusset J, Fajas L (1997) Tissue distribution and quantification of the mRNAs of the peroxisome proliferator activated receptors (PPARs) and liver X receptor (LXR α) in humans: no alteration in adipose tissue of obese and NIDDM patients. *Diabetes* 46:1319–1327
40. Sundvold H, Brzozowska A, Lien S (1997) Characterisation of bovine peroxisome proliferator activated receptors $\gamma 1$ and $\gamma 2$: genetic mapping and differential expression of the two isoforms. *Biochem Biophys Res Commun* 239:857–861
41. Jones JR, Barrick C, Kim KA, Lindner J, Blondeau B, Fujimoto Y, Shiota M, Kesterson RA, Kahn BB, Magnuson MA (2005) Deletion of PPAR gamma in adipose tissues of mice protects against high fat diet-induced obesity and insulin resistance. *Proc Natl Acad Sc USA* 102:6207–6212
42. Nakamura MT, Nara TY (2003) Essential fatty acid synthesis and its regulation in mammals. *Prostaglandins Leukot Essent Fat Acids* 68:145–150
43. Guillou H, Martin P, Jan S, D'Andrea S, Roulet A, Catheline D, Rioux V, Pineau T, Legrand P (2002) Comparative effect of fenofibrate on hepatic desaturases in wild-type and peroxisome proliferator-activated receptor α -deficient mice. *Lipids* 37:981–989
44. Wachira AM, Sinclair LA, Wilkinson RG, Enser M, Wood JD, Fisher AV (2002) Effects of dietary fat source and breed on the carcass composition, n-3 polyunsaturated fatty acid and conjugated linoleic acid content of sheep meat and adipose tissue. *Br J Nutr* 88:697–709

45. Gruffat D, Gobert M, Durand D, Bauchart D (2011) Distinct metabolism of linoleic and linolenic acids in liver and adipose tissues of finishing Normande cull cows. *Animal* 5:1090–1098
46. Latchman DS (1997) Transcription factors: an overview. *Int J Biochem Cell Biol* 29:1305–1312
47. Leonard AE, Kelder B, Bobik EG, Chuang LT, Lewis CJ, Kopchick JJ, Mukerji P, Huang YS (2002) Identification and expression of mammalian long-chain PUFA elongation enzymes. *Lipids* 37:733–740
48. Leonard AE, Bobik EG, Dorado J, Kroeger PE, Chuang LT, Thurmond JM, Parker-Barnes JM, Das T, Huang YS, Mukerji P (2000) Cloning of a human cDNA encoding a novel enzyme involved in the elongation of long-chain polyunsaturated fatty acids. *Biochem J* 350:765–770
49. Qin Y, Dalen KT, Gustafsson JA, Nebb HI (2009) Regulation of hepatic fatty acid elongase 5 by LXR α -SREBP-1c. *Biochim Biophys Acta* 1791:140–147
50. Wang Y, Botolin D, Xu J, Christian B, Mitchell E, Jayaprakasam B, Nair M, Peters JM, Busik J, Olson LK, Jump DB (2006) Regulation of hepatic fatty acid elongase and desaturase expression in diabetes and obesity. *J Lipid Res* 47:2028–2041
51. Leonard AE, Pereira SL, Sprecher H, Huang YS (2004) Elongation of long-chain fatty acids. *Progr Lipid Res* 43:36–54
52. Daley CA, Abbott A, Doyle PS, Nader GA, Larson S (2010) A review of fatty acid profiles and antioxidant content in grass-fed and grain-fed beef. *Nutr J* 9:1–12
53. Wood JD, Enser M, Fisher AV, Nute GR, Sheard PR, Richardson RI, Hughes SI, Whittington FM (2008) Fat deposition, fatty acid composition and meat quality: a review. *Meat Sci* 78:343–358
54. Scott BL, Bazan NG (1989) Membrane DHA is supplied to the developing brain and retina by the liver. *Proc Natl Acad Sci USA* 86:2903–2907
55. Rapoport SI, Rao JS, Igarashi M (2007) Brain metabolism of nutritionally essential polyunsaturated fatty acids depends on both the diet and the liver. *Prostaglandins Leukot Essent Fat Acids* 77:251–261
56. Igarashi M, Ma K, Chang L, Bell JM, Rapoport I (2007) Dietary n-3 PUFA deprivation for 15 weeks upregulates elongase and desaturase expression in rat liver but not brain. *J Lipid Res* 48:2463–2470
57. Lin YH, Salem N Jr (2007) Whole body distribution of deuterated linoleic and α -linolenic acids and their metabolites in the rat. *J Lipid Res* 48:2709–2724
58. Zakim D (1996) Fatty acids enter cells by simple diffusion. *Proc Soc Exp Biol Med* 212:5–14
59. Hajri T, Abumrad NA (2002) Fatty acid transport across membranes: relevance to nutrition and metabolic pathology. *Annu Rev Nutr* 22:383–415
60. Schwenk RW, Holloway GP, Luiken JJFP, Bonen A, Glatz JFC (2010) Fatty acid transport across the cell membrane: regulation by fatty acid transporters. *Prostaglandins Leukot Essent Fat Acids* 82:149–154
61. Glatz JFC, Luiken JJFP, Bonen A (2010) Membrane fatty acid transporters as regulators of lipid metabolism: implications for metabolic disease. *Physiol Rev* 90:367–417
62. Kontrova K, Zidkova J, Bartos B, Skop V, Sajdok J, Kazdova L, Mikulik K, Zidek V, Pravenec M (2007) Effect of RNA interference on biochemical function of protein CD36. *Phys Research* 56:493–496
63. Gavino GR, Gavino VC (1991) Rat liver outer mitochondrial carnitine palmitoyl transferase activity towards long-chain polyunsaturated fatty acids and their CoA esters. *Lipids* 26:266–270
64. Chen CT, Liu Z, Ouellet M, Calon F, Bazinet RP (2009) Rapid β -oxidation of eicosapentaenoic acid in mouse brain: an in situ study. *Prostaglandins Leukot Essent Fat Acids* 80:157–163
65. Saito M, Kubo K (2003) Relationship between tissue lipid peroxidation and peroxidizability index after α -linolenic, eicosapentaenoic, or docosahexaenoic acid intake in rats. *Br J Nutr* 89:19–28

The “HER2–PI3K/Akt–FASN Axis” Regulated Malignant Phenotype of Colorectal Cancer Cells

Nan Li · Xiaodong Bu · Peng Wu · Pingping Wu · Peilin Huang

Received: 21 October 2011 / Accepted: 15 December 2011 / Published online: 6 January 2012
© AOCs 2012

Abstract Recent evidence suggests that HER2 (ErbB2; Her-2/neu) and the related PI3K/Akt signaling pathway substantially affect the malignant phenotype of colorectal cancer cells. Moreover, fatty acid synthase (FASN), which mediates de-novo fatty acid synthesis, is crucially important in the carcinogenesis process of a variety of cancers, including colorectal cancer. The purpose of this study was to investigate the malignant phenotype regulation of colorectal cancer cells via the “HER2–PI3K/Akt–FASN axis”. Caco-2 cells with high expression of HER2 and FASN and high transfection efficiency were selected for functional characterization. The cells were transfected with either HER2-specific RNAi plasmid or negative control RNAi plasmid, followed by Q-RT-PCR and western blot assays to examine expression of HER2, PI3K, Akt, and FASN. MTT and colony-formation assays were used to assess proliferation. Migration was investigated by use of the transwell assay, and apoptosis and cell cycle were assayed by use of flow cytometry. Expression of HER2,

PI3K, Akt, and FASN were downregulated when HER2 was silenced. Proliferation decreased after downregulation of HER2, which was consistent with increased apoptosis. Migration of HER2-silenced cells was also impaired. Loss of HER2 inhibits the activity of the “HER2–PI3K/Akt–FASN axis” of Caco-2 cells, and reduced activity of this axis alters the malignant behavior of Caco-2 cells.

Keywords HER2 · The PI3K/Akt signaling pathway · FASN · Proliferation · Migration · Apoptosis · Caco-2 cells

Abbreviations

FASN	Fatty acid synthase
Q-RT-PCR	Quantitative real-time polymerase chain reaction
MTT	3-(4,5-Dimethylthiazol-2-yl)-2,5-diphenyltetrazolium bromide
RNAi	RNA interference

N. Li · X. Bu · P. Huang (✉)
Department of Internal Medicine, Medical School of Southeast University, Dingjia Qiao 87, Nanjing 210009, People’s Republic of China
e-mail: hplwpp@yahoo.cn

X. Bu · P. Wu · P. Huang
Department of Pathology, Medical School of Southeast University, Nanjing, People’s Republic of China

P. Wu
Department of Internal Medicine, The Tumor Hospital of Jiangsu Province, Nanjing, People’s Republic of China

P. Huang
Department of Internal Medicine, The Second Affiliated Hospital of Southeast University, Nanjing, People’s Republic of China

Introduction

Colorectal cancer is the third most common cause of cancer-related mortality in the world, and the most frequent malignancy of the gastrointestinal tract. Approximately 150,000 new cases are diagnosed annually [1]. HER2 (ErbB2; Her-2/neu) is a member of the epidermal growth factor receptor (EGFR) family of receptor tyrosine kinases (RTKs) that regulates biological functions such as cellular proliferation, transformation, differentiation, motility, and apoptosis [2, 3]. Modulation of HER2 is also tightly regulated in normal cellular function. In-vitro and animal studies have revealed that deregulated HER2 expression/activity is pivotal in oncogenic transformation,

tumorigenesis, and metastasis [4, 5]. Recent studies have provided evidence that HER2 and its family members are overexpressed by colorectal cancer cells, implying it is important in mediating malignant progression [6, 7].

A high-fat diet has been related to the development of many human solid tumors, including colon, breast, and ovarian carcinoma [8]. Fatty acid synthase (FASN) is a multifunctional enzyme that performs seven sequential reactions to convert acetyl-CoA and malonyl-CoA to palmitate and is of central importance in the anabolic conversion of dietary calories into a storage form of energy in mammals [9, 10]. Numerous clinical and basic studies indicate that increased expression of FASN is a common event in breast cancer and in varieties of human solid tumors, particularly those with poor prognosis [11]. Our previous study and recent studies have demonstrated that inhibition of FASN by use of pharmacological inhibitors is selectively cytotoxic to human cancer cells and leads to a significant antitumor effect [12, 13], suggesting that activation of fatty acid synthesis is required for carcinogenesis. Collectively, overexpression of FASN occurs in a wide variety of human cancers and is associated with poor prognosis, suggesting that fatty acid synthesis is an advantage in tumor growth and could be a feature of many human solid tumors and a promising target for chemoprevention or chemotherapy.

It is worthy of note that HER2 has been shown to regulate FASN transcriptional expression by altering the activity of the PI3K/Akt signaling pathway, revealing a molecular connection between HER2 and FASN in breast cancer cells [14]. Inhibition of FASN preferentially induced apoptosis of HER2-overexpressing breast cancer cells [15], suggesting that downregulation of FASN expression might be involved in HER2-mediated cell survival and tumorigenesis. Although lipogenesis has proved to be important for the survival and proliferation of colorectal cancer cells, it remains largely unknown how HER2 regulates lipogenic enzymes (for example FASN), and the factors and mechanisms determining the malignant phenotype of colorectal cancer cells are not yet completely understood. Thus, in this study, we hypothesized that HER2 can regulate FASN expression and change malignant behavior via the PI3K/Akt signaling pathway in colorectal cancer cells.

Materials and Methods

Cell Culture and Target Cell Selection

Four human colorectal cancer cells, Caco-2, HT-29, LoVo, and LS174T, were used in this study. All cells were purchased from the Shanghai Cell Biology Institute of the Chinese Academy of Sciences (Shanghai, China). HT-29,

LoVo, and LS174T cells were cultured in RPMI-1640 medium supplemented with 10% fetal bovine serum (Invitrogen, USA). Caco-2 cells were cultured in minimum essential medium (MEM) supplemented with 10% fetal bovine serum (Invitrogen). All cells were incubated at 37 °C in a humidified atmosphere supplemented with 5% CO₂. HER2 and FASN mRNA expression by the four types of cell were detected by Q-RT-PCR. A negative control RNAi plasmid with scrambled sequences (denoted MR-Neg) (Table 1) was synthesized according to the manufacturer's instructions (Invitrogen), and the four types of cell were transiently transfected with MR-Neg to determine transfection efficiency. HER2 and FASN mRNA expression and transfection efficiency for the four types of cell were integrated for selection of target cells.

HER2-specific RNAi Plasmid Construction and Stable Transfection

Knockdown of HER2 (NCBI reference sequence: NM_001005862.1) was achieved by an RNA interference approach, using pcDNATM 6.2-GW/EmGFP-miR (Invitrogen) to obtain stable clones. Four pairs of HER2-specific RNAi oligos were designed by Block-iTTM RNAi Designer and synthesized (Table 1). After being annealed, connected, and transformed, four different HER2-specific RNAi plasmids (denoted MR-HER2-1 to MR-HER2-4) were synthesized according to the manufacturer's instructions (Invitrogen), and Caco-2 cells were transiently transfected with them. HER2 mRNA expression was detected by Q-RT-PCR to validate the knockdown effect and to choose the most effective HER2-specific RNAi plasmid. Caco-2 cells were then transfected with the most effective HER2-specific RNAi plasmid (MR-HER2-4) and the negative control RNAi plasmid (MR-Neg) by use of Lipofectamine 2000, in accordance with the Invitrogen technical bulletin. Blastidicin (7 µg/ml) was used to select for stable clones.

Experimental Groups

All further experiments were divided into three groups. The experimental group (denoted Caco-2 + MR-HER2): Caco-2 cells were stably transfected with the MR-HER2-4 and collected. Blank control group (denoted Caco-2): Caco-2 cells were cultured normally and collected. Negative control group (denoted Caco-2 + MR-Neg): Caco-2 cells were stably transfected with the MR-Neg and collected.

Quantitative Real-Time Polymerase Chain Reaction

Total RNA was isolated by the TRIzol method (Invitrogen). cDNA was synthesized by use of a reverse

Table 1 The oligo sequences of four HER2-specific RNAi plasmids and the negative control RNAi plasmid

Plasmid		Oligo sequence (5'–3')
MR-HER2-1	Forward	TGCTGTATAGTGGGCACAGGCCACACGTTTTGGCCACTGACTGACGTGTGGCCTGCCACTATA
	Reverse	CCTGTATAGTGGGCAGGCCACACGTCAGTCAGTGGCCAAAACGTGTGGCCTGTGCCACTATAC
MR-HER2-2	Forward	TGCTGTTCAGAGTCAATCATCCAACAGTTTTGGCCACTGACTGACTGTTGGATTTGACTCTGAA
	Reverse	CCTGTTCAGAGTCAAATCCAACAGTCAGTCAGTGGCCAAAACGTGGATGATTGACTCTGAAC
MR-HER2-3	Forward	TGCTGCATTCTGGATGACCACAAAGCGTTTTGGCCACTGACTGACGCTTTGTGCATCCAGAATG
	Reverse	CCTGCATTCTGGATGCACAAAGCGTCAGTCAGTGGCCAAAACGCTTTGTGGTCATCCAGAATGC
MR-HER2-4	Forward	TGCTGTTCGGAGGGTGCCAGTGGAGAGTTTTGGCCACTGACTGACTCTCCACTCACCCTCCGAA
	Reverse	CCTGTTCGGAGGGTGAGTGGAGAGTCAGTCAGTGGCCAAAACGTCTCCACTGGCACCCCTCCGAAC
MR-Neg	Forward	tgctgAAATGTACTGCGCGTGGAGACGTTTTGGCCACTGACTGACGTCTCCACGCAGTACATTT
	Reverse	cctgAAATGTACTGCGTGGAGACGTCAGTCAGTGGCCAAAACGTCTCCACGCAGTACATTTc

transcription kit (Invitrogen) in accordance with the manufacturer's instruction. Gene mRNA expression was verified by use of a fluorescence quantitative PCR system (BioRad, USA). Glyceraldehyde-3-phosphate dehydrogenase (GAPDH) was used as internal standard. The gene primer sequences are listed in Table 2. The cycling conditions were: initial denaturation at 95 °C for 2 min, followed by 40 amplification cycles of 95 °C for 10 s, 60 °C for 30 s, and 70 °C for 45 s. Every real-time PCR assay contained 1.2 µl cDNA template, 0.5 µl SYBR green, and 0.5 µl of every forward and reverse primer in 25 µl reaction mixture. Relative gene mRNA expression was analyzed by use of the $2^{-\Delta\Delta CT}$ method [16]. Every experiment was repeated three times.

Western Blot Analysis

Equal amounts of protein (100 µg per lane) were applied to 4–12% NuPAGE Novex Bis-Tris Mini Gels (Invitrogen) and the separated proteins were transferred on to an Immobilon P PVDF membrane (Invitrogen). The membranes were blotted using primary antibodies directed against human HER2, PI3K, Akt (1:300, 1:400, 1:500;

Signalway Antibody, USA), Phospho-Akt, and FASN (1:500; Cell Signaling Technology, USA). After incubation with the appropriate antirabbit or antimouse horseradish peroxidase-conjugated secondary antibody (1:10,000, Santa Cruz, CA, USA), immunoreactive bands were visualized by chemiluminescence, dissolved, and exposed to X-ray film. GAPDH (1:10,000, Santa Cruz) protein expression was used as a normalization control for protein loading.

Cell Proliferation Assay

Cells ($6 \times 10^3/200$ µl/well) were seeded in 96-well plates. Viable proliferating cells were detected by use of the 3-(4,5-dimethylthiazol-2-yl)-2,5-diphenyltetrazolium bromide (MTT) assay at different times (24, 48, 72, 96, and 120 h), using six wells per time. Cell viability was expressed as optical density (OD), which was detected by use of an enzyme-linked immunoabsorbent assay reader (MK3; Thermo, USA) at 492 nm. Every experiment was repeated three times.

Colony-Formation Assay

Cells ($6 \times 10^2/2$ ml/well) were seeded in 6-well plates, and cultured for 2 weeks to form colonies. The colonies formed were stained with Giemsa, and the colonies containing more than 50 cells were counted under an inverted microscope. Every experiment was repeated three times.

Cell-Migration Assay

Cell migration was measured in 24-well plates by the transwell assay using a chamber containing a poly(ethylene terephthalate) filter membrane with 8-µm pores (Corning, USA). Cells ($6 \times 10^4/200$ µl/chamber) were seeded in the upper chamber with MEM, and 500 µl MEM supplemented with 10% fetal bovine serum was placed in the

Table 2 The gene primer sequences

Gene		Primer sequence (5'–3')
HER2	Forward	CACTGCCAACCGGCCAGAGG
	Reverse	GACTCAGGGTGGCACGGC
PI3K	Forward	TGTAGTGGTGGACGGCGAAGTA
	Reverse	GGGAGGTGTGTTGGTAATGTAGCA
Akt	Forward	GAGAGGAGCGCGTGAGCGTC
	Reverse	TCATCAGCTGGCACTGCGCC
FASN	Forward	CGACAGCACCAGCTTCGCCA
	Reverse	CACGCTGGCCTGCAGCTTCT
GAPDH	Forward	GAAGGTCCGAGTCAACGGATT
	Reverse	CGCTCCTGGAAGATGGTGAT

lower well as a chemoattractant. After incubation for 24 h, the chambers were stained with hematoxylin–eosin (HE). Migrated cells were counted from five randomly selected fields under an inverted microscope. Every experiment was repeated three times.

Cell-Apoptosis Analysis

Cells (5×10^5) were harvested, washed with PBS, and resuspended in binding buffer (Kaijibio, China), followed by mixing with Annexin V-FITC and propidium iodide (Kaijibio). Cells were analyzed by use of a Becton–Dickinson FACSCalibur flow-cytometer provided with CellQuest software (Brentford, MA, USA). Every experiment was repeated three times.

Cell-Cycle Analysis

Cells (1×10^6) were harvested, washed with PBS, and fixed in 70% ethanol. The fixed cells were washed with PBS and resuspended in RNase A (Kaijibio), followed by incubation at 37 °C for 30 min. Cells were stained with PI solution (Kaijibio) and analyzed by use of a Becton–Dickinson FACSCalibur flow-cytometer provided with CellQuest software (Brentford, MA, USA). Every experiment was repeated three times.

Statistical Analysis

Statistical comparisons were performed by use of SAS software, version 9.1 (SAS Institute, Cary, NC, USA). Values are presented as mean \pm standard error of mean (SEM). The statistical significance of differences was determined by one-way ANOVA with a post-hoc test (Student–Newman–Keuls test). Values of $P < 0.05$ were considered to be statistically significant.

Results

Target Cell Selection

HER2, FASN mRNA expression of Caco-2 cells were respectively 138.46 ± 77.6 and 70.52 ± 11.53 . Compared with HT-29, LoVo and LS174T cells, they were both higher (Fig. 1a). After transient transfection with MR-Neg for 24 h (Fig. 1b), transfection efficiency for the four types of cell were observed by use of an inverted fluorescence microscope. Compared with HT-29, LoVo, and LS174T cells, transfection efficiency for Caco-2 cells was, again, higher (Fig. 1c). Hence, Caco-2 cells were selected as the target cells for further experiments.

The Most Effective HER2-specific RNAi Plasmid Selection and Stable Transfection

After transient transfection with four different HER2-specific RNAi plasmids and MR-Neg for 24 h (Figs. 1b, 2a), HER2 mRNA expression of Caco-2 cells was 0.53 ± 0.2 , 0.52 ± 0.07 , 0.31 ± 0.09 , 0.29 ± 0.13 , 1.00. Compared with other groups, HER2 mRNA expression of Caco-2 cells transfected with MR-HER2-4 was the lowest ($P < 0.05$) (Fig. 2b). Therefore, Caco-2 cells were transfected with the most effective HER2-specific RNAi plasmid (MR-HER2-4) and the negative control RNAi plasmid (MR-Neg), and blasticidin ($7 \mu\text{g/ml}$) was used to select for stable clones. The fluorescein signal of stable clones was detected as a granular pattern in the cytoplasm surrounding the nuclei (Fig. 3).

Inhibition of HER2 Expression by RNA Interference-Suppressed FASN Expression of Caco-2 Cells via the PI3K/Akt Signaling Pathway

HER2 mRNA expression by the experimental group was 0.3 ± 0.08 , significantly lower than by the control groups ($P < 0.05$) (Fig. 4a). HER2 protein expression was also reduced compared with the two control groups (Fig. 4b). Interestingly, after inhibiting HER2 expression, PI3K, Akt, and FASN mRNA expression of the HER2–RNAi group were 0.14 ± 0.02 , 0.02, and 0.37 ± 0.03 , all significantly lower than the control groups ($P < 0.05$) (Fig. 4a). Correspondingly, PI3K, Akt, and FASN protein expression also declined dramatically (Fig. 4b). Western blot analysis also revealed a significant decrease in Phospho-Akt (Fig. 4b).

Inhibition of the “HER2–PI3K/Akt–FASN Axis” Blocked the Proliferation and Migration of Caco-2 Cells

To examine possible involvement of the “HER2–PI3K/Akt–FASN axis” in cancer progression, the proliferation and migration of Caco-2 cells after silencing of HER2 were assessed by use of the MTT, colony-formation, and transwell assays. As shown in Fig. 5a, the OD values measured after 5 days showed that proliferation for the experimental group was significantly lower than for the two control groups ($P < 0.05$). Colony-formation by the HER2-silenced group was $4.72 \pm 0.01\%$, and had obviously declined, compared with the blank control group ($11.33\% \pm 0.02$) and the negative control group ($11.78\% \pm 0.02$) ($P < 0.05$) (Fig. 5b). In the transwell assay, HER2-silenced cells migrated less efficiently than control cells ($P < 0.05$) (Fig. 5c). The number of migrating HER2-silenced Caco-2 cells was 158.67 ± 6.51 , compared with 295.33 ± 4.04 for the blank

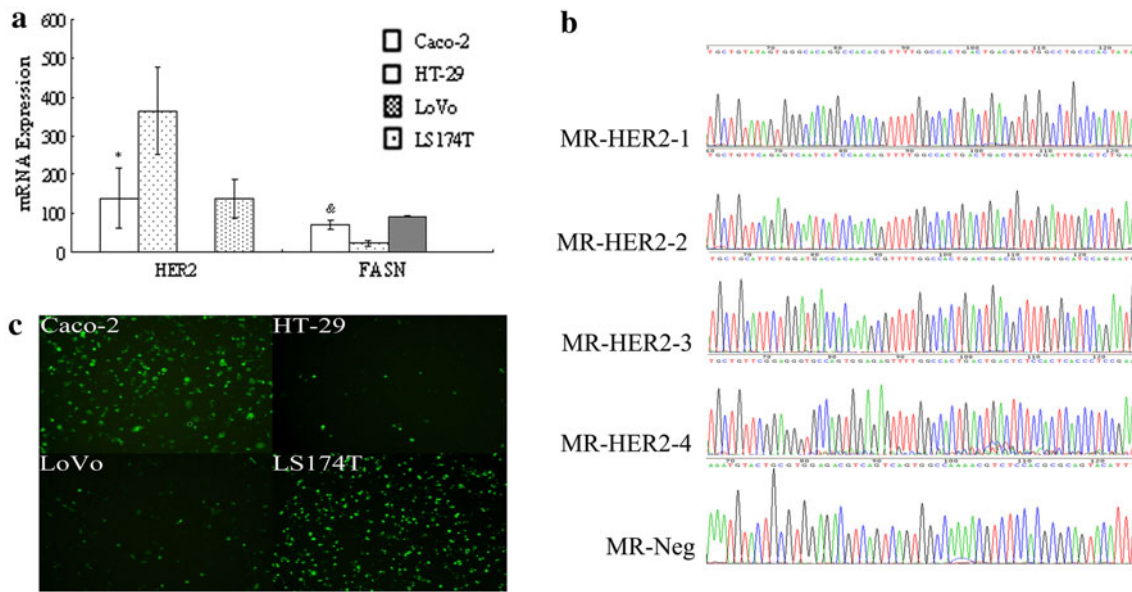


Fig. 1 Target cell selection. **a** HER2 and FASN mRNA expression of Caco-2, HT-29, LoVo, and LS174T cells. *Compared with HT-29 and LoVo cells, $P < 0.05$; Compared with LS174T cells, $P > 0.05$. &Compared with HT-29, LoVo and LS174T cells, $P < 0.05$.

b Sequencing of four different HER2-specific RNAi plasmids and the negative control RNAi plasmid. **c** Fluorescence photograph of Caco-2, HT-29, LoVo, and LS174T cells transiently transfected with the negative control RNAi plasmid for 24 h ($\times 100$ magnification)

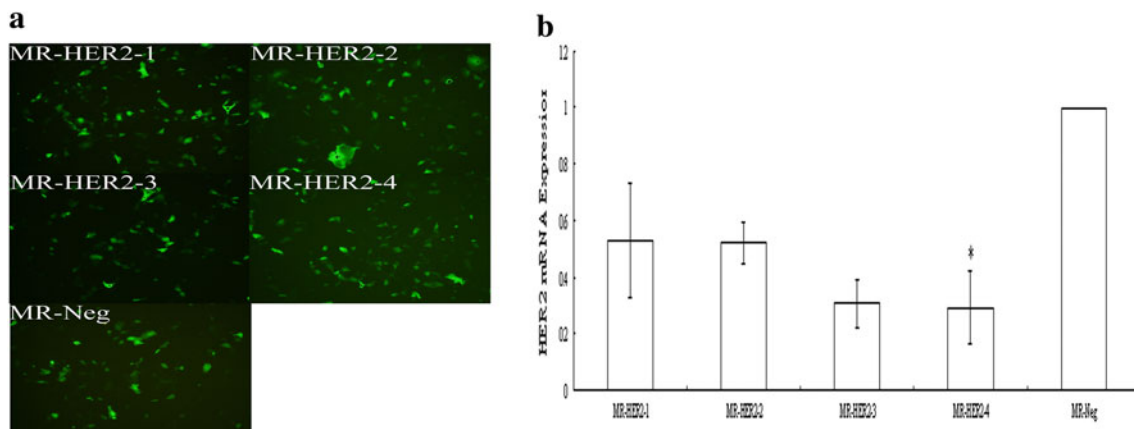


Fig. 2 The most effective HER2-specific RNAi plasmid selection. **a** Fluorescence photograph of Caco-2 cells transiently transfected with four different HER2-specific RNAi plasmids and the negative control RNAi plasmid for 24 h ($\times 100$ magnification). **b** HER2 mRNA

expression of Caco-2 cells transiently transfected with four different HER2-specific RNAi plasmids and the negative control RNAi plasmid for 24 h. *Compared with other groups, $P < 0.05$

control group and 327 ± 14.53 for the negative control group.

RNA Interference-Induced Apoptosis of Caco-2 Cells

HER2 silencing led to a greater early apoptosis ($71.13 \pm 0.04\%$) of Caco-2 cells ($P < 0.05$) (Fig. 6a). There was no difference between late apoptosis of HER2-silenced and control cells ($P > 0.05$) (Fig. 6a) and no significant changes in cell cycle were observed upon HER2 silencing ($P > 0.05$) (Fig. 6b).

Discussion

Historically, HER2 was identified as an oncogene because of its ability to induce the malignant transformation of cultured fibroblasts. HER2 oncogene is highly expressed in different types of human cancer and is linked with poor prognosis of clinical outcome. Therefore, HER2 has become an important therapeutic target in a variety of human tumors for two reasons:

1. HER2 expression closely correlates with the pathogenesis and aggressive behavior of some human tumors; and

Fig. 3 Fluorescence photograph of Caco-2 cells stably transfected with the most effective HER2-specific RNAi plasmid and the negative control RNAi plasmid ($\times 200$ magnification)

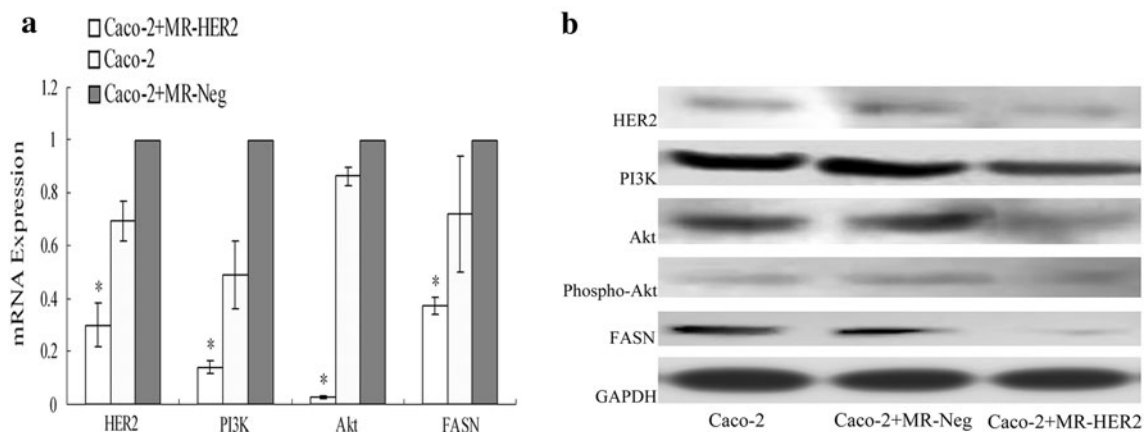
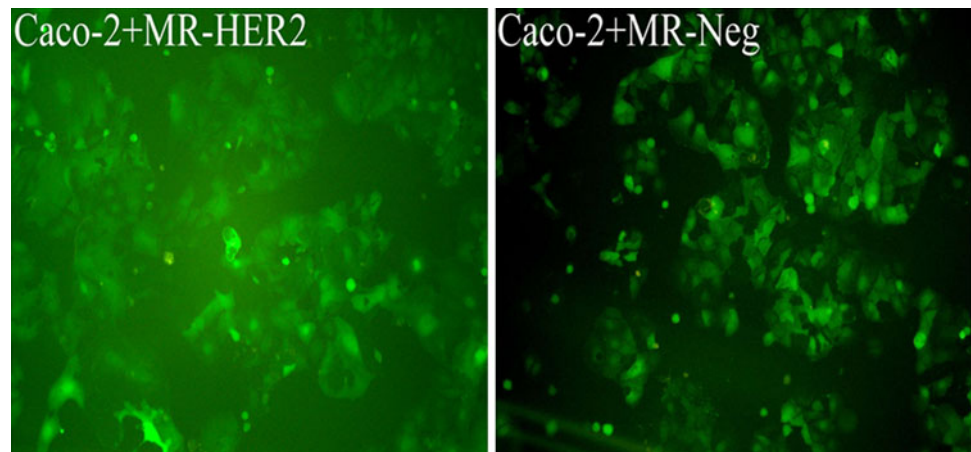


Fig. 4 HER2, PI3K, Akt, and FASN expression of Caco-2 cells by RNA interference. **a** HER2, PI3K, Akt, and FASN mRNA expression. *Compared with the two control groups, $P < 0.05$. **b** HER2, PI3K, Akt, Phospho-Akt, and FASN protein expression

- the expression level of HER2 in human cancer cells with HER2 amplification is higher than in normal tissue, so targeted therapy may reduce its toxicity toward normal tissue.

In this study, we observed that inhibition of HER2 blocked the proliferation and migration of Caco-2 cells and increased apoptosis. This implies that an HER2-mediated pathway essentially controls the malignant behavior of Caco-2 cells, and HER2 overexpression may be a malignant characteristic of colorectal cancer.

Endogenous fatty acid synthesis catalyzed by lipogenic enzymes such as FASN has emerged as an oncogenic stimulus that drives many epithelial malignancies [17, 18]. Intriguingly, recent experimental evidence supports the notion that the oncogenic nature of FASN-mediated lipogenesis largely depends on the activity and/or expression of important cancer-related oncogenes, for example HER2 [19]. HER2 overexpression leads to constitutive upregulation and maintenance of exacerbated FASN-catalyzed endogenous fatty acid synthesis [20, 21];

this “lipogenic benefit” enhances the proliferation, survival, chemoresistance, and metastasis of human cancer cells [22–24], and activation of endogenous fatty acid synthesis in non-cancerous epithelial cells, only, is sufficient to induce a cancer-like phenotype functionally dependent on HER2 activity [17]. Taken together, these findings suggest that HER2 increases the expression of FASN, thereby ensuring hyperactive de-novo fatty acid synthesis which potentiates its oncogenic effect. In this study, we demonstrated that inhibition of HER2 significantly suppressed FASN expression of Caco-2 cells; it further blocked the cell proliferation and cell migration. This implies that HER2 may affect the FASN-mediated lipogenic process and change malignant phenotypes in colorectal cancer cells.

It is well known that aberrant expression of HER2 can trigger the activation of multiple downstream signaling pathways, including the PI3K/Akt signaling pathway and the MAPK signaling pathway, which mediates different aspects of malignancy [25, 26]. PI3K is activated as a result of ligand-dependent activation of HER2, and Akt has

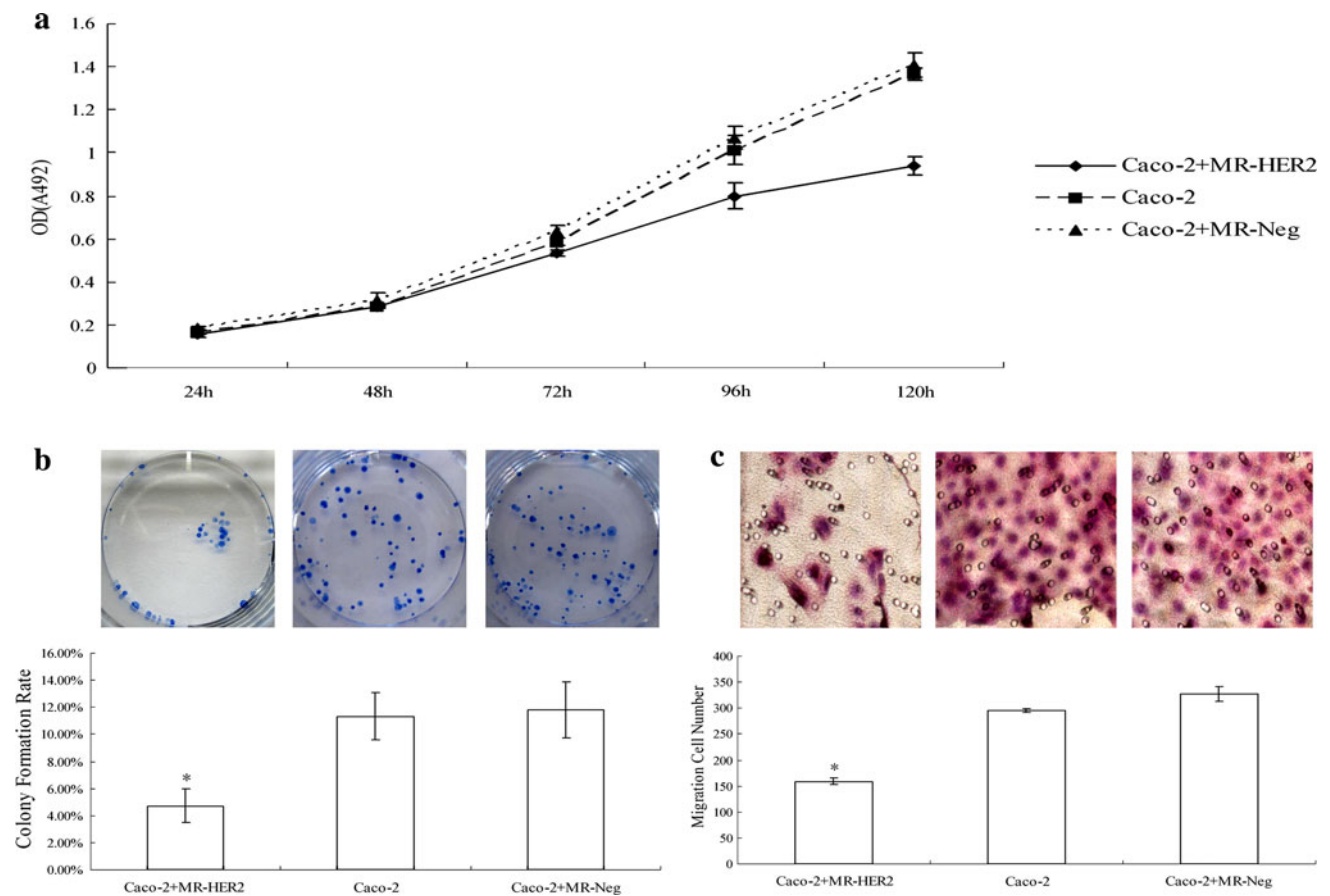


Fig. 5 Proliferation and migration of Caco-2 cells after RNA interference. **a** The proliferation curve. Compared with the two control groups, $P < 0.05$. **b** Colony formation rate. *Compared with the two control groups, $P < 0.05$. **c** Migrating cell number. *Compared with the two control groups, $P < 0.05$ (HE, $\times 200$ magnification)

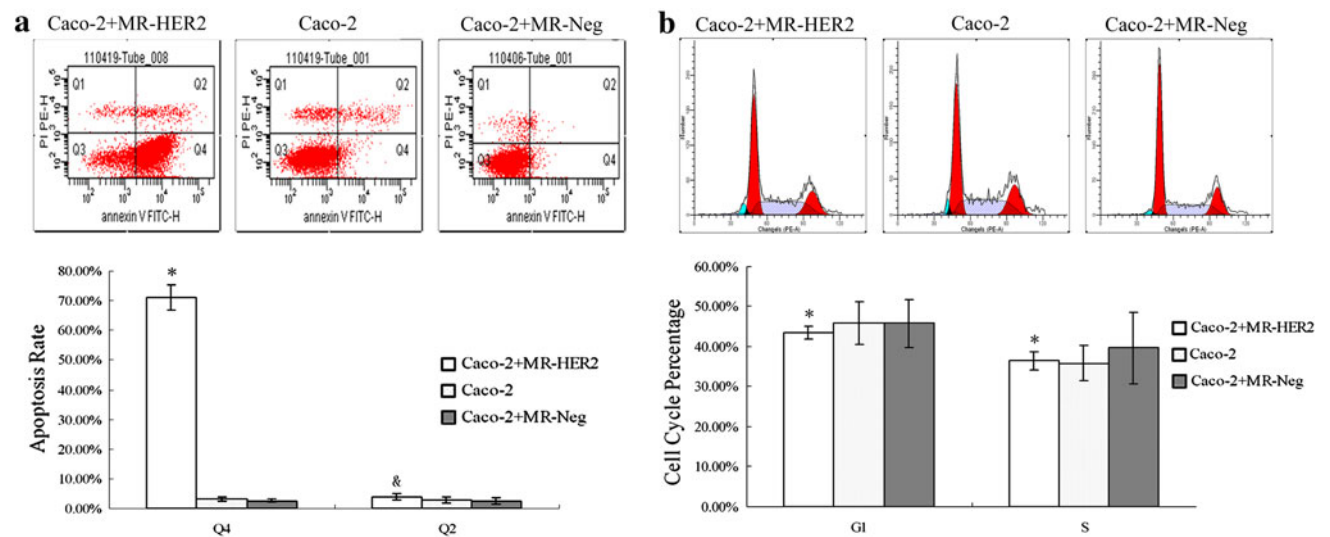


Fig. 6 Apoptosis and cell cycle of Caco-2 cells after RNA interference. **a** Apoptosis rate. *Compared with the two control groups, $P < 0.05$. &Compared with the two control groups, $P > 0.05$. **b** Cell cycle percentage. *Compared with two control groups, $P > 0.05$

emerged as an important regulator of widely divergent cellular processes, including proliferation, apoptosis, differentiation, and metabolism [27]. However, it remains

largely unknown whether specific “effectors” regulated by HER2 ultimately contribute to its tumorigenic effects. There is substantial evidence that the PI3K/Akt signaling

pathway is important in oncogenic transformation and cancer progression, and it has been linked with FASN expression in cancer cells [17, 28]. Kumar-Sinha et al. [14] used a DNA microarray to compare and identify genes induced by HER2 in a mammary epithelial cell line with ectopic HER2 overexpression and in breast cancer cell lines derived from patients with different levels of HER2 expression. They found that HER2 overexpression activated FASN promotion and transcription and increased protein production and activity, whereas inhibitors of HER2, e.g. herceptin and CI-1003, attenuated the effect of HER2 on FASN expression. PI3K activity was thought to be the mediator of HER2 control of FASN expression, because LY294002, a known PI3K inhibitor, abrogated HER2-induced FASN protein production in HER2 overexpressing normal mammary epithelial and breast cancer cells. Thus, transcription of the FASN gene may be induced by HER2 via the PI3K/Akt pathway. Similarly, in our study, we confirmed that inhibition of HER2 expression by RNA interference suppressed FASN expression by Caco-2 cells via the PI3K/Akt signaling pathway, and further blocked the proliferation and migration of Caco-2 cells. This indicates that the “HER2–PI3K/Akt–FASN axis” previously described in breast cancer cells might also exist in colorectal cancer cells, and the axis could be crucially important in the carcinogenesis process of colorectal cancer.

In summary, our results are indicative of the presence of an axis among HER2, the PI3K/Akt signaling pathway, and FASN, and that this “HER2–PI3K/Akt–FASN axis” is crucially important in the carcinogenesis process of colorectal cancer. Elucidating the molecular link between the “HER2–PI3K/Akt–FASN axis” and malignant phenotype of colorectal cancer cells may be important to the development of molecularly targeted therapy against human colorectal cancer.

Acknowledgments This study was supported by the National Natural Science Foundation of China (30973475) and the Natural Science Foundation of Jiangsu Province, China (BK2008305). Lida Zhang, Xiaojin Yu, Xiaoqiang Tian, Yunlang Cai, Qiqiang Long, and Yinghui Lu also contributed to this study.

Conflict of interest The authors declare there is no conflict of interest.

References

- Jemal A, Siegel R, Ward E, Hao Y, Xu J, Murray T, Thun MJ (2008) Cancer statistics. *CA Cancer J Clin* 58(2):71–96
- Yarden Y, Sliwkowski MX (2001) Untangling the ErbB signaling network. *Nat Rev Mol Cell Biol* 2(2):127–137
- Davidson NE (2011) HER2-targeted therapies: how far we’ve come—and where we’ve headed. *Oncology (Williston Park)* 25(5):425–426
- Ménard S, Pupa SM, Campiglio M, Tagliabue E (2003) Biologic and therapeutic role of HER2 in cancer. *Oncogene* 22(42):6570–6578
- Corsi F, Fiandra L, De Palma C, Colombo M, Mazzucchelli S, Verderio P, Allevi R, Tosoni A, Nebuloni M, Clementi E, Prosperi D (2011) HER2 expression in breast cancer cells is downregulated upon active targeting by antibody-engineered multifunctional nanoparticles in mice. *ACS Nano* 5(8):6383–6393
- Porebska I, Harlozinska A, Bojarowski T (2000) Expression of the tyrosine kinase activity growth factor receptors (EGFR, ERB B2, ERB B3) in colorectal adenocarcinomas and adenomas. *Tumour Biol* 21(2):105–115
- LaBonte MJ, Wilson PM, Fazzino W, Russell J, Louie SG, El-Khoueiry A, Lenz HJ, Ladner RD (2011) The dual EGFR/HER2 inhibitor lapatinib synergistically enhances the antitumor activity of the histone deacetylase inhibitor panobinostat in colorectal cancer models. *Cancer Res* 71(10):3635–3648
- Kuhajda FP (2000) Fatty-acid synthase and human cancer: new perspectives on its role in tumor biology. *Nutrition* 16(3):202–208
- Wakil SJ (1989) Fatty acid synthase, a proficient multifunctional enzyme. *Biochemistry* 28(11):4523–4530
- Maier T, Jenni S, Ban N (2006) Architecture of mammalian fatty acid synthase at 4.5 Å resolution. *Science* 311(5765):1258–1262
- Kuhajda FP (2006) Fatty acid synthase and cancer: new application of an old pathway. *Cancer Res* 66(12):5977–5980
- Huang PL, Zhu SN, Lu SL, Dai ZS, Jin YL (2000) Inhibitor of fatty acid synthase induced apoptosis in human colonic cancer cells. *World J Gastroenterol* 6(2):295–297
- Huang CH, Tsai SJ, Wang YJ, Pan MH, Kao JY, Way TD (2009) EGCG inhibits protein synthesis, lipogenesis, and cell cycle progression through activation of AMPK in p53 positive and negative human hepatoma cells. *Mol Nutr Food Res* 53(9):1156–1165
- Kumar-Sinha C, Ignatoski KW, Lippman ME, Ethier SP, Chinnaiyan AM (2003) Transcriptome analysis of HER2 reveals a molecular connection to fatty acid synthesis. *Cancer Res* 63(1):132–139
- Menendez JA, Mehmi I, Verma VA, Teng PK, Lupu R (2004) Pharmacological inhibition of fatty acid synthase (FAS): a novel therapeutic approach for breast cancer chemoprevention through its ability to suppress Her-2/neu (erbB-2) oncogene-induced malignant transformation. *Mol Carcinog* 41(3):164–178
- Livak KJ, Schmittgen TD (2001) Analysis of relative gene expression data using real-time quantitative PCR and the 2(-Delta Delta C(T)) Method. *Methods* 25(4):402–408
- Vazquez-Martin A, Colomer R, Brunet J, Lupu R, Menendez JA (2008) Overexpression of fatty acid synthase gene activates HER1/HER2 tyrosine kinase receptors in human breast epithelial cells. *Cell Prolif* 41(1):59–85
- Migita T, Ruiz S, Fornari A, Fiorentino M, Priolo C, Zadra G, Inazuka F, Grisanzio C, Palescandolo E, Shin E, Fiore C, Xie W, Kung AL, Febbo PG, Subramanian A, Mucci L, Ma J, Signoretti S, Stampfer M, Hahn WC, Finn S, Loda M (2009) Fatty acid synthase: a metabolic enzyme and candidate oncogene in prostate cancer. *J Natl Cancer Inst* 101(7):519–532
- Menendez JA, Lupu R, Colomer R (2005) Targeting fatty acid synthase: potential for therapeutic intervention in her-2/neu-overexpressing breast cancer. *Drug News Perspect* 18(6):375–385
- Chiang CT, Way TD, Tsai SJ, Lin JK (2007) Diosgenin, a naturally occurring steroid, suppresses fatty acid synthase expression in HER2-overexpressing breast cancer cells through modulating Akt, mTOR and JNK phosphorylation. *FEBS Lett* 581(30):5735–5742

21. Grunt TW, Wagner R, Grusch M, Berger W, Singer CF, Marian B, Zielinski CC, Lupu R (2009) Interaction between fatty acid synthase- and ErbB-systems in ovarian cancer cells. *Biochem Biophys Res Commun* 385(3):454–459
22. Horiguchi A, Asano T, Asano T, Ito K, Sumitomo M, Hayakawa M (2008) Pharmacological inhibitor of fatty acid synthase suppresses growth and invasiveness of renal cancer cells. *J Urol* 180(2):729–736
23. Carvalho MA, Zecchin KG, Seguin F, Bastos DC, Agostini M, Rangel AL, Veiga SS, Raposo HF, Oliveira HC, Loda M, Coletta RD, Graner E (2008) Fatty acid synthase inhibition with Orlistat promotes apoptosis and reduces cell growth and lymph node metastasis in a mouse melanoma model. *Int J Cancer* 123(11):2557–2565
24. Liu H, Liu Y, Zhang JT (2008) A new mechanism of drug resistance in breast cancer cells: fatty acid synthase overexpression-mediated palmitate overproduction. *Mol Cancer Ther* 7(2):263–270
25. Marmor MD, Skaria KB, Yarden Y (2004) Signal transduction and oncogenesis by ErbB/HER receptors. *Int J Radiat Oncol Biol Phys* 58(3):903–913
26. Citri A, Yarden Y (2006) EGF–ERBB signalling: towards the systems level. *Nat Rev Mol Cell Biol* 7(7):505–516
27. Kandel ES, Hay N (1999) The regulation and activities of the multifunctional serine/threonine kinase Akt/PKB. *Exp Cell Res* 253(1):210–229
28. Wang HQ, Altomare DA, Skele KL, Poulikakos PI, Kuhajda FP, Di Cristofano A, Testa JR (2005) Positive feedback regulation between AKT activation and fatty acid synthase expression in ovarian carcinoma cells. *Oncogene* 24(22):3574–3582

Maintenance of Arachidonic Acid and Evidence of $\Delta 5$ Desaturation in Cats Fed γ -Linolenic and Linoleic Acid Enriched Diets

Luciano Trevizan · Alexandre de Mello Kessler ·
J. Thomas Brenna · Peter Lawrence ·
Mark K. Waldron · John E. Bauer

Received: 8 June 2011 / Accepted: 16 December 2011 / Published online: 12 January 2012
© AOCS 2012

Abstract Cats have limited $\Delta 6$ desaturase activity. However, γ -linolenate (GLA) feeding may by-pass the $\Delta 6$ desaturase step allowing arachidonate (ARA) accumulation via $\Delta 5$ -desaturation. Alternatively, high dietary linoleate (LNA) may induce limited $\Delta 6$ desaturase also resulting in ARA accumulation. Fatty acid profiles were determined after feeding high LNA, high GLA, or adequate LNA diets. Adult female cats ($n = 29$) were assigned to one of three groups and fed for 8 weeks. Plasma samples were collected at weeks 0, 2, 4 and 8 for plasma triacylglycerol (TAG), total cholesterol (TC), lipoprotein (LP), and plasma and red blood cell membrane phospholipid fatty acid determinations. Time, but no diet, effects were observed for TAG, TC, and LP fractions at weeks 2 and 4 with significant increases likely due to increased dietary fat. However, all values were within feline normal limits. The GLA diet resulted in increased dihomo- γ -linolenic acid (DGLA) and ARA as early as week

2, supporting a $\Delta 5$ desaturase. Further evidence of $\Delta 5$ desaturase was found at high dietary LNA with the appearance of a novel fatty acid, 20:3 $\Delta 7$, 11, 14, apparently formed via $\Delta 5$ desaturation and chain elongation of LNA. However, $\Delta 6$ desaturase induction at high dietary LNA concentration was not observed. Cats are able to maintain plasma and red blood cell ARA when fed a practical diet containing GLA using what appears to be an active $\Delta 5$ desaturase enzyme.

Keywords Δ Arachidonic acid · Dihomo- γ -linolenic acid · Red blood cell membranes · Phospholipid fatty acids

Abbreviations

ARA	Arachidonic acid
BCS	Body condition score
BMR	Body maintenance requirement
BW	Body weight
DGLA	Dihomo- γ -linolenic acid
EFA	Essential fatty acid
GC/MS	Gas chromatography/mass spectroscopy
GLA	γ -Linolenic acid
LNA	Linoleic acid
LP-C	Lipoprotein cholesterol
ME	Metabolizable energy
P/S	Polyunsaturated to saturated fatty acid ratio
PED	Pre-experimental diet
RBC	Red blood cell
TC	Total cholesterol
TAG	Triacylglycerol

L. Trevizan · A. de Mello Kessler
Department of Animal Science, Universidade Federal do Rio Grande do Sul, Porto Alegre, RS 91540-000, Brazil

L. Trevizan · J. E. Bauer (✉)
Comparative Nutrition Laboratory, Department of Small Animal Clinical Science, College of Veterinary Medicine and Biomedical Sciences, Texas A & M University, College Station, TX 77843, USA
e-mail: jbauer@cvm.tamu.edu

Present Address:

L. Trevizan
Laboratório de Ensino Zootécnico, Faculdade de Agronomia, Departamento de Zootecnia, UFRGS, Porto Alegre, RS, Brazil

J. T. Brenna · P. Lawrence
Cornell University, Ithaca, NY 14854, USA

M. K. Waldron
Nestlé Purina Pet Care, St Louis, MO, USA

Introduction

Most mammalian species readily convert linoleic acid (LNA) to arachidonic acid (ARA) utilizing enzyme steps

including $\Delta 6$ desaturation, chain elongation, and $\Delta 5$ desaturation [1]. By contrast, early evidence in cats showed that this species lacked sufficient $\Delta 6$ desaturase activity for this purpose concluding that a dietary source of ARA was necessary for this species [2–5]. Cats fed diets adequate in LNA but deprived of ARA, showed dry, lusterless hair coats, dandruff, behavioral infertility, and hepatic lipid infiltration [2]. A series of studies [2, 3, 6–8] ultimately demonstrated essential fatty acid (EFA) deficiency pointing to the absence of $\Delta 6$ desaturase even though cats had been fed the requisite LNA and α -linolenic acid (ALA) [9].

Further studies involving EFA metabolism of cats were conducted by Sinclair et al. [10] in which an EFA deficient diet was fed using hydrogenated beef tallow. These workers found evidence of Mead acid (i.e. 20:3 $\Delta 5$, 8, 11) even though earlier work had not detected it [3, 4]. It was also noted that, although EFA-deficient rats accumulated Mead acid as a result of $\Delta 6$ and $\Delta 5$ desaturase activities [11], this would likely not occur in feline species because of the limited activity of the $\Delta 6$ desaturase enzyme. Instead, it was hypothesized that the accumulation of Mead acid would more likely be the result of chain elongation of oleic acid followed by $\Delta 8$ and $\Delta 5$ desaturation. However, Frankel and Rivers did not find any evidence of $\Delta 5$ desaturase and no ARA accumulation after feeding a GLA enriched diet [7]. In a following study, however, Sinclair et al. supplemented cats with GLA and reported an increase in ARA as well as the presence of an unknown non-methylene interrupted eicosatrienoic acid that they identified as 20:3 $\Delta 5$, 11, 14. Thus it was concluded that the $\Delta 5$ desaturase was operable in cats [1].

More recently, studies using GC/MS and stable isotope techniques have provided support for the presence of detectable amounts of both $\Delta 6$ and $\Delta 5$ desaturase products in feline liver [12]. In view of the above findings, given the likelihood of a feline $\Delta 5$ desaturase, it was hypothesized, that feeding cats a diet enriched in γ -linolenic acid (GLA) may be a practical way to provide precursors for ARA synthesis via by-passing the limited $\Delta 6$ desaturase step.

Because of the presence of small amounts of $\Delta 6$ desaturase in cats, an additional hypothesis in the present work was that high dietary amounts of LNA with minimal ARA would induce a constitutively low $\Delta 6$ desaturase activity in feline species and thus allow for ARA accumulation as a possible alternative. This question was based on the finding that Pawlosky et al. observed more labeled ARA in cats fed a diet enriched in LNA that was nearly devoid of ARA compared to a commercial dry, extruded diet that contained increased ARA (LNA/ARA ratios of approximately 580 vs. 43 respectively [12]). They attributed their finding to demonstrable $\Delta 6$ desaturation and we therefore wished to test whether it could be induced using a high LNA, low ARA diet.

Materials and Methods

Animals and Diets

Twenty-nine adult, sexually intact female cats ranging in age between 1.5 and 2 years with body weights (BW) between 2.4 and 6.0 kg were used. Cats were individually maintained in kennels according to the American Physiological Society Guidelines for Animal Research, and the protocols were approved by Texas A & M University Animal Care and Use Committee. The cats were assessed to be clinically normal prior to entering the study as indicated by complete blood counts, serum biochemistry profiles, and physical examination. The animals were randomly assigned to one of three groups according to diet fed; high linoleic acid (HL, $n = 9$), formulated with LNA-rich safflower oil; low linoleic acid (LL, $n = 10$), in which safflower oil was replaced by coconut oil to reduce LNA to only adequate levels, and high γ -linolenic acid (GLA, $n = 10$), formulated to contain adequate LNA plus an enriched borage oil containing 70% GLA. The diets were similar in all respects except for fatty acid composition (Table 1). The expected nutrient compositions of the diets were: 35% protein, 18% fat, 7.5% ash, 8% moisture, and 2% crude fiber. The experimental diets were formulated to be complete and balanced in order to meet or exceed minimal nutrient requirements established for adult cats [13, 14] and manufactured by Nestlé Purina PetCare (Saint Louis, MO). Analyses of the diets were performed by Nestlé Purina Laboratories and results were within expected analytical variance for the above targets (Table 2).

Cats were fed according to their individual metabolic body weights ($100 \text{ kcal ME} \times (\text{BW}_{\text{kg}}^{0.67}/\text{day})$) and to maintain a body condition score (BCS) of 5 out of 9 [18]. The cats consumed a pre-experimental diet (PED, Kit N Kaboodle[®], Nestle-Purina Pet Care, minimums, 30% protein and 8% fat; and maximums, 12% moisture and 4.5% crude fiber) for 4 weeks prior to the start of the trial then fed the experimental diets for 8 weeks (see Table 1 for the fatty acid profile of the PED).

Prior to the experimental period, daily food consumption of the PED was measured and determined to be generally sufficient to maintain the animal's body weight at BCS 5. Cat BW and BCS were determined weekly during this time and the cats were allowed to play with paper bags to provide physical activity. The controlled dietary amounts fed and the stimuli to play helped them maintain BCS of 5 and with minimal changes in body weights. In a few cases cats with BCS >5 were provided a reduced calorie allowance to ($80 \text{ kcal ME} \times (\text{BW}_{\text{kg}}^{0.67}/\text{day})$). These animals were maintained in this fashion during the PED period until reaching the desired BCS 5. The animals were fed once daily and food consumption and BMR (Body Maintenance Energy

Table 1 Experimental diet fatty acid profiles

Fatty acid	Diet (g/kg diet as-fed)			
	PED ^a	GLA ^b	HL ^c	LL ^d
<i>Saturated fatty acids</i>				
6:0	nd	0.3	<0.1	0.3
8:0	nd	4.8	1.9	5.0
10:0	nd	4.2	1.9	4.2
12:0	nd	35.0	13.9	36.2
14:0	2.5	14.9	6.4	15.4
15:0	0.4	<0.1	<0.1	<0.1
16:0	25.6	25.3	24.4	24.8
17:0	1.0	0.2	0.2	0.2
18:0	16.8	7.9	7.7	7.6
20:0	0.5	0.2	0.4	0.2
22:0	nd	nd	0.3	nd
24:0	nd	0.2	0.2	0.2
<i>Monounsaturated fatty acids</i>				
14:1	nd	0.2	nd	0.2
16:1n-7	2.7	3.8	3.8	3.7
17:1	0.5	<0.1	<0.1	<0.1
18:1n-9	39.4	31.2	38.6	30.6
18:1n-7	6.0	1.0	2.0	1.5
18:1 isomers	nd	1.1	0.2	0.3
20:1n-11	nd	0.2	0.4	0.2
24:1n-9	nd	nd	0.3	nd
<i>n-6 Polyunsaturated fatty acids</i>				
18:2n-6	22.5	18.5	59.8	17.3
18:2 isomers	<0.1	0.3	0.5	0.2
18:3n-6	<0.1	3.5	0.2	<0.1
20:2n-6	nd	<0.1	<0.1	<0.1
20:3Δ7,11,14	nd	nd	nd	nd
20:3Δ8,11,14	nd	<0.1	<0.1	<0.1
20:4n-6	0.26	0.28	0.29	0.29
22:4n-6	nd	nd	nd	nd
<i>n-3 Polyunsaturated fatty acids</i>				
18:3n-3	1.1	1.3	1.7	1.2
18:4n-3	0.5	<0.1	<0.1	<0.1
20:5n-3	nd	<0.1	<0.1	<0.1
22:5n-3	nd	<0.1	<0.1	<0.1
22:6n-3	nd	<0.1	<0.1	<0.1
UI	nd	1.0	1.1	1.0
Total amount	122.1	156.2	166.1	151.5

Values are the means of duplicate determinations

nd not detected, UI unidentified fatty acids

^a Commercial cat food; Kit N Kaboodle[®], Nestle-Purina Pet Care)

Fat types as follows: ^b Borage oil (γ-linolenic acid 70%) plus coconut oil; ^c Safflower oil; ^d Coconut oil

Requirement (kcal ME)/BW_{kg}^{0.67} day) were recorded daily after 24 h and averaged weekly for statistical analysis. These latter data allowed an allometric factor to be

Table 2 Experimental diet nutrient profiles

Nutrient	Diet (g/kg dry matter)		
	GLA ^a	HL ^b	LL ^c
Crude Protein	346	355	349
Nitrogen-free extract	378	351	378
Fiber	21	18	20
Ash	71	77	70
Fat	185	199	182
Energy, ME kcal/kg ^d	4,417	4,316	4,327

The diets are designated as described in the text. The dry, extruded-type diets were manufactured by Nestlé-Purina Petcare. Diet ingredients (by weight): Brewers milled rice, 35.9%; Soybean protein isolated, 23.3%; Chicken whole carcass and parts, 21.6%; Soybean hulls, 3.67%; Dicalcium phosphate, 2.93%; Coconut oil, 2.80%; Flavor coating, 1.5%; Beef tallow, 0.7%; Potassium chloride, 0.65%; Mineral premix, 0.34%; Choline chloride, 0.32%; Calcium carbonate, 0.29%; Sodium chloride, 0.22%; DL-methionine, 0.18%; Taurine, 0.1%; Vitamin premix, 0.07%; Vitamin E (50%), 0.03%. Vitamin premix contents: 146.32 g/kg nicotinic acid, 10.35 g/kg vitamin A acetate, 90 g/kg DL-α-tocopherol acetate, 84 mg/kg cholecalciferol, 52 g/kg thiamine mononitrate, 51.06 g/kg calcium D-pantothenate, 24.4 g/kg riboflavin, 14.52 g/kg pyridoxine hydrochloride, 6 g/kg folic acid, 508 mg/kg menadione sodium bisulfite, 93 mg/kg vitamin B-12, and 36.8 mg/kg biotin. Mineral mix contents: 65 g/kg zinc as zinc sulfate, 39 g/kg iron as ferrous sulfate, 18.25 g/kg manganese as manganese sulfate, 3.2 g/kg copper as copper sulfate, 651 mg/kg iodine as calcium iodate, and 50 mg/kg selenium as selenium selenite. The remaining percent of each diet were consisted of three dietary oils: Coconut oil, 5.58% in LL diet and Safflower oil, 5.24% in HL diet, which provided the desired fatty acid profiles, Coconut oil 4.85% and Borage oil at 70% GLA, 0.5%. Values are the means of duplicate determinations

^a Borage oil (γ-linolenic acid 70%) plus coconut oil

^b Safflower oil

^c Coconut oil

^d Value obtained by digestibility analyses

calculated for each animal. Individual allometric factors were used to calculate the amount to feed each cat during the subsequent experimental period to maintain a BCS of 5. This allowed each animal to be fed to maintain its ideal body weight and condition. Because of individual variation in caloric needs among outbred cat colonies, individualized feeding was necessary.

Blood Sample Collection and Analyses

Blood samples were obtained from each cat by venipuncture at weeks 0, 2, 4 and 8 during the experimental period. Food had been withheld for 12 h and 7 ml of blood were drawn from a saphenous vein into EDTA-containing tubes. At week 0, complete blood counts and plasma biochemistry profiles were evaluated. Blood samples were centrifuged at 1,800×g for 15 min and plasma was separated from red blood cells (RBC) and frozen at −80 °C in small aliquots

for subsequent analysis. Packed RBC were kept on ice for immediate RBC membrane ghost preparation. The cells were washed with isotonic saline and lysed with deionized water, followed by a sequence of slow speed centrifugation and deionized water washes to isolate membranes. The membranes were suspended in 10 mM phosphate buffer, pH 7.2, and stored at -80°C . Total lipids were then extracted from both plasma and RBC membranes [15]. Total plasma phospholipid fractions were separated by thin layer chromatography, scraped from the plates, and transmethylated to yield fatty acid methyl esters for analysis via gas chromatography [15]. Although some minor fatty acid components in the chromatograms remained unidentified, most of these occurred in samples obtained at week 0 at the start of the feeding study. Nonetheless, identification of all fatty acids including any unique fatty acids eluting in the region between GLA and ARA on the chromatograms were specifically identified using authentic standards and confirmed, when necessary, using covalent adduct chemical ionization gas chromatography/mass spectrometry (CAGC/MS) [16].

Fatty acid data are presented in mol%. Earlier studies in numerous species including cats have found that RBC membrane phospholipid content is unaffected by dietary fat type [17–21]. Also, plasma phospholipid and RBC membrane fatty acids represent similar pools because transfer and exchanges between plasma and RBC membranes are likely the major source of fatty acid enrichment between these two pools in the circulation. Thus it was anticipated that should similar findings between plasma PL and RBC membrane fatty acid profiles occur, they could be readily compared and thus better address the proposed hypotheses in this investigation.

Plasma triacylglycerol (TAG) and total cholesterol (TC) concentrations were determined using enzymatic methods [22]. Lipoprotein cholesterol distributions (LP-C) were determined using freshly isolated plasma via 1% agarose gel electrophoresis and quantified by scanning densitometry [22].

Digestibility Assays

All cats were used for apparent digestibility determinations during week 6 of the feeding period. Complete fecal samples were individually collected twice a day for 5 consecutive days, pooled for each cat, and frozen at -40°C . All samples and diets, were sent to the Nestlé Purina Petcare Laboratory, Saint Louis, for analysis. The parameters evaluated were coefficients of apparent digestibility of crude protein, total fat, crude fiber, ash, and gross energy. The coefficient for digestible energy (DE) and metabolizable energy (ME) were calculated based on DE and urinary loss [13].

Data Analysis

Values presented are means \pm SEM. All data except for the normative BCS data were found to be normally distributed by the Shapiro–Wilks test. The BCS data were analyzed by the nonparametric Kruskal–Wallis one-way ANOVA (SAS 9). Digestibility coefficients were analyzed for main diet and time effects, and diet \times time interactions using Proc GLM ANOVA by SAS ($P < 0.05$). For the other data, statistical significance was determined using repeated measures ANOVA for diet, time, and diet \times time interactions for the following plasma parameters including plasma TAG, TC, LP-C, total phospholipid fatty acid profile, RBC membrane fatty acid profile, food consumption, body weight, and allometric metabolizable energy factor using Proc Mixed by SAS ($P < 0.05$). For all parameters Tukey's multiple comparison of means was performed where appropriate, with the P value set at <0.05 .

Results

Food and Metabolic Energy Consumption

All cats readily consumed the diets when offered and all food was consumed within 4 h. No diet refusals were observed. Diet effects were not observed for either the average weekly energy consumption or amounts of food (g) consumed ($P = 0.77$). A significant time effect for average weekly energy consumption was seen between week 0 and week 5 ($P = 0.05$) (Fig. 1). It should be noted, however, that although the energy densities of the experimental diets were similar, the PED contained less energy per kg (3,200 kcal/kg). Thus, the amount of PED food consumed was higher at week 0 when compared to week 8 ($P = 0.005$) after the experimental diets had been fed.

Body Weights and Body Condition Scores

The cats showed a modest but statistically significant weight loss from week 1 to 8 (overall time effect ($P = 0.0001$)) (Fig. 1) but no changes in BCS were observed (data not shown). The animals' body maintenance requirement (i.e. allometric energy factor) remained stable ($P = 0.14$) except for some minor variation when comparing week 0 to the other time periods ($P < 0.0003$) (Fig. 1).

Plasma TAG, TC, and Lipoprotein Cholesterol Distributions

Time effects but no diet effects were seen for all plasma lipid concentrations. All lipid values were increased at week 4 yet remained within the normal range for adult cats.

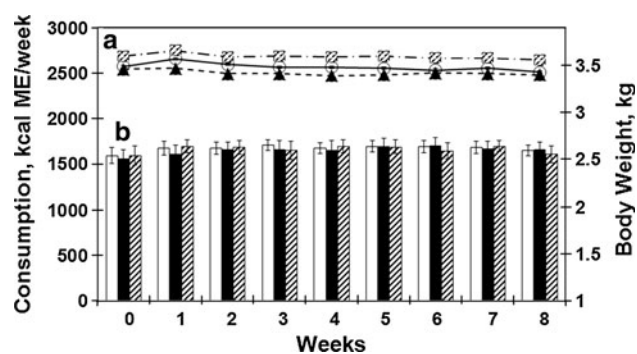


Fig. 1 Average weekly food consumption (left axis, bars) and body weights (right axis, lines) of cats fed the experimental diets. Open bars and symbols GLA diet; closed bars and symbols HL diet; Cross-hatched bars and symbols LL diet. *a* indicates a significant difference in average weekly consumption at week 0 compared to the other weeks by repeated measures ANOVA, $P < 0.05$. *b* indicates a significant difference between week 0 and 5 overall by repeated measures ANOVA, $P < 0.05$

Plasma TC was maximally elevated at week 4 as was the α -LP-C (α -LP-cholesterol) fraction. This fraction was responsible for most of the total plasma cholesterol elevation although the other LP fractions also contributed to a lesser extent to this increase over time (Table 3). The pre- β -LP-C followed a similar pattern with a maximal value achieved at week 2 remaining at week 4 and decreasing thereafter to its initial level at week 8. The β -LP-C fraction also increased but, in this case, remained elevated at week 8 unlike the other LP-C fractions. No diet effect was observed for plasma TAG ($P = 0.25$), but concentrations were significantly different over time ($P = 0.04$) (Table 3). Feeding the experimental diets resulted in statistically significant higher TAG concentrations over baseline values at week 4 which decreased to baseline at week 8 but these elevations were of small magnitude.

Plasma Phospholipid Fatty Acids

Numerous time effects were observed reflecting the fatty acid contents of the experimental diets versus baseline.

However, where diet \times time interactions occurred, additional ANOVA were performed to identify reasons for the differences (Table 4). Compared to the HL diet, both GLA and LL diets resulted in a statistically significant accumulation of 14:0 at weeks 2 and 4 and this increase was maintained at week 8 with the LL diet. Increases in 16:1n-7 were seen with time for all diets and the LL group was higher than GLA and HL groups at all sample times. Increased LNA was found with the HL and LL diets at week 2 which remained elevated throughout the study compared to the GLA diet which showed no change in this fatty acid.

The GLA diet measurably affected 18:3n-6 concentrations. At week 2, this fatty acid increased from 0.26 to 0.82 mol% then slowly decreased but remained significantly higher compared to baseline values. These values were also statistically different compared to the HL and LL diets at all subsequent times. Furthermore, amounts of dihomo- γ -linolenic (DGLA, 20:3 Δ 8, 11, 14) were also significantly elevated with the GLA diet compared to the other groups increasing by more than 5 times at week 2 (i.e. from 1.43 to 7.43 mol%) and continuing to increase to nearly 7 times basal values (9.80 mol%) at week 8. By contrast, amounts of DGLA in the other two groups remained at approximately 1 mol% at all times. It is noteworthy that after week 2, relative amounts of 18:3n-6 decreased at the same time as DGLA increased.

Differences in ARA contents with diet were also observed even though all dietary concentrations were identical. When the GLA diet was fed, ARA was maintained at baseline values while amounts seen in the other two groups were decreased. As such, statistically significant differences were seen at weeks 2, 4 and 8 when the GLA group was compared to the HL group with LL diet fed cats showing intermediate values. The HL diet resulted in decreased plasma PL ARA at all sample times compared with baseline values (approximately 4 vs. 6.8 mol% at baseline). The LL diet also resulted in decreased ARA at week 2 but values recovered somewhat thereafter yet trended downward. It is especially noteworthy that the HL

Table 3 Plasma lipid and lipoprotein-cholesterol concentrations in adult cats during the experimental period

Source	Diet (mg/dL)				Time (week)					Diet versus time P value
	GLA	HL	LL	P value	0	2	4	8	P value	
β -LP-C	21 \pm 1.3	24 \pm 1.7	22 \pm 1.4	0.6860	14 \pm 2.0 ^a	24 \pm 1.3 ^b	27 \pm 2.2 ^b	25 \pm 1.7 ^b	0.0001	0.8445
Pre- β -LP-C	29 \pm 2.1	27 \pm 1.8	31 \pm 1.8	0.5001	25 \pm 2.8 ^a	36 \pm 1.9 ^b	32 \pm 3.0 ^b	24 \pm 2.4 ^a	0.0001	0.4161
α -LP-C	108 \pm 5.8	107 \pm 4.9	108 \pm 6.6	0.9740	81 \pm 4.9 ^a	91 \pm 4.8 ^a	138 \pm 7.8 ^b	122 \pm 8.3 ^c	0.0001	0.5349
Total Cholesterol	158 \pm 7.7	157 \pm 6.5	162 \pm 8.1	0.9586	119 \pm 7.7 ^a	151 \pm 7.3 ^b	196 \pm 9.8 ^c	170 \pm 10.0 ^d	0.0001	0.4002
Triglycerides	25 \pm 1.3	21 \pm 0.8	24 \pm 1.2	0.2452	24 \pm 1.6 ^{a, b}	24 \pm 1.8 ^{a, b}	25 \pm 1.7 ^a	21 \pm 1.5 ^b	0.0372	0.7182

Values are means \pm SEM. GLA (diet $n = 9$), HL diet ($n = 10$) and LL diet ($n = 9$)

Means in a row with superscripts not in common differ, $P < 0.05$. No significant difference was found for diet \times time interactions

Table 4 Cat plasma phospholipid fatty acids (mol%)

Fatty Acid	GLA			HL			LL			Overall SEM	
	Wk 0	Wk 2	Wk 4	Wk 0	Wk 2	Wk 4	Wk 0	Wk 2	Wk 4		Wk 8
	Wk 0	Wk 2	Wk 4	Wk 0	Wk 2	Wk 4	Wk 0	Wk 2	Wk 4		Wk 8
<i>Saturated fatty acids</i>											
12:0	<0.1	<0.1	<0.1	<0.1	<0.1	<0.1	<0.1	<0.1	<0.1	<0.1	<0.1
14:0	0.27 ^{a,1}	0.60 ^{b,1,2}	0.52 ^{b,1,2}	0.16 ^{a,1}	0.36 ^{a,2}	0.31 ^{a,2}	0.32 ^{a,1}	0.65 ^{b,1}	0.67 ^{b,1}	0.51 ^{b,1}	0.05
15:0	0.15	0.13	0.08	0.09	0.12	0.12	0.07	0.10	0.11	0.06	0.02
16:0	14.3	14.9	14.7	13.0	14.8	14.4	12.7	13.3	15.8	13.9	0.56
17:0	0.72	0.47	0.38	0.70	0.30	0.37	0.30	0.68	0.33	0.32	0.04
18:0	29.0	28.0	29.3	29.2	27.7	27.9	26.8	28.5	27.2	27.2	0.66
20:0	0.96	0.74	0.75	0.87	0.96	1.00	1.07	0.88	0.72	0.68	0.07
22:0	0.68	0.40	0.60	0.67	0.52	0.67	0.70	0.57	0.44	0.56	0.06
24:0	0.88 ^a	0.65 ^b	1.10 ^{a,b}	0.93 ^a	0.73 ^b	0.81 ^{a,b}	0.96 ^{a,b}	0.95 ^a	0.60 ^b	0.81 ^{a,b}	0.03
<i>Monounsaturated fatty acids</i>											
16:1n-7	0.39 ^{a,1}	0.62 ^{b,1,2}	0.53 ^{a,1,2}	0.35 ^{a,1}	0.49 ^{b,1}	0.44 ^{b,1}	0.44 ^{b,1}	0.43 ^{a,1}	0.78 ^{b,2}	0.61 ^{b,2}	0.04
17:1	0.05	0.06	0.04	0.06	0.03	0.04	0.03	0.05	0.06	0.04	0.03
18:1n-9	10.8	8.76	8.83	10.7	8.03	7.68	8.52	11.2	9.58	8.86	0.15
18:1n-7	2.34 ^a	2.14 ^{a,b}	2.02 ^{a,b}	2.19 ^a	2.21 ^a	2.27 ^a	2.10 ^a	2.58 ^a	2.55 ^{a,b}	2.15 ^{a,b}	0.30
20:1n-9	0.41	0.42	0.32	0.40	0.39	0.45	0.49	0.44	0.32	0.38	0.04
24:1n-9	1.09	0.75	1.00	1.21	0.93	1.36	1.41	1.19	0.73	0.93	0.11
<i>n-6 Polyunsaturated fatty acids</i>											
18:2n-6	23.8 ^{a,1}	22.8 ^{a,1}	20.5 ^{a,1}	26.0 ^{a,1}	32.2 ^{b,2}	31.9 ^{b,2}	34.0 ^{b,2}	25.6 ^{a,1}	29.2 ^{b,2}	28.3 ^{a,b,2}	0.86
18:3n-6	0.26 ^{a,1}	0.82 ^{b,1}	0.67 ^{b,c,1}	0.21 ^{a,1}	<0.01	<0.01	0.02 ^{a,2}	0.20 ^{a,1}	0.17 ^{a,1}	0.04 ^{a,2}	0.05
20:2n-6	0.66 ^{a,1}	0.52 ^{a,1}	0.55 ^{a,1}	0.66 ^{a,1}	0.89 ^{b,2}	1.02 ^{b,2}	1.24 ^{c,2}	0.65 ^{a,1}	0.64 ^{a,1,2}	0.83 ^{a,1,2}	0.06
20:3Δ7,11,14	0.61 ^{a,1}	0.57 ^{a,1}	0.52 ^{a,1}	0.73 ^{a,b,1}	0.67 ^{a,b,1}	0.66 ^{b,1,2}	0.80 ^{a,2}	0.72 ^{a,1}	0.73 ^{a,1}	0.82 ^{a,2}	0.05
20:3Δ8,11,14	1.43 ^{a,1}	7.43 ^{b,2}	8.45 ^{c,2}	0.97 ^{a,1}	0.92 ^{a,1}	0.99 ^{a,1}	1.03 ^{a,1}	1.04 ^{a,1}	1.42 ^{a,1}	1.68 ^{a,1}	0.18
20:4n-6	6.63 ^{a,1}	5.79 ^{a,1}	6.10 ^{a,1}	6.78 ^{a,1}	4.34 ^{b,1}	4.23 ^{b,2}	4.14 ^{b,2}	6.84 ^{a,1}	5.06 ^{b,1}	5.38 ^{a,b,1,2}	0.35
22:4n-6	1.11 ^a	0.51 ^b	0.59 ^b	1.13 ^a	0.50 ^b	0.52 ^b	0.73 ^b	1.11 ^a	0.47 ^b	0.55 ^b	0.03
<i>n-3 Polyunsaturated fatty acids</i>											
18:3n-3	0.23	0.29	0.30	0.26	0.23	0.28	0.24	0.24	0.32	0.41	0.04
20:5n-3	0.37	0.31	0.14	0.35	0.04	0.08	0.02	0.45	0.16	0.27	0.04
22:5n-3	0.51	0.30	0.56	0.63	0.34	0.41	0.36	0.55	0.37	0.56	0.02
22:6n-3	1.18 ^a	0.74 ^b	0.71 ^b	1.29 ^a	0.58 ^b	0.73 ^b	0.54 ^b	1.26 ^a	0.63 ^b	0.56 ^b	0.04

Mean values and overall SEM

GLA diet ($n = 9$), HL diet ($n = 10$) and LL diet ($n = 9$); superscript letters not in common in a row within a diet group indicate a significant difference between weeks by ANOVA, $P < 0.05$ and superscript numbers not in common in a row within a week indicate a significant difference between diets by ANOVA, $P < 0.05$

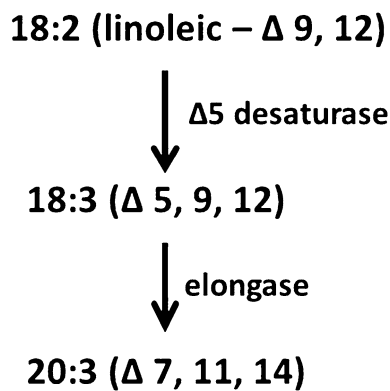


Fig. 2 Summary of the pathway involving Δ5 desaturase for the production of 20:3 Δ7, 11, 14 eicosatrienoic acid from linoleic acid in feline species

diet also showed statistically significant increases of 20:2 Δ11, 14 at weeks 2, 4 and 8 and of 20:3 Δ7, 11, 14 at week 8 compared to the GLA diet at all sample times. The presence of this latter fatty acid was verified by analysis of 8 separate samples from cats in the HL group by CACI-GC-MS/MS. Thus the identity of the peak corresponding to this fatty acid was 20:3 Δ7, 11, 14. One possible pathway for its production from LNA may be Δ5 desaturation followed by elongation (Fig. 2). No 18:3 Δ5, 9, 12 was observed.

Other differences observed were increased amounts of plasma PL LNA in the LL group compared to the GLA group even though both groups contained similar amounts of LNA. Also, depletion of EPA and DHA was observed in all groups during the feeding period; none of the diets contained any appreciable amounts of these fatty acids.

Red Blood Cell Membrane Fatty Acids

As with the plasma PL fatty acid profiles, RBC membrane fatty acids were similarly affected (Table 5). Small, statistically insignificant amounts of 12:0 were found in cats fed the GLA and LL diets both of which contained medium chain fatty acids from coconut oil. Linoleic acid increased in the HL group, achieved maximal values at weeks 2 and 4, then returned to baseline thereafter. Even though ARA concentrations of all experimental diets were identical, differences in this fatty acid were again observed with both the HL and LL diets compared to baseline while ARA values of cats fed the GLA diet were maintained. As expected, the GLA-enriched diet promoted a measurable increase of GLA in the RBC membranes as early as week 2 and also thereafter. In addition, dramatic increases of DGLA were also seen with this diet. Furthermore the GLA diet resulted in increased membrane ARA at week 2 and thereafter compared with the other two diets where decrements were observed. The HL diet again resulted in

significantly higher amounts of 20:3 Δ7, 11, 14 at weeks 4 and 8 compared to the GLA diet group. A significant increase of RBC membrane 20:2 Δ11, 14 was also found with the HL diet at week 4 but not at the other times.

Diet Digestibilities

For all parameters tested, only total fat digestibilities were different among diets ($P = 004$). The HL (92.2%) was significantly different than GLA (94.3%) and LL diets (93.2%).

Discussion

All experimental diets resulted in similar amounts of food consumed, BW, allometric energy factor, and BCS. Food intake during week 0 was somewhat different from the subsequent values because the first week of feeding was used for adaptation to the experimental diets which, for cats, generally requires 4–5 days [13]. After eliminating week 0 values in the analysis, neither time nor diet effects were observed except for a modest decrease in body weight. This latter finding was expected because all cats had been fed to achieve a BCS of 5 out of 9 and began the study at a moderately higher score. The allometric energy factor found for all cats under these maintenance conditions was approximately the same as has been described for adult, intact females in other studies at 104.1 ± 2.8 kcal/(kg body weight)^{0.75} [14].

Plasma TAG, TC and lipoprotein fractions similarly showed no diet effects. However, time effects were observed which were likely due to the increased amount of crude fat present in the experimental diets compared to the PED (i.e. approximately 190 g/kg crude fat in the experimental diets vs. about 130 g/kg crude fat in PED on a dry matter basis). Because cats and dogs primarily transport lipids in circulation via high density lipoprotein fractions [23, 24] the increase in the α-LP-C fraction (i.e. high density lipoprotein cholesterol) observed was consistent with that previously seen in dogs fed higher fat diets. Such partitioning of cholesterol is considered to be protective against atherosclerotic diseases in feline and canine species [23, 24].

Diet effects were clearly observed in the plasma PL and RBC membrane fatty acid fractions. Although two of the diets contained medium chain triacylglycerols, accumulation of shorter chain fatty acids in these fractions was not expected. The reason for this is that long chain fatty acids are generally more readily incorporated due to acyl specificity of the fatty acid synthetase for long chain fatty acids during triacylglycerol esterification [25]. Thus, only small amounts of the shorter chain components were seen.

Table 5 Red blood cell membrane fatty acids during the study (mol%)

Fatty acid	GLA				HL				LL				Overall SEM
	Wk 0		Wk 8		Wk 0		Wk 8		Wk 0		Wk 8		
	Wk 0	Wk 2	Wk 4	Wk 8	Wk 0	Wk 2	Wk 4	Wk 8	Wk 0	Wk 2	Wk 4	Wk 8	
<i>Saturated fatty acids</i>													
12:0	0.01	0.07	0.07	0.11	0.01	0.03	<0.1	0.03	0.01	0.07	0.07	0.08	0.02
14:0	0.25 ^{a,1}	0.63 ^{b,1,2}	0.67 ^{b,2}	0.67 ^{b,1,2}	0.21 ^{a,1}	0.35 ^{a,b,1}	0.38 ^{b,1}	0.51 ^{b,1}	0.24 ^{a,1}	0.72 ^{b,2}	0.85 ^{b,2}	0.88 ^{b,2}	0.02
15:0	0.12	0.05	0.02	<0.01	0.15	0.04	<0.01	<0.01	0.14	0.05	<0.01	<0.01	0.02
16:0	20.2	22.1	21.7	20.1	20.2	20.6	21.3	20.2	19.5	23.4	22.9	21.1	0.86
17:0	0.73	0.51	0.43	0.62	0.71	0.73	0.50	0.92	0.61	0.58	0.48	0.37	0.11
18:0	16.3	14.9	15.8	17.9	16.8	14.2	16.5	17.3	15.8	15.7	16.6	17.1	0.55
20:0	0.61	0.49	0.39	0.27	0.54	0.48	0.45	0.43	0.52	0.73	0.49	0.28	0.04
22:0	0.95	0.77	0.57	0.79	0.91	0.71	0.66	0.79	0.85	0.94	0.65	0.64	0.08
24:0	1.05	1.47	1.32	1.29	0.71	1.20	1.12	1.48	0.96	1.48	1.37	1.63	0.15
<i>Monounsaturated fatty acids</i>													
16:1n-7	0.32	0.34	0.30	0.30	0.34	0.26	0.34	0.27	0.32	0.41	0.38	0.40	0.05
18:1n-7	3.20	3.17	2.68	2.35	2.91	2.85	2.79	2.96	3.02	4.24	2.99	2.55	0.31
18:1n-9	7.60	7.18	7.30	6.43	7.59	7.39	6.81	6.04	8.14	7.33	7.57	7.15	0.25
20:1n-9	0.55	0.41	0.47	0.33	0.53	0.53	0.51	0.39	0.62	0.55	0.48	0.37	0.04
24:1n-9	10.2	10.3	8.26	8.64	8.26	9.68	7.47	9.54	9.05	10.6	8.42	11.1	0.62
<i>n-6 Polyunsaturated fatty acids</i>													
18:2n-6	18.6 ^{a,1}	19.0 ^{a,1}	19.8 ^{a,1}	17.3 ^{a,1}	20.5 ^{a,1}	26.3 ^{b,2}	26.6 ^{b,2}	24.7 ^{a,b,2}	19.9 ^{a,1}	18.8 ^{a,1}	21.2 ^{a,1}	20.8 ^{a,1,2}	0.86
18:3n-6	0.06 ^{a,1}	0.44 ^{b,2}	0.47 ^{b,2}	0.62 ^{b,2}	0.03 ^{a,1}	0.08 ^{a,1,2}	0.03 ^{a,1}	0.19 ^{a,1,2}	0.06 ^{a,1}	0.07 ^{a,1}	<0.01	<0.01	0.07
20:2n-6	0.85 ^{a,1}	0.75 ^{a,1}	0.75 ^{a,1}	0.64 ^{a,1}	0.95 ^{a,1}	1.10 ^{a,b,2}	1.20 ^{b,2}	1.14 ^{a,b,2}	0.96 ^{a,1}	0.82 ^{a,1}	0.93 ^{a,1}	0.73 ^{a,1,2}	0.06
20:3A7,11,14	1.10	1.04	1.10 ¹	0.97 ¹	1.28	1.15	1.54 ²	1.55 ²	1.41	1.08	1.45 ^{1,2}	1.43 ^{1,2}	0.12
20:3A8,11,14	1.39 ^{a,1}	2.57 ^{b,1}	3.73 ^{c,1}	4.43 ^{d,1}	0.86 ^{a,1}	0.78 ^{a,2}	0.77 ^{a,2}	0.52 ^{a,2}	0.87 ^{a,1}	0.77 ^{a,2}	1.11 ^{a,2}	0.93 ^{a,2}	0.11
20:4n-6	11.4 ^{a,1}	10.4 ^{b,1}	12.1 ^{a,b,1}	13.4 ^{a,1}	11.1 ^{a,1}	8.90 ^{b,1}	9.56 ^{a,b}	8.35 ^{b,2}	11.6 ^{a,1}	8.47 ^{b,1}	10.2 ^{a,b,1}	10.5 ^{a,b,2}	0.56
22:4n-6	0.97	1.11	1.22	1.05	0.77	0.75	0.88	0.80	0.94	0.77	0.95	0.67	0.10
<i>n-3 Polyunsaturated fatty acids</i>													
18:3n-3	0.18	0.17	0.29	0.22	0.22	0.15	0.09	0.19	0.23	0.16	0.23	0.16	0.05
20:5n-3	0.31	0.15	0.20	0.09	0.37	0.10	0.08	0.17	0.41	0.19	0.33	0.22	0.06
22:5n-3	0.14	0.17	0.03	<0.01	0.26	0.11	0.04	<0.01	0.16	0.09	0.03	<0.1	0.04
22:6n-3	0.33	0.35	0.22	0.27	0.39	0.33	0.17	0.33	0.39	0.35	0.25	0.01	0.09

Mean values and overall SEM

GLA diet ($n = 9$), HL diet ($n = 10$) and LL diet ($n = 9$); superscript letters not in common in a row within a diet group indicate a significant difference between weeks by ANOVA, a $P < 0.05$ and superscript numbers not in common in a row within a week indicate a significant difference between diets by ANOVA, $P < 0.05$

Increased amounts of LNA in plasma PL and RBC membranes were found with the HL diet but accumulation of GLA was not observed. Although this latter fatty acid is generally presumed to be a short lived metabolite due to rapid chain elongation, its absence in the samples is also consistent with low $\Delta 6$ -desaturase in feline species. In addition, the increase in plasma PL and RBC membrane LNA suggests that dietary amounts of this fatty acid may have saturated the chain elongation step (yielding 20:2 $\Delta 11$, 14) resulting in a modest, yet significant, accumulation of LNA. Competition among substrates for chain elongation may explain, in part, why 20:2 $\Delta 11$, 14, a chain elongation product of LNA, was increased in cats fed the HL and LL diets but not when GLA was fed.

Although the GLA and LL diets contained similar amounts of LNA, plasma PL LNA was increased in the LL group compared to the GLA group. It should be noted that, in general, the P/S ratio of fatty acid profiles will often be nearly constant unless diets are dramatically different (e.g. total EFA deficiency). In the present study, calculated P/S ratios of the plasma PL fractions of the GLA and LL groups were 0.94 and 0.93 respectively. Furthermore, because the GLA group accumulated DGLA, LNA appears to have been substituted by this longer chain derivative and the total amounts of these two plasma PL fatty acids are approximately equivalent among all of the diet groups. It is unknown, however, whether there may have been any increased utilization of LNA when GLA was fed as this was not determined in this study.

The present work confirms the existence of an active $\Delta 5$ desaturase in cats as originally demonstrated by Sinclair et al. [1]. Sinclair et al. [10] also identified 20:3 $\Delta 5$, 11, 14 in feline RBCs and hypothesized that it was formed via chain elongation of 18:1 $\Delta 9$ and $\Delta 8$ desaturation to 20:2 $\Delta 11$, 14 with subsequent $\Delta 5$ desaturation. As such, they hypothesized that ARA might also be formed from LNA using both $\Delta 5$ and $\Delta 8$ desaturase systems. By contrast, in the current study, although 20:2 $\Delta 11$, 14 was observed, we identified the 20:3 isomer as 20:3 $\Delta 7$, 11, 14 and confirmed it by CACI-GC-MS/MS. Our result is consistent with $\Delta 5$ desaturation of LNA followed by chain elongation (Fig. 2) rather than elongation followed by two desaturation steps as proposed by Sinclair et al. [10]. It is also a methylene-interrupted fatty acid species unlike that reported by Sinclair et al.

It is of interest, however, that the $\Delta 5$ desaturase product of LNA, 18:3 $\Delta 5$, 9, 12, was not observed in the present study. This finding is similar to the recent study of Stroud et al. [16] who also observed 20:3 $\Delta 7$, 11, 14, but no 18:3 $\Delta 5$, 9, 12, using $\Delta 6$ desaturase-null mice ($-/-$) fed a high LNA diet similar to the HL diet reported here. In that study, the authors described the pathway noted in Fig. 2 and concluded that $\Delta 5$ desaturation of LNA is likely due to loss

of competition from the absence of $\Delta 6$ desaturation as well as for fatty acid incorporation into phospholipids [16]. The observation of Stroud et al. is consistent with that found here in feline species, a naturally occurring model of absent $\Delta 6$ desaturase. Findings from both models are consistent with $\Delta 5$ desaturation, although the level of activity may be different in cats compared to $\Delta 6$ desaturase-null mice ($-/-$). Nonetheless, taken together, decreases of plasma PL ARA with the HL and LL diets and of RBC membranes with the HL diet along with the maintenance of ARA in the GLA group supports the presence of $\Delta 5$ desaturase activity.

It is possible that both eicosatrienoic acid isomers, 20:3 $\Delta 7$, 11, 14, found in the present study and 20:3 $\Delta 5$, 11, 14, reported by Sinclair et al. [10] may occur depending upon experimental conditions employed. The studies of Sinclair et al. [10] used a combination of GC, silver nitrate thin layer chromatography, ozonolysis with triphenyl phosphine, and separation of aldehyde and aldehyde esters by GC in order to identify their 20 carbon fatty acid. In contrast, the present study employed covalent adduct chemical ionization gas chromatography/mass spectroscopy [14]. Although a tracer study is needed to verify the actual pathway involved, the present findings support the possibility that DGLA, formed when GLA is fed, may be followed by its $\Delta 5$ desaturation thereby providing a functional alternative for maintaining ARA levels using a practical diet in cats. It is of interest that an earlier study of Frankel and Rivers found no ARA accumulation in cats fed 0.73% dietary GLA versus controls [7] and concluded that a $\Delta 5$ desaturase was absent. The present study contained 0.35% dietary GLA but was fed for a longer period which may explain this discrepancy. Also, by comparison, the study of Sinclair et al. [1] fed 6 doses (250 mg each) of GLA for 13 days followed by 6 doses (500 mg each) for the following 13 days and observed marked RBC ARA enrichment in 2 cats. These amounts are roughly equivalent to 160 mg GLA/day per cat overall versus 210 mg GLA/day per cat in the present study.

Cats fed the GLA-enriched diet were thus able to maintain plasma PL and RBC membrane ARA and this difference was statistically significant compared to the HL diet. It should also be noted that ARA trended upward during the feeding period in the GLA group and a longer feeding period may have resulted in further increases. Nonetheless, this difference was statistically significant compared to the HL diet even at week 4. Cats fed the LL diet also appeared not to maintain ARA levels and this result continued trending downward after 8 weeks of feeding. These differences were observed at low, yet identical dietary ARA intake overall. One limitation of this study, however, is that the FA changes observed were relative and not absolute because total FA concentrations were not determined. While unlikely, the possibility exists

that fatty acid pool sizes may have changed given the uniqueness of the cat model and because other plasma lipid alterations were observed over time in this investigation.

Reasons for the downward trend of ARA levels with both the HL and LL diets are unclear given that all diets were formulated to contain minimal, yet adequate, amounts of this fatty acid. The possibility exists that decreased ARA may be related to an effect of LNA on ARA incorporation into PL fractions. For example, Spector et al. [26], using human umbilical vein endothelial cells in culture that also lack $\Delta 6$ desaturase, observed that high concentrations of LNA interfered with the ability of these endothelial cells to maintain adequate ARA. They additionally found that ARA incorporation into PL fractions is reduced as the availability of LA increases [26]. Should these phenomena also occur in $\Delta 6$ desaturase deficient cats, then the 3.5-fold higher LNA concentration of the HL diet would, in part, explain the more marked decrease of ARA in cats fed this highest LNA concentration. Furthermore, plasma PL LNA levels were significantly greater with both the HL and LL diets consistent with the possibility of LNA interference with ARA incorporation as observed by Spector et al. [26]. Finally, although not dramatic, the minimal drop of body weight observed overall by repeated measures ANOVA may have limited actual ARA intake to some extent. If so, cats fed GLA as an alternative precursor for ARA synthesis would maintain ARA levels while animals fed the other two diets may have either consumed less than the minimal ARA requirement or increased its utilization leading to its subsequent depletion.

While a physiologic role for 20:3 $\Delta 7$, 11, 14 is presently unknown, murine macrophage cells have been shown to readily take up pinolenic acid (PNA, 18:3 $\Delta 5$, 9, 12) and elongate it to its respective eicosatrienoic acid. In addition PGE₁ from DGLA and PGE₂ from ARA were both suppressed in that study, presumably due to substrate competition [27]. These authors also suggested that the inhibitory effect of PNA on eicosanoid production may have been the result of competitive incorporation of PNA and 20:3 $\Delta 7$, 11, 14 into phospholipids which reduced the levels of DGLA and ARA available for eicosanoid formation. This possibility may also explain, in part, why ARA was lowest in the HL diet fed cats compared with the GLA and LL groups.

Induction of feline $\Delta 6$ desaturase via increased dietary LNA could not be confirmed in the present study given the decrement of ARA observed in the HL group. Thus, we found no support for the hypothesis that the limited $\Delta 6$ desaturase activity of felines might be induced by high dietary LNA. In rats, feeding high dietary LNA at constant ALA to dams caused reductions in brain and retina ARA in pups as it was transmitted through milk lipid [28]. No effects in plasma and other pools were found, however.

Consequently, feeding high LNA to rats may induce substitution for ARA thereby explaining a drop in ARA. Previous studies in our lab using dogs found no additional accumulation of ARA in either plasma PL or neutrophils when high LNA safflower oil was fed compared to low LNA beef tallow [29]. In addition, a recent review has concluded that increasing dietary LNA content does not increase tissue ARA content in humans consuming a Western-type diet [30]. Such a phenomenon may also be the case in feline species.

As a final point, it was noted that some depletion of EPA and DHA was observed in all groups during the feeding period. This result was not unexpected because the diets did not contain any appreciable amounts of these fatty acids. The 2006 Nutrient Requirements publication for cats has concluded that there are no published studies on an absolute requirement for EPA [14]. However, it does recommend that approximately 0.2% EPA be present. The commercial diet fed to the cats for several months prior to the PED diet contained about 0.2% EPA as determined in our laboratory. However EPA in the commercially available PED (fed for 4 weeks) was not detected and only trace amounts were present in our experimental diets fed for 8 additional weeks. It is unknown whether this would lead to a deficiency over time as optimal amounts of this fatty acid in the diet or concentrations in tissues are not defined in this species.

In summary, the present study demonstrates that GLA-enriched diets are readily consumed by cats without major alteration of BW and BCS or plasma lipid indices. The findings also support the presence of an active $\Delta 5$ desaturase enzyme in feline species. Thus, provision of a dietary vegetable oil source of GLA provides substrate for ARA synthesis in cats most likely via by-passing the $\Delta 6$ desaturation step. The accumulation of DGLA when GLA is fed may also serve as an important precursor for modulation of eicosanoid synthesis in cats. In addition, the $\Delta 6$ desaturase enzyme does not appear to be inducible at high dietary LNA content. Cats are thus a suitable naturally occurring animal model for $\Delta 6$ desaturase deficiency to which experiments involving the null mice ($-/-$) can be compared. Finally, based on these findings, studies employing dietary stearidonic acid to address questions involving longer chain n-3 fatty acid synthesis such as EPA and DPA (n-3) but also including DHA which requires $\Delta 6$ desaturase in a final step, will provide intriguing future investigations.

Acknowledgments Funded by Nestlé-Purina Pet Care, Saint Louis, MO, USA and the Mark L. Morris Professorship of Clinical Nutrition, Texas A & M University, TX USA. The authors wish to acknowledge the Conselho Nacional de Desenvolvimento Científico e Tecnológico (CNPq) from the Brazilian Government for their sponsorship of Luciano Trevizan who helped conduct this study as well as the expert technical assistance of Dr. Wendy Anderson and Ms. Karen Bigley.

J. E. B. and M. K. W. designed research; L. T. conducted research and analyzed data; A. M. K. reviewed data analysis; L. T. and J. E. B. wrote the manuscript; P. L. and J. T. B. provided technical assistance; L. T. and J. E. B. wrote the manuscript and J. E. B. had primary responsibility for final content. M. W. K. is an employee of one of the funding sources.

Conflict of interest None.

References

- Sinclair AJ, McLean JG, Monger EA (1979) Metabolism of linoleic acid in the cat. *Lipids* 14:932–936
- Rivers JPW, Sinclair AJ, Crawford MA (1975) Inability of the cat to desaturate essential fatty acids. *Nature* 258:171–173
- Rivers JPW, Hassam AG, Crawford MA, Brambell MR (1976) The absence of $\Delta 6$ -desaturase activity in cats. *Proc Nutr Soc* 35:69A
- Rivers JPW, Sinclair AJ, Moore DP, Crawford MA (1976) The abnormal metabolism of essential fatty acids in cat. *Proc Nutr Soc* 35:68A
- Rivers JPW, Frankel TL (1980) Fat in the diet of dogs and cats. In: Anderson RS (ed) *Nutrition of the dog and cat*. Pergamon Press, Oxford, pp 67–99
- Hassam AG, Rivers JPW, Crawford MA (1977) The failure of the cat to desaturate linoleic acid: its nutritional implications. *Nutr Metab* 21:321–328
- Frankel T, Rivers JPW (1978) The nutritional and metabolic impact of γ -linolenic acid (18:3 n6) on cats deprived of animal lipid. *Br J Nutr* 39:227–231
- Rivers JPW (1982) Essential fatty acids in cats. *J Small Animal Prac* 23:563–576
- MacDonald ML, Rogers QR, Morris JG (1984) Nutrition of the domestic cat, a mammalian carnivore. *Ann Rev of Nutr* 4:521–562
- Sinclair AJ, Slattery W, McLean JG, Monger EA (1981) Essential fatty acid deficiency and evidence for arachidonate synthesis in the cat. *Br J Nutr* 46:93–96
- Holman RT (1970) Biological activities of polyunsaturated fatty acids. *Prog Chem Fats Lipids* 9:607–6827
- Pawlosky RA, Barnes A, Salem N Jr (1994) Essential fatty acid metabolism in the feline: relationship between liver and brain production of long chain polyunsaturated fatty acids. *J Lipid Res* 35:2032–2040
- Official Publication (2008) Association of American Feed Control Officials (AAFCO), Oxford, pp 159–162
- National Research Council (2006) *Nutrient requirements of dogs and cats*. National Academies Press, Washington, pp 39–44
- Dunbar BL, Bigley KE, Bauer JE (2010) Early and sustained enrichment of serum n-3 long chain polyunsaturated fatty acids in dogs fed a flaxseed supplemented diet. *Lipids* 45:1–10
- Stroud CK, Nara TY, Roqueta-Rivera M, Radlowski EC, Lawrence P, Zhang Y, Cho BH, Segre M, Hess RA, Brenna JT, Haschek WM, Nakamura MT (2009) Disruption of FADS2 gene in mice impairs male reproduction and causes dermal and intestinal ulceration. *J Lipid Res* 50:1870–1880
- Periago JL, Suarez MD, Pita ML (1990) Effect of dietary olive oil, corn oil, and medium chain triglycerides on the lipid composition of rat red blood cell membranes. *J Nutr* 120:986–994
- Brosche T, Heckers H, Platt D, Summa J-D (1986) The effect of different fat supplemented diets on the erythrocyte ghosts and plasma lipid composition of geriatric subjects. *Arch Gerontol Geriatr* 5:83–95
- Degier J, Van Deenan LLM (1963) A dietary investigation of the variations in phospholipid characteristics of red cell membranes. *Biochim Biophys Acta* 84:294–304
- Dougherty RM, Galli C, Ferro-Luzzi A, Iacono M (1987) Lipid and phospholipid fatty acid composition of plasma, red blood cells, and platelets and how they are affected by dietary lipids: a study of normal subjects from Italy, Finland, and the USA. *Am J Clin Nutr* 45:443–455
- Jordan E, Kley S, Len A, Waldron MK, Hoenig M (2008) Dyslipidemia in obese cats. *Domest Anim Endocrinol* 35:290–299
- Wright-Rodgers AS, Waldron MK, Bigley KE, Lees GE, Bauer JE (2005) Dietary fatty acids alter plasma lipids and lipoprotein distributions in dogs during gestation, lactation, and the perinatal period. *J Nutr* 135:2230–2235
- Demacker PNM, Van Heijst PJ, Hak-Lemmers HLM, Stalenhof AFA (1987) A study of the lipid transport system in the cat, *Felix domesticus*. *Atherosclerosis* 66:113–123
- Bauer JE (2004) Lipoprotein-mediated transport of dietary and synthesized lipids and lipid abnormalities in dogs and cats. *JAVMA* 224:668–675
- Papamandjares AA, MacDougall DE, Jones PJH (1998) Medium-chain fatty acids metabolism and energy expenditure: obesity treatment implications. *Life Sci* 62:1203–1215
- Spector AA, Kaduce TL, Hoak JC, Fry GL (1981) Utilization of arachidonic and linoleic acid by cultured human endothelial cells. *J Clin Invest* 68:1003–1011
- Chuang L-T, Tsai P-J, Lee C-L (2009) Uptake and incorporation of pinolenic acid reduces n-6 polyunsaturated fatty acid and downstream prostaglandin formation in murine macrophage. *Lipids* 44:217–224
- Su H-M, Keswick LA, Brenna JT (1996) Increasing dietary linoleic acid in young rats increases and then decreases docosa-hexaenoic acid in retina but not in brain. *Lipids* 31:1289–1298
- Waldron MK, Hannah SS, Bauer JE (2012) Plasma phospholipid fatty acid and ex vivo neutrophil responses are differentially altered in dogs fed fish and linseed oil containing diets at the same n-6:n-3 fatty acid ratio. *Lipids* (in press)
- Rett BS, Whelan J (2011) Increasing dietary linoleic acid does not increase tissue arachidonic acid content in adults consuming western-type diets: a systematic review. *Nutr Metab* 8:36

Plasma Phospholipid Fatty Acid and Ex Vivo Neutrophil Responses are Differentially Altered in Dogs Fed Fish- and Linseed-Oil Containing Diets at the Same n-6:n-3 Fatty Acid Ratio

Mark K. Waldron · Steven S. Hannah ·
John E. Bauer

Received: 11 July 2011 / Accepted: 22 December 2011 / Published online: 18 January 2012
© AOCS 2012

Abstract The effect of diets containing either 18-carbon n-3 fatty acids (FA) or 20/22-carbon n-3 FA on canine plasma and neutrophil membrane fatty acid composition, superoxide and leukotriene B₄ and B₅ production when fed at the same n-6:n-3 fatty acid ratio was investigated. Four groups of ten dogs each were fed a low fat basal diet supplemented with safflower oil (SFO), beef tallow (BTO), linseed oil (LSO), or Menhaden fish oil (MHO) for 28 days. Dietary fat provided 40.8% of energy and the n-6:n-3 of the diets were ~100:1, 9.7:1, 0.38:1, and 0.34:1 for the SFO, BTO, LSO and MHO groups, respectively. The MHO and LSO groups had increased incorporation of EPA and DPA in both the plasma and neutrophil membranes compared to the BTO and SFO groups. DHA was observed in the MHO but not in the LSO group. Neutrophils from the MHO diet fed dogs had less LTB₄ and greater LTB₅ than the other three groups. The LSO group

also showed a reduction in LTB₄ and greater LTB₅ production compared to the SFO and BTO groups. Both LSO and MHO groups had lower superoxide production compared to the SFO and BTO groups. Diets containing 18 or 20/22 carbon n-3 FA fed at the same n-6:n-3 resulted in differential incorporation of long chain n-3 FA into neutrophil membranes. Thus, fatty acid type and chain length individually affect neutrophil membrane structure and function and these effects exist independent of dietary total n-6:total n-3 FA ratios.

Keywords Neutrophils · Canine · n-3 fatty acids · Leukotrienes · Superoxide anion

Abbreviations

AAFCO	Association of American Feed Control Officials
ALA	Alpha-linolenic acid
ARA	Arachidonic acid
BTO	Beef tallow enriched diet
DPAn-3	Docosapentaenoic acid n-3
DHA	Docosahexaenoic acid
EPA	Eicosapentaenoic acid
FA	Fatty acids
FAME	Fatty acid methyl ester(s)
LNA	Linoleic acid
LSO	Linseed oil enriched diet
LTB ₄	Leukotriene B ₄
LTB ₅	Leukotriene B ₅
MHO	Menhaden oil enriched diet
PMA	Phorbol myristic acetate
SAF	Safflower oil enriched diet
SOD	Super oxide dismutase
TBHQ	<i>tert</i> -butylhydroquinone
tot(n-6):tot(n-3)	Total n-6 to total n-3 fatty acid ratio

Presented in part at the 91st annual meeting of the American Oil Chemists' Society (AOCS), 25–28, April, 2000, San Diego, CA. [Waldron, MK, Hannah, SS, Bigley, KE, Dunbar, BL, Bauer, JE, Neutrophil leukotriene synthesis and superoxide production are differentially modulated by type and amount of dietary n-3 polyunsaturated fatty acids. Inform, 11:s118 (abs)].

M. K. Waldron · J. E. Bauer (✉)
Department of Small Animal Clinical Sciences,
College of Veterinary Medicine, Texas A&M University,
College Station, TX 77840, USA
e-mail: jbauer@cvm.tamu.edu

Present Address:

M. K. Waldron
Nestlé Purina PetCare, Checkerboard Square Research,
South, Third Floor, St. Louis, MO 63164, USA

S. S. Hannah
Nestlé Purina PetCare, St. Louis, MO 63164, USA

Introduction

Neutrophils are highly specialized white blood cells essential to the host immune response. When activated, neutrophils adhere to endothelial cells, migrate into tissues (chemotaxis), phagocytose opsonized microbes, and produce toxic compounds [1–3]. Although essential to host defense, neutrophil damage to host tissues is associated with the pathology and progression of specific diseases such as inflammatory bowel diseases, rheumatoid arthritis, coronary heart disease, psoriasis, and ischemic reperfusion injury [1, 2, 4]. The pathophysiology of these diseases is due, in part, to extracellular release of toxic compounds as well as eicosanoid synthesis, including leukotriene B₄ (LTB₄) in the inflammatory response [1–3]. Diets rich in long chain n-3 FA, eicosapentaenoic acid (EPA) and docosahexaenoic acid (DHA), prominent in fish oil, have been shown to have beneficial effects in cardiovascular disease, rheumatoid arthritis, hypertension, renal diseases, and the inflammatory response [5–9] and affect the immune response in mice [10, 11]. These benefits have been attributed, in part, to a reduction in pro-inflammatory leukotrienes produced by neutrophils as well as serving as a substrate for the potent anti-inflammatory compounds known as resolvins [12].

Dietary long chain n-3 FA supplementation results in their incorporation into plasma lipids and phospholipid fractions of circulating immune cells [1, 2, 13–16]. The incorporation of EPA and DHA into neutrophil lipids occurs at the expense of the more pro-inflammatory arachidonic acid (ARA) [17–19]. Furthermore, replacement of ARA with EPA and DHA results in a decrease in neutrophil superoxide production without involvement of the cyclooxygenase pathway and without altering neutrophil lysosomal enzyme release [20]; inhibition of chemotaxin-mediated phosphoinositide formation and chemotaxis [21]; and a decrease of stimulated neutrophil chemiluminescence as an index of production of free oxygen radicals [22]. Membrane fatty acid modifications via diet FA also alter neutrophil leukotriene production. For example, incorporation of EPA and DHA into neutrophil membranes is associated with a reduction in the powerful chemotactic agent, LTB₄, and a corresponding increase in LTB₅, which is 30–100 times less stimulatory than LTB₄ [2, 20, 23–26]. Because polyunsaturated n-3 and n-6 FA compete for insertion into cellular lipids and for enzymes involved in their metabolism [15, 26] the dietary total n-6:total n-3 (tot(n-6):tot(n-3)) ratio rather than absolute amounts of n-6 and n-3 FA have typically been used in studies investigating altered ARA metabolism and eicosanoid synthesis [27–29]. However, it is unlikely that diets rich in plant derived 18-carbon n-3 FA, compared to 20/22-carbon n-3 FA derived from marine

sources, elicit the same anti-inflammatory effects when fed at the same tot(n-6):tot(n-3) ratio. The reason for this is the known limited conversion of 18-carbon n-3 FA precursors to the longer chain derivatives [30, 31, reviewed in 32].

Several studies have examined the effects of fish oil, linseed oil, or fish oil/linseed oil combinations on neutrophil composition and cell functions in laboratory animals and humans [22, 23, 31–36]. Some studies have reported such effects in canine species [37–39]. In addition, one recent work reported the effect of diets containing fish oil on lymphocyte proliferation [40] while another study found that the amount of dietary n-3 fatty acid affected plasma fatty acid profiles of normal dogs independent of the n-6:n-3 FA ratio [41]. However, no investigations to date have examined the separate effects of 18- versus 20/22-carbon dietary n-3 FA on plasma phospholipids, neutrophil fatty acid composition, and cellular functions in canine species when fed at the same n-6:n-3 FA ratios. The present study is the first to address this question.

Materials and Methods

Materials

All chemicals were reagent grade or better and purchased from Sigma Chemical Industries unless otherwise noted.

Experimental Diets

A basal diet was produced by Ralston-Purina Co. (Table 1) and designed to be supplemented with one of the following oils; safflower oil (SFO), beef tallow (BTO), linseed oil (LSO), or menhaden fish oil (MHO) (Table 2). The safflower oil and beef tallow were provided by Ralston-Purina Co (now Nestlé Purina). Cargill Inc. and Zapata Protein (now Omega-Protein, Inc.) supplied the linseed oil and Menhaden fish oil, respectively. Using each of these oil sources, four supplemented diets were prepared daily at the time of feeding containing varying n-6:n-3 FA ratios: The SFO and the BTO supplemented diets had n-6:n-3 of ~100:1 and 9.7:1, respectively and the LSO and MHO diets, had nearly identical n-6:n-3 of 0.38:1 and 0.34:1, respectively. Fatty acid composition of the oil supplemented diets, n-6:n-3, and percentage energy from n-6 and n-3 FA, are summarized (Tables 3 and 4). In addition, total cholesterol contents of the single lot oils were determined and cholesterol concentrations of each oil were equilibrated to that present in the menhaden oil. To inhibit oxidation of the oils the α - and γ -tocopherol contents of the oils were also determined and α - and γ -tocopherols and TBHQ were added to all oils to achieve final concentrations of 1, 1,

Table 1 Composition of the basal diet

Component	Amount (g/kg)
Rice, #4	420.0
SUPRO (Protein Intl., St. Louis, MO)	54.6
Soybean meal	391.2
Meat and bone meal	79.9
NaCl	10.4
Palatability coating	22.6
Vitamin premix	9.32
Phosphorus dicalcium	3.87
L-Lysine	3.00
Mineral mix	3.46
Choline chloride (70%)	1.39
Flavor premix	0.12
Vitamin E (50%)	0.15

The basal diet was a reduced-fat, complete and balanced formula designed to be supplemented with dietary oils at a rate of 18 g/100 g diet. It was prepared by Ralston Purina Co. (presently Nestle-Purina PetCare), St. Louis, MO, USA. The diet ingredients, by weight, included #4 rice, 42.0%; dehulled soybean meal, 39.1%; meat and bone meal, 8.0%; Supro 620[®] protein, 5.5%; flavor coating, 2.3%; sodium chloride, 1.0%; vitamin premix, 0.9%; dicalcium phosphate, 0.4%; choline chloride (70%), 0.15%; vitamin E (50%), 0.02%; and flavor premix, 0.01%. The vitamin premix, contained 146.32 g/kg nicotinic acid, 10.35 g/kg vitamin A acetate, 90 g/kg DL- α -tocopherol acetate, 84 mg/kg cholecalciferol, 52 g/kg thiamine mononitrate, 51.06 g/kg calcium D-pantothenate, 24.4 g/kg riboflavin, 14.52 g/kg pyridoxine hydrochloride, 6 g/kg folic acid, 508 mg/kg menadione sodium bisulfite, 93 mg/kg vitamin B-12, and 36.8 mg/kg biotin. The mineral mix contained 65 g/kg zinc as zinc sulfate, 39 g/kg iron as ferrous sulfate, 18.25 g/kg manganese as manganese sulfate, 3.2 g/kg copper as copper sulfate 655 mg/kg iodine as calcium iodate, and 50 mg/kg selenium as selenium selenite. The remaining 13.3% was provided by various dietary oils which provided the desired fatty acid profiles. Finally, 18 g of beef tallow, safflower oil, linseed oil, or Menhaden fish oil were supplemented/100 g of basal diet at the time of feeding to produce the desired final total fat and n6:n3 fatty acid ratios as described in the text and Table 4

Table 2 Experimental diet nutrient profiles

Nutrient	Basal diet g/kg (as-is basis)	Basal diet + supplement ^a (as-is basis)
Crude protein	364	309
Crude fat	74	215
Nitrogen-free extract	548	465
Ash	14	11
Energy (kJ/g)	16	19

Values are means of duplicate determinations. Energy is calculated based on macronutrient analyses and modified Atwater factors of 14.6, 14.6, 35.6 kJ/g for protein, nitrogen-free extract, and fat respectively

^a 18 g of either beef tallow, safflower oil, linseed oil, or Menhaden fish oil was supplemented/100 g of basal diet at the time of feeding to produce the desired final total fat and n6:n3 fatty acid ratio as described in the text and Table 4

Table 3 Fatty acid content of basal diets plus oil supplements

Fatty acid	BTO (g fatty acid/100 g food)	SFO (g fatty acid/100 g food)	LSO (g fatty acid/100 g food)	MHO (g fatty acid/100 g food)
12:0	nd	nd	nd	0.02
14:0	0.54	0.07	0.04	2.21
14:1	0.09	0.01	0.01	0.01
15:0	0.09	0.01	0.01	0.10
15:1	0.03	nd	nd	0.02
16:0	4.82	2.06	1.76	3.39
16:1	0.50	0.08	0.07	2.58
17:0	0.25	0.01	0.01	0.06
17:1	0.15	0.01	0.01	0.04
18:0	3.49	0.78	0.85	0.75
18:1n-9	7.75	3.36	4.13	2.50
18:1n-7	1.08	0.21	0.21	0.73
18:2n-6	1.64	14.43	4.00	1.31
18:3n-3	0.17	0.14	10.30	0.23
18:3n-6	nd	0.05	nd	0.07
20:0	0.03	0.07	0.03	0.03
20:1n-9 0	0.05	0.05	0.04	0.27
20:2n-6	nd	0.02	nd	0.03
20:3n-6	nd	nd	nd	0.06
20:4n-6	0.01	0.01	0.01	0.12
20:5n-3	nd	nd	nd	3.07
22:0	0.10	0.01	0.01	0.01
22:1n-9	nd	nd	nd	0.19
22:2n-6	nd	nd	nd	0.02
22:4n-6	nd	nd	nd	0.13
22:5n-3	nd	nd	nd	0.48
22:6n-3	nd	nd	nd	1.00
24:0	0.01	0.01	0.01	0.01
Unidentified	0.71	0.13	0.01	2.16
Total	100.00	100.00	100.00	100.00

nd not detected (detection limit, 1 ng)

Table 4 Composition of the oil supplemented basal diets

Diet	Tot(n-6):tot(n-3)	% en fat	% en n-6	% en n-3
BTO	9.69	40.8	3.11	0.32
SFO	101.25	40.8	27.40	0.27
LSO	0.38	40.8	7.60	19.59
MHO	0.34	40.8	2.49	9.16

en% percent energy provided in the diet

and 0.2 g, respectively, per kg oil. Tocopherols and TBHQ were provided by Eastman Chemicals, Kingsport, Tennessee.

Experimental Design

Dogs were individually maintained in kennels according to the American Physiological Society Guidelines for Animal Research and protocols were approved by the Texas A&M University Animal Care and Use Committee. They ranged in bodyweight from 9 to 25.8 kg and in age from 1.5 to 7 years. The study population consisted of 12 hounds, 8 Beagles, and 20 mixed-breed dogs. Because gender effects on canine lipid metabolism are unknown, hounds and Beagles were blocked by breed and gender and randomly assigned to one of four treatment groups. The remaining 20 mixed-breed dogs were blocked by gender and randomly assigned to one of four treatment groups. The feeding trial consisted of four groups of ten dogs each in which the basal diet was supplemented with BTO, LSO, SFO, or MHO at 18 g oil per 100 g of diet and fed for 28 days. Amounts of diets fed were determined based on metabolic body weight of individual dogs. Dogs were weighed weekly and the amount of feed offered adjusted if needed to ensure that weight was maintained. All dogs were healthy and clinically normal based on complete blood counts, serum biochemistry profiles, and serum concentrations of T₃ and T₄ prior to entering the study.

Blood Collection, Plasma Preparation and Neutrophil Isolation

Venous blood samples (30 mL) were collected prior to daily feeding at 9 a.m into tubes containing heparinized saline. Plasma was separated by low speed centrifugation at 150×g for 5 min. Neutrophil isolation was performed according to Markert et al. [42]. Purity of neutrophils was >95% and cell viability, as determined by trypan blue exclusion, was >95%. Cell concentrations were determined microscopically using a hemocytometer.

Lipid Extraction and Fatty Acid Analysis

Plasma and neutrophil total lipids were extracted using chloroform:methanol (2:1, v/v) via a modified Folch procedure [43, 46]. Total plasma phospholipids (PL) were separated via thin layer chromatography, fatty acid methyl esters prepared using the plasma PL and neutrophil lipid extracts, and fatty acid profiles were determined via capillary gas chromatography [45, 47].

Superoxide Production

The determination of superoxide production was performed according to Markert et al. [42]. The release of the superoxide anion (O₂⁻) was measured by the SOD inhibited reduction of ferricytochrome c.

Leukotriene Extraction and Quantitation

Stimulation of neutrophil leukotriene production and fractionation were performed according to Ziboh and Fletcher [33]. Leukotrienes B₄ and B₅ were separated based on retention times of authentic standards (Caymen Chemicals, Ann Arbor, MI, USA) and collected. Samples were stored under N₂ gas at -80 °C until further analysis.

Quantitation of LTB₄ and LTB₅ was performed using an ELISA kit (Amersham Life Science Inc., Arlington Hts., IL, USA) and microplate reader and according to the manufacturer's instructions.

Statistics

Data were analyzed using statistix[®] for windows (Tallahassee, FL, USA). Data are expressed as means ± SD. Data were subjected to one way ANOVA with differences considered significant at *P* < 0.05 or as otherwise noted. Where appropriate, multiple comparisons were conducted by Scheffe's tests. An experiment-wide type I error of 0.05 was maintained. All data were found to follow a normal distribution at *P* < 0.05 using the Shapiro–Wilk test. If variances were non-homogeneous log₁₀ transformed data were analyzed.

Results

Dogs and Diets

The diets were palatable and readily consumed. All dogs remained healthy and body weights were maintained without significant weight gain or loss throughout the study (data not shown).

Plasma Phospholipid FA

Plasma phospholipid FA in the LSO and MHO groups were significantly enriched in EPA with mean values of 4.42 and 10.17 mol% respectively and DPA n-3 at 2.62 and 4.19 mol% respectively. By comparison, neither the BTO nor SFO groups exceeded mean values of 1.44 mol% for these two long chain n-3 FA (*P* < 0.05) (Table 5). The MHO group was also significantly enriched in DHA (6.71 mol%) compared with ≤0.38 mol% in any of the other groups (*P* < 0.05). It is noteworthy that no accumulation of DHA occurred with the LSO diet. For that matter, LSO group mean DHA values were similar to the SFO and BTO groups with no group exceeding 0.38 mol%. The LSO group was the only group to have increased amounts of ALA (2.44 vs. <0.12 g/100 in each of the other groups (*P* < 0.05). Significantly less ARA was observed in the MHO group (i.e. mean value of 10.26 mol% compared

Table 5 Plasma phospholipid fatty acid profiles of dogs fed the diets

Fatty acid	BTO (mol%)	SFO (mol%)	LSO (mol%)	MHO (mol%)
14:0	0.21 ± 0.04 ^a	0.15 ± 0.06 ^b	0.11 ± 0.04 ^b	0.43 ± 0.18 ^c
15:0	0.12 ± 0.07 ^a	0.07 ± 0.01 ^b	0.07 ± 0.04 ^b	0.13 ± 0.03 ^a
16:0	16.31 ± 1.35 ^a	14.04 ± 2.20 ^b	9.39 ± 1.32 ^c	14.95 ± 1.78 ^{a,b}
16:1	0.80 ± 0.11 ^a	0.67 ± 0.19 ^a	0.26 ± 0.15 ^b	0.67 ± 0.27 ^a
17:0	0.97 ± 0.10 ^a	0.64 ± 0.12 ^b	0.73 ± 0.09 ^b	0.90 ± 0.21 ^a
17:1	0.26 ± 0.05 ^a	0.05 ± 0.08 ^b	0.06 ± 0.07 ^b	0.12 ± 0.26 ^b
18:0	25.84 ± 2.21 ^a	28.98 ± 2.08 ^b	32.67 ± 2.23 ^c	30.02 ± 4.59 ^{b,c}
18:1n-9	9.47 ± 1.61 ^a	4.76 ± 0.85 ^b	5.19 ± 0.47 ^b	3.69 ± 0.66 ^c
18:1n-7	2.29 ± 0.25 ^a	2.26 ± 0.25 ^a	2.56 ± 0.44 ^a	3.82 ± 0.69 ^b
18:2n-6	15.92 ± 3.64 ^a	21.72 ± 3.50 ^b	16.90 ± 2.13 ^a	5.84 ± 1.44 ^c
18:3n-3	0.12 ± 0.10 ^a	0.02 ± 0.05 ^a	2.44 ± 1.25 ^b	0.03 ± 0.04 ^a
20:3n-6	1.70 ± 0.39 ^a	1.07 ± 0.48 ^b	1.29 ± 0.25 ^b	0.96 ± 0.27 ^b
20:4n-6	18.61 ± 3.91 ^a	18.10 ± 3.57 ^a	14.57 ± 3.57 ^a	10.26 ± 3.70 ^b
20:5n-3	0.53 ± 0.14 ^a	0.03 ± 0.05 ^a	4.42 ± 1.71 ^b	10.17 ± 1.25 ^c
22:4n-6	1.21 ± 0.41 ^a	1.22 ± 0.37 ^a	0.02 ± 0.05 ^b	0.14 ± 0.06 ^b
22:5n-3	1.44 ± 0.49 ^a	0.79 ± 0.15 ^a	2.62 ± 0.46 ^b	4.19 ± 1.57 ^c
24:0	0.29 ± 0.05 ^a	0.46 ± 0.12 ^b	0.51 ± 0.13 ^b	0.50 ± 0.20 ^b
22:6n-3	0.38 ± 0.08 ^a	0.32 ± 0.13 ^a	0.36 ± 0.10 ^a	6.71 ± 1.96 ^b
24:1n-9	0.63 ± 0.14 ^a	0.98 ± 0.24 ^a	0.75 ± 0.17 ^a	1.84 ± 0.62 ^b

Values given as means ± SD. *nd* not detected, detection limit, 1 ng; *n* = 10 dogs/group

Values within rows with different superscripts are significantly different at $P < 0.05$

to the other three groups ($P < 0.05$). The SFO and BTO groups had higher, yet similar, amounts of ARA with mean values of 18.10 and 18.61 mol% respectively while the LSO group mean was found to be 14.57 mol%. Dogs fed the SFO diet had the highest amount of LNA at 21.72 mol%; the BTO and LSO groups had intermediate and similar values of 15.92 and 16.90 mol% respectively; while the MHO group was found to have the least LNA with only 5.84 mol% of this FA (all $P < 0.05$). Palmitic acid in the LSO group was significantly lower than the other three groups (9.39 vs. ≥ 14.04 mol%) and stearic acid was statistically lower in the BTO group, especially compared with the LSO and MHO diets even though the BTO diet was relatively enriched in this fatty acid compared with the other diets ($P < 0.05$). Oleic acid was significantly increased by approximately 2-fold in the BTO group compared with the other three groups ($P < 0.05$).

Neutrophil Total Lipid Fatty Acid Composition

Significant enrichment of long chain n-3 FA was found in both LSO and MHO groups compared to the BTO and SFO groups (Table 6). The neutrophils of dogs in the MHO group were markedly higher in both EPA and DHA with mean values of 4.21 and 1.79 mol% respectively compared with the BTO and SFO groups where both of these fatty acids were undetected. In the LSO group, a significantly lower mean value of 1.14 mol% for EPA was observed compared to 4.21 mol% in the MHO group ($P < 0.05$). Only small amounts of ALA (mean value, 0.86 mol%) were

seen compared to the other three groups where ALA was undetected. However, no DHA was detected in the LSO group and this was also the case with both the BTO and SFO groups (Table 6). With regard to the n-6 FA, ARA was lower in the LSO group (mean value of 11.96 mol%) compared with 15.00 and 15.64 mol% in the BTO and SFO groups respectively ($P < 0.05$). However, this effect was more pronounced in the MHO group at 9.24 g ARA/100 g ($P < 0.05$). Membrane lipids from SFO were significantly enriched in n-6 fatty acids as follows: an approximate 2-fold increase in 18:2n-6 and 20:3n-6 and a ≥ 5 -fold increase in 20:2n-6. Amounts of 22:4n-6 were also highest with the SFO diet at 3.47 mol% compared with 2.27 with the BTO diet and < 0.5 mol% in both the LSO and MHO groups. Modest, but statistically significant, increases in saturated fatty acids were observed in the BTO group including 15:0, 17:0, and 24:0 compared to all other groups. All groups were also found to have considerable amounts of 24:1n-9 with the MHO group showing the largest increase in this FA (8.21 vs. 5.62, 5.73, and 6.63 mol% in BTO, SFO, and LSO groups respectively ($P < 0.05$)).

Superoxide Production

Supplementation with n-3 FA resulted in significantly less ex vivo superoxide production, presented as $\text{nmol} \times (10 \text{ min})^{-1} \times (10^6 \text{ cells})^{-1} \pm \text{SD}$, in MHO and LSO groups (21.0 ± 2.1 and 21.1 ± 1.2 SD respectively) compared to the BTO and SFO groups (24.4 ± 3.6 and 23.5 ± 4.8 SD respectively) ($P < 0.05$) (Fig. 1).

Table 6 Neutrophil phospholipid fatty acid profiles of dogs fed the diets

Fatty Acid	BTO (mol%)	SFO (mol%)	LSO (mol%)	MHO (mol%)
14:0	0.64 ± 0.56	0.84 ± 0.41	0.68 ± 0.44	0.84 ± 0.26
15:0	1.20 ± 0.75 ^a	0.46 ± 0.16 ^b	0.28 ± 0.37 ^c	0.28 ± 0.26 ^c
16:0	21.42 ± 3.16	21.61 ± 3.58	22.54 ± 4.47	22.09 ± 2.95
16:1	1.34 ± 0.76	0.95 ± 0.72	0.77 ± 0.39	0.84 ± 0.19
17:0	1.11 ± 0.56 ^a	0.69 ± 0.30 ^b	0.30 ± 0.40 ^b	0.59 ± 0.26 ^b
17:1	1.30 ± 0.91 ^a	1.39 ± 0.76 ^a	0.17 ± 0.27 ^b	0.45 ± 0.53 ^b
18:0	17.56 ± 2.83	19.25 ± 3.09	20.21 ± 2.60	17.37 ± 1.95
18:1n-9	10.68 ± 0.75	8.98 ± 1.47	9.44 ± 1.29	9.21 ± 1.12
18:1n-7	1.99 ± 0.31 ^a	1.67 ± 0.25 ^a	1.91 ± 0.67 ^a	3.12 ± 0.45 ^b
18:2n-6	4.86 ± 1.25 ^a	7.38 ± 1.40 ^b	4.90 ± 0.66 ^a	4.07 ± 0.94 ^a
18:3n-3	nd	nd	0.86 ± 0.24	nd
20:0	0.98 ± 0.25	0.72 ± 0.34	0.82 ± 0.25	0.96 ± 0.18
20:1n-9	1.24 ± 0.73	1.20 ± 0.24	1.25 ± 0.60	1.02 ± 0.15
20:2n-6	0.16 ± 0.28 ^a	0.85 ± 0.23 ^b	0.04 ± 0.10 ^a	0.04 ± 0.11 ^a
20:3n-6	0.32 ± 0.41 ^a	0.58 ± 0.27 ^b	0.26 ± 0.25 ^a	0.14 ± 0.18 ^a
20:4n-6	15.00 ± 2.80 ^a	15.64 ± 1.78 ^a	11.96 ± 3.31 ^b	9.24 ± 2.14 ^c
20:5n-3	nd	nd	1.14 ± 0.14 ^a	4.21 ± 1.25 ^b
22:0	0.92 ± 0.36 ^a	1.16 ± 0.64 ^b	1.13 ± 0.27 ^b	0.94 ± 0.40 ^a
22:1n-9	0.96 ± 0.51 ^a	0.66 ± 0.74 ^a	1.61 ± 0.30 ^b	1.90 ± 0.94 ^b
22:2n-6	1.60 ± 0.80	2.05 ± 0.64	1.21 ± 0.70	1.26 ± 0.54
22:4n-6	2.27 ± 0.66 ^a	3.47 ± 0.97 ^b	0.45 ± 0.48 ^c	0.22 ± 0.32 ^c
22:5n-3	nd	nd	2.09 ± 0.83	2.55 ± 0.79
24:0	1.19 ± 0.68 ^a	0.56 ± 0.40 ^b	0.85 ± 0.50 ^b	0.76 ± 0.33 ^b
22:6n-3	nd	nd	nd	1.79 ± 0.31
24:1n-9	5.63 ± 1.30 ^a	5.73 ± 2.14 ^a	6.63 ± 1.92 ^a	8.21 ± 1.97 ^b

Values given as means ± SD; nd not detected; detection limit 1 ng; n = 10 dogs/group. Values within rows with different superscripts are significantly different, $P < 0.05$

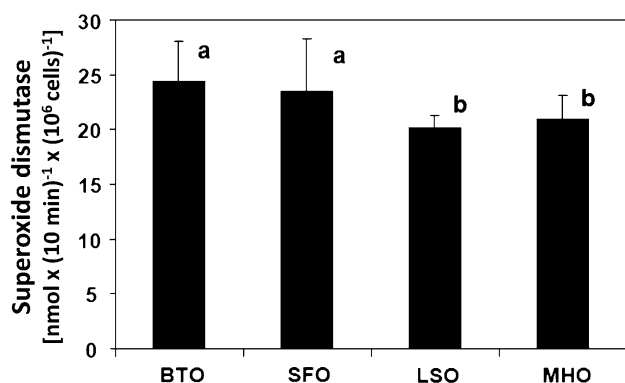


Fig. 1 Superoxide production of phorbol myristic acetate stimulated neutrophils isolated from dogs fed the experimental diets for 28 days, n = 10 dogs/group. The release of the superoxide anion (O_2^-) was measured by the SOD inhibited reduction of ferricytochrome c according to the method as described by Markret et al. [42]. Values are means ± SD. Means without a common letter differ, $P < 0.05$

Leukotriene Production

Neutrophil LTB_4 production, after ex vivo stimulation, expressed as $ng \times (5 \times 10^6 \text{ cells})^{-1} \pm SD$, was lowest in the MHO group at 16.6 ± 3.9 compared to the other groups with the SFO group producing the highest amount,

30.3 ± 7.2 , followed by 26.3 ± 7.2 for BTO and 20.8 ± 7.0 for LSO groups ($P < 0.001$) (Fig. 2a and 2b). By contrast, production of LTB_5 was markedly increased in the MHO and LSO groups at 7.52 ± 2.44 SD and 3.52 ± 2.48 respectively compared to 0.88 ± 0.44 with the BTO diet and 0.69 ± 0.17 in the SFO group ($P < 0.001$). It should be noted that the MHO group LTB_5 increase was more than that observed for the LSO group ($P < 0.001$).

Discussion

Significant differences due to diet were observed in this study for plasma phospholipid and neutrophil total lipid fatty acid compositions, superoxide production, and leukotriene production. Dietary supplementation with linseed or Menhaden fish oil resulted in the enrichment of long chain n-3 FA, consistent with reports in other species [4, 15, 32, 44, 45]. ALA was converted to EPA and further elongated to DPA n-3 but was not converted to DHA. This confirms earlier reports of limited metabolism of n-3 PUFA in dogs [32, 46, 47] and may reflect the inability of adult canine liver to convert DPA to DHA [47]. The modest

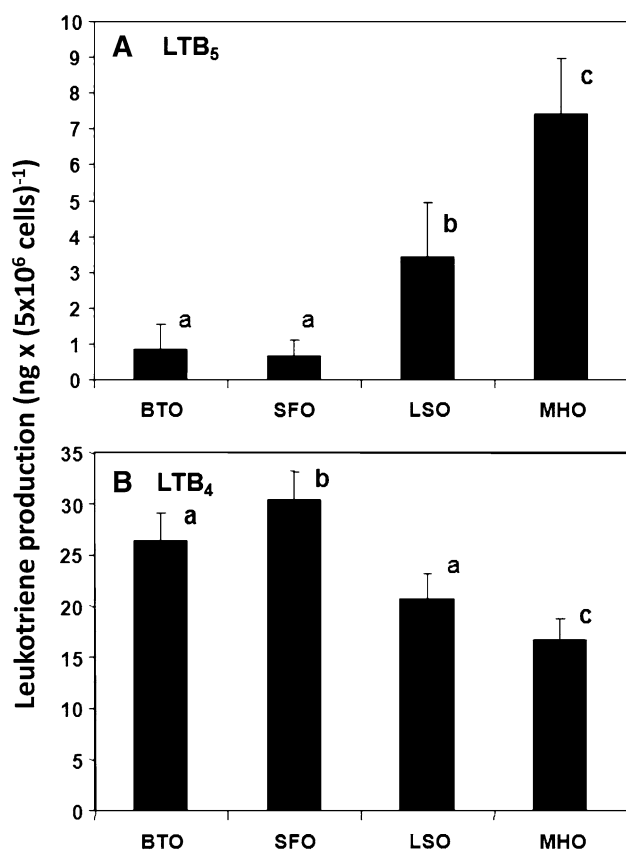


Fig. 2 Leukotriene production of calcium ionophore A23187 stimulated neutrophils isolated from dogs fed the experimental diets for 28 days, $n = 10$ dogs/group. Values are means \pm SD. Stimulation of neutrophil leukotriene production and fractionation were performed according to Ziboh and Fletcher [33]. LTB₄ and LTB₅ were separated by HPLC based on retention times of authentic standards (Caymen Chemicals, Ann Arbor, MI) and collected. Samples were stored under N₂ gas at -80 °C until analysis. Quantitation of LTB₄ and LTB₅ was performed via ELISA (Amersham Life Science Inc., Arlington Hts., IL, USA) and microplate reader. **a** Leukotriene B₅; **b** Leukotriene B₄. Means without a common letter differ, $P < 0.05$

amounts of ALA seen in plasma PL and neutrophil lipids when linseed oil was fed may be the result of either low acyl specificity for esterification or increased utilization. Nonetheless, this finding suggests that only limited amounts of ALA would be available as substrate for further desaturation and elongation. Preferential oxidation of this particular fatty acid exists which may be due to differences in substrate specificity of carnitine palmitoyltransferase I and increased amounts of mRNA for hepatic fatty acyl oxidative enzymes [48]. Such findings have been previously reported in rats and humans where overall conversion of ALA to DHA is limited (reviewed in 32).

As expected, no enrichment of n-3 FA was observed in the BTO and SFO groups. Incorporation of long chain n-3 FA into both plasma PL and neutrophils was significantly greater in the MHO group compared to the LSO group. This effect was seen even though both groups contained

nearly identical n-6:n-3 FA ratios (0.34 vs. 0.38, respectively). Given this observation, it is noteworthy that the LSO diet provided twice as much total n-3 FA. Thus, when diets containing similar (n6):(n3) FA ratios are fed, those containing menhaden fish oil as n-3 FA source more efficiently result in increased long chain n-3 fatty acid accumulation into both plasma and neutrophils. An earlier study by Hall et al. [41] investigated a dietary fish oil dosage effect at constant tot(n-6):tot(n-3) ratio of 1:1 and similar ALA content, but with increasing amounts of fish oil EPA + DHA to geriatric, female Beagles for 12 week. It was found that the dose (and likely type) of n-3 FA was more important than the ratio to achieve maximal EPA and DHA enrichment. The dosage of EPA + DHA in the MHO group of the present study was approximately four times higher than that of the highest n-3 concentration used by Hall et al. and utilized younger dogs of mixed breed and gender. Also, although Hall et al. [41] fed for 12 weeks, we have previously shown that a plasma fatty acid metabolic steady state can be achieved after 4 weeks and remaining so for 12 weeks. An important difference, however, is that the present study compared 18-carbon n-3 FA (i.e. ALA) with 20/22-carbon n-3 FA at the same tot(n-6):tot(n-3) ratio whereas that of Hall et al. fed increasing amounts of 20/22-carbon n-3 at relatively constant ALA. In any case, the present findings are consistent with the earlier study regarding the lack of a contribution of dietary FA ratio to tissue enrichment compared to FA type and dose. It is of interest that relative amounts of 22 carbon highly unsaturated FA, whether n-3 or n-6 FA, were modestly increased and nearly constant among neutrophils of all dietary groups. Both SFO and BTO groups accumulated 22:4n-6 (2.27 and 3.47 mol%, respectively) while the MHO and LSO group had more DPA n-3 (2.09 and 2.55 mol%, respectively). In view of the high dietary polyunsaturated fatty acid concentrations fed each group, resultant chain elongation of the 20 carbon FA (ARA and EPA) appears to have occurred. The possibility exists that these 22 carbon acids may subsequently serve as potential reservoirs of 20 carbon eicosanoid precursors via retroconversion during periods of neutrophil membrane active remodeling. This hypothesis is supported by MacDonald et al. [49] who reported that neutrophil phospholipids undergo extensive turnover with respect to the fatty acyl moiety in their *sn*-2 position. Retroconversion of DHA to EPA at high doses is well documented [50, 51]. The accumulation of DPA found in plasma when n-3 FA are fed may thus represent a central fatty acyl metabolite that may be either retroconverted to EPA in cells such as leukocytes or forward converted to DHA when taken up by neurologic tissues [46, 52].

It is noteworthy that nearly identical incorporation of ARA in plasma PL and neutrophil total lipids occurred when either SFO or BTO diets were fed even though the

SFO diet contained nine times more LNA than the BTO diet. To some extent, increased ARA synthesis and tissue enrichment would be expected as more LNA is fed. However, such an effect was not observed suggesting that other mechanisms may exist that define threshold saturation for AA accumulation even at relatively modest amounts of dietary LNA. Indeed studies by Lands et al. and Bauer et al. [53, 54] have observed such tissue and plasma saturation of ARA as a function of dietary LNA in rats, humans, and dogs. While the physiological significance of this finding is presently unknown, limiting the cellular enrichment of ARA in the presence of high dietary LNA may help prevent the accumulation of deleterious amounts of substrate for eicosanoid synthesis. By contrast, when dietary n-3 FA especially from fish oil are added, the ARA content of neutrophils and plasma was attenuated below this putative saturation level.

It is also of interest that increased amounts of 24:1n-9 were found in neutrophils in all groups and especially in dogs fed the MHO diet. A likely explanation for this observation is active sequential chain elongation of 18:1n-9 occurring in this cell type. By contrast, while 18:1n-9 was increased in plasma PL in the BTO group, 24:1n-9 was not. Thus, this finding appeared to be unique to neutrophils in this study. It should be noted that dietary 18:1n-9 was highest in the BTO diet yet it also contained increased amounts of 16:0 and 18:0 compared to the other diets fed. Because dietary beef tallow has previously been shown in pigs to increase steroyl-CoA desaturase activities [55], a similar effect may have occurred in the BTO diet-fed dogs in the present study leading to desaturation of 18:0.

Enrichment of neutrophil membranes with long chain n-3 FA resulted in a reduction of pro-inflammatory mediators, superoxide anion, and LTB₄. The LSO and MHO groups had approximately a 20% reduction in superoxide production compared to the BTO and SFO groups. This observation is consistent with other reports of the effects of n-3 polyunsaturated fatty acid supplementation on neutrophil superoxide production [56, 57]. This reduction can be attributed to decreased AA because this fatty acid is required for the activation of NADPH oxidase [58]. Abramson et al. reported that ARA, in part, regulates superoxide production by increasing binding of GTP to its regulatory G-protein [59]. Furthermore, these authors concluded that ARA, through its capacity to activate protein kinase C, stimulates NADPH oxidase and activates plasma membrane G-proteins [59].

Because leukotrienes synthesized by neutrophils have a prominent role in the inflammatory response, altering their production by diet is one way in which to modulate the inflammatory response. In the present study it was found that leukotriene production was significantly affected by dietary fat type. Supplementation with linseed oil or

Menhaden fish oil resulted in decreased LTB₄ and increased LTB₅ compared to the SFO and BTO groups. As with long chain n-3 fatty acid enrichment, the decrease in LTB₄ and increase in LTB₅ was significantly greater in the MHO group compared to all other groups. The quantities of leukotrienes produced from isolated canine neutrophils in our study [$\text{ng} \times (5 \times 10^6 \text{ cells})^{-1}$] are consistent with those reported in rats, humans, and one report in dogs [36–38]. By contrast another study investigating the effects of n-3 diets on canine neutrophil leukotriene production reported only 30–100 pg of LTB₄ per 5×10^6 cells [39]. Differences in methodologies used may explain these differences.

The formulation of a low fat basal diet supplemented with either Menhaden fish oil or linseed oil allowed for the creation of diets with nearly identical n-6:n-3 FA ratios. However, these diets differed considerably in their 18-carbon versus 20/22-carbon n-3 FA content. The diets were formulated using ingredients and oils that are commonly used in the manufacture of pet food and could be used for the therapeutic treatment of chronic inflammatory diseases. Given the results of the present study, long chain n-3 FA from marine sources are more efficiently incorporated into neutrophil membranes than diets containing ALA when fed at the same n-6:n-3 ratio. The beneficial effects of n-3 FA due to their competition with n-6 polyunsaturated FA for cellular membrane incorporation has led to the suggestion that the dietary n-6:n-3 ratio be used as a dietary index to modulate cell composition and cellular function [39, 60]. The findings reported here do not support the use of the n-6:n-3 ratio for this purpose. Several workshops have reviewed the health aspects of n-3 PUFA and have concluded that the use of an overall n-6:n-3 ratio is inappropriate [61–65]. Our findings are consistent with this recommendation. Thus, both the type and amount of n-3 FA, but not the n-6:n-3 ratio of diets contribute to alterations in membrane n-3 highly unsaturated fatty acid composition and subsequent changes in cell function.

Acknowledgments The authors wish to thank BL Dunbar, KE Bigley and AL Spencer for technical assistance. Funded by Nestlé Purina PetCare., St. Louis, MO and the Mark L. Morris Professorship in Clinical Nutrition, Texas A&M University, College Station, TX, USA.

Conflict of interest J.E. Bauer has no conflicts of interest. M.K. Waldron and S.S. Hannah are presently employed by Nestlé Purina PetCare., St. Louis, MO, USA.

References

- Weiss SJ (1984) Tissue destruction by neutrophils. *New Engl J Med* 320:365–376
- Smith JA (1984) Neutrophils, host defense, and inflammation: a double edge sword. *J Leukocyte Biol* 56:672–686

3. Chanock SJ, el Benna J, Smith RM, Babior BM (1994) The respiratory burst oxidase. *J Biol Chem* 269:24519–24522
4. Ricevetti G, Mazzone A, Pasotti D, de Servi S, Specchi G (1991) Roles of granulocytes in endothelial injury in coronary heart disease in humans. *Atherosclerosis* 91:1–14
5. Wang C, Harris WS, Chung MM, Lichtenstein AH, Balk EM, Kupelnick B, Jordan HS, Lau J (2006) Fatty acids from fish or fish-oil supplements, but not linolenic acid, benefit cardiovascular disease outcomes in primary and secondary prevention studies; a systematic review. *Am J Clin Nutr* 83:5–17
6. James MJ, Cleland LG (1997) Dietary n-3 FA and therapy for rheumatoid arthritis. *Semin Arthritis Rheum* 27:85–97
7. Appel LJ, Miller ER, Seidler AJ, Whelton PK (1993) Does supplementation of diet with “fish oil” reduce blood pressure? A meta-analysis of controlled clinical trials. *Arch Intern Med* 153:1429–1438
8. De Caterina R, Caprioli R, Giannessi D, Sicari R, Galli C, Lazzarini G, Bernini W, Carr L, Rindi P (1993) n-3 FA reduce proteinuria in patients with chronic glomerular disease. *Kidney Int* 44:843–850
9. Calder PC (2002) Dietary modification of inflammation with lipids. *Proc Nutr Soc* 61:345–358
10. Schwerbrock NM, Karlsson EA, Shi Q, Sheridan PA, Beck MA (2009) Fish oil-fed mice have impaired resistance to influenza infection. *J Nutr* 139:1588–1594
11. Tisset H, Pierre M, Desseyn J-L, Guery B, Beermann C, Galabert C, Gottrand F, Husson M-O (2009) Dietary (n-3) polyunsaturated fatty acids affect the kinetics of anti-inflammatory responses in mice with *Pseudomonas aeruginosa* lung infection. *J Nutr* 139:82–89
12. Broughton KS, Wadde JW (2002) Total fat and (n-3):(n-6) fat ratios influence eicosanoid production in mice. *J Nutr* 132:88–94
13. Serhan CN (2005) Novel eicosanoid and docosanoid mediators: resolvins, docosatrienes, and neuroprotectins. *Curr Opin Clin Nutr Metab Care* 8:115–121
14. Healy DA, Wallace FA, Miles EA, Calder PC, Newsholme P (2000) Effect of low-to-moderate amounts of dietary fish oil on neutrophil lipid composition and function. *Lipids* 35:763–886
15. von Schacky C, Fisher S, Weber PC (1985) Long-term effects of marine ω -3 fatty acids upon plasma and cellular lipids, platelet function, and eicosanoids formation in humans. *J Clin Invest* 76:1626–1631
16. Prisco D, Filippini M, Francalanci I, Paniccia R, Gensine GF, Abbate K, Neri Serneri GG (1996) Effect of n-3 polyunsaturated fatty acid intake on phospholipid fatty acid composition in plasma and erythrocytes. *Am J Clin Nutr* 63:925–932
17. Fisher M, Upchurch KS, Levine OPH, Johnson MH, Vaudruil CH, Natale A, Hoogasian JJ (1986) Effects of dietary fish oil supplementation on polymorphonuclear leukocyte inflammatory potential. *Inflammation* 10:387–392
18. Gibney MJ, Hunter B (1992) The effects of short- and long-term supplementation with fish oil on the incorporation of n-3 polyunsaturated fatty acids into cells of the immune system of healthy individuals. *Eur J Clin Nutr* 47:255–259
19. Terrano T, Seya A, Hirai A, Saito H, Tamura Y, Yoshida S (1987) Effect of oral administration of highly purified eicosapentaenoic acid and docosahexaenoic acid on eicosanoids formation and neutrophil function in healthy subjects. In: Lands WEM (ed) *Polyunsaturated fatty acids and eicosanoids*. American Oil Chemists Society, Champaign, pp 133–138
20. Sperling RI, Benincaso AI, Knoell CT, Larkin JK, Austen KF, Robinson DR (1993) Dietary n-3 polyunsaturated fatty acids FA inhibit phosphoinositide formation and chemotaxis in neutrophils. *J Clin Invest* 91:651–660
21. Luostarinen R, Saldeen T (1996) Dietary fish oil decreases superoxide generation by human neutrophils: Relation to cyclooxygenase pathway and lysosomal enzyme release. *Prost Leuk Essen Fatty Acids* 55:167–172
22. Varming K, Schmidt EB, Svaneborg N, Moller JM, Lervang HH, Grunnet N, Jersild C, Dyerberg J (1995) The effect of n-3 fatty acid on neutrophil chemiluminescence. *Scand J Clin Lab Invest* 55:47–52
23. Sperling RI (1991) Effects of dietary fish oil on leukocyte leukotriene production and PAF generation and on neutrophil chemotaxis. *World Rev Nutr Diet* 66:391–400
24. Charleson S, Evans JF, Leblanc Y, Fitzsimmons BJ, Leveille C, Dupuis P, Ford-Hutchinson AW (1986) Leukotriene B₃, leukotriene B₄ and leukotriene B₅; binding to leukotriene B₄ receptor on rat and human leukocyte membranes. *Prostaglandins* 32:503–516
25. Seya A, Terrano T, Tamura Y, Yoshida S (1988) Comparative effect of leukotriene B₄ and leukotriene B₅ on calcium mobilization in human neutrophils. *Prost Leuk Essen Fatty Acids* 34:47–50
26. Lee TH, Sethi T, Crea AA, Peters W, Arm JP, Horton CE, Walpodtr MJ, Supr BW (1988) Characterization of leukotriene B₃: Comparison of its biological activities with leukotriene B₄ and leukotriene B₅ in complement receptor enhancement, lysosome release and chemotaxis of human neutrophils. *Clin Sci* 74:467–475
27. Payan DG, Wong MYS, Chernow-Rogan T, Valone FH, Pickett WC, Blake VA, Gold WM, Goetzl EJ (1986) Alteration in human leukocyte function induced by ingestion of eicosapentaenoic acid. *J Clin Immunol* 6:402–410
28. Neuringer M, Anderson GJ, Conner WE (1988) The essentiality of the n-3 fatty acids for the development of the retina and the brain. *Annu Rev Nutr* 8:517–541
29. Lee JL, Fukumoto M, Nishida H, Ikeda I, Sugano M (1989) The interrelated effects of n-6/n-3 and polyunsaturated/saturated ratios of dietary fats on the regulation of lipid metabolism in rats. *J Nutr* 119:1893–1899
30. Goyens PLL, Spilker ME, Zock PL, Katan MB, Mensink RP (2005) Compartmental modeling to quantify α -linolenic acid conversion after longer term intake of multiple tracer boluses. *J Lipid Res* 46:1474–1483
31. Su HM, Bernardo L, Mirmiran M, Ma XH, Nathanielsz PW, Brenna JT (1999) Dietary 18:3n-3 and 22:6n-3 as sources of 22:6n-3 accretion in neonatal baboon brain and associated organs. *Lipids* 34:S347–S350
32. Brenna JT, Salem N Jr, Sinclair AJ, Cunnane SC, International Society for the Study of Fatty Acids and Lipids, ISSFAL (2009) Alpha-linolenic acid supplementation and conversion to n-3 long-chain polyunsaturated fatty acids in humans. *Prost Leuk Essen Fatty Acids* 80:85–91
33. Ziboh VA, Fletcher MP (1992) Dose-response effects of dietary α -linoleic acid-enriched oils on human polymorphonuclear-neutrophil biosynthesis of leukotriene B₄. *Am J Clin Nutr* 55:39–45
34. Carletto Bellavite P, Guarinin P, Biasi D, Chirumbolo S, Caramaschi P, Bambara LM, Corrocher R (1996) Changes of fatty acid composition and oxidative metabolism of human neutrophils migrating into inflammatory exudates. *Inflammation* 20:123–127
35. Schneider SM, Fung VS, Palmblad J, Babior BM (2001) Activity of the leukocyte NADPH oxidase in whole neutrophils and cell-free neutrophil preparations stimulated with long-chain polyunsaturated fatty acids. *Inflammation* 1:17–23
36. Gibson RA, Neuman MA, James MJ, Hawkes JS, Hall C, Cleland LG (1992) Effect of n-3 and n-6 dietary fats on the lipoxygenase products from stimulated rat neutrophils. *Prost Leuk Essen Fatty Acids* 46:87–91
37. LeBlanc CJ, Horohov DW, Bauer JE, Hosgood G, Mauldin GE (2008) Effects of dietary supplementation with fish oil on in vivo

- production of inflammatory mediators in clinically normal dogs. *Am J Vet Res* 69:486–493
38. Byrne KP, Campbell KL, Davis CA, Schaffer DJ, Troutt HF (2000) The effects of dietary n-3 vs. n-6 fatty acids on ex vivo LTB₄ generation by canine neutrophils. *Vet Derm* 11:123–131
 39. Vaughn DM, Rheinart GA, Swaim SF, Laurten SD, Garner CA, Boudreaux MK, Spano JS, Hoffman CE, Conner B (1994) Evaluation of dietary n-6 to n-3 fatty acid ratios on leukotriene synthesis in dog skin and neutrophils. *Vet Derm* 5:163–173
 40. LeBlanc CJ, Dietrich MA, Horohov DW, Bauer JE, Hosgood G, Mauldin GE (2007) Effects of dietary fatty fish oil and vitamin E supplementation on canine lymphocyte proliferation evaluated using a flow cytometric technique. *Vet Immunol Immunopath* 119:180–188
 41. Hall JA, Picton RA, Skinner MM, Jewell DE, Wander RC (2006) The (n-3) fatty acid dose, independent of the (n-6) to (n-3) fatty acid ratio, affects the plasma fatty acid profile of normal dogs. *J Nutr* 136:2338–2344
 42. Markert M, Andrews PC, Babior BM (1984) Measurement of O₂⁻ production by human neutrophils. The preparation and assay of NADPH oxidase-containing particles from human neutrophils. *Methods Enzymol* 105:358–365
 43. Folch K, Lees M, Sloane-Stanley GH (1957) A simple method for the isolation and purification of total lipids from animal tissue. *J Biol Chem* 226:497–509
 44. Hansen J-B, Grimsgard S, Nilsen H, Nordoy A, Bonna KH (1999) Effects of highly purified eicosapentaenoic acid and docosahexaenoic acid on fatty acid absorption, incorporation into serum phospholipids and postprandial triglyceridemia. *Lipids* 33:131–138
 45. Burdge GC, Jones AE, Wootton SA (2002) Eicosapentaenoic acid and docosapentaenoic acids are the principal products of α -linolenic acid metabolism in young men. *Br J Nutr* 88:355–363
 46. Bauer JE, Dunbar BL, Bigley KE (1998) Dietary flaxseed in dogs results in differential transport and metabolism of (n-3) polyunsaturated fatty acids. *J Nutr* 128:2641S–2644S
 47. Dunbar BL, Bigley KE, Bauer JE (2010) Early and sustained enrichment of serum n-3 long chain polyunsaturated fatty acids in dogs fed a flaxseed supplemented diet. *Lipids* 45:1–10
 48. Gavino GR, Gavino GC (1991) Rat liver outer mitochondrial carnitine palmitoyltransferase activity toward long chain polyunsaturated fatty acids and CoA esters. *Lipids* 26:266–270
 49. MacDonald JIS, Sprecher H (1991) Phospholipid remodeling in mammalian cells. *Biochim Biophys Acta* 1084:105–121
 50. Brossard N, Croset M, Pachiardi C, Riou JP, Tayot JL, Lagarde M (1996) Retroconversion and metabolism of [¹³C]22:6n-3 in humans and rats after intake of a single dose of [¹³C]22:6n-3 triacylglycerols. *Am J Clin Nutr* 64:577–586
 51. Conquer JA, Holub BJ (1997) Dietary docosahexaenoic acid as a source of eicosapentaenoic acid in vegetarians and omnivores. *Lipids* 32:341–345
 52. Chen H, Ray J, Scarpino V, Acland GM, Aguirre GD, Anderson RE (1999) Synthesis and release of docosahexaenoic acid by the RPE cells of pcd-affected dogs. *Invest Ophthalmol Vis Sci* 10:2418–2422
 53. Lands WEM, Morris A, Libelt B (1990) Quantitative effects of dietary polyunsaturated fats on the composition of fatty acids in rat tissues. *Lipids* 25:505–516
 54. Bauer JE, Waldron MK, Spencer AL, Hannah SS (2002) Predictive equations for the quantitation of polyunsaturated fatty acids in canine plasma and neutrophils from dietary fatty acid profiles. *J Nutr* 132:1642S–1645S
 55. Klingenberg IL, Knabe DA, Smith SB (1995) Lipid metabolism in pigs fed beef tallow or high-oleic acid sunflower oil. *Comp Biochem Physiol Part B* 110:183–192
 56. Carletto A, Bellavite P, Guarinin P, Biasi D, Chirumbolo S, Caramaschi P, Bambara LM, Corrocher R (1996) Changes of fatty acid composition and oxidative metabolism of human neutrophils migrating into inflammatory exudates. *Inflammation* 20:123–127
 57. Schneider SM, Fung VS, Palmblad J, Babior BM (2001) Activity of the leukocyte NADPH oxidase in whole neutrophils and cell-free neutrophil preparations stimulated with long-chain polyunsaturated fatty acids. *Inflammation* 1:17–23
 58. Edwards SW (1994) *Biochemistry physiology of the neutrophil*. Cambridge University Press, New York, pp 1–69
 59. Abramson SB, Leszczynska-Piziak J, Weissmann G (1991) Arachidonic acid as a second messenger: interactions with GTP-binding protein of human neutrophils. *J Immunol* 147:231–236
 60. Harris WS (2006) The omega-6/omega-3 ratio and cardiovascular disease risk: uses and abuses. *Curr Athero Rep* 8:453–459
 61. Stanley JC, Elsom RL, Calder PC, Griffin BA, Harris WS, Jebb SA, Lovegrove JA, Moore CS, Riemersma RA, Sanders TAB (2007) UK food standards agency workshop report: the effects of dietary n-6:n-3 fatty acid ratio on cardiovascular health. *Br J Nutr* 98:1305–1310
 62. Wall R, Ross RP, Fitzgerald GF, Stanton C (2010) Fatty acids from fish: the anti-inflammatory potential of long-chain omega-3 fatty acids. *Nutr Rev* 68:280–289
 63. Anonymous (1992) *Functions of unsaturated fatty acids. In: Unsaturated Fatty Acids: Nutritional and Physiological Significance. The Report of the British Nutrition Foundation's Task Force*, Chapman & Hall, London, pp 48–62
 64. deDeckere EAM, Korver O, Verschuren PM, Katan MB (1998) Health aspect of fish and n-3 polyunsaturated acids from plant and marine origin. *Eur J Clin Nutr* 52:749–753
 65. Simopoulos AP, Leaf A, Salem N Jr (1999) Workshop on the essentiality of and recommended dietary intakes for omega-6 and omega-3 fatty acids. *J Am Coll Nutr* 8:4878–4889

Absorption and Metabolism of *cis-9,trans-11-CLA* and of Its Oxidation Product 9,11-Furan Fatty Acid by Caco-2 Cells

Thorsten Buhrke · Roswitha Merkel ·
Imme Lengler · Alfonso Lampen

Received: 15 August 2011 / Accepted: 22 December 2011 / Published online: 18 January 2012
© The Author(s) 2012. This article is published with open access at Springerlink.com

Abstract Furan fatty acids (furan-FA) can be formed by auto-oxidation of conjugated linoleic acids (CLA) and may therefore be ingested when CLA-containing foodstuff is consumed. Due to the presence of a furan ring structure, furan-FA may have toxic properties, however, these substances are toxicologically not well characterized so far. Here we show that 9,11-furan-FA, the oxidation product of the major CLA isomer *cis-9,trans-11-CLA* (c9,t11-CLA), is not toxic to human intestinal Caco-2 cells up to a level of 100 μ M. Oil-Red-O staining indicated that 9,11-furan-FA as well as c9,t11-CLA and linoleic acid are taken up by the cells and stored in the form of triglycerides in lipid droplets. Chemical analysis of total cellular lipids revealed that 9,11-furan-FA is partially elongated probably by the enzymatic activity of cellular fatty acid elongases whereas c9,t11-CLA is partially converted to other isomers such as c9,c11-CLA or t9,t11-CLA. In the case of 9,11-furan-FA, there is no indication for any modification or activation of the furan ring system. From these results, we conclude that 9,11-furan-FA has no properties of toxicological relevance at least for Caco-2 cells which serve as a model for enterocytes of the human small intestine.

Keywords Furan fatty acid · Conjugated linoleic acid · CLA · Caco-2

Abbreviations

BSA Bovine serum albumin
CLA Conjugated linoleic acid
DMEM Dulbecco's modified Eagle's medium

DMSO Dimethylsulfoxide
FCS Fetal calf serum
Furan-FA Furan fatty acid
GC/MS Gas chromatography/mass spectrometry
LNA Linoleic acid

Introduction

Conjugated linoleic acids (CLA) are polyunsaturated fatty acids that are present in many natural food sources. The term CLA describes a group of positional and geometric isomers of linoleic acid (LNA) derivatives having conjugated double bonds. The conversion from LNA to CLA occurs in the rumen of ruminants by bacterial metabolic activity [1]. Therefore, the main source for CLA taken up by humans is foodstuff derived from ruminants such as milk or meat.

Over the last decade the interest in CLA has arisen because various publications suggested that CLA may have many different positive physiological effects. In vitro, CLA inhibited the growth of various human cancer cells such as colon [2], mammary [3] and prostate [4] cancer cell lines. This anticarcinogenic effect was also determined in vivo where supplementation with CLA resulted in a decreased size of chemically or genetically induced tumors in experimental animals (reviewed in [5]). In addition, CLA seem to prevent atherosclerosis [6, 7, 8] and may improve the immune system [9, 10]. On the other hand, some publications describe negative effects of CLA supplementation, i.e. the induction of non-alcoholic hepatic steatosis in mice [11], the decrease of insulin sensitivity in human subgroups [12], or the increase in proinflammatory cytokines in human adipocytes in vitro [13]. In the past decade,

T. Buhrke (✉) · R. Merkel · I. Lengler · A. Lampen
Department of Food Safety, Federal Institute for Risk
Assessment, Max-Dohrn-Str. 8-10, 10589 Berlin, Germany
e-mail: thorsten.buhrke@bfr.bund.de

attention has predominantly been drawn on a potential anti-adipogenic role of CLA as these substances are proposed to have a positive effect on body composition by decreasing body fat mass and increasing lean muscle mass (reviewed in [14]). In the case of body composition, the CLA isomer *trans*-10, *cis*-12-CLA (t10,c12-CLA) seems to be responsible for reduction of body fat [15]. On the other hand, it was proposed that the isomer *cis*-9,*trans*-11-CLA (c9,t11-CLA) was more effective concerning the inhibition of tumor development [16]. Milk and meat of ruminant animals contain 28 different CLA isomers, and the most abundant isomer in food is the c9,t11-CLA isomer, which represents up to 80% of total CLA.

Due to the reported positive effects of CLA on body mass composition and despite controversial data and some observed negative effects of CLA, these compounds are already available in numerous formulas of food supplements and are currently being discussed for their use as food additives. CLA are classified as “novel foods” in Europe and a premarketing risk assessment of CLA is a mandatory part of the novel food approval. For a reliable risk assessment of CLA it is necessary to focus additionally on the oxidation products of CLA, the furan fatty acids (furan-FA).

Furan-FA are comprised of a furan ring flanked by one alkyl and one carboxyl side chain in the α -positions of the furan ring. It has been shown that in the presence of air CLA can react with dioxygen to form furan-FA [17] (Fig. 1). Therefore, if CLA-containing food supplements are consumed, significant amounts of furan-FA may be taken up by the consumer in parallel. Up to now, hardly anything is known about the toxicological potential of furan-FA. The presence of the aromatic furan ring system in furan-FA gives rise to the assumption that these compounds may have hazard potential since furan itself and numerous furan derivatives have shown themselves to have properties of toxicological relevance (reviewed in [18]). The aim of our study was to investigate the absorption and the metabolism of furan-FA by human intestinal cells. The well-established Caco-2 system was employed for this

study as it is a widely used in vitro model for the intestinal barrier. Differentiated Caco-2 cells are known to form a tight cellular monolayer with morphological and biochemical properties very similar to those of enterocytes of the small intestine [19, 20]. In addition, the Caco-2 system is a well-established model for intestinal lipid metabolism [21].

Experimental Materials and Methods

Chemicals and Fatty Acids

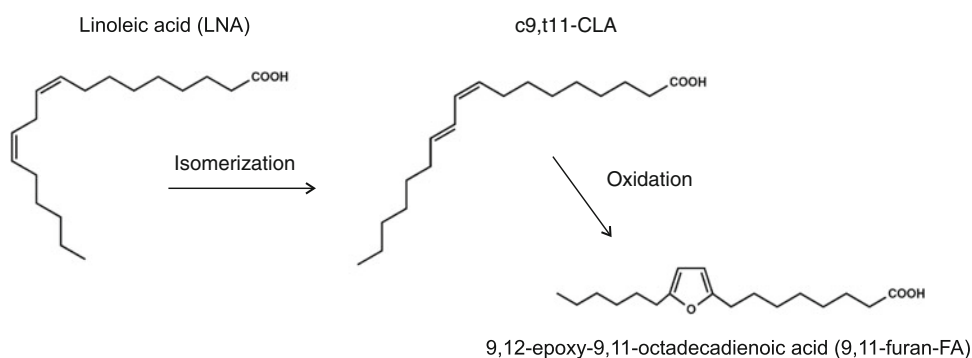
All chemicals were purchased from Merck (Darmstadt, Germany) or Sigma-Aldrich (Taufkirchen, Germany) in the highest available purity. The CLA isomers *cis*-9,*trans*-11-octadecadienoic acid (c9,t11-CLA) and the furan fatty acid 9,12-epoxy-9,11-octadecadienoic acid (9,11-furan-FA) were obtained from Biotrend (Köln, Germany). LNA was purchased from Sigma-Aldrich (Taufkirchen, Germany). All fatty acids were dissolved in DMSO to get 0.1 M stock solutions.

Cell Culture and Treatment with Fatty Acids

Cells were obtained from the European Collection of Cell Culture (ECACC). Culture media and supplements were obtained from PAA Laboratories GmbH (Pasching, Austria). The human adenocarcinoma cell line Caco-2 (ECACC No. 860 10 202) was cultured in Dulbecco's modified Eagle's medium (DMEM) supplemented with 10% fetal calf serum, 100 U/ml penicillin and 100 μ g/ml streptomycin in a humidified atmosphere of 5% CO₂ at 37 °C. Cells were passaged every 3–4 days by treatment with 0.1% trypsin and 0.04% EDTA and then plated at a density of $1.3\text{--}2 \times 10^4$ cells/cm².

For experimentally treatment with fatty acids, cells were allowed to attach by cultivating overnight in medium containing 10% FCS and were then incubated in serum-free medium supplemented with 1% insulin–transferrin–selenium

Fig. 1 Structures of LNA, c9,t11-CLA and 9,11-furan-FA



(ITS, Invitrogen, Karlsruhe, Germany) and 0.1 mg/ml fatty acid-free BSA (Sigma-Aldrich, Taufkirchen, Germany) with various concentrations of the respective fatty acid with a molar ratio of fatty acid to BSA of 4:1.

Oil-Red-O Staining

Caco-2 cells were cultivated on cover slips in 24-well plates with 40,000 cells/well. After 48 h of treatment with fatty acids staining with Oil-Red-O (Sigma-Aldrich, Taufkirchen, Germany) was performed. Cells were washed with Phosphate Buffered Saline (PBS) and fixed with 3.7% formaldehyde for 1 h. 0.3% Oil-Red-O in isopropanol was then added directly to the fixed cells and incubated for 1 h. The microscopy studies were performed with a Axio Observer microscope equipped with a digital camera (Zeiss, Jena, Germany).

Cell Viability Assay

Cells were plated in 96-well plates with 7,500 cells/well for Caco-2 cells in 100 μ l medium. After 2 days of treatment with fatty acids cell viability was estimated by the Cell-Titer-Blue[®] Cell Viability Assay (CTB Assay) (Promega, Madison, WI). Assays were performed by adding 20 μ l of a 1:4 dilution of the CTB reagent in phosphate-buffered saline (PBS) directly to the cells cultured in 100 μ l medium, incubating for 1 h at 37 °C and then measuring fluorescence at 540/590 nm with a Mithras Multimode Reader LB 940 (Berthold Technologies, Vienna, Austria). Values are expressed as percentages of the negative control which was exposed to medium containing 0.1% DMSO and which was taken as 100%. As a positive control for cytotoxicity: cells were exposed to medium containing 0.05% Triton X-100.

Extraction of Total Cellular Lipids and Fatty Acid Derivatization

Caco-2 cells were incubated with 100 μ M of LNA, c9,t11-CLA or 9,11-furan-FA for 48 h. Cells were washed twice with PBS, and after treatment with trypsin/EDTA cells were transferred to reaction tubes. 20 μ l of a 10 mM solution of butylated hydroxytoluene (BHT) in acetonitrile was applied to the cell suspensions to protect the lipids from oxidative damage. Subsequently, cells were lyophilized to completely remove the water and total lipids were extracted twice from the dried cell pellet with 0.7 ml of a 2:1 (v/v) chloroform:methanol mixture. 150 μ l of a 20% solution of BF₃ in methanol was applied to the lipid extracts, and transmethylation was conducted for 10 min at 70 °C. Methylated fatty acids were extracted with 1 ml of hexane, dried over anhydrous sodium sulfate, concentrated in vacuo and finally dissolved in 200 μ l hexane.

GC/MS Analysis

GC/MS analysis was conducted with an Agilent 7890A gas chromatograph coupled to an Agilent MSD 5975C mass spectrometer. Methylated fatty acids were separated with an Rt-2560 column (100 m \times 0.25 mm \times 0.2 μ m; Restek, Bad Homburg, Germany) by using helium as the carrier gas at a flow rate of 1 ml/min. 2 μ l of each samples was applied to the cold injection system (splitless mode, 15 °C) by taking advantage of an MP5 autosampler (Gerstel, Mülheim, Germany). The oven program was as follows: 6 min at 35 °C, ramp to 165 °C at 65 °C/min, 2 min at 165 °C, 1 min at 180 °C, 0.5 min at 190 °C, 1 min at 210 °C. Methylated fatty acids were identified by comparison of retention times with authentic standards and by the fragmentation pattern in the mass spectra. The artificial methylated fatty acid C19:0 was used as the internal standard. Mass spectra were recorded both in the SCAN modus and in the SIM modus to increase sensitivity. The quantitation limit of the method was 0.25 ng/ μ l for each individual fatty acid.

Results

Viability of Caco-2 Cells

In this study we focused on c9,t11-CLA, the major CLA isomer in foodstuff, and on its oxidation product 9,11-furan-FA. Moreover, the metabolic precursor of c9,t11-CLA, LNA, was included in the study.

To analyse potential cytotoxic effects of LNA, c9,t11-CLA and 9,11-furan-FA, Caco-2 cells were incubated with various concentrations of these substances. Subsequently, cellular viability was tested by using the CTB assay. As shown in Fig. 2, incubation of the cells with up to 100 μ M of the respective substance did not affect cellular viability whereas cellular viability was decreased to a level of about 3% upon incubation of the cells with medium containing 0.05% Triton X-100 which was used as positive control. Thus, none of the substances tested in this study displayed cytotoxic potential to Caco-2 cells up to a level of 100 μ M.

Fatty Acid Absorption by Caco-2 Cells

Caco-2 cells have the capacity to absorb free fatty acids and to incorporate them into triglycerides for storage in lipid droplets [22]. To analyze whether the enzymatic machinery of Caco-2 accepts furan-FA as a fatty acid-type substrate at all, lipid droplet staining was conducted with LNA-, CLA- and furan-FA-treated cells in order to visualize cellular absorption of the respective fatty acid. Caco-2 cells were incubated either with LNA, c9,t11-CLA, or

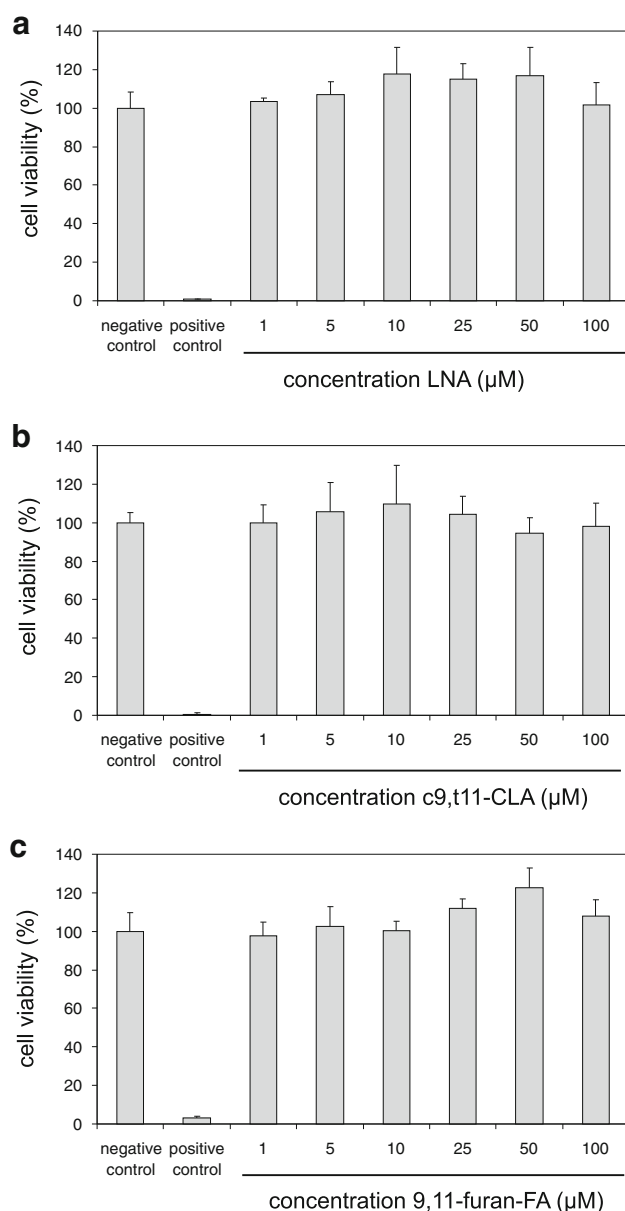


Fig. 2 Viability of Caco-2 cells. Cells were treated with various concentrations of (a) LNA, (b) c9,t11-CLA, and (c) 9,11-furan-FA for 48 h. Cellular viability was determined using the CTB assay and expressed as percentages of negative control which was exposed to medium containing 0.1% DMSO (set as 100%). Data are expressed as the means \pm SD; $n = 5$

9,11-furan-FA, and Oil-Red-O-staining of the cells was conducted after 48 h of incubation in order to visualize the formation of intracellular lipid droplets. In control cells, intracellular red stain was rarely visible, whereas numerous small lipid droplets were stained in cells that had been incubated with 10 μ M LNA, c9,t11-CLA or 9,11-furan-FA (Fig. 3). Incubation of the cells with 100 μ M of the respective free fatty acid yielded cells full of large lipid droplets (Fig. 3). Therefore, Fig. 3 clearly illustrates that

lipid droplet formation in Caco-2 cells increased with increasing concentrations of free fatty acid offered to the cells, independent of the type of fatty acid. Moreover, microscopic inspection of numerous cells indicated that Caco-2 cells treated with 100 μ M of the respective fatty acid tend to be enlarged in size due to lipid droplet formation. In these experiments there was no observation of specific alterations in cell morphology such as shrinking of the cells that might point to toxic effects induced by fatty acid treatment. Thus, in sum, Caco-2 cells seem to absorb 9,11-furan-FA and to store it as triglycerides in lipid droplets as they do with LNA and c9,t11-CLA.

Analysis of Fatty Acid Composition

To follow the fate of the fatty acids taken up by the cells, a GC/MS method was employed to analyze cellular fatty acid composition in more detail. For this purpose, total cellular lipids were extracted from Caco-2 cells that had been incubated with 100 μ M of LNA, c9,t11-CLA, or 9,11-furan-FA, respectively. After lipid hydrolysis and fatty acid derivatization, the resulting mixture of fatty acid methyl esters was separated by gas chromatography. Fatty acid identification was achieved by subsequent MS analysis of individual peaks. The relative amount of the respective fatty acid was calculated from the peak area in relation to the peak area of the internal standard. The results of this analysis are summarized in Table 1.

Incubation of the cells with LNA resulted in an approximately four-fold increase in the relative intracellular content of LNA and in a concomitant relative decrease of the amount of the other fatty acids with two exceptions. Compared to the control cells, the relative amount of the well-known LNA-metabolite 20:4n-6 increased upon incubation of the cells with LNA. In addition, a small amount of t9,t11-CLA was detectable in the samples obtained from LNA-incubated cells.

In the case of c9,t11-CLA, an approx. 20-fold increase in the relative intracellular amount of this substance was observed. In addition, the relative amount of the CLA isomers c9,c11-CLA and t9,t11-CLA increased whereas the relative content of the remaining fatty acids decreased.

Incubation of the cells with 9,11-furan-FA yielded an approx. 20-fold increase in the relative intracellular amount of this compound and a simultaneous decrease of the relative content of all other fatty acids. There was, however, an additional peak in the gas chromatogram that was neither present in the chromatogram of the control cells nor in the chromatograms of the cells incubated with LNA or c9,t11-CLA. The peak area of the additional peak was at a level of about 10% compared to the area of the 9,11-furan-FA peak (data not shown). Comparison of the mass spectra of 9,11-furan-FA and of the unknown substance from the

Fig. 3 Oil-Red-O staining. Caco-2 cells were incubated with LNA, c9,t11-CLA, or 9,11-furan-FA for 48 h. Oil-Red-O staining was conducted as described in the methods section. *Red staining* is indicative of lipid droplets (color figure online)

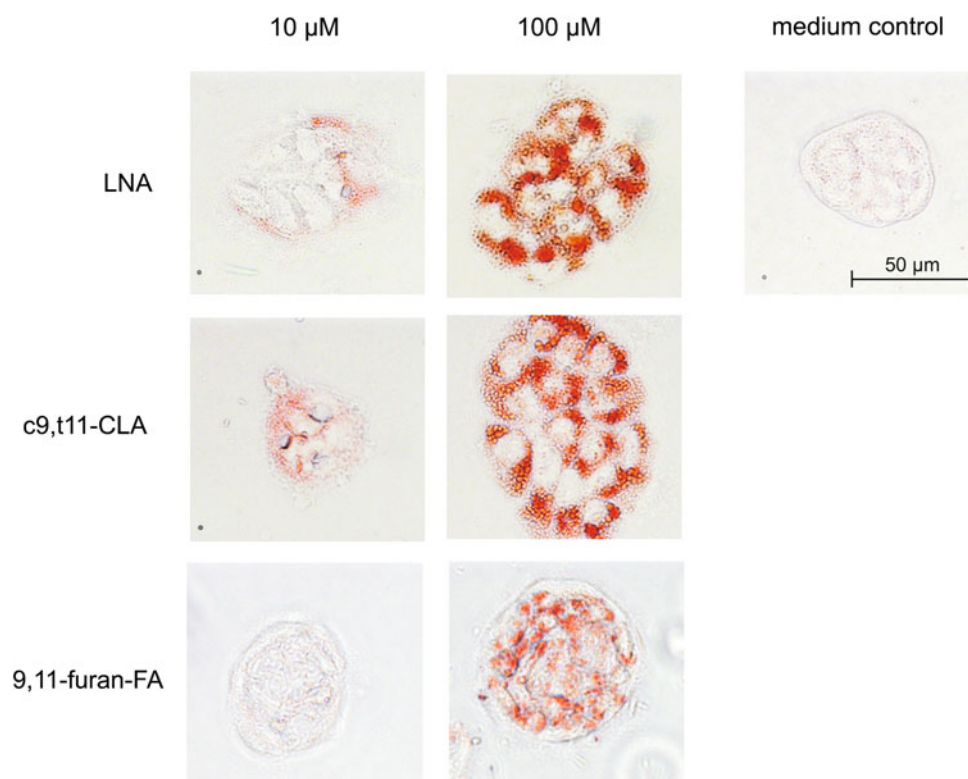


Table 1 Incorporation of LNA, c9,t11-CLA, and 9,11-furan-FA, respectively, into the total cellular lipids of Caco-2 cells after 48 h of incubation

Fatty acid (wt. %)	Control	LNA	c9,t11-CLA	9,11-furan-FA
16:0	6.10 ± 2.72	2.56 ± 1.22	0.92 ± 0.30	0.22 ± 0.06
18:0	50.87 ± 6.41	41.68 ± 4.83	30.21 ± 2.98	13.18 ± 1.61
18:1n-7	5.06 ± 0.57	4.53 ± 0.92	2.31 ± 0.81	2.61 ± 0.44
18:1n-9	5.07 ± 1.54	2.47 ± 0.93	1.98 ± 1.06	1.21 ± 0.33
20:0	4.27 ± 0.55	1.99 ± 0.75	1.31 ± 0.38	0.43 ± 0.14
20:1n-9	3.67 ± 0.46	1.18 ± 0.27	0.78 ± 0.21	0.72 ± 0.22
20:4n-6	12.10 ± 1.37	17.22 ± 3.88	4.00 ± 0.88	3.59 ± 0.52
c9,c11-CLA	nd	nd	2.55 ± 0.88	nd
t9,t11-CLA	nd	0.58 ± 0.26	6.57 ± 1.00	0.07 ± 0.04
LNA	6.44 ± 1.13	23.32 ± 4.29	2.80 ± 0.52	1.03 ± 0.26
c9,t11-CLA	2.19 ± 0.53	1.54 ± 0.49	44.50 ± 4.27	0.20 ± 0.09
9,11-furan-FA	4.23 ± 0.93	2.93 ± 0.79	1.92 ± 0.79	76.71 ± 2.58

nd not detected

additional peak revealed that this substance must be a metabolite of 9,11-furan-FA (Fig. 4). Two major peaks with m/z 165 and m/z 179 in the mass spectrum of 9,11-furan-FA (Fig. 4a) can be explained by the cleavage of the compound between carbon atoms C7 and C8, and between C6 and C7, respectively. Additional β -cleavage of these products between C13 and C14 results in masses of m/z 95 and m/z 107, respectively, additional major peaks in spectrum of Fig. 4a. Since these four masses are also present in the mass spectrum of the unknown metabolite (Fig. 4b), it can be concluded that this metabolite is a derivative of 9,11-furan-FA. Moreover, preservation of

these four masses indicates that the furan ring is still intact in the metabolite and that it was not altered upon cellular metabolic activity.

Since the molecule peak of 9,11-furan-FA with m/z 308 (Fig. 4a) was shifted to a mass of m/z 336 (Fig. 4b), the mass of the metabolite has increased by 28 atomic units (a.u.). In addition, the series of m/z 237, m/z 251, m/z 265 and m/z 277 of Fig. 4a has shifted by 28 a.u. to m/z 265, m/z 279, m/z 293 and m/z 305, respectively, in Fig. 4b. The increase of 28 a.u. can be explained by the addition of two methylene groups to 9,11-furan-FA, resulting in the C20-derivative as depicted in the insert of Fig. 4b.

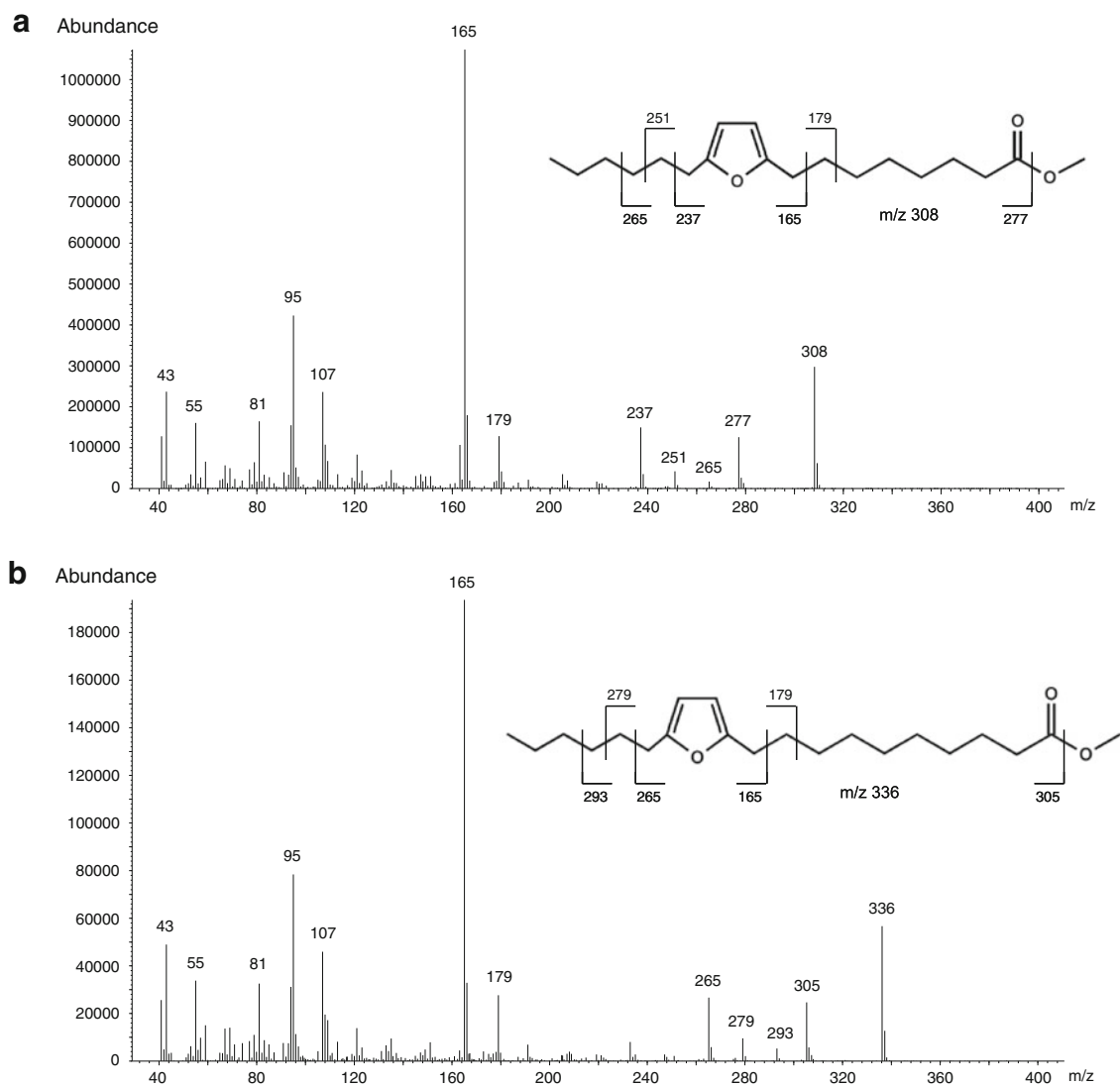


Fig. 4 Mass spectra of (a) 9,11-furan-FA and of (b) the metabolite that was formed upon incubation of Caco-2 cells with 9,11-furan-FA. The masses of the major cleavage products are assigned to the structures of the respective molecule

Discussion

In the past decades, CLA have been intensively investigated in numerous *in vivo* and *in vitro* studies. These substances are supposed to have various positive effects on human health. Therefore, CLA are already available as food supplements, and the risks and benefits of supplementation of foodstuff with CLA are currently under discussion. Surprisingly, the putative presence of furan-FA in CLA preparations plays no role in these discussions so far, although it was shown that furan-FA might arise from auto-oxidation of CLA in the presence of molecular oxygen [17]. From a toxicological point of view, furan-FA are of particular interest because furan-FA harbor a furan ring system, and furan and furan derivatives have been shown to

be toxic compounds (reviewed in [18, 23, 24]). In the liver, furan and furan derivatives are activated by CYP2E1 to form epoxides, and subsequently these epoxides are further converted to yield aldehydes in some cases [25–27]. Epoxides as well as aldehydes can directly react with lipids, proteins or DNA and are therefore toxic to cellular systems. Due to their reactivity to DNA, they are potent mutagens. Therefore, the toxicological characterization of furan-FA has to be conducted in parallel to the current risk and benefit assessment of CLA supplementation.

It is well-known that plants produce furan-FA as secondary metabolites. These furan-FA of plant origin carry methyl groups at one or both β -positions of the furan ring. If these compounds are ingested with food, the methyl groups are converted by liver metabolic activity to carboxylic acid

groups and the resulting urofuran acids are then excreted via the kidney (reviewed in [28]). In contrast to the plant furan-FA, the furan-FA analyzed in this study is an oxidation product of c9,t11-CLA and does not carry substituents at the β -positions of the furan ring. There are only few examples for non-substituted furan-FA in nature. A few non-substituted furan-FA have been isolated only from marine sponges so far, and preliminary in vitro studies revealed considerable cytotoxic potential of these isolates [29, 30]. The furan-FA analyzed in this study, however, showed no cytotoxic effect up to a concentration of 100 μ M.

The Caco-2 cell line used in this study serves as a model for human intestinal enterocytes. Caco-2 cells have been shown to be capable of lipid metabolism including triglyceride synthesis and lipid droplet formation. Moreover, these cells express numerous P450 enzymes and have the capacity to detoxify various compounds. Among others, the CYP2E1 enzyme has shown itself to be expressed by Caco-2 cells [31]. Therefore, the Caco-2 system was the ideal model to study uptake and metabolism of furan-FA by human intestinal cells, because triglyceride formation as well as β -oxidation and CYP-mediated activation of the furan ring could be examined by using this cell line. Our results indicate that furan-FA are taken up by the cells, esterified to triglycerides and stored in lipid droplets. At first glance, there seems to be no difference in the uptake and conversion of LNA, CLA and the corresponding furan-FA by Caco-2 cells. Hydrolysis of total cellular lipids and subsequent fatty acid quantification revealed that LNA and CLA were partly converted to related fatty acids by the cells (Table 1).

In the case of LNA, a relative increase in arachidonic acid (20:4n-6) was observed. It is well-known that mammalian cells have the capacity to use LNA as a precursor for the formation of 20:4n-6. Fatty acid elongation is facilitated by the activity of ELOVL5, a member of the ELOVL (elongation of very long chain fatty acid) protein family [32, 33] followed by the subsequent insertion of two additional double bonds. Thus, based on our lipid analysis, there is some indication that Caco-2 cells do not only take up fatty acid and store them as triglycerides in lipid droplets, but the cells also seem to elongate fatty acids prior to triglyceride formation.

Incubation of the cells with c9,t11-CLA resulted in a relative increase in the CLA isomers c9,c11-CLA and t9,t11-CLA (Table 1). It has recently been shown that the human colon cell line HT-29 can convert t11,t13-CLA into its isomer c9,t11-CLA probably by an enzymatic two-step saturation/desaturation reaction [34]. This might explain the appearance of the c9,c11-CLA isomer in our experiment but can not explain the presence of the t9,t11-CLA isomer as mammalian cells do not introduce *trans* double bonds into fatty acids. We can not exclude that *cis-trans* isomerization

might have occurred chemically during sample preparation or derivatization. By using a solution of c9,t11-CLA in control experiments, however, there was no indication of *cis-trans* isomerization under the given experimental conditions (data not shown). Finally, the unexpectedly high amounts of the different CLA isomers and of 9,11-furan-FA already in the control cells might have been due to the fact that the cells had been incubated in a medium containing 10% fetal calf serum (FCS) that may contain significant amounts of bovine-specific fatty acids.

Lipid extracts from cells incubated with 9,11-furan-FA yielded an additional peak in the gas chromatogram that was not detected with extracts from cells that had been treated with LNA or c9,t11-CLA. Based on the corresponding mass spectrum, we propose a structure for the furan-FA-derived metabolite as presented in Fig. 4b. From a biological point of view, the presence of this compound can simply be explained by the elongation of 9,11-furan-FA probably again by the action of a member of the ELOVL protein family and the subsequent reduction of the condensation product as described for LNA above.

Finally, GC/MS analysis of fatty acid extracts derived from furan-FA-treated Caco-2 cells gave no indication for any modification at the furan ring system. There were no metabolites detected that might have been formed upon epoxide formation or any other modification of the furan ring. Therefore, furan-FA might be either not accepted as a substrate for the cellular CYP machinery, or esterification of furan-FA to form triglycerides and subsequent storage in lipid droplets might be favoured in comparison to the postulated oxidative conversion of the furan ring. In conclusion, furan-FA taken up by human intestinal cells seem to end up preferentially in lipid metabolic pathways such as fatty acid elongation and triglyceride formation, whereas the furan ring present in furan-FA does not seem to be attacked by detoxifying enzymes. In vivo, intestinal cells pack triglycerides into chylomicrons which are VLDL-like particles and secrete them into the blood stream. These chylomicrons are then taken up by liver cells where they are further metabolized. Since our results indicate that the furan ring system of furan-FA was not affected by the metabolic activity of intestinal cells, we will address the question in future studies as to whether the furan ring might be attacked by liver metabolic activity.

Acknowledgments We thank Dr. Lukrecia Benesch-Girke for giving helpful advice in the GC/MS measurements. Linda Brandenburger and Anja Köllner are acknowledged for their technical assistance. This project was funded by the Deutsche Forschungsgemeinschaft (DFG project LA 1177/5-4). There are no conflicts of interest.

Open Access This article is distributed under the terms of the Creative Commons Attribution Noncommercial License which permits any noncommercial use, distribution, and reproduction in any medium, provided the original author(s) and source are credited.

References

- Kepler CR, Hirons KP, McNeill JJ, Tove SB (1966) Intermediates and products of the biohydrogenation of linoleic acid by *Butyrivibrio fibrisolvens*. *J Biol Chem* 241:1350–1354
- Lampen A, Leifheit M, Voss J, Nau H (2005) Molecular and cellular effects of *cis-9,trans-11*-conjugated linoleic acid in enterocytes: effects on proliferation, differentiation, and gene expression. *Biochim Biophys Acta* 1735:30–40
- Chujo H, Yamasaki M, Nou S, Koyanagi N, Tachibana H, Yamada K (2003) Effect of conjugated linoleic acid isomers on growth factor-induced proliferation of human breast cancer cells. *Cancer Lett* 202:81–87
- Kim EJ, Shin HK, Cho JS, Lee SK, Won MH, Kim JW, Park JH (2006) *trans-10, cis-12* conjugated linoleic acid inhibits the G1-S cell cycle progression in DU145 human prostate carcinoma cells. *J Med Food* 9:293–299
- Kelley NS, Hubbard NE, Erickson KL (2007) Conjugated linoleic acid isomers and cancer. *J Nutr* 137:2599–2607
- Lee KN, Kritchevsky D, Pariza MW (1994) Conjugated linoleic acid and atherosclerosis in rabbits. *Atherosclerosis* 108:19–25
- Nicolosi RJ, Rogers EJ, Kritchevsky D, Scimeca JA, Huth PJ (1997) Dietary conjugated linoleic acid reduces plasma lipoproteins and early aortic atherosclerosis in hypercholesterolemic hamsters. *Artery* 22:266–277
- Kritchevsky D, Tepper SA, Wright S, Tso P, Czarnecki SK (2000) Influence of conjugated linoleic acid (CLA) on establishment and progression of atherosclerosis in rabbits. *J Am Coll Nutr* 19:472S–477S
- Cook ME, Miller CC, Park Y, Pariza M (1993) Immune modulation by altered nutrient metabolism: nutritional control of immune-induced growth depression. *Poult Sci* 72:1301–1305
- O'Shea M, Bassaganya-Riera J, Mohede IC (2004) Immunomodulatory properties of conjugated linoleic acid. *Am J Clin Nutr* 79:1199S–1206S
- Clement L, Poirier H, Niot I, Bocher V, Guerre-Millo M, Krief S, Staels B, Besnard P (2002) Dietary *trans-10, cis-12* conjugated linoleic acid induces hyperinsulinemia and fatty liver in the mouse. *J Lipid Res* 43:1400–1409
- Riserus U, Vessby B, Arnlov J, Basu S (2004) Effects of *cis-9,trans-11* conjugated linoleic acid supplementation on insulin sensitivity, lipid peroxidation, and proinflammatory markers in obese men. *Am J Clin Nutr* 80:279–283
- Chung S, Brown JM, Provo JN, Hopkins R, McIntosh MK (2005) Conjugated linoleic acid promotes human adipocyte insulin resistance through NF κ B-dependent cytokine production. *J Biol Chem* 280:38445–38456
- Baddini FA, Fernandes PA, da Ferreira CN, Goncalves RB (2009) Conjugated linoleic acid (CLA): effect modulation of body composition and lipid profile. *Nutr Hosp* 24:422–428
- Park Y, Storkson JM, Albright KJ, Liu W, Pariza MW (1999) Evidence that the *trans-10,cis-12* isomer of conjugated linoleic acid induces body composition changes in mice. *Lipids* 34:235–241
- Churrua I, Fernandez-Quintela A, Portillo MP (2009) Conjugated linoleic acid isomers: differences in metabolism and biological effects. *Biofactors* 35:105–111
- Yurawecz MP, Hood JK, Mossoba MM, Roach JA, Ku Y (1995) Furan fatty acids determined as oxidation products of conjugated octadecadienoic acid. *Lipids* 30:595–598
- Heppner CW, Schlatter JR (2007) Data requirements for risk assessment of furan in food. *Food Addit Contam* 24(Suppl 1): 114–121
- Artursson P, Palm K, Luthman K (2001) Caco-2 monolayers in experimental and theoretical predictions of drug transport. *Adv Drug Deliv Rev* 46:27–43
- Pinto M, Robine-Leon S, Appay MD, Kedinger N, Triadou N, Dussaulx E, Lacroix P, Simon-Assman K, Haffen K, Fogh J, Zwiebaum A (1983) Enterocyte like differentiation and polarization of the human colon carcinoma cell line Caco-2 in culture. *Biol Cell* 47:323–330
- Levy E, Mehran M, Seidman E (1995) Caco-2 cells as a model for intestinal lipoprotein synthesis and secretion. *FASEB J* 9:626–635
- Trotter PJ, Ho SY, Storch J (1996) Fatty acid uptake by Caco-2 human intestinal cells. *J Lipid Res* 37:336–346
- Stich HF, Rosin MP, Wu CH, Powrie WD (1981) Clastogenicity of furans found in food. *Cancer Lett* 13:89–95
- Bakhiya N, Appel KE (2010) Toxicity and carcinogenicity of furan in human diet. *Arch Toxicol* 84:563–578
- Chen LJ, Hecht SS, Peterson LA (1995) Identification of *cis-2-butene-1,4-dial* as a microsomal metabolite of furan. *Chem Res Toxicol* 8:903–906
- Kedderis GL, Carfagna MA, Held SD, Batra R, Murphy JE, Gargas ML (1993) Kinetic analysis of furan biotransformation by F-344 rats in vivo and in vitro. *Toxicol Appl Pharmacol* 123:274–282
- Parmar D, Burka LT (1993) Studies on the interaction of furan with hepatic cytochrome P-450. *J Biochem Toxicol* 8:1–9
- Spiteller G (2005) Furan fatty acids: occurrence, synthesis, and reactions. Are furan fatty acids responsible for the cardioprotective effects of a fish diet? *Lipids* 40:755–771
- Prinsep MR, Blunt JW, Munro MH (1994) Isolation of the furan fatty acid, (8Z,11Z,14Z,17Z)-3,6-epoxyeicos-3,5,8,11,14,17-hexenoic acid from the New Zealand sponge *Hymeniacidon hauraki*. *J Nat Prod* 57:1557–1559
- Shen YC, Prakash CV, Kuo YH (2001) Three new furan derivatives and a new fatty acid from a Taiwanese marine sponge *Plakortis simplex*. *J Nat Prod* 64:324–327
- Lampen A, Bader A, Bestmann T, Winkler M, Witte L, Borlak JT (1998) Catalytic activities, protein- and mRNA-expression of cytochrome P450 isoenzymes in intestinal cell lines. *Xenobiotica* 28:429–441
- Guillou H, Zdravec D, Martin PG, Jacobsson A (2010) The key roles of elongases and desaturases in mammalian fatty acid metabolism: insights from transgenic mice. *Prog Lipid Res* 49:186–199
- Leonard AE, Bobik EG, Dorado J, Kroeger PE, Chuang LT, Thurmond JM, Parker-Barnes JM, Das T, Huang YS, Mukerji P (2000) Cloning of a human cDNA encoding a novel enzyme involved in the elongation of long-chain polyunsaturated fatty acids. *Biochem J* 350(Pt 3):765–770
- Degen C, Ecker J, Piegholdt S, Liebisch G, Schmitz G, Jahreis G (2011) Metabolic and growth inhibitory effects of conjugated fatty acids in the cell line HT-29 with special regard to the conversion of t11, t13-CLA. *Biochim Biophys Acta* 1811:1070–1080

Inhibition of Macrophage Oxidative Stress Prevents the Reduction of ABCA-1 Transporter Induced by Advanced Glycated Albumin

Raphael de Souza Pinto · Gabriela Castilho · Bruno Alves Paim ·
Adriana Machado-Lima · Natalia M. Inada · Edna Regina Nakandakare ·
Aníbal Eugênio Vercesi · Marisa Passarelli

Received: 7 July 2011 / Accepted: 15 December 2011 / Published online: 21 January 2012
© AOCs 2012

Abstract We investigated the role of aminoguanidine and benfotiamine on the inhibition of reactive oxygen species (ROS) generation in macrophages induced by advanced glycated albumin (AGE-albumin) and its relationship with cell cholesterol homeostasis, emphasizing the expression of the ATP binding cassette transporter A-1 (ABCA-1). AGE-albumin was made by incubating fatty acid-free albumin with 10 mM glycolaldehyde. ROS production and ABCA-1 protein level were determined by flow cytometry in J774 macrophages treated along time with control (C) or AGE-albumin alone or in the presence of aminoguanidine or benfotiamine. Mitochondrial function was evaluated by oxygraphy. Compared to C-albumin, AGE-albumin increased ROS production in macrophages, which was ascribed to the activities of NADPH oxidase and of the mitochondrial system. Mitochondrial respiratory chain activity was reduced in cells incubated with AGE-albumin. ROS generation along time was associated with the reduction in macrophage ABCA-1 protein level. Aminoguanidine prevented ROS elevation and restored the ABCA-1 content in macrophages; on the other hand, benfotiamine that promoted a lesser reduction in ROS generation was not able to restore ABCA-1 levels. Inhibition of oxidative stress

induced by AGE-albumin prevents disturbances in reverse cholesterol transport by curbing the reduction of ABCA-1 elicited by advanced glycation in macrophages and therefore may contribute to the prevention of atherosclerosis in diabetes mellitus.

Keywords Advanced glycation end products · Cholesterol efflux · ABCA-1 · Oxidative stress · Aminoguanidine · Benfotiamine

Abbreviations

ABCA-1	ATP binding cassette transporter A-1
ABCG-1	ATP binding cassette transporter G-1
ACAT	Acyl cholesterol acyltransferase
AGE	Advanced glycation end products
AGE-albumin	Advanced glycated albumin
AMG	Aminoguanidine
Apo A-I	Apolipoprotein A-I
BF	Benfotiamine
CML	Carboxymethyllysine
DHE	Dihydroethidium
DM	Diabetes mellitus
DPI	Diphenyleneiodonium
FAFA	Fatty acid free albumin
HDL	High density lipoprotein
LDL	Low density lipoprotein
RAGE	Advanced glycation end products receptor
ROS	Reactive oxygen species

R. de Souza Pinto · G. Castilho · A. Machado-Lima ·
E. R. Nakandakare · M. Passarelli (✉)
Lipids Laboratory (LIM 10), Faculty of Medical Sciences,
University of São Paulo, Av. Dr Arnaldo 455—Room 3305,
São Paulo 01246-000, Brazil
e-mail: mpassere@usp.br

B. A. Paim · N. M. Inada · A. E. Vercesi
Pathology Dept. of Medical Sciences Faculty, UNICAMP,
São Paulo, SP, Brazil

Introduction

Advanced glycation end products (AGE) are prevalent in hyperglycemia, and together with the enhanced glucose

metabolism along the hexosamine, polyol and diacylglycerol-PKC pathways, set up a link between oxidative stress and the development of long-term complications in diabetes mellitus (DM) [1, 2]. By reacting with oxoaldehydes, lipoproteins and albumin can be modified by AGE especially in the postprandial phase in DM as well as in inflammation and in renal chronic disease [3–5]. Atherosclerosis that prevails in DM is associated with serum levels of AGE [6].

Advanced glycated albumin (AGE-albumin) impairs the ATP binding cassette transporter A-1 (ABCA-1) and ATP binding cassette transporter G-1 (ABCG-1) expressions and consequently also the apo A-I and HDL-mediated cholesterol efflux [7–9]. ABCA-1 plays a major role in the first step of the reverse cholesterol transport system by exporting the excess of cell cholesterol to lipid poor apo A-I which ultimately is converted into mature HDL that delivers cholesterol to the liver for bile excretion and to steroidogenic organs [10]. Methylglyoxal, glyoxal and 3-deoxyglucosone can mediate the generation of AGE, although previous reports have demonstrated that glycolaldehyde plays a major role in protein derivatization and in cell lipid efflux damage [7, 8].

Intracellular production of ROS elicited by AGE has mainly been ascribed to NADPH oxidase and to the mitochondrial respiratory chain, leading to the production of vascular adhesion molecules and inflammatory mediators, as well as to the expression of the advanced glycation end products receptor (RAGE) [11–13]. Together, these events are related to endothelial, retinal, renal and neuronal injury in DM [1, 11, 14–16].

To date, there are no data linking intracellular redox imbalance with changes in cholesterol homeostasis elicited by alterations in the expression of ABCA-1. We then investigated whether the AGE-induced ROS generation in macrophages relates to the reduction in ABCA-1 transporter level as well as the role played by anti-AGE and antioxidant compounds, such as aminoguanidine and benfotiamine.

Materials and Methods

This study was approved by The Ethical Committee of the Hospital das Clínicas of the Faculty of Medical Sciences of the University of São Paulo, Brazil (#0807/07). All protocols with humans conformed to the Declaration of Helsinki and animal experiments were done according to the US National Institutes of Health guidelines.

Preparation of AGE-Albumin

AGE-albumin was prepared by incubating bovine fatty acid free albumin (FAFA, 40 mg/mL) with 10 mM

glycolaldehyde (Sigma Chem. Com. St. Louis, MO) for 4 days, at 37 °C, under sterile conditions and a nitrogen atmosphere in a water bath shaker in the dark. Control albumin (C-albumin) was incubated with PBS only. After extensive dialysis, samples were sterilized. Samples contained <50 pg endotoxin/mL as determined by the chromogenic *Limulus amoebocyte* assay (Cape Cod, Falmouth, MA).

Cell Culture

J774 macrophages were cultured in RPMI 1640 containing 10% fetal calf serum (FCS), 1% penicillin–streptomycin and 4 mM L-glutamine and maintained in a 5% CO₂ incubator at 37 °C.

After reaching confluence, cells were treated for different intervals of time with C or AGE-albumin alone (2 mg/mL DMEM) or in the presence of aminoguanidine (AMG) or benfotiamine (BF) to evaluate ABCA-1 protein content, ROS generation and mitochondrial respiration. In all cell culture experiments, cell viability controlled by exclusion with trypan blue was superior to 98%. Apoptosis, assessed by the number of annexin V-FITC positive cells, did not change after exposure to AGE-albumin (data not shown).

Assessment of Carbonyl Content in Macrophages

Lysates from C or AGE-albumin-treated cells were incubated with 10 mM of dinitrophenylhydrazine in 2.5 M HCl for 1 h at room temperature. The reaction was blocked by the addition of 20% trichloroacetic acid (TCA). The pellets were washed twice with absolute ethanol/ethyl acetate (1:1) and once with 10% TCA. The protein pellets were dissolved in 6 M guanidine hydrochloride and the absorption at 370 nm was determined. Carbonyl content was calculated using the molar absorption coefficient of aliphatic hydrazones of 22,000 M⁻¹ cm⁻¹ and expressed as nanomoles carbonyl per milligram of protein.

Immunoblot

J774 macrophages were scraped into Tris buffer saline containing protease inhibitors. Equal amounts of cell protein were applied to a polyacrylamide gel (SDS-PAGE) and CD-36 and RAGE expressions determined using anti-RAGE and anti-CD-36 antibodies (Fitzgerald Industries International, Inc., Concord, MA). The difference between the bands was analyzed in pixels, using the JX-330 Color Image Scanner (Sharp®) and ImageMaster software (Pharmacia Biotech). The results are expressed as arbitrary units, analyzing AGE-albumin versus C-albumin. Ponceau staining was utilized to assure equal protein loading.

Assessment of Carboxymethyllysine Adducts in Control and AGE-Albumin

Equal amounts of C and AGE-albumin were loaded into 10% SDS-PAGE and the content of carboxymethyllysine was determined with an anti-CML antibody (Novus Biologicals, Inc., Littleton, CO). Ponceau staining was also utilized to assure equal protein loading.

Agarose Gel Electrophoresis

Ten micrograms of C and AGE-albumin were subjected to 1% agarose gel electrophoresis and the samples' mobility was determined after 1 h run and staining with Coomassie blue.

Determination of ABCA-1 Protein Level by Flow Cytometry

ABCA-1 content by flow cytometry was analyzed due to the difficulty in attaining a good signal in SDS-PAGE. For this experiment, J774 macrophages previously treated for 24 h with 8-Br cyclic AMP (0.5 mM), were incubated for different intervals of time with C or AGE-albumin in the presence or absence of AMG (5 and 10 mM) or BF (350 μ M). After that, a 10^6 cells concentration was fixed in paraformaldehyde (PFA—4%), incubated with anti-ABCA-1 antibody (Novus Biologicals, Inc., Littleton, CO – 1:250 dilution) for 1 h at room temperature and incubated afterwards with 4 μ g/mL Alexa Fluor 488 antibody (Invitrogen, USA). Cellular fluorescence intensity was evaluated by flow cytometry using a FACS Calibur and the Cellquest software (B. D., San Jose, CA). Under all of the conditions, we corrected for basal cellular fluorescence (without Alexa Fluor 488 antibody).

Reactive Oxygen Species Production

After treatment with C or AGE-albumin, J774 macrophages (1×10^6) were incubated with 5 μ M dihydroethidium (DHE) probe (Molecular Probes, OR) for 45 min. ROS production was evaluated by flow cytometry using a FACS Calibur and the Cellquest software (B.D., San Jose, CA). In order to evaluate the contribution of the NADPH oxidase system to the AGE-induced oxidative stress, cells were incubated for 50 min with DHE in the absence or in the presence of the 10 μ M NADPH oxidase inhibitor, diphenylene iodonium (DPI) (Sigma) and the ROS production was determined.

High-Resolution Respirometry

Respiration rates were recorded with the high-resolution OROBOROS oxygraph (Paar, Innsbruck, Austria) in C and

AGE-albumin-treated macrophages (24 h treatment). The culture medium was maintained in an open chamber at 37 °C (temperature controlled by Pelletier effect), homogenized with a magnetic stirrer (600 rpm), and left to equilibrate with the atmosphere before signal calibration. Oxygen concentration was computed from the partial pressure measured by the electrode. During respiration measurements, each chamber (2-mL working volume) was closed by a piston to prevent oxygen exchange with the atmosphere. Data were recorded at 0.4 s intervals and analyzed by the Datlab Acquisition and Analysis software (Paar). As indicated, 2 μ g/mL of an ATPase inhibitor (oligomycin) was added.

14 C- Acetate Incorporation into Cholesterol and Cholesterol Esterification Rates

After 4 h of treatment of the J774 macrophages with 0.25 mM glycolaldehyde (GAD), the cells were washed twice with PBS containing 1 mg/mL FAFA and incubated for 5 h with 8 μ Ci/mL ($2\text{-}^{14}\text{C}$) sodium acetate (GE-Amersham Biosciences, USA) in DMEM containing 1 mg/mL of FAFA. Cell lipids were extracted with a hexane/isopropanol (3:2, v:v) mixture. The solvent was evaporated under N_2 flow and, after dilution in chloroform, samples were spotted on silica G plates by an automated system (Analtech Inc., USA) for thin layer chromatography development. Lipid standards (Sigma) were utilized and the unesterified and esterified cholesterol bands were isolated in order to measure the associated radioactivity. Cholesterol biosynthesis was expressed as total counts per microgram of cell protein.

Statistical Analysis

Statistical analysis was performed using GraphPad Prism 4.0 software (GraphPad Prism, Inc., San Diego, CA). One-way analysis of variance (ANOVA) and the Newman Keuls post test were utilized to compare differences among groups. Summary data are reported as mean values \pm standard error. A p -value <0.05 was considered statistically significant.

Results

Glycolaldehyde-modified albumin was characterized by the determination of CML content. As shown in Fig. 1a CML was greatly superior in AGE-albumin as compared to C-albumin. In addition, the mobility of AGE-albumin was faster than that of C-albumin on agarose gel electrophoresis (Fig. 1b).

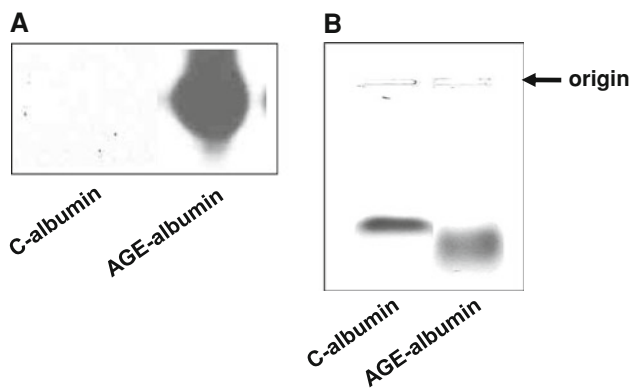


Fig. 1 Carboxymethyllysine content and electrophoretic mobility is increased in AGE-albumin. **a** CML content in albumin modified by 10 mM glycolaldehyde (AGE-albumin) and control albumin (C-albumin) was determined by immunoblot using an anti-CML antibody, **b** electrophoresis mobility was determined in 1% agarose gel and staining with Coomassie blue. *C-albumin* control albumin, *AGE-albumin* advanced glycated albumin

Further, we addressed ROS generation in AGE-albumin-treated cells and its association with the reduction in the ABCA-1 protein level. In macrophages, AGE-albumin induced a higher content of carbonyl derivatives in comparison to C-albumin (Fig. 2a). ROS generation was increased by 24% in J774 macrophages treated with AGE-albumin in comparison to C-albumin and was prevented by incubating cells with a flavoprotein inhibitor, DPI, which is consistent with the role of NADPH oxidase in ROS production in these cells (Fig. 2b).

In an attempt to investigate the oxygen flow along the mitochondrial respiratory chain, C- and AGE-albumin-treated macrophages were evaluated under two different conditions: basal and following the addition of oligomycin. In comparison to C-albumin-treated cells, oxygen flow (pmol/s/mL) was significantly reduced (46%) in cells treated with AGE-albumin (Fig. 2c). In comparison to the basal condition, in the presence of oligomycin, oxygen

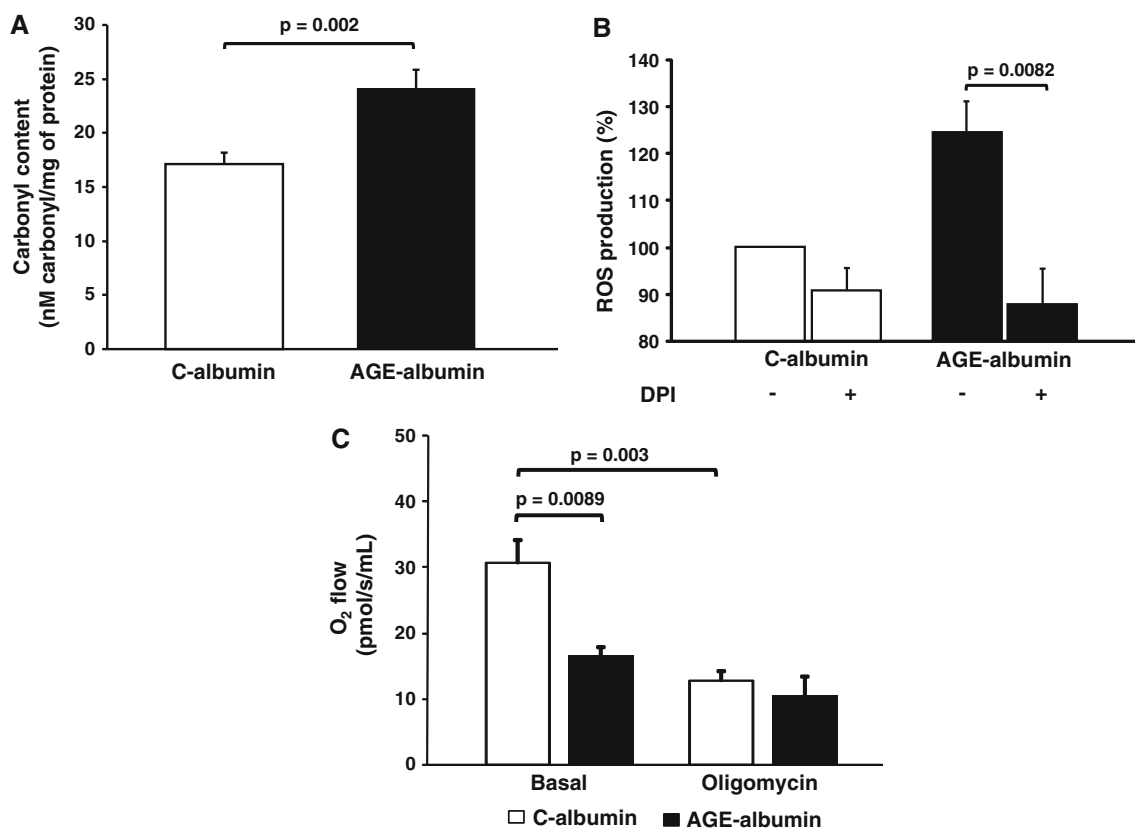


Fig. 2 AGE-albumin enhances carbonyl content and induces ROS production in macrophages: contribution of NADPH oxidase and mitochondria. **a** Carbonyl content was determined in macrophages treated for 24 h with C or AGE-albumin by spectrophotometry, **b** ROS production (mean \pm SE) was determined by flow cytometry in J774 cells treated for 24 h with C or AGE-albumin with the NADPH oxidase inhibitor, DPI ($n = 8$), **c** oxygen consumption rates

(mean \pm SE) were determined in J774 cells after treatment with C or AGE-albumin under basal conditions and after addition of oligomycin (inhibitor of ATP synthase) as indicated ($n = 4$). Results are representative of at least four independent experiments. *C-albumin* control albumin, *AGE-albumin* advanced glycated albumin, *DPI* diphenylene iodonium

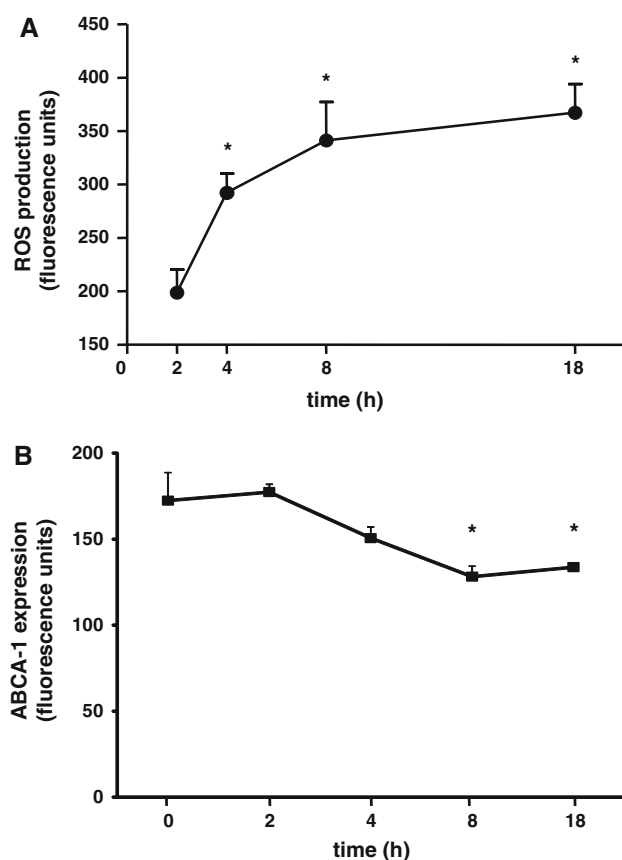


Fig. 3 AGE-albumin increases ROS and decreases ABCA-1 in a time dependent manner. J774 macrophages were treated for different periods of time with C or AGE-albumin. **a** ROS production (mean \pm SE) was determined by flow cytometry (* p < 0.05 compared to 2 h incubation; n = 6, two independent experiments), **b** ABCA-1 protein level was determined by flow cytometry (* p < 0.05 compared to time 0)

flow decreased in C-albumin-treated cells only, with no changes in the cells treated with AGE-albumin.

ROS production was significantly increased along time in AGE-albumin treated macrophages and approached to plateau at the 18th hour (Fig. 3a). ROS generation was accompanied by significant reductions in ABCA-1 protein level after 8 h and 18 h of treatment (Fig. 3b). The association between ROS generation and ABCA-1 reduction was further confirmed by incubating cells with AMG or BF, compounds that function as antioxidants and AGE inhibitors. ROS generation observed in macrophages treated with AGE-albumin alone was reduced 45% by cell incubation with AGE-albumin plus 10 mM AMG (Fig. 4a, inner panel). At this concentration AMG was able to restore the ABCA-1 protein level in macrophages treated with AGE-albumin (Fig. 4a). ROS generation was less inhibited by BF (26%) in cells treated with AGE-albumin (Fig. 4b, inner panel) and, accordingly, BF was not able to restore the ABCA-1 level (Fig. 4b).

It is well-known that reactive oxoaldehydes can be directly formed in the arterial wall. We then measured cholesterol biosynthesis and esterification as well as ROS generation in macrophages directly exposed to glycolaldehyde. Cells subjected to glycooxidation showed a 42% reduction in cholesterol biosynthesis (dpm/ng of cell protein \pm SD) in comparison to control cells (Fig. 5a). In contrast, the cholesterol esterification rate was increased 2.3 fold in macrophages incubated with GAD as compared to control cells (Fig. 5b). In addition, ROS generation was 28% higher in GAD-treated macrophages in comparison to control cells (Fig. 5b, inner panel). These results are in agreement with the observed impairment in the cholesterol efflux elicited by intracellular glycooxidation that subsequently leads to reductions in ABCA-1 protein and intracellular lipid accumulation [8].

Compared to C-albumin, the expression of RAGE and CD-36 were increased by 60 and 35%, respectively, after treatment with AGE-albumin (data not shown).

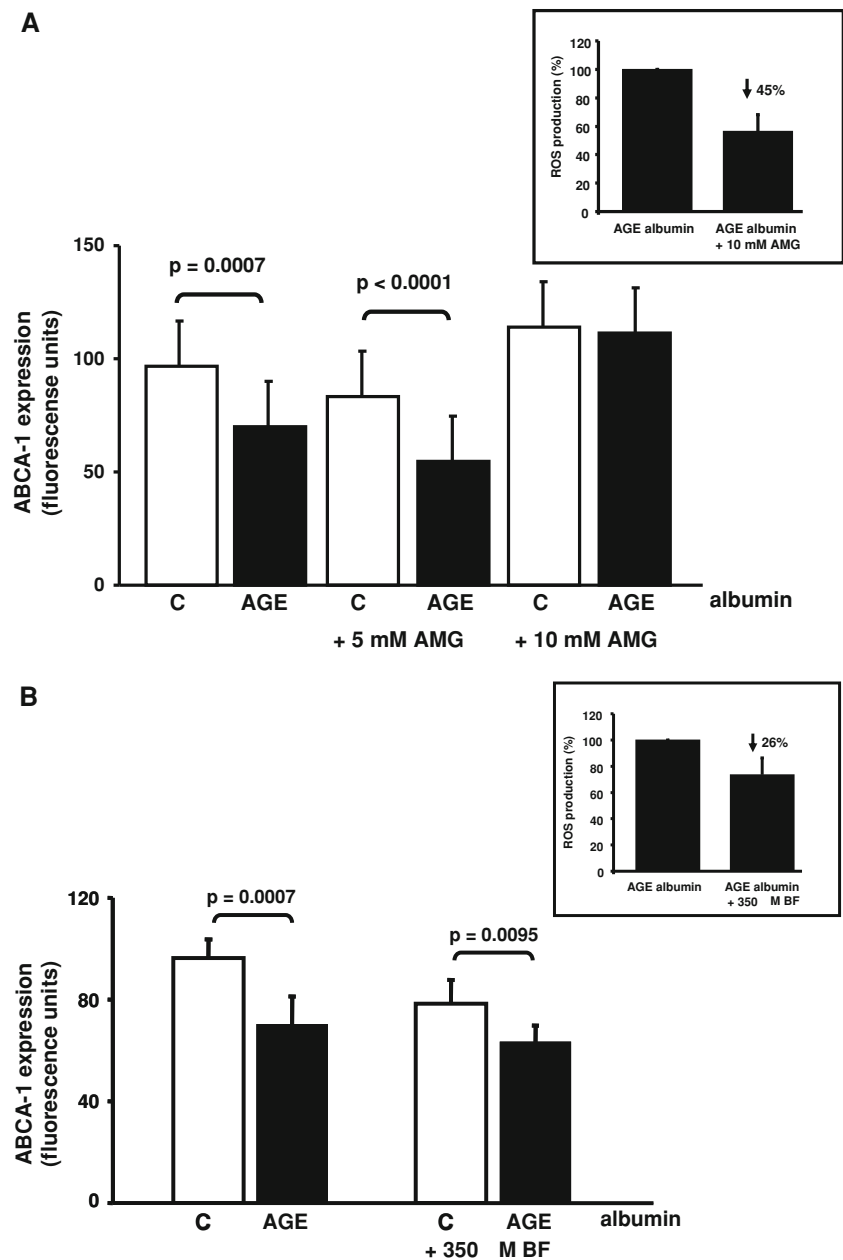
Discussion

Glycated albumin constitutes the overwhelming majority of circulating glycated proteins. AGE-modified albumin is prevalent in DM and disturbs macrophage cholesterol efflux [7]. In the present study, we analyzed the role of control and AGE-albumin on macrophage oxidative stress and its relationship to disturbances in cell cholesterol homeostasis.

Reactive oxygen species were significantly increased in cells treated with AGE-albumin. Our results indicate a combined role of the NADPH oxidase and the mitochondrial respiratory chain in the oxidative stress, although a lower magnitude of ROS levels was detected in our study when compared to data from other authors dealing with different cell types [11, 17].

A diminished mitochondrial respiration contributes to the generation of ROS by mitochondria in consequence of the high reduction state of respiratory chain components [18]. The bulk of mitochondrial ROS generation occurs at the electron transport chain, as a byproduct of respiration. Enhanced electron transport that reflects increased mitochondrial respiratory rates may prevent ROS formation by decreasing oxygen tension in the mitochondrial microenvironment. On the other hand, conditions that lead to lower respiratory rates are frequently accompanied by enhanced ROS release [19]. Then, the contribution of mitochondria to ROS generation and oxidative stress in macrophages exposed to AGE-albumin can be confirmed by the reduction in mitochondrial oxygen flux, increasing both cellular oxygen tension and the reduced state of monoelectronic donors of the respiratory chain. Oligomycin did not show

Fig. 4 Aminoguanidine but not benfotiamine greatly diminishes ROS production in AGE-albumin-treated macrophages and restores ABCA-1 protein level. J774 macrophages were treated with AGE-albumin for 8 h in the presence or absence of **a** 5 and 10 mM aminoguanidine (AMG) or **b** 350 μ M of benfotiamine (BF). ROS production (*inner panels*) and ABCA-1 protein levels were determined by flow cytometry (mean \pm SE; $n = 4$)



an effect in AGE-albumin-treated cells likely because of the already low oxygen consumption rate observed under basal conditions.

The increase in ROS production in macrophages treated with AGE-albumin was accompanied by a severe reduction in ABCA-1 expression. Moreover, the ABCA-1 protein level reduction was consistently observed in several independent experiments. Elevations in ROS were prevented by 10 mM of AMG, a substance that has been shown in identical concentrations to prevent disturbances in cholesterol efflux elicited by AGE by diminishing CML formation [7]. Since no changes in ABCA-1 mRNA levels have been ascribed to cell glycoxidation [8], it is

reasonable to consider that post-transcriptional degradation of ABCA-1 could contribute to its reduction in the AGE-albumin-treated macrophages [20]. In fact, ABCA-1 gene transcription is unaltered by glycoxidative stress [8, 9].

Lipid accumulation can also be worsened in the presence of AGE-albumin due to the enhanced expression of scavenger receptors, LOX-1, CD-36 and RAGE [21, 22] and also by the increased rate of cholesterol esterification by ACAT shown by us. In other words, increased cholesterol flow into cells aggravates atherosclerosis ascribed to an AGE-mediated impairment in the reverse cholesterol transport.

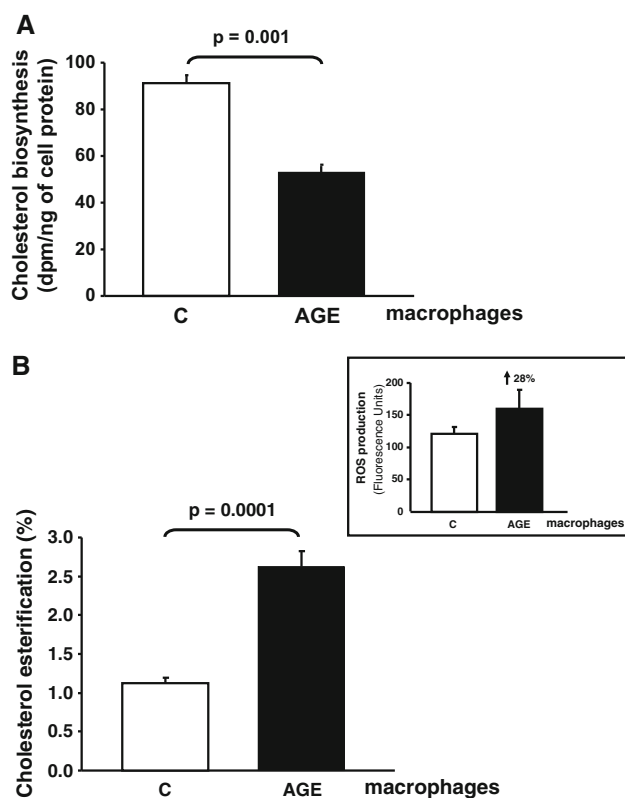


Fig. 5 Glycoxidation reduces cholesterol biosynthesis and enhances cholesterol esterification in macrophages. J774 macrophages were treated with 0.25 mM glycolaldehyde. Control (C) cells were incubated with DMEM only. Cells were treated for 5 h with 8 $\mu\text{Ci}/\text{mL}$ ($2\text{-}^{14}\text{C}$) sodium acetate in order to determine **a** the cholesterol biosynthesis and **b** the percentage of cholesterol esterification (mean \pm SD; $n = 6$). ROS production (*inner panel*) was determined by flow cytometry (mean \pm SE; $n = 5$)

AGE-albumin interacts with RAGE and as consequence of intracellular signal transduction ROS is produced leading to activation of NF- κB that ultimately leads to RAGE expression [22, 23]. Therefore, AGE-albumin is able to generate and propagate oxidative stress in cells, which was also reflected by the increase in cellular carbonyl content.

Our findings are strengthened by the demonstration that serum albumin isolated from uncontrolled type 1 and 2 DM patients reduces the apo A-I and HDL-mediated cholesterol efflux, inducing macrophage lipid accumulation in a similar pattern to that observed in macrophages treated with AGE-albumin (the same in-vitro modified albumin utilized in the present study) [24]. In addition, albumin isolated from DM patients presented a higher amount of CML as compared to albumin isolated from healthy individuals [24]. AGE-albumin utilized in the present study also showed a large amount of CML in comparison to C albumin, although we cannot exclude that other AGE adducts may be present. Besides, taking into account that oxoaldehydes can be generated in the arterial wall, produced in

non-hyperglycemic conditions and are also acquired from food sources, the contribution of AGE-albumin to disturbances in cholesterol homeostasis may be important in a broad spectrum of metabolic conditions. From this point of view, cell lipid accumulation can be minimized by drugs that reduce ROS generation induced by AGE, which should be addressed in future experiments.

Conclusion

AGE-albumin disturbs macrophage lipid homeostasis by increasing the expression of scavenger receptors and diminishing ABCA-1. The reduction in the ABCA-1 protein level elicited by AGE-albumin in macrophages is associated with the oxidative stress via NADPH oxidase system and mitochondria. Anti-AGE and antioxidant compounds known to mitigate greatly the ROS production might hinder the disturbances in the reverse cholesterol transport thus contributing to the prevention of atherosclerosis in DM and other conditions of carbonyl stress such as inflammation and chronic kidney disease.

Acknowledgments This work was supported by a financial grant from Fundação de Amparo à Pesquisa do Estado de São Paulo (FAPESP) to M Passarelli. RS Pinto and A Machado-Lima received scholarships from FAPESP and G Castilho was supported by the Conselho Nacional de Desenvolvimento Científico e Tecnológico (CNPq) and FAPESP, Brazil. The authors are grateful to Eder CR Quintão for his invaluable contribution.

Conflict of interest We declare that no conflict of interest was involved in this study.

References

- Nishikawa T, Edelstein D, Du XL et al (2000) Normalizing mitochondrial superoxide production blocks three pathways of hyperglycaemic damage. *Nature* 404:787–790
- Brownlee M (2001) Biochemistry and molecular cell biology of diabetic complication. *Nature* 414:813–820
- Glomb MA, Monnier VM (1995) Mechanism of protein modification by glyoxal and glycolaldehyde, reactive intermediates of the Maillard reaction. *J Biol Chem* 270:10017–10026
- Wells-Knecht KJ, Brinkman E, Wells-Knecht MC et al (1996) New biomarkers of Maillard reaction damage to protein. *Nephrol Dial Transplant* 11(5):41–47
- Beisswenger PJ, Howell SK, O'Dell RM, Wood MR, Touchette AD, Szwegold BS (2001) alpha-Dicarbonyls increase in the postprandial period and reflect the degree of hyperglycaemia. *Diabetes Care* 24:726–732
- Kilhovd BK, Juutilainen A, Lehto S et al (2007) Increased serum levels of advanced glycation end products predict total, cardiovascular and coronary mortality in women with type 2 diabetes: a population-based 18 year follow-up study. *Diabetologia* 50: 1409–1417
- Machado AP, Pinto RS, Moysés ZP, Nakandakare ER, Quintão EC, Passarelli M (2006) Aminoguanidine and metformin prevent

- the reduced rate of HDL-mediated cell cholesterol efflux induced by formation of advanced glycation end products. *Int J Biochem Cell Biol* 38:392–403
8. Passarelli M, Tang C, McDonald TO et al (2005) Advanced glycation end products precursors impair ABCA1-dependent cholesterol removal from cells. *Diabetes* 54:2198–2205
 9. Isoda K, Folco EJ, Shimizu K, Libby P (2007) AGE-BSA decreases ABCG1 expression and reduces macrophage cholesterol efflux to HDL. *Atherosclerosis* 192:298–304
 10. Oram JF, Vaughan AM (2006) ATP-binding cassette cholesterol transporters and cardiovascular disease. *Circ Res* 99:1031–1043
 11. Basta G, Lazzarini G, Del Turco S, Ratto GM, Schmidt AM, De Caterina R (2005) At least 2 distinct pathways generating reactive oxygen species mediate vascular cell adhesion molecule-1 induction by advanced glycation end products. *Arterioscler Thromb Vasc Biol* 25:1401–1407
 12. Wautier MP, Chappey O, Corda S, Stern DM, Schmidt AM, Wautier JL (2001) Activation of NADPH oxidase by AGE links oxidant stress to altered gene expression via RAGE. *Am J Physiol Endocrinol Metab* 280:E685–E694
 13. Mukherjee TK, Mukhopadhyay S, Hoidal JR (2005) The role of reactive oxygen species in TNF α -dependent expression of the receptor for advanced glycation end products in human umbilical vein endothelial cells. *Biochim Biophys Acta* 1744:213–223
 14. Fernyhough P, Huang TJ, Verkhatsky A (2003) Mechanism of mitochondrial dysfunction in diabetic sensory neuropathy. *J Peripher Nerv Syst* 8(4):227–235
 15. Calcutt NA, Cooper ME, Kern TS, Schmidt AM (2009) Therapies for hyperglycaemia-induced diabetic complications: from animal models to clinical trials. *Nat Rev Drug Discov* 8(5):417–429
 16. Hammes HP, Du X, Edelstein D et al (2003) Benfotiamine blocks three major pathways of hyperglycemic damage and prevents experimental diabetic retinopathy. *Nat Med* 9(3):294–299
 17. Schupp N, Schinzel R, Heidland A, Stopper H (2005) Genotoxicity of advanced glycation end products: involvement of oxidative stress, of angiotensin II type 1 receptors. *Ann NY Acad Sci* 1043:685–695
 18. Cadenas E, Davies KJ (2000) Mitochondrial free radicals generation, oxidative stress, and aging. *Free Radic Biol Med* 29:222–230
 19. Kowaltowski AJ, Souza-Pinto NC, Castilho RF, Vercesi AE (2009) Mitochondria and reactive oxygen species. *Free Rad Bio Med* 47:333–343
 20. Castilho G, Xavier C, Nakandakare E, Laurindo FR, Passarelli M (2009) In vitro macrophage glycoxidation induces cholesterol accumulation due to reticulum endoplasmatic stress. *Atherosclerosis* 10(2):P713
 21. Iwashima Y, Eto M, Hata A, Kaku K, Horiuchi S, Ushikubi F, Sano H (2000) Advanced glycation end products-induced gene expression of scavenger receptors in cultured human monocyte-derived macrophages. *Biochem Biophys Res Commun* 277:368–380
 22. Wautier MP, Chappey O, Corda S, Stern DM, Schmidt AM, Wautier JL (2001) Activation of NADPH oxidase by AGE links oxidant stress to altered gene expression via RAGE. *Am J Physiol Endocrinol Metab* 280:685–694
 23. Yamagishi SI, Maeda S, Matsui T, Ueda S, Fukami K, Okuda S (2011) Role of advanced glycation end products (AGEs) and oxidative stress in vascular complications in diabetes. *Biochim Biophys Acta* (in press)
 24. Machado-Lima A, Pinto R, Holanda C et al (2009) In vivo glycosylated albumin impairs the removal of cholesterol inducing lipid accumulation in macrophages. *Atherosclerosis* 10(2):P1133

Phospholipid Peroxidation: Lack of Effect of Fatty Acid Pairing

Sarah E. Norris · Todd W. Mitchell ·
Paul L. Else

Received: 3 August 2011 / Accepted: 19 December 2011 / Published online: 24 January 2012
© AOCS 2012

Abstract Phospholipids where both fatty acids are polyunsaturated are very rare. Most organisms prefer to couple their polyunsaturated fatty acids (PUFA) with either a saturated (SAT) or a monounsaturated (MUFA) fatty acid. This study examined if these natural couplings are there to protect PUFA from themselves. Specifically, does the coupling of PUFA to SAT or MUFA reduce the potential for increased rates of peroxidation by shrouding these highly peroxidisable fatty acids with less peroxidisable fatty acids? The influence of head group was examined by using the two most common phospholipids found in vertebrate membranes i.e. phosphatidylcholine and phosphatidylethanolamine species. Fatty acid pairings included 16:0/18:2 versus 18:2/18:2 and 16:0/22:6 versus 22:6/22:6. All phospholipids were incorporated into liposomes that were matched for their total PUFA content i.e. 25% PUFA/PUFA or 50% SAT/PUFA with phosphatidylcholine 16:0/16:0 used as the background phospholipid. An iron initiator ($\text{Fe}^{2+}/\text{H}_2\text{O}_2$) was used to induce peroxidation and lipid hydroperoxide production was used to measure peroxidation. The results show that coupling of PUFA together on the same molecule does not increase peroxidation rates and therefore does not support the proposed hypothesis. The lower than expected levels of

peroxidation measured for some phospholipid species (e.g. PtdEtn 22:6/22:6) is possibly due to the partitioning of these molecular species into the inner leaflet of the bilayer.

Keywords Linoleic acid · Docosahexaenoic acid · Lipid peroxidation

Abbreviations

PL	Phospholipid
PUFA	Polyunsaturated fatty acid
LOOH	Lipid hydroperoxide
PtdCho	Phosphatidylcholine
PtdEtn	Phosphatidylethanolamine

Introduction

Hundreds of different phospholipid molecular species constitute the major lipid component of membranes [7]. The breadth of variation in phospholipids is due primarily to the different combinations of fatty acids associated with the major phospholipid classes. For example, in a recent study analysing six major phospholipid classes (PtdCho, PtdEtn, PtdSer, PtdOH, PtdGro and PtdIns), in kidney and brain of three different sized mammals, up to 120 different phospholipid molecular species were found in kidney and up to 66 in the brain [16]. Analysis of the original data used to produce this study shows that virtually no phospholipids (<1%) possess two polyunsaturated fatty acids together on the same molecule, i.e. at both the sn1 and sn2 positions on their glycerol backbones. This presents a rather interesting question, why do organisms tend to avoid the use of PUFA/PUFA phospholipids in their membranes?

S. E. Norris · T. W. Mitchell · P. L. Else (✉)
Metabolic Research Centre, School of Health Sciences,
Illawarra Health and Medical Research Institute (IHMRI),
University of Wollongong, Wollongong,
NSW 2522, Australia
e-mail: pelse@uow.edu.au

S. E. Norris
e-mail: sen965@uowmail.edu.au

T. W. Mitchell
e-mail: toddm@uow.edu.au

Double PUFA phospholipids certainly exist, examples include phospholipids in various microorganisms [25], cephalopod tissues, [21], mitochondrial membranes of oxidative muscle in trout [12] and rod outer segment membrane in higher vertebrates [3]. In these cases docosahexaenoic acid (DHA; 22:6n-3) combines with itself or other PUFA. Macroalgae also possess PUFA/PUFA phospholipids [17] with green algae using 16:3n-3 (hexadecatrienoic acid) and 18:3n-3 (α -linolenic acid, ALA) while brown algae combine 20:4n-6 (arachidonic acid) and 20:5n-3 (eicosapentaenoic acid). These examples of PUFA/PUFA phospholipids are however uncommon. The only commonly known phospholipid that possesses multiple PUFA is cardiolipin (Ptd₂Gro). Cardiolipin is a novel phospholipid found almost exclusively in mitochondria where it binds proteins and is involved, via its oxidation, in initiating apoptosis [20]. Cardiolipin is a diphosphatidylglycerol (a double phospholipid) with four fatty acid tails, and the best-known form of cardiolipin is a tetra linoleic acid (i.e. 4 × 18:2n-6) species that predominates (~85% of cardiolipin) in the heart of mammals [18]. Interestingly in some bivalve molluscs a tetra DHA molecular species is common [11].

One possible explanation for the general lack of PUFA/PUFA phospholipids in membranes is that it presents a peroxidation hazard to the cell. This is because like other molecules within the body, phospholipids are prone to the effects of reactive oxygen species (ROS). But unlike many other molecules, lipid oxidation (or peroxidation) once initiated is self-propagating due to the formation of lipid oxyl (LO[•]) and peroxy (LOO[•]) radical products that can perpetuate the peroxidative process. Another ‘problem’ lipids face is that they also possess very high O₂ solubilities, ~20–30 times more than aqueous media [2] so oxygen is readily available to fuel these reactions in a lipid environment. Most at risk of peroxidation are PUFA because they possess bis-allylic hydrogen’s (hydrogen’s on methylene groups between double bonds) that have lower bond energies meaning that they are more readily removed (or abstracted) by ROS. Therefore, the more double bonds or the greater the level of polyunsaturation (not unsaturation as monounsaturates have no bisallylic hydrogens) the greater the potential for lipid peroxidation. This relationship between the level of polyunsaturation and capacity to peroxidise is expressed in the peroxidation index (see [5]). The peroxidation index is an empirically derived value showing that the oxidizabilities of polyunsaturation fatty acids are dependent upon the number of bis-allylic methylene groups present.

Therefore the coupling of PUFA together on the same phospholipids, and the possibility that these phospholipids might form micro-domains within the membrane has

the potential to fuel rapid, and potentially uncontrollable rates of lipid peroxidation. This could occur as lipid radicals move rapidly from PUFA to PUFA on double PUFA phospholipid molecules forming a peroxidative cascade. Alternatively by coupling PUFA on phospholipids to either a saturated or a monounsaturated fatty acid, peroxidation is likely to be hindered and therefore slower. This could result from ‘steric’ hindrance provided by the presence of far less peroxidisable fatty acids that may act to slow the diffusion of lipid radicals within the lipid environment of the membrane [19], providing time for the normal membrane antioxidant systems to operate.

The aim of this research was to test if phospholipids with PUFA/PUFA combinations of fatty acids display faster rates of peroxidation than phospholipids with the same number and types of PUFA coupled to SAT rather than PUFA. To test this idea liposomes of identical peroxidative capacity were produced using the two most common phospholipid classes found in higher vertebrates i.e. phosphatidylcholine (PtdCho) and phosphatidylethanolamine (PtdEtn). Fatty acid pairings included 16:0/18:2 versus 18:2/18:2 and 16:0/22:6 versus 22:6/22:6. These liposomes were then subject to the same peroxidative stress and the level of peroxidation measured as the amount of lipid hydroperoxide formed.

Materials

All synthetic phospholipids were purchased without any added BHT from Avanti Polar Lipids Inc (Alabama, USA). These included; 1,2-dilinoleyl-sn-glycero-3-phosphatidylcholine (PtdCho 18:2/18:2), 1,2-dilinoleyl-sn-glycero-3-phosphatidylethanolamine (PtdEtn 18:2/18:2), 1,2-didocosahexaenoyl-sn-glycero-3-phosphatidylcholine (PtdCho 22:6/22:6), 1,2-didocosahexaenoyl-sn-glycero-3-phosphatidylethanolamine (PtdEtn 22:6/22:6), 1-palmitoyl-2-linoleoyl-sn-glycero-3-phosphatidylcholine (PtdCho 16:0/18:2), 1-palmitoyl-2-linoleoyl-sn-glycero-3-phosphatidylethanolamine (PtdEtn 16:0/18:2), 1-palmitoyl-2-docosahexaenoyl-sn-glycero-3-phosphatidylcholine (PtdCho 16:0/22:6) and 1-palmitoyl-2-docosahexaenoyl-sn-glycero-3-phosphatidylethanolamine (PtdEtn 16:0/22:6), 1,2 dipalmitoyl-sn-glycero-3-phosphatidylcholine (PtdCho 16:0/16:0) and a mixed phospholipid soy lecithin. All phospholipids were kept in their sealed containers at –20 °C until required. Ammonium ferrous sulphate and xylenol orange were purchased from Sigma-Aldrich (USA). Methanol and chloroform (HPLC grade) were purchased from Crown Scientific (Australia) and sulphuric acid from AJAX Chemicals (Australia). All chemicals used were of analytical grade.

Methods

Liposome Preparation

Liposomes were prepared by mixing various combinations of phospholipids (from stock solutions made-up at 10 mg/mL in 2:1 chloroform:methanol stored at -20°C). Phospholipid mixtures were dried down under N_2 at 37°C for 45 min. These were then immediately rehydrated at 45°C (being above the highest phase transition temperature of 41.5°C for 1,2 dipalmitoyl-sn-glycero-3-phosphatidylcholine (PtdCho16:0/16:0) that was used to form the liposomes) in 140 mM NaCl solution at pH 7.3. This was followed by vigorous vortexing for 10 min. The final concentration of the liposomal suspensions was 0.4 mg of phospholipid/mL. The resuspended phospholipid solutions were subsequently sonicated 3×45 s at an amplitude of 10 μm using a probe-type-sonicator (Sanyo Soniprep 150). Sonication, and the subsequent formation of liposomes, was marked by the opaque phospholipid solutions partially clarifying.

The aim of this investigation was to produce stable liposomes with an identical number of polyunsaturated and saturated fatty acids derived from phospholipids with different ‘geometries’ (i.e. PUFA/PUFA or SAT/PUFA). Liposomes consisted of 75 or 50% PtdCho 16:0/16:0 with either 25% of a phospholipid with a PUFA/PUFA pairings, or 50% of a phospholipid with a PUFA paired with a saturated fatty acid (16:0), respectively. A series of both 18:2 and 22:6 containing phospholipids (both PtdCho and PtdEtn) were compared (in theory the peroxidative capacity of the 22:6 series is five times that of the 18:2 series with the same numbers of fatty acids present [5]). The PUFA/PUFA phospholipids used included: PtdCho 18:2/18:2, PtdEtn 18:2/18:2, PtdCho 22:6/22:6 and PtdEtn 22:6/22:6. The SAT/PUFA phospholipids used included: PtdCho 16:0/18:2, PtdEtn 16:0/18:2, PtdCho 16:0/22:6 and PtdEtn 16:0/22:6. In order to form stable liposomes these peroxidizable phospholipids were combined with the relatively non-oxidisable ‘carrier’ phospholipid PtdCho16:0/16:0 (i.e. 75% for PUFA/PUFA phospholipids and 50% for SAT/PUFA phospholipids).

Liposomes therefore consisted of either 25% of a PUFA/PUFA phospholipid combined with 75% of PtdCho16:0/16:0 or 50% of a SAT/PUFA phospholipid (with the SAT being 16:0) together with 50% PtdCho16:0/16:0. The net result was that all liposomes consisted of 25% PUFA (either 18:2 or 22:6) and 75% SAT (16:0 only). Liposomes were freshly prepared and used immediately following preparation.

Peroxidation

Liposome peroxidation was initiated by using ferrous iron (Fe^{2+}) together with hydrogen peroxide to produce final

reaction concentrations for both products of 10 μM Fe^{2+} / H_2O_2 (hereto referred to as the iron initiator). The final pH of the peroxidation system was 4.4. Ferrous iron (Fe^{2+}) was derived from ammonium ferrous sulphate ($(\text{NH}_4)_2\text{Fe}(\text{SO}_4)_2$) as it was found to be more effective at initiating peroxidation than Fe^{2+} from FeSO_4 . The lower pH of ammonium ferrous sulphate helped to maintain the presence of Fe^{2+} [1] whereas Fe^{2+} from FeSO_4 tended to produce a brown precipitate (assumed due to the conversion of Fe^{2+} to Fe^{3+} and the formation of insoluble Fe^{3+} compounds). Autoperoxidation of the phospholipids was measured by running parallel incubations without the addition of the iron initiator. All peroxidation experiments involved six separate experiments run at 45°C (above 41.7°C being the highest phase transition temperature of PtdCho16:0/16:0) ensuring that all phospholipids in the liposomes were in a liquid state when measured.

Peroxidation was determined by measuring the production of lipid hydroperoxides (i.e. LOOH) using the xylenol orange based method employed in the FOX2 assay. The method used was as previously described by Deiana et al. [6] and reviewed by Bou et al. [4]. The final concentration of the assay medium consisted of 0.25 mM $(\text{NH}_4)_2\text{Fe}(\text{SO}_4)_2$, 0.25 mM H_2SO_4 , 100 μM xylenol orange and 1 mM of butylated hydroxytoluene (added as an antioxidant) in methanol. LOOH production was measured over 3 h with the first measurement made after 10 min. Preliminary measurements at earlier times (2 and 4 min) indicated an essentially linear rate of LOOH for the first 10 min of the experiment. Standard curves were constructed using tert-butyl hydroperoxide (linear range between 0 and 20 nmol; $r^2 = 0.9991$).

Preliminary experiments were conducted on a mixed PtdCho phospholipid i.e. soy lecithin (fatty acid composition: 14.9% 16:0, 3.7% 18:0, 11.4% 18:1, 63% 18:2 and 5.7% 18:3) using the TBARS method (a butylated hydroxytoluene/thiobarbituric acid based assay with tetramethoxypropane used as a standard). Soy lecithin when used with the FOX2 and the TBARS methods produced excellent correlation $r^2 = 0.91$ ($n = 20$) between the methods. However when employed in the current experiment the level of malondialdehyde produced from the phospholipids that contained 18:2 as their only PUFA was very small (as previously found; [10]). This made the use of the TBARS method far less sensitive when liposomes contained linoleic acid as their only PUFA. The formation of dienes during peroxidation was also explored as a means of measuring peroxidation but was found to be too variable whereas the FOX2 method was reliable, highly repeatable and sensitive. Subsequently, the FOX2 method was used to measure peroxidation of the liposomes made from the pure phospholipids. The molecular composition of all PtdCho lipids was confirmed using a QTrap5500 triple quadrupole

linear ion trap mass spectrometer (AB Sciex, Tronto, Canada) equipped with a TriVersa NanoMate automated nanospray source (Advion, Ithica, USA).

Statistical Analysis

Differences in overall peroxidation of liposome with the same head group but different fatty acid couplings were subject to repeated measure ANOVA with one-way ANOVA's at individual time points. A student *t* test was used to compare LOOH present in phospholipids at baseline, those produced during sonication, peroxide present due to the addition of the iron initiator and total peroxides present at initiation of peroxidation. All statistical analysis was performed using SPSS Statistics (v17.0).

Results

Prior to determining the 'peroxidisabilities' of the various liposomes the preexisting level of peroxide present at the various stages of liposome preparation was determined. Figure 1 shows the level of lipid hydroperoxides (LOOH) present at baseline (A), produced during sonication (B), present as a result of the addition of the iron initiator (C), and total levels (D). The baseline values ranged from essentially zero up to 53 nmol LOOH/mg of phospholipid with the PUFA/PUFA phospholipids (i.e. PtdCho 18:2/18:2 PtdEtn 18:2/18:2 and 22:6/22:6) generally displaying significantly higher levels of LOOH than the SAT/PUFA coupled phospholipids (PtdCho and PtdEtn 16:0/18:2 and 16:0/22:6) with the notable exception of PtdCho 22:6/22:6 that had virtually no LOOH present at baseline.

Although preliminary experiments were conducted to minimize LOOH production during sonication the probe sonicator still produced between 22 and 95 nmol of LOOH/mg of PL. PtdEtn 16:0/18:2 and PtdCho 18:2/18:2 generally produced more LOOH than the other phospholipids during sonication. The addition of the iron initiator to the liposomes produced a small and similar (not significant different) rise in peroxide levels across all liposome preparations. This rise in peroxide level was assumed to be due to the presence of H₂O₂ in the iron initiator. The cumulative total of peroxide present in the liposomes varied from 85 to 168 nmol/mg of PL with both PtdCho and PtdEtn 18:2/18:2 having significantly ($p < 0.002$) more peroxide than most of the other phospholipids (e.g. PtdCho 16:0/18:2 and 22:6/22:6 and PtdEtn 16:0/22:6; PtdCho 18:2/18:2 also had higher total levels of peroxide than PtdEtn 22:6/22:6) at the start of the reaction. Subsequently all preparations were normalized by subtracting preexisting total levels of peroxides present for each preparation (with all

preparations except PtdCho and PtdEtn 18:2/18:2 having similar preexisting levels of peroxide) prior to determining the effect of the iron initiator on phospholipid peroxidation.

The subsequent total level of peroxidation for the four different phospholipid pairings (PtdCho and PtdEtn as either 16:0/18:2 versus 18:2/18:2 or 16:0/22:6 versus 22:6/22:6) is shown in Fig. 2. In all cases there was an initial burst of LOOH production followed by either a plateauing or decrease in LOOH production towards the end of the 3 h incubation period. There was no apparent lag phase involved in these experiments presumably due to the pre-existing presence of peroxides that allowed the iron initiator to induce peroxidation immediately upon addition. The phospholipid that produced the greatest total level of LOOH was PtdCho 16:0/22:6. All other lipids produced similar levels of LOOH except for PtdEtn 18:2/18:2 that produced significantly lower total levels of LOOH. It should be noted that both PtdCho and PtdEtn 18:2/18:2 that both had significantly more peroxide at the start of the experiment did not produce more peroxide compared to the other phospholipids following the addition of the iron initiator (especially PtdCho and PtdEtn 16:0/18:2). Since total lipid peroxidation included both an autoperoxidation and an iron initiator component liposome peroxidation was measured either with or without iron initiator to distinguish between the two components.

The profile of autoperoxidation (shown in Fig. 3) was quite different from that found for total peroxidation (shown in Fig. 2). Autoperoxidation displayed an essentially linear profile of peroxide production for all phospholipids over the 3 h of measurement. Interestingly, the fastest rate of peroxidation was found in liposomes that contained 16:0/18:2 followed by phospholipids with 18:2/18:2 then either 16:0/22:6 or 22:6/22:6, irrespective of head group.

To determine the rate and overall level of liposome peroxidation induced by the iron initiator, autoperoxidation was subtracted from total peroxidation. The level of iron-induced peroxidation (shown in Fig. 4) shows increasing levels of LOOH production during the initial 1–2 h of incubation followed by a definite decline in production in the third hour. It was interesting that in preliminary experiments liposomes made using a liposome-maker (from Avanti Polar) tended not to peroxidise as readily as those produced by sonication suggesting that some initial peroxidation (i.e. peroxide production) was required to 'set-off' a continuous peroxidation process. The phospholipid with the highest rate of iron induced peroxidation was PtdCho 16:0/22:6. This phospholipid had significantly higher levels of peroxidation than for the other phospholipids measured. All other phospholipids displayed similar rates and levels of peroxidation (based on LOOH production) except for PtdEtn 18:2/18:2 that had a significantly

Fig. 1 Level of peroxide present at the various stages of liposome production. These include; **a** levels prior to sonication (i.e. at baseline), **b** levels produced during sonication, **c** levels present due to the addition of the iron initiator, and **d** total levels. *Non-identical letters indicate where preparations were different from one another at a significance level of $p < 0.05$. Error bars are SEM, $n = 6$*

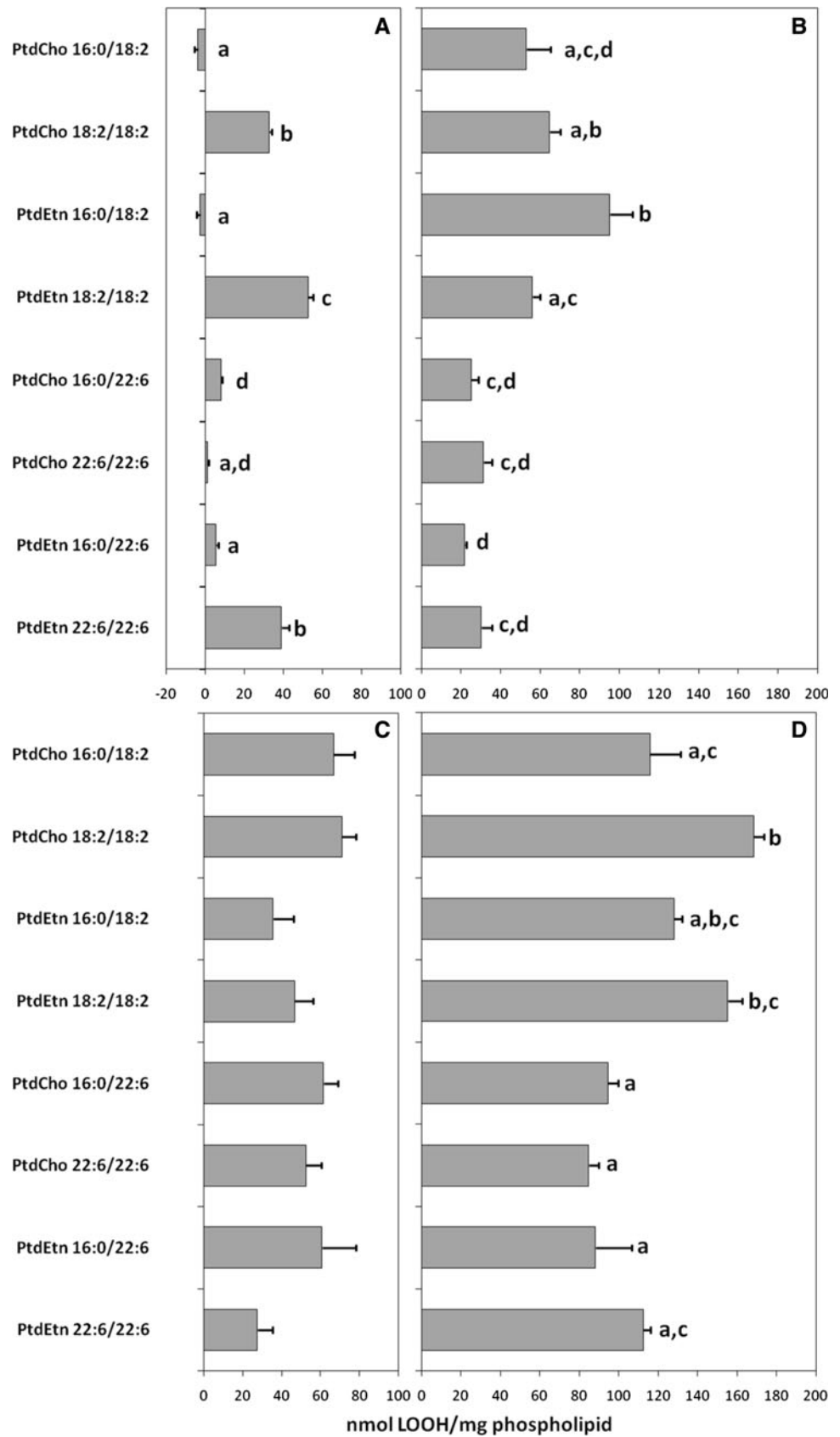
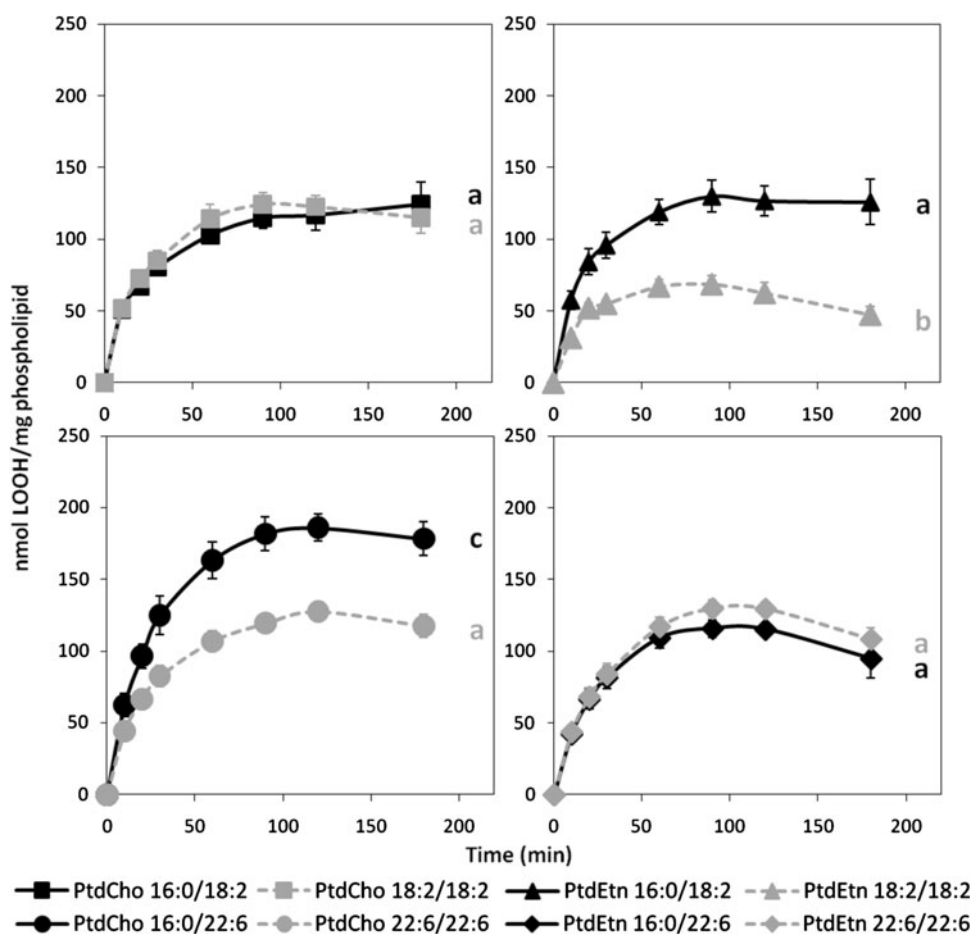


Fig. 2 Total peroxidation of liposomes composed of phosphatidylcholine and phosphatidylethanolamine lipid matched for total PUFA and SAT content but organised either as PUFA/PUFA or as SAT/PUFA pairs. The peroxidation index of 18:2 containing phospholipid was 25 whereas that of phospholipids containing 22:6 was 200. *Non-identical letters indicate preparations different from one another at a significance level of $p < 0.05$. Error bars are SEM, $n = 6$*



lower level of peroxidation, and after 3 h of incubation was displaying virtually no peroxidation as a result of the addition of the iron initiator (Fig. 4).

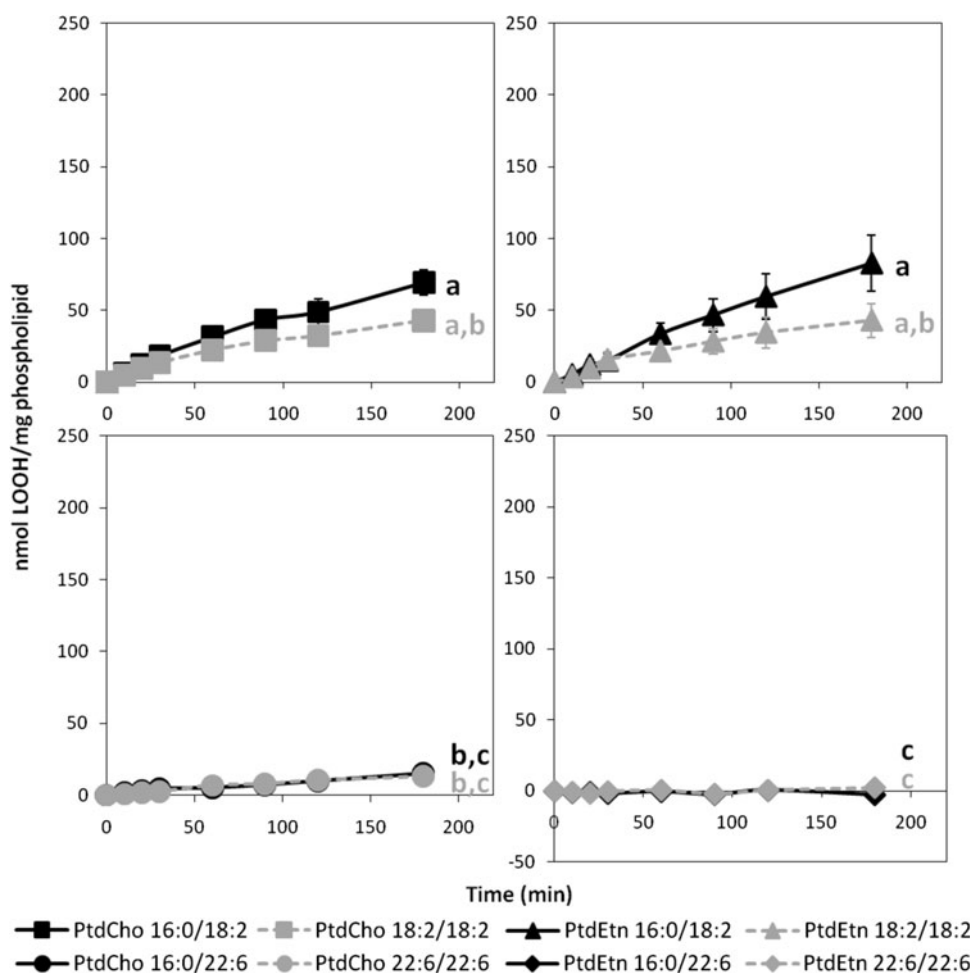
Discussion

There is no clear explanation as to why phospholipids of natural membranes have their PUFA normally coupled to either a SAT or a monounsaturated fatty acid with the pairing of PUFA on the same phospholipid, standing out as something unique and special [22]. This study examined the idea that these natural couplings are there to protect polyunsaturated fatty acids from themselves. That by coupling PUFA to SAT or MUFA the rate of peroxidation of the prone PUFA will be reduced by shrouding them in less peroxidisable fatty acids. In other words, SAT and MUFA hinder the ability of ($LO\cdot$) and ($LOO\cdot$) radicals formed from PUFA, from being able to come in contact with other PUFA and continue their peroxidative cascade. Some support for this idea is found in triglycerides where the peroxidisability of docosahexaenoic acid (22:6n-3) is less likely to occur when in the middle of the molecule (at the sn-2 position) and shrouded by saturates on both sides [24].

The results of the present study however did not support this idea that SAT/PUFA and PUFA/PUFA phospholipids (incorporated into liposomes at the same concentration) peroxidise at different rates. The results show that the peroxidation of phospholipids when matched for PUFA content but derived from different phospholipids with either single or double PUFA pairings overall peroxidise at similar rates and levels. This is at odds with the only other study that has measured peroxidation of phospholipids with SAT/PUFA and PUFA/PUFA pairings [26]. In this study Zerouga and colleagues found PtdCho's composed of 18:0/18:3, 18:0/22:6 and 22:6/22:6 incorporated into liposomes made primarily of PtdCho 18:0/18:1 had quite different levels of peroxidation. They [26] found PtdCho 18:0/22:6 peroxidised at twice the rate of PtdCho 22:6/22:6 and four times more than PtdCho 18:0/18:3, the opposite of that hypothesized and but similar to the present study in that the double PUFA phospholipids did not show increased levels of peroxidation compare to the SAT/PUFA phospholipids.

The Zerouga study [26] used a copper initiator (Cu_2SO_4/H_2O_2) similar to the iron initiator used in the present study. In their study peroxidation was determined by the formation of conjugated dienes in a Tris buffered solution. In our study we found the measurement of conjugated dienes to

Fig. 3 Autoperoxidation (incubated without the iron initiator) of liposomes composed of phosphatidylcholine and phosphatidylethanolamine lipid matched for total PUFA and SAT content but organised either as PUFA/PUFA or as SAT/PUFA pairs. *Non-identical letters* indicate preparations different from one another at a significance level of $p < 0.05$. *Error bars* are SEM, $n = 6$



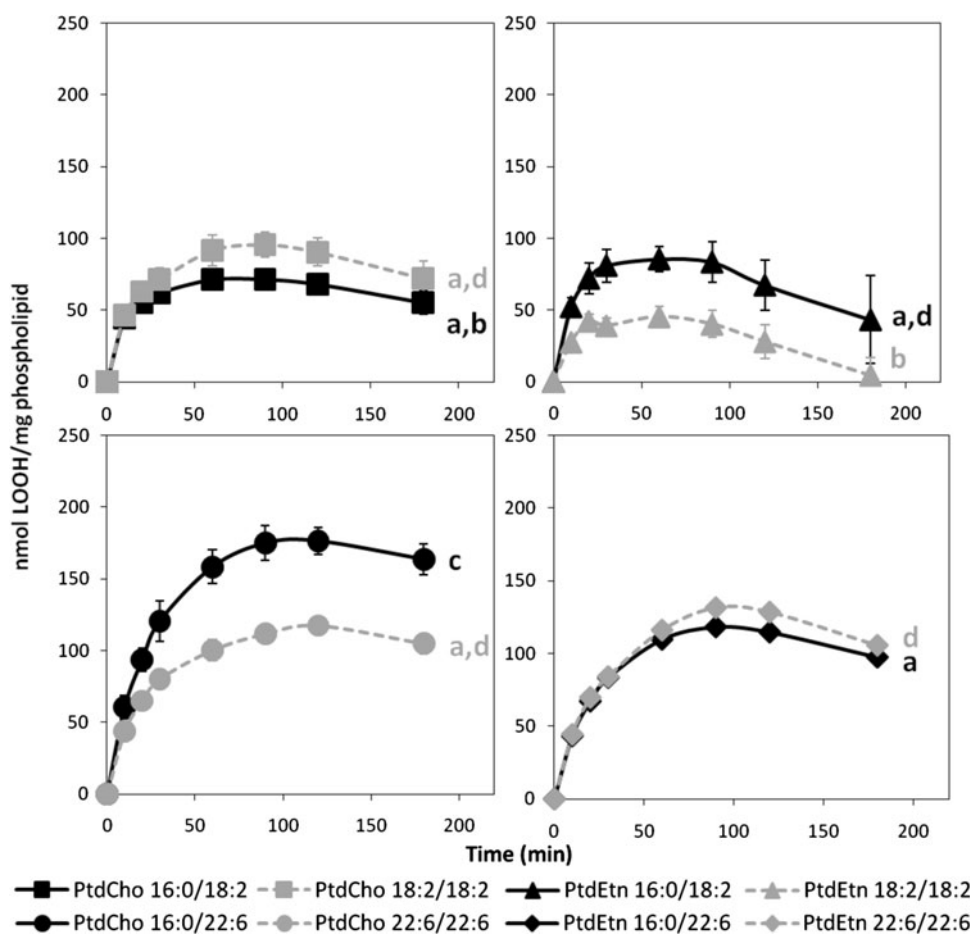
be less precise and that the addition of buffers (HEPES and phosphate) reduced overall peroxidation. This effect of buffers on reducing peroxidation has previously been noted [8, 9] and is why we avoided the use of buffers in the current experiments, alternatively allowing the system to settle at a final pH of ~ 4.4 with the added benefit of helping to maintain iron in its ferrous state.

Prior to performing these experiments we expected that the docosahexaenoic acid containing phospholipids would demonstrate a much higher level of peroxidation than those containing linoleic acid. This was based on the assumption that the level of peroxidation is related to the level of unsaturation, or more specifically to the peroxidation index. The 18:2 containing liposomes in theory have one-fifth of the peroxidative capacity of the 22:6 containing liposomes [5]. Yet peroxidation measured by the production of LOOH showed no major difference between the liposomes. For example, using a linear estimate for LOOH production rate (for the iron initiator component of lipid production) using the time point closest to time zero (i.e. at 10 min), the rate of LOOH production can be estimated as 4.27 ± 0.53 nmol LOOH/mg of PL per minute for the four 18:2 containing phospholipids and 4.81 ± 0.41 nmol

LOOH/mg of PL per minute for the 22:6 containing phospholipids (a non-significant difference).

These estimates for LOOH generation can be used to predict how much of the original PUFA may have been peroxidised over the 3 h of incubation. Using average molecular weights of 738 for 18:2 and 762 for 22:6 containing phospholipids it can be calculated that if these maximal rates continued over the entire 3 h of incubation then 0.774 and 0.864 μmol of LOOH would be produced from the 18:2 and 22:6 containing phospholipids, respectively. If one assumes that one LOOH is produced per PUFA fatty acid (which is theoretically accurate for 18:2 but less than that theoretically capable of being produced by 22:6) then 0.678 and 0.656 μmol of LOOH could be produced from the incubations containing the 18:2 and 22:6 phospholipids, respectively. So in theory most of the 18:2 is likely peroxidised over the 3 h of iron induced peroxidation whereas the 22:6 containing phospholipids would still have a reserve peroxidation capacity. This might account for some of the difference in the peroxidation profiles of the 18:2 and 22:6 containing phospholipids induced by the iron initiator (Fig. 4).

Fig. 4 Peroxidation due to the presence of the iron initiator ($10 \mu\text{M Fe}^{2+}/\text{H}_2\text{O}_2$) derived from total peroxidation minus autoperoxidation of liposomes composed of phosphatidylcholine and phosphatidylethanolamine lipid matched for total PUFA and SAT content but organised either as PUFA/PUFA or as SAT/PUFA pairs. *Non-identical letters indicate preparations different from one another at a significance level of $p < 0.05$. Error bars are SEM, $n = 6$*



The results of the present study imply that both 18:2 and 22:6 form similar amounts of LOOH product per fatty acid molecule rather than that predicted from their peroxidation indices. This is not a new observation. Visioli and colleagues [23] found the yield of peroxidation product from different fatty acids (over 3 h of peroxidation using AAPH—[2,2'-azo-bis(2-amidinopropane)dihydrochloride]) can vary. Visioli et al. found 18:2 produced more LOOH and more conjugated dienes than more highly polyunsaturated fatty acids such as 20:5, 20:4 and 22:6. Whereas they also found that the production of thiobarbituric acid-reacting substances was several fold greater for 22:6, 20:4 and 20:5 than for 18:2 (in our preliminary experiments we also found 18:2 did not produce appreciable amounts of malondialdehyde as measured using TBARS). The conclusion being that different fatty acids differentially contribute to the formation of peroxidation products and that this formation is not necessarily related to their peroxidation capacity. This conclusion may have important physiological implications based on the different roles of these products in organisms. Other studies have also found similar noncompliance [15] between peroxidation products from fatty acids in relationship to their peroxidation capacity.

One reason why 22:6 and 18:2 containing phospholipids might produce similar amounts of LOOH in the present study is that LOOH formed from the 22:6 containing phospholipids decompose at a faster rate than those formed from 18:2. It is interesting to note that the autoperoxidation of the 22:6 containing phospholipids was much lower than those containing 18:2 indicating the possibility of rapid disappearance (or alternatively low production). In fact the low activity of some of the phospholipids, notably PtdCho 22:6/22:6, promoted us to question if these phospholipids may have already peroxidised in storage (i.e. there was no PtdCho 22:6/22:6 left to peroxidise). To test this we analyzed all PtdCho phospholipids (PtdCho 16:0/18:2, PtdCho 18:2/18:2, PtdCho 16:0/22:6, PtdCho 22:6/22:6) using mass spectrometry and found each to contain a single product at the exact mass-to-charge ratio expected of the purified phospholipid. This suggested that the phospholipids had not peroxidised in storage and that the lower than expected rates of peroxidation were real. In the Visioli study [23] the high capacity of 18:2 to produce LOOH was matched by a rapid disappearance of 18:2 as measured using gas chromatography, with only 31% of original fatty acid remaining after 3 h versus 72% of 22:6 remaining

after the same period of peroxidation. Again this tends to support the idea that 18:2 has the capacity to produce high levels of LOOH relative to 22:6.

One of the interesting and unexpected results of the present study was the seemingly lower than expected peroxidation of the phosphatidylethanolamine lipids that contained double PUFA and also PtdCho 22:6/22:6. These phospholipids tended to have lower levels of peroxidation and lost their ability to continue to peroxidise over the 3 h. There are a number of possible explanations for this result. One possibility is that the phosphatidylethanolamines did not solubilize in the aqueous medium and therefore were simply less available in the liposomes (although the more soluble PtdCho 22:6/22:6 also showed a lower than expected peroxidation). Another possibility is that the 'smaller' head group of PtdEtn when combined with two large surface area occupying PUFA fatty acids (18:2/18:2 and 22:6/22:6) might produce molecules with a cone-shape that would tend to partition better into the increased curvature of the inner versus the outer leaflet of the liposome bilayer. This would make these molecules less available for peroxidation and lower their LOOH product formation. Similarly, the increased surface area of two 22:6 PUFA in PtdCho 22:6/22:6, even with its larger headgroup, might also favor its partitioning into the inner leaflet. It is well known that the charge on polar head groups, volume of the phospholipid, curvature of liposomes and molar ratios of phospholipids are all factors that can influence phospholipid distribution in liposomes [13, 14].

In conclusion, this study did not show the hypothesised increased peroxidation of PUFA/PUFA compare to SAT/PUFA phospholipids. The study found that 18:2 and 22:6 containing phospholipids do not produce LOOH in proportion to their peroxidation index. The study also showed that many of the PUFA/PUFA phospholipids seemed to have lower than expected rates of iron-induced peroxidation measured over 3 h, and it was hypothesized that one possible reason for this might be the partitioning of these molecules into the inner leaflet of the liposome bilayer.

Acknowledgments We would like to thank Prof Tony (A. J.) Hulbert and Assoc Prof Steven Blanksby for comments on the original manuscript, also Mr Colin Cortie for helping with some of the experimentation.

References

- Aslamkhan AG, Aslamkhan A, Ahearn GA (2002) Preparation of metal ion buffers for biological experimentation: a methods approach with emphasis on iron and zinc. *J Exp Biol* 292:507–522
- Battino R, Rettich TR, Tominaga T (1983) The solubility of oxygen and ozone in liquids. *J Phys Chem Ref Data* 12:163–178
- Bell MV, Dick JR (1993) The appearance of rods in the eyes of herring and increased di-docosahexaenoyl molecular species of phospholipids. *J Mar Biol Assoc UK* 73(3):679–688
- Bou R, Codony R, Tres A, Decker EA, Guardiola F (2008) Determination of hydroperoxides in foods and biological samples by the ferrous oxidation-xylenol orange method: a review of the factors that influence the methods performance. *Anal Biochem* 377(1):1–15
- Cosgrove JP, Church DF, Pryor WA (1987) The kinetics of the autoxidation of polyunsaturated fatty acids. *Lipids* 22:299–304
- Deiana L, Carru C, Pes G, Tadolini B (1999) Spectrophotometric measurement of hydroperoxides at increased sensitivity by oxidation of Fe²⁺ in the presence of xylenol orange. *Free Radic Res* 31:237–244
- Dowhan W (1997) Molecular basis for membrane phospholipid diversity: why are there so many lipids? *Annu Rev Biochem* 66:199–232
- Fagali N, Catala A (2009) Fe²⁺ and Fe³⁺ initiated peroxidation of sonicated and non-sonicated liposomes made of retinal lipids in different aqueous media. *Chem Phys Lipids* 36(10):88–94
- Fiorentini D, Landi L, Barzanti V, Cabrini L (1989) Buffers can modulate the effect of sonication on egg lecithin liposomes. *Free Radic Res Commun* 6(4):243–250
- Kishida E, Tokumaru S, Ishitani Y, Yamamoto M, Oribe M, Iguchi H, Kojo S (1993) Comparison of the formation of malondialdehyde and thiobarbituric acid-reactive substances from autoxidized fatty acids based on oxygen consumption. *J Agric Food Chem* 41:1598–1600
- Kraffe E, Soudant P, Marty Y, Kervarec N (2005) Docosahexaenoic acid- and eicosapentaenoic acid-enriched cardiolipin in the Manila clam *Ruditapes philippinarum*. *Lipids* 40(6):619–625
- Kraffe E, Yanic M, Guderley H (2007) Changes in mitochondrial oxidative capacities during thermal acclimation of rainbow trout *Oncorhynchus mykiss*: roles of membrane proteins, phospholipids and their fatty acid compositions. *J Exp Biol* 210:149–165
- Kubo K, Sekine S, Saito M (2003) Docosahexaenoic acid-containing phosphatidylethanolamine in the external layer of liposomes protects docosahexaenoic acid from 2,2'-azobis(2-amidinopropane)-dihydrochloride-mediated lipid peroxidation. *Arch Biochem Biophys* 410(1):141–148
- Kubo K, Sekine S, Saito M (2005) Primary aminophospholipids in the external layers of liposomes protect their component polyunsaturated fatty acids from 2,2'-azobis(2-amidinopropane)-dihydrochloride-mediated lipid peroxidation. *J Agric Food Chem* 53(3):750–758
- Napolitano M, Bravo E, Avella M, Chico Y, Ochoa B, Botham KM, Rivabene R (2004) The fatty acid composition of chylomicron remnants influences their propensity to oxidate. *Nutr Metab Cardiovasc Dis* 14:241–247
- Nealon JR, Blanksby SJ, Mitchell TW, Else PL (2008) Systematic differences in membrane acyl composition associated with varying body mass in mammals occur in all phospholipid classes: an analysis of kidney and brain. *J Exp Biol* 211(19):3195–3204
- Saito H, Xue C, Yamashiro R, Moromizato S, Itabashi Y (2010) High polyunsaturated fatty acid levels in two subtropical macroalgae, *Cladosiphon okamuranus* and *Caulerpa lentillifera*. *J Phycol* 46:665–673
- Schlame M, Ren M, Xu Y, Greenburg M, Haller M (2005) Molecular symmetry in mitochondrial cardiolipins. *Chem Phys Lipids* 138:38–49
- Schnitzer E, Pinchuk I, Lichtenberg D (2007) Peroxidation of liposomal lipids. *Eur Biophys J* 36:499–515
- Schug ZT, Gottlieb T (2009) Cardiolipin acts as a mitochondrial signalling platform to launch apoptosis. *Biochim Biophys Acta* 1788:2022–2031

21. Turner N, Hulbert AJ, Else PL (2005) Sodium pump molecular activity and membrane lipid composition in two disparate ectotherms, and comparison with endotherms. *J Comp Physiol B* 175:77–85
22. Valentine RC, Valentine DL (2010) Omega-3 fatty acids and the DHA principle. CRC Press, Boca Raton
23. Visioli F, Colombo C, Galli C (1998) Oxidation of individual fatty acids yields different profiles of oxidation markers. *Biochem Biophys Res Commun* 245:487–489
24. Wijesundera C, Ceccato C, Watkins P, Fagan P, Fraser B, Thienthong N, Perlmutter P (2008) Docosahexaenoic acid is more stable to oxidation when located at the sn-2 position of triacylglycerol compared to sn-1(3). *J Am Oil Chem Soc* 85(6):543–548
25. Yaguchi T, Tanaka S, Yokochi T, Nakahara T, Higashihara T (1997) Production of high yields of docosahexaenoic acid by *Schizochytrium* sp. strain SR21. *J Am Oil Chem Soc* 74(11):1431–1434
26. Zerouga M, Jenki LJ, Stillwell W (1995) Comparison of phosphatidylcholines containing one or two docosahexaenoic acyl chains on properties of phospholipid monolayers and bilayers. *Biochim Biophys Acta* 1236:266–272

Enhancement of Intestinal Permeability Utilizing Solid Lipid Nanoparticles Increases γ -Tocotrienol Oral Bioavailability

Bilal S. Abuasal · Courtney Lucas · Breanne Peyton ·
Alaadin Alayoubi · Sami Nazzal · Paul W. Sylvester ·
Amal Kaddoumi

Received: 3 October 2011 / Accepted: 6 January 2012 / Published online: 24 January 2012
© AOCs 2012

Abstract γ -Tocotrienol (γ -T3), a member of the vitamin E family, has been reported to possess an anticancer activity. γ -T3 is a lipophilic compound with low oral bioavailability. Previous studies showed that γ -T3 has low intestinal permeability. Thus, we have hypothesized that enhancing γ -T3 intestinal permeability will increase its oral bioavailability. Solid lipid nanoparticles (SLN) were tested as a model formulation to enhance γ -T3 permeability and bioavailability. γ -T3 intestinal permeability was compared using in situ rat intestinal perfusion, followed by in vivo relative oral bioavailability studies. In addition, in vitro cellular uptake of γ -T3 from SLN was compared to mixed micelles (MM) in a time and concentration-dependent studies. To elucidate the uptake mechanism(s) of γ -T3 from SLN and MM the contribution of NPC1L1 carrier-mediated uptake, endocytosis and passive permeability were investigated. In situ studies demonstrated SLN has tenfold higher permeability than MM. Subsequent in vivo studies showed γ -T3 relative oral bioavailability from SLN is threefold higher. Consistent with in situ results, in vitro concentration dependent studies revealed γ -T3 uptake from SLN was twofold higher than MM. In vitro mechanistic characterization showed that while endocytosis contributes to γ -T3 uptake from both formulations, the reduced contribution of NPC1L1 to the transport of γ -T3, and passive diffusion enhancement of γ -T3 are primary explanations for its enhanced uptake from SLN. In conclusion, SLN

successfully enhanced γ -T3 oral bioavailability subsequent to enhanced passive permeability.

Keywords Intestinal permeability · Vitamin E · γ -Tocotrienol · Solid lipid nanoparticles · NPC1L1 · In situ intestinal perfusion · Oral absorption · Oral bioavailability

Abbreviations

MM	Mixed micelles
NPC1L1	Niemann-Pick C1-like 1
SLN	Solid lipid nanoparticles
γ -T3	Gamma-tocotrienol

Introduction

γ -Tocotrienol (γ -T3) is a natural form of vitamin E with potential anticancer activity in breast cancer [1–3]. Unfortunately the oral bioavailability of γ -T3 is low [4, 5]. In humans, the absolute bioavailability has not been determined, however in rats γ -T3 oral bioavailability has been found to be as low as 9% [5]. γ -T3 is an oily liquid that is poorly soluble in aqueous solutions [6]. Due to poor aqueous solubility and miscibility, its oral bioavailability can be poor and erratic. As a result, many formulation approaches have been used to enhance its bioavailability by increasing its dissolution including lipid-based formulations, self-emulsifying drug delivery systems (SEDDS), emulsions, and oil solutions [5–8]. However, recent in situ permeability studies in our laboratory have revealed that in addition to the low solubility, γ -T3 intestinal permeability is also low [9]. The results of these studies have demonstrated the intestinal absorption of γ -T3 is a concentration-dependent and saturable process, that is mediated by the

B. S. Abuasal · C. Lucas · B. Peyton · A. Alayoubi ·
S. Nazzal · P. W. Sylvester · A. Kaddoumi (✉)
Department of Basic Pharmaceutical Sciences,
College of Pharmacy, University of Louisiana at Monroe,
Monroe, LA 71201, USA
e-mail: kaddoumi@ulm.edu

transporter Niemann-Pick C1-like 1 (NPC1L1) [9]. Thus, when therapeutic γ -T3 is administered at doses that saturate its own uptake by NPC1L1, γ -T3 oral bioavailability is expected to decrease. To overcome such limitation, it is anticipated that increasing the permeability of γ -T3 using new formulation approaches or structural modifications will enhance its permeability, thus its oral bioavailability.

One of the most promising strategies to increase the absorption is the encapsulation of the drug in a nano-scale delivery system which will facilitate the drug permeability across the intestinal barrier [10, 11]. In this case, bioavailability is not dependent on the physicochemical properties of the drug, but on the properties of the nano-carrier [12–14]. Solid lipid nanoparticles (SLN), a type of submicron particulate drug delivery system, are regarded as an alternative carrier to traditional colloidal systems such as emulsions, liposomes, polymeric microparticles and nanoparticles [15–17]. The natural or artificial synthetic solid lipids are used as carriers with the drug enveloped or dispersed inside the particles to obtain the solid colloidal particles. The particle diameters are in the range of approximately 10–1,000 nm [18]. The advantages of the system include high biocompatibility, high bioavailability, and no problems with multiple routes of administration such as oral, intravenous, pulmonary and transdermal routes [17, 19–22]. Sufficient data implicate the bioavailability of poorly hydrophilic and lipophilic drugs can be improved when these drugs are encapsulated in SLN [10, 19, 23–25]. For example, Nitrendipine, an antihypertensive drug, is a lipophilic drug with poor oral bioavailability ranging from 10 to 20%. When this compound was loaded into SLN and given to rats by intraduodenal administration, the bioavailability of Nitrendipine increased by three- to fourfold compared to that of a Nitrendipine suspension [26]. Following oral administration, nanoparticles have to cross the gastrointestinal barrier either by passive diffusion or by active processes mediated by membrane-bound carriers or membrane-derived vesicles [27].

Recently, SLN has been used in the formulation of γ -T3 [28, 29], however the effect of γ -T3 encapsulation in SLN on its oral bioavailability have not been investigated. γ -T3 is usually administered as an oily solution or in micelle systems [5, 8]. After administration, it will be subjected to digestion and dissolution to form mixed micelles. Mixed micelles (MM) are the end product of intestinal digestion that is most readily available for absorption [30]. In this article the potential of SLN as oral delivery system for γ -T3 will first be illustrated by comparing its intestinal permeability to that from MM utilizing in situ rat intestinal perfusion studies, and relative oral bioavailability of γ -T3; MM preparation was used in the comparative bioavailability and permeability studies to rule out the effect of dissolution rate on γ -T3 absorption process. Then, the

mechanisms of uptake of γ -T3 from both formulations will be demonstrated by elucidating the contribution of carrier-mediated transport by NPC1L1, endocytosis, and passive diffusion to the enhanced uptake of SLN. To address the mechanism of cellular uptake and monitor experimental parameters, in vitro studies utilizing HepG2 cells as a model cell line was chosen. HepG2 cells are human derived hepatocytes with remarkable endogenous expression of NPC1L1 transporter [31].

Materials and Methods

Materials

γ -T3 was provided by First Tech International Co., Ltd. (Hong Kong). Ezetimibe was kindly donated by Schering-Plough Corporation (NJ, USA). Cholesterol and γ -tocopherol were obtained from Sigma (St. Louis, MO). Sodium taurocholate and phosphatidylcholine were purchased from Avanti Polar Lipids, Inc. (Alabaster, AL). [1,2- 14 C]-PEG4000 (polyethylene glycol 4000, Specific activity 0.75 mCi g $^{-1}$) was purchased from American Radiolabeled Chemicals, Inc. (St. Louis, MO). Unlabeled PEG4000 was purchased from Spectrum Chemical (Gardena, CA). Supplies for cell culture were obtained from American Type Cell Culture Collection (ATCC; Manassas, VA). Chlorpromazine was purchased from Sigma. Lutrol $^{\text{®}}$ F62 (poloxamar 188) and compritol ATO were obtained from BASF (Floham Park, NJ). Other chemicals and reagents were obtained from VWR Scientific (West Chester, PA).

Animals

Male Sprague–Dawley rats weighing 260–320 g were acquired from Harlan Laboratories (Houston, TX). All animal experiments were approved by the Institutional Animal Care and Use Committee of the University of Louisiana at Monroe and all surgical and treatment procedures were consistent with the IACUC policies and procedures. Rats were maintained on a 12 h light/dark cycle before the study and were fasted 12–16 h with water ad libitum prior to each experiment.

Formulation of SLN and MM

γ -T3-loaded SLN were prepared as previously described [29]. SLN were manufactured by hot oil/water micro-emulsion using a high shear homogenization technique. In brief, γ -T3, lutrol, and compritol ATO (w/w of the final aqueous dispersion) lipid phase was first prepared by melting compritol ATO at 80 °C to which 0.2% (w/w) γ -T3 was added to form the homogeneous oil phase. In a

separate vial, a 0.2% (w/w) lutrol solution was prepared by dissolving the surfactant in deionized water. The solution was heated to the same temperature as the oil phase. The hot aqueous surfactant solution was then added to the molten lipid phase to form the premix that was further homogenized at 20,000 rpm for 5 min using IKA[®] Ultra-Turrax T8 mixer (IKA[®] Work inc., NC, USA). The formed hot pre-emulsion was then ultrasonicated at 60% pulsar rate for 10 min using an ultra sonic probe homogenizer (Biologics, Inc., VA). Nanoparticles were subsequently formed by cooling the sonicated nano-emulsion overnight at 4 °C. Intensity-weighted mean particle size and population distribution (polydispersity index, PI) of the emulsion were measured by photon correlation spectroscopy (PCS) at 23 °C and a fixed angle of 90° using Nicomp[™] 380 ZLS submicron particle size analyzer (PSS Inc, Santa Barbara, CA). SLN average particle size was 105 nm ($n = 3$ preparations), with polydispersity index (PI) value of 0.134 ± 0.007 .

Mixed micelles were prepared as previously described [32]. γ -T3 diluted in methanol, phosphatidylcholine diluted in methanol, taurocholate diluted in 96% ethanol, and mono- and diglycerides (oleic acid and Capmul dissolved in methanol) were mixed, then evaporated to dryness with mild heating under nitrogen gas. A transport buffer (141 mM NaCl, 4 mM KCl, 1 mM MgSO₄, 10 mM HEPES, 10 mM glucose, and 2.8 mM CaCl₂ adjusted to pH 7.4) was then added to prepare the medium for transport experiments. Final concentrations were: taurocholate 5 μ M, phosphatidylcholine 10 μ M, oleic acid 100 μ M, mono- and diglycerides 300 μ M, and the required γ -T3 concentration in each experiment. The micellar solution was thoroughly vortexed and stirred at 37 °C for 30 min.

In Vitro Studies

Cell Culture

HepG2 cells were cultured in RPMI-1640 supplemented with 10% fetal bovine serum (FBS) and 2.5% antibiotics (penicillin and streptomycin) in a humidified incubator with 5% CO₂ at 37 °C. Cells were plated on 75 cm² flask at a density of 1×10^6 cells/flask and were then harvested at 80% confluence with trypsin–EDTA. Cells were seeded onto a 48-well plate at a density of 50,000 cells/well. When confluent, uptake studies were performed as described below. All experiments were conducted in triplicate.

Time Dependent Studies

On the day of the experiment, SLN and MM were diluted in transport buffer to prepare 2 μ M final concentration of

γ -T3. The media in the incubated plates was discarded, and cells were washed once with warm transport buffer before addition of SLN or MM for 0, 5, 10, 20, 30, 40, 60, 120 min. At the end of the incubation time cells were washed two times with ice cold PBS and lysed with 200 μ l lysis buffer for 2 h before analysis by LC–MS.

Concentration Dependent Studies

Solid lipid nanoparticles and MM were diluted in transport buffer to prepare different concentrations ranging from 1 to 200 μ M. Two hundred microliters from each concentration of SLN and MM were incubated for 60 min. At the end of the experiment, cells were washed twice with ice cold PBS and lysed with 200 μ l lysis buffer for 2 h before analysis by LC–MS.

NPC1L1 Inhibition Studies

To compare the effect of formulation on the carrier-mediated uptake of γ -T3 by NPC1L1, inhibition studies of NPC1L1 by ezetimibe (selective inhibitor of NPC1L1) were performed [9, 33–36]. After washing the cells with warm transport buffer, cells were pre-incubated with rising concentration of ezetimibe at 0, 1, 5, 10, 25, and 50 μ M for 30 min. Cells were then incubated with 4 μ M of γ -T3 prepared as SLN or MM for 60 min with increasing concentration of ezetimibe. After washing with ice cold PBS, cells were lysed with 200 μ l lysis buffer before analysis by LC–MS.

Endocytosis Inhibition Studies

To investigate the contribution of endocytosis to the uptake of SLN and MM, cellular uptake experiment were conducted with and without chlorpromazine (endocytosis inhibitor) [37]. γ -T3, at 5 and 10 μ M, as MM and SLN were prepared. The cells were pre-incubated for 30 min with 0, 25, 50, and 100 μ M of chlorpromazine dissolved in transport buffer, then γ -T3 prepared as SLN or MM was added for 60 min. At the end of the experiments cells were washed and lysed as mentioned above before analysis by LC–MS.

Cellular Uptake Study at 4 °C

At 4 °C, active transport including pinocytic/endocytic uptake of drugs is usually not functioning [38, 39]. Thus, 4 °C experiments will account for passive uptake of SLN and MM. On the day of the experiment, confluent cells were washed and incubated with rising γ -T3 concentrations prepared as SLN or MM as described above in the concentration dependent study; however incubations were conducted at 4 °C. After 60 min incubation, cells were washed, lysed and analyzed by LC–MS.

LC–MS Analysis of γ -T3 in Cellular Uptake Studies

Cell lysates (75 μ l) were mixed with similar volume of acetonitrile in eppendorf tubes and vortex mixed for 30 s. Samples were then centrifuged for 10 min at 10,000g. From the collected supernatant 10 μ l were injected onto the LC–MS system. The chromatographic separation was performed on a 250 \times 4.6 mm Luna 5 μ PFP column (Phenomenex, Torrance, CA) using an Agilent 1100 series LC system (Santa Clara, CA), and 3200 Qtrap LC/MS/MS system (Applied Biosystems, Foster City, CA). The mobile phase consisted of methanol, ethanol and acetonitrile (40:30:30, v/v/v) delivered at 1.0 ml min⁻¹ flow rate with the addition of 0.05% acetic acid. γ -T3 was detected by MS using electrospray ionization (ESI) interface operated in positive mode. γ -T3 was then detected and quantified by MS/MS using multiple-reaction monitoring (MRM) method. The transition (precursor > product) used for quantification was 411 > 151. Protein concentration of the lysate was determined by a BCA kit (Thermo scientific, Rockford, IL). Final samples concentrations were expressed as μ g mg⁻¹ protein.

In Situ Perfusion Studies

In situ rat intestinal perfusion studies were conducted to investigate the difference in the intestinal permeability of γ -T3 loaded in SLN or MM. This experiment was conducted as previously described [9, 40]. In brief, following overnight fasting, rats were anesthetized. The small intestine was then exposed by midline incision and approximately 15 cm of upper jejunum (proximal to the duodenum) was externalized. The isolated segment was flushed with warm normal saline to remove intestinal contents and cannulated with glass cannulas inserted at the inlet and the outlet of the segment. The inlet tubing was connected to a syringe that was placed in an infusion pump. The perfusate was pumped through the lumen at 0.05 ml min⁻¹ flow rate. The perfusate solution consisted of 1 μ M γ -T3 prepared as SLN or MM. [¹⁴C]-PEG4000 (0.02 μ Ci ml⁻¹) with 0.1% cold PEG4000 was added to the perfusate solution as a marker for water secretion or absorption. The perfusate was collected in vials at 20 min intervals for 100 min after 40 min stabilization period. Samples were kept at 4 °C till analysis by HPLC. Effective permeability of γ -T3 from SLN and MM preparations was calculated based on γ -T3 loss from the perfusate according to the equation:

$$P_{\text{eff}} = \frac{-Q \times \ln(C_i/C_0)}{2\pi rL}$$

where Q is the perfusate flow rate through the segment (0.05 ml min⁻¹), r is the radius of the intestinal lumen (0.2 cm), L is the length of the perfused segment (15 cm), C_0 is γ -T3 concentration at the start of perfusion (from the

entry tubing), and C_i is the steady state of γ -T3 concentration exiting the perfused intestinal segment.

In Vivo Relative Bioavailability Experiments

After 12 h fasting, rats were orally gavaged with 10 mg kg⁻¹ γ -T3 prepared as SLN or MM. Rats were anesthetized with intraperitoneal injection of 1.0 g kg⁻¹ urethane dissolved in normal saline. Blood samples were withdrawn from the femoral vein at 1, 2, 3, 4, 5, 6, 8, 10, 12 h. Blood samples were collected in heparinized eppendorf tubes. Samples were then centrifuged at 10,000 rpm for 10 min to separate the plasma. Plasma samples were kept at -20 °C until analysis with HPLC. Following analysis, plasma levels versus time profiles were plotted and fitted using PK-Plus module in GastroplusTM (Simulation Plus, Inc CA). Pharmacokinetic parameters were calculated using non-compartmental analysis.

HPLC Analysis of Intestinal Perfusate and Plasma Samples

Quantification of γ -T3, in the intestinal perfusate was achieved by an isocratic Prominence Shimadzu HPLC system (Columbia, MD) as previously described with some modifications [9, 41]. In brief, perfusate samples were diluted with acetonitrile (1:10 v/v) before injection of 20 μ l into the HPLC. For the extraction of γ -T3 from plasma, 50 μ l plasma and 50 μ l ethanol containing 1% ascorbic acid and 1 μ g ml⁻¹ δ -tocopherol (internal standard) were added in a glass tube and vortex mixed, followed by the addition 1 ml hexane. The mixture was vortex-mixed for 90 s before centrifugation for 10 min at 5,000g. Eight hundred microliters of the supernatant were then transferred to another glass tube and evaporated to dryness by a centrifugal evaporator (Centrivap concentrator, Kansas City, MO, USA) followed by reconstitution with 100 μ l mobile phase before 20 μ l injection onto the HPLC column. The system consisted of SIL 20-AHT autosampler, and LC-20AB pump connected to a DGU-20A3 degasser. Data acquisition was achieved by Shimadzu LC Solution software version 1.22 SP1. The separation was performed at room temperature on an Agilent eclipse XDB-C18 column (5 μ m, 150 \times 4.6 mm id; Agilent Technologies Inc., CA, USA). The mobile phase used for the separation of γ -T3 in perfusate and plasma samples consisted of methanol, ethanol and acetonitrile (85:7.5:7.5, v/v/v) delivered at 1.0 ml min⁻¹ flow rate. UV detection of γ -T3 in perfusate samples was carried out at a wavelength of 210 nm (Shimadzu SPD-20A UV/VIS), while γ -T3 in plasma was detected by fluorescence detection (Shimadzu, RF10A XL) set at 298 nm excitation and 325 nm emission.

Statistical Analysis

Results were expressed as means \pm SEM. Jump[®] software was used to conduct the statistical analysis. A Student's *t* test for the in situ studies, or ANOVA and a *t* test for the endocytosis and NPC1L1 inhibition studies were used for statistical comparison. $p < 0.05$ was considered statistically significant. All animal studies were performed at $n = 3$ per experiment per formulation.

Results

In Situ Perfusion Studies

Results from the in situ perfusion studies revealed that the permeability of γ -T3 prepared as SLN was significantly higher than that from MM. The permeability of γ -T3 delivered as SLN was $9.42 \times 10^{-5} \pm 2.3 \times 10^{-5} \text{ cm s}^{-1}$ while its permeability from MM was $0.9 \times 10^{-5} \pm 0.29 \times 10^{-5} \text{ cm s}^{-1}$ which is approximately tenfold lower than SLN formulation. Results of the in situ perfusion experiments are presented in Fig. 1.

Relative Oral Bioavailability Studies

Following oral administration of a single 10 mg kg^{-1} γ -T3 dose as SLN or MM to fasted rats, γ -T3 plasma concentrations were calculated and plotted versus time (Fig. 2). Peak concentration (C_{max}) and time of peak concentration (T_{max}) were obtained directly from individual plasma concentration–time profile of each rat. The area under the concentration–time curve from time zero to time *t* (AUC_{0-t}) was calculated using the trapezoidal method. The relative bioavailability (F_{rel}) of γ -T3 from SLN compared to MM was calculated using the following equation: $F_{\text{rel}} = (AUC_{0-t}(\text{SLN})/AUC_{0-t}(\text{MM})) \times 100\%$.

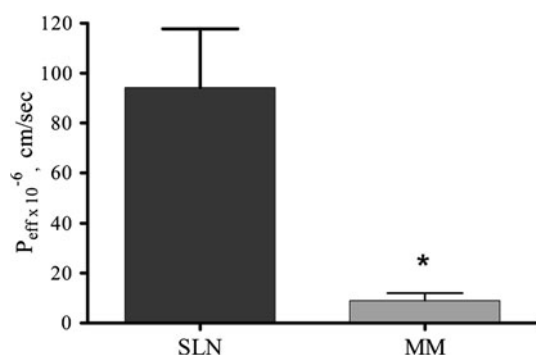


Fig. 1 Effective permeability (P_{eff}) of γ -T3 delivered as SLN or MM using in situ intestinal perfusion ($n = 3$ each). Each value represents the mean \pm SEM ($p < 0.05$)

The AUC of γ -T3 following SLN administration was $12.1 \pm 5.7 \mu\text{g-h ml}^{-1}$ compared to its AUC from MM $3.9 \pm 0.7 \mu\text{g-h ml}^{-1}$ which is approximately threefold lower than SLN ($F_{\text{rel}} = 310\%$). The oral pharmacokinetic parameters of γ -T3 following both formulations are listed in Table 1. As illustrated in Fig. 2 plasma concentration of γ -T3 at all time points are significantly higher for rats administered with SLN formulation compared to MM ($p < 0.05$). The C_{max} value for γ -T3 from SLN was $938 \pm 63 \text{ ng ml}^{-1}$ compared to $212 \pm 111 \text{ ng ml}^{-1}$ from MM. These results demonstrate that incorporation of γ -T3 into SLN significantly increased its absorption thus bioavailability following oral administration.

In Vitro Uptake Studies

Comparative effects of incubation time (5–120 min) on cellular uptake of γ -T3 presented as SLN or MM is shown in Fig. 3a. Results showed significantly preferential and higher uptake of γ -T3 from SLN compared to MM at all examined time points. Comparison of the effect of

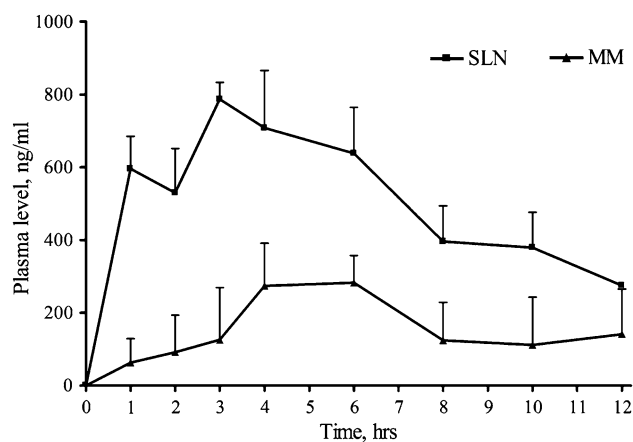


Fig. 2 Plasma concentrations (ng ml^{-1}) versus time (h) profiles of γ -T3 following oral administration of 10 mg kg^{-1} dose of γ -T3 loaded in SLN or MM. Each value represents the mean \pm SEM ($n = 3$)

Table 1 Comparative pharmacokinetic parameters of γ -T3 oral absorption when delivered in SLN or MM following 10 mg kg^{-1} oral administration to rats

Parameter	SLN	MM
AUC ($\mu\text{g ml}^{-1} \text{ h}$)	12.1 ± 5.7	3.9 ± 0.7
C_{max} (ng ml^{-1})	786.4 ± 63	275 ± 111
T_{max} (h)	3 ± 0.9	5 ± 0.9
MRT (h)	15.5 ± 7.5	10.8 ± 2.2
K_e (h^{-1})	0.17 ± 0.1	0.07 ± 0.03

Data are presented as means \pm SEM ($n = 3$)

MRT Mean residence time

K_e Elimination rate constant

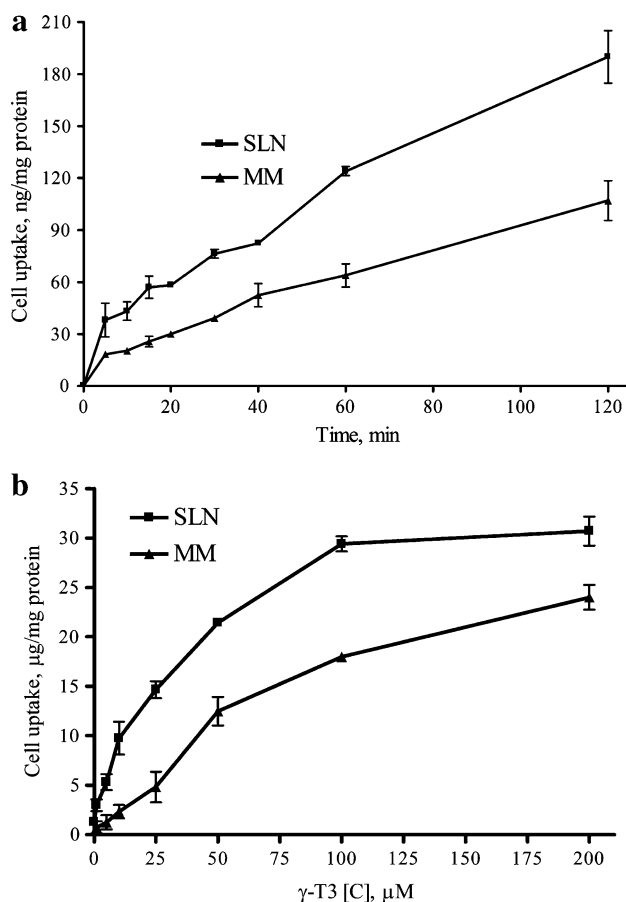


Fig. 3 Comparative effects of **a** incubation time on cellular uptake of 2 μM $\gamma\text{-T3}$ delivered as SLN or MM, and **b** various concentrations of $\gamma\text{-T3}$ -loaded SLN or MM on $\gamma\text{-T3}$ cellular uptake following treatment for 60 min. Each value represents the mean \pm SD from three independent experiments

incubated concentrations of $\gamma\text{-T3}$ -loaded SLN or MM on the cellular uptake following 60 min of treatment is presented in Fig. 3b. For practicality reasons, including sensitivity and less variability, incubation with $\gamma\text{-T3}$ delivered as SLN or MM for 60 min was selected. Results of this experiment revealed a significantly higher concentration dependent uptake of SLN in comparison to MM after 60 min incubation at 37 °C. The results from ezetimibe inhibition studies of $\gamma\text{-T3}$ uptake mediated by NPC1L1 are shown in Fig. 4 and demonstrated a dose-dependent decrease in the uptake of $\gamma\text{-T3}$ after incubation with different ezetimibe concentrations for both SLN and MM. However, while the uptake of $\gamma\text{-T3}$ prepared as SLN is higher than that from MM, the percent decrease in the uptake of $\gamma\text{-T3}$ prepared as MM is more than that from SLN ($p < 0.05$). Maximum inhibition of $\gamma\text{-T3}$ uptake was achieved at ezetimibe concentrations $\geq 10 \mu\text{M}$ for both preparations.

The effect of endocytosis inhibition by chlorpromazine on $\gamma\text{-T3}$ uptake prepared as SLN and MM was also

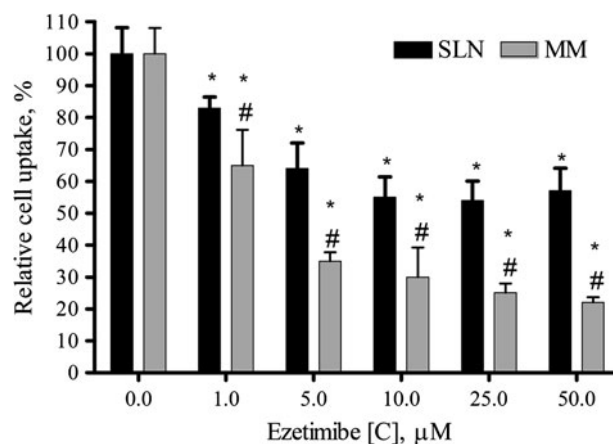


Fig. 4 Effects of NPC1L1 inhibition by ezetimibe on carrier-mediated uptake of 4 μM $\gamma\text{-T3}$ delivered as SLN or MM. Results of this experiment are presented as relative uptake to control (absence of ezetimibe) from three independent experiments. Each value represents the mean \pm SD. Asterisk indicates significantly different from control (absence of ezetimibe), and hash symbol indicates significantly different from SLN, $p < 0.05$

investigated and the results are illustrated in Fig. 5. The results of this experiment revealed that at the two concentrations examined for $\gamma\text{-T3}$ (5 and 10 μM) both SLN and MM were responding to endocytosis inhibition; however the decrease in the uptake of $\gamma\text{-T3}$ from both preparations was similar and low (approximately 25% reduction), but statistically significant (Fig. 5).

It is assumed that at the temperature 4 °C, active carrier-mediated transport and pinocytotic/endocytic uptake of molecules are usually hampered [38, 39]. Thus, studies conducted at 4 °C account for passive uptake of $\gamma\text{-T3}$

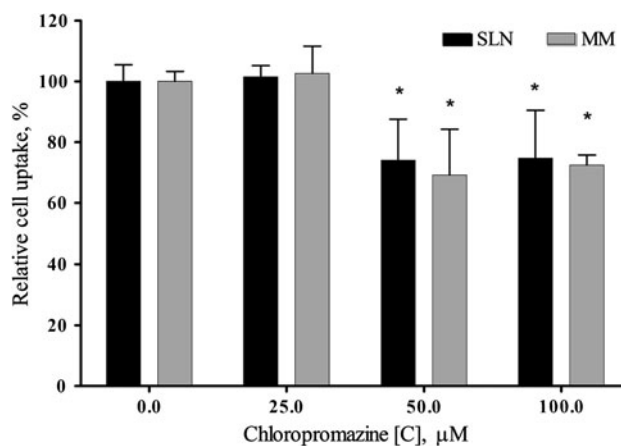


Fig. 5 The effect of endocytosis inhibition by chlorpromazine on the uptake of $\gamma\text{-T3}$ delivered as SLN or MM at 10 μM concentration following treatment for 60 min. Results of this experiment are presented as relative uptake to control (absence of chlorpromazine) from three independent experiments. Each value represents the mean \pm SD. * Significantly different from control (absence of chlorpromazine), $p < 0.05$

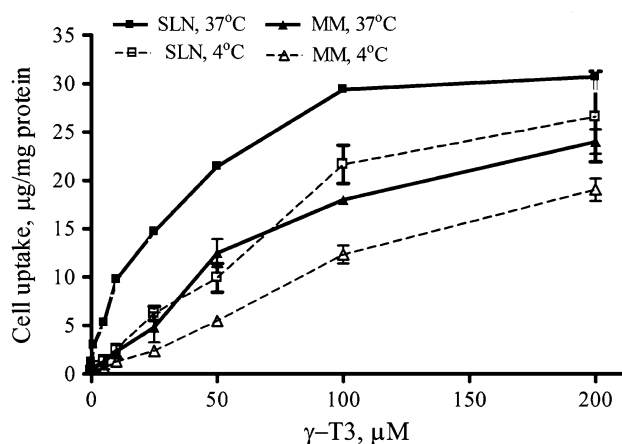


Fig. 6 Concentration dependent uptake studies of γ -T3 delivered as SLN or MM at 37 and 4 °C following treatment for 60 min. Each value represents the mean \pm SD from three independent experiments

loaded in SLN and MM. Comparison of the concentration dependent uptake of γ -T3 at 4 °C and at 37 °C from SLN and MM is presented in Fig. 6. At 4 °C the uptake of γ -T3 delivered as SLN while reduced remains significantly higher than that for MM ($p < 0.05$). In addition, cellular uptake of γ -T3 loaded in SLN and MM at 4 °C was significantly lower than its cellular uptake at 37 °C.

Discussion

The results of this study demonstrated that intestinal permeability and oral absorption of γ -T3 are significantly enhanced when packaged in SLN delivery system compared to MM.

The in situ rat intestinal perfusion model represents an excellent technique to investigate drugs intestinal absorption because it is the closest system to the in vivo physiological conditions. Furthermore, the presence of intact mucosa and drug transporters (e.g. NPC1L1) would accurately predict the in vivo intestinal absorption process. In a previous in situ rat intestinal perfusion study we have demonstrated that the intestinal absorption of γ -T3 is a saturable, dose dependent process and mediated by NPC1L1 [9]. In addition to γ -T3 low solubility, this saturable absorption process by NPC1L1 is believed to contributing to γ -T3 low intestinal permeability thus bioavailability when given in amounts that are higher than NPC1L1 transport capacity.

In the current study, the intestinal permeability and bioavailability of γ -T3 packaged in SLN delivery system were compared to MM preparation. Results from the in situ perfusion studies of γ -T3 demonstrated higher uptake of γ -T3 delivered as SLN compared to MM. This tenfold difference in the permeability of SLN ($9.4 \times 10^{-5} \pm 2.3 \times 10^{-5} \text{ cm s}^{-1}$)

compared to MM ($0.9 \times 10^{-5} \pm 0.29 \times 10^{-5} \text{ cm s}^{-1}$) enhanced the oral bioavailability of γ -T3 administered as SLN by threefold. The above findings confirmed that enhancing γ -T3 intestinal permeability improves its oral bioavailability.

Consistent with in situ studies findings, in vitro HepG2 cellular uptake studies showed significantly higher uptake of γ -T3 delivered as SLN in comparison to MM. HepG2 cell line, derived from hepatocellular liver carcinoma cells, is a pharmacologically validated system for NPC1L1-mediated cholesterol uptake due to its significant endogenous expression of NPC1L1 compared to Caco-2 (derived from human epithelial colorectal adenocarcinoma cells) cell line [42]. Thus, in the current study HepG2 cells were utilized to further investigate the mechanism of enhanced γ -T3 uptake and the contribution of NPC1L1 to γ -T3 carrier-mediated uptake from SLN and MM preparations. The time-dependent studies of 2 μ M γ -T3 delivered as SLN or MM showed a time-dependent preferential cellular uptake of γ -T3 from SLN (Fig. 3a). In addition, concentration dependent studies for 60 min with SLN or MM containing γ -T3 in the range of 1–200 μ M demonstrated a significantly higher cellular uptake of γ -T3 from SLN compared to MM (Fig. 3b). These findings confirm that γ -T3 administered as SLN would have greater intestinal absorption following oral administration.

To explain the enhanced intestinal permeability and cellular uptake of γ -T3 delivered as SLN compared to MM, in vitro mechanistic studies were performed including NPC1L1 carrier-mediated uptake, endocytosis, and passive uptake. Contribution of the carrier-mediated uptake of γ -T3 by NPC1L1 was investigated by treating cells with γ -T3 loaded as SLN or MM with rising concentrations of ezetimibe. Results were expressed as relative uptake of γ -T3 in reference to control (absence of ezetimibe). The results revealed the uptake of γ -T3 loaded in MM was more sensitive to NPC1L1 inhibition by ezetimibe compared to SLN. This was attributed to the fact that γ -T3 delivered as SLN did not efficiently expose γ -T3 to NPC1L1 as it will be impeded inside the SLN matrix (Fig. 4) [29]. As a result, only γ -T3 available on the surface of SLN or released in the media will be exposed to transport by NPC1L1. These findings, thus, demonstrate that the enhanced intracellular uptake of γ -T3 was not attributed to NPC1L1 mediated uptake. On the other hand, the results indicate the important role of NPC1L1 to the cellular uptake of γ -T3 where NPC1L1 inhibition by ezetimibe reduced γ -T3 intracellular levels approximately by 80% for MM and 40% for SLN.

Endocytosis is another proposed mechanism of the uptake of SLN and similar colloidal systems. To investigate the role of endocytosis in the enhanced uptake of SLN, endocytosis inhibition studies with chlorpromazine were conducted. Chlorpromazine is an inhibitor of the clathrin

dependent endocytosis (CDE) pathway. It works by inhibiting clathrin-coated pit formation by a reversible translocation of clathrin and its adapter proteins from the plasma membrane to intracellular vesicles [43]. CDE is the best-characterized endocytic pathway and is believed to be the preferred pathway for microspheres up to 200 nm in size [44]. Thus, in this work it has been considered for evaluation. The inhibition of endocytosis resulted in approximately 25% reduction in γ -T3 uptake from both SLN and MM (Fig. 5). This data revealed that the contribution of endocytosis of both formulations was the same and does not explain the higher uptake of γ -T3 delivered as SLN. While γ -T3 uptake reduction by chlorpromazine does not completely rule out enhanced endocytosis of SLN, for example by clathrin independent pathway, consequent experiments at 4 °C demonstrated an alternative mechanism for the enhanced uptake. Several reports demonstrated cell membrane penetration at 4 °C is related to passive processes [38]. When cells were treated with different concentrations of γ -T3 loaded as SLN or MM and incubated at 4 °C for 60 min, the uptake of γ -T3 from both formulations was reduced. However, the uptake of γ -T3 delivered as SLN remained to be significantly higher than that from MM (Fig. 6), most probably because of the enhanced passive diffusion. SLN surfactants and excipients possibly caused an increase in γ -T3 passive permeability. This assumption was supported by a separate experiment where cells were treated with γ -T3-free SLN (empty vehicle) and γ -T3. The results showed that the cellular uptake of γ -T3 in the presence of SLN vehicle was significantly higher than γ -T3 alone. For example, the addition of SLN vehicle to different concentrations of γ -T3 at 5 and 10 μ M, γ -T3 intracellular level increased from 1.1 ± 0.6 and $1.4 \pm 0.7 \mu\text{g mg}^{-1}$ protein for cells treated with γ -T3 alone, respectively, to 3.4 ± 0.08 and $5.7 \pm 0.04 \mu\text{g mg}^{-1}$ protein for cells treated with γ -T3 and SLN vehicle, respectively. Thus, such data demonstrate that presence of SLN excipients enhanced γ -T3 cellular uptake by approximately fourfold. Furthermore, the data obtained from γ -T3 in the presence of SLN vehicle were comparable to those obtained from γ -T3-loaded SLN at 5 and 10 μ M concentrations and were 3.5 ± 0.03 and $5.3 \pm 0.14 \mu\text{g mg}^{-1}$ protein, respectively.

Collectively, the above results suggest that γ -T3 packaged in SLN delivery system enhanced γ -T3 intestinal permeability and bioavailability by enhancing the passive permeability of γ -T3, and by reducing the contribution of NPC1L1 to the carrier-mediated transport of γ -T3 compared to MM, thus NPC1L1 saturation will occur at higher load of γ -T3 delivered as SLN compared to MM.

In conclusion, at 10 mg kg⁻¹ dose SLN successfully enhanced the oral bioavailability of γ -T3 in comparison to MM. In vitro and in situ studies revealed that the enhanced

bioavailability is mostly related to the enhancement of absorption and permeation across the intestine. Subsequent in vitro uptake studies suggested that enhanced bioavailability of γ -T3 from SLN is primarily a result of its enhanced passive permeability and the reduced contribution of NPC1L1 to the transport of γ -T3.

Conflict of interest All authors acknowledge that they have no personal financial or non-financial conflicts of interest.

References

- Sylvester PW, Shah SJ (2004) Mechanisms mediating the anti-proliferative and apoptotic effects of vitamin E in mammary cancer cells. *Front Biosci* 10:699–709
- Sylvester PW, Shah S (2005) Intracellular mechanisms mediating tocotrienol-induced apoptosis in neoplastic mammary epithelial cells. *Asia Pac J Clin Nutr* 14(4):366–373
- Kline K, Yu W, Sanders BG (2004) Vitamin E and breast cancer. *J Nutr* 134(12 Suppl):3458S–3462S
- Yap SP, Yuen KH, Wong JW (2001) Pharmacokinetics and bioavailability of alpha-, gamma- and delta-tocotrienols under different food status. *J Pharm Pharmacol* 53(1):67–71
- Yap SP, Yuen KH, Lim AB (2003) Influence of route of administration on the absorption and disposition of alpha-, gamma- and delta-tocotrienols in rats. *J Pharm Pharmacol* 55(1):53–58
- Yap SP, Yuen KH (2004) Influence of lipolysis and droplet size on tocotrienol absorption from self-emulsifying formulations. *Int J Pharm* 281(1–2):67–78
- Constantinides PP, Tustian A, Kessler DR (2004) Tocol emulsions for drug solubilization and parenteral delivery. *Adv Drug Deliv Rev* 56(9):1243–1255
- Borowy-Borowski H, Sodja C, Docherty J, Walker PR, Sikorska M (2004) Unique technology for solubilization and delivery of highly lipophilic bioactive molecules. *J Drug Target* 12(7):415–424
- Abuasal B, Sylvester PW, Kaddoumi A (2010) Intestinal absorption of gamma-tocotrienol is mediated by Niemann-Pick C1-like 1: in situ rat intestinal perfusion studies. *Drug Metab Dispos* 38(6):939–945
- Hu L, Tang X, Cui F (2004) Solid lipid nanoparticles (SLNs) to improve oral bioavailability of poorly soluble drugs. *J Pharm Pharmacol* 56(12):1527–1535
- Hu L, Xing Q, Meng J, Shang C (2010) Preparation and enhanced oral bioavailability of cryptotanshinone-loaded solid lipid nanoparticles. *AAPS PharmSciTech* 11(2):582–587
- Peltier S, Oger JM, Lagarce F, Couet W, Benoit JP (2006) Enhanced oral paclitaxel bioavailability after administration of paclitaxel-loaded lipid nanocapsules. *Pharm Res* 23(6):1243–1250
- Zhang Z, Feng SS (2006) Self-assembled nanoparticles of poly(lactide)—vitamin E TPGS copolymers for oral chemotherapy. *Int J Pharm* 324(2):191–198
- Li H, Zhao X, Ma Y, Zhai G, Li L, Lou H (2009) Enhancement of gastrointestinal absorption of quercetin by solid lipid nanoparticles. *J Control Release* 133(3):238–244
- Sun W, Zhang N, Li A, Zou W, Xu W (2007) Preparation and evaluation of N(3)-O-toluyfl-fluorouracil-loaded liposomes. *Int J Pharm* 353(1–2):243–250

16. Muller RH, Mader K, Gohla S (2000) Solid lipid nanoparticles (SLN) for controlled drug delivery—a review of the state of the art. *Eur J Pharm Biopharm* 50(1):161–177
17. zur Muhlen A, Schwarz C, Mehnert W (1998) Solid lipid nanoparticles (SLN) for controlled drug delivery—drug release and release mechanism. *Eur J Pharm Biopharm* 45(2):149–155
18. Shidhaye SS, Vaidya R, Sutar S, Patwardhan A, Kadam VJ (2008) Solid lipid nanoparticles and nanostructured lipid carriers—innovative generations of solid lipid carriers. *Curr Drug Deliv* 5(4):324–331
19. Luo Y, Chen D, Ren L, Zhao X, Qin J (2006) Solid lipid nanoparticles for enhancing vinpocetine's oral bioavailability. *J Control Release* 114(1):53–59
20. Manjunath K, Venkateswarlu V (2005) Pharmacokinetics, tissue distribution and bioavailability of clozapine solid lipid nanoparticles after intravenous and intraduodenal administration. *J Control Release* 107(2):215–228
21. Cavalli R, Gasco MR, Chetoni P, Burgalassi S, Saettone MF (2002) Solid lipid nanoparticles (SLN) as ocular delivery system for tobramycin. *Int J Pharm* 238(1–2):241–245
22. Souto EB, Wissing SA, Barbosa CM, Muller RH (2004) Development of a controlled release formulation based on SLN and NLC for topical clotrimazole delivery. *Int J Pharm* 278(1):71–77
23. Hanafy A, Spahn-Langguth H, Vergnault G, Grenier P, Tubic Grozdanic M, Lenhardt T, Langguth P (2007) Pharmacokinetic evaluation of oral fenofibrate nanosuspensions and SLN in comparison to conventional suspensions of micronized drug. *Adv Drug Deliv Rev* 59(6):419–426
24. Muller RH, Runge S, Ravelli V, Mehnert W, Thunemann AF, Souto EB (2006) Oral bioavailability of cyclosporine: solid lipid nanoparticles (SLN) versus drug nanocrystals. *Int J Pharm* 317(1):82–89
25. Pandita D, Ahuja A, Lather V, Benjamin B, Dutta T, Velpandian T, Khar RK (2011) Development of lipid-based nanoparticles for enhancing the oral bioavailability of paclitaxel. *AAPS Pharm-SciTech* 12(2):712–722
26. Kumar VV, Chandrasekar D, Ramakrishna S, Kishan V, Rao YM, Diwan PV (2006) Development and evaluation of Nitrendipine loaded solid lipid nanoparticles: influence of wax and glyceride lipids on plasma pharmacokinetics. *Int J Pharm* 335(1–2):167–175
27. Fazlollahi F, Angelow S, Yacobi NR, Marchelletta R, Yu AS, Hamm-Alvarez SF, Borok Z, Kim KJ, Crandall ED (2011) Polystyrene nanoparticle trafficking across MDCK-II. *Nanomedicine* 7(5):588–594
28. Ali H, Shirode AB, Sylvester PW, Nazzal S (2010) Preparation, characterization, and anticancer effects of simvastatin-tocotrienol lipid nanoparticles. *Int J Pharm* 389(1–2):223–231
29. Ali H, El-Sayed K, Sylvester PW, Nazzal S (2010) Molecular interaction and localization of tocotrienol-rich fraction (TRF) within the matrices of lipid nanoparticles: evidence studies by Differential Scanning Calorimetry (DSC) and Proton Nuclear Magnetic Resonance spectroscopy (^1H NMR). *Colloids Surf B Biointerfaces* 77(2):286–297
30. Porter CJ, Trevaskis NL, Charman WN (2007) Lipids and lipid-based formulations: optimizing the oral delivery of lipophilic drugs. *Nat Rev Drug Discov* 6(3):231–248
31. Iwayanagi Y, Takada T, Tomura F, Yamanashi Y, Terada T, Inui K, Suzuki H (2011) Human NPC1L1 expression is positively regulated by PPARalpha. *Pharm Res* 28(2):405–412
32. Narushima K, Takada T, Yamanashi Y, Suzuki H (2008) Niemann-pick C1-like 1 mediates alpha-tocopherol transport. *Mol Pharmacol* 74(1):42–49
33. Davis HR, Veltri EP (2007) Zetia: inhibition of Niemann-Pick C1 Like 1 (NPC1L1) to reduce intestinal cholesterol absorption and treat hyperlipidemia. *J Atheroscler Thromb* 14(3):99–108
34. Yamagishi S, Nakamura K, Matsui T, Sato T, Takeuchi M (2006) Inhibition of intestinal cholesterol absorption by ezetimibe is a novel therapeutic target for fatty liver. *Med Hypotheses* 66(4): 844–846
35. Yu L (2008) The structure and function of Niemann-Pick C1-like 1 protein. *Curr Opin Lipidol* 19(3):263–269
36. van Heek M, Farley C, Compton DS, Hoos L, Davis HR (2001) Ezetimibe selectively inhibits intestinal cholesterol absorption in rodents in the presence and absence of exocrine pancreatic function. *Br J Pharmacol* 134(2):409–417
37. Ma Z, Lim LY (2003) Uptake of chitosan and associated insulin in Caco-2 cell monolayers: a comparison between chitosan molecules and chitosan nanoparticles. *Pharm Res* 20(11): 1812–1819
38. Tomoda H, Kishimoto Y, Lee YC (1989) Temperature effect on endocytosis and exocytosis by rabbit alveolar macrophages. *J Biol Chem* 264(26):15445–15450
39. Hu Y, Litwin T, Nagaraja AR, Kwong B, Katz J, Watson N, Irvine DJ (2007) Cytosolic delivery of membrane-impermeable molecules in dendritic cells using pH-responsive core-shell nanoparticles. *Nano Lett* 7(10):3056–3064
40. Amidon GL, Sinko PJ, Fleisher D (1988) Estimating human oral fraction dose absorbed: a correlation using rat intestinal membrane permeability for passive and carrier-mediated compounds. *Pharm Res* 5(10):651–654
41. Abuasal B, Thomas S, Sylvester PW, Kaddoumi A (2011) Development and validation of a reversed-phase HPLC method for the determination of gamma-tocotrienol in rat and human plasma. *Biomed Chromatogr* 25(5):621–627
42. Davies JP, Scott C, Oishi K, Liapis A, Ioannou YA (2005) Inactivation of NPC1L1 causes multiple lipid transport defects and protects against diet-induced hypercholesterolemia. *J Biol Chem* 280(13):12710–12720
43. Wang LH, Rothberg KG, Anderson RG (1993) Mis-assembly of clathrin lattices on endosomes reveals a regulatory switch for coated pit formation. *J Cell Biol* 123(5):1107–1117
44. Rejman J, Oberle V, Zuhorn IS, Hoekstra D (2003) Size-dependent internalization of particles via the pathways of clathrin- and caveolae-mediated endocytosis. *Biochem J* 377(Pt 1):159–169

Tocotrienol Attenuates Triglyceride Accumulation in HepG2 Cells and F344 Rats

Gregor Carpennero Burdeos · Kiyotaka Nakagawa ·
Fumiko Kimura · Teruo Miyazawa

Received: 14 October 2011 / Accepted: 2 February 2012 / Published online: 26 February 2012
© AOCS 2012

Abstract Tocotrienol (T3) is an important phytonutrient found in rice bran and palm oil. T3 has gained much interest for lipid lowering effects, especially for cholesterol (Cho) by inhibiting 3-hydroxy-3-methylglutaryl-coenzyme A reductase. Also, usefulness of T3 in improving triglyceride (TG) profiles has been suggested, but its efficacy and mechanism have been unclear. We investigated how T3 decreases TG concentration in cultured cells and animals. In a cell culture study, human hepatoma cells (HepG2) were incubated in a control or a fat (1 mM oleic acid)-loaded medium containing γ -T3 for 24 h. We found that 10–15 μ M γ -T3 inhibited cellular TG accumulation significantly, especially in the fat-loaded medium. This manifestation was supported by mRNA and protein expressions of fatty acid synthase, carnitine palmitoyltransferase 1, and cytochrome P450 3A4. In concordance with these results, rice bran T3 supplementation to F344 rats (5 or 10 mg T3/day/rat) receiving a high fat diet for 3 weeks significantly reduced TG and the oxidative stress marker (phospholipid hydroperoxides, PLOOH) in the liver and blood plasma. T3 supplementation did not show changes in the Cho level. These results provided new information and the mechanism of the TG-lowering effect of T3. The lipid lowering effects of dietary T3 might be mediated by the reduction of TG synthesis.

Keywords Fatty acid synthase · Tocotrienol · Triglyceride · β -Oxidation · Antioxidant

Abbreviations

BSA	Bovine serum albumin
CL	Chemiluminescence
Cho	Cholesterol
CPT1A	Carnitine palmitoyltransferase 1
CYP3A4	Cytochrome P450 3A4
FASN	Fatty acid synthase
FBS	Fetal bovine serum
HepG2	Human hepatoma cells
HMG-CoAR	3-Hydroxy-3-methylglutaryl-coenzyme A reductase
PCOOH	Phosphatidylcholine hydroperoxide
PEOOH	Phosphatidylethanolamine hydroperoxide
PL	Phospholipid
PLOOH	Phospholipid hydroperoxides
RBT3	Rice bran tocotrienol
RT-PCR	Real-time quantitative reverse transcription-PCR
T-Cho	Total cholesterol
TG	Triglyceride
Toc	Tocopherol
T3	Tocotrienol

Electronic supplementary material The online version of this article (doi:10.1007/s11745-012-3659-0) contains supplementary material, which is available to authorized users.

G. C. Burdeos · K. Nakagawa · F. Kimura · T. Miyazawa (✉)
Food and Biodynamic Chemistry Laboratory,
Graduate School of Agricultural Science,
Tohoku University, Sendai 981-8555, Japan
e-mail: miyazawa@biochem.tohoku.ac.jp

Introduction

In 1922, tocopherol (Toc) was discovered in green leafy vegetables as a micronutrient essential for reproduction [1]. More than 40 years later, tocotrienol (T3) was isolated from latex [2]. Structurally, vitamin E substances differ only in their side chains (Fig. 1). Toc has saturated phytol

side chain, while T3 contains unsaturated isoprenoid tail. To date, eight substances have been found in nature as vitamin E: α -, β -, γ -, and δ -Toc and α -, β -, γ -, and δ -T3. Vitamin E is synthesized in the plastids of plants, and Toc is widely present in a variety of foods such as vegetable oils and nuts. But, T3-containing foods are limited. Rice bran, palm oil, and annatto seed are rich in T3 [3].

Tocopherol and T3 are classified based on their ability (vitamin E activity) to prevent the resorption of rat fetuses. α -Toc displays the highest efficacy among the eight vitamin E substances, whereas α -T3 has about one-third of the activity of α -Toc. Regardless, all forms of vitamin E are able to induce antioxidative effects and to act as protective agents against lipid peroxidation in biological membranes. In some model membrane studies, T3 has been reported to be a more potent antioxidant than Toc [4]. Moreover, T3 has recently gained increasing interest due to its several health-promoting properties that differ somewhat from those of Toc. For example, T3 protects neuronal cells against oxidative damage [5], and suppresses pathological angiogenesis [6, 7] and cancer [8]. These unique effects of T3 could be partly explained by its abilities to induce cell cycle arrest [9], to activate p53 and caspase [10, 11], to suppress adhesion molecules [12], to inhibit nuclear factor- κ B [13], and to down-regulate c-Myc and telomerase [14].

Besides the above activities [5–14], T3 has also gained much attention for its lipid-lowering properties, especially the reduction of cholesterol (Cho). The Cho-lowering effects have been observed in cell culture [15–17], animal [18–21], and human studies [22], and the mechanism may involve a repression of hepatic 3-hydroxy-3-methylglutaryl-coenzyme A reductase through a post-transcriptional process [15, 16]. However, it should be noted that several research groups failed to observe significant changes in serum Cho profiles after supplementation of T3 to hypercholesterolemic patients [23–25] and hyperlipidemic patients with carotid atherosclerosis [26]. Therefore, the effect of T3 on Cho is still controversial and needs further studies.

On the other hand, although little attention has been paid to whether T3 affects other lipids apart from Cho, some earlier studies have suggested a usefulness of T3 in improving triglyceride (TG) profiles. For instance, T3 supplementation has been reported to decrease serum TG levels in healthy human [27] and hypercholesterolemic patients [28]. In support of these results, Zaiden et al. [29] recently reported the ability of T3 to reduce TG biosynthesis in human hepatoma cells (HepG2). Therefore, these studies [27–29] raise a novel possibility that reduction of TG may be a primary role for the lipid-lowering properties of T3. However, because there are few reports in the literature that have evaluated the impact of T3 on TG at gene expression levels, further biological studies are needed to elucidate the mechanism(s) how T3 decreases TG.

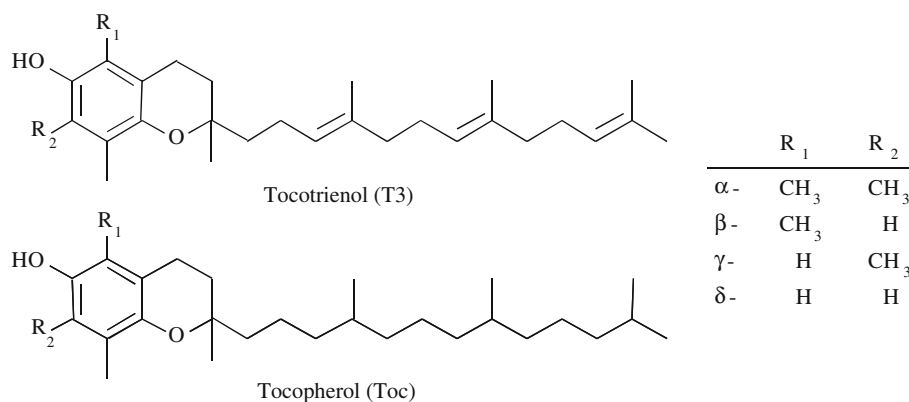
In this study, we aimed to investigate how γ -T3 (most abundant isomer of rice bran T3, RBT3) suppresses TG levels by affecting TG-related gene expressions in a control (normal) and a fat (oleic acid) loaded HepG2. In rats fed a high fat diet, the TG-lowering properties of RBT3 was further evaluated, and compared with the Cho-lowering activity. We confirmed that T3 attenuates TG accumulation by regulating fatty acid synthase (FASN), carnitine palmitoyltransferase 1 (CPT1A), and cytochrome P450 3A4 (CYP3A4) genes and protein expression.

Materials and Methods

Reagents and Cells

α -T3 and γ -T3 were purchased from Chromadex (Santa Ana, CA, USA). α -Toc was obtained from Sigma (St. Louis, MO, USA) and WST-1 reagent from Dojindo Laboratories (Kumamoto, Japan). All other reagents were of analytical grade. RBT3 was kindly provided by Sanwa Yushi Co. Ltd. (Tendo, Yamagata, Japan). RBT3 was composed of 82.3% T3 (31.4% α -T3, 50.5% γ -T3, and

Fig. 1 Chemical structures of T3 and Toc



0.4% δ -T3) and 6.0% Toc (1.9% α -Toc, 2.1% γ -Toc, and 2.0% δ -Toc) (w/w). Vitamin E-stripped corn oil was purchased from Acros Organics (Fairlawn, NJ, USA).

Human hepatoma cells were obtained from the RIKEN cell bank (Tsukuba, Japan). The cells were cultured in RPMI-1640 medium (containing 0.3 g/L L-glutamine and 2.0 g/L sodium bicarbonate, Sigma) supplemented with 10% fetal bovine serum (FBS; Biowest, Paris, France), 100 kU/L penicillin, and streptomycin (100 mg/L) (Gibco BRL, Rockville, MD, USA) at 37 °C in a 5% CO₂/95% air atmosphere in a humidified incubator.

Preparation of Experimental Medium for Cell Culture Study

γ -T3 was dissolved in ethanol at a concentration of 50 μ M. The stock solution was diluted with either 1% bovine serum albumin (BSA; Sigma)/RPMI-1640 (control test medium) or 1% BSA/RPMI-1640 containing 1 mM oleic acid as the fat-loaded medium [30] to achieve the desired final concentration of γ -T3 (0–50 μ M). The final concentration of ethanol in the experimental medium was less than 0.1% (v/v), which did not affect cell viability. A medium with ethanol alone was similarly prepared and used as control medium.

Cell Viability Assay

For cell viability assays, HepG2 (1×10^5) were pre-incubated with 10% FBS/RPMI-1640 in 96 well culture plates. Twenty-four hours later, the cells were washed with PBS and the medium was replaced with the experimental medium. As for the control condition, HepG2 were incubated in the experimental medium without oleic acid together with 0–50 μ M γ -T3. In fat-loaded condition, HepG2 were cultured with experimental medium containing 1 mM oleic acid (as the fat-loaded medium) and γ -T3. After incubation for 24 h, the number of viable cells was determined using WST-1 reagent according to the manufacturer's instructions. In brief, WST-1 reagent (10 μ L) was added to the medium, and incubated at 37 °C for 3 h. Absorbance (450/655 nm) of the medium was measured with a microplate reader (Model 550, Bio-Rad Laboratories, Inc., Hercules, CA, USA). WST-1 is a tetrazolium salt that is converted into the soluble formazan salt by succinate-tetrazolium reductase of the respiratory chain of active mitochondria of viable cells [31].

TG Analysis

Cellular TG concentrations were evaluated using Folch method [32]. Briefly, HepG2 (1×10^5) were pre-incubated with 10% FBS/RPMI-1640 in a 35 mm cell culture

plate for 24 h, and were cultured under control and fat-loaded conditions as described above. After 24 h incubation, cells were washed with PBS and scraped using rubber policeman, transferred into an Eppendorf tube (1.5 mL) and were centrifuged at 1,000g for 3 min. Cell pellets were transferred to a micro smashing tube with the addition of 500 μ L PBS buffer for homogenization. After homogenization, the contents of the cellular protein were determined using the Bradford protein assay (Bio-Rad Laboratories) [33]. Cellular TG was extracted using the Folch method and was measured using a commercial TG kit (Wako).

Isolation of Total RNA and Analysis of mRNA Expression

After 24 h of treatment of HepG2 (1×10^5) with the experimental medium, cells were lysed, scraped with a rubber police man, and transferred into a micro smashing tube. Total RNA was isolated with an RNeasy Plus Mini kit (Qiagen, Valencia, CA, USA) for real-time quantitative reverse transcription-PCR (RT-PCR). cDNA was synthesized using a Ready-To-Go T-Primed First-Strand kit (GE Healthcare, Piscataway, NJ, USA), and PCR amplification was performed with a CFX96 Real-Time PCR Detection System (Bio-Rad Laboratories, NSW, Australia) using SYBR Premix Ex Taq (Takara Bio Inc., Shiga, Japan) and gene-specific primers for FASN, CPT1A, CYP3A4, and β -actin (Table 1). PCR conditions were 95 °C for 60 s, 95 °C for 5 s, and 65 °C for 30 s for 40 cycles.

Western Blotting Analysis

After HepG2 (1×10^5) both in control and fat-loaded conditions were incubated with test medium for 24 h, proteins were separated by SDS-PAGE (4–20% e-PAGEL; Atto, Tokyo, Japan). The protein bands were transferred to polyvinylidene fluoride membranes (Invitrogen, Carlsbad, CA, USA). After blocking for 1 h, the membranes were incubated with primary antibodies for FASN, CPT1A, CYP3A4, and β -actin (Cell Signaling Technology, Beverly, MA, USA), followed by horseradish peroxidase-conjugated secondary antibody (Cell Signaling Technology). ECL Plus (GE healthcare) was used for detection. Band intensities were measured using Image Lab software version 3.0 (BioRad, Hercules, CA, USA).

Animal Experiments

Male F344 rats (6 weeks of age) were obtained from CLEA (Tokyo, Japan), and housed in cages kept at 23 °C with a 12 h light:dark cycle. The rats were acclimated with MF rodent chow (5% of calories from fat; Oriental Yeast,

Table 1 Oligonucleotide primer sequences of HepG2 for real time RT-PCR

Target genes	Primer sequences (5'–3')	Genbank accession no.
FASN, <i>FASN</i>		
Forward	AGCGGCCATTTCCATTGCC	NM_004104
Reverse	CCATGCCCAGAGGGTGGTTG	
CPT1A, <i>CPT1A</i>		
Forward	TTATCTGAGCCTTGGAGATTA	NM_001031847
Reverse	ACCGGTCCAAGCCC	
CYP3A4, <i>CYP3A4</i>		
Forward	CCCGTGAGAAGCAGAGGA	NM_001202855
Reverse	AGCCAAATCTACCTCCTCACACT	
β -Actin, <i>ACTB</i>		
Forward	TGGCACCCAGCACAATGAA	NM_001101
Reverse	CTAAGTCATAGTCGCTAGAAGCA	

FASN fatty acid synthase,
CPT1A carnitine
palmitoyltransferase 1, *CYP3A4*
cytochrome P450 3A4

Tokyo, Japan) and water for 1 week. After acclimatization, rats received ad libitum either MF or high fat diet [35% of calories from fat (powdered beef tallow 15%/100 g and high oleic acid safflower oil 20%/100 g), High Fat Diet HFD32, CLEA]. The high fat treated rats were fed with 5 mg of RBT3 (1.57 mg α -T3, 2.52 mg γ -T3, 0.02 mg δ -T3, 0.10 mg α -Toc, 0.11 mg γ -Toc, and 0.10 mg δ -Toc), 10 mg of RBT3 (3.14 mg α -T3, 5.04 mg γ -T3, 0.04 mg δ -T3, 0.19 mg α -Toc, 0.21 mg γ -Toc, and 0.20 mg δ -Toc), or 10 mg α -Toc once a day for 3 weeks by oral gavage using 200 μ L vitamin E-stripped corn oil as a vehicle. Positive (high fat diet treated) and negative (MF rodent chow treated) control rats received only the vehicle (vitamin E-stripped corn oil). During the feeding period, the weight of rats and food intake were recorded. At the end of the 3-week period, the rats were fasted for 12 h, weighed, and blood samples were collected after decapitation. Blood was treated with EDTA, and plasma was isolated by centrifugation at 1,000g for 15 min at 4 °C. Liver, heart, lung, spleen, kidney, and adipose tissues were removed and weighed. These protocols were reviewed by the Committee on the Ethics of Animal Experiments and carried out in accordance with the Animal Experiment Guidelines of Tohoku University.

Hepatic and Plasma Parameters

Livers were homogenized in an aqueous solution containing 1 mM EDTA and 0.09% NaCl. The liver homogenates were then subjected to lipid extraction by the Folch method [32]. Total lipid extracts were subjected to TG, total Cho (T-Cho), and phospholipid (PL) analyses using commercial kits (Wako).

For plasma samples, TG, T-Cho, and PL were measured by the Mitsubishi Chemical Medicine Corporation (Tokyo, Japan).

Plasma and Liver Phospholipid Hydroperoxides

To examine oxidative stress, phospholipid hydroperoxides (PLOOH) in total lipid extracts from plasma and liver were measured by HPLC with chemiluminescence (CL) detection [34, 35]. PLOOH is a collective term for phospholipid hydroperoxides such as phosphatidylcholine hydroperoxide (PCOOH) and phosphatidylethanolamine hydroperoxide (PEOOH). The column was a Finepak SIL NH2-5 (4.6 \times 250 mm; Japan Spectroscopic Co., Tokyo, Japan), the eluent was 2-propanol–methanol–water (135:45:20, v/v/v), and the flow rate was 1 mL/min. Post-column CL detection was carried out using a CLD-100 detector (Tohoku Electronic Industries Co., Sendai, Japan). A mixture of luminol and cytochrome *c* in 50 mM borate buffer (pH 10.0) was used as a hydroperoxide-specific post-column CL reagent. Calibration was carried out using standard PLOOH.

Statistical Analysis

The data were expressed as means \pm standard deviations (SD). One-way ANOVA was performed, followed by the Bonferroni/Dunn test for multiple comparisons. Differences were considered significant at $P < 0.05$.

Results

Effect of γ -T3 on HepG2 Proliferation

In order to investigate whether T3 affects TG concentrations, an increasing amount of γ -T3 was administered to HepG2 cells for 24 h in both control as well as fat-loaded conditions. Before investigating the effect on TG, cytotoxic activity of γ -T3 was first evaluated. As for the control condition, HepG2 proliferation was somewhat increased by

γ -T3 treatment (1–5 μ M), while 10–15 μ M γ -T3 did not affect on the proliferation (Fig. 2a). As some papers have already reported [36], higher doses (over 15 μ M) of γ -T3 showed a cytotoxic effect (data not shown). A similar effect of γ -T3 was observed under fat-loaded conditions, although under this conditions a more increased proliferation was shown than under the control condition (Fig. 2a). Because 1–15 μ M γ -T3 showed no cytotoxicity except for 15 μ M γ -T3 under the fat-loaded condition showing little decrease in proliferation, we utilized these γ -T3 concentrations in the next experiments for evaluating their effects on TG.

TG Accumulation is Attenuated with γ -T3 by Affecting Fatty Acid Synthase and β -Oxidation Genes and Proteins Expressions in HepG2

TG accumulation in HepG2 was evaluated by the Folch method. For the control condition, 1–5 μ M γ -T3 showed a little effect on TG concentrations (Fig. 2b), probably due to an increase in the proliferation. However, it was found that 10–15 μ M γ -T3 revealed a marked decrease in TG concentration. For the fat-loaded condition, 1–10 μ M γ -T3 treated cells showed an increase in TG concentrations, whereas a significant decrease in TG was observed at 15 μ M. The reason why 1–10 μ M γ -T3 supplementation increases TG concentration may be due increased cell proliferation. These data clearly suggested the TG-lowering effect of T3, and we therefore investigated the effect of γ -T3 on TG-synthesis related gene (FASN) and β -oxidation

genes (CPT1A and CYP3A4). Significant down-regulation of FASN as well as up-regulation of CPT1A and CYP3A4 genes were observed by γ -T3 treatment (over about 10 μ M) in both control and fat-loaded conditions (Fig. 3). Similarly, γ -T3 attenuated the expression of FASN protein and at the same time induced the expression of CPT1A and CYP3A4 proteins (Fig. 4). Therefore, a possible mechanism of the TG-lowering effect of γ -T3 is mediated by down-regulation of FASN and up-regulation of CPT1A and CYP3A4 genes.

Dietary T3 Reduces TG and PLOOH Accumulations in Liver and Plasma of Rats

To verify the TG-lowering effect of T3 in vivo, a rat study was conducted. Rats received either control MF or high fat diet with or without RBT3 for 3 weeks. The high fat diet caused a significant increase in the weight of rats, and the weight tended to decrease ($P = 0.34$) in the 10-mg RBT3 group (Table 2). RBT3 supplementation did not affect the weight of organs, but adipose tissues, especially epididymal and mesenteric fats, showed a reduction in the weight in the 10-mg RBT3 group (Table 2). No differences were observed for food intake (data not shown). For liver parameters, the high fat diet caused significant accumulation of TG and tended to induce PL ($P = 0.11$) accumulation, and also showed a significant accumulation of PLOOH (oxidative stress marker) (Fig. 5). It was found that these accumulations, especially TG and PLOOH, were significantly attenuated in the 10-mg RBT3 supplemented group (Fig. 5).

Fig. 2 Effect of increasing concentrations of γ -T3 on cell proliferation (a) and TG accumulation (b) of HepG2 in control and fat overloaded conditions. Experimental procedures are shown in the “Materials and Methods” section. Data are expressed as means \pm SD ($n = 6$ for cell proliferation and $n = 3$ for TG accumulation). Means without a common letter differ, $P < 0.05$. The “% of control for control condition” represents the fold-increase in cell proliferation under the fat overloaded condition as compared to under the control condition

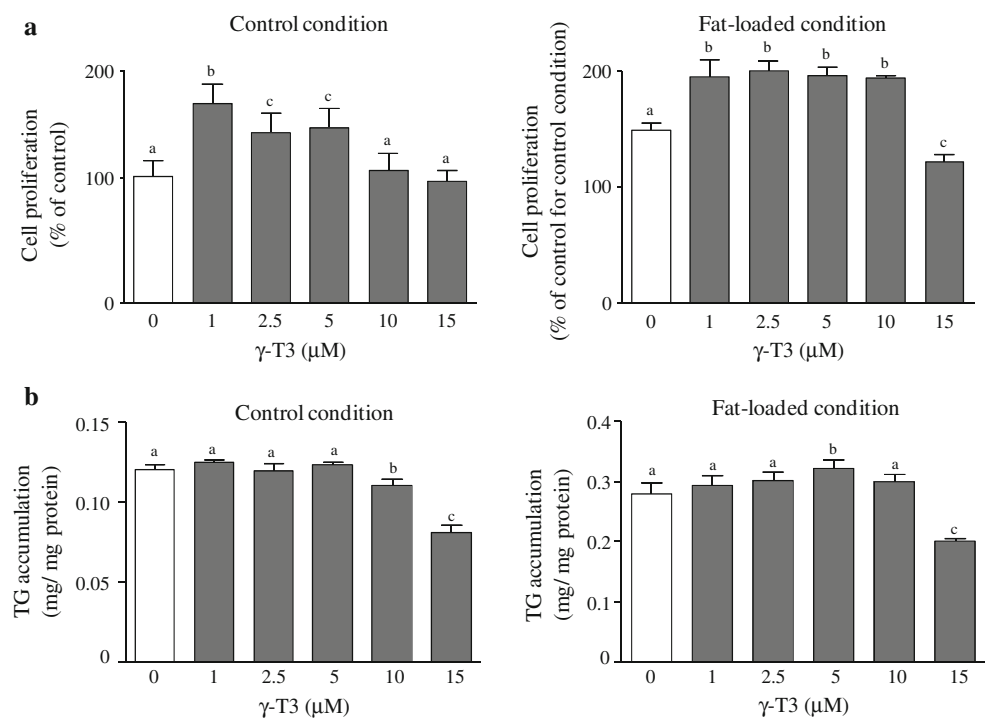
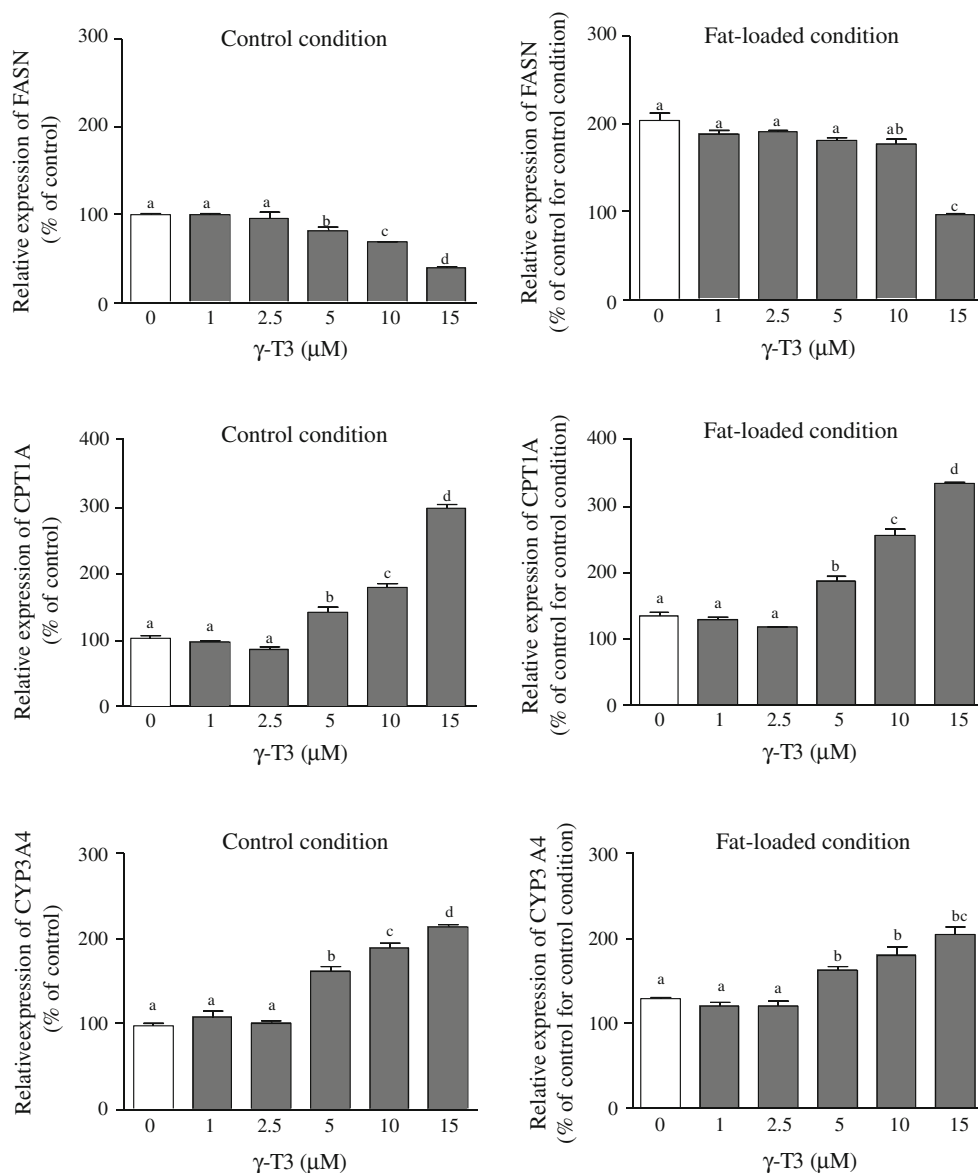


Fig. 3 Effect of increasing concentrations of γ -T3 on mRNA expression of FASN, CPT1A, and CYP3A4 genes in HepG2 in control and fat overloaded conditions. Experimental procedures are shown in the “Materials and Methods” section. Data are expressed as means \pm SD ($n = 6$). Means without a common letter differ, $P < 0.05$. The “% of control for control condition” represents the fold-increase in mRNA expression under fat overloaded conditions as compared to control condition



Similar results were observed for plasma (Fig. 6). In contrast, no significant differences were observed for liver and plasma T-Cho. For the α -Toc supplemented group, no differences were found for lipids and PLOOH parameters in the liver and plasma. These results indicated that the main lipid lowering effects of dietary T3 might be mediated by the reduction of TG, thereby possibly attenuating the TG-induced PLOOH accumulation [37].

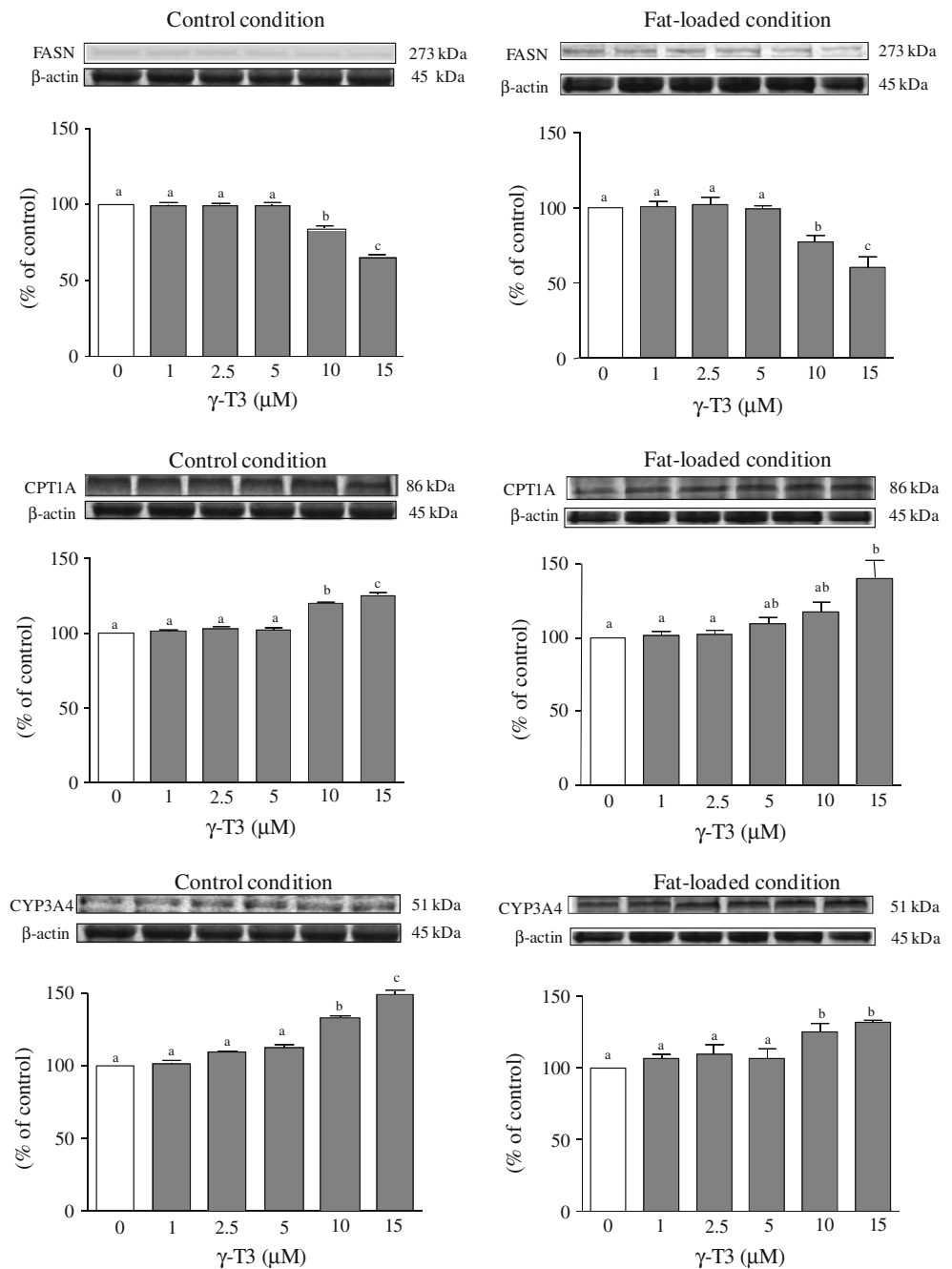
Discussion

TG accumulation has been linked to an increased risk of different afflictions such as coronary artery diseases. In addition, the involvement of oxidative stress (i.e., PCOOH formation) probably due to high TG concentration in vivo has been reported [37]. On the other hand, a novel

possibility pertaining to the attenuating effect of T3 on TG accumulation has been published in some (but not many) studies [27–29]. Since the specific target of T3 in the lipogenic pathway is still vague, further biological studies are needed to elucidate the mechanism(s) on how T3 decreases TG. In the present study, we confirmed the TG-lowering effect of T3 in both in vivo and in vitro studies, and the effect of T3 could be partly explained by its ability to down-regulate the hepatic fatty acid synthase gene and up-regulate β -oxidation genes. These results support a hypothesis that reduction in TG may be the primary benefit caused by dietary T3 [29].

In this study, similar to previous papers [36], a higher dosage of γ -T3 (over 15 μ M) caused cytotoxicity to HepG2 possibly due to apoptosis induction (Fig. 2a). However, low doses of γ -T3 (1–5 μ M) somewhat increased HepG2 proliferation (Fig. 2a). The reasons of the induced cellular

Fig. 4 Effect of increasing concentrations of γ -T3 on expression of FASN, CPT1A, and CYP3A4 proteins in HepG2 under control and fat overloaded conditions. Experimental procedures are shown in the “Materials and Methods” section. Means without a common letter differ, $P < 0.05$. Each Western blot is a representative example of data from three replicate experiments



proliferation still remain unknown, but such increased proliferation was found when cells were incubated with certain antioxidants such as catechin [38]. Consequently, because 1–15 μ M γ -T3 showed no obvious cytotoxicity, we utilized these γ -T3 concentrations in the next experiments for evaluating their effects on TG.

For TG concentration, addition of oleic acid as a fat inducer showed an approximately 1.5 fold increase in TG in HepG2 as compared to the control (Fig. 2b). Such an increase was markedly attenuated by 15 μ M γ -T3. An effect similar to its control condition counterpart was

observed. To date, to the best of our knowledge, there has been one report focusing on the effect of T3 on TG in a cell culture study. Zaiden et al. [29] reported that treatment of γ -T3 and δ -T3 (each 20 μ M) reduces TG synthesis and VLDL secretion in HepG2, however, this study did not measure the actual TG content of the cells. The present study provides quantitative TG results in the cells after administration of γ -T3, and significant attenuation of TG was observed at lower concentrations of γ -T3 (15 μ M).

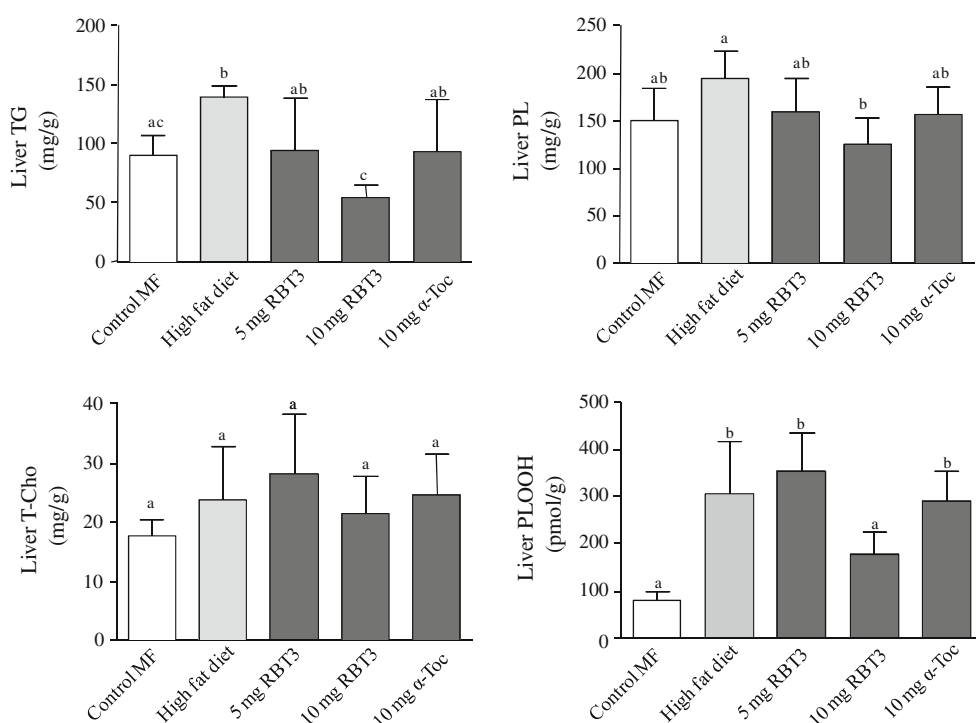
In the present study, we provided new information regarding the possible mechanism of the action of γ -T3 on

Table 2 Body and tissue weights of rats (g)

	Body weight	Liver	Heart	Lung	Spleen	Kidney	Perinephric fat	Mesenteric fat	Epididymal fat
Control MF	192 ± 9.3 ^a	6.54 ± 0.62 ^a	0.70 ± 0.07 ^a	0.83 ± 0.08 ^a	0.47 ± 0.03 ^a	1.26 ± 0.10 ^a	2.50 ± 0.65 ^a	2.24 ± 0.49 ^a	2.81 ± 0.82 ^a
High fat diet	213 ± 10.5 ^b	6.40 ± 0.60 ^a	0.71 ± 0.04 ^a	1.01 ± 0.14 ^a	0.46 ± 0.05 ^a	1.34 ± 0.08 ^a	4.93 ± 0.95 ^b	3.77 ± 0.43 ^b	4.46 ± 0.92 ^b
5 mg RBT3	219 ± 9.7 ^b	6.78 ± 0.71 ^a	0.71 ± 0.05 ^a	1.18 ± 0.22 ^a	0.50 ± 0.03 ^a	1.39 ± 0.09 ^a	4.98 ± 0.31 ^b	3.79 ± 0.27 ^b	4.73 ± 0.68 ^b
10 mg RBT3	206 ± 15.3 ^{ab}	6.19 ± 0.54 ^a	0.67 ± 0.05 ^a	0.88 ± 0.19 ^a	0.46 ± 0.02 ^a	1.30 ± 0.11 ^a	3.73 ± 0.65 ^c	2.97 ± 0.30 ^a	3.93 ± 0.60 ^a
10 mg α -Toc	202 ± 11.8 ^{ab}	6.35 ± 0.51 ^a	0.66 ± 0.06 ^a	1.08 ± 0.16 ^a	0.47 ± 0.04 ^a	1.31 ± 0.07 ^a	3.76 ± 0.59 ^c	3.76 ± 0.81 ^b	3.99 ± 0.61 ^a

Means without a common letter differ, $P < 0.05$

Fig. 5 Effect of RBT3 supplementation on liver lipids (TG, PL, and T-Cho) and oxidative parameter (PLOOH) of rats receiving control MF or high fat diet for 3 weeks. Experimental procedures are shown in the “Materials and Methods” section. Because phosphatidylcholine hydroperoxide (PCOOH) and phosphatidylethanolamine hydroperoxide (PEOOH) are major forms of PLOOH in liver [34, 35], PLOOH is calculated as sum of PCOOH and PEOOH. Data are expressed as means \pm SD ($n = 7$). Means without a common letter differ, $P < 0.05$

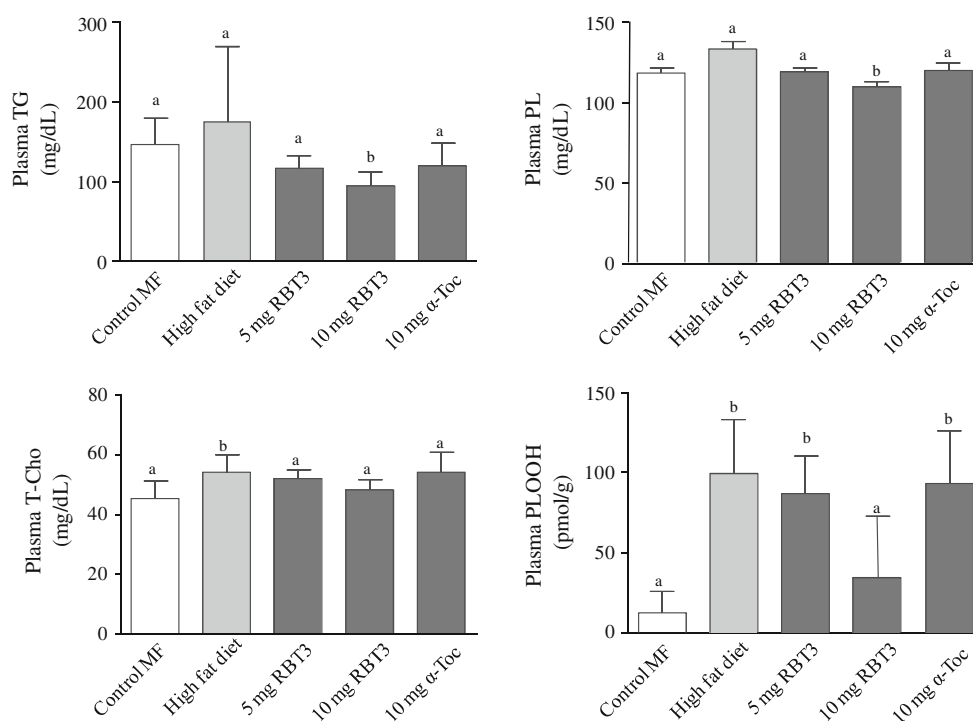


its TG lowering property by down regulation of FASN and up regulation of CPT1A and CYP3A4 in both mRNA and protein levels (Figs. 3, 4). Way et al. [39] showed that by down regulation of FASN, key enzymes for lipogenesis by Pu-erh tea supplementation can attenuate lipid accumulation such as TG in HepG2 cells. On the other hand, β -oxidation genes such as CPT1A and CYP3A4 have different interplaying roles in lipid metabolism. For instance, CPT1A, rate-limiting enzyme for fatty acid oxidation in all tissues was up-regulated in HepG2 upon consumption of polyunsaturated fatty acids, polyphenol and L-carnitine which led to reduced plasma lipid concentrations in a human study [40]. Moreover, CYP3A4, one of the most important enzymes involved in the metabolism of

xenobiotics in the body, has been reported to participate in lipid metabolism by regulation of 25-hydroxycholesterol in mouse liver cells derived cell line [41]. In support to these reports [39–41], administration of γ -T3 in HepG2 significantly down regulated FASN and up-regulated CPT1A and CYP3A4 genes thereby attenuating TG accumulations (Figs. 2b, 3). In addition, similar effects were observed in the protein expression of these genes (Fig. 4).

In support of the cell culture study, the 10-mg RBT3 diet significantly attenuated the accumulation of TG in both liver and plasma of rats (Figs. 5, 6). T3 has been reported to have a potent antioxidative effect [4]. A high fat diet has been reported to increase oxidative stress and resulted in increase in plasma and liver PLOOH [37]. It is therefore

Fig. 6 Effect of RBT3 supplementation on plasma lipids (TG and PL) and oxidative parameter (PLOOH) of rats receiving control MF or high fat diet for 3 weeks. Experimental procedures are shown in the “Materials and Methods” section. Because PCOOH is a major form of PLOOH in plasma [34, 35], PCOOH content is presented as PLOOH. Data are expressed as means \pm SD ($n = 7$). Means without a common letter differ, $P < 0.05$



conceivable that T3 can markedly reduce high fat diet-induced PLOOH accumulation in vivo (Figs. 5, 6). In contrast, dietary RBT3 failed to affect T-Cho concentrations (Figs. 5, 6). Concerning the reported Cho-lowering effect of T3, Quereshi et al. [42] actually demonstrated that the effect of T3 was attenuated by α -Toc. Therefore, the unchanged Cho levels may be due to the presence of α -Toc in the RBT3 (around 0.6 mg for 10 mg RBT3) used in this study. On the other hand, α -Toc did not show any attenuation of TG (Figs. 5, 6). In support of this peculiarity, a study published by Punithavathi et al. [43] showed no effect of α -Toc supplementation alone on TG in an isoproterenol-induced myocardial infarcted Wistar rats. Moreover, our study [44] reported that α -Toc attenuated the cytotoxic effect of δ -T3 in human colorectal adenocarcinoma cells. The present study suggests that among all vitamin E family isomers, a more detailed research between the interactions of these isomers is of great interest. In addition, since the amount of α -T3 present in RBT3 is considerably high, α -T3 was then subjected to proliferation and TG assays to remove any doubt that this T3 isomer might contribute to the TG attenuating effect of T3 (γ -T3). It was found that α -T3 did not show any cytotoxicity nor attenuated the TG accumulations in HepG2 cells (Supplementary Fig. 1). Interestingly, supplementation of RBT3 (10 mg/day) as well as α -Toc showed a significant reduction in the weight of both the perinephric and epididymal fats of rats (Table 2), and therefore we are now investigating the possible mechanism behind this interesting attenuating effect of α -Toc on adipose tissue deposition.

Lipid biosynthesis has a broad array of interplaying genes in its pathway therefore a thorough testing of any possible genes that regulates lipid synthesis and nailing down these genes would provide a more adequate knowledge about the right target for the discovery of medicines for lipid-related diseases. The TG attenuating effect of T3 in both in vivo and in vitro in this study provides novel data about the new TG lowering function of T3.

Acknowledgments A part of this study was supported by KAKENHI (S) (20228002, to T.M.) of JSPS, Japan.

References

- Evans HM, Bishop KS (1922) On the existence of a hitherto unrecognized dietary factor essential for reproduction. *Science* 56:650–651
- Dunphy PJ, Whittle KJ, Pennock JF, Morton RA (1965) Identification and estimation of tocotrienols in *Hevea latex*. *Nature* 207:521–522
- Sookwong P, Nakagawa K, Murata K, Kojima Y, Miyazawa T (2007) Quantitation of tocotrienol and tocopherol in various rice brans. *J Agric Food Chem* 55:461–466
- Serbinova E, Kagan V, Han D, Packer L (1991) Free radical recycling and intramembrane mobility in the antioxidant properties of α -tocopherol and α -tocotrienol. *Free Radic Biol Med* 10:263–275
- Khanna S, Roy S, Slivka A, Craft TKS, Chaki S, Rink C, Notestine MA, DeVries AC, Parinandi NL, Sen CK (2005) Neuroprotective properties of the natural vitamin E α -tocotrienol. *Stroke* 36:2258–2264

6. Nakagawa K, Shibata A, Yamashita S, Tsuzuki T, Kariya J, Oikawa S, Miyazawa T (2007) In vivo angiogenesis is suppressed by unsaturated vitamin E, tocotrienol. *J Nutr* 137:1938–1943
7. Shibata A, Nakagawa K, Sookwong P, Tsuzuki T, Oikawa S, Miyazawa T (2008) Tumor anti-angiogenic effect and mechanism of action of δ -tocotrienol. *Biochem Pharmacol* 76:330–339
8. Hiura Y, Tachibana H, Arakawa R, Aoyama N, Okabe M, Sakai M, Yamada K (2009) Specific accumulation of γ - and δ -tocotrienols in tumor and their antitumor effect in vivo. *J Nutr Biochem* 20:607–613
9. Srivastava JK, Gupta S (2006) Tocotrienol-rich fraction of palm oil induces cell cycle arrest and apoptosis selectively in human prostate cancer cells. *Biochem Biophys Res Commun* 346:447–453
10. Agarwal MK, Agarwal ML, Athar M, Gupta S (2004) Tocotrienol-rich fraction of palm oil activates p53, modulates Bax/Bcl2 ratio and induces apoptosis independent of cell cycle association. *Cell Cycle* 3:205–211
11. Shah S, Sylvester PW (2004) Tocotrienol-induced caspase-8 activation is unrelated to death receptor apoptotic signaling in neoplastic mammary epithelial cells. *Exp Biol Med* 229:745–755
12. Theriault A, Chao JT, Gapor A (2002) Tocotrienol is the most effective vitamin E for reducing endothelial expression of adhesion molecules and adhesion to monocytes. *Atherosclerosis* 160:21–30
13. Ahn KS, Sethi G, Krishnan K, Aggarwal BB (2007) γ -Tocotrienol inhibits nuclear factor- κ B signaling pathway through inhibition of receptor-interacting protein and TAK1 leading to suppression of antiapoptotic gene products and potentiation of apoptosis. *J Biol Chem* 282:809–820
14. Eitsuka T, Nakagawa K, Miyazawa T (2006) Down-regulation of telomerase activity in DLD-1 human colorectal adenocarcinoma cells by tocotrienol. *Biochem Biophys Res Commun* 348:170–175
15. Pearce BC, Parker RA, Deason ME, Qureshi AA, Wright JJ (1922) Hypocholesterolemic activity of synthetic and natural tocotrienols. *J Med Chem* 35:3595–3606
16. Parker RA, Pearce BC, Clark RW, Gordon DA, Wright JJ (1993) Tocotrienols regulate cholesterol production in mammalian cells by post-transcriptional suppression of 3-hydroxy-3-methylglutaryl-coenzyme A reductase. *J Biol Chem* 268:11230–11238
17. Song BL, DeBose-Boyd RA (2006) Insig-dependent ubiquitination and degradation of 3-hydroxy-3-methylglutaryl coenzyme A reductase stimulated by δ - and γ -tocotrienols. *J Biol Chem* 281:25054–25061
18. Watkins T, Lenz P, Gapor A, Struck M, Tomeo A, Bierenbaum M (1993) γ -Tocotrienol as a hypocholesterolemic and antioxidant agent in rats fed atherogenic diets. *Lipids* 28:1113–1118
19. Khor H, Chieng D (1996) Effect of dietary supplementation of tocotrienols and tocopherols on serum lipids in the hamster. *Nutr Res* 16:1393–1401
20. Black TM, Wang P, Maeda N, Coleman RA (2000) Palm tocotrienols protect ApoE $^{+/-}$ mice from diet-induced atheroma formation. *J Nutr* 130:2420–2426
21. Qureshi AA, Salser WA, Parmar R, Emeson EE (2001) Novel tocotrienols of rice bran inhibits atherosclerotic lesions in C57BL/6 ApoE-deficient mice. *J Nutr* 131:2606–2618
22. Qureshi AA, Qureshi N, Wright JJ, Shen Z, Kramer G, Gapor A, Chong YH, DeWitt G, Ong A, Peterson DM (1991) Lowering of serum cholesterol in hypercholesterolemic humans by tocotrienols (palmvitee). *Am J Clin Nutr* 53:1021S–1026S
23. Wahlqvist ML, Krivokuca-Bogetic Z, Lo CS, Hage B, Smith R, Lukito W (1992) Differential serum responses of tocopherols and tocotrienols during vitamin supplementation in hypercholesterolaemic individuals without change in coronary risk factors. *Nutr Res* 12:S181–S201
24. Mensink RP, van Houwelingen AC, Kromhout D, Hornstra G (1999) A vitamin E concentrate rich in tocotrienols had no effect on serum lipids, lipoproteins, or platelet function in men with mildly elevated serum lipid concentrations. *Am J Clin Nutr* 69:213–219
25. O'Byrne D, Grundy S, Packer L, Devaraj S, Baldenius K, Hoppe PP, Kraemer K, Jialal I, Traber MG (2000) Studies of LDL oxidation following α -, γ -, or δ -tocotrienyl acetate supplementation of hypercholesterolemic humans. *Free Radic Biol Med* 29:834–845
26. Tomeo AC, Geller M, Watkins TR, Gapor A, Bierenbaum ML (1995) Antioxidant effects of tocotrienols in patients with hyperlipidemia and carotid stenosis. *Lipids* 30:1179–1183
27. Tan DT, Khor HT, Low WH, Ali A, Gapor A (1991) Effect of a palm-oil-vitamin E concentrate on the serum and lipoprotein lipids in humans. *Am J Clin Nutr* 53:1027S–1030S
28. Qureshi AA, Bradlow BA, Brace L, Manganello J, Peterson DM, Pearce BC, Wright JJ, Gapor A, Elson CE (1995) Response of hypercholesterolemic subjects to administration of tocotrienols. *Lipids* 30:1171–1177
29. Zaiden N, Yap WN, Ong S, Xu CH, Teo VH, Chang CP, Zhang XW, Nesaretnam K, Shiba S, Yap YL (2010) Gamma delta tocotrienols reduce hepatic triglyceride synthesis and VLDL secretion. *J Atheroscler Thromb* 17:1019–1032
30. Gómez-Lechón MJ, Donato MT, Martínez-Romero A, Jiménez N, Castell JV, O'Connor JE (2007) A human hepatocellular in vitro model to investigate steatosis. *Chem Biol Interact* 165:106–116
31. Ishiyama M, Tominaga H, Shiga M, Sasamoto K, Ohkura Y, Ueno K (1996) A combined assay of cell viability and in vitro cytotoxicity with a highly water-soluble tetrazolium salt, neutral red and crystal violet. *Biol Pharm Bull* 19:1518–1520
32. Folch J, Lees M, Stanley GHS (1957) A simple method for the isolation and purification of total lipids from animal tissues. *J Biol Chem* 226:497–509
33. Bradford MM (1976) Rapid and sensitive method for the quantitation of microgram quantities of protein utilizing the principle of protein-dye binding. *Anal Biochem* 72:248–254
34. Miyazawa T, Suzuki T, Fujimoto K, Yasuda K (1992) Chemiluminescent simultaneous determination of phosphatidylcholine hydroperoxide and phosphatidylethanolamine hydroperoxide in the liver and brain of the rat. *J Lipid Res* 33:1051–1059
35. Kinoshita M, Oikawa S, Hayasaka K, Sekikawa A, Nagashima T, Toyota T, Miyazawa T (2000) Age-related increase in plasma phosphatidylcholine hydroperoxide concentrations in normal subjects and patients with hyperlipidemia. *Clin Chem* 46:822–828
36. Wada S, Satomi Y, Murakoshi M, Noguchi N, Yoshikawa T, Nishino H (2005) Tumor suppressive effects of tocotrienol in vivo and in vitro. *Cancer Lett* 2:181–191
37. Asai A, Nakagawa K, Miyazawa T (1999) Antioxidative effects of turmeric, rosemary and capsicum extracts on membrane phospholipid peroxidation and liver metabolism in mice. *Biosci Biotechnol Biochem* 12:2118–2222
38. Zhang D, Al-Hendy M, Richard-Davis D, Montgomery-Rice V, Rajaratnam V, Al-Hendy A (2010) Antiproliferative and proapoptotic effects of epigallocatechin gallate on human leiomyoma cells. *Fertil Steril* 5:1887–1893
39. Way TD, Lin HY, Kuo DH, Tsai SJ, Shieh JC, Wu JC, Lee MR, Lin JK (2009) Pu-erh tea attenuates hyperlipogenesis and induces hepatoma cells growth arrest through activating AMP-activated protein kinase (AMPK) in human HepG2 cells. *J Agric Food Chem* 12:5257–5264
40. Radler U, Stangl H, Lechner S, Lienbacher G, Krepp R, Zeller E, Brachinger M, Eller-Berndl D, Fischer A, Anzur C, Schoerg G, Mascher D, Laschan C, Anderwald C, Lohninger A (2011) A

- combination of (ω -3) polyunsaturated fatty acids, polyphenols and L-carnitine reduces the plasma lipid levels and increases the expression of genes involved in fatty acid oxidation in human peripheral blood mononuclear cells and HepG2. *Ann Nutr Metab* 58:133–140
41. Honda A, Miyazaki T, Ikegami T, Iwamoto J, Maeda T, Hirayama, Saito Y, Teramoto T, Matsuzaki Y (2011) Cholesterol 25-hydroxylation activity of CYP3A4. *J Lipid Res* 52:1509–1516
42. Quereshi AA, Pearce BC, Nor RM, Gapor A, Peterson DM, Elson CE (1996) Dietary α -tocopherol attenuates the impact of γ -tocotrienol on hepatic 3-hydroxy-3-methylglutaryl A reductase activity in chickens. *J Nutr* 126:292–301
43. Punithavathiand VR, Prince PS (2009) Combined effects of quercetin and α -tocopherol on lipids and glycoprotein components in isoproterenol induced myocardial infarcted Wistar rats. *Chem Biol Interact* 181:322–327
44. Shibata A, Nakagawa K, Sookwong P, Tsuduki T, Asai A, Miyazawa T (2010) α -Tocopherol attenuates the cytotoxic effect of δ -tocotrienol in human colorectal adenocarcinoma cells. *Biochem Biophys Res Commun* 397:214–219

Dietary Supplementation with 22-S-Hydroxycholesterol to Rats Reduces Body Weight Gain and the Accumulation of Liver Triacylglycerol

Eili Tranheim Kase · Nataša Nikolić · Nina Pettersen Hessvik · Åse-Karine Fjeldheim · Jørgen Jensen · G. Hege Thoresen · Arild C. Rustan

Received: 21 November 2011 / Accepted: 29 February 2012 / Published online: 18 March 2012
© AOCs 2012

Abstract This study explores the pharmacokinetics of 22-S-hydroxycholesterol (22SHC) in vivo in rats. We also carried out a metabolic study to explore whether the beneficial effects observed of 22SHC on glucose and lipid metabolism in vitro could be seen in vivo in rats. In the pharmacokinetic study, rats were given 50 mg/kg of [³H]22-S-hydroxycholesterol before absorption, distribution and excretion were monitored. In the metabolic study, the effect of 22SHC (30 mg/kg/day for 3 weeks) in rats on body weight gain [chow and high-fat diet (HFD)], serum lipids triacylglycerol (TAG) content and gene expression in liver and skeletal muscle were examined. Results showed that 22SHC was well absorbed after oral administration and distributed to most organs and mainly excreted in feces. Rats receiving 22SHC gained less body weight than their controls regardless whether the animals received chow diet or HFD. Moreover, we observed that animals receiving HFD had elevated levels of serum TAG while this was not observed for animals on HFD supplemented with 22SHC. The amount of TAG in liver was reduced after 22SHC treatment in animals receiving either chow diet or HFD. Gene expression analysis revealed that two genes (carnitine palmitoyltransferase 2 and

uncoupling protein 3) involved in fatty acid oxidation and energy dissipation were increased in liver. Ucp3 expression (both protein and mRNA level) was increased in skeletal muscle, but insulin-stimulated glucose uptake and TAG content were unchanged. In conclusion, 22SHC seems to be an interesting model substance in the search of treatments for disorders involving aberrations in lipid metabolism.

Keywords LXR · 22-S-hydroxycholesterol · In vivo · Ucp3

Abbreviations

22SHC	22-S-hydroxycholesterol
Cd36	Fatty acid transporter
Cpt1a	Carnitine palmitoyltransferase 1a
Cpt1b	Carnitine palmitoyltransferase 1b
Cpt2	Carnitine palmitoyltransferase 2
Lpl	Lipoprotein lipase
Mte-1	Mitochondrial thioesterase-1
Ndufb3	NADH dehydrogenase (ubiquinone) 1 beta subcomplex, 3
Ndufs1	NADH dehydrogenase (ubiquinone) subcomplex, 1
NEFA	Non-esterified fatty acids
LXR	Liver X receptor
Scd1	Stearoyl-CoA desaturase
SREBP1c	Sterol regulatory element-binding protein 1c
TAG	Triacylglycerol
Ucp3	Uncoupling protein 3

E. T. Kase (✉) · N. Nikolić · N. P. Hessvik · Å.-K. Fjeldheim · G. H. Thoresen · A. C. Rustan
Department of Pharmaceutical Biosciences, School of Pharmacy,
University of Oslo, P. O. Box 1068, Blindern,
0316 Oslo, Norway
e-mail: e.t.kase@farmasi.uio.no

J. Jensen
Department of Physical Performance, Norwegian
School of Sport Sciences, Oslo, Norway

J. Jensen
Department of Physiology, National Institute of Occupational
Health, Oslo, Norway

Introduction

Liver X receptors (LXRalpha and LXRbeta) are involved in both cholesterol homeostasis, lipid and glucose

metabolism and have been regarded as possible new drug targets both in the fields of type 2 diabetes (T2D), obesity and atherosclerosis [1]. However, many studies have shown that LXR ligands exert both beneficial effects such as increased reverse cholesterol transport and increased insulin-sensitivity/glucose transport, and undesirable effects such as ectopic lipid accumulation in liver and skeletal muscle [2, 3]. We have previously shown in vitro that the LXR modulator 22-*S*-hydroxycholesterol (22SHC) selectively reduced fatty acid accumulation and lipogenesis in human myotubes [4, 5]. Lipogenesis was also decreased in liver (HepG2) cells, while it was increased in adipocytes (SGBS cells) [6]. Glucose utilization was also increased by 22SHC in human myotubes [4, 5, 14]. Thus, 22SHC have properties that make the substance interesting for drug development.

Transcriptional activation of LXR is dependent of the entry of specific ligands, like certain cholesterol metabolites [7–9]. Oxysterols that activate LXR have a strong hydrogen acceptor at either carbon 22, 24 or 27, illustrated by the fact that 24(*S*), 25-epoxy cholesterol is a potent LXR activator while cholesterol does not affect the receptor [10]. The most abundant cholesterol metabolite in vivo is 27-hydroxycholesterol, which is present in plasma, liver and macrophages [11]. Naturally occurring agonists for LXRs include 24(*S*), 25-epoxycholesterol (liver), 25-hydroxycholesterol, 24-*(S)*-hydroxycholesterol (brain) and 22-*R*-hydroxycholesterol (adrenal gland) [8, 12]. Recently, glucose was also suggested to be an endogenous LXR ligand [13] while the synthetic compound 22SHC can best be described as an LXR modulator [4, 9]. It binds to the LXR receptors, abolish agonist (T0901317) effects on certain genes important for fatty acid metabolism, but not other typical LXR target genes such as ABCA1 and GLUT4 [4, 5].

Previously, we examined the role of LXR on crucial regulatory steps in glucose- and lipid-metabolism both at genetic and functional levels [2, 4–6] Results from experiments performed with myotubes established from matched lean, obese and obese T2D subjects showed that treatment with T0901317 increased lipogenesis more in myotubes established from T2D subjects than in myotubes from lean subjects, and that these effects could be efficiently counteracted by 22SHC [2]. Further studies in human myotubes showed that 22SHC reduced de novo diacylglycerol (DAG) production below basal level, reduced fatty acid uptake and oxidation at the same time as glucose uptake and oxidation were increased [4, 5]. Importantly, 22SHC also decreased the expression of genes involved in cholesterol biosynthesis without altering the expression of the reverse cholesterol transporter ABCA1 [5]. We also showed that de novo lipogenesis was differently affected by 22SHC in vitro depending on the cell type [6].

The previous studies [4–6] showed that 22SHC has the potential to affect lipid and glucose metabolism in vitro. Therefore, this study was conducted to elucidate whether 22SHC can be a model substance in the search of treatments for disorders involving lipid aberrations by exploring the pharmacokinetics of 22SHC and effects of 22SHC on glucose and lipid metabolism in vivo in rats.

Materials and Methods

Bioavailability Study-Pilot

Male Wistar rats (Norwegian Institute of Public Health), 304–316 g, were acclimatized for 1 week and housed in standard stainless-steel cages before two fasted rats were used for oral administration and two fasted rats for intravenous doses of 10 mg (~30 mg/kg) 22-*S*-hydroxycholesterol (22SHC). The 22SHC was dissolved in 45 % water solution of 2-hydroxypropyl- β -cyclodextrin. Blood samples (0.5 ml) were taken before dosing and at 0.3, 1, 3, 7 and 24 h after oral dosing (by gastric tube) and at 5, 30 min and 1.5, 5 and 24 h after i.v. administration.

Determination of 22-*S*-Hydroxycholesterol in Plasma with HPLC–APCI–MS

Plasma (100 μ L) was diluted with 300 μ L 2-propanol. After thorough mixing (15 min) and centrifugation (10 min, 4,000g at 10 °C), an aliquot of 5 μ L was injected from the supernatant into the HPLC system. HPLC was performed with a HP 1100 liquid chromatograph (Agilent Technologies, Palo Alto, CA, USA) interfaced by APCI to a HP mass spectrometric detector (MS) operated in single ion monitoring mode (SIM). 22SHC was separated on a C18, 4.6 mm \times 50 mm reversed phase column at 60 °C. For the pilot study, a three-point analytical curve was made from analysis of albumin solution enriched with known 22SHC concentration. The method was linear from 0.01 to 30 μ g/ml at least and the limit of detection was 5 ng/ml.

Animals for the Pharmacokinetic Study

Male Sprague–Dawley rats (Charles River UK Ltd, Margate, UK), age 6–9 weeks (180–240 g) were used (32). During the acclimatization period, rats were housed in standard stainless-steel cages of up to six rats per group. After dosing, rats were returned to their cages. All rats were weighed before dose administration and again at the time of termination. Diet (VRF1) and drinking water were available to the animals ad libitum. [3 H]22-*S*-hydroxycholesterol ([3 H]22SHC) were administered at doses of

50 mg/kg as single bolus intravenous doses into a caudal vein or as single oral doses. [^3H]22SHC was dissolved in 45 % water solution of 2-hydroxypropyl- β -cyclodextrin. Serial blood samples were collected by venipuncture of a caudal vein and terminal samples were taken by cardiac puncture under isoflurane/oxygen anesthesia. The extent of tritium exchange from [^3H]22SHC following oral administration to two rats was small after 24 h (~ 1.5 %) which means that radio labelled [^3H]22SHC should reflect 22SHC levels in vivo.

Absorption

After single oral and intravenous doses of [^3H]22SHC to three or four subgroups of three male rats, two serial blood samples and one terminal blood sample were taken from each subgroup. Blood samples were taken at 0.25, 0.5, 1, 2, 3, 4, 6, 8 and 24 h after oral dosing and at 5, 10, 15, 30, 45 min and 1, 2, 3, 4, 6, 8 and 24 h after i.v. administration.

Distribution

After administration of single oral doses of [^3H]22SHC to five male rats, one animal was exsanguinated and killed (cervical dislocation) at each of the following time points: 1, 3, 6, 24 and 168 h post-administration. Each terminal blood sample was transferred to a heparinized tube and a portion retained as whole-blood for measurement of radioactivity concentrations. The remainder was immediately centrifuged and the separated plasma transferred into a clean plastic tube; blood cells were retained for analysis. After sacrifice, a selection of tissues and organs were removed or sampled from each carcass.

Excretion

After a single intravenous or oral dose of [^3H]22SHC two groups of three male rats were housed singly in glass metabowls designed to permit the separate collection of urine and feces. Total excreta were collected during 0–168 h post-dose for radioactivity analysis. Urine was collected at 0–6, 6–24 h and subsequently at 24 h intervals up to 168 h post-dose. Feces were collected separately at 24 h intervals during 0–168 h. Expired air (oral dose group) was trapped in purified water and radioactivity monitored. Expired air traps were changed at 24 h intervals and collection continued until <0.1 % of the dose was recovered in two consecutive daily air traps (or until 168 h post-dose). The interiors of the metabolism cages were washed with purified water at 24 h intervals. At 168 h post-dose, the cages were also washed with methanol and all washings were retained for radioactivity measurement.

Animals for the 22-*S*-Hydroxycholesterol-Effect Study

Male Wistar rats were purchased from Scanbur AS, Norway. The rats were fed ad libitum a regular maintenance diet (Special Diets Services (SDS), Witham, Essex, UK) for 5 days after arrival to our animal facilities. Then a feeding regimen was adopted using chow and a high-fat diet (HFD, see “Diets”) for 21 days. The rats were about 9-week-old at the start of the experimental feeding. Wistar rats were randomly divided into four groups with six animals each, receiving either chow \pm 22SHC (30 mg/kg/day) or HFD \pm 22SHC. There were three animals in each cage and they had free access to tap water. The experimental protocol (Id 823) was approved by the National Animal Research Authority.

Diets

The animals were given either chow or HFD. In total, HFD consisted of 1.9 % gelatin, 5.7 % wheat bran, 7.7 % vitamin and mineral mix, 25.1 % cornstarch, 25.7 % casein, 26.8 % beef tallow and 7.1 % sunflower oil. The HFD provided approximately 60 % of the energy from fat.

Experimental Protocol

The rats ($n = 24$) were fed ad libitum on the experimental diets, and the total feed intake of HFD for each group ($n = 6$) was recorded at the end of the experiment. Rats were given 22SHC in 45 % water solution of 2-hydroxypropyl- β -cyclodextrin by gavage. They received 30 mg/kg/day of 22SHC calculated at the beginning of the feeding period. Body weight was registered twice a week. Controls and treated rats were weighed at the same day during the experimental feeding. Blood samples were collected from a vein in the leg in the morning between 08:30 and 09:00 a.m. once a week. Immediately after termination, blood samples (cardiac puncture) and tissues (snap frozen in liquid nitrogen) were collected between 10:00 a.m. and 14:00 p.m. Time-curves of serum analysis are presented only for 0, 1 and 2 weeks since the 3-week samples were collected differently.

Serum Analysis

After anaesthetizing the rats with 20 mg pentobarbital (i.p. 50 mg/ml), blood was collected from all 24 animals by aortic puncture and left in room temperature to coagulate. Serum was prepared and stored at -20 °C prior to analysis. Serum lipids and glucose were measured on the MaxMatPL system (ILS Laboratories Scandinavia AS, Oslo, Norway) using the following kits: glucose, triacylglycerol (TAG), total cholesterol and non-esterified fatty acids (NEFA) (all from ILS Laboratories Scandinavia AS). Serum levels of

insulin were measured by a commercially available ELISA kit (Linco Research, MO, USA).

Determination of Triacylglycerol Content

Frozen tissue samples from all 24 animals were weighed and homogenized in 1 ml ice cold 1 mmol/l EDTA buffer (liver) or 0.2 mmol/l EGTA buffer (gastrocnemius) with Precellys[®]24 bead beater (5,800 beats, 30 s, <http://www.precellys.com>) and spun down for 10 min, 1,000g at 4 °C. The supernatant was transferred to new tubes. Triacylglycerol content was measured with a TG PAP 150-kit (BioMerieux, Marcy l'Etoile, France) according to the supplier's protocol.

Measurement of Glucose Uptake

Epitrochlearis and soleus muscle strips were dissected out from six animals from the HFD control group and six animals for the HFD 22SHC treated group and suspended on holders at their approximate resting length [14]. For in vitro studies, the holders with muscles were placed in test tubes containing Krebs–Henseleit solution (with 5.5 mM glucose, 2 mM sodium pyruvate, 5 mM HEPES (*N*-2-hydroxyethylpiperazine-*N'*-2-ethanesulfonic acid) and 0.1 % bovine serum albumin (BSA, fraction V, Sigma), pH 7.4). All incubations were performed at 30 °C and gas (95 % O₂/5 % CO₂) was continuously bubbled through the buffer. After 30–50 min of preincubation, glucose uptake was determined with [³H]-deoxy-D-glucose [15]. Briefly, 0.25 μCi/ml 2-[1,2-³H(*N*)]-deoxy-D-glucose (20.0 Ci/mmol; DuPont, PerkinElmer) and 0.1 μCi/ml [1-¹⁴C]-D-mannitol (51.5 mCi/mmol; PerkinElmer) were added to the buffer (containing 5.5 mM glucose) and glucose uptake was calculated from the intracellular accumulation of [³H]-2-deoxy-D-glucose as previously described [15]. After incubations, the muscles were blotted on filter paper and frozen in liquid N₂. For measurement of glucose uptake, the muscles were freeze dried, weighed and dissolved in 600 μl 1 M KOH for 20 min at 70 °C. Of the digest, 400 μl was added to 3 ml scintillation solution (Hionic-Fluor, Packard), mixed and counted for radioactivity (TRI-CARB 460C, Packard, USA).

Gene Expression Analysis

Liver and muscle samples (soleus and gastrocnemius) were collected from each rat and snap-frozen in liquid N₂ before storage at –70 °C. The tissues were homogenized in 1 ml lysis buffer with a Precellys[®]24 bead beater (5,800 beats, 30 s) and total RNA was isolated by Agilent Total RNA isolation kit (Agilent Technologies, Santa Clara, CA, USA) or TRIzol[®] (muscle tissue) according to the supplier's total

RNA isolation protocol. RNA samples isolated from TRIzol[®] (Invitrogen, Paisley, Scotland) were treated with TURBO DNA-free[™] (Ambion, Austin, TX, USA) as an additional step after the RNA isolation procedure. Each sample of total RNA was reversely transcribed using Applied Biosystem's High Capacity cDNA Reverse Transcription Kit with RNase inhibitor according to the manufacturer's descriptions. Real time qPCR was performed using an ABI PRISM[®] 7000 Detection System. DNA expression was determined by SYBR[®] Green (Applied Biosystems, Warrington, UK), and primers [36B4 (NM_022402), Gapdh (NM_017008), Lpl (NM_012598), Cd36 (NM_031561), Scd1 (NM_139192), Cpt1a (NM_031559), Cpt1b (NM_013200), Cpt2 (NM_012930), Ndufb3 (NM_001106912), Ndufs1 (NM_001005550), Mte-1 (NM_138907), Ucp3 (NM_013167)] were designed using Primer Express[®] (Applied Biosystems) and purchased from Invitrogen Corp. (<http://www.invitrogen.com>). Each target gene were quantified in triplicates and carried out in a 25 μl reaction volume according to the supplier's protocol. All assays were run for 40 cycles (95 °C for 12 s followed by 60 °C for 60 s). The transcription levels were normalized to the housekeeping control genes 36B4 and GAPDH.

Carnitine Palmitoyltransferase 2 (CPT2) Activity

Frozen tissue samples were homogenized as described above (“[Determination of Triacylglycerol Content](#)”) for six animals from the HFD control group and six animals for the HFD 22SHC treated group. CPT2-activity was measured in total homogenate from liver. The assay contained 25 mM HEPES, 75 mM KCl, 1 M HCl, 6 mM palmitoyl-CoA, 0.4 % Triton X-100 and pH was adjusted to 7.4. The reaction was started by adding 6 mM [methyl-¹⁴C]-L-carnitine (0.1 mCi/ml) (PerkinElmer). The enzymatic activities were analyzed using two identical parallels with 0.5 mg protein for each sample. The samples were extracted twice with water-saturated butanol to separate the substrate from the CPT2 product. The radioactivity was determined by liquid scintillation.

Western Blot Analysis

Tissue samples were homogenized as described above (Determination of triacylglycerol content) for six animals from the HFD control group and six animals for the HFD 22SHC treated group. Total cell lysates prepared in Laemmli buffer were electrophoretically separated on 12 % (w/v) polyacrylamide gels (acrylamide/*N,N'*-bis-methylene acrylamide = 37.5:1) followed by blotting to nitrocellulose membrane and incubation with antibodies recognizing human UCP3 [16]. Immunoreactive bands were visualized with enhanced chemiluminescence and

quantified with Gel-Pro Analyzer (version 2.0) software. Antibody against α -tubulin was used to normalize the UCP3 signal versus the amount of protein loading.

Statistical Methods

Significant difference between the two diet groups was analyzed by Mann–Whitney nonparametric test using a significance level of $p < 0.05$. Statistical comparison between different treatments and days of feeding was performed by linear mixed model (LMM) using SPSS. Correlations are presented with Spearman's correlation coefficient (r).

Results

Pharmacokinetics of 22SHC in Rats

The bioavailability of 22SHC was measured with labeled [^3H]22SHC and non-labeled substance. The bioavailability of 50 mg/kg [^3H]22SHC was found to be $\sim 50\%$ (Fig. 1a; Table 1), and the bioavailability of 30 mg/kg non-labeled 22SHC was $\sim 40\%$ (data not shown). $T_{1/2}$ for [^3H]22SHC was 8.1 and 6.4 h after i.v. and oral administration, respectively. The highest concentration of 22SHC obtained in plasma (C_{max}) after i.v. administration was 22.4 ng/ml after 8 min, while after oral dosing the peak concentration was 7.5 ng/ml after 4 h.

Radiolabeled 22SHC was found in almost all tissues examined and the highest concentrations in most tissues were found after 6 h. The concentration of 22SHC after oral administration was very high throughout the whole

gastrointestinal tract throughout the experimental period and highest after 1 h (Table 2). The organs with the highest concentrations of 22SHC were liver (65 $\mu\text{g/g}$ tissue/6 h), mesenteric lymph nodes (58 $\mu\text{g/g}$ tissue/3 h) and adrenal glands (33 $\mu\text{g/g}$ tissue/6 h). 22SHC levels were also quite high in heart, kidney, lungs, pancreas, bone marrow, and subcutaneous and perirenal fat depots. One week after the oral dose, the highest levels of 22SHC were found in adrenal glands (2.4 $\mu\text{g/g}$ tissue/168 h), subcutaneous fat (1.1 $\mu\text{g/g}$ tissue/168 h) and liver (0.9 $\mu\text{g/g}$ tissue/168 h).

The main part of 22SHC was excreted through feces regardless of oral (89 %) or i.v. (77 %) administration, although a higher fraction was excreted through urine after i.v. administration (Fig. 1b). Also, most of urine excretion was found within 48 h while 22SHC was found in feces also at 96 h (data not shown).

Effects of 22SHC on Body Weight

All animals receiving 22SHC, regardless of diets, gained less body weight than the control animals during the 3-week feeding period (Fig. 2a, b, $p < 0.05$ overall effect). Rats on chow diet receiving 22SHC showed a lower body weight gain compared to control rats during the last week of the experiment (Fig. 2a), while in rats on HFD the 22SHC-induced reduction of body weight gain was apparent already after 1 week (Fig. 2b).

Effects of 22SHC on Serum Lipids, Glucose and Insulin

Treatment with 22SHC did not influence the level of serum triacylglycerol (TAG) in rats on chow diet (Fig. 3a). Serum

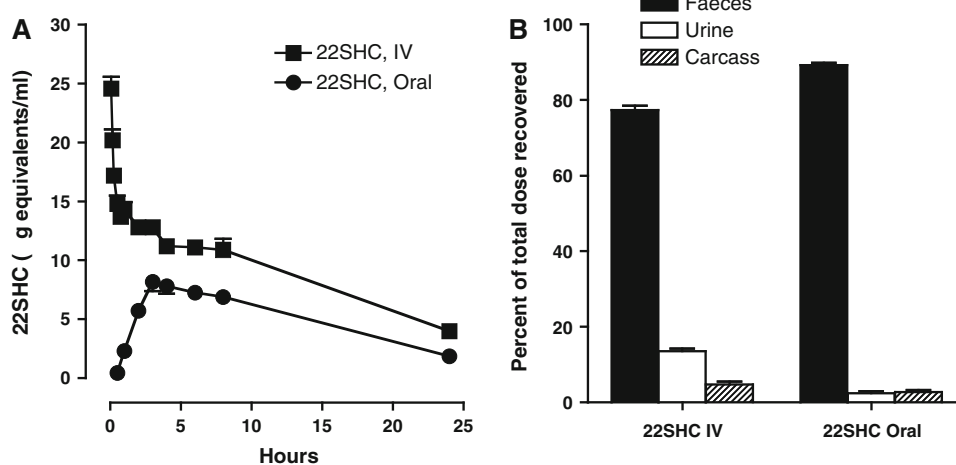


Fig. 1 Absorption (a) and excretion (b) of 22SHC after intravenous and oral administration. Single oral and intravenous (i.v.) doses (50 mg/kg) of [^3H]22SHC were administered to male Sprague–Dawley rats. In a, two serial blood samples and one terminal blood sample were taken from each subgroup. Blood samples were taken at

0.25, 0.5, 1, 2, 3, 4, 6, 8 and 24 h after oral dosing and at 5 min, 10 min, 0.25, 0.5, 0.75, 1, 2, 3, 4, 6, 8 and 24 h after i.v. administration. b Cumulative rates of excretion of radioactivity during 168 h for feces, urine and the remaining carcass. Data in a and b are presented as means \pm SEM ($n = 3$)

Table 1 Pharmacokinetic parameters of non-volatile radioactivity in plasma following single intravenous or single oral doses of [³H]22-*S*-hydroxycholesterol (50 mg/kg) to male rats

Parameter	Intravenous dose (phase A)	Oral dose (phase B)
C_{\max} (ng/ml)	22.4	7.5
T_{\max} (h)	0.08	4
AUC_t (ng h/ml)	174	95.2
AUC (ng h/ml)	195	104
$T_{1/2}$ (h)	8.1	6.4
Extent of tritium exchange (%)	2.8	1.2

C_{\max} highest concentration measured, T_{\max} when C_{\max} is measured, AUC area under curve, $T_{1/2}$ half life

Table 2 Distribution of [³H]22-*S*-hydroxycholesterol in rats

Tissue/organ	μg Equivalents [³ H]22- <i>S</i> -hydroxycholesterol/g tissue				
	1 h	3 h	6 h	24 h	168 h
Plasma (non-lyophilized)	2.72	8.83	7.51	1.81	0.660
Plasma (lyophilized)	2.62	7.30	6.52	0.792	0.045
Whole blood	2.13	5.50	4.92	0.676	0.145
Blood cells	1.48	3.94	3.28	0.367	0.167
Brain	0.586	3.60	4.92	2.81	0.184
Eyes	0.287	1.95	2.47	0.606	0.199
Heart	3.14	13.4	12.2	0.935	0.259
Kidneys	3.33	17.3	19.0	1.65	0.413
Urinary bladder	1.89	4.86	8.18	0.846	0.298
Liver	14.5	63.1	65.0	10.5	0.938
Lungs	12.2	19.5	19.4	1.70	0.353
Spleen	3.63	13.3	11.3	1.22	0.648
Adrenal glands	5.91	32.5	33.0	5.89	2.40
Lymph nodes (mesenteric)	3.00	57.9	36.8	1.99	0.423
Pancreas	2.36	14.7	20.9	2.27	0.320
Thymus	1.01	4.91	6.93	1.09	0.278
Thyroid	18.6	13.9	12.0	1.33	0.799
Prostate	0.719	6.21	7.76	1.75	0.376
Testis	0.267	2.27	3.46	0.996	0.296
Bone marrow	1.73	9.70	10.9	1.30	0.722
Fat (subcutaneous)	1.02	7.06	11.3	9.10	1.05
Fat (perirenal)	4.33	8.67	12.7	10.9	0.759
Muscle (skeletal)	0.783	5.87	7.68	0.692	0.183
Skin	0.574	4.52	6.43	1.93	0.359
Stomach wall	506	257	128	43.9	1.48
Small intestine wall	597	343	252	104	4.47
Large intestine wall	194	247	298	61.6	2.11

levels of TAG were increased by HFD in rats and treatment with 22SHC seemed to completely counteract this elevation of TAG (Fig. 3b, $p < 0.05$ overall effect). Treatment with

22SHC for 3 weeks did not influence serum concentrations of total cholesterol, non-esterified fatty acids (NEFA), glucose or insulin in any of the animal groups (Table 3).

Effects of 22SHC on Levels of Triacylglycerol in Liver and Skeletal Muscle

The concentration of TAG was higher in livers from rats fed HFD than chow diet, and treatment with 22SHC for 3 weeks reduced TAG levels in liver in both treatment groups (Fig. 4a). There were no significant differences in the amount of TAG in gastrocnemius muscle after different diets and treatments (Fig. 4b), however, TAG was correlated negatively with protein levels of UCP3 after 22SHC treatment ($r = -0.822$, $p < 0.05$).

22SHC Did Not Influence Glucose Uptake in Skeletal Muscle Strips

To see if HFD induced insulin-resistance, soleus muscles strips from HFD-fed rats were incubated. Insulin dose-dependently (0, 0.2 and 10 mU/ml insulin) increased glucose uptake (Fig. 5). Furthermore, the insulin-stimulated glucose uptake was not altered after 22SHC treatment compared to control animals.

RNA Expression, UCP3 Protein Level and CPT2-Activity

We wanted to investigate whether the reduced body weight gain (Fig. 2) and reduced concentration of serum and liver TAG (Fig. 4) in the rats receiving the HFD together with 22SHC could be correlated with an increase in mRNA levels of genes involved in fatty acid uptake and oxidation (Fig. 6 Lpl, Cd36, Scd1, Cpt1a (liver), Cpt1b (muscle), Cpt2 (liver), Ndufb3, Ndufs1, Mte-1 (muscle), Ucp3).

In liver we found that the uncoupling protein 3 (Ucp3) mRNA level had increased nearly tenfold (Fig. 6a) by 22SHC, but this was not reflected by increased protein levels of Ucp3 (Fig. 7a). Ucp3 mRNA levels had also increased 2.5-fold in both gastrocnemius (Fig. 6b) and soleus (Fig. 6c) muscles from animals given 22SHC, and protein level of Ucp3 in gastrocnemius had increased 12-fold (Fig. 7a). Hepatic carnitine palmitoyltransferase 2 (Cpt2) mRNA level had increased two-fold (Fig. 6a) while the CPT2-activity only tended to increase (Fig. 7b).

Discussion

Pharmacokinetic studies of 22SHC showed that 22SHC was well absorbed and distributed to different organs after oral administration with a half-life of 6.4 h. Further, administration of 30 mg/kg 22SHC once daily reduced

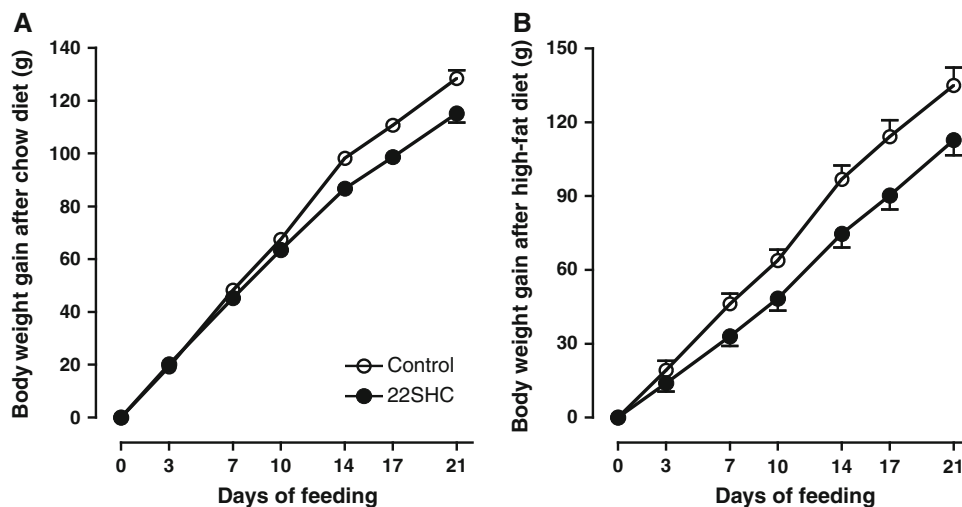


Fig. 2 Body weight gain in Wistar rats during 3 weeks feeding with chow (a) or high-fat diet (b). Rats were randomly divided into four groups with six animals each, receiving either chow (maintenance diet, SDS) \pm 22SHC (30 mg/kg/day) or high-fat diet (HFD) \pm 22SHC (30 mg/kg/day) for 21 days. The rats were given free access

to tap water and were weighed in the morning on day 0, 3, 7, 10, 14, 17 and 21. Data are presented as means \pm SEM ($n = 6$). 22SHC treatment significantly decreased overall body weight gain ($p < 0.05$), linear mixed model, SPSS

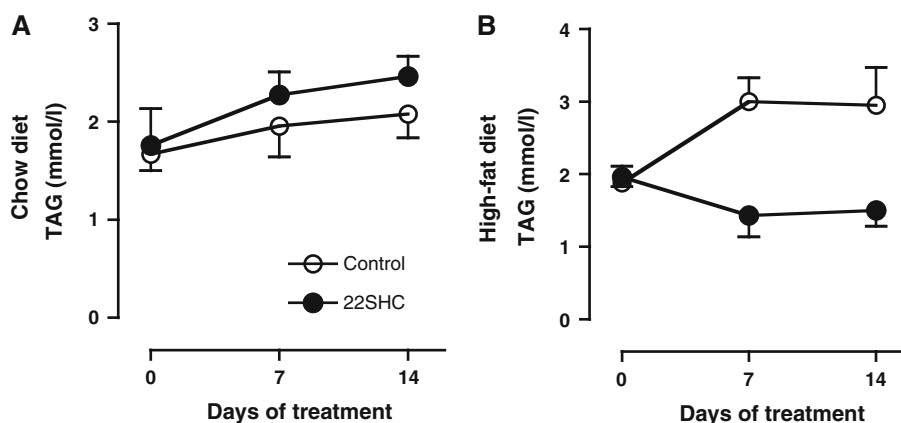


Fig. 3 The concentration of triacylglycerol in serum during feeding chow (a) or high-fat diet (b). Rats were randomly divided into four groups with six animals each, receiving either chow \pm 22SHC or high-fat diet (HFD) \pm 22SHC for 21 days. The rats were given free access to tap water. Blood samples were collected in the morning between 08:30 and 09:00 am once a week at day 0, 7 and 14. Serum

was prepared and stored at -20°C prior to analysis. Serum triacylglycerol (TAG) was measured using the MaxMatPL system as described in “Materials and methods”. Data are presented as means \pm SEM ($n = 6$). 22SHC treatment significantly decreased overall increase of TAG in serum after high-fat diet ($p < 0.05$), linear mixed model, SPSS

body weight gain, and abolished high-fat diet-induced increase of triacylglycerol (TAG) levels in serum. In liver, expression of Cpt2 and Ucp3 was increased and accumulation of TAG was reduced after HFD. In skeletal muscles, Cpt2 and Ucp3 were increased, but 22SHC did not improve insulin-stimulated glucose uptake.

One of the main findings in this study was that rats receiving 22SHC gained less body weight than their controls, regardless of whether the animals received a chow diet or a high-fat diet (HFD). To study the mechanisms

behind these observations, we analyzed mRNA expression of several genes involved in fatty acid transport and oxidation (Lpl, Cd36, Scd1, Cpt, Ndufs, Mte-1, Ucp) in liver and skeletal muscle. 22SHC treatment increased the expression of Cpt2 (liver) and Ucp3. The 22SHC-induced increase of Ucp3 mRNA level was about 10- and 2.5-fold in liver and skeletal muscle, respectively. This response to 22SHC treatment was confirmed by a markedly elevated protein level of Ucp3 in gastrocnemius muscle. Ucp3 is a mitochondrial anion carrier protein with a highly selective

Table 3 Characteristics of the study population

Parameters	Wistar rats (male)			
	Chow	+22SHC	High-fat	+22SHC
Number of animals (<i>n</i>)	6	6	6	6
Start body weight (g)	188 ± 4	187 ± 2	185 ± 3	182 ± 2
Final body weight (g)	317 ± 5	302 ± 6 ^a	320 ± 7	295 ± 7 ^b
Epididymal tissue/final body weight (%)	1.3 ± 0.1	1.2 ± 0.1	2.0 ± 0.2 ^a	1.7 ± 0.2
Liver weight/final body weight (%)	4.2 ± 0.1	4.5 ± 0.1	3.9 ± 0.1	4.1 ± 0.1
Cholesterol (mM)	1.7 ± 0.1	1.6 ± 0.1	2.1 ± 0.1 ^a	2.1 ± 0.1 ^a
Non-esterified fatty acids (mM)	0.31 ± 0.02	0.24 ± 0.04	0.33 ± 0.06	0.22 ± 0.07
Insulin (ng/ml)	4.7 ± 1.1	3.8 ± 0.6	5.0 ± 1.2	4.8 ± 1.3
Glucose (mM)	9.5 ± 0.4	9.3 ± 0.5	10.5 ± 0.4	11 ± 0.3
Feed intake (g/animal/24 h)			16.9	15.2

^a $p < 0.05$ when compared to Wistar rats on chow diet

^b $p = 0.07$

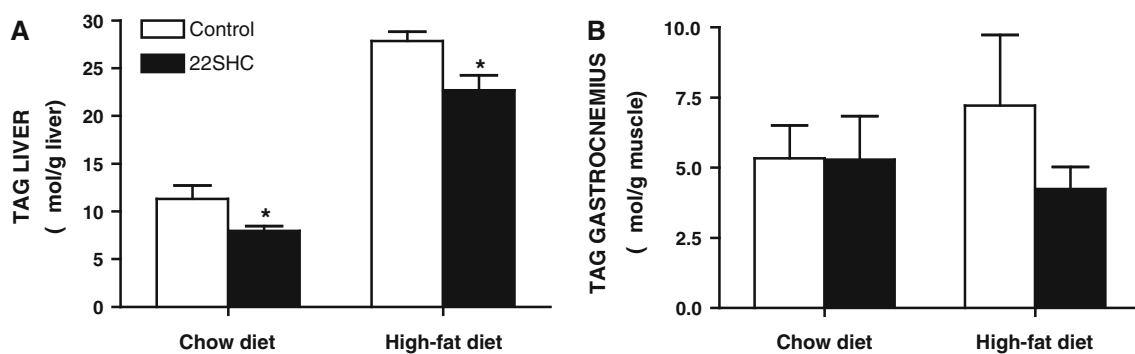


Fig. 4 Triacylglycerol content in liver (a) and gastrocnemius muscle (b) in rats fed chow or high-fat diets. Rats were randomly divided into four groups with six animals each, receiving either chow ± 22SHC or

high-fat diet (HFD) ± 22SHC for 21 days. Tissue samples were prepared as described in “Materials and methods”. Data are presented as means ± SEM ($n = 6$). * $p \leq 0.05$ versus control

expression in skeletal muscle [17]. It has been suggested by in vivo experiments that Ucp3 is involved in fatty acid translocation [17]. Previous research in brown adipose tissue and skeletal muscle from rodents described a strong association between Ucp2 and Ucp3 expression and lipid metabolism [18], and that PPAR γ and PPAR α , transcription factors regulated by lipid metabolites, regulated the expression of Ucp2 and Ucp3 [19, 20]. Further, mice over-expressing human Ucp3 were lean despite overeating, had increased metabolic rate and their skeletal muscle mitochondria showed increased proton conductance [21]. In line with this, Choi et al. [22] have recently shown that wild-type mice fed a high-fat diet were markedly insulin resistant, while mice over-expressing Ucp3 in skeletal muscle were completely protected against lipid-induced defects in insulin signaling and action. These data suggest that the effect on body weight and changes in TAG levels we observed after treatment with 22SHC could partly be mediated through increased expression of Ucp3.

Ectopic accumulated fat, especially in liver and skeletal muscle, promotes the development of mitochondrial

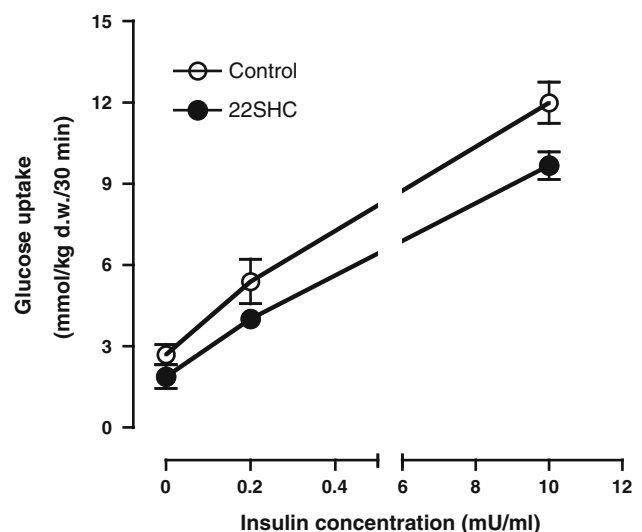


Fig. 5 Glucose transport in soleus muscle strips from rats fed a high-fat diet. Rats were randomly divided into two groups with six animals each, receiving high-fat diet (HFD) ± 22SHC for 21 days. Insulin-stimulated glucose uptake was measured in soleus muscle strips on day 21. Data are presented as means ± SEM ($n = 6$)

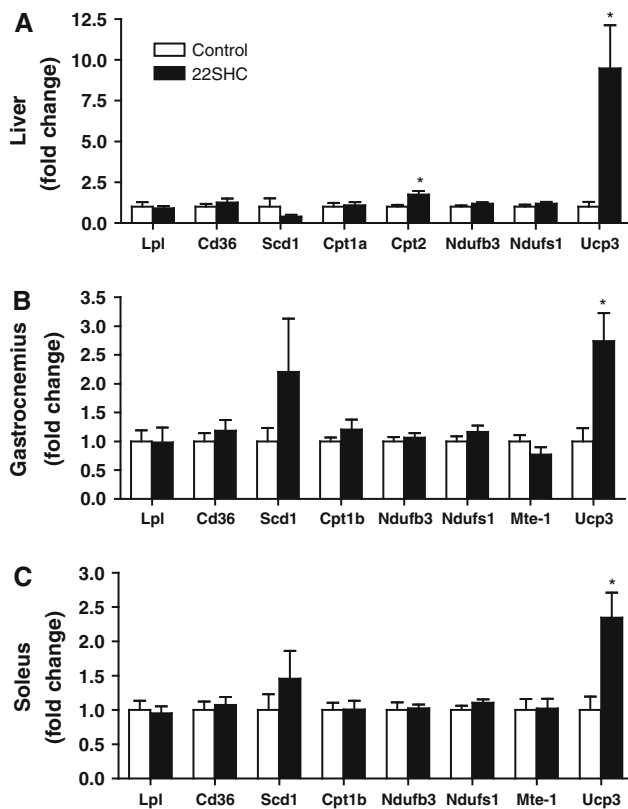


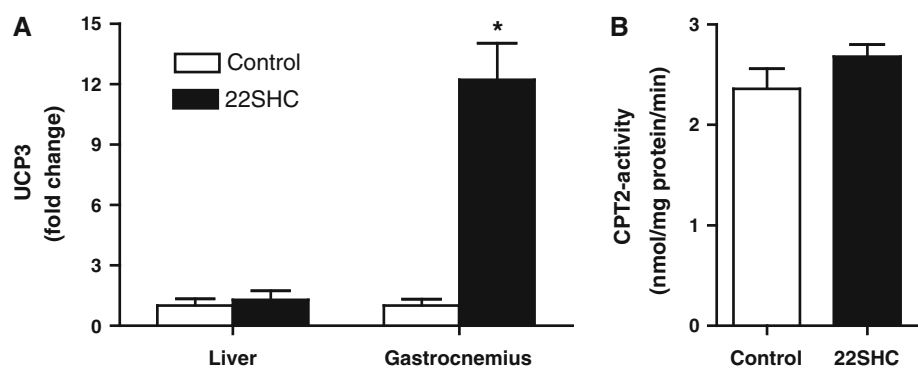
Fig. 6 Gene expression in liver (a), gastrocnemius (b) and soleus muscles (c) from rats fed a high-fat diet. Rats were randomly divided into two groups with six animals each, receiving high-fat diet (HFD) \pm 22SHC for 21 days. Tissue samples were prepared as described in “Materials and methods”. Total RNA was extracted, reversely transcribed and analyzed by RT-qPCR. Results are normalized to levels of GAPDH and presented as means \pm SEM ($n = 6$). *Lpl* lipoprotein lipase, *Cd36* fatty acid transporter, *Scd1* stearoyl-CoA desaturase, *Cpt1a* carnitine palmitoyltransferase 1a, *Cpt1b* carnitine palmitoyltransferase 1b, *Cpt2* carnitine palmitoyltransferase 2, *Ndufb3* NADH dehydrogenase (ubiquinone) 1 beta subcomplex 3, *Ndufs1* NADH dehydrogenase (ubiquinone) subcomplex 1, *Mte-1* mitochondrial thioesterase-1, *UCP3* uncoupling protein 3. * $p \leq 0.05$ versus control

dysfunction and metabolic syndrome [23–25]. Fabbrini et al. [26] have shown that increased level of intrahepatic triacylglycerol (TAG) is an independent indicator of

multiorgan insulin resistance, and that intrahepatic TAG by itself could be directly involved in the pathogenesis of dyslipidemia associated with non-alcoholic fatty liver disease. Therefore, it is possible that visceral adipose tissue itself is not harmful, but is simply an innocent bystander that tracks with intra-hepatic TAG. In our study we observed that the animals receiving only HFD had elevated serum TAG levels while this was not observed for the rats that were treated with 22SHC in combination with the HFD. Interestingly, 22SHC treatment reduced accumulation of TAG in liver compared to control animals, and there was a tendency for reduction in TAG content in gastrocnemius muscle. This is in concordance with recent in vitro data showing reduced de novo lipogenesis in both HepG2 cells (liver cells) and human skeletal muscle cells after 22SHC treatment [6]. Further, the reduction in TAG content was negatively correlated with protein levels of UCP3. This may imply that 22SHC induced a more efficient lipid metabolism by removing TAG from plasma and by increasing fatty acid oxidation and energy dissipation possibly through increased *cpt2* and *Ucp3*-activity. In support of our findings, Changani et al. [27] have shown with MRI technology that UCP3-overexpressing mice weighed less than the control group and most interestingly, since *Ucp3* is mainly expressed in skeletal muscle, they showed no increase in intramuscular fat like the control group. Also, a study on chow-fed UCP3 $^{+/-}$ and UCP3 $^{-/-}$ mice showed that progressive reduction of UCP3 levels resulted in insulin resistance and decreased fatty acid oxidation accompanied by reduced levels of PPAR δ and *Cpt1* [28]. These results also support that UCP3 might be important for an efficient lipid metabolism in vivo.

In vivo *Ucp3*-overexpression animal models with both 2- and 20-fold increase have shown reduced fasting blood glucose [29, 30]. We could neither observe reduced serum glucose in non-fasted animals nor an increase in insulin-stimulated glucose uptake in epitrochlearis muscle strips from rats fed HFD in combination with 22SHC. The lack of effects on glucose metabolism might be caused by the relatively short duration of this in vivo experiment.

Fig. 7 UCP3 protein level (a) and CPT2-activity (b) in tissues from rats fed a high-fat diet. Rats were randomly divided into two groups with six animals each, receiving high-fat diet (HFD) \pm 22SHC for 21 days. Tissue samples were prepared as described in “Materials and methods”. Data are presented as means \pm SEM ($n = 5-6$). * $p \leq 0.05$ versus control



In summary, this study showed that treating rats with 22SHC for 3 weeks resulted in a reduced body weight gain, prevention of an increased concentration of TAG in serum when fed a HFD and a reduction of TAG in liver compared to control animals. We also observed increased gene expression of Ucp3 and Cpt2 in liver and skeletal muscle and increased protein level of Ucp3 in skeletal muscle after 22SHC treatment. To fully understand these results we need a better general understanding of the role of Ucp3 in regulating energy metabolism. Although the mechanisms behind the observed metabolic changes need to be further elucidated, 22SHC seems to be an interesting model substance in the search of treatments for disorders involving lipid aberrations.

Acknowledgments We thank Anne Randi Enget, Mari-Ann Baltzersen, Camilla Stensrud, Kari Williams, Jorid T. Stuenæs and Ada Ingvaldsen for excellent technical assistance. We thank Richard Porter and Lars Henrik Manzke (Trinity College Dublin) for providing us with the UCP3 antibody. Hilde Hyldmo is also thanked for excellent technical assistance with handling of the animals and Vitas AS for analyzing blood samples. This work was supported by grants from the Norwegian Research Council and Birkeland Invention/Inven2 (Project 184019/I10).

References

- Geyeregger R, Zeyda M, Stulnig TM (2006) Liver X receptors in cardiovascular and metabolic disease. *Cell Mol Life Sci* 63:524–539
- Kase ET, Wensaas AJ, Aas V et al (2005) Skeletal muscle lipid accumulation in type 2 diabetes may involve the liver X receptor pathway. *Diabetes* 54:1108–1115
- Schultz JR, Tu H, Luk A et al (2000) Role of LXRs in control of lipogenesis. *Genes Dev* 14:2831–2838
- Kase ET, Andersen B, Nebb HI, Rustan AC, Thoresen GH (2006) 22-Hydroxycholesterols regulate lipid metabolism differently than T0901317 in human myotubes. *Biochim Biophys Acta* 1761:1515–1522
- Kase ET, Thoresen GH, Westerlund S et al (2007) Liver X receptor antagonist reduces lipid formation and increases glucose metabolism in myotubes from lean, obese and type 2 diabetic individuals. *Diabetologia* 50:2171–2180
- Hessvik NP, Bakke SS, Smith R et al (2012) The liver X receptor modulator 22(S)-hydroxycholesterol exerts cell-type specific effects on lipid and glucose metabolism. *J Steroid Biochem Mol Biol* 128:154–164
- Janowski BA, Grogan MJ, Jones SA et al (1999) Structural requirements of ligands for the oxysterol liver X receptors LXRalpha and LXRBeta. *Proc Natl Acad Sci USA* 96:266–271
- Janowski BA, Willy PJ, Devi TR, Falck JR, Mangelsdorf DJ (1996) An oxysterol signalling pathway mediated by the nuclear receptor LXR alpha. *Nature* 383:728–731
- Spencer TA, Li D, Russel JS et al (2001) Pharmacophore analysis of the nuclear oxysterol receptor LXRalpha. *J Med Chem* 44:886–897
- Svensson S, Ostberg T, Jacobsson M et al (2003) Crystal structure of the heterodimeric complex of LXRalpha and RXRBeta ligand-binding domains in a fully agonistic conformation. *EMBO J* 22:4625–4633
- Fu X, Menke JG, Chen Y et al (2001) 27-Hydroxycholesterol is an endogenous ligand for liver X receptor in cholesterol-loaded cells. *J Biol Chem* 276:38378–38387
- Forman BM, Ruan B, Chen J, Schroepfer GJ Jr, Evans RM (1997) The orphan nuclear receptor LXRalpha is positively and negatively regulated by distinct products of mevalonate metabolism. *Proc Natl Acad Sci USA* 94:10588–10593
- Mitro N, Mak PA, Vargas L et al (2007) The nuclear receptor LXR is a glucose sensor. *Nature* 445:219–223
- Franch J, Aslesen R, Jensen J (1999) Regulation of glycogen synthesis in rat skeletal muscle after glycogen-depleting contractile activity: effects of adrenaline on glycogen synthesis and activation of glycogen synthase and glycogen phosphorylase. *Biochem J* 344(Pt 1):231–235
- Aslesen R, Jensen J (1998) Effects of epinephrine on glucose metabolism in contracting rat skeletal muscles. *Am J Physiol* 275:E448–E456
- Kelly OM, McNamara YM, Manzke LH, Meegan MJ, Porter RK (2012) The preservation of in vivo phosphorylated and activated uncoupling protein 3 (UCP3) in isolated skeletal muscle mitochondria following administration of 3,4-methylenedioxymethamphetamine (MDMA aka ecstasy) to rats/mice. *Mitochondrion* 12:110–119
- Bezaire V, Seifert EL, Harper ME (2007) Uncoupling protein-3: clues in an ongoing mitochondrial mystery. *Faseb J* 21:312–324
- Samec S, Seydoux J, Dulloo AG (1998) Role of UCP homologues in skeletal muscles and brown adipose tissue: mediators of thermogenesis or regulators of lipids as fuel substrate? *Faseb J* 12:715–724
- Hwang CS, Lane MD (1999) Up-regulation of uncoupling protein-3 by fatty acid in C2C12 myotubes. *Biochem Biophys Res Commun* 258:464–469
- Brun S, Carmona MC, Mampel T et al (1999) Activators of peroxisome proliferator-activated receptor-alpha induce the expression of the uncoupling protein-3 gene in skeletal muscle: a potential mechanism for the lipid intake-dependent activation of uncoupling protein-3 gene expression at birth. *Diabetes* 48:1217–1222
- Moore GB, Himms-Hagen J, Harper ME, Clapham JC (2001) Overexpression of UCP-3 in skeletal muscle of mice results in increased expression of mitochondrial thioesterase mRNA. *Biochem Biophys Res Commun* 283:785–790
- Choi CS, Fillmore JJ, Kim JK et al (2007) Overexpression of uncoupling protein 3 in skeletal muscle protects against fat-induced insulin resistance. *J Clin Invest* 117:1995–2003
- Chow L, From A, Seaquist E (2010) Skeletal muscle insulin resistance: the interplay of local lipid excess and mitochondrial dysfunction. *Metabolism* 59:70–85
- Lara-Castro C, Garvey WT (2008) Intracellular lipid accumulation in liver and muscle and the insulin resistance syndrome. *Endocrinol Metab Clin North Am* 37:841–856
- Szendroedi J, Roden M (2009) Ectopic lipids and organ function. *Curr Opin Lipidol* 20:50–56
- Fabbrini E, Magkos F, Mohammed BS et al (2009) Intrahepatic fat, not visceral fat, is linked with metabolic complications of obesity. *Proc Natl Acad Sci USA* 106:15430–15435
- Changani KK, Nicholson A, White A et al (2003) A longitudinal magnetic resonance imaging (MRI) study of differences in abdominal fat distribution between normal mice, and lean overexpressors of mitochondrial uncoupling protein-3 (UCP-3). *Diabetes Obes Metab* 5:99–105
- Senese R, Valli V, Moreno M et al (2011) Uncoupling protein 3 expression levels influence insulin sensitivity, fatty acid oxida-

- tion, and related signaling pathways. *Pflugers Arch* 461:153–164
29. Clapham JC, Coulthard VH, Moore GB (2001) Concordant mRNA expression of UCP-3, but not UCP-2, with mitochondrial thioesterase-1 in brown adipose tissue and skeletal muscle in db/db diabetic mice. *Biochem Biophys Res Commun* 287:1058–1062
 30. Costford SR, Chaudhry SN, Salkhordeh M, Harper ME (2006) Effects of the presence, absence, and overexpression of uncoupling protein-3 on adiposity and fuel metabolism in congenic mice. *Am J Physiol Endocrinol Metab* 290:E1304–E1312

Mechanisms Underlying Decreased Hepatic Triacylglycerol and Cholesterol by Dietary Bitter Melon Extract in the Rat

Gamarallage V. K. Senanayake · Nobuhiro Fukuda · Shoko Nshizono · Yu-Ming Wang · Koji Nagao · Teruyoshi Yanagita · Masako Iwamoto · Hideaki Ohta

Received: 30 October 2011 / Accepted: 7 March 2012 / Published online: 29 March 2012
© AOCs 2012

Abstract In these studies, we focused on finding the mechanism(s) underlying the bitter melon (*Momordica charantia* L.) methanol fraction (MF)-dependent reduction in the concentration of hepatic triacylglycerol (TAG) and cholesterol in the rat. Rats were fed diets containing low (5 %) fat for 2 weeks (experiment 1), or low (5 %) and high (15 %) fat for a longer period of 8 weeks (experiment 2). MF was supplemented at 1 % level in both experiments. After feeding, rats were sacrificed, and their livers were

prepared as slices and hepatocytes, followed by incubation with [1(2)-¹⁴C] acetate or [1-¹⁴C] oleic acid (18:1 n-6). Under these conditions, we found that rats fed diets containing MF, as compared to those without MF, showed: (1) no adverse effects on food intake and growth, (2) a decreased hepatic TAG and total cholesterol, irrespective of the difference in dietary fat level or feeding period, and (3) a decreased incorporation of [1(2)-¹⁴C] acetate and [1-¹⁴C] oleic acid into TAG of liver slices and hepatocytes. MF-supplemented rats also showed no altered incorporation of labeled acetate into cholesterol and cholesterol ester, an increased fecal excretion of neutral steroids, but not of acidic steroids, and an enhanced mRNA abundance of carnitine palmitoyltransferase I, which is the rate-limiting enzyme for fatty acid oxidation. These results suggest that dietary MF decreases hepatic TAG synthesis while enhancing fatty acid oxidation, thereby reducing the concentration of hepatic TAG. The liver cholesterol-lowering effect of MF, however, is probably mediated through an increased fecal excretion of neutral steroids, without an effect on cholesterologenesis.

A preliminary part of this study was presented at 11th European Nutrition Conference, Spain, 2011.

G. V. K. Senanayake · N. Fukuda
Department of Biochemistry and Applied Biosciences,
Faculty of Agriculture, University of Miyazaki,
Miyazaki 889-2192, Japan

Present Address:

G. V. K. Senanayake (✉)
Richardson Center for Functional Foods and Nutraceuticals,
University of Manitoba, 196 Innovation Drive,
Winnipeg, MB R3T 2N2, Canada
e-mail: vijitha_senanayake@umanitoba.ca

S. Nshizono
Center for Collaborative Research and Community Cooperation,
University of Miyazaki, Miyazaki 889-2192, Japan

Y.-M. Wang · K. Nagao · T. Yanagita
Department of Applied Biochemistry and Food Science,
Faculty of Agriculture, Saga University, Saga 840-8502, Japan

M. Iwamoto · H. Ohta
Faculty of Nutritional Science,
Nakamura Gakuen University, Fukuoka 814-0198, Japan

Keywords *Momordica charantia* ·
Liver triacylglycerol-lowering effect ·
Liver cholesterol-lowering effect ·
Lipid metabolism

Abbreviations

CPT I Carnitine palmitoyltransferase I
DPS Digitonin precipitable sterol
MF Methanol fraction of *Momordica charantia*
MTP Microsomal transfer protein
PPAR Peroxisome proliferator-activated receptor
STZ Streptozotocin
TAG Triacylglycerol(s)

Introduction

Bitter melon (*Momordica charantia* L.), which is cultivated in countries located in tropical and subtropical areas such as India, Asia, and South America has been traditionally used as a folk medicine for the treatment of diabetes. More recently, favorable effects on glucose metabolism have been demonstrated in cell culture, animal models and human studies [1–8]. It has also been reported that feeding of bitter melon and/or its extract was beneficial in preventing lipid disorders such as hyperlipidemia and diabetic dyslipidemia in both normal rats and in rats with chemically induced diabetes [9]. In a previous series of experiments, we also reported, to our knowledge for the first time, that the freeze-dried powder of bitter melon and its methanol fraction (MF) have potent liver triacylglycerol (TAG)- and cholesterol-lowering activities in rats fed diets with and without cholesterol supplementation [10, 11]. We have also previously examined whether effects of dietary MF on lipid metabolism are reproduced in hamsters fed diets with and without cholesterol supplementation, and found that MF had a potent and dose-dependent lipid-lowering activity in serum, but not in liver, especially in the animals fed diets with cholesterol [12]. Together these data show that bitter melon and its extracts, such as MF, contain bioactive components which favorably modulate TAG and cholesterol metabolism in experimental animals, although there are species-specific differences.

To date, very little information has been reported about the mechanism(s) responsible for the reduced concentration of serum and/or hepatic lipids observed with bitter melon. Bitter melon juice appears to inhibit the synthesis and secretion of TAG in the form of apoB lipoprotein, as well as decrease microsomal transfer protein (MTP) mRNA expression in HepG2 cells [13, 14]. On the other hand, it has been reported that bitter melon extract activates the peroxisome proliferator-activated receptor (PPAR α), and upregulates the expression of acyl CoA oxidase gene in rat hepatoma cells H4IIEC3 [15]. These observations suggest that the triglyceride-lowering effect of bitter melon extract(s) is due to a reciprocal response of TAG synthesis and fatty acid oxidation. There is also a possibility, as reported by Oishi et al. [16] that bitter melon-dependent hypotriglyceridemic action is exerted through an inhibitory effect on digestive enzyme activity in the intestinal tract.

Regarding the mechanism(s) of the hypocholesterolemic and/or liver cholesterol-lowering effects of bitter melon, reduced cholesterol synthesis in the liver and/or increased fecal excretion of steroids seem plausible. However, so far, no information is available to confirm or refute this hypothesis.

In the present studies, we demonstrated for the first time that dietary MF has favorable and independent effects on

TAG and cholesterol metabolism. We also carried out a more detailed mechanistic examination of the effects of dietary MF on TAG and cholesterol metabolism, by using *in vitro* techniques of liver slices and hepatocytes in the presence of radiolabelled acetate and oleic acid (18:1n-6).

Materials and Methods

The bitter melon methanol fraction (MF) was prepared according to the method described previously [10–12]. [1(2)- ^{14}C] sodium acetate (2.18 GBq/mmol) and [1- ^{14}C] oleic acid (18:1 n-9, 2.5 GBq/mmol) were purchased from Amersham Life Sciences (Buckinghamshire, England), and other chemicals were from Wako Chemicals (Osaka, Japan).

Male Sprague–Dawley rats, purchased from a local breeder (Kyudo Co., Kumamoto, Japan), were acclimatized for several days in a temperature and light controlled room (22–24 °C, light on 0700–1900 h). During this period they were fed a pelleted stock chow (Type CE-2, Clea Japan, Tokyo, Japan). They were then divided into two groups (experiment 1) or four groups (experiment 2) with equal body weight (body weight 158 ± 2 g in experiment 1 and 86 ± 1 g in experiment 2). The control diet in experiment 1 was prepared according to the recommendations of the American Institute of Nutrition [17], and contained (by weight): casein, 20 %; corn oil, 5 %; vitamin mixture (AIN 76), 1 %; mineral mixture (AIN 76), 3.5 %; DL-methionine, 0.3 %; choline bitartrate, 0.2 %; cellulose, 5 %; corn starch, 15 %; and sucrose to 100 %. The control diet in experiment 2 was the same as in experiment 1, except for dietary fat levels. In experiment 2, diets were prepared with either 5 % fat (lard 4 % and corn oil 1 %) or 15 % fat (lard 14 % and corn oil 1 %). The fat level in the latter diet was increased at the expense of sucrose. The experimental diet was prepared by adding MF at the 1 % level to the control diets at the expense of sucrose in both experiment 1 and experiment 2. Rats had free access to the diets and water for 2 weeks in experiment 1, and for a longer period of 8 weeks in experiment 2. Food intake and body weight were recorded every other day. In experiment 1, approximately half of the animals were subjected to the liver slice experiments (seven rats for control and eight rats for experimental groups) and the others to hepatocyte experiments (six rats each for control and experimental groups). In experiment 1, the animals were decapitated between 9:00 a.m. and 12:00 p.m., blood was collected, and serum was harvested after centrifugation at 4 °C. The livers were removed immediately, rinsed, dried on filter paper, and weighed. A portion of each liver was cut into small blocks (1.5 \times 1.5 \times 1 cm), sliced (0.5 mm thickness) using a tissue slicer, and immediately transferred to opaque flasks containing ice-cold and oxygenated Krebs–Ringer–Bicarbonate buffer (pH 7.4) and

[1(2)-¹⁴C] sodium acetate. Incubation was carried out for 2 h at 37 °C after flushing with a mixture of O₂:CO₂ (95:5, by vol), and was terminated by addition of 0.1 ml of acetic acid. In the hepatocyte experiments, the rats from control and experimental groups were anesthetized with pentobarbital sodium (64.8 mg/kg BW), and their livers were isolated by a two-step collagenase digestion method [18]. Briefly, anesthetized rats were cleaned and sanitized and placed inside a bio-safety cabinet. The hepatic portal vein was cannulated and the liver was perfused in situ with Krebs–Henseleit buffer (pH 7.4) using a peristaltic pump. A cut was made in the abdominal vena cava just above the level of the kidneys to have an outlet for the drainage of the perfusate. The perfusion was continued until all the lobes of the liver were visibly cleared of blood and blanched. Then the abdominal vena cava was clamped and the thoracic vena cava was cannulated through right atrium and a collagenase solution (0.05 % w/v) in Krebs–Henseleit buffer (pH 7.4) was re-circulated for 10–20 min until the liver lobes gets mildly dispersed. Liver lobes were collected into a sterile beaker with the buffer and sliced. The undispersed parts were filtered out using sterile gauze and the cells were collected into a centrifuge tube. Hepatocytes thus obtained were washed in Hanks buffer and re-suspended in Krebs–Henseleit buffer (pH 7.4) with 10 mM glucose and 2 % bovine serum albumin (fatty acid free, Wako Chemical Co., Japan). All incubations were performed in duplicate for 1 h at 37 °C, in the presence of either [1(2)-¹⁴C] sodium acetate or [1-¹⁴C] oleic acid, under CO₂:O₂ (5:95, by vol) gas. After incubation, cells and medium were separated by low-speed centrifugation (600 rpm for 1 min), followed by washing three times with PBS; cells were then homogenized with a Teflon homogenizer and stored at –80 °C until further analysis for radioactivity in the lipid fractions. Cell viability, as determined by the trypan blue exclusion test, always exceeded 85 %.

All experimental protocols and procedures were approved by the Animal Care and Use Committee of the University of Miyazaki, Japan.

The lipids in the liver and serum were extracted and purified according to the method of Folch et al. [19]. TAG, cholesterol, and phospholipid contents in the lipid extract were measured chemically [10–12]. In the liver slice and hepatocyte experiments, lipids were also extracted by the method of Folch et al. [19] and various lipid fractions were separated by thin layer chromatography on Silica Gel 60G, with a solvent mixture of *n*-hexane/diethyl ether/acetic acid (80:20:1, by vol). The bands corresponding to cholesterol ester, TAG, free fatty acid, partial glycerides (mono- and di-glycerides), and phospholipid were identified with iodine vapor and were scraped into counting vials containing a toluene-based scintillation cocktail. Radioactivity derived from [1(2)-¹⁴C] acetate and [1-¹⁴C] oleic acid in

these lipid fractions was measured in a Wallac 1409 DSA liquid scintillation counter (Wallac Co., The Netherlands). For [1-¹⁴C] acetate incorporation into total fatty acid and digitonin precipitable sterol (DPS), the lipid extract was saponified in methanolic KOH at 75 °C for 30 min, and nonsaponifiable matter was extracted with *n*-hexane three times. After removal of the nonsaponifiable matter, the extracts were acidified with concentrated HCl, and the fatty acids were extracted with *n*-hexane three times. DPS were isolated and purified according to the procedure described previously [20, 21]. Radioactivities for total fatty acid were counted in a toluene-based scintillation cocktail and those for DPS were counted in 1 ml of methanol and Insta Gel.

Feces collected for 2 days before the end of experiment 2 were lyophilized and analyzed for neutral and acidic steroids, as described in detail previously [22].

In experiment 2, the mRNA expression level of liver carnitine palmitoyltransferase I (CPT I) was also measured. Total RNA was extracted from 300 mg of liver, using a TRI ZOL Reagent (Invitrogen, Tokyo, Japan). Extracted RNA was treated with DNase to remove any genomic DNA (gDNA) TaqMan[®] Gene Expression Assays (Applied Biosystems, Tokyo, Japan), Assays-on-Demand[™], Gene Expression Products (Rn00580702_m1 for CPT I, Hs99999901_s1 for 18S RNA; Applied Biosystems, Tokyo, Japan) were used for quantitative real-time RT-PCR analysis of CPT I and 18S RNA expression in the liver. The manufacturer specifies that the assay probes spans an exon junction in the case of CPT I primers and that the assay will not detect gDNA in the case of 18S RNA primers. The amplification was performed with a real-time PCR system (ABI Prism 7000 Sequence Detection System, Applied Biosystems). Results were expressed as a relative value after normalization to 18S RNA expression.

Data were analyzed by Student's *t* test in experiment 1, and by one-way analysis of variance, followed by multiple comparisons with Tukey–Kramer's test (StatView software, Sas Institute, USA) in experiment 2. The statistical significance of the difference of the means in these two experiments was evaluated at the level of *p* < 0.05. In addition, the significance of the interaction of the two treatments was also analyzed by two-factor ANOVA (StatView software, Sas Institute, USA).

Results

Effects of Dietary Bitter Melon Methanol Fraction (MF) on Lipid Metabolism After 2 Weeks of Administration (Experiment I)

Effects of dietary MF, fed for 2 weeks, on growth parameters and the concentration of serum and liver lipids are

Table 1 Effects of *Momordica charantia* methanol fraction (MF) on growth and lipid parameters

	Control (7)	1 % MF (8)
Growth parameter		
Initial body weight (g)	158 ± 2	158 ± 3
Final body weight (g)	275 ± 5	271 ± 4
Food intake (g/day)	21.4 ± 0.5	21.1 ± 0.5
Liver weight (g/100 g BW)	5.76 ± 0.17	5.46 ± 0.09
Serum lipids (mg/dL)		
Triacylglycerol	257 ± 27	260 ± 30
Cholesterol		
Total	86.8 ± 4.1	95.7 ± 4.6
Free	21.0 ± 2.0	22.0 ± 2.3
Ester (%)	75.8 ± 1.9	77.0 ± 2.0
HDL	44.6 ± 2.1	48.0 ± 1.7
Phospholipids	218 ± 12	218 ± 7
Liver lipids (mg/g liver)		
Triglyceride	52.2 ± 6.3	23.8 ± 2.8*
Cholesterol		
Total	2.80 ± 0.11	2.11 ± 0.07*
Free	1.39 ± 0.07	1.35 ± 0.04
Ester (%)	50.2 ± 2.3	35.4 ± 3.3*
Phospholipids	27.6 ± 1.5	29.5 ± 1.4

The values are given as means ± SE of seven to eight rats per group as indicated in parentheses. The rats were fed diets with and without MF for 2 weeks

* Significantly different from the control group at $p < 0.05$

summarized in Table 1. Although dietary MF had no effect on food intake and growth, relative liver weight tended to be lower in rats fed diets with MF than in those fed diets without MF. Effects of dietary MF on serum lipid parameters were marginal; however, dietary MF significantly decreased the concentration of hepatic TAG and total cholesterol by 54.4 and 24.6 %, respectively. The percentage of cholesterol ester in the liver was significantly lowered in rats fed diets with MF as compared to those fed diets without MF. However, the free cholesterol level remained unchanged between the groups, indicating that the marked reduction in hepatic total cholesterol in rats fed diets with MF is due to decreased cholesterol ester. Liver phospholipid concentration was comparable between the groups.

Since hepatic lipid synthesis is one of the regulatory factors responsible for determining the lipid concentration, we first estimated hepatic lipid synthesis by measuring the rate of incorporation of radiolabelled acetate and oleic acid into lipids of both liver slices and hepatocytes prepared from rats fed diets supplemented with and without MF. As shown in Table 2, in the liver slice experiment, the incorporation of [1(2)-¹⁴C] acetate into TAG was 53.1 % lower in rats fed diets with MF compared to those fed diets

Table 2 Effects of *Momordica charantia* methanol fraction (MF) on incorporation of [1(2)-¹⁴C] into lipids of liver slices

	Control (7)	1 % MF (8)
Incorporation of [1(2)- ¹⁴ C]acetate into lipids (liver slice experiment) ^a		
Triacylglycerol	5.14 ± 0.92	2.41 ± 0.81*
Partial glycerides	0.97 ± 0.10	0.89 ± 0.24
Cholesterol	1.56 ± 0.21	1.82 ± 0.22
Cholesterol ester	0.37 ± 0.02	0.38 ± 0.02
Phospholipids	4.49 ± 0.31	6.03 ± 0.61*
Free fatty acid	6.97 ± 0.93	10.1 ± 1.63

The rats were fed diets with and without MF for 2 weeks

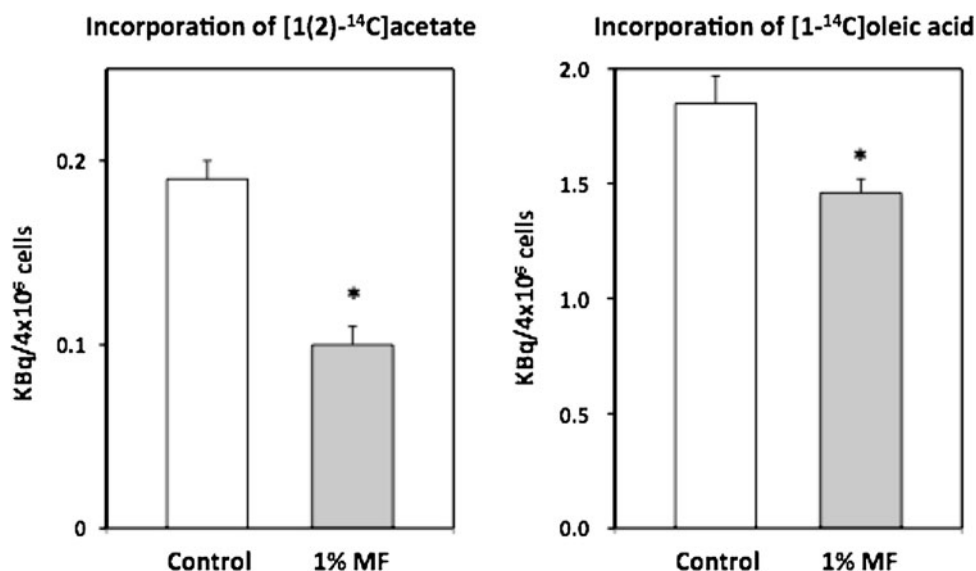
* Significantly different compared to the control group at $p < 0.05$

^a Incorporation of radiolabelled acetate into lipid fractions of liver slices are expressed as kBq/g liver. The values are given as means ± SE of seven rats for control and eight rats for MF group

without MF. The extent of reduction in its incorporation was similar to that of the reduction in liver TAG concentration (54 % reduction in TAG concentration and 53 % reduction in incorporation of [1(2)-¹⁴C] acetate into TAG). On the other hand, incorporation of [1(2)-¹⁴C] acetate into free- and esterified-cholesterol was comparable between the groups, while incorporation of labeled acetate into phospholipids was significantly elevated (1.4-fold) following feeding of MF. Incorporation into free fatty acid fraction tended to be higher in rats fed diets with MF than in those fed diets without MF, but the difference was not significant.

In the hepatocyte experiment, incorporation of [1(2)-¹⁴C] acetate into TAG was 47.3 % lower in liver cells prepared from rats fed diets with MF as compared to those without MF (Fig. 1), while incorporation into both free and esterified cholesterol was comparable between the groups (data not shown). Any effect of dietary MF on the incorporation of [1(2)-¹⁴C] acetate into free fatty acid fraction was also not apparent (data not shown). In this experiment, we further examined the effects of dietary MF on the metabolism of exogenous free fatty acid by using hepatocytes; for this, we used [1-¹⁴C] oleic acid as an exogenous substrate complexed with fatty acid free albumin, and administered to the cells prepared from livers of rats fed with and without dietary MF; dietary MF caused a significantly lowered incorporation of [1-¹⁴C] oleate into TAG fraction (21 % decrease relative to rats fed an MF-free diet) (Fig. 1). On the other hand, no significant differences were observed in incorporation into phospholipids and cholesterol esters between the two groups (data not shown). These results suggest that dietary MF appears to have a potent and specific inhibitory effect on the esterification step of TAG synthesis, but not on de novo synthesis of fatty acids.

Fig. 1 Effect of bitter melon methanol extract (MF) on hepatic TAG synthesis (hepatocyte experiment). Hepatocytes from livers of rats fed diets with and without MF for 2 weeks were incubated in the presence of either [1(2)-¹⁴C] sodium acetate or [1-¹⁴C] oleic acid for 1 h. The values are given as means ± SE of 6 rats per group. *Significantly different from the control group at $p < 0.05$



Effects of Dietary MF on Lipid Metabolism After 8 Weeks of Administration (Experiment 2)

It is known that the level and type of dietary fats are one of the modifying factors for the concentration of serum and liver lipids; in general, high fat diet compared to low fat causes elevated serum and liver lipids. In experiment 2, we examined the effects of dietary MF in rats fed on different fat levels (5 and 15 % fat level) and for prolonged feeding period of 8 weeks. Food intake was comparable in the four groups of rats, as shown in Table 3. However, the final body weight was significantly greater in rats fed high-fat diets than in those fed low-fat diets. Supplementation of MF in the high fat diet, but not in the low fat diet, tended to reduce weight gain. Relative liver weight tended to be lower in rats fed diets with MF, whether rats were fed the high-fat or the low-fat diet. Perirenal and epididymal adipose tissues were significantly heavier in rats fed high-fat diets than in those fed low-fat diets, although supplementation of MF did not influence these parameters. Serum TAG levels were significantly elevated in rats fed high-fat diets compared with those fed low fat diets. Dietary MF in combination with the high-fat diet, but not with the low-fat diet, reduced serum TAG. Neither the concentrations of total- and HDL-cholesterol nor that of phospholipids were influenced by the dietary fat levels or MF supplementation.

Hepatic TAG concentrations were elevated by 1.5-fold in rats fed the high-fat diet compared to those fed the low-fat diet, while supplementation of MF in the low and high-fat diet groups caused reductions in TAG concentration of 44.7 and 52.3 % respectively. The high-fat diet was also associated with an increased concentration of total cholesterol (1.4-fold elevation). Supplementation of MF in the low- and high-fat diets caused reductions of 19.0 and

40.6 %, respectively, in this lipid molecule. The reduction in the concentration of total cholesterol was due to decreases in the concentrations of both free and esterified cholesterol. Phospholipid concentrations were comparable among rats fed high-fat and low-fat diets containing MF and those fed diets without MF.

Fecal excretion of neutral and acidic steroids is shown in Table 4. Fecal weights tended to be heavier in rats fed high-fat diets than in those fed low-fat diets, a further increase in fecal weights was noted in MF-supplemented rats. Although the excretion of bile acids into feces was not different among the groups, that of neutral steroids (coprostanol and cholesterol) was significantly increased in rats fed diets supplemented with MF. The extent of the increase was greater in the high-fat diet group (1.8-fold increase in low-fat diet and 2.3-fold increase in high-fat diet groups, respectively).

In experiment 2, as in experiment 1, we estimated the hepatic lipid synthesis by measuring the incorporation of [1(2)-¹⁴C] acetate into various lipid fractions. Incorporation of labeled acetate into all lipid fractions in the liver was significantly lower in liver slices prepared from rats fed high-fat diets compared to those fed low-fat diets (Table 5). The extent of this reduction was 65.3 % for TAG and 48.8 % for phospholipids. Supplementation of MF in the low fat, but not the high fat diet group resulted in a typical profile of [1(2)-¹⁴C] acetate incorporation into various lipid fractions. Thus, dietary MF caused a significant reduction (45.7 %) in incorporation of labeled acetate into the TAG fraction but incorporation into other fractions (partial glycerides, free- and esterified-cholesterol, and phospholipids) was not affected. In addition, there was no change of incorporation into the free fatty acid fraction between the control and MF groups. To

Table 3 Effect of dietary *Momordica charantia* methanol fraction (MF) on growth and serum lipid parameters in rats

	Low fat		High fat		ANOVA		
	Control (7)	MF (7)	Control (8)	MF (8)	Fat	MF	Interaction
Growth parameter							
Initial body weight (g)	85.4 ± 1.91	85.3 ± 1.61	86.1 ± 1.63	86.2 ± 1.74	NS	NS	NS
Final body weight (g)	483 ± 24.1 ^a	506 ± 9.24 ^{a,b}	558 ± 17.3 ^b	523 ± 12.1 ^{a,b}	<i>p</i> < 0.05	NS	NS
Food intake (g/day)	25.5 ± 1.21	25.3 ± 0.43	25.0 ± 1.22	23.7 ± 0.71	NS	NS	NS
Liver weight (g/100 g BW)	4.24 ± 0.14	4.11 ± 0.09	4.25 ± 0.16	4.04 ± 0.14	NS	NS	NS
Perirenal adipose (g/100 g BW)	2.50 ± 0.42	2.97 ± 0.22	3.51 ± 0.17	3.41 ± 0.34	<i>p</i> < 0.05	NS	NS
Testicular adipose (g/100 g BW)	1.92 ± 0.25	2.02 ± 0.11	2.38 ± 0.11	2.41 ± 0.16	<i>p</i> < 0.05	NS	NS
Serum lipids (mg/dL)							
Triacylglycerols	185 ± 28 ^a	297 ± 35 ^{a,b}	385 ± 61 ^b	287 ± 30 ^{a,b}	<i>p</i> < 0.05	NS	<i>p</i> < 0.05
Cholesterol							
Total	120 ± 13.2	110 ± 11.4	101 ± 6.4	100 ± 6.1	NS	NS	NS
HDL	69.0 ± 5.92	71.0 ± 4.41	71.0 ± 3.52	72.3 ± 5.61	NS	NS	NS
Phospholipids	233 ± 15.2	248 ± 13.1	226 ± 8.45	243 ± 12.1	NS	NS	NS

The rats were fed diets with and without MF for 8 weeks and the values are mean ± SE of seven to eight rats per group as indicated in parentheses

^{a,b} Values not sharing common superscript letters are significantly different at *p* < 0.05

Table 4 Effect of *Momordica charantia* methanol fraction (MF) on liver lipids and fecal steroid excretion in rats

	Low fat		High fat		ANOVA		
	Control (7)	MF (7)	Control (8)	MF (8)	Fat	MF	Interaction
Liver lipids (mg/g)							
Triacylglycerols	60.9 ± 14.1 ^{a,b}	33.7 ± 3.04 ^a	93.2 ± 19.2 ^b	44.5 ± 5.41 ^a	NS	<i>p</i> < 0.05	NS
Cholesterol							
Total	3.36 ± 0.46 ^{a,b}	2.72 ± 0.06 ^a	4.61 ± 0.63 ^b	2.74 ± 0.26 ^a	NS	<i>p</i> < 0.05	NS
Free	1.85 ± 0.23 ^a	1.61 ± 0.10 ^{a,b}	1.70 ± 0.14 ^{a,b}	1.29 ± 0.07 ^b	NS	<i>p</i> < 0.05	NS
Ester (%)	41.8 ± 6.61	40.6 ± 3.93	60.0 ± 4.53	49.2 ± 6.71	<i>p</i> < 0.05	NS	NS
Phospholipids	27.9 ± 1.12	28.1 ± 1.11	27.8 ± 0.62	29.7 ± 0.64	NS	NS	NS
Fecal steroid excretion							
Fecal weight (g/2d)	4.29 ± 0.17 ^a	4.67 ± 0.28 ^{a,b}	4.76 ± 0.23 ^{a,b}	5.26 ± 0.19 ^b	<i>p</i> < 0.05	NS(0.051)	NS
Steroid excretion (mg/2d)							
Bile acids	7.67 ± 0.55	7.27 ± 1.18	8.93 ± 1.28	8.31 ± 1.61	NS	NS	NS
Neutral steroids	13.4 ± 1.53 ^a	24.4 ± 2.01 ^b	14.2 ± 1.83 ^a	32.5 ± 2.31 ^c	<i>p</i> < 0.05	<i>p</i> < 0.0001	NS

The rats were fed diets with and without MF for 8 weeks and the values are mean ± SE of seven to eight rats per group as indicated in parentheses

^{a,b,c} Values not sharing common superscript letters are significantly different at *p* < 0.05

investigate this unexpected finding, we estimated de novo synthesis of fatty acid and cholesterol in liver slices by measuring incorporation of [1(2)-¹⁴C] acetate into total free fatty acid and DPS. Increased dietary fat levels significantly lowered the incorporation of radiolabelled acetate into the total fatty acids and DPS, while there were no significant differences in the incorporation of acetate into total fatty acids due to dietary MF (23.2 ± 3.88 kBq/g for low-fat without MF vs. 21.7 ± 1.53 kBq/g for low-fat

with MF, 10.6 ± 1.73 kBq/g for high-fat without MF vs. 15.1 ± 1.45 for high-fat with MF) and DPS (0.17 ± 0.02 kBq/g for low fat without MF vs. 0.23 ± 0.03 kBq/g for low fat with MF, and 0.05 ± 0.01 kBq/g for high fat without MF vs. 0.10 ± 0.02 kBq/g for high fat with MF). We also checked the expression of CPT I mRNA and found enhanced mRNA abundance following feeding of MF particularly in the low-fat group (data not shown).

Table 5 Effect of dietary *Momordica charantia* methanol fraction (MF) on incorporation of [1(2)-¹⁴C] acetate into liver lipids in rats

	Low fat		High fat		ANOVA		
	Control (7)	MF (7)	Control (8)	MF (8)	Fat (<i>p</i> value)	MF	Interaction
Incorporation of [1(2)- ¹⁴ C] acetate into lipids in liver slices (KBq/g liver)							
Triglycerides	5.91 ± 1.31 ^a	3.21 ± 0.42 ^b	2.05 ± 0.33 ^b	2.45 ± 0.43 ^b	<0.05	NS	<i>p</i> < 0.05
Partial glycerides	1.08 ± 0.18 ^a	1.14 ± 0.09 ^a	0.45 ± 0.08 ^b	0.69 ± 0.14 ^{a,b}	<0.05	NS	NS
Free cholesterol	0.15 ± 0.03 ^{a,b}	0.26 ± 0.05 ^a	0.09 ± 0.02 ^b	0.15 ± 0.03 ^{a,b}	<0.05	<i>p</i> < 0.05	NS
Cholesterol esters	0.23 ± 0.03 ^b	0.22 ± 0.02 ^a	0.13 ± 0.02 ^b	0.15 ± 0.01 ^{a,b}	<0.05	NS	NS
Phospholipids	6.61 ± 0.98 ^a	7.08 ± 0.48 ^a	3.38 ± 0.51 ^b	4.65 ± 0.78 ^{a,b}	<0.05	NS	NS
Free fatty acid	5.95 ± 0.92 ^a	7.03 ± 0.48 ^a	2.81 ± 0.57 ^b	4.71 ± 0.95 ^{a,b}	<0.05	NS	NS

The rats were fed diets with and without MF for 8 weeks and the values are means ± SE of seven to eight rats as indicated in parentheses. Incorporation of radiolabelled acetate into lipid fractions are expressed as kBq/g liver

^{a,b} Values not sharing common superscript letters in the same row are significantly different at *p* < 0.05

Discussion

In the present studies, we show that the methanol fraction (MF) prepared from bitter melon (Koimidori variety), at a 1.0 % dietary level, has potent liver TAG- and cholesterol-lowering activity in rats fed diets containing low (5 %) and high (15 %) fat. In a series of experiments with rats fed diets containing 5 % fat supplemented with or without cholesterol, we had previously reported that feeding of freeze-dried powder prepared from various varieties of bitter melon, especially that from Koimidori, at a 1.0 % dietary level, exhibits potent liver TAG- and cholesterol-lowering potentials, and that its major active principle(s) was localized almost exclusively in the fraction extracted by methanol from Koimidori freeze-dried powder [10, 11]. On the other hand, Ahmed et al. studied the effects of long term feeding (10 wk) of bitter melon juice on plasma and liver lipid profiles in normal and streptozotocin (STZ)-induced Type I diabetic rats, and found that this dietary ingredient exhibits a potent hypolipidemic effects in the STZ-induced diabetic rat [9]. In addition, they also observed the liver TAG-lowering effects of bitter melon juice in non-diabetic normal rat, but not in diabetic rat [9]. These results suggest that bitter melon and/or its extract may be effective in preventing fatty liver and hyperlipidemia caused by high-cholesterol and high-fat diets, as well as the hyperlipidemia induced by diabetes mellitus.

As most studies investigating the biological activity of bitter melon are focused on effects pertaining to plasma glucose and diabetes, or on the mechanism of its hypoglycemic activity [23–25], information regarding the mechanism(s) of its action on serum and/or hepatic lipids is sparse. The present studies therefore focused on understanding the mechanism(s) responsible for the dietary MF-dependent reduction in the concentration of liver TAG and cholesterol. The liver is a major organ regulating the concentrations of serum and/or liver TAG and cholesterol,

through various synthetic and degradative processes (e.g., fatty acid synthesis and oxidation for determining the TAG level, and cholesterologenesis and its elimination into the feces as neutral and acidic steroids for cholesterol level). In the present studies, we calculated the de novo synthesis of lipids by measuring the rate of incorporation of radiolabelled acetate into lipids in liver slices and hepatocytes prepared from rats fed diets with and without MF. In addition, we calculated TAG synthesis by measuring the rate of esterification of exogenous [1-¹⁴C] oleate into the TAG fraction in hepatocytes prepared from these same animals. The appearance of radioactive carbon in hepatic lipids reflects the activation of acetate added to the liver slices and/or hepatocytes to its coenzyme A ester and their subsequent incorporation into glycerolipids and cholesterol. Thus, measuring the rate of incorporation of radioactive acetate into hepatic lipids in the liver slices and hepatocytes is an index of hepatic lipid synthesis and yields valuable information regarding this process, in spite of some limitations such as dilution [26, 27]. In addition, incorporation of [1(2)-¹⁴C] acetate and [1-¹⁴C] oleic acid into hepatic lipids into the liver slices and hepatocytes prepared from rats fed diets with and without MF indicates that these in vitro models of the liver function adequately with respect to lipid synthesis. As shown in Table 1, a marked decrease in TAG concentration in the livers of rats fed diets with MF was concomitantly associated with a decreased incorporation of [1(2)-¹⁴C] acetate into this lipid molecule; the extent of reduction was similar. Further, in experiment 2, this response was reproduced in the liver slices of rats fed, for a longer period of 8 weeks, diets with MF in combination with a low, but not with a high, fat content. On the other hand, incorporation of [1(2)-¹⁴C] acetate into free fatty acid fraction (Tables 2, 4) as well as that into the total fatty acids was not different between the liver slices prepared from rats fed diets with and without MF, suggesting that MF may not be an inhibitor of de novo

fatty acid synthesis. On the other hand, the decrease in the esterification process, as estimated by incorporation of labeled oleate into TAG in hepatocytes, suggested that MF exerts an inhibitory effect on TAG synthesis, rather than fatty acid synthesis. There is no data regarding the effect of bitter melon on fatty acid synthesis, but a few studies have been reported for TAG synthesis. For example, Nerurkar et al. recently reported that HepG2 cells treated with bitter melon juice exhibited reduced cellular TAG synthesis and secretion of TAG into the medium [13, 14]. They also observed that in HepG2 cells treated with bitter melon juice, mRNA expression of MTP was inhibited. MTP plays a pivotal role in the assembly and secretion of apoB-containing lipoproteins, and induces sterol regulatory element-binding protein-1c, which is one of the nuclear transcription factors responsible for modulating lipid and lipoprotein metabolism. The results of these in vitro studies further confirmed in vivo experiments showing that this juice lowers plasma apoB-100 and B-48 in C57BL/6 mice fed high-fat diets [14]. Recently, Chao and Huang observed that bitter melon extract activates PPAR α : an important transcription factor involved in lipid and glucose homeostasis, and upregulates the expression of the acyl CoA oxidase gene in rat hepatoma cells H4IIEC3 [15]. Considering these previous observations in the context of our present results, the mechanism responsible for the observed reduction in the concentration of hepatic TAG by dietary MF is likely to be reduced synthesis of TAG and enhanced fatty acid oxidation.

In these studies, we also measured mRNA expression of carnitine palmitoyltransferase I, which is the rate-limiting enzyme for hepatic mitochondrial fatty acid oxidation. We found, for the first time, that expression of CPT I is enhanced following feeding of MF, particularly in combination with a low fat diet. These results suggest that the diminished concentration of hepatic TAG is directly related to fatty acid oxidation, since an inverse relationship between hepatic TAG content and fatty acid oxidation has been shown [21, 22, 28]. Thus, the mechanism(s) responsible for the observed reduction in the concentration of hepatic TAG may, in part, be attributed to the concomitant elevation of CPT I expression. At present, there has been no direct demonstration that increased enzyme activity accompanies this increase in expression; further studies are needed to determine enzyme activity in animals fed diets with and without MF.

The dietary MF-dependent reduction of hepatic total cholesterol was not accompanied by reduced cholesterol synthesis, as estimated by incorporation of [1(2)-¹⁴C] acetate into both free and esterified cholesterol. Only the reduction in the concentration of cholesterol ester is attributed to decreased synthesis. As shown in Table 4, dietary MF increased fecal excretion of neutral steroids, but

not of acidic steroids, in rats fed low- and high-fat diets, suggesting that MF may influence cholesterol metabolism at the initial stage by inhibiting the absorption of endogenous and exogenous cholesterol. Bitter melon has been reported to contain saponin as an active component [29, 30]; saponin is a known inhibitor of cholesterol absorption in the intestine [31, 32], and thus increases fecal excretion of neutral steroids. Thus, the MF-dependent reduction in the concentration of liver cholesterol may be a consequence of increased fecal excretion of neutral steroids, rather than of altered cholesterologenesis, although further studies are required to elucidate the mechanism.

In summary, bitter melon has active components which may be able to ameliorate the severity of lipid disorders such as hyperlipidemia and fatty liver. The mechanism responsible for the action of bitter melon extracts such as MF is probably the reduced synthesis of liver TAG with a concomitant elevation of fatty acid oxidation. On the other hand, the MF-dependent reduction of liver cholesterol is due to an increase in fecal excretion of neutral sterols. Further studies aimed at characterization of the active component in MF and the precise mechanism(s) responsible for the observed reductions in the liver TAG and cholesterol should be carried out, and this work is in progress in our laboratory.

Acknowledgments G. V. K. Senanayake would like to acknowledge and thank the Japanese Government and the University of Miyazaki for the provision of a Monbusho scholarship grant. The authors wish to thank Mitsuru Maruyama for her excellent technical assistance. We also thank Dr. Melissa Clark in the department of Comparative Biosciences, College of Veterinary Medicine, University of Illinois, Urbana-Champaign, IL, USA, for her valuable comments and for revision of the English in the manuscript.

Conflict of interest The authors declare that there is no conflicts of interest.

References

1. Meir P, Yaniv Z (1985) An in vitro study on the effect of *Momordica charantia* on glucose uptake and glucose metabolism in rats. *Planta Med* 51:12–16
2. Raman A, Lau C (1996) Anti-diabetic properties and phytochemistry of *Momordica charantia* L. (Cucurbitaceae). *Phytomed* 2:349–362
3. Platel K, Srinivasan K (1997) Plant foods in the management of diabetes mellitus: vegetables as potential hypoglycemic agents. *Nahrung* 41:68–74
4. Sitasawad SL, Shewade Y, Bhonde R (2000) Role of bittergourd fruit juice in STZ-induced diabetic state in vivo and in vitro. *J Ethnopharmacol* 73:71–79
5. McCarty MF (2004) Does bitter melon contain an activator of AMP-activated kinase? *Med Hypotheses* 63:340–343
6. Grover JK, Yadav SP (2004) Pharmacological actions and potential uses of *Momordica charantia*: a review. *J Ethnopharmacol* 93:123–132

7. Krawinkel MB, Keding GB (2006) Bitter gourd (*Momordica charantia*): a dietary approach to hyperglycemia. *Nutr Rev* 64:331–337
8. Yin JY, Zhang H, Ye J (2008) Traditional Chinese medicine in treatment of metabolic syndrome. *Endo Metab Immune Disord Drug Targ* 8:99–111
9. Ahmed I, Lakhani MS, Gillett M, John A, Raza H (2001) Hypotriglyceridemic and hypocholesterolemic effects of anti-diabetic *Momordica charantia* (karela) fruit extract in streptozotocin-induced diabetic rats. *Diabetes Res Clin Pract* 51:155–161
10. Jayasooriya AP, Sakono M, Yukizaki C, Kawano M, Yamamoto K, Fukuda N (2000) Effects of *Momordica charantia* powder on serum glucose levels and various lipid parameters in rats fed with cholesterol-free and cholesterol-enriched diets. *J Ethnopharmacol* 72:331–336
11. Senanayake GVK, Maruyama M, Shibuya K, Sakono M, Fukuda N, Morishita T, Yukizaki C, Kawano M, Ohta H (2004) The effect of bitter melon (*Momordica charantia*) on serum and liver triglyceride levels in rats. *J Ethnopharmacol* 91:257–262
12. Senanayake GVK, Maruyama M, Sakono M, Fukuda N, Morishita T, Yukizaki C, Kawano M, Ohta H (2004) The effects of bitter melon (*Momordica charantia*) extracts on serum and liver lipid parameters in hamsters fed cholesterol-free and cholesterol-enriched diets. *J Nutr Sic Vitaminol* 50:253–257
13. Nerurkar PV, Pearson L, Efrid JT, Adeli K, Therault AG, Nerurkar VR (2005) Microsomal triglyceride transfer protein gene expression and apo B secretion are inhibited by bitter melon in HepG2 cells. *J Nutr* 135:702–705
14. Nerurkar PV, Lee YK, Motosue M, Adeli K, Nerurkar VR (2008) *Momordica charantia* (bitter melon) reduces plasma apolipoprotein B-100 and increases hepatic insulin receptor substrate and phosphoinositide-3 kinase interactions. *Br J Nutr* 100:751–759
15. Chao C-Y, Huang C-J (2003) Bitter gourd (*Momordica charantia*) extract activates peroxisome proliferator-activated receptors and upregulates the expression of the acyl CoA oxidase gene in H4IIEC3 hepatoma cells. *J Biomed Sci* 10:782–791
16. Oishi Y, Sakamoto T, Udagawa H, Taniguchi H, Kobayashi-Hattori K, Ozawa Y, Takita T (2007) Inhibition of increases in blood glucose and serum neutral fat by *Momordica charantia* saponin fraction. *Biosci Biotechnol Biochem* 71:735–740
17. American Institute of Nutrition (1977) Report of the American Institute of Nutrition ad hoc committee on standards for nutritional studies. *J Nutr* 107:1340–1348
18. Seglen PO (1973) Preparation of rat liver cells. III. Enzymatic requirements for tissue dispersion. *Exp Cell Res* 82:391–398
19. Folch J, Lees M, Sloane-Stanley GH (1957) A simple method for the isolation and purification of total lipids from animal tissues. *J Biol Chem* 226:497–509
20. Fukuda N, Azain MJ, Ontko JA (1982) Altered hepatic metabolism of free fatty acids underlying hypersecretion of very low density lipoproteins in the genetically obese Zucker rat. *J Biol Chem* 257:14066–14072
21. Fukuda N, Ontko JA (1984) Interactions between fatty acid synthesis, oxidation, and esterification in the reduction of triglyceride-rich lipoproteins by the liver. *J Lipid Res* 25:831–842
22. Fukuda N, Machida M, Oku H, Chinen I (1989) Hypocholesterolemic activity of bagasse alkaline extract in rats fed a high cholesterol diet. *Agric Biol Chem* 53:3097–3098
23. Chen Q, Chan LLY, Li ETS (2003) Bitter melon (*Momordica charantia*) reduces adiposity, lower serum insulin and normalizes glucose tolerance in rats fed a high fat diet. *J Nutr* 133:1088–1093
24. Shih C-C, Lin C-H, Wu J-B (2009) *Momordica charantia* extract on insulin resistance and the skeletal muscle GLUT4 protein in fructose-fed rats. *J Ethnopharmacol* 123:82–90
25. Fuangchan A, Sonthisombat P, Seubnukarn T et al (2011) Hypoglycemic effect of bitter melon compared with metformin in newly diagnosed type 2 diabetes patients. *J Ethnopharmacol* 134:422–428
26. Dietschy JM, McGarry JD (1974) Limitations of acetate as a substrate for measuring cholesterol synthesis in liver. *J Biol Chem* 249:52–58
27. Fears R, Morgan B (1976) Studies on the response of cholesterol biogenesis to feeding in rats. Evidence against the existence of diurnal rhythms. *Biochem J* 158:53–60
28. Fukuda N, Hidaka T, Toda T, Sugano M (1990) Altered hepatic metabolism of free fatty acid in rats fed a threonine-imbalanced diet. *J Nutr Sci Vitaminol* 36:467–474
29. Ng TG, Wong CM, Li WW, Teubg HW (1986) A steryl glycoside fraction from *Momordica charantia* seeds with an inhibitory action on lipid metabolism in vitro. *Biochem Cell Biol* 64:766–771
30. Matsuda H, Shimoda H, Uemura T, Yoshikawa M (1999) Preventive effect of sesquiterpenes from bay leaf on blood ethanol elevation in ethanol-loaded rat: structure requirement and suppression of gastric emptying. *Bioorg Med Chem Lett* 20:2647–2652
31. Malinaow MR, McLaughlin P, Papworth L, Stafford C, Kohler GO, Livingston AL, Cheeke PR (1977) Effect of alfalfa saponins on intestinal cholesterol absorption in rats. *Am J Clin Nutr* 30:2061–2067
32. Francis G, Kerem Z, Makkar HPS, Becker K (2002) The biological action of saponins in animal systems: a review. *Br J Nutr* 88:587–605

Influence of Maternal Diet During Early Pregnancy on the Fatty Acid Profile in the Fetus at Late Pregnancy in Rats

Flavia Spreafico Fernandes · Maria das Graças Tavares do Carmo · Emilio Herrera

Received: 19 September 2011 / Accepted: 6 February 2012 / Published online: 26 February 2012
© AOCS 2012

Abstract The aim of the study was to determine the effects of different dietary fatty acids during the first half of pregnancy on the fatty acid composition of maternal adipose tissue and of maternal and fetal plasma at mid- and late-pregnancy. Pregnant rats received soybean-, olive-, fish-, linseed- or palm-oil diets from conception to day 12 of gestation. Virgin rats receiving the same treatments were studied in parallel. At day 12, some rats were sacrificed and others were returned to the standard diet and studied at day 20. At day 12, the concentrations of most fatty acids in plasma reflected the dietary composition and individual fatty acids in lumbar adipose tissue of pregnant rats correlated with those in the diet. At day 20, the plasma concentration of each fatty acid was higher in pregnant than in both virgin rats and day-12 pregnant rats. The composition in 20-day pregnant (but not in virgin) rats resembled the diet consumed during the first 12 days. Fatty acid concentration in fetal plasma was also influenced by the maternal diet during the first 12 days of pregnancy, and long-chain polyunsaturated fatty acid (LC-PUFA) concentrations correlated with those in the mothers. In conclusion, during the first half of pregnancy maternal adipose tissue stores dietary-derived fatty acids, which are released into blood during late pregnancy enabling LC-PUFA to become available to the fetus.

Keywords Dietary fatty acids · Early pregnancy · Soybean oil · Olive oil · Fish oil · Linseed oil · Palm oil · Rat · Long-chain polyunsaturated fatty acids

Abbreviations

ALA	Alpha-linolenic acid, 18:3 (n-3)
ARA	Arachidonic acid, 20:4 (n-6)
DHA	Docosahexaenoic acid, 22:6 (n-3)
EFA	Essential fatty acid
EPA	Eicosapentaenoic acid, 20:5 (n-3)
F	Fish oil
L	Linseed oil
LA	Linoleic acid, 18:2 (n-6)
LC-PUFA	Long chain polyunsaturated fatty acid
LPL	Lipoprotein lipase
NEFA	Non-esterified fatty acid
O	Olive oil
P	Palm oil
S	Soybean oil
TAG	Triacylglycerol
VLDL	Very low density lipoprotein

Introduction

Evidence in humans suggests that fetal growth is most vulnerable to maternal dietary inadequacies during early pregnancy [1], and recently it has been shown that a high-quality diet in the first trimester of pregnancy is associated with an increase in birth weight and length [2]. In fact, maternal metabolism during pregnancy adapts to benefit the growth and development of the fetus and can be divided into two phases. During the initial two-thirds of gestation, when fetal energy demands are limited, maternal fat stores

Electronic supplementary material The online version of this article (doi:10.1007/s11745-012-3660-7) contains supplementary material, which is available to authorized users.

F. S. Fernandes · M. d. G. Tavares do Carmo
Institute of Nutrition Josué de Castro, Federal University
of Rio de Janeiro, Rio de Janeiro, Brazil

E. Herrera (✉)
Departamento de Biología, Universidad San Pablo CEU,
Madrid, Spain
e-mail: eherrera@ceu.es

increase, both in women [3, 4] and in experimental animals [5, 6]. This is attributable in part to maternal hyperphagia together with increased responsiveness of adipose tissue to insulin [7] and subsequent increased lipoprotein lipase (LPL, EC 3.1.1.34) activity in adipose tissue [8, 9]. During the latter stages of pregnancy this anabolic state switches to a state of catabolism with a marked increase in adipose tissue lipolytic activity and the development of maternal hyperlipidemia, coinciding with the phase of maximal fetal growth [10].

Essential fatty acids (EFA), linoleic acid (LA, 18:2 n-6) and α -linolenic acid (ALA, 18:3 n-3), and their long-chain polyunsaturated derivatives (LC-PUFA) like docosahexaenoic acid (DHA, 22:6 n-3) and arachidonic acid (ARA, 20:4 n-6) are essential for the formation of new tissues during fetal and postnatal development. During intrauterine life, EFA and LC-PUFA must be obtained from maternal circulation by passage across the placenta [11–13]. We previously compared pregnant sows given a dietary supplement of either fish oil (rich in DHA) or olive oil during the first half of gestation only. We found that the proportion of DHA in maternal plasma was higher in the fish oil-fed sows even during the first week postpartum, some 60 days after the supplement had been withdrawn [14].

In the present study, we investigated how differences in the fatty acid composition of diets with normal fat contents offered to rats during the first 12 days of pregnancy, could influence the fatty acid profile in maternal plasma and lumbar adipose tissue. After 12 days, all the animals received the standard pellet diet and we determined how this action modified maternal and fetal plasma fatty acid profiles at day 20 of pregnancy.

Materials and Methods

Animals, Diets, and Experimental Design

Female Sprague–Dawley rats were obtained from the animal quarters at the University San Pablo-CEU, Madrid. The experimental protocol was approved by the Animal Research Committee of the University San Pablo-CEU in Madrid, Spain. The rats were initially fed a standard non-purified diet (B&K Universal, Barcelona, Spain) and housed under controlled light and temperature conditions (12-hour light/dark cycle; 22 ± 1 °C). Rats were mated when they were 3 months old. On the day sperm cells appeared in vaginal smears (day 0 of pregnancy) they were randomly divided into 5 groups, the experimental diets of which contained a characteristic type of non-vitamin fat. In the “S” group, the diet contained 9% soybean oil (rich in LA); in the “O” group, the diet contained 9% olive oil (rich in oleic acid, 18:1 n-9); in the “F” group, the diet

contained 8% fish oil (rich in DHA and Eicosapentaenoic acid, EPA, 20:5 n-3) plus 1% sunflower oil (rich in LA); in the “L” group, the diet contained 8% linseed oil (rich in ALA) plus 1% sunflower oil; and in the “P”, diet contained 8% palm oil (rich in saturated fatty acids, 16:0) plus 1% soy oil. Sunflower oil or soy oil was added to some diets to ensure that the minimum requirement for EFA was met. The experimental design is summarized in Fig. 1. The experimental diets were isoenergetic (4.1 kcal/g) and their composition and the proportional fatty acid profiles are shown in Tables 1 and 2, respectively. In addition, values for the major FA in the diets, expressed as % of total energy intake, are also included in Table 2. The composition of each diet complied with the recommendations of the American Institute of Nutrition [15]. The diets were prepared at the beginning of the experiment and were kept at -20 °C in daily portions until use. Every 24 h fresh diet was provided and the daily food intake was estimated periodically. After 12 days on an experimental diet (day 12 of pregnancy), 6–8 rats from each group were sacrificed; the remaining rats were given the standard pellet diet until day 20, when they too were sacrificed. Rats were always housed in collective cages (3–4 per cage) and had free access to the assigned diet and tap water. Age-matched virgin female rats (V), subjected to the same dietary regimens as the pregnant rats, were studied in parallel. One further group of virgin female rats, that were age-matched to the pregnant rats at the onset of the experiment and that received only the standard pellet diet, was also studied and considered to be the basal group (V0). Rats were sacrificed by decapitation and trunk blood was collected into receptacles containing 1 g $\text{Na}_2\text{EDTA/L}$. The two uterine horns were immediately dissected and weighed with their contents to obtain the maternal weight free of conceptus.

EXPERIMENTAL PROTOCOL DESIGN

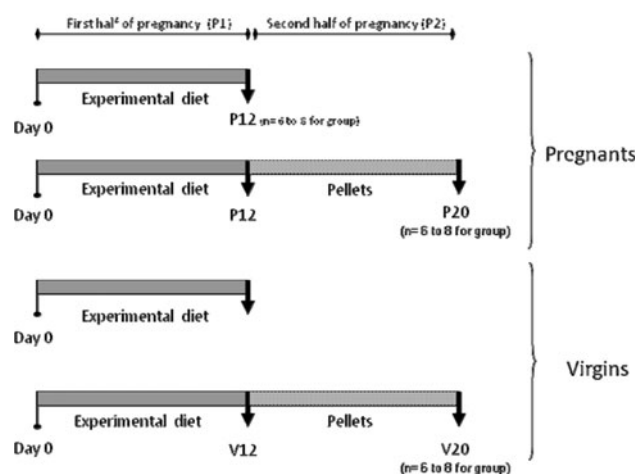


Fig. 1 Schematic experimental design of the study

Table 1 Composition of the diets (g/kg)

Constituents (g/kg of diet)	Soy oil diet	Olive oil diet	Fish oil diet	Linseed oil diet	Palm oil diet
Casein (vitamin free)	200	200	200	200	200
Cornstarch	397.4	397.4	397.4	397.4	397.4
Dextrinized cornstarch	132.0	132.0	132.0	132.0	132.0
Sucrose	80.0	80.0	80.0	80.0	80.0
Cellulose	50.0	50.0	50.0	50.0	50.0
Salt mix ^a	10.0	10.0	10.0	10.0	10.0
Vitamin mix ^b	35.0	35.0	35.0	35.0	35.0
β -Choline	2.5	2.5	2.5	2.5	2.5
Butylhydroquinone-BHT	0.01	0.01	0.01	0.01	0.01
Soy oil	90.0	–	–	–	10.0
Olive oil	–	90.0	–	–	–
Sunflower oil	–	–	10.0	10.0	–
Fish oil	–	–	80.0	–	–
Linseed oil	–	–	–	80.0	–
Palm oil	–	–	–	–	80.0

The experimental diets provided 405 kcal/100 g distributed between carbohydrates (59.7%), proteins (20.7%) and lipids (20%)

^a Salt mix (g/kg diet): copper sulfate 0.1; ammonium molybdate 0.026; sodium iodate 0.0003; potassium chromate 0.028; zinc sulfate 0.091; calcium hydrogen phosphate 0.145; ammonium ferrous sulfate 2.338; magnesium sulfate 3.37; manganese sulfate 1.125; sodium chloride 4; calcium carbonate 9.89; potassium dihydrogen phosphate 14.75

^b Vitamin mix (mg/kg diet): retinyl palmitate 2.4; cholecalciferol 0.025; menadione sodium bisulfite 0.8; biotin 0.22; cyanocobalamin 0.01; riboflavin 6.6; thiamin hydrochloride 6.6; α -tocopherol acetate 100

Lumbar adipose tissue was dissected, placed in liquid nitrogen, and after weighing, kept at -80°C until analysis. In 20-day pregnant rats, fetuses were weighed and decapitated, and the blood collected as indicated above. Fetal liver samples were dissected, immediately placed in liquid nitrogen then stored at -80°C until analysis. Samples from all of the fetuses of the same dam were pooled and processed in parallel to the samples of the adults. Plasma was separated from fresh blood by centrifugation at 1500g for 15 min at 4°C .

Processing of Samples

Plasma triacylglycerols (TAG) and non-esterified fatty acids (NEFA) were determined enzymatically using commercial kits (Spinreact Reactives, Spain and Wako Chemicals, Germany, respectively).

Nonadecenoic acid (19:1) (Sigma Chemical Co.) was added as the internal standard to fresh aliquots of each diet and of frozen plasma, lumbar adipose tissue and fetal liver, which were used for lipid extraction and purification [16]. The final lipid extract was evaporated to dryness under vacuum and the residue resuspended in methanol/toluene and subjected to methanolysis in the presence of acetyl chloride at 80°C for 2.5 h as previously described [17]. Fatty acid methyl esters were separated and quantified on a Perkin-Elmer gas chromatograph (Autosystem) with a

flame ionization detector and a 20 m Omegawax capillary column (internal diameter 0.25 mm). Nitrogen was used as carrier gas, and the fatty acid methyl esters were compared with purified standards (Sigma Chemical Co.). Quantification of the fatty acids in the sample was performed as a function of the corresponding peak areas compared to that of the internal standard. Coefficient of variation values expressed as percentages ranged between 0.0–6.0, giving a mean \pm ES value of $2.28 \pm 0.26\%$ for an arbitrary set of fatty acid analysis. To assess the fatty acid distribution of the different lipid classes (e.g., phospholipids, NEFA, TAG and esterified cholesterol), extracted lipids were separated by thin layer chromatography using Silicagel 60 F₂₅₄ plates (Merck, Darmstadt, Germany) with *n*-heptane/diisopropyl ether/acetic acid (70:30:1, by volume) as the solvent. The bands were visualized with 2',7'-dichlorofluorescein (Supelco, Bellafonte, PA) and eluted from the plate with methanol/toluene and subjected to methanolysis and fatty acid analysis as above.

Statistical Analysis

The values are quoted as mean \pm standard error of the mean (S.E.). Statistical analysis was carried out using SPSS version 17.0 (SPSS Inc., Chicago, IL). Distributions of the studied variables were identified as normal after examination with the Shapiro–Wilk test; therefore, parametric analyses

Table 2 Fatty acid composition in total lipids of experimental and standard diets

Fatty acid	Diet ^a					
	Standard diet (pellets)	Soy oil (S) diet	Olive oil (O) diet	Fish oil (F) diet	Linseed oil (L) diet	Palm oil (P) diet
Palmitic (mg/g of diet)	11.13	10.46	10.35	10.39	5.94	37.31
(as % of total energy)	2.71	2.33	2.31	2.31	1.32	8.29
Stearic (mg/g of diet)	1.17	4.17	3.03	2.66	4.27	4.41
(as % of total energy)	0.29	0.93	0.68	0.59	0.95	0.98
Sum of saturated FA						
(mg/g of diet)	12.53	15.36	13.76	17.84	10.70	42.85
(as % of total energy)	3.05	3.42	3.07	3.97	2.38	9.52
Oleic (mg/g of diet)	14.17	21.80	69.32	22.20	19.84	32.58
(as % of total energy)	3.46	4.86	15.44	4.93	4.41	7.24
Sum of MUFAs						
(mg/g of diet)	14.47	21.94	70.11	47.27	20.06	33.03
(as % of total energy)	3.53	4.89	15.61	10.5	4.46	7.34
LA (mg/g of diet)	41.02	46.48	5.30	7.37	17.78	13.21
(as % of total energy)	10.00	10.35	1.18	1.64	3.95	2.93
ARA (mg/g of diet)	ND	ND	ND	0.44	ND	ND
(as % of total energy)				0.10		
Sum of n-6 PUFAs						
(mg/g of diet)	41.02	46.48	5.36	8.29	17.85	13.21
(as % of total energy)	10.00	10.35	1.19	1.84	3.96	2.93
ALA (mg/g of diet)	2.54	6.01	0.57	0.69	41.24	0.86
(as % of total energy)	0.62	1.34	0.13	0.15	9.16	0.19
EPA (mg/g of diet)	ND	ND	ND	6.85	ND	ND
(as % of total energy)				1.52		
DHA (mg/g of diet)	ND	ND	ND	8.92	ND	ND
(as % of total energy)				1.98		
Sum of n-3 PUFAs						
(mg/g of diet)	2.54	6.01	0.57	16.59	41.38	0.91
(as % of total energy)	0.62	1.34	0.13	3.69	9.20	0.20

Values correspond to the mean of three separate samples processed independently

ND not detected, FA: fatty acid, MUFA monounsaturated FA, PUFA polyunsaturated FA, LA linoleic acid, ARA arachidonic acid, ALA α -linolenic acid, EPA eicosapentaenoic acid, DHA docosahexaenoic acid

^a Experimental diets provided 20% of total energy as fat and standard diet provided 17.2% of total energy as fat

were applied. One-way analysis of variance (ANOVA) was used to compare different diets and three-way ANOVA with physiological status (pregnant or virgin), time (12 or 20 days) and diets as factors was used to compare mean fatty acid values from different dietary treatments. When treatment effects were significantly different ($P < 0.05$), Newman–Keuls simultaneous tests were used to establish statistical differences between individual dietary interventions. Fatty acid compositional data between virgin and pregnant rats were analyzed using an unpaired t test. The Spearman rank correlation analyses were used to investigate associations between fatty acid compositions of experimental diets with those of maternal and fetal plasma, and between maternal plasma and maternal adipose tissue.

Results

Body weight and food intake in pregnant rats were higher than in virgin rats, but no difference was found between the groups of pregnant or of virgin rats receiving the different dietary treatments (data not shown). Both total and conceptus-free body weight in pregnant rats at day 12 (301 ± 3 and 296 ± 4 g; data shown as mean \pm SEM) and at day 20 of pregnancy (395 ± 6 and 315 ± 6 g) were significantly higher ($P < 0.001$) than in age-matched virgin rats on the same day of experimental treatment (267 ± 3 g at day 12 and 273 ± 3 at day 20). Neither the number of embryos or fetuses per dam, nor the body weights of the fetuses, differed between the groups (data not shown).

Fig. 2 Concentration of groups of fatty acids in the plasma of virgin (V) and pregnant (P) rats at 12 and 20 days of the study. Rats were given soy oil-, olive oil-, fish oil-, linseed oil- or palm oil-based diets for 12 days, then from day 12 until day 20 they were given a standard pellet diet. V0 corresponds to age-matched virgin female rats at the onset of the experiment (basal group). Values correspond to mean \pm SEM of 6–8 rats per group. Statistical comparisons between the groups for each fatty acid group are shown by lower-case letters (different letters indicating $P < 0.05$) and comparison between pregnant and virgin rats at the same day of experiment is shown by asterisks (* $P < 0.05$ and ** $P < 0.001$). Saturated fatty acids were calculated as the sum of 14:0, 16:0 and 18:0; monounsaturated fatty acids as the sum of 16:1 (n-7), 18:1 (n-9) and 20:1 (n-9); n-6 PUFA as the sum of 18:2 (n-6), 18:3 (n-6) and 20:4 (n-6); and n-3 PUFA is the sum of 18:3 (n-3), 20:5 (n-3), 22:5 (n-3) and 22:6 (n-3)

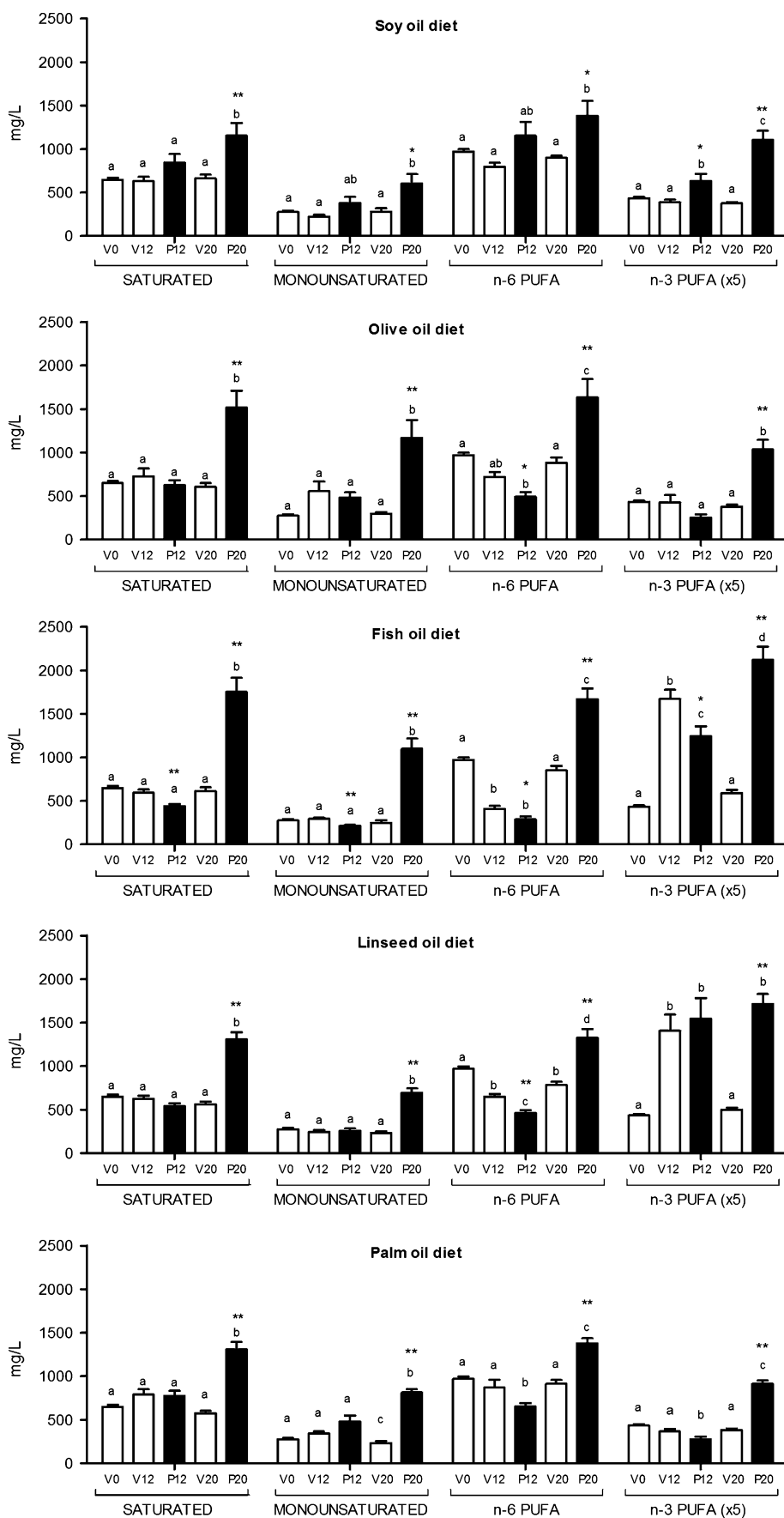


Table 4 Concentrations of specific fatty acids in plasma of virgin (V) and pregnant rats (P) at days 0 (basal), 12 and 20 of the study

Plasma (mg/L)	Soy oil diet						Olive oil diet						Fish oil diet																							
	Virgin		Pregnant		Pregnant		Virgin		Pregnant		Pregnant		Virgin		Pregnant		Pregnant																			
	V0	V20	V12	V20	P12	P20	P20	V12	V20	P12	P20	P20	V12	V20	P12	P20	P20	P20																		
Palmitic	352.8 ± 19.9	340.5 ^{uA} ± 41.7	356.5 ^{uA} ± 20.0	472.2 ^{uA} ± 69.3	765.2 ^{bA} ± 109.5	385.8 ^{gA} ± 67.9	304.9 ^{uA} ± 30.8	357.0 ^{uAB} ± 43.1	1069.0 ^{bAB} ± 149.6	341.8 ^{gA} ± 31.5	318.1 ^{uA} ± 22.4	253.5 ^{gB} ± 19.1	1249.0 ^{gB} ± 134.9	235.8 ± 18.4	188.6 ^{uA} ± 21.5	249.1 ^{uA} ± 36.5	312.4 ^{gAB} ± 41.4	541.9 ^{bA} ± 109.2	516.1 ^{gB} ± 105.7	273.0 ^{uA} ± 17.4	450.6 ^{uA} ± 58.8	1068.8 ^{gB} ± 194.5	233.3 ^{uA} ± 9.7	204.7 ^{uA} ± 26.8	169.6 ^{gB} ± 14.8	974.5 ^{gAB} ± 106.3										
Oleic	446.1 ± 15.97	369.7 ^{uA} ± 24.0	448.0 ^{uA} ± 12.6	694.2 ^{uA} ± 105.4	716.9 ^{uA} ± 131.6	215.3 ^{gB} ± 44.2	371.3 ^{uA} ± 48.1	166.0 ^{gB} ± 23.1	941.8 ^{gA} ± 162.4	194.8 ^{gB} ± 14.0	408.1 ^{gA} ± 21.1	154.9 ^{gB} ± 23.6	1211.0 ^{cA} ± 114.4	469.9 ± 26.2	407.3 ^{gAB} ± 32.7	423.6 ^{uA} ± 20.7	430.0 ^{uA} ± 38.8	445.6 ^{uA} ± 43.2	456.8 ^{gAB} ± 39.6	473.9 ^{uA} ± 24.8	297.5 ^{gB} ± 35.5	489.0 ^{uA} ± 36.4	197.3 ^{gC} ± 19.8	419.7 ^{gA} ± 42.2	118.8 ^{gC} ± 14.0	395.0 ^{bA} ± 26.4										
LA	14.38 ± 1.3	17.7 ^{uA} ± 2.0	15.4 ^{uA} ± 0.8	52.0 ^{gBA} ± 10.8	34.0 ^{bAB} ± 6.0	4.8 ^{gA} ± 0.97	11.0 ^{uA} ± 1.6	6.4 ^{uA} ± 1.0	35.2 ^{gAB} ± 7.2	7.5 ^{uA} ± 0.47	9.7 ^{uA} ± 0.6	5.7 ^{uA} ± 0.8	53.4 ^{gB} ± 5.6	ARA	3.6 ± 1.5	6.6 ^{gBA} ± 0.72	ND ^{uA}	12.5 ^{bA} ± 1.8	5.3 ^{abA} ± 1.0	2.9 ^{gA} ± 1.6	7.0 ^{uA} ± 1.2	174.4 ^{gB} ± 11.8 ^{gB}	132.9 ^{gB} ± 23.2 ^{gB}	23.2 ^{gB} ± 3.4	EPA	53.7 ± 3.0	48.9 ^{uA} ± 4.5	48.9 ^{uA} ± 2.4	51.4 ^{uA} ± 4.0	140.4 ^{bA} ± 13.6	56.7 ^{uA} ± 5.2	54.8 ^{gA} ± 38.9 ^{gA}	123.7 ^{gA} ± 11.1	150.8 ^{gB} ± 91.5 ^{gB}	111.3 ^{gB} ± 12.1	325.2 ^{cB} ± 25.8
DHA																																				

Values correspond to mean ± SEM (*n* = 6–8). Statistical comparisons within the same dietary group (e.g., soy oil group V12 versus V20 versus P12 versus P20) are shown by lower-case superscript letters. Statistical comparisons between dietary groups at the same time of the study (e.g., V12 soy oil diet versus V12 olive oil diet versus V12 fish oil diet versus V12 linseed oil diet versus palm oil diet) are shown by upper-case superscript letters (different letters indicate *P* < 0.05)

ND not detected, V12 virgin rats at day 12 of study, V20 virgin rats at day 20 of study, P12 pregnant rats at day 12 of study, P20 pregnant rats at day 20 of study. MUFA monounsaturated FA, PUFA polyunsaturated FA, LA linoleic acid, ARA arachidonic acid, ALA α -linolenic acid, EPA eicosapentaenoic acid, DHA docosahexaenoic acid

including both LA and ARA in case of the n-6 PUFA and ALA, EPA and DHA in case of n-3 PUFA (Table 4).

The Linseed Oil Diet

Rats on the L diet presented a similar picture to that seen with the F diet in terms of their plasma fatty acid profiles. At day 12 no difference was found in the concentrations of saturated or monounsaturated fatty acids of either virgin or pregnant rats compared to the basal group, and there was a significant decline in n-6 PUFA (Fig. 2), again mostly ARA, and increases in n-3 PUFA, the difference corresponding to both ALA and EPA (Table 4). At day 20, all plasma fatty acids in virgin rats (as on the F diet) returned to basal values, and in pregnant rats there were significant increases compared to the values at day 12. The exception was the n-3 PUFA in the plasma of pregnant rats; the concentration in plasma of pregnant rats at day 20 remained practically the same as in the pregnant rats at day 12. This is accounted for by a decline in EPA and an increase in DHA (Table 4).

The Palm Oil Diet

After 12 days of receiving the P diet, virgin rats did not show any change in fatty acid profile, values remaining stable also at day 20, except for a small but significant decline in monounsaturated fatty acids (Fig. 2). In pregnant rats, however, at day 12 of being on the P diet, higher concentrations of monounsaturated fatty acids (oleic acid) and lower concentrations of both n-6 PUFA and n-3 PUFA were observed (Fig. 2), the difference mainly corresponding to LA and DHA respectively (Table 4). At day 20, pregnant rats of the P group showed increases in the plasma concentrations of all fatty acid groups (Fig. 2); the difference was significant ($P < 0.05$) for virtually all the individual fatty acids, and was especially striking in the case of DHA, which was 3-fold higher than at day 12 (Table 4).

Having described the different responses of pregnant and virgin rats at day 12 and day 20 of the dietary manipulations and taking into account the fact that the experimental diets were only given to the rats during the first 12 days of the 20-day experiment, it is possible to examine the differential responses to the different diets. As shown in Table 4, on the last day of receiving the experimental diets (day 12), most of the changes in plasma fatty acid profile, in both virgin and pregnant rats, mimicked the profiles found in the respective diets, with the exception the values for ARA. ARA is found at very low concentrations in all the diets and at much higher concentrations in all the day-12 plasmas, the effect being less pronounced in the F and L groups. After being fed with standard pellet diet for the last 8 days of experiment (i.e., until day 20), the plasma fatty acid profile in the virgin rats returned to values approaching those observed before the experiment (V0); this is not the case in pregnant rats. Saturated fatty acids were the exception in that they were similar in all the groups. The concentration of monounsaturated fatty acids was highest in the two groups whose diets also contained the most oleic acid, O and F. The two groups with the lowest plasma ARA concentrations were L and F, which also had the highest values of DHA. The day-20 pregnant rats on the L diet had the highest proportions of ALA. None of the rats, with the obvious exception of those on the F diet, had very low plasma levels of DHA, although in pregnant rats of the L group at day 20 were notably higher than the remaining three groups (e.g., S, O and P).

It is to be expected that these different fatty acid profiles in maternal plasma would be reflected in the fetuses at day 20 (see Table 5). Palmitic- and oleic-acid concentrations were highest in the fetuses of dams fed the P diet, the other four groups all being similar to each other. No difference between the groups was found in LA concentrations, whereas ARA was lowest in the fetuses of dams fed either F or L diet, which were also those with the highest values of both EPA and DHA. Concentrations of ALA were

Table 5 Concentrations of specific fatty acids in plasma of 20-day fetuses of dams that were fed an experimental diet during the first 12 days of pregnancy and standard pellet diet from day 12 until day 20

Fatty acid (mg/L)	Soy oil diet	Olive oil diet	Fish oil diet	Linseed oil diet	Palm oil diet
Palmitic	476.7 ^a ± 31.4	465.7 ^a ± 30.8	484.9 ^a ± 29.1	481.6 ^a ± 18.7	596.2 ^b ± 18.7
Oleic	445.6 ^a ± 33.0	480.5 ^a ± 35.0	425.3 ^a ± 24.3	441.9 ^a ± 20.5	582.0 ^b ± 36.3
LA	218.2 ^a ± 20.0	173.2 ^a ± 12.5	202.1 ^a ± 12.9	195.4 ^a ± 10.2	208.7 ^a ± 6.3
ARA	196.2 ^a ± 19.7	178.4 ^{ab} ± 11.4	143.0 ^b ± 11.4	149.5 ^b ± 10.2	248.2 ^c ± 12.9
ALA	7.9 ^a ± 1.4	4.0 ^b ± 0.2	4.8 ^b ± 0.5	6.4 ^{ab} ± 0.9	4.8 ^b ± 0.1
EPA	5.4 ^a ± 0.7	4.5 ^a ± 0.4	13.2 ^b ± 1.1	17.3 ^c ± 1.7	3.7 ^a ± 0.4
DHA	90.9 ^a ± 13.6	64.0 ^a ± 4.4	170.3 ^b ± 15.9	138.4 ^c ± 8.5	79.0 ^a ± 1.2

Values correspond to mean ± SEM ($n = 6-8$). Statistical comparisons are shown by the superscript letters (different letters indicate $P < 0.05$) LA linoleic acid, ARA arachidonic acid, ALA α -linolenic acid, EPA eicosapentaenoic acid, DHA docosahexaenoic acid

highest in fetuses of the S group followed by the L, as compared to the other groups, but were much lower than those of LA in all the groups. In order to determine the potential influence of maternal fatty acids on fetal ones, linear correlation analysis of the concentrations of individual fatty acids between the two sites (Tables 4, 5) was carried out. It was found that only ARA, EPA and DHA showed a significant correlation ($n = 30$, $P < 0.05$, <0.05 and <0.001 , respectively). The proportional distribution of fatty acids in fetal liver of 20 day pregnant rats fed the different diets is shown in supplementary Table 1. The most relevant finding is a lower proportion of ARA and n-6 docosapentaenoic acid and a higher proportion of EPA, n-3 docosapentaenoic acid and DHA in fetuses of the L and F groups as compared to the others. The consistent increase in the concentration of practically all fatty acids in maternal plasma at day 20 compared to all the other groups and the different profiles found in their fetuses, prompted an analysis of the lipid classes that could be carrying them in the plasma.

As shown in Table 6, the lipid class in maternal plasma of all the groups showing the highest proportion of saturated fatty acids was NEFA followed by phospholipids, with smaller proportions in TAG and even smaller in the esterified cholesterol fraction. In the case of monounsaturated fatty acids, the circulating lipid fraction having the highest proportion was TAG, followed by NEFA, then esterified cholesterol or phospholipids. Very differently, the circulating lipid class with the highest proportion of n-6 PUFA (corresponding mainly to ARA) was always esterified cholesterol, followed by either TAG or phospholipids, and the smallest being in the NEFA. In case of n-3 PUFA, phospholipids contained the highest proportion fraction, followed by TAG, esterified cholesterol or NEFA.

In the plasma of fetuses from these same dams (Table 6), none of the fatty acids were detectable as NEFA, but their distribution in the other lipid classes was similar to those in their mothers, albeit with some significant differences. The phospholipids fraction always contained the highest proportion of saturated fatty acid, followed by TAG and esterified cholesterol, which proportion was always higher than in the esterified cholesterol in the corresponding maternal plasma. In fetal plasma, the lipid fraction having the highest proportion of monounsaturated fatty acids was TAG followed by esterified cholesterol and phospholipids; however, the proportion of n-6 PUFA (mainly ARA) in fetal plasma was highest in phospholipids and in esterified cholesterol followed by TAG, and n-3 PUFA represented a higher proportion of the phospholipid fatty acid moieties than did those of esterified cholesterol or TAG, the proportion in NEFA being the lowest. Nevertheless, the proportion of n-3 fatty acids present in each

of the lipid classes analyzed was always lower than the proportions of the other fatty acid families.

In order to test whether maternal adipose tissue represented a store of dietary fatty acids during early pregnancy, the fatty acid profile of lumbar adipose tissue was determined in pregnant rats on the last day of receiving the experimental diet (day 12), and compared to the profile from the basal (V0) group that had received only standard pellets. The results are shown in Table 7. Adipose tissue of the rats on the S diet had higher LA and ALA concentrations than the V0 group; those on the O diet had higher oleic acid but lower LA, ARA and DHA; the rats on the F diet had higher EPA and DHA and lower LA; those on the L diet had higher ALA and EPA; and those on the P diet had higher palmitic acid and oleic acid and lower LA and DHA concentrations than the V0 group.

The similarities observed between the fatty acid composition of the diets (Table 2) and of the lumbar adipose tissue at day 12 of the rats (Table 7) led us to compare the two measurements statistically. A significant linear correlation was found for all the fatty acids except for ARA (which is virtually absent from diets and present at low concentrations in adipose tissue), P values being <0.05 in case of saturated fatty acids and <0.001 for the others (oleic acid, ALA, EPA and DHA).

Discussion

The experiment reported here has shown for the first time that giving rats iso-energetic diets with different fatty acid compositions during just the first 12 days of pregnancy (full term is 22 days) influences the fatty acid profile of maternal adipose tissue greatly, and that these fatty acids are released during late pregnancy even though the rats were returned to a standard diet the second “half” of pregnancy. The experiment further showed that the LC-PUFA in maternal plasma were available to the fetus. This was especially evident when maternal diet during early pregnancy was abundant in n-3 LC-PUFA or n-3 EFA (e.g. ALA), as was the case for the fish oil and linseed oil diets, respectively. In these cases the diet caused a decline in plasma ARA concentrations, which was particularly evident in the fetus.

During the first 12 days of pregnancy in rats, the mother is in an anabolic condition, as shown here by the increased maternal body weight (free of the conceptus) compared to age-matched virgin female rats. Thus, during this early stage of pregnancy, maternal adipose tissue becomes a store of dietary-derived fatty acids, as indicated by the significant linear correlations between the fatty acids in fat pads of day 12 pregnant rats and the composition of the diets as described in the Results section. At this early stage

Table 6 Proportional distribution of groups of fatty acids in different lipid classes in plasma of 20 day-pregnant rats and their fetuses given different experimental diets during the first 12 days of gestation, followed by the standard pellet diet until day 20

Lipid class	Pregnant rats at 20 days				
	Soy oil diet	Olive oil diet	Fish oil diet	Linseed oil diet	Palm oil diet
Phospholipids					
Saturated	49.60 ± 0.29 ^{ab}	48.40 ± 0.24 ^a	53.58 ± 2.35 ^b	51.97 ± 0.70 ^{ab}	48.87 ± 0.53 ^a
Monounsaturated	5.45 ± 0.30 ^a	6.43 ± 0.20 ^a	5.79 ± 0.44 ^a	5.63 ± 0.27 ^a	6.08 ± 0.16 ^a
n-6 PUFA	36.40 ± 1.57 ^a	38.20 ± 0.64 ^a	26.31 ± 1.27 ^b	29.81 ± 0.90 ^c	38.21 ± 1.13 ^a
n-3 PUFA	8.36 ± 0.64 ^a	6.83 ± 0.18 ^a	14.22 ± 0.98 ^b	12.43 ± 0.46 ^c	6.73 ± 0.35 ^a
Triacylglycerols					
Saturated	31.75 ± 0.52 ^a	30.38 ± 0.61 ^a	31.22 ± 0.70 ^a	35.80 ± 5.44 ^a	35.14 ± 3.07 ^a
Monounsaturated	27.53 ± 1.56 ^a	38.97 ± 1.11 ^b	31.71 ± 0.78 ^{ac}	26.76 ± 2.56 ^a	35.21 ± 0.65 ^{bc}
n-6 PUFA	34.28 ± 0.90 ^a	26.95 ± 1.35 ^a	31.10 ± 1.06 ^a	27.90 ± 4.59 ^a	26.14 ± 2.36 ^a
n-3 PUFA	3.59 ± 0.66 ^{ab}	2.43 ± 0.12 ^a	5.42 ± 0.39 ^b	8.88 ± 1.30 ^c	2.30 ± 0.14 ^a
Non-esterified fatty acids					
Saturated	56.34 ± 3.32 ^a	55.16 ± 2.85 ^a	61.35 ± 2.06 ^a	60.89 ± 1.72 ^a	51.38 ± 2.22 ^a
Monounsaturated	20.97 ± 2.27 ^a	28.06 ± 1.50 ^b	20.63 ± 0.95 ^a	20.67 ± 1.09 ^a	25.37 ± 1.67 ^{ab}
n-6 PUFA	18.15 ± 1.66 ^a	13.27 ± 1.34 ^b	14.41 ± 1.12 ^b	14.12 ± 1.08 ^b	19.44 ± 1.30 ^a
n-3 PUFA	3.02 ± 0.52 ^a	3.03 ± 0.55 ^a	3.14 ± 0.37 ^a	3.43 ± 0.49 ^a	2.72 ± 0.57 ^a
Esterified cholesterol					
Saturated	19.15 ± 0.62 ^a	20.76 ± 0.87 ^a	21.90 ± 1.59 ^a	21.12 ± 0.79 ^a	17.60 ± 1.28 ^a
Monounsaturated	9.08 ± 0.28 ^a	15.81 ± 1.98 ^b	12.06 ± 0.70 ^{ab}	10.84 ± 1.21 ^a	11.86 ± 0.96 ^{ab}
n-6 PUFA	67.60 ± 0.58 ^{ab}	62.67 ± 1.50 ^a	62.55 ± 2.81 ^{ab}	61.48 ± 0.84 ^a	68.20 ± 1.73 ^b
n-3 PUFA	4.17 ± 0.34 ^a	0.33 ± 0.05 ^b	4.01 ± 1.06 ^a	6.57 ± 0.32 ^c	2.35 ± 0.39 ^a
<i>Fetal rats at 20 days of pregnancy</i>					
Phospholipids					
Saturated	47.07 ± 0.27 ^a	47.81 ± 0.60 ^a	50.74 ± 2.19 ^a	49.16 ± 0.56 ^a	46.17 ± 0.93 ^a
Monounsaturated	17.55 ± 1.13 ^a	19.36 ± 0.90 ^a	17.64 ± 0.80 ^a	17.97 ± 0.25 ^a	19.37 ± 0.77 ^a
n-6 PUFA	27.95 ± 0.75 ^a	26.81 ± 0.69 ^a	20.48 ± 1.14 ^b	22.90 ± 0.37 ^b	28.37 ± 1.08 ^a
n-3 PUFA	7.43 ± 0.40 ^a	6.01 ± 0.17 ^a	11.15 ± 0.74 ^b	9.97 ± 0.42 ^b	6.09 ± 0.20 ^a
Triacylglycerols					
Saturated	38.95 ± 0.83 ^a	42.29 ± 0.81 ^a	43.80 ± 0.90 ^a	47.94 ± 2.37 ^b	40.49 ± 0.54 ^a
Monounsaturated	35.38 ± 1.93 ^a	39.33 ± 1.63 ^a	36.63 ± 0.84 ^a	34.70 ± 1.59 ^a	38.25 ± 1.39 ^a
n-6 PUFA	23.01 ± 2.10 ^a	16.93 ± 1.52 ^b	14.53 ± 0.40 ^b	13.03 ± 0.80 ^b	17.85 ± 1.10 ^b
n-3 PUFA	3.03 ± 0.34 ^a	1.34 ± 0.12 ^b	5.04 ± 0.35 ^c	4.81 ± 0.51 ^c	1.73 ± 0.24 ^b
Non esterified fatty acids					
Saturated	ND	ND	ND	ND	ND
Monounsaturated	ND	ND	ND	ND	ND
n-6 PUFA	ND	ND	ND	ND	ND
n-3 PUFA	ND	ND	ND	ND	ND
Esterified cholesterol					
Saturated	37.84 ± 1.61 ^a	39.51 ± 2.02 ^a	37.19 ± 0.78 ^a	38.88 ± 0.84 ^a	36.83 ± 2.64 ^a
Monounsaturated	32.87 ± 1.69 ^a	34.15 ± 1.63 ^a	30.86 ± 0.96 ^a	32.91 ± 0.96 ^a	33.79 ± 2.12 ^a
n-6 PUFA	27.10 ± 2.60 ^a	24.64 ± 1.44 ^a	27.02 ± 1.18 ^a	24.77 ± 0.69 ^a	25.85 ± 1.58 ^a
n-3 PUFA	1.77 ± 0.23 ^a	1.51 ± 0.07 ^a	4.71 ± 0.33 ^b	3.49 ± 0.34 ^b	3.03 ± 1.09 ^b

Values are the % composition of fatty acid type within each of the lipid classes and are shown as mean ± SEM ($n = 6-8$). "Saturated" is the sum of the acids 14:0, 16:0 and 18:0; "monounsaturated" is the sum of the acids 16:1 (n-7), 18:1 (n-9), 20:1 (n-9) and 22:1 (n-9); n-6 PUFA are the sum of the n-6 polyunsaturated fatty acids 18:2, 18:3 and 20:4; n-3 PUFA is the sum of n-3 polyunsaturated fatty acids (18:3, 20:5, 22:5, and 22:6). Statistical comparison for each fatty acid group in the different lipid class between dietary groups is shown by superscript letters (different letters indicate $P < 0.05$)

ND not detected

Table 7 Concentration of fatty acids at day-12 of pregnancy in lumbar adipose tissue of rats fed diets containing different fat components

Fatty acid (mg/g of tissue)	Basal (V0)	Soy oil diet	Olive oil diet	Fish oil diet	Linseed oil diet	Palm oil diet
Palmitic	147.0 ± 8.6 ^{ab}	178.1 ± 14.4 ^{bc}	137.5 ± 7.8 ^a	173.6 ± 5.9 ^{bc}	182.2 ± 12.1 ^{bc}	205.8 ± 9.7 ^c
Oleic	205.1 ± 7.1 ^a	231.7 ± 15.2 ^a	330.2 ± 22.8 ^b	216.1 ± 5.5 ^a	256.4 ± 11.1 ^a	298.5 ± 13.9 ^b
LA	188.5 ± 26.2 ^a	237.9 ± 12.7 ^b	97.8 ± 3.3 ^c	128.4 ± 10.6 ^{cd}	178.3 ± 14.8 ^{ad}	134.9 ± 4.3 ^{cd}
ARA	4.3 ± 0.7 ^a	5.5 ± 0.6 ^a	1.9 ± 0.2 ^c	4.0 ± 0.3 ^a	3.7 ± 0.3 ^a	3.3 ± 0.2 ^a
ALA	9.3 ± 1.2 ^a	20.9 ± 1.3 ^b	5.2 ± 0.3 ^a	7.4 ± 0.6 ^a	119.5 ± 6.3 ^c	6.5 ± 0.4 ^a
EPA	2.4 ± 0.5 ^a	0.7 ± 0.0 ^a	0.7 ± 0.1 ^a	10.1 ± 1.0 ^b	3.4 ± 0.3 ^c	0.9 ± 0.1 ^a
DHA	4.9 ± 1.6 ^a	1.7 ± 0.1 ^{ab}	0.3 ± 0.0 ^b	20.8 ± 1.5 ^c	2.9 ± 0.2 ^{ab}	0.7 ± 0.1 ^b

Values correspond to mean ± SEM ($n = 6-8$). Basal (V0) corresponds to sex- and age-matched virgin rats at the onset of the experiment. The statistical comparison between groups for each fatty acid is shown by superscript letters (different letters indicate statistical difference between the groups, $P < 0.05$)

LA linoleic acid, ARA arachidonic acid, ALA α -linolenic acid, EPA eicosapentaenoic acid, DHA Docosahexaenoic acid

of pregnancy, when lipolytic activity in adipose tissue is low due to its increased sensitivity to insulin [7], the fatty acid profile in plasma is the result of three main effects: what has been absorbed from the diet; what is taken up from the blood by the different tissues; and what is released to the blood by the liver, where the highest rate of conversion of EFA to LC-PUFA takes place [18]. Indeed the fatty acid profile in plasma of day 12 pregnant rats indicates that an active conversion of EFA to LC-PUFA is occurring at this stage. Thus, while the linseed oil diet had the highest proportion of ALA and practically no EPA, both virgin and especially pregnant rats on this diet had plasma EPA concentrations that were higher than in all the other groups except those on the fish oil diet, suggesting an active conversion of ALA to EPA. This issue regarding conversion in humans of ALA to longer chain n-3 fatty acids is still subject to significant debate. However, the efficient conversion of ALA to longer chain n-3 fatty acids has been shown to be especially active in women of childbearing age compared to males [19–22]. It has also been shown that estrogen exposure in women increases the conversion of ALA to DHA [20]. Our finding that this conversion is increased in late-pregnant rats is consistent with reports that late pregnancy is a condition where high circulating levels of estrogen are present both in women [23–25] and in rats [26].

Similarly, ARA is practically absent from any of the diets used here, but it was present in the plasma of all the groups, suggesting an active endogenous synthesis from its EFA precursor, LA. However, plasma ARA levels at day 12, in both virgin and pregnant rats, were lower in the fish oil and linseed groups than in any of the other groups. The F and L groups were the ones with the highest contents of n-3 LC-PUFA, either EPA or DHA or both. An inhibitory effect of both of these LC-PUFA on the $\Delta 6$ -desaturase, the key enzyme for ARA synthesis from its essential precursor, LA, has been reported [27, 28]. The findings reported here therefore indicate that the same inhibitory action is

effective in vivo in our rats given the fish oil or the linseed oil diet.

The results from the pregnant rats that were studied at day 20 of pregnancy are of particular interest; the experimental diet of these rats had been discontinued for 8 days and replaced by the standard diet. As well as an increase in both plasma NEFA and TAG, a significant increase in the plasma concentrations of most fatty acid groups was found, when compared to values found both in the virgin rats groups and in pregnant rats at day 12 of gestation. These findings clearly suggest an increased adipose tissue lipolytic activity, which must have contributed to the net release of the dietary fatty acids that were stored in adipose tissue during the first 12 days of pregnancy.

A few exceptions deserve comment, mainly relating to the groups on the fish oil and linseed oil diets. In the fish oil group, plasma EPA concentrations in 20-day pregnant rats decreased compared to values found in 12-day pregnant rats. As the fish oil diet contains very little ALA, the EFA precursor for EPA synthesis, but it is rich in EPA itself, it is proposed that the lower concentration of this fatty acid in 20-day pregnant rats on the F diet could be a consequence of its conversion into DHA, the concentration of which in plasma is about three times higher than in 12-day pregnant rats. Similar reasoning could be used for the situation in the linseed oil group, even though this diet is the richest in ALA. The lower concentration of this fatty acid in 20-day pregnant rats is also followed by a decline in plasma concentrations of EPA and a 5-fold increase in DHA, again suggesting an active synthesis of DHA. The potential effect of high estrogen levels on these activities, referred to above, deserves further direct studies.

These LC-PUFA are transported in maternal plasma mainly as their various esterified forms, such as phospholipids, TAG and esterified cholesterol, with small proportions in the form of NEFA. This agrees with previous findings both in pregnant women [8] and in rats [29], showing that PUFA are carried in plasma associated with the

different lipoprotein fractions rather than in their non-esterified form. This further indicates that, although released from maternal adipose tissue in the form of NEFA, they are rapidly taken up by the liver where they are esterified and incorporated into VLDL to be returned to the circulation. As already proposed [13, 29], maternal lipoproteins seems to be the mechanism of transport by which PUFA arrive at the placenta, where they are taken up and, after hydrolytic release, are transferred to the fetal circulation.

The concentrations of LC-PUFA in fetal plasma and even the proportional distribution of fatty acids in fetal liver were found to be influenced by those in maternal circulation, the relationship being especially evident in the case of the fetuses of dams given PUFA-rich diets during early pregnancy (i.e., soy-, fish- or linseed-oil diets). The same does not appear to be true for the rats given diets rich in saturated and monounsaturated fats (i.e., the palm oil and olive oil diets). The finding probably reflects the fact that the rat fetus carries out fatty acid synthesis *de novo* at this stage of intrauterine life [30], resulting in fetal synthesis of both saturated and monounsaturated acids and presumably lower requirements for their placental transfer.

In conclusion, the findings presented here show that the maternal adipose tissue of rats has the ability to store dietary derived fatty acids during the first half of gestation, which are released into the plasma during late pregnancy from where LC-PUFA become available to the fetus. Although extrapolation of this conclusion to the human condition should be made with caution for obvious reasons, alterations in dietary fatty acid composition during early pregnancy may have consequences in terms of which fatty acids reach the fetus during the stage of its most rapid growth and consequent greatest need of LC-PUFA.

Acknowledgments We thank Milagros Morante for her excellent technical assistance and pp-science-editing.com for editing and linguistic revision of the manuscript. This study was carried out with the financial support of the Spanish Ministry of Science and Innovation (SAF2008-04518), Universidad San Pablo CEU (USP09-12) and the Cooperation Program between Brazil and Universidad San Pablo CEU.

References

1. Wu G, Bazer F, Meininger C, Spencer T (2004) Maternal nutrition and fetal development. *J Nutr* 134:2169–2172
2. Rodríguez-Bernal CL, Rebagliato M, Iñiguez C, Vioque J, Navarrete-Muñoz EM, Murcia M, Bolumar F, Marco A, Ballester F (2010) Diet quality in early pregnancy and its effects on fetal growth outcomes: the infancia y medio ambiente (childhood and environment) mother and child cohort study in Spain. *Am J Clin Nutr* 91:1659–1666
3. Villar J, Cogswell M, Kestler E, Castillo P, Menendez R, Repke JT (1992) Effect of fat and fat-free mass deposition during pregnancy on birth weight. *Am J Obstet Gynecol* 167:1344–1352
4. King JC, Butte NF, Bronstein MN, Kopp LE, Lindquist SA (1994) Energy metabolism during pregnancy: influence of maternal energy status. *Am J Clin Nutr* 59(2 Suppl):439S–445S
5. Lopez-Luna P, Muñoz T, Herrera E (1991) Body fat in pregnant rats at mid- and late-gestation. *Life Sci* 39:1389–1393
6. Moore BJ, Brassel JA (1984) One cycle of reproduction consisting of pregnancy, lactation or no lactation, and recovery: effects on carcass composition in ad libitum-fed and food-restricted rats. *J Nutr* 114:1548–1559
7. Ramos MP, Crespo-Solans MD, Del Campo S, Cacho J, Herrera E (2003) Fat accumulation in the rat during early pregnancy is modulated by enhanced insulin responsiveness. *Am J Physiol Endocrinol Metab* 285:E318–E328
8. Herrera E (2002) Lipid metabolism in pregnancy and its consequences in the fetus and newborn. *Endocrine* 19:43–55
9. Herrera E, Lasunción MA, Martín A, Zorzano A (1992) Carbohydrate-lipid interactions in pregnancy. In: Herrera E, Knopp RH (eds) *Perinatal biochemistry*. CRC Press, Boca Raton, pp 1–18
10. Herrera E, Lasunción MA, Gómez-Coronado D, Aranda P, López-Luna P, Maier I (1988) Role of lipoprotein lipase activity on lipoprotein metabolism and the fate of circulating triglycerides in pregnancy. *Am J Obstet Gynecol* 158:1575–1583
11. Haggarty P (2010) Fatty acid supply to the human fetus. *Ann Rev Nutr* 30:237–255
12. Herrera E, Lasunción MA (2011) Maternal-fetal transfer of lipid metabolites. In: Polin RA, Fox WW, Abman SH (eds) *Fetal and neonatal physiology*, 4th edn. Elsevier Saunders, Philadelphia, pp 441–454
13. Herrera E, Ortega-Senovilla H (2010) Maternal lipid metabolism during normal pregnancy and its implications to fetal development. *Clin Lipidol* 5:899–911
14. Amusquivar E, Laws J, Clark L, Herrera E (2010) Fatty acids in maternal diet during the first or the second half of gestation influences those in sows' milk and piglets' plasma. *Lipids* 45:409–418
15. Reeves PG, Neilesen FH, Fahey GC Jr (1993) AIN-93 purified diets for laboratory rodents: final report of the American Institute of Nutrition ad hoc writing committee on the reformulation of the AIN-76A rodent diet. *J Nutr* 123:1939–1951
16. Folch J, Lees M, Sloane Stanley GH (1957) A simple method for the isolation and purification of total lipids from animal tissues. *J Biol Chem* 22:24–36
17. Amusquivar E, Schiffner S, Herrera E (2011) Evaluation of two methods for plasma fatty acid analysis by GC. *Eur J Lipid Sci Technol* 113:711–716
18. Hassam AG (1977) The influence of α -linolenic acid (18:3 ω 3) on the metabolism of γ -linolenic acid (18:3 ω 6) in the rat. *Br J Nutr* 38:137–140
19. Barcelò-Coblijn G, Murphy EJ (2009) Alpha-linolenic acid and its conversion to longer chain n-3 fatty acids: benefit for human health and a role in maintaining tissue n-3 fatty acid levels. *Prog Lipid Res* 48:355–374
20. Burdge GC, Wootton SA (2002) Conversion of α -linolenic acid to eicosapentaenoic, docosapentaenoic and docosahexaenoic acids in young women. *Br J Nutr* 88:411–420
21. Burdge GC, Jones AE, Wootton SA (2002) Eicosapentaenoic and docosapentaenoic acids are the principal products of α -linolenic acid metabolism in young men. *Br J Nutr* 88:355–363
22. Palowsky R, Hibbeln J, Lin Y, Salem N Jr (2003) n-3 Fatty acid metabolism in women. *Br J Nutr* 90:993–994
23. Darne FJ, McGarrigle HHG, Lachelin GCL (1989) Diurnal variations of plasma and saliva oestrogen, progesterone, cortisol and plasma dehydroepiandrosterone sulphate in late pregnancy. *Eur J Obstet Gynecol Reprod Biol* 32:57–66
24. Pitkin RM, Spellacy WMN (1978) Physiologic adjustments in general. In: Committee on Nutrition of the Mother and Preschool

- Child (ed) Laboratory indices of nutritional status in pregnancy. National Academy Sciences, Washington, pp 1–8
25. Hytten FE, Leitch I (1971) Hormones. In: Hytten FE, Leitch I (eds) *The Physiology of human pregnancy*. Blackwell Scientific Publ, Oxford, pp 179–233
 26. Waynfoth HB, Pope GS, Hosking ZD (1972) Secretion rates of oestrogens into the ovarian venous blood of pregnant rats. *J Reprod Fert* 28:191–196
 27. Garg ML, Thomson ABR, Clandinin MT (1990) Interactions of saturated, n-6 and n-3 polyunsaturated fatty acids to modulate arachidonic acid metabolism. *J Lipid Res* 31:271–277
 28. Raz A, Kamin-Belsky N, Przedeki F, Obukowicz MG (1997) Fish oil inhibits delta 6 desaturase activity in vivo: utility in a dietary paradigm to obtain mice depleted of arachidonic acid. *J Nutr Biochem* 8:558–565
 29. Herrera E, Amusquivar E, López-Soldado I, Ortega H (2006) Maternal lipid metabolism and placental lipid transfer. *Horm Res* 65(suppl. 3):59–64
 30. Lorenzo M, Caldes T, Benito M, Medina JM (1981) Lipogenesis in vivo in maternal and foetal tissues during late gestation in the rat. *Biochem J* 198:425–428

Camelina Meal Increases Egg n-3 Fatty Acid Content Without Altering Quality or Production in Laying Hens

Radhika Kakani · Justin Fowler · Akram-Ul Haq ·
Eric J. Murphy · Thad A. Rosenberger ·
Mark Berhow · Christopher. A. Bailey

Received: 21 June 2011 / Accepted: 10 January 2012 / Published online: 31 January 2012
© AOCS 2012

Abstract *Camelina sativa* is an oilseed plant rich in n-3 and n-6 fatty acids and extruding the seeds results in high protein meal (~40%) containing high levels of n-3 fatty acids. In this study, we examined the effects of feeding extruded defatted camelina meal to commercial laying hens, measuring egg production, quality, and fatty acid composition. Lohmann White Leghorn hens (29 weeks old) were randomly allocated to three dietary treatment groups ($n = 25$ per group) and data was collected over a 12 week production period. All the treatment groups were fed a corn soy based experimental diet containing 0% (control), 5, or 10% extruded camelina meal. We found no significant differences in percent hen-day egg production and feed consumed per dozen eggs. Egg shell strength was significantly higher in both camelina groups compared to the controls. Egg total n-3 fatty acid content increased 1.9- and 2.7-fold in 5 and 10% camelina groups respectively relative to the control. A similar increase in DHA content also occurred. Further camelina meal did not alter

glucosinolate levels and no detectable glucosinolates or metabolic product isothiocyanates were found in the eggs from either the 5 or 10% camelina groups. These results indicate that camelina meal is a viable dietary source of n-3 fatty acids for poultry and its dietary inclusion results in eggs enriched with n-3 fatty acids.

Keywords Laying hens · Camelina meal · Egg quality · n-3 Fatty acids · Egg enrichment

Abbreviations

AHA American Heart Association
ALA Alpha linolenic acid
DHA Docosahexaenoic acid
LNA Linoleic acid
NRC National Research Council

Introduction

There is an increasing interest in converting oil produced from oil seed crops into biofuels in response to the Energy Policy Act, 2005 [1]. However, oil seeds and oil seed meals are used as a source of crude protein and energy in poultry rations. Therefore, the increase in bio-fuel production has created a need to develop ways to use the meal produced following oil extraction that can benefit the poultry industry by producing alternative meals that do not compete with the human diet yet provide an adequate source of energy and protein.

Camelina sativa, also known as gold-of-pleasure or false flax, is an ancient crop native to Northern Europe and Central Asia. The plant belongs to the family Brassicaceae and is considered a versatile crop that requires a low amount of inputs [2, 3]. This annual oil seed crop can be grown with success under different climatic conditions,

R. Kakani (✉) · J. Fowler · A.-U. Haq · Christopher. A. Bailey
Department of Poultry Science, Texas A&M University,
Room 101 Kleberg Center, College Station,
TX 77843-2472, USA
e-mail: kakani@neo.tamu.edu

E. J. Murphy · T. A. Rosenberger
Department of Pharmacology, Physiology, and Therapeutics,
School of Medicine and Health Sciences, University of North
Dakota, Grand Forks, ND, USA

E. J. Murphy
Agragen, LLC, Cincinnati, OH, USA

M. Berhow
National Center for Agricultural Utilization Research,
USDA, Peoria, IL, USA

making it an ideal crop for bio-fuel feedstock. Camelina oil contains high amounts of unsaturated fatty acids with alpha-linolenic (ALA, 18:3n-3) and linoleic (LNA, 18:2n-6) acids accounting for approximately 35 and 15% of the total, respectively [2]. Camelina meal, the by-product of oil extraction, has a crude protein content of 40% and oil content of 10–12% oil of which approximately 5% of the remaining oil is enriched in n-3 fatty acid [4]. Camelina meal can be used as a substitute for soybean meal in animal feeds [4].

Glucosinolates are anti-nutritive compounds generally present in the plants belong to Brassicaceae family which may have negative effects on feed consumption [5, 6]. A reduction in feed intake was reported in turkey poults when camelina meal was included in turkey starter diets at a concentration of more than 5% [7]. In most foods consumed that have glucosinolates these compounds are generally rapidly converted to a variety of degradation products during the course of ingestion and digestion. The most prominent metabolites are isothiocyanates and nitrile forms which are generally believed to have potential biological effects [5, 6]. Low glucosinolate content of camelina makes it a desirable animal feed relative to other Brassicaceae species [4].

Egg yolk composition depends on the dietary nutrient provision. Altering the dietary fatty acid intake of a laying hen can either directly [8] or indirectly due to further acyl chain elongation and desaturation in the liver [9] alter the fatty acid composition of the egg yolk. Feeding poultry diets rich in n-3 fatty acids increases the content of these fatty acids in the egg yolk. [10–17]. Because camelina meal is a rich source of essential fatty acids, it can be incorporated in laying hen diets to enrich the n-3 fatty acid content in eggs.

The modern Western diet is low in n-3 fatty acids resulting in a n-6 to n-3 fatty acid ratio ranging from 15:1 to 20:1 [18], which is proposed to increase the incidence of cardiovascular disease, rheumatoid arthritis, and cancer [18, 19]. There is substantial evidence illuminating health concerns caused by low dietary intake of n-3 fatty acids as well beneficial effects of supplementing diets with long-chain n-3 fatty acids [20–23]. The American Heart Association (AHA) recommends increasing the intake of dietary n-3 fatty acids to reduce the risk of coronary heart disease [24]. Because the available sources of long-chain n-3 fatty acids are limited, additional sources of highly nutritious products must be made available. Because egg fatty acid composition can be increased by altering the poultry diet [8, 9] addition of n-3 rich meals will increase n-3 fatty acid content of eggs. Flax seed is traditionally used to enrich eggs with n-3 fatty acids [14–17], however alternative, lower-cost options are needed. Herein, we propose that extruded defatted camelina meal is an excellent alternative

to flax meal as a source of n-3 fatty acids and protein for laying hen diets. Further, we hypothesize that the inclusion of extruded defatted camelina meal containing 10% residual oil, at levels of 5 and 10% will not alter feed consumption, body weight, egg production, internal egg quality, or sensory quality of eggs, but will increase egg n-3 fatty acid content.

Materials and Methods

One hundred, 25 week-old Lohmann White Laying hens, purchased from Feather Crest Farms, were placed individually into 100 laying hen cages. After a three-week acclimation period, 25 birds were randomly allocated to each of the three treatment blocks at the start of the trial, for a total of 75. Individual bird weights (g) were recorded at day 0 and at the end of each 28 day period (3 periods in total). Birds were caged on one tier in a laying hen house with open windows on two sides and an exhaust fan on one end. An additional fan was placed at the opposite end of the house to provide positive airflow towards the exhaust fan. All the methods used in this study were approved by the Texas A&M University Institutional Animal Care and Use Committee (AUP 2007-250).

A commercial type, phase 1 laying hen diet was formulated according to NRC Poultry [25], (Table 1) including control diet (no camelina meal) and diets that contained 5 and 10% camelina meal. All diets were formulated to be iso-nitrogenous and iso-caloric relative to the basal control diet (Table 1). Diets were formulated based on actual chemical analysis of the mechanically pressed defatted camelina meal (supplied by Great Plain Oil and Exploration) used in this study (Table 2). Feed mixtures were made fresh just prior to each 28 day period. Feed and water were offered ad libitum. No concomitant drug therapy was used during the study. Daily observations were made with regard to general flock condition, temperature, lighting, water, feed, and unanticipated events in the house. Pens were also checked daily for mortality.

The treatment group/block was the unit of measure for egg production and feed consumption. There were 5 hens per treatment within each block for a total of 75 hens. Egg measurements were taken on individual eggs. Weekly egg production was recorded. Egg weight, shell thickness and breaking strength, measured in triplicate, were determined for all eggs laid on one day of each week. Feed consumed per dozen of eggs was calculated based on 28-day periods. During the 2nd feeding period, eggs were collected for determination of interior egg quality. Color and Haugh Units were determined using an Egg AnalyzerTM (Orka Food Technology) at time zero and after 1 and 2 weeks of storage at 4 °C.

Table 1 Diet composition and nutrient content

Ingredient	Control (%)	5% Camelina (%)	10% Camelina (%)
Corn	60.097	58.282	56.466
Dehulled Soybean meal	26.399	23.029	19.659
Camelina meal ^a	0.000	5.000	10.000
DL-Methionine	0.150	0.131	0.111
Fat, AV blend	1.558	1.792	2.026
Limestone	9.712	9.716	9.72
Mono-dicalcium phosphate	1.380	1.344	1.308
Salt	0.403	0.407	0.409
Trace minerals	0.050	0.050	0.050
Vitamin premix	0.250	0.250	0.250
Nutrient content			
Protein	18.00	18.00	18.00
ME (Kcal)	2,800.00	2,800.00	2,800.00
Crude fat	4.10	4.73	5.36
Crude fiber	2.35	2.73	3.11
Calcium	4.00	4.00	4.00
AV phosphate	0.40	0.40	0.40
Sodium	0.18	0.18	0.18
18:3 n-3	0.0616	0.2348	0.4081

^a Mechanically pressed defatted camelina meal

Procedures Used to Measure Egg Lipid Content

Reagents

HPLC grade *n*-hexane, 2-propanol, and anhydrous methanol, methyl formate, and concentrated sulfuric acid were purchased from EM Science (Gibbstown, NJ). Reagent grade sodium methoxide (25 wt%) and ferric chloride hexahydrate was purchased for Sigma-Aldrich (St. Louis, MO). Fatty acid methyl ester and cholesterol standards were purchased from Nu-Chek-Prep (Elysian, MN). All samples were stored at $-80\text{ }^{\circ}\text{C}$ and sample extracts were stored in *n*-hexane/2-propanol (3:2, by Vol.) at $-20\text{ }^{\circ}\text{C}$ prior to use.

Sample Extraction

Yolk samples (0.8–1.0 g) from hard boiled eggs were extracted in *n*-hexane/2-propanol (3:2, by vol.) using a Potter–Elvehjem tissue homogenizer equipped with a Teflon pestle [26]. The final lipid extract was concentrated to zero under a steady-stream of N_2 at $45\text{ }^{\circ}\text{C}$ then re-dissolved in 40 mL *n*-hexane/2-propanol (3:2, by vol.) immediately prior to analysis.

Table 2 Nutrient profile of camelina meal

Nutrient name	Units	Amount
ME poultry	Kcal/kg	2,463.000
Crude protein	PCT	36.000
Crude fat	PCT	10.000
Crude fiber	PCT	11.000
Fatty acids		
Palmitic (16:0)	PCT	1.070
Palmitoleic (16:1)	PCT	0.020
Stearic (18:0)	PCT	0.300
Oleic (18:1)	PCT	2.400
Linoleic (18:2 n-6)	PCT	2.780
α -Linolenic (18:3 n-3)	PCT	3.520
Amino acids		
Cystine	PCT	0.808
Methionine	PCT	0.635
Lysine	PCT	1.760
Tryptophan	PCT	0.340
Threonine	PCT	1.530
Arginine	PCT	2.970
Histidine	PCT	0.880
Valine	PCT	1.910
Leucine	PCT	2.390
Isoleucine	PCT	1.350
Phenylalanine	PCT	1.530
Glycine	PCT	1.914
Phe + Tyr	PCT	2.260
Minerals		
Calcium	PCT	0.276
Phosphorus	PCT	1.140
Sodium	PCT	0.002
Potassium	PCT	1.660
Magnesium	PCT	0.515
Sulphur	PCT	0.931
Iron	mg/kg	160.000
Copper	mg/kg	9.250
Zinc	mg/kg	70.900
Manganese	mg/kg	33.000
Cobalt	mg/kg	0.300
Molybdenum	mg/kg	1.100

Fatty Acid Quantitation and Gas Chromatography

Fatty acid content in the yolk extract was measured in triplicate using a modified method [27]. Briefly, samples were concentrated to zero residual solvent under a steady-stream of nitrogen at $45\text{ }^{\circ}\text{C}$ then transesterified in 2.5% sodium methoxide at $40\text{ }^{\circ}\text{C}$ for 30 min. The reaction was

stopped with the addition of methyl formate and the fatty acid methyl esters were extracted with *n*-hexane. Triheptadecanoin was used as an internal standard to calculate fatty acid mass. Fatty acid content was measured using a Shimadzu 2010 gas chromatograph (Kyoto, Japan) equipped with a flame ionization detector and a capillary column (SP 2330; 30 m × 0.32 mm i.d., Supelco, Bellefonte, PA). Sample runs were initiated at a column temperature of 180 °C followed by a temperature gradient to 200 °C over 8 min starting at 2 min from the beginning of the run. The temperature was held at 200 °C until the end of the run at 20 min. Fatty acid methyl ester standards were used to establish relative retention times and response factors. The internal standard, methyl heptadecanoate, and the individual fatty acids were quantified by peak area analysis and linear regression analysis (Class VP 7.2.1 Datasystem, Kyoto, Japan). The detector response was linear, with correlation coefficients of 0.998 or greater within the sample concentration range for all standards.

Cholesterol Content

The cholesterol content in the yolk lipid extract was measured in triplicate using a colorimetric assay [28]. Briefly, an aliquot of the yolk lipid extract was concentrated to zero under a steady-stream of nitrogen at 45 °C then dissolved in 3 ml absolute ethanol (Pharmco, Brookfield, CT). A 3-ml aliquot of iron working reagent was added to the sample then vigorously mixed for 10 min to bring the reaction to completion. The absorbance of each sample was measured at 550 nm and the concentration was calculated by comparing sample absorbencies to freshly prepared standard curves using linear regression analysis.

Procedures for the Detection of Egg Glucosinolate Content

Methods: Sample Extraction

For HPLC analysis, typically between 0.25 and 0.5 g of defatted chicken feeds, defatted ground camelina seed meals, and defatted freeze dried whole egg powders were extracted with 2–5 mL of methanol. For glucosinolate recovery experiments, 100 µl of a 1.8 µg/µl solution of sinigrin was added to three 5% camelina feed meals and to egg powders. For isothiocyanate analysis, whole egg powders were extracted with dichloromethane.

HPLC Analysis and Quantitation

For intact glucosinolate quantitation, the extract was run on a Shimadzu (Columbia, MD) HPLC System. The column was a C18 Inertsil 250 mm × 4.6 mm; RP C-18, ODS-3,

5µ, column. The glucosinolates were detected by monitoring at 237 nm. The initial mobile phase conditions were 40% methanol/60% aqueous 0.005 M tetrabutylammonium bisulfate (TBS) at a flow rate of 1 ml/min. After injection the initial conditions were held for 40 min, and then up to 100% methanol over another 10 min. Intact glucosinolates were identified by retention time compared to standards and by LC–MS analysis. Extracts from egg powders were confirmed as not having any intact glucosinolates by HPLC and by LC–MS analysis.

Preparation of Glucosinolate Isothiocyanates

The seed meal was defatted with hexane in a Soxhlet extractor for 24 h, after which the residual seed meal was allowed to dry completely. Defatted seed meal (10-g samples) were mixed with 25 ml of 0.05 M Tris buffer, pH 10.0 to convert the glucosinolates into isothiocyanates. Fifty milliliters of dichloromethane was then added to each flask and the flasks were placed in an incubator shaker set at 25 °C and 200 rpm for 8 h. Following hydrolysis, 10 g of sodium chloride and 10 g of anhydrous sodium sulfate were added. The dichloromethane was decanted and filtered, the residual seed meal was extracted for an additional three times with excess dichloromethane. The combined crude dichloromethane extracts were analyzed by gas chromatography–mass spectrometry (GC–MS).

GC–MS Analysis of Isothiocyanates

Gas chromatography–mass spectrometry was performed using a Hewlett-Packard (HP) 6890 GC system attached to an Agilent Systems HP 5972A Mass Selective Detector. The column used was a fused silica HP-5MS capillary (0.25 µm film thickness, 30 m × 0.25 mm ID). The GC operating parameters were as follows: splitless injection mode; temperature programmed from 50 to 325 °C at 10 °C/min with a 5 min interval and final temperature hold; Helium carrier gas flow rate at 1.0 ml/min, with the injector temperature set at 325 °C. Spectra were compared with purified standards prepared in this laboratory. Dichloromethane extracts of camelina seed powders and meals and egg powders were examined by this method and no detectable isothiocyanates were found.

Sensory Evaluation of Eggs

A panel of 28 untrained evaluators (11–68 years of age), who were blinded to treatment groups did sensory evaluation of eggs. All the tasters ate half of a hard-boiled egg, rinsed their pallet and then ate another egg sample. All three treatment groups were eaten in random order. Panelists were asked to rate the taste and aroma of the eggs.

Statistics

Data were analyzed as a one-way ANOVA with 3 treatments using SPSS [29]. Significant differences among treatment means were separated using Duncan's multiple range test at $P < 0.05$.

The fatty acid content of the individual egg samples was measured then these values were used to calculate the average content of fatty acid per sample group. The fatty acid data were analyzed by using one-way ANOVA and a Tukey's post hoc test.

Results

Production

The egg production rate was greater than 95% for all groups with no significant difference in percent hen-day egg production (Table 3). Feed consumed per production of dozen eggs was 1,521, 1,460 and 1,472 g for Control, 5% camelina and 10% camelina groups, respectively. There was no statistical significant difference for the feed consumption and body weight (Table 3). No mortality was observed in any of the treatment groups during the experimental period.

Egg Quality Characteristics

There was no significant difference in egg weight between the Control and 10% camelina groups, however a significant reduction in the egg weight was observed in the 5% camelina group eggs (Table 4). We found a significant difference in the shell strength of eggs among all the groups (Table 4). Egg shell strength was significantly lower for the Control group and higher for the 5% camelina group. Shell thickness for the eggs from 5% camelina group was significantly higher than that of the Control and the 10% camelina groups (Table 4). Overall, shell strength and shell thickness were higher in the 5% group relative to the Control group, whereas shell strength was higher and shell thickness was lower in 10% group relative to control group. There was no significant difference among the treatments in yolk color when analyzed by the Egg analyzerTM at time

Table 4 Effect of camelina meal in laying hen diets on egg characteristics

	Egg weight (g)	Shell strength (Breaking force) (kg)	Shell thickness (mm)
Control	60 ± 4 ^a	4.5 ± 1.0 ^a	0.4019 ± 0.02 ^{a,b}
5% Camelina	58 ± 4 ^b	5.0 ± 1.1 ^c	0.4049 ± 0.02 ^a
10% Camelina	60 ± 5 ^a	4.7 ± 1.1 ^b	0.3997 ± 0.02 ^b

± Standard deviation

^{a,b,c} Means with no common superscript in the same column differ significantly ($P < 0.05$)

zero, one week of cold storage and 2 weeks of cold storage at 4 °C (Data not shown). However, when analyzed for Haugh Unit and Grade, at time zero, eggs from the 5 and 10% camelina groups were graded better [AA] relative to the control eggs [A]. We found no significant difference in the grade when measured after 1 and 2 weeks of cold storage at 4 °C (Table 5).

Egg Fatty Acid Composition

Detailed fatty acid profile of the eggs from three treatment groups is outlined in Table 6. There was a significant increase in the total n-3 fatty acids in the eggs from the 5 and 10% camelina groups, as compared to the Control group. The ratio of n-6 to n-3 fatty acids was also significantly lower in the 10% camelina group (4.3), relative to the 5% camelina group (6.0) and the Control group (12.4). Eggs from the 10% camelina group had on average of 78 mg of DHA per yolk, as compared to 59 mg/yolk from the 5% camelina group and 32 mg/yolk from the Control group. There was a nearly threefold increase in deposition of ALA in the 10% camelina group eggs when compared to the Control group eggs. Cholesterol content of the yolk did not differ significantly between the 5 and 10% camelina groups compared to the Control eggs (data not shown).

Glucosinolate Levels

There were no detectable camelina-derived glucosinolates found in eggs.

Table 3 Effect of camelina meal in laying hen diets on change in body weight, egg production and feed consumption

	Initial wt (g)	Ending wt (g)	Wt change (g)	% Hen day egg production	Feed (g) per dozen eggs
Control	1,438 ± 98	1,632 ± 106	194 ± 76	95.7 ± 3.4	1,521 ± 141
5% Camelina	1,453 ± 82	1,599 ± 82	149 ± 76	95.3 ± 3.2	1,460 ± 123
10% Camelina	1,453 ± 82	1,614 ± 118	161 ± 82	95.3 ± 3.4	1,472 ± 165

± Standard deviation

Table 5 Effect of camelina meal in laying hen diets on Interior Egg Quality—Haugh Unit & [Grade] (Egg AnalyzerTM)

	Time zero	One week cold storage	Two weeks cold storage
Control	71 ± 9 [A]	53 ± 8 [B]	54 ± 8 [B]
5% Camelina	75 ± 5 [AA]	57 ± 11 [B]	57 ± 11 [B]
10% Camelina	75 ± 4 [AA]	57 ± 6 [B]	56 ± 8 [B]

± Standard deviation

Table 6 Effect of camelina meal in laying hen diets on fatty acid profile of eggs

Fatty acid content mg/yolk	Control	5% Camelina	10% Camelina
C14:0	21.2 ± 4.9	11.1 ± 3.3*	8.7 ± 1.8*
C14:1n-5	14.6 ± 2.0	13.6 ± 3.8	11.8 ± 1.8
C16:0	1,168.9 ± 115.4	890.7 ± 156.3*	776.5 ± 100.8*
C16:1n-7	186.7 ± 25.5	133.9 ± 20.4*	106.6 ± 14.0***
C18:0	423.3 ± 51.8	381.2 ± 71.1	395.8 ± 54.1
C18:1n-9	2,028.7 ± 199.6	1,839.5 ± 303.2	1,855.1 ± 249.9
C18:2n-6	522.2 ± 71.4	519.8 ± 96.5	518.6 ± 49.2
C18:3n-6	8.0 ± 1.3	6.5 ± 1.8	7.2 ± 1.2
C18:3n-3	24.6 ± 4.9	50.9 ± 12.8*	73.3 ± 8.0***
C20:1n-9	23.6 ± 3.4	31.2 ± 7.5*	38.4 ± 5.6*
C20:2n-6	8.3 ± 1.1	10.4 ± 2.5	12.8 ± 2.0*
C20:3n-6	10.7 ± 1.5	10.7 ± 1.8	11.9 ± 1.3
C20:4n-6	158.9 ± 18.6	127.6 ± 23.2	129.4 ± 15.4
C20:5n-3	1.0 ± 0.2	1.5 ± 0.4	2.8 ± 0.6
C22:4n-6	5.7 ± 0.6	4.7 ± 0.9	5.0 ± 1.2
C22:5n-6	24.6 ± 1.8	12.5 ± 2.8*	9.6 ± 2.6*
C22:5n-3	2.6 ± 0.4	5.2 ± 1.5*	7.2 ± 1.3***
C22:6n-3	31.8 ± 3.9	59.1 ± 10.5*	77.6 ± 11.2***
Total	4,665.4 ± 456.5	4,110.1 ± 684.5	4,048.3 ± 464.6
Total n-6	738.4 ± 90.7	692.3 ± 125.6	694.5 ± 68.3
Total n-3	60.0 ± 8.1	116.7 ± 23.7*	161.0 ± 19.5***
n-6/n-3	12.4 ± 0.8	6.0 ± 0.2*	4.3 ± 0.1***

± Standard deviation

* Significant from 0% camelina, $P < 0.05$ ** Significant from 5% camelina, $P < 0.05$

Sensory Evaluation

No overt reactions were noted, i.e., facial expressions of poor tasting eggs or really bad tasting eggs, by the panelists. Two individuals noted that the 10% camelina group had a bit of a fishy taste.

Discussion

In this study, we evaluated the use of extruded defatted camelina meal as a protein source rich in n-3 fatty acids on

egg production and quality. In a previous study, when *Camelina sativa* seed oil is added at a level of 5% in laying hen diets, the n-3 fatty acid content of the eggs is increased [30]. Also, the functional properties and sensory quality of the eggs were not negatively affected by the 5% concentration of seed oil demonstrating that the camelina seed oil group scored better than the test group fed with flax seed oil diet [30]. This investigation suggests that *Camelina sativa* seed oil can increase n-3 fatty acid levels in eggs without imparting the same off flavor and odor as flax meal and oil. This is consistent with the results observed in this study.

Camelina meal as a potential feed ingredient in turkey diets at levels above 5% is not recommended as reduction in feed consumption occurs [7]. Feeding camelina meal at levels of 5 or 10% to broilers to enrich tissue n-3 fatty acid content, depresses feed intake and feed conversion ratio during starter phase (0–14 days) while camelina meal did not have any adverse effect on the sensory quality of the meat [31]. Camelina seed does not depress feed consumption at a levels up to 15% in rabbits [32]. Similarly, in our study there was no reduction in the percent hen day production, feed consumption or was there a reduction in hen body weight in the camelina meal fed groups. Because percent hen day egg production is an excellent indicator of health and well-being, the lack of change suggests that neither level of camelina meal had adverse effects on health.

Pekel et al. [33] reported that increasing levels of camelina meal in laying hen diets results in decreased feed consumption, egg production and body weight, however this effect was not observed when camelina meal is fed up to 9% between 22 and 34 weeks. In another report, feeding camelina meal to laying hens at concentrations of 5, 10, and 15% results in a reduction in hen-day egg production at the 15% concentration [34]. This group also reported that yolk weight expressed as a percentage of egg weight was lower for the 10 and 15% camelina groups, but albumin weight expressed as a percentage of egg weight, was higher for these same eggs. Herein, we report that feeding camelina meal up to 10% between 28 and 40 weeks and had no detrimental effects on performance parameters or on egg quality.

We observed a significant difference in the egg weight, shell thickness and shell strength in the 5% camelina group eggs relative to the control group. Our results of egg weight, shell thickness are in contrast to the other study [34], who reported no significant difference in egg weight or shell thickness. The observed reduction in egg weight, increased shell strength and shell thickness in 5% camelina group in the present study may be due to individual bird variation, unknown nutrient interactions or other unexplainable genetic factors because there was no strain difference in the birds used in this study.

As hypothesized, when camelina meal with approximately 12% residual oil is included in hen diets, there is a concomitant increase in total n-3 fatty acid composition from 0.32% in the control eggs to 2.54, 2.69 and 2.99% in 5, 10 and 15% camelina group eggs, respectively [34]. In our study, feeding camelina meal with residual oil content of 10% resulted in a total n-3 fatty acid composition of 2.5 and 3.7% in 5 and 10% camelina group eggs relative to the 1.1% of the control eggs. The net change in total n-3 fatty acids was not the result of a reduction in n-6 fatty acids (Table 6), indicating that inclusion of camelina meal in the diets provided adequate n-6 fatty acid intake. Similar to the other study [34], we also observed a net reduction in saturated fatty acids, but these changes all occurred in a manner that did not alter egg production or egg quality. Diets with moderate levels of ALA and high levels of LA produced increased deposition of DHA in the egg yolk, but not EPA [35]. In the study [35], authors suggested that the increased deposition of DHA may be due to the saturation of the different Δ -unsaturases depending on the level of dietary fat or due to impairment in the conversion of EPA to DHA. However, in the present study we also observed an accretion in the deposition of EPA, but to a very low extent compared to the deposition of DHA. This may be due to the specific action of desaturases to the different dietary source of fat or to the concentration of dietary fat.

Many studies were conducted to investigate the effects of n-3 rich dietary sources in laying hen diets. Using fish meal and fish oil in laying hen diets, both high in n-3 fatty acid content, produced n-3 enriched eggs [11–13, 36–38]. Similarly flax seed meal added to laying hen diets also increases the n-3 fatty acid content although is reported to impart a fishy odor in the egg [14–17]. Herein we propose that camelina meal is a better alternative to flax meal because it is a crop that is much less weather dependent, has more consistent yields, and is cheaper to produce [39]. Thus, camelina meal may offer a less expensive feed ingredient to enrich n-3 fatty acid content in eggs, compared to flax meal.

Addition of camelina meal to laying hen diets at a concentration of 5 and 10% didn't have any detrimental effects on feed consumption and egg production; and there were no detectable glucosinolates in eggs from either treatment groups. Isothiocyanates and nitrile forms are the metabolites of glucosinolates and these are the forms that could possibly have been accumulated in the eggs, but we found no indication of their presence.

Our results indicate that camelina meal can be added as an ingredient to laying hen diets as a source of energy, protein and n-3 fatty acids. Addition of mechanically pressed defatted camelina meal to laying hen diets up to a concentration of 10% did not have any detrimental effects on feed consumption, on hen body weight, on egg production, on

interior quality of eggs and on sensory quality of eggs, while producing n-3 fatty acid enriched eggs.

Acknowledgments This study was funded by Great Plain Oil and Exploration. Camelina meal used in this study was supplied by Great Plain Oil and Exploration.

References

1. US Department of the Interior (Accessed June 2011) <http://www.doi.gov/pam/EnergyPolicyAct2005.pdf>
2. Zubr J (1997) Oil-seed crop: *Camelina sativa*. *Ind Crop Prod* 6:113–119
3. Putnam DH, Budin JT, Field LA, Breene WM (1993) Camelina: a promising low-input oilseed. In: Janick J, Simon JE (eds) *New crops*. Wiley, New York, pp 314–322
4. Pilgeram AL, Sands DC, Boss D, Dale N, Wichman D, Lamb P, Lu C, Barrows R, Kirkpatrick M, Thompson B, Johnson DL (2007) *Camelina sativa*, a Montana omega-3 and fuel crop. In: Janick J, Whipkey A (eds) *Issues in new crops and new uses*. ASHS Press, Alexandria
5. Acamovic T, Gilbert C, Lamb K, Walker KC (1999) Nutritive value of *Camelina sativa* meal for poultry. *Br Poult Sci* 40:S27–S41
6. Tripathi MK, Mishra AS (2007) Glucosinolates in animal nutrition: a review. *Animal Feed Sci Technol* 132:1–27
7. Frame DD, Palmer M, Peterson B (2007) Use of *Camelina sativa* in the diets of young turkeys. *J Appl Poult Res* 16:381–386
8. Watkins BA, Feng S, Strom AK, DeVitt AA, Yu L, Li Y (2003) Conjugated linoleic acids alter the fatty acid composition and physical properties of egg yolk and albumen. *J Agric Food Chem* 51:6870–6876
9. Cherian G, Wolf FW, Sim JS (1996) Dietary oils with added tocopherol: effects on egg or tocopherol, fatty acids, acid oxidative stability. *Poult Sci* 75:423–431
10. Juneja LR (1997) Egg yolk lipids. In: Yamamoto T, Juneja LR, Hatta H, Kim M (eds) *Hen eggs*. CRC Press, Boca Raton, pp 73–98
11. Adams RL, Pratt DE, Lin JH, Stadelman WJ (1989) Introduction of omega-3 polyunsaturated fatty acids into eggs. *Poult Sci* 68(Suppl 1):166
12. Huang ZB, Leibovitz H, Lee CM, Miller R (1990) Effect of dietary fish oil on w-3 fatty acid levels in chicken eggs and thigh flesh. *J Agric Food Chem* 38:743–747
13. Nash DM, Hamilton RMG, Hulan W (1995) The effect of dietary herring meal on the omega-3 fatty acid content of plasma and egg lipids of laying hens. *Can J Anim Sci* 75:247–253
14. Caston L, Leeson S (1990) Research note: dietary flaxseed and egg composition. *Poult Sci* 69:1617–1620
15. Aymond WM, Van Elswyk ME (1995) Yolk thiobarbituric reactive substances and n-3 fatty acids in response to whole and ground flaxseed. *Poult Sci* 74:1358–1394
16. Scheideler SE, Froning GW (1996) The combined influence of dietary flaxseed variety, level, form, and storage conditions on egg production and composition among vitamin E-supplemented hens. *Poult Sci* 75:1221–1226
17. Gonzalez-Esquerra R, Leeson S (2001) Alternatives for enrichment of eggs and chicken meat with n-3 fatty acids. *Can J Anim Sci* 81:295–305
18. Simopoulos AP (2000) Human requirement for n-3 polyunsaturated fatty acids. *Poult Sci* 79:961–970
19. Leaf A, Weber PC (1987) A new era for science in nutrition. *Am J Clin Nutr* 45:1048–1053

20. Connor WE (2000) Importance of n-3 fatty acids in health and disease. *Am J Clin Nutr* 71:171–175
21. Simopoulos AP (1999) Essential fatty acids in health and chronic disease. *Am J Clin Nutr* 70:560–569
22. Kang JX, Leaf A (1996) Antiarrhythmic effects of polyunsaturated fatty acids. *Recent studies. Circulation* 94(7):1774–1780
23. Leaf A, Kang JX, Xiao YF, Billman GE (2003) Clinical prevention of sudden cardiac death by n-3 polyunsaturated fatty acids and mechanism of prevention of arrhythmias by n-3 fish oils. *Circulation* 107(21):2646–2652
24. Kris-Etherton PM, Harris WS, Appel LJ (2002) For the Nutrition Committee. AHA scientific statement. Fish consumption, fish oil, omega-3 fatty acids, and cardiovascular disease. *Circulation* 106:2747–2757
25. Nutrient Requirements of Poultry, Ninth Revised Addition (1994) National Research Council. National Academy Press, Washington
26. Radin NS (1981) Extraction of tissue lipids with a solvent of low toxicity. *Methods Enzymol* 72:5–7
27. Willis S, Samala R, Rosenberger TA, Borges K (2009) Eicosapentaenoic and docosahexaenoic acids are not anticonvulsant or neuroprotective in acute mouse seizure models. *Epilepsia* 50: 138–142
28. Bowman RE, Wolf RC (1962) A rapid and specific ultramicro method for total serum cholesterol. *Clin Chem* 8:302–309
29. SPSS 14.0, SPSS Inc., Chicago, IL
30. Rokka T, Alen K, Valaja J, Ryhanen EL (2002) The effect of a *Camelina sativa* enriched diet on the composition and sensory qualities of hen eggs. *Food Res Int* 35:253–256
31. Ryhanen EL, Perttila S, Tupasela T, Valaja J, Eriksson C, Larkka K (2007) Effect of *Camelina sativa* expeller cake on performance and meat quality of broilers. *J Sci Food Agric* 87:1489–1494
32. Peiretti PG, Mussa PP, Prola L, Meineri G (2007) Use of different levels of false flax (*Camelina sativa* L.) in diets for fattening rabbits. *Livest Sci* 107:192–198
33. Pekel AY, Patterson PH, Hulet RM, Acar N, Cravener TL, Dowler DB, Hunter JM (2009) Production performance of two strains of laying hens fed different levels of camelina meal and flaxseed. *Poult Sci* 88(Suppl 1):31
34. Cherian G, Campbell A, Parker T (2009) Egg quality and lipid composition of eggs from hens fed *Camelina sativa*. *J Appl Poult Res* 18:143–150
35. Grobas S, Mendez J, Lazaro R, De Blas C, Mateos GG (2001) Influence of source and percentage of fat added to diet on performance and fatty acid composition of egg yolks of two strains of laying hens. *Poult Sci* 80:1171–1179
36. Herber SM, Van Elswyk ME (1996) Dietary marine algae promotes efficient deposition of n-3 fatty acids for the production of enriched shell eggs. *Poult Sci* 75:1501–1507
37. Nash DM, Hamilton RMG, Sanford KA, Hulan HW (1996) The effect of dietary menhaden meal and storage on the omega-3 fatty acids and sensory attributes of egg yolk in laying hens. *Can J Anim Sci* 76:377–383
38. Abril R, Barclay W (1998) Production of docosahexaenoic acid-enriched poultry eggs and meat using an algae-based feed ingredient. In: Simopoulos AP (ed) *The return of w-3 fatty acids into the food supply. I. Land-based animal food products and their health effects. World Review in Nutrition and Dietetics*, vol 83. Basel, Switzerland
39. Moloney AP, Woods VB, Crowley JG (1998) A note on the nutritive value of camelina meal for beef cattle. *Ir J Agric Food Res* 37:243–247

Automated High-Throughput Fatty Acid Analysis of Umbilical Cord Serum and Application to an Epidemiological Study

Yu Hong Lin · Norman Salem Jr. · Ellen M. Wells ·
Weiyin Zhou · James D. Loewke · James A. Brown ·
William E. M. Lands · Lynn R. Goldman · Joseph R. Hibbeln

Received: 12 July 2011 / Accepted: 19 February 2012 / Published online: 21 March 2012
© AOCS (outside the USA) 2012

Abstract Large population studies show that polyunsaturated fatty acids are important for human health, but determining relationships between the health benefits and the fatty acid content has been hampered by the unavailability of labor-effective high-throughput technologies. An automated high throughput fatty acid analysis was developed from a previous procedure based on direct transesterification including the automation of chemical procedures, data acquisition and automatic data processing. The method was validated and applied to umbilical cord serum samples in an epidemiological study. The method

was linear in the range of 1–600 $\mu\text{g/mL}$ serum with $r^2 \geq 0.99$. The within-run CV was $<5.4\%$ for 23 fatty acids and a range of recoveries over three concentrations were 76–119% in a low-lipid matrix with the exception of 14:0. The fatty acid concentration as measured by the robotic method for human plasma was in good agreement with the Lepage & Roy method. The fatty acid profile in umbilical cord serum from American subjects ($n = 287$) showed an average of 38.0, 24.9, 32.0 and 4.6% of total fatty acids for saturates, monounsaturates, n-6 and n-3 polyunsaturates, respectively. This is the first report of a complete, validated, cost-effective, automated, high throughput fatty acid measurement method along with application to a population-based study. Automated fatty acid analysis coupled with automated data processing greatly facilitates the high throughput, 72 samples transesterified in 6 h, required for large population-based studies.

Electronic supplementary material The online version of this article (doi:10.1007/s11745-012-3661-6) contains supplementary material, which is available to authorized users.

Y. H. Lin (✉) · N. Salem Jr. · W. Zhou · J. D. Loewke ·
J. A. Brown · W. E. M. Lands · J. R. Hibbeln
Section of Nutritional Neuroscience, Laboratory of Membrane
Biochemistry and Biophysics, National Institute on Alcohol
Abuse and Alcoholism, NIH, 5625 Fishers Lane, Room 3N-07,
MSC 9410, Bethesda, MD 20892-9410, USA
e-mail: yulin@mail.nih.gov

Present Address:

N. Salem Jr.
DSM Nutritional Products, LLC, Columbia, MD, USA

E. M. Wells
Department of Environmental Health Sciences, Case Western
University School of Medicine, Cleveland, OH, USA

E. M. Wells
Department of Environmental Health Sciences, Johns Hopkins
University Bloomberg School of Public Health,
Baltimore, MD, USA

L. R. Goldman
George Washington University School of Public Health and
Health Services, Washington, DC, USA

Keywords Gas chromatography · Automation ·
Robot · Fatty acid · Transesterification

Abbreviations

AA	Arachidonic acid
DHA	Docosahexaenoic acid
EFA	Essential fatty acid
FAME	Fatty acid methyl ester
GC or GC/FID	Gas chromatography/flame ionization detector
GC/MS	Gas chromatography/mass spectrometry
HUFA	Highly unsaturated fatty acid
ISTD	Internal standard
LiHa	Liquid handling arm
pLLD	Pressure-based liquid level detection
PMP	Pressure monitored pipetting
PUFA	Polyunsaturated fatty acid

Robot Automated liquid handling system
VBA Visual Basic Application

Introduction

The content of dietary polyunsaturated fatty acids (PUFA) has been notably associated with human health as reported in several epidemiological studies [1–6] over the past 10 years. In particular, inadequate n-3 PUFA have been implicated in suboptimal neural development [7], increased risk of cardiovascular disease [8], neurodegenerative diseases [9], psychiatric disorders [10], suboptimal IQ [2], as well as other public health related issues [11].

However, the dietary intake of PUFA was usually estimated using food frequency questionnaires [2] which can overestimate and/or underestimate food intake by 20% or more [12]. The relationships between health benefits and n-3 and n-6 PUFA intake and human blood fatty acid content are much needed. The development of the fingertip prick blood sampling [13] and microwave irradiation partial transesterification methodologies [14, 15] has greatly increased the potential for large scale screening of fatty acids in human blood. The further simplification of a one-step, direct transesterification method greatly increased the throughput of fatty acid assays for glycerophospholipids [16]. Nevertheless, the unavailability of automated methodology for labor-saving, high throughput, quantitative and cost-effective fatty acid analysis and the lack of automated data processing have limited the scope of complex n-6 and n-3 fatty acid related clinical studies.

Over the years, we have been developing several techniques to make large scale fatty acid analysis feasible, including a fast gas chromatographic (GC) method [17] and a basic robotic system for the transesterification procedure [18]. This study further developed the robotic procedure and robotic operating script into a working automated, high throughput method for 24 fatty acids in human plasma and serum, and created a Visual Basic Application (VBA) script to automate the data processing. Furthermore, we applied this automated, high throughput technology to umbilical cord sera as part of an epidemiological study.

Materials and Methods

Chemicals and Reagents

All chemicals were of analytical reagent grade and screened for interference with the baseline of chromatograms. Fatty acid standards were purchased from Nu-Chek Prep (Elysian, MN), including docosatrienoic ethyl ester

(22:3n-3) as internal standard (ISTD) and GC reference standard GLC-462 containing 28 fatty acid methyl esters (FAME) of equal weight. GLC-462 was used as the source of individual fatty acid standard in the quality control (QC) samples and validation experiments. Acetyl chloride (Category # 114189) and decane were purchased from Sigma-Aldrich (St. Louis, MO). Toluene and hexane were from EMD Chemicals Inc. (Gibbstown, NJ). Methanol and pentane were from Burdick & Jackson (Muskegon, MI). Stock solutions of standards were prepared in bulk (1–20×) with the addition of butylated hydroxytoluene (BHT, 25 µg/mL) as antioxidant, aliquoted and stored at –80 °C. All solvents were purchased commercially and used without further purification.

Low-Lipid Matrix

A low-lipid matrix was prepared from human serum. The serum lipids were removed using a method modified from Blix [19]; human serum was precipitated with pre-chilled acetone (1:6, by vol) while vortexing, and immediately centrifuged at 1,700g for 3 min at 4 °C. The supernatant fluid was saved and the precipitate was treated twice with the same volume of acetone at –20 °C for 30 min. The pooled precipitates were freeze dried overnight, and stored at –80 °C as a powder for further application in the subsequent experiments. The powder was termed a “low-lipid serum powder”. This powder was dissolved in 0.9% sodium chloride to form a matrix solution with a concentration of 30 mg/mL, containing 8.4% of the original total fatty acids of serum as determined by GC. This matrix solution was applied in QC samples and validation experiments. The supernatant collected as described above was dried under nitrogen, and the total lipid in dried residue was extracted using the Folch method [20]. An aliquot of the extracted total lipids was transesterified, stored at –80 °C and used as a GC reference standard (Ref-LMBB07) along with GLC-462 to identify the retention time of FAME on chromatograms from unknown samples.

Quality Control

Low-lipid matrix serum spiked with fatty acid standards at a low (20 µg of each fatty acid per mL sample), intermediate (100 µg) and high (300 µg) amounts served as QC samples. Reference samples were prepared from 200 mL human serum obtained from a single research blood donor in the Clinical Center of the National Institutes of Health, and then aliquoted and stored at –80 °C. They were measured in 47 replicates in one run, and also in single runs in 12 separated experiments to obtain the mean value of each significant fatty acid. This sample served as a reference sample to monitor the assay performance with a physiological level of fatty acids.

Instrumentation

Automation Liquid Handling System

A Freedom Evo Instrument 200 (TECAN Trading AG, Switzerland) was utilized for automated liquid handling for the transesterification of fatty acids and operated via EVOware[®] software (v2.0, SP1, Patch3). It is referred to as The Robot, and the configuration was as described in detail in a previous report [18]. In brief, the robotic system equipped with a liquid handling arm (LiHa) is placed in a customized fume hood meeting performance criteria described in NIH Design Requirements Manual Chapter 6, Sect. 6-1-00 D.7.d. The robot components are, in order from left to right, a wash station, carriers for disposal tips and samples, reaction blocks, solvent troughs, and GC vial station on a 2-m platform.

The optimal liquid handling parameters required to process each type of liquid, such as aspirate and dispense speeds, pump mechanics, the air gaps separated liquids, and the characteristics of liquids (viscosity, volume, conductivity) etc. were included in liquid class defined within the EVOware script. Each liquid class is identified by a generic name, such as Serum, Solution. In this assay, liquid classes were established for the blood sample and solutions involved during entire run. The liquid class named pressure monitored pipetting-Serum (PMP-Serum) was for sampling serum or plasma, which also included clot detection for possible clots in samples. PMP-Solutions A, B, C, D were for four types of solutions involved in various steps and their respective pipetting parameters. PMP-Extraction was for extracting FAME after direct transesterification through 25 repetitions of mixing by aspiration and dispensing. PMP-FAME was for transferring FAME from reaction test tubes to GC vials prior to being concentrated at 55 °C. The system received preventive maintenance twice a year by the manufacturer and daily maintenance by the trained staff. Robotic pipetting accuracy was calibrated by weighing the deionized water pipetted under the same conditions as those set up for each liquid class. A routine practice was that eight aliquots of solution A-Startup was retained and weighed periodically to verify the accuracy of the ISTD amount.

Gas Chromatography

Three fast gas chromatography (6890 Plus LAN) systems with flame ionization detectors (FID; Agilent Technologies, Inc.; Santa Clara, CA) coupled with customized fused-silica, narrow-bored high-efficiency DB-FFAP capillary columns (Agilent 127-32H2, 15 m × 0.1 mm ID × 0.1 μm film thickness) were employed for chromatographic separation and to acquire the signal of the FAME

as reported previously [17]. GC inlet: 250 °C (split ratio: 50:1), detector: FID (250 °C) with hydrogen 40 mL/min, air 450 mL/min. Carrier gas: hydrogen with pressure of 355 kPa. Make-up gas: nitrogen constant at 10 mL/min. Temperature program: initially 150 °C with a 0.25 min hold with ramp at 35 °C/min to 200 °C, further 8 °C/min to 225 °C with 3.2 min hold, and then 80 °C/min to 245 °C with a 9 min hold to bake off column. Twenty-four fatty acids were eluted in about 8 min in a total run of about 17 min. Typically, GC analyses were completed overnight or were run simultaneously with robotic derivatization for the next batch of samples.

With good sample preparation and chromatographic separation, all the identified peaks were auto-integrated using the ChemStation (B.01.01) built-in integrator. The threshold values for integration parameters, including baseline correction, slope sensitivity, peak width, area reject, height reject, etc. were selected so as to integrate all signals on one chromatogram simultaneously. The merged peaks, sharing the same baseline, were integrated using non-Gaussian calculation. Manual integration was applied for very small peaks where the peak area was <0.05 area unit.

Lepage and Roy Fatty Acids Analysis

One-step direct transesterification developed by Lepage and Roy [21] was applied as a reference fatty acid method. Briefly, 100 μL of plasma or serum were added to 16 × 100 mm disposable borosilicate glass tubes placed in ice containing 1.6 mL of methanol, 0.4 mL of hexane, and 200 μL of acetyl chloride. 10 μg of 22:3n-3 ethyl ester was used as ISTD. The test tubes were capped under nitrogen, heated at 100 °C for 60 min. Afterwards, the tubes were cooled on ice for 10 min and then neutralized by the addition of 5 mL of 6% of Na₂CO₃ solution followed by centrifugation at 1,700g for 4 min. The upper phase containing FAME was collected and the volume was reduced to ~30 μL. An aliquot of 1–3 μL was injected into the GC inlet.

Automatic High Throughput Fatty Acids Analysis

Automation of plasma or serum fatty acid analysis, referred to as the robotic fatty acid assay, was developed from a previous procedure [18] based on Lepage & Roy's direct transesterification in a one-step reaction [21]. The outline of the assay procedure for the current working method and the composition of the various solutions are presented in Fig. 1. The robotic operation script is supplied as Supplemental Material 1.

Solutions were freshly made, stored at room temperature within sealed containers and transferred to solvent troughs

PROCEDURES

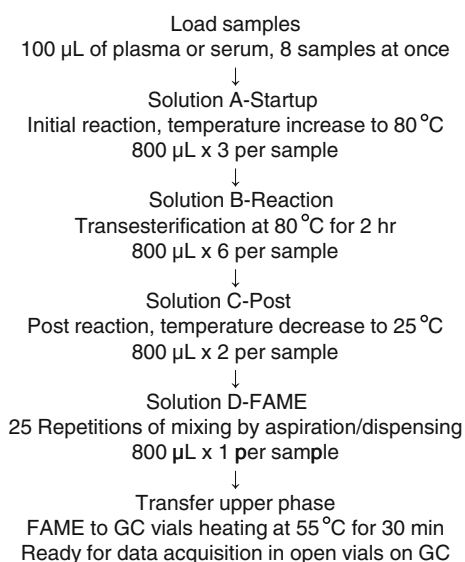


Fig. 1 Outline of the robotic fatty acid analysis procedure. The compositions of four solutions are as followed. A-Startup: methanol (BHT 25 µg/mL):toluene:acetyl chloride (2.0:0.3:0.1; by vol) containing ISTD; B-Reaction: methanol:toluene:acetyl chloride (4.1:0.6:0.1); C-Post:methanol:water (1.4:0.2); D-FAME: decane:pentane (0.08:0.72). FAME fatty acid methyl esters; GC gas chromatography; BHT butylated hydroxytoluene; ISTD internal standard

docked on the automation platform just before the start of the experiment. This guaranteed the accuracy of the concentrations of the ISTD and acetyl chloride. Acetyl chloride was added dropwise to prepare solutions at 0 °C with continuous stirring. Solutions A-Startup, B-Reaction, D-FAME were modified from Stock solutions in the previous procedure [18]. Solution C-Post (methanol:water, 7:1, by vol) was added for a complete reaction and as a key to balance the total reaction time among samples in various locations on the heating block. This also led to a better separation of upper decane/pentane phase containing FAME from the lower aqueous phase which made possible the transferring of the FAME solution to GC vials. BHT was applied as an antioxidant during open tube reactions and remained in the final FAME preparation.

Dissolved plasma or serum in containers was placed in sample carriers. Eight samples of 100 µL of plasma or serum were simultaneously loaded into 13 × 100 mm disposable borosilicate glass tubes preset in Reaction Heating Blocks, referred to as one set of samples. The transesterification reaction started after the addition of solution A-Startup followed by increasing the heating block temperature. The heating block was turned off prior to the addition of solution C-Post. The difference in reaction time between the first set of samples and the last was minimized. There is a maximal 1.6 min difference between

two adjacent sets ($n = 8$ per set) over a 3 h total reaction period. The entire experimental time for the robotic transesterification procedure was nearly independent of the number of samples analyzed, which was about 6 h for up to 72 samples.

Method Validation

The validation and quality control for laboratory robotic fatty acid assay were established in part to be consistent with the Bioanalytical Method Validation in Guidance for Industry by FDA [22] and Clinical Laboratory Improvement Amendments of 1988 [23]. Precision, stability, linearity, recovery and accuracy were examined as follows.

The within-run precision was determined by analysis of 24 fatty acids in 47 replicates of the reference sample. The between-run precision was from one reference sample in each of 12 independent experiments over a 3-month period. The linearity was evaluated by spiking a known amount of fatty acid standard in the low-lipid serum preparation at the concentrations of 1, 5, 10, 25, 50, 100, 200, 400, 600 µg/mL along with 10 µg of ISTD. The peak area ratios of fatty acid to ISTD were determined (endogenous fatty acid amounts from the low-lipid serum were subtracted) and plotted against the concentrations of the added fatty acid. Regression equations and coefficients were then generated. For a routine assay, a one point calibration was applied. The recovery was assessed by spiking a known amount of fatty acid at 20 (low), 100 (intermediate) and 300 µg/mL (high) into the low-lipid serum solution with eight replicates at each concentration. The accuracy was examined by comparing the repeated measurements of human plasma fatty acid concentrations determined by the robotic method ($n = 96$) with the Lepage & Roy method ($n = 16$). The stability of FAME preparations of serum was examined at 1, 2, 3, 8, 12, 18, 24, 30, 60, 90 days after transesterification of 16 reference samples.

In addition, the accuracy and precision for robotic pipetting were also calibrated according to the manufacturer's guidelines.

Epidemiological Study and Subjects

The samples were from the subjects recruited in the Tracking Health Related to Environmental Exposure (THREE) Study. This study was approved by Johns Hopkins University School of Medicine Institutional Review Board (Protocol # 04-04-22-02), reviewed under # NA_00028885 (June 02, 2009). Eligible subjects were singleton, live birth deliveries in the labor and delivery suite at the Johns Hopkins Hospital, Baltimore, Maryland area, during 26 November 2004 and 16 March 2005. Newborns with major congenital anomalies, or whose

mother either gave birth to multiple children, or delivered a single child with an initial twin gestation with fetal loss at ≥ 20 weeks were excluded. Trained clinical staff collected blood from the umbilical cord vein of newborns immediately following delivery. Blood was stored at 4 °C and within 3 h serum was separated by centrifuging at 1,000g for 15 min. Samples were centrifuged to obtain cord serum, aliquoted and stored at -80 °C. Frozen samples were then shipped on dry ice to NIH for fatty acid analysis. Of the 300 samples in the study, 287 had a sufficient quantity of serum to be analyzed for fatty acids. Samples were anonymized so that they could not be linked back to the subjects' identities. Further details regarding methods and population characteristics were reported in a previous publication [24].

Calculation and Automated Data Processing

All the experiments or data described were performed using the robotic method unless otherwise indicated in the text. Data were expressed as the mean concentration \pm standard deviation as μg of fatty acid per mL plasma or serum ($\mu\text{g}/\text{mL}$), or % of each fatty acid of the total weight of the identified fatty acids in each sample (wt%). The fatty acid concentrations in the plasma/serum were calculated by comparing the integrated areas of each fatty acid peak with that of a known amount of ISTD. The percent difference (%Diff) of two experimental values was calculated by dividing the absolute difference of the two values by the average of the two values. Linear regression was analyzed using Microsoft[®] Excel 2003 (Microsoft Corp.; Seattle, WA). The descriptive frequencies analyses were performed in SPSS 13.0 for Windows (SPSS Inc.; Chicago, IL).

The data processing was performed as follows; a calibration table was established providing the GC information for each fatty acid of interest in the reference sample, including peak retention time, signal abundance, integrated area, ISTD amount, etc. According to the number and starting location of the double bonds in the fatty acid carbon chain, a unique identification code was assigned to each fatty acid in the order of elution, as illustrated in Fig. 2a. The Agilent ChemStation software (B.01.01) applied this calibration table to identify fatty acids of interest in all samples in one offline or online sequence and generated a summary report in a text file for all data acquired for further calculation. The above summary reports were imported into an Excel spreadsheet. Fatty acid results were then automatically generated through macro programming (Supplemental Material 2) with Microsoft VBA 6.3 (Microsoft Corp; Seattle, WS), including both concentration ($\mu\text{g}/\text{mL}$) and the proportion of each fatty acid in total fatty acids (wt%).

Results

Robotic High Throughput Fatty Acid Assay Validation

Robotic Pipetting Accuracy and Precision

The calibration parameters offset and factor for the robotic disposal tips were applied to calibrate the net volume specified in the robot script, expressed as calibrated dilutor movement (actual volume) = (net volume \times factor) + offset. The factor for 100 μL is 1.0248, offset as 0; for 2.4 mL is 1.079 and 0. With the calibrated volume, for pipetting of a 100 μL sample, the within-run CV for eight tips was 0.4% with volume 99.9 ± 0.4 μL (mean \pm SD, $n = 5$ for each of eight tips); the between-run CV for five tips was 0.2%, volume ranging from 99.2 to 100.3 μL ($n = 5$). For pipetting 2.4 mL of Solution A, the intra CV was 0.1% with 2.407 ± 0.003 mL ($n = 6$); inter CV 0.4%, volume ranging 2.405–2.411 mL ($n = 6$).

Chromatographic Interference

Noise on the GC chromatograms was significantly reduced in the current robotic method (Fig. 2a) after having replaced the source of the acetyl chloride, the major contributor to the interference observed in Fig. 2b. The chromatogram between 1 and 2.7 min in panel 2a is flatter and has many fewer noise peaks than in panel 2b. The flatter baseline improved the accuracy of automated integration of peaks on one chromatogram and made it possible to automate data processing. In order to evaluate the introduction of extraneous peaks in the blank samples, extensive analyses were performed of all materials used (tubes, pipette tips, etc.), all reagents and solvents and robotic conditions (temperature, duration of reactions, etc.). It was determined that the acetyl chloride reagent was the source of the extraneous peaks and the issue was resolved by switching to a different reagent quality from the same supplier.

A custom, high efficiency capillary column with 10,000 theoretical plates (compared to 4,300 of a conventional column) gave good resolutions for the majority of fatty acid peaks after proper conditioning. The only partial peak co-elution noted were that of 16:1n-7 with an unidentified peak and 18:1n-9 with 18:1n-7, as presented in the insets to Fig. 2a.

Precision and Stability

Measurements of within-run precision indicated a CV $< 5.4\%$ for the concentrations of the measured fatty acids with the exception of 14:0 (14%) (Table 1). Measurements of between-run precision indicated an average CV of

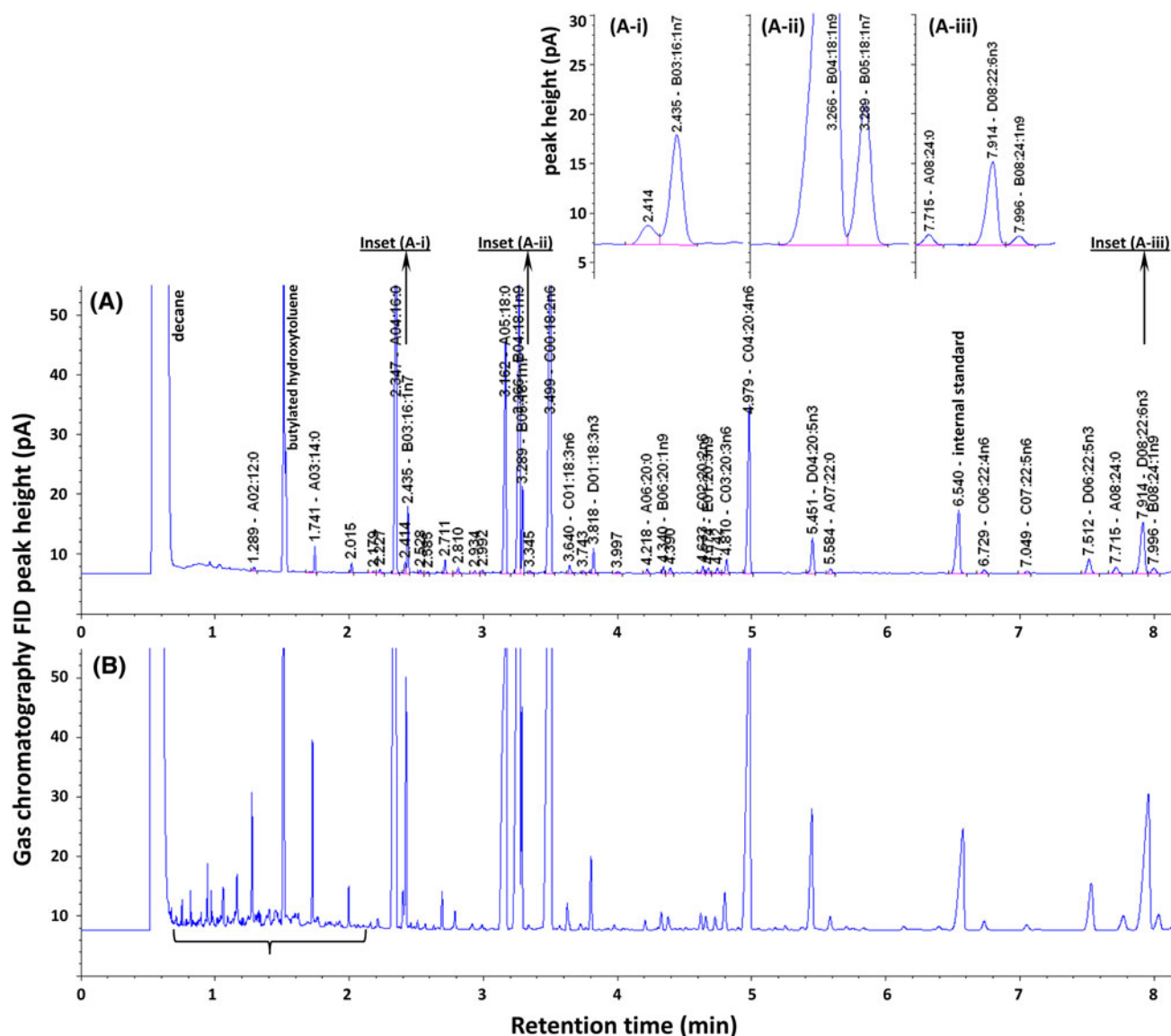


Fig. 2 Gas chromatograms of fatty acid methyl esters from rat plasma using the robotic assay with: **a** newly selected reagents, **b** previously employed reagents. A unique code was assigned to each identified fatty acid. A00 series represent saturates, B00 series for monounsaturates, C00 series for n-6, D00 series for n-3, E00 series for n-9 polyunsaturates. A-i, A-ii, A-iii are insets for **a**. All identified

peaks were auto-integrated using an Agilent ChemStation (B.01.01) built-in integrator. Integration parameters setup was: 1 for slope sensitivity, 0.02 for peak width, 0.05 for area reject, 0.3 for height reject, baseline correction sets advanced, and shoulders set off. *FID*, flame ionization detector

$4.6 \pm 2.0\%$ ($n = 12$) for the wt% of all measured fatty acids (except 14:0, 22:0 and 20:2n-6). The CV values were largely independent of fatty acid concentration, which ranged from 1 to 552 $\mu\text{g/mL}$ serum. The stability of the resultant FAME preparation in decane over 90 days for PUFA and over 30 days for saturates and monounsaturates (stored at -80°C between injections) is presented in Table 1. It was noted that saturated fatty acids and some monounsaturates had decreased beyond 30 days after transmethylation possible due to evaporation during storage. The CV for PUFA concentrations over 90 days was

$2.3 \pm 0.8\%$ with the exception of 5.6% for 20:2n-6, a very small peak that was more difficult to integrate properly. Minimal changes in fatty acid concentrations over a period of 30 days indicate that samples do not have to be analyzed by GC immediately in the case of short-term delays caused by GC malfunction or processing delays.

Linearity

Within the concentration range of 1–600 $\mu\text{g/mL}$ of fatty acids, the r^2 for the calibration curves were >0.996 for

Table 1 Precision, stability and recovery in robotic fatty acid analyses

Analytes	Precision ^a				Stability ^b		Recovery of fatty acids ^c (%)		
	Within-run (<i>n</i> = 47)		Between-run (<i>n</i> = 12)		1–30 days (<i>n</i> = 16)		Added µg fatty acid/sample (<i>n</i> = 8)		
	(µg/mL)	CV (%)	wt%	CV (%)	(µg/mL)	CV (%)	2	10	30
14:0	23.3 ± 3.2	14	1.09 ± 0.17	16	25.7 ± 1.2	4.8	76.6 ± 21	88.1 ± 9	67.8 ± 11
16:0	537.3 ± 29	5.3	21.2 ± 1.00	4.7	561.7 ± 28	5.0	90.7 ± 33	106.7 ± 11	86.1 ± 10
18:0	183.8 ± 6.5	3.5	7.51 ± 0.28	3.7	187.9 ± 4.1	2.2	103.7 ± 16	118.6 ± 7	99.0 ± 6
20:0	8.2 ± 0.2	2.0	0.34 ± 0.02	5.5	8.5 ± 0.2	2.9	100.5 ± 10	99.8 ± 2	95.9 ± 5
22:0	17.5 ± 0.6	3.3	0.70 ± 0.09	12	18.6 ± 0.8	4.5	88.9 ± 7	92.6 ± 2	93.2 ± 6
24:0	14.6 ± 0.5	3.2	0.59 ± 0.06	9.6	15.2 ± 0.6	3.9	77.6 ± 6	83.4 ± 2	85.8 ± 6
16:1n-7	35.5 ± 1.9	5.4	1.53 ± 0.07	4.9	38.4 ± 1.4	3.7	92.4 ± 12	103.2 ± 7	86.6 ± 10
18:1n-9	552.4 ± 20	3.6	23.4 ± 0.59	2.5	578.9 ± 13	2.3	105.3 ± 20	109.3 ± 8	97.1 ± 7
18:1n-7	45.1 ± 1.6	3.5	1.88 ± 0.03	1.5	47.8 ± 1.7	3.6	103.5 ± 12	106.6 ± 6	93.2 ± 7
20:1n-9	3.5 ± 0.1	3.8	0.14 ± 0.01	4.3	3.6 ± 0.1	4.1	96.2 ± 9	100.4 ± 2	96.9 ± 6
22:1n-9	0.9 ± 0.05	5.2	0.04 ± 0.003	8.3	0.9 ± 0.03	3.6	86.0 ± 6	91.7 ± 1	92.3 ± 5
24:1n-9	41.0 ± 1.0	2.5	1.68 ± 0.13	7.8	41.6 ± 0.3	0.8	76.2 ± 6	90.3 ± 2	91.2 ± 5
					1–90 days (<i>n</i> = 16)				
18:2n-6	523.0 ± 20	3.8	22.0 ± 0.63	2.9	546.9 ± 11	2.0	107.6 ± 20	110.5 ± 9	95.4 ± 8
18:3n-6	15.3 ± 0.6	3.9	0.64 ± 0.02	3.2	15.9 ± 0.3	1.6	96.5 ± 10	106.0 ± 6	94.8 ± 7
20:2n-6	3.6 ± 0.2	4.6	0.17 ± 0.03	16	3.7 ± 0.2	5.6	96.0 ± 11	103.3 ± 3	98.0 ± 5
20:3n-6	37.4 ± 0.8	2.3	1.53 ± 0.04	2.9	38.0 ± 0.3	0.9	98.1 ± 10	105.2 ± 4	98.0 ± 6
20:4n-6	250.9 ± 6.6	2.6	10.3 ± 0.25	2.5	255.0 ± 2.0	0.8	104.1 ± 13	105.1 ± 5	96.2 ± 6
22:4n-6	6.3 ± 0.1	1.9	0.26 ± 0.01	4.1	6.1 ± 0.1	2.0	89.1 ± 7	96.0 ± 1	93.8 ± 5
22:5n-6	3.2 ± 0.1	1.9	0.10 ± 0.01	5.4	3.3 ± 0.1	2.9	–	–	–
18:3n-3	6.8 ± 0.3	3.9	0.29 ± 0.01	3.7	7.2 ± 0.2	2.1	97.4 ± 10	104.7 ± 6	94.4 ± 7
20:5n-3	24.3 ± 0.7	2.8	0.96 ± 0.04	4.3	24.7 ± 0.8	3.1	104.8 ± 12	108.9 ± 5	99.0 ± 6
22:5n-3	16.8 ± 0.3	1.6	0.67 ± 0.04	5.5	16.5 ± 0.1	0.8	91.1 ± 7	98.1 ± 2	94.6 ± 5
22:6n-3	70.8 ± 1.2	1.7	2.84 ± 0.14	4.8	69.7 ± 1.2	1.8	90.5 ± 7	98.2 ± 1	94.8 ± 5
20:3n-9	7.2 ± 0.2	2.4	0.30 ± 0.01	4.3	7.4 ± 0.1	1.9	–	–	–
Total fatty acids	2,451 ± 89	3.6			2,498 ± 90	3.6	94.2 ± 11	101.2 ± 4	92.9 ± 6

“–” Indicates data were not available, wt% indicates the proportion of fatty acid of the total weight of the identified fatty acids in one sample

^a Reference samples (human serum) were employed in all experiments

^b Data are expressed as means ± SD

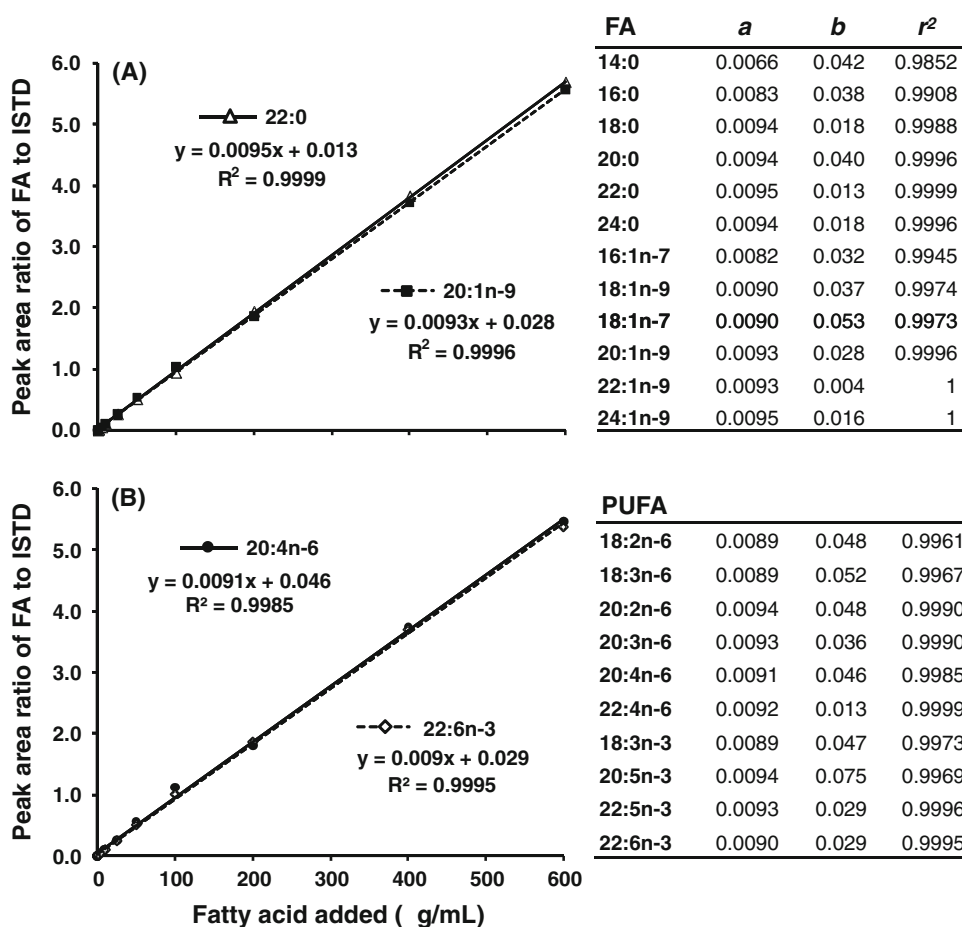
^c Nu-Chek Prep standard mixture GLC-462 was used as the source of the fatty acid standard

PUFA and 0.995 or greater for monounsaturated and saturated fatty acids with the exceptions of 14:0 and 16:0, which were 0.985 and 0.991. As plotted in Fig. 3, 20:4n-6 and 22:6n-3 are presented as the representatives of key PUFA along with examples of saturated (22:0) and monounsaturated (20:1n-9) fatty acids. The slope (*a*), intercept (*b*) and *r*² for the other fatty acids are presented in the same figure. The established calibration curves cover the expected fatty acid concentration range in unknown plasma/serum samples. A few samples with higher concentrations were diluted and re-assayed to increase accuracy.

Recovery and Accuracy

The recoveries ranged from 76 to 119% at low, medium, high concentrations for all fatty acids with the exception of 14:0 which had a low recovery rate (68%) at the high concentration. For PUFA, averages of 97.5 ± 6.4, 103.6 ± 4.8 and 95.9 ± 1.8% for low, intermediate, and high concentrations were observed, respectively (Table 1). The %Diff between the fatty acid concentrations in either decane or hexane was <2.5% (*n* = 5 per group) for 22 fatty acids with the exception of 14:0 (4.7%) (22:5n-6, not available).

Fig. 3 Linear ranges for the robotic fatty acid assay. The area ratios (fatty acid peak referenced to the internal standard) were plotted against the added fatty acid concentrations of 1, 5, 10, 25, 50, 100, 200, 400, 600 $\mu\text{g/mL}$. The regression lines, equations and r^2 of 20:1n-9 and 22:0 were presented in **a** as the examples for the monounsaturates and saturates; 20:4n-6 and 22:6n-3 in **b** are examples for n-6 and n-3 polyunsaturates, respectively. The parameters for the remaining fatty acids are listed alongside the plots. *a* and *b* indicate coefficients for $y = ax + b$. PUFA, polyunsaturated fatty acids



The fatty acid results from the accuracy assessment showed good agreement between the Lepage & Roy method and the robotic method except for some minor fatty acids, as presented in Table 2. The %Diff between lab bench analyses ($n = 16$) and robotic replicates ($n = 96$) was $<5\%$ for the mean values of total saturates, monounsaturates, n-6 highly unsaturated fatty acids (HUFA), n-3 HUFA and total fatty acids. %Diff was $<10\%$ for the majority of fatty acids with the exception of some minor fatty acids—22:0, 18:3n-6, 22:5n-6, 20:3n-9 (10–18%). The 20- and 22-carbon fatty acids with three or more double bonds are categorized as HUFA.

Fatty Acids Profile of Umbilical Cord Serum

The fatty acid profile of the umbilical cord serum from 287 human neonates, as presented in Table 3, had an average of 452 $\mu\text{g/mL}$ (range 272–802) for saturated fatty acids; 298 $\mu\text{g/mL}$ (149–613) for monounsaturated fatty acids; 380 $\mu\text{g/mL}$ (195–636) for n-6 PUFA; 54 $\mu\text{g/mL}$ (24–130)

for n-3 PUFA. These fatty acid classes accounted for 38.0, 24.9, 32.0 and 4.6%, respectively, of all fatty acids measured. Among the essential fatty acids (EFA), the major n-3 fatty acid, docosahexaenoic acid (DHA; 22:6n-3) was 47 $\mu\text{g/mL}$ (21–114), accounting for 4.0% of total fatty acids. Its precursor, 18:3n-3, was 1.8 $\mu\text{g/mL}$ (0.4–18.2) accounting for 0.15% of all fatty acids. The concentrations (in $\mu\text{g/mL}$) of 20:5n-3 was 1.7 and 22:5n-3 was 3.3. However, arachidonic acid (AA; 20:4n-6) averaged 176 $\mu\text{g/mL}$ (84–300), 15.0% of all fatty acids and its precursor, 18:2n-6, was 140 $\mu\text{g/mL}$ (54–390), accounting for 11.6% of all acids. The concentrations (in $\mu\text{g/mL}$) of 20:3n-6 was 33.9 and 22:5n-6 was 12.9. The frequencies of concentration for each PUFA are presented in Fig. 4 as histograms with their Gaussian curves. The percentage of n-3 fatty acids in total HUFA averaged $18.0 \pm 3.5\%$ with a range of 11.3–32.8%. In contrast, the % n-6 in HUFA was $79.7 \pm 3.1\%$ with the highest quintile as 83.5%, and the lowest at 74.9%. The ratio of 20:4n-6 to 20:3n-9 was significantly different between the upper (60.3) and lower (14.9) quintiles.

Table 2 Comparison of repeated measurements of human plasma fatty acid concentrations obtained by either the robotic or Lepage & Roy method

Analytes	Lepage & Roy assay		Robotic assay		Difference (%)
	(n = 16)	CV (%)	(n = 96)	CV (%)	
14:0	21.1 ± 1.4	6.6	21.8 ± 1.7	7.7	3.2
16:0	538.4 ± 29.0	5.4	532.5 ± 27.4	5.1	1.1
18:0	184.4 ± 9.1	4.9	191.3 ± 8.8	4.6	3.7
20:0	5.4 ± 0.3	4.7	6.0 ± 0.4	6.0	9.7
22:0	17.8 ± 0.9	5.0	20.7 ± 1.1	5.1	15.2
24:0	17.7 ± 0.9	4.9	18.4 ± 0.8	4.4	4.0
16:1n-7	41.2 ± 1.9	4.7	39.5 ± 2.1	5.4	4.4
18:1n-9	423.6 ± 20.7	4.9	399.8 ± 16.3	4.1	5.8
18:1n-7	25.5 ± 1.3	5.2	25.6 ± 1.2	4.6	0.6
20:1n-9	3.7 ± 0.2	5.2	3.7 ± 0.2	6.4	1.6
22:1n-9	0.7 ± 0.1	12.7	2.5 ± 0.4	17.4	–
24:1n-9	15.1 ± 0.7	4.6	16.1 ± 0.6	3.7	6.1
18:2n-6	694.1 ± 34.2	4.9	654.6 ± 25.6	3.9	5.9
18:3n-6	15.8 ± 0.6	4.0	14.3 ± 0.6	4.3	10.3
20:2n-6	4.8 ± 0.2	4.8	4.8 ± 0.2	3.8	0.4
20:3n-6	42.4 ± 2.0	4.7	42.2 ± 1.4	3.4	0.5
20:4n-6	132.3 ± 6.3	4.7	130.3 ± 4.4	3.4	1.5
22:4n-6	7.0 ± 0.4	5.1	7.2 ± 0.3	4.2	2.0
22:5n-6	2.7 ± 0.2	5.6	3.2 ± 0.2	6.2	18.1
18:3n-3	15.2 ± 0.8	4.9	14.8 ± 0.6	4.2	2.6
20:5n-3	18.8 ± 0.8	4.3	19.0 ± 0.9	4.6	1.0
22:5n-3	16.5 ± 0.8	4.6	16.7 ± 0.6	3.7	1.5
22:6n-3	27.1 ± 1.3	4.6	27.1 ± 0.8	3.0	0.3
20:3n-9	1.7 ± 0.1	4.2	1.9 ± 0.2	8.0	10.6
Summary					
Saturates	785 ± 41	5.2	791 ± 38	4.8	0.8
Monounsaturates	510 ± 25	4.8	487 ± 20	4.0	4.5
n-6 HUFA	184 ± 9	4.7	183 ± 6	3.3	0.8
n-3 HUFA	62 ± 3	4.5	63 ± 2	3.2	0.6
Total fatty acids	2,271 ± 113	5.0	2,214 ± 89	4.0	2.6

Data are expressed as means ± SD (µg/mL)

Plasma was obtained from a donor at the NIH Clinical Center; 100 µL was used for each assay

The percent difference was calculated by dividing the absolute difference of the two values from the Lepage & Roy and the robotic methods by the average of the two values

HUFA, highly unsaturated fatty acid, indicating 20C or 22C and ≥3 double bonds

Discussion

Here, for the first time, we demonstrated that a complete, validated, automated high throughput method for fatty acid analysis together with the utility of automated data processing can be applied to an observational epidemiology study as an initial step toward demonstrating utility in large population-based studies.

Robotic Fatty Acid Analysis Technical Development

One of the major challenges of this automation assay was to replace traditional vortex mixing in bench-top assays with repeated aspiration and dispensing of the mixture. Our current system had difficulties with repeated cycles of aspiration/dispensing as error messages were generated. This could be remedied by changing the tip but this was a

Table 3 Fatty acid profile in total lipids of umbilical cord venous serum

Analytes	Concentration ($\mu\text{g/mL}$, $n = 287$)				% of Total fatty acid (wt%, $n = 287$)			
	Mean \pm SD	Median	Min	Max	Mean \pm SD	Median	Min	Max
14:0	6.6 \pm 3.4	6.0	1.7	23.4	0.54 \pm 0.22	0.53	0.20	2.52
16:0	293.7 \pm 85.5	277.8	169.8	992.5	24.55 \pm 1.28	24.43	20.76	29.51
18:0	118.1 \pm 26.9	113.2	68.3	244.2	9.99 \pm 0.90	10.05	5.34	12.85
20:0	7.5 \pm 1.8	7.3	4.4	16.1	0.64 \pm 0.12	0.64	0.29	1.01
22:0	13.2 \pm 3.4	12.7	6.8	36.0	1.13 \pm 0.22	1.12	0.59	1.79
24:0	13.1 \pm 3.3	12.6	6.5	30.5	1.12 \pm 0.25	1.10	0.53	2.71
16:1n-7	37.1 \pm 13.9	34.4	12.2	100.1	3.08 \pm 0.66	3.03	1.43	6.17
18:1n-9	200.8 \pm 67.3	186.8	95.1	747.7	16.70 \pm 2.02	16.44	11.34	23.43
18:1n-7	37.1 \pm 10.2	35.5	20.8	74.9	3.12 \pm 0.41	3.09	1.87	4.84
20:1n-9	1.1 \pm 0.5	1.0	0.5	7.2	0.09 \pm 0.02	0.09	0.05	0.20
22:1n-9	0.6 \pm 0.4	0.5	0.3	3.7	0.05 \pm 0.03	0.05	0.02	0.31
24:1n-9	21.2 \pm 6.2	20.4	8.4	59.1	1.82 \pm 0.45	1.80	0.52	3.67
18:2n-6	140.5 \pm 65.2	128.0	54.2	938.6	11.61 \pm 2.15	11.34	6.94	25.56
18:3n-6	4.2 \pm 1.2	4.0	1.8	8.4	0.35 \pm 0.07	0.35	0.19	0.61
20:2n-6	4.5 \pm 1.7	4.1	2.1	13.1	0.38 \pm 0.12	0.35	0.20	1.12
20:3n-6	33.9 \pm 8.1	32.5	12.8	60.6	2.90 \pm 0.56	2.87	1.41	5.44
20:4n-6	176.1 \pm 38.0	173.5	83.7	300.4	14.99 \pm 1.89	15.14	7.54	20.36
22:4n-6	8.0 \pm 2.4	7.6	3.1	20.9	0.68 \pm 0.15	0.67	0.31	1.15
22:5n-6	12.9 \pm 4.8	12.6	3.6	31.2	1.10 \pm 0.35	1.06	0.34	2.14
18:3n-3	1.8 \pm 1.5	1.5	0.4	18.2	0.15 \pm 0.07	0.13	0.04	0.50
20:5n-3	1.7 \pm 1.0	1.5	0.4	7.9	0.15 \pm 0.08	0.13	0.05	0.69
22:5n-3	3.3 \pm 1.5	3.0	1.0	10.1	0.28 \pm 0.11	0.26	0.09	0.73
22:6n-3	47.3 \pm 13.6	45.5	20.7	113.9	4.04 \pm 0.95	3.98	1.83	8.02
20:3n-9	6.3 \pm 3.5	5.4	1.7	25.3	0.54 \pm 0.27	0.47	0.12	1.69
Summary								
Saturates	452 \pm 117	428	272	1,317	38.0 \pm 1.5	37.9	34.5	43.0
Monounsaturates	298 \pm 92	279	149	931	24.9 \pm 2.8	24.6	18.4	32.8
n-6 PUFA	380 \pm 100	368	195	1,317	32.0 \pm 2.4	32.0	25.3	36.9
n-3 PUFA	54 \pm 16	52	24	130	4.6 \pm 1.1	4.5	2.6	9.3
n-6 HUFA	231 \pm 46	229	119	378	19.7 \pm 2.1	19.8	9.8	25.1
n-3 HUFA	52 \pm 15	50	23	127	4.5 \pm 1.1	4.4	2.3	9.1
n6/n3 HUFA	4.6 \pm 1.0	4.5	2.0	7.7	4.6 \pm 1.0	4.5	2.0	7.7
Total fatty acid	1,191 \pm 306	1,128	708	3,672				

Data are expressed as both concentration ($\mu\text{g/mL}$) and the proportion of each fatty acid in the total fatty acid weight (wt%)

PUFA, polyunsaturated fatty acids

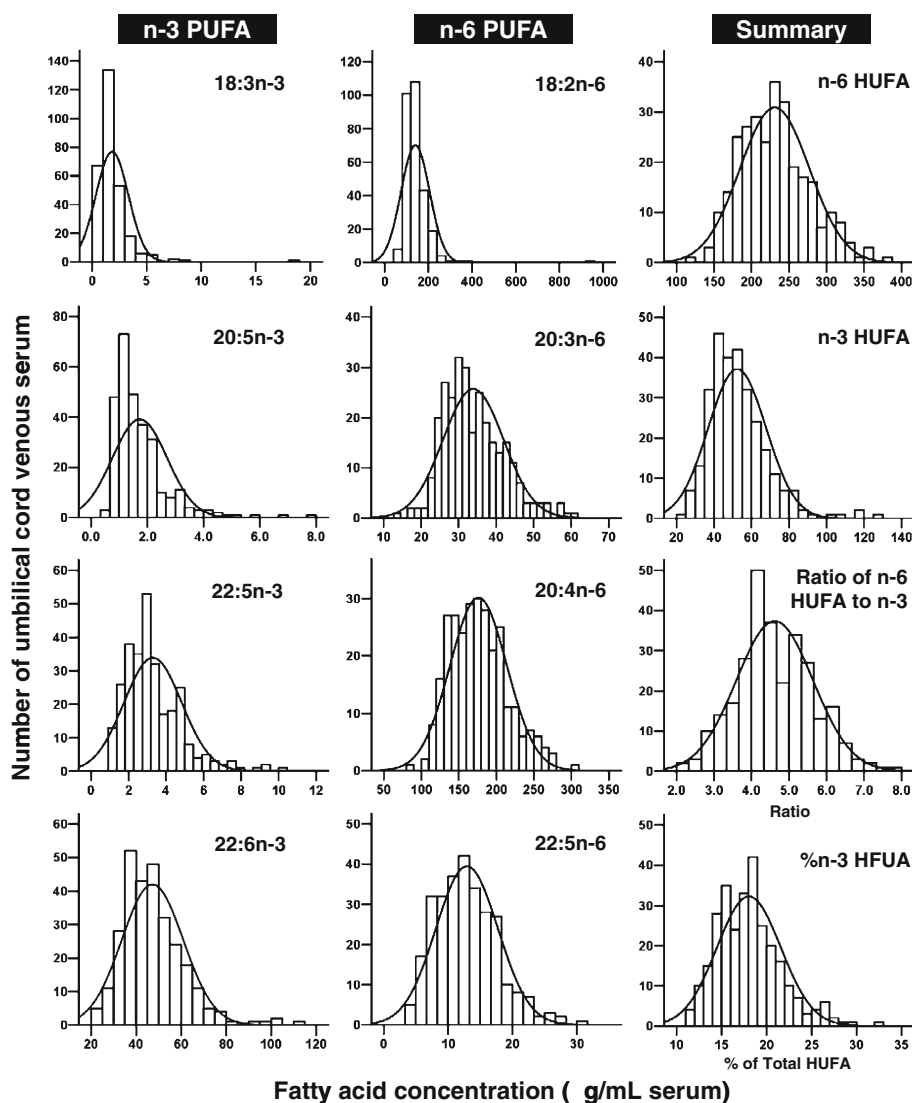
HUFA, highly unsaturated fatty acid, indicating 20C or 22C and ≥ 3 double bonds

slow and expensive solution. This issue was resolved by lowering the under-pressure limit default setting by over tenfold (from -400 to $-5,000$) during the repeated aspiration/dispensing cycle.

The pressure-based liquid level detection (pLLD) is configured for the liquid classes PMP-Serum and PMP-FAME. This detects the liquid surface through a change of

pressure in the air gap between the sample and the system liquid when the pipette tip enters or exits the liquid. One difficulty with our robotic system was that pipetting solution D led to solution dripping and an inaccurate transfer. The dripping could be prevented by pre-rinsing the tip. However, this created a malfunction in the pLLD procedure. This issue was resolved by adding a 5 s delay

Fig. 4 The frequency distribution of polyunsaturated fatty acids (PUFA) in umbilical cord serum ($n = 287$). The concentrations ($\mu\text{g/mL}$) or percentage of n-3 or n-6 in total highly unsaturated fatty acids (HUFA) was plotted as histograms with their normalized curves



following the pre-rinse, which allowed the recovery of pressure in the air gap and provided for normal pLLD.

Acetyl chloride was used as a catalyst for the transesterification with complete derivatization of non-esterified fatty acid, triacylglycerol, cholesterol ester, phospholipid, and sphingomyelin [21]. However, acetyl chloride generates HCl gas that corroded the robot mechanics and electronics. This corrosion was greatly reduced by several steps as follows: addition to two additional preventive maintenance procedures conducted by manufacturer, increasing the air flow of the fume hood enclosing the robot platform; wiping robotic mechanical parts with alcohol before and after assay; parking LiHa rest position near the ventilation exit; removing the used tips and solvent B-Reaction immediately after use. In the longer term, it would be desirable to find an alternative derivatization reagent that is less volatile and/or to significantly reduce the reaction time in the open tube.

Method Validation

A linearity with a regression fit with $r^2 \geq 0.99$ (Fig. 3) demonstrated that this method could be applied for the measurement of endogenous fatty acids in plasma/serum samples over a wide range of concentrations. Good agreement was observed for the fatty acid concentrations determined by the robotic assay compared to those by the reference method with %Diff <10% for the majority of fatty acids and $\leq 2\%$ for n-6 HUFA and n-3 HUFA except 22:5n-6 (Table 2). The much higher concentration for the very minor 22:1n-9 peak in the robotic assay was likely due to an error in peak identification in this specific experiment.

The within-run precision of <5.4% [with the exception of 14:0 (14%)] is well within the range of 1.1–7.9% obtained by GC/FID fatty acid analysis [25] and 4–14% by gas chromatography/mass spectrometry (GC/MS) fatty acid analysis [26]. A higher between-run CV compared to

the within-run was observed in this robotic method as 1.5–12% [with the exceptions of 14:0 and 20:2n-6 (16%)]. It was in comparable to that observed for GC/MS fatty acid analysis (7–17%) [26].

The validation of fatty acid recoveries in plasma samples is inherently difficult due to the widely varying concentrations of various fatty acids within a particular sample. For this reason, recovery experiments were performed at three different concentrations and a plasma matrix with a low lipid content was employed in order to make such an experiment possible. The recoveries thus obtained were comparable to those observed by Quehenberger [26] of 78–115% using a negative chemical ionization GC/MS approach.

Epidemiological Study

The distributions of the various PUFA and the fatty acid compositions were given for the umbilical cord venous serum samples in Fig. 4 and Table 3, respectively, from the Three Study conducted in Baltimore, Maryland. The average concentration of DHA in total lipids in umbilical cord serum was 47.3 ± 13.6 $\mu\text{g/mL}$ (mean \pm SD, $n = 287$) with a median of 45.5. It accounted for $4.0 \pm 0.9\%$ of the weight of total fatty acids. This is in the range of DHA concentrations observed in the umbilical cord plasma/serum total lipids as analyzed by various manually processed fatty acid methods: 40.7 $\mu\text{g/mL}$ ($n = 11$) in the study by Gil-Sanchez et al. [27], 49.9 ($n = 10$) by Lewis [28], and 65.5 $\mu\text{g/mL}$ ($n = 21$) in the study by Denkins [29]. Similarly, for AA, the average concentration was 176 ± 38 $\mu\text{g/mL}$ (15 ± 1.9 wt%) with a median of 174 (15 wt%) and this was again in the range between 79.3 [28] and 271 $\mu\text{g/mL}$ [29]. These values were comparable to those observed in other rather large studies of phospholipid DHA and AA content by Donahue et al. [30] and Kohlboeck [31] as they reported the values of 4.2% (DHA) and 15.5% (AA) in Project Viva ($n = 449$), 7.2% (DHA) and 18.0% (AA) in LISAPLUS Study ($n = 416$). However, both DHA and AA were higher in wt% than the values reported by Pankiewicz [32] of 2.8% DHA and 9.9% AA in total lipids ($n = 38$). The differences in DHA and AA contents are largely dependent on the dietary intake of PUFA among various populations studied and such variations are therefore expected.

Limitation

The robot capital cost, frequent maintenance and the requirement for operation by a well-trained chemist familiar with the operation of GC instruments as well as proficient with automated data calculation would be the major constraint for the establishment of this approach in an analytical laboratory. Multiple fast GC instruments coupled with high efficiency capillary columns are required

to accommodate the larger number of samples that are generated. Manual pipetting would be needed for samples with a very limited volume.

The GC/FID fatty acid assay is generally semi-quantitative since typically one or two internal standards are used for over 20 fatty acids which occur over a wide range of concentrations in a particular plasma sample. More rigorous quantitation may be achieved using a stable isotope labeled analog of a particular fatty acid as internal standard when coupled with GC/MS analysis [26]. In addition, other methodological improvements may also be included in the future. For example, automated sample tracking would speed up work flow, backflushing of the GC injector would serve to shorten the GC run time. The microwave irradiation could potentially reduce the heating and reaction times of transesterification and thus greatly increase the sample throughput and reduce the acid-induced mechanical damage to the robot arm. An automated solid phase extraction separation could be employed to generate fatty acid data for various lipid classes.

Present and Future Applications

In the present application, three fast GC instruments running overnight were needed to support the sample output from a single transesterified robotic system. A single well-trained analyst could operate the robot and GC systems as well as process the data in an automated fashion. The sample output from a typical week was 360 samples analyzed.

This robotic assay has been applied to the fatty acid analyses of 1,600 human sera from active-duty military personnel in a case-control study [33] and 9,581 blood samples from new-born infants and 7-year-old children in a large population study, the Avon Longitudinal Study of Parents and Children (ALSPAC) [34]. The integration of finger prick sampling, robotic derivatization and extraction, fast gas chromatography, and the automated data processing will greatly facilitate fatty acid research. Our present study provides a “proof of principle” that research scale laboratories can perform the thousands of assays per year necessary to support large scale population-based studies concerning the relationship of fatty acid composition to human health and disease.

Acknowledgments This research was supported, in part, by the Intramural Research Program of the National Institute on Alcohol Abuse and Alcoholism, National Institutes of Health; and the National Oceanic and Atmospheric Administration. Thanks to Dr. Shui-Lin Niu for helping with the preparation of the low lipid serum, and Mr. Brian Brown for his assistance with manuscript editing.

Conflict of interest The authors declare that there are no conflicts of interest.

References

- Bakker EC, Ghys AJ, Kester AD, Vles JS, Dubas JS, Blanco CE, Hornstra G (2003) Long-chain polyunsaturated fatty acids at birth and cognitive function at 7 y of age. *Eur J Clin Nutr* 57:89–95
- Hibbeln JR, Davis JM, Steer C, Emmett P, Rogers I, Williams C, Golding J (2007) Maternal seafood consumption in pregnancy and neurodevelopmental outcomes in childhood (ALSPAC study): an observational cohort study. *Lancet* 369:578–585
- Marchioli R, Barzi F, Bomba E, Chieffo C, Di GD, Di MR, Franzosi MG, Geraci E, Levantesi G, Maggioni AP, Mantini L, Marfisi RM, Mastrogiuseppe G, Mininni N, Nicolosi GL, Santini M, Schweiger C, Tavazzi L, Tognoni G, Tucci C, Valagussa F (2002) Early protection against sudden death by n-3 polyunsaturated fatty acids after myocardial infarction: time-course analysis of the results of the Gruppo Italiano per lo Studio della Sopravvivenza nell'Infarto Miocardico (GISSI)-Prevenzione. *Circulation* 105:1897–1903
- Mihrshahi S, Peat JK, Webb K, Tovey ER, Marks GB, Mellis CM, Leeder SR (2001) The childhood asthma prevention study (CAPS): design and research protocol of a randomized trial for the primary prevention of asthma. *Control Clin Trials* 22:333–354
- Seddon JM, George S, Rosner B (2006) Cigarette smoking, fish consumption, omega-3 fatty acid intake, and associations with age-related macular degeneration: the US Twin Study of Age-Related Macular Degeneration. *Arch Ophthalmol* 124:995–1001
- Smithers LG, Collins CT, Simmonds LA, Gibson RA, McPhee A, Makrides M (2010) Feeding preterm infants milk with a higher dose of docosahexaenoic acid than that used in current practice does not influence language or behavior in early childhood: a follow-up study of a randomized controlled trial. *Am J Clin Nutr* 91:628–634
- Salem N Jr, Kim HY, Yeryg JA (1986) Docosahexaenoic acid: membrane function and metabolism. In: Simopoulos AP, Kifer RR, Martin RE (eds) *Health effects of polyunsaturated fatty acids in seafoods*. Academic Press, New York, pp 263–317
- Mozaffarian D (2008) Fish and n-3 fatty acids for the prevention of fatal coronary heart disease and sudden cardiac death. *Am J Clin Nutr* 87:1991S–1996S
- Calon F, Lim GP, Morihara T, Yang F, Ubeda O, Salem N Jr, Frautschy SA, Cole GM (2005) Dietary n-3 polyunsaturated fatty acid depletion activates caspases and decreases NMDA receptors in the brain of a transgenic mouse model of Alzheimer's disease. *Eur J Neurosci* 22:617–626
- Hibbeln JR, Salem N Jr (1995) Dietary polyunsaturated fatty acids and depression: when cholesterol does not satisfy. *Am J Clin Nutr* 62:1–9
- Dunstan JA, Mori TA, Barden A, Beilin LJ, Taylor AL, Holt PG, Prescott SL (2003) Fish oil supplementation in pregnancy modifies neonatal allergen-specific immune responses and clinical outcomes in infants at high risk of atopy: a randomized, controlled trial. *J Allergy Clin Immunol* 112:1178–1184
- Godwin SL, Chambers E, Cleveland L (2004) Accuracy of reporting dietary intake using various portion-size aids in-person and via telephone. *J Am Diet Assoc* 104:585–594
- Marangoni F, Colombo C, Galli C (2004) A method for the direct evaluation of the fatty acid status in a drop of blood from a fingertip in humans: applicability to nutritional and epidemiological studies. *Anal Biochem* 326:267–272
- Armstrong JM, Metherell AH, Stark KD (2008) Direct microwave transesterification of fingertip prick blood samples for fatty acid determinations. *Lipids* 43:187–196
- Banerjee P, Dawson G, Dasgupta A (1992) Enrichment of saturated fatty acid containing phospholipids in sheep brain serotonin receptor preparations: use of microwave irradiation for rapid transesterification of phospholipids. *Biochim Biophys Acta* 1110:65–74
- Glaser C, Demmelmair H, Koletzko B (2010) High-throughput analysis of fatty acid composition of plasma glycerophospholipids. *J Lipid Res* 51:216–221
- Masood A, Stark KD, Salem N Jr (2005) A simplified and efficient method for the analysis of fatty acid methyl esters suitable for large clinical studies. *J Lipid Res* 46:2299–2305
- Masood MA, Salem N Jr (2008) High-throughput analysis of plasma fatty acid methyl esters employing robotic transesterification and fast gas chromatography. *Lipids* 43:171–180
- Blix G (1941) Electrophoresis of lipid-free blood serum. *J Biol Chem* 137:495–501
- Folch J, Lees M, Sloane Stanley GH (1957) A simple method for the isolation and purification of total lipids from animal tissues. *J Biol Chem* 226:497–509
- Lepage G, Roy CC (1986) Direct transesterification of all classes of lipids in a one-step reaction. *J Lipid Res* 27:114–120
- US Food and Drug Administration Guidance for Industry. In: *Bioanalytical method validation*. <http://www.fda.gov/downloads/Drugs/GuidanceComplianceRegulatoryInformation/Guidances/UCM070107.pdf>. Accessed January 2012
- US Department of Health and Human Services (1992) Medicare, Medicaid and CLIA programs: regulations implementing the Clinical Laboratory Improvement Amendments of 1988 (CLIA)—HCFA. Final rule with comment period. *Fed Regist* 57:7002–7186
- Apelberg BJ, Goldman LR, Calafat AM, Herbstman JB, Kuklenyik Z, Heidler J, Needham LL, Halden RU, Witter FR (2007) Determinants of fetal exposure to polyfluoroalkyl compounds in Baltimore, Maryland. *Environ Sci Technol* 41:3891–3897
- Glaser C, Demmelmair H, Koletzko B (2010) High-throughput analysis of total plasma fatty acid composition with direct in situ transesterification. *PLoS One* 5:e12045
- Quehenberger O, Armando AM, Dennis EA (2011) High sensitivity quantitative lipidomics analysis of fatty acids in biological samples by gas chromatography-mass spectrometry. *Biochim Biophys Acta* 1811:648–656
- Gil-Sanchez A, Larque E, Demmelmair H, Acien MI, Faber FL, Parrilla JJ, Koletzko B (2010) Maternal-fetal in vivo transfer of [¹³C] docosahexaenoic and other fatty acids across the human placenta 12 h after maternal oral intake. *Am J Clin Nutr* 92:115–122
- Lewis RM, Hanson MA, Burdge GC (2011) Umbilical venous-arterial plasma composition differences suggest differential incorporation of fatty acids in NEFA and cholesteryl ester pools. *Br J Nutr* 106:463–467
- Denkins YM, Woods J, Whitty JE, Hannigan JH, Martier SS, Sokol RJ, Salem N Jr (2000) Effects of gestational alcohol exposure on the fatty acid composition of umbilical cord serum in humans. *Am J Clin Nutr* 71:300S–306S
- Donahue SM, Rifas-Shiman SL, Olsen SF, Gold DR, Gillman MW, Oken E (2009) Associations of maternal prenatal dietary intake of n-3 and n-6 fatty acids with maternal and umbilical cord blood levels. *Prostaglandins Leukot Essent Fatty Acids* 80:289–296
- Kohlboeck G, Glaser C, Tiesler C, Demmelmair H, Standl M, Romanos M, Koletzko B, Lehmann I, Heinrich J (2011) Effect of fatty acid status in cord blood serum on children's behavioral difficulties at 10 y of age: results from the LISApus Study. *Am J Clin Nutr* 94:1592–1599
- Pankiewicz E, Cretti A, Ronin-Walknowska E, Czeszynska MB, Konefal H, Hnatyszyn G (2007) Maternal adipose tissue, maternal and cord blood essential fatty acids and their long-chain polyunsaturated derivatives composition after elective caesarean section. *Early Hum Dev* 83:459–464
- Lewis MD, Hibbeln JR, Johnson JE, Lin YH, Hyun DY, Loewke JD (2011) Suicide deaths of active-duty US military and omega-3 fatty acid status: a case-control comparison. *J Clin Psychiatry* 72:1585–1590
- Steer CD, Hibbeln JR, Golding J, Smith GD (2012) Polyunsaturated fatty acid levels in blood during pregnancy, at birth and at 7 years: their associations with two common FADS2 polymorphisms. *Hum Mol Genet* (in press)

Statistical Methodological Issues in Handling of Fatty Acid Data: Percentage or Concentration, Imputation and Indices

Roel J. T. Mocking · Johanna Assies · Anja Lok ·
Henricus G. Ruhé · Maarten W. J. Koeter · Ieke Visser ·
Claudi L. H. Bockting · Aart H. Schene

Received: 6 October 2011 / Accepted: 23 February 2012 / Published online: 25 March 2012
© The Author(s) 2012. This article is published with open access at Springerlink.com

Abstract Basic aspects in the handling of fatty acid-data have remained largely underexposed. Of these, we aimed to address three statistical methodological issues, by quantitatively exemplifying their imminent confounding impact on analytical outcomes: (1) presenting results as relative percentages or absolute concentrations, (2) handling of missing/non-detectable values, and (3) using structural indices for data-reduction. Therefore, we reanalyzed an example dataset containing erythrocyte fatty acid-concentrations of 137 recurrently depressed patients and 73 controls. First, correlations between data presented as percentages and concentrations varied for different fatty acids, depending on their correlation with the total fatty acid-concentration. Second, multiple imputation of non-detects resulted in differences in significance compared to zero-substitution or omission of non-detects. Third, patients' chain length-, unsaturation-, and peroxidation-indices were significantly lower compared to controls, which corresponded with patterns interpreted from individual fatty acid tests. In conclusion, results from our example dataset show that statistical methodological choices can have a significant influence on outcomes of fatty acid analysis, which emphasizes the relevance of:

(1) hypothesis-based fatty acid-presentation (percentages or concentrations), (2) multiple imputation, preventing bias introduced by non-detects; and (3) the possibility of using (structural) indices, to delineate fatty acid-patterns thereby preventing multiple testing.

Keywords Multiple imputation · Non-detectable values · Undetectable · Peroxidation index (PI) · Unsaturation index (UI) · Chain length index · Eicosapentaenoic acid (EPA) · Docosahexaenoic acid (DHA) · Polyunsaturated fatty acids (PUFA) · Recurrent major depressive disorder

Introduction

Clinical fatty acid (FA)-research is becoming increasingly performed, but basic statistical methodological issues have remained largely underexposed in scientific literature thus far. We aim to address three of these issues in the handling of FA-data, and provide quantitative examples of their imminent confounding impact on results of FA-analyses, which may confuse the understanding of the roles FA play in (patho)physiology.

First, FA are reported in two ways: as absolute concentrations, or as percentages of the total FA-concentration. The implications of these different presentations have been scarcely addressed. Importantly, the few studies that have investigated this question showed significant differences between both approaches [1–3]. This is conceivable, because an increase in the percentage of one FA automatically results in the decrease in the relative percentage of another FA, even when its absolute concentration remains unchanged [4, 5]. Nevertheless, recent research still seems to opt rather randomly for either presentational method.

R. J. T. Mocking (✉) · J. Assies · A. Lok ·
H. G. Ruhé · M. W. J. Koeter · I. Visser · A. H. Schene
Department of Psychiatry, Academic Medical Center,
University of Amsterdam, Meibergdreef 5,
Amsterdam 1105 AZ, The Netherlands
e-mail: R.J.Mocking@amc.uva.nl

C. L. H. Bockting
Department of Clinical Psychology, University of Groningen,
Grote Kruisstraat 2/1, Groningen 9712 TS, The Netherlands

A second methodological issue is how to handle non-detectable FA-concentrations. In contrast to other research fields [6], FA-research thus far has not addressed this problem. Therefore, possible important analytical consequences remain uninvestigated, which may potentially cause biases in the interpretation of FA-data.

Third, because of the great number and variety of FA, the risk exists that multiple testing induces type-I errors, or the need for strict correction [7, 8]. A solution to this problem could be meaningful data-reduction, decreasing the number of tests needed. One possible way to achieve data-reduction might be the use of indices, delineating distinct FA-patterns by incorporating several FA-concentrations into one variable [9]. Examples of important patterns in FA-research are chain length, unsaturation, and peroxidizability of FA, because these characteristics modulate membrane fluidity and susceptibility to radical attack and are thereby conceivably involved in the pathogenesis of e.g. recurrent depression [10, 11]. Using indices, e.g. the unsaturation index (UI), chain length index (CLI) or peroxidation index (PI) [9], would allow testing of these more complex hypotheses on FA-patterns involving multiple FA, thereby obviating the need to interpret analyses of every individual FA to test your hypothesis. Thus far, most FA-research did not correct for multiple testing [7], and tested indices only in addition to the individual FA. This might potentially have resulted in type-I errors, and thereby bias in the interpretation of FA-analyses.

In this paper, the conceivable confounding effects of these three statistical methodological issues are examined, by providing quantitative examples in a practical research setting, using an example dataset of FA-concentrations of recurrently depressed patient and healthy controls, described previously [10]. This was done on the basis of the following research questions: (1) what is the influence of presentation of results in percentages or concentrations, and how does this differ for different FA, (2) what is the influence of the approach used for missing/non-detectable FA-concentrations on the significances of outcome differences; and (3) what is the influence of the use of indices for data-reduction on outcome differences?

Materials and Methods

To investigate our research questions, we reanalyzed an example dataset consisting of washed erythrocyte FA-concentrations (pmol/10⁶ erythrocytes) from 137 recurrently depressed patients and 73 age- and sex-matched controls, determined by capillary gas chromatography, described in more detail previously [10, 12, 13].

Percentages or Concentrations

To investigate the effects of presentational method, we expressed FA-concentrations both in concentrations (pmol/10⁶ erythrocytes) and molecular percentages (individual FA's concentrations divided by the total FA-concentration). Subsequently, to quantify the difference between the two presentational methods for each FA, we calculated the correlation between its presentation as a percentage or as a concentration using Pearson's r ($r_{\text{absolute-percentage}}$; Table 1). A $r_{\text{absolute-percentage}}$ of 1.00 (perfect correlation) indicates no difference between the two types of FA presentation, while a $r_{\text{absolute-percentage}}$ closer to zero indicates larger differences.

To learn how, for individual FA, presentation as concentrations or percentages results in differential biases, we investigated whether the difference between the two types of presentation (expressed as $r_{\text{absolute-percentage}}$) depended on individual FA-characteristics. Therefore, we performed a second-level analysis exploring the relation between characteristics of the different individual FA and their observed $r_{\text{absolute-percentage}}$. We first calculated each FA's mean concentration ($\text{mean}_{\text{FA}(i)}$; Table 1). Subsequently, for each FA, we calculated the absolute value (non-negative) of the correlation between the specific FA-concentration and the total FA-concentration for an individual subject ($|r_{\text{FA}(i)\text{-concentration-FA-total}}|$; Table 1). Finally, we determined the influence of these individual FA-characteristics ($\text{mean}_{\text{FA}(i)}$ and $|r_{\text{FA}(i)\text{-concentration-FA-total}}|$) by entering these in a stepwise linear regression model as predicting variables with $r(i)_{\text{absolute-percentage}}$ (after Fisher r -to- Z transformation [14]) as dependent variable.

Handling of Non-detectable Values

To examine the influence of the handling of non-detectable/missing values, we compared: (1) substituting non-detectable values with zero, and omitting missing values; (2) omitting both non-detectable and missing values; and (3) using multiple imputation (MI) to estimate both non-detectable and missing values, using the software package Amelia II [15]. Simulation research previously demonstrated that MI was able to provide highly valid estimations of non-measured values, while incorporating the uncertainty involved [6, 16]. MI has been used on missing FA-concentrations before [17, 18], but not on non-detectable FA-concentrations.

To impute non-detectable/missing values, we used information on sex, age, marital status, educational level, social class, Hamilton Depression Rating Scale score, weight, length, waist and hip circumference, smoking, and salivary cortisol and dehydroepiandrosterone sulphate, folic acid, vitamin B₆ and B₁₂, homocysteine, and all other

Table 1 Effects of method of presentation (percentages or concentrations) and handling of non-detectable/missing values on fatty acid (FA) results in example dataset of 137 recurrently depressed patients and 73 non-depressed controls

FA	Presentational effects			Non-detectable/missing values					
	¹ $r_{\text{absolute-percentage}}$	Mean ²	$ r_{\text{FA-total}}^3 $	Zero substitution ⁴		Omission ⁵		Imputation ⁶	
				Patients	Controls	Patients	Controls	Patients	Controls
18:3n-3	0.96	0.83	0.38	0.84	0.81	0.85	0.83	0.83	0.81
18:4n-3	0.99	0.19	0.01	0.21 ⁷	0.035	0.45	0.31	0.24 ⁷	0.08
20:5n-3	0.97	3.55	0.21	3.3	3.9	3.4	3.9	3.3 ⁹	3.9
22:5n-3	0.91	8.87	0.37	7.9 ⁷	10.5	7.9 ⁷	10.5	8.0 ⁷	10.6
22:6n-3	0.95	16.75	0.29	14.8 ⁷	20.1	14.8 ⁷	20.1	14.9 ⁷	20.2
18:2n-6	0.85	66.26	0.66	66	67	66	67	66	67
18:3n-6	0.98	0.52	0.10	0.57 ⁷	0.38	0.61	0.62	0.58 ⁷	0.41
20:3n-6	0.92	9.23	0.37	8.8 ⁹	9.7	8.8 ⁹	9.7	8.9 ⁸	9.8
20:4n-6	0.62	75.22	0.72	71.5 ⁷	81.6	72.1 ⁷	81.6	72.0 ⁷	81.3
22:4n-6	0.91	11.45	0.22	10.7 ⁷	13.0	10.7 ⁷	13.0	10.6 ⁷	13.0
22:5n-6	0.95	1.85	0.14	1.7 ⁷	2.1	1.7 ⁷	2.1	1.7 ⁷	2.1
20:2n-6	0.95	1.33	0.23	1.3	1.3	1.4	1.3	1.3	1.3
22:2n-6	0.99	0.43	0.06	0.37 ⁷	0	0.79	ND	0.51 ⁷	0.26
14:1n-5	0.99	0.42	0.07	0.25 ⁷	0.60	0.57 ⁷	1.15	0.30 ⁷	0.65
16:1n-7	0.98	2.95	0.34	3.0 ⁹	2.5	3.0 ⁹	2.5	3.1 ⁹	2.6
18:1n-7	0.86	7.63	0.72	7.5	7.9	7.6	7.9	7.5	7.9
20:1n-7	0.99	0.29	0.14	0.21	0.27	0.66 ⁷	0.46	0.27	0.34
16:1n-9	1.00	1.27	0.19	0.9 ⁹	1.9	0.9 ⁸	1.9	0.93 ⁸	1.19
18:1n-9	0.69	74.78	0.79	74	75	75	75	75	75
20:1n-9	0.94	1.21	0.31	1.2	1.2	1.2	1.3	1.2	1.2
22:1n-9	0.99	1.96	0.03	1.9	2.1	3.1 ⁸	2.2	1.9	2.1
24:1n-9	0.93	15.47	0.29	13.3 ⁷	19.6	13.3 ⁷	19.6	13.3 ⁷	19.5
20:3n-9	0.99	0.36	0.04	0.36	0.31	0.42	0.40	0.38	0.32
14:0	0.95	3.34	0.34	3.3	3.5	3.3	3.5	3.3	3.5
16:0	0.70	160.7	0.78	164 ⁹	156	164 ⁹	156	163 ⁹	156
18:0	0.30	103.8	0.87	103	104	103	105	103	105
20:0	0.76	2.63	0.59	2.5 ⁷	2.8	2.6 ⁷	2.8	2.5 ⁷	2.8
22:0	0.88	8.26	0.22	7.6 ⁷	9.5	7.6 ⁷	9.5	7.6 ⁷	9.5
24:0	0.93	17.06	0.23	14.8 ⁷	21.3	14.7 ⁷	21.3	14.9 ⁷	21.2

All correlations were calculated using Pearson's r

¹ Correlations between results presented in absolute concentrations (pmol/10⁶ erythrocytes) or relative percentages (FA_(i) concentration divided by the total FA-concentration). All correlations were significant with $P < 0.001$

² Mean concentrations (pmol/10⁶ erythrocytes)

³ Modulus of the correlation between mean FA_(i) concentration and total FA concentration

Differences in concentrations between patients and controls, calculated using independent Student's t tests, after: ⁴ substitution of non-detectable values with zero, ⁵ omission of non-detects, and ⁶ multiple imputation of missing and non-detectable values

Significant compared to controls with ⁷ $P < 0.001$, ⁸ $P < 0.01$, and ⁹ $P < 0.05$

measured FA-concentrations. In addition, for non-detectable values, we assigned range priors in Amelia II indicating that a non-detectable FA concentration must lie between 0.001 and the detection limit of that FA (99 % confidence).

We used differences in erythrocyte FA-concentrations between patients and controls as example outcomes, calculated with independent Student's t tests. We compared

the results of these different approaches to handle non-detectable/missing values to demonstrate their impact.

Calculation of Indices

To investigate the influence of the use of indices on outcome differences we compared two methods. First, we compared the 29 individual FA concentrations in our

example dataset between patients and controls using Student's t tests and a Bonferroni correction. We interpreted the outcome differences to detect patterns of differences in chain length, unsaturation or peroxidizability between patients and controls.

As an alternative to the interpretation of these multiple individual FA-tests, we applied data-reduction using indices, which we compared between patients and controls using Student's t tests. We selected three indices specifically designed to delineate patterns in chain length, unsaturation or peroxidizability.

1. The chain length index (CLI), providing information about FA-chain length. We calculated the CLI by adding the products of each FA's concentration and the number of carbon atoms in their carbon chain and dividing this with the total FA-concentration;
2. The unsaturation index (UI), indicating the number of double bounds per FA. Calculated as follows: $(1 \times \text{monoenoics} + 2 \times \text{dienoics} + 3 \times \text{trienoics} + 4 \times \text{tetraenoics} + 5 \times \text{pentaenoics} + 6 \times \text{hexaenoics}) / \text{total FA-concentration}$;
3. The peroxidation index (PI), showing FA's susceptibility to peroxidation. Calculated as follows: $(0.025 \times \text{monoenoics} + 1 \times \text{dienoics} + 2 \times \text{trienoics} + 4 \times \text{tetraenoics} + 6 \times \text{pentaenoics} + 8 \times \text{hexaenoics}) / \text{total FA-concentration}$.

Subsequently, we compared the results of these index tests to the patterns that emerged from the interpretation of the differences between patients and controls in the individual FA. For this, we compared the index test results to the individual FA-tests on multiply imputed data, and also constructed the indices from imputed data. In this way, we prevented missing values in the original dataset causing many missing values among the indices, which would have reduced statistical power.

Statistical Software

We used PASW statistics 18.0 (SPSS, Inc., 2009, Chicago, IL, USA). MI was performed using Amelia II [15], available via the R software package [19].

Results

Correlation between Percentages and Concentrations

Table 1 shows the difference between percentages and concentrations (expressed as $r_{\text{absolute-percentage}}$) for each FA. Correlations ranged from 0.30 for 18:0 to 1.00 for 16:1n-9.

In the second-level analysis, linear regression showed that $\text{mean}_{\text{FA}(i)}$ was associated with $r(i)_{\text{absolute-percentage}}$

($\beta = -0.685$; $t_{(207)} = -4.882$; $P < 0.001$). This indicates that results presented in percentages or concentrations differed more for FA with higher concentrations.

Furthermore, when $|r|_{\text{FA-concentration-FA-total}}$ was also included in the regression model, it had an independent negative influence on $r_{\text{absolute-percentage}}$ ($\beta = -0.824$; $t_{(207)} = -5.486$; $P < 0.001$; Fig. 1). The influence of $\text{mean}_{\text{FA}(i)}$ on $r_{\text{absolute-percentage}}$ was no longer significant. This indicates that differences between results presented in percentages and concentrations were significantly greater for those FA that have a stronger correlation with the total FA-concentration, and that this influence explained the effect of high FA concentrations on differences between results presented in percentages or concentrations.

Handling of Non-detectable Values

In our example dataset, 21 patients and 8 controls had missing FA-results due to technical reasons. The non-detectable percentage ranged from 0 % for 16:0-24:0, 22:5n-3, 22:6n-3, C18:2n-6, 20:3n-6, 22:4n-6, 22:5n-6, 18:1n-7, 18:1n-9 and 24:1n-9, to 60.5 % for 22:2n-6. The mean non-detectable percentage was 11.1 %.

The impact of different methods to handle missing/non-detectable values on example outcomes are demonstrated in Table 1. Compared to results obtained after MI, substitution of non-detectable values with zero resulted in

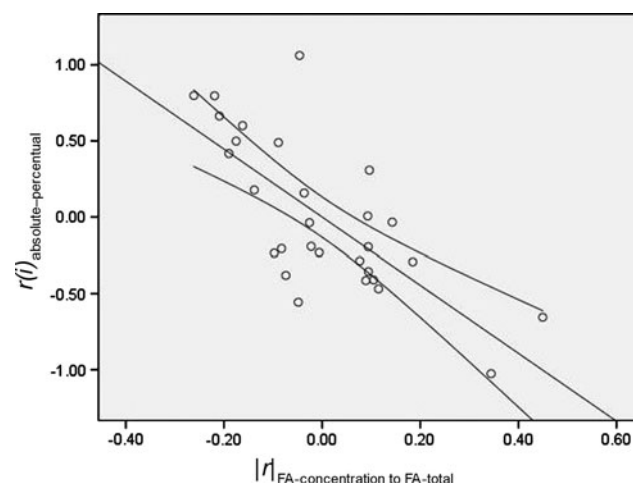


Fig. 1 Second level analysis stepwise partial regression plot of the relationship between $|r|_{\text{FA-concentration to FA-total}}$ [the absolute (non-negative) value of the correlation between the FA-concentration and total FA concentration for an individual subject] with $r(i)_{\text{absolute-percentage}}$ [the correlation between the presentation of a FA as a percentage or as a concentration calculated using Pearson's r (as an indicator of the difference between the two presentational methods)] after Fisher r -to- Z transformation in an example dataset of 29 FA concentration of 137 recurrently depressed patients and 73 healthy controls. Lines represent linear fit and 95 % CI. FA fatty acid, UI unsaturation index, CLI chain length index, PI peroxidation index, MI multiple imputation

different significance-levels for comparisons between patients and controls. Using zero substitution, the difference between patients and controls in 20:5n-3 was not significant, and differences in 20:3n-6 and 16:1n-9 were less significant. Other FA results were comparable, with lower concentrations for FA with non-detectable values, reflecting the expected bias toward zero.

When non-detectable values were omitted and not used in the analyses, the differences between patients and controls in 18:4n-3, 20:5n-3, 18:3n-6, 20:3n-6 were less or no longer significant, while significant differences in 20:1n-7 and 22:1n-9 emerged and differences in 22:2n-6 could not be tested, all compared to results obtained after MI.

Using Indices to Describe FA Patterns

The tests on the 29 individual FA after multiple imputation are listed in the right columns of Table 1. First, a Bonferroni correction for multiple comparisons was performed resulting in a corrected α of $0.05/29 = 0.0017$. After this correction, differences between patients and controls for 20:5n-3, 20:3n-6, 16:1n-7 and 16:0 were no longer significant. Other differences remained significant, with lower concentrations in patients for 22:5n-3, 22:6n-3, 20:3n-6, 20:4n-6, 22:4n-6, 22:5n-6, 14:1n-5, 16:1n-9, 24:1n-9, 20:0, 22:0 and 24:0. Concentrations of 18:4n-3, 18:3n-6, 22:2n-6, 16:1n-7, and 16:0 were higher in patients compared to controls. In analogy to our previous interpretations [10], these results fitted with patterns of reduced chain length, unsaturation and peroxidation for FA of the patients.

After data-reduction using the CLI, UI, and PI, differences between patients and controls were calculated (Table 2). The mean FA values for patients were less unsaturated ($P \sim 1.2 \times 10^{-18}$; Cohen's $d = 2.35$), shorter ($P \sim 7.1 \times 10^{-19}$; Cohen's $d = 1.46$), and less peroxidizable ($P \sim 4.0 \times 10^{-15}$; Cohen's $d = 1.83$).

When comparing the index results to the results of the multiple individual FA-tests, pattern outcomes were similar, with reduced chain length, unsaturation and peroxidation for FA of patients. Using indices resulted in fewer tests, but provided no information on differences in individual FA concentrations between patients and controls.

Discussion

Our results indicate that: (1) presentation of FA in either percentages or concentrations yields different results, particularly for those FA with a stronger correlation with the total FA-concentration, (2) differences in the approach used for non-detectable/missing values influence significance-levels of outcomes of FA-analysis, and (3) the use of the CLI, UI and PI showed differences between patients and controls in FA-patterns, in agreement with interpretations from individual FA-tests.

Differences between data presented in concentrations and percentages imply that these methods are not simply interchangeable. Moreover, differences between percentages and concentrations depended on individual FA-characteristics ($|r|_{\text{FA-concentration to FA-total}}$). This dependency could inflict differential biases in individual FA results. Therefore, our findings emphasize the importance of a hypothesis driven choice of which method to use. Percentages could be used as a measure of the relative importance of a FA set against the total FA concentration; while absolute concentrations could be used for the measurement of a FA itself, independent of the concentration of other FA [3–5, 20].

The appropriate method of presentation could theoretically differ for each research question [21]. For example, concentrations could be most useful to distinguish depressed patients from controls, while percentages might predict disease progression. Therefore, the appropriate presentation method may depend upon which presentation is more (patho)physiologically to the research question under investigation. However, the dearth of research comparing both approaches so far, may—at present—hamper the formation of a hypothesis about which method be more (patho)physiologically relevant. If so, comparison of both methods of presentation could provide a guideline for future research.

Our results show that the way non-detectable/missing values are handled could potentially bias results, because significance levels of differences in example outcomes differed depending on which method was used. However, it should be noted that not only significances of differences, but also magnitudes of differences determine the bias

Table 2 Mean chain length, unsaturation and peroxidation indices compared between recurrently depressed patients and controls

	Patients	SEM	Controls	SEM	<i>t</i>	df	<i>P</i> value
Chain length index	18.32	0.0181	18.55	0.0119	10.96	226.5	$\sim 7.1 \times 10^{-19}$
Unsaturation index	1.29	0.0068	1.39	0.0059	11.14	90.21	$\sim 1.2 \times 10^{-18}$
Peroxidation index	1.10	0.0093	1.22	0.0090	9.241	101.5	$\sim 4.0 \times 10^{-15}$

All differences were calculated using independent Student's *t* test on indices of 137 recurrently depressed patients and 73 controls

SEM standard error of the mean, *df* degrees of freedom

introduced. Nevertheless, if non-detects occur, knowledge of the way they were handled, and discussion of any possible bias that may be inflicted as such, could prevent interpretation errors. Because other research fields already showed superiority of MI compared to other ways of handling non-detectable/missing values [6], this may soon be adapted as the preferred method to handle missing/non-detectable FA-concentrations as well.

By applying data reduction using indices—the CLI, UI and PI—we tested differences between patients and controls in FA-patterns. Index results were similar to the interpretation of the multiple tests on individual FA [10]. This suggests that indices could provide meaningful data-reduction in FA research. Furthermore, from a statistical viewpoint, the use of indices enabled us to test pattern hypotheses more efficiently by using only one outcome variable (CLI, UI or PI), instead of tests of many individual FA. This precluded the need for correction for multiple tests. In our example dataset this was not of specific analytical concern, because differences in individual FA-tests were large and mostly survived the Bonferroni correction. Nevertheless, this advantage may be beneficial in smaller samples or in diseased populations with smaller differences compared with controls. In addition, the indices facilitated quantitative testing of pattern hypotheses, in contrast to the qualitative interpretation of the individual FA tests. The disadvantage of integrating information on multiple FA-concentrations in one index, could be that it might undesirably simplify the underlying complexity of FA-metabolism. In such situations the relevance of an individual FA could be obscured, because differences in individual FA are not tested.

Whether indices should be used in FA-research seems to depend on the hypothesis under investigation. If FA are analyzed in order to test a pattern [e.g. membrane fluidity; unsaturation or peroxidizability; estimated enzyme activity; (inflammation regulating) FA ratios], indices could be used to first test this general pattern hypothesis. Subsequently, based on the index results, new specific hypotheses concerning selected individual FA could be tested. This would reduce the risk for type-I errors, or the need for strict correction for multiple testing [8]. A recent example of the possible usefulness of applying indices is the observation of bimodal distributions of FA unsaturation and chain length patterns in recurrently depressed patients [22]. However, if FA are analyzed to test a hypothesis concerning a specific FA (e.g. EPA), indices have no use, and should not be tested additionally since this would only increase the problem of multiple testing. Future studies are needed to further clarify the applicability of indices in FA-research.

Some additional limitations should be noted. The examples of the possible influences of the presented statistical methodological issues have been presented on the

basis of only one dataset. However, although the size of the biasing effects may differ between different datasets, the basic principles of the issues addressed concern analysis of FA data in general. Second, our example dataset has a moderate sample size when compared to epidemiological studies. This could have influenced the stability of correlation coefficients, and therefore the results. Third, the data presented only concern these three statistical methodological issues, and do not investigate other important factors that may also influence results, e.g. chemical analytical methods, and the nature of the sample (tissue, cell type, lipid fraction, e.g. cholesteryl esters, triacylglycerol, phospholipids) [4]. Finally, because differences in outcome measures were large in our example dataset, the disadvantages of multiple testing—and thereby the advantages of data reduction—could not be clearly exemplified and remain to be further explored in different datasets.

Nevertheless, our study addresses recurrent basic issues in practical FA research. Using a second-level analysis we were able to quantitatively demonstrate the consequences of the various methods of presentation. In addition, we suggested a novel way to handle non-detectable FA-values, using MI. Finally, we showed, to our knowledge for the first time, that indices could be used to delineate differences in FA patterns between depressed patients and controls.

In conclusion, a hypothesis-based choice of the method of FA-presentation (percentages or concentrations) could prevent bias in future FA-research. If it is not clear which method is preferable a priori, comparison of both methods could guide subsequent investigations. Furthermore, MI might prevent bias potentially inducible by missing/non-detectable values. Finally, indices could assist theory based data-reduction, thereby preventing type-I errors associated with multiple testing. Awareness and cautious handling of these statistical methodological issues in future FA-research may further improve interpretation of FA-analyses, and thereby deepen the understanding of the roles FA play in health and disease.

Acknowledgments The authors would like to thank Dr. T.A. Eggelte for his stimulating critique.

Conflict of interest All authors report no biomedical financial interests or potential conflicts of interest.

Open Access This article is distributed under the terms of the Creative Commons Attribution License which permits any use, distribution, and reproduction in any medium, provided the original author(s) and the source are credited.

References

1. Tuna N, Frankhauser S, Goetz FC (1968) Total serum fatty acids in diabetes: relative and absolute concentrations of individual fatty acids. *Am J Med Sci* 225:120–130

2. Schwertner HA, Mosser EL (1993) Comparison of lipid fatty acids on a concentration basis vs weight percentage basis in patients with and without coronary artery disease or diabetes. *Clin Chem* 39:659–663
3. Bradbury KE, Skeaff CM, Green TJ, Gray AR, Crowe FL (2010) The serum fatty acids myristic acid and linoleic acid are better predictors of serum cholesterol concentrations when measured as molecular percentages rather than as absolute concentrations. *Am J Clin Nutr* 91:398–405
4. Hodson L, Skeaff CM, Fielding BA (2008) Fatty acid composition of adipose tissue and blood in humans and its use as a biomarker of dietary intake. *Prog Lipid Res* 47:348–380
5. Chow CK (2009) Fatty acid composition of plasma phospholipids and risk of prostate cancer. *Am J Clin Nutr* 89:1946
6. Baccarelli A, Pfeiffer R, Consonni D, Pesatori AC, Bonzini M, Patterson DG, Bertazzi PA, Landi MT (2005) Handling of dioxin measurement data in the presence of non-detectable values: overview of available methods and their application in the Seveso chloracne study. *Chemosphere* 60:898–906
7. Appleton KM, Rogers PJ, Ness AR (2008) Is there a role for n-3 long-chain polyunsaturated fatty acids in the regulation of mood and behaviour? A review of the evidence to date from epidemiological studies, clinical studies and intervention trials. *Nutr Res Rev* 21:13–41
8. Feise RJ (2002) Do multiple outcome measures require p-value adjustment? *BMC Med Res Methodol* 2:8
9. Hulbert AJ, Pamplona R, Buffenstein R, Buttemer WA (2007) Life and death: metabolic rate, membrane composition, and life span of animals. *Physiol Rev* 87:1175–1213
10. Assies J, Pouwer F, Lok A, Mocking RJT, Bockting CL, Visser I, Abeling NG, Duran N, Schene AH (2010) Plasma and erythrocyte fatty acid patterns in patients with recurrent depression: a matched case-control study. *PLoS one* 14:(5)e10635
11. Piomelli D, Astarita G, Rapaka R (2007) A neuroscientist's guide to lipidomics. *Nat Rev Neurosci* 8:743–754
12. Assies J, Lok A, Weverling GJ, Lieveer R, Visser I, Abeling NNGM, Duran M, Schene AH (2004) Fatty acids and homocysteine levels in patients with recurrent depression: an explorative pilot study. *Prostaglandins Leukot Essent Fatty Acids* 70:349–356
13. Dacremont G, Cocquyt G, Vincent G (1995) Measurements of very long-chain fatty acids, phytanic and prostanoic acid in plasma and cultures fibroblasts by gas chromatography. *J Inherit Metab Dis* 18:77–83
14. Fisher RA (1915) Frequency distribution of the values of the correlation coefficient in samples of an indefinitely large population. *Biometrika* 10:507–521
15. Honaker J, Joseph A, King G, Scheve K, Singh N (2010) AMELIA II: a program for missing data. [Software] Retrieved from <http://gking.harvard.edu/amelia/>
16. Donders AR, van der Heijden GJMG, Stijnen T, Moons KGM (2006) Review: a gentle introduction to imputation of missing values. *J Clin Epidemiol* 59:1087–1091
17. Block RC, Harris WS, Reid KJ, Spertus JA (2008) Omega-6 and trans fatty acids in blood cell membranes: a risk factor for acute coronary syndromes? *Am Heart J* 156:1117–1123
18. Krabbendam L, Bakker E, Hornstra G, van Os J (2007) Relationship between DHA status at birth and child problem behaviour at 7 years of age. *Prostaglandins Leukot Essent Fatty Acids* 76:29–34
19. R Foundation for Statistical Computing (2010) R: a language and environment for statistical computing. Austria, Vienna
20. Schwertner HA (1994) Lipid fatty acids calculated on a concentration vs percentage basis. *Am J Clin Nutr* 59:1093
21. Crowe FL (2009) Reply to CK Chow. *Am J Clin Nutr* 89:1946–1947
22. Mocking RJ, Assies J, Koeter MW, Ruhé HG, Lok A, Schene AH (2012) Bimodal distribution of fatty acids in recurrent major depressive disorder. *Biol Psychiatry* 71:e3–e5

Low Docosahexaenoic Acid Content in Plasma Phospholipids is Associated with Increased Non-alcoholic Fatty Liver Disease in China

Ju-Sheng Zheng · Amei Xu · Tao Huang · Xiaomei Yu · Duo Li

Received: 2 January 2012 / Accepted: 24 March 2012 / Published online: 19 April 2012
© AOCS 2012

Abstract A large proportion of the Chinese population is now at risk of non-alcoholic fatty liver disease (NAFLD). We aimed to investigate the relationship between plasma phospholipids (PL) fatty acids and the risk of NAFLD. One hundred NAFLD patients and 100 healthy subjects were recruited in Hangzhou, China. Plasma PL and selected biochemical and hematological parameters were analyzed by using standard methods. Stepwise logistic regression was used to identify independent risk factors of NAFLD. Plasma PL total saturated fatty acid (SFA), C20:3n-6, serum alanine aminotransferase, high-density lipoprotein cholesterol, and body mass index were independent risk factors of NAFLD. The risk of NAFLD was significantly increased with higher quartiles of plasma PL total SFA (P for trend = 0.028) and C20:3n-6 (P for trend <0.001); plasma PL docosahexaenoic acid (C22:6n-3) was significantly lower in NAFLD patients than in controls (P = 0.032) and the OR of NAFLD in the highest quartile of C22:6n-3 was 0.41 (95 % CI = 0.17–0.97) compared with the lowest quartile. In conclusion, plasma PL total SFA and C20:3n-6 are positively correlated with the risk of NAFLD, while C22:6n-3 is negatively correlated with the risk of NAFLD.

Keywords Non-alcoholic fatty liver disease · Saturated fatty acid · Dihomo-gamma-linolenic acid · Docosahexaenoic acid

Abbreviations

ALP	Alkaline phosphatase
ALT	Alanine aminotransferase
BMI	Body mass index
BUN	Blood urea nitrogen
DBP	Diastolic blood pressure
DBil	Direct bilirubin
GGT	Gamma-glutamyl transferase
HDL-C	High-density lipoprotein cholesterol
IBil	Indirect bilirubin
LDL-C	Low-density lipoprotein cholesterol
MS	Metabolic syndrome
NAFLD	Non-alcoholic fatty liver disease
OR	Odds ratio
PL	Phospholipids
PUFA	Polyunsaturated fatty acid(s)
SBP	Systolic blood pressure
SFA	Saturated fatty acid(s)
TBil	Total bilirubin
TC	Total cholesterol
TG	Triacylglycerol(s)

J.-S. Zheng · A. Xu · T. Huang · D. Li (✉)
Department of Food Science and Nutrition, Zhejiang University,
866 Yuhangtang Road, Hangzhou 310058, China
e-mail: duoli@zju.edu.cn; yuxiaomei_1@hotmail.com

J.-S. Zheng · A. Xu · T. Huang · D. Li
APCNS Centre of Nutrition and Food Safety,
Hangzhou, China

X. Yu
Department of Clinical Laboratory,
Zhejiang Hospital, Hangzhou, China

Introduction

Non-alcoholic fatty liver disease (NAFLD) is a liver disorder characterized by fatty changes of the liver with no apparent history of habitual alcohol intake and is recognized as one of the most common forms of liver diseases [1]. NAFLD encompasses a spectrum of liver disorders

characterized by macrovesicular hepatic fat accumulation (simple steatosis) or accompanied by signs of hepatocyte injury, mixed inflammatory cell infiltrate, and variable hepatic fibrosis in pericellular distribution (non-alcoholic steatohepatitis, NASH) [2, 3]. NAFLD is associated with obesity, type 2 diabetes mellitus, cardiovascular diseases and insulin resistance [4–6], and is therefore considered as the hepatic manifestation of the metabolic syndrome (MS) [7, 8]. The prevalence of NAFLD ranges from 20 to 30 % of the general population in North America, and NAFLD was once assumed to be mainly confined to Western countries [1]. However, the prevalence of NAFLD in China and Japan has nearly doubled in the past two decades [9]. A large proportion of the Chinese population is now at risk of developing NAFLD as the prevalence of obesity, type 2 diabetes mellitus, dyslipidemia, hypertension and MS in China is steadily increasing [9, 10].

Dietary fat and fatty acids regulate hepatic lipid metabolism by modifying gene transcription and might play an important role in people with NAFLD [11]. Dietary saturated fatty acid (SFA) was reported to be positively correlated with NAFLD [12] and dietary n-3 polyunsaturated fatty acids (PUFA) were negatively correlated with NAFLD [13, 14]. Randomized controlled trials [15, 16] showed beneficial effect of n-3 PUFA supplementation on NAFLD. Plasma PL total n-3 PUFA was inversely associated with insulin resistance and MS in the Chinese population [17, 18]. However, the relationship of PL fatty acids with NAFLD in Chinese population is still unclear.

The aim of this study was to investigate the association between plasma PL fatty acids and the risk of NAFLD in a Chinese population in Hangzhou.

Materials and Methods

Subjects and Study Design

The study protocol was approved by the Ethics Committee, College of Biosystem Engineering and Food Science, Zhejiang University, China, and written consent was provided by all the subjects prior to the study.

All the subjects with NAFLD were recruited from Zhejiang Hospital for a health check program during the period of April 2006 to December 2006. The determination of NAFLD was according to the definition of Chinese Liver Disease Association, and the NAFLD was diagnosed when meeting the first five criteria and either the sixth or seventh criterion: (1) those with no alcohol consumption or alcohol consumption <140 g/week for men and <70 g/week for women [19]; (2) those without certain diseases, such as viral hepatitis and drug induced liver disease, which would lead to fatty liver disease; (3) Except for

clinical manifestation of primary disease, nonspecific symptoms such as debilitation, dyspepsia, dull pain in liver and hepatosplenomegaly were allowed; (4) components of metabolic syndrome such as overweight, central obesity, high fasting blood glucose, dyslipidemia and high blood pressure were allowed; (5) Serum transaminase and gamma-glutamyl transferase (GGT) could be moderately increased (less than fivefold), which mainly referred to the increase in alanine aminotransferase (ALT); (6) liver imaging conforming to the imaging diagnosis criteria of diffuse fatty liver; (7) liver biopsy conforming to the histopathological diagnosis criteria of fatty liver. Finally a total of 100 subjects with NAFLD were included and 100 healthy subjects were randomly enrolled as controls. The exclusion criteria of all the NAFLD patients and controls were: (1) those with alcohol consumption ≥ 140 g/week for men and ≥ 70 g/week for women; (2) those with a history of renal disease, cardiovascular disease, diabetes, thyroid disorder and other endocrine diseases; (3) use of weight loss or lipid-lowering medications.

All the enrolled subjects underwent anthropometric measurements including height, body weight and body mass index (BMI) by an interviewer.

Blood Collection

Subjects arrived at the Zhejiang Hospital in the morning following an overnight fast and relaxed for 10 min. Blood pressure was then measured and 10-mL venous blood samples were taken in plain and EDTA vacuum tubes with 20-gauge needles. Serum and plasma were obtained and stored at -20 °C for laboratory analysis.

Laboratory Measurements

Plasma lipids, glucose, serum uric acid, creatinine, blood urea nitrogen (BUN), total bilirubin (TBil), indirect bilirubin (IBil), direct bilirubin (DBil), albumin, immunoglobulin, total protein, ALT, GGT, alkaline phosphatase (ALP) were determined on an autoanalyzer (Olympus AU2700, Tokyo, Japan), via commercially available kits (Olympus). The total lipid content of plasma was extracted with chloroform:methanol (1:1, by vol), and the plasma PL fraction was separated from the total lipids by thin-layer chromatography. The methyl esters of plasma PL fatty acids were prepared by saponification with potassium hydroxide (0.68 mol/L in methanol), which was followed by transesterification with boron trifluoride in methanol [20]. Gas-liquid chromatography was used to separate fatty acid methyl esters as described previously [20].

Definition of MS was according to Fan et al. [2], and the diagnosis of the MS was made when three or more of the following criteria were met: (1) obesity, as BMI ≥ 25 ; (2)

high blood pressure, as blood pressure $\geq 130/85$ mmHg; (3) low high-density lipoprotein-cholesterol (HDL-C), as HDL-C < 1.03 mmol/L for men and HDL-C < 1.29 mmol/L for women; (4) High triacylglycerol (TG), as TG ≥ 1.7 mmol/L; (5) high glucose, as fasting plasma glucose ≥ 6.1 mmol/L.

Statistical Analyses

Continuous variables were presented as means \pm SD. The Kolmogorov–Smirnov test was used to examine the normal distribution of continuous variables. In addition, an independent samples *t* test (for normally distributed variables) or Mann–Whitney *U* test (for non-parametric tests were required) was performed. The Chi-square test was used to compare categorical variables.

Stepwise multivariate logistic regression analysis was used to investigate the independent risk factors associated with risk of NAFLD using the variables which is significant in the univariate analyses, and a total of 20 variables were chosen. Age was introduced into the model as a potential confounder. Glucose, GGT, and TG showed severely skewed distributions and were log-transformed for the logistic regression. To examine the distinctions between NAFLD and MS and their association with plasma PL fatty acids, both the risks of MS and NAFLD according to different quartiles of plasma PL fatty acids (SFA, C20:3n-6, C22:6n-3) were analyzed using a logistical regression model, adjusting for age and gender. Statistical analyses were conducted using SAS for Windows, version 9.1 (SAS Institute). $P < 0.05$ (2-tailed test) was considered statistically significant.

Results

Subject Characteristics and Univariate Analysis

All the subjects enrolled were from the Chinese Han population between 26 and 76 years. As shown in Table 1, there were 100 subjects (85 % male, mean age 44.97 ± 11.27) with NAFLD included in this case–control study, and another 100 subjects (53 % male, mean age 43.37 ± 12.24) were chosen as healthy controls.

The following were significantly higher in the NAFLD group for BMI ($P < 0.001$), total cholesterol (TC, $P = 0.018$), TG ($P < 0.001$), glucose ($P = 0.012$), uric acid ($P < 0.001$), systolic blood pressure (SBP, $P < 0.001$), diastolic blood pressure (DBP, $P = 0.002$), GGT ($P < 0.001$), ALT ($P < 0.001$), ALP ($P = 0.017$), DBil ($P = 0.05$) and creatinine ($P = 0.028$) concentrations, and significantly lower in NAFLD group for high-density lipoprotein cholesterol concentration (HDL-C, $P < 0.001$) compared with the control group. For plasma PL fatty acids (Table 2),

compositions of total SFA ($P = 0.001$) and C20:3n-6 ($P < 0.001$) were significantly higher in NAFLD group than in control group; and docosahexaenoic acid (DHA, C22:6n-3) ($P = 0.032$), C18:1n-7 ($P < 0.001$) and delta-5 desaturase activity (C20:4n-6/C20:3n-6) ($P < 0.001$) in NAFLD group was significantly lower than in the control group.

Multivariate Analysis

Stepwise logistic regression revealed five independent risk factors of NAFLD. The odds ratios (OR) for BMI, ALT, and HDL-C were 1.56 (95 % CI = 1.28–1.90), 1.05 (95 % CI = 1.02–1.09) and 0.05 (95 % CI = 0.01–0.24) respectively. Plasma PL C20:3n-6 (OR = 2.31, 95 % CI = 1.26–4.23) and total SFA (OR = 1.44, 95 % CI = 1.11–1.88) were also risk factors of NAFLD in this study.

Multivariate adjusted analyses (Table 3) showed that the risk of NAFLD was significantly increased with higher tertiles of BMI (P for trend < 0.001) and ALT (P for trend = 0.008), while the risk of NAFLD was lower when HDL-C increased (P for trend = 0.012). For plasma PL fatty acids, age and gender adjusted ORs of NAFLD were increased with higher quartiles of SFA (Fig. 1, P for trend = 0.028) and C20:3n-6 (Fig. 2, P for trend < 0.001). And the OR of NAFLD was 0.41 (95 % CI = 0.17–0.97) for the highest quartile of C22:6n-3 compared with the lowest quartile (Fig. 3).

MS and NAFLD

The prevalence rates of MS and MS components were all significantly higher in the NAFLD group than in the control group (Fig. 4). Age and gender adjusted OR of NAFLD was 17.47 (95 % CI = 4.84–63.04) for MS, 2.10 (95 % CI = 1.00–4.36) for high blood pressure, 4.00 (95 % CI = 2.05–7.80) for high TG, 3.30 (95 % CI = 1.60–6.83) for low HDL-C, and 6.70 (95 % CI = 3.26–13.79) for high BMI (Fig. 5). Multivariate adjusted analyses indicated that OR of MS by quartiles of PL SFA and C22:6n-3 was not significant (P for trend = 0.107 and 0.091, respectively) (data not shown), but for PL C20:3n-6, it was significant (P for trend = 0.028) (data not shown).

Discussion

Epidemiological and dietary intervention studies have shown that the fatty acid profiles of platelet and plasma/serum PL reflected an individual's type of dietary fat intake [21, 22]. This study revealed that plasma PL total SFA and C20:3n-6 were positively correlated with the risk of NAFLD. High plasma PL C22:6n-3 was negatively correlated with the risk of NAFLD.

Table 1 Comparison of clinical and biochemical characteristics in subjects with and without non-alcoholic fatty liver disease (NAFLD)

Variables	Subjects with NAFLD (<i>n</i> = 100)	Subjects without NAFLD (<i>n</i> = 100)	<i>P</i> value
Age (years)	44.97 ± 11.27	43.37 ± 12.24	0.164
Gender (male/female, <i>n</i>)	85/15	53/47	<0.001
Smoking frequency			<0.001
Never (%)	44	76	
Occasional (%)	8	3	
Always (%)	42	21	
Physical activity			0.507
Rarely (%)	33	35	
Occasional (%)	33	21	
Always (%)	33	43	
BMI (kg/m ²)	25.23 ± 2.42	22.07 ± 2.33	<0.001
HDL-C (mmol/L)	1.15 ± 0.27	1.38 ± 0.32	<0.001
LDL-C (mmol/L)	2.64 ± 0.92	2.42 ± 0.63	0.088
TC (mmol/L)	4.99 ± 1.15	4.59 ± 0.75	0.018
TG (mmol/L)	2.18 ± 1.44	1.32 ± 1.11	<0.001
Glucose (mmol/L)	4.92 ± 0.82	4.64 ± 0.62	0.012
Uric acid (μmol/L)	335.71 ± 76.08	288.62 ± 70.08	<0.001
SBP (mmHg)	132.13 ± 20.69	122.13 ± 17.56	<0.001
DBP (mmHg)	80.34 ± 11.98	74.75 ± 9.87	0.002
GGT (U/L)	29.73 ± 20.41	21.05 ± 25.08	<0.001
ALT (U/L)	31.50 ± 16.60	19.50 ± 10.65	<0.001
ALP (U/L)	54.55 ± 13.87	50.80 ± 17.49	0.017
TBil (μmol/L)	16.08 ± 7.34	15.97 ± 6.01	0.645
IBil (μmol/L)	12.83 ± 5.90	13.11 ± 4.90	0.387
DBil (μmol/L)	3.21 ± 1.47	2.87 ± 1.43	0.050
Albumin (g/L)	46.61 ± 2.55	45.95 ± 2.91	0.088
Globulin (g/L)	27.36 ± 3.28	27.07 ± 3.44	0.537
Albumin/globulin	1.73 ± 0.24	1.75 ± 0.23	0.277
Creatinine (μmol/L)	68.98 ± 8.41	66.18 ± 9.40	0.028
BUN (mmol/L)	5.11 ± 1.16	4.92 ± 1.10	0.203
Total protein (g/L)	73.98 ± 4.14	73.01 ± 4.47	0.118

Data are expressed as means ± SD

BMI body mass index, *HDL-C* high-density lipoprotein cholesterol, *LDL-C* low-density lipoprotein cholesterol, *TC* total cholesterol, *TG* triacylglycerol, *SBP* systolic blood pressure, *DBP* diastolic blood pressure, *GGT* gamma-glutamyltransferase, *ALT* alanine aminotransferase, *ALP* alkaline phosphatase, *TBil* total bilirubin, *IBil* indirect bilirubin, *DBil* direct bilirubin, *BUN* blood urea nitrogen

Dietary SFA intake has a great impact on the development of both raised plasma low-density lipoprotein cholesterol (LDL-C) levels and the genesis of NAFLD [23, 24], and it was demonstrated that increased plasma LDL-C by SFA was mainly attributed to reduced hepatic clearance of LDL [24, 25]. Further, increased plasma cholesterol by a high intake of SFA may be a result of down-regulation of hepatic LDL receptor expression, especially through the modulation of activity of SREBP2 gene expression [26]. Previous studies have reported that SFA or percent dietary fat intake was significantly higher for NAFLD than controls [8, 12]; the present study was consistent with previous results [12] and indicated that plasma PL total SFA composition was significantly higher in NAFLD group compared with healthy control group, and also an independent risk factor of NAFLD in the Chinese population. The risk of NAFLD decreased in the quartile 4 compared with quartile 3;

it might be that the sample size is not large enough to get a linear association between SFA and NAFLD risk; however the *P* value for trend was still significant.

N-3 PUFA could stimulate peroxisome proliferator-activated receptor- α activity, which could lead to an increase in TG transportation from hepatocytes; and hepatic lipogenesis could also be inhibited by n-3 PUFA through down-regulation of SREBP1 expression [27]. Results from observational studies [14, 28] and randomized controlled trials [15, 16, 29] also supported that n-3 PUFA may be preventive nutrients for NAFLD. Our results supported that high plasma PL n-3 PUFA (C22:6n-3) was inversely associated with NAFLD risk.

In contrast to n-3 PUFA, PL n-6 PUFA (C20:3n-6) in this study was an independent risk factor of NAFLD. Decrease of delta-5 desaturase activity in subjects with NAFLD might contribute to the increase of C20:3n-6 in the

Table 2 Comparison of plasma phospholipids fatty acid composition in subjects with and without non-alcoholic fatty liver disease (NAFLD)

Variables	Subjects with NAFLD (<i>n</i> = 100)	Subjects without NAFLD (<i>n</i> = 100)	<i>P</i> value
C14: 0	0.38 ± 0.10	0.36 ± 0.11	0.055
C15: 0	0.12 ± 0.04	0.13 ± 0.04	0.404
C16: 0	28.62 ± 1.66	28.26 ± 1.96	0.159
C18: 0	14.63 ± 1.04	14.51 ± 1.26	0.460
C20: 0	0.35 ± 0.07	0.37 ± 0.06	0.029
Total SFA	44.11 ± 1.64	43.47 ± 2.47	0.001
C14: 1	0.36 ± 0.27	0.44 ± 0.33	0.109
C16: 1	0.53 ± 0.21	0.49 ± 0.20	0.088
C17: 1	0.37 ± 0.29	0.35 ± 0.30	0.445
C18: 1n-7	1.13 ± 0.20	1.25 ± 0.20	<0.001
C18: 1n-9	8.47 ± 1.22	8.69 ± 1.19	0.197
C20: 1	0.95 ± 0.76	0.93 ± 0.77	0.511
C22: 1	0.52 ± 0.48	0.45 ± 0.42	0.241
C24: 1	0.79 ± 0.30	0.73 ± 0.29	0.193
Total MUFA	13.10 ± 2.23	13.23 ± 2.15	0.290
C18: 2n-6	21.11 ± 2.88	21.01 ± 2.71	0.799
C18: 3n-6	0.66 ± 0.58	0.61 ± 0.60	0.303
C20: 2n-6	0.38 ± 0.06	0.39 ± 0.08	0.122
C20: 3n-6	2.66 ± 0.73	2.10 ± 0.78	<0.001
C20: 4n-6	8.73 ± 1.74	9.15 ± 2.10	0.121
C22: 2n-6	0.56 ± 0.41	0.78 ± 0.64	0.080
C22: 4n-6	0.22 ± 0.07	0.22 ± 0.06	0.273
C22: 5n-6	0.23 ± 0.08	0.23 ± 0.08	0.791
Total n-6	34.54 ± 2.32	34.29 ± 3.09	0.999
C18: 3n-3	0.16 ± 0.08	0.15 ± 0.07	0.731
C20: 5n-3	1.50 ± 0.56	1.48 ± 0.56	0.839
C22: 5n-3	0.81 ± 0.28	0.79 ± 0.31	0.340
C22: 6n-3	5.45 ± 1.07	5.79 ± 1.15	0.032
Total n-3	7.92 ± 1.49	8.22 ± 1.52	0.208
N-3/n-6	0.23 ± 0.06	0.24 ± 0.07	0.244
Total PUFA	42.45 ± 1.97	42.51 ± 2.67	0.303
Delta-5 desaturase activity (C20:4n-6/C20:3n-6)	3.57 ± 1.36	5.00 ± 2.34	<0.001

Data are expressed as means ± SD

SFA saturated fatty acids, MUFA monounsaturated fatty acids, PUFA polyunsaturated fatty acids

Table 3 Odds ratios (OR) and 95 % confidence interval (CI) for non-alcoholic fatty liver disease (NAFLD) according to the tertiles (T) of BMI, ALT and HDL-C

Variables	T1	T2	T3	<i>P</i> for trend
BMI	20.42	23.71	26.83	
Case/control	12/55	34/32	54/13	
Crude OR	1.00 (ref)	4.87 (2.21–10.72)	19.04 (7.98–45.43)	<0.001
Multivariate OR	1.00 (ref)	3.36 (1.13–10.0)	10.41 (3.20–33.83)	<0.001
ALT	12.22	20.66	42.73	
Case/control	19/46	29/39	52/15	
Crude OR	1.00 (ref)	5.44 (2.46–12.04)	8.77 (2.84–27.14)	<0.001
Multivariate OR	1.00 (ref)	1.43 (0.55–3.74)	4.59 (1.57–13.46)	0.017
HDL-C	0.93	1.24	1.62	
Case/control	47/22	32/33	21/45	
Crude OR	1.00 (ref)	0.45 (0.23–0.92)	0.22 (0.11–0.45)	<0.001
Multivariate OR	1.00 (ref)	0.31 (0.11–0.88)	0.21 (0.07–0.6)	0.012

Multivariate models included BMI, ALT, HDL-C, total SFA, C20:3n-6, age, gender, smoking frequency, and physical activity
BMI body mass index, HDL-C high-density lipoprotein cholesterol, ALT alanine aminotransferase, ref reference

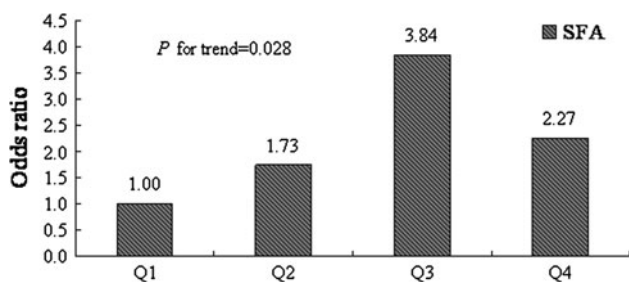


Fig. 1 Odds ratio (OR) of non-alcoholic fatty liver disease (NAFLD) by quartile of plasma phospholipids (PL) total saturated fatty acids (SFA). Adjusted age and gender. The OR of NAFLD was tested using a logistical regression based on quartile of plasma PL total SFA

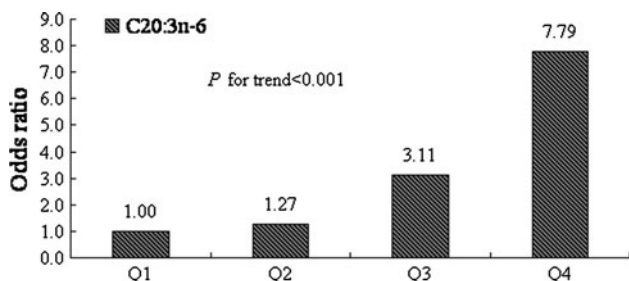


Fig. 2 Odds ratio (OR) of non-alcoholic fatty liver disease (NAFLD) by quartile of plasma phospholipids (PL) C20:3n-6. Adjusted age and gender. The OR of NAFLD was tested using a logistical regression based on quartile of plasma PL C20:3n-6

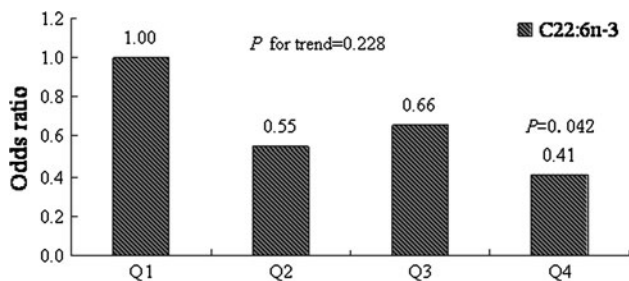


Fig. 3 Odds ratio (OR) of non-alcoholic fatty liver disease (NAFLD) by quartile of plasma phospholipids (PL) C22:6n-3. Adjusted age and gender. The OR of NAFLD was tested using a logistical regression based on quartile of plasma PL C22:6n-3

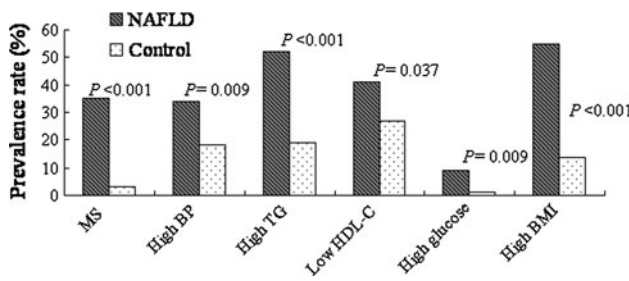


Fig. 4 Prevalence rate (%) of metabolic syndrome (MS) and MS components in the non-alcoholic fatty liver disease (NAFLD) group and the control group

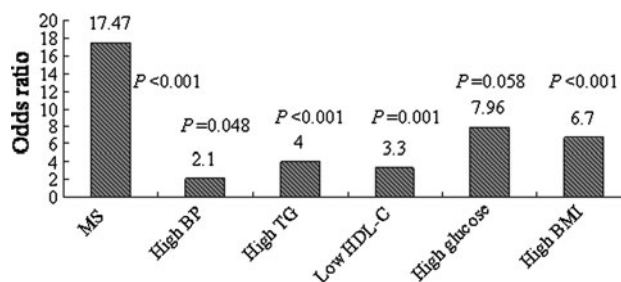


Fig. 5 Odds ratio (OR) of metabolic syndrome (MS) and MS components in the non-alcoholic fatty liver disease (NAFLD) group compared with the control group

present study. Araya et al. [30] reported a marked increase of n-6/n-3 PUFA in the liver of NAFLD patients, and liver PL 20:4n-6 and total long-chain n-6 PUFA were also significantly higher in NAFLD patients than controls. The positive relation between n-6 PUFA and NAFLD was not surprising as n-6 PUFA was reported to be inversely associated with insulin sensitivity [17], and subjects with MS also had significantly higher n-6 PUFA concentration [18]. And both insulin sensitivity and MS are closely related with NAFLD [4, 31]. Further, unbalanced intake of n-6 and n-3 PUFA, which contributed to enhancement of tissue n-6/n-3 PUFA, may inhibit fatty acid from oxidation and secretion and leading to the storage of TG, and then hepatic steatosis [30].

Puri et al. [32] reported that compared with lean normal controls, non-alcoholic fatty liver (NAFL) and NASH subjects had significantly higher plasma C16:1n-7, C18:1n-9, C18:3n-6 and C20:3n-6 contents; plasma C22:5n-3 was also significantly higher in NAFLD subjects compared with controls. However, only C20:3n-6 was found to be significantly higher in NAFLD subjects compared with controls in the present study. It might be that the degree of NAFLD in the present study was different from the previous one; further, different genetic backgrounds of participants may also contribute to the different results in the present study compared with previous ones.

ALT was an independent risk factor of NAFLD in the present study, and this was consistent with previous reports [4, 33, 34]. ALT was once used as a surrogate marker for liver steatosis and to detect NAFLD in the general population [35], however, prevalence of NAFLD may be underestimated by using liver enzymes as a marker of NAFLD [36], and the prevalence of presumed NAFLD was subject to the cut-off ALT value used [37]. The present study showed that the number of subjects with and without an abnormal ALT level (ALT > 30 U/L for men, ALT > 19 U/L for women) was similar in NAFLD patients (49 % of the subjects had abnormal ALT), and this indicated that ALT may be not sensitive enough to predict NAFLD.

People with MS have an increased risk of developing diabetes mellitus, cardiovascular disease and all cause mortality [4–6]. The prevalence rate of MS ranges from 24 to 44 % in the US population [38] and 10 to 30 % in the Asian population [7, 39, 40], but it was significantly higher in people with NAFLD ranging from 41 to 47 % [8, 41, 42]. Obesity and dyslipidemia are two risk factors of NAFLD [2, 9], and these risk factors have also been identified in the present study. Of note, obesity and dyslipidemia are both MS components. NAFLD is a good predictor for the clustering of risk factors for MS [7]. Although the pathogenesis of MS among patients with NAFLD and their interactive impact on survival rate are still unclear, clinically, patients with NAFLD should be screened regularly for the occurrence and development of MS [9]. Another issue of concern in the present study is the ORs across quartiles of plasma PL fatty acids might reflect only the same pathology or successive stages in the same pathology, such as MS. However the prevalence of MS in NAFLD subjects is only 35 % in the present study, less likely to affect the association of NAFLD with plasma PL fatty acids; further, ORs of MS across different plasma PL fatty acids is different from that of NAFLD; for example, there was no significant trend association of plasma PL SFA with MS risk, while it was significant for NAFLD risk.

There are some limitations to this study. First, the sample size chosen was not large enough to get a more definite conclusion, and included a number of women in the NAFLD group that was limited. However, significant differences of many metabolic factors were determined between the two groups and independent risk factors were also identified in the study. In addition, most of the results were gender adjusted, minimizing the effect of gender. Second, using plasma PL fatty acid as the biomarker of dietary fatty acid intake could not reflect the true dietary intake. However the plasma PL fatty acid composition is a common biomarker used to examine the relationship between dietary fatty acid intake and diseases [17, 18], and the correlations between diet and plasma fatty acids remained relatively constant regardless of whether participants were overweight, possessed chronic diseases, were alcohol drinkers or were cigarette smokers [43].

In conclusion, the present study showed that plasma PL total SFA and C20:3n-6 are positively correlated with the risk of NAFLD, while C22:6n-3 is negatively correlated with the risk of NAFLD. Further confirmation of these associations in large randomized controlled studies are needed.

Acknowledgments The study was funded by the National Natural Science Foundation of China (NSFC, No. 30972464), the National Basic Research Program of China (973 Program: 2011CB504002), Natural Science Foundation of Zhejiang Province (Y205709) and Zhejiang University (No. H20091920).

Conflict of interest The authors have declared that there is no potential conflict of interest with respect to this manuscript.

References

- Angulo P (2007) GI epidemiology: nonalcoholic fatty liver disease. *Aliment Pharmacol Ther* 25:883–889
- Fan JG, Farrell GC (2009) Epidemiology of non-alcoholic fatty liver disease in China. *J Hepatol* 50:204–210
- Farrell GC, Chitturi S, Lau GK, Sollano JD (2007) Guidelines for the assessment and management of non-alcoholic fatty liver disease in the Asia-Pacific region: executive summary. *J Gastroenterol Hepatol* 22:775–777
- Riquelme A, Arrese M, Soza A, Morales A, Baudrand R, Perez-Ayuso RM, Gonzalez R, Alvarez M, Hernandez V, Garcia-Zattera MJ, Otarola F, Medina B, Rigotti A, Miquel JF, Marshall G, Nervi F (2009) Non-alcoholic fatty liver disease and its association with obesity, insulin resistance and increased serum levels of C-reactive protein in Hispanics. *Liver Int* 29:82–88
- Goessling W, Massaro JM, Vasan RS, D'Agostino RB Sr, Ellison RC, Fox CS (2008) Aminotransferase levels and 20-year risk of metabolic syndrome, diabetes, and cardiovascular disease. *Gastroenterology* 135:1935–1944
- Targher G (2007) Non-alcoholic fatty liver disease, the metabolic syndrome and the risk of cardiovascular disease: the plot thickens. *Diabet Med* 24:1–6
- Fan JG, Zhu JN, Li XJ, Chen L, Lu YS, Li L, Dai F, Li F, Chen SY (2005) Fatty liver and the metabolic syndrome among Shanghai adults. *J Gastroenterol Hepatol* 20:1825–1832
- Sathiaraj E, Chutke M, Reddy MY, Pratap N, Rao PN, Reddy DN, Raghunath M (2011) A case-control study on nutritional risk factors in non-alcoholic fatty liver disease in Indian population. *Eur J Clin Nutr* 65:533–537
- Fan JG, Saibara T, Chitturi S, Kim BI, Sung JJ, Chutaputti A (2007) What are the risk factors and settings for non-alcoholic fatty liver disease in Asia-Pacific? *J Gastroenterol Hepatol* 22:794–800
- Amarapurkar DN, Hashimoto E, Lesmana LA, Sollano JD, Chen PJ, Goh KL (2007) How common is non-alcoholic fatty liver disease in the Asia-Pacific region and are there local differences? *J Gastroenterol Hepatol* 22:788–793
- Sessler AM, Ntambi JM (1998) Polyunsaturated fatty acid regulation of gene expression. *J Nutr* 128:923–926
- Musso G, Gambino R, De Micheli F, Cassader M, Rizzetto M, Durazzo M, Faga E, Silli B, Pagano G (2003) Dietary habits and their relations to insulin resistance and postprandial lipemia in nonalcoholic steatohepatitis. *Hepatology* 37:909–916
- Zelber-Sagil S, Nitzan-Kaluski D, Goldsmith R, Webb M, Blendis L, Halpern Z, Oren R (2007) Long term nutritional intake and the risk for non-alcoholic fatty liver disease (NAFLD): A population based study. *J Hepatol* 47:711–717
- Oya J, Nakagami T, Sasaki S, Jimba S, Murakami K, Kasahara T, Wasada T, Sekiguchi H, Hasegawa M, Endo Y, Iwamoto Y (2010) Intake of n-3 polyunsaturated fatty acids and non-alcoholic fatty liver disease: a cross-sectional study in Japanese men and women. *Eur J Clin Nutr* 64:1179–1185
- Spadaro L, Magliocco O, Spampinato D, Piro S, Oliveri C, Alagona C, Papa G, Rabuazzo AM, Purrello F (2008) Effects of n-3 polyunsaturated fatty acids in subjects with nonalcoholic fatty liver disease. *Dig Liver Dis* 40:194–199
- Sofi F, Giangrandi I, Cesari F, Corsani I, Abbate R, Gensini GF, Casini A (2010) Effects of a 1-year dietary intervention with n-3 polyunsaturated fatty acid-enriched olive oil on non-alcoholic

- fatty liver disease patients: a preliminary study. *Int J Food Sci Nutr* 61:792–802
17. Huang T, Wahlqvist ML, Xu TC, Xu A, Zhang AZ, Li D (2010) Increased plasma n-3 polyunsaturated fatty acid is associated with improved insulin sensitivity in type 2 diabetes in China. *Mol Nutr Food Res* 54:S112–S119
 18. Huang T, Bhulaidok S, Cai ZZ, Xu TC, Xu F, Wahlqvist ML, Li D (2010) Plasma phospholipids n-3 polyunsaturated fatty acid is associated with metabolic syndrome. *Mol Nutr Food Res* 54:1628–1635
 19. Neuschwander-Tetri BA, Caldwell SH (2003) Nonalcoholic steatohepatitis: summary of an AASLD Single Topic Conference. *Hepatology* 37:1202–1219
 20. Sinclair AJ, O’Dea K, Dunstan G, Ireland PD, Niall M (1987) Effects on plasma lipids and fatty acid composition of very low fat diets enriched with fish or kangaroo meat. *Lipids* 22:523–529
 21. Riboli E, Ronnholm H, Saracci R (1987) Biological Markers of Diet. *Cancer Surv* 6:685–718
 22. Hunter D (1995) Biochemical indicators of dietary intake. In: Willett WC (ed) *Nutritional epidemiology*, Oxford University Press, New York, p 143–203
 23. Larter CZ, Yeh MM, Van Rooyen DM, Teoh NC, Brooling J, Hou JY, Williams J, Clyne M, Nolan CJ, Farrell GC (2009) Roles of adipose restriction and metabolic factors in progression of steatosis to steatohepatitis in obese, diabetic mice. *J Gastroenterol Hepatol* 24:1658–1668
 24. Woollett LA, Spady DK, Dietschy JM (1992) Regulatory effects of the saturated fatty-acids 6-0 through 18-0 on hepatic low-density-lipoprotein receptor activity in the Hamster. *J Clin Invest* 89:1133–1141
 25. Spady DK, Woollett LA, Dietschy JM (1993) Regulation of plasma LDL-cholesterol levels by dietary cholesterol and fatty acids. *Annu Rev Nutr* 13:355–381
 26. Vallim T, Salter AM (2010) Regulation of hepatic gene expression by saturated fatty acids. *Prostaglandins Leukot Essent Fatty Acids* 82:211–218
 27. Yoshikawa T, Shimano H, Yahagi N, Ide T, Amemiya-Kudo M, Matsuzaka T, Nakakuki M, Tomita S, Okazaki H, Tamura Y, Iizuka Y, Ohashi K, Takahashi A, Sone H, Osuga Ji J, Gotoda T, Ishibashi S, Yamada N (2002) Polyunsaturated fatty acids suppress sterol regulatory element-binding protein 1c promoter activity by inhibition of liver X receptor (LXR) binding to LXR response elements. *J Biol Chem* 277:1705–1711
 28. Allard JP, Aghdassi E, Mohammed S, Raman M, Avand G, Arendt BM, Jalali P, Kandasamy T, Prayitno N, Sherman M, Guindi M, Ma DW, Heathcote JE (2008) Nutritional assessment and hepatic fatty acid composition in non-alcoholic fatty liver disease (NAFLD): a cross-sectional study. *J Hepatol* 48:300–307
 29. Tanaka N, Sano K, Horiuchi A, Tanaka E, Kiyosawa K, Aoyama T (2008) Highly purified eicosapentaenoic acid treatment improves nonalcoholic steatohepatitis. *J Clin Gastroenterol* 42: 413–418
 30. Araya J, Rodrigo R, Videla LA, Thielemann L, Orellana M, Pettinelli P, Poniachik J (2004) Increase in long-chain polyunsaturated fatty acid n-6/n-3 ratio in relation to hepatic steatosis in patients with non-alcoholic fatty liver disease. *Clin Sci* 106:635–643
 31. Fan JG, Peng YD (2007) Metabolic syndrome and non-alcoholic fatty liver disease: Asian definitions and Asian studies. *Hepatobiliary Pancreat Dis Int* 6:572–578
 32. Puri P, Wiest MM, Cheung O, Mirshahi F, Sargeant C, Min HK, Contos MJ, Sterling RK, Fuchs M, Zhou H, Watkins SM, Sanyal AJ (2009) The plasma lipidomic signature of nonalcoholic steatohepatitis. *Hepatology* 50:1827–1838
 33. Fu CC, Chen MC, Li YM, Liu TT, Wang LY (2009) The risk factors for ultrasound-diagnosed non-alcoholic fatty liver disease among adolescents. *Ann Acad Med Singap* 38:15–21
 34. Cardoso CRL, Leite NC, Salles GF, Araujo ALE, Villela-Nogueira CA (2009) Prevalence and associated factors of non-alcoholic fatty liver disease in patients with type-2 diabetes mellitus. *Liver Int* 29:113–119
 35. Ruhl CE, Everhart JE (2003) Determinants of the association of overweight with elevated serum alanine aminotransferase activity in the United States. *Gastroenterology* 124:71–79
 36. Zelber-Sagi S, Nitzan-Kaluski D, Halpern Z, Oren R (2006) Prevalence of primary non-alcoholic fatty liver disease in a population-based study and its association with biochemical and anthropometric measures. *Liver Int* 26:856–863
 37. Kim BK, Han KH, Ahn SH (2011) “Normal” range of alanine aminotransferase levels for Asian population. *J Gastroenterol Hepatol* 26:219–220
 38. Ford ES, Giles WH, Dietz WH (2002) Prevalence of the metabolic syndrome among US adults—findings from the third national health and nutrition examination survey. *JAMA* 287:356–359
 39. Nestel P, Lyu R, Low LP, Sheu WH, Nitiyanant W, Saito I, Tan CE (2007) Metabolic syndrome: recent prevalence in East and Southeast Asian populations. *Asia Pac J Clin Nutr* 16:362–367
 40. Li Y, Xu C, Yu C, Xu L, Miao M (2009) Association of serum uric acid level with non-alcoholic fatty liver disease: a cross-sectional study. *J Hepatol* 50:1029–1034
 41. Bajaj S, Nigam P, Luthra A, Pandey RM, Kondal D, Bhatt SP, Wasir JS, Misra A (2009) A case-control study on insulin resistance, metabolic co-variables & prediction score in non-alcoholic fatty liver disease. *Indian J Med Res* 129:285–292
 42. Uchil D, Pipalia D, Chawla M, Patel R, Maniar S, Narayani, Juneja A (2009) Non-alcoholic fatty liver disease (NAFLD)—the hepatic component of metabolic syndrome. *J Assoc Physicians India* 57:201–204
 43. Ma J, Folsom AR, Shahar E, Eckfeldt JH (1995) Plasma fatty-acid composition as an indicator of habitual dietary-fat intake in middle-aged adults. *Am J Clin Nutr* 62:564–571

Exogenous Arachidonate Restores the Dimethoate-Induced Inhibition of Steroidogenesis in Rat Interstitial Cells

Mariana Astiz · Graciela Hurtado de Catalfo ·
María J. T. de Alaniz · Carlos Alberto Marra

Received: 27 November 2011 / Accepted: 19 March 2012 / Published online: 3 April 2012
© AOCs 2012

Abstract The present work studies the potential restorative effect of polyunsaturated fatty acids (PUFA, 5 μ M/24 h) on the dimethoate (DMT)-induced inhibition of testosterone biosynthesis in Leydig cells isolated from rat testes. Various fatty acids (FA) from the n-6 (18:2, 20:3, 20:4, 22:4 and 22:5) and n-3 (18:3, 20:5, 22:5, 22:6) series were assayed in Leydig cells, alone (as delipidated BSA complexes) and in combination with DMT (1 ppm). The n-6 FA stimulated lipid peroxidation (LPO) and inhibited the activities of steroidogenic enzymes (3β - and 17β -hydroxysteroid dehydrogenases). The n-3 FA exerted an anti-oxidant effect, decreasing the production of thiobarbituric-acid reactive substances (TBARS) and inhibiting phospholipase A₂ activity. The biosynthesis of testosterone in DMT-treated cultures was completely normalized by ARA (20:4n-6) and partially restored by the addition of 20:3n-6, increasing ARA content inside the mitochondria. The other FA assayed failed to restore androgenesis. COX-2 protein and prostaglandin F₂ α and E₂ production were stimulated by 20:3n-6, ARA, 18:3n-3 and 20:5 n-3. COX-2 protein decreased upon addition of 22:5n-3 and 22:6n-3. StAR protein was increased by ARA and partially increased by 20:3n-6, likely due to its metabolic conversion into ARA. Both FA increased the mitochondrial cholesterol pool available for testosterone biosynthesis. The rate of androgenesis is likely the result of various regulatory

factors acting concomitantly on the physiology of Leydig cells.

Keywords Arachidonic acid · COX-2 · Dimethoate · Oxidative stress · Prostaglandins · Rat interstitial cells · StAR · PUFA

Abbreviations

ARA	20:4n-6
BSA	Bovine serum albumin
C	Control group
CHOL	Cholesterol
DMT	Dimethoate
FA	Fatty acid(s)
3β HSD	3β -Hydroxysteroid dehydrogenase
17β HSD	17β -Hydroxysteroid dehydrogenase
LPO	Lipid peroxidation
MDA	Malonedialdehyde
MIT	Mitochondrial
OS	Oxidative stress
PEG	Polyethylene glycol-400
PG	Prostaglandin(s)
PL	Phospholipid(s)
PLA ₂	Phospholipase A ₂
ROS	Reactive oxygenated species
StAR	Steroidogenic acute regulatory protein
TBARS	Thiobarbituric acid-reactive substances
TCP	Total cellular protein
Te	Testosterone

M. Astiz · G. Hurtado de Catalfo · M. J. T. de Alaniz ·
C. A. Marra (✉)

INIBIOLP (Instituto de Investigaciones Bioquímicas de La Plata), CCT La Plata, CONICET-UNLP, Cátedra de Bioquímica y Biología Molecular, Facultad de Ciencias Médicas, Universidad Nacional de La Plata, Calles 60 y 120, 1900 La Plata, Argentina
e-mail: camarra@atlas.med.unlp.edu.ar;
contactocarlos@hotmail.com

Introduction

The increasing experimental evidence documenting endocrine dysfunction in the testis has led to the hypothesis that

environmental contaminants adversely affect the male reproductive system [1, 2]. This hypothesis is causally related to the decline in sperm quality observed in developed countries where agrochemicals are used intensively [3]. Many authors have reported that environmental chemicals can mimic estrogen action and also disrupt androgen signaling pathways [4].

Worldwide, dimethoate (DMT) is one of the most commonly used organophosphorus insecticides in horticulture, serving as a systemic insecticide and acaricide for treating gardens, vineyards, and field crops and also applied externally for the control of fly larvae in cattle [5]. Experimental evidence indicates that it impairs fertility, suppresses libido, causes testicular degeneration, and deteriorates semen quality [5].

We found that sub-chronic (5 weeks) administration of DMT to male Wistar rats at low doses (15 mg/kg weight, i.p.) produced evidence toxic effects on testis and modifications in sperm quality [6]. The dosage, similar to the level of pesticide residues in food, caused considerable changes in the appearance, volume and consistence of testes. In agreement with the findings of Sayim et al. [7, 8], the effects included moderate to severe seminiferous tubule degeneration such as sloughing, atrophy and germ cell degeneration, and partial arrest of spermatogenesis. As previously described by Thomas et al. [9], we also found that DMT administration gave rise to a significant increase in the level of circulating gonadotrophins in response to the lower testosterone production. However, previous research proposed that DMT exerts a direct cytotoxic effect unassociated with alterations in LH, FSH, or other hormonal mechanism(s) implicated in androgen biosynthesis [5, 6, 10, 11].

Dimethoate disturbs the pro-oxidant/anti-oxidant balance, causing oxidative stress (OS), a well-known effect of intoxication with environmental contaminants, especially agrochemicals [12–14]. Some of the detrimental effects caused by pesticides in the male reproductive system may therefore be a consequence of the exacerbated free radical production (ROS) [15]. It has been proposed that many pesticides act as pseudosubstrates for the generation of free radicals, which in turn can damage P450 enzymes [4]. However, some research groups dismiss this suggestion since antioxidant supplementation failed to restore testosterone biosynthesis after intoxication by, for example, octylphenols [13]. Our previous results indicated that cultures of interstitial cells isolated from DMT-treated rats have a clear OS condition hallmarked by a general loss of antioxidant capacity and elevation of biomarkers of OS damage [6]. In particular, lipid peroxidation (LPO) is now considered to be the main mechanism by which ROS causes damage leading to impaired cellular function in testis [16]. Mammalian spermatozoa are rich in PUFA,

highly susceptible to OS [4, 8], and the same may be assumed for Leydig cells which are also very rich in PUFA [17]. Induction of OS by DMT has been a focus of research over the last decade in view of its possible role in infertility [4, 18].

We also observed that dimethoate treatment caused a significant loss of PUFA in interstitial cells, especially of 20:4n-6 (ARA), 22:5n-6 and 22:6n-6 fatty acids [6]. As is well known, C₂₂ PUFA are involved in spermatogenesis [19] while ARA is directly linked to the androgenic activity of Leydig cells [20, 21]. Chronic OS may therefore be an important mechanism for the ARA-dependent loss of steroidogenic ability since this fatty acid (FA) is essential for the biological activity of the steroidogenic acute regulatory protein (StAR) [22]. The level of ARA in Leydig cells is controlled by a complex regulatory mechanism involving an acyl-CoA synthetase (ACS4) and a mitochondrial acyl-CoA thioesterase (Acot2). Recent findings show that in steroidogenic cells, ARA release does not operate through the activation of the phospholipase A₂ pathway [23]. In fact, experimental evidence supports the idea that ARA is released from the cholesteryl-ester pool and immediately converted into arachidonoyl-CoA by ACS4 [21]. This thioester binds to the acyl-CoA binding protein (DBI), which in turn binds to the translocator protein (TSPO) located in the outer mitochondrial membrane and possibly facilitates the direct transfer of arachidonoyl-CoA to the mitochondria [22]. In addition, ARA is transformed into lipoxygenated products which induce the transcription of the StAR gene [6, 22]. The conversion of cholesterol to testosterone is limited by the transport of cholesterol from the outer to the inner mitochondrial membrane, which is controlled by StAR activity [24, 25] and the level of ARA [23, 26].

We previously demonstrated that both ARA and cholesterol concentrations are lower in cells isolated from DMT-treated rats [6]. Reduction of ARA, which in turn leads to the reduction of mitochondrial cholesterol content, could be produced by the oxidative destruction of PUFA owing to DMT-induced OS, or increased ARA utilization by the COX-2 pathway (very active in interstitial cells [27]) as the precursor of prostaglandins (PG) G₂, H₂, E₂, D₂ and F_{2 α} [27]. Previous studies performed in mitochondrial fractions subjected to LPO conditions support the assumption that PUFA content can be effectively depleted by overproduction of free radicals [28]. In addition, recent studies from our laboratory indicate that the plasmalogen subfraction is particularly enriched in ARA and highly sensitive to OS [29]. Cyclooxygenase isoenzyme types I (COX-1) and II (COX-2) are key enzymes that function coordinately and are controlled differentially by regulating the amount of ARA and LPO [30]. We observed a significant increase in the level of COX-2 protein in cells

isolated from DMT-treated animals which correlated with the higher concentrations of both PGE₂ and PGF_{2 α} . Concomitantly, StAR protein was diminished at both the gene expression and protein levels. Administration of rofecoxib almost restored the hormonal levels to control values. This specific inhibitor of COX-2 was unable to modify the LPO or the OS condition [6], leading us to conclude that the main target of DMT is related to the increment in COX-2 activity that gives rise to the diminution of ARA, the overproduction of PGE₂ and PGF_{2 α} and the subsequent inhibition of the StAR regulatory mechanism.

In the present work we therefore sought to study the possible restorative effect of polyunsaturated fatty acids (PUFA, 5 μ M/24 h) in cultures of rat Leydig cells on the main mechanistic aspects of the DMT inhibitory effect: (1) LPO status, (2) steroidogenic enzymes activities, (3) mitochondrial cholesterol and ARA levels, (4) PG biosynthesis and (5) StAR and COX-2 expression. We also investigated whether ARA has a specific role in the mechanism of action of DMT or whether there is another long-chain n-6 or n-3 FA that could be biologically active in neutralizing DMT-induced testosterone inhibition. We explored the restorative effect of various fatty acids independently of their relative abundance in the intact cells, since it is well known that in many biological systems there is interaction between the biological effects of members of the two essential series. It is also known that the fatty acid composition of testis (and specifically of interstitial cells) is modified by the quality and quantity of dietary fatty acids. Thus, the final effect on the steroidogenic route depends not only on fatty acid abundance at the basal state, but also on the modifications induced by the fatty acids acquired from the blood stream.

Experimental Procedure

Chemicals

All chemicals used were of reagent grade and obtained from Sigma Chem. Co. (CA, USA, or Buenos Aires, Argentina) or Merck Laboratories (Darmstadt, Germany). Organic solvents were from Carlo Erba (Milano, Italy). Other chemicals employed were of analytical grade and purchased from local commercial sources. Dimethoate (DMT, 2-dimethoxyphosphonylthio-*N*-methylacetamine) was obtained as a gift from INTA (Castelar, Argentina). Pure fatty acids (FA) were obtained from Nu-Chek Prep. (Elysian, MN, USA). All acids were stored in benzene under nitrogen atmosphere at -20°C . Concentrations and purities were routinely checked by capillary gas-liquid chromatography as described in a previous paper [31].

Animals

Male Wistar rats weighing 180 ± 20 g with specific pathogen-free certified status were used. Upon arrival, the rats were allowed to acclimatize for a week before commencing the experiment, during which time they were maintained under controlled conditions of temperature ($25 \pm 2^{\circ}\text{C}$) and a normal photoperiod of 12 h dark and 12 h light. They were fed with standard Purina chow from Ganave S.A. (Santa Fe, Argentina) and water ad libitum. Clinical examination together with body weight evaluation was performed throughout the entire adaptation period. Animal maintenance and handling were in accordance with the NIH guide for the care and use of laboratory animals. All procedures were approved by the local Laboratory Animal Bioethics Committee, Facultad de Ciencias Médicas, UNLP, Argentina.

Cell Culture and Treatment

After killing the rats by rapid decapitation, testes were excised and washed under sterile conditions. The technical procedure for Leydig cell isolation was described in detail in a previous report [32]. Briefly, Leydig cells were removed from the interstitial space of testicular tissue by mechanical shaking with collagenase (Sigma Chem. Co., type IV) in a metabolic incubator, at 34°C , according to Suescon et al. [33]. Cells were suspended in Krebs–Ringer bicarbonate glucose (KRBG) buffer (pH 7.4), examined for viability (90 %) by trypan blue exclusion [34], and counted in a hemocytometer to adjust cell concentration. Aliquots of cell suspensions were subjected to total cellular protein (TCP) determination by the micromethod of Bradford [35]. The homogeneity of cell preparations was assessed by means of the observation of smears fixed in acetone and stained with hematoxylin–eosin. Interstitial cell preparations consisted of 85 % Leydig cells and 15 % spermatids, spermatocytes and small cytoplasmic fragments. Control or DMT-treated cells were divided into experimental sets each containing 6.10^6 cells per sterilized/siliconized Erlenmeyer flask with 20 mL of culture medium in a humidified and oxygenated culture chamber. Flasks with cell suspensions were subjected to soft metabolic agitation in a shaker at 35°C . At zero time, the cells were supplemented with the assayed FA vehiculized as a complex with delipidated serum albumin (FA:BSA; 5:1) at a final concentration of 5 μ M for 24 h. The FA:BSA complexes were sterilized by Millipore (0.22 μ m) ultrafiltration and prepared according to the procedure previously described [36]. Cells treated with FA were divided into two series of 6 flasks each and one series was simultaneously treated with DMT (1 ppm) dissolved in 10 % PEG-400 in PBS (pH 7.40) as vehicle. Aliquots of the added supplements never exceeded 100 μ L per incubation flask.

Cell Viability Tests

Cell viability was assessed at zero time and at the end of the incubation period (24 h) by two methods. Cell suspensions were assayed using exclusion of trypan blue dye according to Jauregui et al. [34]. Samples of culture medium were subjected to centrifugation at 10,000g for 15 min and then ultrafiltered through Millipore membranes (0.22 μ M) in order to discard cell debris, following which they were analyzed by lactate–dehydrogenase (LDH) leakage in the supernatant [34] (Optima-UV-LDH assay kit from Winner Labs., Rosario, Argentina).

Lipid Peroxidation

LPO was assayed as thiobarbituric acid reactive substances (TBARS) and expressed as nmol malondialdehyde (MDA)/mg protein [37].

Immunoblotting

Cells were homogenized by sonication as previously described [6] in Tris/HCl/sucrose buffer with 1 % antiprotease cocktail (Sigma Chem. Co, Bs. As., Argentina) and 2 % SDS. After heating the samples (20 μ g) at 95 °C for 3 min with 10 % mercaptoethanol, aliquots were supplemented with 10 % glycerol and 0.01 % bromophenol blue and loaded on 12 % SDS-PAGE mini-slabs (Mini protean II, Bio-Rad, Hercules, CA, USA). Proteins were electrophoretically transferred overnight to PVDF membranes (Bio-Rad, Hercules, CA, USA) using a transfer buffer containing 25 mM Tris, 190 mM glycine and 20 % methanol. COX-2 protein levels were analyzed using a polyclonal antibody (Santa Cruz Biotechnology Inc., CA, USA) and StAR protein was detected with a rabbit polyclonal antibody generated against amino acids 88–98 of the 30 kDa StAR protein prepared according to Clark et al. [38]. Blots were re-analyzed for α -tubulin as reference protein to control both loading and transfer processes using a polyclonal anti- α -tubulin antibody from Oncogene (San Diego, CA, USA). Immunocomplexes were revealed with peroxidase-labeled secondary antibodies from Amersham Pharmacia Biotech AB (Uppsala, Sweden). Semi-quantitation of Western blots was performed using the GeneGenius gel documentation system and GeneTools software from Syngene (Cambridge, UK). Results were normalized to α -tubulin signal and expressed as “fold change” relative to the control (basal assay), which was assigned a value of 1.

PGF_{2 α} and PGE₂ Assays

For assessment of PGF_{2 α} and PGE₂ content in the interstitial cells, homogenates were centrifuged at 15,000 \times g for

30 min at 2 °C. Supernatants were filtered through Millipore 0.22 μ m filters and concentrated by lyophilization in a Telstar apparatus, Lyobeta Model (Madrid, Spain). The residues were dissolved with HCl 2 N adjusting the pH to 3.5, injected into a 200 mg C₁₈ reverse phase Sep-columns (Peninsula Lab, Belmont, CA, USA) and then eluted with ethyl acetate. The eluted fractions were evaporated to dryness under a nitrogen stream and reconstituted in buffers for enzyme-immuno assay (EIA) determinations. PG were determined using commercially available kits (Prostaglandin F_{2 α} EIA Kit and Prostaglandin E₂ Express EIA Kit from Cayman, Migliore Laclaustra S.R.L. (Buenos Aires, Argentina) with a minimum detection of 4 and 30 pg/mL, respectively. Intra- and inter-assay coefficients of variation were in the range of 8–12 % for both kits.

Lipid Analysis

Aliquots of cell lysates were used to prepare mitochondrial fractions using a combination of low (600 g) and high-speed (11,000 g) centrifugation procedures in a buffer containing HEPES 10 mM/pH 7.50 plus mannitol 200 mM, sucrose 70 mM and EGTA 1 mM according to the recommendation of the kit manufacturer (MITO-ISO1 from Sigma Chem. Co., Buenos Aires). The purity and integrity of the fraction was checked using a CYTOCOX1 kit (Sigma). Total lipids from mitochondrial suspensions were extracted by the method of Folch et al. [39]. The phospholipid fraction was separated from the Folch extracts by the micro-column chromatography method described elsewhere [40] and quantified as phosphorus content [41] after mineralization of an aliquot from the silicic acid partition. GLC of the FAME (fatty acid methyl esters) was performed as indicated in our previous paper [42] except that in this case we used a capillary column mounted on a Hewlett Packard HP 6890 Series GC System Plus (Avondale, PA, USA) equipped with a terminal computer integrator and data station. The FAMES were identified by comparison of their relative retention times with authentic standards and mass distribution was calculated electronically by quantification of the peak areas. To quantify FA content, 21:0 was used as internal standard. Cholesterol (CHOL) content was enzymatically measured according to Allain et al. [43] using a commercial kit from Wiener Lab. (Rosario, Argentina). Testosterone (Te) measurements were performed using a commercial kit KS24CT from Radim (Radim SpA, Pomezia, Italy).

Steroidogenic Enzyme Activities

Appropriate aliquots of homogenate supernatants were employed to determine 3 β -hydroxysteroid-dehydrogenase (3 β HSD) and 17- β -hydroxysteroid-dehydrogenase (17 β

HSD) [EC 1.1.1.51] enzyme activities following the method of Marugesan et al. [44]. In brief, sonicated interstitial cells were centrifuged ($12,000\times g$, 15 min, $1-2\text{ }^{\circ}\text{C}$). Supernatants were mixed with charcoal in order to remove the endogenous steroids and the samples were again centrifuged ($12,000\times g$ 15 min, $2\text{ }^{\circ}\text{C}$). The reaction conditions were defined in preliminary experiments in which enzyme activities were tested by varying the incubation times and concentrations of substrates, protein, and cofactors. Assays were performed under initial velocity conditions in a reaction mixture (250 μL final volume) containing 10 μM of the steroid substrate (Δ^4 -androstenedione or pregnenolone for 17β HSD and 3β HSD, respectively), 1 mM NADPH (17β HSD) or 0.2 mM NAD^+ (3β HSD), and 0.1 M phosphate buffer (pH 7.4). Mixtures were incubated under air in a spectrophotometric cell holder thermostatted at $37\text{ }^{\circ}\text{C}$. The reactions were started by the addition of the supernatant aliquots and OD changes of the nicotinamide cofactor(s) were measured. The incubation mixture deprived of substrate(s) was used as a reagent blank.

PLA₂ Activity

Phospholipase A₂ (PLA₂) activity was determined with [¹⁴C] arachidonoyl-phosphatidylcholine (ARA-PC) (24.0 mCi/mmol, 99 % pure) as substrate according to the method of Hirata et al. [45] with the modifications described in our previous paper [31]. Briefly, cellular homogenates were centrifuged at $15,000\times g$ for 30 min at $2\text{ }^{\circ}\text{C}$ and 20 to 40 μg protein was incubated at $37\text{ }^{\circ}\text{C}$ in a metabolic shaker with 0.5 mL of 50 mM TRIS/glycylglycine buffer (pH 8.0), 0.1 mM Mg Cl_2 , 5 mM *N*-acetylcysteine, and 1 mM ARA-PC biosynthetically prepared in our laboratory. The lipid was previously scattered, under carefully controlled temperature, in cold potassium buffer plus 0.1 mM sodium deoxycholate (grade II, from Sigma Chem. Co.) by means of three 20-s sonication periods with a Heat System-Ultrasonic Sonicator model W-220F (Plainview, NY, USA) equipped with a 1/8-inch diameter microtip at 50 % output. After preincubation at $37\text{ }^{\circ}\text{C}$ for 1 min, the assay was started by the addition of the aliquot assayed. Under these conditions, the reaction was completely linear up to 30 min. It was stopped after 10 min incubation time by the addition of 3 mL isopropyl alcohol/heptane/1 N H_2SO_4 (40:10:1, by vol) followed by 2 mL distilled water plus 2 mL of hexane (Carlo Erba, Milan, Italy) containing 5 μg /tube unlabelled arachidonic acid, thorough mixing and incubation for 10 min at room temperature. Unlabeled acid was added as a carrier to facilitate quantitative extraction. Labeled fatty acids, released by the action of phospholipase A₂, were recovered from the upper phase (at least 95 % yield) and counted by liquid

scintillation (ACS II Scintillation Cocktail, Amersham Pharmacia Biotech., Buckinghamshire, England) using a Wallac Rackbeta Liquid Scintillation Counter (Turku, Finland) with 90 % efficiency for ¹⁴C. Blanks consisted of equivalent aliquot samples boiled at $100\text{ }^{\circ}\text{C}$ for 5 min. Formation of unlabeled lyso-PC was routinely checked by recovering the phospholipid components followed by thin-layer chromatography and radio-scanning (radio-TLC) in a TLC-proportional radioactivity scanner system (Berthold LB-2832, Wildbad, Germany) equipped with a Hewlett-Packard 3396-A Data Station.

Statistical Analysis

Results were analyzed by one way analysis of variance (ANOVA) followed by the Tukey multiple comparison test. Data were expressed as the mean \pm standard deviation (SD) of six independent determinations. They were considered to differ from control data at a level of significance of $*p < 0.01$. Calculations were made with the aid of Systat (version 12.0 for Windows) from SPSS Science (Chicago, IL, USA) and/or Sigma Scientific Graphing Software (version 9.0) from Sigma Chem. Co. (St. Louis, MO, USA).

Results

Each FA assayed was run in parallel with the following control flasks: C (no additions); BSA (delipidated BSA 1 μM) and PEG (an equivalent aliquot of the vehicle used to supplement the flask with DMT). Since there were no statistical differences between the assays, the results routinely refer to C values as the control experiment.

Influence of Treatments on Cell Viability

None of the experimental treatments with DMT alone or in combination with any of the FA assayed in the form of BSA: FA complexes produced significant changes in cell viability by means of either LDH leakage or trypan blue dye exclusion tests (data not shown). Cell viability remained at 95–98 % throughout the incubation period (24 h).

Lipid Peroxidation and Parameters Involved in Lipid Metabolism

DMT produced a significant increase in the TBARS concentration determined in cellular homogenates, confirming previous results from our laboratory (Table 1). TBARS were also higher in mitochondrial suspensions isolated from DMT-treated Leydig cells, increasing from a basal value of 1.9 ± 0.2 nmol MDA/mg mitochondrial protein

to 4.8 ± 0.3 ($P < 0.01$, $n = 6$ independent determinations). TBARS overproduction was sustained in all assays using n-6 FA in combination with DMT, demonstrating a pro-oxidative condition exacerbated by the addition of these kinds of FA. However, n-3-PUFA produced the opposite effect, neutralizing the elevation of TBARS by DMT treatment to almost control values (Table 1). Total lipid extract from mitochondrial fraction was analyzed in terms of the absolute content of CHOL and ARA using a coupled enzymatic procedure with cholesterol oxidase and quantitative capillary gas–liquid chromatography, respectively. The analysis of whole-cell phospholipids demonstrated that total inorganic phosphate content/mg protein was unaffected by dimethoate treatment (data not shown). Similar results were obtained for the phospholipid fraction isolated from the mitochondrial fraction. However, mitochondrial cholesterol content decreased after DMT treatment, this effect being more noticeable in the co-treatment with three FA (18:2n-6, 18:3 n-3 and 20:5 n-3) (Table 1). Addition of 20:3n-6 restored the cholesterol level to control values, whereas ARA was able to significantly increase the concentration of this sterol. ARA content in the phospholipid subfraction extracted from mitochondrial suspensions was almost 30 % lower in DMT-treated cells compared to control data (Table 1). Addition of 20:3n-6 tended to restore the level of ARA and as expected, supplementation with ARA raised the FA concentration ~ 20 % above control values. Incubation in the presence of 18:3n-3 or 20:5n-3 alone (without DMT) produced a slight—although significant—decrease in ARA content compared to control data. Phospholipase A_2 activity was not significantly modified by treatment with DMT or n-6 FA; however, supplementation with n-3 FA alone or in combination with DMT produced significant inhibition of the enzyme activity (Table 1).

Steroidogenesis and Prostaglandin Production

As previously demonstrated in our laboratory, DMT-treated cells exhibit a reduction in 3β and 17β HSD activities (Table 2). The addition of n-6 FA alone produced inhibitory effects per se in both enzymes, reinforced by adding DMT under co-incubation conditions (FA + DMT). However, n-3 FA displayed the opposite effect, stimulating the basal activity of both enzymes and restoring the values to those of the control data or even producing an increase in the presence of DMT. Both prostaglandins (F2 α and E2) increased significantly after DMT treatment. Addition of n-6 FA produced no further changes, with the exception of the 20:3n-6 and ARA FA, whose levels of both PG increased above those of cells with no additions. Incubation with 18:3 and 20:5 FA from the n-3 series increased PG F2 α and E2 whereas the other FA of the same series caused

a decrease in PG concentration compared to control data (Table 2). Under co-incubation conditions with DMT, 20:3n-6 and ARA increased the level of PG E2 compared to that observed with DMT alone. Addition of 22:5n-3 and 22:6n-3 caused a decrease in both PG compared to DMT-treated cells. On the contrary, addition of 20:5n-3 to DMT-treated cells produced a further increase in PG F2 α and E2.

Testosterone Biosynthesis

The concentration of testosterone in Leydig cells was 56 % lower in DMT-treated cells than in the controls. Some FA added alone produced a slight but significant decrease in testosterone biosynthesis (18:2n-6, 22:4n-6 and n-3 FA except 18:3n-3) whereas others (20:3n-6 and ARA) increased the hormone concentration. In co-incubation with DMT, 20:3n-6 tends to normalize Te production whereas ARA not only restores but also stimulates the biosynthesis of androgen beyond control values. All n-3 FA assayed failed to counteract the inhibitory effect displayed by DMT (Table 3).

StAR and COX-2 Expression

The expression of StAR (Fig. 1) and COX-2 (Fig. 2) proteins was tested by Western blotting. Relative quantification of the signals demonstrates that the observed effects strongly depend on the kind of FA tested, whether alone or in combination with DMT. The StAR protein is strongly stimulated by ARA and partially stimulated by its metabolic precursor (20:3n-6). Addition of ARA completely reversed the inhibitory effect caused by DMT. None of the other FA were able to produce this reversion. In the case of 20:5n-3 we also found a more pronounced inhibitory effect than that observed in control cells, especially when the acid was added in combination with DMT. COX-2 protein increased under DMT treatment. Eicosa-8,11,14-trienoic acid also stimulated COX-2 protein over basal levels. In the case of ARA, this stimulation exceeded that observed with DMT treatment. Addition of 18:3n-3 and 20:5n-3 also stimulated COX-2 protein and when the supplemented FA was eicosapentaenoic acid, the effect was additive. On the contrary, treatment with 22:5n-3 and 22:6n-3 FA decreased the COX-2 protein.

Discussion

Previous studies from Carlsen et al. [2] warn about the worldwide decline in semen quality over the past five decades. Retrospective studies performed independently in sperm banks in Paris [46] and London [47] have confirmed

Table 1 Effect of fatty acid (FA) additions on TBARS production, mitochondrial (MIT) araquidonate and cholesterol (CHOL) concentrations, and phospholipase A₂ (PLA₂) activity in rat Leydig cells treated with or without dimethoate (DMT)

Additions	FA	DMT	Parameters			
			TBARS (nmol/mg TCP)	[CHOL] MIT (ng/μg prot.)	[20:4] MIT-PL (μmol/g lipids)	PLA ₂ activity (dpm/min mg prot.)
Control assays	–	–	2.7 ± 0.2	25.5 ± 3.1	37.1 ± 3.8	3,808 ± 131
	–	+	5.1 ± 0.4 ^b	19.4 ± 3.0 ^b	26.6 ± 2.2 ^b	4,201 ± 143
Assays + n-6 FA	18:2	–	3.5 ± 0.2 ^b	26.0 ± 2.2	36.7 ± 4.8	3,911 ± 143
		+	6.4 ± 0.1 ^{a,b}	18.3 ± 2.9 ^{a,b}	25.9 ± 2.9 ^{a,b}	3,845 ± 101
	20:3	–	4.0 ± 0.3 ^b	28.9 ± 1.5	41.8 ± 2.8 ^b	4,025 ± 188
		+	6.6 ± 0.2 ^{a,b}	24.0 ± 1.9 ^a	28.8 ± 1.7 ^{a,b}	3,865 ± 90
	20:4	–	4.3 ± 0.3 ^b	31.2 ± 2.1 ^b	44.1 ± 3.0 ^b	3,919 ± 122
		+	6.1 ± 0.1 ^{a,b}	28.6 ± 1.7 ^b	32.0 ± 1.8 ^{a,b}	3,978 ± 126
	22:4	–	3.9 ± 0.2 ^b	23.2 ± 2.1	35.4 ± 2.5	3,829 ± 111
		+	6.7 ± 0.3 ^{a,b}	20.0 ± 3.1 ^{a,b}	25.9 ± 1.9 ^{a,b}	3,814 ± 105
22:5	–	4.1 ± 0.2 ^b	27.6 ± 2.8	38.0 ± 4.0	3,916 ± 98	
	+	7.0 ± 0.4 ^{a,b}	22.0 ± 2.1 ^{ab}	28.5 ± 2.8 ^{a,b}	4,110 ± 165	
Assays + n-3 FA	18:3	–	2.8 ± 0.1	21.6 ± 2.2 ^b	30.4 ± 2.7 ^b	3,346 ± 107 ^b
		+	3.0 ± 0.2	15.5 ± 1.8 ^{a,b}	21.3 ± 1.8 ^{a,b}	3,400 ± 85 ^b
	20:5	–	2.0 ± 0.2 ^b	22.6 ± 1.1 ^b	29.4 ± 2.0 ^b	3,103 ± 79 ^b
		+	2.5 ± 0.2	16.7 ± 2.2 ^{a,b}	20.7 ± 1.1 ^{a,b}	3,211 ± 70 ^b
	22:5	–	2.1 ± 0.1 ^b	26.8 ± 2.9	35.3 ± 3.5	2,916 ± 122 ^b
		+	3.0 ± 0.1	20.1 ± 1.8 ^{a,b}	24.6 ± 2.4 ^{a,b}	2,975 ± 127 ^b
	22:6	–	2.2 ± 0.1 ^b	27.0 ± 2.3	35.5 ± 1.8	2,713 ± 64 ^b
		+	2.7 ± 0.2	21.1 ± 2.6 ^{a,b}	23.8 ± 3.0 ^{a,b}	2,888 ± 105 ^b

Results were obtained as described in “[Experimental Procedure](#)” (mean ± SD of six independent determinations)

^a Significantly different respect to the corresponding control assay (without DMT addition)

^b Different respect to cells without any additions ($p < 0.01$)

this conclusion. All the experimental and epidemiological evidence points to agrochemicals as the main environmental factor responsible for the decline in sperm quality, especially in those countries where the use of agrochemicals is most widespread [3, 4]. It is almost impossible to draw up an exact scenario of the consequences of environmental pollution on male reproductive functions owing to the lack of adequate data on the level of exposure and precise knowledge of the mechanism of pesticide action on the metabolism of Leydig, Sertoli, and other cells of the germinal and non-germinal series [4, 48].

In the specific case of Leydig cell metabolism, it is well established that there are key events that could produce deleterious effects on the multiple physiological functions of the cells: (1) ROS production in response to toxicants [4, 49], (2) enhancement of COX-2 activity and ARA consumption leading to an increase in F2α and E2 PG [50, 51] and (3) inhibition of StAR activity which internalizes CHOL and regulates the biosynthesis of Te [20, 38]. These factors converge in a complex and not fully understood regulatory mechanism in which ROS, PG and COX-2 (and their metabolites) control the production of Te [12, 21, 50–

52]. In addition, StAR is sensitive to many pesticides [21] and DMT specifically disturbs StAR gene expression in testes [6, 24].

The present work demonstrates that very low doses of DMT added in vitro to Leydig cells were able to produce strong modifications in all the key factors described above that determine the rate of androgenic activity. Interestingly, external supplementation with various n-3 and n-6 FA introduces partial modifications in one or more of the regulatory factors under consideration.

A clear pattern of ROS production was observed in which n-3 FA behave as anti-oxidants and n-6 as pro-oxidants, a finding that is corroborated by other laboratories [53, 54]. As previously stated, detrimental effects of pollutants on the male reproductive system have traditionally been explained in terms of the overproduction of ROS [12–14]. LPO is considered one of main mechanisms by which ROS impairs cell function in testis [16]. Moreover, it has been reported that antioxidants such as curcumin, ascorbate and α-tocopherol [55] may neutralize the androgen imbalance produced by organophosphorates. This hypothesis is supported by the fact that the antioxidant

Table 2 Effect of fatty acid (FA) additions on the steroidogenic enzyme activities and prostaglandin (F2 α and E2) production on rat Leydig cells treated with or without dimethoate (DMT)

Additions	FA	DMT	Parameters			
			3 β HSD (nmol NAD/ min mg prot.)	17 β HSD (nmol NADP/ min mg prot.)	PG F2 α	PG E2
Control assays	–	–	6.2 \pm 0.3	0.7 \pm 0.1	238 \pm 17	76 \pm 5
	–	+	3.7 \pm 0.2 ^b	0.3 \pm 0.04 ^b	496 \pm 31 ^b	144 \pm 10 ^b
Assays + n-6 FA	18:2	–	3.4 \pm 0.1 ^b	0.4 \pm 0.03 ^b	230 \pm 21	81 \pm 7
		+	2.9 \pm 0.05 ^{a,b}	0.1 \pm 0.02 ^{a,b}	481 \pm 27 ^{a,b}	156 \pm 13 ^{a,b}
	20:3	–	4.0 \pm 0.2 ^b	0.4 \pm 0.1 ^b	303 \pm 24 ^b	169 \pm 11 ^b
		+	3.1 \pm 0.1 ^{a,b}	0.2 \pm 0.04 ^{a,b}	501 \pm 42 ^{a,b}	186 \pm 25 ^b
	20:4	–	3.7 \pm 0.1 ^b	0.4 \pm 0.1 ^b	296 \pm 33 ^b	177 \pm 15 ^b
		+	3.0 \pm 0.3 ^b	0.3 \pm 0.03 ^b	489 \pm 18 ^{a,b}	196 \pm 21 ^b
	22:4	–	3.8 \pm 0.2 ^b	0.5 \pm 0.1	233 \pm 29	70 \pm 8
		+	2.9 \pm 0.3 ^{a,b}	0.3 \pm 0.02 ^{a,b}	481 \pm 34 ^{a,b}	141 \pm 12 ^{a,b}
	22:5	–	3.5 \pm 0.2 ^b	0.4 \pm 0.04 ^b	246 \pm 22	78 \pm 6
		+	2.7 \pm 0.2 ^{a,b}	0.2 \pm 0.01 ^{a,b}	503 \pm 40 ^{a,b}	151 \pm 10 ^{a,b}
Assays + n-3 FA	18:3	–	7.5 \pm 0.3	1.0 \pm 0.1 ^b	276 \pm 16 ^b	112 \pm 16 ^b
		+	4.2 \pm 0.1 ^{a,b}	0.4 \pm 0.03 ^{a,b}	521 \pm 29 ^{a,b}	160 \pm 18 ^{a,b}
	20:5	–	7.0 \pm 0.1	1.1 \pm 0.05 ^b	295 \pm 32 ^b	151 \pm 10 ^b
		+	4.5 \pm 0.2 ^{a,b}	0.7 \pm 0.1 ^a	533 \pm 44 ^{a,b}	184 \pm 22 ^{a,b}
	22:5	–	7.7 \pm 0.3 ^b	1.2 \pm 0.2 ^b	206 \pm 17 ^b	65 \pm 5
		+	4.3 \pm 0.1 ^{a,b}	0.6 \pm 0.2 ^a	411 \pm 21 ^{a,b}	98 \pm 9 ^{a,b}
22:6	–	8.1 \pm 0.3 ^b	1.0 \pm 0.1 ^b	218 \pm 15 ^b	60 \pm 4	
		+	5.0 \pm 0.2 ^{a,b}	0.7 \pm 0.1 ^a	395 \pm 18 ^{a,b}	105 \pm 15 ^{a,b}

Results were obtained as described in “Experimental Procedure” (mean \pm SD of 6 independent determinations)

^a Significantly different respect to the corresponding control assay (without DMT addition)

^b Different respect to cells without any additions ($p < 0.01$)

protection of PUFAS, in particular ARA, is directly correlated with better spermatogenesis [19] and androgenic activity in Leydig cells [20, 21]. However, these findings do not correlate with results obtained from our [6] and other [13] laboratories and appear to be an extreme simplification. We previously found that TROLOX[®], administered as a potent antioxidant, provides no substantial protection against DMT-induced changes. In fact Rofecoxib[®], a COX-2 specific inhibitor, partially attenuates DMT-treatment damages [6], leading us to focus on the ARA signaling cascade as another key regulatory feature within the complex scenario of the DMT-inhibition of Te production.

Our findings relating to the changes caused by some FA on COX-2 activity and PG production, in particular the stimulatory effect of ARA and 20:3n-6 [56] and the inhibition exerted by 22:5n-3, 22:6n-3 and 20:5n-3 FA [56–60], have been corroborated by other laboratories. FA are regulators of COX-2 transcription [61] through the PPAR-dependent signaling route. Previous evidence demonstrated that the biosynthesis of androgens is strongly linked to ARA metabolism [20, 21, 62, 63] and it was reported that n-6 PUFA decrease the quality of the sperm without decreasing the number of Leydig cells, probably by altering the ARA cascade [64]. Interestingly, infertile men have

higher levels of n-6 PUFAS in testis and spermatozoa [53]. Studies also demonstrate that the quality and quantity of dietary FA may determine the pattern of PG in testis and fertility performance in men [53, 64, 65], as corroborated in in vitro studies [58, 66]. In addition, 5 α -reductase—a key enzyme in the androgenic pathway—is strongly influenced by the balance between n-3 and n-6 FA [67]. This mechanistic scheme is even more complicated if we consider that PUFA may modify the specific activity of two of the main steroidogenic enzymes, 3 β HSD and 17 β HSD [29, 68]. As previously described by Murugesan [12, 44, 69] and Kostic [70], overproduction of ROS by any mechanism, including PUFA peroxidation, can also inhibit these enzymes. In addition, certain fatty acids per se may influence the activity of these dehydrogenases. In vivo and in vitro experiments on testis and interstitial cells isolated from rats show that a diet of soybean oil reduces 3 β HSD and 17 β HSD activity as compared with a diet containing equivalent amounts of linoleic acid but without significant amounts of linolenic acid (grape seed oil) [29, 71], strongly suggesting that n-3 fatty acids could inhibit 3 β and 17 β steroidogenic activity as reported by other authors [72]. We also demonstrated that independently of the essential series to which they belong, and unlike saturated or monounsaturated fatty acids, PUFA inhibit steroidogenic enzymes

Table 3 Effect of fatty acid (FA) additions on testosterone production of rat Leydig cells treated with or without dimethoate (DMT)

Additions	FA	DMT	Testosterone (pmol/mg TCP)
Control assays	–	–	32.5 ± 2.0
	–	+	14.4 ± 1.0 ^b
Assays + n-6 FA	18:2	–	26.1 ± 2.3 ^b
		+	13.0 ± 0.6 ^{a,b}
	20:3	–	34.1 ± 2.4
		+	22.6 ± 1.7 ^{a,b}
	20:4	–	37.5 ± 2.0 ^b
		+	34.3 ± 2.1
	22:4	–	26.5 ± 2.7 ^b
		+	11.7 ± 0.8 ^{a,b}
22:5	–	27.3 ± 3.0 ^b	
	+	13.4 ± 0.5 ^{a,b}	
Assays + n-3 FA	18:3	–	30.5 ± 2.6
		+	15.1 ± 0.6 ^{a,b}
	20:5	–	26.6 ± 2.0 ^b
		+	13.0 ± 1.1 ^{a,b}
	22:5	–	27.1 ± 0.9 ^b
		+	12.2 ± 1.0 ^{a,b}
	22:6	–	28.4 ± 1.7 ^b
		+	12.6 ± 0.5 ^{a,b}

Results were obtained as described in “[Experimental Procedure](#)” (mean ± SD of 6 independent determinations). TCP, total cellular protein

^a Significantly different respect to the corresponding control assay (without DMT addition)

^b Different respect to cells without any additions ($p < 0.01$)

[29, 71]. This experimental evidence would appear to indicate that ARA decreases testosterone level; however, the inhibitory effect on steroidogenic enzyme activity, although significant, was completely surpassed by the stimulatory action on other main factors determining testosterone biosynthesis, mainly StAR activation.

Availability of ARA depends on its release from phospholipid stores. Although no significant modification in the pool of mitochondrial phospholipids was detected, n-3 PUFA—but not n-6 PUFA—reduced phospholipase A₂ activity to different extents. This finding is in agreement with previous experimental evidence [57, 60] but in apparent contradiction with epidemiological data indicating a reduction of n-3 FA in infertile men [53]. Our results may therefore contribute to understanding why certain n-3 PUFA may have an anti-androgenic effect in Leydig cells.

Many events appear to converge on the central activity of the StAR protein, which ultimately exerts control over the mitochondrial cholesterol pool available for testosterone biosynthesis. The steroidogenic rate is sensitive to small changes in StAR protein activity [24]. It is well

established that translocation of cytoplasmic cholesterol into the mitochondria is controlled by StAR activity [24] and also by the level of ARA [23, 26]. In addition, Diemer et al. [25] reported that ROS per se are able to inhibit StAR activity. Furthermore, PGF2 α significantly depresses StAR activity in porcine, man, rat and human tissues [73–76] and down-regulates 17 β HSD (77). Inhibition of COX-2, on the other hand, significantly increases StAR protein and steroidogenic activity [6, 77].

Whereas our previous findings suggested that the main target of DMT on the steroidogenic route was COX-2 activity, which ultimately modulates the activity of the StAR protein, our present findings lead us to conclude that the mechanism of DMT-induced damage on testosterone biosynthesis in Leydig cells is a multifactorial event with cross-talk among many variables. The resulting rate of biosynthesis is determined by a complex balance between the various factors schematically presented in Fig. 3 (graphical abstract), most of which produce contrary effects, making the final impact difficult to assess. For example, n-3 FA clearly inhibit PLA₂ activity, decreasing the availability of ARA to stimulate the StAR protein, but they simultaneously reduce the overproduction of ROS

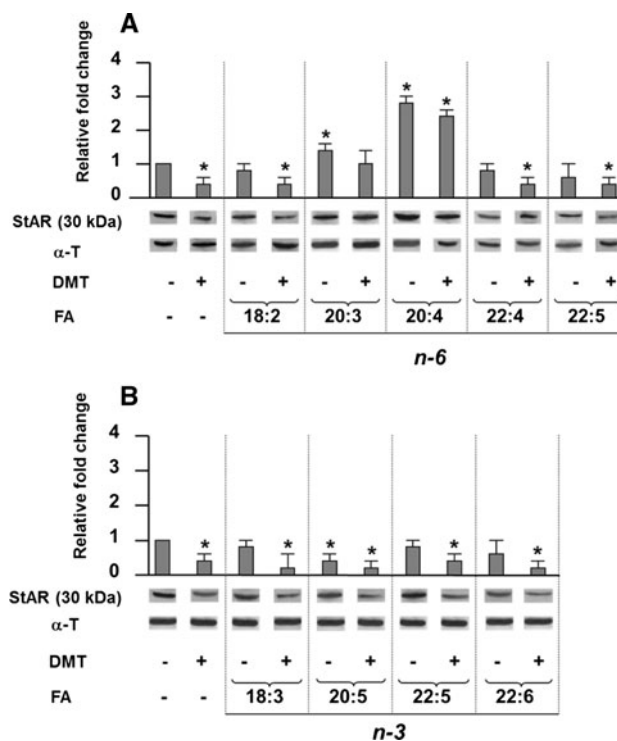


Fig. 1 StAR protein level in interstitial cells treated (24 h) with different fatty acids from n-6 series (*panel a*) or n-3 series (*panel b*) added alone as BSA complexes (5 μ M) or in combination with DMT (1 ppm). Results are representative of six different incubations run in duplicate. See details in “[Experimental Procedure](#)”. (Asterisk) Significantly different with respect to the corresponding control assay (minus DMT)

Clarification of the complex pattern of events that emerges from the present paper may have important connotations in other areas. Disruption of StAR protein activity and the restorative action of PUFA could have implications that go beyond questions of fertility. StAR plays a key role in many other tissues such as adrenal glands, brain, lungs and ovaries, so it is possible that the biosynthetic pathways that regulate mineralo- and glucocorticoids also impact on carbohydrate metabolism, immune function, neuroprotection, water and mineral balance, among others. Further research will help elucidate the detrimental effects of environmental pollutants and their connection with the quantity/quality of PUFA in toxicant-targeted tissues [24, 78–82].

Acknowledgments This study was supported by a grant from Consejo Nacional de Investigaciones Científicas y Técnicas (CONICET), Argentina. We would like to thank Mrs. Agustina Zardis de Cobeñas, Eva Illara de Bozzolo, and Norma Cristalli for their excellent technical assistance.

References

- Cheek AO, McLachlan JA (1998) Environmental hormones and the male reproductive system. *J Androl* 19:5–10
- Carlsen E, Giwercman A, Keiding N, Skakkeback NE (1992) Evidence for decreasing quality of semen during past 50 years. *Biochem Med J* 305:609–613
- Swan SH, Elkin EP, Fenster L (1997) Have sperm densities declined? A reanalysis of global trend data. *Environ Health Perspect* 105:1228–1232
- Saradha B, Mathur PP (2006) Effect of environmental contaminants on male reproduction. *Environ Toxicol Pharmacol* 21:34–41
- Afifi NA, Ramadan A, Ae-Aziz MI, Saki EE (1991) Influence of dimethoate on testicular and epididymal organs, testosterone plasma level and their tissue residues in rats. *Dtsch Tierärztl Wschr* 98:419–423
- Astiz M, Hurtado de Catalfo GE, de Alaniz MJT, Marra CA (2009) Involvement of lipids in dimethoate-induced inhibition of testosterone biosynthesis in rat interstitial cells. *Lipids* 44:703–718
- Sayim F (2007) Histopathological effects of dimethoate on testes of rats. *Bull Environ Contam Toxicol* 78:479–484
- Sayim F (2007) Dimethoate-induced biochemical and histopathological changes in the liver of rats. *Exp Toxicol Pathol* 59:237–243
- Thomas JA, Donovan MD, Schein LG (1978) Biochemical bases for insecticide-induced changes in the male reproductive system. *Toxicol Appl Pharmacol* 45:291–295
- Krause W (1977) Influence of DDT, DDVP, and Malathion on FSH, Lh and testosterone serum levels, and testosterone concentration in testes. *Bull Environ Contam Toxicol* 18:231–242
- Krause W, Homola S (1974) Alterations of the seminiferous epithelium and the Leydig cells of the mouse testis after application of dichlorvos. *Bull Environ Contam Toxicol* 11:429–433
- Murugesan P, Baladaneshi M, Balasubramanian K, Arunakaran J (2007) Effects of polychlorinated biphenyl (Aroclor 1254) on steroidogenesis and antioxidant system in cultured adult rat Leydig cells. *J Endocrinol* 192:325–338
- Murono EP, Derk RC, de León JH (2000) Octylphenol inhibits testosterone biosynthesis by cultured precursor and immature Leydig cells from rat testes. *Reprod Toxicol* 14:275–288
- Murono EP, Derk RC, de León JH (2001) Differential effects of octylphenol, 17 β -estradiol, endosulfan, or bisphenol A on the steroidogenic competence of cultured adult rat leydig cells. *Reprod Toxicol* 15:551–560
- Taylor CT (2001) Antioxidants and reactive oxygen species in human fertility. *Environ Toxicol Pharmacol* 10:189–198
- Cao L, Leers-Sucheta S, Azhar S (2004) Aging alters the functional expression of enzymatic and non-enzymatic anti-oxidant defence systems in testicular rat Leydig cells. *J Steroid Biochem Mol Biol* 88:61–67
- Coniglio JG (1994) Testicular lipids. *Prog Lipid Res* 33:387–401
- Abdollahi M, Shadnia S, Nikfar S, Rezale A (2004) Pesticides and oxidative stress: a review. *Med Sci Monit* 10:RA141–RA147
- Ayala S, Brenner RR, Dumm CG (1977) Effect of polyunsaturated fatty acids of the α -linolenic series on the development of rat testicles. *Lipids* 12:1017–1024
- Payne AH, Hales DB (2004) Overview of steroidogenic enzymes in the pathway from cholesterol to active steroid hormones. *Endocr Rev* 25:947–970
- Cano F, Poderoso C, Cornejo Maciel F, Castilla R, Maloberti P, Castillo F, Neuman I, Paz C, Podestá EJ (2006) Protein tyrosine phosphatases regulate arachidonic acid release, star induction and steroidogenesis acting on a hormone-dependent arachidonic acid-preferring acyl-coA synthetase. *J Steroid Biochem Mol Biol* 99:197–202
- Maloberti P, Maciel FC, Castillo AF, Castilla R, Duarte A, Toledo MF, Meuli F, Mele P, Paz C, Podestá EJ (2007) Enzymes involved in arachidonic acid release in adrenal and Leydig cells. *Mol Cell Endocrinol* 265(266):113–120
- Wang XJ, Dyson MT, Mondillo C, Patrignani Z, Pignataro O, Stocco DM (2002) Interaction between arachidonic acid and cAMP signalling pathways enhances steroidogenesis and stAR gene expression in MA-10 Leydig tumor cells. *Mol Cell Endocrinol* 188:55–63
- Walsh LP, McCornick C, Martin C, Stocco DM (2000) Roundup inhibits steroidogenesis by disrupting steroidogenic acute regulatory (StAR) protein expression. *Environ Health Perspect* 108:769–776
- Diemer T, Allen JA, Hales KH, Hales DB (2003) Reactive oxygen disrupts mitochondria in MA-10 tumor Leydig cells and inhibits steroidogenic acute regulatory (StAR) protein and steroidogenesis. *Endocrinology* 144:2882–2891
- Catalá A (2007) The ability of melatonin to counteract lipid peroxidation in biological membranes. *Curr Mol Med* 7:638–649
- Smith WL, DeWitt DL, Garavito RM (2000) Cyclooxygenases: structural, cellular, and molecular biology. *Annu Rev Biochem* 69:145–182
- Frungeri MB, González-Calvar SI, Parborell F, Albrecht M, Mayerhofer A, Calandra RS (2006) Cyclooxygenase-2 and prostaglandin F_{2 α} in Syrian hamster Leydig cells: inhibitory role on luteinizing hormone/human chorionic-stimulated testosterone production. *Endocrinology* 147:4476–4485
- Hurtado de Catalfo GE, de Alaniz MJT, Marra CA (2008) Dietary lipids modify redox homeostasis and steroidogenic status in rat testis. *Nutrition* 24:717–726
- Frungeri MB, Weidinger S, Meineke V, Köhn FM, Mayerhofer A (2002) Proliferative action of mast-cell tryptase is mediated by PAR2, COX-2, prostaglandins, and PPAR γ : possible relevance to human fibrotic disorders. *Proc Natl Acad USA* 99:15072–15077
- Marra CA, de Alaniz MJT (2005) Neutral and polar lipid metabolism in liver microsomes of growing rats fed a calcium-deficient diet. *Biochim Biophys Acta* 1686:220–237

32. Hurtado de Catalfo GE, Mandon EC, de Gómez Dumm IN (1992) Arachidonic acid biosynthesis in non-stimulated and adrenocorticotropic-stimulated Sertoli and Leydig cells. *Lipids* 27:593–598
33. Suescun MO, González SI, Chiauuzzi VA, Calandra RS (1985) Effects of induced hypoprolactinemia on testicular function during gonadal maturation in the rat. *J Androl* 6:77–82
34. Jauregui HO, Hayner NT, Driscoll JL, Williams-Holland R, Lipsky MH, Galletti PM (1981) Trypan blue dye uptake and lactate dehydrogenase in adult rat hepatocytes—freshly isolated cells, cell suspensions, and primary monolayer cultures. *In Vitro* 17:1100–1110
35. Bradford MM (1976) A rapid and sensitive method for the quantification of microgram quantities of protein utilizing the principle of protein-dye binding. *Anal Biochem* 72:248–254
36. Marra CA, Girón González MD, Suárez Ortega MD (2002) Evidence in Favor of a Specific Transport System for Fatty Acid Uptake in Cultured L6 Cells. (2002) *Lipids* 37: 273–283
37. Yagi K (1976) A simple fluorometric assay for lipoperoxide in blood plasma. *Biochem Med* 15:212–216
38. Clark BJ, Wells J, King SR, Stocco DM (1994) The purification, cloning, and expression of a novel luteinizing hormone-induced mitochondrial protein in MA-10 mouse Leydig tumor cells. Characterization of the androgenic acute regulatory protein (stAR). *J Biol Chem* 269:28314–28322
39. Folch J, Lees M, Sloane GH (1957) A simple method for the isolation and purification of total lipids from animal tissues. *J Biol Chem* 226:497–509
40. Hanahan DJ, Dittner JC, Warashina E (1957) A column chromatographic separation of classes of phospholipids. *J Biol Chem* 228:685–690
41. Chen PS, Toribara TY, Warner H (1956) Microdetermination of phosphorus. *Anal Chem* 33:1405–1406
42. Marra CA, de Alaniz MJT (1989) Influence of testosterone administration on the biosynthesis of unsaturated fatty acids in male and female rats. *Lipids* 24:1014–1019
43. Allain CC, Poon LS, Chan CS, Richmond W, Fu PC (1974) Enzymatic determination of total serum cholesterol. *Clin Chem* 20:470–475
44. Murugesan P, Kanagaraj P, Yuvaraj S, Balasubramanian K, Aruldas MM, Arunakaran J (2005) The inhibitory effects of polychlorinated biphenyl Aroclor 1254 on Leydig cell LH receptors, steroidogenic enzymes and antioxidant enzymes in adult rats. *Reprod Toxicol* 20:117–126
45. Hirata F, Schiffmann E, Venkatasubramanian K, Salomon D, Axelrod J (1980) A phospholipase A₂ inhibitory protein in rabbit neutrophils induced by glucocorticoids. *Proc Natl Acad Sci USA* 77:2533–2536
46. Auger J, Kunstmann JM, Czyglik F, Jouannet P (1995) Decline in semen quality among fertile men in Paris during the past 20 years. *N Eng J Med* 332:281–285
47. Ginsburg J, Okolo S, Prelevic G, Hardiman P (1994) Residence in the London area and sperm density. *Lancet* 343:230
48. Wong C, Kelce WR, Sar M, Wilson EM (1995) Androgen receptor antagonist versus agonist activities of the fungicide vinclozolin relative to hydroxyflutamide. *J Biol Chem* 270:19998–20003
49. Andric NL, Andric SA, Zoric SN, Kostic TS, Stojilkovic SS, Kovacevic RZ (2003) Parallelism and dissociation in the actions of an Aroclor 1260-based transformer fluid on testicular androgenesis and antioxidant enzymes. *Toxicology* 194:65–75
50. Gunnarsson D, Svensson M, Selstam G, Nordberg G (2004) Pronounced induction of testicular PGF_{2α} and suppression of testosterone by cadmium—prevention by zinc. *Toxicology* 200:49–58
51. Wang X, Dyson MT, Jo Y, Stocco DM (2003) Inhibition of cyclooxygenase-2 activity enhances steroidogenesis and steroidogenic acute regulatory gene expression in MA-10 mouse Leydig cells. *Endocrinology* 144:3368–3375
52. Chen H, Liu J, Luo L, Baig MU, Kim JM, Zirkin BR (2005) Vitamin E, aging and Leydig cell steroidogenesis. *Exp Gerontol* 40:728–736
53. Sefarinejad MR, Hosseini SY, Dadkhah F, Asgari MA (2010) Relationship of omega-3 and omega-6 fatty acids with semen characteristics, and anti-oxidant status of seminal plasma: a comparison between fertile and infertile men. *Clin Nutr* 29:100–105
54. Rupasinghe HP, Erkan N, Yasmin A (2010) Antioxidant protection of eicosapentaenoic acid and fish oil oxidation by polyphenolic-enriched apple skin extract. *J Agric Food Chem* 58:1233–1239
55. Sahoo DK, Roy A, Chainy GB (2008) Protective effects of vitamin E and curcumin on L-thyroxine-induced rat testicular oxidative stress. *Chem Biol Interact* 25:121–128
56. Derecka A, Sheldrick EL, Wathes DC, Abayasekara DRE, Flint APF (2008) A PPAR-independent pathway to PUFA-induced COX-2 expression. *Mol Cell Endocrinol* 287:65–71
57. Abayasekara DRE, Wathes DC (1999) Effects of altering dietary fatty acid composition on prostaglandin synthesis and fertility. *Prostaglandins Leukot Essent Fatty Acids* 61:275–287
58. Levine L, Worth N (1984) Eicosapentaenoic acid: its effects on arachidonic acid metabolism by cells in culture. *J Allergy Clin Immunol* 74:430–436
59. Sankaran D, Lu J, Ogborn MR, Aukema HM (2007) COX-2 expression in cystic kidneys is dependent on dietary n-3 fatty acid composition. *J Nutr Biochem* 18:806–812
60. Gravaghi C, La Perle KMD, Ogrodowski P, Kang JX, Quimby F, Lipkin M, Lamprech SA (2011) COX-2 expression, PGE2 and cytokines production are inhibited by endogenously synthesized n-3 PUFA in inflamed colon of fat-1 mice. *J Nutr Biochem* 22:360–365
61. Kim HW, Rao JS, Rapoport SI, Igarashi M (2011) Dietary n-6 PUFA deprivation downregulates arachidonate but upregulates docosahexaenoate metabolizing enzymes in rat brain. *Biochim Biophys Acta* 1811:111–117
62. Wang X, Dyson MT, Jo Y, Stocco DM (2008) Inhibition of cyclooxygenase-2 activity enhances steroidogenesis and steroidogenic acute regulatory gene expression in MA-10 mouse leydig cells. *Endocrinology* 149:851–857
63. Fiedler EP, Plouffe L Jr, Hales DB, Hales KH, Khan I (1999) Prostaglandin F(2alpha) induces a rapid decline in progesterone production and steroidogenic acute regulatory protein expression in isolated rat corpus luteum without altering messenger ribonucleic acid expression. *Biol Reprod* 61:643–650
64. Matzkin ME, Mayerhofer A, Rossi SP, Gonzalez B, Gonzalez CR, Gonzalez-Calvar SI, Terradas C, Ponzio R, Puigdomenech E, Levalle O, Calandra RS, Frungieri MB (2010) Cyclooxygenase-2 in testes of infertile men: evidence for the induction of prostaglandin synthesis by interleukin-1β. *Fertil Steril* 94:1933–1936
65. McVey MJ, Cooke GM, Curran IH, Chan HM, Kubow S, Lok E, Metha R (2008) Effects of dietary fats proteins on rat testicular steroidogenic enzymes and serum testosterone levels. *Food Chem Toxicol* 46:259–269
66. Chene G, Dubourdeau M, Balard P, Escoubet-Lozach L, Orfila C, Berry A, Bernard J, Aries MF, Chavernon M, Pipy B (2007) n-3 and n-6 polyunsaturated fatty acids induce the expression of cox-2 via PPARγ activation in human keratinocyte HaCaT cells. *Biochim Biophys Acta* 1771:576–589
67. Pham H, Ziboh VA (2002) 5-alpha-reductase-catalyzed conversion of testosterone to dihydrotestosterone is increased in prostatic adenocarcinoma cells: suppression by 15-lipoxygenase

- metabolites of gamma-linolenic and eicosapentaenoic acids. *J Steroid Biochem Mol Biol* 82:393–400
68. Fisseha S, Towns R, Harada M, Peegel H, Menon KM (2009) Inhibitory effect of valproic acid on ovarian androgen biosynthesis in rat theca-interstitial cells. *Endocrine* 37:187–193
69. Murugesan P, Senthilkumar J, Balasubramanian K, Aruldas MM, Arunakaran J (2005) Impact of polychlorinated biphenyl Aroclor 1254 on testicular antioxidant system in adult rats. *Hum Exp Toxicol* 24:61–66
70. Kostic TS, Andric SA, Maric D, Kovacevic RZ (2000) Inhibitory effects of stress-activated nitric oxide on antioxidant enzymes and testicular steroidogenesis. *J Steroid Biochem Mol Biol* 75:299–306
71. Huratdo de Catalfo GE, Tacconi de Alaniz MJ, Marra CA (2009) Influence of commercial dietary oils on lipid composition and testosterone production in interstitial cells isolated from rat testis. *Lipids* 44:345–357
72. McVey MJ, Cooke GM, Curran IH, Chan HM, Kubow S, Lok E, Metha R (2007) Effects of dietary fats and proteins on rat testicular steroidogenic enzymes and serum testosterone levels. *Food Chem Toxicol* 46:259–269
73. Diaz FJ, Wiltbank MC (2005) Acquisition of luteolytic capacity involves differential regulation by prostaglandin F₂α of genes involved in progesterone biosynthesis in the porcine corpus luteum. *Domest Anim Endocrinol* 28:172–189
74. Shea-Eaton W, Sandhoff TW, Lopez D, Hales DB, McLean MP (2002) Transcriptional repression of the rat steroidogenic acute regulatory (stAR) protein gene by the AP-1 family member c-Fos. *Mol Cell Endocrinol* 188:161–170
75. Fuchs AR, Chantabraksri U (1981) Prostaglandin F_{2α} regulation of LH-stimulated testosterone production in rat testis. *Biol Reprod* 25:492–501
76. Arakane F, Kallen CB, Watari H, Foster JA, Sepuri NB, Pain D, Stayrook SE, Lewis M, Gerton GL, Strauss JF 3rd (1998) The mechanism of action of steroidogenic acute regulatory protein (stAR). stAR acts on the outside of mitochondria to stimulate steroidogenesis. *J Biol Chem* 273:16339–16345
77. Reinhart AJ, Williams SC, Stocco DM (1999) Transcriptional regulation of the StAR gene. *Mol Cell Endocrinol* 151:161–169
78. Bolognesi C, Morasso G (2000) Genotoxicity of pesticides: potential risk for consumers. *Trends Food Sci Tech* 11:182–187
79. Sivapiriya V, Jayanthisakthisekaran Venkatraman S (2006) Effects of dimethoate (*O,O*-dimethyl *S*-methyl carbamoyl methyl phosphorodithioate) and ethanol in antioxidant status of liver and kidney of experimental mice. *Pest Biochem Physiol* 85:115–121
80. Farag AT, El-Aswad AF, Shaaban NA (2007) Assessment of reproductive toxicity of orally administered technical dimethoate in male mice. *Reprod Toxicol* 23:232–238
81. Latchoumycandane C, Chitra KC, Mathur PP (2002) The effect of 2,3,7,8-tetrachlorodibenzo-*p*-dioxin on mitochondrial and microsomal fractions of rat testis. *Toxicology* 171:127–135
82. Latchoumycandane C, Mathur PP (2002) Effect of methoxychlor on the antioxidant system in mitochondrial and microsome-rich fractions of rat testis. *Toxicology* 176:67–75

Chylomicron Formation and Secretion is Required for Lipid-Stimulated Release of Incretins GLP-1 and GIP

Wendell J. Lu · Qing Yang · Li Yang ·
Dana Lee · David D'Alessio · Patrick Tso

Received: 22 August 2009 / Accepted: 15 December 2011 / Published online: 2 February 2012
© AOCs 2012

Abstract Glucagon-like peptide-1 (GLP-1) and glucose-dependent insulinotropic polypeptide (GIP) are incretins produced in the intestine that play a central role in glucose metabolism and insulin secretion. Circulating concentrations of GLP-1 and GIP are low and can be difficult to assay in rodents. These studies utilized the novel intestinal lymph fistula model we have established to investigate the mechanism of lipid-stimulated incretin secretion. Peak concentrations of GLP-1 and GIP following an enteral lipid stimulus (Liposyn) were significantly higher in intestinal lymph than portal venous plasma. To determine whether lipid-stimulated incretin secretion was related to chylomicron formation Pluronic L-81 (L-81), a surfactant inhibiting chylomicron synthesis, was given concurrently with Liposyn. The presence of L-81 almost completely abolished the increase in lymph triglyceride seen with Liposyn alone ($P < 0.001$). Inhibition of chylomicron formation with L-81 reduced GLP-1 secretion into lymph compared to Liposyn stimulation alone ($P = 0.034$). The effect of L-81 relative to Liposyn alone had an even greater effect on GIP secretion, which was completely abolished ($P = 0.004$). These findings of a dramatic effect of L-81 on lymph levels of GLP-1 and GIP support a strong link

between intestinal lipid absorption and incretin secretion. The relative difference in the effect of L-81 on the two incretins provides further support that nutrient-stimulation of GIP and GLP-1 is via distinct mechanisms.

Keywords Chylomicron · Incretin secretion · Intestinal lipid absorption · Pluronic L-81 · Gut hormones

Introduction

Glucagon-like peptide-1 (GLP-1) and glucose-dependent insulinotropic polypeptide (GIP) are intestinal peptide hormones that are responsible for the incretin effect. The incretins are released after meals and augment postprandial insulin secretion [1]. Glucagon-like peptide-1 is secreted by enteroendocrine L cells located predominantly in the distal small intestine while GIP is secreted by K cells found mainly in the duodenum and jejunum. Both incretins are released into the circulation in response to enteral carbohydrate, fat or mixed nutrient meals [2–4]. Recent findings support an essential role for the incretins in nutrient metabolism and glucose tolerance [5], and advances in pharmacology have led to application of incretin-based drugs to the treatment of diabetes [6].

Glucagon-like peptide-1 and glucose-dependent insulinotropic polypeptide circulate in the plasma in picomolar concentrations and can be difficult to measure accurately in the fasting state. Moreover, GLP-1 does not reach very high concentrations even after meal stimulus. Thus obtaining sufficient blood for serial measurements of GIP and GLP-1 in rodent studies has been challenging. We have established a novel in vivo approach of monitoring GLP-1 and GIP secretion utilizing the lymph fistula rat model.

W. J. Lu (✉) · D. D'Alessio · P. Tso
Department of Molecular and Cellular Physiology,
University of Cincinnati, Cincinnati, OH 45267, USA
e-mail: wendell.lu7@gmail.com

Q. Yang · L. Yang · D. Lee · P. Tso (✉)
Department of Pathology and Laboratory Medicine,
University of Cincinnati, Cincinnati, OH 45267, USA
e-mail: tsopp@email.uc.edu

D. D'Alessio
Department of Medicine,
University of Cincinnati, Cincinnati, OH 45267, USA

Using this approach, we have recently demonstrated [7, 8] that the intestinal lymph is enriched with the gastrointestinal hormone GLP-1 before and after meal intake. We have also demonstrated that the concentrations of GIP and GLP-1 are substantially higher in intestinal lymph than in portal venous plasma [7, 9]. These findings suggest that lymph draining the gut may be a medium through which the function of K and L cells can be examined.

While many studies have focused on the biological effects of GLP-1 and GIP, the mechanisms regulating the release of the incretins in response to nutrients remain to be elucidated. To date, several studies have demonstrated that GIP secretion requires the absorption of glucose in the gut, while GLP-1 release has been reported by some to be stimulated by contact of nutrients with the intestinal lumen and shown by others to require the absorption of nutrients [2, 4, 10–15].

The aim of this study was to examine the role of chylomicron formation and secretion on lipid-stimulated GLP-1 and GIP release *in vivo*. Chylomicrons are synthesized in the intestinal enterocytes during active fat absorption and transported into the lymph. Intestinal formation and transport of chylomicrons is inhibited by a hydrophobic surfactant, Pluronic L-81 (L-81) [16–19]. L-81 is a condensation polymer of polyoxypropylene, which forms a hydrophobic chain that is flanked by the hydrophilic polyoxyethylene. L-81 has been shown to significantly impair the lymphatic transport of triglycerides (TG) [20, 21]. However, L-81 does not inhibit the uptake of lipolytic products of digestion by enterocytes or the reesterification of monoglyceride and fatty acid to form TG [20]. L-81 seems to cause an accumulation of TG in the smooth endoplasmic reticulum and prevents the movement of prechylomicrons from the endoplasmic reticulum into the Golgi complex. A recent report by Fatma et al. [22] showed that L-81 may inhibit the formation of chylomicrons by inhibiting the activity of microsomal triglyceride transfer protein.

Both Pluronic L-81 and Pluronic P-85 (P-85) are difunctional block copolymer surfactant terminating in primary hydroxyl groups. They are both nonionic surfactants composed of a central hydrophobic chain flanked by two hydrophilic chains. L-81 and P-85 have the same sized hydrophobic portion of the molecule, but P-85 has a larger hydrophilic portion than L81. Both Pluronic block copolymers L-81 and P-85 have been examined together in the same studies including lipid-Pluronic interactions [23], cellular uptake of proteins [24], and functional activity of multidrug resistance-associated proteins [25]. Both nonionic surfactants have also been shown to inhibit intestinal P-glycoprotein efflux [26, 27]. In this study, we investigated the effect of the inhibition of chylomicron formation by L-81 and P-85 on the secretion of GLP-1 and GIP, as well as the role of free fatty acids (FFA) on incretin release.

Materials and Methods

Animals

Adult male Sprague–Dawley rats, weighing 240–350 g (Harlan, Indianapolis, IN), were used. Animals were allowed to acclimate to the animal facility for two weeks prior to the experiment. During this period, the animals were fed regular rodent chow (TEKLAD LM485-7912) and housed in a room with a 12/12 light/dark cycle. Both the temperature and the humidity of the room were kept constant.

Surgical Preparation

All procedures were approved by the University of Cincinnati Internal Animal Care and Use Committee and complied with the NIH Guide for the Care and Use of Laboratory Animals. Installation of the lymph duct and intraduodenal cannulae was performed as previously described [8]. Briefly, under halothane anesthesia, the superior mesenteric lymph duct was cannulated with soft vinyl tubing [medical grade; 0.5 mm inner diameter (ID) and 0.8 mm outer diameter (OD) Biocorp Australia Pty Ltd., Melbourne, Australia] according to the method of Bollman et al. [28] with slight modification. Instead of using suture to tie off the lymph duct, a drop of Krazy glue was used to secure the cannula in place. Intraduodenal cannulation was performed by inserting a silicone tube (1.6 mm OD) about 2 cm into the duodenum via a fundal incision of the stomach and the incision was tied off with a purse-string tie and further sealed with a drop of Krazy glue. Post-operatively, animals were kept in Bollman restraining cages and infused with 5% glucose in saline (145 mM NaCl, 4 mM KCl, 0.28 M glucose) at a rate of 3 ml/h and then switched to saline infusion overnight prior to the nutrient absorption study on the following morning. Lymph samples were collected in 0.5 M EDTA and 500 kallikrein inhibitor units/ml aprotinin (Sigma, St. Louis, MO) [7]. Fasting lymph was collected for 1 h before nutrient infusion and then at 30-min intervals for 1 h and then hourly over the subsequent 6 h.

Nutrient Infusate Preparation

Three groups of animals were tested and infused intraduodenally with a single bolus of 3 ml of one of the following four infusates. Except for the saline control group, the infusate for the other three groups had a caloric content of 4.43 kcal/3 ml. The three infusates were: (1) saline (0.9%, control group), (2) Liposyn consisting of 2.215 ml of Liposyn (20%, 2 kcal/ml) and 0.785 ml of saline, (3) L-81 plus Liposyn (12 mg/ml of L-81 in above Liposyn

and saline mixture) this group had an infusion of L-81 alone starting 60 min before the combination of L-81 and Liposyn), (4) P-85 plus Liposyn (12 mg/ml of P-85 in above Liposyn and saline mixture) with an infusion of P-85 alone starting 60 min prior. The caloric load used was based on previous studies which demonstrated that this is sufficient for a robust stimulation of incretin release into lymph [7, 8]. Animals receiving L-81 with their lipid meal were pretreated for 1 h with L-81 alone based on preliminary studies showing that L-81 works most effectively when it is introduced prior to the administration of the L-81 plus Liposyn mixture. L-81 was sonicated together with the appropriate volume of 19 mM sodium taurocholate (NaTC) to form a micellar solution. The L-81 plus Liposyn mixture was sonicated to form an emulsion which was then administered intraduodenally as a single bolus. The P-85 plus Liposyn mixture was also sonicated to form an emulsion and administered in the same manner as the L-81 mixture. P-85 was used as a control to L-81 effect on TG transport and on incretin secretion. Nutrient infusions were followed by infusion of saline at 3 ml per hour. Liposyn (20%) (Abbott Laboratories, North Chicago, IL) consisted of equal amounts of safflower and soybean oil with a caloric content of 2 kcal/ml. L-81 and P-85 were kindly provided to us by BASF (Parsippany, NJ).

GLP-1 Radioimmunoassay

Glucagon-like peptide-1 concentrations in lymph were determined by a commercially available radioimmunoassay (RIA) kit (LINCO Research, St. Louis, MO) as described previously [8]. This kit uses a rabbit anti-GLP-1 serum, GLP-1 (7–36) amide as the standard and ^{125}I -GLP-1 (7–36) amide as tracer. The antiserum used in this RIA recognizes the C-terminus of GLP-1, including both amidated and non-amidated forms (LINCO Research); therefore the assay detects all of the major circulating forms of GLP-1 including GLP-1 (7–36), GLP-1 (7–37), GLP-1 (9–36), GLP-1 (9–37), GLP-1 (1–36) and GLP-1 (1–37) amides in biological fluids.

GIP ELISA

Glucose-dependent insulinotropic polypeptide was determined by ELISA assay kit provided by Linco (St. Louis, MO) that detects both intact GIP and its major metabolite GIP_{3-42} . Briefly, lymph samples were added to wells of a microtiter plate pre-coated with anti-GIP monoclonal antibodies as previously described. A second biotinylated anti-GIP polyclonal antibody was added and then conjugated to streptavidin–horseradish peroxidase. The enzyme activity is measured spectrophotometrically by absorbency at 450 nm.

Chemical Assays

Lymph triglycerides were measured according to the protocol provided by Randox (Randox Laboratories Ltd., Crumlin, UK). This enzymatic assay measured the released glycerol resulting from the hydrolysis of triglycerides. Briefly, 5 μl of lymph was added to 200 μl reagent. After 20 min of incubation at 37 °C, optical density was read at 500 nm. Triglycerides concentration was calculated from the standard solution provided by Randox. Free fatty acids were assayed by a commercial kit from Wako (Wako Diagnostics, Richmond, VA). This enzymatic method involves the acylation of coenzyme A (CoA) by the fatty acids in the presence of added acyl-CoA synthetase. The acyl-CoA product is then oxidized by the added acyl-CoA oxidase to generate hydrogen peroxide. In the presence of peroxidase, a purple colored adduct is formed and can be measured colorimetrically at 550 nm.

Statistical Analysis

All values are expressed as means \pm SE. Two-way repeated-measures ANOVA with Tukey's as a post-test analysis was used to compare all the groups, e.g. L-81 plus Liposyn and Liposyn, throughout the 6 h infusion. The analyses examine the statistical significance between groups and also compare multiple time points within each group. A difference was considered significant if the *P* value was <0.05 . All statistical analyses were performed with the statistics program SigmaStat version 3.5 (SPSS).

Results

Lymph Flow

The lymph flow rate following Liposyn infusion was significantly increased when compared to the saline control group, as reflected by the 30-min time point measure of 4.45 ± 0.38 ml/h for the Liposyn group compared to that of 2.88 ± 0.48 ml/h for the control group ($P = 0.007$, Fig. 1). By 60 min, lymph flow had decreased in the Liposyn group, but at 120 min it was significantly elevated versus the saline control group ($P = 0.001$). The increase remained significant through 180 min ($P = 0.003$) at the rate of 3.84 ± 0.25 ml/h. Addition of L-81 to the Liposyn infusion reduced lymph flow compared to Liposyn alone. In fact, throughout the duration of the 6 h study, the mean lymph flow rate of the L-81 plus Liposyn group, 2.04 ± 0.23 ml/h, was not significantly different from that of the saline control mean, 2.57 ± 0.23 ml/h; however, it was significantly lower than that of the mean flow rate of the Liposyn only group, 3.10 ± 0.25 ml/h ($P = 0.017$).

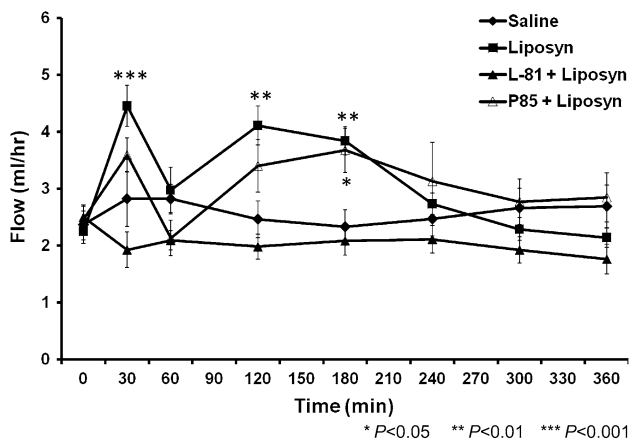


Fig. 1 The lymph flow rate during the 6 h period following administration of intraduodenal infusion of Liposyn (filled boxes), L-81 plus Liposyn (filled triangles), P-85 plus Liposyn (open triangles) or Saline (filled diamonds). Liposyn ($n = 6$), L-81 plus Liposyn ($n = 7$), P-85 plus Liposyn ($n = 4$) or Saline ($n = 6$). Data are presented as means \pm SEM. Asterisks indicate significant differences between the saline group and the Liposyn or P-85 plus Liposyn group, respectively, at specific times. * $P < 0.05$, ** $P < 0.01$, *** $P < 0.001$

Infusion of P-85 plus Liposyn slightly increased the lymph flow rate but it was not significant compared to the saline control except at 180 min. The mean lymph flow rate of the P-85 plus Liposyn group, 2.85 ± 0.17 ml/h, was not significant from that of the control.

Effect of L-81 on Lymphatic Triglycerides and Free Fatty Acids Output

Administration of Liposyn alone induced a significant increase in lymph TG which was evident by 60 min and which peaked at $2,095 \pm 298$ mg/dL 5 h after the bolus of enteral lipid ($P < 0.001$; Fig. 2a). Addition of L-81 (12 mg/ml) together with Liposyn completely abolished the increase in lymph TG, resulting in a profile which was not significantly different from the saline control group. Compared to the L-81 plus Liposyn group, P-85 administration with Liposyn demonstrated a significant increase in lymph TG versus the saline control animals at 180 min ($P = 0.005$) and the increase was sustained and peaked at 300 min ($P < 0.001$) similar to the trend of the Liposyn group. There was a significant difference in lymph TG between the L-81 plus Liposyn and the P-85 plus Liposyn groups starting at 60 min ($P = 0.017$) and all the subsequent time points in this study. The overall mean of the 6 h study for the Liposyn group, $1,206 \pm 67$ mg/dL, was greater than that of the L-81 plus Liposyn group, 59 ± 62 mg/dL ($P < 0.001$). A similar significant difference was observed between the 6 h time course mean of the P-85 plus Liposyn group, 721 ± 82 mg/dL, and that of the L-81 plus Liposyn group ($P < 0.001$).

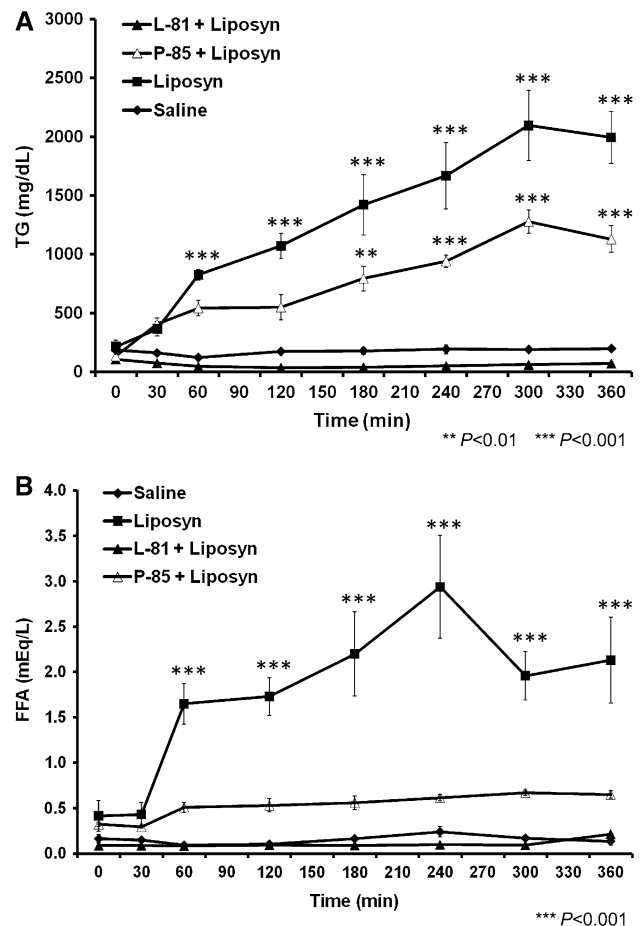


Fig. 2 a Triglycerides content in lymph collected at 30 min and hourly following saline control (filled diamonds) or isocaloric and isovolumetric intraduodenal infusion of Liposyn (filled boxes), Pluronic L-81 (L-81) plus Liposyn (filled triangles) or Pluronic P-85 plus Liposyn (open triangles). Data are means \pm SEM. Asterisks indicate significant elevations of Liposyn group or P-85 plus Liposyn group over the saline values at that time: ** $P < 0.01$, *** $P < 0.001$. **b** Comparison of stimulation of free fatty acids concentrations in response to saline (filled diamonds) or isocaloric and isovolumetric treatment of Liposyn (filled boxes), L-81 plus Liposyn (filled triangles) or P-85 plus Liposyn (open triangle). Data are means \pm SEM. Asterisks indicate significant differences between the saline group and the Liposyn group at specific times: *** $P < 0.001$

Intraduodenal administration of Liposyn alone also stimulated a rapid rise in lymph FFA by 60 min after an initial 30 min period of FFA stability (Fig. 2b). The increase in FFA peaked at 2.93 ± 1.01 mequiv/L 4 h after the Liposyn bolus. The presence of L-81 together with Liposyn completely inhibited the increase in lymph FFA seen with Liposyn alone with the result that levels of FFA in the combined L-81 plus Liposyn group were similar to those in the saline control group which had an average of 0.15 ± 0.15 mequiv/L ($P = 0.891$) over the 6 h study. P-85 infusion with Liposyn showed increased lymph FFA levels after 30 min compared to the saline control and L-81

plus Liposyn but the difference was not significant. The overall mean of the P-85 plus Liposyn group was 0.519 ± 0.16 mequiv/L and the mean of the saline control group was 0.152 ± 0.14 mequiv/L ($P = 0.322$).

Effect of L-81 on Lymph GLP-1 Concentrations and Output

Intraduodenal bolus infusion of Liposyn alone stimulated a rapid peak GLP-1 concentration of 176 ± 29 pM at 30 min (Fig. 3a) and GLP-1 levels remained significantly elevated compared to the saline control through 120 min ($P = 0.042$). The presence of L-81 with Liposyn delayed the postprandial GLP-1 response, resulting in a peak GLP-1 concentration at 120 min rather than 30 min as seen with Liposyn alone. The GLP-1 concentration, although somewhat reduced compared to Liposyn during the first hour, was still significantly higher than the saline controls at all the time points studied up to 240 min with the biggest difference at 120 min when GLP-1 concentration for the combined L-81 plus Liposyn group was 163 ± 47 pM whereas GLP-1 concentration for the saline control was 32 ± 3 pM ($P < 0.001$). Following the combined P-85 plus Liposyn administration, GLP-1 concentration was elevated after 30 min and peaked at 120 min reaching 199 ± 69 pM ($P < 0.001$). Glucagon-like peptide-1 levels were significantly increased versus the saline control from 30 min ($P = 0.001$) through 180 min ($P = 0.005$). The effect of P-85 plus Liposyn on lymph GLP-1 concentration was similar to that of L-81 plus Liposyn both peaking at the same time and had a similar pattern over the 6 h study.

To calculate lymphatic GLP-1 output, post-meal concentrations of the peptide were multiplied by lymph flow. Since lymph concentration of a substrate or of hormones is a function of the release of peptide into the lymph and lymph flow, the lymphatic output serves as a better index of incretin secretion. GLP-1 output following Liposyn administration exhibited a rapid increase by 30 min, peaking at 784 ± 141 fmol/h (Fig. 3b), and then remained elevated for 240 min before decreasing to baseline rates. L-81 plus Liposyn significantly reduced GLP-1 output compared to Liposyn alone initially. At 30 min, when GLP-1 output had reached its maximum in the Liposyn only group, the addition of L-81 decreased GLP-1 secretion by about 75% ($P < 0.001$). However, there was no significant difference between L-81 plus Liposyn and Liposyn groups at 60 min ($P = 0.063$) and subsequent time points. Infusion of P-85 plus Liposyn enhanced GLP-1 secretion to levels similar to Liposyn at 30 min and during the 6 h study. The P-85 plus Liposyn treated animals had greater GLP-1 secretion compared to the saline control group during the first 180 min. The effect of P-85 plus Liposyn was quite similar to that Liposyn alone compared to the

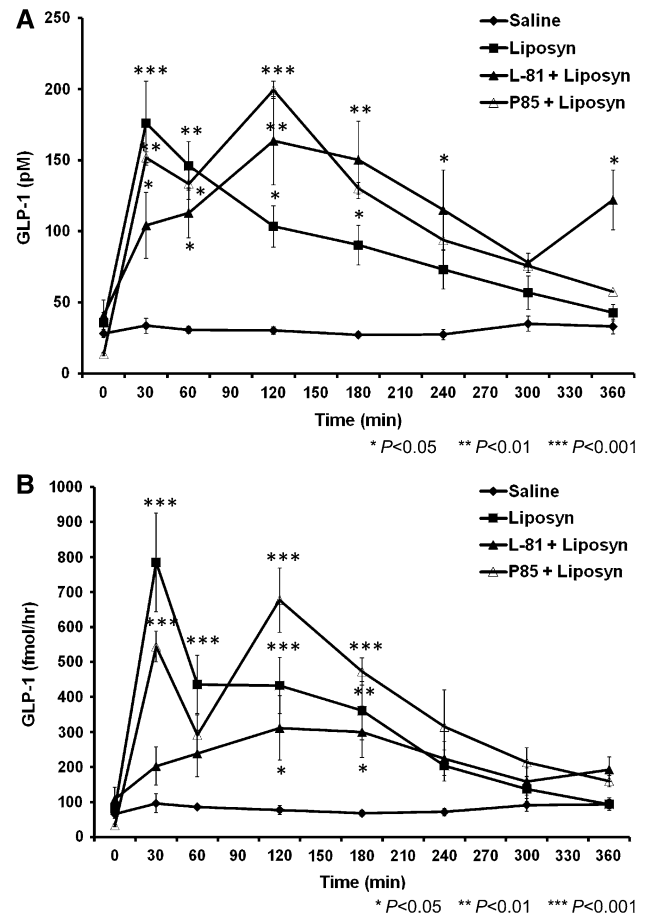


Fig. 3 a Comparison of stimulation of GLP-1 concentrations in response to saline (filled diamonds) or isocaloric and isovolumetric treatment of Liposyn (filled boxes), L-81 plus Liposyn (filled triangles) or P-85 plus Liposyn (open triangles). Liposyn ($n = 6$), L-81 plus Liposyn ($n = 7$), P-85 plus Liposyn ($n = 4$) or Saline ($n = 6$). Data are means \pm SEM. Asterisks indicate significant differences between the saline group and Liposyn group, L-81 plus Liposyn, or P-85 plus Liposyn group, respectively, at specific times. $*P < 0.05$, $**P < 0.01$, $***P < 0.001$. b Lymphatic GLP-1 secretion rate in response to saline (filled diamonds) or isocaloric and isovolumetric treatment of Liposyn (filled boxes), L-81 plus Liposyn (filled triangles) or P-85 plus Liposyn (open triangles). Data are means \pm SEM. Asterisks indicate significant differences between the saline group and Liposyn group, L-81 plus Liposyn, or P-85 plus Liposyn group, respectively, at specific times. $*P < 0.05$, $**P < 0.01$, $***P < 0.001$

effect of L-81 plus Liposyn on GLP-1 secretion. Cumulative lymph GLP-1 secretion during the six hours of the study was calculated by summing the secretion during each hour. The total GLP-1 released following Liposyn alone, Liposyn plus L-81, Liposyn plus P-85, and saline were $2,530 \pm 195$, $1,737 \pm 351$, $2,705 \pm 203$, and 649 ± 52 fmol/h, respectively (Fig. 5a). While L-81 significantly reduced the secretion of GLP-1 in response to Liposyn ($P = 0.034$), the cumulative output was still much greater than the saline controls ($P = 0.005$). Administration of P-85 plus Liposyn generated cumulative GLP-1 output

that was similar to Liposyn by itself and greater than either the L-81 plus Liposyn ($P = 0.042$) or saline control ($P < 0.001$).

Effect of L-81 on Lymph GIP Concentrations and Output

The intraduodenal administration of Liposyn induced a rapid increase in lymph GIP concentration, peaking at 60 min with GIP levels at 488 ± 140 pg/ml. Glucose-dependent insulinotropic polypeptide levels remained elevated throughout the 6 h of study (Fig. 4a). Inhibition of chylomicron formation by the administration of L-81 and Liposyn had a dramatic effect on lymph GIP

concentrations, which changed minimally and did not differ significantly from levels recorded for the saline controls. The mean for the L-81 plus Liposyn group was 93 ± 34 pg/ml compared to the mean for the saline group at 91 ± 40 pg/ml over the entire 6 h time course. Administration of a Pluronic surfactant, which at the same concentration as L-81, has no effect on chylomicron formation such as P-85 together with Liposyn demonstrated no inhibitory effect on lymphatic GIP concentrations. P-85 plus Liposyn induced a rapid increase in GIP levels from 77 ± 22 at fasting to 497 ± 75 pg/ml within 60 min reaching a peak concentration of 529 ± 41 pg/ml at 120 min (Fig. 4a). The P-85 plus Liposyn was significantly elevated compared to the L-81 plus Liposyn group ($P < 0.001$) and to the saline control group ($P < 0.001$) at 60 min. Similar levels of increase was observed for the Liposyn group compared to the L-81 plus Liposyn and saline groups. At 120 min, both the P-85 plus Liposyn and Liposyn groups were still elevated versus the L-81 plus Liposyn and saline control groups ($P < 0.001$). Compared to the L-81 and saline groups, the P-85 plus Liposyn remained increased at 180 min while the Liposyn group started to decrease. The mean for the 6 h time course study of the P-85 plus Liposyn group, 287 ± 45 pg/ml, was also similar to that of the Liposyn group, 289 ± 34 pg/ml.

Glucose-dependent insulinotropic polypeptide secretion was calculated based on the GIP concentration and lymph flow rate. The Liposyn group stimulated a rapid increase in GIP secretion during the first 30 min rising to $1,392 \pm 234$ pg/h and peaked at $1,589 \pm 147$ pg/h by 120 min. Administration of P-85 plus Liposyn induced a more gradual increase in GIP secretion but reached a higher peak of $1,798 \pm 185$ pg/h at the same time point as the Liposyn group at 120 min. Glucose-dependent insulinotropic polypeptide secretion was blocked in the presence of L-81. The L-81 plus Liposyn group only reached a maximum of 348 ± 112 pg/h at 120 min. During the entire time course, the level of GIP secretion stimulated by the L-81 plus Liposyn group was similar to that of the saline control group with overall means of 188 ± 110 and 241 ± 131 pg/h, respectively. There was no difference between the means of the L-81 plus Liposyn and saline control groups with a P value of 0.989. The GIP secretion rate of the Liposyn group was significantly higher than either the L-81 plus Liposyn or saline control group at 30, 60, and 120 min ($P < 0.001$) as well as at 180 min ($P = 0.001$). Without the inhibitory effect of L-81 on chylomicron formation, the surfactant P-85 plus Liposyn demonstrated similar effect as Liposyn showing significant stimulation of GIP secretion rate from 60 to 180 min. The overall means of the P-85 plus Liposyn, 864 ± 147 , and Liposyn, 939 ± 111 pg/h, were also similar having no significant difference ($P = 0.98$). However, the overall

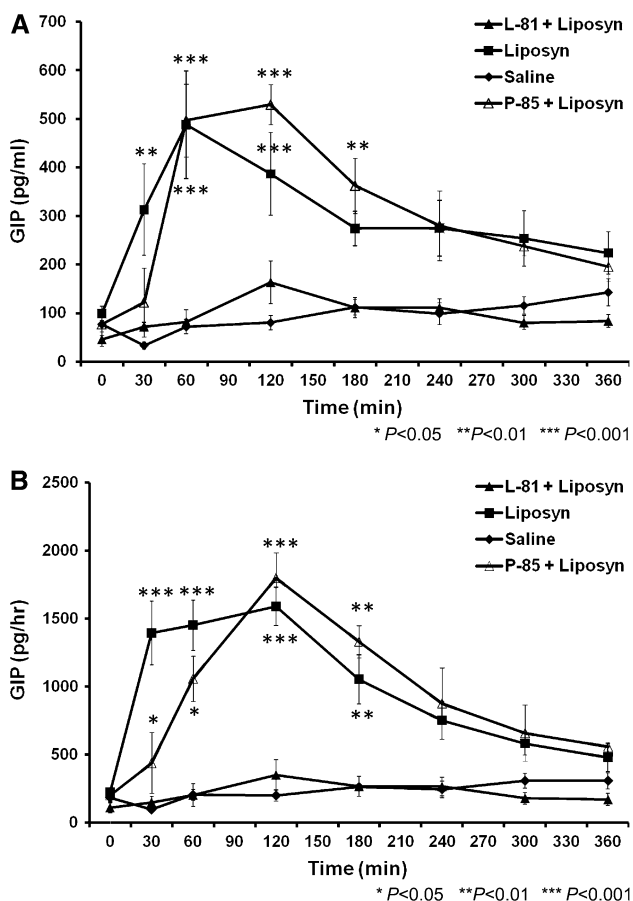


Fig. 4 a Concentrations of GIP in lymph following intraduodenal infusions of Liposyn (filled boxes), L-81 plus Liposyn (filled triangles), P-85 plus Liposyn (open triangles) or saline (filled diamonds). Data are presented as means \pm SEM. Asterisks denote significant differences between the saline group and the Liposyn or P-85 plus Liposyn group, respectively, at that time. * $P < 0.05$, ** $P < 0.01$, *** $P < 0.001$. **b** Lymphatic GIP secretion rate in response to saline (filled diamond) or isocaloric and isovolumetric treatment of Liposyn (filled box), L-81 plus Liposyn (filled triangle) or P-85 plus Liposyn (open triangle). Data are means \pm SEM. Asterisks indicate significant differences between values of the saline group and the Liposyn or P-85 plus Liposyn group, respectively, at that time: * $P < 0.05$, ** $P < 0.01$, *** $P < 0.001$

mean for the 6 h time course of the P-85 plus Liposyn group was much greater than that of the L-81 plus Liposyn group ($P = 0.008$) or the saline control group ($P = 0.024$).

The effect of L-81 on GIP output confirmed the anticipated effect of L-81 in abolishing the secretion of this incretin (Fig. 4b). Furthermore, cumulative lymphatic GIP output in the Liposyn group was $7,510 \pm 1,249$ pg over 6 h whereas the presence of L-81 greatly decreased the output to $1,678 \pm 393$ pg ($P = 0.001$) during the same period (Fig. 5b). Total GIP secretion in the saline control group was $1,929 \pm 258$ pg and was not significantly different from L-81 plus Liposyn ($P = 0.998$). Administration of P-85 together with Liposyn showed similar cumulative

GIP output of $6,909 \pm 1,115$ pg compared to Liposyn ($P = 0.978$). The P-85 plus Liposyn group induced greater lymph GIP output versus that of the L-81 plus Liposyn group ($P = 0.012$) or the saline control group ($P = 0.028$).

Discussion

In previous studies, we showed that the lymph fistula rat model is a useful model for studying the secretion of GLP-1 and GIP in response to glucose and lipid administration. The changes in the concentrations of incretins in intestinal lymph paralleled the changes in plasma levels following carbohydrate, lipid, or mixed nutrient meals [7–9], although lymph concentrations were at much higher levels, suggesting that this model provides a sensitive way of studying gut hormone secretion. In the present study, we took advantage of this newly established conscious rat model to gain insight into the mechanism by which chylomicron formation in the gut stimulates the secretion of incretins by the enteroendocrine cells. By blocking chylomicron formation using Pluronic L-81 (blocking the trafficking of lipoprotein particles from the endoplasmic reticulum to the Golgi apparatus), a relatively distal step in lipid handling by enterocytes, we were able to completely abolish GIP secretion but not GLP-1. Although overall GLP-1 secretion was significantly reduced, the most notable reduction occurred in the initial phase of GLP-1 secretion (first 30 min). The latter phase of GLP-1 secretion was less affected by L-81. The fact that GLP-1 and GIP responses differ is consistent with previous studies suggesting that secretion of the two incretins in response to enteral nutrients occurs via different mechanisms [12].

The near absence of lymph TG when Liposyn was administered in combination with L-81 confirms previous findings which have demonstrated the efficacy of this compound to inhibit the formation and secretion of chylomicron from the small intestine to the lymph [20, 21]. When the incorporation of absorbed TG into chylomicrons is inhibited, the absorbed lipid accumulates in the intestinal epithelial cells as large lipid droplets [20]. Fat digestion and absorption have been shown to occur primarily in the proximal intestine [29–31]. Following the digestion of lipid in the small intestine, free fatty acids and monoglycerides are absorbed by the intestinal enterocytes and re-esterified to TG droplets in the smooth endoplasmic reticulum (ER). L-81 does not affect any of the aforementioned steps, and so, for GIP, the exposure, the uptake, and the re-esterification of the lipid digestion products to form TG is not sufficient to stimulate the K cells to secrete GIP. Our data are consistent with several previous reports that enteral administration of L-81 effectively blocked the postprandial rise in GIP following ingestion of long-chain triglycerides

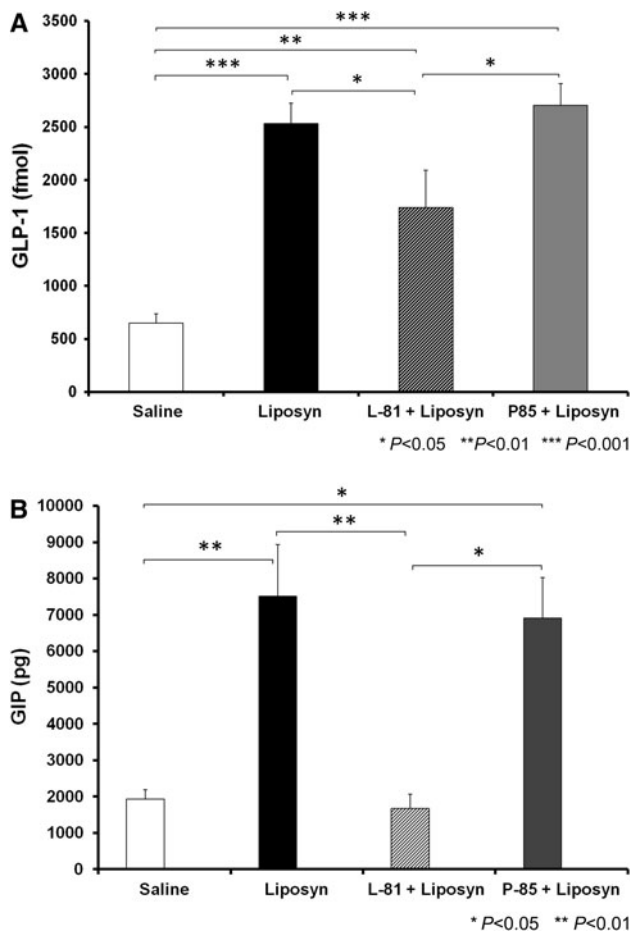


Fig. 5 **a** Cumulative lymphatic GLP-1 output following bolus intraduodenal infusion of Liposyn *black bar*, Liposyn plus L-81 combined *hatched bar*, P-85 plus Liposyn *grey bar* or saline *white bar*. Values are sum of GLP-1 secretion over 6 h time period. Data are means \pm SEM. Asterisks indicate significant differences between respective groups: * $P < 0.05$, ** $P < 0.01$, *** $P < 0.001$. **b** Cumulative GIP output in lymph following bolus intraduodenal infusion of Liposyn *black bar*, Liposyn plus L-81 combined *hatched bar*, P-85 plus Liposyn *grey bar* or saline (white bar). Values are sum of GIP secretion over 6 h time period. Data are means \pm SEM. Asterisks indicate significant differences between respective groups: * $P < 0.05$, ** $P < 0.01$

[32, 33]. Taken together with these findings, our observations that L-81 abolishes the lipid-stimulated rise in GIP indicate that inhibition of chylomicron formation prevents K-cell secretion of GIP.

Under normal circumstances, the TG formed in the ER from absorbed lipid are transported to the Golgi apparatus where the secretory vesicles containing nascent chylomicrons are formed and migrate to the lateral cell membrane. These vesicles subsequently fuse with the lateral plasma-membrane and release the nascent chylomicrons into the intercellular spaces, from where they enter the intestinal lymphatics. In the presence of L-81, however, the trafficking between ER and the Golgi apparatus is prevented which leads to an accumulation of large lipid droplets observable under electron microscopy in distended tubules of smooth endoplasmic reticulum in the apical portion of the enterocytes [20, 34]. Recent data by Fatma et al. [22] showed that L-81 inhibits the microsomal triglyceride transfer activity, a critical component in the trafficking and formation of pre-chylomicrons. This process has a dramatic effect on the secretion of GIP. It is interesting that GIP, produced and secreted almost entirely in the upper intestine, is more affected by L-81 than GLP-1 which is synthesized more distally in the gut. The obvious correlate is that lipid absorption and chylomicron formation is also predominantly a duodenal, upper jejunal process. While we cannot speak to the mechanism whereby GIP, and to a lesser extent GLP-1, secretion is inhibited by L-81, since enteroendocrine cells are not thought to package absorbed lipids into chylomicrons, this effect is likely to be indirect. One plausible explanation is that enterocytes release a factor(s) which stimulate secretion from K-cells. If this is true, the isolation of this factor could be extremely important, not only as it relates to our understanding of the regulation of incretin secretion by macronutrients, but it may also potentially offer a pharmaceutical target for the development of anti-diabetic drugs.

From previous experience we know that L-81 has a profound impact to block chylomicron formation and reduce postprandial TG in lymph and plasma. In this study L-81 reduced incretin secretion, GLP-1 marginally and GIP substantially. Therefore we think it is unlikely that L-81 has an independent effect to stimulate incretin secretion. Even in lymph, concentrations of GIP and GLP-1 are low in the fasting state, and it is unclear that basal secretion has an important physiologic role. Therefore we are not certain that any effect of L-81 alone to reduce incretin secretion would be detectable. For example note the 0 min GLP-1 and GIP levels in the saline and L-81 plus Liposyn groups. The levels are very similar despite infusion of L-81 for 60 min. While not definitive this suggests that administration of L-81 to fasting animals does not have a significant effect on incretin secretion.

The results of our study demonstrated that Pluronic L-81 blocked chylomicron formation induced by Liposyn and the transport of TG to the intestinal lymph. Another Pluronic copolymer examined in the study, P-85, exhibited no inhibitory effect on lymph TG transport at the same dosage administered as L-81. Both L-81 and P-85 have been investigated together in many studies involving cellular uptake of proteins, inhibition of multidrug resistance-associated protein, lipid-Pluronic interactions, and intestinal P-glycoprotein efflux [23–27]. In our study, Pluronic P-85 did not abolish GIP secretion stimulated by Liposyn as Pluronic L-81 did. Pluronic P-85 behaved similarly to Liposyn in stimulating GIP secretion, while Pluronic L-81 behaved similarly to the saline control. The cumulative GIP output induced by P-85 plus Liposyn over the 6 h time course was 4.1 fold greater than that by L-81 plus Liposyn, while cumulative GIP output stimulated by Liposyn alone was 4.5 fold greater than that by L-81 plus Liposyn. Unlike Pluronic L-81, Pluronic P-85 also did not cause a decrease in the initial phase of GLP-1 secretion in response to Liposyn stimulation. The cumulative GLP-1 output induced by P-85 plus Liposyn during the 6 h study was significantly greater than that by either L-81 plus Liposyn or saline control.

In addition to blocking chylomicron secretion, L-81 also prevented the increase in lymphatic free fatty acid output associated with fat absorption as shown in Fig. 3. This raises the possibility that local concentrations of fatty acids in the intestinal mucosa activate K-cells to release GIP. Although possible, we do not believe this to be particularly likely because when we examined lymphatic GIP secretion and lymphatic free fatty acid secretion in a normal animal as depicted in Figs. 4a and 2b, we found that lymphatic GIP secretion peaked much earlier than free fatty acid secretion and also that while lymphatic FFA output gradually increased and before reaching a plateau at 240 min, lymphatic GIP secretion had already started to decrease back to the pre-feeding state before 240 min.

As reflected both by our lymphatic GLP-1 concentration data as well as our GLP-1 secretion data, the presence of L-81 reduced the early phase of GLP-1 secretion by the endocrine cells normally stimulated by fat absorption. While the mechanisms of nutrient-coupling to L-cell secretion are not well understood, it is generally believed that indirect mechanisms account for the early phase of GLP-1 release because GLP-1-producing L-cells are located predominantly in the distal small intestine but plasma levels increase rapidly, within 10 min after meal ingestion [35–37], long before chyme containing the nutrients would be expected to reach the lower gut. Several studies have suggested that neural or humoral mediators are activated by nutrients in the upper gut to signal the release of GLP-1 distally [38–45]. In our study, we found a marked inhibition of GLP-1 secretion during the first 60 min in the

presence of L-81, but the effect of L-81 seemed to diminish from 60 min onwards. From this data, it seems that while the formation and secretion of chylomicrons plays a role in the stimulation of GLP-1 secretion, other factors connected with lipid absorption are important as well. Some have pointed to the activation of G protein coupled receptor 120 by long chain unsaturated fatty acids such as oleic acid and alpha-linolenic acid as one possible mechanism in GLP-1 secretion [45–47]. G protein coupled receptor 120 is distributed widely in the gastrointestinal tract [39]. Bile acids have also been reported to stimulate the release of GLP-1, a process which appears to be mediated by the G protein coupled receptor TGR5 [48]. It is also important to note that only the early secretion of GLP-1 was significantly affected by the presence of L-81. It has been proposed that GIP stimulates the secretion of GLP-1 through activation of the vagus nerve [45]. Because our results show that the increase in GIP secretion following intestinal fat absorption was completely abolished by the addition of L-81, we propose that the lack of the increase in GIP secretion actually resulted in a reduction in the early release of GLP-1 by the endocrine L cells. Thus, L-81 could be a useful tool for the dissection of the relative importance of the different pathways involved in the macronutrient induced secretion of GLP-1. Additional studies would have to be performed to support or refute this interesting notion.

In summary, we have demonstrated that the stimulation of GIP secretion by lipid absorption in the small intestine is dependent on the efficient formation and secretion of chylomicrons and that the inhibition of chylomicron formation by L-81 completely abolishes this stimulation. In contrast, we have shown that GLP-1 secretion by the L-cells is only partially inhibited by L-81, mostly in the early phase of GLP-1 secretion. Another Pluronic copolymer, P-85, examined in our study did not reveal the effect of inhibition of GIP secretion, lymph TG, and the partial reduction of early-phase GLP-1 secretion observed with L-81. We propose that the reduction in the early phase of GLP-1 secretion, believed to be mediated neuronally, is probably a result of the inhibition of GIP secretion. Lastly, our data would suggest that L-81 could be an important and interesting tool in determining the relative importance of the various factors which modulate GLP-1 secretion by intestinal fat absorption.

Acknowledgments This work was supported by grants from the National Institutes of Health, grants DK 56863, ES 14464, DK 56910, DK 76928 and DK 59630.

References

- Kieffer T, Habener J (1999) The glucagon-like peptides. *Endocr Rev* 20:876–913
- Herrmann C, Goke R, Arnold R, Goke B (1995) Glucagon-like peptide-1 and glucose-dependent insulin-releasing polypeptide plasma levels in response to nutrients. *Digestion* 56:117–126
- Ritzel U, Fromme A, Ramadori G (1997) Release of GLP-1 by carbohydrates in the perfused rat ileum. *Acta Diabetol* 34:18–21
- Sugiyama K, Manaka H, Sasaki H (1994) Stimulation of truncated glucagons-like peptide-1 release from the isolated perfused canine ileum by glucose absorption. *Digestion* 55(1):24–28
- Drucker DJ (2006) The biology of incretin hormones. *Cell Metab* 3:153–165
- Ahren B, Schmitz O (2004) GLP-1 receptor agonists and DPP-4 inhibitors in the treatment of type 2 diabetes. *Horm Metab Res* 36:867–876
- D'Alessio D, Lu W, Woods SC, Tso P (2007) Fasting and postprandial concentrations of GLP-1 in intestinal lymph and portal plasma: evidence for selective release of GLP-1 in the lymph system. *Am J Physiol Regul Integr Comp Physiol* 293:2163–2169
- Lu WJ, D'Alessio D, Tso P (2007) The regulation of the lymphatic secretion of glucagon-like peptide-1 (GLP-1) by intestinal absorption of fat and carbohydrate. *Am J Physiol Gastrointest Liver Physiol* 293:963–971
- Lu WJ, D'Alessio D, Tso P (2008) Using the lymph fistula rat model to study the potentiation of GIP secretion by the ingestion of fat and glucose. *Am J Physiol Gastrointest Liver Physiol* 294:1130–1138
- Ebert R, Creutzfeldt W (1987) Gastrointestinal peptides and insulin secretion. *Diabetes Metab Rev* 3:1–26
- Fukase N, Hideo T, Sasaki H (1992) Differences in GLP-1 and GIP responses following sucrose ingestion. *Diabetes Res Clin Pract* 15:187–195
- Schirra J, Arnold R, Goke B (1996) Gastric emptying and release of incretin hormones after glucose ingestion in humans. *J Clin Invest* 97:92–103
- Wachters-Hagedoorn RE, Holst JJ, Vonk RJ (2006) The rate of intestinal glucose absorption is correlated with plasma glucose-dependent insulinotropic polypeptide concentrations in healthy men. *J Nutr* 136:1511–1516
- Ebert R, Creutzfeldt W (1980) Decreased GIP secretion through impairment of absorption. *Front Horm Res* 7:192–201
- Creutzfeldt W, Ebert R, Arnold R, Freichs H, Brown JC (1976) Gastric inhibitory polypeptide (GIP), gastrin and insulin: response to test meal in celiac disease and after duodeno-pancreatectomy. *Diabetologia* 12:279–286
- Nutting D, Hall J, Barrowman JA, Tso P (1989) Further studies on the mechanism of inhibition of intestinal chylomicron transport by Pluronic L-81. *Biochim Biophys Acta* 1004:357–362
- Tso P, Balint JA, Rodgers JB (1980) Effect of hydrophobic surfactant (Pluronic L-81) on lymphatic lipid transport in the rat. *Am J Physiol Gastrointest Liver Physiol* 239:348–353
- Tso P, Black DD, Sabesin SM (1984) Evidence for separate pathways of chylomicron and very low-density lipoprotein assembly and transport by rat small intestine. *Am J Physiol Gastrointest Liver Physiol* 247:G599–G610
- Tso P, Gollamudi SR (1984) Pluronic L-81: a potent inhibitor of the transport of intestinal chylomicrons. *Am J Physiol Gastrointest Liver Physiol* 247:32–36
- Tso P, Balint JA, Bishop MB, Rodgers JB (1981) Acute inhibition of intestinal lipid transport by Pluronic L-81 in the rat. *Am J Physiol Gastrointest Liver Physiol* 241:G487–G497
- Hayashi H, Nutting D, Fujimoto K, Cardelli J, Black D, Tso P (1990) Transport of lipid and apolipoproteins A-I and A-IV in intestinal lymph of the rat. *J Lipid Res* 31:1613–1625
- Fatma S, Yakubov R, Hussain MM et al (2006) Pluronic L81 enhances triacylglycerol accumulation in the cytosol and inhibits chylomicron secretion. *J Lipid Res* 47:2422–2432

23. Krupka TM, Solorio L, Wilson RE, Wu H, Azar N, Exner AA (2010) Formulation and characterization of echogenic lipid-Pluronic nanobubbles. *Mol Pharm* 7:49–59
24. Yi X, Batrakova E, Banks WA, Vinogradov S, Kabanov AV (2008) Protein conjugation with amphiphilic block copolymers for enhanced cellular delivery. *Bioconjug Chem* 19:1071–1077
25. Miller DW, Batrakova EV, Kabanov AV (1999) Inhibition of multidrug resistance-associated protein (MRP) functional activity with Pluronic block copolymers. *Pharm Res* 16:396–401
26. Seeballuck F, Ashford MB, O'Driscoll CM (2003) The effects of Pluronics block copolymers and Cremophor EL on intestinal lipoprotein processing and the potential link with P-glycoprotein in Caco-2 cells. *Pharm Res* 20:1085–1092
27. Batrakova EV, Han HY, VYu Alakhov, Miller DW, Kabanov AV (1998) Effects of Pluronic block copolymers on drug absorption in Caco-2 cell monolayers. *Pharm Res* 15:850–855
28. Bollman JL, Cain JC, Grindlay JH (1949) Techniques for the collection of lymph from the liver, small intestine, or thoracic duct of the rat. *J Lab Clin Med* 33:1349–1352
29. Drover VA, Ajmal M, Nassir F, Davidson NO, Nauli AM, Sahoo D, Tso P, Abumrad NA (2005) CD36 deficiency impairs intestinal lipid secretion and clearance of chylomicrons from the blood. *J Clin Invest* 115:1290–1297
30. Sarda L, Desnuelle P (1958) Actions of pancreatic lipase on esters in emulsions. *Biochim Biophys Acta* 30:513–521
31. Benzonana G, Desnuelle P (1965) Kinetic study of the action of pancreatic lipase on emulsified triglycerides: enzymology assay in heterogeneous medium. *Biochim Biophys Acta* 105:121–136
32. Creutzfeldt W, Ebert R (1993) The enteroinsular axis. In: Go VLW (ed) *The pancreas: biology, pathobiology, and disease*, 2nd edn. Raven Press, New York, pp 769–788
33. Shimotoyodome A, Fukuoka D, Suzuki J, Fujii Y, Mizuno T, Meguro S, Tokimitsu I, Hase T (2009) Coingestion of acylglycerols differentially affects glucose-induced insulin secretion via glucose-dependent insulinotropic polypeptide in C57BL/6 J mice. *Endocrinology* 150:2118–2126
34. Manowitz NR, Tso P, Sabesin SM (1986) Dietary supplementation with Pluronic L-81 modifies hepatic secretion of very low density lipoproteins in the rat. *J Lipid Res* 27:196–207
35. Iritani N, Sugimoto T, Hitoshi I (1999) Oral triacylglycerols regulate plasma glucagons-like peptide-1(7–36) and insulin levels in normal and especially in obese rats. *J Nutr* 129:46–50
36. Qualmann C, Holst JJ, Creutzfeldt W et al (1995) Glucagon-like peptide 1 (7–36 amide) secretion in response to luminal sucrose from the upper and lower gut. *Acta Diabetol* 32:13–16
37. Toft-Nielsen M, Michelsen B, Holst JJ et al (2001) Determinants of the impaired secretion of glucagon-like peptide-1 in type 2 diabetic patients. *J Clin Endocrinol Metab* 86:3717–3723
38. Anini Y, Hansotia T, Brubaker PL (2002) Muscarinic receptors control postprandial release of glucagon-like peptide-1: in vivo and in vitro studies in rats. *Endocrinology* 143:2420–2426
39. Brubaker PL, Anini Y (2003) Direct and indirect mechanisms regulating secretion of glucagon-like peptide-1 and glucagon-like peptide-2. *Can J Physiol Pharmacol* 81:1005–1012
40. Hansen L, Hartmann B, Holst JJ et al (2004) Glucagon-like peptide-1 secretion is influenced by perfusate glucose concentration and by a feedback mechanism involving somatostatin in isolated perfused porcine ileum. *Regul Pept* 118:11–18
41. Hansen L, Lampert S, Holst JJ et al (2004) Neural regulation of glucagon-like peptide-1 secretion in pigs. *Am J Physiol Endocrinol Metab* 287:939–947
42. Hermann-Rinke C, Hess M, Goke B et al (1995) Regulation of glucagon-like peptide-1 secretion from rat ileum by neurotransmitters and peptides. *J Endocrinol* 147:25–31
43. Hermann-Rinke C, McGregor GP, Goke B (2000) Calcitonin gene-related peptide potently stimulates glucagon-like peptide-1 release in the isolated perfused rat ileum. *Peptides* 21:431–437
44. Plaisancie P, Chayvialle J, Cuber J et al (1994) Regulation of glucagon-like peptide-1 (7–36) amide secretion by intestinal neurotransmitters and hormones in the isolated vascularly perfused rat colon. *Endocrinology* 135:2398–2403
45. Rocca AS, Brubaker PL (1999) Role of the vagus nerve in mediating proximal nutrient-induced glucagon-like peptide-1 secretion. *Endocrinology* 140:1687–1694
46. Adachi T, Hirasawa A, Tsujimoto G et al (2005) Free fatty acids administered into the colon promote the secretion of glucagon-like peptide-1 and insulin. *Biochem Biophys Res Commun* 340:332–337
47. Hirasawa A, Miyazaki S, Tsujimoto G et al (2005) Free fatty acids regulate gut incretin glucagon-like peptide 1 secretion through GPR 120. *Nat Med* 11:90–94
48. Katsuma S, Hirasawa A, Tsujimoto G (2005) Bile acids promote glucagon-like peptide-1 secretion through TGR5 in a murine enteroendocrine cell line STC-1. *Biochem Biophys Res Commun* 329:386–390

Beta-Glucosylceramide Administration (i.p.) Activates Natural Killer T cells In Vivo and Prevents Tumor Metastasis in Mice

Masashi Inafuku · Changchun Li · Yasuhiro Kanda ·
Toshihiko Kawamura · Kazuyoshi Takeda ·
Hirosuke Oku · Hisami Watanabe

Received: 9 December 2011 / Accepted: 2 March 2012 / Published online: 20 March 2012
© AOCs 2012

Abstract Natural killer (NK) T cells are well known to play important roles in both tumor rejection and the defense against infectious. Therefore, the antitumor potential of NKT cell-activating antigens have been the focus for the development of NKT cell-based immunotherapies. Up to now, several studies have revealed that the administrations of glycolipids (e.g. α -galactosylceramide) can successfully treat certain metastatic tumors. However, liver injuries appeared upon the application of these antigens. We previously examined the potential of using β -glucosylceramide (β -GlcCer) to inhibit tumor metastasis to the liver. The aim of this study was to determine the antimetastatic effects of β -GlcCer and its impact on the activation of NKT cells. Intraperitoneal administration of β -GlcCer enhanced the production of interferon- γ from hepatic lymphocytes containing NKT cells, and increased

the cytotoxicity of hepatic lymphocytes against tumor cells. Moreover, β -GlcCer administration suppressed the hepatic metastasis of tumors in wild type (WT) mice, but not in $CD1d^{-/-}$ or $J\alpha 18^{-/-}$ mice. The drawback associated with the other glycolipids in liver injury was not noted in WT mice treated with the continuous daily administration of β -GlcCer for 2 weeks. The present study demonstrated that β -GlcCer treatment activates invariant NKT cells, thus resulting in the inhibition of tumor metastasis.

Keywords β -Glucosylceramide · Natural killer T cells · NKT cell-based immunotherapies · Tumor metastasis · Ja18 and CD1d

Abbreviations

GalCer	Galactosylceramide
GlcCer	Glucosylceramide
LacCer	Lactosylceramide
iGb	Isoglobotrihexosylceramide
NK	Natural killer
iNKT	Invariant Natural killer T
TCR	T cell receptor
WT	Wild type
B6	C57BL/6
mAb	Monoclonal antibody
LDH	Lactate dehydrogenase
IFN- γ	Interferon-gamma
IL-4	Interleukin-4

M. Inafuku · C. Li (✉)
Department of Health Sciences, Trans-disciplinary
Research Organization for Subtropics and Island Studies,
University of the Ryukyus, Senbaru 1, Nishihara,
Okinawa 903-0213, Japan
e-mail: changchu@comb.u-ryukyu.ac.jp

Y. Kanda · T. Kawamura
Department of Immunology, Niigata University
School of Medicine, Niigata, Japan

K. Takeda
Department of Immunology, Juntendo University, Tokyo, Japan

H. Oku
Department of Mangroves and Bio-resources,
Center of Molecular Biosciences, University of the Ryukyus,
Okinawa, Japan

H. Watanabe
Department of Tropical Infectious Diseases, Center of Molecular
Biosciences, University of the Ryukyus, Okinawa, Japan

Introduction

Ceramide, a lipid molecule with a sphingoid base backbone, has been shown to play an important role in various

aspects of cancer biology [1, 2]. We previously demonstrated that ceramides with a chain length shorter than C8, but not longer than C12, show tumor-specific cytotoxicity [3]. Glycosylceramide has been shown to induce antitumor immune responses in various cancer models via the activation of natural killer (NK) T cells, which are important immune regulators that can either promote or suppress immunity [4–6]. It has been believed that NKT cells play roles not only in tumor rejection and defense against infectious agents, but also in the regulation of autoimmunity [7]. NKT cells are distinguished from conventional T lymphocytes by their function and T cell receptor (TCR) usage [8]. Most NKT cells recognize glycolipid antigens in the context of the monomorphic major histocompatibility complex class I-like molecule, CD1 [9]. CD1d-restricted NKT cells are further divided by their functions into Types I and II [7, 10, 11]. The antitumor activities of NKT cells have mainly been attributed to the Type I cells, which express an invariant V α 14-J α 18/V β 8 TCR in mice (V α 24-J α 18/V β 11 in humans) and strongly react with the marine sponge-derived glycolipid, α -galactosylceramides (α -GalCer). The administration of α -GalCer results in the rapid and massive activation of NKT cells, and the production of a burst of typical Th1 and Th2 cytokines such as interferon- γ (IFN- γ) and interleukin-4 (IL-4) from these cells [7, 12, 13]. In mice, NKT cells activated by this compound also down-regulate the TCR and NK-1.1 molecule, a NK cell marker, on their cell surface [14, 15], resulting in the apparent disappearance of NK-1.1 positive T cells in vivo.

In most studies for the development of NKT cell-based immunotherapies, the antitumor potential of NKT cell-activating glycolipids has been focused on α -GalCer [16]. Treatment with α -GalCer has been successful for certain metastatic tumors in various studies [17–19]. However, it has been demonstrated that α -GalCer administration can lead to significant liver damage [18, 20, 21]. These liver injuries appear to be a critical drawback to the application of α -GalCer for immunotherapeutic use. Numerous studies have since focused on the development of effective and safe NKT cell-based immunotherapeutics using various compounds, e.g. synthetic analogues of α -GalCer, naturally occurring ligands, and β -anomers of glycosphingolipids. However, the safe and effective ligands that activate NKT cells have not yet been established for the development of NKT cell-based immunotherapies.

β -GlcCer, a naturally occurring glycolipid, is a metabolic intermediate of glucosphingolipids [22]. In our previous study, we demonstrated that β -GalCer (C18:0) and β -GlcCer (C16:0) exert tumor-specific cytotoxicity in vitro [3]. We also reported that intraperitoneal (i.p.) administration of β -GlcCer isolated from malt feed induced a decrease in the proportion of hepatic NK-1.1⁺ T cells in mice, and suppressed the hepatic metastasis of EL-4

lymphoma cells in mice. We therefore suspected that β -GlcCer could contribute to developing NKT cell-based immunotherapies for metastatic tumors. In the present study, we investigated whether treatment with β -GlcCer could enhance antitumor immunity through NKT cells activation, resulting in the suppression of experimental tumor metastasis.

Materials and Methods

Ceramides

Pure ceramides (C4:0 and C8:0), β -GalCer (C18:0), and β -GlcCer (C16:0) were purchased from Avanti Polar Lipid, Inc. (Alabaster, Alabama, USA). In this study, KRN7000 (Kirin Brewery Co., Ltd., Japan) was used as α -GalCer. Malt-feed-derived β -GlcCer (mf- β -GlcCer) was purified as previously described [3]. Chemical structures of these glycosylceramides are summarized in Fig. 1. The ceramides were dissolved in ethanol, and stored at -30°C until use. In this study, 2 and 200 μg of α -GalCer and the other ceramides were used in a single injection, respectively.

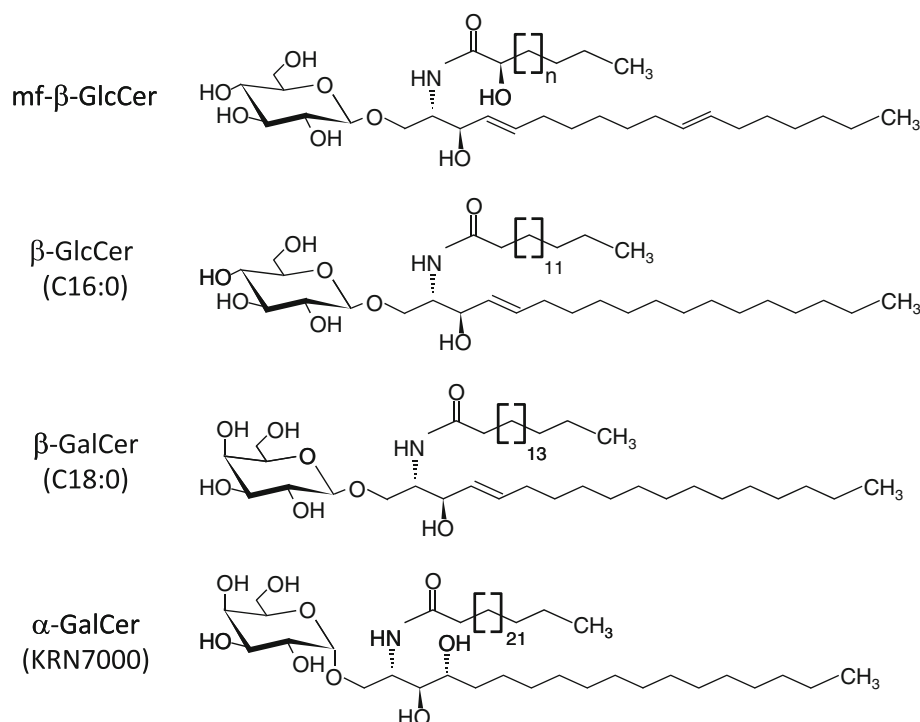
Animals

C57BL/6 (B6) mice (12–16 weeks old) and *CD1d*^{-/-} mice (11–20 weeks old, on a B6 background) were bred and maintained at the University of the Ryukyus and Niigata University, respectively. The *Ja18*^{-/-} mice (14–18 weeks old) on a B6 background were kindly provided by Dr. M. Taniguchi (RIKEN Yokohama Institute, Kanagawa, Japan). All mice were maintained under specific pathogen-free conditions, and given food and water ad libitum. Animal experiments were performed in accordance with the ethical principles and guidelines for the care and use of experimental animals at each university. Their serum and liver were collected at the end of the experiment. The serum IFN- γ levels and the indicator of hepatopathy were measured using commercial ELISA kits purchased from R&D Systems, Inc. (MN, USA) and commercial enzymatic kits (Wako Pure Chemical Industries, Ltd., Osaka, Japan), respectively.

Tumor Metastasis

EL-4 cells, a T-cell lymphoma cell line from a B6 background, were used in this study. These cells (5×10^5 cells/mouse) were intravenously (i.v.) inoculated into B6, *CD1d*^{-/-}, and *Ja18*^{-/-} mice. The mice were administered i.p. injections of ceramides suspended in 200 μL PBS containing 5 % ethanol, 3 days before and on the day of tumor inoculation. A volume of 200 μL of the vehicle

Fig. 1 Chemical structures of glycosylceramides using in this study. In mf- β -GlcCer, Chemical structure of the major-GluCer extracted from malt feed are shown



solution was given as a control at each administration time point. On day 14 after tumor inoculation, the number of tumors visible on the surface of the liver was counted.

Flow Cytometry

The monoclonal antibodies (mAb) used in this study included a FITC-conjugated anti-mouse CD3 ϵ chain (145-2C11) mAb, PE conjugated anti-mouse NK-1.1 (PK136) mAbs, and a biotin-conjugated anti-mouse CD69 (H1.2F3) antibody, which were all purchased from BD Biosciences (CA, USA). The biotin conjugated mAb were detected with Streptavidin-Allophycocyanin reagents (BD Biosciences). To prevent nonspecific Fc receptor-mediated binding of mAbs, the hepatic MNCs were pre-incubated with an anti-CD32/CD16 mAb (2.4G2, BD Biosciences) before staining with the labeled mAbs. The stained cells were analyzed on a FACSCalibur Flow Cytometer and the CellQuest software program (BD Biosciences) was used to analyze the results after gating for cells with the forward and side scatter properties of lymphocytes. Dead cells were excluded by propidium iodide gating.

In Vivo Responses to β -GlcCer in the Liver

At different time points after i.p. treatment with glycosylceramides, the livers were excised from the WT mice. Isolated hepatic MNCs from untreated or treated mice were stained with mAbs followed by a flow cytometric analysis,

or were plated in 96-well round-bottom microculture plates at 5×10^5 cells per well in RPMI-1640 medium (Sigma-Aldrich, Inc.) with 10 % heat-inactivated fetal bovine serum. To assess the levels of cytokine production by the cultured MNCs, the culture supernatants of the MNCs were harvested after 24 h of culture, and the cytokine levels in the culture supernatants were measured.

Cytotoxicity of Hepatic Lymphocytes

NK cell-sensitive YAC-1 lymphoma cells and EL-4 lymphoma cells were used as target cells. Hepatic MNCs (as effector cells) were purified from B6 mice 36 h after i.p. injection of 200 μ g of mf- β -GlcCer, and were suspended in RPMI-1640 medium without Phenol Red (Sigma-Aldrich, Inc.). The serially diluted effector cells were mixed with 1×10^4 target cells in 96-well round-bottom microculture plates. The plates were centrifuged and incubated for 4 h at 37 $^{\circ}$ C. The lactate dehydrogenase (LDH) released from the target cells was colorimetrically measured with an LDH Cytotoxic Test Kit (Wako Pure Chemical Industries). To induce cytotoxicity, poly (I:C), a ligand of toll like receptor 3, was injected (100 μ g/mouse) intraperitoneally into mice 12 h before the cytotoxicity assay.

IFN- γ mRNA Expression in Hepatic NK-1.1 $^{+}$ T Cells

Eighty six mice were sacrificed 24 h after i.p. administration of 200 μ g of mf- β -GlcCer. The isolated hepatic MNCs

were stained with fluorescently labeled anti-CD3 ϵ and anti-NK-1.1 mAbs as described above. The NK-1.1⁺ T cells were then sorted using a FACS Aria II Flow Cytometer (BD Biosciences). Using reverse transcriptase (High Capacity RNA-to-cDNA Kit; ABI, CA, USA), first-strand cDNA was synthesized from 1 μ g of total RNA from the sorted NK-1.1⁺ T cells. The specific primers used in the quantitative real-time PCR analysis were as follows: IFN- γ sense (5'-GAACGCTACACACTGCATC-3'), IFN- γ antisense (5'-GAGCTCATTGAATGCTTGG-3'); β -actin sense (5'-CAGAAGGAGATTACTGCTCTGGCT-3'), and β -actin antisense (5'-GGAGCCACCGATCCACACA-3'). The amplifications were performed with a commercial real-time PCR system (StepOne Real-Time PCR System; ABI). All samples were normalized to the amount of β -actin transcript in each sample.

Recognition of Glycolipid Binding CD1d-Dimer Molecules

Dimeric CD1d molecules (CD1d-dimer) were purchased from BD Biosciences. CD1d-dimer loaded with glycolipids was prepared with a 3- to 10-fold molar excess of glycosylceramides. To detect iNKT cells, hepatic MNCs were labeled with a FITC-conjugated anti-mouse TCR β chain (H57-597) mAb (BD Bioscience) and PE-labeled CD1d-dimer loaded with glycolipids according to the manufacturer's protocol.

Statistical Analyses

All values are expressed as the means \pm S.E.M. The significance of differences in the means between two groups was determined by Student's *t* test. To determine the significance of the differences between means for more than three groups, the data were analyzed by one-way ANOVA,

and then the differences among the mean values were inspected using Tukey-Kramer's multiple comparison tests. Differences were considered to be significant at $P < 0.05$.

Results

We first investigated whether the selective cytotoxicity of ceramides contributes directly to suppressing the metastasis of EL-4 lymphoma cells in B6 mice. The degree of tumor metastasis in mice treated with unglycosylated ceramides showed no significant difference from that in control mice (Fig. 2a, b). However, the treatment with a commercially available pure β -GalCer (C18:0) or β -GlcCer (C16:0) led to the inhibition of tumor metastasis in the liver (Fig. 2c).

As shown in Fig. 3, the proportion of hepatic NK-1.1⁺CD3⁺ cells was significantly decreased in mice treated with α -GalCer. Within the population of NK-1.1⁺CD3⁻ cells (NK cells), the number of CD69 positive cells was also increased. Treatment with mf- β -GlcCer induced a transient decrease in the hepatic NK-1.1⁺CD3⁺ cells proportion and an increase in the proportion of CD69⁺ NK-1.1⁺CD3⁻ cells.

Although the treatment with α -GalCer induced a burst increase in the serum IFN- γ level, the serum IFN- γ level was not altered by mf- β -GlcCer treatment at any of the experimental time points examined in the present study (Fig. 4a). The burst increases in serum IFN- γ and ALT levels induced by α -GalCer treatment were alleviated by the co-administration of mf- β -GlcCer (Fig. 4b). In the mice treated with mf- β -GlcCer, it was observed that there was an increase in the IFN- γ secretion from hepatic MNCs in the mice that were sacrificed 36 h after treatment (Fig. 5a). Using YAC-1 cells as target cells, the cytotoxicity of hepatic MNCs in mice treated with mf- β -GlcCer was significantly enhanced in

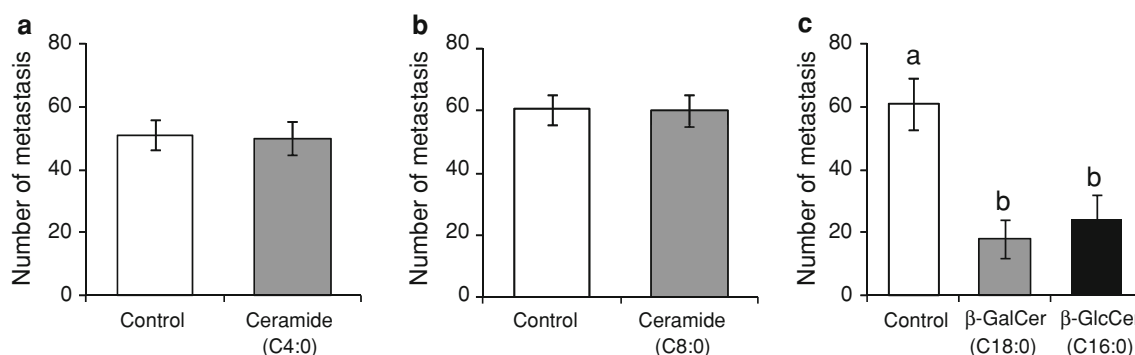
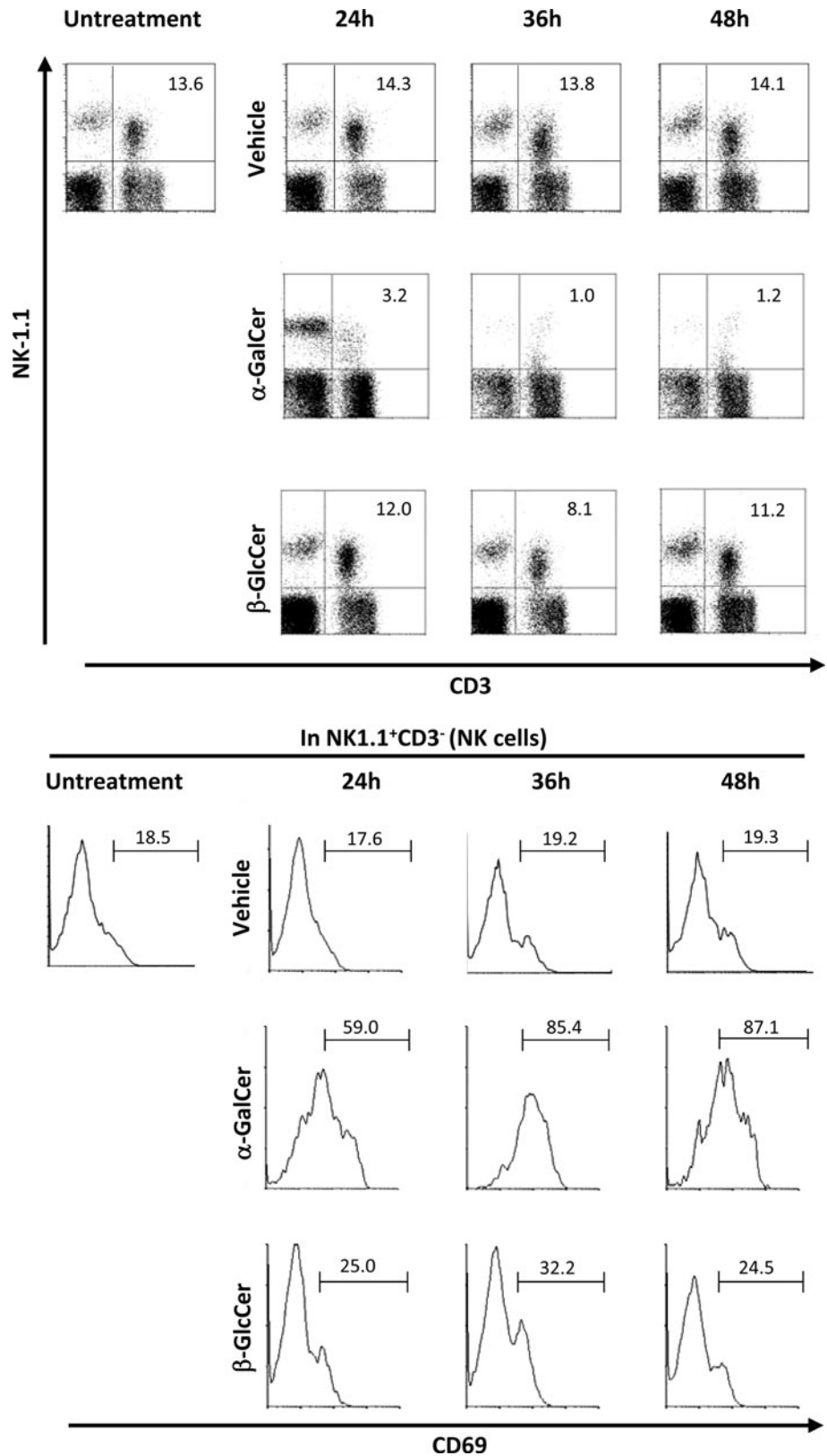


Fig. 2 The antimetastatic activities of ceramides. B6 mice were injected intraperitoneally with 200 μ g of ceramide 3 days before and on the day of intravenous inoculation of EL-4 lymphoma. The mice were then treated with unglycosylceramide with C4:0 and C6:0 fatty acids (a and b, respectively), and with β -GalCer (C18:0) or β -GlcCer

(C16:0) (c). The number of metastatic tumors visible on the liver surface was counted on day 14 after tumor inoculation. The data are presented as the means \pm S.E.M. for six mice. Different letters show significant differences between each experimental group of B6 mice ($P < 0.05$)

Fig. 3 The response of intrahepatic NKT and NK cells to β -GlcCer treatment in B6 mice. Lymphocytes were isolated from the liver at each time point after glycolipid injection. Three color staining for CD3, NK-1.1, and CD69 was conducted. The numbers in the figure indicate the percentages of fluorescence-positive cells in the corresponding areas. The results from one representative experiment out of three are shown



comparison with that in vehicle-treated control mice (Fig. 5b). Similar effect was observed when EL-4 lymphoma cells were used as target cells.

To confirm that β -GlcCer administration activated intrahepatic NKT cells, the IFN- γ production in NKT cells was examined. We thus examined the IFN- γ mRNA

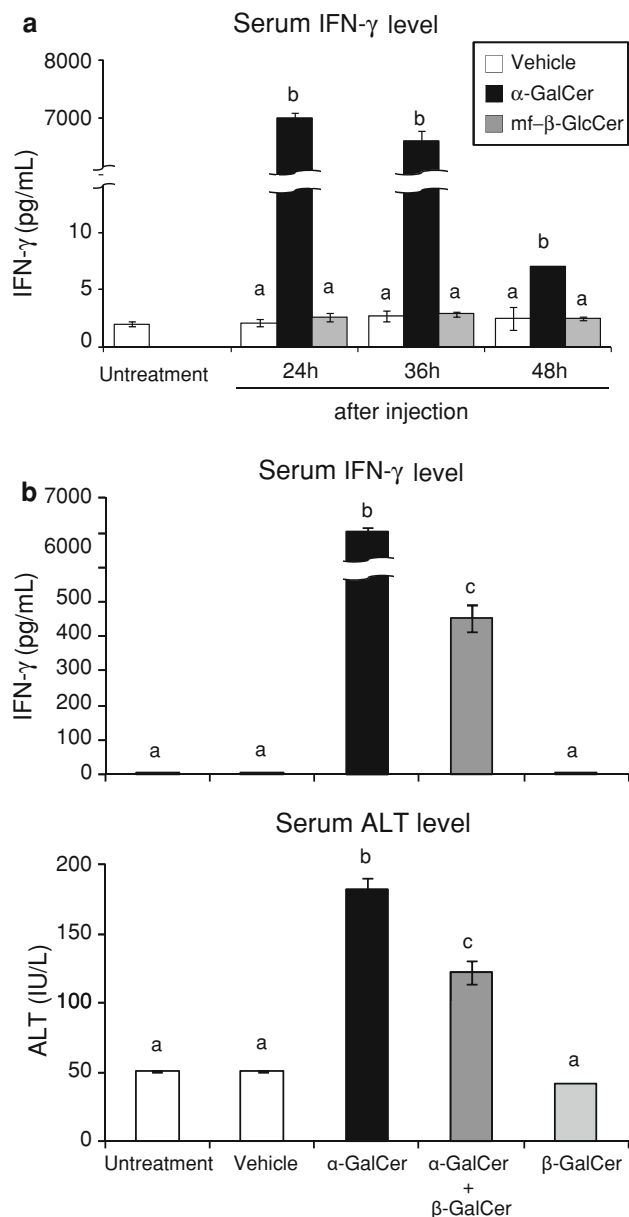


Fig. 4 The in vivo response to β -GlcCer treatment. Sera were collected at each time point after a single i.p. injection of ceramide (a) and 24 h after coadministration of α -GalCer and mf- β -GlcCer to B6 mice (b). The data are expressed as the means \pm S.E.M. for three mice. Different letters show significant differences between each experimental group of B6 mice ($P < 0.05$)

expression in intrahepatic NK-1.1⁺CD3⁺ cells. In this study, all flow cytometry sorting experiments showed >97 % purity (Fig. 6a). Although the mRNA expression of IFN- γ in the sorted NK-1.1⁺CD3⁺ cells was not affected by vehicle treatment, the i.p. injection of mf- β -GlcCer induced a significant enhancement of the IFN- γ mRNA expression (Fig. 6b). In in vitro experiments, the dimeric CD1d molecules loaded with α -GalCer could recognize

invariant NKT cells (Fig. 6c). However, the CD1d-dimer loaded with mf- β -GlcCer did not stain the hepatic MNCs.

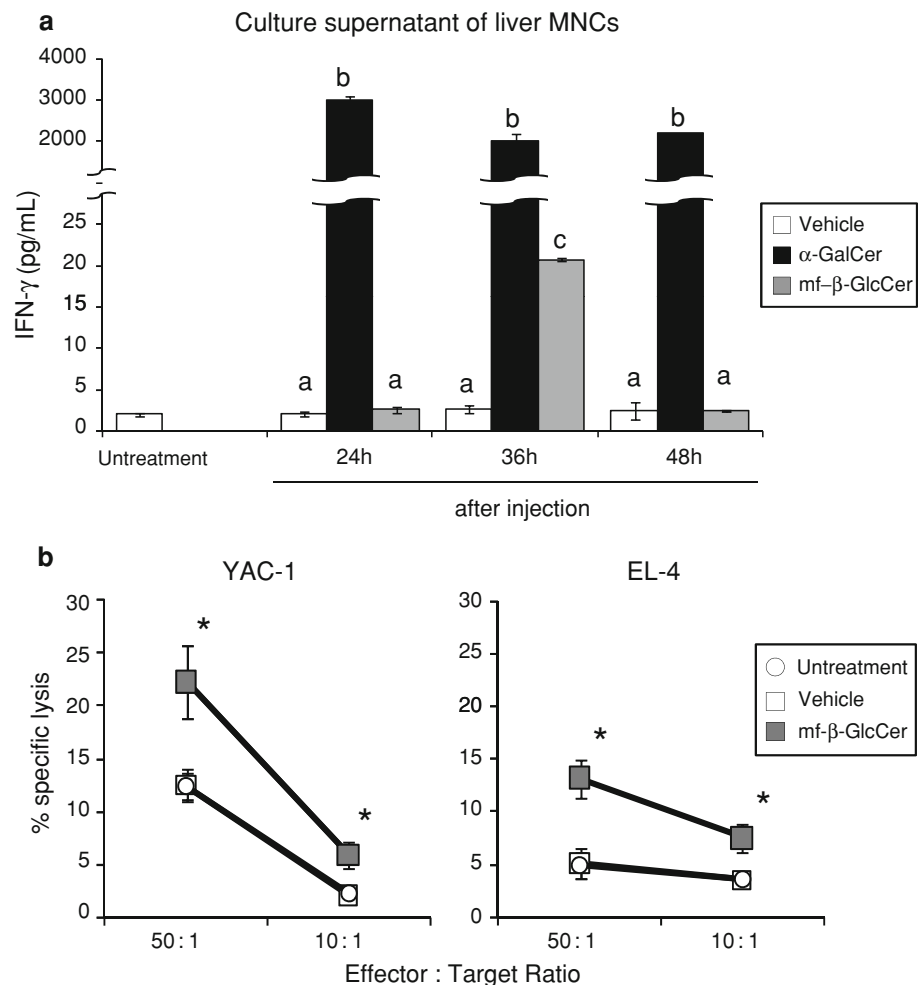
Upon the activation of NKT cells by α -GalCer, CD1d and the V α 14-J α 18/V β 8 TCR are essential molecules on antigen presenting and invariant NKT cells, respectively. Although treatment with mf- β -GlcCer in B6 mice significantly suppressed the number of metastatic tumors on the liver (Fig. 7a), no strong metastatic inhibition by mf- β -GlcCer treatment was observed in the *CD1d*^{-/-} or *Ja18*^{-/-} mice. The daily injection of mf- β -GlcCer (200 μ g/mouse/day) for 7 days did not affect the serum ALT and AST levels in WT mice (Fig. 7b). We also did not note any changes in the histology of the liver during a microscopic evaluation compared to the untreated mice (data not shown).

Discussion

In the present study, the administration of β -GlcCer enhanced the tumor-specific cytotoxicity of hepatic lymphocytes, and the IFN- γ mRNA expression in intrahepatic NKT cells. The β -GlcCer treatment also significantly inhibited the metastasis of experimental EL-4 lymphoma to the liver in WT mice, but not in *CD1d*^{-/-} or *Ja18*^{-/-} mice. The daily administration of β -GlcCer for 7 days did not induce any significant hepatocellular injury, nor any tissue damage as determined by a histological examination. These findings suggest that β -GlcCer, which is widely distributed in the plant kingdom, inhibits an experimental tumor metastasis through NKT cell activation without the critical drawback associated with the application of other antigens for activation of CD1d-restricted NKT cells.

In our previous study [3], the antimetastatic actions of mf- β -GlcCer were suggested to be attributable to two potential mechanisms; the first being their selective cytotoxicity, and the second being the induction of antitumor immunity. Moreover, we did not fully dismiss the possibility that compounds other than β -GlcCer could also contribute to the inhibition of metastasis. We previously reported that unglycosylated ceramides with chain lengths shorter than C8 (C4:0 and C8:0) have more selective cytotoxicity than β -GlcCer [3]. For example, the hepatic metastasis of tumors was inhibited by treatment with glycosylceramides, but not by treatment with unglycosylated ceramide (Fig. 2). The antimetastatic actions of β -GlcCer were not observed in mice with CD1d or J α 18 deficiencies (Fig. 7). These results support that the hypothesis that selective cytotoxicity of β -GlcCer is not required for its antimetastatic activity. This suggests that β -GlcCer injection inhibits tumor metastasis in the liver by enhancing the antitumor immunity.

Fig. 5 The cytokine production and antitumor cytotoxicity of hepatic lymphocytes in response to β -GlcCer treatment in B6 mice **(a)** Hepatic lymphocytes were isolated from B6 mice at each time point after glycolipid injection. The isolated lymphocytes were cultured for 24 h, then the cytokine levels in the culture supernatants were quantified by ELISA. **(b)** Hepatic lymphocytes were isolated from B6 mice 36 h after mf- β -GlcCer injection. To induce cytotoxicity, Poly (I:C) (100 μ g/mouse) was intraperitoneally injected into mice just before the cytotoxicity assay. Each value represents the mean \pm S.E.M. of triplicate cultures. Different letters show significant differences between each experimental group of B6 mice ($P < 0.05$). The asterisks show a significant difference to exist between the vehicle and mf- β -GlcCer treatment groups ($P < 0.05$)



The potential antitumor applications of NKT cell-activating glycolipids have been focused so far on α -GlcCer [16]. Treatment with α -GlcCer has been shown to successfully decrease the growth of certain metastatic tumors [17–19]. With regard to the antimetastatic activity of α -GlcCer in the liver, NK cells are known to be the principal effectors. For example, Nakagawa et al. [18] reported that the IFN- γ produced by α -GlcCer-stimulated hepatic NKT cells plays an essential role in the increase in both the innate antitumor cytotoxicity of NK cells and the adaptive antitumor response of CD8⁺ T cells, thus resulting in the inhibition of tumor metastasis to the liver. Similar to the observations following α -GlcCer treatment, the proportion of hepatic NK-1.1⁺ T cells transiently increased (Fig. 3). Treatment with mf- β -GlcCer also enhanced the IFN- γ mRNA expression in intrahepatic NK-1.1⁺ T cells (Fig. 6b). The expression of CD69, an activation marker, was slightly increased in hepatic NK cells of B6 mice treated with mf- β -GlcCer. As shown in Fig. 5b, the antitumor cytotoxicity of hepatic MNCs against NK cell-sensitive YAC-1 cells was significantly increased in the mice treated with mf- β -GlcCer. The antitumor cytotoxicity of

these cells was also shown when EL-4 lymphoma was used as the target cells. These results suggest that the tumor-specific cytotoxicity of hepatic lymphocytes including NK cells is enhanced by the IFN- γ secreted from the activated NKT cells as a result of β -GlcCer administration.

We noted that β -GlcCer treatment inhibits tumor metastasis in WT mice, but not in *CD1d*^{-/-} and *Ja18*^{-/-} mice (Fig. 7). Therefore, our findings suggest that invariant TCR-expressing T lymphocytes restricted by CD1d molecules, generally referred to as invariant NKT (iNKT) cells, are pivotal effector cells required for the antimetastatic action of β -GlcCer, similar to the observations of α -GlcCer treatment in other studies [17, 18]. Several glycolipids and phospholipids have been identified as natural and endogenous CD1d ligands for NKT cells [23, 24]. For example, Ilan and colleagues examined the effects of β -GlcCer treatment on various animal models. Treatment with β -GlcCer in vivo has been reported to attenuate the tissue damage mediated by Th1-type immune responses in rodent models, including Con A-induced hepatitis, chemically induced hepatic fibrosis, immune-mediated colitis, OVA-induced asthma, and diabetes [25–29]. They also indicated

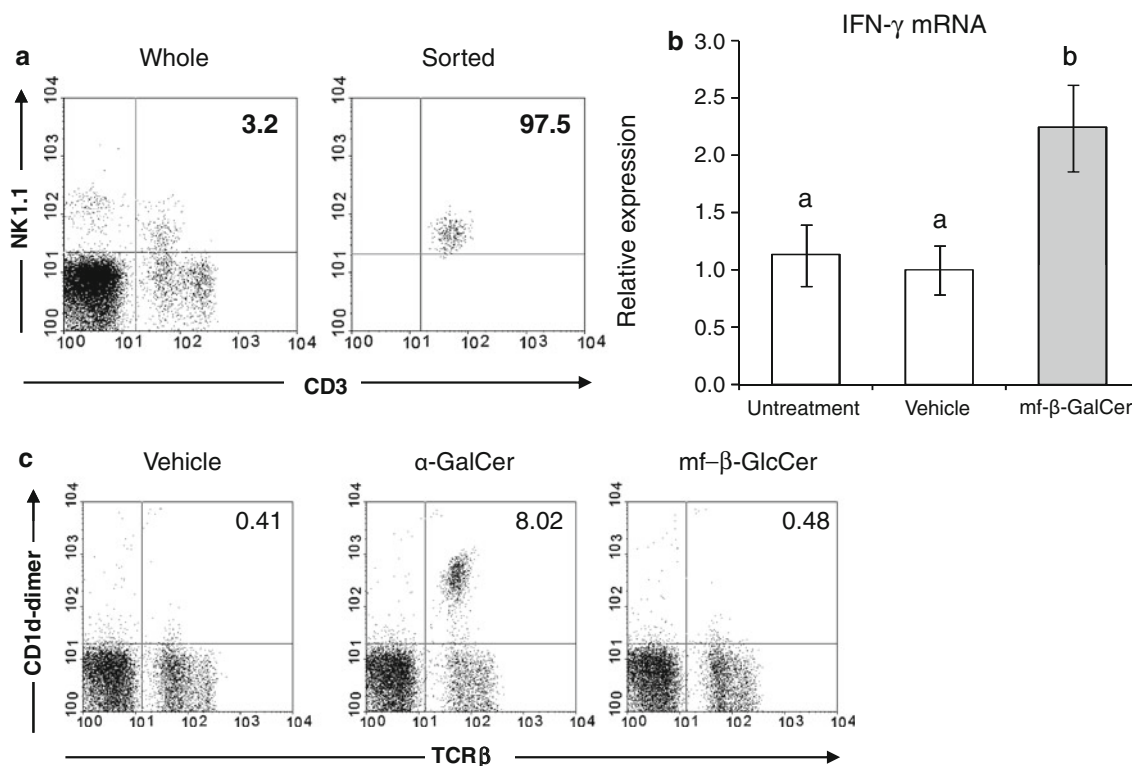


Fig. 6 In vivo response of hepatic NKT cells to β -GlcCer treatment. Hepatic lymphocytes were isolated from B6 mice 24 h after mf- β -GlcCer injection. **a** Two color staining for CD3 and NK-1.1 was conducted, and the NK-1.1⁺CD3⁺ cells were sorted. The numbers in the figure indicate the percentages of fluorescence-positive cells in the corresponding areas. **b** The total RNA was extracted from hepatic NK-1.1⁺ T cells sorted from B6 mice 24 h after treatment, and was

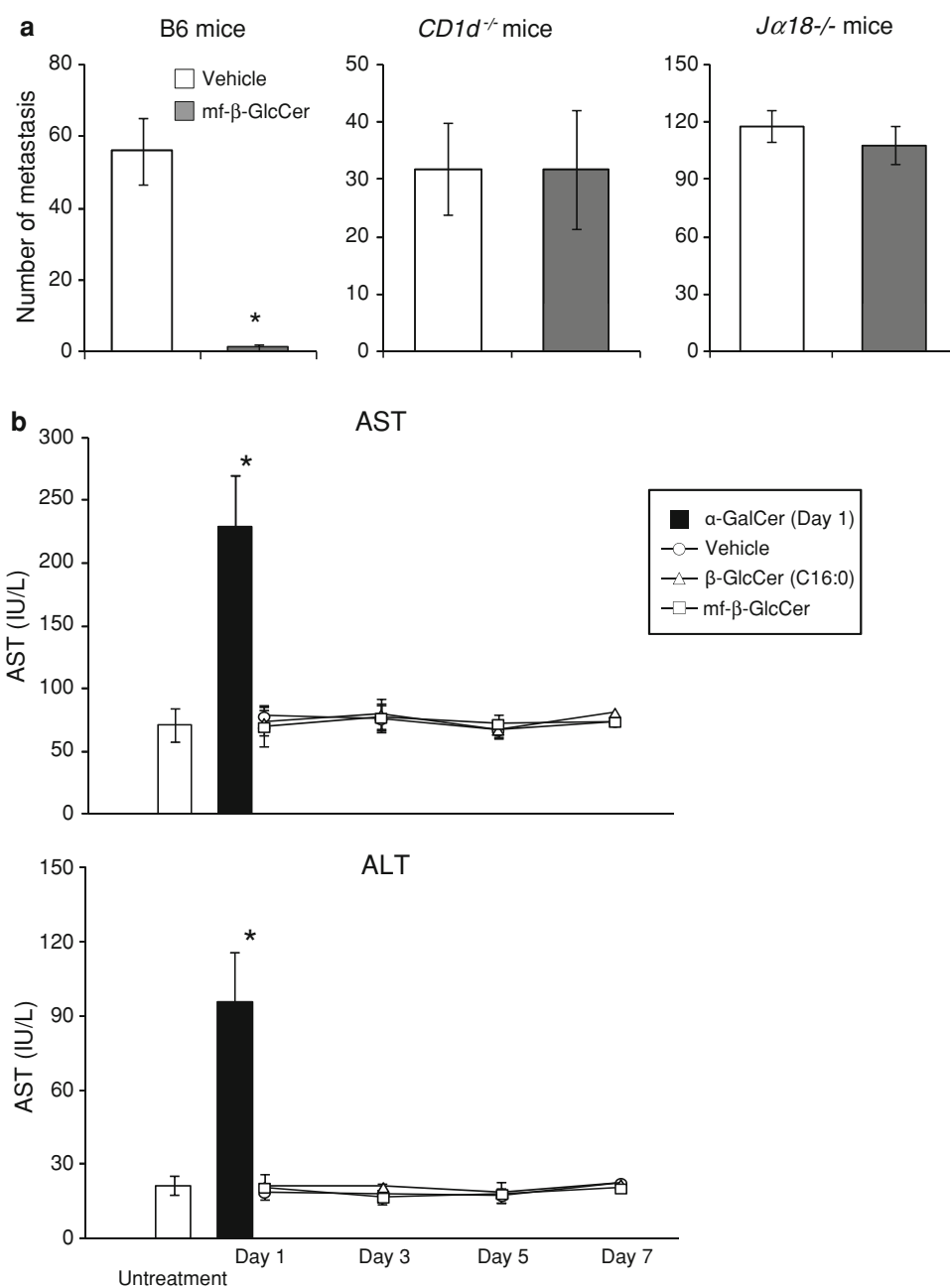
analyzed for the relative expression level of IFN- γ mRNA. The data are expressed as the means \pm S.E.M. for five mice. *Different letters* show significant differences between each experimental group of B6 mice ($P < 0.05$). **c** Hepatic MNCs were stained with anti-TCR β -FITC mAbs and PE-labeled dimeric CD1d molecules loaded with the indicated glycolipids. The *numbers* indicate the percentage of cells within each quadrant. The data are representative of two separate experiments

that the daily i.p. administration of β -GlcCer significantly inhibited in vivo transplanted tumor growth in mice [30]. In mammals, lactosylceramide (LacCer), which consists of β -GlcCer and a galactose residue, is metabolized to isoglobotrihexosylceramide (iGb3) by iGb3 synthase. Since several studies have demonstrated that iGb3 shows in vitro stimulatory activity toward both human and mouse iNKT cells [31, 32], it was suggested that iGb3 may be important for iNKT cell activation. However, the normal development and function of iNKT cells was still observed in mice with iGb3 deficiency [33]. However, Stanic et al. [34] revealed that β -GlcCer synthase deficiency causes the defective presentation of iNKT cells in mice, and found that β -GlcCer binds to CD1d1 but that their complexes are not recognized by human NKT hybridomas. Hence, they predicted that β -GlcCer may be a precursor for the biosynthesis of a natural CD1d-restricted antigen for iNKT cells in mammals. As shown in Fig. 4, the co-administration of mf- β -GlcCer alleviated the burst increase in the serum IFN- γ and ALT levels. Dimeric CD1d loaded with mf- β -GlcCer was not recognized by NKT cells (Fig. 6c).

However, Zigmmond et al. [35] demonstrated that in vitro β -GlcCer treatment induces a significant increase in the IFN- γ /IL-4 ratio from double-negative NKT hybridoma cells. Further studies will be needed to fully understand whether β -GlcCer or their metabolites are responsible for the antimetastatic actions resulting from β -GlcCer treatment.

It was indicated that the growth of transplanted tumors is suppressed in mice treated with β -GlcCer (C12), but not in those treated with β -GlcCer (C8) [30]. Although there is some uncertainty in the chemical structure of the mf- β -GlcCer used in this study in terms of its sphingoid base (Fig. 1), they are mostly composed of the longer saturated fatty acids (>16 carbons) as shown in our previous study [36]. The largest fatty acid component was α -hydroxyeicosanoic acid, which comprises about 50 % of the total amide-linked fatty acids. In this study, antimetastatic activities were observed when mice were administered the pure β -GlcCer (C16:0). Our findings therefore suggest that treatment with β -GlcCer, which are composed of unsaturated fatty acids with more than 16 carbons, has the

Fig. 7 The administration of β -GlcCer exerts antimetastatic activity in wild type mice, but not in $CD1d^{-/-}$ or $Ja18^{-/-}$ mice, and did not induce liver injuries. **a** The mice were injected intraperitoneally with 200 μ g of mf- β -GlcCer 3 days before and on the day of EL-4 lymphoma intravenous inoculation. The number of metastatic tumors visible on the liver surface was counted on day 14 after tumor inoculation. **b** The mice were administered the indicated glycosylceramides by i.p. injection for 7 days. The data are expressed as the means \pm S.E.M. for five or six mice. The asterisk shows a significant difference between the untreated mice and the glycolipid treatment group ($P < 0.05$)



potential to inhibit tumor metastasis through the activation of CD1d-restricted NKT cells, without any significant side effects. With regard to the chemical structure of sphingolipids, a sphingoid base and an acyl chain may be important for their NKT cell activation and for determining their binding affinity of the CD1d/antigen complex [37, 38]. Further studies will be needed to elucidate which chemical structure(s) of β -GlcCer are the most effective. It will also be necessary to understand the exact mechanisms underlying the antimetastatic action of β -GlcCer treatment. In conclusion, the present study demonstrated that intraperitoneal treatment with β -GlcCer activates invariant NKT

cells, resulting in the inhibition of tumor metastasis, and that this apparently lacks the toxicity associated with other glycolipid-based treatments.

References

1. Futerman AH, Hannun YA (2004) The complex life of simple sphingolipids. *EMBO Rep* 5(8):777–782. doi:10.1038/sj.embor.7400208
2. Ogretmen B, Hannun YA (2004) Biologically active sphingolipids in cancer pathogenesis and treatment. *Nat Rev Cancer* 4(8):604–616. doi:10.1038/nrc1411

3. Oku H, Li C, Shimatani M, Iwasaki H, Toda T, Okabe T, Watanabe H (2009) Tumor specific cytotoxicity of beta-glucosylceramide: structure-cytotoxicity relationship and anti-tumor activity in vivo. *Cancer Chemother Pharmacol* 64(3):485–496. doi:[10.1007/s00280-008-0896-2](https://doi.org/10.1007/s00280-008-0896-2)
4. Cerundolo V, Silk JD, Masri SH, Salio M (2009) Harnessing invariant NKT cells in vaccination strategies. *Nat Rev Immunol* 9(1):28–38. doi:[10.1038/nri2451](https://doi.org/10.1038/nri2451)
5. Kobayashi E, Motoki K, Uchida T, Fukushima H, Koezuka Y (1995) KRN7000, a novel immunomodulator, and its antitumor activities. *Oncol Res* 7(10–11):529–534
6. Molling JW, Moreno M, van der Vliet HJ, van den Eertwegh AJ, Scheper RJ, von Blomberg BM, Bontkes HJ (2008) Invariant natural killer T cells and immunotherapy of cancer. *Clin Immunol* 129(2):182–194. doi:[10.1016/j.clim.2008.07.025](https://doi.org/10.1016/j.clim.2008.07.025)
7. Kronenberg M, Gapin L (2002) The unconventional lifestyle of NKT cells. *Nat Rev Immunol* 2(8):557–568. doi:[10.1038/nri854](https://doi.org/10.1038/nri854)
8. Bendelac A, Rivera MN, Park SH, Roark JH (1997) Mouse CD1-specific NK1 T cells: development, specificity, and function. *Annu Rev Immunol* 15:535–562. doi:[10.1146/annurev.immunol.15.1.535](https://doi.org/10.1146/annurev.immunol.15.1.535)
9. Bendelac A, Savage PB, Teyton L (2007) The biology of NKT cells. *Annu Rev Immunol* 25:297–336. doi:[10.1146/annurev.immunol.25.022106.141711](https://doi.org/10.1146/annurev.immunol.25.022106.141711)
10. Jahng A, Maricic I, Aguilera C, Cardell S, Halder RC, Kumar V (2004) Prevention of autoimmunity by targeting a distinct, non-invariant CD1d-reactive T cell population reactive to sulfatide. *J Exp Med* 199(7):947–957. doi:[10.1084/jem.20031389](https://doi.org/10.1084/jem.20031389)
11. Arrenberg P, Halder R, Kumar V (2009) Cross-regulation between distinct natural killer T cell subsets influences immune response to self and foreign antigens. *J Cell Physiol* 218(2):246–250. doi:[10.1002/jcp.21597](https://doi.org/10.1002/jcp.21597)
12. Kawano T, Cui J, Koezuka Y, Toura I, Kaneko Y, Motoki K, Ueno H, Nakagawa R, Sato H, Kondo E, Koseki H, Taniguchi M (1997) CD1d-restricted and TCR-mediated activation of Valpha14 NKT cells by glycosylceramides. *Science* 278(5343):1626–1629
13. Taniguchi M, Harada M, Kojo S, Nakayama T, Wakao H (2003) The regulatory role of Valpha14 NKT cells in innate and acquired immune response. *Annu Rev Immunol* 21:483–513. doi:[10.1146/annurev.immunol.21.120601.141057](https://doi.org/10.1146/annurev.immunol.21.120601.141057)
14. Wilson MT, Johansson C, Olivares-Villagomez D, Singh AK, Stanic AK, Wang CR, Joyce S, Wick MJ, Van Kaer L (2003) The response of natural killer T cells to glycolipid antigens is characterized by surface receptor down-modulation and expansion. *Proc Natl Acad Sci USA* 100(19):10913–10918. doi:[10.1073/pnas.1833166100](https://doi.org/10.1073/pnas.1833166100)
15. Harada M, Seino K, Wakao H, Sakata S, Ishizuka Y, Ito T, Kojo S, Nakayama T, Taniguchi M (2004) Down-regulation of the invariant Valpha14 antigen receptor in NKT cells upon activation. *Int Immunol* 16(2):241–247
16. Schmieg J, Yang G, Franck RW, Tsuji M (2003) Superior protection against malaria and melanoma metastases by a C-glycoside analogue of the natural killer T cell ligand alpha-Galactosylceramide. *J Exp Med* 198(11):1631–1641. doi:[10.1084/jem.20031192](https://doi.org/10.1084/jem.20031192)
17. Nakagawa R, Serizawa I, Motoki K, Sato M, Ueno H, Iijima R, Nakamura H, Shimosaka A, Koezuka Y (2000) Antitumor activity of alpha-galactosylceramide, KRN7000, in mice with the melanoma B16 hepatic metastasis and immunohistological study of tumor infiltrating cells. *Oncol Res* 12(2):51–58
18. Nakagawa R, Nagafune I, Tazunoki Y, Ehara H, Tomura H, Iijima R, Motoki K, Kamishohara M, Seki S (2001) Mechanisms of the antimetastatic effect in the liver and of the hepatocyte injury induced by alpha-galactosylceramide in mice. *J Immunol* 166(11):6578–6584
19. Osada T, Nagawa H, Shibata Y (2004) Tumor-infiltrating effector cells of alpha-galactosylceramide-induced antitumor immunity in metastatic liver tumor. *J Immune Based Ther Vaccines* 2(1):7. doi:[10.1186/1476-8518-2-7](https://doi.org/10.1186/1476-8518-2-7)
20. Fujii H, Seki S, Kobayashi S, Kitada T, Kawakita N, Adachi K, Tsutsui H, Nakanishi K, Fujiwara H, Ikarashi Y, Taniguchi M, Kronenberg M, Ikemoto M, Nakajima Y, Arakawa T, Kaneda K (2005) A murine model of NKT cell-mediated liver injury induced by alpha-galactosylceramide/d-galactosamine. *Virchows Arch* 446(6):663–673. doi:[10.1007/s00428-005-1265-8](https://doi.org/10.1007/s00428-005-1265-8)
21. Biburger M, Tiegs G (2005) Alpha-galactosylceramide-induced liver injury in mice is mediated by TNF-alpha but independent of Kupffer cells. *J Immunol* 175(3):1540–1550 (pii: 175/3/1540)
22. Hannun YA, Luberto C, Argraves KM (2001) Enzymes of sphingolipid metabolism: from modular to integrative signaling. *Biochemistry* 40(16):4893–4903 (pii: bi002836k)
23. Brutkiewicz RR (2006) CD1d ligands: the good, the bad, and the ugly. *J Immunol* 177(2):769–775 (pii: 177/2/769)
24. Zajonc DM, Cantu C 3rd, Mattner J, Zhou D, Savage PB, Bendelac A, Wilson IA, Teyton L (2005) Structure and function of a potent agonist for the semi-invariant natural killer T cell receptor. *Nat Immunol* 6(8):810–818. doi:[10.1038/ni1224](https://doi.org/10.1038/ni1224)
25. Margalit M, Ghazala SA, Alper R, Elinav E, Klein A, Doviner V, Sherman Y, Thalenfeld B, Engelhardt D, Rabbani E, Ilan Y (2005) Glucocerebroside treatment ameliorates ConA hepatitis by inhibition of NKT lymphocytes. *Am J Physiol Gastrointest Liver Physiol* 289(5):G917–G925. doi:[10.1152/ajpgi.00105.2005](https://doi.org/10.1152/ajpgi.00105.2005)
26. Safadi R, Zigmund E, Pappo O, Shalev Z, Ilan Y (2007) Amelioration of hepatic fibrosis via beta-glucosylceramide-mediated immune modulation is associated with altered CD8 and NKT lymphocyte distribution. *Int Immunol* 19(8):1021–1029. doi:[10.1093/intimm/dxm069](https://doi.org/10.1093/intimm/dxm069)
27. Zigmund E, Preston S, Pappo O, Lalazar G, Margalit M, Shalev Z, Zolotarov L, Friedman D, Alper R, Ilan Y (2007) Beta-glucosylceramide: a novel method for enhancement of natural killer T lymphocyte plasticity in murine models of immune-mediated disorders. *Gut* 56(1):82–89. doi:[10.1136/gut.2006.095497](https://doi.org/10.1136/gut.2006.095497)
28. Horani A, Shoseyov D, Doron S, Mruwat R, Amer J, Kerem E, Safadi R (2011) Immune modulation of ovalbumin-induced lung injury in mice using beta-glucosylceramide and a potential role of the liver. *Immunobiology* 216(5):548–557. doi:[10.1016/j.imbio.2010.10.002](https://doi.org/10.1016/j.imbio.2010.10.002)
29. Zigmund E, Zangen SW, Pappo O, Sklair-Levy M, Lalazar G, Zolotarova L, Raz I, Ilan Y (2009) Beta-glycosphingolipids improve glucose intolerance and hepatic steatosis of the Cohen diabetic rat. *Am J Physiol Endocrinol Metab* 296(1):E72–E78. doi:[10.1152/ajpendo.90634.2008](https://doi.org/10.1152/ajpendo.90634.2008)
30. Lalazar G, Ben Ya'acov A, Livovsky DM, El Haj M, Pappo O, Preston S, Zolotarov L, Ilan Y (2009) Beta-glycosphingolipid-induced alterations of the STAT signaling pathways are dependent on CD1d and the lipid raft protein flotillin-2. *Am J Pathol* 174(4):1390–1399. doi:[10.2353/ajpath.2009.080841](https://doi.org/10.2353/ajpath.2009.080841)
31. Zhou D, Mattner J, Cantu C 3rd, Schrantz N, Yin N, Gao Y, Sagiv Y, Hudspeth K, Wu YP, Yamashita T, Teneberg S, Wang D, Proia RL, Lavery SB, Savage PB, Teyton L, Bendelac A (2004) Lysosomal glycosphingolipid recognition by NKT cells. *Science* 306(5702):1786–1789. doi:[10.1126/science.1103440](https://doi.org/10.1126/science.1103440)
32. Xia C, Yao Q, Schumann J, Rossy E, Chen W, Zhu L, Zhang W, De Libero G, Wang PG (2006) Synthesis and biological evaluation of alpha-galactosylceramide (KRN7000) and isoglobotrihexosylceramide (iGb3). *Bioorg Med Chem Lett* 16(8):2195–2199. doi:[10.1016/j.bmcl.2006.01.040](https://doi.org/10.1016/j.bmcl.2006.01.040)
33. Porubsky S, Speak AO, Luckow B, Cerundolo V, Platt FM, Grone HJ (2007) Normal development and function of invariant natural killer T cells in mice with isoglobotrihexosylceramide

- (iGb3) deficiency. *Proc Natl Acad Sci USA* 104(14):5977–5982. doi:[10.1073/pnas.0611139104](https://doi.org/10.1073/pnas.0611139104)
34. Stanic AK, De Silva AD, Park JJ, Sriram V, Ichikawa S, Hirabayashi Y, Hayakawa K, Van Kaer L, Brutkiewicz RR, Joyce S (2003) Defective presentation of the CD1d1-restricted natural Va14Ja18 NKT lymphocyte antigen caused by beta-D-glucosylceramide synthase deficiency. *Proc Natl Acad Sci USA* 100(4):1849–1854. doi:[10.1073/pnas.0430327100](https://doi.org/10.1073/pnas.0430327100)
35. Zigmund E, Shalev Z, Pappo O, Alper R, Zolotarov L, Ilan Y (2008) NKT lymphocyte polarization determined by microenvironment signaling: a role for CD8 + lymphocytes and beta-glycosphingolipids. *J Autoimmun* 31(2):188–195. doi:[10.1016/j.jaut.2008.07.003](https://doi.org/10.1016/j.jaut.2008.07.003)
36. Oku H, Wongtangtintharn S, Iwasaki H, Inafuku M, Shimatani M, Toda T (2007) Tumor specific cytotoxicity of glucosylceramide. *Cancer Chemother Pharmacol* 60(6):767–775. doi:[10.1007/s00280-007-0422-y](https://doi.org/10.1007/s00280-007-0422-y)
37. Miyamoto K, Miyake S, Yamamura T (2001) A synthetic glycolipid prevents autoimmune encephalomyelitis by inducing TH2 bias of natural killer T cells. *Nature* 413(6855):531–534. doi:[10.1038/35097097](https://doi.org/10.1038/35097097)
38. Kobayashi E, Motoki K, Yamaguchi Y, Uchida T, Fukushima H, Koezuka Y (1996) Enhancing effects of alpha-, beta-monoglycosylceramides on natural killer cell activity. *Bioorg Med Chem* 4(4):615–619. (pii: 0968089696000491)

Three New Fatty Acid Esters from the Mushroom *Boletus pseudocalopus*

Ki Hyun Kim · Sang Un Choi · Kang Ro Lee

Received: 1 September 2011 / Accepted: 9 January 2012 / Published online: 24 January 2012
© AOCS 2012

Abstract A bioassay-guided fractionation and chemical investigation of a MeOH extract of the Korean wild mushroom *Boletus pseudocalopus* resulted in the identification of three new fatty acid esters, named calopusins A–C (**1–3**), along with two known fatty acid methyl esters (**4–5**). These new compounds are structurally unique fatty acid esters with a 2,3-butanediol moiety. Their structures were elucidated through 1D- and 2D-NMR spectroscopic data and GC–MS analysis as well as a modified Mosher's method. The new compounds **1–3** showed significant inhibitory activity against the proliferation of the tested cancer cell lines with IC₅₀ values in the range 2.77–12.51 μM.

Keywords *Boletus pseudocalopus* · Boletaceae · Fatty acid esters · Cytotoxicity

Abbreviations

SRB	Sulforhodamine B
HMBC	Heteronuclear multiple bond correlation
HMQC	Heteronuclear multiple quantum coherence
HR	High resolution
ESI	Electrospray ionization
EI	Electron-ionization
MS	Mass spectrometry
NMR	Nuclear magnetic resonance

K. H. Kim · K. R. Lee (✉)
Natural Products Laboratory, School of Pharmacy,
Sungkyunkwan University, 300 Chonchon-dong,
Jangan-ku, Suwon 440-746, Korea
e-mail: krlee@skku.ac.kr

S. U. Choi
Korea Research Institute of Chemical Technology,
Daejeon 305-600, Korea

Introduction

In our continuing search for structurally interesting and bioactive metabolites from Korean wild mushrooms [1–5], we have collected scores of endemic Korean mushroom species in the mountainous areas during the hot humid summer and prepared MeOH extracts of them for antitumor-activity screening tests. Among the collected wild mushrooms, the extract of *Boletus pseudocalopus* (Boletaceae) showed significant cytotoxicity against three human tumor cell lines (A549, Hs746T, and H3122) using a sulforhodamine B (SRB) bioassay [6]. *B. pseudocalopus* is an inedible mushroom with toxicity that is recognized by its yellow fruiting bodies and the blue staining when the fruiting bodies are cut or brushed [7], which is presumably due to the presence of the characteristic bolete pigments such as xerocomic acid, variegatic acid, and variegatorubin [8]. The isolation of cytotoxic grifolin derivatives was reported in a recent phytochemical study of this mushroom [8]. Bioassay-guided fractionation and chemical investigation of the MeOH extract of the fruiting bodies of *B. pseudocalopus* resulted in the isolation of three new fatty acid esters (**1–3**) with a 2,3-butanediol moiety, together with two known fatty acid methyl esters (**4–5**) (Fig. 1). In this study, we describe the isolation and structural elucidation of the three new fatty acid esters (**1–3**) from *B. pseudocalopus*, and the cytotoxic activities of the isolates (**1–5**).

Materials and Methods

General Experimental Procedures

Optical rotations were measured on a Jasco P-1020 polarimeter (Jasco, Easton, MD, USA). IR spectra were

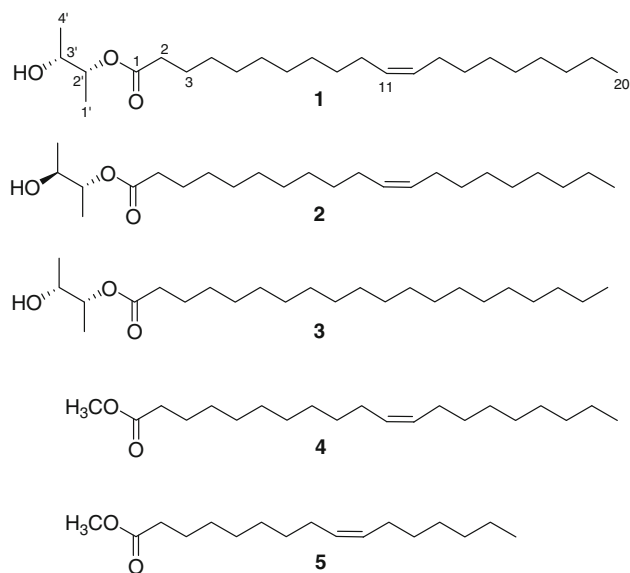


Fig. 1 The structures of the compounds 1–5

recorded on a Bruker IFS-66/S FT-IR spectrometer (Bruker, Karlsruhe, Germany). Electrospray ionization (ESI) and high-resolution (HR)-ESI mass spectra were recorded on a SI-2/LCQ DecaXP liquid chromatography (LC)-mass spectrometer (Thermo Scientific, West Palm Beach, FL, USA). Electron-ionization (EI) mass spectra were obtained on a JEOL JMS700 mass spectrometer (JEOL, Tokyo, Japan). Nuclear magnetic resonance (NMR) spectra were recorded on a Varian UNITY INOVA 500 NMR spectrometer (Varian, Palo Alto, CA, USA) operating at 500 MHz (^1H) and 125 MHz (^{13}C), with chemical shifts given in ppm (δ). Preparative high performance liquid chromatography (HPLC) used a Gilson 306 pump (Gilson, Middleton, WI, USA) with a Shodex refractive index detector (Shodex, New York, NY, USA). Low-pressure liquid chromatography (LPLC) was carried out over a LiChroprep Lobar-A Si 60 column (240×10 mm i.d.; Merck, Darmstadt, Germany) with a FMI QSY-0 pump (Teledyne Isco, Lincoln, NE, USA). Column chromatography was performed with silica gel 60 (Merck, 230–400 mesh). The packing material for molecular sieve column chromatography was Sephadex LH-20 (Pharmacia, Uppsala, Sweden). Merck precoated silica gel F₂₅₄ plates and reversed-phase (RP)-18 F_{254s} plates (Merck, Darmstadt, Germany) were used for thin-layer chromatography (TLC). Spots were detected on TLC under UV light or by heating after spraying with anisaldehyde-sulfuric acid.

Mushroom Material

The fresh fruiting bodies of *Boletus pseudocalopus* Hongo were collected on Mt. Gaya, Hapcheon-Gun of Gyeong-sangnam-do, Korea, in August, 2006. The mushroom was

identified by one of the authors (K.R.L.), according to the taxonomic key of Imazeki and Hongo [9]. A voucher specimen (SKKU 2006–08) was deposited in the herbarium of the School of Pharmacy, Sungkyunkwan University, Suwon, Korea.

Extraction and Isolation

The air-dried (30–40 °C for 20 h) and powdered fruiting bodies of *B. pseudocalopus* (139 g) were extracted twice with 80% aqueous MeOH (each 1.5 L \times 2 day) at room temperature and filtered. The filtrate was evaporated under vacuum to obtain a crude MeOH extract (10 g), which was suspended in distilled water and then successively partitioned with *n*-hexane, CHCl_3 , and *n*-BuOH, yielding 600, 700, and 2,100 mg of residues, respectively. Each fraction was evaluated for cytotoxicity against three human tumor cell lines (A549, Hs746T, and H3122) using an SRB bioassay. We selected the CHCl_3 -soluble fraction for the current phytochemical study, since the CHCl_3 -soluble fraction showed significant cytotoxic activity against the tested tumor cell lines. The CHCl_3 -soluble fraction (700 mg) was separated on a silica gel (230–400 mesh) column chromatography [50 g, 1.5×25 cm, eluted with CHCl_3 -MeOH, 10:1 (1.0 L) and 5:1 (1.0 L)] to yield six fractions [Fr. A, 10:1, 0.3 L; Fr. B, 10:1, 0.3 L; Fr. C, 10:1, 0.4 L; Fr. D, 5:1, 0.3 L; Fr. E, 5:1, 0.3 L; and Fr. F, 5:1, 0.4 L]. Fraction A (350 mg) was subjected to fractionation with Sephadex LH-20 column chromatography [320 g, 3×60 cm, eluted with CH_2Cl_2 -MeOH, 1:1 (2.0 L)] to give three subfractions [Fr. A1, 1:1, 0.7 L; Fr. A2, 1:1, 0.3 L; and Fr. A3, 1:1, 1.0 L]. Subfraction A2 (150 mg) was applied to LPLC on a LiChroprep Lobar-A Si gel 60 column (240×10 mm i.d., 40–63 μm) with a solvent system of CHCl_3 -MeOH (25:1, 800 mL) to give two fractions (A21–A22). Subfraction A21 (50 mg) was purified by preparative normal-phase HPLC using an Apollo Silica column (Alltech, 250 \times 10 mm i.d., 5 μm) with a solvent system of *n*-hexane-EtOAc (15:1, each 800 mL, flow rate; 2 mL/min) to obtain compounds **4** (5 mg) and **5** (7 mg). Subfraction A22 (65 mg) was purified by preparative normal-phase HPLC using an Apollo Silica column (Alltech, 250 \times 10 mm i.d., 5 μm) with a solvent system of *n*-hexane-EtOAc (5:1, each 800 mL, flow rate; 2 mL/min) to afford compounds **1** (4 mg), **2** (3 mg), and **3** (4 mg).

Calopusin A (**1**)

Colorless gum, $[\alpha]_{\text{D}}^{25} +11.6$ (*c* 0.12, CHCl_3); IR (KBr) ν_{max} 3,355 (OH), 2,943, 1,721 (C=O), 1,280, 1,028 cm^{-1} ; ^1H (500 MHz) and ^{13}C (125 MHz) NMR data, see Table 1; ESI-MS (positive mode) m/z 405 $[\text{M} + \text{Na}]^+$; HRESIMS m/z 405.3347 $[\text{M} + \text{Na}]^+$ (calcd. for $\text{C}_{24}\text{H}_{46}\text{NaO}_3$, 405.3345).

Table 1 ^1H (500 MHz) and ^{13}C -NMR (125 MHz) data of **1–3** in CDCl_3 (δ in ppm)^a

Position	1		2		3	
	δ_{H}	δ_{C}	δ_{H}	δ_{C}	δ_{H}	δ_{C}
1		173.7		173.6		173.5
2	2.31 (t, 7.5)	34.8	2.31 (t, 7.5)	34.8	2.31 (t, 7.5)	34.8
3	1.63 (m)	25.2	1.63 (m)	25.2	1.63 (m)	25.2
4	1.25 (br s)	29.8–29.3	1.25 (br s)	29.6–29.3	1.26 (br s)	29.6–29.2
5	1.25 (br s)	29.8–29.3	1.25 (br s)	29.6–29.3	1.26 (br s)	29.6–29.2
6	1.25 (br s)	29.8–29.3	1.25 (br s)	29.6–29.3	1.26 (br s)	29.6–29.2
7	1.25 (br s)	29.8–29.3	1.25 (br s)	29.6–29.3	1.26 (br s)	29.6–29.2
8	1.25 (br s)	29.8–29.3	1.25 (br s)	29.6–29.3	1.26 (br s)	29.6–29.2
9	1.25 (br s)	29.8–29.3	1.25 (br s)	29.6–29.3	1.26 (br s)	29.6–29.2
10	2.01 (m)	27.4	2.01 (m)	27.4	1.26 (br s)	29.6–29.2
11	5.34 (m)	130.2 ^b	5.34 (m)	130.2 ^c	1.26 (br s)	29.6–29.2
12	5.34 (m)	129.9 ^b	5.34 (m)	129.9 ^c	1.26 (br s)	29.6–29.2
13	2.01 (m)	27.4	2.01 (m)	27.4	1.26 (br s)	29.6–29.2
14	1.25 (br s)	29.8–29.3	1.25 (br s)	29.6–29.3	1.26 (br s)	29.6–29.2
15	1.25 (br s)	29.8–29.3	1.25 (br s)	29.6–29.3	1.26 (br s)	29.6–29.2
16	1.25 (br s)	29.8–29.3	1.25 (br s)	29.6–29.3	1.26 (br s)	29.6–29.2
17	1.25 (br s)	29.8–29.3	1.25 (br s)	29.6–29.3	1.26 (br s)	29.6–29.2
18	1.27 (m)	31.4	1.27 (m)	32.1	1.27 (m)	32.1
19	1.30 (m)	22.9	1.30 (m)	22.8	1.32 (m)	22.9
20	0.88 (t, 7.0)	14.3	0.88 (t, 7.0)	14.3	0.88 (t, 7.0)	14.3
1'	1.19 (d, 6.5)	16.5	1.18 (d, 6.5)	14.3	1.19 (d, 6.5)	16.5
2'	4.77 (m)	74.8	4.87 (m)	74.3	4.77 (m)	74.7
3'	3.75 (m)	70.3	3.87 (m)	69.8	3.75 (m)	70.3
4'	1.17 (d, 6.5)	19.3	1.16 (d, 6.5)	18.0	1.17 (d, 6.5)	19.3

^a *J* values are in parentheses and reported in Hz; the assignments were based on HMQC, and HMBC experiments

^{b,c} Assignments may be interchangeable

Calopusin B (2)

Colorless gum, $[\alpha]_{\text{D}}^{25} -10.7$ (*c* 0.14, CHCl_3); IR (KBr) ν_{max} 3,356 (OH), 2,943, 1,720 (C=O), 1,280, 1,028 cm^{-1} ; ^1H (500 MHz) and ^{13}C (125 MHz) NMR data, see Table 1; ESI-MS (positive mode) m/z 405 $[\text{M} + \text{Na}]^+$; HRESIMS m/z 405.3353 $[\text{M} + \text{Na}]^+$ (calcd. for $\text{C}_{24}\text{H}_{46}\text{NaO}_3$, 405.3345).

Calopusin C (3)

Colorless gum, $[\alpha]_{\text{D}}^{25} +13.8$ (*c* 0.18, CHCl_3); IR (KBr) ν_{max} 3,355 (OH), 2,943, 1,721 (C=O), 1,280, 1,028 cm^{-1} ; ^1H (500 MHz) and ^{13}C (125 MHz) NMR data, see Table 1; ESI-MS (positive mode) m/z 407 $[\text{M} + \text{Na}]^+$; HRESIMS m/z 407.3507 $[\text{M} + \text{Na}]^+$ (calcd. for $\text{C}_{24}\text{H}_{48}\text{NaO}_3$, 407.3501).

Alkaline Hydrolysis of 1–3

Hydrolysis of **1–3** (each 1.0 mg) was performed with 5% KOH in MeOH (10 ml) under reflux for 2 h. After cooling,

each reaction mixture was diluted with H_2O and extracted with CHCl_3 . The organic layer was washed with H_2O and filtered. The filtrate was chromatographed by a silica gel Waters Sep-Pak Vac 6 cc (Waters) with a solvent system of *n*-hexane–EtOAc (15:1) to give the fatty acid part. Methyl ester derivatives of fatty acids from **1–3** were prepared by refluxing fatty acids with 1% H_2SO_4 in MeOH (10 ml) for 1 h. The methyl ester mixture was analyzed with GC–MS. The GC–MS analyses were carried out using a Hewlett Packard 6,890–5,973 N GC–MS system operating on electron impact mode (equipped with a HP-5MS UI 60×0.25 mm, 0.25 μm film thickness capillary column). Helium (1.5 ml/min) was used as the carrier gas. The initial temperature of the column was 60 °C, and then heated to 280 °C at a rate of 3 °C/min. The identification of the fatty acid esters was based on comparison of their EI-mass spectra with the NIST/NBS, Wiley library spectra. The aqueous layer was neutralized by passage through an Amberlite IRA-67 column (Rohm and Haas) and was repeatedly evaporated to give each 2,3-butanediol moiety.

The 2,3-butanediol from **1** and **3** showed the negative optical rotation, $[\alpha]_D^{25} - 16.3$ (c 0.07, CHCl_3) and the $^1\text{H-NMR}$ data was consistent with commercial sample (*R,R*)-2,3-butanediol. The $^1\text{H-NMR}$ data of the 2,3-butanediol, $[\alpha]_D^{25} + 10.8$ (c 0.05, CHCl_3) from **2** was consistent with commercial sample, *meso*-2,3-butanediol.

Preparation of the (*R*)- and (*S*)-MTPA Ester Derivatives of **1–3**

To a stirred solution of **1** (1.0 mg) in pyridine (400 μL) was added 4-(dimethylamino)pyridine (1 mg) and (*S*)-(+)- α -methoxy- α -(trifluoromethyl)phenylacetyl chloride (MTPA-Cl, 10 μL). The mixture was stirred at room temperature for 16 h. The reaction mixture was then passed through a silica gel Waters Sep-Pak Vac 6 cc and eluted with *n*-hexane–EtOAc (15:1) to give the respective (*R*)-Mosher ester **1r**. Treatment of **1** (1.0 mg) with (*R*)-MTPA-Cl (10 μL) as described above yielded the corresponding (*S*)-MTPA ester **1s**. Similarly, treatment of **2** and **3** with (*S*)- and (*R*)-MTPA-Cl afforded the respective Mosher esters **2r**, **2s**, **3r**, and **3s** (Table 2).

Cytotoxicity Testing

A sulforhodamine B (SRB) bioassay was used to determine the cytotoxicity of each compound against four cultured human tumor cell lines [6]. The assays were performed at the Korea Research Institute of Chemical Technology. The cell lines used were A549 (lung carcinoma), Hs756T (stomach carcinoma), H3122 (non-small cell lung carcinoma) and HUVEC (human umbilical cord endothelial cells). The cancer cell lines such as A549, Hs756T, and H3122 cells were provided by the National Cancer Institute (NCI). A normal cell line, HUVEC, was purchased from the American Type Culture Collection. Etoposide (purity $\geq 98\%$, Sigma) was used as a positive control. The cytotoxicities of etoposide against the A549, Hs756T, and H3122 cell lines were IC_{50} 0.24, 0.12, and 0.84 μM , respectively. Tested compounds were demonstrated to be pure as evidenced by NMR and HPLC analyses (purity $\geq 95\%$).

Results

The fruiting bodies of *B. pseudocalopus* were extracted with 80% aqueous MeOH. The methanolic extract showed cytotoxicity against some human tumor cell lines using a SRB bioassay in our screening procedures. Bioassay-guided fractionation and chemical investigation of the extract using successive column chromatography over silica gel and Sephadex LH-20, and preparative HPLC resulted in the isolation and identification of three new fatty acid esters (**1–3**), together with two known fatty acid methyl esters (**4–5**) (Fig. 1). Their structures were elucidated as follows.

Compound **1** was isolated as a colorless gum. The molecular formula of **1** was determined to be $\text{C}_{24}\text{H}_{46}\text{O}_3$ by positive mode HRESIMS data at m/z 405.3347 $[\text{M} + \text{Na}]^+$ (calcd. for $\text{C}_{24}\text{H}_{46}\text{NaO}_3$, 405.3345). The IR spectrum indicated that **1** possessed hydroxyl ($3,355\text{ cm}^{-1}$) and carbonyl ($1,721\text{ cm}^{-1}$) groups. The $^1\text{H-NMR}$ spectrum of **1** (Table 1) was similar to that of **4** [10], except that the proton and carbon resonances of a methoxy group in **4** were absent, and the resonances of a 2,3-butanediol moiety at δ_{H} 4.77 (1H, m, H-2'), 3.75 (1H, m, H-3'), 1.19 (3H, d, $J = 6.5\text{ Hz}$, H-1'), and 1.17 (3H, d, $J = 6.5\text{ Hz}$, H-4'); δ_{C} 74.8 (C-2'), 70.3 (C-3'), 19.3 (C-4'), and 16.5 (C-1') were present in **1** [11]. This structure was confirmed by the HMBC spectrum (Fig. 2), where HMBC correlation between H-2' (δ_{H} 4.77) and C-1 (δ_{C} 173.7) indicated the linkage of the 2,3-butanediol unit at C-1. Alkaline hydrolysis of **1** afforded a 2,3-butanediol moiety and a fatty acid unit. The fatty acid unit after esterification with methanol was analyzed as a methyl ester using GC–MS and was identified as methyl 11(*Z*)-eicosenoate (**4**). The double bond position was further confirmed by analysis of the mass fragmentation in the EIMS data (Fig. 2). The absolute configuration of the 2,3-butanediol unit was determined using a modified Mosher's method [12]. Treatment of **1** with (*R*)- and (*S*)-MTPA-Cl gave the (*S*)- and (*R*)-MTPA esters **1s** and **1r**, respectively. The $^1\text{H-NMR}$ signals of the two MTPA esters (Table 2) were assigned on the basis of their $^1\text{H-}^1\text{H-COSY}$ spectra, and the $\Delta\delta$ values ($\delta_{\text{S}} - \delta_{\text{R}}$) were then calculated (Fig. 3). The results indicated that the

Table 2 Partial $^1\text{H-NMR}$ data of the (*S*)- and (*R*)-MTPA esters of **1–3** in CDCl_3 (δ in ppm, 500 MHz)

H	1			2			3		
	(<i>S</i>)-Isomer	(<i>R</i>)-Isomer	$\Delta\delta_{\text{H}(\text{S-R})}$	(<i>S</i>)-Isomer	(<i>R</i>)-Isomer	$\Delta\delta_{\text{H}(\text{S-R})}$	(<i>S</i>)-Isomer	(<i>R</i>)-Isomer	$\Delta\delta_{\text{H}(\text{S-R})}$
1'	1.256	1.315	−0.059	1.255	1.247	+0.008	1.249	1.314	−0.065
2'	5.160	5.185	−0.025	5.335	5.324	+0.011	5.168	5.174	−0.006
3'	4.999	4.987	+0.012	5.171	5.152	+0.019	4.993	4.988	+0.005
4'	1.213	1.143	+0.070	1.135	1.142	−0.007	1.221	1.139	+0.082

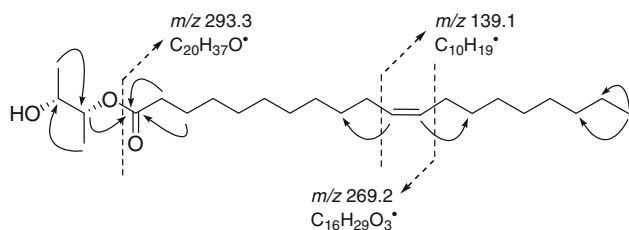
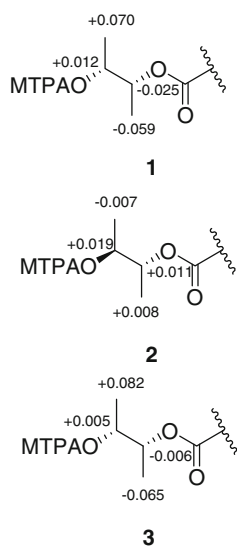


Fig. 2 Key HMBC connectivities and EIMS fragmentation of **1**

absolute configuration of **1** was $3'R$. Moreover, the chemical shifts for H-2' (δ_H 4.77) and H-3' (δ_H 3.75) suggested that these protons have a *cis*-orientation, which was in agreement with that of the monoacetate of *dl*-butane-2,3-diol [δ_H 4.75 (H-2) and δ_H 3.73 (H-3)] [11] and the 2,3-butanediol obtained by hydrolysis of **1** showed the negative optical rotation, $[\alpha]_D^{25} - 16.3$ (*c* 0.07, CHCl_3), in agreement with that of (*R,R*)-2,3-butanediol [13, 14]. Thus, the absolute configuration at C-2' was confirmed to be *R*. In conclusion, the structure of **1** was elucidated as shown in Fig. 1, and named calopusin A.

Compound **2** was obtained as a colorless gum. The molecular formula of **2** was deduced to be $\text{C}_{24}\text{H}_{46}\text{O}_3$ by positive mode HRESIMS data at m/z 405.3353 [$\text{M} + \text{Na}$] $^+$ (calcd. for $\text{C}_{24}\text{H}_{46}\text{NaO}_3$, 405.3345). The ^1H -NMR data of **2** (Table 1) was very similar to that of **1**, except for the chemical shift and splitting pattern of H-2' (δ_H 4.87) and H-3' (δ_H 3.87) in **2** instead of those of H-2' (δ_H 4.77) and H-3' (δ_H 3.75) in **1**, which suggested that compound **2** possessed a *meso*-butane-2,3-diol unit on the basis of the chemical shifts of the monoacetate of *meso*-butane-2,3-diol [δ_H 4.86 (H-2) and δ_H 3.88 (H-3)] [11]. This was further supported by the identical ^1H -NMR data of the 2,3-butanediol obtained by hydrolysis of **2** to commercial sample, *meso*-2,3-butanediol. Analysis of the HMQC and

Fig. 3 $\Delta\delta$ Values ($\delta_S - \delta_R$) in ppm of the two MTPA esters derived from **1–3**



HMBC correlations led to the establishment of the structure for **2**. As described for **1**, the absolute configuration of **2** was determined using a modified Mosher's method [12], which proved the *S*-configuration for C-3' (Fig. 3). Then, the absolute configuration of C-2' was determined to be the *R*-configuration because compound **2** contained a *meso*-butane-2,3-diol unit. Thus, the structure of **2** was assigned as shown in Fig. 1, and named calopusin B.

Compound **3** was isolated as a colorless gum, and had a molecular formula of $\text{C}_{24}\text{H}_{48}\text{O}_3$, as determined by positive mode HRESIMS at m/z 407.3507 [$\text{M} + \text{Na}$] $^+$ (calcd. for $\text{C}_{24}\text{H}_{48}\text{NaO}_3$, 407.3501). The ^1H and ^{13}C -NMR data of **3** (Table 1) were very similar to those of **1**, except for the absence of the chemical shifts attributable to a double bond in **1** [δ_H 5.34 (2H, m, H-11 and H-12); δ_C 130.2 (C-11) and 129.9 (C-12)]. The structure of **3** was confirmed by analysis of 2D-NMR experiments (HMQC and HMBC). As described for **1**, the absolute configuration of **3** was also determined using a modified Mosher's method [12], which proved the *R*-configuration for C-3' (Fig. 3). Then, the absolute configuration of C-2' was assigned as *R* on the basis of the identical chemical shifts for H-2' (δ_H 4.77) and H-3' (δ_H 3.75) of **3** to those of **1**. Thus, the structure of **3** was determined as shown in Fig. 1, and named calopusin C.

The known fatty acid methyl esters were identified as methyl 11(*Z*)-eicosenoate (**4**) [10] and methyl palmitoleate (**5**) [10] by comparison of their spectroscopic data to previously reported values and analysis of GC-MS.

Discussion

The cytotoxic CHCl_3 -soluble fraction from the MeOH extract of *B. pseudocalopus* was separated by repeated column chromatography to obtain compounds **1–5**. Compounds **1–5** were evaluated for their antiproliferative activities against three human cancer cell lines (A549, Hs756T, and H3122) using the SRB bioassay [6]. Compounds **1–3** showed significant inhibitory activity against proliferation of the tested cancer cell lines with IC_{50} values in the range 2.77–12.51 μM (Table 3). However, the known fatty acid methyl esters (**4–5**) without a 2,3-butanediol group were inactive ($\text{IC}_{50} > 20 \mu\text{M}$). In previous studies, the antitumor effect of synthetic 2,3-butanediol fatty acid esters was reported and coixenolide with antitumor activity was isolated from *Coix lacryma-jobi* seeds, which is a mixed ester of palmitoleic acid and vaccenic acid with the 2,3-butanediol [15, 16]. To confirm whether the 2,3-butanediol unit itself is cytotoxic against the tested cell lines, both of (*R,R*)-2,3-butanediol and (*R,S*)-2,3-butanediol obtained by hydrolysis of **1–3** were evaluated for cytotoxicity against three human cancer cell lines

Table 3 Cytotoxicity of fractions and compounds **1–5** against a human normal cell line and three human cancer cell lines using SRB bioassay

Fractions and compounds	IC ₅₀ (μM) ^a			
	A549	Hs746T	H3122	HUVEC
<i>n</i> -hexane-soluble fraction	47.81	37.89	55.43	–
CHCl ₃ -soluble fraction	11.42	6.75	20.15	–
<i>n</i> -BuOH-soluble fraction	63.01	58.92	70.33	–
Fraction A	13.40	5.17	18.62	–
Fraction B	20.86	18.64	17.89	–
Fraction C	32.34	27.47	33.07	–
Fraction D	34.20	40.81	47.90	–
Fraction E	38.71	37.19	48.32	–
Fraction F	26.18	19.54	40.52	–
Fraction A1	18.60	9.45	23.79	–
Fraction A2	10.36	6.28	15.34	–
Fraction A3	21.15	12.42	18.67	–
Fraction A21	15.77	11.16	18.81	–
Fraction A22	7.74	4.82	13.74	–
1	4.97	3.65	12.51	30.97
2	6.02	5.37	9.07	42.92
3	4.04	2.77	8.26	41.71
4	35.30	24.41	66.16	55.27
5	44.59	29.65	60.06	59.59
Etoposide ^b	0.24	0.12	0.84	1.86
Gemcitabine ^c	0.01	0.09	0.01	3.12

^a IC₅₀ value of compounds against each tested cell line, which was defined as the concentration (μM) that caused 50% inhibition of cell growth in vitro

^b Etoposide as a positive control

^c Gemcitabine as a reference compound

(A549, Hs756T, and H3122). But they were inactive (IC₅₀ > 20 μM). These results demonstrate that though the 2,3-butanediol itself is inactive, it improves antitumor activity in such fatty acid esters. To establish whether cytotoxicity exhibited by compounds **1–3** was selective between tumor and normal cells, these compounds were tested against a normal human cell line, HUVEC. The results (Table 3) showed that **1–3** were more cytotoxic against tumor cells than normal cells, indicating that **1–3** exhibited selective toxicity. In particular, compound **3** showed the highest selective cytotoxicity for Hs746T cell line since it exhibited the greatest selectivity index (SI) value of 15.1. The SI value was obtained by dividing the IC₅₀ value for the normal cell line by the IC₅₀ value for the tumor cell line.

In conclusion, we focused our investigation on cytotoxic constituents from the fruiting bodies of *B. pseudocalopus* and identified five fatty acid esters including three new compounds, calopusins A-C (**1–3**) showing significant cytotoxicity. Calopusins A-C (**1–3**), which displayed high selective toxicity against the A549, Hs746T, and H3122 cell lines, may be especially promising for developing an effective drug for lung and stomach cancer in this regard.

Acknowledgments This research was supported by the Basic Science Research Program through the National Research Foundation of Korea (NRF), funded by the Ministry of Education, Science and

Technology (2011-0004672). We thank Drs. E. J. Bang, S. G. Kim, and J. J. Seo at the Korea Basic Science Institute for their assistance with the NMR spectroscopic and mass spectrometric measurements.

Conflict of interest All authors declare that there are no conflicts of interest.

References

- Kim KH, Choi SU, Park KM, Seok SJ, Lee KR (2008) Cytotoxic constituents of *Amanita subjunquillea*. Arch Pharm Res 31: 579–586
- Kim KH, Choi SU, Lee KR (2009) Neomastoidin A, a novel monoacylglycerol with an amino acid moiety from *Macrolepiota neomastoidea*. Chem Lett 38:894–895
- Kim KH, Park KM, Choi SU, Lee KR (2009) Macrolepiotin, a new indole alkaloid from *Macrolepiota neomastoidea*. J Antibiot 62:335–338
- Kim KH, Noh HJ, Choi SU, Park KM, Seok SJ, Lee KR (2010) Russulfoen, a new cytotoxic marasmane sesquiterpene from *Russula foetens*. J Antibiot 63:575–577
- Kim KH, Noh HJ, Choi SU, Park KM, Seok SJ, Lee KR (2010) Lactarane sesquiterpenoids from *Lactarius subvellereus* and their cytotoxicity. Bioorg Med Chem Lett 20:5385–5388
- Skehan P, Storeng R, Scudiero D, Monks A, McMahon J, Vistica D, Warren JT, Bokesch H, Kenney S, Boyd MR (1990) New colorimetric cytotoxicity assay for anticancer-drug screening. J Natl Cancer Inst 82:1107–1112
- Cho DH (2009) Mushrooms and Poisonous Fungi in Korea: Iljinsa Seoul, p 365

8. Song J, Manir MM, Moon SS (2009) Cytotoxic grifolin derivatives isolated from the wild mushroom *Boletus pseudocalopus* (Basidiomycetes). *Chem Biodivers* 6:1435–1442
9. Imazeki R, Hongo T (1989) Colored illustrations of mushrooms of Japan: vol. 2, Hoikusha Osaka, p 159
10. Bernassau JM, Fetizon M (1981) Longitudinal relaxation times and structure elucidation-I: fatty acids and esters. *Tetrahedron* 37:2105–2109
11. Bisht KS, Parmar VS, Crout DHG (1993) Diastereo- and enantio-selective esterification of butane-2,3-diol catalysed by the lipase from *Pseudomonas fluorescens*. *Tetrahedron Asymmetr* 4:957–958
12. Kim KH, Choi SU, Kim YC, Lee KR (2011) Tirucallane triterpenoids from *Cornus walteri*. *J Nat Prod* 74:54–59
13. Tartaglia S, Padula D, Scafato P, Chiummiento L, Rosini C (2008) A chemical/computational approach to the determination of absolute configuration of flexible and transparent molecules: aliphatic diols as a case study. *J Org Chem* 73:4865–4873
14. Bortolini O, Fantin G, Fogagnolo M, Giovannini PP, Guerrini A, Medici A (1997) An easy approach to the synthesis of optically active vic-diols: a new single-enzyme system. *J Org Chem* 62:1854–1856
15. Fukui Y, Yamato M, Umeda N, Kawasaki M (1985) Butanediol derivatives. *Jpn Kokai Tokkyo Koho, JP Patent 60252448*
16. Ukita C, Tanimura A (1961) Studies on the antitumor component in the seeds of *Coix lacryma-jobi* L. var. *ma-yuen* (Roman) Stapf. I. Isolation and anti-tumor activity of coixenolide. *Chem Pharm Bull* 9:43–46

A Novel Fatty Acid, 12,17-Dimethyloctadecanoic Acid, from the Extremophile *Thermogemmatispora* sp. (Strain T81)

M. Vyssotski · J. Ryan · K. Lagutin ·
H. Wong · X. Morgan · M. Stott

Received: 21 December 2011 / Accepted: 13 March 2012 / Published online: 5 April 2012
© AOCS 2012

Abstract The major fatty acids of a novel species of *Thermogemmatispora* sp. (strain T81) from the phylum *Chloroflexi* were identified as *i*18:0 (42.8 % of total fatty acids), *i*19:0 (9.7 %), and *i*17:0 (5.9 %). Also observed was a number of unidentified fatty acids, including a major acid (16.3 %) with ECL of 19.04 (BP1), and 18.76 (TG-WAXMS A). GCMS revealed that this compound is a saturated 20-carbon atom fatty acid. ^1H - and ^{13}C -NMR, with ^1H - ^1H -COSY and ^1H - ^{13}C -HSQC experiments suggested the structure of dimethyl octadecanoic acid with *iso*-branching, and an extra middle-chain methyl group. A pyrrolidide derivative demonstrated the characteristic gaps in GCMS indicating methyl branching at C12 and C17, which was eventually confirmed by a ^1H - ^{13}C -HSQC-TOCSY experiment. This 12,17-dimethyloctadecanoic acid has not been previously detected or described in these organisms. However, a recent description of a phylogenetically related species of *Thermogemmatispora* (Yabe et al., Int J Syst Evol Microbiol 61:903–910, 2010), noted an unidentified 20:0 fatty acid with matching GC behavior and GCMS data to that of strain T81. These data suggest that *Thermogemmatispora* share an ability to synthesize the same fatty acid. A number of other dimethyl-branched fatty

acids, namely 8,14-diMe 15:0; 12,15-diMe 16:0; 10,15-diMe 16:0; 12,16-diMe 17:0; 10,16-diMe 17:0; 12,17-diMe 18:0; 12,18-diMe 19:0; 14,19-diMe 20:0, were also identified in strain T81.

Keywords Extremophile · Bacterial fatty acids · Branched · *Chloroflexi* · *Thermogemmatispora*

Abbreviations

<i>ai</i>	<i>anteiso</i>
BSTFA	<i>N,O</i> -bis(trimethylsilyl)trifluoroacetamide
diMe	Dimethyl
ECL	Equivalent chain length
FAME	Fatty acids methyl esters
HPTLC	High performance thin-layer chromatography
EI	Electron impact
SPE	Solid phase extraction
<i>i</i>	<i>iso</i>

Introduction

Thermogemmatispora sp. T81 (T81 = ICMP 18709^T = DSMZ 45540^T) is a recently described thermophilic, aerobic, Gram-positive bacterium isolated from geothermal soil in Tikitere, New Zealand [1]. It belongs to the phylum *Chloroflexi* in the newly described genus *Thermogemmatispora* in which there are two validly described strains (*T. onikobensis* and *T. foliorum*). Strain T81 grows well on mono and di-saccharide carbon sources as well as lignocellulosic wood pulps, and a wide variety of polysaccharide compounds. The bacteria is able to grow between 45 and 70 °C with an optimum temperature of 50–60 °C, and tolerates pH 3.1–7.1 with an optimum growth pH of

Part of this work was presented at the 102nd AOCS Annual Meeting (Cincinnati, May 2011).

M. Vyssotski (✉) · J. Ryan · K. Lagutin · H. Wong
Industrial Research Limited, PO Box 31-310, Lower Hutt 5040,
New Zealand
e-mail: m.vyssotski@irl.cri.nz

X. Morgan · M. Stott
GNS Science, Extremophiles Research Group, Private Bag 2000,
Taupo 3352, New Zealand

4.6–6.0. Strain T81 differs from the validly described strains of *Thermogemmatispora* in guanine-cytosine content, morphology, salt tolerance, preferred pH, and substrate utilization [unpublished] and is likely to represent a novel *Thermogemmatispora* species.

The fatty acids profiles between strain T81, *T. onikobensis* and *T. foliorum* vary significantly [2]. The major fatty acids in *T. onikobensis* and *T. foliorum*, are *i*17:0 (44.1 and 44.9 %), and *i*19:0 (19.3 and 27.3 %), while in strain T81 these fatty acids are only minor components (5.9 and 9.7 %, respectively). The major fatty acid in T81 is *i*18:0 (42.8 %), which comprises only 2.2 % of the fatty acids of *T. onikobensis* and *T. foliorum*. Both the *T. onikobensis* and *T. foliorum* strains contained relatively high levels of an unidentified fatty acid (26.55 and 14.56 % of total fatty acids, respectively), the methyl ester of which possessed an ECL of 19.032 (on methyl silicone phase). T81 also possesses a number of unidentified fatty acids [3].

The present publication describes fatty acids of this unique organism, including the discovery of a number of novel dimethyl-branched fatty acids, which may be a distinctive feature of *Thermogemmatispora* species.

Materials and Methods

Fermentation

T81 was cultivated under aerobic conditions in both 250-mL Erlenmeyer shake flasks and a 20-L Braun Bioreactor (Biostat C-DCU 20-3 Melsungen, Germany). The growth media used was a modified OP10A liquid mineral salts medium (2.0 g L⁻¹ soluble starch, 1.0 g L⁻¹ yeast extract, 0.8 g L⁻¹ (NH₄)₂SO₄, 0.1 g L⁻¹ KH₂PO₄, 0.04 g L⁻¹ MgSO₄ × 7H₂O, 0.02 g L⁻¹ CaCl₂, 3 mL L⁻¹ FeEDTA solution, 3 mL L⁻¹ methanotrophs trace metal solution, 1 mL L⁻¹ Wolin trace solution) [1]. The biomass produced in the shake flasks which were agitated at 150 rpm and incubated at 60 °C (Infors Multitron 2, Bottmingen, Switzerland) for 72 h. The biomass produced in the 20-L bioreactor was grown at 60 °C with 100 rpm agitation, 5–15 L/min airflow and pH control (5.0) for 72 h. The dry cell weight at the end of 72 h was 1.4 g/L of medium for both shake flasks and bioreactor samples.

Lipid Extraction

The wet biomass from the 100-mL shake flasks was extracted using the method of Bligh and Dyer [4], yielding lipids at 0.2 % by weight. The biomass produced in 20-L fermenters was transmethylated according to Lewis et al. [5].

Fatty Acids Analysis

Fatty acid methyl esters were prepared from small samples of biomass without lipid extraction and analyzed as described by Svetashev et al. [6]. For detailed analysis, fatty acid methyl esters were prepared from the lipid extracts according to the method of Carreau and Dubacq [7], and purified by SPE on a 500-mg Strata SI-1 cartridge (Phenomenex, USA) conditioned with hexane. Hydrocarbons were eluted with 3 mL of hexane, and fatty acids methyl esters were eluted with 6 mL of hexane-diethyl ether (99:1, by v/v). The method used was identical to the procedure presented elsewhere [[8], the third procedure], with the only exception being the use of a solid phase extraction SPE cartridge in place of a Silica gel 60 column. In a separate experiment the lipid extract was fractionated into neutral and polar lipid fractions prior to transesterification. A silica gel SPE cartridge was used, with neutral lipids eluted by chloroform, and polar lipids by methanol.

GLC analysis of fatty acid methyl esters was performed on a TraceGC Ultra instrument (ThermoFinnigan, USA), equipped with FID and 30 m, 0.25 mm i.d. Trace Gold TG-WAXMS A capillary column (Thermo Scientific, USA). Helium was used as the carrier gas; the split ratio was 1:60. Separation temperature was 195 °C. When non-polar BP1 (60 m, 0.32 mm i.d.) methyl silicone capillary column (SGE, Australia) was used, the separation temperature was maintained at 220 °C. Fatty acids were identified by the use of reference compounds, the known ECL values for methyl silicone column [9], and by GCMS (see below). Hydrogenation of fatty acid methyl esters was performed according to Appelqvist [10].

To prepare trimethylsilyl derivatives 30 µL of *N,O*-bis(trimethylsilyl)trifluoroacetamide (BSTFA) with 1 % trimethylchlorosilane (Aldrich, USA) was added to approximately 0.2 mg of the sample in 10 µL of pyridine. The reaction mixture was maintained for 30 min at 60 °C. The sample was either analyzed directly, or was evaporated under a stream of argon and re-dissolved in 0.5 mL of hexane prior to the injection.

Pyrrolidides were prepared according to the procedure described in [11]. Briefly, ~0.1 mg of FAME was dissolved in 50 µL pyrrolidine, 5 µL acetic acid and maintained at 100 °C for 1 h. Unreacted pyrrolidine was removed in the stream of argon. The residue was taken up by 2 mL of hexane-diethyl ether (1:1, by v/v) and washed with 4 × 0.5 mL water. The hexane layer was collected, and the solvent removed under a stream of argon. The residue was dissolved in 1 mL hexane and pyrrolidides analyzed by GCMS.

GCMS analyzes were performed on an Agilent 5890 N gas chromatograph equipped with a 5973 Inert mass-spectrometric detector and HP-5 capillary column (30 m,

0.32 mm i.d.; Hewlett-Packard, USA). Helium was used as the carrier gas. Analysis of FAME and pyrrolidides was initiated at 100 °C (held for 6 min), with the temperature increased at a rate of 5 °C/min up to 160 °C, followed by a rate of 1 °C/min to 240 °C, and then maintained for 25 min.

Preparative HPLC separation of the fatty acids methyl esters was carried out using a Gilson 321 preparative HPLC pump, Agilent 1100 photodiode array detector (at 205 nm), C12 column (Synergy 4 μ Max-RP 80A 250 \times 30.00 mm) with guard column (Phenomenex Security-Guard cartridge C12 15 \times 30.00 mm). Data was collected and analyzed using Gilson Unipoint 3.20 software. Solvents used were: Solvent A: water; Solvent B: acetonitrile. The eluent flow rate was 20 mL/min. The concentration of injected sample was 200 mg/mL in ethanol, 1 mL was injected. The eluent gradient employed was: 0 min—80 % Solvent A, 20 % Solvent B; 8–26 min—10 % Solvent A, 90 % Solvent B; 28 min—100 % Solvent B.

NMR Spectroscopy

All ^1H - and ^{13}C -NMR spectra of fatty acids dissolved in CDCl_3 and referenced to internal TMS at 0 ppm were obtained on a Bruker Avance-III 500 Spectrometer equipped with a Bruker 5-mm broadband probe at 303 K. ^1H , ^{13}C frequencies were 499.8, 125.7 MHz respectively and 90° pulses 13.0, 14.0 μs , respectively. Standard Bruker supplied NMR pulse programs were used for recording all spectra. Pulse program COSYGPMFQF was used to record the gradient selected absolute value proton homonuclear double quantum filtered COSY spectrum. Phase sensitive gradient selected pulse programs HSQCETGP and HSQCETGPMML were used for the two-dimensional (2D) inverse detected ^1H , ^{13}C heteronuclear (HSQC) and HSQC-total correlation (HSQC-TOCSY) spectra with isotropic proton mixing respectively [12].

Parameters for the ^1H spectrum were: sweep width 10,302 Hz, 65,536 data points, 30° excitation pulse, 32 transients taken, each with a 1 s delay time and f.i.d. acquisition time of 3.18 s. Spectra were processed with a standard exponential weighting function with 0.3 Hz line broadening before Fourier transformation. Parameters for the WALTZ ^1H decoupled ^{13}C spectrum were: 30° excitation pulse, sweep width 31,250 Hz, 65,536 data points, 4,192 transients taken each with 0.5 s delay time and f.i.d. acquisition time of 1.05 s for a total acquisition time of 2 h. Spectra were processed with a standard exponential weighting function with 5 Hz line broadening before Fourier transformation. Parameters for the WALTZ ^1H decoupled DEPT90- and DEPT135 ^{13}C spectra were: sweep width 7,530 Hz (narrowed down to focus on the protonated carbon signals of interest), 32,768 data points,

2,048 transients taken each with delay time 0.2 s and f.i.d. acquisition time of 2.18 s for a total acquisition time of 1.5 h. Spectra were processed with a standard exponential weighting function with 5 Hz line broadening before Fourier transformation.

Parameters for the proton homonuclear double quantum filtered COSY spectrum were: two transients taken each with delay time 1.69 s and f.i.d. acquisition time 0.46 s, sweep width F2 2,222 Hz in 2,048 data points, sweep width F1 2,222 Hz in 320 slices for a total acquisition time of 25 min. The absolute value spectrum was processed with a sine bell window function in both directions. Parameters for the HSQC-TOCSY spectrum were: 24 transients taken each with delay time 0.96 s and acquisition time 0.46 s, sweep width F2 2,212 Hz in 1,024 real points, sweep width F1 3,142 Hz in 512 slices, MLEV17 mixing at 8.3 kHz for 60 ms. ^{13}C GARP decoupling (globally optimized alternating phase rectangular pulse) at 3.8 kHz during acquisition for a total spectrum acquisition time of 5 h. Data was processed with a squared cosine bell window function in both directions.

Similar parameters were used for the HSQC spectrum except that 16 scans were taken for 320 slices in the indirect dimension for a total acquisition time of 2 h.

ESI-MS

ESI-MS experiments were performed in negative mode with the use of Waters Q-ToF Premier mass spectrometer working under MassLynx version 4.1 software. Calibration was performed with sodium formate solution. Capillary voltage was 2,500 V, cone voltage 50 V, source temperature 80 °C, desolvation temperature 180 °C, mass range 100–1,000 Da. Typical run duration was between 0.5 and 1 min, with scan time 1 s, and interscan time 0.1 s. Cone gas flow was off, desolvation gas flow was 600 L/h. Collision energy in tandem MS experiments was within the 10–50 eV range.

Results

Fatty Acid Composition of T81

Analysis of fatty acid composition of T81 revealed twenty components present at levels exceeding 0.2 % of total fatty acids. All fatty acids were found to originate from polar lipids. The neutral lipids fraction of T81 produced no FAME upon transmethylation, and was shown to consist only of hydrocarbons [unpublished]. Using the reference compounds, ECL values, and GCMS data eleven of these were identified as saturated fatty acids with straight (14:0, 16:0, 17:0, 18:0), and branched (*i*16:0, *i*17:0, *i*18:0, *i*19:0,

i20:0, *ai17:0*, *ai19:0*) chain. Chemical modifications were used in an attempt to gather initial information on the remaining components, which accounted for 25.1 % of total fatty acids. No changes in fatty acid pattern were observed upon hydrogenation of the sample, suggesting that T81 contains no unsaturated fatty acids. The TLC mobility of FAME and the lack of changes in GC behavior after FAME were treated with BSTFA revealed the absence of hydroxy fatty acids in the sample. The sample

grown in the shake flasks contained 7.6 % of straight chain and 67.3 % of *iso*- + *anteiso*-acids (of total fatty acids). Interestingly, the bacterium grown in the 20 L fermenters demonstrated dramatic changes in straight chain, and *iso*-/*anteiso*- acids content during their growth, which requires further investigation (Table 1).

One more known fatty acid, 12-Me-18:0, was identified on the basis of its ECL [13], GCMS of its methyl ester (a prominent peak at *m/z* 199, accompanied by a weaker ion

Table 1 Fatty acid composition of novel extremophile T81

Fatty acid	ECL _{BP1}	ECL calculated ^c (difference)	ECL _{TG-Wax}	wt %, of total fatty acids		
				100 mL flask	20 L fermenter	
				24 h	48 h	72 h
14:0	13.98		13.98	0.5		
Unidentified	15.77		15.34	0.3		
<i>i16:0</i>	15.64		15.51	2.0	0.6	2.0
8,14-diMe-15:0	16.06	16.03 (0.03)	15.76			0.3
16:0	16.00		16.00	2.9	9.8	1.6
<i>i17:0</i>	16.65		16.52	5.9	12.8	28.2
<i>ai17:0</i>	16.74		16.68	0.9	3.0	5.6
10,15-diMe-16:0	17.06	17.05 (0.01)	16.78	0.6		1.6
12,15-diMe-16:0	17.11	17.11 (0)	16.88	0.2	1.2	0.2
17:0	17.00		17.00	0.2	1.4	0.4
<i>i18:0</i>	17.65		17.52	42.8	4.9	7.8
10,16-diMe-17:0 ^b	18.04	18.00 (0.04)	17.76	5.1		1.6
12,16-diMe-17:0 ^b	18.06	18.07 (−0.01)	17.76			
18:0	18.00		18.00	4.0	39.4	5.6
12-Me 18:0	18.44	18.44 ^d (0)	18.29	1.6	7.6	2.5
<i>i19:0</i>	18.64		18.51	9.7	6.8	14.4
<i>ai19:0</i>	18.72		18.68	4.8	4.8	9.8
12,17-diMe 18:0,"X"	19.04	19.04 (0)	18.76	16.3	8.3	21.6
<i>i20:0</i>	19.63		19.5	1.2		0.5
12,18-diMe-19:0	20.01	n/a	19.72	0.6		
Total				99.6	100.0	99.9
Straight chain				7.6	50.6	7.6
Monomethyl-branched				68.9	39.9	68.9
Dimethyl-branched				22.8	9.5	23.4
With <i>iso</i> -branching				84.4	34	74.4
With <i>anteiso</i> -branching				5.7	7.8	15.4
Odd-carbon chain				51.9	6.3	8.8
Even-carbon chain				47.4	93.7	91.1
Odd number of carbons				28.8	36.4	60.9
Even number of carbons				70.5	63.6	39

Only components accounting for ≥ 0.2 % of total fatty acids are presented

^a A minor component, 14,19-dimethyl-20:0, was also observed by GCMS of pyrrolidides derivatives

^b The ratio of 10,16-diMe-17:0–12,16-diMe-17:0 was approximately 2:3, as revealed by intensities of signals at *m/z* 113 in GCMS of pyrrolidides derivatives

^c For non-polar column, calculated using fractional chain length data from Apon and Nicolaidis [16]

^d As observed by Duque et al. [13] with OV-101 column (similar to BP1 used in the current study)

Fig. 1 GC-MS of pyrrolidides of 12-methyl-18:0 acid from T81. 28 Da gaps indicate the exact position of Me-branching

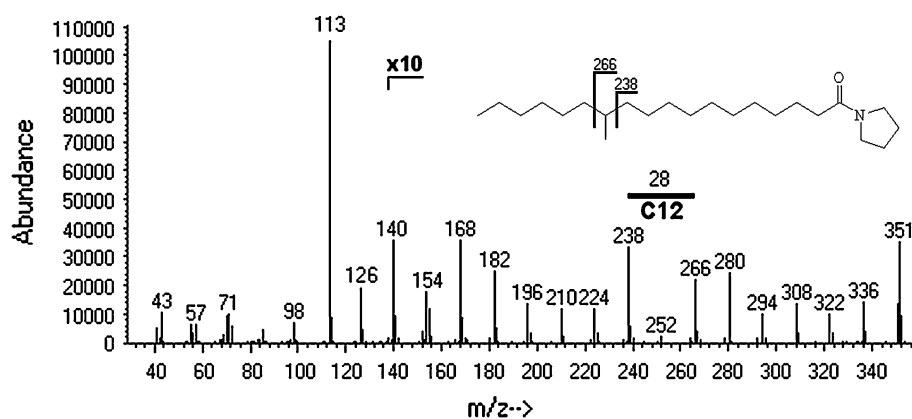
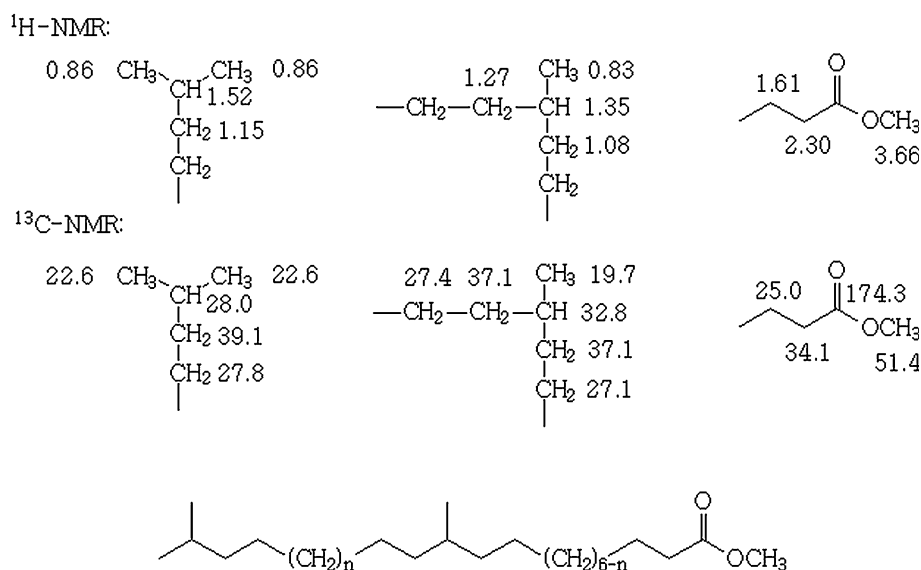


Fig. 2 Fragments of the structure of a methyl ester of a novel fatty acid from T81 suggested by the results of initial NMR experiments. n could vary from 0 to 6. Chemical shifts are given in ppm relative to internal TMS



at m/z 227 expected for FAME of 12-methyl-branched saturated acids), and GCMS of its pyrrolidides (M^+ at m/z 351, and a gap in 28 Da between the ions at m/z 238 and 266, Fig. 1).

Dimethyl-Branched Fatty Acids

The main unknown fatty acid, referred to as “X” in Table 1 was isolated by HPLC with 99 % purity as demonstrated by GC with FID. Its methyl ester possessed an ECL of 19.04 on methyl silicone phase BP1, and 18.76 on a medium polarity phase TG-Wax. GCMS analysis of the corresponding peak (in the form of methyl ester) suggested that this fatty acid is saturated aliphatic twenty carbon atom acid. Negative ion high resolution QToF MS of the free fatty acid anion had an exact mass of 311.2946 that corresponded to $C_{20}H_{39}O_2^-$ (calculated mass 311.2950, difference -1.3 ppm).

A non-integer ECL value for the saturated fatty acid suggested that there was branching present in the molecule. An initial attempt to establish the structure with the use of

GCMS of methyl esters generated a number of alternative structures.

While 21 signals were expected for C20 fatty acid methyl ester in a ^{13}C -NMR spectrum, it contained only 20 signals (in ppm, relative to internal TMS: 19.72, 22.65, 24.97, 27.07, 27.34, 27.76, 27.98, 29.16, 29.25, 29.45, 29.59, 29.67, 30.00, 32.76, 34.13, 37.10, 37.14, 39.11, 51.40 (O-CH₃), and 174.32 (COO)), suggesting that there may be two equivalent carbons. 1H -NMR spectrum contained a doublet at 0.836 (3H, 6.6 Hz, -CH₃), a doublet at 0.863 (6H, 6.6 Hz, two CH₃ groups), a poorly resolved group at 1.0–1.4 ppm (26H, CH₂), a symmetrical 9-component multiplet centered at 1.516 ppm (1H, 6.6 Hz), a multiplet at 1.62 ppm (2H, \sim 7.3 Hz, β -CH₂), a triplet at 2.30 ppm (2H, 7.5 Hz, α -CH₂), and a singlet at 3.66 ppm (3H, -OCH₃). Thus, the presence of the putative fragments shown in Fig. 2 was suggested by NMR.

A very helpful resource, <http://lipidlibrary.aocs.org/>, was used in getting reference spectral data. Since initial 1D-NMR experiments alone were unable to provide a definite structure, we used Reaxys[®] (Elsevier Properties

SA service) and SciFinder[®] (Chemical Abstracts service) to find if there was any spectral information available for fatty acids within the range suggested by NMR (i.e. from 6,17- to 12,17-dimethyloctadecanoic acid). No hits were found for any one of these acids or their derivatives. We also calculated an expected pattern of ions in GC–MS spectra of each possible structure that matched the restrictions presented in Fig. 2, using another page from the above mentioned resource [14]. The best match between calculated four characteristic ions and those present in the experimental spectrum was observed for 12,17-dimethyloctadecanoic acid, with the ions being at m/z 199, 227, and also less intensive ions at m/z 195 (227-MeOH), and 177 (195-H₂O):

GCMS of pyrrolidides (Fig. 3) suggested the structure of 12,17-dimethyloctadecanoic acid as being possible, with 28 Da gaps indicating the points of methyl-branching at C12 and C17. While it was tempting to perceive lower intensity ions at m/z 294 and 308 as another gap indicative of the presence of ethyl- or dimethyl- branching at C14, no evidence of such branching was seen in NMR spectra.

The structural features were investigated further with ¹H-¹H-COSY and ¹H-¹³C-HSQC NMR experiments.

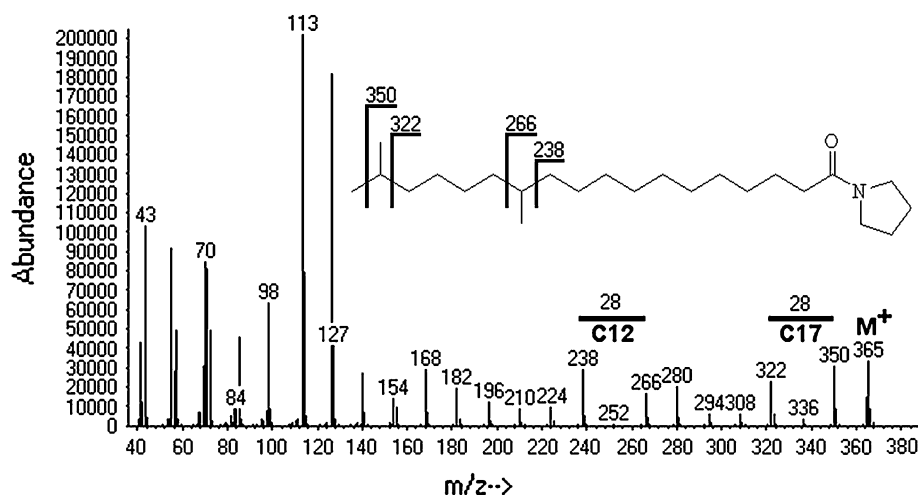
The concerted use of various 1- and 2D-NMR experiments confirmed the structure of 12,17-dimethyl octadecanoic acid. The proton homonuclear 2D correlation (COSY) spectrum is invaluable for tracing connectivity of neighboring protons. Connectivity of the carbon backbone then follows from the proton carbon heteronuclear single quantum (HSQC) spectrum which also confirms the magnetic equivalence of the methylene –CH₂– protons, which is necessary to utilize with confidence, the HSQC-TOCSY spectrum for tracing out the sub-spectral elements of the fatty acid chain. The HSQC-TOCSY results are critical for determining the carbon backbone length between the points of attachment of the methyl groups.

The evidence for the structure assignment of 12,17-dimethyl octadecanoic acid is detailed below. Starting from the ester end of the chain the ¹³C assignment of the carbonyl (C1, 174.32 ppm) and methoxyl (51.40 ppm) can be made on the basis of chemical shift alone. The methoxyl proton signal at 3.66 ppm is easily assigned by the appearance of the intense singlet and confirmed from the HSQC. The characteristic proton signal at 2.30 ppm is readily and uniquely assigned to H2 whereupon the presence of COSY cross peaks progressively identifies H3 (1.61 ppm) and H4 falls into the intractable group of overlapping signals around 1.25 ppm. C2, C3 are then easily identified at 34.1, and 15.0 ppm, respectively from the HSQC spectrum. These values were consistent with those widely published (e.g. in the above mentioned Lipid Library resource).

To assign the C12 to C18 segment of the carbon backbone we initially pinpointed the mid chain attachment point for C19. The intense COSY cross peak to (the three proton integrated intensity, methyl) H19 (0.83 ppm) readily identifies H12 as the broad featureless low intensity hump at 1.35 ppm. The DEPT90 spectrum contains two methine carbons at 28.0 and 32.8 ppm which can be assigned on chemical shift grounds alone to C17, C12 respectively, however conclusive assignment is provided and confirmed from the COSY cross peaks between the attached methyl groups and methine protons, followed by recourse to HSQC.

Carbons C11, C13 can be assigned on chemical shift grounds alone as the almost overlapping pair of signals at 37.10 and 37.15 ppm. This is confirmed by the COSY spectrum from weak cross peaks between H12 (1.35 ppm) to H11 (1.08 ppm) and from H12 to H13 (1.27 ppm). Conclusive discrimination between C11 and C13 rests on the HSQC-TOCSY results to follow. Whilst C11 and C13 are almost overlapping, they are resolvable/discernible at

Fig. 3 GC-MS of pyrrolidides of 12,17-dimethyl-18:0 acid, “X” from T81



high magnification in the HSQC (and HSQC-TOCSY) spectrum.

Starting now from the iso-methyl end of the chain, the H18/H20 (0.86 ppm) proton methyl doublet, H17 is readily assigned to the symmetric 9-component multiplet at 1.516 ppm from the intense cross peak in the COSY spectrum. Similarly H16 (1.16 ppm) is easily and uniquely assigned.

The corresponding carbon assignments for C18/C20, C17 and C16 follow from the HSQC. Although H15 can be identified from the COSY cross peak to H16, it falls into the intractable group of overlapping signals at 1.25 ppm. At this point all that remains is to assign C14 and C15 and the corresponding proton signals. With the confirmed assignment of the carbon backbone extremities from C12- to C18 established, we now resort to results from the HSQC-TOCSY spectrum to complete the identification of the complete backbone segment. For this purpose we seek proton (or carbon) detector signals with intense, sharp, minimalist multiplet patterns to indirectly detect or map out the hoped for continuous chain of totally correlated carbon cross peak signals C18/C20 through to C12 or alternatively traversing the backbone in the opposite direction, from C19 through to C17. Realistically, with the 60 ms proton isotropic mixing time employed in the concatenated TOCSY portion of the pulse program we do not expect to detect a more than five- or six carbon sub spectrum traversal. The methyl doublets H18/H20 or H19 are ideal for this purpose and Fig. 4 shows the corresponding column of ^{13}C cross peaks in the HSQC-TOCSY spectrum. Focusing on the column of cross peaks detected by the very intense H18/H20 methyl doublet, it is noted when looking down at the noise floor that there is no detectable C12 cross peak but a weak cross peak for C13 is visible above the noise. It is therefore reasonable to expect to see the carbon backbone traversal from C18/C20 to C13 but no further. Still focusing on the column of cross peaks detected by H18/H20, the foregoing discussion has detailed the assignments of C18/C20, C17, C16, C13 so ignoring these we are left with two ^{13}C cross peaks at 27.34 and 27.76 ppm which must therefore be C14 and C15. To discriminate between the two it is noted that the 27.76 ppm cross peak is more intense than the 27.34 ppm cross peak so the assignment is C14, C15 at 27.34 and 27.76, respectively.

For the backbone segment from C1 to C11, carbons C1, C2, C3, C11 and their attached protons have already been assigned above. The remaining ^1H signals fall into the intractable region of overlapping signals around 1.25 ppm. Apart from C10, the remaining six carbons fall into the narrow range from 29 to 30 ppm. Assignment of the remaining carbon backbone relies heavily on cross peak intensities in the HSQC-TOCSY spectrum and will not be discussed at length here. Suitable isolated proton detector

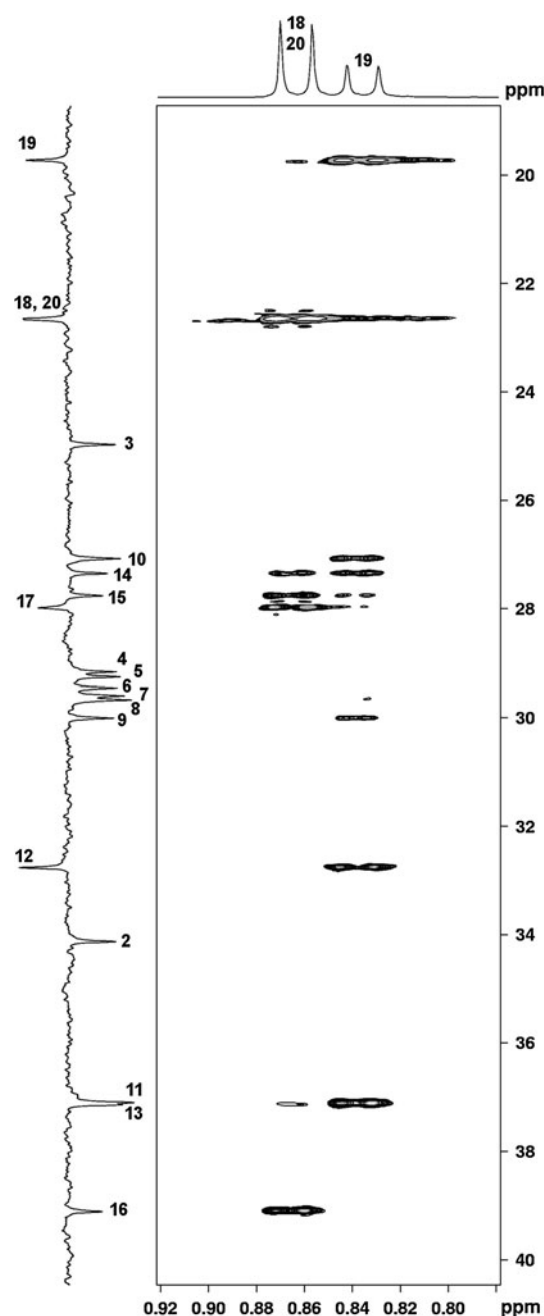
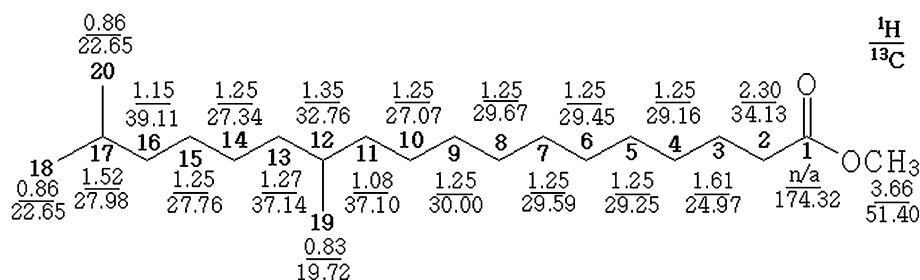


Fig. 4 A fragment of DEPT-TOCSY spectrum of the novel acid from T81. *Horizontal axis* methyl region of ^1H -NMR spectrum, *vertical axis* DEPT spectrum

signals are H2, H3 and H11. The sharp intense H2 triplet is especially informative and the column of ^{13}C cross peaks in the HSQC-TOCSY spectrum immediately provides assignments for: (ppm) C4 (29.16), C5 (29.25), C6 (29.45) and C7 (29.59). From C11 end of the backbone segment, the column of ^{13}C cross peaks detected by the broad H11 multiplet (1.08 ppm) in the HSQC-TOCSY spectrum readily provides assignments for (ppm): C10 (27.07), C9 (30.00) and C8 (29.67) (Fig. 5).

Fig. 5 NMR chemical shifts assignments for 12,17-dimethyloctadecanoic acid methyl ester based on the results of HSQC-TOCSY experiment



The ^{13}C -NMR chemical shifts determined in the current work are in a good agreement with those reported for branched fatty acids by Knothe and Nelsen [15].

Structures of 8,14-diMe 15:0, 10,15-diMe 16:0, 12,15-diMe 16:0, 10,16-diMe 17:0, 12,16-diMe 17:0, 12,17-diMe 18:0, 12,18-diMe 19:0 and 14,19-diMe 20:0 were confirmed by GC-MS of pyrrolidides. Interestingly, spectra of all mentioned fatty acids, except that of 12,15-diMe 16:0, contained similar low intensity ions corresponding to the fragments between *iso*- and middle-chain branching as observed for 12,17-diMe 18:0 (Fig. 3).

To detect methyl esters of 2-methyl fatty acids as possible precursors of mid-chain branched acids, we extracted gas chromatograms for McLafferty ions with m/z 74 (saturated esters without 2-methyl group), and m/z 88 (2-methyl branched esters). While the majority of saturated fatty acids have a base peak with m/z 74 in their positive ion EI mass-spectra, those with 2-methyl substitution possess the base peak at m/z 88 instead [17]. The trace at m/z 88 exactly repeated the pattern of m/z 74 trace, the former having the intensity of all peaks about 1/15 of the latter trace, thus excluding a possibility of a presence of noticeable levels of 2-methyl fatty acids.

Discussion

An impressive feature of T81 fatty acids is the complete lack of unsaturation, and predominance of branched-chain structures. Interestingly, mid-chain branching was only observed with *iso*-acids, and not in the *anteiso*-acids.

The cell morphology of T81 changed significantly between the methods of growth (lateral agitation of the shake flask versus impeller agitation in the 20-L bioreactor) and age of the culture. When the bacterium was agitated through lateral shaking in a temperature controlled shaker incubator, the mycelia grew sparsely (loose pellets) and measurements of dissolved oxygen (data not shown) indicated that the culture medium was oxygen starved. When the bacterium was cultured in a chemostat stirred bioreactor, the morphology changed from loose pellets to dense pellets as the agitation was increased to maintain dissolved oxygen above 30 % (v/v). While no direct link can be

made, the change in the fatty acid profile may be attributed to the change in morphology and growth conditions.

An unidentified fatty acid, seemingly branched 20:0, at levels of 14.6–26.6 % of total fatty acids was reported by Yabe et al. [2] for two species of bacteria also belonging to the class *Ktedonobacteria* of the phylum *Chloroflexi*. The reported ECL on a methyl silicone phase, 19.032, for these two strains was virtually identical to that of the fatty acid we observed in T81. Moreover, the reported fragments of mass-spectrum of its methyl ester matched our data, making it likely that both T81 and the other representatives of the genus *Thermogemmatospira* share the same 12,17-dimethyloctadecanoic fatty acid. A striking difference between fatty acid profiles of these organisms is that the major fatty acid in both of *Thermogemmatospira* species is *i*17:0, while in T81 the dominant fatty acid is *i*18:0. Mid-chain methyl-branched fatty acids are considered to be indicative of actinomycetes (10-methyl-18:0, tuberculos-tearic acid), or sulfate-reducing bacteria (10-methyl-16:0) [18].

There are two viable options for biosynthesis of mid-chain methyl-branched fatty acids: either these acids are formed by methylation of unsaturated *isolanteiso* acids, or by gradual elongation of dimethyl-branched precursors. The former option requires the presence of a corresponding monounsaturated fatty acid, with methyl group supplied by S-adenosyl-methionine [19]. This mechanism is essentially different for the acids with branching close to either terminal methyl or carboxyl group—such fatty acids are synthesized via corresponding primers (short chain branched carboxylic acids, or α -keto-acids for *iso*- and *anteiso*-acids [20], methylmalonic acid for methyl substituents on even-numbered carbons near a carboxyl group [21]). We were unable to detect any unsaturated fatty acids that could serve as precursors for fatty acids containing mid-chain branching in T81.

The latter option requires the participation of a propionate primer at some stage, followed by a series of C2 elongation events. For example, an excess of propionate is required for formation of 2, 4, 6, 8, 10, and 12-methyl tetradecanoic acids, as well as 4,8-dimethyl-substituted acids with chain length from 11 to 15 carbons in mammals [22]. All dimethyl-branched acids we observed in T81

followed one of two patterns: either the acid possessed an odd-carbon chain with an odd number of methylene units between branching points (8,14-diMe 15:0, 10,16-diMe 17:0, 12,16-diMe 17:0, 12,18-diMe 19:0); or an even-carbon chain with an even number of methylene units between branching points (10,15-diMe 16:0, 12,15-diMe 16:0, 12,17-diMe 18:0, 14,19-diMe 20:0). The “odd–odd” pattern may indicate that these acids are synthesized starting from isobutyryl-CoA via a number of C2 elongations followed by formation of methyl-branching due to propionyl-CoA inclusion, followed by a number of C2 elongations. This suggestion is supported by the finding from T81 genome analysis that the organism possesses a complete propionyl-CoA carboxylase set (M. Stott, unpublished data). The “even–even” pattern acids may be synthesized by the similar mechanism, with the only difference being that isovaleryl-CoA serves as a starting block (Fig. 6).

Our data demonstrate that T81 possesses at least four sets of dimethyl branched fatty acids: with branching points separated by two methylene units (12,15-dimethyl-16:0), three methylene units (12,16-dimethyl-17:0), four methylene units (10,15-dimethyl-16:0; 12,17-dimethyl-18:0; 14,19-dimethyl-20:0), and five methylene units (8,14-dimethyl-15:0; 10,16-dimethyl-17:0; 12,18-dimethyl-19:0). The two latter sets suggest that the mid-chain branching is introduced prior to a number of elongation steps. One of the possible precursors for 10,15-dimethyl-16:0/12,17-dimethyl-18:0/14,19-dimethyl-20:0 may be 4,9-dimethyl-decanoic acid, that was reported for halophilic *Bacillus* species [23].

Since fatty acids with three methylene units between specific branching points, namely 4,8-dimethyl-13:0 and 4,8-dimethyl-15:0 were also reported [22], it is not impossible that one yet to be discovered acid, 4,8-dimethyl-9:0, may serve as a precursor for 12,16-dimethyl-17:0. Interestingly, the presence of dimethyl-branched acids was linked to an abnormally soft subcutaneous adipose tissue of lambs reared on diets with a high content of barley [*ibid.*].

Compared with mono-methyl branched and multiple-branched isoprenoid fatty acids, those with two methyl groups are far less reported in the scientific literature. For example, for mycobacteria the acids with one methyl branch in the middle of the chain, or acids with three or four methyl branches at the carboxyl end were reported, but not with two methyl branches [24]. While dimethyl branched fatty acids with one branching point located in the vicinity of carboxyl group and another close to the terminal methyl were relatively more frequently reported for bacteria (e.g. [19]), dimethyl-branched saturated fatty acids with one branching point at the middle of the chain and another close to the terminal methyl are quite rare. Dimethyl-branched fatty acids with three (with 2,6- and 3,7-pattern) and five (with 2,8- and 3,9-pattern) methylene units between the points of branching were reported as constituents of lipids of preen gland in birds [25].

We used Reaxys[®] (Elsevier Properties SA service) and SciFinder[®] (Chemical Abstracts service) to find out if there is any information available about 12,17-dimethyloctadecanoic acid. No findings of this fatty acid have previously been reported, while the only hit found listed this acid among 3,172 branched fatty acids claimed suitable for

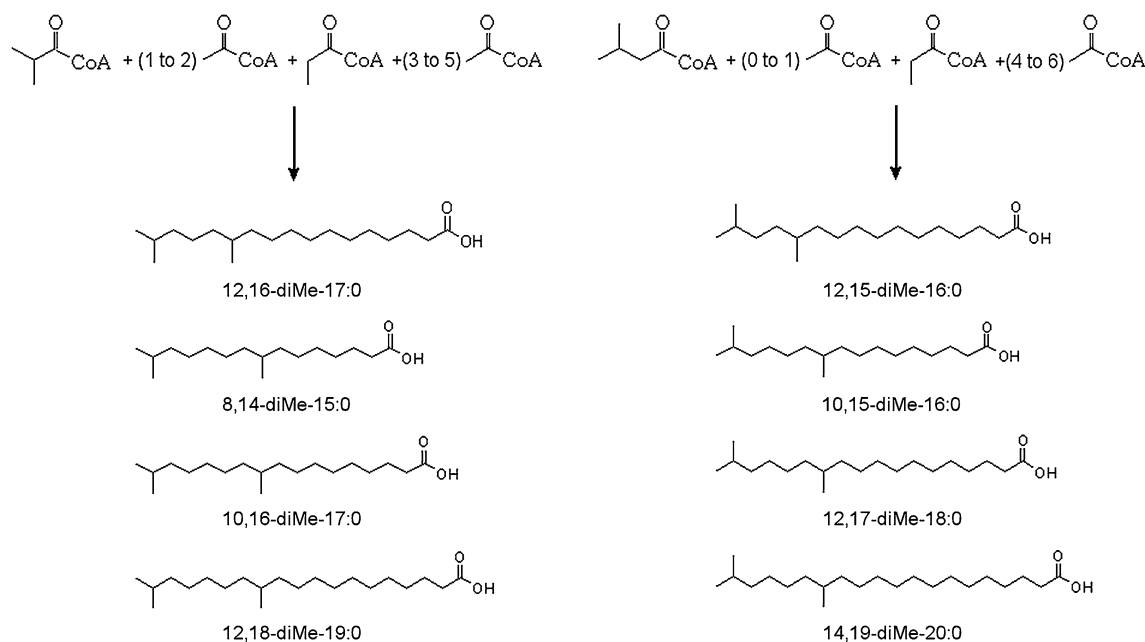


Fig. 6 Dimethyl-branched fatty acids of T81—possible biosynthetic pathways

a range of cleaning and other industrial applications [26]. No example of the synthesis or isolation from a natural source was given in that patent. Some of the other dimethyl-branched acids mentioned in the present work were also listed in that patent: 8,14-dimethyl pentadecanoic; 10,15- and 12,15-dimethyl hexadecanoic acids; and 10,16-dimethyl heptadecanoic acid. The synthesis of 12,16-dimethyl heptadecanoic acid, for use as a reference compound in identification of polymethyl-branched fatty acids, was described by Sen Gupta and Peters [27]. As for the natural occurrence of the dimethyl-branched fatty acids encountered in our study, Hedrick et al. [28] reported that the polar lipids of subsurface sediments collected at a former uranium processing facility contained on average 0.78 % of 10,15-dimethyl hexadecanoic acid. The same acid was found in the hydrolysis products of Gram-negative bacteria *Marinobacter aquaeolei* when *iso*-nonadecane was added to the media [29]. Finally, an unspecified amount of allegedly 8,14-dimethyl pentadecanoic acid was reported [30] to be present in adipose tissue of semi-feral fallow deer, this acid being one of ten with *iso*-branching, the sum of which accounted for 1.05 % of total fatty acids. The latter finding may need better experimental support to be considered reliable, since the structure was deduced using only GCMS data for a peak containing at least three dimethyl-branched isomers. No reports on either synthesis or discovery of 12,18-dimethyl nonadecanoic and 14,18-dimethyleicosanoic acids were found.

Overall, the presence of a group of dimethyl-branched fatty acids with 12,17-dimethyloctadecanoic acid as a major component may serve as a useful taxonomic marker of *Thermogemmatipora* microorganisms.

Acknowledgments Authors are grateful to Dr. Kevin Mitchell for help with HPLC, Dr Yinrong Lu for QToF MS support, Dr. Owen Catchpole for reviewing the manuscript, Alison Speakman for invaluable help in information retrieval (all—IRL). The authors also thank the Tikitere Trust for their on-going support of this research. The study was performed within IRL Capability Fund project “Natural bioactives from NZ extremophile microorganisms”.

Conflict of interest The authors declare that there is no conflict of interest.

References

- Stott MB, Crowe MA, Mountain BW, Smirnova AV, Hou S, Alam M, Dunfield PF (2008) Isolation of novel bacteria, including a candidate division, from geothermal soils in New Zealand. *Environ Microbiol* 10:2030–2041
- Yabe S, Aiba Y, Sakai Y, Hazaka M, Yokota A (2010) *Thermogemmatipora onikobensis* gen. nov., sp. nov. and *Thermogemmatipora foliorum* sp. nov. isolated from geothermal fallen leaves and a description of *Thermogemmatiporaceae* fam. nov. and *Thermogemmatiporales* ord. nov. within the class *Ktedonobacteria*. *Int J Syst Evol Microbiol* 61:903–910
- Vyssotski M, Ryan R, Lagutin K, Wong H, Morgan X, Stott M (2011) Novel fatty acid, 12,17-dimethyloctadecanoic acid, from *Thermogemmatipora* strain T81. 102nd AOCS Annual Meeting and Expo (Cincinnati, Ohio, USA, 1–4 May 2011)
- Bligh EG, Dyer WJ (1959) A rapid method of total lipid extraction and purification. *Can J Biochem Physiol* 37:911–917
- Lewis T, Nichols PD, McMeekin TA (2000) Evaluation of extraction methods for recovery of fatty acids from lipid-producing microheterotrophs. *J Microbiol Methods* 43:107–116
- Svetashev VI, Vysotskii MV, Ivanova EP, Mikhailov VV (1995) Cellular fatty acids of *Alteromonas* species. *Syst Appl Microbiol* 18:37–43
- Carreau JP, Dubacq JP (1978) Adaptation of macro-scale method to the micro-scale for the fatty acid methyl transesterification of biological lipid extracts. *J Chromatogr* 151:384–390
- Cyberlipid (2011) Low pressure fractionation of neutral lipids. <http://www.cyberlipid.org/fraction/frac0006.htm>. Accessed Nov 2011
- Kaneda T (1977) Fatty Acids of the Genus *Bacillus*: an example of branched-chain preference. *Bacteriol Rev* 41:391–418
- Appelqvist LA (1972) A simple and convenient procedure for the hydrogenation of lipids on the micro- and nanomole scale. *J Lipid Res* 13:146–148
- The AOCS Lipid Library (2011) Fatty acids and mass spectrometry. Preparation of nitrogen-containing derivatives for mass spectrometry of fatty acids. <http://lipidlibrary.aocs.org/ms/ms02/index.htm>. Accessed 24 Nov 2011
- Willker W, Leibfritz D, Kerssebaum R, Bermel W (1993) Gradient selection in inverse heteronuclear correlation spectroscopy. *Magn Reson Chem* 31:287–292. doi:10.1002/mrc.1260310315
- Duque C, Cepeda N, Martinez A (1993) The steryl ester and phospholipid fatty acids of the sponge *Agelas conifera* from the Colombian Caribbean. *Lipids* 28:767–769
- The AOCS Lipid Library (2011) Mass spectra of methyl esters of fatty acids. Part 2. Branched-chain fatty acids. <http://lipidlibrary.aocs.org/ms/ms03a/index.htm>. Accessed 24 Nov 2011
- Knothe G, Nelsen TC (1998) Evaluation of the ¹³C-NMR signals of saturated carbon atoms in some long-chain compounds. *J Chem Soc Perkin Trans 2*:2019–2026
- Apon JMB, Nicolaides N (1975) Determination of the position isomers of the methyl branched fatty acid methyl esters by capillary GC/MS. *J Chromatogr Sci* 13:467–473
- Imbs AB, Rodkina SA (2004) Isolation of 2-methyl branched unsaturated very long fatty acids from marine sponge *Halicynthia panicea* and identification of them by GC-MS and NMR. *Chem Phys Lipids* 129:173–181
- White DC, Stair JO, Ringelberg DB (1996) Quantitative comparisons of in situ microbial biodiversity by signature biomarker analysis. *J Ind Microbiol* 17:185–196
- The AOCS Lipid Library (2011) Fatty acids: branched-chain. Structure, occurrence and biosynthesis. http://lipidlibrary.aocs.org/Lipids/fa_branched/index.htm. Accessed 24 Nov 2011
- Kaneda T (1991) *Iso*- and *anteiso*-fatty acids in bacteria—biosynthesis, function, and taxonomic significance. *Microbiol Rev* 55:288–302
- Kolattukudy PE, Bohnet S, Sasaki G, Rogers L (1991) Developmental changes in the expression of S-acyl fatty acid synthase thioesterase gene and lipid composition in the uropygial gland of mallard ducks (*Anas platyrhynchos*). *Arch Biochem Biophys* 284:201–206
- Duncan WRH, Lough AK, Garton GA, Brooks P (1974) Characterization of branched chain fatty acids from subcutaneous triacylglycerols of barley fed lambs. *Lipids* 9:669–673

23. Carballeira NM, Miranda C, Lozano CM, Nechev JT, Ivanova A, Ilieva M, Tzvetkova I, Stefanov K (2001) Characterization of novel methyl-branched chain fatty acids from a halophilic *Bacillus* species. *J Nat Prod* 64:256–259
24. Ramakrishnan T, Murthy PS, Gopinathan KP (1972) Intermediary metabolism of mycobacteria. *Bacteriol Rev* 36:65–108
25. Jacob J, Poltz J (1974) Chemical composition of uropygial gland secretions of owls. *J Lipid Res* 15:243–248
26. Connor DS, Scheibel JJ, Back DJ, Trinh T, Vinson PK, Burckett-St. Laurent JCTR, Sivik MR, Wahl EH, Frankenbach GM, Demeyere HJM (1999) Mid-chain branched fatty acids, soaps, surfactant systems, and consumer products. WO 9920722 A2
27. Sen Gupta AK, Peters H (1966) Isolierung und Strukturaufklärung polyverzweigter Fettsäuren aus Fischöl (Isolation and structure determination of polybranched fatty acids from fish oil). *Fette Seifen Anstrichm* 68:349–360 (In German)
28. Hedrick DB, Peacock AD, Long P, White DC (2008) Multiply methyl-branched fatty acids and diacids in the polar lipids of a microaerophilic subsurface microbial community. *Lipids* 43:843–851
29. Soltani M, Metzger P, Largeau C (2005) Fatty acid and hydroxy acid adaptation in three Gram-negative hydrocarbon-degrading bacteria in relation to carbon source. *Lipids* 40:1263–1272
30. Smith A, Duncan WRH (1979) Characterization of branched-chain fatty acids from fallow deer perinephric triacylglycerols by gas chromatography-mass spectrometry. *Lipids* 14:350–355

The Composition of the Cuticular and Internal Free Fatty Acids and Alcohols from *Lucilia sericata* Males and Females

Marek Gołębiowski · Mieczysława I. Boguś ·
Monika Paszkiewicz · Wioletta Wieloch ·
Emilia Włóka · Piotr Stepnowski

Received: 19 July 2011 / Accepted: 21 February 2012 / Published online: 14 March 2012
© The Author(s) 2012. This article is published with open access at Springerlink.com

Abstract GC, GC–MS, and HPLC–LLSD analyses were used to identify and quantify cuticular and internal lipids in males and females of the blow-fly (*Lucilia sericata*). Sixteen free fatty acids, seven alcohols and cholesterol were identified and quantitatively determined in the cuticular lipids of *L. sericata*. Cuticular fatty acids ranged from C₆ to C₂₀ and included unsaturated entities such as 16:1n-9, 18:1n-9, 20:4n-3 and 20:5n-3. Cuticular alcohols (only saturated and even-numbered) ranged from C₁₂ to C₂₀ in males and C₁₀ to C₂₂ in females. Only one sterol was found in the cuticular lipids of both males and females. 23 free fatty acids, five alcohols and cholesterol were identified in the internal lipids. Internal fatty acids were present in large amounts—7.4 mg/g (female) and 10.1 mg/g (male). Only traces of internal alcohols (from C₁₄ to C₂₆ in males, from C₁₄ to C₂₂ in females) were found in *L. sericata*. Large amounts of internal cholesterol were identified in *L. sericata* males and females (0.49 and 0.97 mg/g of the insect body, respectively).

Keywords Cuticular and internal lipids · HPLC–LLSD · GC–MS · *Lucilia sericata* · *Conidiobolus coronatus* · Fungal infection

Abbreviations

SAM Sabouraud agar medium
TIC Total ion current

SIM	Single ion monitoring
EI	Electron impact
BSTFA	<i>N,O</i> -Bis(trimethylsilyl)trifluoroacetamide
TMCS	Trimethylchlorosilane
M ⁺	Molecular ion
TMSi	Trimethylsilyl derivatives
FFA	Free fatty acids
7-T, 23:1	7-Tricosene
7-P, 25:1	7-Pentacosene
7,11-HD, 27:2	7,11-Heptacosadiene
7,11-ND, 29:2	7,11-Nonacosadiene

Introduction

Lucilia species (Calliphoridae), important pollinators of flowering plants, are distributed worldwide and are the best known species in human infestation in America, Africa, and Asia. These ectoparasites are found in the meat and corpses of animals, and cause myiasis in humans and domestic herbivorous animals [1–3]. In 1826, myiasis caused by *L. sericata* in humans was reported by Magen. It was then that the parasites were isolated from the mouth, eyes, and paranasal sinuses of a hospital patient for the first time.

Unlike the larvae of some other myiasis-causing flies, *L. sericata* larvae rarely invade living healthy tissues surrounding a necrotic wound. Due to this fascinating phenomenon, called facultative myiasis, *L. sericata* larvae have been used since antiquity as a safe and effective wound treatment. The secretions of maggots are known to stimulate in vitro increase in total human fibroblasts [4]

M. Gołębiowski (✉) · M. Paszkiewicz · P. Stepnowski
Institute for Environmental and Human Health Protection,
Faculty of Chemistry, University of Gdańsk,
ul. Sobieskiego 18/19, 80-952 Gdańsk, Poland
e-mail: goleb@chem.univ.gda.pl

M. I. Boguś · W. Wieloch · E. Włóka
Institute of Parasitology, Polish Academy of Sciences,
Twarda 51/55, 00-818 Warsaw, Poland

and have antibacterial properties [5]. Although no in vivo reports regarding wound healing mechanisms of maggot therapy are available, recent data show that fly cuticular fatty acids may play a significant role in this process. Fatty acid extracts of dried *L. sericata* larvae called in traditional Chinese medicine “WuGuChong” and used to treat superficial purulent diseases such as furuncle or carbuncle, can promote murine cutaneous wound healing probably resulting from the powerful angiogenic activity of the extracts [6].

The cuticle of all insects is covered with a very thin epicuticular layer of wax. The cuticle consists of several layers, from the outside to the inside: the epicuticle, the procuticle and the epidermis. The insect cuticle is the first barrier against biological or chemical contact insecticides; it is mostly resistant to enzyme degradation and exhibits characteristic water barrier properties [7].

Naturally occurring entomopathogens are important regulatory factors of insect populations. The potential use of fungal pathogens to control insects is well documented, and the use of fungi as control agents against insect pests has been reviewed [8–12]. Susceptibility or resistance of various insect species to fungal invasion may result from several factors, including differences in the structure and composition of the exoskeleton, the presence of antifungal compounds in the cuticle, as well as the efficiency of cellular and humoral defense reactions of the invaded insect [13]. It is believed that the epicuticular lipid profile of the insect host may be one of pivotal factors determining insect susceptibilities or resistance to fungal attack [14]. The mode of action of entomopathogenic fungi involves the attachment of fungal spores to the cuticle, followed by spore germination and, depending on the fungal species, formation of appressorium or penetrative hyphae. Penetration is then initiated, involving both mechanical and enzymatic mechanisms [15]. Once inside the host, the fungus propagates, consuming nutrients and releases metabolites (some of which might be toxic), which results in mycosis and, ultimately, host death [9, 10].

The ability of the fungus to fully degrade the epicuticular hydrocarbon components of its insect host, utilizing them as an exogenous carbon source, was demonstrated by Napolitano and Juarez [16]. The presence of a wax layer potentially affects spore germination by fungilytic or fungistatic toxicity, or by acting as a barrier to the chitin matrix of the insect exoskeleton, effectively preventing the spore from coming into contact with nutrients or other cues that trigger germination. Thus, the waxy layer produced on the cuticle may act as a first line of defense against fungal pathogens. Little information on both, stimulatory and inhibitory effects of cuticular fatty acids on growth and virulence of insecticidal fungi is available. Medium- and short-chain

fatty acids and alcohols have been demonstrated to be toxic to filamentous fungi, including some that have been isolated specifically from insect cuticle [17, 18], but the toxicity of long-chain fatty acids is unknown. Kerwin [19] demonstrated the toxic effects of 6:0, 7:0, 9:0, 10:0, 18:2 and 18:3 fatty acids on *Entomophthora culicis* conidia. However, 18:1 was found to have a positive effect on spore germination and to mitigate the harmful effects of 18:3 acid. The concentration of fatty acids also had an important impact on fungal growth and conidia development: 0.1% 16:1 was toxic to secondary conidia, but positively affected fungal growth. Cuticular lipids were found to have toxic or inhibitory effects on the conidia of *B. bassiana* and *P. fumosoroseus* when the spores were germinated on nutrient agar in the presence of lipids [19]. Eighteen fatty acids identified in the larval cuticle of three insect species representing differing susceptibilities to *Conidiobolus coronatus* infection [20], were thoroughly tested for effects on the in vitro growth and pathogenicity of this parasitic fungus [21].

This paper describes the cuticular lipid composition of *L. sericata* adults. The surface lipids of flies were separated into classes of compounds using HPLC–LLSD. Qualitative and quantitative analyses were done by GC and GC–MS. The determination of the composition of fly lipids and their impact on the development and pathogenicity of *C. coronatus* may have great practical importance and will allow using this fungus or its metabolites to control insect populations.

Materials and Methods

Insects

Lucilia sericata raised from eggs laid on beef by adult flies, were reared at 25 °C with 50% relative humidity and a 12:12 h photoperiod. Maternal generation was maintained in the same conditions. The insects were fed on beef and it took them approximately 7 days from hatching to puparium formation and another 7 days to the appearance of adult. The insects were exposed for 18 h to fully grown and sporulating fungal colonies. Ten flies were kept in each Petri dish (males and females separately). The adults exposed for 18 h to sterile uninoculated Sabouraud agar supplemented with *G. mellonella* larval extract served as a control. After exposure, the insects were transferred to clean Petri dishes with sugar and water and kept under their growing conditions for 10 days. The condition of the exposed animals was monitored daily. Exposure of tested insects to a *C. coronatus* colony for 18 h was found to be most efficient method resembling the natural infection process [22]. In order to avoid pseudo replication, all

assays of fungi vs. insects were performed with the use of flies from different stocks incubated in three different chambers.

A culture of the wax moth, *Galleria mellonella* was maintained and reared in temperature and humidity controlled chambers (30 °C, 70% r.h.) in constant darkness on an artificial diet [23]. Fully grown larvae were collected before pupation, surface sterilized, homogenized and used as a supplement in fungal cultures.

Fungus

Conidiobolus coronatus, isolate number 3491, originally isolated from *Dendrolaelaps spp.*, was obtained from the collection of Prof. Bałazy (Polish Academy of Sciences, Research Center for Agricultural and Forest Environment, Poznań), routinely maintained in 90-mm Petri dishes at 20 °C with cyclic changes of light (L:D 12:12) on Sabouraud agar medium (SAM) with the addition of homogenized *Galleria mellonella* larvae to a final concentration of 10% wet weight. Addition of homogenized *G. mellonella* larvae enhances SAM cultures of *C. coronatus*. The levels of mycelial growth, conidia production, and virulence were good in hundreds of successive transfers [24] suggesting a stimulatory effect of insect proteins, carbohydrates and lipids on *C. coronatus* growth and insecticidal properties.

Extraction of Insects

Figure 1 shows the scheme for preparing the sample and analysis. Male and female specimens of *L. sericata* were extracted first in petroleum ether for 10 s and then a second time in dichloromethane for 5 min [20]. These two extracts (petroleum extract I and dichloromethane extract II) contained cuticular lipids. The third extraction was a long one with dichloromethane for 10 days (III extract). This third extract contained internal lipids. Then, 0.5 ml of the whole extract was placed in a glass flask and then evaporated under nitrogen to determine the dry mass of the remaining extracted lipids. Table 1 lists the number of adult insects, as well as the masses of the extracts.

High Performance Liquid Chromatography

All lipid extracts of the males and females (I, II and III) were separated into several classes of compounds by HPLC in the normal phase using a Shimadzu LP-6A binary pump in gradient mode. A laser light scattering detector was used as the detection system [25]. To obtain large amounts of lipids for GC–MS analysis the separation was repeated five times. All fractions were evaporated, silylated and analyzed by GC and GC–MS.

Gas Chromatography

The investigations were carried out on a Clarus 500 (Perkin Elmer) gas chromatograph equipped with a Rtx 5 fused silica column (30 m × 0.25 mm i.d., film thickness 0.1 μm) was used. The oven temperature was held at 80 °C for 10 min and then increased at a rate of 4 °C/min to a final temperature of 320 °C [25].

Gas Chromatography–Mass Spectrometry

Gas chromatography–mass spectrometry measurements were carried out by coupling an SSQ 710 (Finnigan Mat) spectrometer to a Hewlett-Packard 5890 gas chromatograph. The samples were introduced through the gas chromatograph equipped with a 30 m × 0.25 mm i.d., Optima-5 silica capillary column and with a 0.25 μm thick film. The oven temperature 80 °C (held for 10 min) was increased to 320 °C at 4 °C/min. The injector temperature was 320 °C and the carrier gas was helium. The ion source was maintained at 220 °C.

The lipids were derivatized by methods described previously [20]. All compounds were identified by comparing the retention time of the analyzed compounds with standards and on the basis of silyl derivative ions. The mass spectrum of trimethylsilyl ethers of fatty acids showed the following ions: M^+ (molecular ion), $[M-15]^+$, and fragment ions at m/z 117, 129, 132, and 145. Cholesterol was identified on the basis of the characteristic ions of silyl derivatives (m/z 458 (M^+), 129, 329, 368, 145, 121 and 353). Characteristic ions of alcohols (trimethylsilyl derivatives) were $[M-15]^+$ and m/z 103 [26].

Statistical Analysis

In order to quantitatively determine each of the compounds analyzed, GC analysis was performed with internal standards (19-methylarachidic acid, 1-octacosanol and sitosterol). Data are presented as the means ± standard deviations of three separate analyses performed on different samples. The data obtained were statistically processed by using the *t* pairwise test for determining significant differences in males and females lipids concentration.

Results

Susceptibility of *L. sericata* to Fungal Infection

Exposure of *L. sericata* adults to the sporulating *C. coronatus* resulted in the prompt death of all tested males and females (Table 2). Both, males and females died around the termination of the 18-h exposure to the fungal culture.

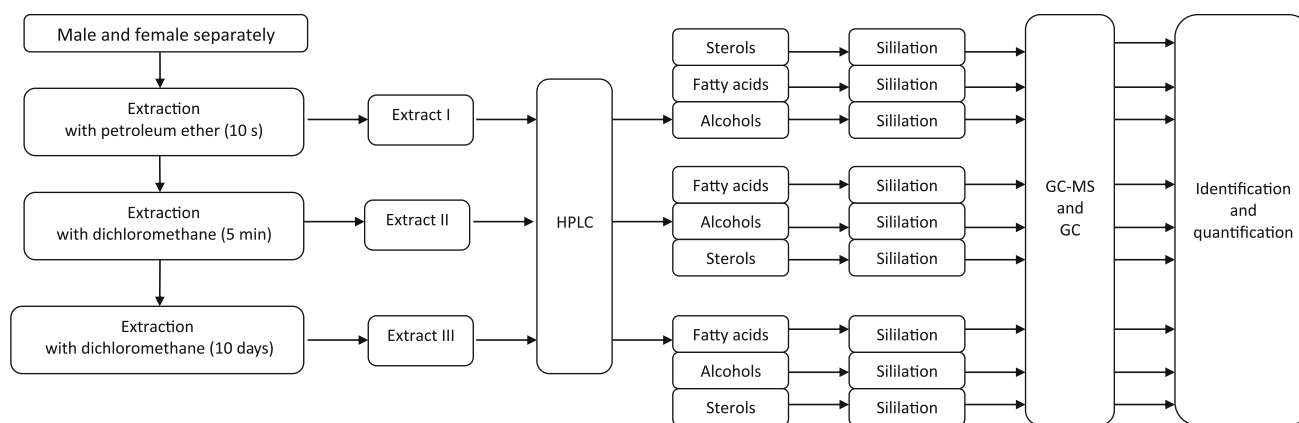


Fig. 1 Scheme of the analysis

Table 1 Quantitative summary of the experiment: numbers and masses of insect; masses of lipids

	Number of insects	Insects (g)	Extracts	Lipids in extracts (mg)	Lipids	
					(mg/insect)	(mg/g of the insect body)
Male	75	1.7	I	5.1	0.07	3.0
			II	1.3	0.02	0.8
			III	42.3	0.56	24.9
Female	80	2.3	I	3.2	0.04	1.4
			II	1.6	0.02	0.7
			III	45.4	0.57	19.7

The lack of resistance of *L. sericata* males and females on *C. coronatus* infection are confirmed by results obtained with the *t* pairwise test. Based on the *t* pairwise test we did not notice any significant differences in males and females susceptibility to fungal infection.

Extraction of *L. sericata* Lipids

This is the first time that the chemical composition of the cuticular and external lipids in the *L. sericata* has been analysed and identified. Three extractions of male and female *L. sericata* were performed. The petroleum ether

(I) and dichloromethane (II) extracts of males yielded 3.0 and 0.8 mg/g of the insect body, respectively. These two extracts consisted of cuticular lipids, so the quantity of lipids amounted to 3.8 mg/g of the insect body. The quantities of male internal lipids yielded 24.9 mg/g of the insect body (0.56 mg/insect). The quantities of cuticular lipid extracts obtained from female *L. sericata* were smaller than those from the males and amounted 2.1 mg/g of the insect body (1.4 and 0.7 mg/g of the insect body in extracts I and II, respectively). Also, the quantities of female internal lipids were less than in the males and yielded 19.7 mg/g of the insect body, but the quantity of internal lipids per insect was almost the same (0.57 mg/female vs. 0.56 mg/male).

Extracts of lipids from male and female *L. sericata* were separated by HPLC–LLSD into fractions containing general groups of chemical entities. The lipids extracted from the males and females contained four fractions: hydrocarbons, triacylglycerols, free fatty acids (FFA) and sterols. The triacylglycerols were present in the internal lipids of male and female (III extracts). They serve as a source of energy stored in fat body. The hydrocarbons were present in cuticular lipids (I and II extracts) in small amounts. They can play an important role as pheromones. In this study were determined compounds with potential antimicrobial activity, including the free fatty acid, alcohol and sterol fractions. These fractions were further analyzed by GC and

Table 2 The susceptibility of *Lucilia sericata* males and females to fungal infection

Developmental stage/treatment	Number of insects	Mortality (%) ^a
Adult females		
Control	30	0
Exposed to <i>C. coronatus</i>	50	100
Adult males		
Control	47	0
Exposed to <i>C. coronatus</i>	50	100

^a Adult insects were exposed to sporulating *C. coronatus* colonies as described in the “Materials and Methods” section. The insect susceptibility to fungal infection is expressed as percentage of mortality in tested populations

Table 3 Chemical composition of the cuticular fatty acids found in males and females of *Lucilia sericata*

FFA	Content ($\mu\text{g}/1\text{ g}$)		Relative content % (w/w)	
	Cuticular FFA (male)	Cuticular FFA (female)	Cuticular FFA (male)	Cuticular FFA (female)
6:0	0.47 \pm 0.04	0.14 \pm 0.02	3.3	1.6
7:0	–	0.15 \pm 0.01	–	1.7
8:0	0.12 \pm 0.02	0.12 \pm 0.01	0.8	1.4
9:0	0.45 \pm 0.03	0.32 \pm 0.04	3.1	3.6
10:0	0.14 \pm 0.02	0.14 \pm 0.01	1.0	1.6
11:0	Traces	Traces	Traces	Traces
12:0	0.26 \pm 0.03	0.28 \pm 0.03	1.8	3.2
14:1n-9	–	–	–	–
14:0	0.31 \pm 0.03	0.31 \pm 0.03	2.2	3.5
15:0	0.14 \pm 0.01	0.15 \pm 0.02	1.0	1.7
16:1n-9	1.48 \pm 0.07	1.34 \pm 0.06	10.3	15.2
16:0	4.2 \pm 0.2	2.8 \pm 0.1	29.4	31.8
17:1n-10	–	–	–	–
17:0	Traces	–	Traces	–
18:2n-6	–	–	–	–
18:1n-9	5.8 \pm 0.4	2.2 \pm 0.1	40.6	25.0
18:0	0.96 \pm 0.05	0.70 \pm 0.05	6.7	8.0
19:0	–	–	–	–
20:5n-3	Traces	0.09 \pm 0.01	Traces	1.0
20:4n-3	Traces	0.14 \pm 0.02	Traces	1.6
20:1n-6	–	–	–	–
20:0	–	Traces	–	Traces
22:0	–	–	–	–
24:0	–	–	–	–
26:0	–	–	–	–
Sum	14.3	8.8	–	–

Cuticular FFA: sum of FFA content in petroleum extract (I), and dichloromethane extract (II)

Data are presented as the means \pm standard deviations of three separate analyses performed on different samples

GC–MS. For qualitative purposes, the instrument was operated in total ion current (TIC) mode and single ion monitoring (SIM) mode for monitoring $[\text{M}–15]^+$ ions (Table 4). Single ion monitoring mode was used to achieve high selectivity and sensitivity. Gas chromatography was used for the quantitative analyses of lipids. Comparisons were made with the lipids extracted from male and female *L. sericata*.

Fatty Acid Composition of Male *L. sericata*

Table 3 summarizes the results obtained during the identification and quantification of FFA in the cuticular lipids of male *L. sericata*. The two cuticular extracts (petroleum ether-I and dichloromethane-II) contained 15 compounds from C_6 to C_{20} . The dominant cuticular fatty acids (all with an even number of carbon atoms) were: 16:1n-9 (10.3%), 16:0 (29.4%), 18:1n-9 (40.6%) and 18:0 (6.7%). The total free fatty acid content in cuticles in males was 14.3 $\mu\text{g}/\text{g}$

(6.1 $\mu\text{g}/\text{g}$ in the petroleum ether extract and 8.2 $\mu\text{g}/\text{g}$ in the dichloromethane extract).

The internal lipids of male *L. sericata* contained 21 FFA (Table 4). The total free fatty acid content in the internal lipids of the male was 10.1 mg/g of the insect body. The fatty acids occurring in the highest concentrations were 16:1n-9 (14.7%), 16:0 (19.5%) and 18:1n-9 (57.4%). The fatty acids 17:1n-10, 18:2n-6, 19:0, 20:1n-6, 20:0, 22:0, 24:0 and 26:0 occurred only in the internal lipids. On the other hand, 10:0 and 11:0 acids occurred only in the cuticular lipids.

Fatty Acid Composition of Female *L. sericata*

The cuticular lipids of female *L. sericata* contained 16 FFA from C_6 to C_{20} (Table 3). Ten FFA from C_8 to C_{18} were identified in the petroleum ether extract (I) and all 16 fatty acids from C_6 to C_{20} in the dichloromethane extract (II). The total free fatty acid content in the cuticle in females was

Table 4 Chemical composition of the internal fatty acids (extract III) found in males and females of *Lucilia sericata*

FFA	Content ($\mu\text{g/l g}$)		Relative content % (w/w)		[M–15] ⁺ Monitored ions (SIM mode)
	Internal FFA (male)	Internal FFA (female)	Internal FFA (male)	Internal FFA (female)	
6:0	1.8 \pm 0.1	1.33 \pm 0.05	<0.1	<0.1	173
7:0	–	0.40 \pm 0.02	–	<0.1	187
8:0	0.86 \pm 0.04	0.96 \pm 0.05	<0.1	<0.1	201
9:0	0.59 \pm 0.03	0.40 \pm 0.02	<0.1	<0.1	215
10:0	–	Traces	–	Traces	229
11:0	–	–	–	–	243
12:0	10.4 \pm 0.8	11.0 \pm 0.5	0.1	0.1	257
14:1n-9	–	Traces	–	Traces	283
14:0	16.4 \pm 0.9	13.1 \pm 0.5	0.2	0.2	285
15:0	1.9 \pm 0.1	2.0 \pm 0.1	<0.1	<0.1	299
16:1n-9	14.8 $\times 10^2 \pm 0.5 \times 10^2$	12.9 $\times 10^2 \pm 0.3 \times 10^2$	14.7	17.5	311
16:0	19.7 $\times 10^2 \pm 0.6 \times 10^2$	15.5 $\times 10^2 \pm 0.5 \times 10^2$	19.5	21.0	313
17:1n-10	6.1 $\times 10^1 \pm 0.3 \times 10^1$	3.9 $\times 10^1 \pm 0.2 \times 10^1$	0.6	0.5	325
17:0	8.2 \pm 0.4	6.6 \pm 0.5	0.1	0.1	327
18:2n-6	2.6 $\times 10^1 \pm 0.1 \times 10^1$	14.7 \pm 0.6	0.3	0.2	337
18:1n-9	5.8 $\times 10^3 \pm 0.2 \times 10^3$	39.3 $\times 10^2 \pm 1 \times 10^2$	57.4	53.2	339
18:0	22.8 $\times 10^1 \pm 0.9 \times 10^1$	16.5 $\times 10^1 \pm 0.7 \times 10^1$	2.3	2.2	341
19:0	Traces	Traces	Traces	Traces	355
20:5n-3	4.2 $\times 10^2 \pm 0.1 \times 10^2$	29.3 $\times 10^1 \pm 0.7 \times 10^1$	4.2	4.0	359
20:4n-3	13.8 $\times 10^1 \pm 0.4 \times 10^1$	8.9 $\times 10^1 \pm 0.3 \times 10^1$	1.4	1.2	361
20:1n-6	Traces	1.23 \pm 0.08	Traces	<0.1	367
20:0	6.5 \pm 0.3	4.6 \pm 0.2	0.1	0.1	369
22:0	1.59 \pm 0.06	0.97 \pm 0.06	<0.1	<0.1	397
24:0	4.7 \pm 0.2	3.0 \pm 0.2	<0.1	<0.1	425
26:0	0.81 \pm 0.03	0.61 \pm 0.03	<0.1	<0.1	453
Sum	10.1 $\times 10^3$	73.9 $\times 10^2$	–	–	–

Data are presented as the means \pm standard deviations of three separate analyses performed on different samples

8.8 $\mu\text{g/g}$ (2.0 $\mu\text{g/g}$ in the petroleum ether extract and 6.8 $\mu\text{g/g}$ in the dichloromethane extract). The percentage contents of fatty acids were very diverse (from traces to 31.2%). The FFA occurring in the highest concentrations were 16:1n-9 (15.2%), 16:0 (31.8%), 18:1n-9 (25.0%) and 18:0 (8.0%).

More fatty acids were present in the internal lipids; they ranged from C₆ to C₂₆ (Table 4) (like the internal lipids in the males). The total free fatty acid content in the internal lipids of the female was 7.4 mg/g of the insect body. Twenty four saturated, monounsaturated and polyunsaturated fatty acids were present in the internal lipids. Saturated (16 compounds) and monounsaturated fatty acids (five compounds) were dominant. The FFA occurring in the highest concentrations were 16:1n-9 (17.5%) 16:0 (21.0%) and 18:1n-9 (53.2%). A similar profile of the major compounds was identified in the cuticular lipids, except that the major compound was 18:1n-9 in the internal lipids and 16:0 in the cuticular lipids. The following acids present in the internal lipids were absent from the cuticular

lipids: 14:1n-9, 17:1n-10, 17:0, 18:2n-6, 19:0, 20:1n-6, 22:0, 24:0 and 26:0. On the other hand, only 11:0 was absent from the internal lipids of female *L. sericata*, whereas the cuticular lipids contains traces of it.

Alcohol Composition of Male *L. sericata*

Table 5 lists the percentage contents of alcohols in the cuticle as well as the alcohol contents calculated per g of insect body. Only five alcohols were found in the cuticular lipids of the males and ranged from C_{12:0} to C_{20:0}. The compound present in the highest concentrations was C_{18:0} (0.37 $\mu\text{g/g}$ of the insect body; relative content 55.2% of total alcohols). The total cuticular alcohol content in male *L. sericata* was only 0.67 $\mu\text{g/g}$. Only traces of five alcohols were found in the internal lipids. These alcohols have more carbon atoms than the cuticular ones, from C_{14:0} to C_{26:0}. The internal lipids contain traces of three alcohols (C_{22:0}, C_{24:0} and C_{26:0}), which were absent from the cuticular

Table 5 Chemical composition of the alcohols found in male of *Lucilia sericata*

Content ($\mu\text{g}/1\text{ g}$)					Relative content % (w/w)	
Alcohols	Cuticular alcohols (male)	Internal alcohols (male)	Cuticular alcohols (female)	Internal alcohols (female)	Cuticular alcohols (male)	Cuticular alcohols (female)
C ₁₀	–	–	Traces	–	–	Traces
C ₁₂	0.05 \pm 0.01	–	0.11 \pm 0.01	–	7.5	13.8
C ₁₄	0.13 \pm 0.01	Traces	0.13 \pm 0.01	Traces	19.4	16.3
C ₁₆	Traces	–	0.03 \pm 0.01	–	Traces	3.8
C ₁₈	0.37 \pm 0.03	–	0.39 \pm 0.03	–	55.2	48.8
C ₂₀	0.12 \pm 0.01	Traces	0.14 \pm 0.01	Traces	17.9	17.5
C ₂₂	–	Traces	Traces	Traces	–	Traces
C ₂₄	–	Traces	–	–	–	–
C ₂₆	–	Traces	–	–	–	–
Sum	0.67	Traces	0.80	Traces	–	–

Cuticular alcohols: sum of alcohols content in petroleum extract (I), and dichloromethane extract (II)

Internal alcohols: content of alcohols in extract III

Data are presented as the means \pm standard deviations of three separate analyses performed on different samples

Table 6 Chemical composition of the cholesterol found in male and female of *Lucilia sericata*

	Content ($\mu\text{g}/1\text{ g}$)	
	Cuticular cholesterol	Internal cholesterol
Male	7.6 \pm 0.4	4.9 $\times 10^2 \pm 0.2 \times 10^2$
Female	11.4 \pm 0.8	9.7 $\times 10^2 \pm 0.3 \times 10^2$

Cuticular cholesterol: sum of cholesterol content in petroleum extract (I), and dichloromethane extract (II)

Internal cholesterol: content of cholesterol in extract III

Data are presented as the means \pm standard deviations of three separate analyses performed on different samples

lipids. All the identified alcohols were saturated, with even-numbered carbon chains.

Alcohol Composition of Female *L. sericata*

The cuticular lipids of the female contained seven saturated alcohols with even-numbered carbon chains from C_{10:0} to C_{22:0} (Table 5). The alcohol C_{18:0} was present in the highest concentrations (48.8%) (the same observation as for the male lipids). The total cuticular alcohol content in females of *L. sericata* was 0.80 $\mu\text{g}/\text{g}$ (a little more than in the males). Only three alcohols (C_{14:0}, C_{20:0} and C_{22:0}) were found in traces in the internal lipids of females.

Cholesterol Content in Male and Female *L. sericata*

The cholesterol contents in the cuticular lipids of males and females were 7.6 and 11.4 $\mu\text{g}/\text{g}$ of the insect body, respectively (Table 6). Considerably more cholesterol was present in the internal lipids of these insects. The quantities

of internal cholesterol in female lipids were double those found in males. The cholesterol was identified on the basis of the characteristic ions (as the trimethylsilyl ether).

Discussion

Free fatty acids of *L. sericata* were present not only in the cuticle; large amounts were also detected in the internal lipids. The efficiency of cuticular and internal lipids extraction differed in *L. sericata* males and females. Amounts of cuticular lipids (mg/g of the insect body) extracted with the use of petroleum ether and dichloromethane from males were 2.1 and 1.1 times higher, respectively, than the amounts of extracts obtained from females. Similarly, amounts of internal lipids extracted from males were 1.3 times higher than analogous extracts obtained from females. The total amounts of extracted lipids (cuticular and internal) comprised 2.99% of male and 2.17% of female wet body weight, respectively. From Gilbert [27] it appears that lipid content in male adults of *Calliphora vicina* (formerly *C. erythrocephala*), closely related to *L. sericata*, and is slightly higher than in females (3.4 vs. 3.3% wet weight). In most insect species the female usually contains more lipids than the male, as a lipid is a most efficient substrate for egg development. However, the reverse may be true for many species and this is especially evident when Lepidoptera are considered [27]. Sexual dimorphism in lipid content in the adult stage was studied in detail in the silk moth *Hyalophora cecropia*. The tissues of *H. cecropia* males contain about five times as much lipid per gram of fresh weight as the tissues of the female. The higher concentration of lipids in the male moth

is most likely correlated with mating behavior, since the male moth flies relatively great distances in search of virgin females while the female does only limited flying after emergence. The silk moth male appears to utilize lipid as a primary substrate for flight while female *H. cecropia* converts a large percentage of her endogenous substrate into eggs [27]. In contrast, adults of *L. sericata* utilize carbohydrates as the main source of flight energy [28]. In spite of intensive studies concerning the flight of *L. sericata* and some other Diptera species, no sexual difference in the flight behavior and biochemistry was evidenced [29, 30].

Cuticular fatty acids in male and female extracts made up ca 0.14 and 0.12% of all lipids, respectively. The amounts of FFA in cuticular lipids can vary with respect to sex, stage and living conditions. It has been shown that FFA comprise from 2.04 to 0.50% of the lipids in the exuviae of *Dendrolimus pini* [31] and only trace amounts of FFA were detected in cuticular lipids from nymphs and exuviae of the Silver leaf whitefly, *Bemisia argentifolii* [32], whereas FFA make up 79.40% of the cuticular lipids of *Calliphora vicina* larvae [20]. Cuticular FFA in males and females of *L. sericata* ranged from C₆ to C₂₀; moreover, they consisted of both odd- and even-numbered carbon chains. Similar profiles were identified in closely related *C. vicina* larvae [20]: the fatty acids in this insect ranged from C₅ to C₂₀, although the typical cuticular fatty acids ranged from C₁₂ to C₂₀. For example, fatty acids in this range were found in lipids from *Frankliniella occidentalis* adults and larvae [33], *Acanthoscelides obtectus* males and females [25], *Liposcelis bostrychophila* [34] and *Fannia canicularis* [35]. In our study, the cuticular fatty acids identified in the adult insects were both saturated and unsaturated. Odd- and even-numbered, saturated and unsaturated fatty acids are typically found in many insect species. The presence of polyunsaturated acids 20:4n-3 and 20:5n-3 in cuticular lipids is rather unusual, although these acids were identified in the lipids of the aquatic insect larvae *Stictochironomus pictulus* [36]. In our work, the females contained these compounds in respective concentrations of 1.6 and 1.0%. Moreover, trace amounts of 20:4n-3 and 20:5n-3 acids were present in the male cuticular lipids. The female extract contained C₇ and C₂₀ acids, which were absent from the male extract. On the other hand, C₁₇ acid occurred only in the male extract.

The profiles of predominant cuticular FFA in males and females of *L. sericata* were similar. The predominant components of males and females consisted of 16:0 and 18:0 and also 16:1n-9 and 18:1n-9 fatty acids. Other cuticular fatty acids were present in much smaller quantities. Only four unsaturated fatty acids were present in both males and females. Internal FFA in males and females of *L. sericata* made up 40.4 and 37.7% of all lipids, respectively.

Free fatty acids were extracted from both sexes of *L. sericata* with carbon numbers ranging from C₆ to C₂₆, so the internal free fatty acid profiles of both adult insects were similar. In this case, the acids present in the highest concentrations in the internal extract were 16:1n-9, 16:0 and 18:1n-9. The contents (%) of 20:5n-3 and 20:4n-3 fatty acids of both sexes were similar; there was a significant difference between the amounts (μg/g) of these acids (male: 0.56 mg/g of the insect body and female: 0.38 mg/g of the insect body). The female extract contained 7:0, and traces of 10:0 and 14:1n-9 acids, which were absent, from the male extract. 22:0, 24:0 and 26:0 acids were present in the internal lipids, which were absent from the cuticular male and female extracts.

The alcohols present in the cuticular lipids of insects usually have an even number of carbons and are saturated [32, 37–39]. In our study, the cuticular lipids of females of *L. sericata* contained seven even-numbered, saturated alcohols from C₁₀ to C₂₂, but the cuticular lipids of the males contained only five such compounds, from C₁₂ to C₂₀. C₁₀ and C₂₂ alcohols were present only in female cuticular lipids. However, the remaining alcohols were identified in both samples at similar levels. The alcohol present in the highest concentrations in males and females was C₁₈ (55.2 and 48.8%, respectively). The alcohols found in our study ranged from C₁₀ to C₂₄, and similar profiles were identified in *Locusta migratoria migratoriodes* (from C₁₀ to C₃₄) and *Schistocerca gregaria* (from C₁₀ to C₃₂) [40]. It is known that the amounts of alcohols in the cuticular lipids of an insect may differ significantly between various species. For example, alcohols made up 42% of all cuticular lipids in pupae of *Heliothis virescens* [37], but only 3 and 4% in nymphs and exuviae of *B. argentifolii* [32]. In our work, the cuticular alcohols in male and female *L. sericata* were <1% of all lipids. Internal lipids of females and males of *L. sericata* respectively contained three (from C₁₄ to C₂₂) and five (from C₁₄ to C₂₆) alcohols in trace quantities.

Diverse biological functions of cuticular alcohols have been reported. In the European honey bee, alcohols may protect against parasite attack. Extracts of *Apis mellifera* cocoons containing alcohols of 17–22 carbons induce a strong arrestment response in the mite *Varroa jacobsoni* [41]. A mixture of short chain alcohols, their acetate derivatives, and (Z)-11-eicosenol secreted by the sting apparatus of the worker honey bee are components of bee alarm pheromones [42]. The sex pheromones of the three most important tortricids of European vineyards, *Eupoecilia ambiguella*, *Sparganothis pilleriana* and *Lobesia botrana*, have been chemically investigated and found to contain up to 15 different straight-chain acetates and alcohols [43]. The role of alcohols found in *L. sericata* remains unknown.

In cuticular and internal lipids of *L. sericata*, cholesterol was identified on the basis of the characteristic ions (m/z 129 (100%), 329 (87%), 145 (38%), 121 (36%), 353 (32%) and M^+ 458) [44] (as the trimethylsilyl ether). Female lipids contained twice as much cholesterol as male lipids. Internal cholesterol in male and female extracts made up 2 and 5% of all lipids, respectively. The respective quantities of cholesterol obtained from male and female *L. sericata* were 0.49 ± 0.02 and 0.97 ± 0.03 mg/g of the insect body, respectively. There was a tenfold higher concentration of cholesterol in internal lipids. Sterols are minor constituents of cuticular lipids [45]. The cholesterol content in cuticular male and female lipids was 7.6 ± 0.4 and 11.4 ± 0.8 $\mu\text{g/g}$, respectively. Assuming that sterols are mandatory for egg production and normal embryonic development, a higher concentration of internal cholesterol in *L. sericata* females seems justified. In contrast, the physiological role of cuticular cholesterol remains obscure.

Naturally occurring entomopathogenic fungi are important regulatory factors of insect populations. *Conidiobolus coronatus*, a cosmopolitan soil fungus causing rapid death of susceptible insects, due to the secretion of toxic metabolites [46, 47] was used in current studies. Exposure of *L. sericata* to sporulating fungal colonies resulted in prompt death of both, males and females while larvae and pupae remained unharmed and developed normally. Similarly, the larvae of closely related *C. vicina* showed amazing resistance to *C. coronatus*, while exposure of two lepidopteran larvae, *G. mellonella* and *D. pini*, resulted in their death. Microscopic studies revealed that the conidia of *C. coronatus* did not germinate on the cuticle of *C. vicina* larvae while the cuticles of both lepidopteran larvae were infiltrated by fungal hyphae [47, 48]. The impressive *C. vicina* resistance to fungus is accompanied by a high resistance of the cuticle to degradation by fungal proteases and a high antiproteolytic capacity of insect hemolymph. On the other hand, the immune system of challenged larvae shows very low activity of both, cellular and humoral components. It seems that the significant protection provided by the *C. vicina* cuticle reduces potentially costly defense responses within the hemocoel. Investment in cuticular protection comes at the cost of low phenoloxidase, lysozyme, encapsulation, and phagocytic activities [48]. The cuticular fatty acids profile of *C. vicina* larvae significantly differs from profiles of *D. pini* and *G. mellonella*. Data from in vitro cultures of *C. coronatus* in media supplemented with various fatty acids showed strong fungistatic effects of 18:2n-6, 18:3n-6, 20:1n-3, and 20:0 [21]. It should be pointed out that all these compounds are missing in the cuticular lipids of *L. sericata* adults (traces of 20:0 were detected in females only). On the other hand, 16:1n-9 stimulating fungal virulence [21] is present at high concentrations in both males and females (10.3 and

15.2% of all cuticular lipids, respectively) suggesting that this compound may be responsible for the prompt death of flies exposed to *C. coronatus* colonies. Analysis of cuticular lipids of *L. sericata* larvae and pupae (currently underway in our laboratories) should provide information on whether the high susceptibility of *L. sericata* adults to fungal infection opposed to the resistance of the larvae and pupae is linked with diverse cuticular lipid profiles. Work on the effects of new compounds found in adults of *L. sericata* on the pathogenicity potential of this entomopathogen is in progress. Knowledge of the role of cuticular lipids in fungal interaction with the insect host can be expected to contribute to a better understanding of the nature of fungal pathogenicity.

Acknowledgments We would like to express our gratitude to Dagmara Gąsiewska for her assistance. Financial support was provided by the Polish Ministry of Science and Higher Education for 2010–2013 grants: N N303 504238 and DS 8110-4-0085-1.

Open Access This article is distributed under the terms of the Creative Commons Attribution License which permits any use, distribution, and reproduction in any medium, provided the original author(s) and the source are credited.

References

- Mateos M, Leon A, Gonzalez-Herranz P, Burgos J, Lopez-Mondejar JA, Baquero F (1990) *Lucilia sericata* infestation of the skin openings for the bone traction device in lengthening of the tibia: apropos of a case [in Spanish]. *Enferm Infecc Microbiol Clín* 8:365–367
- Morsy TA, Fayad ME, Salama MM, Sabry AH, el-Serougi AO, Abdallah KF (1991) Some myiasis producers in Cairo and Giza abattoirs. *J Egypt Soc Parasitol* 21:339–346
- Granz W, Schneider D, Schumann H (1975) Human myiasis in middle Europe [in German]. *Z gesamte innere Med Grenz* 30:293–301
- Prete PE (1996) Growth effects of *Phaenicia sericata* larval extracts on fibroblast: mechanism for wound healing by maggot therapy. *Life Sci* 60:505–510
- Daeschlein G, Mumcuoglu KY, Assadian O, Hoffmeister B, Kramer A (2007) In vitro antibacterial activity of *Lucilia sericata* maggot secretions. *Skin Pharmacol Physiol* 20:112–115
- Zhang Z, Wang S, Diao Y, Zhang J, Lv D (2010) Fatty acid extracts from *Lucilia sericata* larvae promote murine cutaneous wound healing by angiogenic activity. *Lipids Health Dis* 9:24–32
- Hadley NF, Blomquist GJ, Lanham UN (1981) Cuticular hydrocarbons of four species of Colorado Hymenoptera. *Insect Biochem* 11:173–177
- Roberts DR, Hajek AE (1992) Entomopathogenic fungi as bio-insecticides. In: Leatham GF (ed) *Frontiers in industrial mycology*. Chapman and Hall, New York, pp 144–159
- Clarkson JM, Charnley AK (1996) New insight into the mechanisms of fungal pathogenesis in insects. *Trends Microbiol* 4:197–203
- Khachatourians GG (1996) Biochemistry and molecular biology of entomopathogenic fungi. In: Howard DH, Miller JD (eds) *The Mycota VI. Human and animal relationships*. Springer, Berlin, pp 331–363

11. Shah PA, Pell JK (2003) Entomopathogenic fungi as biological control agents. *Appl Microbiol Biotechnol* 61:413–423
12. Faria M, Wraight SP (2007) Mycoinsecticides and mycoacaricides: a comprehensive list with worldwide coverage and international classification of formulation types. *Biol Control* 43:237–256
13. Vilcinskas A, Götz P (1999) Parasitic fungi and their interactions with the insect immune system. *Adv Parasitol* 43:267–313
14. Gillespie JP, Bailey AM, Cobb B, Vilcinskas A (2000) Fungi as elicitors of insect immune responses. *Arch Insect Biochem Physiol* 44:49–68
15. Fargues J, Delmas JC, Lebrun RA (1991) Fecundity and egg fertility in the adult Colorado beetle (*Leptinotarsa decemlineata*) surviving larval infection by the fungus *Beauveria bassiana*. *Entomol Exp Appl* 61:45–51
16. Napolitano R, Juarez MP (1997) Entomopathogenic fungi degrade epicuticular hydrocarbons of *Triatoma infestans*. *Arch Biochem Biophys* 344:208–214
17. Saito T, Aoki J (1983) Toxicity of free fatty acids on the larval surfaces of two lepidopterous insects towards *Beauveria bassiana* (Bals.) Vuill. and *Poecilomyces fumoso-roseus* (Wise) Brown et Smith (Deuteromycetes: Moniliales). *Appl Entomol Zool* 18:225–233
18. Smith RJ, Grula EA (1981) Nutritional requirements for conidial germination and hyphal growth of *Beauveria bassiana*. *J Invertebr Pathol* 37:222–230
19. Kerwin JL (1982) Chemical control of the germination of asexual spores of *Entomophthora culicis*, a fungus parasitic on dipterans. *J Gen Microbiol* 128:2179–2186
20. Gołębowski M, Maliński E, Boguś MI, Kumirska J, Stepnowski P (2008) The cuticular fatty acids of *Calliphora vicina*, *Dendrolimus pini* and *Galleria mellonella* larvae and their role in resistance to fungal infection. *Insect Biochem Mol Biol* 38:619–627
21. Boguś MI, Czygier M, Gołębowski M, Kędra E, Kucińska J, Mazgajska J, Samborski J, Wieloch W, Włóka E (2010) Effects of insect cuticular fatty acids on in vitro growth and pathogenicity of the entomopathogenic fungus *Conidiobolus coronatus*. *Exp Parasitol* 125:400–408
22. Wieloch W, Boguś MI (2005) Exploring pathogenicity potential of *Conidiobolus coronatus* against insect larvae in various infection conditions. *Pesticides* 4:133–137
23. Sehna F (1966) A critical study of the biome and biometry of the wax moth *Galleria mellonella* raised in varying conditions. *Z Wiss Zool* 174:53–82
24. Wieloch W (2006) Toxic metabolites produced by *Conidiobolus coronatus*. Ph.D. thesis. Institute of Parasitology Polish Academy of Sciences, Warszawa, Poland
25. Gołębowski M, Maliński E, Nawrot J, Stepnowski P (2008) Identification and characterization of surface lipid components of the dried-bean beetle *Acanthoscelides obtectus* (Say) (Coleoptera: Bruchidae). *J Stored Prod Res* 44:386–388
26. Gołębowski M, Boguś MI, Paszkiewicz M, Stepnowski P (2011) Cuticular lipids of insects as a potential biofungicides: methods of lipids composition analysis. *Anal Bioanal Chem* 399:3177–3191
27. Gilbert LI (1967) Lipid metabolism and function in insects. In: Beament JW, Treherne JE, Wigglesworth VB (eds) *Advances in insect physiology*. Academic Press, London, pp 69–211
28. Mathur CF, Yurkiewicz WJ (1969) Incorporation of glucose-¹⁴C into lipids of the blowfly during flight. *J Insect Physiol* 15:1567–1571
29. Yurkiewicz WJ, Smyth T (1966) Effect of temperature on flight speed of the sheep blowfly. *J Insect Physiol* 12:189–194
30. Dean TJ (2003) Fastest flyer. In: *Book of insect records*, chap. 1. University of Florida. http://entnemdept.ufl.edu/walker/ufbir/chapters/chapter_01.shtml
31. Gołębowski M, Boguś MI, Paszkiewicz M, Stepnowski P (2010) The composition of the free fatty acids from *Dendrolimus pini* exuviae. *J Insect Physiol* 56:391–397
32. Buckner JS, Hagen MM, Nelson DR (1999) The composition of the cuticular lipids from nymphs and exuviae of the silver leaf whitefly, *Bemisia argentifolii*. *Comp Biochem Physiol* 124B:201–207
33. Gołębowski M, Maliński E, Nawrot J, Szafranek J, Stepnowski P (2007) Identification of the cuticular lipid composition of the western flower thrips *Frankliniella occidentalis*. *Comp Biochem Physiol* 147B:288–292
34. Howard RW, Lord JC (2003) Cuticular lipids of the booklouse, *Liposcelides bostrychophola*: hydrocarbons, aldehydes, fatty acids, and fatty acid amides. *J Chem Ecol* 29:615–627
35. Kerwin JL (1984) Fatty acid regulation of the germination of *Erynia variabilis* conidia on adults and puparia of the lesser housefly, *Fannia canicularis*. *Can J Microbiol* 30:158–161
36. Kiyashko SI, Imbs AB, Narita T, Svetashev VI, Wada E (2004) Fatty acid composition of aquatic insect larvae *Stictochironomus pictulus* (Diptera: Chironomidae): evidence of feeding upon methanotrophic bacteria. *Comp Biochem Physiol* 139B:705–711
37. Buckner JS, Mardaus MC, Nelson DR (1996) Cuticular lipid composition of *Heliothis virescens* and *Helicoverpa zea* pupae. *Comp Biochem Physiol* 114B:207–216
38. Buckner JS, Nelson DR, Mardaus MC (1994) The lipid composition of the wax particles from adult whiteflies, *Bemisia tabaci* and *Trialeurodes vaporariorum*. *Insect Biochem Mol Biol* 24:977–987
39. Nelson DR, Fatland CL, Buckner JS, Freeman TP (1999) External lipids of adults of the giant whitefly, *Aleurodicus dugesii*. *Comp Biochem Physiol* 123B:137–145
40. Orah VS, Lockey KH (1990) Cuticular lipids of *Locusta migratoria migratoriodes*, *Schistocerca gregaria* and other orthopteran species. Polar components. *Comp Biochem Physiol* 95B:603–608
41. Donze G, Schnyder-Candrian S, Bogdanov S, Diehl PA, Guerin PM, Kilchenmann V, Monachon F (1998) Aliphatic alcohols and aldehydes of the honey bee cocoon induce arrestment behavior in *Varroa jacobsoni* (Acari: Mesostigmata), an ectoparasite of *Apis mellifera*. *Arch Insect Biochem Physiol* 37:129–145
42. Pickett JA, Williams IH, Martin AP (1982) (Z)-11-eicosen-1-ol, an important new pheromonal component from the sting of the honey bee, *Apis mellifera* L. (Hymenoptera, Apidae). *J Chem Ecol* 8:163–175
43. Arn H, Rauscher S, Guerin P, Buser HR (1998) Sex pheromone blends of three tortricid pests in European vineyards. *Agric Ecol Environ* 21:111–117
44. Steel G, Henderson W (1972) Rapid method for detection and characterization of steroids. *Anal Chem* 44:1302–1304
45. Lockey KH (1988) Lipids of the insect cuticle: origin, composition and function. *Comp Biochem Physiol B* 89:595–645
46. Boguś MI, Scheller K (2002) Extraction of an insecticidal protein fraction from the pathogenic fungus *Conidiobolus coronatus*. *Acta Parasitol* 47:66–72
47. Boguś MI, Kędra E, Bania J, Szczepanik M, Czygier M, Jabłoński P, Pasztaleniec A, Samborski J, Mazgajska J, Polanowski A (2007) Different defense strategies of *Dendrolimus pini*, *Galleria mellonella*, and *Calliphora vicina* against fungal infection. *J Insect Physiol* 53:909–922
48. Boguś MI, Szczepanik M (2000) Histopathology of *Conidiobolus coronatus* infection in *Galleria mellonella* larvae. *Acta Parasitol* 45:48–54

Lipid Class and Fatty Acid Content of the *Leptocephalus* Larva of Tropical Eels

D. Deibel · C. C. Parrish · P. Grønkjær ·
P. Munk · T. Gissel Nielsen

Received: 26 September 2011 / Accepted: 23 March 2012 / Published online: 17 April 2012
© AOCS 2012

Abstract The leptocephalus larva of eels distinguishes the elopomorph fishes from all other bony fishes. The leptocephalus is long lived and increases in size primarily through the synthesis and deposition of glycosaminoglycans. Energy stored during the larval stage, in the form of glycosaminoglycan and lipids, is required to fuel migration, metamorphosis and metabolism of the subsequent glass eel stage. Despite the importance of energy storage by leptocephali for survival and recruitment, their diet, condition and lipid content and composition is essentially unknown. To gain further insight into energy storage and condition of leptocephali, we determined the lipid class and fatty acid concentration of larvae collected on a cross-shelf transect off Broome, northwestern Australia. The total lipid concentration of two families and four sub-families of leptocephali ranged from 2.7 to 7.0 mg g wet weight⁻¹, at the low end of the few published values. Phospholipid and triacylglycerol made up ca. 63 % of the total lipid pool. The triacylglycerol:sterol ratio, an index of nutritional condition, ranged from 0.9 to 3.7, indicating that the leptocephali were in good condition. The predominant fatty acids were 16:0 (23 mol%), 22:6n-3 (docosahexaenoic acid, DHA, 16 mol%), 18:0 (8.2 mol%), 20:5n-3 (eicosapentaenoic

acid, EPA, 6.7 mol%), 18:1n-9 (6.4 mol%) and 16:1n-7 (6.3 mol%). The DHA:EPA ratio ranged from 2.4 to 2.9, sufficient for normal growth and development of fish larvae generally. The leptocephali had proportions of bacterial markers >4.4 %, consistent with the possibility that they consume appendicularian houses or other marine snow that is bacteria rich.

Keywords Eel · *Leptocephalus* · Total lipid · Fatty acid · Lipid class · Triacylglycerol · DHA · EPA · Galathea 3

Abbreviations

ARA	Arachidonic acid
AMPL	Acetone mobile polar lipid(s)
ANOVA	Analysis of variance
CV	Coefficient of variation
DHA	Docosahexaenoic acid
EFA	Essential fatty acid(s)
EPA	Eicosapentaenoic acid
FA	Fatty acid(s)
FAME	Fatty acid methyl ester(s)
FFA	Free fatty acid(s)
GAG	Glycosaminoglycans(s)
GC-FID	Gas chromatography with flame ionization detection
HPLC	High performance liquid chromatography
LI	Lipolysis index
MUFA	Monounsaturated fatty acid(s)
PL	Phospholipid(s)
P/S	Polyunsaturated/saturated fatty acid ratio
PUFA	Polyunsaturated fatty acid(s)
SFA	Saturated fatty acid(s)
SL	Standard length
SPSS	Statistical Package for the Social Sciences
ST	Sterol(s)

D. Deibel (✉) · C. C. Parrish
Ocean Sciences Centre, Memorial University
of Newfoundland, St. John's, NL A1C 5S7, Canada
e-mail: ddeibel@mun.ca

P. Grønkjær
Department of Bioscience, Aarhus University,
Ole Worms Allé 1, 8000 Aarhus C, Denmark

P. Munk · T. G. Nielsen
National Institute of Aquatic Resources, Technical University
of Denmark, Kavalergården 6, 2920 Charlottenlund, Denmark

TAG	Triacylglycerol(s)
TLC-FID	Thin layer chromatography with flame ionization detection
WW	Blotted wet weight

Introduction

The life history of elopomorph fishes (i.e. bonefish, ladyfish, tarpon and true eels) differs from that of all other fishes because of the presence of a long lived, gelatinous larval stage known as the leptocephalus [1]. While most fish larvae have a development time of days to a few weeks, leptocephali may live for a few weeks, several months, or >1 year [1–3]. This raises many questions concerning the adaptations of leptocephali enabling such a long pre-metamorphic existence, including predator avoidance behavior and food acquisition. How they feed has been a mystery for centuries [4], as most leptocephali collected in nature have empty guts [5]. It has been suggested that they feed on marine snow, including larvacean tunicate houses [6], perhaps supplemented by direct uptake of dissolved nutrients from seawater solution [5]. New genetic data of gut contents suggests that small leptocephali of the European eel *Anguilla anguilla* feed on a variety of zooplanktonic prey in the Sargasso Sea, dominated by gelatinous taxa such as the hydrozoans, some species of which are commonly known as jellyfish [7].

While there is some knowledge of pre-metamorphic lipid dynamics of the leptocephali of bonefish [8], little is known about the nutritional state or biochemical condition of eel leptocephali in the field. Essentially nothing is known of pre-metamorphic energy storage by eel leptocephali or of changes in lipid and fatty acid content and composition during metamorphosis [9]. Both migration by leptocephali and their metamorphosis into juvenile eels require considerable quantities of energy. Bonefish leptocephali obtain the energy for metamorphosis by catabolizing endogenous reserves, primarily lipids and carbohydrates, which are stored during the pre-metamorphic time period. Most of these reserves are stored in the acellular, gelatinous matrix of the leptocephali [10] which is composed of various sulfated glycosaminoglycans (GAG) [11]. Glycosaminoglycans make up most of the organic mass of bonefish and eel leptocephali, which have a water content >90 % [2, 11]. As leptocephali approach the time of metamorphosis to the glass eel stage, GAG are metabolized, leading to a considerable decrease in water content (ca 80 %) and to body shrinkage by up to 75 % [10]. However, it has been suggested that bonefish leptocephali also lose ca. 50 % of their total lipids during

metamorphosis, providing ca. 80 % of the energy required to undertake this crucial life history transformation [8, 11]. Furthermore, it has been suggested that the endogenous energy reserves of the glass eel stage are provided by the leptocephali depot lipids which remain following metamorphosis [12]. Thus, energy storage during the leptocephalus stage is of crucial importance not only for metamorphosis, but also for the critical post-metamorphic stage, when glass eels may be under nutritional stress [12].

This paper reports the first determination of the lipid class and fatty acid content and composition of eel leptocephali. We explored the following questions of pre-metamorphic leptocephali: (1) what is the total lipid, lipid class and fatty acid content and composition of eel leptocephali? (2) How do lipid and fatty acid content and composition vary among several families and sub-families of leptocephali? (3) Is there evidence of lipid storage, and which lipid classes and fatty acids are accumulated? (4) What is the nutritional condition of the leptocephali? These questions are significant because lipids and fatty acids are important in leptocephalus nutrition, to the fueling of larval metamorphosis [8], and as dietary indicators. The true eels (Anguilliformes) are distributed throughout tropical and temperate waters worldwide [1]. They inhabit ecosystems from the coastal zone to the deep sea, with more than 600 species globally [1]. Eel leptocephali can be highly concentrated in specific oceanic environments, and often many different species of leptocephali can be collected within a relatively small area [1].

Methods

Leptocephali were collected at eight stations from 9 to 15 November 2006 on a cross-shelf transect off Broome, Australia, eastern Indian Ocean (stations 3–10) (Fig. 1). The stations ranged in depth from 87 to 1,699 m (Table 1). This transect was part of leg 7 of the Galathea 3 expedition on board the Danish Navy surveillance frigate “F359” Vædderen.

Water column properties were characterized by a Sea-bird SBE 9/11 CTD Sealogger equipped with 12, 30-l bottles on a rosette sampler. Rosette casts from the surface to within 10 m of the bottom were performed prior to each net tow. Tows for fish larvae were made using a ring net with a mouth diameter of 2 m and a mesh size of 0.55 mm. The gear was lowered from the surface to within 10 m of the bottom, or a maximum of 200 m, and then retrieved. Tow velocity was ca. 1 ms⁻¹ for a duration of 30–45 min, resulting in a range of tow volumes from 5,101 to 14,130 m³ (Table 1). All samples presented in this paper were collected between sunset and midnight.

When the gear was on deck, the cod end contents were immediately washed into plastic buckets and taken to the

Fig. 1 Station locations on the Broome transect off the coast of northwest Australia. Also shown are bathymetric contours, 50, 100, 150, 250, 500 and 1,000 m (map courtesy of R. Brushett). Bathymetry is approximate. For more accurate depth values see Table 1

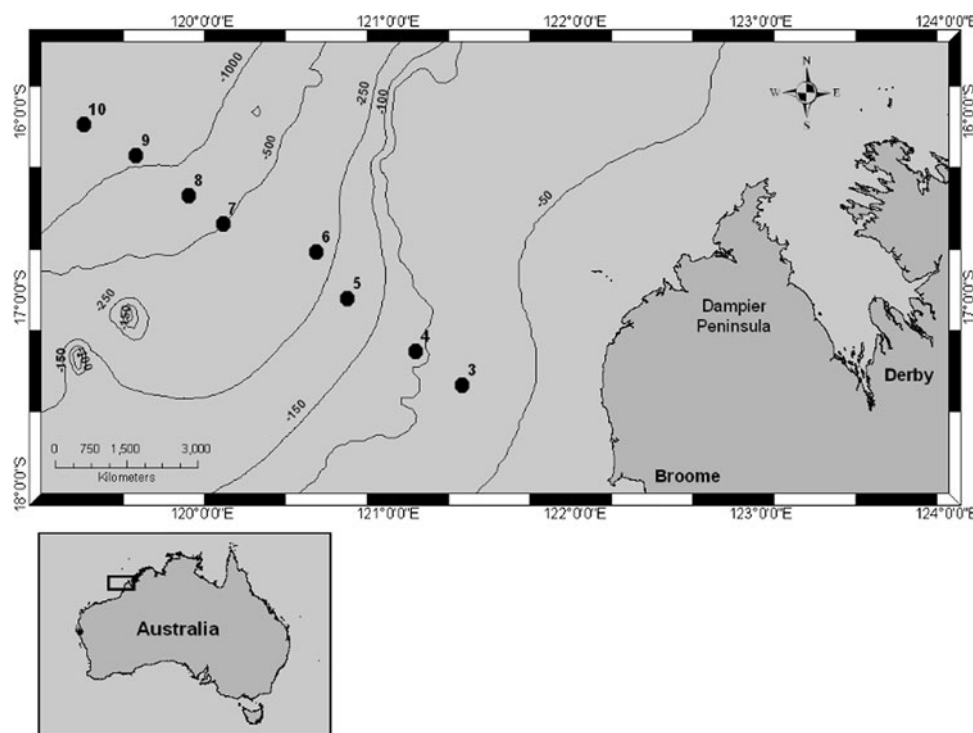


Table 1 Summary of station and ring net tow information on the Broome transect for the collection of eel leptocephalus larvae

Station	Date (dd/mm/yy)	Latitude (S, dd.mm.ss)	Longitude (E, ddd.mm.ss)	Depth (m)	Time of ring net tow (hhmm, local)	Profile of ring net tow (m)	Volume of ring net tow (m ³)
3	09/11/06	17.27.75	121.24.08	87	2200	0-77-0	6,038
4	10/11/06	17.17.12	121.09.18	113	2300	0-103-0	6,969
5	11/11/06	17.00.20	120.46.56	170	2100	0-160-0	10,892
6	12/11/06	16.45.20	120.36.76	364	2200	0-200-0	8,491
7	13/11/06	16.36.40	120.07.25	460	2000	0-200-0	11,865
8	13/11/06	16.27.49	119.56.38	589	2100	0-200-0	14,130
9	14/11/06	16.13.55	119.39.32	1,162	2000	0-200-0	8,457
10	15/11/06	16.03.96	119.21.95	1,699	2000	0-200-0	5,101
Mean (±sd)				581 ± 571			8,993 ± 3,088

A map of the station transect is shown in Fig. 1

laboratory for sorting. Within an hour, the leptocephali were sorted and placed in plastic trays containing pre-chilled seawater. The trays were stored in a refrigerator at ca. 5 °C for 1–2 h before further sample processing.

Next, each leptocephalus was removed from its sorting tray and identified to the lowest taxonomic level possible (family or sub-family) following the descriptions of Miller and Tsukamoto [1]. Standard length (SL) was determined to the nearest 0.1 mm using a dissecting microscope with an ocular micrometer. The larvae were then rinsed in filtered seawater and placed into small, plastic weighing boats. Guts were examined for particulate content with a dissecting microscope and documentary photomicrographs taken. After all leptocephali were identified and measured

at a particular station, they were blotted dry and wet weight was determined to the nearest 10 mg. The leptocephali were then placed in a freezer at –20 °C until further processing.

Leptocephali were selected haphazardly from the trays for lipid extraction, making sure to obtain a representative range of body sizes at each station. They were removed from the freezer, rinsed on each side with distilled water and placed in lipid-cleaned, glass test tubes. High performance liquid chromatography (HPLC)-grade chloroform was added sufficient to cover the larvae. The test tubes were then placed on ice until all animals had been processed. The head space of each tube was then purged for 15 s with N₂ and the caps wrapped with Teflon tape to

ensure a tight seal. The purged tubes were stored at $-20\text{ }^{\circ}\text{C}$ onboard ship, and returned to the laboratory in an insulated container on dry ice. Total system blanks were run at each station to monitor sample contamination.

Laboratory Analyses

Extractions

Lipid samples were extracted according to Parrish [13]. Samples were homogenized in a 2:1 mixture of ice-cold chloroform:methanol using a Polytron PCU-2-110 homogenizer (Brinkmann Instruments, Rexdale, ON, Canada). Chloroform-extracted water was added to bring the ratio of chloroform:methanol:water to 8:4:3. The sample was sonicated for 10 min in an ice bath and centrifuged at 5,000 rpm for 2 min. The bottom organic layer was removed using a double pipetting technique, placing a long lipid-cleaned Pasteur pipette inside a short one, to remove the organic layer without disturbing the top aqueous layer. Chloroform was then added back to the extraction test tube and the entire procedure repeated three times. All the organic layers were pooled into a lipid-cleaned vial. The samples were concentrated using a flash-evaporator (Buchler Instruments, Fort Lee, N.J.).

Lipid class composition was determined using an Iatroscan Mark V thin layer chromatograph with flame ionization detection (TLC-FID), silica-coated Chromarods and a three-step development method [14]. The lipid extracts were applied to the Chromarods and focused to a narrow band using 100 % acetone. The first development system was hexane:diethyl ether:formic acid (99.95:1:0.05). The rods were developed for 25 min, removed from the system for 5 min and replaced for 20 min. The second development was for 40 min in hexane:diethyl ether:formic acid (79:20:1). The final development system had two steps, the first was 100 % acetone for two, 15-min time periods, followed by two 10-min periods in chloroform:methanol:chloroform-extracted water (5:4:1). Before being exposed to each solvent system the rods were equilibrated in a constant humidity chamber. After each development system, the rods were scanned in the Iatroscan and the three scans were joined using the T data scan 3.10 chromatography analysis program (RSS Inc., Bennis, Tenn., USA). The Chromarods were calibrated using standards from Sigma Chemicals (St. Louis, MO, USA). Blanks were run exactly as were the samples, and were subtracted from the sample lipid class values before statistical analysis and plotting. Blank values were generally $<1\%$ of sample values for most lipid classes. Lipids were quantitatively extracted from a known wet mass of sample and individual class amounts were calibrated using standards. The lipid masses were divided by the wet weight of the sample after

blank correction. In this paper, values are reported both as lipid concentration ($\mu\text{g g wet weight}^{-1}$), and as lipid proportion [(mass of each lipid class/mass of total lipids) $\times 100\%$].

Lipid extracts were transesterified using 14 % BF_3/MeOH for 1.5 h at $85\text{ }^{\circ}\text{C}$. Using TLC-FID, we found that this method derivatized over 90 % of the acyl lipids in leptocephalus larvae. A majority of the fatty acid methyl esters (FAME) were analysed on a HP 6890 gas chromatograph with flame ionization detection (GC-FID) equipped with a 7683 autosampler. The GC column was a ZB wax+ (Phenomenex, USA). The column length was 30 m with an internal diameter of $0.25\text{ }\mu\text{m}$. The column temperature began at $65\text{ }^{\circ}\text{C}$ which was maintained for 0.5 min. The temperature ramped to $195\text{ }^{\circ}\text{C}$ at a rate of $40\text{ }^{\circ}\text{C min}^{-1}$, held for 15 min, then ramped to a final temperature of $220\text{ }^{\circ}\text{C}$ at a rate of $2\text{ }^{\circ}\text{C min}^{-1}$. This final temperature was held for 3.25 min. The carrier gas was hydrogen supplied at a rate of 2 ml min^{-1} . The injector temperature started at $150\text{ }^{\circ}\text{C}$ and ramped to a final temperature of $250\text{ }^{\circ}\text{C}$ at a rate of $200\text{ }^{\circ}\text{C min}^{-1}$. The detector temperature stayed constant at $260\text{ }^{\circ}\text{C}$. Peaks were identified using retention times from standards purchased from Supelco, 37 component FAME mix (product number 47885-U), bacterial fatty acid ester mix (product number 47080-U), polyunsaturated fatty acid (PUFA) 1 (product number 47033) and PUFA 3 (product number 47085-U). A majority of our fatty acid identifications were based on standards for which we have GC-MS data on file. The remainder were identified with reference to Ackman [15]. Chromatograms were integrated using either the HP ChemStation Chromatography Software (Version B00.00) or Varian Galaxie software (Version 1.9). Individual fatty acids were blank corrected and expressed as a proportion of total fatty acids (mol/mol). Blank values were generally $<1\%$ of sample values for all fatty acids.

Statistics

Lipid, lipid class and fatty acid concentration ($\text{mg g wet weight}^{-1}$) and proportion (% of total lipids or mol% of total fatty acids) are expressed as mean values ± 1 standard deviation. Seven of the 100 lipid class samples were removed from the data set before analysis, due either to accidental loss or insufficient sample weight. Four of the fatty acid samples were removed for similar reasons. Many of the means were non-normally distributed. Therefore, all data were transformed into ranks before statistical analyses (non-parametric). Differences in the mean rank of all variables among taxa were examined using single factor analysis of variance (ANOVA) with six levels (i.e. the taxonomic groups, Table 2). The ANOVA conclusions were double checked using the Brown-Forsythe robust test

which adjusts the F values for unequal variances (Statistical Package for the Social Sciences, SPSS). A post hoc Hochberg's GT2 test was used to determine which taxa had mean values significantly different from one another. The reject criterion for all statistical tests was $p < 0.05$. Statistical analyses were done using SPSS ver. 18.0.2. Figure 2 was made using SigmaPlot ver. 10.0.

Results

The Leptocephali

Total lipid, lipid class and fatty acid data are reported for leptocephali from six eel families or sub-families; Bathymyrinae (Conger eels), Congrinae (Conger eels), Muraenesocidae (Pike Conger eels), Myrophinae (Worm eels), Ophichthinae (Snake eels), and Nettastomatidae (Duck Bill eels) (Table 2). The larvae ranged in SL from 22 to 150 mm and in blotted wet weight (WW) from 0.02 to 2.30 g (Fig. 2). Wet weight increased exponentially with increasing SL. Most of the larvae analyzed for lipids and fatty acids were <75 mm long and <0.3 g WW. The Bathymyrinae were by far the most abundant and common larvae, and were the only family collected at all eight stations, covering the full range of size and weight of all the larvae (Fig. 2).

The Myrophinae were both the shortest and lightest larvae, with a mean SL of ca. 45.8 mm and WW of 0.09 g, whereas the Muraenesocidae were the largest and heaviest, with a mean SL of 132 mm and weight of 1.40 g (Table 3). These mean SL and WW were significantly different from one another. The mean SL of the Bathymyrinae, Nettastomatidae and Ophichthinae ranged from 66.0 to 73.2 mm and were not significantly different from one another.

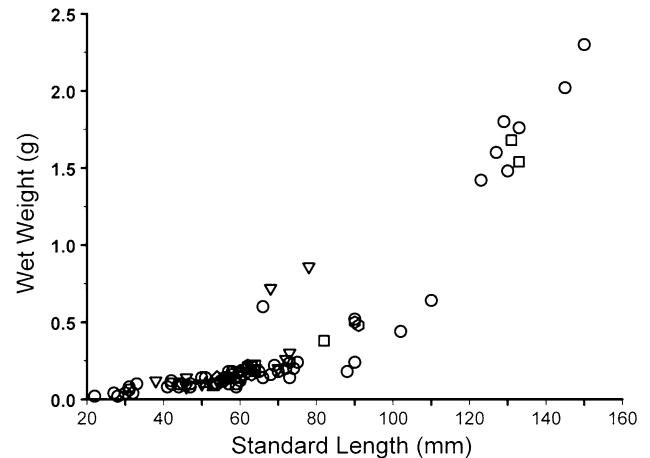


Fig. 2 Wet weight (g) versus standard length (mm) of eel leptocephali collected on the Broome transect. Note that the X axis begins at a standard length of 20 mm. Data points for leptocephali taxa are: circle Bathymyrinae, square Congrinae, diamond Muraenesocidae, hexagon Myrophinae, diamond up Nettastomatidae, diamond down Ophichthinae. The power equation describing this relationship is $WW (g) = 1.3 \times 10^{-5} SL (mm)^{2.34}$ ($n = 88$, $r^2 = 0.86$)

Except for the above mentioned difference in WW between the Muraenesocidae and Myrophinae, the WW of the remaining four taxa ranged from 0.21 to 0.41 g, and were not significantly different from one another.

Total Lipid Concentration and Lipid Class Composition

The mean total lipid concentration per taxon ranged from 2.7 to 7.0 mg g WW⁻¹, with an overall mean for all samples of 3.7 ± 2.4 mg g WW⁻¹ (Table 3). Assuming that eel larvae are ca. 93 % water [1, 16], this overall mean value of total lipids would be equivalent to ca. 5.2 % of dry weight. The Ophichthinae had the highest mean lipid concentration and the Bathymyrinae the lowest (Table 3).

Table 2 Common names, and adult eel habitat characteristics and migratory behavior of the six families and sub-families of eel leptocephali collected on the Broome transect

Family	Subfamily	Common name	Habitat	Migrate
Congridae	Bathymyrinae (shelf)	Conger	Tropical-temperate/sand and mud bottoms/shallow/few species on slope to 2,000 m depth	Short or none/no further than shelf break
	Congrinae (shelf)	Conger	Ditto	Ditto
Muraenesocidae (coastal)	–	Pike congers	Coastal waters <100 m	?
Ophichthidae (coastal)	Myrophinae Ophichthinae	Snake and worm eels	Tropical/intertidal to 750 m/sand, grass, tidal creeks, estuaries	Yes, likely spawn near shelf break
Nettastomatidae (deep slope)	–	Duckbill	Deep water only/slope	?

Information was abstracted from Miller and Tsukamoto [1]. The taxa in bold face are the names that are used in this paper. The “?” indicates cells for which we could not find the pertinent information

Table 3 Mean (\pm sd) standard length, blotted wet weight, and total lipid and lipid class concentrations of six taxa of eel leptocephalus larvae selected haphazardly from ring net samples on the Broome transect (see Table 1; Fig. 1)

	Bathymyrinae	Congrinae	Muraenesocidae	Myrophinae	Nettastomatidae	Ophichthinae	Overall mean
Standard length (mm)	66.0 ^{ab} \pm 28.8 [59]	52.3 ^a \pm 20.6 [6]	132 ^b \pm 1.5 [2]	43.0 ^a \pm 16.6 [5]	72.3 ^{ab} \pm 2.5 [3]	73.2 ^{ab} \pm 18.9 [13]	66.7 \pm 28.1 [88]
Wet weight (g)	0.36 ^{ab} \pm 0.54 [59]	0.41 ^{ab} \pm 0.35 [6]	1.62 ^b \pm 0.20 [2]	0.08 ^a \pm 0.05 [5]	0.21 ^{ab} \pm 0.03 [3]	0.21 ^{ab} \pm 0.16 [13]	0.38 \pm 0.53 [91]
Total lipids (mg g WW ⁻¹)	2.7 ^a \pm 0.9 [59]	5.6 ^{ab} \pm 2.2 [6]	4.1 ^{ab} \pm 2.1 [6]	4.4 ^{ab} \pm 3.3 [4]	4.1 ^{ab} \pm 1.3 [3]	7.0 ^b \pm 3.9 [14]	3.7 \pm 2.4 [93]
Neutral fraction (mg g WW ⁻¹)							
Hydrocarbons	0.04 ^{ab} \pm 0.07 [59] (1.6 %)	0.06 ^{ab} \pm 0.02 [6] (1.1 %)	0.07 ^b \pm 0.04 [6] (1.9 %)	0.11 ^b \pm 0.13 [4] (2.5 %)	0 ^a [3] (0 %)	0.08 ^b \pm 0.06 [14] (1.4 %)	0.05 \pm 0.07 [92] (1.5 %)
Steryl esters + wax esters	0.03 \pm 0.03 [60] (1.0 %)	0.04 \pm 0.06 [6] (0.7 %)	0.05 \pm 0.03 [6] (1.2 %)	0.09 \pm 0.16 [4] (2.0 %)	0.01 \pm 0.008 [3] (0.22 %)	0.04 \pm 0.02 [14] (0.6 %)	0.03 \pm 0.05 [93] (0.9 %)
Ethyl esters	0.007 \pm 0.003 [60] (0.3 %)	0.008 \pm 0.01 [6] (0.1 %)	0.003 \pm 0.008 [6] (0.04 %)	0 [4] (0 %)	0 [3] (0 %)	0.01 \pm 0.02 [14] (0.1 %)	0.007 \pm 0.02 [93] (0.2 %)
Methyl esters	0.004 \pm 0.02 [60] (0.1 %)	0 [6] (0 %)	0.006 \pm 0.008 [6] (0.2 %)	0 [4] (0 %)	0.005 \pm 0.007 [3] (0.28 %)	0.007 \pm 0.01 [14] (0.1 %)	0.004 \pm 0.02 [93] (0.1 %)
Ethyl ketones	0.02 \pm 0.06 [60] (0.8 %)	0.03 \pm 0.04 [6] (0.6 %)	0.03 \pm 0.04 [6] (0.47 %)	0.15 \pm 0.27 [4] (3.4 %)	0.02 \pm 0.02 [3] (0.49 %)	0.03 \pm 0.05 [14] (0.5 %)	0.03 \pm 0.08 [93] (0.8 %)
Methyl ketone	0.004 \pm 0.01 [60] (0.2 %)	0.01 \pm 0.02 [6] (0.2 %)	0.0002 \pm 0.0005 [6] (0.007 %)	0.01 \pm 0.03 [4] (0.2 %)	0.02 \pm 0.02 [3] (0.46 %)	0.009 \pm 0.03 [14] (0.1 %)	0.006 \pm 0.02 [93] (0.2 %)
Diacylglycerol ethers	0.004 \pm 0.02 [60] (0.2 %)	0 [6] (0 %)	0.0003 \pm 0.0008 [6] (0.01 %)	0.006 \pm 0.01 [4] (0.1 %)	0 [3] (0 %)	0.002 \pm 0.007 [14] (0.03 %)	0.003 \pm 0.01 [93] (0.1 %)
Triacylglycerols	0.5^a \pm 0.3 [60] (19 %)	2.1^b \pm 1.4 [6] (35 %)	1.3^{ab} \pm 0.8 [6] (31 %)	0.72^{ab} \pm 0.66 [4] (16 %)	0.9^{ab} \pm 1.0 [3] (22 %)	2.0^b \pm 1.9 [14] (25 %)	0.89 \pm 1.0 [93] (21 %)
Free fatty acids	0.2 \pm 0.2 [60] (5.6 %)	0.2 \pm 0.1 [6] (2.9 %)	0.2 \pm 0.1 [6] (3.5 %)	0.37 \pm 0.29 [4] (8.4 %)	0.3 \pm 0.3 [3] (6.4 %)	0.4 \pm 0.2 [14] (6.9 %)	0.22 \pm 0.20 [93] (5.6 %)
Alcohols	0.03 \pm 0.06 [60] (0.9 %)	0.03 \pm 0.03 [6] (0.4 %)	0.002 \pm 0.004 [6] (0.02 %)	0.11 \pm 0.13 [4] (2.5 %)	0.005 \pm 0.007 [3] (0.10 %)	0.03 \pm 0.06 [14] (0.5 %)	0.03 \pm 0.06 [93] (0.8 %)
Sterols	0.5^{ab} \pm 0.2 [60] (18 %)	0.6^{bc} \pm 0.1 [6] (12 %)	0.3^a \pm 0.2 [6] (8.4 %)	0.85^c \pm 0.23 [4] (19 %)	0.6^{bc} \pm 0.6 [3] (14 %)	0.7^{bc} \pm 0.2 [12] (12 %)	0.54 \pm 0.21 [93] (17 %)
Diacylglycerols	0.03 \pm 0.09 [60] (1.0 %)	0.09 \pm 0.01 [6] (0.2 %)	0.03 \pm 0.04 [6] (0.43 %)	0.13 \pm 0.27 [4] (3.0 %)	0.05 \pm 0.07 [3] (1.5 %)	0.07 \pm 0.08 [14] (1.1 %)	0.04 \pm 0.02 [93] (1.0 %)
Polar fraction (mg g WW ⁻¹)							
Acetone-mobile polar lipids	0.25 \pm 0.19 [60] (9.1 %)	0.3 \pm 0.2 [6] (5.2 %)	0.3 \pm 0.2 [6] (7.0 %)	0.37 \pm 0.26 [4] (8.4 %)	0.3 \pm 0.03 [3] (7.6 %)	0.7 \pm 0.7 [14] (11 %)	0.34 \pm 0.37 [93] (9.0 %)
Phospholipids	1.1 \pm 0.4 [60] (42 %)	2.2 \pm 7.4 [6] (41 %)	1.8 \pm 0.8 [6] (46 %)	1.5 \pm 1.5 [4] (34 %)	1.9 \pm 2.0 [3] (47 %)	2.8 \pm 1.4 [14] (41 %)	1.5 \pm 0.9 [93] (42 %)
Ratios							
Neutral/total lipids	0.49 \pm 0.09 [59]	0.54 \pm 0.07 [6]	0.47 \pm 0.05 [6]	0.67 \pm 0.19 [4]	0.47 \pm 0.47 [3]	0.49 \pm 0.05 [14]	0.49 \pm 0.09 [93]
Polar/total lipid	0.51 \pm 0.09 [59]	0.46 \pm 0.07 [6]	0.53 \pm 0.05 [6]	0.33 \pm 0.19 [4]	0.53 \pm 0.53 [3]	0.52 \pm 0.05 [14]	0.51 \pm 0.09 [93]
Triacylglycerols/ sterols	1.26 ^{ab} \pm 1.02 [60]	3.36 ^{bc} \pm 2.31 [6]	3.74 ^c \pm 0.85 [6]	0.85 ^a \pm 0.63 [4]	1.51 ^{abc} \pm 1.61 [3]	2.40 ^{abc} \pm 1.37 [14]	1.68 \pm 1.38 [93]
Sterols/phospho lipids	0.47 ^b \pm 0.28 [60]	0.33 ^{ab} \pm 0.15 [6]	0.19 ^a \pm 0.02 [6]	2.6 ^b \pm 3.2 [4]	0.34 ^{ab} \pm 0.32 [3]	0.32 ^{ab} \pm 0.18 [14]	0.51 \pm 0.78 [93]
Lipolysis index	0.08 \pm 0.07 [60]	0.04 \pm 0.03 [6]	0.04 \pm 0.02 [6]	0.17 \pm 0.13 [4]	0.08 \pm 0.08 [3]	0.09 \pm 0.04 [14]	0.08 \pm 0.06 [93]

Table 3 continued

	Bathymyrinae	Congrinae	Muraenesocidae	Myrophinae	Nettastomatidae	Ophichthinae	Overall mean
SEWE/ SEWE + TAG	0.07 ± 0.13	0.02 ± 0.02	0.04 ± 0.03	0.32 ± 0.47	0.01 ± 0.01	0.02 ± 0.02	0.06 ± 0.15
	[59]	[6]	[6]	[4]	[3]	[14]	[92]

The values in square brackets are the number of samples used to calculate each mean [n] and for lipid classes the values in parentheses represent the mean % of total lipids. The lipolysis index was calculated as $[\text{free fatty acids} + \text{alcohols} (\text{acyl lipids} + \text{alcohols})^{-1}] \times 100$, where acyl lipids = the sum of the concentrations of steryl esters + wax esters, ethyl esters, methyl esters, glyceryl ethers, triacylglycerols, diacylglycerols, free fatty acids, acetone mobile polar lipids and phospholipids. All ratios are w/w and are without units. Numbers in bold face are the three predominant lipid classes in each taxon. Superscripts indicate values not significantly different from one another (single factor ANOVA by ranks). A response variable without superscripts indicates that all means in that particular row are not significantly different from one another. When $n < 4$, the standard deviation was replaced by 50 % of the range of the data

This difference was significant. The mean lipid concentrations of the remaining taxa were not significantly different from one another.

Over all taxa and stations the most abundant lipid classes were phospholipids (PL) (42 % of total lipids), triacylglycerol (TAG) (21 %), sterols (ST) (17 %), acetone mobile polar lipids (AMPL) (9 %) and free fatty acids (FFA) (5.6 %) (Table 3). These five lipid classes accounted for ca. 95 % of total lipids. Across all taxa, ST and PL concentration were most conserved, with coefficients of variation (CV) of overall mean values of 39 and 60 %, respectively. Triacylglycerols and AMPL were most variable, with CV of 112 and 109 %, respectively. Sample contamination and hydrolysis appear to have been minimal, as both hydrocarbons and FFA had overall mean proportions < 7 % of total lipids (Table 3). The Bathymyrinae and Myrophinae were the only two families with TAG proportions ≤ 20 %.

Among the polar lipids, phospholipid (PL) mean concentrations ranged from 1.1 to 2.8 mg g WW⁻¹, but were not significantly different as a function of taxon (Table 3). The PL proportion was essentially identical in five of the six taxa, ranging from 41 to 47 % of total lipids. The Myrophinae was the only taxon with a PL proportion < 40 % of total lipids.

Ratios of Lipid Classes

Neutral and polar lipids made essentially equal contributions to the total lipid pool, with taxon-specific mean values ranging from a low of 47 % neutral of total lipids for the Muraenesocidae and Nettastomatidae, to a high of 54 % neutral of total lipids for the Congrinae (Table 3). The differences among the mean values of neutral and polar lipid content were not significantly different among the six taxa.

The TAG:ST ratio is often used as an indication of nutritional condition of heterotrophs, i.e. an index of the energy storage-to-cell structure ratio [17]. The mean

TAG:ST ratio varied ca. fourfold among the six families of leptocephali, from a low of 0.85 for the Myrophinae to a maximum of 3.7 for the Muraenesocidae (Table 3).

The lipolysis index [LI, i.e., $\text{FFA} + \text{alcohols} (\text{acyl lipids} + \text{alcohols})^{-1}$] provides an indication of the breakdown of neutral and polar lipids [18]. The mean LI was uniformly low for the six families of leptocephali, generally < 0.10 , except for the Myrophinae, which had a mean LI of 0.16 (Table 3). Post hoc analysis indicated that the mean LI for the Myrophinae was significantly greater than was that of the Congrinae and the Muraenesocidae.

Fatty Acids

The six most common fatty acids were 16:0 (overall mean = 23 mol%), 22:6n-3 (docosahexaenoic acid, DHA, 16 mol%), 18:0 (8.2 mol%), 20:5n-3 (eicosapentaenoic acid, EPA, 6.7 mol%), 18:1n-9 (6.4 mol%) and 16:1n-7 (6.3 mol%) (Table 4). Thus, these six fatty acids (FA) accounted for a mean of 67 mol% of total FA. The fatty acids 16:0 and DHA were clearly predominant, together accounting for ca. 40 mol% of total FA. The fatty acids 16:0, 18:0, EPA and DHA were among the six most common in all six leptocephali taxa. The only qualitative difference in the most common FA occurred in the Muraenesocidae and Ophichthinae, in which 16:1n-7 replaced 18:1n-9 as one of the six most common FA (Table 4).

Twenty-four of the 38 FA shown in Table 4 had significant among-taxon differences in mean proportion, including the six most common FA. 16:0 was particularly highly conserved, with a coefficient of variation of the overall mean of only 10 %. The essential fatty acid (EFA) DHA was more variable, with a CV of the overall mean of 23 %. Taxon-specific mean values of DHA proportion ranged from 15 mol% for the Bathymyrinae to 20 mol% for the Congrinae and Nettastomatidae. This difference in DHA proportion was statistically significant.

Table 4 Mean (\pm sd) mol% fatty acids of total fatty acids and fatty acid marker ratios of six taxa of eel leptocephalus larvae selected at random from ring net samples on the Broome transect (see Table 1; Fig. 1)

Fatty acid or marker ^{A,B}	Bathymyrinae [62]	Congrinae [6]	Muraenesocidae [6]	Myrophinae [6]	Nettastomatidae [3]	Ophichthinae [13]	Overall mean [96]
14:0	5.6 ^{ab} \pm 1.3	4.8 ^a \pm 0.7	6.9 ^b \pm 0.7	3.9 ^a \pm 0.8	4.2 ^a \pm 0.8	4.9 ^a \pm 1.0	5.4 \pm 1.3
15:0	1.8 ^{ab} \pm 0.2	1.9 ^b \pm 0.1	1.8 ^{ab} \pm 0.0	1.5 ^a \pm 0.4	1.6 ^a \pm 0.1	1.5 ^a \pm 0.2	1.8 \pm 0.3
<i>i</i> 16:0 ^C	0.1 \pm 0.2	0.1 \pm 0.0	0.1 \pm 0.0	0.1 \pm 0.1	0.1 \pm 0.0	0.1 \pm 0.0	0.1 \pm 0.1
<i>ai</i> 16:0	0.1 \pm 0.2	0.2 \pm 0.2	0.0 \pm 0.0	0.3 \pm 0.5	0.2 \pm 0.3	0.0 \pm 0.1	0.1 \pm 0.2
16:0	24^{ab} \pm 2.4	22^{ab} \pm 0.8	21^a \pm 0.6	22^{ab} \pm 2.4	24^b \pm 1.9	22^{ab} \pm 2.5	23 \pm 2.4
16:1n-9? ^C	0.7 \pm 0.2	0.7 \pm 0.1	0.7 \pm 0.3	0.6 \pm 0.1	0.8 \pm 0.1	0.6 \pm 0.1	0.7 \pm 0.2
16:1n-7	6.4^{ab} \pm 0.9	6.3^{ab} \pm 0.9	7.2^b \pm 1.0	4.3^a \pm 1.0	4.6^a \pm 0.7	6.6^b \pm 2.1	6.3 \pm 1.3
16:2n-4	1.0 ^{ab} \pm 0.5	1.4 ^{ab} \pm 0.4	1.5 ^b \pm 0.5	0.6 ^a \pm 0.3	0.9 ^{ab} \pm 0.4	1.3 ^{ab} \pm 0.5	1.0 \pm 0.5
Phytanic? ^C	0.6 \pm 0.7	0.1 \pm 0.2	0.2 \pm 0.3	0.6 \pm 0.6	0.3 \pm 0.2	0.2 \pm 0.2	0.5 \pm 0.6
17:0	1.4 \pm 0.2	1.4 \pm 0.1	1.5 \pm 0.1	1.4 \pm 0.1	1.4 \pm 0.1	1.4 \pm 0.2	1.4 \pm 0.2
16:3n-4?	0.4 \pm 0.4	0.2 \pm 0.4	0.2 \pm 0.3	0.2 \pm 0.4	0.4 \pm 0.6	0.2 \pm 0.3	0.3 \pm 0.4
17:1a	0.4 \pm 0.4	0.5 \pm 0.4	0.4 \pm 0.2	0.5 \pm 0.3	0.4 \pm 0.4	0.5 \pm 0.3	0.5 \pm 0.4
18:0	8.3^{ab} \pm 1.6	6.9^a \pm 0.8	6.8^a \pm 0.7	9.6^b \pm 2.1	8.2^{ab} \pm 1.6	8.0^{ab} \pm 1.4	8.2 \pm 1.6
18:1n-9 ^C	6.8 \pm 1.1	6.6 \pm 0.2	5.1 \pm 0.9	6.6 \pm 1.1	5.9 \pm 1.2	5.2 \pm 1.4	6.4 \pm 1.3
18:1n-7	3.6 ^{bc} \pm 0.6	2.8 ^{ab} \pm 0.3	4.0 ^c \pm 0.7	3.1 ^{abc} \pm 0.6	2.6 ^a \pm 0.3	4.2 ^c \pm 1.3	3.6 \pm 0.7
18:1n-6?	0.1 \pm 0.4	0.0 \pm 0.0	0.0 \pm 0.0	0.1 \pm 0.3	0.3 \pm 0.5	0.1 \pm 0.2	0.1 \pm 0.4
18:1n-5?	0.3 \pm 1.0	0.1 \pm 0.1	0.1 \pm 0.1	0.1 \pm 0.1	0.4 \pm 0.5	0.1 \pm 0.1	0.2 \pm 0.8
18:2n-6	3.5 ^b \pm 0.5	2.5 ^a \pm 0.4	3.2 ^{ab} \pm 0.2	2.9 ^a \pm 0.3	2.7 ^a \pm 0.5	2.9 ^a \pm 0.2	3.3 \pm 0.5
18:2n-4	0.3 ^{ab} \pm 0.2	0.5 ^{bc} \pm 0.1	0.7 ^c \pm 0.2	0.4 ^{abc} \pm 0.1	0.3 ^a \pm 0.0	0.6 ^{bc} \pm 0.3	0.4 \pm 0.2
18:3n-4	0.1 \pm 0.3	0.0 \pm 0.0	0.1 \pm 0.1	0.1 \pm 0.1	0.1 \pm 0.1	0.0 \pm 0.1	0.1 \pm 0.2
18:3n-3	0.9 ^a \pm 0.2	1.0 ^{ab} \pm 0.2	1.9 ^b \pm 0.2	1.2 ^{ab} \pm 0.3	2.0 ^b \pm 0.6	1.7 ^b \pm 0.6	1.1 \pm 0.5
18:4n-3	1.1 ^a \pm 0.3	2.3 ^b \pm 0.5	1.8 ^b \pm 0.4	2.5 ^b \pm 0.3	3.0 ^b \pm 0.9	2.1 ^b \pm 0.7	1.5 \pm 0.7
18:4n-1?	0.1 \pm 0.3	0.0 \pm 0.0	0.0 \pm 0.0	0.0 \pm 0.0	0.3 \pm 0.6	0.1 \pm 0.1	0.1 \pm 0.3
20:1n-9	0.1 \pm 0.2	0.1 \pm 0.1	0.1 \pm 0.1	0.0 \pm 0.0	0.0 \pm 0.0	0.1 \pm 0.1	0.1 \pm 0.1
20:1n-7? ^C	0.1 \pm 0.4	0.1 \pm 0.1	0.1 \pm 0.1	0.0 \pm 0.0	0.1 \pm 0.1	0.2 \pm 0.2	0.1 \pm 0.3
20:2a?	0.1 \pm 0.4	0.0 \pm 0.0	0.0 \pm 0.0	0.0 \pm 0.1	0.0 \pm 0.0	0.0 \pm 0.0	0.1 \pm 0.3
20:2b?	0.1 \pm 0.3	0.0 \pm 0.0	0.1 \pm 0.1	0.0 \pm 0.1	0.0 \pm 0.0	0.1 \pm 0.4	0.1 \pm 0.3
20:4n-6	3.4 ^b \pm 0.8	2.6 ^{ab} \pm 0.1	2.3 ^a \pm 0.4	2.1 ^a \pm 0.2	2.1 ^a \pm 0.4	1.9 ^a \pm 0.4	2.9 \pm 0.9
20:3n-3 ^C	0.2 \pm 0.5	0.0 \pm 0.0	0.2 \pm 0.1	0.5 \pm 0.8	0.0 \pm 0.1	0.2 \pm 0.1	0.2 \pm 0.5
20:4n-3	0.5 ^{ab} \pm 0.3	0.8 ^{abc} \pm 0.2	1.9 ^c \pm 0.2	0.4 ^a \pm 0.5	0.4 ^a \pm 0.2	1.3 ^{bc} \pm 0.7	0.7 \pm 0.6
20:5n-3	6.3^a \pm 0.9	8.5^b \pm 0.8	6.8^{ab} \pm 0.9	7.7^{ab} \pm 0.8	7.3^{ab} \pm 1.7	7.0^{ab} \pm 1.7	6.7 \pm 1.2
22:1n-9	0.7 ^b \pm 0.6	0.4 ^{ab} \pm 0.3	0.1 ^a \pm 0.1	1.4 ^b \pm 1.2	0.3 ^{ab} \pm 0.2	0.3 ^{ab} \pm 0.2	0.6 \pm 0.6
21:5n-3?	0.0 ^a \pm 0.0	0.1 ^a \pm 0.1	0.2 ^b \pm 0.0	0.0 ^a \pm 0.1	0.1 ^a \pm 0.1	0.4 ^{ab} \pm 1.3	0.1 \pm 0.5
22:5n-6	1.6 \pm 0.3	1.7 \pm 0.1	1.6 \pm 0.2	1.6 \pm 0.2	1.4 \pm 0.1	1.7 \pm 0.3	1.6 \pm 0.3
22:5n-3	0.7 ^{ab} \pm 0.3	1.0 ^{bc} \pm 0.3	1.7 ^c \pm 0.2	0.5 ^a \pm 0.3	0.6 ^{ab} \pm 0.0	1.1 ^{bc} \pm 0.5	0.8 \pm 0.4
24:0	0.4 \pm 1.0	0.1 \pm 0.1	0.0 \pm 0.1	0.1 \pm 0.2	0.0 \pm 0.1	0.4 \pm 0.6	0.3 \pm 0.9
22:6n-3	15^a \pm 3.1	20^b \pm 1.0	17^{ab} \pm 1.7	19^{ab} \pm 2.5	20^b \pm 1.9	18^{ab} \pm 4.0	16 \pm 3.6
24:1	0.5 \pm 1.7	0.1 \pm 0.1	0.0 \pm 0.0	0.7 \pm 1.7	0.6 \pm 1.0	0.0 \pm 0.1	0.4 \pm 1.4
Bacterial	4.8 \pm 0.7	5.0 \pm 0.4	4.5 \pm 0.3	4.5 \pm 0.8	4.6 \pm 0.5	4.4 \pm 0.9	4.7 \pm 0.7
Sum Saturated ^C	43 \pm 3.7	38 \pm 1.6	39 \pm 1.4	41 \pm 3.9	41 \pm 3.0	39 \pm 3.8	42 \pm 3.9
Sum MUFA	20 ^b \pm 1.9	18 ^{ab} \pm 1.3	18 ^{ab} \pm 1.6	18 ^{ab} \pm 1.0	17 ^a \pm 1.5	19 ^{ab} \pm 3.4	20 \pm 2.3
Sum PUFA	36 ^a \pm 4.7	43 ^b \pm 1.9	42 ^{ab} \pm 2.9	41 ^{ab} \pm 3.7	42 ^{ab} \pm 4.2	42 ^{ab} \pm 6.8	38 \pm 5.5
P/S	0.8 ^a \pm 0.2	1.1 ^b \pm 0.1	1.1 ^{ab} \pm 0.1	1.0 ^{ab} \pm 0.2	1.0 ^{ab} \pm 0.2	1.1 ^{ab} \pm 0.3	0.9 \pm 0.2
Sum n-3	25 ^a \pm 3.8	33 ^b \pm 1.8	31 ^b \pm 2.8	32 ^b \pm 3.1	33 ^b \pm 4.1	32 ^b \pm 6.4	27 \pm 5.5
Sum n-6	9.3 ^b \pm 1.2	7.9 ^{ab} \pm 0.2	8.2 ^{ab} \pm 0.7	7.4 ^a \pm 0.6	7.0 ^a \pm 0.4	7.2 ^a \pm 0.6	8.6 \pm 1.3
C ₁₆ PUFA ratio	4.8 \pm 1.7	5.6 \pm 1.6	6.1 \pm 2.0	4.1 \pm 1.4	5.1 \pm 1.0	5.3 \pm 1.3	5.0 \pm 1.6

Table 4 continued

Fatty acid or marker ^{A,B}	Bathymyrinae [62]	Congrinae [6]	Muraenesocidae [6]	Myrophinae [6]	Nettastomatidae [3]	Ophichthinae [13]	Overall mean [96]
Sum 20:1n-9, 22:1n-11, 22:1n-9	0.8 ^b ± 0.6	0.5 ^{ab} ± 0.3	0.1 ^a ± 0.1	1.4 ^b ± 1.2	0.4 ^{ab} ± 0.2	0.4 ^{ab} ± 0.4	0.7 ± 0.6
Terrestrial (18:3n-3+18:2n-6)	4.4 ^{abc} ± 0.5	3.6 ^a ± 0.4	5.2 ^c ± 0.3	4.1 ^{ab} ± 0.6	4.7 ^{bc} ± 0.9	4.6 ^{bc} ± 0.6	4.4 ± 0.6

The number of samples used to calculate each mean is shown in square brackets in row no. 1. Bacterial fatty acid marker = *i15:0* + *ai15:0* + 15:0 + 15:1 + *i16:0* + *ai16:0* + *i17:0* + *ai17:0* + 17:0 + 17:1. *Sum MUFA* the sum of monounsaturated fatty acids, *Sum PUFA* the sum of polyunsaturated fatty acids, *P/S* the ratio of polyunsaturated to saturated fatty acids, *Sum n-3* the sum of all n-3 fatty acids, *Sum n-6* the sum of all n-6 fatty acids. *C₁₆ PUFA ratio* (a diatom marker) = (16:2n-4 + 16:3n-4 + 16:4n-3 + 16:4n-1)/(16:0 + 16:1n-7 + 16:1n-5 + 16:2n-4 + 16:3n-4 + 16:4n-3 + 16:4n-1) × 100 %. All ratios are mol/mol and are without units. Numbers in bold face are the five predominant fatty acids in each taxon. Superscripts indicate values not significantly different from one another (single factor ANOVA by ranks). If a particular response variable lacks superscripts this indicates that all means in that particular row are not significantly different from one another. A ‘?’ following a particular fatty acid indicates that commercial standards were not available and identification was done by comparison with Ackman [15]

^A The following fatty acids were below detection limits in all samples: 18:2a, 18:2b, 22:2NMIDa?, 22:2NMIDb?

^B The following fatty acids and fatty acid markers were present at proportions <0.99 mol% and were not included in the above table: trimethyltridecanoic acid (TMTD), 14:1, *i15:0*, *ai15:0*, 15:1, pristanic acid?, 16:1n-11?, 16:1n-5, *i17:0*, *ai17:0*, 17:1b, 16:4n-3?, 16:4n-1, 18:1n-11?, 18:3n-6, 19:0, 20:0, 18:5n-3, 20:1n-11?, 20:2n-6, 20:3n-6, 21:0, 22:0, 22:1n-7, 22:1n-11(13), 23:0, 22:4n-6?, 22:4n-3?, and free fatty acids as a % of wet weight

^C Fatty acid or marker with statistically significant difference among means (one way ANOVA by ranks, *p* < 0.05) but only a single homogeneous group using Hochberg’s GT-2 multiple comparison test (*p* > 0.05). Therefore, superscripts could not be assigned to taxonomic groups for these fatty acids and markers

Fatty Acid Sums, Ratios and Markers

The sums of saturated FA and PUFA were essentially equal across all six taxa of leptocephali, each constituting ca. 40 mol% of the total FA (Table 4). This was reflected in the polyunsaturated/saturated (P/S) fatty acid ratio, which had an overall mean value of 0.9. The only significant differences among the taxa were in the sum of PUFA, which was lower in the Bathymyrinae (36 mol%) than in the Congrinae (43 mol%).

The low sum PUFA value for the Bathymyrinae was also reflected in the sum of n-3 FA (25 mol%), which was significantly lower than that of the five other taxa, which was ≥31 mol% (Table 4). The sum of n-6 FA ranged from 7.0 mol% for the Nettastomatidae to 9.3 mol% for the Bathymyrinae. The n-6 FA pool was dominated by the EFA arachidonic acid (20:4n-6, ARA, 2.9 mol%) and 18:2n-6 (3.3 mol%) (Table 4). The sum of n-6 FA for the eel leptocephali collected off Broome was ca. 1/3 that of n-3 FA, giving a range of n-3:n-6 FA of 2.7 for the Bathymyrinae to ≥3.8 for the other five taxa (data not shown).

The DHA:EPA ratio has been shown to be related to egg hatchability and larval development of marine fish, generally with higher ratios being associated with high quality eggs and normal development. The DHA:EPA ratio of the eel leptocephali we collected ranged from 2.4 to 2.7 for all six taxa (data not shown).

The bacterial fatty acid marker (*i15:0* + *ai15:0* + 15:0 + 15:1 + *i16:0* + *ai16:0* + *i17:0* + *ai17:0* + 17:0 +

17:1), and the sum of 18:2n-6 and 18:3n-3, which has been used as a terrestrial plant marker in cold water coastal environments [30, 34], made essentially equal contributions to total fatty acids (i.e. 4.7 and 4.4 mol%, respectively) (Table 4). While the bacterial marker was not significantly different among taxa, the Muraenesocidae had significantly more of the terrestrial FA markers (5.2 mol%) than did the Congrinae (3.6 mol%) and the Myrophinae (4.1 mol%). There was little evidence of carnivory by the leptocephali, as the sum of 20:1n-9 + 22:1n-11 + 22:1n-9 (a proxy for copepod prey) [19] was <1.4 mol% for all taxa (Table 4). The *C₁₆* PUFA ratio (a common diatom marker) [(16:2n-4 + 16:3n-4 + 16:4n-3 + 16:4n-1)/(16:0 + 16:1n-7 + 16:1n-5 + 16:2n-4 + 16:3n-4 + 16:4n-3 + 16:4n-1) × 100 %] was relatively variable within taxa, with an overall mean of 5.0 % (Table 4).

Discussion

The Leptocephali

The eel taxa examined in this study are all strictly marine throughout their life histories, and reside in tropical and sub-tropical continental shelf waters, from near the coast (Ophichthinae) to over the continental slope (Nettastomatidae) [1, 20]. Their migratory behavior is poorly known, but the Ophichthinae may carry out seasonal migration across the continental shelf to spawn near the shelf break

[1]. The size and WW of the taxa collected off Broome are typical of published values for eel leptocephali around the world. Furthermore, the relationship between SL and WW of the taxa we examined is similar to that published for *Paraconger caudilimbatus* from the Gulf of Mexico [2]. For example, the difference in WW predicted by the power equation in Fig. 2 and that of Bishop et al. [2] for a larva 70 mm long is 39 % of the mean value.

Total Lipid Concentration and Lipid Class Composition

Congrid, muraenid and ophichthid leptocephali from the Gulf of Mexico had 2–3 times greater mean lipid concentration than did the larvae we collected off Broome, ranging from 0.8 to 1.0 % of WW [2]. However, leptocephali of *Ariosoma balaericum* collected in the Gulf of Mexico, ranging in length from 20 to 200 mm (very similar to the range in Table 3), had total lipid concentrations ranging from 0.3 to 1.2 % of WW, overlapping values we determined for leptocephali collected on the Broome transect of 0.3–0.7 %. Type II elopomorph larvae are distinguished from the Type I larvae of the other bony fishes primarily by the deposition of large quantities of GAG during the second half of the larval period. Thus, lipid concentration generally decreases in eel larvae with increasing age due to the deposition of large quantities of GAG [16]. However, lipid accumulation rates larva⁻¹ actually increase with increasing age in preparation for the energy demands of metamorphosis [8, 16, 21]. Thus, the relatively low lipid concentrations we have determined suggest that our samples were dominated by relatively old leptocephali with large deposits of GAG. Lipid class and fatty acid data indicate that the low total lipid concentrations were not due to starvation (see below).

The lipid class composition of the leptocephali was similar to that of other fish larvae. PL, ST and TAG were also the top three lipid classes in non-eel fish larvae we have examined recently, accounting for 82–99 % of total lipids in larvae of haddock, Pacific cod, and Atlantic cod [22, 23]. Gadoid PL was generally a higher proportion than in the eel leptocephali (53–85 %); while TAG was generally lower (3–12 %). Thus, although the leptocephali collected off Broome were part of a relatively lipid-poor tropical food web, they accumulated TAG to greater proportions than do the Type I larvae of temperate and boreal gadoids. TAG are generally the most important neutral energy storage depot in marine fish larvae [24].

Ratios of Lipid Classes

Triacylglycerol:sterol ratios <0.2 are generally considered to indicate severe starvation in the early life stages of a variety of marine fish species [17, 25]. Thus, the values we

have determined indicate that all of the taxa except the Myrophinae were in excellent nutritional condition and that none of the leptocephali, including those of the Myrophinae, were suffering severe starvation at the time of sampling.

The LI is defined in Table 3, and provides an index of lipid breakdown. The low values of the LI confirm little lipid breakdown during sample processing, shipment and storage, and likely reflect in situ lipid catabolism by the leptocephali before collection. The relatively high LI of the Myrophinae leptocephali accords with the low TAG:ST ratio noted above, and suggests accelerated catabolism of storage lipids in this taxon in the immediate pre-collection period.

Fatty Acids

We could find no comparative information on the FA composition of leptocephali in the literature. The only information available was for the FA composition of leptocephali of the bonefish *Abula* sp. collected in the Gulf of California, which also had 16:0 and DHA as the two predominant FA (Table 5) [8]. In fact, the FA profiles of the bonefish and eel leptocephali are remarkably similar, with the largest differences being for the relatively minor 18:2n-6, 20:3n-3 and 20:4(n-6?) (Table 5). The fatty acid 16:0 is generally among the most common of marine invertebrates and vertebrates, and was strongly conserved among all six taxa of leptocephali we examined. The EFA DHA was more variable among the leptocephali indicating some degree of nutritional differentiation among the taxa. Within the plankton, DHA originates primarily from flagellates and dinoflagellates [26, and references therein], indicating strong linkage of eel leptocephali off Broome to these microplankton which are abundant at the base of tropical marine food webs. The DHA:EPA ratio is often assumed to reflect nutritional condition in marine heterotrophs, with values >2 considered to indicate good conditions for development and growth. The DHA:EPA ratio of the leptocephali we examined was >2.4, nearly in the middle of the DHA:EPA ratio of bonefish leptocephali in the neutral (1.7) and polar fractions (4.1) [8], and satisfactory for normal development. It also indicates that the leptocephali are relatively high quality prey in terms of DHA content.

Fatty Acid Sums, Ratios and Markers

Both the sum of saturated fatty acids (SFA) and sum of PUFA fall within the published range for bonefish leptocephali (Table 5). The sum of monounsaturated fatty acids (MUFA) was essentially identical with MUFA in the neutral lipid fraction of bonefish leptocephali (Table 5). The high values of SFA and PUFA, and low values of MUFA, are typical of Type I and II marine fish larvae generally [27].

Table 5 Comparison of the fatty acid composition (wt% of total FA) in late stage bonefish leptocephali from Padrón et al. [8] and the overall mean proportions of six taxa of eel leptocephali off Broome, Australia (from Table 4)

Fatty acid	Bonefish neutral lipids	Bonefish polar lipids	Eels (this study) total lipids
14:0	7.1	2.4	4.4
14:1	1.3	0	–
16:0	22	38	21
16:1n-7	8.2	3.0	5.7
18:0	4.2	9.7	8.2
18:1n-9	6.4	3.6	6.4
18:1n-7	3.0	3.3	3.6
18:2n-6	2.7	1.2	3.3
18:3n-3	4.2	1.2	1.1
18:4n-3	4.8	0	1.5
20:3n-6	0.9	2.7	–
20:3n-3	1.0	0.6	0.2
20:4	3.0	2.1	3.2
20:5n-3	10	6.0	7.1
22:4n-6	1.0	0	–
22:5n-3	1.7	1.5	1.0
22:6n-3	17	25	19
Saturated	34	50	39
Monoenes	19	9.9	19
PUFA	47	40	42
n-3:n-6	8.6	8.7	3.3

Column 1 follows the format and nomenclature of Padrón et al. [8]. Dashed lines indicate FA proportions <1 wt% in all samples

It has been shown that n-3 and n-6 FA have mutually inhibitory effects on incorporation and bioconversion [28]. Thus, the n-3:n-6 ratio has been shown to be important for the development of fish larvae [28]. The values we observed are lower than the mean for bonefish leptocephali (i.e. 8.6–8.7, Table 5), suggesting a relatively high proportion of n-6 FA in the leptocephali off Broome. The n-6 FA are particularly abundant in tropical marine food webs relative to n-3 FA [27, 29], perhaps accounting for the low values of this ratio in the leptocephali we collected. Possible sources of n-6 FA include benthic macroalgae and sea grasses [26, 30], as well as some species of phytoplankton [31].

There were relatively high levels of bacterial and terrestrial FA markers in the leptocephali, perhaps reflecting their near-shore, tropical habitat. In comparison, the primarily herbivorous Arctic copepod *Calanus hyperboreus* had maximum bacterial marker levels of 1.5 % [32] and omnivorous adult *Mysis mixta* and *Acanthostephia malmgreni* from the benthic boundary layer of Conception Bay, Newfoundland, had bacterial FA marker levels ranging from 2 to 6 % and terrestrial FA marker levels

from 1 to 3 % [33]. Thus, the epipelagic leptocephali have similar levels of bacterial FA markers and higher levels of terrestrial FA markers than do near-bottom detritivorous crustaceans. However, a potential confounding factor is the occurrence of 18:3n-3 and 18:2n-6 in some phytoplankton [31] and sea grasses [30]. Although we have shown these FA to be robust makers of terrestrial source material in boreal waters [30, 34], we have not confirmed their efficacy on the Broome transect. The high level of bacterial markers in the eel leptocephali collected off Broome relative to planktonic copepods we have studied [32], is consistent with the possible feeding of leptocephali on bacteria-rich appendicularian houses and marine snow aggregates [6, 7].

The C₁₆ PUFA ratio is a marker of nutrient replete marine diatoms [35]. This ratio was highly variable within the taxa we examined (i.e. CV from 20 to 35 %), and relatively low overall (i.e. an overall mean of 5 %). This value is much lower than that we have determined for herbivorous copepods feeding during the spring bloom (C₁₆ PUFA ratio = 23 %) [36], but similar to a variety of carnivorous invertebrates feeding on sinking spring bloom material (C₁₆ PUFA ratio from 4 to 5 % for the amphipods *A. malmgreni*, *Anonyx* spp. and *Parathemisto* spp., the shrimp *Pandalus borealis*, and the chaetognath *Parasagitta elegans*) [36]. Thus, the leptocephali collected off Broome are only weakly connected with diatom production in the euphotic zone.

Our interest in the lipid and fatty acid content of tropical eel leptocephali (Type II larva) was to better understand their nutrition, energy storage and diet, and thus their ecology and physiological adaptations to an extended larval period. Perhaps not surprising is the complexity of our results, with some biochemical similarities between eel leptocephali and the larvae of non-eel fishes, and some important differences. We determined relatively low total lipid concentrations ranging from 2.7 to 7.0 mg g WW⁻¹, suggesting that the WW of the leptocephali off Broome was dominated by large deposits of GAG. However, PL, TAG and ST were the dominant lipid classes, which is also typical of the Type I larvae we have studied recently.

Although the leptocephali off Broome have an extended life span and had just come through the austral winter, the TAG:ST and DHA:EPA ratios indicated that they were in good condition and were growing and developing normally. The predominant fatty acids were 16:0, 22:6n-3 (DHA), 18:0, and 20:5n-3 (EPA), typical of marine fish larvae feeding at a low trophic level. However, the leptocephali were relatively enriched in n-6 fatty acids and poor in long chain monoenes, both typical of tropical waters. The leptocephali had proportions of bacterial markers >4 %, consistent with the possibility that they may have been consuming bacteria-rich appendicularian houses or other marine snow.

Acknowledgments The present work was carried out as part of the Galathea 3 expedition under the auspices of the Danish Expedition Foundation. We thank the Captain of HMDS ‘Vædderen’, Carsten Schmidt, and his crew for excellent assistance with our sampling. The authors thank J.T. Christensen, B. Søborg and A. Sampey for technical assistance onboard HMS Vædderen. J. Wells carried out the lipid and fatty acid analyses. The project was supported by grants from Knud Højgaards Fond and the Danish Natural Sciences Research Council, and by a Discovery Grant from the Natural Sciences and Engineering Research Council of Canada (DD). This paper is Galathea 3 contribution no. P87.

References

- Miller MJ, Tsukamoto K (2004) An introduction to leptocephali biology and identification. Ocean Research Institute, University of Tokyo, 90 pp
- Bishop RE, Torres JJ, Crabtree RE (2000) Chemical composition and growth indices in leptocephalus larvae. *Mar Biol* 137:205–214
- Robinet T, Lecomte-Finiger R, Escoubeyrou K, Feunteun E (2003) Tropical eels *Anguilla* spp. recruiting to Réunion Island in the Indian Ocean: taxonomy, patterns of recruitment and early life histories. *Mar Ecol Prog Ser* 259:263–272
- Bishop RE, Torres JJ (2001) Leptocephalus energetics: assembly of the energetics equation. *Mar Biol* 138:1093–1098
- Otake T, Nogami K, Maruyama K (1993) Dissolved and particulate organic matter as possible food sources for eel leptocephali. *Mar Ecol Prog Ser* 92:27–34
- Mochioka N, Iwamizu M (1996) Diet of anguillid larvae: leptocephali feed selectively on larvacean houses and fecal pellets. *Mar Biol* 125:447–452
- Riemann L, Alfredsson H, Hansen MM et al (2010) Qualitative assessment of the diet of European eel larvae in the Sargasso Sea resolved by DNA barcoding. *Biol Lett* 6:819–822
- Padrón D, Lindley VA, Pfeiler E (1996) Changes in lipid composition during metamorphosis of bonefish (*Albula* sp.) leptocephali. *Lipids* 31:513–519
- Miller MJ (2009) Ecology of anguilliform leptocephali: remarkable transparent fish larvae of the ocean surface layer. *Aq BioSci Monogr* 2:1–94
- Lecomte-Finiger R, Maunier C, Khafif M (2004) Les larves leptocephales, ces méconnues. *Cybium* 28:83–95
- Pfeiler E (1984) Glycosaminoglycan breakdown during metamorphosis of larval bonefish *Abula*. *Mar Biol Lett* 5:241–249
- Kawakami Y, Mochioka N, Kimura R, Nakazono A (1999) Seasonal changes of the RNA/DNA ratio, size and lipid contents and immigration adaptability of Japanese glass-eels, *Anguilla japonica*, collected in northern Kyushu, Japan. *J Exp Mar Biol Ecol* 238:1–19
- Parrish CC (1999) Determination of total lipid, lipid classes, and fatty acids in aquatic samples. In: Arts MT, Wainman B (eds) *Lipids in freshwater ecosystems*, pp 4–20
- Parrish CC (1987) Separation of aquatic lipid classes by Chromarod thin-layer chromatography with measurement by Iatroscan flame ionization detection. *Can J Fish Aquat Sci* 44:722–731
- Ackman RG (1986) WCOT (capillary) gas-liquid chromatography. In: Hamilton RJ and Rossell JB (eds) *Analysis of oils and fats*, Elsevier, New York, pp 137–206
- Donnelly J, Torres JJ, Crabtree RE (1995) Proximate composition and nucleic acid content of premetamorphic leptocephalus larvae of the congrid eel *Ariosoma balearicum*. *Mar Biol* 123:851–858
- Hilton Z, Poortenaar CW, Sewell MA (2008) Lipid and protein utilisation during early development of yellowtail kingfish (*Seriola lalandi*). *Mar Biol* 154:855–865
- Parrish CC, McKenzie CH, MacDonald BA, Hatfield EA (1995) Seasonal studies of seston lipids in relation to microplankton species composition and scallop growth in South Broad Cove, Newfoundland. *Mar Ecol Prog Ser* 129:151–164
- Cripps GC, Atkinson A (2000) Fatty acid composition as an indicator of carnivory in Antarctic krill, *Euphausia superba*. *Can J Fish Aquat Sci* 57:31–37
- Ma T, Miller MJ, Shinoda A, Minagawa G, Aoyama J, Tsukamoto K (2005) Age and growth of *Saurenhelys* (Nettastomatidae) and *Dysomma* (Synphobranchidae) leptocephali in the East China Sea. *J Fish Biol* 67:1619–1630
- Pfeiler E (1986) Towards an explanation of the developmental strategy in leptocephalous larvae of marine teleost fishes. *Env Biol Fish* 15:3–13
- Garcia AS, Parrish CC, Brown JA, Johnson SC, Leadbeater S (2008) Use of differently enriched rotifers, *Brachionus plicatilis*, during larviculture of haddock, *Melanogrammus aeglefinus*: effects on early growth, survival and body lipid composition. *Aquacult Nutr* 14:431–444
- Laurel BJ, Copeman LA, Hurst TP, Parrish CC (2010) The ecological significance of lipid/fatty acid synthesis in developing eggs and newly hatched larvae of Pacific cod (*Gadus macrocephalus*). *Mar Biol* 157:1713–1724
- Rainuzzo JR, Reitan KI, Olsen Y (1997) The significance of lipids at early stages of marine fish: a review. *Aquaculture* 155:103–115
- Håkanson JL (1989) Analysis of lipid components for determining the condition of anchovy larvae, *Engraulis mordax*. *Mar Biol* 102:143–151
- Dalsgaard J, St. John M, Kattner G, Muller-Navarra D, Hagen W (2003) Fatty acid trophic markers in the pelagic marine environment. *Adv Mar Biol* 46:278–340
- de Silva SS, Gunasekera RM, Collins R, Ingram BA, Austin CM (1997) Changes in the fatty acid profile of the Australian shortfin eel in relation to development. *J Fish Biol* 50:992–998
- Furuita H, Unuma T, Nomura K, Tanaka H, Okuzawa K, Sugita T, Tamamoto T (2006) Lipid and fatty acid composition of eggs producing larvae with high survival rate in the Japanese eel. *J Fish Biol* 69:1178–1189
- Piché J, Iverson SJ, Parrish FA, Dollar R (2010) Characterization of forage fish and invertebrates in the Northwestern Hawaiian Islands using fatty acid signatures: species and ecological groups. *Mar Ecol Prog Ser* 418:1–151
- Copeman LA, Parrish CC, Gregory RS, Jamieson RE, Wells J, Whittaker MJ (2009) Fatty acid biomarkers in coldwater eelgrass meadows: elevated terrestrial input to the food web of age-0 Atlantic cod *Gadus morhua*. *Mar Ecol Prog Ser* 386:237–251
- Viso A-C, Marty J-C (1993) Fatty acids from 28 marine microalgae. *Phytochem* 34:1521–1533
- Stevens CJ, Deibel D, Parrish CC (2004) Copepod omnivory in the North Water Polynya (Baffin Bay) during autumn: spatial patterns in lipid composition. *Deep Sea Res I* 51:1637–1658
- Richoux NB, Deibel D, Thompson RJ, Parrish CC (2005) Seasonal and developmental variation in the fatty acid composition of *Mysis mixta* (Mysidacea) and *Acanthostephia malmgreni* (Amphipoda) from the hyperbenthos of a cold-ocean environment (Conception Bay, Newfoundland). *J Plank Res* 27:719–733
- Budge SM, Parrish CC, McKenzie CH (2001) Fatty acid composition of phytoplankton, settling particulate matter and sediments at a sheltered bivalve aquaculture site. *Mar Chem* 76:285–303
- Parrish CC, Thompson RJ, Deibel D (2005) Lipid classes and fatty acids in plankton and settling matter during the spring bloom in a cold ocean coastal environment. *Mar Ecol Prog Ser* 286:57–68
- Parrish CC, Deibel D, Thompson RJ (2009) Effect of sinking spring phytoplankton blooms on lipid content and composition in suprabenthic and benthic invertebrates in a cold ocean coastal environment. *Mar Ecol Prog Ser* 391:33–51

Proximate and Fatty Acid Composition of Some Commercially Important Fish Species from the Sinop Region of the Black Sea

Demet Kocatepe · Hülya Turan

Received: 10 May 2011 / Accepted: 20 January 2012 / Published online: 11 February 2012
© AOCS 2012

Abstract The proximate and fatty acid compositions of the commercially important fish species (*Engraulis encrasicolus*, *Alosa alosa*, *Belone belone*, *Scorpaena porcus*, *Pomatomus saltatrix*, *Mullus barbatus*) from the Sinop region of the Black Sea were examined. The fat contents ranged from 1.26% (for scorpion fish) to 18.12% (for shad). The protein contents were min 14.54% (for red mullet) and maximum 20.26% (for belone). The fatty acid compositions of the fish ranged from 27.83 to 35.91% for saturated fatty acids, 19.50–33.80% for monounsaturated fatty acids and 15.25–40.02% for polyunsaturated fatty acids. Among the saturated fatty acids, palmitic acid (16:0) (17.75–22.20%) was the dominant fatty acid for all the fish species. As a second saturated fatty acid, myristic acid (14:0) was observed in four of the fish species and its content ranged from 4.72 to 7.31%. Whereas, for the other two fish species, the second saturated fatty acid was stearic acid (18:0) ranging between 4.54 and 10.64%. Among the monounsaturated fatty acids, those occurring in the highest proportions were oleic acid (18:1n-9c) (11.67–22.45%) and palmitoleic acid (16:1) (4.50–9.40%). Docosahexaenoic acid (22:6n-3) (5.41–28.52%), eicosapentaenoic acid (20:5n-3) (4.68–11.06) and linoleic acid (18:2n-6) (1.38–3.49%) were dominant polyunsaturated fatty acids, respectively. All the

species, in particular the belone, the anchovy and the shad had high levels of the n-3 series.

Keywords Fish · Fatty acids · EPA · DHA · Anchovy · Belone · Shad · Scorpion fish · Bluefish · Red Mullet

Abbreviations

ALA	Alpha-linolenic acid (18:3n-3)
DHA	Docosahexaenoic acid (22:6n-3)
DPA	Docosapentaenoic acid (22:5n-3)
EPA	Eicosapentaenoic acid (20:5n-3)
LNA	Linoleic acid (18:2n-6)
MUFA	Monounsaturated fatty acid(s)
OLA	Oleic acid (18:1n-9)
PAM	Palmitic acid (16:0)
PUFA	Polyunsaturated fatty acid(s)
SFA	Saturated fatty acid(s)
STA	Stearic acid (18:0)

Introduction

Fatty acids serve a wide variety of metabolic functions, critical to all forms of life. Polyunsaturated fatty acids (PUFA), particularly the n-3 and n-6 series, play an important role in non-energy-producing biological functions. n-3 PUFA, namely eicosapentaenoic acid, 20:5n-3 (EPA) docosapentaenoic acid, 22:5n-3 (DPA) and docosahexaenoic acid, 22:6n-3 (DHA) plays numerous roles within the human body [1].

The health benefits of the long-chain n-3 PUFA such as 20:5n-3 and 22:6n-3 have been well observed in scientific studies such as the prevention or reduction of human coronary artery disease [2–7], a significant decrease in total cholesterol and high density lipoprotein levels [8], in

D. Kocatepe
Department of Food and Beverage Management,
Sinop University, School of Tourism and Hotel Management,
57000 Sinop, Turkey
e-mail: dkocatepe@sinop.edu.tr

H. Turan (✉)
Department of Fishing and Processing Technology,
Sinop University, Fisheries Faculty, 57000 Sinop, Turkey
e-mail: hturan@sinop.edu.tr

peripheral arterial disease, improvement in endothelial functions [9] improvement in depressive symptoms in parkinsonian patients [10], a reduction in the risk of breast cancer [11, 12] and a reduction in the risk of prostate cancer [13].

Long-chain n-3 PUFA cannot be easily synthesized by humans and must be ingested in the diet [14]. Most of the PUFA of fish lipids occur as the n-3 type. The contents of different fatty acids in fish lipids depend on numerous factors, such as diet, the geographic location, the environmental temperature, the time of year, the body length, the lipid content, etc. [15].

Sinop is one of the important port cities on the Black Sea. In particular, anchovy is of utmost importance for commercial fishing in this area. Additionally, the other commercial fish species in this region are bonito, shad, belone, turbot, scorpion fish, horse mackerel, blue fish, red mullet and whiting. Knowledge of the fatty acid composition and nutritional value of commercially important fish species is needed. Therefore, this paper presents the fatty acid compositions and other nutritional values of a variety of commercial fish species found in the Sinop region of the Black Sea.

Materials and Methods

Sample Preparation

For this research, 2 kg each of six different species of commercially important fish were chosen and purchased from the local fish market in January 2011. These were anchovy (*Engraulis encrasicolus*), shad (*Alosa alosa*), belone (*Belone belone*), scorpion fish (*Scorpaena porcus*), bluefish (*Pomatomus saltatrix*), and red mullet (*Mullus barbatus*). The average weights of the fish were 6.18 ± 0.3 g for anchovy, 229.60 ± 10.83 g for shad, 73.31 ± 4.75 g for belone, 87.82 ± 9.91 g for scorpion fish, 110.37 ± 8.17 g for bluefish, and 10.29 ± 0.56 g for red mullet. A minimum of nine fish from each individual species were gutted, filleted and minced for analysis.

Analysis

The moisture and ash contents were determined as described by AOAC [16], and the protein content was determined by the Kjeldahl method [16]. The crude lipid content was performed by acid digestion prior to petroleum ether extraction (boiling point 40–60 °C) in a Soxtec system [17]. These analyses were performed in triplicate. After the fish carbohydrate value was calculated [carbohydrate value = $100 - (\text{water} + \text{lipid} + \text{protein} + \text{ash})$] the energy value was calculated according to the Atwater

method [18]. The fatty acid content was determined using the IUPAC II.D.19 method [19]. The fatty acids were analyzed using a Perkin Elmer Auto System XL gas chromatograph (Perkin-Elmer, Beaconsfield, UK) equipped with a SP-2330 column and a flame ionization detector. The separation of the fatty acids methyl esters was achieved using a fused silica capillary column (30 m \times 0.25 mm \times 0.20 μm film thickness). The oven temperature was set at 120 °C for 2 min, then increased to 220 °C with a ramp rate of 5 °C/min, and then held for 15 min. The injector and detector temperatures were maintained at 240 and 250 °C, respectively. The carrier gas was helium at 10 psi with a split ratio of 1/50. The air and hydrogen pressures were 338 and 45 ml/min, respectively. The results were determined by the percentage of each fatty acid with respect to the total fatty acids. The fatty acid analyses were conducted in two replicates and the results were expressed in GC area % as mean values \pm standard error. For identification of the fatty acids, their retention times were compared to those of the standard methyl esters (Supelco 37-Component FAME Mix). For conversion of the percentile values to units of weight, the formula recommended originally by Weihrauch et al. [20] and then Paul and Southgate [21] and Soriguier et al. [22] was employed. The formula for fish is as follows: Factor (fish) = $0.933 - (0.143/\text{total fat})$. The conversion factor (CF) for the n-3 FA of *E. encrasicolus*: CF = $0.933 - (0.143/13.90) = 0.92$; $(0.92 \times 28.40)/100 = 0.26$ g/100 g of n-3 (Table 3).

Statistical Analysis

The results of the analyses were presented as means \pm standard errors. Statistical analysis was conducted with the Minitab Statistical Software package (Minitab Release, 13). A one-way analysis of the variance (ANOVA) was used to verify the differences between the species and significance of those differences were tested with the Tukey Test. The significance level was $P < 0.05$.

Results and Discussion

Proximate Composition

Table 1 shows the proximate composition of the six species of fish.

The main chemical components of fish meat are water, crude protein, and lipids. Together they make up approximately 98% of the total mass of flesh. The other constituents, i.e., carbohydrates, vitamins, and minerals, are present in minor quantities. The contents of the main components in the fish body depend primarily on the

Table 1 Proximate composition of six fish species (expressed on a wet weight basis (%))

Fish species	Moisture (%)	Protein (%)	Fat (%)	Ash (%)	Carbohydrate (%)	Energy cal/g
<i>Engraulis encrasicolus</i> (anchovy)	66.95 ± 0.64 ^a	16.31 ± 0.17 ^{a, c}	13.90 ± 0.44 ^a	1.03 ± 0.05 ^a	1.94 ± 0.02 ^a	201.77 ± 2.50 ^a
<i>Alosa alosa</i> (shad)	59.79 ± 1.01 ^b	19.09 ± 0.05 ^b	18.12 ± 0.13 ^b	0.86 ± 0.02 ^{b, d}	1.25 ± 0.29 ^{a, b}	243.74 ± 2.51 ^b
<i>Belone belone</i> (belone)	73.97 ± 0.20 ^c	20.26 ± 0.13 ^b	3.64 ± 0.04 ^c	1.25 ± 0.02 ^c	0.71 ± 0.18 ^b	116.77 ± 0.66 ^c
<i>Scorpaena porcus</i> (scorpion fish)	80.10 ± 0.14 ^d	16.91 ± 0.04 ^a	1.26 ± 0.08 ^d	0.92 ± 0.02 ^{a, b}	0.95 ± 0.04 ^b	82.84 ± 1.26 ^d
<i>Pomatomus saltatrix</i> (blue fish)	70.87 ± 0.59 ^e	15.24 ± 0.55 ^{c, d}	12.29 ± 0.28 ^e	0.76 ± 0.04 ^d	0.87 ± 0.07 ^b	176.73 ± 5.35 ^e
<i>Mullus barbatus</i> (red mullet)	75.25 ± 0.25 ^c	14.54 ± 0.00 ^d	8.32 ± 0.24 ^f	1.14 ± 0.04 ^{a, c}	0.66 ± 0.11 ^b	133.95 ± 1.54 ^f

Data are the mean values of three replicates ± standard errors

Within a column values with different superscript letters are significantly different ($P < 0.05$)

(Sample size: 2 kg for each fish species)

species, the stage of maturity, the sex, the spawning cycle, the environment, the season, and the nutritional condition of the animal [15, 23, 24]. Flesh from healthy fish contains 60–84% water, 15–24% protein and 0.1–22% fat; minerals usually constitute 1–2%. The proportions of the constituents are species-specific and the main variations between species are in the fat content. Fish are often classified according to fat content. Lean fish have <0.5% fat, semi-fat fish contain 0.5–2% and fatty fish have more than 2% [25]. In this study, the lipid content ranged from 1.26% for scorpion fish to 18.12% for shad. The scorpion fish could be classified as a semi-fat fish. All the remaining fish could be classified as fatty fish. However, between the fatty fish, the highest fat content was determined in the shad flesh ($P < 0.05$). The fat contents were shad > anchovy > blue fish > red mullet > belone > scorpion fish ($P < 0.05$). Sorting by the moisture content was scorpion fish > red mullet ≥ belone > blue fish > anchovy > shad ($P < 0.05$). In general, there is an inverse relationship between the amount of fat and moisture in the flesh. As shown in Table 1, the moisture content in deep water species (scorpion fish and red mullet) was more than in the pelagic species.

The protein content tends to vary much less widely from one species to another. Most fish contain approximately 20% protein [25]. Also, in this research, the protein content of the fish varied from 14.54 to 20.26%. The ash content ranged from 0.76% for the blue fish to 1.25% for the belone.

The major carbohydrate in fish muscle is glycogen, which is a polymer of glucose. A typical muscle in a live fish may contain between 0.1 and 1% glycogen [25]. In this research, the lowest carbohydrate content was obtained from the red mullet (0.66%) however, it was similar to the carbohydrate value of the other fish except for the anchovy ($P < 0.05$). The energy value of the fish ranged from 82.84 to 243.74 cal ($P < 0.05$), and the fat content together with the energy value, was determined as a linearly relationship ($r = 0.99$).

Similar food compositions for the fish observed in this research have been determined by several other researchers [26–30].

Fatty Acid Composition

Table 2 shows the fatty acid composition of six fish species.

The fatty acids composition of the fish species ranged from 27.83 to 35.91% saturated fatty acid (SFA), 19.50–33.80% monounsaturated fatty acid (MUFA) and 15.25–40.02% PUFA. It was observed that the proportion of these fatty acids changed significantly between the six fish species ($P < 0.05$). Among them, those occurring in the highest proportions were myristic acid (14:0), palmitic acid (16:0) (PAM), stearic acid (18:0) (STA), palmitoleic acid (16:1), oleic acid (18:1n-9) (OLA), linoleic acid (18:2n-6) (LNA), alpha-linolenic acid (18:3n-3) (ALA), eicosapentaenoic acid (20:5n-3) (EPA) and docosahexaenoic acid (22:6n-3) (DHA). These results are in line with previous studies on the fatty acids of other species [27–29, 31–38]. It was also observed that the proportion of these fatty acids vary among the species.

The SFA values were significantly different ($P < 0.05$) for the six fish species. The highest SFA value was obtained from the scorpion fish (35.91%) whose fat content was the lowest in all fish. This was followed by anchovy (35.07%), blue fish (32.86%) and red mullet (30.46%), belone (29.56%) and shad (27.83%). Güner et al. [27] reported SFA ratios 40.77% for anchovy, 38.16% for red mullet, 35.87% for belone, 31.77% for shad. SFA ratios of anchovy by Kaya and Turan [28] were declared as 38.62, 35.20, and 33.57% in November, December and January, respectively. Öksüz and Özyılmaz [29] reported that SFA ratios of anchovy ranged from 37.91 to 34.04% (from October to April). Tanakol et al. [31] determined SFA ratios 42.2% for anchovy, 34.4% for bluefish and 34.7% for belone. Bayır et al. [32] found SFA ratios in bluefish,

Table 2 Fatty acid composition of fish species (% fatty acids methyl ester/total of the methyl esters)

Fatty acids	<i>Engraulis encrasicolus</i> (anchovy)	<i>Alosa alosa</i> (shad)	<i>Belone belone</i> (belone)	<i>Scorpaena porcus</i> (scorpion fish)	<i>Pomatomus saltatrix</i> (blue fish)	<i>Mullus barbatus</i> (red mullet)
12:0	0.08 ± 0.00 ^a	0.05 ± 0.01 ^b	nd	nd	0.06 ± 0.01 ^b	0.07 ± 0.00 ^{a, b}
13:0	0.08 ± 0.00 ^a	0.05 ± 0.01 ^b	nd	nd	0.05 ± 0.00 ^b	0.03 ± 0.00 ^c
14:0	7.31 ± 0.02 ^a	4.72 ± 0.00 ^b	5.12 ± 0.05 ^c	3.07 ± 0.00 ^d	5.43 ± 0.04 ^c	2.59 ± 0.00 ^f
15:0	1.05 ± 0.01 ^a	0.63 ± 0.01 ^b	nd	nd	0.74 ± 0.01 ^c	0.95 ± 0.00 ^d
16:0	19.97 ± 0.07 ^a	17.75 ± 0.07 ^b	19.51 ± 0.06 ^c	22.20 ± 0.07 ^d	19.34 ± 0.02 ^c	20.05 ± 0.05 ^a
17:0	1.58 ± 0.01 ^a	1.25 ± 0.01 ^b	nd	nd	1.46 ± 0.00 ^c	1.47 ± 0.01 ^c
18:0	3.83 ± 0.03 ^a	3.06 ± 0.01 ^b	4.38 ± 0.06 ^c	10.64 ± 0.05 ^d	4.99 ± 0.02 ^e	4.54 ± 0.01 ^c
20:0	0.93 ± 0.01 ^a	0.35 ± 0.00 ^b	0.57 ± 0.03 ^c	nd	0.49 ± 0.00 ^d	0.32 ± 0.00 ^b
22:0	0.26 ± 0.00 ^a	nd	nd	nd	0.25 ± 0.00 ^b	0.12 ± 0.00 ^c
23:0	nd	nd	nd	nd	0.07 ± 0.01 ^a	0.33 ± 0.01 ^b
ΣSFA	35.07 ± 0.10 ^a	27.83 ± 0.09 ^b	29.56 ± 0.04 ^c	35.91 ± 0.03 ^d	32.86 ± 0.01 ^c	30.46 ± 0.08 ^f
14:1	0.17 ± 0.00 ^a	0.12 ± 0.00 ^b	nd	nd	0.14 ± 0.00 ^c	0.26 ± 0.01 ^d
16:1	5.99 ± 0.02 ^a	4.50 ± 0.02 ^b	7.07 ± 0.03 ^c	5.23 ± 0.01 ^d	6.20 ± 0.11 ^a	9.40 ± 0.14 ^e
18:1n-9c	11.67 ± 0.08 ^a	22.08 ± 0.04 ^b	20.68 ± 0.19 ^c	17.32 ± 0.01 ^d	22.45 ± 0.05 ^b	20.49 ± 0.05 ^c
20:1n-9	1.38 ± 0.01 ^a	2.54 ± 0.02 ^a	2.59 ± 0.07 ^a	1.65 ± 0.00 ^a	1.53 ± 1.14 ^a	1.73 ± 0.01 ^a
24:1	0.31 ± 0.01 ^a	1.02 ± 0.00 ^b	nd	1.60 ± 0.01 ^c	0.19 ± 0.00 ^d	1.94 ± 0.01 ^e
ΣMUFA	19.50 ± 0.08 ^a	30.26 ± 0.04 ^b	30.34 ± 0.10 ^b	25.79 ± 0.01 ^c	30.50 ± 1.08 ^b	33.80 ± 0.10 ^d
18:2n-6t	0.16 ± 0.00	nd	nd	nd	nd	nd
18:2n-6	2.52 ± 0.02 ^a	2.16 ± 0.01 ^b	3.49 ± 0.06 ^c	2.41 ± 0.01 ^a	2.15 ± 0.00 ^b	1.38 ± 0.00 ^d
18:3n-3	1.25 ± 0.00 ^a	1.57 ± 0.01 ^b	1.69 ± 0.03 ^c	3.95 ± 0.00 ^d	1.17 ± 0.02 ^e	0.41 ± 0.00 ^f
18:3n-6	0.19 ± 0.01 ^a	0.14 ± 0.00 ^b	nd	nd	0.15 ± 0.00 ^b	0.11 ± 0.00 ^c
20:2 cis	0.29 ± 0.00 ^a	0.30 ± 0.00 ^b	nd	nd	0.33 ± 0.00 ^c	0.66 ± 0.00 ^d
20:3n-3	0.11 ± 0.00 ^a	0.12 ± 0.00 ^b	nd	nd	0.12 ± 0.00 ^c	0.27 ± 0.00 ^d
22:2	0.88 ± 0.06 ^a	0.35 ± 0.01 ^b	1.65 ± 0.02 ^c	5.04 ± 0.04 ^d	0.48 ± 0.02 ^b	1.30 ± 0.04 ^e
20:5n-3 cis	11.06 ± 0.03 ^a	5.73 ± 0.02 ^b	4.68 ± 0.04 ^c	6.08 ± 0.04 ^d	4.70 ± 0.01 ^c	5.52 ± 0.00 ^e
22:2n-9	nd	nd	nd	nd	0.32 ± 0.01 ^a	0.20 ± 0.01 ^b
22:6n-3 cis	15.99 ± 0.07 ^a	17.31 ± 0.06 ^b	28.52 ± 0.11 ^c	8.91 ± 0.01 ^d	10.75 ± 0.04 ^e	5.41 ± 0.02 ^f
ΣPUFA	32.43 ± 0.08 ^a	27.67 ± 0.11 ^b	40.02 ± 0.13 ^c	26.38 ± 0.01 ^d	20.15 ± 0.05 ^e	15.25 ± 0.01 ^f
Σn-3	28.40 ± 0.10 ^a	24.72 ± 0.08 ^b	34.89 ± 0.18 ^c	18.94 ± 0.05 ^d	16.73 ± 0.04 ^e	11.60 ± 0.02 ^f
Σn-6	2.87 ± 0.02 ^a	2.30 ± 0.01 ^b	3.49 ± 0.06 ^c	2.41 ± 0.01 ^b	2.30 ± 0.00 ^b	1.49 ± 0.00 ^d
n-3/n-6	9.91 ± 0.05 ^a	10.77 ± 0.05 ^b	10.01 ± 0.24 ^a	7.87 ± 0.00 ^c	7.27 ± 0.02 ^d	7.79 ± 0.01 ^{c, d}
DHA/EPA	1.45 ± 0.00 ^a	3.02 ± 0.00 ^b	6.10 ± 0.02 ^c	1.47 ± 0.00 ^a	2.29 ± 0.00 ^d	0.98 ± 0.00 ^e
Total	86.99 ± 0.10 ^a	85.76 ± 0.24 ^{a, c}	99.91 ± 0.01 ^b	88.08 ± 0.05 ^a	83.51 ± 1.14 ^c	79.5 ± 0.00 ^d
Unidentified	13.01 ± 0.10 ^a	14.25 ± 0.24 ^{a, c}	0.09 ± 0.01 ^b	11.93 ± 0.05 ^a	16.49 ± 1.14 ^c	20.50 ± 0.00 ^d

Data are the mean values of two replicates ± standard errors

nd Not detected

Within a row values with different superscript letters are significantly different ($P < 0.05$)

anchovy and belone of 38.35, 37.81, and 28.89%, respectively. Palmitic acid was the primary SFA, contributing to 57–66% of the total SFA content of lipids for all the fish species. These result is in line with previous studies on the fatty acids of other species [27–29, 31, 32]. The highest 16:0 content was detected in the scorpion fish, whereas the lowest value was found in the shad. The palmitic acid content in the anchovy and red mullet; belone and the blue fish were similar ($P > 0.05$). Myristic acid was the

secondary fatty acid for the pelagic fish species (anchovy > blue fish > belone > shad, $P < 0.05$), whereas 18:0 was the secondary fatty acid for the deep water species (10.64% for scorpion fish, 4.54% for red mullet).

The MUFA values were significantly different ($P < 0.05$) for all six fish species. The highest MUFA value was obtained from the red mullet (33.80%), followed by the blue fish (30.50%), belone (30.34%) and then the shad (30.26%) ($P > 0.05$), whereas the lowest value was

found in the anchovy (19.50%) ($P < 0.05$). This result is in accordance with Güner et al. [27] who found that anchovy showed the lowest percentage (24.80%) of MUFA in other fish (red mullet, belone and shad). Öksüz and Özyılmaz [29] reported monthly changes (25.91–31.51%) in the levels of the MUFA component throughout the catching season of anchovy. Oleic acid was the most represented of the MUFA, accounting for 60–74% of the total MUFA for all the fish. The highest 18:1n-9 contents were obtained from the blue fish (22.45%) and the shad (22.08%) ($P > 0.05$), followed by belone (20.68%), the scorpion fish (17.32%) and the red mullet (20.49%) ($P > 0.05$), whereas the lowest value was found in the anchovy (11.67%) ($P < 0.05$). While the highest 16:1 value was obtained from the red mullet (9.40%), the lowest value was found for the shad (4.50), and its contents were similar to the anchovy and the blue fish ($P > 0.05$). This two fatty acid (18:1n-9 and 16:1) were determined as the major fatty acids in MUFA in also other studies [27–29, 31, 32].

The PUFA values were significantly different ($P < 0.05$) for the six fish species. The highest PUFA value was obtained from the belone (40.02%), followed by anchovy (32.43%), shad (27.67%), scorpion fish (26.38%), and blue fish (20.15%), whereas the lowest value was found in the red mullet (15.25%). This result is in accordance with Güner et al. [27] who found that red mullet showed the lowest percentage (16.72%) of PUFA in other fish (belone, shad, and anchovy). The major fatty acids, identified as PUFA, were 22:6n-3 and 20:5n-3, respectively. The highest proportion of 22:6n-3 in the total PUFA was obtained from the belone (71%), followed by shad (62%), blue fish (53%) and anchovy (49%), whereas, the scorpion fish (34%) and red mullet (35%) contained lower 22:6n-3 contents. Güner et al. [27] also determined a lower 22:6n-3 content in red mullet than anchovy, belone and shad. It was observed that the proportion of 22:6n-3 in the pelagic fish (belone, shad, blue fish and anchovy) was higher than those in the deep water fish (scorpion fish and red mullet). Similarly, the high proportion of 20:5n-3 was detected in the red mullet (36% of total PUFA) and anchovy (34%), followed by the scorpion fish (23%), blue fish (23%), shad (21%), whereas the belone (12%)

contained lower 20:5n-3 than the other fish. However, the 20:5n-3 values were anchovy > scorpion fish > shad > red mullet > blue fish \geq belone. The 20:5n-3 values in the fish (anchovy, red mullet, belone and shad) studied here were higher than those in the fish (anchovy, red mullet, belone and shad) studied by Güner et al. [27]. Also, the 22:6n-3 values in red mullet, belone and shad except for anchovy were higher than those in the fish studied by Güner et al. [27]. In the PUFA, the 18:2n-6 contents ranged from 1.38% (for red mullet) to 3.49% (for belone). The linoleic acid contents were similar to that of the anchovy (2.52%) with the scorpion fish at (2.41%), shad (2.16%) with blue fish (2.15%), ($P > 0.05$), whereas the 18:3n-3 contents were significantly different in all the fish species, with a content range from 0.41% (for red mullet) to 3.95% (for scorpion fish).

The British Nutrition Foundation [39] recommended that people who have a balanced and healthy diet consume 0.2 g of EPA and DHA daily. The American Heart Association (AHA) recommends that all adults should include fish in their diet at least twice a week, especially oily fish [40–42], and for patients with documented coronary heart disease, the AHA recommends \approx 1 g of EPA + DHA (combined) per day [40, 41]. This may be obtained from the consumption of oily fish or from n-3 fatty acid capsules, although the decision to use the latter should be made in consultation with a physician [40, 41].

Table 3 shows the amounts of EPA + DHA in fish from this research.

As shown in Table 3, the highest EPA + DHA value was obtained from the belone (0.29), followed by anchovy (0.25) and shad (0.21), whereas the lowest values were found for the scorpion fish (0.12), blue fish (0.14) and red mullet (0.15). To meet the EPA and DHA recommendations according to the British Nutrition Foundation, 100 g of belone, anchovy and shad is enough but scorpion fish, blue fish and red mullet should be consumed in amounts higher than 100 g. This research indicates that very oily fish such as anchovy and shad have more EPA + DHA than semi-fat fish such as scorpion fish. However, belone is shown to be a very good source of EPA + DHA, despite the low amount of fat (Table 3).

Table 3 Σ SFA, Σ MUFA, Σ PUFA, EPA, DHA content of fish species (g/100 g fish)

Species	Lipid (%)	Σ SFA	Σ MUFA	Σ PUFA	n-6	n-3	EPA	DHA	EPA + DHA
<i>E. encrasicolus</i> (anchovy)	13.90	0.32	0.18	0.30	0.03	0.26	0.10	0.15	0.25
<i>A. alosa</i> (shad)	18.12	0.26	0.28	0.26	0.02	0.23	0.05	0.16	0.21
<i>B. belone</i> (belone)	3.64	0.26	0.27	0.36	0.03	0.31	0.04	0.25	0.29
<i>S. porcus</i> (scorpion fish)	1.26	0.29	0.21	0.22	0.02	0.16	0.05	0.07	0.12
<i>P. saltatrix</i> (blue fish)	12.29	0.30	0.29	0.19	0.02	0.15	0.04	0.10	0.14
<i>M. barbatus</i> (red mullet)	8.32	0.28	0.31	0.14	0.01	0.11	0.05	0.10	0.15

In the present study, it was observed that all the species had high levels of the n-3 series, ranging from 11.60% for red mullet and 34.89% for belone ($P < 0.05$) (Table 2). However, the level of the n-6 series was detected as being low; ranging from 1.49% for the red mullet and 3.49% for belone. The level of the n-6 series of the shad, scorpion fish and blue fish were similar ($P > 0.05$). Excessive amounts of n-6 PUFA and a very high n-6/n-3 ratio, as is found in today's Western diets, promote the pathogenesis of many diseases; including cardiovascular disease, hypertension, depression, cancer, and inflammatory and autoimmune diseases, whereas increased levels of n-3 PUFA (a low n-6/n-3 ratio) exert suppressive effects [1, 43–47]. Because of the low content of n-6 fatty acids in marine fish, the ratio of the total n-3–n-6 fatty acids (essential fatty acid ratio) is high, varying from about 5, and reaching a ratio of more than 10 [48]. In this research, the highest value of n-3/n-6 ratio was obtained from the shad (10.77), followed by belone (10.01) and anchovy (9.91), whereas the lowest values were detected in the scorpion fish (7.87), red mullet (7.79) and blue fish (7.27) (Table 2).

In conclusion, this research indicated that the belone, anchovy and shad in particular, are excellent food sources for EPA + DHA. In addition, the red mullet, blue fish and scorpion fish are also good sources of EPA + DHA.

References

- Wanasundara UN, Wanasundara J, Shahidi F (2002) Omega-3 fatty acid concentrates: a review of production technologies. In: Alasalvar C (ed) *Seafood—quality, technology and nutraceutical applications*. Springer, Berlin
- Hu FB, Bronner L, Willett WC, Stampfer MJ, Rexrode KM, Albert CM, Hunter D, Manson JE (2002) Fish and omega-3 fatty acid intake and risk of coronary heart disease in women. *JAMA—J Am Med Assoc* 287:1815–1821
- Von Schacky C, Harris WS (2007) Cardiovascular risk and the omega-3 index. *J Cardiovasc Med* 8(Suppl 1):46–49
- Yamagishi K, Iso H, Date C, Fukui M, Wakai K, Kikuchi S, Inaba Y, Tanabe N, Tamakoshi A, Japan Collaborative Cohort Study for Evaluation of Cancer Risk Study Group (2008) Fish, ω -3 polyunsaturated fatty acids, and mortality from cardiovascular diseases in a nationwide community-based cohort of Japanese men and women the JACC (Japan Collaborative Cohort Study for Evaluation of Cancer Risk) study. *J Am Coll Cardiol* 52(12):988–996
- Chattapakorn N, Settakorn J, Petsophonsakul P, Suwannahoi P, Mahakranukrauh P, Srichairatanakool S, Chattapakorn SC (2009) Cardiac mortality is associated with low levels of omega-3 and omega-6 fatty acids in the heart of cadavers with a history of coronary heart disease. *Nutr Res* 29:696–704
- Park Y, Lim J, Kwon Y, Lee J (2009) Correlation of erythrocyte fatty acid composition and dietary intakes with markers of atherosclerosis in patients with myocardial infarction. *Nutr Res* 29:391–396
- Amano T, Matsubara T, Uetani T, Kato M, Kato B, Yoshida T, Harada K, Kumagai S, Kunimura A, Shinbo Y, Kitagawa K, Ishii H, Murohara T (2011) Impact of omega-3 polyunsaturated fatty acids on coronary plaque instability: an integrated backscatter intravascular ultrasound study. *Atherosclerosis*. doi:10.1016/j.atherosclerosis.2011.05.030
- Emsley R, Niehaus DJH, Oosthuizen PP, Koen L, Ascott-Evans B, Chiliza B, Van Rensburg SJ, Smit RM (2008) Safety of the omega-3 fatty acid, eicosapentaenoic acid (EPA) in psychiatric patients: results from a randomized, placebo-controlled trial. *Psychiatr Res* 161:284–291
- Schiano V, Laurenzano E, Brevetti G, De Maio JJ, Lanero S, Scopacasa F, Chiariello M (2008) Omega-3 polyunsaturated fatty acid in peripheral arterial disease: effect on lipid pattern, disease severity, inflammation profile, and endothelial function. *Clin Nutr* 27:241–247
- Da Silva TM, Munhoz RP, Alvarez C, Naliwaiko K, Kiss Á, Andreatini R, Ferraz AC (2008) Depression in Parkinson's disease: a double-blind, randomized, placebo-controlled pilot study of omega-3 fatty-acid supplementation. *J Affect Disord* 111:351–359
- Maillard V, Bougnoux P, Ferrari P, Jourdan ML, Pinault M, Lavillonnière F, Body G, Le Floch O, Chajès V (2002) N-3 and N-6 fatty acids in breast adipose tissue and relative risk of breast cancer in a case-control study in tours, France. *Int J Cancer* 98(1):78–83
- Kaur B, Jørgensen A, Duttaroy AK (2009) Fatty acid uptake by breast cancer cells (MDA-MB-231): effects of insulin, leptin, adiponectin, and TNF α . *PLEFA* 80:93–99
- Shannon J, O'Malley J, Mori M, Garzotto M, Palma AJ, King IB (2010) Erythrocyte fatty acids and prostate cancer risk: a comparison of methods. *PLEFA* 83:161–169
- Alasalvar C, Shahidi F, Quantick P (2002) Food and health applications of marine nutraceuticals: a review. In: Alasalvar C (ed) *Seafoods—quality, technology and nutraceutical applications*. Springer, Berlin
- Sikorski ZE, Kołakowska A, Pan BS (1990) The nutritive composition of the major groups of marine food organisms. In: Sikorski ZE (ed) *Seafood: resources, nutritional composition, and preservation*. CRC Press, Boca Raton
- AOAC (1995) *Official methods of analysis of the association of official analytical chemists*, 16th edn. Author, Arlington
- AOAC (2005) *Official methods of analysis of the association of official analytical chemists*, 18th edn. Author, Gaithersburg
- Falch E, Overrien I, Solberg C, Slizyte R (2010) Composition and calories. In: Nolle LML, Toldrá F (eds) *Seafood and seafood product analysis*. CRC Press Taylor and Francis Group, Boca Raton
- IUPAC (1979) *Standard methods for analysis of oils, fats and derivatives*, 6th edn. (5th edn. Method II.D.19). Pergamon Press Oxford, Oxford
- Weihrauch JL, Posati LP, Anderson BA, Exler J (1977) Lipid conversion factors for calculating fatty acid contents of foods. *J Am Oil Chem Soc* 54:36–40
- Paul AA, Southgate DAT (1988) In: McCance A, Widdowson F (eds) *The composition of foods*. HMSO, London, pp 16–17
- Soriguer F, Serna S, Valverde E, Hernando J (1997) Lipid, protein, calorie content of different Atlantic and Mediterranean fish shellfish and molluscs commonly eaten in the south of Spain. *Eur J Epidemiol* 13:451–463
- Ockerman HW (1992) *Fishery by-products*. In: Hall GM (ed) *Fish processing technology*. Blackie Academic and Professional, New York
- Hylidig G, Larsen E, Green-Petersen D (2007) Fish and sensory analysis in the fish Chain. In: Nolle LML (ed) *Handbook of meat, poultry and seafood quality*. Blackwell Publishing Professional, USA
- Clucas IJ, Ward AR (1996) *Post-harvest fisheries development: a guide to handling, preservation, processing and quality*. Natural Resources Institute, UK

26. Karaçam H, Düzgüneş E (1988) Hamsi Balıklarında Net Et Verimi ve Besin Analizleri Üzerine Bir Araştırma. Ege Üniversitesi, Su Ürünleri Dergisi 5(19–20):100–107
27. Güner S, Dincer B, Alemdag N, Colak A, Tüfekci M (1998) Proximate composition and selected mineral content of commercially important fish species from the Black Sea. J Sci Food Agric 78:337–342
28. Kaya Y, Turan H (2008) Comparison of protein, lipid and fatty acids composition of anchovy (*Engraulis encrasicolus* L. 1758) during the commercial catching season. J Muscle Foods 21:474–483
29. Öksüz A, Özyılmaz A (2010) Changes in fatty acid compositions of Black Sea anchovy (*Engraulis encrasicolus* L. 1758) during catching season. Turk J Fish Aquat Sci 10:381–385
30. Kocatepe D, Turan H, Taşkaya G, Kaya Y, Erden R, Erdoğan F (2011) Effects of cooking methods on the proximate composition of Black Sea anchovy (*Engraulis encrasicolus*, Linnaeus 1758). Gıda 36(2):71–75
31. Tanakol R, Yazıcı Z, Şener E, Sencer E (1999) Fatty acid composition of 19 species of fish from the Black Sea and the Marmara Sea. Lipids 34(3):291–297
32. Bayır A, Haliloğlu Hİ, Sirkecioğlu AN, Aras NM (2006) Fatty acid composition in some selected marine fish species living in Turkish waters. J Sci Food Agric 86:163–168
33. Özogul Y, Özogul F (2007) Fatty acid profiles of commercially important fish species from the Mediterranean, Aegean and Black Seas. Food Chem 100:1634–1638
34. Özogul Y, Özogul F, Alagoz S (2007) Fatty acid profiles and fat contents of commercially important seawater and freshwater fish species of Turkey: a comparative study. Food Chem 103:217–223
35. Özogul Y, Özogul F, Çiçek E, Polat A, Kulay E (2009) Fat content and fatty acid compositions of 34 marine water fish species from the Mediterranean Sea. Int J Food Sci Nutr 60(6):464–475
36. Dunne PG, Cronin DA, Brennan, MH, Gormley TR (2010) Determination of the total lipid and the long chain omega-3 polyunsaturated fatty acids, EPA and DHA, in deep-sea fish and shark species from the north-east Atlantic. JFisheriesScienc.com 4(3):269–281
37. Memon NN, Talpur FN, Bhangar MI, Balouch A (2011) Changes in fatty acid composition in muscle of three farmed carp fish species (*Labeo rohita*, *Cirrhinus mrigala*, *Catla catla*) raised under the same conditions. Food Chem 126:405–410
38. Usydus Z, Szlinder-Richert J, Adamczyk M, Szatkowska U (2011) Marine and farmed fish in the Polish market: comparison of the nutritional value. Food Chem 126:78–84
39. British Nutrition Foundation (1992) Unsaturated fatty acids. Nutritional and physiological significance. Report of British Nutrition Foundation. Chapman and Hall, London
40. Kris-Etherton PM, Harris WS, Appel LJ (2002) AHA Scientific Statement: fish consumption, fish oil, omega-3 fatty acids, and cardiovascular disease. Circulation 106:2747–2757
41. Kris-Etherton PM, Harris WS, Appel LJ (2003) Omega-3 fatty acids and cardiovascular disease: new recommendations from the American Heart Association. Arterioscler Thromb Vasc Biol 23:151–152
42. Lichtenstein AH, Appel LJ, Brands M, Carnethon M, Daniels S, Franch HA, Franklin B, Kris-Etherton P, Harris WS, Howard B, Karanja N, Lefevre M, Rudel L, Sacks F, Van Horn L, Winston M, Wylie-Rosett J (2006) Diet and lifestyle recommendations revision 2006: A scientific statement from the American Heart Association Nutrition Committee. Circulation 114:82–96
43. Simopoulos AP (2002) The importance of the ratio of omega-6/omega-3 essential fatty acids. Biomed Pharmacother 56:365–379
44. Simopoulos AP (2004) Omega-6/Omega-3 essential fatty acid ratio and chronic diseases. Food Rev Int 20(1):77–90
45. Simopoulos AP (2006) Evolutionary aspects of diet, the omega-6/omega-3 ratio and genetic variation: nutritional implications for chronic diseases. Biomed Pharmacother 60:502–507
46. Simopoulos AP (2008) The omega-6/omega-3 fatty acid ratio, genetic variation, and cardiovascular disease. Asia Pac J Clin Nutr 17(S1):131–134
47. Candela CG, Lopez LMB, Kohen VL (2011) Importance of a balanced omega 6/omega3 ratio for the maintenance of health, nutritional recommendations. Nutr Hosp 26(2):323–329
48. Valfré F, Caprino F, Turchini GM (2003) The health benefit of seafood. Vet Res Commun 27(Suppl 1):507–512

Oral Supplementation with Dihomo- γ -Linolenic Acid (DGLA)-Enriched Oil Increases Serum DGLA Content in Healthy Adults

Takao Tanaka · Saki Kakutani · Chika Horikawa · Hiroshi Kawashima · Yoshinobu Kiso

Received: 17 January 2012 / Accepted: 28 February 2012 / Published online: 14 March 2012
© AOCs 2012

Abstract Dihomo- γ -linolenic acid (DGLA) is one of the polyunsaturated fatty acids, and is expected to show anti-allergic activity. We examined the effects of supplementation with DGLA-enriched oil (450 mg as free DGLA) for 4 weeks in healthy adults in a randomized controlled study. The DGLA composition in the total fatty acids of serum phospholipids increased from 2.0 to 3.4 %, and returned to the initial level after a 4-week washout. No side effects or changes in blood biochemical parameters were observed. These results indicate that serum DGLA content can be safely increased by supplementation with 450 mg DGLA under these conditions.

Keywords Polyunsaturated fatty acid · Dihomo- γ -linolenic acid · DGLA · Atopic dermatitis · Human

Abbreviations

AD	Atopic dermatitis
ARA	Arachidonic acid
DGLA	Dihomo- γ -linolenic acid
DGLA oil	DGLA-enriched triglyceride
DHA	Docosahexaenoic acid
GLA	γ -Linolenic acid

Introduction

Dihomo- γ -linolenic acid (20:3n-6; DGLA, 8,11,14-eicosatrienoic acid) is one of the polyunsaturated fatty acids and

a constituent of cell membranes. It is metabolized to eicosanoids, such as 1-series prostaglandins and 15-hydroxyeicosatrienoic acid, which exhibit anti-inflammatory or anti-platelet-aggregation effects [1, 2]. Recently, a new fermentation technique was established using a fungus, *Mortierella alpina*, enabling industrial production of DGLA-enriched triglyceride (DGLA oil) [3]. The DGLA content of this oil is very high, reaching approximately 40 % in total fatty acids. We used this oil to investigate the effects of DGLA administration in rodents. Oral administration of DGLA oil markedly reduced clinical skin severity scores and scratching behavior in NC/Nga mice, the standard model for human atopic dermatitis (AD) [4]. This is consistent with the evidence that the DGLA concentration in serum phospholipids in AD patients was significantly lower than that in healthy volunteers [5]. DGLA was also revealed to have an anti-atherosclerotic effect in apoE-deficient mice [6]. Therefore, the application of DGLA oil for human use is expected. Previously, we found that serum DGLA content in healthy men can increase by supplementation with DGLA oil (50 or 150 mg as free DGLA) [7]. The increase of DGLA composition in serum phospholipids was 0.67 % by supplementation with 150 mg, but there was no significant increase by supplementation with 50 mg. To determine if a higher serum DGLA content can be achieved safely, we investigated the effects of supplementation with DGLA-enriched oil (450 mg as free DGLA) for 4 weeks in healthy Japanese participants in a randomized controlled study.

Materials and Methods

The study design was a randomized, double-blind and placebo-controlled parallel group intervention trial. This study was approved by the Institutional Review Boards of

T. Tanaka · S. Kakutani · C. Horikawa · H. Kawashima (✉) · Y. Kiso

Institute for Health Care Science, Suntory Wellness Ltd., 1-1-1 Wakayamadai, Shimamoto, Osaka 618-8503, Japan
e-mail: hiroshi_kawashima@suntory.co.jp

Suntory Ltd. (Osaka, Japan), and performed according to the Helsinki declaration. Healthy Japanese participants (25–44 years old) were recruited after assessment of medical and dietary histories. Each participant provided written informed consent after receiving a thorough explanation of the study. This double-blind, placebo-controlled study included 4-week supplementation and a subsequent 4-week washout, which together formed the test period. The participants were randomly divided into two groups. The DGLA group received six capsules, which contained 1,215 mg of DGLA oil per six capsules per day (corresponding to 450 mg of DGLA per day). The DGLA oil was extracted from a biomass of submerged fermented *M. alpina* and refined by high-purification processes [3]. The placebo group received six capsules containing 1,215 mg of olive oil per day without DGLA. Blood samples were obtained three times, on the day before supplementation began, after the 4 weeks of supplementation, and after the 4-week washout. Sampling was performed from 09:00 to 11:00 after approximately 12 h of fasting. The physical characteristics of participants were measured, and blood and urine were collected for determination of biochemical parameters, fatty acid analysis, and urinalysis. Hematological, blood biochemical, and urinalysis parameters were assayed in the usual manner. Lipids in the serum were extracted by the Folch method [8], and were separated into phospholipids and triacylglycerols by thin-layer chromatography with silica gel 60 (Merck, Darmstadt, Germany). The solvent system consisted of hexane/diethyl ether (7/3, v/v). Fatty acid residues in the phospholipid and triacylglycerol fractions were analyzed as described previously [9]. Findings were examined by repeated ANOVA and Dunnett's test for intra-group comparison and by student *t* test for inter-group

Table 1 Baseline characteristics of the participants who completed the study

Characteristics	Placebo group	DGLA group
Number	10	10
Male/female	7/3	7/3
Age (years)	30.6 ± 4.8	31.7 ± 7.6
Height (cm)	168.1 ± 7.0	171.0 ± 7.1
Body weight (kg)	62.3 ± 10.0	63.8 ± 9.3
DGLA in PL (%) ^a	2.01 ± 0.45	1.99 ± 0.43

Values are the means ± SD. There were no differences between the groups

^a DGLA content in total fatty acids of serum phospholipids

comparison, using the Statistical Package for the Social Sciences for Windows version 17.0 (SPSS Inc., Chicago, IL). *P* value of less than 0.05 was considered to indicate statistical significance.

Results and Discussion

Twenty-six healthy volunteers were originally enrolled. Five of them did not participate because of personal reasons (2 participants) or meeting the exclusion criteria (3 participants). Twenty-one participants (8 males and 3 females in the DGLA group, 7 males and 3 females in the placebo group) were administered the sample, and 20 participants completed the trial (1 male in the DGLA group was withdrawn due to having a cold). There were no significant differences in the baseline characteristics (Table 1). There were no side effects during the study period, and all adverse events observed were considered unrelated to supplementation.

The fatty acid composition of the serum phospholipids is shown in Fig. 1. The mean DGLA composition (±SD) in

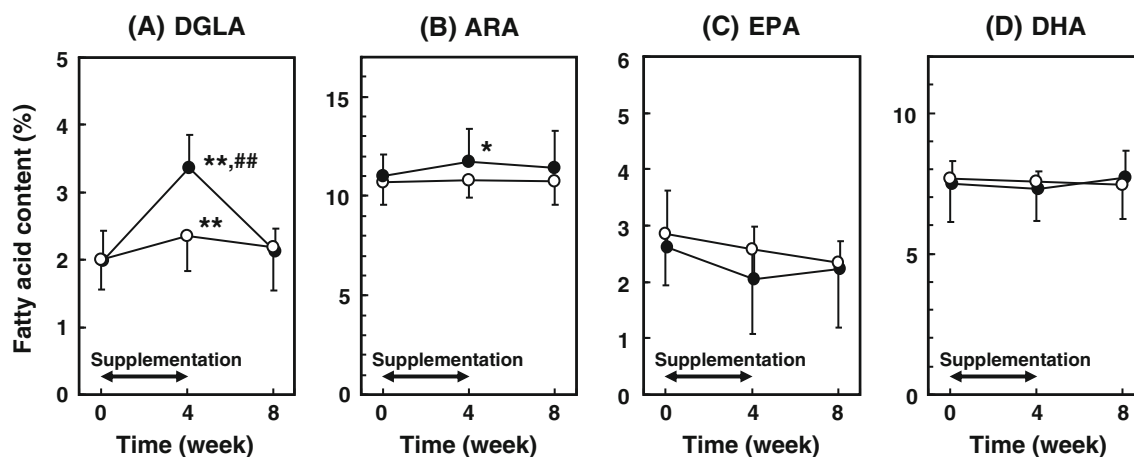


Fig. 1 Fatty acid content of DGLA (a), ARA (b), EPA (c) and DHA (d) in total fatty acids of serum phospholipids. Each value represents the mean ± SD (*N* = 10 (placebo group, open circles) and *N* = 10 (DGLA group, closed circles)). **P* < 0.05, ***P* < 0.01 versus

baseline in the group (repeated ANOVA and Dunnett's test). ##*P* < 0.01 versus placebo group in the case that the change from baseline is significantly different in each time point (unpaired *t* test)

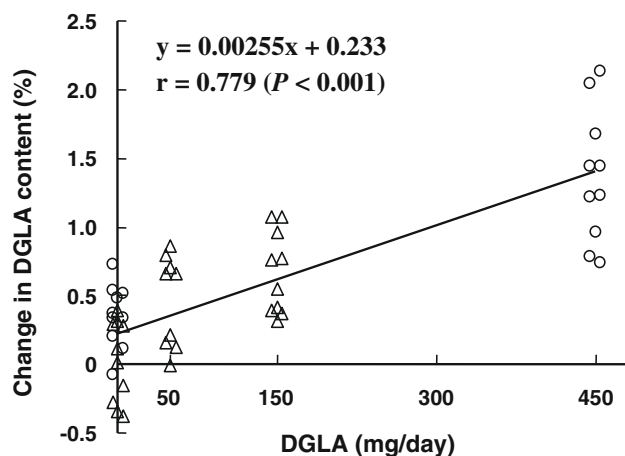


Fig. 2 Correlation of the DGLA dose and the change in DGLA content in serum phospholipids. *Open circles* are the individual data in this study, and *open triangles* are those in a previous study [7]

total fatty acids of serum phospholipids increased from 1.99 (± 0.43) to 3.36 (± 0.50) % in the DGLA group, whereas it was unchanged in the placebo group over the

test period. The increase in DGLA content was 1.37 % in the DGLA group, which was larger than the increases of 0.67 and 0.46 % by the supplementation with 150 and 50 mg DGLA, respectively [7]. This is also more effective than the supplementation with γ -linolenic acid (GLA), the precursor of DGLA, since the increase in DGLA content was only 1.1 % by the administration of GLA-containing oil (900 mg/day, as free GLA) [10]. After the 4-week washout, the DGLA content returned to 2.12 (± 0.35) %, indicating that DGLA levels can be easily returned to the initial levels by discontinuation of DGLA ingestion, and that continuous DGLA ingestion is needed to maintain an increased DGLA level. The major polyunsaturated fatty acids in the serum phospholipids other than DGLA and arachidonic acid (ARA) were unchanged throughout the test period. The ARA increase was probably due to the conversion of DGLA to ARA, but the activity of conversion seemed not so high under the conditions since the increase (0.76 %) was small. There were no effects on serum contents of eicosapentaenoic acid (EPA) and docosahexaenoic acid (DHA). These data suggest that

Table 2 Blood biochemical and hematological parameters

Parameter		Placebo group (N = 10)			DGLA-group (N = 10)		
		Baseline	Week 4	Week 8	Baseline	Week 4	Week 8
AST	IU/l	17.9 \pm 3.1	17.3 \pm 2.4	17.4 \pm 2.7	18.0 \pm 5.3	17.6 \pm 3.1	17.5 \pm 3.5
ALT	IU/l	13.9 \pm 4.5	15.5 \pm 4.7	15.3 \pm 4.3	17.5 \pm 10.4	15.4 \pm 6.2	15.7 \pm 7.3
ALP	IU/l	187 \pm 57	186 \pm 56	182 \pm 59	172 \pm 64	172 \pm 56	165 \pm 52
LDH	IU/l	190 \pm 43	167 \pm 50**	169 \pm 40**	169 \pm 26	157 \pm 26**	156 \pm 22**
γ -GTP	IU/l	23.3 \pm 7.3	24.2 \pm 7.5	25.1 \pm 9.5	24.6 \pm 19.8	27.2 \pm 23.6	27.8 \pm 25.0
Albumin	g/dl	4.7 \pm 0.3	4.6 \pm 0.3**	4.6 \pm 0.3	4.8 \pm 0.2	4.7 \pm 0.2	4.6 \pm 0.1
TP	g/dl	7.3 \pm 0.3	7.2 \pm 0.3	7.3 \pm 0.3	7.3 \pm 0.3	7.2 \pm 0.2	7.3 \pm 0.2
T-Bil	mg/dl	1.0 \pm 0.4	1.0 \pm 0.3	1.1 \pm 0.3	1.0 \pm 0.2	1.0 \pm 0.2	1.0 \pm 0.2
UA	mg/dl	5.7 \pm 2.0	5.4 \pm 2.2	5.7 \pm 2.2	6.0 \pm 1.1	6.1 \pm 1.1	6.1 \pm 1.0
BUN	mg/dl	12.9 \pm 2.7	12.0 \pm 2.6	13.2 \pm 3.0	11.0 \pm 3.3	11.8 \pm 2.8	11.9 \pm 2.8
CRE	mg/dl	0.8 \pm 0.1	0.8 \pm 0.1	0.8 \pm 0.1	0.8 \pm 0.2	0.8 \pm 0.2	0.8 \pm 0.1
CPK	IU/l	127 \pm 67	101 \pm 40	117 \pm 59	126 \pm 76	96 \pm 36	94 \pm 28
T-CHO	mg/dl	175 \pm 31	174 \pm 32	184 \pm 35	172 \pm 22	174 \pm 20	181 \pm 20*
TG	mg/dl	70.4 \pm 33.4	90.0 \pm 55.1	87.9 \pm 61.2	80.8 \pm 49.0	81.9 \pm 38.3	82.6 \pm 33.9
Glu	mg/dl	85.4 \pm 6.3	84.6 \pm 5.3	85.0 \pm 7.1	85.9 \pm 7.3	85.5 \pm 4.6	85.3 \pm 6.2
WBC	$10^3/\text{mm}^3$	5.3 \pm 0.8	5.2 \pm 0.7	5.0 \pm 0.8	5.0 \pm 0.8	4.8 \pm 0.8	5.0 \pm 1.2
RBC	$10^6/\text{mm}^3$	4.9 \pm 0.5	4.7 \pm 0.5**	4.8 \pm 0.4	4.9 \pm 0.4	4.8 \pm 0.4	4.8 \pm 0.4
Hb	g/dl	14.6 \pm 1.6	14.3 \pm 1.6	14.6 \pm 1.5	14.6 \pm 1.1	14.6 \pm 1.0	14.75 \pm 1.1
Ht	%	44.6 \pm 4.0	43.6 \pm 4.1*	44.3 \pm 3.6	45.0 \pm 3.0	44.3 \pm 2.9	44.5 \pm 3.0
Platelet	$10^4/\text{mm}^3$	24.4 \pm 2.3	24.5 \pm 3.5	24.0 \pm 3.7	25.2 \pm 5.1	24.1 \pm 3.7	24.7 \pm 4.7

Values are the means \pm SD

AST aspartate aminotransferase; ALT alanine aminotransferase; ALP alkaline phosphatase; LDH lactate dehydrogenase; γ -GTP γ -glutamyl transpeptidase; TP total protein; T-Bil total bilirubin; UA uric acid; BUN blood urea nitrogen; CRE creatinine; CPK creatine phosphokinase; T-CHO total cholesterol; TG triglycerides; Glu glucose; WBC white blood cells; RBC red blood cells; Hb hemoglobin; Ht hematocrit

* $P < 0.05$, ** $P < 0.01$ versus baseline in the group (repeated ANOVA and Dunnett's test). There were no differences in the change from baseline between the groups

supplementation with DGLA oil is very useful in increasing serum DGLA content, because the activity of conversion of both GLA to DGLA and DGLA to ARA seems low in humans. The increase in serum DGLA content (1.37 %) observed in the present study is considered enough to demonstrate clinical efficacy, because GLA administration seemed effective against AD when the increase in serum DGLA content was more than approximately 1 % [11, 12]. Anti-dermatitis effects were also shown in the NC/Nga mice model when the increase in serum DGLA content was approximately 1.5 % [4]. The correlation of the DGLA dose and the increase of serum DGLA is shown in Fig. 2. The plots are individual values in this study and a previous study [7]. Positive correlation was observed, indicating that the increase of DGLA composition in serum phospholipids is 0.255 % per 100 mg supplementation with DGLA for 4 weeks.

Blood biochemical and hematological parameters are shown in Table 2. There were no significant differences between the groups. Some significant differences compared to the baseline values were observed (lactate dehydrogenase, albumin, total cholesterol, red blood cells and hematocrit), but they were within the normal ranges for healthy Japanese adults. Diastolic and systolic blood pressures, coagulation parameters (prothrombin time, activated partial thromboplastin time and antithrombin III) and urinalysis parameters (protein, sugar, and urobilinogen) were also within the normal ranges and showed no significant differences between the groups (data not shown).

In conclusion, these findings show that the human serum DGLA content can be safely increased by supplementation with DGLA oil (corresponding to 450 mg of DGLA per day) for 4 weeks. We can control the human serum DGLA content by supplementation with various doses of DGLA oil, containing from 50 to 450 mg of DGLA as the free fatty acid. Further investigation is expected in supplementation with DGLA oil to patients with atopic dermatitis or symptoms of allergy.

References

1. Dooper MM, Wassink L, M'Rabet L, Graus YM (2002) The modulatory effects of prostaglandin-E on cytokine production by human peripheral blood mononuclear cells are independent of the prostaglandin subtype. *Immunology* 107:152–159
2. Iversen L, Fogh K, Kragballe K (1992) Effect of dihomogammalinolenic acid and its 15-lipoxygenase metabolite on eicosanoid metabolism by human mononuclear leukocytes in vitro: selective inhibition of the 5-lipoxygenase pathway. *Dermatol Res* 284:222–226
3. Kawashima H, Akimoto K, Higashiyama K, Fujikawa S, Shimizu S (2000) Industrial production of dihomogamma-linolenic acid by a $\Delta 5$ desaturase-defective mutant of *Mortierella alpina* 1S-4 fungus. *J Am Oil Chem Soc* 77:1135–1138
4. Kawashima H, Tateishi N, Shiraishi A, Teraoka N, Tanaka T, Tanaka A, Matsuda H, Kiso Y (2008) Oral administration of dihomogamma-linolenic acid prevents development of atopic dermatitis in NC/Nga mice. *Lipids* 43:37–43
5. Manku MS, Horrobin DF, Morse N, Kyte V, Jenkins K (1982) Reduced levels of prostaglandin precursors in the blood of atopic patients: defective delta-6-desaturase function as a biochemical basis for atopy. *Prostaglandins Leukot Med* 9:615–628
6. Takai S, Jin D, Kawashima H, Kimura M, Shiraishi-Tateishi A, Tanaka T, Kakutani S, Tanaka K, Kiso Y, Miyazaki M (2009) Anti-atherosclerotic effects of dihomogamma-linolenic acid in apoE-deficient mice. *J Atheroscler Thromb* 16:480–489
7. Teraoka N, Kawashima H, Shiraishi-Tateishi A, Tanaka T, Nakamura J, Kakutani S, Kiso Y (2009) Oral supplementation of dihomogamma-linolenic acid (DGLA)-enriched oil alters serum fatty acids in healthy men. *Biosci Biotechnol Biochem* 73:1453–1455
8. Sakuradani E, Kobayashi M, Shimizu S (1999) $\Delta 9$ -Fatty acid desaturase from arachidonic acid-producing fungus: a unique gene sequence and its heterologous expression in a fungus, *Aspergillus*. *Eur J Biochem* 260:208–216
9. Folch J, Lees M, Stanley GHS (1957) A simple method for the isolation and purification of total lipids from animal tissues. *J Biol Chem* 226:497–509
10. Henz BM, Jablonska S, van de Kerkhof PC, Stingl G, Blaszczyk M, Vandervalk PG, Veenhuizen R, Muggli R, Raederstorff D (1999) Double-blind, multicentre analysis of the efficacy of borage oil in patients with atopic eczema. *Br J Dermatol* 140:685–688
11. Schalin-Karrila M, Mattila L, Jansen CT, Uotila P (1987) Evening primrose oil in the treatment of atopic eczema: effect on clinical status, plasma phospholipid fatty acids and circulating blood prostaglandins. *Br J Dermatol* 117:11–19
12. Hederos CA, Berg A (1996) Epogam evening primrose oil treatment in atopic dermatitis and asthma. *Arch Dis Child* 75:494–497

Trans Fatty Acids: Induction of a Pro-inflammatory Phenotype in Endothelial Cells

Kevin A. Harvey · Candace L. Walker ·
Zhidong Xu · Phillip Whitley · Rafat A. Siddiqui

Received: 31 January 2012 / Accepted: 14 May 2012 / Published online: 9 June 2012
© AOCs 2012

Abstract Epidemiological data have shown an association of the intake of industrial produced *trans* fatty acids (TFA) and sudden cardiac death. The present study examines the impact of elaidic acid (*t*18:1n-9) and linoelaidic acid (*t*18:2n-6) on the human aortic endothelial cell functional response. *Trans* fatty acids predominately incorporated into the phospholipid component while only a minute fraction of the total fatty acids (FA) incorporated into triacylglycerol. *Trans* fatty acids incorporated into the plasma membranes at the expense of the saturated-FA, stearic, palmitic, and to a lesser extent, myristic acid. Both *t*18:1n-9 and *t*18:2n-6 induced a pro-inflammatory response by elevating surface expression of intercellular adhesion molecule-1 (ICAM-1). Neither oleic nor linoleic evoked a pro-inflammatory phenotype under the maximal 50 μ M treatments. Both TFA and stearic acid increased phosphorylation of the ICAM-1 transcriptional regulator, nuclear factor- κ B (NF- κ B), while oleic and linoleic acids did not appear to alter the phosphorylation status. Elaidic acid minimally affected endothelial cell growth, whereas linoelaidic acid completely inhibited growth at 100 μ M and imparted limited cytotoxicity up to 300 μ M. Stearic

acid induced cytotoxicity at concentrations above 75 μ M, while oleic and linoleic acids evoked gradual dose-dependent growth inhibition with cytotoxicity occurring only at linoleic acid concentrations greater than 200 μ M. In conclusion, *t*18:1n-9 and *t*18:2n-6 fatty acids effectively incorporated into the phospholipid component of endothelial cells and subsequently induce a pro-inflammatory phenotype.

Keywords *Trans* fatty acids · Endothelial cells · Inflammation · NF κ B · Lipid droplets

Abbreviations

ANOVA	Analysis of variance
BCA	Bicinchoninic acid
BSA	Bovine serum albumin
CHD	Coronary heart disease
CO ₂	Carbon dioxide
EBM2	Endothelial basal medium
EC	Endothelial cell(s)
FA	Fatty acid(s)
FBS	Fetal bovine serum
GAPDH	Glyceraldehyde 3-phosphate dehydrogenase
HAEC	Human aortic endothelial cell(s)
HUVEC	Human umbilical vein endothelial cell
ICAM-1	Intercellular adhesion molecule-1
IP-TFA	Industrially produced- <i>trans</i> fatty acid(s)
NF- κ B	Nuclear factor- κ B
PE	Phycoerythrin
PL	Phospholipid(s)
RP-TFA	Ruminant produced- <i>trans</i> fatty acid(s)
SFA	Saturated fatty acid(s)
<i>t</i> 18:1n-9	<i>Trans</i> Δ 9-octadeca-monoenoic acid (elaidic acid)
<i>t</i> 18:2n-6	<i>Trans</i> Δ 9,12-octadeca-dienoic acid (linoelaidic acid)

K. A. Harvey · C. L. Walker · Z. Xu · P. Whitley ·
R. A. Siddiqui
Cellular Biochemistry Laboratory, Methodist Research Institute,
Indianapolis, IN 46202, USA

R. A. Siddiqui
Department of Medicine, Indiana University School of
Medicine, Indianapolis, IN 46202, USA

R. A. Siddiqui (✉)
Indiana University Health–Methodist Hospital,
Methodist Research Institute, 1800 N. Capital Ave–E504,
Indianapolis, IN 46202, USA
e-mail: rsiddiqu@iuhealth.org

TAG	Triacylglycerol(s)
TBST	Tris buffered saline-tween 20
TFA	<i>Trans</i> fatty acid(s)
VCAM-1	Vascular cell adhesion molecule-1

Introduction

Trans fatty acid sources are either industrially produced (IP-TFA) or ruminant produced (RP-TFA). Industrially produced-*trans* fatty acids are generated by the partial hydrogenation of vegetable fats and, to lesser extent, fish oils using a high heat source, hydrogen gas, and a metal catalyst. Industrially produced-*trans* fatty acids account for a majority of the *trans* fats in the western diet, and the IP-TFA content of partially hydrogenated fat could reach as high as 60 % [1]. Naturally occurring RP-TFA arise from the bio-hydrogenation in ruminant animals, which are present in beef and sheep products, such as milk and cheese. The RP-TFA present in meat and dairy products comprise a maximum of 6 % of the fat content [1]. In European countries, such as Denmark, aggressive measures have drastically reduced IP-TFA in food products; as a result, their major source of TFA is ruminant produced. The RP-TFA intake in the general Danish population consists of 85 % dairy products and the remaining 15 % in ruminant meat products [2]. Conversely, TFA consumption in the USA population is estimated to account for 4–12 % of the total dietary fat intake, which equates to 13 g of TFA/person/day based on the highest daily intake of TFA [3]. Despite recent trends to drastically reduce *trans* fatty acids from dietary intake in European countries, IP-TFA are readily present in the western diet, particularly in the USA. *Trans* fatty acid intake in Canada was as high as 8.4 g/person/day in the mid-1990s; however, following the health Canada's 2007 request to voluntarily reduce the quantity of IP-TFA by food manufacturers, the average daily intake dropped to 3.4 g/person/day (1.4 % food energy) in 2008 [4]. Even with the significant reduction, the TFA intake continues to exceed the World Health Organizations recommendations of <1 % of food energy consumption.

Epidemiological evidence has established a correlation of TFA consumption with the risk of death from coronary heart disease, primarily due to IP-TFA sources [5–7]. Mozaffarian et al. [8] performed a meta-analysis of four prospective cohort studies investigating the association of TFA intake with the incidence of coronary heart disease (CHD) that resulted in a pooled relative risk of 1.23 (95 % CI, 1.11–1.37; $P < 0.0001$). Furthermore, these investigators evaluated TFA consumption and the risk of nonfatal myocardial infarction in three retrospective case-control studies, which assessed the TFA content in adipose tissue.

With the inclusion of these retrospective studies, the meta-analysis enhanced the association between TFA consumption and the risk of developing CHD (pooled relative risk 1.29; 95 % CI, 1.11–1.49; $P < 0.0001$). Mozaffarian et al. [8] cautions that although the correlation between TFA intake and the risk of CHD are predominantly due to IP-TFA, RP-TFA consumption could be as detrimental if consumed in significant quantities. In a Danish 18-year follow-up study, there was no indication of an association of RP-TFA intake and the risk of CHD in men. In fact, indications of an inverse correlation were observed in women [9]. Additional studies should be performed in this controversial relationship of RP-TFA consumption and the risk of developing cardiovascular disease.

While most investigations have focused on the impact of IP-TFA, Motard-Bélanger and colleagues [10] reported that both IP- and RP-TFA consumption adversely affects cholesterol homeostasis. Mozaffarian et al. [11] reviewed the effects of TFA consumption on CHD. *Trans* fatty acid consumption disrupts cholesterol homeostasis, resulting in increased low-density lipoprotein cholesterol with a corresponding decrease in high-density lipoprotein cholesterol levels. Additional evidence outlined in their review emphasizes the pro-inflammatory impact of TFA, including elevated levels of tumor necrosis factor- α , interleukin-6, and C-reactive protein [11]. Bendsen et al. [12] conducted a 16-week intervention study examining the effect of IP-TFA consumption on biomarkers of inflammation in overweight postmenopausal women. Elevated IP-TFA intake increased TNF- α levels as well as soluble forms of the TNF receptors. The investigators conclude that IP-TFA consumption may involve the activation of TNF- α as a possible mechanism leading to the development of cardiovascular disease.

Saturated fatty acids (SFA), stearic acid in particular, are believed to contribute to CHD by invoking lipid-mediated vascular cell dysfunction [13–17]. In a population-based cross-sectional study aimed at determining the effects of SFA and TFA intake on the mean carotid artery intimal medial thickness, elevated consumption of both of these fatty acid classes were independently associated with increased intimal medial thickness [18]. The authors conclude that elevated intake of SFA and TFA may lead to an increased risk of subclinical atherosclerosis. Based on the limited amount of evidence available, previously published data suggest linoelaidic acid is more responsible for CHD than elaidic acid [11, 19]; however, no direct assessment has been performed in primary cells derived from the vasculature. Endothelial cells (EC) are an integral component of the development and progression of CHD, which is hypothesized to possibly be the end result of chronic systemic inflammation. Previous reports published from our laboratory emphasized the significant role of long-

chain saturated fatty acids in the generation of a pro-inflammatory endothelial cell phenotype [20, 21]. In the present study, we initiated *in vitro* studies to directly evaluate the deleterious effects of two commonly consumed TFA, elaidic and linoelaidic acids, in comparison to their saturated counterpart, stearic acid. As previously reported [22], TFA structurally resemble saturated fatty acids. We hypothesized that TFA-supplemented endothelial cells would develop a pro-inflammatory phenotype similar to cellular responses following long-chain saturated fatty acids, as previously reported [20, 21]. In this investigation, we initiated *in vitro* studies to compare the direct effects of the TFA, elaidic and linoelaidic acids, as well as stearic acid supplementation on the phenotypic and functional responses in human aortic endothelial cells.

Materials and Methods

Materials

Human-derived aortic endothelial cells as well as the growth medium comprised of EGM-2MV bullet kits (endothelial growth medium-2 microvascular) were purchased from Lonza Walkersville Inc. (Walkersville, MD, USA). Fetal bovine serum was obtained from Invitrogen Corporation (Carlsbad, CA, USA). Consumable tissue culture materials were purchased from Fisher Scientific (Pittsburgh, PA, USA). Western blot antibodies were acquired from Cell Signaling Technology (Danvers, MA). Fluorescently coupled antibodies were obtained from BD Pharmingen (San Diego, CA, USA). All fatty acids were purchased from Nu-Chek Prep Inc. (Elysian, MN, USA). Gas chromatography standards were purchased from Restek Corporation, Bellefonte, PA, USA). Additional chemicals and reagents were obtained from Sigma Chemical Company (St. Louis, MO, USA), unless otherwise noted.

Human Aortic Endothelial Cell Culture

Primary human aortic endothelial cells (HAEC) were maintained in endothelial basal medium-2 (EBM2) supplemented with 5 % fetal bovine serum (FBS) and bullet kit materials as specified by the manufacturer. Cell culture passages of less than ten were experimentally utilized at 80–90 % confluence. Human aortic endothelial cells were maintained at 37 °C in a humidified atmosphere in the presence of 5 % CO₂.

Fatty Acid Incorporation into Endothelial Cells

Fatty acid stock solutions (1 mM) were prepared by complexing fatty acid free-bovine serum albumin (BSA) with

individual free fatty acids [23]. Sub-confluent endothelial monolayers were cultured for 24 h in the presence or absence of albumin bound-fatty acids (50 μM). Following treatments, cells were trypsinized and washed in phosphate buffered saline (PBS) supplemented with 0.1 % fatty acid free-BSA. Cell pellets were resuspended in calcium and magnesium-free PBS and sonicated to lyse the cells. Internal standards (C23:0, phospholipid and triglyceride) were added to a known volume of cell lysate, whereas protein content was determined with the remaining lysate using a bicinchoninic acid (BCA) protein assay kit (R and D Systems, Elysian, MN).

Lipids were extracted using the Folch method with chloroform:methanol (2:1) [24]. Fractionation of the lipid classes into phospholipids (PL) and triacylglycerols (TAG) was performed using thin layer chromatography using a hexane: diethyl ether: acetic acid (70:30:1; by volume) solvent system. The scraped lipid fractions were subjected to acid-catalyzed esterification by heating for 90 min at 100 °C in a boron trifluoride-methanol solution (14 %). The fatty acid methyl esters were separated by gas chromatography (Shimadzu GC2010; Shimadzu, Columbia, MD, USA) as previously described [25]. Fatty acid peaks were identified by retention times in comparison to authentic standards. Data were analyzed with Shimadzu's GC solutions software and quantified as the mean quantity of each fatty acid normalized to reflect the protein concentration of each sample.

Lipid Droplet Visualization

Excess triglycerides and cholesterol esters are often packaged and stored intracellularly in the form of lipid droplets. Human aortic endothelial cells were cultured in 4-well Permanox chamber slides in EBM-2 complete medium supplemented with albumin-bound fatty acids for 24 h. The cellular neutral lipids were stained using an oil red O staining kit as described by the manufacturer. These cells were counterstained with modified Mayer's hematoxylin for visualization using an Olympus BX40 upright microscope at 500× magnification with an oil immersion objective.

Flow Cytometric Analysis of HAEC Adhesion Molecule Expression

Treated HAEC were trypsinized, washed in PBS containing 0.5 % BSA, and resuspended in the same buffer for antibody labeling. Cells were labeled with 0.25 μg phycoerythrin (PE)-conjugated intercellular adhesion molecule-1 (ICAM-1), which is also known as CD54, for 20 min at room temperature in the dark. Subsequently, the cells were washed with PBS containing 0.5 % BSA and

resuspended in 300 μ L of the wash buffer. In order to ensure binding specificity, an isotope control was established for each data set. Data analysis was performed on a FACSCalibur flow cytometer (Becton–Dickinson, San Jose, CA, USA) equipped with a 15 mW air-cooled argon-ion laser emitting at a 488 nm wavelength. The PE signal was detected through a 585 nm band pass filter and quantified using CellQuest Software (Becton–Dickinson). Results indicate the mean fluorescent intensity of gated endothelial cells, which excluded cellular debris and particles.

Western Blot Analysis

Subconfluent HAEC were grown in six-well tissue culture-treated plates in the presence or absence of albumin-bound fatty acids in EBM-2 complete medium for 24 h under standard tissue culture conditions. Treated cells were rinsed in cold PBS and lysed on ice for 15 min in a 20 mM Tris–HCl (pH 7.4) buffer containing 137 mM NaCl, 100 mM NaF, 2 mM Na_3VO_4 , 10 % glycerol, 1 % Nonidet P-40, 2 mM PMSF, 1 μ g/ml leupeptin, 0.15 units/ml aprotinin, and 2.5 mM diisopropyl fluorophosphate. Protein content was determined using a BCA protein assay kit following centrifugation of the detergent solubilized extracts to remove insoluble matter. Proteins were electrophoretically separated in 4–12 % polyacrylamide gradient gels and transferred onto nitrocellulose membranes. Membranes were blocked for 30 min at room temperature in 10 % Roche Western Blocking reagent in Tris-buffered saline supplemented with 0.1 % Triton X-100 (TBST). Blots were probed with primary antibodies according to the manufacturer's recommendations. Secondary antibodies were peroxidase-conjugated for protein detection using an enhanced chemiluminescence (ECL) system (Amersham Pharmacia Biotechnology, Piscataway, NJ, USA). Nitrocellulose membranes were stripped in 62.5 mM Tris–HCl (pH 6.8) buffer containing 2 % SDS and 100 mM β -mercaptoethanol for 30 min at 50 °C. Stripped blots were washed six times in TBST, blocked, and reprobed with an alternative antibody.

Growth Inhibition and Cytotoxicity Assay

Determination of the influence of fatty acids on cellular growth inhibition and cytotoxicity was evaluated as previously described [20, 21]. Endothelial cells (5,000 cells/well) were plated in a 96-well flat bottom plate and maintained in EBM-2 complete medium for 6 h to permit cell adherence. A subset of established wells were utilized to determine cellular growth (X; baseline at day zero) by administering WST-1 reagent (10 μ L/well) and recording optical density readings at 450 nm following a 90-minute

incubation under standard tissue culture conditions. All other wells were replaced with EBM-2 complete medium supplemented with varying concentrations of albumin-bound fatty acids. Cell cultures were maintained for an additional 48 h at 37 °C in humidified 5 % CO_2 . Following the addition of WST-1 and 90-minute incubation, optical density values were used to calculate growth inhibition or cell loss based on the day zero baseline readings. Vehicle controls (EBM-2 complete medium supplemented with fatty acid free bovine serum albumin) determined the total growth potential (Y). Cell growth (Z) was normalized to 100 % using the formula $((Y - X / X) \times 100)$. Effects of fatty acid supplementation were ascertained by comparing to Z values. Values from 100 to zero indicated growth inhibition, whereas values less than zero indicated cell loss. Results are expressed as the means \pm standard deviations of at least four determinations.

Apoptosis Detection

Endothelial cells (1.0×10^5) were cultured in six-well plates overnight in EBM-2 complete medium. Spent media was replaced with EBM-2 complete medium supplemented with albumin-bound fatty acids and cultured under typical conditions for 24 h. Following treatments, the cells were rinsed in PBS and trypsinized from the plates. All spent medium, PBS washes, and trypsinized cells were collectively combined to ensure both adherent and non-adherent cells were harvested for analysis. Cell pellets were labeled in a solution containing Annexin V Fluorescein and propidium iodide, which was prepared as described by the manufacturer (Roche Applied Science, Indianapolis, IN). Cell suspensions were labeled in the dark at room temperature for 20 min. Analysis was performed on a FACSCalibur flow cytometer (Becton–Dickinson, San Jose, CA) equipped with a 15 mW air-cooled argon-ion laser emitting at a 488 nm wavelength. Annexin V was detected through a 530 nm band pass filter, while propidium iodide was detected through a 650 nm long pass filter. Data were quantified using CellQuest software (Becton–Dickinson). Data represent the mean \pm standard deviation of three determinations.

Statistical Analysis

Data represent the mean \pm the standard deviation of at least three determinations. Fatty acid profiles were compared between control and experimental groups using Student *t* tests. To account for multiple comparisons to a single control group, significance levels were adjusted using the Bonferroni correction, meaning differences were only considered significant when $P \leq 0.025$. For the apoptosis/necrosis data, where group variances were

similar, analysis of variance (ANOVA) was used for initial comparisons across all groups. If a significant difference was detected across all groups, then Dunnett's multiple comparison test was used to compare each experimental group to control. Group variances for the ICAM-1 expression data were not assumed to be equal, so multiple Student *t* tests for unequal variances (Welch's *t* test) were used to compare treatment groups to control. To account for the multiple comparisons to a single control group, the Bonferroni correction was used to adjust the significance levels. Here differences were only considered significant if $P \leq 0.017$. Significant differences between treatment and control groups are indicated with an asterisk in the tables.

Results

Cellular Incorporation of *Trans* Fatty Acids

Endothelial cells were supplemented for 24 h with *trans* fatty acids (50 μ M) prior to extraction and fractionation into phospholipids and triacylglycerols. Table 1a summarizes the fatty acid distribution in the EC phospholipids. Both elaidic and linoelaidic cellular levels constitute a minor component of the overall fatty acid profile in vehicle-treated cells; however, both of the TFA were readily incorporated into cellular phospholipids (40–54 % of total FA content). This resulted in a 190-fold ($P < 0.025$) and 275-fold ($P < 0.025$) enrichment of *t18:1n-9* and *t18:2n-6*, respectively. Importantly, this incorporation coincides with noteworthy and significant ($P < 0.025$) decreases in saturated fatty acids (SFA) namely myristic acid (36 % vehicle-treated vs. 17 % TFA-treated), palmitic (32 % vehicle-treated vs. 15 % TFA-treated), +stearic (18 % vehicle-treated vs. 8 % TFA-treated), and monounsaturated fatty acid (MUFA) namely oleic acid (28 % vehicle-treated vs. 10–20 % TFA-treated) levels. The decrease in long-chain polyunsaturated fatty acids (LC-PUFA) was also significant ($P < 0.05$) but it was to a lesser extent than that of SFA and MUFA (approximately 12–25 %). The treatment of *t18:2n-6* reduced n-3 and n-6 PUFA to approximately an equal extent, whereas effect of *t18:1n-9* was very minimal on n-6 PUFA reduction than that of n-3 PUFA. Interestingly, the incorporation of TFA did not result in any significant increase in the total fatty acid content in the phospholipid fraction. Table 1b summarizes the fatty acid distribution in the EC triacylglycerols. The fatty acid amounts present in the TAG fraction remained relatively low (2 % of total FA) to that of the phospholipid fraction in vehicle-treated cells. Both TFA were also able to increase incorporation into TAGs by 30–40 % of total fatty acid content. This resulted in an enrichment of *t18:1n-9* by 33-fold and *t18:2n-6* by 60-fold. There appears to be a

small decrease (non-significant) in palmitic acid (12–17 %), but this decrease appears to be compensated by an increase in myristic acid, resulting in no overall change in LC-SFA. It therefore appears that unlike their incorporation into phospholipids, the TFA did not incorporate at the expense of other fatty acids; rather they simply accumulated, causing an increase of total FA in TAGs by 40 or 80 % on *t18:1n-9* or *t18:2n-6* treatment, respectively. Furthermore, TFA also enhanced some accumulation of LC-PUFA, particularly n-3 PUFA. The overall increase in FA in TAG contributes to an increase of 3–3.5 % of total cellular fatty acids.

Lipid droplet formation is indicative of an accumulation of TAGs being packaged and stored intracellularly. Figure 1 depicts representative oil red O- and hematoxylin-stained EC supplemented with varying fatty acids (50 μ M). Stearic acid-supplemented cells lacked the presence of detectable lipid droplets, which corresponded to the vehicle control cells. As indicated with arrows, lipid droplet accumulation was readily visible in oleic- and linoleic-supplemented EC. The *trans* fatty acids, elaidic and linoelaidic, did present lipid droplets; however, the abundance of these droplets was substantially less apparent than their *cis* fatty acid counterparts.

Effect of *Trans* Fatty Acid Supplementation on Pro-inflammatory Responses in EC

Adhesion molecule surface expression is indicative of the inflammatory status of EC; therefore, our laboratory quantified intercellular adhesion molecule-1 (ICAM-1; CD54) levels in fatty acid supplemented EC. Cultured EC have basal levels of ICAM-1 surface expression under standard tissue culture conditions. Endothelial cells were supplemented with various fatty acids for 24 h prior to flow cytometric analysis. Table 2 summarizes the results of the relative abundance of ICAM-1 surface expression. Our laboratory previously identified the pro-inflammatory impact of saturated fatty acids, namely stearic acid, on HAEC. *Trans* fatty acid-supplementation met or exceeded ICAM-1 expression levels in comparison to stearic acid. The highest level of ICAM-1 expression was observed with elaidic acid (50 μ M); however, it is important to note that the quantity of ICAM-1 basal expression is only a percentage of the cell's ability to respond to cytokine stimulation. *cis* fatty acid supplementation did not significantly elevate basal ICAM-1 expression in comparison to the vehicle.

Although linked to various signaling mechanisms, phosphorylation of NF- κ B has been associated with the pathway leading to ICAM-1 transcription and subsequent deployment to the plasma membrane [20, 21]. Following a 24-hour fatty acid supplementation, EC lysates were

Table 1 Analysis of the phospholipid fatty acid profile (A) and triacylglycerol fatty acid profile (B)

Fatty acid	Vehicle	Elaidic (50 μ M)	Linoelaidic (50 μ M)
A			
10:0 (capric acid)	0.05 \pm 0.01	0.10 \pm 0.05	0.09 \pm 0.02
12:0 (lauric acid)	0.11 \pm 0.01	0.09 \pm 0.06	0.14 \pm 0.02
14:0 (myristic acid)	9.39 \pm 0.59	4.76 \pm 0.23 ^b	3.76 \pm 0.11 ^b
16:0 (palmitic acid)	83.11 \pm 4.68	41.87 \pm 2.10 ^b	38.40 \pm 0.57 ^b
18:0 (stearic acid)	48.87 \pm 3.40	21.78 \pm 1.04 ^b	24.26 \pm 0.64 ^b
<i>t</i> 18:1n-9 (elaidic acid)	0.31 \pm 0.09	107.27 \pm 5.09 ^b	0.65 \pm 0.35
18:1n-9 (oleic acid)	75.02 \pm 2.90	51.12 \pm 1.24 ^b	30.19 \pm 0.61 ^b
<i>t</i> 18:2n-6 (linoelaidic acid)	0.25 \pm 0.02	0.12 \pm 0.08	153.74 \pm 23.18 ^b
18:2n-6 (linoleic acid)	4.06 \pm 0.02	4.43 \pm 0.19	3.59 \pm 0.15 ^b
20:0 (arachidic acid)	0.37 \pm 0.04	0.22 \pm 0.01	0.19 \pm 0.04
18:3n-6 (γ -linolenic acid)	0.23 \pm 0.01	0.11 \pm 0.00 ^b	0.06 \pm 0.01
18:3n-3 (α -linolenic acid)	0.75 \pm 0.08	0.43 \pm 0.04 ^b	0.38 \pm 0.05 ^b
20:4n-6 (arachidonic acid)	27.82 \pm 2.60	24.46 \pm 1.51	21.10 \pm 1.74
20:5n-3 (eicosapentaenoic acid)	2.96 \pm 0.30	1.88 \pm 0.07	1.70 \pm 0.03 ^b
22:6n-3 (docosahexaenoic acid)	9.19 \pm 1.14	7.95 \pm 0.41	6.50 \pm 0.73
Total	262.48 \pm 15.89	266.61 \pm 12.12	284.73 \pm 28.22
B			
10:0 (capric acid)	0.20 \pm 0.07	0.13 \pm 0.02	0.11 \pm 0.03
12:0 (lauric acid)	0.05 \pm 0.00	0.09 \pm 0.01	0.14 \pm 0.08
14:0 (myristic acid)	0.48 \pm 0.04	0.62 \pm 0.22	0.43 \pm 0.04
16:0 (palmitic acid)	2.42 \pm 0.35	2.01 \pm 0.1	2.13 \pm 0.09
18:0 (stearic acid)	0.93 \pm 0.21	0.89 \pm 0.2	0.99 \pm 0.09
<i>t</i> 18:1n-9 (elaidic acid)	0.05 \pm 0.04	2.39 \pm 0.91 ^a	0.01 \pm 0.01
18:1n-9 (oleic acid)	1.24 \pm 0.38	1.62 \pm 0.57	1.57 \pm 0.11
<i>t</i> 18:2n-6 (linoelaidic acid)	0.02 \pm 0.02	0.01 \pm 0.00	4.40 \pm 0.47 ^b
18:2n-6 (linoleic acid)	0.16 \pm 0.02	0.15 \pm 0.05	0.21 \pm 0.01
20:0 (arachidic acid)	0.04 \pm 0.01	0.04 \pm 0.01	0.05 \pm 0.02
18:3n-6 (γ -linolenic acid)	0.01 \pm 0.01	0.01 \pm 0.01	0.01 \pm 0.01
18:3n-3 (α -linolenic acid)	0.03 \pm 0.01	0.04 \pm 0.00	0.05 \pm 0.02
20:4n-6 (arachidonic acid)	0.06 \pm 0.01	0.07 \pm 0.07	0.12 \pm 0.03
20:5n-3 (eicosapentaenoic acid)	0.04 \pm 0.02	0.04 \pm 0.03	0.04 \pm 0.01
22:6n-3 (docosahexaenoic acid)	0.02 \pm 0.02	0.02 \pm 0.01	0.04 \pm 0.01
Total	5.78 \pm 1.21	8.14 \pm 2.21	10.34 \pm 1.03

Endothelial cells were treated with fatty acids (50 μ M) for 24 h under standard culture conditions prior to analysis

Phospholipids and triacylglycerols were resolved using thin layer chromatography and extracted as described in the methods

Fatty acid quantification was based on an internal standard and normalized to protein content

Results are expressed as the mean \pm the standard deviation of three experiments

^a, ^b Denotes statistically significant differences at $P \leq 0.05$, $P \leq 0.25$, respectively in comparison to the vehicle control

Values are expressed in μ g/mg protein \pm SD

electrophoretically separated, transferred, and probed using a phospho-specific (Ser468) antibody for NF- κ B in comparison to GAPDH loading controls. As shown in Fig. 2, EC supplemented with the TFA, elaidic and linoelaidic, demonstrated dose-dependent increases in NF- κ B phosphorylation. With the exception of only a very slight increase in the

phospho-NF- κ B levels observed following 50 μ M oleic acid supplementation, oleic and linoleic acid-supplementation did not substantially enhance the phosphorylation status of NF- κ B. As previously reported by our laboratory, stearic acid-supplemented HAEC also increased NF- κ B phosphorylation in a dose-dependent manner [20].

Fig. 1 Effect of fatty acid supplementation on the accumulation of neutral lipid storage. Human aortic endothelial cells were supplemented with 50 μM of each individual fatty acid for 24 h at 37 $^{\circ}\text{C}$ in 5 % CO_2 . As described in the methods, lipid droplets containing triacylglycerols were stained with oil red O, and nuclei were counterstained with hematoxylin for cellular definition ($\times 500$ magnification). Treatments included **a** vehicle, **b** stearic acid, **c** oleic acid, **d** elaidic acid, **e** linoleic acid and **f** linoelaidic acid. Lipid droplets are indicated by the arrows. No excess accumulation of lipid droplets was observed when HAEC were co-supplemented with both fatty acids

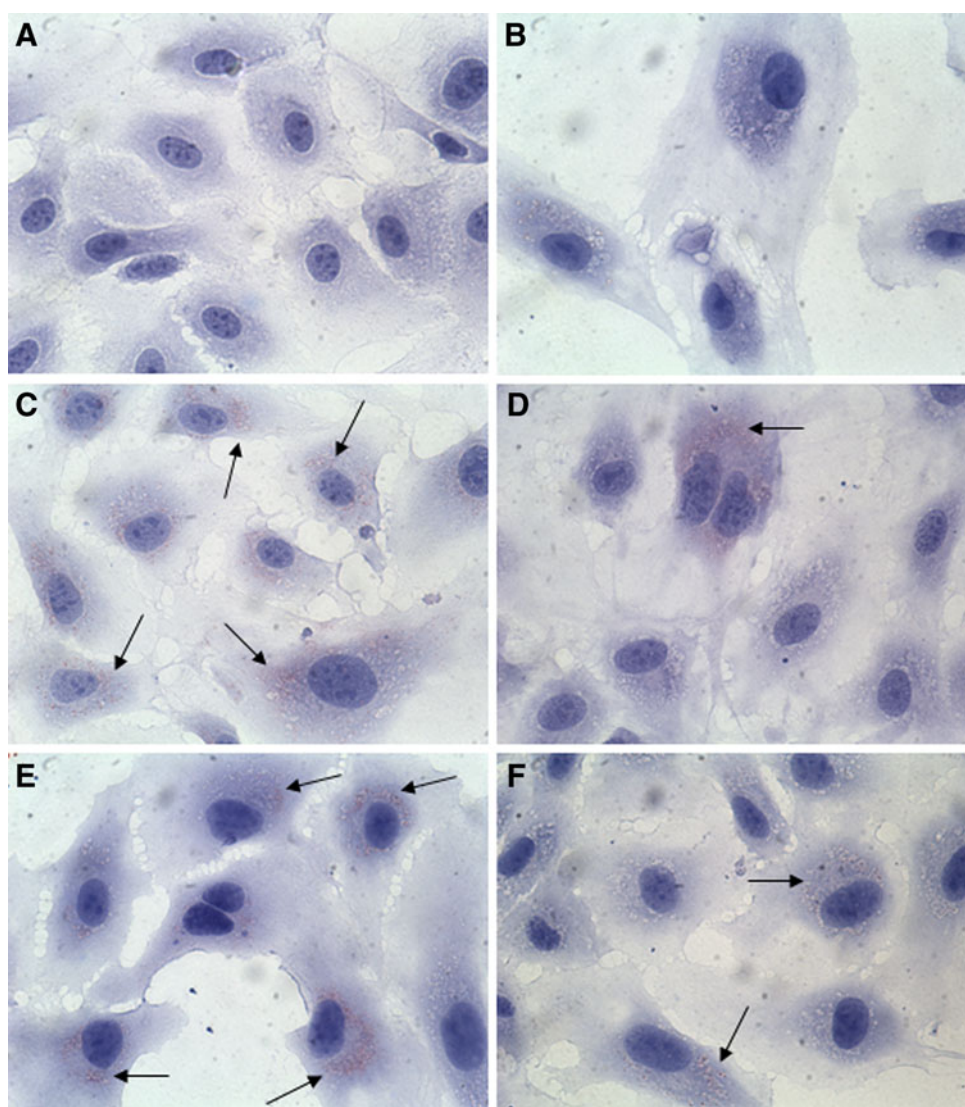


Table 2 Effect of fatty acid supplementation on HAEC ICAM-1 expression

Fatty Acid	Concentration		
	5 μM	25 μM	50 μM
Vehicle	194.3 \pm 20.5		
Elaidic	239.6 \pm 4.1	328.3 \pm 11.0 ^a	422.8 \pm 10.0 ^a
Linoelaidic	270.5 \pm 2.4	325.4 \pm 13.1 ^a	383.3 \pm 21.2 ^a
Stearic	206.3 \pm 12.3	246.3 \pm 7.4	386.1 \pm 13.8 ^a
Oleic	191.1 \pm 18.3	217.6 \pm 1.0	216.8 \pm 4.3
Linoleic	181.1 \pm 2.6	229.9 \pm 2.4	219.3 \pm 3.5

Endothelial cells were supplemented with varying concentrations of fatty acids for 24 h under standard culture conditions

Relative ICAM-1 membrane expression levels were quantified by flow cytometry and are presented as the mean fluorescent intensity \pm the standard deviation of three determinations

^a Denotes statistically significant differences ($P \leq 0.017$) in comparison to the vehicle control

Effect of *Trans* Fatty Acid Supplementation on HAEC Growth Inhibition and Cytotoxicity

In Fig. 3a the effect of TFA supplementation on EC growth is compared to stearic acid. Stearic acid-induced total growth inhibition was observed at 50 μM and significant cytotoxicity occurred at concentrations greater than 75 μM . While linoelaidic acid did invoke a low degree of EC cytotoxicity at the highest concentrations, a steady dose-dependent effect on growth inhibition was observed at concentrations greater than 25 μM . Elaidic acid minimally impacted EC growth and demonstrated no indication of affecting cellular cytotoxicity. Oleic and linoleic acid, the *cis* counterparts to the TFA, did negatively influence the growth potential of the EC, especially at concentrations greater than 150 μM . Linoleic acid supplementation was more potent than oleic, resulting in cell loss at the highest concentrations.

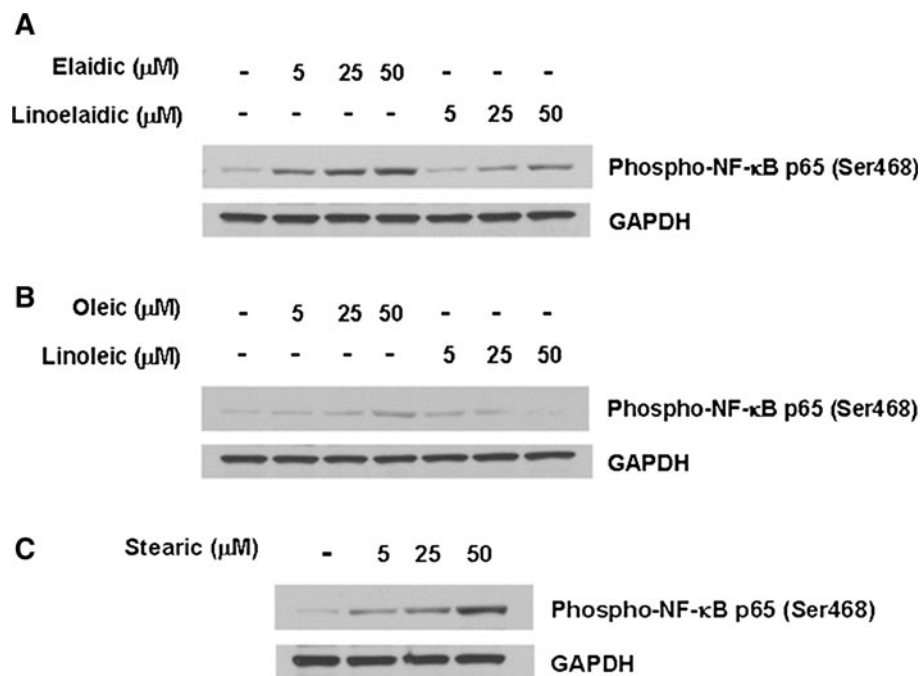


Fig. 2 Effect of fatty acid supplementation on the phosphorylation of the transcriptional regulator of ICAM-1, NF- κB . Human aortic endothelial cells were supplemented with varying concentrations of fatty acids for 24 h under typical tissue culture conditions. Endothelial cell lysates (15 $\mu\text{g}/\text{sample}$) were electrophoretically separated in a 4–12 % polyacrylamide gradient gel and subsequently transferred

onto nitrocellulose membranes. Using phospho-specific antibodies to detect the activation state of the transcriptional activator, NF- κB , the relative impact of each fatty acid was ascertained. **a** Elaidic and linoelaidic, **b** oleic and linoleic, **c** and stearic acid-supplemented cells were compared. Glyceraldehyde 3-phosphate dehydrogenase (GAPDH) was used as the protein loading control

Effect of Fatty Acid Supplementation on HAEC Apoptosis/Necrosis

To obtain evidence to support the observations in the growth inhibition and cytotoxicity studies, EC were supplemented with fatty acids (either 75 or 100 μM) for 24 h prior to assessing cell viability. Table 3 compares individual fatty acid treatments with a vehicle control in terms of the percentages of cells classified as viable, apoptotic, or necrotic. The TFA, elaidic and linoelaidic acid, slightly affected the overall viability of the cell population, which corresponded with elevated percentages of apoptotic and necrotic cells, particularly at the 100 μM dose. Oleic and linoleic supplementation affected cellular viability to a lesser extent with the exception of an unexplained shift in the population dynamics following linoelaidic acid (75 μM) supplementation. Stearic acid supplementation clearly demonstrated a significant decrease in cell viability with corresponding increases in apoptotic and necrotic events. This evidence reinforces the findings from the growth inhibition and cytotoxicity studies.

Discussion

Endothelial cells supplemented with either elaidic or linoelaidic fatty acids significantly altered the cellular

profile. Interestingly, these fatty acids incorporated into cellular phospholipids, mainly at the expense of myristic, palmitic, and stearic acids, without causing any net gain in total fatty acid levels. Our laboratory previously reported [20] that stearic acid also incorporated into the phospholipid fraction at the expense of palmitic acid without causing any net increase in total fatty acid content in this fraction. However, in the triacylglycerol fraction, incorporation of TFA was minimal (2–4 $\mu\text{g}/\text{mg}$ proteins) compared to phospholipids (100–150 $\mu\text{g}/\text{mg}$ protein) and did not occur at the expense of any other fatty acid. As shown previously [20], stearic acid incorporation into the TAG fraction was minimal (8 $\mu\text{g}/\text{mg}$ protein) compared to its incorporation into phospholipids (70 $\mu\text{g}/\text{mg}$ protein). In contrast to saturated and *trans* fatty acids, oleic acid, a *cis* fatty acid, incorporated substantially in both phospholipid (80 $\mu\text{g}/\text{mg}$ protein) and TAG (20 $\mu\text{g}/\text{mg}$ proteins) fractions. This data clearly demonstrates that TFA not only structurally resemble saturated fatty acids but they also incorporate into the cell in a similar fashion to that of saturated fatty acids. The fatty acid incorporation results are consistent with the formation of lipid droplets, which are comprised of TAGs and cholesterol esters. Elaidic and linoelaidic fatty acids did generate a few lipid droplets, whereas vehicle and stearic acid supplemented cells were devoid of oil red O-stained droplets. This data suggests that

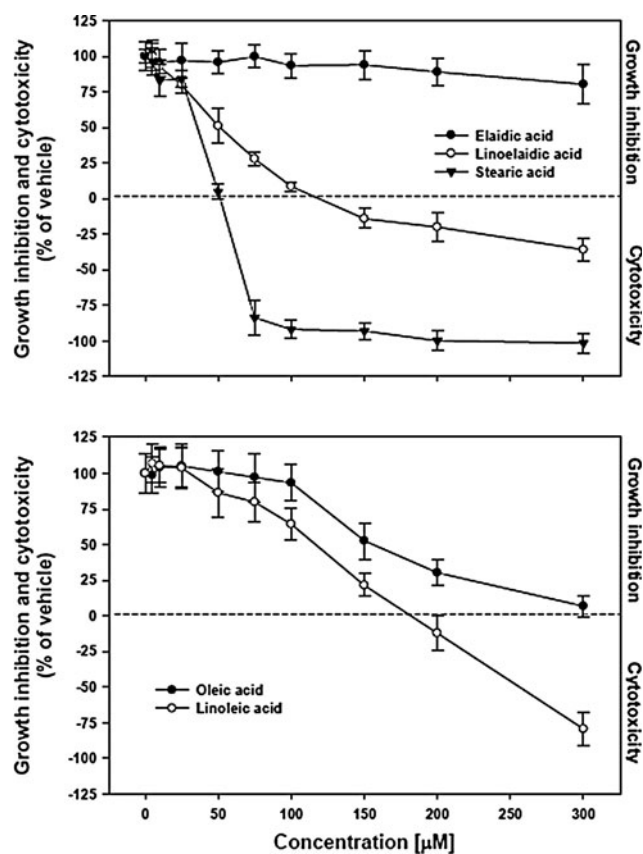


Fig. 3 Effect of fatty acid supplementation on HAEC growth inhibition and cytotoxicity. Human aortic endothelial cells were supplemented with albumin-bound fatty acids at varying concentrations for 48 h at 37 °C in 5 % CO₂. Cells were administered WST-1 assay reagent, as described in the methods, to ascertain the metabolic activity. Values less than 100, but above 0, represent growth inhibition, whereas values falling below 0 indicate cell loss in comparison to the day 0 initial population. Calculations of these values are described in the methods. **a** Elaidic, linoelaidic, and stearic acids are shown, whereas **b** oleic and linoleic acids portray the *cis* counterparts to the TFA. Data represent the mean ± the standard deviation of at least four determinations

the polyunsaturated fatty acids, oleic and linoleic, efficiently converted excess fatty acid accumulation into the neutral lipid packages, whereas TFA have a limited capacity for being incorporated into lipid droplets. This further suggests that TFA act more like saturated fatty acids.

Next we compared the functional properties of saturated and *cis/trans* unsaturated fatty acids. We have previously reported the pro-inflammatory effects of long-chain saturated fatty acids, particularly stearic acid [21]. Within this report, we demonstrated that elevated phosphorylation of NF- κ B (Ser468) corresponded with increased ICAM-1 surface expression in non-challenged endothelial cells. Both elaidic and linoelaidic acids induced phosphorylation of the transcriptional regulator, NF- κ B, consistent with stearic acid. The phosphorylation levels corresponded to

Table 3 Effect of fatty acid supplementation on endothelial cell apoptosis/necrosis

	Apoptosis/necrosis detection (mean percentage ± SD)		
	Viable	Apoptotic	Necrotic
Vehicle	78.0 ± 2.0	9.0 ± 1.3	13.1 ± 0.7
Elaidic (μM)			
75	74.3 ± 3.8	12.6 ± 2.0	13.2 ± 1.8
100	70.6 ± 1.6 ^a	12.8 ± 1.2 ^a	16.6 ± 2.5
Linoelaidic (μM)			
75	73.0 ± 3.6	12.2 ± 0.6 ^a	14.8 ± 3.1
100	69.6 ± 3.1 ^a	13.7 ± 0.6 ^a	16.7 ± 2.7
Linoleic (μM)			
75	72.5 ± 2.2 ^a	11.2 ± 1.9	16.4 ± 0.5 ^a
100	75.6 ± 1.3	10.7 ± 1.2	13.8 ± 2.3
Oleic (μM)			
75	74.2 ± 2.6	13.4 ± 2.6	12.4 ± 3.1
100	76.0 ± 2.0	11.3 ± 3.4	12.8 ± 1.4
Stearic (μM)			
75	66.4 ± 5.2 ^a	20.3 ± 3.6 ^a	13.6 ± 1.3
100	50.2 ± 3.2 ^a	32.8 ± 2.2 ^a	17.0 ± 1.0 ^a

Prior to apoptosis/necrosis analysis using flow cytometry, endothelial cells were supplemented with individual fatty acids for 24 h at 37 °C in 5 % CO₂

The data reflects the percentage of cells observed in each classification. Results are expressed as the mean ± the standard deviation of three determinations

^a Denotes significant differences ($P \leq 0.025$) in comparison to the vehicle control

increased non-challenged ICAM-1 surface expression. Importantly, the TFA enhanced ICAM-1 expression to levels equal to or surpassing those of stearic acid-supplemented cells. The *cis* counterparts did not appear to alter the phosphorylation status or the corresponding ICAM-1 surface expression. These results portray a pro-inflammatory endothelial cell phenotype that is consistent with our previous findings, which focused primarily on linoelaidic acid [25, 26]. Sanadgol et al. [27] reported that elaidic acid supplementation did not diminish tumor necrosis factor- α or lipopolysaccharide-induced upregulation of ICAM-1, whereas oleic acid supplementation suppressed the inflammatory response. This evidence suggests that TFA not only invoke a pro-inflammatory response, but they also assist in maintaining the activation status. Furthermore, Rezamond et al. [28] found elevated mRNA expression of pro-inflammatory markers, including interleukin-1 β and ICAM-1, in bovine mammary epithelial cells supplemented with elaidic acid. In a cross-sectional study of 730 women from the nurses' health study I cohort, TFA intake was associated with elevated plasma levels of C-reactive protein, soluble tumor necrosis factor receptor-2, E-selectin, soluble ICAM-1, and soluble VCAM-1 [29]. The authors

conclude that elevated TFA intake could lead to a chronic pro-inflammatory endothelial cell phenotype, which could progress into CHD.

Consistent with our previous reports, stearic acid-supplemented endothelial cells invoke cytotoxicity at concentrations surpassing 75 μM [20, 21]. Unlike stearic acid, elaidic and linoelaidic acids do not adhere to the same growth inhibition and cytotoxicity observations. Elaidic acid appears to be well tolerated in terms of endothelial cell growth inhibition, whereas linoelaidic acid did significantly inhibit growth at concentrations $>50 \mu\text{M}$ and limited cell loss was apparent at concentrations exceeding 150 μM . Flow cytometric determination of apoptosis and/or necrosis clearly demonstrated the negative impact of stearic acid supplementation on endothelial cell viability; moreover, premature cell loss in the stearic acid-supplemented EC likely skewed the overall percentages, thereby minimizing the negative impact. *Trans* fatty acids did slightly impact endothelial apoptosis/necrosis albeit at relatively low percentage alterations. A recent report by Qiu et al. [30] claimed that relatively high concentrations of elaidic acid induced apoptosis in HUVEC cells. This TFA-induced apoptosis involved the activation of caspases 3, 8, and 9. Zapolska-Downar et al. [31] also assessed TFA's ability to induce apoptosis in HUVEC by comparing both elaidic and linoelaidic fatty acids. They also describe a caspase-3 dependent induction of apoptosis; however, the concentrations used in this study were exceedingly high (up to 5 mM). Consistent with our observations, linoelaidic acid appeared to be potentially more detrimental than elaidic acid.

In conclusion, both elaidic and linoelaidic fatty acids incorporate into endothelial cell phospholipids, and TFA are capable of being incorporated into triacylglycerols to a limited extent. Elaidic acid-supplemented endothelial cells portrayed the most pro-inflammatory phenotype. Furthermore, in contrast to stearic acid (as shown previously) [20], elaidic acid did not negatively impact human aortic endothelial cell growth; however, cellular incorporation of TFA from industrially produced dietary sources into the vasculature could lead to a sustained inflammatory state as elaidic acid is significantly more abundant than linoelaidic in the IP-TFA. The concentration of *trans* fatty acids (5–50 μM) used in the present study were within the physiological range found in fasting 20-years-old non-Hispanic white individuals (30–103 μM) [32]. The pro-inflammatory effects observed in this *in vitro* study, therefore, suggest an association of dietary TFA with CHD.

Acknowledgments The authors wish to thank Ms. Elaine Bammerlin for the editorial assistance and Mr. Colin Terry for the help in the statistical analysis of the data. The work was supported by a Methodist Research Institute's summer student internship to Mr. Phillip Whitley.

Conflict of interest The authors declare that they have no conflict of interest.

References

1. Stender S, Astrup A, Dyerberg J (2008) Ruminant and industrially produced *trans* fatty acids: health aspects. *Food Nutr Res* 52. doi: 10.3402/fnr.v52i0.1651
2. Jakobsen MU, Bysted A, Andersen NL, Heitmann BL, Hartkopp HB, Leth T, Overvad K, Dyerberg J (2006) Intake of ruminant *trans* fatty acids in the Danish population aged 1–80 years. *Eur J Clin Nutr* 60:312–318
3. Allison DB, Denke MA, Dietschy JM, Emken EA, Kris-Etherton P, Nicolosi RJ (1995) *Trans* fatty acids and coronary heart disease risk. Report of the expert panel on *trans* fatty acids and coronary heart disease. *Am J Clin Nutr* 62:655S–708S
4. Ratnayake WM, L'Abbe MR, Farnworth S, Dumais L, Gagnon C, Lampi B, Casey V, Mohottalage D, Rondeau I, Underhill L, Vigneault M, Lillycrop W, Meleta M, Wong LY, Ng T, Gao Y, Kwong K, Chalouh S, Pantazopoulos P, Gunaratna H, Rahardja A, Blagden R, Roscoe V, Krakalovich T, Neumann G, Lombaert GA (2009) *Trans* fatty acids: current contents in Canadian foods and estimated intake levels for the Canadian population. *J AOAC Int* 92:1258–1276
5. Willett WC, Stampfer MJ, Manson JE, Colditz GA, Speizer FE, Rosner BA, Sampson LA, Hennekens CH (1993) Intake of *trans* fatty acids and risk of coronary heart disease among women (see comment). *Lancet* 341:581–585
6. Pietinen P, Ascherio A, Korhonen P, Hartman AM, Willett WC, Albanes D, Virtamo J (1997) Intake of fatty acids and risk of coronary heart disease in a cohort of Finnish men. The alpha-tocopherol, beta-carotene cancer prevention study. *Am J Epidemiol* 145:876–887
7. Ascherio A (2004) *Trans* fatty acids and coronary heart disease. *Harvard School of Public Health* 1–8
8. Mozaffarian D, Katan MB, Ascherio A, Stampfer MJ, Willett WC (2006) *Trans* fatty acids and cardiovascular disease. *N Engl J Med* 354:1601–1613
9. Jakobsen MU, Overvad K, Dyerberg J, Heitmann BL (2008) Intake of ruminant *trans* fatty acids and risk of coronary heart disease. *Int J Epidemiol* 37:173–182
10. Motard-Belanger A, Charest A, Grenier G, Paquin P, Chouinard Y, Lemieux S, Couture P, Lamarche B (2008) Study of the effect of *trans* fatty acids from ruminants on blood lipids and other risk factors for cardiovascular disease. *Am J Clin Nutr* 87:593–599
11. Mozaffarian D, Aro A, Willett WC (2009) Health effects of *trans* fatty acids: experimental and observational evidence. *Eur J Clin Nutr* 63(Suppl 2):S5–S21
12. Bendsen NT, Stender S, Szecsi PB, Pedersen SB, Basu S, Hellgren LI, Newman JW, Larsen TM, Haugaard SB, Astrup A (2011) Effect of industrially produced *trans* fat on markers of systemic inflammation: evidence from a randomized trial in women. *J Lipid Res* 52:1821–1828
13. Schaffer JE (2003) Lipotoxicity: when tissues overeat. *Curr Opin Lipidol* 14:281–287
14. Unger RH (2002) Lipotoxic diseases. *Annu Rev Med* 53:319–336
15. Sheehan MT, Jensen MD (2000) Metabolic complications of obesity. Pathophysiologic considerations. *Med Clin North Am* 84:363–385
16. Eckel RH, Barouch WW, Ershow AG (2002) Report of the National Heart, Lung, and Blood Institute–National Institute of Diabetes and Digestive and Kidney Diseases working group on the pathophysiology of obesity-associated cardiovascular disease. *Circulation* 105:2923–2928

17. Jakobsen MU, O'Reilly EJ, Heitmann BL, Pereira MA, Balter K, Fraser GE, Goldbourt U, Hallmans G, Knekt P, Liu S, Pietinen P, Spiegelman D, Stevens J, Virtamo J, Willett WC, Ascherio A (2009) Major types of dietary fat and risk of coronary heart disease: a pooled analysis of 11 cohort studies. *Am J Clin Nutr* 89:1425–1432
18. Merchant AT, Kelemen LE, de Koning L, Lonn E, Vuksan V, Jacobs R, Davis B, Teo KK, Yusuf S, Anand SS (2008) Interrelation of saturated fat, *trans* fat, alcohol intake, and subclinical atherosclerosis. *Am J Clin Nutr* 87:168–174
19. Lemaitre RN, King IB, Mozaffarian D, Sotoodehnia N, Rea TD, Kuller LH, Tracy RP, Siscovick DS (2006) Plasma phospholipid *trans* fatty acids, fatal ischemic heart disease, and sudden cardiac death in older adults: the cardiovascular health study. *Circulation* 114:209–215
20. Harvey KA, Walker CL, Xu Z, Whitley P, Pavlina TM, Hise M, Zaloga GP, Siddiqui RA (2010) Oleic acid inhibits stearic acid-induced inhibition of cell growth and pro-inflammatory responses in human aortic endothelial cells. *J Lipid Res* 51:3470–3480
21. Harvey KA, Walker CL, Pavlina TM, Xu Z, Zaloga GP, Siddiqui RA (2010) Long-chain saturated fatty acids induce pro-inflammatory responses and impact endothelial cell growth. *Clin Nutr* 29:492–500
22. Roach C, Feller SE, Ward JA, Shaikh SR, Zerouga M, Stillwell W (2004) Comparison of *cis* and *trans* fatty acid containing phosphatidylcholines on membrane properties. *Biochemistry* 43:6344–6351
23. van Greevenbroek MM, Voorhout WF, Erkelens DW, van Meer G, de Bruin TW (1995) Palmitic acid and linoleic acid metabolism in Caco-2 cells: different triglyceride synthesis and lipoprotein secretion. *J Lipid Res* 36:13–24
24. Folch J, Lees M, Stanley GHS (1957) A simple method for the isolation and purification of total lipids from animal tissue. *J Biol Chem* 226:497–509
25. Harvey KA, Arnold T, Rasool T, Antalis C, Miller SJ, Siddiqui RA (2008) *Trans* fatty acids induce pro-inflammatory responses and endothelial cell dysfunction. *Br J Nutr* 99:723–731
26. Siddiqui RA, Harvey KA, Ruzmetov N, Miller SJ, Zaloga GP (2009) n-3 fatty acids prevent whereas *trans* fatty acids induce vascular inflammation and sudden cardiac death. *Br J Nutr* 102:1811–1819
27. Sanadgol N, Mostafaie A, Bahrami G, Mansouri K, Ghanbari F, Bidmeshkipour A (2010) Elaidic acid sustains LPS and TNF- α induced ICAM-1 and VCAM-1 expression on human bone marrow endothelial cells (HBMEC). *Clin Biochem* 43:968–972
28. Rezamand P, McGuire MA (2011) Effects of *trans* fatty acids on markers of inflammation in bovine mammary epithelial cells. *J Dairy Sci* 94:316–320
29. Lopez-Garcia E, Schulze MB, Meigs JB, Manson JE, Rifai N, Stampfer MJ, Willett WC, Hu FB (2005) Consumption of *trans* fatty acids is related to plasma biomarkers of inflammation and endothelial dysfunction. *J Nutr* 135:562–566
30. Qiu B, Hu JN, Liu R, Fan YW, Li J, Li Y, Deng ZY (2011) The caspase pathway of elaidic acid (9t-C18:1)—induced apoptosis in human umbilical vein endothelial cells. *Cell Biology International* (in press)
31. Zapolska-Downar D, Kosmider A, Naruszewicz M (2005) *Trans* fatty acids induce apoptosis in human endothelial cells. *J Physiol Pharmacol* 56:611–625
32. Vesper HW, Kuiper HC, Mirel LB, Johnson CL, Pirkle JL (2012) Levels of plasma *trans* fatty acids in non-Hispanic white adults in the United States in 2000 and 2009. *JAMA* 307:562–563

Trans Isomers of EPA and DHA in Omega-3 Products on the European Market

Caterina Sciotto · Svein A. Mjøs

Received: 13 December 2011 / Accepted: 3 April 2012 / Published online: 9 May 2012
© AOCS 2012

Abstract The levels of *trans* isomers of eicosapentaenoic (EPA) acid and docosahexaenoic acid (DHA) in 77 omega-3 products on the European market have been studied. Fatty acids were analyzed as fatty acid methyl esters by gas chromatography with a flame ionization detector, using a cyanopropyl coated stationary phase. The amount of mono-*trans* EPA isomers relative to the corresponding all-*cis* isomer ranged from 0.19 to 4.5 %. The corresponding values for mono-*trans* DHA relative to the all-*cis* isomer ranged from 0.25 to 5.9 %. There was a strong correlation between the degree of isomerization of EPA and DHA, showing that DHA was 1.26 times more isomerized than EPA. Division of the samples into different product groups showed that samples with a low degree of isomerization were found in all groups, except one. This shows that a high degree of isomerization is avoidable, and also points to deodorization of the oils as the main source of *trans* isomers.

Keywords Omega-3 supplements · Fish oil · Fish oil concentrates · EPA · DHA · *Trans* fatty acids · Thermal isomerization

Abbreviations

ALA	Alpha linolenic acid (18:3n-3)
DHA	Docosahexaenoic acid (22:6n-3)
DPA	Docosapentaenoic acid (22:5n-3)
DI	Degree of isomerization
EPA	Eicosapentaenoic acid (20:5n-3)
FAME	Fatty acid methyl ester
GC	Gas chromatography
MS	Mass spectrometry

Introduction

Eicosapentaenoic acid (EPA, 20:5n-3) and docosahexaenoic acid (DHA, 22:6n-3) are the two major long chain omega-3 fatty acids in most fats and oils of marine origin. They are known for their positive health effects, such as protection against cardiovascular disease [1, 2] and their critical role in brain function and neurodevelopment [2–4]. There are also claims of reduced inflammation [5, 6], as well as positive effects on psychological and cognitive function [2, 3].

Recommendations for the intake of EPA and DHA vary [2, 7, 8], and so does consumption of fish and other sources of long chain omega-3 fatty acids. But there is a general gap between the recommendations and the average intake of EPA and DHA in western diets [7, 9].

As a consequence, a large number of food supplements and fortified foods containing EPA and DHA in varying amounts are on the market. These products are typically

Electronic supplementary material The online version of this article (doi:10.1007/s11745-012-3672-3) contains supplementary material, which is available to authorized users.

C. Sciotto · S. A. Mjøs (✉)
Department of Chemistry, University of Bergen,
P.O. Box 7803, 5020 Bergen, Norway
e-mail: svein.mjøs@kj.uib.no

C. Sciotto
Dipartimento Farmaco-chimico, Facoltà di Farmacia,
Università di Messina, viale Annunziata,
98168 Messina, Italy

S. A. Mjøs
Nofima BioLab, Kjerreidviken 16,
5141 Fyllingsdalen, Norway

omega-3 rich fish oils or fish oils where EPA and DHA have been concentrated, e.g., by distilling off shorter fatty acids. Some products are also of algal origin, or contain oils from other marine sources, such as krill. Many of the products are blends of different oils, including common vegetable oils.

It has been shown in previous studies that the processing conditions commonly used for deodorization of oils may lead to the formation of *trans* isomers of EPA and DHA through thermal isomerization [10–13]. Another possible source of these *trans* isomers may be the distillation used for concentrating EPA and DHA in fish oils. Thermal isomerization does not lead to positional isomerism of the double bonds [11–13], and the number of possible *trans* isomers that can be formed is therefore equal to 2^n , where n is the number of double bonds in the molecule, i.e., $2^5 = 32$ for EPA and $2^6 = 64$ for DHA. However, under normal operating conditions, only minor amounts of isomers with more than one *trans* double bond are formed [11–13].

It was shown in [14] that *trans* isomers of EPA or DHA were present in four commercial fish oils and three products of algal origin, but no comprehensive study of the levels in products on the market has been conducted. The purpose of this study has been to evaluate the levels of EPA and DHA *trans* isomers in omega-3 products on the European market, and 77 food supplements or pharmaceutical products claiming to contain EPA and DHA were studied.

Materials and Methods

Samples

Omega-3 products claiming to contain EPA, DHA or both were purchased over the counter in pharmacies or other retail stores in Norway (25 products), Italy (7 products), Spain (13 products), Germany (12 products), UK (15 products) and France (1 product). In addition, four products were purchased over the Internet from Norwegian suppliers. The products were selected so that there would not be replicates of the same product and brand name in the study. However, it is common that products from the same manufacturer are sold under different product and brand names in different markets. It is therefore likely that some of the products in the study may come from the same process and raw material. All products were capsules, except for one of the cod liver oils, which was purchased as a bottled liquid. The products were stored refrigerated and taken out of the refrigerator the day before analysis. All products were within the shelf life when analyzed.

Analysis

Fatty acid methyl esters were prepared from 32 ± 8 mg of the products (1–2 drops, depending on viscosity) by heating at 100 °C for 5 min in 1.5 mL 0.5 N methanolic NaOH followed by heating at 100 °C after addition of 2.0 mL 12 % methanolic BF_3 . Samples were thereafter vortex mixed for 30 s after addition of 1 mL isooctane, 5 mL saturated aqueous NaCl solution was added, the samples were vortexed again and the isooctane layer was collected. The extraction with isooctane was thereafter repeated and the isooctane layer was combined with the first aliquot. The parameters were as described in AOCS Ce 1b-89 [15], except that 5 min reaction time was applied in the BF_3 step and that the saturated methyl ester 21:0 was added as internal standard. Two capsules of each product were analyzed.

The samples were analyzed using an Agilent 7890 gas chromatograph equipped with a flame ionization detector (GC-FID), a split-splitless injection port and a 7673 automatic liquid sampler (Agilent, Santa Clara, CA, USA). The chromatographic conditions were based on the methodology described in [13]. To achieve optimal resolution this reference proposes separate methods for *trans* isomers of EPA and DHA, respectively. Both methods used a BPX-70 column with $L = 60$ m, i.d. = 0.25 mm and $d_f = 0.25$ μm (SGE, Ringwood, Australia). Helium (99.999 %) was used as the carrier gas at an estimated velocity of 26 cm/s, the injector temperature was 250 °C, the detector temperature was 260 °C, and 1 μL sample was injected in the splitless mode. EPA isomers were analyzed by the following temperature program: injection was done at 60 °C, after 4 min the temperature was increased by 30 °C/min to 180 °C followed by 1 °C/min to 220 °C. DHA isomers were analyzed by injection at 60 °C, after 4 min the temperature was increased by 30 °C/min to 160 °C, followed by 1 °C/min to 220 °C. The chromatographic system was controlled by GC Chemstation B.03.02 (Agilent). Integration of chromatographic peaks, quantification and reporting were done in Chrombox C 11-09 (<http://www.chrombox.org>) running under Matlab 6.5 (Mathworks, Natick, MA, USA).

Blank samples and a reference fish oil were prepared daily to check the quality of the reagents. Chromatographic areas were corrected by empirical response factors based on the reference mixture GLC-793 (Nu-Chek Prep. Elysian, MN, USA) that was run as every 10th sample in the analytical sequence. The composition of the reference sample is given as supplementary material (Table S1). Approximately 2 ng of each FAME in the mixture was applied on the column. Response factors of compounds that were not in the reference mixture were calculated from response factors of similar compounds with respect to the

number of double bonds and carbons. The response factors for the EPA and DHA *trans* isomers were set equal to the corresponding *cis* isomers. Qualitative reference mixtures of mono-*trans* EPA and mono-*trans* DHA, prepared as described in [16], were analyzed at regular intervals. The largest peaks in these mixtures corresponded to approximately 3.5 ng on the column.

Because of the great variation of the sample composition it was necessary to analyze the samples twice to adjust the concentration to an appropriate amount for separation and quantification of the peaks. The concentration was scaled after EPA or DHA, depending on which of these that was in largest amounts. The concentration was scaled so that the largest peak corresponded to approximately 15 ng on the column.

To identify the peaks in the region around EPA and DHA, a subset of the samples were also analyzed by gas chromatography–mass spectrometry (GC–MS) at chromatographic conditions described as Program 1 in [17]. The GC–MS system was a HP-5890 GC connected to a HP-5972 mass spectrometer (Agilent). Both short scans (m/z 50–110) and full scans (m/z 50–438) were applied. The peaks were identified in Chrombox Q 11-08 (<http://www.chrombox.org>) using libraries of mass spectra and ECL values downloaded from [18], and by interpretation rules summarized in [19].

Principal component analysis of the fatty acid profiles were performed using Unscrambler 9.8. The variables were standardized prior to the calculation (mean centered and divided by the standard deviation). Other calculations were performed in Microsoft Excel 2002 for Windows.

Results

Chromatographic Resolution

Chromatographic patterns of the region around EPA and DHA of the mono-*trans* reference mixtures and three selected products are shown in Fig. 1. The three products shown were the products with a degree of isomerization closest to the mean value of typical “18/12 oil”, a “33/23 concentrate” and the seal and cod liver oils, which are similar in composition. The three products shown are therefore significantly isomerized, but they are not extreme. See Sect. “Product Groups” for further details.

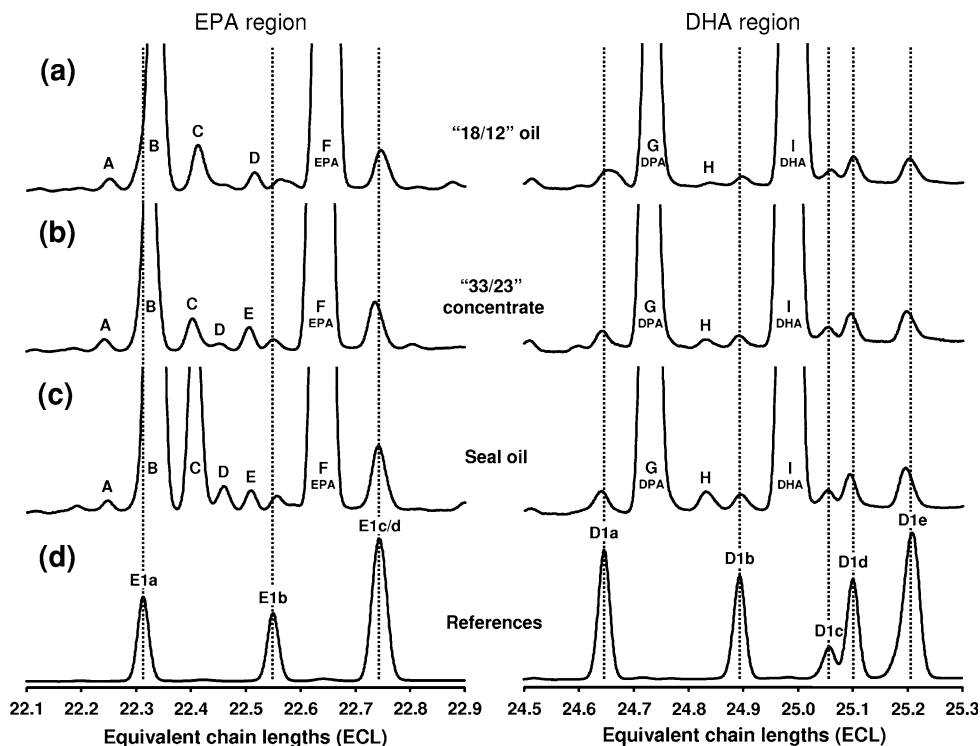
The resolution shown in Fig. 1 shows the same chromatographic pattern as presented in [16] and [13], and the naming of the mono-*trans* isomers (E1a–d and D1a–e) are according to the same references. The patterns presented in these papers show that the five *trans* isomers of EPA elute in three peaks, and that the six *trans* isomers of DHA elute in five peaks. In these works, the analyses were performed by GC–MS.

As can be seen from the chromatograms, there is a significant overlap between some of the *trans* isomers and other FAME, particularly in the case of EPA. The peaks labelled A–I in the figure has been completely or partially identified by GC–MS using conditions described in [16, 19] and MS libraries and ECL-patterns presented at [18]. Peak A was partially identified as a polyunsaturated FAME, but the quality of the mass spectrum was not sufficient to elucidate further details. Minor amounts of n-4 polyunsaturated fatty acids have previously been reported in marine lipids [17, 19, 20], and a possible structure is 20:4n-4 since it elutes immediately before 20:4n-3, but a non-methylene interrupted 20:4 has also been reported in the same region [18]. Peak B is a mixture of the E1a isomer with 20:4n-3 and 22:1n-11. Both these are common in marine lipids. Peak C is 22:1n-9, which is also a common fatty acid and present in the reference mixture. Peak D was identified as a polyunsaturated FAME, but the quality of the mass spectrum was not sufficient to elucidate further details. A possible structure is 20:4n-1. This fatty acid has previously been reported in marine lipids [17, 19, 21]. Peak E was identified as a monounsaturated FAME, The structure was assigned to the 22:1n-7 based on the distance to the n-9 isomer and ECL values reported at [18]. Peaks F and G are the all-*cis* EPA and all-*cis* DPA (22:5n-3) FAME. Peak H was identified by mass spectrometry as a polyunsaturated FAME. This peak appears in samples that has relatively large amounts of all-*cis* DPA and also a significant degree of isomerization. It has previously been reported as *trans* isomers of DPA corresponding to the E1c/d peak from EPA [13]. Peak I is all-*cis* DHA.

It has been shown that the apparent polarity of cyanopropyl columns increase with temperature [22]. The overlap between the 22:1 monoenes and the *trans* isomers of EPA can therefore be solved by using higher temperature gradients or lower carrier gas velocity, which will increase the elution temperature of the compounds. However, it has also been shown that the chromatographic selectivity on cyanopropyl phases depends basically on the number of *cis* double bonds in the molecule [17]. The overlaps between the 20:4 isomers and mono-*trans* EPA is therefore more difficult to resolve since the molecules have the same number of carbons and *cis* double bonds. Increasing the temperatures to move the EPA isomers away from the 22:1 isomers will lead to a general decrease in separation efficiency and move all-*cis* EPA closer to the E1c/d peak, because all-*cis* EPA have more *cis* double bonds.

Trans isomers of EPA and DHA have previously been separated on BPX-70 [13, 16], SP-2560 [16], CP-Sil 88 [11, 12, 14] and BP-20 [23] capillary columns. None of the previous works has shown that it is possible to separate all the *trans* isomers from possible interferents in a broad range of samples. However, it has been shown in previous

Fig. 1 Chromatographic patterns around EPA and DHA of (a) “18/12 oil”, b “33/23 concentrate”, c seal oil and d the qualitative reference mixtures of mono-*trans* EPA and mono-*trans* DHA. See text in “Chromatographic Resolution” for explanation of the identities of peaks A to I



works that the major *trans* EPA peak E1c/d and the two last *trans* DHA peaks, D1d and D1e, can be expected to be free of interferences [13, 16]. Quantification in this work is therefore based on these peaks.

Quantification and Quality Criteria

It should be emphasized that the chromatographic conditions in the study were optimized for quantification of mono-*trans* EPA and mono-*trans* DHA isomers. Other *trans* fatty acids may be present in low amounts in the products, either as a result of thermal isomerization in fish oil, or because some of the products in the study are blends with vegetable oils, which often contain *trans* isomers of C18 fatty acids. One of the products in the study also had a chromatographic pattern that indicated presence of hydrogenated vegetable oil. Minor amounts of di-*trans* EPA and di-*trans* DHA may also be formed during refining, but amounts are insignificant compared to mono-*trans* isomers [13]. Other *trans* fatty acids than mono-*trans* isomers of EPA and DHA have not been quantified in this study. The term total *trans* in this paper therefore refers to the sum of quantified EPA and DHA mono-*trans* isomers. *Trans* EPA and *trans* DHA refer to the estimated sum of mono-*trans* isomers. For simplicity, *cis* EPA/DHA is used to refer to the naturally occurring all-*cis* isomers.

Because recommendations of daily intake given on packages of omega-3 products are usually adjusted after the content of EPA and DHA the results are reported as percent *trans* isomers relative to the *cis* analog. These

values are denoted *trans* EPA_{%cis} and *trans* DHA_{%cis} for EPA and DHA, respectively. Total content of EPA and DHA *trans* isomers are reported as percent relative to the total fatty acid content and denoted total *trans*_{%FA}.

As shown in previous works, three of the mono-*trans* peaks can be expected to be free of interferences and therefore suitable for quantification of trace amounts [13, 16]. This is the largest *trans* EPA peak, eluting after the *cis* isomer (E1c/d), and the two largest *trans* DHA peaks eluting after the *cis* DHA peak (D1d and e). In [13] it was shown that the largest *trans* EPA peak contained approximately 77.4 % of the *trans* EPA isomers, and that the two largest *trans* DHA peaks respectively contained 28.5 and 37.4 % of the *trans* DHA isomers. It was also shown that with a moderate degree of isomerization, these relationships were quite constant. The sums of *trans* EPA were therefore estimated by multiplying the amounts calculated from the last *trans* EPA peak by 1.29 and the sums of *trans* DHA were estimated by multiplying the amounts calculated from two last *trans* DHA peaks with 1.52. These values were thereafter divided by the amounts of the corresponding all *cis* isomers and multiplied by 100 % to get the mass percent *trans* isomers relative to the *cis* isomers (*trans* EPA_{%cis} and *trans* DHA_{%cis}). Since the quantification is based on empirically derived correction factors the amounts of all the *trans* peaks relative to the all-*cis* isomers are reported as supplementary material (Tables S2 and S3).

The criterion for the acceptance of the results was that the percentage of *trans* isomers relative to the *cis* analogs should not differ by more than 20 % in the two replicates.

For one of the samples it was not possible to establish acceptable values for the EPA isomers. This was a sample with almost zero *cis* EPA. Results for EPA are therefore reported for 76 samples, compared to 77 samples for DHA.

Degree of Isomerization

The term degree of isomerization (DI) has been used in previous studies of thermal isomerization of polyunsaturated fatty acids as a measure of the fraction or percentage of the original *cis* isomers that have been isomerized [13, 24–27]. The DI of fatty acid *x*, expressed as a percentage, is calculated according to Eq. 1 below:

$$DI_{\%(x)} = 100 \frac{m_{(x)trans}}{m_{(x)cis} + m_{(x)trans}} = 100 \frac{trans\ x_{\%cis}}{100 + trans\ x_{\%cis}} \quad (1)$$

where *m* is the mass of *trans* isomers relative to the corresponding *cis* isomer. As long as the $DI_{\%}$ is low, the value will be close to $trans\ x_{\%cis}$.

The DI of DHA is plotted against the DI of EPA in Fig. 2. As can be expected if the *trans* isomers are formed by the same process, there is a strong correlation between the DI values. The slope of the regression line is 1.26, meaning that DHA in the studied products is 26 % more isomerized than EPA. The isomerization mechanisms of polyunsaturated fatty acids are not fully understood, but studies on the isomer formation of 18:3 acids [25–29], EPA [12–14] and DHA [12–14] have shown that double bonds in different positions isomerize to a different degree. Comparisons of the reaction rates of 18:2 and 18:3 acids [24, 27, 29], as well as EPA and DHA [13, 14] have shown

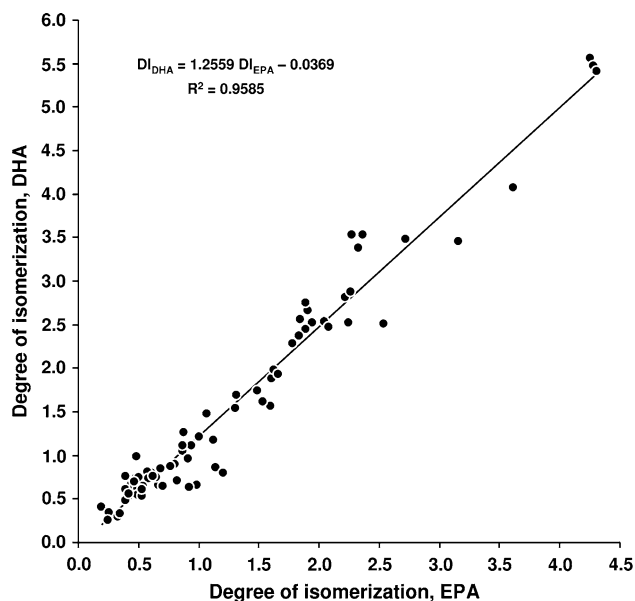


Fig. 2 Degree of isomerization of DHA versus degree of isomerization of EPA

that reaction rates tend to increase more than the number of double bonds, and that the number of methylene-groups between methylene-interrupted double bonds may be of importance. The relationship 1.26 corresponds well with the ratio of double bond enclosed methylene groups, which is 5/4 for DHA/EPA. However, the slope corresponds less well with the results in [13], which predicts that DHA isomerize 1.6 times faster than EPA. However, these predictions were partially based on experimental conditions that gave extreme DI values compared to those we see in products on the market. Fournier et al. [14] studied four commercial fish oils and found DI_{DHA} over DI_{EPA} varying from 1.26 to 1.53, which is more in accordance with what we observed in this study.

Distributions

The distributions of % *trans* EPA and % *trans* DHA relative to the corresponding *cis* isomers and total *trans* isomers relative to sum fatty acids are shown in Fig. 3, and the values are far from being normally distributed.

$Trans\ EPA_{\%cis}$ ranged from 0.19 to 4.5 % and $trans\ DHA_{\%cis}$ ranged from 0.25 to 5.9 %. The median values were slightly below 1 % for both distributions, meaning that more than half of the products has less than 1 % *trans* isomers relative to the *cis* analogs. But there are also a significant number of samples with severe isomerization. The values for total *trans* relative to total fatty acids show a similar distribution. However, because of the large variation in the content of EPA and DHA in the samples, it is emphasized that samples that are high in $trans\ EPA_{\%cis}/DHA_{\%cis}$ are not necessarily the same samples that are high in total *trans* relative to total FA. In the following discussion, samples within the first quartile of the distribution (lowest 25 %) will be denoted low *trans* and samples in the third quartile (highest 25 %) will be denoted high *trans* (See Fig. 3 for values).

Product Groups

Based on the product labelling, the amount of EPA and DHA in the products (Fig. 4), and principal component analysis of the complete fatty acid profiles, the products were assigned to different product groups. Figure 4 shows four dense groups. One of the groups with 15 objects consists of typical South American “18/12 oils” containing approximately 18 % EPA and 12 % DHA. Three products in the study was labelled salmon oil, but it was not possible to distinguish these products from the 18/12 oils by the principal component analysis of the fatty acid profiles. These were therefore also assigned to the 18/12 oils. Two other dense groups were formed by the cod liver oils (6 objects) and the seal oils (4 objects).

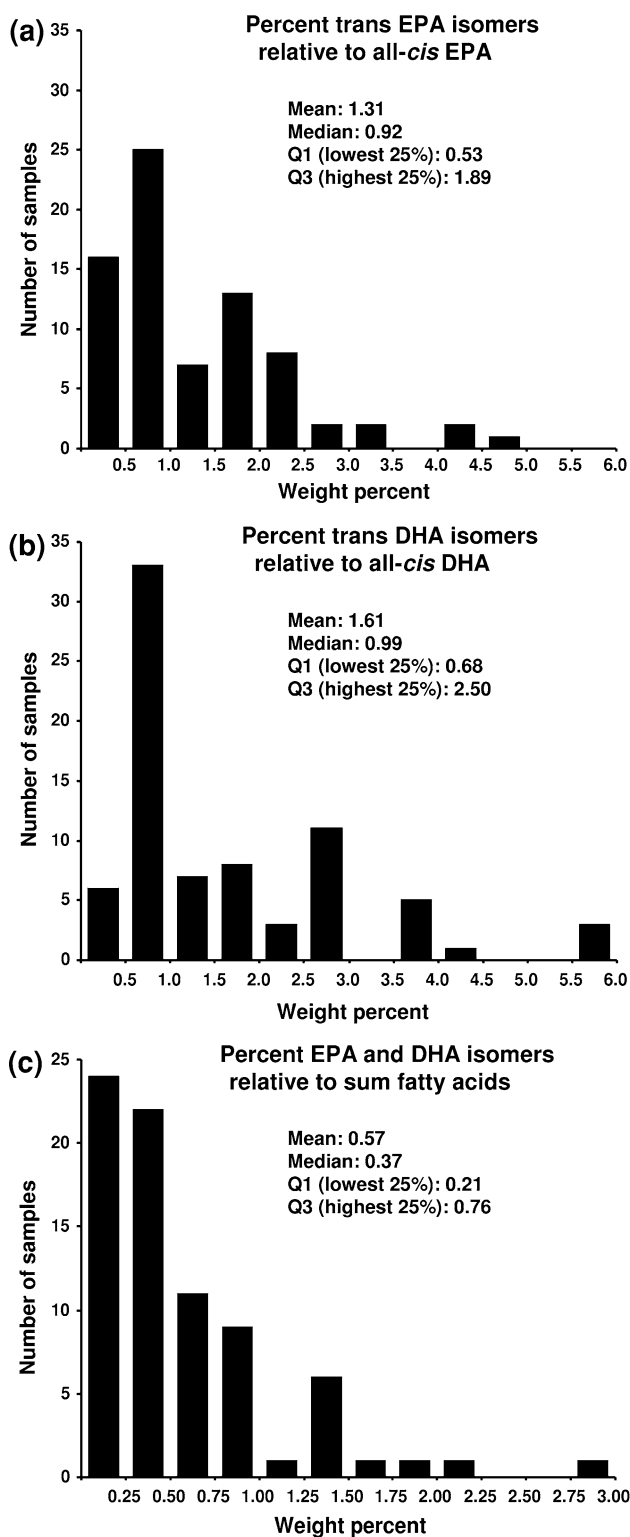


Fig. 3 Distribution and statistics of (a) *trans* EPA isomers relative to *cis* EPA, (b) *trans* DHA isomers relative to *cis* DHA, and (c) sum of *trans* EPA and *trans* DHA isomers relative to total fatty acids

The largest group (25 objects) consists of products with approximately 33 % EPA and 23 % DHA. They are therefore labelled as “33/23 concentrates”. These had

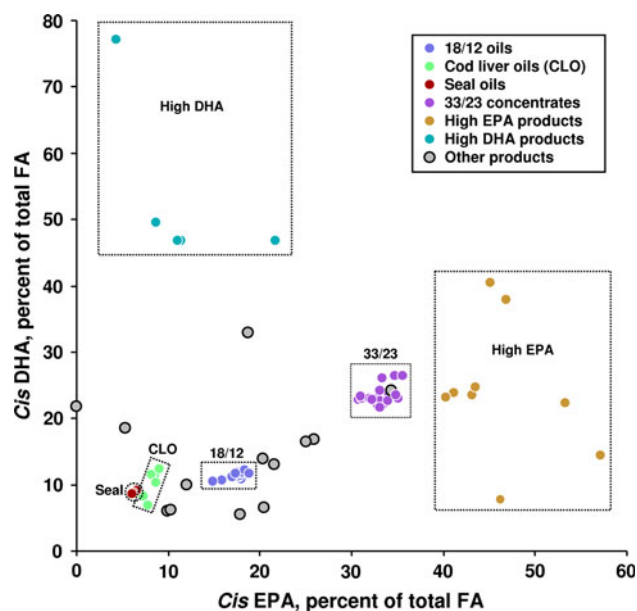


Fig. 4 Weight percent of *cis* EPA and *cis* DHA relative to total fatty acids in the samples

approximately the same EPA/DHA relationships as the 18/12 oils and low levels of short fatty acids, indicating that they are made by distilling off the shorter fatty acids from 18/12 oils.

Products with more than 40 % EPA (9 objects) or more than 40 % DHA (5 objects) were assigned to “high EPA products” and “high DHA products”, respectively. One of the products in the high EPA group also had DHA levels slightly above 40 %. Both these groups had a high variation in the fatty acid profiles, indicating that they are made from different raw materials and by different processes.

Some products (13 objects) could not be assigned to any of these groups based on the fatty acid profile. Inspection of the labelling of these products showed that they were either blends of different marine oils or blends of marine oils with vegetable oils.

Statistics for the different groups are given in Table 1. One of the product groups showed a particularly high degree of isomerization. All four seal oil products were in the high *trans* EPA and high *trans* DHA category, and four of the five most isomerized samples in the study were seal oils. The average *trans* EPA and *trans* DHA levels were 4.0 and 4.8, respectively. However, because the amounts of EPA and DHA in seal oils are rather low compared to the other products in the study, the amount of *trans* isomers relative to total fatty acids were moderate. All seal oil products in the study were purchased on the Norwegian market.

For the other groups there were no trends. There were large variations in the degree of isomerization within each group, and all groups except the seal oils contained objects

Table 1 Isomerization data for specific product groups

	“18/12” oils	Cod liver oils	Seal oils	“33/23” concentrates	High EPA products	High DHA products	Other products
% <i>cis</i> EPA/total FA							
range	14.86–18.85	7.37–8.99	6.07–6.57	30.76–35.58	40.31–57.12	4.34–21.64	0.03–25.86
mean ± SD	17.39 ± 0.97	8.26 ± 0.62	6.23 ± 0.23	33.02 ± 1.31	46.30 ± 5.57	11.41 ± 6.37	15.80 ± 7.74
% <i>trans</i> EPA/ <i>cis</i> EPA							
range	0.47–2.80	0.49–1.95	3.24–4.51	0.33–4.44	0.19–2.61	0.67–1.99	0.39–2.38
mean ± SD	1.02 ± 0.70	1.17 ± 0.62	4.00 ± 0.60	1.20 ± 0.94	0.78 ± 0.81	1.22 ± 0.65	1.53 ± 0.72
% <i>cis</i> DHA/total FA							
range	10.52–12.18	6.80–12.35	8.58–9.00	21.55–26.44	7.63–40.46	46.70–77.10	5.51–32.96
mean ± SD	11.35 ± 0.47	10.04 ± 2.15	8.72 ± 0.19	23.31 ± 1.25	24.16 ± 10.17	53.39 ± 13.31	13.77 ± 7.79
% <i>trans</i> DHA/ <i>cis</i> DHA							
range	0.61–3.61	0.63–2.83	3.58–5.79	0.29–5.89	0.25–2.58	0.66–2.63	0.54–3.66
mean ± SD	1.30 ± 0.89	1.42 ± 1.07	4.83 ± 1.10	1.48 ± 1.26	0.86 ± 0.78	1.53 ± 0.98	1.84 ± 1.10
% <i>trans</i> isomers/total FA							
range	0.17–0.90	0.12–0.45	0.54–0.77	0.18–2.76	0.19–1.86	0.45–2.08	0.15–1.41
mean ± SD	0.32 ± 0.22	0.23 ± 0.14	0.67 ± 0.12	0.74 ± 0.60	0.54 ± 0.54	1.00 ± 0.73	0.51 ± 0.42
Number of samples							
<i>n</i> samples in group	15	6	4	25	9	5	13
<i>n</i> low <i>trans</i> EPA	2	1	0	9	6	0	1
<i>n</i> high <i>trans</i> EPA	2	2	4	4	1	1	5
<i>n</i> low <i>trans</i> DHA	2	3	0	6	6	1	1
<i>n</i> high <i>trans</i> DHA	2	2	4	4	1	2	4
<i>n</i> low total <i>trans</i>	7	4	0	1	1	0	6
<i>n</i> high total <i>trans</i>	1	0	1	10	2	2	3

with a high degree of isomerization as well as objects with a low degree of isomerization.

Discussion

The strong correlation between DI of EPA and DHA in Fig. 2 indicates that the quantified peaks are free of significant chromatographic interferences. The correlation also indicates that *trans* isomers of EPA and DHA are formed by the same process.

EPA and DHA isomerize rapidly compared to linolenic (18:3n-3) and oleic acids (18:2n-6), of which there have been reports showing significant amounts of *trans* isomers in products on the market [25, 30, 31]. The distributions in Fig. 3 and the number of samples with a DI below 1 % indicates that the majority of manufacturers have focus on the degree of isomerization and are careful when refining the oils, but there are quite a large number of exceptions.

The fact that samples with low *trans* EPA and low *trans* DHA were found in all product groups except the seal oils, shows that products with a large DI can be avoided. The large number of samples with low *trans* EPA and *trans* DHA in the concentrates also show that formation of *trans*

isomers in the distillation process, which requires a high temperature in a short period, is probably insignificant compared to deodorization of the oils. The percentage of samples with low *trans* EPA and low *trans* DHA was higher in the “33/23 concentrates” and “high EPA concentrates” than in the “18/12 oils”.

There is limited information on the biological effects of the *trans* isomers of EPA and DHA. The majority of research on *trans* fatty acids has been carried out on *trans* isomers of C18 fatty acids, and in particular on isomers of 18:1 (oleic acid). Considering the great difference in function of the *cis* analogs, *trans* isomers of EPA and DHA should not be expected to have similar effects as the *trans* C18 fatty acids. Taking into consideration that very small differences in structure and geometry of molecules often have large effects in toxicological studies, the five *trans* EPA isomers and the six *trans* DHA isomers may also differ from each other in function. *Trans* EPA and DHA isomers should therefore be regarded as 11 chemical compounds for which there is limited knowledge about effects. There is some information on biological effects available in the scientific literature, mostly on EPA isomers. *Trans* EPA isomers are elongated and desaturated into *trans* 22:5 and 24:5 fatty acids, and *trans* isomers of

EPA behave differently than *cis* EPA in the eicosanoid synthesis [32]. It has also been shown that *trans* EPA and *trans* DHA have different effects than their *cis* analogs on platelet aggregation [33, 34]. *Trans* isomers of EPA and DHA has been detected in human platelets [35] and in liver lipids of rats [36], possibly as result of intake of 18:3n-3 (alpha linolenic acid) that is elongated and desaturated in the body [35, 36]. Intake of isomerized 18:3n-3 has also led to incorporation of *trans* DHA isomers in the retina and cerebral phospholipids in rats [37, 38]. In this respect it should be emphasized that the *trans* isomers of EPA and DHA that result from metabolism of isomerized 18:3n-3 are basically the isomers with *trans* geometry in the n-3 position (*trans*-17 EPA and *trans*-19 DHA), which are not among the major *trans* isomers formed from heat induced isomerization of EPA and DHA [13].

Currently, we do not have the necessary knowledge to assess whether the levels seen in this study pose any negative effects on human health. There is therefore a need for further studies of the biological effects of *trans* isomers of EPA and DHA. In the meantime there may be good reasons for authorities, consumers and manufacturers to pay attention to the levels of these isomers in the omega-3 products and foods fortified with such products.

Conclusions

The content of mono-*trans* EPA relative to the *cis* isomer (*trans* EPA_{%cis}) varied from 0.19 to 4.5 % in the studied products, with a mean value of 1.31 % and a median value of 0.92 %. Corresponding values for DHA (*trans* DHA_{%cis}) were 0.25, 5.9, 1.61 and 0.99 %. The fact that samples with low *trans* EPA and low *trans* DHA were found in all product groups, except the seal oils, shows that products with large degree of isomerization can be avoided. The distribution also indicates that the process of concentrating EPA and DHA by distillation is not a significant source of *trans* isomers compared to the deodorization of the crude oils. There is currently not enough information about the biological effects of the isomers to assess whether the levels found in this study can have any significant effects on consumer health.

References

1. von Schacky C (2003) The role of omega-3 fatty acids in cardiovascular disease. *Curr Atheroscler Rep* 5:139–145
2. Mozaffarian D, Rimm EB (2006) Fish intake contaminants and human health—evaluating the risks and the benefits. *J Am Med Assoc* 296:1885–1899
3. Fontani G, Corradeschi F, Felici A, Alfatti F, Migliorini S, Lodi L (2005) Cognitive and physiological effects of omega-3 polyunsaturated fatty acid supplementation in healthy subjects. *Eur J Clin Invest* 35:691–699
4. Morris MC, Evans DA, Bienias JL, Tangney CC, Bennett DA, Wilson RS, Aggarwal N, Schneider J (2003) Consumption of fish and n-3 fatty acids and risk of incident Alzheimer disease. *Arch Neur* 60:940–946
5. Lands WEM (1992) Biochemistry and physiology of n-3 fatty acids. *FASEB J* 6:2530–2536
6. Wall R, Ross RP, Fitzgerald GF, Stanton C (2010) Fatty acids from fish: the anti-inflammatory potential of long-chain omega-3 fatty acids. *Nutr Rev* 68:280–290
7. Patterson AC, Stark KD (2008) Direct determinations of the fatty acid composition of daily dietary intakes—incorporating nutraceuticals and functional food strategies to increase n-3 highly unsaturated fatty acids. *J Am Coll Nutr* 27:538–546
8. Simopoulos AP, Leaf A, Salem N (2000) Workshop statement on the essentiality of and recommended dietary intakes for omega-6 and omega-3 fatty acids. *Prostag Leukotr Ess* 63:119–121
9. Kris-Etherton PM, Taylor DS, Yu-Poth S, Huth P, Moriarty KM, Fishell V, Hargrove RL, Zhao G, Etherton TD (2000) Polyunsaturated fatty acids in the food chain in the United States. *Am J Clin Nutr* 71:179S–188S
10. Wijesundera RC, Ratnayake WMN, Ackman RG (1989) Eicosapentaenoic acid geometrical isomer artifacts in heated fish oil esters. *J Am Oil Chem Soc* 66:1822–1830
11. Fournier V, Destaillets F, Juanéda P, Dionisi F, Lambelet P, Sébédio JL, Berdeux O (2006) Thermal degradation of long-chain polyunsaturated fatty acids during deodorization of fish oils. *Eur J Lipid Sci Technol* 108:33–42
12. Fournier V, Juanéda P, Destaillets F, Dionisi F, Lambelet P, Sébédio JL, Berdeux O (2006) Analysis of eicosapentaenoic acid and docosahexaenoic acid geometrical isomers formed during fish oil deodorization. *J Chromatogr A* 1129:21–28
13. Mjøs SA, Solvang M (2006) Geometrical isomerisation of EPA and DHA at high temperatures. *Eur J Lipid Sci Technol* 108:589–597
14. Fournier V, Destaillets F, Hug B, Golay PA, Joffre F, Juanéda P, Sémon E, Dionisi F, Lambelet P, Sébédio JL, Berdeux O (2007) Quantification of eicosapentaenoic and docosahexaenoic acid geometrical isomers formed during fish oil deodorization by gas-liquid chromatography. *J Chromatogr A* 1154:353–359
15. Official methods and recommended practices of the American Oil Chemists' Society (1998) 5th edn. AOCS Press, Champaign, IL (USA)
16. Mjøs SA (2005) Properties of *trans* isomers of eicosapentaenoic acid and eicosahexaenoic acid methyl esters on cyanopropyl stationary phases. *J Chromatogr A* 1100:185–192
17. Mjøs SA (2004) Two-dimensional fatty acid retention indices. *J Chromatogr A* 1061:201–209
18. <http://www.chrombox.org/data> (Accessed 01.Feb.2012)
19. Mjøs SA (2004) The prediction of fatty acid structure from selected ions in electron impact mass spectra of fatty acid methyl esters. *Eur J Lipid Sci Technol* 106:550–560
20. Mjøs SA (2003) Identification of fatty acids in gas chromatography by application of different temperature and pressure programs on a single capillary column. *J Chromatogr A* 1015:151–161
21. Mjøs SA, Grahl-Nielsen O (2006) Prediction of gas chromatographic retention of polyunsaturated fatty acid methyl esters. *J Chromatogr A* 1110:171–180
22. Castello G, Vezzani S, D'Amato G (1997) Effect of temperature on the polarity of some stationary phases for gas chromatography. *J Chromatogr A* 779:275–286
23. Mjøs SA (2008) Retention behavior of *trans* isomers of eicosapentaenoic and docosahexaenoic acid methyl esters on a polyethylene glycol stationary phase. *Eur J Lipid Sci Technol* 110:547–553

24. Hénon G, Kemény Z, Recseg K, Zwobada F, Kovari K (1999) Deodorization of vegetable oils—part I: modelling the geometrical isomerization of polyunsaturated fatty acids. *J Am Oil Chem Soc* 75:73–81
25. Wolff RL (1993) Further studies on artificial geometrical isomers of alpha-linolenic acid in edible linolenic acid-containing oils. *J Am Oil Chem Soc* 70:219–224
26. Wolff RL (1993) Heat-induced geometrical isomerization of alpha-linolenic acid: effect of temperature and heating time on the appearance of individual isomers. *J Am Oil Chem Soc* 70:425–430
27. Kemény Z, Recseg K, Hénon G, Kóvari K, Zwobada F (2001) Deodorization of vegetable oils: prediction of trans polyunsaturated fatty acid content. *J Am Oil Chem Soc* 78:973–979
28. Wolff RL, Nour M, Bayard CC (1996) Participation of the *cis*-12 ethylenic bond to *cis-trans* isomerization of the *cis*-9 and *cis*-15 ethylenic bonds in heated alpha-linolenic acid. *J Am Oil Chem Soc* 73:327–332
29. Wolff RL *Cis-trans* isomerization of octadecatrienoic acids during heating—study of pinolenic (*cis*-5 *cis*-9 *cis*-12 18:3) acid geometrical isomers in heated pine seed oil. *J Am Oil Chem Soc* 71:1129–1134
30. Wolff RL (1992) Trans-polyunsaturated fatty acids in French edible rapeseed and soybean oils. *J Am Oil Chem Soc* 69:106–110
31. Martin CA, Visentainer JV, de Oliveira AN, de Oliveira CC, Matsushita M, de Souza NE (2008) Fatty acid contents of Brazilian soybean oils with emphasis on trans fatty acids. *J Braz Chem Soc* 19:117–122
32. Loï C, Chardigny JM, Cordelet C, Leclere L, Genty M, Ginies C, Noël JP, Sébédio JL (2000) Incorporation and metabolism of *trans* 20:5 in endothelial cells—effect on prostacyclin synthesis. *Lipids* 35:911–918
33. Loï C, Chardigny JM, Berdeaux O, Vatele JM, Poullain D, Noël JP, Sébédio JL (1998) Effects of three *trans* isomers of eicosapentaenoic acid on rat platelet aggregation and arachidonic acid metabolism. *Thromb Haemost* 80:656–661
34. O'Keefe SF, Lagarde M, Grandgirard A, Sebedio JL (1990) Trans n-3 eicosapentaenoic and docosahexaenoic acid isomers exhibit different inhibitory effects on arachidonic acid metabolism in human platelets compared to the respective *cis* fatty acids. *J Lipid Res* 31:1241–1246
35. Chardigny JM, Sébédio JL, Juanéda P, Vatele JM, Grandgirard A (1993) Occurrence of N-3 trans polyunsaturated fatty acids in human platelets. *Nutr Res* 13:1105–1111
36. Chardigny JM, Sebedio JL, Grandgirard A, Martine L, Berdeaux O, Vatele JM (1996) Identification of novel trans isomers of 20:5n-3 in liver lipids of rats fed a heated oil. *Lipids* 31:165–168
37. Chardigny JM, Bron A, Sébédio JL, Juaneda P, Grandgirard A (1994) Kinetics of incorporation of N-3 trans fatty acid in rat retina. *Nutr Res* 14:909–917
38. Acar N, Bonhomme B, Joffre C, Bron AM, Creuzot-Garcher C, Bretillon L, Doly M, Chardigny JM (2006) The retina is more susceptible than the brain and the liver to the incorporation of *trans* isomers of DHA in rats consuming trans isomers of alpha-linolenic acid. *Reprod Nutr Dev* 5:515–525

Oral Supplementation of Butyrate Reduces Mucositis and Intestinal Permeability Associated with 5-Fluorouracil Administration

Talita Mayra Ferreira · Alda Jusceline Leonel · Marco Antônio Melo ·
Rosana R. G. Santos · Denise Carmona Cara · Valbert N. Cardoso ·
Maria I. T. D. Correia · Jacqueline I. Alvarez-Leite

Received: 27 November 2011 / Accepted: 23 April 2012 / Published online: 31 May 2012
© AOCs 2012

Abstract Mucositis affects about 40 % of patients undergoing chemotherapy. Short chain fatty acids (SCFA), mainly butyrate, are claimed to improve mucosal integrity, reduce intestinal permeability and act as anti-inflammatory agents for the colon mucosa. We evaluated the effects of oral administration of SCFA or butyrate in the 5FU-induced mucositis. Mice received water, SCFA or butyrate during all experiment (10 days) and a single dose of 5FU (200 mg/kg) 3 days before euthanasia. We evaluated inflammatory and histological score by morphometry, and

by activity of enzymes specific to neutrophil, eosinophil and macrophage and TLR-4, TNF-alpha and IL6 expressions. Intestinal permeability and tight junction protein ZO-1 expression were evaluated. Mice from the 5FU (5-Fluorouracil) group presented weight loss, ulcerations and inflammatory infiltration of neutrophils and eosinophils, increased expression of IL6 and TNF-alpha and increased intestinal permeability. SCFA minimized intestinal damage, reduced ulcerations without affecting intestinal permeability. Butyrate alone was more efficient at improving those parameters than in SCFA solution and also reduced intestinal permeability. The expression of pro-inflammatory cytokines and ZO-1 tended to be higher in the SCFA supplemented but not in the butyrate supplemented group. We showed the beneficial effects of butyrate on intestinal mucositis and its promising function as an adjuvant in the treatment of diseases not only of the colon, but also of the small intestine.

Keywords Mucositis · Inflammation · Short-chain fatty acids · Butyrate · 5-Fluorouracil · Lipids

Abbreviations

5FU	5-Fluorouracil
CCL2/MCP-1	Monocyte chemotactic protein-1
DMSO	Dimethyl sulfoxide
DTPA	Diethyleneaminopentacetic acid
EPO	Eosinophil peroxidase
GLP-2	Glucagon-like peptide-2
MCT	Monocarboxylate transporters
MPO	Myeloperoxidase
NAG	N-Acetylglucosaminidase
SCFA	Short-chain fatty acid
TJ	Tight junctions
(ZO)-1	Zonula occludens-1

T. M. Ferreira · A. J. Leonel · M. A. Melo · J. I. Alvarez-Leite
Departamento de Bioquímica e Imunologia,
Instituto de Ciências Biológicas, Universidade Federal de Minas
Gerais, Av. Antônio Carlos, 6627, Pampulha, Belo Horizonte,
MG CEP 31270-901, Brazil

T. M. Ferreira · A. J. Leonel · M. A. Melo ·
R. R. G. Santos · D. C. Cara · V. N. Cardoso ·
M. I. T. D. Correia · J. I. Alvarez-Leite
Departamento de Morfologia, Instituto de Ciências Biológicas,
Universidade Federal de Minas Gerais, Av. Antônio Carlos,
6627, Pampulha, Belo Horizonte, MG CEP 31270-901, Brazil

R. R. G. Santos · D. C. Cara · V. N. Cardoso
Departamento de Análises Clínicas e Toxicológicas,
Faculdade de Farmácia, Universidade Federal de Minas Gerais,
Av. Antônio Carlos, 6627, Pampulha, Belo Horizonte,
MG CEP 31270-901, Brazil

M. I. T. D. Correia
Departamento de Cirurgia, Faculdade de Medicina,
Universidade Federal de Minas Gerais, Av. Antônio Carlos,
6627, Pampulha, Belo Horizonte, MG CEP 31270-901, Brazil

J. I. Alvarez-Leite (✉)
Universidade Federal de Minas Gerais, Caixa Postal 486,
Belo Horizonte CEP 30161-970, Brazil
e-mail: jalvarezleite@gmail.com

Introduction

Short-chain fatty acids (SCFA) mainly acetate, propionate and butyrate are produced by bacterial fermentation, particularly of dietary fiber and carbohydrate in the large intestine. They are readily absorbed and are metabolized in the liver, producing energy. Butyrate, the 4-carbon fatty acid, has been tested as one of the therapeutic options for colon inflammatory diseases but was not previously tested for small intestine conditions, such as mucositis. Several in-vitro and in-vivo studies have shown that butyrate stimulates cell proliferation, inhibits inflammatory mediator production, reduces intestinal permeability and induces apoptosis in colon cancer cells [11, 19, 22, 28]. Moreover, SCFA and butyrate enemas have been considered in the therapy of ulcerative colitis [10, 15, 28].

Mucositis secondary to 5FU chemotherapy is related to alterations in intestinal permeability, causing bacterial translocation and changes in the intestinal immune status. Gut barrier disruption could be related to reduction of cell proliferation or an increase in apoptosis, both influenced by the presence of butyrate in the intracellular milieu. Intestinal paracellular permeability is regulated by the tight junctions [26] which consist of junctional protein complexes located in the apical portion of enterocytes and formed by transmembrane as well as peripheral membrane proteins such as occludin, claudin-1 and zonula occludens (ZO)-1.

Our group has previously shown the beneficial effect of a solution of SCFA (acetate, propionate and butyrate) in the clinical manifestations of ARA-C induced mucositis in mice [20]. In that study, the mechanism of such an action and the specific fatty acid responsible for this effect was not investigated. Due to its metabolic relevance on cell metabolism butyrate is the more promising candidate for such an effect.

Considering the significant clinical impact of mucositis and the beneficial effects of the SCFA solution on the small intestinal mucosa, we aimed to characterize the effects of oral administration of either SCFA or butyrate solutions on

the amelioration of intestinal mucosa after 5-fluorouracil (5FU) administration.

Materials and Methods

Four-week-old female Swiss mice from animal facility of the Federal University of Minas Gerais (Brazil) received water, SCFA or butyrate solutions (replacing drink water) ad libitum for 10 days Table 1. On the 7th day, animals were injected intraperitoneally with a single dose of 5-fluorouracil (5FU, 200 mg/kg, Eurofarma[®], Brazil) or PBS. The SCFA solution was prepared according to Ramos et al. [20] and contained 35 mM of acetate, 15 mM of propionate, and 9 mM of butyrate (Sigma-Aldrich, USA). The butyrate solution had a concentration of 9 mM. The pH of all solutions was adjusted to 7.4 by adding sodium hydroxide (50 %).

The animals were subdivided into 6 groups: 1, control group ($n = 12$): no mucositis induction and receiving water; 2, 5FU group: with mucositis and receiving water; 3, SCFA group ($n = 4$): no mucositis induction and receiving SCFA solution; 4, 5FU + SCFA group ($n = 18$): with mucositis and receiving SCFA solution, 5, Butyrate group ($n = 18$): no mucositis induction and receiving butyrate solution and 6, 5FU + butyrate group ($n = 18$): with mucositis and receiving butyrate solution.

On the 10th experimental day, all animals were anesthetized and euthanized for blood and organ collection. Body weight, liquid intake and food intake were measured on the 1st and 10th experimental days. The energy intake was calculated, taking into consideration calories from food and solutions. The protocol was approved by the Animal Care Committee of Universidade Federal de Minas Gerais (UFMG), CETEA # 46/2008.

Histological Analysis

The small intestine and colon were removed from the pylorus to the ileocecal valve and from the cecum to the rectum, respectively. The organs were washed, gently perfused with

Table 1 Experimental groups of Swiss mice receiving water or experimental solutions and chow diet during 10 days

Group	Liquid intake	Treatment (single dose)
Control	Water	PBS ^a
SCFA	C ₂ (35 mM) + C ₃ (15 mM) + C ₄ (9 mM) ^b	PBS
Butyrate	Butyrate (9 mM)	PBS
5FU	Water	5FU (200 mg/kg)
5FU + SCFA	C ₂ (35 mM) + C ₃ (15 mM) + C ₄ (9 mM)	5FU (200 mg/kg)
5FU +Butyrate	Butyrate (9 mM)	5FU (200 mg/kg)

^a PBS or 5-fluorouracil (5FU) were intraperitoneally administered on the 7th experimental day. The pH of all solutions was 7.4 ± 0.2

^b C₂, acetate; C₃, propionate; C₄, butyrate

PBS and measured with an inextensible millimeter ruler. The intestine was divided into the duodenum, jejunum and ileum and then fixed in paraformaldehyde (4 %) for 15 min. The segments were opened along their longitudinal axes, fixed in Bouin's solution for 6 h, embedded in paraffin and cut into 5 μ m thick sections before being stained with hematoxylin-eosin (H&E). Images were obtained using a JVC TK-1270/RGB microcamera and the KS300 software built into a Kontron Elektronick/Carl Zeiss image analyzer. Ten fields from H&E sections were randomly chosen for villi height measurement.

Alterations of the mucosal architecture (general structure, cell distribution, mucosa and submucosa aspect), ulcerations, inflammation, villus height and inflammatory infiltration were used to determine the histological score. The samples were coded and then scored by a trained pathologist. The score ranged from zero (no alteration) to 3 (severe alteration) according to Soares et al. [24]. The results are presented as the sum of the score obtained for each parameter.

Neutrophil, Macrophage and Eosinophil infiltrations were evaluated by analyzing the enzyme activity of myeloperoxidase (MPO), *N*-acetylglucosaminidase (NAG) and eosinophil peroxidase (EPO), respectively. Samples were homogenized and centrifuged, and precipitates were used for quantification of enzyme activities as previously described [28]. Briefly, precipitates were dissolved in HETAB 0.5 % (Sigma-Aldrich[®], USA) in phosphate buffer and centrifuged.

For EPO quantification, 75 μ L of supernatant was added to 75 μ L of OPD (Sigma-Aldrich[®], USA), diluted in Tris-HCl and H₂O₂ and incubated at 37 °C for 30 min. The reaction was stopped by adding 50 μ L H₂SO₄ before being read at wavelength 492 nm in a microplate spectrophotometer (TermoPlate, Brazil).

For MPO quantification, 25 μ L of supernatant was added to 25 μ L of TMB in DMSO (Sigma-Aldrich[®], USA). After addition of 100 μ L H₂O₂, the solution was incubated at 37 °C for 5 min. The reaction was stopped by adding H₂SO₄ before being read at 450 nm in a microplate spectrophotometer (TermoPlate, Brazil).

For NAG quantification, precipitates were dissolved in 0.1 % Triton X-100 (Sigma-Aldrich[®], USA) and centrifuged before the supernatant was added to *p*-nitrophenyl-*N*-acetyl- β -D-glucosamine solution in citrate/phosphate. After incubation, the reaction was stopped by the addition of glycine buffer and read at 400 nm in a microplate spectrophotometer (TermoPlate, Brazil). Results were expressed in arbitrary units (based on absorbance) by 100 mg of tissue.

Study of Intestinal Permeability

We studied intestinal permeability using ^{99m}Tc diethyle-neaminopentacetic acid (DTPA). Because DTPA is not

absorbed by the healthy small intestine, its presence in the blood is proportional to the increase in the damage of intestinal paracellular permeability. Animals were gavaged with 0.1 mL of DTPA labeled with 3.7 MBq ^{99m}technetium in the form of sodium pertechnetate (Na^{99m}TcO₄), obtained by a ⁹⁹molybdenum/^{99m}technetium generator (IPEN/CNEMA, São Paulo, Brazil) [7]. Four hours after gavage, animals were anesthetized and exsanguinated by the axillary plexus. The radioactivity of the standard dose and blood samples was determined in an automatic pit scintillator (ANSR, Abbott[®], USA), and the percentage of recovered dose in each animal was calculated as follows: radioactivity of blood/radioactivity of standard dose \times 100. The average of the control group values was used as a reference. The results were presented as the increase seen in experimental groups over the control group (expressed as a percent).

RT-PCR

The total RNA from the ileum was extracted using the TRIzol[®] reagent according to the manufacturer's protocol. The reverse transcription was performed using 2 μ g of the total RNA, 200 U of the reverse transcriptase, 2.5 μ L of the 5 \times RT buffer, 1.8 μ L of the 10 mM dNTPs, 0.2 μ L of the 10,000 U/mL RNasin, and 1.0 μ L of the 50 μ M oligo dT. The temperature settings for this reaction were 70 °C for 5 min, on ice for 2 min, 42 °C for 60 min, 70 °C for 15 min and 4 °C for the final step. The resulting cDNA was used for real-time PCR as described below. The specific primers were designed using the Primer Express software and synthesized by IDT. Real time PCR was carried out on a StepOne sequence detection system (Applied Biosystems) using the Power SYBR Green PCR Master Mix (Applied Biosystems). The dissociation curve indicated that only one product was obtained in each reaction. The relative levels of gene expression were determined using the $\Delta\Delta$ Cycle threshold method as described by the manufacturer, in which data for each sample is normalized to the β -actin expression. The PCR results were analyzed with the SDS 2.1 software (Applied Biosystems), and the amount of mRNA of each gene of interest was normalized to the amount of the murine β -actin gene. mRNA expression levels were calculated as the fold difference relative to the housekeeping gene: relative expression = $2^{-(CT_{\text{target gene}} - CT_{\text{[}\beta\text{-actin-1]})}$.

The sequences of the primers used are as follows:

TNF α : 5'CGTCGTAGCAAACCACCAAG3' and 5'GAGATAGCAAATCGGCTGACG3'

IL6: 5'ACAACCACGGCCTTCCCTACTT-3' and 5'CA CGATTTCCAGAGAACATGTG3'

TLR4: 5'TGACAGGAAACCCTATCCAGAGTT3' and 5'TCTCCACAGCCACCAGATTCT3'

ZO-1: 5'CCAGCTTATGAAAGGGTTGTTTC3' and 5'TCCTCTCTTGCCAACCTTTTCTC3'

β-actin: 5'CTGCCTGACCAAGTC3' and 5'CAAGAAGGAAGGCTGGAAAGG A3'

Statistical Analysis

Statistical analysis was performed using the Graph Pad Prism 7.0[®] software (San Diego CA). The results were tested for outliers (Grubbs' test) and normality using the Kolmogorov–Smirnov test. The one-way ANOVA and the Newman–Keuls multiple comparison post-test were used for all parameters except for architecture alteration and villus height (non-parametric distribution), which were instead analyzed by the Kruskal–Wallis and Dunn's post-test. To compare gene expression of a specific group with the control group, an unpaired *t* test or a Mann–Whitney test was used. A significant difference was defined as $p \leq 0.05$.

Results

Initially we compared the effect of the three control groups (control, SCFA and butyrate groups) on weight gain and intestinal morphology. The results showed that the three groups presented the same weight evolution and intestinal

mucosa aspect (data not shown), demonstrating that SCFA and butyrate administrations do not interfere with intestinal mucosa integrity. For this reason, we omitted data from SCFA and butyrate control groups, presenting only the results of control mice (without SCFA or butyrate supplementation).

Energy and Hydric Intake and Ponderal Evolution

Total liquid intake was similar among all experimental groups, although food intake was reduced in the 5FU group compared to the control group (Fig. 1a, b). Yet, as expected, animals from the 5FU group lost weight. However, animals receiving the SCFA solution lost less weight, and those treated with butyrate did not lose any (Fig. 1c), suggesting that these solutions, mainly butyrate solution, attenuate aggression induced by 5FU. Intestinal length, one of the mucositis characteristics, was reduced in the 5FU group and presented an intermediated level after SCFA and butyrate supplementation (Fig. 1d).

Histological Analyses

Histological analyses of the 5FU group showed the mucositis picture with tissue damage, a reduction in villus height, the presence of inflammatory cells and ulcerations all along the small intestine, which was more

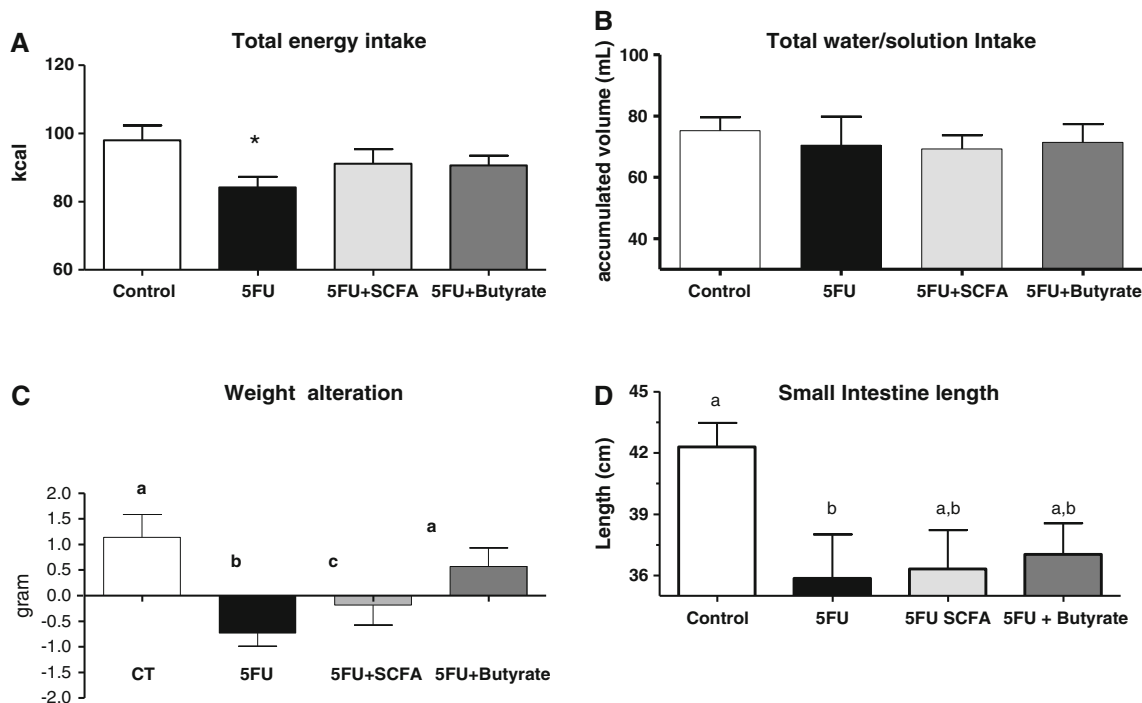


Fig. 1 Energy (a) and liquid (b) intake, weight variation (c) and intestinal length (d) of control mice and mice treated with 5FU (IP) and receiving water (5FU group), SCFA (5FU + SCFA group) or

butyrate (5FU + butyrate group) for 10 days. $n = 15$ – 18 /group. Bars represent average and vertical lines represent standard error. Different letters indicate a statistical difference ($p < 0.05$)

intense in the ileal segment (Fig. 2a). On the other hand, animals receiving SCFA or butyrate solutions presented less intense tissue damage, preservation of villi length in all segments of the small intestine and a lack of mucosa ulceration (Fig. 2a). These results of histological analyses

confirm the more effective protection of butyrate compared to SCFA. Colon histology did not reveal any inflammation (data not shown), reinforcing the fact that the tissue damage driven by 5FU is restricted to the small intestine.

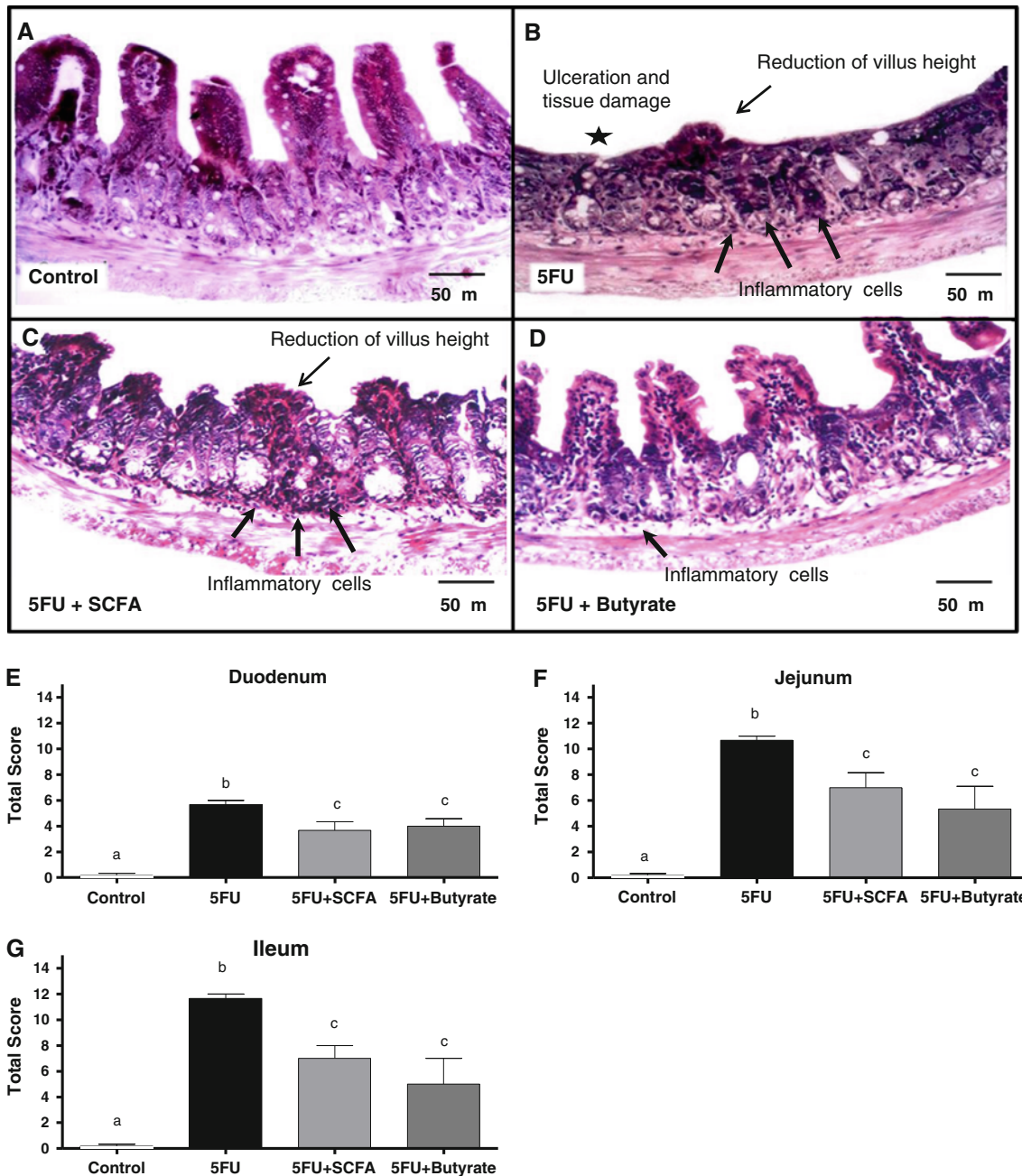


Fig. 2 (Refer to the on-line version for this figure in color) Morphology of the ileum of **a** control mice and mice treated with 5FU (IP) and receiving **b** water, **c** SCFA solution or **d** butyrate solution replacing water for 10 days. In 5FU group: tissue damage with loss of villi, presence of inflammatory cells and ulceration. 5FU + SCFA group: reduction of tissue damage with relative preservation of mucosa villi length and architecture. Inflammatory cells are still seen in mucosa and submucosa. 5FU + butyrate group:

improvement of general architecture and villus height. Inflammatory infiltration (*arrow heads*) is still present in mucosa and submucosa. Histological scores of duodenum (**e**), jejunum (**f**) and ileum (**g**) of control, 5FU, 5FU + SCFA or 5FU + butyrate groups. $n = 6$ per group. In **e**, **f** and **g** the results are the sum of the score obtained for each parameter. *Bars* represent average and *vertical lines* represent the standard error. *Different letters* indicate a statistical difference ($p < 0.05$)

Histological Score

Mucosa improvement was confirmed by the worse histological score for 5FU-treated animals compared to the control animals (Fig. 2b–d). When each intestinal segment was analyzed separately, the duodenum was moderately affected by 5FU treatment, while the inflammation score was intense for both the jejunum and ileum of mice from the 5FU group. Nonetheless, after SCFA and butyrate treatment, the histological score was reduced in all intestinal segments (Fig. 2b, c).

Next, we individually analyzed the four parameters used for the histological score. Mucosa ulceration and general architecture as well as the villus length contribute to the intestinal mucosa recovering following SCFA and butyrate supplementation (Fig. 3). Interestingly, inflammatory infiltration did not decrease after SCFA or butyrate supplementation.

Leukocyte Infiltration and Cytokine Expression

Because no differences were observed in the inflammatory infiltration between groups, we evaluated the activity of neutrophils, macrophages and eosinophils in the intestines of all animals through the determination of MPO, NAG and EPO enzyme activities, respectively. Neutrophil infiltration, as measured by MPO activity was increased as a consequence of 5FU treatment (Fig. 4). Following the results of

the inflammatory score, neither SCFA nor butyrate altered MPO activity (neutrophil infiltration). NAG activity (macrophage infiltration) was similar among groups, including the control group, suggesting it is not relevant to the damage induced by 5FU in this phase of inflammation (Fig. 4). Regarding EPO activity (eosinophil infiltration), it increased 4 times with 5FU treatment compared to the control group. Nevertheless, EPO returned to the control levels after SCFA and butyrate treatments (Fig. 5).

Amplification of mRNA of Pro-Inflammatory Molecules

Gene expression of TLR-4, IL-6 and TNF- α was analyzed by RT-PCR. The TLR4 expression presented a strong tendency ($p = 0.06$) to be higher in 5FU mice compared to controls but it was not different between supplemented groups (Fig. 5a). Regarding TNF- α and IL-6 expressions, a strong tendency ($p = 0.057$) of increased values was seen in 5FU and 5FU + SCFA, but not in 5FU + butyrate (Fig. 5b).

Intestinal Permeability

5FU damage is associated with an increase in intestinal permeability, which can be detected by the blood recovery of $^{99m}\text{Tc-DTPA}$ after an oral dose. For animals in all 5FU groups, intestinal permeability was higher than the control group, which was not reversed by SCFA. However,

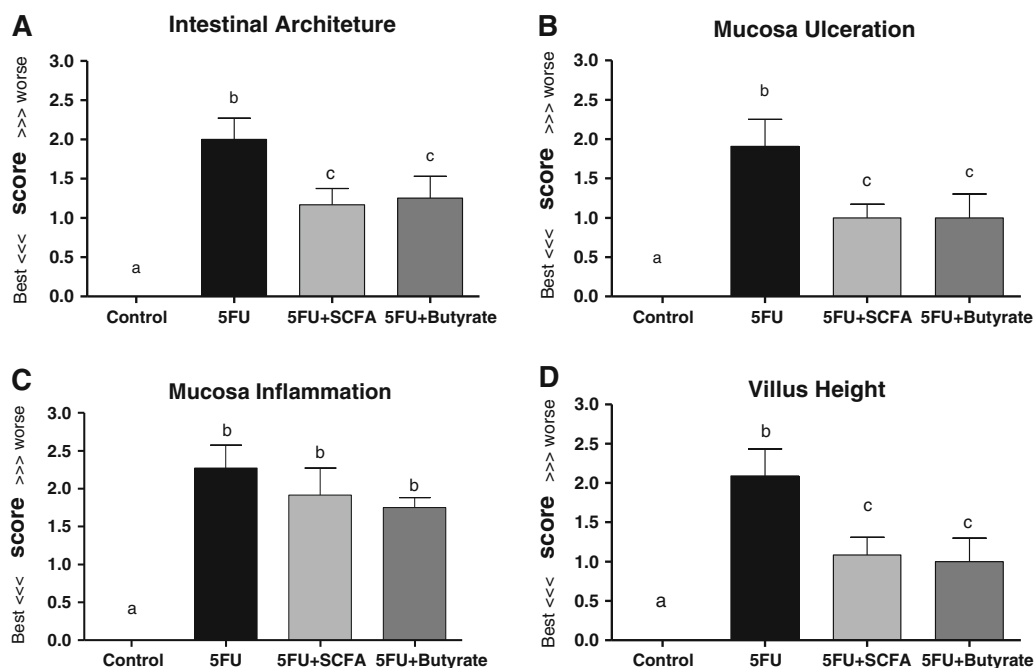


Fig. 3 Evaluation of mucosa architecture alteration (a), mucosa ulcerations (b), inflammatory infiltration (c) and villus height (d) of duodenum, jejunum and ileum of control mice or mice treated with 5FU and receiving water (5FU group), SCFA (5FU + SCFA group)

or butyrate (5FU + butyrate group) for 10 days. $n = 6$ per group. Bars represent average and lines represent standard error. Different letters indicate a statistical difference ($p < 0.05$)

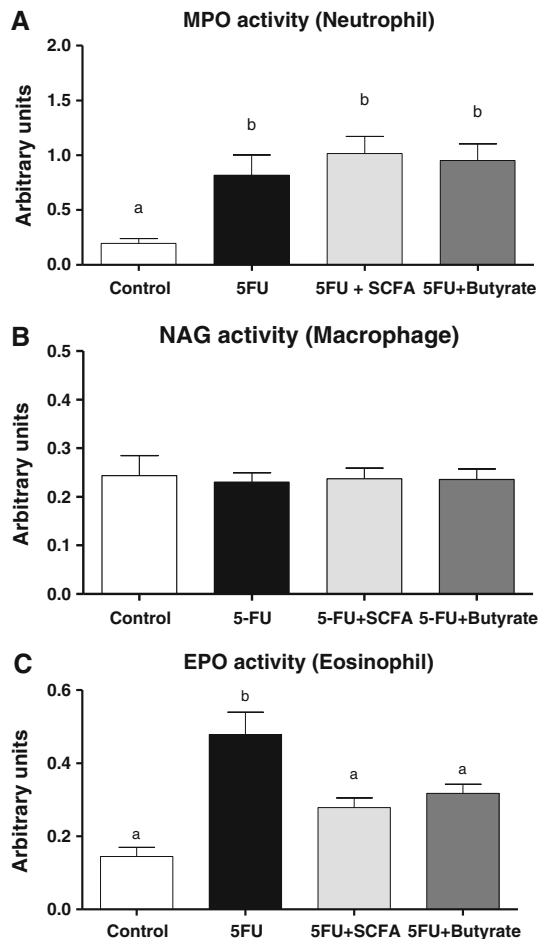


Fig. 4 Evaluation of the enzyme activity of MPO, NAG and EPO, as indirect determination of neutrophil (a), macrophage (b) and eosinophil (c) infiltration, respectively, in the small intestine of control mice or mice treated with 5FU (IP) and receiving water (5FU group), SCFA (5FU + SCFA group) or butyrate (5FU + butyrate group) for 10 days. $n = 7/\text{group}$. Bars represent average and vertical lines represent standard error. Different letters indicate a statistical difference ($p < 0.05$)

butyrate administration reduced intestinal permeability to levels that were closer to those of the control groups (Fig. 6).

Since paracellular permeability is linked to tight junction protein interactions, ZO-1 protein expression was also investigated, also showing a strong tendency to increased expression in 5FU ($p = 0.056$) and 5FU + SCFA ($p = 0.09$) groups. Once again, 5FU + butyrate mice presented ZO-1 expression closer to control ones.

Discussion

In the current study, we have shown that SCFA and, in particular, butyrate are effective in improving mucosa

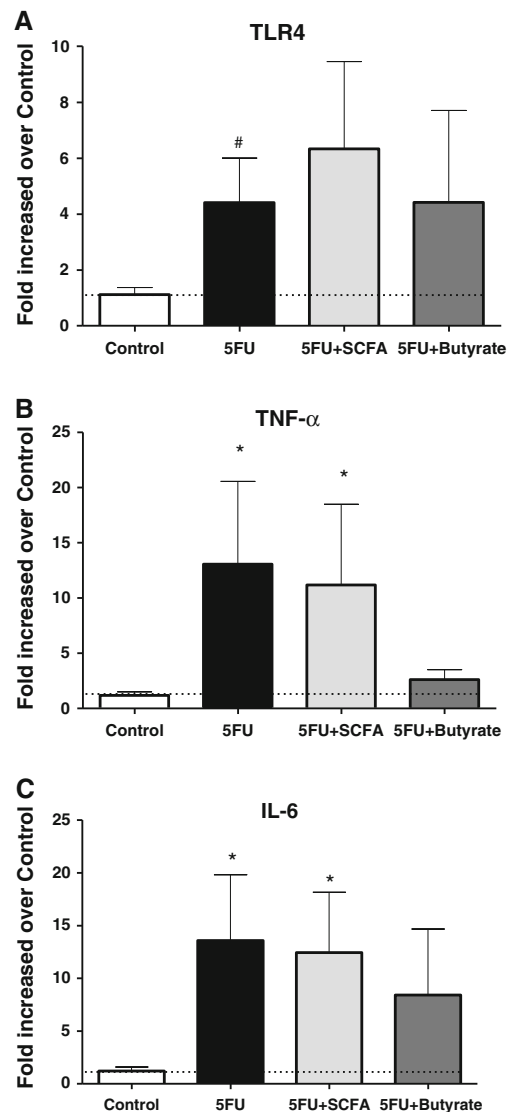


Fig. 5 TLR4 (a), TNF- α (b) and IL-6 (c) mRNA amplifications in the ileum of control mice or mice treated with 5FU (IP) and receiving water (5FU group), SCFA (5FU + SCFA group) or butyrate (5FU + butyrate group) for 10 days. Bars represent average and lines represent standard error. $N = 4/\text{group}$. # $p = 0.061$ and * $p = 0.057$ compared to the control group

integrity and reducing inflammation in an experimental model of mucositis. Moreover, these effects were obtained by the oral supplementation of fatty acids rather than rectal via as is usually done. In a previous study, we showed that SCFA solution improves intestinal manifestation of mucositis [20]. However, we did not evaluate the effects of butyrate used alone and limited our analyses to the histological aspects of the intestinal mucosa. As far as we know, the current study is the first one to address the effect of butyrate supplementation on the evolution of chemotherapy-induced intestinal mucositis.

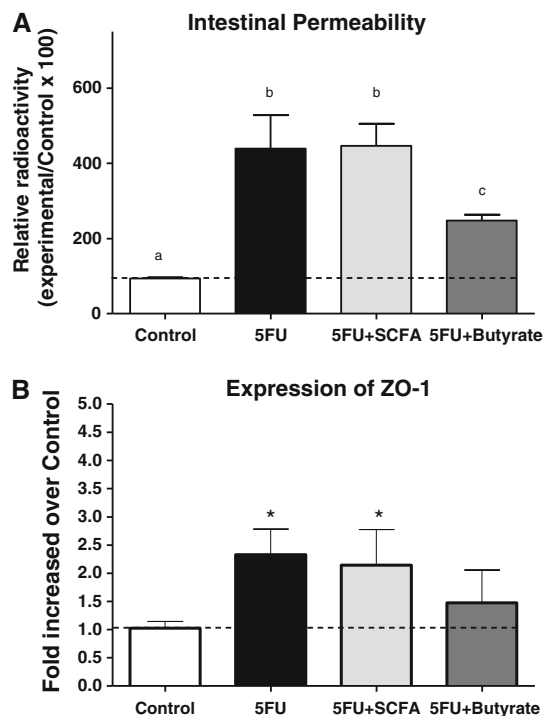


Fig. 6 Evaluation of intestinal permeability after oral administration of Tc^{99} labeled DTPA (a). Results represent the increase in the percentage of the radioactivity recovered in the blood of 5FU, 5FU + SCFA and 5FU + butyrate groups compared to the control group. $n = 7$ /group. Different letters indicate a statistical difference ($p < 0.05$). **b** ZO-1 mRNA amplification in the ileum of control mice or mice treated with 5FU (IP) and receiving water (5FU group), SCFA (5FU + SCFA group) or butyrate (5FU + butyrate group) for 10 days. Bars represent average and lines represent standard error. $N = 4$ /group. * $p = 0.057$ and 0.091 for 5FU and 5FU + SCFA groups, respectively compared to control group

Role of SCFA and Butyrate on the Intestinal Integrity

Although the SCFA and butyrate solutions had beneficial effects on mucositis, the butyrate solution was the most effective. While it contained the same concentration of butyrate as the butyrate-alone solution, the SCFA solution only partially reduced weight loss and did not prevent permeability alteration or reduced the pro-inflammatory cytokine expression in the intestine. We believe that, rather than presenting deleterious effects, the presence of acetate and propionate in the SCFA solution reduced the intestinal absorption of butyrate via the border brush transporter. The transport of butyrate through monocarboxylate transporters (MCT) is saturable, coupled with H^+ and inhibited by several monocarboxylates, such as acetate, propionate, pyruvate, L-lactate and α -ketobutyrate [8]. We hypothesize that the higher concentration of acetate (35 mM) and propionate (15 mM) in contrast to the lower concentration of butyrate (9 mM) in the SCFA solution could compete with the butyrate transport by MCT and/or another intestinal

transporter, resulting in a smaller absorption and, consequently, a smaller post absorptive effect of butyrate in the SCFA solution compared to the butyrate alone.

Anti-Inflammatory Action

The mucosa analyses showed that neutrophil infiltration, as measured by MPO activity had increased in 5FU-treated animals and that SCFA or butyrate solutions did not interfere in this aspect. Moreover, macrophage infiltration, as measured by NAG activity, was not different in any 5FU-treated groups compared to the control group. This latter result could be explained by the pattern of cell migration towards the inflammatory site. Neutrophils are the first cells arriving at the inflammatory site causing an increase in MPO activity in the first hours after administration of 5FU as seen in the current study [3, 24]. In contrast, macrophages are effector cells, most frequently seen in later inflammatory stages, mainly after 3 days of inflammatory stimulus [30]. Our mice were euthanized 3 days after the administration of 5FU, which may explain the lack of differences in macrophage concentration between the control and 5FU groups. Regarding eosinophils, we found an intense infiltration related to mucositis that was prevented by SCFA and butyrate supplementation. Although the role of eosinophils in mucositis is seldom studied, the detection of eosinophils in the intestinal mucosa of patients with inflammatory intestinal diseases, even in small quantities, has been associated with adverse clinical consequences, such as weight loss, malabsorption and shortening of large intestine crypts [21, 31]. Thus, a reduction of these cells in the groups treated with SCFA and butyrate is considered a sign of a better prognosis.

The expression of the pro-inflammatory molecules TLR4, IL6 and $TNF\alpha$ tended to be higher in the 5FU group. This increase was possibly due to the inflammation caused by 5FU itself and due to the rupture of the intestinal barrier permitting bacterial translocation and LPS-induced TLR4 activation. In concordance to the permeability data and MPO activity, 5FU + butyrate group kept cytokine expression closer to the control group. These data suggest that the better intestinal trophism seen in this group attenuates the inflammatory stimulus secondary to LPS and bacterial translocations, reducing activation of mucosal immune cells.

The absence of differences between the 5FU and butyrate groups for NAG and MPO activities as well as inflammatory score suggest that a trophic rather than immunologic effect is the main mechanism for both butyrate and SCFA protection. Nonetheless, butyrate demonstrated a more intense effect on the intestinal barrier that could be due to its metabolic effect as an energetic source associated to its action on gene expression. The results of

butyrate on cytokines and TLR4 expressions compared to SCFA are in agreement with the improvement of intestinal permeability which will reduce bacterial translocation and LPS induced immune response activation.

Intestinal Permeability

Cell infiltration and intestinal permeability are important markers of tissue damage and mucosal inflammation [2, 17]. We have observed that butyrate reduced the alteration in intestinal permeability that is typically seen in 5FU mice. Our results are in agreement with other in-vitro studies showing the improvement of intestinal permeability with butyrate solutions [14, 19, 27]. The mechanism of this effect can be linked to gene expression of tight junction proteins, since butyrate and trichostatin A, an inhibitor of histone acetylase decreased tight junction permeability in Caco-2 cells via lipoxynase activation [18].

ZO-1 is a TJ protein that interacts with occludin, ZO-2, ZO-3 and actin, reducing intestinal permeability and inducing cell differentiation. Since 5FU treatment induced the increase of intestinal permeability, one would expect a reduction in ZO-1 protein in tight junctions [13, 16, 23]. However, our results showed that ZO-1 expression was increased in groups which presented an increase in permeability (5FU and 5FU + SCFA) compared to the control. We believe that this higher expression of ZO-1 reflects the more intense mucosal repair after 5FU-induced damage. ZO-1 protein and expression are generally tested under conditions of continuous inflammatory stimuli such as cell incubation with pro-inflammatory agents [23] or animal models with chronic inflammatory diseases [13, 16]. This continuous inflammatory stimulus maintains ZO-1 expression down-regulated in those models, avoiding the repair of the intestinal barrier. However, in our mucositis model, 5FU that has a short half-life [4] was given as a single dose 3 days before euthanasia of the mice. Since intestinal mucosa is renewed every 3–4 days, we believe that new intestinal cells formed after 5FU injection overexpressed ZO-1 in order to compensate the important intestinal barrier disruption. In the 5FU + butyrate group, mucosal damage was lower (as seen by the reduction in intestinal permeability and mucosa recovery) compared to the 5FU non-supplemented group, reducing the necessity of a compensatory ZO-1 expression. Probably, ZO-1 expression, intestinal permeability in the 5FU + butyrate group was closer to the control group, reinforcing our hypothesis. Moreover, ZO-1 altered expression in the 5-FU and 5FU + SCFA groups can be related to the ZO-1 translocation from the cell boundary (tight junction location) to the cytoplasm as previously described [23]

Possible Mechanisms of Action

The mechanisms of action of SCFA and butyrate on intestinal cells are not totally understood. Oral administration of SCFA exposes the stomach and small intestine mucosa to these fatty acids before reaching the colon [25, 29] and are transported to the liver [8]. There, they can be metabolized to glutamate, glutamine and acetoacetate [5] important fuels for enterocytes [1, 5, 6]. Butyrate also increases the pancreatic secretion and the activity of jejunal brush-border enzymes [9], increasing availability of nutrients for enterocyte regeneration, stimulates of Glucagon-like peptide-2 (GLP-2) [32], a pleiotropic intestinotrophic hormone that enhances digestive and absorptive capacity [12]. All these components propitiate the mucosa integrity, protecting cells from 5FU damage, including the increase in intestinal permeability. As a consequence, the bacterial translocation is reduced, minimizing the inflammatory response.

In conclusion, the results presented here highlight, for the first time, the potential use of butyrate in inflammatory diseases of the small intestine, such as mucositis. Oral administration of butyrate contributes to rebuilding the intestinal mucosa by quickly repairing ulcerated and inflamed tissue.

Acknowledgments This study was supported by grants from the Conselho Nacional de Desenvolvimento Científico e Tecnológico (CNPq); Coordenação de Aperfeiçoamento de Nível Superior (CAPES), Fundação de Amparo a Pesquisa de Minas Gerais (FAP-EMIG) e Pro-Reitoria de Pesquisa (PRPq) da UFMG. The authors are grateful to Maria Helena Alves, for taking care of the animals.

Conflict of interest The authors declare that they have no conflict of interest.

References

1. Bergman EN (1990) Energy contributions of volatile fatty acids from the gastrointestinal tract in various species. *Physiol Rev* 70:567–590
2. Blijlevens NM, Van't Land B, Donnelly JP, M'Rabet L, de Pauw BE (2004) Measuring mucosal damage induced by cytotoxic therapy. *Support Care Cancer* 12:227–233
3. Broughton G 2nd, Janis JE, Attinger CE (2006) The basic science of wound healing. *Plast Reconstr Surg* 117:12S–34S
4. Chu E, Sartorelli AC (2012) Cancer chemotherapy. In: Katzung BG, Masters SB, Trevor AJ (eds) *Basic and clinical pharmacology*, chap 54, 12th edn. McGraw-Hill, New York
5. Desmoulin F, Canioni P, Cozzone PJ (1985) Glutamate–glutamine metabolism in the perfused rat liver. ¹³C-NMR study using (2-¹³C)-enriched acetate. *FEBS Lett* 185:29–32
6. Duee PH, Darcy-Vrillon B, Blachier F, Morel MT (1995) Fuel selection in intestinal cells. *Proc Nutr Soc* 54:83–94
7. Generoso SV, Viana M, Santos R, Martins FS, Machado JA, Arantes RM, Nicoli JR, Correia MI, Cardoso VN (2010) *Saccharomyces cerevisiae* strain UFMG 905 protects against

- bacterial translocation, preserves gut barrier integrity and stimulates the immune system in a murine intestinal obstruction model. *Arch Microbiol* 192:477–484
8. Guilloteau P, Martin L, Eeckhaut V, Ducatelle R, Zabielski R, Van Immerseel F (2010) From the gut to the peripheral tissues: the multiple effects of butyrate. *Nutr Res Rev* 23:366–384
 9. Guilloteau P, Savary G, Jaguelin-Peyrault Y, Rome V, Le Normand L, Zabielski R (2010) Dietary sodium butyrate supplementation increases digestibility and pancreatic secretion in young milk-fed calves. *J Dairy Sci* 93:5842–5850
 10. Hamer HM, Jonkers D, Venema K, Vanhoutvin S, Troost FJ, Brummer RJ (2008) Review article: the role of butyrate on colonic function. *Aliment Pharmacol Ther* 27:104–119
 11. Hinnebusch BF, Meng S, Wu JT, Archer SY, Hodin RA (2002) The effects of short-chain fatty acids on human colon cancer cell phenotype are associated with histone hyperacetylation. *J Nutr* 132:1012–1017
 12. Hornby PJ, Moore BA (2011) The therapeutic potential of targeting the glucagon-like peptide-2 receptor in gastrointestinal disease. *Expert Opin Ther Targets* 15:637–646
 13. Hudcovic T, Kolinska J, Klepetar J, Stepankova R, Rezanka T, Srutkova D, Schwarzer M, Erban V, Du Z, Wells JM, Hrnčir T, Tlaskalova-Hogenova H, Kozakova H (2012) Protective effect of *Clostridium tyrobutyricum* in acute dextran sodium sulphate-induced colitis: differential regulation of tumour necrosis factor- α and interleukin-18 in BALB/c and severe combined immunodeficiency mice. *Clin Exp Immunol* 167:356–365
 14. Kinoshita M, Suzuki Y, Saito Y (2002) Butyrate reduces colonic paracellular permeability by enhancing PPAR γ activation. *Biochem Biophys Res Commun* 293:827–831
 15. Luhrs H, Gerke T, Muller JG, Melcher R, Schaubert J, Boxberger F, Scheppach W, Menzel T (2002) Butyrate inhibits NF- κ B activation in lamina propria macrophages of patients with ulcerative colitis. *Scand J Gastroenterol* 37:458–466
 16. Martinez C, Vicario M, Ramos L, Lobo B, Mosquera JL, Alonso C, Sanchez A, Guilarte M, Antolin M, de Torres I, Gonzalez-Castro AM, Pigrau M, Saperas E, Azpiroz F, Santos J (2012) The jejunum of diarrhea-predominant irritable bowel syndrome shows molecular alterations in the tight junction signaling pathway that are associated with mucosal pathobiology and clinical manifestations. *Am J Gastroenterol*
 17. Melo ML, Brito GA, Soares RC, Carvalho SB, Silva JV, Soares PM, Vale ML, Souza MH, Cunha FQ, Ribeiro RA (2008) Role of cytokines (TNF- α , IL-1 β and KC) in the pathogenesis of CPT-11-induced intestinal mucositis in mice: effect of pentoxifylline and thalidomide. *Cancer Chemother Pharmacol* 61(5):775–784
 18. Ohata A, Usami M, Miyoshi M (2005) Short-chain fatty acids alter tight junction permeability in intestinal monolayer cells via lipoxygenase activation. *Nutrition* 21:838–847
 19. Peng L, He Z, Chen W, Holzman IR, Lin J (2007) Effects of butyrate on intestinal barrier function in a Caco-2 cell monolayer model of intestinal barrier. *Pediatr Res* 61:37–41
 20. Ramos MG, Bambirra EA, Cara DC, Vieira EC, Alvarez-Leite JI (1997) Oral administration of short-chain fatty acids reduces the intestinal mucositis caused by treatment with Ara-C in mice fed commercial or elemental diets. *Nutr Cancer* 28:212–217
 21. Rothenberg ME (2004) Eosinophilic gastrointestinal disorders (EGID). *J Allergy Clin Immunol* 113:11–28 quiz 29
 22. Sanderson IR (2007) Dietary modulation of GALT. *J Nutr* 137:2557S–2562S
 23. Sappington PL, Han X, Yang R, Delude RL, Fink MP (2003) Ethyl pyruvate ameliorates intestinal epithelial barrier dysfunction in endotoxemic mice and immunostimulated caco-2 enterocytic monolayers. *J Pharmacol Exp Ther* 304:464–476
 24. Soares PM, Mota JM, Gomes AS, Oliveira RB, Assreuy AM, Brito GA, Santos AA, Ribeiro RA, Souza MH (2008) Gastrointestinal dysmotility in 5-fluorouracil-induced intestinal mucositis outlasts inflammatory process resolution. *Cancer Chemother Pharmacol* 63:91–98
 25. Souba WW, Scott TE, Wilmore DW (1985) Intestinal consumption of intravenously administered fuels. *JPN J Parenter Enteral Nutr* 9:18–22
 26. Turner JR (2009) Intestinal mucosal barrier function in health and disease. *Nat Rev Immunol* 9:799–809
 27. Van Deun K, Pasmans F, Van Immerseel F, Ducatelle R, Haesebrouck F (2008) Butyrate protects Caco-2 cells from *Campylobacter jejuni* invasion and translocation. *Br J Nutr* 100:480–484
 28. Vieira EL, Leonel AJ, Sad AP, Beltrao NR, Costa TF, Ferreira TM, Gomes-Santos AC, Faria AM, Peluzio MC, Cara DC, Alvarez-Leite JI (2012) Oral administration of sodium butyrate attenuates inflammation and mucosal lesion in experimental acute ulcerative colitis. *J Nutr Biochem* (in press)
 29. Windmueller HG, Spaeth AE (1978) Identification of ketone bodies and glutamine as the major respiratory fuels in vivo for postabsorptive rat small intestine. *J Biol Chem* 253:69–76
 30. Xavier RJ, Podolsky DK (2007) Unravelling the pathogenesis of inflammatory bowel disease. *Nature* 448:427–434
 31. Yan BM, Shaffer EA (2009) Primary eosinophilic disorders of the gastrointestinal tract. *Gut* 58:721–732
 32. Yazbeck R, Howarth GS, Abbott CA (2009) Growth factor based therapies and intestinal disease: is glucagon-like peptide-2 the new way forward? *Cytokine Growth Factor Rev* 20:175–184

Lipid Transfer to HDL is Higher in Marathon Runners than in Sedentary Subjects, but is Acutely Inhibited During the Run

Mauro Vaisberg · André L. L. Bachi ·
Conceição Latrilha · Giuseppe S. Dioguardi ·
Sergio P. Bydlowski · Raul C. Maranhão

Received: 28 December 2011 / Accepted: 17 May 2012 / Published online: 9 June 2012
© AOCs 2012

Abstract Although exercise increases HDL-cholesterol, exercise-induced changes in HDL metabolism have been little explored. Lipid transfer to HDL is essential for HDL's role in reverse cholesterol transport. We investigated the effects of acute exhaustive exercise on lipid transfer to HDL. We compared plasma lipid, apolipoprotein and cytokine levels and in vitro transfer of four lipids from a radioactively labeled lipid donor nanoemulsion to HDL in sedentary individuals ($n = 28$) and in marathon runners ($n = 14$) at baseline, immediately after and 72 h after a

marathon. While HDL-cholesterol concentrations and apo A1 levels were higher in marathon runners, LDL-cholesterol, apo B and triacylglycerol levels were similar in both groups. Transfers of non-esterified cholesterol [6.8 (5.7–7.2) vs. 5.2 (4.5–6), $p = 0.001$], phospholipids [21.7 (20.4–22.2) vs. 8.2 (7.7–8.9), $p = 0.0001$] and triacylglycerol [3.7 (3.1–4) vs. 1.3 (0.8–1.7), $p = 0.0001$] were higher in marathon runners, but esterified-cholesterol transfer was similar. Immediately after the marathon, LDL- and HDL-cholesterol concentrations and apo A1 levels were unchanged, but apo B and triacylglycerol levels increased. Lipid transfer of non-esterified cholesterol [6.8 (5.7–7.2) vs. 5.8 (4.9–6.6), $p = 0.0001$], phospholipids [21.7 (20.4–22.2) vs. 19.1 (18.6–19.3), $p = 0.0001$], esterified-cholesterol [3.2 (2.2–3.8) vs. 2.3 (2–2.9), $p = 0.02$] and triacylglycerol [3.7 (3.1–4) vs. 2.6 (2.1–2.8), $p = 0.0001$] to HDL were all reduced immediately after the marathon but returned to baseline 72 h later. Running a marathon increased IL-6 and TNF- α levels, but after 72 h these values returned to baseline. Lipid transfer, except esterified-cholesterol transfer, was higher in marathon runners than in sedentary individuals, but the marathon itself acutely inhibited lipid transfer. In light of these novel observations, further study is required to clarify how these metabolic changes can influence HDL composition and anti-atherogenic function.

M. Vaisberg
Department of Otorhinolaryngology,
Federal University of São Paulo, São Paulo, Brazil

A. L. L. Bachi
Department of Microbiology and Immunology,
Federal University of São Paulo, São Paulo, Brazil

C. Latrilha · R. C. Maranhão
The Heart Institute (InCor), University of São Paulo,
São Paulo, Brazil

G. S. Dioguardi
Dante Pazzanese Institute of Cardiology, São Paulo, Brazil

S. P. Bydlowski
Department of Internal Medicine, University of São Paulo
Medical School, São Paulo, Brazil

R. C. Maranhão
Faculty of Pharmaceutical Sciences, University of São Paulo,
São Paulo, Brazil

R. C. Maranhão (✉)
Laboratório de Metabolismo de Lípidos,
Instituto do Coração (InCor) do Hospital das Clínicas,
FMUSP, Av. Dr. Enéas de Carvalho Aguiar, 44, 1° subsolo,
São Paulo, SP 05403-000, Brazil
e-mail: ramarans@usp.br

Keywords Cholesteryl ester transfer protein (CETP) · HDL metabolism · Cholesterol · Exercise training and lipids · Nanoemulsions · Cytokines

Abbreviations

HDL High-density lipoprotein
LDL Low-density lipoprotein
HDL-C High-density lipoprotein cholesterol

LDL-C	Low-density lipoprotein cholesterol
VLDL	Very low-density lipoprotein
IDL	Intermediate-density lipoprotein
Apo	Apolipoprotein
CETP	Cholesteryl ester transfer protein
PLTP	Phospholipid transfer protein
NEC	Non-esterified cholesterol
EC	Esterified cholesterol
PL	Phospholipids
TAG	Triacylglycerol(s)
IL	Interleukin
TNF	Tumor necrosis factor
CHD	Coronary heart disease
PON	Paraoxonase
BMI	Body mass index
NaCl	Sodium chloride
KBr	Potassium bromide

Introduction

The beneficial effects of moderate exercise training on the cardiovascular system and on the major risk factors related to cardiovascular disease, such as plasma lipid concentration, have been well established [1]. However, the underlying mechanisms of the protective effects of exercise remain largely unknown [2]. Regular aerobic exercise training decreases low-density lipoprotein cholesterol (LDL-C) and triacylglycerol (TAG) levels and increases high-density lipoprotein cholesterol (HDL-C) levels [3–6]. This leads to a characteristically anti-atherogenic lipid profile and is accompanied by an increase in apolipoprotein (apo) A1 and a decrease in apo B, the main apolipoproteins present in HDL and LDL particles, respectively [7]. Exhaustive, high-intensity exercise, such as that practiced by female marathon runners, elicits strong increases in HDL-C, but unlike moderate exercise, the effects on LDL-C and TAG levels are not significant [8]. This isolated increase in HDL-C is apparently not sufficient to protect from atherosclerosis as it has been shown that marathon runners do not have better coronary artery calcification indexes than sedentary individuals [9]. An important factor influencing exercise-induced plasma lipid changes is the effect of cytokines such as interleukin-6 (IL-6) and tumor necrosis factor alpha (TNF- α), since both cytokines inhibit the activity of lipoprotein lipase and their concentrations increase acutely during exhaustive exercise [10, 11].

HDL-C is an important protective factor against atherosclerosis and an important marker of longevity [12]. The inverse correlation between HDL-C concentration and the likelihood of coronary heart disease (CHD) is well-known, but the protective action of HDL, such as its role in reverse

cholesterol transport, is only partially reflected by its concentration [13, 14]. In reverse cholesterol transport, cholesterol from peripheral tissues is transferred to HDL and transported to the liver, where it is excreted by the bile [15]. HDL also has antioxidant activity—mostly due to paraoxonase 1 (PON 1), which is linked to HDL—and anti-inflammatory, antithrombotic and vasodilatory activities, which may account for the antiatherogenic role of this lipoprotein [16, 17].

HDL metabolism is complex. This lipoprotein is formed in the circulation by the lipidation of apo A1 to produce a disk-shaped nascent form of HDL, which is then transformed into the mature, round form. HDL is continuously remodeled, and lipid transfer to and from this lipoprotein is an essential part of its metabolism and atheroprotective functions, such as the promotion of reverse cholesterol transport [18]. Transfer of lipids is facilitated by transfer proteins such as cholesteryl ester transfer protein (CETP) and phospholipid transfer protein (PLTP), which are involved in the transfer of core lipids (cholesteryl esters and TAG) and surface lipids (PL and free cholesterol), respectively [19–21]. To date, the role of CETP and PLTP in atherogenesis is not completely understood, but HDL-C status is clearly more affected by lipid transfer than very low-density lipoprotein (VLDL) and low-density lipoprotein (LDL) status.

In this study we aimed to investigate whether the transfer to HDL of the four main lipids in the circulation, namely, NEC, EC, PL and TAG, as estimated by an *in vitro* assay [22] is affected by the practice of high-intensity exercise, such as marathon running, and whether marathon running causes an acute change in these transfers. Our results show that there is indeed a marked difference in the lipid transfer process between marathon runners and sedentary individuals. Furthermore, running a marathon acutely inhibits lipid transfer in these athletes.

Materials and Methods

Study Subjects

Fourteen male recreational marathon runners aged 25–50 years and 28 male sedentary individuals were recruited for the study. The two groups were paired for age and BMI (data shown in Table 1). None of the participants were smokers, addicted to alcohol consumption or obese or had systemic arterial hypertension or liver, renal, metabolic, inflammatory or neoplastic diseases. None were using lipid-lowering medications.

The Ethics Committee of the Federal University of São Paulo approved the study, and written informed consent was obtained from all subjects after they were provided with a complete description of the protocol.

Blood samples of the marathon runners were collected at rest (baseline), immediately after and 72 h after the

Table 1 Physical (mean \pm S.D.) and laboratory (median and interquartile range) data for sedentary subjects at rest and marathon runners on three different occasions: at rest (baseline), immediately after and 72 h after a marathon

Variables	Sedentary ($n = 28$)	Marathon runners ($n = 14$)		
		Baseline	Immediately after	72 h after
Age (y)	37.5 \pm 4	38 \pm 7		
Body mass index (kg/m ²)	24.8 \pm 2.0	23.7 \pm 3.3		
Hematocrit (%)	15.4 [14.5–15.9]	14.9 [14.3–15.5]	15.2 [14.9–15.9]	14.4 [13.8–15]*
Hemoglobin (g/dL)	46.1 [43.8–47.9]	44.5 [43.2–45.9]	46.7 [45.2–47.8]*	43.2 [41.7–44.5]*
Total bilirubin (mg/dL)	0.56 [0.34–0.84]	0.62 [0.44–1.01]	0.88 [0.57–1.14]*	0.54 [0.44–0.95]*
Cholesterol (mg/dL)				
Total	170 [154–210]	198 [175–217]	185 [165–234]	173.5 [148–195]
HDL	43 [38–51]	61 [46–74] [#]	58 [50–72]	62 [46–76]
LDL	107 [88–140]	119 [101–134]	105 [79–132]	92 [84–116]
Triglycerides (mg/dL)	98 [77–114]	66 [55–104]	107 [69–148]*	87 [56–136]
Apolipoprotein (g/L)				
A ₁	142 [121–157]	161 [143–185] [#]	153 [124–171]	170 [138–202]
B	78 [71–96]	74 [64–85]	83 [61–101]*	87 [67–99]

[#] p value between sedentary \times marathon runners (baseline)

* Statistical significant difference in comparison to baseline value

marathon race. Blood was also collected at rest from sedentary people. Blood draws for all the individuals were performed after 12 h of fasting. Marathon runners trained an average of 80–100 km/week to prepare for the race, or an average of 2 h/day. The last training session was performed 24 h before the blood draw. We recommended that all marathon runners ingested 500 mL of water before the marathon. Water was provided by the marathon organizers during the race.

Plasma Lipids

Plasma total cholesterol (measured by the CHOD–PAP method) and total bilirubin levels were determined using commercial kits (Kovalente, São Gonçalo, Brazil), and the results were analyzed with an automated system (Dimension[®] RxL Max[®] Integrated Chemistry System, Siemens, Deerfield, IL). HDL-C and TAG concentrations were determined using commercial kits and an automated analysis system (ADVIA[®] 2,400 Chemistry System, Siemens Healthcare Diagnostics Inc., Deerfield, IL). LDL-C was estimated by the Friedewald formula [23]. Apo A1 and B were measured by rate nephelometry on an Image[®] Immunochemistry System (Beckman Coulter, Brea, CA).

Nanoemulsion Preparation and Lipid Transfer Assay

The lipid donor nanoemulsion used in this study mimics the LDL lipid structure, which consists of a surface monolayer of PL and NEC surrounding a core of

cholesteryl esters also containing residual TAG. The nanoemulsion was prepared from a lipid mixture composed of 40 mg cholesteryl oleate, 20 mg egg phosphatidylcholine, 1 mg triolein and 0.5 mg cholesterol purchased from Sigma Chemical Company (St. Louis, MO). Emulsification of lipids by prolonged ultrasonic irradiation in aqueous media and the two-step procedure of ultracentrifuging the crude emulsion and adjusting its density with KBr to obtain the nanoemulsion was carried out as described previously [22, 24]. The nanoemulsion fraction was dialyzed against 0.9 % NaCl solution. Trace amounts of cholesteryl [1-¹⁴C] oleate and glycerol tri [9, 10 (n)-³H] oleate or [7(n)-³H] cholesterol and L-3-phosphatidylcholine, 1-stearoyl-2-[1-¹⁴C] arachidonyl (Amersham, Little Chalfont, Buckinghamshire, UK) were added to the initial solution.

The *in vitro* assay to measure lipid transfer from the nanoemulsion to HDL was previously described by Lo Prete et al. [25]; briefly a nanoemulsion labeled with ³H-CE and ¹⁴C-PL or with ¹⁴C-NEC and ³H-TAG is incubated with whole plasma. This incubation is followed by chemical precipitation of the nanoemulsion and apo B containing lipoproteins. The radioactivity of the supernatant containing the lipids that shifted from the nanoemulsion to HDL is then measured by liquid scintillation counting. Transfer of radioactive material from the nanoemulsion to HDL is expressed as the radioactivity in the HDL-containing supernatant as a percentage of the total radioactivity of the nanoemulsion incubated with the plasma [25].

Determination of CETP and PLTP Activity

Serum CETP and PLTP activity was measured using commercially available CETP and PLTP activity assay kits (BioVision Inc, Mountain view, CA) and serum samples of marathon runners collected before (baseline), immediately after and 72 h after a marathon race, following the manufacturer's instructions.

Serum Cytokine Concentration

The concentrations in pg/mL of cytokines IL-6 and TNF- α in the serum of marathon runners collected before (baseline), immediately after and 72 h after a marathon race and in sedentary individuals at rest were measured using the Luminex bead-based system for human cytokines and the LINCoplex kit for simultaneous multi-analyte detection (Linco Research, St Charles, MO).

Statistical Analysis

The Mann–Whitney test was used to determine if the differences between the results for sedentary individuals and those for marathon runners at rest were significant. The Friedman test and Müller–Dunn post-test were used to determine if the differences between the baseline results for the marathon runners and the results immediately after and 72 h after the marathon were significant. The significance level was set to 5 % ($p < 0.05$). Age and BMI data are expressed as means \pm standard deviations. Other parameters evaluated are expressed as median and interquartile range.

Results

As shown in Table 1, there were no significant differences in baseline values of hematocrit, hemoglobin and total bilirubin levels between marathon runners and sedentary individuals.

The results for serum lipids showed that HDL-C concentration was higher in the marathon runners group than in the sedentary group ($p = 0.001$), but there was no statistically significant difference between the two groups for either LDL-C or TAG. When measured in conjunction with HDL-C, levels of apo A1 ($p = 0.04$), which is the major apo in the HDL fraction, were also higher in marathon runners, whereas there was no statistically significant difference in apo B levels between the groups.

Figure 1 shows that transfers of NEC [6.8 (5.7–7.2) vs. 5.2 (4.5–6), $p = 0.001$], PL [21.7 (20.4–22.2) vs. 8.2 (7.7–8.9), $p = 0.0001$] and TAG [3.7 (3.1–4) vs. 1.3 (0.8–1.7), $p = 0.0001$] were higher in marathon runners

than in sedentary individuals but that transfer of EC [3.2 (2.2–3.8) vs. 2.7 (2.2–3), not significant (NS)] was statistically the same.

As hemoconcentration could eventually lead to increased plasma lipid concentration, hematocrit percentages were measured immediately after the marathon and were found to be unchanged (Table 1), indicating that the athletes were adequately hydrated during the race. The increases in hemoglobin levels ($p = 0.01$) and total bilirubin ($p = 0.03$) observed here could be related to acute episodes of hemolysis, which frequently occur in marathon races [26].

As also shown in Table 1, LDL and HDL-C values did not change from baseline to immediately after the marathon, but TAG levels increased by roughly 60 % ($p = 0.001$). Apo B, which is mainly an LDL marker but is also present in VLDL, increased after the race ($p = 0.02$) whereas apo A1 was unchanged.

As shown in Fig. 1, transfers of NEC [6.8 (5.7–7.2) vs. 5.8 (4.9–6.6), $p = 0.0001$], PL [21.7 (20.4–22.2) vs. 19.1 (18.6–19.3), $p = 0.0001$], EC [3.2 (2.2–3.8) vs. 2.3 (2–2.9), $p = 0.02$] and TAG [3.7 (3.1–4) vs. 2.6 (2.1–2.8), $p = 0.0001$] to HDL were all reduced after running a marathon.

It can be seen from Table 1 that all the lipid and apolipoprotein values had already returned to baseline levels 72 h after the marathon ended. The same occurred with the lipid transfer values, which are shown in Fig. 1: transfers of NEC [6.4 (5.8–6.9) vs. 6.8 (5.7–7.2), NS], EC [2.6 (2.1–3.1) vs. 3.2 (2.2–3.8), NS] and PL [20.9 (19.8–22.1) vs. 21.7 (20.4–22.2), NS] were not statistically different from baseline transfer values, except for the transfer of TAG [3 (2.6–3.5) vs. 3.7 (3.1–4), $p = 0.005$], which increased but was still significantly different from baseline values.

Figure 2 shows CETP (a) and PLTP (b) activity in serum of marathon runners on three occasions: at rest (baseline), immediately after and 72 h after the marathon finished. CETP activity was unchanged and PLTP activity ($p = 0.001$) was elevated immediately after the marathon but returned to baseline levels after 72 h.

Figure 3 shows serum concentrations of IL-6 (a) and TNF- α (b) in sedentary individuals at rest and the change in cytokine levels in marathon runners from baseline to immediately after and 72 h after the marathon. IL-6 baseline values for marathon runners and sedentary individuals were statistically equal. However, TNF- α concentrations in marathon runners were lower than in sedentary individuals at rest ($p = 0.001$). Running a marathon race led to a pronounced increase in the concentrations of both IL-6 ($p = 0.0004$) and TNF- α ($p = 0.004$), which returned to baseline levels 72 h after the marathon ended.

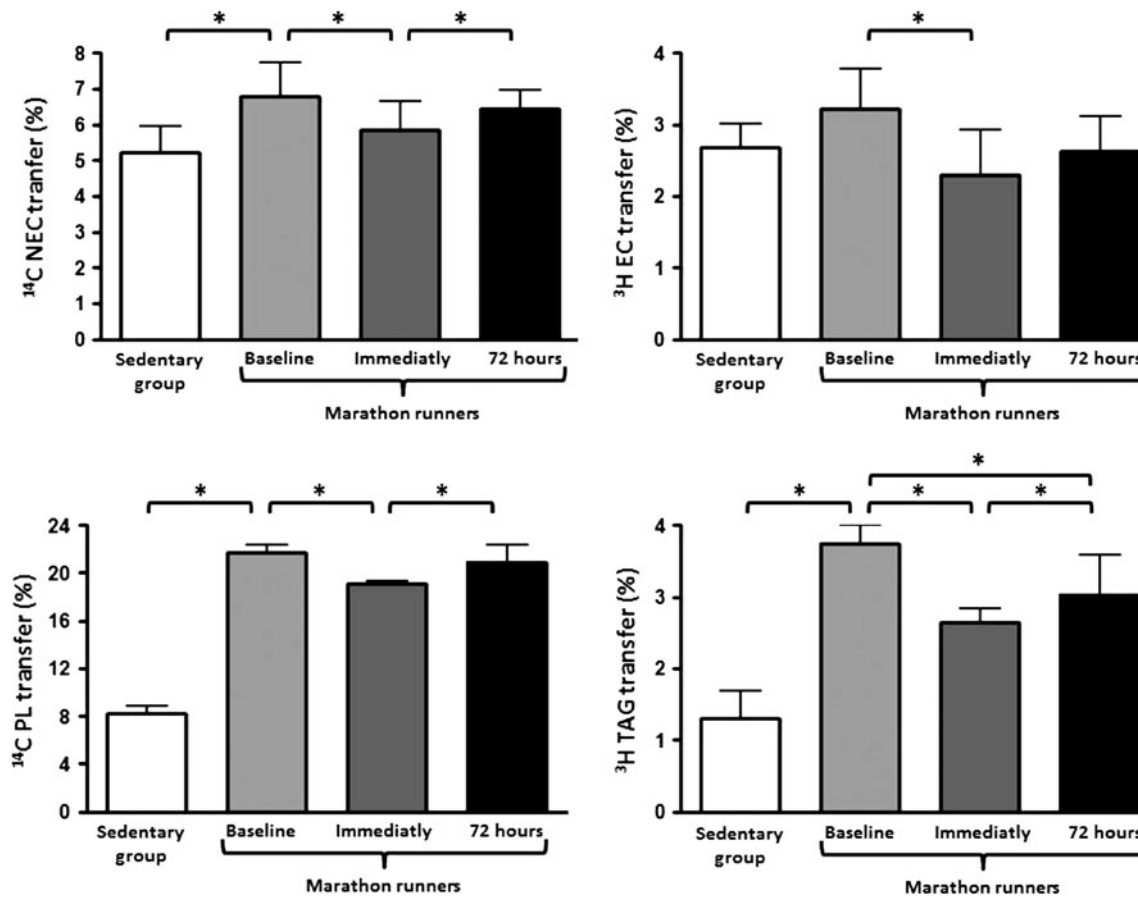
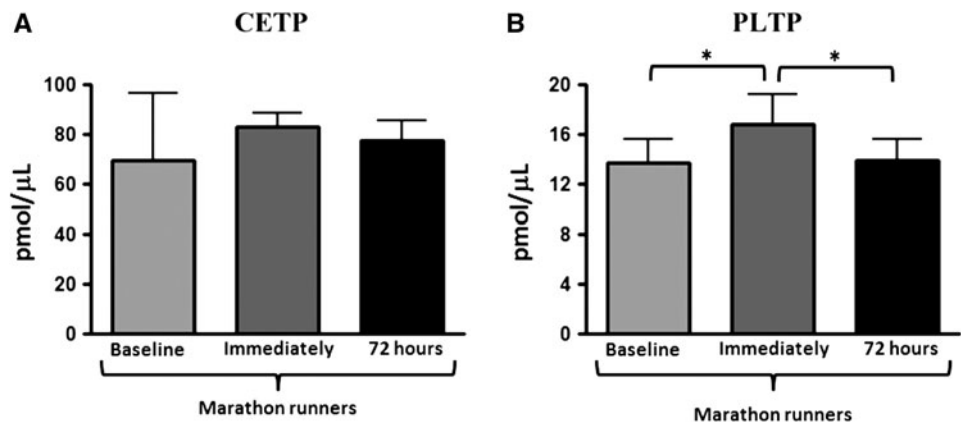


Fig. 1 In vitro transfer of radiolabeled NEC (non-esterified cholesterol) and EC (esterified-cholesterol), PL (phospholipids) and TAG (triacylglycerol) from a donor lipid nanoemulsion to HDL in a group of sedentary subjects at rest and a group of marathon runners

measured on three different occasions: at rest (baseline), immediately after and 72 h after a marathon. Data are presented as medians and interquartile ranges, with a significance level of $*p < 0.05$

Fig. 2 Serum CETP and PLTP activity (pmol/ μ L/h) in a group of marathon runners measured on three different occasions: at rest (baseline), immediately after and 72 h after a marathon. Data are presented as medians (interquartile range) with a significance level of $*p < 0.05$

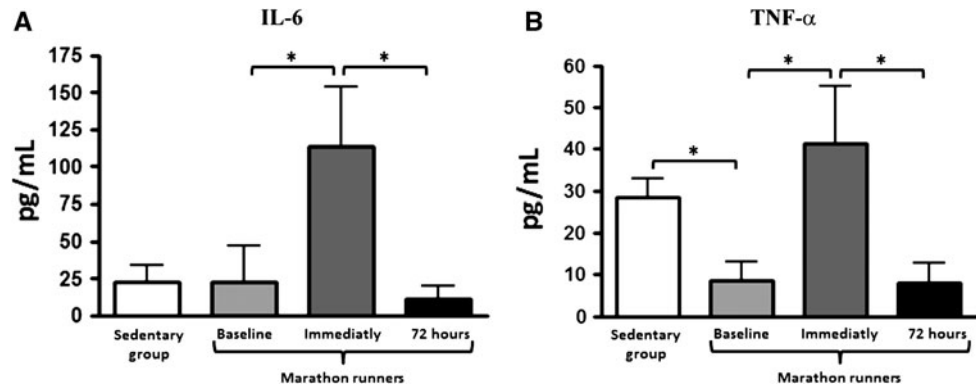


Discussion

The results of this study show that while levels of HDL-C and apo A1 (the main HDL apolipoprotein) in marathon runners were different from those in sedentary individuals, LDL-C and apo B were statistically the same. This is in agreement with the findings of other studies showing that regular exercise

training in general and intensive training in particular increase HDL-C [5]. However, training does not guarantee reductions in LDL-C or apo B [27–29], although high-intensity exercise, such as an endurance triathlon, often elicits a decrease in triacylglyceridemia [30, 31]. In the current study, no differences were found in either LDL-C or TAG levels between marathon runners and sedentary individuals.

Fig. 3 Serum concentrations (pg/mL) of cytokines IL-6 (a) and TNF- α (b) in a group of sedentary subjects at rest and in a group of marathon runners measured on three different occasions: at rest (baseline), immediately after and 72 h after a marathon. Data are presented as medians (interquartile range) with a significance level of $*p < 0.05$



It has been reported that, after an ultramarathon or marathon, HDL-C may increase acutely [32] or, as occurred in our study, remain unchanged [33], with large inter-individual variations [32, 33].

A novel finding of this study was that the transfer of lipids to HDL was higher in marathon runners than in sedentary individuals at rest, except for the transfer of EC. This effect could be ascribed to marathon runners having higher HDL-C concentrations, favoring an increase in lipid transfer [25]. It is also possible that increases in CETP and PLTP enhanced the transfers of TAG and PL, respectively. PLTP can also facilitate NEC transfer [34]. While enrichment of HDL with PL is considered beneficial in terms of reverse cholesterol transfer, enrichment with TAG may destabilize the HDL particles [35] and, contrary to what was observed in the present study, lead to a decrease in HDL. However, the fact that more of these lipids were transferred to HDL in marathon runners than in sedentary people does not imply that lipid enrichment occurred, as lipid transfer is bidirectional and in the present study only transfers from the donor nanoemulsion to HDL were measured. Conceivably, compositional changes in the HDL fraction may also change the ability of this lipoprotein to take up lipids from other lipoprotein classes or, as is the case here, from a standard donor nanoemulsion. Recently, our group showed that in subjects that had precocious coronary artery disease the *in vitro* transfer of NEC to HDL was reduced [36, 37]. Since HDL is the main cholesterol esterification site in the circulation and this reaction is essential for stabilization of the plasma cholesterol pool and for reverse cholesterol transport, reduction in NEC transfer to HDL may affect important functions of this lipoprotein, increasing cardiovascular risk. Therefore, we can speculate that the increased transfer of NEC to HDL in marathon runners may play an important role in cardiovascular disease prevention.

The acute effects of running a marathon on lipid and lipoprotein profiles and on lipid transfer to HDL have also been documented. The effects on triacylglycerol-rich lipoproteins such as VLDL were remarkable, as fasting

TAG levels increased more than twofold in female runners [38]. In contrast, HDL-C levels, as well as levels of the HDL marker apo A1, were unchanged and even though previous studies have shown that LDL-C levels were reduced after exhaustive exercise such as an ultra-marathon or bicycle marathon [33, 39], here LDL-C levels were unchanged. Thus, the increase in the LDL marker apo B was due to the marked increase in VLDL, as apo B is also present in the VLDL fraction [40]. The fact that HDL levels were unchanged shortly after the marathon while lipid transfer had decreased suggests that HDL was structurally more stable during the exercise.

Our data confirm previous findings that TNF- α is lower in athletes than in sedentary subjects [41, 42] and that TNF- α and IL-6 increase after a training session of intense exercise [43, 44]. As both TNF- α and IL-6 inhibit lipoprotein lipase [45–50], the transient post-marathon hypertriacylglyceridemia observed in this study can be ascribed to the increase in these cytokines.

HDL-C and apo A1 levels were not acutely changed immediately after the marathon, but the transfer rates of all four lipids to HDL were reduced. Although a decrease in lipid transfer could be attributed to a reduction in CETP and PLTP activity, this did not occur in our study [7, 39, 51]. These findings are similar to those in acute inflammatory response, which elicits an increase in PLTP activity [52] without a change in CETP [53] and interferes with the antioxidant action of HDL, the HDL-associated enzyme paraoxonase-1 (PON1) and apo A1 [53–55]. This effect, also observed in the presence of IL-6 and TNF- α [56] increases phospholipids oxidation [55], possibly leading to a decrease in the capacity of HDL to take up lipids. Another factor leading to decreased lipid transfer to HDL is the increase in triacylglycerol-rich lipoproteins such as VLDL or IDL reflected in marathon-induced hypertriacylglyceridemia [57]. This could have increased the transfer of the nanoemulsion lipids to VLDL at the expense of HDL. An increase in transfers to HDL in conjunction with a return of TAG to pre-marathon levels, as observed 72 h after the run, suggests that this mechanism could have

contributed to the reduction in lipid transfer immediately after the marathon.

While the small number of participants in this study could be considered a limitation, especially when data for the runners at rest are compared with those for the sedentary subjects, the great difference in the results for the lipid transfer assay mitigates this drawback. Furthermore, this is not a limitation in the experiments comparing the acute effects of a marathon run because the data for each participant were compared before and after the marathon, with marked differences found between pre- and post-marathon results for all the individual participants.

In conclusion, lipid transfer to HDL, an important element of HDL metabolism and function, was remarkably increased in individuals who practiced exhaustive exercise. However, running a marathon inhibited lipid transfer transiently, an effect that is possibly related to the increase in serum cytokines. Since HDL has a role in inflammatory processes and is affected by intensive exercise training, our findings may have important physiological implications. Further research is required to establish the mechanisms behind the phenomena described here.

Acknowledgments The authors are grateful to Dr. Jeferson Silva for contributing to the discussion of the manuscript. This study was supported by the Fundação de Amparo à Pesquisa de São Paulo (FAPESP), São Paulo, Brazil. Prof. Maranhão has a research grant from the Conselho Nacional de Desenvolvimento Científico e Tecnológico (CNPq, 475819/2010-1), Brasília, Brazil.

Conflict of interest All the authors participated in the design of the study, interpretation of the data and writing of the manuscript. The authors declare that there are no conflicts of interest.

References

- Kokkinos P, Sheriff H, Kheirbek R (2011) Physical inactivity and mortality risk. *Cardiol Res Pract* 2011:924945. doi:10.4061/2011/924945
- Meissner M, Nijstad N, Kuipers F, Tietge UJ (2010) Voluntary exercise increases cholesterol efflux but not macrophage reverse cholesterol transport in vivo in mice. *Nutr Metab (Lond)* 7:54. doi:10.1186/1743-7075-7-54
- Kobayashi Y, Takeuchi T, Hosoi T, Yoshizaki H, Loepky JA (2005) Effect of a marathon run on serum lipoproteins, creatine kinase, and lactate dehydrogenase in recreational runners. *Res Q Exerc Sport* 76:450–455
- Ring-Dimitriou S, von Duvillard SP, Paulweber B, Stadlmann M, Lemura LM, Peak K, Mueller E (2007) Nine months aerobic fitness induced changes on blood lipids and lipoproteins in untrained subjects versus controls. *Eur J Appl Physiol* 99: 291–299
- Tambalis K, Panagiotakos DB, Kavouras SA, Sidossis LS (2009) Responses of blood lipids to aerobic, resistance, and combined aerobic with resistance exercise training: a systematic review of current evidence. *Angiology* 60:614–632
- Herzberg GR (2004) Aerobic exercise, lipoproteins, and cardiovascular disease: benefits and possible risks. *Can J Appl Physiol* 29:800–807
- Serrat-Serrat J, Ordonez-Llanos J, Serra-Grima R, Gomez-Gerique JA, Pellicer-Thoma E, Payes-Romero A, Gonzalez-Sastre F (1993) Marathon runners presented lower serum cholesteryl ester transfer activity than sedentary subjects. *Atherosclerosis* 101: 43–49
- Skinner ER, Watt C, Maughan RJ (1987) The acute effect of marathon running on plasma lipoproteins in female subjects. *Eur J Appl Physiol Occup Physiol* 56:451–456
- Mohlenkamp S, Lehmann N, Breuckmann F, Brocker-Preuss M, Nassenstein K, Halle M, Budde T, Mann K, Barkhausen J, Heusch G, Jockel KH, Erbel R (2008) Running: the risk of coronary events: Prevalence and prognostic relevance of coronary atherosclerosis in marathon runners. *Eur Heart J* 29:1903–1910
- Mathur N, Pedersen BK (2008) Exercise as a mean to control low-grade systemic inflammation. *Mediators Inflamm* 2008: 109502
- Pedersen BK, Febbraio MA (2008) Muscle as an endocrine organ: focus on muscle-derived interleukin-6. *Physiol Rev* 88:1379–1406
- Landi F, Russo A, Cesari M, Pahor M, Bernabei R, Onder G (2007) HDL-cholesterol and physical performance: results from the ageing and longevity study in the Sirente geographic area (iSIRENTE Study). *Age Ageing* 36:514–520
- Khera AV, Cuchel M, de la Llera-Moya M, Rodrigues A, Burke MF, Jafri K, French BC, Phillips JA, Mucksavage ML, Wilensky RL, Mohler ER, Rothblat GH, Rader DJ (2011) Cholesterol efflux capacity, high-density lipoprotein function, and atherosclerosis. *N Engl J Med* 364:127–135
- Heinecke J (2011) HDL and cardiovascular-disease risk—time for a new approach? *N Engl J Med* 364:170–171
- von Eckardstein A, Nofer JR, Assmann G (2001) High density lipoproteins and arteriosclerosis. Role of cholesterol efflux and reverse cholesterol transport. *Arterioscler Thromb Vasc Biol* 21:13–27
- Meyers CD, Kashyap ML (2004) Pharmacologic elevation of high-density lipoproteins: recent insights on mechanism of action and atherosclerosis protection. *Curr Opin Cardiol* 19:366–373
- Wang M, Briggs MR (2004) HDL: the metabolism, function, and therapeutic importance. *Chem Rev* 104:119–137
- Kontush A, Chapman MJ (2011) Antiatherogenic function of HDL particle subpopulations: focus on antioxidative activities. *Curr Opin Lipidol* 21:312–318
- Tall A (1995) Plasma lipid transfer proteins. *Annu Rev Biochem* 64:235–257
- Chapman MJ, Le Goff W, Guerin M, Kontush A (2011) Cholesteryl ester transfer protein: at the heart of the action of lipid-modulating therapy with statins, fibrates, niacin, and cholesteryl ester transfer protein inhibitors. *Eur Heart J* 31:149–164
- Maranhao RC, Roland IA, Hirata MH (1990) Effects of Triton WR 1339 and heparin on the transfer of surface lipids from triglyceride-rich emulsions to high density lipoproteins in rats. *Lipids* 25:701–705
- Maranhao RC, Cesar TB, Pedroso-Mariani SR, Hirata MH, Mesquita CH (1993) Metabolic behavior in rats of a nonprotein microemulsion resembling low-density lipoprotein. *Lipids* 28:691–696
- Friedewald WT, Levy RI, Fredrickson DS (1972) Estimation of the concentration of low-density lipoprotein cholesterol in plasma, without use of the preparative ultracentrifuge. *Clin Chem* 18:499–502
- Ginsburg GS, Small DM, Atkinson D (1982) Microemulsions of phospholipids and cholesterol esters. Protein-free models of low density lipoprotein. *J Biol Chem* 257:8216–8227

25. Lo Prete AC, Dina CH, Azevedo CH, Puk CG, Lopes NH, Hueb WA, Maranhao RC (2009) In vitro simultaneous transfer of lipids to HDL in coronary artery disease and in statin treatment. *Lipids* 44:917–924
26. Kratz A, Lewandrowski KB, Siegel AJ, Chun KY, Flood JG, Van Cott EM, Lee-Lewandrowski E (2002) Effect of marathon running on hematologic and biochemical laboratory parameters, including cardiac markers. *Am J Clin Pathol* 118:856–863
27. Durstine JL, Grandjean PW, Cox CA, Thompson PD (2002) Lipids, lipoproteins, and exercise. *J Cardiopulm Rehabil* 22:385–398
28. Mackinnon LT, Hubinger LM (1999) Effects of exercise on lipoprotein(a). *Sports Med* 28:11–24
29. Angelopoulos TJ, Sivo SA, Kyriazis GA, Caplan JD, Zoeller RF, Lowndes J, Seip RL, Thompson PD (2007) Do age and baseline LDL cholesterol levels determine the effect of regular exercise on plasma lipoprotein cholesterol and apolipoprotein B levels? *Eur J Appl Physiol* 101:621–628
30. Graham TE (2004) Exercise, postprandial triacylglyceridemia, and cardiovascular disease risk. *Can J Appl Physiol* 29:781–799
31. Lamou-Fava S, McNamara JR, Farber HW, Hill NS, Schaefer EJ (1989) Acute changes in lipid, lipoprotein, apolipoprotein, and low-density lipoprotein particle size after an endurance triathlon. *Metabolism* 38:921–925
32. Skinner ER, Black D, Maughan RJ (1985) Variability in the response of different male subjects to the effect of marathon running on the increase in plasma high density lipoprotein. *Eur J Appl Physiol Occup Physiol* 54:488–493
33. Wu HJ, Chen KT, Shee BW, Chang HC, Huang YJ, Yang RS (2004) Effects of 24 h ultra-marathon on biochemical and hematological parameters. *World J Gastroenterol* 10:2711–2714
34. Tzotzas T, Desrumaux C, Lagrost L (2009) Plasma phospholipid transfer protein (PLTP): review of an emerging cardiometabolic risk factor. *Obes Rev* 10:403–411
35. Chatterjee C, Sparks DL (2011) Hepatic lipase, high density lipoproteins, and hypertriglyceridemia. *Am J Pathol* 178:1429–1433
36. Azevedo CH, Wajngarten M, Prete AC, Diament J, Maranhao RC (2011) Simultaneous transfer of cholesterol, triglycerides, and phospholipids to high-density lipoprotein in aging subjects with or without coronary artery disease. *Clinics (Sao Paulo)* 66:1543–1548
37. Maranhao RC, Freitas FR, Strunz CM, Santos RD, Mansur AJ, Mansur AP (2011) Lipid transfers to HDL are predictors of precocious clinical coronary heart disease. *Clin Chim Acta* 413:502–505
38. Goodyear LJ, Van Houten DR, Fronsoe MS, Rocchio ML, Dover EV, Durstine JL (1990) Immediate and delayed effects of marathon running on lipids and lipoproteins in women. *Med Sci Sports Exerc* 22:588–592
39. Foger B, Wohlfarter T, Ritsch A, Lechleitner M, Miller CH, Dienstl A, Patsch JR (1994) Kinetics of lipids, apolipoproteins, and cholesteryl ester transfer protein in plasma after a bicycle marathon. *Metabolism* 43:633–639
40. Goncalves RP, Hungria VT, Chiattono CS, Pozzi DB, Maranhao RC (2003) Metabolism of chylomicron-like emulsions in patients with Hodgkin's and with non-Hodgkin's lymphoma. *Leuk Res* 27:147–153
41. Rubin DA, Hackney AC (2010) Inflammatory cytokines and metabolic risk factors during growth and maturation: influence of physical activity. *Med Sport Sci* 55:43–55
42. Szostak J, Laurant P (2011) The forgotten face of regular physical exercise: a 'natural' anti-atherogenic activity. *Clin Sci (Lond)* 121:91–106
43. Pedersen BK, Steensberg A, Schjerling P (2001) Exercise and interleukin-6. *Curr Opin Hematol* 8:137–141
44. Nieman DC, Henson DA, Smith LL, Utter AC, Vinci DM, Davis JM, Kaminsky DE, Shute M (2001) Cytokine changes after a marathon race. *J Appl Physiol* 91:109–114
45. Eder K, Baffy N, Falus A, Fulop AK (2009) The major inflammatory mediator interleukin-6 and obesity. *Inflamm Res* 58:727–736
46. Yudkin JS, Kumari M, Humphries SE, Mohamed-Ali V (2000) Inflammation, obesity, stress and coronary heart disease: is interleukin-6 the link? *Atherosclerosis* 148:209–214
47. Morisset AS, Huot C, Legare D, Tchernof A (2008) Circulating IL-6 concentrations and abdominal adipocyte isoproterenol-stimulated lipolysis in women. *Obesity (Silver Spring)* 16:1487–1492
48. Nomura K, Noguchi Y, Yoshikawa T, Kondo J (1997) Plasma interleukin-6 is not a mediator of changes in lipoprotein lipase activity in cancer patients. *Hepatogastroenterology* 44:1519–1526
49. Wu G, Brouckaert P, Olivecrona T (2004) Rapid downregulation of adipose tissue lipoprotein lipase activity on food deprivation: evidence that TNF-alpha is involved. *Am J Physiol Endocrinol Metab* 286:E711–E717
50. Kern PA, Saghizadeh M, Ong JM, Bosch RJ, Deem R, Simsolo RB (1995) The expression of tumor necrosis factor in human adipose tissue. Regulation by obesity, weight loss, and relationship to lipoprotein lipase. *J Clin Invest* 95:2111–2119
51. Seip RL, Moulin P, Coker T, Tall A, Kohrt WM, Mankowitz K, Semenovich CF, Ostlund R, Schonfeld G (1993) Exercise training decreases plasma cholesteryl ester transfer protein. *Arterioscler Thromb* 13:1359–1367
52. Cheung MC, Brown BG, Marino Larsen EK, Frutkin AD, O'Brien KD, Albers JJ (2006) Phospholipid transfer protein activity is associated with inflammatory markers in patients with cardiovascular disease. *Biochim Biophys Acta* 1762:131–137
53. Jahangiri A (2010) High-density lipoprotein and the acute phase response. *Curr Opin Endocrinol Diabetes Obes* 17:156–160
54. Navab M, Berliner JA, Subbanagounder G, Hama S, Lusis AJ, Castellani LW, Reddy S, Shih D, Shi W, Watson AD, Van Lenten BJ, Vora D, Fogelman AM (2001) HDL and the inflammatory response induced by LDL-derived oxidized phospholipids. *Arterioscler Thromb Vasc Biol* 21:481–488
55. Navab M, Anantharamaiah GM, Reddy ST, Van Lenten BJ, Fogelman AM (2009) HDL as a biomarker, potential therapeutic target, and therapy. *Diabetes* 58:2711–2717
56. Van Lenten BJ, Wagner AC, Navab M, Fogelman AM (2001) Oxidized phospholipids induce changes in hepatic paraoxonase and ApoJ but not monocyte chemoattractant protein-1 via interleukin-6. *J Biol Chem* 276:1923–1929
57. Magkos F, Wright DC, Patterson BW, Mohammed BS, Mittenborfer B (2006) Lipid metabolism response to a single, prolonged bout of endurance exercise in healthy young men. *Am J Physiol Endocrinol Metab* 290:E355–E362

8-[2-(2-Pentyl-Cyclopropylmethyl)-Cyclopropyl]-Octanoic Acid and Its Diastereomers Improve Age-Related Cognitive Deterioration

Takeshi Kanno · Takahiro Yaguchi ·
Tadashi Shimizu · Akito Tanaka · Tomoyuki Nishizaki

Received: 9 January 2012 / Accepted: 23 April 2012 / Published online: 15 May 2012
© AOCS 2012

Abstract Racemic 8-[2-(2-pentyl-cyclopropylmethyl)-cyclopropyl]-octanoic acid (DCP-LA), a linoleic acid derivative with cyclopropane rings instead of *cis*-double bonds, contains possible four diastereomers such as α,α -, α,β -, β,α -, and β,β -DCP-LA. The present study examined the effect of racemic and diastereomeric DCP-LA on age-related learning and memory disorders using accelerated-senescence-prone mice 8 (SAMP8) and accelerated-senescence-resistant mice 1 (SAMR1). In the water maze test, the acquisition and retention latencies for SAMP8 mice were significantly longer than the latency for SAMR1 mice, indicating spatial learning and memory impairment for SAMP8 mice. All the racemic (1 mg/kg, *per os*) and diastereomeric DCP-LA (0.25 mg/kg, *per os*) significantly shortened the acquisition latency for SAMP8 mice, and racemic, α,α - and α,β -DCP-LA significantly shortened the retention latency, with the advantage greater than the acetylcholine (ACh) esterase inhibitor galanthamine. The results of the present study show that all the racemic and diastereomeric DCP-LA, has the potential to improve age-related learning and memory deterioration, the potential varying among them.

Keywords DCP-LA · Diastereomer · Learning and memory decline · Aging · SAMP8 mice

Abbreviations

DCP-LA	8-[2-(2-Pentyl-cyclopropylmethyl)-cyclopropyl]-octanoic acid
ACh	Acetylcholine
PKC	Protein kinase C
GABA	γ -Aminobutyric acid
CaMKII	Ca ²⁺ /Calmodulin-dependent protein kinase II
PP1	Protein phosphatase-1
AMPA	α -Amino-3-hydroxy-5-methyl-4-isoxazole propionic acid
LTP	Long-term potentiation
SAMP8	Accelerated-senescence-prone mice 8
SAMR1	Accelerated-senescence-resistant mice 1
PEG	Polyethylene glycol
<i>Per os</i>	Oral administration

Introduction

We have synthesized the linoleic acid derivative with cyclopropane rings instead of *cis*-double bonds, 8-[2-(2-pentyl-cyclopropylmethyl)-cyclopropyl]-octanoic acid (DCP-LA), for the purpose of developing an anti-dementia drug [1]. DCP-LA serves as a selective and direct activator of protein kinase C (PKC)- ϵ [2]. DCP-LA stimulates glutamate release from presynaptic terminals in a PKC- and presynaptic $\alpha 7$ ACh receptor-dependent manner, thereby leading to a long-lasting facilitation of hippocampal synaptic transmission [3]. DCP-LA, alternatively, still stimulates the release of γ -aminobutyric acid (GABA) from hippocampal interneurons by targeting $\alpha 7$ ACh receptors under the control of PKC [4]. Moreover, DCP-LA activates Ca²⁺/calmodulin-dependent protein kinase II (CaMKII) by

T. Kanno · T. Yaguchi · T. Nishizaki (✉)
Division of Bioinformation, Department of Physiology,
Hyogo College of Medicine, 1-1 Mukogawa-cho,
Nishinomiya 663-8501, Japan
e-mail: tomoyuki@hyo-med.ac.jp

T. Shimizu · A. Tanaka
Laboratory of Chemical Biology, Advanced Medicinal Research
Center, Hyogo University of Health Sciences, Kobe, Japan

inhibiting protein phosphatase-1 (PP-1), to promote exocytosis of the α -amino-3-hydroxy-5-methyl-4-isoxazole propionic acid (AMPA) receptor subunits GluR1 and GluR2, resulting in the increased membrane surface localization of AMPA receptors on postsynaptic cells in the hippocampus [5]. This DCP-LA action also contributes to facilitation of hippocampal synaptic transmission. DCP-LA improves spatial learning and memory impairment induced by intraperitoneal injection with scopolamine or intraventricular injection with amyloid β_{1-40} peptide and age-related cognitive decline [6, 7]. Additionally, DCP-LA neutralizes and improves impairment of long-term potentiation (LTP), a cellular model of learning and memory, in the in-vivo hippocampus and spatial learning deficits, that are induced by a considerably low dose of mutant amyloid β_{1-42} peptide lacking glutamate-22 [8].

So far, we have carried out those experiments using racemic modification of DCP-LA. Racemic DCP-LA consists of at least four diastereomers such as α,α -, α,β -, β,α -, and β,β -DCP-LA. To assess characteristics of each diastereomer, we have separately synthesized DCP-LA diastereomers (Fig. 1). α,β -DCP-LA selectively and directly activated PKC- ϵ and stimulated release of transmitters such as glutamate, dopamine, and serotonin from rat hippocampal slices in a PKC- and $\alpha 7$ ACh receptor-dependent manner, with the highest potency among four diastereomers [9].

The present study was conducted to assess the effect of racemic and diastereomeric DCP-LA on age-related learning and memory impairment using accelerated-senescence-prone mice 8 (SAMP8), that reveal early onset and irreversible advancement of senescence, and accelerated-senescence-resistant mice 1 (SAMR1) with normal aging [10], and to compare the potential for DCP-LA to improve learning and memory decline with that for galanthamine, an ACh esterase inhibitor, that has been developed as an anti-dementia drug and is now available for treatment of Alzheimer's dementia. We show here that all the racemic and diastereomeric DCP-LA could ameliorate age-related learning and memory deterioration, with the beneficial effect being greater than with galanthamine.

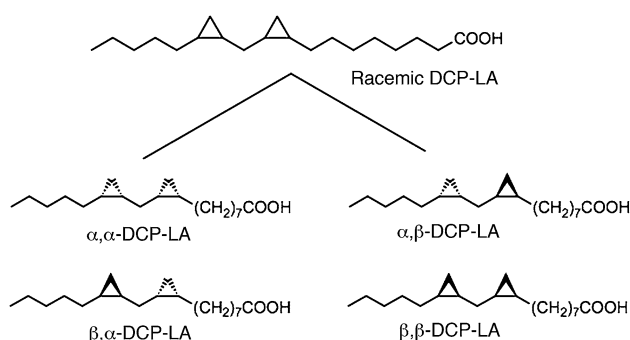


Fig. 1 Structures of racemic and diastereomeric DCP-LA

Materials and Methods

Animal Care

All procedures have been approved by the animal care and use committee at Hyogo College of Medicine and were in compliance with the National Institutes of Health Guide for the Care and Use of Laboratory Animals.

Animals

Animal preparation: male SAMP8 and SAMR1 mice (age, 22–25 weeks) were obtained from Takeda Pharmaceutical Co. (Osaka, Japan). Mice were individually housed in cages at 23 ± 1 °C, with a 12-h light/dark cycle (light phase beginning at 7:00 a.m.), and had free access to pellet food and water. All the tests here were carried out between 9:00 a.m. and 5:00 p.m.

Construction of Racemic and Diastereomeric DCP-LA

Racemic and diastereomeric DCP-LA were constructed by the method described previously [9]. We previously examined the effect of racemic DCP-LA on synaptic transmission in the in-vivo rat hippocampus at doses ranging from 0.01 to 1 mg/kg, where the most beneficial effect was obtained with intraperitoneal injection with 1 mg/kg of racemic DCP-LA. Racemic DCP-LA contains each diastereomer at the ratio of 1:1:1:1. We, therefore, administered racemic DCP-LA at a dose of 1 mg/kg and each diastereomer at a dose of 0.25 mg/kg to mice in the present experiments.

Administration with DCP-LA or Galanthamine

DCP-LA and galanthamine were dissolved with polyethylene glycol (PEG). Racemic DCP-LA, each diastereomeric DCP-LA, galanthamine, or PEG was directly administered by an oral sonde (*per os*) 1 h prior to each behavioral trial.

Open Field Test

Open field box, that is a cube constructed of 30×30 cm plastic plate, covered with a wooden box to shut out light, was prepared for an open field test. The open-field arena was illuminated at 110 lx by an incandescent lamp fixed on the roof of the box. To avoid outer noise, a fan, producing a noise of 45 dB, was fixed on the wall of the box. Two infrared beams ran from two walls 2 cm above the floor with a 10 cm interval, making cross stripes in parallel with the floor. Numbers to break the beams were regarded as locomotion activity. Twelve infrared beams, on the other

hand, ran 4.5 cm above the floor with a 2.5-cm interval. Numbers to break the beams were regarded as rearing activity. Mice were allowed to move freely in the open-field arena. The test was performed under the light conditions for 10 min. The initial half time of the test was performed under the light conditions, and the latter half time of the test under the dark conditions.

Water Maze Test

A circular plastic water tank 90 cm in diameter and 36 cm deep was used for a water maze test. The entire inside of the pool was painted black, and the pool was filled up to 20 cm from the bottom with murky water containing Indian ink at 22 °C. A platform (11 cm in diameter) painted black was placed in the water, the top sinking 0.5 cm below the water surface. The pool was put in a test room, where there were several marks that mice were able to see from the pool. The position of the marks remained unchanged throughout testing. A platform was located in the constant position, i.e., in the middle of one quadrant, equidistant from the center and edge of the pool. Mice facing the wall of the pool were placed into water at one of five positions selected at random, and time from start to escape onto the platform (acquisition latency) was measured. When they had succeeded, mice were allowed to stay on the platform for 10 s. When mice failed to find the platform within 90 s, the trial was stopped and mice were put on the platform for 10 s. Two trials were carried out a day, and the second trial began 2 min after the end of the first trial. Mice received the task for consecutive 8 days, and the mean latency from 2 consecutive days was calculated. Seven days later, the platform was removed and the retention latency (time from the start to arrival to the place where the platform had been set, 30 s in maximum) was measured.

Passive Avoidance Test

A two-compartment step-through passive avoidance apparatus; a front illuminated chamber (10 × 10 cm floor and a wall height of 20 cm) and a rear dark chamber (10 × 10 cm floor and a wall height of 20 cm) was used for a passive avoidance test. Each chamber was separated by a guillotine door and grids were attached on both the floors. When mice entered the dark chamber, the guillotine door was locked and in turn, electrical stimulation of 0.36 mA for 3 s was applied to their feet, thereafter leaving mice in the chamber for 30 s. Mice were initially put in the light chamber, and moving time from the light chamber to the dark chamber was measured as acquisition latency. The same trial was tested 24 h later, and staying time in the light chamber (maximum, 300 s) was measured as retention latency.

Statistical Analysis

The same mice were used throughout open field test, water maze test, and passive avoidance test. Statistical analysis was carried out using Dunnett's test, analysis of variance (ANOVA), Fisher's Protected Least Significant Difference (PLSD) test, and unpaired *t* test.

Results

Effects of DCP-LA and Galanthamine on Motor Activity

In the open field test to assess motor activity, locomotion and rearing activities under the light conditions for SAMP8 mice significantly increased as compared with the activities for SAMR1 mice ($P = 0.010$ and 0.020 , respectively, unpaired *t* test), while there was no significant difference in the those activities under the dark conditions between SAMP8 and SAMR1 mice (Table 1). This accounts for higher motor activity for SAMP8 mice under the light conditions.

For SAMR1 and SAMP8 mice, racemic DCP-LA (1 mg/kg, *per os*), each diastereomeric DCP-LA (0.25 mg/kg, *per os*), or galanthamine (2.5 mg/kg, *per os*) had no effect on locomotion and rearing activities both under the light and dark conditions as compared with those activities for control mice with PEG administration (Table 1). The locomotion activity for SAMR1 and SAMP8 mice with galanthamine was significantly lower than that for SAMR1 mice with α,β -DCP-LA under the dark conditions ($P = 0.042$, Dunnett's test) or for SAMP8 mice with α,β -DCP-LA under the light conditions ($P = 0.038$, Dunnett's test) and β,β -DCP-LA under the dark conditions ($P = 0.012$, Dunnett's test, Table 1). Moreover, the rearing activity for SAMR1 and SAMP8 mice with galanthamine was significantly lower than that for SAMR1 mice with β,α -DCP-LA under the light ($P = 0.029$, Dunnett's test) and dark conditions ($P = 0.018$, Dunnett's test) or for SAMP8 mice with racemic ($P = 0.009$, Dunnett's test), α,α - ($P = 0.006$, Dunnett's test), β,α - ($P = 0.036$, Dunnett's test), and β,β -DCP-LA under the dark conditions ($P = 0.034$, Dunnett's test, Table 1). Collectively, galanthamine might tend to reduce motor activities, with the potential greater than at least some types of DCP-LA, although galanthamine or DCP-LA does not significantly influence basal motor activities.

Effects of DCP-LA and Galanthamine on Spatial Learning and Memory

To assess spatial learning and memory, water maze test was carried out. There was significant difference in the

Table 1 Motor activity

Locomotion	SAMR1		SAMP8	
	Light	Dark	Light	Dark
	#			
Control	51 ± 18	67 ± 11	125 ± 13	69 ± 13
Racemic DCP-LA	49 ± 16	47 ± 17	100 ± 11	62 ± 16
α,α -DCP-LA	39 ± 7	41 ± 8	138 ± 19	56 ± 6
α,β -DCP-LA	36 ± 4	44 ± 5	133 ± 14	66 ± 28
β,α -DCP-LA	46 ± 6	56 ± 16	124 ± 20	75 ± 13
β,β -DCP-LA	43 ± 1 *	28 ± 6	103 ± 10 *	92 ± 12
Galanthamine	29 ± 9	25 ± 6	93 ± 11	49 ± 12 *
	#			
	Light	Dark	Light	Dark
Control	104 ± 23	171 ± 32	179 ± 12	207 ± 37
Racemic DCP-LA	119 ± 19	182 ± 37	144 ± 21	213 ± 16
α,α -DCP-LA	70 ± 19	121 ± 31	185 ± 12	245 ± 12 **
α,β -DCP-LA	96 ± 10	181 ± 27	179 ± 10	220 ± 40 **
β,α -DCP-LA	119 ± 9	297 ± 26	202 ± 68	229 ± 34
β,β -DCP-LA	96 ± 17 *	230 ± 41 *	154 ± 8	220 ± 32 *
Galanthamine	71 ± 16	172 ± 43	221 ± 45	145 ± 13 *

$P < 0.05$, unpaired t test;
 * $P < 0.05$, ** $P < 0.01$,
 Dunnett's test; Each $N = 5$
 mice

acquisition latency between SAMR1 and SAMP8 groups in the ANOVA test, and the latency for SAMP8 mice was significantly prolonged as compared with the latency for SAMR1 mice (Fisher's PLSD test, Fig. 2a). In addition, the retention latency for SAMP8 mice was also significantly longer than the latency for SAMR1 mice (unpaired t test, Fig. 2b). These findings confirm age-related spatial learning and memory impairment for SAMP8 mice.

For SAMR1 mice, β,β -DCP-LA (0.25 mg/kg, *per os*) significantly shortened the acquisition latency (ANOVA followed by Fisher's PLSD test), while racemic DCP-LA (1 mg/kg, *per os*), the remaining DCP-LA diastereomers (0.25 mg/kg, *per os*), or galanthamine (2.5 mg/kg, *per os*) had no effect (Fig. 3a). This suggests that β,β -DCP-LA could serve as a learning enhancer for normal subjects. In contrast, the retention latency for SAMR1 mice was not affected by any DCP-LA or galanthamine (Fig. 3b).

For SAMP8 mice, all the racemic (1 mg/kg, *per os*) and diastereomeric DCP-LA (0.25 mg/kg, *per os*) significantly shortened the acquisition latency as compared with control mice with PEG administration (ANOVA followed by Fisher's PLSD test), but galanthamine (2.5 mg/kg, *per os*) otherwise exhibited no beneficial effect (Fig. 4a). Notably, a significant difference in the acquisition latency for SAMP8 mice was obtained between DCP-LA group and galanthamine group (ANOVA). All the racemic, α,α -, α,β -, β,α -, and β,β -DCP-LA significantly shortened the acquisition latency for SAMP8 mice, with $P = 0.022$ for racemic DCP-LA group and $P < 0.001$ for each diastereomeric DCP-LA group as compared with the latency for galanthamine group (Fig. 4a).

For SAMP8 mice, racemic (1 mg/kg, *per os*), α,α - (0.25 mg/kg, *per os*), and α,β -DCP-LA (0.25 mg/kg, *per os*) significantly shortened the retention latency (Dunnett's

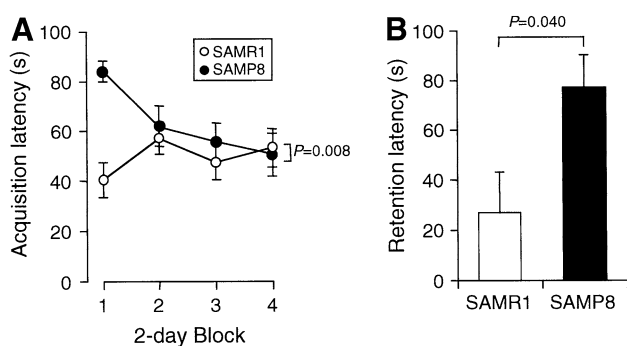


Fig. 2 Spatial learning and memory for SAMR1 and SAMP8 mice. The water maze test was carried out in SAMR1 and SAMP8 mice 1 h after oral administration with 0.1 ml of PEG. **a** Acquisition latency. In the graph, each point represents the mean (\pm SEM) latency from a 2-day block ($n = 5$ mice). *P* value, Fisher's PLSD test. **b** Retention latency. In the graph, each column represents the mean (\pm SEM) latency ($n = 5$ mice). *P* value, unpaired *t* test

test) as compared with control mice with PEG, but no significant effect was found with the remaining diastereomeric DCP-LA (0.25 mg/kg, *per os*) and galanthamine (2.5 mg/kg, *per os*, Fig. 4b). The retention latency for SAMP8 mice with racemic or α,α -DCP-LA was significantly shorter than the latency for mice with galanthamine (Dunnett's test, Fig. 4b). Taken together, these results indicate that all the racemic and diastereomeric DCP-LA could ameliorate spatial learning and memory deterioration for SAMP8 mice, the potential varying among them, with the advantage of efficacy greater than galanthamine.

Effects of DCP-LA and Galanthamine on Anxiety Behavior

In the passive avoidance test to assess anxiety behavior, the acquisition and retention latencies for SAMP8 mice was significantly shorter than the latencies for SAMR1 mice ($P = 0.046$ and $P = 0.033$, respectively unpaired *t* test, Table 2). This suggests lowered anxiety for SAMP8 mice.

Subsequently, the passive avoidance test was carried out in SAMR1 and SAMP8 mice after oral administration with PEG, racemic DCP-LA (1 mg/kg), each diastereomeric DCP-LA (0.25 mg/kg), or galanthamine (2.5 mg/kg). There was no significant difference in the latencies between control with PEG and any group with racemic DCP-LA, each diastereomeric DCP-LA, or galanthamine (Table 2). This indicates that all the DCP-LA and galanthamine have no effect on anxiety behavior.

The acquisition latency for SAMP8 mice with α,α - (0.25 mg/kg, *per os*) and α,β -DCP-LA (0.25 mg/kg, *per os*), however, was significantly longer than the latency for mice with galanthamine (2.5 mg/kg, *per os*; $P = 0.036$ and 0.009, respectively, Dunnett's test; Table 2). Moreover, the

retention latency for SAMP8 mice with β,α -DCP-LA (0.25 mg/kg, *per os*) was also significantly longer than the latency for mice with galanthamine (2.5 mg/kg, *per os*; $P = 0.040$, Dunnett's test; Table 2). Overall, galanthamine might tend to enhance age-related anxiety, to a extent greater than at least some types of DCP-LA.

Discussion

Racemic DCP-LA contains four possible diastereomers, and we have established roots for selective optical resolution from racemic DCP-LA and succeeded in synthesizing four diastereomers, namely α,α -, α,β -, β,α -, and β,β -DCP-LA [9]. Each individual diastereomer might exhibit unexpected effects distinct from racemic DCP-LA, as is the case with thalidomide that had been developed as a hypnotic; of two enantiomers such as (*S*)- and (*R*)-form. The (*S*)-form of thalidomide caused the serious side-effect teratogenesis [11]. Accordingly, it is very critical to check the characteristics of each DCP-LA diastereomer.

In the water maze test, the acquisition and retention latencies for SAMP8 mice were significantly longer than the latencies for SAMR1 mice, indicating age-related spatial learning and memory impairment for SAMP8 mice. For SAMP8 mice, all the racemic and diastereomeric DCP-LA significantly shortened the acquisition latency and further, racemic, α,α -, and α,β -DCP-LA significantly shortened the retention latency as compared with the latencies for control mice with PEG, although the potentials varied depending upon DCP-LA types. This implies that racemic and diastereomeric DCP-LA could improve age-related learning and memory deterioration. Interestingly, β,β -DCP-LA significantly shortened the acquisition latency still for SAMR1 mice, while it did not affect the retention latency. This suggests that β,β -DCP-LA could enhance learning ability for normal subjects too.

In the open field test, locomotion and rearing activities under the light conditions for SAMP8 mice significantly increased as compared with the activities for SAMR1 mice, indicating higher motor activities for SAMP8 mice. Racemic and diastereomeric DCP-LA had no remarkable effect on locomotion and rearing activities under both the light and dark conditions for SAMP8 and SAMR1 mice. This interprets that improvement of spatial learning and memory disorder for SAMP8 mice induced by racemic and diastereomeric DCP-LA is not due to alterations of motor activities for SAMP8 mice. Moreover, we had earlier confirmed that eyesight for SAMP8 and SAMR1 mice functions normally [7]. This indicates that improvement of spatial learning and memory disorder for SAMP8 mice induced by racemic and diastereomeric DCP-LA is not due to alterations to the eyesight of SAMP8 mice.

Fig. 3 Effects of DCP-LA and galanthamine on spatial learning and memory for SAMR1 mice. Water maze test was carried out in SAMR1 mice 1 h after oral administration with 0.1 ml of PEG alone, racemic DCP-LA (1 mg/kg), each diastereomeric DCP-LA (0.25 mg/kg), or galanthamine (2.5 mg/kg). **a** Acquisition latency. In the graphs, each point represents the mean (\pm SEM) latency from a 2-day block ($n = 5$ mice). P values, Fisher's PLSD test. **b** Retention latency. In the graph, each column represents the mean (\pm SEM) latency ($n = 5$ mice)

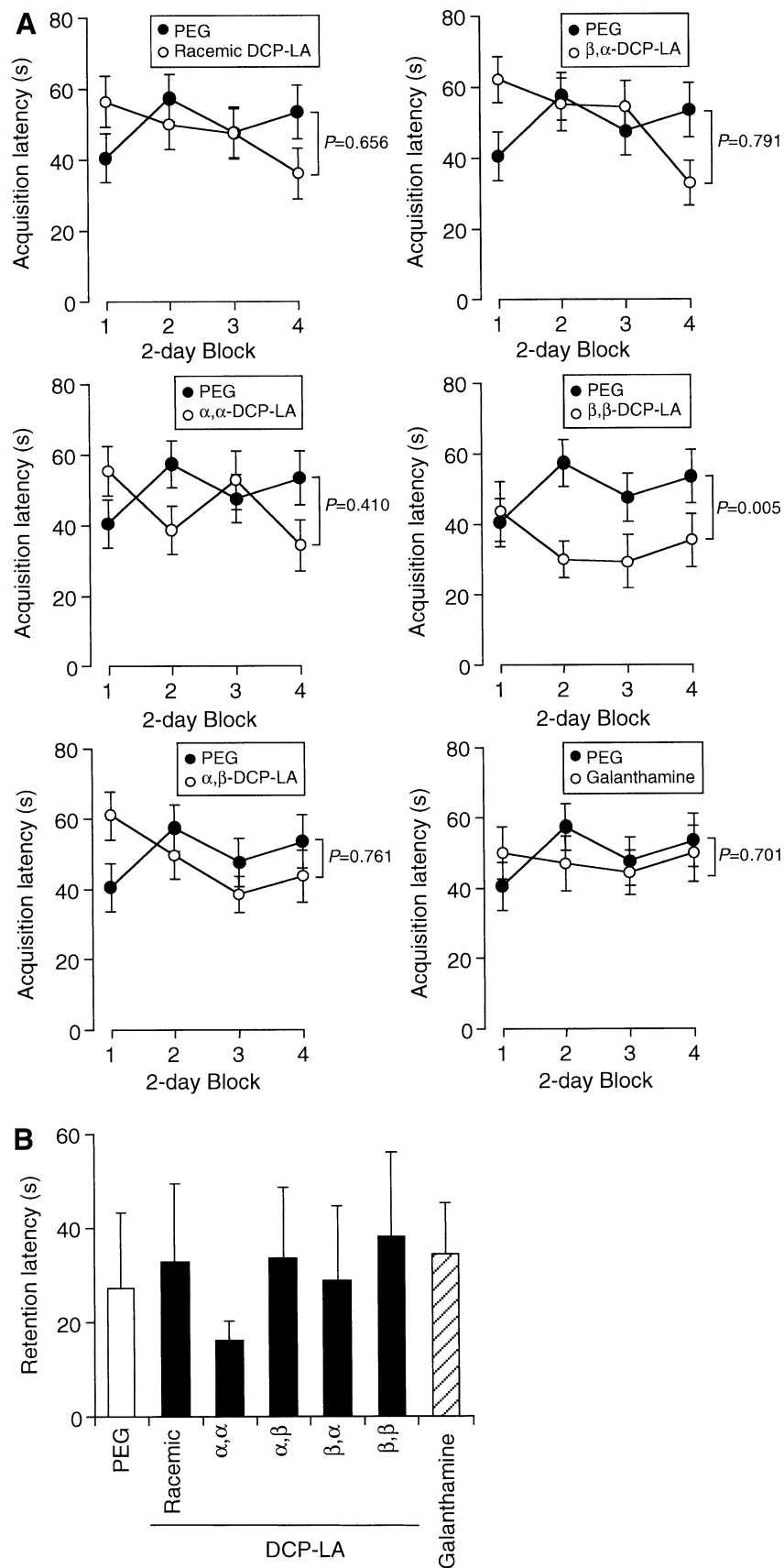


Fig. 4 Effects of DCP-LA and galanthamine on spatial learning and memory for SAMP8 mice. The water maze test was carried out in SAMP8 mice 1 h after oral administration with 0.1 ml of PEG alone, racemic DCP-LA (1 mg/kg), each diastereomeric DCP-LA (0.25 mg/kg), or galanthamine (2.5 mg/kg). **a** Acquisition latency. In the graphs, each point represents the mean (\pm SEM) latency from a 2-day block ($n = 5$ mice). P values, Fisher's PLSD test. **b** Retention latency. In the graph, each column represents the mean (\pm SEM) latency ($n = 5$ mice). P values, Dunnett's test

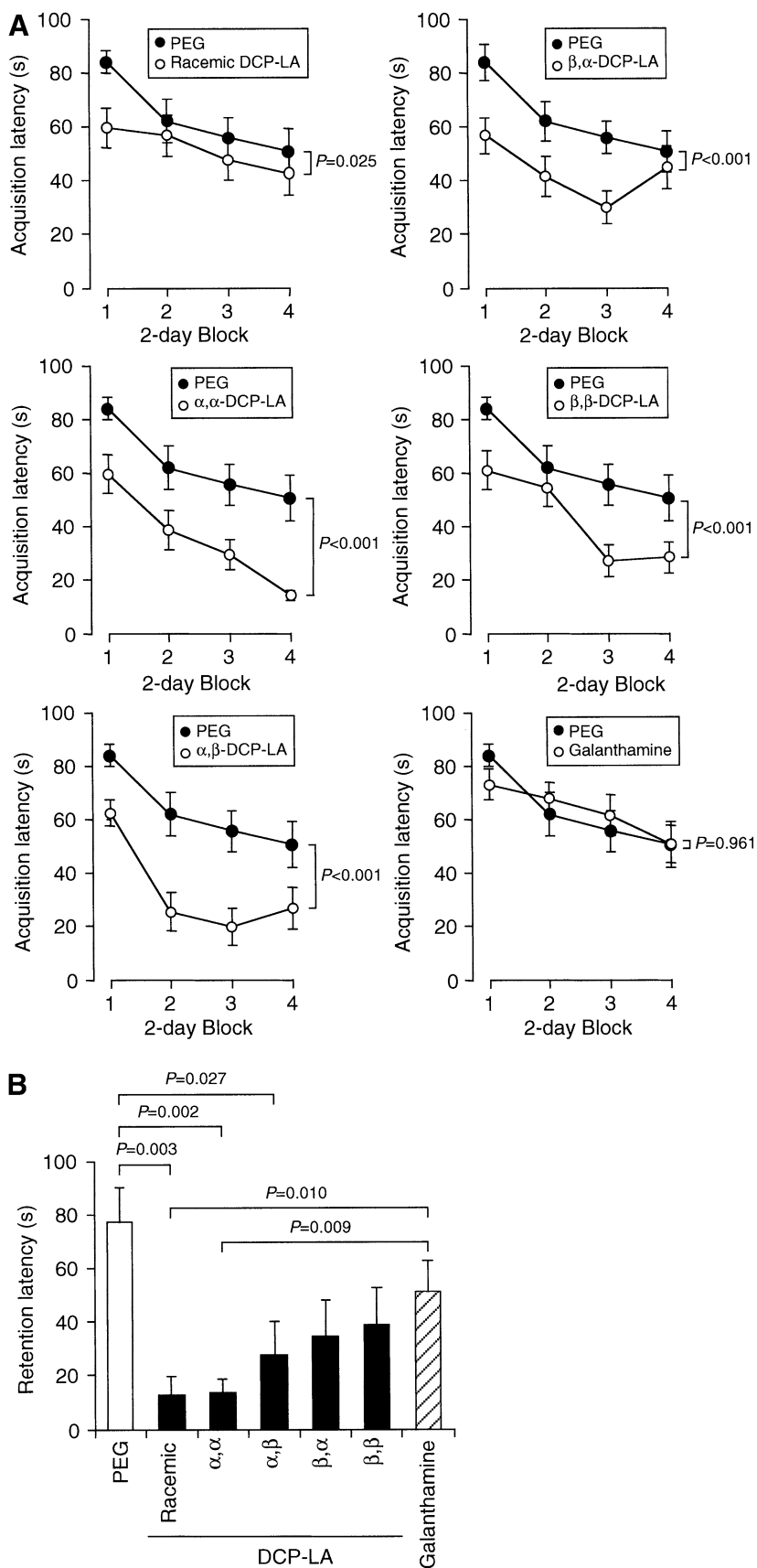


Table 2 Anxiety behavior

	SAMR1	SAMP8
Acquisition (s)		
	#	
Control	21 ± 2	14 ± 2
Racemic DCP-LA	16 ± 3	13 ± 2
α,α -DCP-LA	32 ± 10	16 ± 2
α,β -DCP-LA	20 ± 4	18 ± 1
β,α -DCP-LA	15 ± 3	16 ± 3
β,β -DCP-LA	18 ± 2	10 ± 1
Galanthamine	23 ± 7	9 ± 1
Retention (s)		
	#	
Control	188 ± 62	26 ± 10
Racemic DCP-LA	241 ± 59	23 ± 7
α,α -DCP-LA	209 ± 63	23 ± 7
α,β -DCP-LA	185 ± 70	24 ± 7
β,α -DCP-LA	300<	36 ± 15
β,β -DCP-LA	228 ± 64	68 ± 36
Galanthamine	193 ± 55	13 ± 2

$P < 0.05$, unpaired t test;
 * $P < 0.05$, ** $P < 0.01$,
 Dunnett's test; Each $N = 5$
 mice

In the passive avoidance test, the acquisition and retention latencies for SAMP8 mice was significantly shorter than the latencies for SAMR1 mice, indicating reduced anxiety for SAMP8 mice. Racemic and diastereomeric DCP-LA had no significant effect on the acquisition and retention latencies for SAMP8 mice. This explains that improvement in spatial learning and memory disorder for SAMP8 mice induced by racemic and diastereomeric DCP-LA is not related to alterations in the anxiety behavior of SAMP8 mice.

Galanthamine, an inhibitor of acetylcholine esterase, is considered to be a promising drug for treatment with Alzheimer's dementia and it is now available clinically for its treatment [12, 13]. No beneficial effect of galanthamine

on age-related learning and memory impairment, however, was obtained here. In contrast, racemic and diastereomeric DCP-LA significantly shortened the acquisition and retention latencies for SAMP8 mice more than galanthamine. This suggests that DCP-LA has the potential to ameliorate age-related learning and memory deterioration, with the advantage of efficacy greater than galanthamine.

The sites of action for DCP-LA are absolutely different to those for galanthamine. In explanation for the anti-dementia action, galanthamine increases ACh concentrations in the synaptic cleft by preventing ACh hydrolysis, thereby facilitating cholinergic transmissions, with no selectivity on G protein-linked muscarinic ACh receptors or nicotinic ACh receptors including $\alpha 7$ ACh receptors.

One of the major action sites for DCP-LA is PKC- ϵ , that is enriched in the presynaptic terminals. DCP-LA increases glutamate release from presynaptic terminals by targeting presynaptic $\alpha 7$ ACh receptors through selective activation of PKC- ϵ , leading to a long-lasting facilitation of hippocampal synaptic transmission [1–3, 9]. This could account for DCP-LA-induced improvement of spatial learning and memory disorders in a variety of animal models, as previously shown [6–8], and again in the present study. Surprisingly, racemic and diastereomeric DCP-LA stimulate the release of not only glutamate but dopamine and serotonin in a PKC- and $\alpha 7$ ACh receptor-dependent manner, although the potential varies depending on the DCP-LA types [9]. This raises the possibility that DCP-LA could have beneficial effects on a variety of forms of dementia including Alzheimer disease, neurodegenerative diseases such as Parkinson disease and diffuse Lewy body disease, extrapyramidal disorders, and psychiatric impairments such as depression, panic disorder, and mental irritation, which are caused by a reduction in or a deficiency of dopamine or serotonin. To address these points, we are currently carrying out further behavioral experiments using different animal models.

In conclusion, the results of the present study show that all the racemic and diastereomeric DCP-LA could ameliorate age-related learning and memory decline, with a beneficial efficacy greater than galanthamine.

References

1. Tanaka A, Nishizaki T (2003) The newly synthesized linoleic acid derivative FR236924 induces a long-lasting facilitation of hippocampal neurotransmission by targeting nicotinic acetylcholine receptors. *Bioorg Med Chem Lett* 13:1037–1040
2. Kanno T, Yamamoto H, Yaguchi T, Hi R, Mukasa T, Fujikawa H, Nagata T, Yamamoto S, Tanaka A, Nishizaki T (2006) The linoleic acid derivative DCP-LA selectively activates PKC- ϵ , possibly binding to the phosphatidylserine binding site. *J Lipid Res* 47:1146–1156
3. Yamamoto S, Kanno T, Nagata T, Yaguchi T, Tanaka A, Nishizaki T (2005) The linoleic acid derivative FR236924 facilitates hippocampal synaptic transmission by enhancing activity of presynaptic $\alpha 7$ acetylcholine receptors on the glutamatergic terminals. *Neuroscience* 130:207–213
4. Kanno T, Yaguchi T, Yamamoto S, Yamamoto H, Fujikawa H, Nagata T, Tanaka A, Nishizaki T (2005) 8-[2-(2-Pentyl-cyclopropylmethyl)-cyclopropyl]-octanoic acid stimulates GABA release from interneurons projecting to CA1 pyramidal neurons in the rat hippocampus via pre-synaptic $\alpha 7$ acetylcholine receptors. *J Neurochem* 95:695–702
5. Kanno T, Yaguchi T, Nagata T, Tanaka A, Nishizaki T (2009) DCP-LA stimulates AMPA receptor exocytosis through CaMKII activation due to PP-1 inhibition. *J Cell Physiol* 221:183–188
6. Nagata T, Yamamoto S, Yaguchi T, Iso H, Tanaka A, Nishizaki T (2005) The newly synthesized linoleic acid derivative DCP-LA ameliorates memory deficits in animal models treated with amyloid- β peptide and scopolamine. *Psychogeriatrics* 5:122–126
7. Yaguchi T, Nagata T, Mukasa T, Fujikawa H, Yamamoto H, Yamamoto S, Iso H, Tanaka A, Nishizaki T (2006) Linoleic acid derivative DCP-LA improves learning impairment in SAMP8. *Neuroreport* 17:105–108
8. Nagata T, Tomiyama T, Mori H, Yaguchi T, Nishizaki T (2009) DCP-LA neutralizes mutant amyloid β peptide-induced impairment of long-term potentiation and spatial learning. *Behav Brain Res* 206:151–154
9. Shimizu T, Kanno T, Tanaka A, Nishizaki T (2011) α, β -DCP-LA selectively activates PKC- ϵ and stimulates neurotransmitter release with the highest potency among 4 diastereomers. *Cell Physiol Biochem* 27:149–158
10. Takeda T, Hosokawa M, Higuchi K (1991) Senescence-accelerated mouse (SAM): a novel murine model of accelerated senescence. *J Am Geriatr Soc* 39:911–919
11. Blaschke G, Kraft HP, Fickentscher K, Köhler F (1979) Chromatographische Racemattrennung von Thalidomid und Teratogene Wirkung der Enantiomere. *Arzneimittelforschung* 29:1640–1642
12. Salomone S, Caraci F, Leggio GM, Fedotova J, Drago F (2011) New pharmacological strategies for treatment of Alzheimer's disease: focus on disease-modifying drugs. *Br J Clin Pharmacol*. doi:10.1111/j.1365-2125.2011.04134.x
13. Wu TY, Chen CP, Jinn TR (2010) Alzheimer's disease: aging, insomnia and epigenetics. *Taiwan J Obstet Gynecol* 49:468–472

Partially Hydrolyzed Guar Gums Reduce Dietary Fatty Acid and Sterol Absorption in Guinea Pigs Independent of Viscosity

Jonathan Santas · Jordi Espadaler ·
Jordi Cuñé · Magda Rafecas

Received: 15 December 2011 / Accepted: 15 May 2012 / Published online: 6 June 2012
© AOCS 2012

Abstract This study investigated the effect of two partially hydrolyzed guar gums (PHGG) on fatty acid and sterol excretion. PHGG were obtained by chemical hydrolysis of guar gum (GG) with H₂O:EtOH (1:1) at 100 °C for 1 h (PHGG1) or 2 h (PHGG2). The viscosity of the PHGG in a 1 % (w/v) aqueous solution corresponded to that of a pseudoplastic fluid and was higher for PHGG1 than PHGG2. Guinea pigs (*n* = 8 per group) were fed high fat diets (17/100 g) that contained 12/100 g of cellulose, PHGG1, or PHGG2 for 4 weeks. Despite the differences in viscosity, the two PHGG exerted similar physiological effects. Compared to the control cellulose group, the body weight gain was lower in animals fed PHGG, although no effect on food consumption was observed. PHGG increased the excretion of fatty acids and neutral sterols, but not bile acids. Consumption of PHGG did not alter the fecal fatty acid profile, while intestinal bioconversion of sterols tended to increase in response to PHGG2. A reduction in the viscosity within the range tested did not correlate with losses in the hypocholesterolemic capacity of PHGG as both were effective in reducing plasma cholesterol. Thus, we conclude that the chemical hydrolysis of guar gum renders the gum suitable for inclusion in food products without significantly altering its beneficial health effects.

Keywords Dietary fiber · Partially hydrolyzed guar gum · Fatty acids · Cholesterol · Bile acids

Abbreviations

BA	Bile acid(s)
CA	Cholic acid
CDCA	Chenodeoxycholic acid
CE	Cellulose
DCA	Deoxycholic acid
FA	Fatty acid(s)
FAME	Fatty acid methyl ester(s)
FID	Flame ionization detector
GG	Guar gum
LCA	Lithocholic acid
LDL	Low density lipoprotein
MUFA	Monounsaturated fatty acid(s)
NS	Neutral sterol(s)
PHGG	Partially hydrolyzed guar gum
PHGG1	Partially hydrolyzed guar gum for 1 h
PHGG2	Partially hydrolyzed guar gum for 2 h
PUFA	Polyunsaturated fatty acid(s)
SEM	Standard error of the mean
SFA	Saturated fatty acid(s)
TSFA	Total saturated fatty acids
TUFA	Total unsaturated fatty acids
UDCA	Ursodeoxycholic acid
UFA	Unsaturated fatty acid(s)

Introduction

Guar gum (GG) is a natural polysaccharide that consists of a (1 → 4)- α -D-mannopyranose backbone with single units of linked α -D-galactopyranose. Given its hypolipidemic and hypoglycemic effects, this gum is considered one of the most promising water-soluble dietary fibers [1, 2]. There is

J. Santas · M. Rafecas (✉)
Department of Nutrition and Food Science, XaRTA-INSA,
University of Barcelona, 08028 Barcelona, Spain
e-mail: magdarafecas@ub.edu

J. Santas · J. Espadaler · J. Cuñé
AB-Biotics, S.A., Parc Tecnològic del Vallès,
08290 Cerdanyola del Vallès, Spain

strong evidence that GG decreases the incidence of factor risks associated with cardiovascular diseases, such as high levels of plasma triglycerides and cholesterol, mainly LDL-cholesterol [2, 3]. The hypolipidemic effects of this gum are attributed to its capacity to decrease the absorption of dietary fat and cholesterol, reduce bile acid reabsorption in the small intestine, and produce short chain fatty acids by partial fermentation in the cecum [4, 5].

GG is widely known for its water-soluble characteristics and viscosity [4, 6]. In manufactured or processed foods, gums are commonly used as thickeners and emulsifiers. However, the high viscosity of GG may limit its use at physiologically effective concentrations in some food products [7]. Partial hydrolysis has recently been reported to improve the inclusion of this gum in food products and increase consumer acceptance [8]. For instance, Sunfiber® is a PHGG product that is commercially available and has GRAS status (Generally Recognized As Safe) in the USA [7]. The viscosity of enzymatically hydrolyzed GG can be as low as 10 mPa s in a 5 % aqueous solution, while that of commercially available GG is about 2,000–3,000 mPa s in a 1 % aqueous solution [7]. Nevertheless, it has been reported that the health benefits of partially hydrolyzed GG (PHGG) are similar to those of intact GG [7, 9]. Therefore, it has been proposed that the health benefits of PHGG do not appear to be exclusively dependent on its molecular weight or viscosity and that hypolipidemic mechanisms other than viscosity may be involved [8].

Various studies have reported the capacity of dietary fiber to reduce fat absorption. However, dietary fat exerts a range of effects on lipid metabolism depending on its sterol and fatty acid composition [10]. In general, *trans* fatty acids and most saturated fatty acids (SFA) are considered hyperlipidemic. For instance, lauric (C12:0), myristic (C14:0) and palmitic (C16:0) acids increase the plasma concentration of LDL-cholesterol mainly by decreasing the activity of its receptors in the liver [11]. In contrast to SFA, monounsaturated (MUFA) and polyunsaturated fatty acids (PUFA) decrease LDL-cholesterol by a series of mechanisms, such as enhancing the hepatic uptake of LDL particles or the activity of 7 α -hydroxylase [12]. To our knowledge, only a few studies have addressed the effect of functional ingredients on the absorption of individual fatty acids. Interestingly, some of these ingredients exert selective fat-binding capacity, thereby affecting plasma and liver lipid profiles [13, 14]. Given all these considerations, the study of the effect of dietary fiber on each fatty acid is relevant.

Here, we examined the effect of chemically hydrolyzed guar gum on lipid excretion in order to provide new insights into its hypolipidemic mechanism. The effect of PHGG on fat excretion was studied longitudinally and an exhaustive analysis of fecal sterols and fatty acids was

conducted to assess the effect of fiber on fat excretion over time. For this purpose, we used the guinea pig as it is widely accepted as a more reliable model of human lipid metabolism than other more commonly used animals, such as mice or rats, and because, in contrast to hamsters, guinea pigs do not ferment fiber in their stomachs [15].

Materials and Methods

Materials

Fatty acid methyl ester (FAME) standards were of 99 % or higher purity. Oleic acid (C18:1n-9), linolenic acid (C18:3n-3) and heneicosanoate acid (C21:0) were purchased from Larodan Fine Chemical AB (Malmö, Sweden). The remaining FAME standards, bile acids, Sylon BTZ (3:2:3, BSA + TMCS + TMSI) and anhydrous pyridine were from Sigma Chemical Co. (St. Louis, MO, USA). Sterol standards were supplied by Steraloids (Newport, Rhode Island, USA).

Sodium methylate 0.5 N was prepared by dissolving 17 g of sodium in 1 L of dry methanol. *N*-hexane and boron trifluoride (20 % in anhydrous methanol) were purchased from Merck (Darmstadt, Germany). Sodium chloride and anhydrous sodium sulfate were from Panreac (Barcelona, Spain) whereas chloroform, cyclohexane, methanol, ethanol and diethyl ether were purchased from Scharlau Chemie S.A. (Sentmenat, Spain). All solvents and reagents were of analytical grade or higher and double distilled water was used throughout the study.

Production of PHGG

PHGG was obtained by chemical hydrolysis of natural GG from *Cyamopsis tetragonoloba*. The hydrolysis was conducted in a reactor vessel with H₂O:EtOH (1:1) at 100 °C, 4 bar and constant magnetic stirring at 700 rpm. GG was added into the pre-warmed reactor at a concentration of 15 % (w/v) and hydrolyzed for either 1 h (PHGG1) or 2 h (PHGG2). After hydrolysis, the reactor vessel was allowed to cool to 50 °C and samples were passed through a filter plate of porosity No. 2 (40–100 μ m, Vidrafoc, S.A., Barcelona, Spain). The residue was subsequently washed twice with 100 mL of EtOH 95 % and allowed to dry for 5 h at 40 °C in a vacuum oven.

Determination of Viscosity and Rheological Properties of PHGG

The viscosity of 1 % aqueous dispersions of PHGG was determined using a First RM Rheometer from Lamy Rheometers (Champagne au Mont d'Or, France). Homogeneous

polymer dispersions were prepared by sprinkling a given amount of product into deionised water at 40 °C with vigorous magnetic stirring (1,000 rpm). After 1 h of incubation, the preparations were sonicated at 40 °C for 10 min and finally allowed to stand at room temperature for 4 h. The viscoelastic properties of the PHGG dispersions were determined in the same day at 25 °C at shear rates ranging from 1 to 250 s⁻¹.

Diets

Three isocaloric diets were obtained by adding experimental fiber sources (12/100 g of diet) to a non-fiber basal diet prepared by Teklan Harlan (Madison, WI, USA) (Table 1). The fiber used for the control group was cellulose (CE) (Teklan Harlan, Madison, WI, USA) while PHGG1 and PHGG2 were used for the experimental

Table 1 Composition of diets fed to guinea pigs

Component	CE (g/100 g)	PHGG1 (g/100 g)	PHGG2 (g/100 g)	Energy ^a (%)
Protein	18.1	18.1	18.1	18.0
Fat mix ^b	16.9	16.9	16.9	37.9
Sugars ^c	44.3	44.3	44.3	44.1
Mineral mix ^d	4.6	4.6	4.6	
Vitamin mix ^c	1.0	1.0	1.0	
Cellulose	12.0			
Guar gum 1 h		12.0		
Guar gum 2 h			12.0	

CE cellulose, PHGG1 partially hydrolyzed guar gum (1-h hydrolysis), PHGG2 partially hydrolyzed guar gum (2-h hydrolysis)

^a Percentage of energy provided for each nutrient in the experimental diets, being the same for each experimental diet

^b Fat mix contained olive oil/palm kernel oil/safflower oil (1:2:1.8)

^c Added as cornstarch/sucrose (1:1.43)

^d Mineral and vitamin mix were adjusted to meet National Research Council requirements for guinea pigs. Mineral mix composition (g/100 g): calcium phosphate 38.7, potassium acetate 29.9, calcium carbonate 9.2, magnesium oxide 9.2, potassium chloride 7.4, sodium chloride 3.7, ferric citrate 1.1, manganese sulfate, monohydrate 0.6, zinc carbonate 0.203, cupric sulfate 0.055, potassium iodate 0.002, chromium potassium sulfate, dodecahydrate 0.018, sodium selenite, pentahydrate 0.002, ammonium paramolybdate, tetrahydrate 0.006. Vitamin mix composition (g/100 g): *p*-aminobenzoic acid 1.10, vitamin-C (ascorbic acid) 10.17, biotin 0.004, vitamin B₁₂ (0.1 % in mannitol) 0.30, calcium pantothenate 0.66, choline dihydrogen citrate 34.97, folic acid 0.02, inositol 1.10, vitamin K₃ (menadione) 0.50, pyridoxine HCl 0.99, niacin 0.22, riboflavin 0.22, thiamin HCl 0.22, vitamin A: palmitate (500,000 IU g⁻¹) 0.40, vitamin D₃: cholecalciferol (500,000 IU g⁻¹) 0.04, vitamin E: DL-alpha tocopheryl acetate (500 IU g⁻¹) 2.42, corn starch 46.67

Table 2 Fatty acid and sterol composition of diets fed to guinea pigs

	CE (mg/g)	PHGG1 (mg/g)	PHGG2 (mg/g)
Fatty acids			
C12:0	28.55 ± 1.48	26.99 ± 0.41	28.49 ± 0.53
C14:0	10.20 ± 0.50	9.77 ± 0.11	10.11 ± 0.18
C16:0	14.25 ± 0.70	13.64 ± 0.13	14.19 ± 0.24
C17:0	0.12 ± 0.00	0.11 ± 0.00	0.11 ± 0.00
C18:0	14.20 ± 0.72	13.56 ± 0.09	14.32 ± 0.26
C20:0	0.52 ± 0.02	0.50 ± 0.00	0.51 ± 0.01
C22:0	0.43 ± 0.02	0.41 ± 0.01	0.42 ± 0.01
C24:0	0.28 ± 0.02	0.25 ± 0.02	0.25 ± 0.01
TSFA	68.54 ± 3.44	65.24 ± 0.76	68.42 ± 1.13
C18:1n-9	19.93 ± 0.92	18.69 ± 0.12	19.19 ± 0.41
C18:1n-7	1.40 ± 0.06	1.33 ± 0.01	1.36 ± 0.03
MUFA	21.33 ± 0.97	20.02 ± 0.13	20.55 ± 0.43
C18:2n-6	64.89 ± 3.11	61.41 ± 0.54	63.58 ± 1.30
C18:3n-3	2.73 ± 0.13	2.58 ± 0.03	2.69 ± 0.05
PUFA	67.62 ± 3.24	63.99 ± 0.57	66.26 ± 1.36
TUFA	88.95 ± 4.20	84.01 ± 0.70	86.82 ± 1.78
TSFA/TUFA	0.77 ± 0.00	0.78 ± 0.00	0.79 ± 0.01
n-6/n-3	23.74 ± 0.03	23.80 ± 0.05	23.68 ± 0.03
Sterols (mg/100 g)			
Cholesterol	38.57 ± 0.02	38.35 ± 0.48	39.51 ± 0.76
Campesterol	8.85 ± 0.03	8.63 ± 0.24	7.86 ± 0.20
β-Sitosterol	21.18 ± 0.37	20.71 ± 0.43	21.37 ± 0.52
Sitostanol	6.11 ± 0.69	5.33 ± 0.43	4.20 ± 0.45

Results expressed as mean ± SEM for quadruplicated analysis. No statistical differences were found among treatments (*P* > 0.1)

CE cellulose, PHGG1 partially hydrolyzed guar gum (1-h hydrolysis), PHGG2 partially hydrolyzed guar gum (2-h hydrolysis), TSFA total saturated fatty acids, MUFA monounsaturated fatty acids, PUFA polyunsaturated fatty acids, TUFA total unsaturated fatty acids

groups. The fat mix content of diets was olive oil/palm-kernel oil/safflower oil (1:2:1.8). Detailed fatty acid and sterol composition of the diets are present in Table 2.

Animals

Female Dunkin-Hartley guinea pigs were supplied by Harlan Interfauna Ibérica (Barcelona, Spain). Animals weighing 300–400 g were randomly assigned to the treatment groups (8 animals/group) after 1 week of acclimation, when all animals were fed with control CE diet. Two guinea pigs were kept per stainless steel cage, which was wire-bottomed to avoid coprophagia. Animals were housed in a room with a controlled light-cycle (light from 0800 to 2000 hours) at 22 ± 1 °C for 4 weeks of treatment. Food and water were consumed ad libitum. Every 48 h, feces were collected, animals weighed and food consumption controlled. Feces were manually cleaned from sawdust contamination, weighed, homogenized, freeze-dried and

stored at $-20\text{ }^{\circ}\text{C}$. After isoflurane anesthesia, non-fasted guinea pigs were killed by heart puncture and blood samples were collected in heparinized tubes. Plasma was separated after centrifugation at $1,500\times g$ for 15 min at $4\text{ }^{\circ}\text{C}$ and stored at $-80\text{ }^{\circ}\text{C}$ until analysis. All procedures were approved by the Animal Care and Use Committee of the University of Barcelona.

Determination of Fatty Acid Content in Feces and Diets

Fatty acids (FA) of diets and feces were determined by gas chromatography. FAME were obtained directly from lyophilized samples by in situ basic–acidic derivatization as previously described [16]. Heneicosanoate acid (C21:0) was used as the internal standard.

Determination of Neutral Sterols and Bile Acids

Neutral sterols (NS) and bile acids (BA) were extracted as previously described by Keller et al. [17]. 5α -Cholestane and 23-nor-cholic acid were used as internal standards for NS and BA, respectively. Extracts were evaporated at $30\text{ }^{\circ}\text{C}$ under nitrogen flux, dried in a vacuum desiccator overnight and stored at $-20\text{ }^{\circ}\text{C}$ in a nitrogen atmosphere until silanization and injection. Silanization was carried out by dissolving the samples in an appropriate amount of anhydrous pyridine and adding an equal volume of Sylon BTZ. Samples were injected after silanization for 30 min at room temperature.

GC Conditions

The FAME were analyzed using an Agilent 4890D gas chromatograph, equipped with a flame ionization detector (FID). A split–splitless injector was used with a split ratio of 1:30 and the injection volume was $1\text{ }\mu\text{L}$. The injector and detector temperatures were kept at 270 and $300\text{ }^{\circ}\text{C}$, respectively. FAME were separated in a fused-silica capillary column ($60\text{ m}\times 0.25\text{ mm i.d.}, 0.2\text{ }\mu\text{m}$) from Supelco (Bellefonte, PA, USA). The oven temperature was programmed as follows: an initial temperature of $140\text{ }^{\circ}\text{C}$ for 3 min, followed by an increase of $6\text{ }^{\circ}\text{C min}^{-1}$ to $180\text{ }^{\circ}\text{C}$, then $2\text{ }^{\circ}\text{C min}^{-1}$ to $200\text{ }^{\circ}\text{C}$ and $7\text{ }^{\circ}\text{C min}^{-1}$ to $240\text{ }^{\circ}\text{C}$ and it was finally left to stand for 5 min at $240\text{ }^{\circ}\text{C}$. Helium was used as carrier gas and nitrogen as makeup gas to increase the sensitivity of the detector.

NS and BA were analyzed using a Perkin Elmer Auto-system gas chromatograph equipped with a FID. One microliter of sample and a split ratio of 1:12.5 were used for injection. The injector and detector temperatures were kept at 290 and $350\text{ }^{\circ}\text{C}$, respectively. NS and BA were separated with a 5 % polysilarylene–95 % polydimethylsiloxane capillary column ($60\text{ m}\times 0.25\text{ mm i.d.},$

$0.25\text{ }\mu\text{m}$) from Phenomenex (Torrance, CA, USA). Oven temperature was programmed with an initial temperature of $245\text{ }^{\circ}\text{C}$ during 30 s, a rate of $5\text{ }^{\circ}\text{C}$ until 290° and it was finally left to stand at this temperature for 30 min.

Chromatographic peaks were identified by comparing the retention times with those of known standards and by co-chromatography. FAME, NS and BA were quantified by the internal standard addition method and using calibration curves with $R^2 > 0.99$.

Determination of Plasma Lipids

Total cholesterol, HDL-chol, LDL-chol and triglycerides were enzymatically determined with a Modular DPE Hitachi auto-analyzer from Roche Diagnostics (Mannheim, Germany).

Statistical Analysis

Data were analyzed by SPSS v.17 for Windows. Significant differences between treatments were determined by one-way ANOVA and the exact nature of the differences between groups by Duncan's multirange test. Differences between initial and final values for each treatment were determined by the Student's *t* test after assessing equality of variances by Leven's test. Results are expressed as means \pm standard error (SEM). A confidence coefficient of 95 % was used.

Results

Viscosity Measurements

The flow curves of 1 % PHGG aqueous solutions at shear rates ranging from 1 to 250 s^{-1} are shown in Fig. 1. Viscosity of solutions at these rates ranged from 2,884 to 184 and from 1,720 to 110 mPa s for PHGG1 and PHGG2, respectively. The flow curves corresponded to pseudo-plastic fluids as the viscosity was dependent on shear rate, being lower at higher rates. The viscosity of PHGG dispersions was not time-dependent and showed neither thixotropic nor rheopectic behavior.

Body Weight and Food Consumption

All animals gained weight during the study, although the gain was significantly lower in the PHGG groups than the control (Table 3). However, food consumption was not affected by dietary fiber. This observation implies that food efficiency was reduced by PHGG ingestion. Food efficiency was slightly lower in animals fed PHGG1 than those on PHGG2, but differences were not statistically significant.

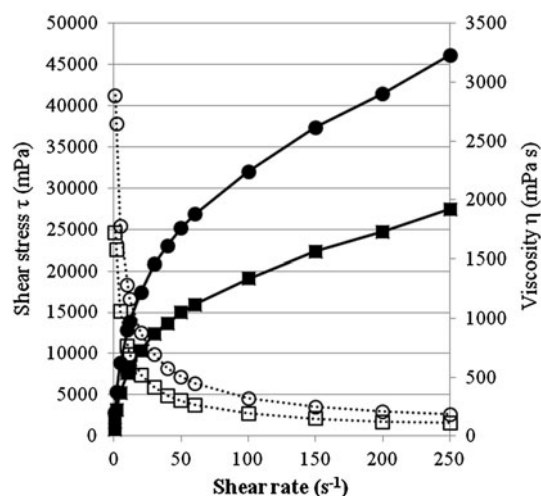


Fig. 1 Rheological measurements of PHGG dispersions. Values of shear stress (τ) at various shear rates are expressed in mPa for partially hydrolyzed guar gum (1-h hydrolysis) (filled circles) and partially hydrolyzed guar gum (2-h hydrolysis) (filled squares) in 1 % aqueous solution. Values of viscosity are expressed in mPa s for partially hydrolyzed guar gum (1-h hydrolysis) (open circles) and partially hydrolyzed (2-h hydrolysis) (open squares)

Fatty Acid Excretion

Fecal dry weight was not significantly altered by PHGG compared to CE during the study (Table 3). In contrast, FA concentration in feces of the PHGG groups was increased compared to the control group (Fig. 2). SFA and UFA concentration in feces were highly increased by PHGG during the first week of treatment. After this time, the concentration in feces tended to stabilize, although a continuous slight increment in SFA concentration in feces of all groups was observed.

Table 4 shows the concentration of fecal FA at the end of the experiment. SFA concentration in feces was higher than that of UFA. The results reveal a higher excretion of SFA, especially palmitic (C16:0) and stearic (C18:0) acids,

than of UFA. The concentration of all SFA was increased by PHGG1 and PHGG2 compared to CE. Among UFA, fecal MUFA were accounted for mainly by oleic acid (C18:1n-9), whereas linoleic acid (C18:2n-6) was the most abundant PUFA. As observed for SFA, the consumption of the PHGG increased the excretion of MUFA and PUFA. As a result, the FA profile as well as the TSFA/TUFA ratio in feces was not altered by PHGG. The same results were observed for the n-6/n-3 PUFA isomer ratio. In general, the effect of PHGG2 on FA excretion was slightly greater than that of PHGG1, although differences were not statistically significant.

NS Excretion

The concentration of fecal NS is shown in Table 5. The overall excretion was increased in all groups after 4 weeks on high fat diets. However, the increment in animals fed either PHGG1 or PHGG2 was higher than that of CE, reaching final values of 16.07 ± 0.41 , 17.98 ± 0.58 and 10.92 ± 0.73 mg of NS per animal and day for PHGG1, PHGG2 and CE, respectively. PHGG consumption increased the excretion of cholesterol, but especially the excretion of its major metabolic products. We calculated the coprostanol/cholesterol and the secondary metabolites of cholesterol/cholesterol ratios in order to assess the effect of experimental fibers on the intestinal bioconversion of cholesterol. No statistical differences for these parameters were found between treatments, although the bioconversion in feces of animals fed PHGG2 was slightly higher. No effect was observed on phytosterol excretion ($P > 0.05$).

BA Excretion

Fecal BA are shown in Table 6. Secondary BA were the most abundant BA in feces and were accounted for mainly by lithocholic acid. Total BA excretion was only slightly

Table 3 Body weight, food consumption and excretion

	<i>n</i>	CE	PHGG1	PHGG2
Initial body weight (g)	8	346.3 \pm 7.2	353.3 \pm 5.9	352.1 \pm 3.5
Final body weight (g)	8	445.8 \pm 11.4 ^a	392.1 \pm 16.7 ^b	402.5 \pm 13.4 ^b
Weight gain (g)	8	99.5 \pm 6.8 ^a	38.7 \pm 13.6 ^b	50.5 \pm 13.5 ^b
Food consumption (g animal ⁻¹ day ⁻¹)	4	27.5 \pm 1.2	27.6 \pm 1.1	28.2 \pm 1.6
Food efficiency (g of animal 100 g consumed ⁻¹) ^A	8	13.1 \pm 1.0 ^a	5.0 \pm 1.8 ^b	6.2 \pm 1.5 ^b
Initial fecal dry weight (g of feces animal ⁻¹ day ⁻¹)	4	2.0 \pm 0.5	2.7 \pm 0.3	2.2 \pm 0.7
Final fecal dry weight (g of feces animal ⁻¹ day ⁻¹)	4	1.9 \pm 0.4	2.3 \pm 0.7	2.7 \pm 0.3

Results are expressed as means \pm SEM. Results in the same row not sharing a common superscript are significantly different based on Duncan's multirange test at $P < 0.05$

CE cellulose, PHGG1 partially hydrolyzed guar gum (1-h hydrolysis), PHGG2 partially hydrolyzed guar gum (2-h hydrolysis)

^A Consumption was assumed to be equal for each animal in the same cage

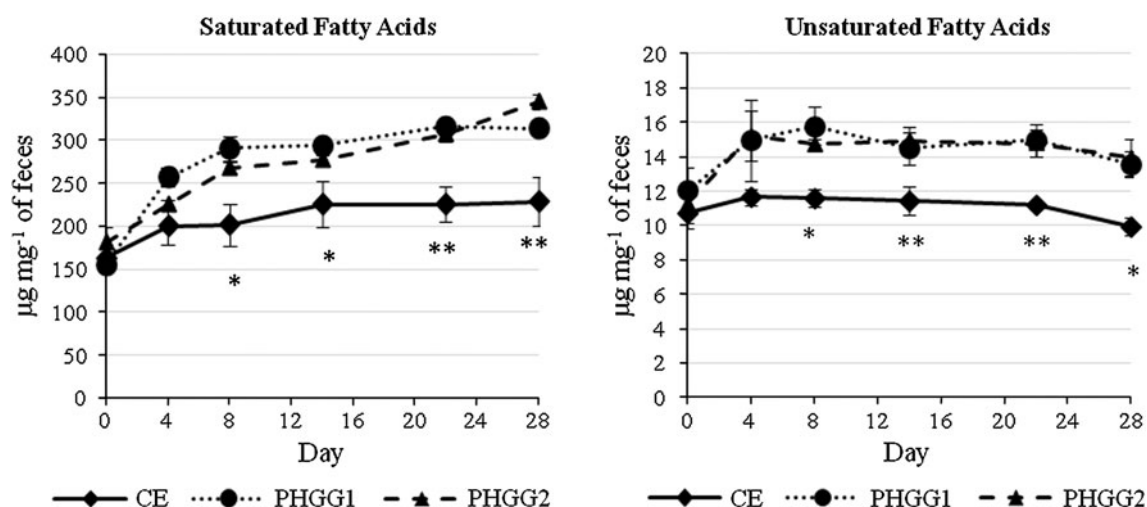


Fig. 2 Concentration of saturated and unsaturated fatty acids in feces during the study. Results are expressed as mean \pm SEM in mg of fatty acids per animal and day ($n = 4$). Differences between

treatments are denoted as * for $P < 0.05$ and ** for $P < 0.01$. CE cellulose, PHGG1 partially hydrolyzed guar gum (1-h hydrolysis), PHGG2 partially hydrolyzed guar gum (2-h hydrolysis)

Table 4 Fatty acid concentration in feces at the end of the treatment

	CE	PHGG1	PHGG2
C12:0	4.23 \pm 0.46 ^a	7.04 \pm 0.61 ^b	8.05 \pm 0.45 ^b
C14:0	8.76 \pm 1.12 ^a	13.31 \pm 1.08 ^b	15.66 \pm 1.18 ^b
C16:0	49.07 \pm 7.99 ^a	70.11 \pm 4.29 ^{ab}	84.05 \pm 8.50 ^b
C17:0	0.75 \pm 0.08 ^a	1.02 \pm 0.02 ^b	0.91 \pm 0.00 ^b
C18:0	159.59 \pm 20.37 ^a	214.99 \pm 3.14 ^b	229.28 \pm 3.99 ^b
C20:0	2.71 \pm 0.22	3.21 \pm 0.10	2.91 \pm 0.13
C22:0	2.18 \pm 0.09 ^a	2.53 \pm 0.06 ^b	2.36 \pm 0.07 ^{ab}
C24:0	1.55 \pm 0.08 ^a	1.82 \pm 0.05 ^b	1.69 \pm 0.05 ^{ab}
TSFA	228.84 \pm 28.57 ^a	314.02 \pm 3.10 ^b	344.91 \pm 8.76 ^b
C18:1n-9	3.99 \pm 0.22 ^a	4.76 \pm 0.36 ^{ab}	5.70 \pm 0.72 ^b
C18:1n-7	1.12 \pm 0.32	1.90 \pm 0.33	2.22 \pm 0.35
MUFA	5.11 \pm 0.51 ^a	6.66 \pm 0.50 ^{ab}	7.92 \pm 0.76 ^b
C18:2n-6	4.50 \pm 0.28 ^a	6.45 \pm 0.49 ^b	5.50 \pm 0.35 ^{ab}
C18:3n-3	0.34 \pm 0.04 ^a	0.47 \pm 0.03 ^b	0.54 \pm 0.03 ^b
PUFA	4.85 \pm 0.25 ^a	6.92 \pm 0.48 ^b	6.04 \pm 0.39 ^{ab}
TUFA	9.96 \pm 0.51 ^a	13.58 \pm 0.76 ^b	13.96 \pm 1.08 ^b
Total	238.78 \pm 28.90 ^a	327.60 \pm 2.84 ^b	358.85 \pm 7.73 ^b
TSFA/ TUFA	22.88 \pm 2.50	23.36 \pm 1.43	25.29 \pm 2.52
n-6/n-3	13.95 \pm 2.36	13.94 \pm 1.31	10.18 \pm 0.10

Results are expressed as means \pm SEM in μg of FA mg^{-1} of feces ($n = 4$). Results in the same row not sharing a common superscript are significantly different based on Duncan's Multirange test at $P < 0.05$

CE cellulose, PHGG1 partially hydrolyzed guar gum (1-h hydrolysis), PHGG2 partially hydrolyzed guar gum (2-h hydrolysis), TSFA total saturated fatty acids, MUFA monounsaturated fatty acids, PUFA polyunsaturated fatty acids, TUFA total unsaturated fatty acids

increased by PHGG1 compared to CE and PHGG2. This increase led to augmented chenodeoxycholic and lithocholic acid excretion. However, differences were not statistically significant. The bioconversion of chenodeoxycholic acid to its secondary metabolite lithocholic acid was increased in PHGG groups; however, this increment was statistically significant only for PHGG2 ($P < 0.029$).

Plasma Lipids

Plasma lipids at the end of the experiment are shown in Table 7. Plasma triglycerides were not significantly altered by PHGG compared to CE. In contrast, total plasma cholesterol was lower in PHGG groups, mainly due to a reduction in LDL cholesterol ($P < 0.05$). As a result, the HDL/LDL ratio was improved in animals fed PHGG diets.

Discussion

The physiological beneficial effects of GG are commonly attributed to its water-soluble and high viscosity characteristics [5, 6]. Several studies have reported that the gel-forming properties of GG reduce the rate of gastric emptying and increase satiation. These effects may decrease food consumption—advocated as the main mechanism responsible for a lower weight gain in animals fed GG [6, 18]. The viscosity of fluids is highly dependent on various factors, such as temperature, pH, pressure, shear rate and time. Given these influences, it is difficult to

Table 5 Excretion of neutral sterols

	CE	PHGG1	PHGG2
Cholesterol			
Initial	2.20 ± 0.23	2.80 ± 0.31	2.08 ± 0.19
Final	2.02 ± 0.31 ^a	3.56 ± 0.54 ^b	3.23 ± 0.49 ^{ab}
Coprostanol			
Initial	3.51 ± 0.39	4.52 ± 0.45	3.36 ± 0.60
Final	5.04 ± 0.91 ^a	7.40 ± 0.44 ^{b**}	9.78 ± 0.57 ^{c**}
Cholestanol			
Initial	1.02 ± 0.11	1.26 ± 0.14	0.94 ± 0.13
Final	1.11 ± 0.16 ^a	1.48 ± 0.06 ^b	1.76 ± 0.04 ^{b**}
Cholestanone			
Initial	0.97 ± 0.12	1.20 ± 0.11	1.01 ± 0.11
Final	1.25 ± 0.14 ^a	1.90 ± 0.24 ^{ab**}	2.01 ± 0.26 ^{b**}
β-Sitosterol			
Initial	1.11 ± 0.08	1.36 ± 0.11	1.09 ± 0.12
Final	1.16 ± 0.10	1.27 ± 0.10	0.83 ± 0.19
Sitostanol			
Initial	0.46 ± 0.03	0.55 ± 0.06	0.44 ± 0.05
Final	0.35 ± 0.13	0.47 ± 0.02	0.37 ± 0.12
Total sterols			
Initial	9.27 ± 0.80	11.68 ± 0.98	8.91 ± 1.07
Final	10.92 ± 0.73 ^a	16.07 ± 0.41 ^{b**}	17.98 ± 0.58 ^{c**}
Copr./chol.^A			
Initial	1.64 ± 0.22	1.66 ± 0.23	1.59 ± 0.15
Final	2.86 ± 0.84	2.33 ± 0.57	3.28 ± 0.59
Secd./chol.^B			
Initial	2.57 ± 0.35	2.56 ± 0.33	2.53 ± 0.17
Final	3.74 ± 1.09	3.34 ± 0.69	4.48 ± 0.68

Results are expressed as means ± SEM in mg of sterol animal⁻¹ day⁻¹ ($n = 4$). Results in the same row that do not share a common superscript are significantly different based on Duncan's multirange test at $P < 0.05$. Differences between initial and final values based on Student's t test are denoted as * for $P < 0.05$ or** for $P < 0.01$. Campesterol was found only in trace amounts

CE cellulose, PHGG1 partially hydrolyzed guar gum (1-h hydrolysis), PHGG2 partially hydrolyzed guar gum (2-h hydrolysis)

^A Ratio of coprostanol/cholesterol

^B Ratio of secondary metabolites of cholesterol (coprostanol, cholestanol and cholestanone)/cholesterol

compare data from studies that have applied distinct methodologies and conditions. It has been proposed that oral perception of fluid viscosity correlates well with the viscosity of the fluid at a shear rate of 10 s⁻¹ [19]. At this rate, the viscosity of PHGG was significantly different, registering 1,285 and 766 mPa s for PHGG1 and PHGG2, respectively. This difference can be attributed to the higher degree of hydrolysis of the latter. However, the viscosity of PHGG obtained by chemical hydrolysis appears to be considerably higher than that of enzymatically hydrolyzed GG, which has been published to be about 10 mPa s in 5 %

Table 6 Bile acid excretion

	CE	PHGG1	PHGG2
Primary			
CA			
Initial	tr	tr	tr
Final	tr	tr	tr
CDCA			
Initial	0.32 ± 0.12	0.44 ± 0.09	0.31 ± 0.12
Final	0.24 ± 0.07	0.39 ± 0.10	0.37 ± 0.07
Secondary			
DCA			
Initial	nd	nd	nd
Final	nd	nd	nd
LCA			
Initial	2.11 ± 0.62	2.58 ± 0.52	2.14 ± 1.00
Final	1.63 ± 0.43	2.87 ± 0.90	3.15 ± 0.50
UDCA			
Initial	1.05 ± 0.39	0.99 ± 0.13	1.00 ± 0.41
Final	0.53 ± 0.15	0.69 ± 0.15	0.66 ± 0.07
Total BA			
Initial	3.48 ± 1.13	4.00 ± 0.72	3.45 ± 1.53
Final	2.41 ± 0.51	3.96 ± 1.12	4.18 ± 0.63
LCA/CDCA			
Initial	8.04 ± 1.63	6.00 ± 0.54	6.12 ± 0.64
Final	7.16 ± 1.92	7.14 ± 0.99	8.79 ± 0.69*

Results are expressed as means ± SEM in mg of bile acid animal⁻¹ day⁻¹ ($n = 4$). No statistical differences were found between treatments ($P > 0.05$). * Differences between initial and final values based on Student's t test ($P < 0.01$)

CE cellulose, PHGG1 partially hydrolyzed guar gum (1-h hydrolysis), PHGG2 partially hydrolyzed guar gum (2-h hydrolysis), CA cholic acid, CDCA chenodeoxycholic acid, DCA deoxycholic acid, LCA lithocholic acid, UDCA ursodeoxycholic acid, Total BA total bile acids, nd not detected, tr traces

Table 7 Plasma lipids

	CE	PHGG1	PHGG2
Triglycerides	0.63 ± 0.07	0.63 ± 0.07	0.56 ± 0.08
Total cholesterol	2.59 ± 0.68 ^b	1.38 ± 0.20 ^a	0.93 ± 0.11 ^a
HDL-col	0.20 ± 0.06	0.15 ± 0.02	0.11 ± 0.01
LDL-col	2.68 ± 0.74 ^b	1.26 ± 0.19 ^a	0.89 ± 0.11 ^a
HDL/LDL	0.08 ± 0.01 ^a	0.13 ± 0.01 ^{ab}	0.14 ± 0.02 ^b

Results are expressed as means ± SEM in mmol L⁻¹ ($n = 8$). Results in the same row that do not share a common superscript are significantly different based on Duncan's multirange test at $P < 0.05$

CE cellulose, PHGG1 partially hydrolyzed guar gum (1-h hydrolysis), PHGG2 partially hydrolyzed guar gum (2-h hydrolysis)

aqueous solution [7]. Chemical hydrolysis of GG allowed us to compare the physiological benefits of two PHGG with distinct degrees of viscosity. The rheological experiments

of 1 % PHGG aqueous solutions revealed pseudoplastic (shear-thinning) behavior. Previous studies have reported similar findings for aqueous solutions of GG [20].

In our study, both PHGG reduced body weight gain to a similar extent. However, this decrease was not correlated with changes in food consumption, which is consistent with the findings of other studies [18]. A reduction in the absorption of nutrients and thus the calories they provide can be partially responsible for the lower food efficiency of diets containing PHGG.

In good agreement with previous reports, fat excretion was increased by ingestion of PHGG [21]. The longitudinal study of PHGG consumption reveals that the effect occurred from the beginning of the treatment and stabilized after 1 week. Therefore, no accumulative effect was observed after the first week.

As previously reported [13], the concentrations of medium and long chain SFA in feces, especially C16:0 and C18:0, were higher when compared to its concentration in diets. This finding is mainly attributed to the low digestibility of these FA [22]. The FA profile in feces was not altered by PHGG consumption in a similar way to other dietary fibers such as pectin [23] and in contrast to others such as hydroxypropyl methylcellulose [14].

Another hypocholesterolemic property commonly attributed to soluble dietary fiber is its capacity to increase the excretion of BA and endogenous and exogenous cholesterol. In vitro [8] and in vivo studies [24] have shown that PHGG conserves the capacity of the native GG to increase cholesterol excretion. In our study, NS excretion was greater after consumption of PHGG, mainly as a result of an increment in cholesterol metabolites such as coprostanol and cholestanol. Thus, the bioconversion of cholesterol tended to increase in animals ingesting PHGG2. Although it is widely accepted that GG increases BA excretion, thus decreasing its reabsorption [24, 25], controversial results have been reported for PHGG. Our results are consistent with the findings of Favier et al. [21], who reported that total BA excretion was not significantly altered by PHGG ingestion. However, as seen for NS, the consumption of PHGG2 increased the bioconversion of primary BA to their secondary metabolites. Similar results on BA bioconversion were observed by Gallaher et al. [26], who reported that the lithocholic/chenodeoxycholic ratio in feces of hamsters fed low viscosity GG was higher than that of animals on native GG. However, that study was performed in hamsters, which partially ferment GG in the pregastric pouch of the stomach [26] and have a distinct BA profile in feces to that of guinea pigs [27]. Our results show that this effect is also present in guinea pigs, a more suitable model for the study of lipid metabolism. GG and PHGG are partially fermented in the intestine, thus favoring increased endogenous bacterial population and activity

[28, 29]. For instance, the growth of intestinal bacteria such *Lactobacillus* spp. and *Bifidobacterium* spp. is enhanced in humans after PHGG consumption [30]. Hence, an increase in bacterial activity may result in greater sterol bioconversion. The lower viscosity of PHGG2 could explain its higher pre-biotic effect as it favors interaction with intestinal microbiota.

Based on these results, the increase in NS excretion appears to be one of the main mechanisms responsible for the lower total plasma cholesterol in animals fed PHGG diets. In addition, it is plausible that the fermentability of PHGG can contribute to its hypocholesterolemic effect due to the production of short chain fatty acids, mainly propionate, which can decrease the endogenous synthesis of cholesterol [29, 31].

On balance, within the degree of hydrolysis tested, a reduction in the viscosity of PHGG did not correlate with a loss of hypolipidemic capacity. Current evidence indicates that consumption of viscous fibers such as GG can alter the viscosity of digesta in the gastrointestinal tract and thereby decrease the bioaccessibility of fat and cholesterol [6, 26, 32]. Nevertheless, it remains questionable whether alterations on in vitro viscosity may result in proportional physiological responses [32, 33]. For instance, Gallaher et al. [32] observed that although only small increments in viscosity were necessary to decrease plasma cholesterol, further increments did not result in larger reductions of plasma cholesterol. In addition, it has been suggested that other mechanisms not attributed to viscosity can be complementarily responsible for the hypolipidemic effect of PHGG. The bioaccessibility of fat and cholesterol was previously studied by Minekus et al. [8] using a dynamic model of the gastrointestinal tract. The authors concluded that PHGG can also reduce lipid absorption by a depletion-flocculation mechanism, which is typical of polymers that do not show surface activity. Since the polysaccharide does not adsorb to the fat droplets, this can result in a region around the droplet where the concentration of the polysaccharide is lower than in the bulk solution. This phenomenon could cause an osmotic pressure that would favor the fat droplets flocculating and coalescing. As a result, it may reduce the emulsifying effect of bile acids and therefore the bioaccessibility of fat and cholesterol.

In conclusion, both PHGG reduced body weight gain and plasma cholesterol, regardless of their in vitro viscosity within the ranges tested. Thus, the chemical hydrolysis can improve the suitability of GG for use in food products without affecting their rheology or palatability and conserving most of its hypolipidemic properties.

Acknowledgments J. Santas was granted a Torres Quevedo fellowship. The authors thank A. Aldanondo, S. Scapucci and A. Gonciarz for their support during sample analysis.

References

- Ellis PR, Wang Q, Rayment P, Ren Y, Ross-Murphy S (2001) Guar gum. In: Handbook of Dietary Fiber. CRC Press, USA
- Butt MS, Shahzadi N, Sharif MK, Nasir M (2007) Guar gum: a miracle therapy for hypercholesterolemia, hyperglycemia and obesity. *Crit Rev Food Sci Nutr* 47(4):389–396
- Shahzadi N, Butt MS, Sharif MK, Nasir M (2007) Effect of guar gum on the serum lipid profile of Sprague Dawley rats. *LWT Food Sci Technol* 40(7):1198–1205
- Theuwissen E, Mensink RP (2008) Water-soluble dietary fibers and cardiovascular disease. *Physiol Behav* 94(2):285–292
- Gunness P, Gidley MJ (2010) Mechanisms underlying the cholesterol-lowering properties of soluble dietary fibre polysaccharides. *Food Funct* 1(2):149–155
- Dikeman CL, Fahey GC (2006) Viscosity as related to dietary fiber: a review. *Crit Rev Food Sci* 46(8):649–662
- Yoon S-, Chu D-, Juneja LR (2008) Chemical and physical properties, safety and application of partially hydrolyzed guar gum as dietary fiber. *J Clin Biochem Nutr* 42(1):1–7
- Minikus M, Jelier M, Xiao JZ, Kondo S, Iwatsuki K, Kokubo S, Bos M, Dunnewind B, Havenaar R (2005) Effect of partially hydrolyzed guar gum (PHGG) on the bioaccessibility of fat and cholesterol. *Biosci Biotechnol Biochem* 69(5):932–938
- Slavin JL, Greenberg NA (2003) Partially hydrolyzed guar gum: clinical nutrition uses. *Nutrition* 19(6):549–552
- Erkkila A, de Mello VDF, Riserus U, Laaksonen DE (2008) Dietary fatty acids and cardiovascular disease: an epidemiological approach. *Prog Lipid Res* 47(3):172–187
- Fernandez ML, West KL, Roy S, Ramjiganesh T (2001) Dietary fat saturation and gender/hormonal status modulate plasma lipids and lipoprotein composition. *J Nutr Biochem* 12(12):703–710
- Fernandez ML, West KL (2005) Mechanisms by which dietary fatty acids modulate plasma lipids. *J Nutr* 135(9):2075–2078
- Brufau G, Canela MA, Rafecas M (2006) A high-saturated fat diet enriched with phytosterol and pectin affects the fatty acid profile in guinea pigs. *Eur J Lipid Sci Tech* 41(2):159–168
- Yokoyama W, Anderson WHK, Albers DR, Hong Y-, Langhorst ML, Hung S-, Lin J-, Young SA (2011) Dietary hydroxypropyl methylcellulose increases excretion of saturated and *trans* fats by hamsters fed fast food diets. *J Agric Food Chem* 59(20):11249–11254
- Fernandez ML, Volek JS (2006) Guinea pigs: a suitable animal model to study lipoprotein metabolism, atherosclerosis and inflammation. *Nutr Metab* 3(17). doi:10.1186/1743-7075-3-17
- López-López A, Castellote-Bargalló AI, López-Sabater MC (2000) Comparison of two direct methods for the determination of fatty acids in infant feces. *Anal Biochem* 282(2):250–255
- Keller S, Jahreis G (2004) Determination of underivatized sterols and bile acid trimethyl silyl ether methyl esters by gas chromatography–mass spectrometry–single ion monitoring in faeces. *J Chromatogr B* 813(1–2):199–207
- Yamada K, Tokunaga Y, Ikeda A, Ohkura K-, Kaku-Ohkura S, Mamiya S, Beong OL, Tachibana H (2003) Effect of dietary fiber on the lipid metabolism and immune function of aged Sprague–Dawley rats. *Biosci Biotechnol Biochem* 67(2):429–433
- Cutler AN, Morris ER, Taylor LJ (1983) Oral perception of viscosity in fluid foods and model systems. *J Texture Stud* 14(4):377–395
- Nandhini Venugopal K, Abhilash M (2010) Study of the hydration kinetics and rheological behaviour of guar gum. *Int J Pharma Sci Res* 1(1):28–39
- Favier M-, Bost P-, Demigné C, Rémésy C (1998) The cholesterol-lowering effect of guar gum in rats is not accompanied by an interruption of bile acid cycling. *Lipids* 33(8):765–771
- Baer DJ, Judd JT, Kris-Etherton PM, Zhao G (2003) Stearic acid absorption and its metabolizable energy value are minimally lower than those of other fatty acids in healthy men fed mixed diets. *J Nutr* 133(12):4129–4134
- Brufau G (2007) Phytosterols, but not pectin, added to a high-saturated-fat diet modify saturated fatty acid excretion in relation to chain length. *J Nutr Biochem* 18(9):580–586
- Favier M-, Bost P-, Guittard C, Demigné C, Rémésy C (1997) The cholesterol-lowering effect of guar gum is not the result of a simple diversion of bile acids toward fecal excretion. *Lipids* 32(9):953–959
- Overton PD, Furlonger N, Beety JM, Chakraborty J, Tredger JA, Morgan LM (1994) The effects of dietary sugar-beet fiber and guar gum on lipid-metabolism in Wistar rats. *Br J Nutr* 72(3):385–495
- Gallaher DD, Hassel CA, Lee K-, Gallaher CM (1993) Viscosity and fermentability as attributes of dietary fiber responsible for the hypocholesterolemic effect in hamsters. *J Nutr* 123(2):244–252
- Kasbo J, Saleem M, Perwaiz S, Mignault D, Lamireau T, Tuchweber B, Yousef I (2002) Biliary, fecal and plasma deoxycholic acid in rabbit, hamster, guinea pig, and rat: comparative study and implication in colon cancer. *Biol Pharm Bull* 25(10):1381–1384
- Flickinger EA, Wolf BW, Garleb KA, Chow J, Leyer GJ, Johns PW, Fahey GC Jr (2000) Glucose-based oligosaccharides exhibit different in vitro fermentation patterns and affect in vivo apparent nutrient digestibility and microbial populations in dogs. *J Nutr* 130(5):1267–1273
- Yoon S-, Chu D-, Juneja LR (2006) Physiological functions of partially hydrolyzed guar gum. *J Clin Biochem Nutr* 39(3):134–144
- Okubo T, Ishihara N, Takahashi H, Fujisawa T, Kim M, Yamamoto T, Mitsuoka T (1994) Effects of partially hydrolyzed guar gum intake on human intestinal microflora and its metabolism. *Biosci Biotechnol Biochem* 58(8):1364–1369
- Velázquez M, Davies C, Maret R, Slavin JL, Feirtag JM (2000) Effect of oligosaccharides and fibre substitutes on short-chain fatty acid production by human faecal microflora. *Anaerobe* 6(2):87–92
- Gallaher DD, Hassel CA, Lee K- (1993) Relationships between viscosity of hydroxypropyl methylcellulose and plasma cholesterol in hamsters. *J Nutr* 123(10):1732–1738
- Ellis PR, Dawoud FM, Morris ER (1991) Blood glucose, plasma insulin and sensory responses to guar-containing wheat breads: effects of molecular weight and particle size of guar gum. *Br J Nutr* 66(3):363–379

The Fatty Acid 8,11-Diol Synthase of *Aspergillus fumigatus* is Inhibited by Imidazole Derivatives and Unrelated to PpoB

Fredrik Jernerén · Ernst H. Oliw

Received: 5 March 2012 / Accepted: 6 April 2012 / Published online: 28 April 2012
© AOCS 2012

Abstract (8*R*)-Hydroperoxy-(9*Z*,12*Z*)-octadecadienoic acid (8-HPODE) is formed by aspergilli as an intermediate in biosynthesis of oxylipins with effects on sporulation. 8-HPODE is transformed by separate diol synthases to (5*S*,8*R*)-dihydroxy- and (8*R*,11*S*)-dihydroxy-(9*Z*,12*Z*)-octadecadienoic acids (5,8- and 8,11-DiHODE). The former is formed by the cytochrome P450 (P450) domain of 5,8-linoleate diol synthase (5,8-LDS or PpoA). Our aim was to characterize the 8,11-diol synthase of *Aspergillus fumigatus*, which is prominent in many strains. The 8,11-diol synthase was soluble and had a larger molecular size (>100 kDa) than most P450. Miconazole, ketoconazole, and 1-benzylimidazole, classical inhibitors of P450, reduced the biosynthesis of 8,11-DiHODE from 8-HPODE (apparent IC₅₀ values ~0.8, ~5, and ~0.6 μM, respectively), but did not inhibit the biosynthesis of 5,8-DiHODE. Analysis of hydroperoxides of regioisomeric C₁₈ and C₂₀ fatty acids showed that the 8,11-diol synthase was specific for certain hydroperoxides with *R* configuration. The suprafacial hydrogen abstraction and oxygen insertion at C-11 of 8-HPODE was associated with a small deuterium kinetic isotope effect ($^Hk_{cat}/^Dk_{cat} \sim 1.5$), consistent with P450-catalyzed oxidation. The genome of *A. fumigatus* contains over 70 P450 sequences. The reaction mechanism, size, and solubility of 8,11-diol synthase pointed to PpoB, a homologue of 5,8-LDS, as a possible candidate of this activity. Gene deletion of *ppoB* of *A. fumigatus* strains

AF:Δku80 and J272 did not inhibit biosynthesis of 8,11-DiHODE and recombinant PpoB appeared to lack diol synthase activity. We conclude that 8,11-DiHODE is formed from 8-HPODE by a soluble and substrate-specific 8,11-diol synthase with catalytic characteristics of class III P450.

Keywords Gene deletion · Sporulation · Animal heme peroxidase · LC–MS/MS · Insect cells · Protein expression

Abbreviations

CV	Column volume
CP	Chiral phase
CYP	Cytochrome P450
DiHODE	Dihydroxyoctadecadienoic acid
DOX	Dioxygenase
ΔppoB	Deletion of <i>ppoB</i>
HOME	Hydroxyoctadecenoic acid
HPOME	Hydroperoxyoctadecenoic acid
HPODE	Hydroperoxyoctadecadienoic acid
HPOTrE	Hydroperoxyoctadecatrienoic acid
LDS	Linoleate diol synthase
P450	Cytochrome P450
ppo	Psi producing oxygenase
RP	Reversed phase
TIC	Total ion current

Introduction

Unsaturated fatty acids can be oxidized to biological mediators in fungi as well as in plants and animals, and some of them are formed by homologous enzymes [1–3]. The animal heme peroxidase gene family contains members which oxidize fatty acids to hydroperoxides, as the

Electronic supplementary material The online version of this article (doi:10.1007/s11745-012-3673-2) contains supplementary material, which is available to authorized users.

F. Jernerén · E. H. Oliw (✉)
Department of Pharmaceutical Biosciences, Uppsala Biomedical Center, Uppsala University, 75124 Uppsala, Sweden
e-mail: Ernst.Oliw@farmbio.uu.se

first event in a chain of further transformations. The prototypes are cyclooxygenase-1 and -2 of animals, but the pathogen induced α -dioxygenase (α -DOX) of plants, 7,8-linoleate diol synthase (7,8-LDS) of the Take-all fungus, and psi-producing oxygenase A (PpoA) and C (PpoC) of aspergilli belong to this group [4–8], and possibly also psi producing oxygenase B (PpoB) [7–9].

The biological significance of fungal oxylipins was discovered by Champe et al. [10], who found that oxygenated metabolites of linoleic acid induced premature sexual sporulation of *Aspergillus nidulans*. These hormones were designated precocious sexual inducers (psi), and two were identified as (8*R*)-hydroxy-(9*Z*,12*Z*)-octadecadienoic acid (8-HPODE) and 5*S*,8*R*-dihydroxy-(9*Z*,12*Z*)-octadecadienoic acid (5,8-DiHODE) [10, 11]. The list of fungal oxylipins has since been expanded to include hydroperoxy C₁₈ fatty acids, epoxy alcohols, aldehydes, and allene oxides [1, 2, 12, 13].

The fatty acid heme-dioxygenases have a common reaction mechanism, which is based on oxidation of their heme iron with formation of a tyrosyl radical [4, 6, 14, 15]. The substrates and products differ. Cyclooxygenases convert arachidonic acid via an 11-peroxyl radical intermediate to prostaglandin endoperoxides, α -DOX oxidizes a wide range of fatty acids to unstable (2*R*)-hydroperoxy metabolites, whereas 7,8-LDS oxidizes linoleic acid sequentially to 8-HPODE and (7*S*,8*S*)-dihydroxy-(9*Z*,12*Z*)-octadecadienoic acid (7,8-DiHODE) [4, 6, 16]. The latter is formed by the diol synthase of the C-terminal P450 domain of 7,8-LDS [17], which is a member of the class III P450 [17–19].

Cloning and characterization of 7,8-LDS contributed to the discovery of three related proteins of aspergilli, viz., PpoA (also designated 5,8-LDS), PpoB, and PpoC (also designated 10*R*-DOX) [7, 8, 12, 20, 21]. 5,8-LDS forms two of the psi factors described by Champe and colleagues above [12, 20], whereas 10*R*-DOX oxidizes 18:2*n*-6 to 10*R*-hydroperoxy-(8*E*,12*Z*)-octadecadienoic acid (10*R*-HPODE) and 18:1*n*-9 to 8*R*-hydroperoxy-(9*Z*)-octadecadienoic acid (8-HPOME) [12, 22]. 5,8-LDS and 10*R*-DOX have been characterized from *A. nidulans* and *A. fumigatus* by gene deletion and expression [12, 17, 19, 22, 23]. Some aspergilli biosynthesize (8*R*,11*S*)-dihydroxy-(9*Z*,12*Z*)-octadecadienoic acid (8,11-DiHODE) from 8-HPODE [9, 12, 24] and this metabolite is not formed by recombinant 5,8-LDS or 10*R*-DOX. PpoB could possibly be related to biosynthesis of 8,11-DiHODE, at least in some aspergilli. The deduced PpoB protein sequences form a relatively heterogeneous group and the function of PpoB may therefore differ between aspergilli (Supplemental data, Fig. S1).

8,11-DiHODE was first identified in the fungus *Lepidotitius lacteus* [25]. Enzymes in lamellae of the field mushroom and mycelia of some filamentous fungi were

later found to transform 8-HPODE to 8,11-DiHODE [9, 12, 24, 26, 27]. These investigations showed that 8,11-DiHODE is formed from 8-HPODE in analogy with the intramolecular formation of 5,8-DiHODE [12], as outlined in Fig. 1. The biological function of 8,11-DiHODE in aspergilli has been difficult to evaluate, as we lack information on the 8,11-diol synthase and its gene. 8,11-DiHODE could have effects on sporulation in analogy with the psi factors of *A. nidulans*.

Biosynthesis of 8,11-DiHODE was observed in *A. fumigatus* Fresen., but significant biosynthesis was not detected in the sequenced *A. fumigatus* strain AF293 [12]. Our first objective was to determine whether 8,11-DiHODE biosynthesis occurred in *A. fumigatus* A1163, the second sequenced strain [28], or in other isolates. The second objective was to investigate the biochemical properties of the 8,11-diol synthase of *A. fumigatus* and establish its characteristics in relation to class III P450, which do not require an electron donor [18]. We therefore partly purified the 8,11-diol synthase activity, studied its substrate specificity, oxygenation mechanism, and effects of P450 inhibitors. The third objective was to investigate whether it was possible to link the biosynthesis of 8,11-DiHODE to a specific P450 out of over 70 P450 sequences in the genome. *ppoB* seemed to be a promising gene candidate as discussed above. *ppoB* has been subject to gene deletion, but unfortunately only in *A. nidulans* and *A. fumigatus* AF293, which lack significant capacity to form 8,11-DiHODE [7, 12]. We therefore decided to express recombinant PpoB and to disrupt *ppoB* in strains of *A. fumigatus* with prominent

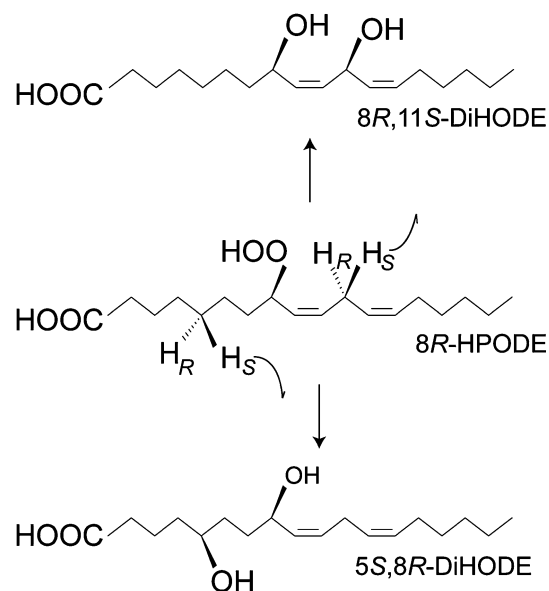


Fig. 1 Overview of the isomerization of 8*R*-HPODE to 5*S*,8*R*- and 8*R*,11*S*-DiHODE

8,11-diol synthase activity, and we chose to use *Agrobacterium tumefaciens*-mediated transformation [27, 29].

Materials and Methods

Materials

Fatty acids (99 %) and [U-¹³C]18:2n-6 (98 %) were from Merck, Sigma, and Larodan, and stored at 50–100 mM in ethanol (–20 °C). 8*R*-HPODE and [U-¹³C]8*R*-HPODE were prepared by biosynthesis [17], purified by TLC [5], and the integrity was confirmed by LC–MS/MS analysis. 8*S*-HPOME and 11-hydroperoxyocta-(9*Z*)-decenoic (11-HPOME) acids were obtained by autoxidation of 18:1n-9, and purified by NP-HPLC and CP-HPLC [30]. 13-Hydroperoxyoctadeca-(9*Z*,11*E*)-dienoic acid (13-HPODE) and 13-hydroperoxyoctadeca-(9*Z*,11*E*,12*Z*)-trienoic acid (13-HPOTrE) were obtained by biosynthesis and used as internal standards [31]. [11*S*-²H]18:2n-6 (>98 %) and [11,11-²H₂]18:2n-6 (>98 %) were a generous gift of Dr. Hamberg, Karolinska Institutet. Chemically competent *Escherichia coli* (Top10), mouse anti-V5-epitope antibody, Superscript III Kit, hygromycin B, InsectSelect System with pIZ/V5-His, Cellfectin, and phleomycin (Zeocin) were from Invitrogen. Restriction enzymes were from New England BioLabs and Fermentas. Plasmid Midi kit, and QIAquick gel extraction kit were from Qiagen. *Pfu* DNA polymerase and CloneJet PCR cloning kit were from Fermentas. Phusion and Phire DNA Polymerases were from Finnzymes. ECL Advance Western Blotting Detection kit, dNTPs, and horseradish peroxidase labeled anti-mouse IgG antibodies were from GE Healthcare. pGEM7Zf+ was from Promega. pCAMBIA0380 was obtained from CAMBIA (Canberra, Australia). Cefotaxime, RNaseA, ampicillin, kanamycin, 3,5-dimethoxy-4-hydroxyacetophenone, 1-benzylimidazole, ozagrel, fluconazole, ketoconazole, miconazole, troleandomycine, α -naphthoflavone, sulfaphenazole, metyrapone and voriconazole were from Sigma-Aldrich. Ex-Cell 420 insect serum free medium was purchased from SAFB-Biosciences (Hampshire, United Kingdom). Gentamycin sulfate and *Spodoptera frugiperda* (*Sf*21) cells were obtained locally. Primers were obtained from Cybergene (Huddinge, Sweden). Sequencing was performed at Uppsala Genomic Center (Rudbeck Laboratories, Uppsala University). *Agrobacterium tumefaciens* (strain AGL-1) was kindly supplied by Dr. Sesma (Centre for Plant Biotechnology and Genomics, Madrid, Spain). *A. fumigatus* strains pyrG⁺AF::Delta ku80 (AF:Δku80) and A1163 were from Fungal Genetics Stock Center (FGSC#1151 and FGSC#1163). J272 (CBS 287.95) was a kind gift from Dr. Melin (SLU, Uppsala, Sweden), and

H237 was obtained locally. 7,8-LDS was prepared from mycelium of *Magnaporthe oryzae* as described [27].

Fungal Growth

A. fumigatus strains were grown in malt extract medium, usually for 1–3 days at 37 °C followed by 2–5 days at room temperature under cycles of 8 h in dark and 16 h in fluorescent light (True-light). Mycelia were harvested by filtration through one layer of Miracloth (Calbiochem), and washed with saline. Mycelia were ground into a fine powder in liquid nitrogen, and stored at –80 °C. The nitrogen powder was homogenized (glass-Teflon, 10 passes; +4 °C) in 10 vols. (w/v) of 0.1 mM KHPO₄ (pH 7.3)/2 mM EDTA/0.04 % Tween-20, centrifuged at 13,000×g (2 min, +4 °C). The supernatant was designated nitrogen powder homogenate and used immediately for enzyme assays (biosynthesis of products, test of stability, effects of drugs) and for further purification.

Enzyme Assays

Recombinant PpoB or nitrogen powder homogenate was incubated with 100 μM of unsaturated fatty acid for 40 min on ice, or with 2 μM [U-¹³C]8-HPODE. The reaction (0.3–0.5 ml) was terminated with ethanol (4 vols.), an internal standard (13-HODE) was added in some experiments, and proteins were precipitated by centrifugation. The metabolites were extracted on octadecyl silica (SepPak/C₁₈), eluted with ethyl acetate, evaporated to dryness, and dissolved in 40–50 μl of 75 or 100 % methanol; 5–10 μl was subject to LC–MS/MS analysis. 50–100 μM 18:1n-7, 8*S*- and 11-HPOME were incubated in the same way. The kinetic isotope effect was assayed with 100 μM unlabeled and deuterated linoleic acids ([11*S*-²H]18:2n-6 or [11,11-²H₂]18:2n-6) in separate incubations in triplicate (20 min, +4 °C). After termination, 13*R*-HOTrE was added an internal standard, and the metabolites were extracted and analyzed as above.

Gel Filtration of 8,11-Diol Synthase

The subcellular localization of the 8,11-diol synthase activity (along with the 5,8-diol synthase activity) was determined by differential centrifugation (10,000×g, 15 min; 100,000×g, 60 min; +4 °C) and assayed with [U-¹³C]18:2n-6 as a substrate. The stability of the diol synthase activities at +4 °C were determined with [U-¹³C]8-HPODE as a substrate, and compared with the stability of 8-DOX with [U-¹³C]18:2n-6 as substrate.

Purification of the 8,11-linoleate diol synthase activity was achieved by homogenization (glass-Teflon, 10 passes;

+4 °C) of nitrogen powder in 10 vols. (w/v) of 0.05 mM KHPO₄ buffer (pH 7.35)/0.04 % Tween-20. The homogenate was clarified by centrifugation at 13,000×g (10 min, +4 °C), and the supernatant was filtered and centrifuged (55,000×g, 35 min; +4 °C). The supernatant was loaded onto a Q-Sepharose column (column volume (CV) 12 ml) at a flow-rate of 1 ml/min (ÄKTA FPLC system, GE Healthcare). The column was washed with three CVs 0.05 mM KHPO₄ buffer (pH 7.35)/0.04 % Tween-20 and the protein was subsequently eluted by step-wise increase in the concentration of NaCl (0.25 M, 1 CV; 0.5 M, 1 CV; 0.75 M, 1 CV; 1 M, 3 CV).

Fractions with enzyme activity converting 8-HPODE to 8,11-DiHODE were pooled, and the volume was reduced by ultrafiltration (Amicon Ultracel, 30 kDa) and washed with 0.05 mM KHPO₄ buffer (pH 7.35)/150 mM NaCl/0.04 % Tween-20. The concentrate was separated by size-exclusion chromatography (Superdex 200 HR 10/30, GE Healthcare) with a flow-rate of 0.4 ml/min. 1 ml fractions were analyzed for enzyme activity using [U-¹³C]8-HPODE as a substrate.

Effects of P450 Inhibitors on the Diol Synthase Activities

The effect of a series of P450 inhibitors on the 5,8- and 8,11-diol synthase activities of *A. fumigatus* AF:Δku80 was investigated in triplicate by LC–MS/MS analysis. Miconazole, fluconazole, voriconazole, ketoconazole, ozagrel, 1-benzylimidazole, troleandomycine, α-naphthoflavone, sulfaphenazole, or metyrapone was added to an aliquot of nitrogen powder homogenate in concentrations ranging from 0.3 to 100 μM. The reactions were started by the addition of 100 μM [U-¹³C]18:2n-6, proceeded for 40 min on ice, and were terminated with 4 vols. of ethanol containing the internal standard (13-HODE). The metabolites were extracted as described above. The inhibitory effects of these substances were assessed by LC–MS/MS analysis of the carboxylate anions with monitoring of the ratios of the specific fragment ions (*m/z* 329 → 224 for [U-¹³C]8,11-DiHODE; *m/z* 329 → 120 for [U-¹³C]5,8-DiHODE, *m/z* 313 → 165 for [U-¹³C]8-HODE; and *m/z* 313 → 193 for [U-¹³C]10-HODE) and the internal standard, 13-HODE (*m/z* 295 → 195). The inhibition of the 8,11-diol synthase activity was also confirmed with 2 μM [U-¹³C]8-HPODE as a substrate.

Cloning of *ppoB* and Expression in Insect Cells

Total RNA was isolated from nitrogen powder of *A. fumigatus* J272 [22]. The full length cDNA was obtained by PCR technology and cloned into pIZ/V5-His expression vector using KpnI/XbaI generating pIZ_ppoB, with primers listed in the Supplementary data (Table S1).

Plasmid-driven expression was performed by transfection of *Sf21* cells with pIZ_ppoB or pIZ/V5-His_ppoB and Cellfectin as described [32]. Cells were harvested after 48 h, suspended in lysis buffer (50 mM KHPO₄ (pH 7.4)/1 mM EDTA/1 mM GSH/5 % glycerol/0.04 % Tween-20) and sonicated (Branson sonifier cell disrupter B15, max. power 20 %, 3 × 5 s pulses; +4 °C). The cell debris was spun down (15,000×g, 30 min; +4 °C) and the supernatant was used for enzyme assay.

Gene Deletion of *ppoB* and PCR Analysis of Fungal Transformants

Two separate constructs for gene deletion of *ppoB* were prepared in pCAMBIA0380 (Fig. 2). In the first construct, nucleotides 1,247–1,938 of *ppoB*, which include the catalytically important tyrosine residue for hydrogen abstraction, was replaced with a 1,424-bp hygromycin B resistance cassette under the control of the TrpC promoter of *A. nidulans*. The cassette was flanked by sequences of 1,324-bp (upstream) and 1,098-bp (downstream) to ensure homologous recombination and targeted insertion. These flanking sequences were obtained by PCR technology from genomic DNA of *A. fumigatus* by using primers Afum_F-5'-reg/Afum_R-5'-reg and Afum_F-3'-reg/Afum_R-3'-reg, respectively (Table S1). This construct was designated pCAMB_Δ*ppoB*(1). In the second construct, pCAMB_Δ*ppoB*(2), nucleotides 1247–3724 of *ppoB* was replaced with the TrpC/*hph* cassette, flanked by the same upstream sequence as above, and a new downstream sequence

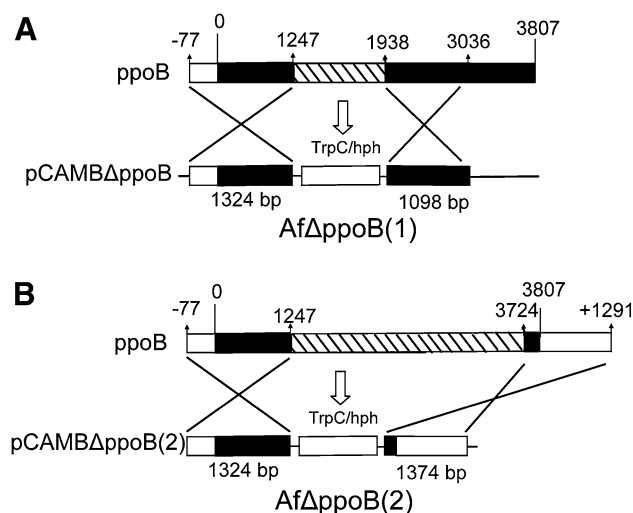


Fig. 2 Overview of two constructs used for deletion of *ppoB*. **a** The construct AfΔ*ppoB*(1) replaced the DOX domain with a hygromycin B cassette under the control of the TrpC promoter of *A. nidulans* (TrpC/*hph* cassette). **b** The construct AfΔ*ppoB*(2) replaced both the DOX and the P450 domains with the hygromycin B cassette and the TrpC promoter

(1,374-bp), amplified using primers Afum_F-3'-2 and Afum_R-3'-2. This ensured that both the DOX domain and the heme binding region of the P450 domain were deleted (Fig. 2).

Fungal conidia were prepared from 8 to 12-days-old mycelia grown on *Aspergillus* minimal medium [33] at 22 °C under 16 h light/8 h dark cycles of fluorescent light (True-light). Conidia were harvested with 4 ml distilled water using a glass spreader and were filtered through Miracloth. Competent *A. tumefaciens* containing either the pCAMB_Δ*ppoB*(1) or Δ*ppoB*(2) constructs were used to transform obtained *A. fumigatus* J272 or AF:Δku80, respectively, according to Sugui et al. [29] with minor modifications. *Aspergillus* minimal medium agar plates were used, supplemented with 250 μg/ml hygromycin B to select transformed conidia, and 200 μM cefotaxime to eliminate *A. tumefaciens*.

Fungal genomic DNA was prepared by incubating nitrogen powder in an equal amount of extraction buffer (200 mM Tris/HCl (pH 8.5)/250 mM NaCl/25 mM EDTA/0.5 % SDS) at 70 °C for 30 min. Samples were centrifuged, and the supernatant treated with RNaseA, extracted with phenol and chloroform. Genomic DNA was precipitated with isopropanol, collected by centrifugation, and re-suspended in deionized water. Three primer pairs were used to distinguish whether the transformants were the result of homologous recombination with deletion of the *ppoB* gene (Table S1). Primers F-*hph* and R-*hph*, which amplified 971-bp from the *hph* gene, were used for initial screening and were positive in all transformants. Primers F-Δ*ppoB*-Af and R-Δ*ppoB*-Af amplified a fragment of 1,775-bp from transformants resulting from targeted transformation, while F-Δ*ppoB*2-Af and R-Δ*ppoB*2-Af amplified 1,708-bp. These primer pairs would generate different amplicons, or no amplicons at all, in ectopic transformants without simultaneous targeted disruption of *ppoB*. Primers Δ*ppoB*-Af and R-Af-*ppoB*-wt generated amplicons of 1,845-bp from strains containing an intact *ppoB*. Primers F-Δ*ppoB*-Af and R-Δ*ppoB*2-Af amplified a 6,455-bp fragment covering the entire genomic insert, which was subsequently sequenced.

LC/MS Analysis

Reversed phase-HPLC (RP-HPLC) with MS/MS analysis was performed on an octadecyl silica column (5 μm; 2 × 150 mm with a guard cartridge 2 × 4 mm; Phenomenex), which was usually eluted with methanol/water/acetic acid, 800/200/0.05, at 0.3 ml/min, with aid of Surveyor MS pump (ThermoFisher). The effluent was subject to electrospray ionization in a linear ion trap mass spectrometer (LTQ, ThermoFisher). The heated transfer capillary was set at 315 °C, the ion isolation width at 1.5, the collision energy at 50 (arbitrary scale), and the tube lens at

90–130 V. Prostaglandin $F_{1\alpha}$ was infused for tuning. Data were analyzed by the Xcalibur software.

Results

Biosynthesis of 8,11-DiHODE by Strains of *A. fumigatus*

All eight strains of *A. fumigatus* except AF293 oxygenated linoleic acid to significant amounts of 8,11-DiHODE, and all strains formed 5,8-DiHODE (Table 1). The oxygenase activities varied between preparations of the same strain. This made comparison between strains difficult, but we could not find any major differences between the strains (except AF293).

The genomes of AF293 and A1163 have been sequenced [34]. The latter oxidized linoleic acid to 8,11-DiHODE (Fig. 3). This was the only noticeable difference, as both AF293 and A1163 formed 5,8-DiHODE, 8-HODE, and 10-HODE (cf. [12]). We found that growing mycelia of A1163 in a liquid medium at room temperature for a few days yielded pronounced expression of the 8,11-diol synthase activity, as 8,11-DiHODE was often formed as the main metabolite (Fig. 3).

The 8,11-Diol Synthase Activity

As endogenous linoleic acid was oxidized during enzyme preparation, we used [U-¹³C]-labeled substrates. We found that ~90 % of the 8,11-diol synthase activity was present in the cytosolic fraction after differential centrifugation with only ~10 % associated with the microsomal pellet.

We next examined the stability of the 8,11-diol synthase and the 8-DOX and 5,8-diol synthase activities. The 8-DOX activity decreased rapidly and was absent after

Table 1 Summary of *A. fumigatus* ssp. analyzed for biosynthesis of 8,11-DiHODE

Strain	Comments	8,11-DiHODE biosynthesis	Strain Refs
AF293	Wild type	–	[12]
Fresen	Wild type	+	[12]
A1163	CEA17 (pyrG+)	+	[28]
H237	Wild type, clinical isolate	+	[46]
J272 (CBS 287.95)	Wild type	+	This study
AF:Δku80	CEA17 (pyrG+)	+	[47]
J272 Δ <i>ppoB</i>	DOX deletion	+	This study
AF:Δku80Δ <i>ppoB</i>	DOX-CYP deletion	+	This study

– Not detected; + 8,11-DiHODE was formed as a major metabolite

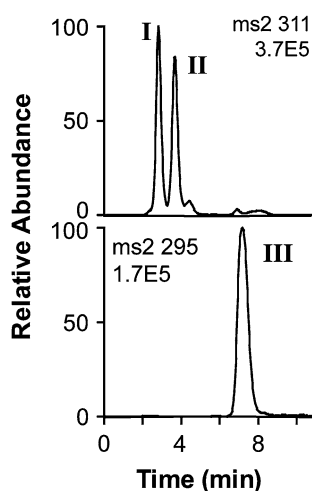


Fig. 3 RP-HPLC–MS/MS analysis of products formed from linoleic acid by *A. fumigatus* A1163. The metabolites were formed by nitrogen powder preparation of mycelia. Peak I, 8,11-DiHODE; peak II, 5,8-DiHODE; peak III contained a mixture of 8- and 10-HODE

24 h on ice as judged from incubations with [U-¹³C]18:2n-6, whereas the 5,8- and 8,11-diol synthase activities with [U-¹³C]8-HPODE as substrate appeared to be unaffected. After 72 h on ice, the 5,8-diol synthase activity was lost, while most of the 8,11-diol synthase activity remained.

Substrate specificities of the 8-DOX and the 5,8- and 8,11-diol synthase activities of *A. fumigatus* Fresen have been described previously [12], but we extended the substrate specificities as follows. We found that 18:1n-7 (vacenic acid) was oxidized to 10-HPOME by the AF:Δku80 strain and isomerized to 10,13-DiHOME. In contrast to 8*R*-HPOME, we found that 8*S*-HPOME and 11-HPOME were not transformed to 8,11-DiHOME, which demonstrates the substrate specificity of the 8,11-diol synthase.

We compared the rate of oxidation of 18:2n-6, [11*S*-²H]18:2n-6, and [11,11-²H₂]18:2n-6 to 8,11-DiHODE by nitrogen powder of *A. fumigatus*. The deuterium label at position 11*S* is abstracted in the transformation to 8,11-DiHODE (Fig. 1). With aid of an internal standard, we found by LC–MS analysis of the molecular ions that the primary deuterium kinetic isotope effect was small ($k_{cat}^H/k_{cat}^D \sim 1.5$) and the secondary kinetic isotope effect was insignificant. This is in agreement with the non-competitive deuterium kinetic isotope effects of CYP3A4 and the 5,8-diol synthase of PpoA of *A. nidulans* [35, 36].

Effects of P450 Inhibitors on 8,11- and 5,8-Diol Synthase Activities

1-Benzylimidazole, miconazole, ketoconazole, and ozagrel reduced the biosynthesis of [U-¹³C]8,11-DiHODE from [U-¹³C]18:2n-6 at μM concentrations. The inhibitory actions of the drugs were confirmed with 2 μM [U-¹³C]

8-HPODE as substrate. The apparent IC₅₀ values were ~0.6, ~0.8, ~5, and ~30 μM, respectively. The dose-dependent reduction of 8,11-DiHODE biosynthesis by miconazole is shown in Fig. 4. Two related drugs, voriconazole and fluconazole, which lack the imidazole moiety, appeared to be considerably less active (<20 % inhibition at 100 μM). Several drugs did not inhibit the oxygenation of linoleic acid to 5,8- and 8,11-diols by *A. fumigatus* at 100 μM concentrations (metyrapone, sulfaphenazole, alfa-naphthoflavone, and troleandomycin).

In contrast, the biosynthesis of 5,8-DiHODE and 8-H(P)ODE by 5,8-LDS and 10-H(P)ODE by 10*R*-DOX appeared to be largely unaffected by 100 μM of the six inhibitory drugs discussed above. For example, the ratio of [U-¹³C]5,8-DiHODE/[U-¹³C]8-HODE formed in the presence of 100 μM of a potent inhibitor of 8,11-diol synthase, miconazole, was only 10 % lower than in the controls. We confirmed that these drugs did not reduce the 8-DOX and 7,8-diol synthase activities of 7,8-LDS of *M. oryzae*, suggesting that the potent inhibition by imidazole derivatives could be specific for the 8,11-diol synthase.

Gel Filtration of the 8,11-Diol Synthase Activity

The 8,11- and 5,8-diol synthase activities were followed during anion-exchange chromatography (Q-Sepharose; Fig. 5a). Fractions with detectable diol synthase activities (LC–MS analysis) were combined and reduced to ~200 μl by ultrafiltration; an aliquot isomerized [U-¹³C]HPODE readily to ~80 % 8,11-DiHODE and ~20 % 5,8-DiHODE. The concentrate was analyzed by gel filtration (Superdex 200 HR) and fractions were assayed for biosynthesis of 8,11-DiHODE. Low 8,11-DiHODE biosynthesis

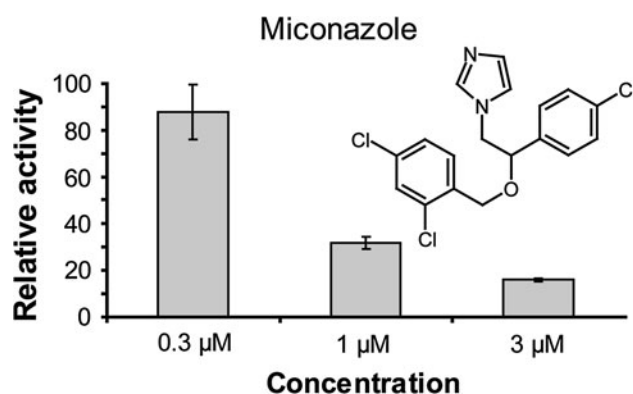


Fig. 4 Inhibition of 8,11-DiHODE biosynthesis in *A. fumigatus* by miconazole. All incubations of subcellular fractions of strain AF:Δku80 were conducted in triplicates with [U-¹³C]linoleic acid as substrate, corrected for the recovery of the internal standard (13-HODE), and are presented as mean values ±SD ($n = 3$). Relative activity refers to formation of [U-¹³C]8,11-DiHODE without miconazole. The biosynthesis of [U-¹³C]8-HPODE was not influenced by the miconazole. The insert shows the structure of miconazole

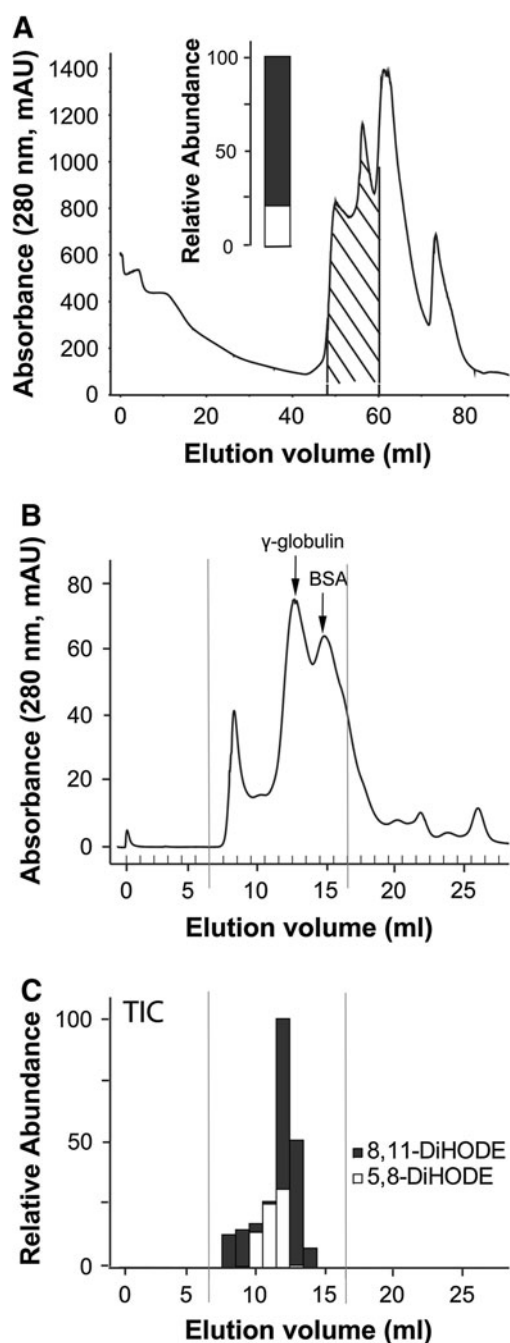


Fig. 5 Purification of the linoleate diol synthase activities of *A. fumigatus*. **a** Anion-exchange chromatography (Q-Sepharose) of material from AF: Δ ku80. Active fractions (hatched) were combined, concentrated, and analysed for biosynthesis of diols from 8-HPODE. The inset shows that 8,11-DiHODE (black) and 5,8-DiHODE (white) were formed in a ratio of 4:1. **b** Gel filtration. The material from anion-exchange chromatography in **a** was separated by gel filtration (Superdex 200HR), and fractions between the horizontal lines were analyzed for diol synthase activities. The elution volumes of γ -globulin (\sim 156 kDa) and BSA (\sim 67 kDa) are indicated by arrows. **c** Assay of diol synthase activities. The fractions between the vertical lines in **b** and **c** were assayed for diol synthase activities, and the formation of 8,11-DiHODE (black) and 5,8-DiHODE (white), relative to the peak fraction at 12 min, is indicated by the bars

Table 2 Differences in the deduced protein sequences of PpoB of *A. fumigatus* AF293, A1163, and J272. The PpoB of the latter was expressed in this study

Amino acid position	AF293	A1163	J272
229	Ala	Pro	Pro
244	Ile	Val	Ile
663	Pro	Ala	Pro
1059	Thr	Ala	Thr
1104	Ser	Pro	Pro

GenBank ID: AF293, XP_746438; A1163, EDP47075; J272, HQ832882

was evident in the front fractions, but peak 8,11-DiHODE biosynthesis was noted between 12 and 13 ml with approximately the same elution volume as γ -globulin (\sim 156 kDa, Fig. 5b). Peak 5,8-DiHODE biosynthesis was present at 11–12 ml, suggesting that 5,8-LDS (\sim 120 kDa) mainly eluted as a monomer or dimer. Gel filtration demonstrated that the 8,11- and 5,8-diol synthase activities partly overlapped on this column.

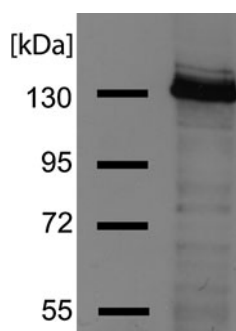
Cloning and Expression of ppoB

With RT-PCR we obtained the full-length cDNA of *ppoB* from J272 (GenBank ID: HQ832882). We found that the intron–exon borders of *ppoB* of J272 were as predicted for *ppoB* of the two sequenced strains, AF293 and A1163. The deduced protein sequence of this PpoB differed at two positions from the PpoB of strain AF293 and three positions from PpoB of strain A1163 (Table 2). Inspection of the J272 sequence shows these replacements were not unique, but PpoB of AF293 differed at two positions (Ala229 and Ser1004) from both of the other two PpoB sequences.

We confirmed that PpoB was expressed in insect cells by Western blot analysis of the V5 epitope, as shown in Fig. 6. We next examined recombinant PpoB for enzymatic activity. We incubated recombinant PpoB expressed in insect cells with linoleic acid, α -linolenic acid, and oleic acid, but we could not detect significant formation of hydroxy- or hydroperoxy metabolites. Attempts to detect diol synthase activities with 8-HPODE as a substrate were also unsuccessful. Recombinant protein expression can give inactive enzymes as expression artefacts, although the insect expression system has worked well for this class of enzymes, e.g., recombinant LDS (*A. fumigatus* [17], *M. oryzae*,¹ and *Gaeumannomyces graminis* [17]) and 10R-DOX (*A. fumigatus* [22]). We therefore decided to delete *ppoB* as this could provide unequivocal information on its relation to 8,11-diol synthase.

¹ Jernerén F., unpublished observation.

Fig. 6 Western blot analysis of PpoB expressed in insect cells. The detected band corresponds approximately to the expected size of ppoB (~133 kDa). An anti-V5 antibody was used for detection, and the markers of the protein ladder are indicated



Gene Deletion of *ppoB*

Gene deletion was performed with two constructs, Af Δ ppoB(1) and Af Δ ppoB(2), as summarized in Fig. 2. This yielded two gene deletion strains (J272 Δ ppoB and AF: Δ ku80 Δ ppoB, respectively; Table 1). We confirmed homologous recombination with PCR technology, as illustrated for the largest deletion construct in Fig. 7. In addition, a PCR-fragment, covering the entire genomic insert, was amplified from genomic DNA of a transformant. The targeted insertion of the construct was verified by sequencing of this PCR product.

Incubation of the two Δ ppoB strains with linoleic acid consistently showed that the 8,11-diol synthase activity was unaffected, and so were the activities of 5,8-LDS and 10-DOX. We conclude that gene deletion of *ppoB* did not influence the biosynthesis of 8,11-DiHODE. Southern blot hybridization is traditionally used to identify ectopic insertions, but PCR analysis is informative in identifying homologous recombination [37]. Since the biosynthesis of 8-HPODE and 8,11-DiHODE were unaffected by *ppoB* deletion, the possibility of an additional ectopic integration event was not further investigated.

Characteristics of the Δ ppoB Mutants

Radial growth rate and asexual sporulation capacity of J272 Δ ppoB and AF: Δ ku80 Δ ppoB appeared to be unchanged. These results are in agreement with the effects of *ppoABC*-RNA silencing and *ppoB* gene deletion experiments performed in the AF293 strain [8, 38], which does not produce significant amounts of 8,11-DiHODE (Table 1).

Discussion

We report that 8,11-diol synthase likely belongs to the class III P450 with specificity for certain fatty acid hydroperoxides with *R* configuration. The oxygenation mechanism with a small deuterium kinetic isotope effect and strong inhibition by imidazole derivatives are typical

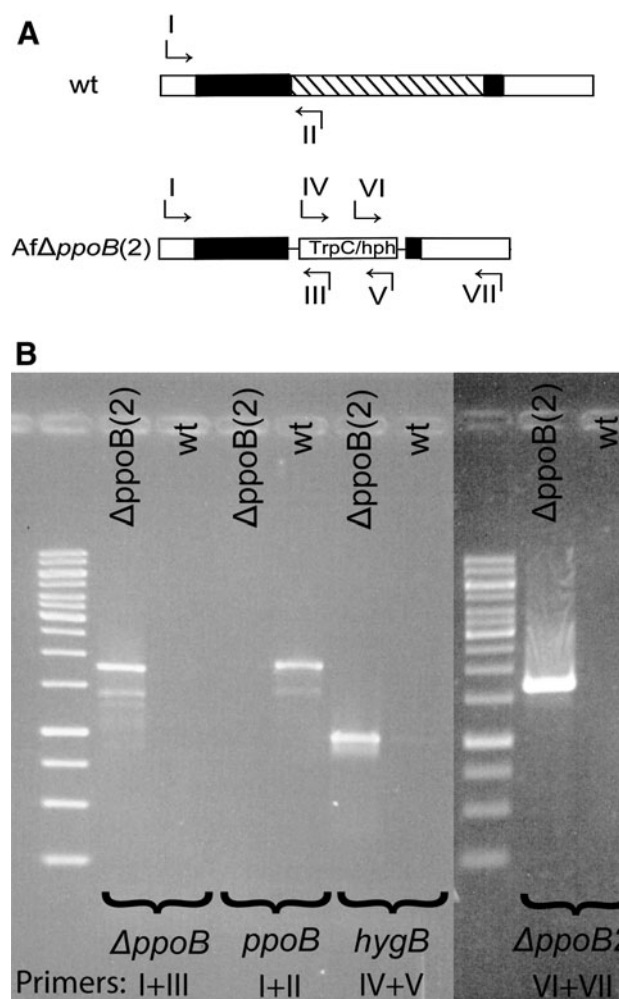


Fig. 7 PCR analysis of *A. fumigatus* AF: Δ ku80 Δ ppoB. **a** Specific primer pairs were designed to distinguish between targeted gene deletion (primers I + III and VI + VII) and for intact *ppoB* gene (primers I + II) and for integration of the hygromycin B cassette (primers IV + V). **b** PCR was performed with genomic DNA from *A. fumigatus* AF: Δ ku80 (wt) and gene deletion strain AF: Δ ku80 Δ ppoB [Af Δ ppoB(2)], yielding the expected product patterns. See text and Table S1 for details

of P450. The distribution of the 8,11-diol synthase to the soluble cell fraction and its apparent molecular size differ from many class III P450, but not significantly from 5,8-LDS. It was therefore unexpected that 8,11-diol synthase of *A. fumigatus* could not be linked to PpoB in spite of sequence similarities with 5,8-LDS.

Biosynthesis of 8,11-DiHODE has only been observed in aspergilli in connection with 5,8-LDS, which oxidizes 18:2n-6 to the precursor, 8*R*-HPODE. The 8,11-diol synthase activity is prominent in all investigated strains except AF293 (Table 1). The 8,11-diol synthase readily transforms the 8*R*-hydroperoxy metabolite of C₁₈ fatty acids (18:1n-9, 18:2n-6, 18:3n-3) and the 10*R*-hydroperoxy metabolite of vaccenic acid (18:1n-7) to 1,4-diols, but 8*S*-HPOME or

11-HPOME were not transformed. The 8,11-diol synthase thus appears to be both regio- and stereospecific. Pharmacological analysis revealed striking differences between 8-11-diol synthase and 5,8- and 7,8-diol synthases.

We found that miconazole, ketoconazole, and 1-benzylimidazole inhibited the 8,11-diol synthase activity with apparent IC₅₀ values at low μM concentrations. These drugs are used to treat aspergillosis by inhibition of lanosterol 14 α -demethylase (CYP51) or to reduce platelet aggregation [inhibition of thromboxane synthase (CYP5A)] [39, 40]. The CYP5A inhibitor ozagrel also inhibited the 8,11-diol synthase, but voriconazole and fluconazole were less active. 8,11-Diol synthase was inhibited by drugs with an imidazole as functional group, which blocks catalysis by ligation to the ferric heme iron [40–42]. None of these drugs inhibited the diol synthase activity of 5,8- and 7,8-LDS even at high concentrations (0.1 mM). The selective inhibition of 8,11-diol synthase suggests structural differences in the P450 heme environment of the three diol synthases.

What is the biological function of 8,11-DiHODE? *A. nidulans* is traditionally a model organism for studies of oxylipin effects on sexual and asexual sporulation [10, 43]. *A. nidulans* does not form 8,11-DiHODE, and its biological effects should therefore be investigated in other aspergilli, e.g., *A. fumigatus*, *A. clavatus*, or *A. niger* [9, 12, 24]. 8,11-DiHODE might conceivably affect the sexual cycle of *A. fumigatus*, which was discovered only recently [44], and might be implicated in pathogen-host interactions in analogy with other oxylipins [3].

Recombinant PpoB of *A. fumigatus* J272, which was expressed in insect cells, lacked detectable 8,11-diol synthase activity and did not oxygenate linoleic acid or other unsaturated C₁₈ fatty acids. This insect cell expression system has been used to successfully express 5,8- and 7,8-LDS as well as 10R-DOX [17, 22]. The two sequenced strains of *A. fumigatus*, AF293 and A1163, differ markedly in biosynthesis of 8,11-DiHODE, although their PpoB sequences are similar to PpoB of J272 (Table 2). It therefore seems likely that PpoB may have other catalytic functions, but we cannot rule out loss of activity due to expression artifacts. We therefore chose to study the potential relationship between PpoB and 8,11-diol synthase by gene deletion.

We disrupted *ppoB* with two different constructs, using *Agrobacterium tumefaciens*-mediated transformation, and confirmed the gene deletions by PCR technology and sequencing. Gene deletion of *ppoB* did not affect the biosynthesis of 8,11-DiHODE. This unexpected finding has gained recent support. *A. clavatus* is closely related to *A. fumigatus*, and it has a prominent capacity to synthesize 8,11-DiHODE [9]. While this work was in progress, we found that PpoB of *A. clavatus* contains a serine at the

position of the conserved heme-thiolate (cysteine) residue of its P450 domain [9]. Point mutation of this cysteine residue to serine or alanine is commonly used to abolish P450 catalysis [17, 19, 45]. Replacement of this critical cysteine residue of PpoB during evolution of *A. clavatus* and gene deletion of *ppoB* in *A. fumigatus* both left the biosynthesis of 8,11-DiHODE unaffected.

In addition to 5,8-LDS and 10R-DOX homologues, some aspergilli may also express PpoB and one or two additional DOX-CYP enzymes. These orphan enzymes all contain the characteristic YRWH motif in their DOX domains [13, 24]. In analogy with cyclooxygenases, the Tyr and His residues of this sequence likely represent the catalytically important Tyr residue for hydrogen abstraction and the proximal heme ligand [32, 46]. The orphan DOX-CYP enzymes could therefore be dioxygenases or peroxidases. 9R-HPODE is formed by *A. terreus* [13], and work is now in progress to clone and express its three orphan DOX-CYP enzymes in pursuit of the 9R-DOX activity.

Acknowledgments This work was supported by grants from the Swedish Research Council (03X-06523), the Knut and Alice Wallenberg Foundation (KAW 2004.123), and by Uppsala University. We thank Dr. Melin for the generous gift of aspergilli strains, and Dr. Hamberg for the gift of stereospecifically deuterated fatty acids.

References

- Christensen SA, Kolomiets MV (2011) The lipid language of plant–fungal interactions. *Fungal Gen Biol* 48:4–14
- Brodhun F, Feussner I (2011) Oxylipins in fungi. *FEBS J* 278: 1047–1063
- Tsitsigiannis DI, Keller NP (2007) Oxylipins as developmental and host-fungal communication signals. *Trends Microbiol* 15: 109–118
- Smith WL, Urade Y, Jakobsson PJ (2011) Enzymes of the cyclooxygenase pathways of prostanoid biosynthesis. *Chem Rev* 111:5821–5865
- Su C, Oliw EH (1996) Purification and characterization of linoleate 8-dioxygenase from the fungus *Gaeumannomyces graminis* as a novel hemoprotein. *J Biol Chem* 271:14112–14118
- Hamberg M, Ponce de Leon I, Rodriguez MJ, Castresana C (2005) Alpha-dioxygenases. *Biochem Biophys Res Commun* 338: 169–174
- Tsitsigiannis DI, Kowieski TM, Zarnowski R, Keller NP (2005) Three putative oxylipin biosynthetic genes integrate sexual and asexual development in *Aspergillus nidulans*. *Microbiology (Reading, England)* 151:1809–1821
- Tsitsigiannis DI, Bok JW, Andes D, Nielsen KF, Frisvad JC, Keller NP (2005) *Aspergillus* cyclooxygenase-like enzymes are associated with prostaglandin production and virulence. *Infect Immun* 73:4548–4559
- Jermerén F, Garscha U, Hoffmann I, Hamberg M, Oliw EH (2010) Reaction mechanism of 5,8-linoleate diol synthase, 10R-dioxygenase and 8,11-hydroperoxide isomerase of *Aspergillus clavatus*. *Biochim Biophys Acta* 1801:503–507
- Champe SP, el-Zayat AA (1989) Isolation of a sexual sporulation hormone from *Aspergillus nidulans*. *J Bacteriol* 171:3982–3988

11. Mazur P, Meyers HV, Nakanishi K, El-Zayat AAE, Champe SP (1990) Structural elucidation of sporogenic fatty acid metabolites from *Aspergillus nidulans*. *Tetrahedron Lett* 31:3837–3840
12. Garscha U, Jernerén F, Chung D, Keller NP, Hamberg M, Oliw EH (2007) Identification of dioxygenases required for *Aspergillus* development. Studies of products, stereochemistry, and the reaction mechanism. *J Biol Chem* 282:34707–34718
13. Jernerén F, Hoffmann I, Oliw EH (2010) Linoleate 9R-dioxygenase and allene oxide synthase activities of *Aspergillus terreus*. *Arch Biochem Biophys* (Erratum 2010; 500; 210) 495:67–73
14. Su C, Sahlin M, Oliw EH (1998) A protein radical and ferryl intermediates are generated by linoleate diol synthase, a ferric heme protein with dioxygenase and hydroperoxide isomerase activities. *J Biol Chem* 273:20744–20751
15. Fielding AJ, Brodhun F, Koch C, Pievo R, Denysenkov V, Feussner I, Bennati M (2011) Multifrequency electron paramagnetic resonance characterization of PpoA, a CYP450 fusion protein that catalyzes fatty acid dioxygenation. *J Am Chem Soc* 133:9052–9062
16. Hamberg M, Zhang LY, Brodowsky ID, Oliw EH (1994) Sequential oxygenation of linoleic acid in the fungus *Gaeumannomyces graminis*: stereochemistry of dioxygenase and hydroperoxide isomerase reactions. *Arch Biochem Biophys* 309:77–80
17. Hoffmann I, Jernerén F, Garscha U, Oliw EH (2011) Expression of 5,8-LDS of *Aspergillus fumigatus* and its dioxygenase domain. A comparison with 7,8-LDS, 10-dioxygenase, and cyclooxygenase. *Arch Biochem Biophys* 506:216–222
18. Werck-Reichhart D, Feyereisen R (2000) Cytochromes P450: a success story. *Genome Biol* 1:reviews3003.3001–3003.3009
19. Brodhun F, Göbel C, Hornung E, Feussner I (2009) Identification of PpoA from *Aspergillus nidulans* as a fusion protein of a fatty acid heme dioxygenase/peroxidase and a cytochrome P450. *J Biol Chem* 284:11792–11805
20. Tsitsigiannis DI, Zarnowski R, Keller NP (2004) The lipid body protein, PpoA, coordinates sexual and asexual sporulation in *Aspergillus nidulans*. *J Biol Chem* 279:11344–11353
21. Tsitsigiannis DI, Kowieski TM, Zarnowski R, Keller NP (2004) Endogenous lipogenic regulators of spore balance in *Aspergillus nidulans*. *Eukaryot Cell* 3:1398–1411
22. Garscha U, Oliw EH (2009) Leucine/valine residues direct oxygenation of linoleic acid by (10R)- and (8R)-dioxygenases: expression and site-directed mutagenesis of (10R)-dioxygenase with epoxyalcohol synthase activity. *J Biol Chem* 284:13755–13765
23. Brodhun F, Schneider S, Göbel C, Hornung E, Feussner I (2010) PpoC from *Aspergillus nidulans* is a fusion protein with one active heme. *Biochem J* 425:553–565
24. Wadman MW, de Vries RP, Kalkhove SI, Veldink GA, Vliegthart JF (2009) Characterization of oxylipins and dioxygenase genes in the asexual fungus *Aspergillus niger*. *BMC Microbiol* 9:1–9
25. Fox SR, Akpinar A, Prabhune AA, Friend J, Ratledge C (2000) The biosynthesis of oxylipins of linoleic and arachidonic acids by the sewage fungus *Leptomitus lacteus*, including the identification of 8R-Hydroxy-9Z,12Z-octadecadienoic acid. *Lipids* 35:23–30
26. Wadman MW, van Zadelhoff G, Hamberg M, Visser T, Veldink GA, Vliegthart JF (2005) Conversion of linoleic acid into novel oxylipins by the mushroom *Agaricus bisporus*. *Lipids* 40:1163–1170
27. Jernerén F, Sesma A, Franceschetti M, Hamberg M, Oliw EH (2010) Gene deletion of 7,8-linoleate diol synthase of the rice blast fungus: studies on pathogenicity, stereochemistry, and oxygenation mechanisms. *J Biol Chem* 285:5308–5316
28. Fedorova ND, Khaldi N, Joardar VS, Maiti R, Amedeo P, Anderson MJ, Crabtree J, Silva JC, Badger JH, Albarraq A, Angiuoli S, Bussey H, Bowyer P, Cotty PJ, Dyer PS, Egan A, Galens K, Fraser-Liggett CM, Haas BJ, Inman JM, Kent R, Lemieux S, Malavazi I, Orvis J, Roemer T, Ronning CM, Sundaram JP, Sutton G, Turner G, Venter JC, White OR, Whitty BR, Youngman P, Wolfe KH, Goldman GH, Wortman JR, Jiang B, Denning DW, Nierman WC (2008) Genomic islands in the pathogenic filamentous fungus *Aspergillus fumigatus*. *PLoS Genet* 4:e1000046
29. Sugui JA, Chang YC, Kwon-Chung KJ (2005) *Agrobacterium tumefaciens*-mediated transformation of *Aspergillus fumigatus*: an efficient tool for insertional mutagenesis and targeted gene disruption. *Appl Environ Microbiol* 71:1798–1802
30. Oliw EH, Wennman A, Hoffmann I, Garscha U, Hamberg M, Jernerén F (2011) Stereoselective oxidation of regioisomeric octadecenoic acids by fatty acid dioxygenases. *J Lipid Res* 52:1995–2004
31. Oliw EH (2002) Plant and fungal lipoxygenases. *Prostaglandins Other Lipid Mediat* 68–69:313–323
32. Garscha U, Oliw EH (2008) Critical amino acids for the 8(R)-dioxygenase activity of linoleate diol synthase. A comparison with cyclooxygenases. *FEBS Lett* 582:3547–3551
33. Tsai HF, Chang YC, Washburn RG, Wheeler MH, Kwon-Chung KJ (1998) The developmentally regulated alb1 gene of *Aspergillus fumigatus*: its role in modulation of conidial morphology and virulence. *J Bacteriol* 180:3031–3038
34. Arnaud MB, Chibucos MC, Costanzo MC, Crabtree J, Inglis DO, Lotia A, Orvis J, Shah P, Skrzypek MS, Binkley G, Miyasato SR, Wortman JR, Sherlock G (2010) The *Aspergillus* Genome Database, a curated comparative genomics resource for gene, protein and sequence information for the *Aspergillus* research community. *Nucleic Acids Res* 38:D420–D427
35. Nadler A, Koch C, Brodhun F, Wehland JD, Tittmann K, Feussner I, Diederichsen U (2011) Influence of substrate dideuteriation on the reaction of the bifunctional heme enzyme psi factor producing oxygenase A (PpoA). *Chem BioChem* 12:728–737
36. Krauser JA, Guengerich FP (2005) Cytochrome P450 3A4-catalyzed testosterone 6beta-hydroxylation stereochemistry, kinetic deuterium isotope effects, and rate-limiting steps. *J Biol Chem* 280:19496–19506
37. Frandsen RJ, Frandsen M, Giese H (2012) Targeted gene replacement in fungal pathogens via *Agrobacterium tumefaciens*-mediated transformation. *Methods Mol Biol* 835:17–45
38. Dagenais TR, Chung D, Giles SS, Hull CM, Andes D, Keller NP (2008) Defects in conidiophore development and conidium-macrophage interactions in a dioxygenase mutant of *Aspergillus fumigatus*. *Infect Immun* 76:3214–3220
39. Leung KC, Li MY, Leung BC, Hsin MK, Mok TS, Underwood MJ, Chen GG (2010) Thromboxane synthase suppression induces lung cancer cell apoptosis via inhibiting NF-kappaB. *Exp Cell Res* 316:3468–3477
40. Warrilow AG, Melo N, Martel CM, Parker JE, Nes WD, Kelly SL, Kelly DE (2010) Expression, purification, and characterization of *Aspergillus fumigatus* sterol 14-alpha demethylase (CYP51) isoenzymes A and B. *Antimicrob Agents Chemother* 54:4225–4234
41. Noble MA, Quaroni L, Chumanov GD, Turner KL, Chapman SK, Hanzlik RP, Munro AW (1998) Imidazolyl carboxylic acids as mechanistic probes of flavocytochrome P-450 BM3. *Biochemistry* 37:15799–15807
42. Ishitsuka Y, Moriuchi H, Isohama Y, Tokunaga H, Hatamoto K, Kurita S, Irikura M, Iyama K, Irie T (2009) A selective thromboxane A2 (TXA2) synthase inhibitor, ozagrel, attenuates lung injury and decreases monocyte chemoattractant protein-1 and interleukin-8 mRNA expression in oleic acid-induced lung injury in guinea pigs. *J Pharmacol Sci* 111:211–215

43. Calvo AM, Hinze LL, Gardner HW, Keller NP (1999) Sporogenic effect of polyunsaturated fatty acids on development of *Aspergillus* spp. *Appl Environ Microbiol* 65:3668–3673
44. O’Gorman CM, Fuller HT, Dyer PS (2009) Discovery of a sexual cycle in the opportunistic fungal pathogen *Aspergillus fumigatus*. *Nature* 457:471–474
45. Vatsis KP, Peng HM, Coon MJ (2002) Replacement of active-site cysteine-436 by serine converts cytochrome P450 2B4 into an NADPH oxidase with negligible monooxygenase activity. *J Inorg Biochem* 91:542–553
46. Koch C, Fielding AJ, Brodhun F, Bennati M, Feussner I (2011) Linoleic acid positioning in psi factor producing oxygenase A, a fusion protein with an atypical cytochrome P450 activity. *FEBS J*. doi:10.1111/j.1742-4658.2011.08352.x (e-Pub 7 Oct 2011)
47. da Silva Ferreira ME, Kress MR, Savoldi M, Goldman MH, Hartl A, Heinekamp T, Brakhage AA, Goldman GH (2006) The akuB(KU80) mutant deficient for nonhomologous end joining is a powerful tool for analyzing pathogenicity in *Aspergillus fumigatus*. *Eukaryot Cell* 5:207–211

Improved Extraction of Saturated Fatty Acids but not Omega-3 Fatty Acids from Sheep Red Blood Cells Using a One-Step Extraction Procedure

Edward H. Clayton · Catherine E. Gulliver ·
John W. Piltz · Robert D. Taylor · Robert J. Blake ·
Richard G. Meyer

Received: 3 February 2012 / Accepted: 17 April 2012 / Published online: 10 May 2012
© AOCS 2012

Abstract Several methods are available to extract total lipid and methylate fatty acids from a range of samples including red blood cells (RBC). Fatty acid analysis of human RBC can be undertaken using a two-step extraction and methylation or a combined one-step extraction and methylation procedure. The lipid composition of sheep RBC differs significantly from that of humans and may affect their extraction. The purpose of the current study

was to examine the efficiency of extraction of lipid and detection of fatty acids from sheep RBC using a one-step procedure. Fatty acids were analysed using a one-step extraction and methylation procedure using methanol:toluene and acetyl chloride in comparison with a two-step procedure involving extraction of lipid using chloroform:methanol and separate methylation. Concentrations of saturated fatty acids including C16:0 and C18:0 were significantly higher (42.6 and 33.9 % respectively) following extraction using the one-step procedure compared with the two-step procedure. However, concentrations of some polyunsaturated fatty acids, including C20:5n-3 and C22:6n-3 were not significantly different between either procedure. The improved detection of fatty acids may be related to the ability of different solvents to extract different lipid fractions. The differential extraction of lipids and detection of fatty acids from sheep RBC may have important implications in studies examining the effect of dietary treatment on the possible health benefits of fatty acids.

E. H. Clayton (✉) · J. W. Piltz · R. G. Meyer
NSW Department of Primary Industries, Wagga Wagga
Agricultural Institute, Pine Gully Rd, Wagga Wagga,
NSW 2650, Australia
e-mail: edward.clayton@dpi.nsw.gov.au

E. H. Clayton · C. E. Gulliver · J. W. Piltz
EH Graham Centre for Agricultural Innovation, an alliance
between NSW DPI and Charles Sturt University, Wagga Wagga,
NSW, Australia

C. E. Gulliver
School of Animal and Veterinary Science, Charles Sturt
University, Wagga Wagga, NSW 2678, Australia

C. E. Gulliver
Future Farm Industries CRC, The University of Western
Australia, Crawley, WA 6009, Australia

R. D. Taylor
Australian Livestock Research, Charlestown Rd, Kotara South,
NSW 2289, Australia

R. J. Blake
Hunter New England Area Health Service, John Hunter Hospital,
Lookout Rd, New Lambton, NSW 2305, Australia

R. J. Blake
School of Biomedical Sciences, University of Newcastle,
Callaghan, NSW 2308, Australia

Keywords FAME · Methanol · Toluene · Chloroform ·
Extraction · Sheep · Red blood cells · Omega-3 · Omega-6

Abbreviations

FAME	Fatty acid methyl esters
FID	Flame ionisation detector
LoD	Limit of detection
LCn-3PUFA	Long-chain omega-3 polyunsaturated fatty acids
LCn-6PUFA	Long-chain omega-6 polyunsaturated fatty acids
MUFA	Monounsaturated fatty acids
RBC	Red blood cells
SFA	Saturated fatty acids

Introduction

Concentrations of fatty acids in red blood cells (RBC) reflect long-term dietary intake [1, 2], particularly long-chain omega-3 polyunsaturated fatty acids [LCn-3PUFA] [3]. Changes in the concentrations of LCn-3PUFA in plasma of ruminants have been reported following changes in diet, particularly, after the introduction of grain to sheep and cattle [4, 5]. The effect of diet on the concentrations of LCn-3PUFA in RBC of sheep, however, has not previously been reported.

The analysis of fatty acids in RBC typically involves a two-step procedure, firstly, extraction of lipids and, secondly, saponification and methylation [6]. There are several methods available to extract total lipids from RBC, including the Folch procedure [7], the modified procedure of Bligh and Dyer using altered solvent ratios and volumes [8] and procedures using less toxic solvents, including isopropanol [9, 10]. Lipid samples then have to be methylated separately, which lengthens the time required for analysis. A one-step extraction and methylation procedure is also available for the analysis of fatty acids in a range of tissues, including RBC of humans and rats [11]. The main advantage of this procedure is that it is less time consuming compared with the two-step procedure.

The efficiency of extraction of lipid and analysis of fatty acid methyl esters (FAME) from RBC may be differentially affected by the method of lipid extraction. The analysed concentrations of C16:0 and C18:0 but not C18:2n-6 and C20:5n-3 were significantly higher when fatty acids were analysed in the RBC of humans using the one-step procedure of Lepage and Roy compared with extraction using the Folch procedure [12]. This differential extraction may influence the results obtained when examining the effects of dietary treatments on changes in RBC fatty acid profiles.

The lipid composition of ruminant RBC differs significantly from humans. While human and ruminant RBC are comprised of approximately 26–30 % cholesterol and 50–70 % phospholipid [13, 14], ruminant RBC is comprised predominantly of sphingomyelin and lacks phosphatidyl choline [14]. Sphingomyelin accounts for approximately 54 % of phospholipid and 30 % of total lipids in sheep and cattle RBC [14]. No previous studies have examined the use of the one-step extraction and methylation procedure for the analysis of FAME in RBC of sheep. Therefore, the aims of the current study were, firstly, to determine whether the analysis of fatty acids in sheep RBC could be undertaken using the one-step extraction and methylation procedure developed by Lepage and Roy [11] compared with a two-step procedure and, secondly, to determine whether changes in RBC fatty acids following dietary treatment were affected by the method of analysis.

Materials and Methods

Experimental Design

Animals in the current study were part of a larger study examining the influence of omega-3 polyunsaturated fatty acids (PUFA) on reproductive performance (Gulliver et al. submitted) and were fed one of two dietary treatments differing in total omega-3 and omega-6 PUFA. The current study consisted of two parts. The first part of the study compared two methods for the analysis of fatty acids in sheep RBC at baseline prior to dietary treatment and the second part of the study determined whether changes in RBC fatty acids following dietary treatment differed between analytical methods.

Animals and Feeding

Thirty Merino × Border Leicester first cross ewes (mean bodyweight = 86.8 ± 1.4 kg) were randomly allocated to one of two groups using a stratified block randomisation procedure with animals stratified to block based on bodyweight. Ewes in Group 1 (high omega-3 PUFA, $n = 15$) were offered a ration containing 100 % cereal silage (n-6:n-3 ratio = 0.36), while ewes in Group 2 (high omega-6 PUFA, $n = 15$) were offered a ration containing 70 % oat grain, 22 % cereal silage and 8 % cottonseed meal (n-6:n-3 ratio = 5.28).

The study was approved by the Charles Sturt University Animal Care and Ethics Committee (Protocol No: 09/123) and was compliant with the NSW Animal Research Act 1985 (as amended) in accordance with the ethical principles that have their origins in the Australian Code of Practice for the Care and Use of Animals for Scientific Purposes [15].

Blood samples were collected from all animals at baseline prior to the introduction of experimental rations and again 2 weeks following introduction. Blood was collected from the jugular vein into a 10-mL VacutainerTM containing lithium heparin. Following centrifugation at $1,500 \times g$ for 10 min, plasma was decanted and RBC were collected as described previously [3].

Reagents and Standards

Chloroform, methanol, toluene, acetyl chloride, potassium carbonate (K_2CO_3) and sodium chloride (NaCl) were all purchased from Sigma. FAME standards were purchased from Nu-Chek Prep (GLC68C, Elysian, MN USA), Supelco (37 Component FAME Mix, Cat No. 47885-U and C18:1n-7, Cat No. 4-6904, Supelco, Bellefonte, PA) and Sigma (C18:3n-6, Cat No. L6503-100MG, C20:5n-3, Cat No. E2012-5MG and C22:2n-6, Cat No. D4034-25MG, St

Louis, MO). The nonadecanoic acid methyl ester (C19:0) internal standard was also purchased from Sigma (Cat No. N5377-1G, St Louis, MO).

Lipid Extraction Using the Folch Procedure

Total lipids were extracted from RBC using the method of Folch [7] with slight modifications. In brief, 200 μL of RBC was added to a round-bottomed centrifuge tube and 5.0 mL of a chloroform:methanol (2:1 v/v) mixture was added to give a final solvent:sample ratio of 25:1 [16]. Tubes were capped and samples were vortexed vigorously for 30 s. Following agitation for 15 min using an orbital shaker, samples were centrifuged for 15 min at $1,500\times g$. The supernatant was transferred to a conical centrifuge tube and 1.0 mL of 0.9 % NaCl added to facilitate the separation of layers. Samples were centrifuged for 10 min at $600\times g$ and the lower chloroform layer containing total lipids was transferred by aspiration to an 8.0 mL glass culture tube with a Teflon-lined lid (Elm Scientific). The remaining solvent was evaporated under nitrogen at 40 °C. The total lipid component was then methylated using the Lepage and Roy procedure outlined below.

Direct Extraction and Methylation—Lepage and Roy

Total RBC lipids were extracted and fatty acids were methylated using the one-step procedure of Lepage and Roy [11]. In brief, 100 μL of RBC (or total lipid extracted using the Folch procedure described above) was added to an 8.0-mL glass culture tube and exactly 2.0 mL of methanol:toluene (4:1 v/v) containing C19:0 (0.02 mg/mL) internal standard was added and vortexed vigorously. Fatty acids were methylated by adding 200 μL acetyl chloride drop-wise while vortexing, followed by heating to 100 °C for 1 h. After cooling, the reaction was stopped by slowly adding 5 mL of 6 % K_2CO_3 while mixing by vortex. The sample was centrifuged at $1,500\times g$ for 10 min to facilitate the separation of the layers. The upper toluene layer containing the FAME was transferred to a 2-mL glass vial and sealed with a Teflon-lined screw-cap for subsequent analysis by gas chromatography.

FAME Analysis

Individual FAME were identified using an Agilent 6890 N gas chromatograph (GC) with a flame ionisation detector (FID). FAME were separated using a fused carbon–silica column, coated with cyanopropylphenyl (BPX70, 30 m \times 0.25 mm i.d. and 0.25 μm film thickness, SGE Analytical Science, Ringwood, Victoria, Australia, P/N 054622). The carrier gas was helium with a total flow rate of

12.4 mL min^{-1} , a split ratio of 10:1 and a column flow of 0.9 mL min^{-1} . The inlet temperature was 250 °C, the inlet pressure was 107.8 kPa and the injection volume was 3 μL into a focus inlet liner (4 mm i.d. SGE Analytical Science, P/N 092002) that was changed at least every 50 injections. The oven temperature was set at 150 °C and held for 0.5 min, increased at 10 °C min^{-1} to 180 °C, increased at 1.5 °C min^{-1} to 220 °C and then increased at 30 °C min^{-1} up to 260 °C and maintained for 5 min to give a total run time of 36.5 min. The FID temperature was set at 280 °C with the following gas flow rates; hydrogen = 35 mL min^{-1} , instrument air = 350 mL min^{-1} and nitrogen make-up gas = 30 mL min^{-1} . Sample FAME peaks were identified by comparing their retention times with those of a standard mixture of genuine FAME (as described above) and quantitated using Agilent Chemstation Version B.01.03 and Microsoft Excel using a four point standard curve for each FAME using C19:0 as the internal standard. In addition, some peaks for branched-chain fatty acids, for which standard FAME were not available, were identified by comparison with published data as described previously [17]. All results were calculated as $\mu\text{g}/\text{mL}$ RBC or $\text{g}/100$ g total identified FAME.

The lower limit of detection (LoD) was calculated from three times the standard deviation of the estimated peak area:internal standard peak area ratio for a concentration equal to 0 interpolated from the four standards [18]. The LoD was less than 0.01 $\mu\text{g}/\text{mL}$ for all FAME analysed. The co-efficient of variation for the analyses ranged between 3.1–8.2 % for the two-step procedure and 1.1–2.2 % for the one-step procedure.

Statistical Analyses

Prior to analysis, data were assessed for homoscedasticity and normality assumptions using the Scatterplot and Explore options of the Statistical Package for Social Sciences (SPSS) version 14.0 for Windows [19]. Differences in concentrations of FAME between methods at baseline and over time were analysed by repeated measures analysis using the Mixed Model procedure in the SAS statistical program [20]. The restricted maximum likelihood (REML) estimation used “animal” nested within “method” as the individual experimental unit and “animal” nested within “method” as a random effect [3, 21]. The most appropriate covariance structure for each analysis was determined by reference to the Schwarz’s Bayesian Information Criterion (BIC) [22]. The analysis determined the fixed effects of “analytical method”, “dietary treatment” and “time” as well as the interaction between fixed effects. The relationship between RBC FAME concentrations between analytical methods were analysed by Pearson correlation using SAS.

The mean percentage change in each of the major FAME over time following dietary treatment was also analysed using the Mixed Model procedure in SAS. The analysis determined the fixed effects of “analytical method” and “dietary treatment”. Data for percentage change in FAME over time were positively skewed and were transformed prior to analysis ($Y = \log_{10} C18:0 + 17.5$, $Y = \log_{10} C18:2n-6 + 13.5$, $Y = \log_{10} C18:3n-3 + 33.8$, $Y = \log_{10} n-6:n-3 \text{ ratio} + 48.6$) [23].

One ewe offered the high omega-6 PUFA diet refused to eat oats and was, therefore, withdrawn from the study and data from that ewe were excluded from all analyses. An alpha of 0.05 was used for all statistical tests.

Results

Baseline FAME Concentrations

The mean concentration of the major saturated fatty acids (SFA) including C16:0, C18:0 and C22:0 was significantly ($p < 0.01$) higher when RBC FAME were analysed using the one-step procedure compared with the two-step procedure (Table 1). Conversely, concentrations of RBC omega-3 PUFA including C18:3n-3, C20:5n-3 and C22:5n-3 were not significantly ($p > 0.05$) different when RBC FAME were analysed using the one-step compared with the two-step procedure (Table 1). Mean concentrations of C18:0 were underestimated by approximately 26.9 % when fatty acids were analysed using the two-step procedure compared with the one-step procedure of Lepage and Roy, while concentrations of C18:2n-6 were underestimated by approximately 18.9 % using the two-step procedure. The SFA percentage as a proportion of total FAME was higher, while the percentage of monounsaturated fatty acids (MUFA), n-3 and n-6 PUFA were lower when RBC FAME were analysed using the one-step compared with the two-step procedure (data not shown).

Concentrations of RBC FAME analysed using the one-step and two-step procedures were significantly ($p < 0.001$) positively correlated. The relationship between analytical procedures was higher for C18:3n-3 ($r^2 = 0.92$) and C18:2n-6 ($r^2 = 0.78$) compared with C18:0 ($r^2 = 0.57$, Fig. 1).

Change in FAME Concentrations Following Dietary Treatment

Mean concentrations of C18:0 (141.3 ± 2.76 versus 131.7 ± 2.65 , $p = 0.015$) and C18:2n-6 (93.2 ± 2.17 versus 81.2 ± 2.08 , $p < 0.001$) and the ratio of n-6:n-3 fatty acids (3.53 ± 0.07 versus 2.81 ± 0.07 , $p < 0.001$) were significantly higher when sheep consumed a diet high in omega-6 PUFA compared with omega-3 PUFA for

14 days. Conversely, the mean concentration of RBC C18:3n-3 was significantly ($p < 0.001$) lower when sheep consumed a diet high in omega-6 PUFA (11.95 ± 0.47 compared with omega-3 PUFA (17.27 ± 0.45)).

The response to dietary treatment was not significantly different when RBC FAME were analysed using either the one-step or two-step procedure (analytical method \times dietary treatment \times time interaction, $p > 0.05$). The interaction between analytical method and dietary treatment was also not significant in the analysis of percentage change in any FAME over time, however, the percentage decrease in n-6:n-3 ratio when ewes were fed a diet high in omega-3 PUFA (but not the diet high in omega-6 PUFA) was significantly ($p = 0.008$) greater when FAME were analysed using the two-step procedure (re-transformed mean = -35.9%) compared with the one-step procedure (re-transformed mean = -25.5% , Fig. 2).

Discussion

The differential analysis of fatty acids from sheep RBC using the one-step compared with the two-step procedure observed in the current study agrees with previous findings examining the extraction of lipids from a range of tissues. The concentration of a number of fatty acids, in particular SFA, was higher in human RBC [12], milk [24] and plasma [11] when lipids were extracted and FAME were analysed using the one-step procedure compared with extraction of lipid using the Folch procedure.

Concentrations of fatty acids were not always higher when the one-step procedure was employed in the current study, which also agrees with previous comparisons. For example, concentrations of the LCn-3PUFA C20:5n-3 and C22:5n-3 were not significantly different between methods in the current study which is similar to findings with human RBC [12]. The differential detection of SFA compared with MUFA, LCn-3PUFA and LCn-6PUFA resulting in changes in the percentage of FAME as a proportion of total FAME has important implications for the analysis of FAME in RBC. The relationship between RBC FAME and health markers of disease may be affected differentially by the method of analysis used, if the proportions of FAME are considered.

Although concentrations of FAME were significantly different between the two analytical methods, the change in FAME concentrations over the period of feeding experimental diets that differed in omega-3 PUFA and omega-6 PUFA did not differ significantly between methods. The reduction in the n-6:n-3 ratio when ewes consumed a diet high in omega-3 PUFA, however, was significantly greater when the two-step procedure was used compared with the one-step procedure. This differential analysis has important

Table 1 Mean concentration ($\mu\text{g/mL}$) of fatty acid methyl esters (FAME) in the red blood cells of ewes at baseline prior to dietary treatment using the one-step procedure of Lepage and Roy compared with a two-step procedure including Folch lipid extraction

FAME	Method of extraction		
	Two-step procedure (Folch)	One-step procedure (Lepage)	<i>p</i> values
SFA			
C10:0	0.23 (± 0.10)	0.97 (± 0.10)	<0.001
C11:0	13.13 (± 0.70)	2.14 (± 0.71)	<0.001
C12:0	0.35 (± 0.06)	1.42 (± 0.07)	<0.001
C14:0	4.06 (± 0.14)	4.36 (± 0.14)	0.144
iC15:0	1.40 (± 0.06)	1.06 (± 0.06)	<0.001
aiC15:0	0.87 (± 0.04)	1.36 (± 0.04)	<0.001
C15:0	3.28 (± 0.12)	5.10 (± 0.12)	<0.001
C16:0	138.5 (± 3.95)	196.1 (± 4.02)	<0.001
iC17:0	4.07 (± 0.17)	5.34 (± 0.17)	<0.001
aiC17:0	2.99 (± 0.25)	3.83 (± 0.26)	0.023
C17:0	11.39 (± 0.41)	16.63 (± 0.42)	<0.001
C18:0	105.4 (± 3.18)	144.2 (± 3.23)	<0.001
C20:0	1.43 (± 0.07)	1.75 (± 0.07)	0.001
C21:0	1.90 (± 0.09)	0.94 (± 0.09)	<0.001
C22:0	11.91 (± 0.45)	17.05 (± 0.46)	<0.001
C23:0	4.45 (± 0.14)	5.97 (± 0.15)	<0.001
C24:0	25.23 (± 0.96)	37.26 (± 0.98)	<0.001
Total SFA	330.5 (± 7.78)	446.2 (± 7.92)	<0.001
MUFA			
C14:1n-7	0.39 (± 0.10)	0.56 (± 0.10)	0.223
C15:1n-4	0.61 (± 0.16)	0.38 (± 0.17)	0.321
C16:1n-7	7.57 (± 0.27)	9.89 (± 0.28)	<0.001
C17:1n-6	6.31 (± 0.40)	2.03 (± 0.41)	<0.001
C18:1n9t	2.59 (± 0.09)	1.78 (± 0.09)	<0.001
C18:1n-9	309.9 (± 9.16)	382.5 (± 9.33)	<0.001
C18:1n-7	13.57 (± 1.15)	22.48 (± 1.17)	<0.001
C20:1n-9	3.15 (± 0.15)	5.14 (± 0.15)	<0.001
C22:1n-9	1.62 (± 0.07)	2.20 (± 0.07)	<0.001
C24:1n-9	140.9 (± 6.56)	200.5 (± 6.69)	<0.001
Total MUFA	486.6 (± 15.56)	627.5 (± 15.86)	<0.001
n-3 PUFA			
C18:3n-3	11.36 (± 0.55)	12.06 (± 0.56)	0.379
C20:3n-3	0.61 (± 0.05)	0.85 (± 0.05)	0.001
C20:5n-3	6.30 (± 0.55)	6.76 (± 0.56)	0.554
C22:5n-3	5.07 (± 0.31)	4.90 (± 0.32)	0.703
C22:6n-3	3.75 (± 0.21)	4.68 (± 0.22)	0.003
Total n-3 PUFA	27.09 (± 1.40)	29.25 (± 1.42)	0.279
n-6 PUFA			
C18:2n-6t	1.97 (± 0.11)	0.71 (± 0.11)	<0.001
C18:2n-6	63.16 (± 2.56)	77.87 (± 2.61)	<0.001
C18:3n-6	0.83 (± 0.14)	1.20 (± 0.15)	0.069
C20:2n-6	0.96 (± 0.06)	2.08 (± 0.06)	<0.001
C20:3n-6	1.04 (± 0.06)	1.32 (± 0.06)	0.002
C20:4n-6	8.32 (± 0.54)	8.68 (± 0.55)	0.636
C22:2n-6	0.59 (± 0.13)	1.91 (± 0.14)	<0.001
Total n-6 PUFA	83.19 (± 3.17)	94.60 (± 3.22)	0.014
Total Identified FAME	921.1 (± 24.72)	1195.4 (± 25.19)	<0.001
n-6:n-3 Ratio	3.14 (± 0.08)	3.27 (± 0.09)	0.300

FAME fatty acid methyl esters, SFA saturated fatty acids, MUFA monounsaturated fatty acids, n-3 PUFA omega-3 polyunsaturated fatty acids, n-6 PUFA omega-6 polyunsaturated fatty acids

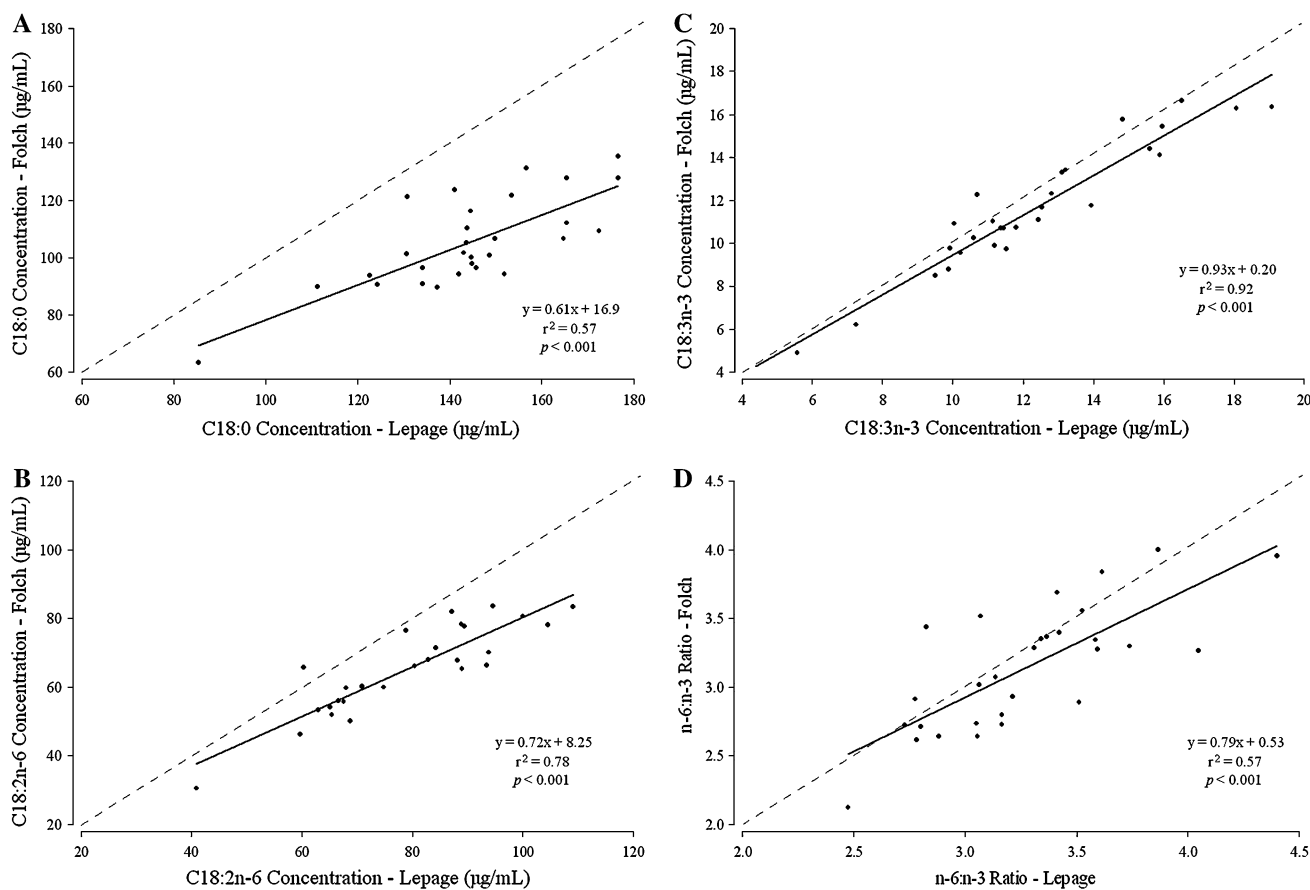


Fig. 1 Correlation between the concentration of **a** C18:0, **b** C18:2n-6, **c** C18:3n-3 ($\mu\text{g/mL}$) and **d** the ratio of omega-6:omega-3 polyunsaturated fatty acids (n-6:n-3 ratio) in the red blood cells (RBC) of sheep following analysis of fatty acids using the one-step

extraction and methylation procedure of Lepage and Roy [11] or the two-step procedure including a Folch extraction [7]. Data are baseline concentrations prior to dietary treatment

implications, particularly in research projects examining the effects of dietary treatment on health benefits of LCn-3PUFA in both animal or human studies, as the n-6:n-3 ratio may be the most closely related marker for several diseases, including cardiovascular disease [25] and mental health disorders such as depression [26].

The differential analysis of FAME from RBC observed in the current study was likely due to the different polarity of solvents used to extract different lipid fractions. The extraction of non-polar lipids such as cholesteryl esters and triglycerides is expected to be greater when a lower polarity solvent mixture is used, such as that used in the Folch extraction (chloroform:methanol (2:1 v/v), dielectric constant = 14.2), compared with a higher polarity solvent mixture used in the Lepage and Roy extraction (methanol:toluene (4:1 v/v), dielectric constant = 26.9) [6]. Conversely, extraction of polar lipids such as phospholipid is expected to be greater when a higher polarity solvent is used.

The proportion of fatty acids that are expected to be contained in different lipid fractions of sheep [27] or cattle

[28] RBC and the expected proportion of different lipid fractions in sheep RBC [14, 27, 29] were estimated from previous studies. These estimates were used to calculate the proportion of each fatty acid likely to be found in the phospholipid fraction of RBC and compared with the differential analysis of fatty acids between methods in the current study (Fig. 3). The improved detection of FAME with the one-step compared with the two-step procedure in the current study was significantly positively correlated ($r^2 = 0.58$, $p < 0.01$) with the estimated proportion of each fatty acid contained in phospholipid (Fig. 3). The detection of C22:0, C24:0 and C24:1n-9 that is contained solely in the phospholipid fraction of RBC was approximately 30 % higher when FAME was analysed with the one-step compared with the two-step procedure.

Similar improvements in the detection of fatty acids contained predominantly in phospholipids have been found in previous studies when higher polarity solvents were used. For example, the concentration of a number of fatty acids including C16:0 and C18:0 in beef [30], human plasma [31] and human RBC [10] was significantly higher

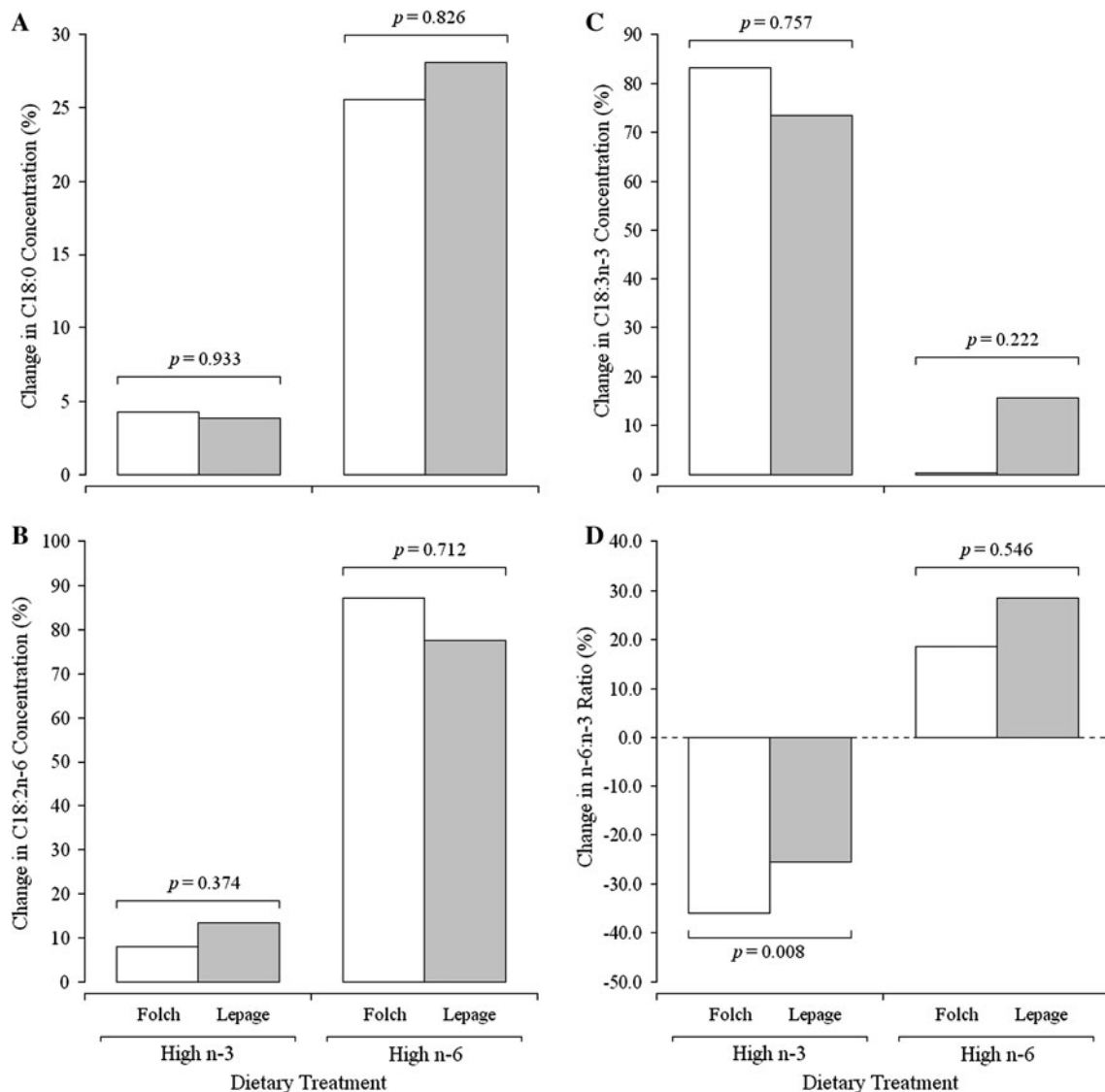


Fig. 2 Mean percentage change in the concentration of **a** C18:0, **b** C18:2:n-6, **c** C18:3:n-3 and **d** the ratio of omega-6:omega-3 fatty acids (n-6:n-3 ratio) in the red blood cells (RBC) of sheep following the consumption of a diet high in omega-3 or omega-6 polyunsaturated fatty acids for 14 days. Fatty acids were analysed using the one-step extraction and methylation procedure of Lepage and Roy

[11] (shaded bars) or the two-step procedure including a Folch extraction [7] (unshaded bars). Values are re-transformed least squares means (transformations prior to analysis; $Y = \log_{10} \text{C18:0} + 17.5$, $Y = \log_{10} \text{C18:2n-6} + 13.5$, $Y = \log_{10} \text{C18:3n-3} + 33.8$, $Y = \log_{10} \text{n-6:n-3 ratio} + 48.6$)

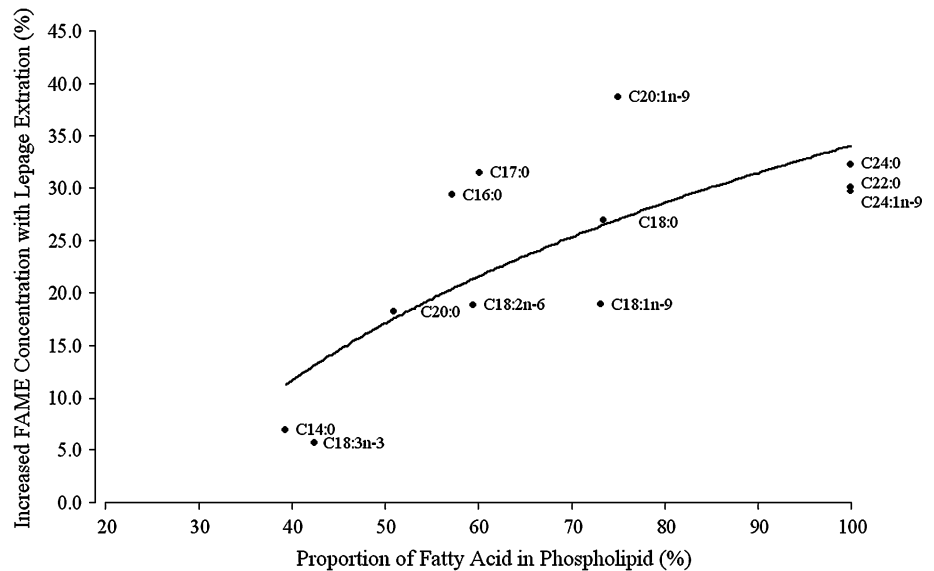
when methanol or hexane:isopropanol were used compared with chloroform:methanol.

The lower detected concentrations of FAME in RBC when the Folch lipid extraction procedure was used could also be due to physical effects of the solvents on RBC membranes. For example, low polarity chloroform may have led to clotting of membrane-bound proteins and a reduction in the ability of the solvents to extract membrane bound fatty acids [10]. The Folch extraction procedure may need to be undertaken if individual lipid fractions need to be separated, therefore, it may be necessary to improve the extraction of fatty acids using this procedure. The

extraction of total lipid from RBC may be improved if RBC are mixed initially with ice-cold methanol alone and then chloroform is added in the correct proportion following the initial extraction with methanol [13]. The extraction of lipid and SFA may also be improved with additional chloroform washes [16], however, this would add considerable time to an already lengthy procedure. Further research is required to determine whether the extraction of total lipid from sheep RBC can be improved with modifications to the Folch procedure.

There are limitations to the one-step extraction and methylation procedure that need to be addressed during

Fig. 3 Relationship between the proportion of total fatty acid in phospholipid and the percentage increase in fatty acid methyl ester (FAME) concentration at baseline prior to dietary treatment using the one-step extraction and methylation procedure of Lepage and Roy [11] compared with extraction of lipid using the Folch procedure [7]. Increased FAME concentration with Lepage extraction (%) = $[56.2 \times \log_{10} \text{proportion of fatty acid in phospholipid (\%)}] - 78.43$, $r^2 = 0.58$, $p < 0.01$. Proportion of fatty acid in phospholipid derived from data in sheep [27] or cattle (C24:0 and C24:1n-4) [28]



chromatography analysis. For example, the chromatography resolution degrades following multiple injections which can increase the limit of detection. While this degradation in resolution can be overcome by changing the inlet liner at least every 50 injections, this adds an additional cost to the analysis. Different inlet liners can also alter the resolution and, therefore, correct inlet liner selection is critical to the analysis.

Conclusions

The analysis of fatty acids from sheep RBC using the one-step Lepage and Roy procedure resulted in higher analysed concentrations of a number of fatty acids, primarily SFA, compared with lipid extraction using the Folch procedure prior to methylation. The observed difference in fatty acid concentration was most likely due to improved extraction of phospholipids using higher polarity solvents in the one-step procedure. The effect of dietary treatment on RBC FAME was similar when the one-step and two-step procedures were used, however, the effect of dietary treatment on the n-6:n-3 ratio of RBC was significantly different between analytical methods. This differential detection of omega-6 PUFA compared with omega-3 PUFA may have important implications in studies examining the effect of dietary treatment on the health benefits of different fatty acids where the primary outcome of importance is the n-6:n-3 ratio.

Acknowledgments We thank Greg Clark, Steven Huckell, Michael Loiterton, Rex Edis, Craig Rodham, John Wilkins, Susan Robertson, the Gulliver family, Jessica Rose, John Broster and Dr Stephanie Knott for technical assistance during the conduct of the study. We also thank Jamie Ayton for providing assistance with the gas chromatography.

This study was conducted without dedicated external funding. This study was supported by in-kind provision of equipment by the Diagnostic and Analytical Systems division of NSW DPI.

Conflict of interest None.

References

- Brown AJ, Pang E, Roberts DC (1991) Persistent changes in the fatty acid composition of erythrocyte membranes after moderate intake of n-3 polyunsaturated fatty acids: study design implications. *Am J Clin Nutr* 54(4):668–673
- Marckmann P, Lassen A, Haraldsdottir J, Sandstrom B (1995) Biomarkers of habitual fish intake in adipose tissue. *Am J Clin Nutr* 62(5):956–969
- Clayton EH, Hanstock TL, Kable CJ, Hirneth SJ, Garg ML, Hazell PL (2008) Long-chain omega-3 polyunsaturated fatty acids in the blood of children and adolescents with juvenile bipolar disorder. *Lipids* 43(11):1031–1038
- Duckett SK, Wagner DG, Yates LD, Dolezal HG, May SG (1993) Effects of time on feed on beef nutrient composition. *J Anim Sci* 71(8):2079–2088
- Scollan ND, Choi NJ, Kurt E, Fisher AV, Enser M, Wood JD (2001) Manipulating the fatty acid composition of muscle and adipose tissue in beef cattle. *Br J Nutr* 85(1):115–124
- Christie WW (2003) *Lipid analysis: isolation, separation, identification and structural analysis of lipids*, 3rd edn. The Oily Press, Bridgwater
- Folch J, Lees M, Sloane Stanley GH (1957) A simple method for the isolation and purification of total lipids from animal tissues. *J Biol Chem* 226(1):497–509
- Bligh EG, Dyer WJ (1959) A rapid method of total lipid extraction and purification. *Can J Biochem Physiol* 37(8):911–917
- Hara A, Radin NS (1978) Lipid extraction of tissues with a low-toxicity solvent. *Anal Biochem* 90(1):420–426
- Bocking C, Nockher WA, Schreiner M, Renz H, Pfefferle PI (2010) Development and validation of a combined method for the biomonitoring of omega-3/6 fatty acids and conjugated linoleic acids in different matrices from human and nutritional sources. *Clin Chem Lab Med* 48(12):1757–1763

11. Lepage G, Roy CC (1986) Direct transesterification of all classes of lipids in a one-step reaction. *J Lipid Res* 27(1):114–120
12. Rodriguez-Palmero M, Lopez-Sabater MC, Castellote-Bargallo AI, De la Torre-Boronat MC, Rivero-Urgell M (1997) Comparison of two methods for the determination of fatty acid profiles in plasma and erythrocytes. *J Chromatogr A* 778(1–2):435–439
13. Ways P, Hanahan DJ (1964) Characterization and quantification of red cell lipids in normal man. *J Lipid Res* 5(3):318–328
14. Nelson GJ (1967) Lipid composition of erythrocytes in various mammalian species. *BBA Lipid Lipid Met* 144(2):221–232
15. NHMRC (2004) Australian code of practice for the care and use of animals for scientific purposes, 7th edn. Australian Government, Canberra
16. Iverson SJ, Lang SL, Cooper MH (2001) Comparison of the Bligh and Dyer and Folch methods for total lipid determination in a broad range of marine tissue. *Lipids* 36(11):1283–1287
17. Or-Rashid MM, Fisher R, Karrow N, AlZahal O, McBride BW (2010) Fatty acid profile of colostrum and milk of ewes supplemented with fish meal and the subsequent plasma fatty acid status of their lambs. *J Anim Sci* 88(6):2092–2102
18. NATA (2009) Technical Note 17 - Guidelines for the validation and verification of chemical test methods. National Association of Testing Authorities Available online: http://www.nata.asn.au/phocadownload/publications/Technical_publications/Technotes_Infopapers/technical_note_17_apr09.pdf. Accessed 1 Dec 2011
19. Coakes SJ, Steed LG (2001) SPSS: analysis without anguish, version 10.0 for windows. Wiley, Sydney
20. SAS Institute Inc (1997) SAS/STAT Software: changes and enhancements through release 6.12. SAS Institute Inc, Cary
21. Littell RC, Henry PR, Ammerman CB (1998) Statistical analysis of repeated measures data using SAS procedures. *J Anim Sci* 76(4):1216–1231
22. Wang Z, Goonewardene LA (2004) The use of MIXED models in the analysis of animal experiments with repeated measures. *Can J Anim Sci* 84(1):1–11
23. Tabachnick BG, Fidell LS (2001) Using multivariate statistics, 4th edn. Allyn and Bacon, Sydney
24. Lepage G, Roy CC (1984) Improved recovery of fatty acid through direct transesterification without prior extraction or purification. *J Lipid Res* 25(12):1391–1396
25. Simopoulos AP (1999) Essential fatty acids in health and chronic disease. *Am J Clin Nutr* 70(3 Suppl):S560–S569
26. Clayton EH, Hanstock TL, Garg ML, Hazell PL (2007) Long-chain omega-3 polyunsaturated fatty acids in the treatment of psychiatric illnesses in children and adolescents. *Acta Neuro-psych* 19(2):92–103
27. Connellan JM, Masters CJ (1965) Fatty acid components of ovine erythrocyte lipids. *Aust J Biol Sci* 18:445–447
28. Hanahan DJ, Watts RM, Papajohn D (1960) Some chemical characteristics of the lipids of human and bovine erythrocytes and plasma. *J Lipid Res* 1(5):421–432
29. Nelson GJ (1967) Composition of neutral lipids from erythrocytes of common mammals. *J Lipid Res* 8(4):374–379
30. Rule DC (1997) Direct transesterification of total fatty acids of adipose tissue, and of freeze-dried muscle and liver with boron-trifluoride in methanol. *Meat Sci* 46(1):23–32
31. Araujo P, Nguyen TT, Froyland L, Wang JD, Kang JX (2008) Evaluation of a rapid method for the quantitative analysis of fatty acids in various matrices. *J Chromatogr A* 1212(1–2):106–113

LC–ESI–MS/MS Identification of Polar Lipids of Two Thermophilic *Anoxybacillus* Bacteria Containing a Unique Lipid Pattern

Tomáš Řezanka · Margarita Kambourova ·
Anna Derekova · Irena Kolouchová ·
Karel Sigler

Received: 15 February 2012 / Accepted: 12 April 2012 / Published online: 8 May 2012
© AOCS 2012

Abstract Phospholipids and glycolipids from two recently described species belonging to the thermophilic genus *Anoxybacillus* were analyzed by liquid chromatography–electrospray tandem mass spectrometry (LC/ESI–MS/MS). Analysis of total lipids from the facultatively anaerobic *A. bogrovensis* on a HILIC (Hydrophilic Interaction LIquid Chromatography) column succeeded in separating diacyl- and plasmalogen phospholipids. The LC/ESI–MS/MS analysis of the strict aerobe *A. rupsiensis* revealed the presence of different unique polar lipids, predominantly alanyl-, lysyl-, and glucosyl-phosphatidylglycerols and cardiolipins. Each of the classes of polar lipids was then analyzed by means of the ESI–MS/MS and more than 140 molecular species of six lipid classes from *A. bogrovensis* and nearly 200 molecular species of nine classes of polar lipids from *A. rupsiensis* were identified. Five classes of unidentified polar lipids were detected in both strains. Plasmalogens were thus determined for the first time in a facultatively anaerobic bacterium, i.e. *A. bogrovensis*.

Electronic supplementary material The online version of this article (doi:10.1007/s11745-012-3675-0) contains supplementary material, which is available to authorized users.

T. Řezanka (✉) · K. Sigler
Institute of Microbiology, Academy of Sciences of the Czech Republic, Vídeňská 1083, 142 20 Prague, Czech Republic
e-mail: rezanka@biomed.cas.cz

M. Kambourova · A. Derekova
Institute of Microbiology, Bulgarian Academy of Science,
acad. G. Bonchev str. 26, 1113 Sofia, Bulgaria

I. Kolouchová
Department of Biotechnology, Institute of Chemical Technology
Prague, Technická 5, 166 28 Prague, Czech Republic

Keywords *Anoxybacillus* · Plasmalogens · *O*-Aminoacylphosphatidylglycerols · *O*-Aminoacyl cardiolipins · Liquid chromatography–electrospray tandem mass spectrometry · HILIC column

Abbreviations

ACN	Acyl carbon number
APtdGro	Acyl-phosphatidylglycerol
BMP	Bismonoacylglycerophosphate
CID	Collision-induced dissociation
Ptd ₂ Gro	Cardiolipin or diphosphatidylglycerol, or more precisely 1,3-bis(<i>sn</i> -3'-phosphatidyl)- <i>sn</i> -glycerol
FA	Fatty acid
FAME	Fatty acid methyl ester
GC–MS	Gas chromatography–mass spectrometry
HILIC	Hydrophilic Interaction LIquid Chromatography
LC/ESI–MS/MS	Liquid chromatography–electrospray ionization tandem mass spectrometry
PlsEtn	Ethanolamine plasmalogen
PlsGro	Glycerol plasmalogen
PlsOH	Plasmalogen phosphatidic acid
PtdEtn	Phosphatidylethanolamine
PtdGro	Phosphatidylglycerol
PtdOH	Phosphatidic acid
TLC	Thin layer chromatography

Introduction

Thermophilic bacteria are type extremophiles that are adapted to life at high temperature (optimum growth above 50 °C). They inhabit separate permanently hot niches such as

areas with geothermal and volcanic activity. They were among the first inhabitants of Earth and hold the lowest branches in the global phylogenetic tree of life; their study is thus intimately related with the question of the origin of life and biological evolution. Thermophilic adaptation to severe conditions resulted in the development of several unique mechanisms, one of which is a specific composition of microbial membranes, which form the lipid bilayer permeability barrier of cells. The ability of bacteria to control and modify the biophysical properties of their membrane is achieved by a change of phospholipid composition in response to environmental changes. As an adaptation to the fluidizing effects of increased growth temperature, it is common to observe an increase in the proportion of long chain and saturated fatty acids within the membrane [1].

The efforts to identify new lipids, which may extend the scientific knowledge and have potential practical application, include the isolation and study of new microorganisms in long-known genera. The genus *Bacillus* has a long taxonomic history. Since it was described by Cohn in 1872, its systematics has undergone major revisions [2]. Based on the large number of novel endo-spore forming bacteria described in the 1990-s, Zeigler [3] described 15 genera as *Bacillus* sensu lato (*Bacillus*-like group) and predicted the list of approved *Bacillus*-like genera to expand rapidly during the new decade. One of the recently described genera in this clade is the genus *Anoxybacillus*; its representatives are thermophilic and alkaliphilic or alkalitolerant, chemorganotrophic bacteria. Though representatives of *Anoxybacillus* have been first identified as anaerobes [4], an additional amendment [5] referred to them as aerotolerant anaerobes. Further, most of these species have been found to be facultative anaerobes and even for some species anaerobic growth was registered only in some conditions [6]. The genus comprises currently 15 species [7] isolated from different geographical areas—Russia, Belgium, Turkey, Mongolia, etc. Two of the species, *A. rupiensis* [8] and *A. bogrovensis* [9] were recently isolated from Bulgarian hot springs and novel molecules of lipids including, e.g., plasmalogens were envisaged in these new microorganisms.

Plasmalogens are any derivatives of *sn*-glycero-3-phosphoric acid that contain *O*-alk-1'-enyl residue attached to the glycerol moiety at *sn*-1 position and a polar head made of a nitrogenous base or glycerol moiety. Their occurrence is limited to strictly anaerobic bacteria and they have not yet been identified in aerobic or facultatively anaerobic bacteria. They are common constituents of animal lipids from invertebrates to humans [10] and are found mostly as plasmalogen phosphatidylcholine, plasmalogen ethanolamine (PlsEtn), plasmalogen phosphatidylglycerol (PlsGro), and plasmalogen phosphatidic acid (PlsOH).

Phosphatidylglycerol (PtdGro) and cardiolipin (Ptd₂Gro) are the major anionic membrane lipids in most bacteria [11].

Forms of PtdGro and Ptd₂Gro modified by different amino acids have been described; for instance, lysyl-phosphatidylglycerol (lysyl-PtdGro) and other aminoacyl esters of PtdGro, such as alanyl-PtdGro, or ornithyl-PtdGro, are major membrane lipids in several Gram-positive bacteria (Firmicutes) [12]. Lysyl-PtdGro constitutes a major membrane lipid in different strains of bacteria [13, 14] such as *Bacillus subtilis* [15], *B. anthracis* [16], and *Listeria monocytogenes* [17]. Alanyl-PtdGro was isolated from *Clostridium perfringens* [14]. A large variety of PtdGro-derived lipids are present in *Enterococcus faecalis* (formerly known as *Streptococcus faecalis*) which probably has alanyl-PtdGro, 2'-lysyl-PtdGro, 3'-lysyl-PtdGro, 2',3'-dilysyl-PtdGro, arginyl-PtdGro, and a diglucosyl derivative of PtdGro [18].

Lysyl-, alanyl-, and glucosyl-Ptd₂Gro have also been described in bacteria [19]. The paper by Peter-Katalinic and Fischer [20], who identified α -D-glucopyranosyl-, D-alanyl- and L-lysylcardiolipin from Gram-positive bacteria (*Streptococcus* sp., *Vagococcus fluvialis* or from *Listeria welshimeri*), can be considered a basic study in the field of mass spectrometry of these polar lipids. A detailed structural study of a cardiolipin and an integral membrane protein was reported for *Rhodobacter sphaeroides* AM260W, which is able to grow heterotrophically via fermentation and aerobic and anaerobic respiration [21].

Identification of these polar lipids is relatively difficult. Many studies using two-dimensional TLC identified only some of the spots while other spots remained unidentified. Other methods of choice are HPLC, especially in combination with mass spectrometry, or mass spectrometry alone, including tandem mass spectrometry [22]. These methods were used for identifying 16 bacterial strains, e.g. *Bacillus subtilis* or *Staphylococcus aureus* [23].

Further, amphiphilic molecules such as phospholipids can be separated on a Hydrophilic Interaction LIquid Chromatography (HILIC) column, but this method has been described in only a few papers, with relatively controversial results concerning especially the elution of individual phospholipid classes [24–26].

This report is part of our investigation of bacterial lipids within the framework of a comprehensive program on the analysis and biosynthesis of lipids [27, 28]. We present here the separation and identification by LC–ESI/MS² of intact plasmalogen phospholipids from diacyl phospholipids of the facultatively anaerobic bacterium *A. bogrovensis*, and nearly 200 molecular species of nine classes of polar lipids from *A. rupiensis*.

Results and Discussion

The total lipid extracts prepared from *A. bogrovensis* by the modified Bligh and Dyer method [29] have been

pre-fractionated by using a cartridge with aminopropyl silica-based polar bonded phase, and further separated on a HILIC column into the individual lipid classes [28]. The chromatographic conditions have been optimized to provide the best separation of all lipid classes. The composition of mobile phase is crucial for the separation of lipid classes. Good resolution of lipid classes was obtained with the mixture of hexane/2-propanol/aqueous ammonium acetate [30] but better selectivity, chromatographic resolution and low background noise were observed in a mobile phase containing methanol–acetonitrile–water with ion-pairing agents such as ammonium salts [24]. The concentration of water and salts including the pH value of mobile phase are crucial parameters for separation and identification of ionic lipids. The use of ion-pairing agents (e.g., ammonium acetate or formate) significantly improves the chromatographic resolution and ionization efficiency of lipids. The best separation and signal intensity have been achieved in mobile phases with 1 mM aqueous ammonium acetate at pH 7 [28]. Lipids from *A. bogrovensis* were separated (Fig. 1) and quantified based on the negative-ion ESI mass spectra [Table 1S (Supplement)]. The retention times of eluted lipids are based on their adsorptions (electrostatic forces) on the HILIC column and showed that lipids with higher polarity or stronger dissociation are more retained. Most lipid classes were baseline separated but some lipids were co-eluted and five peaks were not identified (U1–U5); see Fig. 1 and Table 1S (Supplement).

Individual strains of genus *Bacillus* are being continuously reclassified on the basis of 16S rRNA gene sequence analysis [31]. This is the probable reason why older papers about lipids of bacilli describe considerable heterogeneity in the lipid content [32]. On the other hand, it should be noted that the polar lipids of most bacilli have not yet been

identified. Most of the authors are satisfied with the identification of 3–4 polar lipids on the basis of matching the R_f of two-dimensional TLC [33, 34]. Other spots on the TLC plate remain unidentified; thus Minana-Galbis et al. [33] described eight spots, Khianngam et al. [35] four spots and Kampfer et al. [36] did not identify four, i.e. half of the total number of spots.

The two species of the genus *Anoxybacillus* that we analyzed differ in the composition of their polar lipids. The major phospholipids present are Ptd₂Gro and PtdGro, which confirms that these species belong to the bacilli [12]. Preliminary papers describing the polar lipid composition of the genus *Anoxybacillus* indicated that the strains contain a large number of unidentified polar lipids [33, 37] and share a similar chemical composition. The chemical composition of our two strains also centers around the presence of three polar lipid classes (Ptd₂Gro, PtdGro, PtdEtn), and the dominance of iso- and anteiso-fatty acids (Table 1; see Ref. [8, 9]). Similar observations on *Anoxybacillus* fatty acids were reported by other authors [38, 39].

As seen in Tables 3S–11S, the facultatively anaerobic *A. bogrovensis* was found to contain a total of 12 identified polar lipid classes with 172 molecular species, whereas the aerobic *A. rupiensis* contains six identified polar lipid classes with a total of 195 molecular species. Both species contain five classes of polar lipids that could not be identified. We shall deal in detail only with those Tables that are not given in Supplements.

Individual classes of separated phospholipids were identified by ESI–MS. Based on literature data [40, 41] and our previous results we were able to identify and quantify individual molecular species, see Tables 3–7. The only potential uncertainty concerned the identification of PtdGro

Fig. 1 LC/ESI chromatogram of the phospholipids from *A. bogrovensis*

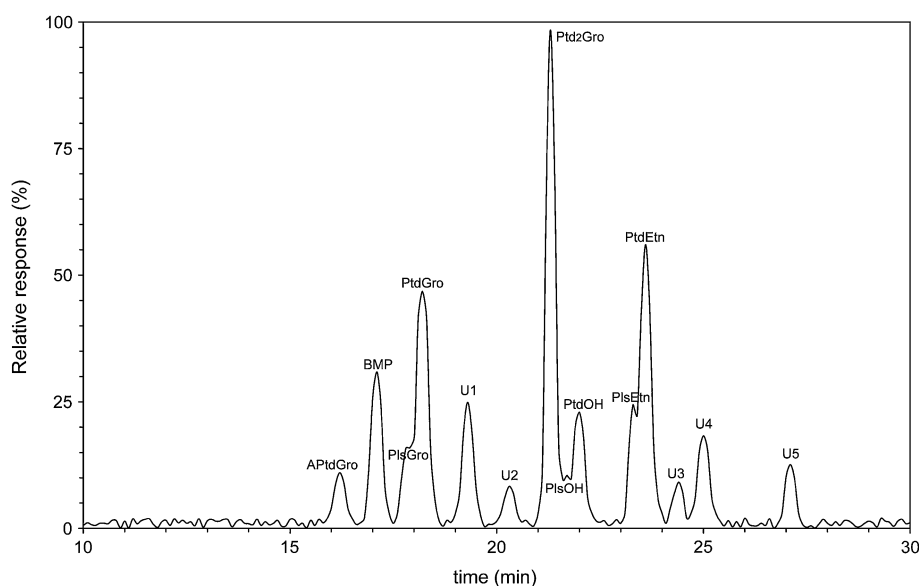


Table 1 Fatty acid compositions (weight percentages) of *A. bogrovensis* and *A. rupsiensis* as determined by GC–MS

Fatty acid	<i>A. bogrovensis</i>	<i>A. rupsiensis</i>
14:0 ^a	0.3	0.2
i-15:0	22.9	26.6
ai-15:0	5.3	1.5
15:0	0.4	0.2
i-16:0	13.3	15.0
16:0	8.9	10.5
i-17:0	20.2	28.3
ai-17:0	21.5	4.6
17:0	0.3	0.2
i-18:0	0.5	0.2
18:0	6.4	12.6
20:0	tr	0.1
22:0	tr	nd

^a First numeral, number of carbon atoms in the chain; second numeral, number of double bond; *i* isoacid; *ai* anteisoacid
tr traces (between 0.01 and 0.1 % of total FAs)

nd not detected (below 0.01 % of total FAs)

and BMP [26, 42]. However, the HILIC column provided a base-line separation without any problems.

Both phospholipids contain two acids, two glycerol moieties and one phosphodiester and the only difference between them is thus in the position of one of the acyls. For this reason the two phospholipids cannot be distinguished by mass spectrometry alone and it is necessary to use HPLC for their separation [26, 42].

Tandem mass spectrum of PtdGro 15:0/15:0 and BMP 15:0/15:0 in negative-ion mode produced similar fragmentation for both compounds, making specific determination of either lipid in the presence of the other difficult. Intense product ions were observed for the acyl (m/z 241) and for the glycerophosphate fragment at m/z 153. Minor differences in the intensities were observed for the ions at m/z 451 and 469 corresponding to the neutral loss of the $[M-H-ketene]^-$ and $[M-H-R_2COOH]^-$. One clear distinction between PtdGro and BMP was the ability of PtdGro to lose the glycerol moiety without the loss of a fatty acid, i.e. a daughter ion of mass $[M-H-74]^-$ was always observed only for PtdGro but not for the compound with retention time 17.1 min. Thus, the neutral loss of 74 Da, i.e. ion at m/z 619, is specific for the 15:0/15:0 PtdGro species [43] and we concluded that this peak must contain BMP, for which it holds that each of the two glycerol moieties is esterified by one fatty acid.

Plasmenyl phospholipids were identified on the basis of our previously described fragmentation [28] and the method described by Hsu and Turk [44]. Briefly, the mass spectrum of all plasmenyl phospholipids is dominated by a set of RCO^- , $[M-H-R_2COOH]^-$, $[M-H-R'CH=C=O]^-$,

and $[M-H]^-$ ions that identify the fatty acid substituent. Ions reflecting the 1-*O*-alk-1'-enyl moiety are minor or not present but complete structural characterization of plasmenyl phospholipids can be carried out on the basis of the above ions.

Quantification of individual molecular species of the four classes of plasmalogens is given in Tables 3S–5S. Although the base-line separation of diacyl and alkenylacyl (plasmalogen) of the appropriate class of phospholipid was not successful, we succeeded in quantifying individual molecular species by using the method of Hsu and Turk [44]. Briefly, dissociation of the $[M-H-R_2COOH-polar\ head\ group]^-$ ions from the $[M-H]^-$ ions of plasmalogen phospholipid that have undergone consecutive losses of the fatty acid substituent at *sn*-2 and the polar head group readily gives the structural information about the radical group at *sn*-1, resulting in semiquantification of appropriate molecular species. This is essentially a neutral loss scan with a mass offset that correlates with the mass of the specified neutral losses, i.e. fatty acid at *sn*-2 position and polar head group of the phospholipid.

Analysis of *A. rupsiensis* lipids (Fig. 2) showed that the content of complex lipids is markedly different from that in *A. bogrovensis*. Based on previously published data [45] it can be assumed that the major peaks in the chromatogram are mainly PtdGro and Ptd₂Gro or their derivatives (Figs. 3, 4). As seen from the chromatogram, five other peaks could not be identified. The molecular species of nine identified classes of phospholipids are mentioned in Tables 12S–18S.

Only a few papers are devoted to the analysis of substituted PtdGro or Ptd₂Gro by mass spectrometry in Gram-positive bacteria. Peter-Katalinic and Fischer [20] fundamentally contributed to the identification of cardiolipin derivatives, i.e. Ptd₂Gro substituted on the *sn*-2 hydroxyl of the middle glycerol with α -D-glucopyranosyl- (gluco-Ptd₂Gro), D-alanyl- (alanyl-Ptd₂Gro), or L-lysyl- (lysyl-Ptd₂Gro) moieties. A review describing the presence of glucosyl-Ptd₂Gro, lysyl-Ptd₂Gro, alanyl-Ptd₂Gro, lysyl-PtdGro, etc. was published by Geiger et al. [11].

Analysis of PtdGro and Ptd₂Gro derivatives consisted in their separation on a HILIC column and identification by mass spectrometry. Mass spectra of derivatives of Ptd₂Gro have been described by, e.g., Peter-Katalinic and Fischer [20], who used positive and negative FAB to identify α -D-glucopyranosyl-, D-alanyl- and L-lysylcardiolipins. Negative ionization was more convenient in all cases since, due to the decreased formation of an alkali ion adduct, the negative-ion mass spectrum of the substituted-Ptd₂Gros provided a less complicated pattern than the positive-ion-mode and yielded sufficient information for elucidating the structure of most peaks in the chromatogram.

Based on literature data we assumed that all substituted derivatives of both PtdGro (Table 2) and Ptd₂Gro (Table 3)

Fig. 2 LC/ESI chromatogram of the phospholipids from *A. rupiensis*

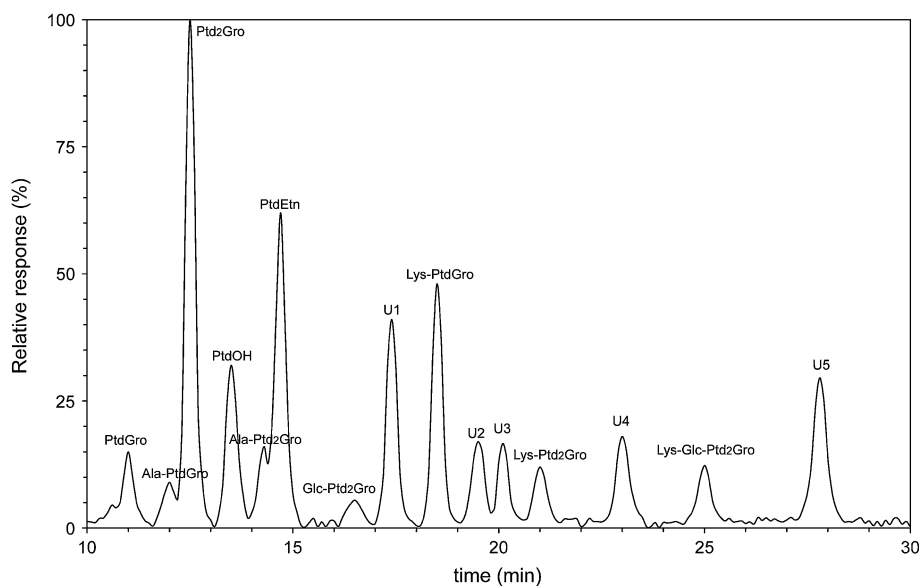
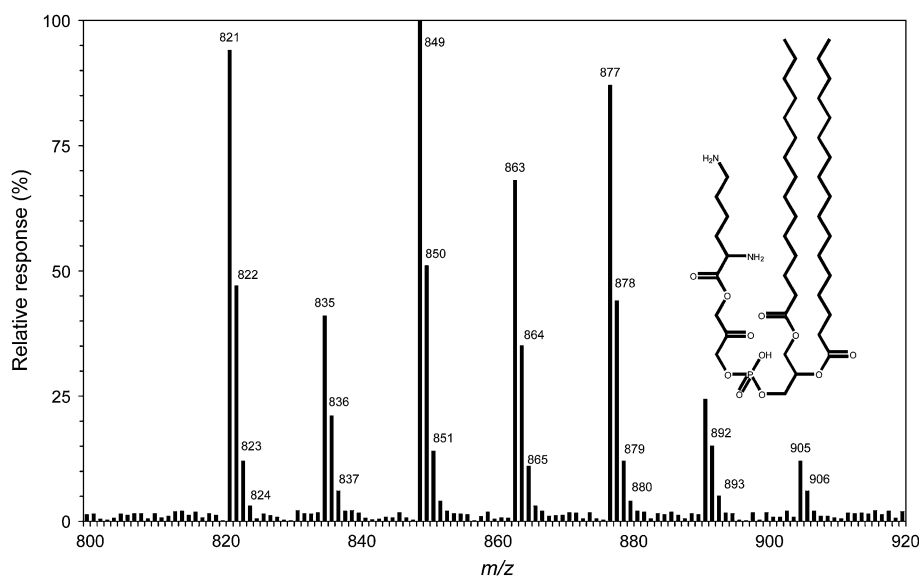


Fig. 3 ESI-mass spectrum of Lys-PtdGro from *A. rupiensis* in negative ion mode including structure of the major molecular species, i.e. 15:0/17:0-Lys-PtdGro having $[M-H]^-$ at 849 Da



will exhibit similar behavior, i.e. cleavage of a polar substituent—glucose or amino acid. For instance, the MS² product-ion spectrum of 17:0/15:0-lysyl-PtdGro (Fig. 5) shows $[M-H]^-$ ion at m/z 849, which was observed in the negative-ESI; this gives rise to the ion at m/z 721 arising from loss of a lysine (128 Da) from deprotonated ion of a substituted-PtdGro.

The MS/MS spectrum of alanyl-PtdGro (15:0/17:0-alanyl-PtdGro) also shows two ions. One of them, at m/z 88, corresponds to the anion of alanine while the other, at m/z 718, arises by neutral loss of 88 Da (alanine) from 15:0/17:0-alanyl-PtdGro ($[M-H]^-$ at m/z 806).

The splitting off of a neutral moiety will transform the unsubstituted PtdGro to a simpler structure and further fragmentation in mass spectrometer is thus identical with

the fragmentation of unsubstituted PtdGro [46] described above.

The structure of lysyl-PtdGro was further confirmed by the presence of ion at m/z 647 originating from the loss of the dehydrated glycerol head group (74 Da), along with the ion at m/z 405, arising from m/z 479 by loss of dehydrated glycerol or from m/z 497 by loss of a glycerol residue (92 Da). The structure was further confirmed by the presence of the ions at m/z 269 and at m/z 241 corresponding to C17 and C15 saturated carboxylate anions, respectively. The ions at m/z 479 and m/z 497 arise from losses of the C15 acyls as an acid or a ketene, respectively, along with the ions at m/z 451 and m/z 469 corresponding to the analogous losses of C17 fatty acid moiety. Differentiation of *sn*-1 and *sn*-2 position was based on the abundance of

Fig. 4 ESI-mass spectrum of Lys-Ptd₂Gro from *A. rufipes* in negative ion mode including structure of the major molecular species, i.e. 15/17/17/15-Lys-Ptd₂Gro having [M–H][–] at 1,480.05 Da. Asterisk Ion at 1407.02 Da arises by splitting of lysine from [M–H][–] at 1,536.12 Da

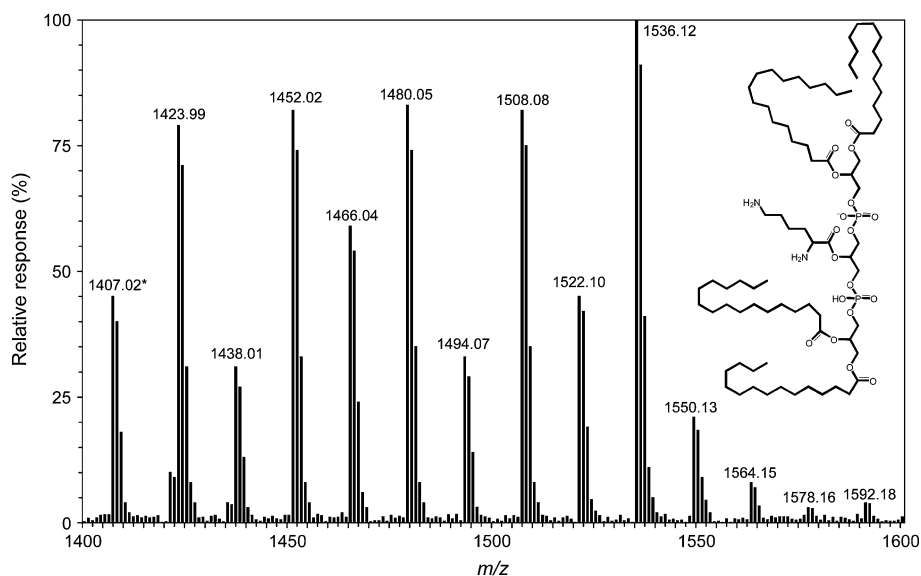


Table 2 Lys-PtdGro identified in *A. rufipes*, the masses of protonated molecules ([M–H][–]), their ACN, and relative quantities of appropriate molecular species (%), including total %

[M–H] [–]	ACN	Mol spec	%	Mol spec	%	Total %
821	30	15/15	21.9			21.9
835	31	15/16	9.6			9.6
849	32	15/17	19.7	16/16	3.5	23.2
863	33	15/18	7.5	16/17	8.2	15.7
877	34	16/18	3.1	17/17	17.0	20.1
891	35	17/18	6.7			6.7
905	36	18/18	2.8			2.8

two pairs of ions: those at m/z 479/497 were, respectively, more abundant than those at m/z 451/469; this documents that C17 FA is present in position *sn*-1 and C15 FA in position *sn*-2. Based on the above findings, the given molecular species can be determined as 17:0/15:0-lysyl-PtdGro. The situation was complicated by the presence of an isobaric molecule, i.e. 16:0/16:0-lysyl-PtdGro having characteristic ions at m/z 255, 391, 465, 483, etc., see also Fig. 5. Further aminoacyl-PtdGros or aminoacyl-Ptd₂Gros derivatives were identified in a similar way.

The major fragmentation pathway of Lys-Ptd₂Gro (Fig. 6) derivative gives an [M–H][–] ion at m/z 1479, which is shown in Fig. 7. As noted above, both Lys-PtdGro and Lys-Ptd₂Gro undergo the neutral loss of a lysine moiety; the complex lipid (Lys-Ptd₂Gro) has thus in fact been translated into the simplified structure (Ptd₂Gro) and analyzed as previously described [27, 47], see also Fig. 7.

The structure of hexosyl-Ptd₂Gro was deduced on the basis of knowledge of negative mass spectra published previously by several authors [20, 47, 48].

The major derivative of hexosyl-Ptd₂Gro gives an [M–H][–] ion at m/z 1514 and an [M–2H]^{2–} ion at m/z 756. CID of the [M–2H]^{2–} ions at m/z 756 at a collision energy of 50 eV yields two carboxylate anions at m/z 241 and m/z 269, reflecting the two fatty acyl moieties, i.e. both saturated C15 and C17 acids, in the molecule. As observed before in the detection of fragment ions due to the neutral loss of a hexose moiety, a fragmentation type was not detected in the MS/MS experiment using the [M–2H + Na][–] as a precursor ion but only for [M–H][–] [48]. The whole demonstration of hexosyl-Ptd₂Gro structure has thus in fact been translated into the simplified structure (Ptd₂Gro) and analyzed as previously described [47], see also above.

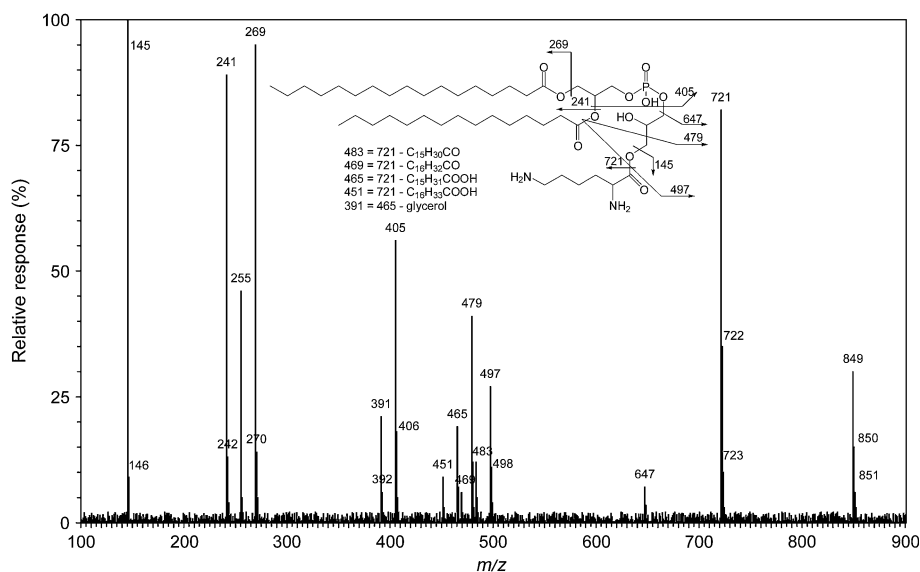
Table 3, which presents 29 molecular species of Lys-Ptd₂Gro, which is in agreement with the content of total FAs. A similar picture emerges in Table 2 describing the content of Lys-PtdGro, which also shows 15/15-, 17/17- and 15/17-Lys-PtdGro as major molecular species.

The peak with retention time 25.0 min (Fig. 2) is assumed to belong to glucosyl-Ptd₂Gro, in which some of the hydroxyls of glucose are esterified by an amino acid (lysine). Due to an insufficient amount of biomass we could not determine the complete structure and its full determination, as well as that of the as yet unknown peaks, will be the topic of our forthcoming study.

So far, not a single paper has appeared which would describe the separation and subsequent identification of any complex lipid having both straight- and branched-chain FAs in the molecule. In a previous study [28] we succeeded in separating synthetic triacylglycerols differing only in straight- and branched chain FAs (specifically 17:0/17:0/17:0 from ai-17:0/ai-17:0/ai-17:0). Unfortunately, because the mass spectra of both triacylglycerols are identical, the

Table 3 Lys-Ptd₂Gro identified in *A. rupiensis*, the masses of protonated molecules ($[M-H]^-$), their ACN, and relative quantities of appropriate molecular species (%), including total %

$[M-H]^-$	ACN	Mol spec	%	Mol spec	%	Mol spec	%	Mol spec	%	Mol spec	%	Total %
1423	60	15/15/15/15	12.6									12.6
1437	61	15/15/15/16	5.0									5.0
1451	62	15/15/16/16	2.0	15/15/15/17	11.0							13.0
1465	63	15/16/16/16	0.8	15/15/15/18	4.3	15/15/16/17	4.3					9.4
1479	64	15/17/17/15	12.5	15/16/16/17	0.7							13.2
1493	65	16/16/16/17	0.7	15/15/17/18	3.8	15/16/16/18	0.7					5.2
1507	66	15/17/17/17	8.3	16/16/17/17	1.5	16/16/16/18	0.3	15/15/18/18	1.5	15/16/17/18	1.5	13.1
1521	67	16/17/17/17	3.3	15/17/17/18	3.3	16/16/17/18	0.6					7.2
1535	68	17/17/17/17	14.4	16/17/17/18	1.3	16/16/18/18	0.2					15.9
1549	69	15/18/18/18	0.5	17/17/17/18	2.8							3.3
1563	70	17/17/18/18	1.1	16/18/18/18	0.2							1.3
1577	71	17/18/18/18	0.4									0.4
1591	72	18/18/18/18	0.6									0.6

Fig. 5 The tandem ESI product-ion spectrum of the $[M-H]^-$ ion of 16/16-Lys-PtdGro and 17/15-Lys-PtdGro including fragmentation

individual molecular species shown in all tables and figures can contain straight- and branched-chain FAs. The only exception is the separation and identification of straight- and branched-chain FAs as methyl esters by GC-MS (Table 2), which presented no problems.

In this study we demonstrated that the ability of one species, i.e. *A. bogrovensis* to grow under facultatively anaerobic conditions quite clearly affects both qualitative and quantitative composition of lipids. The majority of lipids in the two strains under study was qualitatively the same but the strain of *A. rupiensis* cultivated under aerobic conditions showed a much wider range of polar lipids, i.e. aminoacyl-phospholipids, including as yet undescribed amino-phospho-glyco-lipid. In addition, to our knowledge we are the first to determine plasmalogens in a facultatively anaerobic bacterium. The recent

review about plasmalogens [11] still refers to this as unproven.

We believe that the ability to synthesize many different lipids must also be seen in a taxonomic and evolutionary context of classification of this genus. Our study points to the value of chemotaxonomy within the bacilli and to the need for including such analyses in all future taxonomic work on this and other groups [49].

Experimental

The standard lipid 1-palmitoyl-2-oleoyl-*sn*-glycero-3-[phospho-*rac*-(1-glycerol)] (16:0, 18:1 PtdGro) used in the experiments to verify the bacterial compound structure was purchased from Avanti Polar Lipids (Alabaster, AL, USA).

atmospheric oxygen. Cells were harvested after centrifugation (4,000 rpm for 20 min) and two washes with distilled water, and lyophilized. The dry biomass after lyophilization of both strains was 0.367 g/L for *A. rupiensis* and 0.233 g/L media for *A. bogrovensis*.

The extraction procedure was based on the method of Bligh and Dyer [29], except that 2-propanol was substituted for methanol, since isopropanol does not serve as a substrate for phospholipases [50]. The alcohol-water mixture was cooled, one part chloroform was added and the lipids were extracted for 30 min. Insoluble material was sedimented by centrifugation and the supernatant was separated into two phases. The aqueous phase was aspirated off and the chloroform phase was washed three times with two parts 1 M KCl each. The resulting chloroform phase was evaporated to dryness under reduced pressure.

First, total lipid extracts were applied to Sep-Pak Cartridge Vac 35 cc (Waters; with 10 g of aminopropylsilica-based polar bonded phase), and from the cartridge were subsequently eluted nonacidic lipids with 40 mL of chloroform–methanol (7:3), and acidic lipids with 30 mL of chloroform–methanol–concentrated aqueous ammonia (70:30:2) containing 0.4 % (w/v) ammonium acetate. The eluate was reduced in volume and subjected to LC–MS.

HPLC equipment consisted of a 1090 Win system, PV5 ternary pump and automatic injector (HP 1090 series, Hewlett Packard, USA), and two Ascentis[®] Express HILIC HPLC columns [2.7 μ m particle size, L \times I.D. 15 cm \times 2.1 mm (Supelco, Prague)] connected in series. LC was performed at a flow rate of 0.45 mL/min for the phospholipids from the *A. bogrovensis* and 0.58 mL/min for the phospholipids from the *A. rupiensis*, respectively, with a linear gradient from mobile phase containing methanol/acetonitrile/aqueous 1 mM ammonium acetate (50:30:20, v/v/v) to methanol/acetonitrile/aqueous 1 mM ammonium acetate (10:70:20, v/v/v) for 60 min. The whole HPLC flow was introduced into the ESI source without any splitting.

The detector was an Applied Biosystems Sciex API 4000 mass spectrometer (Applied Biosystems Sciex, Ontario, Canada) using electrospray mass spectra. The ionization mode was negative, the nebulizing gas (N₂) pressure was 350 kPa and the drying gas (N₂) flow and temperature were 9.2 L/min and 310 °C, respectively. The electrospray needle was at ground potential, whereas the capillary tension was held at 4,000 V. The cone voltage was kept at 250 V. The mass resolution was 0.1 Da and the peak width was set to 5 s. For an analysis, total ion currents (full scan) were acquired from 80 to 2,000 Da.

Mass spectra of CID ions were acquired by colliding the Q1 selected precursor ions with Ar gas at a collision target gas and applying collision energy of 50 eV in Q2. Scanning range of Q3 was m/z 80–2,000 with a step size of m/z 0.25 and a dwell time of 1 ms. A peak threshold of 0.2 %

intensity was applied to the mass spectra. The instrument was interfaced to a computer running Applied Biosystems Analyst version 1.4.1 software.

Gas chromatography–mass spectrometry of FAME was done on a GC–MS system consisting of Varian 450-GC, Varian 240-MS ion trap detector with external ionization (EI), and CombiPal autosampler (CTC, USA). The sample was injected onto a 25 m \times 0.25 mm \times 0.1 μ m Ultra-1 capillary column (Supelco, Czech Republic) under a temperature program: 5 min at 50 °C, increasing at 10 °C min⁻¹ to 320 °C and 15 min at 320 °C. Helium was the carrier gas at a flow of 0.52 mL min⁻¹. All spectra were scanned within the range m/z 50–600.

Comparison of retention times of commercially obtained standards [Bacterial Acid Methyl Ester (BAME) Mix (Supelco, Prague)] and previously published results [51] were used for identification.

Acknowledgments The research was supported by GACR P503/11/0215, by the Institutional Internal Project RVO61388971, and by a bilateral agreement between the Institute of Microbiology, Bulgarian Academy of Sciences, Bulgaria and Novozymes, Denmark.

References

- Denich TJ, Beaudette LA, Lee H, Trevors JT (2003) Effect of selected environmental and physico-chemical factors on bacterial cytoplasmic membranes. *J Microbiol Methods* 52:149–182
- Stackebrandt E, Swiderski J (2002) From phylogeny to systematics: the dissection of the genus *Bacillus*. In: Berkeley R, Heyndrickx M, Logan NA, De Vos P (eds) Applications and systematics of *Bacillus* and relatives. Blackwell Publishing, Oxford, pp 8–22
- Zeigler DR (2001) The genus *Geobacillus*. Introduction and strain catalog. In: Zeigler DR (eds) Catalog of strains, vol. 3, 7th edn. *Bacillus* Genetic Stock Center, The Ohio State University, USA
- Pikuta E, Lysenko A, Chuvilskaya N, Mendrock U, Hippe H, Suzina N, Nikitin D, Osipov G, Laurinavichius K (2000) *Anoxybacillus pushchinensis* gen. nov., sp. nov., a novel anaerobic, alkaliphilic, moderately thermophilic bacterium from manure, and description of *Anoxybacillus flavithermus* comb. nov. *Int J Syst Evol Micro* 50:2109–2117
- Pikuta E, Cleland D, Tang J (2003) Aerobic growth of *Anoxybacillus pushchinoensis* K1^T: emended descriptions of *A. pushchinoensis* and the genus *Anoxybacillus*. *Int J Syst Evol Micro* 53:1561–1562
- Yumoto I, Hirota K, Kawahara T, Nodasaka Y, Okuyama H, Matsuyama H, Yokota Y, Nakajima K, Hoshino T (2004) *Anoxybacillus voinovskiensis* sp. nov., a moderately thermophilic bacterium from a hot spring in Kamchatka. *Int J Syst Evol Microbiol* 54:1239–1242
- Cihan AC, Ozcan B, Cokmus C (2011) *Anoxybacillus salavatliensis* sp. nov., an α -glucosidase producing, thermophilic bacterium isolated from Salavatli Turkey. *J Basic Microb* 51:136–146
- Derekova A, Sjöholm C, Mandeva R, Kambourova M (2007) *Anoxybacillus rupiensis* sp. nov., a novel thermophilic bacterium isolated from Rupi basin (Bulgaria). *Extremophiles* 11:577–583

9. Atanassova M, Derekova A, Mandeva R, Sjöholm C, Kambourova M (2008) *Anoxybacillus bogrovensis* sp. nov., a novel thermophilic bacterium isolated from a hot spring in Dolni Bogrov Bulgaria. *Int J Syst Evol Micr* 58:2359–2362
10. Goldfine H (2010) The appearance, disappearance and reappearance of plasmalogens in evolution. *Prog Lipid Res* 49:493–498
11. Geiger O, Gonzalez-Silva N, Lopez-Lara IM, Sohlenkamp C (2010) Amino acid-containing membrane lipids in bacteria. *Prog Lipid Res* 49:46–60
12. O'Leary WM, Wilkinson SG (1988) Gram-positive bacteria. In: Ratledge S, Wilkinson SG (eds) *Microbial lipids*. Academic Press, London, pp 117–201
13. Nahaie MR, Goodfellow M, Minnikin DE, Hajek V (1984) Polar lipid and isoprenoid quinone composition in the classification of *Staphylococcus*. *J Gen Microbiol* 130:2427–2437
14. Roy H, Ibba M (2008) RNA-dependent lipid remodeling by bacterial multiple peptide resistance factors. *Proc Natl Acad Sci USA* 105:4667–4672
15. Op den Kamp JA, Redai I, van Deenen LL (1969) Phospholipid composition of *Bacillus subtilis*. *J Bacteriol* 99:298–303
16. Samant S, Hsu FF, Neyfakh AA, Lee H (2009) The *Bacillus anthracis* protein MprF is required for synthesis of lysylphosphatidylglycerols and for resistance to cationic antimicrobial peptides. *J Bacteriol* 191:1311–1319
17. Fischer W, Leopold K (1999) Polar lipids of four *Listeria* species containing L-lysylcardiolipin, a novel lipid structure, and other unique phospholipids. *Int J Syst Bacteriol* 49:653–662
18. dos Santos Mota JM, den Kamp JA, Verheij HM, van Deenen LL (1970) Phospholipids of *Streptococcus faecalis*. *J Bacteriol* 104:611–619
19. Schlame M (2008) Cardiolipin synthesis for the assembly of bacterial and mitochondrial membranes. *J Lipid Res* 49:1607–1620
20. Peter-Katalinic J, Fischer W (1998) α -D-Glucopyranosyl-, D-alanyl- and L-lysylcardiolipin from gram-positive bacteria: analysis by fast atom bombardment mass spectrometry. *J Lipid Res* 39:2286–2292
21. McAuley KE, Fyfe PK, Ridge JP, Isaacs NW, Cogdell RJ, Jones MR (1999) Structural details of an interaction between cardiolipin and an integral membrane protein. *PNAS* 96:14706–14711
22. Vaidyanathan S, Kell DB (2002) Flow-injection electrospray ionization mass spectrometry of crude cell extracts for high-throughput bacterial identification. *J Am Soc Mass Spectrom* 13:118–128
23. Zhang JI, Talaty N, Costa AB, Xia Y, Tao WA, Bell R, Callahan JH, Cooks RG (2011) Rapid direct lipid profiling of bacteria using desorption electrospray ionization mass spectrometry. *Int J Mass Spectr* 301:37–44
24. Schwalbe-Herrmann M, Willmann J, Leibfritz D (2010) Separation of phospholipid classes by hydrophilic interaction chromatography detected by electrospray ionization mass spectrometry. *J Chromatogr A* 1217:5179–5183
25. Kamleh A, Barrett MP, Wildridge D, Burchmore RJS, Scheltema RA, Watson DG (2008) Metabolomic profiling using Orbitrap Fourier transform mass spectrometry with hydrophilic interaction chromatography: a method with wide applicability to analysis of biomolecules. *Rapid Commun Mass Spectrom* 22:912–918
26. Scherer M, Schmitz G, Liebisch G (2010) Simultaneous quantification of cardiolipin, bis(monoacylglycerophosphate and their precursors by hydrophilic interaction LC–MS/MS including correction of isotopic overlap. *Anal Chem* 82:8794–8799
27. Rezanka T, Siristova L, Melzoch K, Sigler K (2009) Direct ESI–MS analysis of *O*-acyl glycosylated cardiolipins from the thermophilic bacterium *Alicyclobacillus acidoterrestris*. *Chem Phys Lipids* 161:115–121
28. Rezanka T, Siristova L, Matoulkova D, Sigler K (2011) Hydrophilic interaction liquid chromatography: ESI–MS/MS of plasmalogen phospholipids from *Pectinatus* bacterium. *Lipids* 46:765–780
29. Bligh ED, Dyer WJ (1959) A rapid method of total lipid extraction and purification. *Can J Biochem Biophysiol* 37:911–917
30. Lisa M, Cifkova E, Holcapek M (2011) Lipidomic profiling of biological tissues using off-line two-dimensional high-performance liquid chromatography–mass spectrometry. *J Chromatogr A* 1218:5146–5156
31. Ash C, Farrow JAE, Wallbanks S, Collins MD (1991) Phylogenetic heterogeneity of the genus *Bacillus* revealed by comparative analysis of small-subunit-ribosomal RNA sequences. *Lett Appl Microbiol* 13:202–206
32. Clejan S, Krulwich TA, Mondrus KR, Seto-Young D (1986) Membrane lipid composition of obligately and facultatively alkaliphilic strains of *Bacillus* spp. *J Bacteriol* 168:334–340
33. Minana-Galbis D, Pinzon DL, Loren JG, Manresa A, Oliart-Ros RM (2010) Reclassification of *Geobacillus pallidus* (Scholz et al. 1988) Banat et al. 2004 as *Aeribacillus pallidus* gen. nov., comb. nov. *Int J Syst Evol Micr* 60:1600–1604
34. Dinsdale AE, Halket G, Coorevits A, van Landschoot A, Busse H, de Vos P, Logan NA (2011) Emended descriptions of *Geobacillus thermoleovorans* and *Geobacillus thermocatenuatus*. *Int J Syst Evol Micr* 61:1802–1810
35. Khiangngam S, Tanasupawat S, Akaracharanya A, Kim KK, Lee KC, Lee J-S (2010) *Cohnella thailandensis* sp. nov., a xylanolytic bacterium from Thai soil. *Int J Syst Evol Micr* 60:2284–2287
36. Kampfer P, Rosselló-Mora R, Falsen E, Busse H-J, Tindall BJ (2006) *Cohnella thermotolerans* gen. nov., sp. nov., and classification of '*Paenibacillus hongkongensis*' as *Cohnella hongkongensis* sp. nov. *Int J Syst Evol Micr* 56:781–786
37. Gul-Guven R, Guven K, Poli A, Nicolaus B (2008) *Anoxybacillus kamchatkensis* subsp. asaccharedens subsp. nov., a thermophilic bacterium isolated from a hot spring in Batman. *J Gen Appl Microbiol* 54:327–334
38. Belduz AO, Dulger S, Demirbag Z (2003) *Anoxybacillus gonensis* sp. nov., a moderately thermophilic, xylose-utilizing, endospore-forming bacterium. *Int J Syst Evol Micr* 53:1315–1320
39. Dulger S, Demirbag Z, Belduz AO (2004) *Anoxybacillus ayderensis* sp. nov. and *Anoxybacillus kestanbolensis* sp. nov. *Int J Syst Evol Micr* 54:1499–1503
40. Hsu FF, Turk J (2000) Characterization of phosphatidylethanolamine as a lithiated adduct by triple quadrupole, tandem mass spectrometry with electrospray ionization. *J Mass Spectrom* 35:596–606
41. Hsu FF, Turk J (2009) Electrospray ionization with low-energy collisionally activated dissociation tandem mass spectrometry of glycerophospholipids: mechanisms of fragmentation and structural characterization. *J Chromatogr B* 877:2673–2695
42. Meikle PJ, Duplock S, Blacklock D, Whitfield PD, Macintosh G, Hopwood JJ, Fuller M (2008) Effect of lysosomal storage on bis(monoacylglycerophosphate). *Biochem J* 411:71–78
43. Retra K, Bleijerveld OB, van Gestel RA, Tielens AG, van Helmond JJ, Brouwers JF (2008) A simple and universal method for the separation and identification of phospholipid molecular species. *Rapid Commun Mass Spectrom* 22:1853–1862
44. Hsu FF, Turk J (2007) Differentiation of 1-*O*-alk-1'-enyl-2-acyl and 1-*O*-alkyl-2-acyl glycerophospholipids by multiple-stage linear ion-trap mass spectrometry with electrospray ionization. *J Am Soc Mass Spectrom* 18:2065–2073
45. Siristova L, Melzoch K, Rezanka T (2009) Fatty acids, unusual glycerophospholipids and DNA analyses of thermophilic bacteria isolated from hot springs. *Extremophiles* 13:101–109

46. Hsu FF, Turk J (2001) Studies on phosphatidylglycerol with triple quadrupole tandem mass spectrometry with electrospray ionization: fragmentation processes and structural characterization. *J Am Soc Mass Spectrom* 12:1036–1043
47. Hsu FF, Turk J, Rhoades ER, Russell DG, Shi Y, Groisman EA (2005) Structural characterization of cardiolipin by tandem quadrupole and multiple-stage quadrupole ion-trap mass spectrometry with electrospray ionization. *J Am Soc Mass Spectrom* 16:491–504
48. Beckedorf AI, Schaffer Ch, Messner P, Peter-Katalinic J (2002) Mapping and sequencing of cardiolipins from *Geobacillus stearothermophilus* NRS 2004/3a by positive and negative ion nanoESI-QTOF-MS and MS/MS. *J Mass Spectrom* 37:1086–1094
49. Wayne LG, Brenner DJ, Colwell RR, Grimont PAD, Kandler O, Krichevsky MI, Moore WEC, Murray RGE, Stackebrandt E, Starr MP, Trüper HG (1987) Report of the Ad Hoc Committee on reconciliation of approaches to bacterial systematics. *Int J Syst Bacteriol* 37:463–464
50. Kates M (1986) Techniques of lipidology: isolation, analysis and identification of lipids. In: Work TS, Work E (eds) *Laboratory techniques in biochemistry and molecular biology*, 2nd edn. Elsevier, Amsterdam, pp 220–223
51. Rezanka T, Podojil M (1984) The very long-chain fatty-acids of the green-alga, *Chlorella kessleri*. *Lipids* 19:472–473

Analysis of Fatty Acids in 12 Mediterranean Fish Species: Advantages and Limitations of a New GC-FID/GC-MS Based Technique

Teresina Nevigato · Maurizio Masci ·
Elena Orban · Gabriella Di Lena · Irene Casini ·
Roberto Caproni

Received: 20 January 2012 / Accepted: 28 April 2012 / Published online: 30 May 2012
© AOCS 2012

Abstract When fatty acids in fish are analyzed, results in percentage form (profile analysis) are mostly reported. However, the much more useful results expressed as mg/100 g (absolute analysis) is the main information required. Absolute methods based on calibration curves are of good accuracy but with a high degree of complexity if applied to a great number of analytes. Procedures based on the sequence profile analysis–total FA determination–absolute analysis may be suitable for routine use, but suffer from a number of uncertainties that have never been really resolved. These uncertainties are mainly related to the profile analysis. In fact, most profile analyses reported in the literature disagree about the number and type of fatty acids monitored as well as about the total percentage to assign to their sum so leading to possible inaccuracies; in addition the instrumental response factor for all FAME (fatty acid methyl esters) is often considered as a constant, but this is not exactly true. In this work, a set of 24 fatty acids was selected and studied on 12 fish species in the Mediterranean area (variable in lipid content and month of sampling): in our results, and in these species, this set constitutes, on average, 90 ± 3 % of the total fatty acid content. Moreover the error derived from the assumption of a unique response factor was investigated. Two different detection techniques (GC-FID and GC-MS) together with two capillary columns (different in length and polarity) were used in order to acquire complementary data on the same sample. With the protocol here proposed absolute analyses on the 12 cited species are easily achievable by

the total FA determination procedure. The accuracy of this approach is good in general, but in some cases (DHA for example) is lower than the accuracy of calibration-based methods. The differences were evaluated on a case by case basis.

Keywords Fatty acids · Fish · Quantitative analysis · Gas chromatography · Mass spectrometry · Flame ionization detector · Omega-3 fatty acids

Abbreviations

FAME	Fatty acid methyl ester(s)
GC-FID	Gas chromatography with flame ionization detector
GC-MS	Gas chromatography mass spectrometry
EI	Electron ionization
DHA	Docosahexaenoic acid (22:6n-3)
FA	Fatty acid(s)
SFA	Saturated fatty acid(s)
EPA	Eicosapentaenoic acid (20:5n-3)
PUFA	Polyunsaturated fatty acid(s)
LC-PUFA	Long chain polyunsaturated fatty acid(s)
RF	Response factor

Introduction

Fatty acids (FA) are major components of lipids. They are carboxylic acids present as esters in glycerides. In sphingolipids they are linked via an amide bond to a sphingoid base. Double C–C bonds variable in number and in position may be present in the FA molecule (Fig. 1a): in animals and plants, their configuration is prevalently *cis*- (more correctly *Z*-configuration).

T. Nevigato (✉) · M. Masci · E. Orban · G. Di Lena ·
I. Casini · R. Caproni
National Research Institute for Food and Nutrition (INRAN),
Via Ardeatina 546, 00178 Rome, Italy
e-mail: nevigato@inran.it

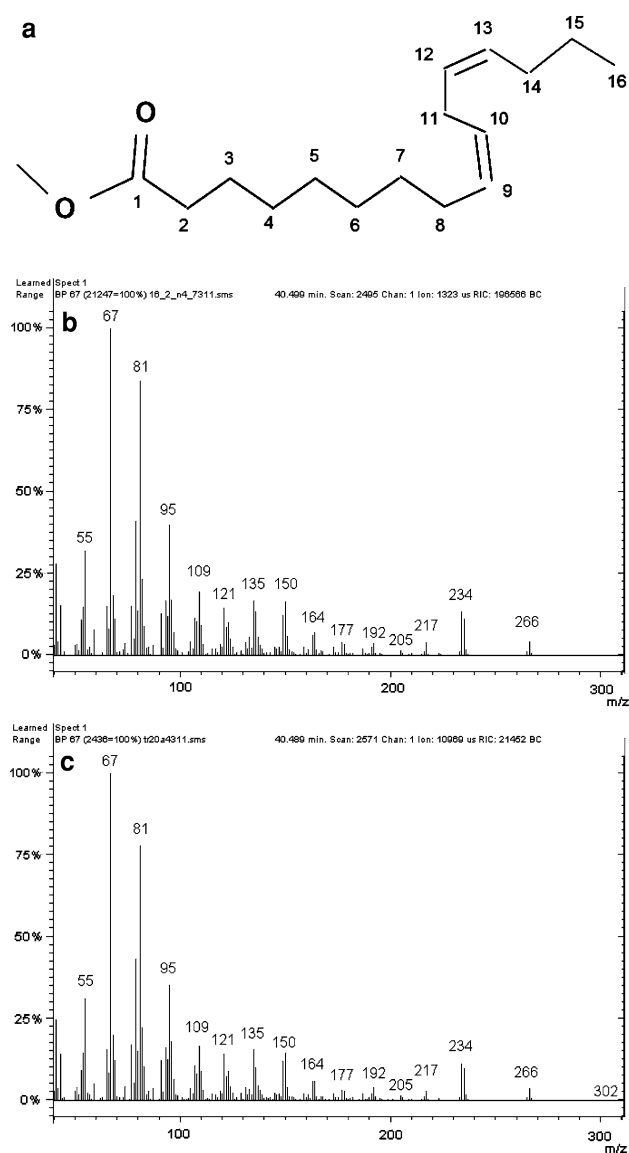


Fig. 1 **a** Molecular structure of the fatty acid 16:2n-4 (or 16:2 ω -4) in methyl ester form. IUPAC name: (9Z,12Z)-hexadecadienoic acid methyl ester. **b** Mass Spectrum of the peak obtained by injecting the authentic methylated standard of 16:2n-4. **c** Mass Spectrum of a peak with the same t_R and obtained by injecting a rainbow trout sample

The consumption of fat in the modern age is remarkable compared to the past and major causes of death in Western societies such as degenerative cardiovascular diseases and cancer are linked to aspects of dietary fat intake. This led to the recommendation that dietary intake of unsaturated FA be increased relative to that of all SFA (saturated fatty acids) [1], together with the reduction of total fat intake [2]. A number of studies reported the benefits derived from the consumption of omega-3 fatty acids and positive effects on health were observed [3]. A great attention was devoted to 20:5n-3 (EPA) and 22:6n-3 (DHA) fatty acids [4] and the recommended dosing that provides maximal cardio

protection [5] is reported. PUFA (polyunsaturated fatty acids) with special emphasis to EPA and DHA, are largely present in fish [6, 7] and fish consumption is associated with a significantly lower risk of fatal and total coronary heart diseases [8]. Recent studies focused on n-6/n-3 PUFA ratio as an important parameter towards a number of pathologies [9, 10]. Other authors suggested that the sum EPA + DHA has to be used instead of the n-6/n-3 ratio being more adequate in evaluating for coronary artery disease risk [11]. It is evident that the content of each fatty acid as mg/100 g edible portion is the main information needed.

In a complex fat matrix like a fish oil up to 100 different fatty acids, or more, can be present and detected, in dependence on the instrumental sensitivity available. In fish lipid analyses only a limited number of them is generally selected (the more important). Quantitative analysis in fish oils can be carried out at two different levels:

1. Profile analysis, that means the determination of each selected FAME as percent of total FAME
2. Absolute analysis, i.e., the assessment of the exact quantity of each selected FAME as mg/100 g edible portion

The level 1 is very often the reported result [6, 7, 12–16]. In fact the profile analysis is relatively easy to carry out if compared with the absolute analysis.

If absolute analysis is achieved with the use of calibration curves [17] it is required that certified quantitative standards are used for calibration, but degradation problems affect PUFA analytical standards when stored, even for a short period of time, and some authors suggest that even by using authentic standards, calibration could be difficult [18]. Absolutely fresh standards should have to be used every time. Moreover, the number of calibrations involved, time, and operator expertise needed make calibration curve approach undoubtedly complex.

A much more affordable method for absolute analysis could be the sequence profile analysis–total FA determination–absolute analysis. Total FA determination can be experimentally achieved by saponification that forms carboxylate ions. Then free fatty acids are reconstituted. This allows that the total fatty acid content as mg/100 g edible portion is known. The same information can also be obtained by applying a widely used conversion factor [19]. However the procedure profile analysis–total FA determination–absolute analysis requires that profile analysis is carried out with great accuracy to avoid errors in the subsequent absolute analysis. However, there is no agreement in the literature on how profile analysis in fish samples has to be conducted. This is an old problem. Due to complexity of requested work various approximations were applied. Most authors selected a number of fatty acids and considered

them as the 100 %. But number and kind of selected FAME vary a lot from one author to another: some considered 33 FAME as 100 % [15] others 17 FAME [16] or 37 FAME [13] as 100 %. Some works considered all peaks in the Chromatograms as FAME, i.e., the 100 % [12], but this is not always true as ascertained in our research by means of mass spectrometry: on 21 fish samples we recognized a mean number of 16 peaks as not-FAME (with a maximum of 32 not-FAME peaks in a European hake sample). Another problem in profile analyses is that the instrumental response factor is often considered as a constant.

In the present work the absolute analysis via total FA determination was carefully set up by executing a complete study of 12 different fish species from the Mediterranean area both of freshwater and marine origin. A set of 24 FAME was selected and compared with all FAME present in samples in order to ascertain the true percentage of their sum over total fatty acids. To our knowledge this is the first time this task has been carried out. The error derived from the assumption of a unique response factor is evaluated.

Materials and Methods

Chemicals and Reagents

The 24 monitored FAME are listed in Tables 3, 4, 5, 7. Methanol, *n*-hexane, potassium hydroxide, ethanol (96° ACS reagent), hydrochloric acid, and chloroform were purchased from Carlo Erba Reagenti, Milano, Italy. Boron trifluoride (BF₃) methanol solution (14 %) and sodium methoxide were purchased from Sigma Aldrich, St. Louis, MO, USA. Ethanolic KOH was prepared weekly by dissolving 10 g of potassium hydroxide in 20 mL of distilled water in a refrigerated 100 mL volumetric flask; after the solution became cool, the volume was brought up to the final 100 mL with ethanol. Analytical standards of triglycerides, individual analytical standards of the 24 FAME studied, FAME mixtures (Me95, Me96), and certified materials (PUFA-1 marine source, PUFA-3 Menhaden oil) were purchased either from Sigma Aldrich, St. Louis, MO, USA or from Larodan, Malmö, Sweden. The Standard Reference Material “1946 lake superior fish tissue” (fillets from adult lake trout, *Salvelinus namaycush*) was purchased from NIST[®], National Institute of Standards and Technology, Gaithersburg, MD, USA. The FAPAS[®] test material T1475, cod liver oil, was from The Food and Environment Research Agency, Sand Hutton, UK.

Fish Samples

Fish samples were collected directly by us or by well-trained personnel, stored on ice, and transported to our

Institute. Here they were filleted as reported in our previous works [6, 7]. Three or more individuals were always pooled in all samplings.

Lipid Extraction

Lipids were extracted from the fish fillets by means of a methanol–chloroform procedure based on the method of Bligh and Dyer [20] modified by Kinsella et al. [21]. A 30–35-g amount of homogenized sample was used for lipid extraction.

Derivatization (Transesterification)

An aliquot of oil coming from the lipid extraction step was derivatized. FA were GC-analyzed as FAME (methyl derivatives): due to the negligible difference the percentage of a single FA was considered as coincident with the percentage of that FA methyl-derivated (FAME). Transesterification (methyl derivatization) was conducted by transferring 10 mg of extracted oil in a 20-mL amber tube with a Teflon-lined screw cap. Then 150 µL of chloroform was added and the tube was shaken by means of a Vortex Mixer (Heidolph, Schwabach, Germany), then 1.5 mL of BF₃ 14 % methanol solution, and 1.5 mL of methanol were added and a second shaking was carried out. The tube was immersed in a water bath for 18 min at 65 °C and then in a tap-water bath: 1.5 mL of distilled water was immediately added while 3 mL of *n*-hexane were added only after the solution had cooled. The tube was shaken and the upper layer was transferred in a 5-mL amber glass vial with a Teflon-lined screw cap and a cone shape at the end, then the solvent was evaporated under a stream of nitrogen.

The 3-mL addition of *n*-hexane in the 20-mL amber tube (and the evaporation from the 5-mL vial, after transferring) was repeated for other two times.

Finally in the 5-mL vial, brought to dryness, 200 µL of *n*-hexane were introduced: this solution was ready for GC injections.

Appropriate derivatizations of blank material were also carried out.

Alternative procedures were tested both for lipid extraction and for derivatization (sodium methoxide) and no differences in fatty acid profile were observed if compared with procedures normally used in this work.

Instrumental

GC-FID (Flame Ionization Detector)

The hexanic solution of FAME coming from derivatization step was injected in a 6890 Agilent gas chromatograph with flame ionization detector (GC-FID), equipped with a

SPBTM PUFA fused silica capillary column (Supelco inc., Bellefonte PA, USA) 30 m × 0.25 mm I.D., 0.20 μm film thickness. Helium as the carrier gas was used in ramp flow mode and was programmed as follows: 0.8 mL/min for 20 min, then increasing to 1 mL/min at a rate of 0.2 mL/min², 20 min hold, then increasing to 1.2 mL/min, at a rate of 0.2 mL/min² until the end of the analysis. Operating conditions for the oven temperature were: initial temperature 50 °C, 2-min hold, increasing to 210 °C, at a rate of 9 °C/min; this last temperature was maintained for 40 min. The post run temperature was 210 °C, 5-min hold. Injector temperature was 200 °C, while FID temperature was 275 °C. Injections were made in split mode (1:50) with an injection volume of 2 μL.

GC–MS (Mass Spectrometry)

The same hexanic solution of FAME coming from derivatization step was injected in GC–MS. Instrument used was a Varian 3900 GC connected to the mass spectrometer Saturn 2100T equipped with an Ion Trap analyzer. The column installed was a CP-WAX 52 CB (60 m × 0.32 mm I.D., 0.50 μm film thickness, 0.45 mm O.D.) from Chrompack, Middelburg, the Netherlands. Injections were made in split mode (1:100) with an injection volume of 0.5 ± 0.1 μL and by using 1 μL of *n*-hexane as a plug. The column oven temperature was settled at an initial value of 50 °C (2 min hold), increased to 140 °C (0 min hold, ramp of 22.5 °C/min), and finally increased to 228 °C (29 min hold, ramp of 2.0 °C/min). Helium as the carrier gas was used at a variable flow regulated by the applied pressure in this way: initial pressure 4.4 psi (0 min hold, observed column flow: 1.0 mL/min), increase to 10.0 psi (0 min hold, ramp of 1.40 psi/min, observed column flow at 10.0 psi: 1.1 mL/min), increase to 14.4 psi (0 min hold, ramp of 0.10 psi/min, observed flow at 14.4 psi: 1.1 mL/min), and finally increase to 29.2 psi (24.90 min hold, ramp of 3.70 psi/min, observed flow at 29.2 psi: 2.5 mL/min). Total runtime was of 79 min. Injector temperature was 220 °C. Mass spectra were obtained in EI (Electron Ionization) mode at 70 eV. Ion trap temperature was 180 °C. For quantitative analyses only full scan chromatograms (TIC: total ion current, also named RIC: reconstructed ion current) were used and the selected mass to charge ratio to acquire was in the 40–440 *m/z* range. SIS (selected ion storage, also named SIM: selected ion monitoring) measures were sometimes used only for qualitative evaluations. In such cases the desired ion mass was selected together with an isolation window of ±2.0 *m/z*. Examples of mass spectra obtained in full scan mode are shown in Fig. 1b and c.

We cite here that most fatty acid libraries are done with a Quadrupole instrument instead of Ion Trap. For this reason we created a “personal” fatty acid library by using

authentic standards with the Ion Trap: this library was used to confirm spectra obtained from peaks in fish samples. In any case no relevant differences were observed between spectra in our personal library and spectra present in the NIST[®] MS database installed on the Varian[®] Workstation.

Total Fatty Acid Determination

A second aliquot of oil (0.1 g) coming from the lipid extraction step was subjected to saponification to experimentally calculate the total FA. Saponification was conducted according to the method of Kinsella et al. [21]. The recovery was assessed by processing a known amount of the standard triglyceride tripalmitolein (tri-16:1n-7): at the end of the analysis the observed recovery was of 99.9 %.

Alternatively the total FA can be calculated by means of a conversion factor without carrying out experimental measures: it relates the total FA amount to the total lipids. This factor was developed by Weihrauch et al. [19] and is also used by the U.S. Department of Agriculture [22].

Results and Discussion

The procedure profile analysis–total FA determination–absolute analysis is based on the accurate percentage assessment of each FA (profile analysis) to be subsequently related with the total FA content in the sample (if, for example, the FA X is 20 % of total FA and the total FA content is 1,000 mg/100 g edible portion then the FA X is 200 mg/100 g edible portion).

Response Factor (RF)

The response factor (RF) is not mentioned at all in many fish fatty acid profile studies [6, 7, 12–16], especially when FID is used as the detector. This implies that a unique FID response factor for all fish fatty acids is tacitly assumed and that area percentage is assumed as coincident with mass percentage. On the other hand some works demonstrated that FID response factors for different FAME are not equal [23], thus contradicting this assumption. The use of an appropriate correction for each FAME in order to convert the percentages of peak areas into mass percentages could be needed or not in dependence of the desired degree of accuracy as clarified later. The EU Commission Regulation 2568/91 [24] reports an example of how such a correction could be made. Obviously the response factor is not a problem if calibration curves are used.

We investigated the FID response factor for 10 representative FAME for which absolutely fresh standards were used. We optimized experimental conditions and, on the basis of observations made by Schreiner [18] and the

AOCS method [25] some precautions were taken. Split injections were used both at GC-FID and GC-MS instrument (1:50 and 1:100 respectively), while the injection temperature was maintained not below 200–220 °C. In addition a WAX-type capillary column and an amount of solvent in the injection syringe, ahead of a 0.5- μ L sample, were used in the GC-MS system (1 μ L of solvent was loaded in the syringe before sample loading). It has been proposed in fact that the injection technique, especially in vaporizing injectors, is the main source of error in response factor evaluation of long chain PUFA (for example the attribution of a low RF only to FID behavior when also an incorrect injection may contribute). This error can be minimized by reducing discrimination effects in the injector [18]. In Table 1 they are reported RFs measured in this work and RFs measured by Schreiner for three long chain (LC)-PUFA these last normalized to 18:0 RF (normalized RF do not depend from the IS (internal standard) employed in measuring RF, but only from the FAME chosen for normalization; normalized RF are used for general comparisons between different research works). Normalized RF to 18:0 for the same three LC-PUFA but analyzed with our instrumental conditions are reported too: there is a good agreement between the two works.

Our research confirms what previously reported: even when injection errors are minimized we see that the FID response towards different FAME is not exactly the same. The magnitude of this difference can be evaluated. Among the 10 FAME we studied all kinds are comprised (from

short-chain SFA to long-chain PUFA) therefore the set may be considered as representative of FAME in general. We can see in Table 1 that GC-FID response factors for these 10 FAME vary in the range of 4 % RSD (relative standard deviation) with a significant negative deviation from the mean of 22:6n-3 RF.

In the present method a mean error of about 7 % over all FAME analyzed was observed in the final results (Tables 4, 7). With reference to the same Tables 4 and 6, the underestimation on 22:6-3 could be evaluated at about 14–18 % but more frequently the underestimation on 22:6n-3 reaches a value of 20–21 %. This was caused also by the above cited trend of RFs (together with other sources of error). We can affirm, therefore, that using a unique FID response factor for all FAME, as most analysts do and as we did in this work, leads, together with other sources of error, to a mean error of 7 % with the conditions used here. Obviously if other sources of error increase also the final mean error increases (such as, for example, attributing to the studied FAME the 100 % of FAME present in the sample, as is usually done; in some fortunate cases overestimation due to this wrong assumption could be compensated by the underestimation caused by a low response factor considered as constant but this is certainly not a scientific procedure). The inability to isolate the error caused by RF from other sources of error leads us to specify that 7 % is to be intended as the possible maximum mean error derived from RF with the conditions used in this work. This error may be judged as acceptable in most

Table 1 Response factors (RFs)

FAME	GC-FID response factors measured in the present study				GC-MS response factors measured in the present study				GC-FID response factors normalized to 18:0 (RF _{18:0} = 1): comparison with the work of Schreiner	
	Conc. (mg/L)	Mean FAME peak area ^a (counts)	Mean IS ^b peak area (counts)	RF ^c	Conc. (mg/L)	Mean FAME peak area ^a (counts)	Mean IS ^d peak area (counts)	RF ^c	Present study	Schreiner [18]
12:0	16.25	9.9	837.1	0.91	280.28	263,326	494,665	0.94		
13:0	11.25	6.5	763.6	0.95	218.59	219,213	494,665	1.00		
14:0	2,500.00	1,384.8	779.8	0.89	836.65	830,340	494,665	0.99		
14:1n-5	22.50	14.0	837.1	0.93	266.36	253,764	494,665	0.95		
16:0	4,375.00	2,770.3	844.6	0.94	836.62	847,822	494,665	1.01		
18:0	2,000.00	1,020.5	690.5	0.92	669.29	732,382	494,665	1.09		
18:2n-6	1,375.00	820.4	837.1	0.89	585.63	597,756	494,665	1.02	0.97	0.99
20:1n-9	625.00	321.7	685.7	0.94	552.11	575,680	494,665	1.04		
20:4n-6	500.00	298.6	825.0	0.90	557.75	528,317	494,665	0.94	0.98	0.96
22:6n-3	4,125.00	2,122.6	765.2	0.84	1,104.22	848,957	494,665	0.77	0.91	0.93

^a $n = 3$: each FAME standard solution was prepared in triplicate and injected once

^b 15:1n-5 fatty acid methyl ester was added as IS (internal standard) at a concentration of 1,250.00 mg/L

^c $RF = R_A C_S / R_S C_A$ where: R_A = analyte response (peak area), C_S = internal standard concentration, R_S = internal standard response, C_A = analyte concentration

^d 21:0 fatty acid methyl ester was added as IS (internal standard) at a concentration of 492.96 mg/L

nutritional evaluations. If a better accuracy is requested it must be taken into account an increase in procedure complexity. One way can be the assessment and the use of corrections for analytes studied as cited above [24] by employing absolutely fresh standards of FAME: this procedure was applied in the present work to correct DHA. In our conditions we observed that the correction factor to convert the percentage of DHA peak area into mass percentage is equal to 1.26. This factor works very well when the real percentage of the 24 selected FAME is near to 90 % that is the case of most samples (19 on 21 samples, see Table 2). In Tables 4, 5, and 7 there is a separate row with the corrected DHA value.

Another way is the calculation and the use of theoretical response factors [18].

As regards GC–MS full scan response factors they are reported in Table 1 together with GC–FID values. We can see that RFs have the same reciprocal relations on the two instruments; namely, they are different from each other but vary in a not very broad range, with the exception of DHA that confirms a noticeable negative deviation also in GC–MS. The unusual overestimation of GC–FID for the 16:0 FAME, with respect GC–MS, is not caused by a very different MS response factor but it is due to one or more

peaks that coelute with 16:0 on FID column, as shown in Fig. 2 and explained below.

Qualitative Analysis

In this work an investigated FAME had to match the retention time (t_R) of the pure certified standard both on FID column and MS column if the presence of that FAME had to be confirmed. Further verifications completed the identification step, such as the comparison of mass spectrum with that of the pure standard injected by us and with the spectrum present in the NIST[®] MS database. When necessary injections in SIS, selected ion storage (otherwise named SIM, selected ion monitoring) were carried out for qualitative evaluations.

A double profile analysis FID-based and MS-based was always achieved and this quantitative cross control allowed that the purity of GC–FID peaks was checked, as explained below. First of all we accurately verified that the GC–MS peaks did not coelute with other peaks. Under our conditions, GC–FID and GC–MS generally showed the same percent result for a certain FAME in a chosen sample. Being the GC–MS peaks certainly not interfered it follows that GC–FID peaks are also not interfered, but when a

Table 2 Sum of the 24 selected FAME (% of total FAME) in 12 Mediterranean fish species together with the total lipid content and the collecting season

Sample	Origin	Total lipid content (g/100 g)	Month of fish sampling	Sum of the 24 selected FAME (% of total FAME)
Thinlip mullet (<i>Liza ramada</i>)	Latium region, Italy	3.93	July	83.43
Gilthead seabream (<i>Sparus aurata</i>)	Greece (farmed)	7.22	May	91.69
European seabass (<i>Dicentrarchus labrax</i>)	Northern Italy (farmed)	8.00	October	90.54
European seabass (<i>Dicentrarchus labrax</i>)	Southern Italy (farmed)	6.92	December	90.25
European seabass (<i>Dicentrarchus labrax</i>)	Central Italy (farmed)	9.00	December	90.44
Rainbow trout (<i>Oncorhynchus mykiss</i>)	Central Italy (farmed)	5.24	September	92.26
Bogue (<i>Boops boops</i>)	Puglia region, Italy	1.06	March	89.40
Dogtooth grouper (<i>Epinephelus caninus</i>)	Mediterranean Sea	1.20	February	88.35
European hake (<i>Merluccius merluccius</i>)	Italy (Adriatic Sea)	1.24	January	87.25
European hake (<i>Merluccius merluccius</i>)	Italy (Tyrrhenian Sea)	0.81	February	89.32
Shade-fish (<i>Argyrosomus regius</i>)	Orbetello, Italy (farmed)	2.55	March	92.24
Shade-fish (<i>Argyrosomus regius</i>)	Ansedonia, Italy (farmed)	1.71	November	92.93
Gilthead seabream (<i>Sparus aurata</i>)	Southern Italy	3.89	October	82.18
Gilthead seabream (<i>Sparus aurata</i>)	Civitavecchia, Italy (farmed)	5.80	June	91.66
Gilthead seabream (<i>Sparus aurata</i>)	Gaeta, Italy (farmed)	14.54	February	92.39
Turbot (<i>Psetta maxima</i>)	Spain (farmed)	2.00	July	88.96
Brook trout (<i>Salvelinus fontinalis</i>)	Northern Italy (farmed)	6.50	June	91.35
Common sole (<i>Solea solea</i>)	Central Italy (farmed)	5.88	December	89.19
Tench (<i>Tinca tinca</i>)	Poirino, Italy (farmed)	4.30	June	91.69
Rainbow trout (<i>Oncorhynchus mykiss</i>)	Northern Italy (farmed)	7.64	November	89.75
Rainbow trout (<i>Oncorhynchus mykiss</i>)	Italy (farmed)	3.99	March	91.24

Results obtained by GC–MS measurements and by applying the (1E) equation

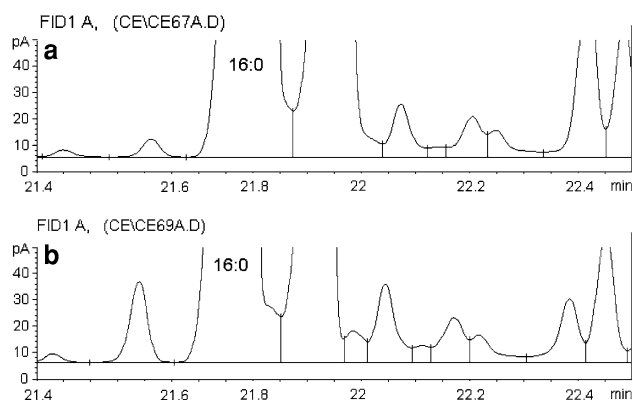


Fig. 2 GC-FID chromatogram of two different fish samples. **a** In this fish sample there are coeluting peaks with 16:0 as revealed by the FID overestimation with respect GC-MS, but they are not visible. **b** In this sample there is the same FID overestimation and one of the coeluting peaks with 16:0 it is also visible

relevant disagreement in the sense of quantitative overestimation by GC-FID is present a GC-FID coelution was detected. With this technique we discovered a frequent GC-FID coelution that can be inferred from Tables 3, 4, and 7 and is shown in Fig. 2. FAME peak coelutions not detectable on GC-FID equipment is cited in the literature as a real event [26]. Alternatively we had the possibility of using the same capillary columns on both instruments: this would make possible a more immediate control of coelutions on GC-FID equipment. Nevertheless, we preferred to use two different columns for qualitative purposes as the following explains. Due to molecular FAME characteristics, EI (electron ionization)-GC-MS often does not show adequate specificity toward particular C-C double bond positional isomers. In some cases, retention times are of primary importance and the double instrumental analysis with the use of two columns different in length and polarity was chosen so as to acquire complementary data, as recommended [24].

The good resolution of GC-MS Chromatograms can be observed in Figs. 3 and 4 (24:1n-9 fatty acid, normally detectable in fish samples, is completely separated from 22:6, with a shorter retention time: it is not visible in Fig. 3 due to its low intensity).

The 24 Selected FAME: Their Total Amount in Samples

The exact percentage of an investigated FAME can be assessed only when the number and the amount of all FAME present in the sample are known. To solve this problem we carried out a complete study on the 12 species shown in Table 2. Mass spectrometry has identification power and sensitivity enough to detect the presence of FAME even in trace quantities. Even if the possible

Table 3 FAME profile analysis of a gilthead seabream sample (*Sparus aurata*)

FAME	Profile analysis (% of total FAME)	
	GC-FID ^a	GC-MS ^b
12:0	0.042 ± 0.001	0.040 ± 0.001
13:0	0.0176 ± 0.0004	0.019 ± 0.001
14:0	3.80 ± 0.09	3.51 ± 0.12
15:0	0.27 ± 0.01	0.30 ± 0.01
16:0	13.40 ± 0.32	11.39 ± 0.38
17:0	0.207 ± 0.005	0.28 ± 0.01
18:0	4.61 ± 0.11	3.65 ± 0.12
20:0	0.192 ± 0.005	0.283 ± 0.01
14:1n-5	0.069 ± 0.002	0.079 ± 0.003
16:1n-7	5.81 ± 0.14	5.34 ± 0.18
18:1n-9	20.28 ± 0.48	20.28 ± 0.68
18:1n-7	2.64 ± 0.06	3.16 ± 0.11
20:1n-9	1.90 ± 0.04	2.42 ± 0.08
22:1n-9	0.390 ± 0.009	0.50 ± 0.02
22:1n-11	1.18 ± 0.03	1.41 ± 0.05
16:2n-4	0.46 ± 0.01	0.54 ± 0.02
18:2n-6	14.65 ± 0.35	14.92 ± 0.50
18:3n-3	1.88 ± 0.04	2.07 ± 0.07
18:4n-3	0.79 ± 0.02	0.80 ± 0.03
20:2n-6	0.46 ± 0.01	0.64 ± 0.02
20:4n-6	0.56 ± 0.01	0.68 ± 0.02
20:5n-3	4.73 ± 0.11	5.11 ± 0.17
22:5n-3	3.65 ± 0.09	3.66 ± 0.12
22:6n-3	8.00 ± 0.19	8.92 ± 0.30

The same gilthead seabream sample listed in Table 2, second row

^a Number of GC-FID transesterifications = 2, number of GC-FID injections per transesterification = 1

^b Number of GC-MS transesterifications = 1, number of GC-MS injections per transesterification = 1

isomers indicated by the NIST[®] MS database could be more than one, nevertheless, after that Mass Spectrum was examined, the attribution, or not, of the investigated peak to the FAME class was always very clear. By considering all FAME in the sample (with a signal to noise ratio >3) GC-MS chromatograms of fish samples generally showed a number of FAME of about 80, but in some cases this number was 100 or more.

For each species the global amount of the 24 selected FAME was obtained as follows:

$$\text{global amount of the 24 selected FAME (\% of total FAME)} = \frac{(\text{sum of peak areas of the 24 selected FAME}) \times 100}{\text{sum of peak areas of all FAME revealed}} \quad (1E)$$

Results are shown in Table 2. For the 12 species examined in this study we may see that the mean

Table 4 Complete FAME analysis of a thinlip mullet sample (*Liza ramada*)

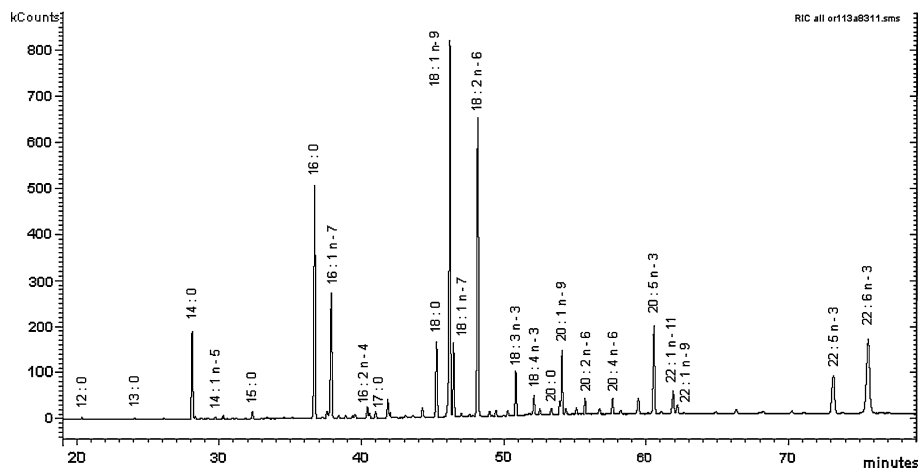
FAME	Profile analysis (% of total FAME)		Absolute analysis (mg/100 g)		
	GC-FID ^a	GC-MS ^b	Profile used: GC-FID ^c	Procedure used: calibration curves	Error (%)
12:0	0.112 ± 0.003	0.131 ± 0.004	3.9 ± 0.1	4.3 ± 0.2	-9
13:0	0.049 ± 0.001	0.068 ± 0.002	1.7 ± 0.1	1.9 ± 0.2	-11
14:0	4.12 ± 0.10	4.57 ± 0.15	143.7 ± 4.8	154.3 ± 33.4	-7
15:0	0.69 ± 0.02	0.83 ± 0.03	24.2 ± 0.8		
16:0	20.59 ± 0.49	17.85 ± 0.59	719.0 ± 24.1		
17:0	0.55 ± 0.01	0.66 ± 0.02	19.3 ± 0.6		
18:0	3.89 ± 0.09	4.27 ± 0.14	135.7 ± 4.5		
20:0	0.201 ± 0.005	0.28 ± 0.01	7.0 ± 0.2		
14:1n-5	0.069 ± 0.002	0.100 ± 0.003	2.4 ± 0.1	2.4 ± 0.1	0
16:1n-7	10.85 ± 0.26	11.08 ± 0.37	378.9 ± 12.7	348.7 ± 37.9	+9
18:1n-9	7.94 ± 0.19	8.73 ± 0.29	277.2 ± 9.3		
18:1n-7	3.28 ± 0.08	3.87 ± 0.13	114.6 ± 3.8		
20:1n-9	0.56 ± 0.01	0.73 ± 0.02	19.5 ± 0.7	19.7 ± 9.5	-1
22:1n-9	0.072 ± 0.002	0.146 ± 0.005	2.5 ± 0.1		
22:1n-11	0.203 ± 0.005	0.071 ± 0.002	7.1 ± 0.2		
16:2n-4	0.93 ± 0.02	1.01 ± 0.03	32.3 ± 1.1		
18:2n-6	2.81 ± 0.07	3.08 ± 0.10	98.2 ± 3.3	103.4 ± 5.6	-5
18:3n-3	4.61 ± 0.11	4.53 ± 0.15	160.9 ± 5.4		
18:4n-3	5.72 ± 0.13	5.21 ± 0.17	199.7 ± 6.7		
20:2n-6	0.24 ± 0.01	0.41 ± 0.01	8.4 ± 0.3		
20:4n-6	1.12 ± 0.03	1.16 ± 0.04	38.9 ± 1.3	36.2 ± 10.9	+7
20:5n-3	8.88 ± 0.21	8.74 ± 0.29	310.1 ± 10.4	325.7 ± 34.2	-5
22:5n-3	1.84 ± 0.04	1.75 ± 0.06	64.4 ± 2.2		
22:6n-3	10.68 ± 0.25	10.73 ± 0.36	372.8 ± 12.5	452.7 ± 49.7	-18
Mean error (absolute value)					7
22:6n-3 corrected [24]			469.7 ± 15.7		+4

The same thinlip mullet sample listed in Table 2, first row

^a Number of GC-FID transesterifications = 2, number of GC-FID injections per transesterification = 1

^b Number of GC-MS transesterifications = 1, number of GC-MS injections per transesterification = 1

^c Number of total FA determinations by saponification = 2. Total measured FA = 3,491.6 ± 34.5 mg/100 g. Total measured lipids = 3.93 ± 0.02 g/100 g

Fig. 3 GC-MS chromatogram of the gilthead seabream sample of Table 3

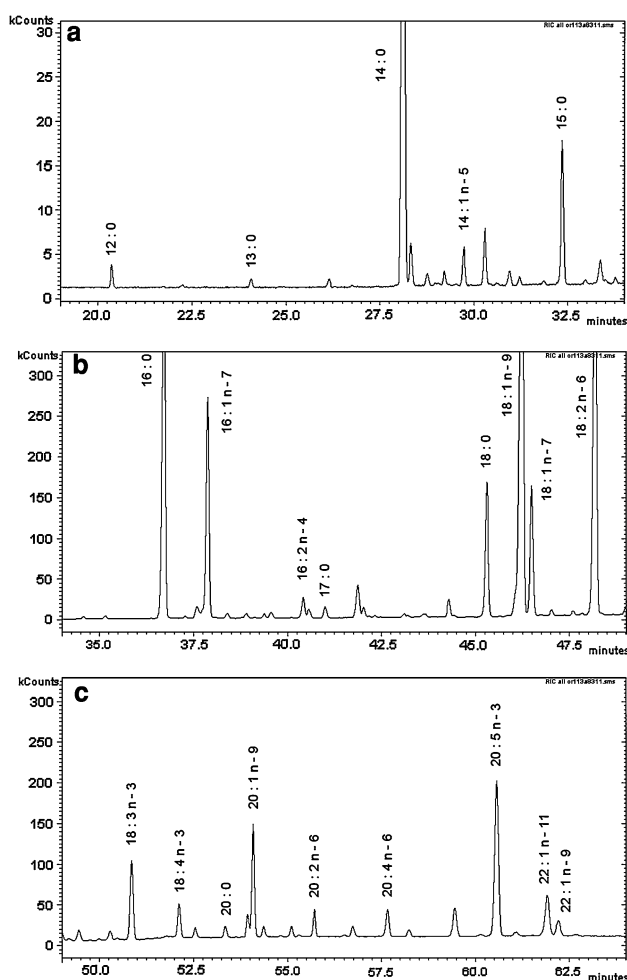
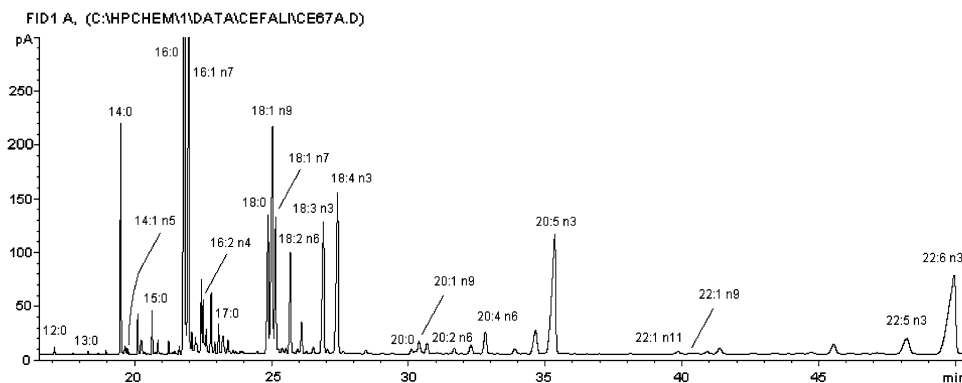


Fig. 4 Magnification of chromatogram of Fig. 3. **a** 19–34 min segment. **b** 34–49 min segment. **c** 49–64 min segment

percentage of the 24 selected FAME, over total FAME, is 89.8 ± 2.8 . On the basis of all observations made by us in our work we can round the sum of the 24 selected FAME to 90 ± 3 % of total FAME. This value can be usefully employed whenever one of the 12 species is investigated for the FAME Profile and will be used in any calculation of this work.

Fig. 5 GC-FID chromatogram of the thinlip mullet sample of Table 4



Profile Analysis (Percentages)

The 24 selected peaks represent the 90 ± 3 % of total FAME in samples, as cited above, and this value was used as reference in calculating the amount of each FAME:

$$\text{amount of the investigated FAME in the sample (\%)} = \frac{(\text{peak area of the investigated FAME}) \times 90}{\text{sum of peak areas of the 24 selected FAME}} \quad (2E)$$

In Eqs. (1E) and (2E) area percentages were approximated to mass percentages by taking into account considerations exposed in the response factor paragraph reported above. Table 3 shows the profile analysis for the gilthead sea bream sample of Figs. 3 and 4. Results were obtained by applying the (2E) equation both to GC-FID and GC-MS peak areas. Other Profile analyses are shown in Tables 4 and 7. The good agreement generally observed between percentages coming from GC-FID and coming from GC-MS, made it possible that the profile used to carry out the subsequent absolute analysis was generally that obtained by GC-FID.

Absolute Analysis (mg/100 g Edible Portion)

Total FA Determination

From the results expressed as percentages (profile analysis) the content of each FA in mg/100 g of edible portion can be obtained if the exact amount of total FA in mg/100 g of edible portion is known. We experimentally determined this quantity by means of saponification achieved as reported in “Materials and Methods”. An aliquot of oil, from the total extracted, was taken for saponification. The total FA in mg/100 g of edible portion can be obtained according to the following equation:

$$m = \frac{F}{T} \times P \times 1,000 \quad (3E)$$

where m is the total FA in 100 g of edible portion (mg/100 g of edible portion), T is the aliquot of oil weighed for

Table 5 Amount of each fatty acid (mg/100 g edible portion) in 20 Mediterranean fish samples

FAME	Gilthead seabream	European seabass	European seabass	European seabass	Rainbow trout	Bogue	Dogtooth grouper	European hake	European hake	Shade-fish
12:0	2.8	4.0	2.7	4.7	2.6	0.7	1.0	1.1	0.4	1.4
13:0	1.2	1.7	1.6	2.4	1.0	0.4	0.3	0.5	0.2	0.6
14:0	250.7	307.1	353.8	457.8	166.7	16.1	30.6	40.0	9.3	103.7
15:0	17.9	22.2	26.5	30.1	12.0	5.4	5.1	7.3	2.7	7.8
16:0	883.6	1,117.1	1,054.5	1,374.3	664.1	172.5	214.3	186.1	110.4	430.9
17:0	13.7	15.2	16.0	19.7	9.8	7.0	11.1	8.4	4.6	7.2
18:0	304.2	213.8	194.4	255.7	205.3	65.5	89.9	57.5	44.5	156.8
20:0	12.7	9.6	7.2	6.5	5.8	2.6	3.1	3.7	1.5	4.4
14:1n-5	4.6	4.6	4.3	5.4	0.8	0.3	0.4	0.4	0.1	0.8
16:1n-7	383.1	332.3	420.3	613.8	176.9	23.7	98.5	67.7	17.2	112.5
18:1n-9	1,337.1	1,386.3	1,149.3	1,351.8	693.7	68.8	94.4	96.6	59.1	257.7
18:1n-7	174.0	171.3	161.2	221.7	111.1	23.2	40.5	39.7	15.8	48.5
20:1n-9	125.6	303.4	211.9	157.1	75.0	5.3	3.9	6.2	3.2	37.4
22:1n-9	25.7	26.3	19.4	13.0	7.3	0.7	0.3	1.2	0.8	5.6
22:1n-11	77.8	273.9	152.1	90.0	73.4	2.5	2.5	2.7	1.1	37.7
16:2n-4	30.3	27.6	32.5	54.5	16.4	0.7	5.0	3.9	1.1	12.3
18:2n-6	965.6	1,004.2	539.0	739.0	1,059.1	10.3	10.9	16.2	15.8	320.8
18:3n-3	124.2	171.1	126.7	112.0	121.7	4.0	10.3	8.3	2.6	27.5
18:4n-3	51.8	108.5	79.3	133.8	50.0	3.6	2.5	8.8	2.6	17.5
20:2n-6	30.6	39.9	31.6	42.7	41.0	3.3	1.6	4.6	5.1	5.0
20:4n-6	37.0	33.1	34.3	53.8	23.7	28.1	39.9	24.7	20.4	29.6
20:5n-3	311.8	394.2	398.8	809.8	211.8	38.5	31.8	99.6	37.0	156.9
22:5n-3	240.9	94.6	114.7	142.7	72.1	13.8	53.8	16.5	7.5	47.6
22:6n-3	527.2	527.1	549.8	736.1	470.2	264.3	127.2	211.0	188.5	182.6
22:6n-3 corrected [24]	664.3	664.2	692.8	927.5	592.5	333.0	160.2	265.8	237.5	230.0
<i>m</i> value from Weihrauch conversion	6,593.3	7,321.0	6,313.4	8,254.0	4,745.9	846.0	976.6	1,013.9	612.7	2,236.1

FAME	Shade-fish	Gilthead seabream	Gilthead seabream	Gilthead seabream	Turbot	Brook trout	Common sole	Tench	Rainbow trout	Rainbow trout
12:0	0.5	3.9	1.7	6.8	0.6	4.6	3.9	3.2	4.3	2.2
13:0	0.3	1.1	1.2	3.0	0.4	2.0	2.4	1.3	2.7	1.0
14:0	22.7	62.5	168.1	583.5	73.4	341.0	347.5	57.0	447.7	156.5
15:0	3.7	26.1	13.1	40.1	6.4	21.0	27.2	15.1	29.9	11.4
16:0	255.6	810.5	660.0	1,907.0	284.2	919.1	886.8	783.5	1,107.2	593.2
17:0	5.4	40.4	14.1	24.9	5.2	14.3	16.2	11.6	19.8	9.1
18:0	115.3	352.0	236.0	566.8	58.2	223.9	159.3	262.9	261.6	180.5
20:0	3.7	6.3	9.1	19.4	2.6	6.1	6.4	6.3	8.6	3.1
14:1n-5	0.5	2.8	3.9	15.4	0.5	4.9	4.8	2.2	3.7	0.6
16:1n-7	50.5	312.2	265.0	826.9	111.6	431.5	469.5	250.4	364.7	180.8
18:1n-9	158.2	669.0	854.1	3,432.9	194.7	859.2	641.0	817.9	923.9	485.3
18:1n-7	35.1	132.5	129.1	340.4	54.7	187.0	170.5	65.4	156.5	88.7
20:1n-9	13.0	31.0	47.7	310.7	23.7	81.5	30.0	23.3	341.7	22.3
22:1n-9	1.3	6.3	11.9	54.7	3.6	8.5	6.1	0.9	29.7	3.0
22:1n-11	7.4	8.8	31.9	205.1	8.5	39.7	18.9	3.8	448.0	8.4
16:2n-4	4.4	9.9	30.7	47.5	10.7	43.7	52.9	4.9	35.1	19.9
18:2n-6	155.4	43.1	1,183.5	1,589.6	121.0	881.2	300.2	833.2	748.0	637.3
18:3n-3	9.9	30.0	122.0	343.4	15.1	73.8	45.3	107.5	112.3	76.8

Table 5 continued

FAME	Shade-fish	Gilthead seabream	Gilthead seabream	Gilthead seabream	Turbot	Brook trout	Common sole	Tench	Rainbow trout	Rainbow trout
18:4n-3	10.5	23.5	38.6	107.1	27.9	55.5	73.1	14.7	116.2	25.2
20:2n-6	4.2	12.5	28.5	57.3	7.6	43.5	8.9	25.7	28.3	26.8
20:4n-6	47.1	85.9	29.7	39.9	22.2	35.8	43.1	44.6	29.9	22.6
20:5n-3	134.8	167.4	274.9	427.0	204.5	354.4	345.7	44.0	299.9	204.6
22:5n-3	38.1	101.3	193.7	320.6	73.0	150.8	510.9	15.6	99.3	78.3
22:6n-3	229.5	198.5	392.8	810.7	240.4	546.5	638.0	87.2	667.5	384.3
22:6n-3 corrected [24]	289.2	250.1	494.9	1,021.4	303.0	688.6	803.9	109.9	841.1	484.2
<i>m</i> value from Weihrauch conversion	1,452.4	3,486.4	5,268.4	13,422.8	1,723.0	5,921.5	5,343.0	3,868.9	6,985.1	3,579.7

Profile used: GC-FID. The samples are the same as those listed in Table 2. Results for thinlip mullet are shown in Table 4

saponification (g), F is the total FA found in the aliquot T by saponification (g), P is the lipids in edible portion weighed (g/100 g).

In Table 4 the total FA content (m) was determined in a thinlip mullet sample by applying the Eq. (3E). The value of m (total FA) was found to be $3,491.6 \pm 34.5$ mg/100 g of edible portion. If, on the same sample, the factor for finfish derived by Weihrauch et al. [19] is applied (this factor provides the FA amount in a sample without executing the saponification step) we obtain $m = 3,525.2$ mg/100 g. It can be seen that the Weihrauch conversion procedure fits very well with the experimental value so confirming its validity.

Absolute Amount of Each FA

In the same thinlip mullet sample of Table 4 the absolute amount of each FA (mg/100 g of edible portion) was determined by applying the Eq. (4E) reported below:

$$\begin{aligned} & \text{amount of the investigated FAME in the sample (mg/100g)} \\ & = \frac{[\text{percentage of the investigated FAME in the sample (\%)}] \times m}{100} \end{aligned} \quad (4E)$$

In Fig. 5 the GC-FID gas chromatogram obtained for the thinlip mullet sample cited here is shown.

In the 20 remaining fish samples other than thinlip mullet the absolute amount of each FA (mg/100 g of edible portion) was determined by using the factor derived by Weihrauch et al. [19]. Results are listed in Table 5 where the value of m for each sample, obtained by using the Weihrauch conversion, is also reported.

Validation and Analytical Quality Control

The certified reference material “FAPAS® T1475-cod liver oil” was used to validate the profile analysis as described in

this paper. It was analyzed in the exact way exposed above (“Results and Discussion”, profile analysis). If we take into account that this material is not strictly within the field of method applicability (cod liver instead of fish fillet) result can be viewed as good (see Table 6) with the expected error either on 22:6n-3 (uncorrected value) and on the other three LC-PUFA.

The Standard Reference Material “NIST® 1946 Lake Superior Fish Tissue” was used to validate the entire approach profile analysis–total FA determination–absolute analysis as proposed in this work. It was analyzed in the exact way exposed above (“Results and Discussion”, absolute analysis). The result is reported in Table 7. In the present research (and with the GC-FID column used) we observed that the 16:0 fatty acid percentage is constantly overestimated by GC-FID with respect GC-MS. This is due to a coelution, see Fig. 2. For example the FID value for 16:0 in the reference material is 14.68 % and the obtained MS value is 12.51 %. The same situation can be observed in Tables 3 and 4.

One of the most important controls we performed was the analysis of the thinlip mullet sample of Table 4 by employing a method calibration curve-based we executed specifically for this purpose. As in the case of the Standard Reference Material NIST® this control was used to validate the entire approach profile analysis–total FA determination–absolute analysis. We used fresh standards and replicate measures. In order to achieve this objective 10 FAME were dissolved in such a way that solutions at four different concentrations were obtained. Each one, of the four concentrations, was prepared in triplicate and GC-FID injected for a total number of 120 dilutions that led to 10 calibration curves (peak area vs. concentration). Recovery analyses were carried out on standard triglycerides that were transesterified as described in “Materials and Methods”. Results showed the same recovery for different FA with a mean value of 45 ± 1 %. Peak areas observed in GC-FID

Table 6 FAME profile analysis of CRM (Certified Reference Material) “FAPAS® T1475-Cod Liver Oil” with the proposed method

FAME	Amount detected (%) GC-FID ^a	Amount declared (% of total FAME)		Amount detected (%) GC-MS ^b	Distance from satisfactory range	
		Assigned value	Satisfactory range		GC-FID (%)	GC-MS (%)
18:3n-3	0.96 ± 0.02	0.95	0.86–1.05	0.96 ± 0.03	0	0
20:5n-3	10.83 ± 0.26	12.93	11.64–14.23	10.49 ± 0.35	-7	-10
22:5n-3	1.52 ± 0.04	1.88	1.69–2.07	1.53 ± 0.05	-10	-9
22:6n-3	7.88 ± 0.19	10.66	9.59–11.73	8.02 ± 0.27	-18	-16

^a GC-FID: number of transesterifications = 2, number of injections per transesterification = 1

^b GC-MS: number of transesterifications = 1, number of injections per transesterification = 1

Table 7 Analysis of SRM (Standard Reference Material) “NIST® 1946-Lake Superior Fish Tissue (Trout: *Salvelinus namaycush*)” with the proposed method

FAME	Profile analysis (% of total FAME)		Absolute analysis (mg/100 g)		
	GC-FID ^a	GC-MS ^b	Profile used: GC-FID ^c	Amount declared	Error (%)
12:0	0.058 ± 0.001	0.077 ± 0.003	5.4 ± 0.4	5.55 ± 0.51	-3
13:0	0.0188 ± 0.0004	0.020 ± 0.001	1.8 ± 0.1	Not declared	
14:0	3.19 ± 0.08	3.34 ± 0.11	297.1 ± 24.3	316 ± 9	-6
15:0	0.30 ± 0.01	0.38 ± 0.01	28.2 ± 2.3	28.5 ± 1.6	-1
16:0	14.68 ± 0.35	12.51 ± 0.42	1,367.6 ± 111.4	1,220 ± 40	+12
17:0	0.203 ± 0.005	0.29 ± 0.01	18.9 ± 1.5	22.5 ± 2.3	-16
18:0	2.87 ± 0.07	3.77 ± 0.13	267.4 ± 21.8	263 ± 11	+2
20:0	0.114 ± 0.003	0.19 ± 0.01	10.6 ± 0.9	10.0 ± 1.2	+6
14:1n-5	0.084 ± 0.002	0.116 ± 0.004	7.8 ± 0.6	Not declared	
16:1n-7	8.80 ± 0.21	8.62 ± 0.29	819.9 ± 66.8	816 ± 26	+1
18:1n-9	27.85 ± 0.66	24.21 ± 0.81	2,594.3 ± 211.3	2,640 ± 80	-2
18:1n-7	4.15 ± 0.10	5.15 ± 0.17	386.4 ± 31.5	373 ± 5	+4
20:1n-9	1.46 ± 0.03	1.86 ± 0.06	135.9 ± 11.1	132 ± 12	+3
22:1n-9	0.240 ± 0.006	0.34 ± 0.01	22.4 ± 1.8	26.6 ± 6.0	-16
22:1n-11	0.079 ± 0.002	0.046 ± 0.002	7.4 ± 0.6	Not declared	
16:2n-4	0.34 ± 0.01	0.28 ± 0.01	31.2 ± 2.5	Not declared	
18:2n-6	3.98 ± 0.09	4.69 ± 0.16	371.0 ± 30.2	348 ± 23	+7
18:3n-3	2.23 ± 0.05	2.41 ± 0.08	207.4 ± 16.9	221 ± 25	-6
18:4n-3	1.05 ± 0.02	1.02 ± 0.03	98.0 ± 8.0	106 ± 13	-8
20:2n-6	1.03 ± 0.02	1.42 ± 0.05	95.9 ± 7.8	99.0 ± 4.3	-3
20:4n-6	2.14 ± 0.05	2.33 ± 0.08	199.5 ± 16.3	212 ± 19	-6
20:5n-3	3.24 ± 0.08	3.62 ± 0.12	302.1 ± 24.6	296 ± 19	+2
22:5n-3	3.42 ± 0.08	3.78 ± 0.13	318.3 ± 25.9	335 ± 26	-5
22:6n-3	8.49 ± 0.20	9.52 ± 0.32	790.7 ± 64.4	920 ± 100	-14
Mean error (absolute value)					6
22:6n-3 corrected [24]			996.3 ± 81.2		+8

^a GC-FID: number of transesterifications = 2, number of injections per transesterification = 1

^b GC-MS: number of transesterifications = 1, number of injections per transesterification = 1

^c Number of total FA determinations by saponification = 5. Total measured FA = 9,316.7 ± 539.4 mg/100 g. Total measured lipids = 10.34 ± 1.30 g/100 g. Total declared lipids = 10.17 ± 0.48 g/100 g

Chromatograms of the thinlip mullet sample of Table 4 were used in combination with calibration curves and measured recoveries to evaluate the content of each FAME

(mg/100 g edible portion). Results obtained with calibration curves were compared with results obtained with the method proposed in this work. Table 4 shows a good

agreement between the two independent techniques, if we except DHA, for which accuracy is at the level discussed in this work. The calibration approach was used also to evaluate the content of 22:6n-3 in the Standard Reference Material NIST[®] of Table 7: result was of 873 mg/100 g. This means an error of -5 % with respect to the declared value so confirming a better accuracy of methods calibration-based. These validation measures indicate that the procedure profile analysis–total FA determination–absolute analysis as conducted here can be usefully employed as an alternative to the procedure calibration-based when one of the 12 Mediterranean fish species cited above is analyzed. With some advantages and disadvantages to be taken into account. A great advantage lies in complexity reduction: when GC-FID and GC-MS Chromatograms of the sample are obtained is sufficient to apply the value of 90 ± 3 % and the conversion factor of Weihrauch et al. [19] as exposed above to obtain the absolute final result. Absolutely fresh standards of FAME are not necessary in each analysis. This makes it possible that absolute analyses can be readily conducted on a routine basis on fish samples and for a significant number of fatty acids. The main disadvantage is that the method is probably of lower accuracy with respect to methods that are calibration-based, especially in some cases. Nevertheless accuracy is enough for most nutritional evaluations being of the 7 % mean error associated with results under the conditions used here.

References

- Krogmann A, Staiger K, Haas C, Gommer N, Peter A, Heni M, Machicao F, Häring HU, Staiger H (2011) Inflammatory response of human coronary artery endothelial cells to saturated long-chain fatty acids. *Microvasc Res* 81:52–59
- Paisley C, Lloyd H, Sparks P, Mela DJ (1995) Consumer perceptions of dietary changes for reducing fat intake. *Nutr Res* 5:1755–1766
- Moyad MA (2005) An introduction to dietary/supplemental omega-3 fatty acids for general health and prevention: part II. *Urol Oncol Semin O I* 23:36–48
- Torrejon C, Jung UJ, Deckelbaum RJ (2007) n-3 Fatty acids and cardiovascular disease: actions and molecular mechanisms. *Prostag Leukotr Ess* 77:319–326
- Lavie CJ, Milani RV, Mehra MR, Ventura HO (2009) Omega-3 polyunsaturated fatty acids and cardiovascular diseases. *J Am Coll Cardiol* 54:585–594
- Orban E, Masci M, Navigato T, Di Lena G, Casini I, Caproni R, Gambelli L, De Angelis P, Rampacci M (2006) Nutritional quality and safety of whitefish (*Coregonus lavaretus*) from Italian lakes. *J Food Compos Anal* 19:737–746
- Orban E, Navigato T, Masci M, Di Lena G, Casini I, Caproni R, Gambelli L, De Angelis P, Rampacci M (2007) Nutritional quality and safety of European perch (*Perca fluviatilis*) from three lakes of Central Italy. *Food Chem* 100:482–490
- Whelton SP, He J, Whelton PK, Muntner P (2004) Meta-analysis of observational studies on fish intake and coronary heart disease. *Am J Cardiol* 93:1119–1123
- Williams CD, Whitley BM, Hoyo C, Grant DJ, Iraggi JD, Newman KA, Gerber L, Taylor LA, McKeever MG, Freedland SJ (2011) A high ratio of dietary n-6/n-3 polyunsaturated fatty acids is associated with increased risk of prostate cancer. *Nutr Res* 31:1–8
- Kalogeropoulos N, Panagiotakos DB, Pitsavos C, Chrysoshoou C, Rousinou G, Toutouza M, Stefanadis C (2010) Unsaturated fatty acids are inversely associated and n-6/n-3 ratios are positively related to inflammation and coagulation markers in plasma of apparently healthy adults. *Clin Chim Acta* 411:584–591
- Harris WS, Assaad B, Poston WC (2006) Tissue omega-6/omega-3 fatty acid ratio and risk for coronary artery disease. *Am J Cardiol* 98:19i–26i
- Memon NN, Talpur FN, Bhanger MI, Balouch A (2011) Changes in fatty acid composition in muscle of three farmed carp fish species (*Labeo rohita*, *Cirrhinus mrigala*, *Catla catla*) raised under the same conditions. *Food Chem* 126:405–410
- Jabeen F, Chaudhry AS (2011) Chemical compositions and fatty acid profiles of three freshwater fish species. *Food Chem* 125:991–996
- Njinkoué JM, Barnathan G, Miralles J, Gaydou EM, Samb A (2002) Lipids and fatty acids in muscle, liver and skin of three edible fish from the Senegalese coast: *Sardinella maderensis*, *Sardinella aurita* and *Cephalopholis taeniodops*. *Comp Biochem Phys B* 131:395–402
- Pacetti D, Alberti F, Boselli E, Frega NG (2010) Characterisation of furan fatty acids in Adriatic fish. *Food Chem* 122:209–215
- Jalali-Heravi M, Vosough M (2004) Characterization and determination of fatty acids in fish oil using gas chromatography–mass spectrometry coupled with chemometric resolution techniques. *J Chromatogr A* 1024:165–176
- Juárez M, Juárez A, Aldai N, Avilés C, Polvillo O (2010) Validation of a gas–liquid chromatographic method for analysing samples rich in long chain n-3 polyunsaturated fatty acids: application to seafood. *J Food Compos Anal* 23:665–670
- Schreiner M (2005) Quantification of long chain polyunsaturated fatty acids by gas chromatography. Evaluation of factors affecting accuracy. *J Chromatogr A* 1095:126–130
- Weihrauch JL, Posati LP, Anderson BA, Exler J (1977) Lipid conversion factors for calculating fatty acids contents of foods. *J Am Oil Chem Soc* 54:36–40
- Bligh EG, Dyer WJ (1959) A rapid method of total lipid extraction and purification. *Can J Biochem Phys* 37:911–917
- Kinsella JE, Shimp JL, Mai J, Weihrauch J (1977) Fatty acid content and composition of freshwater finfish. *J Am Oil Chem Soc* 54:424–429
- US Department of Agriculture, Agricultural Research Service (2009) Composition of foods. Raw, processed, prepared. USDA National Nutrient Database for Standard Reference, Release 22:18
- Dodds ED, McCoy MR, Rea LD, Kennish JM (2005) Gas chromatography quantification of fatty acids methyl esters: flame ionization detector vs. electron impact mass spectrometry. *Lipids* 40:419–428
- European Union Regulation, Commission regulation (EEC) No 2568/91 (1991) Analysis by gas chromatography of methyl esters of fatty acids: use of correction factors. Official Newspaper of the European Community 1991R2568:59–60
- AOCS (1989) Official method Ce 1b-89. In: Firestone D (ed) Official methods and recommended practices of the American oil chemists' society. Champaign, IL
- Thurnhofer S, Vetter W (2005) A gas chromatography/electron ionization–mass spectrometry–selected ion monitoring method for determining the fatty acid pattern in food after formation of fatty acid methyl esters. *J Agric Food Chem* 53:8896–8903

Erratum to: Daily Intake of Cod or Salmon for 2 Weeks Decreases the 18:1n-9/18:0 Ratio and Serum Triacylglycerols in Healthy Subjects

Vibeke H. Telle-Hansen · Laila N. Larsen ·
Arne T. Høstmark · Marianne Molin ·
Lisbeth Dahl · Kari Almendingen · Stine M. Ulven

Published online: 17 May 2012
© AOCs 2012

Erratum to: Lipids (2012) 47:151–160
DOI 10.1007/s11745-011-3637-y

In the original version of the article, the values of the control and cod groups were incorrectly published. The correct version of Table 3 is given below.

The online version of the original article can be found under doi:[10.1007/s11745-011-3637-y](https://doi.org/10.1007/s11745-011-3637-y).

V. H. Telle-Hansen · M. Molin · K. Almendingen ·
S. M. Ulven (✉)
Department of Health, Nutrition and Management,
Faculty of Health Sciences, Oslo and Akershus University
College of Applied Sciences, Postbox 4, St. Olavsplass,
0130 Oslo, Norway
e-mail: StineMarie.Ulven@hioa.no

V. H. Telle-Hansen
Department of Nutrition, Institute of Basic Medical Sciences,
Faculty of Medicine, University of Oslo, Postbox 1046,
Blindern, 0316 Oslo, Norway

L. N. Larsen
EpiGen Institute, Research Centre, Akershus University
Hospital, Postbox 26, 1478 Lørenskog, Norway

A. T. Høstmark
Section of Preventive Medicine and Epidemiology,
University of Oslo, Postbox 1130, Blindern, 0318 Oslo, Norway

M. Molin
Institute of Basic Medical Sciences, Faculty of Medicine,
University of Oslo, Postbox 1110, Blindern, 0317 Oslo, Norway

L. Dahl
National Institute of Nutrition and Seafood Research (NIFES),
Postbox 2029, Nordnes, 5817 Bergen, Norway

K. Almendingen
Unit of Clinical Research, Research Centre, Akershus University
Hospital, Postbox 26, 1478 Lørenskog, Norway

Table 3 Fatty acids in plasma phospholipids at baseline and at end of study [median (25–75 percentile)]

Parameter (mg/ml)	Treatment	<i>n</i>	Baseline	End of study	<i>P</i> value ^a	<i>P</i> value ^b
Palmitic acid (16:0)	Control	10	0.282 (0.231–0.323)	0.281 (0.255–0.327)	0.05	
	Cod	9	0.276 (0.245–0.323)	0.282 (0.268–0.316)	NS	NS
	Salmon	11	0.267 (0.221–0.401)	0.295 (0.228–0.345)	NS	0.04
Stearic acid (18:0)	Control	10	0.115 (0.099–0.138)	0.129 (0.120–0.141)	NS	
	Cod	9	0.125 (0.112–0.145)	0.127 (0.121–0.137)	NS	NS
	Salmon	11	0.132 (0.107–0.149)	0.144 (0.118–0.153)	NS	NS
Sum SFA	Control	10	0.409 (0.327–0.459)	0.409 (0.379–0.468)	0.05	
	Cod	9	0.404 (0.366–0.461)	0.412 (0.397–0.445)	NS	NS
	Salmon	11	0.393 (0.334–0.575)	0.418 (0.354–0.498)	NS	NS
Oleic acid (18:1)	Control	10	0.079 (0.068–0.094)	0.086 (0.071–0.096)	NS	
	Cod	9	0.087 (0.079–0.102)	0.080 (0.073–0.086)	NS	0.03
	Salmon	11	0.095 (0.059–0.116)	0.063 (0.052–0.075)	0.005	0.001
Linoleic acid (18:2)	Control	10	0.215 (0.181–0.227)	0.254 (0.202–0.265)	0.05	
	Cod	9	0.205 (0.182–0.236)	0.221 (0.200–0.238)	NS	NS
	Salmon	11	0.243 (0.200–0.295)	0.189 (0.164–0.221)	0.004	0.001
Arachidonic acid (20:4)	Control	10	0.074 (0.062–0.089)	0.081 (0.066–0.087)	NS	
	Cod	9	0.080 (0.075–0.103)	0.085 (0.078–0.101)	NS	NS
	Salmon	11	0.077 (0.056–0.099)	0.078 (0.059–0.083)	NS	0.04
Sum n-6	Control	10	0.285 (0.253–0.313)	0.319 (0.294–0.338)	0.05	
	Cod	9	0.291 (0.268–0.331)	0.306 (0.299–0.330)	NS	NS
	Salmon	11	0.297 (0.268–0.386)	0.262 (0.221–0.308)	0.06	0.001
EPA	Control	10	0.006 (0.000–0.009)	0.008 (0.007–0.009)	NS	
	Cod	9	0.007 (0.003–0.009)	0.012 (0.008–0.013)	0.03	NS
	Salmon	11	0.009 (0.006–0.010)	0.057 (0.043–0.073)	0.003	<0.001
DHA	Control	10	0.052 (0.046–0.063)	0.053 (0.050–0.058)	NS	
	Cod	9	0.052 (0.042–0.066)	0.066 (0.061–0.070)	0.01	0.003
	Salmon	11	0.078 (0.054–0.089)	0.092 (0.078–0.108)	0.003	0.001
Sum n-3	Control	10	0.054 (0.052–0.065)	0.061 (0.058–0.066)	NS	
	Cod	9	0.056 (0.050–0.072)	0.077 (0.074–0.082)	0.01	0.008
	Salmon	11	0.088 (0.054–0.099)	0.141 (0.123–0.181)	0.003	<0.001

^a Wilcoxon test for within-group changes from baseline to end of study

^b Mann–Whitney *U* test for between-group changes (the cod and salmon groups compared to control group) (baseline adjusted values)

Plasma Levels of FABP4, but not FABP3, Are Associated with Increased Risk of Diabetes

Luc Djoussé · J. Michael Gaziano

Received: 24 January 2012 / Accepted: 25 May 2012 / Published online: 16 June 2012
© AOCs 2012

Abstract Little is known about the association between plasma concentrations of fatty acid binding protein 3 and 4 and the risk of diabetes in population-based cohorts. In a prospective nested case–control design, we studied 149 cases of diabetes and 149 matched controls from the Physicians’ Health Study. Plasma fatty acid binding proteins were measured on frozen specimens collected between 1995 and 2001 by ELISA. Cases of diabetes were self-reported and validated in a subsample via review of medical records. We used conditional logistic regression to estimate multivariable relative risks. The mean age at baseline was 64.9 years and median plasma fatty acid binding protein 3 and 4 were 2.12 ng/ml (IQR 1.62–2.66) and 15.32 ng/ml (IQR 12.14–18.73), respectively. In separate models, each fatty acid binding protein was positively associated with the risk of diabetes in a conditional logistic regression adjusting for matching variables, smoking, and hypertension. However, upon adjustment for each other, only fatty acid binding protein 4 (but not 3) was positively

associated with the risk of diabetes [relative risk (95 % CI) 1.0 (reference), 2.73 (1.08–6.89), 2.66 (1.11–6.42), and 6.89 (2.83–16.80) across consecutive quartiles of fatty acid binding protein 4, *P* for trend <0.0001]. The FABP4–diabetes association was modified by body mass index (*P* interaction 0.03). Our data showed a positive association between plasma fatty acid binding protein 4 but not 3 and the risk of diabetes in US male physicians. The interaction with body mass index warrants further investigations.

Keywords Diabetes · Epidemiology · Fatty acid binding proteins · Adipokines · Risk factors

Abbreviations

CI	Confidence interval
DM	Type 2 diabetes
ELISA	Enzyme-linked immunosorbent assay
FABP	Fatty acid binding protein
RR	Relative risk
SD	Standard deviation

L. Djoussé (✉) · J. M. Gaziano
Division of Aging, Department of Medicine, Brigham and Women’s Hospital and Harvard Medical School,
1620 Tremont St, 3rd Floor, Boston, MA 02120, USA
e-mail: ldjouss@partners.org

L. Djoussé · J. M. Gaziano
Geriatric Research, Education, and Clinical Center,
Boston Veterans Affairs Healthcare System, Boston, MA, USA

L. Djoussé · J. M. Gaziano
Massachusetts Veterans Epidemiology and Research
Information Center, Boston Veterans Affairs Healthcare System,
Boston, MA, USA

J. M. Gaziano
Division of Preventive Medicine, Brigham and Women’s
Hospital, Boston, MA, USA

Introduction

Type 2 diabetes (DM) is a major health issue with worldwide health consequences [1–4]. It is estimated that more than 350 million people will be diagnosed with DM by 2030 [5]. Complex secular trends in nutrition and physical activity have led to a dramatic increase in the prevalence of being overweight and obesity [6] with resulting increased prevalence of DM [4, 7, 8]. Adipocytes are known to produce various adipokines, which can influence inflammation, lipids, and glucose metabolism, all of which are relevant in the development of DM [9, 10]. Fatty-acid-

binding proteins (FABPs) are a family of carrier proteins for fatty acids and other lipophilic substances such as eicosanoids and retinoids [11–13]. Of the 9+ members of FABPs [14], FABP4 is mainly expressed by adipocytes and macrophages whereas FABP3 is expressed by skeletal and heart muscle. Mice lacking FABP4 gene gain weight under high-fat diet but do not develop insulin resistance as would be the case in wild type mice [15]. This observation suggests that FABP4 may play a role in the obesity–DM association. Such a hypothesis is supported by the fact that expression of FABP4 leads to insulin resistance in animals [16–18]. While other studies have reported cross-sectional associations between FABP4 and the prevalence of metabolic syndrome [12, 19, 20], only one prospective study has suggested a positive association between plasma FABP4 and incident DM [21]. No previous study has examined the association between FABP3 and the risk of DM and it is unclear whether FABP3 and FABP4 are independently associated with the risk of DM. Hence, we sought to assess whether plasma concentrations of FABP3 and FABP4 are independently associated with the risk of DM in US male physicians.

Materials and Methods

Study Population

Participants in these analyses were members of the Physicians' Health Study I and II who provided blood samples between 1995 and 2001. The Physicians' Health Study I was a completed randomized, double-blind, placebo-controlled trial designed to study the use of low-dose aspirin and beta-carotene for the primary prevention of cardiovascular disease and cancer [22, 23]. The Physicians' Health Study II started in 2001 and was a randomized trial assessing the effects of vitamins on the risk of cardiovascular disease and cancer [24, 25]. Current analyses used a prospective nested case–control design with a risk set sampling technique to select subjects. All eligible subjects were free of DM at the time of blood collection. For each case of incident DM occurring during follow up, we randomly selected a control among participants who were alive and free of DM at the time of diagnosis of the index case (risk set) and matched to the case on age at blood collection (within 1 year), race, year of birth (same), and time of blood collection (within 30 days). From the total pairs identified, we randomly selected 150 pairs for the current study. Because one control did not have data on FABP3 and FABP4, our final sample consisted of 149 matched pairs. Each participant signed an informed consent form and the Institutional Review Board at Brigham and Women's Hospital approved the study protocol.

Measurement of Fatty Acid Binding Protein 3 and 4

Plasma FABP4 was measured using the Human Adipocyte FABP ELISA (Human FABP4 ELISA) from BioVendor LLC (Candler, NC). In this assay, samples and standards are added to microplate wells coated with immobilized polyclonal anti-human AFABP antibody. After incubation and washing, biotin-labeled polyclonal anti-human AFABP antibody is added. Following a second wash, streptavidin-HRP conjugate is added. After a final wash, tetramethylbenzidine is added to the wells. An acidic stop solution terminates the reaction. The optical density of the wells is measured on a SpectraMax spectrophotometer (Molecular Devices, Sunnyvale, CA) at 450 and 630 nm. The intensity of the color formed by the enzymatic reaction is directly proportional to the concentration of FABP4 in the sample and concentration is determined from a standard curve. The inter-assay coefficient of variations were 2.6–5.1 %.

Plasma FABP3 was measured using the Human H-FABP ELISA (Human FABP3 ELISA) from Cell Sciences, Inc (Canton, MA). In this assay, samples and standards are added to microplate wells coated with immobilized anti-human HFABP antibody. After incubation peroxidase conjugated antibody is added. Following a wash, tetramethylbenzidine is added to the wells. An acidic stop solution terminates the reaction. The optical density of the wells is measured on a SpectraMax spectrophotometer (Molecular Devices, Sunnyvale, CA) at 450 and 630 nm. The intensity of the color formed by the enzymatic reaction is directly proportional to the concentration of FABP3 in the sample and concentration is determined from a standard curve.

Ascertainment of Incident DM in the PHS

Ascertainment of DM and other endpoints in the PHS has been achieved using annual follow-up questionnaires. We have validated the diagnosis of self-reported DM in a sample of men by reviewing their medical records. In the PHS, a systematic request of medical records is available for the trial primary endpoints (myocardial infarction, stroke, cancer, death, and pulmonary embolus). For the validation study of DM, we selected all participants who reported a diagnosis of DM on the follow-up questionnaires and had a subsequent diagnosis of myocardial infarction. The rationale for selecting myocardial infarction was that medical records for this event are more likely to contain pertinent information on past medical history, laboratory measurements, and current medications. In contrast, records to confirm cancer or death events are limited mostly to histological reports or death certificates, respectively. Of the 186 subjects who suffered myocardial infarction after a self-reported diagnosis of type 2 diabetes,

we randomly selected half (93 people) for chart review. Medical records were available for 60 subjects. Two physicians independently reviewed these charts. A diagnosis of DM was made if there was sufficient evidence in the chart defined as one of the following: (a) diagnosis of DM on the discharge summary, (b) current treatment with insulin or oral hypoglycemic agents, or (c) fasting glucose above 126 mg/dl or non-fasting glucose above 200 mg/dl. Using these criteria, DM was confirmed in 59 out of 60 cases (98.3 %). There was an excellent agreement between the two examiners ($\kappa = 100\%$).

Other Variables

Demographic information was obtained through self-reports. At baseline, each subject provided information on exercise (how often do you exercise vigorously enough to work up sweat? Possible answers included rarely/never, 1–3/month, 1/week, 2–4/week, 5–6/week, and daily); smoking (never, former, and current smoker); and alcohol intake (rarely/never, 1–3/month, 1/week, 2–4/week, 5–6/week, daily, and 2+/day). Self-reported baseline weight and height were used to compute body mass index (weight in kilograms divided by height in meters squared). Information on prevalent hypertension and coronary heart disease was collected at baseline and through follow-up questionnaires. An endpoint committee of the Physicians' Health Study reviewed the medical records to confirm the diagnosis of myocardial infarction and coronary bypass or angioplasty.

Statistical Analyses

Due to the non-Gaussian distribution of FABP3/4, we use the natural logarithm to normalize their distributions. We created quartiles of log(FABP3) and log(FABP4) using the distribution of these biomarkers in the control series. Means and percentages of baseline characteristics of the study participants are presented according to diabetes status. We used conditional logistic regression to estimate the relative risk of diabetes using the lowest quartile of each biomarker as the reference category. The multivariable adjusted model controlled for matching variables (race, age, time of blood collection, and year of birth), cigarette smoking, hypertension, and mutual control for FABP3 and FABP4. We also evaluated confounding by prevalent coronary heart disease (myocardial infarction, coronary bypass or angioplasty). Additional control for exercise and alcohol consumption did not alter the conclusions (data not shown). Furthermore, we modeled FABP4 and FABP3 as continuous variables using the logarithmic transformed values and estimated relative risks associated with each standard deviation higher log-FABP4 or log-FABP3 using

the models described above. We considered effect measure modification by body mass index given our prior findings of interaction between body mass index and FABP4 in older adults [26], by including product terms of both main exposures (FABP3/4) and body mass index and main effects in the regression model. To obtain a *P* value for linear trend, we created a new variable that was assigned the median value of FABP3/4 in each quartile within the control series and fitted such a variable in the conditional logistic regression. All analyses were performed using SAS (SAS version 9.3, NC) and the alpha level was set at 0.05. All *P* values were two-sided.

Results

The mean age was 64.9 years and 84.6 % were Caucasians. FABP3 and FABP4 were not normally distributed (skewness and kurtosis were 2.92 and 12.2, respectively, for FABP3; corresponding values for FABP4 were 1.84 and 5.60). Subjects who developed DM had a higher body mass index, higher prevalence of coronary heart disease, higher plasma concentrations of FABP3 and 4, lower prevalence of vigorous exercise and hypertension, and were more likely to be current smokers than controls (Table 1). Body mass index was positively correlated with log-transformed FABP4 (Spearman correlation coefficient = 0.44, $P < 0.0001$) but not with log(FABP3) (Spearman correlation coefficient = -0.02, $P = 0.78$). Spearman correlation coefficient between log(FABP3) and log(FABP4) was 0.23 ($P = 0.005$). In a conditional logistic regression model adjusting for matching factors, log(FABP3) was positively associated with diabetes [relative risk (95 % CI) of 1.0 (ref), 0.68 (0.30–1.54), 1.11 (0.56–2.23), and 2.24 (1.09–4.59) across consecutive quartiles of log(FABP3), P for trend 0.008]. Additional adjustment for hypertension and smoking had little effect on the results (P for trend 0.012). Likewise, log(FABP4) was positively associated with DM in the basic model [relative risk (95 % CI) 1.0 (ref), 1.62 (0.73–3.61), 1.84 (0.85–4.01), and 5.20 (2.40–11.27) across consecutive quartiles of log(FABP4), P for trend <0.0001]. Additional adjustment for hypertension and smoking strengthened the results [RR (95 % CI) 1.0 (ref), 2.08 (0.88–4.89), 2.32 (1.01–5.31), and 6.23 (2.75–14.10), respectively]. When both FABP4 and FABP3 were included in the fully adjusted model, FABP4 but not FABP3 was associated with the risk of DM (Table 2). Additional adjustment for prevalent coronary heart disease had minimal effect on the odds ratios [e.g., relative risks were 1.0 (ref), 2.70 (1.06–6.87), 2.87 (1.16–7.01), and 6.87 (2.82–16.76) across consecutive quartiles of FABP4]. Each standard deviation increment of log(FABP4) was associated with 80 % increased risk of

Table 1 Characteristics of 298 male physicians according to diabetes status

Characteristics	Diabetes cases (<i>N</i> = 149)	Controls (<i>N</i> = 149)
Age (years) ^a	64.9 ± 8.1	64.9 ± 8.1
Race (% Caucasian) ^a	84.6	84.6
Body mass index (kg/m ²)	28.3 ± 4.6	25.5 ± 3.5
log(FABP3)	0.87 ± 0.58	0.75 ± 0.49
log(FABP4)	2.98 ± 0.42	2.73 ± 0.38
Current smokers (%)	7.4	3.4
Former smokers (%)	41.6	41.6
Current alcohol drinkers (%)	80.1	84.5
Vigorous exercise (%)	48.3	68.7
Hypertension (%)	29.5	36.9
Prevalent coronary heart disease (%)	13.4	10.1

Data are presented as mean ± standard deviation or percentage

FABP fatty acid binding protein

^a Matching variables

DM (95 % CI 37–137 %), Table 2). There was evidence for interaction between body mass index and FABP4 (*P* for interaction 0.03) but not FABP3 (*P* = 0.29) in the fully adjusted model. Unfortunately, we did not have adequate data (i.e. only 17 matched pairs with body mass index <25 kg/m²) for stratified analyses by body mass index.

Discussion

In this prospective nested case–control study, we found a positive and linear association between plasma FABP4 and FABP3 on the risk of DM among United State male physicians when examined individually. However, only

FABP4 (but not FABP3) was independently associated with the risk of DM upon mutual adjustment for the other FABP. The risk of DM was nearly seven fold higher in the fourth compared to the first quartile of FABP4 adjusting for confounders and FABP3. Lastly, the FABP4–diabetes association was modified by body mass index whereas no interaction was seen between body mass index and FABP3. This is the first study to show that FABP4 is positively related to DM risk, independent of FABP3 in a large sample of humans.

Several animal studies have examined the effects of FABP4 insulin resistance and DM risk [13, 15, 16, 27]. However, only limited data is available in humans. In cross-sectional studies, FABP4 was associated with a higher prevalence of metabolic syndrome [10, 12, 19, 20, 28]. Furthermore, in a small Chinese population, a higher concentration of FABP4 was associated with a two-fold increased risk of DM after 10 years of follow up [21]. Those findings are consistent with a positive association between plasma FABP4 and incident DM among US older adults (65+ years at baseline) [26]. However, neither of the previous studies examined the role of FABP3 on the FABP4–DM association for further comparison. The current study suggests that FABP3 may not be as important as FABP4 in the development of DM. The effect modification observed between FABP4 and body mass index is consistent with data from the Cardiovascular Health Study showing similar interaction [26]. We had inadequate data to conduct stratified analyses by body mass index in our study. However, the Cardiovascular Health Study reported a 78 % higher risk of diabetes (95 % CI 13–181 %) per standard deviation higher FABP4 in men with body mass index below 25 kg/m² but no significant relation in overweight [1.03 (0.71–1.49)] or obese [1.43 (0.90–2.28)] men

Table 2 Relative risk (95 % CI) for diabetes according to quartiles and standard deviation increase of fatty acid binding protein

FABP3				FABP4			
Quartiles	Cases/ <i>N</i>	Model 1 ^a	Model 2 ^b	Quartiles	Cases/ <i>N</i>	Model 1 ^a	Model 2 ^b
≤2.485	31/67	1.00 (ref)	1.00 (ref)	≤0.471	15/50	1.00 (ref)	1.00 (ref)
2.486–2.728	24/61	0.48 (0.20–1.18)	0.37 (0.15–0.96)	0.472–0.745	25/63	1.96 (0.85–4.52)	2.73 (1.08–6.89)
2.729–2.930	32/70	0.82 (0.38–1.77)	0.85 (0.38–1.89)	0.746–0.978	28/66	2.05 (0.91–4.62)	2.66 (1.11–6.42)
≥2.930	62/100	1.31 (0.58–2.95)	1.13 (0.48–2.67)	≥0.979	81/119	5.31 (2.35–12.00)	6.89 (2.83–16.80)
<i>P</i> for trend		0.23	0.36			<0.0001	<0.0001
Per SD increase of log(FABP3)		1.07 (0.81–1.41)	1.03 (0.77–1.37)	Per SD increase of log(FABP4)		1.74 (1.34–2.25)	1.80 (1.37–2.37)

FABP fatty acid binding protein, SD standard deviation

^a Model 1: Conditional logistic regression adjusted for matching factors (age, race, time of blood collection, and year of birth) and the fatty acid binding protein

^b Model 2: Additional adjustment for hypertension and cigarette smoking

[26]. It is possible that being overweight/obesity confers a higher background rate for diabetes, thereby making it more difficult to detect a small increment in diabetes risk in such a high-risk population. In contrast, with a lower background risk of diabetes in lean subjects, a small increase in diabetes risk conferred by FABP4 might be readily detectable. Our working hypothesis is that FABP4 is downstream of obesity and future work is needed for further investigation.

Data from the Nurse's Health and Health Professionals Follow-up Studies [17] showed that a functional mutation (T-87C) in the FABP4 gene was associated with a reduced expression of FABP4 in adipocytes and a lower risk of DM (especially among obese subjects). Those data also suggest a possible interaction between body composition and FABP4 on DM risk and are consistent with the interaction observed in the current study. In contrast, other investigators did not show a major effect of FABP4 gene on diabetes risk [29]. At this point, little is known about potential pathways by which FABP4 may influence the risk of DM in humans.

FABP3 and 4 are transport proteins and play an important role in lipid metabolism and perhaps glucose utilization [30, 31]. FABP4-knockout mice remain insulin sensitive despite the development of adiposity under a high-fat diet [15]. In contrast, wild type mice develop insulin resistance and adiposity under a high-fat diet. A working hypotheses could be that FABP4 might mediate obesity-induced insulin resistance and subsequent development of DM. Alternatively, FABP4 may promote lipolysis by removing fatty acids that inhibit hepatic sensitive lipase [27, 32]. Lastly, FABP4 may increase the risk of DM by interfering with key enzymes in the de novo lipogenesis [33, 34]. Unfortunately, we did not have appropriate data to explore further the role of FABP4 on DM risk in our study. At this point, we cannot eliminate the possibility that elevated plasma FABP4 could just be a marker of metabolic derangement associated with metabolic syndrome, obesity, or diabetes. Consistent with this hypothesis, the PREDI-MED data suggest that elevated plasma FABP4 predicts atherogenic dyslipidemia in 578 volunteers after a median follow up of 4 years [35]. FABP4 has also been reported as a biomarker of atherogenic dyslipidemia, independent of obesity and insulin resistance [36]. Though our subjects were free of DM at the time of blood collection, we cannot exclude the prevalence of metabolic syndrome or abnormal glucose tolerance at the time of blood collection.

Our study has some limitations. The fact that all participants were male physicians, most of whom were Caucasians, limits the generalizability of the current findings. Our validation of diabetes was limited to a subsample in this cohort, hence, we cannot exclude the possibility of

misclassification of DM. Such misclassification of DM cases is more likely to be non-differential with respect to FABP3 and 4 concentrations and would likely have led to an underestimation of the true association. As an observational study, we cannot rule out chance, residual or unmeasured confounding as alternative explanation of our results. On the other hand, the use of risk set technique, matching to minimize confounding, the availability of several potential covariates, and standardized methods for follow-up and cases ascertainment are strengths of the present study.

In summary, our data suggest that FABP4 but not FABP3 is positively associated with a higher risk of DM. Such an association appears to be modified by body mass index. If confirmed in other studies, FABP4 may offer a new pharmacological targets in the management of diabetes and/or risk stratification.

Acknowledgments Dr Djoussé has full access to all of the data in the study and takes responsibility for the integrity of the data and the accuracy of the data analysis. We are indebted to the participants in the PHS for their outstanding commitment and cooperation and to the entire PHS staff for their expert and unfailing assistance. The Physicians' Health Study is supported by grants CA-34944, CA-40360, and CA-097193 from the National Cancer Institute and grants HL-26490 and HL-34595 from the National Heart, Lung, and Blood Institute, Bethesda, MD.

Conflict of interest None to disclose.

References

1. Wirehn AB, Andersson A, Ostgren CJ, Carstensen J (2008) Age-specific direct healthcare costs attributable to diabetes in a Swedish population: a register-based analysis. *Diabet Med* 25:732–737
2. Marchant K (2008) Diabetes and chronic kidney disease: a complex combination. *Br J Nurs* 17:356–361
3. Vijan S, Hofer TP, Hayward RA (2000) Cost-utility analysis of screening intervals for diabetic retinopathy in patients with type 2 diabetes mellitus. *JAMA* 283:889–896
4. King H, Aubert RE, Herman WH (1998) Global burden of diabetes, 1995–2025: prevalence, numerical estimates, and projections. *Diabetes Care* 21:1414–1431
5. Wild S, Roglic G, Green A, Sicree R, King H (2004) Global prevalence of diabetes: estimates for the year 2000 and projections for 2030. *Diabetes Care* 27:1047–1053
6. Flegal KM, Carroll MD, Ogden CL, Johnson CL (2002) Prevalence and trends in obesity among US adults, 1999–2000. *JAMA* 288:1723–1727
7. Howard BV, Rodriguez BL, Bennett PH, Harris MI, Hamman R, Kuller LH, Pearson TA, Wylie-Rosett J (2002) Prevention conference VI: diabetes and cardiovascular disease: writing group I: epidemiology. *Circulation* 105:e132–e137
8. Mokdad AH, Bowman BA, Ford ES, Vinicor F, Marks JS, Koplan JP (2001) The continuing epidemics of obesity and diabetes in the United States. *JAMA* 286:1195–1200
9. Kershaw EE, Flier JS (2004) Adipose tissue as an endocrine organ. *J Clin Endocrinol Metab* 89:2548–2556

10. Bagheri R, Qasim AN, Mehta NN, Terembula K, Kapoor S, Braunstein S, Schutta M, Iqbal N, Lehrke M, Reilly MP (2010) Relation of plasma fatty acid binding proteins 4 and 5 with the metabolic syndrome, inflammation and coronary calcium in patients with type-2 diabetes mellitus. *Am J Cardiol* 106:1118–1123
11. Makowski L, Hotamisligil GS (2004) Fatty acid binding proteins—the evolutionary crossroads of inflammatory and metabolic responses. *J Nutr* 134:2464S–2468S
12. Stejskal D, Karpisek M (2006) Adipocyte fatty acid binding protein in a Caucasian population: a new marker of metabolic syndrome? *Eur J Clin Invest* 36:621–625
13. Yang R, Castriota G, Chen Y, Cleary MA, Ellsworth K, Shin MK, Tran JL, Vogt TF, Wu M, Xu S, Yang X, Zhang BB, Berger JP, Qureshi SA (2011) RNAi-mediated germline knockdown of FABP4 increases body weight but does not improve the deranged nutrient metabolism of diet-induced obese mice. *Int J Obes (Lond)* 35:217–225
14. Chmurzynska A (2006) The multigene family of fatty acid-binding proteins (FABPs): function, structure and polymorphism. *J Appl Genet* 47:39–48
15. Hotamisligil GS, Johnson RS, Distel RJ, Ellis R, Papaioannou VE, Spiegelman BM (1996) Uncoupling of obesity from insulin resistance through a targeted mutation in aP2, the adipocyte fatty acid binding protein. *Science* 274:1377–1379
16. Boord JB, Maeda K, Makowski L, Babaev VR, Fazio S, Linton MF, Hotamisligil GS (2004) Combined adipocyte-macrophage fatty acid-binding protein deficiency improves metabolism, atherosclerosis, and survival in apolipoprotein E-deficient mice. *Circulation* 110:1492–1498
17. Tuncman G, Erbay E, Hom X, De Vivo I, Campos H, Rimm EB, Hotamisligil GS (2006) A genetic variant at the fatty acid-binding protein aP2 locus reduces the risk for hypertriglyceridemia, type 2 diabetes, and cardiovascular disease. *Proc Natl Acad Sci USA* 103:6970–6975
18. Simon I, Escote X, Vilarrasa N, Gomez J, Fernandez-Real JM, Megia A, Gutierrez C, Gallart L, Masdevall C, Vendrell J (2009) Adipocyte fatty acid-binding protein as a determinant of insulin sensitivity in morbid-obese women. *Obesity (Silver Spring)* 17:1124–1128
19. Hsu BG, Chen YC, Lee RP, Lee CC, Lee CJ, Wang JH (2010) Fasting serum level of fatty-acid-binding protein 4 positively correlates with metabolic syndrome in patients with coronary artery disease. *Circ J* 74:327–331
20. Xu A, Wang Y, Xu JY, Stejskal D, Tam S, Zhang J, Wat NM, Wong WK, Lam KS (2006) Adipocyte fatty acid-binding protein is a plasma biomarker closely associated with obesity and metabolic syndrome. *Clin Chem* 52:405–413
21. Tso AW, Xu A, Sham PC, Wat NM, Wang Y, Fong CH, Cheung BM, Janus ED, Lam KS (2007) Serum adipocyte fatty acid binding protein as a new biomarker predicting the development of type 2 diabetes: a 10-year prospective study in a Chinese cohort. *Diabetes Care* 30:2667–2672
22. (1988) Findings from the aspirin component of the ongoing Physicians' Health Study. *N Engl J Med* 318:262–264
23. (1989) Final report on the aspirin component of the ongoing Physicians' Health Study. Steering Committee of the Physicians' Health Study Research Group. *N Engl J Med* 321:129–135
24. Christen WG, Gaziano JM, Hennekens CH (2000) Design of Physicians' Health Study II—a randomized trial of beta-carotene, vitamins E and C, and multivitamins, in prevention of cancer, cardiovascular disease, and eye disease, and review of results of completed trials. *Ann Epidemiol* 10:125–134
25. Sesso HD, Buring JE, Christen WG, Kurth T, Belanger C, MacFadyen J, Bubes V, Manson JE, Glynn RJ, Gaziano JM (2008) Vitamins E and C in the prevention of cardiovascular disease in men: the Physicians' Health Study II randomized controlled trial. *JAMA* 300:2123–2133
26. Djousse L, Khawaja O, Bartz TM, Biggs ML, Ix JH, Ziemann SJ, Kizer JR, Tracy RP, Siscovick DS, Mukamal KJ (2012) Plasma fatty acid binding protein 4, non-esterified fatty acids, and incident diabetes in older adults. *Diabetes Care*. doi:10.2337/dc11-1690
27. Leff T, Granneman JG (2010) Adipose tissue in health and disease. Wiley-Blackwell, New York
28. Xu A, Tso AW, Cheung BM, Wang Y, Wat NM, Fong CH, Yeung DC, Janus ED, Sham PC, Lam KS (2007) Circulating adipocyte-fatty acid binding protein levels predict the development of the metabolic syndrome: a 5-year prospective study. *Circulation* 115:1537–1543
29. Mansego ML, Martinez F, Martinez-Larrad MT, Zabena C, Rojo G, Morcillo S, Soriguer F, Martin-Escudero JC, Serrano-Rios M, Redon J, Chaves FJ (2012) Common variants of the liver Fatty Acid binding protein gene influence the risk of type 2 diabetes and insulin resistance in Spanish population. *PLoS One* 7:e31853
30. Furuhashi M, Hotamisligil GS (2008) Fatty acid-binding proteins: role in metabolic diseases and potential as drug targets. *Nat Rev Drug Discov* 7:489–503
31. Krusinova E, Pelikanova T (2008) Fatty acid binding proteins in adipose tissue: a promising link between metabolic syndrome and atherosclerosis? *Diabetes Res Clin Pract* 82(Suppl 2):S127–S134
32. Shen WJ, Liang Y, Hong R, Patel S, Natu V, Sridhar K, Jenkins A, Bernlohr DA, Kraemer FB (2001) Characterization of the functional interaction of adipocyte lipid-binding protein with hormone-sensitive lipase. *J Biol Chem* 276:49443–49448
33. Roberts R, Hodson L, Dennis AL, Neville MJ, Humphreys SM, Harnden KE, Micklem KJ, Frayn KN (2009) Markers of de novo lipogenesis in adipose tissue: associations with small adipocytes and insulin sensitivity in humans. *Diabetologia* 52:882–890
34. Erbay E, Babaev VR, Mayers JR, Makowski L, Charles KN, Snitow ME, Fazio S, Wiest MM, Watkins SM, Linton MF, Hotamisligil GS (2009) Reducing endoplasmic reticulum stress through a macrophage lipid chaperone alleviates atherosclerosis. *Nat Med* 15:1383–1391
35. Cabre A, Babio N, Lazaro I, Bullo M, Garcia-Arellano A, Masana L, Salas-Salvado J (2012) FABP4 predicts atherogenic dyslipidemia development. The PREDIMED study. *Atherosclerosis* 222(1):229–234
36. Cabre A, Lazaro I, Girona J, Manzanares JM, Marimon F, Plana N, Heras M, Masana L (2008) Plasma fatty acid binding protein 4 is associated with atherogenic dyslipidemia in diabetes. *J Lipid Res* 49:1746–1751

A Single Bout of Exercise Increases the Expression of Glucose but not Fatty Acid Transporters in Skeletal Muscle of IL-6 KO Mice

B. Łukaszuk · I. Białuk · J. Górski ·
M. Zajączkiewicz · M. M. Winnicka ·
A. Chabowski

Received: 10 January 2012 / Accepted: 2 May 2012 / Published online: 24 May 2012
© The Author(s) 2012. This article is published with open access at Springerlink.com

Abstract IL-6 is a biologically active cytokine released during exercise by contracting skeletal muscles. It appears to be highly involved in the regulation of muscles energy substrate utilization. Whether an ablation of IL-6 (IL-6 KO) in mice subjected to a single bout of exercise affects lipid and/or glucose metabolism is currently unknown. In the present study we examined fatty acid (FAT/CD36, FABPpm, FATP-1, FATP-4) as well as glucose (GLUT-1, GLUT-4) transporters expression in IL-6 KO mice. In addition, intramuscular glycogen and lipid content was also evaluated. The expression of all fatty acid transporters (FAT/CD36: +25 %; FATP-1: +31 %; FABPpm: +12.7 %; FATP-4: +7.2 %) was increased in muscles from IL-6 KO mice compared to wild type (WT) mice. Accordingly intramuscular lipid content was also increased in these muscles (FFA: +38 %; DAG: +36 % and TAG: +160 %). Interestingly, IL-6 deficiency had only minor effect on glucose transporters expression (GLUT-1: -4 %, and GLUT-4: -5.1 %), with no apparent difference in muscular glycogen content. A single bout of exercise increased the glucose transporters (GLUT-1: +8 %; GLUT-4: +15 %) as well as FA transporters (FAT/CD36: +13 %; FABPpm: +4.5 %; FATP: +2.5 %, FATP-4: +10 %) expression but only in WT skeletal muscles. In muscles from IL-6 KO mice exercise induced changes only in glucose (GLUT-1: +20 %; GLUT-4: +35 %) but not in the content of FA transporters. Concomitantly, IL-6 KO

mice displayed shorter time toward exhaustion with more pronounced reductions in intramuscular lipid and glycogen content. We may speculate, that IL-6 deficiency provokes more pronounced glucose utilization over lipid oxidation during a single bout of exhausting exercise.

Keywords IL-6 · Skeletal muscle · Lipids · Glycogen · FA transporters · Glucose transporters

Abbreviations

AMPK	AMP-activated protein kinase
DAG	Diacylglycerols
DNA	Deoxyribonucleic acid
FA	Fatty acids
FABPpm	Plasma membrane associated fatty acid binding protein
FAT/CD36	Fatty acid translocase
FATP-1	Fatty acid transport protein isoform 1
FATP-4	Fatty acid transport protein isoform 4
FFA	Free fatty acids
GLUT-1	Glucose transporter isoform 1
GLUT-4	Glucose transporter isoform 2
IL-6	Interleukin-6
KO	Knock-out animals
PCR	Polymerase chain reaction
SEM	Standard error of the mean
SOCS	Suppressor of cytokine signaling
TAG	Triacylglycerols
WT	Wild type animals

B. Łukaszuk · J. Górski · A. Chabowski (✉)
Department of Physiology, Medical University of Białystok,
ul. Mickiewicza 2C, 15-222 Białystok, Poland
e-mail: adrian@umwb.edu.pl

I. Białuk · M. Zajączkiewicz · M. M. Winnicka
Department of General and Experimental Pathology,
Medical University of Białystok, Białystok, Poland

Introduction

In the last few years, evidence has accumulated showing that interleukin-6 (IL-6) is an important molecule involved

not only in immune regulation, hematopoiesis or inflammation but also in glucose and lipid metabolism [1]. IL-6 is synthesized by skeletal muscle and its secretion is markedly augmented during contractile activity [1, 2]. The resultant increase in IL-6 serum concentration positively correlates with increased glucose uptake and fatty acid (FA) oxidation in skeletal muscles. Likely both seem to be mediated by activation of AMPK (AMP-activated protein kinase) [1, 3, 4]. The activation of AMPK, which increases usage of energy substrates is commonly implicated in insulin sensitizing actions in skeletal muscles. However, this view has been recently challenged since serum IL-6 elevation was commonly observed in patients with metabolic disorders such as obesity and/or diabetes [5–7]. There is no evident explanation for this discrepancy. It might be speculated that IL-6 is also a potent activator of SOCS (suppressor of cytokine signaling) and thus increased activation of SOCS3 in skeletal muscles and liver leads to insulin resistance commonly observed in patients with obesity and diabetes [8].

At rest, skeletal muscles use both glucose and fatty acids (FA) as an equivalent energy source [9, 10]. However during exercise, the type of substrate used depends mainly on the intensity and the duration of exercise [2, 11]. It is generally well accepted that, with increased intensity of the exercise, there is a substantial enhancement in glucose utilization. Importantly, a crucial (but not exclusive) rate-limiting process in myocytes glucose utilization, involves transport of glucose across the sarcolemma. The process, that is specifically mediated by membrane glucose transporter proteins belonging to the facilitative GLUT/SLC2A family [12]. In contrary, fatty acids (FA), due to their hydrophobic nature, are able to rapidly traverse the lipid bilayer of the cell membrane by simple diffusion [13]. However, in addition to passive diffusion, a considerable evidence has accumulated to support the existence and importance of a protein-mediated FA transport [14–16]. In skeletal muscles a number of FA transporters have been identified, including (1) a family of fatty acid transport proteins (i.e. FATP-1,4), (2) plasma membrane associated fatty acid binding protein (FABPpm) and (3) fatty acid translocase (FAT/CD36) [17–19].

Given that IL-6 is an important muscle derived factor highly involved in myocyte energy substrate metabolism, we sought to investigate the effect of IL-6 ablation on glucose (GLUT-1, 4) and FA transporters (FAT/CD36, FABPpm, FATP-1,4) expression in skeletal muscle challenged by exercise. Additionally, intramuscular lipids and the glycogen contents were assessed. Aware of the age influence in IL-6 KO phenotype, we investigated the effect of a single bout of exhausting exercise in older mice (12 months).

Materials and Methods

Animals and Experimental Model

Male mice, wild type (C57B4/6J) and IL-6 KO (C57B4/6J IL-6^{tm1^{Kopf}}–/–) were randomly allocated into two groups: sedentary and exercised till exhaustion (swimming). Until the day of experiment (12 months) mice were bred on site in an approved animal holding facility with free access to food and water. The study was conducted in accordance to guidelines of local ethic committee for animal care.

Methods

Genotyping

IL-6 KO mice was tested using genomic DNA and PCR method to confirm deficiency of IL-6 gene as described elsewhere [20, 21]. Briefly, “Genomic mini” kit (A&A Biotechnology, Gdansk, Poland) was used to isolate DNA from mouse tails followed by PCR [applied custom made primers: F 5'-AAGTGCATCATCGTTGTTCA TAC3'; R 5'-CCATCCAGTTGCCTTCTTG-3' and commercially available DNA polymerase Taq “Marathon” (A&A Biotechnology, Gdansk, Poland)]. Subsequently DNA was separated on the 1 % agarose gel with ethidium bromide by means of electrophoresis. As a result we gained material from WT animals' encompassed DNA fragments with size ca. 900 bp, whereas DNA fragments originate from knock-out mice (size about 1400 bp) additionally contained a fragment of neomycin cassette.

Exercise Protocol

Animals were used after 7 days of acclimatization to the laboratory conditions. They were maintained in a temperature-controlled environment (22 ± 1 °C) with a 12-h light–dark cycles beginning at 7 a.m. Experiments took place between 1.00 p.m. and 4.00 p.m. in the air-conditioned, sound-isolated room with the possibility of an accurate control of the light intensity. A single bout of exercise was carried out in a tank consisted of a circular, galvanized and painted in white steel pool (120 cm in diameter, 30 cm height) filled up to 26 cm depth with water maintained at 30 ± 1 °C. The mice were submitted to swimming exercise carrying load (lead fish sinkers, attached to the tail) corresponding to 5 % of their body weight. Animals were assessed to be fatigued when they remained under the water surface for 5 s [16].

Intramuscular FA (FAT/CD36, FABPpm, FATP-1,4), Glucose (GLUT-1, GLUT-4) Transporters and pAMPK/AMPK Protein Expression

The protein expression of FAT/CD36, FABPpm, FATP 1, FATP 4 and GLUT-1, GLUT-4 (50 μ g) as well as AMPK and pAMPK (90 μ g) was determined in muscle homogenates (soleus). Western blotting technique was used to detect the protein content as described by us and others [22, 23]. Briefly, the total protein content in each sample was determined by bicinchoninic acid method with BSA serving as a protein standard. Then, the proteins in each sample were separated using 10 % SDS-polyacrylamide gel electrophoresis and transferred to the nitrocellulose membrane. Equal protein concentrations were loaded in each lane as confirmed by Ponceau staining the blot membrane. In the next step membranes were immunoblotted with selected primary antibodies (FAT/CD36, FATP 1, FATP 4 (Abcam, EU) and GLUT-1, GLUT-4 and β -actin (Santa Cruz Biotechnology, US) as well as AMPK, pAMPK (Thr172) (Cell Signaling, US). Quantification of the selected protein content was achieved by densitometry [Optical Density (OD); Biorad, Poland]. The protein expression (FAT/CD36, FATP 1, FATP 4, GLUT-1 and GLUT-4) was related to β -actin and then to the control (WT sedentary or IL-6 KO sedentary, appropriately as indicated in the legends of figures) that was set to 100 %. Finally, each experimental group was expressed relatively (%) to the control. In addition, AMPK activation was expressed as pAMPK/AMPK ratio. Accordingly, Western Blots were made in triplicates.

Intramuscular Lipid Content

The mice were killed by cervical dislocation and immediately samples of soleus muscle were taken. Afterwards, the samples were rapidly cleaned from any visible non-muscle tissue, frozen in liquid nitrogen and finely powdered. Next the powder was transferred to a glass tube for consequent lipids extraction using the Folch et al. method [24] with modifications of van der Vusse et al. [25]. Gas liquid chromatography (Hewlett-Packard 5890 Series II gas chromatograph, HP-INNOWax capillary column) was used for identification and quantification of individual fatty acid methyl esters, whereas the total FFA, TAG, DAG concentration was estimated as the sum of particular fatty acid species content of the assessed fraction. The value was expressed as nanomoles per gram of wet tissue.

Intramuscular Glycogen Content

Soleus glycogen content was determined as described recently [23, 26]. Skeletal muscles were digested in 30 %

KOH for 20 min and then, a spectrophotometric assay was used to qualify the content of free glucose. Glycogen level is expressed in μ mol of glucose/g of wet tissue.

Statistics

All data are expressed as means \pm SEM. Statistical differences between groups were tested with analysis of variance (one way ANOVA) to determine the statistical significance, and appropriate post hoc test. Statistical significance was set at $p \leq 0.05$.

Results

Genotyping confirmed the deficiency of the functional IL-6 gene in the IL-6 KO mice as shown previously [20, 21]. IL-6 KO and wild type (WT) mice displayed no differences in body weight and serum glucose or FFA levels (data not shown, [21]).

Effect of IL-6 KO Genotype on Basal Skeletal Muscle Fatty Acid Transporters Expression and Lipid Content

In sedentary groups, the expression of fatty acid transporters (FAT/CD36: +25 %; FABPpm: +12.7 %; FATP-1: +31 %; $p \leq 0.05$; FATP-4: +7.2 %; $p > 0.05$) was increased in muscles from IL-6 KO mice compared to wild type mice (Fig. 1a–d). Accordingly intramuscular lipid content was also increased in these muscles (FFA: +38 %; DAG: +36 % and TAG: +160 %; $p \leq 0.05$) (Fig. 2a, b).

Effect of IL-6 KO Genotype on Basal Skeletal Muscle Glucose Transporters Expression and Glycogen Content

Interestingly, IL-6 deficiency had only minor effect on: (1) glucose transporters expression (GLUT-1: -4 %, and GLUT-4: -5.1 %; $p > 0.05$; Fig. 3a, b) and (2) glycogen content in soleus muscle compared to control (-7 %; $p > 0.05$; Fig 3c).

Effect of Single Bout of Exhausting Exercise and IL-6 KO Genotype on Skeletal Muscle Fatty Acid Transporters Expression and Lipid Content

A single bout of exhausting exercise induced a small but significant increase in expression of both FAT/CD36 and FATP-4 (+13 and +10 %; $p \leq 0.05$; Fig. 4a), with no apparent change in FABPpm and FATP-1 (+4.5 and +2.5 %; $p > 0.05$) in WT mice. No significant changes in FA transporters expression induced by exercise were observed in the IL-6 KO group (Fig. 4b).

Fig. 1 The effect of IL-6 deficiency on the expression of fatty acid transporters (**a** FAT/CD36, **b** FABPpm, **c** FATP-1, **d** FATP-4) in soleus muscle of sedentary mice. Representative Western Blots present a relative change in the protein expression related to β -actin content. ($n = 8$; asterisk WT Sed vs. IL-6 KO Sed, $P < 0.05$; OD optical density; control (WT Sed) set at 100 %)

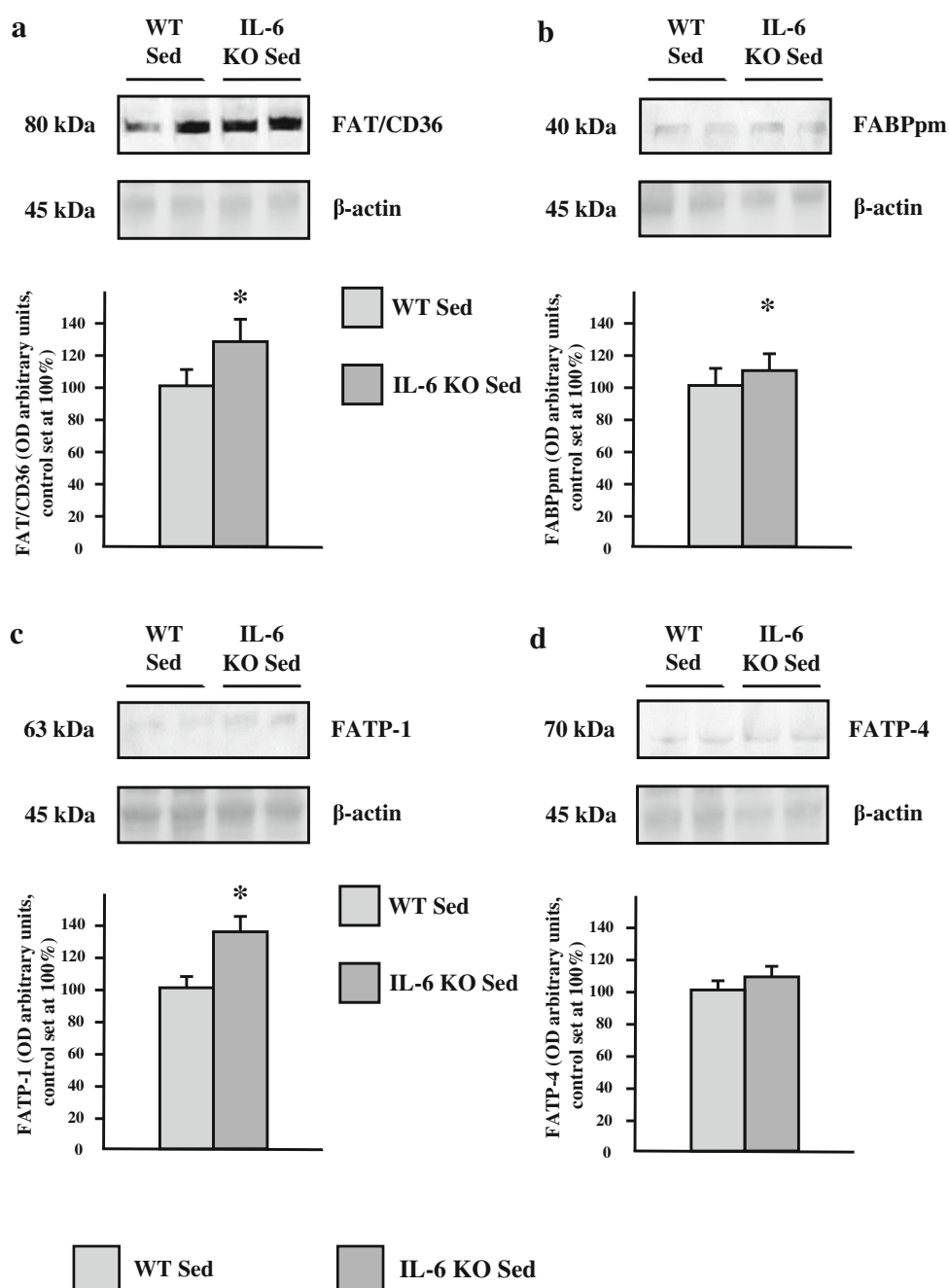


Fig. 2 The effect of IL-6 deficiency on intramuscular lipid content (**a** FFA, DAG; **b** TAG), in soleus muscle tissue of sedentary mice. ($n = 8$; asterisk WT Sed vs. IL-6 KO Sed, $P < 0.05$, FFA free fatty acids, DAG diacylglycerols, TAG triacylglycerols)

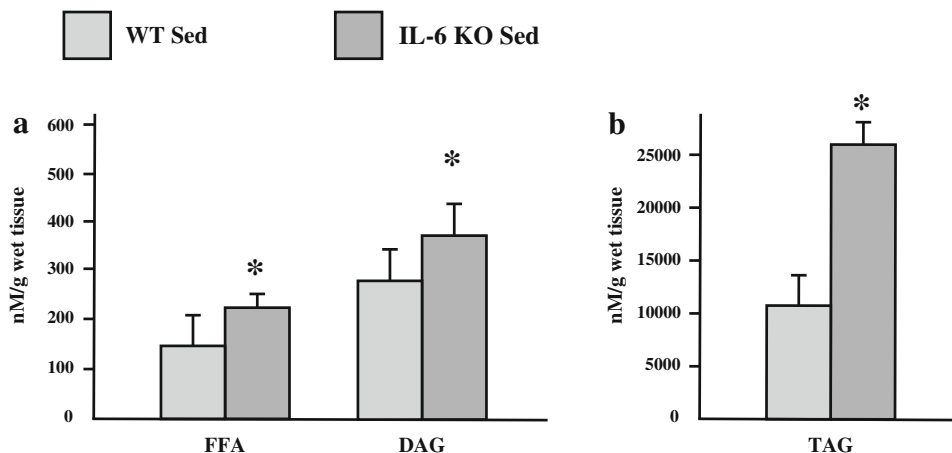
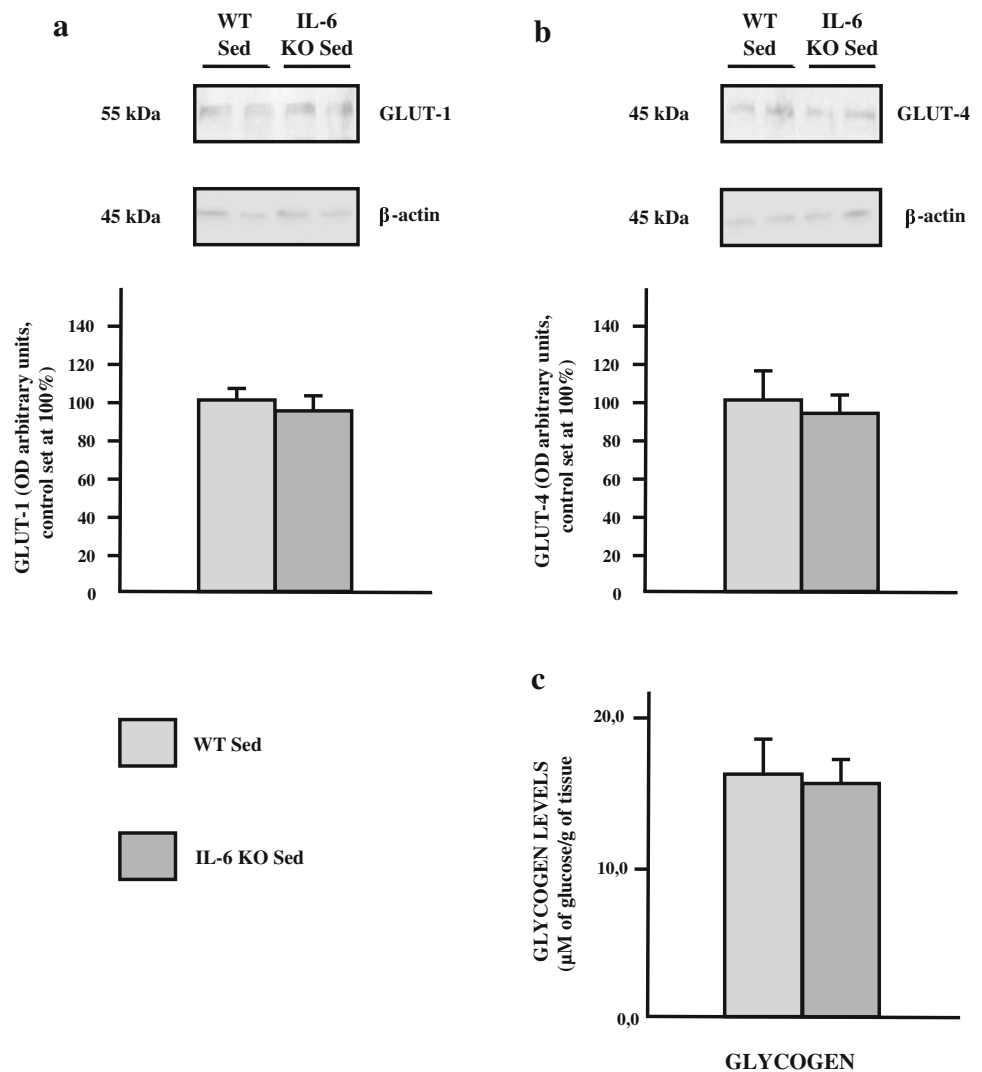


Fig. 3 The effect of IL-6 deficiency on the expression of glucose transporters (**a** GLUT-1, **b** GLUT-4) in soleus muscle of sedentary mice. Representative Western Blots present a relative change in the protein expression related to β -actin content. ($n = 8$; asterisk WT Sed vs. IL-6 KO Sed, $P < 0.05$; OD optical density; control (WT Sed) set at 100 %)



Applied exercise induced a significant reduction in intramuscular FFA and TAG content with more pronounced depletion in IL-6 KO group (-30 and -50 % in WT vs. -45 and -65 % in IL-6 KO group respectively; $p \leq 0.05$; Fig. 5a, b). Apparently, not significant changes were observed in DAG fraction in both groups studied regardless the genotype.

Effect of Single Bout of Exhausting Exercise and IL-6 KO Genotype on Skeletal Muscle Glucose Transporters Expression and Glycogen Content

Exercise induced a significant increase in glucose transporters (GLUT-1: $+8$ %, GLUT-4: $+15$ %; $p \leq 0.05$; Fig. 6a) in WT mice, with more pronounced changes in IL-6 KO littermates ($+20$ and $+35$ %; $p \leq 0.05$; Fig. 6b).

In both WT and IL-6 KO mice, exhausting exercise induced significant reduction in soleus muscle glycogen level (-30 and 60 %, respectively; $p \leq 0.05$ Fig. 7a, b).

Effect of Single Bout of Exhausting Exercise and IL-6 KO Genotype on Skeletal Muscle AMPK Activation

Exercise-induced AMPK activation as shown by increased the pAMPK/AMPK ratio ($+40$ %; $p \leq 0.05$; Fig. 8), but only in WT mice, since we observed relatively lower (-10 %; $p > 0.05$; AMPK activation in IL-6 KO mice).

Effect of Single Bout of Exhausting Exercise and IL-6 KO Genotype on Time Performance of Exercise

IL-6 KO mice had a significantly reduced endurance capacity compared to WT mice. The swimming duration time for knock-out animals was much shorter (51 min),

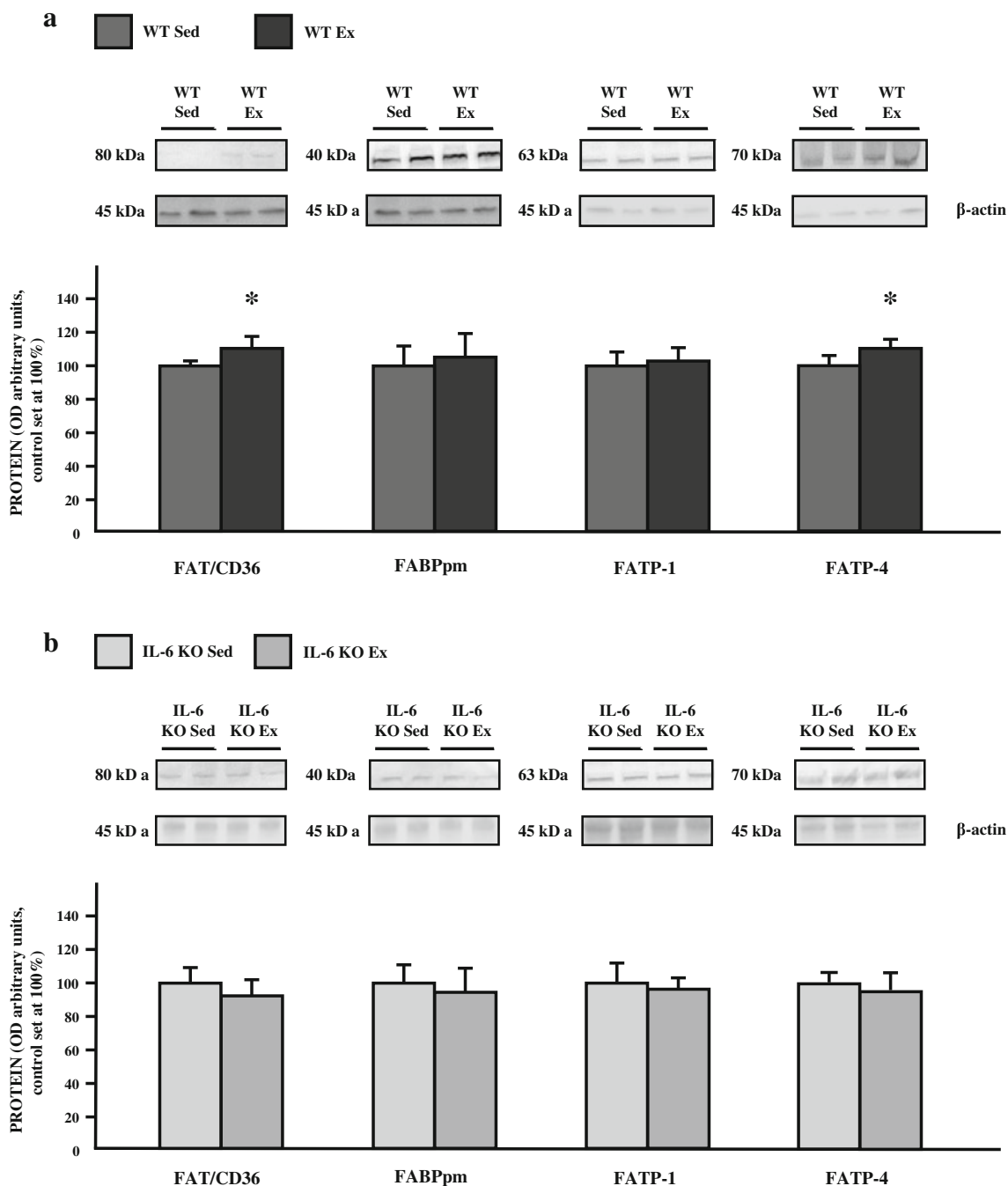


Fig. 4 The effect of a single bout of exhausting exercise on the expression of fatty acid transporters (FAT/CD36, FABPpm, FATP-1, FATP-4) in soleus muscle of WT (**a**) and IL-6 KO mice (**b**). Representative Western Blots present a relative change in the protein

expression related to β -actin content. ($n = 8$; asterisk **a** WT Sed vs. WT Ex, $P < 0.05$; control (WT Sed) set at 100 %); asterisk **b** IL-6 KO Sed vs. IL-6 KO Ex, control (IL-6 KO Sed) set at 100 %)

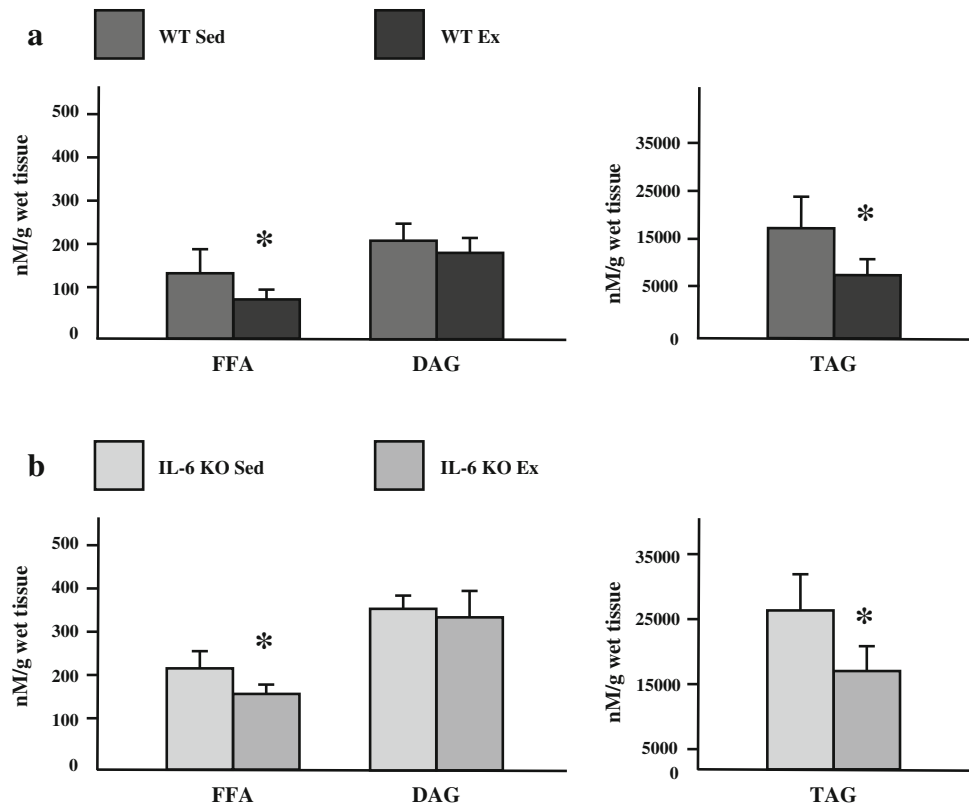
comparing with WT littermates (95 min) ($p \leq 0.05$; Fig. 9).

Discussion

The present study revealed that skeletal muscles from IL-6 deficient mice, when challenged by exercise, respond by:

(1) increased expression of glucose (mainly GLUT-4), but not FA transporters and (2) increased reliance on intramuscular energy depots (-65% TAG and -60% glycogen reductions). These are accompanied by a lack of significant changes in the expression of AMPK kinase, when compared to WT littermates. Along with the findings, IL-6 KO mice displayed much shorter time till exhaustion

Fig. 5 The effect of a single bout of exhausting exercise on the fatty acid content (FFA, DAG, TAG), in soleus muscle of WT (a) and IL-6 KO mice (b). ($n = 8$; asterisk WT vs. IL-6 KO, $P < 0.05$, FFA free fatty acids, DAG diacylglycerols, TAG triacylglycerols)



during intense swimming. We confirmed also our earlier findings indicating a higher intramuscular lipid content (TAG, FFA, DAG) together with greater FA transport protein expression (FAT/CD36, FABPpm and FATP-1) in IL-6 KO mice [21]. However, despite intramuscular lipid accumulation and increased expression of FA transporters, IL-6 KO mice displayed no other features of obese phenotype (as shown in our previous study) [21, 27].

A growing amount of evidence implicates IL-6 as an important regulator of skeletal muscle metabolism. It seems likely that interleukin-6 exerts its effect on glucose uptake and FA oxidation in skeletal muscles via activation of AMPK (AMP-activated protein kinase) [4, 28]. Studies in vitro [29], ex vivo [30] and in vivo [31, 32] indicate a direct link between IL-6 and AMPK activation. The present study confirmed the existence of such a relations as evidenced by lower activation of AMPK during exercise in IL-6 KO mice comparing to WT littermates. Therefore, we may speculate also that, at rest, lack of functional IL-6 could significantly decreased basal AMPK activation, which in turn, resulted in decreased FA oxidation and subsequent accumulation of intramuscular lipids. This, together with an increased fatty acid transporters expression in skeletal muscle, was likely the cause of fatty acids accumulation in TAG and FFA fractions (present study and [21]). Additionally, functional IL-6 deficiency when

challenged by exercise, induced a smaller reduction in intramuscular lipids that, again, can be attributed to the lack of significant AMPK activation (and AMPK-related FA oxidation). Based on the above, we may speculate that IL-6 deficiency diminishes the AMPK activation during exercise and it seems likely, that exercise-induced activation of AMPK does not directly require IL-6 [33]. During exercise IL-6 serum levels may be increased as much as 100-fold) [34, 35] and in WT mice greater AMPK activation results not only in a response to the increased ratio of AMP/ATP but is additionally triggered by an IL-6 dependent pathway [36]. An open question remains, whether these effects are additive in skeletal muscles. Our findings suggest such a possibility, since, in WT mice, exhausting exercise induced not only a depletion of endogenous energy stores (a reduction in TAG and glycogen), but also induced glucose and fatty acid transporters expression, exacerbating exogenous energy substrates flux into the muscles. It is well known that AMPK activation results in robust energy provision and many studies have shown both: increased FA and glucose oxidation as well as enhanced FA and glucose transporters expression [14, 37, 38]. The present study suggests that with IL-6 deficiency, at least when AMPK activation is diminished, FA flux and subsequent FA oxidation are reduced. Concomitantly, this genetic lack of functional IL-6, associated with diminished

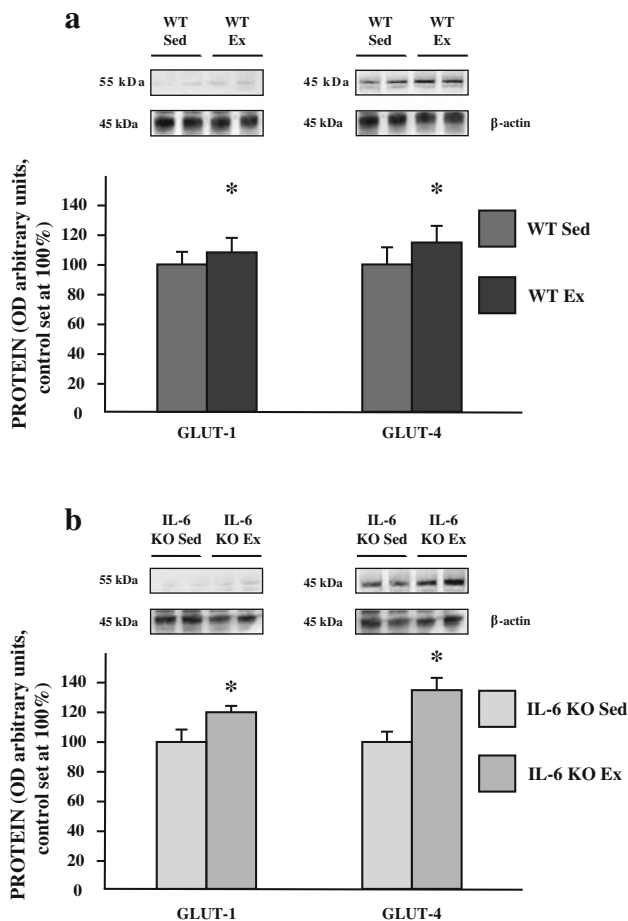


Fig. 6 The effect of a single bout of exhausting exercise on the expression of glucose transporters: GLUT-1, GLUT-4 in soleus muscle of WT (**a**) and IL-6 KO mice (**b**). Representative Western Blots present a relative change in the protein expression related to β -actin content. ($n = 8$; asterisk **a** WT Sed vs. WT Ex, $P < 0.05$; control (WT Sed) set at 100 %); asterisk **b** IL-6 KO Sed vs. IL-6 KO Ex, control (IL-6 KO Sed) set at 100 %)

exercise-induced AMPK activity, resulted in the increased expression of GLUT-4. It leaves an open discussion for other factors that may also be involved in favoring glucose metabolism over FA oxidation. Furthermore, IL-6 deficient animals exhibited diminished capacity for endurance performance. Likely, it is related to the respiratory exchange ratio (RER), since others reported that during exercise IL-6 KO mice reveal decreased exercise capacity [39]. Likewise, decreased AMPK activation (present study and [39]) could contribute to the shorter time till exhaustion as it was shown in mice expressing a dominant negative AMPK [40].

Along with this idea are studies showing that IL-6 may play a significant role in angiogenesis processes [41]. Thus, IL-6 deficiency may cause a decreased oxygen supply that

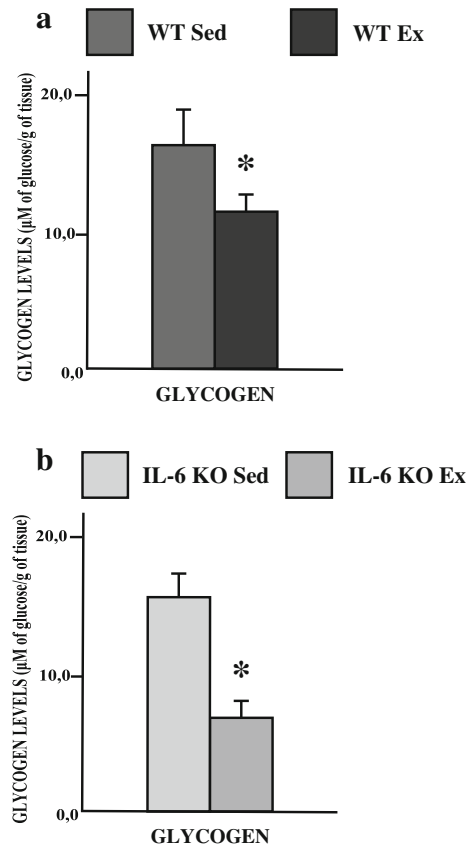


Fig. 7 The effect of a single bout of exhausting exercise on the glycogen content (μ M of glucose/g of tissue) in soleus muscle of WT (**a**) and IL-6 KO mice (**b**). ($n = 8$; asterisk **a** WT Sed vs. WT Ex and **b** IL-6 KO Sed vs. IL-6 KO Ex, $P < 0.05$)

contributes to the decreased lipid utilization [42]. It has also been suggested that IL-6 released from contracting skeletal muscles stimulates the release of glucose and FA from the liver and adipose tissue [1, 2] and lack of functional IL-6 may result in a reduced plasma energy substrate availability. We may speculate this may account for greater reliance on intramuscular energy depots observed in IL-6 KO mice (a higher reduction of intramuscular glycogen and TAG). Nevertheless, the exact mechanism responsible for decreased endurance capacity in IL-6 deficient mice needs to be clarified.

Summing up, the present study has provided several novel findings. We confirmed greater expression of FA transport proteins and accumulation of intramuscular lipids in soleus from IL-6 KO sedentary mice. We found also that IL-6 deficiency results in shorter time till exhaustion accompanied by pronounced intramuscular glycogen depletion, with substantial changes in glucose but not fatty acid transporters expression.

Fig. 8 The effect of a single bout of exhausting exercise on pAMPK/AMPK protein expression in soleus muscle of WT (a) and IL-6 KO (b) mice. ($n = 8$; double asterisks a WT Sed vs. WT Ex, $P < 0.05$; control (WT Sed) set at 100 %; asterisk b IL-6 KO Sed vs. IL-6 KO Ex, control (IL-6 KO Sed) set at 100 %)

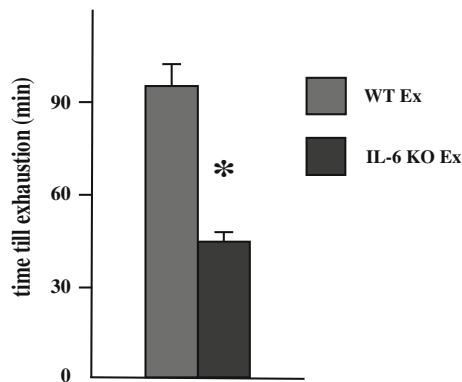
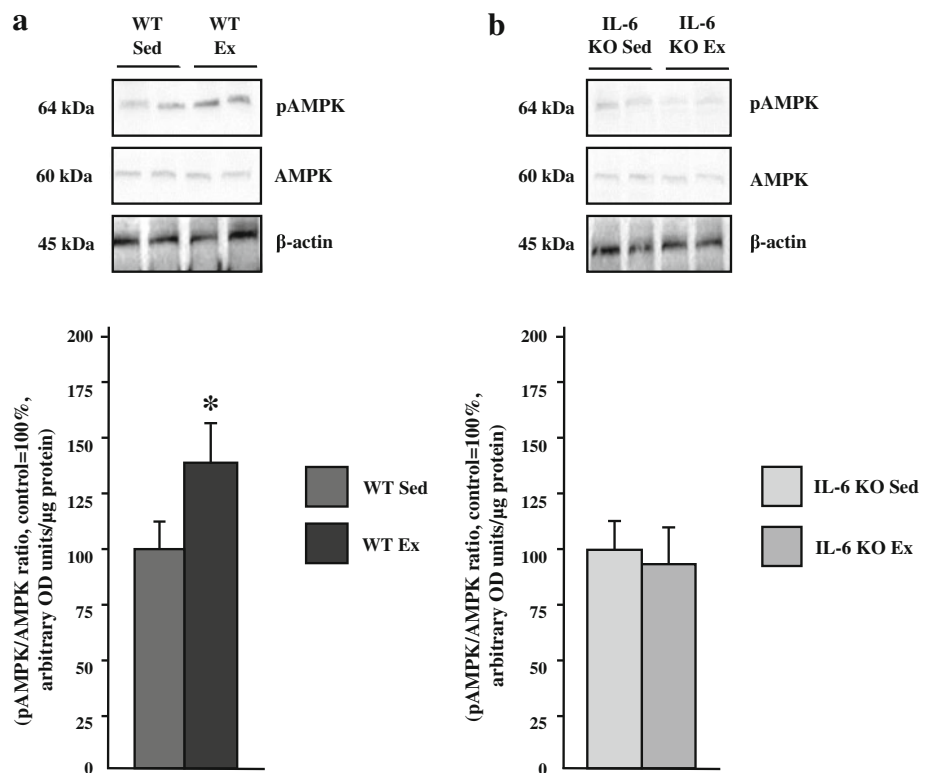


Fig. 9 The effect of a single bout of exhausting exercise on the swimming duration time ($n = 8$; asterisk WT Ex vs. IL-6 KO Ex, $P < 0.05$)

Acknowledgments This work was supported by the Medical University of Białystok (# 3-18613L and 113-18669L).

Conflict of interest The authors declare that there is no conflict of interest.

Open Access This article is distributed under the terms of the Creative Commons Attribution License which permits any use, distribution, and reproduction in any medium, provided the original author(s) and the source are credited.

References

- Pedersen BK (2011) Muscles and their myokines. *J Exp Biol* 214:337–346
- Pedersen BK, Febbraio MA (2008) Muscle as an endocrine organ: focus on muscle-derived interleukin-6. *Physiol Rev* 88:1379–1406
- Ruderman NB, Keller C, Richard AM, Saha AK, Luo Z, Xiang X, Giralt M, Ritov VB, Menshikova EV, Kelley DE, Hidalgo J, Pedersen BK, Kelly M (2006) Interleukin-6 regulation of AMP-activated protein kinase. Potential role in the systemic response to exercise and prevention of the metabolic syndrome. *Diabetes* 55 (Suppl 2):S48–S54
- Carey AL, Steinberg GR, Macaulay SL, Thomas WG, Holmes AG, Ramm G, Prelovsek O, Hohnen-Behrens C, Watt MJ, James DE, Kemp BE, Pedersen BK, Febbraio MA (2006) Interleukin-6 increases insulin-stimulated glucose disposal in humans and glucose uptake and fatty acid oxidation in vitro via AMP-activated protein kinase. *Diabetes* 55(10):2688–2697
- Vozarova B, Weyer C, Hanson K, Tataranni PA, Bogardus C, Pratley RE (2001) Circulating interleukin-6 in relation to adiposity, insulin action, and insulin secretion. *Obes Res* 9(7):414–417
- Bastard JP, Jardel C, Bruckert E, Blondy P, Capeau J, Laville M, Vidal H, Hainque B (2000) Elevated levels of interleukin 6 are reduced in serum and subcutaneous adipose tissue of obese women after weight loss. *J Clin Endocrinol Metab* 85(9):3338–3342
- Kern PA, Ranganathan S, Li C, Wood L, Ranganathan G (2001) Adipose tissue tumor necrosis factor and interleukin-6 expression in human obesity and insulin resistance. *Am J Physiol Endocrinol Metab* 280(5):E745–E751
- Senn JJ, Klover PJ, Nowak IA, Zimmers TA, Koniaris LG, Furlanetto RW, Mooney RA (2003) Suppressor of cytokine signaling-3 (SOCS-3), a potential mediator of interleukin-6-dependent insulin resistance in hepatocytes. *J Biol Chem* 278(16):13740–13746
- Bickel PE (2004) Metabolic fuel selection: the importance of being flexible. *J Clin Invest* 114(11):1547–1549

10. Weber JM (2011) Metabolic fuels: regulating fluxes to select mix. *J Exp Biol* 214(Pt 2):286–294
11. Spriet LL (1998) Regulation of fat/carbohydrate interaction in human skeletal muscle during exercise. *Adv Exp Med Biol* 441:249–261
12. Ryder JW, Kawano Y, Galuska D, Fahlman R, Wallberg-Henriksson H, Charron MJ, Zierath JR (1999) Postexercise glucose uptake and glycogen synthesis in skeletal muscle from GLUT4-deficient mice. *FASEB J* 13(15):2246–2256
13. Kamp F, Hamilton JA, Westerhoff HV (1993) Movement of fatty acids, fatty acid analogues, and bile acids across phospholipid bilayers. *Biochemistry* 32:11074–11086
14. Glatz JF, Luiken JJ, Bonen A (2010) Membrane fatty acid transporters as regulators of lipid metabolism: implications for metabolic disease. *Physiol Rev* 90(1):367–417
15. Holloway GP, Bonen A, Spriet LL (2009) Regulation of skeletal muscle mitochondrial fatty acid metabolism in lean and obese individuals. *GP Holloway*. *Am J Clin Nutr* 89(1):455S–462S
16. Bonen A, Chabowski A, Luiken JJ, Glatz JF (2007) Is membrane transport of FFA mediated by lipid, protein, or both? Mechanisms and regulation of protein-mediated cellular fatty acid uptake: molecular, biochemical, and physiological evidence. *Physiology (Bethesda)* 22:15–29
17. Schaffer JE, Lodish HF (1994) Expression cloning and characterization of a novel adipocyte long chain fatty acid transport protein. *Cell* 79:427–436
18. Holloway GP, Lally J, Nickerson JG, Alkhateeb H, Snook LA, Heigenhauser GJ, Calles-Escandon J, Glatz JF, Luiken JJ, Spriet LL, Bonen A (2007) Fatty acid binding protein facilitates sarcolemmal fatty acid transport but not mitochondrial oxidation in rat and human skeletal muscle. *J Physiol* 582:393–405
19. Marotta M, Ferrer-Martinez A, Parnau J, Turini M, Macé K, Gomez-Foix AM (2004) Fiber type- and fatty acid composition-dependent effects of high-fat diets on rat muscle triacylglyceride and fatty acid transporter protein-1 content. *Metabolism* 53:1032–1036
20. Kopf M, Baumann H, Freer G, Freudenberg M, Lamers M, Kishimoto T, Zinkernagel R, Bluethmann H, Köhler G (1994) Impaired immune and acute-phase responses in interleukin-6-deficient mice. *Nature* 368:339–342
21. Chabowski A, Zmijewska M, Gorski J, Bonen A, Kaminski K, Kozuch M, Winnicka MM (2008) IL-6 deficiency increases fatty acid transporters and intramuscular lipid content in red but not white skeletal muscle. *J Physiol Pharmacol* 59(Suppl 7):105–117
22. Dube JJ, Bhatt BA, Dedousis N, Bonen A, O'Doherty RM (2007) Leptin, skeletal muscle lipids, and lipid-induced insulin resistance. *Am J Physiol Regul Integr Comp Physiol* 293(2):R642–R650
23. Chabowski A, Górski J, Calles-Escandon J, Tandon NN, Bonen A (2006) Hypoxia-induced fatty acid transporter translocation increases fatty acid transport and contributes to lipid accumulation in the heart. *FEBS Lett* 580(15):3617–3623
24. Folch J, Lees M, Sloane Stanley GH (1957) A simple method for the isolation and purification of total lipids from animal tissues. *J Biol Chem* 226(1):497–509
25. van der Vusse GJ, Roemen TH, Reneman RS (1980) Assessment of fatty acids in dog left ventricular myocardium. *Biochim Biophys Acta* 617(2):347–349
26. Carroll NV, Longley RW, Roe JH (1956) The determination of glycogen in liver and muscle by use of anthrone reagent. *J Biol Chem* 220(2):583–593
27. Chabowski A, Zmijewska M, Górski J, Bonen A, Kamiński K, Winnicka MM (2007) Effect of IL-6 deficiency on myocardial expression of fatty acid transporters and intracellular lipid depots. *J Physiol Pharmacol* 58(1):73–82
28. Wolsk E, Mygind H, Grøndahl TS, Pedersen BK, van Hall G (2010) IL-6 selectively stimulates fat metabolism in human skeletal muscle. *Am J Physiol Endocrinol Metab* 299(5):E832–E840
29. Nieto-Vazquez I, Fernández-Veledo S, de Alvaro C, Lorenzo M (2008) Dual role of interleukin-6 in regulating insulin sensitivity in murine skeletal muscle. *Diabetes* 57(12):3211–3221
30. Bruce CR, Dyck DJ (2004) Cytokine regulation of skeletal muscle fatty acid metabolism: effect of interleukin-6 and tumor necrosis factor- α . *Am J Physiol Endocrinol Metab* 287(4):E616–E621
31. van Hall G, Steensberg A, Sacchetti M, Fischer C, Keller C, Schjerling P, Hiscock N, Møller K, Saltin B, Febbraio MA, Pedersen BK (2003) Interleukin-6 stimulates lipolysis and fat oxidation in humans. *J Clin Endocrinol Metab* 88(7):3005–3010
32. Ruderman NB, Keller C, Richard AM, Saha AK, Luo Z, Xiang X, Giralt M, Ritov VB, Menshikova EV, Kelley DE, Hidalgo J, Pedersen BK, Kelly M. (2006) Interleukin-6 regulation of AMP-activated protein kinase. Potential role in the systemic response to exercise and prevention of the metabolic syndrome. *Diabetes* 55 (Suppl 2):S48–S54
33. Hiscock N, Fischer CP, Sacchetti M, van Hall G, Febbraio MA, Pedersen BK (2005) Recombinant human interleukin-6 infusion during low-intensity exercise does not enhance whole body lipolysis or fat oxidation in humans. *Am J Physiol Endocrinol Metab* 289(1):E2–E7
34. Nieman DC, Dumke CL, Henson DA, McNulty SR, Gross SJ, Lind RH (2005) Muscle damage is linked to cytokine changes following a 160-km race. *Brain Behav Immun* 19:398–403
35. Suzuki K, Yamada M, Kurakake S, Okamura N, Yamaya K, Liu Q, Kudoh S, Kowatari K, Nakaji S, Sugawara K (2000) Circulating cytokines and hormones with immunosuppressive but neutrophil-priming potentials rise after endurance exercise in humans. *Eur J Appl Physiol* 81:281–287
36. Kelly M, Keller C, Avilucea PR, Keller P, Luo Z, Xiang X, Giralt M, Hidalgo J, Saha AK, Pedersen BK (2004) AMPK activity is diminished in tissues of the IL-6 knockout mice: the effect of exercise. *Biochem Biophys Res Commun* 320:449–454
37. Luiken JJ, Coort SL, Willems J, Coumans WA, Bonen A, van der Vusse GJ, Glatz JF (2003) Contraction-induced fatty acid translocase/CD36 translocation in rat cardiac myocytes is mediated through AMP-activated protein kinase signaling. *Diabetes* 52(7):1627–1634
38. Thomson DM, Winder WW (2009) AMPK control of fat metabolism in skeletal muscle. *Acta Physiol (Oxf)* 196(1):147–154
39. Földt J, Wernstedt I, Fitzgerald SM, Wallenius K, Bergström G, Jansson JO (2004) Reduced exercise endurance in Interleukin-6-deficient mice. *Endocrinology* 145(6):2680–2686
40. Mu J, Barton ER, Birnbaum MJ (2003) Selective suppression of AMP-activated protein kinase in skeletal muscle: update on 'lazy mice'. *Biochem Soc Trans* 31(Pt 1):236–241
41. Wei LH, Kuo ML, Chen CA, Chou CH, Lai KB, Lee CN, Hsieh CY (2003) Interleukin-6 promotes cervical tumor growth by VEGF-dependent angiogenesis via a STAT3 pathway. *Oncogene* 22(10):1517–1527
42. McArdle WD, Katch FI, Katch VL (2006) Measuring and evaluating human energy generating capacities during exercises. In: McArdle WD, Katch FI, Katch VL (eds) *Essentials of exercise physiology*, Tom 1, 3rd edn. Lippincott Williams & Wilkin, pp 223–259

Increased Glyceride–Glycerol Synthesis in Liver and Brown Adipose Tissue of Rat: In-Vivo Contribution of Glycolysis and Glyceroneogenesis

Valéria E. Chaves · Danúbia Frasson ·
Maria A. R. Garófalo · Luiz C. C. Navegantes ·
Renato H. Migliorini · Isis C. Kettelhut

Received: 6 January 2012 / Accepted: 16 May 2012 / Published online: 10 June 2012
© AOCS 2012

Abstract We have previously shown that a high-protein, carbohydrate-free diet can decrease the production of glycerol-3-phosphate (G3P) from glucose and increase glyceroneogenesis in both brown (BAT) and epididymal (EAT) adipose tissue. Here, we utilized an in-vivo approach to examine the hypothesis that there is reciprocal regulation in the G3P synthesis from glucose (via glycolysis) and glyceroneogenesis in BAT, EAT and liver of fasted rats and cafeteria diet-fed rats. Glyceroneogenesis played a prominent role in the generation of G3P in the liver (~70 %) as well as in BAT and EAT (~80 %) in controls rats. The cafeteria diet induced an increase in the total glyceride-glycerol synthesis and G3P synthesis from glucose and a decrease in glyceroneogenesis in BAT; this diet did not affect either the total glyceride-glycerol synthesis or G3P generation from glyceroneogenesis or glycolysis in the liver or EAT. Fasting induced an increase in total glyceride-glycerol synthesis and glyceroneogenesis and a decrease in G3P synthesis from glucose in the liver but did not affect either the total glyceride-glycerol synthesis or G3P

synthesis from glyceroneogenesis in BAT and EAT, despite a reduction in glycolysis in these tissues. These data demonstrate that reciprocal changes in the G3P generation from glucose and from glyceroneogenesis in the rat liver and BAT occur only when the synthesis of glycerides–glycerol is increased. Further, our data suggest that this increase may be essential for the systemic recycling of fatty acids by the liver from fasted rats and for the maintenance of the thermogenic capacity of BAT from cafeteria diet-fed rats.

Keywords Glyceroneogenesis · Glycerol-3-phosphate · Glycolysis · Phosphoenolpyruvate carboxykinase · Epididymal adipose tissue · Brown adipose tissue · Liver

Abbreviations

BAT	Brown adipose tissue
BW	Body weight
EAT	Epididymal adipose tissue
FA	Fatty acids
FFA	Free fatty acids
G3P	Glycerol-3-phosphate
IBAT	Interscapular brown adipose tissue
PEPCK	Phosphoenolpyruvate carboxykinase
SpA	Specific activity
TAG	Triacylglycerol
WAT	White adipose tissue

Electronic supplementary material The online version of this article (doi:10.1007/s11745-012-3683-0) contains supplementary material, which is available to authorized users.

V. E. Chaves (✉)
Laboratory of Physiology and Pharmacology, Federal University of São João del-Rei, Avenida Sebastião Gonçalves Coelho, 400, Chanadour, Divinópolis, Minas Gerais, Brazil
e-mail: valeria.chaves@gmail.com

D. Frasson · R. H. Migliorini · I. C. Kettelhut
Department of Biochemistry-Immunology, Faculty of Medicine, University of São Paulo, Ribeirão Preto, São Paulo, Brazil

M. A. R. Garófalo · L. C. C. Navegantes
Department of Physiology, Faculty of Medicine, University of São Paulo, Ribeirão Preto, São Paulo, Brazil

Introduction

Liver, white (WAT) and brown (BAT) adipose tissues are directly involved in the maintenance of lipidic homeostasis. In a fed state, the liver stores glucose as glycogen and

excess nutrients are converted into triacylglycerol (TAG), which is then secreted into the bloodstream as TAG-enriched lipoproteins (VLDL) [1]. WAT stores energy as TAG in the post-prandial state and mobilizes fatty acids (FA) in situations of energy demand. More recently, the interest in understanding the WAT physiology has been renewed. This tissue can also participate in the maintenance of the body homeostasis by its capacity to synthesize and to release adipokines [2]. Leptin, the first adipokine described, contributes toward central control of energetic balance, inhibiting food intake and stimulating BAT thermogenesis [2]. Although the physiologic role of BAT in adult humans remains undefined, recent findings indicate that BAT is present and active in a significant number of adults [3]. It is known that the first step in the sequence of metabolic events leading to the activation of BAT thermogenesis is the hydrolysis of endogenous TAG. The FA thus produced, apart from being the main substrates for heat production, are natural uncouplers of oxidative phosphorylation, activating UCP-1, the uncoupling protein specific of BAT mitochondria [3]. The maintenance of adequate stores of TAG is, therefore, essential for a normal functioning of liver, WAT and BAT. TAG production requires a continuous supply of glycerol-3-phosphate (G3P) to esterify newly synthesized or preformed FA. G3P can be formed from three precursors: (1) from glucose via dihydroxyacetone in the glycolytic pathway and conversion to G3P by glycerophosphate dehydrogenase; (2) from glycerol, produced by hydrolysis of stored triacylglycerol (TAG) or taken up by tissue from the circulation, which is converted to G3P by glycerokinase; and (3) from three-carbon intermediates (such as lactate and pyruvate) by glyceroneogenesis, which forms phosphoenolpyruvate via the dicarboxylic shuttle and subsequently produces G3P by a partial reversion of glycolysis (Fig. 1). Only in the last decade, has the importance of glyceroneogenesis as a

supplier of G3P for lipid metabolism been recognized [4, 5]. Recently, in-vivo experiments have indicated that glyceroneogenesis in rat WAT is the major pathway for glyceride–glycerol synthesis [6–8]. In vitro studies have suggested that glyceroneogenesis is also physiologically significant in BAT and liver [9–11].

The experiments described in the present study were motivated by previous findings in rats: (1) adapted to a high-protein, carbohydrate free, (2) fed a cafeteria diet, (3) fasted and (4) diabetic. All these experimental conditions have been used for many years in this laboratory to investigate the nutritional and hormonal control of energy-linked metabolic processes. Our experiments have demonstrated that the adaptation of rats to a high-protein, carbohydrate-free diet induces a reduction in plasma insulin levels [12] and an increase in WAT glyceroneogenic activity, as evidenced by an increased activity of phosphoenolpyruvate carboxykinase (PEPCK) [13] and increased rates of incorporation of non-glucose substrates into TAG-glycerol in vivo [14] and in vitro, in tissue fragments [13] or in adipocytes [15]. Because the use of glucose in vivo and the glycolytic flux are reduced in WAT from rats fed the high-protein, carbohydrate-free diet [16], the increased glyceroneogenesis may represent a compensatory mechanism for the reduced generation of G3P via glycolysis [14]. Similar findings were obtained in BAT from rats fed the high-protein, carbohydrate-free diet [17]. In contrast, cafeteria diet feeding induces a decrease in glyceroneogenesis, which was indicated by reduced PEPCK activity and by decreased rates of ^{14}C -pyruvate incorporation into TAG-glycerol in vitro by isolated white adipocytes or BAT fragments, and an increase in the in-vivo glucose uptake in epididymal adipose tissue (EAT) and BAT [9, 18]. In hepatic tissue, glyceroneogenesis and gluconeogenesis can be simultaneously evaluated in vitro by the rate of incorporation of ^{14}C -pyruvate into glyceride–glycerol and by the amount of glucose released into the incubation

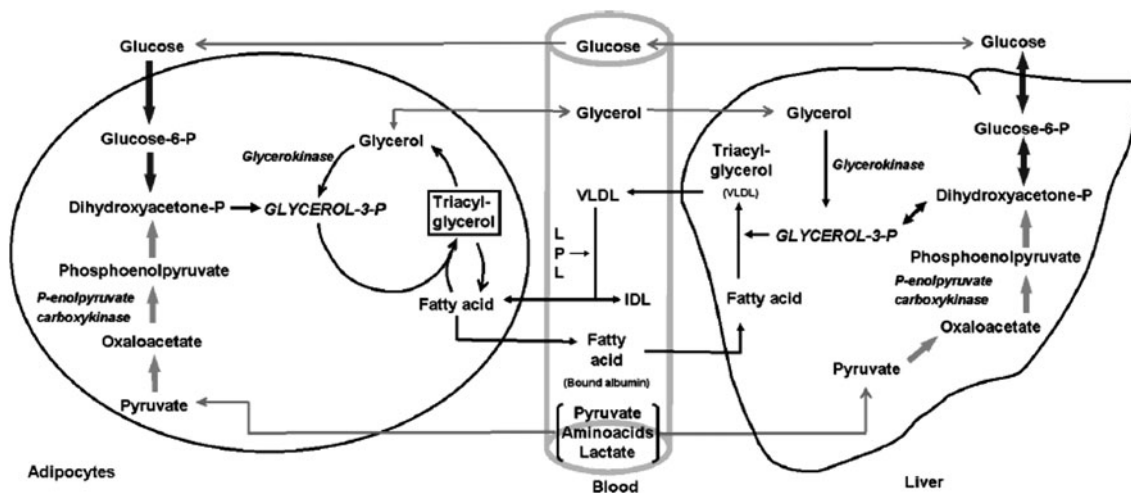


Fig. 1 Sources and pathways of glycerol-3-phosphate generation in adipose tissue and the liver and possible systemic recycling of fatty acids

Table 1 Brown and white adipose tissue weights, free fatty acid and insulin plasma concentrations of fasted, cafeteria-fed or control diet-fed rats

	Control	Fasted	Cafeteria diet
Interscapular brown adipose tissue (g)	0.18 ± 0.01	0.17 ± 0.01	0.36 ± 0.02*
Epididymal adipose tissue (g)	1.00 ± 0.03	0.77 ± 0.01*	2.15 ± 0.11*
Free fatty acid (mmol/L)	0.35 ± 0.03	0.97 ± 0.04*	0.42 ± 0.04
Insulin (μU/mL)	37.4 ± 4.00	14.96 ± 2.60*	60.78 ± 5.89*

Data are means ± SEM from 10 rats

* $P < 0.05$ vs. control

medium, respectively; both pathways are increased in the liver from fasted and diabetic rats [11]. In both situations, the glycolytic flux (estimated by the amount of ^3H recovered from water after incubation of liver slices in medium containing ^3H -glucose) and the generation of G3P from glucose (assayed by the rate of ^{14}C -glucose incorporation into glyceride–glycerol) are reduced in the liver slices [11]. These primarily in vitro findings from WAT, BAT and liver suggest that glyceroneogenesis and glycolysis would be reciprocally regulated to ensure the generation of G3P that is necessary for FA esterification and TAG synthesis. However, further in-vivo experimentation is needed to firmly establish this hypothesis.

In this work, we examined the in-vivo changes induced by fasting and feeding of a cafeteria diet on glyceroneogenesis and glycolysis in hepatic tissue, EAT and BAT. Fasting and feeding of a cafeteria diet are two physiological conditions that induce opposite effects on the plasma insulin levels (Table 1) and rates of cellular glucose uptake. In addition, fasting results in an increase in adipose tissue lipolysis and FA uptake by the liver. The purpose of this study was to directly assess whether G3P production from glucose or gluconeogenic precursors is reciprocally regulated in liver tissue and adipose tissue.

Materials and Methods

Animals

Male Wistar rats (9–12 animals) were housed in suspended wire-bottom cages in a room maintained at 25 ± 2 °C with a 12 h light/12 h dark cycle. For the fasting experiments, rats weighing 230–250 g were left without food but had free access to water for 48 h. For the cafeteria diet feeding experiments, rats initially weighing 45–55 g were fed a cafeteria diet for 3 weeks, which consisted of a standard balanced diet [Nuvilab CR1, Nuvital, Brazil (22 % protein,

55 % carbohydrate and 4.5 % lipid)] that was supplemented each day with four different lipid-rich, palatable items selected from a list of 12 foods, including bacon, caramel candy, cashew nuts, cookies, cornstarch biscuits, cheese biscuits, chocolate rolls, chocolate wafers, nougat, peanut candy, potato chips, and toast. In addition, the water offered to these rats contained 20 % sucrose. Control rats were only fed a commercial diet, and they consumed water ad libitum. The energy intake of the control rats, estimated from the daily intake and composition of the commercial diet, was 209 ± 4 kJ 100 g $^{-1}$ body weight (bw) d $^{-1}$ (mean ± SEM). In rats that were fed the cafeteria diet, the energy intake, which included the amount and composition of palatable items and the volume of water consumed, was approximately 40 % higher (293 ± 13 kJ 100 g $^{-1}$ bw d $^{-1}$) than that of the control rats. In cafeteria diet-fed rats, protein contributed 15 ± 1 %, carbohydrate 65 ± 1 % and lipid 20 ± 1 % of the total energy intake, compared to contributions of 25, 63 and 12 %, respectively, in rats that were fed the control diet. All rats weighed 220–240 g during the experiments, which were always performed between 08:00 and 10:00 hours. The rat care and treatment protocols received prior institutional approval by the Ethical Committee of the University of São Paulo (protocol number 174/2007).

Label Injection

The labeled molecules [^{14}C]-glucose (10 μCi) and $^3\text{H}_2\text{O}$ (3 mCi) were dissolved in 0.5 mL of saline and injected into non-anesthetized rats, freely moving in its cage, through a catheter that was inserted under anesthesia into the right jugular vein 2 days before the experiments. After flushing the catheter with saline, 0.2 mL blood samples were taken 1, 5, 15, 30 and 60 min after label injection for determination of [^{14}C]-glucose specific activity (SpA). Immediately after obtaining the 60-min sample, which was also used to determine the water SpA (^3H DPM ÷ g atom of water hydrogen), each animal was killed by cervical dislocation, and the liver, interscapular BAT (IBAT) and EAT were rapidly removed. IBAT was carefully cleaned free of adhering fat and muscle. All tissue were weighed and suspended in chloroform:methanol (2:1).

Isolation of Tissue Glyceride–Glycerol

The total lipids from liver, IBAT and EAT samples were extracted with 2:1 chloroform:methanol by the procedure described in Folch [19]. Labeled $^3\text{H}_2\text{O}$ was removed from the inferior phases (predominantly chloroform) by washing three times with a superior-phase mixture. After each wash, the tubes were briefly centrifuged to sharpen the phase boundary, and the superior phase was aspirated and discarded. The chloroform phase was evaporated to dryness, and the

saponifiable lipids were hydrolyzed with ethanolic KOH for 1 h at 70 °C. After extraction of the nonsaponifiable lipids and acidification with 6 % H₂ClO₄, the ¹⁴C-³H-FA were extracted with petroleum ether, and the extract was evaporated to dryness in a scintillation vial and dissolved in SX22-5 scintillation liquid (Fisher Scientific®). The aqueous hydrolysate containing ¹⁴C-³H-glycerol was dissolved in SX20-5 scintillation liquid (Fisher Scientific®).

Determination of Plasma Glucose and Water Specific Radioactivity

Plasma was deproteinized with 6 % H₂ClO₄, and after neutralization, the supernatant was applied to a Dowex column (1 × 8; 100–200 mesh; formate form) to separate [U-¹⁴C]-glucose from [¹⁴C]-pyruvate and [¹⁴C]-lactate. The compounds that were retained by the column were recovered by thoroughly washing the column with 1 N NaOH. The concentration of plasma glucose was determined enzymatically using a commercial kit from Labtest® (Lagoa Santa, Brazil). Water SpA was determined directly from aliquots of diluted (1:50) plasma dissolved in SX20-5 scintillation liquid (Fisher Scientific®).

Radioactivity Measurements

The degree of quenching in each sample was obtained to enable radioactivity calculation in dpm. Simultaneous liquid scintillation counting of the ³H and ¹⁴C contents of FA or glycerol was performed using a channels ratio method [20] on a Packard Tri-Carb 2100 TR spectrometer.

Experimental Approach

The synthesis of glycerol and FA of glycerides was evaluated in the same animal by simultaneously determining the rate of conversion of ³H from tritiated water, which estimates the total synthesis from all carbon sources, and ¹⁴C from glucose in two fractions (glycerol and FA) of glycerides in the liver, BAT and EAT. The transformation rates of glucose carbon into tissue glyceride-glycerol or glyceride-FA were estimated using the semi-compartmental approach described by Baker and Huebotter [21], which is a modification of the non-compartmental approach of Shipley [22]. The semi-compartmental analysis, which combines features of both the non-compartmental and the compartmental analyses, requires measurement of the SpA time curve for glucose after a single injection of a radioactive tracer (as in the method of Shipley [22]) and measurement of the radioactivity of an “end product” at any time point (60 min in this study). The rates of glyceride-glycerol synthesis from glucose were calculated as described in [21] and [22], using the factor 0.036 to convert

μg of glucose carbon to nmol of glycerol synthesized. The assumptions and supportive arguments for the adequacy of ³H₂O for measuring lipid synthesis from all carbon sources have been presented by Windmueller and Spaeth [23] and Jungas [24]. The rates of glyceride-glycerol synthesis from ³H₂O were estimated assuming that each glycerol that was incorporated into glyceride contained 3.3 atoms of ³H when glycerol was formed from glucose via glycolysis [24] and 5 atoms of ³H when glycerol was formed from non-glucose substrates via glyceroneogenesis [25].

The curves of plasma glucose SpA (corrected by mg of carbon glucose) were fitted to two-term exponential equations (Fig. 2) and whose parameters were used in the calculations [21]. The actual formulae are provided in supplemental material.

Other Methods of Chemical Analysis

Plasma FFA levels were determined by the method described by Dole and Meinertz [26] and the concentration of plasma insulin by radioimmunoassay was measured using a commercial kit (Coat-a-Count Insulin) from DPC (Diagnostic Products Corporation).

Statistical Methods

The results are expressed as means ± SEM, and the differences between the means were analyzed using the Student's *t* test with *P* < 0.05 as the criterion of significance.

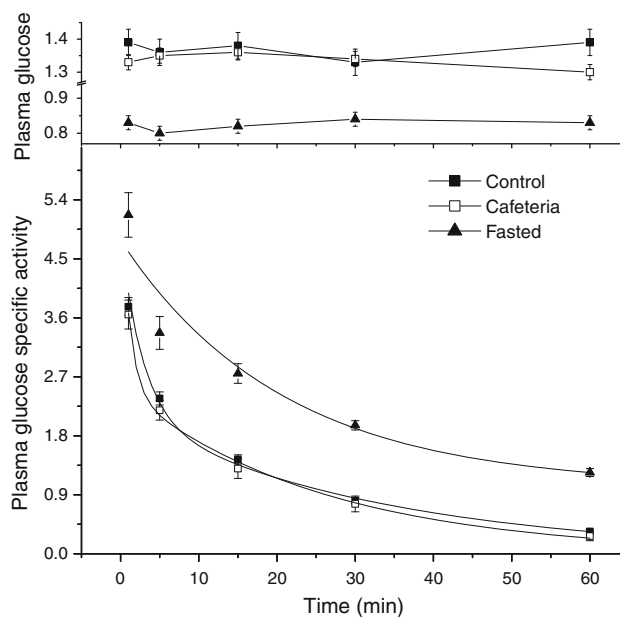


Fig. 2 Plasma glucose (mg mL⁻¹) and plasma glucose specific activity (% of injected dose mg of glucose carbon⁻¹) after intravenous injection of tracer ¹⁴C-glucose into either fasted, cafeteria-fed or control diet-fed rats. Each point is the mean ± SEM of 9–12 rats

Results

Fasting induced an approximately 30 % reduction in EAT weight but did not affect IBAT weight. Conversely, the cafeteria diet induced a significant increase (~100 %) in both EAT and IBAT weights. The plasma FFA levels were increased approximately 170 % in fasting rats but did not change in rats fed a cafeteria diet (Table 1). The plasma insulin levels were lower (60 %) in fasting rats and higher (63 %) in cafeteria-diet-fed rats (Table 1).

When compared with rats that were fed the control diet, de novo synthesis of FA was markedly reduced in the liver tissue (~74 %), IBAT (~59 %) and EAT (~65 %) from fasted rats and clearly increased in liver tissue (~124 %), IBAT (~380 %) and EAT (~770 %) from rats fed the cafeteria diet (Fig. 3). G3P generation from glucose and non-glucose sources was evaluated in vivo by simultaneously determining the rate of $^3\text{H}_2\text{O}$ and ^{14}C -glucose incorporation into glyceride–glycerol within the same animal. Total glyceride–glycerol synthesis was significantly increased in the liver tissue (~110 %) from fasted rats and in IBAT (~78 %) from cafeteria-diet-fed rats compared to control rats (Fig. 4). The increase in total glyceride–glycerol synthesis induced by fasting in the liver tissue was due to an increase in G3P generation via glyceroneogenesis (~180 %), despite the decrease in glycolytic flux (~66 %) (Fig. 4). In contrast, the increase in total glyceride–glycerol synthesis in IBAT induced by the cafeteria diet was due to an increase in G3P synthesis via glycolytic flux (~670 %), even though there was a reduction in synthesis via glyceroneogenesis (~42 %) (Fig. 4). Fasting also induced a decrease in glyceride–glycerol synthesis from glucose in IBAT (~88 %) and EAT (~85 %) without affecting the total synthesis of glyceride–glycerol and glyceroneogenesis (Fig. 4). The cafeteria diet did not affect the rates of glyceride–glycerol synthesis from glucose via glycolysis or from non-glucose substrates via glyceroneogenesis in the liver tissue or in EAT (Fig. 4). During the 60 min experimental period, injected ^{14}C -glucose could be converted into ^{14}C -pyruvate and ^{14}C -lactate. We found that the plasma concentrations of these latter compounds remained constant (approximately 0.07 % of the injected ^{14}C -glucose). Because the consumption of these compounds by tissues was negligible compared with the use of glucose (varying from 1.70 to 0.42 %), we assumed that there was no appreciable turnover of ^{14}C -labeled product during the experimental period.

Discussion

The data presented here clearly show that, compared to glycolysis, the in-vivo glyceroneogenic pathway played a

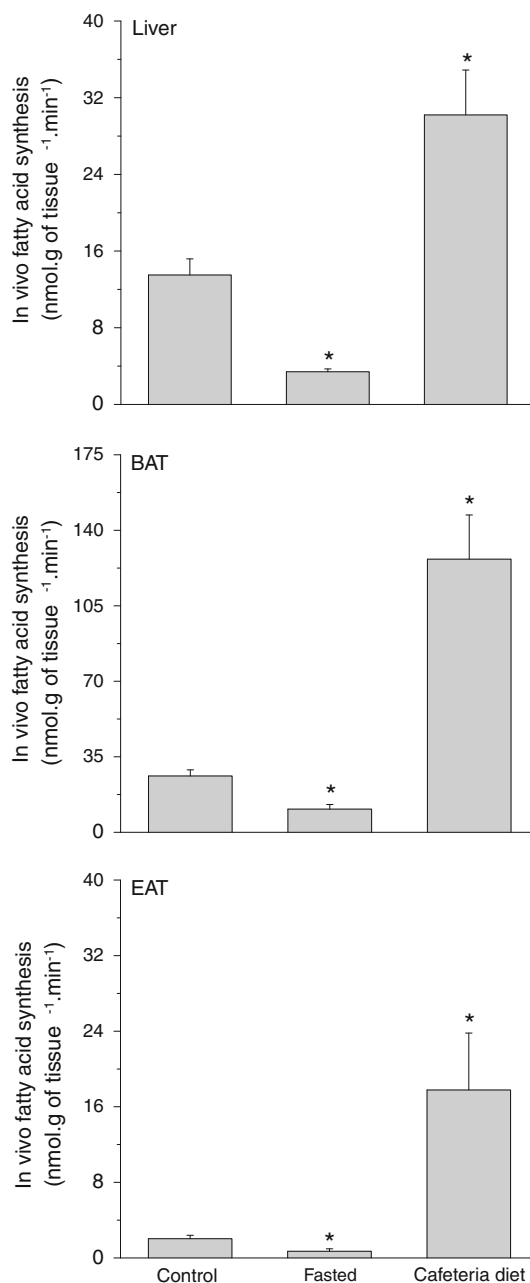


Fig. 3 Effect of fasting and cafeteria diet feeding on the in-vivo rate of de novo fatty acid synthesis in the liver and brown and epididymal adipose tissues. Bars are means \pm SEM of 9–12 rats. * $P < 0.05$ vs. control

prominent role in the generation of G3P in the liver tissue (73 ± 5 %), IBAT (83 ± 8 %), and EAT (80 ± 6 %) in control rats. Previous in-vivo studies have shown that glyceroneogenesis is the major pathway for G3P synthesis in the WAT of rodents [6–8, 14, 17]. The present work is the first in-vivo evidence that fasting and a cafeteria diet can induce reciprocal changes in G3P generation from glyceroneogenesis and glucose (via glycolysis). Glyceroneogenesis was reduced and glycolysis and total

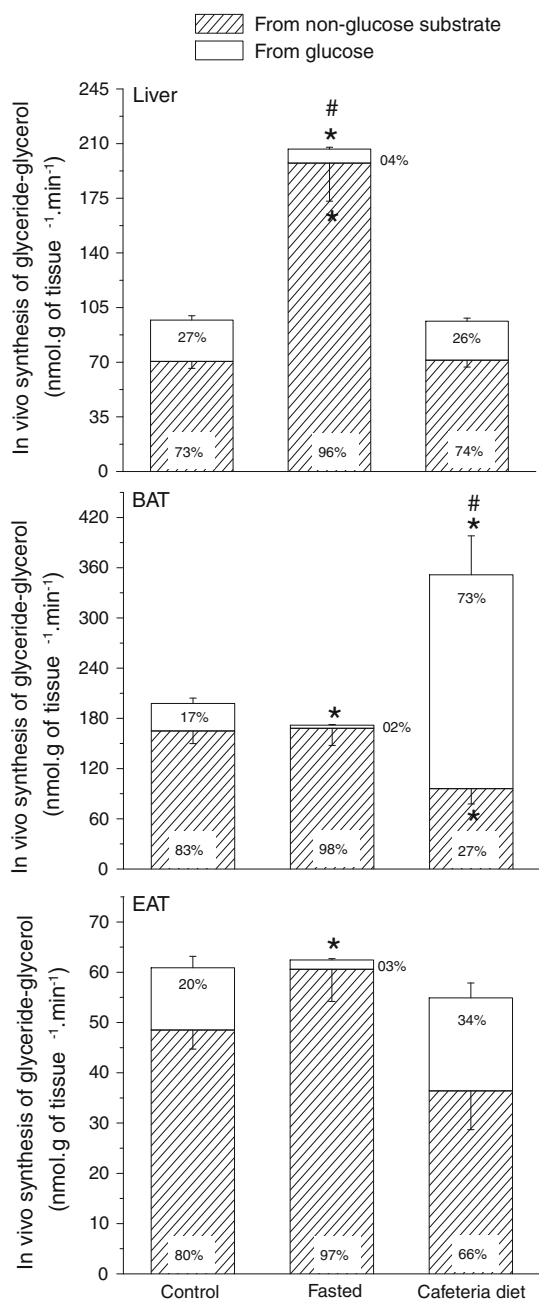


Fig. 4 Effect of fasting and cafeteria diet feeding on the in-vivo synthesis of glyceride-glycerol from glucose (via glycolysis) and non-glucose substrates (via glyceroneogenesis) in rat liver and brown and epididymal adipose tissue. Bars are means \pm SEM of 9–12 rats. The values in the bars represent the percent contribution of each pathway for the total glyceride-glycerol synthesis. * $P < 0.05$ relative to glycolysis or glyceroneogenesis versus control. # $P < 0.05$ relative to total glyceride-glycerol synthesis versus control

glyceride-glycerol (G3P) synthesis were increased in BAT from rats fed the cafeteria diet, thus the relative contribution of glyceroneogenesis for total G3P synthesis was significantly lower ($27 \pm 5\%$, $P < 0.05$ vs. control, Fig. 4). Glyceroneogenesis and total G3P synthesis were

increased and glycolysis was decreased in the liver tissue of fasted rats, thus the contribution of glyceroneogenesis for total glyceride-glycerol synthesis was $96 \pm 12\%$ ($P = 0.09$ vs. control, Fig. 4). Previous in vitro experiments have shown that a reduction in the G3P generation via glycolysis is accompanied by a significant activation of glyceroneogenesis in liver slices during fasting [11]. We have also previously demonstrated in vitro that G3P synthesis from glucose is increased and glyceroneogenesis is reduced in IBAT from cafeteria-diet-fed rats [9]. The cafeteria diet did not affect either the in-vivo synthesis of G3P from glucose (via glycolysis) or glyceroneogenesis in the liver tissue and EAT (Fig. 4). This finding confirms our hypothesis that there is an in-vivo reciprocal regulation of G3P synthesis between these pathways. This reciprocal change in G3P generation by glyceroneogenesis and glycolysis is important to maintain an adequate supply of the G3P needed for TAG formation and to ensure normal tissue function. In contrast, fasting did not affect either the glyceroneogenesis or the total glyceride-glycerol synthesis in these tissues, although there was a reduction in G3P synthesis from glucose. Previous in vitro studies have shown that fasting induces a reduction in the PEPCK activity and a decrease in the rate of incorporation of [$1-^{14}\text{C}$] pyruvate into glyceride-glycerol in IBAT and EAT [10, 27, 28]. Recent in-vivo experiments also demonstrated that glyceroneogenesis does not change in EAT in response to 48 h of fasting [8]. The low insulin levels and high FFA levels in fasted rats are expected to increase transcription of the PEPCK gene [29–31], and this increase could stimulate BAT and EAT glyceroneogenesis. However, our findings suggest that there is not a good correlation between gene expression or maximal enzymatic activity and actual flux through the metabolic pathway. Recently, it was demonstrated in vivo that the reduction in plasma insulin levels did not induce changes in EAT glyceroneogenesis in rats fed a low-protein, high-carbohydrate diet [6]. There are several possible explanations for the different responses observed in vivo and in vitro. Notably, in-vivo experiments are capable of evaluating metabolic pathways in conditions that cannot be reproduced in vitro, mainly because a blood supply and sympathetic activity are connected to each tissue.

The effect of the cafeteria diet or fasting on total FA synthesis correlates with the insulin levels in the animals; cafeteria-diet-fed rats showed increases in liver, BAT and EAT, while fasting rats showed decreases in all three tissues (Fig. 3). Using the data for the synthesis of de novo FA and glyceride-glycerol, we can estimate the amount of glycerol used to esterify preformed FA. The fraction of glycerol used for esterification of preformed FA can be obtained by disregarding the glycerol used to esterify de novo synthesized FA, which corresponds to one-third of the glyceride-FA synthesized from $^3\text{H}_2\text{O}$. We assume that

3 mol FA is esterified by 1 mol glycerol because approximately 90 % of the lipids found in adipose tissue are TAG; however, this percentage is lower in the liver. When compared with control diet-fed rats, this estimate shows an increase in the amount of glycerol used to esterify preformed FA in the liver tissue (~ 120 %) of fasted rats ($205 \pm 24 \text{ nmol g}^{-1} \text{ min}^{-1}$ vs. 92 ± 5 in control, $P < 0.05$) and in the IBAT (~ 60 %) of cafeteria-diet-fed rats ($309 \pm 49 \text{ nmol g}^{-1} \text{ min}^{-1}$ vs. 189 ± 22 in control, $P < 0.05$). The cafeteria diet also resulted in an increase in the esterification rate of de novo FA synthesized in the liver tissue, EAT and IBAT, while fasting induced a decrease in the three tissues (Fig. 3). The rate of glycerol used to esterify preformed FA was elevated in liver (~ 90 %), BAT (~ 90 %) and EAT (~ 95 %), even in control rats. Previous studies also showed an elevated rate of glycerol used to esterify preformed FA in liver, BAT and EAT from rats fed a balanced, purified diet (94, 89 and 64 %, respectively) or from rats fed a high-protein, carbohydrate-free diet (96, 96 and 94 %, respectively) [14, 17]. Direct in vivo measurements of the rates of TAG synthesis and degradation in adipose tissue showed that, despite very active TAG synthesis, lipid degradation occurs at a substantial rate. TAG degradation is approximately 50 % of the lipid synthesis rate in EAT from mice fed a low-fat, high-carbohydrate or high-fat, low-carbohydrate diet [32]. It has been hypothesized that the adipose tissue could play a crucial role in buffering the flux of FA in the circulation in the postprandial period, analogous to the roles of the liver and skeletal muscle in buffering postprandial glucose fluxes. Adipose tissue provides its buffering action by suppressing the release of FFA into the circulation and by increasing TAG clearance [33]. Our results support this hypothesis, indicating that the use of preformed FA, which are recycled after the hydrolysis of endogenous TAG and taken up from the circulating lipoproteins, for glyceride synthesis is markedly high in the liver and adipose tissues.

We agree that the increase in total glycerol synthesis in the liver tissue of fasted rats, which is accompanied by a reduction in the de novo synthesis of FA, is necessary to guarantee the esterification of preformed FA. Fasting induces an increase in the mobilization of WAT FA to meet the energy demands of peripheral tissues. However, a fraction of the FFA is removed from the bloodstream by the liver and converted to TAG, which are either stored in hepatocytes or released from the liver into the circulation as VLDL (Fig. 1). Our results are the first to suggest that this systemic recycling of FA exists in vivo between the WAT and the liver. In contrast, the increase in the total glycerol synthesis in the BAT of cafeteria-diet-fed rats is sufficient to ensure the esterification of preformed FA and de novo synthesized FA, which have increased levels. The cafeteria diet induces BAT thermogenesis [9], stimulating the hydrolysis of endogenous

TAG and subsequently producing FA, which are both substrates and uncoupling messengers for BAT mitochondria. Therefore, the maintenance of adequate TAG stores by the esterification of FA seems to be essential for normal BAT function. Our results indicate that the esterification of de novo synthesized FA is not sufficient to guarantee adequate stores of TAG (and thermogenesis) in the BAT from cafeteria-diet-fed rats and that the reesterification of preformed FA is necessary. The major fraction of preformed FA that are esterified is probably recycled after hydrolysis of endogenous TAG because lipoprotein lipase activity is reduced in the BAT of rats that are fed the cafeteria diet [9].

In summary, the data of our present study, assayed in vivo, suggest that the reciprocal changes in the generation of glycerol-3-phosphate from glucose (via glycolysis) and from glyceroneogenesis occur only when the synthesis of total glyceride-glycerol is increased in the tissue. This increased synthesis seems to be essential for the systemic recycling of FA by the liver from fasted rats and for the maintenance of the thermogenic capacity of the BAT from cafeteria-diet-fed rats.

Acknowledgments We thank V.D. Galban, N.M. Zanon and E.A. Filippin for their technical assistance. We also thank Renato Hélio Migliorini in memoriam for being an exemplary scientist and professor. This work was supported by grants from Fundação de Amparo à Pesquisa do Estado de São Paulo (FAPESP) and Conselho Nacional de Pesquisa (CNPq).

References

1. Ferré P, Foufelle F (2010) Hepatic steatosis: a role for de novo lipogenesis and the transcription factor SREBP-1c. *Diabetes Obes Metab* 12:83–92
2. Vázquez-Vela ME, Torres N, Tovar AR (2008) White adipose tissue as endocrine organ and its role in obesity. *Arch Med Res* 39:715–728
3. Nedergaard J, Bengtsson T, Cannon B (2011) Three years with adult human brown adipose tissue. *Ann N Y Acad Sci* 1212:E20–E36
4. Reshef L, Olswang Y, Cassuto H, Blum B, Croniger CM, Kalhan SC, Tilghman SM, Hanson RW (2003) Glyceroneogenesis and the triglyceride/fatty acid cycle. *J Biol Chem* 278:30413–30416
5. Hanson RW, Reshef L (2003) Glyceroneogenesis revisited. *Biochimie* 85:1199–1205
6. Buzelle SM, Santos MP, Baviera AM, Lopes CF, Garófalo MAR, Navegantes LCC, Kettelhut IC, Chaves VE, Kawashita NH (2010) A low-protein, high-carbohydrate diet increases the adipose lipid content without increasing the glycerol-3-phosphate or fatty acid content in growing rats. *Can J Physiol Pharmacol* 88:1157–1165
7. Bederman IR, Foy S, Chandramouli V, Alexander JC, Previs SF (2009) Triglyceride synthesis in epididymal adipose tissue: contribution of glucose and non-glucose carbon sources. *J Biol Chem* 284:6101–6108
8. Nye CK, Hanson RW, Kalhan SC (2008) Glyceroneogenesis is the dominant pathway for triglyceride glycerol synthesis in vivo in the rat. *J Biol Chem* 283:27565–27574

9. Chaves VE, Frasson D, Martins-Santos ME, Navegantes LC, Galban VD, Garófalo MAR, Kettelhut IC, Migliorini RH (2008) Fatty acid synthesis and generation of glycerol-3-phosphate in brown adipose tissue from rats fed a cafeteria diet. *Can J Physiol Pharmacol* 86:416–423
10. Festuccia WTL, Kawashita NH, Garófalo MAR, Moura MAF, Brito SRC, Kettelhut IC, Migliorini RH (2003) Control of glyceroneogenic activity in rat brown adipose tissue. *Am J Physiol Regul Integr Comp Physiol* 285:R177–R182
11. Martins-Santos ME, Chaves VE, Frasson D, Boschini RP, Garófalo MA, Kettelhut IC, Migliorini RH (2007) Glyceroneogenesis and the supply of glycerol-3-phosphate for glyceride-glycerol synthesis in liver slices of fasted and diabetic rats. *Am J Physiol Endocrinol Metab* 293:E1352–E1357
12. Kawashita NH, Moura MAF, Brito MN, Brito SMRC, Garófalo MAR, Kettelhut IC, Migliorini RH (2002) Relative importance of sympathetic outflow and insulin in the reactivation of brown adipose tissue lipogenesis in rats adapted to a high-protein diet. *Metabolism* 51:343–349
13. Botion LM, Kettelhut IC, Migliorini RH (1995) Increased adipose tissue glyceroneogenesis in rats adapted to a high protein, carbohydrate-free diet. *Horm Metab Res* 27:310–313
14. Botion LM, Brito MN, Brito NA, Brito SR, Kettelhut IC, Migliorini RH (1998) Glucose contribution to in vivo synthesis of glyceride-glycerol and fatty acids in rats adapted to a high-protein, carbohydrate-free diet. *Metabolism* 47:1217–1221
15. Brito SC, Festuccia WL, Kawashita NH, Moura MF, Xavier AR, Garófalo MA, Kettelhut IC, Migliorini RH (2006) Increased glyceroneogenesis in adipose tissue from rats adapted to a high-protein, carbohydrate-free diet: role of dietary fatty acids. *Metabolism* 55:84–89
16. Brito SRC, Moura MAF, Kawashita NH, Brito MN, Kettelhut IC, Migliorini RH (2001) Glucose uptake and glycolytic flux in adipose tissue from rats adapted to a high-protein, carbohydrate-free diet. *Metabolism* 50:1208–1212
17. Brito MN, Brito NA, Brito SR, Moura MA, Kawashita NH, Kettelhut IC, Migliorini RH (1999) Brown adipose tissue triacylglycerol synthesis in rats adapted to a high-protein, carbohydrate-free diet. *Am J Physiol* 276:R1003–R1009
18. Chaves VE, Frasson D, Martins-Santos ME, Boschini RP, Garófalo MAR, Festuccia WTL, Kettelhut IC, Migliorini RH (2006) Glyceroneogenesis is reduced and glucose uptake is increased in adipose tissue from cafeteria diet-fed rats independently of tissue sympathetic innervations. *J Nutr* 136:2475–2480
19. Folch J, Lees M, Stanley GA (1957) A simple method for the isolation and purification of total lipids from animal tissues. *J Biol Chem* 226:497–509
20. Hendler RW (1964) Procedure for simultaneous assay of two β -emitting isotopes with the liquid scintillation counting technique. *Anal Biochem* 7:110–120
21. Baker N, Huebotter RJ (1972) Compartmental and semicompartamental approaches for measuring glucose carbon flux to fatty acids and other products in vivo. *J Lipid Res* 13:716–724
22. Shipley RA, Chudzik EB, Gibbons AP, Jongedyk K, Brummond DO (1967) Rate of glucose transformation in the rat by whole-body analysis after glucose- ^{14}C . *Am J Physiol* 213:1149–1158
23. Windmueller HG, Spaeth AE (1966) Perfusion in situ with tritium oxide to measure hepatic lipogenesis and lipid secretion. *J Biol Chem* 241:2891–2899
24. Jungas RL (1968) Fatty acid synthesis in adipose tissue incubated in tritiated water. *Biochemistry* 7:3708–3717
25. Moura MA, Festuccia WT, Kawashita NH, Garófalo MA, Brito SR, Kettelhut IC, Migliorini RH (2005) Brown adipose tissue glyceroneogenesis is activated in rats exposed to cold. *Pflugers Arch* 449:463–469
26. Dole VP, Meinertz H (1960) Microdetermination of long-chain fatty acids in plasma and tissues. *J Biol Chem* 235:2595–2599
27. Gorin E, Tal-Or Z, Shafrir E (1969) Glyceroneogenesis in adipose tissue of fasted, diabetic and triamcinolone treated rats. *Eur J Biochem* 8:370–375
28. Reshef L, Hanson RW, Ballard FJ (1969) Glyceride-glycerol synthesis from pyruvate. Adaptive changes in phosphoenolpyruvate carboxykinase and pyruvate carboxylase in adipose tissue and liver. *J Biol Chem* 244:1994–2001
29. Chakravarty K, Cassuto H, Reshef L, Hanson RW (2005) Factors that control the tissue-specific transcription of the gene for phosphoenolpyruvate carboxykinase-C. *Crit Rev Biochem Mol Biol* 40:129–154
30. Antras-Ferry J, Le Bigot G, Robin P, Robin D, Forest C (1994) Stimulation of phosphoenolpyruvate carboxykinase gene expression by fatty acids. *Biochem Biophys Res Commun* 203:385–391
31. Duplus E, Glorian M, Tordjman J, Berge R, Forest C (2002) Evidence for selective induction of phosphoenolpyruvate carboxykinase gene expression by unsaturated and nonmetabolized fatty acids in adipocytes. *J Cell Biochem* 85:651–661
32. Brunengraber DZ, McCabe BJ, Kasumov T, Alexander JC, Chandramouli V, Previs SF (2003) Influence of diet on the modeling of adipose tissue triglycerides during growth. *Am J Physiol Endocrinol Metab* 285:E917–E925
33. Frayn KN (2002) Adipose tissue as a buffer for daily lipid flux. *Diabetologia* 45:1201–1210

Metabolism of Anandamide into Eoxamides by 15-Lipoxygenase-1 and Glutathione Transferases

Pontus K. A. Forsell · Åsa Brunnström ·
Malin Johannesson · Hans-Erik Claesson

Received: 21 November 2011 / Accepted: 14 May 2012 / Published online: 9 June 2012
© AOCs 2012

Abstract Human 15-lipoxygenase-1 (15-LO-1) can metabolize arachidonic acid (ARA) into pro-inflammatory mediators such as the eoxins, 15-hydroperoxyeicosatetraenoic acid (HPETE), and 15-hydroxyeicosatetraenoyl-phosphatidylethanolamine. We have in this study investigated the formation of various lipid hydroperoxide by either purified 15-LO-1 or in the Hodgkin lymphoma cell line L1236, which contain abundant amount of 15-LO-1. Both purified 15-LO-1 and L1236 cells produced lipid hydroperoxides more efficiently when anandamide (AEA) or 2-arachidonoyl-glycerol ester was used as substrate than with ARA. Furthermore, L1236 cells converted AEA to a novel class of cysteinyl-containing metabolites. Based on RP-HPLC, mass spectrometry and comparison to synthetic products, these metabolites were identified as the ethanolamide of the eoxin (EX) C₄ and EXD₄. By using the epoxide EXA₄-ethanol amide, it was also found that platelets have the capacity to produce the ethanolamide of EXC₄ and EXD₄. We suggest that the ethanolamides of the eoxins should be referred to as eoxamides, in analogy to the ethanolamides of prostaglandins which are named prostamides. The metabolism of AEA into eoxamides might engender molecules with novel biological

effects. Alternatively, it might represent a new mechanism for the termination of AEA signalling.

Keywords 15-Lipoxygenase-1 · Anandamide · Endocannabinoid · Inflammation · Pain · Arachidonic acid · Glutathione

Abbreviations

LO	Lipoxygenase
ARA	Arachidonic acid
AEA	Anandamide
EX	Eoxin
LT	Leukotriene
2-AG	2-Arachidonoyl-glycerol ester
PPAR	Peroxisome proliferator-activated receptor
GSH	Glutathione
GST	Glutathione-S-transferase

Introduction

Lipoxygenases (LOs) are a family of enzymes catalyzing the positional as well as stereo-specific introduction of molecular oxygen into *cis*-1,4-pentadiene structures found in unsaturated fatty acids or derivatives thereof [1–3] leading to the formation of a hydroperoxide. Oxidation of arachidonic acid (ARA) by 5-lipoxygenase (5-LO) (EC 1.13.11.34), the key enzyme in leukotriene synthesis, leads to the formation of the unstable epoxide leukotriene (LT) A₄. This compound can be conjugated with glutathione to form LTC₄ by LTC₄ synthase (EC 4.4.1.20) [4] or hydrolyzed by LTA₄ hydrolase (EC 3.3.2.6) to form LTB₄. Leukotriene C₄, and its metabolites LTD₄ and LTE₄, are proinflammatory agents, potent bronchoconstrictors and

P. K. A. Forsell · Å. Brunnström · M. Johannesson ·
H.-E. Claesson
Orexo AB, Uppsala, Sweden

P. K. A. Forsell (✉) · Å. Brunnström
Department of Neuroscience, Innovative Medicine, CNSP,
AstraZeneca R&D, 151 85 Sodertalje, Sweden
e-mail: Pontus.Forsell@astrazeneca.com

Å. Brunnström · H.-E. Claesson
Department of Medicine, Solna and Karolinska Institutet,
Karolinska University Hospital, Stockholm, Sweden

inducers of plasma leakage [5] whereas LTB_4 is a potent chemoattractant [5]. In analogy to the formation LTC_4 , a pathway for the formation of eoxins, a class of structurally related pro-inflammatory lipid mediators, has been described [6, 7]. The oxidation of ARA, catalyzed by human 15-lipoxygenase-1 (15-LO-1) (EC 1.13.11.33), leads in two consecutive steps to the unstable epoxide eoxin (EX) A_4 which can be conjugated to glutathione to yield EXC_4 , a reaction very similar to the formation of LTC_4 [6, 8]. The conjugation of glutathione to lipid epoxides is performed by glutathione transferases, including LTC_4 -synthase (LTC_4S), microsomal glutathione S-transferase 2 (mGST-2) and soluble glutathione transferases [6, 9–11].

In contrast to 5-LO, less is known about the physiological or pathological role of 15-LO-1. Thus, the finding that eoxins are proinflammatory might shed some light onto the role of 15-LO-1 in inflammatory processes. Furthermore, 15-HPETE and 15-HETE-phosphatidylamine have also been found to possess pro-inflammatory effects [12, 13]. On the other hand, 15-LO-1 metabolites have also been demonstrated to possess anti-inflammatory roles [14]. The expression of human 15-LO is selective and cells such as human eosinophils, airway epithelial cells, reticulocytes, mast cells and dendritic cells has been demonstrated to express 15-LO-1 [7, 15, 16]. The enzyme 15-LO-1, or its rodent ortholog 12/15-LO, has been implicated in pro- as well as anti-inflammatory processes [3, 17]. Two reports describe that ovalbumin sensitized 12/15-LO null mice have reduced airway inflammation, reduced cytokine production and less proliferation of airway epithelial cells after exposure of allergen [18, 19]. Other pathological processes where 15-LO-1 has been suggested to play a role includes cytokine release from airway epithelial cells [20], cardiac inflammation [21], propagation of cancer metastasis [22], atherosclerosis [23–25], Alzheimer's disease [26], insulin resistance and diabetic nephropathy [27, 28]. Furthermore, pharmacological evidence suggests that 15-LO-1 is involved in neuronal cell death induced by oxidative stress [29]. Unlike 5-LO, 15-LO-1 and 12/15-LO has a broad substrate specificity [15] and the enzyme can metabolize membrane bound phospholipids [27] and other conjugated lipids like endocannabinoids and vanilloids to their corresponding mono-hydroxy metabolites [30–35].

Endocannabinoids are a family of endogenous lipid-derived mediators of which arachidonyl ethanolamide (AEA) (anandamide) and 2-arachidonoylglycerol (2-AG) are amongst the most characterized substances. Both AEA and 2-AG are agonists of the G-protein coupled cannabinoid receptors (CB) 1 and 2 [36, 37]. AEA and other endocannabinoids also bind to the vanilloid receptor channel TRPV-1 (VR-1), an ion channel that mediates the pungent effect of the red hot chilli pepper component capsaicin [37, 38].

Oxygenation of endocannabinoids or vanilloids by lipoxygenases has been described in several reports and the monohydroxy derivatives of AEA seem to signal through CB1/2, TRPV-1 and PPAR- α [30–35]. The lipid class *N*-acyltaurines (NAT) was recently discovered and arachidonoyltaurine has also been shown to function as a substrate for lipoxygenases but not for cyclooxygenases [39]. On the other hand, cyclooxygenase-2 (COX-2) (EC 1.14.99.1) has been reported to metabolize AEA and 2-AG to their corresponding prostaglandin-ethanolamide and glycerol esters with high efficiency [40–42]. The pharmacology of these COX-2 metabolites is rapidly being defined and they are now collectively called prostamides [43]. The oxygenation of endocannabinoids by either cyclooxygenases or lipoxygenases is an expanding research area and there is a great likelihood that the oxygenation pathways for endocannabinoids will intersect with eicosanoid pathways [44, 45].

We report herein the in-vitro identification of a novel class of cysteinyl-containing eoxin-like metabolites derived from AEA, i.e. eoxin-ethanolamides, which in analogy to the prostamides are named eoxamides. This pathway of AEA metabolism may lead to a new class of biological active endocannabinoid metabolites or alternatively, a new pathway for terminating AEA signalling.

Materials and Methods

Materials

ARA, AEA and LNA were purchased from NuCheck. HPLC solvents were from Rathburn Chemicals (Walkerburn UK). Synthetic 13-hydroxyoctadeca-9Z,11E-dienoic acid (13-HODE) and 15-hydroxyeicosa-5Z,8Z,11Z,13E-tetraenoic acid (15-HETE) were from Biomol. Diphenyl-1-pyrenylphosphine (DPPP) was from Molecular Probes, Invitrogen. Tissue culture medium, antibiotics, fetal calf serum and Dulbeccos phosphate buffered saline (D-PBS) were from Gibco (Paisley, Scotland, UK). 14,15-epoxy-5,8,10,12 (*Z,Z,E,E*)-eicosatetraenoyl-EA (EXA_4 -EA) was provided by Mats Hamberg (Karolinska Institutet, Sweden). All other chemicals and reagents were from Sigma-Aldrich.

Chemical Synthesis of Eoxin Amides

14-Glutathionyl-15-hydroxy-5,8,10,12(*Z,Z,E,E*)-eicosatetraenoyl-EA (EXC_4 -EA) was synthesized from EXA_4 -EA by conjugation to glutathione under alkaline conditions. Briefly, EXA_4 -EA was dried under nitrogen and resuspended in 50 mM NaOH and 5 mM GSH to a final

concentration of 1 mM. The reaction was allowed to proceed for at least 3 h at room temperature. The purity and quantization of the produced EXC₄-EA was performed with RP-HPLC and mass spectrometry. 14(*R*)-cysteinylglycyl-15(*S*)-hydroxy-5,8,10,12 (*Z,Z,E,E*)-eicosatetraenoyl-EA (EXD₄-EA) was synthesized as described above with the exception that glutathione was exchanged for Cys-Gly (Sigma-Aldrich, Sweden).

15-LO-1 Fluorescent Enzyme Assay

The 15-LO-1 activity was measured in 96-well black plates (Optiplate, Corning) essentially as described [46]. Briefly, purified 15-LO-1 diluted in D-PBS at 3.18 µg/mL (2.8 µg/mL final concentration) or D-PBS alone was added to each well. Thereafter was 5 µL 2 mM LNA added to each well and the plate was incubated at room temperature for 10 min. The reaction was terminated with 1 volume of methanol containing 0.25 mM DPPP for fluorescent detection of lipid hydroperoxides or with one volume of methanol without DPPP for RP-HPLC-analysis of metabolites as described below. Fluorescence was measured 30 min after the addition of DPPP using a Spectramax Gemini fluorescence plate reader (Molecular Devices) with an excitation wavelength of 363 nm and an emission wavelength of 380 nm.

15-LO-1 Cell-based Assay

The human Hodgkin lymphoma cell line L1236 was grown in a humidified atmosphere at 5 % CO₂ in RPMI 1640 medium supplemented with 10 % heat-inactivated fetal calf serum and L-glutamine. The cells were washed twice in D-PBS before suspension in D-PBS at a final concentration of 10 × 10⁶ cells/mL. Substrate diluted in ethanol was added to yield a final concentration of 50 µM (or as indicated) and the samples were thereafter incubated for typically 2 min at 37 °C. The reaction was terminated by the addition of two volumes of methanol and the samples were stored at –20 °C for at least 60 min before RP-HPLC analysis.

Analysis of Lipoxygenase Products by RP-HPLC

Plates were centrifuged at 2,500 rpm for 5 min to remove precipitated proteins. The resulting supernatants was used for the analysis of monohydroxy acids, eoxins and cysteinyl-containing metabolites of AEA by injecting an aliquot of the supernatant onto a Onyx Monolithic C18 column (100 × 4.6 mm from Phenomenex) at a flow rate of 1.2 mL/min using a Waters Alliance 2795 system. Products were eluted by a 1-min isocratic period followed by a 20-min linear gradient from 20:27:53:0.8 to 35:35:30:0.8 (acetonitrile:methanol:H₂O:acetic acid (pH adjusted to 5.6 with NH₃) (by volume)). The retention times for all metabolites were compared

to authentic standards and qualitative measurements were performed using a 2996 photodiode-array (PDA) detector to verify the spectrum of peaks.

Analysis of products from cellular incubations with EXA₄-EA were performed by injecting an aliquot of the supernatant onto a C18 NovaPak (3.9 × 150 mm) column from Waters coupled to a Waters Alliance 2695 system equipped with a 2996 PDA UV-detector using a flow rate of 1.2 mL/min. Products were eluted by a 4-min isocratic period followed by a 10-min linear gradient from 25:15:60:0.8 to 45:45:10:0.8 [acetonitrile:methanol:H₂O:acetic acid (pH adjusted to 5.6 with NH₃) (by volume)]. In cases with large sample volumes, the supernatants were evaporated under reduced pressure and the residues dissolved in methanol and transferred to a test tube. Samples were thereafter evaporated to dryness under a stream of nitrogen, and finally resuspended in 300 µl of the appropriate mobile phase.

Nanospray Mass Spectrometry Analysis

After termination of incubations, samples were centrifuged (1400×g, 6 min) and the supernatants were diluted with water to contain maximum 25 % methanol and transferred to a washed and equilibrated extraction cartridge, Oasis HLB 1 cc 10 mg (Waters AB, Sweden). The columns were washed with water and eluted with 200 µl methanol to retrieve the metabolites. Reverse phase HPLC was performed on a Waters Alliance 2690 with a Nova Pak C₁₈ column (2.1 × 150 mm, Waters AB). The initial mobile phase was 100 % A (0.01 % acetic acid adjusted to pH 5.6 with ammonia) at a flow rate at 0.4 mL/min. A linear gradient was started after 5 min, reaching 36 % B (60:40 acetonitrile: methanol) at 20 min. The mobile phase was isocratic at 64:36, A:B for 100 min. Column effluent was monitored using diode array detection (PDA 996, Waters AB, Sweden). UV spectra were acquired between 200 and 340 nm. The material in the peaks I and II was collected with a fraction collector (FC II, Waters AB, Sweden) and further analyzed by mass spectrometry. The collected fractions were dried to some extent under N₂ and subsequently dissolved in methanol:water (1:1). Mass spectrometry was performed on a Quattro Micro or a Quattro Ultima triple quadrupole mass spectrometer (Micromass, Manchester, UK) operating in positive ion mode with a capillary voltage at 2.2 kV. MS/MS were obtained using collision energy of 20 eV using argon as the collision gas.

Statistical Analysis

Raw data were imported into Graph Pad PRISM 5.0 and all graphs and chromatograms were generated by the use of this software. Statistical analyses were performed by Students two-tailed unpaired paired *t* test.

Results

Comparison of Different Lipid-derivatives as Substrate for Human 15-LO-1

Human 15-LO-1 is known to use a variety of lipids as substrates, albeit with different efficient substrate utilization, i.e. different K_m and V_{max} [47]. We have previously described a fluorescent method for detecting 15-LO-1 derived lipid hydroperoxides [46]. We used this method to investigate different conjugated neutral derivatives of ARA and LNA, i.e. ethanolamides and glycerol esters, as substrates for 15-LO-1. Purified human enzyme was incubated with different substrates as outlined in Fig. 1. The fluorescence intensity obtained with ethanolamide of ARA and LNA was significantly higher than the fluorescence obtained with the free fatty acid. Incubation of the glycerol ester of ARA, but not that of LNA, led to significant higher fluorescence as compared to the free acid. The difference between ARA and AEA as substrate for 15-LO-1 was further investigated in a cellular assay by dose–response curves followed by analysis of the monohydroxy products using RP-HPLC. We have previously described that the Hodgkin lymphoma cell line L1236 express high levels of active endogenous 15-LO-1 and that the cells can produce eoxins [8]. Thus, L1236 cells were incubated with various concentrations of ARA or AEA and as depicted in Fig. 2, both substrates induced a robust formation of 15-HETE and 15-HETE-EA, respectively. The apparent K_m ($K_{m(app)}$) was calculated to 108 or 39 μM when using AEA or ARA, respectively. The difference observed in the formation of lipid-hydroperoxides as judged by fluorescence (Fig. 1) could not be observed in the cell-based assay. The cause

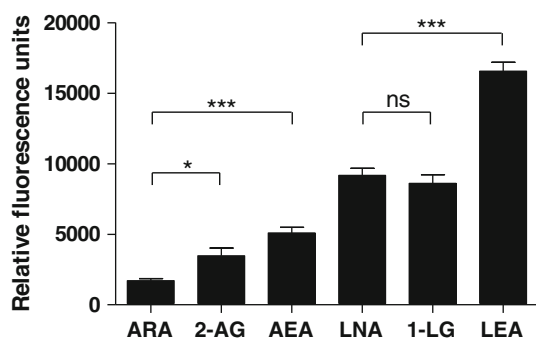


Fig. 1 Formation of lipid hydroperoxides by 15-LO-1. Purified human 15-LO-1 was incubated with 200 μM of the indicated substrate. The reaction was quenched with one volume of methanol containing 125 μM DPPP after 10 min and the lipid hydroperoxide was allowed to react with DPPP for 30 min before the fluorescence was determined. The results are the means \pm SEM from three independent experiments each performed in triplicates. ARA arachidonic acid, 2-AG 2-arachidonoylglycerol, AEA anandamide, LNA linoleic acid, 1-LG 1-linoleoyl-glycerol, LEA linoleoylethanolamide

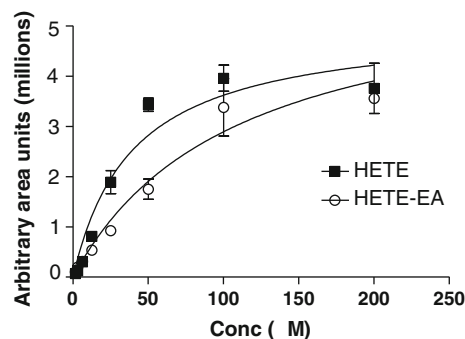


Fig. 2 Formation of monohydroxy metabolites in L1236 cells. L1236 cells (5×10^6 cells/mL) were incubated with the indicated concentrations of ARA or AEA. The amount of 15-HETE or 15-HETE-EA as well as 12-HETE or 12-HETE-EA was quantified by RP-HPLC. The formation of 15- and 12-HETE is presented as the sum of the two metabolites and the results are the means \pm SEM ($n = 3$) from two independent experiments. Open circles indicate the sum of 12- and 15-HETE-EA and solid squares indicate the sum of 12- and 15-HETE

for this might be that the lipid-hydroperoxides were not metabolized in the enzyme assay due to the fact that they were rapidly reduced to the monohydroxy metabolites in the presence of DPPP. The metabolism of the lipid-hydroperoxides in the cell-based assay is most likely very different as compared to the metabolism using purified enzyme. Epoxides could be formed by dehydration or hydroperoxide isomerize activity of 15-LO-1. Furthermore, the epoxides might be non-enzymatically hydrolysed to several dihydroxy products or conjugated to glutathione by a glutathione transferase, as described for the formation of eoxins in L1236 cells [7].

Analysis of Anandamide Metabolites in L1236 Cells

The characterization of ARA metabolites in L1236 cells has been described [8] but no report have so far characterized metabolism of AEA in L1236 cells. In order to characterize the metabolism of AEA in L1236 cells, we investigated the formation of dihydroxy-AEA such as 8(*S*),15(*S*)-, 8(*R*),15(*S*)- and 14(*R*),15(*S*)-dihydroxy-AEA as well as putative cysteinyl-containing AEA metabolites by RP-HPLC after incubation of cells with AEA. As shown in Fig. 3, incubations with AEA led to the formation of metabolites with a characteristic UV-absorbance maximum at 270 nm with two shoulders, thus indicating the presence of a conjugated triene in these samples (Fig. 3, peaks 4–6). These metabolites are thus likely to be dihydroxy-metabolites of AEA. Interesting was the fact that we observed two major and one minor metabolite with an UV-absorbance maximum at 280 nm and two shoulders after incubation of L1236 cells with AEA (Fig. 3, peaks 1–3). These characteristics of the UV-spectrum indicate a triene conjugated with glutathione. The retention time of these mediators were

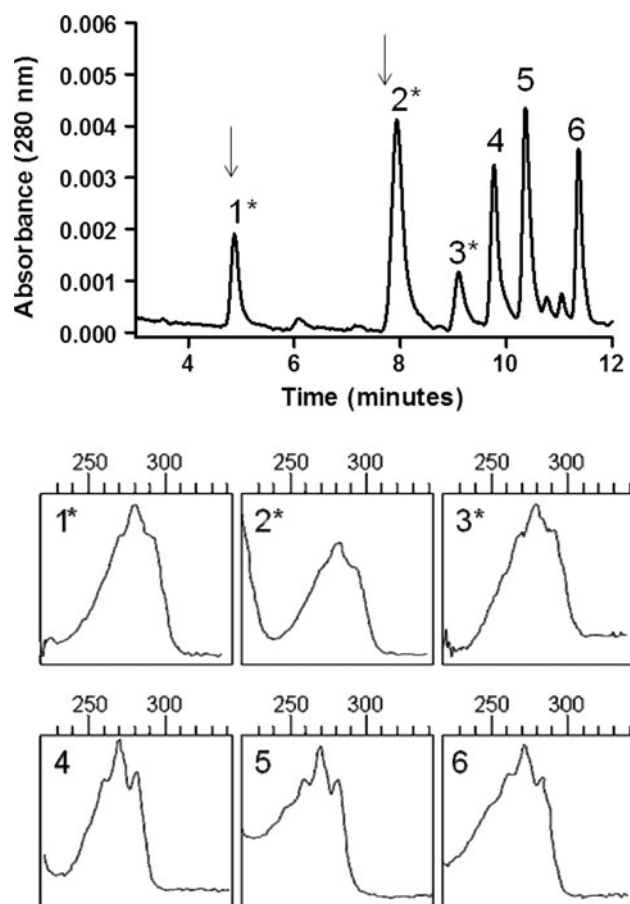


Fig. 3 Chromatographic profile of anandamide metabolites in L1236 cells. L1236 cells (1.0×10^7 cells/mL) were incubated with $50 \mu\text{M}$ of AEA. An aliquot of the supernatant ($200 \mu\text{L}$) was injected onto a Onyx monolithic C18 column and the formation of eluting cysteinyl-containing metabolites was analyzed by their absorbance at 280 nm. *Upper panel* shows the elution profile and absorbance at 280 nm. *Asterisks* at peaks 1, 2 and 3 denote products with UV-absorbance maximum at 280 nm. The elution of synthetic $\text{EXC}_4\text{-EA}$ and $\text{EXD}_4\text{-EA}$ were analyzed using the same chromatographic system and the elution times are indicated by *arrows*. *Lower panel* shows the UV-spectra for the indicated peaks

different from other cysteinyl-containing ARA-derivates such as the cysteinyl-containing leukotrienes or the eoxins (data not shown), indicating that these metabolites were unique metabolites of AEA. The most polar AEA metabolite formed with a UV-absorbance maximum at 280 nm (peak 1) was analyzed by mass spectrometry. In a positive ion mode MS scan it had the 669 m/z present, which correspond to AEA conjugated with glutathione. The material in peak 1 gave rise to a MS/MS daughter ion spectrum, containing 308 m/z which correspond to the glutathione part (Fig. 4a). The fragmentation occurred mainly in the peptide part. Thus, this gives no information about the position of glutathione in the fatty acid, although nothing in the MS/MS spectra contradicts the theory that the glutathione is positioned on the omega-7 carbon.

In order to verify the identity of the products in peak 1, we synthesized 14,15-epoxy-eicosatetraenoyl-EA and chemically conjugated glutathione. RP-HPLC and MS/MS analysis of this synthetic compound demonstrated identical retention time and UV-spectrum after RP-HPLC analysis (data not shown) as well as identical molecular mass and similar MS/MS fragmentation pattern (Fig. 4b) to the product in peak 1, thus demonstrating that the product in peak 1 is indistinguishable to synthetic 14-glutathionyl-15-hydroxy-5,8,10,12(*Z,Z,E,E*)-eicosatetraenoyl-EA ($\text{EXC}_4\text{-EA}$). The stereochemistry at carbon 14 and 15 has not yet been determined. The stereochemistry of the double bonds is based upon the UV-spectrum and has not yet been experimentally verified.

A second AEA-metabolite with a UV-spectrum similar to $\text{EXC}_4\text{-ethanol amide}$ and a retention time of 8 min was also observed after incubation of L1236 cells with AEA (Fig. 3, peak 2). The mechanism of formation and metabolism of leukotrienes and eoxins suggested that this metabolite could be the ethanol amide equivalent of EXD_4 . Thus, we synthesized $\text{EXD}_4\text{-EA}$ from 14,15-epoxy-eicosatetraenoyl-EA by conjugating the dipeptide Cys-Gly (by a similar addition as described for the conjugation of glutathione). The product of this reaction displayed a similar retention time and UV-spectrum as observed for the less polar compound eluting at 8 min (data not shown) thus suggesting that this metabolite is the $\text{EXD}_4\text{-ethanol amide}$ ($\text{EXD}_4\text{-EA}$) metabolite of AEA (Fig. 5).

Furthermore, a third metabolite with similar UV-spectrum as the other AEA-metabolites was also detectable in L1236 cells after incubation with AEA (Fig. 3, peak 3). The identity of this minor metabolite is unclear but our hypothesis is that this metabolite is $\text{EXE}_4\text{-EA}$. EXE_4 , another cysteinyl-containing eoxin, was identified after incubations of L1236 cells with EXA_4 [8]. The retention time and UV-spectrum of the third product suggests that the identity of this metabolite is $\text{EXE}_4\text{-EA}$.

Based upon the structural similarity to the eoxins, we suggest that these novel AEA-metabolites should be called eoxamides, in analogy to the nomenclature for prostaglandins and the corresponding prostaglandin-ethanol amides, i.e. the prostamides.

Comparison Between the Formation of Eoxins and Eoxamides in L1236 Cells

In order to compare the capacity of L1236 cells to produce cysteinyl-containing 15-LO-1 metabolites derived from ARA or AEA, we quantified the formation of eoxins and eoxamides by RP-HPLC analysis. Since incubation of 15-LO-1 with 2-arachidonoyl glycerol (2-AG) led to significantly higher fluorescence (Fig. 1) than ARA, presumably through the formation of 2-AG lipid hydroperoxides,

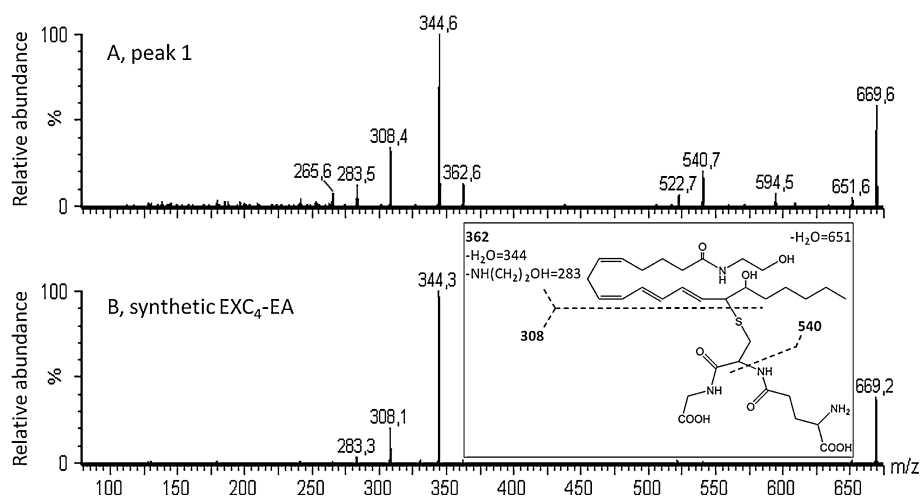


Fig. 4 Identification of anandamide metabolites by MS/MS. L1236 cells were incubated with AEA and the samples were thereafter purified by solid phase extraction and analyzed with RP-HPLC. Peak 1 were collected and further analyzed by mass spectrometry. Peak 1 and synthetic EXC₄-EA had corresponding retention times. The samples were introduced to a triple quadrupole mass spectrometer by nanospray infusion. The MS spectra contained a [M + H]⁺ at 669

and subsequently MS/MS daughter ion scan at *m/z* 669 was performed. The MS/MS spectra of the material in peak 1 are displayed in *panel a*. *Panel b* shows spectrum of components in the fraction collected from the HPLC analysis of synthetic EXC₄-EA. The insert in *panel b* also shows the structure and suggested fragments of synthetic EXC₄-EA. Spectra A were recorded on a Quattro Ultima (Waters) and spectrum B on a Quattro Micro (Waters)

we also included 2-AG in our studies of cysteinyl-containing 15-LO-1 metabolites. As summarized in Fig. 6, addition of 50 μM of substrate to cells led to a robust formation of cysteinyl-containing metabolites of both ARA and AEA. The cells had higher capacity to convert AEA to EXC₄/D₄-EA than to metabolize ARA to EXC₄/D₄. However, considerably lower amount of cysteinyl-containing 2-AG metabolites were detected.

Metabolism of EXA₄-Ethanol Amide by Human Platelets and L1236 cells

Platelets are well-known producers of eicosanoids and especially TXA₂ and 12-HETE through the actions of COX1/TXAS and 12-LO, respectively [48]. Platelets express LTC₄-synthase and can convert exogenous added LTA₄ to LTC₄ [49]. Thus, to further characterize the extent of eoxamide formation in other cells, we incubated human platelets with EXA₄-EA and analyzed the metabolites formed by RP-HPLC. As demonstrated in Fig. 7, platelets readily produced both EXC₄-EA and EXD₄-EA upon incubation with EXA₄-EA as indicated by the presence of two metabolites with an UV-absorbance maximum at 280 nm (Fig. 7, peak 1 and 4) that co-eluted with synthetic standards of EXC₄-EA and EXD₄-EA (indicated by arrows in Fig. 7). Furthermore, several metabolites with UV-absorbance maximum at 270 nm could be detected after incubation of platelets with EXA₄-EA. These metabolites (peaks 2, 3 and 5) are likely to be dihydroxy metabolites of AEA. Figure 8 shows the profile of cysteinyl-containing EXA₄-EA metabolites formed at different incubation

period in both platelets (Fig 8a) and in L1236 cells (Fig. 8b). The major product formed in platelets at all time points was EXD₄-EA (Figs. 7, 8a). The metabolism of EXC₄-EA and EXD₄-EA in L1236 appeared to be more extensive than in platelets since formation of a third less polar metabolite, presumably EXE₄-EA, was observed to a higher extent in L1236 cells than in platelets (Figs. 3, 7, 8b). This metabolite could only be observed in platelets at incubation times of 10 min or longer, and then only to a low extent. The total formation of cysteinyl-containing metabolites of EXA₄-EA was higher in incubations with L1236 cells than in incubations with platelets. However, the amount of protein is different in L1236 cells as compared to platelets and the values are not corrected for the amount of protein in each cell. Thus, the efficacy of the cells to form eoxamides cannot be judged from these data. Studies using purified glutathione transferases in order to identify enzymes capable of synthesizing eoxamides and to investigate enzyme kinetics are currently ongoing.

Discussion

Endocannabinoids have, since their discovery, been the subject of extensive research as well as pharmaceutical intervention [50]. The tonus of AEA is regulated by de novo synthesis as well as with hydrolyses by FAAH or monoacylglycerol lipases and it has been demonstrated that pharmaceutical blockade of AEA hydrolysis have analgesic effects [51–54]. By blocking the degradation of AEA, one would anticipate higher levels of AEA and thus also

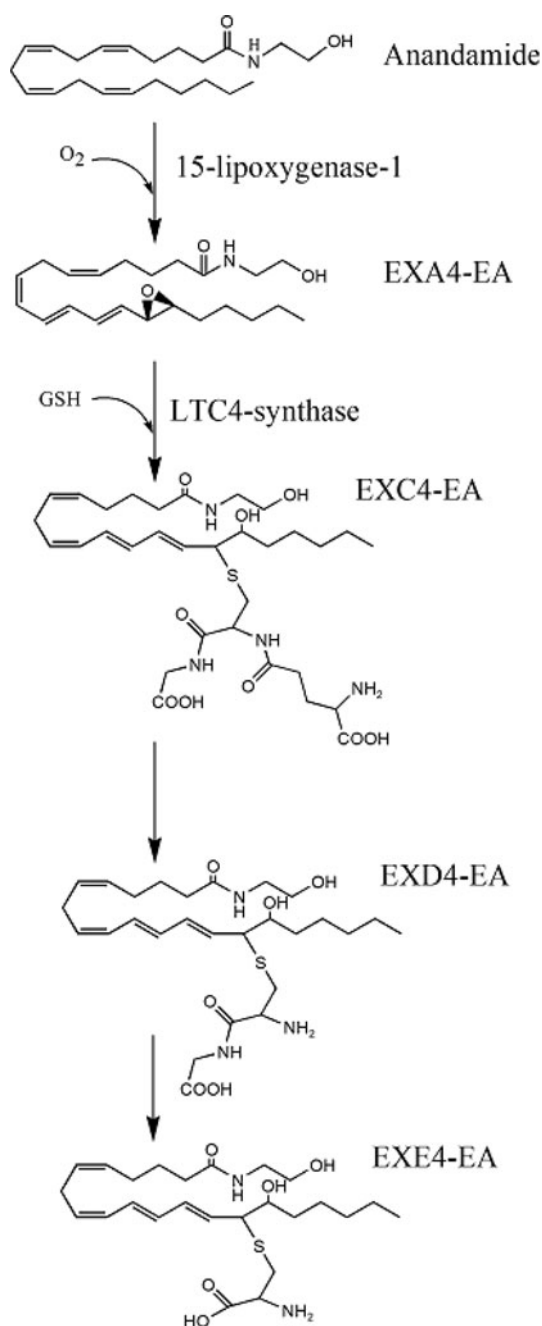


Fig. 5 Pathway for the formation of eoxamides

several applications for these pharmaceuticals in disorders where AEA signalling is involved in the pathophysiology of the disease. Neuropathic pain is one area where intervention of endocannabinoids might prove to be efficacious [55]. Our finding that 15-LO-1 can utilize neutral lipids such as AEA and 2-AG to the same extent, or even better than the corresponding free fatty acid (Figs. 1, 2), indicates that 15-LO-1 mediated oxygenation of endocannabinoids can be extensive as compared to metabolism of ARA in cells expressing 15-LO-1. Furthermore, we describe herein

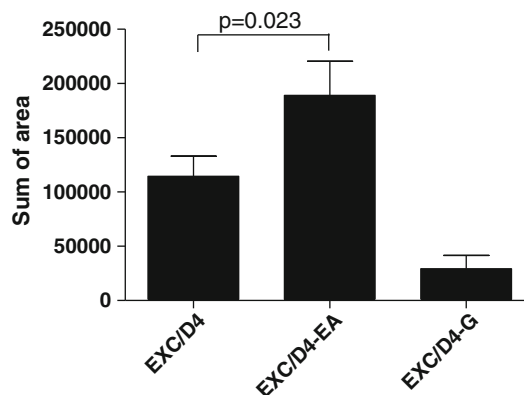


Fig. 6 Relative cellular formation of cysteinyl-containing metabolites formed from ARA, AEA or 2-AG in L1236 cells. L1236 cells (1.0×10^7 cells/mL) were incubated with 50 μ M of ARA, AEA or 2-AG. An aliquot of the supernatant (200 μ L) was analyzed RP-HPLC. The formation of cysteinyl-containing metabolites were analyzed by their absorbance at 280 nm and by comparison of retention times to synthetic standards. The results are presented as the sum of cysteinyl-containing metabolites \pm SEM ($n = 3$) from three individual experiment, each performed in duplicate

the formation of previously unknown cysteinyl-containing metabolites of AEA by the concerted action of 15-LO-1 and a glutathione transferase (Figs. 3, 4 and 5). The formation of cysteinyl-containing metabolites of AEA exceeded the formation of cysteinyl-containing metabolites from ARA (Fig. 6), supporting the fact that 15-LO-1 mediated metabolism of AEA can be extensive. Apart from the L1236 cells, platelets were also identified as a cellular source of eoxamides (Figs. 7, 8), but only if provided with the epoxide-precursor 14,15-LTA₄-EA. This is analogous to the formation of LTC₄ by platelets after addition of exogenous LTA₄ [56], so-called transcellular metabolism. Cells that express both 15-LO-1 and an appropriate glutathione transferase can indeed synthesize eoxamides from endogenous sources, as seen in L1236 cells. Platelets which lack 15-LO-1 are dependent on transcellular metabolism of EXA₄ for EXC₄ synthesis. If transcellular metabolism also occurs for eoxamides remains to be determined. The fact that there is metabolism of EXC₄-EA to EXD₄-EA and possibly also to EXE₄-EA (Figs. 3, 8) suggests that the pathway for metabolism of eoxamides are similar to the metabolism of cysteinyl-leukotrienes. The metabolism of eoxamides to a stable end-product such as EXE₄-EA could lead to a way to measure the formation of these novel metabolites in vivo.

Endocannabinoids have been described as having multiple effects within the CNS of which some are due to binding of endocannabinoids to cannabinoid-receptor expressing neurons whereas other effects are due to neuroinflammation [50]. The recent finding that monoacylglycerol lipase (MAGL) can hydrolyze 2-arachidonoylglycerol to generate

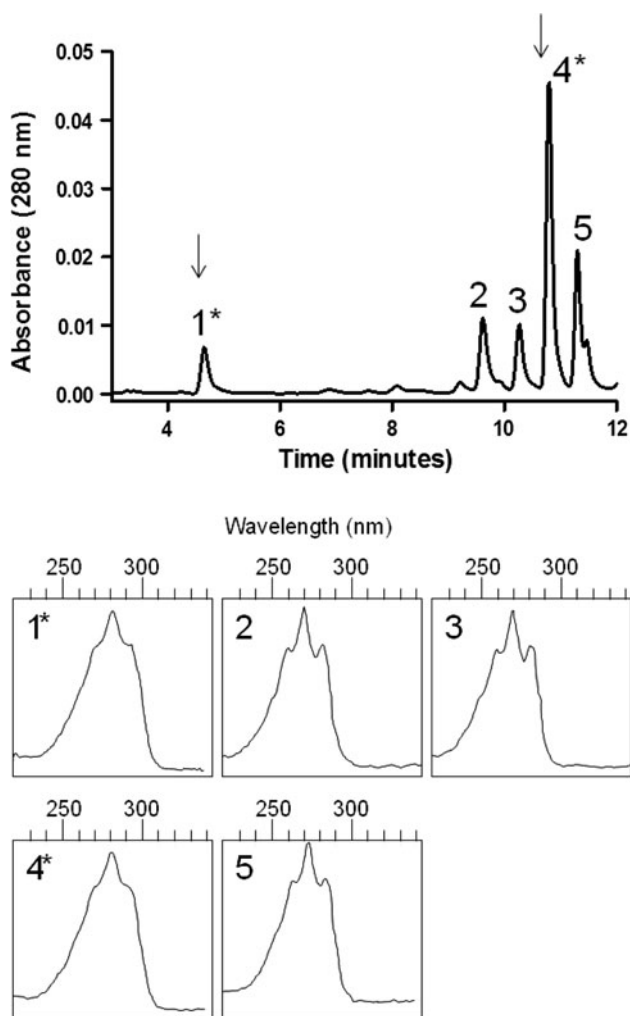


Fig. 7 Chromatographic profile of metabolites formed in platelets after addition of EXA₄-EA. Human washed platelets (approximately 4.0×10^8 cells/mL) were incubated with 50 μ M of EXA₄-EA for 5 min before termination with acidic methanol. After centrifugation, an aliquot of the supernatant (200 μ L) was injected onto a Nova Pak C18 RP-HPLC column. Metabolites were eluted using a different gradient as compared to Fig. 3 (described in “Materials and Methods”). Upper panel shows the elution profile and absorbance at 280 nm. The formation of metabolites was analyzed by comparing their retention times to synthetic standards as well as their absorbance at 280 or 270 nm. Asterisks at peak 1 and 4 denote products with UV-absorbance maximum at 280 nm. The elution times of synthetic EXC₄-EA and EXD₄-EA are indicated by arrows at 4.7 and 11 min, respectively. The lower panel shows the UV-spectra for the indicated peaks

ARA as a precursor for neuroinflammatory prostaglandins has also shed light on the role of endocannabinoids in neuroinflammation [45]. It is noteworthy that 15-LO-1 is expressed within the CNS [26] and that formation of leukotrienes in the CNS has been known for a long time [57, 58]. The recent finding that leukotriene receptor antagonists is effective in an animal model of multiple sclerosis [59]

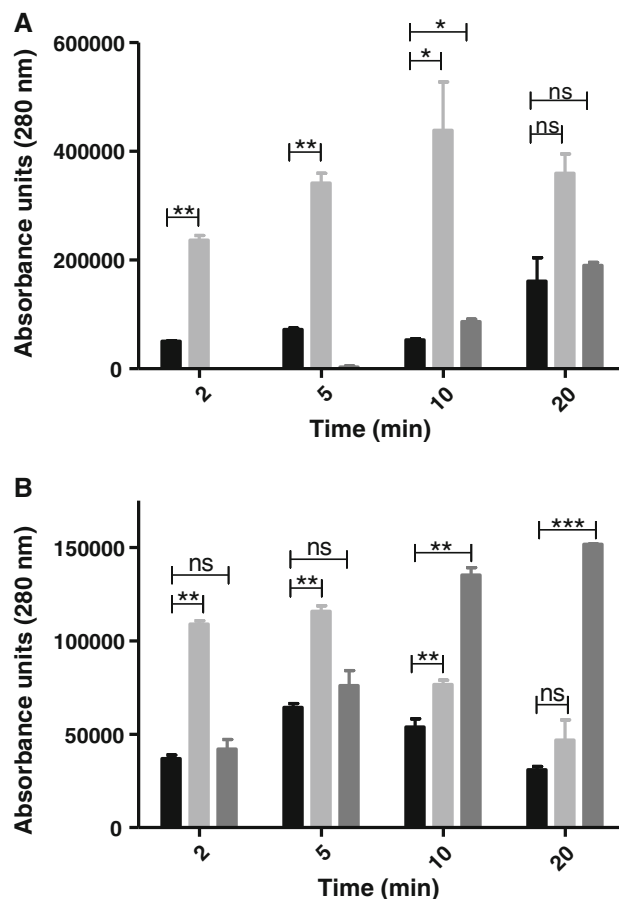


Fig. 8 Comparison between the cellular formation of eoxamides in platelets and L1236 cells after addition of EXA₄-EA. Human washed platelets (approximately 4.0×10^8 cells/mL) (a) or L1236 cells (1.0×10^7 cells/mL) (b) were incubated with 50 μ M of EXA₄-EA for the indicated times before termination with acidic methanol. The formation of cysteinyl-containing metabolites were analyzed by comparing their retention times to synthetic standards as well as their absorbance at 280 nm. The results are presented as the sum of cysteinyl-containing metabolites \pm SEM ($n = 3$) from one representative experiment out of two. Black bars EXC₄-EA, light dark grey bars EXD₄-EA and dark grey bars EXE₄-EA

further highlights the link between CNS, neuroinflammation and cysteinyl-containing leukotrienes.

The Hodgkin lymphoma cell line L1236 has high endogenous expression of 15-LO-1. The expression of 15-LO-1 has also been confirmed in several Reed-Sternberg positive cells by immunohistochemistry [8] and one hypothesis could be that 15-LO-1 plays a regulatory role in controlling immunological responses in the inflammatory process. Apart from their role within the CNS, cannabinoids are also known to be able to affect the immune system and CB1 and 2 are expressed in immune cells with B-lymphocytes being one of the cell types that most abundantly express CB1 and 2 [60, 61]. Polymorphonuclear neutrophils, T-cells and monocytes have also been shown to express CB1 and 2. Thus, the possibility for

immunomodulatory functions for enzymes/receptors involved in endocannabinoid signalling, or termination thereof, is evident. Several pharmacological active compounds that interfere with the endocannabinoid system display plethoric effects affecting both systemic as well as peripheral processes including body weight control, neuropathic pain, inflammation and cytokine release [50]. Our finding of the eoxamides identifies a new pathway for the formation of AEA metabolites. If these unique compounds display any biological role themselves remains to be investigated. However, it is interesting to note that several metabolites of AEA such as the lipoxygenase derived monohydroxy acids [62] or the cyclooxygenases derived prostamides bind to existing receptors or exerts their effect through yet unidentified receptors.

The catabolism of endocannabinoids by FAAH can have a profound effect on pain sensation in animals [53]. The formation of eoxamides is a new example of the catabolism of AEA and the concerted action of 15-LO-1 and glutathione S-transferases or LTC₄-synthase to yield EXC₄-EA might be a new mechanism to terminate AEA signalling. Given the fact that 15-LO-1 has an expression profile restricted to higher primates and rabbits [47], the described metabolism of AEA in this report could be unique to man and other species that express 15-LO-1. We suggest that the described peroxidation and subsequent glutathionylation of AEA should be considered as an alternative pathway to FAAH/MAGL-pathways for elimination and secretion of AEA and as a new pathway for the generation of novel and potentially biological active AEA-metabolites.

Acknowledgments Dr. Mats Hamberg (Karolinska Institutet, Sweden) is gratefully acknowledged for providing synthetic metabolites. This study was supported by grants from the Swedish Cancer Society, Karolinska Institutet and an unrestricted grant from Orexo.

References

- Radmark O (2002) Arachidonate 5-lipoxygenase. *Prostaglandins Other Lipid Mediat* 68–69:211–234
- Yoshimoto T, Takahashi Y (2002) Arachidonate 12-lipoxygenases. *Prostaglandins Other Lipid Mediat* 68–69:245–262
- Kuhn H, Walther M, Kuban R (2002) Mammalian arachidonate 15-lipoxygenases structure, function, and biological implications. *Prostaglandins Other Lipid Mediat* 68–69:263–290
- Lam B (2003) Leukotriene C₄ synthase. *Prostaglandins Leukot Essent Fatty Acids* 69(2–3):111–116
- Claesson H, Dahlen S (1999) Asthma and leukotrienes: antileukotrienes as novel anti-asthmatic drugs. *J Intern Med* 245(3):205–227
- Feltenmark S, Gautam N, Brunnstrom A, Griffiths W, Backman L, Edenius C, Lindbom L, Bjorkholm M, Claesson H-E (2008) Eoxins are proinflammatory arachidonic acid metabolites produced via the 15-lipoxygenase-1 pathway in human eosinophils and mast cells. *PNAS* 105(2):680–685. doi:10.1073/pnas.0710127105
- Claesson H-E (2009) On the biosynthesis and biological role of eoxins and 15-lipoxygenase-1 in airway inflammation and Hodgkin lymphoma. *Prostaglandins Other Lipid Mediat* 89(3–4):120–125
- Claesson H, Griffiths W, Brunnstrom A, Schain F, Andersson E, Feltenmark S, Johnson H, Porwit A, Sjoberg J, Bjorkholm M (2008) Hodgkin Reed-Sternberg cells express 15-lipoxygenase-1 and are putative producers of eoxins in vivo: novel insight into the inflammatory features of classical Hodgkin lymphoma. *FEBS J* 275(16):4222–4234
- Lam BK, Austen FK (2000) Leukotriene C₄ synthase. A pivotal enzyme in the biosynthesis of the cysteinyl leukotrienes. *Am J Respir Crit Care Med* 161(2):S16–S19
- Sjostrom M, Jakobsson PJ, Heimburger M, Palmblad J, Haeggstrom JZ (2001) Human umbilical vein endothelial cells generate leukotriene C₄ via microsomal glutathione S-transferase type 2 and express the CysLT(1) receptor. *Eur J Biochem* 268(9):2578–2586
- Brunnstrom A, Hamberg M, Griffiths W, Mannervik B, Claesson H (2011) Biosynthesis of 14,15-hexoxilins in human 11236 Hodgkin lymphoma cells and eosinophils. *Lipids* 46(1):69–79
- Conrad M, Sandin A, Forster H, Seiler A, Friehoff J, Dagnell M, Bornkamm GW, Radmark O, van Huijsduijnen RH, Aspenstrom P, Bohmer F, Ostman A (2010) 12/15-lipoxygenase-derived lipid peroxides control receptor tyrosine kinase signaling through oxidation of protein tyrosine phosphatases. *PNAS* 107(36):15774–15779. doi:10.1073/pnas.1007909107
- Zhao J, O'Donnell VB, Balzar S, St. Croix CM, Trudeau JB, Wenzel SE (2011) 15-Lipoxygenase 1 interacts with phosphatidylethanolamine-binding protein to regulate MAPK signaling in human airway epithelial cells. *PNAS*, 108(34): 14246–14251. doi:10.1073/pnas.1018075108
- Serhan CN, Brain SD, Buckley CD, Gilroy DW, Haslett C, O'Neill LAJ, Perretti M, Rossi AG, Wallace JL (2006) Resolution of inflammation: state of the art, definitions and terms. *FASEB J*: fj.06-7227com. doi:10.1096/fj.06-7227com
- Kuhn H, O'Donnell V (2006) Inflammation and immune regulation by 12/15-lipoxygenases. *Prog Lipid Res* 45(4):334–356
- Gulliksson M, Brunnstrom A, Johannesson M, Backman L, Nilsson G, Harvima I, Dahlen B, Kumlin M, Claesson H (2007) Expression of 15-lipoxygenase type-1 in human mast cells. *Biochim Biophys Acta* 1771(9):1156–1165
- Van Dyke TE, Serhan CN (2003) Resolution of Inflammation: a new paradigm for the pathogenesis of periodontal diseases. *J Dent Res* 82(2):82–90. doi:10.1177/154405910308200202
- Andersson C, Claesson H-E, Rydell-Tormanen K, Swedmark S, Hallgren A, Erjefalt JS (2008) Mice lacking 12/15-lipoxygenase have attenuated airway allergic inflammation and remodeling. *Am J Respir Cell Mol Biol* 39(6):648–656. doi:10.1165/rncmb.2007-0443OC
- Hajek A, Lindley A, Favoreto S, Carter R, Schleimer R, Kuperman D (2008) 12/15-Lipoxygenase deficiency protects mice from allergic airways inflammation and increases secretory IgA levels. *J Allergy Clin Immunol* 122(3):633–639.e3
- Liu C, Xu D, Liu L, Schain F, Brunnstrom A, Bjorkholm M, Claesson H-E, Sjoberg J (2009) 15-Lipoxygenase-1 induces expression and release of chemokines in cultured human lung epithelial cells. *Am J Physiol Lung Cell Mol Physiol* 297(1):L196–L203. doi:10.1152/ajplung.00036.2008
- Kayama Y, Minamino T, Toko H, Sakamoto M, Shimizu I, Takahashi H, Okada S, Tateno K, Moriya J, Yokoyama M, Nojima A, Yoshimura M, Egashira K, Aburatani H, Komuro I (2009) Cardiac 12/15 lipoxygenase-induced inflammation is involved in heart failure. *J Exp Med* 206(7):1565–1574. doi:10.1084/jem.20082596
- Kerjaschki D, Bago-Horvath Z, Rudas M, Sexl V, Schneckenthner C, Wolbank S, Bartel G, Krieger S, Kalt R, Hantusch B,

- Keller T, Nagy-Bojarszky K, Huttary N, Raab I, Lackner K, Krautgasser K, Schachner H, Kaserer K, Rezar S, Madlener S, Vonach C, Davidovits A, Nosaka H, Hammerle M, Viola K, Dolznig H, Schreiber M, Nader A, Mikulits W, Gnant M, Hirakawa S, Detmar M, Alitalo K, Nijman S, Offner F, Maier T, Steinhilber D, Krupitza G (2011) Lipoxygenase mediates invasion of intrametastatic lymphatic vessels and propagates lymph node metastasis of human mammary carcinoma xenografts in mouse. *J Clin Invest* 121(5):2000–2012
23. Cornicelli J (1998) 15-lipoxygenase inhibitors as anti-atherosclerosis agents. *IDrugs* 1(2):206–213
 24. Bocan T, Rosebury W, Mueller S, Kuchera S, Welch K, Daugherty A, Cornicelli J (1998) A specific 15-lipoxygenase inhibitor limits the progression and monocyte-macrophage enrichment of hypercholesterolemia-induced atherosclerosis in the rabbit. *Atherosclerosis* 136(2):203–216
 25. Zhao L, Pratico D, Rader D, Funk C (2005) 12/15-Lipoxygenase gene disruption and vitamin E administration diminish atherosclerosis and oxidative stress in apolipoprotein E deficient mice through a final common pathway. *Prostaglandins Other Lipid Mediat* 78(1–4):185–193
 26. Pratico D, Zhukareva V, Yao Y, Uryu K, Funk CD, Lawson JA, Trojanowski JQ, Lee VM-Y (2004) 12/15-Lipoxygenase is increased in Alzheimer's disease: possible involvement in brain oxidative stress. *Am J Pathol* 164(5):1655–1662
 27. Vahsen S, Rakowski K, Ledwig D, Dietze-Schroeder D, Swifka J, Sasson S, Eckel J (2006) Altered GLUT4 translocation in skeletal muscle of 12/15-lipoxygenase knockout mice. *Horm Metab Res* 38(6):391–396
 28. Xu Z, Li S, Lanting L, Kim Y, Shanmugam N, Reddy M, Narayan R (2006) Relationship between 12/15-lipoxygenase and COX-2 in mesangial cells: potential role in diabetic nephropathy. *Kidney Int* 69(3):512–519
 29. van Leyen K, Arai K, Jin G, Kenyon V, Gerstner B, Rosenberg P, Holman T, Lo E (2008) Novel lipoxygenase inhibitors as neuroprotective reagents. *J Neurosci Res* 86(4):904–909
 30. Ueda N, Yamamoto K, Yamamoto S, Tokunaga T, Shirakawa E, Shinkai H, Ogawa M, Sato T, Kudo I, Inoue K (1995) Lipoxygenase-catalyzed oxygenation of arachidonyl ethanolamide, a cannabinoid receptor agonist. *Biochim Biophys Acta* 1254(2):127–134
 31. Kozak KR, Gupta RA, Moody JS, Ji C, Boeglin WE, DuBois RN, Brash AR, Marnett LJ (2002) 15-lipoxygenase metabolism of 2-arachidonylglycerol. Generation of a peroxisome proliferator-activated receptor alpha agonist. *J Biol Chem* 277(26):23278–23286
 32. Moody J, Kozak K, Ji C, Marnett L (2001) Selective oxygenation of the endocannabinoid 2-arachidonylglycerol by leukocyte-type 12-lipoxygenase. *Biochemistry* 40(4):861–866
 33. Hampson A, Hill W, Zan-Phillips M, Makriyannis A, Leung E, Eglén R, Bornheim L (1995) Anandamide hydroxylation by brain lipoxygenase: metabolite structures and potencies at the cannabinoid receptor. *Biochim Biophys Acta* 1259(2):173–179
 34. Edgmond WS, Hillard CJ, Falck JR, Kearn CS, Campbell WB (1998) Human platelets and polymorphonuclear leukocytes synthesize oxygenated derivatives of arachidonyl ethanolamide (anandamide): their affinities for cannabinoid receptors and pathways of inactivation. *Mol Pharmacol* 54(1):180–188
 35. Prusakiewicz J, Turman M, Vila A, Ball H, Al-Mestarihi A, Di Marzo V, Marnett L (2007) Oxidative metabolism of lipoamino acids and vanilloids by lipoxygenases and cyclooxygenases. *Arch Biochem Biophys* 464(2):260–268
 36. Sugiura T, Waku K (2002) Cannabinoid receptors and their endogenous ligands. *J Biochem* 132(1):7–12
 37. Howlett AC, Barth F, Bonner TI, Cabral G, Casellas P, Devane WA, Felder CC, Herkenham M, Mackie K, Marti BR, Mechoulam R, Pertwee RG (2002) International union of pharmacology. XXVII. Classification of Cannabinoid Receptors. *Pharmacol Rev* 54(2):161–202. doi:10.1124/pr.54.2.161
 38. De Petrocellis L, Di Marzo V (2005) Lipids as regulators of the activity of transient receptor potential type VI (TRPV1) channels. *Life Sci* 77(14):1651–1666
 39. Turman M, Kingsley P, Rouzer C, Cravatt B, Marnett L (2008) Oxidative metabolism of a fatty acid amide hydrolase-regulated lipid, arachidonoyltaurine. *Biochemistry* 47(12):3917–3925
 40. Yu M, Ives D, Ramesha CS (1997) Synthesis of prostaglandin E2 ethanolamide from anandamide by cyclooxygenase-2. *J Biol Chem* 272(34):21181–21186. doi:10.1074/jbc.272.34.21181
 41. Kozak KR, Rowlinson SW, Marnett LJ (2000) Oxygenation of the endocannabinoid, 2-arachidonylglycerol, to glyceryl prostaglandins by cyclooxygenase-2. *J Biol Chem* 275(43):33744–33749. doi:10.1074/jbc.M007088200
 42. Kozak KR, Crews BC, Morrow JD, Wang LH, Ma YH, Weinander R, Jakobsson PJ, Marnett LJ (2002) Metabolism of the endocannabinoids, 2-arachidonylglycerol and anandamide, into prostaglandin, thromboxane, and prostacyclin glycerol esters and ethanolamides. *J Biol Chem* 277(47):44877–44885
 43. Woodward D, Liang Y, Krauss A (2008) Prostaglandins (prostaglandin-ethanolamides) and their pharmacology. *Br J Pharmacol* 153(3):410–419
 44. Rouzer C, Marnett L (2011) Endocannabinoid oxygenation by cyclooxygenases, lipoxygenases, and cytochromes P450: crosstalk between the eicosanoid and endocannabinoid signaling pathways. *Chem Rev* 111(10):5899–5921
 45. Nomura DK, Morrison BE, Blankman JL, Long JZ, Kinsey SG, Marcondes MCG, Ward AM, Lichtman AH, Conti B, Cravatt BF (2011) Endocannabinoid hydrolysis generates brain prostaglandins that promote neuroinflammation. *Science*. doi:10.1126/science.1209200
 46. Dahlstrom M, Forsstrom D, Johannesson M, Huque-Andersson Y, Bjork M, Silfverplatz E, Sanin A, Schaal W, Pelcman B, Forsell PKA (2010) Development of a fluorescent intensity assay amenable for high-throughput screening for determining 15-lipoxygenase activity. *J Biomol Screen* 15(6):671–679. doi:10.1177/1087057110373383
 47. Johannesson M, Backman L, Claesson H, Forsell P (2010) Cloning, purification and characterization of non-human primate 12/15-lipoxygenases. *Prostaglandins Leukot Essent Fatty Acids* 82(2–3):121–129
 48. Forsell P, Olsson A, Andersson E, Nallan L, Gelb M (2005) Polychlorinated biphenyls induce arachidonic acid release in human platelets in a tamoxifen sensitive manner via activation of group IVA cytosolic phospholipase A2-alpha. *Biochem Pharmacol* 71(1–2):144–155
 49. Edenius C, Stenke L, Tornhamre S, Heidvall K, Forsberg I, Nasman-Glaser B, Lindgren J (1991) Metabolism of granulocyte-derived leukotriene A4 in human platelets and respiratory tissue: transcellular formation of lipoxins and leukotrienes. *Adv Exp Med Biol* 314:281–288
 50. Di Marzo V (2008) Targeting the endocannabinoid system: to enhance or reduce? *Nat Rev Drug Discov* 7(5):438–455
 51. Chang L, Luo L, Palmer J, Sutton S, Wilson S, Barbier A, Breitenbucher J, Chaplan S, Webb M (2006) Inhibition of fatty acid amide hydrolase produces analgesia by multiple mechanisms. *Br J Pharmacol* 148(1):102–113
 52. Jhaveri MD, Richardson D, Kendall DA, Barrett DA, Chapman V (2006) Analgesic effects of fatty acid amide hydrolase inhibition in a rat model of neuropathic pain. *J Neurosci* 26(51):13318–13327. doi:10.1523/jneurosci.3326-06.2006
 53. Naidu PS, Kinsey SG, Guo TL, Cravatt BF, Lichtman AH (2010) Regulation of inflammatory pain by inhibition of fatty acid amide hydrolase. *J Pharmacol Exp Ther* 334(1):182–190. doi:10.1124/jpet.109.164806

54. Trang T (2007) Inhibition of fatty acid amide hydrolase: a potential treatment for neuropathic pain. *J Neurosci* 27(13):3364–3365. doi:[10.1523/jneurosci.0583-07.2007](https://doi.org/10.1523/jneurosci.0583-07.2007)
55. Dray A (2008) Neuropathic pain: emerging treatments. *Br J Anaesth* 101(1):48–58. doi:[10.1093/bja/aen107](https://doi.org/10.1093/bja/aen107)
56. Edenius C, Heidvall K, Lindgren J (1988) Novel transcellular interaction: conversion of granulocyte-derived leukotriene A4 to cysteinyl-containing leukotrienes by human platelets. *Eur J Biochem* 178(1):81–86
57. Lindgren J, Hulting A, Hokfelt T, Dahlen S, Eneroth P, Werner S, Patrono C, Samuelsson B (1985) Evidence for leukotriene formation and a neuroendocrine role for leukotriene C4 in rat brain. *Adv Prostaglandin Thromboxane Leukot Res* 15:561–564
58. Schalling M, Neil A, Terenius L, Lindgren J, Miamoto T, Hokfelt T, Samuelsson B (1986) Leukotriene C4 binding sites in the rat central nervous system. *Eur J Pharmacol* 122(2):251–257
59. Wang L, Du C, Lv J, Wei W, Cui Y, Xie X (2011) Antiasthmatic drugs targeting the cysteinyl leukotriene receptor 1 alleviate central nervous system inflammatory cell infiltration and pathogenesis of experimental autoimmune encephalomyelitis. *J Immunol* 187(5):2336–2345. doi:[10.4049/jimmunol.1100333](https://doi.org/10.4049/jimmunol.1100333)
60. Rayman N, Lam K, Van Leeuwen J, Mulder A, Budel L, Lowenberg B, Sonneveld P, Delwel R (2007) The expression of the peripheral cannabinoid receptor on cells of the immune system and non-Hodgkin's lymphomas. *Leuk Lymphoma* 48(7):1389–1399
61. Rayman N, Lam KH, Laman JD, Simons PJ, Lowenberg B, Sonneveld P, Delwel R (2004) Distinct expression profiles of the peripheral cannabinoid receptor in lymphoid tissues depending on receptor activation status. *J Immunol* 172(4):2111–2117
62. van der Stelt M, van Kuik J, Bari M, van Zadelhoff G, Leeftang B, Veldink G, Finazzi-Agro A, Vliegenthart J, Maccarrone M (2002) Oxygenated metabolites of anandamide and 2-arachidonoylglycerol: conformational analysis and interaction with cannabinoid receptors, membrane transporter, and fatty acid amide hydrolase. *J Med Chem* 45(17):3709–3720

Fatty Acid Composition of the Brain, Retina, Liver and Adipose Tissue of the Grey Mouse Lemur (*Microcebus murinus*, Primate)

Fabien Pifferi · Martine Perret · Philippe Guesnet ·
Fabienne Aujard · Jean-Marc Alessandri

Received: 27 January 2012 / Accepted: 17 May 2012 / Published online: 10 June 2012
© AOCs 2012

Abstract The particular interest in supplementing human foods with n-3 fatty acids has arisen from the findings that this series of polyunsaturated fatty acids (PUFA) have an impact on neuronal functions. Indeed vertebrates, including humans, preferentially use docosahexaenoic acid (DHA, 22:6n-3) over other long-chain n-3 PUFA for the genesis of their neuronal and retinal membranes. The grey mouse lemur is a nocturnal prosimian primate originating from Madagascar. The increased use of this omnivorous primate in nutritional studies (chronic caloric restriction, n-3 fatty acids supplementation), justifies the interest of determining their fatty acids body composition. In the present study, we report the fatty acid composition in lipid classes from the main target tissues (brain, retina, liver and adipose tissue) of six adult mouse lemurs raised under laboratory nutritional conditions. Among the main findings, n-6-docosapentaenoic acid (n-6-DPA; 22:5n-6) is very low in the brain cortex and retina, whereas there is a very high accumulation of docosahexaenoic acid (DHA, 22:6n-3) in the neural tissues compared to liver and plasma. In particular, DHA accounts for about one half of the total fatty acids in the retina ethanolamine glycerophospholipids. This high concentration clearly indicates that DHA is efficiently

transferred from blood lipids to the outer segment of the mouse lemur retina. We conclude that the mouse lemur n-3 PUFA metabolism efficiently drives DHA to neural tissues, through the blood–brain barrier and the blood–retina barrier.

Keywords Brain · Docosahexaenoic acid (DHA; 22:6n-3) · Docosapentaenoic acid (n-6-DPA; 22:5n-6) · Mouse lemur · Polyunsaturated fatty acids · Retina

Abbreviations

ALA	α -Linolenic acid
ARA	Arachidonic acid
CNS	Central nervous system
ChoGpl	Choline glycerophospholipids
DHA	Docosahexaenoic acid
DMA	Dimethylacetals
n-6DPA	Docosapentaenoic acid
EPA	Eicosapentaenoic acid
ETA	Eicosatrienoic acid
EtnGpl	Ethanolamine phosphoglycerolipids
LNA	Linoleic acid
MUFA	Monounsaturated fatty acids
NL	Neutral Lipids
NPD1	Neuroprotectin D1
PUFA	Polyunsaturated fatty acids
PtdSer	Phosphatidylserine
SFA	Saturated fatty acids

F. Pifferi (✉) · M. Perret · F. Aujard
Mécanismes Adaptatifs et Evolution, UMR 7179 Centre
National de la Recherche Scientifique, Muséum National
d'Histoire Naturelle, Brunoy, France
e-mail: pifferi@mnhn.fr

P. Guesnet
PG Consulting, 19 rue Montbaouron, 78000 Versailles, France

J.-M. Alessandri
Département Alimentation Humaine, Institut National de la
Recherche Agronomique, Domaine de Vilvert, bât. 230,
Nurélice UR 909, 78352 Jouy-en-Josas, France

Introduction

The particular interest in supplementing human foods with n-3 fatty acids has arisen from the findings that this series

of polyunsaturated fatty acids (PUFA) has an impact on neuronal functions. Indeed vertebrates, including humans, preferentially use docosahexaenoic acid (DHA, 22:6n-3) over other long-chain n-3 PUFA for the genesis of their neuronal and retinal membranes (review in [1]). Moreover, when n-3 fatty acids are adequately supplied by the diet, the central nervous system (CNS) membranes of the newborn and adult mammals have higher concentrations in DHA than in n-6 fatty acids, a particular fatty acid composition that is not found in the other tissues. On the other side, if the n-3 fatty acids are chronically low or inadequate in the diet, there is a DHA collapse in the CNS membranes which is almost exactly compensated by the rise of a long-chain derivative of the n-6 series, docosapentaenoic acid (n-6-DPA), to maintain the membrane content of 22C PUFA [2]. This n-6 substitute of DHA is synthesized in the liver from its essential precursor linoleic acid (LNA, 18:2n-6) of oleaginous plant origin, transported in blood lipids and distributed as an end-product to the DHA-deprived tissues including brain and retina [3]. However, the structural replacement of DHA by n-6-DPA has been shown to underlie alterations of retina and brain functions, indicating that the specific accretion of DHA during development is essential for the proper functioning of the mammalian CNS (review in [2]). Regarding the specific roles of DHA, one of the major findings of this decade is that DHA may be converted in response to oxidative stress into oxygenated derivatives which exert potent protective action through the inhibition of pro-apoptotic genes and the induction of anti-apoptotic and anti-inflammatory genes [4]. The synthesis and bioactivity of a lipoxxygenated derivative of DHA, neuroprotectin D1 (NPD1), were formerly evidenced in a rat model of brain ischemia [5]. NPD1 has been also shown to promote retinal pigment epithelial cell survival during oxidative stress [6] and to abrogate genotoxic and oxidative damage in a rat model of liver injury [7].

Docosahexaenoic acid may be directly provided under the esterified form in triacylglycerols (mainly in fish oils and marine products) or may be synthesized from the n-3 precursor, α -linolenic acid (ALA, 18:3 ω 3), through the same hepatic enzyme pathway as that producing ω 6-DPA from LNA upon n-3 deficiency [8, 9]. Therefore, the balance between DHA and ω 6-DPA in blood lipids and in cell membranes, especially those of neurones and retinal cells, will result from both the ratio of n-3 to n-6 in the dietary lipids and from the capacity of liver to convert the plant-issued precursors into their respective long-chain derivatives.

The grey mouse lemur (Fig. 1) is a nocturnal prosimian primate originating from Madagascar. In captivity, this non-human primate has a life expectancy of around 8 years (Languille et al. 2012) [10] and presents specific



Fig. 1 The grey mouse lemur (*Microcebus murinus*)

characteristics, e.g., omnivorous dietary habits and small size and weight (80–120 g). Grey mouse lemurs display a common pattern of cognitive alteration during ageing with humans which makes it a good model to evaluate the effects of dietary treatments on behavioral outcomes, especially in relation to aging or during dietary interventions [11, 12]. Specific tasks have been developed and adapted in our laboratory [10] offering the possibility of evaluating, in this small primate, the impact on longevity or cognitive functions of dietary supplements such as antioxidants [13] or n-3 fatty acids [14].

This nocturnal primate exhibits biological seasonal rhythms that are photoperiodically driven characterized in particular by a winter body mass gain and decreased resting metabolic rate [15]. The increase in body mass can represent close to 50 % of the summer acclimated body mass and is mainly due to fat accumulation [16]. Until now, the tissue fatty acid composition of the grey mouse lemur has not been analyzed and it is thus not known whether the DHA status of this primate raised on an experimental regimen made of milk, eggs, cereals and fruits is adequate. In the present study, we report the fatty acid composition in phospholipids from the main target tissues, brain, retina, liver and adipose tissue of the mouse lemur raised under standard nutritional conditions and acclimated to a winter-like photoperiod.

Materials and Methods

Animals and Ethics Statement

The experiment was performed in accordance with the Principles of Laboratory Animal Care (National Institutes of Health publication 86–23, revised 1985) and the European Communities Council Directive (86/609/EEC). The research was conducted under the authorization # 91–305

Table 1 Concentration (mg FA/100 g diet) of fatty acids in the experimental diet

	SFA	MUFA	n-6 PUFA	n-3 PUFA
6:0	28.9	14:1n-5	10.1	18:2n-6
8:0	20.7	16:1n-9	6.3	18:3n-6
10:0	43.4	16:1n-7	16.8	20:2n-6
12:0	38.8	18:1n-9	225.2	20:3n-6
14:0	89.8	18:1n-7	18.0	20:4n-6
15:0	2.6	20:1n-9	1.4	22:4n-6
16:0	317.1	20:1n-7	0.2	22:5n-6
17:0	4.1	22:1n-11	0.2	Total
18:0	78.3	22:1n-9	0.3	109.3
20:0	1.7	22:1n-7	0.3	
22:0	0.7	24:1n-9	0.7	
24:0	2.2	Total	279.5	
Total	628.3			

SFA saturated fatty acids,
MUFA monounsaturated fatty acids,
PUFA polyunsaturated fatty acids

from the “Direction Départementale de la Protection des Populations” and the internal review board of the UMR 7179. The experiment was done under personal license (authorization number 91–460, issued 5 June, 2009) delivered by the Ministry of Education and Science. Nociception was minimized as much as possible. Six adult female grey mouse lemurs (*M. murinus*, Cheirogaleidae, primates) acclimated to winter-like photoperiod aged of 23 ± 4 months were raised on fresh fruits and a laboratory daily-made mixture of cereals, milk and egg given ad libitum. The fatty acid composition of this meal is reported in Table 1. It contained about 1 g of total fatty acids per 100 g of meal. PUFA from both series were present, mainly in the form of 18 carbons precursors, LNA (103.8 mg/100 g) and ALA (9.9 mg/100 g). The long-chain PUFA were also present, mainly ARA (3.2 mg/100 g) and DHA (1.4 mg/100 g).

Tissues Collection

Animals were anesthetized by ketamine lethal injection. Blood samples were drawn via the saphenous vein and the animals were killed. The liver and frontal cortex were rapidly removed and frozen in liquid nitrogen then stored at -80°C until analysis. A sample of white adipose tissue was excised from the tail (white adipose tissue being mainly located in the tail during winter mass gain).

The outer retinas (containing the rod outer segments of the photoreceptor cells) were prepared according to the method of Chen et al. [17]. The eyes were removed, and the retinas were detached from the retinal pigment epithelium (RPE) by incubating the eyecups in a calcium-free Ringer buffer (pH 7.4) containing 118 mmol NaCl/L, 4.7 mmol KCl/L, 1.17 mmol KH_2PO_4 /L, 1.17 mmol MgSO_4 /L, 5.6 mmol D-glucose/L, 35 mmol NaHCO_3 /L, and 1 mmol EDTA/L with gentle stirring at room

temperature. The two retinas by animal were pooled and the six preparations were stored at -80°C .

Separation of Phospholipid Classes and Fatty Acid Composition Analysis

The total lipids were extracted from the outer retina and from dilacerated samples of around 50 mg of cerebral cortex and liver with 4 ml of chloroform–methanol (2:1, by vol). The fatty acid composition of the diet was analyzed by the same experimental procedure with a known amount of 19:0-TAG as internal standard. The liver neutral lipids (NL) and the three main phospholipid classes from liver, cerebral cortex and retina, phosphatidylserine (PtdSer), choline glycerophospholipids (ChoGpl), and ethanolamine phosphoglycerolipids (EtnGpl) were isolated by solid-phase extraction on a 500 mg aminopropyl bonded silica cartridge [18]. The cartridges were equilibrated beforehand with eluent I (isopropanol/chloroform, 1:2, by vol). Each sample of total lipids was dried under nitrogen, resolubilized in 250 μl of eluent I and deposited onto a single-use cartridge. It was eluted with 3 ml of eluent I to recover the NL, then with 3 ml of diethylether/acetic acid (98:2, by vol) (discarded), 1 ml of acetonitrile (discarded) and 8 ml of acetonitrile/*n*-propanol (3:1, by vol) to recover the ChoGpl fraction. The cartridge was then eluted with 2 ml of acetonitrile/*n*-propanol (1:1, by vol) (discarded) and 3 ml of methanol to recover the EtnGpl fraction, consisting in a mixture of phosphatidylethanolamine and 1-*O*-alkylenyl-2-acyl glycerophosphoethanolamine. Upon transmethylolation (see below), the latter compound generates fatty acid methyl esters from the *sn*-2 position and dimethylacetals (DMA) from the *sn*-1 position. The PtdSer fraction was recovered at the end of the procedure by eluting with anhydrous isopropanol/methanolic HCl 3N (4:1, by vol). The three phospholipid fractions were dried

under a nitrogen flux and transmethylated by methanol at 90 °C in the presence of 10 % BF₃ to generate fatty acid methyl esters and DMA, which were both extracted with hexane. The samples were analyzed by gas liquid chromatography using a 50 m × 0.20 mm capillary column (CP-Wax 52CB, Varian, Les Ulis, France) and a one-stage temperature program, from 54 to 212 °C at 3 °C/min [19]. The resulting peaks were identified by comparison of their retention times to those of a mix of standard compounds (mix GLC-68A from Nu-Chek-Prep, MN). The proportion of each fatty acid was automatically computed from the ratio of its peak area to the sum of total areas, including DMA, and expressed in mol% (peaks having a surface <0.1 % of total were not computed). The theoretical maximum value of DHA (DHAm_{max}) was calculated as the sum of DHA + n-6 DPA. The desaturation index of n-3 and n-6 series was also calculated. The desaturation index of each series is computed from the content (expressed in % by weight) of the corresponding fatty acid (n-6 or n-3) balanced by the number of its double-bond. The global value obtained within each series results from the sum of the individual indices. It gives an indication of the total unsaturation level in membranes brought about by the n-6 or by the n-3 series.

Statistical Analysis

All values are expressed as means ± SEM. Paired Student's *t* test analyses were used to ascertain the significant differences in the fatty acid content between tissues. Comparisons were considered to differ significantly with *p* < 0.05. All statistical computations were performed with Prism 5 for Windows XP (Graphpad software).

Results

Adipose Tissue and Plasma (Table 2)

The total lipids of the adipose tissue mainly contains saturated fatty acids (SFA) and monounsaturated fatty acids (MUFA) which together accounts for 96 % of the total fatty acids, reflecting the role of lipid energy storage of this tissue. The PUFA, especially DHA, are extremely low, suggesting that the adipose tissue is not a DHA supplier for other organs. Moreover, the level of the two essential PUFA, linoleic (18:2n-6) and α -linolenic (18:3n-3), were also low, representing 2.1 and 0.2 mol%, respectively. The MUFA are less concentrated in the plasma phospholipids (PL) than in the adipose tissue. DHA and n-6-DPA are both present in the plasma PL (4.6 and 1.2 mol%, respectively) indicating that the blood concentration of DHA issued from metabolism in the present condition of feeding matches

Table 2 Fatty acid composition (mol%) in adipose tissue total lipids (TL) and in plasma phospholipids (PL)

	Adipose tissue (TL)	Plasma (PL)
8:0	2.1 ± 0.1	nd
10:0	0.1 ± 0.0	nd
12:0	0.7 ± 0.1	0.6 ± 0.2
14:0	8.1 ± 0.5	0.3 ± 0.1
15:0	0.2 ± 0.0	0.2 ± 0.0
16:0	23.6 ± 1.7	25.6 ± 0.9
17:0	0.1 ± 0.0	0.4 ± 0.1
18:0	3.6 ± 0.6	16.4 ± 1.2
20:0	0.1 ± 0.0	0.2 ± 0.0
22:0	nd	0.1 ± 0.0
24:0	0.1 ± 0.1	0.1 ± 0.0
14:1n-5	0.3 ± 0.0	nd
16:1n-9	0.7 ± 0.1	0.2 ± 0.0
16:1n-7	6.5 ± 0.6	0.4 ± 0.1
18:1n-9	48.5 ± 0.8	8.9 ± 0.0
18:1n-7	2.1 ± 0.3	1.6 ± 0.0
20:1n-11	0.1 ± 0.0	0.1 ± 0.0
20:1n-9	0.2 ± 0.1	0.1 ± 0.0
20:3n-9	0.1 ± 0.1	0.1 ± 0.0
18:2n-6	2.1 ± 0.4	12.1 ± 2.0
20:2n-6	nd	0.2 ± 0.0
20:3n-6	nd	2.1 ± 0.1
20:4n-6	0.2 ± 0.1	13.6 ± 0.1
22:4n-6	0.1 ± 0.0	1.1 ± 0.4
22:5n-6	nd	1.2 ± 0.3
18:3n-3	0.2 ± 0.1	0.1 ± 0.0
20:5n-3	nd	0.2 ± 0.0
22:5n-3	0.1 ± 0.1	1.3 ± 0.4
22:6n-3	0.1 ± 0.0	4.6 ± 0.9
Σ SFA	38.7 ± 1.4	43.9 ± 0.0
Σ MUFA	58.6 ± 1.2	11.3 ± 0.0
Σ n-6 PUFA	2.4 ± 0.5	30.2 ± 1.1
Σ n-3 PUFA	0.3 ± 0.2	6.1 ± 1.3
Σ DMA	nd	1.5 ± 0.2

nd not detected, SFA saturated fatty acids, MUFA monounsaturated fatty acids, PUFA polyunsaturated fatty acids, DMA dimethylacetals

about 80 % of its theoretical maximum value (DHAm_{max}, 5.8 mol%). Eicosatrienoic acid (ETA, 20:3 n-9), a long-chain derivative of the n-9 series marker of total PUFA deficiency, is present at low level.

Liver (Table 3)

The EtnGpl fraction of liver contains 9.8 % DHA and 2.9 mol% n-6-DPA. The relatively high level of n-6-DPA suggests that DHA might reach higher values (theoretically 12.7 mol%) under optimized conditions of n-3 supplies.

Table 3 Fatty acid composition (mol%) of the liver Neutral Lipids (NL), choline glycerophospholipids (ChoGpl) and ethanolamine glycerophospholipids (EtnGpl)

	NL	ChoGpl	EtnGpl
14:0	5.8 ± 1.0	0.24 ± 0.1	0.1 ± 0.0
16:0	21.9 ± 1.8	27.3 ± 0.9	15.4 ± 0.7
17:0	0.3 ± 0.1	0.3 ± 0.1	0.3 ± 0.0
18:0	2.4 ± 0.5	15.2 ± 0.6	22.9 ± 2.2
19:0	0.3 ± 0.1	0.2 ± 0.1	0.1 ± 0.1
20:0	0.3 ± 0.1	0.1 ± 0.0	0.1 ± 0.0
16:1n-9	0.8 ± 0.1	0.1 ± 0.0	0.0 ± 0.0
16:1n-7	5.0 ± 0.8	0.6 ± 0.1	0.3 ± 0.1
18:1n-9	50.3 ± 3.3	11.2 ± 1.5	7.9 ± 1.5
18:1n-7	2.7 ± 0.5	3.0 ± 1.1	2.2 ± 0.6
20:1n-11	0.2 ± 0.1	0.1 ± 0.0	0.1 ± 0.0
20:1n-9	0.2 ± 0.0	0.1 ± 0.0	0.1 ± 0.0
20:3n-9	0.1 ± 0.0	0.2 ± 0.1	0.2 ± 0.1
18:2n-6	5.7 ± 1.3	12.6 ± 2.5	4.6 ± 1.3
18:3n-6	0.2 ± 0.1	0.1 ± 0.0	0.0 ± 0.0
20:3n-6	0.3 ± 0.1	1.7 ± 0.4	0.7 ± 0.1
20:4n-6	1.9 ± 0.7	19.2 ± 1.7	28.3 ± 1.0
22:4n-6	0.2 ± 0.1	0.7 ± 0.2	1.0 ± 0.2
22:5n-6	0.1 ± 0.1	1.2 ± 0.2	2.9 ± 0.3
18:3n-3	0.7 ± 0.1	0.2 ± 0.2	0.1 ± 0.0
20:5n-3	0.1 ± 0.1	0.6 ± 0.1	0.6 ± 0.1
22:5n-3	0.4 ± 0.1	1.5 ± 0.9	2.1 ± 0.4
22:6n-3	0.2 ± 0.1	3.6 ± 0.9	9.8 ± 1.0
Σ SFA	31.0 ± 1.6	43.3 ± 1.0	39.0 ± 2.9
Σ MUFA	59.3 ± 3.1	15.4 ± 1.3	10.9 ± 2.0
Σ n-6 PUFA	8.3 ± 1.7	35.4 ± 1.3	37.5 ± 1.1
Σ n-3 PUFA	1.4 ± 0.2	5.9 ± 0.5	12.6 ± 0.7
Σ DMA	1.1 ± 0.4	0.7 ± 0.1	1.7 ± 0.2
Desat. index			
n-6	24.3 ± 4.8	126.7 ± 4.5	152.1 ± 4.5
n-3	7.9 ± 1.3	39.2 ± 3.2	82.8 ± 4.6

nd not detected, SFA saturated fatty acids, MUFA monounsaturated fatty acids, PUFA polyunsaturated fatty acids, DMA dimethylacetals

The ChoGpl fraction contains DHA and n-6-DPA at lower levels (3.6 and 1.2 mol%, respectively), while the NL contains very low amounts of these long-chain derivatives, 0.2 and 0.1 mol% respectively. The major fatty acids in liver NL are SFA (31.0 mol%) and MUFA (59.3 mol%), mainly present in the form of palmitic acid (16:0) and of oleic acid (18:1n-9). Briefly, the main PUFA in the liver phospholipids are the long-chain derivatives, arachidonic acid (ARA, 20:4n-6) and DHA, while the NL store their respective precursors, LNA (5.7 mol% 18:2n-6) and ALA (0.7 mol% 18:3n-3). The highest contents in ARA and DHA are found in the EtnGpl fraction which consequently has a high level of total unsaturation, with a double-bond index for the n-6 and n-3 series equal to 152 and 83

respectively (vs. 127 and 39 in ChoGpl). There is no substantial accumulation of ETA in liver lipid classes (≤ 0.2 %).

Brain Cortex (Table 4)

The major fatty acids in the ChoGpl fraction from the brain cortex are palmitic acid (52.1 mol%) and oleic acid (17.5 mol%), while DHA is relatively low (4.3 mol%). By contrast, DHA is the major fatty acid in the EtnGpl fraction (32.0 mol%) and the second major fatty acid in PtdSer (24.9 mol%). In the three phospholipid classes, DHA takes account for 98 % of the total n-3 PUFA, a proportion that is

Table 4 Fatty acid composition (mol%) of the brain cortex phospholipids choline glycerophospholipids (ChoGpl), ethanolamine glycerophospholipids (EtnGpl) and phosphatidylserine (PtdSer)

	ChoGpl	EtnGpl	PtdSer
14:0	1.4 ± 0.1	0.2 ± 0.0	0.2 ± 0.0
16:0	52.1 ± 0.3	9.2 ± 0.2	3.5 ± 0.3
17:0	0.3 ± 0.1	0.4 ± 0.1	0.3 ± 0.1
18:0	8.5 ± 0.4	23.3 ± 0.5	40.8 ± 0.7
19:0	0.1 ± 0.1	0.1 ± 0.0	0.1 ± 0.0
20:0	0.1 ± 0.0	0.1 ± 0.0	0.1 ± 0.0
16:1n-9	1.1 ± 0.1	0.3 ± 0.0	0.1 ± 0.0
16:1n-7	0.9 ± 0.1	0.4 ± 0.0	1.1 ± 0.1
18:1n-9	17.5 ± 0.3	9.9 ± 0.6	14.2 ± 1.1
18:1n-7	7.7 ± 0.3	3.3 ± 0.1	3.7 ± 0.2
20:1n-11	0.0 ± 0.0	0.1 ± 0.0	0.0 ± 0.0
20:1n-9	0.4 ± 0.0	1.5 ± 0.2	0.8 ± 0.1
20:3n-9	0.1 ± 0.0	0.3 ± 0.1	0.1 ± 0.0
18:2n-6	0.4 ± 0.1	0.1 ± 0.0	0.7 ± 0.1
18:3n-6	0.0 ± 0.0	0.1 ± 0.0	0.0 ± 0.0
20:3n-6	0.1 ± 0.0	0.2 ± 0.0	0.4 ± 0.0
20:4n-6	4.4 ± 0.2	12.9 ± 0.9	4.3 ± 0.1
22:4n-6	0.3 ± 0.0	3.3 ± 0.2	2.1 ± 0.2
22:5n-6	0.2 ± 0.0	1.8 ± 0.2	2.0 ± 0.3
18:3n-3	0.0 ± 0.0	0.0 ± 0.0	0.0 ± 0.0
20:5n-3	0.0 ± 0.0	0.0 ± 0.0	0.2 ± 0.0
22:5n-3	0.1 ± 0.0	0.3 ± 0.1	0.3 ± 0.1
22:6n-3	4.3 ± 0.3	32.0 ± 1.7	24.9 ± 1.2
Σ SFA	62.4 ± 0.4	33.3 ± 0.7	45.2 ± 0.6
Σ MUFA	27.8 ± 0.5	15.8 ± 1.0	20.1 ± 1.5
Σ n-6 PUFA	5.4 ± 0.2	18.5 ± 1.1	9.5 ± 0.4
Σ n-3 PUFA	4.4 ± 0.3	32.4 ± 1.7	25.3 ± 1.2
Σ DMA	0.4 ± 0.1	17.9 ± 0.9	1.2 ± 0.2
Desat. index			
n-6	25.1 ± 1.1	66.3 ± 4.7	41.5 ± 2.1
n-3	32.9 ± 2.0	178.3 ± 10.4	172.4 ± 7.4

nd not detected, SFA saturated fatty acids, MUFA monounsaturated fatty acids, PUFA polyunsaturated fatty acids, DMA dimethylacetals

characteristic for neural tissues of mammals. Besides, the brain EtnGpl contains 10-times more DMA in comparison with the liver counterpart, reflecting the specifically high concentration of ether-phospholipids (plasmalogens) in the CNS membranes. In comparison with DHA, the n-6-DPA content is low (1.8 mol% in EtnGpl, $p < 0.001$), indicating that the cerebral needs in DHA are almost fully covered (on the basis that DHA alone takes account for around 95 % of the sum DHA + n-6-DPA). The PtdSer fraction presents the same high DHA content as that in EtnGpl (25.9 mol%), which is a further indication that the brain requirements in DHA are almost fully covered in these animals. The high DHA contents result in high levels of n-3 double-bond index in EtnGpl and PtdSer (178 and 172), values typical for cerebral phospholipids.

Retina (Table 5)

The retina has the highest DHA content (24.7, 37.8 and 47.3 mol% in the ChoGpl, PtdSer and EtnGpl fractions, respectively) whereas the content in n-6-DPA is, in comparison, very low (<2 mol%, $p < 0.001$ for all phospholipids classes). It may be noted that, as in rodents, DHA takes account for almost one half of the whole fatty acids esterified in the retinal EtnGpl of the mouse lemur. This is a clear indication that DHA in the photoreceptor cells of these animals is about at its maximum level. The other major fatty acids are 16:0, 18:0 and ARA in EtnGpl and PtdSer, and SFA and MUFA in ChoGpl. The high DHA content in the retina phospholipids results in very high values of the n-3 double-bond index, i.e., 178 in ChoGpl, 287 in EtnGpl and 258 in PtdSer.

Discussion

This work provides the first analysis of the fatty acid composition in neural and peripheral tissues of the mouse lemur. We examined in particular the DHA status in animals raised on an experimental home-made diet, especially in the brain cortex and retina, the main target tissues, but also in the liver, the main organ ensuring the synthesis of DHA from its precursor.

The home-made diet contained traces of n-6-DPA (0.03 % of total dietary fatty acids), probably from the milk or egg lipids. Notwithstanding, the presence of this long-chain end product of the n-6 series in the hepatic and plasma phospholipids at a substantial level may be indicative of an endogenous synthesis, which would be due to a moderate inadequacy of the amount of n-3 PUFA in diet. α -LNA in the adipose tissue is a marker of dietary α -LNA intake. The very low content of α -LNA in the adipose tissue of the grey mouse lemur (0.2 mol%), compared to

Table 5 Fatty acid composition (mol%) in the retinal phospholipids choline glycerophospholipids (ChoGpl), ethanolamine glycerophospholipids (EtnGpl) and Phosphatidylserine (PtdSer)

	ChoGpl	EtnGpl	PtdSer
14:0	1.1 ± 0.1	0.1 ± 0.0	0.5 ± 0.1
16:0	30.5 ± 0.8	4.8 ± 0.3	5.6 ± 0.8
17:0	0.2 ± 0.0	0.3 ± 0.0	0.5 ± 0.1
18:0	20.4 ± 1.2	27.5 ± 1.9	32.8 ± 0.9
19:0	0.1 ± 0.0	0.1 ± 0.0	0.1 ± 0.1
20:0	0.3 ± 0.0	0.5 ± 0.1	0.4 ± 0.1
16:1 n-9	0.6 ± 0.1	0.1 ± 0.0	0.1 ± 0.0
16:1 n-7	0.4 ± 0.0	0.1 ± 0.0	0.9 ± 0.1
18:1 n-9	13.5 ± 1.2	4.0 ± 0.3	8.1 ± 0.9
18:1 n-7	2.2 ± 0.2	1.2 ± 0.1	2.4 ± 0.2
20:1 n-11	0.0 ± 0.0	0.0 ± 0.0	0.0 ± 0.0
20:1 n-9	0.2 ± 0.0	0.3 ± 0.1	0.3 ± 0.1
20:3 n-9	0.0 ± 0.0	0.1 ± 0.0	0.0 ± 0.0
18:2 n-6	0.3 ± 0.1	0.2 ± 0.0	0.8 ± 0.1
18:3 n-6	0.0 ± 0.0	0.1 ± 0.0	0.0 ± 0.0
20:3 n-6	0.2 ± 0.0	0.3 ± 0.0	0.3 ± 0.0
20:4 n-6	3.8 ± 0.2	9.3 ± 1.0	4.6 ± 0.2
22:4 n-6	0.3 ± 0.0	1.3 ± 0.1	2.1 ± 0.2
22:5 n-6	0.8 ± 0.1	1.8 ± 0.2	1.4 ± 0.2
18:3 n-3	0.0 ± 0.0	0.0 ± 0.0	0.1 ± 0.0
20:5 n-3	0.1 ± 0.0	0.1 ± 0.0	0.3 ± 0.1
22:5 n-3	0.3 ± 0.0	0.6 ± 0.1	0.9 ± 0.1
22:6 n-3	24.7 ± 1.9	47.3 ± 2.5	37.8 ± 2.0
Σ SFA	52.5 ± 1.2	33.2 ± 2.4	39.9 ± 1.0
Σ MUFA	17.0 ± 1.5	5.7 ± 0.4	11.9 ± 1.2
Σ n-6 PUFA	5.3 ± 0.2	13.0 ± 0.9	9.2 ± 0.5
Σ n-3 PUFA	25.1 ± 1.9	48.0 ± 2.5	39.0 ± 1.9
Σ DMA	0.4 ± 0.0	8.7 ± 0.8	1.3 ± 0.3
Desat. index			
n-6	23.5 ± 1.1	50.5 ± 3.9	38.6 ± 2.2
n-3	178.1 ± 11.6	287.5 ± 14.8	257.6 ± 11.3

nd not detected, SFA saturated fatty acids, MUFA monounsaturated fatty acids, PUFA polyunsaturated fatty acids, DMA dimethylacetals

that found in rat fed an α -LNA adequate diet (1 %) [19], is also indicative of a relative inadequacy in n-3 in the diet. However, the very low amount of ETA (a biomarker of PUFA deficiency) indicates that total PUFA intakes are sufficient [19]. In addition, adipose tissue contains very high levels of 16:0 (23.6 ± 1.7 mol%) and 18:1n-9 (48.5 ± <0.8 mol%). These amounts of saturated and monounsaturated fatty acids in adipose tissue can be linked to the seasonal fattening and reduced resting metabolic rate exhibited during winter by this species [15, 20]. In addition, it is noteworthy that grey mouse lemurs are seasonal primates that exhibit an important fattening during winter, with an increase in body mass that can represent close to

50 % of the summer acclimated body mass [16]. During the winter, the fat mass represents 35 % of the animal's body weight whereas it represents only 10 % during summer [16]. The present results must be interpreted taking into account that fatty acid compositions have been determined in winter acclimated animals. Very few studies have investigated the fatty acid composition of tropical primates, and more particularly heterotherms. Fietz and colleagues [21] reported the fatty acids composition of the fat-tailed dwarf lemur (*Cheirogaleus medius*), a small primate belonging to the family of *Cheirogaleidae* like the grey mouse lemur. In this species, white adipose tissue contains around 67 % monounsaturated fatty acids, a level higher but comparable to that found in our study (60 %). In both species, 18:1n-9 was the main fatty acid of adipose tissue. As suggested by Fietz et al. [21], because of its high prevalence, 18:1n-9 is probably the main fuel provider during hypothermia in both species.

n-6-DPA is very low in the brain cortex and retina, whereas there is a dramatic biomagnification of DHA in the neural tissues compared to liver and plasma (Fig. 2). In the brain cortex EtnGpl, DHA represents 32.0 ± 1.7 mol%, and 9.8 ± 1.0 in the liver EtnGpl ($p < 0.001$; $t = 25.97$; $df = 5$), and only 4.6 ± 0.9 in the plasma TL ($p = 0.005$, $t = 4.301$; $df = 5$, when compared to liver). In particular, DHA accounts for about one half of the total fatty acids in the retina EtnGpl (47.3 ± 2.5 mol%, $p < 0.001$; $t = 15.63$; $df = 5$, when compared to brain cortex EtnGpl). This high concentration clearly indicates that DHA is efficiently transferred from blood lipids to the outer segment of the mouse lemur retina. It has been demonstrated in the frog and rat retina that DHA is translocated from blood lipoproteins to photoreceptor cells across the choriocapillaris, the Bruch's membrane and the RPE [22]. The RPE cells

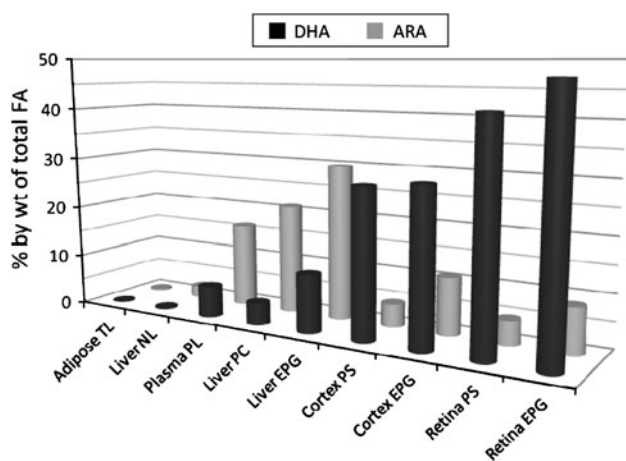


Fig. 2 Biomagnification of docosahexaenoic acid (DHA, black bars) and arachidonic acid (ARA, grey bars) in the brain and retinal phospholipids of the mouse lemur, in comparison with liver and plasma

release DHA in the interphotoreceptor matrix (IPM) from which it passes into the photoreceptor inner segment where it is incorporated into phospholipids, mainly EtnGpl and PtdSer, for the biogenesis of new membranes, notably those of the photoreceptor disks formed at the outer segment basement. The older disks are phagocytized at the tip of the outer segment by the RPE phagosome, the released DHA molecules being secreted into the IPM for a new cycle of disk biogenesis. RPE cells are capable by themselves of synthesizing DHA from its upstream metabolic precursors (translocated from blood lipids), providing an additional supply for the photoreceptor cells [23]. Thus, the RPE plays a crucial role in the DHA synthesis and recycling, allowing the photoreceptor disks to maintain—in spite of their permanent renewal—the highest DHA concentration of the organism. Similarly to rats, the mouse lemur is a nocturnal species whose vision recruits rod photoreceptor cells [24]. The high concentration of DHA in the outer segment of the mouse lemur retina, similar to that found in that of rats raised on standard diets, strongly suggests that DHA is crucial for the optimum functioning of the lemur rod photoreceptor cells. On the basis of former studies performed on membrane models [25], it may be supposed that DHA-rich phospholipid species (EtnGpl and PtdSer) of the mouse lemur retina ensure a high level of disorder in the membrane environment of the rhodopsin molecules, facilitating the photo-induced conformational change of rhodopsin and the subsequent activation of the G-protein cascade.

The brain cortex phospholipids are also rich in DHA, although at a lower level than in the retina. We have previously shown in rat submitted to a dose-response effect that the retina and brain phospholipids have their own and specific maximum of DHA incorporation (DHAm_{ax}), even though DHA continues to increase in diet [18]. In the rat EtnGpl fraction, the DHAm_{ax} values were equal to 29 % in the frontal cortex and 46 % in the retina. The values which we found in the mouse lemur, 29 and 47 % respectively ($p < 0.001$; $t = 14.75$; $df = 5$), clearly show that the incorporation of DHA into the outer retina is highly similar in the two animal models. Thus, the mouse lemur raised on the home-made diet efficiently metabolizes the dietary n-3 PUFA for the optimum modeling of his cortical and retinal membranes. Therefore, the relative inadequacy of n-3 supplies in the home-made diet, that we may infer from the presence of n-6-DPA in liver and plasma, is fully compensated by the very efficient transfer of DHA to the avid neural tissues, excluding on the contrary n-6-DPA.

However, we recently showed that mouse lemurs receiving the home-made diet supplemented with tuna oil, rich in DHA, had their level of anxiety significantly lowered in comparison with animals receiving a placebo supplementation (olive oil) [14]. The behavioral and cognitive

tests evidenced a beneficial effect of the tuna oil-supplemented diet on the brain functions of the grey mouse lemur, which may a priori suggest an improvement in their cerebral DHA status. However, on the basis of the present data in animals placed under standard feeding, which have low levels of n-6-DPA in their brain phospholipids and DHA values close to those of the rat DHAm_{ax}, it is likely that the requirements for DHA of the neural tissues are almost fully covered with the standard diet. If this speculation is correct, supplementing the diet of adult animals with tuna oil would result in only a modest gain of DHA in the neural tissues. However, our previous study showed that animals fed the tuna oil-supplemented diet had much higher concentrations of EPA, n-3-DPA and DHA in their blood plasma phospholipids than those fed the standard diet [14]. These preformed long-chain n-3 PUFA are potential substrates for the synthesis of an array of bioactive lipids, eicosanoids, docosanoids, maresins and neuroprostanes. Docosanoids mainly include NPD1, a novel DHA-derived stereoselective mediator of signaling, especially in brain and retina cells [4]. It has been shown that NPD1 elicits potent anti-inflammatory actions and prohomeostatic bioactivity, is anti-angiogenic, promotes corneal nerve regeneration, and induces brain cell survival [4]. Whether the lowering of anxiety that we evidenced in DHA-supplemented mouse lemurs is related to activation of the NPD1 signaling pathway and to an improvement of the neuroinflammatory status opens a new field of investigation.

The consumption of n-6 and n-3 fatty acids in equilibrated proportions is crucial in the regulation of cellular physiology and in the prevention of pathologies such as cardiovascular, autoimmune and inflammatory diseases, diabetes and obesity or certain neuropsychiatric affections [2]. Indeed, the dietary intake of n-3 fatty acid (α -linolenate and also DHA) are crucial parameters in the development of retinal and neural function during the perinatal period [2]. On the other hand, a high ratio of n-6/n-3 fatty acids in cell membranes due to an excessive consumption of n-6 fatty acids and a relative n-3 fatty acid deficiency, may promote the pathogenesis of several diseases, including cardiovascular diseases, metabolic syndrome, inflammatory disorders and obesity [1, 4]. These health implications of fatty acids are of major importance when considering that the mouse lemur is becoming an emerging model in nutritional, metabolic and aging studies [10].

We conclude that the mouse lemur n-3 PUFA metabolism efficiently drives DHA to neural tissues, through the blood–brain barrier and the blood–retina barrier. The mouse lemur offers an emerging non-human primate model for n-3 PUFA metabolism studies and nutritional intervention in humans.

Acknowledgments The authors thank Laurine Haro for tissue preparation and Alain Linard and Marie-Sylvie Lallemand for the fatty acids analysis. This work was financially supported by the Groupe Lipides et Nutrition, the Centre National de la Recherche Scientifique/Muséum National d'Histoire Naturelle, and the Institut National de la Recherche Agronomique. The contributors to the funding had no role in the study design, data collection and analysis, decision to publish, or preparation of the manuscript.

References

- Arterburn LM, Hall EB, Oken H (2006) Distribution, interconversion, and dose response of n-3 fatty acids in humans. *Am J Clin Nutr* 83:1467S–1476S
- Alessandri JM, Guesnet P, Vancassel S, Astorg P, Denis I, Langelier B, Aid S, Poumès-Ballihaut C, Champeil-Potokar G, Lavielle M (2004) Polyunsaturated fatty acids in the central nervous system: evolution of concepts and nutritional implications throughout life. *Reprod Nutr Dev* 44(6):509–538
- Kim HW, Rao JS, Rapoport SI, Igarashi M (2011) Regulation of rat brain polyunsaturated fatty acid (PUFA) metabolism during graded dietary n-3 PUFA deprivation. *Prostaglandins Leukot Essent Fatty Acids* 85:361–368
- Bazan NG, Molina MF, Gordon WC (2011) Docosahexaenoic acid signalolipidomics in nutrition: significance in aging, neuroinflammation, macular degeneration, Alzheimer's, and other neurodegenerative diseases. *Annu Rev Nutr* 31:321–351
- Marcheselli VL, Hong S, Lukiw WJ, Tian XH, Gronert K, Musto A, Hardy M, Gimenez JM, Chiang N, Serhan CN, Bazan NG (2003) Novel docosanoids inhibit brain ischemia-reperfusion-mediated leukocyte infiltration and pro-inflammatory gene expression. *J Biol Chem* 278:43807–43817
- Calandria JM, Bazan NG (2010) Neuroprotectin D1 modulates the induction of pro-inflammatory signaling and promotes retinal pigment epithelial cell survival during oxidative stress. *Adv Exp Med Biol* 664:663–670
- González-Pérez A, Planagumà A, Gronert K, Miquel R, López-Parra M, Titos E, Horrillo R, Ferré N, Deulofeu R, Arroyo V, Rodés J, Clària J (2006) Docosahexaenoic acid (DHA) blunts liver injury by conversion to protective lipid mediators: protectin D1 and 17S-hydroxy-DHA. *FASEB J* 20:2537–2539
- Rapoport SI, Igarashi M, Gao F (2010) Quantitative contributions of diet and liver synthesis to docosahexaenoic acid homeostasis. *Prostaglandins Leukot Essent Fatty Acids* 82:273–276
- Gao F, Kim HW, Igarashi M, Kiesewetter D, Chang L, Ma K, Rapoport SI (2011) Liver conversion of docosahexaenoic and arachidonic acids from their 18-carbon precursors in rats on a DHA-free but α -LNA-containing n-3 PUFA adequate diet. *Biochim Biophys Acta* 1811:484–489
- Languille S, Blanc S, Blin O, Canale CI, Dal-Pan A, Devau G, Dhenain M, Dorieux O, Epelbaum J, Gomez D, Hardy I, Henry PY, Irving EA, Marchal J, Mestre-Francis N, Perret M, Picq JL, Pifferi F, Rahman A, Schenker E, Terrien J, Théry M, Verdier JM, Aujard F (2012) The grey mouse lemur: a non-human primate model for ageing studies. *Ageing Res Rev* 11:150–162
- Picq JL, Aujard F, Volk A, Dhenain M (2012) Age-related cerebral atrophy in nonhuman primates predicts cognitive impairments. *Neurobiol Aging* 33:1096–1109
- Picq JL (2007) Aging affects executive functions and memory in mouse lemur primates. *Exp Gerontol* 42:223–232
- Dal-Pan A, Pifferi F, Marchal J, Picq JL, Aujard F, RESTRIKAL Consortium (2011) Cognitive performances are selectively enhanced during chronic caloric restriction or resveratrol supplementation in a primate. *PLoS ONE* 6:e16581

14. Vinot N, Jouin M, Lhomme-Duchadeuil A, Guesnet P, Alessandri JM, Aujard F, Pifferi F (2011) Omega-3 fatty acids from fish oil lower anxiety, improve cognitive functions and reduce spontaneous locomotor activity in a non-human primate. *PLoS ONE* 6:e20491
15. Perret M, Aujard F (2001) Daily hypothermia and torpor in a tropical primate: synchronization by 24-h light-dark cycle. *Am J Physiol Regul Integr Comp Physiol* 281:R1925–R1933
16. Giroud S, Perret M, Stein P, Goudable J, Aujard F, Gilbert C, Robin JP, Le Maho Y, Zahariev A, Blanc S, Momken I (2010) The grey mouse lemur uses season-dependent fat or protein sparing strategies to face chronic food restriction. *PLoS ONE* 5(1):e8823
17. Chen H, Wiegand RD, Anderson RE (1992) Decreased docosahexaenoic acid levels in retina and pigment epithelium of frogs fed crickets. *Exp Eye Res* 54:885–892
18. Alessandri JM, Poumès-Ballihaut C, Langelier B, Perruchot MH, Raguénez G, Lavialle M, Guesnet P (2003) Incorporation of docosahexaenoic acid into nerve membrane phospholipids: bridging the gap between animals and cultured cells. *Am J Clin Nutr* 78:702–710
19. Guesnet P, Lallemand SM, Alessandri JM, Jouin M, Cunnane SC (2011) Alpha-linolenate reduces the dietary requirement for linoleate in the growing rat. *Prostaglandins Leukot Essent Fatty Acids* 85:353–360
20. Perret M, Aujard F (2006) Aging and biological rhythms in primates. *Med Sci (Paris)* 22:279–283 (review French)
21. Fietz J, Tataruch F, Dausmann KH, Ganzhorn JU (2003) White adipose tissue composition in the free-ranging fat-tailed dwarf lemur (*Cheirogaleus medius*; Primates), a tropical hibernator. *J Comp Physiol B* 173:1–10
22. Wang N, Anderson RE (1993) Transport of 22:6n-3 in the plasma and uptake into retinal pigment epithelium and retina. *Exp Eye Res* 57:225–233
23. Wang N, Anderson RE (1993) Synthesis of docosahexaenoic acid by retina and retinal pigment epithelium. *Biochemistry* 32:13703–13709
24. Dkhissi-Benyahya O, Szel A, Degrip WJ, Cooper HM (2001) Short and mid-wavelength cone distribution in a nocturnal Strepsirrhine primate (*Microcebus murinus*). *J Comp Neurol* 438:490–504
25. Litman BJ, Mitchell DC (1996) A role for phospholipid polyunsaturation in modulating membrane protein function. *Lipids* 31:S193–S197

Oral Administration of Oleic or Linoleic Acids Modulates the Production of Inflammatory Mediators by Rat Macrophages

Juliana Magdalon · Marco A. R. Vinolo · Hosana G. Rodrigues · Vivian A. Paschoal · Rosângela P. Torres · Jorge Mancini-Filho · Philip C. Calder · Elaine Hatanaka · Rui Curi

Received: 16 January 2012 / Accepted: 23 May 2012 / Published online: 14 June 2012
© AOCs 2012

Abstract Oleic (OLA) and linoleic (LNA) acids are commonly consumed fatty acids and they can modulate the inflammatory response, in which macrophages play an important role. The aim of this study was to investigate the effects of these two fatty acids on the production of inflammatory mediators by macrophages. Rats received oral administration of water (control), OLA or LNA (0.22 g/kg body weight) daily for 10 days and peritoneal resident macrophages were then isolated. Subsequently, they were seeded in culture plates and the production of various inflammatory mediators was assessed. Oral administration with OLA decreased the production of IL-1 β , IL-6 and CINC-2 $\alpha\beta$ by resident macrophages and LNA decreased the production of IL-1 β , IL-6 and VEGF in the absence of lipopolysaccharide (LPS), although it

accelerated IL-1 β release and decreased IL-10 synthesis when cells were stimulated with LPS. Neither fatty acid affected the production of superoxide anion, hydrogen peroxide, nitrite, TNF- α , PGE₂, LTB₄ or 15(S)-HETE. Thus, OLA and LNA influence the production of several inflammatory mediators by macrophages.

Keywords Fatty acids · Inflammation · ROS · RNS · Cytokines · VEGF · Eicosanoids

Abbreviations

15(S)-HETE	15(S)-hydroxyeicosatetraenoic acid
C	Control
CINC-2 $\alpha\beta$	Cytokine-induced neutrophil chemoattractant-2 $\alpha\beta$
IL-1 β	Interleukin-1 β
IL-6	Interleukin-6
IL-10	Interleukin-10
LNA	Linoleic acid
LPS	Lipopolysaccharide
LTB ₄	Leukotrienes B ₄
OLA	Oleic acid
PGE ₂	Prostaglandin E ₂
PMA	Phorbol myristate acetate
ROS	Reactive oxygen species
RNS	Reactive nitrogen species
TNF- α	Tumor necrosis factor- α
VEGF	Vascular endothelial growth factor

Electronic supplementary material The online version of this article (doi:10.1007/s11745-012-3687-9) contains supplementary material, which is available to authorized users.

J. Magdalon (✉) · M. A. R. Vinolo · H. G. Rodrigues · V. A. Paschoal · R. Curi
Departamento de Fisiologia e Biofísica, Instituto de Ciências Biomédicas, Universidade de São Paulo, Av. Prof. Lineu Prestes, 1524, 1º andar, sala 105. Cidade Universitária, CEP 05508-900, SP, Sao Paulo, Brazil
e-mail: jumagdalon@ig.com.br; magdalon@icb.usp.br

R. P. Torres · J. Mancini-Filho
Faculty of Pharmaceutical Sciences, University of Sao Paulo, Sao Paulo, Brazil

P. C. Calder
Faculty of Medicine, Institute of Human Nutrition, University of Southampton, Southampton, UK

E. Hatanaka
Institute of Physical Activity and Sport Sciences, University Cruzeiro do Sul, Sao Paulo, Brazil

Introduction

Macrophages are mononuclear phagocytes that derive from blood monocytes. They play a central role in the initiation, perpetuation and resolution of inflammatory responses

through the strictly regulated release of inflammatory mediators, such as reactive oxygen species (ROS), reactive nitrogen species (RNS), cytokines, eicosanoids and growth factors [1]. Inflammation is triggered by infection or tissue injury. An effective inflammatory response is key to eliminating pathogens. Resolution of inflammation serves to reduce infiltration and activity of inflammatory cells, to clear apoptotic leukocytes, and to promote wound healing and tissue repair. Non-resolution of inflammation is associated with the development of various pathological states [2].

There is on-going interest in the effects of fatty acids on aspects of inflammation [3–5]. Many *in vitro* studies with pure fatty acids have been performed. Dietary studies have tended to use fats and oils rich in particular fatty acids or fatty acid classes, with few dietary investigations of pure fatty acids. Oleic (OLA) and linoleic (LNA) acids are abundant fatty acids in western diets [6]. The former is found in meat, eggs, milk and olive oil, whereas the latter is found in soybean, sunflower, safflower and corn oils, which can be used in food manufacture and animal feeding [7, 8]. Effects of pure OLA or LNA on inflammatory processes are poorly explored. Recently, we have observed that oral administration of OLA or LNA to rats improved wound healing and modulated the inflammatory phase of wound repair [9] and influenced the function of neutrophils [10]. Here we continue this work by exploring the effects of oral administration of pure OLA or LNA on macrophage functions.

Materials and Methods

Reagents and Chemicals

Oleic and linoleic acids, lipopolysaccharide (LPS) from *Escherichia coli* serotype 026:B6, phorbol myristate acetate (PMA), sodium bicarbonate, L-glutamine, HEPES, lucigenin, cell growth determination kit, propidium iodide and horseradish peroxidase (HRP) Type II were purchased from Sigma-Aldrich Co. (St. Louis, MO, USA). RPMI 1640, penicillin–streptomycin (Pen Strep), fetal bovine serum (FBS) and Amplex[®] Ultrared were purchased from Invitrogen (Carlsbad, CA, USA). DuoSet kits for cytokine determination were purchased from R&D Systems (Minneapolis, MN, USA). Kits for eicosanoid quantification were purchased from Cayman Chemical Co. (Ann Arbor, MI, USA).

Animals and Oral Administration of Fatty Acids

The Animal Care Committee of the Institute of Biomedical Sciences, University of Sao Paulo, approved the experimental procedure (Protocol number: 86). Male Wistar rats (180 ± 20 g) were obtained from the Department of Physiology and Biophysics, Institute of Biomedical

Sciences, University of Sao Paulo, Brazil and were maintained at 23 °C under a light:dark cycle of 12:12 h. Animals received non-purified diet (Nuvital, Curitiba, Brazil; providing 3.0 kcal total metabolizable energy/g), whose composition is presented in Table 1, and water *ad libitum*. The fatty acid composition of the chow is presented elsewhere [10]. Rats were treated daily for 10 days by gavage with 0.22 g/kg body weight of water (control), OLA or LNA. This supplementation adds 23 and 10 % of OLA and LNA, respectively, to the amount of such fatty acids deriving from chow. Animals were sacrificed approximately 1 h after the last supplementation. The fatty acid administration did not change food, calorie or water intake [10].

Isolation of Peritoneal Resident Macrophages

Peritoneal cells were obtained by intraperitoneal lavage with 50 mL PBS (136.8 mM sodium chloride, 2.7 mM potassium chloride, 0.9 mM potassium phosphate, 6.4 mM sodium phosphate dibasic, pH 7.4). The cells were collected by centrifugation (500g, 4 °C, 10 min). Erythrocytes were lysed in 5 mL hypotonic solution (150 mM ammonium chloride, 10 mM sodium bicarbonate, 0.1 mM EDTA, pH 7.4). Remaining cells were collected by centrifugation, resuspended in 1 mL PBS and counted in a hemocytometer under an optical microscope. Finally cells were again centrifuged and then suspended in RPMI 1640 medium culture supplemented with 10 % FBS, 100 U/mL penicillin, 100 µg/mL streptomycin, 24 mM sodium bicarbonate, 2 mM L-glutamine and 20 mM HEPES. They were then seeded (cell concentration based on the experiment) and maintained in a humidified incubator at 37 °C in an atmosphere of 5 % CO₂. After 1 h, non-adherent cells were removed by washing with culture medium culture; remaining adherent cells were above 90 % macrophages, as described elsewhere [11–13].

Table 1 Composition of the diet

Nutrients	g/kg diet
Carbohydrate	408
Protein	220
Fat	45
Fiber	80
Calcium	14
Phosphate	8
Mix of vitamins and minerals ^a	100
Moisture	125

^a Vitamin A 12,000 UI, vitamin D3 1,800 UI, vitamin E 30 mg; vitamin K3 3 mg, vitamin B1 5 mg, vitamin B2 6 mg, vitamin B6 7 mg, vitamin B12 20 mcg, niacin 60 mg, pantothenic 20 mg, folic acid 1 mg, biotin 0.05 mg, choline 600 mg, iron 50 mg, zinc 60 mg, copper 10 mg, iodine 2 mg, manganese 60 mg, selenium 0.05 mg, cobalt 1.5 mg

Cell Viability Determined by MTT Assay

The MTT assay was used to determine cell viability; the assay reflects functional mitochondria. MTT was added to culture plates of adherent macrophages (4×10^5 cells) and the plates were incubated for 3 h at 37 °C (100 μ L of final volume). Then the medium was removed and 100 μ L 0.1 N HCl in anhydrous isopropanol added. Absorbance was measured at 570 and 690 nm and plotted as the difference between the readings found at the two wavelengths, as specified by the manufacturer.

Determination of DNA Fragmentation

DNA fragmentation in macrophages was determined using propidium iodide staining. Briefly, cells (10^6) were resuspended in 200 μ L lysis buffer (0.1 % sodium citrate and 0.1 % Triton X-100) with 20 μ g/mL propidium iodide and were then incubated in the dark for 30 min. Subsequently, cells were analyzed (10,000 cells/sample) in a flow cytometer (FACSCalibur, Becton–Dickinson, San Juan, CA, USA) using Cell Quest software. Fluorescence was measured using FL2 channel (orange-red fluorescence-585/42 nm).

Lipid Extraction and Determination of Fatty Acid Composition in Plasma by Gas Chromatography

Plasma was collected 1 h after animal treatment. Derivatization of plasma lipid extract was performed according to AOAC Official Methods 996.06 [14], with some modifications. Aliquots of 1 mL from each plasma sample were added to a screw-cap test tube and 5 mg pyrogalllic acid, 0.1 mL standard (5 mg/mL tritridecanoic C13:0 in chloroform), 0.1 mL ethanol, 0.5 mL HCl 8.3 M and some glass beads were added. The tubes were placed in a water bath at 75 °C for 40 min and then cooled at room temperature. Subsequently, 1 mL ethyl ether and 1 mL petroleum ether were added and samples were centrifuged at 10,000 rpm for 5 min. Top phase was transferred to another tube and ether was evaporated under N_2 in a water bath (below 40 °C). Methylation was performed by addition of 1 mL BF_3 (7 % in methanol) and 0.5 mL toluene and subsequent boiling at 100 °C for 45 min. After cooling at room temperature, 2.5 mL water, 1 mL hexane and approximately 0.5 g Na_2SO_4 anhydrous were added. The tubes were left to rest to allow phase separation and then the top phase was transferred to a vial containing anhydrous Na_2SO_4 and evaporated under N_2 . Before injection into the chromatograph, 0.2 mL hexane was added to each sample. Samples were analyzed using gas chromatography on a GC 17A (Shimadzu) equipped with a flame-ionization detector (FID), automatic injector AOC-20 and a

Workstation Class GC10. Fatty acid separation was achieved using a fused-silica column SP-2560 (bis-cyano-propyl polysiloxane) (100 m \times 0.25 mm \times 0.2 μ m; Supelco, Bellefonte, USA). The column temperature was programmed as follows: 140 °C for 5 min; heating at 4 °C/min until 240 °C; 240 °C for 30 min. The injector and detector were at 250 °C, and helium was used as the carrier gas at a 1 mL/min flow rate. The split ratio was 1/10. Two microliters of derivatized lipid extract was injected and the fatty acid methyl ester peaks were identified by comparison of retention times of fatty acid methyl ester standards and the chromatograms viewed in the Ce 1 h-05 methods [15].

ROS Production as Determined by Lucigenin-Amplified Chemiluminescence Assay

The lucigenin-amplified chemiluminescence assay is able to measure ROS, mostly superoxide anion, since lucigenin releases energy in the form of light when excited by superoxide anion. After 1 h incubation of macrophages (4×10^5 cells in a final volume of 200 μ L), the culture medium was discarded and PBS supplemented with 10 % FBS, 10 mM glucose, 1.5 mM magnesium chloride, 1 mM calcium chloride and 1 mM lucigenin was added in the absence or presence of PMA (positive control-10 nM) (250 μ L of final volume). Chemiluminescence was measured in luminometer (Synergy HT Multi-Mode Microplate Reader, BioTek Instruments, Inc., Winooski, VT, USA) during 1 h at 37 °C [16]. Results were expressed as chemiluminescence during 1 h, subtracting blank values.

ROS Production as Determined by Amplex[®] Ultrared Fluorescence Assay

Amplex[®] Ultrared fluorescence assay is also able to measure ROS, but it detects mainly hydrogen peroxide. The product of Amplex[®] (*N*-acetyl-3,7-dihydroxyphenoxazine) oxidation, after HRP-catalyzed reduction of hydrogen peroxide, is named resorufin. This is a red, stable and fluorescent compound that can be measured by fluorometry, indicating the relative amount of hydrogen peroxide in the sample [17]. After 1 h incubation (4×10^5 cells in a final volume of 200 μ L), culture medium was discarded and PBS supplemented with 10 % FBS, 10 mM glucose, 1.5 mM magnesium chloride, 1 mM calcium chloride, 50 μ M Amplex[®] Ultrared and 0.1 U/mL HRP type II was added in the absence or presence PMA (positive control—10 nM) (200 μ L of final volume). The plate was then incubated in the dark for 1 h at 37 °C, followed by measurement in a fluorimeter (Synergy HT Multi-Mode Microplate Reader, BioTek Instruments, Inc., Winooski, VT, USA) (excitation 530 nm/emission 590 nm). Results were expressed as fluorescence during 1 h, subtracting blank values.

Nitrite Quantification

Macrophages (10^6 cells) were incubated in RPMI medium in a final volume of 1 mL for 24 h in the absence or presence of LPS (positive control—5 $\mu\text{g}/\text{mL}$). For quantification of nitrite, 100 μL Griess reagent (1 % sulfanilamide in 5 % H_3PO_4 and 0.1 % α -naphthyl ethylenediamine in distilled water, mixed 1:1) was added to 100 μL cell culture supernatant in a 96-well plate. The standard curve was determined by different concentrations of sodium nitrite (0–80 μM) and sample absorbance was measured in spectrophotometer (Synergy HT Multi-Mode Microplate Reader, BioTek Instruments, Inc., Winooski, VT, USA) at 550 nm [18]. Results were expressed as nitrite production (μM).

Cytokine and VEGF Quantification in Culture Supernatants

Macrophages (10^6 cells) were incubated in RPMI medium in a final volume of 250 μL for 5 h or 1 mL for 24 h in the absence or presence of LPS (positive control—5 $\mu\text{g}/\text{mL}$). Tumor necrosis factor- α (TNF- α), interleukin-1 β (IL-1 β), interleukin-6 (IL-6), cytokine-induced neutrophil chemoattractant-2 $\alpha\beta$ (CINC-2 $\alpha\beta$ /CXCL3), interleukin-10 (IL-10) and vascular endothelial growth factor (VEGF) quantifications were performed in sample supernatants using DuoSet kits (Minneapolis, MN, USA), as described by the manufacturer. Sample absorbance was measured in a spectrophotometer (Synergy HT Multi-Mode Microplate Reader, BioTek Instruments, Inc., Winooski, VT, USA) at 450 nm.

Eicosanoid Quantification in Culture Supernatants

Macrophages (10^6 cells) were incubated in RPMI medium in a final volume of 1 mL for 24 h in the absence or presence of LPS (positive control—5 $\mu\text{g}/\text{mL}$). Prostaglandin E_2 (PGE $_2$), leukotrienes B_4 (LTB $_4$) and 15(*S*)-hydroxyeicosatetraenoic acid (15(*S*)-HETE) quantifications were performed in culture supernatants using Cayman kits (Ann Arbor, MI, USA), as described by the manufacturer. Sample absorbance was measured in a spectrophotometer (Synergy HT Multi-Mode Microplate Reader, BioTek Instruments, Inc., Winooski, VT, USA) at 412 nm.

Statistical Analysis

Results are presented as means \pm standard error means (SEM). Comparison between control (C) and fatty acid treated groups was performed using one way ANOVA and Dunnett post hoc test. Significant difference was considered when $p < 0.05$.

Results

Viability of Macrophages

There were no differences between groups with respect to macrophage viability determined by the MTT assay or macrophage DNA fragmentation (data not shown).

Plasma Fatty Acid Composition

Animals treated with OLA presented an increase in plasma OLA by 71 %, whereas treatment with LNA increased plasma LNA by 48 and stearic acid by 40 % (Supplementary Table 1), confirming that oral administration with fatty acids changed plasma fatty acid composition.

ROS and Nitrite Production by Macrophages

There were no differences between groups with respect to production of ROS (Fig. 1) or nitrite (Fig. 2).

Cytokine and VEGF Production by Macrophages

Cytokine and VEGF concentrations were measured in the supernatant of cells incubated for 5 or 24 h and with or without LPS stimulation. There was no significant difference in TNF- α production between groups. Linoleic acid increased IL-1 β release by 34 % when macrophages were stimulated with LPS during 5 h compared with the control group. After 24 h of incubation, unstimulated macrophages from rats that received either OLA or LNA showed a reduction by 50 and 62 %, respectively, in IL-1 β release. Oleic acid decreased by 54 and 45 % IL-6 release, in the absence and presence of LPS, respectively, after 5 h of incubation. Linoleic acid decreased IL-6 production by unstimulated macrophages after 5 and 24 h by 45 and 55 %, respectively. Oleic acid decreased CINC-2 $\alpha\beta$ production by unstimulated macrophages by 43 % after 5 h. Linoleic acid decreased IL-10 production by LPS-stimulated macrophages by 49 % after 24 h (Fig. 3). LPS did not increase VEGF release (data not shown). Neither OLA nor LNA changed VEGF production after 5 h of incubation, whereas after 24 h, LNA caused a reduction by 31 % (Fig. 4).

Eicosanoid Production by Macrophages

Neither OLA nor LNA altered production of PGE $_2$, LTB $_4$ or 15(*S*)-HETE after 24 h (Fig. 5).

Discussion

Oleic and linoleic acids are two commonly consumed fatty acids in the human diet and they can influence the immune

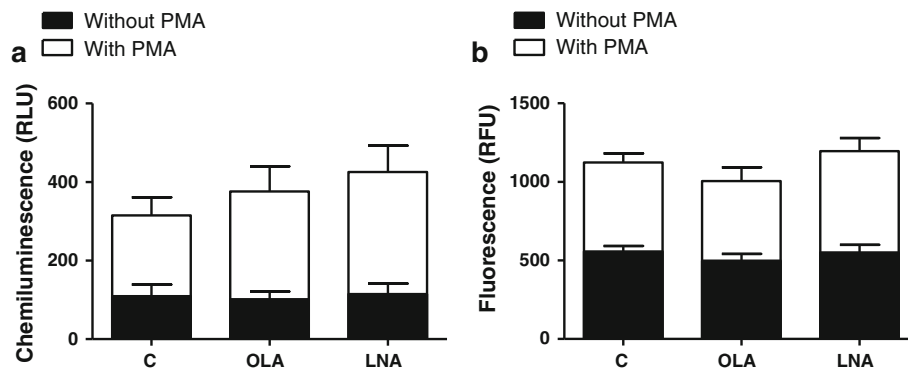


Fig. 1 Effects of oleic or linoleic acids on ROS production by macrophages from the different groups in the absence or presence of PMA. **a** Mainly superoxide is measured. **b** Mainly hydrogen peroxide is measured. Peritoneal macrophages (4×10^5 cells) from rats treated

for 10 days with water (control), oleic or linoleic acids were cultured for 1 h in the absence or presence of PMA (10 nM). Results are presented as means \pm SEM, $n = 9$ –13 samples

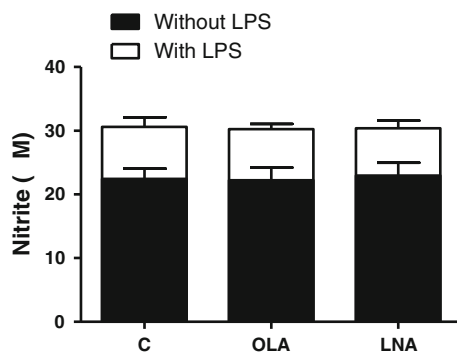


Fig. 2 Effects of oleic or linoleic acids on nitrite production by macrophages from the different groups in the absence or presence of LPS. Peritoneal macrophages (10^6 cells) from rats treated for 10 days with water (control), oleic or linoleic acids were cultured for 24 h in the absence or presence of LPS ($5 \mu\text{g}/\text{mL}$). Results are presented as mean \pm SEM, $n = 9$ samples

response [3–5]. Moreover, oral administration of either fatty acid improves the wound healing process of rats [9], in which macrophages play an important role. The present study has shown that the oral administration of OLA or LNA modulates macrophage function, i.e., decreases the production of $\text{IL-1}\beta$, IL-6 , $\text{CINC-2}\alpha\beta$, IL-10 and VEGF . The production of superoxide anion, hydrogen peroxide, nitrite, $\text{TNF-}\alpha$, PGE_2 , LTB_4 and $15(S)\text{-HETE}$, however, remained unchanged. The findings are summarized in Table 2.

The lack of effect of fatty acids on the MTT assay and DNA fragmentation indicates that the functional effects of the fatty acids observed here do not relate to an altered viability of the macrophages.

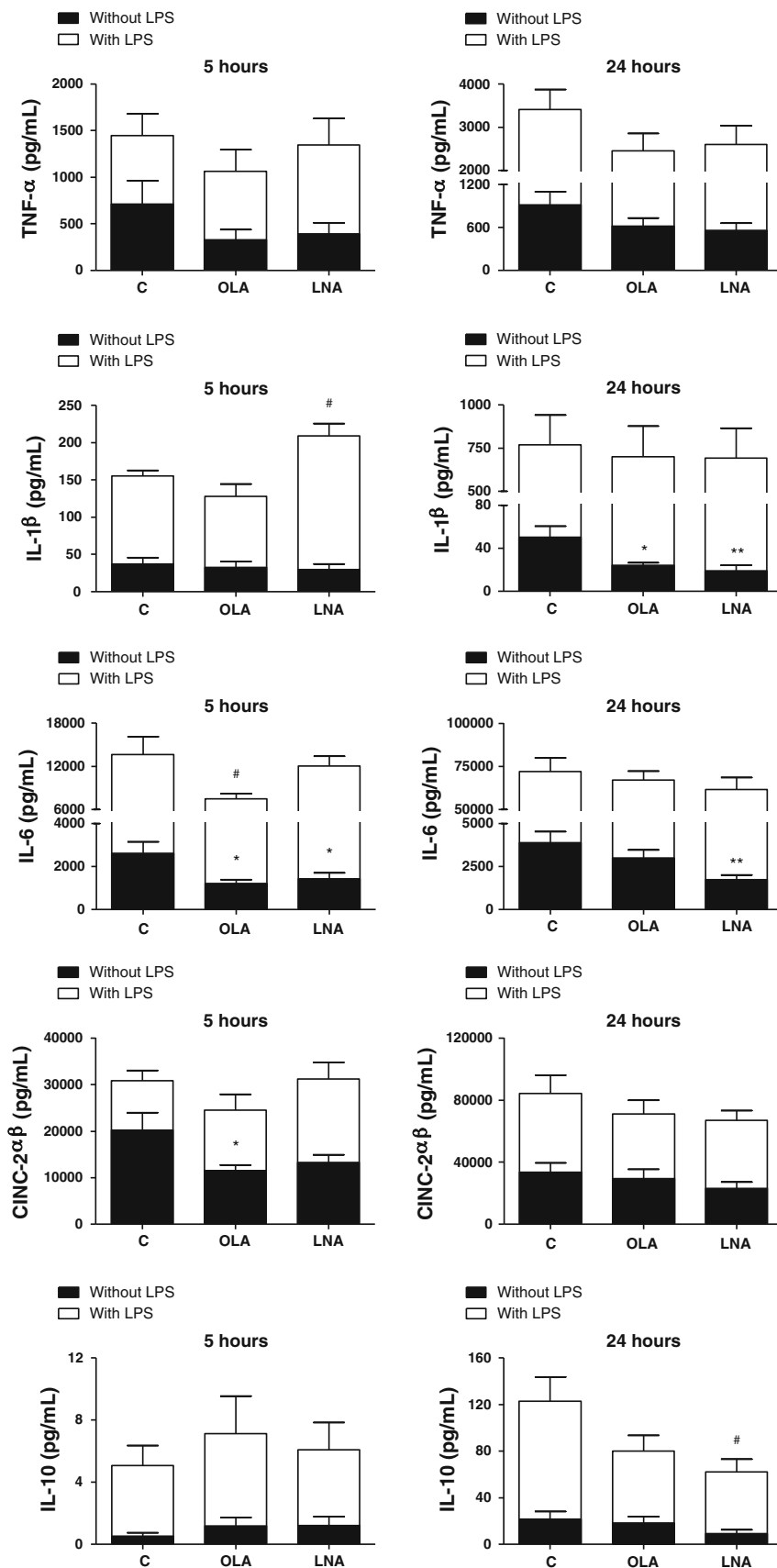
The lack of effect of the two fatty acids on production of superoxide, hydrogen peroxide and nitrite (a surrogate for nitric oxide produced by inducible nitric oxide synthase) indicates that some of the fundamental aspects of host defense associated with macrophages remain intact after

exposure to these two fatty acids. However, these mediators are associated with inflammation, so these components of the inflammatory response seem unaffected by the two fatty acids, as used here. In previous studies, feeding mice olive oil (a source of OLA) or safflower oil (a source of LNA) for a period of 8 weeks increased nitric oxide production by LPS-stimulated peritoneal macrophages [19], whereas feeding for 16 weeks decreased it [20]. Such conflicting observations may be explained by differences in treatment period, consumed doses of fatty acids, or effects of other compounds present in the oils that influence macrophage function.

During the inflammatory response, several cytokines are secreted by macrophages and other cells, as a result of pattern recognition receptor (PRR) activation by microorganisms. $\text{TNF-}\alpha$ is one of the first cytokines to be secreted during inflammation and it elicits various reactions in the organism, including leukocyte activation and migration to the inflammatory site, cell proliferation, differentiation and apoptosis [21, 22]. There was no significant difference between cells isolated from control animals and those treated orally with OLA or LNA with regard to $\text{TNF-}\alpha$ production. Feeding olive or safflower oils for 6 or 8 weeks reduced $\text{TNF-}\alpha$ secretion by thioglycolate-elicited peritoneal macrophages stimulated with LPS [19, 20, 23]. It should be noted, however, that the activation state of the cells influences such response, since peritoneal resident macrophages stimulated with LPS did not present alteration in $\text{TNF-}\alpha$ production when animals were fed these same oils [23].

$\text{IL-1}\beta$ is secreted mainly by macrophages and monocytes and is synthesized as its precursor, pro- $\text{IL-1}\beta$ [24]. Treatment with LNA accelerated $\text{IL-1}\beta$ release when macrophages were stimulated with LPS, since despite the increase after 5 h of incubation, $\text{IL-1}\beta$ level was similar to control after 24 h of incubation. However, in the absence

Fig. 3 Effects of oleic or linoleic acids on TNF- α , IL-1 β , IL-6, CINC-2 $\alpha\beta$, IL-10 production by macrophages from the different groups in the absence or presence of LPS. Peritoneal macrophages (10^6 cells) from rats treated for 10 days with water (control), oleic or linoleic acids were cultured for 5 or 24 h in the absence or presence of LPS (5 $\mu\text{g}/\text{mL}$). Results are presented as mean \pm SEM, $n = 7$ –15 samples. * $p < 0.05$, ** $p < 0.01$, compared to control without LPS; # $p < 0.05$, comparing to control with LPS (One way ANOVA and Dunnett post hoc test)



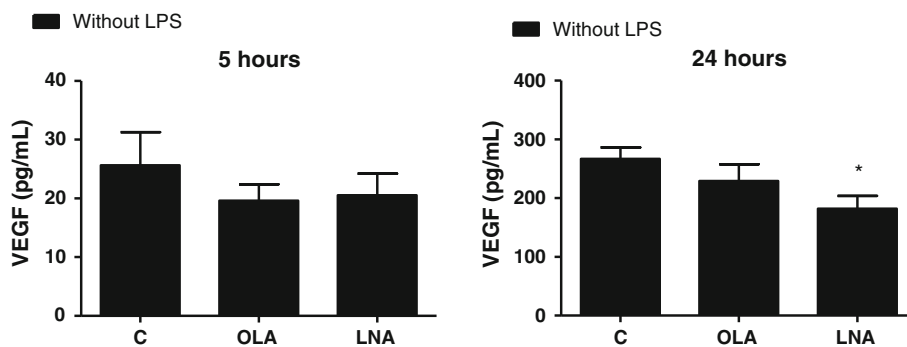
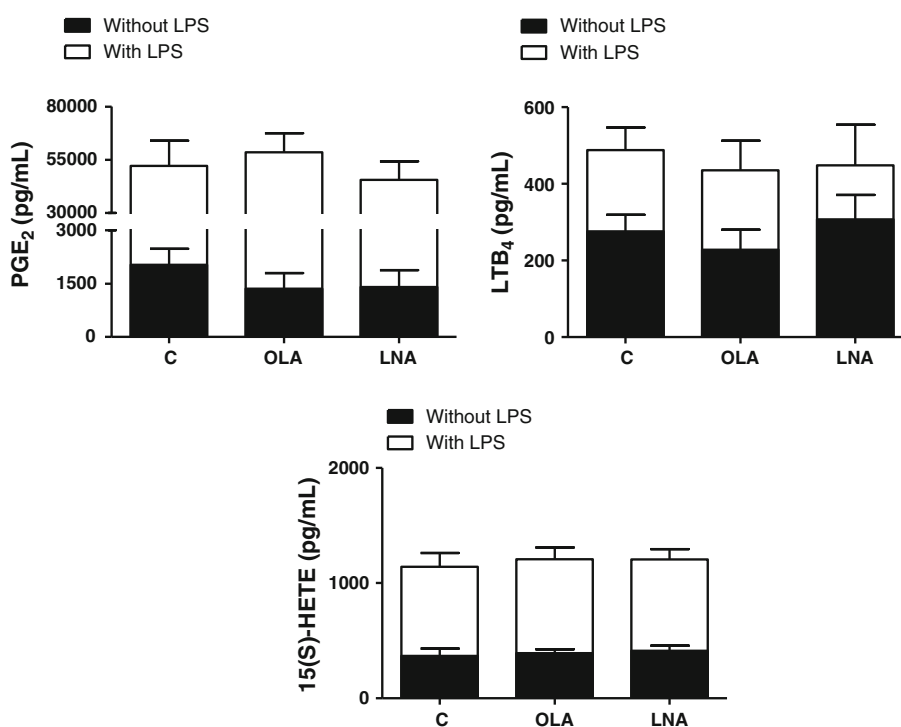


Fig. 4 Effects of oleic or linoleic acids on VEGF production by macrophages from the different groups in the absence or presence of LPS. Peritoneal macrophages (10^6 cells) from rats treated for 10 days with water (control), oleic or linoleic acids were cultured for 5 or 24 h

in the absence of LPS. Results are presented as mean \pm SEM, $n = 10$ – 14 samples. * $p < 0.05$, compared to control (One way ANOVA and Dunnett post hoc test)

Fig. 5 Effects of oleic or linoleic acids on PGE₂, LTB₄ and 15(S)-HETE production by macrophages from the different groups in the absence or presence of LPS. Peritoneal macrophages (10^6 cells) from rats treated for 10 days with water (control), oleic or linoleic acids were cultured for 5 or 24 h in the absence or presence of LPS (5 μ g/mL). Results are presented as mean \pm SEM, $n = 9$ – 11 samples



of LPS, a suppressive effect of OLA or LNA on IL-1 β production was only observed after 24 h incubation. Considering that IL-1 β is an important mediator of inflammation, since it stimulates signaling pathways that trigger the expression of other cytokines, chemokines, adhesion molecules, acute phase proteins and proteases [25, 26], the acceleration of its release may hasten the resolution of the inflammatory response. Other studies demonstrated that IL-1 β release is not altered by macrophages isolated from animals supplemented with olive and safflower oils and stimulated with LPS [19, 23].

In addition to TNF- α and IL-1 β , macrophages also produce IL-6 in response to microorganism recognition and together they modulate local and systemic inflammation

[27]. Oleic acid delayed IL-6 production by macrophages stimulated or not with LPS, since its level was lower than control after 5 h of incubation but was similar to control after 24 h. Linoleic acid decreased IL-6 release only in the absence of LPS and this effect was maintained until 24 h. Although several studies have demonstrated a suppressive effect of the in vivo treatment with (n-3) fatty acids [28–30] on IL-6 production by macrophages, this is the first in which the same effects have been demonstrated with OLA and LNA. Among several actions, IL-6 stimulates the synthesis of acute phase proteins, modulates cytotoxic T lymphocyte proliferation and differentiation, induces antibody production by B lymphocytes and stimulates the resolution of inflammation. However, its overproduction is

Table 2 Summary of the effects of oleic and linoleic acids on the production of inflammatory mediators by macrophages

	Oleic acid		Linoleic acid	
	Without stimulus	With stimulus	Without stimulus	With stimulus
O ₂ ⁻	↔	↔	↔	↔
H ₂ O ₂	↔	↔	↔	↔
Nitrite	↔	↔	↔	↔
TNF- α 5 h	↔	↔	↔	↔
TNF- α 24 h	↔	↔	↔	↔
IL-1 β 5 h	↔	↔	↔	↑
IL-1 β 24 h	↓	↔	↓	↔
IL-6 5 h	↓	↓	↓	↔
IL-6 24 h	↔	↔	↓	↔
CINC-2 $\alpha\beta$ 5 h	↓	↔	↔	↔
CINC-2 $\alpha\beta$ 24 h	↔	↔	↔	↔
IL-10 5 h	↔	↔	↔	↔
IL-10 24 h	↔	↔	↔	↓
VEGF 5 h	↔	↔	↔	↔
VEGF 24 h	↔	↔	↓	↔
PGE ₂	↔	↔	↔	↔
LTB ₄	↔	↔	↔	↔
15(S)-HETE	↔	↔	↔	↔

↔ unaltered, ↓ decreased, ↑ increased

15(S)-HETE 15(S)-hydroxyeicosatetraenoic acid, CINC-2 $\alpha\beta$ cytokine-induced neutrophil chemoattractant-2 $\alpha\beta$, IL-1 β interleukin-1 β , IL-6 interleukin-6, IL-10 interleukin-10, LTB₄ leukotrienes B₄, PGE₂ prostaglandin E₂, TNF- α tumor necrosis factor- α , VEGF vascular endothelial growth factor

associated with Crohn's disease, Castleman's disease, multiple myeloma and rheumatoid arthritis [31, 32].

The release of cytokines such as TNF- α , IL-1 β and IL-6 at inflammatory sites stimulates chemokine expression [33]. Among the different chemokines, the CXC chemokines are the main chemoattractants of neutrophils during inflammation, which then migrate toward areas with higher concentration of chemokines [34]. Oral administration of OLA delayed CINC-2 $\alpha\beta$ production, as observed by the lower concentration compared to control after 5 h of incubation followed by a similar one after 24 h. In contrast, neutrophils from rats treated with LNA showed higher production of CINC-2 $\alpha\beta$ after 4 h of incubation but a reduction in such production after 18 h [10]. A similar response was observed in the wound tissue of animals treated with LNA [9]. Opposite effects on neutrophils and macrophages may assure an appropriate inflammatory response, as they have distinct but complementary features and kinetics [35].

After eliminating microorganisms, macrophages are stimulated to ingest apoptotic cells. This process triggers the release of inflammation-resolving cytokines such as IL-10 and TGF- β [2]. IL-10 is a central cytokine during resolution of inflammation and acts by repressing the pro-

inflammatory response from innate and adaptive immunity and thus prevents tissue damage caused by these cytokines. On the other hand, increased expression of IL-10 has been associated with chronic infectious state, since the inflammatory response is repressed [36]. Therefore, the lower production of IL-10 caused by oral treatment with linoleic acid in the presence of LPS after 24 h incubation may lead to a higher microbicidal activity of these cells. There are very few studies assessing the effect of fatty acids on IL-10 production and most of them used (n-3) fatty acids. Dietary fish oil decreases IL-10 release by murine peritoneal macrophages, when compared to a corn oil diet [37].

The synthesis of VEGF is also essential for the resolution of inflammation and tissue repair, since it stimulates the formation of new blood vessels and thus enables the supply of nutrients and oxygen to the tissue. VEGF is mainly secreted by macrophages and keratinocytes in response to hypoxia and acts on endothelial cells from local blood vessels. Therefore, its synthesis must be strictly controlled, otherwise it can trigger fibrosis and cancer [1, 38, 39]. This is the first study to analyze the effect of fatty acids on VEGF production by macrophages and it was observed that the oral administration of OLA or LNA decreased VEGF production after 24 h incubation.

Lipid mediators are mostly derived from arachidonic acid and also play a central role in the inflammatory response such that those that are synthesized during the beginning of inflammation are gradually switched to others with anti-inflammatory and inflammation-resolving properties [40]. In addition to its effect on the cardinal signs of acute inflammation, PGE₂ also acts as an anti-inflammatory mediator depending on the context, whereas LTB₄ stimulates the recruitment of neutrophils and lipoxins promote resolution of inflammation [40–42]. There was no effect of the in vivo treatment with OLA or LNA on eicosanoid synthesis. In agreement with our observations, feeding mice olive or safflower oils had no effect on eicosanoid production by resident macrophages when stimulated with LPS [23]. Likewise, a diet rich in LNA did not change PGE₂ and LTB₄ production by macrophages after infection with *Mycobacterium tuberculosis* [43]. 15(S)-HETE is one of the precursors of lipoxins and its synthesis is catalyzed by 15-lipoxygenase, present in various types of cells including macrophages [44]. Therefore, the effects of fatty acids on 15(S)-HETE production might indicate alterations on lipoxin synthesis. This is the first study to assess the effect of OLA or LNA on 15(S)-HETE production by macrophages. The lack of effect of these two fatty acids on eicosanoid production may mean that arachidonic acid levels in macrophages were not altered by these fatty acids. However, fatty acid composition of the cells was not assessed here, so this explanation cannot be confirmed.

In conclusion, OLA decreased the production of IL-1 β , IL-6 and CINC-2 $\alpha\beta$ by resident macrophages, indicating that this fatty acid may be therapeutically used to control inflammation. Linoleic acid decreased the production of IL-1 β , IL-6 and VEGF in the absence of LPS, although it accelerated IL-1 β release and decreased IL-10 synthesis when cells were stimulated with LPS. The mechanisms of action of the fatty acids in exerting these actions are unknown and were not investigated here. It could be speculated that part of their actions occurs through activation/inhibition of transcription factors, such as NF- κ B, AP-1 or PPARs, but further investigations are needed. The present study makes an important contribution to the elucidation of the effects of OLA or LNA on the production of several inflammatory mediators by macrophages and it is tempting to suggest that they might be used for treating pathological states in which macrophages play a central role, such as wound healing.

Acknowledgments This study was supported by Fundação de Amparo à Pesquisa do Estado de São Paulo (FAPESP), Conselho Nacional de Desenvolvimento Científico e Tecnológico (CNPq) and Coordenação de Aperfeiçoamento de Pessoal de Nível Superior (CAPES).

Conflict of interest The authors declare that they have no conflict of interest.

References

- Laskin DL, Sunil VR, Gardner CR, Laskin JD (2011) Macrophages and tissue injury: agents of defense or destruction? *Annu Rev Pharmacol Toxicol* 51:267–288
- Nathan C, Ding AH (2010) Nonresolving Inflammation. *Cell* 140(6):871–882
- Yaquob P (2002) Monounsaturated fatty acids and immune function. *Eur J Clin Nutr* 56(Suppl 3):S9–S13
- Calder PC, Grimble RF (2002) Polyunsaturated fatty acids, inflammation and immunity. *Eur J Clin Nutr* 56(Suppl 3):S14–S19
- Galli C, Calder PC (2009) Effects of fat and fatty acid intake on inflammatory and immune responses: a critical review. *Ann Nutr Metab* 55(1–3):123–139
- Nutrient Intakes from Food: Mean Amounts Consumed per Individual, by Gender and Age, What We Eat in America, NHANES 2007–2008 (2010) US Department of Agriculture, Agricultural Research Service. www.ars.usda.gov/ba/bhnrc/fsrg
- Calder PC (2008) Polyunsaturated fatty acids, inflammatory processes and inflammatory bowel diseases. *Mol Nutr Food Res* 52(8):885–897
- British Nutrition Foundation (1992) Unsaturated fatty acids: nutritional and physiological significance. The Report of the British Nutrition Foundation Task Force, Chapman & Hall, London
- Rodrigues HG, Vinolo MAR, Magdalon J, Vitzel K, Nachbar RT, Pessoa AFM, Santos MF, Hatanaka E, Calder PC, Curi R (2012) Oral administration of oleic or linoleic acid accelerates the inflammatory phase of wound healing. *J Invest Dermatol* 132(1):208–215
- Rodrigues HG, Vinolo MA, Magdalon J, Fujiwara H, Cavalcanti DM, Farsky SH, Calder PC, Hatanaka E, Curi R (2010) Dietary free oleic and linoleic acid enhances neutrophil function and modulates the inflammatory response in rats. *Lipids* 45(9):809–819
- Bustos R, Sobrino F (1992) Stimulation of glycolysis as an activation signal in rat peritoneal-macrophages—effect of glucocorticoids on this process. *Biochem J* 282:299–303
- Rabinovich G, Castagna L, Landa C, Riera CM, Sotomayor C (1996) Regulated expression of a 16-kd galectin-like protein in activated rat macrophages. *J Leukoc Biol* 59(3):363–370
- Letari O, Nicosia S, Chiavaroli C, Vacher P, Schlegel W (1991) Activation by bacterial lipopolysaccharide causes changes in the cytosolic free calcium-concentration in single peritoneal-macrophages. *J Immunol* 147(3):980–983
- AOAC (2002) Official methods of analysis. AOAC International, Gaithersburg
- AOCS (2005) Official Method Ce 1 h-05. Determination of *cis*-, *trans*-, saturated, monounsaturated, and polyunsaturated fatty acids in vegetable or non-ruminant animal oils and fats by capillary GLC. AOCS Press, Champaign
- Hatanaka E, Levada-Pires AC, Pithon-Curi TC, Curi R (2006) Systematic study on ROS production induced by oleic, linoleic, and gamma-linolenic acids in human and rat neutrophils. *Free Radic Biol Med* 41(7):1124–1132
- Zhou M, Diwu Z, Panchuk-Voloshina N, Haugland RP (1997) A stable nonfluorescent derivative of resorufin for the fluorometric determination of trace hydrogen peroxide: applications in detecting the activity of phagocyte NADPH oxidase and other oxidases. *Anal Biochem* 253(2):162–168
- Grando FC, Felicio CA, Twardowschy A, Paula FM, Batista VG, Fernandes LC, Curi R, Nishiyama A (2009) Modulation of peritoneal macrophage activity by the saturation state of the fatty acid moiety of phosphatidylcholine. *Braz J Med Biol Res* 42(7):599–605

19. Yaqoob P, Calder P (1995) Effects of dietary lipid manipulation upon inflammatory mediator production by murine macrophages. *Cell Immunol* 163(1):120–128
20. Wallace FA, Neely SJ, Miles EA, Calder PC (2000) Dietary fats affect macrophage-mediated cytotoxicity towards tumour cells. *Immunol Cell Biol* 78(1):40–48
21. Tracey KJ, Cerami A (1993) Tumor necrosis factor: an updated review of its biology. *Crit Care Med* 21(10 Suppl):S415–S422
22. Locksley RM, Killeen N, Lenardo MJ (2001) The TNF and TNF receptor superfamilies: integrating mammalian biology. *Cell* 104(4):487–501
23. Wallace FA, Miles EA, Calder PC (2000) Activation state alters the effect of dietary fatty acids on pro-inflammatory mediator production by murine macrophages. *Cytokine* 12(9):1374–1379
24. Stylianou E, Saklatvala J (1998) Interleukin-1. *Int J Biochem Cell Biol* 30(10):1075–1079
25. Braddock M, Quinn A, Canvin J (2004) Therapeutic potential of targeting IL-1 and IL-18 in inflammation. *Expert Opin Biol Ther* 4(6):847–860
26. Bird S, Zou J, Wang TH, Munday B, Cunningham C, Secombes CJ (2002) Evolution of interleukin-1 beta. *Cytokine Growth F R* 13(6):483–502
27. Medzhitov R (2007) Recognition of microorganisms and activation of the immune response. *Nature* 449(7164):819–826
28. Bonilla DL, Ly LH, Fan YY, Chapkin RS, McMurray DN (2010) Incorporation of a dietary omega 3 fatty acid impairs murine macrophage responses to *Mycobacterium tuberculosis*. *PLoS ONE* 5(5):e10878
29. Shi Y, Pestka JJ (2009) Mechanisms for suppression of interleukin-6 expression in peritoneal macrophages from docosahexaenoic acid-fed mice. *J Nutr Biochem* 20(5):358–368
30. Jia Q, Zhou HR, Shi Y, Pestka JJ (2006) Docosahexaenoic acid consumption inhibits deoxynivalenol-induced CREB/ATF1 activation and IL-6 gene transcription in mouse macrophages. *J Nutr* 136(2):366–372
31. Assier E, Boissier MC, Dayer JM (2010) Interleukin-6: from identification of the cytokine to development of targeted treatments. *Joint Bone Spine* 77(6):532–536
32. Rose-John S, Scheller J, Elson G, Jones SA (2006) Interleukin-6 biology is coordinated by membrane-bound and soluble receptors: role in inflammation and cancer. *J Leukoc Biol* 80(2):227–236
33. Gouwy M, Struyf S, Proost P, Van Damme J (2005) Synergy in cytokine and chemokine networks amplifies the inflammatory response. *Cytokine Growth Factor Rev* 16(6):561–580
34. Olson TS, Ley K (2002) Chemokines and chemokine receptors in leukocyte trafficking. *Am J Physiol Regul Integr Comp Physiol* 283(1):R7–R28
35. Silva MT (2010) When two is better than one: macrophages and neutrophils work in concert in innate immunity as complementary and cooperative partners of a myeloid phagocyte system. *J Leukoc Biol* 87(1):93–106
36. Ouyang W, Rutz S, Crellin NK, Valdez PA, Hymowitz SG (2011) Regulation and functions of the IL-10 family of cytokines in inflammation and disease. *Annu Rev Immunol* 29:71–109
37. Petursdottir DH, Olafsdottir I, Hardardottir I (2002) Dietary fish oil increases tumor necrosis factor secretion but decreases interleukin-10 secretion by murine peritoneal macrophages. *J Nutr* 132(12):3740–3743
38. Tonnesen MG, Feng X, Clark RA (2000) Angiogenesis in wound healing. *J Investig Dermatol Symp Proc* 5(1):40–46
39. Hoeben A, Landuyt B, Highley MS, Wildiers H, Van Oosterom AT, De Bruijn EA (2004) Vascular endothelial growth factor and angiogenesis. *Pharmacol Rev* 56(4):549–580
40. Levy BD, Clish CB, Schmidt B, Gronert K, Serhan CN (2001) Lipid mediator class switching during acute inflammation: signals in resolution. *Nat Immunol* 2(7):612–619
41. Serhan CN, Chiang N, Van Dyke TE (2008) Resolving inflammation: dual anti-inflammatory and pro-resolution lipid mediators. *Nat Rev Immunol* 8(5):349–361
42. Funk CD (2001) Prostaglandins and leukotrienes: advances in eicosanoid biology. *Science* 294(5548):1871–1875
43. Mayatepek E, Paul K, Leichsenring M, Pfisterer M, Wagner D, Domann M, Sonntag HG, Bremer HJ (1994) Influence of dietary (n-3)-polyunsaturated fatty acids on leukotriene B4 and prostaglandin E2 synthesis and course of experimental tuberculosis in guinea pigs. *Infection* 22(2):106–112
44. Petasis NA, Akritopoulou-Zanze I, Fokin VV, Bernasconi G, Keledjian R, Yang R, Uddin J, Nagulapalli KC, Serhan CN (2005) Design, synthesis and bioactions of novel stable mimetics of lipoxins and aspirin-triggered lipoxins. *Prostaglandins Leukot Essent Fatty Acids* 73(3–4):301–321

Thermo-induced Vesicular Dynamics of Membranes Containing Cholesterol Derivatives

Tsuyoshi Yoda · Mun'delanji C. Vestergaard ·
Tsutomu Hamada · Phuc Thi Minh Le ·
Masahiro Takagi

Received: 8 May 2012 / Accepted: 8 June 2012 / Published online: 1 July 2012
© AOCs 2012

Abstract Membrane structural organization is an intrinsic property of a cell membrane. Any changes in lipid composition, and/or any stimuli that affect molecular packing induce structural re-organization. It membrane dynamics provide a means by which changes in structure organization can be determined, upon a change in the membrane internal or external environment. Here, we report on the effect of thermo-stress on membranes containing cholesterol liquid crystal (LC) compounds cholesterol benzoate (BENZO) and oxidized cholesterols. We have (1) revealed that lipid vesicles containing this artificial cholesterol derivative (BENZO) is thermo-responsive, and that this thermo-sensitivity is significantly similar to naturally oxy-cholesterols (2) elucidated the mechanism behind the membrane perturbation. Using Langmuir monolayer experiments, we have demonstrated that membrane perturbation was due to an increase in the molecular surface area, (3) discussed the similarities between cholesterol benzoate in the cholesterol LC state and in lipid bilayer membranes. Last, (4) drawing from previously reported findings, our new data on membrane dynamics, and the discussion above, we propose that artificial cholesterol derivatives such as BENZO, open new possibilities for controlled and tailored design using model membrane systems. Examples could include the development of

membrane technology and provide a trigger for progress in thermo-tropical liquid crystal engineering.

Keywords Lipid vesicles · Membrane dynamics · Cholesterol (CHOL) · Cholesterol liquid crystal (LC) · Oxidized cholesterol (OxyCHOL) · Thermo-responsive · Cholesterol benzoate (BENZO)

Abbreviations

DOPC	1,2-Dioleoyl- <i>sn</i> -glycero-3-phosphocholine
CHOL	Cholesterol
7KC	7-Ketocholesterol
7 β HC	7 β -Hydroxycholesterol
25HC	25-Hydroxycholesterol
CHOL	OC cholesterol oleyl carbonate
CHOL	PA cholesterol pelargonate
LC	Liquid crystal
RT	Room temperature
BENZO	Cholesterol benzoate
OxyCHOL	Oxidized cholesterol(s)

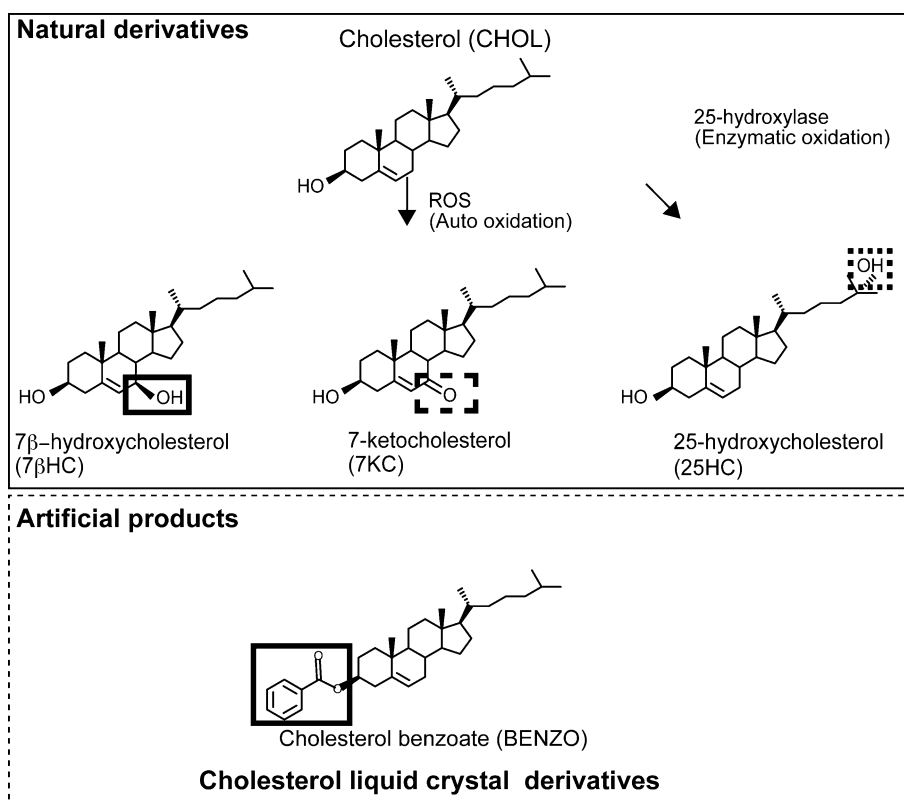
Introduction

Structural organization such as lipid packing, is an intrinsic property of cell membranes, and contributes to biophysical processes such as endo- and exocytosis, that are important for normal cellular function [1]. Cholesterol (CHOL) contributes about 30–40 % (mol%) to the total lipid composition of the membrane lipid bilayer [2]. Any changes in its molecular composition may induce membrane restructuring. In fact, it has been reported that oxidized cholesterol (OxyCHOL) renders membranes unstable more than non-oxidized cholesterol-containing systems [3, 4].

Electronic supplementary material The online version of this article (doi:10.1007/s11745-012-3695-9) contains supplementary material, which is available to authorized users.

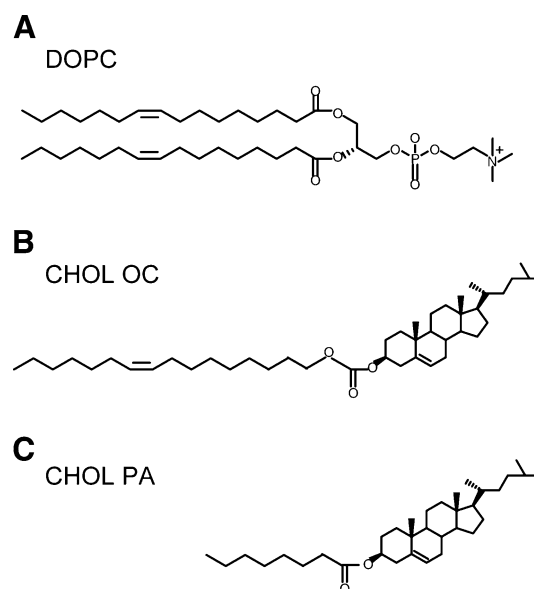
T. Yoda · M. C. Vestergaard (✉) · T. Hamada ·
P. T. M. Le · M. Takagi
School of Materials Science Japan Advanced Institute
of Science and Technology (JAIST), 1-1 Asahidai,
Nomi, Ishikawa 923-1292, Japan
e-mail: munde@jaist.ac.jp

Scheme 1 Cholesterol derivatives. Cholesterol can be oxidized either non-enzymatically or enzymatically. 7-Ketocholesterol (7KC) and 7 β HC are produced by reactive oxygen species. 25-Hydroxycholesterol (25HC) is oxidized enzymatically [5, 16]. BENZO is an artificial cholesterol derivative [18]



In a recent study, we investigated the thermo-responsiveness of OxyCHOL in lipid vesicles [5]. We observed changes in membrane perturbation and we proposed a mechanism behind the change in stability. In this study, we have elucidated the mechanism we had proposed. Further, we have investigated the effect of an artificial cholesterol derivative, cholesterol benzoate (BENZO, Scheme 1), on membrane stability. Since BENZO can form a cholesterol liquid crystal (LC) state, when in the presence of other natural cholesterol derivatives such as Cholesterol oleyl carbonate (CHOL OC) and Cholesterol pelargonate (CHOL PA) (Scheme 2) [6, 7] we aimed to investigate its effect on membrane dynamics. In particular, our choice was motivated by the similarities in structure between DOPC lipid and CHOL PA, CHOL OC. We investigated how the dynamics may relate to those induced by physiologically relevant OxyCHOL and the possible implications.

Membrane structural re-organization and re-packing can be induced by various forms of stimuli such as oxidation, light, and temperature [5, 8–12]. Rafts are considered to be a form of order–disorder phase separation that develop due to the interaction between lipid molecules. Ordered domains are cholesterol rich domains [1, 12, 13], and CHOL is one of the most important components of biological membranes. Oxidation of lipids, lipid peroxidation is a biomarker of cellular oxidative stress [14]. It has long been recognized as contributing to oxidative damage resulting from inflammatory processes, chemical and



Scheme 2 Similarity of structure between cholesterol liquid crystal CHOL PA and CHOL OC and phospholipid DOPC. Some natural cholesterol derivatives have been known to form cholesterol liquid crystal state. These include, CHOL OC (b) and CHOL PA (c). The structure of DOPC (a) acyl chains is similar to structure of esters in CHOL PA and CHOL OC with sterol backbones

reperfusion injury, and chronic diseases such as atherosclerosis and cancer [15]. Recent studies have suggested that cholesterol is an important target of oxidative stress in

membrane components [8, 14, 15]. Auto-oxidation of cholesterol at the C7 position produces 7-ketocholesterol (7KC), and 7 β -hydroxycholesterol (7 β HC), the major oxidized cholesterol species in atherosclerotic plaques [6]. Enzymatically oxidized derivatives of cholesterol are generated mainly on the iso-octyl side chain makes some products such as 24- and 25-hydroxycholesterols (Scheme 1) for production of these OxyCHOL [16]. Some cholesterol derivatives have been known to generate a LC phase [6, 17]. These compounds are used in fluorescence films for membrane technologies, exploiting their liquid crystalline properties [18]. We imagined that properties of membranes containing liquid crystals might be affected by temperature. Heterogeneous membrane containing cholesterol glycol lipid derivatives were reported to be thermo-responsive compounds [19].

In a recent study, Akiyama and colleagues investigated the effect of cholesterol glycolipids, at various temperatures, on domain stability [19]. Another group reported that increased levels of OxyCHOL in brain areas undergoing neuroinflammation may enhance exocytosis and neurotransmitter release, thereby aggravating excitotoxicity [20]. However, there is lot yet to be understood about membrane dynamic processes. Cell-sized lipid vesicles have been used to study the effect of different types of stresses on membrane stability [5, 8, 9, 21–24]. The cell-sized vesicles allow real-time observation of dynamic morphological changes to be clearly visualized, without compromising the “controllable” analytical advantage [2]. They also mimic the physiological environment closely in terms of the spatio-temporal scale at which interactions take place, thus allowing understanding and clarification of mechanisms [22, 25, 26]. In this study, we used such vesicles.

We had reported that 7KC was one of major derivatives of cholesterol after oxidative stress [5]. It has been reported that this OxyCHOL is related to crystal formation on macrophages and even muscles [27]. The crystal domain has been investigated on model membranes and cultured cells [28, 29]. Further, phase transitions of cholesterol derivatives were observed to influence liquid order domain stabilities [30]. However, as far as we are aware, membrane vesicular dynamics of BENZO known to form the LC state have not been reported. Here, we studied the dynamics of vesicles containing BENZO upon a slight increase in temperature. Using the Langmuir monolayer experiment, we analyzed changes in the molecular area in response to applied pressure by measuring the Π – A curve. We discussed the common mechanism between the lipid vesicles containing BENZO and those with OxyCHOL.

Materials and Methods

Materials

1,2-Dioleoyl-*sn*-glycero-3-phosphocholine (DOPC) and cholesterol (CHOL) were purchased from Avanti Polar Lipids (Alabaster, USA). Cholesterol benzoate (BENZO), 7 β -hydroxycholesterol (7 β HC), 7-ketocholesterol (7KC) and 25-hydroxycholesterol (25HC) were purchased from Sigma-Aldrich (USA). Chloroform was purchased from Kanto chemical (Japan). Methanol was from Nacalai Tesuque (Japan). Deionized water obtained from a Millipore Milli-Q purification system was used to prepare the reagents.

Preparation of Lipid Vesicles

Lipid vesicles were prepared by the natural swelling method from dry lipid films [5, 8]. Lipid mixtures (DOPC, CHOL, BENZO) dissolved in chloroform or chloroform/methanol (2:1, vol/vol) in a glass test tube. They were dried under a vacuum for 3 h to form thin lipid films. The films were then hydrated overnight with deionized water at room temperature (RT) to final concentrations of 0.2 mM lipids. During the course of this study, RT was approximately 22.0 ± 2.0 °C.

Microscopic Observation Conditions

The lipid vesicle solution (5 μ L) was placed in a silicon-well (0.2 mm) on a slide glass, and covered with a smaller cover slip. We observed changes in membrane morphology with a phase-contrast microscope (Olympus BX50, Japan), at RT. The silicon-well and the cover slip ensured that evaporation of the solution did not occur over the duration of the experiment. The images were recorded on a hard-disc drive at 30 frames/s.

Effect of Temperature on Membrane Fluctuation

We prepared two membrane systems composed of DOPC/CHOL (DOPC/CHOL (1:1 molar ratio), BENZO (DOPC/CHOL/BENZO 100:87.5:12.5). Lipid vesicles were prepared and observed as above. While on the stage, temperature was carefully changed using a thermal controller (Tokai-Hit MATS-5550RA-BT; Japan), from 22 to 40 °C. The samples were subjected to a temperature increase at a rate of 1.0 °C/min from 25 to 40 °C [5].

Effect of Temperature on Molecular Area of Monolayer Membranes

A Filgen LB-400 (Aichi, Japan) instrument (Kuhn type) was used to measure the π -A isotherms [32]. DOPC/CHOL (1:1) was dissolved in chloroform to a final concentration of 2 mM lipids and 5 μ L of this solution was added to 100 ml of Milli-Q pure water at each temperature. Temperatures were controlled by attaching the system to the instrument. Waiting for least 10 min, after each temperature was confirmed, the π -A isotherms were measured. Their π -A isotherms were measured using the same procedure and conditions as those of DOPC, DOPC/CHOL/BENZO (50:43.75:6.25), DOPC/CHOL/7KC (50:43.75:6.25), DOPC/CHOL/7 β HC (50:43.75:6.25), DOPC/CHOL/25HC (50:43.75:6.25) and OXY is DOPC/CHOL/7 β HC/7KC (50:43.75:3.75:2.5).

Results

Thermo-responsiveness of BENZO-containing Lipid Vesicles

First we prepared lipid vesicles containing BENZO at 6.25 % (molar ratio) of total lipids. We then investigated the thermo-responsiveness of the lipid vesicles containing BENZO. In this paper, we use the term thermo-responsiveness to describe the response by the lipid vesicles induced by the change in temperature [5]. Lipid vesicles were prepared using a natural swelling method [8] to a final lipid concentration of 0.2 mM. An unsaturated phospholipid 1,2-Dioleoyl-*sn*-glycero-3-phosphocholine (DOPC) constituted 50 % of the total. The other 50 % was

composed of cholesterol (CHOL) for DOPC/CHOL vesicles. For DOPC/CHOL lipid vesicles with BENZO or other cholesterol derivatives, the derivatives constituted 6.25 %, in line with our previous findings [5]. Scheme 1 shows the structures of the lipids, cholesterol and cholesterol derivatives used in this study. Figure 1 shows typical images of lipid vesicles containing DOPC/CHOL/BENZO and DOPC/CHOL upon increases in temperature. The bottom graphs show the degree of membrane fluctuation at 22 °C (black), 23 °C (gray) as a function of radius and its distribution. We plotted the value of radius of $r - \langle r \rangle$ in each θ ($\theta = \pm\pi/n$, $n = 1, 2, 3, \dots, 100$). The images and graphs clearly show that both lipid vesicles were spherical in

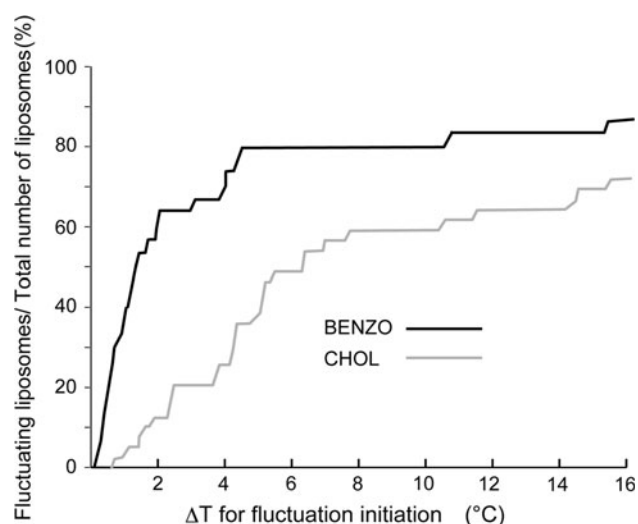


Fig. 2 Membrane fluctuation of lipid vesicles. Temperature was increased from RT to 25.0 °C, using a thermo-controller percentage of lipid vesicles, which started fluctuating at a given level of temperature increase, BENZO (black) and CHOL (gray) ($n = 30$)

Fig. 1 Membrane fluctuation of lipid vesicles. Temperature was increased from RT to 25.0 °C, using a thermo-controller. Images of a typical lipid vesicle captured using a phase-contrast microscope. The scale bar is 10 μ m. These graphs show membrane fluctuation at 22 °C (black), 23 °C (gray) as a function of radius and its distribution. Plotted the value of radius of $r - \langle r \rangle$ in each θ ($\theta = \pm\pi/n$, $n = 1, 2, 3, \dots, 100$) [5, 8, 21–23]. BENZO (a) and CHOL (b)

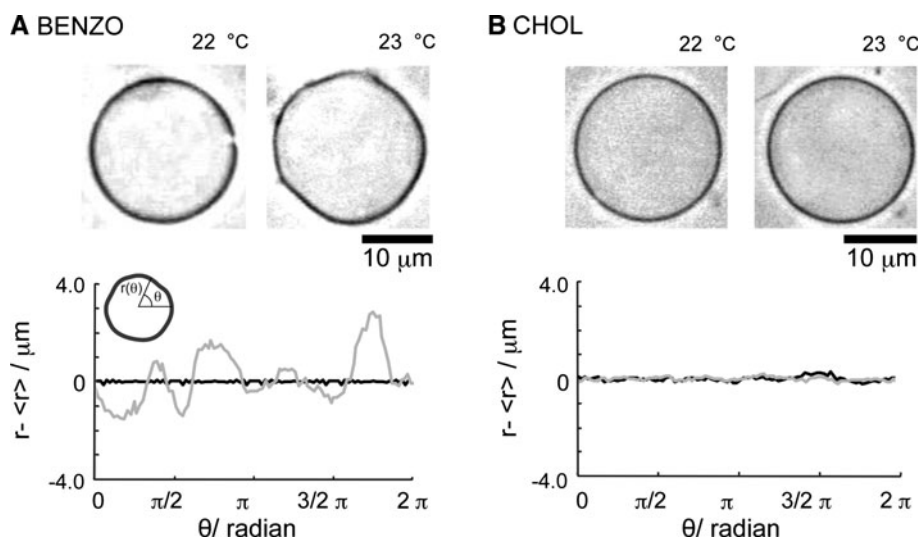


Table 1 The effect of temperature increase on membrane fluctuation. The values represent the increase in temperature (\uparrow temp.) required for 50 % of the lipid vesicles to start fluctuating. Some of data was reported previously [5]. We carried out >30 lipids vesicles per membrane type

Membrane system	Increase in temperature (\uparrow temp) ($^{\circ}$ C)
Cholesterol (CHOL)	6.4
7 β -Hydroxycholesterol (7 β HC)	2.5
7-Ketocholesterol (7KC)	1.7
25-Hydroxycholesterol (25HC)	1.7
OXY (7 β HC + 7KC)	0.5
Cholesterol benzoate (BENZO)	1.1

shape at 22 $^{\circ}$ C. At 23 $^{\circ}$ C, the DOPC/CHOL/BENZO vesicles started to fluctuate, in contrast to the DOPC/CHOL vesicle whose stability was not affected at this temperature.

We then studied membrane responses over a wider range of temperatures. Interestingly, even a small increase in temperature ($\Delta T \sim 2.0$ $^{\circ}$ C) was enough to actuate membrane fluctuation in more than half of the lipid vesicles

containing BENZO. We widened our temperature window even further (between 9 and 29 $^{\circ}$ C) in order to establish a response pattern. BENZO-containing membranes were more thermo-responsive than lipid vesicles without BENZO (Fig. 2). The degree of thermo-responsiveness for lipid vesicles containing the BENZO (which forms LC state at RT in mixture with other compounds [6, 7]), was comparable to that of vesicles containing auto- and enzymatically oxidized (that is, of direct physiological relevance) OxyCHOL [5] (Table 1).

Effect of Temperature on the Molecular Area of BENZO-Containing Lipid Membranes

Thermo-tropism of lipid vesicles containing BENZO although not new [18] is interesting when we consider that the vesicular stability was dramatically affected with a small increase in temperature, and the membrane perturbation was observed in real-time. We attempted to further our understanding by investigating the chemo-physical mechanism behind the changes in stability. Previously, we

Fig. 3 Thermal responsiveness of lipid monolayer membranes. DOPC, CHOL [DOPC/Chol (1:1)] and BENZO [DOPC/CHOL/BENZO (50:43.75:6.25)] are shown. Surface pressure (p)–area per molecule (A) at 30 mN/m, at each temperature from 9 to 29 $^{\circ}$ C. **a** Shows the typically p–A curves of membranes at each temperatures 9, 13, 17, 21, 25 $^{\circ}$ C respectively. Increases in molecular area correspond to the increasing temperature. DOPC (gray) CHOL (white) and BENZO (black) of **b**

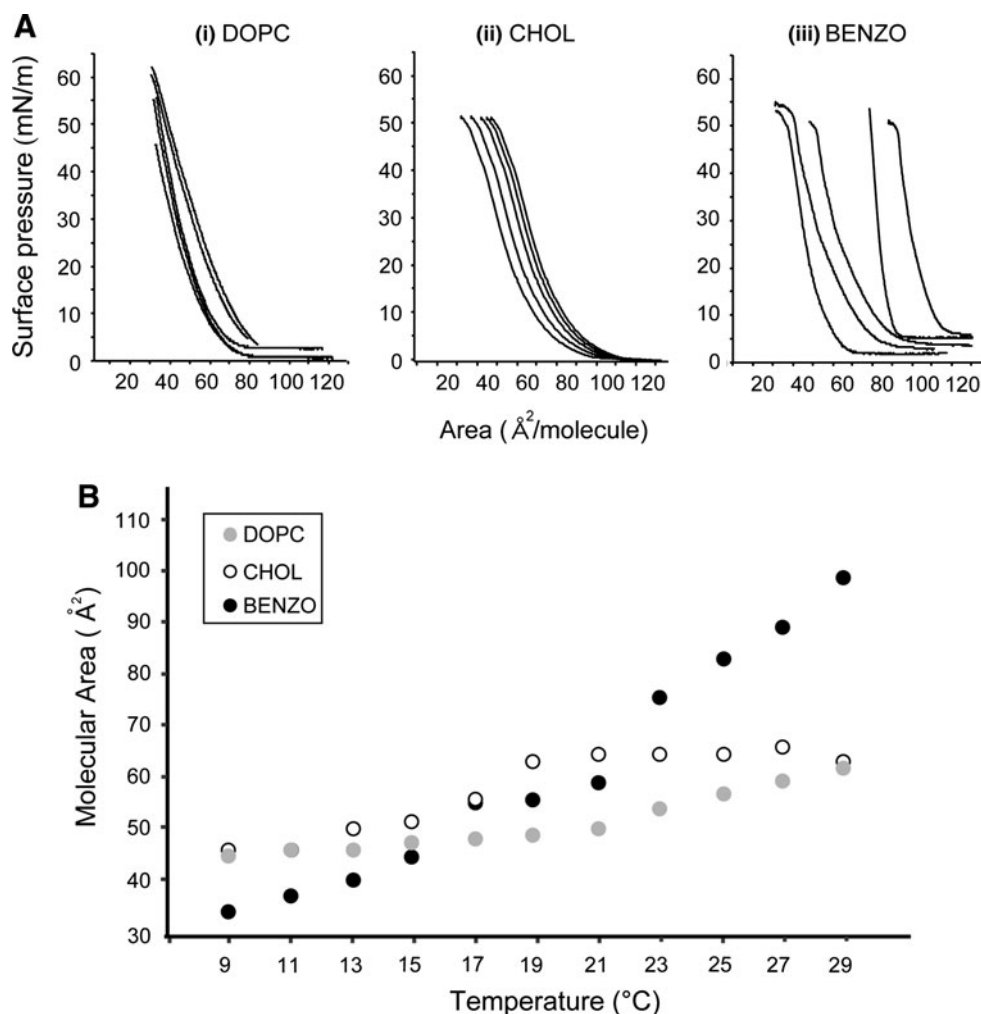
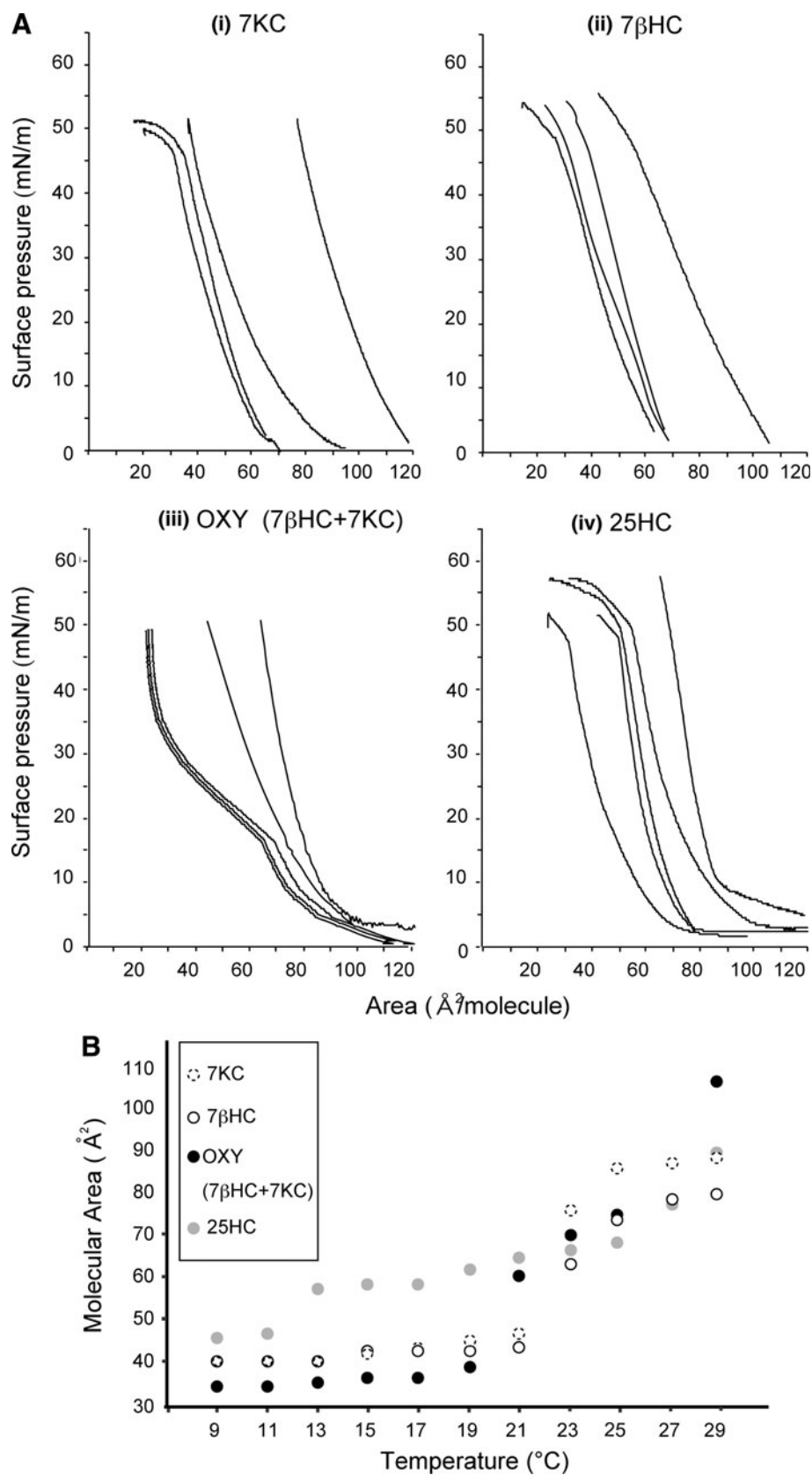


Fig. 4 Typical thermal responsiveness of lipid monolayer oxidized cholesterol-containing membranes, 7KC [DOPC/CHOL/7KC (50:43.75:6.25)], 7 β HC [DOPC/CHOL/7 β HC (50:43.75:6.25)] OXY [DOPC/CHOL/7 β HC/7KC (50:43.75:3.75:2.5)], 25HC [DOPC/CHOL/25HC (50:43.75:6.25)]. Surface pressure (p)–area per molecule (a) at 30 mN/m, at each temperature 9–29 °C. **a** Shows the typically P–A curves of a membrane at each temperatures 9, 13, 17, 21, 25 °C respectively ($n = 10$). However, data of 7KC and 7 β HC at 9, 13 were nearly equal value, we have omitted data at 9 °C. As increasing shown **b** that are 7KC (*dashed-circles*), 7 β HC (*white-circles*), OXY (7 β HC + 7KC, *black-circles*), and 25HC (*gray-circles*)



had hypothesized that the membrane dynamics induced by changes in temperature, were a consequence of an increase in molecular area [5]. We, therefore, studied the effect of temperature on the molecular area of monolayer membranes using the Langmuir monolayer membrane method. We prepared membrane systems composed of singular (unitary), binary and ternary mixtures of lipids (DOPC, DOPC/CHOL and DOPC/CHOL/BENZO membrane systems). First, we used the DOPC only system as an instrumental control. The control values agreed closely with previous reports (Fig. 3a) [31]. Subsequently, we conducted the monolayer experiments using these membrane systems. Assuming that the bilayer membrane consists of monolayers, the lateral pressure in the lipid bilayer would normally be 30–40 mN/m [32].

BENZO-containing monolayer membranes exhibited a relatively bigger increase in molecular area upon increasing temperature. The response pattern was quasi-linear. In agreement with the vesicular fluctuation reported above, cholesterol-only membrane systems showed only a slight increase in molecular area (Fig. 3b).

Effect of Temperature on Molecular Area of OxyCHOL-Containing Lipid Membranes

Recently, we studied the thermo-responses of lipid vesicles containing OxyCHOL to changes in temperature, and had hypothesized that the membrane perturbation we had observed was due to the increase in temperature [5]. Similar to BENZO-containing lipid vesicles, we followed up on our previous study and investigated the cause, using the Langmuir monolayer experiment. Indeed, we confirmed that thermo-induced fluctuation was due to an increase in molecular surface area (Fig. 4). Further, we established that the thermo-response of these two membrane systems (BENZO- and OxyCHOL-containing) is strikingly similar. Previously, it had been reported that a 3 % increase in a membrane surface area is enough to induce liposome fluctuation [23]. BENZO-containing membranes had a \approx 3 % molecular area increase at temperatures <2.0 °C (between 21 and 23 °C). Taken together, the results are in good agreement with the onset of fluctuation upon an increase in temperature (Fig. 2).

Discussion

We can now discuss these similarities of the two membrane systems, and the possible implications. First, we consider the following: (1) BENZO is known to form a LC state, at RT, when in the presence of other natural cholesterol derivatives such as CHOL OC and CHOL PA (Scheme 2) [6, 7]; (2) the self-ordering of the phospholipid bilayer in

membranes is a lyotropic liquid crystalline behavior, that is, phospholipid bilayers form a LC state [33, 34]; (3) the experimental conditions which include a mixing ratio of DOPC/CHOL/Cholesterol derivatives are similar to those of CHOL PA/CHOL OC/BENZO [7]. We calculated the correlation coefficient ($r = 0.83$) between the two membrane systems based on the numbers of carbons, hydrogen, and cholesterol molecule; (4) the structure of DOPC acyl chains is similar to structure of esters in CHOL PA and CHOL OC with sterol backbones (Scheme 2). Despite the knowledge that a cholesterol (twisted nematic) LC state can not exist in a physiological membrane, the facts above strongly suggest that at a molecular level, molecular interactions between BENZO in the DOPC/CHOL membranes are similar to BENZO's association in CHOL PA/CHOL OC. In addition, given our findings that the dynamics of BENZO- and OxyCHOL-containing membrane systems have significantly similar temperature sensitivity, we can now consider the lyotropic nature of BENZO in model membrane systems, and its possible exploitation for tailored design in model membranes.

To summarize, we have (1) succeeded in producing cell-sized membrane containing cholesterol liquid crystal BENZO, (2) revealed that lipid vesicles containing this artificial cholesterol derivative is thermo-responsive, and that this thermo-sensitivity is significantly similar to natural OxyCHOL, (3) elucidated the mechanism behind the membrane fluctuations. Using Langmuir monolayer experiments we have demonstrated that membrane perturbation was due to an increase in molecular surface area, (4) discussed the similarities between BENZO in the cholesterol LC state and in lipid bilayer membranes. Last, (5) drawing from previously reported findings, our new data on membrane dynamics, and the discussion above, we propose that artificial cholesterol derivatives such as BENZO, open new possibilities for controlled and tailored design using model membrane systems.

Acknowledgments We gratefully acknowledge Ms. Ryoko Sugimoto for technical support. We are grateful to Dr. Masaomi Hatakeyama for providing technical assistance with the analysis of membrane fluctuation. T.Y. is supported by a research fellowship from the Japan Society for the Promotion of Science (JSPS) for Young Scientists (no. 10297). This work was supported by a Grant-in-Aid for Scientific Research B, C and Young Scientists B from the JSPS and on Scientific Research on Priority Areas “Soft Matter Physics”, “Bio Manipulation”, and “Soft Interfaces” from the MEXT of Japan.

References

1. Simons K, Ikonen E (1997) Functional rafts in cell membranes. *Nature* 387:569–572
2. Vestergaard M, Hamada T, Takagi M (2008) Using model membranes for the study of amyloid beta: lipid interactions and neurotoxicity. *Biotechnol Bioeng* 99:753–763

3. Kim DH, Frangos JA (2008) Effects of amyloid β -peptides on the lysis tension of lipid bilayer vesicles containing oxysterols. *Biophys J* 95:620–628
4. Massey JB, Pownall HJ (2005) The polar nature of 7-ketocholesterol determines its location within membrane domains and the kinetics of membrane microsolvubilization by Apolipoprotein A-I. *Biochemistry* 44:10423–10433
5. Vestergaard MC, Yoda T, Hamada T, Akazawa-Ogawa Y, Yoshida Y, Takagi M (2011) The effect of oxysterols on thermo-induced membrane dynamics. *Biochim Biophys Acta* 1808:2245–2251
6. Small DM (1998) George Lyman Duff memorial lecture. Progression and regression of atherosclerotic lesions. Insights from lipid physical biochemistry. *Arterioscler Thromb Vasc Biol* 8:103–129
7. Elser W, Ennulat RD (1976) Selective reflection of cholesteric liquid crystal. In: Brown GH (ed) *Advanced in liquid crystals*, vol 2. Academic Press, New York, pp 73–172
8. Yoda T, Vestergaard MC, Akazawa-Ogawa Y, Yoshida Y, Hamada T, Takagi M (2010) Dynamic response of a cholesterol-containing model membrane to oxidative stress. *Chem Lett* 39:1273–1274
9. Hamada T, Sugimoto R, Vestergaard MC, Nagasaki T, Takagi M (2010) Membrane disk and sphere: controllable mesoscopic structures for the capture and release of a targeted object. *J Am Chem Soc* 132:10528–10532
10. Kas J, Sackmann E (1991) Shape transitions and shape stability of giant phospholipid vesicles in pure water induced by area-to-volume changes. *Biophys J* 60:825–844
11. Julien H, Bommeau S (2009) Asymmetric oxidation of giant vesicles triggers curvature-associated shape transition and permeabilization. *Biophys J* 97:2904–2912
12. Hamada T, Sugimoto R, Nagasaki T, Takagi M (2011) Photochemical control of membrane raft organization. *Soft Matter* 7:220–224
13. Hancock J (2006) Lipid rafts: contentious only from simplistic standpoints. *Nat Rev Mol Cell Biol* 7:456–462
14. Saito Y, Yoshida Y, Niki E (2007) Cholesterol is more susceptible to oxidation than linoleates in cultured cells under oxidative stress induced by selenium deficiency and free radicals. *FEBS Lett* 581:4349–4354
15. Dargel R (1992) Lipid-peroxidation—a common pathogenetic mechanism. *Exp Toxicol Pathol* 44:169–181
16. Doukyu N (2009) Characteristics and biotechnological applications of microbial cholesterol oxidases. *Appl Microbiol Biotechnol* 83:825–837
17. Golovina NA, Zagainova LI, Polishchuk AP, Puchkovskaya GA, Tatarinov SI (1988) Ordering and conformational transitions in cholesteryl benzoate. *J Appl Spectrosc* 49:1196–1202
18. Hussain A, Pina A, Roque A (2009) Bio-recognition and detection using liquid crystals. *Biosens Bioelectron* 25:1–8
19. Akiyama H, Hamada T, Nagatsuka Y, Kobayashi S, Hirabayashi Y, Murakami-Murofushi K (2011) Molecular diversity and functions of glycosylated lipids in biological membranes. *Cytologia* 76:19–25
20. Ma M, Zhang J, Farooqui AA, Chen P, Ong W (2010) Effects of cholesterol oxidation products on exocytosis. *Neurosci Lett* 476:36–41
21. Hamada T, Hirabayashi Y, Ohta T, Takagi M (2009) Rhythmic pore dynamics in a shrinking lipid vesicle. *Phys Rev E* 80:051921–051927
22. Morita M, Vestergaard MC, Hamada T, Takagi M (2010) Real-time observation of model-membrane dynamics induced by Alzheimer's amyloid beta. *Biophys Chem* 147:81–86
23. Ishii K, Hamada T, Hatakeyama M, Sugimoto R, Nagasaki T, Takagi M (2009) Reversible control of exo- and endo-budding transitions in a photosensitive lipid membrane. *ChemBioChem* 10:251–256
24. Hamada T, Kishimoto Y, Nagasaki T, Takagi M (2011) Photochemical control of membrane raft organization. *Soft Matter* 7:9061–9068
25. Takiguchi K, Negishi M, Takiguchi YT, Homma M, Yoshikawa K (2011) Transformation of ActoHMM assembly confined in cell-sized liposome. *Langmuir* 27:11528–11535
26. Hamada T, Hagihara H, Morita M, Vestergaard MC, Tsujino Y, Takagi M (2012) Physicochemical profiling of surfactant-induced membrane dynamics in a cell-sized liposome. *J Phys Chem Lett* 3:430–435
27. Phillips JE, Geng YJ, Mason RP (2001) 7-Ketocholesterol forms crystalline domains in model membranes and murine aortic smooth muscle cells. *Atherosclerosis* 8:125–135
28. Geng YJ, Phillips JE, Mason RP, Casscells SW (2003) Cholesterol crystallization and macrophage apoptosis: implication for atherosclerotic plaque instability and rupture. *Biochem Pharmacol* 66:1485–1492
29. Mason RP, Tulenko TN, Jacob RF (2003) Direct evidence for cholesterol crystalline domains in biological membranes: role in human pathobiology. *Biochim Biophys Acta* 1610:198–207
30. Ziblat R, Leiserowitz L, Addadi L (2010) Crystalline domain structure and cholesterol crystal nucleation in single hydrated DPPC:cholesterol:POPC bilayers. *J Am Chem Soc* 132:9920–9927
31. Park JW, Ahn DJ (2008) Temperature effect on nanometer-scale physical properties of mixed phospholipid monolayers. *Colloids Surf B* 62:157–161
32. Hamada T, Sato Y, Nagasaki T, Yoshikawa K (2005) Reversible photo-switching in a cell-sized vesicle. *Langmuir* 21:7626–7628
33. Steim JM, Tourtellotte ME, Reinert JC, McElhaney RN, Rader RL (1969) Calorimetric evidence for the liquid crystalline state of lipids in a biomembrane. *Proc Natl Acad Sci USA* 63:104–109
34. Tsong TY (1975) Transport of 8-anilino-1-naphthalenesulfonate as a probe of the effect of cholesterol on the phospholipid bilayer structures. *Biochemistry* 14:5409–5414

Evaluating the In Vitro Metabolism of Docosahexaenoic Acid in Sheep Rumen Fluid

Noelia Aldai · Gonzalo Hervás · Álvaro Belenguer ·
Pilar Frutos · Angel R. Mantecón · John K. G. Kramer

Received: 6 October 2011 / Accepted: 25 May 2012 / Published online: 14 June 2012
© AOCS 2012

Abstract Rumen metabolism (e.g., biohydrogenation) of dietary unsaturated fatty acids (FA) is one of the main reasons why ruminant fats tend to be highly saturated and contain many isomerized FA intermediates. The process by which long-chain (20- to 24-carbon FA) polyunsaturated FA (LC-PUFA) are metabolized by rumen bacteria is not as well understood as that of linoleic or linolenic acids. In order to better understand the fate of LC-PUFA in the rumen several concentrations of docosahexaenoic acid (DHA) were evaluated in in vitro batch incubations ranging from 100 to 1,500 µg per 6 mL of incubation volume using rumen fluid from sheep and incubated for 0, 1, 2, 3, and 6 h. From the results, it was shown that DHA was extensively metabolized at low (100 to 300 µg/6 mL incubation volume), but not at high level of inclusion (800 µg). At 300 µg of DHA most of the depleted DHA was recovered as LC-DHA metabolites within the first 6 h of incubation, and at the lowest levels (100 µg of incubation volume) further metabolism is apparent at 6 h. Using SP-2560 GC columns several LC-DHA metabolites were shown to elute after 24:0 and just past DHA, a region generally free of interfering FA. The present in

vitro study would appear to be a useful method to evaluate the production of DHA metabolites in combination with its depletion.

Keywords Fatty acid metabolism · DHA · Biohydrogenation · GC · Metabolites · Incubation

Abbreviations

DHA	Docosahexaenoic acid
EPA	Eicosapentaenoic acid
FA	Fatty acid(s)
FAME	Fatty acid methyl ester(s)
GC	Gas chromatography
h	Hour(s)
LC-PUFA	Long chain-polyunsaturated fatty acid(s)

Introduction

Over the last decade, numerous attempts have been made to enrich beef and milk products with docosahexaenoic acid (DHA) and eicosapentaenoic acid (EPA) [1, 2], because of the reported health benefits of these long-chain polyunsaturated fatty acids (LC-PUFA) [3]. The results of an extensive review have shown that the transfer efficiency of LC-PUFA into milk averaged about 4.1 % for DHA and 2.6 % for EPA [4]. A low transfer efficiency into meat lipids [5] is also consistent with the low levels of LC-PUFA leaving the rumen and entering the omasal canal in cows fed dietary fish oil supplements [6]. This raises the question of what is happening to LC-PUFA in the rumen to account for its disappearance. Dietary linoleic and linolenic acids are known to be extensively biohydrogenated [7], and a similar isomerization and reduction process to 22:0 have

N. Aldai (✉)
Food Science and Technology, Faculty of Pharmacy,
Universidad del País Vasco/Euskal Herriko Unibertsitatea,
01006 Vitoria, Spain
e-mail: noeliaaldai@gmail.com; noelia.aldai@ehu.es

G. Hervás · Á. Belenguer · P. Frutos · A. R. Mantecón
Instituto de Ganadería de Montaña, CSIC-ULE, Finca Marzanas,
24346 Grulleros, León, Spain

J. K. G. Kramer
Guelph Food Research Centre, Agriculture and Agri-Food
Canada, Guelph, ON N1G 5C9, Canada
e-mail: jkgkramer@rogers.com

been suggested recently for DHA [8]. A different process has also been proposed for the metabolism of LC-PUFA that involves the reduction and/or isomerization of double bonds closest to the carboxyl group [9]. To further investigate the metabolism of DHA in the rumen, a preliminary *in vitro* study was undertaken where several levels of unesterified DHA were incubated with total rumen fluid from sheep over a time period from 0 to 6 h (h) maximum.

Materials and Methods

Animals and Diet

Three dry ewes (2 Assaf and 1 Merino breed) averaging 60 ± 6.2 kg body weight were fitted with ruminal cannula and served as donors of rumen contents. Sheep were fed 1.1 kg dry matter per day of oats hay in one morning meal for over 2 weeks.

In Vitro Incubations

Between 100 and 200 mL of rumen content were collected pre-feeding from each ewe and transferred to the laboratory in pre-warmed thermo flasks. The rumen contents were strained through a double layer of muslin, pooled together (same volume from each ewe), and kept under CO₂ flushing.

Batch-cultures were performed using 15-mL Hungate tubes. The incubated substrate was composed of a proportional mixture of glucose, cellobiose, maltose, corn starch, and casein in order to avoid confounding effects of other fat or carbohydrate sources. Each tube contained 36 mg of the substrate mix (7.2 mg of each ingredient) and unesterified DHA (U-84-A from Nu-Chek Prep, Elysian, MN, USA) dissolved in ethanol (10 µg/µL).

In one trial, 10, 30, and 80 µL of the DHA solution were added to separate sets of tubes. These gave a final DHA content of 100, 300 or 800 µg per tube or 16.7, 50, or 133.3 µg/mL, respectively. The total incubation volume was of 6 mL, composed of 2 mL of rumen fluid plus 4 mL of phosphate-bicarbonate buffer. The buffer solution was prepared as described by Goering and Van Soest [10], with the exception that no trypticase was added. In order to have the same amount of ethanol in all tubes, 70 and 50 µL of ethanol were added to the tubes containing 16.7 and 50 µg of DHA/mL, respectively. As reported by Morgavi et al. [11], these low volumes of ethanol should not affect fermentation, and not considered toxic to the rumen microorganisms. Each set of tubes (single tube per DHA level and incubation period) was incubated under anaerobic conditions for 0, 1, 2, 3, and 6 h in an incubator set at 39 °C, and tubes were individually agitated every hour.

After each incubation time, the reaction was stopped by placing the tubes in ice-water for 15 min and then storing them at -80 °C. An exception was made for tubes at 0 h in which the appropriate amount of DHA was added after the tubes containing all the other ingredients were placed into the ice-water in order to avoid any possible reaction. An additional tube with no DHA was also frozen at 0 h (control) to determine the natural content of DHA and other fatty acids (FA) in rumen fluid as determined by GC in the region from 24:0 to DHA.

Fatty Acid Analysis

Samples were freeze-dried and, in the same tube, the samples were transesterified using consecutive base and acid catalysts [12] as follows: first 1.5 mL of methanol was added to each tube that was subsequently sonicated for 10 min to rupture cells. After vortexing, the tubes were placed in the sonicator for another 5 min and then 0.4 mL of 0.25 N NaOCH₃ was added, vortexed and tubes were placed in a thermoblock at 50 °C for 30 min. After cooling, 1.5 mL of 10 % (v/v) H₂SO₄ in methanol was added, vortexed and heated at 80 °C for 15 min. After cooling, 1 mL of distilled H₂O was added and the methylated lipids were extracted with 2 mL of hexane. Tubes were then centrifuged at 2,000 rpm (~ 800 g) for 5 min (20 °C) to clarify the layers. The upper hexane layer was transferred to a clean test tube containing approximately 1 g of anhydrous sodium sulphate. The extraction step was repeated with another 2 mL of hexane. The combined hexane was evaporated under a stream N₂ at 37 °C, and the FA methyl esters (FAME) were reconstituted in hexane and analyzed by gas chromatography (GC) (Agilent Technologies 7890A GC System), using a 100 m SP-2560 column (Supelco, Bellefonte, PA, USA). At this point 10 µL of an internal standard (10 µg/µL of 13:0 methyl ester, N-13-M from Nu-Chek Prep, Elysian, MN, USA) was added. Samples were analyzed using the temperature program plateauing at 175 °C [13] and H₂ was used as carrier gas. GC reference standards #463 and #603, and the FAME of 21:0, 23:0 and 26:0 (Nu-Chek Prep Inc., Elysian, MN) were used to identify the FAME peaks. The purity of the DHA was tested after esterifying the free DHA using the aforementioned acid catalyst and analyzing the FAME by GC under the same conditions described above.

Results and Discussion

The partial GC chromatogram from 22:2n-6 to just past DHA for the sheep rumen fluid incubated with 300 µg DHA per tube from 0 to 6 h is shown in Fig. 1. This region was selected because LC-DHA metabolites would be

expected to elute here if the first steps of DHA metabolism involves the formation of one *trans* double bond, loss of 1 or 2 double bonds, or loss of 1 or 2 carbon atoms. Such LC-PUFA metabolites arising from DHA were recently reported to occur in the omasal canal of cows fed fish oil [9]. The GC region from 24:0 to just past DHA at time 0 h showed only minor peaks of 24:0, 15*c*-24:1 and 26:0 both with and without DHA; only the graph with DHA is shown (Fig. 1, 0 h). The DHA used in the incubation studies had only trace amounts of a few DHA isomers (Fig. 1, DHA). It is evident from the GC results in Fig. 1 that numerous peaks in the region from 57 to 70 min appeared during the 6 h incubation, and are suspected to be LC FAME metabolites formed from DHA (or LC-DHA metabolites).

Figure 2 shows DHA depletion (%) and LC-DHA metabolite formation (%) relative to DHA incubated over the 6 h period of incubation. For these calculations baseline DHA and other peak areas at 0 h (control) were subtracted from the rest of the chromatograms. The results show a decrease in DHA and an increase in total LC-DHA metabolites when DHA was added to the incubation tubes.

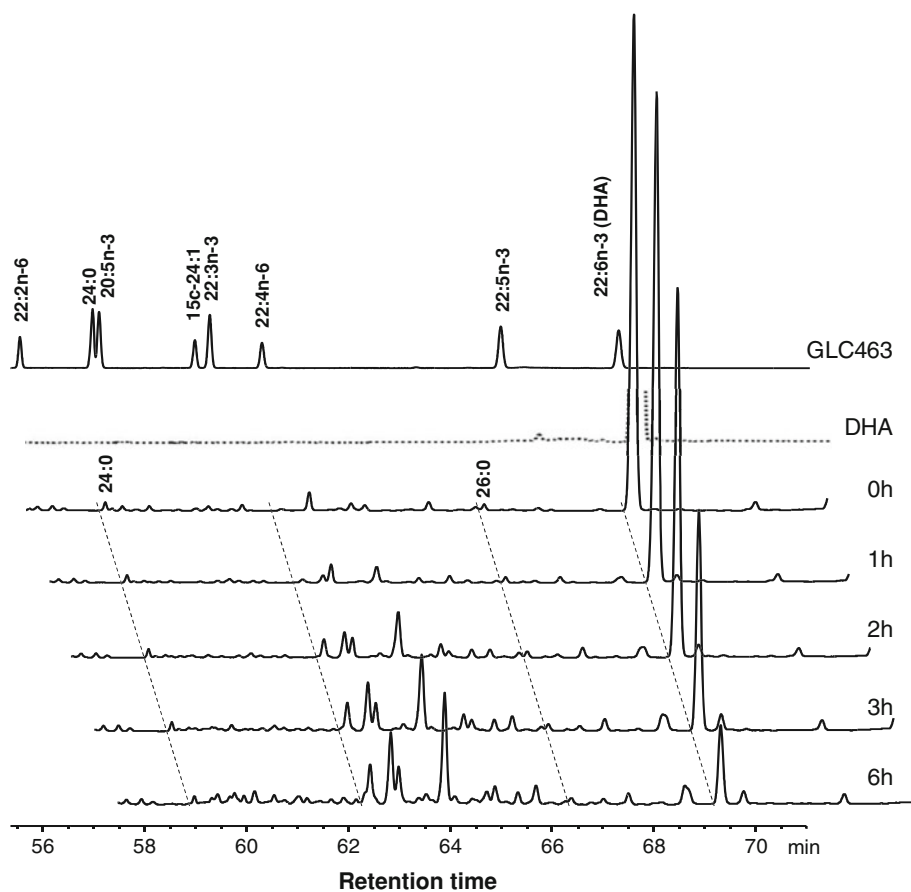
At the lowest DHA levels approximately 90 % of the incubated DHA was depleted after 6 h with extensive production of LC-DHA metabolites. Most of the depleted DHA was recovered as LC-DHA metabolites within the

first 3 h when 100 μg were incubated per tube. However, after 3 h the content of LC-DHA metabolites dropped which suggests further metabolism to DHA to metabolites which eluted before 24:0. In the present study, the drop was not observed when 300 μg was incubated. In a separate experiment 150 and 1,500 μg per incubation tube were added using the same protocol and conditions. The results using 150 μg were similar to 100 μg in the present study, but at 1,500 μg per incubation tube very little metabolism of DHA was evident even after 6 h (data not shown).

The results of this preliminary study indicate that the amount of DHA incubated with rumen fluid, as well as the incubation times are factors affecting DHA metabolism. A wide range of FA concentrations and lengths of incubation times have been reported in batch studies using total rumen fluid [8, 14–16]. High concentrations of free FA are known to be toxic to rumen microbes [17, 18]. Maia et al. [19] showed that several ruminal bacteria species exhibited growth inhibition at 50 $\mu\text{g}/\text{mL}$ of PUFA in the media. This agrees with our study which shows that at the lowest levels of DHA inclusion (100 and 300 μg per tube), the DHA level decreased dramatically. However, higher levels of DHA showed moderate metabolism after 6 h of incubation.

The results of this *in vitro* study with rumen fluid imply that DHA metabolism is concentration dependent. At low

Fig. 1 Partial GC chromatograms from 22:2n-6 to past DHA selected from rumen incubation with 300 μg DHA per 6 mL over 0, 1, 2, 3, and 6 h. A reference GC standard (GLC 463) was included for comparison as well as the free DHA that was methylated



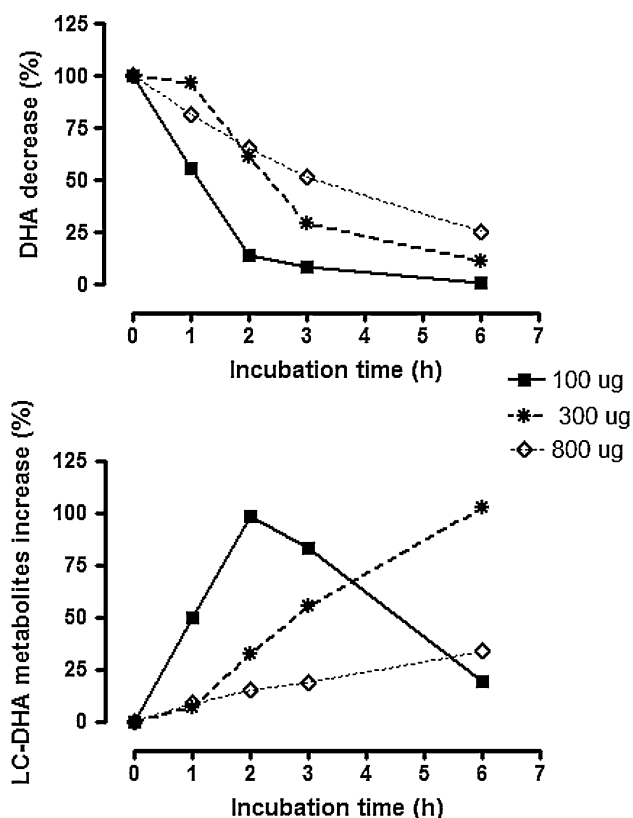


Fig. 2 Calculated DHA depletion (%) and long-chain (LC) DHA metabolite production (%) relative to DHA incubated for each level (100, 300 and 800 µg per tube) and incubation time (0, 1, 2, 3 and 6 h)

levels of DHA addition (≤ 300 µg per tube or 50 µg/mL) extensive metabolism occurred as evident by its depletion and formation of LC-DHA metabolites that elution in the GC region between 24:0 and DHA. There appears to be evidence of further metabolism of the LC-DHA metabolites after 3 h when 100 µg DHA per tube was incubated. It was recently suggested that DHA may be isomerized and reduced to 22:0 by similar pathways as observed for the 18-carbon polyunsaturated FA like linoleic and linolenic acids to 18:0 [8]. However, we did not observe an increase in 22:0 content (data not shown), in agreement with others [9], but that may be due to the much shorter incubation times used in the present study of 6 versus 48 h. Extensive metabolism of DHA at low levels of addition would help to explain the low transfer efficiency of DHA into ruminant tissues, but it is not clear whether a higher supplementation of DHA would result in increased accretion of DHA into meat and milk. Addition of low levels of DHA to the diet of ruminants has recently been used to increase the level of rumenic and vaccenic acids rather than increasing the level of DHA per se [20, 21], because this addition increases the production of *trans*-18:1 isomers in rumen fluid [22]. The 6-h incubation period coupled with analysis of the

LC-DHA metabolites by GC would provide a useful method to evaluate the fate of DHA in ruminants.

Acknowledgments This research was funded by a Marie Curie International Outgoing Fellowship within the 7th European Community Framework Programme (SPACANBEEF, PIOF-GA-2008-220730). N. Aldai thanks the Spanish Ministry of Science and Innovation for the contract provided through the 'Ramón y Cajal' (RYC-2011-08593) program. Technical help of the staff from the research farm and the laboratories of the IGM (CSIC-ULE) is very much appreciated. We thank Dr. J.K. Lee from the FDA (College Park, Maryland) for his statistical advice and suggestions.

References

- Lock AL, Bauman DE (2004) Modifying milk fat composition of dairy cows to enhance fatty acids beneficial to human health. *Lipids* 39:1197–1206
- Scollan N, Hocquette J-F, Nuernberg K, Dannenberger D, Richardson I, Moloney A (2006) Innovations in beef production systems that enhance the nutritional and health value of beef lipids and their relationship with meat quality. *Meat Sci* 74:17–33
- FAO/WHO (2008) Interim summary of conclusions and dietary recommendations on total fat & fatty acids. From the Joint FAO/WHO Expert Consultation on fats and fatty acids in human nutrition, 10–14 November 2008. WHO, Geneva
- Chilliard Y, Glasser F, Ferlay A, Bernard L, Rouel J, Doreau M (2007) Diet, rumen biohydrogenation and nutritional quality of cow and goat milk fat. *Eur J Lipid Sci Technol* 109:828–855
- Ashes JR, Siebert BD, Gulati SK, Cuthbertson AZ, Scott TW (1992) Incorporation of n-3 fatty acid of fish oil into tissue and serum lipids of ruminants. *Lipids* 27:629–631
- Shingfield KJ, Ahvenjärvi S, Toivonen V, Ärölä A, Nurmela KVV, Huhtanen P, Grünari JM (2003) Effect of dietary fish oil on biohydrogenation of fatty acids and milk fatty acid content in cows. *Anim Sci* 77:165–179
- Harfoot CG, Hazlewood GP (1997) Lipid metabolism in the rumen. In: Hobson PN, Stewart CS (eds) *The rumen microbial ecosystem*. Blackie, London, pp 382–426
- Klein CM, Jenkins TC (2011) Docosahexaenoic acid elevates *trans*-18:1 isomers but is not directly converted into *trans*-18:1 isomers in ruminal batch cultures. *J Dairy Sci* 94:4676–4683
- Kairenius P, Toivonen V, Shingfield KJ (2011) Identification and ruminal outflow of long-chain fatty acid biohydrogenation intermediates in cows fed diets containing fish oil. *Lipids* 46:587–606
- Goering MK, Van Soest PJ (1970) Forage fiber analysis (apparatus, reagents, procedures and some applications). In: *Agriculture handbook no 379*. USDA, Washington, DC
- Morgavi DP, Boudra H, Jouany JP, Michalet-Doreau B (2004) Effect and stability of gliotoxin, an *Aspergillus fumigatus* toxin, on in vitro rumen fermentation. *Food Addit Contam* 21:871–878
- Kramer JKG, Fellner V, Dugan MER, Sauer FD, Mossoba MM, Yurawecz MP (1997) Evaluating acid and base catalysts in the methylation of milk and rumen fatty acids with special emphasis on conjugated dienes and total *trans* fatty acids. *Lipids* 32:1219–1228
- Kramer JKG, Hernandez M, Cruz-Hernandez C, Kraft J, Dugan MER (2008) Combining results of two GC separations partly achieves determination of all *cis* and *trans* 16:1, 18:1, 18:2 and 18:3 except CLA isomers of milk fat as demonstrated using Ag-ion SPE fractionation. *Lipids* 43:259–273
- Mosley EE, Powell GL, Riley MB, Jenkins TC (2002) Microbial biohydrogenation of oleic acid to *trans* isomers in vitro. *J Lipid Res* 43:290–296

15. Laverroux S, Glasser F, Gillet M, Joly C, Doreau M (2011) Isomerization of vaccenic acid to *cis* and *trans* C18:1 isomers during biohydrogenation by rumen microbes. *Lipids* 46:843–850
16. Maia MRG, Correia CAS, Alves SP, Fonseca AJM, Cabrita ARJ (2011) Technical note: stearidonic acid metabolism by mixed ruminal microorganisms in vitro. *J Anim Sci* 90:900–904
17. Noble RC, Moore JH, Harfoot CG (1974) Observations on the pattern on biohydrogenation of esterified and unesterified linoleic acid in the rumen. *Br J Nutr* 31:99–108
18. Body DR (1976) The occurrence of *cis*-octadec-15-enoic acid as a major biohydrogenation product from methyl linolenate in bovine rumen liquor. *Biochem J* 157:741–744
19. Maia MRG, Chaudhary LC, Figueres L, Wallace RJ (2007) Metabolism of polyunsaturated fatty acids and their toxicity to the microflora of the rumen. *Antonie Leeuwenhoek* 91:303–314
20. Cruz-Hernandez C, Kramer JKG, Kennely JJ, Glimm DR, Sorensen BM, Okine EK, Goonewardene LA, Weselake RJ (2007) Evaluating the conjugated linoleic acid and *trans* 18:1 isomers in milk fat of dairy cows fed increasing amounts of sunflower oil and a constant level of fish oil. *J Dairy Sci* 90:3786–3801
21. Bernard L, Mouriot J, Rouel J, Glasser F, Capitan P, Pujos-Guillot E, Chardigny J-M, Chilliard Y (2010) Effects of fish oil and starch added to a diet containing sunflower-seed oil on dairy goat performance, milk fatty acid composition and in vivo $\Delta 9$ -desaturation of [^{13}C] vaccenic acid. *Br J Nutr* 104:346–354
22. AbuGhazaleh AA, Jenkins TC (2004) Short communication: docosahexaenoic acid promotes vaccenic acid accumulation in mixed rumen cultures when incubated with linoleic acid. *J Dairy Sci* 87:1047–1050

Novel Heneicosadienoic and Tricosadienoic Acid Isomers in Ovaries of Marine Archaeogastropods

Hideki Kawashima · Masao Ohnishi

Received: 23 April 2012 / Accepted: 1 June 2012 / Published online: 26 June 2012
© AOCS 2012

Abstract To investigate unusual odd-chain fatty acids (FA) from gonads of archaeogastropods, limpets *Cellana grata* and *Cellana toreuma*, a subfraction enriched in FA with two double bonds extracted from the gonads was obtained by using argentation thin-layer chromatography. The resulting fraction was analyzed by using capillary gas chromatography–mass spectrometry of its methyl esters, 3-pyridylcarbinol esters and pyrrolidide derivatives. Six novel all-*cis* diene isomers were identified as 7,18-heneicosadienoic (21:2Δ7,18), 8,14-tricosadienoic (23:2Δ8,14), 9,15-tricosadienoic (23:2Δ9,15), 7,18-tricosadienoic (23:2Δ7,18), 9,18-tricosadienoic (23:2Δ9,18), and 9,20-tricosadienoic (23:2Δ9,20) acids. In the present study, the differences in the proportion of tricosadienoic acid isomers between the ovary lipids of *C. grata* and *C. toreuma* were recognized.

Keywords Archaeogastropods · Gonad · Non-methylene-interrupted fatty acid · Odd-chain fatty acid

Abbreviations

EI	Electron impact
FA	Fatty acid(s)
FID	Flame ionization detector
GLC	Gas-liquid chromatography
GC–MS	Gas chromatography–mass spectrometry

MS	Mass spectrum
NMI	Non-methylene-interrupted
TAG	Triacylglycerol(s)
TLC	Thin-layer chromatography

Introduction

Non-methylene-interrupted (NMI) fatty acids (FA) with even-chain lengths, especially straight-chain NMI dienoic FA with 20 and 22 carbon atoms, are commonly present in small amounts in mollusks, echinoderms, and sponges, but their biological role and function are not fully understood [1]. In contrast to straight even-chain NMI dienoic FA, to date, studies of the occurrence of straight odd-chain NMI dienoic FA with 21 and 23 carbon atoms from living organisms are limited [2–7], because of their usually very minor amounts less than straight even-chain NMI FA. Of the nine different straight odd-chain NMI FA identified from living organisms, both 21:2Δ7,13 and 21:2Δ7,15 as minor components have been reported from the edible bivalve *Megangulus zyanoensis* and gonads of limpets *Cellana grata* and *Collisella dorsuosa* [2, 4]. In addition to these isomers, both 21:2Δ5,9 and 21:2Δ7,16 are also found in very small amounts in the limpet gonads of *C. grata* [3], but 21:2Δ5,9 is present in some marine sponges [1]. Four NMI heneicosadienoic acids 21:2Δ5,13, 21:2Δ5,15, 21:2Δ5,16, and 21:2Δ5,20 are distributed in a cold-seep clam of the genus *Calyplogena* [5, 6]. To date, only a straight-chain NMI tricosadienoic acid from marine invertebrates has been identified as 23:2Δ5,9, which is widely distributed in minor amounts (<0.3 % of total FA) in sponges, sea anemones, nudibranchs and limpet gonads [1, 3]. However, other straight-chain NMI

H. Kawashima (✉)
Bioscience Laboratory, Miyako College, Iwate Prefectural University, Miyako 027-0039, Japan
e-mail: ajoe@iwate-pu.ac.jp

M. Ohnishi
Department of Agriculture and Life Science, Obihiro University of Agriculture and Veterinary Medicine, Obihiro 080-8555, Japan

heneicosadienoic and tricosadienoic acids from living organisms may not have been reported.

In our study of the occurrence and structure of NMI FA from the gonads of limpets of marine archaeogastropods, we showed that the structural diversity of NMI FA with 20, 21, 22, and 24 carbon atoms in the ovaries of *C. grata* comprises a wide range of unusual positional isomers [2, 3, 7]. In the present study, to further clarify the detailed odd-chain NMI dienoic FA at relatively low concentrations in the two archaeogastropod limpets *C. grata* and *C. toreuma*, we investigated the structures of these FA by using a combination of argentation thin-layer chromatography (TLC) and capillary gas chromatography–mass spectrometry (GC–MS). Here, we describe the identification of novel heneicosadienoic and tricosadienoic acids detected at trace levels exclusively (<0.05 % of total FA) in ovary lipids and differences in the proportion of tricosadienoic acids between triacylglycerols (TAG) and polar lipids in both limpet species. Furthermore, a possible biosynthetic pathway for novel odd-chain NMI FA is discussed. These findings may provide insight into whether some NMI FA participate in the ecological and physiological roles of marine mollusks.

Experimental Procedures

Reagents

Methyl heneicosanoate (H3265) and tricosanoic acid (T6543) were purchased from Sigma-Aldrich Co. (St. Louis, MO, USA). All solvents used here were of top grade.

Sampling of Limpets and Extraction of Lipids

Limpets *C. grata* (mean shell length, 37.9 ± 4.6 mm, $n = 95$) and *C. toreuma* (mean shell length, 34.4 ± 2.6 mm, $n = 120$) from Kirikiri, Iwate Prefecture, north-eastern Japan, were sampled between August and October, from 2008 to 2010. After sampling, all limpets were immediately dissected in the laboratory. The sex was determined by microscopic examination, and the gonads were distinguished as male or female. Pooled male or female gonads (15–20 g wet weight) were suspended in 50 mL chloroform–methanol (2:1, v/v) and were homogenized for 1 min at 16,000 rpm by using an IKA Ultra-Turrax T25 basic (IKA Japan KK, Nara, Japan). Lipids were extracted by the method of Bligh and Dyer [8].

Fractionation of TAG and Polar Lipids

Triacylglycerols and polar lipids from lipid extracts were separated on silica gel 60 TLC plates (Merck KGaA.,

Darmstadt, Germany) using *n*-hexane/diethyl ether/acetic acid (80:30:1, v/v/v) as the developing solvent. The lipids were detected by brief exposure to iodine vapor and were marked. TAG and polar lipids were recovered from the scraped silica bands by elution with chloroform/methanol (1:1, v/v).

Preparation of FA Methyl Esters, 3-Pyridylcarbinol Esters and Pyrrolidide Derivatives

Fatty acid methyl esters and 3-pyridylcarbinol esters were prepared as described previously [2]. Pyrrolidide derivatives were prepared according to the method of Andersson and Holman [9].

Fractionation of FA Methyl Esters by Argentation TLC

Fatty acid methyl esters prepared from TAG and polar lipids were separated by argentation TLC (5 % AgNO₃–silica gel 60) into six fractions having zero to five double bonds, using *n*-hexane/diethyl ether (80:20, v/v) as the mobile phase with double development, according to the degree of unsaturation. FA methyl ester bands were located by spraying with a 0.2 % (w/v) solution of 2',7'-dichloro-fluorescein in ethanol and were viewed under UV light at 366 nm. The migration solvent used to confirm geometrical diene isomers was a mixture of *n*-hexane/diethyl ether (90:10, v/v). FA methyl esters were recovered from the scraped silica bands by elution with *n*-hexane [4], and were analyzed by using GLC and GC–MS.

Catalytic Hydrogenation of Unsaturated FA Methyl Esters

An aliquot of fractionated unsaturated FA methyl esters was hydrogenated by stirring at 20 °C for 2 h in *n*-hexane (3 mL) with 18 mg of palladium black (Wako Pure Chemical Industries, Ltd., Osaka, Japan) [4]. The resulting mixture was analyzed by using GLC and GC–MS.

GLC and GC–MS Analyses

FA methyl esters were analyzed by using GLC with a Shimadzu GC-1700 gas chromatograph (Shimadzu, Kyoto, Japan) equipped with an FID and an Omegawax-320 column (30 m × 0.32 mm i.d., 0.25 μm film thickness; Supelco, Bellefonte, PA, USA). The column temperature was isothermal at 220 °C. The injector and detector temperatures were 260 °C, and the carrier gas was helium, at a flow rate of 1.0 mL/min.

GC–MS analyses were done by using a Shimadzu GCMS-QP2010 coupled with a Shimadzu 2010 GC equipped with either the same column as described for

GLC analysis on an SAC-5 column (30 m × 0.25 mm i.d., 0.25 μm film thickness; Supelco, Bellefonte, PA, USA). The carrier gas was helium, at a flow rate of either 0.6 or 1.5 mL/min, and pressure programming was used in constant flow mode. The oven temperature was programmed as follows: isothermal at 200 °C for 2 min, increased from 200 to 270 °C (3 °C/min) and maintained at 270 °C for 50 min. Electron impact (EI) mass spectra of FA methyl esters, 3-pyridylcarbinol esters and pyrrolidide derivatives were recorded at an ionization energy of 70 eV and an ion source at 200 °C. Split injection was done with a split ratio of either 1:10 or 1:25. All samples of gonad lipids were analyzed in duplicate.

Results and Discussion

In this study, eight different dienoic FA with 21 carbon atoms, seven of which (21:2Δ5,9, 21:2Δ7,13, 21:2Δ7,15, 21:2Δ7,16, 21:2Δ11,14, 21:2Δ12,15, and 21:2Δ13,16) had been reported by us previously [2, 3], and seven different dienoic FA with 23 carbon atoms, including 23:2Δ5,9 which had been described previously [1, 3], were detected in scanty amounts in gonads of the limpet *C. grata*. Tables 1 and 2 list six novel odd-chain dienoic acids, which were classified as a group of NMI FA, identified by using capillary EI GC–MS of their pyrrolidide derivatives and 3-pyridylcarbinol esters.

The mass spectrum (MS) of the novel methyl ester 21:2Δ7,18 showed a molecular ion at m/z 336 and a fragment ion at m/z 305 due to a loss of OCH₃, suggesting a heneicosadienoic acid. After complete hydrogenation of the FA, a newly formed peak displayed a molecular ion at m/z 340, assigning a saturated FA with 21 carbon atoms. The retention time and MS of the peak agreed with those of authentic heneicosanoic acid. The structure of 21:2Δ7,18 was

confirmed by the MS of its pyrrolidide derivative, which had a molecular ion at m/z 375, and the double bond position was assigned by gaps of 12 amu between m/z 168 and 180 and between m/z 320 and 332 (Fig. 1a). Similarly, MS data for the 3-pyridylcarbinol ester confirmed the structure of 21:2Δ7,18 at m/z 413 [M]⁺, corresponding to a heneicosadienoic acid, and at m/z 206, 232, 358, and 384, indicating the presence of double bonds at Δ7 and Δ18 (Fig. 1b).

The MS of each individual methyl ester of tricosadienoic acid isomers showed a molecular ion at m/z 364 and a characteristic ion at m/z 333 due to a loss of OCH₃, suggesting a tricosadienoic acid. After complete hydrogenation of the diene isomers, a newly formed peak gave a molecular ion at m/z 368, indicating a saturated FA with 23 carbon atoms. The retention time and MS of the methyl ester of the peak were identical to those of authentic tricosanoic acid. From these results, seven isomers detected in this study were straight-chain dienoic FA isomers with 23 carbon atoms. The MS of all pyrrolidide derivatives of the isomers yielded a molecular ion at m/z 403 that corresponded to a tricosadienoic acid (Table 1). However, of the seven tricosadienoic acids, including 23:2Δ5,9 as a known FA, detected in this study, only one was not identified because of its very small amounts. The MS given in Fig. 2a resembles that of 18:2Δ8,12 as illustrated in the lipid library [10] and that of 18:2Δ8,13 from the sponge *Leuconia johnstoni* [11]. The MS of the pyrrolidide derivative of 23:2Δ8,14 gave gaps of 12 amu between m/z 182 and 194 and between m/z 264 and 276, indicating double bond positions at Δ8 and Δ14. The MS of the pyrrolidide derivative of 23:2Δ9,15 had gaps of 12 amu between m/z 196 and 208 and between m/z 278 and 290, indicating double bond positions at Δ9 and Δ15. This MS of the diagnostic fragment ions was the same for that of 18:2Δ9,15 [12]. In the MS of the pyrrolidide derivative of 23:2Δ7,18, the fragment ions for double bond positions

Table 1 EI–MS data for pyrrolidide derivatives of heneicosadienoic and tricosadienoic acids from the limpet gonads of *Cellana grata*

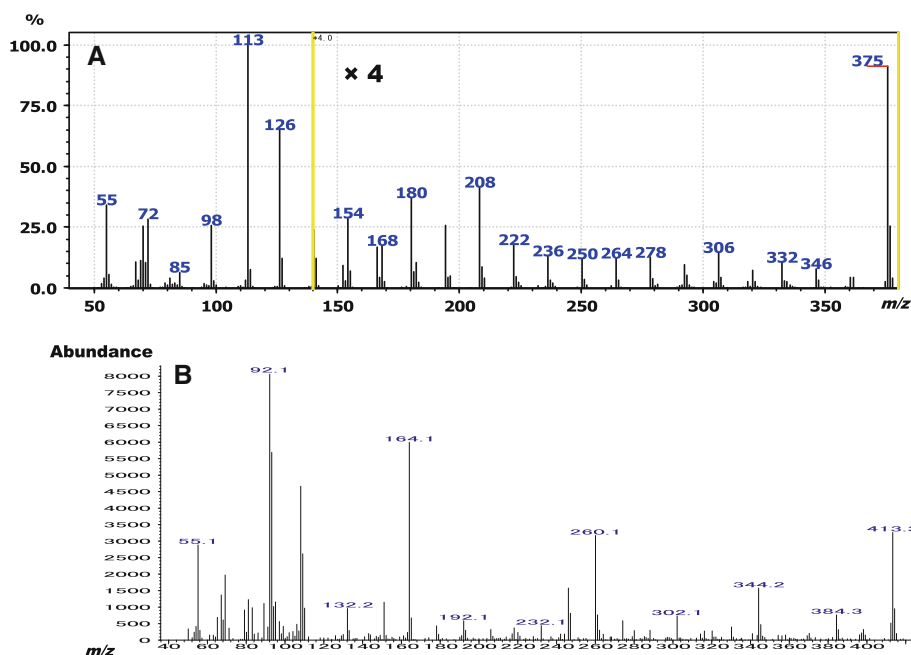
Fatty acid	t_R (min)	m/z (relative ion intensity %)
21:2Δ7,18	17.79	113 (100), 126 (57), 140 (5.8), 154 (5.9), 168 (4.1) , 180 (7.5) , 194 (5.0), 208 (7.8), 222 (3.8), 236 (2.8), 250 (2.7), 264 (3.1), 278 (3.1), 292 (2.2), 306 (2.6), 320 (1.4) , 332 (2.2) , 346 (1.7), 360 (0.8), 375 ([M] ⁺ , 17)
23:2Δ8,14	21.94	113 (100), 126 (67), 140 (3.7), 154 (4.1), 168 (10), 182 (5.4) , 194 (5.1) , 208 (6.2), 222 (4.6), 236 (6.3), 250 (8.7), 264 (2.3) , 276 (2.0) , 290 (2.9), 304 (3.1), 318 (1.9), 332 (2.2), 346 (1.2), 360 (1.7), 374 (1.2), 388 (0.3), 403 ([M] ⁺ , 17)
23:2Δ9,15	22.19	113 (100), 126 (60), 140 (5.6), 154 (5.5), 168 (3.0), 182 (7.0), 196 (2.9) , 208 (4.5) , 222 (2.7), 236 (4.1), 250 (4.8), 264 (6.7), 278 (4.5) , 290 (1.8) , 304 (1.9), 318 (2.7), 332 (1.0), 346 (3.4), 360 (2.2), 374 (1.7), 388 (0.1), 403 ([M] ⁺ , 17)
23:2Δ7,18	22.36	113 (100), 126 (64), 140 (5.6), 154 (4.4), 168 (4.3) , 180 (5.6) , 194 (4.7), 208 (7.7), 222 (3.2), 236 (4.6), 250 (4.4), 264 (2.9), 278 (2.2), 292 (1.5), 306 (4.4), 320 (1.5) , 332 (1.3) , 346 (1.5), 360 (4.6), 374 (3.0), 388 (0.6), 403 ([M] ⁺ , 17)
23:2Δ9,18	22.41	113 (100), 126 (58), 140 (5.8), 154 (3.1), 168 (4.4), 182 (8.5), 196 (2.4) , 208 (2.4) , 222 (4.0), 236 (5.2), 250 (5.8), 264 (1.6), 278 (1.5), 292 (1.7), 306 (5.3), 320 (1.4) , 332 (1.2) , 346 (2.0), 360 (3.4), 374 (2.5), 388 (0.5), 403 ([M] ⁺ , 26)
23:2Δ9,20	22.64	113 (100), 126 (58), 140 (4.5), 154 (2.8), 168 (2.0), 182 (5.1), 196 (2.7) , 208 (4.4) , 222 (1.8), 236 (4.6), 250 (5.1), 264 (3.5), 278 (2.7), 292 (1.9), 306 (3.1), 320 (2.5), 334 (2.4), 348 (1.4) , 360 (1.4) , 374 (1.8), 388 (0.4), 403 ([M] ⁺ , 26)

Fragment ions given in boldface correspond to diagnostic ones

Table 2 EI–MS data for 3-pyridylcarbinol esters of heneicosadienoic and tricosadienoic acids from the limpet gonads of *Cellana grata*

Fatty acid	t_R (min)	m/z (relative ion intensity %)
21:2 Δ 7,18	53.44	92 (100), 108 (58), 164 (72), 206 (5.4) , 232 (6.5) , 246 (18), 260 (40), 344 (20), 358 (1.5) , 384 (6.4) , 398 (6.4), 413 ([M] ⁺ , 41)
23:2 Δ 8,14	67.21	92 (100), 108 (68), 164 (81), 220 (14) , 246 (5.1) , 260 (11), 274 (28), 302 (7.1) , 328 (12) , 342 (24), 426 (3.3), 441 ([M] ⁺ , 28)
23:2 Δ 9,15	67.85	92 (100), 108 (61), 164 (68), 234 (7.6) , 260 (12) , 274 (19), 288 (20), 316 (7.7) , 342 (9.1) , 356 (18), 426 (2.6), 441 ([M] ⁺ , 31)
23:2 Δ 7,18	68.57	92 (100), 108 (58), 164 (51), 206 (8.0) , 232 (4.8) , 246 (11), 260 (29), 344 (25), 358 (2.4) , 384 (8.9) , 398 (19), 426 (5.7), 441 ([M] ⁺ , 47)
23:2 Δ 9,18	69.89	92 (100), 108 (76), 164 (68), 234 (6.1) , 260 (6.8) , 274 (24), 288 (29), 344 (20), 358 (1.8) , 384 (7.9) , 398 (24), 426 (1.6), 441 ([M] ⁺ , 40)
23:2 Δ 9,20	70.70	92 (100), 108 (64), 164 (92), 234 (6.4) , 260 (11) , 274 (19), 288 (29), 372 (32), 386 (8.4) , 412 (6.8) , 426 (10), 441 ([M] ⁺ , 45)

Fragment ions given in boldface correspond to diagnostic ones

Fig. 1 EI–MS of the pyrrolidide derivative (a) and 3-pyridylcarbinol ester (b) of 7,18-heneicosadienoic acid (21:2 Δ 7,18)

were identical to those of the pyrrolidide derivative 21:2 Δ 7,18 as described above. As shown in Fig. 3a, the MS of the pyrrolidide derivative of 23:2 Δ 9,18 showed gaps of 12 amu between m/z 196 and 208 and between m/z 320 and 332, indicating double bond positions at Δ 9 and Δ 18. Finally, in the MS of the pyrrolidide derivative of 23:2 Δ 9,20, which is a homologue of 21:2 Δ 7,18, as compared to the fragment ions of double bonds for 23:2 Δ 9,15 and 23:2 Δ 9,18, an ion for the double bond at Δ 9 was the same, but a gap of 12 amu for the double bond position at Δ 20 was between m/z 348 and 360. In addition, double bond positions in five novel tricosadienoic acids from limpet gonads were also determined by using capillary GC–MS of their 3-pyridylcarbinol esters. In the mass spectra of the 3-pyridylcarbinol esters of all tricosadienoic acid isomers, their double bond locations were identified by searching for a gap of 26 amu from the fragmentation ions.

Of five mass spectra of the 3-pyridylcarbinol esters of tricosadienoic FA, the spectra of 23:2 Δ 8,14 and 23:2 Δ 9,18, as unusual major FA in limpet gonads (Table 3), are shown in Figs. 2b and 3b, respectively. The MS of the 3-pyridylcarbinol ester of 23:2 Δ 8,14 had diagnostic peaks at m/z 441 [M]⁺ and 220, 246, 302, and 328 for double bond positions at Δ 8 and Δ 14. The MS of the 3-pyridylcarbinol ester of 23:2 Δ 9,18 had a molecular ion at m/z 441, and the double bonds were identified individually by ions that differed by 26 amu from m/z 234 to 260 and 358 to 384. Furthermore, the mass spectra of the 3-pyridylcarbinol esters of 23:2 Δ 7,18, 23:2 Δ 9,18 and 23:2 Δ 9,20 were compared with those of 24:2 Δ 7,17 and 26:2 Δ 9,19 as shown in the lipid library [13]. The mass data clearly show that each individual double bond position in the 3-pyridylcarbinol esters of these isomers was identical to that in the pyrrolidide derivatives.

Fig. 2 EI-MS of the pyrrolidide derivative (a) and 3-pyridylcarbinol ester (b) of 8,14-tricosadienoic acid (23:2 Δ 8,14)

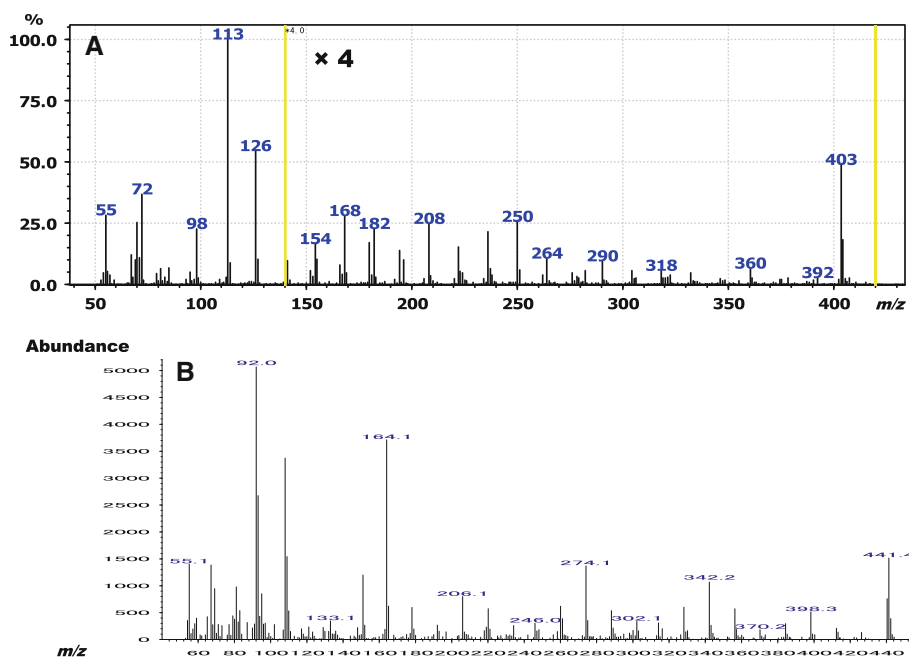
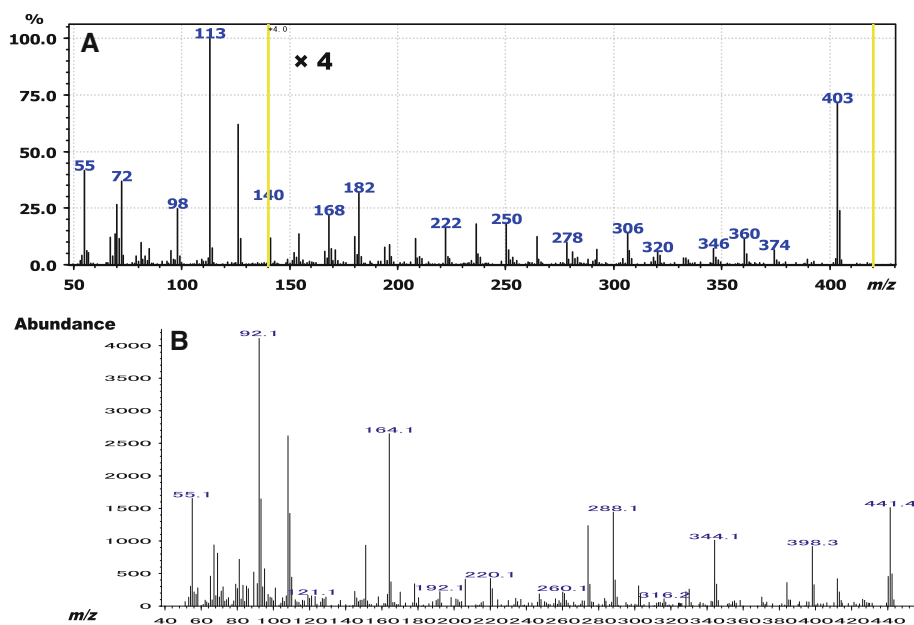


Fig. 3 EI-MS of the pyrrolidide derivative (a) and 3-pyridylcarbinol ester (b) of 9,18-tricosadienoic acid (23:2 Δ 9,18)



In this study, six novel dienoic FA co-eluted with 22:2 Δ 7,13 and 22:2 Δ 7,15 with *cis*-configurations shown by argentation TLC, indicating that their double bonds would have the *cis*-configuration. To the best of our knowledge, these FA were identified from nature for the first time. The most interesting series of the FA was a family of these NMI tricosadienoic acids with first double bonds at either Δ 7, Δ 8, or Δ 9, but 23:2 Δ 5,9, the only NMI tricosadienoic acid isomer in marine invertebrates, had been reported previously [1, 7].

To further clarify the distribution of unusual tricosadienoic acids in TAG and polar lipids (mainly phosphatidylcholine

and phosphatidylethanolamine) of gonads of limpet species, FA of *C. grata* and *C. toreuma* were analyzed. However, tricosadienoic acids from both TAG and polar lipids of all testes were not detected in this study (data not shown). In contrast, clear differences were found in the proportion of tricosadienoic acid composition between the TAG and polar lipids in the two limpet species. The predominant isomer in TAG was 23:2 Δ 9,18 and 23:2 Δ 8,14 for *C. grata* and *C. toreuma*, respectively, but the proportion of 23:2 Δ 9,15 in both *Cellana* species was almost the same (Table 3). Similarly, differences in proportion of

Table 3 Distribution of tricosadienoic acid isomers (%) in ovaries of *C. grata* and *C. toreuma*

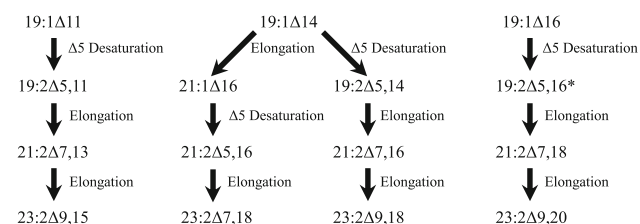
Fatty acid	Triacylglycerols		Polar lipids	
	<i>C. grata</i>	<i>C. toreuma</i>	<i>C. grata</i>	<i>C. toreuma</i>
23:2Δ5,9	5.1	–	–	50.1
23:2Δ8,14	16.8	54.2	51.0	32.4
23:2Δ9,15	20.0	20.9	49.0	17.5
23:2Δ7,18	11.7	6.4	–	–
23:2Δ9,18	33.5	18.5	–	–
23:2Δ9,20	10.3	–	–	–
23:2Δx,y	2.6	–	–	–

The proportion of each isomer was calculated from the total isomers

tricosadienoic acid composition of polar lipids were also recognized, and the abundant isomer was 23:2Δ8,14 and 23:2Δ5,9 for *C. grata* and *C. toreuma*, respectively. The structural variety of odd-chain NMI FA was also recognized in this study, but why a number of unusual NMI FA found only in the ovaries of limpets, which are one of the most primitive gastropod families, is still unknown.

From our results, biosynthetic pathways for the novel tricosadienoic acids belonging to a group of NMI FA were also discussed. The pathway of odd-chain NMI dienoic FA is thought to be basically similar to that of even-chain NMI dienoic FA (Fig. 4). Thus, among tricosadienoic acids, 23:2Δ9,15, 23:2Δ9,18 and 23:2Δ9,20 might be derived from initial precursors 19:1Δ11, 19:1Δ14 and 19:1Δ16, respectively, by Δ5 unsaturation and two successive chain elongation reactions. Similarly, 23:2Δ7,18 might be synthesized from 19:1Δ14, the same initial precursor for 23:2Δ9,18, by chain elongation and sequential Δ5 unsaturation reactions and finally by chain elongation reaction. In contrast, only 23:2Δ8,14 may be formed from 24:2Δ9,15, which is present in limpet gonads [2], by an α-oxidation reaction. But proof or corroboration of this hypothesis requires additional studies.

More interestingly, a 1:2 mixture of all-*cis* dienoic FA, 23:2Δ5,9 and 24:2Δ5,9, isolated from the Turkish sponge *Agelas oroides* inhibits the activity of an enoyl-acyl carrier protein reductase in *Plasmodium falciparum*, which causes

**Fig. 4** Possible biosynthetic pathways for novel tricosadienoic FA. Asterisk not found in organisms

malaria in humans, and in *Escherichia coli* [14]. Furthermore, 23:2Δ14,17 with all *cis*-configuration from the extract of the root of *Angelica dahurica* inhibits a novel proto-oncogenic protein, Shp2, and colony formation of HepG2 cells, and strongly induce poly (ADP-ribose) polymerase cleavage [15]. In our previous study, we showed that a series of rare NMI FA with 24 carbon atoms (24:2Δ5,9, 24:2Δ9,15, 24:2Δ9,17, 24:3Δ5,9,15, 24:3Δ5,9,17, 24:3Δ9,15,18, 24:4Δ5,9,15,18, and 24:5Δ5,9,15,18,21) is especially rich in the ovaries of *C. grata* [8]. Therefore, limpet gonads may be possible marine resources of unique unsaturated FA, but in minor amounts. Because some NMI FA contain further unusual double bond positions in their chemical structures, they could be potential substances for key bioactive compounds, as well as some biomarkers in the marine food web, in future research.

Acknowledgments We are grateful to the two anonymous referees for their helpful comments on the manuscript. This study was supported by the Cooperative Program (No. 118, 2012) of the Atmosphere and Ocean Research Institute, The University of Tokyo.

References

- Barnathan G (2009) Non-methylene-interrupted fatty acids from marine invertebrates: occurrence, characterization and biological properties. *Biochimie* 91:671–678
- Kawashima H (2005) Unusual minor nonmethylene-interrupted di-, tri-, and tetraenoic fatty acids in limpet gonads. *Lipids* 40:627–630
- Kawashima H, Ohnishi M, Ogawa S, Matsui K (2008) Unusual fatty acid isomers of triacylglycerols and polar lipids in female limpet gonads of *Cellana grata*. *Lipids* 43:559–567
- Kawashima H, Ohnishi M (2004) Identification of minor fatty acids and various nonmethylene-interrupted diene isomers in mantle, muscle, and viscera of the marine bivalve *Megangulus zyoensis*. *Lipids* 39:265–271
- Saito H, Osako K (2007) Confirmation of a new food chain utilizing geothermal energy: unusual fatty acids of a deep-sea bivalve, *Calypptogena phaseoliformis*. *Limnol Oceanogr* 52:1910–1918
- Saito H (2009) Japanese patent (Japan Koukai Tokkyo Kouhou) JP 2009-197195 A 2009.9.3
- Kawashima H, Ohnishi M (2006) Occurrence of novel non-methylene-interrupted C24 polyenoic fatty acids in female gonad lipids of the limpet *Cellana grata*. *Biosci Biotechnol Biochem* 70:2575–2578
- Bligh EG, Dyer WJ (1959) A rapid method of total lipid extraction and purification. *Can J Biochem Physiol* 37:911–917
- Andersson BÅ, Holman RT (1974) Pyrrolidides for mass spectrometric determination of the position of the double bond in monounsaturated fatty acids. *Lipids* 9:185–190
- Christie WW. (2012) AOCS lipid library. http://lipidlibrary.aocs.org/ms/arch_pyr/index.htm. Accessed 18 May 2012
- Quévrain E, Barnathan G, Meziane T, Domart-Coulon I, Rabe-saotra V, Bourguet-Kondracki ML (2012) New 2-methyl-13-icosenoic acid from the temperate calcisponge *Leuconia johnstoni*. *Lipids* 47:345–353
- Andersson BÅ (1978) Mass spectrometry of fatty acid pyrrolidides. *Prog Chem Fats Other Lipids* 16:279–308

13. Christie WW. (2012) AOCS lipid library. http://lipidlibrary.aocs.org/ms/arch_pic/index.htm. Accessed 18 May 2012
14. Tasdemir D, Topaloglu B, Perozzo R, Brun R, O'Neill R, Carballeira NM, Zhang X, Tonge PJ, Linden A, Rüedi P (2007) Marine natural products from the Turkish sponge *Agelas oroides* that inhibit the enoyl reductases from *Plasmodium falciparum*, *Mycobacterium tuberculosis* and *Escherichia coli*. *Bioorg Med Chem* 15:6834–6845
15. Liu D, Kong G, Chen QC, Wang G, Li J, Xu Y, Lin T, Tian Y, Zhang X, Yao X, Feng G, Lu Z, Chen H (2011) Fatty acids as natural specific inhibitors of the proto-oncogenic protein Shp2. *Bioorg Med Chem Lett* 21:6833–6837

Correcting the Effects of $-20\text{ }^{\circ}\text{C}$ Storage and Aliquot Size on Erythrocyte Fatty Acid Content in the Women's Health Initiative

James V. Pottala · Mark A. Espeland ·
Jason Polreis · Jennifer Robinson · William S. Harris

Received: 31 January 2012 / Accepted: 18 May 2012 / Published online: 11 July 2012
© AOCS 2012

Abstract Red blood cell (RBC) fatty acid (FA) patterns have been shown to predict risk for cardiovascular and other chronic diseases. As part of a project analyzing RBC samples from the Women's Health Initiative Memory Study (WHIMS) we observed implausibly low levels of highly unsaturated fatty acids (HUFA) suggestive of degradation. This was hypothesized to be due to short term storage (<1 month) at $-20\text{ }^{\circ}\text{C}$ during sample aliquoting. The purpose of this study was to measure the extent of degradation that occurs under these conditions, and then to use regression calibration equations with multiple

imputations to correct the biases. Samples from the Women's Health Initiative that had always been stored at $-80\text{ }^{\circ}\text{C}$ were obtained and subjected to similar conditions as the WHIMS samples. General linear mixed models were used to develop bias-corrected calibration equations for each fatty acid. Sample degradation occurred at $-20\text{ }^{\circ}\text{C}$ with the average HUFA loss of 3.5 to 5.9 % per week depending on aliquot size (250 and 80 μL , respectively). Using the ratio of HUFA to saturated fatty acids (HUFA/SAT) as a marker of degradation, this bias-correction method raised the HUFA/SAT from 0.70 to 0.81, which was similar to that (0.78) seen in another large study with optimal processing. In summary, RBC samples should always be stored at $-80\text{ }^{\circ}\text{C}$. The FA compositions of the degraded RBC samples from WHIMS were rehabilitated by application of regression calibration equations and multiple imputations, and these imputed datasets should be used in all future WHIMS studies.

J. V. Pottala · J. Polreis · W. S. Harris (✉)
OmegaQuant LLC, Sioux Falls, SD, USA
e-mail: bill@omegaquant.com

M. A. Espeland
Department of Biostatistical Sciences,
Wake Forest School of Medicine,
Winston-Salem, NC, USA

J. Robinson
Departments of Epidemiology and Medicine,
University of Iowa College of Public Health,
Iowa City, IA, USA

W. S. Harris
Cardiovascular Health Research Center,
Sanford Research, Sioux Falls, SD, USA

W. S. Harris
Department of Medicine, Sanford School of Medicine,
University of South Dakota, Sioux Falls, SD, USA

W. S. Harris
Health Diagnostic Laboratory Inc.,
Richmond, VA, USA

Keywords Erythrocyte · Gas chromatography ·
n-3 Fatty acids · n-6 Fatty acids · Multiple imputations ·
WHIMS

Abbreviations

BHT	Butylated hydroxyl toluene
CVD	Cardiovascular disease
HUFA	Highly unsaturated fatty acid(s)
SAT	Saturated fatty acid(s)
RBC	Red blood cell(s)
WHI	Women's Health Initiative
WHIMS	WHI Memory Study
FA	Fatty acid(s)
PUFA	Polyunsaturated fatty acid(s)
GC	Gas chromatography
C_p	Process capability index

Background

There is an increasing interest in defining the relations between fatty acid patterns and risk for chronic disease. Fatty acids have long been known to have both positive and negative effects on metabolism and physiology. Higher intakes (and thus blood levels) of saturated and *trans* fatty acids exacerbate dyslipidemia and inflammatory processes and increase risk for cardiovascular disease (CVD). The polyunsaturated fatty acids (PUFA) of both the n-3 and n-6 classes reduce risk for CVD [1, 2], and inverse relations between the n-3 levels with prevalent [3] and incident [4] dementia have been reported. Erythrocytes (red blood cells, RBC) have become the sample of choice for assessing fatty acid status because they are readily available, represent the composition of other membranes [5], have low biological variability [6] and reflect relatively long term exposure to fatty acids [7]. Other sample types that have been used to assess n-3 fatty acid status include whole blood, whole plasma, plasma lipid classes (phospholipids, cholesteryl esters, triacylglycerol), platelets, leukocytes and buccal cells.

The Women's Health Initiative Memory Study (WHIMS) was an ancillary study of the Women's Health Initiative (WHI), which was a randomized trial to test the effects of hormone therapy on cognitive outcomes [8]. As part of a project using gas chromatography (GC) to analyze frozen RBC samples collected by the WHI among women who had enrolled in WHIMS, we noticed marked variability in the highly unsaturated fatty acids (HUFA, those fatty acids with 20 or more carbons and three or more double bonds) with a proportion of samples having very low to non-existent HUFA levels (Fig. 1). While low n-3 fatty acid levels (i.e., 20:5n-3 and 22:6n-3) could reflect a low fish intake, very low levels of the most prominent HUFA in RBC membranes, 20:4n-6, cannot be thus explained. Membrane levels of 20:4n-6 are known to be tightly metabolically regulated and largely independent of intake of 18:2n-6, the primary n-6 fatty acid in the diet [9]. This apparent loss of HUFA was most likely due to oxidative degradation since they contain 3–6 methylene-interrupted double bonds.

We hypothesized that a period of storage at -20°C (instead of -80°C), which occurred during the sample aliquoting phase prior to shipment to the research laboratory, may have been responsible for the loss of HUFA. Others have described storage of RBC at this temperature as being a potential problem [10–12]. We also considered the aliquot size as a possible factor since it appeared that the original 80 μL aliquots of RBC were more likely to be affected than the later received 250 μL aliquots. The purpose of this study was to characterize the effects of storage at -20°C on all RBC FA levels for both aliquot sizes used, with a view towards developing regression

calibration equations that could be used to correct the biased measures in the WHIMS data set. Additional experiments using antioxidant preservatives were conducted to document that oxidation was the probable cause of the loss of HUFA in these samples.

Experimental Methods

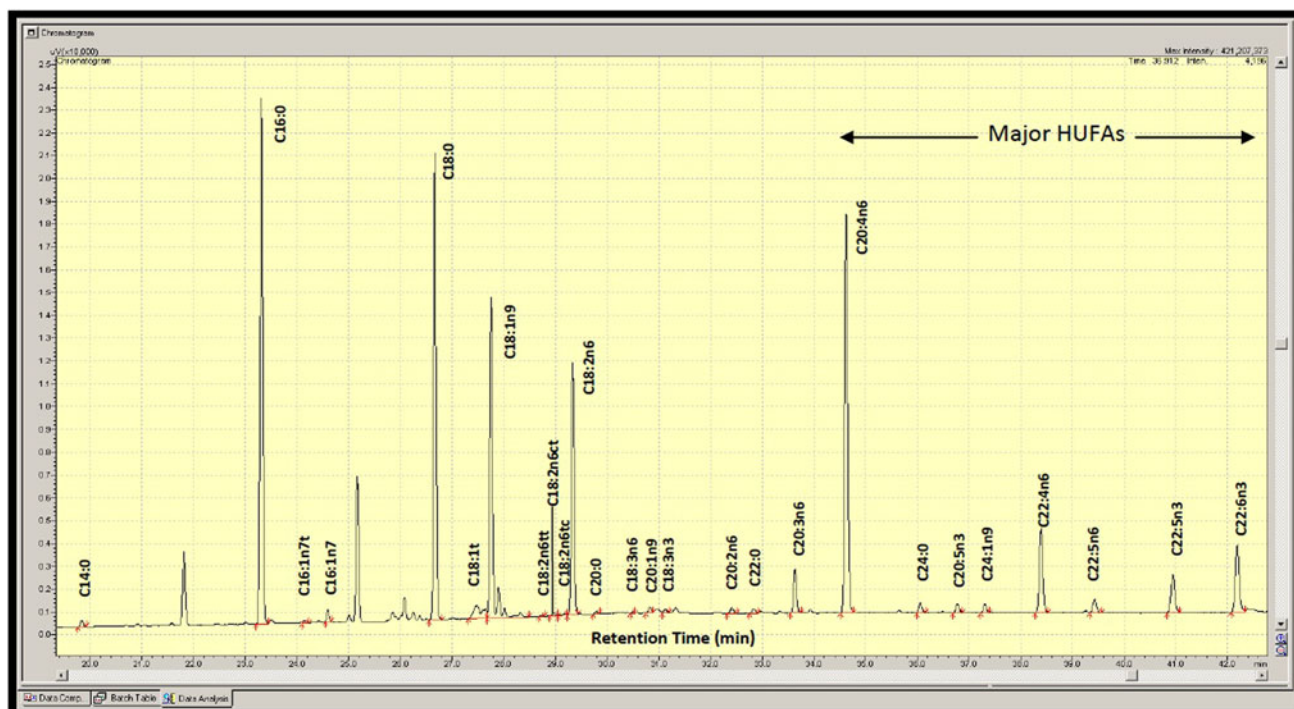
Subjects

The study design, eligibility criteria, and recruitment procedures of the WHI hormone therapy clinical trial have been described elsewhere [13]. Briefly, in 1992 WHI began enrolling postmenopausal women aged 50–79 at forty clinical centers nationwide to study cardiovascular disease, cancer, and osteoporotic fractures. It included three clinical trials, i.e., dietary modification (low-fat), calcium and vitamin D, and hormone therapy. WHIMS began enrollment in 1996 for women aged 65–80 at 39 of the clinical centers to test the hypothesis that hormone therapy reduces the incidence of dementia and cognitive decline [8]. The National Institutes of Health and the institutional review boards for all participating institutions approved the WHI and WHIMS protocols and consent forms, and all participants provided written informed consent.

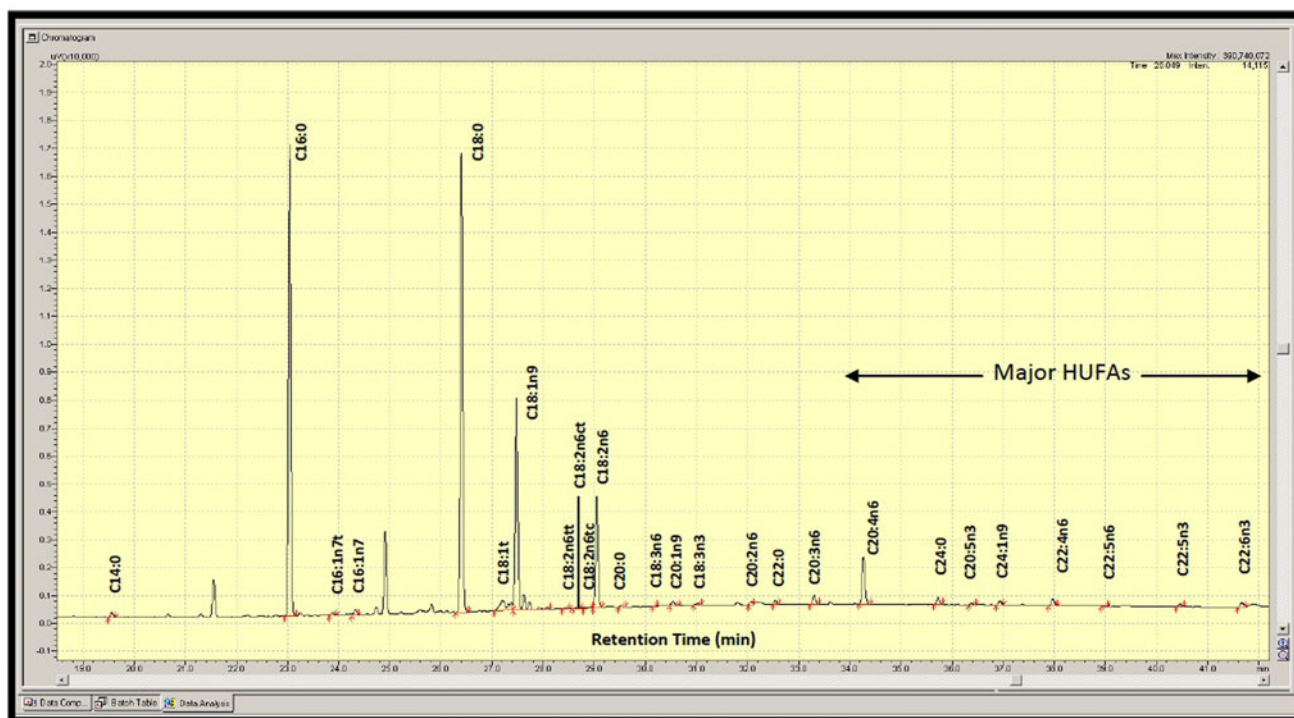
Sample Collection and Processing

The following is a summary of the steps used in the collection, shipment, storage, and aliquoting of RBC samples in the WHI:

1. Fasting blood samples were drawn from consenting participants at WHI field centers and processed for plasma, buffy coat, and RBC within 1 h of collection. A single 1.8 mL aliquot (primary vial) of unwashed packed RBC was prepared for each participant.
2. Aliquots were placed in a -70°C freezer within 2 h of collection.
3. Frozen samples were packed on dry ice and shipped on a weekly basis to the central biorepository Fisher, in Rockville, MD.
4. Samples were placed into -80°C freezers at the central repository and stored for up to 16 years.
5. Samples for analysis were pulled from the biorepository and shipped to the sample processing lab (SPL; Seattle, WA) on dry ice.
6. Samples were removed from the shipping box and placed into a -20°C freezer until they were ready for processing (6–16 days).
7. Samples were removed from the -20°C freezer and thawed on ice. An 80- μL aliquot of RBC was



A



B

Fig. 1 Representative chromatograms illustrating the difference between (a) “normal” and (b) “degraded” samples

transferred to a secondary vial (2 mL) and the rest of the primary vial was dispensed in 250- μ L aliquots into 2-mL vials for re-deposit at the biorepository.

8. The 80- and 250- μ L aliquots were again stored at -20°C until shipped to the research laboratory and biorepository, respectively, on dry ice (4–15 days).

9. Upon receipt at the research laboratory and biorepository, the samples were placed in a -80°C freezer.

-80 to -20°C (Pre-Thaw) Experiment

To study the effect of RBC processing step 5 (i.e., shifting the frozen samples from -80 to -20°C), 25 pairs of 1.8 mL fresh RBC samples were collected from subjects undergoing routine clinical testing and frozen for 1 day at -80°C . Then one set of 25 samples was shifted to -20°C , while the other set remained at -80°C . After 14 days all samples were analyzed for fatty acid composition.

Degradation Experiment

In order to determine the combined effects of storage temperature and aliquot size on the apparent loss of HUFA (processing steps 6–7), we obtained 100 RBC samples from women who had consented and had been screened for participation in WHI, but who were ultimately not enrolled. Hence, they had been stored at -80°C just as long as the WHIMS samples. To make the samples even more representative of the WHIMS cohort, they were cross-stratified by subject's race, age, geographic region, and then randomly selected. These 1.8-mL RBC aliquots were shipped directly to the research lab on dry ice. Upon receipt, the samples were placed in a -80°C freezer until the experiment began. At that time, samples were thawed and one aliquot was taken for immediate FA analysis. The rest of the sample was divided into six aliquots: three (80 μL) and

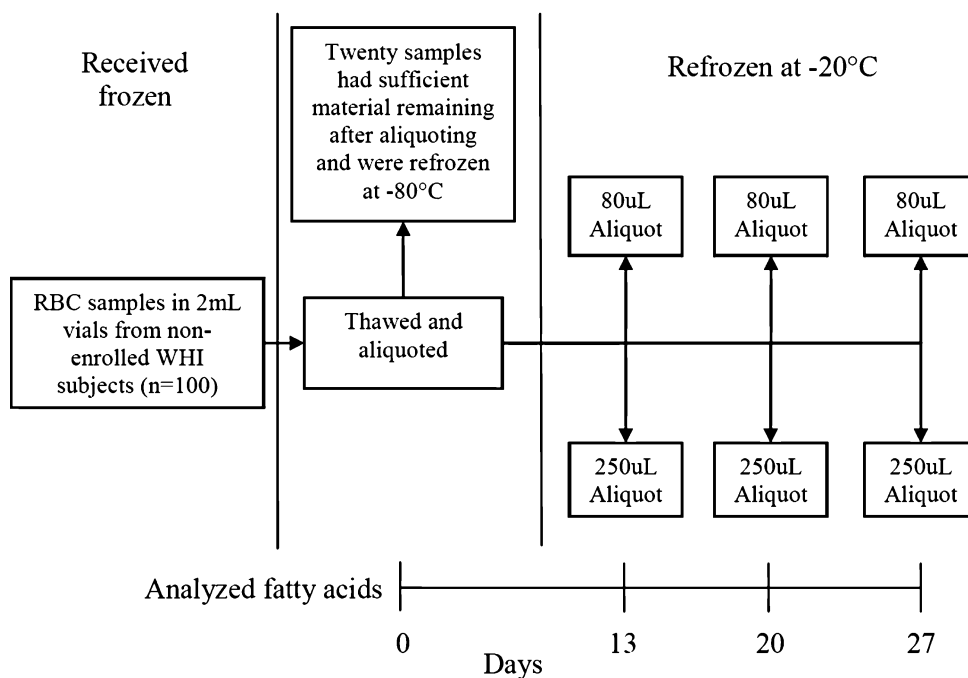
three (250 μL). (The 80- μL aliquot size was used since this was the size originally requested by the investigators, and the analysis required only 25 μL of RBC. The 250- μL aliquot size was used because, once degradation was suspected during the original analysis, we retrieved backup aliquots from the biorepository for repeat testing, and these were 250- μL aliquot sizes. These had also been stored for a time at -20°C like the 80- μL aliquots (see WHI sample processing described in above).

Hence, the final WHIMS RBC FA dataset included 80- and 250- μL aliquots, all of which had been subjected to some storage at -20°C .) The six aliquots were all placed at -20°C , and the 20 samples with RBC left over were immediately re-frozen at -80°C . After 13 days of -20°C storage, one 80- μL and one 250- μL sample were removed and analyzed for FA composition. Other aliquot pairs were removed and analyzed on days 20 and 27. The 20 samples refrozen at -80°C were reanalyzed after 12 weeks of storage (Fig. 2).

Antioxidant Experiment

We conducted an experiment to determine whether inclusion of an antioxidant (BHT) would prevent the RBC HUFA degradation. A 500-mg/L solution of BHT was prepared in methanol and added to the RBC sample (at 4 μL BHT/100 μL RBC) as described by Otto et al. [11]. We obtained five fresh RBC samples and treated each as follows: freeze at -80°C for 1 day, thaw on day 2, analyze for baseline FA composition, and prepare three, 80- μL aliquots. Each sample had one aliquot stored at -80°C

Fig. 2 Degradation (i.e., post-thaw) and -80°C storage experimental design



(control) and the other two at $-20\text{ }^{\circ}\text{C}$, with or without BHT. After 20 days of storage, the vials were removed and analyzed for FA composition.

RBC Fatty Acid Analysis

Red blood cells fatty acid composition was analyzed using GC with flame ionization detection using a modification of the direct methylation method of Arajuo et al. [14]. Unwashed, packed RBC (25 μL) were transferred to a screw-cap glass vial. Methanol containing 14 % boron trifluoride (Sigma-Aldrich, St. Louis, MO) and hexane (EMD Chemicals, USA) were added sequentially, 250 μL

summed and referred to as 18:1 *trans*. Fatty acid composition was expressed as a weight percent of total identified fatty acids. The coefficient of variation for the major HUFA (18:2n-6, 20:4n-6, 22:5n-3, 22:4n-6, 22:6n-3, and 20:5n-3) was <6.5 %.

Statistical Methods

The degradation experiment involving storage temperature and aliquot size was conducted to mimic the conditions of the WHIMS RBC samples. As a marker of sample integrity we used the ratio of HUFA to saturated fatty acids (HUFA/SAT).

$$\frac{\text{HUFA}}{\text{SAT}} = \frac{20:3n6 + 20:4n6 + 22:4n6 + 20:5n3 + 22:5n3 + 22:5n6 + 22:6n3}{14:0 + 16:0 + 18:0 + 20:0 + 22:0 + 24:0}$$

of each. The vial was briefly vortexed and then placed in an aluminum bead hot bath at $100\text{ }^{\circ}\text{C}$ for 10 min. After cooling, 250 μL of HPLC grade water was added, the tubes were recapped, vortexed and centrifuged for 3 min at 3,000 rpm to separate layers. A 50- μL aliquot of the hexane (upper) layer was transferred to a GC vial. GC was carried out using a G2010 Gas Chromatograph (Shimadzu Corporation, Columbia, MD) equipped with a SP2560, 100-m fused silica capillary column (0.25 mm internal diameter, 0.2 μm film thickness; Supelco, Bellefonte, PA). Run conditions were: carrier gas, hydrogen; linear velocity, 22.0 cm/s; injector temperature, $230\text{ }^{\circ}\text{C}$; oven program, initial temperature of $140\text{ }^{\circ}\text{C}$ hold for 5 min, ramp temperature at a rate of $4\text{ }^{\circ}\text{C}/\text{min}$ to $240\text{ }^{\circ}\text{C}$ and hold for 15 min (total run time 45 min); detector temperature, $240\text{ }^{\circ}\text{C}$. Fatty acids were identified by comparison with a standard mixture of fatty acids characteristic of RBC (GLC 782, NuCheck Prep, Elysian, MN) which was also used to determine individual fatty acid response factors. The following 24 fatty acids (by class) were identified: saturated (14:0, 16:0, 18:0, 20:0, 22:0 24:0); *cis* monounsaturated (16:1, 18:1, 20:1, 24:1); *cis* n-6 polyunsaturated (18:2, 18:3, 20:2, 20:3, 20:4, 22:4, 22:5); and *cis* n-3 polyunsaturated [18:3, 20:5, 22:5, 22:6]. The omega-3 index is defined as the sum of 20:5n-3 and 22:6n-3. The chromatographic conditions used in this study were sufficient to isolate the 16:1 *trans* isomers and the 18:2 Δ 9t-12c, 9t-12t, and 9c-12t isomers (which were summed and expressed as 18:2 *trans*). However, each individual 18:1 *trans* molecular species (i.e., 18:1 Δ 6 to Δ 13) could not be individually identified but appeared as two blended peaks that eluted just before oleic acid. The areas of these two peaks were

General linear mixed models (GLMM) were used to model the degradation mean response over time by aliquot size for the individual fatty acids and the HUFA/SAT ratio. The models included a random intercept to incorporate the sample clustering among the repeated aliquots. The statistical parameters were estimated using restricted maximum likelihood with the ‘sandwich’ variance estimator; these standard errors are robust to misspecification of the covariance structure [15]. The mean response was modeled allowing a differential slope by aliquot sizes. Fatty acids with mean abundances <1 % were transformed using natural logarithm to improve normality and homoscedasticity of the residuals. General linear mixed models were also used to analyze the HUFA/SAT ratio for the pre-thaw, $-80\text{ }^{\circ}\text{C}$ storage, and antioxidant experiments.

The negative of the slope estimates from the degradation experiment were used to form calibration equations, to restore the WHIMS samples using lognormal or normal linear regression, corresponding to whether the fatty acid was log transformed or not. Since these equations are estimated rather than known, it is important to include the imprecision due to this estimation in the bias-corrected data. Values were imputed by making stochastic draws from the bias-corrected sampling distributions as described by Rubin [16] for data missing at random. The algorithm for the multiple imputation method is shown in Fig. 3. This was repeated for the entire sample ten times, which has been shown by Rubin to have high relative efficiency compared to an infinite number of imputations even with a large fraction of missing information. Analyses were performed using SAS[®] software (version 9.2; SAS Institute Inc., Cary, NC).

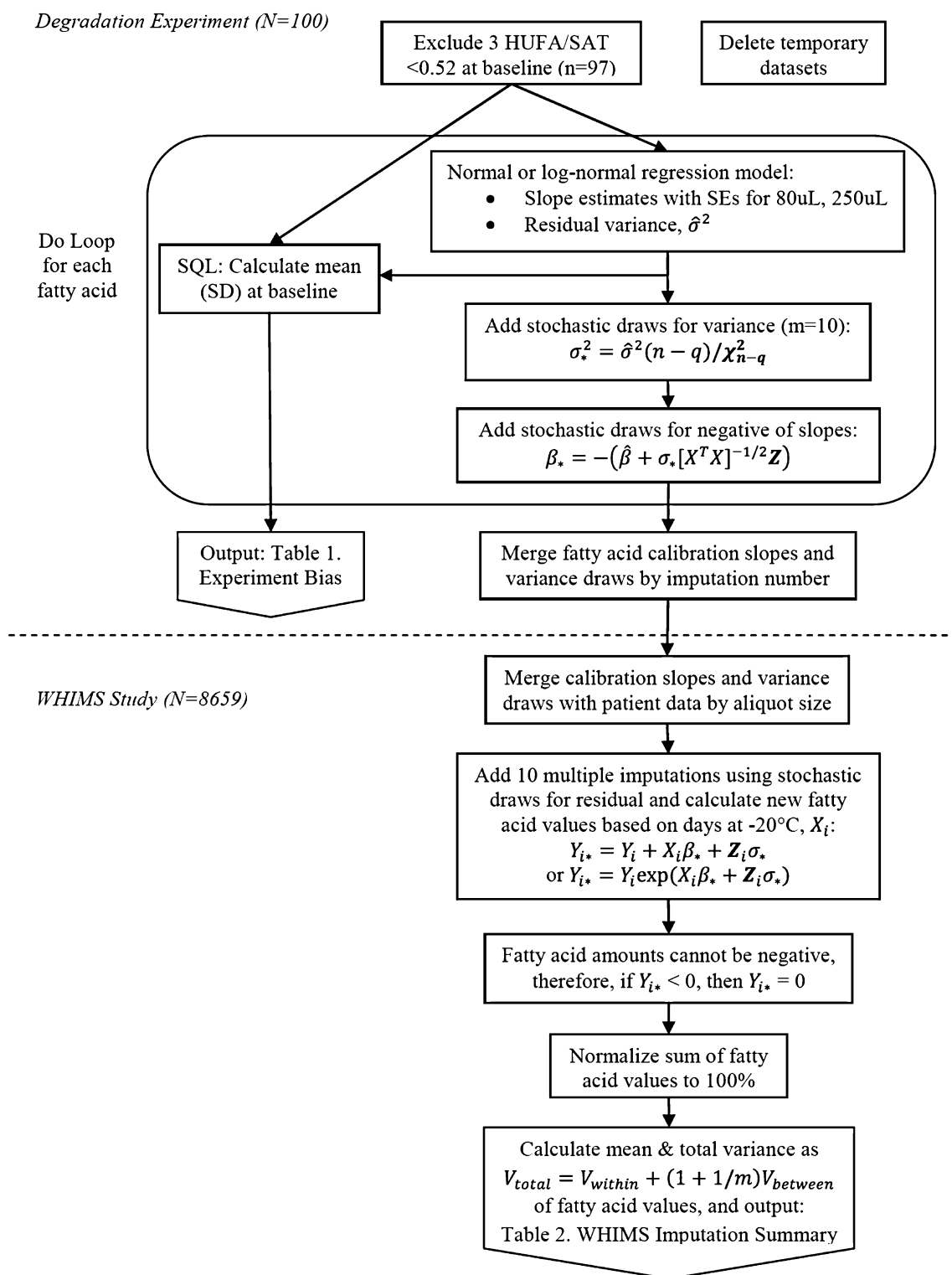


Fig. 3 Statistical methods algorithm for multiple imputations using explicit linear mixed models

Results

A minimum threshold for RBC FA analytical quality was established in a large cohort study (Framingham Heart

Study, $n = 3,197$, unpublished data) where RBC samples were frozen at -80°C on the day of collection and kept at that temperature until the day of analysis about 2 years later. The HUFA/SAT ratio in this dataset was 0.7767 ± 0.0564 .

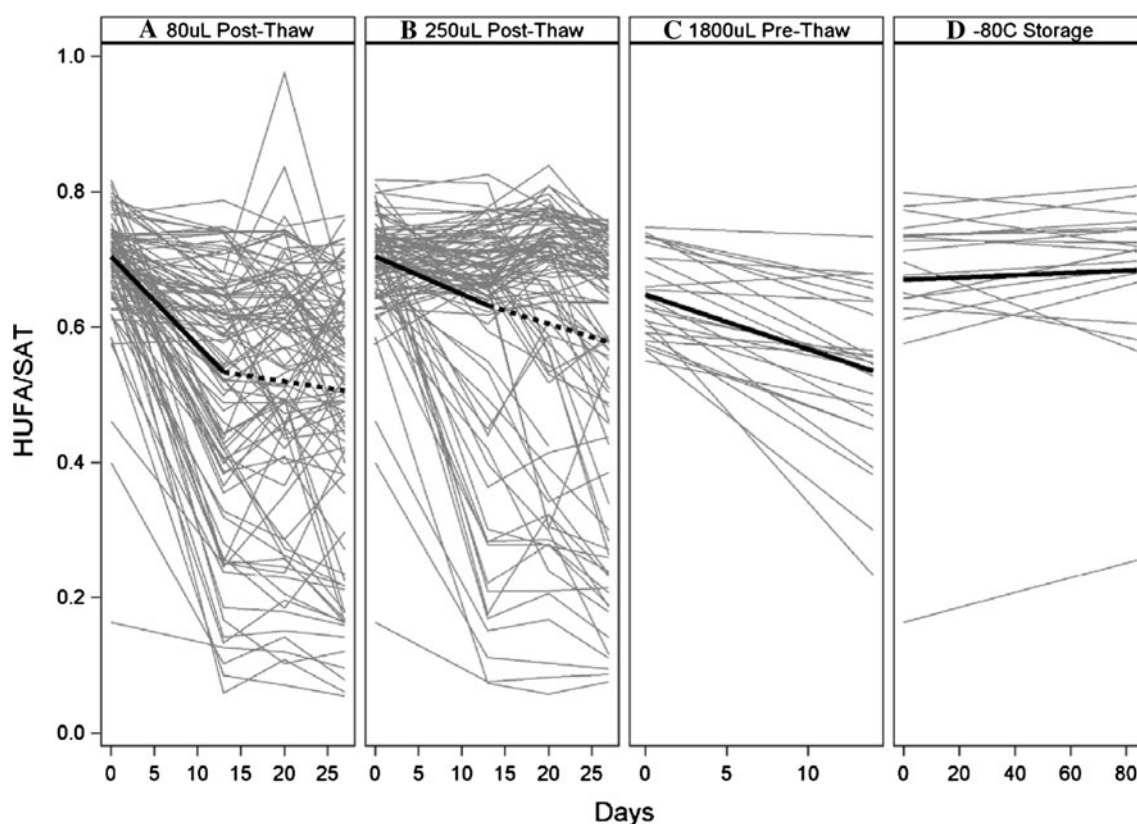


Fig. 4 Individual response profiles of HUFA/SAT ratio (which is comprised of 13 fatty acids). **a, b** The 80 and 250 μL results were from the degradation experiment at $-20\text{ }^{\circ}\text{C}$. Linear regression is shown for weeks 0–2 (*solid, bold*) and weeks 2–4 (*dashed, bold*). **c** The 1,800 μL aliquot was from the pre-thaw experiment at $-20\text{ }^{\circ}\text{C}$

(see “[Experimental Methods](#)”). Over the first 2 weeks the 250- μL post-thaw and 1,800- μL pre-thaw slopes were similar ($p = 0.34$); however, the 80- μL post-thaw may degrade at a faster rate than the 1,800- μL pre-thaw ($p = 0.06$). **d** The last panel shows there was no degradation in samples stored at $-80\text{ }^{\circ}\text{C}$ for 12 weeks ($p = 0.27$)

In order to establish a minimum HUFA/SAT ratio for use in detecting degraded samples, we employed the process capability index (C_p) [17]. Process capability index is a quality control metric commonly used in manufacturing, and is defined as $C_p = (\text{mean} - \text{lower limit})/3\text{SD}$. Setting the C_p to 1.5, which is recommended for critical parameters of stable processes (like GC analysis of fatty acids), and solving for the ‘lower limit’ returns a HUFA/SAT ratio of 0.52 ($0.7767 - 4.5 \cdot (0.0564) = 0.52$). Therefore, if the HUFA/SAT ratio is less than 0.52 the sample is deemed to be degraded. Note: this threshold was derived based on the particular RBC fatty acid analysis method given above, and may not be accurate for fatty acid data generated by other analytical methods.

The effects of storage at $-20\text{ }^{\circ}\text{C}$ on HUFA/SAT ratios are shown in Fig. 4a, b for the 100 WHI RBC samples in 80- and 250- μL aliquot sizes, respectively. There were three samples with HUFA/SAT < 0.52 at baseline, and thus these were excluded from the regression analysis. There were a total of 94 samples with paired data for 80- and 250- μL aliquots at days 0 and 13, three samples did not have 250- μL aliquots due to insufficient material. Out of

these samples, 34 (36 %) of the 80- μL aliquots degraded between days 0 and 13, and 16 (17 %) of the 250- μL aliquots that did the same. Importantly 20 of the degraded 80- μL aliquots had matching 250- μL aliquots that did not degrade, while there were only two samples which degraded in the 250- μL but not the 80- μL aliquot (McNemar’s test $p < 0.0001$). In summary, although a substantial number of samples degraded at $-20\text{ }^{\circ}\text{C}$, the 80- μL aliquots were more likely to degrade than the larger 250- μL aliquots.

Some loss of HUFA occurred even in the 1,800- μL aliquot, simply by shifting the frozen vials from -80 to $-20\text{ }^{\circ}\text{C}$ without thawing to room temperature (Fig. 4c). When comparing the 250 μL (post-thaw processing steps 6–7) to the 1,800 μL (pre-thaw processing step 5) from different experiments at $-20\text{ }^{\circ}\text{C}$, the changes were similar in the HUFA/SAT ratios over the first 2 weeks (Fig. 4b, c). The weekly slopes (SE) for the 250 and 1,800 μL were -0.0387 (0.0091) and -0.0566 (0.0090), respectively, $p = 0.34$. However, the 80- μL post-thaw slope (SE) was -0.0919 (0.0092), which may degrade at a faster rate than the 1,800- μL pre-thaw over the first 2 weeks ($p = 0.06$).

Table 1 Bias (% mean change per week) of RBC fatty Acids (by weight%) in -20 °C storage degradation experiment, N = 97

	Baseline		% Bias	
	Mean	SD	250 µL	80 µL
14:0 Myristic	0.44	0.11	(1.1)	(0.7)
16:0 Palmitic	23.08	1.34	1.6	3.6
18:0 Stearic	17.48	1.02	1.9	4.1
20:0 Eicosanoic	0.11	0.08	1.9	1.7
22:0 Docosanoic	0.06	0.02	11.5	14.8
24:0 Lignoceric	0.13	0.05	8.5	12.0
16:1 Palmitoleic	0.51	0.21	1.0	1.3
18:1 Oleic	14.17	1.07	1.4	2.0
20:1 Eicosenoic	0.22	0.05	1.7	3.8
24:1 Nervonic	0.09	0.03	15.2	16.5
16:1t Palmitoleic <i>trans</i>	0.22	0.04	9.7	3.3
18:1t Oleic <i>trans</i>	2.20	0.65	0.0	0.3
18:2t Linoleic <i>trans</i>	0.59	0.16	(0.8)	(1.6)
18:2n-6 Linoleic	11.09	1.72	(0.4)	(1.9)
20:2n-6 Eicosadienoic	0.29	0.05	(1.1)	(0.6)
18:3n-3 Alpha linolenic	0.17	0.07	(0.2)	(3.3)
18:3n-6 Gamma linolenic	0.11	0.05	(12.6)	(14.4)
20:3n-6 Eicosatrienoic	1.66	0.37	(0.5)	(2.8)
20:4n-6 Arachidonic	15.51	1.36	(3.2)	(5.7)
22:4n-6 Docosatetraenoic	3.81	0.78	(4.0)	(6.2)
20:5n-3 Eicosapentaenoic	0.66	0.46	(6.1)	(7.9)
22:5n-3 Docosapentaenoic	2.38	0.38	(3.7)	(6.5)
22:5n-6 Docosapentaenoic	0.68	0.20	(3.5)	(6.1)
22:6n-3 Docosahexaenoic	4.34	1.42	(3.4)	(6.2)

Negative values are shown in parentheses

Twenty samples from the degradation experiment had sufficient material remaining after making the six aliquots to test their stability when stored at -80 °C for 12 weeks. As expected there was no degradation (Fig. 4d) and the mean HUFA/SAT ratio was unchanged ($p = 0.27$). These results, and those from the pre-thaw experiment, indicate that a freeze/thaw cycle did not alter the fatty acid profiles; but the storage temperature did.

Storage of RBC samples at -20 °C caused a loss of all HUFA, and the relative proportion of saturated and monounsaturated fatty acids increased (since the total amount of fatty acids is constrained to 100 %) (Table 1). Although the rise in the non-HUFA was presumed to be due to the constraint of reporting FA abundances as a percent of total, it was possible that the rise in their abundance was due to the potential co-elution of some HUFA degradation products with the SATs. This possibility was, however, discounted by analysis of degraded samples by GC-mass spectroscopy which confirmed that no other molecular species were present in the major saturated and monounsaturated fatty acid peaks (data not shown).

The average weekly decreases in HUFA content were - 3.5 and -5.9 % for the 250- and 80-µL aliquots, respectively. The two most abundant saturated fatty acids 16:0

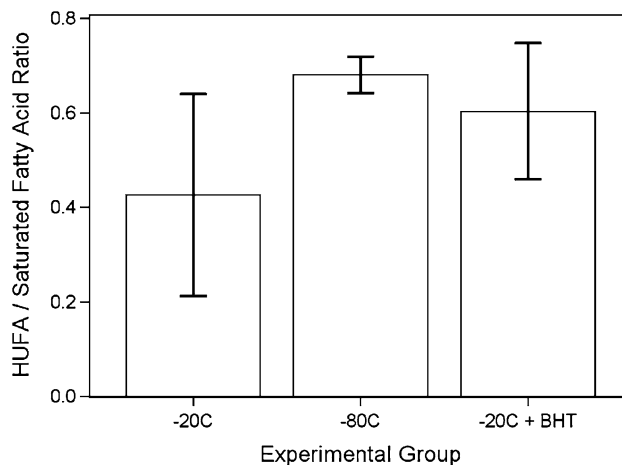


Fig. 5 Triplicate 80-µL aliquots were stored at -80 (control), -20, and -20 °C with butylated hydroxytoluene (BHT), an antioxidant, for five RBC samples over 20 days (overall $p = 0.003$). Mean with 95 % confidence intervals are shown

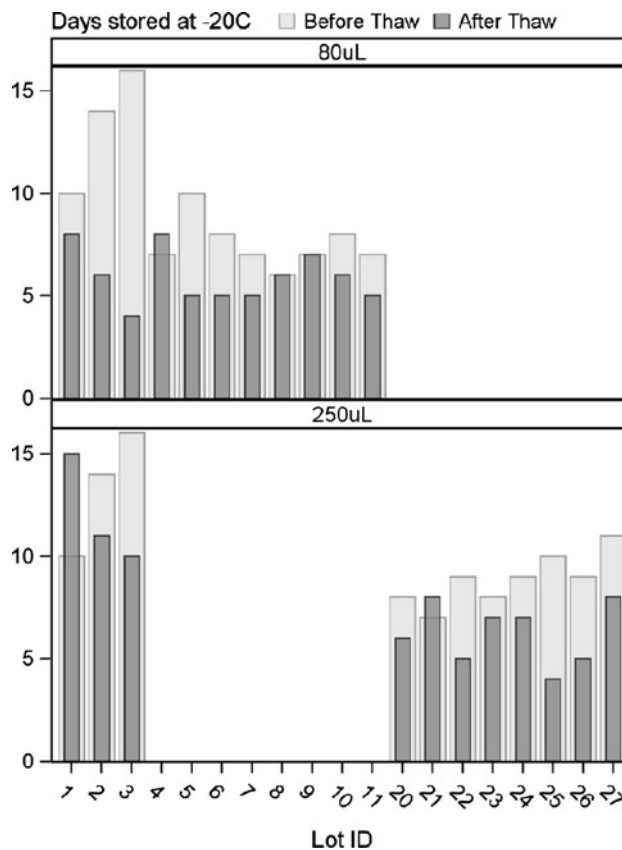


Fig. 6 Distribution of days WHIMS RBC samples were exposed to -20 °C storage before and after thawing, by shipping lot identification number (N = 8,659)

and 18:0 accounted for about 40 % of the total fatty acids, and demonstrated the inverse effect of the loss of HUFA as noted above. They increased (as a percentage of total) by an average of 1.8 and 3.9 % per week in the 250- and 80- μ L aliquots, respectively.

In the 20-day, 80- μ L antioxidant experiment there was a significant difference among the groups, i.e., -80 (control), -20 , and -20 °C with BHT, $p = 0.003$ (Fig. 5). The HUFA/SAT ratio decreased from 0.68 to 0.43 between the -80 and -20 °C samples (Dunnnett adjustment $p = 0.008$), but HUFA/SAT ratios were similar between the -80 and -20 °C + BHT samples ($p = 0.17$). The antioxidant experiment demonstrated that the loss of HUFA in the RBC samples during storage at -20 °C was very likely due to oxidation.

All WHIMS RBC samples ($N = 8,659$) were exposed to some period of -20 °C storage before and after thawing (processing steps 5–7 listed above; Fig. 6). The results from the pre-thaw experiment demonstrated that the 1,800- and 250- μ L aliquot sizes degraded similarly over time at -20 °C. Since the degradation experiment included actual WHI RBC samples representative of the WHIMS samples, the slopes for the individual fatty acids from the 250 μ L were used for the pre-thaw exposure duration in the regression calibration. However, the regression calibration slopes for the post-thaw exposure duration corresponded with their aliquot size, 80 or 250 μ L. Multiple imputations ($m = 10$) of the regression calibration equations were applied to all WHIMS RBC samples. While these techniques are well suited to correct bias, the cost is increased

Table 2 Descriptive statistics for WHIMS RBC fatty acids raw data and imputed values ($N = 8,659$, $m = 10$ imputations)

Variable	Weight%				% Bias ^b	Mol%			
	Raw data		Imputation			Raw data		Imputation	
	Mean	SD	Mean	SD ^a		Mean	SD	Mean	SD ^a
14:0 Myristic	0.36	0.10	0.38	0.12	(3.3)	0.29	0.08	0.30	0.10
16:0 Palmitic	22.24	2.17	21.13	2.61	5.3	19.91	1.94	18.86	2.33
18:0 Stearic	17.68	1.91	16.70	2.33	5.9	17.56	1.90	16.53	2.31
20:0 Eicosanoic	0.13	0.05	0.13	0.06	0.3	0.14	0.05	0.14	0.07
22:0 Docosanoic	0.20	0.11	0.17	0.12	19.0	0.24	0.13	0.20	0.14
24:0 Lignoceric	0.41	0.20	0.35	0.24	15.0	0.53	0.26	0.45	0.31
16:1 Palmitoleic	0.48	0.22	0.48	0.23	1.3	0.43	0.20	0.43	0.20
18:1 Oleic	14.65	1.20	14.14	1.40	3.6	14.45	1.18	13.90	1.38
20:1 Eicosenoic	0.24	0.08	0.23	0.09	3.7	0.26	0.09	0.25	0.10
24:1 Nervonic	0.37	0.19	0.29	0.21	27.5	0.47	0.24	0.37	0.27
16:1t Palmitoleic <i>trans</i>	0.16	0.09	0.16	0.15	(0.7)	0.14	0.08	0.14	0.13
18:1t Oleic <i>trans</i>	2.11	0.64	2.10	0.67	0.4	2.08	0.63	2.06	0.66
18:2t Linoleic <i>trans</i>	0.41	0.13	0.43	0.18	(4.8)	0.40	0.13	0.42	0.18
18:2n-6 Linoleic	11.60	1.73	11.80	1.85	(1.7)	11.36	1.69	11.52	1.81
20:2n-6 Eicosadienoic	0.29	0.07	0.30	0.10	(4.1)	0.30	0.07	0.31	0.10
18:3n-3 Alpha linolenic	0.15	0.05	0.16	0.08	(6.4)	0.15	0.05	0.16	0.08
18:3n-6 Gamma linolenic	0.11	0.07	0.17	0.16	(35.6)	0.11	0.07	0.16	0.16
20:3n-6 Eicosatrienoic	1.72	0.41	1.76	0.45	(2.4)	1.84	0.44	1.88	0.48
20:4n-6 Arachidonic	15.45	2.27	16.69	2.74	(7.4)	16.43	2.41	17.69	2.90
22:4n-6 Docosatetraenoic	3.58	0.79	3.97	0.93	(9.7)	4.16	0.92	4.59	1.08
20:5n-3 Eicosapentaenoic	0.57	0.29	0.69	0.40	(16.6)	0.60	0.31	0.73	0.42
22:5n-3 Docosapentaenoic	2.24	0.46	2.47	0.56	(9.3)	2.59	0.53	2.84	0.64
22:5n-6 Docosapentaenoic	0.71	0.20	0.80	0.30	(11.3)	0.82	0.23	0.92	0.35
22:6n-3 Docosahexaenoic	4.14	1.35	4.50	1.48	(8.1)	4.75	1.55	5.15	1.69
Omega-3 index ^c	4.71	1.56	5.19	1.73	(9.2)	–	–	–	–
HUFA/SAT ratio	0.70	0.12	0.81	0.15	(13.2)	–	–	–	–

Negative values are shown in parentheses

^a Imputation SD = SQRT (within imputation variance + $(1 + 1/m) \times$ between imputation variance)

^b (Raw data weight% mean/imputation weight% mean–1) \times 100 %

^c The omega-3 index is calculated as 20:5n-3 + 22:6n-3

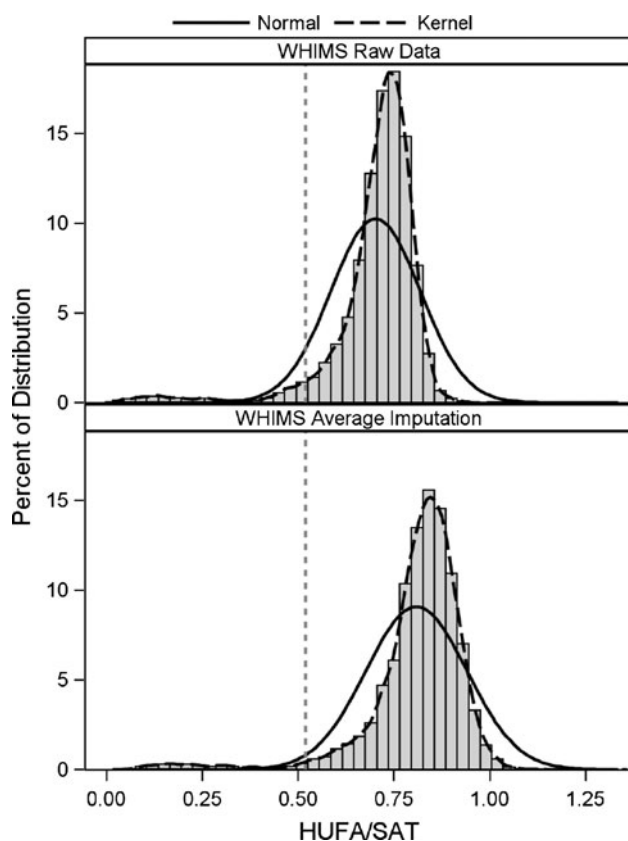


Fig. 7 Histograms including normal and kernel distributions. **a** WHIMS HUFA/SAT original measurements ($N = 8,659$); which included 466 (5.4 %) below the quality threshold HUFA/SAT = 0.52. **b** WHIMS HUFA/SAT averages from ten imputations; 272 (3.1 %) were below the quality threshold

total variability in the imputed data. Since originally the fatty acid measurements summed to 100 %, this constraint was likewise imposed on each imputation. The raw means and standard deviations (SD) are shown in Table 2 by weight% and mol% along with the bias-corrected means and SDs. The distribution of the HUFA/SAT ratio for the entire WHIMS cohort is shown before and after multiple imputations; the mean has been shifted to the right with added variability (Fig. 7). Even after implementing these techniques some samples remained degraded with average imputation HUFA/SAT < 0.52 ($n = 272$; 3.1 %).

Discussion

As creators of the fatty acid database for WHIMS, the authors have a responsibility to release a final dataset that can be used in future analyses by other investigators employing standard statistical methods. When significant sample degradation was finally detected and confirmed, we conducted the experiments described here in order to correct the degradation bias with a view towards generating as

accurate a data set as possible. In these experiments, we used well-preserved WHI samples (always kept at $-80\text{ }^{\circ}\text{C}$) and exposed them to similar conditions as the WHIMS samples experienced. The explicit regression calibration equations based on this experiment were used for bias correction.

There was marked variation among the WHI experimental samples with respect to their susceptibility to degradation, and the reason why one sample degraded and another did not is unclear. Three of the 100 test samples were degraded before receipt in the laboratory, although they were stored at $-80\text{ }^{\circ}\text{C}$ in the repository there may have been different handling protocols among the multiple field collection centers. By day 13 of storage at $-20\text{ }^{\circ}\text{C}$, 37 and 17 % of samples were degraded in the 80- and 250- μL aliquots, respectively. In an attempt to determine why these samples degraded and the others did not, we examined the fatty acid profiles using multivariate analyses techniques, i.e., principal components analysis and stepwise discriminant analysis (data not shown). We found nothing in the fatty acid profiles that distinguished degraded from preserved samples. One limitation of this study is that we did not measure endogenous levels of RBC antioxidant defense systems (vitamins C and E, glutathione, superoxide dismutase, etc.) [18]. Variations in these factors might have explained the differential susceptibility to degradation that we observed. We also determined in a subset of 3,600 samples that the duration of storage at $-80\text{ }^{\circ}\text{C}$ (within the range of 10–16 years) did not influence the likelihood of a sample being degraded (data not shown). Presumably the reason why the 80- μL aliquots were more susceptible than the 250- μL aliquots in the 2-mL storage vials relates to greater proportion of surface area to sample volume exposed to air in the smaller aliquot size. The ability of antioxidants to prevent degradation also supports the hypothesis that the loss of PUFA was due to oxidation. As noted earlier, others have reported that storage at $-20\text{ }^{\circ}\text{C}$ is insufficient for protection of RBC FA composition [10–12], but that this applied even to samples moved from -80 to $-20\text{ }^{\circ}\text{C}$ without an intervening thaw had not been appreciated.

Since single imputation methods using the best predicted value underestimate variability, multiple imputations were implemented by replacing each fatty acid value with ten instances from a distribution of possible values. Over the last two decades the multiple imputation technique has been used in health care research, and was developed for releasing health care public use datasets [19]. The Third National Health and Nutritional Examination Survey (NHANES III) was completed in 1994 and was the first implementation of multiple imputation ($m = 5$) for that survey, replacing the previous method of reweighting for unit non-response and leaving item non-response values

as missing [20]. Multiple imputation methods have also been implemented in the National Health Interview Survey [19], and are recommended for clinical research [20].

Application of these techniques to the original WHIMS dataset increased the HUFA levels and correspondingly decreased the saturated and monounsaturated FA levels. We believe that these remediated values best represent the fatty acid composition of RBC in WHIMS. The imputed fatty acid datasets generated as described herein should be used in all future studies examining the relationships between RBC fatty acids and any outcomes from WHIMS. A description of how these imputed data sets may be utilized in WHIMS analyses is included in “Appendix 1”. In conclusion, RBC samples destined for fatty acid analysis should always be stored at -80°C .

Acknowledgments The authors wish to thank several people at the WHI Clinical Coordinating Center (Fred Hutchinson Cancer Research Center, Seattle, WA); Sue Mann for her detailed project management, Joe Larson for his SAS data management, and Megan Skinner for her assistance with stratified random sampling. This study was supported in part under a contract with the NHLBI (BAA 19). The WHI program is funded by the National Heart, Lung, and Blood Institute, National Institutes of Health, US Department of Health and Human Services through contracts HSN268201100046C, HHSN268201100001C, HHSN268201100002C, HSN268201100003C, HHSN268201100004C, and HHSN271201100004C.

Appendix 1

This section is specifically for biostatisticians who will be working with the WHIMS RBC fatty acid data sets to test a variety of hypotheses in this study. All samples were exposed to -20°C , which is why all samples were subjected to the calibration equations and multiple imputations. However, some samples remained degraded with average imputation HUFA/SAT <0.52 after correction, and these samples should be excluded from analyses ($n = 272$; 3.1 %). For the remaining samples, standard statistical methods can be applied to the complete data by imputation. For a single inference the set of parameter estimates can be combined into an overall inference by calculating the parameter’s average variance over the repeated imputations (within variability) + the variance of the parameter’s mean (between variability) multiplied by $(1 + (1/m))$ for a finite number of imputations [21]. For multiple inferences future WHIMS investigators analyzing these RBC data should use the SAS[®] procedure PROC MIANALYZE, which implements Rubin’s technique and calculates confidence intervals for the overall inference by using as inputs the covariance matrix and parameter estimates from general linear mixed models or generalized linear models. Rubin developed the multiple imputation method using Bayesian statistics, and then evaluated the technique in randomization-based

statistics using interval estimation [16]. His results show that the final inference is valid as a randomization based confidence interval or a Bayesian probability interval with the same nominal coverage.

Appendix 2: Short List of WHI Investigators

Program Office (National Heart, Lung, and Blood Institute, Bethesda, Maryland) Jacques Rossouw, Shari Ludlam, Joan McGowan, Leslie Ford, and Nancy Geller.

Clinical Coordinating Center (Fred Hutchinson Cancer Research Center, Seattle, WA) Garnet Anderson, Ross Prentice, Andrea LaCroix, and Charles Kooperberg.

Investigators and Academic Centers (Brigham and Women’s Hospital, Harvard Medical School, Boston, MA) JoAnn E. Manson; (MedStar Health Research Institute/Howard University, Washington, DC) Barbara V. Howard; (Stanford Prevention Research Center, Stanford, CA) Marcia L. Stefanick; (The Ohio State University, Columbus, OH) Rebecca Jackson; (University of Arizona, Tucson/Phoenix, AZ) Cynthia A. Thomson; (University at Buffalo, Buffalo, NY) Jean Wactawski-Wende; (University of Florida, Gainesville/Jacksonville, FL) Marian Limacher; (University of Iowa, Iowa City/Davenport, IA) Robert Wallace; (University of Pittsburgh, Pittsburgh, PA) Lewis Kuller; (Wake Forest University School of Medicine, Winston-Salem, NC) Sally Shumaker.

Women’s Health Initiative Memory Study (Wake Forest University School of Medicine, Winston-Salem, NC) Sally Shumaker.

References

- Harris WS, Mozaffarian D, Rimm EB, Kris-Etherton PM, Rudel LL, Appel LJ, Engler MM, Engler MB, Sacks FM (2009) Omega-6 fatty acids and risk for cardiovascular disease: a science advisory from the American Heart Association Nutrition Committee. *Circulation* 119:902–907
- Kris-Etherton PM, Harris WS, Appel LJ (2002) Fish consumption, fish oil, omega-3 fatty acids, and cardiovascular disease. *Circulation* 106:2747–2757
- Cherubini A, Andres-Lacueva C, Martin A, Lauretani F, Iorio AD, Bartali B, Corsi A, Bandinelli S, Mattson MP, Ferrucci L (2007) Low plasma N-3 fatty acids and dementia in older persons: the INCHIANTI study. *J Gerontol A Biol Sci Med Sci* 62:1120–1126
- Dullemeijer C, Durga J, Brouwer IA, van de RO, Kok FJ, Brummer RJ, van Boxtel MP, Verhoef P (2007) n-3 Fatty acid proportions in plasma and cognitive performance in older adults. *Am J Clin Nutr* 86:1479–1485
- Harris WS, Sands SA, Windsor SL, Ali HA, Stevens TL, Magalski A, Porter CB, Borkon AM (2004) Omega-3 fatty acids in cardiac biopsies from heart transplant patients: correlation with erythrocytes and response to supplementation. *Circulation* 110:1645–1649

6. Harris WS, Thomas RM (2009) Biological variability of blood omega-3 biomarkers. *Clin Biochem* 43:338–340
7. Katan MB, Deslypere JP, van Birgelen AP, Penders M, Zegwaard M (1997) Kinetics of the incorporation of dietary fatty acids into serum cholesteryl esters, erythrocyte membranes, and adipose tissue: an 18-month controlled study. *J Lipid Res* 38:2012–2022
8. Shumaker SA, Reboussin BA, Espeland MA, Rapp SR, McBee WL, Dailey M, Bowen D, Terrell T, Jones BN (1998) The Women's Health Initiative Memory Study (WHIMS): a trial of the effect of estrogen therapy in preventing and slowing the progression of dementia. *Control Clin Trials* 19:604–621
9. Rett BS, Whelan J (2011) Increasing dietary linoleic acid does not increase tissue arachidonic acid content in adults consuming western-type diets: a systematic review. *Nutr Metab (London)* 8:36–51
10. Magnusardottir AR, Skuladottir GV (2006) Effects of storage time and added antioxidant on fatty acid composition of red blood cells at -20°C . *Lipids* 41:401–404
11. Otto SJ, Foreman-von Drongelen MM, von Houwelingen AC, Hornstra G (1997) Effects of storage on venous and capillary blood samples: the influence of deferoxamine and butylated hydroxytoluene on the fatty acid alterations in red blood cell phospholipids. *Eur J Clin Chem Clin Biochem* 35:907–913
12. Di Marino L, Maffettone A, Cipriano P, Celentano E, Galasso R, Iovine C, Berrino F, Panico S (2000) Assay of erythrocyte membrane fatty acids. Effects of storage time at low temperature. *Int J Clin Lab Res* 30:197–202
13. The Women's Health Initiative Study Group (1998) Design of the women's health initiative clinical trial and observational study. The Women's Health Initiative Study Group. *Control Clin Trials* 19:61–109
14. Araujo P, Nguyen TT, Froyland L, Wang J, Kang JX (2008) Evaluation of a rapid method for the quantitative analysis of fatty acids in various matrices. *J Chromatogr A* 1212:106–113
15. Fitzmaurice GM, Laird NM, Ware JH (2004) *Applied Longitudinal Analysis*. John Wiley, Hoboken
16. Rubin DB (1987) *Multiple imputation for non-response in surveys*. John Wiley, New Jersey
17. Montgomery DC (2001) *Introduction to statistical quality control*, 4th edn. John Wiley, New York
18. Pandey KB, Rizvi SI (2011) Biomarkers of oxidative stress in red blood cells. *Biomed Pap Med Fac Univ Palacky Olomouc Czech Repub* 155:131–136
19. Rubin DB, Schenker N (1991) Multiple imputation in health-care databases: an overview and some applications. *Stat Med* 10:585–598
20. Schafer JL, Ezzati-Rice TM, Johnson W, Khare M, Little RJA, Rubin DB (1996) The NHANES III multiple imputation project. In: *Proceeding of the Survey Research Methods Section, American Statistical Association*, pp 28–37
21. Rubin DB (1996) Multiple imputation after 18+ years. *J Am Stat Assoc* 91:473–489

Myocardial Infarction Changes Sphingolipid Metabolism in the Uninfarcted Ventricular Wall of the Rat

Małgorzata Knapp · Małgorzata Żendzian-Piotrowska · Krzysztof Kurek · Agnieszka Błachnio-Zabielska

Received: 6 April 2012 / Accepted: 16 May 2012 / Published online: 26 July 2012
© AOCs 2012

Abstract It is known that the ratio, the level of sphingosine-1-phosphate (S1P)/the level of ceramide (CER) determines survival of the cells. The aim of the present study was to examine the effect of myocardial infarction on the level of different sphingolipids in the uninfarcted area. The experiments were carried out on male Wistar rats: 1, control; 2, after ligation of the left coronary artery (infarct) and 3, sham operated. Samples of the uninfarcted area of the left ventricle were taken in 1, 6 and 24 h after the surgery. The level of sphingolipids, S1P, CER, sphingosine (SPH), sphinganine-1-phosphate (SPA1P) and sphinganine (SPA) was determined. The control values were (ng/mg), S1P- 0.33 ± 0.03 , SPH- 1.02 ± 0.13 , SPA1P- 0.11 ± 0.01 , SPA- 0.28 ± 0.04 , total CER- 20.3 ± 1.8 . In infarct, the level of S1P in the uninfarcted area was reduced by ~ 3 times in 1 and 6 h and decreased further in 24 h. The level of SPH decreased in 1 h and returned to the control thereafter. The total level of CER decreased in 6 h after the infarction. Sham surgery also produced changes in the level of certain sphingolipids. The ratio, the level of S1P/the level of CER was markedly reduced at each time point after the infarction. It is concluded that the reduction in the S1P/CER ratio could be responsible for increased apoptosis in the uninfarcted area after the myocardial infarction in the rat.

Keywords Myocardial infarction · Uninfarcted area · Sphingolipids · Rat

Abbreviations

S1P	Sphingosine-1-phosphate
CER	Ceramide
SPH	Sphingosine
SPA1P	Sphinganine-1-phosphate
SPA	Sphinganine

Introduction

It has been well documented that sphingosine-1-phosphate (S1P) exerts cardioprotective effect against ischemia as well ischemia/reperfusion injury. On the contrary, another sphingolipid namely ceramide (CER) increases apoptosis of cardiomyocytes in consequence of the procedures. These results were obtained mostly by adding either S1P or a short-chain CER in vitro or in isolated, perfused heart or by changing in the activity of enzymes involved in synthesis/catabolism of the compounds in myocardium [1–4]. Ischemia/reperfusion was shown to reduce the level of S1P in the isolated perfused rat heart by over 50 %, the effect being partially prevented by ischemic preconditioning [5]. In another study ischemia/reperfusion did not affect the heart S1P level. However, it was markedly elevated by ischemic preconditioning. Further elevation in its content was produced by following ischemia/reperfusion procedure [7]. The data concerning the level of CER clearly show that ischemia/reperfusion increases its level in isolated, perfused heart [1, 5, 7, 9, 11] and in the rat heart in vivo [10]. This increase was partially prevented by ischemic preconditioning [5, 8]. Examination of the behavior of individual CER in isolated perfused rat heart after ischemia/reperfusion showed elevation in the level of 7 out of 14 identified species [11].

M. Knapp (✉)
Department of Cardiology, Medical University of Białystok,
Skołodowskiej-Curie 24a, 15-276 Białystok, Poland
e-mail: malgo33@interia.pl

M. Żendzian-Piotrowska · K. Kurek · A. Błachnio-Zabielska
Department of Physiology, Medical University of Białystok,
Białystok, Poland

Ischemia itself also elevated the level of CER in the isolated, perfused heart [7, 8] and in the ischemic area in vivo [10] although no effect was also reported [9].

The uninfarcted portion of the left ventricle is subjected to increased workload as a result of exclusion of the infarcted area from contractile activity. It results in dysfunction of the left ventricle and subsequent elevation in the left ventricular end diastolic pressure and reduction of the left ventricular developed pressure. Surprisingly, there are only very few data available on the metabolism of sphingolipids in the uninfarcted area after myocardial infarction. In one of the above-mentioned studies [9] ischemia/reperfusion was shown not to affect the level of CER in the uninfarcted area. On the contrary, another one [10] reported that the level of CER in the nonischemic area was stable after 30 min ischemia, but it was elevated after subsequent reperfusion as well after 210 min ischemia itself.

The aim of the present study was to examine the level of S1P, CER, sphingosine (SPH), sphinganine (SPA) and sphinganine-1-phosphate (SPA1P) in the uninfarcted area of the left ventricle in 1, 6 and 24 h after ligation of the left coronary artery in the rat.

Methods

The experimental procedure was approved by the Ethical Committee on the Animal Research at the Medical University of Białystok. Male Wistar rats, 200–220 g body weight were used. They were divided into three groups: 1, control; 2, after myocardial infarction (infarct) and 3, after sham surgery (sham). The rats of the infarct group were anaesthetized with thiopental (80 mg/100 g of body weight). The thoracic cavity was opened in the left 5th intercostal space. The lungs were ventilated by frequent air puffs administered manually by means of a small rubber balloon connected with the rat's nose by means of a plastic tube. The heart was exteriorized, the pericardium was cut open and the left coronary artery was ligated with a 6-0 monofilament polypropylene suture thread (Surgipro). Thereafter, the heart was placed back in the thoracic cavity, the thorax was sutured and the rat started to breath spontaneously. After the surgery the rats were placed in their home cages. The same procedure was applied in the sham group with the exception that the coronary artery was not ligated. The rate of survival of the rats subjected to the myocardial infarction was 60 %. In separate rats ($N = 3$) the ischemic area was determined in 24 h after ligation of the left coronary artery using Evans blue dye (1 ml, 2 %, iv). The hearts were excised, frozen and cut into thin slices (2 mm). The ischemic area (expressed as a percentage of left ventricle area) was determined using a stereoscopic microscope (Motic SMZ-143-N2GG, Xiamen, China)

equipped with a digital camera [12]. The ischemic area encompassed 36.3 % of the left ventricle.

At 1, 6 and 24 h after ligation of the coronary artery the rats were anaesthetized again and a sample of the left ventricle next to the interventricular septum, as far as possible from the ischemic area was taken and frozen in liquid nitrogen. In 24 h after the surgery, samples from the center of visible ischemic area were taken from three rats. Also a sample from similar area of a control rat was taken. The samples were fixed in Bouin's fluid for 48 h in +4 °C and embedded in paraffin in a routine way. Next they were cut in 4 µm slices (Leica 2025 Autocut) and stained with haematoxylin–eosin (H + E) for histological examination. Typical pictures are presented at the Fig. 1.

Determination of Sphingolipids

The level of sphingolipids was measured using a UPLC/MS/MS approach according to Blachnio-Zabielska et al. [13]. Briefly, frozen tissue (~20 mg) was homogenized three times in homogenization buffer containing 0.25 M sucrose, 20 mM KCl, 50 mM Tris and 0.5 mM EDTA, pH 7.4. Immediately afterwards 50 µl of the internal standard solution (17C-SPH and 17C-S1P, and 17C16:0-Cer Avanti Polar Lipids) as well as 1.5 ml of an extraction mixture (isopropanol:water:ethyl acetate, 35:5:60 v:v:v) were added to each homogenate. The mixture was vortexed, sonicated and then centrifuged for 10 min at 4,000 rpm. The supernatant was transferred to a new tube and pellet was re-extracted. After centrifugation supernatants were combined and evaporated under nitrogen. The dried sample was reconstituted in 100 µl of LC Solvent A for LC/MS/MS analysis. The following sphingolipids were quantified: Sph, dhSph, S1P, dhS1P, C14:0-Cer, C16:0-Cer, C18:1-Cer, C18:0-Cer, C20:0-Cer, C22:0-Cer, C24:1-Cer, C24:0-Cer. Sphingolipids were analyzed by means of an Agilent 6460 triple quadrupole mass spectrometer using positive ion electrospray ionization (ESI) source with multiple reaction monitoring (MRM). The chromatographic separation was performed using an Agilent 1290 Infinity Ultra Performance Liquid Chromatography (UPLC). The analytical column was a reverse-phase Zorbax SB-C8 column 2.1 × 150 mm, 1.8 µm. Chromatographic separation was conducted in binary gradient using 2 mM ammonium formate, 0.15 % formic acid in methanol Sigma-Aldrich (St. Louis, MO) as Solvent A and 1.5 mM ammonium formate, 0.1 % formic acid in water Sigma-Aldrich (St. Louis, MO) as Solvent B at the flow rate of 0.4 ml/min.

Statistical analysis

The data are presented as means ± SD, $N = 8$. $N = 8$ rats for each time point in either group. Data were analyzed by

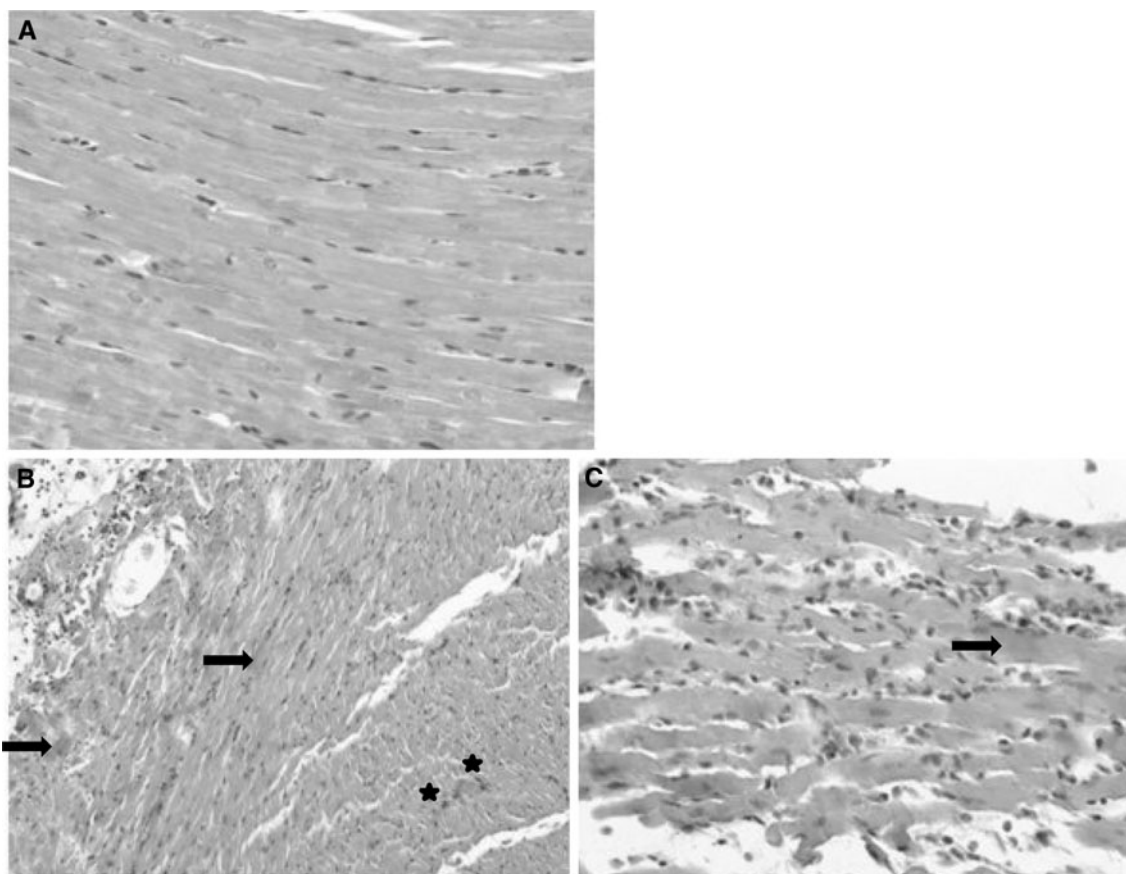


Fig. 1 Microscopic pictures of the heart. H&E stain, original magnification: **a, b** $\times 100$, **c** $\times 200$. **a** control rat. Regular arrangement of myocardial fibers is seen. **b, c** 24 h after ligation of the left coronary artery. Microscopic images demonstrating the main histopathological changes of the myocardium: interstitial hemorrhage

(*asterisks*), myofiber degeneration (hypereosinophilia, loss of transversal striation and fragmenting nuclei *arrows*), infiltrating leucocytes and macrophages are apparent. (To view this figure in color, please consult the online version of this paper)

ANOVA with Tukey HSD (Honestly Significant Difference) post hoc test for unequal sample size. $P < 0.05$ is regarded as significant.

Results

Sphingosine-1-phosphate (Fig. 2a)

The infarction (infarct) resulted in a profound reduction in the level of SIP as early as 1 h after. It stabilized in 6 h and declined further in 24 h as compared to 1 h. After sham surgery (sham) the level of SIP in 1 h remained stable and decreased in 6 and 24 h in comparison to the control. It was higher from the respective value in infarct at each time point.

Sphingosine (Fig. 2b)

The level of SPH decreased in 1 h in infarct and returned to the control thereafter. Sham resulted in a $\sim 50\%$ reduction

in the level of the compound in 24 h compared to the control value.

Sphinganine-1-phosphate (Fig. 3a)

The level of SPA1P in infarct decreased in 1 h and then remained stable. There was gradual elevation in the level of the compound in sham.

Sphinganine (Fig. 3b)

The level of sphinganine was unchanged in infarct. In sham, it was reduced in 1 and 24 h after operation. In infarct, the level of sphinganine in 6 and 24 h was higher than the respective value in sham.

Ceramide (Table 1)

The total level of CER in infarct was reduced in 6 h and returned to the control level in 24 h. It remained stable in

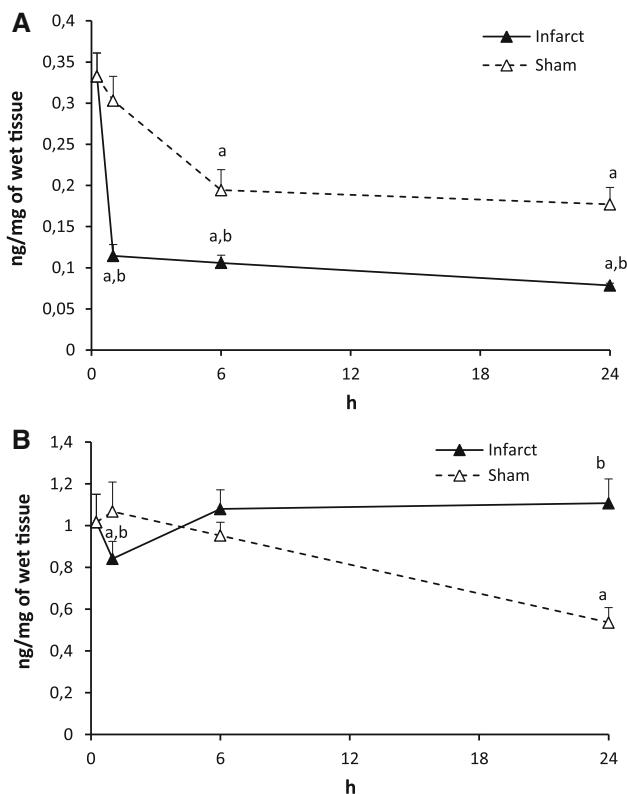


Fig. 2 The impact of myocardial infarction (filled triangles) or sham operation (open triangles) on the level of sphingosine-1-phosphate (a) and sphingosine (b) in the left ventricle of the heart. Black vertical bars represent SD ($N = 8$ per group). ^a $P < 0.05$ as compared to the control, ^b $P < 0.05$ as compared to appropriate sham group

sham. There are also several changes in the level of individual Cer, but they do not form a uniform picture.

Discussion

This is the first study showing a dramatic reduction in the level of S1P in the uninfarcted area of the left ventricle early after the myocardial infarction. S1P is produced by phosphorylation of SPH by the enzyme SPH kinase. It is degraded by two enzymes: sphingoid base-1-phosphate phosphatase and S1P lyase [14, 15]. If the reduction in the content of S1P was a consequence of reduced phosphorylation of SPH one could expect an accumulation of the latter which was not the case with the exception of a small, though significant, elevation in its content in 24 h in infarct group. S1P was shown to be transported from different cells including erythrocytes and platelets, the process being increased upon stimulation [16–19]. It is therefore possible that increased transport of the compound from the cardiomyocytes to the blood was activated in the uninfarcted area resulting in the reduction in its content in the ventricle wall. As mentioned in the introduction elevation in S1P content

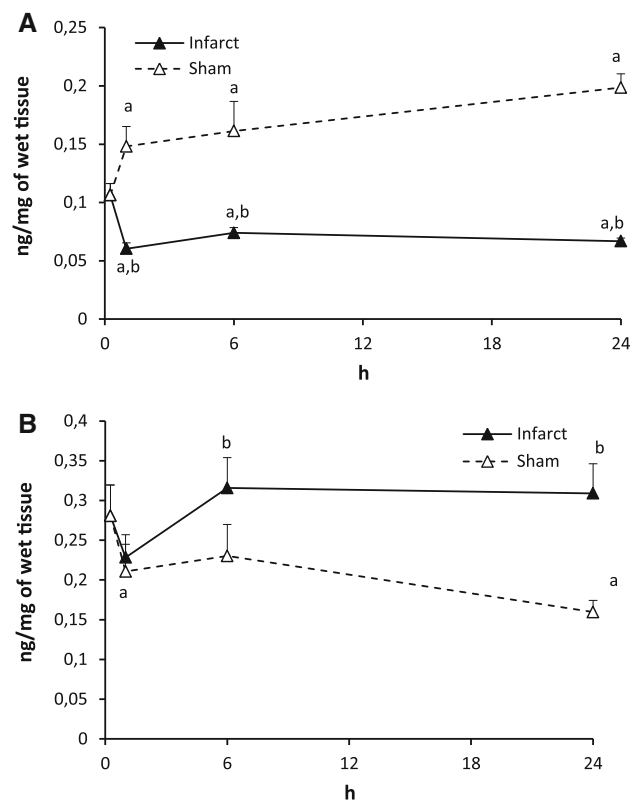


Fig. 3 The impact of myocardial infarction (filled triangles) or sham operation (open triangles) on the level of sphinganine-1-phosphate (a) and sphinganine (b) in the left ventricle of the heart. Black vertical bars represent SD ($N = 8$ per group). When bars not visible, SD smaller than the size of the marker. ^a $P < 0.05$ as compared to the control, ^b $P < 0.05$ as compared to appropriate sham group

was repeatedly shown to protect the heart against ischemia/reperfusion injury, whereas reduction of its level had opposite effect. The cardioprotective impact of S1P includes increased survivability of cardiomyocytes during ischemia in vitro, reduction of the infarct size and left ventricular developed pressure and elevation in the left ventricular end diastolic pressure in isolated, perfused heart subjected to ischemia or ischemia/reperfusion procedure [1–4]. Therefore it may be expected that the profound reduction in the level of S1P in the uninfarcted area of the left ventricle could contribute to the insufficiency of this area after the myocardial infarction.

Sphinganine-1-phosphate is a product of phosphorylation of sphinganine a precursor of CER on the de novo synthesis pathway. We are not aware of any data on the level of SPA1P in the heart. The present data indicate that it is much lower than the level of S1P. Similar relation was reported in plasma, erythrocytes and platelets [17, 20]. The myocardial infarction reduced the level of SPA1P in the uninfarcted ventricle though to a lesser degree than the level of S1P. It was not accompanied by a reduction in the level of sphinganine. It indicates that the reduction in its

Table 1 Effect of myocardial infarction on the level (ng/mg) of ceramides in the uninfarcted ventricular wall of the rat

Ceramide	Control	1 h		6 h		24 h	
C14	0.013 ± 0.003	I	0.018 ± 0.004 ^a	I	0.012 ± 0.002 ^b	I	0.014 ± 0.002
		S	0.016 ± 0.001	S	0.015 ± 0.002	S	0.016 ± 0.001 ^a
C16	3.773 ± 0.621	I	3.105 ± 0.438 ^a	I	3.217 ± 0.366	I	3.760 ± 0.243
		S	3.124 ± 0.310	S	3.118 ± 0.466	S	3.363 ± 0.434
C18	1.358 ± 0.146	I	1.380 ± 0.139	I	1.255 ± 0.106	I	1.325 ± 0.156 ^b
		S	1.586 ± 0.133	S	1.379 ± 0.200	S	0.917 ± 0.086 ^a
C18:1	0.689 ± 0.088	I	0.613 ± 0.073	I	0.606 ± 0.048	I	0.485 ± 0.049 ^a
		S	0.667 ± 0.054	S	0.606 ± 0.058	S	0.513 ± 0.036 ^a
C20	1.558 ± 0.138	I	1.378 ± 0.168	I	1.123 ± 0.134 ^{a, b}	I	1.189 ± 0.177 ^a
		S	1.254 ± 0.135 ^a	S	1.371 ± 0.153	S	0.971 ± 0.091 ^a
C22	3.596 ± 0.433	I	2.971 ± 0.337 ^a	I	2.806 ± 0.304 ^a	I	2.978 ± 0.242 ^a
		S	3.576 ± 0.443	S	3.173 ± 0.448	S	3.260 ± 0.259
C24	6.352 ± 0.797	I	6.988 ± 0.598	I	5.830 ± 0.405	I	6.498 ± 0.648
		S	6.533 ± 0.611	S	6.296 ± 0.714	S	6.667 ± 0.306
C24:1	2.965 ± 0.365	I	3.353 ± 0.466	I	2.544 ± 0.289 ^b	I	3.055 ± 0.349
		S	3.543 ± 0.183	S	3.137 ± 0.311	S	2.990 ± 0.239
Total	20.304 ± 1.815	I	19.805 ± 1.666	I	17.080 ± 1.133 ^a	I	19.303 ± 1.322
		S	20.299 ± 0.613	S	19.095 ± 1.464	S	18.698 ± 0.499

values are means ± SD, $N = 8$

I infarct, S sham operated

^a $P < 0.05$ as compared to the control

^b $P < 0.05$ as compared to the respective value in the sham group

level was rather a consequence of increased transport of the compound from the cells. Interestingly in sham the level of SPA1P increased and the elevation was mirrored by reduction in the level of sphinganine. It would indicate that phosphorylation of sphinganine increased in this case. A mechanism behind these changes remains to be explored. A role of SPA1P is only poorly recognized. It binds to S1P receptors and mimics most effects of S1P [21]. Since its level is much lower than the level of S1P a consequence of its reduction is probably also much weaker.

A factor triggering changes in sphingolipid metabolism in the uninfarcted area of the myocardium remains obscure. It was previously shown that acute exercise produces several changes in sphingolipid metabolism in the heart [22] and skeletal muscles [23]. However, a mechanism responsible for the changes hasn't been studied so far. Increased work output during exercise may be such a factor. As indicated in the introduction, the uninfarcted area of the left ventricle is subjected to increased work load. It may be presumed that this factor is responsible for the changes in the sphingolipid metabolism described presently in the area.

Interestingly, the sham surgery produced also changes in the level of sphingolipids. At present, there are no reliable data for explanation of the phenomenon. However, it is well known that a number of stress factors, cytokines and

steroid hormones affect sphingolipid metabolism [15, 28]. Therefore, it may be presumed that thoracotomy and exteriorization of the heart in the sham group was a stress factor producing the observed changes.

Ligation of the left coronary artery in the rat was shown to induce apoptosis of cardiomyocytes in the uninfarcted ventricular wall and interventricular septum early (3 h) after ligation reached its peak at 1–2 days and decreased thereafter. At 1 day after the infarction a decrease in the expression of bcl-2 and an increase in the expression of bax took place (earlier than 1 day data were not reported). The authors pointed out that an increased mechanical load triggered the programmed cell death [24]. In another study in the rat, increased apoptosis in the uninfarcted area in 3 h after myocardial infarction was observed and the process persisted for 28 days. It was accompanied by activation of caspase-3 and proapoptotic shift of the Bcl-2/Bax ratio [25]. Increased apoptosis of cardiomyocytes in the uninfarcted area of the left ventricle in 24 h after infarction was also reported. Contrary to the above study, it persisted up to 4 weeks [26]. It should be added that 30 min ischemia followed by reperfusion did not increase apoptosis in the nonischemic area either of rabbit [8] or rat heart in vivo [10]. It is well established that CER exerts very strong proapoptotic action [27–29]. A factor triggering apoptosis in the uninfarcted area hasn't been recognized so far.

The present study showed a transient (in 6 h after the infarction) reduction in the level of CER in the examined sample of the ventricle. This would indicate that CER itself could not contribute to the activation of apoptosis in the rat heart reported above. However, the level of pro-survival S1P was deeply reduced at the same time. It was postulated that it is the ratio: the level of S1P/the level of CER which plays a crucial role in regulation of apoptosis [21]. In the present study the ratio decreased by 63.75 % in 1 h, by 61.25 % in 6 h and by 75 % in 24 h after ligation of the artery. Such a shift in the ratio would favor apoptosis. Therefore, it is a good reason to conclude that this mechanism may be responsible for at least early activation of apoptosis in the uninfarcted area of the left ventricle after ligation of the left coronary artery in the rat.

In summary, we showed that myocardial infarction induced profound changes in sphingolipid metabolism in the uninfarcted area of the left ventricle of the rat. Specifically, it deeply reduced the S1P/CER ratio. It is concluded that the reduction in the ratio could be responsible for the early activation of apoptosis in the uninfarcted area of the left ventricle after myocardial infarction.

Acknowledgments This work was supported by UMB grants 113-18664L, 114-18874L. We greatly appreciate Prof. Irena Kasacka for microscopic examination of the myocardium and Dr. Justyna Marciniak for determination of the ischemic area.

References

- Karliner JS (2009) Sphingosine kinase and sphingosine-1-phosphate in cardioprotection. *J Cardiovasc Pharmacol* 53:189–197. doi:10.1097/FJC.0b013e3181926706
- Kennedy S, Kane KA, Pyne NJ, Pyne S (2009) Targeting sphingosine-1-phosphate signalling for cardioprotection. *Curr Opin Pharmacol* 9:194–201. doi:10.1016/j.coph.2008.11.002
- Knapp M (2011) Cardioprotective role of sphingosine-1-phosphate. *J Physiol Pharmacol* 62:601–607
- Gundewar S, Lefer DJ (2008) Sphingolipid therapy in myocardial ischemia-reperfusion injury. *Biochim Biophys Acta* 1780:571–576. doi:10.1016/j.bbagen.2007.08.014
- Vessey DA, Kelley M, Li L, Huang Y, Zhou HZ, Zhu BQ, Karliner JS (2006) Role of sphingosine kinase activity in protection of heart against ischemia reperfusion injury. *Med Sci Monit* 12:BR318–BR324
- Cui J, Engelman RM, Maulik N, Das DK (2004) Role of ceramide in ischemic preconditioning. *J Am Coll Surg* 198:770–777. doi:10.1016/j.jamcollsurg.2003.12.016
- Cordis GA, Yoshida T, Das DK (1998) HPTLC analysis of sphingomyelin, ceramide and sphingosine in ischemic/reperfused rat heart. *J Pharm Biomed Anal* 16:1189–1193. doi:10.1016/S0731-7085(97)00260-4
- Argaud L, Prigent A-F, Chalabreysse L, Loufouat J, Lagarde M, Ovize M (2004) Ceramide in the antiapoptotic effect of ischemic preconditioning. *Am J Physiol Heart Circ Physiol* 286:H246–H251. doi:10.1152/ajpheart.00638.2003
- Zhang DX, Fryer RM, Hsu AK, Gross GJ, Campbell WB, Li P-L (2001) Production and metabolism of ceramide in normal and ischemic-reperfused myocardium of rats. *Basic Res Cardiol* 96:267–274. doi:10.1007/s00395-012-0266-4
- Bielawska AE, Shapiro JP, Jiang L, Melkonyan HS, Piot C, Wolfe CL, Tomei D, Hannun YA, Umansky SR (1997) Ceramide is involved in triggering of cardiomyocyte apoptosis induced by ischemia and reperfusion. *Am J Pathol* 151:1257–1263
- Beręsewicz A, Dobrzyń A, Górski J (2002) Accumulation of specific ceramides in ischemic/reperfused rat heart: effect of ischemic preconditioning. *J Physiol Pharmacol* 53:371–382
- Lupiński SL, Schlicker E, Pędzińska-Betiuk A, Malinowska B (2011) Acute myocardial ischemia enhances the vanilloid TRPV1 and serotonin 5-HT(3) receptor-mediated Bezold-Jarisch reflex in rats. *Pharmacol Rep* 63:1450–1459
- Błażnio-Zabielska AU, Persson XM, Koutsari C, Zabielski P, Jensen MD (2012) An LC/MS/MS method for measuring the in vivo incorporation of plasma free fatty acids into intramyocellular ceramides in humans. *Rapid Commun Mass Spectrom* 26:1134–1140. doi:10.1002/rcm.6216
- Gault CR, Obeid LM, Hannun YA (2010) An overview of sphingolipid metabolism: from synthesis to breakdown. *Adv Exp Med Biol* 688:1–23
- Riboni L, Viani P, Bassi R, Prinetti A, Tettamanti G (1997) The role of sphingolipids in the process of signal transduction. *Prog Lipid Res* 36:153–195. doi:10.1016/S0163-7827(97)00008-8
- Ito K, Anada Y, Tani M, Ikeda M, Sano T, Kihara A, Igarashi Y (2007) Lack of sphingosine 1-phosphate degrading enzymes in erythrocytes. *Biochem Biophys Res Commun* 357:212–217. doi:10.1016/j.bbrc.2007.03.123
- Hänel P, Andréani P, Gräler MH (2007) Erythrocytes store and release sphingosine 1-phosphate in blood. *FASEB J* 21:1202–1209. doi:10.1096/fj.06-7433com
- Kim RH, Takabe K, Milstien S, Spiegel S (2009) Export and functions of sphingosine-1-phosphate. *Biochim Biophys Acta* 179:692–696. doi:10.1016/j.bbalip.200902011
- Yatomi Y, Ruan F, Hakomori S, Igarashi Y (1995) Sphingosine-1-phosphate: a platelet-activating sphingolipid released from agonist-stimulated human platelets. *Blood* 86:193–202
- Andréani P, Gräler MH (2006) Comparative quantification of sphingolipids and analogs in biological samples by high-performance liquid chromatography after chloroform extraction. *Anal Biochem* 358:239–246. doi:10.1016/j.ab.2006.08.027
- Spiegel S, Milstien S (2002) Sphingosine-1-phosphate, a key cell signaling molecule. *J Biol Chem* 277:25851–25854. doi:10.1074/jbc.R200007200
- Baranowski M, Zabielski P, Błażnio A, Górski J (2008) Effect of exercise duration on ceramide metabolism in the rat heart. *Acta Physiol* 192:519–529. doi:10.1111/j.1748-1716.2007.01755.x
- Dobrzyń A, Górski J (2002) Effect of acute exercise on the content of free sphinganine and sphingosine in different skeletal muscle types of the rat. *Horm Metab Res* 34:523–529. doi:10.1055/s-2002-34793
- Cheng W, Kajstura J, Nitahara JA, Li B, Teiss K, Liu Y, Clark WA, Krajewski S, Reed JC, Olivetti G, Anversa P (1996) Programmed myocyte cell death affects the viable myocardium after infarction in rats. *Exp Cell Res* 226:316–327. doi:10.1006/excr.1996.0232
- Simonis G, Wiedemann S, Schwarz K, Christ T, Sedding DG, Yu X, Marquetant R, Braun-Dullaeus RC, Ravens U, Strasser RH (2008) Chelerythine treatment influences the balance of pro and anti-apoptotic signaling pathways in the remote myocardium after infarction. *Mol Cell Biochem* 310:119–128. doi:10.1007/s11010-007-9672-6
- Palojoki E, Saraste A, Ericsson A, Pulkki K, Kallajoki M, Voipio-Pulkki LM, Tikkanen I (2001) Cardiomyocyte apoptosis and ventricular remodeling after myocardial infarction in rats. *Am J Physiol Heart Circ Physiol* 280:H2726–H2731

27. Gangoiti P, Camacho L, Arana L, Ouro A, Granado MH, Brizuela L, Casas J, Fabriás G, Abad JL, Delgado A, Gómez-Muñoz A (2010) Control of metabolism and signaling of simple bioactive sphingolipids: implications in disease. *Prog Lipid Res* 49:316–334. doi:[10.1016/j.plipres.2010.02.004](https://doi.org/10.1016/j.plipres.2010.02.004)
28. Huwiler A, Kotler T, Pfeilschifter J, Sandhoff K (2000) Physiology and pathophysiology of sphingolipid metabolism and signaling. *Biochem Biophys Acta* 1485:63–69. doi:[10.1016/S1388-1981\(00\)00042-1](https://doi.org/10.1016/S1388-1981(00)00042-1)
29. Bartke N, Hannun YA (2009) Bioactive sphingolipids: metabolism and function. *J Lipid Res* 50:S91–S96. doi:[10.1194/jlr.R800080-JLR200](https://doi.org/10.1194/jlr.R800080-JLR200)

trans-10,*cis*-12 Conjugated Linoleic Acid Enhances Endurance Capacity by Increasing Fatty Acid Oxidation and Reducing Glycogen Utilization in Mice

Jun Ho Kim · Jonggun Kim · Yeonhwa Park

Received: 12 March 2012 / Accepted: 24 June 2012 / Published online: 11 July 2012
© AOCS 2012

Abstract The supplementation of conjugated linoleic acid (CLA) has been shown to improve endurance by enhancing fat oxidation during exercise in rodents and humans. This study was designed to investigate the isomer-specific effects of CLA on endurance capacity and energy metabolism in mice during exercise. Male 129Sv/J mice were divided into three dietary groups and fed treatment diet for 6 weeks; control, 0.5 % *cis*-9,*trans*-11 (*c9,t11*) CLA, or 0.5 % *trans*-10,*cis*-12 (*t10,c12*) CLA. Dietary *t10,c12* CLA induced a significant increase in maximum running time and distance until exhaustion with a dramatic reduction of total adipose depots compared to a control group, but there were no significant changes in endurance with the *c9,t11* CLA treatment. Serum triacylglycerol and non-esterified fatty acid concentrations were significantly lower in the *t10,c12* fed mice after exercise compared to control and the *c9,t11* CLA fed-animals. Glycogen contents in livers of the *t10,c12* fed-mice were higher than those in control mice, concomitant with reduction of serum L-lactate level. There were no differences in non-exercise physical activity among all treatment groups. In addition, the mRNA expression levels of carnitine palmitoyl transferase 1 β , uncoupling protein 2 and peroxisome proliferator-activated receptor δ (PPAR δ) in skeletal muscle during exercise were significantly up-regulated by the *t10,c12* CLA but not the *c9,t11* CLA. These results suggest that the *t10,c12* CLA is responsible for improving endurance exercise capacity by promoting fat oxidation with a reduction of the consumption of stored liver glycogen, potentially mediated via PPAR δ dependent mechanisms.

Keywords Conjugated linoleic acid · Exercise · Fat oxidation · Endurance · Mice

Abbreviations

AMPK	AMP-activated protein kinase
BUN	Blood urea nitrogen
CLA	Conjugated linoleic acid
CPT1 β	Carnitine palmitoyl transferase 1 β
IL-6	Interleukin 6
LPL	Lipoprotein lipase
NEFA	Non-esterified fatty acid
NEPA	Non-exercise physical activity
PPAR δ	Peroxisome proliferator-activated receptor δ
TAG	Triacylglycerol
UCP2	Uncoupling protein 2

Introduction

One of the major determinants of endurance capacity is increasing fat oxidation, which leads to the sparing of muscle glycogen [1, 2]. Fatty acid β -oxidation in muscle mitochondria followed by aerobic respiration is required to adequately generate ATP for muscular energy during exercise [3]; thus, enhanced fat oxidation, while decreasing carbohydrate utilization as an energy source, results in increased endurance capacity during prolonged exercise.

Conjugated linoleic acid (CLA) is an anti-obesity bioactive compound that plays a key role in enhanced fatty acid β -oxidation in skeletal muscle, suggesting preferential usage of fat over glucose as an energy source in muscle during exercise [4, 5]. In fact, previous short- (1 week) and long-term (10 weeks) feeding studies with CLA showed that dietary CLA enhances maximum swimming or

J. H. Kim · J. Kim · Y. Park (✉)
Department of Food Science, University of Massachusetts,
102 Holdsworth Way, Amherst, MA 01003, USA
e-mail: ypark@foodsci.umass.edu

running capacity by increasing fat oxidation in mice [6, 7]. The CLA preparation used in these studies consisted primarily two major CLA isomers, *cis*-9,*trans*-11 (*c9,t11*) and *trans*-10,*cis*-12 (*t10,c12*) isomers. Previous studies suggested the roles and interactions between these two isomers on a number of biological functions of CLA, however, no research has reported the effects of different isomers of CLA on endurance exercise performance and related energy metabolism [8].

Among these two major CLA isomers, the *t10,c12* CLA isomer has been shown to be responsible for body fat reduction along with increased fatty acid oxidation via carnitine palmitoyl transferase 1 β (CPT1 β) and uncoupling protein 3 in skeletal muscle [9, 10]. These reports led us to hypothesize that the *t10,c12* CLA isomer may be responsible for improving endurance capacity as well. Thus we investigated the isomer-specific effects of CLA on endurance capacity and related physiological metabolism in mice as well as determined non-exercise physical activity (NEPA) in this study. This research may provide an important basis for developing CLA as a novel ergogenic aid for future human applications.

Materials and Methods

Materials

cis-9,*trans*-11 (*c9,t11*) and *t10,c12* CLA were provided by Natural Lipids Ltd. AS (Hovdebygda, Norway). The compositions of the CLA isomers were 90 % *c9,t11* isomer (90.1 % *c9,t11*, 3.8 % *t10,c12*, 2.5 % other CLA isomers, and 3.3 % oleic acid) and 94 % *t10,c12* isomer (2.0 % *c9,t11*, 94.4 % *t10,c12*, 2.9 % other CLA isomers, and 0.4 % oleic acid). Semi-purified powdered diet (TD04460, 94 % basal mix) was purchased from Harlan Teklad (Madison, WI). Serum total cholesterol, triacylglycerol (TAG) and glucose assay kits were purchased from Genzyme Diagnostics (Charlottetown, PE, Canada). Non-esterified fatty acid (NEFA) and L-lactate assay kits were purchased from BioAssay Systems (Hayward, CA). Blood urea nitrogen (BUN) and glycogen assay kits were purchased from BioQuant (San Diego, CA) and Cayman Chemical Company (Ann Arbor, MI), respectively. Other chemicals used were purchased from either Sigma Chemical Co. (St. Louis, MO) or Fisher Scientific (Pittsburgh, PA).

Animals and Diet

All animal procedures were approved by the Institutional Animal Care and Use Committee at the University of Massachusetts, Amherst (Protocol ID 2010-0032). Forty

male 129Sv/J mice (5-week-old) were obtained from breeding colonies maintained at the University of Massachusetts Amherst. Animals were housed in individual wire-bottomed cages in a windowless room with a 12-h light–dark cycle. During a 1-week adaptation period, all mice were fed a control diet and were subjected to running exercise three times (velocity of 10 m/min on 0° inclination for 15 min with shock grid OFF, followed by 10 min with shock grid ON) to acclimate to the treadmill. At the end of the adaptation period, all animals were subjected to an endurance test for the measurement of their baselines on the running time to exhaustion. To minimize individual variations on endurance capacity baseline, we selected 18 mice with the closest value to the mean baseline from the original 40. Finally, selected mice were randomly divide into three groups and fed control diet or diet containing 0.5 % of *c9,t11* or *t10,c12* CLA isomer for 6 weeks. The diet composition is shown in Table 1. Body weight and feed intake were recorded weekly. At the end of study, the mice were fasted for 4 h, ran for 40 min according to the endurance protocol, and then immediately sacrificed by CO₂ asphyxiation. Blood was collected by cardiac puncture, and internal organs (liver, heart, kidney, spleen and adipose tissues) were also weighed.

Exercise Training and Endurance Protocol

During the experimental period, all animals were trained three times a week on a motorized treadmill (Columbus Instrument, Columbus, OH). Training was performed for a total 15 min (10 min at 10 m/min, then an increase of 1 m/min every minute for 5 min) on 10° inclination with shock grid ON. Mice were encouraged to run with the use of an electric grid placed at the end of the treadmill (0.97 mA, 1 Hz).

Table 1 Composition of experimental diets

Ingredient	g/kg
Casein, 'vitamin-free' tested	194
L-Cystine	3
Sucrose	87.5
Cornstarch	373.5
Maltodextrin	132
Cellulose	50
Soybean oil	95
Soybean oil or <i>c9,t11</i> CLA or <i>t10,c12</i> CLA	5
Mineral mix <i>w/o</i> Ca	35
CaCO ₃	12.5
Vitamin mix	10
Choline bitartrate	2.5
<i>tert</i> -Butylhydroquinone	0.02
Total	1,000

Endurance capacity was determined every other week by placing animals on an individual treadmill at room temperature. The exercise regimen was started with shock grid ON and 10° inclination at 10 m/min for 10 min, speed was increased by 1 m/min up to 25 m/min (15 min with increase speed), and then held at 25 m/min until exhaustion. Based on previous studies, which measured treadmill endurance capacity [11–13], mice were defined as exhausted if they were willing to sustain on the shock grid three times for more than 2 s or remain on the shock grid for five consecutive seconds. At the moment of exhaustion the mouse was removed from the treadmill. The total running time and distance until exhaustion were recorded and used as the index of endurance capacity.

Non-Exercise Physical Activity (Voluntary Movement)

The NEPA was monitored using LoliTrack Quatro Video Tracking Software Version 1.0 (Loligo Systems, Tjele, Denmark) with an infrared camera. The mice were placed in cages (30 × 46 × 40 cm) individually from 12:00 p.m. to 9:00 a.m. the next day with free access to diet and water (provided as HydroGel[®], Clear H₂O, Portland, ME) twice during the experimental period. The mice to be tracked were placed against a contrasting background and the software assigned an *X*, *Y* coordinate pair to the center of the contrasting objects. The program found all pixels within the range of 640 × 480 pixels and calculated the center *X* and *Y* coordinates of these pixels. The time-stamped *X*, *Y*-coordinates were written into a data file to 5 times/s, and then the data was imported into Excel for analysis. Movement data for 19 h (light cycle, 2:00 p.m.–6:00 p.m. and next day 6:00 a.m.–9:00 a.m.; dark cycle, 6:00 p.m.–6:00 a.m. next day) except 2 h (12:00 p.m.–2:00 p.m.) of early phase for adapting to surroundings was analyzed. Voluntary movements were expressed as total travel distance (m).

Biochemical Parameters

Serum was separated by centrifugation at 3,000g for 20 min at 4 °C. Serum samples were used for determination of TAG, glucose, total cholesterol, NEFA, L-lactate and BUN using commercial kits as specified by the manufacturer. The glycogen contents in gastrocnemius muscle and liver were measured by the enzymatic method using a commercial kit.

Real Time PCR

Gastrocnemius muscle was homogenized in 1 mL of TRIzol reagent and then total RNA was isolated according to the TRIzol protocol. Total RNA was reverse transcribed

to cDNA using a High Capacity cDNA Reverse Transcription kit (Applied Biosystems, Foster, CA), as described in the manufacture's protocol. cDNA was used as a template for the relative quantitation for the selected target genes [CPT1 β (Mm00487200_m1), uncoupling protein 2 (UCP2, Mm00627597_m1), lipoprotein lipase (LPL, Mm00434764_m1), interleukin 6 (IL-6, Mm00446190_m1), peroxisome proliferator-activated receptor δ (PPAR δ , Mm00803184_m1)] with predesigned TaqMan gene expression assay kits. Each 20 μ L reaction contained 100 ng cDNA, 2 \times TaqMan Gene Expression Mastermix, forward and reverse primers and TaqMan probe. All reactions were carried out in triplicate with the StepOnePlus Real-Time PCR System (Applied Biosystems, Foster, CA) using the following conditions: 50 °C for 2 min and 95 °C for 10 min followed by forty cycles of 95 °C for 15 s and 60 °C for 1 min. Results were normalized to glyceraldehyde-3-phosphate dehydrogenase (GAPDH, Mm99999915_g1) as an internal standard, and relative quantities of each gene were presented in terms of $2^{-\Delta\Delta C_t}$, calculated using the ΔC_t and $\Delta\Delta C_t$ values.

Statistical Analyses

Data were analyzed by one-way ANOVA of the SAS software for Windows release 9.2 (SAS Institute Inc., Cary, NC) on the W32_VSHOME platform. For the body weight, feed intake, feed efficiency ratio, endurance time, endurance distance and NEPA data, one-way ANOVA with repeated measures were performed for the data analysis. To test for differences in total adipose depot and organ weight among the experimental groups, analysis of covariance (ANCOVA) with final body mass as covariates was used. Homogeneity of regression assumptions of the ANCOVA model was tested. This assumption was met for organ weight data, but violated for total adipose data. For total adipose depot data, ANCOVA analysis was performed for each of three levels of final body mass (minimum, mean and maximum) [14]. The least squares means option using a Tukey–Kramer adjustment was used for the multiple comparisons among the experimental groups. Data are shown as the mean \pm SE. *P* values <0.05 are reported as statistically significant.

Results

Body Weights and Feed Intake

No significant differences were observed in body weights between treatments in regular running-exercised mice during the experimental period (Fig. 1a). Feed intake in the *t10,c12* CLA fed mice steadily increased from Week 3 and showed a significant difference compared to control group

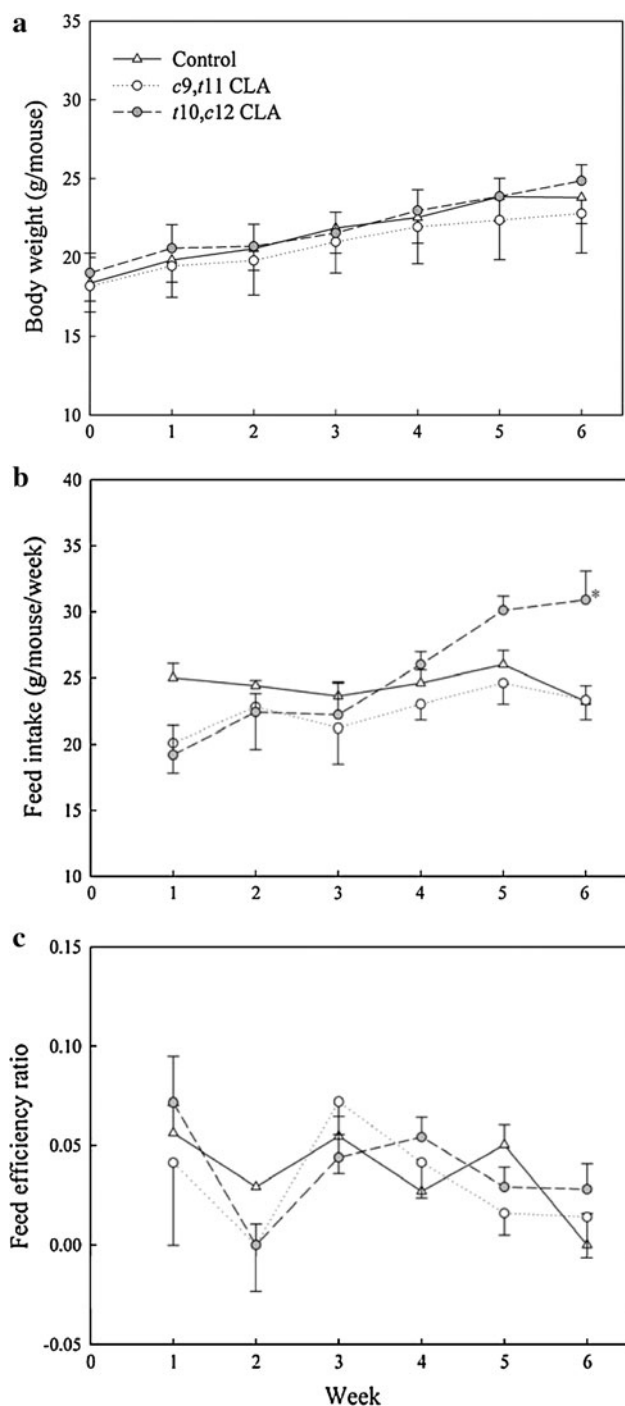


Fig. 1 Effects of CLA isomers on body weight (a), feed intake (b) and feed efficiency ratio (c). Mice were fed one of the treatment diets for 6 weeks. Feed efficiency ratio was calculated as weight gain (g/mouse/week)/feed intake (g/mouse/week). Values represent mean \pm SE ($n = 6$). *Significantly different from control ($P < 0.05$)

at Week 6, but there was no significant difference in feed intake between the *c9,t11* CLA and control groups during the entire experimental period (Fig. 1b). Feed efficiency ratio did not show significant differences among all treatment groups (Fig. 1c).

Adipose Depots and Organ Weights

Adipose tissue weights including epididymal, mesenteric and retroperitoneal fat were adjusted for body size variation at three levels of final body mass (minimum, mean and maximum) as a covariate (Fig. 2). These were necessary since ANCOVA has an underlying assumption of homogeneity of regression, which was not satisfied by our data. This suggests that the dietary effect for adipose tissue weight depends on whole body mass in this study. The ANCOVA analysis showed a significant reduction of adipose depots by the *t10,c12* CLA compared to control at the levels of mean and maximum of final body mass, although it was not significant at minimum level. The ANCOVA analysis showed overall increases in organ weights including liver, heart, kidney and spleen in the *t10,c12* CLA fed mice compared to other groups (Table 2).

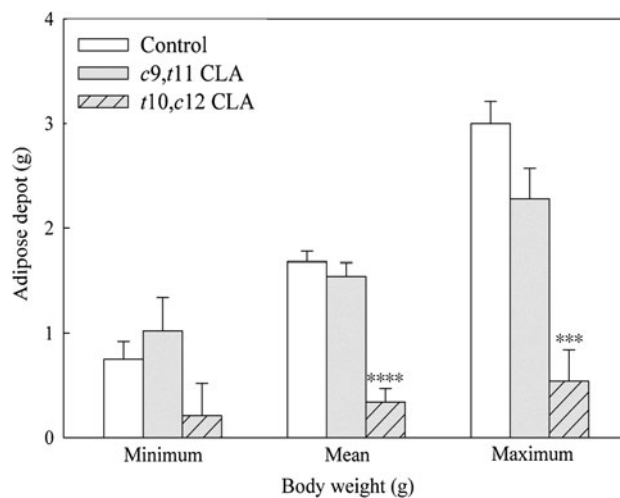


Fig. 2 Effects of CLA isomers on adipose depot. Mice were fed one of the treatment diets for 6 weeks. Adipose depot includes epididymal, mesenteric and retroperitoneal fat. Homogeneity of regression slopes in ANCOVA model was violated (there was a significant interaction between dietary effect on adipose depot and final body mass), and means were adjusted for each of three levels of final body mass (minimum, mean and maximum) [14]. Values represent means \pm SE ($n = 6$). *Significantly different from control ($***P < 0.001$, $****P < 0.0001$)

Table 2 Organ weights

Organ (g)	Dietary group		
	Control	<i>c9,t11</i> CLA	<i>t10,c12</i> CLA
Liver	0.86 \pm 0.14 ^b	0.85 \pm 0.14 ^b	2.27 \pm 0.16 ^a
Heart	0.11 \pm 0.00 ^b	0.12 \pm 0.00 ^b	0.13 \pm 0.00 ^a
Kidney	0.37 \pm 0.02 ^b	0.38 \pm 0.02 ^b	0.45 \pm 0.02 ^a
Spleen	0.05 \pm 0.00 ^b	0.05 \pm 0.00 ^b	0.08 \pm 0.00 ^a

Values represent means \pm SE ($n = 6$). Means are adjusted for final body mass using the ANCOVA analysis. Means with different superscripts within the same row are significantly different ($P < 0.05$)

Endurance Capacity and Non-Exercise Physical Activity

Endurance capacities of mice were determined by the maximum running time and distance recorded on the treadmill. The maximum running time and distance were significantly increased in the *t10,c12* CLA group compared to control mice at Week 2 and Week 6, but there were no significant differences between the *c9,t11* CLA group and control during the experimental period (Fig. 3a, b). Dietary supplementation of the *t10,c12* CLA brought on increases of approximately 2.7-fold in maximum time and 4.8-fold in maximum distance at Week 2 compared to their baseline. Control mice showed increases of approximately 1.5-fold (time) and 2.5-fold (distance) at Week 2 compared to their baseline, indicating the effects of other contributing factors such as body weight and running training on endurance capacity.

The NEPA was individually monitored in special cages during both light and dark cycles. In contrast with endurance capacity, the NEPA decreased over time in all treatment

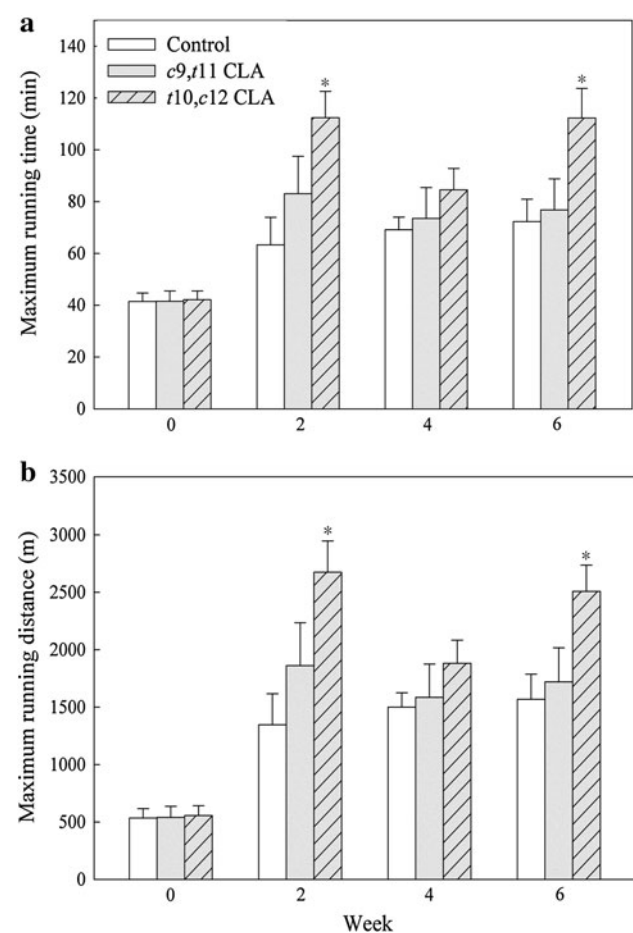


Fig. 3 Effects of CLA isomers on maximum running time (a) and distance (b). Endurance capacity was evaluated with treadmill exercise every 2 weeks. Values represent mean \pm SE ($n = 6$). *Significantly different from control ($P < 0.05$)

groups, and neither CLA isomer caused significant changes in NEPA of mice during the experimental period (Fig. 4).

Serum Parameters and Glycogen Contents

The serum concentrations of major metabolic substrates after 40 min of endurance exercise are shown in Table 3. There were no marked differences in serum parameters between the control and the *c9,t11* CLA groups. However, the serum TAG, NEFA and L-lactate concentrations in the *t10,c12* CLA group were significantly lower than those in the control group. The serum glucose level was the highest in the *t10,c12* CLA group, but not significant. Supplementation of the *t10,c12* CLA significantly increased the total cholesterol level compared to other groups, and there were no differences in the serum BUN levels among all treatment groups.

The glycogen concentrations of the gastrocnemius muscle and liver after 40 min of endurance exercise in the *t10,c12* CLA fed mice tended to be higher than those in other tested mice, although a significant difference compared to control mice was observed only in liver (Table 4).

mRNA Expressions

To determine the mRNA expression levels of key enzymes involved in lipid and energy expenditure metabolism, selected mRNA levels were measured in gastrocnemius muscle after exercise (Fig. 5). The expressions of CPT1 β , UCP2 and PPAR δ in muscle after exercise significantly increased in the *t10,c12* CLA fed animals compared to those of the control, indicating the *t10,c12* CLA controls energy metabolism by up-regulating the muscle

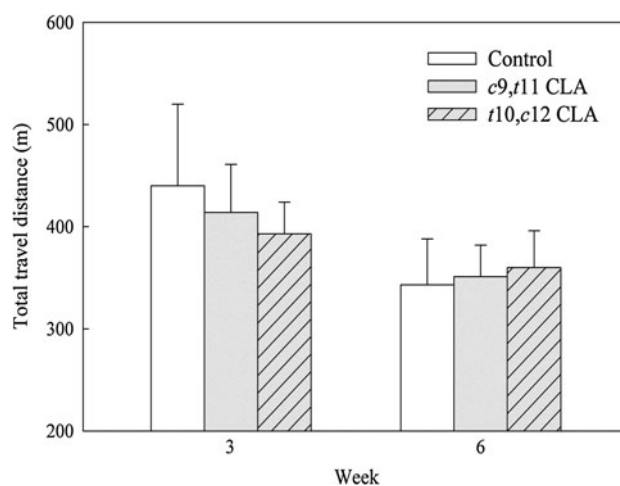


Fig. 4 Effects of CLA isomers on non-exercise physical activity. Non-exercise physical activity was monitored in individual clear cages during light and dark cycles (19 h) twice throughout the experimental period. Values represent means \pm SE ($n = 6$)

Table 3 Serum parameters

mmol/L	Dietary group		
	Control	<i>c9,t11</i> CLA	<i>t10,c12</i> CLA
TAG	1.39 ± 0.08 ^a	1.27 ± 0.15 ^a	0.83 ± 0.07 ^b
Glucose	10.7 ± 1.4	10.0 ± 1.3	15.0 ± 2.0
Total cholesterol	2.78 ± 0.16 ^b	2.93 ± 0.11 ^b	4.11 ± 0.44 ^a
NEFA	2.08 ± 0.08 ^a	2.07 ± 0.14 ^a	1.19 ± 0.04 ^b
L-Lactate	6.83 ± 0.39 ^a	6.52 ± 0.31 ^{ab}	5.75 ± 0.10 ^b
BUN	13.8 ± 0.9	12.6 ± 0.6	11.9 ± 0.5

At the end of study, the mice ran for 40 min according to the endurance protocol and were sacrificed by CO₂ asphyxiation. Values represent means ± SE (*n* = 6). Means with different superscripts within the same row are significantly different (*P* < 0.05)

Table 4 Glycogen contents in muscle and liver

Tissue (mg/g)	Dietary group		
	Control	<i>c9,t11</i> CLA	<i>t10,c12</i> CLA
Gastrocnemius muscle	0.90 ± 0.21	0.79 ± 0.15	1.58 ± 0.59
Liver	22.9 ± 2.3 ^b	25.8 ± 2.3 ^{ab}	33.3 ± 3.5 ^a

At the end of study, the mice ran for 40 min according to the endurance protocol and were sacrificed by CO₂ asphyxiation. Values represent means ± SE (*n* = 6). Means with different superscripts within the same row are significantly different (*P* < 0.05)

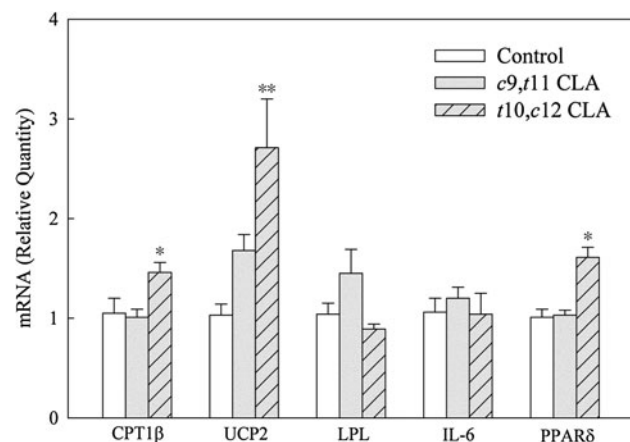


Fig. 5 Effects of CLA on expressions of selected genes from skeletal muscle. *CPT1β* carnitine palmitoyl transferase, *UCP2* uncoupling protein 2, *LPL* lipoprotein lipase, *IL-6* interleukin 6, *PPARδ* peroxisome proliferator-activated receptor δ . Relative quantities of each gene were presented in terms of $2^{-\Delta\Delta C_t}$, calculated using the ΔC_t and $\Delta\Delta C_t$ values. Values represent means ± SE (*n* = 6). *Significantly different from control (**P* < 0.05, ***P* < 0.01)

expressions of *CPT1β*, *UCP2* and *PPARδ* during exercise, effects not seen with the *c9,t11* CLA. The expression levels of *LPL* and *IL-6* were not different with treatments of either CLA isomer compared to control.

Discussion

There is much evidence that the wide range of CLA's activities results from interaction between the two major CLA isomers, *c9,t11* and *t10,c12*; additive, independent, or antagonistic effects [8]. In the present study, we investigated the isomer-specific effects of these major CLA isomers on endurance capacity and utilization of metabolic substrates during prolonged exercise. Among these two isomers, the effect of CLA on fatty acid oxidation and body fat reduction is known to be due to the independent effect of the *t10,c12* CLA isomer [9, 15]. Consistently, our current research confirmed that the adipose depots were significantly reduced in *t10,c12* CLA fed mice but not in *c9,t11* fed mice. In addition, our results showed that the *t10,c12* isomer increased endurance capacity in mice.

The body weights did not show differences among all treatment groups during the experimental period, but the feed intake was significantly higher in the *t10,c12* CLA group than other groups at Week 6. These results indicate that the overall balances between energy intake and expenditure were similarly maintained among all treatment groups, when the mice were subjected to the regular exercise in this study. In addition, the reduction of body fat with the constant increases in feed intake in the latter half of the experiment in the *t10,c12* CLA group may potentially indicate overall increases in lean mass as previously suggested [16].

It is well known that increased fat utilization during endurance exercise enables athletes to improve endurance capacity by a sparing effect on the glycogen stores, although the impact of muscle glycogen on endurance is not clear in rodents [17, 18]. The two major repositories of glycogen are the liver and skeletal muscle, and the relative proportion of muscle glycogen is lower, up to tenfold, in mice than in humans [19, 20]. Fernandez et al. [17] suggested that one determining factor for the endurance capacity in mice could be the amount of glycogen stored in liver, rather than that stored in muscle. In the present study, glycogen contents were increased in muscle and liver of the *t10,c12* CLA fed mice, but significance was observed only in liver. This conservation of glycogen consumption accompanied the decreases of serum concentrations of TAG and L-lactate in the *t10,c12* CLA fed mice, suggesting the *t10,c12* CLA could enhance endurance capacity of mice by increasing fat utilization and reducing the consumption of stored liver glycogen. Although we did not include a non-exercise group in this study, Mizunoya et al. [6] showed that the changes of biochemical parameters including serum glucose, TAG and NEFA after prolonged exercise were greater in CLA-fed mice than control mice. Therefore, it is possible that dietary CLA with exercise has a combination effect on biological responses during

exercise. Alternatively, we cannot exclude the possibility that these responses are due to the acute bout of exercise [21].

The CPT1 β is a rate-limiting enzyme of mitochondrial fatty acid β -oxidation, and UCP2 has been shown to be associated with energy expenditure by dissipating the chemiosmotic gradient in mitochondria [22, 23]. In the present study, the mRNA expression levels of CPT1 β and UCP2 were significantly up-regulated by the *t10,c12* CLA, while the *c9,t11* CLA did not induce any significant changes in these genes over the control. Therefore, these results suggest that the *t10,c12* CLA regulates energy metabolism beneficially for the endurance by enhancing fatty acid β -oxidation in muscle during exercise. Additionally, IL-6 is released in large amounts from skeletal muscle during prolonged exercise and IL-6 deficient mice showed reduced endurance and energy expenditure during exercise [24]. Chung et al. [25] reported that the *t10,c12* CLA increases the expression and secretion of IL-6 in human adipocytes, but there was no CLA effect on muscle IL-6 expression in mice in this study.

One of interesting results here is that *t10,c12* CLA significantly up-regulated the muscle mRNA level of PPAR δ . Muscle oxidative capacity is a crucial factor for determining endurance, and PPAR δ is a key regulator of lipid and carbohydrate metabolism in the muscle [26]. In fact, Wang et al. [27] demonstrated that the targeted activation of the PPAR δ gene in muscle leads to muscle fiber transformation to increased mitochondria-rich type I muscle, which mainly uses oxidative metabolism for energy production. In the same report, PPAR δ -null mice showed a remarkably decreased endurance capability compared to their wild type counterparts. Therefore, our present results suggest that *t10,c12* CLA could improve endurance by stimulating oxidative metabolism via PPAR δ regulation in skeletal muscle.

Alternatively, CLA's effect is mediated by AMP-activated protein kinase (AMPK), which is known to be the main regulator of exercise-mediated responses in the skeletal muscle, and PPAR δ is one of the primary downstream targets of AMPK [28–30]. The activation of both AMPK and PPAR δ is associated with the ability to promote endurance [28]. Indeed, it was demonstrated that a PPAR δ agonist and exercise training show synergistic activity of increasing oxidative myofibers and running endurance in mice [28]. Moreover, others recently reported no influence on PPAR δ by CLA [31]. The major difference between our current study and this report is the presence of exercise training in ours. This suggests potential combination/synergistic effects of *t10,c12* CLA with exercise training on improving exercise performance via AMPK and/or PPAR δ -dependent pathways. However, further studies are required to confirm if effects of CLA on endurance capacity involves AMPK and PPAR δ , including its effects on mitochondrial biogenesis.

We have to point out that our results in Fig. 5, only measuring mRNA expressions of selected markers, may be rather limited. However, it has been previously reported that there is a positive correlation between the increased mRNA expression of PPAR δ and its protein expression as well as the correlation between increased mRNA levels of CPT1 β and UCP2 on increased fat oxidation [32, 33]. Nonetheless, we cannot exclude the possibility of regulations of CLA occurring during post-transcriptional and post-translational periods and their activities.

CLA has been shown to enhance energy expenditure, supported by increased oxygen consumption [34, 35] and the expression of uncoupling proteins [36, 37]. Ohnuki et al. [38] reported that the oral administration of a CLA mixture increased serum concentrations of adrenalin and noradrenalin in mice, suggesting stimulation of the sympathetic nervous system. Therefore, CLA isomers may contribute to energy expenditure by inducing the enhancement of NEPA (grooming, feeding, walking around, etc.) as well as exercise performance. However, our data here showed that neither CLA isomer induced a significant change in NEPA during 6 weeks of dietary supplementation. By contrast, CLA supplementation increased NEPA previously when no extensive exercise regime was used [39]. This discrepancy suggests an interaction between NEPA and extensive exercise regime. Thus, further investigations are needed to understand the effects of CLA on NEPA, especially interaction between NEPA and extensive exercise.

There are currently seven human clinical studies reporting on CLA and exercise performance currently [40–46]. Four reported that CLA supplementation resulted in positive effects on at least one of exercise outcomes compared to control [40–43]. Others primarily evaluated effects of CLA on strength or capacity. Blankson et al. [40] reported increased training hours with CLA supplementation, which is consistent with our current observation. The present findings along with the previous studies suggest that CLA could boost the effects of exercise training on endurance capacity, and our results confirmed that the *t10,c12* CLA is responsible for those effects. However, others reported no changes in exercise outcomes with CLA in humans [44–46].

The NEFA is one of major fuels available with glycogen and glucose for oxidative metabolism during exercise [17]. Many researches demonstrated improved endurance capacity by increasing fat utilization during exercise and have shown increased serum level of NEFA during and/or after exercise with improved endurance [17, 47–49]. This might have resulted from increases of lipolysis in white adipose tissue, hydrolysis of very low-density lipoprotein TAG, or hydrolysis of intramyocellular triglyceride stores [17]. However, a previous study using CLA mixture

showed an improved endurance by promoting fat oxidation, with decreased serum concentrations of NEFA [6]. Others have consistently reported, as does this study, that CLA mix or *t10,c12* isomer showed reduced serum levels of NEFA with enhanced endurance by CLA [7]. The decreases of circulating NEFA by CLA supplementation could be most likely explained by the modulation of hepatic lipid metabolisms such as fatty liver. Fatty liver associated with CLA is primarily found in animal studies, and is believed to be due to tremendous fat mobilization from adipocytes and enhanced hepatic lipogenesis [50–52].

In conclusion, the present study demonstrated that *t10,c12*, but not *c9,t11*, CLA supplementation with exercise training enhances the running endurance capacity of mice by increasing muscle fat oxidation and reducing the consumption of stored glycogen during prolonged exercise. The increased expression level of PPAR δ in skeletal muscle indicates enhanced muscle oxidative metabolism by *t10,c12* CLA with exercise training. These findings provide important information for the application of CLA as a novel ergogenic aid.

Acknowledgments The authors thank Prof. Daeyoung Kim at the Department of Mathematics and Statistics, University of Massachusetts, Amherst for help with statistical assistance. We also thank Ms. Jayne M. Storkson for help preparing this manuscript and Ms. Dayeh Lee and Eunji Choi for assistance with the experiments. This material is based on work supported by the National Institute of Food and Agriculture, US Department of Agriculture, the Massachusetts Agricultural Experimental Station and the Department of Food Science under Project No. MAS0201001529. Dr. Yeonhwa Park is one of the inventors of CLA use patents that are assigned to the Wisconsin Alumni Research Foundation.

References

- Mancini D, Benaminovitz A, Cordisco ME, Karmally W, Weinberg A (1999) Slowed glycogen utilization enhances exercise endurance in patients with heart failure. *J Am Coll Cardiol* 34:1807–1812
- Jung K, Kim IH, Han D (2004) Effect of medicinal plant extracts on forced swimming capacity in mice. *J Ethnopharmacol* 93:75–81
- Fushiki T, Matsumoto K, Inoue K, Kawada T, Sugimoto E (1995) Swimming endurance capacity is increased by chronic consumption of medium-chain triglycerides. *J Nutr* 125:531–539
- Rahman SM, Wang YM, Yotsumoto H, Cha JY, Han SY, Inoue S, Yanagita T (2001) Effects of conjugated linoleic acid on serum leptin concentration, body-fat accumulation, and β -oxidation of fatty acid in OLETF rats. *Nutrition* 17:385–390
- Kennedy SR, Leaver MJ, Campbell PJ, Zheng X, Dick JR, Tocher DR (2006) Influence of dietary oil content and conjugated linoleic acid (CLA) on lipid metabolism enzyme activities and gene expression in tissues of Atlantic salmon (*Salmo salar* L.). *Lipids* 41(5):423–436
- Mizunoya W, Haramizu S, Shibakusa T, Okabe Y, Fushiki T (2005) Dietary conjugated linoleic acid increases endurance capacity and fat oxidation in mice during exercise. *Lipids* 40:265–271
- Kim JH, Park HG, Pan JH, Kim SH, Yoon HG, Bae GS, Lee H, Eom S-H, Kim YJ (2010) Dietary conjugated linoleic acid increases endurance capacity of mice during treadmill exercise. *J Med Food* 13(5):1057–1060
- Park Y, Pariza MW (2007) Mechanisms of body fat modulation by conjugated linoleic acid (CLA). *Food Res Int* 40:311–323
- Park Y, Storkson JM, Albright KJ, Liu W, Pariza W (1999) Evidence that the *trans*-10,*cis*-12 isomer of conjugated linoleic acid induces body composition changes in mice. *Lipids* 34:235–241
- Ribot J, Portillo MP, Picó C, Teresa Macarulla M, Palou A (2007) Effects of *trans*-10, *cis*-12 conjugated linoleic acid on the expression of uncoupling proteins in hamsters fed an atherogenic diet. *Br J Nutr* 97:1074–1082
- Fueger PT, Shearer J, Krueger TM, Posey KA, Bracy DP, Heikkinen S, Laakso M, Rottman JF, Wasserman DH (2005) Hexokinase II protein content is a determinant of exercise endurance capacity in the mouse. *J Physiol* 566(2):533–541
- Lightfoot JT, Turner MJ, Knab AK, Jedlicka AE, Oshimura T, Marzec J, Gladwell W, Leamy LJ, Kleeberger SR (2007) Quantitative trait loci associated with maximal exercise endurance in mice. *J Appl Physiol* 103:105–110
- Koch LG, Meredith TA, Fraker TD, Metting PJ, Britton SL (1998) Heritability of treadmill running endurance in rats. *Am J Physiol* 275:R1455–R1460
- Milliken GA, Johnson DE (2002) Analysis of covariance. In: Analysis of messy data, vol III. Chapman and Hall/CRC Press, Boca Raton, pp 123–160
- de Deckere EA, van Amelsvoort JM, McNeill GP, Jones P (1999) Effects of conjugated linoleic acid (CLA) isomers on lipid levels and peroxisome proliferation in the hamster. *Br J Nutr* 82(4):309–317
- Park Y, Albright KJ, Liu W, Storkson JM, Cook ME, Pariza MW (1997) Effect of conjugated linoleic acid on body composition in mice. *Lipids* 32:853–858
- Fernandez C, Hansson O, Nevsten P, Holm C, Klint C (2008) Hormone-sensitive lipase is necessary for normal mobilization of lipids during submaximal exercise. *Am J Physiol Endocrinol Metab* 295:E179–E186
- Pederson BA, Cope CR, Schroeder JM, Smith MW, Irimia JM, Thurberg BL, DePaoli-Roach AA, Roach PJ (2005) Exercise capacity of mice genetically lacking muscle glycogen synthase. *J Biol Chem* 280(17):17260–17265
- Kasuga M, Ogawa W, Ohara T (2003) Tissue glycogen content and glucose intolerance. *J Clin Invest* 111:1282–1284
- Hribal ML, Oriente F, Accili D (2002) Mouse models of insulin resistance. *Am J Physiol Endocrinol Metab* 282(5):E977–E981
- Hamada T, Arias EB, Cartee GD (2006) Increased submaximal insulin-stimulated glucose uptake in mouse skeletal muscle after treadmill exercise. *J Appl Physiol* 101:1368–1376
- Echtay KS, Winkler E, Frischmuth K, Klingenberg M (2001) Uncoupling proteins 2 and 3 are highly active H(+) transporters and highly nucleotide sensitive when activated by coenzyme Q (ubiquinone). *Proc Natl Acad Sci USA* 98:1416–1421
- Son C, Hosoda K, Matsuda J, Fujikura J, Yonemitsu S, Iwakura H, Masuzaki H, Ogawa Y, Hayashi T, Itoh H, Nishimura H, Inoue G, Yoshimasa Y, Yamori Y, Nakao K (2001) Up-regulation of uncoupling protein 3 gene expression by fatty acids and agonists for PPARs in L6 myotubes. *Endocrinology* 142:4189–4194
- Faldt J, Wernstedt I, Fitzgerald SM, Wallenius K, Bergstrom G, Jansson JO (2004) Reduced exercise endurance in interleukin-6-deficient mice. *Endocrinology* 145(6):2680–2686
- Chung S, Brown JM, Provo JN, Hopkins R, McIntosh MK (2005) Conjugated linoleic acid promotes human adipocyte insulin

- resistance through NF κ B-dependent cytokine production. *J Biol Chem* 280(46):38445–38456
26. Krämer DK, Al-Khalili L, Guigas B, Leng Y, Garcia-Roves PM, Krook A (2007) Role of AMP kinase and PPARdelta in the regulation of lipid and glucose metabolism in human skeletal muscle. *J Biol Chem* 282(27):19313–19320
 27. Wang YX, Zhang CL, Yu RT, Cho HK, Nelson MC, Bayuga-Ocampo CR, Ham J, Kang H, Evans RM (2004) Regulation of muscle fiber type and running endurance by PPAR δ . *PLoS Biol* 2(10):e294
 28. Narkar VA, Downes M, Yu RT, Emblar E, Wang YX, Banayo E, Mihaylova MM, Nelson MC, Zou Y, Juguilon H, Kang H, Shaw RJ, Evans RM (2008) AMPK and PPARdelta agonists are exercise mimetics. *Cell* 134(3):405–415
 29. Canto C, Auwerx J (2010) AMP-activated protein kinase and its downstream transcriptional pathways. *Cell Mol Life Sci* 67:3407–3423
 30. Matsakas A, Narkar VA (2010) Endurance exercise mimetics in skeletal muscle. *Curr Sports Med Rep* 9(4):227–232
 31. Parra P, Serra F, Palou A (2012) Transcriptional analysis reveals a high impact of conjugated linoleic acid on stearoyl-coenzyme A desaturase 1 mRNA expression in mice gastrocnemius muscle. *Genes Nutr*. doi:10.1007/s12263-011-0279-x
 32. Amengual J, Ribot J, Bonet ML, Palou A (2008) Retinoic acid treatment increases lipid oxidation capacity in skeletal muscle of mice. *Obesity* 16(3):585–591
 33. Tanaka T, Yamamoto J, Iwasaki S, Asaba H, Hamura H, Ikeda Y, Watanabe M, Magoori K, Ioka RX, Tachibana K, Watanabe Y, Uchiyama Y, Sumi K, Iguchi H, Ito S, Doi T, Hamakubo T, Naito M, Auwerx J, Yanagisawa M, Kodama T, Sakai J (2003) Activation of peroxisome proliferator-activated receptor delta induces fatty acid beta-oxidation in skeletal muscle and attenuates metabolic syndrome. *Proc Natl Acad Sci USA* 100(26):15924–15929
 34. Terpstra AH, Javadi M, Beynen AC, Kocsis S, Lankhorst AE, Lemmens AG, Mohede ICM (2003) Dietary conjugated linoleic acids as free fatty acids and triacylglycerols similarly affect body composition and energy balance in mice. *J Nutr* 133:3181–3186
 35. Nagao K, Wang YM, Inoue N, Han SY, Buang Y, Noda T, Kouda N, Okamatsu H, Yanagita T (2003) The 10trans, 12cis isomer of conjugated linoleic acid promotes energy metabolism in OLETF rats. *Nutrition* 19:652–656
 36. Peters JM, Park Y, Gonzalez FJ, Pariza MW (2001) Influence of conjugated linoleic acid on body composition and target gene expression in peroxisome proliferator-activated receptor alpha-null mice. *Biochim Biophys Acta* 1533:233–242
 37. Choi JS, Jung MH, Park HS, Song J (2004) Effect of conjugated linoleic acid isomers on insulin resistance and mRNA levels of genes regulating energy metabolism in high-fat-fed rats. *Nutrition* 20:1008–1017
 38. Ohnuki K, Haramizu S, Oki K, Ishihara K, Fushiki T (2001) A single oral administration of conjugated linoleic acid enhanced energy metabolism in mice. *Lipids* 36:583–587
 39. Park Y, Park Y (2012) Conjugated fatty acids increase energy expenditure in part by increasing voluntary movement in mice. *Food Chem* 133:400–409
 40. Blankson H, Stakkestad JA, Fagertun H, Thom E, Wadstein J, Gudmundsen O (2000) Conjugated linoleic acid reduces body fat mass in overweight and obese humans. *J Nutr* 130:2943–2948
 41. Pinkoski C, Chilibeck PD, Candow DG, Eslinger D, Ewaschuk JB, Facci M, Farthing JP, Zello GA (2006) The effects of conjugated linoleic acid supplementation during resistance training. *Med Sci Sports Exerc* 38(2):339–348
 42. Tarnopolsky M, Zimmer A, Paikin J, Safdar A, Aboud A, Pearce E, Roy B, Doherty D (2007) Creatine monohydrate and conjugated linoleic acid improve strength and body composition following resistance exercise in older adults. *PLoS One* 10:e991
 43. Cornish SM, Candow DG, Jantz NT, Chilibeck PD, Little JP, Forbes S, Abeysekera S, Zello GA (2009) Conjugated linoleic acid combined with creatine monohydrate and whey protein supplementation during strength training. *Int J Sport Nutr Exerc Metab* 19(1):79–96
 44. Kreider RB, Ferreira MP, Greenwood M, Wilson M, Almada AL (2002) Effects of conjugated linoleic acid supplementation during resistance training on body composition, body density, strength and selected hematologic markers. *J Strength Cond Res* 16:325–334
 45. Colakoglu S, Colakoglu M, Taneli F, Cetinoz F, Turkmen M (2006) Cumulative effects of conjugated linoleic acid and exercise on endurance development, body composition, serum leptin and insulin levels. *J Sports Med Phys Fit* 46:570–577
 46. Diaz ML, Watkins BA, Li Y, Anderson RA, Campbell WW (2008) Chromium picolinate and conjugated linoleic acid do not synergistically influence diet- and exercise-induced changes in body composition and health indexes in overweight women. *J Nutr Biochem* 19:61–68
 47. Oh TW, Ohta F (2003) Dose-dependent effect of capsaicin on endurance capacity in rats. *Br J Nutr* 90:515–520
 48. Murase T, Haramizu S, Shimotoyodome A, Nagasawa A, Tokimitsu I (2005) Green tea extract improves endurance capacity and increases muscle lipid oxidation in mice. *Am J Physiol Regul Integr Comp Physiol* 288:R708–R715
 49. Minegishi Y, Haramizu S, Hase T, Murase T (2011) Red grape leaf extract improves endurance capacity by facilitating fatty acid utilization in skeletal muscle in mice. *Eur J Appl Physiol* 111:1983–1989
 50. Pariza MW (2004) Perspective on the safety and effectiveness of conjugated linoleic acid. *Am J Clin Nutr* 79:1132S–1136S
 51. Clement L, Poirier H, Niot I, Bocher V, Guerre-Millo M, Krief S, Staels B, Besnard P (2002) Dietary *trans*-10,*cis*-12 conjugated linoleic acid induces hyperinsulinemia and fatty liver in the mouse. *J Lipid Res* 43:1400–1409
 52. Poirier H, Niot I, Clement L, Guerre-Millo M, Besnard P (2005) Development of conjugated linoleic acid (CLA)-mediated lipotrophic syndrome in the mouse. *Biochimie* 87:73–79

Free Fatty Acid Derivative HUHS2002 Potentiates $\alpha 7$ ACh Receptor Responses Through Indirect Activation of CaMKII

Takeshi Kanno · Tadashi Shimizu · Akito Tanaka · Takaaki Nishimoto · Tomoyuki Nishizaki

Received: 9 May 2012 / Accepted: 28 June 2012 / Published online: 21 July 2012
© AOCs 2012

Abstract The present study examined the effect of 4-[4-(Z)-hept-1-enyl-phenoxy] butyric acid (HUHS2002), a free fatty acid derivative, on $\alpha 7$ acetylcholine (ACh) receptor responses. HUHS2002 potentiated whole-cell membrane currents through $\alpha 7$ ACh receptors expressed in *Xenopus* oocytes in a concentration (1–100 nM)-dependent manner, reaching about 140 % of the original amplitude at 100 nM 50 min after a 10-min treatment. The HUHS2002 effect was prevented by KN-93, an inhibitor of Ca^{2+} /calmodulin-dependent protein kinase II (CaMKII), while it was not affected by GF109203X, an inhibitor of protein kinase C (PKC), or H-89, an inhibitor of protein kinase A (PKA). In the in situ CaMKII assay using cultured rat hippocampal neurons, HUHS2002 activated CaMKII and the activation was abolished by KN-93. In the cell-free assay of protein phosphatase 1 (PP1), HUHS2002 partially inhibited PP1 activity. Taken together, these results indicate that HUHS2002 potentiates $\alpha 7$ ACh receptor responses by indirectly activating CaMKII, possibly via inhibition of PP1.

Keywords $\alpha 7$ ACh receptor · Free fatty acid · Derivative · CaMKII · PP1

Abbreviations

HUHS2002	4-[4-(Z)-hept-1-enyl-phenoxy] butyric acid
ACh	Acetylcholine
CaMKII	Ca^{2+} /calmodulin-dependent protein kinase II
PKC	Protein kinase C
PKA	Protein kinase A
PP1	Protein phosphatase 1
DCP-LA	8-[2-(2-Pentyl-cyclopropylmethyl)-cyclopropyl]-octanoic acid
HEPES	4-(2-Hydroxyethyl)-1-piperazineethanesulfonic acid
EGTA	Ethylene glycol-bis-(β -aminoethyl ether)- <i>N,N,N',N'</i> -tetraacetic acid
PBS	Phosphate-buffered saline
HPLC	High-performance liquid chromatography
PLSD	Protected least significant difference

Introduction

Of neuronal nicotinic acetylcholine (ACh) receptors, a class of ligand-gated cation channels, $\alpha 7$ ACh receptor is preferentially localized at presynaptic terminals in the brain and regulates neurotransmitter release [1–8]. An enhancement in presynaptic nicotinic ACh receptors including $\alpha 7$ ACh receptor induces a long-lasting facilitation of hippocampal synaptic transmission by stimulating glutamate release [1–5]. Alzheimer disease is characterized by impairment in hippocampus-based episodic memory function. The cholinergic systems appear to be selectively disrupted in brain tissues from Alzheimer's patients [9–11]. Intriguingly, amyloid- β peptide, a critical factor proposed for the pathogenesis of Alzheimer disease, is bound to $\alpha 7$

T. Kanno · T. Nishimoto · T. Nishizaki (✉)
Division of Bioinformation, Department of Physiology,
Hyogo College of Medicine, 1-1 Mukogawa-cho,
Nishinomiya 663-8501, Japan
e-mail: tomoyuki@hyo-med.ac.jp

T. Shimizu · A. Tanaka
Laboratory of Chemical Biology, Advanced Medicinal Research
Center, Hyogo University of Health Sciences, 1-3-6 Minatojima,
Chuo-ku, Kobe 650-8530, Japan

ACh receptor [12]. Nicotinic ACh receptors, alternatively, decrease in the aging brain [13]. In the light of these facts, $\alpha 7$ ACh receptor could be a useful target for development of anti-dementia drugs [14].

So far we have found that *cis*-unsaturated free fatty acids such as arachidonic, linoleic, and linolenic acid potentiate nicotinic ACh receptor responses via a protein kinase C (PKC) pathway [14–18]. PKC is the major intracellular signaling messenger to regulate and modulate a wide-variety of bioreactions. PKC isozymes include conventional PKCs such as PKC- α , - β I, - β II, and - γ , novel PKCs such as PKC- δ , - ϵ , - η , - θ , and - μ , and atypical PKCs such as PKC- λ / i for mouse/human, - ζ and - ν [19]. All the PKC isozymes share a conserved kinase domain, but the regulatory domain differs among three classes of PKCs; the regulatory domain for conventional PKCs contains the C1A/C1B and C2 domains, that for nPKCs contains the C2-like and C1A/C1B domains, and that for atypical PKCs contains the PB1 and C1 domains [20]. *Cis*-unsaturated free fatty acids are capable of activating novel PKCs in a Ca^{2+} - and diacylglycerol-independent manner. When systemically applied, the free fatty acids are promptly metabolized and decomposed. We, therefore, synthesized the linoleic acid derivative 8-[2-(2-pentyl-cyclopropylmethyl)-cyclopropyl]-octanoic acid (DCP-LA), that exhibits stable bioactivities still in *in vivo* systems [4]. Of particular interest is that DCP-LA serves as a selective and direct activator of PKC- ϵ , that is preferentially localized in pre-synaptic terminals in the brain [21]. DCP-LA enhances responses of presynaptic $\alpha 7$ ACh receptors by activating PKC- ϵ , causing an increase in the release of neurotransmitters such as glutamate, γ -aminobutyric acid, serotonin, and dopamine [5, 7, 8].

Unexpectedly, oleic acid, a *cis*-unsaturated free fatty acid, enhances *Torpedo* ACh receptor responses via a Ca^{2+} /calmodulin-dependent protein kinase II (CaMKII) pathway, regardless of PKC activation [22]. Arachidonic acid enhances currents through Ca^{2+} -permeable AMPA receptors under the control of CaMKII [23]. Moreover, DCP-LA indirectly activates CaMKII by inhibiting protein phosphatase 1 (PP1), thereby promoting AMPA receptor delivery toward the membrane surface [24]. These findings suggest that *cis*-unsaturated free fatty acids are still implicated in CaMKII activation.

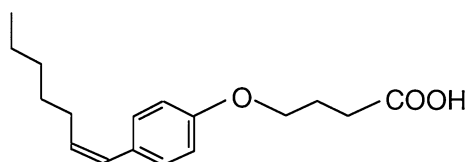


Fig. 1 Structure of HUHS2002

To gain further insight into bioactivities of free fatty acids, we newly synthesized HUHS2002 (Fig. 1), a free fatty acid derivative, and examined the effect on $\alpha 7$ ACh receptor responses. We show here that HUHS2002 potentiates $\alpha 7$ ACh receptor responses by indirectly activating CaMKII, possibly through inhibition of PP1.

Materials and Methods

Animal Care

All procedures were approved by the Animal Care and Use Committee at Hyogo College of Medicine and were in compliance with the National Institutes of Health Guide for the Care and Use of Laboratory Animals.

In Vitro Transcription and Translation

The rat $\alpha 7$ ACh receptor cDNA was kindly provided from Dr. James W. Patrick (Baylor College of Medicine, USA). The mRNA coding the rat $\alpha 7$ ACh receptor subunit was synthesized by *in vitro* transcription. Mature *Xenopus* oocytes were surgically removed from female frogs under ether anesthesia and manually separated from the ovary. Collagenase (0.5 mg/ml) treatment was carried out to remove the follicular cell layer, and 24 h later oocytes were injected with approximately 50 nl of the $\alpha 7$ ACh receptor subunit mRNA (1 mg/ml), and incubated in Barth's solution [in mM: 88 NaCl, 1 KCl, 2.4 NaHCO_3 , 0.82 MgSO_4 , 0.33 $\text{Ca}(\text{NO}_2)_2$, 0.41 CaCl_2 , and 7.5 Tris, pH 7.6] at 18 °C.

Two-Electrode Voltage-Clamp Recording

Oocytes were transferred to a recording chamber 2–3 days after injection of the $\alpha 7$ ACh receptor subunit mRNA and continuously superfused at 22 °C in a standard extracellular solution [in mM: 88 NaCl, 2 KCl, 1.8 CaCl_2 , and 5 HEPES, pH 7.0] or Ca^{2+} -free extracellular solution [in mM: 88 NaCl, 2 KCl, 1 EGTA, and 5 HEPES, pH 7.0]. ACh (100 μM) was bath-applied to oocytes at 10 min intervals before and after 10-min treatment with HUHS2002, and ACh-evoked currents were recorded, i.e., the sampling rate was once every 10 min. It was confirmed that repetitive applications with ACh at 10-min intervals have no effect on ACh-evoked current amplitude. In a two-electrode voltage-clamp configuration, whole-cell membrane currents were recorded with a GeneClamp-500 amplifier (Axon Instruments, Inc., Foster City, CA, USA), filtered at 20–50 Hz, and analyzed on a microcomputer using pClamp software (version 6.0.3, Axon Instruments, Inc.). The electrode used, with the resistance of 2–3 $\text{M}\Omega$, was filled with 2 M KCl.

Cell Culture

The hippocampus was removed from the embryonic Wistar rat brain (gestational age, 18 days). Dissociated hippocampal cells were seeded on 96-well plates and grown in a culture medium: neurobasal with the supplement B27 (50:1), 2.5 mM glutamine, 50 μ M glutamate, penicillin (final concentration, 100 U/ml), and streptomycin (final concentration, 0.1 mg/ml) in a humidified atmosphere of 5 % CO₂ and 95 % air at 37 °C. Two days later, cytosine arabinoside (5 μ M) was added to the culture medium to suppress glial cell proliferation.

In Situ CaMKII Assay

CaMKII activity in cultured rat hippocampal neurons after 7 days in vitro was assayed by the method as previously described [24]. Cultured neurons were treated with HUHS2002 in the presence and absence of KN-92 or KN-93 at 37 °C for 10 min in an extracellular solution [137 mM NaCl, 5.4 mM KCl, 10 mM MgCl₂, 0.3 mM Na₂HPO₄, 0.4 mM K₂HPO₄, and 20 mM HEPES, pH 7.2]. Then, cells were rinsed with 100 μ l Ca²⁺-free phosphate-buffered saline (PBS) and incubated at 30 °C for 15 min in 50 μ l of the extracellular solution containing 50 μ g/ml digitonin, 25 mM glycerol 2-phosphate, 200 μ M ATP, and 100 μ M Autocamtide-2 (Lys-Lys-Ala-Leu-Arg-Arg-Gln-Glu-Thr-Val-Asp-Ala-Leu; MW 1,527.8) (Calbiochem, San Diego, CA, USA), a synthetic CaMKII substrate peptide. The supernatants were collected and boiled at 100 °C for 5 min to terminate the reaction. An aliquot of the solution (20 μ l) was loaded onto a reversed phase high-performance liquid chromatography (HPLC) (LC-10ATvp, Shimadzu Co., Kyoto, Japan). A substrate peptide peak and a new product peak were detected at an absorbance of 214 nm (SPD-10Avp UV-vis detector, Shimadzu Co.). Molecular weights for each peak were calibrated from the two standard spectrums, bradykinin (MW 1,060.2) and neurotensin (MW 1,672.9). In the analysis of matrix-assisted laser desorption ionization time of flight mass spectrometry (Voyager DE-STR, PE Biosystems Inc., Foster City, CA, USA), a substrate peak and a new product peak revealed a molecular weight of 1,527 and 1,607, respectively. This explains why a new product peak corresponds to phosphorylated substrate peptide, since a molecular weight of 1,607 is consistent with total molecular weight of unphosphorylated substrate peptide (MW 1,527) plus HPO₃ (MW 80). Areas for unphosphorylated and phosphorylated CaMKII substrate peptide were measured (the total area corresponds to the concentration of CaMKII substrate peptide used here). The amount of phosphorylated substrate peptide (pmol/min/ μ g cell protein) was calculated and used as an index of CaMKII activity.

Cell-Free Assay for CaMKII and PP1 Activity

For cell-free CaMKII assay, a synthetic CaMKII substrate peptide (10 μ M) was reacted with CaMKII (5 U) (Calbiochem) in a reaction medium (25 μ l, pH 8.0) containing 40 mM HEPES, 5 mM Mg-acetate, 0.4 mM CaCl₂, 0.1 mM ATP, 0.1 mM EGTA, 1 μ M calmodulin (Calbiochem) in the presence and absence of HUHS2002 at 35 °C for 10 min. For a cell-free PP1 assay, a synthetic CaMKII substrate peptide (10 μ M) was reacted with CaMKII (5 U) and PP1 (5 mU) (Sigma, St. Louis, MO, USA) in the same reaction medium as for CaMKII assay in the presence and absence of microcystin (Sigma) or HUHS2002 at 35 °C for 10 min. Each reaction was terminated at 100 °C for 5 min. An aliquot of each solution (15 μ l) was injected onto the column (250 mm \times 4.6 mm) (COSMOSIL 5C18-AR-II, Nacalai Tesque, Kyoto, Japan), and loaded onto a reversed phase HPLC system (LC-10ATvp, Shimadzu Co.). Unphosphorylated peptide and phosphorylated peptide were detected at an absorbance of 214 nm (SPD-10Avp UV-vis detector, Shimadzu Co.). Phosphorylated substrate peptide (pmol/min) was used as an index of CaMKII activity. Dephosphorylated substrate peptide (the amount of phosphorylated substrate peptide in the absence of PP1 minus the amount in the presence of PP1 together with and without microcystin or HUHS2002) (Δ pmol/min) was used as an index of PP1 activity. As is the case with DCP-LA [24], much higher concentrations of HUHS2002 in the cell-free system than in the in-situ system were used to detect the activity of CaMKII and PP1.

Statistical Analysis

Statistical analysis was carried out using Fisher's protected least significant difference (PLSD) test and Dunnett's test.

Results

HUHS2002 Potentiates Currents Through α 7 ACh Receptors in a CaMKII-Dependent Manner

For *Xenopus* oocytes, expressing α 7 ACh receptors, bath-application with ACh (100 μ M) generated inward whole-cell membrane currents at a holding potential of -60 mV (Fig. 2). HUHS2002 (100 nM) potentiated the currents to approximately 150 % of the original amplitude, the effect being evident 50 min after a 10-min treatment (Fig. 2). The potentiating effect of HUHS2002 was concentration (1–100 nM) dependent (Fig. 3).

α 7 ACh receptor channels are highly permeable to calcium. In the *Xenopus* oocyte expression system, ACh-evoked currents are composed of currents through α 7 ACh receptor channels and endogenous chloride channels that are

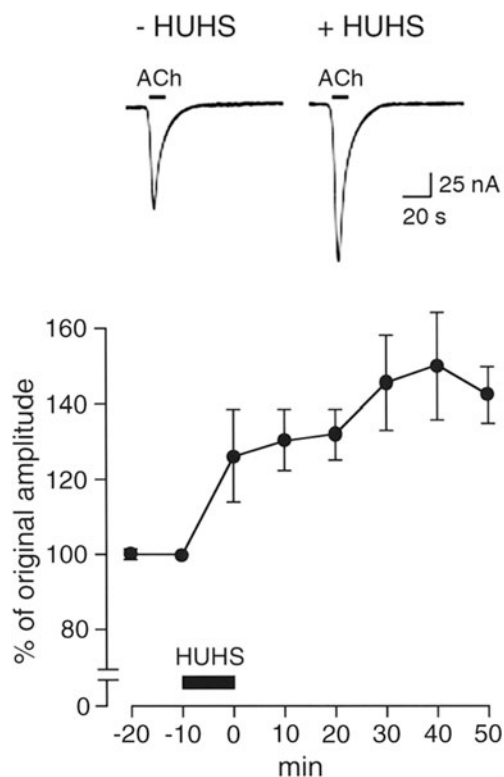


Fig. 2 HUHS2002-induced potentiation of $\alpha 7$ ACh receptor currents. $\alpha 7$ ACh receptors were expressed in *Xenopus* oocytes, and ACh (100 μM) was bath-applied to oocytes for 10 s at a 10-min interval before and after a 10-min treatment with HUHS2002 (HUHS) (100 nM) in Ca^{2+} -containing extracellular solution. The holding potential was -60 mV. Application with ACh is indicated by bars. Typical currents recorded 10 min before and 50 min after treatment with HUHS2002 are shown. In the graph, each point represents the mean (\pm SEM) percentage of the original amplitudes (-10 min) ($n = 8$ independent experiments)

activated by Ca^{2+} influx through $\alpha 7$ ACh receptor channels. HUHS2002 (100 nM) still potentiated ACh-evoked currents in Ca^{2+} -free extracellular solution (Fig. 3). This indicates that HUHS2002-induced potentiation of ACh-evoked currents is due to an enhancement in $\alpha 7$ ACh receptor channel currents but not in Ca^{2+} -sensitive chloride channel currents.

HUHS2002 (100 nM)-induced potentiation of $\alpha 7$ ACh receptor channel currents was significantly inhibited by KN-93 (3 μM), an inhibitor of CaMKII ($P < 0.001$ as compared with the currents after HUHS2002 treatment in the absence of CaMKII, Fisher's PLSD test), while the potentiation was not affected by GF109203X (100 nM), an inhibitor of PKC, or H-89 (1 μM), an inhibitor of PKA (Fig. 4). This suggests that HUHS2002 potentiates $\alpha 7$ ACh receptor channel currents by activating CaMKII.

HUHS2002 Activates CaMKII Due to PP1 Inhibition

Our next attempt was to obtain evidence for HUHS2002-induced CaMKII activation. To address this point, we

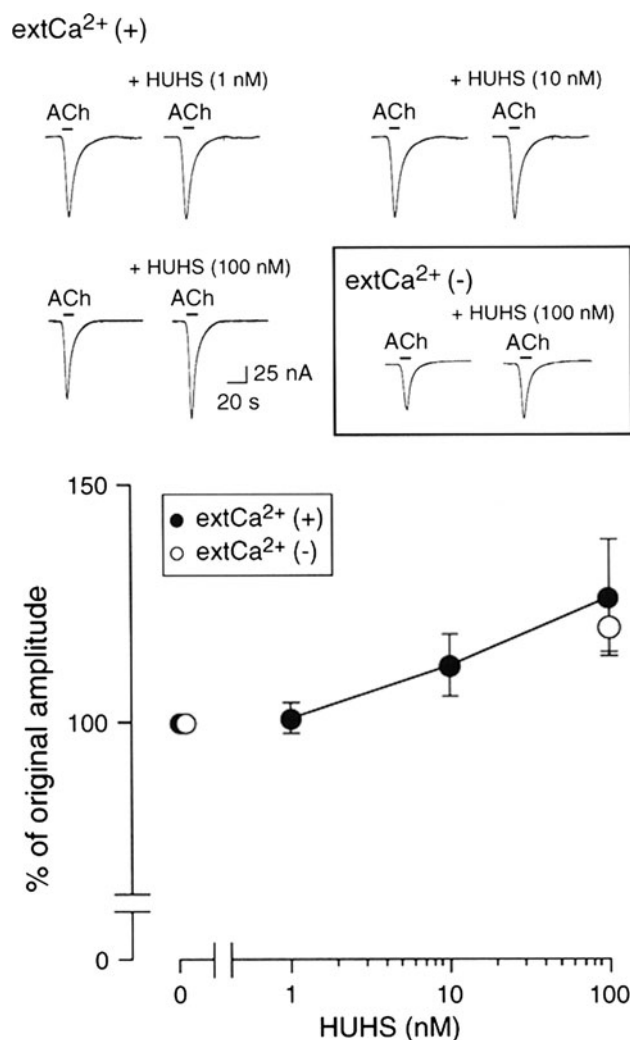


Fig. 3 HUHS2002 concentration-dependent potentiation of $\alpha 7$ ACh receptor currents. ACh (100 μM)-evoked whole-cell membrane currents were monitored from oocytes expressing $\alpha 7$ ACh receptors 10 min before and 10 min after 10-min treatment with HUHS2002 (HUHS) at concentrations as indicated in Ca^{2+} -containing [ext Ca^{2+} (+)] and Ca^{2+} -free extracellular solution [ext Ca^{2+} (-)]. Typical currents are shown in the upper panel. In the graph, each point represents the mean (\pm SEM) percentage of original amplitudes (-10 min) ($n = 5$ –8 independent experiments)

assayed CaMKII activity with a reversed phase HPLC. HUHS2002 (100 nM) significantly enhanced CaMKII activity in cultured rat hippocampal neurons, and the HUHS2002 effect was significantly inhibited by KN-93 (3 μM), an inhibitor of CaMKII, but not KN-92 (3 μM), an inactive form of KN-93 (Fig. 5a). This provides evidence that HUHS2002 is actually capable of activating CaMKII. In the cell-free system, however, no activation of CaMKII was obtained with HUHS2002 at any concentration ranging from 1 nM to 10 μM (Fig. 5b). This implies that HUHS2002 does not directly activate CaMKII.

CaMKII is activated through its own autophosphorylation, but otherwise activated CaMKII is inactivated through

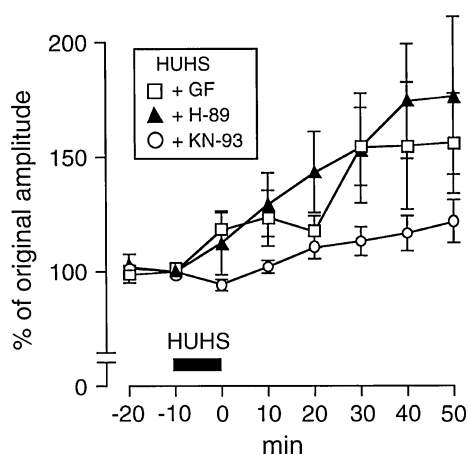


Fig. 4 HUHS2002-induced potentiation of $\alpha 7$ ACh receptor currents via a CaMKII pathway. ACh (100 μ M)-evoked whole-cell membrane currents were monitored from oocytes expressing $\alpha 7$ ACh receptors 10 min before and after 10-min treatment with HUHS2002 (HUHS) (100 nM) in the presence of GF109203X (GF) (100 nM), H-89 (1 μ M), or KN-93 (3 μ M). In the graph, each point represents the mean (\pm SEM) percentage of original amplitudes (-10 min) ($n = 5$ independent experiments)

dephosphorylation catalyzed by PP1. Then, we postulated that HUHS2002 might indirectly activate CaMKII by inhibiting PP1. In the cell-free PP1 assay, microcystin (1 μ M), an inhibitor of PP1, markedly suppressed PP1 activity (Fig. 6). Likewise, HUHS2002 (10 μ M) significantly inhibited PP1 activity (Fig. 6). Taken together, the results indicate that HUHS2002 could indirectly activate CaMKII by inhibiting PP1.

Discussion

In the present study, the free fatty acid derivative HUHS2002 potentiated currents through $\alpha 7$ ACh receptors expressed in *Xenopus* oocytes, and the effect was clearly inhibited by the CaMKII inhibitor KN-93. This indicates that HUHS2002 enhances $\alpha 7$ ACh receptor responses via a CaMKII pathway. To our knowledge, this is the first showing CaMKII-dependent enhancement in $\alpha 7$ ACh receptor responses.

To obtain evidence for HUHS2002-induced CaMKII activation, we assayed CaMKII activity. HUHS2002 activated CaMKII in cultured rat hippocampal neurons, but no activation of CaMKII was obtained under the cell-free conditions. This accounts for indirect CaMKII activation by HUHS2002. Then, the question addressing is how HUHS2002 activates CaMKII. PP1 is recognized to dephosphorylate and inactivate CaMKII. In the present study, HUHS2002 reduced PP1 activity under the cell-free conditions, although the inhibition was partial in comparison to the known inhibitor microcystin. This indicates that

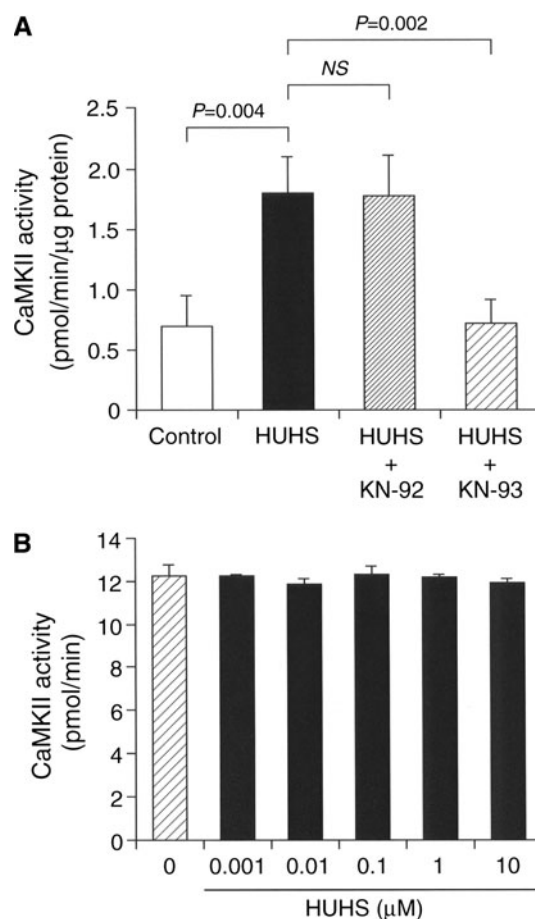


Fig. 5 HUHS2002-induced CaMKII activation. **a** Cultured rat hippocampal neurons were untreated or treated with HUHS2002 (HUHS) (100 nM) in the absence (Control) and presence of KN-92 (3 μ M) or KN-93 (3 μ M). Phosphorylated substrate peptide (pmol/min/ μ g cell protein) was used as an index of CaMKII activity. In the graph, each column represents the mean (\pm SEM) CaMKII activity ($n = 10$ independent experiments). P values, Dunnett's test. *NS*, not significant. **b** CaMKII activity was assayed under the cell-free conditions in the absence and presence of HUHS2002 (HUHS) at concentrations as indicated. In the graph, each column represents the mean (\pm SEM) CaMKII activity (pmol/min) ($n = 6$ independent experiments)

HUHS2002 is capable of activating CaMKII at least in part by inhibiting PP1. How HUHS2002 inhibits PP1, however, is presently unknown. A plausible explanation for this includes that HUHS2002 directly binds to and inhibits PP1 or HUHS2002 promotes transit from inactive inhibitor-1 to active inhibitor-1 through PKA phosphorylation, to suppress PP1 activity.

$\alpha 7$ ACh receptor has no CaMKII phosphorylation site [25], and therefore, the HUHS2002-induced potentiation of $\alpha 7$ ACh receptor responses is not due to modulation of the receptor channel properties through CaMKII phosphorylation. HUHS2002 might stimulate $\alpha 7$ ACh receptor exocytosis in a CaMKII-dependent manner, to increase membrane surface localization of the receptors, thereby

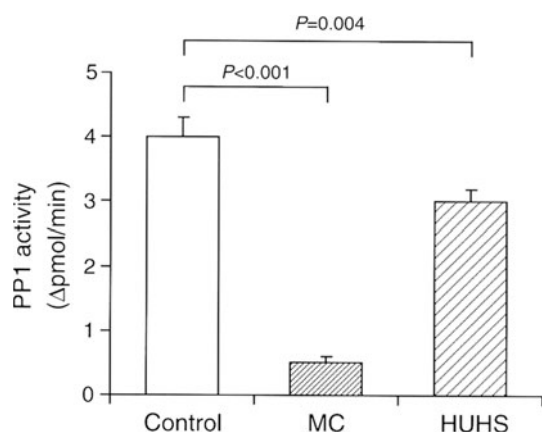


Fig. 6 HUHS2002-induced PP1 inhibition. PP1 activity was assayed in the cell-free systems in the absence (Control) and presence of microcystin (MC) (1 μ M) or HUHS2002 (HUHS) (10 μ M). In the graph, each column represents the mean (\pm SEM) PP1 activity ($n = 8$ independent experiments). P values, Dunnett's test

enhancing whole-cell $\alpha 7$ ACh receptor responses. A recent study, however, shows that inhibition of plasma membrane calcium-ATPase pump isoform 2 promotes internalization of $\alpha 7$ ACh receptor through a CaMKII-dependent mechanism [26]. It is presently unknown how CaMKII activated by HUHS2002 acts on $\alpha 7$ ACh receptors, to enhance the receptor responses. To address this question, we are probing CaMKII targets responsible for potentiation of $\alpha 7$ ACh receptor responses.

Evidence has pointed to the interaction of *cis*-unsaturated free fatty acids such as arachidonic, oleic, linoleic, linolenic, and docosahexaenoic acid with PKC [19]. We have found that a variety of *cis*-unsaturated free fatty acids and the linoleic acid derivative DCP-LA potentiate nicotinic ACh receptor responses by activating PKC [2, 4, 5, 8, 15–18]. In the preliminary study, HUHS2002 also activated PKC. HUHS2002-induced potentiation of $\alpha 7$ ACh receptor responses here, however, was not inhibited by the PKC inhibitor GF109203X, ruling out the implication of PKC in the HUHS2002 effect. Why PKC activated by HUHS2002 does not participate in potentiation of $\alpha 7$ ACh receptor responses remains to be explored.

In conclusion, the results of the present study suggest that the free fatty acid derivative HUHS2002 potentiates $\alpha 7$ ACh receptor responses by indirectly activating CaMKII at least in part due to PP1 inhibition. This may represent a novel pathway linking lipid signaling to $\alpha 7$ ACh receptor responses.

References

1. Nishizaki T, Nomura T, Matsuyama S, Kondoh T, Fujimoto E, Yoshii M (2001) Critical role of presynaptic nicotinic ACh

receptor in the formation of long-term potentiation: implication of development of anti-dementia drug. *Psychogeriatrics* 1:209–217

2. Nishizaki T, Nomura T, Matsuoka T, Enikolopov G, Sumikawa K (1999) Arachidonic acid induces a long-lasting facilitation of hippocampal synaptic transmission by modulating PKC activity and nicotinic ACh receptors. *Mol Brain Res* 69:263–272
3. Nishizaki T, Nomura T, Matsuoka T, Kondoh T, Enikolopov G, Sumikawa K, Watabe S, Shiotani T, Yoshii M (2000) The anti-dementia drug nefiracetam facilitates hippocampal synaptic transmission by functionally targeting presynaptic nicotinic ACh receptors. *Mol Brain Res* 80:53–62
4. Tanaka A, Nishizaki T (2003) The newly synthesized linoleic acid derivative FR236924 induces a long-lasting facilitation of hippocampal neurotransmission by targeting nicotinic acetylcholine receptors. *Bioorg Med Chem Lett* 13:1037–1040
5. Yamamoto S, Kanno T, Nagata T, Yaguchi T, Tanaka A, Nishizaki T (2005) The linoleic acid derivative FR236924 facilitates hippocampal synaptic transmission by enhancing activity of presynaptic $\alpha 7$ acetylcholine receptors on the glutamatergic terminals. *Neuroscience* 130:207–213
6. Kanno T, Yaguchi T, Yamamoto S, Nagata T, Yamamoto H, Fujikawa H, Nishizaki T (2005) Bidirectional regulations for glutamate and GABA release in the hippocampus by $\alpha 7$ and non- $\alpha 7$ ACh receptors. *Biochem Biophys Res Commun* 338:742–747
7. Kanno T, Yaguchi T, Yamamoto S, Yamamoto H, Fujikawa H, Nagata T, Tanaka A, Nishizaki T (2005) 8-[2-(2-pentyl-cyclopropylmethyl)-cyclopropyl]-octanoic acid stimulates GABA release from interneurons projecting to CA1 pyramidal neurons in the rat hippocampus via pre-synaptic $\alpha 7$ acetylcholine receptors. *J Neurochem* 95:695–702
8. Shimizu T, Kanno T, Tanaka A, Nishizaki T (2011) α, β -DCP-LA selectively activates PKC- ϵ and stimulates neurotransmitter release with the highest potency among 4 diastereomers. *Cell Physiol Biochem* 27:149–158
9. Aubert I, Araujo DM, Cécycy D, Robitaille Y, Gauthier S, Quirion R (1992) Comparative alterations of nicotinic and muscarinic binding sites in Alzheimer's and Parkinson's diseases. *J Neurochem* 58:529–541
10. Perry EK, Perry RH, Smith CJ, Dick DJ, Candy JM, Edwardson JA, Fairbairn A, Blessed G (1987) Nicotinic receptor abnormalities in Alzheimer's and Parkinson's diseases. *J Neurol Neurosurg Psychiatry* 50:806–809
11. Whitehouse PJ, Martino AM, Wagster MV, Price DL, Mayeux R, Atack JR, Kellar KJ (1988) Reductions in [3 H]nicotinic acetylcholine binding in Alzheimer's disease and Parkinson's disease: an autoradiographic study. *Neurology* 38:720–723
12. Parri HR, Hernandez CM, Dineley KT (2011) Research update: $\alpha 7$ nicotinic acetylcholine receptor mechanisms in Alzheimer's disease. *Biochem Pharmacol* 82:931–942
13. Nordberg A (1994) Human nicotinic receptors—their role in aging and dementia. *Neurochem Int* 25:93–97
14. Hernandez CM, Dineley KT (2012) $\alpha 7$ nicotinic acetylcholine receptors in Alzheimer's disease: neuroprotective, neurotrophic or both? *Curr Drug Targets* 13:613–622
15. Ikeuchi Y, Nishizaki T, Matsuoka T, Sumikawa K (1996) Arachidonic acid potentiates ACh receptor currents by protein kinase C activation but not by receptor phosphorylation. *Biochem Biophys Res Commun* 221:716–721
16. Nishizaki T, Ikeuchi Y, Matsuoka T, Sumikawa K (1997) Short-term depression and long-term enhancement of ACh-gated channel currents induced by linoleic and linolenic acid. *Brain Res* 751:253–258
17. Nishizaki T, Matsuoka T, Nomura T, Sumikawa K (1998) Modulation of ACh receptor currents by arachidonic acid. *Mol Brain Res* 57:173–179

18. Yaguchi T, Yamamoto S, Nagata T, Kanno T, Tanaka A, Nishizaki T (2005) Effects of *cis*-unsaturated free fatty acids on PKC- ϵ activation and nicotinic ACh receptor responses. *Mol Brain Res* 133:320–324
19. Nishizuka Y (1995) Protein kinase C and lipid signaling for sustained cellular responses. *FASEB J* 9:484–496
20. Steinberg SF (2008) Structural basis of protein kinase C isoform function. *Physiol Rev* 88:1341–1378
21. Kanno T, Yamamoto H, Yaguchi T, Hi R, Mukasa T, Fujikawa H, Nagata T, Yamamoto S, Tanaka A, Nishizaki T (2006) The linoleic acid derivative DCP-LA selectively activates PKC- ϵ , possibly binding to the phosphatidylserine binding site. *J Lipid Res* 47:1146–1156
22. Nishizaki T, Ikeuchi Y, Matsuoka T, Sumikawa K (1997) Oleic acid enhances ACh receptor currents by activation of Ca²⁺/calmodulin-dependent protein kinase II. *NeuroReport* 8:597–601
23. Nishizaki T, Matsuoka T, Nomura T, Enikolopov G, Sumikawa K (1999) Arachidonic acid potentiates currents through Ca²⁺-permeable AMPA receptors by interacting with a CaMKII pathway. *Mol Brain Res* 67:184–189
24. Kanno T, Yaguchi T, Nagata T, Tanaka A, Nishizaki T (2009) DCP-LA stimulates AMPA receptor exocytosis through CaMKII activation due to PP1 inhibition. *J Cell Physiol* 221:183–188
25. Moss SJ, McDonald BJ, Rudhard Y, Schoepfer R (1996) Phosphorylation of the predicted major intracellular domains of the rat and chick neuronal nicotinic acetylcholine receptor $\alpha 7$ subunit by cAMP-dependent protein kinase. *Neuropharmacol* 35:1023–1028
26. Gómez-Varela D, Schmidt M, Schoellerman J, Peters EC, Berg DK (2012) PMCA2 via PSD-95 controls calcium signaling by $\alpha 7$ -containing nicotinic acetylcholine receptors on aspiny interneurons. *J Neurosci* 32:6894–6905

Macrophages Alter the Differentiation-Dependent Decreases in Fibronectin and Collagen I/III Protein Levels in Human Preadipocytes

AnneMarie Gagnon · Michelle N. Yarmo ·
Anne Landry · Alexander Sorisky

Received: 5 April 2012 / Accepted: 21 June 2012 / Published online: 12 July 2012
© AOCs 2012

Abstract Adipose tissue of obese individuals is characterized by increased fibrosis and macrophage infiltration. Extensive remodeling of the extracellular matrix (ECM) that occurs during adipogenesis can be influenced by macrophages, but it remains unclear how macrophage-secreted factors alter preadipocyte ECM protein expression under non-adipogenic versus adipogenic conditions. Confluent human subcutaneous abdominal preadipocytes were cultured for 14 days, with or without adipogenic inducers, in either control medium, medium conditioned by THP-1 monocytes (THP-1-MonCM), or medium conditioned by THP-1 macrophages (THP-1-MacCM). Under non-adipogenic conditions in THP-1-MacCM, collagen I/III and fibronectin protein levels rose by 40 and 70 %, respectively ($p < 0.05$, $n = 3$; compared to control non-adipogenic medium). When preadipocytes were exposed to adipogenic inducers in THP-1-MacCM, collagen I/III levels increased by 50 %, but those of fibronectin fell by 48 %, both compared to non-adipogenic THP-1-MacCM conditions. The rise in collagen I/III levels contrasts with the 51 % decrease in collagen I/III that occurs with induction of differentiation in control medium, whereas, the decrease in fibronectin is more modest, but consistent in THP-1-MacCM (48 %) and control medium (92 %). A similar effect on fibronectin levels occurred using medium conditioned by LPS-treated human monocyte-derived macrophages (MD-MacCM). Our data indicate macrophage-derived factors regulate levels of collagen I/III and fibronectin in preadipocytes

under non-adipogenic and adipogenic conditions. Further studies are needed to determine if these changes in these ECM proteins contribute to the anti-adipogenic action of MacCM.

Keywords Preadipocyte · Adipogenesis · Fibronectin · Collagen · Extracellular matrix · Macrophage

Abbreviations

BMI	Body mass index
ECM	Extracellular matrix
ERK1/2	Extracellular signal-regulated kinase 1/2
FABP4/aP2	Fatty acid binding protein 4
IL-1 β	Interleukin-1 β
IOD	Integrated optical density
LPS	Lipopolysaccharide
MacCM	Macrophage-conditioned medium
MMP	Matrix metalloproteinase
MD	Monocyte-derived
MonCM	Monocyte-conditioned medium
PPAR γ	Peroxisome proliferator-activated receptor γ
TG	Triacylglycerol
TIMP	Tissue inhibitor of matrix metalloproteinase
TNF α	Tumor necrosis factor α
TPA	12- <i>O</i> -Tetradecanoylphorbol-13-acetate

Introduction

Under conditions of chronic nutrient excess, adipose tissue expands by hypertrophy and hyperplasia, the latter through a process of recruitment and differentiation of preadipocytes called adipogenesis [1]. A deficit in adipogenesis may arise in this context, resulting in exaggerated adipocyte

A. Gagnon · M. N. Yarmo · A. Landry · A. Sorisky (✉)
Chronic Disease Program, Ottawa Hospital Research Institute,
Departments of Medicine and of Biochemistry, Microbiology
and Immunology, University of Ottawa, General Campus
C-4421, 501 Smyth Rd, Ottawa, ON K1H 8L6, Canada
e-mail: asorisky@ohri.ca

hypertrophy that is associated with insulin resistance and inflammation [2, 3]. Macrophages accumulate in adipose tissue of obese individuals [4–6], and they may negatively influence adipogenesis. Indeed, impairment of mouse and human adipocyte differentiation by macrophage-secreted factors has been previously reported by us and others [7, 8]. The mechanisms by which macrophages exert their anti-adipogenic effect remain elusive, but the extracellular matrix (ECM) could be a target.

The ECM is a physiological regulator of adipogenesis and adipose tissue remodeling [9–11]. The preadipocyte ECM consists mainly of fibrillar collagens (types I and III) and fibronectin. Upon differentiation, these proteins are down-regulated, and a laminar basement membrane structure emerges, mainly composed of collagen IV, entactin and laminin [12]. Matrix metalloproteinases (MMPs), tissue inhibitor of matrix metalloproteinases (TIMPs), and adhesion receptors of the integrin family influence adipogenesis [13–15]. Obesity is associated with a progressive elevation in the expression of several collagens, resulting in adipose tissue fibrosis [11].

Previous studies on the effects of macrophage-secreted factors on ECM protein expression have not clearly distinguished between changes occurring in the presence versus the absence of adipogenic inducers [8]. Here, we have examined the influence of human macrophage-secreted factors on the differentiation-associated changes in the levels of fibrillar collagens (I and III), and fibronectin in human preadipocytes. In particular, we have carefully compared the changes in these ECM proteins induced by macrophages under adipogenic versus non-adipogenic conditions.

Experimental Procedure

Cell Culture of Human THP-1 Macrophages and Preparation of MonCM and MacCM

As previously described [7], THP-1 monocytes were resuspended at 1×10^6 cells/mL in RPMI supplemented with 2 mM L-glutamine, 4.5 g/L HEPES, 1 mM sodium pyruvate, 10 % FBS, 0.05 mM β -mercaptoethanol, and antibiotics (100 U/mL penicillin and 0.1 mg/mL streptomycin). THP-1-monocytes were differentiated into adherent macrophages with 100 nM 12-*O*-tetradecanoylphorbol-13-acetate (TPA) for 24 h (>95 % conversion). The medium was then replaced with fresh growth medium (no TPA present) and, after another 24 h, the macrophage conditioned medium (THP-1-MacCM) was collected and centrifuged at $150 \times g$ for 5 min. Supernatants were transferred and frozen at -20°C until use. Medium conditioned by THP-1 monocytes (THP-1-MonCM), as well as medium

never exposed to THP-1 cells (control medium), were processed in parallel as controls.

Isolation and Culture of Monocyte-Derived (MD) Macrophages and Preparation of MD-MacCM

Blood was obtained from three healthy volunteers (approved by the Ottawa Hospital Research Ethics Board #2008445-01H). Blood samples were diluted with PBS supplemented with 2 mM EDTA and layered onto Ficoll-Hypaque (GE Healthcare; Uppsala, Sweden). Peripheral blood mononuclear cells were isolated by density-gradient centrifugation ($400 \times g$ for 30 min). The buffy coat was removed and placed in culture in RPMI supplemented with antibiotics, and monocytic cells were allowed to adhere for 1 h. Floating cells were then removed through several washes with PBS/2 mM EDTA; remaining adherent cells were placed in RPMI supplemented with 10 % FBS and antibiotics in the presence or absence of 1 $\mu\text{g}/\text{mL}$ LPS for 24 h to generate MD-MacCM and LPS-MD-MacCM. Each medium was collected, centrifuged at $150 \times g$ for 5 min, and the supernatant was frozen at -20°C until use. Medium supplemented or not with LPS, and not exposed to cells, was processed in parallel as control.

Isolation of Human Abdominal Subcutaneous Stromal Preadipocytes and Adipogenic Induction

Subcutaneous adipose tissue samples were obtained from six weight-stable female patients (age ranged from 34 to 53 years; BMI ranged from 22.4 to 43.1) undergoing elective abdominal surgery (approved by the Ottawa Hospital Research Ethics Board #1995023-01H). Patients receiving insulin or steroid treatment were excluded. Preadipocytes were isolated and differentiated as described [7]. In brief, adipose tissue was dissected away from connective tissue and capillaries, then digested with collagenase CLS type I (600 U/g of tissue). Preadipocytes, obtained following progressive size filtration and centrifugation, were grown in DMEM supplemented with 10 % FBS, antibiotics, and 50 U/mL nystatin (growth medium). For differentiation, preadipocytes were seeded on plastic dishes (immunoblot analysis) or on glass coverslips (immunocytochemistry) at 3×10^4 cells/cm² and grown to confluence in growth medium. Confluent preadipocytes were placed in THP-1-MacCM, THP-1-MonCM, MD-MacCM, or control medium supplemented or not with adipogenic inducers: 5 $\mu\text{g}/\text{mL}$ insulin, 100 μM indomethacin, 0.5 μM dexamethasone, and 0.25 mM isobutylmethylxanthine for 14 days. Cells were photographed and processed for triacylglycerol (TG) and protein measurement, followed by immunoblot analysis. Alternatively, cells seeded on coverslips were processed for immunocytochemistry.

Any contamination with macrophage or endothelial cells is $<2\%$ under our culture conditions.

TG Assay

Cellular TG was extracted using a solution of 2:3 (vol/vol) isopropanol:heptane. TG accumulation was quantified using a colorimetric assay [7]. Cellular remains were solubilized in Laemmli buffer [16]. Protein was quantified using the modified Lowry assay (Bio-Rad Protein Assay Kit, Mississauga, Canada) with bovine serum albumin (BSA) as a standard. TG values were normalized to protein content.

Immunoblot Analysis

Following TG extraction, equal amounts of solubilized protein from the cellular remains were resolved by SDS-PAGE and transferred to nitrocellulose membrane. Membranes were blocked, then probed with primary antibodies directed against: collagen I/III (1/500, rabbit polyclonal; EMD Biosciences), fibronectin (1/10,000 mouse monoclonal; BD Biosciences), peroxisome proliferator-activated receptor γ (2 $\mu\text{g}/\text{mL}$, PPAR γ , rabbit polyclonal, Santa Cruz), fatty acid binding protein 4 (0.1 $\mu\text{g}/\text{mL}$, FABP4/aP2, goat polyclonal, R&D Systems), or extracellular

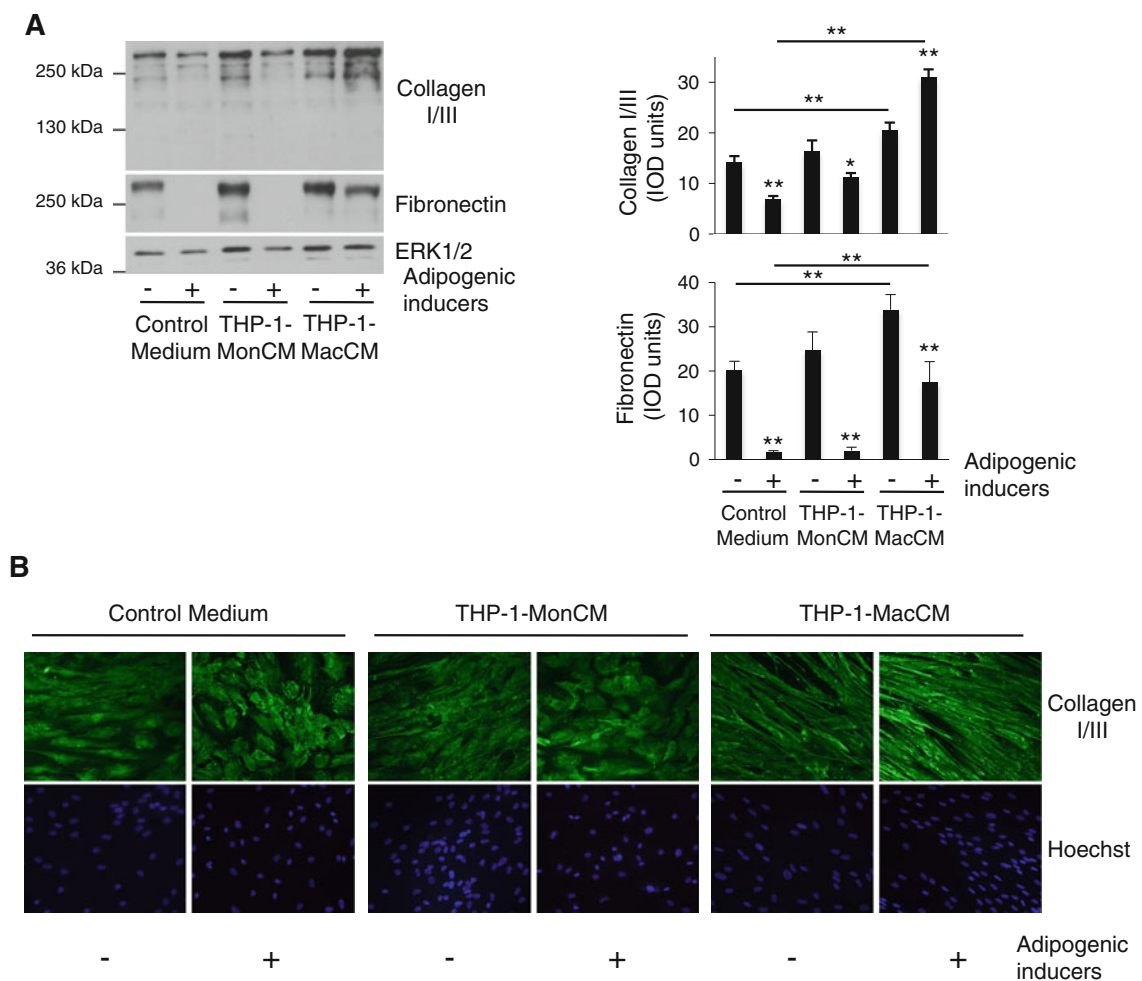


Fig. 1 Changes in levels of collagen I/III and fibronectin protein in preadipocytes cultured in THP-1-MacCM under non-adipogenic and adipogenic conditions. Confluent human abdominal subcutaneous preadipocytes were exposed (+) or not (–) to adipogenic inducers in control medium, THP-1-MonCM, or THP-1-MacCM for 14 days. **a** Solubilized protein was immunoblotted with the indicated antibodies. Representative immunoblots from one patient are shown. Densitometric data are the mean \pm SE of 3 separate patient samples. * $p < 0.05$ and ** $p < 0.01$ compared to the same condition without adipogenic inducers or between indicated pairs, assessed by two-way

ANOVA with replications, followed by Tukey post-tests. ERK1/2 serves as a loading control. **b** Confluent human abdominal subcutaneous preadipocytes were seeded on glass coverslips prior to exposure (+) or not (–) to adipogenic inducers in control medium, THP-1-MonCM, or THP-1-MacCM for 14 days. Cells were fixed and stained with collagen I/III antibodies and Hoechst dye. Immunoreactivity was detected with AlexaFluor488-conjugated IgGs. Representative photomicrographs from one patient sample are shown. Similar results were obtained with three other patients

signal-regulated kinase 1/2 (0.5 $\mu\text{g}/\text{mL}$, ERK1/2, rabbit polyclonal, Chemicon). Following incubation with appropriate peroxidase-conjugated secondary antibodies (1:2,000 for PPAR γ , 1:10,000 for collagen I/III, and 1:50,000 for others), signal intensity was assessed by chemiluminescence and a digital imaging system. Quantitative results are expressed as integrated optical density (IOD) units.

Immunocytochemistry

Cells were fixed with methanol:acetone (3:7, v/v) for 15 min. Cells were extensively washed, and antigenic sites were blocked with PBS supplemented with 2 % BSA. Fixed cells were then incubated with collagen I/III antibodies (1:50) or blocking solution (non-specific) binding, followed by incubation with AlexaFluor488-conjugated secondary antibodies (1 $\mu\text{g}/\text{mL}$). Nuclei were stained with Hoechst dye, as previously described [17]. Coverslips were mounted on glass slides and fluorescence was visualized with a Zeiss Axioplan 2 microscope.

Results

The Effect of THP-1-MacCM on Levels of Collagen I/III and Fibronectin

We measured levels of collagen I/III and fibronectin protein in human preadipocytes that were cultured either in non-adipogenic or adipogenic conditions in either control, THP-1-MonCM, or THP-1-MacCM (Fig. 1a).

Under non-adipogenic conditions, THP-1-MacCM raised the levels of collagen I/III and fibronectin in preadipocytes, by 40 and 70 %, respectively, versus non-adipogenic control medium. THP-1-MonCM had no effect; the averaged ERK1/2 signal was significantly higher for this condition, but normalization did not alter the result that ECM protein expression is not affected by THP-1-MonCM.

Adipogenic induction in control medium led to a reduction in collagen I/III and fibronectin levels by 51 and 92 %, respectively, versus non-adipogenic control

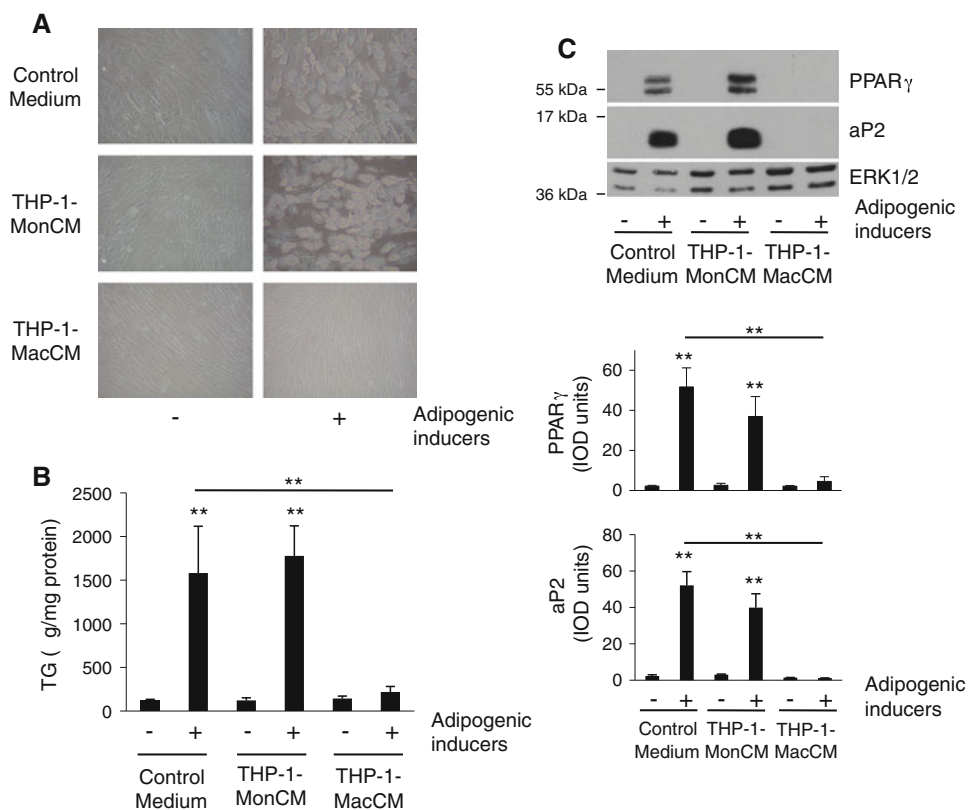


Fig. 2 The effect of THP-1-MacCM on human adipocyte differentiation. Confluent human abdominal subcutaneous preadipocytes were exposed (+) or not (–) to adipogenic inducers in control medium, THP-1-MonCM, or THP-1-MacCM for 14 days. **a** Representative photomicrographs for one patient sample are shown. Similar results were obtained with two other patients **b** TG was extracted, quantified, and normalized to protein content. Results are the mean \pm SE of

three separate patient samples. **c** Solubilized protein was immunoblotted with the indicated antibodies. Representative immunoblots from one patient are shown. Densitometric data are the mean \pm SE of three separate patient samples. ** $p < 0.01$ compared to the same condition without adipogenic inducers or between indicated pairs, assessed by two-way ANOVA with replications, followed by Tukey post-tests. ERK1/2 serves as a loading control

conditions. When preadipocytes were exposed to adipogenic inducers in THP-1-MacCM, fibronectin levels followed a similar pattern, but to a more modest degree, falling by 48 %. This level of fibronectin was comparable to that of preadipocytes in non-adipogenic control medium. In contrast, collagen I/III levels did not decrease at all, but instead increased further by another 50 % in the presence of adipogenic inducers, compared to the timed non-adipogenic control condition.

Given the progressive rise of collagen I/III levels even in the presence of adipogenic inducers in the THP-1-MacCM, we assessed collagen I/III organization by immunocytochemistry in human preadipocytes under non-adipogenic and adipogenic conditions (Fig. 1b). Under non-adipogenic conditions, THP-1-MacCM induced a more elongated, spindly morphology of human preadipocytes compared to control or THP-1-MonCM. In the presence of adipogenic inducers, the cells in THP-1-MacCM were even more elongated and organized, in keeping with the progressive increase in collagen I/III noted by immunoblot analysis. Cells in control medium or THP-1-MonCM became more polygonal in shape, consistent with the adipogenic process that occurred under those conditions.

Concomitant with these effects on fibronectin and collagen I/III levels, adipogenesis was potently inhibited by THP-1-MacCM, but not THP-1-MonCM, as assessed by morphology, TG accumulation, and adipogenic gene expression (Fig. 2).

The Effect of LPS-MD-MacCM on Levels of Fibronectin

Although the human THP-1 cell line is a well-accepted model of human monocyte-macrophage biology [18, 19], we extended our studies to examine the effects of conditioned medium from primary human monocyte-derived macrophages that were or were not treated with LPS (Fig. 3).

Under non-adipogenic conditions, LPS-MD-MacCM had no effect on fibronectin levels compared to control medium. Addition of adipogenic inducers to the LPS-MD-MacCM caused fibronectin levels to decrease by 51 %, consistent with, but less potent than the 92 % reduction that occurred with adipogenesis in the control medium. LPS-MD-MacCM effectively inhibited adipogenesis, as assessed by morphology, TG accumulation, and adipogenic markers PPAR γ and aP2 (Fig. 4). MD-MacCM, generated without prior LPS treatment, had no effect on fibronectin levels compared to control medium, with or without adipogenic inducers, consistent with its inability to inhibit adipogenesis.

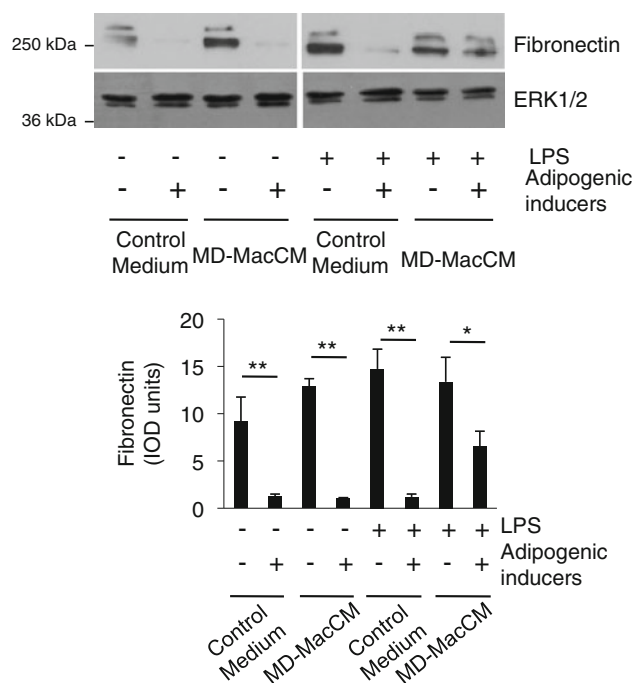


Fig. 3 Changes in levels of fibronectin protein in preadipocytes cultured in MD-MacCM under non-adipogenic and adipogenic conditions. Confluent human abdominal subcutaneous preadipocytes were exposed (+) or not (–) for 14 days, to adipogenic inducers in control medium or CM generated from adherent monocytes (MD-MacCM) activated or not with LPS. Solubilized proteins were immunoblotted with the indicated antibodies. Representative immunoblots from one patient are shown. Densitometric data are the mean \pm SE of three separate patient samples. * p < 0.05 and ** p < 0.01 between indicated pairs, assessed by two-way ANOVA with replications, followed by Tukey post-tests. ERK1/2 serves as a loading control

Discussion

Although the anti-adipogenic action of MacCM has been reported by several groups, using a variety of experimental models, the precise mechanism through which this occurs is not well-understood [7, 8, 20–22]. The ECM proteins produced by adipose cells have been suggested to be targets of MacCM [8, 23]. However, the effect of MacCM on preadipocytes in non-adipogenic versus adipogenic conditions has not been systematically studied. Therefore, we compared collagen I/III and fibronectin levels under both conditions, using human preadipocytes and two human macrophage models, THP-1 macrophages and primary monocyte-derived macrophages.

Previously, human preadipocytes treated with adipogenic inducers in the presence of macrophage-secreted factors for 10–12 days were reported to have higher levels of fibronectin protein compared to cells that were differentiated under control conditions [8]. However, their

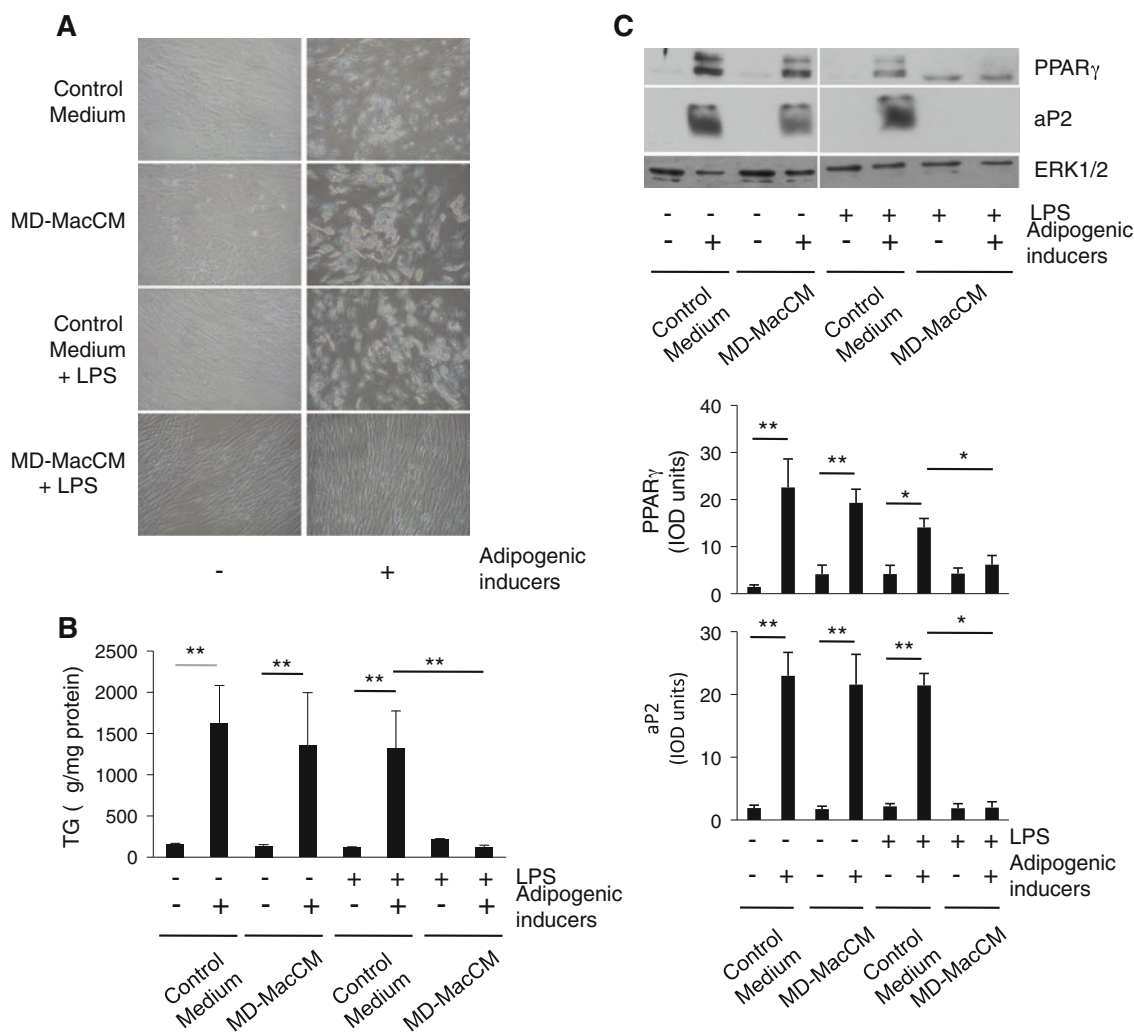


Fig. 4 The effect of human MD-MacCM on human adipocyte differentiation. Confluent human abdominal subcutaneous preadipocytes were exposed (+) or not (–) for 14 days, to adipogenic inducers in control medium or CM generated from adherent monocytes (MD-MacCM) activated or not with LPS. **a** Representative photomicrographs for one patient sample are shown. Similar results were obtained with two other patients. **b** TG was extracted, quantified, and

normalized to protein content. Results are the mean \pm SE of three separate patient samples. **c** Solubilized proteins were immunoblotted with the indicated antibodies. Representative immunoblots from one patient are shown. Densitometric data are the mean \pm SE of three separate patient samples. * p < 0.05 and ** p < 0.01 between indicated pairs, assessed by two-way ANOVA with replications, followed by Tukey post-tests. ERK1/2 serves as a loading control

analysis of the effect of the macrophages on fibronectin levels did not include a timed control study of preadipocytes cultured under non-adipogenic conditions. Therefore, the effect of macrophage factors on cellular fibronectin levels in non-adipogenic versus adipogenic conditions was not assessed. Here, we have undertaken this comparison using either THP-1-MacCM or MD-MacCM.

In the case of THP-1-MacCM, fibronectin levels rose under non-adipogenic conditions, whereas, with MD-MacCM, fibronectin levels remained constant. This difference could be due to variations in the quantity or type of factors released by the two macrophage models. With the results of this non-adipogenic timed control treatment as a comparator, it can be observed that fibronectin levels

are actually lower in preadipocytes cultured in either THP-1-MacCM or MD-MacCM in the presence of the adipogenic inducers. However, the reduction in fibronectin levels that occurs with adipogenic inducers in MacCM is weaker than in control medium. Over time, this results in relatively higher levels of fibronectin in preadipocytes in MacCM, compared to control medium, both under adipogenic conditions. A reduction in fibronectin levels is an established component of the adipogenic program [24]. The attenuation in the fall of fibronectin might be a direct effect of MacCM on fibronectin itself, but might also be an indirect consequence of the overall inhibition of adipogenesis caused by MacCM, perhaps through actions on other targets.

A reduction in fibrillar collagen is also a key part of the ECM remodeling that occurs with adipocyte differentiation [25]. Our comparison of non-adipogenic and adipogenic conditions demonstrates that THP-1 MacCM has a distinct effect on collagen I/III, promoting an ongoing rise in levels, even in the presence of adipogenic inducers. This was observed by immunoblot analysis and supported by cellular imaging. The basis for this divergence in behavior of collagen I/III versus fibrinogen in response to MacCM is not known at present. Examining the levels of these ECM proteins released into the medium by the adipose cells might also be informative. With the small number of donors in this study, there was no apparent effect of age or weight on the responses we measured; it is possible that such potential influences could be detected if the number of donors was larger. Due to detection problems for collagen I/III immunoblots using a smaller number of human preadipocytes to match the limited volume of MD-MacCM, we could not compare collagen I/III versus fibronectin for this model.

The expression of collagen I/III and fibronectin can be regulated by pro-inflammatory cytokines, such as tumor necrosis factor α (TNF α) and interleukin-1 β (IL-1 β), both found in MacCM. However, neutralization of these factors on an individual basis yields only minimal reversal of the inhibition of adipogenesis, despite a reduction in adipose cell inflammation [8, 22]. It remains possible that many factors released by macrophages, including Wnt molecules [26], are competent to prevent adipogenesis. ERK1/2 and NF- κ B signaling pathways are activated in preadipocytes exposed to macrophage-secreted factors, and their pharmacological inhibition reverses the negative effect of MacCM on adipogenesis [20, 27]. These pathways could be involved in the regulation of genes implicated in ECM remodeling. However, at this time, it is not known whether the inhibition of the anti-adipogenic effect of macrophage-secreted factors by interfering with these signaling pathways is linked to normalization of ECM protein levels. More work is needed to determine if the anti-adipogenic effect of MacCM depends on alterations in preadipocyte ECM proteins.

Our data using cell culture models of human macrophages and preadipocytes describe changes in ECM proteins under non-adipogenic and adipogenic conditions. They should be interpreted in context with *in vivo* adipose tissue remodeling, which involves complex interactions of its cellular population, including adipocytes, preadipocytes, and infiltrating immune cells. Macrophage-secreted factors not only alter the physiology of preadipocytes and adipocytes within the adipose tissue, they also modify the extracellular environment to promote a fibrotic state. The role of the altered ECM environment on preadipocyte growth survival, and differentiation, as well as on adipocyte function requires further investigation, and may be important for metabolic health.

Acknowledgments This work was supported by a grant to AS from the Heart and Stroke Foundation of Canada (Ontario) NA 6634. We thank Fiona Frappier and Dr. J B Angel (OHRI) for assistance with production of MD-MacCM, and patients and surgeons of The Ottawa Hospital for their participation in acquiring adipose tissue samples.

References

- Lee MJ, Wu Y, Fried SK (2010) Adipose tissue remodeling in pathophysiology of obesity. *Curr Opin Clin Nutr Metab Care* 13:371–376
- Heilbronn L, Smith SR, Ravussin E (2004) Failure of fat cell proliferation, mitochondrial function and fat oxidation results in ectopic fat storage, insulin resistance and type 2 diabetes mellitus. *Int J Obesity* 28:S12–S21
- Arner E, Westermark PO, Spalding KL, Britton T, Ryden M, Frisen J, Bernard S, Arner P (2010) Adipocyte turnover: relevance to human adipose tissue morphology. *Diabetes* 59:105–109
- Weisberg SP, McCann D, Desai M, Rosenbaum M, Leibel RL, Ferrante AWJ (2003) Obesity is associated with macrophage accumulation in adipose tissue. *J Clin Invest* 112:1796–1808
- Xu H, Barnes GT, Yang Q, Tan G, Yang D, Chou CJ, Sole J, Nichols A, Ross JS, Tartaglia LA, Chen H (2003) Chronic inflammation in fat plays a crucial role in the development of obesity-related insulin resistance. *J Clin Invest* 112:1821–1830
- Osborn O, Olefsky JM (2012) The cellular and signaling networks linking the immune system and metabolism in disease. *Nat Med* 18:363–374
- Constant VA, Gagnon A, Landry A, Sorisky A (2006) Macrophage-conditioned medium inhibits the differentiation of 3T3-L1 and human abdominal preadipocytes. *Diabetologia* 49:1402–1411
- Lacasa D, Taleb S, Keophiphath M, Miranville A, Clement K (2007) Macrophage-secreted factors impair human adipogenesis: involvement of proinflammatory state in preadipocytes. *Endocrinology* 148:868–877
- Halberg N, Wernstedt-Asterholm I, Scherer PE (2008) The adipocyte as an endocrine cell. *Endocrinol Metab Clin North Am* 37:753–768
- Henegar C, Tordjman J, Achard V, Lacasa D, Cremer I, Guerre-Millo M, Poitou C, Basdevant A, Stich V, Viguier N, Langin D, Bedossa P, Zucker JD, Clement K (2008) Adipose tissue transcriptomic signature highlights the pathological relevance of extracellular matrix in human obesity. *Genome Biol* 9:R14
- Khan T, Muise ES, Iyengar P, Wang ZV, Chandalia M, Abate N, Zhang BB, Bonaldo P, Chua S, Scherer PE (2009) Metabolic dysregulation and adipose tissue fibrosis: role of collagen VI. *Mol Cell Biol* 29:1575–1591
- Gregoire FM, Smas CM, Sul HS (1998) Understanding adipocyte differentiation. *Physiol Rev* 78:783–809
- Meissburger B, Stachorski L, Röder E, Rudofsky G, Wolfrum C (2011) Tissue inhibitor of matrix metalloproteinase 1 (TIMP1) controls adipogenesis in obesity in mice and in humans. *Diabetologia* 54:1468–1479
- Chun TH, Hotary KB, Sabeh F, Saltiel AR, Allen ED, Weiss SJ (2006) A pericellular collagenase directs the 3-dimensional development of white adipose tissue. *Cell* 15:429–431
- Liu J, DeYoung S, Zhang M, Zhang M, Cheng A, Saltiel AR (2005) Changes in integrin expression during adipocyte differentiation. *Cell Metab* 2:165–177
- Laemmli UK (1970) Cleavage of structural proteins during the assembly of the head of bacteriophage T4. *Nature* 227:680–685
- Papineau D, Gagnon A, Sorisky A (2003) Apoptosis of human abdominal preadipocytes before and after differentiation into adipocytes in culture. *Metabolism* 52:987–992

18. Auwerx J (1991) The human leukemia cell line, THP-1: a multifunctional model for the study of monocyte-macrophage differentiation. *Experientia* 47:22–31
19. Kohro T, Tanaka T, Murakami T, Wada Y, Aburatani H, Hamakubo T, Kodama T (2004) A comparison of differences in the gene expression profiles of phorbol 12-myristate 13-acetate differentiated THP-1 cells and human monocyte-derived macrophages. *J Atheroscler Thromb* 11:88–97
20. Yarmo MN, Gagnon A, Sorisky A (2010) The anti-adipogenic effect of macrophage-conditioned medium requires the IKK β /NF- κ B pathway. *Horm Metab Res* 42:831–836
21. Stienstra R, Duval C, Keshkar S, van der Laak J, Kersten S, Müller M (2008) Peroxisome proliferator-activated receptor γ activation promotes infiltration of alternatively activated macrophages into adipose Tissue. *J Biol Chem* 283:22620–22627
22. Lu C, Kumar PA, Fan Y, Sperling MA, Menon RK (2010) A novel effect of growth hormone on macrophage modulates macrophage-dependent adipocyte differentiation. *Endocrinology* 151:2189–2199
23. Keophiphath M, Achard V, Henegar C, Rouault C, Clément K, Lacasa D (2009) Macrophage-secreted factors promote a profibrotic phenotype in human preadipocytes. *Mol Endocrinol* 23: 11–24
24. Spiegelman BM, Ginty CA (1983) Fibronectin modulation of cell shape and lipogenic gene expression in 3T3-adipocytes. *Cell* 35:657–666
25. Weiner FR, Shah A, Smith PJ, Rubin CS (1989) Regulation of collagen gene expression in 3T3-L1 cells. *Biochemistry* 28: 4094–4099
26. Bilkovski R, Schulte DM, Oberhauser F, Mauer J, Hampel B, Gutschow C, Krone W, Laudes M (2011) Adipose tissue macrophages inhibit adipogenesis of mesenchymal precursor cells via wnt-5a in humans. *Int J Obes* 35:1450–1454
27. Constant VA, Gagnon A, Yarmo M, Sorisky A (2008) The anti-adipogenic effect of macrophage-conditioned medium depends on ERK1/2 activation. *Metabolism* 57:465–472

Dynamics of the Lipid Content and Biomass of *Calanus finmarchicus* (copepodite V) in a Norwegian Fjord

Maria Bergvik · Øystein Leiknes · Dag Altin ·
Kjersti Rennan Dahl · Yngvar Olsen

Received: 22 December 2011 / Accepted: 5 July 2012 / Published online: 24 July 2012
© AOCS 2012

Abstract *Calanus finmarchicus* is the dominant zooplankton species in the North Atlantic. This zooplankton is also of interest for commercial harvesting due to its high abundance and biochemical contents. In the present study, copepodite stage V of *C. finmarchicus* was sampled at different depths from January to June in 2009, 2010 and 2011 in the Trondheimsfjord (63°29'N 10°18'E). The fatty acid composition was analyzed in individual copepods and in the seston. It was found that the fatty acid profile of copepods was related to the fatty acid profile of potential food sources. This study indicates that the onset of vertical migration of stage V, which was observed in May, has a strong link to the production of phytoplankton and lipid accumulation in *C. finmarchicus*. The content of 14:0 and 16:0 fatty acids in the specimens did not increase from February to May in surface waters. This suggests that these fatty acids in the diet were used as precursors for the biosynthesis of 20:1n-9 and 22:1n-11 fatty acids and fatty alcohols. A potential harvesting season of *C. finmarchicus* could be when the species is abundant in surface waters; the content of n-3 fatty acids will vary throughout this season. The peak abundance of *C. finmarchicus* in the spring varied substantially between the years studied.

Keywords *Calanus finmarchicus* · Lipids · Fatty acids · PUFA · Wax esters · Phytoplankton lipids · Lipid metabolism · Spring variation · Vertical migration

Abbreviations

Chl <i>a</i>	Chlorophyll <i>a</i>
C5	Copepodite stage five
MUFA	Mono unsaturated fatty acid(s)
PUFA	Poly unsaturated fatty acid(s)
TFA	Total fatty acid(s)

Introduction

Calanus finmarchicus (Gunnerus, 1765) is the dominant zooplankton species in the Norwegian and Barents Seas [1]. The annual production in the Nordic Seas is roughly estimated to be 74 million tons by wet weight [2]. The copepod has a generation time of 1–2 years in the Norwegian Sea and a dormancy period in deep waters during the winter [3, 4]. *C. finmarchicus* hatch as nauplius larvae and progress through six naupliar stages and five copepodite stages before reaching sexual maturity. The females spawn at the time of the spring bloom, and the offspring feed to obtain large lipid deposits in summer and autumn [5]. The storage lipids of late copepodites and adults are in the form of wax esters, which are fatty acids esterified with fatty alcohols. Wax esters are the most common storage lipids in herbivorous zooplankton feeding on short blooms of phytoplankton followed by long periods of food shortage [6]. The phospholipids mainly consist of phosphatidyl choline and phosphatidyl ethanolamine [7] and contain a high proportion of the fatty acids 22:6n-3 and 20:5n-3 [8, 9].

Due to its abundance and biochemical components, *C. finmarchicus* is a promising marine raw material and an interesting source for commercial use. World aquaculture has grown steadily in the last 50 years, with an annual growth rate of 8.7 % (excluding China) since 1970.

M. Bergvik (✉) · Ø. Leiknes · K. R. Dahl · Y. Olsen
Department of Biology, Norwegian University of Science
and Technology, 7491 Trondheim, Norway
e-mail: maria.bergvik@bio.ntnu.no

D. Altin
Biotrix, 7022 Trondheim, Norway

Meanwhile, in the last 10–15 years, most global fisheries have become fully or overexploited, and the maximum sustainable catch has probably been reached, of which 20–30 % is used for animal feed [10]. Further growth in the aquaculture of carnivorous fish and crustaceans will require alternative sources of feed ingredients. Vegetable sources can replace part of the fishmeal and oil used today, but the need for n-3 long chain polyunsaturated fatty acids (LC-PUFA) like 22:6n-3 and 20:5n-3 will require new marine lipid sources [11, 12]. Harvesting zooplankton could be one alternative to meet the increased demand for n-3 LC-PUFA in the aquaculture industry. Atlantic salmon (*Salmo salar*) is capable of utilizing oil from *C. finmarchicus* in its diet [13–16], demonstrating the suitability of *C. finmarchicus* as a new marine ingredient in fish feed. Phospholipids in *C. finmarchicus* have high proportions of 22:6n-3 and 20:5n-3, and could meet the dietary demands of early marine fish larvae, as they require phospholipids [17] in addition to a high content of 22:6n-3 and 20:5n-3 fatty acids [18]. Moreover, there has been increasing awareness of the importance of marine lipids in human nutrition, and beneficial health effects have been documented for the consumption of n-3 LC-PUFA, which are mainly provided by marine lipids [19]. *C. finmarchicus* could also be an interesting additive for human nutrition. Wax esters from *C. finmarchicus* have a low melting point and contain long chain, monounsaturated fatty alcohols, which make this material interesting for cosmetics, lubricants, and pharmaceuticals, as discussed by Sargent and Henderson [20].

In the present study, we examined the size and fatty acid content of copepodite stage V (C5) of *C. finmarchicus* sampled at different depths at a fixed location in the Trondheimsfjord (63°29'N 10°18'E), from January to June in 2009–2011. The main food sources of zooplankton are phytoplankton and protozoa. The stock and condition of *C. finmarchicus* will therefore naturally be affected by changes in phytoplankton composition. In the Trondheimsfjord, the first spring bloom consists mainly of diatoms, while later, dinoflagellates and flagellates dominate the bloom [21]. The dominant fatty acids of diatoms are 16:0, 16:1n-7 and 20:5n-3 [22], whilst dinoflagellates have variable levels of 16:0, 18:4n-3, 18:5n-3, 20:5n-3 and 22:6n-3 [23, 24]. The profile of the fatty acids in the wax esters of *C. finmarchicus* will reflect the fatty acid composition of the dietary phytoplankton [25], but copepods are also dispersed by currents, which provides spatial and depth variation.

In addition to dietary fatty acids, *C. finmarchicus* are capable of de novo synthesis of fatty alcohols from carbohydrates and proteins [26]. Wax esters contain fatty alcohols synthesized de novo, esterified with fatty acids, and the fatty alcohols contain fairly stable content of 20:1n-9 and 22:1n-11 [27, 28] in addition to 14:0 and 16:0, while their fatty acid composition partly reflects the diet of the

copepods. The fatty acids 20:1n-9 and 22:1n-11 are also a prominent component of wax esters [20, 27] and are synthesized de novo by *C. finmarchicus* [26]. However, field observations for documenting biosynthesis are scarce and more detailed information from both field and laboratory studies are needed.

The fatty acid composition of *C. finmarchicus* at different depths could also provide more information on the vertical migration and dormancy of this copepod in the Trondheimsfjord. This zooplankton needs sufficient lipid storage to overcome dormancy and to undertake vertical upward migration, molting and the production of gonads [29]. A threshold lipid level is among several theories suggested as a trigger for vertical migration and dormancy in *C. finmarchicus* [30].

The aim of the present study was to study the lipid variations in *C. finmarchicus* from January to June, before and during the spring phytoplankton blooms, in the Trondheimsfjord. The copepods sampled from different depths were compared on the individual level with regard to fatty acid composition and size, and compared to the fatty acid profile of the phytoplankton present at the time of collection.

Materials and Methods

Sampling Procedure

Plankton samples were collected in 2009, 2010 and 2011 (Table 1) at a fixed position in the Trondheimsfjord (63°29'N 10°18'E) between 10:00 h and 14:00 h, from the vessel R/V Gunnerus. The sample location was chosen because it is fairly representative of the water masses in the main body of the fjord [31]. The samples were collected using a multiple opening and closing net system (patent no. NO318542, square opening 0.0625 m², 200- μ m mesh) mounted on a conductivity temperature depth instrument (CTD, Seabird Electronics Inc., USA). The multinet was hauled vertically and each separate net was opened and closed at selected depth intervals (440 (seabed)–300 m, 300–100 m, 100–50 m and 50–0 m) operated by an on-board control unit. The sampling was repeated three times for the subsequent analyses.

Samples for the determination of species, stage composition and enumeration for an estimate of abundance and stage composition were preserved with buffered formalin (4 %) in seawater and stored at room temperature.

Samples for lipid analysis of *C. finmarchicus* were collected as described above, but kept alive in containers with seawater until arrival at the laboratory for further subsampling (10 °C). Viable *C. finmarchicus* from each depth range (5–10 individuals), if available, were then transferred

Table 1 Overview of the sampling dates of copepods for lipid analyses and biometric measurements and the seston for lipid analyses in 2009–2011

Years	Month	Seston samples for lipid analyses	Copepod samples for lipid analyses	Copepod samples for biometric measurements
2009	Feb		23.02.09	
	March	13.03.09	30.03.09	
		17.03.09		
		24.03.09		
	April	01.04.09	27.04.09	
		22.04.09		
		28.04.09		
	May	19.05.09	18.05.09	
		25.05.09		
	June	03.06.09		
2010	Jan		26.01.10	
	Feb	28.02.10	18.02.10	18.02.10
	Mar	26.03.10	02.03.10	02.03.10
			15.03.10	
	Apr	07.04.10	06.04.10	
		28.04.10	28.04.10	
	May	18.05.10	18.05.10	18.05.10
	June	09.06.10		
2011	Jan		25.01.11	25.01.11
	Feb		14.02.11	
	Mar	09.03.11	07.03.11	
		15.03.11	22.03.11	
		29.03.11		
	Apr	07.04.11	26.04.11	
		05.05.11		
	May	09.05.11	09.05.11	
		30.05.11	30.05.11	
		20.06.11	20.06.11	20.06.11

to vials and stored at -80°C under a nitrogen atmosphere (N_2) until analysis.

Samples for biometric measurements using image analysis were collected as described above and kept in containers of seawater (approximately 20 L) until arrival at the laboratory for further processing. The containers were placed at 4°C ($\pm 2^{\circ}\text{C}$) until sampling for biometry.

Seston samples for lipid analysis (Table 1) of the surface water were obtained from seawater pumped from a depth of approximately 1.5 m into a reservoir. The water was screened through a plankton net (mesh size $200\ \mu\text{m}$) before feeding into a flow-through centrifuge by gravity at a flow rate of $0.65\text{--}0.85\ \text{L}\ \text{min}^{-1}$. The centrifuge was spun at 5,500 rpm, and the seston was removed from the centrifugal bowl ($D = 10.5\ \text{cm}$) at intervals. Samples for lipid and fatty acid analysis were immediately frozen and stored

at -80°C under N_2 . Water samples collected at 0, 3 and 10 m for the analysis of chlorophyll *a* (Chl *a*) were collected using Niskin water bottles (30 L), screened with a plankton net (nominal $200\ \mu\text{m}$) and kept in dark containers until filtration. The seston was harvested using Whatman GF/F glass fiber filters.

Analytical Procedure

Live *C. finmarchicus* were classified according to developmental stage under a dissecting microscope (Leica MZ6, Leica Microsystems GmbH, Wetzlar, Germany) based on morphological criteria [32] and size [33]. We did not separate *C. finmarchicus* from *C. helgolandicus* when sorting live copepods, but analyses of the curvature of the basiopod of the fifth pair of swimming legs in *Calanus* sp. from the fixed samples showed a very low abundance of *C. helgolandicus* (0–10 % compared to *C. finmarchicus*) [34, 35].

For biometric analysis *C. finmarchicus* was placed under a dissecting microscope (Leica MZ125, Leica Microsystems, GmbH, Wetzlar, Germany). Images were captured at fixed magnifications with a still-video camera (Sony DFW-SX900, Sony Corp, Japan) controlled by the software Fire-i v.3.01.0.111 (Unibrain Inc., San Diego, USA) operated by a computer after anesthetizing the copepods with tricaine methanesulfonate (FinquelTM, Argent Laboratories, Redmond, USA; 1.5 g/L stock solution in seawater) and orienting them in a fixed position. Biometric analysis of the copepods were done manually using the software ImageJ 1.43u (National Institutes of Health, Bethesda, USA) with the aid of a graphic tablet (Cintiq 12wx, Wacom Co. Ltd., Saitama, Japan). The volume of the oil sac and prosome was calculated according to Miller et al. [36] based on the measurement of the length of the prosome and oil sac as well as the corresponding area of the two compartments. The software was scaled by measuring an image on a calibration slide (E. Leitz, Wetzlar, Germany) captured at the same magnification as the copepods.

Chlorophyll *a* was extracted in methanol and quantified using a fluorometer (Turner Designs) according to Strickland and Parsons [37].

Total lipids of the seston were extracted and determined gravimetrically according to Bligh and Dyer [38] with modifications described by Jakobsen et al. [39]. Fatty acid methyl esters from extracted lipids were prepared according to Metcalfe et al. [40] and were analyzed in duplicate. A modified direct transmethylation procedure from Abdulkadir and Tsuchiya [41] was used to analyze the fatty acids of individual *C. finmarchicus*. Individual copepods were weighed (UMX2 Ultra-microbalance, Mettler Toledo, Columbus, USA), added to 0.5 mL isooctane with C19:0 as an internal standard (Nu-Chek Prep, Japan) followed by

0.2 mL 14 % BF_3 in methanol, and heated for 2 h (100 °C). The tube was cooled on ice, then 0.1 mL isooctane and 0.2 mL distilled water were added and mixed using a vortex mixer for 1 min. After centrifugation (1,640g, 3 min), the upper isooctane phase was transferred to vials and analyzed on a gas chromatograph (Perkin Elmer AutoSystem XL) running TotalChrom v.6.3.1 software (both Perkin Elmer Inc., Waltham, USA). The instrumental conditions were identical to those used in the study by Bergvik et al. [42]. Direct methylation for preparing the fatty acids of individual *C. finmarchicus* was validated by comparing with the conventional methods of Bligh and Dyer [38] and Metcalfe [40]. Five individuals of *C. finmarchicus* were analyzed by direct methylation and three batches with 10 individuals each were analyzed using the conventional method. Direct methylation showed a slightly higher content of total fatty acids compared to the conventional method, indicating that the method was more efficient at extracting fatty acids from *C. finmarchicus*.

Statistics

The Kolmogorov–Smirnov test was used to test for normality. Some groups of samples were not normally distributed even after log transformation, and the homogeneity of variances were not equal. Non-parametric analyses were therefore used for all the statistical analysis in this study. Kruskal–Wallis test was used to compare samples, and the Mann–Whitney *U* test was used to compare all samples for significant differences when the Kruskal–Wallis test indicated a significant difference ($P < 0.05$). The significance level for differences using the Mann–Whitney *U* test was adjusted with the Bonferroni correction and resulted in significance levels of $P < 0.008$ for six groups and $P < 0.013$ for four groups. The sample groups varied in size, and the lowest and highest number included in each group is specified in each figure. All statistical analyses were performed using SPSS Statistics v. 17.0 (SPSS Inc., Chicago, USA). Samples are presented as the mean and error bars indicate standard error of the mean (SEM). All figures were made using SigmaPlot v. 10.0 (Systat Software Inc., San Jose, USA).

Results

C. finmarchicus was sampled from January to June for 3 years (2009–2011) in the Trondheimsfjord at four different depth intervals. The concentration of chlorophyll *a* (Chl *a*) was also measured throughout the sampling period to follow phytoplankton biomass fluctuations. The females spawned early in the spring and the smaller stages of *C. finmarchicus* (copepodite stage 1–3) were registered in

April in all years of the study. The appearance of the smaller stages coincided with the maximum concentration of Chl *a*, although the Chl *a* concentration was low in 2010 compared to the other 2 years (Fig. 1a). The highest abundance of *C. finmarchicus* (sum of all stages) was observed in April

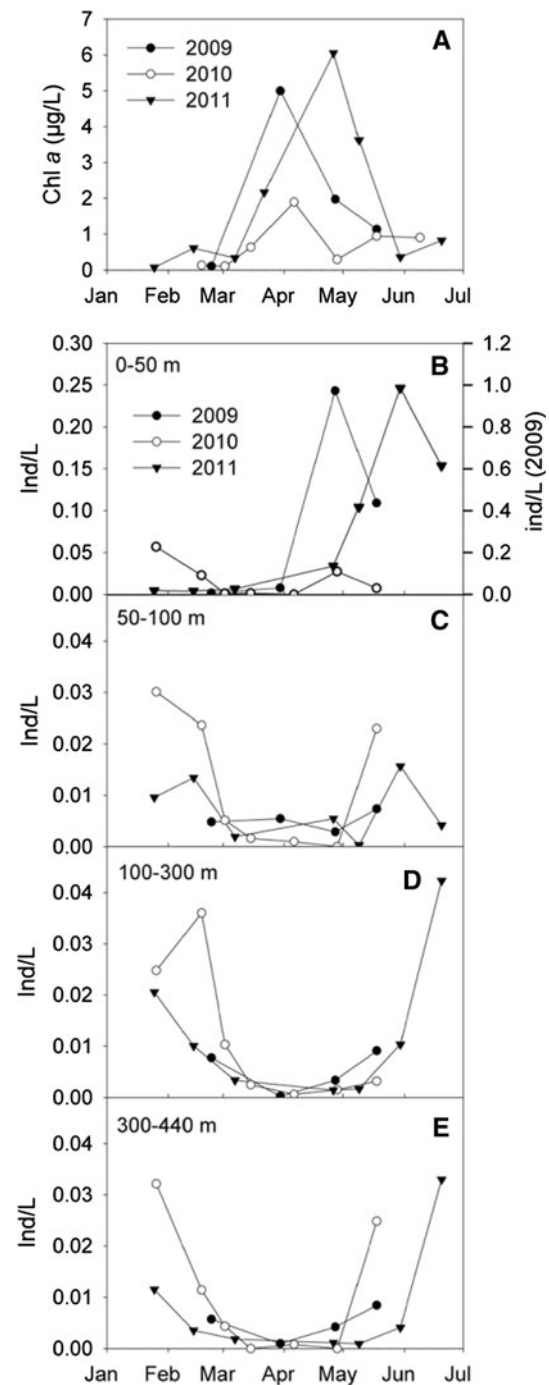


Fig. 1 Concentration of Chl *a* (µg/L) in the upper 10 m from January to June in 2009–2011 **a**. Abundance of *C. finmarchicus* (sum of copepodite stage 4 (C4), copepodite stage 5 (C5), females and males) (ind/L) at 0–50 m **b** from January to June in 2009–2011

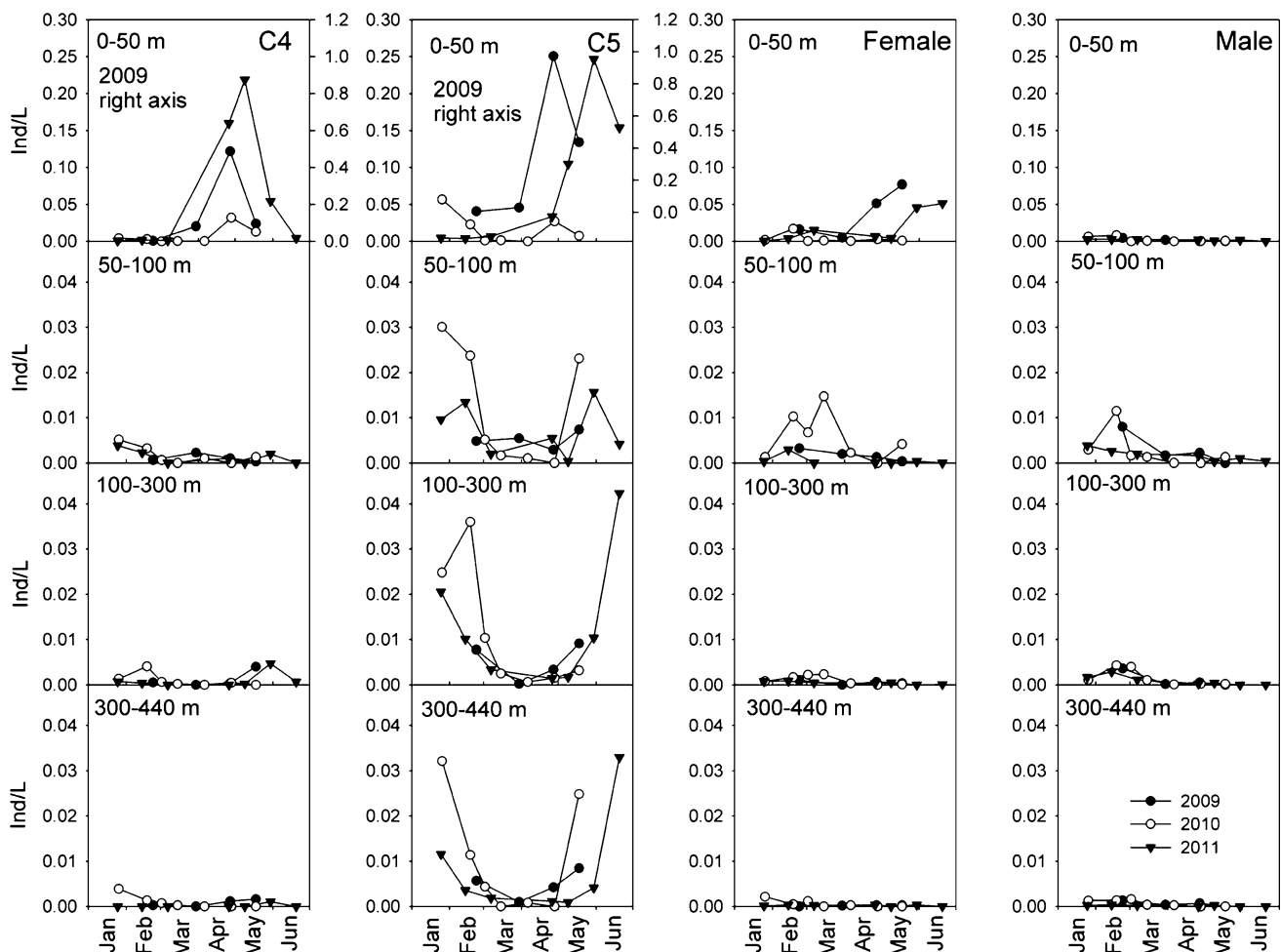


Fig. 2 Abundance of copepodite stage 4 (C4), copepodite stage 5 (C5), females (F) and males (M) (ind/L) at 0–50 m, 50–100 m, 100–300 m and 300–440 m from January to June in 2009–2011

and May in 2009 and 2011 (Fig. 1b), whereas there was a minimal number of *C. finmarchicus* in 2010, similar to the concentration of Chl *a*. The maximum numbers of *C. finmarchicus* were four times higher in 2009 compared to 2011. The concentration of chlorophyll *a* (Chl *a*) in the upper 10 m (Fig. 1a) was positively correlated with the abundance of *C. finmarchicus* in the upper 50 m; the phytoplankton bloom measured as Chl *a* was followed by an increase in the number of *C. finmarchicus*. The abundance of copepodite stage 4 (C4), copepodite stage 5 (C5), females and males (Fig. 2) in the surface (0–50 m) shows that C4 and C5 peaked in late April and May in all years. Following the peak of C5, there was a smaller peak of females, simultaneous with the increase in the number of C5 in deeper waters (50–440 m). The number of males was low and showed little variation, but a small increase was seen in February and March from a depth of 300 m to the surface. The females also showed a small increase in February and March. In January and February of all years, C5 resided mainly in intermediate and deeper layers, and were present

in low numbers in April and May, but increased again from May to June when some of the C5 started their migration to deeper layers. C5 was the dominant stage in the deepest layer. The variation between years in the numbers of C5 at intermediate depths and close to the seabed were not as pronounced, compared to the variation at the surface.

The total lipid content (Fig. 3a) and total fatty acid (TFA) content (Fig. 3b) of the seston showed pronounced variations both through the year and between years. The lipid content was highest in April 2009, in May 2010 and in June 2011 and ranged from 2 to 12 % dry weight (dw). TFA comprised on average 29 % of the total lipids.

The average content of total fatty acids (TFA, mg/g dw) in C5 from both 0–50 m (Fig. 4a) and 300–440 m (Fig. 4b) did not change considerably from January to June in 2009–2011. The dry weight per individual C5 in the upper 50 m increased steadily from February to June (Fig. 4c). The dry weight in January was higher compared to February, but not statistically different from that in April to June (Fig. 4c). The dry weight of C5 close to the seabed

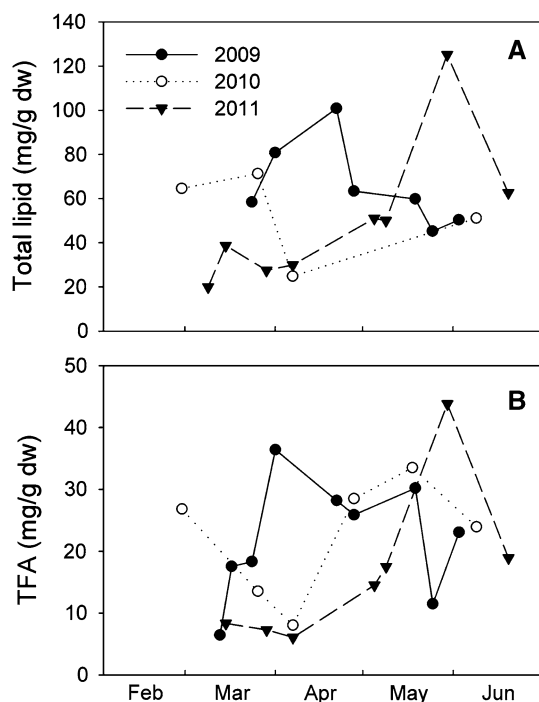


Fig. 3 Content of total lipids (mg/g dw) **a** and total fatty acids (TFA) (mg/g dw) **b** in the seston from March to June in 2009–2011

(300–440 m) also increased from January to May, but showed the same dry weight in June (Fig. 4d). The content of total fatty acids (TFA) per individual at the surface and close to the seabed showed a similar pattern of variation as the dry weight (Fig. 4e, f), and a correlation was found between individual dry weight and TFA content ($r_s = 0.87$, $N = 389$, $P < 0.001$) (Fig. 4g). The body volume of C5 also correlated with the oil sac volume ($r_s = 0.80$, $N = 393$, $P < 0.001$) (Fig. 4h). The dry weights of C5 were significantly lower at the surface (0–50 m) compared to both at intermediate depths and close to the seabed (Fig. 5a). The same trend was apparent for the mean body volume (Fig. 5b) and the individual content of TFA and the oil sac volume, which both increased from the surface toward deeper water layers (Fig. 5c, d).

The fatty acid composition of the seston showed a similar pattern of variation for all years, although with some variation between years (Fig. 6a). The dominant fatty acids in the seston were 22:6n-3, 20:5n-3, 18:4n-3, 16:1n-7, 18:1n-9, 18:0, 16:0 and 14:0. The fraction of the flagellate fatty acid, 18:4n-3 showed the highest variation between years, with a share of 18:4n-3 of 5 % in 2010 and 25 % in 2009. The content of the diatom fatty acid 16:1n-7 showed the same pattern in the spring in all 3 years, with a higher content in the middle of April and at the start of June.

The content of the n-3 polyunsaturated fatty acids (PUFA) 22:6n-3, 20:5n-3 and 18:4n-3 in the surface C5 individuals decreased from January to February, but

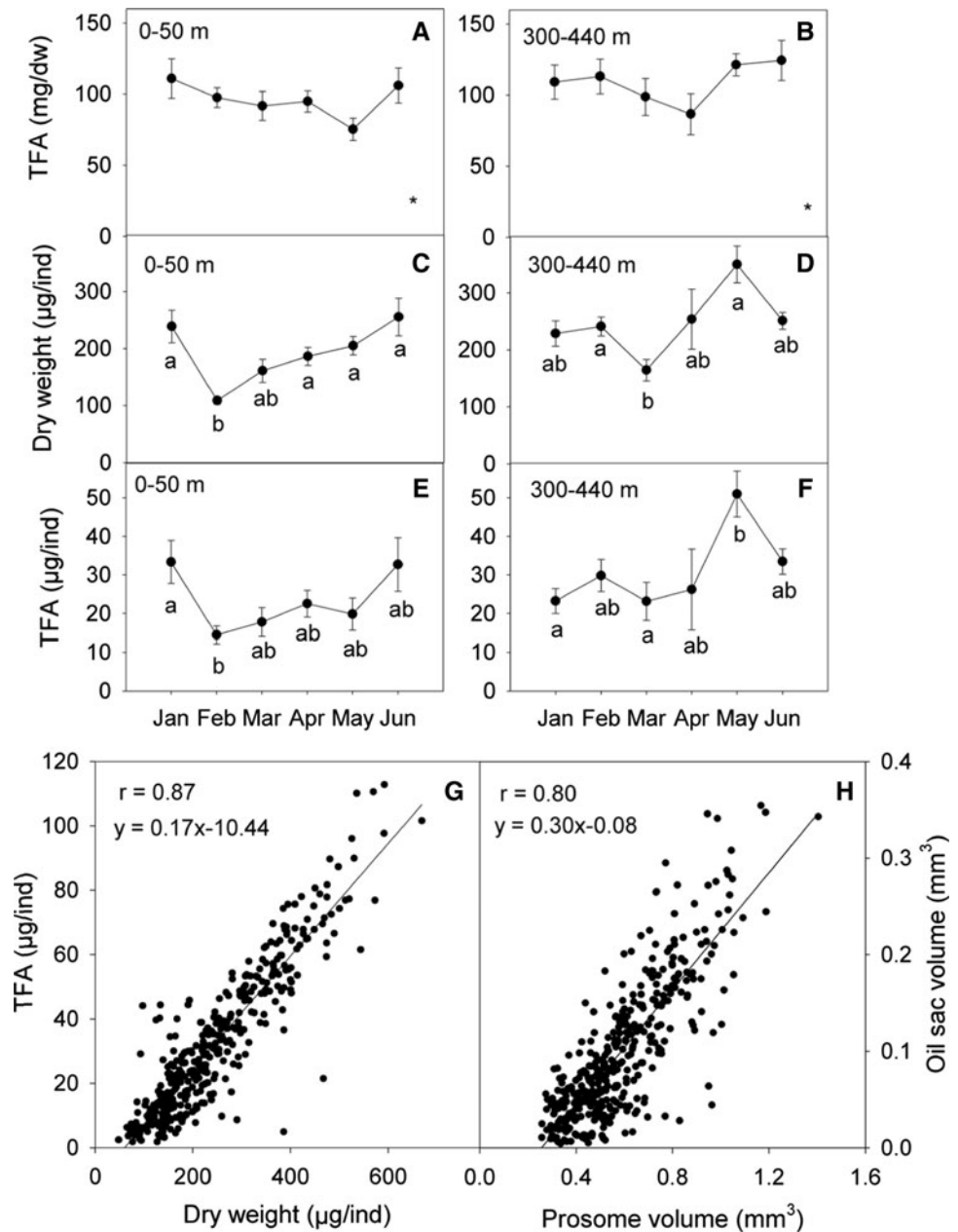
increased from February to March and remained relatively stable until June (Fig. 6b). The content of 16:1n-7, 18:1n-9, 14:0 and 16:0 decreased from January to February and increased again in June. The minor fatty acids constituting on average less than 1 % of TFA are not presented. The content of the different fatty acids in C5 close to the seabed (Fig. 6c) showed a general increase in fatty acids originating from the diet. The fatty acids 16:1n-7 and 18:4n-3 are fatty acids derived from diatoms and flagellates, respectively. Most evident was the increase in 18:4n-3 in April, May and June, reaching 13 % of TFA from zero, suggesting that surface C5 that had grazed on the spring bloom of phytoplankton had migrated toward the seabed. An increase was also seen in the content of 22:6n-3, 20:5n-3 and 16:1n-7 in May. The content of 18:1n-9, 14:0 and 16:0 showed no significant differences from January to June.

The content of 20:1n-9 and 22:1n-11 in C5 at the surface declined from January to February (Fig. 7a, c). From February to June, there were no changes in the content of these fatty acids at a depth of 0–50 m, but we found a higher level of 20:1n-9 and 22:1n-11 close to the seabed (Fig. 7b, d). There was a significant increase in 20:1n-9 and 22:1n-11 from the surface to deeper waters (Fig. 7e).

The fraction of n-3 PUFA of TFA (Fig. 8a) in C5 *C. finmarchicus* declined from January to February, followed by a 61 % increase in March. The percentage composition remained unchanged until a decline took place in June. The decline from January to February was caused by a reduced content of 18:4n-3, while the contents of the fatty acids 20:5n-3 and 22:6n-3 did not change. The fatty acid 20:5n-3 was the cause of the considerable increase in n-3 PUFA from February to March, while 22:6n-3 gradually increased until May. The proportion of mono-unsaturated fatty acids (MUFA) (Fig. 8b) in C5 decreased slightly from January to April, after which it remained unchanged. The percentage content of 20:1n-9 and 16:1n-7 did not change much over this period, but the proportion of 22:1n-11 showed a similar pattern of variation over time as MUFA.

The dry weights of C5 at each depth in the individual months are shown in Fig. 9a. Similar for all months except March, the smallest amounts of C5 were found at the surface, and the largest amounts were found at intermediate depths in January and June. The dynamics of 18:4n-3, 20:5n-3 and 22:6n-3 are shown in Fig. 9b. In January, the content of 18:4n-3 was low at all depths, while the content of 20:5n-3 and 22:6n-3 was higher and stable. In February, the content of these fatty acids decreased at all depths; this pattern was also seen with dry weight and lipid content (Fig. 9a). In March, the same fatty acids increased at the surface as fatty acids became available in the seston. In April, there was an increase in 18:4n-3, 20:5n-3 and 22:6n-3 in the intermediate layers, which could indicate the vertical migration of some C5 from the surface. In May, these fatty acids also

Fig. 4 Average total fatty acids ($\mu\text{g/g dw}$) in *C. finmarchicus* C5 in 0–50 m (a) and 300–440 m (b) from January to June in 2009–2011. Average dry weight ($\mu\text{g/ind}$) of *C. finmarchicus* C5 at 0–50 m c and 300–440 m (d) from January to June in 2009–2011. Average total fatty acids ($\mu\text{g/ind}$) in *C. finmarchicus* C5 at 0–50 m e and 300–440 m (f) from January to June in 2009–2011. Correlation ($r_s = 0.91$, $p < 0.001$, $N = 389$) between dry weight ($\mu\text{g/ind}$) and TFA ($\mu\text{g/ind}$) in all *C. finmarchicus* C5 in this study (g). Correlation ($r_s = 0.80$, $p < 0.001$, $N = 393$) between prosome volume (mm^3) and oil sac volume (mm^3) in all *C. finmarchicus* C5 with biometric measurements (h). Lower case letters indicate significant differences and stars indicate no significant difference. The sample sizes in a, c and e ranged from 10 to 36 individuals, and in b, d and f the sample sizes ranged from 5 to 20 individuals



increased in the deepest layer. The content of the fatty acids 20:1n-9 and 22:1n-11 in C5 (Fig. 9c) was lower at the surface in all months. The content at the surface decreased from January to February, but remained high in deeper layers. In March, the content of 20:1n-9 and 22:1n-11 also decreased in deeper layers. In April and May, the content of these fatty acids increased in deeper layers, but remained low at the surface.

Discussion

The content of lipids and fatty acids in C5 of *C. finmarchicus* in the present work revealed an interaction between

phytoplankton and *C. finmarchicus*, and that lipid and fatty acid accumulation in C5 could be the trigger for vertical migration in the spring. Several theories on the mechanism that triggers the onset of dormancy in *C. finmarchicus* have been suggested, in which food availability, temperature, photoperiod and lipid accumulation are among the suggested cues for entering dormancy [30, 43, 44]. In the present study, there was an increased abundance of C5 in deep waters (300–440 m) in May, indicating the start of vertical migration. We found that the individual size of C5 in surface waters was smaller than the individuals from deep waters, as found in previous studies [5, 45]. The total fatty acid content and volume of the oil sac of C5 also increased from the surface waters toward deeper waters.

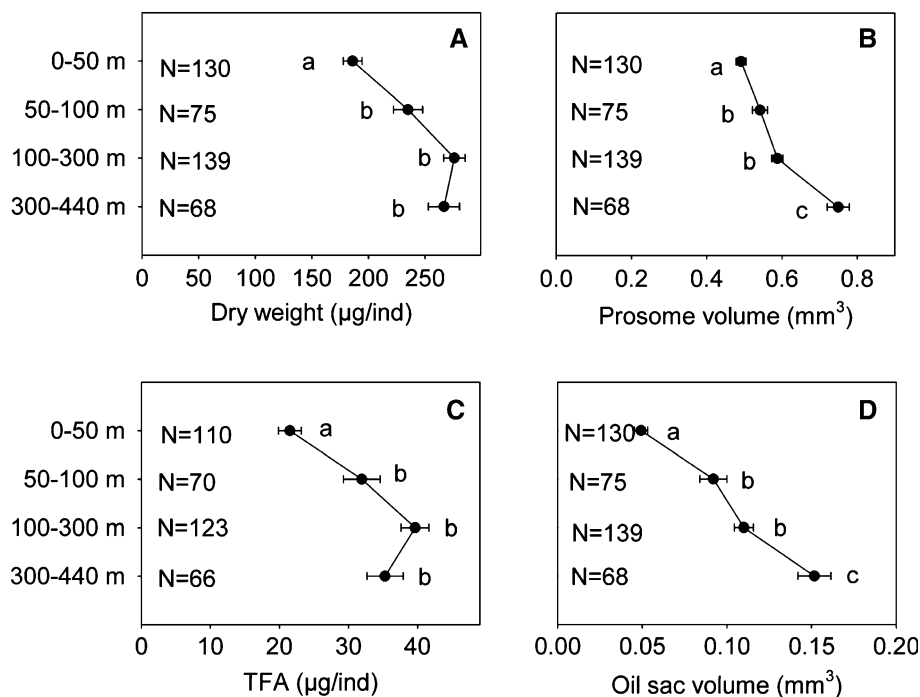
This has been observed previously for both C5 [29, 46, 47] and females [48], and Hirche [45] found larger C5 in deep waters compared to those residing in surface waters. *C. finmarchicus* is dependent on a large lipid reserve to survive dormancy, undertake upward migration, and to have enough energy for molting and gonad formation [29]. The size and lipid content at each depth in May increased both in the deepest layer as compared to the values in April. This suggests that C5 that migrating toward deeper layers had a higher lipid content and were bigger compared to the C5 remaining in the surface waters. The lipid level could thus be the trigger for vertical migration and the onset of dormancy, as discussed by Irigoien [30].

The fatty acid composition of C5 stages of *C. finmarchicus* can also contribute to a better understanding of the onset of dormancy and the relationship between *C. finmarchicus* and the phytoplankton present. The fatty acids of the seston clearly showed the signature fatty acids of diatoms and flagellates over the season (16:1n-7 and 18:4n-3 respectively), revealing a bloom of diatoms at the end of March and a bloom of flagellates at the beginning of June. Sakshaug and Mykkestad [21] found a bloom of diatoms in the Trondheimsfjord at the end of March both in 1970 and in 1971. Spring blooms of dinoflagellates were highly variable between the 2 years of their study, but dinoflagellate blooms followed the diatom blooms in both years. *C. finmarchicus* feeds mainly on phytoplankton, and the signature fatty acids of phytoplankton are directly incorporated in their wax esters [25, 49]. We found that 22:6n-3, 20:5n-3, 18:4n-3 and 16:1n-7 were the dominant fatty acids

Fig. 6 Composition of fatty acids (% of TFA) in the seston (a) from March to June in 2009–2011. Average content of fatty acids ($\mu\text{g}/\text{ind}$) in *C. finmarchicus* C5 from January to June at 0–50 m (b) and 300–440 m (c). In addition to 20:1n-9 and 22:1n-11, the composition of these fatty acids was on average over 1 % of TFA in *C. finmarchicus*. Lower case letters indicate significant differences and stars indicate no significant difference. The sample sizes in b ranged from 10 to 28 individuals and in c the sample sizes ranged from 5 to 19 individuals

from the phytoplankton that were incorporated into the C5 of *C. finmarchicus*. The increase in these fatty acids in *C. finmarchicus* was thereby related to the available fatty acids in the seston, indicating that both diatoms and dinoflagellates were important components of their diet. The importance of diatoms and flagellates in the diet of *C. finmarchicus* revealed as an increased content of the signature fatty acids (16:7n-1 and 18:4n-3 for diatoms and flagellates respectively), have been shown in several studies [47, 50]. The increase in the main n-3 PUFA, 18:4n-3, 20:5n-3 and 22:6n-3, in the deep waters close to the seabed was pronounced in May, suggesting that the deep water C5 had recently fed on phytoplankton at the surface. Most prominent was the content of 18:4n-3, which was nearly absent in January to March close to the seabed, but then reached 15 % of TFA in May. The content of 18:4n-3 and 20:5n-3 was in fact higher in C5 from deep waters compared to those in surface waters. This might suggest that when C5 copepods at the surface reach a certain content of wax esters after the accumulation of phytoplankton, they will migrate toward deeper waters. The onset of migration was about 1 month after the

Fig. 5 Average dry weight ($\mu\text{g}/\text{ind}$) (a), prosome volume (mm^3) (b), TFA ($\mu\text{g}/\text{ind}$) (c) and oil sac volume (mm^3) (d) in *C. finmarchicus* C5 at 0–50 m, 50–100 m, 100–300 m and 300–440 m. Lower case letters indicate significant differences and stars indicate no significant difference. *N* equals the number of replicates



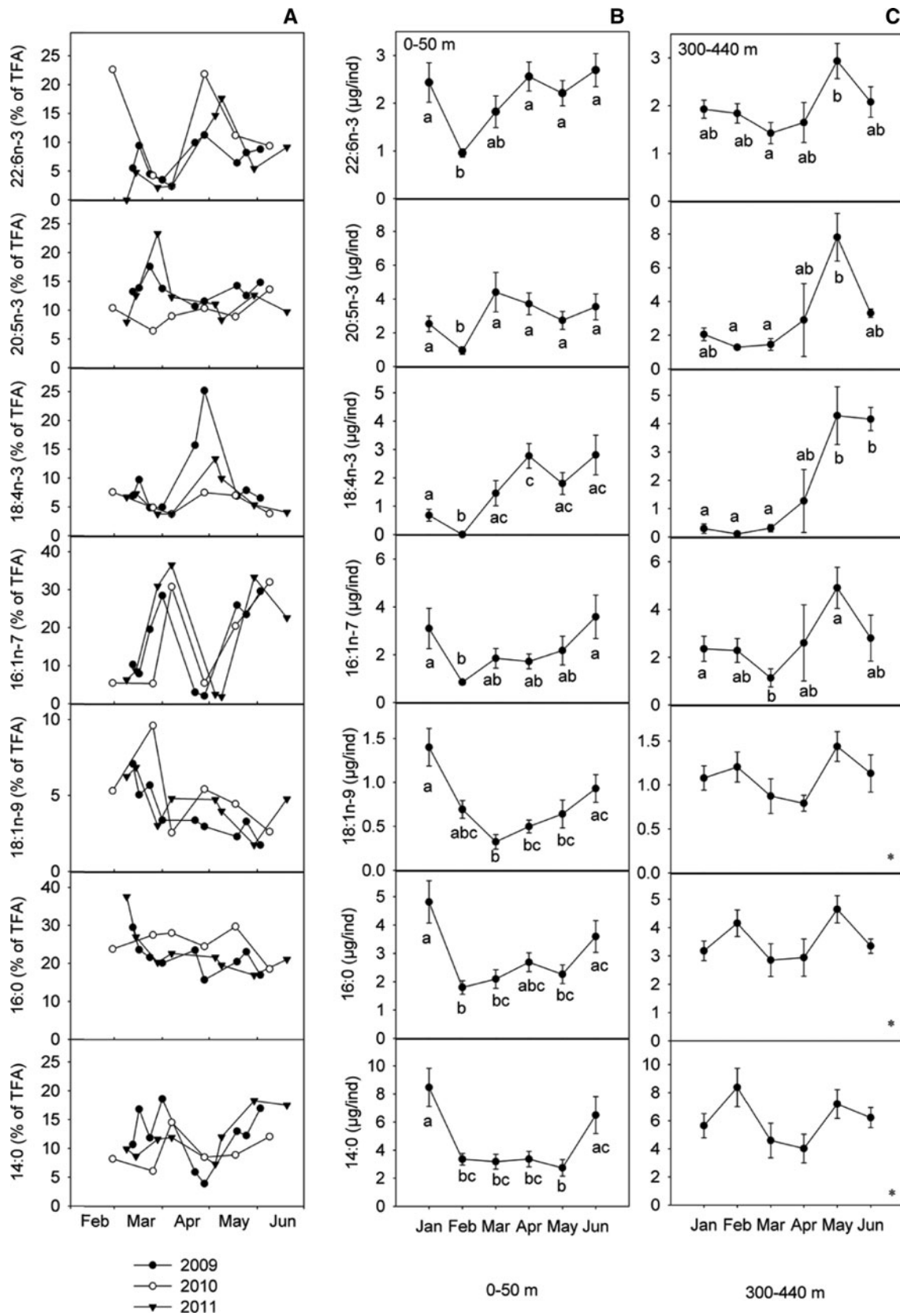
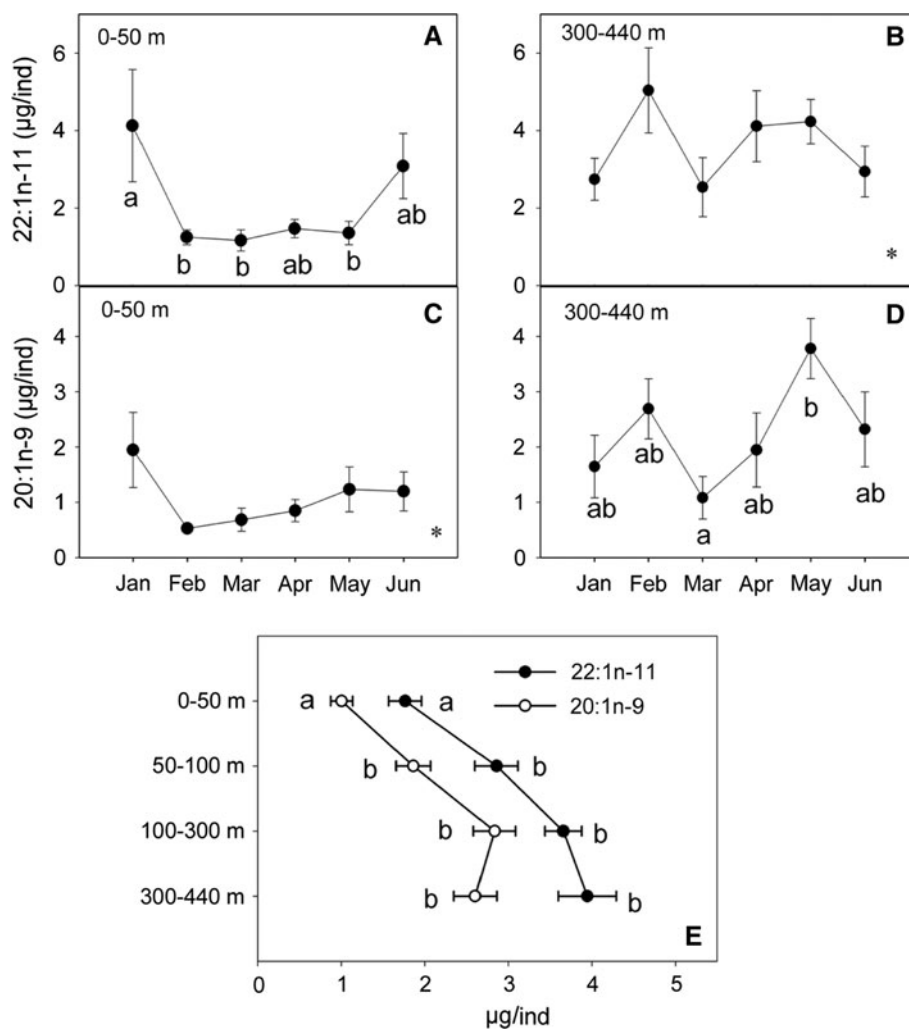


Fig. 7 Average content of the fatty acid 22:1n-11 in *C. finmarchicus* C5 from January to June through 0–50 m (a) and 300–440 m depth (b). Average content of the fatty acid 20:1n-9 in *C. finmarchicus* C5 from January to June through 0–50 m (c) and 300–440 m depth (d). Average content of 20:1n-9 and 22:1n-11 in C5 through all depths: 0–50 m, 50–100 m, 100–300 m and 300–440 m. Lower case letters indicate significant differences and star indicates no significant difference. The sample sizes in a and c ranged from 10 to 28 individuals, in b and d the sample sizes ranged from 5 to 19 individuals and in e the sample sizes ranged from 66 to 123 individuals



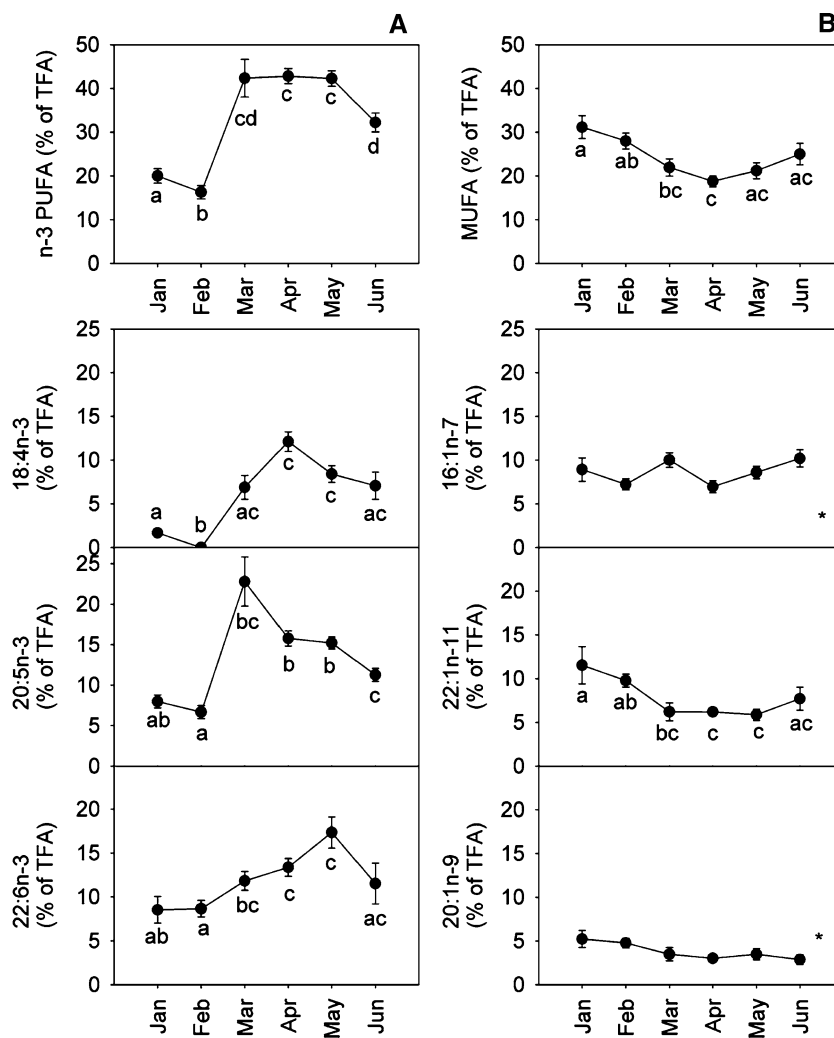
phytoplankton bloom, suggesting a strong link between the production of phytoplankton, lipid accumulation and the onset of migration.

Although some C5 descended to deeper waters in May, there was a concurrent increase in the number of females at the surface. This could indicate that while some C5 start their vertical migration, others molt to females, and was also found in the Irminger Sea [47]. We suggest that the lipid content will decide whether a C5 will migrate or molt. If the lipid content is above a certain level, the C5 will descend to deeper waters. If the requisite lipid level has not been reached, the C5 will molt to females which will start a new generation of *C. finmarchicus*. Miller et al. [36] found that large C5 in the surface waters in December molted to females while the smaller C5 remained in surface waters waiting for food until March, when they again found larger C5 which they attributed to a new generation of C5. The results from our study suggest that lipid accumulation has a strong connection with the onset of dormancy. Johnson et al. [51] did not find an environmental factor that

explained the onset of dormancy in *C. finmarchicus*, and suggested that lipid accumulation could be an explanation.

In our study, most of the fjord population of *C. finmarchicus* had ascended to the surface by March. C5 stages of *C. finmarchicus* that have ascended from deeper water will probably use their lipid reserves to molt into adults and develop gonads. Gatten et al. [52] showed that one half of the wax ester reserves in *C. helgolandicus* were utilized when C5 matured to females and formed gonads. Jonasdottir [29] also suggested that the main part of the lipid reserve was used for vertical migration and gonad formation in *C. finmarchicus*. The lipid content and the size of C5 in our study decreased from January to February, but this could also be the result of a lack of food at the surface. Copepods in surface waters have been shown to have a higher energy demand compared to copepods in deeper waters [5] because metabolism is slow during dormancy in deeper water [45]. Therefore, *C. finmarchicus* would have to catabolize wax esters to meet increased energy demand at the surface [53]. Other authors have also found a

Fig. 8 Fraction of n-3 polyunsaturated fatty acids (PUFA) (a) and monounsaturated fatty acids (MUFA) (% of TFA) (b) in *C. finmarchicus* C5 at 0–50 m from January to June in 2009–2011. The main n-3-PUFA and MUFA are also included. Lower case letters indicate significant differences and stars indicate no significant difference. The sample sizes in a and b ranged from 10 to 28 individuals

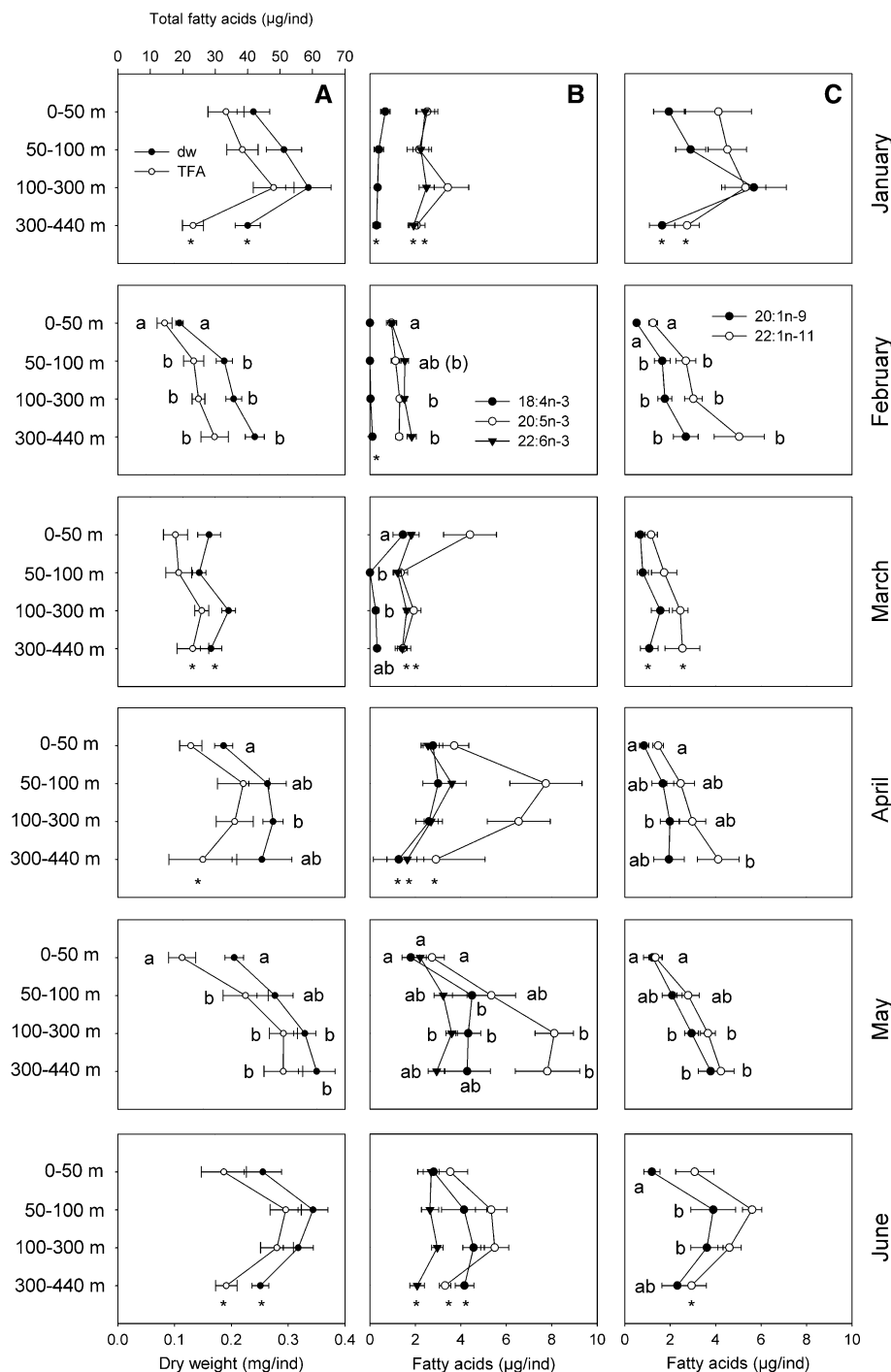


decrease in size and lipid content, but this occurred from December to January [29, 54, 55] and from February to May [46]. Irigoien et al. [56] also found a decrease in the carbon content of *C. finmarchicus* before the spring bloom appeared. Our data show a small increase in females at the surface and in intermediate waters and an increase in males in intermediate waters in February. We suggest that lipid-rich C5 ascend to the surface water and molt into females, while the remaining C5, with a lower lipid content, must wait for phytoplankton production in order to molt. The difference in the time of lipid depletion in the studies mentioned above could have been the result of different locations of study, which could result in a shift in the time for upward migration. An earlier upward migration would lead to an earlier depletion of lipids. Females have been shown to produce eggs prior to the phytoplankton bloom [57], suggesting that the lipid reserves are used for the production of eggs. However, Koski et al. [58] have shown that the fatty acid profile of eggs from *C. finmarchicus* resembled the fatty acid profile of the seston. The smaller copepodite stages (CI–CIII) were observed in April in all

3 years of our study, coincident with the phytoplankton bloom, suggesting that egg production took place before the phytoplankton bloom. The new generation of C5 may be present as soon as late April, given that a sufficient amount of food is present.

The content of the fatty acids 20:1n-9 and 22:1n-11 in individual C5 at the surface was low, but the content was significantly higher closer to the seabed. When *C. finmarchicus* accumulates energy reserves as wax esters in the spring, the formation of fatty alcohols is a necessary step of that synthesis. The proposed route of biosynthesis for fatty alcohols is the synthesis of fatty acids and further conversion of fatty acids into fatty alcohols by fatty acyl coenzyme A oxido-reductase [20, 59]. The production of wax esters by copepods is in fact thought to be limited by this synthesis of fatty alcohols from fatty acids [59, 60]. *C. finmarchicus* contains high amounts of the fatty alcohols 20:1n-9 and 22:1n-11 [27, 28, 61]. The fatty acids 20:1n-9 and 22:1n-11 are synthesized first with subsequent reduction to the corresponding fatty alcohols during lipid accumulation. The content of these fatty acids was scarce

Fig. 9 Dry weight (mg/ind), total fatty acids (TFA, $\mu\text{g}/\text{ind}$) (a), content of 18:4n-3, 20:5n-3 and 22:6n-3 ($\mu\text{g}/\text{ind}$) (b) and content of 20:1n-9 and 22:1n-11 ($\mu\text{g}/\text{ind}$) (c) in C5 of *C. finmarchicus* at 0–50 m, 50–100 m, 100–300 m and 300–440 m from January to June. Note the two *x*-axes in a, where dry weight is indicated by the lower *x*-axis and TFA is indicated by the upper *x*-axis. All numbers are the average of values from 2009 to 2011. The sample sizes ranged from 10 to 15 in January, 13–25 in February, 12–26 in March, 5–27 in April, 19–36 in May and 5–10 in June



during the phase of lipid accumulation in surface waters in the present study, and we can assume that all of the synthesized 20:1n-9 and 22:1n-11 was converted to the fatty alcohols 20:1n-9 and 22:1n-11. When *C. finmarchicus* descends to deeper waters, the copepods have accumulated enough wax esters to enter dormancy and to hibernate through the winter. They no longer require biosynthesis of fatty alcohols and they may instead accumulate the fatty acids 20:1n-9 and 22:1n-11 in their wax esters. The present

study shows that the content of long-chain MUFA increases in copepods at depths of 50–100 m and more.

The fatty acids 20:1n-9 and 22:1n-11 are thought to be synthesized de novo from carbohydrate- and protein precursors [6] with the intermediates 14:0, 16:0 and 18:0, which are further elongated and desaturated to form 20:1n-9 and 22:1n-11. Also, Henderson and Sargent [62] have shown that the carnivorous copepod *Euchaeta norvegica* uses glucose and amino acids in the de novo biosynthesis

of fatty alcohols. In the present study, 14:0, 16:0 and 18:0 were present in the phytoplankton at high levels, e.g. the content of 18:0 was 20 % of TFA in March and April and the content of 14:0 and 16:0 was on average 30–50 % of TFA throughout the sampling period. The content of these fatty acids in the copepods, however, did not increase from February to May and the content of 18:0 was scarce. At the same time, the contents of 18:4n-3, 20:5n-3 and 22:6n-3 in the copepods increased, suggesting that phytoplankton was ingested. The saturated fatty acids 14:0 and 16:0 could then either be catabolized for energy or they could be used as precursors for fatty alcohol synthesis of the longer mono-unsaturated fatty alcohols, 14:0 and 16:0. Some evidence of the incorporation of dietary 14:0 into wax esters has been provided, as well as incorporation into fatty alcohol in *C. helgolandicus* [60]. Sargent and Falk-Petersen [53] suggested the possibility of a further elongation of dietary 14:0 and 16:0, but no evidence was found to support this. Graeve et al. [63] showed that *C. finmarchicus* retained PUFA from a ^{13}C labeled diatom diet, and converted 16:1n-7 from the diet to the corresponding fatty alcohol. This suggests that *C. finmarchicus* selectively accumulates and retains fatty acids in accordance with its metabolic requirements [63]. Sargent and Falk-Petersen [53] also suggested the possibility that the synthesis of wax esters is a flexible system in such a way that zooplankton can switch de novo synthesis in relation to a variable diet.

The individual content of 20:5n-3 and 22:6n-3 decreased from January to February, while the content of the same fatty acids per dry weight was unchanged. From February to March, there was a significant increase in 20:5n-3 and a tendency for an increase in 22:6n-3. The phytoplankton in the surface water contained high fractions of 20:5n-3 and low fractions of 22:6n-3, in agreement with the different increase of these fatty acids in copepods. Phospholipids in *C. finmarchicus* consist mainly of 20:5n-3 and 22:6n-3 in a 1:2 ratio [8, 64]. 22:6n-3 is an essential fatty acid that is important for maintaining specific cellular functions, and Scott et al. [65] have discussed 22:6n-3 as an important factor in the mobility and migration of *C. finmarchicus*. This fatty acid has also been shown to be important in the reproductive capability of copepods [66]. Marine copepods have shown poor capability for the synthesis of 22:6n-3 and 20:5n-3, but the need for n-3 PUFA is vital in their phospholipids and for reproduction. Bell et al. [67] showed that female *C. finmarchicus* have a poor ability to convert 18:3n-3 to 20:5n-3 and 22:6n-3, but this does not rule out the possibility that *C. finmarchicus* can synthesize 22:6n-3 if requirements are not met through the diet. Koski et al. [58] showed that the fatty acid composition of *Calanus* eggs reflected the diet of the females, and furthermore suggested that hatching success was limited by the lipid or PUFA content in the

eggs. This further supports the idea that these specimens did not have the ability to efficiently synthesize n-3 PUFA. Nutritional studies on *C. finmarchicus* should be performed in order to better understand lipid metabolism in this species and the importance of 20:5n-3 and 22:6n-3 during ontogenic development.

We suggest that *C. finmarchicus* could be a new source of marine raw material in the future. *C. finmarchicus* is abundant in surface waters in the spring and summer when phytoplankton or other potential zooplankton food is present, and can be found in very high concentrations. This short time-window is the most likely period for commercial harvest. The content of n-3 fatty acids in *C. finmarchicus* will vary considerably depending on the phytoplankton present during this period. The content of 20:5n-3 will be most dominant during the diatom bloom, and the content of 18:4n-3 and 22:6n-3 will increase later in the spring, caused by a bloom of diatoms and other flagellates (e.g. *Phaeocystis pouchetii*). The content of wax esters will also increase during the spring, indirectly shown as an increase in total fatty acids in the present work. We suggest that C5 will start their vertical migration when a significant lipid level has been reached, and that C5 with lower lipid levels after the phytoplankton bloom will molt to females at the surface and start a new generation. The vertical migration of C5 is in May in the Trondheimsfjord, and a possible harvest should exploit *C. finmarchicus* in the period when it is most abundant and before the majority of the copepods descend to deeper water. However, the concentration of *C. finmarchicus* at the surface can vary greatly between years in the Trondheimsfjord, which may also be the case in other fjords. When this copepod is present in low numbers in a fjord, harvesting can have an impact on the predators of zooplankton, and harvesting of a sparse population would probably not be sustainable. However, when *C. finmarchicus* is abundant, harvesting could even be a positive input for the population, leaving more food for the remaining stock. Our results suggest that fjords are not a suitable harvesting area for *C. finmarchicus*, at least not when the abundance is low.

Acknowledgments This work was supported by the Norwegian Research Council (projects 172641/S40 and 178447). Thanks to the crew of R/V Gunnerus for assisting with sampling and to Ida Fines for performing the biometric analysis. We wish to thank the anonymous reviewers and the associate editor who helped with improving the manuscript.

References

1. Planque B, Batten SD (2000) *Calanus finmarchicus* in the North Atlantic: the year of *Calanus* in the context of interdecadal change. ICES J Mar Sci 57:1528–1535. doi:10.1006/jmsc.2000.0970

2. Aksnes DL, Blindheim J (1996) Circulation patterns in the North Atlantic and possible impact on population dynamics of *Calanus finmarchicus*. *Ophelia* 44:7–28
3. Tande KS, Hopkins CCE (1981) Ecological investigations of the zooplankton community of Balsfjorden, Northern Norway: The genital system in *Calanus finmarchicus* and the role of gonad development in overwintering strategy. *Mar Biol* 63:159–164. doi:10.1007/bf00406824
4. Diel S, Tande K (1992) Does the spawning of *Calanus finmarchicus* in high latitudes follow a reproducible pattern? *Mar Biol* 113:21–31. doi:10.1007/bf00367634
5. Marshall SM and Orr AP (1955) *The Biology of a Marine Copepod*. Oliver & Boyd Ltd., London, pp 81–96
6. Sargent JR, Gatten RR, Henderson RJ (1981) Marine Wax Esters. *Pure Appl Chem* 53:867–871. doi:10.1351/pac198153040867
7. Fraser AJ, Sargent JR, Gamble JC (1989) Lipid class and fatty-acid composition of *Calanus finmarchicus* (Gunnerus), *Pseudocalanus* sp and *Temora longicornis* Muller from a nutrient-enriched seawater enclosure. *J Exp Mar Biol Ecol* 130:81–92. doi:10.1016/0022-0981(89)90020-8
8. Farkas T, Storebakken T, Bhosie NB (1988) Composition and physical state of phospholipids in calanoid copepods from India and Norway. *Lipids* 23:619–622. doi:10.1007/BF02535608
9. Evjemo JO, Reitan KI, Olsen Y (2003) Copepods as live food organisms in the larval rearing of halibut larvae (*Hippoglossus hippoglossus* L.) with special emphasis on the nutritional value. *Aquaculture* 227:191–210. doi:10.1016/S0044-8486(03)00503-9
10. FAO (2008) *The state of world fisheries and aquaculture 2008*. Food and agricultural organization of the United Nations
11. Turchini GM, Torstensen BE, Ng W (2009) Fish oil replacement in finfish nutrition. *Rev Aquac* 1:10–57. doi:10.1111/j.1753-5131.2008.01001.x
12. Olsen Y (2011) Resources for fish feed in future mariculture. *Aquac Environ Interact* 1:187–200. doi:10.3354/aei00019
13. Olsen RE, Henderson RJ, Sountama J, Hemre G, Ringo E, Melle W, Tocher DR (2004) Atlantic salmon, *Salmo salar*, utilizes wax ester-rich oil from *Calanus finmarchicus* effectively. *Aquaculture* 240:433–449. doi:10.1016/j.aquaculture.2004.07.017
14. Hynes N, Egeland ES, Koppe W, Baardsen G, Kiron V (2009) *Calanus* oil as a natural source for flesh pigmentation in Atlantic salmon (*Salmo salar* L.). *Aquac Nutr* 15:202–208. doi:10.1111/j.1365-2095.2008.00584.x
15. Oxley A, Bøgevik AS, Henderson RJ, Waagbø R, Tocher DR, Olsen RE (2009) Digestibility of *Calanus finmarchicus* wax esters in Atlantic salmon (*Salmo salar*) freshwater psmolts and seawater postsmolts maintained at constant water temperature. *Aquac Nutr* 15:459–469. doi:10.1111/j.1365-2095.2008.00611.x
16. Bøgevik AS, Tocher DR, Langmyhr E, Waagbø R, Olsen RE (2009) Atlantic salmon (*Salmo salar*) postsmolts adapt lipid digestion according to elevated dietary wax esters from *Calanus finmarchicus*. *Aquac Nutr* 15:94–103. doi:10.1111/j.1365-2095.2008.00571.x
17. Tocher DR, Bendiksen EA, Campbell PJ, Bell JG (2008) The role of phospholipids in nutrition and metabolism of teleost fish. *Aquaculture* 280:21–34. doi:10.1016/j.aquaculture.2008.04.034
18. Sargent JR, Tocher DR, Bell JG (2002) The lipids. In: John EH, Ronald WH (eds) *Fish nutrition*, 3rd edn. Academic Press, San Diego
19. Larsen R, Eilertsen K-E, Elvevoll EO (2011) Health benefits of marine foods and ingredients. *Biotechnol Adv* 29:508–518. doi:10.1016/j.biotechadv.2011.05.017
20. Sargent JR, Henderson RJ (1986) Lipids. In: Corner EDS, O'Hara SCM (eds) *The biological chemistry of marine copepods*. Oxford University Press, Oxford
21. Sakshaug E, Myklesstad S (1973) Studies on the phytoplankton ecology of the trondheimsfjord. III. Dynamics of phytoplankton blooms in relation to environmental factors, bioassay experiments and parameters for the physiological state of the populations. *J Exp Mar Biol Ecol* 11:157–188. doi:10.1016/0022-0981(73)90053-1
22. Kates M, Volcani BE (1966) Lipid components of diatoms. *Biochim Biophys Acta* 116:264–278. doi:10.1016/0005-2760(66)90009-9
23. Harrington GW, Beach DH, Dunham JE, Holz GG (1970) The polyunsaturated fatty acids of marine Dinoflagellates. *J Eukaryot Microbiol* 17:213–219. doi:10.1111/j.1550-7408.1970.tb02359.x
24. Reitan KI, Rainuzzo JR, Olsen Y (1994) Effect of nutrient limitation on fatty acid and lipid content of marine microalgae. *J Phycol* 30:972–979. doi:10.1111/j.0022-3646.1994.00972.x
25. Lee RF, Barnett AM, Hirota J (1971) Distribution and importance of wax esters in marine copepods and other zooplankton. *Deep-Sea Res Oceanogr Abstr* 18:1147–1165. doi:10.1016/0011-7471(71)90023-4
26. Sargent JR (1978) Marine wax esters. *Sci Prog* 65:437–458
27. Kattner G, Krause M (1989) Seasonal variations of lipids (wax esters, fatty-acids and alcohols) in calanoid copepods from the North Sea. *Mar Chem* 26:261–275. doi:10.1016/0304-4203(89)90007-8
28. Falk-Petersen S, Sargent JR, Tande KS (1987) Lipid composition of zooplankton in relation to the sub-arctic food web. *Polar Biol* 8:115–120. doi:10.1007/BF00297065
29. Jónasdóttir SH (1999) Lipid content of *Calanus finmarchicus* during overwintering in the Faroe-Shetland Channel. *Fish Oceanogr* 8:61–72. doi:10.1046/j.1365-2419.1999.00003.x
30. Irigoien X (2004) Some ideas about the role of lipids in the life cycle of *Calanus finmarchicus*. *J Plankton Res* 26:259–263
31. Tokle NE (2006) Are the ubiquitous marine copepods limited by food or predation? Experimental and field-based studies with main focus on *Calanus finmarchicus*, in Department of Biology, Norwegian University of Science and Technology, Trondheim
32. Mauchline J (1998) The biology of calanoid copepods. In: Blaxter JHS, Southward AJ, Tyler PA (eds) *Advances in marine biology*, vol 33. Academic Press, San Diego
33. Unstad KH, Tande KS (1991) Depth distribution of *Calanus finmarchicus* and *Calanus glacialis* in relation to environmental conditions in the Barents sea. *Polar Res* 10:409–420
34. Frost BW (1974) *Calanus marshallae*, a new species of calanoid copepod closely allied to the sibling species *C. finmarchicus* and *C. glacialis*. *Mar Biol* 26:77–99. doi:10.1007/bf00389089
35. Fleminger A, Hulsemann K (1977) Geographical range and taxonomic divergence in North Atlantic *Calanus* (*C. helgolandicus*, *C. finmarchicus* and *C. glacialis*). *Mar Biol* 40:233–248. doi:10.1007/bf00390879
36. Miller CB, Morgan CA, Prah FG, Sparrow MA (1998) Storage lipids of the copepod *Calanus finmarchicus* from Georges Bank and the Gulf of Maine. *Limnol Oceanogr* 43:488–497
37. Strickland JDH, Parsons TR (1972) *A practical handbook of seawater analysis*, 2nd edn. Bulletin 167, Fisheries Research Board of Canada, Ottawa
38. Bligh EG, Dyer WJ (1959) A rapid method of total lipid extraction and purification. *Can J Biochem Physiol* 37:911–917
39. Jakobsen AN, Aasen IM, Josefsen KD, Strom AR (2008) Accumulation of docosahexaenoic acid-rich lipid in thraustochytrid *Aurantiochytrium* sp strain T66: effects of N and P starvation and O-2 limitation. *Appl Microbiol Biotechnol* 80:297–306. doi:10.1007/s00253-008-1537-8
40. Metcalfe LD, Schmitz AA, Pelka JR (1966) Rapid preparation of fatty acid esters from lipids for gas chromatographic analysis. *Anal Chem* 38:514–515. doi:10.1021/ac60235a044
41. Abdulkadir S, Tsuchiya M (2008) One-step method for quantitative and qualitative analysis of fatty acids in marine animal samples. *J Exp Mar Biol Ecol* 354:1–8. doi:10.1016/j.jembe.2007.08.024

42. Bergvik M, Overrein I, Bantle M, Evjemo JO, Rustad T (2012) Properties of *Calanus finmarchicus* biomass during frozen storage after heat inactivation of autolytic enzymes. *Food Chem* 132:209–215. doi:[10.1016/j.foodchem.2011.10.058](https://doi.org/10.1016/j.foodchem.2011.10.058)
43. Miller CB, Cowles TJ, Wiebe PH, Copley NJ, Grigg H (1991) Phenology in *Calanus finmarchicus*—hypotheses about control mechanisms. *Mar Ecol Prog Ser* 72:79–91
44. Hind A, Gurney WSC, Heath M, Bryant AD (2000) Overwintering strategies in *Calanus finmarchicus*. *Mar Ecol Prog Ser* 193:95–107
45. Hirche HJ (1983) Overwintering of *Calanus finmarchicus* and *Calanus helgolandicus*. *Mar Ecol Prog Ser* 11:281–290. doi:[10.3354/meps011281](https://doi.org/10.3354/meps011281)
46. Pasternak A, Arashkevich E, Tande K, Falkenhaus T (2001) Seasonal changes in feeding, gonad development and lipid stores in *Calanus finmarchicus* and *C. hyperboreus* from Malangen, northern Norway. *Mar Biol* 138:1141–1152. doi:[10.1007/s002270100553](https://doi.org/10.1007/s002270100553)
47. Heath MR, Rasmussen J, Ahmed Y, Allen J, Anderson CIH, Brierley AS, Brown L, Bunker A, Cook K, Davidson R, Fielding S, Gurney WSC, Harris R, Hay S, Henson S, Hirst AG, Holliday NP, Ingvarsdottir A, Irigoien X, Lindeque P, Mayor DJ, Montagnes D, Moffat C, Pollard R, Richards S, Saunders RA, Sidey J, Smerdon G, Speirs D, Walsham P, Waniek J, Webster L, Wilson D (2008) Spatial demography of *Calanus finmarchicus* in the Irminger Sea. *Prog Oceanogr* 76:39–88. doi:[10.1016/j.pocean.2007.10.001](https://doi.org/10.1016/j.pocean.2007.10.001)
48. Jonasdottir SH, Richardson K, Heath, Ingvarsdottir A, Christoffersen A (2008) Spring production of *Calanus finmarchicus* at the Iceland-Scotland ridge. *Deep-Sea Res PT I* 55:471–489. doi:[10.1016/j.dsr.2007.12.009](https://doi.org/10.1016/j.dsr.2007.12.009)
49. Graeve M, Kattner G, Hagen W (1994) Diet-induced changes in the fatty-acid composition of Arctic herbivorous copepods—experimental-evidence of trophic markers. *J Exp Mar Biol Ecol* 182:97–110
50. Pepin P, Parrish CC, Head EJJ (2011) Late autumn condition of *Calanus finmarchicus* in the northwestern Atlantic: evidence of size-dependent differential feeding. *Mar Ecol Prog Ser* 423:155–166. doi:[10.3354/meps08952](https://doi.org/10.3354/meps08952)
51. Johnson CL, Leising AW, Runge JA, Head EJJ, Pepin P, Plourde S, Durbin EG (2008) Characteristics of *Calanus finmarchicus* dormancy patterns in the Northwest Atlantic. *ICES J Mar Sci: Journal du Conseil* 65:339–350. doi:[10.1093/icesjms/fsm171](https://doi.org/10.1093/icesjms/fsm171)
52. Gatten RR, Sargent JR, Forsberg TEV, Ohara SCM, Corner EDS (1980) On the nutrition and metabolism of zooplankton. 14. Utilization of lipid by *Calanus helgolandicus* during maturation and reproduction. *J Mar Biol Assoc UK* 60:391–399
53. Sargent JR, Falk-Petersen S (1988) The lipid biochemistry of calanoid copepods. *Hydrobiologia* 167–168:101–114. doi:[10.1007/bf00026297](https://doi.org/10.1007/bf00026297)
54. Miller CB, Crain JA, Morgan CA (2000) Oil storage variability in *Calanus finmarchicus*. *ICES J Mar Sci* 57:1786–1799. doi:[10.1006/jmsc.2000.0975](https://doi.org/10.1006/jmsc.2000.0975)
55. Kattner G, Krause M (1987) Changes in lipids during the development of *Calanus finmarchicus* s.l. from copepodid I to adult. *Mar Biol* 96:511–518. doi:[10.1007/BF00397968](https://doi.org/10.1007/BF00397968)
56. Irigoien X, Head R, Klenke U, Meyer-Harris B, Harbour D, Niehoff B, Hirche HJ, Harris R (1998) A high frequency time series at weathership M, Norwegian Sea, during the 1997 spring bloom: feeding of adult female *Calanus finmarchicus*. *Mar Ecol Prog Ser* 172:127–137
57. Niehoff B, Klenke U, Hirche HJ, Irigoien X, Head R, Harris R (1999) A high frequency time series at Weathership M, Norwegian Sea, during the 1997 spring bloom: the reproductive biology of *Calanus finmarchicus*. *Mar Ecol Prog Ser* 176:81–92. doi:[10.3354/meps176081](https://doi.org/10.3354/meps176081)
58. Koski M, Yebra L, Dutz J, Jónasdóttir S, Vidoudez C, Jakobsen H, Pohnert G, and Nejstgaard J (2012) The effect of egg versus seston quality on hatching success, naupliar metabolism and survival of *Calanus finmarchicus* in mesocosms dominated by *Phaeocystis* and diatoms. *Mar Biol* 159:643–660. doi:[10.1007/s00227-011-1843-z](https://doi.org/10.1007/s00227-011-1843-z)
59. Pascal JC, Ackman RG (1976) Long chain monoethylenic alcohol and acid isomers in lipids of copepods and capelin. *Chem Phys Lipids* 16:219–223. doi:[10.1016/0009-3084\(76\)90029-3](https://doi.org/10.1016/0009-3084(76)90029-3)
60. Lee RF, Nevenzel JC, Paffenhöfer GA (1972) The presence of wax esters in marine planktonic copepods. *Naturwissenschaften* 59:406–411
61. Volkmann JK, Everitt DA (1986) Some analyses of lipid classes in marine organisms, sediments and seawater using thin-layer chromatography—flame ionisation detection. *J Chromatogr A* 356:147–162. doi:[10.1016/S0021-9673\(00\)91474-2](https://doi.org/10.1016/S0021-9673(00)91474-2)
62. Henderson RJ, Sargent JR (1980) Biosynthesis of neutral lipids by *Euchaeta norvegica*. *Mar Biol* 56:1–6. doi:[10.1007/BF00390587](https://doi.org/10.1007/BF00390587)
63. Graeve M, Albers C, Kattner G (2005) Assimilation and biosynthesis of lipids in Arctic *Calanus* species based on feeding experiments with a C-13 labelled diatom. *J Exp Mar Biol Ecol* 317:109–125. doi:[10.1016/j.jembe.2004.11.016](https://doi.org/10.1016/j.jembe.2004.11.016)
64. Overrein I (2010) Copepod lipids in aquaculture, in Department of Biotechnology. Norwegian University of Science and Technology, Trondheim
65. Scott CL, Kwasniewski S, Falk-Petersen S, Sargent JR (2002) Species differences, origins and functions of fatty alcohols and fatty acids in the wax esters and phospholipids of *Calanus hyperboreus*, *C. glacialis* and *C. finmarchicus* from Arctic waters. *Mar Ecol Prog Ser* 235:127–134. doi:[10.3354/meps235127](https://doi.org/10.3354/meps235127)
66. Evjemo JO, Tokle N, Vadstein O, Olsen Y (2008) Effect of essential dietary fatty acids on egg production and hatching success of the marine copepod *Temora longicornis*. *J Exp Mar Biol Ecol* 365:31–37. doi:[10.1016/j.jembe.2008.07.032](https://doi.org/10.1016/j.jembe.2008.07.032)
67. Bell MV, Dick JR, Anderson TR, Pond DW (2007) Application of liposome and stable isotope tracer techniques to study polyunsaturated fatty acid biosynthesis in marine zooplankton. *J Plankton Res* 29:417–422. doi:[10.1093/plankt/fbm025](https://doi.org/10.1093/plankt/fbm025)

Sesamin Modulates Gene Expression Without Corresponding Effects on Fatty acids in Atlantic Salmon (*Salmo salar* L.)

A. Schiller Vestergren · L. Wagner ·
J. Pickova · G. Rosenlund · A. Kamal-Eldin ·
S. Trattner

Received: 21 February 2012 / Accepted: 21 June 2012 / Published online: 13 July 2012
© AOCS 2012

Abstract This study examined the effects of sesamin inclusion in vegetable oil-based diets fed to Atlantic salmon (*Salmo salar* L.). The diets used differed in n-6/n-3 fatty acid (FA) ratio (0.5 and 1) and sesamin content (high 5.8 g/kg, low 1.16 g/kg and no sesamin). The oils used in the feeds were a mixture of rapeseed, linseed and palm oil. Fish were fed for 4 months. Fatty acids and expression of hepatic genes involved in transcription, lipid uptake, desaturation, elongation and β -oxidation were measured. No major effects on the percentage of DHA in white muscle, liver triacylglycerol and phospholipid fraction were detected. Genes involved in β -oxidation, elongation and desaturation were affected by sesamin addition. Limited effects were seen on any of the transcription factors tested and no effect was seen on the expression of peroxisome proliferator-activated receptors (PPAR). Expression of both SREBP-1 and SREBP-2 increased with sesamin addition. It was concluded that supplementation of fish feed with a high level of sesamin had a negative effect on the growth rate and live weight and did not alter the proportions of DHA in tissues even though gene expression was

affected. Thus, more studies are needed to formulate a diet that would increase the percentage of DHA in fish without negative effects on fish growth.

Keywords Elongation · Desaturation · DHA · β -Oxidation · PGC-1 α · Vegetable oil · n-6/n-3 Fatty acid ratio

Abbreviations

ARA	Arachidonic acid (20:4n-6)
ACO	Acyl-CoA oxidase
ALA	Alpha-linolenic acid (18:3n-3)
CPT1	Carnitine palmitoyl transferase I
Δ 5 fad	Delta 5 fatty acid desaturase
Δ 6 fad	Delta 6 fatty acid desaturase
DHA	Docosahexaenoic acid (22:6n-3)
DTA	Dodecylthioacetic acid
ELOVL	Elongation of very long chain fatty acids gene
EPA	Eicosapentaenoic acid (20:5n-3)
FAME	Fatty acid methyl ester(s)
FA	Fatty acid(s)
FCR	Feed conversion ratio
FO	Fish oil
K	Condition factor
LNA	Linoleic acid (18:2n-6)
LCPUFA	Long chain polyunsaturated fatty acid(s)
LXR α	Liver X receptor α
MUFA	Monounsaturated fatty acid(s)
n-3	Omega-3
n-6	Omega-6
n-6/n-3	n-6/n-3 PUFA
PUFA	Polyunsaturated fatty acid(s)
PPAR	Peroxisomal proliferator-activated receptor(s)
PGC-1 α	Peroxisome proliferator activated receptor γ coactivator-1 α

A. Schiller Vestergren and L. Wagner contributed equally.

A. Schiller Vestergren · L. Wagner (✉) · J. Pickova ·
A. Kamal-Eldin · S. Trattner
Department of Food Science, Swedish University of Agricultural
Sciences (SLU), Uppsala BioCenter, P.O. Box 7051,
75007 Uppsala, Sweden
e-mail: liane.wagner@slu.se

G. Rosenlund
Skretting ARC, P.O. Box 48, 4001 Stavanger, Norway

S. Trattner
Department of Wildlife, Fish and Environmental Studies,
SLU, Umeå, Sweden

PL	Phospholipid(s)
SFA	Saturated fatty acid(s)
SD	Standard deviation
SGR	Specific growth rate
SR-B1	Scavenger receptor class B1
SREBP	Sterol regulatory element binding protein
TAG	Triacylglycerol
TTA	Tetradecylthioacetic acid
VO	Vegetable oil

Introduction

Atlantic salmon (*Salmo salar* L.) is well known for being rich in omega-3 (n-3) long chain polyunsaturated fatty acids (LCPUFA, defined as $\geq C20$) [1, 2]. These n-3 fatty acids (FA) are important for the prevention of cardiovascular disease and brain development, and have anti-inflammatory properties [3].

The expansion in aquaculture production over the last 50 years and the static or even decreasing supply of fish oil (FO) for fish feed production have created a need for alternative vegetable oils (VO) for use in farmed fish feeds. Studies have suggested that replacing FO with VO does not affect fish growth or taste. However, VO are devoid of n-3 LCPUFA and can therefore decrease the amount of these FA in fish muscle [2, 4, 5]. To compensate for the negative effect of lower LCPUFA content, several studies have suggested improving the conversion of α -linolenic acid (ALA, 18:3n-3) to LCPUFA by adding modulators of lipid metabolism to fish feed [2, 6–11]. Sesamin, an oil-soluble lignan found in sesame seeds, is suggested to possess such modulatory properties. In both Atlantic salmon and rainbow trout (*Oncorhynchus mykiss*), the biosynthesis of LCPUFA from ALA to DHA has been well described [12–15]. The genes coding for the enzymes involved in elongation and desaturation have been isolated and characterized in salmonids [16, 17]. In previous studies by our group, a mixture of sesamin/episesamin increased the proportion of docosahexaenoic acid (22:6n-3, DHA) in rainbow trout, [8] and decreased the levels of ALA in Atlantic salmon [18]. Furthermore, in Atlantic salmon hepatocytes, it has been shown that synthesis of n-3 LCPUFA, particularly DHA, increases in the presence of sesamin/episesamin mixture [6]. Sesamin is known to increase gene expression and enzyme activity involved in mitochondrial and peroxisomal β -oxidation [19–25] and to inhibit the $\Delta 5$ -fatty acid desaturation of n-6 FA in rodents [26]. It has been suggested [20, 27] that sesamin triggers these actions through ligand binding to the peroxisomal proliferator-activated receptors (PPARs).

One co-activator of the PPARs is peroxisome proliferator-activated receptor- γ co-activator-1 α (PGC-1 α). PGC-1 α together with PPAR α is involved in the fine-tuning of transcriptional responses in the β -oxidation pathway to environmental variations [28].

In addition, PPAR α has been shown to activate the gene coding for carnitine palmitoyltransferase 1 (CPT-1) by binding to a peroxisome proliferator response elements upstream in the promoter region of the gene, thereby playing an important role in regulating β -oxidation in rodents [29], humans [30] and fish [31]. Similarly, PPAR α activate acyl-CoA oxidase (ACO) the first and rate-limiting enzyme of peroxisomal β -oxidation [30].

Expression of the genes coding for the very long chain fatty acids 5 (ELOVL5) elongase, $\Delta 6$ fatty acid desaturase ($\Delta 6$ fad) and $\Delta 5$ fatty acid desaturase ($\Delta 5$ fad) is regulated by sterol regulatory element binding protein 1c (SREBP-1c). Sterol regulatory element binding protein 2 (SREBP-2) is another transcription factor that regulates lipid homeostasis, including LCPUFA biosynthesis and cholesterol metabolism [32]. Liver X receptor α (LXR α) and LXR β have been shown to activate SREBP-1c in rodents [33, 34]. SREBP-1c, SREBP-2 and LXR α [34] have been isolated and characterized in salmonids.

Recently ELOVL4 has been isolated and characterized in Atlantic salmon. ELOVL4 has been shown to elongate C20 and C22 polyunsaturated fatty acids and to convert eicosapentaenoic acid (20:5n-3, EPA) and 22:5n-3 to 24:5n-3, an intermediate substrate for DHA biosynthesis [35].

In addition, the main high-density lipoprotein (HDL) receptor, scavenger receptor class B1 (SRB-1), responsible for regulating lipid levels from peripheral tissues to the liver [36], has been investigated together with CD36, a gene coding for fatty acid translocase involved in lipid uptake over the membrane [37].

The aim of this study was to investigate possible effects of dietary sesamin in combination with different n-6/n-3 ratios in the diet on post smolt Atlantic salmon muscle and liver in seawater. The different n-6/n-3 ratios were included for comparison of effects by substrate availability on elongation and desaturation.

Fish performance, FA composition and expression of genes involved in lipid pathways were examined. The gene expressions described above were studied in order to determine salmonid responses to sesamin.

Materials and Methods

Animals and Diets

Atlantic salmon were fed seven different experimental diets as shown in Table 1, all produced by Skretting ARC

Feed Technology Plant (Stavanger, Norway). Prior to the trial, the fish were fed a commercial diet (Skretting Transfer 3.0; Skretting, Stavanger, Norway). Each diet was formulated to give an n-6/n-3 FA ratio of either 0.5 (V0.5) or 1.0 (V1), the analyzed n-6/n-3 ratio for V1 was 0.9, however referred to as V1. Different n-6/n-3 ratios were chosen based on the study from Trattner et al. [6] on rainbow trout, which showed increased effects by sesamin at the higher n-6/n-3 ratio. The diets were combined with two different levels of sesamin; high dose (SH) = 5.8 g/kg feed [6], low dose (SL) = 1.16 g/kg feed or a control without sesamin (S0) = 0 g/kg feed. This means that V0.5SL indicates a vegetable oil-based diet with an n-6/n-3 fatty acid ratio of 0.5 and low inclusion of sesamin. The level of added sesamin was chosen to match the concentration of lignan in sesame oil and different dietary levels assuming different dietary inclusion rates. The high level of 5.8 g/kg feed is equivalent to 20 % sesame oil inclusion [6]. The low dose was 20 % of 5.8 g/kg corresponding to 1.16 g/kg. As an additional control, a diet with only fish oil (FO) and no sesamin added was also used.

The dry sesamin powder was added to the feed mix together with the premixes prior to extrusion. Three different batches with increasing sesamin amounts were produced and the different oils were then coated on. Sesamin (98 % purity) was obtained from KEB Biotech (Beijing, China). The experimental diets contained fish meal (Scandinavian LT meal, Skretting, Stavanger) (320 g/kg), wheat gluten (107.4 g/kg), soya concentrate (243.2 g/kg), wheat (89.5 g/kg), premixes (9 g/kg) and sesamin (0, 1.16 and

5.8 g/kg). Fish oil (238.5 g/kg) was added to the control diet (FO) (Skretting, Stavanger), whereas a mixture of vegetable oils was added to diets V0.5S0, V0.5SL and V0.5SH to give 53.5 g rapeseed oil/kg feed (Skretting, Stavanger), 135 g linseed oil/kg feed (Elbe Fetthandel GmbH, Hamburg, Germany) and 50 g palm oil/kg feed (Fritex 24, Aarhuskarlshamn Sweden AB, Karlshamn, Sweden). The other three diets (V1) contained 138.5 g/kg rapeseed oil, 40 g/kg linseed oil and 60 g/kg palm oil. Pellet size was 4 mm. The FA composition of the experimental diets is shown in Table 1.

The feeding trial was carried out at Skretting ARC Fish Trials Station (Stavanger, Norway) in circular tanks (1 m diameter) supplied with flow-through seawater at 12 °C. Each tank was stocked with 35 Atlantic salmon (initial weight 104.6 ± 9.9 g) individually tagged with micro-transponders (Trac ID Systems AS, Stavanger, Norway). The fish were fed in single tanks twice per day for 4 months (November–March) by means of automatic feeders. Fish was fed ad libitum and uneaten feed was removed. At slaughter (average fish weight 553.6 ± 88.1 g), liver and white muscle from eight fish per diet were sampled, frozen in liquid nitrogen and stored at -80 °C for further analysis. The specific growth rate (SGR) was calculated as: $SGR = 100 \times (W_2^{1/3} - W_1^{1/3}) D^{-1}$ with W_2 being final, W_1 the initial weight and D the number of days [38]. The feed conversion ratio (FCR) was calculated as g feed eaten (as feed matter basis) divided by g biomass increase obtained from the 4-month period between samplings. The condition factor (K) was calculated as: $K = 100 \times (WL^{-3})$ with W is live

Table 1 Diet codes, oil (g/kg), fatty acid composition (%) and sesamin levels in the experimental diets

	V0.5S0	V0.5SL	V0.5SH	V1S0	V1SL	V1SH	FO
n-6/n-3	0.5	0.5	0.5	0.9	0.9	0.9	0.3
Linseed oil	135	135	135	40	40	40	–
Rapeseed oil	53.5	53.5	53.5	138.5	138.5	138.5	–
Palm oil	50	50	50	60	60	60	–
Fish oil	–	–	–	–	–	–	238.5
Sesamin (g/kg)	0	0.16	5.80	0	1.16	5.80	0
LNA	14.7	14.3	14.7	15.1	15.4	15.3	4.9
ALA	27.8	27.2	27.6	13.2	13.0	13.1	2.4
ARA	0.2	0	0	0.1	0	0.1	0.4
EPA	1.2	1.1	1.1	1.4	1.3	1.3	6.9
DHA	1.6	1.6	1.6	1.8	1.8	1.8	9.7
SFA	17.5	17.4	17.5	18.7	18.7	18.8	24.8
MUFA	34.2	33.9	33.8	46.8	47.1	47.1	41.5
n-6 PUFA	15.0	15.5	15.6	16.2	15.8	15.7	6.2
n-3 PUFA	31.1	30.7	30.9	17.1	16.7	16.8	23.3
Unknown	2.1	2.4	2.1	1.3	1.5	1.8	4.4

SFA saturated fatty acids (14:0, 16:0, 18:0), MUFA monounsaturated fatty acids (16:1n-7, 18:1n-9, 18:1n-7, 20:1, 22:1), PUFA polyunsaturated fatty acids

body weight (g) and L is fork length (cm) of each fish [39]. The liver samples used for gene expression analysis were transferred to RNAlater-ICE (AM7030, Applied Biosystems Part of Life Technologies, Carlsbad, CA, US) directly before storage at $-20\text{ }^{\circ}\text{C}$.

Lipid Analysis

The samples were prepared by skinning and deboning the fillets. The white muscle was then dissected from the region between the dorsal and ventral fins. For each group liver ($n = 8$) and muscle ($n = 6$) samples were analyzed in duplicate. Total lipids were extracted according to Trattner et al. [6]. After drying, the lipids were weighed to determine the lipid content and stored in hexane at $-80\text{ }^{\circ}\text{C}$ until further analysis. All chemicals and other solvents used for analyses were purchased from Merck (Darmstadt, Germany) except for chloroform (Sigma Chemicals Co. St. Louis, MO, USA). The solvents were used without further purification.

Total lipids in muscle tissue and liver were separated by thin-layer chromatography according to Pickova et al. [40]. Fatty acid methyl esters (FAME) from both triacylglycerols (TAG) and phospholipids (PL) were prepared according to the method described by Appelqvist [41].

FAME were analyzed by gas chromatography using a CP 3800 instrument (Varian AB, Stockholm, Sweden) equipped with a flame ionization detector and split injector and fitted with a fused silica capillary column BPX 70 (SGE, Austin, Tex.), length 50 m id. 0.22 mm, 0.25 μm film thickness [42]. The peaks were identified by comparing their retention times with those of the standard mixture GLC-68 A (Nu-check Prep, Elysian, USA). Peak areas were integrated using Galaxie chromatography data system software version 1.9 (Varian AB, Stockholm, Sweden). Fatty acids were quantified using the internal standard (C17:1) methyl-15-methylheptadecanoate (Larodan Fine Chemicals AB, Malmö, Sweden).

Gene Expression Analysis

Gene expression in the liver was investigated by quantitative real-time PCR using an array of target genes coding for enzymes involved in lipid homeostasis.

Total RNA was isolated from the liver of 6 individual fish from each treatment using the spin purification method SV Total RNA Isolation System (Z3105, Promega, Madison, Wisconsin, USA). Each liver was cut in $5 \times 5\text{ mm}$ pieces and approximately 1.7 mg of each liver was randomly collected. Each liver sample was then homogenized and lysed. The isolation and DNase procedures were performed according to the manufacturer's instructions. Total RNA was quantified using a GeneQuantTM 1300 Spectrophotometer (GE Healthcare Life Sciences, Uppsala, Sweden).

Reverse transcription first strand cDNA was synthesized using the High-Capacity cDNA Archive kit (Applied Biosystems Part of Life Technologies, Carlsbad, CA, USA). The protocol was scaled up to from 20- to 100- μl reactions. The kit components were mixed according to the manufacturer's instructions and the reverse transcription reaction was carried out on a Veriti[®] 96-Well Fast Thermal Cycler (Applied Biosystems Part of Life Technologies, Carlsbad, CA, USA). The RT conditions were as follows: 1 cycle at $37\text{ }^{\circ}\text{C}$ (60 min) and 1 cycle at $95\text{ }^{\circ}\text{C}$ (5 min). The cDNA samples were diluted 1:100 before use.

Real-time PCR analysis of relative abundance of mRNA was carried out using a Fast SYBR[®] Green Master Mix (Applied Biosystems Part of Life Technologies, Carlsbad, CA, USA). The PCR reaction mix (20 μl) consisted of 0.9 μl of each forward and reverse primer (final concentration of 0.5 μM), 6 μl cDNA (approximately 20 ng/sample) and 10 μl master mix diluted with RNase-free water in accordance with the manufacturer's instructions. The primers used for real-time PCR analysis with the corresponding GenBank[®] accession numbers are listed in Table 2. The primers were designed based on available Atlantic salmon sequences from the online version of GenBank[®] (NCBI) using Primer Express[®] software (Applied Biosystems Part of Life Technologies, Carlsbad, CA, USA) [8] or copied from literature references and custom-made at Invitrogen Part of Life Technologies (Carlsbad, CA, USA). Real-time PCR was performed using the StepOnePlusTM Real-time PCR System (Applied Biosystems of Life Technologies, Foster City, CA, USA). The samples were denatured at $95\text{ }^{\circ}\text{C}$ for 20 s, followed by 40 cycles of annealing and elongation ($95\text{ }^{\circ}\text{C}$ for 3 s and $60\text{ }^{\circ}\text{C}$ for 30 s) and melt curve analysis to ensure that only a single product was amplified.

All samples were run simultaneously for each gene in triplicate, with a non-template control on each plate. Elongation factor 1a (EF1 α), NADH-ubiquinone oxidoreductase (NUOR), eukaryotic translation initiation factor 3 (ETiF) and RNA polymerase II polypeptide (RPL2) were evaluated for their stability across all experimental variables and samples using the DataAssist software version 2.0 (Applied Biosystems of Life Technologies, Foster City, CA, USA). RPL2 was chosen as the most stable reference gene (results not shown). ΔC_T was calculated by subtracting the C_T for RPL2 from the C_T for the target gene. The relative expression was then calculated by comparing the ΔC_T values for fish fed with or without addition of sesamin using the term $2^{-\Delta\Delta C_T}$ and reported as arbitrary -fold change units [43]. At the end of each real-time PCR run, melt curve analysis was carried out to ensure that only a single product was amplified.

Table 2 Sequences of primers used in analyses and their GenBank accession numbers

Primer	Forward primer (5'-3')	Reverse primer (5'-3')	GenBank Acc. no
RPL2	TAACGCCCTGCTCTTCACGTTGA	ATGAGGGACCTTGTAGCCAGCAA	CA049789
EF1- α^a	CACCACCGCCATCTGATCTACAA	TCAGCAGCCTCCTTCTCGAACTTC	AF321836
NUOR ^d	CAACATAGGGATTGGAGAGCTGTACG	TTCAGAGCCTCATCTTGCCTGCT	DW532752
ETiF ^g	CAGGATGTTGTTGCTGGATGGG	ACCCAAGTGGGAGGTCAGAA	DW542195
PPAR α^a	TCCTGGTGGCCTACGGATC	CGTTGAATTCATGGCGAACT	DQ294237
PPAR β 1A ^b	GAGACGGTCAGGGAGCTCAC	CCAGCAACCCGTCCTTGTT	AJ416953
PPAR γ (long/short) ^b	CATTGTCAGCCTGTCCAGAC	ATGTGACATTCCCACAAGCA	AJ292963
PGC-1 α	CAACCACCTTGCCACTTCCT	CGGTGATCCCTTGTTGGTCAT	FJ710605.1
CD36 ^d	GGATGAACTCCCTGCATGTGA	TGAGGCCAAAGTACTCGTCGA	AY606034
$\Delta 5$ fad ^d	GAGAGCTGGCACCGACAGAG	GAGCTGCATTTTCCCATGG	AF478472
$\Delta 6$ fad ^d	AGAGCGTAGCTGACACAGCG	TCCTCGGTTCTCTCTGCTCC	AY458652
ACO ^b	CCTTCATTGTACCTCTCCGCA	CATTTCAACCTCATCAAAGCCAA	DQ364432
CPT1 ^d	GTACCAGCCCCGATGCCTTCAT	TCTCTGTGCGACCCTCTCGGAA	AM230810
LXR ^e	GCCGCCGCTATCTGAAATCTG	CAATCCGGCAACCAATCTGTAGG	FJ470290
SREBP-1	GACAAGGTGGTCCAGTTGCT	CACACGTTAGTCCGCATCAC	NM001195818
SREBP-2 ^h	TCGCGCCTCTGATGATT	AGGGCTAGGTGACTGTTCTGG	NM001195819
SR-B1 ^b	AACTCAGTGAAGAGGCCAACTTG	TGCGGCGGTGATGATG	DQ266043
ELOVL5a ^c	ACAAGACAGGAATCTCTTTCAGATTAA	TCTGGGGTACTGTGCTATAGTGTAC	AY170327
ELOVL5b ^c	ACAAAAAGCCATGTTTATCTGAAAGA	CACAGCCCCAGAGACCCACTT	DW546112
ELOVL2 ^c	CGGGTACAAAATGTGCTGGT	TCTGTTTCCGATAGCCATT	TC91192
ELOVL4 ⁱ	TTGTCAAATTGGTCTCTGTGC	TAAAAGCCCTTTGGGATGA	HM208347

RPL2 RNA polymerase II polypeptide, EF1- α elongation factor 1 α , NUOR NADH-ubiquinone oxidoreductase, ETiF eukaryotic translation initiation factor 3, PPAR peroxisome proliferator-activated receptor, PGC-1 α proliferator-activated receptor gamma coactivator 1 alpha, CD 36 cluster of differentiation 36, $\Delta 5$ $\Delta 5$ desaturase, $\Delta 6$ $\Delta 6$ desaturase, ACO acyl-CoA oxidase, CPT1 carnitin palmitoyl transferase I, LXR liver X receptor α , SREBP sterol regulatory element binding protein, SR-B1 scavenger receptor class BI, ELOVL elongation of very long chain fatty acids gene

Already designed and validated in ^a[62] ^b[48] ^c[16] ^d[8] ^e[34] ^f[63] ^g[64] ^h[65] ⁱ[35]

Statistical Analyses

Relative expressions of the different genes, in relation to the reference gene, were determined using the DataAssist software version 2.0 (Applied Biosystems, Foster City, CA, USA). All data are presented as mean values \pm standard deviation (SD) and differences were regarded as significant at $p < 0.05$. Data were analyzed with the general linear model (GLM) procedure (SAS Institute Inc., Cary, NC, USA, version 9.2) [44] with diet as the fixed factor and individual fish as the experimental unit. Tukey's test was used to determine differences between the diets of interest; particularly, VO diets were compared with FO diet, and VOSL/VOSH diets were compared with control VO diets.

Results

Fish Performance

No mortality occurred during the feeding experiment. The mean weight of the fish increased from 104.6 ± 9.9 g to

553.6 ± 88.1 g. The final weight and specific growth rate (SGR) of fish fed with VO diet was not significantly different from that of the FO control. However, there were significant ($p < 0.05$) differences in both final weight and SGR between the control without sesamin (S0) and the high sesamin (SH) group (Table 3). The FCR for the whole trial was similar in all tanks. The average K in the fish at the end of the trial was 1.31 ± 0.09 and was similar in all groups (Table 3).

Fat Content and Fatty Acid Composition

Muscle fat content did not differ between the groups, ranging from 1.4 to 1.8 %. In the liver, lipid content was significantly increased from 5.0 to 7.4 % and 8.0 % in the V0.5SH and V1SH groups, respectively, compared with the groups without sesamin. The FA composition of TAG and PL fractions in white muscle are shown in Table 4 and Table 5, respectively. The FA composition in tissues of control fish fed a fish oil-based diet differed significantly from that of other groups fed vegetable oil-based diets.

Table 3 Initial, final weight (g), specific growth rate (SGR, %/day), feed conversion ratio (FCR, g feed/g body weight increase) and condition factor (*K*) of Atlantic salmon fed seven experimental diets for 4 months, mean values \pm SD, $n = 8$

	V0.5S0	V0.5SL	V0.5SH	V1S0	V1SL	V1SH	F0
Initial weight	103.4 \pm 10.7	105.5 \pm 10.7	106.3 \pm 10.2	103.8 \pm 10.6	103.1 \pm 11.4	105.6 \pm 9.2	105.8 \pm 9.7
Final weight	557 \pm 101 ^a	543 \pm 84 ^{ab}	514 \pm 92 ^b	582 \pm 71 ^a	553 \pm 92 ^{ab}	530 \pm 76 ^{bc}	587 \pm 82 ^a
SGR	1.57 \pm 0.14 ^a	1.49 \pm 0.13 ^{abc}	1.43 \pm 0.13 ^c	1.58 \pm 0.10 ^a	1.53 \pm 0.13 ^{ab}	1.47 \pm 0.13 ^{bc}	1.56 \pm 0.12 ^a
FCR	0.74	0.75	0.75	0.73	0.74	0.76	0.72
<i>K</i>	1.32 \pm 0.08	1.31 \pm 0.09	1.28 \pm 0.10	1.31 \pm 0.11	1.28 \pm 0.08	1.32 \pm 0.08	1.28 \pm 0.07

For abbreviations see Table 1

^{abc} Mean values across rows with different superscripts are significantly different ($p < 0.05$)

White Muscle

Some of the FA in white muscle were significantly affected by sesamin supplementation of the diet, depending on the n-6/n-3 ratio (Table 4). In the TAG fraction of fish fed sesamin and a diet with an n-6/n-3 ratio of 0.5 (V0.5SH), the level of 20:3n-3 increased, while EPA and 22:5n-3 decreased compared with V0.5S0. In the V1SH group (n-6/n-3 = 1; high sesamin level), the content of 18:0 and 18:1n-9 decreased and 18:2n-6 increased (compared with V1S0). When comparing the two n-6/n-3 ratios, V0.5 (n-6/n-3 = 0.5) showed higher levels of 18:0, 18:3n-3, 18:4n-3, 20:3n-3 and 22:1n-11 and lower levels of 18:1n-9 and 20:1n-9 than V1 (n-6/n-3 = 1). The addition of sesamin significantly increased PUFA at the n-6/n-3 ratio of 1. In the PL fraction the proportions of 16:0, 18:1n-9, 18:2n-6, 20:1n-9, 20:3n-6 and 20:4n-6 were significantly lower, while the proportions of 18:3n-3, 20:3n-3 and 22:1n-11 were higher in V0.5 compared with V1. The presence of sesamin in the feed increased the proportion of 20:3n-3 (V0.5SH) and decreased that of 20:5n-3 (V0.5SH), 20:3n-6 (V1SH) and 22:5n-3 (V0.5SH and V1SH) in the muscle PL.

Liver

The FA composition in both TAG and PL fractions of the liver differed considerably between the dietary groups (Table 5). In the TAG fraction and diets with an n-6/n-3 ratio of 0.5, the percentage of 18:2n-6 (V0.5SL), 18:3n-3 (V0.5SL) and 20:3n-3 (V0.5SH) increased and that of 18:0 (V0.5SL) and 22:5n-3 (V0.5SH) decreased with sesamin addition compared with V0.5S0. Diets with an n-6/n-3 ratio of 1 (V1) and containing sesamin decreased the proportion of the following FA: 16:1n-7 (V1SL and V1SH), 18:1n-9 (V1SL, V1SH), 20:3n-6 (V1SH), 22:1n-11 (V1SL), 20:5n-3 and 22:5n-3 (V1SH). The percentage of the FA 18:1n-9 was lower and that of 18:3n-3 and 20:3n-3 higher in the liver from fish fed V0.5 compared with V1. In the PL fraction the level of 14:0 (V0.5SL, V0.5SH) decreased,

while that of 18:1n-9 (V0.5SH) and 18:3n-3 (V0.5SL, V0.5SH) increased after consumption of a sesamin-enriched diet with an n-6/n-3 ratio of 0.5. Diets with an n-6/n-3 ratio of 1 and high sesamin addition resulted in a decreased percentage of 20:3n-6 and 20:4n-6 (V1SH compared with V1S0). In diets with added sesamin, the percentage of 18:2n-6, 20:1n-9 and 20:3n-3 increased significantly, while that of 20:5n-3 and 22:5n-3 decreased with both n-6/n-3 ratios. The proportion of 20:4n-6 was lower and that of 16:0, 18:0, 18:3n-3, 18:4n-3 and 20:3n-3 higher in V0.5 compared with V1. The linoleic acid (LNA, 18:2n-6)/n-6 LCPUFA ratio in the PL fraction increased with the high amount of sesamin and was higher in the V0.5 diet than in the V1 diet. The ALA/(18:4n-3 + n-3 LCPUFA) ratio in the TAG fraction (V0.5SH and V1) and in the PL fraction (V0.5SH) increased after high inclusion of sesamin. PUFA increased in groups with low sesamin addition (V0.5SL) and an n-6/n-3 ratio of 0.5 in both fractions (TAG and PL).

Gene Expression

Transcription Factors

The expression profiles of transcription factors involved in lipid homeostasis (PPAR α , PPAR β 1A, PPAR γ (long/short), PGC-1 α , SREBP-1, SREBP-2 and LXR α) assessed in relation to the reference gene RPL2 are shown in Fig. 1a.

Expression of PPAR α was not affected by any addition of sesamin or by different n-6/n-3 ratios. Similarly, expression of PPAR β 1A was not affected significantly by VO diets with increased n-6/n-3 ratios. However, there was a tendency for lower PPAR β 1A mRNA levels with the VO diet compared with the FO diet. The PPAR β 1A mRNA levels were significantly lower with the higher amount of sesamin in diets with both n-6/n-3 ratios. For the higher n-6/n-3 ratio, the decrease in expression was significant compared with FO, as well as the V1S0 diet. Comparing the PPAR γ long expression rate, a significant increase ($p < 0.05$) was observed for tissue samples from the group fed the highest concentrations of sesamin in combination

Table 4 Fat content (%) and fatty acid composition (%) in the triacylglycerol and phospholipid fractions of white muscle from Atlantic salmon fed seven experimental diets, mean value \pm SD, $n = 6$

	V0.5S0	V0.5SL	V0.5SH	V1S0	V1SL	V1SH	F0
Fat content	1.6 \pm 0.4 ^a	1.4 \pm 0.2 ^a	1.5 \pm 0.3 ^a	1.6 \pm 0.4 ^a	1.6 \pm 0.4 ^a	1.8 \pm 0.5 ^a	1.6 \pm 0.3 ^a
Fatty acid	Triacylglycerol						
14:0	0.81 \pm 0.05 ^c	0.87 \pm 0.05 ^{bc}	0.78 \pm 0.02 ^c	0.88 \pm 0.03 ^{bc}	0.98 \pm 0.09 ^b	0.94 \pm 0.06 ^b	4.53 \pm 0.11 ^a
16:0	13.6 \pm 0.7 ^c	13.8 \pm 0.3 ^c	13.6 \pm 0.4 ^c	14.6 \pm 0.2 ^b	14.8 \pm 0.2 ^b	14.2 \pm 0.3 ^{bc}	17.9 \pm 0.4 ^a
16:1n-7	0.89 \pm 0.04 ^d	0.91 \pm 0.04 ^{cd}	0.85 \pm 0.04 ^d	1.00 \pm 0.02 ^{bc}	1.01 \pm 0.06 ^b	1.00 \pm 0.08 ^{bc}	4.67 \pm 0.06 ^a
18:0	3.9 \pm 0.1 ^a	3.8 \pm 0.1 ^a	3.8 \pm 0.1 ^a	3.5 \pm 0.1 ^b	3.4 \pm 0.1 ^b	3.1 \pm 0.1 ^c	3.1 \pm 0.2 ^c
18:1n-9	32.3 \pm 0.5 ^c	32.1 \pm 0.3 ^c	31.9 \pm 0.4 ^c	43.0 \pm 0.3 ^a	42.4 \pm 0.4 ^{ab}	42.1 \pm 0.3 ^b	22.3 \pm 0.4 ^d
18:2n-6	13.8 \pm 0.22 ^{abc}	13.6 \pm 0.22 ^{bc}	13.9 \pm 0.22 ^{ab}	13.5 \pm 0.18 ^c	13.6 \pm 0.17 ^{bc}	14.1 \pm 0.33 ^a	5.05 \pm 0.16 ^d
18:3n-3	19.7 \pm 0.5 ^a	19.3 \pm 0.6 ^a	20.2 \pm 0.8 ^a	8.3 \pm 0.3 ^b	8.2 \pm 0.1 ^b	8.7 \pm 0.5 ^b	2.3 \pm 0.2 ^c
18:4n-3	2.1 \pm 0.2 ^a	2.1 \pm 0.3 ^a	2.1 \pm 0.4 ^a	1.2 \pm 0.2 ^b	1.2 \pm 0.3 ^b	1.4 \pm 0.2 ^b	1.3 \pm 0.1 ^b
20:1n-9	1.9 \pm 0.2 ^c	2.1 \pm 0.1 ^c	2.0 \pm 0.1 ^c	3.0 \pm 0.2 ^b	3.0 \pm 0.2 ^b	3.0 \pm 0.1 ^b	6.4 \pm 0.1 ^a
20:3n-6	0.41 \pm 0.04 ^{bc}	0.39 \pm 0.04 ^{bc}	0.35 \pm 0.06 ^c	0.53 \pm 0.04 ^a	0.56 \pm 0.08 ^a	0.48 \pm 0.07 ^{ab}	Trace
20:4n-6	0.07 \pm 0.05 ^c	Trace	Trace	0.16 \pm 0.01 ^b	0.17 \pm 0.02 ^b	0.14 \pm 0.04 ^b	0.39 \pm 0.03 ^a
20:3n-3	1.0 \pm 0.1 ^b	1.1 \pm 0.2 ^{ab}	1.3 \pm 0.1 ^a	0.5 \pm 0.1 ^c	0.5 \pm 0.1 ^c	0.6 \pm 0.1 ^c	0.3 \pm 0.0 ^d
22:1n-11	2.5 \pm 0.1 ^b	2.7 \pm 0.1 ^b	2.7 \pm 0.3 ^b	2.0 \pm 0.0 ^a	2.0 \pm 0.1 ^a	2.0 \pm 0.1 ^a	9.8 \pm 0.3 ^c
20:5n-3	1.0 \pm 0.2 ^b	0.8 \pm 0.2 ^{bc}	0.6 \pm 0.1 ^c	0.6 \pm 0.1 ^c	0.7 \pm 0.1 ^{bc}	0.5 \pm 0.1 ^c	3.7 \pm 0.4 ^a
22:5n-3	0.39 \pm 0.04 ^b	0.38 \pm 0.04 ^{bc}	0.30 \pm 0.03 ^d	0.32 \pm 0.02 ^{cd}	0.32 \pm 0.03 ^{bcd}	0.26 \pm 0.03 ^d	1.57 \pm 0.07 ^a
22:6n-3	2.3 \pm 0.2 ^b	2.4 \pm 0.2 ^b	2.2 \pm 0.2 ^b	2.0 \pm 0.2 ^b	2.1 \pm 0.2 ^b	2.2 \pm 0.2 ^b	10.6 \pm 0.4 ^a
n-6 desat ratio ^e	9.9 \pm 0.7 ^a	10.0 \pm 0.5 ^a	10.8 \pm 1.5 ^a	7.5 \pm 0.5 ^b	6.8 \pm 0.6 ^{bc}	7.4 \pm 0.7 ^b	5.7 \pm 0.5 ^c
n-3 desat ratio ^f	2.9 \pm 0.2 ^a	2.9 \pm 0.3 ^a	3.2 \pm 0.4 ^a	1.8 \pm 0.2 ^b	1.7 \pm 0.1 ^b	1.7 \pm 0.2 ^b	0.1 \pm 0.0 ^c
SFA	18.5 \pm 0.8 ^c	18.6 \pm 0.5 ^{bc}	18.3 \pm 0.4 ^c	19.3 \pm 0.2 ^{bc}	19.4 \pm 0.2 ^b	18.7 \pm 0.3 ^{bc}	26.3 \pm 0.8 ^a
MUFA	39.9 \pm 0.5 ^d	40.2 \pm 0.3 ^d	39.8 \pm 0.6 ^d	52.5 \pm 0.2 ^a	51.8 \pm 0.3 ^{ab}	51.6 \pm 0.2 ^b	48.0 \pm 0.8 ^c
PUFA	41.6 \pm 0.4 ^a	41.2 \pm 0.5 ^a	41.9 \pm 0.5 ^a	28.3 \pm 0.4 ^c	28.7 \pm 0.3 ^{bc}	29.7 \pm 0.5 ^b	25.7 \pm 1.1 ^d
n-3	26.4 \pm 0.3 ^a	26.1 \pm 0.3 ^a	26.6 \pm 0.4 ^a	13.0 \pm 0.4 ^c	13.1 \pm 0.3 ^c	13.7 \pm 0.3 ^c	19.7 \pm 0.9 ^b
n-6	15.2 \pm 0.2 ^c	15.0 \pm 0.2 ^c	15.2 \pm 0.2 ^c	15.3 \pm 0.1 ^{bc}	15.6 \pm 0.2 ^b	16.0 \pm 0.2 ^a	5.94 \pm 0.2 ^d
n-3/n-6	1.74 \pm 0.02 ^b	1.74 \pm 0.02 ^b	1.75 \pm 0.02 ^b	0.85 \pm 0.02 ^c	0.84 \pm 0.02 ^c	0.85 \pm 0.02 ^c	3.32 \pm 0.07 ^a
Fatty acid	Phospholipids						
14:0	0.19 \pm 0.02 ^c	0.19 \pm 0.05 ^c	0.21 \pm 0.04 ^{bc}	0.25 \pm 0.04 ^{bc}	0.21 \pm 0.04 ^{bc}	0.30 \pm 0.05 ^b	1.10 \pm 0.11 ^a
16:0	18.3 \pm 0.48 ^c	19.0 \pm 0.72 ^c	18.8 \pm 0.73 ^c	20.2 \pm 0.48 ^b	20.1 \pm 0.68 ^b	20.5 \pm 0.59 ^b	22.4 \pm 0.45 ^a
16:1n-7	0.15 \pm 0.03 ^{cd}	0.14 \pm 0.03 ^d	0.14 \pm 0.06 ^{cd}	0.20 \pm 0.01 ^{bc}	0.20 \pm 0.02 ^{bc}	0.23 \pm 0.02 ^b	0.94 \pm 0.05 ^a
18:0	3.16 \pm 0.20 ^{ab}	3.71 \pm 0.70 ^a	3.30 \pm 0.29 ^{ab}	3.10 \pm 0.28 ^{ab}	2.92 \pm 0.32 ^b	3.04 \pm 0.32 ^{ab}	2.80 \pm 0.51 ^b
18:1n-9	11.4 \pm 0.7 ^b	11.2 \pm 0.9 ^b	11.1 \pm 0.6 ^b	15.2 \pm 0.6 ^a	15.0 \pm 0.9 ^a	14.9 \pm 1.3 ^a	7.71 \pm 0.5 ^c
18:2n-6	6.6 \pm 0.3 ^b	6.4 \pm 0.5 ^b	6.7 \pm 0.6 ^b	8.5 \pm 0.4 ^a	8.3 \pm 0.4 ^a	8.4 \pm 0.7 ^a	1.9 \pm 0.1 ^c
18:3n-3	12.4 \pm 1.0 ^a	11.8 \pm 0.9 ^a	11.8 \pm 1.1 ^a	6.8 \pm 0.4 ^b	6.5 \pm 0.4 ^b	6.6 \pm 0.6 ^b	1.5 \pm 0.1 ^c
18:4n-3	0.84 \pm 0.13 ^a	0.76 \pm 0.09 ^{ab}	0.67 \pm 0.08 ^{ab}	0.60 \pm 0.10 ^b	0.61 \pm 0.10 ^b	0.62 \pm 0.07 ^b	0.18 \pm 0.08 ^c
20:1n-9	0.36 \pm 0.05 ^c	0.38 \pm 0.10 ^c	0.46 \pm 0.11 ^c	0.73 \pm 0.07 ^b	0.77 \pm 0.13 ^b	0.71 \pm 0.10 ^b	1.11 \pm 0.08 ^a
20:3n-6	1.1 \pm 0.1 ^c	1.1 \pm 0.1 ^c	1.0 \pm 0.1 ^c	1.8 \pm 0.1 ^a	1.8 \pm 0.2 ^a	1.5 \pm 0.1 ^b	0.1 \pm 0.0 ^d
20:4n-6	0.7 \pm 0.1 ^b	0.7 \pm 0.1 ^b	0.6 \pm 0.1 ^b	1.1 \pm 0.1 ^a	1.1 \pm 0.1 ^a	1.0 \pm 0.1 ^a	1.0 \pm 0.1 ^a
20:3n-3	1.59 \pm 0.15 ^b	1.68 \pm 0.34 ^b	2.03 \pm 0.31 ^a	0.96 \pm 0.11 ^c	0.91 \pm 0.09 ^c	0.96 \pm 0.10 ^c	0.29 \pm 0.02 ^d
22:1n-11	3.2 \pm 0.2 ^a	3.3 \pm 0.2 ^a	3.4 \pm 0.5 ^a	2.1 \pm 0.1 ^b	2.1 \pm 0.2 ^b	2.0 \pm 0.1 ^b	1.7 \pm 0.1 ^b
20:5n-3	7.3 \pm 0.7 ^{ab}	6.7 \pm 0.8 ^{bc}	5.8 \pm 0.6 ^c	6.4 \pm 0.5 ^{bc}	6.6 \pm 0.4 ^{bc}	5.7 \pm 0.4 ^c	8.0 \pm 0.7 ^a
22:5n-3	2.16 \pm 0.23 ^b	1.92 \pm 0.10 ^{bc}	1.67 \pm 0.09 ^{cd}	1.86 \pm 0.14 ^c	1.88 \pm 0.10 ^c	1.55 \pm 0.15 ^d	2.87 \pm 0.20 ^a
22:6n-3	28.0 \pm 2.4 ^b	28.6 \pm 1.4 ^b	29.6 \pm 1.7 ^b	27.0 \pm 1.0 ^b	27.6 \pm 2.2 ^b	28.5 \pm 2.0 ^b	42.7 \pm 1.5 ^a
n-6 desat ratio ^e	2.44 \pm 0.13 ^{ab}	2.41 \pm 0.26 ^{ab}	2.56 \pm 0.26 ^a	2.18 \pm 0.13 ^b	2.15 \pm 0.17 ^b	2.39 \pm 0.27 ^{ab}	1.36 \pm 0.09 ^c
n-3 desat ratio ^f	0.3 \pm 0.0 ^a	0.3 \pm 0.0 ^a	0.3 \pm 0.0 ^a	0.2 \pm 0.0 ^b	0.2 \pm 0.0 ^b	0.2 \pm 0.0 ^b	0.0 \pm 0.0 ^c
SFA	21.6 \pm 0.1 ^c	22.9 \pm 1.3 ^{bc}	22.3 \pm 1.0 ^{bc}	23.5 \pm 0.5 ^b	23.2 \pm 0.9 ^b	23.8 \pm 0.6 ^b	26.7 \pm 0.9 ^a
MUFA	16.9 \pm 0.9 ^b	16.7 \pm 1.3 ^b	16.9 \pm 0.8 ^b	20.4 \pm 0.7 ^a	20.6 \pm 0.8 ^a	20.4 \pm 1.4 ^a	14.5 \pm 0.9 ^c
PUFA	61.5 \pm 1.1 ^a	60.5 \pm 0.3 ^{ab}	60.9 \pm 0.6 ^a	56.1 \pm 0.7 ^c	56.2 \pm 1.6 ^c	55.8 \pm 1.4 ^c	58.8 \pm 1.1 ^b

Table 4 continued

	V0.5S0	V0.5SL	V0.5SH	V1S0	V1SL	V1SH	F0
n-3	52.2 ± 1.2 ^b	51.4 ± 0.6 ^b	51.5 ± 0.9 ^b	43.6 ± 0.9 ^c	44.0 ± 1.8 ^c	43.9 ± 1.9 ^c	55.4 ± 1.1 ^a
n-6	9.26 ± 0.4 ^b	9.04 ± 0.4 ^b	9.32 ± 0.6 ^b	12.5 ± 0.4 ^a	12.2 ± 0.3 ^a	11.9 ± 0.6 ^a	3.36 ± 0.1 ^c
n-3/n-6	5.65 ± 0.3 ^b	5.70 ± 0.3 ^b	5.55 ± 0.4 ^b	3.50 ± 0.2 ^c	3.62 ± 0.2 ^c	3.71 ± 0.4 ^c	16.5 ± 0.6 ^a

For abbreviations see Table 1

SFA include 14:0, 15:0, 16:0, 17:0, 18:0, 20:0, 22:0

MUFA include 14:1, 16:1n-7, 17:1, 18:1n-9, 18:1n-7, 18:1n-5, 20:1n-9, 22:1n-11, 22:1n-9, 24:1

PUFA include 18:2n-6, 18:3n-3, 18:3n-6, 18:4n-3, 20:2n-6, 20:3n-6, 20:4n-6, 20:3n-3, 20:5n-3, 22:5n-3, 22:6n-3

^{a–d} Mean values across rows with different superscripts are significantly different ($p < 0.05$)

^e n-6 desat ratio = $18:2n-6 / (20:2n-6 + 20:3n-6 + 20:4n-6)$

^f n-3 desat ratio = $18:3n-3 / (18:4n-3 + 20:3n-3 + 20:5n-3 + 22:5n-3 + 22:6n-3)$

with the highest n-6/n-3 level compared with both the FO control and the V1S0 control.

The mRNA levels for PGC-1 α were significantly downregulated for both n-6/n-3 ratios compared with FO. No change was seen when sesamin was added to the low n-6/n-3 diet. However, for the group fed the diet with an n-6/n-3 ratio of 1 and inclusion of sesamin, the mRNA levels were similar to PGC-1 α expression in the FO diet.

SREBP-1 and SREBP-2 were significantly downregulated in the V0.5S0 group compared with the FO control. In groups fed sesamin together with low n-6/n-3 ratio (V0.5SL and V0.5SH), the mRNA expressions of SREBP-1 and SREBP-2 were significantly upregulated compared with V0.5S0, on the same level or higher than for FO (V0.5SL, V0.5SH and V1SL significantly different from V0.5S0; $p < 0.05$). The highest concentration of sesamin in combination with an n-6/n-3 ratio of 1 (V1) did not result in any significant change in expression of SREBP-1 and -2. The expression levels of SREBP-1 were significantly lower in the V1 groups, but did not change when sesamin was added. Gene expression level for SREBP-2 did not change from that of FO in tissue samples from V1 groups, nor did inclusion of sesamin change the mRNA levels compared with the FO group.

Expression of LXR α in tissues from fish fed V0.5 diets was significantly decreased compared with fish fed the FO diet. However, with addition of sesamin, LXR α was significantly upregulated for both levels, returning to the same level as for fish fed the FO diet. For fish fed V1 diets with or without sesamin, no change in LXR α expression was seen compared with the FO control.

Lipid Uptake

CD36 mRNA levels remained unchanged in tissues from fish fed the VO diet compared with the FO diet. Addition of sesamin decreased expression of CD36 significantly in fish fed the high n-6/n-3 diet compared with both the FO

control and the VO control (V1S0). SR-B1 expression was not affected by changes in n-6/n-3 ratio or addition of sesamin (Fig. 1b).

Desaturation and Elongation

The effects on desaturation and elongation genes are shown in Fig. 1c. Expression of $\Delta 6$ fad and $\Delta 5$ fad was significantly downregulated in the V0.5 diets compared with FO. The levels of $\Delta 6$ fad mRNA were significantly upregulated in liver of fish fed V0.5SL and V0.5SH compared with V0.5S0 and exceeded the levels seen in the FO control ($p < 0.05$). This trend was consistent for the results observed for $\Delta 5$ fad (except for V0.5SL; $p < 0.05$). The V1S0 diet significantly increased expression of $\Delta 6$ fad and $\Delta 5$ fad, compared with FO. However, when sesamin was included in the V1 diet, the levels of $\Delta 6$ fad mRNA decreased ($p < 0.05$).

The levels of ELOVL5b (V0.5S0 and V1S0; $p < 0.05$) and ELOVL2 (V1S0; $p < 0.05$) increased in both VO diets irrespective of the n-6/n-3 ratio. Sesamin also decreased expression of ELOVL5b in V1SL compared with V1S0. Sesamin lowered expression of ELOVL2 in the diets with an n-6/n-3 ratio of 1 (V0.5SH and V1SH; $p < 0.05$).

The transcription level of ELOVL5a was not affected by VO compared with FO. Expression of ELOVL5a was increased by the addition of sesamin for fish fed the diets with lower n-6/n-3 ratio (V0.5SH; $p < 0.05$). No effect of sesamin on ELOVL5a was seen in the diets with higher n-6/n-3 ratio.

When sesamin was added, expression of ELOVL4 was upregulated for V0.5SL and V1SH compared with V0.5S0 and V1S0.

β -Oxidation

CPT1 mRNA expression increased significantly in liver samples from fish fed diets with higher n-6/n-3 ratios. However, when sesamin was added to V0.5 diets (V0.5SL

Table 5 Fat content (%) and fatty acid composition (%) in the triacylglycerol and phospholipid fractions of liver from Atlantic salmon fed seven experimental diets, mean value \pm SD, $n = 8$

	V0.5S0	V0.5SL	V0.5SH	V1S0	V1SL	V1SH	F0
Fat content	5.00 \pm 0.45 ^c	4.93 \pm 0.59 ^c	7.38 \pm 1.83 ^{ab}	5.05 \pm 0.56 ^c	5.72 \pm 0.93 ^{bc}	8.03 \pm 2.29 ^a	4.18 \pm 0.41 ^c
Fatty acid	Triacylglycerol						
14:0	1.2 \pm 0.6 ^b	0.8 \pm 0.2 ^b	0.7 \pm 0.1 ^b	0.9 \pm 0.1 ^b	0.8 \pm 0.2 ^b	0.7 \pm 0.1 ^b	2.9 \pm 0.1 ^a
16:0	8.5 \pm 2.6 ^b	7.9 \pm 2.1 ^b	6.3 \pm 0.9 ^b	7.9 \pm 1.0 ^b	6.8 \pm 2.0 ^b	5.8 \pm 0.9 ^b	13.1 \pm 2.1 ^a
16:1n-7	1.4 \pm 0.1 ^c	1.3 \pm 0.2 ^c	1.3 \pm 0.2 ^c	1.7 \pm 0.1 ^b	1.4 \pm 0.1 ^c	1.3 \pm 0.2 ^c	4.8 \pm 0.3 ^a
18:0	7.01 \pm 1.02 ^a	5.36 \pm 0.74 ^{bc}	6.04 \pm 1.12 ^{ab}	5.77 \pm 0.75 ^{abc}	5.03 \pm 0.70 ^{bcd}	4.72 \pm 0.83 ^{cd}	3.83 \pm 0.50 ^d
18:1n-9	46.5 \pm 3.4 ^c	44.3 \pm 4.3 ^c	47.6 \pm 2.2 ^c	61.7 \pm 1.5 ^a	54.9 \pm 3.6 ^b	54.6 \pm 1.0 ^b	33.0 \pm 3.6 ^d
18:2n-6	11.0 \pm 1.18 ^b	12.5 \pm 1.01 ^a	11.8 \pm 0.89 ^{ab}	10.8 \pm 0.67 ^b	11.8 \pm 0.87 ^{ab}	11.9 \pm 0.81 ^{ab}	5.71 \pm 0.36 ^c
18:3n-3	11.1 \pm 1.85 ^b	13.7 \pm 2.35 ^a	12.4 \pm 1.44 ^{ab}	5.29 \pm 0.72 ^c	5.30 \pm 1.01 ^c	5.45 \pm 0.40 ^c	2.58 \pm 0.26 ^d
18:4n-3	0.79 \pm 0.34 ^{ab}	1.04 \pm 0.35 ^a	0.67 \pm 0.17 ^{ab}	0.52 \pm 0.03 ^b	0.47 \pm 0.21 ^b	0.40 \pm 0.15 ^b	0.93 \pm 0.36 ^a
20:1n-9	4.09 \pm 0.59 ^{ef}	4.03 \pm 0.75 ^f	4.91 \pm 0.46 ^{de}	6.09 \pm 0.38 ^{bc}	5.58 \pm 0.55 ^{cd}	6.61 \pm 0.58 ^{ab}	7.29 \pm 0.39 ^a
20:3n-6	0.56 \pm 0.10 ^{bcd}	0.49 \pm 0.10 ^{cd}	0.43 \pm 0.08 ^d	0.78 \pm 0.11 ^a	0.66 \pm 0.11 ^{ab}	0.57 \pm 0.08 ^{bc}	Trace
20:4n-6	Trace	Trace	Trace	0.21 \pm 0.02	Trace	0.18 \pm 0.01	0.44 \pm 0.08
20:3n-3	1.42 \pm 0.25 ^b	1.73 \pm 0.43 ^b	2.19 \pm 0.36 ^a	0.66 \pm 0.06 ^{cd}	0.72 \pm 0.15 ^{cd}	0.97 \pm 0.16 ^c	0.47 \pm 0.06 ^d
22:1n-11	0.32 \pm 0.03 ^{cd}	0.31 \pm 0.02 ^d	0.31 \pm 0.02 ^d	0.42 \pm 0.05 ^b	0.33 \pm 0.06 ^{cd}	0.38 \pm 0.04 ^{bc}	0.61 \pm 0.05 ^a
20:5n-3	0.79 \pm 0.21 ^{bc}	0.89 \pm 0.17 ^b	0.44 \pm 0.14 ^{cd}	0.72 \pm 0.18 ^{bc}	0.51 \pm 0.16 ^{cd}	0.36 \pm 0.14 ^d	4.07 \pm 0.46 ^a
22:5n-3	0.27 \pm 0.09 ^{bc}	0.33 \pm 0.10 ^b	0.17 \pm 0.01 ^d	0.28 \pm 0.08 ^{bc}	0.20 \pm 0.11 ^{cd}	0.23 \pm 0.01 ^d	2.47 \pm 0.22 ^a
22:6n-3	1.2 \pm 0.5 ^{bc}	1.5 \pm 0.6 ^b	0.5 \pm 0.2 ^c	1.3 \pm 0.4 ^{bc}	0.8 \pm 0.5 ^{bc}	0.7 \pm 0.3 ^{bc}	10.6 \pm 1.0 ^a
n-6 desat ratio ^g	5.4 \pm 0.8 ^{ab}	6.6 \pm 1.9 ^a	5.0 \pm 0.5 ^{bc}	3.8 \pm 0.5 ^c	5.0 \pm 0.8 ^{bc}	4.5 \pm 0.3 ^{bc}	4.2 \pm 0.7 ^{bc}
n-3 desat ratio ^h	2.57 \pm 0.57 ^b	2.55 \pm 0.36 ^b	3.25 \pm 0.34 ^a	1.60 \pm 0.39 ^c	2.18 \pm 0.51 ^{bc}	2.33 \pm 0.37 ^b	0.14 \pm 0.01 ^d
SFA	16.6 \pm 3.79 ^b	14.0 \pm 1.82 ^{bcd}	13.1 \pm 1.64 ^{cd}	14.8 \pm 1.47 ^{bc}	12.7 \pm 1.71 ^{cd}	11.3 \pm 1.22 ^d	20.5 \pm 2.32 ^a
MUFA	54.5 \pm 3.7 ^c	52.4 \pm 5.2 ^c	56.6 \pm 2.6 ^c	73.6 \pm 1.8 ^a	65.3 \pm 4.2 ^b	66.2 \pm 1.5 ^b	51.4 \pm 3.8 ^c
PUFA	28.6 \pm 2.95 ^b	33.6 \pm 3.63 ^a	30.3 \pm 2.92 ^{ab}	22.4 \pm 1.31 ^c	22.1 \pm 2.60 ^c	22.5 \pm 1.48 ^c	28.2 \pm 1.53 ^b
n-3	15.5 \pm 2.00 ^b	19.1 \pm 3.11 ^a	16.2 \pm 1.99 ^b	8.72 \pm 0.95 ^c	7.89 \pm 1.89 ^c	7.86 \pm 0.79 ^c	21.1 \pm 1.34 ^a
n-6	13.0 \pm 1.16 ^b	14.4 \pm 0.76 ^a	14.1 \pm 1.04 ^{ab}	13.7 \pm 0.58 ^{ab}	14.2 \pm 0.86 ^{ab}	14.6 \pm 0.92 ^a	7.09 \pm 0.30 ^c
n-3/n-6	1.2 \pm 0.1 ^b	1.3 \pm 0.2 ^b	1.2 \pm 0.1 ^b	0.6 \pm 0.1 ^c	0.6 \pm 0.1 ^c	0.5 \pm 0.1 ^c	3.0 \pm 0.2 ^a
Fatty acid	Phospholipids						
14:0	0.7 \pm 0.2 ^b	0.3 \pm 0.0 ^c	0.4 \pm 0.0 ^c	0.3 \pm 0.0 ^c	0.3 \pm 0.0 ^c	0.3 \pm 0.0 ^c	1.1 \pm 0.1 ^a
16:0	17.0 \pm 0.98 ^a	16.9 \pm 0.55 ^a	16.9 \pm 0.91 ^a	15.7 \pm 0.65 ^b	15.8 \pm 0.53 ^b	14.8 \pm 0.72 ^b	17.3 \pm 0.71 ^a
16:1n-7	0.36 \pm 0.04 ^b	0.34 \pm 0.04 ^{bc}	0.32 \pm 0.05 ^{bc}	0.34 \pm 0.03 ^{bc}	0.33 \pm 0.05 ^{bc}	0.29 \pm 0.04 ^c	1.09 \pm 0.05 ^a
18:0	9.0 \pm 0.8 ^a	8.5 \pm 0.6 ^a	8.6 \pm 0.7 ^a	7.2 \pm 0.4 ^b	7.2 \pm 0.6 ^b	7.2 \pm 0.3 ^b	6.7 \pm 0.5 ^b
18:1n-9	14.8 \pm 0.87 ^b	14.9 \pm 0.43 ^b	16.2 \pm 0.99 ^a	16.2 \pm 0.81 ^a	16.6 \pm 0.51 ^a	17.0 \pm 0.87 ^a	10.5 \pm 0.42 ^c
18:2n-6	6.4 \pm 0.5 ^c	7.1 \pm 0.5 ^{ab}	7.3 \pm 0.4 ^{ab}	6.8 \pm 0.2 ^{bc}	6.9 \pm 0.2 ^{ab}	7.4 \pm 0.4 ^a	2.1 \pm 0.1 ^d
18:3n-3	4.07 \pm 0.58 ^b	4.80 \pm 0.56 ^a	5.13 \pm 0.48 ^a	1.82 \pm 0.14 ^c	2.06 \pm 0.22 ^c	2.24 \pm 0.30 ^c	0.55 \pm 0.06 ^d
18:4n-3	0.21 \pm 0.10 ^a	0.28 \pm 0.04 ^a	0.20 \pm 0.12 ^a	0.10 \pm 0.02 ^b	0.10 \pm 0.05 ^b	n.d	0.21 \pm 0.02 ^a
20:1n-9	1.47 \pm 0.27 ^d	1.59 \pm 0.29 ^{cd}	1.98 \pm 0.19 ^b	1.96 \pm 0.21 ^b	1.92 \pm 0.14 ^{bc}	2.61 \pm 0.26 ^a	2.66 \pm 0.20 ^a
20:3n-6	2.3 \pm 0.2 ^{cd}	2.2 \pm 0.1 ^d	2.0 \pm 0.3 ^d	3.1 \pm 0.2 ^a	2.8 \pm 0.3 ^{ab}	2.6 \pm 0.3 ^{bc}	0.3 \pm 0.0 ^e
20:4n-6	2.3 \pm 0.2 ^c	2.3 \pm 0.3 ^c	2.0 \pm 0.2 ^c	3.9 \pm 0.3 ^a	3.9 \pm 0.4 ^a	3.3 \pm 0.5 ^b	4.0 \pm 0.1 ^a
20:3n-3	1.11 \pm 0.20 ^b	1.30 \pm 0.16 ^b	1.64 \pm 0.23 ^a	0.51 \pm 0.05 ^d	0.56 \pm 0.06 ^{cd}	0.77 \pm 0.12 ^c	0.29 \pm 0.02 ^e
20:5n-3	8.9 \pm 1.1 ^a	8.9 \pm 1.0 ^a	6.8 \pm 0.9 ^{bc}	7.7 \pm 0.9 ^{ab}	7.6 \pm 0.5 ^{ab}	6.1 \pm 1.0 ^c	8.7 \pm 0.9 ^a
22:5n-3	2.05 \pm 0.36 ^b	1.89 \pm 0.26 ^{bc}	1.59 \pm 0.22 ^{cd}	1.87 \pm 0.19 ^{bc}	2.00 \pm 0.22 ^b	1.42 \pm 0.26 ^d	2.73 \pm 0.21 ^a
22:6n-3	27.1 \pm 2.30 ^d	28.1 \pm 0.82 ^{cd}	26.3 \pm 1.71 ^d	29.9 \pm 1.03 ^{bc}	29.2 \pm 0.79 ^{bc}	30.6 \pm 1.31 ^b	38.5 \pm 1.09 ^a
n-6 desat ratio ^g	1.0 \pm 0.1 ^{bc}	1.2 \pm 0.1 ^{ab}	1.2 \pm 0.1 ^a	0.8 \pm 0.1 ^e	0.8 \pm 0.1 ^{de}	0.9 \pm 0.1 ^{cd}	0.4 \pm 0.0 ^f
n-3 desat ratio ^h	0.10 \pm 0.02 ^b	0.12 \pm 0.02 ^b	0.14 \pm 0.01 ^a	0.05 \pm 0.00 ^c	0.05 \pm 0.01 ^c	0.06 \pm 0.01 ^c	0.01 \pm 0.00 ^d
SFA	26.7 \pm 1.3 ^a	25.8 \pm 0.4 ^a	25.9 \pm 1.4 ^a	23.1 \pm 0.7 ^b	23.3 \pm 0.9 ^b	22.3 \pm 0.8 ^b	25.6 \pm 0.6 ^a
MUFA	17.5 \pm 0.90 ^d	17.7 \pm 0.67 ^d	19.4 \pm 1.16 ^c	19.6 \pm 0.82 ^c	19.9 \pm 0.53 ^{bc}	21.1 \pm 1.01 ^b	32.3 \pm 0.66 ^a
PUFA	55.8 \pm 1.8 ^{bc}	58.4 \pm 0.5 ^a	54.7 \pm 1.9 ^c	57.3 \pm 0.3 ^{ab}	56.8 \pm 0.7 ^{ab}	56.5 \pm 0.6 ^b	58.3 \pm 0.8 ^a
n-3	43.4 \pm 1.48 ^c	45.3 \pm 0.44 ^b	41.6 \pm 1.87 ^d	41.9 \pm 0.37 ^{cd}	41.5 \pm 0.80 ^d	41.1 \pm 0.60 ^d	51.0 \pm 0.72 ^a

Table 5 continued

	V0.5S0	V0.5SL	V0.5SH	V1S0	V1SL	V1SH	FO
n-6	12.5 ± 0.35 ^c	13.2 ± 0.30 ^b	13.1 ± 0.45 ^b	15.4 ± 0.37 ^a	15.3 ± 0.36 ^a	15.4 ± 0.39 ^a	7.28 ± 0.18 ^d
n-3/n-6	3.48 ± 0.07 ^b	3.44 ± 0.08 ^{bc}	3.17 ± 0.19 ^c	2.72 ± 0.08 ^d	2.72 ± 0.10 ^d	2.68 ± 0.09 ^d	7.01 ± 0.19 ^a

For abbreviations see Table 1

SFA include 14:0, 15:0, 16:0, 17:0, 18:0, 20:0, 22:0

MUFA include 14:1, 16:1n-7, 17:1, 18:1n-9, 18:1n-7, 18:1n-5, 20:1n-9, 22:1n-11, 22:1n-9, 24:1

PUFA include 18:2n-6, 18:3n-3, 18:3n-6, 18:4n-3, 20:2n-6, 20:3n-6, 20:4n-6, 20:3n-3, 20:5n-3, 22:5n-3, 22:6n-3

^{a–f} Mean values across rows with different superscripts are significantly different ($p < 0.05$)

^g n-6 desat ratio = $18:2n-6 / (20:2n-6 + 20:3n-6 + 20:4n-6)$

^h n-3 desat ratio = $18:3n-3 / (18:4n-3 + 20:3n-3 + 20:5n-3 + 22:5n-3 + 22:6n-3)$

and V0.5SH), the levels of CPT1 mRNA decreased (V0.5SH; $p < 0.05$) (Fig. 1d). There was an equivalent decrease for the highest concentration of sesamin in the V1 diet (V1SH; $p < 0.05$).

Gene expression of ACO increased 2.7-fold when sesamin was added at the higher concentration compared with FO in diets with an n-6/n-3 ratio of 0.5, but decreased 0.6-fold ($p < 0.05$) when the n-6/n-3 ratio was 1.

Discussion

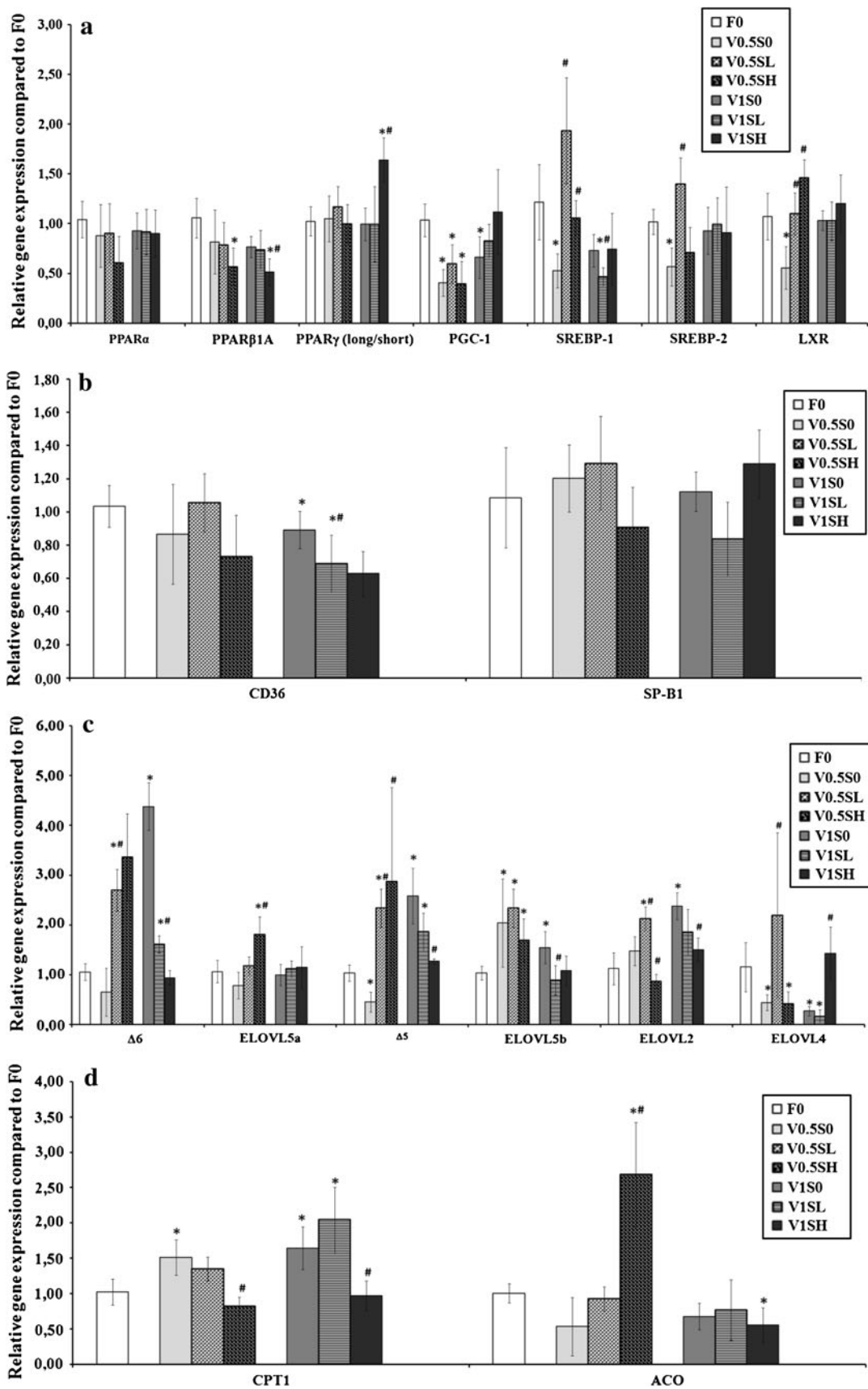
The main objective of this study was to investigate whether Atlantic salmon responded differently to sesamin addition depending on n-6/n-3 ratio in the diet.

Replacement of FO with VO did not affect growth performance measured as weight, K factor and FCR in the present study. Inclusion of sesamin had a dose-dependent negative effect on growth, but only the highest inclusion resulted in significantly reduced weight and SGR of the fish. The results do not suggest diet dependent differences in feed utilization of feeds with and without sesamin (overall K factor was 1.31 ± 0.09). VO has been shown not to affect growth performance in studies on Atlantic salmon [2, 4, 45] and rainbow trout [6]. The inclusion of sesamin showed no effect on growth performance in Baltic Atlantic salmon [46], rainbow trout [6] and carp [47]. The reduced growth in the high sesamin groups is in agreement with studies on other bioactive compounds e.g. dodecylthioacetic acid (DTA) and tetradecylthioacetic acid (TTA) at 5 °C [48], and Moya-Falcon et al. [49] showed that a TTA diet (0.6 % TTA to FO) lowers the body weight of Atlantic salmon at 12 °C. The Atlantic salmon white muscle lipid content was approximately 1.6 % in all groups. No effects on palatability of feeds containing any of these bioactive compounds have been reported so far. Liver fat content was significantly increased by addition of the high level of sesamin, confirming previous findings in rats [18]. In contrast, the liver lipid content is reported to be

unaffected by the addition of TTA to Atlantic salmon diets [49]. As expected, replacement of FO with VO reduced the proportion of DHA five-fold in muscle TAG and ten-fold in liver TAG, but in the PL fraction by only approximately 1.5-fold in both muscle and liver. Sesamin affected FA involved in the synthesis of DHA, e.g. 20:3n-3 increased, EPA and 22:5n-3 decreased and a slight increase in DHA was detected (non significant). Increased levels of 18:2n-6 and 18:3n-3 were also observed as an effect of VO inclusion compared with FO. These results are in agreement with Bell et al. [4], who found that replacement of FO with rapeseed oil (100 %) lowered the proportion of DHA in liver by more than fourfold, but in muscle lipids by only twofold. Similarly, Kleveland et al. [48] showed that dietary TTA increased 18:2n-6 and that DTA increased EPA and 22:5n-3 in white muscle. In the previous study, a significant increase in DHA was observed on addition of a dietary sesamin/episesamin mixture [17].

These different responses to bioactive compounds could be explained by several factors: (1) The physiological response to sesamin may vary between fish size or species. It is well known that in freshwater fish, ALA is converted to EPA and then to DHA [15, 50]. (2) Within the same species, variations in the response to sesamin may depend on age, gender and possibly environmental conditions such as temperature and feed composition. The feeding period could also affect physiological response to sesamin. In the present study, the experimental diets were fed to fish for 4 months, which is longer than in previous studies (8–11 weeks) [6, 18, 47]. Furthermore, seawater stage fish have a lower capacity to convert ALA to DHA than freshwater fish [50–52]. (3) In our study pure sesamin was used,

Fig. 1 Relative expression of genes shown as fold change in liver of fish fed the fish oil (FO) diet and experimental diets with and without sesamin (S). (a) Transcription factors, (b) uptake, (c) elongation, desaturation and (d) β -oxidation. * Denotes significant difference from fish fed the FO diet ($p < 0.05$), n = 6; # Denotes significant difference from fish fed the vegetable oil (VO) diet without sesamin ($p < 0.05$), n = 6. For abbreviations see Tables 1 and 2



whereas Trattner et al. [6, 18] supplemented the fish diet with an equi-mixture of sesamin/episesamin for rainbow trout and Baltic Atlantic salmon. The same mixture was used in a study on Atlantic salmon hepatocytes [8]. It has previously been shown in mammals that episesamin might be more effective in modulating the activity of enzymes involved in lipid metabolism. Therefore, the presence of episesamin in the diet of fish may be important for modulation of FA composition.

The two different n-6/n-3 ratios had an impact on n-3 FA content in fish, mainly in that the higher ratio resulted in lower amounts of ALA. This decrease was not reflected in the percentage of DHA and EPA. The addition of sesamin to diets with low n-6/n-3 ratio increased desaturation index (ALA/(18:4n-3 + n-3 LCPUFA)) in the TAG and PL fractions of liver more than muscle. The desaturation index also increased in the TAG fraction of the liver for diets with high n-6/n-3 ratio. The significant increase in elongation and desaturation index for V0.5 diet could be explained by the higher substrate availability compared with the V1 diet.

Very limited responses were seen for all transcription factors tested. No effect was seen on PPAR α expression. In the case of PPAR γ long, significant upregulation was seen when sesamin was added to higher n-6/n-3 ratio diets, while for PPAR β 1A sesamin decreased the mRNA expression level. This could indicate that the effect of sesamin is not caused by ligand binding to the PPARs. Cloning analysis of the ligand binding regions of PPAR α and PPAR γ genes in Atlantic salmon have revealed that they contain additional amino acid residuals, which could suggest that the ligand binding properties in salmon PPARs can differ from those seen in rodents [53]. This could explain the deviation from findings in rodents [20].

Since both PPAR α and PPAR γ have been shown to induce the transcription of CD36 and SR-B1 [54–56], it was not surprising that the effects on these genes were limited. Only CD36 was significantly downregulated in tissues from fish fed the higher dietary ratio of n-6/n-3 with sesamin added.

Expression of SREBP-1 and SREBP-2 was significantly increased by sesamin addition to the low n-6/n-3 ratio diets, and in fish fed these diets the SREBP target genes desaturases and elongases were also significantly upregulated. It has been shown in liver hepatocytes of rodents that ELOVL5 elongase, Δ 6 fad and Δ 5 fad desaturase expression are regulated by both PPAR α and SREBP-1c [57, 58]. In agreement with this, the present study showed increased expression of SREBP, elongases and desaturases.

The transcription rate of all elongases except ELOVL5a was increased in the liver of salmon fed VO, irrespective of the n-6/n-3 ratio, compared with that of fish fed a FO diet. This is in line with Morais et al. [16] who reported that expression of ELOVL5b and ELOVL2, but not that of ELOVL5a, was significantly increased in both liver and

intestine when Atlantic salmon were fed VO instead of FO. ELOVL5b codes for genes involved in the elongation of C18 to C20 PUFA and ELOVL2 for genes involved in the elongation of C20 to C22 [16, 17]. The increase in ELOVL5b and ELOVL2 in fish fed the VO diet (V0.5) with low sesamin addition was accompanied by upregulation of SREBP-1c and a non significant increase in the amount of 20:3n-3 and DHA in both the TAG and the PL fractions. However, PPAR α expression was not affected by sesamin inclusion. Fish fed the V0.5SL and V0.5SH diets showed increased expression of LXR compared with fish fed the V0.5S0 diet. This could indicate that sesamin acts on SREBP-1c directly, or indirectly by activation of liver X receptor α (LXR α). The increased expression of LXR α and SREBP can also be associated, since LXR α and LXR β have been shown to activate SREBP-1c in rodents [33, 34].

Expression of desaturation and elongation genes increased significantly with addition of sesamin. The effect of sesamin seemed to be influenced by the n-6/n-3 ratio in the feed. For the lower n-6/n-3 ratio sesamin increased desaturation and elongation, while for the higher n-6/n-3 ratio sesamin decreased both desaturation and elongation. This is similar to results reported by Trattner et al. [8]. A possible interaction between feed FA composition and sesamin content could explain the different results between the groups in the present study.

Earlier studies in rats [20, 59] and in salmon hepatocytes [8] found that sesamin positively influenced the activity and gene expression of both ACO and CPT1, which are involved in peroxisomal and mitochondrial β -oxidation, respectively. In the low n-6/n-3 ratio groups we found similar results for ACO but not for CPT1. However, in our study both ACO and CPT1 were significantly downregulated after high sesamin addition in the high n-6/n-3 ratio diet. This might indicate that the n-6/n-3 ratio influenced the response of β -oxidation genes to sesamin.

The lack of correlation between desaturase expression and LCPUFA biosynthesis may also indicate that the effect of sesamin was mediated through other mechanisms not yet understood.

Several studies have shown that the enzymes and the genes involved in the biosynthesis of highly unsaturated FA are upregulated after VO feeding [60, 61]. In our study, sesamin inclusion in both VO diets increased DHA levels in the TAG and PL fractions. This is in agreement with findings reported for Atlantic salmon and rainbow trout [6, 8, 46].

Conclusions

The addition of sesamin to vegetable oil-based diets affected the expression of genes involved in the lipid metabolism and had minor effects on fatty acids. The

response to sesamin was affected by the dietary n-6/n-3 ratio. High sesamin inclusion had a negative effect on growth rate but did not affect the feed conversion ratio or the condition factor.

References

- Gordon Bell J, James Henderson R, Tocher DR, McGhee F, Dick JR, Porter A, Smullen RP, Sargent JR (2002) Substituting fish oil with crude palm oil in the diet of Atlantic salmon (*Salmo salar*) affects muscle fatty acid composition and hepatic fatty acid metabolism. *J Nutr* 132:222–230
- Torstensen BE, Bell JG, Rosenlund G, Henderson RJ, Graff IE, Tocher DR, Lie Ø, Sargent JR (2005) Tailoring of Atlantic salmon (*Salmo salar* L.) flesh lipid composition and sensory quality by replacing fish oil with a vegetable oil blend. *J Agric Food Chem* 53:10166–10178
- Sargent J, McEvoy L, Estevez A, Bell G, Bell M, Henderson J, Tocher DR (1999) Lipid nutrition of marine fish during early development: current status and future directions. *Aquaculture* 179:217–229
- Bell JG, McEvoy J, Tocher DR, McGhee F, Campbell PJ, Sargent JR (2001) Replacement of fish oil with rapeseed oil in diets of Atlantic salmon (*Salmo salar*) affects tissue lipid compositions and hepatocyte fatty acid metabolism. *J Nutr* 131:1535–1543
- Bell JG, Henderson RJ, Tocher DR, Sargent JR (2004) Replacement of dietary fish oil with increasing levels of linseed oil: modification of flesh fatty acid compositions in Atlantic salmon (*Salmo salar*) using a fish oil finishing diet. *Lipids* 39:223–232
- Trattner S, Kamal-Eldin A, Brännäs E, Moazzami AA, Žlábek V, Larsson P, Ruyter B, Gjøen T, Pickova J (2008) Sesamin supplementation increases white muscle docosahexaenoic acid (DHA) levels in rainbow trout (*Oncorhynchus mykiss*) fed high alpha-linolenic acid (ALA) containing vegetable oil: metabolic actions. *Lipids* 43:989–997
- Trattner S, Pickova J, Park KH, Rinchar J, Dabrowski K (2007) Effects of alpha-lipoic and ascorbic acid on the muscle and brain fatty acids and antioxidant profile of the South American pacu *Piaractus mesopotamicus*. *Aquaculture* 273:158–164
- Trattner S, Ruyter B, Ostbye TK, Gjøen T, Zlabek V, Kamal-Eldin A, Pickova J (2008) Sesamin increases alpha-linolenic acid conversion to docosahexaenoic acid in Atlantic salmon (*Salmo salar* L.) hepatocytes: role of altered gene expression. *Lipids* 43:999–1008
- Kennedy SR, Bickerdike R, Berge RK, Porter AR, Tocher DR (2007) Influence of dietary conjugated linoleic acid (CLA) and tetradecylthioacetic acid (TTA) on growth, lipid composition and key enzymes of fatty acid oxidation in liver and muscle of Atlantic cod (*Gadus morhua* L.). *Aquaculture* 264:372–382
- Vegusdal A, Gjøen T, Berge RK, Thomassen MS, Ruyter B (2005) Effect of 18:1n-9, 20:5n-3, and 22:6n-3 on lipid accumulation and secretion by Atlantic salmon hepatocytes. *Lipids* 40:477–486
- Vegusdal A, Østbye T-K, Tran TN, Gjøen T, Ruyter B (2004) β -Oxidation, esterification, and secretion of radiolabeled fatty acids in cultivated Atlantic salmon skeletal muscle cells. *Lipids* 39:649–658
- Buzzi M, Henderson RJ, Sargent JR (1996) The desaturation and elongation of linolenic acid and eicosapentaenoic acid by hepatocytes and liver microsomes from rainbow trout (*Oncorhynchus mykiss*) fed diets containing fish oil or olive oil. *Biochim Biophys Acta Lipids Lipid Metab* 1299:235–244
- Tocher DR, Dick JR (1990) Polyunsaturated fatty acid metabolism in cultured fish cells: incorporation and metabolism of (n-3) and (n-6) series acids by Atlantic salmon (*Salmo salar*) cells. *Fish Physiol Biochem* 8:311–319
- Buzzi M, Henderson RJ, Sargent JR (1997) Biosynthesis of docosahexaenoic acid in trout hepatocytes proceeds via 24-carbon intermediates. *Comp Biochem Physiol B: Biochem Mol Biol* 116:263–267
- Bell MV, Dick JR, Porter AEA (2001) Biosynthesis and tissue deposition of docosahexaenoic acid (22:6n-3) in rainbow trout (*Oncorhynchus mykiss*). *Lipids* 36:1153–1159
- Morais S, Monroig O, Zheng XZ, Leaver MJ, Tocher DR (2009) Highly Unsaturated Fatty Acid Synthesis in Atlantic Salmon: characterization of ELOVL5- and ELOVL2-like Elongases. *Mar Biotechnol* 11:627–639
- Hastings N, Agaba MK, Tocher DR, Zheng X, Dickson CA, Dick JR, Teale AJ (2004) Molecular cloning and functional characterization of fatty acyl desaturase and elongase cDNAs involved in the production of eicosapentaenoic and docosahexaenoic acids from α -linolenic acid in Atlantic salmon (*Salmo salar*). *Mar Biotechnol* 6:463–474
- Trattner S, Ruyter B, Ostbye TK, Kamal-Eldin A, Moazzami A, Pan J, Gjoen T, Brannas E, Zlabek V, Pickova J (2011) Influence of dietary sesamin, a bioactive compound on fatty acids and expression of some lipid regulating genes in Baltic Atlantic salmon (*Salmo salar* L.) juveniles. *Physiol Res* 60:125–137
- Ide T, Nakashima Y, Iida H, Yasumoto S, Katsuta M (2009) Lipid metabolism and nutrigenomics—Impact of sesame lignans on gene expression profiles and fatty acid oxidation in rat liver. *Forum Nutr* 61:10–24
- Ashakumary L, Rouyer I, Takahashi Y, Ide T, Fukuda N, Aoyama T, Hashimoto T, Mizugaki M, Sugano M (1999) Sesamin, a sesame lignan, is a potent inducer of hepatic fatty acid oxidation in the rat. *Metab Clin Exp* 48:1303–1313
- Lim JS, Adachi Y, Takahashi Y, Ide T (2007) Comparative analysis of sesame lignans (sesamin and sesamol) in affecting hepatic fatty acid metabolism in rats. *Br J Nutr* 97:85–95
- Kiso Y, Tsuruoka N, Kidokoro A, Matsumoto I, Abe K (2005) Sesamin ingestion regulates the transcription levels of hepatic metabolizing enzymes for alcohol and lipids in rats. *Alcoholism Clin Exp Res* 29:116S–120S
- Tsuruoka N, Kidokoro A, Matsumoto I, Abe K, Kiso Y (2005) Modulating effect of sesamin, a functional lignan in sesame seeds, on the transcription levels of lipid- and alcohol-metabolizing enzymes in rat liver: a DNA microarray study. *Biosci Biotechnol Biochem* 69:179–188
- Kiso Y (2004) Antioxidative roles of sesamin, a functional lignan in sesame seed, and its effect on lipid- and alcohol-metabolism in the liver: a DNA microarray study. *BioFactors* 21:191–196
- Kushiro M, Masaoka T, Hageshita S, Takahashi Y, Ide T, Sugano M (2002) Comparative effect of sesamin and episesamin on the activity and gene expression of enzymes in fatty acid oxidation and synthesis in rat liver. *J Nutr Biochem* 13:289–295
- Fujiyamafujiwara Y, Umedasawada R, Kuzuyama M, Igarashi O (1995) Effects of sesamin on the fatty-acid composition of the liver of rats fed N-6 and N-3 fatty acid-rich diet. *J Nutr Sci Vitam* 41:217–225
- Arachchige PG, Takahashi Y, Ide T (2006) Dietary sesamin and docosahexaenoic and eicosapentaenoic acids synergistically increase the gene expression of enzymes involved in hepatic peroxisomal fatty acid oxidation in rats. *Metabolism Clin Exp* 55:381–390
- LeMoine CMR, Genge CE, Moyes CD (2008) Role of the PGC-1 family in the metabolic adaptation of goldfish to diet and temperature. *J Exp Biol* 211:1448–1455

29. McGarry JD, Brown NF (1997) The mitochondrial carnitine palmitoyltransferase system. From concept to molecular analysis. *Eur J Biochem* 244:1–14
30. Varanasi U, Chu R, Huang Q, Castellon R, Yeldandi AV, Reddy JK (1996) Identification of a peroxisome proliferator-responsive element upstream of the human peroxisomal fatty acyl coenzyme A oxidase gene. *J Biol Chem* 271:2147–2155
31. Boukouvala E, Leaver MJ, Favre-Krey L, Theodoridou M, Krey G (2010) Molecular characterization of a gilthead sea bream (*Sparus aurata*) muscle tissue cDNA for carnitine palmitoyltransferase 1B (CPT1B). *Comp Biochem Physiol B: Biochem Mol Biol* 157:189–197
32. Leaver MJ, Villeneuve LAN, Obach A, Jensen L, Bron JE, Tocher DR, Taggart JB (2008) Functional genomics reveals increases in cholesterol biosynthetic genes and highly unsaturated fatty acid biosynthesis after dietary substitution of fish oil with vegetable oils in Atlantic salmon (*Salmo salar*). *BMC Genomics* 9:299
33. Zhou J, Febbraio M, Wada T, Zhai Y, Kuruba R, He J, Lee JH, Khadem S, Ren S, Li S et al (2008) Hepatic fatty acid transporter Cd36 is a common target of LXR, PXR, and PPAR[gamma] in promoting steatosis. *Gastroenterology* 134(556–567):e551
34. Cruz-Garcia L, Minghetti M, Navarro I, Tocher DR (2009) Molecular cloning, tissue expression and regulation of liver X Receptor (LXR) transcription factors of Atlantic salmon (*Salmo salar*) and rainbow trout (*Oncorhynchus mykiss*). *Comp Biochem Physiol B: Biochem Mol Biol* 153:81–88
35. Carmona-Antoñanzas G, Monroig Ó, Dick JR, Davie A, Tocher DR (2011) Biosynthesis of very long-chain fatty acids ($C > 24$) in Atlantic salmon: cloning, functional characterisation, and tissue distribution of an Elovl4 elongase. *Comp Biochem Physiol B: Biochem Mol Biol* 159:122–129
36. Kleveland EJ, Syvertsen BL, Ruyter B, Vegusdal A, Jørgensen SM, Gjøen T (2006) Characterization of scavenger receptor class B, type I in Atlantic salmon (*Salmo salar* L.). *Lipids* 71:1017–1027
37. Zhou J, Stubhaug I, Torstensen BE (2010) Trans-membrane uptake and intracellular metabolism of fatty acids in Atlantic salmon (*Salmo salar* L.) hepatocytes. *Lipids* 45:301–311
38. Brannas E, Chaix T, Nilsson J, Eriksson LO (2005) Has a 4-generation selection programme affected the social behaviour and growth pattern of Arctic charr (*Salvelinus alpinus*)? *Appl Anim Behav Sci* 94:165–178
39. Busacker GP, Adelman IR, Goolish EM (1990) Growth. In: Schreck CB, Moyle PB (eds) *Methods for fish biology*. American Fisheries Society, Bethesda, pp 363–388
40. Pickova J, Dutta PC, Larsson PO, Kiessling A (1997) Early embryonic cleavage pattern, hatching success, and egg-lipid fatty acid composition: comparison between two cod (*Gadus morhua*) stocks. *Can J Fish Aquat Sci* 54:2410–2416
41. Appelqvist L-Å (1968) Rapid methods of lipid extraction and fatty acid methyl ester preparation for seed and leaf tissue with special remarks on preventing the accumulation of lipid contaminants. *Arkiv För Kemi* 28:551–570
42. Eriksson SF, Pickova J (2007) Fatty acids and tocopherol levels in M-Longissimus dorsi of beef cattle in Sweden—A comparison between seasonal diets. *Meat Sci* 76:746–754
43. Livak KJ, Schmittgen TD (2001) Analysis of relative gene expression data using real-time quantitative PCR and the $2^{-\Delta\Delta CT}$ method. *Methods* 25:402–408
44. Nelder JA, Wedderburn RWM (1972) Generalized Linear Models. *J R Stat Soc Ser A (General)* 135:370–384
45. Torstensen BE, Øyvind L, Frøyland L (2000) Lipid metabolism and tissue composition in Atlantic salmon (*Salmo salar* L.)—Effects of capelin oil, palm oil, and oleic acid-enriched sunflower oil as dietary lipid sources. *Lipids* 35:653–664
46. Trattner S, Ruyter B, Østbye TK, Kamal-Eldin A, Moazzami A, Pan J, Gjøen T, Brännäs E, Zlabek V, Pickova J (2011) Influence of dietary sesamin, a bioactive compound on fatty acids and expression of some lipid regulating genes in Baltic Atlantic salmon (*Salmo salar* L.) juveniles. *Physiol Res* 60:125–137
47. Mraz J, Schlechtriem C, Olohan LA, Fang YX, Cossins AR, Zlabek V, Samuelsen T, Pickova J (2010) Sesamin as a potential modulator of fatty acid composition in common carp (*Cyprinus carpio*). *Aquac Res* 41:e851–e861
48. Kleveland EJ, Ruyter B, Vegusdal A, Sundvold H, Berge RK, Gjøen T (2006) Effects of 3-thia fatty acids on expression of some lipid related genes in Atlantic salmon (*Salmo salar* L.). *Comp Biochem Physiol B: Biochem Mol Biol* 145:239–248
49. Moya-Falcón C, Hvattum E, Dyrøy E, Skorve J, Stefansson SO, Thomassen MS, Jakobsen JV, Berge RK, Ruyter B (2004) Effects of 3-thia fatty acids on feed intake, growth, tissue fatty acid composition, β -oxidation and Na^+ , K^+ -ATPase activity in Atlantic salmon. *Comp Biochem Physiol B: Biochem Mol Biol* 139:657–668
50. Zheng X, Seiliez I, Hastings N, Tocher DR, Panserat S, Dickson CA, Bergot P, Teale A (2004) Characterization and comparison of fatty acyl Delta 6 desaturase cDNAs from freshwater and marine teleost fish species. *Comp Biochem Physiol B-Biochem Mol Biol* 139:269–279
51. Sargent JR, Tacon AGJ (1999) Development of farmed fish: a nutritionally necessary alternative to meat. *Proc Nutr Soc* 58:377–383
52. Sales J (2010) Quantification of the differences in flesh fatty acid components between farmed and wild fish. *J Aquat Food Prod Technol* 19:298–309
53. Andersen Ø, Eijsink VGH, Thomassen M (2000) Multiple variants of the peroxisome proliferator-activated receptor (PPAR) [gamma] are expressed in the liver of Atlantic salmon (*Salmo salar*). *Gene* 255:411–418
54. Burri L, Thoresen GH, Berge RK (2010) The role of PPAR α activation in liver and muscle. *PPAR Res* 2010, article ID 542359
55. Motojima K, Passilly P, Peters JM, Gonzalez FJ, Latruffe N (1998) Expression of putative fatty acid transporter genes are regulated by peroxisome proliferator-activated receptor α and γ activators in a tissue- and inducer-specific manner. *J Biol Chem* 273:16710–16714
56. Poirier H, Niot I, Monnot MC, Braissant O, Meunier-Durmort C, Costet P, Pineau T, Wahli W, Willson TM, Besnard P (2001) Differential involvement of peroxisome-proliferator-activated receptors α and δ in fibrate and fatty-acid-mediated inductions of the gene encoding liver fatty-acid-binding protein in the liver and the small intestine. *Biochem J* 355:481–488
57. Qin YF, Dalen KT, Gustafsson J-Å, Nebb HI (2009) Regulation of hepatic fatty acid elongase 5 by LXR α -SREBP-1c. *Biochim Biophys Acta Mol Cell Biol Lipids* 1791:140–147
58. Matsuzaka T, Shimano H, Yahagi N, Amemiya-Kudo M, Yoshikawa T, Hasty AH, Tamura Y, Osuga JI, Okazaki H, Iizuka Y et al (2002) Dual regulation of mouse $\Delta 5$ - and $\Delta 6$ -desaturase gene expression by SREBP-1 and PPAR α . *J Lipid Res* 43:107–114
59. Jeng KCG, Hou RCW (2005) Sesamin and sesamol: nature's Therapeutic Lignans. *Curr Enzyme Inhib* 1:11–20
60. Zheng X, Tocher DR, Dickson CA, Bell JG, Teale AJ (2005) Highly unsaturated fatty acid synthesis in vertebrates: new insights with the cloning and characterization of a $\Delta 6$ desaturase of Atlantic salmon. *Lipids* 40:13–24
61. Tocher DR, Bell JG, MacGlaughlin P, McGhee F, Dick JR (2001) Hepatocyte fatty acid desaturation and polyunsaturated fatty acid composition of liver in salmonids: effects of dietary vegetable oil. *Comp Biochem Physiol B-Biochem Mol Biol* 130:257–270

62. Jorgensen SM, Kleveland EJ, Grimholt U, Gjoen T (2006) Validation of reference genes for real-time polymerase chain reaction studies in Atlantic salmon. *Mar Biotechnol* 8:398–408
63. Bahuaud D, Mørkøre T, Østbye TK, Veiseth-Kent E, Thomassen MS, Ofstad R (2010) Muscle structure responses and lysosomal cathepsins B and L in farmed Atlantic salmon (*Salmo salar* L.) pre- and post-rigor fillets exposed to short and long-term crowding stress. *Food Chem* 118:602–615
64. Castro V, Grisdale-Helland B, Helland SJ, Kristensen T, Jørgensen SM, Helgerud J, Claireaux G, Farrell AP, Krasnov A, Takle H (2011) Aerobic training stimulates growth and promotes disease resistance in Atlantic salmon (*Salmo salar*). *Comp Biochem Physiol Mol Integr Physiol* 160:278–290
65. Minghetti M, Leaver MJ, Tocher DR (2011) Transcriptional control mechanisms of genes of lipid and fatty acid metabolism in the Atlantic salmon (*Salmo salar* L.) established cell line, SHK-1. *Biochim Biophys Acta Mol Cell Biol Lipids* 1811:194–202

Isolation of a $\Delta 5$ Desaturase Gene from *Euglena gracilis* and Functional Dissection of Its HPGG and HDASH Motifs

Dana Walters Pollak · Michael W. Bostick · Hyeryoung Yoon ·
Jamie Wang · Dieter H. Hollerbach · Hongxian He · Howard G. Damude ·
Hongxiang Zhang · Narendra S. Yadav · Seung-Pyo Hong ·
Pamela Sharpe · Zhixiong Xue · Quinn Zhu

Received: 10 November 2011 / Accepted: 18 May 2012 / Published online: 24 June 2012
© The Author(s) 2012. This article is published with open access at Springerlink.com

Abstract Delta (Δ) 5 desaturase is a key enzyme for the biosynthesis of health-beneficial long chain polyunsaturated fatty acids such as arachidonic acid (ARA, C20:4n-6), eicosapentaenoic acid (C20:5n-3) and docosahexaenoic acid (C22:6n-3) via the “desaturation and elongation” pathways. A full length $\Delta 5$ desaturase gene from *Euglena gracilis* (*Eg $\Delta 5D$*) was isolated by cloning the products of polymerase chain reaction with degenerate oligonucleotides as primers, followed by 5' and 3' rapid amplification of cDNA ends. The whole coding region of *Eg $\Delta 5D$* was 1,350 nucleotides in length and encoded a polypeptide of 449 amino acids. BlastP search showed that *Eg $\Delta 5D$* has about 39 % identity with a $\Delta 5$ desaturase of *Phaeodactylum tricornutum*. In a genetically modified dihomogamma-linoleic acid (DGLA, C20:3n-6) producing *Yarrowia lipolytica* strain, *Eg $\Delta 5D$* had strong $\Delta 5$ desaturase activity with DGLA to ARA conversion of more than 24 %. Functional dissection of its HPGG and HDASH motifs demonstrated that both motifs were important, but not necessary in the exact form as encoded for the enzyme activity of *Eg $\Delta 5D$* . A double mutant *Eg $\Delta 5D$ -34G158G* with altered sequences within both HPGG and HDASH motifs was generated and exhibited $\Delta 5$ desaturase activity similar to the wild type *Eg $\Delta 5D$* . Codon optimization of the

N-terminal region of *Eg $\Delta 5D$ -34G158G* and substitution of the arginine with serine at residue 347 improved substrate conversion to 27.6 %.

Keywords $\Delta 5$ desaturase · HPGG motif · HDASH motif · Double mutant · Fatty acid biosynthesis · *Yarrowia lipolytica*

Abbreviations

ALA	Alpha-linolenic acid (ALA 18:3n-3)
ARA	Arachidonic acid (C20:4n-6)
ATCC	American Type Culture Collection (Rockville, MD)
DAG	Diacylglycerol
Dd $\Delta 5D$	$\Delta 5$ Desaturase of <i>Dictyostelium discoideum</i>
DGLA	Dihomo-gamma-linoleic acid (C20:3n-6)
DHA	Docosahexaenoic acid (C22:6n-3)
DPA	Docosapentaenoic acid (22:5n-3)
Eg $\Delta 4D$	$\Delta 4$ Desaturase of <i>Euglena gracilis</i>
Eg $\Delta 5D$	$\Delta 5$ Desaturase of <i>Euglena gracilis</i>
Eg $\Delta 8D$	$\Delta 8$ Desaturase of <i>Euglena gracilis</i>
EG Media	<i>Euglena</i> growth media
FFA	Unesterified fatty acids
FOA	5-Fluoro-orotic acid FOA
EPA	Eicosapentaenoic acid (C20:5n-3)
ETA	Eicosatetraenoic acid (C20:4n-3)
GC	Gas chromatography
HGM	High glucose media
His-rich motif	Histidine-rich motif
Ig $\Delta 5D$	$\Delta 5$ Desaturase of <i>Isochrysis galbana</i>
LC-PUFA	Long chain polyunsaturated fatty acids
LNA	Linoleic acid (18:2n-6)
Ma $\Delta 5D$	$\Delta 5$ Desaturase of <i>Mortierella alpina</i>
MMLeu	Minimal media + leucine

Electronic supplementary material The online version of this article (doi:10.1007/s11745-012-3690-1) contains supplementary material, which is available to authorized users.

D. W. Pollak · M. W. Bostick · H. Yoon · J. Wang ·
D. H. Hollerbach · H. He · H. G. Damude · H. Zhang ·
N. S. Yadav · S.-P. Hong · P. Sharpe · Z. Xue · Q. Zhu (✉)
Biochemical Sciences and Engineering, Central Research
and Development, E. I. du Pont de Nemours and Company,
Wilmington, DE 19880, USA
e-mail: quinn.zhu@usa.dupont.com

NL	Neutral lipids
Ot Δ 5D	Δ 5 Desaturase of <i>Ostreococcus tauri</i>
PCR	Polymerase chain reaction
Pi Δ 5D	Δ 5 Desaturase of <i>Pythium irregulare</i>
PL	Phospholipids
PI Δ 8D	Δ 8 Desaturase of <i>Pavlova lutheri</i>
Pm Δ 5D	Δ 5 Desaturase of <i>Phytophthora megasperma</i>
Pt Δ 5D	Δ 5 Desaturase of <i>Phaeodactylum tricornutum</i>
PUFA	Polyunsaturated fatty acids
RACE	Rapid amplification of cDNA ends
TAG	Triacylglycerol
Ta Δ 5D	Δ 5 Desaturase of <i>Thraustochytrium aureum</i>
Ts Δ 8D	Δ 8-Sphingolipid desaturase of <i>Thalassiosira pseudonana</i>

List of symbols

α	Alpha
γ	Gamma
Δ	Delta
#	Number

Introduction

There is increasing interest in the recognized health benefits of long chain polyunsaturated fatty acids (LC-PUFA) such as arachidonic acid (ARA, C20:4n-6), eicosapentaenoic acid (EPA, C20:5n-3) and docosahexaenoic acid (DHA, C22:6n-3) for both humans and animals [1–3]. Since mammals lack delta (Δ) 12- and Δ 15-desaturases, ARA, EPA and DHA cannot be synthesized de novo and must be obtained either in the diet or synthesized through “desaturation and elongation” pathways (Fig. 1) from essential fatty acids linoleic acid (LNA, 18:2n-6) and/or alpha (α)-linolenic acid (ALA 18:3n-3). These LC-PUFA are important fatty acids for human growth and development. For example, ARA, a precursor of EPA, is abundant in the brain and muscles. As a lipid second messenger ARA is involved in cellular signaling and is a key inflammatory intermediate [3]. EPA is a precursor of DHA, and induces a broad anti-inflammatory response [1–3]. DHA is a major ω -3 fatty acid in the mammalian central nervous system and enhances synaptic activities in neuronal cells [1–4]. EPA and DHA are the precursors of E- and D-series resolvins, respectively. These two classes of resolvins have distinct structural, biochemical and pharmacological properties [5, 6]. ARA and DHA together play critical roles for neurological development and health [4, 7]. Dietary EPA and DHA can effectively reduce the level of blood triglycerides in human [8]. Increased intake of EPA-rich

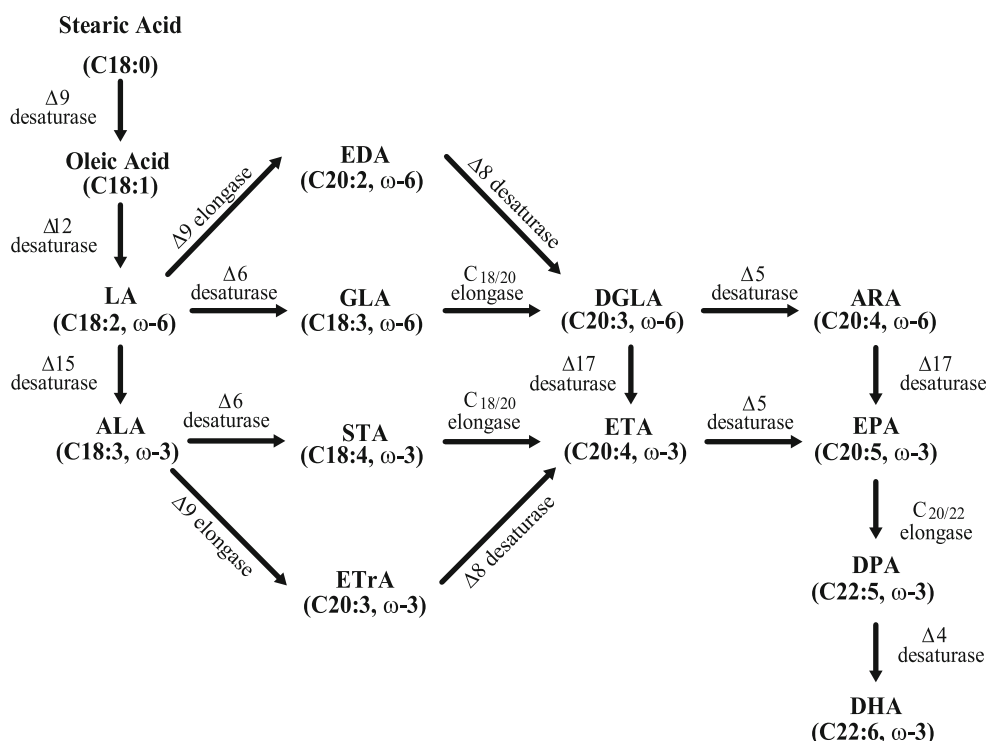
supplement has beneficial effects on coronary heart disease, high blood pressure, inflammatory disorders and mental illness [9, 10].

Currently, the primary source of EPA and DHA is marine fish oil. Most of the EPA and DHA in fish oil are from their cold-water oceanic microalgae food sources. More than 85 % of isolated fish oil is used for aquaculture. In the case of salmon-farming, fish oils from approximately 4 pounds of fish are needed to raise one pound of salmon filet, the fish-in and fish-out ratio is about 4:1. In today’s environment, wild-caught fish often contain contaminants such as methylmercury, polychlorinated biphenyls, dioxins and several other halogenated persistent organic pollutants [11]. With ever-growing human populations, and limited sources of ocean fish, there is growing concern about the quality, quantity and sustainability of fish oil.

In the last two decades, great efforts have been focused on developing different hosts for production of LC-PUFA. Wild type *Mortierella alpina* has been developed for commercial production of ARA [12], while *Cryptocodinium cohnii* and *Schizochytrium* have been developed for commercial production of DHA [13]. The ARA and DHA oils produced from these organisms have been largely used in infant formulas. *Yarrowia lipolytica* has been genetically engineered to contain an EPA biosynthesis pathway [14] allowing for the commercial production of EPA oil, NewHarvest™ (<http://www.newharvest.com>). The EPA oil has been used as a human nutritional supplement. Additionally, EPA-rich *Yarrowia* biomass has been used to feed a brand of farmed salmon, Verlasso™ (<http://www.verlasso.com>), with a fish-in and fish-out ratio of about 1:1. However, the current production scale and cost of ARA, EPA and DHA cannot meet the market demand.

Various organisms use different pathways to synthesize ARA, EPA and DHA. *Cryptocodinium* and *Schizochytrium* synthesize EPA and DHA through a polyketide-based pathway [15], while some species of algae, fungi, and protists synthesize ARA, EPA and DHA through fatty acid “desaturation and elongation” pathways [16, 17]. All “desaturation and elongation” pathways (Fig. 1) require LNA and/or ALA as a substrate, followed by the “ Δ 9 elongase and Δ 8 desaturase” pathway or the “ Δ 6 desaturase and C_{18/20} elongase” pathway to synthesize ARA, EPA and DHA by orchestrated elongation and desaturation reactions. So far, genetic engineering has mainly employed these “desaturation and elongation” pathways to modify hosts such as plants and yeast to produce ARA, EPA and DHA [14, 18–23]. Production of ARA, EPA and DHA through “desaturation and elongation” pathways requires gene expression of Δ 5 desaturase to catalyze the conversion of di-homo- γ -linolenic acid (DGLA, C20:3n-6) to ARA, with a similar activity of converting eicosatetraenoic acid (ETA, C20:4n-3) to EPA. Since the isolation of Δ 5

Fig. 1 Biosynthetic pathways for ARA, EPA and DHA via “desaturation and elongation” pathways



desaturase gene from *Mortierella alpina* (*MaΔ5D*, 24, 25), several $\Delta 5$ desaturase genes have been isolated [26], however, there is little research about their structure/function relationship. Additionally, more efficient $\Delta 5$ desaturase genes are needed to ensure engineered organisms may produce high levels of ARA, EPA and DHA.

$\Delta 5$ desaturases are known as “front-end” desaturases, wherein desaturation occurs between a pre-existing double bond and the carboxyl terminus of the fatty acid [26–29]. Like other desaturases, $\Delta 5$ desaturase is an iron-containing and membrane-bound enzyme that requires both molecular oxygen and an electron transfer to introduce double bonds into an existing acyl chain. Microsomal cytochrome b_5 serves as electron donor to desaturase enzymes [26, 29, 30]. Fatty acid desaturation can be carried out via concerted action of multiple enzymes including NADH reductase, the desaturase enzyme, and cytochrome b_5 reductase. Alternatively, many desaturases contain both a cytochrome b_5 domain and a desaturase domain. For example, $\Delta 4$, $\Delta 5$, $\Delta 6$ and $\Delta 8$ desaturases have a cytochrome b_5 domain at their N-terminus [26]; $\Delta 9$ desaturase has a cytochrome b_5 domain at its C-terminus [30]. The cytochrome b_5 domain of all desaturases has a heme-binding “HPGG” motif. Previous studies using molecular dynamics simulations suggest the “HPGG” motif is important for heme group assembly and desaturase function [31, 32].

The active site of desaturases has been characterized as a diiron cluster that is bound to the enzyme by three regions

of highly conserved histidine-rich (His-rich) motifs [27, 30]. These three His-rich motifs $H(X)_{3-4}H$, $H(X)_{2-3}HH$, and $H/Q(X)_{2-3}HH$ are conserved among all front-end desaturases, and the eight histidine residues of these three motifs are essential for catalytic activity [33]. In the case of $\Delta 5$ desaturase from *MaΔ5D* [24, 25], the exact amino acid sequence of the first His-rich motif ($H(X)_{3-4}H$) is HDASH, which has been suggested as one of the characteristics of $\Delta 5$ desaturases and necessary for its function to convert DGLA to ARA [34]. Recent studies find that several $\Delta 5$ desaturases (GenBank accession #: AAL82631, AAL13311, AAL92562, AAM09687, CAJ07076) do not contain the exact HDASH sequence. Due to the important role of $\Delta 5$ desaturases in LC-PUFA biosynthesis, a detailed understanding of the functional significance of the conserved HPGG and HDASH motifs may contribute to improvements in hosts biologically engineered to produce commercially valuable LC-PUFA.

We report the isolation of a $\Delta 5$ desaturase gene from *Euglena gracilis* (*EgΔ5D*). Expression of *EgΔ5D* in a genetically modified DGLA producing *Y. lipolytica* strain revealed that *EgΔ5D* had strong $\Delta 5$ desaturase activity. Functional dissection of HPGG and HDASH motifs demonstrated that neither the HPGG nor the HDASH motif is necessary in the exact form as encoded for enzyme activity of *EgΔ5D*. Various mutants, within HPGG or HDASH motif alone, or within both HPGG and HDASH motifs, are functionally equivalent or have higher $\Delta 5$ desaturase activity than the wild type *EgΔ5D*. Codon optimization of

the N-terminal region of a double mutant *EgΔ5D-34G158G* and substitution of the arginine with serine at residue 347 effectively improved the enzyme's substrate conversion.

Materials and Methods

Strains, Media and Growth Conditions

E. gracilis was kindly provided by Dr. Richard Triemer of Michigan State University (East Lansing, MI). *Euglena* growth (EG) media (per liter): 1 g sodium acetate, 1 g of beef extract, 2 g of Bacto® tryptone and 2 g of Bacto® yeast extract in 970 mL of water. After filter sterilizing, 30 mL of soil–water supernatant was aseptically added. A 1-mL aliquot of *E. gracilis* culture was transferred into 250 ml of EG Medium in a 500-mL glass bottle. The cultures were grown at 23 °C with a 16 h light, 8 h dark cycle for 2 weeks with no agitation.

Y. lipolytica strain Y2224 is a 5-fluoroorotic acid (FOA) resistant mutant of wild type strain American Type Culture Collection (ATCC, Rockville, MD) #20362 (Fig. 2a) with a mutation in the *URA3* gene (Genbank accession#: No. AJ306421). *Y. lipolytica* strain Y4036U (Zhu et al., unpublished data) is a genetically modified strain with a *Leu*⁻ and *Ura*⁻ phenotype, also originated from the wild type strain ATCC #20362. Strain Y4036U produced

approximately 18 % DGLA of total fatty acids (Fig. 2b) and is composed of heterologous genes encoding Δ12 desaturase of *Fusarium moniliforme* [35]; C16/18 elongase of *M. alpina* [36]; Δ9 elongase of *E. gracilis* [37] and synthetic mutant of Δ8 desaturase [38] derived from *E. gracilis*. Minimal Media + Leucine (MMLeu), High Glucose Media (HGM) and YPD medium were used as required for *Y. lipolytica* strains and cultured at 30 °C. MMLeu (per liter): 20 g of glucose; 1.7 g yeast nitrogen base without amino acids or ammonium sulfate; 0.1 g proline; 0.1 g leucine; pH 6.1. HGM (per liter): 80 g glucose, 2.58 g KH₂PO₄, 5.36 g K₂HPO₄, pH 7.5. YPD medium (per liter): 10 g of yeast extract, 20 g of Bacto peptone, and 20 g of glucose. Agar plates were prepared by addition of 20 g/l agar to liquid media.

General Techniques for Molecular Biology

Recombinant DNA techniques were used according to standard methods [39, 40]. Site-directed mutagenesis was performed according to the manufacturer's protocol (QuikChange™, Stratagene; San Diego, CA). When PCR or site-directed mutagenesis was involved in the generation of mutants and/or cloning, DNA was sequenced to verify that no additional mutations were introduced.

Total RNA was extracted from the *E. gracilis* cells using the RNA STAT-60™ reagent (Amsbio LLC., Lake forest, CA). 85 μg of mRNA was purified from 1 mg of total RNA using the mRNA Purification Kit (Amersham Biosciences, Piscataway, NJ). Synthesis of cDNA from the *E. gracilis* mRNA was carried out using the adapter primer AP of 3'-RACE kit from Invitrogen (Carlsbad, CA) and the Smart IV oligonucleotide of BD-Clontech Creator™ Smart™ cDNA library kit (Mississauga, ON, Canada) as primers. The reverse transcription was performed with Superscript II reverse transcriptase of Invitrogen.

PCR reactions were carried out in a 50 μl total volume comprising: PCR buffer (containing 10 mM KCl, 10 mM (NH₄)₂SO₄, 20 mM Tris–HCl (pH 8.75), 2 mM MgSO₄, 0.1 % Triton X-100), 100 μg/mL BSA, 200 μM each deoxyribonucleotide triphosphate, 10 pmol of each primer, 10 ng cDNA of *E. gracilis* and 1 μl of Taq DNA polymerase (Epicentre Technologies, Madison, WI). The thermocycler conditions were set for 35 cycles at 95 °C for 1 min, 56 °C for 30 s and 72 °C for 1 min, followed by a final extension at 72 °C for 10 min. The DNA band with expected size was isolated from a 1 % agarose gel and cloned into pGEM-T easy vector (Promega, Madison, WI).

Modified 5' and 3' RACE techniques were used to obtain the full length *EgΔ5D*. The cDNA product from *E. gracilis* mRNA was used as template, and all the primers used in the 5' and 3' RACE are listed in Supplemental Table S1. Specifically, a gene specific primer ODMWP480

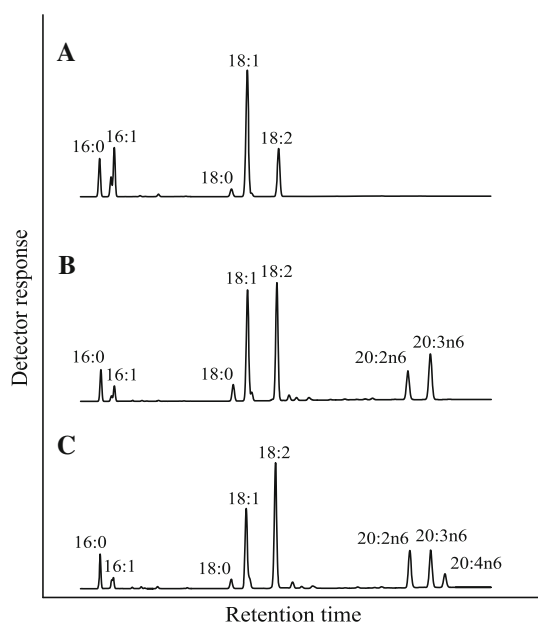


Fig. 2 Chromatograms of the fatty acid profiles. Fatty acid profile of wild type *Y. lipolytica* strain ATCC#20362 (a). Fatty acid profile of Y4036U strain, producing about 8 % HGLA (b). Fatty acid profile of Y4036U strain transformed with pDMW367-M4, producing about 3.7 % ARA of total lipids (c)

and a generic primer CDSIII 5' were used in the first round of 5' RACE. The PCR amplifications were carried out in a 50 μ l total volume, comprising: 25 μ l of *LA Taq*TM pre-mix (TaKaRa Bio Inc., Otsu, Shiga, 520-2193, Japan), 10 pmol of each primer and 1 μ l of Taq DNA polymerase (Epicentre Technologies, Madison, WI). The thermocycler conditions were the same as described above. One micro liter of this product was directly used in a second amplification, which differed from the first only in that the primers used, ODMWP479 and the generic primer DNR CDS 5' were internal to the first set of primers. As no translation initiation codon was found in the product of the first round of 5' RACE, the entire modified 5' RACE protocol was repeated using gene specific primers YL791 and YL792 as primers instead of the primers used in the first round.

A variation of a 3' RACE technique was used to isolate the C-terminal fragment of *Eg Δ 5D*. The combinations of primers ODMW469 and AUAP, and then YL470 and AUAP were used in the initial amplification and second round reaction, respectively. The PCR reactions were the same as those described for the 5' RACE.

Yarrowia Expression Vector and Transformation

Yarrowia expression vector pDMW367 contained autonomous replication sequence 18 [41] and a *URA3* gene (Genbank accession#: No. AJ306421) of *Y. lipolytica*. It also contains a *FBAIN::Eg Δ 5D:Pex20* chimeric gene. The *FBAIN* is a promoter derived from the fructose-bisphosphate aldolase gene (*FBA1*) of *Y. lipolytica* [42]. The *Eg Δ 5D* is the coding region of a wild type Δ 5 desaturase of *E. gracilis*, in which the amino acid at position 347 is arginine. The *Pex20* was a terminator sequence of *PEX20* gene (Genbank accession#: AF054613) of *Y. lipolytica*. Transformation of *Y. lipolytica* strain Y4036U was carried out as described by Chen et al. [43].

Cultivation of *Y. lipolytica* Transformants and Fatty Acid Analysis by Gas Chromatography

The *Yarrowia* expression plasmid and its derivatives were used to transform strain Y4036U individually. Transformants from each transformation were streaked onto new MMLeu plates and kept in a 30 °C incubator for 2 days. Cells from streaked plates were cultivated in 24 well blocks with 3 mL MMLeu, and incubated for 2 days at 30 °C with shaking at 200 rpm. The cells were then collected by centrifugation and resuspended in 3 mL HGM. The cells were incubated another 5 days at 30 °C with shaking at 200 rpm.

Fatty acid methyl esters from 1 ml cell culture of *Y. lipolytica* or *E. gracilis* were prepared as described [44],

except that the fatty acid methyl esters were extracted with 0.5 ml of heptane and separated by Agilent 7890A GC using hydrogen as carrier gas supplied by a hydrogen generator (Parker Hannifin, Cleveland, OH). The oven temperature was programmed from 200 to 240 °C at a rate of 25 °C/min. The proportion of each fatty acid was based on the integrated peak area of the corresponding fatty acid methyl ester as a percent relative to the sum of all integrated peaks as calculated by Agilent ChemStation Software.

Results

Isolation of Δ 5 Desaturase Gene from *E. gracilis*

Fatty acid profile analyses showed that there were moderate amounts of EDA, DGLA, ARA, EPA, docosapentaenoic acid (DPA 22:5n-3) and DHA produced in *E. gracilis* (data not shown), confirming that there was a " Δ 9 elongase/ Δ 8 desaturase" pathway in *E. gracilis* [16, 38, 45]. The genes encoding the Δ 9 elongase, Δ 8 desaturase [16, 38], Δ 5 desaturase, Δ 17 desaturase, C20/22 elongase and Δ 4 desaturase [45] were responsible for the production of EDA, DGLA, ARA, EPA, DPA and DHA, respectively (Fig. 1).

After comparison of four Δ 5 desaturase genes, *Pi Δ 5D* from *Pythium irregulare* [46], *Pm Δ 5D* from *Phytophthora megasperma* (Genbank accession #: CAD53323), *Pt Δ 5D* from *Phaeodactylum tricorutum* [47], and *Dd Δ 5D* from *Dictyostelium discoideum* (Genbank accession #: XP_640331) as well as two Δ 8 desaturase genes, *Eg Δ 8D* from *E. gracilis* [16, 38] and *Pl Δ 8D* from *Pavlova lutheri* [48], two conserved regions, GHH(I/V)YTN and N(Y/F)Q(V/D)EHH (Fig. 3) were selected to design primers to amplify a portion of *Eg Δ 5D*. To reduce the degeneracy of the primers, four primers (Supplemental Table S1: 5-1A to 1D) were generated for conserved region 1 and four primers (Supplemental Table S1: 5-5AR to 5-5DR) for the anti-sense strand of conserved region 2. One DNA fragment amplified with primers 5-1B and 5-5DR was cloned into pGEM-T Easy vector to generate pT-F10-1. DNA sequence showed that a 590 bp insert of pT-F10-1 encoded an amino acid sequence with 38 % identity and 53 % similarity to the amino acid sequence of the Δ 8-sphingolipid desaturase of *Thalassiosira pseudonana* (*Ts Δ 8D*, Genbank accession #: AAX14502), and 37 % identity and 52 % similarity with *Pt Δ 5D* [47]. These data suggested that the 590 bp DNA fragment might be a part of a desaturase gene of *E. gracilis*. This gene was designated as putative *Eg Δ 5D*.

5' and 3' RACE techniques were used to extend the 590 bp region of the putative *Eg Δ 5D* (Fig. 4). A 797 bp

A

	Position	Conserved Region 1	Position
PtΔ5D	208	QHWT-HHAYTNHAE MDPD	222
PmΔ5D	228	QHVVGH HHIYTNVAGADPD	245
PiΔ5D	207	QHVVGH HHIYTNVAGADPD	224
DdΔ5D	210	QHVI GHHLYTNV RNADPD	227
EgΔ8D	182	RHNA-HHSA TNVQGHDPD	198
PvΔ8D	208	RHNT-HHVC TNE DGS DDPD	224

B

	Position	Conserved Region 2	Position
PtΔ5D	292	TGGLN FQVEHHLFPRMSS	409
PmΔ5D	407	TGALNYQVTHHLFPGV SQ	424
PiΔ5D	386	CGALNYQVTHHLYPGI SQ	403
DdΔ5D	394	SGGLNLQVTHHCFPTIAQ	411
EgΔ8D	352	FGGLNYQIEHHLWPTLPR	369
PvΔ8D	362	TGFISLQTEHHLFPMMP T	379

Fig. 3 Alignment of the conserved regions among some Δ5 and Δ8 desaturases. The amino acid sequence alignment was performed with Clustal W analysis (MegAlign™ program of DNASTAR software). Identical residues are shaded in black. PtΔ5D, Δ5 desaturase from *P. tricorutum* (29, GenBank accession #: AAL92562); PmΔ5D, Δ5 desaturase from *P. megasperma* (GenBank accession #: CAD53323); PiΔ5D, Δ5 desaturase from *P. irregulare* (30, GenBank accession #: AAL13311); DdΔ5D, Δ5 desaturase from *D. discoideum* (GenBank accession #: XP_640311); EgΔ8D, Δ8 desaturase from *E. gracilis* (24, GenBank accession #: AAD45877) and PvΔ8D, Δ8 desaturase from *P. lutheri* [48]

DNA fragment with no translation initiation codon was isolated by the first round of 5' RACE. This 797 bp DNA fragment had a 238 bp overlap with the 5' end of the 590 bp fragment of pT-F10-1 and provided 559 bp of 5' upstream sequence. A 273 bp DNA fragment was generated by the second round 5' RACE experiment. This 273 bp DNA fragment had 253 bp overlap with the 5' part of the 797 bp DNA fragment and provided 20 bp of 5' upstream sequence. Seventeen [17] bp of the 20 bp encoded the N-terminal portion of the putative *EgΔ5D*, including the translation initiation codon. A 464 bp DNA sequence was identified by one round of 3' RACE. The first 184 bp of the 464 bp fragment encoded the C-terminal coding region, including the translation stop codon, of the putative *EgΔ5D*.

Assembly of the 5' region, the original 590 bp fragment and the 3' region resulted in a 1,633 bp contig, comprising the complete coding region with additional untranslated 5' and 3' ends (Fig. 4). The coding region of the putative *EgΔ5D* is 1,350 bp in length and encodes a peptide of 449 amino acids. BlastP searches using the full length putative *EgΔ5D* as the query sequence showed that it shares 39 % identity and 56 % similarity with PtΔ5D [47]; 37 % identity and 55 % similarity with TsΔ8D (Genbank accession #: AAX14502). Amino acid sequence alignment performed with the Clustal W analysis (MegAlign™

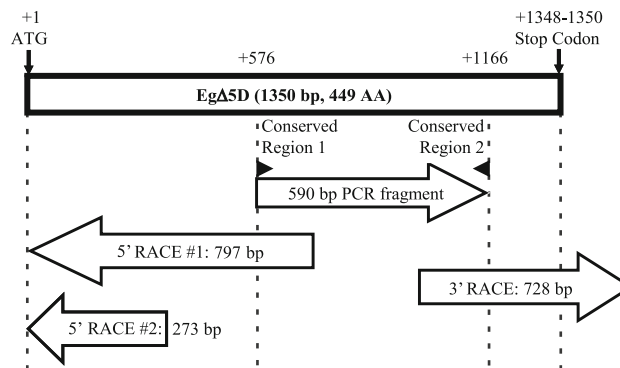


Fig. 4 Graphical representation of the assembly of full length *EgΔ5D*. A 590 bp DNA fragment encoding a portion of *EgΔ5D* was isolated by PCR amplification with degenerate primers. The N-terminal part was isolated by two round of 5' RACE, and the C-terminal portion was isolated by one round of 3' RACE

program of DNASTAR software) showed that *EgΔ5D* has <30 % identity with some represent Δ5 desaturases such as *IgΔ5D* from *I. galbana* (AEA72469); *MaΔ5D* from *M. alpina* [24, 25, 34]; *PiΔ5D* [46]; *OtΔ5D* from *O. tauri* (Genbank accession #: XP_003082424) and *TaΔ5D* from *T. aureum* [49]. Further analyses showed that *EgΔ5D* has only 20 % and 25.5 % identity with *EgΔ8D* [16] and *EgΔ4D* [45] desaturases of *E. gracilis*, respectively. It was found that the PCR products for the full length coding region of putative *EgΔ5D* had two versions, both having identical nucleotide sequence except at base pair positions 1,039 and 1,041. This disagreement resulted in a codon change from CGA to AGC. As such, one PCR product indicated arginine at position 347, whereas the second indicated serine. It was hypothesized that this discrepancy was raised at the stage of PCR amplification or during cDNA generation.

Determination of Δ5 Desaturase Activity and Topology Model of *EgΔ5D*

To study the function of the putative *EgΔ5D*, plasmid pDMW367 was generated to express the *EgΔ5D* coding region under the control of the strong constitutive FBAIN promoter [42] from *Y. lipolytica*. The four restriction sites (i.e., *Bgl*II, *Eco*RI, *Hind*III and *Nco*I) inside the coding region of *EgΔ5D* in pDMW367 were removed by site-directed mutagenesis to generate pDMW367-M4 (Supplemental Fig. S1). The amino acid sequence of *EgΔ5D* is identical in pDMW367 and pDMW367-M4 constructs, and the amino acid at position 347 is an arginine.

The pDMW367 and pDMW367-M4 constructs were used to transform DGLA producing strain Y4036U. There was no ARA produced in the parent strain Y4036U (Fig. 2b), while there was about 3.7 % ARA and 11.5 % DGLA produced in transformants of Y4036U with either

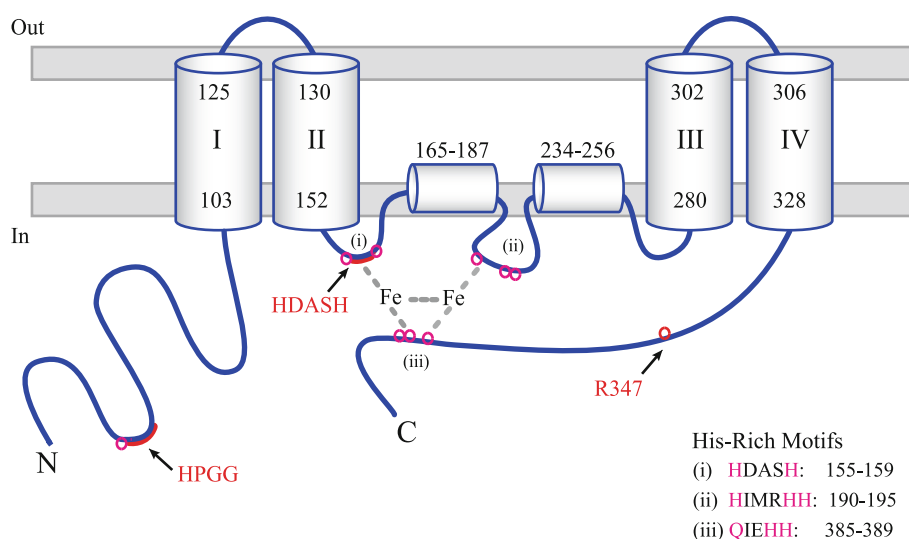


Fig. 5 Topology model of *EgΔ5D*. *EgΔ5D* is a membrane diiron protein with three His-rich motifs. The $HX_{(3,4)}H$ motif, HDASH, is located from residues 155 to 159; the $HX_{(2,3)}HH$ motif, HIMRHH, located from residues 190 to 195, and the $(H/Q)X_{(2,3)}HH$ motif,

QIEHH, located from residues 385 to 389. *EgΔ5D* has four transmembrane domains (I–IV) and two hydrophobic stretches (residues from 165 to 187, and 234 to 256). Its N-terminal cytochrome b_5 domain and C-terminal region are located in the cytoplasm

the pDMW367 or pDMW367-M4 construct (Fig. 2c). These results demonstrated that *EgΔ5D* indeed encodes a $\Delta 5$ desaturase. *EgΔ5D* could convert DGLA to ARA with a conversion of about 24.3 %. The conversion of DGLA to ARA was calculated according to the formula: $([ARA \text{ product}]/[DGLA \text{ substrate} + ARA \text{ product}])$. The pDMW367 and pDMW367-M4 constructs were also used to transform strain Y2224, a FOA resistant mutant of wild type strain ATCC#20362. There was no GLA produced in the transformants with either the pDMW367 or pDMW367-M4 construct (data not shown). These results demonstrated that *EgΔ5D* does not have $\Delta 6$ desaturase activity; it is not a bifunctional enzyme.

Like other fatty acid desaturases, *EgΔ5D* is also a membrane-bound enzyme and belongs to a super-family of membrane di-iron proteins with three His-rich motifs: $HX_{(3,4)}H$, $HX_{(2,3)}HH$ and $(H/Q)X_{(2,3)}HH$. These His residues have been predicted to be located in the cytoplasmic face of the membrane and have been shown to be very important for enzyme activity [33]. Within *EgΔ5D*, these 3 His-rich motifs are the HDASH motif located from residue 155 to 159, the HIMRHH motif located from residue 190 to 195, and the QIEHH motif located from residue 385 to 389. The third His-rich motif contains a glutamine substitution that is common to other front-end desaturases. Based on transmembrane domain analysis (TMHMM Server v. 2.0, Center for Biological Sequence Analysis, BioCentrum-DTU, Technical University of Denmark, DK-2800 Lyngby, Denmark) and the location of the His-rich motifs, a topology model of *EgΔ5D* was developed (Fig. 5). The model shows that the N-terminal cytochrome b_5 domain is located in the

cytosol. The topology model also predicts that *EgΔ5D* has a total of four transmembrane regions (amino acid residues 103–125, 130–152, 280–302 and 306–328) and two hydrophobic regions (amino acid residues 165–187, and 234–256). These hydrophobic segments are not membrane-spanning, and may represent hydrophobic patches located closed to the di-iron active site. Because the substrates for the desaturase is highly hydrophobic, they will likely partition into the lipid bilayer. Therefore we purport that the di-iron active site assembled from these His-clusters may occur at or very near the membrane surface.

The HPGG Motif is Important, but not Necessary for $\Delta 5$ Desaturase Activity of *EgΔ5D*

It has been suggested that the highly conserved HPGG motif plays a crucial role in heme group assembly, protein folding and stabilization in cytochrome b_5 proteins, with the histidine residue functioning as an axial heme ligand where a peptide chain reversal occurs [50]. Previous studies have demonstrated that the heme-binding HPGG motif, and in particular, the histidine residue, is essential for enzyme activity of desaturases with cytochrome b_5 domain [51–53]. Although sequence divergence in the vicinity of the HPGG motif is normal, the HPGG motif itself has been conserved throughout the evolution of all the $\Delta 5$ desaturase genes [54]. Thus it was claimed to be a characteristic of $\Delta 5$ desaturases and necessary for its function to convert DGLA to ARA [34].

To assess the functional significance of the HPGG motif (position 33–36) of *EgΔ5D*, we first elected the proline

Table 1 $\Delta 5$ Desaturase activity of *EgΔ5D* with HxGG mutations

Gene name	Sequence of HPGG motif	$\Delta 5$ Conversion (%)	% of wild type <i>EgΔ5D</i>
<i>EgΔ5D</i>	HPGG	24.2	100
<i>EgΔ5D-34A</i>	HaGG	22.7	93.5
<i>EgΔ5D-34C</i>	HcGG	22.6	93.2
<i>EgΔ5D-34D</i>	HdGG	12.5	51.6
<i>EgΔ5D-34E</i>	HeGG	14.7	60.5
<i>EgΔ5D-34F</i>	HfGG	17.9	73.9
<i>EgΔ5D-34G</i>	HgGG	23.8	98.2
<i>EgΔ5D-34H</i>	HhGG	21.3	87.8
<i>EgΔ5D-34I</i>	HiGG	18.3	75.4
<i>EgΔ5D-34K</i>	HkGG	22.7	93.8
<i>EgΔ5D-34L</i>	HlGG	17.0	70.0
<i>EgΔ5D-34M</i>	HmGG	19.0	78.4
<i>EgΔ5D-34N</i>	HnGG	19.8	81.5
<i>EgΔ5D-34Q</i>	HqGG	19.8	81.7
<i>EgΔ5D-34R</i>	HrGG	19.4	79.9
<i>EgΔ5D-34S</i>	HsGG	20.4	84.1
<i>EgΔ5D-34T</i>	HtGG	19.6	80.7
<i>EgΔ5D-34V</i>	HvGG	20.2	83.4
<i>EgΔ5D-34W</i>	HwGG	22.2	91.7
<i>EgΔ5D-34Y</i>	HyGG	17.7	73.1

Average of 6 samples for each construct containing different mutations

residue at position 34 (P34) as a target for amino acid substitution. Single amino acid mutations were carried out to generate all 19 amino acid substitution mutants (HxGG). Table 1 shows that the P34 residue could be substituted with several different amino acids without significantly impacting the $\Delta 5$ desaturase activity of *EgΔ5D*. The *EgΔ5D-34A*, *EgΔ5D-34C*, *EgΔ5D-34K* or *EgΔ5D-34W* mutants exhibited >90 % of the wild type *EgΔ5D* activity. The *EgΔ5D-34G* mutant was functionally equivalent to the wild type *EgΔ5D*.

Next, we studied the significance of the second glycine residue at position 36 (G36) within the HPGG motif of *EgΔ5D* using the same approach as that for P34. Table 2 shows that the G36 residue within the HPGG motif could be substituted with several different amino acids without significantly impacting the $\Delta 5$ desaturase activity of *EgΔ5D*. The *EgΔ5D-36S* or *EgΔ5D-36D* mutant had about 100.8 or 99.2 % of $\Delta 5$ desaturase activity when compared to *EgΔ5D*, respectively.

The above functional studies at the P34 and G36 positions within the HPGG motif of *EgΔ5D* demonstrated that the HPGG motif could be changed without impacting the $\Delta 5$ desaturase activity. Specifically, the *EgΔ5D-34G*, *EgΔ5D-36S* and *EgΔ5D-36D* mutants were functionally equivalent to the wild type *EgΔ5D*. Comparison of the

Table 2 $\Delta 5$ Desaturase activity of *EgΔ5D* with HPGx mutations

Gene name	Sequence of HPGG motif	$\Delta 5$ Conversion (%)	% of wild type <i>EgΔ5D</i>
<i>EgΔ5D</i>	HPGG	24.2	100
<i>EgΔ5D-36A</i>	HPGa	18.3	75.6
<i>EgΔ5D-36C</i>	HPGc	6.5	26.8
<i>EgΔ5D-36D</i>	HPGd	24.0	99.2
<i>EgΔ5D-36E</i>	HPGe	21.1	86.9
<i>EgΔ5D-36F</i>	HPGf	3.3	13.4
<i>EgΔ5D-36H</i>	HPGh	18.1	74.8
<i>EgΔ5D-36I</i>	HPGi	1.5	6.4
<i>EgΔ5D-36K</i>	HPGk	19.0	78.3
<i>EgΔ5D-36L</i>	HPGl	9.1	37.7
<i>EgΔ5D-36M</i>	HPGm	13.4	55.2
<i>EgΔ5D-36N</i>	HPGn	19.5	80.3
<i>EgΔ5D-36P</i>	HPGp	18.0	74.1
<i>EgΔ5D-36Q</i>	HPGq	19.9	82.1
<i>EgΔ5D-36R</i>	HPGr	15.5	63.8
<i>EgΔ5D-36S</i>	HPGs	24.4	100.8
<i>EgΔ5D-36T</i>	HPGt	22.8	93.9
<i>EgΔ5D-36V</i>	HPGv	1.9	8.0
<i>EgΔ5D-36W</i>	HPGw	15.1	62.2
<i>EgΔ5D-36Y</i>	HPGy	11.2	46.3

Average of 6 samples for each construct containing different mutations

ARA in unesterified fatty acid (FFA), phospholipid (PL) and neutral lipid (NL) pools of *Yarrowia* transformants with *EgΔ5D* and *EgΔ5D-34G* showed that the P34G mutation did not affect the ARA distribution in these pools (Supplemental Fig. S2).

Improvement of $\Delta 5$ Desaturase Activity of *EgΔ5D* by Amino Acid Substitution Within the HDASH Motif

The HDASH motif was also claimed as one of the characteristics of $\Delta 5$ desaturases and necessary for its function to convert DGLA to ARA [34]. To test the hypothesis that the exact sequence of the HDASH motif (position 155–159) of *EgΔ5D* was required, we first selected the alanine residue at position 157 (A157) as a target. The $\Delta 5$ desaturase activity attributed to each mutation at A157 is summarized in Table 3. The data showed that almost all mutations at A157 greatly reduced the $\Delta 5$ desaturase activity of *EgΔ5D*. However, the *EgΔ5D-157G* and *EgΔ5D-157S* mutants retained about 96 and 94 % activity of wild type *EgΔ5D*, respectively.

We also studied the significance of the serine residue at position 158 (S158) within the HDASH motif of *EgΔ5D*. Table 4 shows that the S158 could be substituted with either an alanine or a glycine without substantially

Table 3 $\Delta 5$ Desaturase activity of *Eg* $\Delta 5D$ with HDxSH mutations

Gene name	Sequence of HDASH motif	$\Delta 5$ Conversion (%)	% of wild type <i>Eg</i> $\Delta 5D$
<i>Eg</i> $\Delta 5D$	HDASH	24.8	100
<i>Eg</i> $\Delta 5D$ -157C	HDcSH	10.7	43.1
<i>Eg</i> $\Delta 5D$ -157D	HDdSH	1.0	4.0
<i>Eg</i> $\Delta 5D$ -157E	HDeSH	0.9	3.6
<i>Eg</i> $\Delta 5D$ -157F	HDfSH	1.0	4.0
<i>Eg</i> $\Delta 5D$ -157G	HDgSH	23.8	96
<i>Eg</i> $\Delta 5D$ -157H	HDhSH	1.0	4.0
<i>Eg</i> $\Delta 5D$ -157I	HDiSH	0.9	3.6
<i>Eg</i> $\Delta 5D$ -157K	HDkSH	1.0	4.0
<i>Eg</i> $\Delta 5D$ -157L	HDlSH	1.1	4.4
<i>Eg</i> $\Delta 5D$ -157M	HDmSH	1.0	4.0
<i>Eg</i> $\Delta 5D$ -157N	HDnSH	1.1	4.4
<i>Eg</i> $\Delta 5D$ -157P	HDpSH	2.3	9.3
<i>Eg</i> $\Delta 5D$ -157Q	HDqSH	0.6	2.4
<i>Eg</i> $\Delta 5D$ -157R	HDrSH	0.8	3.2
<i>Eg</i> $\Delta 5D$ -157S	HDsSH	23.3	94
<i>Eg</i> $\Delta 5D$ -157T	HDtSH	1.0	4.0
<i>Eg</i> $\Delta 5D$ -157V	HDvSH	0.3	1.2
<i>Eg</i> $\Delta 5D$ -157W	HDwSH	0.9	3.6
<i>Eg</i> $\Delta 5D$ -157Y	HDySH	0.7	2.8

Average of 3 samples for each construct containing different mutations

impacting the $\Delta 5$ desaturase activity of *Eg* $\Delta 5D$. Specifically, the *Eg* $\Delta 5D$ -158A mutant had about 100.9 % activity of wild type *Eg* $\Delta 5D$, while the *Eg* $\Delta 5D$ -158G mutation had about 107.7 % activity of wild type *Eg* $\Delta 5D$. These data demonstrated that the HDASH motif could be changed without significantly reducing the $\Delta 5$ desaturase activity. In fact, the enzyme activity of *Eg* $\Delta 5D$ could be improved by substitution of the S158 within the HDASH motif with a glycine residue.

Both HPGG and HDASH Motifs were not Necessary in the Exact Form as Encoded for $\Delta 5$ Desaturase Activity of *Eg* $\Delta 5D$

In order to study whether *Eg* $\Delta 5D$ could maintain strong $\Delta 5$ desaturase activity with mutations in both HPGG and HDASH motifs, we generated a series of double mutants. The results (Table 5) demonstrate that $\Delta 5$ desaturases could be constructed having variant HPGG and HDASH motifs that retain at least 64 % of $\Delta 5$ desaturase activity when compared to the wild type.

The proline residue within the HPGG motif can be substituted with glycine with simultaneous substitution of either (1) the alanine residue within the HDASH motif for glycine or (2) the serine residue within the HDASH motif

Table 4 $\Delta 5$ Desaturase activity of *Eg* $\Delta 5D$ with HDxH mutations

Gene name	Sequence of HDASH motif	$\Delta 5$ Conversion (%)	% of wild type <i>Eg</i> $\Delta 5D$
<i>Eg</i> $\Delta 5D$	HDASH	23.3	100
<i>Eg</i> $\Delta 5D$ -158A	HDAaH	23.5	100.9
<i>Eg</i> $\Delta 5D$ -158C	HDAcH	17.9	76.8
<i>Eg</i> $\Delta 5D$ -158D	HDA dH	2.8	12.0
<i>Eg</i> $\Delta 5D$ -158E	HDAeH	1.9	8.2
<i>Eg</i> $\Delta 5D$ -158F	HDAfH	1	4.3
<i>Eg</i> $\Delta 5D$ -158G	HDAgH	25.1	107.7
<i>Eg</i> $\Delta 5D$ -158H	HDAhH	1.6	6.9
<i>Eg</i> $\Delta 5D$ -158I	HDaiH	1.1	4.7
<i>Eg</i> $\Delta 5D$ -158K	HDAkH	1	4.3
<i>Eg</i> $\Delta 5D$ -158L	HDAlH	1.1	4.7
<i>Eg</i> $\Delta 5D$ -158M	HDAmH	2.3	9.9
<i>Eg</i> $\Delta 5D$ -158N	HDA nH	16.5	70.8
<i>Eg</i> $\Delta 5D$ -158P	HDApH	1.2	5.2
<i>Eg</i> $\Delta 5D$ -158Q	HDAqH	10.4	44.6
<i>Eg</i> $\Delta 5D$ -158R	HDArH	10.0	42.9
<i>Eg</i> $\Delta 5D$ -158T	HDA tH	9.6	41.2
<i>Eg</i> $\Delta 5D$ -158V	HDAvH	1.5	6.4
<i>Eg</i> $\Delta 5D$ -158W	HDAwH	9.3	40.0
<i>Eg</i> $\Delta 5D$ -158Y	HDAyH	1.1	4.7

Average of 3 samples for each construct containing different mutations

for alanine or glycine. The proline residue within the HPGG motif can also be substituted with histidine with simultaneous substitution of the serine residue within the HDASH motif for either alanine or glycine. And, the second glycine residue within the HPGG motif can be substituted with serine with simultaneous substitution of the serine residue within the HDASH motif for either alanine or glycine. Specifically, the *Eg* $\Delta 5D$ -34G/157G, *Eg* $\Delta 5D$ -34G/158A and *Eg* $\Delta 5D$ -34H/158G double mutants had more than 80 % of the $\Delta 5$ desaturase activity of *Eg* $\Delta 5D$, while *Eg* $\Delta 5D$ -34G/158G had about 97 % $\Delta 5$ desaturase activity of *Eg* $\Delta 5D$. Further analyses showed that the ARA distribution in FFA, PL and NL pools of *Yarrowia* transformants with *Eg* $\Delta 5D$ -34G/158G was similar to *Yarrowia* transformants with *Eg* $\Delta 5D$ -34G or *Eg* $\Delta 5D$ (Supplemental Fig. S2), suggesting that the simultaneous substitutions (P34G and S158G) within HPGG and HDASH motifs did not change desaturase substrate specificity.

Increased Substrate Conversion of *Eg* $\Delta 5D$ -34G/158G with Double Mutations in HPGG and HDASH Motifs

In order to increase the substrate conversion of *Eg* $\Delta 5D$ -34G/158G, we optimized the codon usage of the

Table 5 $\Delta 5$ Desaturase activity of *Eg $\Delta 5D$* with mutants simultaneously comprising mutations within HPGG and HDASH motifs

Gene name	Sequence of HPGG motif	Sequence of HDASH motif	$\Delta 5$ Conversion (%)	% of wild type <i>Eg$\Delta 5D$</i>
<i>Eg$\Delta 5D$</i>	HPGG	HDASH	27.5	100
<i>Eg$\Delta 5D$-34G157G</i>	HgGG	HDgSH	22.9	83
<i>Eg$\Delta 5D$-34G158A</i>	HgGG	HDAaH	24.3	88
<i>Eg$\Delta 5D$-34G158G</i>	HgGG	HDAgH	26.8	97
<i>Eg$\Delta 5D$-34H158A</i>	HhGG	HDAaH	18.7	68
<i>Eg$\Delta 5D$-34H158A</i>	HhGG	HDAgH	22	80
<i>Eg$\Delta 5D$-36S158A</i>	HPGs	HDAaH	17.5	64
<i>Eg$\Delta 5D$-36S158G</i>	HPGs	HDAgH	18.9	69

Average of 6 samples for each construct containing different mutations

N-terminal portion of the gene for expression in *Y. lipolytica*. The codon-optimized *Eg $\Delta 5D$ -34G/158G*, designated as “*Eg $\Delta 5M$ ””, had 48 bp changed in the first 204 bp of the coding region (23.5 %; Fig. 6), which resulted in optimization of 43 codons of the first 68 amino acids within the N-terminus of the protein (63.2 %). The amino acid sequence encoded by the codon-optimized *Eg $\Delta 5M$* was identical to that of the *Eg $\Delta 5D$ -34G/158G*. *Eg $\Delta 5M$* was used to replace the *Eg $\Delta 5D$* of pDMW367-M4 to generate pDMW367-5M, containing a *FBAIN::Eg $\Delta 5M$::Pex20* chimeric gene.*

We then studied the importance of the arginine or serine at position 347 that were found in the original clones of *Eg $\Delta 5D$* . Based on *Eg $\Delta 5M$* , the CGA codon for arginine at position 347 was changed to AGC codon to encode for serine, which was designated as *Eg $\Delta 5M1$* . The synthetic *Eg $\Delta 5M1$* was used to replace the *Eg $\Delta 5D$* of pDMW367-M4 to generate pDMW367-5M1, containing an *FBAIN::Eg $\Delta 5M1$::Pex20* chimeric gene.

The $\Delta 5$ desaturase activity of *Eg $\Delta 5D$* , *Eg $\Delta 5M$* and *Eg $\Delta 5M1$* is summarized in Table 6. GC analyses determined that there were about 3.6 % ARA and 10.8 % DGLA, 4.0 % ARA and 11.2 % DGLA, and 4.1 % ARA and 10.8 % DGLA of total fatty acids produced in the *Yarrowia* transformants with pDMW367-M4, pDMW367-5M, and pDMW367-5M1, respectively. It showed that the wild-type *Eg $\Delta 5D$* converted about 24.8 % of DGLA to ARA; *Eg $\Delta 5M$* converted 26.7 % of DGLA to ARA; and, *Eg $\Delta 5M1$* converted 27.6 % of DGLA to ARA. The fatty acid profile of *Yarrowia* transformants with *Eg $\Delta 5M1$* was

<i>Eg$\Delta 5D$-34G158G</i>	ATGGCTCTCAGTCTTACCACAGAACAGCTG	30
<i>Eg$\Delta 5M$</i>	ATGGCCCTGTCTCTCACTACCAGAACAGCTC	30
<i>Eg$\Delta 5D$-34G158G</i>	TTAGAACGCCCTGATTTGGTTGCGGATTTGAT	60
<i>Eg$\Delta 5M$</i>	CTGGAGCGACCTGATCTCGTTCGCTATCGAT	60
<i>Eg$\Delta 5D$-34G158G</i>	GGCATCCTCTACGACCTTGAAAGGGCTTGCC	90
<i>Eg$\Delta 5M$</i>	GGTATCCTGTACGACCTCGAGGGCCTTGCC	90
<i>Eg$\Delta 5D$-34G158G</i>	AAAAGTTCATGGTGGAGGAGATTTGATTCTC	120
<i>Eg$\Delta 5M$</i>	AAGGTGCATGGTGGTGGAGACCTCATTCTG	120
<i>Eg$\Delta 5D$-34G158G</i>	GCTTCTGGTGCCTTGATGCCTCCCTCTC	150
<i>Eg$\Delta 5M$</i>	GCCTCTGAGCCTCCGACGCCTCTCCCTC	150
<i>Eg$\Delta 5D$-34G158G</i>	TTTTATTCAATGCATCCATACGTCAAACCG	180
<i>Eg$\Delta 5M$</i>	TTCTACTCTATGCATCCCTACGTCAAAGCC	180
<i>Eg$\Delta 5D$-34G158G</i>	GAGAACTCCAAATTGCTTCACACAG	204
<i>Eg$\Delta 5M$</i>	GAGAACTCCAAGCTCTGCACCAA	204

Fig. 6 Comparison of the 5' portion (204 bp) of *Eg $\Delta 5D$ -34G158G* and its codon optimized version, *Eg $\Delta 5M$* . The DNA sequence alignment was performed with Clustal W analysis (MegAlign™ program of DNASTAR software). Identical residues are shaded in black

almost identical to the profile of *Yarrowia* transformants with pDMW367-M4 as shown in Fig. 2c, except that more ARA was produced. These data demonstrated that the codon optimization of *Eg $\Delta 5D$* improved its substrate conversion efficiency. Further, the amino acid at position 347 did affect the $\Delta 5$ desaturase activity of *Eg $\Delta 5D$* , with a serine residue preferred over an arginine residue.

Discussion

Y. lipolytica has an established history of robust fermentation performance at commercial scale for processes including the production of food-grade citric acid for human consumption and single-cell protein for animal feeds [55]. Recently, *Y. lipolytica* has been used as a host for production of lipid-based compounds [14, 56, 57]. Some *Y. lipolytica* strains are oleaginous organisms that are able to accumulate up to 40 % dry cell weight as oil when starved for nitrogen in the presence of excess glucose as carbon source. However, LNA is the only PUFA that *Y. lipolytica* can synthesize de novo (Fig. 2a). Therefore, it

Table 6 $\Delta 5$ Desaturase activity of *Eg $\Delta 5D$* and codon optimized *Eg $\Delta 5M$* and *Eg $\Delta 5M1$*

Gene name	Sequence of HPGG motif	Sequence of HDASH motif	Sequence at residue 347	$\Delta 5$ Conversion (%)
<i>Eg$\Delta 5D$</i>	HPGG	HDASH	R	24.8
<i>Eg$\Delta 5M$</i>	HgGG	HDAgH	R	26.5
<i>Eg$\Delta 5M1$</i>	HgGG	HDAgH	S	27.6

Average of 6 samples for each construct containing different mutations

is necessary to isolate genes encoding enzymes for every step of the “desaturation and elongation” pathways (Fig. 1) before genetically engineering *Y. lipolytica* to produce ARA, EPA and DHA oil. $\Delta 5$ desaturase is the enzyme responsible for the conversion of DGLA to ARA, and ETA to EPA. Although several $\Delta 5$ desaturase genes have been isolated from various organisms [26], more effective enzymes may help to improve the production of commercially important LC-PUFA.

Previous studies have indicated that *Euglena* was able to synthesize ARA, EPA and DHA through the “ $\Delta 9$ elongase/ $\Delta 8$ desaturase” pathway [16, 38, 45]. In this report, the gene encoding a $\Delta 5$ desaturase from *E. gracilis* was isolated and characterized. Our results indicated two nucleotide sequences with a difference of two base pairs that would result in either arginine or serine at position 347. This discrepancy was most likely generated from PCR amplification or during cDNA generation. BlastP searches showed that the amino acid sequence of *Eg $\Delta 5D$* shares <40 % identity with any $\Delta 5$ desaturase found in Genbank; *Pt $\Delta 5D$* [47] was the most similar one (about 39 %), suggesting that the primary structure of *Eg $\Delta 5D$* is quite different from those $\Delta 5$ desaturase genes previously isolated. Amino acid sequence alignment also shows that *Eg $\Delta 5D$* has about 20 % identity with *Eg $\Delta 8D$* [16, 38] and about 25.5 % identity with *Eg $\Delta 4D$* [45]. These data suggest that *Eg $\Delta 5D$* is evolutionary closer to $\Delta 5$ desaturase than the $\Delta 4$ or $\Delta 8$ desaturases. Functional analyses of *Eg $\Delta 5D$* in *Y. lipolytica* strains Y4036U and Y2224 revealed that it has strong $\Delta 5$ desaturase activity, with more than 24 % substrate conversion of DGLA to ARA, and it is not a $\Delta 5/\Delta 6$ bifunctional enzyme.

The HPGG motif is expected to be on the cytochrome b_5 surface, in contact with the heme through van der Waals interactions [27]. The conserved HPGG motif was thought to be essential in maintaining cytochrome b_5 electron transfer function, with the histidine serving as a heme axial ligand [50]. Substitution of the histidine residue of the HPGG motif with alanine in the $\Delta 6$ desaturase cytochrome b_5 domain of starflower, rat and algae abolished $\Delta 6$ desaturase activity [51–53]. It is expected that H33 of *Eg $\Delta 5D$* should also be essential for its function.

The HPGG motif itself has a unique structure. The proline residue of the HPGG stretch is located in a turn between two consecutive helices (Fig. 5) and was thought to be important in protein folding and in maintaining cytochrome b_5 protein stability [32]. The three-carbon side chain of proline is bonded to both the nitrogen and the carbon of the peptide backbone to form a five-member ring that greatly restricted its conformational freedom. The nonpolar characteristic of this ring structure may create a hydrophobic spot within the HPGG motif. On the other hand, the glycine possesses the smallest amino acid side

chain, hydrogen, which can allow for greater flexibility in local structure. It is likely that the combination of proline and glycine residues within the cytochrome b_5 HPGG motif is an important factor affecting both the structural position of the hydrophobic heme pocket and the appropriate orientation of the heme group within the heme pocket relative to the desaturase catalytic site. Surprisingly, our results indicate that the proline residue of the HPGG motif is not essential for electron transfer from the heme group of the cytochrome b_5 domain to the catalytic diiron cluster of *Eg $\Delta 5D$* . Most substitution mutants at P34 displayed at least 70 % of the wild type *Eg $\Delta 5D$* activity. The *Eg $\Delta 5D$ -34G* (HgGG) mutant had greater than 98 % of the wild type *Eg $\Delta 5D$* activity, demonstrating that the proline residue of HPGG motif is not required for the enzyme activity of *Eg $\Delta 5D$* (Table 1).

It is noteworthy that aspartate substitutions in *Eg $\Delta 5D$ -34D* and *Eg $\Delta 5D$ -36D* exhibit different effects on desaturase activity. Compared to free cytochrome b_5 , while there are several conserved acidic amino acids, there is a characteristic reduction in the number of aspartate and glutamate residues in the vicinity of the HPGG motif of cytochrome b_5 domain of desaturases. This reduced number of acidic residues around the heme pocket is thought to contribute to stabilizing nonpolar intermolecular interactions between the cytochrome b_5 and desaturase domains [27, 54]. Substitutions involving aspartate or glutamate residues in the HPGG motif may affect the interface geometry of electron donor/acceptor docking that is exhibited in desaturase activity due to altered electron transfer. We also found that substitutions for G36 of *Eg $\Delta 5D$* resulted in mutants with strong $\Delta 5$ desaturase activity. The most functional mutants were the small, slightly polar serine replacement, *Eg $\Delta 5D$ -36S*, and the acidic substitution with aspartate, *Eg $\Delta 5D$ -36D*. The activities of these two mutants are about the same as the wild type *Eg $\Delta 5D$* (Table 2).

The amino acid sequence of the first His-rich motif, HX_(3, 4)H, of *Eg $\Delta 5D$* is HDASH located from residues 155 to 159. The HDASH motif has been suggested as one of the characteristics of $\Delta 5$ desaturases and necessary for its function to convert DGLA to ARA in any transformed organisms [34]. Sequence analyses showed that there are natural variants of the HDASH motif in $\Delta 5$ desaturases, for example, *Pt $\Delta 5D$* [46] has the sequence of HDsSH, the $\Delta 5$ desaturase from *Thraustochytrium sp.* ATCC 21685 (GenBank accession #: AAM09687) has the sequence of HemgH, the $\Delta 5$ desaturase from *Leishmania major strain Friedlin* (GenBank accession #: CAJ07076) has the sequence of HeAgH, the $\Delta 5$ desaturase from Atlantic salmon (GenBank accession #: AAL82631) has the sequence of HDyGH, and *Pt $\Delta 5D$* [47] has the sequence of HDAnH in the corresponding location. This suggests that the HDASH

motif is not an invariant characteristic of $\Delta 5$ desaturases, and may be not required for $\Delta 5$ desaturase activity. We suggest that the two His residues of HDASH motif participate in the coordination of the diiron center (Fig. 5), but the other three residues (DAS) residues between the two His residues can be modified.

Systemic substitution studies (Tables 3, 4) at positions A157 and S158 within the HDASH motif of *EgΔ5D* demonstrated that these two residues could be replaced, and the mutants retained good $\Delta 5$ desaturase activity. The *EgΔ5D-157G* and *EgΔ5D-157S* mutants had about 96 and 94 % of the wild type *EgΔ5D* activity, respectively. Since *PiΔ5D* has an HDsSH motif [46], it is not surprising that *EgΔ5D-157S* with sequence HDsSH functioned well in *Yarrowia*. We also found that S158 could be substituted with either alanine or glycine. The alanine, glycine and serine are interchangeable within the HDASH motif of *EgΔ5S*; furthermore, the enzyme activity of *EgΔ5D* could be improved with a motif of HDAGH instead of HDASH (Table 4).

To determine whether at least one motif, HPGG or HDASH, is required for the enzyme activity of *EgΔ5D*, a series of mutants with mutations in both the HPGG and HDASH motifs was generated (Table 5). Some double mutants such as *EgΔ5D-34G/157G*, *EgΔ5D-34G/158A* and *EgΔ5D-34H/158G* had more than 80 % of wild type *EgΔ5D* activity, while *EgΔ5D-34G/158G* had almost the same activity as wild type *EgΔ5D*. Therefore, neither the HPGG nor the HDASH motif is necessary in the exact form as encoded for the activity of *EgΔ5D*.

Distribution analyses (Supplemental Fig. S2) of ARA in FFA, PL and NL pools of *Yarrowia* transformants with *EgΔ5D* shows that more ARA loaded in PL pool than that in FFA pool, suggesting that *EgΔ5D* is also an acyl-lipid desaturase, just like other front-end desaturases from lower plants, fungi and algae [26]. ARA distribution comparison of *Yarrowia* transformants with *EgΔ5D-34G* and *EgΔ5D-34G/158G* with wild type *EgΔ5D* shows that either single mutation within HPGG motif (P34G), or simultaneous mutations within HPGG (P34G) and HDASH (S158G) motifs does not change its fatty acid distribution pattern (Supplemental Fig. S2), and therefore these changes in *EgΔ5D* do not affect its substrate specificity.

An effective $\Delta 5$ desaturase is required for efficient conversion of DGLA to ARA or ETA to EPA (Fig. 1) in engineered *Y. lipolytica* or other organisms to produce commercially valuable LC-PUFA. We employed two approaches to improve the enzyme activity of the double mutant *EgΔ5D-34G/158G*. The optimization (Fig. 6) of the 43 codons of the 68 amino acids within the N-terminal portion of *EgΔ5D-34G/158G*, *EgΔ5M*, improved substrate conversion (Table 6). This improvement may relate to the rate of translation. Recent reports suggest that sequence at

the beginning of a gene can influence translation, and the mRNA structure at the 5' end of an mRNA can affect protein levels [58, 59]. Next, we substituted the arginine residue at position 347 with the serine which was identified in our original PCR products. Surprisingly, this R347S substitution in codon optimized *EgΔ5MI* further improved substrate conversion (Table 6). These data suggest that some un-conserved amino acids among different $\Delta 5$ desaturases may be good targets for protein evolution to generate improved enzymes. At this stage, the improved *EgΔ5D*, both *EgΔ5M* and *EgΔ5MI* should enable us to engineer *Yarrowia* and other organisms to produce high levels of ARA, EPA and DHA.

In conclusion, our studies suggest that the exact sequences of the HPGG and HDASH motifs are not necessary for the function of *EgΔ5D*. Several amino acids within these two motifs can be changed individually, or simultaneously, without significantly reducing the enzyme activity or altering its substrate specificity. In some cases such as *EgΔ5D-36D*, *EgΔ5D-36S*, and *EgΔ5D-158G* mutants, the $\Delta 5$ desaturase activity can be improved. In order to fully understand the function of *EgΔ5D*, the roles of the $HX_{(2,3)}HH$ and $(H/Q)X_{(2,3)}HH$ motifs as well as the un-conserved amino acids need to be studied in the future.

Acknowledgments We are grateful to Ethel Jackson and Henry Bryndza for their strong support. We thank every member of our Omega-3 team for their suggestions and discussions, Raymond Jackson and the DNA sequencing lab for their technical service, and Kelley Norton and Arthur Kruckeberg for critical reading of this manuscript.

Conflict of interest There are no actual or potential conflicts of interest.

Open Access This article is distributed under the terms of the Creative Commons Attribution License which permits any use, distribution, and reproduction in any medium, provided the original author(s) and the source are credited.

References

- Riediger ND, Othman RA, Suh M, Moghadasian MH (2009) A systemic review of the roles of n-3 fatty acids in health and disease. *J Am Diet Assoc* 109:668–679
- Freeman LM (2010) Beneficial effects of omega-3 fatty acids in cardiovascular disease. *J Small Anim Pract* 51:462–470
- Mourek J, Mourek J Jr (2011) Developmentally dependent and different roles of fatty acids OMEGA-6 and OMEGA-3. *Prague Med Rep* 112:81–92
- Mayurasakorn K, Williams JJ, Ten VS, Deckelbaum RJ (2011) Docosahexaenoic acid: brain accretion and roles in neuroprotection after brain hypoxia and ischemia. *Curr Opin Clin Nutr Metab Care* 14:158–167
- Uddin M, Levy BD (2011) Resolvins: natural agonists for resolution of pulmonary inflammation. *Prog Lipid Res* 50:75–88

6. Serhan CN (2007) Resolution phase of inflammation: novel endogenous anti-inflammatory and proresolving lipid mediators and pathways. *Annu Rev Immunol* 25:101–137
7. Kiso Y (2011) Pharmacology in health foods: effects of arachidonic acid and docosahexaenoic acid on the age-related decline in brain and cardiovascular system function. *J Pharmacol Sci* 115:471–475
8. Weitz D, Weintraub H, Fisher E, Schwartzbard AZ (2010) Fish oil for the treatment of cardiovascular disease. *Cardiol Rev* 18:258–263
9. Yokoyama M, Origasa H, Matsuzaki M, Matsuzawa Y, Saito Y, Ishikawa Y, Oikawa S, Sasaki J, Hishida H, Itakura H, Kita T, Kitabatake A, Nakaya N, Sakata T, Shimada K, Shirato K (2007) Effects of eicosapentaenoic acid on major coronary events in hypercholesterolaemic patients (JELIS): a randomised open-label, blinded endpoint analysis. *Lancet* 369:1090–1098
10. Féart C, Peuchant E, Letenneur L, Samieri C, Montagnier D, Fourrier-Reglat A, Barberger-Gateau P (2008) Plasma eicosapentaenoic acid is inversely associated with severity of depressive symptomatology in the elderly: data from the Bordeaux sample of the three-city study. *Am J Clin Nutr* 87:1156–1162
11. Costa LG (2007) Contaminants in fish: risk-benefit considerations. *Arh Hig Rada Toksikol* 58:567–574
12. Streekstra H (2010) Arachidonic acid: fermentative production by *Mortierella* fungi. In: Cohen Z, Ratledge C (eds) *Single cell oils*, 2nd edn. AOCS Press, Urbana
13. Barclay W, Weaver C, Metz J, Hansen J (2010) Development of a docosahexaenoic acid production technology using *Schizochytrium*: historical perspective and update. In: Cohen Z, Ratledge C (eds) *Single cell oils*, 2nd edn. AOCS Press, Urbana
14. Zhu Q, Xue Z, Yadav N, Damude H, Pollak D, Rupert R, Seip J, Hollerbach D, Macool D, Zhang H (2010) Metabolic engineering of an oleaginous yeast for the production of omega-3 fatty acids. In: Cohen Z, Ratledge C (eds) *Single cell oils*, 2nd edn. AOCS Press, Urbana
15. Metz JG, Roessler P, Facciotti D, Levering C, Dittrich F, Lassner M, Valentine R, Lardizabal K, Domergue F, Yamada A, Yazawa K, Knauf V, Browse J (2001) Production of polyunsaturated fatty acids by polyketide synthases in both prokaryotes and eukaryotes. *Science* 293:290–293
16. Wallis JG, Browse J (1999) The $\Delta 8$ -desaturase of *Euglena gracilis*: an alternate pathway for synthesis of 20-carbon polyunsaturated fatty acids. *Arch Biochem Biophys* 365:307–316
17. Pereira SL, Leonard AE, Mukerji P (2003) Recent advances in the study of fatty acid desaturases from animals and lower eukaryotes. *Prostaglandins Leukot Essent Fatty Acids* 68:97–106
18. Qiu X, Hong H, MacKenzie SL (2001) Identification of a delta 4 fatty acid desaturase from *Thraustochytrium* sp. involved in the biosynthesis of docosahexanoic acid by heterologous expression in *Saccharomyces cerevisiae* and *Brassica juncea*. *J Biol Chem* 276:31561–31566
19. Qi B, Fraser T, Mugford S, Dobson G, Sayanova O, Butler JJ, Napier A, Stobart AK, Lazarus CM (2004) Production of very long chain polysaturated omega-3 and omega-6 fatty acids in plants. *Nat Biotechnol* 22:739–745
20. Kajikawa M, Yamato KT, Kohzu Y, Nojiri M, Sakuradani E, Shimizu S, Sakai Y, Fukuzawa H, Ohyama K (2004) Isolation and characterization of delta(6)-desaturase, an ELO-like enzyme and delta(5)-desaturase from the liverwort *Marchantia polymorpha* and production of arachidonic and eicosapentaenoic acids in the methylotrophic yeast *Pichia pastoris*. *Plant Mol Biol* 54:335–352
21. Damude HG, Kinney AJ (2008) Engineering oilseeds to produce nutritional fatty acids. *Physiol Plant* 132:1–10
22. Venegas-Calero M, Sayanova O, Napier JA (2010) An alternative to fish oils: metabolic engineering of oil-seed crops to produce omega-3 long chain polyunsaturated fatty acids. *Prog Lipid Res* 49:108–119
23. Tavares S, Grotkjær T, Obsen T, Haslam RP, Napier JA, Gunnarsson N (2011) Metabolic engineering of *Saccharomyces cerevisiae* for production of eicosapentaenoic acid, using a novel {delta}5-desaturase from *Paramecium tetraurelia*. *Appl Environ Microbiol* 77:1854–1861
24. Michaelson LV, Lazarus CM, Griffiths G, Napier JA, Stobart AK (1998) Isolation of a delta5-fatty acid desaturase gene from *Mortierella alpina*. *J Biol Chem* 273:19055–19059
25. Knutzon DS, Thurmond JM, Huang YS, Chaudhary S, Bobik EG Jr, Chan GM, Kirchner SJ, Mukerji P (1998) Identification of delta5-desaturase from *Mortierella alpina* by heterologous expression in bakers' yeast and canola. *J Biol Chem* 273:29360–29366
26. Meesapyodsuk D, Qiu X (2012) The front-end desaturase: structure, function, evolution and biotechnological use. *Lipids* 47:227–237
27. Sperling P, Heinz E (2001) Desaturases fused to their electron donor. *Eur J Lipid Sci Technol* 103:158–180
28. Napier JA, Michaelson LV, Sayanova O (2003) The role of cytochrome *b*₅ fusion desaturases in the synthesis of polyunsaturated fatty acids. *Prostaglandins Leukot Essent Fatty Acids* 68:135–143
29. Schenkman JB, Jansson I (2003) The many roles of cytochrome *b*₅. *Pharmacol Ther* 97:139–152
30. Stuke JE, McDonough VM, Martin CE (1990) The OLE1 gene of *Saccharomyces cerevisiae* encodes the delta 9 fatty acid desaturase and can be functionally replaced by the rat stearoyl-CoA desaturase gene. *J Biol Chem* 265:20144–20149
31. Shanklin J, Guy JE, Mishra G, Lindqvist Y (2009) Desaturases: emerging models for understanding functional diversification of diiron-containing enzymes. *J Biol Chem* 284:18559–18563
32. Lin YW, Ying TL, Liao LF (2009) Dynamic consequences of mutating the typical HPGG motif of apocytochrome *b*₅ revealed by computer simulation. *Chin Chem Let* 200:631–634
33. Shanklin J, Whittle E, Fox BG (1994) Eight histidine residues are catalytically essential in a membrane-associated iron enzyme, stearoyl-CoA desaturase, and are conserved in alkane hydroxylase and xylene monooxygenase. *Biochemistry* 33:12787–12794
34. Knutzon D, Mukerji P, Huang YS, Thurmond J, Chaudhary S (1999) Methods and compositions for synthesis of long chain poly-unsaturated fatty acids. US Patent 5,972,664
35. Yadav NS, Zhu Q, Zhang H (2009) $\Delta 12$ desaturases suitable for altering levels of polyunsaturated fatty acids in oleaginous yeast. US Patent 7,504,259
36. Macool DJ, Xue Z, Zhu Q (2008) A *Mortierella alpina* *c*_{16/18} fatty acid elongase. US Patent 7,470,532
37. Damude HG, McGonigle B, Zhu Q, Xue Z (2011) Delta-9 elongases and their use in making polyunsaturated fatty acids. US Patent 8,049,062
38. Damude HG, He H, Liao D-I, Zhu Q (2011) Mutant delta-8 desaturase genes engineered by targeted mutagenesis and their use in making polyunsaturated fatty acids. US Patent 8,026,089
39. Sambrook J, Fritsch EF, Maniatis T (1989) *Molecular cloning: a laboratory manual*, 2nd edn. Cold Spring Harbor Laboratory, Cold Spring Harbor
40. Ausubel FM, Brent R, Kingston RE, Moore DD, Seidman JG, Smith JA, Struhl K (2010) *Current protocols in molecular biology*. Wiley, New York
41. Fournier P, Abbas A, Chasles M, Kudla B, Ogrydziak D, Yaver D, Xuan JW, Peito A, Ribe AM, He F, Gaillardin CC (1993) Colocalization of centromeric and replicative functions on autonomously replicating sequences isolated from the yeast *Yarrowia lipolytica*. *Proc Natl Acad Sci USA* 90:4912–4916

42. Hong S-Y, Seip J, Walters-Pollak D, Rupert R, Jackson R, Xue Z, Zhu Q (2011) Engineering *Yarrowia lipolytica* to express secretory invertase with strong FBA1IN promoter. *Yeast* 29:59–72
43. Chen DC, Beckerich JM, Gaillardin C (1997) One-step transformation of the dimorphic yeast *Yarrowia lipolytica*. *Appl Microbiol Biotechnol* 48:232–235
44. Cahoon EB, Ripp KG, Hall SE, Kinney AL (2001) Formation of conjugated Δ^8 , Δ^{10} -double bonds by Δ^{12} -oleic acid desaturase-related enzymes: biosynthetic origin of calendic acid. *J Biol Chem* 276:2637–2643
45. Meyer A, Cirpus P, Ott C, Schlecker R, Zahringer U, Heinz E (2003) Biosynthesis of docosahexaenoic acid in *Euglena gracilis*: biochemical and molecular evidence for the involvement of a delta4-fatty acyl group desaturase. *J Biochem* 42:9779–9788
46. Hong H, Datla N, MacKenzie SL, Qiu X (2002) Isolation and characterization of a $\Delta 5$ FA desaturase from *Pythium irregulare* by heterologous expression in *Saccharomyces cerevisiae* and oilseed crops. *Lipids* 37:863–868
47. Domergue F, Lerchl J, Zahringer U, Heinz E (2002) Cloning and functional characterization of *Phaeodactylum tricorutum* front-end desaturases involved in eicosapentaenoic acid biosynthesis. *Eur J Biochem* 269:4105–4113
48. Damude H, Zhu Q (2007) Delta-8 desaturase and its use in making polyunsaturated fatty acids. US Patent 7,943,823
49. Kobayashi T, Sakaguchi K, Matsuda T, Abe E, Hama Y, Hayashi M, Honda D, Okita Y, Sugimoto S, Okino N, Ito M (2011) Increase of eicosapentaenoic acid in thraustochytrids through thraustochytrid ubiquitin promoter-driven expression of a fatty acid {delta}5 desaturase gene. *Appl Environ Microbiol* 77:3870–3876
50. Lederer F (1994) The cytochrome b4-fold: an adaptable module. *Biochimie* 76:674–692
51. Sayanova O, Shewry PR, Napier JA (1999) Histidine-41 of the cytochrome b₅ domain of the borage delta6 fatty acid desaturase is essential for enzyme activity. *Plant Physiol* 121:641–646
52. Guillou H, D'Andrea S, Rioux V, Barnouin R, Dalaine S, Pedrono F, Jan S, Legrand P (2004) Distinct roles of endoplasmic reticulum cytochrome b₅ and fused cytochrome b₅-like domain for rat $\Delta 6$ -desaturase activity. *J Lipid Res* 45:32–40
53. Hongsthong A, Subudhi S, Sirijuntarut M, Kurdrud P, Cheevadhanarak S, Tanticharoen M (2006) Revealing the complementation of ferredoxin by cytochrome b₅ in the *Spirulina-Δ6*-desaturation reaction by N-terminal fusion and co-expression of the fungal-cytochrome b₅ domain and *Spirulina-Δ6*-acyl-lipid desaturase. *Appl Microbiol Biotechnol* 72:1192–1201
54. Gostincar C, Turk M, Gunde-Cimerman N (2010) The evolution of fatty acid desaturases and cytochrome b₅ in eukaryotes. *J Membr Biol* 233:63–72
55. Ratledge C (2010) Single cell oils for the 21st century. In: Cohen Z, Ratledge C (eds) *Single cell oils*, 2nd edn. AOCS Press, Urbana
56. Beopoulos A, Nicaud JM, Gaillardin C (2011) An overview of lipid metabolism in yeasts and its impact on biotechnological processes. *Appl Microbiol Biotechnol* 90:1193–1206
57. Sabirova JS, Haddouche R, Van Bogaert IN, Mulaa F, Verstraete W, Timmis KN, Schmidt-Dannert C, Nicaud JM, Soetaert W (2011) The 'LipoYeasts' project: using the oleaginous yeast *Yarrowia lipolytica* in combination with specific bacterial genes for the bioconversion of lipids, fats and oils into high-value products. *Microb Biotechnol* 4:47–54
58. Kudla G, Murray AW, Tollervey D, Plotkin JB (2009) Coding sequence determinants of gene expression in *Escherichia coli*. *Science* 324:255–258
59. Kahali B, Ahmad S, Ghosh TC (2011) Selective constraints in yeast genes with differential expressivity: codon pair usage and mRNA stability perspectives. *Gene* 481:76–82

Serum Autotaxin is not a Useful Biomarker for Ovarian Cancer

Kazuhiro Nakamura · Koji Igarashi · Ryunosuke Ohkawa · Hiromitsu Yokota · Akiko Masuda · Shunsuke Nakagawa · Tetsu Yano · Hitoshi Ikeda · Junken Aoki · Yutaka Yatomi

Received: 2 March 2012 / Accepted: 22 May 2012 / Published online: 15 June 2012
© AOCs 2012

Abstract Autotaxin (ATX) is a glycoprotein that was first identified in the conditioned medium of human melanoma cells as an autocrine motility factor. It possesses lysophospholipase D activity, producing the bioactive lipid mediator lysophosphatidic acid (LPA) from lysophosphatidylcholine. Enhanced expression of ATX mRNA has been reported in various cancer cells and tissues, and it has been speculated that ATX overexpression in cancer cells may be associated with aberrant LPA production. LPA and ATX have been implicated in cancer progression and metastasis, and ovarian

cancer is a representative example. In the present study, we measured the serum ATX antigen levels in patients with ovarian cancer and evaluated the usefulness of this parameter for clinical laboratory testing. The serum ATX antigen levels were not increased in ovarian cancer patients as compared with the levels in healthy subjects, and the serum ATX may not be useful as a biomarker for ovarian cancer.

Keywords Autotaxin · Clinical laboratory testing · Immunoenzymetric assay · Lysophosphatidic acids · Ovarian cancer · Tumor marker

K. Nakamura · A. Masuda · H. Ikeda · Y. Yatomi (✉)
Department of Clinical Laboratory Medicine,
Graduate School of Medicine, The University of Tokyo,
7-3-1 Hongo, Bunkyo-ku, Tokyo 113-8655, Japan
e-mail: yatoyuta-tky@umin.ac.jp

K. Nakamura
e-mail: nakamurak.lab@gmail.com

K. Igarashi
Bioscience Division, Reagent Development Department,
AIA Research Group, TOSOH Corporation, Kanagawa, Japan

R. Ohkawa · H. Yokota · A. Masuda · H. Ikeda · Y. Yatomi
Department of Clinical Laboratory, The University of Tokyo
Hospital, Tokyo, Japan

S. Nakagawa · T. Yano
Department of Obstetrics and Gynecology, Graduate School
of Medicine, The University of Tokyo, Tokyo, Japan

J. Aoki
Department of Molecular and Cellular Biochemistry,
Graduate School of Pharmaceutical Sciences,
Tohoku University, Miyagi, Japan

J. Aoki
PRESTO, Japan Science and Technology Corporation,
Saitama, Japan

Abbreviations

LPA	Lysophosphatidic acid
ATX	Autotaxin
LysoPLD	Lysophospholipase D
CA125	Cancer antigen 125

Introduction

Lysophosphatidic acid (1- or 2-acyl-*sn*-glycero-3-phosphatidic acid, LPA) is a simple lysophospholipid, and is attracting great attention as a lysophospholipid mediator. This bioactive lipid exerts important biological actions, including cell proliferation, migration and survival [1]. The multiple actions of LPA are explained by its binding to and activation of specific G-protein-coupled receptors (LPA1-6), leading to subsequent stimulation of the small GTPases, Ras, Rho and Rac [1–3].

The precise mechanism underlying the extracellular production of LPA has been elucidated in recent studies. In the plasma, autotaxin (ATX) plays a pivotal role in the production of LPA [1, 4]. ATX is a glycoprotein which was

first discovered in the conditioned medium of human A2058 melanoma cells as an autocrine motility factor [1]. Later, it was revealed that ATX possesses lysophospholipase D (lysoPLD) activity, which hydrolyzes lysophosphatidylcholine to produce LPA [4].

LPA has been shown to be involved in several cellular processes such as proliferation, progression and invasion in in-vitro studies [1, 5–7]. On the other hand, enhanced expression of ATX mRNA has also been reported in various metastatic cancer cells and tissues [1, 7–10], and it has been speculated that ATX overexpression in cancer cells may be associated with aberrant LPA production. Together with these findings, not only LPA, but also ATX are likely to play critical roles in the pathophysiology of cancers.

Several studies have indicated that ATX and LPA are also related to the development/progression of ovarian cancer. For example, LPA and ATX have been demonstrated to promote ovarian cancer progression and invasion [6, 7]. ATX has been shown to delay apoptosis induced by carboplatin in ovarian cancer cells [8]. In addition, ATX and LPA receptors have been shown to be expressed in these cells [7, 8]. These studies clearly suggest that ATX and LPA are involved in the onset/progression of ovarian cancer.

Previous studies have investigated whether LPA can serve as a potential biomarker for ovarian cancer. The plasma LPA levels have been found to be increased in patients with ovarian cancer [11]. However, another group reported no difference in the plasma LPA levels between patients with ovarian cancer and healthy controls [12]. At present, whether plasma LPA might serve as a useful marker of ovarian cancer is still controversial. One of the reasons for this discrepancy is the difficulty in plasma LPA measurement. We previously reported that measurement of the plasma LPA concentration for clinical purposes has the critical and difficult problem; plasma levels of LPA can be easily altered during the sample preparation and preservation [13]. Therefore, re-examination conducted under stringent conditions to minimize any increase of the LPA level after sampling is needed for evaluation of the usefulness of plasma LPA measurement for ovarian cancer.

While plasma/serum LPA increases dramatically if samples are not handled properly, the serum ATX/lysoPLD remains relatively stable [13]. Serum ATX measurement seems to allow easier handling of the samples than plasma LPA measurement, and we confirmed that the ATX/lysoPLD antigen concentration and activity were well correlated with the plasma LPA concentration [10, 14–16]. Therefore, the plasma LPA can be estimated from the serum ATX. In the present study, we measured the serum ATX antigen levels in patients with ovarian cancer and evaluated the usefulness of this parameter for clinical laboratory testing.

Methods

The serum samples used in this study were residual samples of those obtained for laboratory analyses (for medical checkups). The study was conducted with the approval of the Institutional Research Ethics Committee of the Faculty of Medicine, the University of Tokyo. Informed consent from the patients was obtained for the use of the samples. Commercially available serum of ovarian cancer patients and healthy subjects were obtained from SLR Research Corporation (Carlsbad, CA, USA), BioTheme Research Solutions, Inc. (Davie, FL, USA) and ProMedDx, LLC (Norton, MA, USA).

The ATX antigen levels in the serum were determined by a two-site immunoenzymetric assay using the ATX assay reagent and the TOSOH AIA system (TOSOH, Tokyo, Japan) [14]. Serum cancer antigen 125 (CA125) levels were also analyzed by a two-site immunoenzymetric assay. The statistical significance of the differences between two groups was determined by an unpaired Student's *t* test. The correlations were evaluated by linear regression analysis. $p < 0.05$ was considered to be indicative of statistical significance.

Results

We first compared the ATX antigen concentrations in residual serum samples between ovarian cancer patients and healthy subjects (Table 1-A). No significant difference in the mean serum ATX level was observed between the patients and healthy subjects ($p = 0.946$). We then examined the correlation between the serum ATX and the serum CA125 in ovarian cancer patients. CA125 is believed to be the best biomarker for ovarian cancer, and is increased to above 35 U/mL in about 80 % of women with epithelial ovarian cancer [17]. No significant correlation was observed between ATX and CA125 ($p = 0.797$, Table 1-A). Similarly, no significant difference of the ATX level was observed between the patients and healthy subjects when commercially available sera were employed ($p = 0.110$, Table 1-B). Slight but significant correlation was detected between ATX and CA125 in commercially available serum ($r = 0.347$, $p < 0.001$) although its significance remains to be solved. When we analyzed the relationship between the serum ATX concentrations and the clinical course in two patients with ovarian cancer, no changes in the serum ATX were detected after chemotherapy, while the serum CA125 levels markedly decreased after chemotherapy (data not shown).

Table 1 Serum ATX concentrations in serum samples from patients with ovarian cancer and healthy subjects

	No. of patients	Age (years) mean \pm 2SD	ATX antigen levels mean \pm 2SD (mg/L)	CA125 levels mean \pm 2SD (U/mL)	Linear regression analysis	
					<i>r</i>	<i>p</i>
(A) Residual serum samples						
Ovarian cancer patients	21	53 \pm 24	0.856 \pm 0.376	438 \pm 969	0.060	0.797
Healthy subjects	46	37 \pm 18	0.859 \pm 0.353			
(B) Commercially available serum						
Ovarian cancer patients	101	64 \pm 30	1.122 \pm 0.754	970 \pm 4,261	0.347	<0.001
Healthy subjects	56	38 \pm 18	1.031 \pm 0.537			

There was no significant difference in the mean ATX concentration between ovarian cancer patients and healthy subjects, as determined using an unpaired Student's *t* test. No significant correlation between the serum ATX and serum CA125 was observed in ovarian cancer patients in residual serum samples, while significant correlation was detected between these parameters in commercially available serum, as determined using linear regression analysis. The reference value for CA125 is below 30 U/mL.

Discussion

In this study, we measured the serum ATX concentrations in ovarian cancer patients based on our initial supposition that the serum ATX levels might be increased in these cancer patients. However, no significant differences were detected in the serum ATX concentrations between patients with ovarian cancer and healthy subjects (Table 1). No significant correlation was detected between ATX and CA125 in our residual serum samples, while slight but significant correlation was detected when commercially available sera were assayed; its significance remains to be solved based on the fact that no significant differences were detected in the serum ATX concentrations between patients with ovarian cancer and healthy subjects despite a major difference for CA125.

Based on our present data, it seems unlikely that the serum ATX is useful as a tumor marker for ovarian cancer. In this study, we measured only the serum ATX antigen since its concentration is well correlated with the serum lysoPLD activity and since ATX assay is actually more promising than the lysoPLD activity measurement for routine laboratory testing. We, however, admit the limitation of our data since we did not confirm the correlation between the levels of ATX antigen and lysoPLD activity using samples from ovarian cancer patients, which should be important future tasks.

ATX was originally identified as a tumor cell motility factor and has been reported to be expressed in several cancer cells [1, 7–10]. Therefore, it was deemed that the serum ATX may reflect the pathological condition and be elevated in cancer patients. Contrary to this expectation, not many reports have clarified the clinical significance of serum ATX measurement in these patients. The (patho)physiological conditions associated with marked aberrant elevation of the serum ATX induced by cancer cells appear to be limited to follicular lymphoma and

pancreatic cancer, at least at present [10, 18]. In addition to ovarian cancer, we also confirmed that the serum ATX antigen was unsuitable as a tumor marker for prostate cancer (data not shown), as had been shown by measuring lysoPLD activity [9]. Considering the specificity of the rise of the serum ATX in these conditions, measurement of the serum ATX may be extremely useful for the diagnosis of follicular lymphoma and pancreatic cancer.

As described above, we could not confirm the clinical significance of the serum ATX assay in ovarian cancer patients despite that ATX is reportedly involved in the onset/progression of ovarian cancer. Our present data may indicate that ovarian cancer cells do not produce sufficient amounts of ATX to cause an elevation of the serum ATX concentrations. Although the serum ATX is not increased in ovarian cancer patients, this does not exclude the possibility of ATX involvement in ovarian cancer, since ATX, which produces LPA, may locally play an important role in its pathophysiology.

Acknowledgments This work was supported by a Grant-in-Aid for Scientific Research from the Ministry of Education, Culture, Sports, Science and Technology, Japan, and the Japanese Society of Laboratory Medicine Fund for the Promotion of Scientific Research.

References

1. Moolenaar WH, van Meeteren LA, Giepmans BN (2004) The ins and outs of lysophosphatidic acid signaling. *BioEssays* 26: 870–881
2. Lee CW, Rivera R, Gardell S, Dubin AE, Chun J (2006) GPR92 as a new G12/13- and Gq-coupled lysophosphatidic acid receptor that increases cAMP, LPA5. *J Biol Chem* 281:23589–23597
3. Yanagida K, Masago K, Nakanishi H, Kihara Y, Hamano F, Tajima Y, Taguchi R, Shimizu T, Ishii S (2009) Identification and characterization of a novel lysophosphatidic acid receptor, p2y5/LPA6. *J Biol Chem* 284:17731–17741
4. Umezu-Goto M, Kishi Y, Taira A, Hama K, Dohmae N, Takio K, Yamori T, Mills GB, Inoue K, Aoki J, Arai H (2002) Autotaxin

- has lysophospholipase D activity leading to tumor cell growth and motility by lysophosphatidic acid production. *J Cell Biol* 158:227–233
5. Xu Y, Fang XJ, Casey G, Mills GB (1995) Lysophospholipids activate ovarian and breast cancer cells. *Biochem J* 309(Pt 3): 933–940
 6. Jeong KJ, Park SY, Cho KH, Sohn JS, Lee J, Kim YK, Kang J, Park CG, Han JW, Lee HY (2012) The Rho/ROCK pathway for lysophosphatidic acid-induced proteolytic enzyme expression and ovarian cancer cell invasion. *Oncogene* (in press)
 7. Ptaszynska MM, Pendrak ML, Bandle RW, Stracke ML, Roberts DD (2008) Positive feedback between vascular endothelial growth factor-A and autotaxin in ovarian cancer cells. *Mol Cancer Res* 6:352–363
 8. Vidot S, Witham J, Agarwal R, Greenhough S, Bamrah HS, Tigyi GJ, Kaye SB, Richardson A (2010) Autotaxin delays apoptosis induced by carboplatin in ovarian cancer cells. *Cell Signal* 22:926–935
 9. Nakamura K, Takeuchi T, Ohkawa R, Okubo S, Yokota H, Tozuka M, Aoki J, Arai H, Ikeda H, Ohshima N, Kitamura T, Yatomi Y (2007) Serum lysophospholipase D/autotaxin may be a new nutritional assessment marker: study on prostate cancer patients. *Ann Clin Biochem* 44:549–556
 10. Masuda A, Nakamura K, Izutsu K, Igarashi K, Ohkawa R, Jona M, Higashi K, Yokota H, Okudaira S, Kishimoto T, Watanabe T, Koike Y, Ikeda H, Kozai Y, Kurokawa M, Aoki J, Yatomi Y (2008) Serum autotaxin measurement in haematological malignancies: a promising marker for follicular lymphoma. *Br J Haematol* 143:60–70
 11. Xu Y, Shen Z, Wiper DW, Wu M, Morton RE, Elson P, Kennedy AW, Belinson J, Markman M, Casey G (1998) Lysophosphatidic acid as a potential biomarker for ovarian and other gynecologic cancers. *JAMA* 280:719–723
 12. Baker DL, Morrison P, Miller B, Riely CA, Tolley B, Westermann AM, Bonfrer JM, Bais E, Moolenaar WH, Tigyi G (2002) Plasma lysophosphatidic acid concentration and ovarian cancer. *JAMA* 287:3081–3082
 13. Nakamura K, Ohkawa R, Okubo S, Tozuka M, Okada M, Aoki S, Aoki J, Arai H, Ikeda H, Yatomi Y (2007) Measurement of lysophospholipase D/autotaxin activity in human serum samples. *Clin Biochem* 40:274–277
 14. Nakamura K, Igarashi K, Ide K, Ohkawa R, Okubo S, Yokota H, Masuda A, Oshima N, Takeuchi T, Nangaku M, Okudaira S, Arai H, Ikeda H, Aoki J, Yatomi Y (2008) Validation of an autotaxin enzyme immunoassay in human serum samples and its application to hypoalbuminemia differentiation. *Clin Chim Acta* 388:51–58
 15. Watanabe N, Ikeda H, Nakamura K, Ohkawa R, Kume Y, Aoki J, Hama K, Okudaira S, Tanaka M, Tomiya T, Yanase M, Tejjima K, Nishikawa T, Arai M, Arai H, Omata M, Fujiwara K, Yatomi Y (2007) Both plasma lysophosphatidic acid and serum autotaxin levels are increased in chronic hepatitis C. *J Clin Gastroenterol* 41:616–623
 16. Hosogaya S, Yatomi Y, Nakamura K, Ohkawa R, Okubo S, Yokota H, Ohta M, Yamazaki H, Koike T, Ozaki Y (2008) Measurement of plasma lysophosphatidic acid concentration in healthy subjects: strong correlation with lysophospholipase D activity. *Ann Clin Biochem* 45:364–368
 17. Bast RC Jr, Klug TL, St John E, Jenison E, Niloff JM, Lazarus H, Berkowitz RS, Leavitt T, Griffiths CT, Parker L, Zurawski VR Jr, Knapp RC (1983) A radioimmunoassay using a monoclonal antibody to monitor the course of epithelial ovarian cancer. *N Engl J Med* 309:883–887
 18. Nakai Y, Ikeda H, Nakamura K, Kume Y, Fujishiro M, Sasahira N, Hirano K, Isayama H, Tada M, Kawabe T, Komatsu Y, Omata M, Aoki J, Koike K, Yatomi Y (2011) Specific increase in serum autotaxin activity in patients with pancreatic cancer. *Clin Biochem* 44:576–581

***Trans* Fatty Acid Intakes and Food Sources in the U.S. Population: NHANES 1999–2002**

Penny M. Kris-Etherton · Michael Lefevre ·
Ronald P. Mensink · Barbara Petersen ·
Jennifer Fleming · Brent D. Flickinger

Received: 16 November 2011 / Accepted: 19 July 2012 / Published online: 18 August 2012
© The Author(s) 2012. This article is published with open access at Springerlink.com

Abstract Because of efforts to decrease *trans* fatty acids (TFA) in the food supply, intake should be assessed in the population to establish a baseline TFA intake. The 1999–2002 National Health and Nutrition Examination Survey (NHANES) was used to identify a benchmark for TFA intake. TFA was estimated by mean, median, and quintile of intake, TFA intake data were weighted using the NHANES 4-year sample weights. The main outcome measures included TFA intake in grams per day and

percentage of energy in the top 25 food sources of TFA. Data are reported for 16,669 individuals ≥ 3 years of age. Median TFA intake was 2.3 % of calories (5 g/day) with 0.9–4.5 % of energy (1.5–13.1 g/day) over different quintiles of intake. Mean TFA intake was 2.5 % of energy (6.1 g/day). The range of TFA intake in the fifth quintile was very large, i.e., 3.5–12.5 % of energy or 8.8–92.4 g/day. Increasing quintiles of TFA intake were associated with increases in total fat (26.7–37.6 % of energy), saturated fat (7.6–10.5 % of energy), and calories (for those >20 years of age: 2,416–2,583 for men and 1,679–1,886 for women). Major food sources of dietary TFA were cakes, cookies, pies, and pastries. Based on current dietary guidance to consume as little industrial TFA as possible, much progress is needed to attain this goal, including food industry efforts to remove TFA from the food supply and educating the public about making healthy food choices.

For the ILSI North America Technical Committee on Dietary Lipids.

P. M. Kris-Etherton (✉) · J. Fleming
Department of Nutritional Sciences, 319 Chandlee Laboratory,
The Pennsylvania State University, University Park,
PA 16802, USA
e-mail: pmk3@psu.edu

J. Fleming
e-mail: jas58@psu.edu

M. Lefevre
Department of Nutrition, Dietetics and Food Science, Utah State
University, 9815 Old Main Hill, Logan, UT 84322-9815, USA
e-mail: michael.lefevre@usu.edu

R. P. Mensink
Department of Human Biology, Nutrition and Toxicology
Research Institute Maastricht, Maastricht University,
P.O. Box 616, 6200 MD Maastricht, The Netherlands
e-mail: r.mensink@HB.unimaas.nl

B. Petersen
Exponent, Inc., 1150 Connecticut Ave NW, Suite 1100,
Washington, DC 20036, USA
e-mail: bpetersen@exponent.com

B. D. Flickinger
Archer Daniels Midland Company, Randall Research Center,
1001 N. Brush College Rd., Decatur, IL 62521, USA
e-mail: flickinger@adm.com

Keywords *Trans* fatty acid intake · Industrial *trans* fatty acid intake · Fatty acid intake · Quintiles of *trans* fatty acid intake · Food sources of *trans* fatty acids · NHANES 1999–2002

Abbreviations

CSFII	Continuing Survey of Food Intakes by Individuals
FARE	Foods Analysis and Residue Evaluation Program
FDA	U.S. Food and Drug Administration
MUFA	Monounsaturated fatty acids
NHANES	National Health and Nutrition Examination Survey
SFA	Saturated fatty acids
TFA	<i>Trans</i> fatty acids
USDA	U.S. Department of Agriculture

Introduction

Dietary recommendations have been made in the United States and globally to decrease *trans* fatty acids (TFA) produced by partial hydrogenation of vegetable oils [1, 2]. These recommendations are based on numerous studies demonstrating many adverse health effects of TFA [3]. Multiple strategies have been invoked in the United States to decrease dietary TFA, including nutrition labeling of TFA on the Nutrition Facts Panel (law passed in 2003; enacted in 2006), as well as passage of legislation banning or restricting use of fats and oils containing TFA in some states and cities [4, 5]. In 2009, legislation to limit TFA in the food supply was enacted in 1 state and proposed in 13 states and the District of Columbia [6]. Based on the success of this approach in New York, it seems that legislative strategies may be an effective strategy for decreasing TFA in foods [7]. Mozaffarian and Stampfer [7] estimated that a 1 % reduction in TFA intake could prevent 72,000 cardiovascular disease-related deaths per year. The U.S. Food and Drug Administration (FDA) have also suggested that the removal of TFA from just 3 % of breads and cakes and 15 % of cookies and crackers would save up to US \$59 billion in health care costs over the next 20 years [8]. Consequently, the food industry is actively lowering TFA in the food supply by developing new fats and oils and modifying existing ones [9, 10].

The last comprehensive analysis of TFA intake was published by Allison et al. [11] in 1999, using 1989–1991 data collected from the U.S. Department of Agriculture's (USDA) Continuing Survey of Food Intakes by Individuals (CSFII). At that time, the average TFA intake in the United States was 2.6 % of calories, or 5.3 g/day [11]. Since the work by Allison et al. was published, many food products have had TFA removed and/or reduced appreciably [5, 12]. Much of this has happened as the result of legislation (announced on January 9, 2003) mandating TFA labeling on the Nutrition Facts Panel by January 1, 2006. Clearly, there is a need to evaluate the effects of this announcement and legislation on current TFA intake, and this needs to be done in the context of the most current TFA intake prior to the FDA's announcement. Consequently, it is important to benchmark current TFA intake against intake that is more recent than the 1989–1991 data to evaluate the impact of legislation enacted to decrease TFA intake.

The purpose of this study was to assess TFA intake in different population groups in the United States using more recent intake data from the 1999–2002 National Health and Nutrition Examination Survey (NHANES) just prior to the time that legislation was passed for TFA to be listed on the Nutrition Facts Panel. We also evaluated food sources of TFA in different population groups. A better understanding

of the major food sources of TFA would be helpful for ongoing efforts to markedly lower TFA in the food supply.

Materials and Methods

Estimation of TFA Intake During 1999–2002

To estimate dietary intake of TFA, we used 1999–2002 NHANES consumption data as well as the Foods Analysis and Residue Evaluation Program (FARE) software (v.7.997; Exponent, Washington, DC). FARE is proprietary data processing software that was developed to facilitate the mining of the thousands of individual intake records in the NHANES database. A more detailed description of the analysis done by using the FARE program is described by DiRienzo et al. [13]. FARE is used by the FDA, the USDA, the California Office of Environmental Health Hazard Assessment, and the Health Canada Pest Management Regulatory Agency to derive estimates of food, nutrient, and contaminant intakes based on NHANES and CSFII consumption data.

Dietary assessment in NHANES 1999–2002 was conducted using two 24-h dietary recalls, one in person and a second one by telephone [14]. The TFA content of foods was derived from the NHANES dataset. The NHANES used the *Trans* Fatty Acid Database (laboratory analyses completed between 1990 and 1993) that was released in 1995 as “Special table 1: Fat and fatty acid content of selected foods containing *trans* fatty acids.” This is referred to as the USDA Nutrient Database for Standard Reference (Release 15) which was used to map the *trans* fat content of analyzed foods to the foods reported in the 1999–2002 NHANES. Total dietary TFA intakes were calculated by multiplying the amount of food consumed by the concentration of TFA in that food, and were expressed as a percentage of individual energy intakes per day. The TFA intake data were weighted using the NHANES 4-year sample weights as a means to ensure that the results are representative of the US population (aged ≥ 3 years). Two separate analyses were required to determine the quintile cutoff points for grams per day as well as percentage of energy. The quintiles for the analyses expressed as grams per person per day were calculated based upon grams per day of TFA intake. A second set of population quintile groups was calculated for the percentage of energy analyses based upon the per capita TFA intake expressed as a percentage of energy. The values provided within each quintile are the mean nutrient intakes of that quintile of the population. The inter-quintile ranges of TFA intake from the total diet for each quintile are provided. The unweighted sample sizes are not exactly the same for each quintile; however, the quintiles are balanced after applying

the statistical weights. Populations were defined by age and gender according to the criteria used by Allison et al. [11] so that results could be compared.

Estimation of Food Sources of TFA

Twenty-five food categories were established based on pre-established food groupings in NHANES (e.g., grains and salty snacks, milk and milk products, etc.) and then further sub-divided to allow identification of categories of foods as eaten (e.g., ready-to-eat breakfast cereals) or that were mentioned in previous studies to be contributors to TFA intakes. The amount of TFA in food (g/100 g) was derived from NHANES recipes as described above.

Results

The mean, median, 90th percentile, and quintiles of TFA intake, as well as other fatty acids, total fat (in grams per day), and energy in the U.S. population (aged ≥ 3 years), are reported for 16,669 subjects (Table 1; Fig. 1) as well as percentages of energy (Table 2). It is apparent that males aged 12–19 years have the highest mean TFA intake expressed as grams per day compared with the other populations for each quintile. When expressed as a percentage of energy, the intake of TFA was similar in all population groups. Subjects were stratified on the basis of total TFA intake as grams per day or percentage of energy, thereby explaining why the number of subjects differs within a quintile between tables for all population groups. The median TFA intake between 1999 and 2002 was 2.3 % of calories (5 g/day) with a range of 0.9–4.5 % of energy (1.5–13.1 g/day) over the different quintiles of intake. The mean TFA intake was 2.5 % of energy (6.1 g/day). There was a remarkable range of TFA intake in the top quintile (3.5–12.5 % of energy, or 8.8–92.4 g/day). Increasing quintiles of TFA intake were associated with increases in total fat (range, 26.7–37.6 % of energy), saturated fat (range, 7.6–10.5 % of energy), as well as calories (for men and women aged >20 years: 2,416–2,583 for men and 1,679–1,886 for women). Interestingly, intakes of *cis*-monounsaturated fatty acid (MUFA) and linoleic acid (both as grams per day and percentage of energy) also increased with increasing TFA intake. Notably, from the first to the fifth quintile, energy intakes increased approximately twofold in each cohort, whereas TFA increased 5- to 8-fold across the quintiles for all cohorts. On a percentage-of-energy basis, TFA increased about 4.5- to 5-fold across the quintiles for all cohorts. This suggests that food choices varied and dietary patterns differed across the TFA quintiles. Likewise, as a percentage of energy, TFA intake also increased concomitant with increases in

percentage of energy from total fat, saturated fatty acids (SFA), MUFA, and polyunsaturated fatty acids, with the increases in TFA being proportionally greater. Specifically, TFA increased 4- to 5-fold across quintiles of TFA intake, whereas energy intake increased from 7 to 17 %. Trends for TFA intakes were similar for all population groups studied (Tables 1, 2), with median TFA intake ranging from 2.1 to 2.5 % of calories (4.4–6.6 g/day). The mean TFA intake ranged from 2.3 to 2.7 % of calories (5.0–7.8 g/day). Intakes of TFA (as a percentage of calories), as well as SFA, oleic acid, linoleic acid, and alpha-linolenic acid, were similar among the different cohorts studied (Fig. 2).

The top 25 food categories that accounted for 79 % of TFA intake in the United States were identified on the basis of gram quantity of TFA consumed (Fig. 3). In our analysis, the major source of dietary TFA in the total population aged ≥ 3 years was cakes, cookies, pies, and pastries (Fig. 3), accounting for approximately 19 % of total TFA intake. Importantly, this food source of TFA was approximately 2-fold higher than the next three leading sources, which include yeast breads, French fries (commercial), and grain mixtures/ethnic mixed dishes. The fifth highest contributor was tortilla chips (accounting for 5.5 % of total TFA). Stick margarine provided 2.9 % of total TFA, and was ranked eighth in TFA intake. The 10 major food sources of TFA across the different population cohorts were very similar (Table 3).

A comparison of the above data with the 1989–1991 CSFII data [11] showed that the mean and median values were similar across cohorts, whereas TFA intake at the 90th percentile was higher (Table 4) in our analysis. In terms of the percentage of calories from TFA in 1989–1991, all cohorts in the 90th percentile of TFA intake consumed approximately 3.2 % of calories. In contrast, using the 1999–2002 NHANES data, TFA intake was 4.1–4.7 % of calories in similar cohorts. These results clearly indicate that consumption of TFA food sources increased considerably between 1991 and 2002 in individuals in the 90th percentile of TFA intake.

Discussion

The mean TFA intake in children and adults in the United States between 1999 and 2002 was 5.0–7.8 g/day (2.3–2.7 % of energy). In all cohorts, the range in TFA intake from the first quintile (1.3–2.0 g/day) to the fifth quintile (9.6–16.5 g/day) varied by approximately 5- to 8-fold. On a percentage-of-calories basis, TFA consumption ranged from 0.8–1.2 % (quintile 1) to 4.4–5.0 % of calories (quintile 5). For all population groups, there was remarkable variation in the range of TFA intake on a

Table 1 Per capita total dietary intakes of *trans* fatty acids, energy, fat, and select fatty acids (g/day)^a

Population, energy, and nutrient	Mean	Median	90th percentile	Q1 ^b	Q2	Q3	Q4	Q5
Children aged 3–5 years								
Participants (<i>n</i>)	1,034			220	206	216	198	194
IQR				0–2.50	2.50–3.75	3.75–5.28	5.28–7.24	7.24–35.13
Total <i>trans</i> fatty acids	5.0	4.5	8.9	1.7	3.2	4.5	6.1	9.6
Energy (kcal) ^c	1,650	1,591	2,360	1,130	1,438	1,644	1,867	2,169
Total fat	59.6	56.5	91.4	36.3	48.6	59.1	69.7	84.1
SFA (14:0, 6:0,18:0)	18.8	17.8	30.6	11.5	16.0	19.0	21.9	25.8
14:0	2.1	1.9	3.9	1.4	2.0	2.2	2.4	2.6
16:0	11.1	10.5	17.9	6.8	9.4	11.2	13.0	15.1
18:0	5.6	5.3	9.2	3.2	4.5	5.6	6.5	8.1
18:1c	17.3	16.2	28.0	10.5	13.6	16.9	20.4	24.9
18:2c	6.3	5.5	11.1	3.8	5.1	6.4	7.5	8.7
18:3c	0.5	0.4	0.9	0.4	0.4	0.5	0.6	0.7
Children aged 6–11 years								
Participants (<i>n</i>)	2,124			444	432	368	416	464
IQR				0–3.04	3.04–4.60	4.60–6.10	6.10–8.60	8.60–35.01
Total <i>trans</i> fatty acids	6.1	5.2	10.8	2.1	3.8	5.3	7.3	12.2
Energy (kcal) ^c	1,996	1,883	2,952	1,427	1,717	1,864	2,214	2,757
Total fat	73.9	68.4	116.1	46.4	60.6	69.6	82.7	110.4
Total SFA	22.9	21.2	37.1	14.9	19.2	21.9	26.6	31.8
14:0	2.4	2.1	4.3	1.7	2.1	2.5	3.0	2.7
16:0	13.6	12.6	21.9	9.1	11.5	13.0	15.7	18.9
18:0	6.9	6.3	11.3	4.2	5.6	6.4	8.0	10.3
18:1c	22.0	20.2	34.9	13.9	18.0	20.0	24.3	33.6
18:2c	8.7	7.1	15.6	5.6	7.0	8.0	9.1	14.0
18:3c	0.7	0.5	1.3	0.5	0.5	0.6	0.7	1.0
Males aged 12–19 years								
Participants (<i>n</i>)	2,252			480	477	467	429	399
IQR				0–3.28	3.28–5.49	5.49–8.06	8.06–11.79	11.79–92.41
Total <i>trans</i> fatty acids	7.8	6.6	14.7	2.0	4.4	6.7	9.7	16.5
Energy (kcal) ^c	2,672	2,484	4,238	1,702	2,075	2,633	3,078	3,872
Total fat	95.8	87.1	162.1	44.6	72.0	93.4	115.5	149.2
SFA (14:0, 16:0, 18:0)	29.7	26.8	51.4	15.6	23.0	29.5	36.0	44.5
14:0	3.0	2.5	6.0	1.7	2.5	3.0	3.7	4.1
16:0	17.8	16.0	31.1	9.5	13.9	17.7	21.4	26.3
18:0	9.0	8.2	15.6	4.4	6.6	8.8	10.9	14.1
18:1c	28.9	25.6	49.0	14.7	21.6	28.2	34.8	45.0
18:2c	11.6	9.8	21.5	5.9	9.1	11.8	13.3	18.0
18:3c	0.9	0.7	1.7	0.5	0.7	0.9	1.1	1.4
Females aged 12–19 years								
Participants (<i>n</i>)	2,263			473	443	445	453	449
IQR				0–2.59	2.59–4.24	4.24–6.06	6.06–8.94	8.94–36.39
Total <i>trans</i> fatty acids	6.1	5.2	11.7	1.5	3.4	5.2	7.4	12.7
Energy (kcal) ^c	1,987	1,882	3,095	1,268	1,692	1,910	2,293	2,761
Total fat	71.5	65.7	119.4	36.6	55.4	67.6	86.6	110.8
SFA (14:0, 16:0, 18:0)	21.7	19.6	38.4	11.4	17.7	20.7	26.5	32.1
14:0	2.2	1.8	4.5	1.2	1.9	2.2	2.8	2.9
16:0	13.0	11.7	22.9	7.0	10.6	12.4	15.7	18.9

Table 1 continued

Population, energy, and nutrient	Mean	Median	90th percentile	Q1 ^b	Q2	Q3	Q4	Q5
18:0	6.6	6.0	11.6	3.2	5.1	6.1	8.0	10.2
18:1c	21.1	19.2	35.5	11.1	16.2	19.8	25.1	33.0
18:2c	9.3	7.5	18.4	5.3	7.1	8.8	11.0	14.2
18:3c	0.8	0.6	1.5	0.5	0.6	0.8	0.8	1.1
Males aged ≥ 20 years								
Participants (<i>n</i>)	4,236			967	963	878	753	675
IQR				0–2.75	2.75–4.64	4.64–7.01	7.01–10.20	10.20–59.78
Total <i>trans</i> fatty acids	6.8	5.6	13.1	1.7	3.7	5.7	8.3	14.7
Energy (kcal) ^c	2,596	2,440	3,959	1,772	2,178	2,505	2,874	3,647
Total fat	95.8	86.7	161.4	51.6	74.1	91.5	109.2	152.6
SFA (14:0, 16:0, 18:0)	28.0	25.0	50.0	14.4	21.8	27.6	32.2	44.2
14:0	2.6	2.1	5.3	1.3	2.1	2.7	3.0	3.9
16:0	16.9	15.0	29.8	8.9	13.2	16.6	19.4	26.3
18:0	8.5	7.5	15.1	4.1	6.4	8.3	9.8	14.0
18:1c	28.8	25.9	49.9	15.6	21.9	27.5	32.9	45.8
18:2c	12.3	10.2	23.4	6.7	9.2	11.5	14.4	19.4
18:3c	1.1	0.8	2.2	0.7	0.8	1.0	1.2	1.6
Females aged ≥ 20 years								
Participants (<i>n</i>)	4,760			1,039	1,007	953	873	888
IQR				0–2.15	2.15–3.62	3.62–5.25	5.25–7.56	7.56–35.0
Total <i>trans</i> fatty acids	5.2	4.4	9.8	1.3	2.9	4.4	6.3	10.9
Energy (kcal) ^c	1,838	1,736	2,830	1,243	1,590	1,768	2,010	2,579
Total fat	68.4	61.8	116.2	37.8	53.8	65.6	78.3	106.4
SFA (14:0, 16:0, 18:0)	19.5	17.4	34.6	10.3	15.7	18.9	22.6	30.0
14:0	1.9	1.5	3.8	1.0	1.6	1.8	2.2	2.6
16:0	11.7	10.5	20.9	6.3	9.5	11.4	13.5	17.9
18:0	5.9	5.3	10.4	2.9	4.6	5.7	6.8	9.6
18:1c	20.1	18.0	34.8	11.0	15.5	19.2	22.8	31.7
18:2c	9.4	7.7	18.0	5.3	7.1	9.1	10.8	14.6
18:3c	0.8	0.6	1.7	0.5	0.7	0.8	0.9	1.2

^a Per capita estimates are based on food consumption data for all individuals who responded during the one NHANES survey day. This analysis includes all foods in the diet. Conducted in FARE version 7.997

^b Quintiles calculated based upon per capita total *trans* fatty acid consumption. Number of participants indicates the unweighted sample size, interquintile range (*IQR*) indicates cutoff values of trans fat intake, and mean intake values are reported within each quintile

^c Energy units are kcal/day

Fig. 1 Dietary TFA (g/day) in all demographic groups by quintile of intake

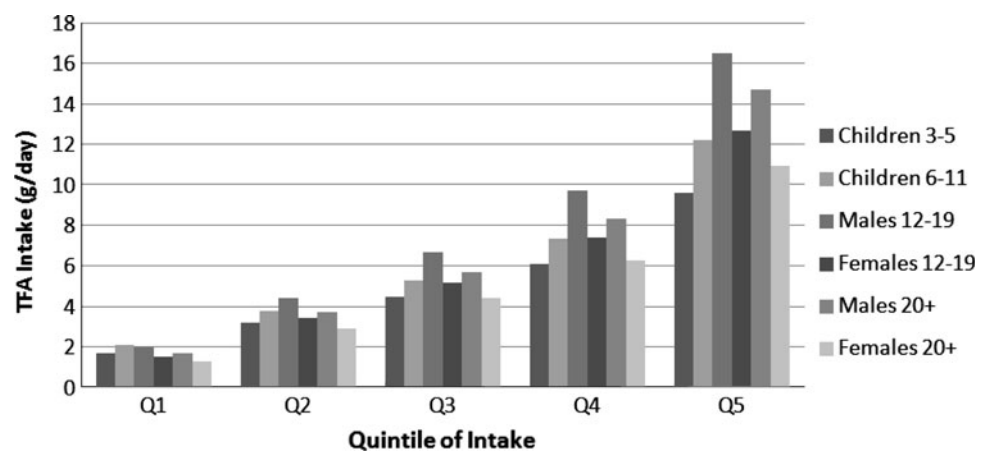


Table 2 Per capita total dietary intakes of *trans* fatty acids, fat, select fatty acids, and energy (% total energy)^a

Population, nutrient	Mean	Median	90th percentile	Q1 ^b	Q2	Q3	Q4	Q5
Children aged 3–5 years								
Participants (<i>n</i>)	1,034			231	218	186	210	189
IQR				0–1.65	1.65–2.31	2.31–2.79	2.79–3.61	3.61–8.83
Total <i>trans</i> fatty acids	2.7	2.5	4.4	1.2	2.0	2.5	3.1	4.6
Total fat	32.4	32.0	42.1	28.1	31.3	32.5	33.9	35.9
Sum 14:0, 16:0, 18:0	10.2	10.0	14.4	9.1	10.3	10.5	10.9	10.2
14:0	1.2	1.1	2.0	1.2	1.3	1.2	1.2	0.9
16:0	6.0	5.9	8.4	5.4	6.1	6.2	6.4	6.0
18:0	3.0	3.0	4.2	2.5	2.9	3.1	3.3	3.3
18:1c	9.4	9.2	13.0	8.1	8.9	9.2	10.0	10.7
18:2c	3.5	3.1	5.6	2.8	3.5	3.4	3.7	3.8
18:3c	0.3	0.2	0.5	0.3	0.3	0.3	0.3	0.3
Energy (kcal) ^c	1,650	1,591	2,360	1,525	1,604	1,742	1,668	1,703
Children aged 6–11 years								
Participants (<i>n</i>)	2,124			435	433	402	432	422
IQR				0–1.64	1.64–2.26	2.26–2.88	2.88–3.73	3.73–8.54
Total <i>trans</i> fatty acids	2.7	2.5	4.4	1.2	2.0	2.6	3.3	4.7
Total fat	33.1	33.2	42.9	29.9	31.6	33.2	34.1	36.6
Total SFA	10.3	10.1	14.2	9.6	10.2	10.4	10.5	10.7
14:0	1.1	1.0	1.8	1.1	1.2	1.1	1.0	1.0
16:0	6.1	6.1	8.5	5.8	6.0	6.2	6.2	6.3
18:0	3.1	3.1	4.3	2.7	2.9	3.1	3.2	3.4
18:1c	9.8	9.6	13.6	8.9	9.1	10.0	10.2	11.0
18:2c	3.9	3.4	6.4	3.6	3.6	4.0	4.1	4.3
18:3c	0.3	0.3	0.5	0.3	0.3	0.3	0.3	0.3
Energy (kcal) ^c	1,996	1,883	2,952	1,806	2,067	2,057	2,058	1,989
Males aged 12–19 years								
Participants (<i>n</i>)	2,252			454	445	443	446	464
IQR				0–1.47	1.47–2.09	2.09–2.76	2.76–3.62	3.62–9.90
Total <i>trans</i> fatty acids	2.6	2.4	4.4	1.0	1.8	2.4	3.2	4.7
Total fat	32.0	32.5	42.3	25.8	31.1	32.3	34.7	36.2
Sum 14:0, 16:0, 18:0	9.9	9.9	14.0	8.3	10.3	10.2	10.6	10.2
14:0	1.0	0.9	1.8	0.9	1.1	1.0	1.1	0.8
16:0	5.9	5.9	8.3	5.0	6.2	6.1	6.3	6.1
18:0	3.0	3.0	4.1	2.3	3.0	3.0	3.2	3.3
18:1c	9.6	9.7	13.3	7.7	9.4	9.7	10.3	11.1
18:2c	3.9	3.5	6.5	3.2	3.6	4.0	4.3	4.3
18:3c	0.3	0.3	0.6	0.3	0.3	0.3	0.3	0.3
Energy (kcal) ^c	2,672	2,484	4,238	2,390	2,740	2,793	2,727	2,704
Females 12–19 years								
Participants (<i>n</i>)	2,263			457	431	443	485	447
IQR				0–1.49	1.49–2.10	2.10–2.80	2.80–3.88	3.88–12.46
Total <i>trans</i> fatty acids	2.7	2.5	4.7	1.0	1.8	2.4	3.3	5.0
Total fat	32.0	32.0	43.6	25.9	30.6	32.3	34.2	37.2
Sum 14:0, 16:0, 18:0	9.7	9.6	14.1	8.2	9.8	10.0	10.3	10.2
14:0	1.0	0.9	1.8	0.9	1.1	1.1	1.0	0.8
16:0	5.8	5.7	8.3	5.0	5.9	6.0	6.1	6.1
18:0	2.9	2.9	4.3	2.3	2.8	3.0	3.2	3.3

Table 2 continued

Population, nutrient	Mean	Median	90th percentile	Q1 ^b	Q2	Q3	Q4	Q5
18:1c	9.5	9.4	13.3	7.7	9.0	9.3	10.2	11.2
18:2c	4.2	3.6	7.0	3.7	4.0	4.1	4.5	4.7
18:3c	0.3	0.3	0.6	0.3	0.3	0.3	0.3	0.4
Energy (kcal) ^c	1,987	1,882	3,095	1,746	1,952	2,099	2,095	2,045
Males aged ≥ 20 years								
Participants (<i>n</i>)	4,236			837	918	864	825	792
IQR				0–1.21	1.21–1.82	1.82–2.46	2.46–3.37	3.37–10.51
Total <i>trans</i> fatty acids	2.3	2.1	4.1	0.8	1.5	2.1	2.9	4.4
Total fat	32.8	32.7	45.0	26.2	31.31	33.19	35.1	38.1
Sum 14:0, 16:0, 18:0	9.5	9.5	14.1	7.3	9.4	10.0	10.3	10.6
14:0	0.9	0.8	1.6	0.7	0.9	1.0	0.9	0.8
16:0	5.8	5.8	8.4	4.5	5.7	6.0	6.2	6.3
18:0	2.9	2.9	4.3	2.1	2.8	3.0	3.2	3.5
18:1c	9.9	9.7	14.3	7.9	9.5	10.0	10.6	11.6
18:2c	4.3	3.7	7.2	3.5	3.9	4.2	4.5	5.1
18:3c	0.4	0.3	0.7	0.3	0.4	0.4	0.4	0.4
Energy (kcal) ^c	2,596	2,440	3,959	2,416	2,605	2,603	2,772	2,583
Females aged ≥ 20 years								
Participants (<i>n</i>)	4,760			962	1,013	968	926	891
IQR				0–1.31	1.31–1.98	1.98–2.66	2.66–3.52	3.52–10.00
Total <i>trans</i> fatty acids	2.5	2.3	4.3	0.9	1.7	2.3	3.0	4.5
Total fat	33.0	33.0	45.5	26.6	31.8	33.2	35.4	38.2
Sum 14:0, 16:0, 18:0	9.4	9.2	14.1	7.3	9.3	9.8	10.2	10.4
14:0	0.9	0.8	1.7	0.7	1.0	1.0	1.0	0.8
16:0	5.7	5.5	8.4	4.5	5.6	5.9	6.1	6.2
18:0	2.8	2.8	4.2	2.1	2.7	2.9	3.1	3.4
18:1c	9.7	9.6	14.1	7.7	9.2	9.8	10.4	11.5
18:2c	4.6	4.0	8.2	3.6	4.3	4.5	5.1	5.3
18:3c	0.4	0.3	0.8	0.4	0.4	0.4	0.4	0.4
Energy (kcal) ^c	1,838	1,736	2,830	1,679	1,816	1,893	1,918	1,886

^a Per capita estimates are based on food consumption data for all individuals who responded during the one NHANES survey day, whether they reported eating the food(s) or ingredient(s) of interest. Percentage of energy for total fat and the individual fatty acids should be determined per individual and grouped within quintiles based on *trans* intake as %en. Conducted in FARE version 7.99

^b Quintiles calculated based upon % energy from total *trans* fatty acid consumption. Interquintile range (*IQR*) indicates cutoff values of *trans* fat intake, and mean intake values are reported within each quintile

^c Energy units are kcal/day. The values for each quintile are the mean kcal/day consumed by the participants who consumed the amount *trans* fat as a % of energy listed in the interquintile range

grams-per-day basis, as well as a percentage-of-energy basis in quintile 5. Variation was greatest in males aged 12–19 years, with intake that varied from 12 to 92 g/day in quintile 5. Collectively, these data illustrate that some individuals consume large quantities of TFA (in quintile 5), whereas there are others who eat little TFA (in quintile 1). Interestingly, as TFA intakes increased across quintiles, energy, total fat, and SFA intakes also increased in all populations. However, there were important differences in the magnitude of increases for each of these dietary constituents. Although there were noticeable increases in total fat and SFA intake across quintiles, as well as somewhat

modest increases in energy intake across quintiles (specifically for the fatty acid data presented as percentages of energy in Table 2), the proportional increase in TFA was dramatically greater.

Collectively, our results indicate a change in dietary patterns across quintiles. Specifically, TFA-containing foods were either added to the diet or substituted for non-TFA-containing foods. Given that the proportional increase in dietary TFA was greater than the increase in energy, it seems that substitution of TFA-containing foods was more common. Thus, a high TFA intake reflects a different dietary pattern compared with a lower TFA intake. In fact,

Fig. 2 Fatty acid intake (% of calories) by demographic group. *SFA* saturated fatty acid, *LA* linoleic acid, *ALA* alpha-linolenic acid, *TFA* *trans* fatty acid

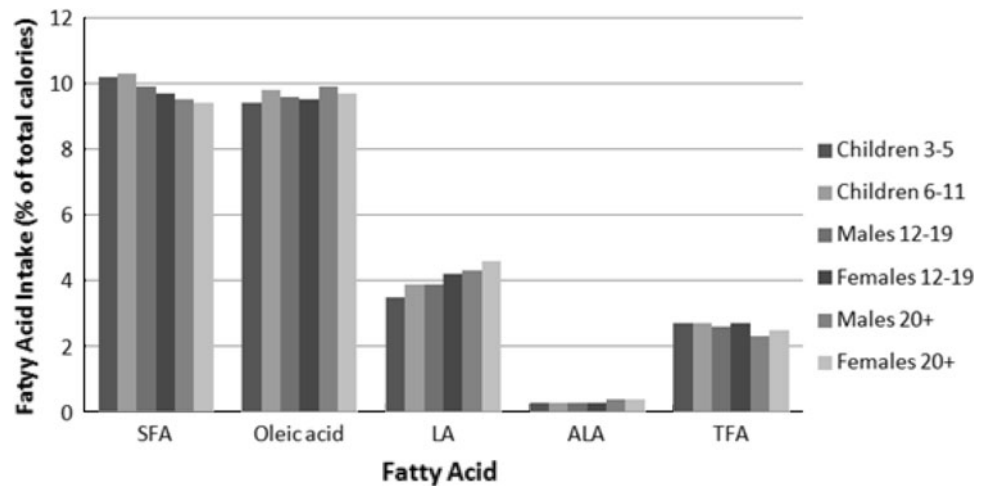
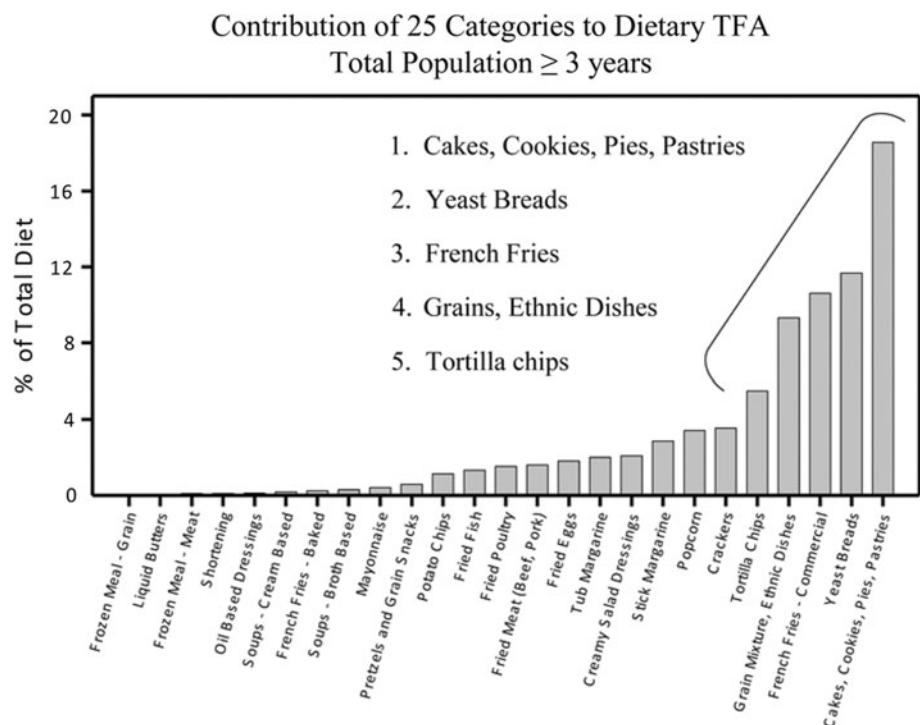


Fig. 3 Contribution of 25 food categories to dietary TFA. The Y axis represents the percentage of total TFA contributed by the respective food category



starting with quintile 2, it appears that the dietary patterns are shifting because of increases in the proportions of TFA, SFA, and total fat (as a percentage of energy) relative to the increase in energy intake. However, although all population groups showed similar changes in fatty acids and energy across quintiles, it can be concluded that dietary patterns within a quintile are likely comparable among the different population groups.

It is telling that the results of this study show that the population evaluated in 1999–2002 consumed similar amounts of TFA compared to the U.S. population surveyed in 1989–1991 [11]. In fact, the mean and median TFA intakes are similar in both studies. However, what is striking between the two studies is the increase in TFA intake in the

90th percentile. As Table 4 shows, there were approximately 20 and 27 % higher TFA intakes in men and women, respectively, in the 1999–2002 database versus the earlier survey. Collectively, this finding suggests that there is a relatively large cohort of individuals in the population who have made changes in their diet in a manner that is incongruent with current dietary recommendations. It is important to appreciate that the large gap between the 99.9th and 100th percentiles of TFA intake (34 vs. 92 g/day) most likely represents only a very small group of high-TFA consumers, which would be expected to slightly skew the results for this cohort. Nonetheless, these findings indicate that there are individuals who follow extreme dietary practices, putting them at high risk for chronic disease and malnutrition.

Table 3 Top 10 food group contributors to *trans* fat intake in different population groups

All, ≥ 3 years	Children, 3–5 years	Children, 6–11 years	Males, 12–19 years	Females, 12–19 years	Males, ≥ 20 years	Females, ≥ 20 years
Cakes, cookies, pies, pastries	Cakes, cookies, pies, pastries	Cakes, cookies, pies, pastries	Cakes, cookies, pies, pastries	Cakes, cookies, pies, pastries	Cakes, cookies, pies, pastries	Cakes, cookies, pies, pastries
Yeast breads	French fries	Grains	French fries	French fries	Yeast breads	Yeast breads
French fries	Grains	French fries	Grains	Grains	French fries	French fries
Grains	Yeast breads	Yeast breads	Yeast breads	Yeast breads	Grains	Grains
Tortilla chips	Tortilla chips	Tortilla chips	Tortilla chips	Tortilla chips	Tortilla chips	Crackers
Crackers	Crackers	Crackers	Popcorn	Crackers	Stick margarine	Tortilla chips
Popcorn	Popcorn	Popcorn	Crackers	Popcorn	Popcorn	Popcorn
Stick margarine	Stick margarine	Stick margarine	Fried meat (beef, pork)	Stick margarine	Crackers	Stick margarine
Creamy salad dressing	Tub margarine	Tub margarine	Stick margarine	Creamy salad dressing	Fried eggs	Creamy salad dressing
Tub margarine	Fried eggs	White potatoes	Fried poultry	Fried poultry	Fried meat (beef, pork)	Tub margarine

Table 4 Comparison of *trans* fatty acid intake in 1989–1991 and 1999–2002 (g/day)

Population	CSFII ^a (1989–1991)	NHANES (1999–2002)
Children, 3–5 years		
Mean	4.1	5.0
Median	3.9	4.5
90th percentile	6.6	8.9
Males, 12–19 years		
Mean	7.1	7.8
Median	6.7	6.6
90th percentile	11.4	14.7
Females, 12–19 years		
Mean	5.1	6.1
Median	4.9	5.2
90th percentile	8.6	11.7
Males 20–49 years, 50–69 years; males ≥ 20 years ^a		
Mean	6.6/5.8	6.8
Median	5.9/5.1	5.6
90th percentile	11.6/10.2	13.1
Females 20–49 years, 50–69 years; females ≥ 20 years ^a		
Mean	4.6/4.2	5.2
Median	4.2/3.7	4.4
90th percentile	8.0/7.4	9.8

^a CSFII adult data were divided into subgroups of 20–49 and 50–69 years; NHANES reported all adults in one group (≥ 20 years)

The food sources of dietary TFA are similar among the different population groups studied. The major TFA sources were cakes, cookies, pies, and pastries, as well as yeast breads, French fries, grains and ethnic dishes, and tortilla chips. It is important to note that many food sources of TFA are also major contributors of SFA [8], such as

grain-based desserts, savory snacks, ethnic dishes, and French fries/fried potatoes. Many of these foods are typically classified as discretionary calories and consequently should be limited in the diet. Reducing these foods would not only decrease TFA but also SFA and excess calories.

Our analysis provides useful information about TFA intake and food sources in the United States prior to the onset of legislative action intended to decrease TFA in the food supply. The data presented here are important as a benchmark to track changes in TFA intake in the future as the result of these sweeping legislative mandates to decrease TFA in the food supply. It will be important to monitor changes in fatty acid intake in the population because of the concerted effort to remove TFA from the food supply. Much progress has occurred in food science and lipid chemistry to appreciably decrease industrially produced TFA in the food supply in recent years. In fact, a new study reported an average population intake of 1.3 g/day of industrially produced TFA using analysis of 2003–2006 NHANES data [15]. In many instances, oils high in MUFA are replacing conventional fats that are high in TFA (e.g., for liquid fat food applications), whereas in other situations, fat sources of SFA are replacing solid fats rich in TFA (e.g., for solid fat food applications). One caveat to be mindful of is that efforts to decrease TFA should not result in increases in SFA intake in the population. Consistent with this, the American Heart Association [16] has recommended that TFA and SFA in unmodified foods not be greater than total SFA in modified foods. It is clear that there are currently countless fats that differ in their fatty acid profiles that could be substituted for TFA. It will be important that fats devoid of TFA be selected to achieve current dietary fatty acid guidelines and, thereby, realize a public health benefit. This has been

reported in a recent modeling exercise by Lefevre et al. [17]. The last point that must be emphasized is to acknowledge that many of the foods that deliver industrially produced TFA are “extras in the diet,” and even if they are modified to have a fatty acid profile that is consistent with current dietary recommendations, their intake should be limited within the context of a healthy diet that meets current food-based and nutrient recommendations. Limiting intake of these fatty acid-modified foods will also help control calories, which is a pressing societal need.

A limitation of this study is that the analysis of TFA intake was based on NHANES 1999–2002 data. The TFA data were derived from the 1995 *Trans* Fatty Acid Database and the USDA Nutrient Database for Standard Reference (Release 15). Consequently, changes that were made in foods in the marketplace (with respect to TFA content) between 1993 (when the TFA analyses of foods were completed) and 1999–2002 are not reflected in this analysis. This is a well-recognized limitation of the available nutrient databases and underscores the importance of continuously updating them. Another potential limitation is the use of two 24-h recalls. According to Allison et al. [11], 3 days of intake data provide a better assessment of usual intake. Moreover, the present study only evaluated industrial TFA and not other sources of TFA, which could have important health implications [18]. Despite these limitations, however, this study provides useful information about TFA intake in the population and important food sources prior to collective efforts by the food industry to decrease TFA in the food supply.

In summary, in all population groups studied, TFA intake between 1999 and 2002 was 5.0–7.8 g/day (2.3–2.7 % of energy). Much of the TFA consumed was derived from energy-dense and nutrient-poor foods such as cakes, cookies, pies, pastries, and savory snacks (i.e., chips). Strikingly, there was a population, albeit small, with an extremely high intake of TFA (males aged 12–19 years in the fifth quintile, who consumed 11.8–92.4 g/day) as well as SFA (and also energy). Obviously, this reflects very poor dietary practices. In fact, as TFA intake increased in the population groups studied, there was a trend toward poorer dietary practices. Ongoing nutrition intervention efforts must be directed at decreasing TFA and also promoting healthy dietary patterns.

Acknowledgments This research was funded by ILSI North America.

Conflict of interest Penny Kris-Etherton, Michael Lefevre and Ronald Mensink received financial support from ILSI North America for disseminating the research findings.

Open Access This article is distributed under the terms of the Creative Commons Attribution License which permits any use, distribution, and reproduction in any medium, provided the original author(s) and the source are credited.

References

1. U.S. Department of Agriculture, U.S. Department of Health and Human Services (2010) Dietary guidelines for Americans, 2010. <http://www.cnpp.usda.gov/DGAs2010-PolicyDocument.htm>. Accessed 28 July 2011
2. Food and Agriculture Organization of the United Nations (2010) Fats and fatty acids in human nutrition: report of an expert consultation. <http://foris.fao.org/preview/25553-0e4cb94ac52f9a25af77ca5cfba7a8c.pdf>. Accessed 28 July 2011
3. Mozaffarian D, Katan MB, Ascherio A, Stampfer MJ, Willett WC (2006) Trans fatty acids and cardiovascular disease. *N Engl J Med* 354:1601–1613
4. Micha R, Mozaffarian D (2008) Trans fatty acids: effects on cardiometabolic health and implications for policy. *Prostaglandins Leukot Essent Fatty Acids* 79:147–152
5. Remig V, Franklin B, Margolis S, Kostas G, Nece T, Street JC (2010) Trans fats in America: a review of their use, consumption, health implications, and regulation. *J Am Diet Assoc* 110:585–592
6. National Conference of State Legislatures (2009) Trans fat and menu labeling legislation. <http://www.ncsl.org/programs/health/transfatmenulabelingbills.htm>. Accessed 24 Jan 2011
7. Mozaffarian D, Stampfer MJ (2010) Removing industrial *trans* fat from foods. *BMJ* 340:c1826
8. U.S. Department of Agriculture (June 15, 2010) Report of the dietary guidelines Advisory Committee on the Dietary Guidelines for Americans, 2010. <http://www.cnpp.usda.gov/DGAs2010-DGACReport.htm>. Accessed 24 Jan 2011
9. Tarrago-Trani MT, Phillips KM, Lemar LE, Holden JM (2006) New and existing oils and fats used in products with reduced *trans*-fatty acid content. *J Am Diet Assoc* 106:867–880
10. Crupkin M, Zambelli A (2008) Detrimental impact of *trans* fats on human health: Stearic acid-rich fats as possible substitutes. *Comp Rev Food Sci Food Safety* 7:271–279
11. Allison DB, Egan SK, Barraj LM, Caughman C, Infante M, Heimbach JT (1999) Estimated intakes of *trans* fatty and other fatty acids in the US population. *J Am Diet Assoc* 99:166–174
12. Eckel RH, Borra S, Lichtenstein AH, Yin-Piazza SY, *Trans Fat Conference Planning Group* (2007) Understanding the complexity of *trans* fatty acid reduction in the American diet: American Heart Association *Trans Fat Conference 2006*: report of the *Trans Fat Conference Planning Group*. *Circulation* 115:2231–2246
13. DiRienzo MA, Astwood JD, Petersen BJ, Smith KM (2006) Effect of substitution of low linolenic acid soybean oil for hydrogenated soybean oil on fatty acid intake. *Lipids* 41:149–157
14. Wright JD, Borrud LG, McDowell MA, Wan C-Y, Radimer K, Johnson CL (2007) Nutrition assessment in the National Health and Nutrition Examination Survey 1999–2002. *J Am Diet Assoc* 107:822–829
15. Doell D, Folmer D, Lee H, Honigfort M, Carberry S (2012) Updated estimate of *trans* fat intake by the US population. *Food Addit Contam Part A Chem Anal Control Expo Risk Assess* 29:861–874
16. American Heart Association (2008) *Trans fat policy position statement*. http://www.heart.org/idc/groups/heart-public/@wcm/@adv/documents/downloadable/ucm_301697.pdf. Accessed 2 Nov 2011
17. Lefevre M, Mensink RP, Kris-Etherton PM, Peterson B, Smith K, Flickinger BD (2012) Estimated cardiovascular disease risk reduction with alternatives to soybean oil containing *trans* fatty acids. *Lipids* (in press)
18. Brouwer IA, Wanders AJ, Katan MB (2010) Effect of animal and industrial *trans* fatty acids on HDL and LDL cholesterol levels in humans—a quantitative review. *PLoS One* 5:e9434

Dietary *trans*-Fatty Acid Induced NASH is Normalized Following Loss of *trans*-Fatty Acids from Hepatic Lipid Pools

Brent A. Neuschwander-Tetri · David A. Ford ·
Sahaja Acharya · George Gilkey · Metin Basaranoglu ·
Laura H. Tetri · Elizabeth M. Brunt

Received: 1 January 2012 / Accepted: 27 July 2012 / Published online: 26 August 2012
© AOCs 2012

Abstract Previous experiments in mice showed that dietary *trans*-fats could play a role in non-alcoholic steatohepatitis (NASH) yet little is known about the accumulation *trans*-fats in hepatic lipid pools in relationship to liver injury. NASH is also associated with obesity yet improves with only modest weight loss. To distinguish the role of obesity versus sustained consumption of a *trans*-fat containing diet in causing NASH, mice with obesity and NASH induced by consuming a high *trans*-fat diet for 16 weeks were subsequently fed standard chow or maintained on *trans*-fat chow for another 8 weeks. The accumulation, partitioning and loss of *trans*-fats in the major hepatic lipid pools during and after *trans*-fat consumption were

determined. Obese mice switched to standard chow remained obese but steatohepatitis improved. *trans*-fats were differentially incorporated into the major hepatic lipid pools and the loss of *trans*-fats after crossover to control chow was greatest in the cholesteryl ester pool. In summary, dietary changes can improve the biochemical and histopathological changes of NASH despite persistent obesity in mice. Analysis of hepatic lipids confirmed that dietary *trans*-fats accumulate in the major lipid pools and are released differentially with diet normalization. The substantial loss of *trans*-fats from the cholesteryl ester pool in parallel with improvement in NASH suggests that this pool of *trans*-fats could play a role in the pathogenesis of NASH.

B. A. Neuschwander-Tetri · M. Basaranoglu · L. H. Tetri
Division of Gastroenterology and Hepatology, Department
of Internal Medicine, Saint Louis University, Saint Louis, USA

B. A. Neuschwander-Tetri
Liver Center, Saint Louis University, Saint Louis, USA

B. A. Neuschwander-Tetri (✉)
3635 Vista Ave., Saint Louis, MO 63110, USA
e-mail: tetrica@slu.edu

D. A. Ford
Department of Biochemistry and Molecular Biology,
Saint Louis University, Saint Louis, USA

D. A. Ford
Center for Cardiovascular Research, Saint Louis University,
Saint Louis, USA

S. Acharya · G. Gilkey
School of Medicine, Saint Louis University,
Saint Louis, USA

E. M. Brunt
Department of Pathology and Immunology,
Washington University, Saint Louis, USA

Keywords High fructose corn syrup · Fatty liver ·
Obesity · Leptin · Resistin

Abbreviations

NASH	Nonalcoholic steatohepatitis
ALIOS	American lifestyle induced obesity syndrome
ALT	Alanine aminotransferase
MUFA	Monounsaturated fatty acid(s)
PUFA	Polyunsaturated fatty acid(s)
HFCS	High fructose corn syrup
EDTA	Ethylenediaminetetraacetic acid
FAME	Fatty acid methyl ester(s)
VLDL	Very low density lipoprotein
SCD	Stearoyl-CoA desaturase
XO	Crossover

Introduction

Lifestyle modifications that include caloric restriction to achieve both weight loss and increased physical activity

are the primary therapeutic interventions recommended to patients with nonalcoholic steatohepatitis (NASH) [1, 2]. Because clinical case series have identified obesity as a major risk factor for NASH and the degree of obesity correlates with the severity of disease [3, 4], normalization of weight to a healthy range might be needed to achieve significant improvement in liver disease. However, available clinical data suggest otherwise. Several studies have shown that patients can have improved histopathological findings with only a modest weight reduction of 5–10 % [5–7] and a large community intervention trial demonstrated improved nonalcoholic liver disease (NAFLD) measured by magnetic resonance spectroscopy with exercise and just 3 % weight loss [8].

To examine the effects of the rodent equivalent of therapeutic lifestyle modifications on NASH, we normalized the diet for 8 weeks in mice with obesity and NASH induced by the American lifestyle induced obesity syndrome (ALIOS) model for an initial period of 16 weeks. The ALIOS model includes feeding male C57BL/6 mice with high fat, *trans*-fat enriched chow and consumption of high fructose corn syrup resulting in a NASH-like liver histological phenotype [9]. We had previously shown that the *trans*-fat component of the ALIOS model is the primary factor responsible for the development of NASH in the ALIOS mouse model [9] and this has been confirmed by *trans*-fat feeding without inclusion of high fructose corn syrup [10, 11]. The liver pathology that develops in this model may be strain specific as AKR/J mice did not develop significant steatohepatitis when fed a similar diet [12] and the abnormalities may also be dependent on the source of fat used to prepare the partially hydrogenated vegetable oil [13]. In the current study, we show that despite persistent obesity, continued excessive caloric intake and an abnormal adipokine profile, obese ALIOS mice changed to standard rodent chow had marked improvement in the biochemical and histological evidence of NASH. Determination of the incorporation and subsequent release of *trans*-fats in the major hepatic lipid pools during and after *trans*-fat consumption confirmed *trans*-fat incorporation in all major pools but differential release with the cholesterol ester pool of *trans*-fats being the most labile.

Materials and methods

Animal Treatment

Male C57BL/6 mice initially 6–8 weeks old (Harlan, Indianapolis, IN) were treated as approved by the Animal Care Committee of Saint Louis University (protocol #1573). Mice were kept on a 12 h:12 h light:dark schedule

at 23 °C, housed in cages of five, and weighed weekly. All animals received humane care according to the criteria outlined in the “Guide for the Care and Use of Laboratory Animals” prepared by the National Academy of Sciences and published by the National Institutes of Health (NIH publication 86-23 revised 1985).

ALIOS mice were fed a diet similar in composition to an American fast food diet with 45 % calories in the chow from fat in the form of partially hydrogenated soybean oil (28 % of fatty acids as saturated, 57 % MUFA and 13 % PUFA; *trans*-fat custom diet TD06303, Harlan Teklad). The *trans*-fat content of the partially hydrogenated soybean oil used to prepare the chow was approximately 30 % and mostly in the form of elaidic acid according to the supplier. ALIOS mice were also given high fructose corn syrup equivalent (HFCS, 55 % fructose, 45 % glucose by weight) in their drinking water at a concentration of 42 g/l. The drinking water was provided as gel–water [93 % water, 2.8 % gelatin (Pork skin gelatin, Type A, Sigma, St. Louis) and 4.2 % HFCS] in dishes on the cage floor. In order to discourage physical activity in ALIOS mice, the wire racks were removed from the cages. Control mice were given standard rodent chow containing 13.6 % of calories from fat in the form of soybean oil (15 % of fatty acids as saturated fat, 23 % MUFA and 61 % PUFA; 2018S, Harlan Teklad, Madison, WI). Control mice ($n = 10$) fed standard chow were kept in cages with wire racks and were given gel–water without HFCS. After 16 weeks of ALIOS conditions, one group of mice ($n = 10$) continued with ALIOS conditions for an additional 8 weeks while a second identical group ($n = 10$) was crossed over to control conditions for an additional 8 weeks. Food and water consumption were measured by weighing new and remaining food and water 3 times weekly between treatment weeks 10 and 16 and then again from weeks 19 to 24.

Mice were sacrificed after ketamine and xylazine anesthesia. Plasma prepared with EDTA was separated and frozen at -80 °C. Livers were removed, weighed and divided into sections that were either fixed in 10 % phosphate buffered formalin (Sigma Aldrich, St. Louis, MO) or frozen in liquid nitrogen. Formalin fixed, paraffin-embedded tissue was sectioned (5 μ m) and stained with hematoxylin and eosin, Sirius red and Masson’s trichrome.

Chemistry

Plasma alanine aminotransferase (ALT), aspartate aminotransferase (AST), total cholesterol (free and esterified), and triglycerides were measured using a calibrated clinical analyzer (Cobas Mira Plus Chemistry Analyzer, Roche Diagnostics, Indianapolis, IN). Liver triglyceride content was measured using an endpoint glycerol phosphate oxidase method (Pointe Scientific, Lincoln Park, MI). Plasma

leptin and resistin were measured by multiplexed immunoassay (Linco Diagnostics, St. Charles, MO).

Plasma and Liver Lipidomics

Samples of liver (40–50 mg) were homogenized in 500 μ l phosphate buffered saline, and lipids were extracted from 100 μ l of the liver homogenate in the presence of internal standards for each lipid class [14]. Lipid classes were separated by thin layer chromatography using silica gel Gas stationary phase and a mobile phase comprised of petroleum ether/ethyl ether/acetic acid (80/20/1, v/v/v) [15]. Subsequently, fatty acid methyl esters (FAME) were prepared by acid methanolysis [15] and subjected to gas chromatography (GC) on an SP-2560 fused silica capillary column (100 m \times 0.25 mm, 0.2 μ m film thickness) with flame ionization detection (FID) [16]. FAME were quantified by comparisons with FAME derived from internal standards added during liver lipid extraction.

Statistical Analysis

The data were analyzed for statistical significance with ANOVA and post hoc two-tailed *t* tests with significance being $P < 0.05$. Results are reported as mean \pm standard deviation (SD).

Results

Mice treated with the ALIOS conditions of a high *trans*-fat and high fructose corn syrup diet for 16 weeks became obese and weighed 31 % more than control mice. Little further weight gain occurred during the ensuing 8 weeks in ALIOS or control mice (Fig. 1). Crossover to control chow and unrestricted activity was not associated with weight loss and crossover mice weights were not significantly different from ALIOS mice at any of the subsequent time points examined. The measured energy consumption based on combined food and HFCS consumption was 24 % higher in ALIOS mice compared to control mice during weeks 10–16 but was similar when measured from weeks 19 to 24 (Table 1). The obese crossover mice had the same energy consumption as the mice continued on the ALIOS diet despite eating control chow.

Despite persistent excessive energy consumption and obesity in the crossover (XO) mice, liver weights and liver triglyceride content were substantially lower after crossover to standard chow and unrestricted activity (Fig. 2). The mean liver weight of ALIOS mice doubled to 2.19 ± 0.56 g compared to control mice at 24 weeks. The liver weight of ALIOS mice at 16 weeks was 1.81 ± 0.41 g as previously reported [9]; the further increase at 24 weeks in these mice

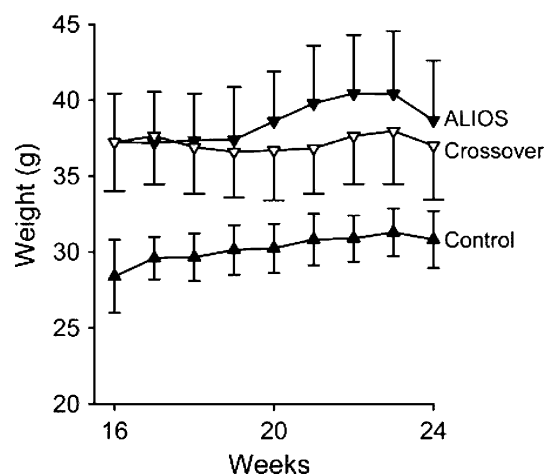


Fig. 1 Mean body weight after crossover from ALIOS conditions to control conditions (standard chow and water, no activity restrictions) for another 8 weeks compared to the weight of mice that remained on ALIOS conditions or were treated with control conditions for the entire 24 weeks. When feeding began at week 0, all mice weighed the same (18.4 ± 0.9 g). By week 16, the ALIOS mice weighed substantially more than control mice [37.2 ± 3.2 g ($n = 30$) vs. 28.4 ± 3.2 g ($n = 20$), $P < 0.001$]. Crossover at week 16 did not result in subsequent weight loss although there was no further weight gain ($n = 10$). A trend towards continued weight gain was evident in mice that remained on ALIOS conditions ($n = 10$). The weights at the final time point tended to be reduced compared to the previous week because of overnight fasting before sacrifice. The mean weights of ALIOS mice and crossover mice were significantly greater than control mice ($n = 10$) at all time points whereas there was not significant differences between ALIOS and crossover mice at any of these time points ($P < 0.05$; $n = 10$ mice in each group, error bars denote SD)

Table 1 Energy consumption by mice before and after crossover to control chow

	kcal/mouse/day (\pm SD)		
	Control	ALIOS	Crossover
Weeks 10–16	8.9 ± 1.4	$11.0 \pm 1.7^*$	
Weeks 19–24	9.5 ± 1.5	10.1 ± 2.2	10.1 ± 1.0

* $P < 0.001$ compared to control chow consumption during week 10 to 16

was not statistically significant ($P = 0.13$). The liver weight of control mice did increase from 0.91 ± 0.08 g at 16 weeks to 1.09 ± 0.07 g at 24 weeks ($P < 0.001$). The lower liver weight at 24 weeks after 8 weeks of crossover to control conditions compared to mice remaining on the ALIOS diet correlated with substantially lower liver triglyceride content as well, suggesting that the mobilization of liver triglyceride was largely responsible for the loss of liver weight. Similarly, biochemical evidence of hepatocellular injury as assessed by the plasma ALT level was reduced in the crossover group compared to the ALIOS group (Fig. 3). Plasma ALT was fourfold elevated at 24 weeks in ALIOS with a mean of

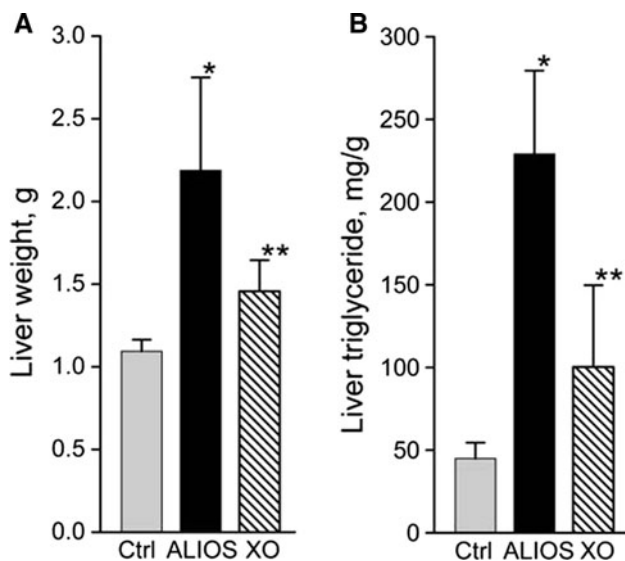


Fig. 2 Liver weight (a) and triglyceride content (b) at 24 weeks. Crossover to control conditions from weeks 16 to 24 (XO) caused reduction in liver weight and triglyceride content approaching normal levels (* $P < 0.05$ compared to control and crossover, ** $P < 0.05$ compared to control and ALIOS; $n = 10$ mice per group; error bars denote SD)

122 U/l. This was elevated to the same degree as previously described at 16 weeks, a time point at which the mean ALT was 119 U/l [9]. Plasma AST exhibits a high baseline level in mice but was also significantly elevated at 24 weeks of ALIOS conditions to 250 U/l. As observed with ALT, AST levels were nearly normal after 8 weeks of crossover to control feeding conditions.

Changes in total plasma cholesterol and triglyceride levels were discordant during ALIOS treatment and subsequent crossover to control conditions (Fig. 4). Whereas total plasma cholesterol was elevated in ALIOS mice and returned to normal following crossover to control chow, plasma triglycerides were not elevated during *trans*-fat feeding yet became elevated after crossover to control chow. This, in conjunction with decreased levels of hepatic triglyceride after crossover, is supportive of the mobilization of hepatic triglyceride in the crossover mice.

Plasma levels of the adipokines leptin and resistin were elevated in ALIOS mice and remained elevated after treatment with control conditions (Fig. 5), consistent with adipose tissue being the source of these adipokines, and the fact that the crossover mice remained obese. A decline of plasma resistin levels between 16 and 24 weeks was noted in both the control mice and the ALIOS mice.

Examination of liver histology in the ALIOS mice at 24 weeks demonstrated substantial accumulation of steatosis as a mix of large and small droplet fat (Fig. 6, Panel B). Similar to the abnormalities seen at 16 weeks [9], striking zonation of steatosis was noted with large droplet

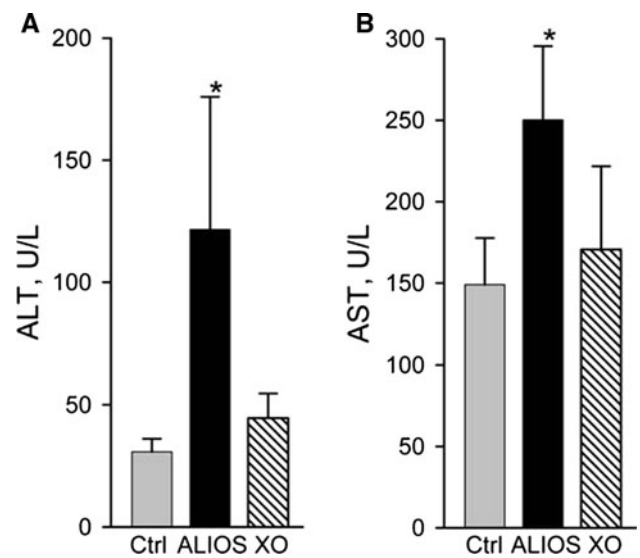


Fig. 3 Plasma ALT (a) and AST (b) levels were increased after 24 weeks of ALIOS conditions but returned to near normal in crossover mice (* $P < 0.05$ compared to control and crossover; $n = 10$ mice per group; error bars denote SD)

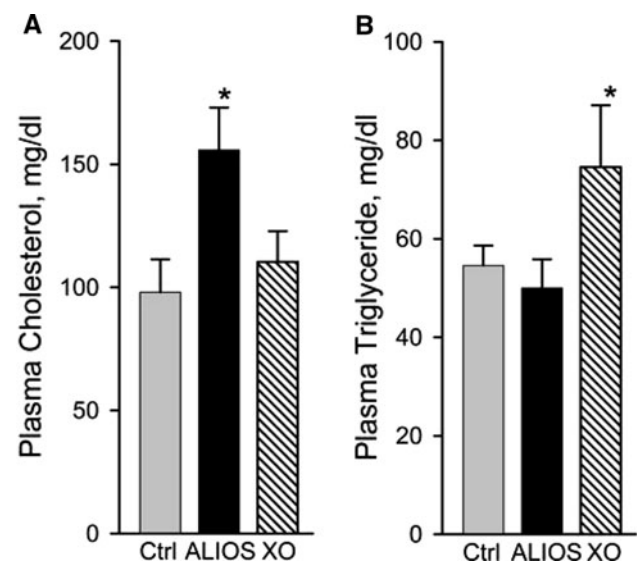


Fig. 4 Plasma total cholesterol levels (a) were increased by 59 % in ALIOS mice at 24 weeks and were near normal in crossover mice (* $P < 0.05$ compared to control and crossover by ANOVA; $n = 10$ mice per group; error bars denote SD). In contrast, plasma triglyceride levels (b) were unchanged in ALIOS mice but were increased by 36 % after 8 weeks of crossover conditions (* $P < 0.05$ compared to control and ALIOS; $n = 5$ mice per group; error bars denote SD)

fat most notably in zone 1 areas and small droplet fat being localized to zone 3 regions. Scattered lobular foci of mixed inflammatory infiltrates were evident. Hepatocellular ballooning and necrosis were not observed by routine light microscopy. In mice crossed over to control conditions for 8 weeks, variable but often substantial resolution of

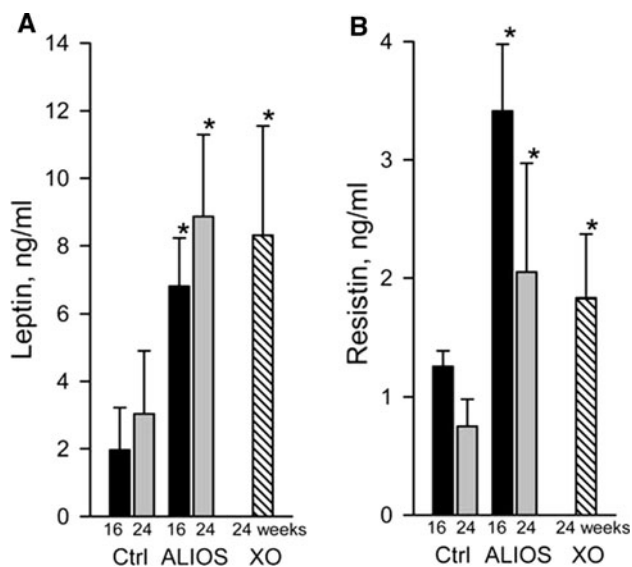


Fig. 5 Plasma leptin (a) and resistin (b) levels were increased in ALIOS mice at 16 and 24 weeks compared to control levels at the same time point (denoted by asterisks). Levels did not normalize with crossover to control chow. Resistin levels at 24 weeks were lower than at 16 weeks in both the control mice and ALIOS mice ($P < 0.05$). * $P < 0.05$ compared to control at the same time point; $n = 5$ mice per group; error bars denote SD

steatosis was present (Fig. 6, Panel C). Fibrosis was not identified in ALIOS mice at 24 weeks or in mice crossed over to control conditions by Masson's trichrome or Sirius red staining.

The incorporation of dietary *trans*-fats into triglyceride, phospholipid and cholesteryl ester pools in the liver and the clearance of esterified *trans*-fats from these pools following

elimination of dietary *trans*-fats were also evaluated and is reported as the percent of total fatty acids that are *trans* 18:1 plus *trans* 18:2. Other *trans*-fat species were present in comparatively negligible amounts. Extraction of liver lipids followed by separation into free fatty acid, triglyceride, polar lipid (e.g. phosphatidylcholine) and cholesteryl ester pools and analysis of FAME derived from each lipid pool by gas chromatography-flame ionization detection was performed to assess the effect of the ALIOS diet on liver lipids and the reversibility of these changes. The *trans*-fat content in the chow was similarly measured and found to be 30.8 % of fatty acids by weight monounsaturated *trans*-fat acids (*trans* 18:1) and 6.8 % *trans* 18:2, similar to what was reported by the manufacturer. In the mouse livers after 24 weeks of *trans*-fat feeding, the fraction of fatty acids as *trans*-fats in hepatic lipid pools ranged from 5 to 8.9 % (Fig. 7). *trans*-fats were not found in control animal livers consistent with finding that *trans* 18:1 and *trans* 18:2 were each less than 0.1 % of liver fatty acids in normal rats [17]. The polar lipid pool was the most enriched at 8.9 % of fatty acids as *trans*-fats and appeared to be the slowest to turn over with about half the *trans*-fat content after 8 weeks of a *trans*-fat free diet compared to mice fed the *trans*-fat diet for 24 weeks. The cholesteryl ester pool on the other hand appeared to turn over rapidly as the *trans*-fat content after crossover to control chow was only 3 % of that in mice continued on the *trans*-fat diet.

The effect of the ALIOS diet on types of fatty acids in the major hepatic lipid pools was also examined. Both the triglyceride and cholesteryl ester pools were expanded whereas the polar lipid pool, likely comprised primarily of membrane lipids was relatively unchanged (Fig. 8). The

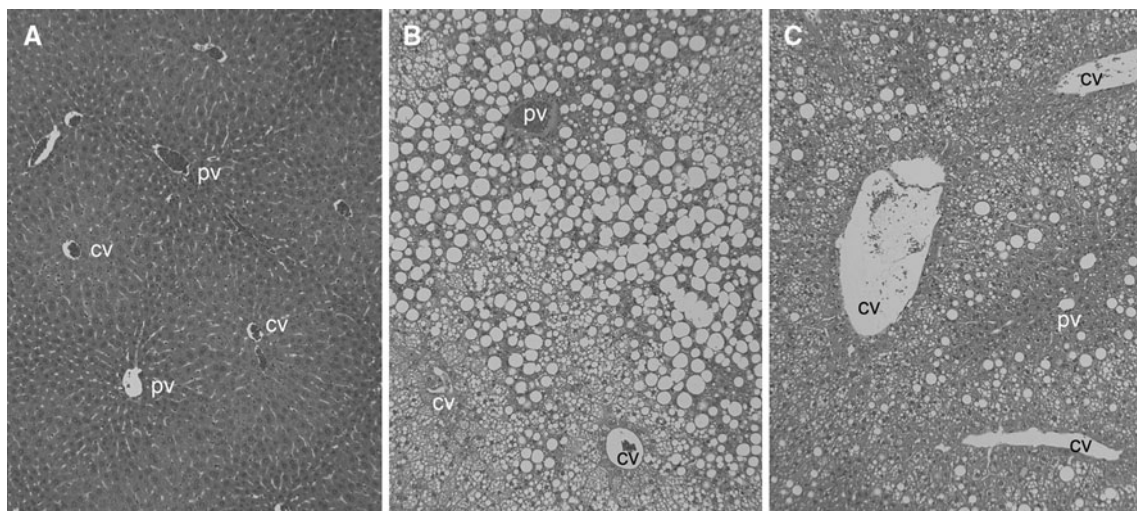


Fig. 6 Representative liver histology from control (a), ALIOS (b) and crossover (c) mice at 24 weeks. ALIOS livers at 24 weeks are characterized by extensive zone 1 macrovesicular steatosis around the portal venules (pv) and microvesicular steatosis are the central venules (cv) similar to that described previously at 16 weeks. Most of

the macrovesicular fat was gone after 8 weeks of crossover to control chow leaving a ring of macrovesicular fat in zone 2 and residual microvesicular fat in zone 3. Hematoxylin and eosin stain, $\times 20$ original magnification

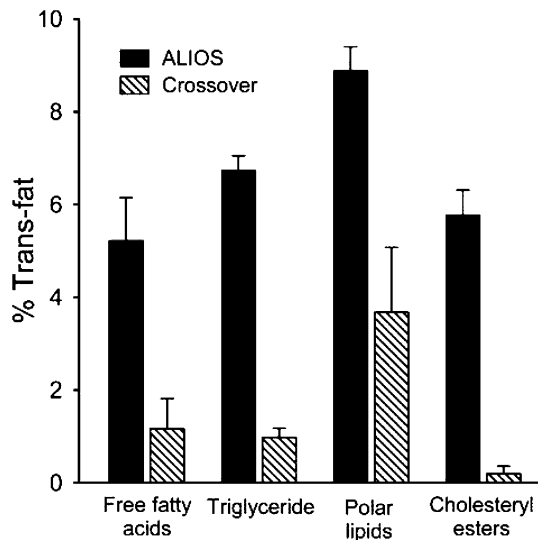


Fig. 7 Incorporation of *trans*-fats into the free fatty acid, triglyceride, polar lipid and cholesteryl ester pools of fatty acid containing hepatic lipids after *trans*-fat feeding for 24 weeks or after *trans*-fat feeding for 16 weeks followed by crossover to control chow for a further 8 weeks. No *trans*-fats were detectable in any of the pools in control mice fed standard chow for the 24 week period (not shown). The polar lipid pool, mostly phosphatidylcholine, was the most *trans*-fat enriched pool in the liver and retained the greatest amount after crossover to control chow. The cholesteryl ester pool by comparison was mostly devoid of *trans*-fats after crossover to control chow, suggesting rapid turnover. The data represents the mean of analyses of 5–9 mice per group, error bars indicate standard deviation; the percent *trans*-fat incorporation into the fatty acids pools was significantly less in the crossover group compared to the ALIOS group for each lipid pool ($P < 0.001$ for all groups)

C16:1/C16:0 desaturation index was markedly increased in the cholesteryl ester and free fatty acid pools indicating increased formation or retention of monounsaturated fatty acids during feeding in these pools. These changes partially reversed after normalization of the diet. By comparison, there was little effect of the diet on the desaturation index of fatty acids incorporated into the triglyceride and polar lipid pools.

Discussion

Even if effective pharmacological therapies are developed for NASH, the initial recommendations for treatment will likely remain lifestyle modifications to reduce caloric intake, improve the quality of food eaten and increase aerobic activity. Although a number of small studies of lifestyle interventions have indicated that this approach is generally effective in reversing NASH if the changes can be maintained, major clinical studies have not been reported to validate this treatment approach [2, 18]. Weight reduction to the point of normalization of body mass index

is difficult to accomplish and is rarely sustained by most overweight individuals [19, 20]. However, available studies that indicate NASH can improve with relatively small amounts of weight loss in the range of 5–10 % [21], although this remains controversial [22].

One goal of these experiments was to determine if changing to a normal diet and activity level could lead to improvement in the extensive hepatic steatosis and elevated ALT levels that are characteristic of NASH and which develop in sedentary mice consuming a diet high in *trans*-fats. Surprisingly, markedly improved liver histology and ALT levels occurred with normalization of the diet for a relatively short period despite the continued consumption of the same number of calories and a lack of weight loss. The failure to lose weight was also observed in a more prolonged diet induced obesity model in rats [23] and has disconcerting implications for success with diet interventions for human obesity. The mechanisms controlling satiety and feeding behavior are only beginning to be understood [24, 25] and further evaluating the role of these mechanisms in preventing weight loss was beyond the scope of this study. Leptin has anorexic effects but leptin levels remained elevated after crossover, suggesting that central nervous system leptin resistance could play a role in preventing the normal response to this adipokine [26].

Despite sustained obesity with elevated resistin and leptin levels, the liver disease in mice crossed over to control conditions improved with reductions in liver fat content and decreased biochemical evidence of hepatocellular injury. This observation indicates that obesity per se and dysregulated leptin responsiveness are not the cause of NASH in this model. Instead, it suggests that ongoing dietary factors or the abnormalities in lipid trafficking related to the diet are primarily responsible. Thus obesity and liver disease may occur as parallel processes in response to a poor diet rather than obesity being a direct cause of liver disease.

Previous analysis of the ALIOS model found that the inclusion of a high level of *trans*-fats in the ALIOS diet is the major determinant of the resultant liver disease while the presence of high fructose corn syrup resulted in slightly greater consumption of the fat-containing chow [9]. Subsequent studies of mice fed *trans*-fats have also demonstrated the development of NASH [10, 11, 27] and an increase in hepatocellular ballooning was noted even with a relatively low dose of dietary *trans*-fats in one study [10]. A subsequent study using AKR/J mice found that *trans*-fat feeding caused elevated aminotransferases but in contrast to the previous studies, significant liver histological changes were not identified in this mouse strain [12]. A potential source of confusion in understanding the effects of *trans*-fat feeding in causing liver disease was a recent report indicating that mice fed *trans*-fats developed

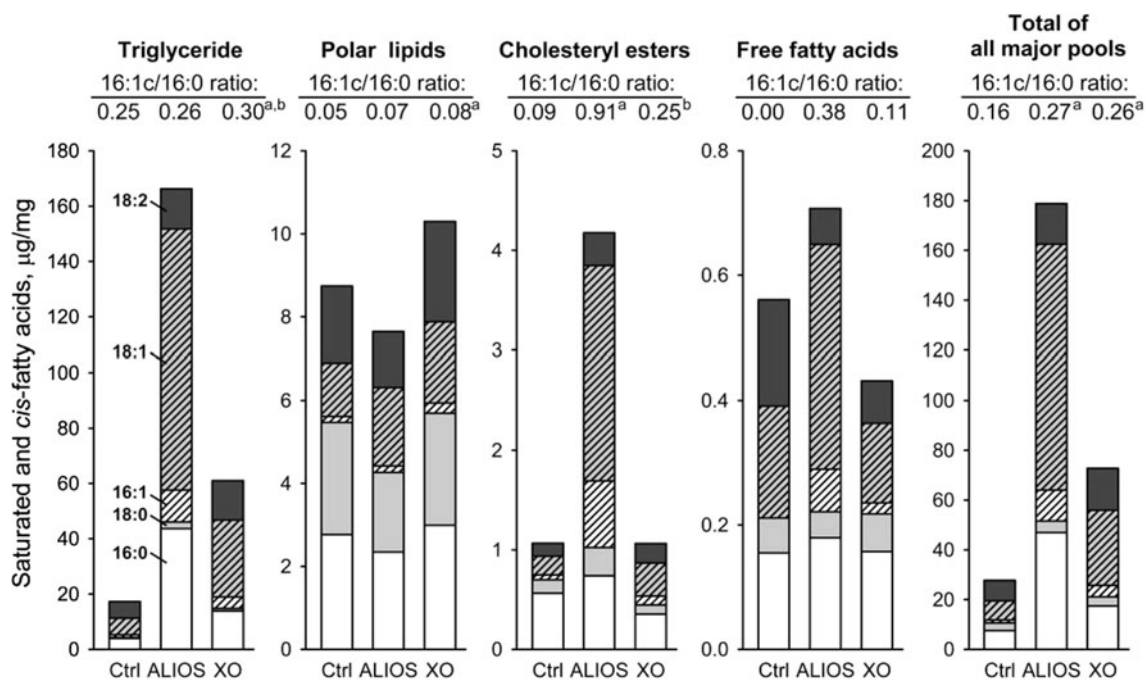


Fig. 8 Saturated and *cis*-unsaturated C16 fatty acids incorporation into triglyceride, polar lipids, cholesteryl esters or present as free fatty acids in the liver in control, ALIOS and crossover (XO) mice at 24 weeks. The identities of species represented by segments of the stacked bars are shown on the *left panel*. The monounsaturated pool (MUFA) was expanded in the ALIOS mice, especially in the cholesteryl ester pool. The polar lipid pool, representing membrane lipids was relatively unchanged. All pools contracted proportionally after crossover to control chow for 8 weeks. The essential fatty acid

linoleic acid (18:2) was increased in the triglyceride and cholesteryl ester pools and remained increased in the triglyceride pool after crossover to control chow. The desaturation index (the ratio of 16:1c/16:0) was increased in the cholesteryl ester and free fatty acid pools under ALIOS conditions. The data represents the mean of analyses of 5–9 mice per group; *a* the ratio is significantly different from control; *b* TF-HC and XO ratios are significantly different; non-significance is indicated by *no letter*; significance is defined as $P < 0.05$ by *t* test

features of NASH [28] but the fat source was fully hydrogenated coconut oil containing no detectable *trans*-fats [29].

The causal role of dietary components rather than obesity in causing NASH may also explain why relatively small amounts of weight loss in the range of 5–10 % have been associated with improved NASH in clinical trials. It may be that adhering to a healthier diet with the intent of achieving weight reduction could be directly beneficial to the liver independent of actual weight reduction. Clinical trials testing the hypothesis that *trans*-fats could play a role in lipotoxic liver injury have not been reported. A possible exception is a trial of excessive fast food consumption by student volunteers that led to elevations of serum ALT levels within weeks despite trivial changes in liver fat content [30]. However, the actual *trans*-fat content of this diet was not reported and other dietary factors could play a role in this worrisome finding.

The normal plasma triglyceride levels observed in ALIOS mice suggest that despite substantial hepatic accumulation of fat, either a secretory block prevents its release from the liver as VLDL or robust mechanisms of triglyceride removal from the blood prevent hypertriglyceridemia despite increased secretion. The observation that

plasma triglycerides became elevated in mice after being returned to control conditions supports the former hypothesis because this occurred at a time when hepatic steatosis was resolving.

There is no data on the incorporation and turnover of *trans*-fats in hepatic lipid pools with respect to the associated liver pathology. Previous studies have shown that *trans*-fats may be poor substrates for enzymatic incorporation into triglyceride compared to their *cis* analogues whereas they may be better substrates for peroxisomal oxidative pathways [31, 32]. Earlier studies also suggested that *trans*-fats are less facile substrates for mitochondrial beta-oxidation [31, 33–36], although this has been disputed [32]. The diminished ability of *trans*-fats to be handled by enzymatic pathways may explain the disproportionately low *trans*-fat incorporation into liver lipid pools compared to the dietary exposure in which more than 30 % of the fat was *trans*-fat.

The incorporation of *trans*-fats into the major hepatic lipid pools was evaluated to determine if changes in specific pools correlated with changes in the pathological findings after resumption of regular chow. An earlier study demonstrated incorporation of *trans*-fats into all major lipid pools to varying degrees when given to rats as free

fatty acids [37] but conflicting data suggested that little *trans*-fat was incorporated into triglyceride when given as triglyceride [38]. Studies have also shown that *cis* to *trans* isomerization can be facilitated by thiyl radicals under severe oxidant stress such as occurs with carbon tetrachloride administration to rats or gamma irradiation of tissue homogenates [17]. Whether the trace amounts of endogenously produced of *trans*-fats found in that previous study contributed to the accumulation of *trans*-fats in liver lipid pools in the ALIOS model cannot be determined in the present experiment. Such a contribution would seem unlikely however since the accumulation following substantial free radical stress was still less than 1 %.

The present study demonstrates that with crossover to control chow, the cholesteryl ester pool appeared to be the most labile with near complete loss of *trans*-fat cholesteryl esters after 8 weeks of control chow. By comparison, the polar lipid pool, representing membrane lipids such as phosphatidylcholine, retained its *trans*-fats to a substantial degree. Incorporation of *trans*-fats into membrane phospholipids can have important physiologic effects. For example, *trans*-fats increase membrane cholesterol content and alter G-protein coupled receptor activation [39, 40] and *trans*-fat incorporation into adipocyte membranes was found to impair insulin signaling and regulation of lipolysis [41]. However, the substantial persistence of *trans*-fats in the polar lipid pool at a time when liver injury is markedly improving after crossover to control chow suggests that membrane incorporation of *trans*-fats may not be the primary mechanism of *trans*-fat induced NASH in this model. On the other hand, the *trans*-fat incorporation into the cholesteryl ester pool was substantially diminished with consumption of control chow. The observation that this parallels the improvement in liver injury suggests that the role of *trans*-fat cholesteryl esters deserve further study in the pathogenesis of NASH. Somewhat surprising was the lability of the *trans*-fat content of the triglyceride pool, an observation also made in an earlier study [38]. This suggests that the accumulation and degradation of triglyceride in the liver is a highly dynamic process in contrast to adipocyte triglyceride which has a much slower turnover [42]. If the loss of triglyceride after normalization of the diet simply reflected a flow of fatty acids out of the pool, then the fraction of *trans*-fat in this pool would be relatively stable. Alternatively, triglyceride containing *trans*-fats may be preferentially degraded by the lipases responsible for hepatocyte triglyceride turnover.

Upregulation of stearoyl-CoA desaturase (SCD) is a common feature in diet induced obesity models and metabolic disease [43]. Once thought to play a role in metabolic disease [44, 45], this compensatory response of the liver to handle an increased burden of saturated fat is now thought to play a protective role in the liver by increasing

the ability to store fatty acids inertly by forming triglycerides [46], and thus avert lipotoxic injury from fatty acid metabolites [47]. Increased SCD activity can be estimated by the increased desaturation index of C16 fatty acids [48]. Indeed, mice fed the ALIOS diet demonstrated increased desaturation of C16 fatty acids in the cholesteryl ester pool. By comparison, there was a relative lack of a corresponding increase in the desaturation index of fatty acids incorporated into the triglyceride, polar lipid and free fatty acid pools. Understanding the implications of the uniquely marked increase in desaturation of fatty acids esterified to cholesterol in response to *trans*-fat feeding requires further investigation.

In summary, normalization of diet promoted improvement in NASH caused by a high *trans*-fat diet despite persistent obesity in mice. *trans*-fats were differentially incorporated into hepatic lipid pools and were released from these pools at different rates after stopping *trans*-fat consumption. The significance of these changes in the pathogenesis and potential for reversal of NASH warrants further investigation.

Acknowledgments This research was supported by NIH grant HL 74214 (DAF) and the Saint Louis University Liver Center.

References

- Bugianesi E, Marzocchi R, Villanova N, Marchesini G (2004) Non-alcoholic fatty liver disease/non-alcoholic steatohepatitis (NAFLD/NASH): treatment. *Baillieres Best Pract Res Clin Gastroenterol* 18:1105–1116
- Neuschwander-Tetri BA (2009) Lifestyle modification as the primary treatment of NASH. *Clin Liver Dis* 13:649–665
- Haynes P, Liangpunsakul S, Chalasani N (2004) Nonalcoholic fatty liver disease in individuals with severe obesity. *Clin Liver Dis* 8:535–547
- Silverman JF, O'Brien KF, Long S, Leggett N, Khazanie PG, Pories WJ, Norris HT, Caro JF (1990) Liver pathology in morbidly obese patients with and without diabetes. *Am J Gastroenterol* 85:1349–1355
- Ueno T, Sugawara H, Sujaku K, Hashimoto O, Tsuji R, Tamaki S, Torimura T, Inuzuka S, Sata M, Tanikawa K (1997) Therapeutic effects of restricted diet and exercise in obese patients with fatty liver. *J Hepatol* 27:103–107
- Petersen KF, Dufour S, Befroy D, Lehrke M, Hendler RE, Shulman GI (2005) Reversal of nonalcoholic hepatic steatosis, hepatic insulin resistance, and hyperglycemia by moderate weight reduction in patients with type 2 diabetes. *Diabetes* 54:603–608
- Harrison SA, Day CP (2007) Benefits of lifestyle modification in NAFLD. *Gut* 56:1760–1769
- Schäfer S, Kantartzis K, Machann J, Venter C, Niess A, Schick F, Machicao F, Häring HU, Fritsche A, Stefan N (2007) Lifestyle intervention in individuals with normal versus impaired glucose tolerance. *Eur J Clin Invest* 37:535–543
- Tetri LH, Basaranoglu M, Brunt EM, Yerian LM, Neuschwander-Tetri BA (2008) Severe NAFLD with hepatic necroinflammatory changes in mice fed *trans* fats and a high-fructose corn syrup equivalent. *Am J Physiol Gastrointest Liver Physiol* 295:G987–G995

10. Obara N, Fukushima K, Ueno Y, Wakui Y, Kimura O, Tamai K, Kakazu E, Inoue J, Kondo Y, Ogawa N, Sato K, Tsuduki T, Ishida K, Shimosegawa T (2010) Possible involvement and the mechanisms of excess *trans*-fatty acid consumption in severe NAFLD in mice. *J Hepatol* 53:326–334
11. Machado RM, Stefano JT, Oliveira CP, Mello ES, Ferreira FD, Nunes VS, de Lima VM, Quintão EC, Catanozi S, Nakandakare ER, Lottenberg AM (2010) Intake of *trans* fatty acids causes nonalcoholic steatohepatitis and reduces adipose tissue fat content. *J Nutr* 140:1127–1132
12. Koppe SW, Elias M, Moseley RH, Green RM (2009) *trans* fat feeding results in higher serum alanine aminotransferase and increased insulin resistance compared with a standard murine high-fat diet. *Am J Physiol Gastrointest Liver Physiol* 297:G378–G384
13. Kraft J, Spiltoir JI, Salter AM, Lock AL (2011) Differential effects of the *trans*-18:1 isomer profile of partially hydrogenated vegetable oils on cholesterol and lipoprotein metabolism in male F1B hamsters. *J Nutr* 141:1819–1826
14. Bligh EG, Dyer WJ (1959) A rapid method of total lipid extraction and purification. *Can J Biochem Physiol* 37:911–917
15. Ford DA, Gross RW (1988) Identification of endogenous 1-*O*-alk-1'-enyl-2-acyl-*sn*-glycerol in myocardium and its effective utilization by choline phosphotransferase. *J Biol Chem* 263:2644–2650
16. Shirasawa S, Sasaki A, Saida Y, Satoh C (2007) A rapid method for *trans*-fatty acid determination using a single capillary GC. *J Oleo Sci* 56:53–58
17. Zambonin L, Ferreri C, Cabrini L, Prata C, Chatgialiloglu C, Landi L (2006) Occurrence of *trans* fatty acids in rats fed a *trans*-free diet: a free radical-mediated formation? *Free Radic Biol Med* 40:1549–1556
18. Bouneva I, Kirby DF (2004) Management of nonalcoholic fatty liver disease: weight control. *Clin Liver Dis* 8:693–713
19. Elmer PJ, Obarzanek E, Vollmer WM, Simons-Morton D, Stevens VJ, Young DR, Lin P-H, Champagne C, Harsha DW, Svetkey LP, Ard J, Brantley PJ, Proschan MA, Erlinger TP, Appel LJ, Premier Collaborative Research Group (2006) Effects of comprehensive lifestyle modification on diet, weight, physical fitness, and blood pressure control: 18-month results of a randomized trial. *Ann Intern Med* 144:485–495
20. Sacks FM, Bray GA, Carey VJ, Smith SR, Ryan DH, Anton SD, McManus K, Champagne CM, Bishop LM, Laranjo N, Leboff MS, Rood JC, de Jonge L, Greenway FL, Loria CM, Obarzanek E, Williamson DA (2009) Comparison of weight-loss diets with different compositions of fat, protein, and carbohydrates. *N Engl J Med* 360:859–873
21. Harrison SA, Fecht W, Brunt EM, Neuschwander-Tetri BA (2009) Orlistat for overweight subjects with nonalcoholic steatohepatitis: a randomized, prospective trial. *Hepatology* 49: 80–86
22. Ahima RS (2007) Insulin resistance: cause or consequence of nonalcoholic steatohepatitis? *Gastroenterology* 132:444–446
23. Hill JO, Lin D, Yakubu F, Peters JC (1992) Development of dietary obesity in rats, influence of amount and composition of dietary fat. *Int J Obes Relat Metab Disord* 16:321–333
24. Morton GJ, Cummings DE, Baskin DG, Barsh GS, Schwartz MW (2006) Central nervous system control of food intake and body weight. *Nature* 443:289–295
25. Kelesidis T, Kelesidis I, Chou S, Mantzoros CS (2010) Narrative review: the role of leptin in human physiology: emerging clinical applications. *Ann Intern Med* 152:93–100
26. Shapiro A, Mu W, Roncal C, Cheng KY, Johnson RJ, Scarpace PJ (2008) Fructose-induced leptin resistance exacerbates weight gain in response to subsequent high-fat feeding. *Am J Physiol Regul Integr Comp Physiol* 295:R1370–R1375
27. Collison KS, Maqbool Z, Saleh SM, Inglis A, Makhoul NJ, Bakheet R, Al-Johi M, Al-Rabiah R, Zaidi MZ, Al-Mohanna FA (2009) Effect of dietary monosodium glutamate on *trans* fat-induced nonalcoholic fatty liver disease. *J Lipid Res* 50: 1521–1537
28. Kohli R, Kirby M, Xanthakos SA, Softic S, Feldstein AE, Saxena V, Tang PH, Miles L, Miles MV, Balistreri WF, Woods SC, Seeley RJ (2010) High-fructose, medium chain *trans* fat diet induces liver fibrosis and elevates plasma coenzyme Q9 in a novel murine model of obesity and nonalcoholic steatohepatitis. *Hepatology* 52:934–944
29. Neuschwander-Tetri BA (2011) No trans fats. *Hepatology* 54:750–751
30. Kechagias S, Ernerson Å, Dahlqvist O, Lundberg P, Lindström T, Nystrom FH, for the Fast Food Study Group (2008) Fast-food-based hyper-alimentation can induce rapid and profound elevation of serum alanine aminotransferase in healthy subjects. *Gut* 57:649–654
31. Beare-Rogers JL (1970) The deposition of polyunsaturated fatty acids in the rat fed partially hydrogenated vegetable oil. *J Am Oil Chem Soc* 47:487–489
32. Guzmán M, Klein W, Gómez del Pulgar T, Geelen MJ (1999) Metabolism of *trans* fatty acids by hepatocytes. *Lipids* 34:381–386
33. Lawson LD, Holman RT (1981) β -Oxidation of the geometric and positional isomers of octadecenoic acid by rat heart and liver mitochondria. *Biochim Biophys Acta* 665:60–65
34. Lawson LD, Kummerow FA (1979) β -Oxidation of the coenzyme A esters of elaidic, oleic, and stearic acids and their full-cycle intermediates by rat heart mitochondria. *Biochim Biophys Acta* 573:245–254
35. Lawson LD, Kummerow FA (1979) β -Oxidation of the coenzyme A esters of vaccenic, elaidic, and petroselaidic acids by rat heart mitochondria. *Lipids* 14:501–503
36. Ide T, Watanabe M, Sugano M, Yamamoto I (1987) Activities of liver mitochondrial and peroxisomal fatty acid oxidation enzymes in rats fed *trans* fat. *Lipids* 22:6–10
37. Wood R, Chumbler F, Wiegand R (1977) Incorporation of dietary *cis* and *trans* isomers of octadecenoate in lipid classes of liver and hepatoma. *J Biol Chem* 252:1965–1970
38. Moore CE, Alfin-Slater RB, Aftergood L (1980) Incorporation and disappearance of *trans* fatty acids in rat tissues. *Am J Clin Nutr* 33:2318–2323
39. Roach C, Feller SE, Ward JA, Shaikh SR, Zerouga M, Stillwell W (2004) Comparison of *cis* and *trans* fatty acid containing phosphatidylcholines on membrane properties. *Biochemistry* 43:6344–6351
40. Niu SL, Mitchell DC, Litman BJ (2005) *trans* fatty acid derived phospholipids show increased membrane cholesterol and reduced receptor activation as compared to their *cis* analogs. *Biochemistry* 44:4458–4465
41. Ibrahim A, Natrajan S, Ghafoorunnissa R (2005) Dietary *trans*-fatty acids alter adipocyte plasma membrane fatty acid composition and insulin sensitivity in rats. *Metabolism* 54:240–246
42. Hirsch J, Farquhar JW, Ahrens EH Jr, Peterson ML, Stoffel W (1960) Studies of adipose tissue in man. A microtechnic for sampling and analysis. *Am J Clin Nutr* 8:499–511
43. Flowers MT (2009) The $\Delta 9$ fatty acid desaturation index as a predictor of metabolic disease. *Clin Chem* 55:2071–2073
44. Attie AD, Krauss RM, Gray-Keller MP, Brownlie A, Miyazaki M, Kastelein JJ, Lusis AJ, Stalenhoef AF, Stoehr JP, Hayden MR, Ntambi JM (2002) Relationship between stearoyl-CoA desaturase activity and plasma triglycerides in human and mouse hypertriglyceridemia. *J Lipid Res* 43:1899–1907
45. Hulver MW, Berggren JR, Carper MJ, Miyazaki M, Ntambi JM, Hoffman EP, Thyfault JP, Stevens R, Dohm GL, Houmard JA,

- Muoio DM (2005) Elevated stearoyl-CoA desaturase-1 expression in skeletal muscle contributes to abnormal fatty acid partitioning in obese humans. *Cell Metab* 2:251–261
46. Li ZZ, Berk M, McIntyre TM, Feldstein AE (2009) Hepatic lipid partitioning and liver damage in nonalcoholic fatty liver disease: role of stearoyl-CoA desaturase. *J Biol Chem* 284:5637–5644
47. Neuschwander-Tetri BA (2010) Hepatic lipotoxicity and the pathogenesis of nonalcoholic steatohepatitis: the central role of nontriglyceride fatty acid metabolites. *Hepatology* 52:774–788
48. Peter A, Cegan A, Wagner S, Lehmann R, Stefan N, Königsrainer A, Königsrainer I, Häring HU, Schleicher E (2009) Hepatic lipid composition and stearoyl-coenzyme A desaturase 1 mRNA expression can be estimated from plasma VLDL fatty acid ratios. *Clin Chem* 55:2113–2120

Predicted Changes in Fatty Acid Intakes, Plasma Lipids, and Cardiovascular Disease Risk Following Replacement of *trans* Fatty Acid-Containing Soybean Oil with Application-Appropriate Alternatives

Michael Lefevre · Ronald P. Mensink ·
Penny M. Kris-Etherton · Barbara Petersen ·
Kim Smith · Brent D. Flickinger

Received: 6 March 2012 / Accepted: 18 July 2012 / Published online: 18 August 2012
© The Author(s) 2012. This article is published with open access at Springerlink.com

Abstract The varied functional requirements satisfied by *trans* fatty acid (TFA)—containing oils constrains the selection of alternative fats and oils for use as potential replacements in specific food applications. We aimed to model the effects of replacing TFA-containing partially hydrogenated soybean oil (PHSBO) with application-appropriate alternatives on population fatty acid intakes, plasma lipids, and cardiovascular disease (CVD) risk. Using the National Health and Nutrition Examination Survey 24-hour dietary recalls for 1999–2002, we selected 25 food categories, accounting for 86 % of soybean oil (SBO) and 79 % of TFA intake for replacement modeling. Before modeling, those in the middle quintile had a mean PHSBO TFA intake of 1.2 % of energy. PHSBO replacement in applications requiring thermal stability by either

low-linolenic acid SBO or mid-oleic, low-linolenic acid SBO decreased TFA intake by 0.3 % of energy and predicted CVD risk by 0.7–0.8 %. PHSBO replacement in applications requiring functional properties with palm-based oils reduced TFA intake by 0.8 % of energy, increased palmitic acid intake by 1.0 % of energy, and reduced predicted CVD risk by 0.4 %, whereas replacement with fully hydrogenated interesterified SBO reduced TFA intake by 0.7 % of energy, increased stearic acid intake by 1.0 % of energy, and decreased predicted CVD risk by 1.2 %. PHSBO replacement in both thermal and functional applications reduced TFA intake by 1.0 % of energy and predicted CVD risk by 1.5 %. Based solely on changes in plasma lipids and lipoproteins, all PHSBO replacement models reduced estimated CVD risk, albeit less than previously reported using simpler replacement models.

For the ILSI North America Technical Committee on Dietary Lipids.

M. Lefevre (✉)

Department of Nutrition, Dietetics and Food Science,
Utah State University, 9815 Old Main Hill, Logan,
UT 84322-9815, USA
e-mail: michael.lefevre@usu.edu

R. P. Mensink

Department of Human Biology, NUTRIM School for Nutrition,
Toxicology and Metabolism, Maastricht University, Maastricht,
The Netherlands

P. M. Kris-Etherton

Department of Nutritional Sciences, The Pennsylvania State
University, University Park, PA 16802, USA

B. Petersen · K. Smith

Exponent Inc, Washington, DC 20036, USA

B. D. Flickinger

Nutritional Science, Archer Daniels Midland Company,
Randall Research Center, Decatur, IL 62521, USA

Keywords *trans* fatty acid · Partially hydrogenated soybean oil (PHSBO) · Cardiovascular disease · Linolenic acid

Abbreviations

CVD	Cardiovascular disease
FA	Fatty acid
FARE	Foods Analysis and Residue Evaluation
FDA	US Food and Drug Administration
FH-IE	Fully hydrogenated interesterified
HDL-C	High-density lipoprotein cholesterol
LDL-C	Low-density lipoprotein cholesterol
NHANES	National Health and Nutrition Examination Survey
PHSBO	Partially hydrogenated soybean oil
SBO	Soybean oil
TC	Total cholesterol

TFA *trans* fatty acid
USDA US Department of Agriculture

Introduction

On July 9, 2003, the US Food and Drug Administration (FDA) mandated that food manufacturers list the content of *trans* fatty acid (TFA) on the Nutrition Facts panel of foods and dietary supplements by January 1, 2006. Subsequently, additional legislation banning or restricting the use of fats and oils containing TFA has been passed in California as well as major US metropolitan areas such as New York City and Philadelphia, and has been considered in 23 other states [1]. These actions occurred in response to compelling evidence that dietary TFA increases the risk for cardiovascular disease (CVD) [2], most notably by raising total cholesterol (TC) and low-density lipoprotein cholesterol (LDL-C) while lowering high-density lipoprotein cholesterol (HDL-C) [3].

The food manufacturing and restaurant industries have responded by reformulating products and recipes to minimize their TFA content. Although the ensuing reduction in the population intake in TFA is predicted to reduce the risk for CVD, the extent of this risk reduction is dependent on the choice of TFA replacement fats. In 2005, prior to TFA labeling requirements, per capita availability of margarine and shortening totaled 33.1 lbs/year (15.05 kg/year) or 370 kcal/person/day [4]. Thus, the choice of alternative oils used to replace margarines and shortening has the potential to affect health by changing a substantial portion of the population's fatty acid (FA) intake in addition to that of TFA alone.

The choice of TFA replacements within a given food is constrained by the desired functionality. TFA-containing fats and oils have two desirable properties: thermal stability for use in frying and an appropriate melting profile for use as shortening or margarine when solid fats are required. Consequently, a single replacement option for TFA is unlikely to satisfy the broad array of applications currently filled by TFA-containing oils. Furthermore, TFA replacement oils need to be available in sufficient amounts to meet domestic consumption demands, estimated in 2005 to be 8.6×10^9 billion pounds (3.9×10^9 kg) alone for soybean oil (SBO) used in baking, frying, and margarine applications [5].

As efforts to replace TFA-containing oils continue, guidance is needed with respect to which oils, or combination of oils, would likely provide the greatest improvements in CVD risk. In the present study, we model the effects of five application-appropriate TFA replacement

scenarios on population intakes of FA. The choice of oils used in our replacement scenarios was based on both functional suitability and availability as TFA replacements. Issues of availability limited our choices to replacements based on either soy bean or palm oil. In food applications requiring oils with enhanced thermal stability (e.g., for fried foods) we selected two low linolenic acid soy bean oils alternatives: (1) a low linolenic acid soy bean oil in which the linolenic acid is reduced and replaced with linoleic acid; and (2) a low linolenic acid, mid oleic acid soybean oil in which both the linolenic and linoleic acid are reduced and replaced with oleic acid. In food applications requiring solid fats to provide functional properties (e.g., for pie crusts and margarines), we selected two solid fat alternatives with different fatty acid profiles: (1) palm oil in which the predominant saturated fatty acid is palmitic acid; and (2) interesterified, fully hydrogenated soybean oil in which the predominant saturated fatty acid is stearic acid. This modeling exercise enabled us to predict the effect of these replacement scenarios on reductions in CVD risk mediated by changes in plasma lipid/lipoprotein levels.

Materials and Methods

Modeling of Changes in Dietary FA Intake Following PHSBO Replacement

The methods for estimating SBO intake, TFA intake, and changes in dietary FA intakes following application-appropriate substitution of replacement oils and fats for PHSBO are essentially identical to those previously published [6, 7] and are detailed below.

Estimation of TFA Intake During 1999–2002

Dietary intake of whole foods was estimated using food consumption data from the 1999–2002 National Health and Nutrition Examination Survey (NHANES) [8], which included 9,965 participants in 1999–2000 and 11,039 participants in 2001–2002. All estimates were derived using the NHANES 4-year medical examination center statistical weights and adjusting for survey design.

NHANES researchers used two US Department of Agriculture (USDA) databases—the 1993 *trans* Fatty Acid Database [9] and the Nutrient Database for Standard Reference [10], in which many foods are the same—to map the TFA content of analyzed foods to the foods reported in the 1999–2002 NHANES. All analyses, including the total dietary TFA intakes, were calculated using the NHANES food consumption data and TFA content of individual foods using Foods Analysis and Residue Evaluation

(FARETM) software (version 7.997; Exponent, Washington, DC). TFA consumption for individuals was calculated using the following formula:

$$E_{\text{TFA}} = \sum_i (\text{Fc})_i (\text{TFA}_f)_i$$

where E_{TFA} is the total intake of TFA, i is the number of different food types consumed daily, Fc is the amount of food consumed (g/day), and TFA_f is the TFA content of food (g/100 g food).

Estimation of SBO Content of NHANES Foods

The SBO content of food (including both nonhydrogenated and PHSBO) was determined using the USDA-developed recipes that translate foods reported in the NHANES “as eaten” into their component ingredients (raw agricultural commodities) for purposes of nutrient analysis [8]. The recipes used in the FARE program are based on the USDA recipes but have been made more user friendly for use in additional kinds of intake analyses, including ingredients, additives, or contaminants. For example, the USDA recipes break foods down from the food reported as consumed (e.g., pizza) into the ingredients (e.g., dough, tomato sauce, and cheese). The final recipes were further broken down into the raw agricultural commodities (e.g., wheat flour, tomatoes, olive oil, milk-based fat, etc.). The final recipes have been quality checked and approved by the USDA and are currently used by the FDA.

The calculation for the SBO from foods reported consumed in the NHANES is similar to the formula presented earlier except that the amount of food consumed was multiplied by the amount of SBO in food (derived from NHANES recipes) to estimate individual SBO intakes.

Selection of Food Categories for TFA Replacement Modeling

All NHANES foods were assigned to 1 of 59 broad food categories. These categories are based on the NHANES tiered food coding (i.e., all foods in the diet are grouped into three tiers starting with nine broad food categories and 263 additional subcategories). The selection of these categories was based on prior knowledge of their SBO content and degree of hydrogenation as communicated by the industry members of the ILSI North America Technical Committee on Dietary Lipids. The calculations for total dietary SBO and TFA intake within each food category were estimated as described above but on a food category basis. Based on these analyses, 25 food categories, accounting for 86 % of SBO intake and 79 % of TFA

intake, were further considered for inclusion in our replacement models (Table 1).

Reference Consumption of FA from SBO

For the purposes of this analysis, we defined the consumption of FA from the SBO fraction of foods during the 1999–2002 NHANES survey period as our “reference.” This period was selected because it immediately preceded significant efforts by the food industry to remove TFA from products.

The NHANES database does not include the FA composition of the individual components (e.g., SBO) of foods. The SBO used in foods is either liquid (nonhydrogenated) or partially hydrogenated to a particular level. The FA composition of the SBO will vary depending on the level of hydrogenation. Because it would be impossible to make assumptions regarding the specific TFA composition of the oils used for several thousand foods containing SBO, we simplified our analysis by assigning a SBO with a specified degree of hydrogenation and TFA content to each of the targeted 25 broad food categories. We then used the category-assigned SBO composition to estimate the SBO FA composition for all individual foods within each category.

The 1993 USDA *trans* Fatty Acid Database [9] and the USDA Nutrient Database for Standard Reference (Release 15) [10] were used to assign the FA content (including TFA) of SBO to each of the selected 25 broad food categories. The USDA *trans* Fatty Acid Database has FA profiles for the oil in 214 foods. When this database did not provide the FA profiles for specific varieties of SBO used in target food groups, these FA were estimated using information from the food industry (ILSI North America Technical Committee on Dietary Lipids). The FA data for SBO within the 25 broad food categories were chosen to reflect what was in the food marketplace during the 1999–2002 NHANES survey years (Table 1).

When a specific oil was not listed in a food recipe for oils, margarines, or shortenings, a Monte Carlo approach was used to select an oil for this food. Oil varieties used in the analysis were based on the USDA oil production statistics [11]. The SBO used to estimate reference FA intakes ranged in TFA content from 0.7 % of FA (liquid SBO, not hydrogenated) to 43.3 % of FA (for popcorn) (Table 1).

Individual SBO TFA intakes from both nonhydrogenated and partially hydrogenated SBO (henceforth combined and collectively referred to as PHSBO) were determined and the population was subsequently grouped by quintiles of PHSBO TFA intake. Once an NHANES respondent was assigned to a particular quintile in the reference analysis, we computed the mean intakes of the

Table 1 Fatty acid profiles of soybean oils assigned to broad food categories used for replacement models

Food categories	NHANES intake		Assigned soybean oil fatty acid composition (percentage of total fatty acids)						Assigned replacement fat
	TFA (g/day)	SBO (g/day)	16:0	18:0	18:1c	18:2n6	18:3n3	18:1t	
1. Frozen plate meals with grain mixture as major ingredient ^a	0.001	0.01	10.5	6.5	26.3	35.0	3.6	12.7	F1A; F2A
2. Squeeze or liquid butters ^a	0.003	0.02	10.1	3.6	21.2	51.3	6.8	0.7	Not replaced
3. Frozen or shelf-stable plate meals with meat, poultry, fish as major ingredient ^a	0.006	0.02	11.5	6.0	24.7	34.6	3.0	6.6	F1A; F2A
4. Cooking fats (shortening) ^a	0.006	0.15	10.5	6.5	26.3	35	3.6	12.7	F1A; F2A
5. Salad dressings, oil based ^{2a}	0.007	0.63	10.1	3.6	21.2	51.3	6.8	0.7	Not replaced
6. Soups, creamed based ^a	0.011	0.06	11.1	9.3	30.2	15.0	0.8	23.1	F1A; F2A
7. French fries, baked from frozen ^a	0.015	0.02	11.5	10.4	28.3	6.2	0.3	34.2	H1; H2
8. Soups, broth based ^a	0.018	0.12	10.1	3.6	21.2	51.3	6.8	0.7	Not replaced
9. Mayonnaise ^a	0.024	1.18	10.1	3.6	21.2	51.3	6.8	0.7	Not replaced
10. Pretzels and other grain snacks ^a	0.036	0.06	11.1	9.3	30.2	15.0	0.8	23.1	F1A; F2A
11. White potatoes, chips and sticks ^a	0.069	0.13	11.1	9.3	30.2	15.0	0.8	23.1	H1; H2
12a. Fried fish including breaded and fried, commercially fried ^a	0.080	0.41	11.1	9.3	30.2	15.0	0.8	23.1	H1; H2
12b. Fried fish including breaded and fried, home fried ^b	Included in 12a		10.4	5.5	24.1	39.3	4.8	8.1	H1; H2
13a. Fried poultry including breaded and fried, commercially fried ^a	0.092	0.43	11.1	9.3	30.2	15.0	0.8	23.1	H1; H2
13b. Fried poultry including breaded and fried, home fried ^b	Included in 13a		10.4	5.5	24.1	39.3	4.8	8.1	H1; H2
14a. Fried beef, veal, and pork, including breaded and fried, commercially fried ^a	0.097	0.12	11.1	9.3	30.2	15.0	0.8	23.1	H1; H2
14b. Fried beef, veal, and pork, including breaded and fried, home fried ^b	Included in 14a		10.4	5.5	24.1	39.3	4.8	8.1	H1; H2
15a. Fried eggs, commercially fried ^a	0.110	0.53	11.1	9.3	30.2	15.0	0.8	23.1	H1; H2
15b. Fried eggs, home fried ^b	Included in 15a		10.4	5.5	24.1	39.3	4.8	8.1	H1; H2
16. Tub margarine ^b	0.122	0.60	17.9	9.2	24.8	17.8	2.5	11.7	F1B; F2B
17. Salad dressings, cream based ^a	0.126	1.36	10.1	3.6	21.2	51.3	6.8	0.7	Not replaced
18. Stick margarine ^b	0.174	0.66	13.7	7.9	22.4	19.4	2.2	18.7	F1C; F2C
19. Popcorn ^b	0.207	0.43	11.1	13.5	22.0	4.0	0.2	43.3	F1A; F2A
20. Crackers ^a	0.215	0.63	11.1	9.3	30.2	15.0	0.8	23.1	F1A; F2A
21. Tortilla chips and other corn-based snacks ^a	0.333	1.05	10.8	7.9	28.3	25.0	2.2	17.9	H1; H2
22. Grain mixtures, ethnic dishes (Mexican, Puerto Rican, Asian, Italian) ^a	0.565	2.82	11.1	9.3	30.2	15.0	0.8	23.1	F1A; F2A
23. French fries, commercial ^b	0.643	2.02	11.2	9.7	29.6	12.1	0.6	26.7	H1; H2
24a. Yeast bread, including breaded non-fried meats, excluding sweet rolls and biscuits ^b	0.708	4.18	10.2	4.4	22.4	47.2	6.0	3.7	Not replaced
24b. Sweet rolls and biscuits ^b	Included in 23a		11.3	9.9	29.3	10.6	0.6	28.6	F1A; F2A
25. Cakes, cookies, pies, pastries, pancakes, waffles, French toast ^a	1.125	4.02	11.1	9.3	30.2	15.0	0.8	23.1	F1A; F2A
Sum of 25 categories	4.8	21.7							
Total diet	6.1	25.2							

Table 1 continued

Food categories	NHANES intake		Assigned soybean oil fatty acid composition (percentage of total fatty acids)					Assigned replacement fat
	TFA (g/day)	SBO (g/day)	16:0	18:0	18:1c	18:2n6	18:3n3	
25 categories as % of total diet	79 %	86 %						

NHANES, National Health and Nutrition Examination Survey; SBO, soybean oil; TFA, *trans* fatty acid. For replacement fats: *F1A* functional model 1A, *F2A* functional model 2A, *F1B* functional model 1B, *F2B* functional model 2B, *F1C* functional model 1C, *F2C* functional model 2C, *H1* heat-stable model 1, *H2* heat-stable model 2

^a Fatty acid composition for the PHSBO used in the products derived from the USDA *Trans* Fatty Acid Database [9]

^b Fatty acid composition for the PHSBO used in the products assigned by ILSI Technical Committee on Fatty Acids based on member companies' estimate of product composition in the marketplace between 1999 and 2002

major FA within each quintile of PHSBO TFA intake. Respondents remained in the same population quintile for all subsequent replacement model analyses.

Consumption of FA Following PHSBO Oil Replacement

To determine the dietary impact of substituting new oils for existing partially PHSBO in the diet, five application-appropriate replacement models were considered.

Heat-Stable Model 1 A nonhydrogenated low-linolenic acid SBO was substituted in applications requiring thermal stability (e.g., frying). Foods included were tortilla chips and other corn-based baked snacks; commercially and home fried meat, fish, poultry, eggs, and French fries; home-baked French fries; and potato chips.

Heat-Stable Model 2 A nonhydrogenated mid-oleic, low-linolenic acid SBO was substituted in the same foods as in heat-stable model 1.

Functional Model 1 Palm-based oils were substituted in applications requiring specific functional characteristics (e.g., melting profile and shortening applications). Foods included were stick and tub margarines; shortening; baked goods; crackers, pretzels, and other grain snacks; creamy soups; grain mixed dishes; sweet rolls and biscuits; popcorn; and frozen meals.

Functional Model 2 Fully hydrogenated interesterified (FH-IE)-based SBO, high in stearic acid, were substituted in the same foods as in functional model 1.

Complete Model A 50:50 ratio of the oils used in the heat-stable models 1 and 2 was substituted in thermal applications and a 50:50 ratio of the oils used in functional models 1 and 2 was substituted in functional applications.

To simplify our analyses, only the PHSBO portion of the food within the 25 food categories was subject to replacement modeling. The FA composition of the oils used in the replacement models, along with that of non-hydrogenated SBO and a typical PHSBO, are presented in

Table 2. A review of the TFA content of the 25 categories revealed a number of categories that would have had a low degree of SBO hydrogenation between 1999 and 2002 [12]. These categories included “squeeze or liquid butters,” “soups, broth based,” “salad dressing, oil based,” “salad dressing, creamed based,” “mayonnaise,” and “yeast breads—other than sweet rolls and biscuits” (Table 1). Consequently, the reference FA composition of these categories was retained throughout all replacement scenarios.

Once the PHSBO replacements were made, we computed the predicted mean intakes of each of the FA within each quintile of reference PHSBO TFA intake.

Calculation of 20-Year CVD Risk

Predicted changes in FA intake from reference values were estimated within each PHSBO TFA quintile for each of the five replacement models. Using published regression equations [3], we calculated the predicted mean change in TC, LDL-C, HDL-C, triglycerides, and the TC/HDL-C ratio based on dietary FA replacements. From the TC/HDL-C ratio, we estimated the 20-year risk for developing CVD from equations provided by Anderson et al. [13]. Predicted change in relative risk was defined as follows: (model 20-year CVD risk)/(reference 20-year CVD risk)—1.

Data Management and Statistical Analyses

All NHANES data management, TFA replacement modeling, and estimates of means, medians, and percentile distributions for dietary FA intakes under each replacement model were accomplished using FARE software. Estimates of changes in lipid levels and coronary heart disease risk associated for each replacement model were calculated using an Excel (Microsoft, Redmond, WA) spreadsheet populated with the relevant equations and coefficients.

Table 2 Nutrient profiles of reference SBO and oils used in replacement models

Replacement oil	Application	C16:0	C18:0	C18:1c	C18:2n6	C18:3n3	C18:1t
Reference: soybean oil	Frying	10.5	4.4	22.6	50.4	6.8	0.0
Reference: typical PHSBO	Frying and shortening	11.1	9.3	30.2	15.0	0.8	23.1
Heat-stable 1: low-linolenic acid, SBO based	Frying	10.5	4.4	25.9	56.1	2.0	0.7
Heat-stable 2: mid-oleic, low-linolenic acid SBO	Frying	9.5	3.5	50.0	35.0	2.8	0.7
Functional 1A: palm oil based	Shortening	42.0	4.0	40.5	10.0	0.0	1.0
Functional 2A: FH-IE SBO based	Shortening	11.5	35.1	15.2	30.4	2.5	3.9
Functional 1B: palm oil based	Tub margarine	18.1	3.7	23.9	37.3	4.8	0.8
Functional 2B FH-IE SBO based	Tub margarine	10.3	11.0	21.3	46.3	5.9	1.5
Functional 1C: palm oil based	Stick margarine	24.3	2.8	40.2	11.7	3.7	0.9
Functional 2C: FH-IE SBO based	Stick margarine	9.1	17.8	26.5	35.5	5.5	2.2

Data are the percentages of total fatty acid

FH-IE, fully hydrogenated interesterified; PHSBO, partially hydrogenated soybean oil; SBO, soybean oil

Results

Population TFA Intake

Based on the USDA *trans* Fatty Acid Database and the USDA Nutrient Database for Standard Reference, the mean population total TFA intake during 1999–2002 was 2.5 % of energy with a 90th percentile intake at 4.3 % of energy (Table 3). Those in the highest quintile of TFA intake had a mean total TFA intake of 4.5 % of energy with a range between 3.5 and 12.5 % of energy.

Estimated mean TFA intake from PHSBO in the top 25 SBO-containing food categories was 1.4 % of energy, accounting for 56 % of the value derived for the population total TFA intake (Table 3). The 90th percentile for PHSBO TFA was 3.0 % of energy (70 % of the value derived for the population total TFA intake). Taking into account naturally occurring TFA from beef and dairy products (estimated at 21 % of total TFA intake) [10], the estimated

mean TFA intake from PHSBO in the top 25 SBO-containing food categories accounted for 71 % of the population total TFA intake from hydrogenated vegetable oils.

Predicted Effects of Application-Appropriate PHSBO Replacement on Product FA Composition

The predicted effects of the replacement of PHSBO with application-appropriate oils on FA classes for selected food product groups are shown in Fig. 1. The food product groups in Fig. 1 were selected to indicate a representative range of predicted changes in FA composition. Net predicted change in TFA content (as a percentage of total FA) ranged from a net reduction of approximately 10 % of FA for tub margarine to >40 % of FA for popcorn with most other products ranging between 20 and 25 % of FA. For popcorn, cakes, cookies, pies, and pastries that require PHSBO for functional properties, replacement of PHSBO with either palm-based oils or FH-IE SBO increased

Table 3 Estimated and modeled per capita intake of TFA for the U.S. population (aged ≥ 3 years) as a percentage of total energy

Replacement model	Mean	90th percentile	TFA intake quintile ^a				
			1	2	3	4	5
TFA intake from NHANES 1999–2002 data	2.5	4.3	0.9 (0–1.3)	1.7 (1.3–2.0)	2.3 (2.0–2.6)	3.0 (2.6–3.5)	4.5 (3.5–12.5)
Reference TFA intake from PHSBO	1.4	3.0	0.2 (0–0.4)	0.7 (0.4–0.9)	1.2 (0.9–1.5)	1.9 (1.5–2.3)	3.2 (2.3–10.5)
Heat-stable 1: low-linolenic SBO	1.1	2.5	0.1	0.5	0.9	1.4	2.5
Heat-stable 2: mid-oleic, low-linolenic SBO	1.1	2.5	0.1	0.5	0.9	1.4	2.5
Functional 1: palm-based oil	0.5	1.3	0.1	0.3	0.4	0.6	0.9
Functional 2: FH-IE SBO	0.6	1.4	0.1	0.3	0.5	0.8	1.2
Combined: both heat-stable and functional replacements	0.2	0.4	0.1	0.2	0.2	0.2	0.3

FH-IE, fully hydrogenated interesterified; PHSBO, partially hydrogenated soybean oil; SBO, soybean oil; TFA, *trans* fatty acid

^a For quintiles, data are mean (range)

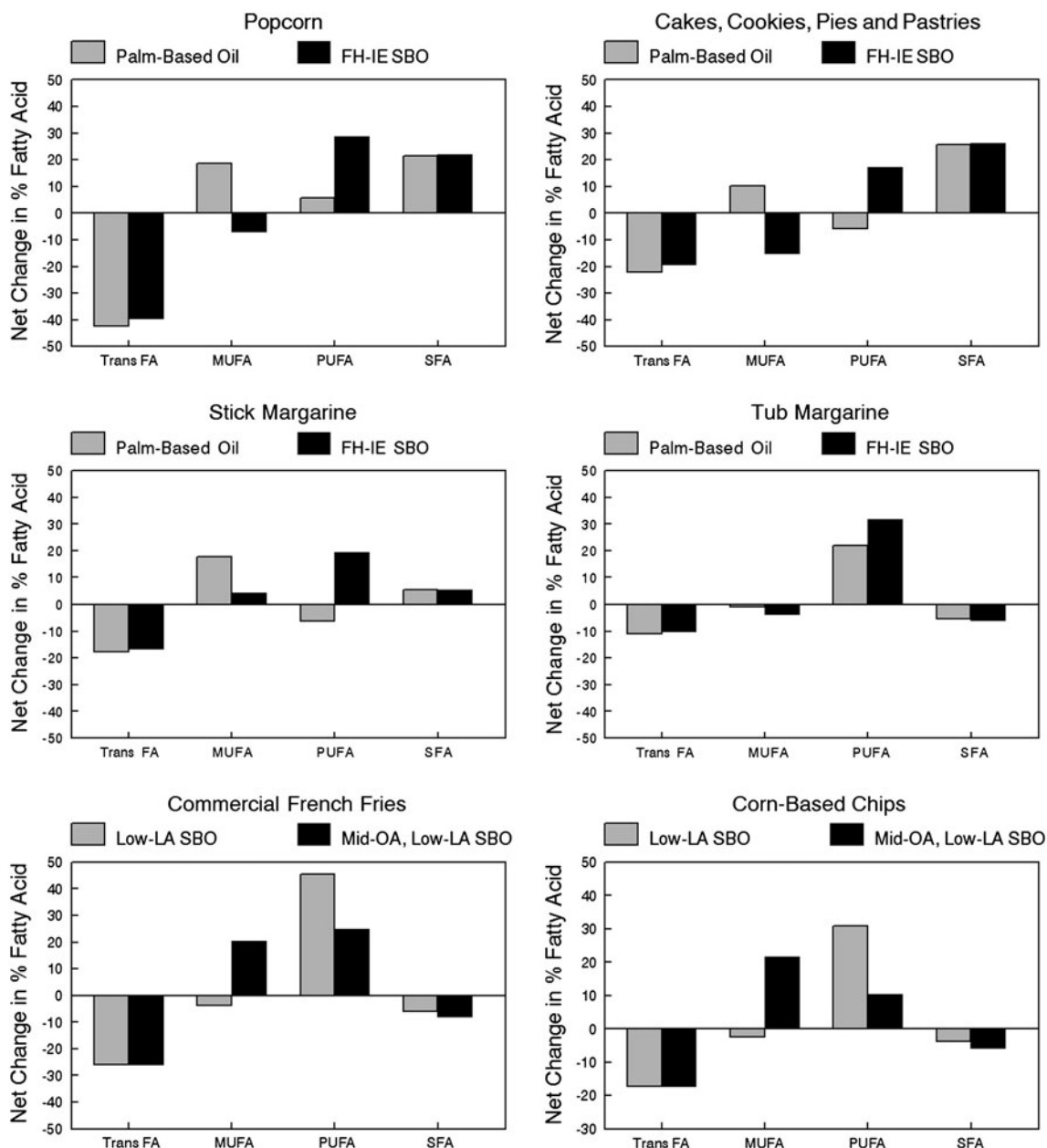


Fig. 1 Predicted change in fatty acid content of selected food categories with replacement of partially hydrogenated soybean oil (PHSBO) with application-appropriate oils. Graphs show the predicted net changes (as a percentage of total fatty acids) in *trans* fatty acid (TFA), MUFA, PUFA, and SFA following replacement of PHSBO with either palm-based oils or fully hydrogenated interesterified

soybean oil in foods requiring a functional fat (popcorn, cakes, cookies, pies, pastries, stick margarine, tube margarine) or with low-linolenic acid soybean oil or mid-oleic, low-linolenic acid soybean oil in foods requiring heat-stable oils (commercial French fries, corn-based chips)

predicted total saturated FA (SFA) by 20–25 % of FA. In contrast, replacement of PHSBO with either palm-based oils or FH-IE SBO in stick margarine is predicted to result in a moderate net increase in SFA by approximately 5 % of FA, whereas in tub margarines SFA are predicted to decrease by approximately 5 % of FA.

For products in which PHSBO is used for thermal stability (French fries, corn chips) replacement of PHSBO with

low-linolenic acid SBO (heat-stable model 1) increased predicted PUFA levels between 30 and 45 % of FA, whereas predicted *cis*-MUFA levels were largely unchanged. In the same applications, replacement of PHSBO with mid-oleic, low-linolenic acid SBO (heat-stable model 2) increased predicted PUFA levels by 10–25 % of FA, whereas predicted MUFA levels increased by approximately 20 %.

Effect of Application-Appropriate PHSBO Replacement on Population FA Intakes

Replacement of PHSBO in applications requiring thermal stability with either low-linolenic acid SBO (heat-stable model 1) or mid-oleic, low-linolenic acid SBO (heat-stable model 2) produced identical predicted reductions in mean PHSBO TFA intakes of 0.3 % of energy (25 % decrease) in the middle and 0.7 % of energy (22 % decrease) in the upper quintile of PHSBO TFA intake (Table 3). Both heat-stable replacement models increased predicted linoleic acid intake, whereas the use of mid-oleic, low-linolenic SBO predictably increased oleic acid intake. Modest reductions in total SFA were predicted in the high TFA consumers, whereas linolenic acid was not predicted to change with either heat-stable replacement oil (Table 4).

Replacement of PHSBO used in functional applications with palm-based oils reduced predicted PHSBO TFA intake by 0.8 % of energy (67 % decrease) in the middle and 2.3 % of energy (72 % decrease) in the upper quintiles of PHSBO TFA intake (Table 3). These predicted reductions in PHSBO TFA were accompanied by 1.0 and 3.0 % predicted increases in energy from palmitic acid in the middle and upper PHSBO TFA intake quintiles (Table 4). Use of palm-based oils also produced slight predicted reductions in linoleic and linolenic acid and increases in oleic acid.

Because of its residual TFA content (as provided for commercial food ingredient products at the time), replacement of PHSBO used in functional applications with FH-IE SBO produced smaller predicted reductions in PHSBO TFA intakes than observed with palm-based oil.

Replacement of PHSBO with FH-IE SBO reduced predicted mean PHSBO TFA intake by 0.7 % of energy (58 % decrease) in the middle and 2.0 % of energy (63 % decrease) in the upper quintiles of SBO TFA intake (Table 3). These predicted reductions in SBO TFA were accompanied by 0.9 and 2.4 % predicted increases in energy intake from stearic acid in the middle and upper quintiles, whereas predicted changes in total SFA were identical to those observed in the palm-based oil replacement model (Table 4). Use of FH-IE SBO also produced predicted reductions in oleic acid and increases in linoleic acid intakes.

Combined replacement of PHSBO used in both thermal and functional applications with equal contributions from each application-appropriate oil produced the greatest predicted reduction in PHSBO TFA intake. Predicted PHSBO TFA intake decreased by 83 % (1.0 % of energy) in the middle quintile, whereas predicted intake decreased by 91 % (2.9 % of energy) in the upper quintile (Table 3). These predicted changes in PHSBO TFA intakes were accompanied by predicted increases in palmitic, stearic, and linoleic acids with virtually no predicted change in either oleic or linolenic acids (Table 4).

Effect of Application-Specific PHSBO Replacement on Estimated 20-Year CVD Risk

From predicted changes in FA intakes relative to reference values, we calculated predicted changes in TC, LDL-C, HDL-C, and the TC/HDL-C ratio. With the exception of replacement with palm-based oil, LDL-C was predicted to decrease in all models (Fig. 2a). All replacement models

Table 4 Estimated mean fatty acid intakes from SBO (including PHSBO) at reference and under five application-appropriate replacement models for the middle and upper population quintiles for PHSBO TFA intake

Replacement model	Population quintile	C16:0	C18:0	C18:1c	C18:2n6	C18:3n3	Total SFA (C14:0-C18:0)
Reference	3rd	1.0	0.6	2.4	3.1	0.4	1.6
Heat-stable 1: low-linolenic SBO	3rd	1.0	0.6	2.4	3.6	0.4	1.6
Heat-stable 2: mid-oleic; low-linolenic SBO	3rd	1.0	0.5	2.7	3.3	0.4	1.5
Functional 1: palm-based oil	3rd	2.0	0.5	2.8	2.9	0.3	2.5
Functional 2: FH-IE SBO	3rd	1.0	1.5	2.0	3.7	0.4	2.5
Combined: both heat-stable and functional replacements	3rd	1.5	0.9	2.5	3.7	0.4	2.4
Reference	5th	1.8	1.4	4.7	4.0	0.4	3.2
Heat-stable 1: low linolenic SBO	5th	1.8	1.2	4.5	5.3	0.4	3.0
Heat-stable 2: mid-oleic; low linolenic SBO	5th	1.8	1.2	5.3	4.6	0.5	3.0
Functional 1: palm oil based	5th	4.8	0.9	5.9	3.7	0.3	5.7
Functional 2: FH-IE SBO	5th	1.9	3.8	3.5	5.7	0.6	5.7
Combined: both heat-stable and functional replacements	5th	3.2	2.1	4.8	5.6	0.5	5.3

Data are for the US population (aged ≥ 3 years) as a percentage of total energy

FH-IE, fully hydrogenated interesterified; PHSBO, partially hydrogenated soybean oil; SBO, soybean oil; SFA, saturated fatty acid; TFA, *trans* fatty acid

showed a predicted increase in HDL-C (Fig. 2b) and decrease in the TC/HDL-C ratio (Fig. 2c). Predicted 20-year CVD risk (derived from changes in TC/HDL-C) declined with each of the five replacement models (Fig. 3). Predicted changes in CVD risk were similar with both heat-

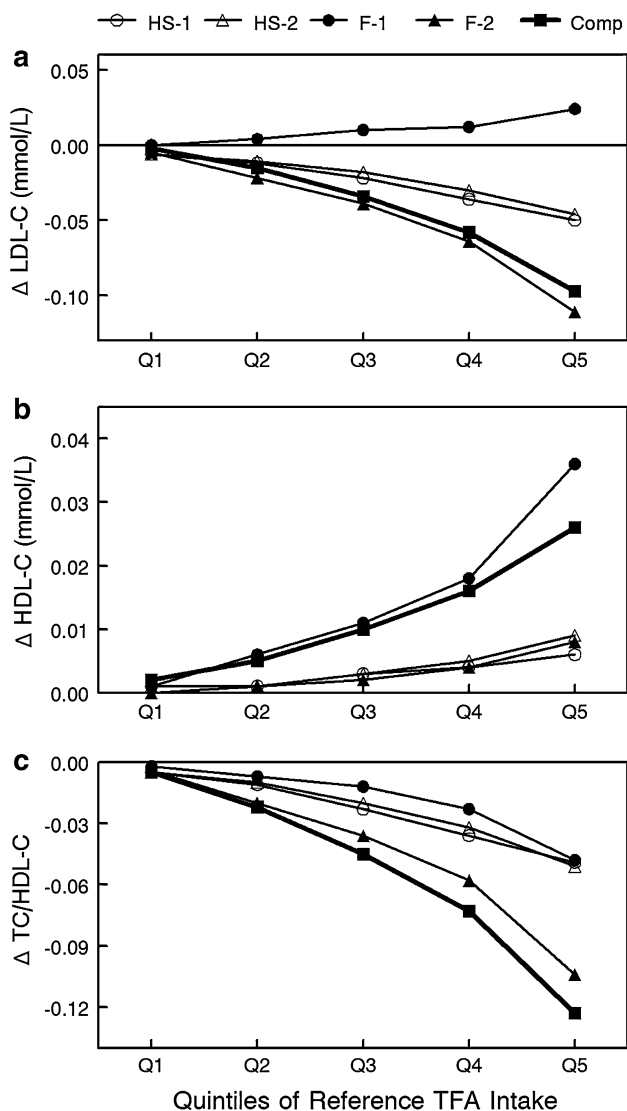


Fig. 2 Predicted change in **a** low-density lipoprotein cholesterol, **b** high-density lipoprotein cholesterol, and **c** total cholesterol/high-density lipoprotein cholesterol ratio for each quintile of reference *trans* fatty acid intake. HS-1, heat-stable model 1 using nonhydrogenated low-linolenic acid soybean oil (SBO) as a replacement in applications requiring thermal stability; HS-2, heat-stable model 2 using nonhydrogenated mid-oleic, low-linolenic acid SBO as a replacement in applications requiring thermal stability; F-1, functional model 1 using palm-based oils in applications requiring specific functional characteristics; F-2, functional model 2 using fully hydrogenated interesterified-based SBO in applications requiring specific functional characteristics; Comp, complete replacement using a 50:50 ratio of the oils used in heat-stable models 1 and 2 and a 50:50 ratio of the oils used in functional models 1 and 2 in their appropriate applications

stable replacement models with risk declining by 0.7–0.8 % in the middle and 1.6–1.7 % in the upper quintiles of SBO TFA intake. In contrast, estimated CVD reduction differed between the two functional replacement models. Use of a palm-based oil reduced predicted CVD risk by 0.4 % in middle and by 1.6 % in the upper quintiles. In contrast, the FH-IE SBO reduced predicted CVD risk by 1.2 % in the middle and 3.4 % in the upper quintiles. The complete replacement model reduced predicted CVD risk by 1.5 % in the middle and 4.0 % in the upper quintiles.

Discussion

Our study shows for the first time the predicted changes in the population intake of dietary FA associated with achievable application-appropriate replacements for PHSBO. With near complete replacement of PHSBO used in thermal and functional applications with an equal mix of likely available options, we predicted that TFA intake would decline by >90 % (2.9 % of energy) in the upper quintile of TFA users with increases in palmitic acid (1.4 %

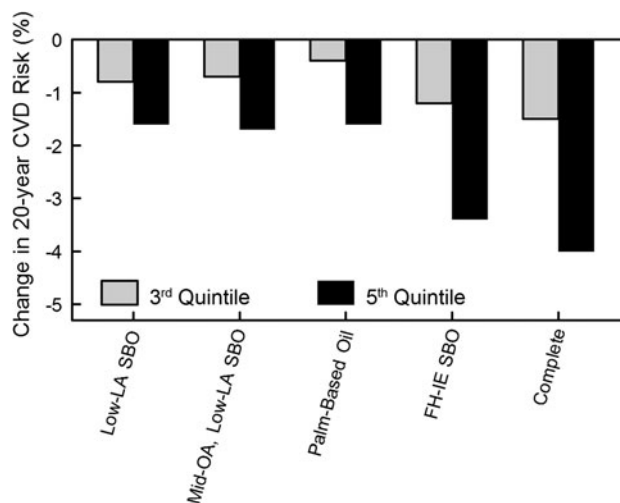


Fig. 3 Predicted change in 20-year cardiovascular disease (CVD) risk following near complete replacement of partially hydrogenated soybean oil (PHSBO) with application-appropriate oils across quintiles of reference soybean oil *trans* fatty acid intake. Reference risk assumed a 40-year-old man without diabetes, hypertension, or left ventricular hypertrophy with a total cholesterol (TC) level of 200 mg/dL and an high-density lipoprotein cholesterol (HDL-C) level of 45 mg/dL. Changes in risk are based on predicted changes in the TC/HDL-cholesterol ratio subsequent to changes in predicted fatty acid intake following PHSBO replacement. *Low-LA SBO* low-linolenic acid soybean oil, *Mid-OA, Low-LA SBO* mid-oleic, low-linolenic acid soybean oil, *FH-IE SBO* fully hydrogenated interesterified soybean oil; complete, for heat-stable applications: 50:50 use of low-linolenic acid soybean oil and mid-oleic, low-linolenic acid soybean oil and for functional applications: 50:50 use of palm-based oils and fully hydrogenated interesterified soybean oil

of energy), stearic acid (0.7 % of energy), and linoleic acid (1.6 % of energy) intakes and no appreciable change in oleic or linolenic acid intakes. Based exclusively on predicted changes in TC/HDL-C levels, we estimated that these changes in dietary FA would result in a 20-year CVD risk reduction of 1.5 % in the middle and 4.0 % in upper TFA quintiles.

Our choice of using TC/HDL-C as our primary metric is justified based on observations that unlike saturated FA, TFA both increase LDL-C and decrease HDL-C, resulting in uniquely unfavorable increases in the TC/HDL-C [3]. Indeed, the ability of TFA to increase TC/HDL-C has been used as a primary rationale in the call for its reduction in the diet [14]. The use of the TC/HDL-C ratio as the primary metric to evaluate changes in CVD risk associated with replacement of TFA in the diet is also supported in the World Health Organization scientific update on TFA [15].

The time period used for our reference analysis (1999–2002 NHANES survey), coupled with industry data for TFA content of foods in the marketplace at that time, allowed us to estimate the effects of TFA replacement prior to significant product reformulation. Our estimate of a mean total TFA intake of 2.5 % of energy agrees with a previous estimate of 2.6 % of energy from the Continuing Survey of Food Intakes of Individuals data for 1989–1991 [16] and 1994–1996 [12].

The mean SBO TFA content during the reference time period for the foods used in our replacement model was 56 % of that derived from the NHANES data, a difference due to several factors. To simplify our analysis, we focused only on SBO as the TFA source. Thus, partially hydrogenated oils from other sources (e.g., corn, canola, and cottonseed), which may contribute up to 18 % of partially hydrogenated oil consumption [17], were not considered in our analysis. Second, in selecting only the 25 SBO-containing food categories for analysis, we largely excluded TFA from animal sources, which may account for 21 % of TFA intake [12]. Finally, we updated the TFA content of selected foods, including items such as creamy salad dressings and sauces in which the TFA content reported in the USDA *trans* Fatty Acid Database was likely to be substantially higher than what was present in the marketplace during 1999–2002 [12].

Changes in selected food product FA composition in the United States between 2005 and 2008 resulting from replacement of TFA have been reported [18]. Analysis of changes in microwave popcorn FA composition indicated a net reduction of approximately 40 % in TFA and a net increase of 24 % in SFA. This compares favorably with our estimates of a net reduction of 40–42 % in TFA and a net increase of 22 % in SFA. For cakes and cookies, our predicted changes in TFA and SFA are approximately half of that reported to have occurred (estimated 40 % net

reduction in TFA and 60 % net increase in SFA for the United States). These differences could reflect the selection of products higher in TFA for longitudinal FA analysis as opposed to the broader spectrum of foods within the cakes and cookies categories used in our estimates. Finally, our predicted changes in the product categories also are consistent with reported reductions in TFA + SFA and increases in *cis*-unsaturated FA following product reformulation in Canada [19]. With the exception of a predicted modest 3–7 % net increase in TFA + SFA levels in the cakes, cookies, pies, and pastries category, predictions for all other food categories indicated a net decrease in the TFA and SFA levels and a net increase in the *cis*-unsaturated FA levels (data not shown).

Our analysis accounted for approximately 71 % of TFA from vegetable sources. The remaining 29 % likely comes from hydrogenated corn, canola, and cottonseed oil not included in our replacement model. Assuming that these were similarly subjected to replacement would further decrease predicted CVD risk by an additional 40 % relative to our original estimates resulting in a 20-year CVD risk reduction of 2.1 % in the middle and 5.6 % in the upper TFA quintiles. However, even after corrections for unaccounted TFA from vegetable sources, our estimate for CVD risk reduction based on changes in the TC/HDL-C ratio is less than half of that predicted by others (estimated at 6 % for the population average) [2]. Most of this difference can be traced to the choice of specific replacement oils. Earlier studies [2, 20] modeled the health effects of TFA replacement using simpler approaches in which all dietary TFA are replaced with a single class of FA (MUFA, PUFA, or SFA). Although this approach has been useful in providing guidance about the preferred FA to replace TFA to achieve maximum CVD risk reduction, it fails to consider certain practical issues for commercial food production.

Our approach was fundamentally different from previous studies in three respects. First, to reflect the food reformulation process more accurately, the unit of exchange in our analysis was whole oils and not individual FA. This approach adds complexities by taking into consideration changes in FA beyond TFA in terms of what is removed with the TFA-containing oil and what is added with the replacement oil.

Second, our approach considers the functional attributes required of the replacement oil to effectively substitute for TFA-containing oils within a given broad application. Thus, although oils high in PUFA or MUFA may be considered suitable replacements for many frying applications (accounting for approximately 25 % of TFA intake), they would not provide the desired functional characteristics in many baking applications.

Finally, because of the magnitude of TFA usage, particularly as PHSBO, the options for oil replacement are

limited by availability and economics. Although both corn and sunflower oil have been used to replace TFA-containing oils for frying applications, their combined domestic production in 2006 was only 15 % of that of SBO [21] and supply reliability for commercial use is questionable [17]. The emergence of trait-enhanced SBO low in linolenic acid with or without increased oleic acid levels [17] suggests that they will likely constitute a substantial fraction of the oils used to replace TFA in frying applications. For functional applications, palm-based oil replacements have been used in Europe for over a decade and are currently available in sufficient quantities to meet demand [22]. However, because of the magnitude of domestic SBO production, we included FH-IE SBO in our models because it is likely that functional limitations with FH-IE SBO will shortly be overcome and it will be available as an alternative to palm oil.

Our estimates for CVD risk reduction are based only on the predicted effects of changes in individual FA on circulating lipoproteins. Our models do not consider possible effects on other CVD risk factors including inflammation and hemostatic factors, lipoprotein[a], and endothelial function, all of which are affected by TFA and other FA [2]. Thus, the actual reduction in CVD risk associated with TFA replacements may be greater than our estimates. Indeed, employing simpler substitution models, the estimates for CVD risk reduction based on data from prospective studies have been approximately four times higher than that predicted from changes in the TC/HDL-C ratio [2]. Based on changes in FA classes (and not individual FA) and published regression coefficients from prospective studies [23], our data would predict a reduction in CVD events of 11 % in the middle and 29 % in the upper quintiles of TFA users under the complete replacement model.

It is important to note that each of the proposed replacement strategies has uncertainties. The use of less thermally stable frying oils may result in increased consumption of oxidized and thermally degraded FA with potential adverse health effects [24]. Expanded use of low-linolenic SBO beyond that needed for applications requiring thermal stability (e.g., salad and cooking oils) may decrease population intakes of this beneficial n3-FA. Although oils high in oleic acid are generally considered to be healthy, some have cautioned against their increased consumption because of a similar atherogenic potential when compared to saturated fat in animal models [25], and recent data suggest that MUFA may actually increase coronary heart disease risk relative to SFA [26]. As a TFA replacement for functional applications, FH-IE SBO would seem to be preferred, largely because of the high content of

cholesterol-neutral stearic acid. However, very high stearic acid (10.9 % of energy) intakes may increase fibrinogen levels [27]. Furthermore, the randomization of FA in the glycerol moiety of the triglyceride molecule by the inter-esterification process may adversely affect glucose metabolism at very high stearic acid intakes (12 % of energy) [28]. As a tropical oil, palm oil markedly increases LDL-C due to its high palmitic acid content [3]. These uncertainties warrant a continuing assessment of the health effects of new fats and oils introduced into the marketplace.

Finally, not considered in the current study was replacement of TFA-containing foods with other foods, rather than replacing their TFA-containing oils. Indeed, replacement of cakes, cookies, pies, French fries, chips, and other such foods with fruits, vegetables, and whole grains to achieve a dietary pattern consistent with current recommendations [29] would be expected to provide the greatest reduction in CVD risk.

In summary, all TFA replacement strategies evaluated changed the fatty acid profile in a manner that is projected to decrease CVD risk, albeit to different extents based on the specific selection of the replacement oils. The combined use of mid-oleic, low-linolenic SBO for frying applications and fully hydrogenated interesterified SBO for functional application is predicted to provide the greatest reduction in CVD risk. Nonetheless, our estimates of this CVD risk reduction, which are based solely on the predicted changes in plasma lipid profile, are lower than previous estimates due in large part to the real-world constraints associated with the selection of the TFA replacement oils. As more data are developed regarding the quantitative relationship between changes in dietary fatty acid composition and changes in a broader spectrum of CVD risk factors, the modeling employed in this study would be expected to provide even better estimates of the health consequences associated with population-wide changes in the use oils in the food supply. Such detailed modeling would be increasingly valuable as a tool to guide both policy makers and the food industry as further changes in the production, availability and use of alternate dietary oils are contemplated in efforts to provide a healthier food supply.

Acknowledgments This project was funded by the ILSI North America Technical Committee on Dietary Lipids. The members (and affiliated companies) of the ILSI North America Technical Committee on Dietary Lipids who participated in this project are as follows: Brent Flickinger, PhD (Archer Daniels Midland Company); Kristin Reimers, MS, RD (ConAgra Foods Inc); Satya S. Jonnalagadda, PhD (General Mills Inc); Amy Griel, PhD, RD (The Hershey Company); Kristin Herron Rubin, PhD (Kraft Foods Inc); Steven Rizk, PhD (Masterfoods USA); Shawna Lemke, PhD (Monsanto Company); Zdenek Kratky, PhD (Nestlé USA); Sanjiv Agarwal, PhD (Sara Lee); and Fran Seligson, PhD, RD (consultant for The Hershey Company).

Conflict of interest Michael Lefevre serves as a scientific advisor to the ILSI North America Technical Committee on Dietary Lipids and the Soy Nutrition Institute; is a member of Kraft Foods Worldwide Health and Wellness Advisory Council; has served as a consultant for Archer Daniels Midland, Almond Board of California, ConAgra, Egg Nutrition Council, Frito-Lay, The Hershey Company, Mars, and Monsanto; and has research support from General Mills. Penny M. Kris-Etherton received funding from the United Soybean Board to conduct a literature review on the health effects of stearic acid. She also has grant support from General Mills for a whole grain study and had support from The Hershey Company to conduct a study on macadamia nuts. Brent D. Flickinger is employed by Archer Daniels Midland, a member of the ILSI North America Technical Committee on Dietary Lipids. Ronald P. Mensink, Barbara Petersen, and Kim Smith have no reported conflicts. Michael Lefevre, Ronald P. Mensink and Penny M. Kris-Etherton have received honoraria to support the preparation of this manuscript.

Open Access This article is distributed under the terms of the Creative Commons Attribution License which permits any use, distribution, and reproduction in any medium, provided the original author(s) and the source are credited.

References

- National Conference of State Legislatures (accessed 2008 Jul 22) Trans fat and menu labeling legislation. <http://www.ncsl.org/programs/health/transfatmenulabelingbills.htm>
- Mozaffarian D, Katan MB, Ascherio A, Stampfer MJ, Willett WC (2006) Trans fatty acids and cardiovascular disease. *N Engl J Med* 354:1601–1613
- Mensink RP, Zock PL, Kester AD, Katan MB (2003) Effects of dietary fatty acids and carbohydrates on the ratio of serum total to HDL cholesterol and on serum lipids and apolipoproteins: a meta-analysis of 60 controlled trials. *Am J Clin Nutr* 77:1146–1155
- U.S. Department of Agriculture, Economic Research Service (2007 February 15; accessed July 22, 2008) Added fats and oils: Per capita availability. <http://www.ers.usda.gov/Data/FoodConsumption/Spreadsheets/fats.xls>
- U.S. Census Bureau (2006) Fats and oils: Production, consumption, and stocks: 2005. Washington, DC: U.S. Census Bureau. Report No. M311K(05)-13
- DiRienzo MA, Astwood JD, Petersen BJ, Smith KM (2006) Effect of substitution of low linolenic acid soybean oil for hydrogenated soybean oil on fatty acid intake. *Lipids* 41:149–157
- DiRienzo MA, Lemke SL, Petersen BJ, Smith KM (2008) Effect of substitution of high stearic low linolenic acid soybean oil for hydrogenated soybean oil on fatty acid intake. *Lipids* 43:451–456
- Centers for Disease Control and Prevention, National Center for Health Statistics (accessed August 2007). The National Health and Nutrition Examination Survey (NHANES) 1999–2002. Public Data Release 1999–2002. http://www.cdc.gov/nchs/nhanes/nhanes1999-2000/nhanes99_00.htm
- U.S. Department of Agriculture, Agricultural Research Service (2004; accessed August 2007) Selected foods containing trans fatty acids. <http://www.nal.usda.gov/fnic/foodcomp/Data/Classics/index.html#trans>
- U.S. Department of Agriculture, Agricultural Research Service (2010) Nutrient Database for Standard Reference. <http://www.nal.usda.gov/fnic/foodcomp/search/2010>
- U.S. Department of Agriculture, Economics, Statistics and Market Information System (2005; accessed July 23, 2008) Oil Crops Yearbook 2005. <http://usda.mannlib.cornell.edu/MannUsda/homepage.do>
- Food US, Administration Drug (2003) Food labeling: *trans* fatty acids in nutrition labeling, nutrient content claims, and health claims. *Fed Regist* 68:41434–41506
- Anderson KM, Wilson PW, Odell PM, Kannel WB (1991) An updated coronary risk profile. A statement for health professionals. *Circulation* 83:356–362
- Institute of Medicine (2002) Dietary reference intakes for energy, carbohydrate, fiber, fat, fatty acids, cholesterol, protein, and amino acids. In: *Dietary Fats: Total and Fatty Acids*. National Academies Press, Washington, DC, pp 422–541
- Uauy A, Aro A, Ghafoorunissa R, L'Abbá M, Mozaffarian D, Skeaff M, Stender S, Tavella M (2009) WHO scientific update on *trans* fatty acids: summary and conclusions. *Eur J Clin Nutr* 63:S68–S75
- Allison DB, Egan SK, Barraj LM, Caughman C, Infante M, Heimbach JT (1999) Estimated intakes of trans fatty and other fatty acids in the US population. *J Am Diet Assoc* 99:166–174
- Eckel RH, Borra S, Lichtenstein AH, Yin-Piazza SY (2007) Understanding the complexity of trans fatty acid reduction in the American diet: American Heart Association Trans Fat Conference 2006: report of the Trans Fat Conference Planning Group. *Circulation* 115:2231–2246
- Stender S, Astrup A, Dyerberg J (2009) What went in when trans went out? *N Engl J Med* 361:314–316
- Ratnayake WM, L'Abbe MR, Mozaffarian D (2009) Nationwide product reformulations to reduce trans fatty acids in Canada: when trans fat goes out, what goes in? *Eur J Clin Nutr* 63:808–811
- Hu FB, Stampfer MJ, Manson JE, Rimm E, Colditz GA, Rosner BA, Hennekens CH, Willett WC (1997) Dietary fat intake and the risk of coronary heart disease in women. *N Engl J Med* 337:1491–1499
- U.S. Department of Agriculture/Economics, Statistics and Market Information System (2008; accessed July 23, 2008) Oil Crops Yearbook 2008. <http://usda.mannlib.cornell.edu/MannUsda/homepage.do>
- U.S. Department of Agriculture (Nov. 2007). World Agricultural Production. Report No. WAP 11–07. USDA, Washington, DC
- Mozaffarian D, Clarke R (2009) Quantitative effects on cardiovascular risk factors and coronary heart disease risk of replacing partially hydrogenated vegetable oils with other fats and oils. *Eur J Clin Nutr* 63(Suppl 2):S22–S33
- Williams MJ, Sutherland WH, McCormick MP, de Jong SA, Walker RJ, Wilkins GT (1999) Impaired endothelial function following a meal rich in used cooking fat. *J Am Coll Cardiol* 33:1050–1055
- Brown JM, Shelness GS, Rudel LL (2007) Monounsaturated fatty acids and atherosclerosis: opposing views from epidemiology and experimental animal models. *Curr Atheroscler Rep* 9:494–500
- Jakobsen MU, O'Reilly EJ, Heitmann BL, Pereira MA, Balter K, Fraser GE, Goldbourt U, Hallmans G, Knekt P, Liu S, Pietinen P, Spiegelman D, Stevens J, Virtamo J, Willett WC, Ascherio A (2009) Major types of dietary fat and risk of coronary heart disease: a pooled analysis of 11 cohort studies. *Am J Clin Nutr* 89:1425–1432
- Baer DJ, Judd JT, Clevidence BA, Tracy RP (2004) Dietary fatty acids affect plasma markers of inflammation in healthy men fed controlled diets: a randomized crossover study. *Am J Clin Nutr* 79:969–973
- Sundram K, Karupaiah T, Hayes KC (2007) Stearic acid-rich interesterified fat and trans-rich fat raise the LDL/HDL ratio and plasma glucose relative to palm olein in humans. *Nutr Metab (Lond)* 4:3
- Lichtenstein AH, Appel LJ, Brands M, Carnethon M, Daniels S, Franch HA, Franklin B, Kris-Etherton P, Harris WS, Howard B, Karanja N, Lefevre M, Rudel L, Sacks F, Van Horn L, Winston M, Wylie-Rosett J (2006) Diet and lifestyle recommendations revision 2006: a scientific statement from the American Heart Association Nutrition Committee. *Circulation* 114:82–96

Serum Small Dense Low-density Lipoprotein Concentrations are Elevated in Patients with Significant Coronary Artery Stenosis and are Related to Features of the Metabolic Syndrome

Shima Yazdandoust · Seyyed Mohammad Reza Parizadeh · Mohsen Moohebbati · Parichehreh Yaghmaei · Amir Ali Rahsepar · Shima Tavallaie · Mohammad Soukhtanloo · Roshanak Khojasteh · Roghayeh Paydar · Afsoon Fazlinezhad · Homa Falsoleiman · Mashalla Dehghani · Majid Ghayour-Mobarhan · Gordon A. Ferns

Received: 17 February 2012 / Accepted: 30 July 2012 / Published online: 18 August 2012
© AOCs 2012

Abstract Serum small dense low-density lipoprotein (sd-LDL) concentrations were measured in patients with angiographically defined coronary artery disease (CAD) and compared to concentrations in healthy subjects. Five hundred and seventy patients with stable CAD were divided into CAD⁻ and CAD⁺ based on angiography. Patients in whom stenosis was <50 % in diameter were classified as having a ‘normal’ angiogram (CAD⁻), otherwise the patients were allocated to the CAD⁺ group. The CAD⁺ group was further subcategorized into single-, double- and triple-vessel disease (VD). Serum sd-LDL concentrations were significantly lower in controls compared with CAD⁺ and CAD⁻ patients ($P < 0.001$). Moreover, CAD⁺ patients had higher concentrations of sd-LDL than

CAD⁻ patients ($P < 0.01$). sd-LDL levels were not significantly associated with severity of CAD defined by the number of stenosed coronary arteries ($P = 0.245$). All participants were also categorized into subgroups with or without metabolic syndrome. Subjects with metabolic syndrome had higher levels of sd-LDL than subjects without metabolic syndrome ($P < 0.01$). Multiple linear regressions showed that in CAD patients, triacylglycerol, total-cholesterol, body mass index, and waist circumferences were the most important determinants of serum sd-LDL concentrations. We found that sd-LDL levels were significantly higher in patients presenting with symptoms of CAD. Moreover, patients with significant stenosis of their coronary arteries (>50 % stenosis) had higher levels of sd-LDL compared to patients without significant lesions.

Keywords Small dense low-density lipoprotein · Coronary artery disease · Severity · Metabolic syndrome · Angiography

S. Yazdandoust · P. Yaghmaei
Department of Biology, Faculty of Basic Sciences, Science Research Campus of Islamic Azad University, Tehran, Iran

S. Yazdandoust · S. M. R. Parizadeh · A. A. Rahsepar · S. Tavallaie · M. Soukhtanloo · R. Khojasteh · M. Ghayour-Mobarhan (✉)
Faculty of Medicine, Biochemistry of Nutrition Research Center, Mashhad University of Medical Science, Mashhad, Iran
e-mail: ghayourm@mums.ac.ir

M. Moohebbati · A. A. Rahsepar · S. Tavallaie · R. Paydar · A. Fazlinezhad · H. Falsoleiman · M. Dehghani · M. Ghayour-Mobarhan
Faculty of Medicine, Cardiovascular Research Center, Mashhad University of Medical Science, Mashhad, Iran

G. A. Ferns
Faculty of Health, Institute for Science and Technology in Medicine, University of Keele, Staffordshire, UK

Abbreviations

AHA/NHLBI	American Heart Association/National Heart, Lung and Blood Institute
ANOVA	One-way analysis of variance
BMI	Body mass index
CVD	Cardiovascular disease
CAD	Coronary artery Disease
FBG	Fasting blood glucose
HDL-C	High density lipoprotein cholesterol
hs-CRP	High sensitive C-reactive protein
MS	Metabolic syndrome
Sd-LDL	Small-dense low-density lipoprotein
SPECT	Single photon emission computed tomography
SVD	Single vessel disease

Introduction

A high serum low-density lipoprotein cholesterol (LDL-C) is a well established risk factor for cardiovascular disease (CVD) [1]. However, the qualitative features of LDL particles also appear to play an important role in the development of CVD as a novel risk factor, particularly the size spectrum of LDL-C particles and the predominance of small dense LDL (sd-LDL) particles. Several studies have investigated the possible role of sd-LDL in the pathogenesis of CVD and most have reported a positive association between the sd-LDL levels and the presence and severity of CVD [2–6].

It has been previously reported that the mean LDL particle size is smaller in those patients with proven coronary artery disease (CAD) based on angiography than for healthy controls; the authors observed that after multiple regression analysis the presence of high levels of sd-LDL was a significant and independent risk factor for CAD [2]. Moreover, it has been reported that men with an LDL particle size <25.6 nm had a significantly higher (2.2-fold increase) in the 5-year rate of ischemic heart disease compared with those men having an LDL particle size >25.6 nm [6] and hence it has been proposed that the presence of high concentrations of sd-LDL particles is a potent risk factor for CVD [3]. Previous studies have reported that there is a linear correlation between the sd-LDL concentrations and the risk of development of cardiovascular events [4, 5]. It has also been demonstrated that in healthy middle-age individuals the predominance of sd-LDL particles is associated with increased proinflammatory activation of peripheral mononuclear cells [7]. There is also evidence that sd-LDL is associated with the metabolic syndrome [8, 9]. In the present study, we aimed to evaluate the association between sd-LDL concentrations and severity of atherosclerosis defined by number of stenosed vessels in Persian population and also to assess the relationship between sd-LDL concentrations and several components of the metabolic syndrome.

Methods

Study Population

The study participants were selected from those subjects who underwent coronary angiography in the Quem Hospital, Mashhad in the north-eastern region of Iran. Angiography was principally indicated for stable angina, in patients who were positive for at least one objective test of myocardial ischemia including: exercise stress test, dobutamine stress echocardiography, and thallium SPECT (single photon emission computed tomography). The

exclusion criteria for the study were as follows; oral contraceptives or hormone replacement therapy, pregnancy, prior history of coronary angioplasty or coronary artery bypass graft, having overt clinical features of infection or chronic inflammatory disease, and all subjects were negative for viral markers of hepatitis and anti-HIV antibody. Moreover, patients with myocardial infarction within the previous 3 months, renal, hepatic or malignant diseases were excluded. Finally, 570 patients fulfilled the inclusion criteria and blood samples were collected from all of them prior to the procedure. These patients included those with a primary diagnosis of CAD and included diabetic patients. Patients who were diagnosed with CAD were treated with a statin, and those who were diagnosed as diabetic were treated with anti-diabetic drugs. No subjects in the control group were treated with statins, whilst 22.6 and 32.4 % of patients in CAD– and CAD+ group were previously treated with statins respectively.

Coronary angiograms were performed using routine procedures using a femoral approach on patients who were fasted prior to the procedure. Analysis of the angiograms was performed offline by a specialist cardiologist. The presence of one or more stenoses ≥ 50 % in diameter of at least one major coronary artery (left main, right coronary artery, left anterior descending, circumflex) was considered evidence of significant CAD [10]. Patients in whom stenosis was <50 % in diameter were categorized as having a ‘normal’ angiogram (CAD–). The CAD+ patients were sub-classified according to the number of significantly affected stenotic vessels into: single-vessel ($n = 114$), double-vessel ($n = 123$), and triple-vessel ($n = 174$) disease groups. One-hundred and nine healthy volunteers were also recruited as a normal control group. The control group comprised subjects who had never experienced any symptom nor had any signs of CVD. These subjects had no other apparent major disease. Information on smoking, drug use and family history of CAD was obtained via a questionnaire. The study protocol was approved by the Ethics Committee of Mashhad University of Medical Sciences (MUMS) and written informed consent was obtained from each participant.

Definition of Metabolic Syndrome

The American Heart Association/National Heart, Lung and Blood Institute (AHA/NHLBI) guideline was used to categorize subjects into metabolic syndrome-positive and metabolic syndrome-negative subgroups [11]. Metabolic syndrome was defined as the co-occurrence of at least three of the following five metabolic abnormalities: (1) elevated serum fasting glucose (≥ 100 mg/dl) or use of medication for hyperglycemia; (2) elevated serum triacylglycerols (≥ 150 mg/dl); (3) reduced serum high density lipoprotein-

cholesterol (HDL-C) (<40 mg/dl in males and <50 mg/dl in females); (4) elevated systolic (≥ 130 mmHg) or diastolic (≥ 85 mmHg) blood pressure or use of medication for hypertension; and (5) elevated waist circumference (≥ 102 cm in males and ≥ 88 cm in females).

Anthropometric and Other Measurements

Anthropometric parameters including weight, height, and body mass index (BMI) were measured in all subjects. Weight was measured with the subjects dressed in light clothing after an overnight fasting using a standard scale. BMI was calculated as weight (in kg) divided by height squared (in square meters). Blood pressure was measured twice while the patients were seated and rested, using a standard mercury sphygmomanometer. The systolic blood pressure was defined as the appearance of the first sound (Korotkoff phase 1), and the diastolic blood pressure was defined as the disappearance of the sound (Korotkoff phase 5) during deflation of the cuff.

Blood Sampling and Biochemical Analysis

Blood samples were taken from each patient for analysis prior to the procedure. Following venipuncture, blood samples were collected into Vacutainer[®] tubes and centrifuged at 15,000g for 15 min at 4 °C. After separation, aliquots of serum were frozen at –80 °C until analysis. A full fasted lipid profile comprising total-cholesterol, triacylglycerols, HDL-C and LDL-C were determined for each subject. Serum lipid and fasting blood glucose (FBG) concentrations were measured enzymatically with the use of commercial kits using a BT-3000 autoanalyzer (Biotechnica, Rome, Italy). High sensitive C-reactive protein (hs-CRP) was measured by a PEG-enhanced immunoturbidimetry method with an Alcyon[®] analyzer (ABBOTT, Chicago, IL, USA).

Determination of Serum sd-LDL Levels

Serum sd-LDL concentrations were determined using a method previously described in detail by Hirano et al. [12]. Briefly, a precipitation reagent (150 U/ml heparin-sodium salt and 90 mmol/l MgCl₂) was added to 0.5 ml of serum sample, mixed and incubated for 10 min at 37 °C. The samples were placed in an ice bath and allowed to stand for 15 min, and centrifuged at 15,000 rpm for 15 min at 4 °C. An aliquot of the clear supernatant was removed for LDL-cholesterol and apo B analyses. The LDL-C in the heparin-Mg²⁺ supernatant (containing HDL and sd-LDL) was directly and selectively determined by a homogeneous method. The concentration of the sd LDL-apoB in the heparin-Mg²⁺ supernatant was measured by an

immunoturbidimetric assay (Apo-B, Biosystems). In this method, as has been previously described, the cholesterol and apo-B values obtained by the precipitation method were similar to those obtained in the lipoprotein separated by ultracentrifugation, and the authors have found there was an excellent correlation between the two methods for sd LDL-cholesterol and apoB [12]. The coefficients of variation of inter- and intra-assay for the precipitation method were 1.3–1.6 and 1.7–3.7 %, respectively.

Statistical Analysis

All statistical analyses were performed using the SPSS for Windows[™], version 16 software package (SPSS Inc., Chicago, IL, USA). Data were expressed as means \pm SD (for parameters with a normal distribution) or median and interquartile range (for non-normally distributed data). Data that were normally distributed were analyzed using Student's *t* test (for 2 groups) or one-way analysis of variance (ANOVA) (for >2 groups). Data found to be non-normally distributed were analyzed using the non-parametric Mann–Whitney test (for 2 groups) or Kruskal–Wallis (for >2 groups). Categorical data were compared using the Chi-square test. A two-sided *P* value <0.05 was considered statistically significant. A Bonferroni correction was applied in the comparison of sd-LDL values between control, CAD– and CAD+ groups. Bivariate correlations between different parameters and sd-LDL levels were performed using Spearman's rank correlation and Kendall's test. Stepwise multiple linear regression analysis was used to determine which of the conventional risk factors could influence sd-LDL values. The predictor variables classified as dichotomous (1 = yes/0 = no) including diabetes mellitus, hyperlipidemia, hypertension, sex and smoking were entered into the initial model. Height, weight, FBG, waist circumference, hip circumference, HDL-C, LDL-C, systolic and diastolic blood pressure, triacylglycerol and number of narrowed vessels were entered as continuous variables in the same model. The effect of statin therapy was also analyzed as a covariate variable.

Results

Demographic Characteristics

Clinical and biochemical characteristics of all 3 groups (CAD+, CAD–, and control) are summarized in Table 1. LDL-C values were found to be significantly higher in controls than for patients. This may be attributed to the fact that a proportion of the CAD patients were on treatment with a statin, whilst none of controls were on statin treatment. With regard to the subgroups of CAD+ patients with

Table 1 Demographic and clinical characteristics of CAD positive and negative and control participants

	CAD-positive	CAD-negative	Controls	<i>P</i> value
Number	411	159	109	
Gender (M/F)	260/151	48/111	49/60	<0.001
DM (%)	40.3	27.8	0.9	<0.001
Smoking (%)	46	26.6	3.7	<0.001
HTN (%)	69.1	72.8	4.2	<0.001
HLP (%)	40.8	34.8	0	<0.001
Statin (%)	32.4	22.6	0	<0.001
Age (year)	58.31 ± 10.72	52.71 ± 11.53	56.52 ± 6.70	<0.001
Height (cm)	161.10 ± 10.32	157.80 ± 9.76	162.88 ± 7.26	<0.001
Weight (kg)	70.54 ± 14.51	68.45 ± 13.46	71.95 ± 10.76	0.262
BMI (kg/m ²)	27.40 ± 8.02	27.62 ± 5.74	27.14 ± 3.95	0.799
WC/HC ratio	0.95 ± 0.09	0.92 ± 0.09	0.94 ± 0.07	<0.01
WC (cm)	91.63 ± 13.42	89.93 ± 14.33	97.95 ± 10.62	<0.05
HC (cm)	95.75 ± 12.08	97.43 ± 12.77	103.53 ± 7.54	<0.001
FBG (mg/dl)	126.92 ± 63.13	110.69 ± 45.89	80.53 ± 10.74	<0.001
TC (mg/dl)	176.29 ± 49.62	179.51 ± 48.04	185.68 ± 39.75	0.054
LDL-C (mg/dl)	102.91 ± 37.21	102.03 ± 40.01	120.79 ± 29.21	<0.001
HDL-C (mg/dl)	43.16 ± 13.03	44.01 ± 11.96	48.63 ± 39.47	0.133
TAG (mg/dl)	131.00 (94.00–188.00)	121.50 (86.00–179.00)	109.00 (93.00–139.00)	0.003
hs-CRP (mg/dl)	3.25 (1.33–7.72)	1.89 (1.00–6.28)	2.20 (1.40–3.01)	<0.001
SBP (mmHg)	142.47 ± 30.51	142.84 ± 26.47	121.84 ± 12.38	<0.01
DBP (mmHg)	78.29 ± 13.68	76.38 ± 14.46	76.58 ± 9.13	0.371
Sd-LDL (mg/dL)*	34.42 (19.68–53.37)	30.21 (16.52–46.52)	16.52 (11–27.5)	<0.001

Values are presented as means ± SD or median (interquartile range). Comparisons between controls, CAD+ and CAD– patients were performed using ANOVA or Kruskal–Wallis and Chi-square test

CAD coronary artery disease, *sd-LDL* small dense low density lipoprotein, *DM* diabetes mellitus, *HTN* hypertension, *HLP* hyperlipidemia, *WC* waist circumference, *HC*; hip circumference, *FBG* fasting blood glucose, *BMI* body mass index, *TC* total-cholesterol, *LDL-C* low-density lipoprotein cholesterol, *HDL-C* high-density lipoprotein cholesterol, *TAG* triacylglycerol, *hs-CRP* high-sensitive C-reactive protein, *SBP* systolic blood pressure, *DBP* diastolic blood pressure

* Means before covariate analysis

different number of stenosed vessels [single-vessel disease (SVD), double-vessel disease (2VD), and triple-vessel disease (3VD)], no significant differences in demographic parameters were observed between different subgroups ($P > 0.05$, Table 2) except age. All subjects were divided into those with or without metabolic syndrome, based on AHA/NHLBI criteria. These data have been summarized in Table 3.

Sd-LDL Values Among Different Groups

Median sd-LDL values in the control group were [16.52 (11–27.5) (mg/dl)], being significantly lower than CAD– [30.21 (16.52–46.52) (mg/dl)] and CAD+ patients [34.42 (19.68–53.37) (mg/dl)] (comprising SVD, 2VD and 3VD) ($P < 0.001$). The results remained significant after Bonferroni correction. Moreover, CAD– patients had statistically lower median sd-LDL values in comparison with

patients with SVD, 2VD and 3VD ($P < 0.01$). In the CAD+ group, median sd-LDL values were [36.26 (20.60–54.42) (mg/dl)], [29.16 (18.63–49.16) (mg/dl)] and [35.73 (19.55–57.05) (mg/dl)] in SVD, 2VD and 3VD patients respectively. Median sd-LDL levels were not significantly different among SVD, 2VD and 3VD patients ($P = 0.245$). Gender and smoking status did not alter the sd-LDL values significantly between controls, CAD+ and CAD– patients ($P > 0.05$).

The subjects were also divided into those with or without co-existing metabolic syndrome. As would be expected, the sd-LDL levels were significantly higher in patients with metabolic syndrome [33.9 (19.16–52.31) (mg/dl)] in comparison with patients without metabolic syndrome [27.6 (16.52–45.34) (mg/dl)] ($P = 0.006$). Sd-LDL levels were evaluated based on different components of the metabolic syndrome. In those subjects with several components of the metabolic syndrome such as increased waist circumference,

Table 2 Demographic and clinical characteristics of CAD positive participants

	1VD	2VD	3VD	P value
Number	114	123	174	
Gender (M/F)	66/48	83/40	111/63	0.305
DM (%)	38.4	42.9	39.8	0.855
Smoking (%)	50.0	45.8	43.5	0.664
HTN (%)	65.2	70.6	70.6	0.840
HLP (%)	33.9	44.5	42.7	0.391
Statin (%)	28.9	27.6	37.9	0.384
Age (years)	55.24 ± 10.78	57.67 ± 10.29	60.79 ± 10.44	<0.001
Height (cm)	162.18 ± 9.85	160.94 ± 12.12	160.51 ± 9.18	0.344
Weight (kg)	71.31 ± 14.74	71.58 ± 16.49	69.31 ± 12.77	0.786
BMI (kg/m ²)	27.14 ± 5.19	28.38 ± 12.69	26.89 ± 4.51	0.981
WC/HC ratio	0.95 ± 0.07	0.95 ± 0.12	0.96 ± 0.07	0.301
WC (cm)	92.26 ± 13.14	91.09 ± 15.46	91.58 ± 12.07	0.963
HC (cm)	97.14 ± 12.59	95.49 ± 12.93	94.99 ± 11.08	0.494
FBG (mg/dl)	122.23 ± 51.82	129.29 ± 69.54	128.20 ± 65.09	0.821
TC (mg/dl)	173.26 ± 44.48	169.86 ± 42.89	182.94 ± 56.43	0.214
LDL-C (mg/dl)	95.93 ± 35.75	104.17 ± 35.29	106.54 ± 39.11	0.118
HDL-C (mg/dl)	44.12 ± 12.91	42.75 ± 11.08	42.83 ± 14.44	0.652
TAG (mg/dl)	135.00 (91.75–193.00)	130.00 (92.00–183.00)	135.00 (96.25–189.75)	0.929
hs-CRP (mg/dl)	2.41 (1.14–5.69)	4.02 (1.22–15.08)	3.32 (1.55–7.67)	0.167
SBP (mmHg)	138.65 ± 32.52	143.85 ± 29.62	144.01 ± 29.72	0.290
DBP (mmHg)	78.22 ± 12.67	78.42 ± 14.39	78.24 ± 13.88	0.984
Sd-LDL (mg/dL)	36.26 (20.60–54.42)	29.16 (18.63–49.16)	35.73 (19.55–57.05)	0.245

Values are presented as means ± SD or median (interquartile range). Comparisons between 1VD, 2VD and 3VD patients were performed using ANOVA or Kruskal–Wallis and Chi-square test

CAD coronary artery disease, *sd-LDL* small dense low density lipoprotein, *DM* diabetes mellitus, *HTN* hypertension, *HLP* hyperlipidemia, *WC* waist circumference, *HC* hip circumference, *FBG* fasting blood glucose, *BMI* body mass index, *TC* total-cholesterol, *LDL-C* low-density lipoprotein cholesterol, *HDL-C* high-density lipoprotein cholesterol, *TAG* triacylglycerol, *hs-CRP* high-sensitive C-reactive protein, *SBP* systolic blood pressure, *DBP* diastolic blood pressure, *VD* vessel disease

reduced HDL-C, and hypertension had significantly higher levels of sd-LDL in comparison with those subjects without above components (Table 4). This was not however the case for hyperglycemia and hypertriacylglycerolemia. When the females and males with and without metabolic syndrome were analyzed separately, it was found that females ($P = 0.006$) but not in males ($P = 0.108$), sd-LDL levels were significantly different between patients with and without metabolic syndrome.

Covariate Analysis

The effects of statin therapy were analyzed as a covariate variable. We found that in the present study, statin therapy had a covariate effect in 3 groups of CAD+, CAD– and control subjects, whilst we did not observe this effect in the CAD+ subgroups. After covariate analysis, we found similar results, as CAD+ and CAD– patients had significantly higher levels of sd-LDL than controls ($P < 0.001$).

Moreover, a significant difference was observed between patients with and without metabolic syndrome ($P < 0.05$). Covariate analysis also confirmed our previous results indicating that only in females ($P < 0.01$) but not in males ($P = 0.137$), sd-LDL levels were significantly different between patients with and without metabolic syndrome.

Correlation Between sd-LDL Values and CAD Risk Factors

Among the risk factors for CAD, in the CAD+ group waist and hip circumferences, waist/hip ratio, FBG, LDL-C, HDL-C, triacylglycerol (positively) and systolic blood pressure (inversely) were related to sd-LDL levels, however in CAD– patients sd-LDL levels were not associated with any of the classical CAD risk factors except waist circumference and triacylglycerol. In controls, FBG and triacylglycerol (positively) and LDL-C and hs-CRP (inversely) was associated with sd-LDL levels. No association was

Table 3 Demographic and clinical characteristics of patients with and without metabolic syndrome

	Total (<i>n</i> = 587)	MS+ (<i>n</i> = 215)	MS– (<i>n</i> = 372)	<i>P</i> value
Sd-LDL (mg/dL)*	29.7 (17–47.6)	33.9 (19.16–52.31)	27.6 (16.52–45.34)	0.006
Gender (F) (%)	47.4 %	61.4 %	34.9 %	<0.001
Age (years)	56.73 ± 10.60	57.50 ± 10.05	55.95 ± 11.36	0.091
Height (cm)	160.30 ± 10.15	158.24 ± 11.42	161.91 ± 9.23	<0.01
Weight (cm)	70.05 ± 14.09	74.06 ± 16.14	67.90 ± 12.40	<0.01
BMI (kg/m ²)	27.45 ± 7.31	29.96 ± 10.18	25.95 ± 4.71	<0.001
WC/HC ratio	0.94 ± 0.09	0.96 ± 0.07	0.93 ± 0.10	<0.001
WC (cm)	91.48 ± 13.63	96.63 ± 11.77	87.79 ± 13.55	<0.001
HC (cm)	96.58 ± 12.20	99.83 ± 10.24	94.30 ± 12.79	<0.001
FBG (mg/dl)	115.54 ± 56.58	135.71 ± 69.23	103.60 ± 41.47	<0.001
TC (mg/dl)	178.48 ± 47.91	177.00 ± 48.34	177.08 ± 44.99	0.937
LDL-C (mg/dl)	105.98 ± 37.12	102.64 ± 38.77	105.51 ± 36.35	0.191
HDL-C (mg/dl)	44.35 ± 20.56	37.89 ± 9.18	49.16 ± 25.44	<0.001
TAG (mg/dl)	124 (93.00–175.00)	166.5 (127.75–210.25)	105 (84.00–145.00)	<0.001
hs-CRP (mg/dl)	2.54 (1.26–6.20)	2.66 (1.26–6.22)	2.75 (1.26–6.88)	0.801
SBP (mmHg)	141.87 ± 29.26	155.67 ± 27.89	132.48 ± 26.42	<0.001
DBP (mmHg)	77.72 ± 13.77	81.99 ± 14.47	74.94 ± 12.55	<0.001
1VD (%)	16.8	29.4	27.6	0.895
2VD (%)	18.1	28.0	30.6	0.696
3VD (%)	25.6	42.7	41.8	0.914

Values are presented as means ± SD or median (interquartile range). Comparisons between patients with and without metabolic syndrome were performed using Student's *t* test or Mann–Whitney and Chi-square tests

Sd-LDL Small dense low density lipoprotein, *MS* metabolic syndrome, *WC* waist circumference, *HC* hip circumference, *FBG* fasting blood glucose, *BMI* body mass index, *TC* total-cholesterol, *LDL-C* low-density lipoprotein cholesterol, *HDL-C* high-density lipoprotein cholesterol, *TAG* triacylglycerol, *hs-CRP* high-sensitive C-reactive protein, *SBP* systolic blood pressure, *DBP* diastolic blood pressure, *VD* vessel disease

* Means before covariate analysis

Table 4 Sd-LDL values in subgroups with and without metabolic syndrome components

	Statin	MS– (<i>n</i> = 372)	MS+ (<i>n</i> = 215)	<i>P</i> value
Hypertriacylglycerolemia	No	23.37 (12.84–38.63)	32.31 (19.68–50.34)	0.129
	Yes	20.21 (8.5–38.23)	42.58 (19.68–61.13)	
Reduced HDL-C	No	23.37 (15.74–39.16)	32.84 (19.68–50.21)	<0.001
	Yes	19.68 (10.21–27.05)	36.79 (17.31–52.58)	
Elevated WC	No	31.79 (19.16–52.84)	33.89 (19.68–50.73)	0.005
	Yes	29.16 (17.71–47.71)	39.95 (22.58–56.79)	
Hypertension	No	43.10 (25.74–56.52)	33.37 (16.5–52.31)	0.002
	Yes	45.47 (24.95–58.63)	42.58 (27.97–60.73)	
Hyperglycemia	No	24.95 (11–44.95)	32.05 (17.01–48.89)	0.583
	Yes	28.10 (18.24–62.58)	44.68 (22.71–61.13)	

Group comparisons were performed using Kruskal–Wallis test with Bonferroni correction. As statin therapy was as a covariate variable, patients who were treated with stains were analyzed separately

Sd-LDL small dense low density lipoprotein, *MS* metabolic syndrome *HDL-C* high density lipoprotein-C, *WC* Waist circumference

found for traditional CAD risk factors such as diabetes mellitus, smoking, hypertension and hyperlipidemia with sd-LDL in 3 groups (Data have not been shown).

When the association between different biochemical and CAD risk factors with sd-LDL levels were assessed among

the 3 subgroups of CAD patients (SVD, 2VD and 3VD), we found that LDL-C and triacylglycerol (positively) and smoking (inversely) were associated with serum sd-LDL concentrations in patients with SVD. In the 2VD subgroup, only triacylglycerol was associated with the sd-LDL

concentrations; whilst in the 3VD subgroup, waist and hip circumference, waist/hip ratio, FBG, LDL-C, HDL-C, triacylglycerol (positively) and systolic blood pressure (inversely) were associated with the sd-LDL concentrations (Data not shown).

Association Between sd-LDL Values and CAD Risk Factors

Stepwise multiple linear regressions in CAD patients yielded the following equation for the prediction of serum

sd-LDL values [sd-LDL values = 0.115 (triacylglycerol) + 0.154 (total-cholesterol) – 0.891 (BMI) + 0.306 (waist circumferences)] (Table 5). Moreover, in patients with metabolic syndrome, the regression model yielded the following equation for the prediction of serum sd-LDL values in patients with metabolic syndrome [sd-LDL values = 0.149 (triacylglycerol) + 0.173 (total-cholesterol)] (Table 6). In patients without metabolic syndrome, the following equation for the prediction of serum sd-LDL values was found [sd-LDL values = 0.148 (total-cholesterol) + 9.07 (gender) + 0.061 (triacylglycerol) + 0.107

Table 5 Stepwise multiple linear regressions of factors affecting sd-LDL levels in CAD patients

Independent variable	Before covariate analysis			After covariate analysis		
	β	% Variation	<i>P</i> values	β	% Variation	<i>P</i> values
Triacylglycerol	0.115	16	0.0001	0.115	16.1	<0.001
Total-cholesterol	0.154	5.6	0.0001	0.16	6.1	<0.001
Body mass index	–0.891	1.2	0.002	–0.904	1.2	0.002
Waist circumferences	0.306	1.3	0.024	0.319	1.3	0.019

Diabetes mellitus, hyperlipidemia, hypertension, sex and smoking were entered into the initial model. Height, weight, fasting blood glucose, waist and hip circumference, high and low density lipoprotein-cholesterol, systolic and diastolic blood pressure blood pressure, triacylglycerol and number of narrowed vessels were entered as continuous variables in the same model. Regression analyses were performed before entering the effect of statin consumption as covariate variable

Sd-LDL small dense low density lipoprotein

Table 6 Stepwise multiple linear regressions of factors affecting sd-LDL levels in subjects with metabolic syndrome

Independent variable	Before covariate analysis			After covariate analysis		
	β	% Variation	<i>P</i> values	β	% Variation	<i>P</i> values
Triacylglycerol	0.149	19.6	0.0001	0.146	19.5	<0.001
Total-cholesterol	0.173	5.9	0.002	0.177	6.2	0.002

Diabetes mellitus, hyperlipidemia, hypertension, sex and smoking were entered into the initial model. Height, weight, fasting blood glucose, waist and hip circumference, high and low density lipoprotein-cholesterol, systolic and diastolic blood pressure blood pressure, triacylglycerol and number of narrowed vessels were entered as continuous variables in the same model. Regression analyses were performed before entering the effect of statin consumption as covariate variable

Sd-LDL small dense low-density lipoprotein

Table 7 Stepwise multiple linear regressions of factors affecting sd-LDL levels in subjects without metabolic syndrome

Independent variable	Before covariate analysis			After covariate analysis		
	β	% Variation	<i>P</i> values	β	% Variation	<i>P</i> values
Total-cholesterol	0.148	10.7	0.0001	0.146	10.5	<0.001
Sex	9.07	4.2	0.006	9.223	4.4	0.006
Triacylglycerol	0.061	2.5	0.015	0.062	2.7	0.015
Systolic blood pressure	0.107	1.9	0.043	–	–	–

Diabetes mellitus, hyperlipidemia, hypertension, sex and smoking were entered into the initial model. Height, weight, fasting blood glucose, waist and hip circumference, high and low density lipoprotein-cholesterol, systolic and diastolic blood pressure blood pressure, triacylglycerol and number of narrowed vessels were entered as continuous variables in the same model. Regression analyses were performed before entering the effect of statin consumption as covariate variable

Sd-LDL small dense low density lipoprotein

(systolic blood pressure)] (Table 7). After regression analysis and entering statin consumption as a covariate variable, we found similar results in all three regression analysis, but only in patients without metabolic syndrome systolic blood pressure lost its significance.

Discussion

To our knowledge, the predominance of the sd-LDL phenotype has not previously been studied in Persian CAD patients. We have however recently found higher levels of sd-LDL in SVD versus 3VD patients among 204 patients presenting with acute coronary syndrome [13]. Thus, we aimed to evaluate the possible relationship between the severity of CAD and sd-LDL concentrations within a larger sample size in which CAD was defined angiographically. In the present study, we found higher levels of sd-LDL concentrations in CAD+ patients compared with CAD– and healthy controls. Moreover, the sd-LDL values were significantly higher in CAD– patients, who had no significant stenosis in their coronary arteries based on angiography results, than healthy controls.

There have been previous studies that have reported a positive association between the sd-LDL levels, LDL particle size and the presence and severity of CVD [2–6]. It has also been reported that the mean LDL size was smaller in those patients with proven CAD based on angiography results than the healthy controls; Moreover, after multiple regression analysis, the presence of sd-LDL was found to be an important and independent risk factor for CAD development apart from the traditional cardiovascular risk factors [2]. Furthermore, it has been reported that men with an LDL particle size <25.6 nm had a significant 2.2-fold increase in the 5-year rate of ischemic heart disease compared with those men having an LDL particle size >25.6 nm [6] and it has been proposed that sd-LDL particles and high concentrations of sd-LDL are both important risk factors for CVD [3]. Previous reports indicate that there is a linear correlation between the sd-LDL concentrations and the risk of development of cardiovascular events [4, 5].

It has been proposed that sd-LDL may be involved in the pathogenesis of CVD via several mechanisms. Sd-LDL is one of the most atherogenic lipoprotein classes, and in comparison with larger-sized lipoproteins, sd-LDL particles have (1) a lower affinity for the LDL-receptors [14], (2) higher susceptibility to oxidative modification and (3) lesser antioxidants concentrations [15], (4) longer retention time in the circulation [16] and (5) enter the arterial wall more easily [17].

Although our method is less precise than the recently developed quantitative angiographic techniques such as

those using the Gensini coronary atherosclerosis scores and angiography itself may not accurately measure the CAD severity, but based on the number of stenosed vessels, we did not find any association between sd-LDL levels and severity of CAD; LDL- and total-cholesterol levels were comparable between patients with SVD, 2VD and 3VD. Some studies have reported results consistent with ours. Koba et al. [18] found that LDL size is not related to the severity and extent of coronary lesions determined by Gensini score. In other study by Kwon et al. [2], it was found that patients with more extensive CAD had smaller LDL particles. In other study, both sd-LDL mass concentrations and also sd-LDL particle size were measured simultaneously in patients with CAD and their association with severity of disease (based on Gensini score) was determined. The authors found that high sd-LDL concentrations were closely related to the CAD severity independently of classical coronary risk factors, while LDL particle size was not related. Thus, they suggested that the progression of CAD is closely linked to the amount of sd-LDL but not with the LDL particle size [3].

There is also strong evidence suggesting that sd-LDL is independently associated with the metabolic syndrome; Haffner et al. [19] have reported a decreased LDL size in subjects with multiple metabolic disorders. Moreover, several studies have suggested sd-LDL as a valuable marker for diagnosis and severity of the metabolic syndrome [8, 9]. It has been previously reported that increased plasma triacylglycerol and decreased HDL-C concentrations are usually accompanied by the presence of sd-LDL particles comprising together the atherogenic lipoprotein phenotype [20, 21]. Furthermore, in regard to important role of triacylglycerol in the composition and metabolic fate of lipoproteins, it has been reported that 80 % of patients with serum triacylglycerols above 1.5 mmol/L are characterized by the presence of sd-LDL subfraction pattern [22]. In the present study, as would be expected the subjects with metabolic syndrome had higher levels of sd-LDL values compared with subjects without metabolic syndrome. Moreover, when sd-LDL levels were analyzed with respect to metabolic syndrome components separately and statin therapy analyzed as a covariate variable, we found that all of metabolic syndrome components except hypertriacylglycerolemia and hyperglycemia appear to affect sd-LDL levels significantly. In a recent cross-sectional study by Kathiresan et al. [23], the number of sd-LDL particles was found to be greater in patients with metabolic syndrome and to increase with the number of components of metabolic syndrome.

In addition, multiple linear regressions showed that triacylglycerol, total-cholesterol, BMI, and waist-circumferences were the most important determinants of sd-LDL levels in CAD patients. Increased plasma triacylglycerol

plays a critical role in preponderance of sd-LDL in CAD patients, as our results and other studies support that LDL particle size is associated with serum triacylglycerol level [24]. Hirano et al. [12] have reported that sd-LDL is positively associated with LDL-C and triacylglycerol and inversely with HDL-C. When the females and males with and without metabolic syndrome were analyzed separately, it was found that only in females but not in males, sd-LDL levels were significantly different. As Coresh et al. [25], have previously reported, this finding can be explained by the fact that female subjects had significantly higher levels of HDL-C and lower levels of triacylglycerol in comparison with the male subjects.

In the present study, the regression model showed that sd-LDL levels were negatively associated with BMI in the CAD patients. While it would be expected that patients with a high BMI, would have high levels of sd-LDL, the regression model did not show this in our sample population. This may be explained by this notion that more than 30 % of the subjects in CAD group were treated with statins. Moreover, it has been previously revealed that statin therapy does not decrease the proportion of sd-LDL among total LDL particles, but in fact increases it, while predictably reducing total LDL-C, absolute amounts of sd-LDL, and absolute amounts of large, buoyant LDL [26]. It has been proposed that statins are able to up-regulate the activity of LDL receptor and decreases large, buoyant LDL more than sd-LDL, as statins increase LDL receptor activity; large, buoyant LDL is a better ligand for the LDL receptor than sd-LDL [27]. Hence, it may be concluded that those patients who have higher BMI, are more prone to development of CAD and these patients usually receive statins lifelong. Thus, it could be possible those patients, who have higher BMI and are treated with statins, would have lower sd-LDL values.

In conclusion, we found that sd-LDL levels are significantly higher in patients presenting with symptoms of CAD. Moreover, patients with evident stenosis in their coronary arteries had also higher levels of sd-LDL levels compared with those patients without overt lesions. Due to our results, sd-LDL concentrations are not associated with severity of CAD defined by number of stenosed coronary arteries. In addition to assessing the impact of lipid-lowering agents on sd-LDL size further studies are needed to assess the effect of lipid lowering drugs in reduction of sd-LDL concentrations.

Limitations

This study has a number of limitations; first, it was not possible to control for the dosage, or type of statin in our subgroups of our patients. It is possible that patients with more severe disease were on higher doses of statin, or more

potent statins, and this will cause increasing effects on sd-LDL. We did not examine the size distribution of sd-LDL. It is not clear whether the LDL size profile or sd-LDL concentration is the better risk marker. There was a potential problem of selection bias in our study, as patients included were those with extant CAD rather than an unselected metabolic syndrome population. As we looked at a rather selected group of patients with metabolic syndrome, that may not be representative of all patients with metabolic syndrome. We hope future studies provide more information about this that which one (size or concentrations of sd-LDL) would be more useful in clinical practice.

Acknowledgments The Mashhad University of Medical Science has provided the financial supports for this study. We are particularly grateful to the patients and their family members who volunteered to participate in this study. We are particularly grateful to Ms. Zahra Gharai Sheyda for data analysis. The results presented in this work have been taken from Shima Yazdandoust's thesis in Mashhad University of Medical Science.

Conflict of interest None.

References

- Ross R (1999) Atherosclerosis—an inflammatory disease. *N Engl J Med* 340:115–126
- Kwon SW, Yoon SJ, Kang TS, Kwon HM, Kim JH, Rhee J et al (2006) Significance of small dense low-density lipoprotein as a risk factor for coronary artery disease and acute coronary syndrome. *Yonsei Med J* 47:405–414
- Koba S, Hirano T, Ito Y, Tsunoda F, Yokota Y, Ban Y et al (2006) Significance of small dense low-density lipoprotein-cholesterol concentrations in relation to the severity of coronary heart diseases. *Atherosclerosis* 189:206–214
- Gardner CD, Fortmann SP, Krauss RM (1996) Association of small low-density lipoprotein particles with the incidence of coronary artery disease in men and women. *JAMA* 276:875–881
- St-Pierre AC, Cantin B, Dagenais GR, Mauriege P, Bernard PM, Despres JP et al (2005) Low-density lipoprotein subfractions and the long-term risk of ischemic heart disease in men: 13-year follow-up data from the Quebec Cardiovascular Study. *Arterioscler Thromb Vasc Biol* 25:553–559
- Lamarche B, St-Pierre AC, Ruel IL, Cantin B, Dagenais GR, Despres JP (2001) A prospective, population-based study of low density lipoprotein particle size as a risk factor for ischemic heart disease in men. *Can J Cardiol* 17:859–865
- Norata GD, Raselli S, Grigore L, Garlaschelli K, Vianello D, Bertocco S et al (2009) Small dense LDL and VLDL predict common carotid artery IMT and elicit an inflammatory response in peripheral blood mononuclear and endothelial cells. *Atherosclerosis* 206:556–562
- Krayenbuehl PA, Wiesli P, Schmid C, Lehmann R, Spinass GA, Berneis K (2008) Insulin sensitivity in type 2 diabetes is closely associated with LDL particle size. *Swiss Med Wkly* 138:275–280
- Gazi I, Tsimihodimos V, Filippatos T, Bairaktari E, Tselepis AD, Elisaf M (2006) Concentration and relative distribution of low-density lipoprotein subfractions in patients with metabolic syndrome defined according to the National Cholesterol Education Program criteria. *Metabolism* 55:885–891

10. Marroquin OC, Kip KE, Kelley DE, Johnson BD, Shaw LJ, Bairey Merz CN et al (2004) Metabolic syndrome modifies the cardiovascular risk associated with angiographic coronary artery disease in women: a report from the Women's Ischemia Syndrome Evaluation. *Circulation* 109:714–721
11. Grundy SM, Brewer HB Jr, Cleeman JI, Smith SC Jr, Lenfant C (2004) Definition of metabolic syndrome: Report of the National Heart, Lung, and Blood Institute/American Heart Association conference on scientific issues related to definition. *Circulation* 109:433–438
12. Hirano T, Ito Y, Saegusa H, Yoshino G (2003) A novel and simple method for quantification of small, dense LDL. *J Lipid Res* 44:2193–2201
13. Emadzadeh MR, Alavi MS, Soukhtanloo M, Mohammadpour T, Rahsepar AA, Tavallaie S et al (2012) Changes in small dense low-density lipoprotein levels following acute coronary syndrome. *Angiology*, s1–7. doi:[10.1177/0003319712441855](https://doi.org/10.1177/0003319712441855)
14. Chen GC, Liu W, Duchateau P, Allaart J, Hamilton RL, Mendel CM et al (1994) Conformational differences in human apolipoprotein B-100 among subspecies of low density lipoproteins (LDL). Association of altered proteolytic accessibility with decreased receptor binding of LDL subspecies from hypertriglyceridemic subjects. *J Biol Chem* 269:29121–29128
15. Tribble DL, Rizzo M, Chait A, Lewis DM, Blanche PJ, Krauss RM (2001) Enhanced oxidative susceptibility and reduced antioxidant content of metabolic precursors of small, dense low-density lipoproteins. *Am J Med* 110:103–110
16. Packard CJ, Demant T, Stewart JP, Bedford D, Caslake MJ, Schwertfeger G et al (2000) Apolipoprotein B metabolism and the distribution of VLDL and LDL subfractions. *J Lipid Res* 41:305–318
17. Bjornheden T, Babyi A, Bondjers G, Wiklund O (1996) Accumulation of lipoprotein fractions and subfractions in the arterial wall, determined in an in vitro perfusion system. *Atherosclerosis* 123:43–56
18. Koba S, Hirano T, Kondo T, Shibata M, Suzuki H, Murakami M et al (2002) Significance of small dense low-density lipoproteins and other risk factors in patients with various types of coronary heart disease. *Am Heart J* 144:1026–1035
19. Haffner SM, Mykkanen L, Robbins D, Valdez R, Miettinen H, Howard BV et al (1995) A preponderance of small dense LDL is associated with specific insulin, proinsulin and the components of the insulin resistance syndrome in non-diabetic subjects. *Diabetologia* 38:1328–1336
20. Rizzo M, Berneis K (2006) Low-density lipoprotein size and cardiovascular risk assessment. *QJM* 99:1–14
21. Austin MA, King MC, Vranizan KM, Krauss RM (1990) Atherogenic lipoprotein phenotype. A proposed genetic marker for coronary heart disease risk. *Circulation* 82:495–506
22. Demacker PN, Veerkamp MJ, Bredie SJ, Marcovina SM, de Graff J, Stalenhoef AF (2000) Comparison of the measurement of lipids and lipoproteins versus assay of apolipoprotein B for estimation of coronary heart disease risk: a study in familial combined hyperlipidemia. *Atherosclerosis* 153:483–490
23. Kathiresan S, Otvos JD, Sullivan LM, Keyes MJ, Schaefer EJ, Wilson PW et al (2006) Increased small low-density lipoprotein particle number: a prominent feature of the metabolic syndrome in the Framingham Heart Study. *Circulation* 113:20–29
24. Tsunoda F, Koba S, Hirano T, Ban Y, Iso Y, Suzuki H et al (2004) Association between small dense low-density lipoprotein and postprandial accumulation of triglyceride-rich remnant-like particles in normotriglyceridemic patients with myocardial infarction. *Circ J* 68:1165–1172
25. Coresh J, Kwiterovich PO Jr, Smith HH, Bachorik PS (1993) Association of plasma triglyceride concentration and LDL particle diameter, density, and chemical composition with premature coronary artery disease in men and women. *J Lipid Res* 34:1687–1697
26. Choi CU, Seo HS, Lee EM, Shin SY, Choi UJ, Na JO et al (2010) Statins do not decrease small, dense low-density lipoprotein. *Tex Heart Inst J* 37:421–428
27. Nigon F, Lesnik P, Rouis M, Chapman MJ (1991) Discrete subspecies of human low density lipoproteins are heterogeneous in their interaction with the cellular LDL receptor. *J Lipid Res* 32:1741–1753

Synthesis and Characterization of Novel n-9 Fatty Acid Conjugates Possessing Antineoplastic Properties

Azmat A. Khan · Ahmad Husain · Mumtaz Jabeen ·
Jamal Mustafa · Mohammad Owais

Received: 18 November 2011 / Accepted: 30 July 2012 / Published online: 26 August 2012
© AOCS 2012

Abstract The present study enumerates the synthesis, spectroscopic characterization, and evaluation of anticancer potential of esters of two n-9 fatty acids viz., oleic acid (OLA) and ricinoleic acid (RCA) with 2,4- or 2,6-diisopropylphenol. The synthesis strategy involved esterification of the hydroxyl group of diisopropylphenol (propofol) to the terminal carboxyl group of n-9 fatty acid. The synthesized propofol-n-9 conjugates having greater lipophilic character were tested initially for cytotoxicity in-vitro. The conjugates showed specific growth inhibition of cancer cell lines whereas no effect was observed in normal cells. In general, pronounced growth inhibition was found against the human skin malignant melanoma cell line (SK-MEL-1). The anticancer potential was also determined by testing the effect of these conjugates on cell migration, cell adhesion and induction of apoptosis in SK-MEL-1 cancer cells. Propofol-OLA conjugates significantly induced apoptosis

in contrast to propofol-RCA conjugates which showed only weak signals for cytochrome *c*. Conclusively, the synthesized novel ester conjugates showed considerable moderation of anti-tumor activity. This preliminary study places in-house synthesized conjugates into the new class of anticancer agents that possess selectivity toward cancer cells over normal cells.

Keywords Ester conjugates · Antineoplastic · Apoptosis · Caspase-3 · Cytochrome *c* · Cytotoxicity · Cancer cell line

Abbreviations

A549	Human lung carcinoma
ARA	Arachidonic acid
DCC	<i>N,N</i> -dicyclohexylcarbodiimide
DMAP	4-(Dimethyl amino pyridine)
HepG2	Human liver hepatocellular carcinoma
HFL1	Human lung fibroblast
HL-60	Human leukemia
IC-50	Concentration of a test compound that reduces 50 % of cell viability
LNA	Linoleic acid
MDA-MB-361	Ductal breast carcinoma
MUFA	Monounsaturated fatty acid(s)
OLA	Oleic acid
Propofol	Diisopropylphenol
PUFA	Polyunsaturated fatty acid(s)
RCA	Ricinoleic acid
RPMI	Rosewell Park Memorial Institute
SK-MEL-1	Human skin malignant melanoma
UFA	Unsaturated fatty acid(s)
2,4P-OLA	2,4-Diisopropylphenol-oleic acid
2,6P-OLA	2,6-Diisopropylphenol-oleic acid
2,4P-RCA	2,4-Diisopropylphenol-ricinoleic acid
2,6P-RCA	2,6-Diisopropylphenol-ricinoleic acid

Electronic supplementary material The online version of this article (doi:10.1007/s11745-012-3707-9) contains supplementary material, which is available to authorized users.

A. A. Khan (✉) · M. Owais
Interdisciplinary Biotechnology Unit, Aligarh Muslim
University, Aligarh 202002, India
e-mail: azmatbiotech@gmail.com

A. Husain
Department of Chemistry, Aligarh Muslim University,
Aligarh 202002, India

M. Jabeen
Department of Zoology, Aligarh Muslim University,
Aligarh 202002, India

J. Mustafa
University Polytechnic, Aligarh Muslim University,
Aligarh 202002, India

Introduction

Dietary constituents are reported to be one of the main safety factors in the prevention and pathobiology of cancer [1]. They are now being used effectively as an alternative to the conventional anticancer drugs. A range of natural sources like castor oil, olive oil, almonds, peanuts, red meat, fish oil, etc., contains the *n*-hydroxy unsaturated fatty acids (UFA). These fatty acids have been shown to play an important role in inhibition of various type of cancer and manifest less side-effects when compared to standard chemotherapeutic agents [2, 3]. The UFA are taken up rapidly by tumor cells [4] and their hydrophobic nature facilitates their rapid incorporation into the lipid bilayer of cells [5, 6] resulting in disruption of membrane structure and fluidity [7]. Considering these characteristics of UFA, they are now being used exogenously to enhance the anticancer activity of various chemotherapeutic agents [8, 9] and for tumor-targeting drug delivery.

To achieve effective tumor-specific drug delivery, the UFA have been chemically modified to enhance their specificity, potent biological activity and reduction in toxicity against a range of therapeutic targets [10]. Previously, we had demonstrated efficient synthesis of *n*-6 polyunsaturated fatty acid (PUFA)-esters where PUFA was conjugated with propofol in order to enhance its activity, lipid-solubility, bioavailability, and decrease its side-effects [11]. Propofol (diisopropylphenol) is one of the most popular chemical agents used for induction of anesthesia and is non-toxic to humans at high concentrations (3–8 µg/ml; 20–50 µM) [12]. The presence of two isopropyl groups at the ortho position with respect to the hydroxyl group in propofol exerts a steric hindrance that prevents access of hydrophilic molecules to the hydroxyl group. This makes the molecule highly hydrophobic. Although it is an intravenous sedative-hypnotic agent, propofol also shows preferential scavenging of organo-radical species. Clinically relevant concentrations of propofol are reported to decrease the metastatic potential of human cancer cells [13] and have been shown to induce apoptosis involving both extrinsic and intrinsic pathways [14]. Our preliminary studies showed a noticeable feature of selective inhibition of cancerous cells by the novel PUFA-ester conjugates [11]. These results encouraged the present work, which is directed towards the synthesis of a new class of *n*-9 monounsaturated fatty acid (MUFA)-ester conjugates possessing anticancer activity.

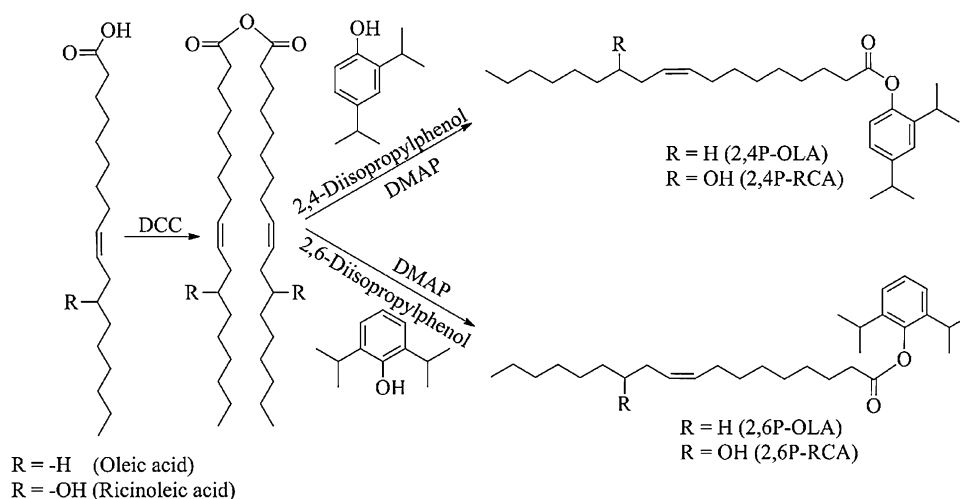
Amongst UFA, the MUFA, despite being crucial to the body, have received less attention than *n*-3 and *n*-6 PUFA counterparts. Primarily, MUFA offer major health benefits

viz., promotes healthy blood lipid profiles, mediates blood pressure, improves insulin sensitivity and regulates glucose levels [15]. The major MUFA in human diets is oleic acid (OLA; *cis*-9-octadecenoic acid). It is found in several animal and vegetable oils; olive oil being its richest source. High concentrations of OLA are found to lower the levels of cholesterol, atherosclerosis and aid in cancer prevention [16–18]. Curiosity has been stimulated in OLA since the discovery of its role in protection from breast cancer [19–23]. Various epidemiological and animal model studies have correlated the consumption of OLA rich olive oil with reduction in cancer incidences [24–27]. In-vitro studies conducted by Menendez et al. [19] have shown the use of OLA in synergistically enhancing the effectiveness of various anticancer agents. The higher concentration of OLA has been revealed to induce DNA fragmentation and loss of membrane structure of various cancer cell lines [28]. Recently, Brinkmann et al. [29] suggested that OLA has a great potential to lyse the membrane of target cells and also induce apoptosis in cancer cells. The augmentation of the antiproliferative effect of OLA can be ascribed partly to its unique structure. The presence of one double bond (monounsaturated) at the 9th position in a 18-carbon chain makes it much less susceptible to oxidation and thereby imparts higher stability.

Ricinoleic acid (RCA; *cis*-12-hydroxyoctadec-9-enoic acid), the other MUFA has not yet been investigated for its role in cancer prevention. In yeast, RCA is a possible intermediate in the conversion of oleic acid to linoleic acid [30]. RCA produced through the hydrolysis of castor oil is a pharmacologically active molecule [31]. Structurally RCA is similar to OLA, but with a slight difference, where one hydroxyl group is present at the 12th carbon position. Unlike other UFA, the presence of an additional hydroxyl group provides several interesting properties to RCA by which it can be converted to useful chemical analogs. A study on the biological action of RCA has shown that it does not exert any hyper-analgesic effect towards heat and chemical nociceptive stimuli [32]. These properties render RCA as a promising analgesic and anti-inflammatory agent for local application. The surfactant properties of RCA have been considered to impart its antibacterial activity [33]. Moreover, its chemical structure has been used as a basis for the development of novel capsaicin-like compounds [34].

Here, we report the synthesis of four novel *n*-9 MUFA-ester derivatives (Scheme 1). The conjugates were spectroscopically analyzed to establish their chemical structures, followed by evaluation of their in-vitro anticancer efficacy. These conjugates were tested for their ability on apoptosis, cell migration and cell adhesion.

Scheme 1 Schematic representation of chemical synthesis of propofol-OLA and propofol-RCA conjugates



Materials and Methods

Materials

Oleic acid, ricinoleic acid, 2,6-diisopropylphenol, 2,4-diisopropylphenol, *N,N*-dicyclohexylcarbodiimide (DCC), 4-dimethylaminopyridine (DMAP), Rosewell Park Memorial Institute (RPMI)-1640 medium, Eagle's Minimum Essential Medium (EMEM); 2-[4-(2 hydroxyethyl)piperazine-1-yl]ethane sulfonic acid (HEPES); phenylmethylsulfonyl fluoride (PMSF); EDTA; dithiothreitol (DTT); 3,4,5-dimethylthiazol-2-yl-2, 5-diphenyl-tetrazolium bromide (MTT), propidium iodide, sodium dodecyl sulphate (SDS) were acquired from Sigma-Aldrich. Fetal calf serum (FCS) was procured from Bio-Whittaker. Thin-layer chromatography plates (60A, 0.2 mm thick) and silica gel (60–120 mesh) were purchased from Fisher Scientific. Dichloromethane (DCM), methanol, ethanol, chloroform, *n*-hexane, diethyl ether, sucrose, KCl, MgCl₂, dimethyl sulfoxide (DMSO) and acetic acid were procured from Merck. Cell migration and adhesion kits were obtained from Cell Biolabs, Inc.

Monoclonal antibodies such as anti-caspase-3, anti-cytochrome *c* and anti- β -actin were purchased from BD Biosciences (San Diego, CA). Secondary anti-mouse peroxidase-conjugated antibody was from Amersham Pharmacia Biotech. A chemiluminescence detection kit was purchased from GE healthcare.

Cell Lines and Culture Conditions

Cell lines SK-MEL-1 (ATCC# HTB-67), HepG2 (ATCC# HB-8065), MDA-MB-361 (ATCC# HTB-27), A549 (ATCC# CCL-185), HL 60 (ATCC# CCL-240) and non-cancerous HFL1 (ATCC# CCL-153) were obtained from the American Type Culture Collection (Rockville, MD). SK-MEL-1 and HepG2 cell lines were maintained in

EMEM whereas MDA-MB-361, A549, HL-60 and HFL1 were maintained in RPMI medium. To make the complete growth medium, both types of media were supplemented with 10 % (v/v) heat-inactivated FCS, 2 mM L-glutamine, 100 U/ml penicillin and 100 μ g/ml streptomycin. All cells were maintained at 37 °C in a 95 % humidified atmosphere containing 5 % CO₂. Cells were screened periodically for mycoplasma contamination.

Synthesis and Purification of Propofol-*n*-9 Conjugates

A synthesis approach was conceived using the protocol of Siddiqui et al. [35]. However, several modifications were incorporated in our lab for synthesis of the final product [11]. A 1 mmol amount of the respective MUFA was dissolved in 5 ml dichloromethane (DCM). To this mixture, 0.45 mmol of coupling reagent *N,N*-dicyclohexylcarbodiimide (DCC) was added and the reaction mixture was stirred for 10 min at room temperature (23–25 °C). Finally, 1 mmol of one of the propofol isomers (2,6-propofol/2,4-propofol) was added and the reaction mixture was esterified in the presence of a catalyst, 0.152 mmol 4-dimethylaminopyridine (DMAP). The reaction mixture was stirred for a period of 10 h in the dark. The reaction was stopped by filtration and the filtrate was concentrated under reduced pressure to yield the product. The progress of the reaction was monitored on thin layer chromatography (TLC) in iodine vapour. Finally, the synthesized product was purified by silica gel column chromatography with solvent system *n*-hexane and diethyl ether (1:1).

2,4-Diisopropylphenol-Oleic Acid (2,4P-OLA)

Yield 82 %; ¹H NMR (CDCl₃, δ _H): 0.88 (*t*, *J* = 3.76 Hz, 3H), 1.20 (*d*, *J* = 6.92 Hz, 12H), 1.25–1.46 (*m*, 22H), 1.79

(*quin*, $J = 7.32$ Hz, 2H), 2.0 (*q*, 2H), 2.6 (*t*, $J = 7.64$ Hz, 2H), 2.8 (*t*, $J = 6.68$ Hz, 1H), 2.9 (*m*, 1H), 5.3 (*m*, 2H), 7.14 (*d*, $J = 2.2$ Hz, 1H), 7.16 (*s*, 1H), 7.20 (*d*, $J = 2.88$ Hz, 1H); ^{13}C NMR (CDCl_3 , δ_{C}): 14.1, 22.6, 25.06, 25.66, 27.23, 27.53, 29.18–29.63, 31.55, 34.22, 123.87, 126.42, 127.91, 128.12, 130.02, 130.25, 140.32, 145.62, 172.38. FAB-MS: $[\text{M}]^+$ 442. Anal. calc. for $\text{C}_{30}\text{H}_{50}\text{O}_2$: C, 81.39; H, 11.38. Found: C, 80.93; H, 11.43. IR (KBr, cm^{-1}): 2926, 2860, 1758, 1460, 1137.

2,6-Diisopropylphenol-Oleic Acid (2,6P-OLA)

Yield 85 %; ^1H NMR (CDCl_3 , δ_{H}): 0.88 (*t*, $J = 3.92$ Hz, 3H), 1.19–1.43 (*m*, 34H), 1.76 (*m*, 2H), 2.0 (*m*, 2H), 2.57 (*t*, $J = 7.48$ Hz, 2H), 2.9 (*m*, 2H), 5.35 (*m*, 2H), 6.89 (*d*, $J = 5.96$ Hz, 2H), 7.0 (*t*, $J = 6.08$ Hz, 1H); ^{13}C NMR (CDCl_3 , δ_{C}) 14.23, 22.71, 24.31, 24.97, 27.22, 27.50, 29.15–29.79, 33.56, 34.13, 121.90, 124.08, 124.37, 130.06, 130.25, 140.32, 146.52, 172.68. FAB-MS: $[\text{M}]^+$ 442. Anal. calc. for $\text{C}_{30}\text{H}_{50}\text{O}_2$: C, 81.39; H, 11.38. Found: C, 80.99; H, 11.47. IR (KBr, cm^{-1}): 2929, 2863, 1757, 1453, 1142, 786, 720.

2,4-Diisopropylphenol-Ricinoleic Acid (2,4P-RCA)

Yield 84 %; ^1H NMR (CDCl_3 , δ_{H}): 0.88 (*t*, $J = 9.88$ Hz, 3H), 1.19–1.48 (*m*, 30H), 1.77 (*m*, 2H), 2.07 (*q*, 2H), 2.23 (*t*, $J = 13.72$ Hz, 2H), 2.56 (*t*, $J = 15.0$ Hz, 2H), 2.8 (*m*, 1H), 2.9 (*m*, 1H), 3.6 (*m*, 1H), 5.4 (*m*, 1H), 5.5 (*m*, 1H), 6.88–6.90 (*d*, $J = 5.76$ Hz, 1H), 7.04 (*d*, $J = 8.0$ Hz, 1H), 7.12 (*s*, 1H); ^{13}C NMR (CDCl_3 , δ_{C}): 71.58, 125.24, 133.42, 134.1, 141.02, 150.93, 172.73. FAB-MS: $[\text{M}]^+$ 458, $[\text{M}-17]^+$ 441. Anal. calc. for $\text{C}_{30}\text{H}_{50}\text{O}_3$: C, 78.55; H, 10.99. Found: C, 78.93; H, 11.23. IR (KBr, cm^{-1}): 2955, 2874, 1735, 1499, 1447, 1252, 1174, 817, 740, 634, 544.

2,6-Diisopropylphenol-Ricinoleic Acid (2,6P-RCA)

Yield 86 %; ^1H NMR (CDCl_3 , δ_{H}): 0.80 (*t*, $J = 6.96$ Hz, 3H), 1.11–1.40 (*m*, 30H), 1.68–1.72 (*m*, 2H), 1.98 (*q*, 2H), 2.1 (*t*, $J = 13.6$ Hz, 2H), 2.54 (*t*, $J = 15.08$ Hz, 2H), 2.8 (*m*, 2H), 3.5 (*m*, 1H), 5.3 (*m*, 1H), 5.5 (*m*, 1H), 6.80–6.82 (*d*, $J = 15.44$ Hz, 1H), 6.9 (*t*, $J = 7.6$ Hz, 1H); ^{13}C NMR (CDCl_3 , δ_{C}) 71.52, 120.6, 123.87, 126.42, 133.67, 139.54, 145.61, 172.40. FAB-MS: $[\text{M}-17]^+$ 441. Anal. calc. for $\text{C}_{30}\text{H}_{50}\text{O}_3$: C, 78.55; H, 10.99. Found: C, 78.98; H, 11.13. IR (KBr, cm^{-1}): 2934, 2869, 1749, 1452, 1364, 1171, 820, 733.

Spectral Analysis of Propofol-n-9 Conjugates

The formation of propofol-n-9 conjugates was confirmed by various spectroscopic studies. The presence of diisopropyl-phenolate in the synthesized conjugates was

assessed by UV spectroscopy on a UV Mini-1240 spectrophotometer. The absorption spectra were measured between 200 and 600 nm. The infrared spectra of the conjugates were recorded on a Nicolet-6700 FT-IR instrument. An aliquot (ten microliter of $1\ \mu\text{g}/\mu\text{l}$) of the conjugate was deposited exactly within the cell limit and scanned as a thin film after evaporation of solvent. Absorption peaks of synthesized conjugates were observed at 1757.40/1758.73 (2,6P-OLA/2,4P-OLA) and 1740.07/1735.00 (2,6P-RCA/2,4P-RCA). The presence of $\nu(\text{C}=\text{O})$, $\nu(\text{C}-\text{O})$, aromatic C–H (propofol) and aliphatic C–H bond and absence of hydroxyl ($-\text{OH}$) absorption peak corresponds to the data published previously [11]. The formation of new conjugates was elucidated with ^1H - and ^{13}C -NMR spectra on a BRUKER AVANCE II 400 NMR spectrometer. The FAB-MS spectra were recorded on a JEOL SX 102 Mass Spectrometer/Data System using Argon/Xenon (6 kV, 10 mA) as the FAB gas.

Analysis of Growth Inhibition of Cancer Cells

The conjugates were examined for their cytotoxicity against five different types of cancer cell lines viz., SK-MEL-1 (human skin malignant melanoma), HepG2 (human liver hepatocellular carcinoma), MDA-MB-361 (human ductal carcinoma, breast), A549 (human lung carcinoma), HL-60 (human leukemia, acute promyelocytic) as well as one non-cancerous HFL1 (human lung fibroblast) using a standard MTT reduction assay. Cells in exponential growth were seeded into 96-well plates at a concentration of 5×10^5 cells/200 μl /well and allowed to grow in their respective medium containing 5 % FCS. After 24 h, cells were treated with different concentrations of test conjugate or parent controls (OLA and RCA only/propofol only) at a concentration range of 0–15 μM . Vehicle control (ethanol only) and positive control (doxorubicin) cells were cultured using the same conditions. Following 94 h incubation, the medium was removed and replaced with fresh medium. MTT reagent (5 mg/ml in PBS) was added to each well at a volume of 1:10 and incubated for 2–3 h at 37 °C. After treatment, 100 μl of DMSO was added to each well after carefully aspirating the supernatants. Absorbance was measured at 620 nm in a multi-well plate reader. Triplicate wells were prepared for each individual concentration. Dose–response curves were plotted as percentages of the cell absorbance. Drug sensitivity was expressed in terms of the concentration of drug required for a 50 % reduction in cell viability (IC_{50}).

Toxicity Analysis of Propofol-n-9 Conjugates

Preliminary acute toxicity of conjugates was tested through erythrocyte lysis test wherein hemoglobin, released as a

result of membrane leakage or disruption caused by exposure to high doses of the drug, was measured spectrophotometrically [36]. Fresh human blood in heparin was subjected to centrifugation at 1,000g for 15 min at 4 °C. Buffy coat as well as plasma was discarded. The washed erythrocytes were diluted with isotonic buffer (10 mM phosphate buffer, 150 mM NaCl) and 50 % hematocrit was prepared. To study the extent of haemolysis, the suspension of RBCs was incubated with 150 μ M (dose that induces cytotoxicity concentrated ten times) of conjugates, propofol only as well as OLA and RCA only at 37 °C for 1 h. Ethanol was taken as the vehicle control. After 1 h, the reaction mixture was centrifuged at 1,500g and the supernatant was collected and analyzed by UV–Visible spectroscopy ($\lambda_{\text{max}} = 576$ nm) for released hemoglobin.

Analysis of Cancer Cell Migration

Cell migration was performed with CytoSelect 24-Well Cell Migration Assay (Cell Biolabs, Inc.). Under sterile conditions, the 24-well migration plate was allowed to warm up at room temperature for 10 min. The lower well of the migration plate was supplemented with 500 μ l of EMEM containing 10 % fetal bovine serum with or without (control) test conjugates. To the inside of each insert 100 μ l of SK-MEL-1 (0.5–1.0 $\times 10^6$ cells/ml) cell suspension was added. The plates were incubated for 8 h at 37 °C in a humidified CO₂ incubator. After incubation, the media from inside the inserts was carefully aspirated and the non-migratory cells were removed using cotton-tipped swabs. The inserts were transferred to a clean well containing 400 μ l of cell stain solution and incubated for 10 min at room temperature. The stained inserts were gently washed several times and then transferred again to an empty well. Finally, 200 μ l of extraction solution per well was added and incubated for 10 min on an orbital shaker. From each sample, 100 μ l was taken in a 96-well microtiter plate and the absorbance at 560 nm was read in a plate reader.

Analysis of Cancer Cell Adhesion

The cell adhesion assay was performed with a CytoSelect 24-Well Cell Adhesion Assay kit (Cell Biolabs, Inc.). Under sterile conditions, the ECM adhesion plate was allowed to warm up at room temperature for 10 min. Then 150 μ l of the SK-MEL-1 cell suspension (0.1–1.0 $\times 10^6$ cells/ml) in serum free media with control or test conjugates was added to each well. The plates were incubated for 30–90 min in a CO₂ incubator. The wells were washed three times with PBS and the adhered cells were stained with 200 μ l of cell stain solution for 10 min at room temperature. The excess stain was removed by washing

4–5 times with distilled water. After air drying the wells, 200 μ l of extraction solution per well was added and then incubated for 10 min on an orbital shaker. Then 150 μ l from each extracted sample was transferred to a 96-well microtiter plate and the absorbance at 560 nm was read in a plate reader. Absorbance of dye in the control (vehicle-treated) cells was regarded as 100 % adherence and the percentage adherence of treated cells was calculated in comparison with that of the control cells.

Apoptosis Assay

Cancer cells (1 $\times 10^7$ cells per well) were grown in 6-well plates in a serum free culture medium (respective to the cell line used) in a humidified CO₂ incubator at 37 °C. After 24 h, confluent cells were treated with control (ethanol only) or parent control (OLA/RCA only/propofol only) or test conjugates and incubated for 24 h again. Following incubation, cells were harvested and washed twice in PBS. The cells were suspended in 50 μ l of ice-cold TNN buffer containing 50 mM Tris–HCl pH 7.4, 100 mM NaCl, 5 mM EDTA, 0.5 % Nonidet P-40, 1 μ g/ml pepstatin, 0.5 mM EGTA, 200 μ M PMSF, 0.5 mM DTT and 1 μ g/ml of leupeptin and homogenized in a Teflon homogenizer. A post-nuclear fraction was prepared by centrifugation for 5 min at 2,000 rpm at 4 °C. The supernatant was further centrifuged for 20 min at 10,000 rpm at 4 °C and the resultant cytosolic fraction was used for detecting the expression of two apoptotic factors; cytochrome *c* and caspase-3.

Western Blotting

Equal amounts of protein in SDS sample buffer were subjected to 10 % SDS-polyacrylamide gel electrophoresis [37]. Immunoblotting of resolved proteins was done on a nitrocellulose membrane. Nonspecific binding on the nitrocellulose membrane was minimized by blocking for 1 h at room temperature with PBS-T [PBS (pH 7.5) and 0.05 % Tween-20] containing 5 % (w/v) non-fat dry milk. The treated membrane was washed in PBS-T and then incubated overnight at 4 °C with specific primary antibodies (monoclonal anti-cytochrome-*c* or monoclonal anti-caspase-3) in PBS-T containing 5 % (w/v) BSA. The membranes were again washed in PBS-T, anti-mouse peroxidase-conjugated secondary antibodies in PBS-T were added for 2 h, and immunoreactive bands were detected by enhanced chemiluminescence detection kit. Blots were re-probed with an antibody for β -actin to control for equal protein loading and transfer. Densitometric values of protein bands were quantified using Alpha Image Analysis software on Alpha Image Gel Documentation System.

Protein Determination

Protein content was determined by the BCA method [38]. The mixture of solutions A and B (1:49) of BCA reagent was added to the protein sample and further incubated at 37 °C for 45 min. The absorbance was measured at 562 nm and the protein concentration was calculated using a standard curve of BSA.

Statistical Analysis

Results are expressed as the means \pm SD of three experiments for each treatment and were plotted accordingly. Individual treatments were tested against the control by using the Student *t* tests. Significant differences from controls were considered at $P < 0.05$. Analyses were conducted with SPSS version 13.0.

Results

Chemistry

The two isomers of propofol viz. 2,4-propofol and 2,6-propofol were conjugated with OLA and RCA separately. The four novel propofol-n-9 conjugates were obtained from the esterification of hydroxyl ($^1\text{C-OH}$) group of propofol with the terminal carboxylic group of MUFA in the presence of DCC and DMAP. The reaction sequences are outlined in Scheme 1. The newly synthesized ester derivatives of propofol-OLA and propofol-RCA were located at specific *RF* values when subjected to thin layer chromatography analysis (Supplementary Fig. 1). The *RF* values of the products significantly differ from those of the parent controls viz. OLA/RCA and propofol. The conjugates were synthesized in good yield and had a colorless viscous liquid (oily) consistency at room temperature.

Spectral Characterization of Propofol-n-9 Conjugates

UV Absorbance

Propofol-OLA conjugates The spectra of parent OLA (Fig. 1a, b) showed an absorption peak at 268 nm whereas, absorption peaks of 2,4-propofol and 2,6-propofol were observed at 282.8 and 286 nm, respectively. In 2,4P-OLA and 2,6P-OLA conjugates, the characteristic peaks appeared at 263 and 266 nm, respectively.

Propofol-RCA conjugates The spectra of parent RCA (Fig. 1c, d) showed two absorption peaks at 255 and 270 nm whereas, absorption peaks of 2,4-propofol and 2,6-propofol were observed at 281.2 and 285.3 nm,

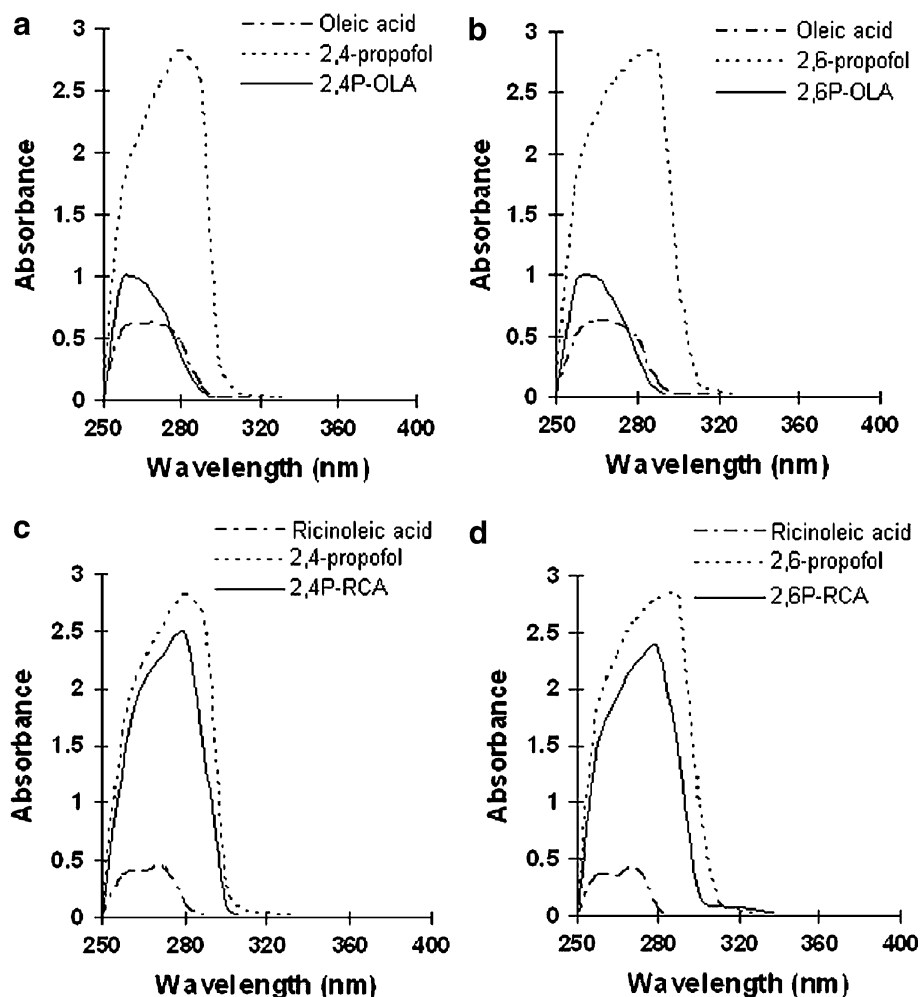
respectively. These peaks were shifted to 278 and 279 nm, for 2,4P-RCA and 2,6P-RCA conjugates, respectively.

Nuclear Magnetic Resonance Spectral Studies

Propofol-OLA and propofol-RCA conjugates The formation of propofol-OLA and propofol-RCA conjugates was further confirmed with the ^1H - and ^{13}C -NMR spectra. Assignments of the signals are based on the chemical shift and intensity pattern. The absence of a signal of the hydroxyl group confirms the synthesis of 2,4P-OLA and 2,6P-OLA (Supplementary Fig. 2a, b, respectively). The two olefinic protons of 2,4P-OLA and 2,6P-OLA (*k* and *i*) were observed as a multiplet at δ_{H} 5.36 while that of 2,4P-RCA and 2,6P-RCA (*l* and *k*) were resonating as multiplet at δ_{H} 5.4 ppm and 5.5 ppm respectively (Supplementary Fig. 2c, d) [39]. Due to the proximity of the hydroxy group to the double bond, the signal of the olefinic protons of 2,4P-RCA and 2,6P-RCA were split, with the downfield signal being assigned to the *k* proton at C-10 and the upfield signal assigned to the *l* proton at C-9 [40]. The $-\text{OH}$ proton is exchangeable with deuterium and might not always be visible as in our case. A triplet was observed at 0.88 ppm corresponding to the terminal methyl protons of the fatty acid chain. A conspicuous multiplet corresponding to the methylene protons of the fatty acid chain appeared in the range 1.25–1.46 ppm. The methyl protons of the isopropyl chain of the ring of 2,4P-OLA were observed as a doublet at 1.20 ppm while the signal corresponding to methyl protons of a isopropyl chain of 2,6P-OLA, 2,4P-RCA and 2,6P-RCA was merged with the methylene protons appearing as a strong multiplet at 1.19–1.48 ppm range. The methylene groups ($-\text{CH}_2-\text{CH}=\text{CH}-\text{CH}_2-$) attached to the olefinic carbons were resonating as a quartet at 2.00–2.07 ppm (relatively at lower field) as a consequence of olefinic bond. The methylene protons $-\text{CH}=\text{CH}-\text{CH}_2-\text{CH}(\text{OH})-$ of 2,4P-RCA and 2,6P-RCA were observed at 2.23 ppm as triplet with a coupling of 13.72 Hz. The $-\text{CH}_2-\text{CH}(\text{OH})-\text{CH}_2-$ protons of 2,4P-RCA and 2,6P-RCA resonate at 3.62 ppm as multiplet, since it is attached to the $-\text{OH}$ group, therefore is shifted downfield from the others. The $-\text{COCH}_2-$ protons adjacent to a carbonyl group resonate in the range 2.50–2.60 ppm, while the $-\text{CO}-\text{CH}_2-\text{CH}_2-$ protons were resonating in the range 1.75–1.85 ppm as a multiplet. In the case of 2,4P-OLA and 2,4P-RCA, $\text{Ar}-\text{CH}<$ gives two signals in the range 2.9–2.6 ppm [12] while for 2,6P-OLA and 2,6P-RCA, it gives a single signal at 2.9 ppm [41–43]. The aromatic protons appear in the usual range 6.80–7.30 ppm.

In the ^{13}C -NMR spectra, the assignments of the ^{13}C signal for $>\text{C}=\text{O}$ group of an ester is quite straightforward

Fig. 1 UV absorbance spectra of propofol-OLA and propofol-RCA conjugates. **a** 2,4P-OLA, **b** 2,6P-OLA, **c** 2,4P-RCA, **d** 2,6P-RCA. Absorbance of parent controls is also shown



and were observed in the range of 172.0–173.0 ppm [41, 43, 44]. The terminal methyl groups gave signals in 14–15 ppm range. Olefinic carbons were recorded at 133–125 ppm [39, 40, 45]. The $-\text{CH}(\text{OH})-$ carbon of 2,4P-RCA and 2,6P-RCA was recorded at 71.58 ppm. Assignment of other significant carbon signals has been shown in the Supplementary Fig. 2a–d.

FAB-MS Studies

Propofol-OLA and propofol-RCA conjugates The mass spectrum and fragmentation pattern of the 2,4P-OLA, 2,6P-OLA, 2,4P-RCA and 2,6P-RCA are illustrated in Supplementary Fig. 3a–d, respectively. They are typical in that they have a prominent ion peak at $m/z = 163$, 177, 264, 265 and 281, which are all fragments about the ester group. The molecular ion $[\text{M} + 3\text{H}]^+$ ($m/z = 445$), $[\text{M} + \text{H}]^+$ ($m/z = 443$) and $[\text{M}]^+$ ($m/z = 458$) are easily distinguished. The base peak was observed at $m/z = 177$ with its isotopic peak at $m/z = 178$ and represents a cleavage in the ester group. There is an ion at $m/z = 163$ representing loss

of the terminal carbon as a methylene group from the base peak of propofol [46].

Analysis of Growth Inhibition

Consistent with a previous report [11], the newly synthesized conjugates significantly inhibited cancer cell growth in a dose-dependent manner. All tested cells after treatment with the conjugates showed variable growth inhibitions till a maximum tested concentration of 15 μM was reached, making them potent, less potent or equipotent (IC_{50} values: Table 1). However, SK-MEL-1 was observed to be the most sensitive to all the four conjugates (Figs. 2, 3). The conjugates showed statistically significant ($P < 0.05$) anticancer activity in comparison with the vehicle control. The in-vitro evaluation revealed that structural modifications of propofol and MUFA resulted in conjugates that were non-toxic to non-cancerous HFL1 cells. This feature imparts extra edge to the synthesized products and put them into the class of anticancer agents in terms of selectivity and specificity. Although conjugates of propofol-linoleic acid and

Table 1 Analysis of cytotoxic effect of propofol-n-9 conjugates in several cancer cell lines

Conjugates	Cell lines (IC ₅₀ , μM)					
	HepG2	MDA-MB-361	SK-MEL-1	A549	HL-60	HFL1
2,4P-OLA	3.9	3.1	2.5	3.7	3.4	NA
2,6P-OLA	2.8	2.6	2.3	3.7	3.2	NA
2,4P-RCA	4.8	LA	4.1	LA	7.4	NA
2,6P-RCA	4.2	LA	3.9	LA	5.4	NA
2,4P-LNA	4.1	3.2	4.9	LA	LA	NA
2,6P-LNA	3.3	2.7	4.1	LA	LA	NA
2,4P-ARA	3.7	7.5	LA	5.3	4.4	LA
2,6P-ARA	3.1	7.2	LA	4.6	3.9	LA
Doxorubicin	2.2	2.0	1.9	3.6	3.1	NA

The highest concentration tested was 15 μM. Values are the means of three observations

NA not active, LA less active, SK-MEL-1 human skin malignant melanoma, HepG2 human liver hepatocellular carcinoma, MDA-MB-361 ductal breast carcinoma, A549 human lung carcinoma, HL-60 human leukemia, HFL1 human lung fibroblast

propofol-arachidonic acid, (previously synthesized in our laboratory) [11] were also reported to be significantly cytotoxic to cancer cell lines (Table 1), the propofol-oleic acid conjugates synthesized in the present study were also found to be more potent anticancer molecules.

Toxicity Level of Propofol-n-9 Conjugates

The toxicity levels of conjugates were determined by in-vitro hemolysis testing. Figure 4 displays lysis of erythrocytes by various conjugates expressed as a percentage of total lysis (100 % lysis) induced with Triton X-100. The propofol-OLA conjugates caused negligible RBC lysis as compared to propofol-RCA conjugates. Among various conjugates 2,6P-OLA (~8 % hemolysis) and 2,4P-OLA (~10 % hemolysis) imparted less toxicity to erythrocytes than does 2,6P-RCA (~18 % hemolysis) and 2,4P-RCA (~19 % hemolysis). The intrinsic lytic ability of the propofol only, OLA and RCA only was also tested. RCA (~21 % hemolysis) caused a higher toxicity than OLA (~6 % hemolysis), propofol (~17 % hemolysis) and ethanol (~4 % hemolysis) thereby resulting in significant hemolysis of RBCs.

Note: Further in-vitro evaluations of anticancer efficacy of propofol-n-9 conjugates were done on the SK-MEL-1 skin cancer cell line since it was observed to be more prone to the cytotoxic effect of conjugates.

Effect of Propofol-n-9 Conjugates on SK-MEL-1 Cancer Cell Migration

The results shown in Fig. 5 demonstrate that OLA, RCA and propofol alone had a minimal effect on skin cancer cell migration. On the other hand, propofol-OLA and propofol-RCA inhibited cell migration by about 50 % ($P < 0.05$) and 30 % respectively to that of the control group.

Effect of Propofol-n-9 Conjugates on SK-MEL-1 Cancer Cell Adhesion

We also tested the effect of the propofol-OLA and propofol-RCA conjugates on the adhesion of the skin cancer cells to a fibronectin surface. While, OLA and RCA or propofol alone did not significantly affect skin cancer cell adhesion (Fig. 6), in contrast, propofol-OLA and propofol-RCA inhibited cell adhesion by ~40 % (significant at $P < 0.05$) and 35 %, respectively.

Effect of Propofol-n-9 Conjugates on Induction of Apoptotic Factors

Protein fractions of SK-MEL-1 cancer cells after incubation with n-9 or propofol alone or with test conjugates individually were screened by Western blotting after 24 h of treatment. Propofol-OLA conjugates were able to induce apoptosis in SK-MEL-1 cells at 15 μM concentration whereby a significant increase in the expression of cytochrome *c* and caspase-3 was distinctly visualized (Fig. 7a, lanes 4 and 5). Whereas, weak signals of cytochrome *c* and no signals of caspase-3 were recorded with propofol-RCA conjugates (data not shown).

Mean densitometric values of individual bands of cytochrome *c* and caspase-3 were quantified using image analysis gel documentation system software. Each value was mean of three experiments. At 15 μM tested concentration, increased expression of both apoptotic factors was recorded with slight variations in the activity of 2,4P-OLA and 2,6P-OLA conjugates. Release of 32.8 and 36.6 % cytochrome *c* and expression of 28.7 and 34.1 % caspase-3 was observed after treatment with 2,4P-OLA and 2,6P-OLA, respectively (Fig. 7b, c).

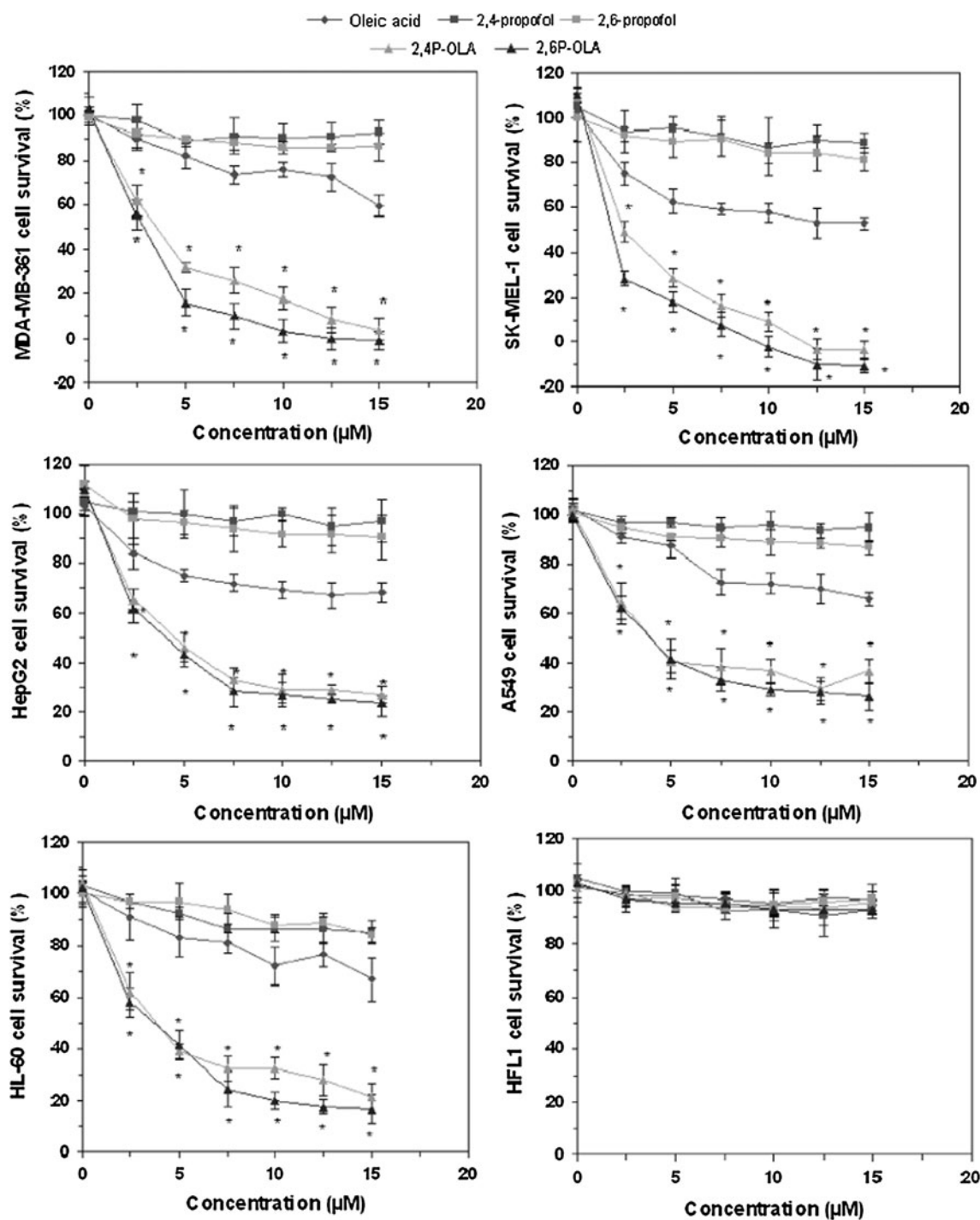


Fig. 2 Viability assessment of various cell lines after treatment with propofol-OLA conjugates. The effects of novel esters along with parent OLA and 2,4-/2,6-propofol are expressed as the means \pm SD of three experiments

Discussion

Efforts made in medicinal and combinatorial chemistry continue to give rise to a wide range of anticancer agents with remarkable therapeutic potential. A number of studies have concluded that chemically modified fatty acid

molecules possess more specific and potent biological activity, in addition to possibly affecting a wider range of therapeutic targets [10]. Over the last decade several attempts have been made to synthesize novel anticancer compounds by conjugating fatty acids with various anti-cancer drugs [35, 45, 47–49]. Many of these agents have

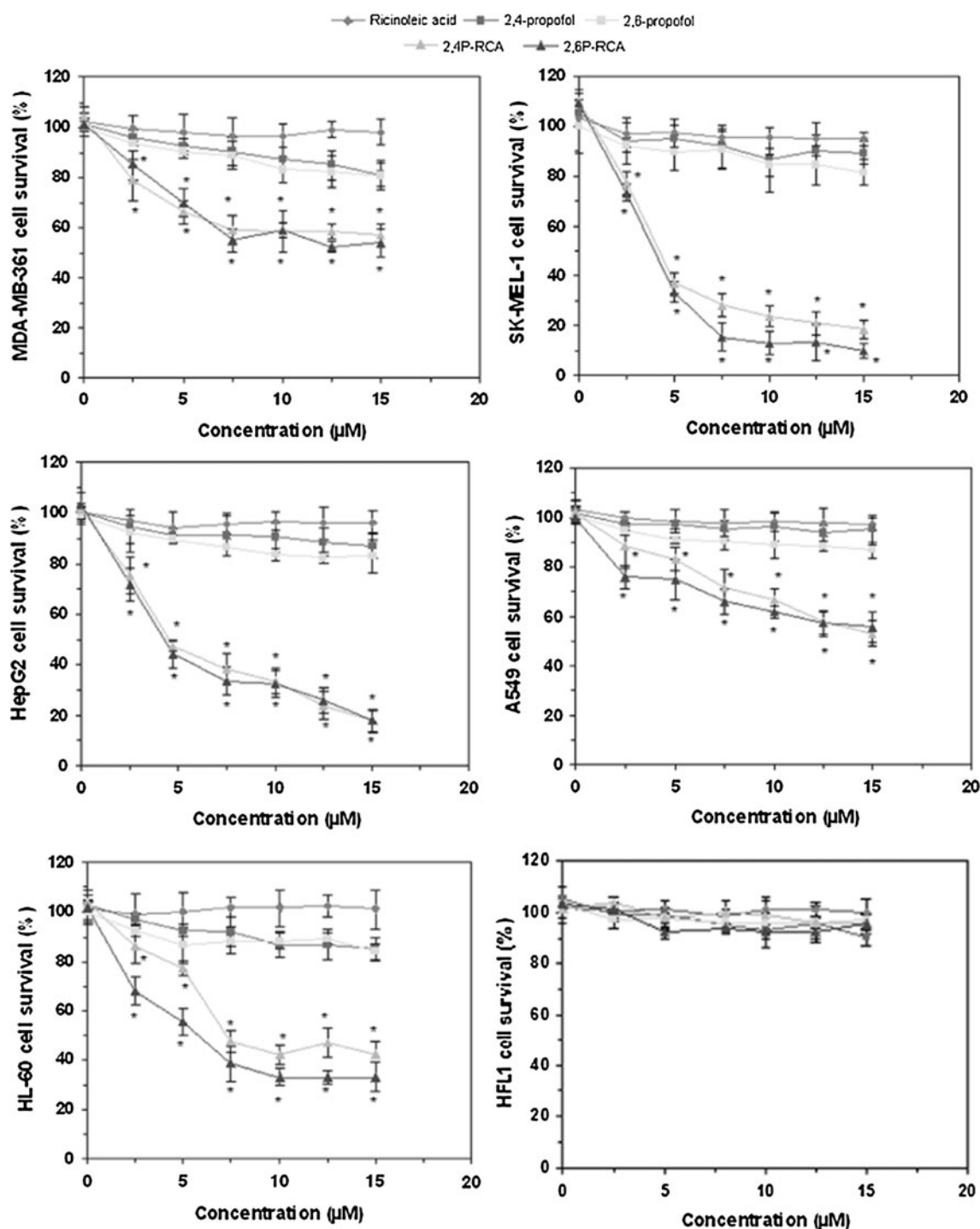


Fig. 3 Viability assessment of various cell lines after treatment with propofol-RCA conjugates. The effects of novel esters along with parent RCA and 2,4-/2,6-propofol are expressed as the means \pm SD of three experiments

solubility, stability or toxicological issues, which hamper their development into viable treatment strategies. To overcome these issues, the administration of antioxidants such as propofol is speculated to enhance the impact of chemotherapy. The co-administration of propofol with chemotherapeutic UFA, is supposed to enhance the

cytotoxicity and inhibit the oxidative damage, thereby inhibiting the growth of tumors. The cytotoxicity of different propofol-fatty acid esters have been investigated previously [11, 35, 50]. The present work is based on the chemical conjugation of MUFA with propofol isomers. The presence of DMAP (catalyst) and DCC (coupling

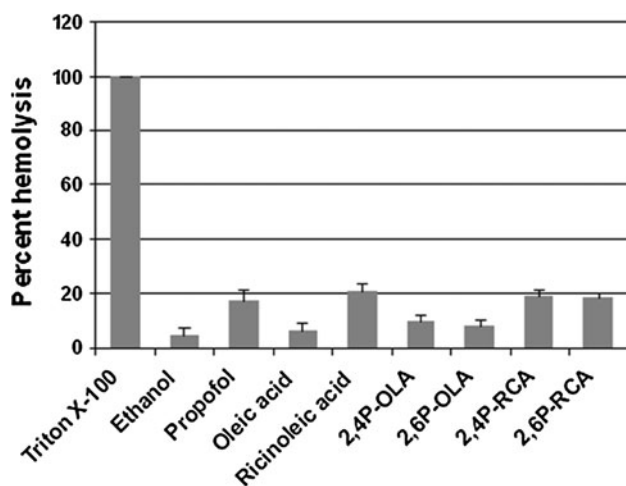


Fig. 4 The extent of damage caused to blood erythrocytes by propofol-n-9 conjugates was measured as the percentage lysis of the total red blood cells added. The data are the means \pm SD of three sets of different experiments

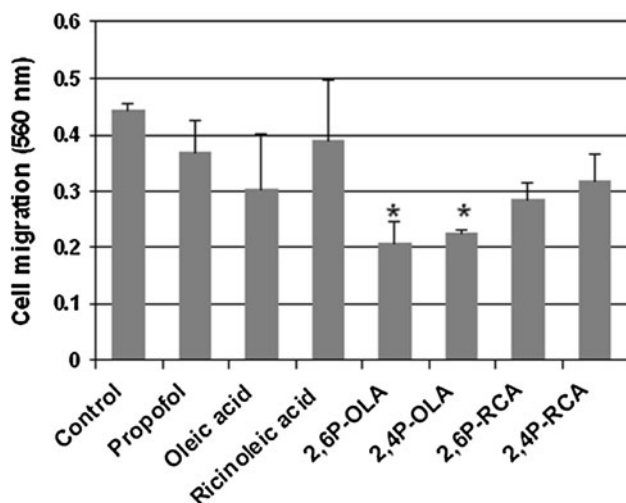


Fig. 5 Effect of propofol-n-9 conjugates on migration of SK-MEL-1 cancer cells. Results are the means \pm SD for three experiments. The level of significance for various data when compared to control ($P < 0.05$) is indicated with an *asterisk*

reagent) was a pre-requisite for esterification of novel conjugates. The use of the DCC/DMAP method was found to be a more suitable synthetic route under milder reaction conditions, giving a higher yield and providing convenient product purification strategies. The chemical nature of the four novel MUFA-esters reported in this study show absorption peaks in the ultraviolet range, which were quite distinct from the reactant parent controls (Fig. 1). The presence of an ester bond, aromatic C–H bond, and absence of the free –OH group as visualized by FT-IR, confirmed the formation of conjugates. Elemental analysis of conjugates showed the values for ‘CHN’ within ± 0.4 % of the theoretical ones.

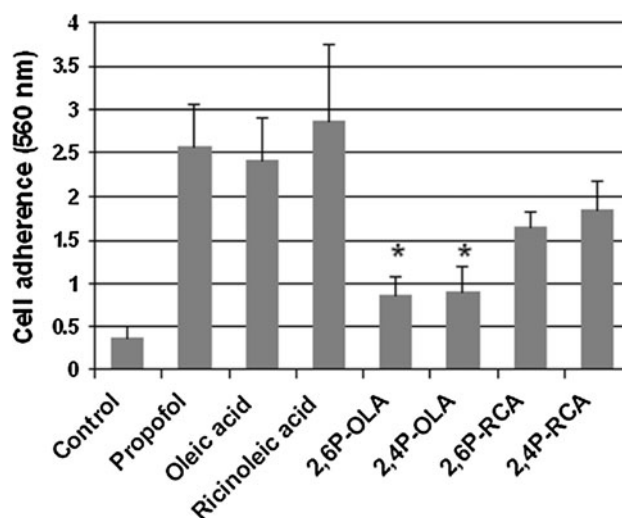


Fig. 6 Effect of propofol-n-9 conjugates on adhesion of SK-MEL-1 cancer cells. Results are the means \pm SD for three experiments. The level of significance from the control ($P < 0.05$) is indicated with an *asterisk*

When the NMR signals of the conjugates were compared with the parent propofol [35], the hydroxyl proton signal at about 4.82 ppm in propofol was not visualized in the spectra of conjugates. The absence of hydroxyl group signal in $^1\text{H-NMR}$ spectra of the conjugates confirms the synthesis of new product, distinct from parent controls. The overall shift in signals indicates that the ester bond was formed at C-19 hydroxyl group of propofol. The molecular mass of the novel MUFA-ester derivatives determined by mass spectrometry was very close to the theoretically calculated molecular mass values viz., 442.47 Da for propofol-OLA conjugates and 458 Da for propofol-RCA conjugates.

After establishing the structures of the conjugates, their inherent toxicity in terms of cell membrane lysis was determined. The in-vitro erythrocyte lysis test showed that the newly synthesized esters cause only negligible damage to RBCs (Fig. 5). The four novel MUFA-esters were also screened for potential anticancer activities against a range of human cancer cell lines (Figs. 2, 3). The cytotoxic efficacy of these conjugates is expressed in terms of IC_{50} values, as shown in Table 1. Among various esters synthesized, propofol-OLA conjugates showed greater in-vitro anticancer activity with IC_{50} values ranging from 2.3 μM for SK-MEL-1 cells to 3.9 μM for HepG2 cells. Propofol-RCA conjugates however, moderately inhibited various cancer cells and showed negligible inhibition against MDA-MB-361 and A549 (IC_{50} values ranging from 3.9 μM for SK-MEL-1 cells to 7.4 μM for HL-60 cells). The propofol-n-9 conjugates were non-toxic to the normal HFL1 cells up to the highest concentration screened (15 μM).

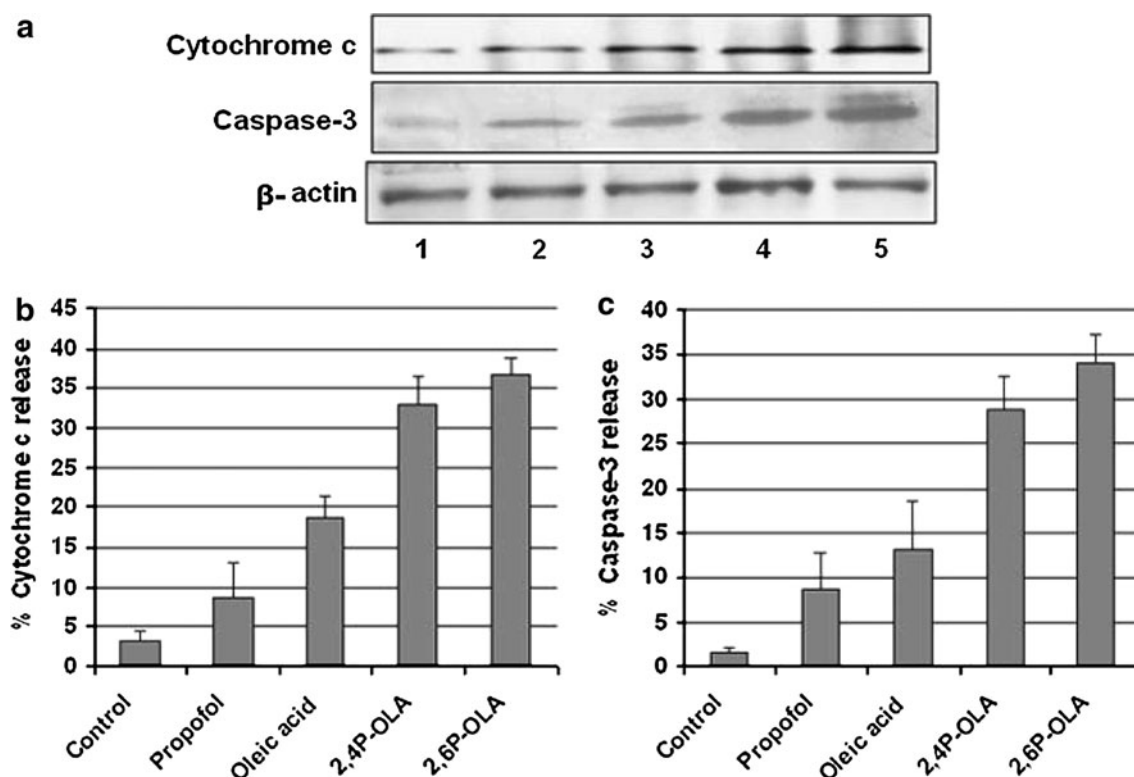


Fig. 7 **a** Immunoblots showing relative distribution of cytochrome *c*, caspase-3 in SK-MEL-1 (human skin malignant melanoma) cells after treatment with (1) control; (2) oleic acid; (3) propofol; (4) 2,4P-OLA; (5) 2,6P-OLA. β -actin expression was manifested as loading control.

b, c Densitographs showing relative density of cytochrome *c* and caspase-3 respectively, in the nitrocellulose blots. Results are mean values \pm SD in triplicates

Since, the conjugates revealed optimum cytotoxicity against SK-MEL-1 cells; we used this cell line for further studies. Cell migration and adhesion are essential processes in tumor metastasis [51]. In the present study, cell migration and cell adhesion assay revealed that the conjugates were able to inhibit the metastatic potential of SK-MEL-1 cells (Figs. 5, 6) where parent controls were not effective. Selective apoptosis of malignant cells is the most commonly analyzed attribute in chemotherapeutic studies. Modulation of expression of apoptotic factors must be tightly regulated for normal cellular functioning. Therefore, we also analyzed the effect of the conjugates on the induction of apoptosis by assaying for caspase-3 activation and cytochrome *c* release (Fig. 7). The 2,6P-OLA conjugate showed increased expression of both cytochrome *c* (36.6 %) and caspase-3 (34.1 %) in comparison with 2,4P-OLA (Fig. 7b, c). On the other hand, very weak signals for cytochrome *c* were detected when SK-MEL-1 cells were treated with propofol-RCA conjugates (data not shown). Interestingly, no signal of caspase-3 was recorded upon treatment of SK-MEL-1 cells with propofol-RCA conjugates. Thus, among the four conjugates, propofol-OLA conjugates promote apoptotic

cell death at doses of 15 μ M. Our current findings, thus demonstrate that propofol-OLA conjugates can induce the apoptosis by induction of a novel pathway through which n-9 MUFA putatively modulate the aggressive behavior of skin cancer.

Conclusion

The present study has shown the synthesis of four novel propofol-n-9 ester conjugates revealing unique cytotoxic action against various cancer cell lines. The conjugates are able to inhibit the growth of cancer cells in a dose-dependent manner. Positive results in the inhibition of cancer cell migration and adhesion further established their anticancer potential. Although, propofol-RCA conjugates are observed to be weak candidates in initiating apoptosis, the propofol-OLA conjugates induce a cell signaling pathway, that eventually leads to apoptotic cell death in skin cancer cells. Our preliminary data strongly suggest that the synthesized conjugates possess potent anticancer activity. However, the exact mechanism by which these conjugates modulate the apoptotic pathway in cancer cells

selectively, while sparing the non-malignant cells needs further investigation.

Acknowledgments We are thankful to Prof. M. Saleemuddin, Co-ordinator, Interdisciplinary Biotechnology Unit, Aligarh Muslim University, Aligarh, India for providing the central instrumentation facility to carry out the experiments. We also thank the Sophisticated Analytical Instrumentation Facility (SAIF) of the Central Drug Research Institute, Lucknow, India for providing the NMR and mass spectra facility. The study was conducted with the financial support given to Mr. Azmat Ali Khan by the University Grants Commission (India).

Conflict of interest All authors declare that there is no conflict of interest.

References

- Das UN (2006) Essential fatty acids a review. *Curr Pharm Biotechnol* 7:467–482
- Menéndez JA, del Mar Barbacid M, Montero S, Sevilla E, Escrich E, Solanas M, Cortés-Funes H, Colomer R (2001) Effects of gamma-linolenic acid and oleic acid on paclitaxel cytotoxicity in human breast cancer cells. *Eur J Cancer* 37(3):402–413
- Menéndez JA, Ropero S, del Barbacid MM, Montero S, Solanas M, Escrich E, Cortes-Funes H, Colomer R (2002) Synergistic interaction between virorelbine and gamma-linolenic acid in breast cancer cells. *Breast Cancer Res Treat* 72(3):203–219
- Sauer LA, Dauchy RT (1992) The effect of omega-6 and omega-3 fatty acids on 3H-thymidine incorporation in hepatoma 7288CTC perfused in situ. *Br J Cancer* 66(2):297–303
- Dratz EA, Deese AJ (1986). In: Simopoulos AP, Kifer RR, Martin RE, Orlando FL (eds) Health effects of polyunsaturated fatty acids in seafoods, Academic Press, pp 319–351
- Salem NJ, Kim HY, Yergey JA (1986) In: Simopoulos, AP, Kifer RR, Martin RE, Orlando FL (eds) Health effects of polyunsaturated fatty acids in seafoods, Academic Press, pp 263–317
- Grammatikos SI, Subbaiah PV, Victor TA, Miller WM (1994) n-3 and n-6 fatty acid processing and growth effects in neoplastic and non-cancerous human mammary epithelial cell lines. *Br J Cancer* 70(2):219–227
- Miyazawa A, Igarashi M, Kameyama T, Inoue Y. (2000) Conjugated polyunsaturated fatty acid compositions for killing cancer cells. *Jpn. Kokai Tokky Koho, Application: JP 99-129045 19990330*, 10
- Menendez JA, Ropero S, Lupu R, Colomer R (2004) Dietary fatty acids regulate the activation status of Her-2/neu (c-erb B-2) oncogene in breast cancer cells. *Ann Oncol* 15:1719–1721
- Tronstad KJ, Berge K, Berge RK, Bruserud O (2003) Modified fatty acid and their possible therapeutic targets in malignant diseases. *Expert Opin Ther Targets* 7:663–677
- Khan AA, Alam M, Tufail S, Mustafa J, Owais M (2011) Synthesis and characterization of novel PUFA esters exhibiting potential anticancer activities: an in vitro study. *Eur J Med Chem* 46:4878–4886
- Coetzee JF, Glen JB, Wium CA, Boshoff L (1995) Pharmacokinetic model selection for target controlled infusions of propofol. Assessment of three parameter sets. *Anesthesiology* 82:1328–1345
- Mammoto T, Mukai M, Mammoto A, Yamanaka Y, Hayashi Y, Mashimo T, Kishi Y, Nakamura H (2002) Intravenous anesthetic, propofol inhibits invasion of cancer cells. *Cancer Lett* 184:165–170
- Tsuchiya M, Asada A, Arita K, Utsumi T, Yoshida T, Sato EF, Utsumi K, Inoue M (2002) Induction and mechanism of apoptotic cell death by propofol in HL-60 cells. *Acta Anaesthesiol Scand* 46:1068–1074
- Gillingham LG, Harris-Janzen S, Jones PJ (2011) Dietary mono-unsaturated fatty acids are protective against metabolic syndrome and cardiovascular disease risk factors. *Lipids* 46(3):209–228
- Parthasarathy S, Khoo JC, Miller E, Barnett J, Witztum JL, Steinberg D (1990) Low density lipoprotein rich in oleic acid is protected against oxidative modification: implications for dietary prevention of atherosclerosis. *Proc Natl Acad Sci USA* 87:3894–3898
- Win DT (2005) Oleic acid—the anti-breast cancer component in olive oil. *Au J T* 9:75–78
- Natali F, Siculella L, Salvati S, Gnoni GV (2007) Oleic acid is a potent inhibitor of fatty acid and cholesterol synthesis in C6 glioma cells. *J Lipid Res* 48:1966–1975
- Menendez JA, Vellon L, Colomer R, Lupu R (2005) Oleic acid, the main monounsaturated fatty acid of olive oil, suppresses Her-2/neu (erb B-2) expression and synergistically enhances the growth inhibitory effects of trastuzumab (Herceptine) in breast cancer cells with Her-2/neu oncogene amplification. *Ann Oncol* 16:359–371
- Noguchi M, Minami M, Yagasaki R, Kinoshita K, Earashi M, Kitagawa H, Taniya T, Miyazaki I (1997) Chemoprevention of DMBA induced mammary carcinogenesis in rats by low-dose EPA and DHA. *Br J Cancer* 75:348–353
- Rose DP, Connolly JM (1990) Effects of fatty acids and inhibitors of eicosanoid synthesis on the growth of a human breast cancer cell line in culture. *Cancer Res* 50:7139–7144
- Rose DP, Connolly JM, Coleman M (1996) Effect of omega-3 fatty acids on the progression of metastases after the surgical excision of human breast cancer cell solid tumors growing in nude mice. *Clin Cancer Res* 2:1751–1756
- Rose DP, Connolly JM (1999) Anti angiogenicity of docosahexaenoic acid and its role in the suppression of breast cancer cell growth in nude mice. *Int J Oncol* 15:1011–1015
- Lipworth L, Martinez ME, Angell J, Hsieh CC, Trichopoulos D (1997) Olive oil and human cancer: an assessment of the evidence. *Prev Med* 26:181–190
- Simonsen NR, Fernandez-Crehuet Navajas J, Martin-Moreno JM, Strain JJ, Huttunen JK, Martin BC, Thamm M, Kardinaal AF, van't Veer P, Kok FJ, Kohlmeier L (1998) Tissue stores of individual monounsaturated fatty acids and breast cancer: the EURAMIC study. *Am J Clin Nutr* 68:134–141
- Solanas M, Hurtado A, Costa I, Moral R, Menendez JA, Colomer R, Escrich E (2002) Effects of high olive diet on the clinical behavior and histopathological features of rat DMBA-induced mammary tumors compared with a high corn oil diet. *Int J Oncol* 21:745–753
- Moral R, Solanas M, Garcia G, Colomer R, Escrich E (2003) Modulation of EGFR and neu expression by n-6 and n-9 high-fat diets in experimental mammary adenocarcinomas. *Oncol Rep* 10:1417–1424
- Andrade LN, Lima TM, Curi R, Castrucci AM (2005) Toxicity of fatty acids on murine and human melanoma cell lines. *Toxicol In Vitro* 19:553–560
- Brinkmann CR, Heegaard CW, Petersen TE, Jensenius JC, Thiel S (2011) The toxicity of bovine α -lactalbumin made lethal to tumor cells is highly dependent on oleic acid and induces killing in cancer cell lines and noncancer-derived primary cells. *FEBS J* 278(11):1955–1967
- Yuan C, Bloch K (1961) Conversion of oleic acid to linoleic acid. *J Biol Chem* 236:1277–1279

31. Borsotti G, Guglielmetti G, Spera S, Battistel E (2001) Synthesis of phosphatidylcholines containing ricinoleic acid. *Tetrahedron* 57:10219–10227
32. Vieira C, Evangelista S, Cirillo R, Terraciano R, Lippi A, Maggi CA, Manzini S (2000) Antinociceptive activity of ricinoleic acid, a capsaicin-like compound devoid of pungent properties. *Eur J Pharmacol* 407:109–116
33. Gaginella TS, Haddad AC, Go VLW, Phillips SF (1977) Cytotoxicity of ricinoleic acid (castor oil) and other intestinal secretagogues on isolated intestinal epithelial cells. *J Pharmacol Exp Ther* 201:259–266
34. Klopman G, Li J-Y (1995) Quantitative structure–agonist activity relationship of capsaicin analogues. *J Comp Aid Mol Des* 9:283–294
35. Siddiqui RA, Zerouga M, Wu M, Castillo A, Harvey KA, Zaloga GP, Stillwell W (2005) Anticancer properties of propofol-docosahexaenoate and propofol-eicosapentaenoate on breast cancer cells. *Breast Cancer Res* 7:R645–R654
36. Owais M, Masood AK, Faisal SM, Haque W (2002) Immunomodulator tuftsin augments antifungal activity of Amphotericin B against experimental murine candidiasis. *J Drug Target* 10(3): 185–192
37. Laemmli UK (1970) Cleavage of structural proteins during the assembly of the head of bacteriophage T4. *Nature (London)* 227:680–685
38. Stoscheck CM (1990) Quantitation of protein. *Meth Enzymol* 182:50–69
39. Magrioti V, Constantinou-Kokotou V (2002) Synthesis of (*S*)- α -amino oleic acid. *Lipids* 37:223–228
40. Klemm LH, Taylor DR (1980) Alumina-catalyzed reactions of hydroxyarenes and hydroaromatic ketones. 9. Reaction of phenol with 1-propanol. *J Org Chem* 45:4326–4329
41. Brown ML, Eidam HA, Paige M, Jones PJ, Patel MK (2009) Comparative molecular field analysis and synthetic validation of a hydroxyamide-propofol binding and functional block of neuronal voltage-dependent sodium channels. *Bioorg Med Chem* 17:7056
42. Malkov AV, Stewart-Liddon AJP, Teply F, Kobr L, Muir KW, Haigh D, Ko-covsky P (2008) New pinene-derived pyridines as bidentate chiral ligands. *Tetrahedron* 64:4011–4025
43. Zhang W, Dichtel WR, Stieg AZ, Benitez D, Gimzewski JK, Heath JR, Stoddart JF (2008) Folding of a donor-acceptor polyrotaxane by using noncovalent bonding interactions. *Proc Natl Acad Sci USA* 105:6514–6519
44. Davletbakova M, Baibulatova NZ, Dokichev VA, Yunusov MS (2001) Catalytic synthesis of the methyl ester of (9Z,12R)-12-(Methoxycarbonylmethoxy)-octadec-9-enoic acid. *Chem Nat Comp* 37:93–94
45. Mustafa J, Khan SI, Ma G, Walker LA, Khan IA (2004) Synthesis and anticancer activities of fatty acid analogs of podophyllotoxin. *Lipids* 39:167–172
46. Christie WW (1998) Gas chromatography–mass spectrometry methods for structural analysis of fatty acids. *Lipids* 33:343–353
47. Takahashi M, Fukutake M, Isoi T, Fukuda K, Sato H, Yazawa K, Sugimura T, Wakabayashi K (1997) Suppression of azoxymethane induced rat colon carcinoma development by a fish oil component, docosahexaenoic acid (DHA). *Carcinogenesis* 18:1337–1342
48. Bradley MO, Swindell CS, Anthony FH, Witman PA, Devanesan P, Webb NL, Baker SD, Wolff AC, Donehower RCJ (2001) Tumor targeting by conjugation of DHA to paclitaxel. *Controlled Release* 74:233–236
49. Mustafa J, Khan SI, Ma G, Walker LA, Khan IA (2005) Synthesis and in vitro cytotoxic activity of N-, F-, and S-ether derivatives of podophyllotoxin fatty acid adducts. *Lipids* 40:375–382
50. Harvey KA, Xu Z, Whitley P, Davisson VJo, Siddiqui RA (2010) Characterization of anticancer properties of 2,6-diisopropylphenol–docosahexaenoate and analogues in breast cancer cells. *Bioorg Med Chem* 18:1866–1874
51. Bogenrieder T, Herlyn M (2003) Axis of evil: molecular mechanisms of cancer metastasis. *Oncogene* 22:6524–6536

Reduction of Rat Cardiac Hypertrophy by Osthol is Related to Regulation of Cardiac Oxidative Stress and Lipid Metabolism

Feng Zhou · Wen Zhong · Jie Xue ·
Zhen-lun Gu · Mei-lin Xie

Received: 19 March 2012 / Accepted: 8 August 2012 / Published online: 24 August 2012
© AOCs 2012

Abstract The objective of this study was to examine the therapeutic effect of osthol, a coumarin compound isolated from the fruit of *Cnidium monnieri* (L.) Cusson, on cardiac hypertrophy in rats and investigate its potential mechanisms. The rats with cardiac hypertrophy induced by renovascular hypertension were given osthol orally by gavage for 4 weeks. The results showed that in the osthol 20 mg/kg group, the blood pressure, heart weight index and myocardial malondialdehyde content were lowered ($p < 0.001$, $p = 0.002$ and $p = 0.025$, respectively), the myocardial superoxide dismutase and glutathione peroxidase contents were increased ($p < 0.001$), and the elevated unesterified fatty acids and triacylglycerols in myocardial tissues were decreased ($p = 0.017$ and $p = 0.004$, respectively). At the same time, the myocardial peroxisome proliferator-activated receptor (PPAR)- α and carnitine palmitoyltransferase (CPT)-1a mRNA expressions were increased and the myocardial diacylglycerol acyltransferase (DGAT) mRNA expression was decreased in the osthol 20 mg/kg group ($p < 0.001$). Osthol treatment was associated with a decreased cross-sectional area of cardiomyocytes ($p < 0.001$). These findings suggest that osthol may exert a therapeutic effect on cardiac hypertrophy in rats, and its mechanisms may be related to the improvement of myocardial oxidative stress and lipid metabolism

via regulation of PPAR α -mediated target gene expressions including an increase in CPT-1a mRNA expression and a decrease in DGAT mRNA expression.

Keywords Osthol · Cardiac hypertrophy · Hypertension · Oxidative stress · Lipid metabolism

Abbreviations

CPT-1a	Carnitine palmitoyltransferase-1a
DGAT	Diacylglycerol acyltransferase
FFA	Unesterified fatty acids
GAPDH	Glyceraldehyde phosphate dehydrogenase
GSH-Px	Glutathione peroxidase
MDA	Malondialdehyde
PPAR	Peroxisome proliferator-activated receptor
RT-PCR	Reverse transcription polymerase chain reaction
SOD	Superoxide dismutase
TAG	Triacylglycerol(s)

Introduction

Hypertension is now recognized as the most common cause of cardiac hypertrophy. The formation and development of cardiac hypertrophy is not only due to an adaptive response of the heart to pressure overload but also be due to myocardial oxidative stress and energy metabolism imbalance [1–3]. In vivo and in vitro studies indicate an association of myocardial oxidative stress with myocardial remodeling [4–6]. Myocardial energy metabolism gradually switches from fatty acids to glucose utilization during the formation of cardiac hypertrophy [2, 3, 7]. This metabolic shift can be viewed as an adaptive response, because it may decrease

F. Zhou · W. Zhong · J. Xue · M. Xie (✉)
Department of Pharmacology, College of Pharmaceutical
Sciences, Soochow University, Suzhou 215123, China
e-mail: xiemeilin@suda.edu.cn

Z. Gu
Suzhou Institute of Chinese Materia Medica,
Soochow University, Suzhou 215123, China

oxygen consumption per mole of ATP generated [8]. However, it finally leads to certain maladaptive features including increased lipid accumulation in the heart due to impaired oxidation of fatty acids.

Osthol is a coumarin compound isolated from the fruit of *Cnidium monnieri* (L.) Cusson (Apiaceae), a traditional Chinese medicine. Recently, numerous studies have revealed that osthol exhibits various pharmacological activities such as anti-inflammation [9], anti-osteoporosis [10], an estrogen-like effect [11], hypoglycemic activity [12], inhibition of hepatic oxidative stress [13] and cellular apoptosis [14], and cardiovascular effects including anti-thrombosis and platelet aggregation [15], a decrease in blood pressure [16] and myocardial fibrosis [17]. It was also reported that osthol might be a dual agonist of peroxisome proliferator-activated receptor (PPAR)- α/γ [12, 18, 19], which are known to regulate the myocardial energy and lipid homeostasis [20]. Moreover, osthol could also regulate the downstream target genes of PPAR α/γ , such as carnitine palmitoyltransferase (CPT)-1a and diacylglycerol acyltransferase (DGAT) [13]. The former is a rate-limiting enzyme mediating the entrance of fatty acids into the mitochondria [21], and the latter is a key enzyme in the process of triacylglycerol (TAG) biosynthesis [22].

From these data, we hypothesized that osthol may reduce the cardiac hypertrophy induced by renovascular hypertension via regulation of PPAR α -mediated target genes involved in lipid metabolism and inhibition of myocardial oxidative stress. In the present study, the antioxidant enzymes superoxide dismutase (SOD) and glutathione peroxidase (GSH-Px), as well as a stable terminal metabolite of lipid peroxidation malondialdehyde (MDA) were used as the indicators of oxidative stress.

Materials and Methods

Drugs and Reagents

Osthol was kindly provided by Dr. Jia Zhou of Xi'an Green Fount Natural Product Co. Ltd. (China), the purity was >98 % as determined by high performance liquid chromatography. The assay kits for SOD, GSH-Px, MDA, unesterified fatty acids (FFA) and TAG were manufactured by Nanjing Jiancheng Bioengineering Institute (Nanjing, China). Trizol was a product of Invitrogen (Carlsbad, CA, USA). Reverse transcriptase, dNTP Mix and Taq DNA Polymerase were products of Fermentas (Vilnius, Lithuania). The primers used for amplification by reverse transcription polymerase chain reaction (RT-PCR) were synthesized by Sangon Gene Company (Shanghai, China).

Animals

Sprague–Dawley rats (male, 250 ± 20 g) used in this study were supplied by the Animal Breeding Center of Soochow University (Suzhou, China). Housing conditions of the animals were maintained at a temperature (22–24 °C) and humidity (55–60 %), with a 12 h light/dark cycle. The experimental rats were allowed free access to food and water. The animal study was approved by the Ethics Committee of Soochow University and conducted in accordance with the regulations for the use and care of experimental animals at Soochow University (number of Ethic Committee: 2010-85). These rats were randomized into 4 groups ($n = 8$): namely, control (surgical intervention but not ligation), model (left renal artery ligation), osthol 10 and 20 mg/kg groups (treatment with osthol 10 and 20 mg/kg after left renal artery ligation).

Preparation of Rat Renovascular Hypertensive Model

The rat renovascular hypertensive model induced by two kidney-one clip method was prepared as previously described [23]. For preparation of the animal model, the rats were anesthetized with sodium pentobarbital (i.p. 50 mg/kg). The incision in the left flank was made above the left kidney. A blunt glass needle was used to divide the left renal artery, and then the left renal artery was clipped together with a silver clip (0.2 mm in diameter), which was then removed to generate the renal arteriostenosis and later hypertension. Rats in the control group underwent the same operation but not clipped. After 4 weeks, medicine-treated rats were given osthol 0.2 ml/100 g/day orally by gavage, and the control and model rats were orally given an equivalent volume of 0.5 % sodium carboxymethyl cellulose solution. Ogawa et al. [16] reported that osthol could decrease blood pressure and improve hepatic lipid metabolism in spontaneously hypertensive rats after administration for 4 weeks. Therefore, all of rats were sacrificed after treatment with osthol for 4 weeks. The blood and heart were collected for measurement of design parameters. The partial left ventricles were taken, put into a freezing tube, then weighed and quickly frozen in liquid nitrogen and stored at -80 °C for RT-PCR. The weight of the partial left ventricles equaled the total weight minus the weight of the empty tube. The rest of the heart was obtained and weighed for measurement of related parameters.

Measurement of Systolic Blood Pressure

The systolic blood pressure of rat tail artery was measured in rats that were awake using the CODA 4 tail-cuff non-invasive blood pressure system (Kent Scientific Corporation, Torrington, USA) and once every 2 weeks after

renovascular ligation. The room temperature of the measurement was kept at about 30 °C. The rats were acclimated to the acrylic holders and tail-cuff apparatus, specifically designed for the non-invasive blood pressure system, for 5 min before each rat measurement. The blood pressure measurements were performed at the same time of day (9:00–13:00) in order to avoid the influence of the circadian cycle, and the blood pressure values were obtained by calculation of the average reading of five measurements.

Measurement of Heart Weight Indexed to Body Weight

The heart was immediately excised and weighed. The absolute heart weight was obtained by the calculation, namely, the weight of partial left ventricles plus the weight of the rest of heart. The heart weight index was calculated according to absolute heart weight (g) divided by body weight (g).

Measurement of Myocardial SOD, GSH-Px, and MDA Levels

The heart was excised and partial right ventricles were rapidly cut into pieces in ice-cold saline, then a tissue homogenate (10 %, W/V) was prepared. The contents of myocardial SOD, GSH-Px, MDA and protein were determined by colorimetric methods, respectively. All procedures completely complied with the manufacturer's instructions.

Measurement of Myocardial FFA and TAG Levels

The partial left ventricles were rapidly cut into pieces, the tissue homogenate (10 %, W/V) was prepared using a chloroform/methanol mixed solution (1:1, V:V) to extract the myocardial lipid, the prepared sample was then

centrifuged at 1,200×g for 10 min, the substratum obtained was used for measurement of FFA and TAG levels according to the colorimetric methods following the manufacturer's instructions.

Morphological Observation

The partial specimens of left ventricles were fixed in 10 % formaldehyde solution, embedded in paraffin, and sectioned on a microtome for hematoxylin–eosin staining, and then examined under a light microscope to evaluate the size of cardiomyocytes. The perimeters of 100 cells from every section were traced and analyzed by the Image J 1.44p software system, which was used to calculate the mean cross-sectional area.

RT-PCR

Total RNA was extracted from frozen rat myocardial tissues using trizol reagent, and RT-PCR was performed according to the manufacturer's instructions. The concentration and purity of the RNA were determined spectrophotometrically by the absorbance ratio 260:280 nm. Then total RNA (5 µg) was used for the RT reaction performed in 40 µl of the final volume at 42 °C for 60 min. The PCR was carried out by the following conditions: one cycle of 94 °C for 3 min, followed by 35 cycles of denaturation at 94 °C for 30 s, annealing (the temperature was seen in Table 1) for 60 s, and extension at 72 °C for 30 s. A final extension was 72 °C for 10 min. The RT-PCR was used for measurement of PPAR α , CPT-1a, DGAT, and glyceraldehyde phosphate dehydrogenase (GAPDH) mRNA expressions in rat myocardial tissues. The specific primers used for PCR amplification were seen in Table 1. GAPDH was used as an internal control. Data were expressed as a ratio of the signals of interest mRNA to that of GAPDH mRNA.

Table 1 The specific primers used for PCR amplification to determine the gene expression in rat myocardial tissues

Gene	Primer sequence	bp	Annealing temperature (°C)
PPAR α			
Sense	5'-CCTGGCAATGCACTGAACATCG-3'	509	59
Antisense	5'-ACGCCGTTGGCTACCATCTTG-3'		
CPT-1a			
Sense	5'-GGATGGCTATGGTCAAGGT-3'	392	52
Antisense	5'-CAGTATGGCGTGGATGGT-3'		
DGAT			
Sense	5'-CTTTCTGCTACGGCGGGTTCTT-3'	493	59
Antisense	5'-CAGTGGGACCTGAGCCATCATT-3'		
GAPDH			
Sense	5'-ATGACTCTACCCACGGCAAGT-3'	704	57
Antisense	5'-GGAGACAACCTGGTCCTCAGT-3'		

Statistical Analysis

The data are expressed as means \pm SEM. The *F* test and Kolmogorov–Smirnov test were performed to test for homogeneity of variance and normality of distribution, respectively. The normally distributed variables were analyzed using one-way analysis of variance (ANOVA) followed by a post hoc LSD test. The variables that are not normally distributed and/or displayed homogeneity of variance were analyzed using one-way ANOVA followed by a post hoc Games–Howell test. The statistical analysis was conducted using SPSS 18.0 software. $p < 0.05$ was considered statistically significant.

Results

Effect on Systolic Blood Pressure

The results are shown in Table 2. Compared with the control group, the systolic blood pressure in the model group was higher after the second week subsequent to renovascular ligation and steadily maintained at the high level ($p < 0.001$), suggesting that rat hypertension had developed. The systolic blood pressure was reduced with osthol 20 mg/kg/day treatment at 2 and 4 weeks ($p < 0.001$), and the expected reduction in systolic blood pressure was also observed after treatment with osthol 10 mg/kg/day for 4 weeks ($p = 0.023$).

Effect on Heart Weight Indexed to Body Weight

The results are shown in Table 3. The absolute heart weights and heart weights indexed to body weight in the model group were higher than those in the control group ($p = 0.038$ and $p < 0.001$, respectively). Indexed heart weight was lower in the animals treated for 4 weeks with osthol 20 mg/kg/day compared to the model animals ($p = 0.002$).

Table 3 Changes of absolute heart weight, body weight, and heart weight indexed to body weight after treatment with osthol for 4 weeks in renovascular hypertensive rats

Group	Absolute heart weight (g)	Body weight (g)	Heart weight indexed to body weight (g/g)
Control	1.290 \pm 0.032	444.1 \pm 9.4	0.00291 \pm 0.00005
Model	1.390 \pm 0.029 [#]	440.1 \pm 5.9	0.00318 \pm 0.00004 [#]
Osthol 20 mg/kg	1.332 \pm 0.030	450.8 \pm 7.5	0.00295 \pm 0.00005*
Osthol 10 mg/kg	1.388 \pm 0.044	451.4 \pm 4.8	0.00308 \pm 0.00010

Data are presented as means \pm SEM; $n = 8$

[#] $p < 0.05$ versus control group

* $p < 0.05$ versus model group

Effect on Myocyte Cross-Sectional Area

The results are presented in Fig. 1. Compared with the control group, the myocyte cross-sectional area in the model group was higher ($p < 0.001$). After treatment with osthol 10 and 20 mg/kg/day for 4 weeks, the myocyte cross-sectional area was lower ($p < 0.001$), showing a cardiomyocyte smaller in size.

Effects on Myocardial SOD, GSH-Px, and MDA Contents

The results shown in Table 4 indicate that in the model group, the myocardial SOD and GSH-Px contents were lowered ($p = 0.002$ and $p = 0.027$, respectively), and the MDA content had increased as compared with the control group ($p = 0.019$). After administration for 4 weeks, the SOD and GSH-Px contents in myocardial tissues were increased in the osthol 10 mg/kg ($p = 0.035$ and $p < 0.001$, respectively) and 20 mg/kg ($p < 0.001$) groups, but the MDA content was only lowered in the osthol 20 mg/kg group ($p = 0.025$).

Table 2 Changes of systolic blood pressure of rat tail artery after renovascular ligation for 8 weeks and later treatment with osthol for 4 weeks in rats (mmHg)

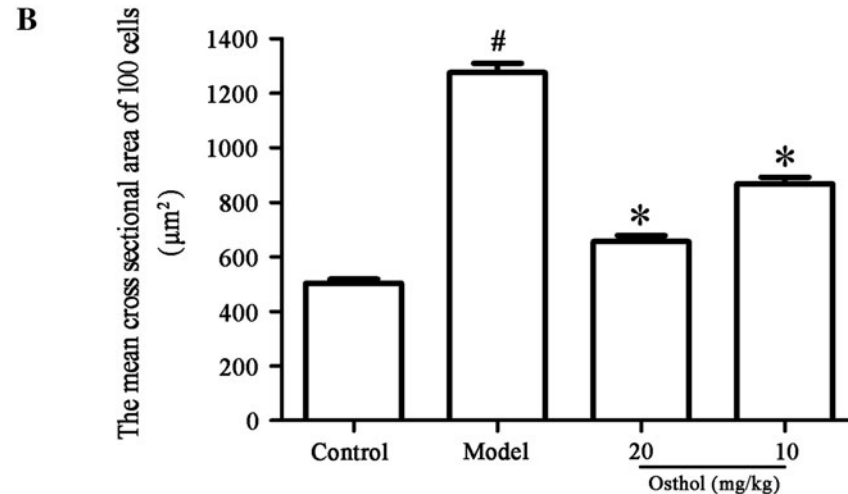
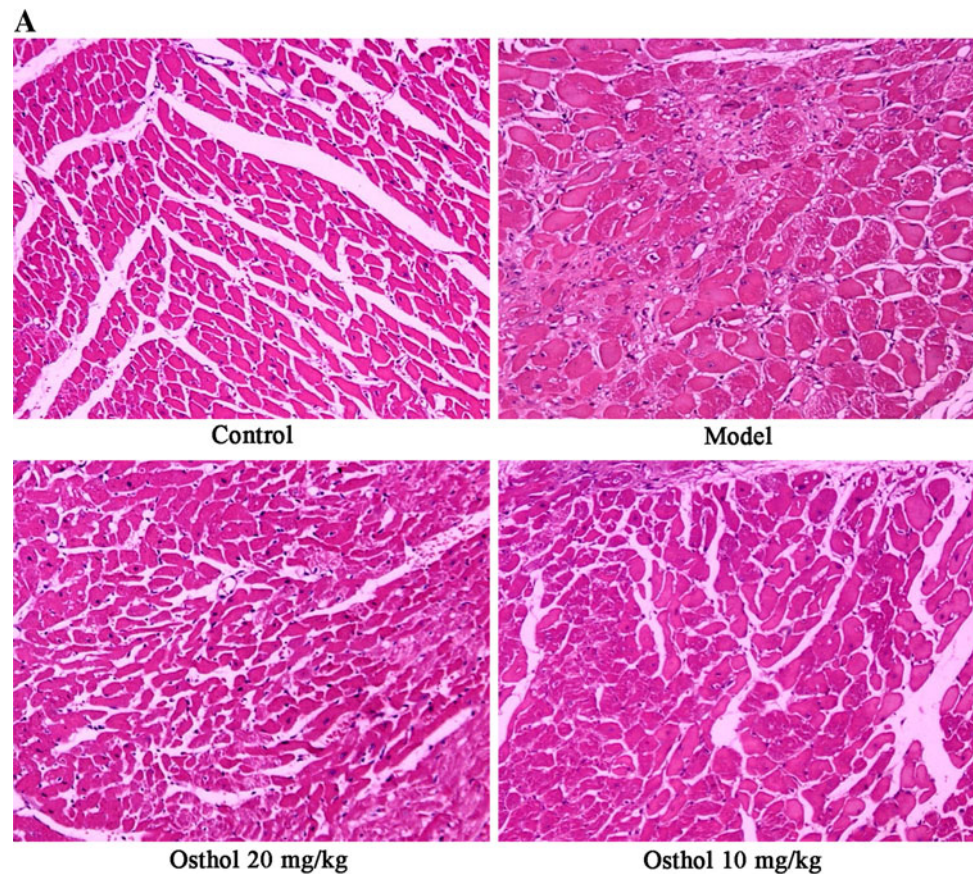
Group	Pre-treatment with osthol			Post-treatment with osthol	
	0	2nd week	4th week	2nd week	4th week
Control	133.0 \pm 0.6	133.9 \pm 1.8	125.8 \pm 1.6	131.0 \pm 1.7	125.2 \pm 1.8
Model	132.2 \pm 1.5	158.6 \pm 3.6 [#]	161.9 \pm 2.7 [#]	162.2 \pm 2.0 [#]	161.1 \pm 1.9 [#]
Osthol 20 mg/kg	130.4 \pm 1.1	154.0 \pm 2.4 [#]	160.1 \pm 2.6 [#]	133.4 \pm 3.0*	129.4 \pm 2.0*
Osthol 10 mg/kg	134.1 \pm 0.8	156.9 \pm 2.1 [#]	158.8 \pm 2.9 [#]	159.0 \pm 2.6 [#]	153.5 \pm 2.2 ^{#,*}

Data are presented as means \pm SEM; $n = 8$

[#] $p < 0.05$ versus control group

* $p < 0.05$ versus model group

Fig. 1 Myocardial histological changes after treatment with osthol for 4 weeks in renovascular hypertensive rats. **a** The images of myocardium (hematoxylin–eosin staining, $\times 100$). **b** The mean cross-sectional area of 100 cardiomyocytes. Data are presented as means \pm SEM; $n = 8$. $\#p < 0.05$ versus control group; $*p < 0.05$ versus model group



Effects on Myocardial FFA and TAG Levels

The results are presented in Table 5. In the model group, the levels of myocardial FFA and TAG were higher compared with the control group ($p < 0.001$ and $p = 0.008$, respectively). After treatment with osthol for 4 weeks, the elevated FFA and TAG were lowered in the osthol 20 mg/kg group ($p = 0.017$ and $p = 0.004$, respectively), but not affected in the osthol 10 mg/kg group.

Effects on Myocardial PPAR α , CPT-1a, and DGAT mRNA Expressions

As shown in Fig. 2, the myocardial PPAR α and CPT-1a mRNA expressions had been lowered in the model group ($p < 0.001$) and increased in the osthol 10 mg/kg ($p = 0.003$ and $p = 0.012$, respectively) and 20 mg/kg ($p < 0.001$) groups. The myocardial DGAT mRNA expression was increased in the model group compared to

Table 4 Levels of SOD, GSH-Px, and MDA in myocardial tissues after treatment with osthol for 4 weeks in renovascular hypertensive rats

Group	SOD (U/mg protein)	GSH-Px ($\mu\text{mol/mg protein}$)	MDA (nmol/mg protein)
Control	170.1 \pm 4.2	77.0 \pm 2.0	0.469 \pm 0.018
Model	144.2 \pm 5.0 [#]	70.8 \pm 1.4 [#]	0.574 \pm 0.035 [#]
Osthol 20 mg/kg	166.8 \pm 2.6*	88.8 \pm 1.5*	0.467 \pm 0.024*
Osthol 10 mg/kg	162.7 \pm 6.2*	87.5 \pm 2.3*	0.486 \pm 0.022

Data are presented as means \pm SEM; $n = 8$

[#] $p < 0.05$ versus control group

* $p < 0.05$ versus model group

Table 5 Levels of myocardial FFA and TAG after treatment with osthol for 4 weeks in renovascular hypertensive rats

Group	FFA ($\mu\text{mol/g protein}$)	TAG (mg/g protein)
Control	27.51 \pm 1.42	0.963 \pm 0.074
Model	48.82 \pm 3.79 [#]	1.232 \pm 0.045 [#]
Osthol 20 mg/kg	37.98 \pm 2.04*	1.034 \pm 0.037*
Osthol 10 mg/kg	48.36 \pm 5.40	1.250 \pm 0.039

Data are presented as means \pm SEM; $n = 8$

[#] $p < 0.05$ versus control group

* $p < 0.05$ versus model group

the control group ($p < 0.001$), and decreased in the osthol 20 mg/kg group ($p < 0.001$) and unchanged in the osthol 10 mg/kg group compared to the model group.

Discussion

The two kidney-one clip method is generally acknowledged as a conventional model of hypertension, which may cause an increase in the angiotensin II release via the activation of renin-angiotensin system, and leads to an increase in the blood pressure and oxidative stress, and final cardiac hypertrophy [4, 23, 24]. Our experimental results indicated that in the model group, the blood pressure, heart weight index, myocyte cross-sectional area and myocardial MDA content were increased, the myocardial SOD and GSH-Px contents were decreased, suggesting that the rat cardiac hypertrophy induced by renovascular hypertension had successfully developed, and the animal model might result in myocardial oxidative stress.

Hypertension is generally recognized as a major risk for cardiac hypertrophy. Ogawa et al. [16] observed that osthol could lower the elevated blood pressure in stroke-prone spontaneously hypertensive rats. In the present study, our

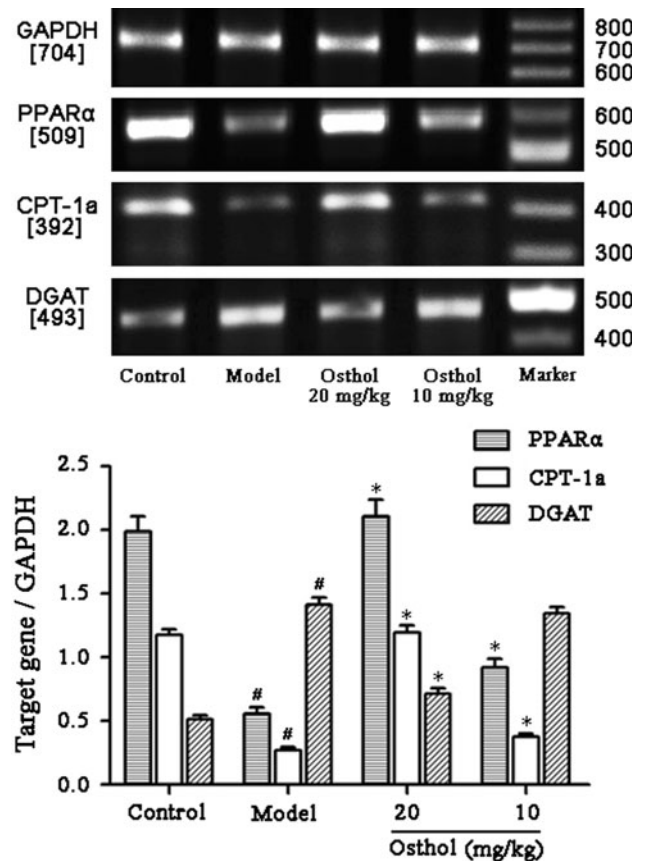


Fig. 2 Effects of osthol on myocardial PPAR α , CPT-1a and DGAT mRNA expressions after administration for 4 weeks in renovascular hypertension-induced cardiac hypertrophic rats. Data are presented as means \pm SEM; $n = 5$. [#] $p < 0.05$ versus control group; * $p < 0.05$ versus model group

experimental results further demonstrated that osthol was effective in lowering blood pressure. The mechanism might be related to its Ca²⁺ channel-blocking property and the elevation of the cGMP level in vascular smooth muscle [25].

Recently, it has been reported that oxidative stress is involved in hypertensive development in the two kidney-one clip animal model [26] and plays a critical role in the progression of cardiac hypertrophy [1, 4, 27–29]. It is known that oxidative stress may lead to the accumulation of the lipid peroxidation product MDA, and cause cellular dysfunction. The antioxidants may play an important role in cellular defense against oxidative stress and it has been proposed that they prevent the development of cardiac hypertrophy [30, 31]. In the present study, the results showed that osthol at 20 mg/kg/day was associated with a reduced MDA content and increased the SOD and GSH-Px contents in the heart, demonstrating an inhibitory effect on the myocardial oxidative stress. The results were in accordance with our previous observation [13], which might be one of mechanisms for the observed antihypertrophic effect.

Under normal physiological condition, the main substrates of myocardial energy metabolism are from fatty acids. Recent studies have shown that the myocardium of cardiac hypertrophy might switch from fatty acids to glucose utilization [2, 3, 7], which results in the decrement of myocardial fatty acid oxidation and the accumulation of fatty acids and TAG in the heart. This conversion may initially be a compensatory mechanism, but the continuous accumulation of fatty acids in the heart may lead to further oxidative stress and severe cardiac hypertrophy [1]. In our present study, the results also showed that the levels of myocardial FFA and TAG were higher in the model group. After treatment with osthol, the elevated lipid levels in myocardium were lower, suggesting that osthol might reduce the cardiac hypertrophy via regulation of myocardial lipid metabolism.

PPAR α plays an important role in regulating lipid metabolic genes including CPT-1a and DGAT [20]. In the present study, we found that after treatment with osthol, the myocardial PPAR α and CPT-1a mRNA expressions were increased, while the myocardial DGAT mRNA expression was decreased, suggesting that osthol might enhance myocardial fatty acid oxidation and suppress myocardial TAG biosynthesis, and that the reduction in myocardial TAG in osthol-treated rats was consistent with reduced DGAT mRNA expression.

In conclusion, our present study demonstrated that osthol is effective at alleviating renovascular hypertension-induced cardiac hypertrophy in rats, and the mechanisms of its effect might be related to the reduction in myocardial oxidative stress and an improvement in myocardial lipid metabolism via regulation of PPAR α -mediated target genes CPT-1a and DGAT. However, there were some deficiencies in the present study. It would be best to investigate the exact effects of osthol on protein expressions of PPAR α , CPT-1a and DGAT. On the other hand, the inflammatory cytokines also participates in the pathogenesis of cardiac hypertrophy [32], thus the therapeutic effect of osthol may be attributed partly to its anti-inflammatory property. Our previous studies have observed that osthol could inhibit myocardial inflammatory factors like nuclear factor- κ B and transforming growth factor β 1 in myocardial fibrotic mice [17]. Therefore, further research is also needed to clarify this.

Acknowledgments This work was supported by grants from the Science and Technology Fund of Suzhou City (no. SWG0903) and the Priority Academic Program Development of Jiangsu Higher Education Institutions, China. The authors gratefully acknowledge associate Professor Min Deng for her assistance in histopathological analysis.

Conflict of interest The authors declare that there are no conflicts of interest.

References

- Purushothaman S, Nair RR, Harikrishnan VS, Fernandez AC (2011) Temporal relation of cardiac hypertrophy, oxidative stress, and fatty acid metabolism in spontaneously hypertensive rat. *Mol Cell Biochem* 351:59–64
- Bishop SP, Altschuld RA (1970) Increased glycolytic metabolism in cardiac hypertrophy and congestive failure. *Am J Physiol* 218:153–159
- Takeyama D, Kagaya Y, Yamane Y, Shiba N, Chida M, Takahashi T, Ido T, Ishide N, Takishima T (1995) Effects of chronic right ventricular pressure overload on myocardial glucose and free fatty acid metabolism in the conscious rat. *Cardiovasc Res* 29:763–767
- Polizio AH, Balestrasse KB, Yannarelli GG, Noriega GO, Gorzalczy S, Taira C, Tomaro ML (2008) Angiotensin II regulates cardiac hypertrophy via oxidative stress but not antioxidant enzyme activities in experimental renovascular hypertension. *Hypertens Res* 31:325–334
- Adiga IK, Nair RR (2007) A positive association between cardiomyocyte volume and serum malondialdehyde levels. *Int J Cardiol* 115:246–248
- Liu C, Cao F, Tang QZ, Yan L, Dong YG, Zhu LH, Wang L, Bian ZY, Li H (2010) Allicin protects against cardiac hypertrophy and fibrosis via attenuating reactive oxygen species-dependent signaling pathways. *J Nutr Biochem* 21:1238–1250
- Bernardo BC, Weeks KL, Pretorius L, McMullen JR (2010) Molecular distinction between physiological and pathological cardiac hypertrophy: experimental findings and therapeutic strategies. *Pharmacol Therapeut* 128:191–227
- Agrawal R, Agrawal N, Koyani CN, Singh R (2010) Molecular targets and regulators of cardiac hypertrophy. *Pharmacol Res* 61:269–280
- Liu JX, Zhang WP, Zhou L, Wang XR, Lian QS (2005) Anti-inflammatory effect and mechanism of osthol in rats. *J Chin Med Mater* 28:1002–1006
- Zhang QY, Qin LP, He WD, Van Puyvelde L, Maes D, Adams A, Zheng HC, De Kimpe N (2007) Coumarins from *Cnidium monnieri* and their antiosteoporotic activity. *Planta Med* 73:13–19
- Kuo PL, Hsu YL, Chang CH, Chang JK (2005) Osthole-mediated cell differentiation through bone morphogenetic protein-2/p38 and extracellular signal-regulated kinase 1/2 pathway in human osteoblast cells. *J Pharmacol Exp Ther* 314:1290–1299
- Liang HJ, Suk FM, Wang CK, Hung LF, Liu DZ, Chen NQ, Chen YC, Chang CC, Liang YC (2009) Osthole, a potential antidiabetic agent, alleviates hyperglycemia in db/db mice. *Chem Biol Interact* 181:309–315
- Zhang JJ, Xue J, Wang HB, Zhang Y, Xie ML (2010) Osthole improves alcohol-induced fatty liver in mice by reduction of hepatic oxidative stress. *Phytother Res* 25:638–643
- Okamoto T, Kawasaki T, Hino O (2003) Osthole prevents anti-fas antibody-induced hepatitis in mice by affecting the caspase-3-mediated apoptotic pathway. *Biochem Pharmacol* 65:677–681
- Chen R, Xie ML, Zhou J (2005) Experimental study of osthole on inhibition of thrombosis and platelet aggregation. *Chin Pharmacol Bull* 21:440–443
- Ogawa H, Sasai N, Kamisako T, Baba K (2007) Effects of osthole on blood pressure and lipid metabolism in stroke-prone spontaneously hypertensive rats. *J Ethnopharmacol* 112:26–31
- Chen R, Xue J, Xie ML (2011) Reduction of isoprenaline-induced myocardial TGF- β 1 expression and fibrosis in osthole-treated mice. *Toxicol Appl Pharmacol* 256:168–173
- Zhang Y, Xie ML, Xue J, Gu ZL (2007) Osthole improves fat milk-induced fatty liver in rats, modulation of hepatic

- PPAR- α / γ -mediated lipogenic gene expression. *Planta Med* 73:718–724
19. Zhang Y, Xie ML, Xue J, Gu ZL (2008) Osthonol regulates enzyme protein expression of CYP7A1 and DGAT2 via activation of PPAR α / γ in fat milk-induced fatty liver rats. *Asian Nat Prod Res* 10:807–812
 20. Yang QL, Li YH (2007) Roles of PPARs on regulating myocardial energy and lipid homeostasis. *J Mol Med* 85:697–706
 21. Morifuji M, Sanbongi C, Sugiura K (2006) Dietary soya protein intake and exercise training have an additive effect on skeletal muscle fatty acid oxidation enzyme activities and mRNA levels in rat s. *Br J Nutr* 96:469–475
 22. Yen CLE, Stone SJ, Koliwad S, Harris C, Farese RV (2008) DGAT enzymes and triacylglycerol biosynthesis. *J Lipid Res* 49:2283–2301
 23. Sharifi AM, Akbarloo N, Heshmatian B, Ziai A (2003) Alteration of local ACE activity and vascular responsiveness during development of 2K1C renovascular hypertension. *Pharmacol Res* 47:201–209
 24. Okamura T, Miyazaki M, Inagami T, Toda N (1986) Vascular rennin-angiotensin system in two-kidney one clip hypertensive rats. *Hypertension* 8:560–565
 25. Ko FN, Wu TS, Liou MJ, Huang TF, Teng CM (1992) Vasorelaxation of rat thoracic aorta caused by osthole isolated from *Angelica pubescens*. *Eur J Pharmacol* 219:29–34
 26. Oliveira-Sales EB, Dugaich AP, Carillo BA, Abreu NP, Boim MA, Martins PJ, D'Almeida V, Dolnikoff MS, Bergamaschi CT, Campos RR (2008) Oxidative stress contributes to renovascular hypertension. *Am J Hypertens* 21:98–104
 27. Foussal C, Lairez O, Calise D, Pathak A, Guilbeau-Frugier C, Valet P, Parini A, Kunduzova O (2010) Activation of catalase by apelin prevents oxidative stress-linked cardiac hypertrophy. *FEBS Lett* 584:2363–2370
 28. Jaiswal A, Kumar S, Seth S, Dinda AK, Maulik SK (2010) Effect of U50, 488H, a κ -opioid receptor agonist on myocardial α - and β -myosin heavy chain expression and oxidative stress associated with isoproterenol-induced cardiac hypertrophy in rat. *Mol Cell Biochem* 345:231–240
 29. Dai DF, Johnson SC, Villarin JJ, Chin MT, Nieves-Cintrón M, Chen T, Marcinek DJ, Dorn GW, Kang YJ, Prolla TA, Santana LF, Rabinovitch PS (2011) Mitochondrial oxidative stress mediates angiotensin II-induced cardiac hypertrophy and G α q overexpression-induced heart failure. *Circ Res* 108:837–846
 30. Tsujimoto I, Hikoso S, Yamaguchi O, Kashiwase K, Nakai A, Takeda T, Watanabe T, Taniike M, Matsumura Y, Nishida K, Hori M, Kogo M, Otsu K (2005) The antioxidant edaravone attenuates pressure overload-induced left ventricular hypertrophy. *Hypertension* 45:921–926
 31. Sheng R, Gu ZL, Xie ML, Zhou WX, Guo CY (2007) EGCG inhibits cardiomyocyte apoptosis in pressure overload-induced cardiac hypertrophy and protects cardiomyocytes from oxidative stress in rats. *Acta Pharmacol Sin* 28:191–201
 32. Shiota N, Rysa J, Kovanen PT, Rusokaho H, Kokkonen JO, Lindstedt KA (2003) A role for cardiac mast cells in the pathogenesis of hypertensive heart disease. *J Hypertens* 21:1935–1944

Pluronic Block Copolymers Inhibit Low Density Lipoprotein Self-Association

Alexandra A. Melnichenko · Denis V. Aksenov · Veronika A. Myasoedova ·
Oleg M. Panasenko · Alexander A. Yaroslavov · Igor A. Sobenin ·
Yuri V. Bobryshev · Alexander N. Orekhov

Received: 25 April 2012 / Accepted: 28 June 2012 / Published online: 14 July 2012
© AOCs 2012

Abstract Little is known about exogenous inhibitors of low-density lipoprotein (LDL) aggregation. The search for nontoxic and bioavailable inhibitors of LDL aggregation is of interest, especially considering that the suppression of the aggregation of LDL might represent a therapeutic approach. We hypothesized that amphiphilic copolymers of propylene oxide and ethylene oxide, the so-called Pluronic block copolymers, can be used to influence the aggregation of LDL. In this work we used Pluronic® P85, L61 and F68. A comparative study of the effects of Pluronic block copolymers with various hydrophilic–lipophilic properties on the aggregation process of LDL showed that Pluronic copolymers with strong hydrophobic properties (P85 and L61) at concentrations close to or greater than the respective critical concentration of micelle formation inhibited the aggregation process of LDL; however, the “hydrophilic” Pluronic F68 had no effect on the aggregation of

LDL at any concentration. Thus, the study demonstrated for the first time that Pluronic® block copolymers inhibit LDL self-association. The possibility of modulating the aggregation of LDL by various Pluronic copolymers can be regarded as a prerequisite in the creation of new types of anti-atherosclerotic drugs.

Keywords Low density lipoproteins · LDL · Aggregation · Atherosclerosis · Pluronic block copolymers

Abbreviations

ApoA	Apolipoprotein
ApoA-I	High-density lipoprotein apolipoprotein
BSA	Bovine serum albumin
HDL	High-density lipoprotein(s)
EO	Ethylene oxide
LDL	Low-density lipoprotein(s)
PO	Propylene oxide
VLDL	Very low-density lipoprotein(s)

A. A. Melnichenko · V. A. Myasoedova · A. N. Orekhov
Institute of General Pathology and Pathophysiology, Russian
Academy of Medical Sciences, Moscow, Russia

D. V. Aksenov · V. A. Myasoedova · O. M. Panasenko ·
I. A. Sobenin · Y. V. Bobryshev · A. N. Orekhov
Skolkovo Innovative Centre, Institute for Atherosclerosis
Research, Russian Academy of Natural Sciences,
Moscow, Russia

A. A. Yaroslavov
Department of Chemistry, M.V. Lomonosov Moscow State
University, Moscow, Russia

Y. V. Bobryshev (✉)
Faculty of Medicine, School of Medical Sciences,
St Vincent’s Hospital Sydney, University of New South Wales,
Kensington, NSW 2052, Australia
e-mail: y.bobryshev@unsw.edu.au

Introduction

One of the earliest manifestations of atherosclerosis at the cellular level is the accumulation of lipids, particularly cholesterol esters, in the intima of the arteries [1–4]. The source of the lipids that accumulate in the intima of blood vessels is the low-density lipoproteins (LDL) circulating in the blood [4, 5]. It is known that native LDL circulating in the blood cannot cause lipid accumulation in cultured cells and thus, native LDL are not atherogenic [6–8]. However, modified LDL do become atherogenic [8–11]. In vitro, LDL can be modified by various ways (acetylated, treated with malondialdehyde, vortexed) [8–11].

It is also known that native LDL do not form aggregates and do not possess atherogenic properties, which means LDL do not cause the intracellular accumulation of lipids [12]. Aggregated LDL acquire atherogenic properties as shown in *in vitro* experiments [10–12]. The binding affinity of LDL (–) to human aortic proteoglycans depends on their aggregation level [13]. It is a general assumption that *in vivo*, native LDL (which are not modified or aggregated) do not possess atherogenic properties. This explains interest in the search for modulators of the LDL aggregation process.

For this reason, there is heightened interest in the search for modulators of the LDL aggregation process.

There are several known endogenous inhibitors of the aggregation of LDL [10, 14], such as 17 beta-estradiol (E2), a specific ligand to apoB-100, stabilizes apoprotein, and the E2-stabilized LDL is resistant to aggregation [15], lipoprotein-deficient serum, bovine serum albumin (BSA), high-density lipoprotein (HDL) from healthy donors and primary HDL apolipoprotein (ApoA-I). These inhibitors all have amphiphilic properties, and presumably by interacting with hydrophobic regions on the surface of the LDL, these inhibitors prevent an interaction between LDL particles and inhibit aggregation. Little is known about exogenous inhibitors of LDL aggregation. Therefore, the search and studies of nontoxic and bioavailable inhibitors of LDL aggregation are of great interest, especially considering that the suppression of the aggregation of LDL might represent a therapeutic approach.

In this work, we hypothesized that amphiphilic copolymers of propylene oxide (PO) and ethylene oxide (EO), the so-called Pluronic block copolymers, can be used to this end. In this study, we examined the ability of various Pluronic copolymers to influence the aggregation of LDL.

Materials and Methods

We used Pluronic® P85, L61 and F68 (BASF; Wyandotte, MI). The study complied with institutional ethical use protocols. The total LDL fraction was isolated by ultracentrifugation using a two-step density gradient of NaBr from the serum of patients with cardiovascular disease (men aged 40–74 years with early asymptomatic carotid atherosclerosis) [16]. The protein concentration in the LDL samples was determined using the Lowry method.

To study the aggregation of LDL, the suspension was first freed from those in spontaneously formed aggregates by filtering the sample through a filter with a pore diameter of 0.45 µm (Nalgene, USA). LDL at a concentration of 0.5 mg protein/ml were incubated at 37 °C in isotonic phosphate buffer (IFB; GIBCO; Paisley, UK; KCl 0.2 g/l, KH₂PO₄ 0.2 g/l, NaCl 8 g/l, and Na₂HPO₄ 1.15 g/l,

pH 7.2) with constant stirring at 100 rpm. The degree of aggregation of LDL was assessed by recording light transmission fluctuations through a laser light beam at a wavelength of 860 nm using an Aggregometer (Aggregation analyzer; Biola, RF, USA) [17]. The method is based on the fact that the relative dispersion of the optical density fluctuations caused by random changes in the number of particles entering the optical path of the laser beam reflects the deviations from their average size; in other words, the degree of LDL aggregation. At regular intervals, the fluctuation of light transmission was recorded.

The average size of the aggregates formed was estimated by quasi-elastic scattering of the laser on an Autosizer 2 Malvern (Malvern Instruments, UK). For this measurement, samples of LDL at a concentration of 2.5 mg protein/ml were incubated at 37 °C in isotonic phosphate buffer with constant stirring at 1,000 rpm. At regular intervals, the particle size measurement was performed. The addition of EDTA did not affect the association of LDL.

Results

Low-density lipoprotein particles are prone to spontaneous aggregation. The so-called spontaneous aggregation of LDL, which is not induced by external factors, occurs during the incubation of LDL particle suspensions at 37 °C with constant stirring. We used two methods to assess the aggregation of LDL and the influence of Pluronic copolymers on this process, the transmission method and the fluctuations of the quasi-elastic laser scattering method. In all cases, the results obtained using the two methods to evaluate the aggregation of LDL fully coincided. This finding is well illustrated in Figs. 1 and 2.

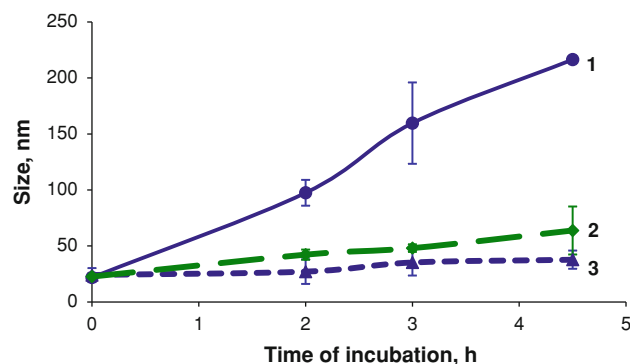


Fig. 1 Kinetic curves showing changes in the average particle size of LDL under the influence of Pluronic P85. The incubation medium was IFB at pH 7.4, the concentration of LDL was 2.5 mg protein/ml, incubation temperature was 37 °C, and a stirring speed of 1,000 r/min was used. Curve (1), suspension of LDL in the absence of Pluronic P85; curves (2 and 3) in the presence of 0.01 and 0.1 % Pluronic P85, respectively

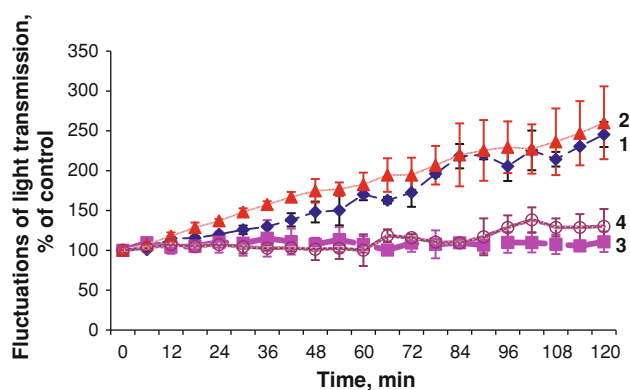


Fig. 2 Kinetic curves of changes in the fluctuations of light transmission of the suspension under the influence of Pluronic P85. The incubation medium was IFB at pH 7.4, the concentration of LDL was 0.5 mg protein/ml, incubation temperature was 37 °C, and a stirring speed of 100 r/min was used. Curve (1), suspension of LDL in the absence of Pluronic P85; curves (2–4) in the presence of 0.005, 0.1 and 0.01 % Pluronic P85, respectively

We conducted a comparative study of Pluronic block copolymers with various hydrophilic–lipophilic properties on the aggregation process of LDL. For these experiments, we used Pluronic F68, which has a high hydrophilic–lipophilic balance (HLB 29) and pronounced hydrophilic properties, Pluronic L61, which is characterized by a large hydrophobic balance (HLB 3), and Pluronic P85, which has a moderate hydrophilic and lipophilic balance (HLB 16).

Figure 1 shows representative kinetic curves of changes in the average particle size of LDL in the event of spontaneous aggregation and in the presence of Pluronic P85. We observed an increase in the average particle size during spontaneous aggregation that depends on the incubation time (Fig. 1). At the same time, the addition of various concentrations of Pluronic P85 significantly inhibited the formation of LDL aggregates. Therefore, the addition of Pluronic P85 at a concentration of 0.1 % (v/v%) to a suspension of LDL before incubation inhibited the aggregation by 93 % after 4.5 h of incubation (Fig. 1). This suppression effect was dependent on the concentration of Pluronic P85, and when the concentration of Pluronic P85 was used at 0.01 %, aggregation was suppressed by 79 % after 4.5 h of incubation (Fig. 1).

Similar data were obtained in the fluctuations of light transmission. Figure 2 shows typical curves of variation of light transmission fluctuations in the suspension of LDL in the presence of various concentrations of Pluronic copolymers in the incubation medium. As shown in Fig. 2, the lowest concentration of Pluronic P85 (0.005 %) had no effect on the aggregation process of LDL. Thus, it is clear that Pluronic P85 was an inhibitor of the aggregation of LDL only at a concentration close to or greater than

Table 1 Properties of the used pluronics

Pluronic	Molecular mass (Da)	Critical micelle concentration (%)	Hydrophilic–lipophilic balance
L61	2,000	>0.022	3
P85	4,600	0.005–0.05	16
F68	8,400	>0.4	29

the critical concentration of micelle formation (CCM) (Table 1), which is 0.03 % for Pluronic P85.

When Pluronic P85 was added to a suspension of LDL during incubation (when the process of aggregation of the particles had already been initiated), an increase in the average particle size of LDL was inhibited (Fig. 3). Pluronic P85 was added to a suspension of LDL at a concentration of 0.1 % after the first and second hour of incubation. In both cases, no further increase in the average particle size was observed, and aggregation was fully suppressed. It should be noted that the addition of Pluronic P85 did not cause any decrease in the average particle size; therefore, one can assume that the action of Pluronic P85 did not induce disaggregation of the LDL aggregates. Consequently, the aggregation of LDL is irreversible and is likely to merge LDL particles.

In addition to Pluronic P85, we examined the ability of two other Pluronic copolymers to inhibit the aggregation of LDL. It was shown that Pluronic F68, which is characterized by pronounced hydrophilic properties and a high value of HLB, has no influence on the aggregation process of LDL particles. Figure 4 shows representative kinetic curves of changes in light transmission fluctuations in the presence of Pluronic F68 at a concentration of 0.4 % and in the absence of Pluronic copolymers (Fig. 4). In addition, using a higher concentration of Pluronic F68 (4 %) did not

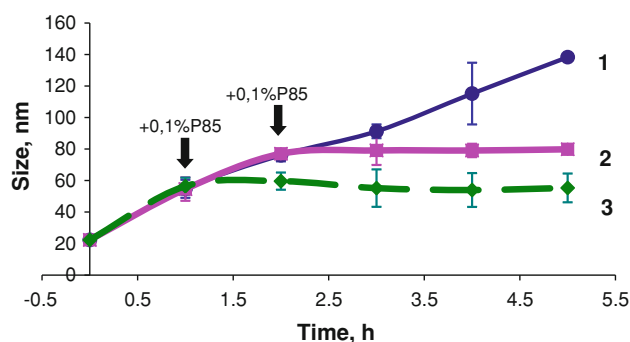


Fig. 3 Kinetic curves of changes in the average particle size of LDL under the influence of Pluronic P85. The incubation medium was IFB at pH 7.4, the concentration of LDL was 2.5 mg protein/ml, incubation temperature was 37 °C, and a stirring speed of 1,000 r/min was used. Curve (1), suspension of LDL in the absence of Pluronic P85; curve (2), in the presence of 0.1 % Pluronic P85 added after 2 h of incubation; and curve (3), in the presence of 0.1 % Pluronic P85 added after 1 h of incubation

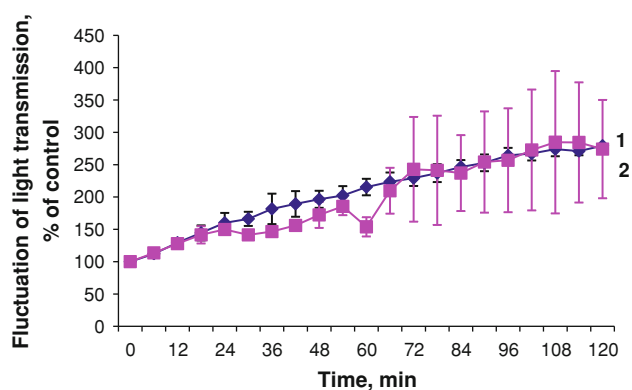


Fig. 4 Kinetic curves of changes in the fluctuations of light transmission of the suspension of LDL under the influence of Pluronic F68. The incubation medium was IFB at pH 7.4, the concentration of LDL was 0.5 mg protein/ml, incubation temperature was 37 °C, and a stirring speed of 100 r/min was used. Curve (1), suspension of LDL in the absence of Pluronic F68; and curve (2), in the presence of 0.4 % Pluronic F68

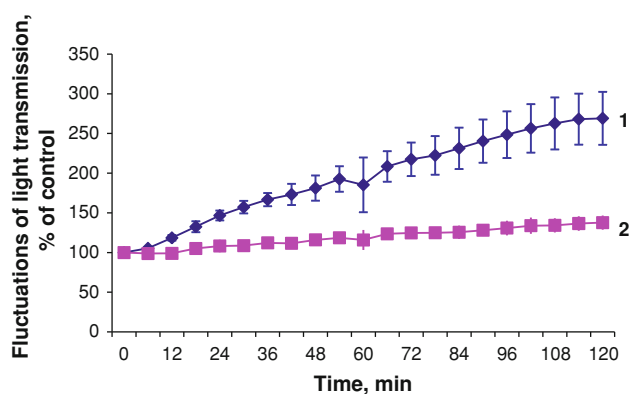


Fig. 5 Kinetic curves of changes in the fluctuations of light transmission of the suspension of LDL under the influence of Pluronic L61. The incubation medium was IFB at pH 7.4, the concentration of LDL was 0.5 mg protein/ml, the incubation temperature was 37 °C, and a stirring speed of 100 r/min was used. Curve (1), suspension of LDL in the absence of Pluronic L61; and curve (2) in the presence of 0.022 % Pluronic L61

lead to inhibition of the aggregation process of LDL (data not shown). However, the application of Pluronic L61, which has pronounced hydrophobic properties and a low HLB value, led to the suppression of the aggregation of LDL. Thus, at a concentration of 0.022 %, Pluronic L61 inhibited the growth of fluctuations in the transmittance of the suspension of LDL after 2 h of incubation at 78 % (Fig. 5). Using a higher concentration of Pluronic L61, 0.22 %, led to an almost complete suppression of LDL aggregation, and the use of a lower concentration, 0.0022 %, had no effect on the aggregation of LDL particles (data not shown). Therefore, Pluronic copolymers with strong hydrophobic properties (P85 and L61) at concentrations close to or greater than the respective CCM

inhibited the aggregation process of LDL; however, the “hydrophilic” Pluronic F68 had no effect on the aggregation of LDL at any concentration.

Discussion

Aggregation of LDL particles can be expressed as a reversible aggregation of particles and as the irreversible fusion of modified LDL particles. The mechanism of LDL particle aggregation is still not completely understood. There is evidence that modifications of LDL change the hydrophilic surface layers of the particles, thereby disturbing their hydrate-solvate shell and leading to increased hydrophobicity of the particles, resulting in the loss of stability in solution [10, 14]. Therefore, it is assumed that the aggregation of LDL particles is due to hydrophobic interactions of modified LDL particles. A number of more recent studies dealing with LDL aggregation have reported findings important for the further understanding of the mechanisms of LDL aggregation. In particular, studies by Parassasi et al. [18], Bancells et al. [13, 19, 20], Greco et al. [21], Llorente-Cortes et al. [22, 23], Öörni et al. [24], Plihtari et al. [25], Lahdesmaki et al. [26] have contributed to enhancing the knowledge on different aspects of the molecular mechanisms involved in LDL aggregation and on the role that LDL aggregation plays in atherosclerosis.

We studied the effect of Pluronic copolymers on the LDL aggregation process. Pluronic copolymers consist of a lipophilic part, which is formed by PO, and a hydrophilic part, which is built with EO, and these copolymers have the following structure: $(EO)_N-(PO)_M-(EO)_N$. This structure defines the basic properties of the Pluronic copolymer, including the ability to interact with biological membranes and induce structural changes [27]. Important characteristics of Pluronic copolymers are the CCM above which the assembly of individual copolymers into micelles occurs and the HLB, which reflects the ratio of hydrophilic and hydrophobic substances. Currently, there are many different Pluronic copolymers that differ in the number of monomers of EO and PO and are characterized by different hydrophilic and lipophilic properties, molecular weight and PFC [28]. Thus, the polymers that are characterized by a significant number of PO molecules and a small number of EO molecules are highly lipophilic and have a relatively low CCM and HLB, such as Pluronic L61. In contrast, Pluronic copolymers with large number of EO are dominated by hydrophilic interactions and are characterized by high CCM values and HLB, such as Pluronic F68. Lastly, there is a group of Pluronic copolymers with intermediate properties, such as P85.

We investigated the ability of Pluronic P85, L61 and F68 with different CCM and HLB characteristics

(Table 1). Our results suggest that the ability of amphiphilic copolymers of propylene oxide and ethylene oxide to inhibit the aggregation of LDL is directly dependent on the degree of hydrophobicity in the Pluronic copolymer. Pluronic copolymers with severe and moderate hydrophobic properties, such as L61 and P85, can significantly inhibit the aggregation of LDL; however, this happens only at concentrations close to the CCM. In this study, we conclude that it is the micellar form of Pluronic copolymers that are capable of inhibiting LDL particle aggregation, and Pluronic individual molecules inhibitory properties do not possess this property. These data support the hypothesis first made by Khoo and coworkers [10] on the role of hydrophobic interactions in the aggregation of LDL. Presumably, during incubation with constant mixing, conformational changes in the structure of LDL occur and lead to exposure of hydrophobic sites on the surface of the particles. Therefore, this change begins an interaction of hydrophobic regions between different particles and leads to the aggregation of LDL. When amphiphilic substances are present in a suspension of LDL, the lipophilic part of the amphiphilic molecules can interact with the hydrophobic domains on the LDL particle surface, which prevents the aggregation process of LDL.

Taking into account the importance of the aggregation of LDL in the pathogenesis of atherosclerosis [9–11], the possibility of suppressing LDL aggregation with Pluronic copolymers can stimulate the development of new approaches in therapy and prevention of atherosclerosis. In addition, actively investigating the possibility of using Pluronic copolymers as carriers of drugs in cases with low bioavailability is another potential role for Pluronic copolymers. For example, in the treatment of multi-drug resistant tumors [29], Pluronic micelles with a medicine show a much higher cytotoxicity toward cancer cells than do the drug without the addition of the Pluronic micelles. Pluronic P85 is also used when the penetration of drugs across the blood–brain barrier is necessary [30].

Various Pluronic copolymers have long been used as “carriers” of drugs, which promote the transport of drugs in an unchanged form; however, their role is much more significant. We studied the mechanisms of action of Pluronic copolymers on multi-drug resistant cells. It was shown that the Pluronic copolymers can reduce the microviscosity of the cell membrane, significantly increase ATP levels in cancer and adjacent cells, and reduce the efflux of drugs among other roles [31]. Furthermore, Pluronic copolymers exhibit diverse biological activities, including the ability to affect lipid metabolism. Therefore, when Pluronic L81 inhibited the assembly and secretion of chylomicrons, it helped to reduce LDL cholesterol and lipoproteins in very low-density lipoproteins (VLDL) and prevented the development of diet-induced

hypercholesterolemia and atherosclerosis in rats [16]. However, it has been reported that Pluronic P-407 causes hyperlipidemia in mice [32].

Obviously, before any Pluronic block copolymer can be considered as an anti-atherosclerotic agent, it would be necessary to investigate whether the association of this Pluronic copolymer to LDL (assuming that it is irreversibly bound) would not interfere with normal LDL metabolism.

Conclusion

This research work demonstrates, for the first time, that Pluronic® block copolymers inhibit LDL self-association. Obviously, further studies are needed in order to examine the applicability of the finding for atherosclerosis therapeutic intervention. The possibility of modulating the aggregation of LDL by various Pluronic copolymers can be regarded as a prerequisite in the creation of new types of anti-atherosclerotic drugs.

Acknowledgments This study was supported by the Russian Ministry of Education and Science.

Conflict of interest No conflict of interest is declared by the authors.

References

1. Anitschkow NN, Chatalov S (1913) Über experimentelle Cholesterinsteatose und ihre Bedeutung für die Entstehung einiger pathologischer Prozesse. *Zentralbl Allg Pathol* 24:1–9
2. Smith EB (1974) The relationship between plasma and tissue lipids in human atherosclerosis. *Adv Lipid Res* 12:1–49
3. Mahley RW, Innerarity TL, Weisgraber KH, Oh SY (1979) Altered metabolism (in vivo and in vitro) of plasma lipoproteins after selective modification of lysine residues of apoproteins. *J Clin Invest* 64:743–750
4. Alaupovic P (1971) Apolipoproteins and lipoproteins. *Atherosclerosis* 13:141–146
5. Bobryshev YV (2006) Monocyte recruitment and foam cell formation in atherosclerosis. *Micron* 37:208–222
6. Bates SR, Wissler RW (1976) Effect of hyperlipemic serum on cholesterol accumulation in monkey aortic medial cells. *Biochim Biophys Acta* 450:78–88
7. Ross R, Harker L (1976) Hyperlipidemia and atherosclerosis. *Science* 193:1094–1100
8. Goldstein JL, Ho YK, Basu SK, Brown MS (1979) Binding site on macrophages that mediates uptake and degradation of acetylated low density lipoprotein, producing massive cholesterol deposition. *Proc Natl Acad Sci USA* 76:333–337
9. Fogelman AM, Shechter I, Seager J, Hokom M, Child JS, Edwards PA (1980) Malondialdehyde alteration of low density lipoproteins leads to cholesteryl ester accumulation in human monocyte-macrophages. *Proc Natl Acad Sci USA* 77:2214–2218
10. Khoo JC, Miller E, McLoughlin P, Steinberg B (1990) Prevention of low density lipoprotein aggregation by high density lipoprotein or apolipoprotein A-I. *J Lipid Res* 31:645–652

11. Lopes-Virella MF, Klein RL, Lyons TJ, Stevenson HC, Witztum JL (1988) Glycosylation of low-density lipoprotein enhances cholesteryl ester synthesis in human monocyte-derived macrophages. *Diabetes* 37:550–557
12. Tertov VV, Sobenin IA, Gabbasov ZA, Popov EG, Orekhov AN (1989) Lipoprotein aggregation as an essential condition of intracellular lipid caused by modified low density lipoproteins. *Biochem Biophys Res Commun* 16:489–494
13. Bancells C, Benítez S, Jauhainen M, Ordóñez-Llanos J, Kovanen PT, Villegas S, Sánchez-Quesada JL, Öörni K (2009) High binding affinity of electronegative LDL to human aortic proteoglycans depends on its aggregation level. *J Lipid Res* 50:446–455
14. Talbot RM, del Rio JD, Weinberg PD (2003) Effect of fluid mechanical stresses and plasma constituents on aggregation of LDL. *J Lipid Res* 44:837–845
15. Brunelli R, Balogh G, Costa G, De Spirito M, Greco G, Mei G, Nicolai E, Vigh L, Ursini F, Parasassi T (2010) Estradiol binding prevents ApoB-100 misfolding in electronegative LDL(-). *Biochemistry* 49:7297–7302
16. Tertov VV, Kaplun VV, Sobenin IA, Orekhov AA (1998) Low-density lipoprotein modification occurring in human plasma possible mechanism of in vivo lipoprotein desialylation as a primary step of atherogenic modification. *Atherosclerosis* 138:183–195
17. Tertov VV, Sobenin IA, Gabbasov ZA, Popov EG, Jaakkola O, Solakivi T, Nikkari T, Smirnov VN, Orekhov AN (1992) Multiple-modified desialylated low density lipoproteins that cause intracellular lipid accumulation. Isolation, fractionation and characterization. *Lab Invest* 67:665–675
18. Parasassi T, De Spirito M, Mei G, Brunelli R, Greco G, Lenzi L, Maulucci G, Nicolai E, Papi M, Arcovito G, Tosatto SC, Ursini F (2008) Low density lipoprotein misfolding and amyloidogenesis. *FASEB J* 22:2350–2356
19. Bancells C, Villegas S, Blanco FJ, Benítez S, Gállego I, Beloki L, Pérez-Cuellar M, Ordóñez-Llanos J, Sánchez-Quesada JL (2010) Aggregated electronegative low density lipoprotein in human plasma shows a high tendency toward phospholipolysis and particle fusion. *J Biol Chem* 285:32425–32435
20. Bancells C, Benítez S, Ordóñez-Llanos J, Öörni K, Kovanen PT, Milne RW, Sánchez-Quesada JL (2011) Immunochemical analysis of the electronegative LDL subfraction shows that abnormal N-terminal apolipoprotein B conformation is involved in increased binding to proteoglycans. *J Biol Chem* 286:1125–1133
21. Greco G, Balogh G, Brunelli R, Costa G, De Spirito M, Lenzi L, Mei G, Ursini F, Parasassi T (2009) Generation in human plasma of misfolded, aggregation-prone electronegative low density lipoprotein. *Biophys J* 97:628–635
22. Llorente-Cortés V, Badimon L (2005) LDL receptor-related protein and the vascular wall: implications for atherothrombosis. *Arterioscler Thromb Vasc Biol* 25:497–504
23. Llorente-Cortés V, Otero-Viñas M, Camino-López S, Costales P, Badimon L (2006) Cholesteryl esters of aggregated LDL are internalized by selective uptake in human vascular smooth muscle cells. *Arterioscler Thromb Vasc Biol* 26:117–123
24. Öörni K, Pentikäinen MO, Ala-Korpela M, Kovanen PT (2000) Aggregation, fusion, and vesicle formation of modified low density lipoprotein particles: molecular mechanisms and effects on matrix interactions. *J Lipid Res* 41:1703–1714
25. Plihtari R, Kovanen PT, Öörni K (2011) Acidity increases the uptake of native LDL by human monocyte-derived macrophages. *Atherosclerosis* 217:401–406
26. Lähdesmäki K, Öörni K, Alanne-Kinnunen M, Jauhainen M, Hurt-Camejo E, Kovanen PT (2012) Acidity and lipolysis by group V secreted phospholipase A(2) strongly increase the binding of apoB-100-containing lipoproteins to human aortic proteoglycans. *Biochim Biophys Acta* 1821:257–267
27. Vinogradov SV, Batrakova EV, Li S, Kabanov AV (2004) Mixed polymer micelles of amphiphilic and cationic copolymers for delivery of antisense oligonucleotides. *J Drug Target* 12:517–526
28. Batrakova EV, Li S, Alakhov VY, Miller DW, Kabanov AV (2003) Optimal structure requirements for pluronic block copolymers in modifying P-glycoprotein drug efflux transporter activity in bovine brain microvessel endothelial cells. *Farmacol Exp Ther* 304:845–854
29. Alakhova DY, Rapoport NY, Batrakova EV, Timoshin AA, Li S, Nicholls D, Alakhov VY, Kabanov AV (2010) Differential metabolic responses to pluronic in MDR and non-MDR cells: a novel pathway for chemosensitization of drug resistant cancers. *J Controlled Release* 142:89–100
30. Batrakova EV, Li S, Li Y, Alakhov VY, Kabanov AV (2004) Effect of pluronic P85 on ATPase activity of drug efflux transporters. *Pharm Res* 21:2226–2233
31. Batrakova EV, Li S, Li Y, Alakhov VY, Elmquist WF, Kabanov AV (2004) Distribution kinetics of a micelle-forming block copolymer Pluronic P85. *J Controlled Release* 100:389–397
32. Johnston TP, Baker JC, Hall D, Jamal AS, Emeson EE, Palmer WK (1999) Potential downregulation of HMG-CoA reductase following chronic administration of P-407 to C57BL/6 mice. *J Cardiovasc Pharmacol* 34:831–842

Comparison of Free Fatty Acids Composition of Cuticular Lipids of *Calliphora vicina* Larvae and Pupae

Marek Gołębiowski

Received: 11 March 2012 / Accepted: 11 July 2012 / Published online: 7 August 2012
© AOCS 2012

Abstract The chemical characterization of the free fatty acid (FFA) fractions of the cuticular lipids of *Calliphora vicina* larvae and pupae was performed by separating the FFA fraction using high-performance liquid chromatography with laser light scattering detection (HPLC–LLSD) and quantitatively analyzing the FFA using gas chromatography–electron impact mass spectrometry (GC–MS). Thirty-two saturated and unsaturated FFA were identified and quantified in the insect lipids. Cuticular FFA profiles of *C. vicina* larvae and pupae were compared. Cuticular FFA of larvae and pupae accounted for 70.8 and 77.8 % of the total lipids, respectively. The cuticular lipids of *C. vicina* larvae contained 24 FFA ranging from 8:0 to 24:0, whereas the cuticular lipids of pupae contained 32 FFA ranging from 6:0 to 26:0. The cuticular lipids of the larvae contained 16 saturated, five monounsaturated, one diunsaturated, and two polyunsaturated FFA. The cuticular lipids of the pupae contained 18 saturated, nine monounsaturated, two diunsaturated, and three polyunsaturated FFA. The major cuticular FFA in *C. vicina* larvae and pupae was 18:1 (47.6 and 41.7 %, respectively). The highest amounts of total cuticular FFA were detected in larvae of *C. vicina* (1.7 mg/g of the insect body). The quantities of total cuticular FFA in pupae were smaller (1.4 mg/g of the insect body).

Keywords *Calliphora vicina* · Free fatty acids · HPLC–LLSD · GC–MS

Abbreviations

TIC	Total ion current
SIM	Single ion monitoring
EI	Electron impact
BSTFA	<i>N,O</i> -Bis(trimethylsilyl) trifluoroacetamide
TMCS	Trimethylchlorosilane
M ⁺	Molecular ion
TMSi	Trimethylsilyl derivatives
FFA	Free fatty acids

Introduction

The cuticular lipids constitute the initial passive barrier to desiccation [1] as well as to fungal and bacterial infection [2], and they may reduce the penetration of toxins and chemicals [3]. Cuticular lipids are also involved in various types of chemical communication [4]. For example, insects use components of the surface lipids as contact pheromones when they encounter each other. The cuticular lipids in pheromones are hydrocarbons, short-chain unsaturated aldehydes, ketones, fatty acids, and acetate esters of short-chain unsaturated alcohols.

The insects belonging to the Calliphoridae, Sarcophagidae, and Muscidae families often colonize a human corpse [5], and are often very important elements in forensic investigation. For example, *Calliphora vicina* is considered as a synanthropic species and larvae of this species are used in criminal investigations to determine the post-mortem interval (PMI), i.e., the time from death to discovery of the corpse.

In view of the great importance of *C. vicina*, it was decided to identify and assign the components of the free fatty acid (FFA) mixtures found on the surface layers of the

M. Gołębiowski (✉)
Faculty of Chemistry, Institute for Environmental and Human
Health Protection, University of Gdańsk, ul. Sobieskiego 18/19,
80-952 Gdańsk, Poland
e-mail: goleb@chem.univ.gda.pl

cuticle in larvae and pupae. Susceptibility or resistance of various insect species to fungal infection may be caused by several factors. The most important of them are differences in the structure and composition of the exoskeleton. The exudation of ammonia and allantoin is very significant in cleansing the insects' microhabitat. The bacteriostatic effects of the heat generated by accumulations of actively feeding larvae, the presence of antifungal compounds in the cuticle, especially FFA [6], as well as the cellular and humoral defense reactions of insect are also important [7, 8]. Susceptibility to penetration by fungal pathogen depends on mechanical barriers which either prevent or reduce infection and chemical barriers which inhibit or kill the pathogen. For example, FFA possess the ability to kill or inhibit the growth of fungi and bacteria [6, 9–13]. The antibacterial and antifungal effects of FFA are frequently observed during bioassay of extracts from a variety of organisms [13–15]. The activity of each FFA is influenced by its structure, especially the length of the carbon chain and the presence, number, orientation, and position of double bonds, and the presence the hydroxyl group is important for the antibacterial activity of FFA [16]. Unsaturated FFA are more active than saturated FFA with the same carbon chain length [16, 17] and unsaturated FFA are more active against Gram-positive bacteria than Gram-negative [18]. Additionally, FFA with the double bonds in the *cis* orientation have greater antibacterial activity than FFA with double bonds in the *trans* orientation [10, 12].

The most popular techniques used for the identification and quantification of cuticular lipids are TLC [19], column chromatography [20], HPLC/LLSD [21], GC-FID [22], GC-MS-TIC [23, 24], GC-MS-SIM [25], and MALDI [26]. For analysis, relatively volatile compounds solid-phase microextraction (SPME) [27, 28] or solid injection (SI) [29] coupled to the GC or GC-MS are often used [30].

This paper describes the qualitative and quantitative comparisons of cuticular and internal FFA profiles of larvae and pupae. These results provide baseline data for further studies on the possible role of FFA in the resistance to microbial attack. The lipids of flies were separated into classes of compounds using high-performance liquid chromatography with laser light scattering detector (HPLC-LLSD). Qualitative and quantitative analyses were done by gas chromatography combined with mass spectrometry (GC-MS).

Methods and Material

Insects

A total of 140 larvae and 302 pupae of *C. vicina* were obtained from the Institute of Parasitology, Polish

Academy of Sciences in Warsaw (Poland). The insects, raised from eggs laid on beef by adult flies, were reared at 28 °C with 70 % relative humidity and a 12:12 h photoperiod. Maternal generation was maintained in the same conditions. For experiments, 1-day-old larvae and freshly emerged pupae were used. All insects were quickly frozen and kept at –20 °C until being used.

Extraction of Lipids

The cuticular and internal lipids were extracted by methods described previously [24]. All larvae and pupae were first extracted separately by stirring in 20 ml of petroleum ether for 10 s (extracts 1L and 1P). All primarily extracted larvae and pupae were separately extracted for a second time in 20 ml of dichloromethane for 1 min (extracts 2L and 2P). Finally, the insects were extracted with 50 ml dichloromethane for 10 days (extracts 3L and 3P). The obtained extract was filtered (0.45 µm) and collected into a glass vial. A 1-ml aliquot of this extract was further taken and placed into a tared glass flask, and then evaporated under nitrogen in order to determine the dry mass of extracted lipids. For example, extracts 1L and 2L contained cuticular lipids, and extract 3L contained internal lipids of larvae.

High-Performance Liquid Chromatography with Laser Light Scattering Detector

The lipids were separated by methods described previously [31]. All lipid extracts (larvae and pupae) were separated using HPLC-LLSD. Separation in the normal phase (five replicates) was performed on a silica gel column (Econosil Silica 5 Micron, Alltech, 25 cm × 4.6 mm i.d.). Binary gradient elution with eluent A (hexane) and eluent B (15 % of acetone in dichloromethane) was applied with a linear gradient from A to B within 35 min. Total flow was maintained at 0.8 ml/min. The FFA fractions obtained by HPLC were silylated with 100 µl of a mixture of 99 % bis(trimethylsilyl)acetamide and 1 % chlorotrimethylsilane (Sigma Aldrich) for 1 h at 100 °C and then analyzed by GC-MS.

Gas Chromatography Mass Spectrometry

GC-MS analysis of each FFA fraction was performed with a Finnigan Mat SSQ 710 mass spectrometer coupled to a Hewlett-Packard 5890 gas chromatograph. Compounds were separated on a 30 m × 0.25 mm i.d., film thickness 0.25 µm, HP-5 capillary column. Helium was used as the carrier gas at a flow rate of 1 ml/min. The injector temperature was 320 °C and the column oven temperature cycle was 60 °C for 10 min, then 60–320 °C at 4 °C/min; the final temperature was then held for 20 min. Electron-impact

ionization (electron energy 70 eV, ion source temperature 200 °C) was used.

In order to quantitatively determine each of the analyzed FFA, GC–MS analysis was performed with an internal standard (19-methylarachidonic acid). The contents of the compounds in the analyzed samples were calculated from the chromatogram peak areas. The results were expressed as mean \pm standard deviation of three GC–MS analyses.

Results

Total Lipids and Free Fatty Acids

The total quantity of cuticular and internal lipids larvae was 20.4 and 461.8 mg, which comprised 0.2 and 5.4 % of the total fresh weight of the biological material, respectively (Table 1). The percentage content of cuticular and internal lipids in pupae was similar. The total quantity of cuticular and internal lipids of pupae was 30.0 and 514.9 mg, which comprised less than 0.2 and 3.1 % of the total fresh weight of the biological material, respectively (Table 1). Cuticular FFA of larvae and pupae accounted for 70.8 and 77.8 % of the total lipids, respectively, whereas internal FFA of larvae and pupae made up 5.2 and 21.3 % of the total lipids, respectively.

Free fatty acid fractions obtained as a result of the HPLC–LLSD separations were then subjected to further GC–MS analysis. GC–MS in total ion current (TIC) mode was used to identify unknown components, and single ion monitoring mode (SIM) to verify recognized molecular ions. FFA in the cuticular and internal lipids of *C. vicina* larvae and pupae were identified on the basis of the characteristic ions: 73, 128, 132, 145, $M-15^+$, and M^+ (molecular ion).

The amount of cuticular FFA isolated from larvae was 1.7 mg/g. The results obtained from pupae were similar: 1.4 mg/g of the insect body. The total mass of internal FFA

Table 1 Quantitative summary of the experiment: numbers and masses of insect (*Calliphora vicina*); masses of lipids

Stages	Number of insects	Masses of insects (g)	Masses of lipids in extracts (mg)	Extracts	Masses of lipids (mg/g of the insect body)
Larvae	140	8.5	9.2 \pm 0.1	1L	1.1
			11.2 \pm 0.1	2L	1.3
			461.8 \pm 5.5	3L	54.3
Pupae	302	16.6	11.6 \pm 0.1	1P	0.7
			18.4 \pm 0.2	2P	1.1
			514.9 \pm 6.2	3P	31.0

1L and 1P, petroleum extracts (10 s), 2L and 2P dichloromethane extracts (5 min), 3L and 3P, dichloromethane extracts (10 days)

was greater in pupae (6.6 mg/g). This last quantity is about twice the average in larvae (2.8 mg/g).

Cuticular Free Fatty Acids in Larvae

Cuticular lipids of larvae contained 24 FFA ranging from 8:0 to 24:0 (Table 2). Among cuticular FFA of larvae, 15 saturated, seven unsaturated with even-numbered, and two unsaturated with odd-numbered carbon chains FFA were present. The major FFA in *C. vicina* larvae were 18:1n-9 (47.6 %), 16:1n-9 (20.0 %), 16:0 (19.4 %), and 18:0 (9.4 %). FFA occurring in smaller quantities (from greater than 0.1 to 1 %) were 12:0 (0.4 %), 14:1n-9 (0.6 %), 14:0 (0.3 %), 17:1n-10 (0.8 %), 17:0 (0.6 %), and 18:2n-6 (0.9 %). The cuticular lipids also contained 14 FFA present in concentrations from traces to less than 0.1 %.

Cuticular Free Fatty Acids in Pupae

Table 2 lists the FFA contents calculated per gram of pupae body. Among 32 cuticular FFA of pupae, 18:1n-9 (41.7 %), 16:0 (19.3 %), 16:1n-9 (16.4 %), 18:0 (8.6 %), and 18:2n-6 (6.9 %) were the most abundant compounds. One fatty acid is present in a smaller amount (14:0, 2.4 %). Other FFA were detected in very small and comparable amounts from 0.7 % (26:1) to less than 0.1 % (e.g., 6:0). Cuticular lipids of pupae contained 18 saturated FFA, among which seven fatty acids are odd-numbered, and also 14 unsaturated FFA, among which three fatty acids are odd-numbered.

Comparison of Free Fatty Acids Composition of Cuticular Lipids of *C. vicina* Larvae and Pupae

The presence of six FFA with 20 carbon atoms in the chain, namely, 20:0, 20:1n-6, 20:2n-6, 20:3n-6, 20:4n-3, and 20:5n-3, in the cuticular lipids of pupae is very interesting. On the other hand, only four FFA with 20 carbon atoms in the chain were present in the cuticular lipids of larvae.

The following free acids present in the cuticular lipids of pupae were absent from the cuticular lipids of larvae: 6:0, 7:0, 19:1n-10, 20:3n-6, 20:2n-6, 22:1n-9, 26:1n-9, and 26:0. The percentage contents of cuticular 14:0 and 18:2n-6 in pupae were significantly higher than those of cuticular lipids in larvae and compromised 2.4 vis 0.3 % and 6.9 vis 0.9 %, respectively.

In cuticular lipids of larvae, the relative content of 16:1n-9 was higher than the relative content of 16:0. On other hand, in cuticular lipids of pupae, the relative content of 16:1n-6 was lower than the relative content of 16:0.

Internal Free Fatty Acids in Larvae

Internal lipids of larvae *C. vicina* contained 26 FFA ranging from 6:0 to 22:0 (Table 2). In the internal lipids 15

Table 2 Chemical composition of the fatty acids found in larvae and pupae of *Calliphora vicina*

FFA	Larvae		Pupae	
	Cuticular FFA	Internal FFA	Cuticular FFA	Internal FFA
Masses of free fatty acids ($\mu\text{g/g}$ of fresh weight of insect)				
6:0	–	0.55 ± 0.06	0.13 ± 0.02	–
7:0	–	0.47 ± 0.07	0.14 ± 0.01	5.1 ± 0.5
8:0	0.28 ± 0.03	0.95 ± 0.08	0.48 ± 0.04	$1.3 \times 10^1 \pm 0.1 \times 10^1$
9:0	2.1 ± 0.2	0.91 ± 0.07	0.52 ± 0.04	4.7 ± 0.4
10:0	0.89 ± 0.06	0.51 ± 0.06	0.33 ± 0.03	0.78 ± 0.04
11:0	1.5 ± 0.1	1.01 ± 0.09	0.77 ± 0.09	Traces
12:0	7.4 ± 0.6	8.4 ± 0.7	2.4 ± 0.2	$1.6 \times 10^1 \pm 0.1 \times 10^1$
13:0	0.69 ± 0.06	1.36 ± 0.09	0.53 ± 0.04	$1.8 \times 10^1 \pm 0.2 \times 10^1$
14:1n-9	10.4 ± 0.8	$3.5 \times 10^1 \pm 0.3 \times 10^1$	7.8 ± 0.5	$6.3 \times 10^1 \pm 0.5 \times 10^1$
14:0	4.5 ± 0.4	$1.9 \times 10^2 \pm 0.2 \times 10^2$	$3.3 \times 10^1 \pm 0.2 \times 10^1$	$3.4 \times 10^2 \pm 0.3 \times 10^2$
15:1n-10	0.98 ± 0.07	–	0.92 ± 0.06	–
15:0	8.7 ± 0.4	$1.9 \times 10^1 \pm 0.1 \times 10^1$	5.8 ± 0.5	$1.8 \times 10^2 \pm 0.1 \times 10^2$
16:1n-9	$3.4 \times 10^2 \pm 0.2 \times 10^2$	$6.5 \times 10^2 \pm 0.5 \times 10^2$	$2.3 \times 10^2 \pm 0.2 \times 10^2$	$1.2 \times 10^3 \pm 0.1 \times 10^3$
16:0	$3.3 \times 10^2 \pm 0.2 \times 10^2$	$3.8 \times 10^2 \pm 0.2 \times 10^2$	$2.7 \times 10^2 \pm 0.2 \times 10^2$	$1.6 \times 10^3 \pm 0.1 \times 10^3$
17:1n-10	$1.4 \times 10^1 \pm 0.1 \times 10^1$	$6.5 \times 10^1 \pm 0.5 \times 10^1$	2.2 ± 0.2	$9.1 \times 10^1 \pm 0.8 \times 10^1$
17:0	10.3 ± 0.6	10.7 ± 0.6	8.8 ± 0.6	$1.4 \times 10^2 \pm 0.1 \times 10^2$
18:2n-6	$1.5 \times 10^1 \pm 0.1 \times 10^1$	–	$9.6 \times 10^1 \pm 0.6 \times 10^1$	–
18:1n-9	$8.1 \times 10^2 \pm 0.6 \times 10^2$	$1.5 \times 10^3 \pm 0.1 \times 10^3$	$5.7 \times 10^2 \pm 0.4 \times 10^2$	$2.7 \times 10^3 \pm 0.2 \times 10^3$
18:0	$1.6 \times 10^2 \pm 0.1 \times 10^2$	$4.4 \times 10^1 \pm 0.4 \times 10^1$	$1.2 \times 10^2 \pm 0.1 \times 10^2$	$3.2 \times 10^2 \pm 0.2 \times 10^2$
19:1n-10	–	4.2 ± 0.3	2.3 ± 0.2	–
19:0	0.36 ± 0.03	Traces	0.59 ± 0.05	–
20:5n-3	1.4 ± 0.1	$1.6 \times 10^1 \pm 0.1 \times 10^1$	3.9 ± 0.4	$1.3 \times 10^1 \pm 0.1 \times 10^1$
20:4n-3	0.96 ± 0.08	$1.6 \times 10^1 \pm 0.1 \times 10^1$	4.3 ± 0.4	$1.0 \times 10^1 \pm 0.1 \times 10^1$
20:3n-6	–	1.7 ± 0.2	0.36 ± 0.02	–
20:2n-6	–	0.34 ± 0.02	0.24 ± 0.02	–
20:1n-6	0.94 ± 0.06	1.16 ± 0.09	3.0 ± 0.2	–
20:0	1.5 ± 0.1	2.1 ± 0.1	6.0 ± 0.4	–
22:1n-9	–	–	1.4 ± 0.1	–
22:0	0.21 ± 0.03	0.48 ± 0.05	3.4 ± 0.2	2.3 ± 0.2
24:0	Traces	–	1.19 ± 0.08	2.2 ± 0.2
26:1n-9	–	–	$1.0 \times 10^1 \pm 0.1 \times 10^1$	–
26:0	–	–	1.5 ± 0.2	0.33 ± 0.03
Sum	1.7×10^3	2.8×10^3	1.4×10^3	6.6×10^3

Cuticular FFA, sum of FFA content in petroleum extract (1L and 1P) and dichloromethane extract (2L and 2P). Internal FFA, dichloromethane extract (3L and 3P). Data are presented as the mean \pm standard deviation of three separate analyses performed on different samples

saturated, six monounsaturated, one diunsaturated, and four polyunsaturated FFA have been identified. Only three acids are present in high concentrations (more than 10 %): 16:0 (13.6 %), 16:1n-9 (23.2 %), and 18:1n-9 (53.6 %). Other acids amounted to from less than 0.1 to 6.8 %. Among saturated acids, the following are the most abundant: 16:0 (13.6 %), 14:0 (6.8 %), and 18:0 (1.6 %). Among unsaturated acids, the following are the most abundant: 18:1n-9 (53.6 %), 16:1n-9 (23.2 %), and 17:1n-10 (2.3 %). Internal lipids of larvae contained six FFA with 20 carbon atoms in

the chain: 20:0, 20:1n-6, 20:2n-6, 20:3n-6, 20:4n-3, and 20:5n-3.

Internal Free Fatty Acids in Pupae

Internal lipids of pupae *C. vicina* contained 20 FFA ranging from 7:0 to 26:0 (Table 2). FFA occurring in the highest quantities were 16:1n-9 (18.2 %), 16:0 (24.2 %), and 18:1n-9 (40.9 %). Except for 16:1n-9 and 18:1n-9, which occurred in large amounts, the following unsaturated FFA

are present in smaller quantities: 14:1n-9 (1.0 %), 17:1n-10 (1.4 %), 20:5n-3 (0.2 %), and 20:4n-3 (0.2 %). Among saturated free acids, only C16:0 is present in large amount (24.2 %). Four saturated FFA are present from 2.1 % (17:0) to 5.2 % (14:0). Other saturated FFA occur in smaller quantities.

Comparison of Free Fatty Acids Composition of Internal Lipids of *C. vicina* Larvae and Pupae

The following acids present in the larvae lipids were absent in the pupae lipids: 6:0, 11:0, 19:1n-10, 19:0, 20:3n-6, 20:2n-6, 20:1n-6, and 20:0. On the other hand, only 13:0, 24:0, and 26:0 were absent from the internal lipids of larvae *C. vicina*.

In the internal lipids of larvae, the relative content of 16:1n-9 was higher than the relative content of 16:0. However, in the internal lipids of pupae, the relative content of 16:1n-6 was lower than that of 16:0. The same situation is observed in cuticular lipids of larvae and pupae.

Internal lipids of larvae contained six FFA with 20 carbon atoms in the chain but internal lipids of pupae contained only two of those compounds (20:4n-3 and 20:5n-3).

The percentage contents of internal 15:0 and 18:0 in pupae were significantly higher than those of internal lipids in larvae and compromised 5.2 vis 0.7 % and 4.8 vis 1.6 %, respectively.

Discussion

The major components of the cuticular lipid coating of insects are often hydrocarbons, such as *n*-alkanes, monomethylalkanes, dimethylalkanes, and alkenes [32], FFA [31], alcohols [33], aldehydes [34], wax esters [35], fatty acid methyl esters [32], and acylglycerols [36].

In our work, we stated that cuticular lipids of *C. vicina* larvae contained FFA from 8:0 to 24:0 and pupae from 6:0 to 26:0. Table 3 lists the FFA identified in insect cuticular lipids. For example, in the cuticular lipids the following FFA were identified: from 10:0 to 22:1 in *Locusta migratoria migratoriodes* adult [37], from 10:0 to 20:1 in *Schistocerca gregaria* adult [37], from 14:0 to 18:1 in *Frankliniella occidentalis* larvae [32], from 16:0 to 18:3 in *Acanthoscelides obtectus* female [21], and from 16:0 to 36:0 in *Apis mellifera* [38].

In our study, the major cuticular FFA were: 16:1n-9, 16:0, 18:2n-6, 18:1n-9 and 18:0 in pupae and 16:1n-9, 16:0, 18:1n-9 and 18:0 in larvae.

In the other insects species, the major FFA were 14:0 (40 %) in *Acyrtosiphon pisum* [42], 16:0 (25 %) in *L. migratoria migratoriodes* adult, (64 %) in *S. gregaria*

adult, (63 %) in *F. occidentalis* larvae, (36 %) in *Fannia canicularis* adult [40], (38 and 30 %) in *Attagenus megatoma* 6.8- and 32-week-old larvae, respectively [43], 18:0 (58 %) in *A. megatoma* adult [41], (33 %) in *Lasioderma serricornis* larvae [44], (40 %) in *Dendrolimus pini* larvae [6], (49–52 %) in *Galleria mellonella* larvae [6] and (51 %) in *A. obtectus* female [21], 18:3 (28 %) in *Melanoplus sanguinipes* and *M. packardii* adult [36], 24:0 (29 %) in *A. mellifera* [38], and 28:0 (34 %) in *D. pini* exuviae [31]. On the basis of these results, we stated that two major FFA (16:0 and 18:1) were present in many insect species. Other major FFA are atypical (14:0, 24:0, and 24:0). In our study, the major compound in cuticular lipids of larvae and pupae, i.e., 18:1n-9, is typical.

Saturated, unsaturated, and even-numbered FFA ranging from 12 to 20 are typically found in many insect species [30, 33, 45], whereas the presence of FFA ranging from 5 to 11 and from 21 to 26 are unusual. In particular odd-numbered FFA and polyunsaturated FFA such as 15:1n-10, 17:1n-10, 20:5n-3, and 20:4n-3 identified in lipids of *C. vicina* are unusual. Only typical cuticular FFA ranging from 12:0 to 20:0 are present in cuticular lipids of larvae *F. occidentalis* [32], adult *F. canicularis* [40], *L. bostrychophila* [34], and female *A. obtectus* [21].

In our study, the FFA (in the range from 5:0 to 11:0) 8:0, 9:0, 10:0, and 11:0 in larvae and additionally 6:0 and 7:0 in pupae were identified in the cuticular lipids. Similar cuticular lipids ranging from 5:0 to 11:0 were identified in the lipids of *D. pini* exuviae [31], *L. migratoria migratoriodes* adult, *S. gregaria* adult [39], and *A. pisum* [42]. The numbers of fatty acids in this range are not large: one compound in the cuticular lipids of *L. migratoria migratoriodes*, *S. gregaria*, and *A. pisum* and four FFA in *D. pini* exuviae.

Cuticular lipids of *C. vicina* larvae and pupae contained several odd-numbered FFA. Among this group the following acids are present: 9:0, 11:0, 13:0, 15:0, 17:0, and 19:0 in larvae and pupae and additionally 7:0 in pupae. All of these FFA are minor constituents. Those compounds were identified in the cuticular lipids of some insects. For example, 9:0, 11:0, 21:0, 15:0, 17:0, 19:0, and from 23:0 to 33:0 were present in *D. pini* exuviae [31]. The 15:0, 17:0, and 19:0 entities were identified in *S. gregaria* adult [39] and 15:0 and 17:0 were present in the cuticular lipids of *L. migratoria migratoriodes* adult [39].

Among odd-numbered and unsaturated acids only 15:1n-10 and 17:1n-10 in larvae and 15:1n-10, 17:1n-10, and 19:1n-10 in pupae of *C. vicina* are present in small amounts. These FFA (17:1 and 19:1) were also identified in cuticular lipids of *S. gregaria* adult [39]. Moreover, the presence of polyunsaturated and odd-numbered fatty acid (21:3) in cuticular lipids of *L. migratoria migratoriodes* was detected. However, its biological function needs additional research.

Table 3 The composition of the fatty acids found in lipids of insects

Insect species/references																				
FFA	Lm [39]	Sg [39]	Fo [32]	Fc [40]	Am [41]	Ap [42]	Am [38]	Ms [36]	Mp [36]	Lb [34]	Am [43]	Am [43]	Am [43]	Ls [44]	Cv [6]	Dp [6]	Gm [6]	Ao [21]	Dp [31]	
C _{5:0}															Tr					
C _{6:0}															Tr					
C _{8:0}															Tr					Tr
C _{9:0}															Tr					0.1
C _{10:0}	1	4			2										Tr					0.1
C _{11:0}															Tr					0.1
C _{12:0}	7	5			Tr	4		2	2						Tr					0.1
C _{12:1}		<1																		0.2
C _{13:0}																				
C _{14:0}	14	12	5	1	5	70		2	1				2	3	1.7		Tr			0.1
C _{14:1}	<1	<1																		0.5
C _{15:0}	14	<1																		
C _{16:0}	25	64	63	36	26	4	7	13	10	+	38	30	17	23	25.3	17.7	32.7–38.9	12.6		2.2
C _{16:1}	1	<1	4	16	3	2		3	4	+	4	5	19	4	22.6		Tr			
C _{16:2}													<1							
C _{17:0}	<1	<1																		0.4
C _{17:1}		1																		
C _{18:0}	14	12	12	18	10	4	7	6	5	+	16	11	3	9	1.6	8.8	14.5–6.6	7.3		1.7
C _{18:1}	<1	<1	17	25	22	5		21	23	+	17	26	58	33	23.2	39.8	49.2–51.9	50.9		
C _{18:2}	3	Tr		4	20	7		24	26	+		2		18	24.0	19.2	3.6–2.7	18.4		
C _{18:3}	<1	<3		Tr	2	2		28	28		2	3		1		14.6		10.7		
C _{19:0}		Tr																		0.4
C _{19:1}		Tr																		
C _{20:0}	5	Tr			1			Tr				<1	<1	3	1.7		Tr			4.7
C _{20:1}	<1	Tr															Tr			
C _{21:0}																				0.4
C _{21:3}	4																			
C _{22:0}	3				2		4	Tr				2	2	2		2				9.5
C _{22:1}	6																			
C _{23:0}					9		29				15	14		<1						0.1
C _{24:0}																				2.2
C _{25:0}																				0.3
C _{26:0}							12				3	5								6.7
C _{27:0}																				0.6

Table 3 continued

FFA	Lm [39]	Sg [39]	Fo [32]	Fc [40]	Am [41]	Ap [42]	Am [38]	Ms [36]	Mp [36]	Lb [34]	Am [43]	Am [43]	Am [43]	Ls [44]	Cv [6]	Dp [6]	Gm [6]	Ao [21]	Dp [31]	
C _{28:0}			11																	34.1
C _{29:0}																				1.5
C _{30:0}					9															27.5
C _{31:0}																				0.4
C _{32:0}					9															5.2
C _{33:0}																				0.1
C _{34:0}					9															0.7
C _{36:0}					3															

Concentration given in % lipid total

+, compound present in the lipids; FFA, free fatty acids; Tr, traces; Lm, the migratory locust, *Locusta migratoria migratorides* adult; Sc, the desert locust, *Schistocerca gregaria* adult; Fo, the western flower thrips, *Frankliniella occidentalis* larvae; Fc, the lesser housefly, *Fannia canicularis* adult; Ame, the black carpet beetle, *Attagenus megatoma* larvae; Ac, the pea aphid, *Acyrtosiphon pisum*; Am, the honey bee, *Apis mellifera*; Ms, the migratory grasshopper, *Melanoplus sanguinipes* adult; Mp, the packard grasshopper, *Melanoplus packardii* adult; Lb, the booklouse, *Liposcelis bostrychophila*; Am, *Attagenus megatoma* 6.8- and 32-week-old larvae adult; Ls, the cigarette beetle, *Lasioderma serricorne* larvae; Cv, the blowfly, *Calliphora vicina* larvae; Gm, the wax moth, *Galleria mellonella* larvae; Dp, the pine-tree lappet moth, *Dendrolimus pini* larvae; Ao, the bean weevil, *Acanthoscelides obtectus* female; Dp, *Dendrolimus pini* exuviae

Free fatty acids with molecular weight from 20:0 to 26:0 (only even-numbered) are present in cuticular lipids of *C. vicina* larvae and pupae, but all of these compounds are minor constituents: in larvae from traces to 0.1 % and in pupae from less than 0.1 to 0.7 %. Cuticular FFA in range from 20:0 to 26:0 were detected in the cuticular lipids of *M. sanguinipes* adult [36], *G. mellonella* larvae [6], and *S. gregaria* adult [39]. Eight FFA even-numbered and ranging from 22:0 to 36:0 were present in cuticular lipids of *A. mellifera* [38] and three FFA ranging from 22:0 to 26:0 were identified in cuticular lipids of *A. megatoma* 6.8- and 32-week-old larvae [43] and also two compounds are present in *A. megatoma* larvae [41] and *L. sarricorne* larvae [44].

In our previous work [6] it was shown that the cuticular fatty acid profiles of *C. vicina* larvae (last-instar wandering larvae) differ from the profile of *C. vicina* larvae analyzed here. The major difference was the content of 18:1n-9 and 18:2n-6 in the cuticle. In our previous work, the relative content of 18:1 and 18:2 was 23.2 and 24.0 %, respectively, whereas in the present work, the relative content of 18:1n-9 and 18:2n-6 was 47.6 and 0.9 %, respectively. The concentrations of FFA of last-instar wandering larvae were circa eight times higher than those of the final instar larvae. Changes in the composition of cuticular lipids during development have been studied in only a few insects. For example, total cuticular lipid of *A. megatoma* increased from 4.1 to 13.7 µg/larvae for the 6.8- and 32-week-old larvae, respectively [43]. The amount of 16:0 and 18:0 decreased while 18:1 increased in the older *A. megatoma* larvae. The presence of 18:2 and 20:0 in 32-week-old larvae of *A. megatoma* is interesting, whereas these compounds were absent in the 6.8-week-old larvae. Additionally, the FFA profile in the adult insects is different: 18:3, 22:0, 24:0, and 26:0 were not found in the adult insects whereas they were present in both groups of larvae. A similar change in composition was also found during development of the *G. mellonella* larvae. The fatty acid profile in the VIIth larval instar of *G. mellonella* from 0–2 h to 8 days after molting is different [6]. In this case, the concentrations of 16:0, 18:0, 18:1, and 18:2 in the extracts of this larvae were found to increase significantly during this period. Evidently, the lipid composition is determined by sex, developmental stage, and age [43]. Moreover, the lipid composition depends on the living conditions, i.e., temperature, dryness, and available food [46, 47]. In this study, the number of FFA identified by GC–MS analysis of cuticular extracts of *C. vicina* larvae is higher than that reported in our previous work on this fly species. Besides changes in the composition of cuticular lipids during development, this observation may be consistent with the fact that in the present study we used more a sensitive mass spectrometer with lower limits of

detection and quantification. Both results (present and earlier) showed the similar qualitative fatty composition, although data were obtained using different extraction methods and GC–MS equipments.

Free fatty acids present in the cuticular surface of insect larvae and pupae could be inhibitory to germination and growth of conidia and penetration of the integument by entomopathogenic fungi. In our previous work [37] fungistatic effects of 16:0, 16:1, 18:0, 18:1, 18:2, 18:3, 20:0, and 20:1 were shown. The cuticular lipids of larvae and pupae *C. vicina* contained FFA in this range, with the exception of 18:3. Also medium- and short-chain fatty acids which are present in cuticular lipids of larvae and pupae of *C. vicina* were demonstrated to present toxicity to filamentous fungi, including some that had been isolated specifically from insect cuticle [48, 49]. FFA might be engaged in protecting larvae from fungal pathogens, whereas the presence of, for example, 15:0 stimulated *C. coronatus* growth [37]. The determination of the cuticular fatty acid profiles and information on which particular fatty acids support the fungal assault and which contribute to insect resistance to entomopathogenic fungi is of great importance and requires a better understanding of the physiological aspects of fungal growth and virulence factors.

In conclusion, the conducted analyses exposed qualitative and quantitative differences in FFA chemical composition of the examined developmental stages. The major differences are cuticular lipids of pupae contained 6:0, 7:0, 19:1n-10, 20:3n-6, 20:2n-6, 22:1n-9, 26:1n-9, and 26:0, which were not found in larvae; In the cuticular lipids of larvae, the relative content of 16:1n-9 was higher than the relative content of 16:0. On other hand, in cuticular lipids of pupae, the relative content of 16:1n-9 was lower than that of 16:0.

Differences in FFA chemical composition of larvae and pupae may be responsible for susceptibility or resistance to fungal infection. Experiments which are currently ongoing in our laboratories will show which of the identified compounds possess antimicrobial activity. Hopefully the results described here revealing the chemical composition of fatty acids of *C. vicina* will be an important contribution to further studies of the taxonomy and physiology of insects.

Acknowledgments I would like to thank Prof. Mieczysława I. Boguś for providing the insects to analyze. I would like to express my gratitude to Anna Grubba for her assistance. Financial support was provided by the Polish Ministry of Research and Higher Education for 2010–2013 (grant N N303 504238) and the University of Gdansk (grant DS 8110-4-0085-1).

References

- Hadley NF (1994) Water relations of terrestrial arthropods. Academic, San Diego
- St. Leger R (1991) Integument as a barrier to microbial infections. In: Binnington K, Retnakaran A (eds) Physiology of the insect epidermis. CSIRO, Australia, pp 284–306
- Gilby AR (1984) Cuticle and insecticides. In: Bereiter-Hahn J, Matoltsy AG, Richards KS (eds) Biology of the integument. Invertebrates, vol 1. Springer-Verlag, Berlin, pp 694–702
- Howard RW (1993) Cuticular hydrocarbons and chemical communication. In: Stanley-Samuelson DW, Nelson DR (eds) Insect lipids: chemistry, biochemistry and biology. University of Nebraska Press, Lincoln, pp 179–226
- Bonacci T, Vercillo V, Brandmayr P, Fonti A, Tersaruolo C, Brandmayr TZ (2009) A case of *Calliphora vicina* Robineau-Desvoidy, 1830 (Diptera, Calliphoridae) breeding in a human corpse in Calabria (southern Italy). *Legal Med* 11:30–32
- Gołębowski M, Maliński E, Boguś MI, Kumirska J, Stepnowski P (2008) The cuticular fatty acids of *Calliphora vicina*, *Dendrolimus pini* and *Galleria mellonella* larvae and their role in resistance to fungal infection. *Insect Biochem Mol Biol* 38:619–627
- Vilcinskas A, Götz P (1999) Parasitic fungi and their interactions with the insect immune system. *Adv Parasitol* 43:267–313
- Park JW, Lee BL (2012) Insect immunology. In: Gilbert LI (ed) Insect molecular biology and biochemistry. Elsevier, Amsterdam, pp 480–512
- Bergsson G, Arnfinnsson J, Steingrímsson Ó, Thormar H (2001) Killing of Gram-positive cocci by fatty acids and monoglycerides. *APMIS* 109:670–678
- Kabara JJ, Swieczkowski DM, Conley AJ, Truant JP (1972) Fatty acids and derivatives as antimicrobial agents. *Antimicrob Agents Chemother* 2:23–28
- Kabara JJ, Vrable R, Lie Ken Jie MSF (1977) Antimicrobial lipids: natural and synthetic fatty acids and monoglycerides. *Lipids* 12:753–759
- Feldlaufer MF, Knox DA, Lusby WR, Shimanuki H (1993) Antimicrobial activity of fatty acids against *Bacillus* larvae, the causative agent of American foulbrood disease. *Apidologie* 24:95–99
- Benkendorff K, Davis AR, Rogers CN, Bremner JB (2005) Free fatty acids and sterols in the benthic spawn of aquatic molluscs, and their associated antimicrobial properties. *J Exp Mar Biol Ecol* 316:29–44
- Wille JJ, Kydonieus A (2003) Palmitoleic acid isomer (C16:1Δ6) in human skin sebum is effective against Gram-positive bacteria. *Skin Pharmacol Appl Skin Physiol* 16:176–187
- Harada K-I, Suomalainen M, Uchida H, Masui H, Ohmura K, Kiviranta J, Niku-Paavola M-L, Ikemoto T (2000) Insecticidal compounds against mosquito larvae from *Oscillatoria agardhii* strain 27. *Environ Toxicol* 15:114–119
- Zheng CJ, Yoo JS, Lee TG, Cho HY, Kim YH, Kim WG (2005) Fatty acid synthesis is a target for antibacterial activity of unsaturated fatty acids. *FEBS Lett* 579:5157–5162
- Desbois AP, Lebl T, Yan L, Smith VJ (2008) Isolation and structural characterisation of two antibacterial free fatty acids from the marine diatom, *Phaeodactylum tricorutum*. *Appl Microbiol Biotechnol* 81:755–764
- Galbraith H, Miller TB, Paton AM, Thompson JK (1971) Antibacterial activity of long chain fatty acids and the reversal with calcium, magnesium, ergocalciferol and cholesterol. *J Appl Bacteriol* 34:803–813
- Maliński E, Hebanowska E, Szafranek J, Nawrot J (1986) The composition of the hydrocarbons of the larvae of the Khapra beetles, *Trogoderma granarium*. *Comp Biochem Physiol* 84B:211–215
- Hebanowska E, Maliński E, Latowska A, Dubis E, Pihlaja K, Oksman P, Nawrot J, Szafranek J (1990) A comparison of

- cuticular hydrocarbons of larvae and beetles of the *Tribolium destructor*. Comp Biochem Physiol 96B:815–819
21. Gołębiowski M, Maliński E, Nawrot J, Stepnowski P (2008) Identification and characterization of surface lipid components of the dried-bean beetle *Acanthoscelides obtectus* (Say) (Coleoptera: Bruchidae). J Stored Prod Res 44:386–388
 22. Nelson DR, Buckner JS, Fatland CL (1994) The composition of external lipids of adult whiteflies, *Bemisia tabaci* and *Trialeurodes vaporariorum*. Comp Biochem Physiol 109B:293–303
 23. Buckner JS, Mardaus MC, Nelson DR (1996) Cuticular lipid composition of *Heliothis virescens* and *Helicoverpa zea* pupae. Comp Biochem Physiol 114B:207–216
 24. Gołębiowski M, Boguś MI, Paszkiewicz M, Wieloch W, Włóka E, Stepnowski P (2012) The composition of the cuticular and internal free fatty acids and alcohols from *Lucilia sericata* males and females. Lipids 47:613–622
 25. Gołębiowski M, Paszkiewicz M, Grubba A, Gąsiewska D, Boguś MI, Włóka E, Wieloch W, Stepnowski P (2012) Cuticular and internal n-alkane composition of *Lucilia sericata* larvae, pupae, male and female imagines: application of HPLC–LLSD and GC/MS–SIM. Bull Entomol Res 102:453–460
 26. Vrkoslav V, Muck A, Cvacka J, Svatoš A (2010) MALDI imaging of neutral cuticular lipids in insects and plants. J Am Soc Mass Spectrom 21:220–231
 27. Pasquale C, Guarino S, Peri E, Alonzo G, Colazza S (2007) Investigation of cuticular hydrocarbons from *Begrada hilaris* ganders by SPME/GC–MS. Anal Bioanal Chem 389:1259–1265
 28. Villaverde ML, Girotti JR, Mijailovsky SJ, Pedrini N, Juárez MP (2009) Volatile secretions and epicuticular hydrocarbons of the beetle *Ulomoides dermestoides*. Comp Biochem Physiol 154B:381–386
 29. Turillazzi S, Sledge MF, Cremer S, Heinze J (2002) A method for analysing small-size specimens in GC–MS. J Insect Soc Life 4:169–175
 30. Gołębiowski M, Boguś MI, Paszkiewicz M, Stepnowski P (2011) Cuticular lipids of insects as a potential biofungicides: methods of lipids composition analysis. Anal Bioanal Chem 399:3177–3191
 31. Gołębiowski M, Boguś MI, Paszkiewicz M, Stepnowski P (2010) The composition of the free fatty acids from *Dendrolimus pini* exuviae. J Insect Physiol 56:391–397
 32. Gołębiowski M, Maliński E, Nawrot J, Szafranek J, Stepnowski P (2007) Identification of the cuticular lipid composition of the Western Flower Thrips *Frankliniella occidentalis*. Comp Biochem Physiol 147B:288–292
 33. Gołębiowski M, Dawgul M, Kamysz W, Boguś MI, Wieloch W, Włóka E, Paszkiewicz M, Przybysz E, Stepnowski P (2012) The antimicrobial activity of the alcohols from *Musca domestica*. J Exp Biol. doi:10.1242/jeb.073155
 34. Howard RW, Lord JC (2003) Cuticular lipids of the booklouse, *Liposcelis bostrychophila*: hydrocarbons, aldehydes, fatty acids, and fatty acid amides. J Chem Ecol 29:615–627
 35. Buckner JS, Hagen MM, Nelson DR (1999) The composition of the cuticular lipids from nymphs and exuviae of the silverleaf whitefly, *Bemisia argentifolii*. Comp Biochem Physiol 124B:201–207
 36. Soliday CL, Blomquist GJ, Jackson LL (1974) Cuticular lipids of insects. VI. Cuticular lipids of the grasshoppers *Melanoplus sanguinipes* and *Melanoplus packardii*. J Lipid Res 15:399–405
 37. Boguś MI, Czygier M, Gołębiowski M, Kędra E, Kucińska J, Mazgajska J, Samborski J, Wieloch W, Włóka E (2010) Effects of insect cuticular fatty acids on in vitro growth and pathogenicity of the entomopathogenic fungus *Conidiobolus coronatus*. Exp Parasitol 125:400–408
 38. Blomquist GJ, Chu AJ, Remaley S (1980) Biosynthesis of wax in the honeybee, *Apis mellifera* L. Insect Biochem 10:313–321
 39. Orah V, Lockey KH (1990) Cuticular lipids of *Locusta migratoria migratoriodes*, *Schistocerca gregaria* (Acrididae) and other Orthopteran species-I. Polar components. Comp Biochem Physiol 95B:603–608
 40. Kerwin JL (1984) Fatty acid regulation of the germination of *Erynia variabilis* conidia on adults and puparia of the lesser housefly, *Fannia canicularis*. Can J Microbiol 30:158–161
 41. Baker JE (1978) Cuticular lipids of larvae *Attagenus megatoma*. Insect Biochem 8:287–292
 42. Brey PT, Ohayon Lesourd M, Castex H, Roucace J, Latge JP (1985) Ultrastructure and chemical composition of the outer layers of the cuticle of the pea aphid *Acyrtosiphon pisum* (HARRIS). Comp Biochem Physiol A 82:401–411
 43. Baker JE (1979) Developmental changes in cuticular lipids of the black carpet beetle, *Attagenus megatoma*. Insect Biochem 9:335–339
 44. Baker JE, Sukkestad DR, Nelson DR, Fatland CL (1979) Cuticular lipids of larvae and adults of the cigarette beetle, *Lasioderma serricorne*. Insect Biochem 9:603–611
 45. Lockey KH (1988) Lipids of the insect cuticle: origin, composition and function. Comp Biochem Physiol 89B:595–645
 46. Szafranek B, Paszkiewicz M, Gołębiowski M, Stepnowski P (2011) Gas chromatographic analysis of plant and insect surface compounds: cuticular waxes and terpenoids. In: Gas chromatography/book 2. In Tech. ISBN 979-953-307-736-8
 47. Espelie KE, Bernays EA (1989) Diet-related differences in the cuticular lipids of *Manduca sexta* larvae. J Chem Ecol 15:2003–2017
 48. Saito T, Aoki J (1983) Toxicity of free fatty acids on the larval surfaces of two lepidopterous insects towards *Beauveria bassiana* (Bals.) Vuill. And *Poecilomyces fumoso-roseus* (Wize) Brown et Smith (*Deuteromycetes: Moniliales*). Appl Entomol Zool 18:225–233
 49. Smith RJ, Grula EA (1981) Nutritional requirements for conidial germination and hyphal growth of *Beauveria bassiana*. J Invertebr Pathol 37:222–230

Development of a Method to Measure pre β HDL and α HDL apoA-I Enrichment for Stable Isotopic Studies of HDL Kinetics

Xuefei Li · Michael Stolinski · A. Margot Umpleby

Received: 23 March 2012 / Accepted: 12 July 2012 / Published online: 11 August 2012
© AOCs 2012

Abstract Our understanding of HDL metabolism would be enhanced by the measurement of the kinetics of pre β HDL, the nascent form of HDL, since elevated levels have been reported in patients with coronary artery disease. Stable isotope methodology is an established technique that has enabled the determination of the kinetics (production and catabolism) of total HDL apoA-I in vivo. The development of separation procedures to obtain a pre β HDL fraction, the isotopic enrichment of which could then be measured, would enable further understanding of the pathways in vivo for determining the fate of pre β HDL and the formation of α HDL. A method was developed and optimised to separate and measure pre β HDL and α HDL apoA-I enrichment. Agarose gel electrophoresis was first used to separate lipoprotein subclasses, and then a 4–10 % discontinuous SDS-PAGE used to isolate apoA-I. Measures of pre β HDL enrichment in six healthy subjects were undertaken following an infusion of L-[1- 13 C-leucine]. After isolation of pre β and α HDL, the isotopic enrichment of apoA-I for each fraction was measured by gas chromatography–mass spectrometry. Pre β HDL apoA-I enrichment

was measured with a CV of 0.51 % and α HDL apoA-I with a CV of 0.34 %. The fractional catabolic rate (FCR) of pre β HDL apoA-I was significantly higher than the FCR of α HDL apoA-I ($p < 0.005$). This methodology can be used to selectively isolate pre β and α HDL apoA-I for the measurement of apoA-I isotopic enrichment for kinetics studies of HDL subclass metabolism in a research setting.

Keywords Pre β HDL · α HDL · apoA-I kinetics · Stable isotopes · Mass spectrometry · Electrophoresis · Human

Abbreviations

2-DE	2-Dimensional electrophoresis
α -KIC	α -Ketoisocaproate
α HDL	Alpha High density lipoprotein
AP	Alkaline phosphatase
APE	Atom percent excess
ApoA-I	Apolipoprotein A-I
CAD	Coronary artery disease
CETP	Cholesterol ester transfer protein
FCR	Fractional catabolic rate
FPLC	Gel filtration fast protein liquid chromatography
FSR	Fractional secretion rate
GC–MS	Gas chromatography–mass spectrometry
HDL	High density lipoprotein
HDL-C	High density lipoprotein cholesterol
LCAT	Lecithin-cholesterol acyltransferase
m/z	Mass to charge ratio
PR	Production rate
pre β HDL	Prebeta high-density lipoprotein
SDS-PAGE	Sodium dodecylsulfate polyacrylamide gel electrophoresis
TAG	Triacylglycerol

X. Li (✉) · A. M. Umpleby
Diabetes and Metabolic Medicine, Faculty of Health
and Medical Sciences, University of Surrey,
Guildford, UK
e-mail: xuefei.li@surrey.ac.uk

M. Stolinski
School of Life Sciences, Faculty of Science,
Engineering and Computing, Kingston University,
London, UK
e-mail: m.stolinski@kingston.ac.uk

Introduction

High-density lipoproteins (HDL) are heterogeneous particles, varying in shape, size, density and composition [1]. The main apolipoproteins of human HDL are apoA-I and apoA-II, which comprise 70 and 20 % of total HDL proteins, respectively. The mature forms of HDL are spherical, while nascent HDL, which is a minor component of total HDL, is discoidal [2]. Discoidal HDL is converted into the spherical form by lecithin-cholesterol acyltransferase (LCAT).

The heterogeneity of HDL extends to variations in surface charge resulting in differences in electrophoretic mobility. When separated by agarose gel electrophoresis, HDL has either prealpha (pre α), alpha (α), prebeta (pre β) or gamma (γ) migration [3]. The α -migrating HDL particles comprise the major proportion of HDL in plasma and exist as mature, spherical forms which include the HDL₂ and HDL₃ subfractions [1]. Pre β HDL comprises of one or two molecules of apoA-I combined with phospholipids and unesterified cholesterol and includes not only nascent HDL but also recycled lipid-poor apoA-I from the remnants of large HDL particles [2, 4].

Increasing the total level of HDL is regarded as a potential therapeutic target to prevent coronary artery disease (CAD). However, the failed trial of the cholesterol ester transfer protein (CETP) inhibitor torcetrapib challenged the concept that higher HDL cholesterol (HDL-C) would necessarily result in low heart disease risk [5]. Therefore, being able to understand the kinetics of HDL subclasses is essential to understanding their metabolism, as the biological functionality of individual HDL subclasses may be the key determinant of their cardiovascular protective properties. The heterogeneous characteristics of HDL and the bidirectional inter-conversion between HDL subclasses make its metabolism complicated. There is, therefore, an increased interest in measuring the kinetics of individual HDL subfractions. There is evidence that HDL subclass distribution changes in pathological conditions such as type 2 diabetes, dyslipidemia and CAD [6–8]. Previous studies indicate that pre β HDL increases dramatically in patients with CAD, hypertriglyceridemia and hypercholesterolemia [6, 9, 10]. Cheung et al. [7] have shown that the abnormal distribution of HDL subclasses is more strongly associated with the risk of CAD than a low level of HDL-C.

Stable isotope methodology is an established technique that enables determination of the kinetics of HDL apoA-I in vivo [11]. Our understanding of HDL metabolism would be considerably enhanced by the measurement of the discrete HDL subclass kinetics and in particular the kinetics of pre β HDL. Ultracentrifugation is a robust and effective

method for the separation of lipoproteins and has been used to determine the kinetics of HDL apoA-I [12]. However, a combination of high salt concentrations and high centrifugal forces may damage the integrity of certain HDL subpopulations and lead to the dissociation of apoA-I from HDL [13, 14]. Pre β HDL, therefore, cannot be recovered in the density range of $1.063 < d < 1.21$ g/ml, but is present in the density range of $d > 1.21$ g/ml [15]. Furthermore, apoA-I at a density higher than 1.21 g/ml may not only originate from pre β HDL in the plasma but may also include that disassociated from mature α HDL during ultracentrifugation, causing inaccuracies in the interpretation of kinetic data if all apoA-I at this density is assumed to be pre β HDL. Ultracentrifugation cannot, therefore, be used to isolate pre β HDL. Thus, it is necessary to develop an alternative method that avoids disturbing HDL subpopulation integrity and also avoids contamination of the pre β HDL subclass so that an accurate determination of pre β HDL apoA-I kinetics can be obtained. Therefore, in this article, we have described a procedure which can be used to isolate individual HDL subclasses and thereby improve specificity for the determination of HDL apoA-I kinetics. Our methodology utilises an initial agarose separation followed by SDS-PAGE to enable the isolation of apoA-I from the separated pre β HDL and α HDL particles. This process enables the measurement of individual enrichment levels of apoA-I in each of the subpopulations. This is likely to be an important area of research given the progress in clinical studies on HDL-based interventions, where manipulating HDL levels are seen as a target for reducing the risk of atherosclerosis.

Materials and Methods

Materials were from Sigma-Aldrich, Gillingham, Dorset, UK, Fisher Scientific UK, Loughborough, Leicestershire, UK, and Bio-Rad Laboratories, Richmond, CA, USA, unless otherwise stated.

Clinical Protocol

The study protocol was approved by the West Kent Local Research Ethics Committee and the University of Surrey Ethics Committee. All the subjects gave written informed consent. Six healthy subjects (4 females and 2 males) were recruited for this study. Following an overnight fast, a primed (1 mg/kg) constant (1 mg/kg/h) infusion of L-[1-¹³C] leucine (15 mg/ml, ¹³C enrichment 99 %; Cambridge Isotopes, MA, USA) was administered intravenously for 9 h using an IVAC 560 pump (IVAC, Hampshire, UK). Blood samples were taken at baseline and

every hour for 9 h. Samples for α -ketoisocaproate (α -KIC) were taken at 0, 4, 6, 7, 8 and 9 h.

Blood for pre β HDL and α HDL separation and plasma apoA-I concentration was collected in tubes containing EDTA at a final concentration of 0.1 %. Blood samples for α -KIC enrichment were collected in tubes containing lithium heparin. Plasma was separated from red blood cells at 2,500 rpm for 10 min at 4 °C by centrifugation (Sorvall legend RT centrifuge; Thermo Fisher Scientific, Waltham, MA, USA). Plasma samples for α HDL and pre β HDL separation, lipid profiles, apoA-I concentration and α -KIC enrichment were stored at -80 °C. It has previously been shown that there is no significant difference in the percent distribution of pre β HDL and α HDL between fresh plasma and plasma stored at -80 °C for up to 1 year [5]. In the current study, the separation of α HDL and pre β HDL by agarose gel electrophoresis was completed within 2 weeks of each metabolic study.

Isolation of pre β HDL and α HDL by Agarose Gel Electrophoresis

To separate α HDL and pre β HDL, 160 μ l plasma diluted with sample buffer (4:1 v:v, 50 % glycerol, 125 mM Tris, 125 mM tricine, 0.005 % bromophenol blue, pH 8.6) was loaded onto a 0.6 % agarose gel (low electroendosmosis agarose with a high gelling temperature; Fluka, Buchs, Switzerland) prepared with 25 mM, pH 8.6 Tris-tricine buffer (Tricine from Acros Organics, Geel, Belgium). Agarose gel electrophoresis used a flat-bed gel cassette with water cooling system placed on ice, (CHU20 max-cooled horizontal gel unit; Sie-plas, Southam, Warwickshire, UK), run at 25 mM, pH 8.6 Tris-tricine buffer at 170 V for 3 h. Samples were loaded on alternate lanes to avoid contamination between samples.

The agarose gel was stained with 0.05 % coomassie blue R250 (BDH, Corston, Bath, UK) prepared in methanol acetic acid solution (methanol:H₂O:acetic acid, 9:9:1, by vol) and stained for 3–4 h or until the bands were well developed. Excess dye was then removed by destaining with the same methanol acetic acid solution.

Extraction and Delipidation of Proteins from pre β HDL and α HDL

After destaining the agarose gel, individual α HDL and pre β HDL bands were excised and freeze-dried (ModulyoD Freeze Dryer; Thermo Fisher Scientific) overnight. Proteins were extracted from α HDL and pre β HDL bands with 3 ml of 1 % SDS solution for four and three times, respectively, at room temperature and then concentrated by freeze-drying. To precipitate and purify the HDL proteins from SDS, coomassie blue R250 and lipid, 4 ml ice-cold ethanol was

added to precipitate proteins on ice for 1 h. The samples were then centrifuged at 4,000 rpm for 1 h at 1 °C and the supernatant discarded. The remaining lipid in the samples was removed by adding 4 ml ice-cold diethyl ether and the samples again centrifuged as described above.

Isolation of apoA-I from pre β HDL and α HDL by SDS-PAGE

After delipidation, α HDL and pre β HDL samples were dissolved in 70 μ l sample buffer (0.15 M sodium phosphate, 12.5 % glycerol, 2 % SDS, 5 % β -mercaptoethanol, 0.001 % bromophenol blue, pH 6.8). ApoA-I was isolated by 4–10 % discontinuous SDS-PAGE (40 % polyacrylamide/Bis, 37.5:1) run with Tris–glycine buffer (0.25 M glycine, 25 mM Tris-base, 0.1 % SDS, w/v, pH 8.5) in a PROTEAN II gel Cell (Bio-Rad Laboratories) at 80 V for 16 h. Samples were loaded on alternate lanes to avoid contamination between samples. A low pH tris base-SDS buffer system (0.25 M Tris base, 0.2 % SDS, w/v, pH 6.8) was used for the 4 % stacking gel and a high pH tris base-SDS buffer system (0.75 M Tris base, 0.2 % SDS, w/v, pH 8.8) for the 10 % resolving gel. SDS-PAGE was stained using a silver staining kit following the manufacturer's protocol. The apoA-I bands were then excised from the gel and hydrolysed in 1 ml 6 M HCl at 120 °C for 24 h. The hydrolysed samples were purified by ion exchange chromatography (Polypropylene columns from Evergreen Scientific, CA, USA; AG50W-X8 cation exchange resin 100–200 mesh; BioRad Laboratories). Pre β HDL apoA-I has a low concentration in plasma. This makes background noise significant when isotopic enrichment is determined by a sensitive GC–MS method. A previous study has indicated that contamination can originate from reagents, gels and glassware [16]. All methodological steps— isolation by SDS-PAGE, hydrolysis, amino acid purification with ion exchange chromatography and derivatisation for GC–MS—have the potential to introduce contamination and their contribution to this effect was investigated. The largest source of contamination was found to be associated with the PAGE gel itself. The process of silver staining did not introduce any leucine contaminants. Pilot studies had shown that leucine contamination from fragments of gel was proportional to the extracted gel size. The samples processed in this study were all obtained from a single 1 cm² gel sample which was excised using a plastic corer thereby ensuring consistency in gel size extraction. Contamination experiments showed that reducing gel areas to 1 cm² areas and maximising sample volume by using 160 μ l plasma for each sample accounted for contamination levels of no more 1.6 % of the peak responses for pre β HDL. In each study, enrichment at each time point was

corrected for baseline enrichment which would correct for any contamination from the gel.

Derivatization of Amino Acids for GC–MS

After purification by ion exchange chromatography, apoA-I hydrolysed samples were freeze-dried and then derivatised with 100 μ l TFA/TFAA (1:1, by vol; Fluka) at 110 °C for 5 min. Toluene (0.5 ml) and H₂O (1 ml) were added and after vortexing, samples were centrifuged briefly and the top layer containing the derivatised amino acids in toluene transferred into GC vials. Isotopic enrichment of ¹³C leucine was analysed by GC–MS (7890A GC system, Agilent 5975 inert XL MSD; Agilent Technologies, Wokingham, Berkshire, UK) in negative chemical ionisation mode with methane as the reagent gas, monitoring ions *m/z* 209 (*m*) and 210 (*m* + 1). The GC was equipped with a Rtx-5, 30 m, 0.25 mm inner diameter (ID), 0.25 μ m film capillary column (Thames Restek, Bucks, UK) using helium as the carrier gas at a flow rate of 1 ml/min.

Determination of Plasma α -KIC Isotopic Enrichment

Isotopic enrichment of α -KIC was determined by a modified method of Ford et al. [17] with selected ion monitoring of fragments at *m/z* 259 (*m*) and 260 (*m* + 1) in electron ionisation mode by GC–MS equipped with same column as described above.

Measurement of apoA-I Concentration

Plasma apoA-I concentration was measured by an immunoturbidimetric method using an ABX Mira Plus (Horiba ABX, Northampton, UK). ApoA-I concentration from pre β HDL and α HDL was measured by western blotting. After agarose gel electrophoresis, the pre β HDL and α HDL bands were transferred to a 0.2- μ m nitrocellulose membrane (Amersham Pharmacia Biotech, Bucks, UK) and run overnight at 30 V in a glycine-tris (25 mM tris-base, 200 mM glycine pH 8.3) running buffer [18]. The membrane was incubated with a specific primary antibody (1:10,000, goat polyclonal to human apoA-I; Abcam, Cambridge, UK) and then incubated with secondary antibody [1:2,500, donkey polyclonal to goat IgG-H&L; Abcam] linked with the enzyme alkaline phosphatase (AP). ApoA-I was immuno-localised by staining the membrane with AP Conjugate Substrate Kit. The relative apoA-I ratio of pre β HDL and α HDL was calculated after scanning the western blotting membrane by a densitometer (GS800; Bio-Rad Laboratories). The concentrations of pre β HDL and α HDL apoA-I were then calculated from the total plasma apoA-I concentration. The CV for pre β HDL apoA-I

α HDL apoA-I concentration measured with this method was 2.3 and 0.27 %, respectively (*n* = 3).

Measurement of Lipid Concentration

Plasma and HDL TAG and cholesterol were measured using an ABX Mira Plus analyser using TAG and cholesterol assay kits (Horiba ABX).

Data Analysis

The atom percent excess (APE) of ¹³C-leucine and ¹³C α -KIC was calculated from the peak area ratio corrected for the baseline. It has recently been shown that APE rather than the tracer:tracee ratio is the correct method for expressing enrichment when calculating lipoprotein fluxes [19].

$$\text{APE (\%)} = [(R_t - R_0)/(R_t - R_0 + 1)] \times 100$$

where *R_t* and *R₀* are the isotopic area ratios of (*m* + 1)/*m* (210/209 for leucine, 260/259 for α -KIC) for the sample at time *t* and baseline sample at time zero, respectively. The fractional secretion rate (FSR) of HDL apoA-I in each subclass was calculated using linear regression as used previously for the measurement of total HDL apoA-I kinetics [20].

$$\text{FSR (pools/day)} = (\text{Slope of the apoA-I APE time curve} / \text{KIC}_{\text{APE}}) \times 24$$

where plasma α -ketoisocaproate enrichment (KIC_{APE}) is a measure of hepatic intracellular leucine enrichment [17]. In a steady state, the FSR is equal to fractional catabolic rate (FCR). The production rate (PR) was calculated from the product of the FSR and the pool size. ApoA-I pool size was calculated by the concentration of apoA-I of each subclass multiplied by plasma volume. Plasma volume was calculated as described by Pearson et al. [21].

Statistical Analysis

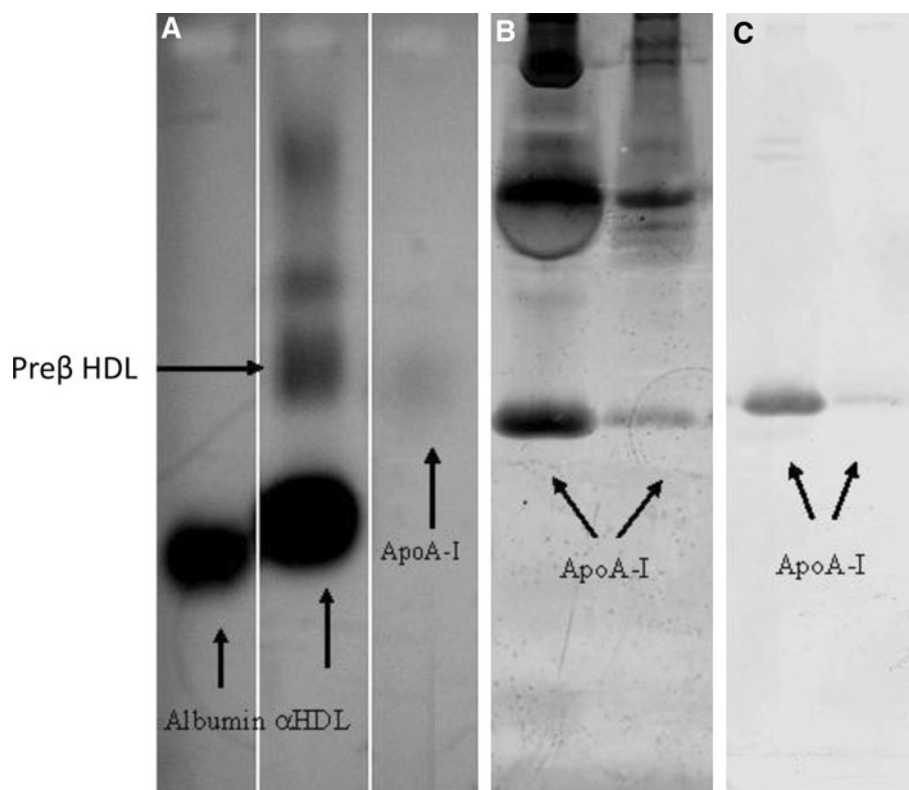
Results are presented as mean \pm SEM. Statistical differences in HDL subclass variables were analysed by paired two-tailed *t* test using the software SPSS 16.0 (SPSS, USA). In all the comparisons, *P* < 0.05 was considered statistically significant.

Results and Discussion

Development of Electrophoresis Methodology

A modified 2-dimensional electrophoresis (2-DE) method was used to separate α HDL and pre β HDL apoA-I directly

Fig. 1 **a** Plasma separation on agarose gel with coomassie blue staining. **b** ApoA-I separated by 4–10 % discontinuous SDS-PAGE with silver staining. **c** Western blot of SDS-PAGE



from plasma. This method of separation is based on both surface charge and molecular weight. The method avoided the use of ultracentrifugation to prevent possible structural and compositional changes of HDL. The protocol combines a non-denatured first-dimensional agarose gel step which separates lipoprotein particles on the basis of surface charge with a denatured second-dimensional SDS-PAGE separation. This separates proteins based on molecular weight. With this method, a relatively large plasma sample (160 μ l) was loaded onto an agarose gel (Fig. 1a). Purified apoA-I has pre β -migrating mobility and was used to identify the position of pre β HDL [22]. Albumin has α -migrating mobility and was used to identify the position of α -migrating HDL. After separation of pre β HDL and α HDL by agarose gel electrophoresis, individual bands of pre β HDL and α HDL were excised. The effects of high plasma TAG on agarose gel electrophoresis and potential contamination from non-HDL apoA-I containing particles such as from VLDL pre β apoAI were not investigated in this study. However, precipitation of apoB containing lipoproteins by magnesium chloride/heparin [23] as a process to avoid any confounding effects could be developed. This could prevent plasma samples with broad β -mobility from interfering with the pre β band and could also eliminate any potential contamination from VLDL pre β apoA-I.

Efficient extraction of the proteins in these bands was necessary before loading onto SDS-PAGE. A 1 % SDS solution was found to be an effective method for the extraction of proteins from the agarose gel bands. The effectiveness of a freeze-drying step prior to the SDS extraction procedure was also investigated. Results indicated that freeze-drying the bands improved the SDS extraction procedure. The sample volumes used for the extraction of apo A-I were approximately 10 and 12 ml for pre β HDL and α HDL, respectively. It was necessary to reduce these sample volumes and remove the SDS as well as any lipids and Coomassie blue before reconstitution in sample buffer. This was achieved by an ethanol precipitation to remove the SDS and Coomassie blue, followed by a diethyl ether extraction to remove any remaining lipids. This process allowed the isolation of apoA-I from both α HDL and pre β HDL for SDS-PAGE (Fig. 1b). When developing the method, the migrating position of apoA-I was confirmed by western blotting (Fig. 1c).

Optimising pre β HDL Concentration for GC–MS

The average peak area of α HDL was 28 times higher than that of pre β HDL. The relatively smaller peak areas of pre β HDL made it difficult to measure the 13 C-leucine isotopic enrichment accurately. To overcome this issue, the

derivatised samples of pre β HDL were adjusted to provide similar areas for both fractions.

To test the precision of the measurement of the isotopic enrichment of pre β HDL and α HDL apoA-I by GC-MS, pre β HDL and α HDL were isolated from six identical plasma samples (taken 9 h after the ^{13}C leucine infusion) using 2-DE. Pre β HDL and α HDL apoA-I isotopic enrichment had a CV of 0.51 and 0.34 %, respectively.

Pre β HDL and α HDL apoA-I Concentration Measured by Western Blotting

It is technically difficult to independently measure pre β HDL and α HDL apoA-I concentration directly from plasma, and, therefore, concentrations were estimated using the relative ratio of pre β HDL and α HDL apoA-I as detected by western blotting. Pre β HDL apoA-I, as a percentage of total apoA-I was 10.1 ± 0.35 % while α HDL was 89.9 ± 0.35 %. This is similar to a previous study which reported that pre β HDL and α HDL were 10.6 and 89.7 %, respectively, of total apoA-I in healthy subjects [8]. Pre β HDL apoA-I concentration was significantly lower than α HDL apoA-I concentration (0.15 ± 0.13 and 1.18 ± 0.083 mg/ml, respectively, $p = 0.005$).

Pre β HDL and α HDL apoA-I Kinetics

The possibility of using this two-dimensional electrophoresis method to measure the kinetics of apoA-I in α HDL and pre β HDL following isotopic labelling with ^{13}C leucine was explored in six healthy volunteers. The subject characteristics are shown in Table 1. All subjects with the exception of one had normal lipid levels. Pre β HDL apoA-I enrichment increased more rapidly than α HDL apoA-I enrichment and the FCR of pre β HDL apoA-I (0.20 ± 0.017 pools/day) was significantly higher than the FCR of α HDL apoA-I

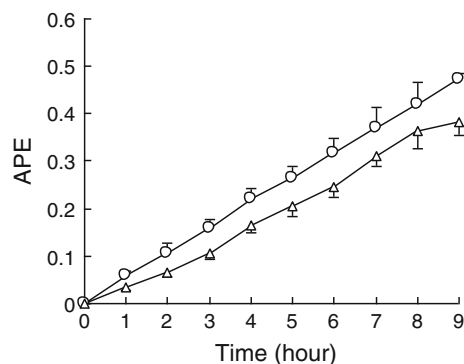


Fig. 2 Enrichment (APE) of pre β HDL apoA-I (open circle) and α HDL apoA-I (open triangle). Results are presented as mean \pm SEM ($n = 6$)

(0.17 ± 0.016 pools/day, $p < 0.005$) (Fig. 2). Pre β HDL and α HDL kinetics have only been previously measured by one research group after separation by gel filtration fast protein liquid chromatography (FPLC) [24]. Both studies utilised a continuous infusion of stable isotopically labelled leucine to determine kinetics of pre β and α HDL in six healthy individuals. Individuals from both studies had similar plasma α HDL apoA-I and pre β -HDL concentrations and were fairly well matched, although the previous study infused [$5,5,5\text{-}^2\text{H}_3$] labelled leucine over a longer period of 14 h in males only. The current study infused 1- ^{13}C leucine for 9 h and also included two women. Pre-menopausal women generally have higher levels of HDL-C than age-matched men [25]. Pre β HDL apoA-I FCR in the current study ($0.124\text{--}0.237$ pools/day) was slightly lower than that measured by FPLC ($0.142\text{--}0.367$ pools/day), while α HDL apoA-I FCR in the current study ($0.107\text{--}0.209$ pools/day) was slightly higher than that measured by FPLC ($0.076\text{--}0.148$ pools/day) [24]. Differences in these results may have also been due to the type of kinetic analysis used; the previous study utilised a multicompartmental analysis,

Table 1 Subject characteristics ($n = 6$)

	1	2	3	4	5	6	Mean \pm SEM
Age (years)	30	33	41	53	34	35	37.67 ± 3.4
Gender	F	F	M	F	M	F	–
BMI (kg/m^2)	25.60	22.40	25.80	20.40	22.10	26.80	23.85 ± 1.04
Insulin (pmol/L)	59.03	108.34	90.98	43.06	83.34	138.90	87.28 ± 14.01
Plasma-TAG (mmol/L)	0.50	0.69	0.65	0.63	2.00	1.00	0.91 ± 0.23
Plasma-C (mmol/L)	4.15	3.69	4.71	4.58	3.54	5.85	4.42 ± 0.34
HDL-TAG (mmol/L)	0.06	0.10	0.05	0.08	0.12	0.07	0.08 ± 0.011
HDL-C (mmol/L)	1.40	1.36	1.20	1.98	0.78	1.04	1.29 ± 0.16
Plasma apoA-I (mg/ml)	1.33	1.32	1.35	1.73	1.04	1.17	1.32 ± 0.094
α HDL apoA-I (mg/ml)	1.18	1.19	1.20	1.54	0.93	1.05	1.18 ± 0.083
pre β HDL apoA-I (mg/ml)	0.16	0.13	0.14	0.19	0.11	0.12	0.15 ± 0.13

F female, M male, BMI body mass index, TAG triacylglycerol, C cholesterol, HDL high-density lipoprotein, ApoA-I apolipoprotein A-I

and also had a longer clinical protocol. However, of importance is that the current study avoids the possibility of any overlap between subclasses which could occur when separating whole plasma α and pre β HDL with FPLC. Even though the previous study demonstrated the purity of apoA-I in pre β and α HDL populations as isolated by FPLC, the authors acknowledged that, in order to analyse pure subclasses, 10 FPLC fractions containing both pre β and α HDL had to be omitted [24].

The PR of pre β HDL apoA I (1.03 ± 0.06 mg/kg/day) was lower than the PR of α HDL (6.73 ± 0.4 mg/kg/day, $P < 0.001$). This was unexpected since pre β HDL is considered to be the precursor pool for α HDL. However, pre β HDL is a mixture of nascent HDL, recycled lipid-poor apoA-I and remnants of large HDL particles [2, 4]. Thus, the nascent HDL apoA-I enrichment, the precursor of α HDL, could be diluted by the recycling of apoA-I. An explanation for recycling of apoA-I possibly leading to a lower production rate could be related to the activity of plasma factors such as enzymes and receptors associated with the dissociation of apoA-I from more mature HDL. Pre β HDL can be subdivided into pre β 1 and pre β 2 fractions. These particles have been shown to have different sizes and may represent particles which are metabolised differently. In this context, the metabolism of pre β 1 has been more extensively investigated [26]. The isolation of pre β HDL fractions using two-dimensional separation techniques, also utilising sequential agarose and PAGE techniques, has been previously described [27]. These authors utilised pulse chase labelling techniques to show the preferential incorporation of labelled cholesterol from cultured fibroblasts into different pre β HDL particles which had been isolated from human blood. These particles (Pre β 1 and pre β 2) also showed differences in the rate of accumulation of enriched cholesterol. A similar approach could be incorporated with the kinetic study described here, measuring both labelled apoA-I and cholesterol fluxes to further elucidate the kinetics of the different HDL subpopulations, providing a more complete description of particles kinetics in relation to providing an explanation for the lower production rate of pre β HDL particles.

This protocol was adopted since it could be conducted in 1 day, and the primary aim was to generate samples for the development of a robust working method for the separation of apoA-I whose enrichment could be measured. ApoA-I has a relatively slow turnover rate with a mean residence time of approximately 5 days [28], so a much longer study needs to be undertaken with blood sampling over 1–2 weeks in order to develop a suitable model of HDL subclass kinetics [29]. This would only be possible using an intravenous bolus of isotopically labelled leucine rather than an infusion and would provide more information about the inter-conversion between HDL subclasses. Future

studies could also involve the separation of distinct pre β subclasses and could describe the kinetics of these particles utilising multicompartmental analysis. Multi-compartmental analysis is the most appropriate form of modelling to use, as it can provide data related to the recycling of the tracer which cannot be obtained by linear regression [30]. The use of multicompartmental techniques would enable the determination of the contribution of the recycling of unlabelled apoA-I from larger particles in addition to the production rate of nascent pre β HDL. The paper describes the use of a two-dimensional electrophoresis method for the complete separation of pre β HDL and α HDL apoA-I, which can be used to measure pre β HDL and α HDL apoA-I enrichment after isotopic labelling of apoA-I in human kinetic studies. Further studies need to be undertaken to develop a suitable clinical protocol which, when combined with this preparative methodology, can provide a robust measure of HDL subclass kinetics in a research setting.

Acknowledgments Xuefei Li was the recipient of a University of Surrey PhD scholarship. We are grateful to Mrs J. Batt for her technical assistance.

References

1. Barter PJ (2000) Hugh sinclair lecture: the regulation and remodelling of HDL by plasma factors. *Atheroscler Suppl* 4(3): 39–47
2. Rye KA, Barter PJ (2004) Formation and metabolism of prebeta-migrating, lipid-poor apolipoprotein A-I. *Arterioscler Thromb Vasc Biol* 24:421–428
3. Huang Y, von Eckardstein A, Wu S, Maeda N, Assmann G (1994) A plasma lipoprotein containing only apolipoprotein E and with gamma mobility on electrophoresis releases cholesterol from cells. *Proc Natl Acad Sci USA* 91:1834–1838
4. Miida T, Sakai K, Ozaki K, Nakamura Y, Yamaguchi T, Tsuda T, Kashiwa T, Murakami T, Inano K, Okada M (2000) Bezafibrate increases prebeta 1-HDL at the expense of HDL2b in hypertriglyceridemia. *Arterioscler Thromb Vasc Biol* 20:2428–2433
5. Moyad MA, Merrick GS (2007) Cholesterol, cholesterol-lowering agents/statins, and urologic disease: part VI—the recent rise and fall of the HDL-boosting drug torcetrapib. *Urol Nurs* 27:169–173
6. Asztalos BF, Roheim PS, Milani RL, Lefevre M, McNamara JR, Horvath KV, Schaefer EJ (2000) Distribution of ApoA-I-containing HDL subpopulations in patients with coronary heart disease. *Arterioscler Thromb Vasc Biol* 20:2670–2676
7. Cheung MC, Brown BG, Wolf AC, Albers JJ (1991) Altered particle size distribution of apolipoprotein A-I-containing lipoproteins in subjects with coronary artery disease. *J Lipid Res* 32:383–394
8. Xu Y, Fu M (2003) Alterations of HDL subclasses in hyperlipidemia. *Clin Chim Acta* 332:95–102
9. Miida T, Yamaguchi T, Tsuda T, Okada M (1998) High prebeta1-HDL levels in hypercholesterolemia are maintained by probucol but reduced by a low-cholesterol diet. *Atherosclerosis* 138:129–134
10. Yang Y, Yan B, Fu M, Xu Y, Tian Y (2005) Relationship between plasma lipid concentrations and HDL subclasses. *Clin Chim Acta* 354:49–58

11. Cohn JS, Wagner DA, Cohn SD, Millar JS, Schaefer EJ (1990) Measurement of very low density and low density lipoprotein apolipoprotein (Apo) B-100 and high density lipoprotein Apo A-I production in human subjects using deuterated leucine. Effect of fasting and feeding. *J Clin Invest* 85(3):804–811
12. Ikewaki K, Rader DJ, Schaefer JR, Fairwell T, Zech LA, Brewer HB Jr (1993) Evaluation of apoA-I kinetics in humans using simultaneous endogenous stable isotope and exogenous radio-tracer methods. *J Lipid Res* 34:2207–2215
13. Kunitake ST, Kane JP (1982) Factors affecting the integrity of high density lipoproteins in the ultracentrifuge. *J Lipid Res* 23:936–940
14. Cheung MC, Wolf AC (1988) Differential effect of ultracentrifugation on apolipoprotein A-I-containing lipoprotein subpopulations. *J Lipid Res* 29:15–25
15. Cheung MC, Albers JJ (1979) Distribution of cholesterol and apolipoprotein A-I and A-II in human high density lipoprotein subfractions separated by CsCl equilibrium gradient centrifugation: evidence for HDL subpopulations with differing A-I/A-II molar ratios. *J Lipid Res* 20:200–207
16. Dwyer KP, Barrett PH, Chan D, Foo JI, Watts GF, Croft KD (2002) Oxazolinone derivative of leucine for GC-MS: a sensitive and robust method for stable isotope kinetic studies of lipoproteins. *J Lipid Res* 43:344–349
17. Ford GC, Cheng KN, Halliday D (1985) Analysis of (1–¹³C)leucine and (¹³C)KIC in plasma by capillary gas chromatography/mass spectrometry in protein turnover studies. *Bio-med Mass Spectrom* 12:432–436
18. Ishida BY, Frolich J, Fielding CJ (1987) Prebeta-migrating high density lipoprotein: quantitation in normal and hyperlipidemic plasma by solid phase radioimmunoassay following electrophoretic transfer. *J Lipid Res* 28:778–786
19. Ramakrishnan R (2006) Studying apolipoprotein turnover with stable isotope tracers: correct analysis is by modeling enrichments. *J Lipid Res* 47:2738–2753
20. Umpleby AM, Das S, Stolinski M, Shojaae-Moradie F, Jackson NC, Jefferson W, Crabtree N, Nightingale P, Shahmanesh M (2005) Low density lipoprotein apolipoprotein B metabolism in treatment-naive HIV patients and patients on antiretroviral therapy. *Antivir Ther* 10:663–670
21. Pearson TC, Guthrie DL, Simpson J, Chinn S, Barosi G, Ferrant A, Lewis SM, Najean Y (1995) Interpretation of measured red cell mass and plasma volume in adults: Expert Panel on Radio-nuclides of the International Council for Standardization in Haematology. *Br J Haematol* 89:748–756
22. Asztalos BF, Sloop CH, Wong L, Roheim PS (1993) Two-dimensional electrophoresis of plasma lipoproteins: recognition of new apo A-I-containing subpopulations. *Biochim Biophys Acta* 41(1169):291–300
23. Wieland H, Seidel D (1973) Improved techniques for assessment of serum lipoprotein patterns. II. Rapid method for diagnosis of type III hyperlipoproteinemia without ultracentrifugation. *Clin Chem* 19:1139–1141
24. Chétiveaux M, Ouguerram K, Zair Y, Maugère P, Falconi I, Nazih H, Krempf M (2004) New model for kinetic studies of HDL metabolism in humans. *Eur J Clin Invest* 34(4):262–267
25. Collins P (2008) HDL-C in post-menopausal women: an important therapeutic target. *Int J Cardiol* 124(3):275–282
26. Nakamura Y, Kotite L, Gan Y, Spencer TA, Fielding CJ, Fielding PE (2004) Molecular mechanism of reverse cholesterol transport: reaction of pre-beta-migrating high-density lipoprotein with plasma lecithin/cholesterol acyltransferase. *Biochemistry* 43(46):14811–14820
27. Castro GR, Fielding CJ (1988) Early incorporation of cell-derived cholesterol into pre-beta-migrating high-density lipoprotein. *Biochemistry* 27(1):25–29
28. Schaefer EJ, Zech LA, Jenkins LL, Bronzert TJ, Rubalcaba EA, Lindgren FT, Aamodt RL, Brewer HB Jr (1982) Human apolipoprotein A-I and A-II metabolism. *J Lipid Res* 23:850–862
29. Fisher WR, Venkatakrishnan V, Zech LA, Hall CM, Kilgore LL, Stacpoole PW, Diffenderfer MR, Friday KE, Sumner AE, Marsh JB (1995) Kinetic evidence for both a fast and a slow secretory pathway for apolipoprotein A-I in humans. *J Lipid Res* 36:1618–1628
30. Chan DC, Barrett PH, Watts GF (2004) Lipoprotein transport in the metabolic syndrome: methodological aspects of stable isotope kinetic studies. *Clin Sci (Lond)* 107(3):221–232

Docosahexanoic Acid Improves Chemotherapy Efficacy by Inducing CD95 Translocation to Lipid Rafts in ER⁻ Breast Cancer Cells

Julia B. Ewaschuk · Marnie Newell · Catherine J. Field

Received: 28 July 2011 / Accepted: 31 August 2012 / Published online: 7 October 2012
© AOCs 2012

Abstract Docosahexanoic acid (DHA) and eicosapentaenoic acid (EPA) have been shown to possess anti-carcinogenic properties in mammary cancers, both in vitro and in vivo. The objective of this study was to investigate the effect of treating three different breast cancer cell lines with DHA or EPA on cellular growth, chemotherapy efficacy, and CD95 expression and localization in the cell. MDA-MB-231, MCF-7 and SKBr-3 cells were incubated with EPA or DHA with or without chemotherapy agents [doxorubicin (dox), Herceptin]. Cell growth was assessed by WST-1 assay and CD95 expression was investigated using flow cytometry, Western blotting and confocal microscopy. DHA and EPA inhibited the growth of all three breast cancer cell lines in a dose-dependent fashion ($P < 0.05$). DHA, and to a lesser extent EPA, induced the movement and raft clustering of CD95 in the cell membrane (via confocal microscopy) and the surface expression (via flow cytometry) in MDA-MB-231 cells. Neither fatty acid altered the growth/metabolic activity of the non-transformed MCF-12A breast cell line. Pre-treatment with DHA, but not EPA, improved the efficacy of dox in estrogen receptor negative MDA-MB-231 cells ($P < 0.05$), but not in the other two cell lines. Pre-treating cells with DHA increased CD95 surface expression (threefold) and the plasma membrane raft content of CD95 (2fold) and FADD (>4-fold) after dox treatment, compared to dox treatment alone ($P < 0.05$). This study demonstrated that pre-treatment of estrogen receptor negative MDA-MB-231 cells with DHA increased the anti-cancer effects of dox and

presents evidence to suggest that this may be mediated in part by CD95-induced apoptosis.

Keywords Breast cancer · n-3 Polyunsaturated fatty acids · CD95 · Chemotherapy · Cell death · Apoptosis · FADD

List of symbols

Abbreviations

DAPI	4',6'-Diamidino-2-phenylindole
DHA	Docosahexanoic acid
DISC	Death-inducing signaling complex
EPA	Eicosapentaenoic acid
ER	Estrogen receptor
FADD	Fas-associated death domain-containing protein
LNA	Linoleic acid
OLA	Oleic acid
PUFA	Polyunsaturated fatty acid(s)

Introduction

The long chain polyunsaturated fatty acids (PUFA) n-3 fatty acids, eicosapentaenoic acid (EPA) and docosahexanoic acid (DHA) have been shown to exert a number of beneficial biological properties, including anti-cancer effects [1–4]. Our group and others have demonstrated that DHA and EPA decrease the in vitro growth of breast cancer cells, including estrogen receptor (ER)-negative [4–9] and ER-positive [10–14] cell lines. Considerable research exists demonstrating that oral intake of EPA and DHA inhibits the growth of mammary tumors in animal models [3, 9]. While it is recognized that n-3 PUFA alter tumor growth in cell and animal models, current

J. B. Ewaschuk · M. Newell · C. J. Field (✉)
Department of Agricultural, Food and Nutritional Sciences,
4-126A Li Ka Shing Health Research Innovation Centre,
University of Alberta, Edmonton, AB T6G 2E1, Canada
e-mail: Catherine.Field@ualberta.ca

understanding of the cellular mechanisms is incomplete. Several candidate mechanisms have been proposed for the action of n-3 PUFA on breast cancer cells, including alterations in membrane structure and composition, as well as changes in membrane-mediated functions and signals (e.g., lipid rafts, lipid second messengers, signaling proteins, downstream transcription factors, and lipid peroxides) [9]. The cell membrane is a dynamic, asymmetric, heterogeneous structure containing lipid rafts. These microdomains are enriched in saturated fatty acids, sphingolipids, cholesterol and glycosylphosphatidylinositol-linked proteins [15, 16]. Rafts also contain an abundance of signaling proteins [17], suggesting a role in signal transduction, possibly by facilitating the interaction of signaling molecules with their corresponding receptors [18]. EPA and DHA are known to be readily incorporated into tumor cell membranes when provided in the diet or in cell culture media [2, 19–21] and to alter lipid raft organization [22]. Studies from our laboratory show that EPA and DHA are also incorporated into lipid rafts of MDA-MB-231 [5] and MCF-7 (unpublished data) breast cancer cells in vitro, and this is associated with reduced raft epidermal growth factor receptor expression in MDA-MB-231 cells [5].

There is evidence that suggests that long chain n-3 PUFA may also augment chemotherapy treatment of breast cancer. For example, breast cancer patients with a higher concentration of DHA in breast adipose tissue respond more favorably to chemotherapy than those with lower adipose DHA [23]. A recent open-label, single-arm, phase II study demonstrated that a daily intake of 1.8 g of DHA during anthracycline-based chemotherapy in breast cancer patients resulted in the longest overall survival for patients with the highest plasma DHA [24]. Correspondingly, there are in vitro and rodent-model studies indicating that n-3 PUFA sensitize breast cancer cells to the effects of chemotherapy (reviewed in [9, 25]).

A detailed understanding of the cellular processes responsible for the effects of DHA and EPA, not only on cell growth, but also on the action of chemotherapy drugs is lacking. We previously demonstrated that n-3 PUFA induced cell death through an apoptotic mechanism, the initiation of which is unknown [4]. The transmembrane death receptor CD95 (APO-1/Fas) is the best characterized member of the death receptors that activate the extrinsic apoptosis pathway [26]. Activation results in CD95 aggregation in the plasma membrane, followed closely by recruitment of Fas-associated death domain-containing protein (FADD) and caspase-8 to the CD95 receptor, forming the death-inducing signaling complex (DISC) [27]. Treatment of tumor cells with doxorubicin (dox), a widely used antineoplastic drug therapy, has been shown to induce apoptosis and the movement of DISC to membrane rafts [28, 29]. Given the ability of DHA and EPA to alter

lipid raft structure and function, we hypothesized that EPA and/or DHA may initiate cell-death by altering lipid raft-CD95 co-localization.

To increase the understanding of the mechanisms of action of n-3 PUFA on breast cancer cells, this study aimed to determine the impact on cell growth of treating three human cancer cell lines in vitro with DHA or EPA with and without dox and to identify the impact on the cellular content and location of the CD95 death receptor.

Materials and Methods

Cell Culture

Cell lines were obtained from the American Type Culture Collection (Rockville, MD). MDA-MB-231 cells were maintained in Iscove's modified Dulbecco's medium, MCF-7 cells in minimum essential medium, MCF-12A in Dulbecco's modified Eagle medium with 20 ng/ml epidermal growth factor, 100 ng/ml 1 cholera toxin, 10 µg/ml insulin and 500 ng/ml hydrocortisone, and SKBr-3 cells in McCoy's 5A medium. All media were supplemented with penicillin and streptomycin, and 5 % v/v fetal calf serum (all media components from Gibco Invitrogen Corporation, Burlington, ON, Canada). Cells were grown at 37 °C in 5 % CO₂ at 98 % relative humidity. Cells were seeded at 1×10^6 cells per flask (75 cm²) in 15 ml of medium and allowed 48 h to adhere prior to the application of experimental conditions. For WST-1 viability experiments cells were seeded in 96-well plates, and for immunofluorescence experiments cells were grown on coverslips in 12-well plates. All experiments were initiated at 75–80 % confluence of cells.

Conjugated Fatty Acids

Fatty acids were purchased from NuChek Prep Inc. (Elysian, MN). Fatty acids were conjugated to bovine serum albumin (BSA, Sigma Aldrich) as follows: fatty acids were solubilized in ethanol, dried under nitrogen gas and resuspended in 1 ml potassium hydroxide (0.1 M and incubated and 50 °C for 10 min). BSA was added drop-wise (9 ml, 7.5 %) and incubated overnight at 4 °C. Solutions were filtered through a 0.22 µm syringe filter and stored at –20 °C.

Control Conditions and Experimental Design

A series of preliminary experiments comparing the fatty acid profiles of human breast tissue to that of cultured cell lines indicated that the fatty acids supplied in the culture media described above were not sufficient to optimize cell growth and the supply of n-6 fatty acids (data not shown). To ameliorate this deficiency we supplemented all

conditions with 40 μM oleic acid (OLA) and 40 μM linoleic acid (LNA); this was considered the control condition (rather than plain culture media). Neither of these fatty acids exerts cytotoxic effects at those concentrations or even tenfold higher concentrations (data not shown). After 48 h of incubation in fatty acid-free medium, the culture medium was replaced with 15 ml of fresh medium containing the experimental fatty acids (on a background of 40 μM OLA/40 μM LNA) and the cells were further incubated for 48 h (treatments were reapplied after 24 h). For chemotherapy and other subsequent experiments, EPA and DHA concentrations were selected to yield approximately equivalent effects on cell death among differing cell lines. For chemotherapy experiments, after this initial 48 h fatty-acid pre-treatment, the fatty acids were removed and chemotherapy agents, specific for the cell lines, were added for 24 h. To choose concentrations of chemotherapy agents, preliminary experiments were conducted to yield equivalent cell death (approximately 20 %) in each of the studied cell lines in response to chemotherapy at 24 h (data not shown; 1.5×10^{-6} M dox for MCF-7, 4.1×10^{-7} M for MDA-MB-231, and 11 $\mu\text{g}/\text{ml}$ of HerceptinTM for the dox-resistant HER2/c-erb-2 over-expressing SKBr-3 cell line). Cells were then harvested using trypsin-ethylenetriaminetetraacetic acid (Gibco Invitrogen Corporation, Burlington, ON).

Assessment of Cell Growth via Cellular Viability

Cellular viability was assessed using the cell proliferation reagent, WST-1 (Roche Applied Science, Laval, PQ), according to manufacturer's instructions. Previous studies with the MTT assay confirmed that incubation with DHA and EPA reduced cell numbers [5]. Preliminary studies were conducted to confirm that reduction in WST-1 activity after incubation with DHA or EPA was consistent with a reduced number of MCF-7 or MDA-MB-231 cells. To confirm that viability was due to a decrease in cell numbers, cell counts were performed ($n = 3$) for EPA at 100 μM and DHA at 60 μM for 48 h and compared to 100 μM OLA for both the MCF-7 and MDA-MB-231 cells.

Immunofluorescence and Confocal Microscopy

Cells were seeded (5×10^5 cells/well) onto sterile coverslips in 12-well culture plates and incubated until 80 % confluence was reached. Fatty acid and chemotherapy treatment was carried out as described above. Cells were fixed in 4 % paraformaldehyde, and after 1 h of blocking with 1 % BSA in PBS, were incubated with the monoclonal antibodies anti-CD95 (Abcam, San Francisco, CA, USA) and Alexafluor 555-conjugated cholera toxin subunit

B (CTxB) (Invitrogen, Burlington, ON, Canada) for 1 h at room temperature. After washing with PBS, Alexafluor 488-conjugated goat anti-mouse secondary antibody was added. Nuclei were stained with 4',6'-diamidino-2-phenylindole (DAPI). Coverslips were inverted onto microscope slides, in mounting medium Fluorsave. Slides were examined with a Zeiss Axiovert 100 M confocal microscope coupled with a Zeiss LSM510 laser scanning system (Germany). Images were taken with a 63 \times Plan-apochromat n.a. 1.4 with a zoom factor of 2. Alexafluor 488 was scanned with an argon laser (excitation wavelength, 488 nm; emission wavelength, 505 nm), and Alexafluor 555-labeled CTxB with a HeNe laser (excitation wavelength 543 nm, emission wavelength 560 nm). For DAPI staining, a Coherent Mira 2-Photon laser tuned at 780 nm was used, and emission was collected with a BP 390–465 IR. Confocal reflectance images were obtained by reflecting excitation wavelengths to a confocal detector.

Lipid Raft Isolation

Lipid rafts were isolated as previously described [5]. The sucrose gradient(s) containing rafts were identified by measuring raft markers Gzi (using anti-Gzi antibody, Oncogene Research Products, CedarLane Laboratories) by Western blotting, as previously described [5].

Western Blotting

Whole cell and lipid raft protein lysates were prepared from cells as previously described [4]. Protein content was determined by bicinchoninic acid protein assay (Sigma). Equal amounts of protein (60 μg) from each treatment were separated by sodium dodecyl sulfate polyacrylamide gel electrophoresis as previously described [4, 5]. Precision Plus ProteinTM All blue (BioRad Laboratories Ltd., Mississauga, ON, Canada) molecular weight standards were used to monitor protein separation. Ponceau S staining was used to confirm transfer and even protein loading. Anti-Gz (i) (Cell Signaling Technology, New England Biolabs, ON, Canada) was used to identify rafts. Membranes were blocked for 1 h at room temperature in Tris-buffered saline plus Tween-20 (TBST: 0.01 M Tris-HCl pH 6.8, 0.15 M NaCl, 0.1 % v/v Tween-20) and 5 % w/v powdered milk. After rinsing with TBST, membranes were incubated overnight at 4 °C with anti-CD95 or anti-FADD (Abcam) or anti-glyceraldehyde-3-phosphate dehydrogenase (Cell Signaling Technology, Danvers MA) as a loading control, diluted 1:10,000 in TBST containing 5 % BSA. A 1:2,500 dilution of the secondary antibody, horseradish peroxidase-conjugated donkey anti-rabbit IgG (Jackson Immuno-research Labs, Cedarlane Laboratories), or goat anti-mouse IgG (Invitrogen, Burlington, ON, Canada) in TBST and 5 %

w/v powdered milk was incubated with the membranes for 1 h at room temperature. Membranes were developed using enhanced chemiluminescence (ECL Plus™) western blotting detection reagents (Amersham Biosciences, GE Healthcare, Baie d'Urfe, QC, Canada) and read on a Typhoon™ Trio+ variable mode imager (Amersham Biosciences). The intensity of target bands was quantified using ImageQuant™ TL software (Amersham Biosciences).

Flow Cytometry

Cells were treated as indicated, harvested with 0.5 % trypsin and suspended in 4 % FCS-PBS. After 30 min of incubation with anti-CD95 or isotype controls at 4 °C, cells were washed twice and resuspended in phosphate buffered saline containing paraformaldehyde (10 g/l plus Na azide) and analyzed on a FACScan (Becton–Dickinson, Sunnyvale, CA, USA) according to the relative fluorescence intensity using CellQuest software. Resulting percentages were corrected for background fluorescence (0–5 %) determined by incubating the cells with appropriate isotype placebos (IgG1).

Statistical Analyses

All statistical analyses were carried out using SAS, version 9.1 (SAS Institute, Cary, NC, USA). For cell culture experiments, a minimum of three separate experiments were conducted. Data were tested for normal distribution and, once confirmed, analyzed by one-way or one-way repeated measures ANOVA, followed by post hoc analysis using Tukey's test to identify significant ($P < 0.05$) differences among fatty acid and chemotherapy treatments.

Results

Cell Viability

Treatment with DHA (Fig. 1a), and to a lesser extent, EPA (Fig. 1b), significantly ($P < 0.05$) reduced cellular viability (assessed by using the WST-1 assay) of all cancer cell lines tested compared to either incubation with no fatty acids or a control fatty acid treatment of similar concentration (data not shown). The cell viability of non-transformed breast epithelial cell line MCF-12A was not significantly affected by either fatty acid (Fig. 1a, b). In additional experiments it was confirmed that the decrease in the WST-1 assay was consistent with a decrease in cell number. Incubation of MCF-7 cells with EPA (100 μ M) or DHA (60 μ M), compared to cells incubated with a control fatty acid mixture (OLA/ALA) for 48 h resulted in reduced cell numbers by 52 ± 4 and 42 ± 4 %, respectively). For

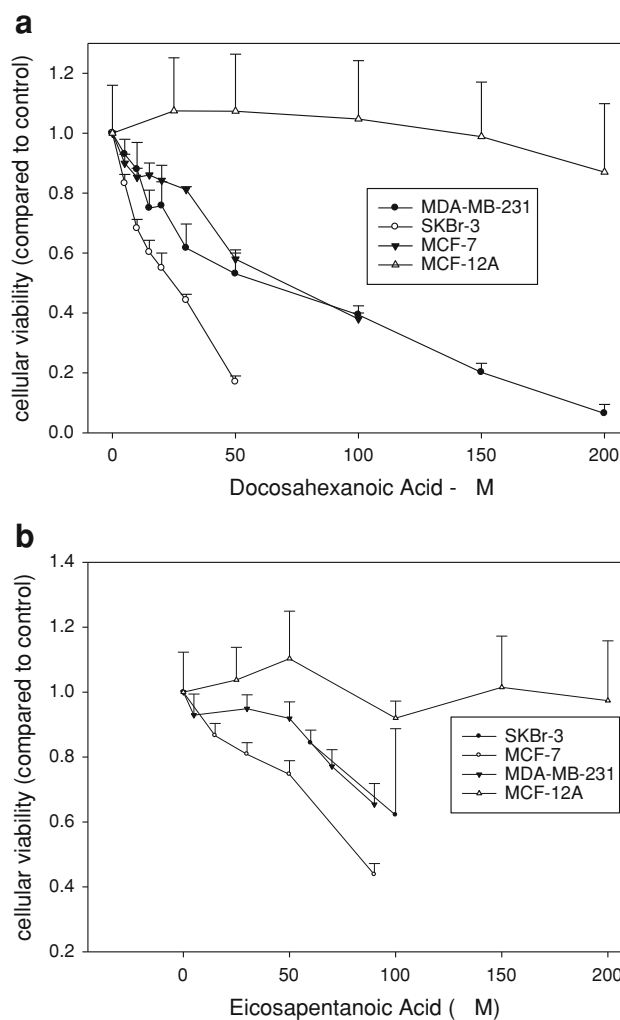


Fig. 1 Cellular viability in response to n-3 polyunsaturated fatty acid treatment in normal and transformed human breast cell lines. Viability was assessed in response to increasing concentrations of **a** DHA and **b** EPA. MDA-MB-231, MCF-7, SKBr-3 breast cancer cells and non-transformed MCF-12A cells were incubated for 72 h in the presence of varying concentrations of albumin-conjugated DHA or EPA. Viability was assessed using the WST-1 assay. Viability of transformed cells was significantly decreased with increasing concentrations of DHA and EPA ($P < 0.05$). The growth of non-malignant breast cells (MCF-12A) was not affected until concentrations ≥ 200 μ M for DHA and 300 μ M for EPA. For transformed cells, $n = 6$ –8 cell passages, for MCF-12A, $n = 3$

MDA-MB-231 cells, the same EPA and DHA concentration resulted in reduced cell counts by 59 ± 3 and 59 ± 4 %.

Interaction with Chemotherapeutic Agents

Pre-treatment with EPA at 100 μ M and DHA at all concentrations tested (25, 50 and 100 μ M) significantly reduced the growth of SKBr-3 cells but neither fatty acid increased the effect of Herceptin on tumor cell viability (Table 1). At 25 and 50 μ M, EPA significantly reduced the

Table 1 Effect of n-3 fatty acid incubation on the response to Herceptin in SKBr-3 cells

Fatty acid (μM)	Drug treatment		Comparison –Herceptin versus +Herceptin ($P <$)
	–Herceptin	+Herceptin (11 $\mu\text{g}/\text{ml}$)	
0	–	0.73 ± 0.12^a	
25 EPA	0.94 ± 0.04^a	0.68 ± 0.03^a	0.03
50 EPA	0.91 ± 0.05^a	0.70 ± 0.07^a	0.03
100 EPA	0.58 ± 0.09^b	0.50 ± 0.04^b	NS
25 DHA	0.68 ± 0.06^b	0.77 ± 0.05^a	NS
50 DHA	0.53 ± 0.05^b	0.62 ± 0.05^b	NS
100 DHA	0.39 ± 0.04^c	0.37 ± 0.03^c	NS

Cells were incubated with the fatty acid treatment for 48 h. This was followed by a 24 h incubation) or without (–Herceptin) with (+Herceptin). Values are mean \pm SEM ($n = 4$ independent replications/treatment). Within a column, means that do not share a common superscript are significantly different ($P < 0.05$). The comparison of the cells treated with and without Herceptin is indicated in the column labeled comparison

Table 2 Effect of n-3 fatty acid incubation on the response to dox in MCF-7 cells

Fatty acid (μM)	Drug treatment		Comparison –dox versus +dox ($P <$)
	–dox	+dox (0.85 $\mu\text{g}/\text{ml}$)	
0	–	0.84 ± 0.08^a	
25 EPA	0.89 ± 0.03^a	0.88 ± 0.04^a	NS
50 EPA	0.88 ± 0.08^a	0.82 ± 0.08^a	NS
100 EPA	0.60 ± 0.07^b	0.66 ± 0.10^b	NS
25 DHA	0.87 ± 0.07^a	0.84 ± 0.09^a	NS
50 DHA	0.41 ± 0.04^c	0.57 ± 0.04^c	NS
100 DHA	0.20 ± 0.01^d	All dead	

Cells were incubated with the fatty acid treatment for 48 h. This was followed by a 24 h incubation without (–dox) or with (+dox). Values are means \pm SEM ($n = 4$ independent replications/treatment). Within a column, means that do not share a common superscript are significantly different ($P < 0.05$). The comparison of the cells treated with and without dox is indicated in the column labeled Comparison. All dead indicates that there were no cells left to measure

Table 3 Effect of n-3 fatty acid incubation on the response to dox in MDA-MB-231 cells

Fatty acid (μM)	Drug treatment		Difference –dox versus +dox ($P <$)
	–dox	+dox (0.22 $\mu\text{g}/\text{ml}$)	
0	–	0.82 ± 0.05^a	
30 EPA	0.94 ± 0.05^a	0.81 ± 0.05^a	NS
60 EPA	0.84 ± 0.04^b	0.69 ± 0.05^a	NS
100 EPA	0.62 ± 0.09^c	0.43 ± 0.25^b	0.005
30 DHA	0.92 ± 0.08^a	0.75 ± 0.06^a	NS
60 DHA	0.50 ± 0.11^c	0.08 ± 0.15^c	0.05
100 DHA	0.19 ± 0.01^d	All dead	

Cells were incubated with the fatty acid treatment for 48 h. This was followed by a 24 h incubation without (–dox) or with (+dox). Values are means \pm SEM ($n = 4$ independent replications/treatment). Within a column, means that do not share a common superscript are significantly different ($P < 0.05$). The comparison of the cells treated with and without dox is indicated in the column labeled comparison. All dead indicates that there were no cells left to measure

viability of Herceptin-treated SKBr-3 cells compared with EPA treatment alone ($P = 0.03$). Incubation with EPA at 100 μM and DHA at all concentrations tested (25, 50 and 100 μM) significantly reduced the growth of MCF-7 cells but pre-incubation with either fatty acid did not

significantly change the effect of dox treatment on cell viability (Table 2). Incubation with EPA at 100 μM and DHA at all concentrations tested (30, 60, and 100 μM) significantly reduced the cell viability of MDA-MB-231 cells. Preincubation with EPA at 100 μM and DHA at

>60 μM increased the effect of dox on reducing the metabolic activity of MDA-MB-231 cells (Table 3). Based on the results in Table 3, EPA incubation for 48 h at 100 μM and DHA at 60 μM was used in all subsequent experiments. Cell counting experiments ($n = 3$) were also performed in the MDA-MB-231 cell line to confirm that the decrease seen in the WST-1 assay was consistent with a decrease in the number of cells. Compared to pre-incubation with OLA/LNA (control), 48 h of treatment with DHA reduced cell numbers by $66 \pm 1\%$ ($P < 0.05$). Pre-treating MDA-MB-231 cells with control fatty acids for 48 h before dox (0.22 $\mu\text{g/ml}$ for 24 h) resulted in reduced cell numbers ($76 \pm 6\%$), while pre-treatment with DHA (50 μM) resulted in a significantly greater cell loss ($45 \pm 1\%$, $P < 0.05$).

CD95 Localization in Tumor Cells

Localization of CD95 was determined in MDA-MB-231 cells (Fig. 2a) and MCF-7 cells (Fig. 2b) by examining the overlay (D panels; yellow regions indicate areas of colocalization) of CD95 (A panels, green) with the lipid raft marker cholera toxin subunit B (B panels, red). Blue nuclei (C panels) are included to indicate the location of nuclei. Under control conditions (Box 1) and with dox treatment (Box 2), no colocalization of CD95 and cholera toxin subunit B was observed, indicating that CD95 is intracellular under these conditions. Membrane organization was disrupted in dox treated cells (Boxes 2B, 4B, 6B). There was also a suggestion of lipid raft clustering after incubation with DHA or EPA (panels 3D/5D and 4D/6D with and without dox in MDA-MB-231 cells. When DHA (Box 3) and DHA+dox (Box 4) were applied, CD95 co-localized with the lipid raft marker in both cell lines (panels 3D, 4D) after DHA treatment. This appeared more dramatic in MDA-MB-231 (Fig. 2a) cells than in MCF-7 cells (Fig. 2b). EPA (Box 5) and EPA+dox (Box 6) did not appear to induce CD95 translocation to the cell membrane.

n-3 PUFA and Dox Effects on CD95 in MDA-MB-231 Cells

The surface expression (mean fluorescence) of CD95 increased with EPA, DHA or dox treatment (control treatment not shown in Fig. 3a). Treatment with DHA or dox increased CD95 surface expression significantly more than EPA (Fig. 3a, b). However, pre-treatment with DHA (Fig. 3a, b), but not EPA (Fig. 3a) before treatment with dox, resulted in a significantly greater (threefold increase) CD95 surface expression on MDA-MB-231 cells. The total amount of CD95 (Fig. 3c) or FADD (data not shown) in cells did not change with any of these treatments. However, both DHA and dox treatment increased the relative amount

Fig. 2 Immunolocalization of CD95 in MDA-MB-231 (Fig. 3a) and MCF-7 cells (Fig. 3b). Cells were pretreated for 48 h with either no n-3 PUFA (box 1, 2) 60 μM DHA (box 3, 4) or 100 μM EPA (box 5, 6), followed by a 24 h treatment with dox (boxes 2, 4 and 6). CD95 was labeled with Alexafluor-488 conjugated antibody (green) and was intracellular under control conditions and upon treatment with dox. Membrane organization was disrupted in dox-treated cells, as indicated by the Alexa-fluor 555-conjugated lipid raft marker, cholera toxin subunit B (red). When DHA and DHA + dox were applied, CD95 appeared to co-localize with lipid rafts, observed in the yellow portions of the overlay. To a lesser extent, EPA also induced CD95 translocation to lipid rafts. Stack size: $73 \times 73 \mu\text{m}$. Images are representative of the results of three separate experiments

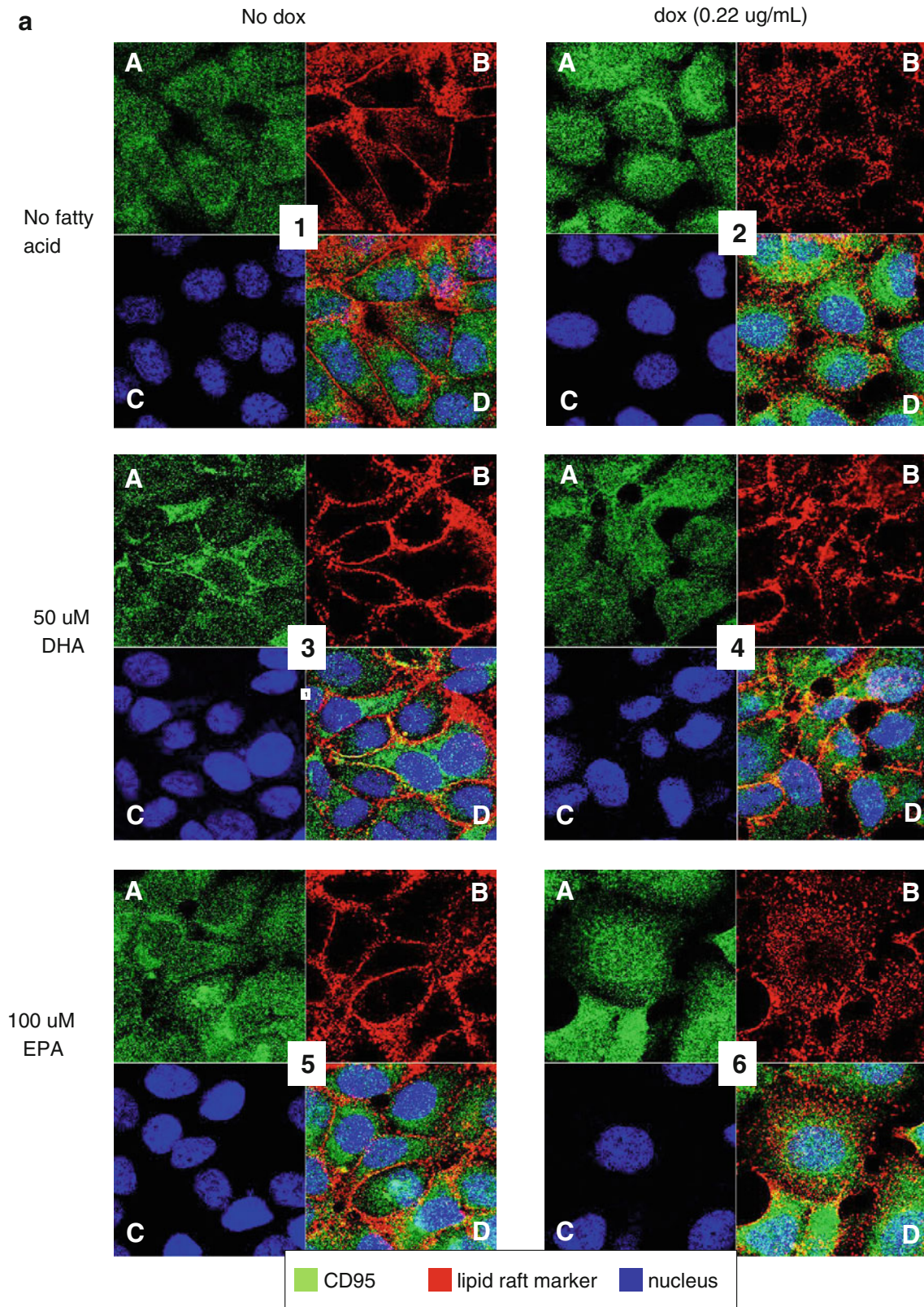
of CD95 (Fig. 3d), but not FADD (Fig. 3e) in membrane rafts compared to the control fatty acid treatment (statistics not illustrated on Fig. 3). Pre-treating cells with DHA resulted in significantly more CD95 (Fig. 3d) and FADD (Fig. 3e) in lipid rafts after dox treatment, compared to all the other treatments.

Discussion

Consistent with previous studies [9, 30, 31], in the present study we demonstrated the growth-inhibitory effects of DHA and EPA on human breast cell cancers. Our studies demonstrate that DHA and EPA, even at high concentrations, do not affect the growth and metabolic activity of the non-transformed breast cell line MCF-12A. In the conditions in this study, DHA induced cell death at lower concentrations than EPA in all transformed cell lines. We also showed that DHA and EPA (albeit at higher concentrations) enhanced the efficacy of the chemotherapy drug, dox, in MDA-MB-231 cells. Lastly, we determined that at least a portion of the cytotoxic effect of DHA and its beneficial effects on the action of dox may be due to the movement of the CD95 (Fas) and FADD, two key proteins in DISC, into the lipid raft portion of the membrane in MDA-MB-231 cells.

Effect of EPA and DHA on the Selective Effect on the Growth of Human Breast Cancer Cells

Long-chain n-3 PUFA have been shown to reduce the viability of breast cancer cells, both in vitro and in animal models [3, 12, 23, 32, 33]. Consistent with these observations, the current study demonstrates the dose-responsive cytotoxic properties of DHA and EPA on transformed breast cells, and is the first, to our knowledge, to confirm the lack of effect of these PUFA, even at high concentrations, on the growth/metabolism of non-transformed breast cells. This observation has the potential to be of clinical importance as most of the current therapies for malignant cells have negative effects on healthy cells. The



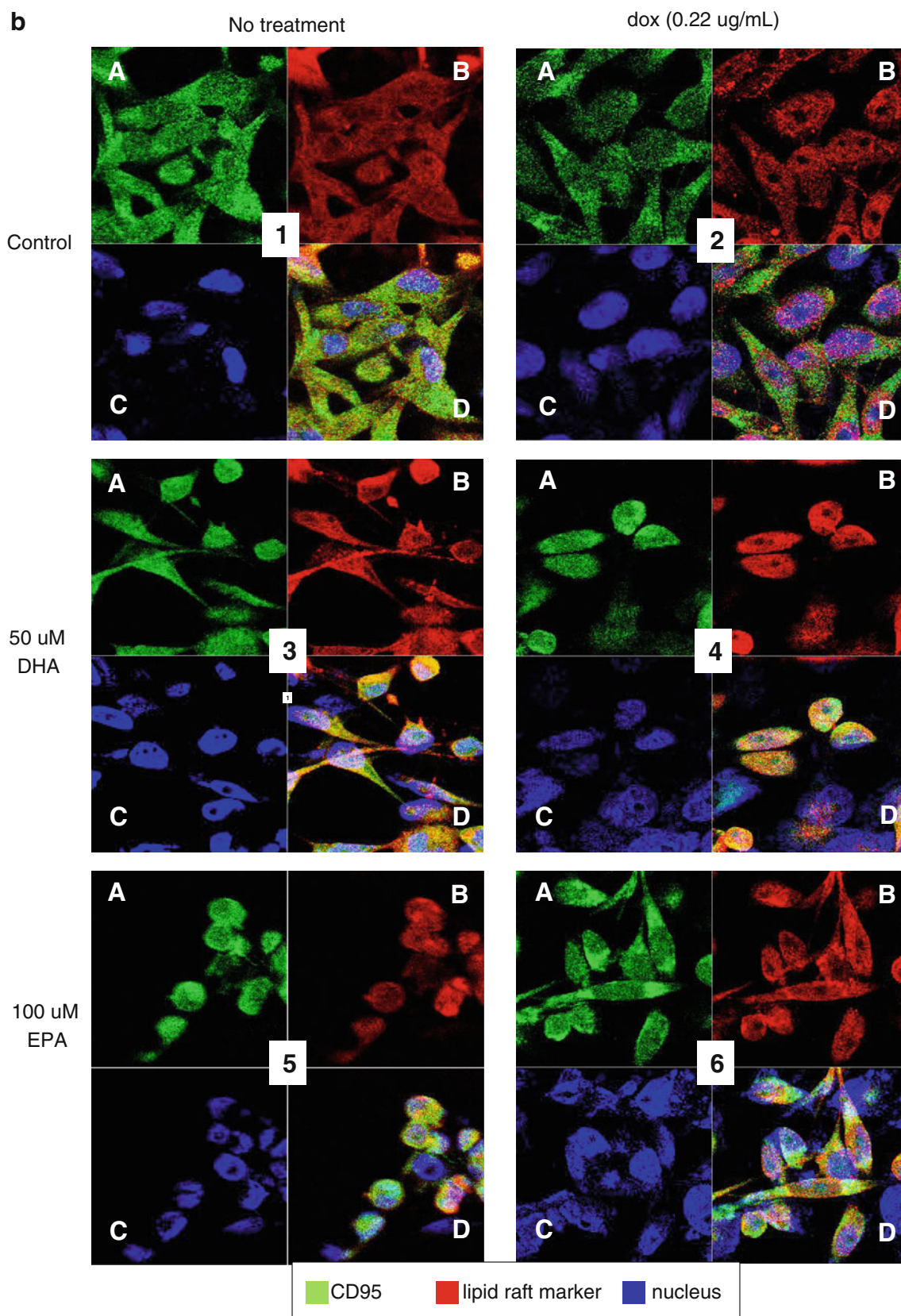


Fig. 2 continued

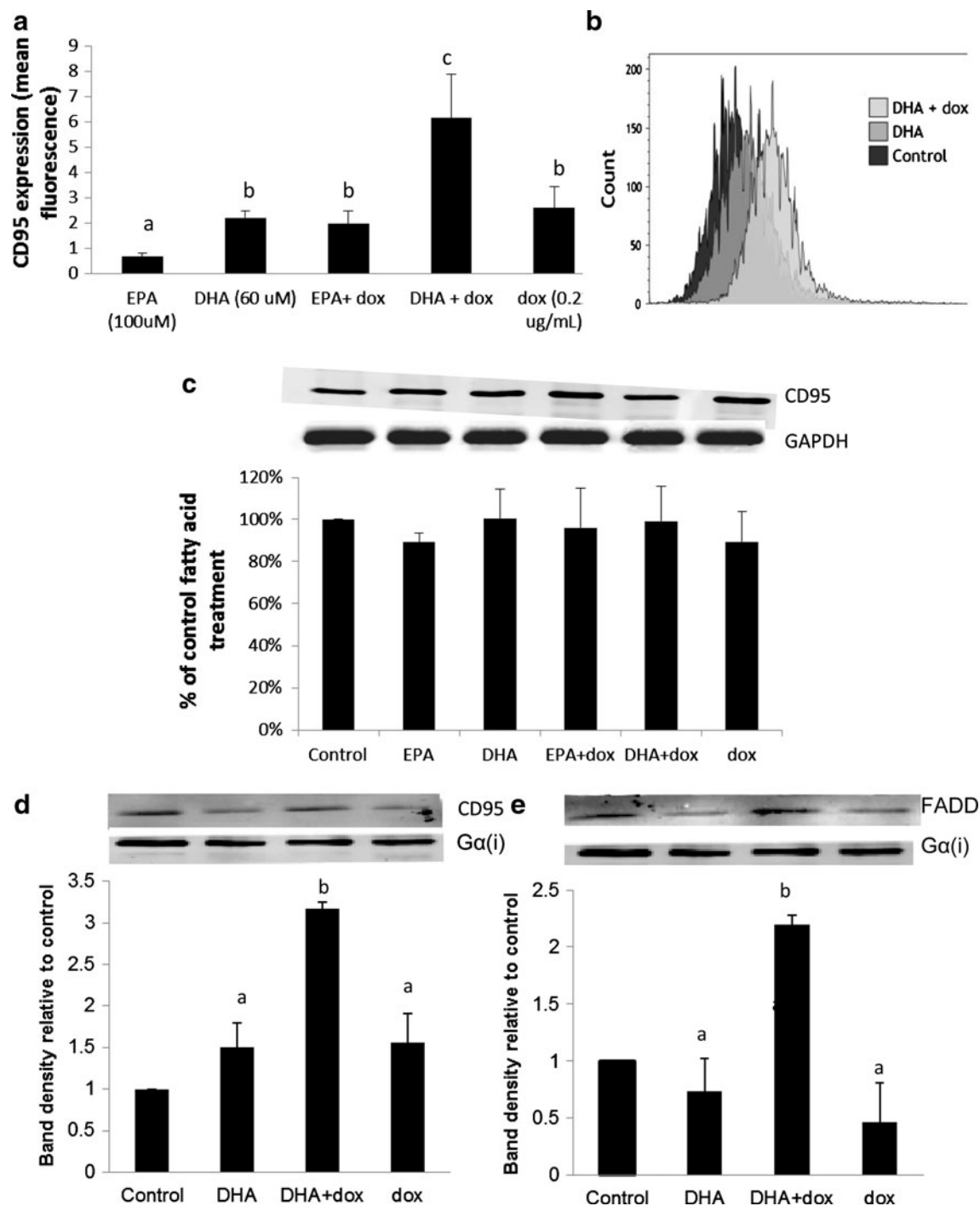


Fig. 3 CD95 expression in MDA-MB-231 breast cancer cells exposed to DHA, EPA, with and without dox. **a** MDA-MB-231 cells were pretreated for 48 h with either 60 μ M DHA or 100 μ M EPA, followed by a 24 h treatment with or without dox (0.22 μ g/ml). Cells were analyzed for CD95 surface expression by flow cytometry. Mean \pm SEM ($n = 3$) that do not share a common letter are significantly different ($P < 0.05$). **b** The shift in mean fluorescence in the flow cytometry analysis after treatment with a representative control fatty acid mixture (OLA + LNA), DHA or DHA followed by dox [as described in **a**]. **c** Cells were treated as in **a**, except CD95

analysis was carried out on whole-cell protein by Western blot and expressed as a percent of the band density of the control fatty acid treatment. There was no significant difference between groups [mean \pm SEM ($n = 3$)]. **d** Cells were treated with DHA, DHA + dox or dox as described in **a**. Lipid rafts were isolated and raft **d** CD95 and **e** FADD content was determined by Western blot and expressed as a percent of the band density of the control fatty acid treatment. Mean \pm SEM ($n = 3$) that do not share a common letter are significantly different ($P < 0.05$)

concentration of DHA or EPA needed to induce anti-cancer effects *in vivo* is unknown, but our previous work has demonstrated that the concentrations selected in the current study for the drug experiments result in a fatty acid composition of n-3 and n-6 fatty acids [5] similar to concentrations reached in mammary tumor phospholipids when rodents are fed a high fish oil diet (EPA and DHA) [21].

A number of mechanisms have been proposed to explain the effects of n-3 PUFA on the growth and death of breast cancer cells [4, 34, 35]. Most hypothesized mechanisms involve the fatty acids being incorporated into the cell membrane. Previous work by our group [4] has demonstrated that DHA/EPA treatment of human breast cancer cells increases apoptosis and alters the composition of lipid rafts [5]. The FAS receptor, also known as CD95, is a receptor on the surface of cells that regulates apoptosis in cancer cells [36]. Upon activation, CD95 moves to lipid rafts in the plasma membrane [37]. Cancer cells have been demonstrated to under-express CD95 [29] and inducing expression is a mechanism by which many anticancer drugs work [27]. Incorporation of n-3 fatty acids alters other receptors in breast cancer cells [5] and DHA has been shown to induce caspase-8 activation [32], which is an early step in the CD95 pathway.

Using the immunofluorescent overlay of CD95 with cholera toxin subunit B; used to identify lipid rafts [38, 39], our data suggests that the anti-growth effects of DHA, and to a much lesser extent EPA, may in part be due to movement of CD95 to the raft. With fluorescent microscopy there was an indication of raft clustering after treatment with DHA in the MDA-MB-231 cells but not the MCF-7 which may have contributed to the effects on growth. Modified clustering of lipid rafts, and an increase in their size has been shown in response to DHA, but not EPA, in EL4 cells [40]. Further studies using the MDA-MB-231 cell line demonstrated that incubation with DHA resulted in increased surface expression of CD95 and increased CD95 in the membrane rafts; further supporting that DHA may mediate some of its cytotoxic effect on highly metastatic ER⁻ tumor cells via activation of the death receptor complex on the cell surface. A recent nutrigenomic study investigating the effects of EPA on breast cancers differing in ER status concluded that the ER status of breast cancer cells may play a role in breast cancer cell response to treatments with n-3 and n-6 fatty acids [41]. In the present study, the similar rate of cytotoxicity (reduced metabolic activity) after treatment with DHA and EPA between the MDA-MB-231 cells (ER⁻) and the MCF-7 cells (ER⁺), suggest that ER status may not be the major mechanism by which n-3 PUFA act, at least *in vitro*. SKBr-3 cells over-express Her2, a growth receptor that is part of the epidermal growth receptor family. We have previously demonstrated that treatment with a mixture of

DHA and EPA reduced the movement of the epidermal growth receptor into lipid rafts in MDA-MB-231 cells [5] suggesting a mechanism by which EPA and DHA inhibit the growth of SKBr-3 cells in the current study. This may also be the mechanism responsible for the increased cell death we observed in response to low concentrations of EPA (25 and 50 μ M) and Herceptin. It is unclear why higher concentrations of EPA do not induce the same effects; further investigation of growth receptor expression and localization in response to EPA and Herceptin treatment is warranted.

To our knowledge, this is the first report of CD95 membrane co-localization in response to n-3 PUFA in breast cancer cells; but is consistent with what has been reported to occur in T-cells from fish oil-fed mice [42]. Conversely, a study of migration and metastasis in MDA-MB-231 cells reported that DHA treatment (at concentrations similar to those used in the current study) also alter the structure of lipid rafts, but described this disruption in a manner similar to what occurs after treatment with methyl-beta-cyclodextrin [43]. In the current study, we demonstrate that treatment with DHA (and to a lesser extent EPA) resulted in the movement of a key signaling molecules, CD95, to the membrane in two human breast cancer cell lines.

Effect of Pre-treatment with EPA or DHA on Dox Sensitivity

Pre-treatment with either EPA or DHA did not significantly increase the cytotoxic effect of Herceptin or dox in SKBr-3 cells and MCF-7 (except perhaps when pre-treated with 100 μ M DHA). However, for MDA-MB-231 cells there was a higher toxicity of dox when cells had been pre-treated with EPA (100 μ M) or DHA (>50 μ M), suggesting a potential therapeutic benefit of providing this fatty acid prior to treatment with chemotherapy drugs. Vibet et al. [44] also observed that treating MCF-7 cells with DHA did not increase the sensitization to dox [44], which suggests that activity of the drug is not influenced by changes in membrane composition in this ER⁺ cell line. Our study is the first report, to our knowledge, examining the potential effect of n-3 fatty acids on the action of Herceptin, a mAb that blocks the binding to the Her2 receptor.

Pre-treatment with DHA and EPA (albeit at higher concentrations), significantly improved the anti-growth/metabolic effect of dox treatment on MDA-MB-231 cells. This was accompanied by a higher surface expression of CD95 (threefold) and content of CD95 (twofold) in the lipid raft fraction (twofold) over DHA or dox treatments alone. As we were unable to detect changes in total cellular CD95 protein, our results suggest that the combination of DHA and dox causes intracellular CD95 to move into the

lipid rafts in the cell membrane. CD95 aggregation is known to result in the recruitment of FADD to the CD95 receptor in membrane rafts, forming the CD95-DISC, which activates the apoptotic cascade initiated by caspase-8 [27]. Consistent with the literature [28, 29], in the present study, dox treatment increases FADD content in the rafts. Our data extends this by demonstrating that pre-treatment with DHA increases (fourfold) the amount of FADD that moves into the raft.

Although identifying the mechanism to explain how pre-treatment with DHA increases the co-localization of CD95/FADD in the raft, it is logical to predict that this may occur via an increase in the DHA content of the rafts. We have previously reported that providing DHA (with EPA) significantly increases the content of DHA in plasma membrane rafts in MDA-MB-231 cells [5]. Similarly, we have fed DHA to rodents and produced changes in the DHA content of the rafts in immune cells that were similar to what would have occurred in the tumor cells in the current study. JCR:LA-cp rats fed a diet containing 28 g fish oil/kg diet enriched the lipid raft DHA concentration to approximately 1.0 ± 0.1 % of total fatty acids [45]. Treating MDA-MB-231 cells with $40 \mu\text{M}$ DHA yielded a raft DHA concentration of 2.6 ± 0.4 % ($n = 6$) for total fatty acids (unpublished results).

A change in ceramide content in the cells could also contribute to the anti-cancer properties of DHA as DHA treatment results in a decreased sphingomyelin content and increased ceramide content in rafts from MDA-MB-231 cells [5]. A change in the cellular content of ceramide in tumors increases the content of CD95 and DISC in the membrane [46] and has been demonstrated to induce apoptosis [47]. Additionally, dox treatment has been reported to increase ceramide synthesis in tumor cells [48]. DHA treatment has also been demonstrated to facilitate the ability of dox to induce oxidative stress in tumor cells [44], supporting another membrane associated mechanism for improved sensitization.

Our findings are of potential clinical relevance as treatment with the anthracycline-based antibiotic, dox, is one of the drugs of choice for treatment of highly invasive metabolically active breast tumors, which are modeled by the MDA-MB-231 cell line [29, 49]. There is clinical evidence to support our findings. Breast cancer patients with higher concentrations of DHA in breast adipose tissue at the time of diagnosis were reported to respond more favorably to chemotherapy (i.e., had greater tumor regression) [23]. There is also preliminary evidence suggesting that treatment/feeding DHA might improve/prevent some of the side effects (both clinical and the development of drug resistance) of several chemotherapy drugs (reviewed by [9, 25]). In support of this, a phase II study examining effects of DHA supplementation on epirubicin (optical isomer of dox) efficacy in patients with highly

metastatic breast cancer found DHA treatment was associated with improved survival [24].

In summary, our study provides evidence that pre-treatment with DHA prior to treatment with a commonly used breast cancer drug, can increase the anti-cancer effects of the drug in an ER⁻, highly invasive human breast tumor. Our data suggests that increased membrane raft localization and aggregation of CD95 and formation of DISC, an important signal of apoptosis, may be one of the mechanisms to explain this increased sensitivity. Future studies aimed at linking changes in the cell mediated by DHA pre-treatment will assist in understanding the potential role that DHA supplementation could have as adjuvant treatment for breast cancer.

Acknowledgments Study funding provided by the Canadian Institutes of Health Research (CIHR). J. Ewaschuk was a recipient of a CIHR post-doctoral fellowship.

Conflict of interest The authors have no conflict of interest to report.

References

- Bougnoux P, Maillard V, Chajes V (2005) Omega-6/omega-3 polyunsaturated fatty acids ratio and breast cancer. *World Rev Nutr Diet* 94:158–165
- Karmali RA, Marsh J, Fuchs C (1984) Effect of omega-3 fatty acids on growth of a rat mammary tumor. *J Natl Cancer Inst* 73:457–461
- Rose DP, Connolly JM (1999) Omega-3 fatty acids as cancer chemopreventive agents. *Pharmacol Ther* 83:217–244
- Schley PD, Jijon HB, Robinson LE, Field CJ (2005) Mechanisms of omega-3 fatty acid-induced growth inhibition in MDA-MB-231 human breast cancer cells. *Breast Cancer Res Treat* 92:187–195
- Schley PD, Brindley DN, Field CJ (2007) (n-3) PUFA alter raft lipid composition and decrease epidermal growth factor receptor levels in lipid rafts of human breast cancer cells. *J Nutr* 137:548–553
- Bernard-Gallon DJ, Vissac-Sabatier C, Antoine-Vincent D, Rio PG, Maurizis J-C, Fustier P, Bignon Y-J (2002) Differential effects of n-3 and n-6 polyunsaturated fatty acids on *BRCA1* and *BRCA2* gene expression in breast cell lines. *Br J Nutr* 87:281–289
- Baumgartner M, Sturlan S, Roth E, Wessner B, Bachleitner-Hofmann T (2004) Enhancement of arsenic trioxide-mediated apoptosis using docosahexaenoic acid in arsenic trioxide-resistant solid tumor cells. *Int J Cancer* 112:707–712
- Menendez JA, Roper S, Mehmi I, Atlas E, Colomer R, Lupu R (2004) Overexpression and hyperactivity of breast cancer-associated fatty acid synthase (oncogenic antigen-519) is insensitive to normal arachidonic fatty acid-induced suppression in lipogenic tissues but it is selectively inhibited by tumoricidal alpha-linolenic and gamma-linolenic fatty acids: a novel mechanism by which dietary fat can alter mammary tumorigenesis. *Int J Oncol* 24:1369–1383
- Biondo PD, Brindley DN, Sawyer MB, Field CJ (2008) The potential for treatment with dietary long-chain polyunsaturated n-3 fatty acids during chemotherapy. *J Nutr Biochem* 19:787–796
- Grammatikos SI, Subbaiah PV, Victor TA, Miller WM (1994) n-3 and n-6 fatty acid processing and growth effects in neoplastic and non-cancerous human mammary epithelial cell lines. *Br J Cancer* 70:219–227

11. Chajes V, Sattler W, Stranzl A, Kostner GM (1995) Influence of n-3 fatty acids on the growth of human breast cancer cells in vitro: relationship to peroxides and vitamin-E. *Breast Cancer Res Treat* 34:199–212
12. Begin ME, Eells G, Horrobin DF (1988) Polyunsaturated fatty acid-induced cytotoxicity against tumor cells and its relationship to lipid peroxidation. *J Natl Cancer Inst* 80:188–194
13. Yamamoto D, Kiyozuka Y, Adachi Y, Takada H, Hioki K, Tsubura A (1999) Synergistic action of apoptosis induced by eicosapentaenoic acid and TNP-470 on human breast cancer cells. *Breast Cancer Res Treat* 55:149–160
14. Tsujita-Kyutoku M, Yuri T, Danbara N, Senzaki H, Kiyozuka Y, Uehara N, Takada H, Hada T, Miyazawa T, Ogawa Y, Tsubura A (2004) Conjugated docosahexaenoic acid suppresses KPL-1 human breast cancer cell growth in vitro and in vivo: potential mechanisms of action. *Breast Cancer Res* 6:R291–R299
15. Simons K, Toomre D (2000) Lipid rafts and signal transduction. *Nat Rev Mol Cell Biol* 1:31–39
16. Shaw AS (2006) Lipid rafts: now you see them, now you don't. *Nat Immunol* 7:1139–1142
17. Foster LJ, De Hoog CL, Mann M (2003) Unbiased quantitative proteomics of lipid rafts reveals high specificity for signaling factors. *Proc Natl Acad Sci USA* 100:5813–5818
18. Brown DA, London E (1998) Functions of lipid rafts in biological membranes. *Annu Rev Cell Dev Biol* 14:111–136
19. Hatala MA, Rayburn J, Rose DP (1994) Comparison of linoleic acid and eicosapentaenoic acid incorporation into human breast cancer cells. *Lipids* 29:831–837
20. Rose DP, Connolly JM, Rayburn J, Coleman M (1995) Influence of diets containing eicosapentaenoic or docosahexaenoic acid on growth and metastasis of breast cancer cell in nude mice. *J Natl Cancer Inst* 87:587–592
21. Robinson LE, Clandinin MT, Field CJ (2002) The role of dietary long-chain n-3 fatty acids in anti-cancer immune defense and R3230AC mammary tumor growth in rats: influence of diet fat composition. *Breast Cancer Res Treat* 73:145–160
22. Rockett BD, Franklin A, Harris M, Teague H, Rockett A, Shaikh SR (2011) Membrane raft organization is more sensitive to disruption by (n-3) PUFA than nonraft organization in EL4 and B cells. *J Nutr* 141:1041–1048
23. Bougnoux P, Germain E, Chajes V, Hubert B, Lhuillery C, Le FO, Body G, Calais G (1999) Cytotoxic drugs efficacy correlates with adipose tissue docosahexaenoic acid level in locally advanced breast carcinoma. *Br J Cancer* 79:1765–1769
24. Bougnoux P, Hajjaji N, Ferrasson MN, Giraudeau B, Couet C, Le FO (2009) Improving outcome of chemotherapy of metastatic breast cancer by docosahexaenoic acid: a phase II trial. *Br J Cancer* 101:1978–1985
25. Siddiqui RA, Harvey KA, Xu Z, Bammerlin EM, Walker C, Altenburg JD (2011) Docosahexaenoic acid: a natural powerful adjuvant that improves efficacy for anticancer treatment with no adverse effects. *BioFactors* 37:399–412
26. Barnhart BC, Alappat EC, Peter ME (2003) The CD95 type I/type II model. *Semin Immunol* 15:185–193
27. Fulda S, Strauss G, Meyer E, Debatin KM (2000) Functional CD95 ligand and CD95 death-inducing signaling complex in activation-induced cell death and doxorubicin-induced apoptosis in leukemic T cells. *Blood* 95:301–308
28. Bollinger CR, Teichgraber V, Gulbins E (2005) Ceramide-enriched membrane domains. *Biochim Biophys Acta* 1746:284–294
29. Kim HS, Lee YS, Kim DK (2009) Doxorubicin exerts cytotoxic effects through cell cycle arrest and Fas-mediated cell death. *Pharmacology* 84:300–309
30. Blanckaert V, Ulmann L, Mimouni V, Antol J, Brancquart L, Chenais B (2010) Docosahexaenoic acid intake decreases proliferation, increases apoptosis and decreases the invasive potential of the human breast carcinoma cell line MDA-MB-231. *Int J Oncol* 36:737–742
31. Patterson RE, Flatt SW, Newman VA, Natarajan L, Rock CL, Thomson CA, Caan BJ, Parker BA, Pierce JP (2011) Marine fatty acid intake is associated with breast cancer prognosis. *J Nutr* 141:201–206
32. Kang KS, Wang P, Yamabe N, Fukui M, Jay T, Zhu BT (2010) Docosahexaenoic acid induces apoptosis in MCF-7 cells in vitro and in vivo via reactive oxygen species formation and caspase 8 activation. *PLoS One* 5:e10296
33. Shaikh IA, Brown I, Schofield AC, Wahle KW, Heys SD (2008) Docosahexaenoic acid enhances the efficacy of docetaxel in prostate cancer cells by modulation of apoptosis: the role of genes associated with the NF-kappaB pathway. *Prostate* 68:1635–1646
34. Sawyer M, Field CJ (2010) Possible mechanisms for omega-3 (n-3) the anti-tumour action. In: Carviello G, Serini S (eds) *Diet and Cancer*. Springer, New York
35. Wendel M, Heller AR (2009) Anticancer actions of omega-3 fatty acids—current state and future perspectives. *Anticancer Agents Med Chem* 9:457–470
36. Rickert RC, Jellusova J, Miletic AV (2011) Signaling by the tumor necrosis factor receptor superfamily in B-cell biology and disease. *Immunol Rev* 244:115–133
37. Grassme H, Jekle A, Riehle A, Schwarz H, Berger J, Sandhoff K, Kolesnick R, Gulbins E (2001) CD95 signaling via ceramide-rich membrane rafts. *J Biol Chem* 276:20589–20596
38. Blank N, Schiller M, Krienke S, Wabnitz G, Ho AD, Lorenz HM (2007) Cholera toxin binds to lipid rafts but has a limited specificity for ganglioside GM1. *Immunol Cell Biol* 85:378–382
39. Kenworthy AK, Petranova N, Edidin M (2000) High-resolution FRET microscopy of cholera toxin B-subunit and GPI-anchored proteins in cell plasma membranes. *Mol Biol Cell* 11:1645–1655
40. Shaikh SR, Rockett BD, Salameh M, Carraway K (2009) Docosahexaenoic acid modifies the clustering and size of lipid rafts and the lateral organization and surface expression of MHC class I of EL4 cells. *J Nutr* 139:1632–1639
41. Alquobaili F, Miller SA, Muhie S, Day A, Jett M, Hammamieh R (2010) Estrogen receptor-dependent genomic expression profiles in breast cancer cells in response to fatty acids. *J Carcinog* 8:17
42. Fan YY, Ly LH, Barhoumi R, McMurray DN, Chapkin RS (2004) Dietary docosahexaenoic acid suppresses T cell protein kinase C theta lipid raft recruitment and IL-2 production. *J Immunol* 173:6151–6160
43. Altenburg JD, Siddiqui RA (2009) Omega-3 polyunsaturated fatty acids down-modulate CXCR4 expression and function in MDA-MB-231 breast cancer cells. *Mol Cancer Res* 7:1013–1020
44. Vibet S, Goupille C, Bougnoux P, Steghens JP, Gore J, Maheo K (2008) Sensitization by docosahexaenoic acid (DHA) of breast cancer cells to anthracyclines through loss of glutathione peroxidase (GPx1) response. *Free Radic Biol Med* 44:1483–1491
45. Ruth MR, Proctor SD, Field CJ (2009) Feeding long-chain n-3 polyunsaturated fatty acids to obese leptin receptor-deficient JCR:LA-cp rats modifies immune function and lipid-raft fatty acid composition. *Br J Nutr* 101:1341–1350
46. Carpinteiro A, Dumitru C, Schenck M, Gulbins E (2008) Ceramide-induced cell death in malignant cells. *Cancer Lett* 264:1–10
47. Ogretmen B, Hannun YA (2004) Biologically active sphingolipids in cancer pathogenesis and treatment. *Nat Rev Cancer* 4:604–616
48. Kawase M, Watanabe M, Kondo T, Yabu T, Taguchi Y, Umehara H, Uchiyama T, Mizuno K, Okazaki T (2002) Increase of ceramide in adriamycin-induced HL-60 cell apoptosis: detection by a novel anti-ceramide antibody. *Biochim Biophys Acta* 1584:104–114
49. Dawood S, Ueno NT, Valero V, Woodward WA, Buchholz TA, Hortobagyi GN, Gonzalez-Angulo AM, Cristofanilli M (2011) Identifying factors that impact survival among women with inflammatory breast cancer. *Ann Oncol* 23(4):870–875

Fish Oil Supplementation Reduces Cachexia and Tumor Growth While Improving Renal Function in Tumor-Bearing Rats

Isabela Coelho · Fernando Casare · Danielle C. T. Pequito · Gina Borghetti · Ricardo K. Yamazaki · Gleisson A. P. Brito · Marcelo Kryczyk · Luiz Claudio Fernandes · Terezila M. Coimbra · Ricardo Fernandez

Received: 17 May 2012 / Accepted: 24 August 2012 / Published online: 27 September 2012
© AOCS 2012

Abstract The objective of the present work was to study the renal function of healthy and tumor-bearing rats chronically supplemented with fish oil (FO), a source of n-3 polyunsaturated fatty acids. Weanling male rats were divided in two groups, one control (C) and another orally supplemented for 70 days with FO (1 g/kg body weight). After this time, half the animals of each group were injected in the right flank with a suspension of Walker 256 tumor cells (W and WFO). The W group had less proteinemia reflecting cachectic proteolysis, FO reversed this fact. Tumor weight gain was also reduced in WFO. Glomerular filtration rate (GFR) was not different in FO or W compared to C, but was higher in WFO. Renal plasma flow (RPF) was higher in the FO supplemented groups. The W group had lower plasma osmolality than the C group, but FO supplementation resulted in normalization of this parameter. Fractional sodium excretion (FE_{Na^+}) of FO rats was similar to C. Proximal Na^+ reabsorption, evaluated by lithium clearance, was similar among the groups. Urinary thromboxane B_2 (TXB_2) excretion was lower in the supplemented groups.

Electronic supplementary material The online version of this article (doi:10.1007/s11745-012-3715-9) contains supplementary material, which is available to authorized users.

I. Coelho · F. Casare · D. C. T. Pequito · G. Borghetti · R. K. Yamazaki · G. A. P. Brito · M. Kryczyk · L. C. Fernandes · R. Fernandez (✉)
Departamento de Fisiologia, Setor de Ciências Biológicas, Universidade Federal do Paraná (UFPR) Centro Politécnico s/n.–Jd. das Américas, Post Box 19031, Curitiba, PR 81531-990, Brazil
e-mail: ricfer@ufpr.br

T. M. Coimbra
Departamento de Fisiologia–Faculdade de Medicina de Ribeirão Preto, Universidade de São Paulo (USP), Ribeirão Preto, SP, Brazil

The number of macrophages in renal tissue was higher in W compared to C rats, but was lower in WFO rats compared to W rats. In conclusion, FO supplementation resulted in less tumor growth and cachexia, and appeared to be renoprotective, as suggested by higher RPF and GFR.

Keywords Fish oil supplementation · Fatty acid · Renal function · Cachexia · Glomerular filtration · Sodium excretion

Abbreviations

FO	Fish oil
PUFA	Polyunsaturated fatty acid(s)
EPA	Eicosapentaenoic acid
DHA	Docosahexaenoic acid
ARA	Arachidonic acid
PG	Prostaglandins
TX	Thromboxanes
AVP	Arginine-vasopressin hormone
C	Control rats
W	Walker 256 tumor-bearing rats
WFO	Walker 256 tumor-bearing rats supplemented with fish oil
PAH	<i>p</i> -Aminohippuric acid
RBF	Renal plasma flow
GFR	Glomerular filtration rate
FE_{Na^+}	Fractional sodium excretion
C_{Li^+}	Lithium clearance
PFR_{Na^+}	Proximal fractional reabsorption of Na^+
$PPFR_{Na^+}$	Post-proximal fractional excretion of Na^+
DD_{Na^+}	Na^+ distal delivery
MCP-1	Chemokine monocyte chemoattractant protein 1
TAG	Serum triacylglycerol
COX	Cyclooxygenase

Introduction

The n-3 and n-6 polyunsaturated fatty acid (PUFA) families are derived from the desaturation and elongation of the α -linolenic and linoleic acids that are ingested as components of food. While the principal members of the n-3 PUFA family are eicosapentaenoic acid (EPA) and docosahexaenoic acid (DHA), arachidonic acid (ARA) is the main derivate in the n-6 PUFA family [8]. Over the past 150 years, human beings have significantly increased their consumption of saturated and n-6 PUFA, while reducing the intake of n-3 PUFA. Consumption of a high n-6:n-3 PUFA ratio promotes elevated concentrations of potential proinflammatory, thrombotic and vasoconstrictor mediators that are associated with high incidence of chronic diseases such as hypertension, diabetes, and cancer [46, 50]. Diet supplementation with fish oil (FO), which is rich in n-3 PUFA, has reduced the incidence of these diseases [32, 46, 50]. In particular, epidemiologic and experimental studies have shown that long-chain n-3 PUFA (n-3 PUFA) have the ability to chemoprevent and chemosuppress the growth of tumors as well as the tumor-associated syndrome cachexia [22, 40]. Cachexia is characterized by anorexia, weight loss, early satiety, changes in taste perception, weakness, anemia and edema, depletion of carbohydrates, protein and lipid stores, and skeletal muscle wasting [36, 54]. Impaired salt-water excretion is a well-known systemic effect of cancer cachexia that has been studied in several animal models, including Walker 256 tumor-bearing rats [5, 28, 45]. In addition to alterations in hydro-electrolyte metabolism, some forms of carcinomas show a glomerular disease, which is mainly manifested as heavy proteinuria or progressive renal failure [57]. In a previous study, we investigated the effect of lifelong consumption of FO on hydroelectrolyte metabolism and renal function in cachectic rats; the animals' diet was supplemented with FO throughout gestation and lactation and into adulthood. A renoprotective effect was observed, but glomerular hemodynamics and tubular functions were not analyzed [24].

In the kidney, the cyclooxygenase enzyme system is the major pathway for ARA metabolism, leading to the formation of prostaglandins (PG) and thromboxanes [43]. These products modulate the actions of the other hormones or autacoids, in particular, physiological actions on renal vascular tone, mesangial and glomerular functions, and handling of salt and water [31, 43]. Inhibition of cyclooxygenase activity in the absence of exogenous administration or endogenous release of hormones such as angiotensin II (AII) or arginine-vasopressin (AVP) has little effect on renal functional parameters [33, 39]. On the other hand, the products of cyclo-oxygenase metabolism have been implicated as mediators of renal functional changes observed in several disorders: glomerular injury

(IgA nephropathy, lupus nephritis, etc.), various forms of acute and chronic renal failure, allograft rejection, cyclosporine nephrotoxicity, hepatorenal syndrome, diabetic nephropathy, and renal hypertension [30, 49]. FO-supplemented diets lead to competition among the substrates involved in ARA oxygenation pathways, leading to the formation of biologically less active end products [12, 43]. This mechanism explains the preventive effects of FO-supplemented diets on the various pathologies cited above [4, 7, 9, 17, 26]. The effect of a diet supplemented with FO on renal functional parameters in healthy subjects has been less studied, and available reports are contradictory [16, 19, 43].

Therefore, the objective of this study was to investigate the renal function of healthy and tumor-bearing rats chronically supplemented with FO.

Materials and Methods

Animals and Study Design

All experimental procedures were carried out in accordance with the ethical principles established by the Experimental Brazilian Council (COBEA), and with the requirements of the "Guide for the care and use of experimental animals (Canadian Council on Animal Care)". The local Animal Ethics Committee approved the experimental protocols used in this study (protocol no. 243). Weanling male Wistar rats (aged 21 days) were maintained under controlled temperature (22 ± 3 °C) and humidity, in a 12 h/12 h light/dark cycle and divided into two groups. One group received a standard commercial chow [carbohydrate 63,4 %kcal, protein 25,6 %kcal and lipid 11 %kcal, where the fatty acid composition represented (% of fatty acid): palmitic acid (16:0) 20.7, stearic acid (18:0) 2.3, oleic acid (18:1n-9) 19.5, linoleic acid (18:2n-6) 51.3, α -linolenic (18:3n-3) 5.0 and arachidonic acid (20:4n-6) 0.1] (Nurilab CR1, Nuvital Nutrients Ltda., Curitiba, PR, Brazil) diet ad libitum and the other was fed the same chow diet but were also orally supplemented with FO (kindly donated by the Herbarium Foundation for Health and Research, Curitiba, PR, Brazil). The FO used was a mixed marine triacylglycerol preparation containing 180 g eicosapentaenoic acid (EPA) and 120 g docosahexaenoic acid (DHA) per kg. EPA and DHA were not detectable in regular chow. The oil supplement was administered at a dose of 1 g/kg body weight per day and was given orally as a single bolus using a precision microliter pipette. This dose represents approximately 1.25 % (w/w) of the diet. At 90 days of age half the animals of each group were injected into the right flank with a sterile suspension of 2×10^7 Walker 256 tumor cells

obtained from an ascitic tumor-bearing rat, and the other animals were injected with 1.0 mL 0.9 % (w/v) NaCl without anesthesia, as previously described [23]. The amount injected ensured that the tumor mass was 5–8 % of the carcass weight at the time of the measurements (the 14th day after inoculation). The following groups were set up: control and supplemented with FO (C and FO, respectively), and group tumor-bearing and tumor-bearing supplemented with FO (W and WFO, respectively). Body weight was determined every two days during the experimental time.

As the animals to be supplemented with FO were handled every day this could induce certain level of stress. To rule out this effect a pilot study was performed with a control oil supplement, coconut fat (rich in saturated fatty acids), at a dose of 1 g/kg body weight per day. In healthy rats supplemented with coconut fat the body weight gain was similar to that observed in C and FO groups, but in tumor-bearing rats they present similar weight loss and tumor mass weight than W group, the opposite to that observed in WFO (see Electronic supplementary material).

Kidney Function

The rats were prepared for kidney function measurements as follows. Half of animals were housed individually in metabolic cages (EB 309 Insight[®], Riberão Preto, SP, Brazil) for 2 days prior to killing (day 14th after tumor inoculation). The cages facilitated accurate collection of urine not contaminated with feces or food. Fourteen hours before the renal test, 1 mL LiCl (60 mmol LiCl/100 g body wt) was given by means of gavage. The rats had free access to tap water but no food. Spontaneously voided urine was collected under oil into a graduated centrifuge tube, and urinary volume was determined gravimetrically. Next day the animals were injected with pentobarbital sodium 150 mg/kg for blood collection by cardiac puncture and after were killed with an overdose of pentobarbital. The tumor and kidney were removed, weighed and frozen at -80°C for analysis. Plasma was collected by blood centrifugation at 2,000g. Plasma and urine were used for the determination of creatinine, urea, electrolyte (Na^+ , K^+ and Li^+), total protein content, and osmolality.

Clearance Studies

The glomerular filtration rate (GFR) was determined by inulin clearance and renal plasma flow (RPF) by *p*-aminohippuric acid (PAH) clearance. The animals were anesthetized with 65 mg/kg and 10 mg/kg body weight (wt) of sodium pentobarbital and ketamine, respectively, administered intraperitoneally. After anesthesia the rats were

prepared for clearance experiments. In brief, a tracheotomy was performed and the left jugular vein was also cannulated with another catheter for infusion of inulin, PAH and fluids. To collect urine samples, the urinary bladder was cannulated by a suprapubic incision with a double catheter allowing air injection to expedite emptying. The urine was collected under oil, and the volume determined gravimetrically. Following the surgical procedure, an initial dose of inulin (30 mg/100 g body wt diluted in 0.9 % NaCl) and PAH (0.02 mg/mL of extracellular fluid, assuming extracellular fluid at 20 % of body wt) were administered through the jugular vein. Subsequently, a constant infusion of inulin, PAH and 3 % mannitol in saline was infused at a rate of 0.1 mL/min throughout the experiment. After 40 min of stabilization urine and blood samples (by cardiac puncture) were collected twice with approximately 30 min of interval. The values for renal clearance were derived from the average of the two collection periods. The results are reported as means \pm SEM per kg body wt. At the end of the experiment, the right kidney was removed and frozen at -80°C .

Plasma and Urine Analysis

Plasma and urine creatinine and urea were measured by a colorimetric method (picric acid) and the Bergmeyer method, respectively (Labtest Diagnostica, Lagoa Santa, MG, Brazil). Total plasma and urine protein content was determined by the biuret method (Labtest Diagnostica, Lagoa Santa, MG, Brazil). Inulin in plasma and urine was measured by the anthrone method [27]. PAH in plasma and urine was determined by a modification of Smith's method [51]. Sodium, potassium and lithium concentrations were measured by flame photometry (CELM, FC180, São Paulo, Brazil). Osmolality of plasma and urine was measured by a vapor pressure osmometer (MicroOsmometer–Vapro5520[®], WESCOR-USA).

Calculations

Renal clearances and fractional excretions were calculated by standard techniques. Fractional electrolyte (Na^+ , K^+ and lithium) excretion (FE_{ion^+}) (%) was calculated as $C_{\text{ion}^+}/C_{\text{Cr}}$, where C_{ion^+} is Na^+ , K^+ or lithium clearance and C_{Cr} is creatinine clearance. Lithium clearance (C_{Li^+}) was used to assess proximal tubule output [53]. It should be noted that lithium is assumed to be reabsorbed in the proximal tubules in parallel with sodium and water, and that it is neither secreted nor reabsorbed beyond the proximal tubule [6]. Proximal Fractional Reabsorption of Na^+ (PFR_{Na^+}) and Post-Proximal Fractional Excretion of Na^+ ($\text{PPFR}_{\text{Na}^+}$) were calculated as $(\text{CF}_{\text{Na}^+} - \text{DD}_{\text{Na}^+})/\text{CF}_{\text{Na}^+}$ % and $(C_{\text{Na}^+}/C_{\text{Li}^+}) \times 100$, respectively. Where, DD_{Na^+} is Distal

Delivery of sodium ($C_{Li+} \times P_{Na+}$, $\mu\text{equiv}/\text{min}$); C_{Li+} , C_{Na+} and C_{Cr} are lithium, sodium and creatinine clearance (mL/min), respectively; and P_{Na+} is plasma sodium concentration (mequiv/L). Osmolality measurements were using to determinate osmolar clearance (C_{osm}) (mL/min) and free water clearance (C_{H_2O}) (mL/min), which C_{H_2O} as $C_{osm} - V_u$, where V_u is urinary flow (mL/min).

Immunohistochemical Studies

At the end of RBF and GFR experiments, the animals were killed by an intravenous injection of thiopental (100 mg/kg body wt). Renal tissue samples were fixed in 9 % formalin NaCl, stocked at 70 °C ethanol, and then embedded in paraffin. For renal histology evaluation, longitudinal sections of 5 μm of thickness were stained with trichrome. For immunostaining of macrophages, a monoclonal mouse anti-rat ED-1 antibody that only reacts against antigens present in the cytoplasm of macrophages and monocytes (anti-ED1, 1:1,000; Serotec, Oxford, United Kingdom) was used. Desmin staining was performed with a monoclonal mouse anti-rat antibody (anti-desmin 1:100; Dako, Glostrup, Denmark). These sections were incubated for 60 min at room temperature. After washing, the sections were incubated with rabbit anti-mouse immunoglobulin with low affinity for rat IgG (1:200; Dako, Glostrup, Denmark). The reaction product was detected with avidin–biotin–peroxidase complex (Vector Laboratories, CA). The color reaction was developed with 3,3'-diaminobenzidine (Sigma Chemical Co.) supplemented with hydrogen peroxide, and the material was then counterstained with methyl green, dehydrated, and mounted. Negative controls were created by replacing the primary monoclonal antibody with equivalent concentrations of normal mouse IgG. The extent of ED1-positive cell infiltration in glomerulus and tubular cells was evaluated in 30 microscopic fields (measuring 0.245 mm^2 each), and mean values per kidney were calculated. In the evaluation of immunoperoxidase staining for desmin, each glomerulus or field of renal cortex (each measuring 0.245 mm^2) was graded semiquantitatively under light microscopy (40 \times), and the mean score per kidney (ranging from 0 to 4) was calculated. Each score primarily reflected changes in the extent, rather than the intensity, of staining and depended on the percentage of the grid field showing positive staining: absence of staining or less than 5 % = 0; 5 to 25 % = 1; 25 to 50 % = 2; 50 to 75 % = 3; and more than 75 % = 4. This semiquantitative scoring system has been reported to be reproducible among different observers, and highly correlated with those obtained by computerized morphometry and evaluated using light microscopy (40 \times).

Determination of PGE₂ and TXB₂ Concentration in Urine

Urine PGE₂ and TXB₂ concentrations were determined by an enzyme immunoassay kit according to the manufacturer's instructions (Cayman Chemical Co, Ann Arbor, MI, USA). Standard curves were constructed by serially diluting PGE₂ and TXB₂ in buffer at concentrations between 7.8 and 1,000 pg/mL . Data were expressed in pg/min , where the concentrations were normalized by urinary flow.

Statistical Analysis

Data are reported as means \pm SEM. All data were initially tested for normality by the Kolmogorov–Smirnov test. Statistical comparisons were made by analysis of variance (ANOVA) followed by Tukey's multiple comparison test, using the statistical software GraphPad Prism version 5.00 for Windows (GraphPad Inc, San Diego, CA, USA), and the level of significance was set at $p < 0.05$.

Results

The body and tumor weight of the different groups are shown in Table 1. In healthy rats the body weight gain in the FO group was similar to the control group (C), but for the Walker 256 tumor-bearing rats (W) it was significantly lower than control ($p < 0.05$). FO supplementation was able to modify weight loss of tumor-bearing animals, where the FO tumor-bearing group (WFO) presented body weight gain when compared to the W group. FO supplementation also reduced tumor mass weight by 60 % compared to the W group ($p < 0.05$) (Table 1). Kidney weight of the W group was significantly lower than control, however when kidney weight was normalized by animal weight this difference was not observed (Table 1). The FO supplementation did not modify this parameter significantly.

The tumor-bearing group showed a clear signal of cancer cachexia, i.e., a depletion of protein stores. Proteinemia was significantly lower in the W group compared to the C and FO groups. On the other hand, the FO tumor-bearing group (WFO) was similar to the C and FO groups (see Table 2). Urinary excretion of proteins was not modified by FO supplementation or tumor presence.

Glomerular filtration was determinate by inulin clearance. This parameter did not present significant changes in the FO group or in the W group if compared to control group (see Table 2). At the same time, FO supplementation in tumor presence (WFO group) increased the GFR significantly compared with W ($p < 0.05$). Despite the differences observed in GFR, plasma creatinine concentration was similar among the groups (see Table 2). In the same

Table 1 Effect of FO supplementation on animal body weight before and after tumor inoculation

	C (<i>n</i> = 14)	FO (<i>n</i> = 12)	W (<i>n</i> = 12)	WFO (<i>n</i> = 11)
Weight (g) before tumor inoculation	325.3 ± 8.2	295.2 ± 10.4	297.4 ± 13.8	308.2 ± 10.8
Weight (g) after 14 days of tumor inoculation	334.4 ± 14.2	306.1 ± 12.8	302.7 ± 11.7	317.1 ± 8.5
Tumor weight (g)	–	–	15.8 ± 0.9	6.4 ± 2.1 ^b
Weight gain (g) for 14 days	9.1 ± 2.6	10.9 ± 3.05	(−10.57 ± 1.68 ^a)	(2.46 ± 1.69 ^b)
Kidney weight (g)	1.16 ± 0.04	1.14 ± 0.03	1.01 ± 0.03 ^a	1.14 ± 0.03
Kidney weight (g/kg wt)	3.24 ± 0.08	3.41 ± 0.11	3.26 ± 0.11	3.62 ± 0.12

The values in parentheses represent the weight gain calculated considering only the carcass weight (body weight on the 14th day minus tumor weight). Data are presented as means ± SEM

^a *p* < 0.05 vs C group

^b *p* < 0.05 vs W group

Table 2 Effect of FO supplementation on renal function

	C	FO	W	WFO
GFR (mL/min/kg of body wt)	10.57 ± 0.87 (<i>n</i> = 13)	11.59 ± 0.93 (<i>n</i> = 13)	9.11 ± 0.96 (<i>n</i> = 8)	11.68 ± 0.75 ^b (<i>n</i> = 8)
RPF (mL/min/kg of body wt)	24.74 ± 1.21 (<i>n</i> = 13)	38.19 ± 2.06 ^a (<i>n</i> = 13)	18.60 ± 3.05 (<i>n</i> = 8)	35.56 ± 3.03 ^b (<i>n</i> = 8)
Filtration fraction (%)	41.2 ± 4.4 (<i>n</i> = 13)	32.6 ± 3.0 (<i>n</i> = 13)	39.7 ± 5.6 (<i>n</i> = 8)	32.4 ± 3.0 (<i>n</i> = 8)
Proteinemia (g/dL)	5.2 ± 0.2 (<i>n</i> = 10)	5.6 ± 0.1 (<i>n</i> = 10)	4.5 ± 0.1 ^a (<i>n</i> = 12)	5.1 ± 0.2 (<i>n</i> = 11)
Plasma creatinine (mg/dL)	0.36 ± 0.06 (<i>n</i> = 9)	0.34 ± 0.03 (<i>n</i> = 9)	0.34 ± 0.04 (<i>n</i> = 9)	0.45 ± 0.06 (<i>n</i> = 10)
Plasma urea (mg/dL)	41.0 ± 2.0 (<i>n</i> = 9)	41.9 ± 1.9 (<i>n</i> = 9)	40.9 ± 1.65 (<i>n</i> = 9)	45.1 ± 2.23 (<i>n</i> = 10)
Urinary excretion of protein (mg/day)	0.41 ± 0.08 (<i>n</i> = 8)	0.28 ± 0.06 (<i>n</i> = 8)	0.21 ± 0.05 (<i>n</i> = 8)	0.29 ± 0.09 (<i>n</i> = 8)
Urinary TXB ₂ (ng/min)	30 ± 4 (<i>n</i> = 8)	18 ± 1 ^a (<i>n</i> = 9)	35 ± 3 (<i>n</i> = 8)	23 ± 1 ^b (<i>n</i> = 9)
Urinary PGE ₂ (ng/min)	53 ± 9 (<i>n</i> = 8)	39 ± 9 (<i>n</i> = 8)	47 ± 13 (<i>n</i> = 8)	48 ± 1 (<i>n</i> = 8)

Data are presented as means ± SEM

GFR glomerular filtration rate (mL/min/kg of body wt), RPF renal plasma flow (mL/min/kg of body wt)

^a *p* < 0.05 vs C group

^b *p* < 0.05 vs W group

way, plasma urea concentration was similar among the groups (Table 2).

The values of *p*-aminohippuric acid clearance represent RPF. FO supplementation increased the blood flow significantly in the control and tumor-bearing groups (*p* < 0.05), where FO promoted a rise of 54 % compared with C and WFO a rise of 91 % in relation to W (see Table 2). These results indicate that FO supplementation was able to modify renal hemodynamic, inducing vasodilatation. Despite the changes observed in RPF, the filtration fraction data were not changed significantly by FO supplementation or tumor presence (Table 2).

The tumor-bearing group (W) had less plasma osmolality compared to control rats (C) (see Table 3). This alteration in plasma osmolality was reverted in supplemented animals (WFO). Despite these differences, urine osmolality and osmolar clearance were similar among the different groups. Moreover, the free water clearance presents negative values in all groups, indicating that the distal segments keep the ability of water reabsorption (Table 3).

Table 4 shows renal handling of sodium and potassium. Na⁺ and K⁺ urinary excretion were not significantly modified by FO supplementation or tumor presence. The FE_{Na+} of control rats supplemented with FO was similar to control. FE_{Na+} in W group was nominally lower than control groups but not statistically significant (see Table 4). Plasma sodium concentration of supplemented and tumor-bearing groups was similar to the control group. The lithium clearance method was used to calculate the amounts of water and sodium delivered from the end of the proximal straight tubule. Table 4 shows the values of fractional lithium excretion (FE_{Li}), Na⁺ Distal Delivery (DD_{Na+}), Proximal Fractional Reabsorption of Na⁺ (PFR_{Na+}) and C_{Na+}/C_{Li} ratio (expressing the post-proximal fractional excretion of Na⁺). FE_{Li} and PFR_{Na+} were not modified by FO supplementation or tumor presence, indicating that proximal Na⁺ reabsorption was similar among the groups. C_{Na+}/C_{Li} ratio represents post-proximal fractional excretion of sodium, and this parameter is utilized to estimate the distal sodium reabsorption. So, an increase in

Table 3 Effect of FO supplementation on plasma osmolality (P_{OSM}), urine osmolality (U_{OSM}), osmolar (C_{OSM}) and free water clearance (C_{H_2O})

	C ($n = 12$)	FO ($n = 13$)	W ($n = 10$)	WFO ($n = 13$)
P_{OSM} (mOsm/kgH ₂ O)	281.3 ± 3.4	288.2 ± 3.4	266.4 ± 6.3 ^a	284.5 ± 6.5
U_{OSM} (mOsm/kgH ₂ O)	858.5 ± 104.7	839.7 ± 85.2	879.4 ± 120.0	1,030 ± 122.3
C_{OSM} (mL/min)	0.041 ± 0.005	0.032 ± 0.004	0.032 ± 0.004	0.035 ± 0.003
C_{H_2O} (mL/min)	-0.027 ± 0.005	-0.018 ± 0.002	-0.023 ± 0.002	-0.022 ± 0.002

Data are presented as means ± SEM

^a $p < 0.05$ vs C group

post-proximal fractional excretion of sodium, an increase in C_{Na^+}/C_{Li} ratio, indicates that the distal sodium reabsorption was reduced. C_{Na^+}/C_{Li} ratio was not modified by FO supplementation in control rats, indicating that fractional sodium reabsorption beyond the proximal tubule was equivalent between these groups. However, FO supplementation significantly reversed the tendency to increase in fractional distal sodium reabsorption observed in tumor-bearing rats (W), as indicated by the increased value for C_{Na^+}/C_{Li} ratio in the WFO group (see Table 4).

Urinary excretion of TXB₂ in control animals averaged 30 ± 4 ng/min and decreased by 40 % to 18 ± 1 ng/min ($p < 0.05$), $n = 9$, after FO supplementation. FO supplementation in tumor-bearing rats was also able to reduce urinary excretion of TXB₂ (see Table 2). Despite the differences observed in TXB₂ excretion, urinary excretion of PGE₂ was similar among groups (Table 2).

Immunohistochemical Studies

In kidneys that underwent histological studies, no significant differences in appearance were found in glomerular or tubulointerstitium morphology among the different groups (data not shown). The number of macrophages/monocytes in renal tissue was evaluated by immunolocalization of

ED1 positive cells. In glomerulus, the number of ED1 (macrophages/monocytes)-positive cells were similar in C and FO groups: 0.79 ± 0.16 and 1.17 ± 0.07, respectively, $p > 0.05$ (see Fig. 1). However, for tumor-bearing rats it was significantly higher: 5.57 ± 1.82 positive cells number, a value that was reduced to control levels by FO supplementation (WFO): 2.32 ± 0.56 positive cells number/field, $p < 0.05$ (Fig. 1). A similar profile was observed in tubulointerstitium cortical area (see Fig. 2).

The expression of desmin at glomerular edge was not significantly modified by FO supplementation or tumor presence (Fig. 3). The group mean score was 0.078 ± 0.078 in C, 0.024 ± 0.017 in FO, 0.65 ± 0.41 in W, and 0.30 ± 0.10 in WFO. In most rat strains, glomerular expression of desmin is confined to mesangial cells, and podocytes only express it following injury. Therefore, higher desmin expression at glomerular edge can be considered as a marker of podocyte damage.

Discussion

This study shows that dietary supplementation with FO of only 1.25 % w/w resulted in a slight modification in renal function of healthy rats (an increase in renal blood flow).

Table 4 Effect of FO supplementation on plasma Na⁺ and K⁺ level (P_{Na^+} and P_{K^+}), Na⁺ and K⁺ excretion load, fractional Na⁺ and lithium excretion (FE), proximal fractional reabsorption of Na⁺

(PFR_{Na^+}), post-proximal fractional excretion of Na⁺ (C_{Na^+}/C_{Li} ratio), and Na⁺ distal delivery (DD_{Na^+}) (μequiv/min)

Groups	C ($n = 12$)	FO ($n = 12$)	W ($n = 12$)	WFO ($n = 12$)
P_{Na^+} (mequiv/L)	152.6 ± 3.3	148.8 ± 3.5	153.3 ± 3.0	148.9 ± 4.1
Na ⁺ excretion load (μequiv/min)	1.15 ± 0.15	0.82 ± 0.18	0.77 ± 0.15	0.97 ± 0.11
P_{K^+} (mequiv/L)	3.19 ± 0.19	3.68 ± 0.30	3.03 ± 0.16	3.17 ± 0.16
K ⁺ excretion load (μequiv/min)	1.04 ± 0.21	0.93 ± 0.19	1.10 ± 0.18	1.09 ± 0.16
FE _{Na⁺} (%)	1.24 ± 0.36	1.25 ± 0.40	0.87 ± 0.21	1.61 ± 0.38
FE _{Li} (%)	58.76 ± 6.16	63.55 ± 9.49	60.53 ± 5.87	58.81 ± 7.70
PFR_{Na^+} (%)	41.24 ± 6.16	36.45 ± 9.49	40.80 ± 6.76	41.19 ± 7.70
C_{Na^+}/C_{Li} ratio (%)	1.38 ± 0.20	1.24 ± 0.19	0.90 ± 0.19	1.69 ± 0.23 ^a
DD_{Na^+} (μequiv/min)	94.08 ± 11.86	82.08 ± 7.87	76.94 ± 11.51	76.55 ± 8.51

Data are presented as means ± SEM

^a $p < 0.05$ vs W group

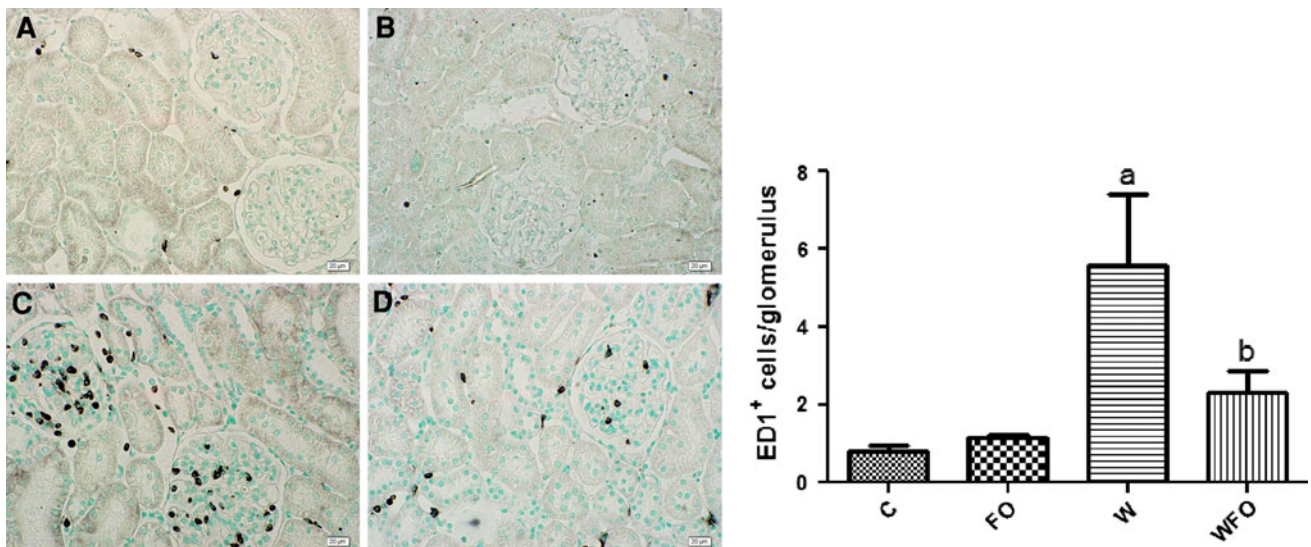


Fig. 1 Number of ED1-positive cells (macrophages/monocytes) in the glomerulus from control rats C, control rats supplemented with fish oil FO, Walker 256 tumor-bearing rats W and Walker 256 tumor-bearing rats supplemented with fish oil WFO. *a* $p < 0.05$ compared

with C group; *b* $p < 0.05$ vs W group. Immunolocalization of ED1 cells of: **a** Groups C ($n = 3$), **b** Groups FO ($n = 3$), **c** Groups W ($n = 4$) and **d** Groups WFO ($n = 5$). Note that the number of ED1-positive cells is higher in **c** than in **a** and **b** ($40\times$)

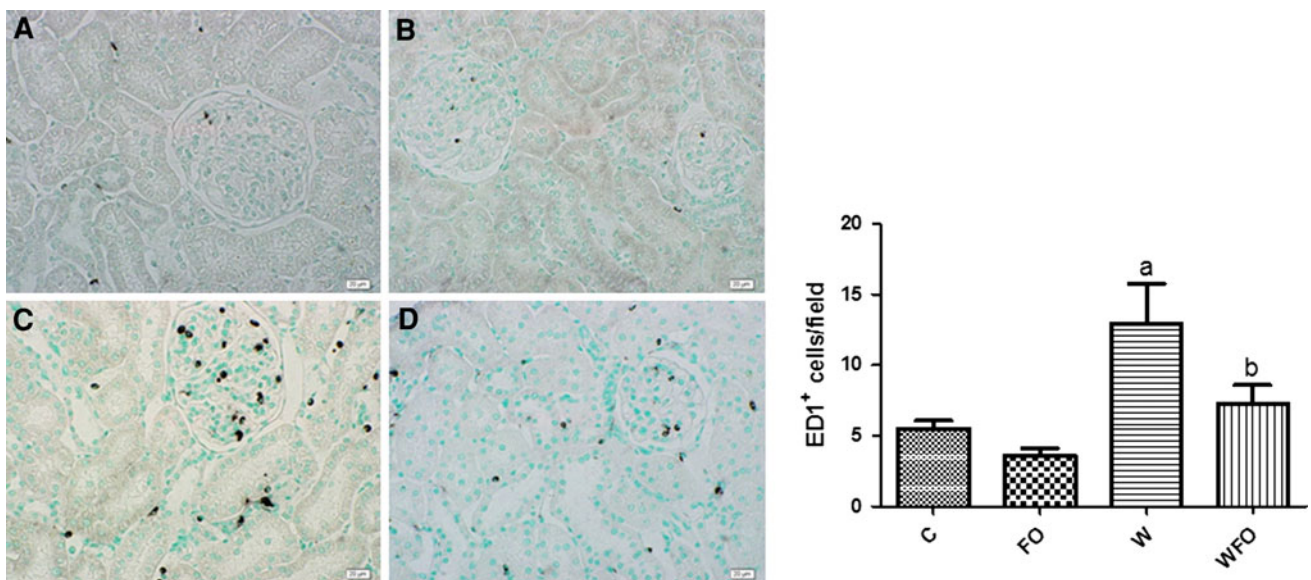


Fig. 2 Number of ED1-positive cells (macrophages/monocytes) in tubulointerstitial area in the renal cortex from control rats C, control rats supplemented with fish oil FO, Walker 256 tumor-bearing rats W and Walker 256 tumor-bearing rats supplemented with fish oil WFO.

a $p < 0.05$ vs C group; *b* $p < 0.05$ vs W group. Immunolocalization of ED1 cells of: **a** Groups C ($n = 3$), **b** FO ($n = 3$), **c** W ($n = 4$) and **d** WFO ($n = 5$). Note that the number of ED1-positive cells is higher in **c** than in **a** and **b** ($40\times$)

However, in tumor-bearing rats, the same diet led to a decrease in tumor growth and a renoprotective effect accompanied by a rise in RPF and the preservation of glomerular filtration.

Over the past 20 years, several studies have suggested the efficacy and potential clinical utility of n-3 fatty acid dietary supplementation in human renal diseases such as idiopathic immunoglobulin A nephropathy, lupus nephritis,

cyclosporine A toxicity, vascular access thrombosis of end-stage renal disease, and idiopathic calcium urolithiasis [3, 13, 18, 21]. The most accepted hypothesis explaining the multifaceted actions of n-3 fatty acids on kidney diseases relates to the activities of the metabolites derived from EPA as opposed to those derived from ARA. The n-3 fatty acids compete with ARA in the cellular membrane, ultimately reducing inflammatory, thrombotic, and aggregation

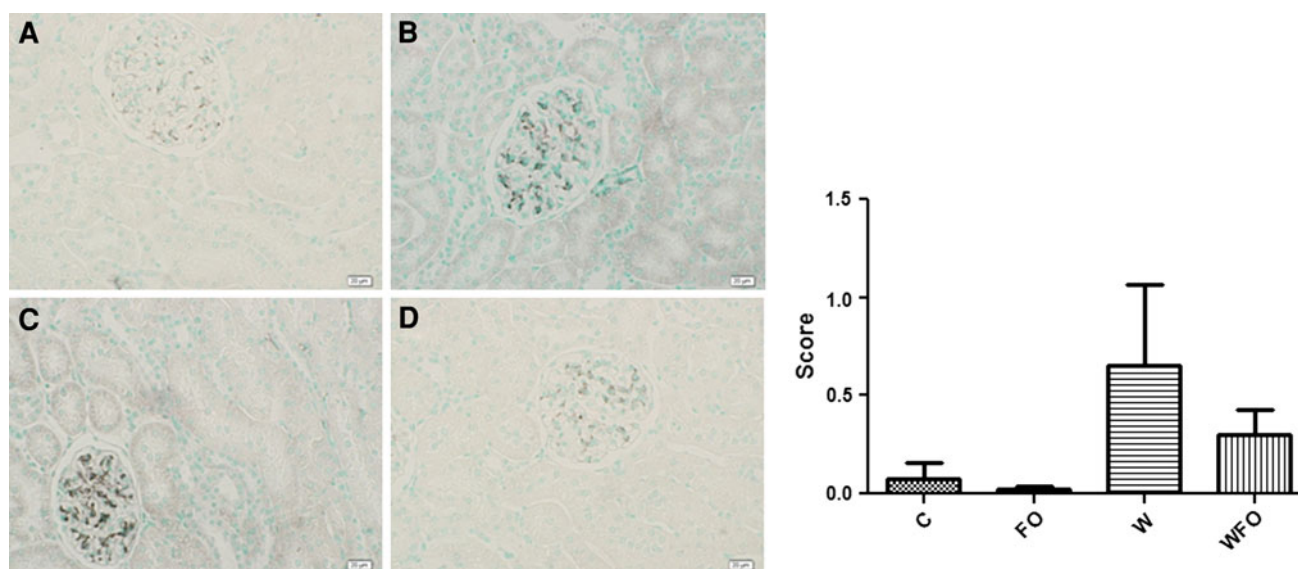


Fig. 3 Score for desmin at glomerular edge in the renal cortex of rats from C, FO, W and WFO groups. Immunolocalization of desmin at glomerular edge: **a** Groups C ($n = 2$), **b** FO ($n = 4$), **c** W ($n = 3$) and **d** WFO ($n = 4$) ($40\times$)

mediators such as PGE_2 and TXB_2 , and increasing mediators such as PGE_3 and TXB_3 , which attenuate these processes [2, 34].

Despite numerous studies devoted to several different kinds of renal diseases, few investigations have examined the effects of n-3 fatty acid dietary supplementation on renal function in healthy animals or humans [19, 35, 48]. In the present work, we observed that chronic dietary supplementation with n-3 fatty acids in rats did not significantly alter the GFR, but did promote a rise of 91 % in renal blood flow, suggesting preferential vasodilatation of efferent arteriole. However, Schmitz et al. [48] observed a significant increase in the single-nephron glomerular filtration rate (SNGFR) when glomerular hemodynamics was evaluated in rats by using micropuncture. The elevated SNGFR was primarily due to a marked increase in single-nephron plasma flow, which was associated with a significant reduction in efferent arteriolar resistance. The increase in RPF observed in the groups fed with supplemented diet could be explained by competition between n-3 fatty acid metabolism and the production of ARA-derived prostanoids in the kidney [2]. FO, which is rich in EPA, generates series 3 prostanoids (PGI_3 , PGE_3 , and TBX_3) and series 5 leukotrienes, with vasodilating characteristics. In contrast, arachidonic acid derivatives such as thromboxanes (TBX_2) have vasoconstrictive actions [1, 31]. Potent renal vasodilators include PGI_3 and PGE_3 , whereas TBX_3 has little effect on vascular smooth muscle tone. In the present work, we observed a significant reduction in the urinary excretion of TBX_2 in n-3 fatty acid-supplemented animals, suggesting a fatty acid-mediated decrease in TBX_2 synthesis. Despite the reduction

observed in TBX_2 excretion, urinary excretion of PGE_2 was similar among the groups. The EIA methodology utilized in this study has a limitation resulting from cross reactivity between TXB_2 and TXB_3 , and between PGE_2 and PGE_3 . The lack of effect on urinary excretion of PGE_2 can be explained by this limitation. On the other hand, Logan et al. [35] observed that feeding FO for 1 month to rats had no effect on the mean GFR (as determined using inulin clearance) or RPF. In a similar manner, we reported in a previous study that FO supplementation in the diet fed to female rats throughout pregnancy and lactation, and then in their offspring post-weaning diet for 10 weeks, also did not modify glomerular filtration [24].

The discrepancies observed between our study and others could be attributed to the differences in experimental design, such as duration of supplementation period and amount of FO added to the experimental diets. The study by Schmitz et al. [48] was performed after 4–6 weeks of n-3 fatty acid dietary supplementation, whereas the present study was conducted after 10–12 weeks. Furthermore, the animals described in the Schmitz publication were fed standard laboratory chow supplemented with 18 % (w/w) of FO, whereas the chow used in our study was supplemented with approximately 1.25 % (w/w) FO. Despite the observed changes in renal hemodynamics in the FO group, other parameters like renal handling of sodium and potassium were not modified by the supplementation. Previous studies with healthy humans have also reported that inhibition of COX-derived prostanoids have minimal effects on renal hemodynamics and tubular function [15, 52].

Cachexia-anorexia syndrome (a devastating state of malnutrition) is a common manifestation of cancer and

non-malignant chronic diseases such as AIDS, advanced congestive heart failure, chronic obstructive pulmonary disease, and rheumatoid arthritis, among others [20, 29]. Epidemiological studies have shown a link between fat-rich diets and incidence of cancer [10, 40]. Tumor growth demands energy, which must be provided by the host. As a consequence, depletion of energy stores (glycogen in the liver and muscles; protein in the muscles; triacylglycerol in the adipose tissue) of the host ensues. In the current study, tumor growth was associated with reduced animal growth and reduced total serum protein concentration. Thus, this model induced cancer cachexia. Supplementation with FO significantly reversed the reduction in weight gain observed in the Walker 256 tumor-bearing rats, reduced tumor growth, and increased total serum protein concentrations. In previous studies by our group, we observed that several “cachectic” serum parameters such as glucose, lactate, cholesterol, and HDL-C returned to normal levels in Walker 256 tumor-bearing rats supplemented with FO [38, 56]. The mechanisms used by n-3 PUFA to combat neoplastic cells are yet to be elucidated. Modifications in prostaglandin biosynthesis, cyclooxygenase-2 activity, and angiogenesis, and modulation of the immune function and lipid peroxidation have all been suggested to play a significant role [32]. There is an alternative hypothesis of reducing weight loss in cachexia from an increase in lipid in the diet. An increase in total caloric intake leads to a rise in fat stores or reduced depletion of energy stores potentially relieving the reliance on protein catabolism. FO supplementation increases total caloric intake in only 3.3 %, an amount unlikely to explain the effect observed in weight loss.

The progression of renal injury depends on many factors such as immune cell recruitment, inflammatory mediators, and cellular proliferation [44, 59]. Monocyte/macrophage recruitment in the renal tissue is the initial stage of the injury process, and this recruitment is mainly initiated by a chemokine monocyte chemoattractant protein 1 (MCP-1) [14, 47]. In the present study, we observed an increase in macrophage recruitment by the renal tissue (glomerular and interstitial) of tumor-bearing rats (W group), indicating renal disease in its initial stages. Despite these inflammatory signals, renal hemodynamical parameters were preserved in these rats. Macrophage recruitment was reversed in the WFO group, suggesting an increase in the production of anti-inflammatory mediators or inhibition of pathways involved in renal injury. An et al. [2] demonstrated that anti-inflammatory effects of FO in the kidney may be explained by decreased MCP-1 expression; this is suggested in a 5/6 nephrectomy model, where FO reduced renal injury, as well as the activation of ERK and NF- κ B, and MCP-1 expression, which are pathway participants in the progression of fibrosis. Similar results were also observed by Peake et al. [41] in a model of obstructive

renal injury in rats. As discussed above, FO supplementation decreased the production of ARA-derived prostanoids with vasoconstrictive actions, like TBX₂. This explains the significant reduction observed in urinary excretion of TBX₂ in this group. Another factor that could contribute to the increase in GFR induced by FO supplementation is reduction in whole blood viscosity due to reduced serum lipid levels. In a previous study, we observed that Walker 256 tumor-bearing rats given a FO-supplemented diet displayed reduced serum triacylglycerol (TAG) levels in contrast to the W group, but similar to the control rats [42]. Therefore, FO dietary supplementation may have caused a reduction in plasma and/or whole blood viscosity, which likely contributed to the observed decrease in renal vascular resistance. On the other hand, control rats on the same diet had serum TAG and cholesterol levels similar to the non-treated control animals [56]. Thus, the small effects of this supplementation on the GFR in control animals that were observed in the present work could be explained in part by the constancy of plasma lipid levels, and in part, by the slight effect of inhibition of cyclooxygenase products on the renal parameters of normal rats and humans [39, 58].

Injury of foot process and the glomerular barrier can be detected by desmin immunostaining [11]. We observed that desmin expression was not significantly modified by FO supplementation or tumor presence. In animal models of renal damage, an increase in desmin expression in the glomerulus is usually indicative of glomerular sclerosis and loss of glomerular selectivity to macromolecules such as proteins [25]. These lesions could result in marked and persistent proteinuria; however, proteinuria was not observed in the present study.

As Walker 256 carcinoma progresses in control rats (W), their water intake is sustained despite their progressive decline in food consumption [24]. This apparent excessive water intake has been attributed to retention of water associated with the known retention of sodium ions due to increased secretion of aldosterone, and/or inappropriate antidiuretic hormone secretion [5, 37]. The reduced plasma osmolality observed in the tumor-bearing rats in the present study corroborates this tendency to retain water. Another factor to be considered is the decrease in total serum protein concentration, which caused a reduction in the blood colloid oncotic pressure, favoring the movement of water from the vascular to the interstitial space, resulting in hypovolemia and renal preservation of salt and water [55]. Other authors have reported a decrease in urinary Na⁺ excretion by W rats, as observed in the present study [24, 45, 55]. Supplementation with FO reversed the alterations caused by tumor growth on renal fractional excretion of sodium. The tumor-bearing animals that were fed FO also had a plasma osmolality similar to the control group, indicating a reversal in the tendency to retain water that accompanies cancer cachexia.

In summary, dietary supplementation with FO (1,25 % w/w) induced only slight modifications in renal hemodynamics in control animals. Interestingly, in tumor-bearing rats, this change in n-3 PUFA intake caused a remarkable reduction in tumor growth and cachexia, and had a reno-protective function as well.

Acknowledgments Authors thank Dr. Carolina A. Freire for the osmolality readings and useful suggestions. Research supported by Fundação Araucária, Paraná, Brasil. Luiz C. Fernandes and Terezila M. Coimbra were supported by grants of the Conselho Nacional de Pesquisas (CNPq), Brasil.

Conflict of interest The authors declare that they have no conflict of interest.

References

- Aguila MB, Pinheiro AR, Aquino JC, Gomes AP, Mandarim-De-Lacerda CA (2005) Different edible oil beneficial effects (canola oil, fish oil, palm oil, olive oil, and soybean oil) on spontaneously hypertensive rat glomerular enlargement and glomeruli number. *Prostaglandins Other Lipid Mediat* 76:74–85
- An WS, Kim HJ, Cho K, Vaziri ND (2009) Omega-3 fatty acid supplementation attenuates oxidative stress, inflammation, and tubulointerstitial fibrosis in the remnant kidney. *Am J Physiol Renal Physiol* 297:F895–F903
- Baggio B, Budakovic A, Priante G, Gambaro G, Manzato E, Khan S (2002) Dietary fatty acid supplementation modulates the urinary excretion of calcium and oxalate in the rat. Insight into calcium lithogenesis. *Nephron* 91:486–491
- Bayorh MA, Williams EF, Ogbolu EC, Walker CE, Manor EL, Brown LG, Chenault VM (1996) Effects of MaxEPA on salt-induced hypertension: relationship to [³H]nitrobenzylthioinosine binding sites. *Clin Exp Hypertens* 18:37–49
- Blackburn GL, Maini BS, Bistran BR, Mcdermmott WV Jr (1977) The effect of cancer on nitrogen, electrolyte and mineral metabolism. *Cancer Res* 37:2348–2353
- Boer WH, Fransen R, Shirley DG, Walter SJ, Boer P, Koomans HA (1995) Evaluation of lithium clearance method: direct analysis of tubular lithium handling by micropuncture. *Kidney Int* 47:1023–1030
- Brown SA, Brown CA, Crowell WA, Barsanti JA, Kang C, Allen T, Cowell C, Finco DR (2000) Effects of dietary polyunsaturated fatty acid supplementation in early renal insufficiency in dogs. *J Lab Clin Med* 135:275–286
- Calder PC (2006) Polyunsaturated fatty acids and inflammation. *Prostaglandins Other Lipid Mediat* 75:197–202
- Câmara NO, Martins JO, Landgraf RG, Jancar S (2009) Emerging roles for eicosanoids in renal diseases. *Curr Opin Nephrol Hypertens* 18:21–27
- Caygill CPJ, Charlett A, Hill MJ (1996) Fat, fish, fish oil and cancer. *Br J Cancer* 74:159–164
- Coimbra TM, Janssen U, Gröne HJ, Ostendorf T, Kunter U, Schmidt H, Brabant G, Floege J (2000) Early events leading to renal injury in obese Zucker (fatty) rats with type II diabetes. *Kidney Int* 57:167–182
- Culp BR, Titus BG, Lands WE (1979) Inhibition of prostaglandin biosynthesis by eicosapentaenoic acid. *Prostaglandins Med* 3:269–278
- De Caterina R, Endres S, Kristensen SD, Schmidt EB (1994) N-3 fatty acids and renal diseases. *Am J Kidney Dis* 24:397–415
- Diaz Encarnacion MM, Warner GM, Cheng J, Gray CE, Nath KA, Grande JP (2011) N-3 Fatty acids block TNF- α -stimulated MCP-1 expression in rat mesangial cells. *J Physiol Renal Physiol* 300:1142–1151
- DiBona GF (1986) Prostaglandins and nonsteroidal anti-inflammatory drugs. Effects on renal hemodynamics. *Am J Med* 17:12–21
- Dolegowska B, Piłkuła E, Safranow K, Olszewska M, Jakubowska K, Chlubek D, Gutowski P (2006) Metabolism of eicosanoids and their action on renal function during ischaemia and reperfusion: the effect of alprostadil. *Prostaglandins Other Lipid Mediat* 75:403–411
- Donadio JV, Grande JP (2004) The role of fish oil/omega-3 fatty acids in the treatment of IgA nephropathy. *Semin Nephrol* 24:225–243
- Donadio JV (2001) N-3 Fatty acids and their role in nephrologic practice. *Curr Opin Nephrol Hypertens* 10:639–642
- Dusing R, Struck A, Göbel BO, Weisser B, Vetter H (1990) Effects of n-3 fatty acids on renal function and renal prostaglandin E metabolism. *Kidney Int* 38:315–319
- Evans WJ, Morley JE, Argilés J, Bales C, Baracos V, Guttridge D, Jatoi A, Kalantar-Zadeh K, Lochs H, Mantovani G, Marks D, Mitch WE, Muscaritoli M, Najand A, Ponikowski P, Rossi Fanelli F, Schambelan M, Schols A, Schuster M, Thomas D, Wolfe R, Anker SD (2008) Cachexia: a new definition. *Clin Nutr* 27:793–799
- Fassett RG, Gobe GC, Peake JM, Coombes JS (2010) Omega-3 polyunsaturated fatty acids in the treatment of kidney disease. *Am J Kidney Dis* 56:728–742
- Fearon KCH, Barber MD, Moses AG, Ahmedzai SH, Taylor GS, Tisdale MJ, Murray GD (2006) Double-blind, placebo-controlled, randomized study of eicosapentaenoic acid diester in patients with cancer cachexia. *J Clin Oncol* 24:3401–3407
- Fernandes LC, Carpinelli AR, Hell NS, Curi R (1991) Improvement of cancer cachexia and decrease of Walker 256 tumor growth by insulin administration in rats. *Cancer Ther Control* 1:259–268
- Fernandez R, Piechnik J, Fabris R, Malnic G, Fernandes LC (2004) Effect of chronic fish oil supplementation on renal function of normal and cachectic rats. *Braz J Med Biol Res* 37:1481–1489
- Franciscato HDC, Marin ECS, Cunha FQ, Costa RS, Silva CGA, Coimbra TM (2011) Role of endogenous hydrogen sulfide on renal damage induced by adriamycin injection. *Arch Toxicol* 85:1597–1606
- Friedman A, Moe S (2006) Review of the effects of omega-3 supplementation in dialysis patients. *Clin J Am Soc Nephrol* 1:182–192
- Fuehr J, Kaczmarczyk J, Kruttgen CD (1955) A simple colorimetric method of inulin determination in renal clearance studies on metabolically normal subjects and diabetics. *Klin Wochenschr* 33:729–730
- Giacosa A, Frascio F, Sukkar SG, Roncella S (1996) Food intake and body composition in cancer cachexia. *Nutrition* 12:S20–S23
- Grossberg AJ, Scarlett JM, Marks DL (2010) Hypothalamic mechanisms in cachexia. *Physiol Behav* 100:478–489
- Hao C, Breyer MD (2007) Physiologic and pathophysiologic roles of lipid mediators in the kidney. *Kidney Int* 71:1105–1115
- Hao C, Breyer MD (2008) Physiological regulation of prostaglandins in the kidney. *Ann Rev Physiol* 70:357–377
- Jiang WG, Bryce RP, Horrobin DF (1998) Essential fatty acids: molecular and cellular basis of their anti-cancer action and clinical implications. *Crit Rev Oncol Hematol* 27:179–209

33. Kim G (2008) Renal effects of prostaglandins and cyclooxygenase-2 inhibitors. *Electrolyte Blood Press* 6:35–41
34. Lauretani F, Semba RD, Bardinelli S, Miler ER, Ruggiero C, Cherubini A, Guralnik JM, Ferrucci L (2008) Plasma polyunsaturated fatty acids and the decline of renal function. *Clin Chem* 54:475–481
35. Logan JL, Michael UF, Benson B (1992) Dietary fish oil interferes with renal arachidonic acid metabolism in rats: correlations with renal physiology. *Metabolism* 41:382–389
36. Luft FC (2007) Cachexia has only one meaning. *J Mol Med* 85:783–785
37. Morrison AR (1986) Biochemistry and pharmacology of renal arachidonic acid metabolism. *Am J Med* 80:3–11
38. Mund RC, Pizato N, Bonatto S, Nunes EA, Vicenzi T, Tanhoffer R, de Oliveira HH, Curi R, Calder PC, Fernandes LC (2007) Decreased tumor growth in Walker 256 tumor-bearing rats chronically supplemented with fish oil involves COX-2 and PGE2 reduction associated with apoptosis and increased peroxidation. *Prostaglandins Other Lipid Mediat* 76:113–120
39. Munger K, Baylis C (1988) Sex differences in renal hemodynamics in rats. *Am J Physiol* 254:223–231
40. Pandalai PK, Pilat MJ, Yamazaki K (1996) The effects of omega-3 and omega-6 fatty acids on in vitro prostate cancer growth. *Anticancer Res* 16:815–820
41. Peake J, Gobe G, Fassett R, Coombes J (2011) The effects of dietary fish oil on inflammation, fibrosis and oxidative stress associated with obstructive renal injury in rats. *Mol Nutr Food Res* 55:400–410
42. Pinto JA Jr, Folador A, Bonato SJ, Aikawa J, Yamazaki RK, Pizato N, Facin M, Grohs H, de Oliveira HH, Naliwaiko K, Ferraz AC, Nishiyama A, Fernandez R, Curi R, Fernandes LC (2004) Fish oil supplementation in F1 generation associated with naproxen, clenbuterol, and insulin administration reduce tumor growth and cachexia in Walker 256 tumor-bearing rats. *J Nutr Biochem* 15:358–365
43. Raymond C, Harris Jr, Matthew D, Breyer BM (2008) Arachidonic Acid Metabolites and the Kidney. In: *The Kidney*, chap. 11
44. Remuzzi G, Bertani T (1998) Pathophysiology of progressive nephropathies. *N Engl J Med* 339:1448–1456
45. Rettori O, Vieira-Matos AN, Gontijo JR (2000) Re-assessment of the renal hydrosaline dysfunction in rats bearing the Walker-256 tumor. *Ren Fail* 22:769–784
46. Ruxton CHS, Reed SC, Simpson MJA, Millington KL (2004) The health benefits of omega-3 polyunsaturated fatty acids: a review of the evidence. *J Hum Nutr Diet* 17:449–459
47. Schlondorff D (1995) The role of chemokines in the initiation and progression of renal disease. *Kidney Int* 47:S44–S47
48. Schmitz PG, O'donnell MP, Kasiske BL, Keane WF (1991) Glomerular hemodynamic effects of dietary polyunsaturated fatty acid supplementation. *J Lab Clin Med* 18:129–135
49. Shapiro H, Theilla M, Attal-Singer J, Singer P (2011) Effects of polyunsaturated fatty acid consumption in diabetic nephropathy. *Nat Rev Nephrol* 7:110–121
50. Simopoulos AP (2008) The importance of the omega-6/omega-3 fatty acid ratio in cardiovascular disease and other chronic diseases. *Exp Biol Med* 233:674–688
51. Smith H, Finkelstein N, Aliminoso L, Crawford B, Graber M (1945) The renal clearances of substituted hippuric acid derivatives and other aromatic acids in dog and man. *J Clin Invest* 24:388–404
52. Svendsen KB, Bech JN, Sørensen TB, Pedersen EB (2000) A comparison of the effects of etodolac and ibuprofen on renal haemodynamics, tubular function, rennin, vasopressin and urinary excretion of albumin and α -glutathione-S-transferase in healthy subjects: a placebo-controlled cross-over study. *Eur J Clin Pharmacol* 56:383–388
53. Thomsen K, Nielsen CB, Flyvbjerg A (2002) Effects of glycine on glomerular filtration rate and segmental tubular handling of sodium in conscious rats. *Clin Exp Pharmacol Physiol* 29:449–454
54. Tisdale MJ (2009) Mechanisms of cancer cachexia. *Physiol Rev* 89:381–410
55. Toal JN, Millar FK, Brooks RH, White J (1961) Sodium retention by rats bearing the Walker carcinosarcoma 256. *Am J Physiol* 200:175–181
56. Togni V, Ota CC, Folador A, Júnior OT, Aikawa J, Yamazaki RK, Freitas FA, Longo R, Martins EF, Calder PC, Curi R, Fernandes LC (2003) Cancer cachexia and tumor growth reduction in walker 256 tumor-bearing rats supplemented with n-3 polyunsaturated fatty acids for one generation. *Nutr Cancer* 46:52–58
57. Usalan C, Emry S (1998) Membranoproliferative glomerulonephritis associated with small cell lung carcinoma. *Int Urol Nephrol* 30:209–213
58. Zipser RD (1985) Effects of selective inhibition of thromboxane synthesis on renal function in humans. *Am J Physiol* 248:753–756
59. Zoja C, Abbate M, Remuzzi G (2006) Progression of chronic kidney disease: insights from animal models. *Curr Opin Nephrol Hypertens* 15:250–257

Oleic Acid Attenuates *trans*-10,*cis*-12 Conjugated Linoleic Acid-Mediated Inflammatory Gene Expression in Human Adipocytes

Meaghan Reardon · Semone Govern ·
Kristina Martinez · Wan Shen · Tanya Reid ·
Michael McIntosh

Received: 24 May 2012 / Accepted: 13 August 2012 / Published online: 2 September 2012
© AOCS 2012

Abstract The weight loss supplement conjugated linoleic acid (CLA) consists of an equal mixture of *trans*-10,*cis*-12 (10,12) and *cis*-9,*trans*-11 (9,11) isomers. However, high levels of mixed CLA isomers, or the 10,12 isomer, causes chronic inflammation, lipodystrophy, or insulin resistance. We previously demonstrated that 10,12 CLA decreases de novo lipid synthesis along with the abundance and activity of stearoyl-CoA desaturase (SCD)-1, a δ -9 desaturase essential for the synthesis of monounsaturated fatty acids (MUFA). Thus, we hypothesized that the 10,12 CLA-mediated decrease in SCD-1, with the subsequent decrease in MUFA, was responsible for the observed effects. To test this hypothesis, 10,12 CLA-treated human adipocytes were supplemented with oleic acid for 12 h to 7 days, and inflammatory gene expression, insulin-stimulated glucose uptake, and lipid content were measured. Oleic acid reduced inflammatory gene expression in a dose-dependent manner, and restored the lipid content of 10,12 CLA-

treated adipocytes without improving insulin-stimulated glucose uptake. In contrast, supplementation with stearic acid, a substrate for SCD-1, or 9,11 CLA did not prevent inflammatory gene expression by 10,12 CLA. Notably, 10,12 CLA impacted the expression of several G-protein coupled receptors that was attenuated by oleic acid. Collectively, these data show that oleic acid attenuates 10,12 CLA-induced inflammatory gene expression and lipid content, possibly by alleviating cell stress caused by the inhibition of MUFA needed for phospholipid and neutral lipid synthesis.

Keywords Conjugated linoleic acid · Adipocytes · Oleic acid · Inflammatory gene expression · Stearoyl-CoA desaturase · Monounsaturated fatty acids · G-protein receptors

Abbreviations

AP-1	Activator protein
ATF	Activating transcription factor 3
BMI	Body mass index
BSA	Bovine serum albumin
9,11 CLA	<i>cis</i> -9, <i>trans</i> -11 Conjugated linoleic acid
10,12 CLA	<i>trans</i> -10, <i>cis</i> -12 Conjugated linoleic acid
COX	Cyclooxygenase
DOG	Deoxy-glucose
DEX	Dexamethasone
ER	Endoplasmic reticulum
ERK	Extracellular signal-regulated kinase
FFA	Free fatty acid(s)
GAPDH	Glyceraldehyde-3-phosphate dehydrogenase
GPRC	G-protein coupled receptors
GPR	G-protein receptors
JNK	c-Jun-NH ₂ -terminal kinase
LXR	Liver X receptor

M. Reardon · S. Govern · K. Martinez · W. Shen · T. Reid ·
M. McIntosh (✉)
Department of Nutrition, University of North Carolina
at Greensboro, 318 Stone Building, PO Box 26170,
Greensboro, NC 27402-6170, USA
e-mail: mkmcinto@uncg.edu

M. Reardon
e-mail: mareardo@uncg.edu

S. Govern
e-mail: semone.ayala@gmail.com

K. Martinez
e-mail: kbmarti2@uncg.edu

W. Shen
e-mail: w_shen@uncg.edu

T. Reid
e-mail: TMGELLY@uncg.edu

MAPK	Mitogen-activated protein kinase
MCP	Monocyte chemoattractant protein
MEK	Mitogen-activated protein kinase kinase
MUFA	Monounsaturated fatty acid(s)
NF- κ b	Nuclear factor kappa B
PPAR	Peroxisome proliferator activated receptor
SCD	Stearoyl-CoA desaturase
SREBP	Sterol regulatory element binding protein
SV	Stromal vascular
TG	Triglyceride(s)

Introduction

Losing body fat without reducing food intake or increasing physical activity is attractive to many who want to lose weight. One approach is consumption of conjugated linoleic acid (CLA), a fatty acid found in dairy products and ruminant meats and in supplements and fortified foods marketed worldwide for weight loss. Indeed, a meta-analysis of 18 clinical studies revealed that adults that consumed daily an average of 3.2 g of an equal mixture of two CLA isomers, *cis*-9,*trans*-11 (9,11) and *trans*-10,*cis*-12 (10,12) lost approximately 0.2 lb of body fat per week without changing food intake [1]. Intriguingly, mice consuming higher amounts of CLA than humans lose body fat more rapidly, but may concurrently develop side effects including chronic inflammation, insulin resistance, or lipodystrophy [2].

Only the 10,12 isomer reduces adiposity or delipidated adipocytes. However, at high doses 10,12 CLA alone and an equal mixture of 10,12 and 9,11 CLA has been reported to cause inflammation, lipodystrophy, or insulin resistance in mice [2] and human subjects [3, 4]. In contrast, the 9,11 isomer alone has anti-inflammatory and adipogenic properties, and improves insulin sensitivity in mice [5, 6]. Proposed anti-obesity mechanisms of 10,12 CLA include regulation of (1) energy metabolism, (2) adipogenesis, (3) lipid metabolism, (4) inflammation, and (5) adipocyte apoptosis (reviewed in [7]). However, direct linkages of these potential mechanisms to body fat loss, especially inflammation, are unclear.

One potential mechanism by which CLA decreases adiposity is by repressing the expression or activity of lipogenic enzymes such as stearoyl-CoA desaturase-1 (SCD-1), the rate-limiting enzyme required for the synthesis of monounsaturated fatty acids (MUFA), thereby reducing the synthesis of phospholipids and neutral lipids. Such reductions in these lipids could cause cell stress given their important role in regulating membrane function and eicosanoid synthesis. Consistent with this hypothesis, 10,12 CLA alone or a mixture of 10,12 and 9,11 CLA decreases the levels of MUFA in rodents [8, 9], 3T3L1 adipocytes [10], and primary human

adipocytes [11, 12]. We also recently found in primary human adipocytes that (1) 10,12 CLA decreased the expression of SCD-1 and of two transcription factors that regulate SCD-1 transcription, sterol regulatory element binding protein (SREBP)-1C and liver X receptor (LXR) α , within 5–7 h of treatment, and (2) 10,12, but not 9,11 CLA completely ablated the protein levels of SCD-1 after 12 h of treatment [12]. However, 10,12 CLA supplementation reduced body weight in SCD-1 knockout mice, simultaneously increasing the ratio of C16:0/16:1 fatty acids and decreasing the ratio of C18:0/18:1 fatty acids [13], suggesting CLA's reduction in adiposity is independent of SCD-1.

Consequences of inhibiting SCD-1 activity include increasing the ratio of saturated fatty acids to MUFA, which is known to cause inflammation and insulin resistance (reviewed in [14]). Thus, we hypothesized that supplementing 10,12 CLA-treated cultures with the MUFA oleic acid (C18:1) would overcome this anticipated blockade of MUFA synthesis, thereby mitigating cell stress associated with deficiencies in phospholipids and neutral lipids. To test this hypothesis, we supplemented 10,12 CLA-treated primary human adipocytes with micromolar levels oleic acid for 12 h to 7 days, and measured inflammatory gene and protein expression, insulin-stimulated glucose uptake, lipid content, and the expression of several G protein receptors (GPR). To show the specificity of MUFA, we also pretreated cultures with stearic acid, a substrate for SCD-1, and 9,11 CLA. Consistent with our hypothesis, oleic acid reduced inflammatory gene expression in a dose-dependent manner, and restored the lipid content of 10,12 CLA-treated adipocytes without improving insulin-stimulated glucose uptake. In contrast, supplementation with stearic acid, a substrate for SCD-1, or 9,11 CLA did not prevent increased inflammatory gene expression by 10,12 CLA. Lastly, 10,12 CLA affected the expression of several GPR, cell surface receptors that respond to extracellular stimuli including free fatty acids (FFA), which was attenuated by oleic acid. Collectively, these data show that oleic acid supplementation attenuates 10,12 CLA-induced inflammatory gene expression and lipid content, possibly by alleviating cell stress caused by the inhibition of MUFA needed for phospholipid and neutral lipid synthesis.

Materials and Methods

Materials

All cell-culture wares and Hyclone fetal bovine serum were purchased from Fisher Scientific. Adipocyte medium (AM-1) was purchased from Zen-Bio. Isomers of CLA (+98 % pure) were purchased from Matreya (Pleasant Gap, PA). Gene expression assays for interleukin-1 β (IL-1 β), IL-6, IL-8, cyclooxygenase-2 (COX-2), monocyte chemoattractant

protein-1 (MCP-1), and glyceraldehyde-3-phosphate dehydrogenase (GAPDH) were purchased from Applied Biosystems Inc. (Foster City, CA). The polyclonal antibody for anti-GAPDH and activating transcription factor (ATF)3 were obtained from Santa Cruz Biotechnology (Santa Cruz, CA). Anti-total or anti-phospho (P) JNK, ERK, I κ B α , and P-cJun antibodies were purchased from Cell Signaling Technologies (Beverly, MA). GW9508 was purchased from Tocris Bioscience (Ellisville, MO). All other chemicals and reagents were purchased from Sigma unless otherwise stated.

Cell Culture Model

Abdominal adipose tissue was obtained from non-diabetic Caucasian and African–American females between the ages of 20 and 50 years old with a body mass index ≤ 32.0 who had undergone elective surgery as previously described [15]. These selection criteria allow for reduced variation in gender, age, and obesity status. Institutional Review Board approval was granted through the University of North Carolina at Greensboro and the Moses H. Cone Memorial Hospital. Stromal vascular (SV) cells from human adipose tissue were isolated via collagenase digestion and subsequently grown as described previously [15]. Cells were differentiated in differentiation media [i.e., AM-1 supplemented with 250 μ M isobutylmethylxanthine and 1 μ M rosiglitazone (BRL49653; a PPAR γ agonist generously provided by Dr. Per Sauerberg at Novo Nordisk A/S, Copenhagen, Denmark)] for 3 days. Subsequently, differentiated cultures were maintained in AM-1 only for 7–14 days. These cultures contain approximately 50 % adipocytes and 50 % preadipocytes by day 7. CLA isomers were given at physiological levels [16, 17]. Oleic acid was given at micromolar levels given its abundance in human blood [18] and adipocytes [11]. Fatty acids were complexed to fatty acid-free (>98 %) bovine serum albumin (BSA; Sigma A7030, lot #040M1649) at a 4:1 molar ratio. This BSA was chosen based on its decreased capacity to increase inflammatory gene expression compared to other BSA samples tested (unpublished data). BSA levels were normalized to the highest fatty acid treatment so that all cultures contained the same amount of BSA vehicle. Fatty acid treatments were added at the same time. Each experiment was repeated in triplicate using a mixture of cells from at least two different subjects unless otherwise indicated.

RNA Isolation and Real-Time Quantitative PCR (qPCR)

Primary human SV cells were seeded in 35-mm dishes at 0.4×10^6 cells per dish and differentiated for 3 days. The media was changed on days 3 and 6. Cells were treated on

day 7 with fatty acids or BSA vehicle control. After 18 h RNA was isolated from cell cultures using the RNeasy mini kit (Qiagen, Valencia, CA) following the manufacturer's protocol for human adipocytes. For real time qPCR, 2 μ g of total RNA was used to generate first strand cDNA using the Applied Biosystems high capacity cDNA archive kit. qPCR was performed using a 7500 fast real-time PCR system (Applied Biosystems) using Taqman[®] universal PCR master mix and Taqman gene expression assays. To account for possible variation related to cDNA input amounts or the presence of PCR inhibitors, the endogenous reference gene GAPDH was quantified simultaneously for each sample in separate wells of the same 96-well plate.

Lipid Content Determination

Primary human SV cells were seeded in 12-well plates at 2×10^6 cells per plate and differentiated for 3 days. The media was changed to AM-1 on days 3 and 6. Cells were treated on days 7 and 11 with fatty acids or BSA control. On day 14, the media was removed and cell cultures were washed with Hank's balanced salt solution (HBSS). The presence of intracellular lipid was visualized by staining the cultures with oil red O, and lipid content was quantified based on absorbance levels at 540 nm as we previously described [11].

Immunoblotting

Immunoblotting using 20 μ g of protein per lane was conducted using 4–12 % NuPage Pre-Cast Gels (Invitrogen) as previously described [19]. Briefly, PVDF membranes were blocked with 5 % milk in TBST for 1 h and washed 3 \times in TBST for 5 min. Blots were incubated overnight at 4 $^{\circ}$ C with primary antibodies targeting I κ B α , P-cJun, P-JNK, P-ERK, total cJun, total ERK, and ATF3 at a dilution of 1:1,000, and subsequently incubated in the respective horseradish peroxidase-conjugated secondary antibody at a dilution of 1:5,000 at room temperature for 1 h. Primary and secondary antibodies targeting GAPDH were used at a 1:5,000 dilution. After washing, blots were treated with chemiluminescence reagent for 1 min and film was exposed using a SRX-101A Konica Minolta film developer. Densitometry was performed using a Kodak image station 440 CF by Perkin Elmer and Kodak molecular imaging software version 4.0.

Insulin-Stimulated 2-[³H]Deoxy-glucose (2-DOG) Uptake

Primary human SV cells were seeded in 12-well plates at 1.6×10^5 per well and differentiated for 12 days. On day 12, media were changed to serum free low glucose

(5 mmol/L) media. Twenty-four hours later, cultures were pretreated with fatty acids or BSA control. The culture media was removed and replaced with 0.5 mL of HBSS without or with 100 nmol/L human insulin for 10 min. After insulin preincubation, 4 nM 2-DOG (0.5 μ Ci per well) was added to each well and incubated at 37 °C for 90 min. Basal and insulin-stimulated 2-DOG uptake were measured as described previously [11].

Statistical Analysis

Data are expressed as means \pm SEM. Data were analyzed using one-way analysis of variance followed by Student's *t* tests for each pair for multiple comparisons. Differences were considered significant if $p < 0.05$. All analyses were performed using JMP IN version 9.0 software (SAS Institute, Cary, NC).

Results

Oleic Acid Attenuates 10,12 CLA-Mediated Inflammatory Gene Expression and Delipidation

In order to determine the extent to which 10,12 CLA-induced inflammatory gene expression was caused by inhibition of SCD-1-mediated MUFA synthesis [11, 12], we co-supplemented 10,12 CLA-treated primary human adipocytes with oleic acid. Oleic acid and 9,11 CLA alone had no effect on inflammatory gene expression (Fig. 1). Consistent with our hypothesis, 10,12 CLA-mediated increases in the expression of IL-6, IL-8, COX-2, and II-1 β were decreased in a dose-dependent manner by co-supplementation with oleic acid (Fig. 1). However, oleic acid did not prevent 10,12 CLA-mediated activation of ERK, JNK, cJun, or I κ B α or increased abundance of ATF3 (data not shown). Given the decrease in the inflammatory response by oleic acid, we speculated that oleic acid would also attenuate 10,12 CLA-induced delipidation. Indeed, 10,12 CLA-mediated delipidation was blocked by co-supplementation with oleic acid (Fig. 2). However, oleic acid did not prevent 10,12 CLA-mediated insulin resistance (data not shown).

Stearic Acid or 9,11 CLA Supplementation do not Attenuate 10,12 CLA-Mediated Inflammatory Gene Expression or Delipidation

In order to determine the specificity of oleic acid inhibition of inflammatory gene expression in 10,12 CLA-treated cultures, primary human adipocytes were co-supplemented with stearic acid, a substrate for SCD-1 and a precursor to oleic acid. Unlike oleic acid, stearic acid alone increased

the expression of IL-6, IL-8, and COX-2 (Fig. 3), consistent with the reported effects of saturated fatty acids on markers of inflammation (reviewed in [14]). Furthermore, stearic acid co-supplementation did not attenuate 10,12-mediated inflammatory gene expression (Fig. 3). In fact, the two highest levels of stearic acid exacerbated 10,12 CLA-mediated induction of inflammatory genes.

Because of the reported anti-inflammatory and anti-diabetic properties of 9,11 CLA [5], we co-supplemented 10,12 CLA-containing cultures with 9,11 CLA. Although 9,11 CLA alone did not increase inflammatory gene expression, its inclusion in the 10,12 CLA-treated cultures did not prevent 10,12 CLA-mediated inflammatory gene expression (Fig. 4) or delipidation (data not shown). These data demonstrate that the 9,11 CLA isomer does not directly prevent 10,12 CLA-mediated inflammatory gene expression or delipidation in vitro. Collectively, these data suggest that CLA-mediated inflammatory gene expression is due, in part, to lack of oleic acid, an abundant MUFA [11, 18] required by mammalian cells for the synthesis of phospholipids and neutral lipids.

Oleic Acid Influences the Effects of 10,12 CLA on GPR Expression

Free fatty acids activate FFA receptors, including G-protein-coupled receptors (GPCR) and GPR, that impact inflammatory signaling and metabolism (reviewed in [20]). Notably, activation of GPR120 has anti-inflammatory properties. Therefore, we examined the effects of 10,12 CLA in the absence and presence of oleic acid on the expression of several GPR expressed in adipocytes. Interestingly, 10,12 CLA decreased the expression of GPR120, but increased the expression of GPR56 and GPRC5A (Fig. 5a). Furthermore, the GPR40/120 agonist GW9508 attenuated 10,12 CLA-mediated increase of inflammatory gene expression and suppression of lipogenic gene expression (Fig. 5b). Intriguingly, oleic acid supplementation attenuated 10,12 CLA-mediated suppression of GPR120, and induction of GPRC5A (Fig. 5c), but not GPR56 (data not shown). Taken together, these data suggest that 10,12 CLA influences specific GPR that impact signaling pathways involved in inflammation and lipogenesis.

Discussion

Consistent with our hypothesis, oleic acid supplementation attenuated 10,12 CLA-induced inflammatory gene expression (Fig. 1) and delipidation (Fig. 2) in primary human adipocytes. In contrast, stearic acid, a substrate for SCD-1, or 9,11 CLA did not prevent 10,12 CLA-mediated increase

Fig. 1 Cultures of primary human adipocytes were treated without or with 30–300 μM oleic acid (OA), 50 μM 9,11 CLA, or 50 μM 10,12 CLA for 12 h. Subsequently, mRNA levels of IL-8, IL-6, IL-1 β , COX-2, and GAPDH (load control) were measured using qPCR. Data were normalized to BSA vehicle controls (OA, 0, -CLA). Means \pm SE ($n = 3$ –4) not sharing a common superscript (a–e) are significantly different ($p < 0.05$). Data are representative of three independent experiments

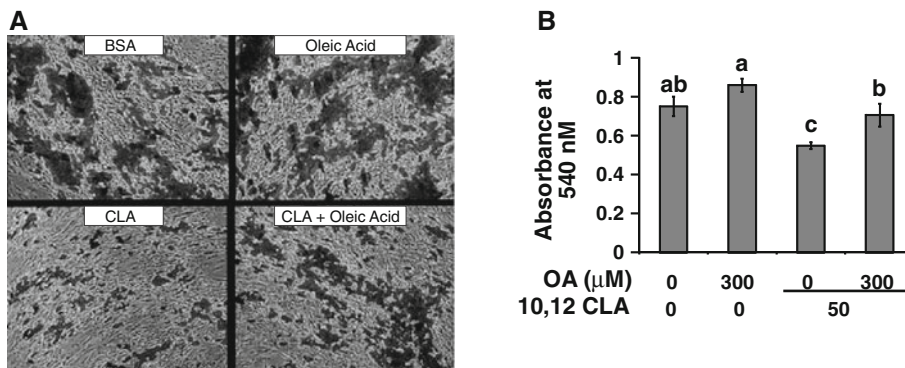
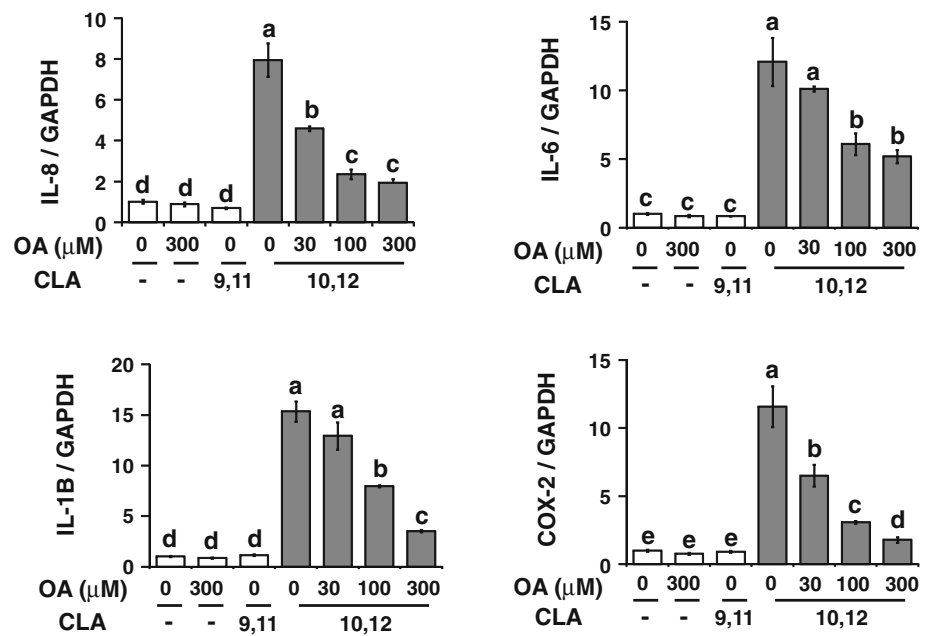


Fig. 2 Cultures of primary human adipocytes were treated without or with 300 μM oleic acid (OA), 50 μM 10,12 CLA, or BSA vehicle (0 OA, 0 CLA) for 7 days. Subsequently, **a** cultures were stained with oil red O and photographed using an Olympus inverted microscope

with a 20 \times objective and **b** the stain concentration was quantified. **b** Means \pm SE ($n = 3$) not sharing a common superscript (a–c) are significantly different ($p < 0.05$). Data are representative of two independent experiments

in inflammatory gene expression (Figs. 3, 4) or delipidation (data not shown). These data are consistent with our previous findings in primary human adipocytes showing that 10,12 CLA decreased (1) de novo lipid synthesis within 24–72 h, (2) the MUFA/saturated fatty acid ratio within 24 h, (3) the mRNA and protein levels of SCD-1 within 7 h in an isomer-specific fashion, and (4) the expression of LXR α and SREBP-1c within 5 h [12]. They are also consistent with data obtained from mice [8, 9], and murine [10, 21–23] or porcine [24] (pre)adipocytes, suggesting that 10,12 CLA rapidly reduces the abundance or activity of SCD-1. Collectively, these data suggest that by reducing the abundance or levels of lipogenic transcription factors that control SCD-1 (i.e., LXR α , SREBP-1c, PPAR γ), 10,12 CLA suppresses the synthesis of MUFA needed for phospholipid and neutral lipid synthesis, storage, or

metabolism. Such a scenario could conceivably cause cell stress that impairs the adipocyte's capacity to sequester, synthesize, and store lipids. Consistent with this hypothesis, we previously demonstrated that 10,12 CLA, but not 9,11 CLA, decreased de novo lipid synthesis of triglycerides (TG), FFA, diacylglycerol, cholesterol esters, cardiolipin, phospholipids, and ceramides in human adipocytes within 3–24 h [12].

Ntambi first proposed that 10,12 CLA-mediated inhibition of SCD-1 in mice [10, 21, 22] and in humans [23] is important for its anti-lipogenic effects. SCD-1 and diacylglycerol transferase-2 (DGAT2) have been shown to colocalize in the ER and be important for TG synthesis [25]. Dietary and endogenous palmitate (C16:0) and stearate (C18:0) are desaturated by SCD-1 and channeled to DGAT2 for the final step in TG synthesis in the ER. This

Fig. 3 Cultures of primary human adipocytes were treated without or with 10–100 μM stearic acid (SA), 50 μM 9,11 CLA, or 50 μM 10,12 CLA for 12 h. Subsequently, mRNA levels of IL-8, IL-6, IL-1 β , COX-2, and GAPDH (load control) were measured using qPCR. Data were normalized to BSA vehicle controls (SA, 0, -CLA). Mean \pm SE ($n = 3\text{--}4$) not sharing a common superscript (a–e) are significantly different ($p < 0.05$). Data are representative of two independent experiments

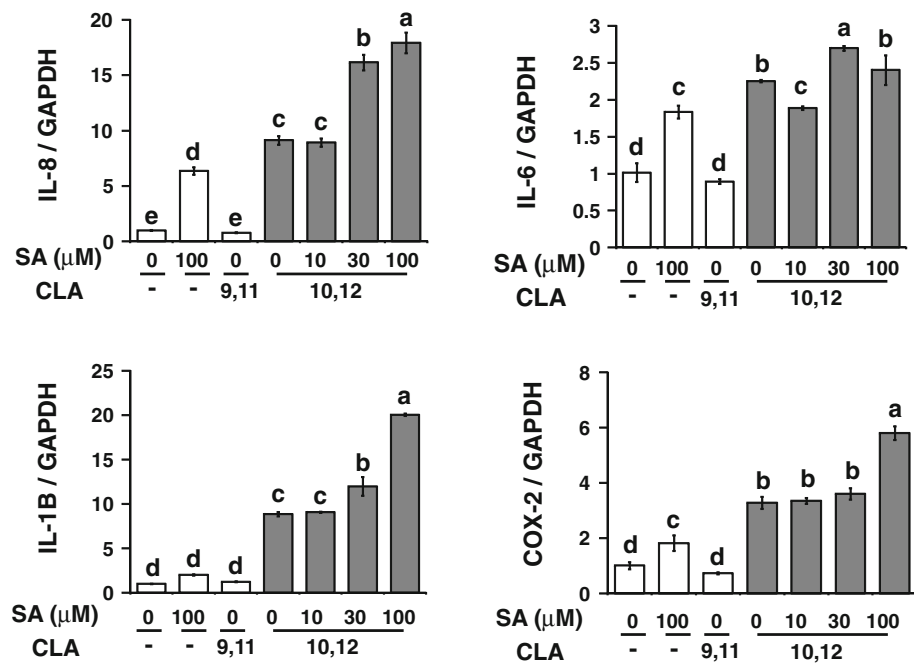
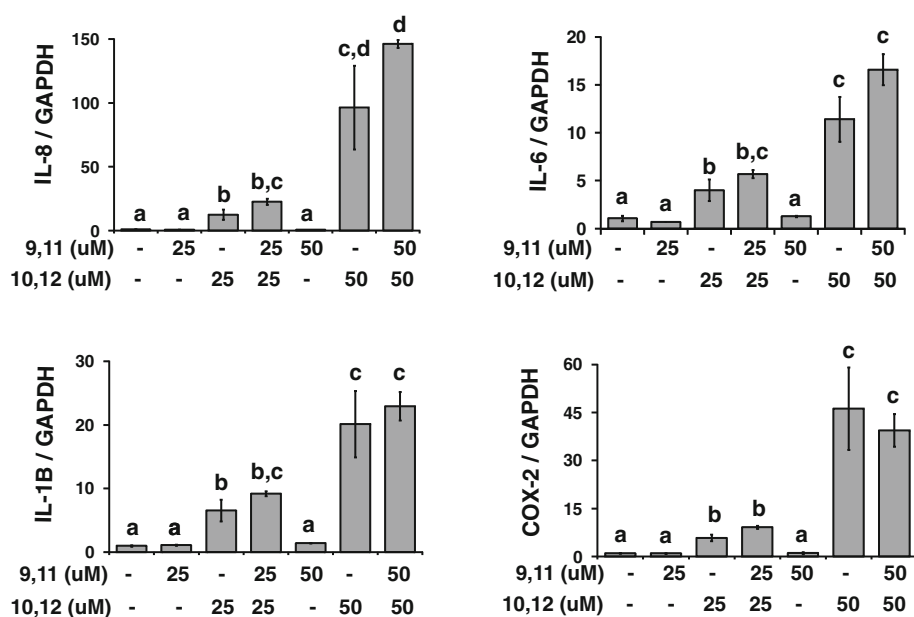


Fig. 4 Cultures of primary human adipocytes were treated without or with 25–50 μM 9,11 CLA, or 10,12 CLA for 18 h. Subsequently, mRNA levels of IL-8, IL-6, IL-1 β , COX-2, and GAPDH (load control) were measured using qPCR. Data were normalized to BSA vehicle controls (–9,11, –10,12 CLA). Mean \pm SE ($n = 3\text{--}4$) not sharing a common superscript (a–e) are significantly different ($p < 0.05$). Data are representative of three independent experiments



close association between SCD-1 and DGAT2 enhances the efficiency of TG synthesis [25]. However, 10,12 CLA-mediated reduction in body fat mass was similar in SCD-1 knockout and wild type mice, suggesting that the reduction in adiposity by 10,12 CLA is independent of SCD-1 in mice [13]. Indeed, SCD-1 is not the only lipogenic gene suppressed by 10,12 CLA, given its antagonism of the key lipogenic transcription factors LXR α , SREBP-1c, and PPAR γ (reviewed in [7]).

We anticipated that, because oleic acid supplementation attenuated inflammatory gene expression, it would also

decrease the activation of upstream transcription factors and mitogen-activated protein kinases (MAPK) controlling the expression of these genes. However, 10,12 CLA-mediated activation of ERK, JNK, cJun, ATF3, and NF- κ B was not inhibited by oleic acid supplementation (data not shown). Reasons for this lack of inhibition of inflammatory transcription factors and MAPK are unclear, as we have previously shown that inhibiting 10,12 CLA-mediated activation of NF- κ B [26], cJun [27], ERK [15], and JNK [19] attenuates 10,12 CLA-mediated inflammatory gene expression. Perhaps 10,12 CLA's reported increase in the

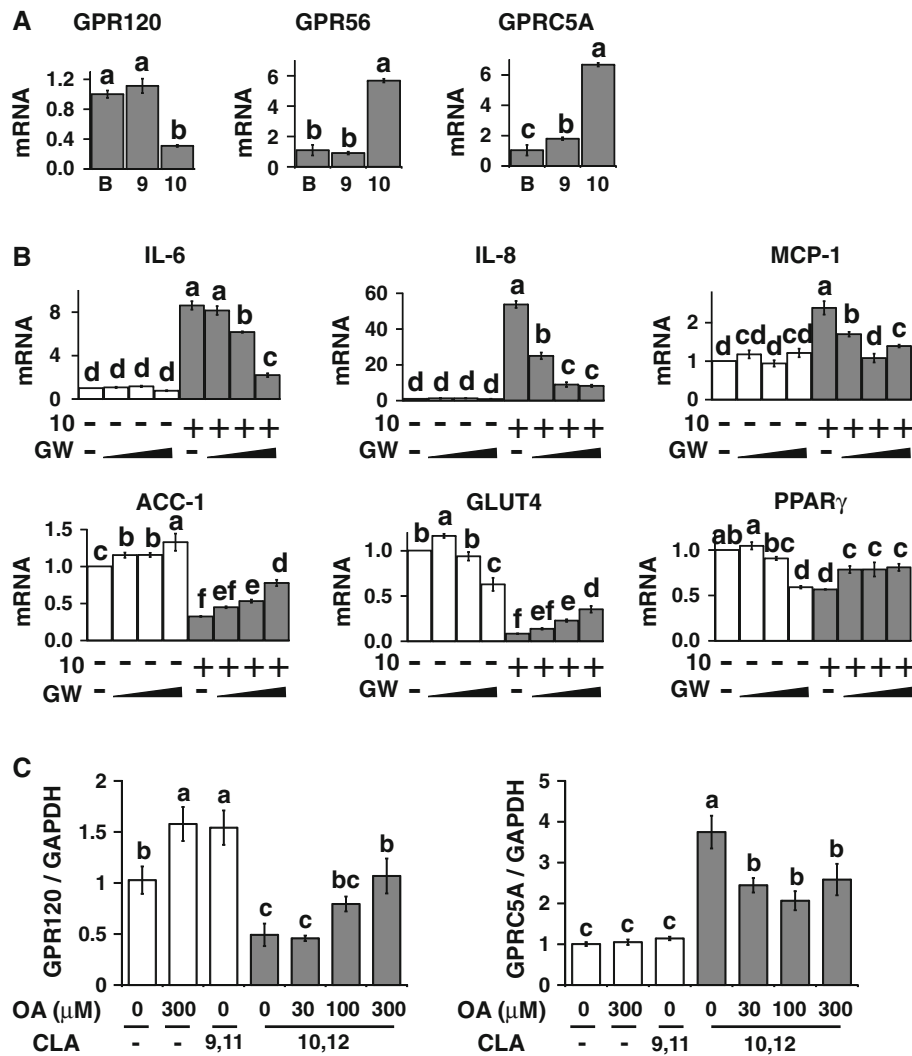


Fig. 5 Cultures of primary human adipocytes were treated without or with: **a** 50 μ M 9,11 CLA, 10,12 CLA, or BSA vehicle for 12 h; **b** 50 μ M 10,12 CLA or 1, 10, or 100 μ M GW9508 for 18 h; or **c** 30–300 μ M oleic acid (OA), 50 μ M 9,11 CLA, or 50 μ M 10,12 CLA for 12 h. Subsequently, mRNA levels of candidate genes were measured using

qPCR. Data were normalized to BSA vehicle controls. Means \pm SE ($n = 3-4$) not sharing a common superscript (**a-f**) are significantly different ($p < 0.05$). Data are representative of at least two independent experiments

typical integrated stress response [28] or atypical ER stress response [29] contributes to the induction of inflammatory gene expression independent of NF- κ B, AP-1, or MAPK.

Alternatively, oleic acid may attenuate 10,12 CLA-mediated inflammatory gene expression by impacting specific GPCR or GPR that regulate inflammatory signaling and delipidation. GPR40, 84, 119, and 120 are classically activated by long chain FFA, and GPR41 and 43 by short chain FFA. Importantly, (1) cell surface, FFA receptors [30–32] and putative GPCR [33–35] activated by FFA impact on cell signaling, (2) CLA reduces FFA transport in tumors and white adipose tissue by activating specific GPCR [36, 37], (3) CLA increased pancreatic insulin release via islet GPR40 [38], and (4) we found that impairing coupling between GPCR and Gi/o with pertussis

toxin blocked 10,12 CLA's suppression of PPAR γ target gene expression and lipid metabolism in adipocytes [15].

Notably, long chain unsaturated FFA such as docosahexanoic acid activate GPR120, which is highly expressed in adipose tissue and contributes to their anti-inflammatory properties [30]. GPR120 also binds other mono- and polyunsaturated fatty acids including oleic acid [39]. Consistent with these data, we found that (1) oleic acid increased GPR120 expression (Fig. 5c), (2) 10,12 CLA decreased the expression of GPR120 (Fig. 5a,c), which was attenuated by supplementation with oleic acid (Fig. 5c), (3) the GPR40/120 agonist GW9508 attenuated 10,12 CLA-mediated inflammatory gene expression and suppression of lipogenic gene expression (Fig. 5b), (4) oleic acid supplementation inhibited 10,12 CLA-mediated suppression of

GPR120 (Fig. 5c), and (5) 10,12 CLA had no effect on the expression of GPR40 (data not shown), which had very low levels of expression in primary human adipocytes. These data suggest that 10,12 CLA's pro-inflammatory effects may be linked upstream to its inhibition of GPR120. Studies on the activity of GPR120 in cells treated with 10,12 CLA are needed to test this hypothesis.

We also measured the expression of GPR56 and GPRC5A, members of the non-classical adhesion [40] and tumor suppressor [41] families reported to be expressed in inflamed tissues [42], respectively, that we identified as CLA-induced candidates in a microarray assay (unpublished data). Indeed, 10,12 CLA increased the expression of GPRC5A and GPR56 (Fig. 5a), and oleic acid supplementation decrease this response for GPRC5A (Fig. 5c). Aside from the fact that these GPR are expressed in inflamed tissues, the physiological significance of these GPR findings in primary human adipocytes is unclear at this time.

Taken together, these data demonstrate that oleic acid supplementation attenuates 10,12 CLA-induced inflammatory gene expression and delipidation in primary human adipocytes, possibly by alleviating cell stress [28, 29] caused by the inhibition of SCD-1 [11, 12]. Our previous findings showed that 10,12 CLA rapidly reduces de novo lipid synthesis proceeded by inhibition of transcriptional regulators of lipogenesis and their downstream targets, including SCD-1 [12]. Therefore, we hypothesize that these changes impair MUFA synthesis needed for phospholipid and neutral lipid accumulation, thereby delipidating human adipocytes.

Acknowledgments This work was supported by grants from the National Institute of Health (NIH) National Institute of Diabetes and Digestive and Kidney Diseases/Office of Dietary Supplements (NIDDK/ODS) (5R01-DK063070) to MM, the NIH F31DK084812 to KM, and the UNCG Undergraduate Research Assistantship Program to MR and SG.

Conflict of interest None.

References

1. Whigham LD, Watras AC, Schoeller DA (2007) Efficacy of conjugated linoleic acid for reducing fat mass: a meta-analysis in humans. *Am J Clin Nutr* 85:1203–1211
2. Poirier H, Niot I, Clement L, Guerre-Millo M, Besnard P (2005) Development of conjugated linoleic acid (CLA)-mediated lipotrophic syndrome in the mouse. *Biochimie* 87:73–79
3. Risérus U, Arner P, Brismar K, Vessby B (2002) Treatment with dietary *trans*-10,*cis*-12 conjugated linoleic acid causes isomer specific insulin resistance in obese men with the metabolic syndrome. *Diabetes Care* 25:1516–1521
4. Tholstrup T, Raff M, Staarup E, Lund P, Basu S, Bruun JM (2008) An oil mixture with *trans*-10,*cis*-12 conjugated linoleic acid increases markers of inflammation and in vivo lipid peroxidation compared with *cis*-9,*trans*-11 conjugated linoleic acid in postmenopausal women. *J Nutr* 138:1445–1451
5. Moloney F, Toomey S, Noone E, Nugent A, Allan B, Loscher CE, Roche HM (2007) Antidiabetic effects of *cis*-9,*trans*-11 conjugated linoleic acid may be mediated via anti-inflammatory effect in white adipose tissue. *Diabetes* 56:574–582
6. Halade G, Halade GV, Rahman MM, Fernandes G (2010) Differential effects of conjugated linoleic acid isomers in insulin-resistant female C57bl/6j mice. *J Nutr Biochem* 21:332–337
7. Kennedy A, Martinez K, Schmidt S, Mandrup S, Lapoint K, McIntosh M (2010) Antiobesity mechanisms of action of conjugated linoleic acid. *J Nutr Biochem* 21:171–179
8. Martin JC, Grégoire S, Siess MH, Genty M, Chardigny JM, Berdeaux O, Juaneda P, Sébédio JL (2000) Effects of conjugated linoleic acid isomers on lipid metabolizing enzymes in male rats. *Lipids* 35:91–98
9. House RL, Cassady JP, Eisen EJ, Eling TE, Collins JB, Grissom SF, Odle J (2005) Functional genomic characterization of delipidation elicited by *trans*-10,*cis*-12 conjugated linoleic acid (t10c12-CLA) in a polygenic obese line of mice. *Physiol Genomics* 21:351–361
10. Choi Y, Kim YC, Han YB, Park Y, Pariza MW, Ntambi JM (2000) The *trans*-10,*cis*-12 isomer of conjugated linoleic acid downregulates stearoyl-CoA desaturase-1 gene expression in 3T3-L1 adipocytes. *J Nutr* 130:1920–1924
11. Brown M, Sandberg-Boysen M, Skov S, Morrison R, Storkson J, Lea-Currie R, Pariza M, Mandrup S, McIntosh M (2003) Isomer specific regulation of metabolism and PPAR γ by conjugated linoleic acid (CLA) in human preadipocytes. *J Lipid Res* 44:1287–1300
12. Obsen T, Faergeman N, Chung S, Martinez K, Gobern S, Loreau L, Wabitsch L, Mandrup SM, McIntosh M (2012) *trans*-10,*cis*-12 Conjugated linoleic acid decreases de novo lipid synthesis in human adipocytes. *J Nutr Biochem* 23:580–590
13. Kang K, Miyazaki M, Ntambi JM, Pariza MW (2004) Evidence that the antiobesity effect of conjugated linoleic acid is independent of effects on stearoyl-CoA desaturase-1 expression and enzyme activity. *Biochem Biophys Res Commun* 315:532–537
14. Kennedy A, Martinez K, Chuang CC, LaPoint K, McIntosh M (2009) Saturated fatty acid-mediated inflammation and insulin resistance in adipose tissue—mechanisms of actions and implications. *J Nutr* 139:1–4
15. Brown JM, Boysen MS, Chung S, Fabyi O, Morrison RF, Mandrup S, McIntosh M (2004) Conjugated linoleic acid induces human adipocyte delipidation: autocrine/paracrine regulation of MEK/ERK signaling by adipocytokines. *J Biol Chem* 279:26735–26747
16. Mougios V, Matsakas A, Petridou A, Ring S, Sagredos A, Melissopoulous A, Tsigilis N, Nikolaidis M (2001) Effect of supplementation with conjugated linoleic acid on human serum lipids and body fat. *J Nutr Biochem* 12:585–594
17. Petridou A, Mougios V, Sagredos A (2003) Supplementation with CLA: isomer incorporation into serum lipids and effect on body fat of women. *Lipids* 38:805–811
18. Martinez K, Kennedy A, McIntosh M (2011) JNK inhibition by SP600125 attenuates *trans*-10,*cis*-12 conjugated linoleic acid-mediated regulation of inflammation and lipogenic gene expression. *Lipids* 46:885–892
19. Samieri C, Feart C, Proust-Lima C, Peuchant E, Tzourio C, Stapf C, Berr C, Barberger-Gateau P (2011) Olive oil consumption, plasma oleic acid, and stroke incidence. *Neurology* 77:418–425
20. Oh DY, Lagakos WS (2011) The role of G-protein-coupled receptors in mediating the effects of fatty acids on inflammation and insulin sensitivity. *Curr Opin Clin Nutr Metab Care* 14:322–327

21. Lee K, Pariza M, Ntambi J (1998) Conjugated linoleic acid decreases hepatic stearoyl CoA desaturase mRNA expression. *Biochem Biophys Res Commun* 248:817–821
22. Park Y, Storkson J, Ntambi J, Cook M, Sih C, Pariza M (2000) Inhibition of hepatic stearoyl-CoA desaturase activity by *trans*-10,*cis*-12 CLA and its derivative. *Biochem Biophys Acta* 1486:285–292
23. Choi Y, Park Y, Pariza M, Ntambi J (2001) Regulation of stearoyl-CoA desaturase activity by *trans*-10,*cis*-12 CLA in HepG2 cells. *Biochem Biophys Res Commun* 284:689–693
24. Brandebourg TD, Hu CY (2005) Isomer-specific regulation of differentiating pig preadipocytes by conjugated linoleic acids. *J Anim Sci* 83:2096–2105
25. Man WC, Miyazaki M, Chu K, Ntambi J (2006) Co-localization of SCD1 and DGAT2: implying preference for endogenous monounsaturated fatty acids in triglyceride synthesis. *J Lipid Res* 47:1928–1939
26. Chung S, Brown JM, Provo JN, Hopkins R, McIntosh M (2005) Conjugated linoleic acid promotes human adipocyte insulin resistance through NFκB-dependent cytokine production. *J Biol Chem* 280:38445–38456
27. Martinez K, Kennedy A, West T, Milatovic D, Aschner M, McIntosh M (2010) *trans*-10,*cis*-12 Conjugated linoleic acid instigates inflammation in human adipocytes compared to preadipocytes. *J Biol Chem* 285:17701–17712
28. LaRosa P, Riethoven J, Chen H, XIA Y, Zhou YL, Chen M, Miner J, Fromm M (2007) *trans*-10,*cis*-12 Conjugated linoleic acid activates the integrated stress response pathway in adipocytes. *Physiol Genomics* 31:544–553
29. Ou L, Wu Y, Ip C, Meng X, Hsu Y, Ip M (2008) Apoptosis induced by t10,c12 conjugated linoleic acid is mediated by an atypical endoplasmic reticulum stress response. *J Lipid Res* 49:985–994
30. Oh DY, Talukdar SE, Bae J, Imamura T, Morinaga H, Fan W, Li P, Lu WJ, Watkins SM, Olefsky SM (2010) GPR120 is an omega-3 fatty acid receptor mediating potent anti-inflammatory and insulin-sensitizing effects. *Cell* 142:687–698
31. Kotarsky K, Nilsson NE, Flodgren E, Owman C, Olde B (2003) A human cell surface receptor activated by free fatty acids and thiazolidinedione drugs. *Biochem Biophys Res Commun* 301:406–410
32. Soto-Guzman A, Robledo T, Lopez-Perez M, Salazar EP (2008) Oleic acid induces Erk1/2 activation and Ap-1 DNA binding activity through a mechanism involving Src kinase and EGFR transactivation in breast cancer cells. *Mol Cell Endocrinol* 294:81–91
33. Briscoe CP, Tadayyon M, Andrews JL, Benson WG, Chambers JK, Eilert MM, Ellis C, Elshourbagy NA, Goetz AS, Minnick DT, Murdock PR, Sauls HR, Shabon U, Spinage LD, Strum JC, Szekeres PG, Tan KB, Way JM, Ignar DM, Wilson S, Muir AI (2003) The orphan G protein-coupled receptor GPR40 is activated by medium and long chain fatty acids. *J Biol Chem* 278:11303–11311
34. Qanbar R, Bouvier M (2003) Role of palmitoylation/depalmitoylation reactions in G-protein-coupled receptor function. *Pharmacol Ther* 97:1–33
35. Itoh Y, Kawamata Y, Harada M, Kobayashi M, Fujii R, Fukusumi S, Ogi K, Hosoya M, Tanaka Y, Uejima H, Tanaka H, Maruyama M, Satoh R, Okubo S, Kizawa H, Komatsu H, Matsumura F, Noguchi Y, Shinohara T, Hinuma S, Fujisawa Y, Fujino M (2003) Free fatty acids regulate insulin secretion from pancreatic beta cells through GPR40. *Nature* 422:173–176
36. Sauer LA, Dauchy RT, Blask DE, Krause JA, Davidson LK, Dauchy EM, Welham KJ, Coupland K (2004) Conjugated linoleic acid isomers and *trans* fatty acids inhibit fatty acid transport in hepatoma 7288ctc and inguinal fat pads in buffalo rats. *J Nutr* 134:1989–1997
37. Hsu YC, Ip M (2011) Conjugated linoleic acid-induced apoptosis in mouse mammary tumor cells is mediated by both G protein-coupled receptor-dependent activation of the AMP-activated protein kinase pathway and by oxidative stress. *Cell Signal* 23:2013–2020
38. Schmidt J, Liebscher K, Merten N, Grundmann M, Mielenz J, Sauerwein H, Chistiansen E, Due-Hansen M, Ulven T, Ullrich S, Gomeza J, Drewke C, Kostenis E (2011) Conjugated linoleic acids mediate insulin release through islet G protein coupled receptor FFA1/GPR40. *J Biol Chem* 286:11890–11894
39. Hirasawa A, Tsumaya K, Awaji T, Katsuma S, Adachi T, Yamada M, Sugimoto Y, Miyazaki S, Tsujimoto G (2005) Free fatty acids regulate gut incretin glucagon-like peptide-1 secretion through GPR120. *Nat Med* 11:90–94
40. Paavola K, Stephenson J, Ritter S, Alter S, Hall R (2011) The N terminus of the adhesion G protein-coupled receptor GPR56 control receptor signaling activity. *J Biol Chem* 33:28914–28921
41. Deng J, Fukimoto J, Ye X, Men T, Van Pelt C, Chen Y, Lin X, Kadara H, Tao Q, Lotan D, Lotan R (2010) Knockout of the tumor suppressor gene GPRC5a in mice leads to NF-κB activation in airway epithelium and promotes lung inflammation and tumorigenesis. *Cancer Prev Res* 3:424–436
42. Chiesa D, Falco M, Parolini F, Bellora F, Petretto A, Romeo E, Balsamo M, Gambarotti M, Scordamaglia F, Tabellini G, Facchetti F, Vermi W, Bottino C, Moretta A, Vitale M (2010) GPR56 as a novel marker for identifying the CD56null CD16+ NK cell subset both in blood stream and in inflamed peripheral tissues. *Int Immun* 22:91–100

Of those with chronic infection, 20–30 % develop cirrhosis and hepatocellular carcinoma (HCC) [1]. Interferon (IFN)-based treatment regimens have been widely used, but these treatment regimens have side effects, require long-term therapy, and are expensive. Estimation of the effectiveness of IFN-based therapy prior to treatment would be beneficial.

The velocity of decrease in viral load during IFN-based therapy is a good indicator for the prediction of sustained virological response (SVR). High SVR rates are predicted by rapid virological response (RVR) and early virological response (EVR) [2, 3]. Although mechanisms of treatment failure are poorly understood, previous reports have proposed IFN-stimulated genes and the inability to develop effective anti-HCV immunity as possible explanations [4].

Recently, fatty acids have been implicated in the pathogenesis of several diseases associated with metabolic disorders (such as obesity, diabetes and cardiovascular disease) [5, 6] and in immunological response [7]. In liver diseases, especially in non-alcoholic steatohepatitis, the effect of impaired peroxisomal polyunsaturated fatty acid metabolism and nonenzymatic oxidation on fatty acid constitution is associated with disease progression [8]. It has been reported that HCV core protein has effects on fatty acid synthesis, and that fatty droplets in the liver are related to development of disease [9, 10]. Although there have been reports about the role of fatty acids in liver in patients with HCV [9, 10], the relationship between serum fatty acids and efficacy of IFN-based antiviral therapy against HCV remains controversial.

The aims of the present study were to evaluate whether the composition of serum fatty acids could predict RVR, EVR, or SVR from IFN-based therapy in patients with HCV. Data from HCV patients were collected and in-vitro assays were performed using HCV-replication cell culture systems.

Patients and Methods

Patients

Consecutive patients with HCV treated with IFN-based therapy at Ehime University Hospital were enrolled prospectively from December 2008 to December 2010. Moreover, 10 healthy volunteers (age range 26–70 years) were enrolled in this study as healthy subjects. This study was carried out in accordance with the Declaration of Helsinki, and the institutional review board of Ehime University Hospital approved this study (Approval # 0710004). Written informed consent was provided by study participants.

Patients with chronic HCV infection, with creatinine clearance >50 mL/min, and who had not been previously

treated with antiviral or immunosuppressive agents within the 3 months preceding enrollment were included. Patients with other liver disease such as autoimmune hepatitis, primary biliary cirrhosis, hepatitis B virus (HBV) infection, or HCC; co-infection with human immunodeficiency virus; poorly controlled cardiovascular, hematologic or pulmonary disease; pregnancy; autoimmune disease; severe depression or other psychiatric disorders; and/or active substance abuse were excluded. To exclude HBV infection, hepatitis B surface antigen (HBs-Ag) and anti-hepatitis B core (HBc) antibody were checked. Patients with positive HBs-Ag or a high titer of anti-HBc antibody were excluded.

Interferon and Ribavirin Combination Therapy

Patients received one of four treatment regimens: [1] pegylated interferon (PEG-IFN) α -2b 1.0 μ g/kg/week or 1.5 μ g/kg/week subcutaneously in combination with oral ribavirin (RBV) dosed by body weight (40–65 kg, 800 mg/day; >65 –85 kg, 1,000 mg/day; >85 –105 kg, 1,200 mg/day; >105 –125 kg, 1,400 mg/day), [2] PEG-IFN α -2a 180 μ g/week subcutaneously plus oral RBV dosed as above, [3] PEG-IFN α -2a 180 μ g/week subcutaneously, or [4] IFN- β 600 million IU/day intravenously plus oral RBV dosed as above. In order to identify the levels of fatty acids that could have an important role in the response to treatment with IFN, all patients who had been treated with IFN were enrolled. After informing potential subjects about the costs, estimated adverse events, and effects of each treatment protocol according the Japanese guidelines for anti-HCV treatment [11], the required treatment regimen was chosen and treatment was started.

Laboratory Assessment

Patients' serum samples were collected around 6 a.m. after fasting on day 2 of the study before IFN-based treatment. Additionally, fasting serum was collected at the end of IFN-based treatment. Serum samples were frozen and stored at -80 °C within 4 h of collection and then thawed at the time of measurement. Fatty acid concentrations in total serum lipids was measured with liquid chromatography (SRL Co. Ltd., Tokyo, Japan). Subjects were diagnosed as having dyslipidemia if they had TC ≥ 220 mg/dL, and/or HDL-c ≤ 40 mg/dL, and/or TG ≥ 150 mg/dL [12], and/or taking lipid-lowering agents.

The HCV genotype was determined by the polymerase chain reaction (PCR) using a mixed primer set derived from nucleotide sequences from the nonstructural-5 (NS5) region (SRL Co. Ltd.) [13]. HCV RNA was measured quantitatively before and during therapy using PCR (Cobas Amplicor HCV monitor v 2.0 using the tenfold dilution method, Roche Diagnostics, Mannheim, Germany). The

lower level of detection for this assay was less than 1.2 log₁₀ IU/mL. Undetectable serum HCV RNA on testing was considered a negative test. RVR was defined as undetectable serum HCV RNA within 4 weeks from the start of the treatment. EVR was defined as undetectable serum HCV RNA within 12 weeks from the start of the treatment. SVR was defined as undetectable serum HCV RNA within 24 weeks after the end of treatment.

The HCV genotype recovered from patients was determined using the Illumina Human610-quad BeadChip (Illumina, San Diego, CA, USA) as previously described [14, 15]. Amino acid substitutions of aa70 or aa91 in the core region of HCV genotype 1b were evaluated by agarose gel electrophoresis using mutation-specific primers for wild-type (aa70: arginine, aa91: leucine) and mutant (aa70: glutamine/histidine, aa91: methionine) viruses (SRL Co. Ltd.) [16]. In this study, the pattern of arginine (wild-type) at aa70 and leucine (wild-type) at aa91 was evaluated as double wild-type, while the other patterns were non-double wild-type. The nucleotide sequence of the interferon sensitivity-determining region (ISDR) in the HCV NS5A region was determined by direct sequencing through PCR-amplified materials [17]. Wild-type ISDR was defined as having no amino acid substitutions based on the HCV-J strain of genotype 1b.

Assay for Detecting Single Nucleotide Polymorphisms of Interleukin-28B (IL-28B)

Two single nucleotide polymorphisms of interleukin-28B (rs8099917 [14] and rs12979860 [15]) were examined using the TaqMan assay. The sequence of the probe and primers for the TaqMan assay for detecting rs8099917 was provided by Dr. Yasuhito Tanaka (Department of Virology and Liver Unit, Nagoya City University Graduate School of Medical Sciences, Nagoya, Japan), and rs12979860 was provided by Dr. David B. Goldstein (Center for Human Genome Variation, Duke University, Durham, NC, USA). Patient DNA was isolated from blood samples. For rs8099917 [14], homozygotes (T/T) were defined as having the IL-28B major allele, and heterozygotes (T/G) or homozygotes (G/G) were defined as having the minor allele. For rs12979860 [25], homozygotes (C/C) were defined as having the major allele, and heterozygotes (T/C) or homozygotes (T/T) were defined as having the minor allele.

Preparation of the In-Vitro Replication System

The human hepatoma cell lines Huh7 (Japanese Collection of Research Bioresources, Osaka, Japan) and Huh7.5.1 (provided by Dr. Francis V. Chisari; Department of Immunology and Microbial Science, The Scripps Research

Institute, La Jolla, CA, USA) were cultured with Dulbecco's modified Eagle's medium (DMEM) (Sigma Chemical, St. Louis, MO, USA) containing 10 % fetal bovine serum (Filtron PTY LTD, Brooklyn, Australia).

For the in-vitro assay of HCV genotype 1, the plasmid-based binary HCV replication system was used [18, 19], in which the plasmid contained the infectious full-length genotype 1a cDNA sequence corresponding to the H77 prototype strain with the T7 promoter sequence (pT7-flHCV-Rz, provided by Dr. Raymond T. Chung (Gastrointestinal Unit, Massachusetts General Hospital, Boston, MA, USA). pT7-flHCV-Rz cells were transfected to Huh7 cells by using Lipofectamine (Invitrogen, Carlsbad, CA, USA). Subsequently, the T7 polymerase was delivered by using a replication-defective adenovirus vector (Ad-T7pol) at a multiplicity of infection of 10.

For the in-vitro assay of HCV genotype 2, the HCV replication system pJFH1-full that encodes HCV genotype 2a JFH1 sequence was used, which was provided by Dr. Takaji Wakita (Department of Virology II, National Institute of Infectious Diseases, Tokyo, Japan) [20]. HCV RNA was synthesized using the Megascript T7 kit (Ambion, Austin, TX, USA), with the linearized pJFH1-full as template. After DNase I (Ambion) treatment, the transcribed HCV RNA was purified using ISOGEN-LS (Nippon Gene, Tokyo, Japan). For RNA transfection, Huh 7.5.1 cells were resuspended in Opti-MEM I (Invitrogen) containing 10 µg of HCV RNA and subjected to an electric pulse (960 µF and 260 V) using the Gene Pulser II apparatus (Bio-Rad, Richmond, CA, USA). After electroporation, the cell suspension was cultured under normal conditions with DMEM.

Evaluation of Effect of Palmitic Acid In Vitro

For the in-vitro assay, palmitic acid (Sigma Chemical), myristic acid (Sigma Chemical), stearic acid (Sigma Chemical), and oleic acid (Sigma Chemical), were solubilized in ethanol with albumin as a stock solution of 20 mM and stored at -20 °C, as described previously [21, 22]. These fatty acid-albumin complex solutions were freshly prepared before each experiment. Subsequently, preliminary experiments were performed using 10–500 µM solutions of fatty acids in order to assess the concentrations of fatty acids that would not compromise cell viability. Cell viability was not compromised when 10–100 µM fatty acids were used in the MTS assay (cytotoxicity assay using 3-(4,5-dimethylthiazol-2-yl)-5-(3-carboxymethoxyphenyl)-2-(4-sulfophenyl)-2H-tetrazolium, CellTiter 96 Aqueous One Solution cell proliferation assay[®], Promega, Madison, WI) [18]; thus, 100 µM fatty acids were used for culture experiments. Fatty acids were added after the preparation of H77 and JFH1 HCV replication cells, and then IFN-α2b

(100 IU/mL) and RBV (50 μ M) were added to the culture medium of those cells. In the control samples, solubilized solutions were added without fatty acids.

Quantitative Real-Time Reverse-Transcription PCR

Cellular mRNA was extracted by TRIzol (Invitrogen), and levels of HCV replication were quantified by real-time reverse transcription-PCR with SYBR green I dye (Roche Diagnostics) and primers encoded for the 5'UTR of HCV using LightCycler technology (Roche Diagnostics) as described previously [18, 19]. Glyceraldehyde-3-phosphate dehydrogenase (GAPDH) (Roche Diagnostics) was detected using primer sets under the recommended conditions. Data are expressed as copy numbers of HCV RNA or cellular mRNA per molecule of GAPDH mRNA.

Statistical Analysis

Data are expressed as means \pm standard deviations or as means \pm standard errors of mean. The Wilcoxon test was used to analyze continuous variables. The Chi-square test was used for analysis of categorical data. Group comparisons involving more than two independent groups were performed using the Kruskal–Wallis test. Multivariate analysis was performed using a logistic regression model with stepwise method. The relationships between palmitic acid and the other parameters were analyzed with the Pearson product-moment correlation coefficient. Each cutoff point for continuous variables was decided by receiver operating characteristics (ROC) curve analysis. The RVR, EVR, and SVR rates of patients with low levels of palmitic acid were defined as positive predictive value (PPV) in the prediction of RVR, EVR, and SVR. Non-RVR, non-EVR, and non-SVR rates in patients with high levels of palmitic acid were defined as the negative predictive value (NPV) for prediction of non-RVR, non-EVR, and non-SVR. A *P* value of less than 0.05 was considered statistically significant. Statistical analyses were performed using JMP version 9 software (SAS Institute Japan, Tokyo, Japan).

Results

Patient Characteristics

A total of 55 patients with HCV were included. There were 27 men and 28 women. The mean age was 53.59 ± 11.15 years (range 22–69 years). The baseline characteristics of the study population are shown in Supplemental Table 1. Thirty-seven patients were infected with genotype 1 (all genotype 1b) and 18 patients with genotype 2

(14 with genotype 2a and four with genotype 2b). There was no significant difference between two groups in serum lipid composition (Table 1).

Response to Treatment

Among patients with genotype 1, 22 % (8/37) of patients received PEG-IFN α -2a plus RBV, 16 % (6/37) received PEG-IFN α -2a, 51 % (19/37) received PEG-IFN α -2b plus RBV, and 11 % (4/37) received IFN- β plus RBV. Among patients with genotype 2, 6 % (1/18) of patients received PEG-IFN α -2a plus RBV, 22 % (4/18) received PEG-IFN α -2a, 67 % (12/18) received PEG-IFN α -2b plus RBV, and 6 % (1/18) received IFN- β plus RBV.

RVR was achieved in 35 % (19/55) of patients overall. Twenty-seven percent (10/37) of patients with HCV genotype 1, and 50 % (9/18) with genotype 2 achieved RVR. EVR occurred in 64 % (35/55) of patients. EVR was achieved in 51 % (19/37) of patients with HCV genotype 1, and in 89 % (16/18) of patients with genotype 2.

For assessment of SVR, four patients dropped out of the treatment because of depression (2/4), general fatigue (3/4), and retinopathy (1/4). SVR was achieved in 69 % (35/51) of patients overall, in 56 % (19/34) of patients with HCV genotype 1, and in 94 % (16/17) of patients with genotype 2 evaluated by the above described protocol.

Predictors of Virological Response

Univariate analysis was performed for factors associated with RVR, EVR, and SVR (Supplemental Table 2). For RVR, a low serum triglyceride level was identified as a contributing factor. For EVR, low body mass index (BMI) and HCV genotype 2 were identified as contributing factors. For SVR, low BMI, total cholesterol, and HCV genotype 2 were identified as contributing factors. Further analysis was performed to examine the relationship of fatty acid levels to RVR, EVR, and SVR (Table 2). Table 2 shows the fatty acids significantly associated with virological response to IFN-based therapy by univariate analysis (*P* < 0.05). Other than the listed fatty acids, lauric acid, arachidic acid, behenic acid, lignoceric acid, myristoleic acid, eicosenoic acid, erucic acid, linoleic acid, γ -linolenic acid, arachidonic acid, and eicosapentaenoic acid were evaluated; however, those fatty acids were not significantly associated with any treatment response (RVR, EVR, or SVR). For RVR, low levels of myristic acid, palmitic acid, stearic acid, oleic acid, α -linolenic acid, eicosadienoic acid, adrenic acid, docosapentaenoic acid, and docosahexaenoic acid were identified as significant contributing factors. For EVR, palmitic acid and nervonic acid were identified as significant contributing factors. For SVR, myristic acid, palmitic acid, palmitoleic acid,

Table 1 Total serum lipid composition ($\mu\text{g/mL}$) in 55 patients infected with HCV

Genotype	All ($n = 55$)	1b ($n = 37$)	2a or b ($n = 18$)	<i>P</i> value (1b vs. 2a, b)
Saturated fatty acid				
Lauric acid (12:0)	1.31 \pm 1.1	1.2 \pm 0.81	1.53 \pm 1.54	0.73
Myristic acid (14:0)	24.68 \pm 17.47	21.91 \pm 8.38	30.37 \pm 27.75	0.37
Palmitic acid (16:0)	614.44 \pm 138.03	598.02 \pm 133.65	648.19 \pm 144.58	0.35
Stearic acid (18:0)	186.63 \pm 43.27	180.76 \pm 40.53	198.71 \pm 47.32	0.25
Arachidic acid (20:0)	5.98 \pm 1.3	5.84 \pm 1.34	6.27 \pm 1.19	0.25
Behenic acid (22:0)	15.75 \pm 3.97	15.31 \pm 3.81	16.63 \pm 4.25	0.29
Lignoceric acid (24:0)	14.11 \pm 3.23	13.88 \pm 3.13	14.59 \pm 3.47	0.62
Monounsaturated fatty acid				
Palmitoleic acid (16:1n7)	66.96 \pm 26.69	63.96 \pm 27.34	73.14 \pm 24.92	0.23
Oleic acid (18:1n9)	537.07 \pm 151.73	510.11 \pm 126.91	592.48 \pm 184.90	0.21
Eicosenoic acid (20:1n9)	4.65 \pm 1.59	4.42 \pm 1.28	5.11 \pm 2.04	0.22
Erucic acid (22:1n9)	1.39 \pm 0.51	1.35 \pm 0.42	1.47 \pm 0.66	0.31
Nervonic acid (24:1n9)	33.25 \pm 5.8	33.34 \pm 6.04	33.07 \pm 5.44	0.94
Polyunsaturated fatty acid				
Linoleic acid (18:2n6)	693.88 \pm 151.44	680.31 \pm 155.32	721.76 \pm 143.32	0.23
γ -Linolenic acid (18:3n6)	7.57 \pm 3.84	7.15 \pm 3.62	8.44 \pm 4.24	0.3
α -Linolenic acid (18:3n3)	19.31 \pm 8.26	18.14 \pm 7.12	21.73 \pm 10.01	0.27
Eicosadienoic acid (20:2n6)	5.72 \pm 1.51	5.72 \pm 1.56	5.71 \pm 1.45	0.91
Mead acid (20:3n9)	2.18 \pm 1.19	2.25 \pm 1.33	2.02 \pm 0.84	0.80
Dihomo- γ -linolenic acid (20:3n6)	35.68 \pm 11.75	35.14 \pm 12.76	36.8 \pm 9.57	0.6
Arachidonic acid (20:4n6)	140.91 \pm 36.63	139.61 \pm 39.44	143.58 \pm 30.91	0.61
Eicosapentaenoic acid (20:5n3)	45.5 \pm 26.19	44.28 \pm 24.04	48 \pm 30.74	0.67
Adrenic acid (22:4n6)	4.59 \pm 1.56	4.53 \pm 1.69	4.71 \pm 1.27	0.50
Docosapentaenoic acid (22:5n3)	17.63 \pm 6.64	18.08 \pm 5.72	18.77 \pm 8.30	0.75
Docosahexaenoic acid (22:6n3)	123.37 \pm 44	120.5 \pm 39.73	129.28 \pm 52.46	0.7

Values are expressed as means \pm standard deviation

P values were determined by the Wilcoxon test

nervonic acid, mead acid, dihomogamma-linolenic acid, and adrenic acid were identified as significant contributing factors. Only a low level of palmitic acid was found to contribute significantly to all of RVR, EVR, and SVR. In Table 2, the odds ratio for each fatty acid was near 1.0, because the range of palmitic acid was wide (from 370.8 to 955.9) compared to the value of the treatment effect of RVR, EVR, and SVR (from 0 to 1).

Multivariate logistic regression analysis was conducted in order to determine independent predictive variables associated with virological response. With regard to fatty acids, palmitic acid was selected for multivariate analysis because it was a significant factor for RVR, EVR, and SVR by univariate analysis. Palmitic acid concentration was found to be significantly correlated with total cholesterol, triglycerides, and 12 fatty acids by the Pearson product-moment correlation in patients with HCV (Supplemental Table 3). Moreover, the serum levels of palmitic acid were not different statistically by the regimen of IFN based

treatment ($554.2 \pm 96.4 \mu\text{g/mL}$ in PEG-IFN α -2a + RBV, $556.4 \pm 95.8 \mu\text{g/mL}$ in PEG-IFN α -2a, $643.6 \pm 140.7 \mu\text{g/mL}$ in PEG-IFN α -2b + RBV, and $658.3 \pm 209.4 \mu\text{g/mL}$ in IFN β + RBV).

For additional factors for multivariate analysis, seven factors were selected that had been identified in previous reports: age, gender, BMI, serum alanine aminotransferase, genotype, viral load, and a history of IFN therapy [23–26]. As a result of stepwise multivariate analysis, only low levels of palmitic acid and HCV genotype 2 were found to be significant contributing factors for RVR, EVR, and SVR (Table 3).

Evaluation of Palmitic Acid Level as a Predictor of Virological Response

ROC curves were constructed and areas under curves (AUC) were calculated (Table 4). A graph of the AUC for RVR, EVR, and SVR is shown in Supplemental Fig. 1. As

Table 2 Fatty acids ($\mu\text{g}/\text{mL}$) associated with virological response to interferon-based therapy identified by univariate analysis

	RVR ($n = 55$)		EVR ($n = 55$)		SVR ($n = 51$)	
	OR (95 % CI)	<i>P</i> value	OR (95 % CI)	<i>P</i> value	OR (95 % CI)	<i>P</i> value
Saturated fatty acid						
Myristic acid (14:0)	0.88 (0.79–0.96)	0.01	0.96 (0.902–1.002)	0.16	0.93 (0.86–0.99)	0.04
Palmitic acid (16:0)	0.99 (0.983–0.996)	0.003	0.9956 (0.9909–0.9998)	0.049	0.995 (0.9899–0.9995)	0.04
Stearic acid (18:0)	0.98 (0.96–0.99)	0.01	0.991 (0.978–1.004)	0.19	0.988 (0.973–1.002)	0.1
Monounsaturated fatty acid						
Palmitoleic acid (16:1n7)	0.98 (0.95–0.99998)	0.07	0.99 (0.97–1.01)	0.36	0.976 (0.953–0.998)	0.04
Oleic acid (18:1n9)	0.993 (0.987–0.998)	0.004	0.9992 (0.9955–1.003)	0.68	0.998 (0.994–1.002)	0.38
Nervonic acid (24:1n9)	0.96 (0.86–1.06)	0.41	0.9 (0.8–0.99)	0.04	0.85 (0.75–0.95)	0.01
Polyunsaturated fatty acid						
α -Linolenic acid (18:3n3)	0.86 (0.74–0.96)	0.02	0.98 (0.92–1.05)	0.6	0.97 (0.89–1.04)	0.38
Eicosadienoic acid (20:2n6)	0.47 (0.25–0.78)	0.01	0.76 (0.5–1.09)	0.15	0.71 (0.45–1.05)	0.11
Mead acid (20:3n9)	0.68 (0.37–1.13)	0.17	0.73 (0.44–1.17)	0.2	0.51 (0.27–0.86)	0.02
Dihomo- γ -linolenic acid (20:3n6)	0.949 (0.898–0.998)	0.05	0.957 (0.908–1.004)	0.08	0.92 (0.86–0.97)	0.01
Adrenic acid (22:4n6)	0.62 (0.38–0.93)	0.03	0.84 (0.58–1.2)	0.33	0.67 (0.43–0.98)	0.048
Docosapentaenoic acid (22:5n3)	0.74 (0.59–0.88)	0.003	0.96 (0.88–1.04)	0.35	0.93 (0.82–1.03)	0.18
Docosahexaenoic acid (22:6n3)	0.98 (0.95–0.99)	0.03	0.988 (0.972–1.001)	0.1	0.98 (0.959–0.997)	0.02

Bold values are statistically significant ($P < 0.05$)

RVR rapid virological response, EVR early virological response, SVR sustained virological response, OR odds ratio, CI confidence interval

Table 3 Factors associated with virological response to interferon-based therapy identified by multivariate analysis

Factor	Category	RVR ($n = 55$)		EVR ($n = 55$)		SVR ($n = 51$)	
		OR (95 % CI)	<i>P</i> value	OR (95 % CI)	<i>P</i> value	OR (95 % CI)	<i>P</i> value
Genotype	1. 1b	1		1		1	
	2. 2a, b	0.38 (0.16–0.8)	0.01	0.24 (0.008–0.57)	0.005	0.993 (0.987–0.998)	0.01
Palmitic acid (16:0)		0.988 (0.979–0.994)	0.001	0.993 (0.987–0.998)	0.01	0.993 (0.987–0.998)	0.01

Only variables that achieved statistical significance ($P < 0.05$) on multivariate logistic regression are shown

RVR rapid virological response, EVR early virological response, SVR sustained virological response, OR odds ratio, CI confidence interval

is seen in Table 4, AUC, cutoff value, sensitivity, specificity, PPV, NPV, and diagnostic accuracy of prediction in RVR were 0.79, 569.1 $\mu\text{g}/\text{mL}$, 73.68, 77.78, 63.64, 84.85, and 76.36 %, respectively; in EVR were 0.7, 586.7 $\mu\text{g}/\text{mL}$, 60, 80, 84, 53.33, and 67.27 %, respectively; and in SVR were 0.7, 587.7 $\mu\text{g}/\text{mL}$, 63.64, 77.78, 84, 53.84, and 68.63 %, respectively. Low levels of palmitic acid in RVR were associated with high specificity and NPV, while low levels of palmitic acid in EVR and SVR were associated high specificity and PPV.

Serum levels of palmitic acid in patients with HCV were significantly higher than those in healthy subjects (614.44 ± 138.03 vs. 480.67 ± 117.53 $\mu\text{g}/\text{mL}$, respectively, $P = 0.01$). Ninety-one percent (50/55) of patients with HCV had higher levels of palmitic acid compared to the mean level of palmitic acid in healthy subjects. Additionally, serum levels of palmitic acid were evaluated between patients with SVR and patients without SVR. The levels of palmitic acid were

significantly lower in patients with SVR compared to patients without SVR (554.3 ± 138.6 vs. 668.5 ± 183 $\mu\text{g}/\text{mL}$, respectively, $P = 0.01$).

Genetic Analysis

The relationship between palmitic acid and IL-28B polymorphism was investigated in the 37 patients with genotype 1 HCV infection. The level of palmitic acid was compared between major and minor polymorphisms. There were no significant differences between the two groups (Table 5). Amino acid substitution in the core region of HCV and mutated nucleotide sequence of ISDR were not associated with serum levels of palmitic acid (Table 5).

In patients with HCV genotype 1 infection, further analysis was performed in order to evaluate whether the level of palmitic acid could be a predictive factor of the efficacy of anti-HCV treatment. Univariate logistic

Table 4 Sensitivity, specificity, positive predictive value (PPV), negative predictive value (NPV), and diagnostic accuracy of palmitic acid for prediction of virological response to interferon-based therapy

	AUC (95 % CI)	Cutoff value ($\mu\text{g/mL}$)	Sensitivity (%)	Specificity (%)	PPV (%)	NPV (%)	Diagnostic accuracy (%)
RVR ($n = 55$)	0.79 (0.66–0.89)	569.1	73.68	77.78	63.64	84.85	76.36
EVR ($n = 55$)	0.7 (0.56–0.82)	586.7	60	80	84	53.33	67.27
SVR ($n = 51$)	0.7 (0.56–0.82)	587.7	63.64	77.78	84	53.84	68.63

Each value was determined by receiver operating characteristic curve analysis

AUC area under curve, RVR rapid virological response, EVR early virological response, SVR sustained virological response

Table 5 Palmitic acid concentration at baseline in 37 patients infected with genotype 1 HCV

			<i>P</i> value
IL28B polymorphism ^a			
rs8099917	Major ($n = 30$)	Minor ($n = 7$)	0.32
	580.8 \pm 123.42	672.24 \pm 210.48	
rs12979860	Major ($n = 29$)	Minor ($n = 8$)	0.14
	575.54 \pm 104.62	679.51 \pm 195.95	
Amino acid substitutions in the core region ^b			
aa 70	Wild ($n = 28$)	Non-wild ($n = 9$)	0.47
	588.21 \pm 123.42	628.54 \pm 166.08	
aa 91	Wild ($n = 21$)	Non-wild ($n = 16$)	0.24
	571.56 \pm 112.74	632.74 \pm 153.80	
aa 70 and aa 91	Double-wild ($n = 16$)	Non-double-wild ($n = 21$)	0.154
	561.71 \pm 109.88	625.68 \pm 145.73	
Nucleotide sequence of ISDR ^c			
	0–1 ($n = 15$)	≥ 2 ($n = 21$)	0.14
	615.12 \pm 115.07	564.77 \pm 170.04	

Data are given as means \pm standard deviations

HCV hepatitis C virus, IL-28B interleukin-28B, ISDR interferon sensitivity-determining region, PCR polymerase chain reaction

P value was determined by the Wilcoxon test

^a For IL-28B, the major allele of rs8099917 was defined as TT, and the minor allele was defined as T/G or G/G. The major allele of rs12979860 was defined as C/C, and the minor allele was defined as T/C or T/T

^b Amino acid substitutions were evaluated in pretreatment serum by PCR with mutation-specific primers. Wild-type at aa 70 and wild-type at aa 91 were evaluated as double-wild-type, while the other patterns were considered non-double-wild-type

^c In ISDR, 0–1 was defined as having no amino acid substitutions or one substitution, ≥ 2 was defined as containing two or more amino acid substitutions

regression analysis was performed for IL-28B polymorphisms (rs8099917 and rs12979860), amino acid substitution in HCV core 70 and 91, mutated nucleotide sequence of ISDR, and palmitic acid level (Supplementary Table 4). Analysis revealed that palmitic acid level and the ISDR mutation could be significant predictive factors for RVR ($P = 0.03$ and $P = 0.02$, respectively). For EVR and SVR,

only the palmitic acid level was identified as a significant predictive factor ($P = 0.01$ for both EVR and SVR). Moreover, multivariate logistic regression analysis revealed that the level of palmitic acid was the only significant contributing factor for EVR (odds ratio = 0.988, 95 % confidence interval 0.979–0.996; $P = 0.01$); however, it was not a significant factor for RVR or SVR (Table 6).

Effect of Fatty Acids In Vitro

The effect of palmitic acid on HCV replication was assessed in vitro using transfected cultured cells expressing H77 (Fig. 1a) or JFH1 (Fig. 1b) HCV clones. In both cell lines, levels of HCV RNA were not altered with the addition of palmitic acid alone. However, anti-HCV effects of IFN and RBV were diminished by addition of palmitic acid ($P = 0.028$ and $P = 0.038$ for H77 and JFH1, respectively, by Wilcoxon test). Moreover, other saturated fatty acids (such as myristic acid and stearic acid) and unsaturated fatty acids (such as oleic acid) were assessed. Myristic acid, stearic acid, and oleic acid did not affect HCV replication, and did not alter the treatment effect of IFN and RBV (Supplementary Fig. 2A, 2B).

Discussion

The present study suggests that low serum levels of palmitic acid could be a predictive factor for virological response to IFN-based therapy in both HCV genotype 1 and 2 infections. In addition, it was also suggested that palmitic acid impairs the anti-HCV effects of IFN and RBV in vitro.

Several studies have shown that HCV core protein disrupts fatty acid homeostasis [9, 26]. HCV core protein has been shown to significantly increase the proportion of C18:1 fatty acids (such as oleic and vaccenic acids), but not palmitic acid, in the livers of patients with HCV infection [9, 10]. Irmisch et al. [27] compared fatty acids in serum of patients with untreated chronic HCV infection with those in treated patients and healthy controls. They showed that

Table 6 Factors associated with virological response to interferon-based therapy in patients with genotype 1 identified by multivariate analysis

Factor	Category	RVR		EVR	
		OR (95 % CI)	<i>P</i> value	OR (95 % CI)	<i>P</i> value
Palmitic acid (16:0)		0.992 (0.982–0.999)	0.07	0.989 (0.98–0.996)	0.01
Nucleotide sequence of ISDRs ^a	0–1	1		1	
	≥2	5.56 (0.95–38.08)	0.06	5.3 (0.86–48.08)	0.09

Only variables that achieved $P < 0.1$ on multivariate logistic regression with stepwise method are shown. In SVR, there was no significant factor, which achieved $P < 0.1$. Total variables include palmitic acid, nucleotide sequence of ISDRs

HCV hepatitis C virus, OR odds ratio, CI confidence interval, RVR rapid virological response, EVR early virological response, ISDR interferon sensitivity-determining region, SVR sustained virological response, IL-28B interleukin-28B, PCR polymerase chain reaction

^a In ISDR, 0–1 was defined as having no amino acid substitutions or one substitution, ≥2 was defined as containing two or more amino acid substitutions

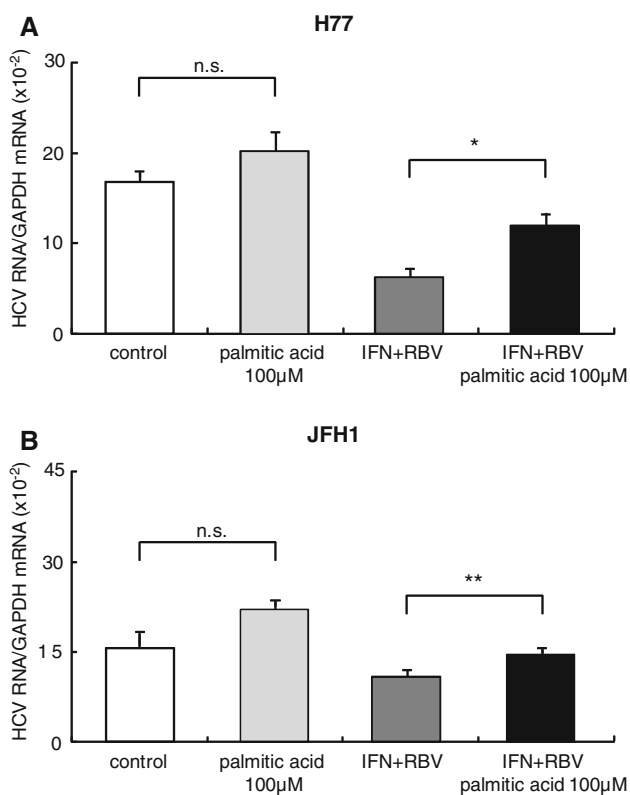


Fig. 1 Effects of palmitic acid on in-vitro viral replication and activity of interferon- α plus ribavirin. Levels of HCV RNA were measured after adding interferon- α (IFN- α) and ribavirin (RBV) with or without 100 μ M palmitic acid. H77 plasmid-based replication (HCV genotype 1a) (a). JFH1 HCV replication system (HCV genotype 2a) (b). * $P = 0.028$. ** $P = 0.038$. Data are mean \pm standard error of the mean (SEM) of six independent experiments. The Wilcoxon test was used to analyze the data. $P < 0.05$ was considered statistically significant. *ns* not significant

women who responded to treatment and healthy controls had significantly higher levels of eicosapentaenoic and arachidonic acid than did untreated HCV patients. There was no significant difference in palmitic acid among the three groups [27]. However, the study did not use

pretreatment serum of treated HCV patients and was not a comparison between treated HCV patients who responded to anti-HCV therapy and those who did not. The study compared patients who responded to anti-HCV treatment and untreated patients (including patients who would have responded to anti-HCV treatment if they had received it).

Kapadia et al. and Leu et al. [21, 22] found that both an increase in saturated fatty acids, including palmitic acid, and an increase in monounsaturated fatty acids enhanced HCV replication, whereas increases in polyunsaturated fatty acids such as arachidonic acid suppressed HCV replication in vitro. Huang et al. [28] showed that arachidonic acid inhibited HCV replication by increasing lipid peroxidation, resulting in a decrease in the amount of HCV RNA. In addition, Leu et al. [22] showed that when arachidonic acid was added to IFN- α , a strong synergistic anti-HCV effect was observed in vitro; however, the mechanism of this effect is not well understood.

In the present study, it was found that the concentration of arachidonic acid in the serum of patients infected with HCV was not associated with a change in the effect of IFN-based therapy (data not shown). In fact, the quantity of HCV RNA did not correlate significantly with concentrations of any fatty acids, including palmitic acid, in the serum of HCV patients (data not shown). The present in-vitro data obtained with HCV cell culture systems also indicated that there is no association between saturated fatty acids (including palmitic acid and unsaturated acids such as oleic acid) and HCV replication. However, in this in-vitro system, palmitic acid had an inhibitory effect on IFN-based therapy against HCV. These clinical and in vivo results indicate that inhibitory effects of palmitic acid against IFN-based therapy may be direct effects on hepatocytes.

Another potential explanation for the decreased effect of IFN-based therapy associated with palmitic acid would be the inability of patients to develop effective anti-HCV immunity [29]. It was previously been reported that

palmitic acid can induce inflammation and impair the antigen-specific function of dendritic cells (DC) in humans and mice [7]. These conditions might be comparable to chronic HCV infection. Function of DC is impaired in HCV infection [30, 31]. High levels of palmitic acid might further impair the function of DC, reducing anti-HCV immunity. Further studies are needed to identify the mechanisms underlying the effects of palmitic acid, including immunomodulatory effects.

Multiple factors have been reported to be associated with a poor response to IFN-based treatment. Viral factors [including HCV genotype, quantity of HCV RNA, nucleotide sequence of ISDR, and amino acid substitutions in the core region (core aa70 and aa91)] have been shown to affect response to IFN-based therapy [17, 23, 24, 32–34]. On the host side, older age, male gender, obesity, insulin resistance or metabolic syndrome, low density lipoprotein, race, and either steatosis or advanced fibrosis on liver biopsy have all been reported as factors associated with poor response to IFN-based therapy [24–26, 33, 34]. Recently, IL-28B polymorphism has received attention as a potential factor affecting response to therapy [14].

Based on the present results, previously reported factors that have been shown to influence the effect of IFN therapy were not associated with the level of palmitic acid. Based on the results of univariate and multivariate analyses, the level of palmitic acid was a significant independent predictive factor of response to IFN-based therapy in patients with HCV genotypes 1 and 2. However, a validation study with a larger number of patients with HCV is needed.

In conclusion, this study is the first to report that the serum level of palmitic acid could be a pretreatment predictive factor of virological response with IFN-based therapy in patients with HCV infection. According to the present findings, pretreatment serum concentration of palmitic acid could be used to select patients more likely to respond to IFN-based therapy. It is possible that a special diet or drugs that lower levels of palmitic acid might improve response to IFN-based therapy in patients with HCV infection.

Acknowledgments This work was supported in part by a Grant-in-Aid for Scientific Research [JSPS KAKENHI 23700907 to T.M.; JSPS KAKENHI 21590848 to Y.H.] from the Japanese Ministry of Education, Culture, Sports, Science and Technology, and a Grant-in-Aid for Scientific Research and Development from the Japanese Ministry of Health, Labor and Welfare to Y.H. We thank Ms. Satomi Yamanaka, Ms. Chie Matsugi and Ms. Sakiko Inoh for excellent technical assistance. The sequence of the probe and primers for the TaqMan assay for detecting rs8099917 was kindly provided by Dr. Yasuhito Tanaka (Department of Virology and Liver Unit, Nagoya City University Graduate School of Medical Sciences, Nagoya, Japan), and rs12979860 was provided by Dr. David B. Goldstein (Center for Human Genome Variation, Duke University, Durham, NC, USA). The HCV replication system with pJFH1-full was kindly provided by Dr. Takaji Wakita (Department of Virology

II, National Institute of Infectious Diseases, Tokyo, Japan), and that with pT7-flHCV-Rz was provided by Dr. Raymond T. Chung (Gastrointestinal Unit, Massachusetts General Hospital, Boston, MA, USA). We also thank Dr. Francis V. Chisari (Department of Immunology and Microbial Science, The Scripps Research Institute, La Jolla, CA, USA) for providing the Huh7.5.1 human cancer cell lines.

Conflict of interest None.

References

- Lavanchy D (2009) The global burden of hepatitis C. *Liver Int* 29:74–81
- Manns MP, McHutchison JG, Gordon SC, Rustgi VK, Shiffman M, Reindollar R, Goodman ZD, Koury K, Ling M, Albrecht JK (2001) Peginterferon alpha-2b plus ribavirin compared with interferon alpha-2b plus ribavirin for initial treatment of chronic hepatitis C: a randomized trial. *Lancet* 358:958–965
- Davis GL, Wong JB, McHutchison JG, Manns MP, Harvey J, Albrecht J (2003) Early virologic response to treatment with peginterferon alpha-2a plus ribavirin in patients with chronic hepatitis C. *Hepatology* 38:645–652
- Feld JJ, Nanda S, Huang Y, Chen W, Cam M, Pusek SN, Schweigler LM, Theodore D, Zacks SL, Liang TJ, Fried MW (2007) Hepatic gene expression during treatment with peginterferon and ribavirin: identifying molecular pathways for treatment response. *Hepatology* 46:1548–1563
- Hotamisligil GS (2006) Inflammation and metabolic disorders. *Nature* 444:860–867
- Anderson SG, Sanders TA, Cruickshank JK (2009) Plasma fatty acid composition as a predictor of arterial stiffness and mortality. *Hypertension* 53:839–845
- Miyake T, Akbar SM, Yoshida O, Chen S, Hiasa Y, Matsuura B, Abe M, Onji M (2010) Impaired dendritic cell functions disrupt antigen-specific adaptive immune responses in mice with nonalcoholic fatty liver disease. *J Gastroenterol* 45:859–867
- Puri P, Wiest MM, Cheung O, Mirshahi F, Sargeant C, Min HK, Contos MJ, Sterling RK, Fuchs M, Zhou H, Watkins SM, Sanyal AJ (2009) The plasma lipidomic signature of nonalcoholic steatohepatitis. *Hepatology* 50:1827–1838
- Moriya K, Todoroki T, Tsutsumi T, Fujie H, Shintani Y, Miyoshi H, Ishibashi K, Takayama T, Makuuchi M, Watanabe K, Miyamura T, Kimura S, Koike K (2001) Increase in the concentration of carbon 18 monosaturated fatty acids in the liver with hepatitis C: analysis in transgenic mice and humans. *Biochem Biophys Res Commun* 281:1207–1212
- Miyoshi H, Moriya K, Tsutsumi T, Shinzawa S, Fujie H, Shintani Y, Fujinaga H, Goto K, Todoroki T, Suzuki T, Miyamura T, Matsuura Y, Yotsuyanagi H, Koike K (2011) Pathogenesis of lipid metabolism disorder in hepatitis C: polyunsaturated fatty acids counteract lipid alterations induced by the core protein. *J Hepatol* 54:432–438
- Akuta N, Kumada H (2008) Treatment guideline for HCV infection. *Nihon Shokakibyō Gakkai Zasshi* (in Japanese) 105:186–190
- Examination Committee of Criteria for ‘Obesity Disease’ in Japan, Japan Society for the Study of Obesity (2002) New criteria for ‘obesity disease’ in Japan. *Circ J* 66:987–992
- Chayama K, Tsubota A, Arase Y, Saitoh S, Koida I, Ikeda K, Matsumoto T, Kobayashi M, Iwasaki S, Koyama S, Morinaga T, Kumada H (1993) Genotypic subtyping of hepatitis C virus. *J Gastroenterol Hepatol* 8:150–156

14. Tanaka Y, Nishida N, Sugiyama M, Kurosaki M, Matsuura K, Sakamoto N, Nakagawa M, Korenaga M, Hino K, Hige S, Ito Y, Mita E, Tanaka E, Mochida S, Murawaki Y, Honda M, Sakai A, Hiasa Y, Nishiguchi S, Koike A, Sakaida I, Imamura M, Ito K, Yano K, Masaki N, Sugauchi F, Izumi N, Tokunaga K, Mizokami M (2009) Genome-wide association of IL28B with response to pegylated interferon-alpha and ribavirin therapy for chronic hepatitis C. *Nat Genet* 41:1105–1109
15. Ge D, Fellay J, Thompson AJ, Simon JS, Shianna KV, Urban TJ, Heinzen EL, Qiu P, Bertelsen AH, Muir AJ, Sulkowski M, McHutchison JG, Goldstein DB (2009) Genetic variation in IL28B predicts hepatitis C treatment-induced viral clearance. *Nature* 461:399–401
16. Okamoto K, Akuta N, Kumada H, Kobayashi M, Matsuo Y, Tazawa H (2007) A nucleotide sequence variation detection system for the core region of hepatitis C virus-1b. *J Virol Methods* 141:1–6
17. Enomoto N, Sakuma I, Asahina Y, Kurosaki M, Murakami T, Yamamoto C, Ogura Y, Izumi N, Marumo F, Sato C (1996) Mutations in the nonstructural protein 5A gene and response to interferon in patients with chronic hepatitis C virus 1b infection. *N Engl J Med* 334:77–81
18. Hiasa Y, Kuzuhara H, Tokumoto Y, Konishi I, Yamashita N, Matsuura B, Michitaka K, Chung RT, Onji M (2008) Hepatitis C virus replication is inhibited by 22beta-methoxyolean-12-ene-3beta, 24(4beta)-diol (ME3738) through enhancing interferon-beta. *Hepatology* 48:59–69
19. Hiasa Y, Blackard JT, Lin W, Kamegaya Y, Horiike N, Onji M, Schmidt EV, Chung RT (2006) Cell-based models of sustained, interferon-sensitive hepatitis C virus genotype 1 replication. *J Virol Methods* 132:195–203
20. Wakita T, Pietschmann T, Kato T, Date T, Miyamoto M, Zhao Z, Murthy K, Habermann A, Kräusslich HG, Mizokami M, Bartenschlager R, Liang TJ (2005) Production of infectious hepatitis C virus in tissue culture from a cloned viral genome. *Nat Med* 11:791–796
21. Kapadia SB, Chisari FV (2005) Hepatitis C virus RNA replication is regulated by host geranylgeranylation and fatty acids. *Proc Natl Acad Sci USA* 102:2561–2566
22. Leu GZ, Lin TY, Hsu JT (2004) Anti-HCV activities of selective polyunsaturated fatty acids. *Biochem Biophys Res Commun* 318:275–280
23. Poynard T, Marcellin P, Lee SS, Niederau C, Minuk GS, Ideo G, Bain V, Heathcote J, Zeuzem S, Trepo C, Albrecht J (1998) Randomised trial of interferon alpha2b plus ribavirin for 48 weeks or for 24 weeks versus interferon alpha2b plus placebo for 48 weeks for treatment of chronic infection with hepatitis C virus. International Hepatitis Interventional Therapy Group (IHIT). *Lancet* 352:1426–1432
24. Barnes E, Webster G, Whalley S, Dusheiko G (1999) Predictors of a favorable response to alpha interferon therapy for hepatitis C. *Clin Liver Dis* 3:775–791
25. Bressler BL, Guindi M, Tomlinson G, Heathcote J (2003) High body mass index is an independent risk factor for nonresponse to antiviral treatment in chronic hepatitis C. *Hepatology* 38:639–644
26. Arase Y, Kumada H, Chayama K, Tsubota A, Koida I, Ikeda K, Saitoh S, Matsumoto T, Kobayashi M (1994) Interferon retreatment of nonresponders with HCV-RNA-positive chronic hepatitis C. *J Gastroenterol* 29:299–304
27. Irmisch G, Hoepfner J, Thome J, Richter J, Fernow A, Reisinger EC, Lafrenz M, Loebermann M (2011) Serum fatty acids, antioxidants, and treatment response in hepatitis C infection: greater polyunsaturated fatty acid and antioxidant levels in hepatitis C responders. *J Clin Lipidol* 5:288–293
28. Huang H, Chen Y, Ye J (2007) Inhibition of hepatitis C virus replication by peroxidation of arachidonate and restoration by vitamin E. *Proc Natl Acad Sci USA* 104:18666–18670
29. Salem ML, El-Demellawy M, El-Azm AR (2010) The potential use of toll-like receptor agonists to restore the dysfunctional immunity induced by hepatitis C virus. *Cell Immunol* 262:96–104
30. Hiasa Y, Horiike N, Akbar SM, Saito I, Miyamura T, Matsuura Y, Onji M (1998) Low stimulatory capacity of lymphoid dendritic cells expressing hepatitis C virus genes. *Biochem Biophys Res Commun* 249:90–95
31. Hiasa Y, Takahashi H, Shimizu M, Nuriya H, Tsukiyama-Kohara K, Tanaka T, Horiike N, Onji M, Kohara M (2004) Major histocompatibility complex class-I presentation impaired in transgenic mice expressing hepatitis C virus structural proteins during dendritic cell maturation. *J Med Virol* 74:253–261
32. Enomoto N, Sakuma I, Asahina Y, Kurosaki M, Murakami T, Yamamoto C, Izumi N, Marumo F, Sato C (1995) Comparison of full-length sequences of interferon-sensitive and resistant hepatitis C virus 1b. Sensitivity to interferon is conferred by amino acid substitutions in the NS5A region. *J Clin Invest* 96:224–230
33. Akuta N, Suzuki F, Kawamura Y, Yatsuji H, Sezaki H, Suzuki Y, Hosaka T, Kobayashi M, Kobayashi M, Arase Y, Ikeda K, Kumada H (2007) Predictive factors of early and sustained responses to peginterferon plus ribavirin combination therapy in Japanese patients infected with hepatitis C virus genotype 1b: amino acid substitutions in the core region and low-density lipoprotein cholesterol levels. *J Hepatol* 46:403–410
34. Akuta N, Suzuki F, Sezaki H, Suzuki Y, Hosaka T, Someya T, Kobayashi M, Saitoh S, Watahiki S, Sato J, Kobayashi M, Arase Y, Ikeda K, Kumada H (2006) Predictive factors of virological non-response to interferon-ribavirin combination therapy for patients infected with hepatitis C virus of genotype 1b and high viral load. *J Med Virol* 78:83–90

concentrations compared to a diet high in polyunsaturated fatty acids (PUFA) [1–8]. As circulating levels of cholesterol are related to heart disease, including elevated levels of LDL, the ability to reduce plasma cholesterol levels with dietary intervention has been the focus of many studies over the past few decades.

Dietary cholesterol can play a role in modulating plasma cholesterol levels. An increase in dietary cholesterol often leads to an increase in plasma cholesterol levels [9, 10]. The impact of dietary cholesterol on plasma cholesterol levels begin with its uptake by enterocytes of the small intestine. Intraluminal cholesterol, dietary as well as biliary cholesterol, is solubilized into micelles containing fatty acids, phospholipids, and monoacylglycerols. The micelles cross the unstirred water layer where they are taken up by protein-mediated processes, i.e. NPC1L1, or passively diffuse into the enterocytes. These chylomicrons reach the systemic circulation where smaller chylomicron remnants are produced which are then taken up by the liver by way of the LDL receptor-related protein (LRP). As most chylomicron remnants are taken up by the liver, a majority of diet-derived cholesterol is taken up by the liver. The diet-derived hepatic cholesterol can then be stored as cholesteryl ester, utilized for cellular maintenance and regulatory processes, or be secreted back into the circulation as VLDL. Circulating VLDL is converted to LDL within the circulation after lipase hydrolysis of core triacylglycerols. The LDL particles are cleared primarily via the LDL receptor [11]. HDL is formed in the circulation as the result of apo AI-mediated efflux of cholesterol from cells with some HDL secreted from the intestine [12, 13]. HDL-cholesterol also can be obtained from VLDL after transfer of ester by way of cholesteryl ester transfer protein (CETP). HDL is taken up by a number of tissues, including the liver and steroidogenic tissues via SR-BI [14]. Various intraluminal factors influence cholesterol absorption, independent of genetic effects on cholesterol transporters. For example, a change in luminal bile acid concentrations and composition can affect cholesterol absorption by altering micellar formation [15–19]. Indeed, we showed that humans given a cholic acid supplement had increased intraluminal bile acid concentrations and consequently more cholesterol carried in non-vesicles, likely micelles [20]. We further showed that cholesterol is absorbed when carried in micelles and not vesicles [21]. A high fat diet also enhances cholesterol absorption, possibly by increasing substrates for micellar formation [22].

Though the relationship between the amount of dietary fat consumed and cholesterol absorption is well known, the effect of dietary fatty acid composition on cholesterol absorption in humans is uncertain. The impact of different fatty acids on cholesterol absorption can be several-fold. First, fatty acids could theoretically affect micellar

formation. Dietary SFA could remain relatively insoluble, making poor micelles, and/or cholesterol could partition into the undigested lipid. Either effect would result in reduced absorption or reduced plasma lipid levels with SFA, which seems unlikely. In addition, dietary fatty acids can affect expression of genes involved in processes of cholesterol absorption. The PPARs are known mediators of dietary PUFA, as they are activated by PUFA [23]. Recent studies have shown that PPAR α can enhance cholesterol absorption by way of NPC1L1 [24].

Though some studies using human subjects have shown a decrease in absorption of cholesterol with diets enriched in PUFA versus SFA [9, 10, 22], the studies have either used indirect measurements of cholesterol absorption (plant sterols), sterol balance measurements, or used non-physiological diets, i.e. liquid diets or diet that contain extremely large amounts of cholesterol. Thus, the purpose of the current study was to directly measure cholesterol absorption using stable isotopes in humans fed a solid diet. Cholesterol fractional synthetic rates were also measured as these will often be inversely affected by cholesterol absorption. As verification of results, plant sterol and cholesterol biosynthetic intermediate levels were measured as well, as was intraluminal levels of micelles and/or vesicles.

Subjects and Methods

Subjects

The study was a randomized cross over study and healthy adult males and females of any race ($n = 20$), ages 18–40 were recruited by advertisement at the University of Cincinnati, College of Medicine and the Cincinnati Children's Hospital Medical Center (CCHMC). The protocol was approved by the Institutional Review Board of CCHMC as well as the Scientific Advisory Committee of the General Clinical Research Center (GCRC) of CCHMC, Cincinnati, OH, USA (Protocol number #2008-0298). Subjects were screened for any evidence of cardiovascular, pulmonary, renal, gastrointestinal, hepatobiliary diseases or soy allergy and excluded if any conditions were found. Subjects with diabetes mellitus, chronic usage of any medication including oral contraceptives and plasma total and LDL cholesterol exceeding 200 and 120 mg/dl, respectively, were also excluded. Only subjects with Apo AIV 1/1 and Apo E 3/3 genotypes were enrolled in order to reduce the genotypic influence. Apo E and AIV gene expressions could affect cholesterol absorption and account for inter-individual variation in total serum cholesterol concentrations [10, 25, 26]. Females were non-pregnant and not planning pregnancy during the course of the study.

Experimental Design

After fulfillment of inclusion/exclusion criteria and a complete verbal explanation of the study, subjects signed the consent form. Subjects provided a 3-day diet diary. Based upon caloric intakes from the diet diary, total calories required to maintain steady body weight were estimated and diet menus were made on a 3 day rotating schedule. During the study, subjects consumed a diet consisting of P/S ratio of 2:1 or a similar diet with a P/S ratio of 0.5:1. The dietary compositions for the two experimental diets are shown in Table 1. Subjects were randomized to diet using a random number table and stratified by age (<30, ≥30) because of perceived differences in metabolic rates between these age groups. At baseline (day 0) physical examination was performed on the subjects and blood drawn for measuring plasma TAG, total, LDL and HDL cholesterol concentrations. Subjects visited the center daily or every third day to pick up prepared diets which were frozen after preparation. Diets were prepared by the research dietitian on the GCRC at the CCHMC. During each week of the study period, subjects' body weights were obtained to ensure maintenance of basal weight. Subjects were advised not to eat anything other

than the foods provided. Subjects were also instructed to follow the dietary instructions such as eating all the meals on time and to maintain their physical activity to be same throughout the study. No alcohol was permitted during the whole study period. During and at the end (day 14 and 19, respectively) of each phase, fasting blood samples were collected for analysis and urine for pregnancy testing for females.

After 2 weeks on the diet (day 14), fasting blood samples were collected from study subjects for analysis. Plasma was separated for measuring TAG, as well as total, LDL and HDL cholesterol concentration measurements. 2 days later (day 16) subjects were provided with an intravenous injection of 15 mg [25,26,26,26,27,27,27-D₇] cholesterol and a 75-mg oral dose of [3,4-¹³C] cholesterol for cholesterol absorption analysis according to the method of Bosner et al. [27], as originally proposed by Zilversmit [28] and as described previously [29]. The ratio of ingested 3,4-¹³C cholesterol to injected 25,26,26,26,27,27,27-D₇ cholesterol enrichment in red blood cells (RBC) cholesterol after 48, and 72 h was taken as an indicator of the cholesterol fractional absorption rate. Cholesterol synthesis rates were also measured using the deuterium incorporation approach. On day 19, after an overnight fast, baseline blood was drawn for RBC cholesterol isotope measurement. Subjects were given oral deuterated water, and the next day (day 20) blood was obtained at the same time as the isotope administration on day 19. On completion of first dietary period, subjects participated in the alternative arm of the study after a washout period of at least 4 weeks. Thereafter, the same sequence of events was performed as described for the first phase of the study.

Table 1 Composition of the experimental diets

Composition	Low P/S	High P/S
Proteins (g/100 kcal)	5.04	4.94
Carbohydrates (g/100 kcal)	12.56	12.59
Fats (g/100 kcal)	3.28	3.32
Cholesterol (mg/100 kcal)	15.05	12.05
Fatty acids (g/100 g of fat)		
6:0	0.07	0.10
8:0	0.11	0.10
10:0	0.21	0.15
12:0	0.21	0.30
14:0	1.82	0.94
16:0	22.15	19.77
18:0	10.43	8.48
20:0	0.04	0.05
16:1	2.85	1.82
18:1	32.94	27.76
20:1	0.14	0.20
18:2	23.18	34.27
18:3	2.88	3.50
SFA (g/100 kcal)	1.09	0.55
PUFA (g/100 kcal)	0.56	1.14
MUFA (g/100 kcal)	1.37	1.29

P/S polyunsaturated/saturated fatty acids, SFA saturated fatty acids, PUFA polyunsaturated fatty acids, MUFA monounsaturated fatty acids

Plasma Lipid Concentrations

Blood samples after collection were centrifuged at 1,500 rpm for 15 min to separate RBC and plasma. Separated aliquots were immediately stored at −80 °C until analysis. Plasma total and HDL cholesterol and TAG concentrations were measured enzymatically by Quest Diagnostics Nichols Institute, a certified Center for Disease Control (CDC) Lipid Research Clinic.

Desmosterol and lathosterol levels were measured in plasma as markers for cholesterol synthesis and campesterol and β-sitosterol levels were measured as cholesterol absorption markers [30]. Sterol concentrations were determined by gas liquid chromatography (GLC), as described by Ntanos and Jones [31], using 5α-cholestane (Sigma-Aldrich Canada Ltd, Oakville, ON, Canada) as an internal standard. Briefly, after saponification, non-saponified materials were extracted and derivatized with TMSi reagent [pyridine-hexamethyl disilazantrimethyl chlorosilane (9:3:1,

vol:vol)] [32]. Sterols were identified using known standards (Sigma-Aldrich Canada Ltd, Oakville, ON, Canada).

Cholesterol Absorption

Free cholesterol was extracted from RBC according to established methods [33]. ^{13}C cholesterol enrichments in RBC lipid extracts were determined using on-line gas chromatography/combustion/isotope ratio mass spectrometry approach (Agilent 6890N chromatograph interfaced with a Finnigan Delta V Pulse isotope ratio mass spectrometer (Bremen, Germany)). Isotope abundance, expressed in delta (d) per mil (‰), was calculated using CO_2 as a reference gas and further corrected against the international reference standard, Pee Dee Belemnite limestone. The measurement of free-cholesterol deuterium enrichment was performed using online gas chromatography/pyrolysis/isotope ratio mass spectrometry and expressed relative to standard mean ocean water and a series of standards of known enrichment. Isotope abundance, expressed in d ‰, was calculated using H_2 as reference gas. The average ^{13}C and D_7 enrichments of 48 and 72 h RBC free cholesterol relative to baseline samples were used to calculate the cholesterol absorption coefficient using the ratio of orally ingested ^{13}C cholesterol to intravenously administered D_7 cholesterol as described by Bosner et al. [27] and by us [29].

Cholesterol Fractional Synthetic Rate

Cholesterol synthesis rates were assessed after 24 h of deuterium water administration using the deuterium incorporation approach [34] as described before [29]. This method measures cholesterol synthesis as the rate of deuterium incorporation from body water into RBC membrane free cholesterol over a 24 h period. Deuterium enrichment was measured in both RBC free cholesterol and plasma water as described above. Enrichments were expressed relative to standard mean ocean water using a calibration curve of working standards. FSR is taken to represent RBC free-cholesterol deuterium enrichment values relative to the corresponding mean plasma water sample enrichment after correcting for the free-cholesterol pool. FSR represents that fraction of the cholesterol pool that is synthesized in 24 h and is calculated as per the equation [34].

Intraluminal Cholesterol Solubilization

After blood collection on day 14, duodenal aspirates were collected and treated as described [29]. Topical anesthesia was applied to the nose and throat, and sedation was used with intravenous midazolam if subjects wished. A nasoduodenal tube was placed with fluoroscopic guidance with

the tube tip placed at the ligament of Trietz, and 12–20 ml of duodenal drainage was collected by siphonage for 15 min (–15 to 0 time). Subjects then ingested a meal consisting of olive oil, egg and egg white, sucrose, vanilla extract and 0.15 M NaCl in 240 ml water [29]. Duodenal drainage was collected in 15 min intervals for 90 min and then one 30 min interval. Anti-microbial and anti-bacterial compounds were added as samples were collected. After completion of collection periods, 0.5 ml aliquots were saved to measure lipids in luminal contents and remaining 12–15 ml separated into the subphase. The subphase was separated into vesicles and non-vesicles by size-exclusion column chromatography as described [35]. Cholesterol was measured directly in the total and subphase intraluminal contents by GLC; the ratio of subphase to total cholesterol was considered solubilized cholesterol. Cholesterol was also measured in the fractions from the size exclusion columns mostly by GLC. Vesicular cholesterol was that which came off the column in the void volume and non-vesicular cholesterol, including micellar cholesterol, was that which was eluted from the column after the initial vesicular fraction.

Apolipoprotein Genotypes

DNA from peripheral blood was isolated according to instructions provided in the High Pure PCR Template Preparation Kit (Boehringer Mannheim, Indianapolis, IN, USA). ApoE and ApoA-IV genotypes were determined as described by earlier [36, 37].

Statistical Analysis

Results were expressed as means \pm SEM obtained from ANOVA using the root mean square error to estimate the pooled standard error. End point variables were tested for statistical significance by student's t test and repeated measures ANOVA with $p < 0.05$. The correlations among plasma lipid profile, cholesterol absorption and synthesis, cholesterol precursors, sterols and their ratios were analyzed using Pearson correlations. All statistical measures were analyzed using Statistical Package for the Social Sciences (SPSS) version 10.0.

Results

Seventeen subjects (8 males and 9 females) with an average of 26.5 ± 3.6 years of age, 70.9 ± 16.6 kg and BMI of 24.3 ± 3.3 kg/m² (Table 2) started the study of which 16 completed both phases of study. Fifteen Caucasians and one African subject participated. One subject withdrew from the study after completing first phase which was a

Table 2 Baseline characteristics of subjects

Variables	Subjects (n = 17)
Age (years)	26.47 ± 3.57
Body weight (kg)	70.89 ± 16.65
Height (cm)	169.63 ± 13.01
Body mass index (kg/m ²)	24.3 ± 3.27
Total cholesterol (mg/dl)	163.4 ± 26.5
LDL (mg/dl)	95.1 ± 21.9
HDL (mg/dl)	51.0 ± 19.47
Triglycerides (mg/dl)	89.0 ± 34.6

high ratio P/S diet due to personal reasons and not related to the study. No adverse events were recorded during the study due to the diet.

No significant changes were observed in body weights when comparing both between the phases and between the baseline and end points of each phase. Plasma total cholesterol ($P = 0.015$) and LDL-cholesterol ($P = 0.014$) concentrations were reduced as early as 14 days of consumption of a diet with a high P/S ratio (Table 3). By day 19 of the study, a further reduction in total ($P = 0.011$) and LDL-cholesterol concentrations ($P = 0.003$) occurred such that total cholesterol was reduced $\approx 8\%$ and LDL-cholesterol was reduced $\approx 12\%$ (Table 3). No impact of diet on HDL-cholesterol or TAG concentrations was observed at either time point after diet consumption.

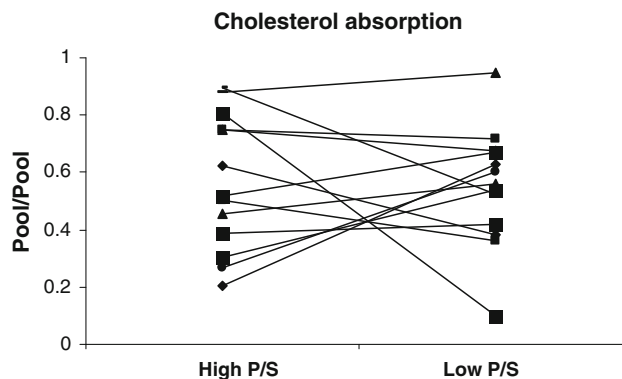
No significant difference was found in fractional cholesterol absorption determined by dual stable isotope kinetics measurement (Fig. 1). Cholesterol absorption markers including β -sitosterol and campesterol showed no significant changes in their concentrations as well their ratios with cholesterol in plasma between high and low P/S ratio diet phases (Table 4). In parallel with results, there was no difference in the solubilized cholesterol in the

Table 3 Lipid profile of subjects during and after consuming a high or low P/S ratio diet

Variables	Total cholesterol (mg/dl)	LDL (mg/dl)	HDL (mg/dl)	TG (mg/dl)
High P/S (day 14) ^a	147.2 ± 7.5*	83.4 ± 6.3*	47.7 ± 4.0	81.1 ± 6.0
Low P/S (day 14) ^a	158.6 ± 7.6	94.4 ± 6.4	47.1 ± 3.4	87.0 ± 6.9
High P/S (day 19) ^b	144.1 ± 9.2*	79.9 ± 7.1*	49.3 ± 4.5	74.7 ± 6.8
Low P/S (day 19) ^b	155.8 ± 9.8	91.8 ± 7.4	49.5 ± 4.5	74.6 ± 8.5

Values are expressed as means ± SEM

* Significant at $P < 0.05$ compared with low P/S ratio diet at same time points ^a $n = 16$, ^b $n = 13$

**Fig. 1** Cholesterol absorption for each subject fed a high or low P/S ratio diet ($n = 13$)**Table 4** Plasma sterols concentration in plasma and their ratios with cholesterol and cholesterol precursors in subjects after consuming a high or low P/S ratio diet

Variables	Low P/S	High P/S
Campesterol ($\mu\text{mol/l}$)	11.3 ± 1.0	11.6 ± 0.7
β -Sitosterol ($\mu\text{mol/l}$)	6.7 ± 0.8	7.0 ± 0.7
Campesterol + β -sitosterol ($\mu\text{mol/l}$)	18.0 ± 1.5	18.6 ± 1.2
Campesterol:cholesterol ($\mu\text{mol}/\text{mmol}$)	2.4 ± 0.3	2.9 ± 0.2
β -Sitosterol:cholesterol ($\mu\text{mol}/\text{mmol}$)	1.4 ± 0.2	1.8 ± 0.2
(Campesterol + β -sitosterol):cholesterol ($\mu\text{mol}/\mu\text{mol}$)	3.8 ± 0.4	4.6 ± 0.3
Lathosterol:campesterol ($\mu\text{mol}/\mu\text{mol}$)	1.0 ± 0.2	1.0 ± 0.2
Lathosterol: β -sitosterol ($\mu\text{mol}/\mu\text{mol}$)	1.7 ± 0.4	1.6 ± 0.4

Values are expressed as means ± SEM ($n = 10$)

lumen of the subjects containing either diet (Fig. 2a). As might be expected, the percentage of non-vesicular cholesterol also remained similar between all subjects (Fig. 2b).

No apparent change was seen in cholesterol absorption, or fractional synthetic rate of cholesterol with different dietary fatty acid composition (Fig. 3). Indirect measures of cholesterol synthesis, plasma cholesterol precursor levels, i.e. desmosterol and lathosterol, failed to significantly differ between groups (Table 5).

Discussion

Our results confirm that diets consisting of greater P/S ratios had reduced plasma cholesterol concentrations, specifically LDL-cholesterol [3, 5, 38–40]. Importantly, our results specifically show that the decrease in LDL-cholesterol levels was not due to an effect of dietary fatty acid composition on cholesterol absorption or synthetic rate. Support for these results was confirmed by indirect

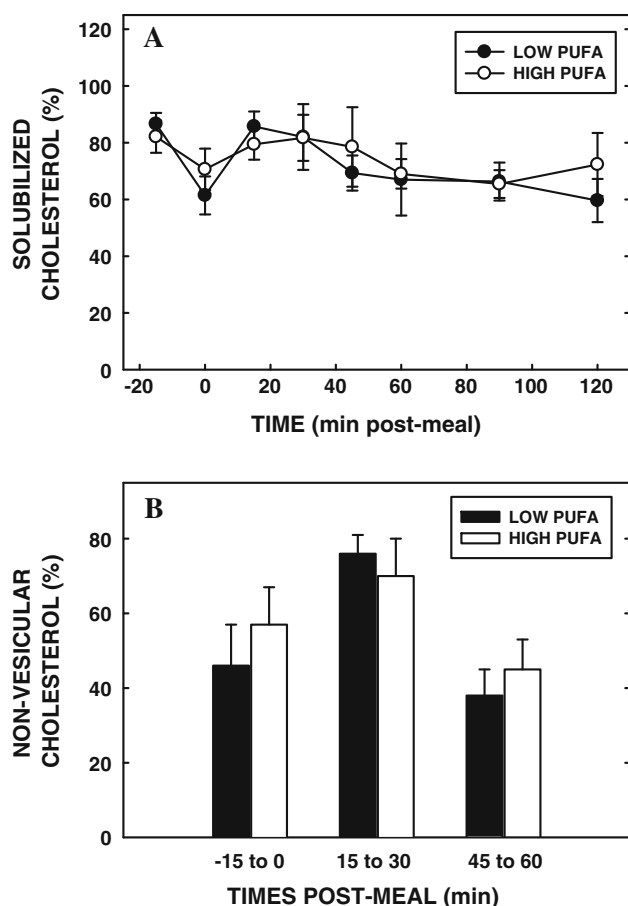


Fig. 2 The amount of cholesterol solubilized in the aqueous fraction (subphase) of the luminal samples of subjects fed low or high PUFA diets. After an overnight fast, a naso-duodenal tube was placed at the ligament of Trietz and 15–20 ml of luminal sample collected. Subjects consumed a liquid meal as described in the study design section of the Research Plan, and samples collected from the lumen every 15 min for 2 h and then for 30 min. Samples were spun to separate the subphase from total contents. The amount of cholesterol in the total and subphase was measured by GLC and amount solubilized shown (a). The percentages of total cholesterol present as non-vesicular cholesterol in the subphase at –15 to 0, 15 to 30, and 45 to 60 min post-meal are shown (b). Data are presented as means \pm SEM ($n = 16$)

measurements of cholesterol trafficking. Specifically, the extent of non-vesicular cholesterol, likely present as micelles, was the same in lumens of subjects on either diet. As cholesterol needs to be packaged into micelles prior to absorption [21], it is not surprising that cholesterol absorption was not different. Likewise, circulating plant sterol concentrations were similar, an indication of similar cholesterol absorption [30]. For cholesterol synthesis, cholesterol biosynthetic precursors in the circulation were similar as well [30].

Until now, the relationship between dietary fat composition and cholesterol absorption in humans has remained unclear since methods used included different indirect

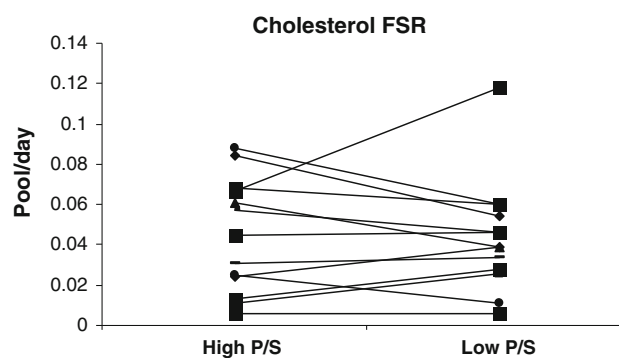


Fig. 3 Cholesterol fractional synthesis rate for each subject fed a high or low P/S ratio diet ($n = 13$)

Table 5 Plasma cholesterol precursor concentration in plasma and their ratios with cholesterol in subjects after consuming a high or low P/S ratio diet

Variables	Low P/S	High P/S
Desmosterol ($\mu\text{mol/l}$)	12.0 ± 0.9	11.6 ± 1.1
Lathosterol ($\mu\text{mol/l}$)	11.6 ± 1.5	11.14 ± 1.6
Desmosterol:cholesterol ($\mu\text{mol/mmol}$)	2.5 ± 0.3	2.9 ± 0.2
Lathosterol:cholesterol ($\mu\text{mol/mmol}$)	2.5 ± 0.4	2.7 ± 0.3

Values are expressed as means \pm SEM ($n = 10$)

absorption measurements, variably controlled subject populations, and variations in dietary cholesterol. Unlike our study, in which dietary cholesterol was rigorously controlled, subjects were normolipemic, subjects from specific apo E genotypes, and cholesterol absorption measured by the dual isotope method; most previous studies were much less carefully controlled using state-of-the-art methods at the time of publication. McNamara et al. [9] evaluated the effect of a dietary cholesterol challenge within diets containing either saturated or polyunsaturated fat. Fractional cholesterol absorption was not affected by the P/S ratio, regardless of amount of cholesterol fed. Grundy and Ahrens directly compared cholesterol absorption in subjects given SFA versus high P/S diets containing relatively high levels of dietary cholesterol and observed no differences in fractional cholesterol absorption and marked variability [41]. Using a cross over design, Wood et al. [22] studied the effect of liquid formula containing dietary fat as predominantly saturated or unsaturated fat plus high levels of cholesterol in five normolipidemic adults and found decreased cholesterol absorption when subjects received diets containing predominantly unsaturated fat. Finally, Miettinen et al. discovered that cholesterol absorption decreased when changing from a diet relatively high in cholesterol and fat (38 % calories) with mostly saturated fat (P/S = 0.28) to one with half as much cholesterol and less fat (24 % calories) with a higher P/S

ratio (0.72). Even though there was less amount of fat and cholesterol in the diet, impact of changes with dietary fat composition on cholesterol was very large [10].

A number of additional studies have been completed in which sterol synthesis was measured. As reduced cholesterol absorption will lead to increased sterol synthesis, these studies could also help delineate the effect of dietary fatty acid on cholesterol absorption. Interestingly, a number of studies found that the fractional synthetic rate for cholesterol was higher in subjects fed PUFA-containing diets compared to baseline diets or diets containing high SFA [40, 42–45]. If PUFA only affected absorption, these studies would suggest that PUFA affected cholesterol absorption in subjects of these other studies. However, other variables exist that can lead to a separation of the two processes. For example, different fatty acids can have direct impact upon metabolism. Likewise, some of these studies used hypercholesterolemic or obese subjects. In support of our absorption data, we detected no differences in cholesterol synthesis by stable isotope or by cholesterol biosynthetic intermediate concentrations.

Cholesterol absorption measurements have also been carried out in various animal models. Studies in rats and rabbits have shown that dietary PUFA either increased or decreased cholesterol absorption [46–48]. Mott et al. showed cholesterol absorption to be similar in baboons fed diets containing either saturated or unsaturated fat independent of cholesterol content [49, 50], whereas Tanaka and Portman [51] showed that PUFA versus SFA-enriched diets lead to increased cholesterol absorption in squirrel monkeys. Part of the differences in the various models are likely due to variations in cholesterol metabolism [50], making the current studies important and relevant as they were completed in humans.

Even though there was no effect on cholesterol absorption in the current studies, plasma cholesterol concentrations were still reduced in subjects consuming a greater P/S ratio. Over the years, several different processes have been shown to be affected by dietary PUFA. Daumerie et al. [52] demonstrated a reduction in hepatic LDL receptor activity and elevated LDL cholesterol production rate in hamsters fed with a SFA-enriched diet compared to one enriched in PUFA or MUFA, ultimately leading to increased plasma LDL-cholesterol concentrations [52–54]. Perhaps SFA have a greater effect on increasing plasma cholesterol versus the impact of PUFA on decreasing plasma cholesterol levels, depending on the baseline or comparison. This is actually supported by equations devised by Keys et al. [55] and Hegsted et al. [2] and more recently by Etherton and colleagues [56] that gives a relative change in plasma cholesterol based on the nature of the fat fed. Other effects of lipids on metabolism might also occur. In addition, high PUFA containing diets

lead to reduced activities of lipogenic enzymes such as phosphatidase, phosphohydrolase and diacylglycerol acyl-transferase compared with low PUFA containing olive oil and thereby decrease serum lipid concentrations [57]. Consumption of a diet with high P/S ratio also increases postprandial fat oxidation [42, 58]. Thus, some of these non-absorptive effects of PUFA must have played a role in the reduction of plasma cholesterol when higher P/S diets are fed to normocholesterolemic subjects.

In conclusion, consumption of a high P/S ratio diet did not affect cholesterol absorption or synthesis in normolipidemic subjects, despite a decrease in total and LDL cholesterol concentrations. Results indicate that high P/S diets alter lipids through mechanisms other than cholesterol absorption and synthesis in normolipidemic subjects.

Acknowledgments We thank YenMing Chan, Richardson Centre for Functional Foods and Nutraceuticals, and Dr. Scot Harding, adjunct professor, Department of Human Nutritional Sciences, University of Manitoba for their help with the analytical part of the study. We also thank Suzanne Summer and the staff of the Body Composition Core of the General Clinical Research Center for their help with dietary management for the study. We were also supported by the National Institute of Health RR 08084 and DK 068463.

Conflict of interest No authors have any conflict of interest with the current study.

References

- Ahrens EH Jr, Insull W Jr, Blomstrand R, Hirsch J, Tsaltas TT, Peterson ML (1957) The influence of dietary fats on serum-lipid levels in man. *Lancet* 272:943–953
- Hegsted DM, McGandy RB, Myers ML, Stare FJ (1965) Quantitative effects of dietary fat on serum cholesterol in man. *Am J Clin Nutr* 17:281–295
- Mattson FH, Grundy SM (1985) Comparison of effects of dietary saturated, monounsaturated, and polyunsaturated fatty acids on plasma lipids and lipoproteins in man. *J Lipid Res* 26:194–202
- Mensink RP, Katan MB (1989) Effect of a diet enriched with monounsaturated or polyunsaturated fatty acids on levels of low-density and high-density lipoprotein cholesterol in healthy women and men. *N Engl J Med* 321:436–441
- Hodson L, Skeaff CM, Chisholm WA (2001) The effect of replacing dietary saturated fat with polyunsaturated or monounsaturated fat on plasma lipids in free-living young adults. *Eur J Clin Nutr* 55:908–915
- Montoya MT, Porres A, Serrano S, Fruchart JC, Mata P, Gerique JA, Castro GR (2002) Fatty acid saturation of the diet and plasma lipid concentrations, lipoprotein particle concentrations, and cholesterol efflux capacity. *Am J Clin Nutr* 75:484–491
- Lecerf JM (2009) Fatty acids and cardiovascular disease. *Nutr Rev* 67:273–283
- Buyken AE, Flood V, Rochtchina E, Nestel P, Brand-Miller J, Mitchell P (2010) Modifications in dietary fat quality are associated with changes in serum lipids of older adults independently of lipid medication. *J Nutr* 140:88–94
- McNamara DJ, Kolb R, Parker TS, Batwin H, Samuel P, Brown CD, Ahrens EH Jr (1987) Heterogeneity of cholesterol

- homeostasis in man. Response to changes in dietary fat quality and cholesterol quantity. *J Clin Invest* 79:1729–1739
10. Miettinen TA, Gylling H, Vanhanen H, Ollus A (1992) Cholesterol absorption, elimination, and synthesis related to LDL kinetics during varying fat intake in men with different apolipoprotein E phenotypes. *Arterioscler Thromb* 12:1044–1052
 11. Dietschy JM (1998) Dietary fatty acids and the regulation of plasma low density lipoprotein cholesterol concentrations. *J Nutr* 128:444S–448S
 12. Brunham LR, Kruit JK, Iqbal J, Fievet C, Timmins JM, Pape TD, Coburn BA, Bissada N, Staels B et al (2006) Intestinal ABCA1 directly contributes to HDL biogenesis in vivo. *J Clin Invest* 116:1052–1062
 13. Timmins JM, Lee JY, Boudyguina E, Kluckman KD, Brunham LR, Mulya A, Gebre AK, Coutinho JM, Colvin PL et al (2005) Targeted inactivation of hepatic Abca1 causes profound hypoalphalipoproteinemia and kidney hypercatabolism of apoA-I. *J Clin Invest* 115:1333–1342
 14. Acton S, Rigotti A, Landschulz KT, Xu S, Hobbs HH, Krieger M (1996) Identification of scavenger receptor SR-BI as a high density lipoprotein receptor. *Science* 271:518–520
 15. Hernell O, Stagers JE, Carey MC (1990) Physical-chemical behavior of dietary and biliary lipids during intestinal digestion and absorption. 2. Phase analysis and aggregation states of luminal lipids during duodenal fat digestion in healthy adult human beings. *Biochemistry* 29:2041–2056
 16. Swell L, Trout EC Jr, Hopper JR, Field H Jr, Treadwell CR (1958) Specific function of bile salts in cholesterol absorption. *Proc Soc Exp Biol Med* 98:174–176
 17. Holt PR, Fairchild BM, Weiss J (1986) A liquid crystalline phase in human intestinal contents during fat digestion. *Lipids* 21:444–446
 18. Hofmann AF, Borgstrom B (1962) Physico-chemical state of lipids in intestinal content during their digestion and absorption. *Fed Proc* 21:43–50
 19. Donovan JM, Timofeyeva N, Carey MC (1991) Influence of total lipid concentration, bile salt:lecithin ratio, and cholesterol content on inter-mixed micellar/vesicular (non-lecithin-associated) bile salt concentrations in model bile. *J Lipid Res* 32:1501–1512
 20. Woollett LA, Buckley DD, Yao L, Jones PJ, Granholm NA, Tolley EA, Tso P, Heubi JE (2004) Cholic acid supplementation enhances cholesterol absorption in humans. *Gastroenterology* 126:724–731
 21. Woollett LA, Wang Y, Buckley DD, Yao L, Chin S, Granholm N, Jones PJ, Setchell KD, Tso P, Heubi JE (2006) Micellar solubilization of cholesterol is essential for absorption in humans. *Gut* 55:197–204
 22. Wood PD, Shioda R, Kinsell LW (1966) Dietary regulation of cholesterol metabolism. *Lancet* 2:604–607
 23. Jump DB, Botolin D, Wang Y, Xu J, Christian B, Demeure O (2005) Fatty acid regulation of hepatic gene transcription. *J Nutr* 135:2503–2506
 24. Iwayanagi Y, Takada T, Tomura F, Yamanashi Y, Terada T, Inui K, Suzuki H (2011) Human NPC1L1 expression is positively regulated by PPARalpha. *Pharm Res* 28:405–412
 25. Gylling H, Miettinen TA (1992) Cholesterol absorption and synthesis related to low density lipoprotein metabolism during varying cholesterol intake in men with different apoE phenotypes. *J Lipid Res* 33:1361–1371
 26. McCombs RJ, Marcadis DE, Ellis J, Weinberg RB (1994) Attenuated hypercholesterolemic response to a high-cholesterol diet in subjects heterozygous for the apolipoprotein A-IV-2 allele. *N Engl J Med* 331:706–710
 27. Bosner MS, Ostlund RE Jr, Osofisan O, Grosklos J, Fritschle C, Lange LG (1993) Assessment of percent cholesterol absorption in humans with stable isotopes. *J Lipid Res* 34:1047–1053
 28. Zilversmit DB (1972) A single blood sample dual isotope method for the measurement of cholesterol absorption in rats. *Proc Soc Exp Biol Med* 140:862–865
 29. Woollett LA, Buckley DD, Yao L, Jones PJ, Granholm NA, Tolley EA, Heubi JE (2003) Effect of ursodeoxycholic acid on cholesterol absorption and metabolism in humans. *J Lipid Res* 44:935–942
 30. Nissinen MJ, Miettinen TE, Gylling H, Miettinen TA (2009) Applicability of non-cholesterol sterols in predicting response in cholesterol metabolism to simvastatin and fluvastatin treatment among hypercholesterolemic men. *Nutr Metab Cardiovasc Dis* 20:308–316
 31. Ntanos FY, Jones PJ (1998) Effects of variable dietary sitostanol concentrations on plasma lipid profile and phytosterol metabolism in hamsters. *Biochim Biophys Acta* 1390:237–244
 32. Lutjohann D, Meese CO, Crouse JR 3rd, von Bergmann K (1993) Evaluation of deuterated cholesterol and deuterated sitostanol for measurement of cholesterol absorption in humans. *J Lipid Res* 34:1039–1046
 33. Folch J, Lees M, Sloane Stanley GH (1957) A simple method for the isolation and purification of total lipides from animal tissues. *J Biol Chem* 226:497–509
 34. Jones PJ, Leitch CA, Li ZC, Connor WE (1993) Human cholesterol synthesis measurement using deuterated water. Theoretical and procedural considerations. *Arterioscler Thromb* 13:247–253
 35. Yao L, Heubi JE, Buckley DD, Fierra H, Setchell KD, Granholm NA, Tso P, Hui DY, Woollett LA (2002) Separation of micelles and vesicles within luminal aspirates from healthy humans: solubilization of cholesterol after a meal. *J Lipid Res* 43:654–660
 36. Hixson JE, Powers PK (1991) Restriction isotyping of human apolipoprotein A-IV: rapid typing of known isoforms and detection of a new isoform that deletes a conserved repeat. *J Lipid Res* 32:1529–1535
 37. Hixson JE, Vernier DT (1990) Restriction isotyping of human apolipoprotein E by gene amplification and cleavage with HhaI. *J Lipid Res* 31:545–548
 38. Diniz YS, Cicogna AC, Padovani CR, Santana LS, Faine LA, Novelli EL (2004) Diets rich in saturated and polyunsaturated fatty acids: metabolic shifting and cardiac health. *Nutrition* 20:230–234
 39. Mensink RP (1994) Dietary monounsaturated fatty acids and serum lipoprotein levels in healthy subjects. *Atherosclerosis* 110(Suppl):S65–S68
 40. Mazier MJ, Jones PJ (1997) Diet fat saturation and feeding state modulate rates of cholesterol synthesis in normolipidemic men. *J Nutr* 127:332–340
 41. Grundy SM, Ahrens EH Jr (1970) The effects of unsaturated dietary fats on absorption, excretion, synthesis, and distribution of cholesterol in man. *J Clin Invest* 49:1135–1152
 42. Jones PJ, Ridgen JE, Phang PT, Birmingham CL (1992) Influence of dietary fat polyunsaturated to saturated ratio on energy substrate utilization in obesity. *Metabolism* 41:396–401
 43. Jones PJ, Lichtenstein AH, Schaefer EJ (1994) Interaction of dietary fat saturation and cholesterol level on cholesterol synthesis measured using deuterium incorporation. *J Lipid Res* 35:1093–1101
 44. Jones PJ, Lichtenstein AH, Schaefer EJ, Namchuk GL (1994) Effect of dietary fat selection on plasma cholesterol synthesis in older, moderately hypercholesterolemic humans. *Arterioscler Thromb* 14:542–548
 45. Jones PJ, Ausman LM, Croll DH, Feng JY, Schaefer EA, Lichtenstein AH (1998) Validation of deuterium incorporation against sterol balance for measurement of human cholesterol biosynthesis. *J Lipid Res* 39:1111–1117

46. Sheehe DM, Green JB, Green MH (1980) Influence of dietary fat saturation on lipid absorption in the rat. *Atherosclerosis* 37:301–310
47. Thomson AB, Keelan M, Garg ML, Clandinin MT (1989) Influence of dietary fat composition on intestinal absorption in the rat. *Lipids* 24:494–501
48. Meijer GW, Lemmens AG, Versluis A, Van Zutphen LF, Beynen AC (1991) The hypercholesterolemic effect of dietary coconut fat versus corn oil in hypo- or hyperresponsive rabbits is not exerted through influencing cholesterol absorption. *Lipids* 26:340–344
49. Mott GE, Jackson EM, Morris MD (1980) Cholesterol absorption in baboons. *J Lipid Res* 21:635–641
50. Eggen DA (1974) Cholesterol metabolism in rhesus monkey, squirrel monkey, and baboon. *J Lipid Res* 15:139–145
51. Tanaka N, Portman OW (1977) Effect of type of dietary fat and cholesterol on cholesterol absorption rate in squirrel monkeys. *J Nutr* 107:814–821
52. Daumerie CM, Woollett LA, Dietschy JM (1992) Fatty acids regulate hepatic low density lipoprotein receptor activity through redistribution of intracellular cholesterol pools. *Proc Natl Acad Sci USA* 89:10797–10801
53. Woollett LA, Spady DK, Dietschy JM (1992) Saturated and unsaturated fatty acids independently regulate low density lipoprotein receptor activity and production rate. *J Lipid Res* 33:77–88
54. Woollett LA, Spady DK, Dietschy JM (1989) Mechanisms by which saturated triacylglycerols elevate the plasma low density lipoprotein-cholesterol concentration in hamsters. Differential effects of fatty acid chain length. *J Clin Invest* 84:119–128
55. Keys A, Anderson JT, Grande F (1965) Serum cholesterol response to changes in the diet: IV. Particular saturated fatty acids in the diet. *Metabolism* 14:776–787
56. Derr J, Kris-Etherton PM, Pearson TA, Seligson FH (1993) The role of fatty acid saturation on plasma lipids, lipoproteins, and apolipoproteins: II. The plasma total and low-density lipoprotein cholesterol response of individual fatty acids. *Metabolism* 42:130–134
57. Takeuchi H, Nakamoto T, Mori Y, Kawakami M, Mabuchi H, Ohishi Y, Ichikawa N, Koike A, Masuda K (2001) Comparative effects of dietary fat types on hepatic enzyme activities related to the synthesis and oxidation of fatty acid and to lipogenesis in rats. *Biosci Biotechnol Biochem* 65:1748–1754
58. Clandinin MT, Wang LC, Rajotte RV, French MA, Goh YK, Kielo ES (1995) Increasing the dietary polyunsaturated fat content alters whole-body utilization of 16:0 and 10:0. *Am J Clin Nutr* 61:1052–1057

of them related to cardiac or cerebral ischemia [1]. In most cases, atherosclerosis is the pathology behind cardiovascular complications. Atherosclerosis is a complex systemic disorder with a progressive development involving various cell types [2]. Among them, vascular smooth muscle cells (VSMC) play important roles throughout the slow progression of the pathology. Indeed, VSMC migration and proliferation from the media toward the intima of the vessel wall contribute to stable plaque development. They also synthesize extracellular matrix proteins, part of building blocks of a thick fibrous cap. In advanced lesions, VSMC apoptosis favors plaque instability by thinning the fibrous cap, increasing thereby risks of plaque rupture and thrombosis [3, 4].

Among risk factors of CVD, type 2 diabetes (T2D) has become a widespread concern. The American Centers for Disease Control and Prevention have approximated in the 2011 National Diabetes Fact Sheet that 25.8-million people, 8.3 % of the population in USA, were affected by diabetes in 2010 [5]. A major cardiovascular complication of T2D is an accelerated process of atherosclerosis pathogenesis, associated with metabolic syndrome and insulin resistance [6]. Hyperinsulinemia and a high plasma level of free fatty acids (FFA) are well known characteristics of these conditions. While hyperinsulinemia affects the proliferation, migration and contractility of VSMC [7–9], it is recognized that FFA at high concentration, and according to their nature, can play various roles on VSMC functions.

Saturated fatty acids (SFA) are present in high proportion in the Western diet, associated with increased risk of developing CVD [10, 11]. Many studies have demonstrated that SFA have a negative impact on different cell types, principally by inducing apoptosis. Indeed, it has been reported that SFA such as palmitic or stearic acids cause higher level of apoptosis in VSMC [12, 13], but also in endothelial cells [14, 15], hepatocytes [16], β -cells [17, 18] and cardiomyocytes [19, 20]. On the other hand, monounsaturated fatty acids (MUFA), which are more abundant in the Mediterranean diet, are recognized for their protective impact against CVD [21–23]. MUFA such as palmitoleic or oleic acids can reduce the impact of SFA on apoptosis [13, 15, 16]. It has also been demonstrated in different studies that oleic acid (OLA) promotes VSMC proliferation and migration [24–26]. Thus, OLA seems to have an important protective role in late stages of atherosclerosis, by preventing plaque thinning.

Most of these studies were performed with individual FFA or with a combination of two, but rarely with complex mixes, although dietary fatty acids are composed of a group of FFA rather than being limited to one or two of them. Therefore, the role of FFA on VSMC apoptosis when they are combined in groups of various proportions is still unclear. In one of our previous studies, we found that

VSMC apoptosis level was higher when cells were treated with adipocyte supernatants isolated from male mice fed with a high-fat diet from animal origin richer in SFA (named AD, for animal diet) than when treated with adipocyte supernatants from male mice fed with a high-fat diet from vegetal origin richer in MUFA (named VD, for vegetal diet) [27]. This level was further increased when adipocytes were stimulated with a high dose of insulin (unpublished data). With these results in mind, we hypothesized that in a hyperinsulinemic state, a combination of synthetic FFA with a higher proportion of SFA (hSFA) would induce more elevated VSMC apoptosis rates than a combination of FFA with a higher proportion of MUFA (hMUFA).

Thus, this work aims to assess the impact of these two FFA combinations, derived from both diets in our previous studies, on the proliferation and apoptosis of VSMC in the presence or not of a high insulin dose. The two combinations tested contain the same FFA but in different proportions. Our results show that the FFA combinations have a pro-apoptotic impact on VSMC, principally due to SFA. The presence of OLA in these combinations reduces VSMC apoptosis rates induced by SFA, even more than when OLA was alone. Such an effect was modulated by the FFA ratios and the presence or not of a high insulin dose. In the presence of a competition between pro- and anti-apoptotic mechanisms, these results suggest that the relative concentration of each FFA in a combination (SFA vs. MUFA) is as important as their total concentrations to determine their impact on VSMC functions.

Materials and Methods

Cell Isolation and Culture

VSMC were isolated from the aortas of 10-week old male mice C57BL/6 (Charles River, Montreal, Canada) using a method modified from Ray et al. [28]. Briefly, mice were euthanized by a ketamine/xylazine mix and full length aortas, from aortic arch to kidneys, were extracted. Freshly isolated aortas were dissected into 2–3 mm pieces and digested with type II collagenase (Invitrogen, Carlsbad, CA, USA) for 5 h at 37 °C, 5 % CO₂. The digested aortas were then washed twice by centrifugation for 5 min at 300×g to remove all traces of collagenase. The obtained VSMC were put in culture to be amplified in Dulbecco's Modified Eagle Medium (DMEM) low glucose (Invitrogen), 1 % penicillin–streptomycin (Invitrogen), 10 % fetal bovine serum (FBS) (PAA Laboratories, Pasching, Austria), 0.5 ng/ml EGF and 2 ng/ml FGF-basic (Pepro-Tech, Rocky Hill, NJ, USA), at 37 °C, 5 % CO₂. The smooth muscle cell phenotype was confirmed by a positive

staining for alpha smooth muscle actin (rabbit monoclonal antibody, ab32575, 1:400) and for SM-22 α (rabbit polyclonal antibody, ab14106, 1:100) (Abcam, Cambridge, MA, USA), both specific markers of smooth muscle cells. Positive stains were visualized by immunofluorescence with a confocal microscope (LSM510) and analysed with a Zeiss LSM Image Browser System (Zeiss, Toronto, Canada). Cells at passage 4 or 5 were used throughout this study. All animal procedures in this protocol (#2010-59-1) were approved by the Animal Ethics Committee of the Montreal Heart Institute.

Fatty Acid Preparation and VSMC Stimulations

Palmitic [C16:0, PAM], palmitoleic [C16:1n-7, PAL], stearic [C18:0, STA], oleic [C18:1n-9, OLA], linolenic [C18:3n-3, ALA] and arachidonic [C20:4n-6, ARA] acids (Sigma-Aldrich, St. Louis, MO, USA) were dissolved at 50 mM in 80 °C water containing a 10 % excess of NaOH 1 N (55 mM). After dissolution, each free fatty acid (FFA) was immediately added to a 20 % fatty acid-free bovine serum albumin (FA-free BSA) (PAA Laboratories) solution that has been pre-heated at 45 °C to obtain 10 mM FFA stock solutions with a molar ratio of 3.3:1 FFA/BSA. The FFA-BSA complexes were stirred at 45 °C until complete dissolution, filter sterilized and stored in aliquots at –20 °C until usage. For VSMC stimulations, cells were treated whether with a combination of FFA at a final concentration of 900 μ M or with individual FFA at the concentration found in each combination. The two combinations used contained the same mix of fatty acids but at different ratios and were derived from diets with fat of animal origin (AD, D12492, Research Diets, New Brunswick, NJ, USA) and vegetal origin (VD, D06061202, Research Diets) used in our previous studies [27]. The concentrations of each FFA present in both combinations are shown in Table 1. For the control condition, cells were treated with a BSA solution without FFA. The VSMC stimulations were done for 24 or 72 h, depending on the measured parameter, in the presence or not of 1 nM insulin (Sigma) in 1 % FBS DMEM medium.

Proliferation Assays by Manual Counts

The effects of fatty acid combinations and insulin on proliferation were evaluated by manual cell counts. VSMC were plated into 24-well culture plates at a seeding density of 1×10^4 cells/well and allowed to grow for 24 h. After an overnight starvation in a 0.1 % FBS DMEM medium and 72 h of stimulation with the fatty acid combinations, with or without insulin, cells in each well were trypsinized and re-suspended in 100 μ l of 20 % FBS DMEM medium for cell count. Live and dead cells were counted by Trypan

Table 1 Molar ratios of the two fatty acid combinations

Fatty acid (μ M/900 μ M)	hSFA combination	hMUFA combination
C16:0 PAM	244	135
C16:1n-7 PAL	39	1.8
C18:0 STA	139	106
C18:1n-9 OLA	443	650
C18:3n-3 ALA	18	8.1
C20:4n-6 ARA	17.1	0
Total SFA	383	241
Total MUFA <i>cis</i>	482	652
Total PUFA <i>cis</i>	35.1	8.1

PAM palmitic acid, PAL palmitoleic acid, STA stearic acid, OLA oleic acid, ALA alpha-linolenic acid, ARA arachidonic acid, SFA saturated fatty acids, MUFA monounsaturated fatty acids, PUFA polyunsaturated fatty acids

blue stain (Invitrogen) exclusion with a hemocytometer under a phase-contrast microscope.

Apoptosis Induction as Measured by Caspase-3 Assays

To determine the level of apoptotic VSMC, cells were seeded in a black 96-well plate with a clear flat bottom (Corning Inc., Corning, NY, USA) at 2.6×10^4 cells/well and stimulated for 24 h with the fatty acid combinations or with individual FFA, with or without insulin. Caspase-3 activity was evaluated with the Apo-ONE Homogeneous Caspase 3/7 Assay Kit (Promega, Madison, WI, USA), according to the manufacturer's instructions. After 2 to 4 h of incubation, the activity was measured on a microplate reader (Synergy 2 Multi-Mode, Biotek, Winooski, VT, USA) at 520 nm, the fluorescent emission wavelength of the substrate cleaved by caspase-3.

Cell Cycle Analysis by Flow Cytometry

To determine the impact of fatty acid combinations and insulin on cell cycle phase modulation, VSMC were plated into 6-well plates at a seeding density of 4×10^4 cells/well and stimulated for 24 h as mentioned above. After trypsinization and washing in PBS-BSA 0.5 %, cells were permeabilized with 0.1 % saponin in PBS for 10 min and then fixed in a 1:1 acetone/methanol mix at –20 °C for another 10 min. For DNA staining, after 3 washing steps, 50 μ g/ml propidium iodide (Sigma) in PBS-BSA 0.5 % containing 5 μ g/ml of ribonuclease A (Sigma) was added to cells for 30 min. Following 2 washing steps, cell cycle phases were evaluated on a flow cytometer with a 488-nm wavelength argon laser (Coulter EPICS XL, Beckman Coulter, Brea, CA, USA) and analyzed with the Weasel software (Walter and Eliza Hall Institute of Medical

Research, Parkville, Australia). Data are presented as the percentage of cells in each phase of cell cycle.

Statistical Analysis

In all experiments, data are expressed as means \pm SEM and each group of data was compared using one-way ANOVA with Tukey–Kramer or Dunnett multiple comparison tests. The Tukey–Kramer comparison test was used to compare groups of data between themselves, while the Dunnett comparison test was used to compare each testing group to the control group. Data from Figs. 1 (hSFA vs. hMUFA), 2 (hSFA vs. hMUFA), 3 (hSFA vs. hMUFA), 4 (vs. PAM or STA) and 5 (vs. PAM + 0 μ M OLA or STA + 0 μ M OLA) were analyzed with Tukey–Kramer test whereas data from Figs. 1 (vs. BSA controls), 2 (vs. BSA controls), 3 (vs. BSA controls), 4 (vs. hSFA or hMUFA combinations) and 5 (vs. OLA alone) were evaluated with the Dunnett test. A $P < 0.05$ was considered statistically significant.

Results

Fatty Acid Combinations Inhibit VSMC Proliferation

A 72-h treatment with either hSFA or hMUFA FFA combination at 900 μ M decreased by 35–40 % the number of cells when compared to BSA alone (Fig. 1). This decrease was significant for hSFA and hMUFA when combined with a 1 nM insulin stimulation (hSFA: 18,587 \pm 1,575 cells/well and hMUFA: 17,810 \pm 720 cells/well vs. BSA: 30,175 \pm 2,200 cells/well, $P < 0.0001$) whereas in absence

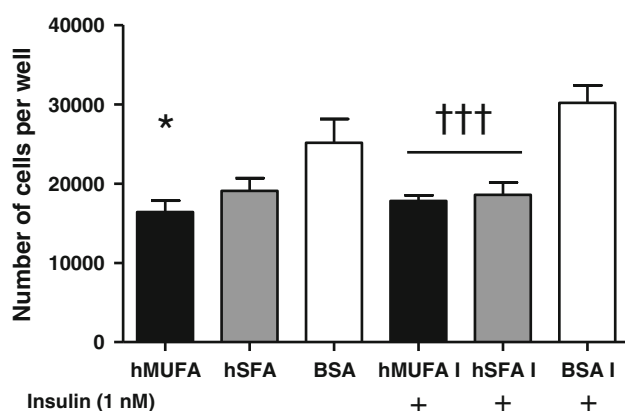


Fig. 1 Effect of fatty acid combinations on VSMC proliferation. Cells were stimulated for 72 h with either hSFA or hMUFA fatty acid combinations at 900 μ M, in the presence or not of 1 nM insulin. Cell proliferation was evaluated by manual counts. Data are means \pm SEM and represent the number of cells per well of a culture plate ($n = 7$). * $P < 0.05$ versus BSA. ††† $P < 0.001$ versus BSA I

of insulin, it was significant only for hMUFA (hMUFA: 16,413 \pm 1,446 cells/well vs. BSA: 25,143 \pm 3,024 cells/well, $P = 0.0285$).

Both hSFA and hMUFA FFA combinations cause the induction of apoptosis of VSMC. The observed inhibition of proliferation was related to an enhanced apoptosis rate. Indeed, a 24-h treatment with both FFA combinations at 900 μ M significantly increased caspase-3 activity compared to BSA control condition (hSFA: 2.90 \pm 0.21-fold, hMUFA: 3.00 \pm 0.24-fold vs. BSA without insulin, $P < 0.0001$; Fig. 2a and hSFA: 2.73 \pm 0.25-fold, hMUFA: 3.65 \pm 0.17-fold vs. BSA with insulin, $P < 0.0001$; Fig. 2b). While caspase-3 activity was the same between

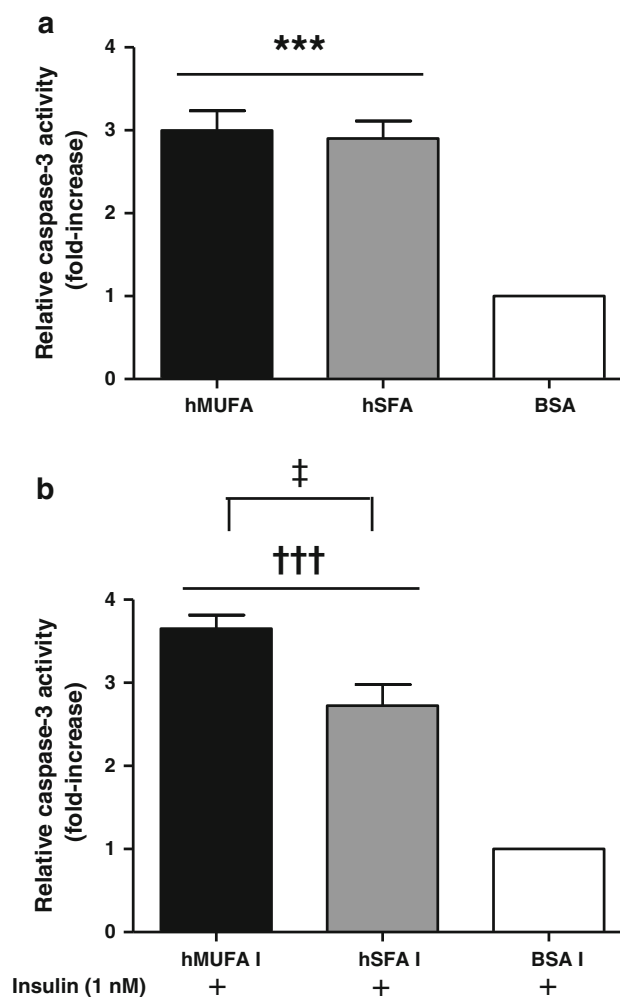


Fig. 2 Impact of fatty acid combinations on the induction of apoptosis of VSMC. Cells were treated for 24 h with either hSFA or hMUFA fatty acid combinations at 900 μ M in the absence (a) or presence (b) of a co-treatment with 1 nM insulin. The induction of apoptosis was measured by caspase-3 activity. Data are means \pm SEM and represent the relative caspase-3 activity (fold-increase) compared to BSA controls ($n = 4$). *** $P < 0.001$ versus BSA, ††† $P < 0.001$ versus BSA I, ‡ $P < 0.05$ hSFA I versus hMUFA I

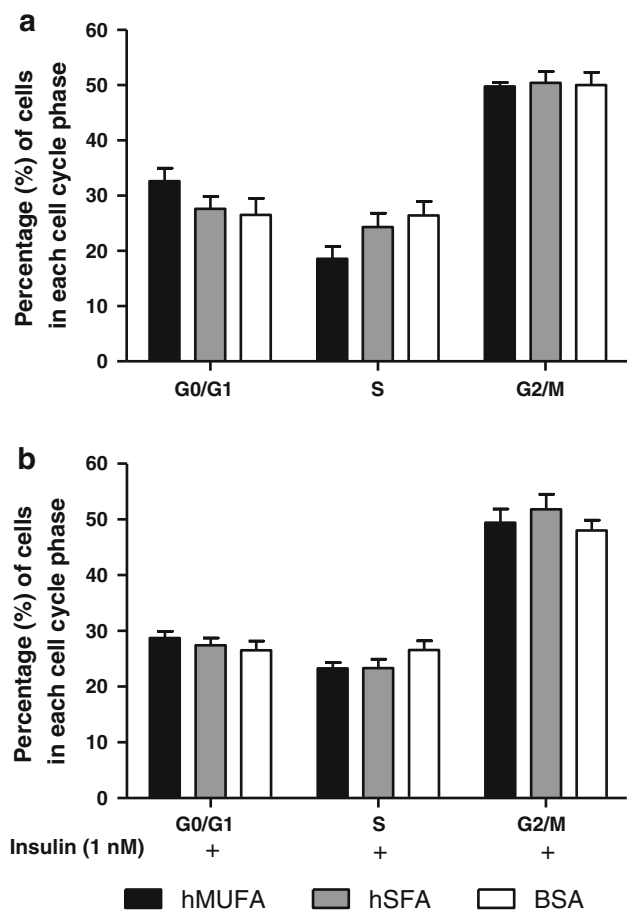


Fig. 3 Influence of fatty acid combinations on the modulation of VSMC cell cycle phases. Cells were treated for 24 h with either hSFA or hMUFA fatty acid combinations at 900 μ M in the absence (a) or presence (b) of a co-treatment with 1 nM insulin. Cell cycle modulation was evaluated by flow cytometry with a PI staining. Data are means \pm SEM and are expressed as the percentage of cells in each cell cycle phase ($n = 4$). The black bars represent the hMUFA combination, the gray bars are for the hSFA combination and the white bars for BSA

hSFA and hMUFA stimulations in absence of insulin, a co-treatment with 1 nM insulin increased it for hMUFA compared to hSFA ($P = 0.0220$; Fig. 2b). Since this difference between the two FFA combinations was not observed in the inhibition of proliferation (Fig. 1), the increased level of apoptotic VSMC with hMUFA stimulation combined with insulin may be due to a blockage in a cell cycle phase. However, analysis of PI stained cells by flow cytometry revealed no significant difference in the cell cycle phases between stimulations with hSFA and hMUFA FFA combinations in absence or presence of insulin (Fig. 3a and b). Therefore, enhanced apoptosis following VSMC stimulation with the hMUFA FFA combination in the presence of insulin was not related to a cell cycle blockage.

Saturated Fatty Acids are the Main Inducers of Apoptosis in hSFA and hMUFA Combinations

To investigate the contribution to apoptosis induction of the different FFA, VSMC were also stimulated with each single fatty acid for 24 h at the same concentration as the one found either in hSFA or in hMUFA combinations (Table 1). Caspase-3 activity was mainly induced by palmitic (PAM) and stearic (STA) acids, both SFA, at the concentrations found in hSFA (PAM: 75 ± 5 RFU, $P < 0.01$ vs. PAL and ARA, $P < 0.001$ vs. ALA), (STA: 86 ± 5 RFU, $P < 0.05$ vs. OLA, $P < 0.001$ vs. PAL, ALA and ARA) when compared with caspase-3 activity caused by MUFA and polyunsaturated fatty acids (PUFA) (OLA: 52 ± 8 RFU, PAL: 27 ± 7 RFU, ALA: 2 ± 10 RFU, ARA: 20 ± 8 RFU) (Fig. 4a). Similar results were demonstrated at the concentrations found in hMUFA (PAM: 116 ± 15 RFU, $P < 0.001$ vs. OLA: 29 ± 2 RFU, PAL: 0 ± 10 RFU and ALA: -4 ± 6 RFU), (STA: 168 ± 2 RFU, $P < 0.001$ vs. OLA, PAL and ALA) (Fig. 4b). When stimulations with individual FFA were combined with 1 nM insulin, a similar pattern was obtained for concentrations present in hSFA (PAM: 120 ± 3 RFU, $P < 0.01$ vs. PAL: 60 ± 13 RFU, $P < 0.001$ vs. OLA: 33 ± 4 RFU, ALA: 26 ± 2 RFU and ARA: 25 ± 14 RFU), (STA: 141 ± 6 RFU, $P < 0.001$ vs. OLA, PAL, ALA and ARA) (Fig. 4c) and hMUFA (PAM: 131 ± 5 RFU, $P < 0.001$ vs. OLA: 20 ± 2 RFU, PAL: 0.33 ± 1.20 RFU and ALA: 29 ± 7 RFU), (STA: 145 ± 5 RFU, $P < 0.001$ vs. OLA, PAL and ALA) (Fig. 4d).

Saturated Fatty Acids Alone Induce Higher Caspase-3 Activity than When Combined in hSFA and hMUFA

SFA induced much higher apoptosis at concentrations found in both hSFA and hMUFA when added alone to the culture media than when mixed in the combinations. PAM induced a 6.8-fold-increase (75 ± 5 RFU), STA a 7.9-fold-increase (86 ± 5 RFU) and, interestingly, the MUFA OLA a 4.8-fold-increase (52 ± 8 RFU) in caspase-3 activity compared to the hSFA combination (11 ± 2 RFU, $P < 0.001$ vs. PAM and STA, $P < 0.05$ vs. OLA; Fig. 4a). In contrast, apoptosis was increased by 16-fold with PAM (116 ± 15 RFU) and by 23-fold with STA (168 ± 2 RFU) compared to the hMUFA combination (7.3 ± 0.3 RFU, $P < 0.001$; Fig. 4b). In presence of 1 nM insulin, similar results were obtained at hSFA concentrations for PAM (7.1-fold-increase, 120 ± 3 RFU) and for STA (8.3-fold-increase, 141 ± 6 RFU) compared to the hSFA combination (17 ± 0.6 RFU, $P < 0.01$), but not significant with OLA stimulation (1.9-fold-increase, 33 ± 4 RFU vs. hSFA combination) (Fig. 4c). A similar pattern was induced with single FFA at hMUFA concentrations (PAM: 20-fold-increase,

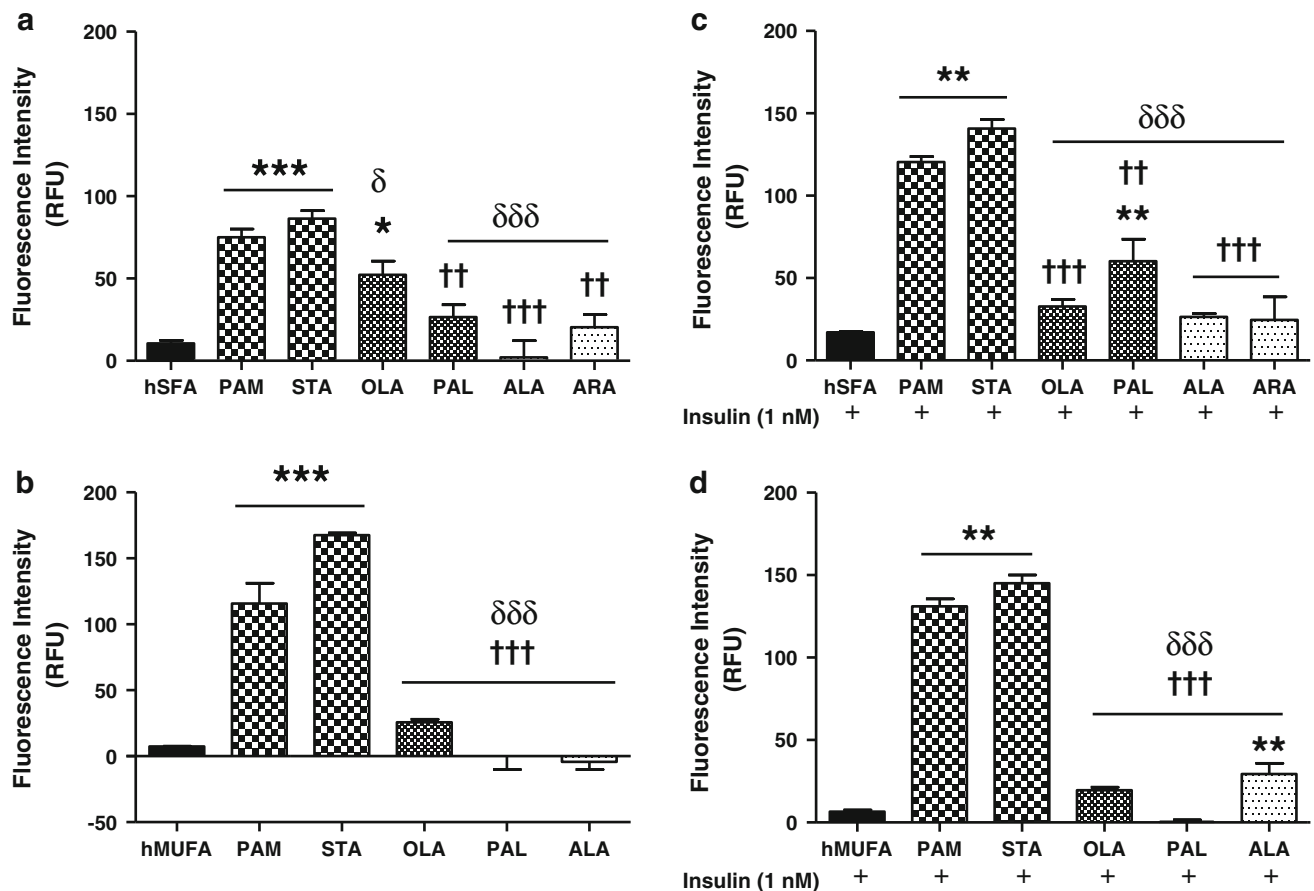


Fig. 4 PAM and STA are the main inducers of VSMC apoptosis in the fatty acid combinations. Cells were stimulated for 24 h with individual fatty acids present in the combinations found in hSFA combination (**a, c**) or hMUFA combination (**b, d**) in the absence (**a, b**) or presence (**c, d**) of a co-treatment with 1 nM insulin. The induction of apoptosis was measured by caspase-3 activity. Data are means \pm SEM (BSA control values for each fatty acid were subtracted) and represent the relative fluorescence intensity

131 \pm 5 RFU and STA: 22-fold-increase, 145 \pm 5 RFU) compared to the hMUFA combination (6.7 \pm 0.9 RFU, $P < 0.01$; Fig. 4d).

OLA Attenuates the Impact of Saturated Fatty Acids on the Apoptosis Level in a Dose-Dependent Manner

VSMC were stimulated for 24 h with PAM or STA at the same concentrations as those in hSFA and hMUFA combinations. These stimulations were made alone or combined with increasing doses of OLA until reaching the concentration of this fatty acid in hSFA (443 μ M) or hMUFA (650 μ M). OLA reduces the impact of SFA on caspase-3 activity in a dose-dependent manner at both hSFA and hMUFA concentrations. At hSFA concentrations of SFA, OLA, at the two highest doses tested, significantly attenuated the effect of PAM (PAM 244 μ M + OLA

(RFU) of the product of Z-DEVD-R110 substrate, cleaved by the active caspase-3 into its R110 fluorescent form ($n = 3$). The *black bars* represent hSFA or hMUFA combination, the bars with a large grid are for SFA, those with a small grid for MUFA and the *dotted bars* are for PUFA. * $P < 0.05$, ** $P < 0.01$ and *** $P < 0.001$ versus hSFA or hMUFA combination. †† $P < 0.01$ and ††† $P < 0.001$ versus PAM, $\delta P < 0.05$ and $\delta\delta\delta P < 0.001$ versus STA

225 μ M: 49 \pm 9 RFU, +OLA 443 μ M: 35 \pm 1 RFU vs. PAM 244 μ M: 106 \pm 5 RFU, $P < 0.05$; Fig. 5a) and at all doses tested for STA (STA 139 μ M + OLA 50 μ M: 79 \pm 3 RFU, +OLA 100 μ M: 77 \pm 12 RFU, +OLA 225 μ M: 62 \pm 12 RFU, +OLA 443 μ M: 44 \pm 10 RFU vs. STA 139 μ M: 137 \pm 5 RFU, $P < 0.01$; Fig. 5a). When combined with SFA at hMUFA concentrations, all doses of OLA significantly attenuated the level of apoptosis for both PAM and STA (PAM 135 μ M + OLA 50 μ M: 45 \pm 9 RFU, +OLA 100 μ M: 40 \pm 4 RFU, +OLA 225 μ M: 34 \pm 1 RFU, +OLA 443 μ M: 30 \pm 1 RFU, +OLA 650 μ M: 27 \pm 2 RFU vs. PAM 135 μ M: 152 \pm 15 RFU, $P < 0.001$) (STA 106 μ M + OLA 50 μ M: 65 \pm 1 RFU, +OLA 100 μ M: 49 \pm 6 RFU, +OLA 225 μ M: 38 \pm 1 RFU, +OLA 443 μ M: 31 \pm 2 RFU, +OLA 650 μ M: 32 \pm 0.3 RFU vs. STA 106 μ M: 207 \pm 2 RFU, $P < 0.001$) (Fig. 5b).

With a 1 nM insulin co-treatment, the reducing effect of OLA on PAM at hSFA concentration was significant for all doses (PAM 244 μM + OLA 50 μM: 48 ± 7 RFU, +OLA 100 μM: 32 ± 2 RFU, +OLA 225 μM: 30 ± 1 RFU, +OLA 443 μM: 24 ± 2 RFU vs. PAM 244 μM: 150 ± 3 RFU, *P* < 0.01; Fig. 5c) and, as already observed without insulin, on STA too (STA 139 μM + OLA 50 μM: 68 ± 9 RFU, +OLA 100 μM: 41 ± 4 RFU, +OLA 225 μM: 33 ± 1 RFU, +OLA 443 μM: 31 ± 2 vs. STA 139 μM: 178 ± 6 RFU, *P* < 0.01; Fig. 5c). At hMUFA concentrations in presence of insulin, OLA maintained its capacity to reduce SFA-induced caspase-3 activity (PAM 135 μM + OLA 50 μM: 53 ± 4 RFU, +OLA 100 μM: 43 ± 2 RFU, +OLA 225 μM: 40 ± 0.3 RFU, +OLA 443 μM: 34 ± 1 RFU, +OLA 650 μM:

32 ± 1 RFU vs. PAM 135 μM: 174 ± 5 RFU, *P* < 0.01) (STA 106 μM + OLA 50 μM: 48 ± 1 RFU, +OLA 100 μM: 42 ± 1 RFU, +OLA 225 μM: 40 ± 2 RFU, +OLA 443 μM: 37 ± 2 RFU, +OLA 650 μM: 34 ± 2 RFU vs. STA 106 μM: 199 ± 5 RFU, *P* < 0.01) (Fig. 5d).

The Combination of OLA with SFA has a Higher Reducing Effect than OLA Alone on the Apoptosis Level at hSFA Concentrations

When PAM and OLA were combined at concentrations present in hSFA, the caspase-3 activity was significantly lower than with OLA alone (PAM 244 μM + OLA 443 μM: 35 ± 1 RFU vs. OLA 443 μM: 74 ± 8 RFU, *P* < 0.05; Fig. 5a). In presence of 1 nM insulin, this

Fig. 5 Protective effect of OLA on VSMC apoptosis induced by SFA. Cells were stimulated for 24 h with PAM or STA alone or combined with increasing doses of OLA in the absence (a, b) or presence (c, d) of 1 nM insulin. Concentrations used for PAM, STA and for maximal doses of OLA were those found in hSFA (a, c) or hMUFA (b, d) combinations. The induction of apoptosis was measured by caspase-3 activity. Data are means ± SEM and represent the relative fluorescence intensity (RFU) formed by active caspase-3 (*n* = 3). †*P* < 0.05, ††*P* < 0.01, †††*P* < 0.001 versus PAM. δδ*P* < 0.01, δδδ*P* < 0.001 versus STA. **P* < 0.05, ***P* < 0.01, ****P* < 0.001 versus OLA alone (black bars)

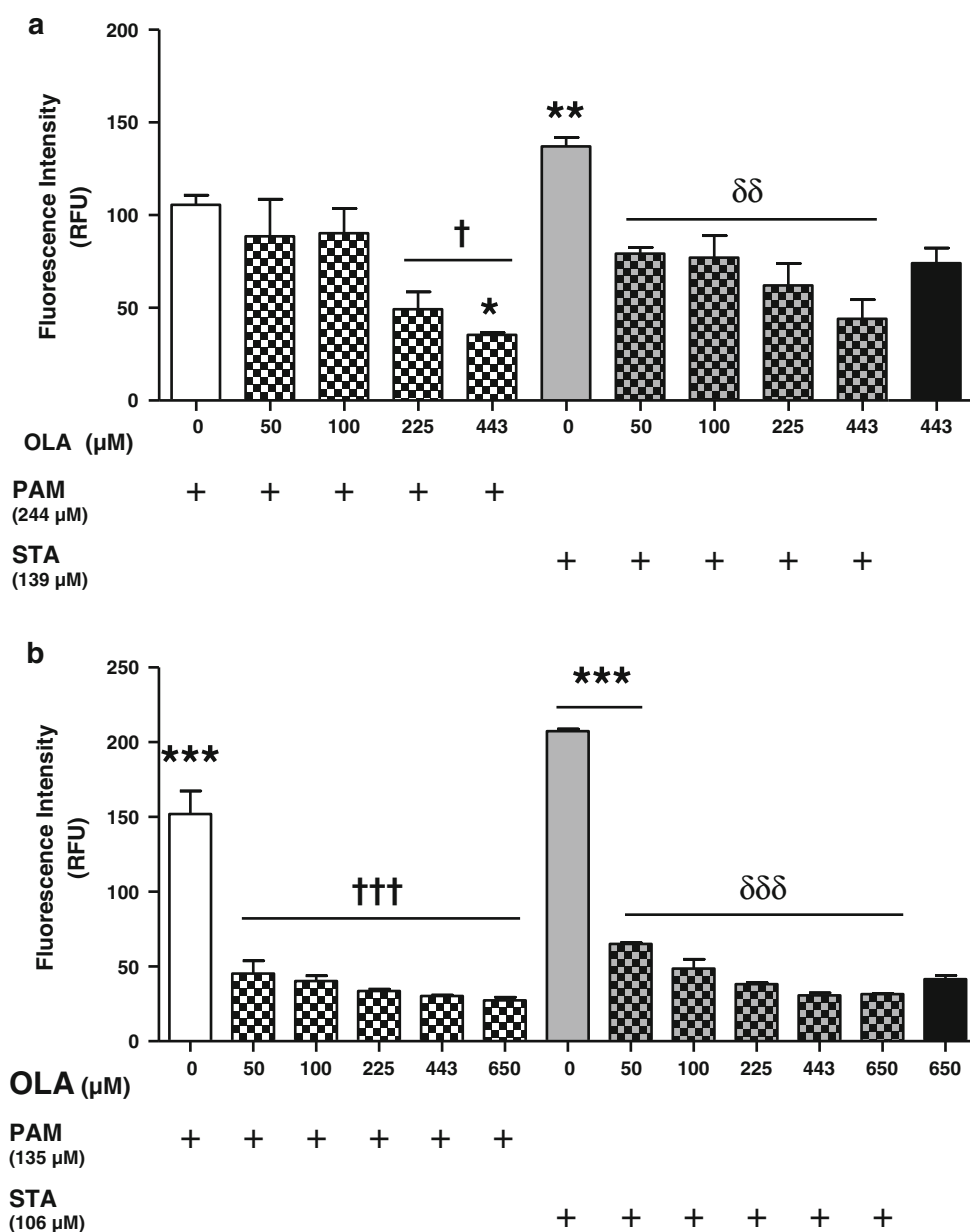
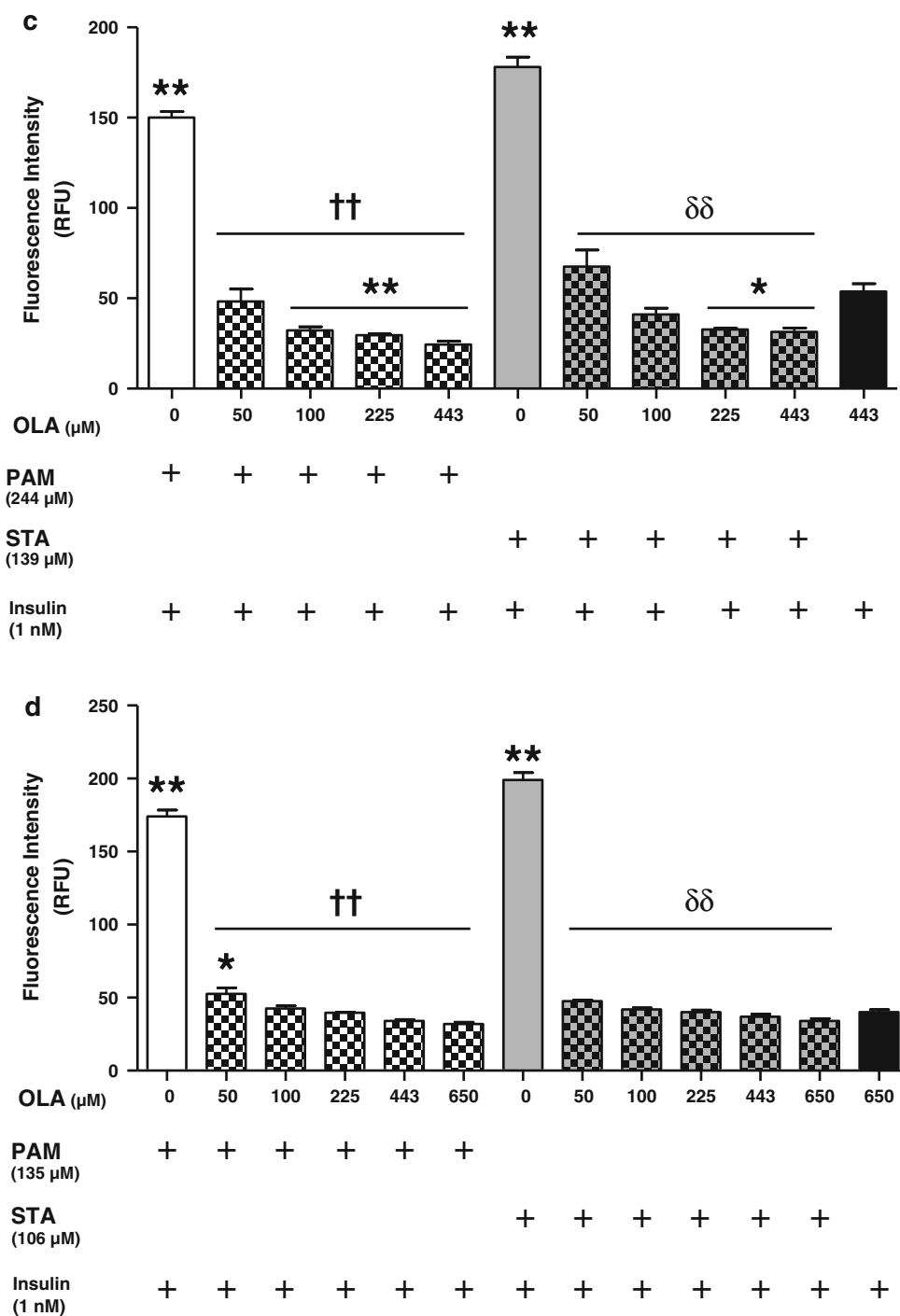


Fig. 5 continued



phenomenon was observed starting from 100 μM OLA when combined with PAM (PAM 244 μM + OLA 100 μM: 32 ± 2 RFU, +OLA 225 μM: 30 ± 1 RFU, +OLA 443 μM: 24 ± 2 RFU vs. OLA 443 μM: 54 ± 4 RFU, $P < 0.01$; Fig. 5c) and from 225 μM OLA when combined with STA (STA 139 μM + OLA 225 μM: 33 ± 1 RFU, +OLA 443 μM: 31 ± 2 RFU vs. OLA 443 μM, $P < 0.05$; Fig. 5c). This observation was not

made at hMUFA concentrations, either with or without insulin.

Discussion

A high plasma concentration of FFA is a common feature in patients suffering atherosclerosis in combination with

T2D. It is generally accepted that SFA, known to induce apoptosis in many cell types, have a pro-atherogenic role on vascular cells [17, 20]. In contrast, MUFA have a protective impact with an anti-apoptotic effect [13, 15]. Since most studies are conducted with only one or two FFA at a time, little is known about the impact of relevant complex groups of FFA on vascular cells. In this study, we assessed the impact of two FFA combinations, containing the same FFA but in different proportions, on VSMC viability. The hSFA combination was richer in SFA than the hMUFA combination, which contained a higher proportion of MUFA. The hSFA combination was inspired by the Western diet composition, while the hMUFA combination was rather modeled on the Mediterranean diet. The hyperinsulinemia found in diabetic and atherosclerotic patients was reproduced by the addition of insulin to FFA combinations in the cellular assays.

The first parameter evaluated was VSMC proliferation. Since BSA, used for FFA solubility, and insulin are individually known to be pro-proliferative [29, 30], an enhanced mitogenic action was expected with those mixed proteins. However, the detectable FFA effects *in vitro* exceeded the BSA effects, as published studies have demonstrated pro-proliferative impacts of FFA such as oleic acid [25] and anti-proliferative impacts of FFA such as stearic acid [15] compared to BSA controls. When using FFA combinations, we rather observed an inhibition of VSMC proliferation, significant with hMUFA combination in absence of insulin. The anti-mitotic effect of hSFA combination became apparent in the hyperinsulinemic condition. This observation suggests that insulin cannot counteract the impact of FFA combinations on VSMC proliferation. Indeed, the pro-proliferative effect of insulin alone on VSMC is relatively low, with around 20 % increase in proliferation for cells treated 72 h with insulin doses from 0.5 to 5 nM compared to untreated cells (data not shown).

Since a large proportion of FFA in the combinations used for this study was composed of pro-apoptotic SFA, we hypothesized that the observed inhibition of VSMC proliferation could be due to an induction of apoptosis. With individual FFA, at concentrations found in hSFA and hMUFA combinations, the highest caspase-3 activity was associated to SFA. Also, the apoptosis rate of VSMC was much lower with mixed FFA than with the majority of individual FFA, except for the PUFA. This important observation suggests the presence in the combinations of one or more FFA with a protective impact on cell viability. Because oleic acid is the most abundant FFA in the combinations and is well known for its anti-apoptotic activity, we postulated that it may be primarily responsible for the protective effect. We confirmed the anti-apoptotic dose-dependent properties of oleic acid on VSMC stimulated

with palmitic or stearic acids at concentrations found in both combinations. This effect could be due to an enhanced SFA internalization into triacylglycerol (TAG) vesicles by oleic acid. It was reported that internalized oleic acid is preferentially integrated into cellular TAG vesicles. In contrast, SFA are rather metabolized in their active form involved in lipotoxicity effects. However, the combination of SFA with oleic acid favors the integration of SFA into TAG vesicles, with an inverse correlation between FFA lipotoxicity and storage levels into TAG [15, 31, 32].

Furthermore, oleic acid attenuated VSMC apoptosis levels more strongly when combined with a SFA than when used alone, but only at hSFA concentrations. This observation suggests a competition between pro- and anti-apoptotic mechanisms that relies on given relative concentrations of SFA and MUFA. At hSFA concentrations, the phenomenon was significant only when oleic acid was almost two times more abundant (1.82-fold) than palmitic acid. With stearic acid, a similar ratio was reached with 225 μM oleic acid (1.62-fold). In this case, significant inhibition of caspase-3 activity was not reached most probably because of the higher pro-apoptotic potential of stearic acid compared to palmitic acid. A better protective effect was obtained at a 3:1 ratio (oleic acid/stearic acid), without being significant, although very close. At hMUFA concentrations, oleic acid combined with a SFA tends to have the same effect. However, since the apoptosis level with the hMUFA concentration of oleic acid (650 μM) alone was initially lower than at hSFA concentration, it became difficult to further reduce it when added with SFA. This could explain why the effect seems to be more important at hSFA concentrations. It also highlights the importance of MUFA in the hSFA combination, which is rich in harmful SFA.

In the presence of insulin, the basal apoptosis rate observed with oleic acid was lower than without insulin. This combined protective effect was transposed in a further reduction of VSMC apoptosis when single SFA was added at hSFA concentration. This effect was observed this time with both palmitic and stearic acids even with lower oleic acid doses. It is known that insulin increases fatty acid transporter CD36 translocation on cell surface, increasing therefore FFA uptake [33]. Since it has been demonstrated that there is no specific preference for FFA binding to CD36 [34], this probably did not have an impact on oleic acid uptake compared to SFA uptake. However, as an anabolic hormone, insulin is known to reduce palmitic acid β -oxidation and to increase its esterification into TAG in skeletal muscles [35]. Thus, oleic acid could be more effective in presence of insulin in VSMC due to a combined promotion of SFA integration into TAG vesicles rather than to a preferential cellular uptake.

Besides oleic acid and SFA, hSFA and hMUFA combinations contained other FFA such as palmitoleic, linolenic and arachidonic acids. These three FFA were in much lower proportions, but still could have affected VSMC viability. Indeed, palmitoleic and linolenic acids are recognized to reduce the pro-apoptotic impact of SFA in different cell types by inhibiting endoplasmic reticulum stress [16, 36–38]. In our previous studies, palmitoleic acid was present in the diets used for our experiments and we added this fatty acid to our present combinations to reproduce the same composition [27]. It was added since it is the only other MUFA apart from oleic acid in our combinations. More importantly, the ratio of this FFA between the two diets used previously was very different (approximately 20 times more in hSFA). It is possible though, that the concentration of palmitoleic acid in hMUFA combination was too low to have a detectable impact on cell viability. We have focused our study on oleic acid, as it is present in a much higher proportion in the combinations and as many studies have demonstrated its protective roles. However, it would be of great interest to repeat the experiments with palmitoleic acid combined with a SFA in our future works, to see if it has the same impact as oleic acid on reducing VSMC apoptosis rates.

When testing for linolenic acid, we observed an apoptosis level similar to the one obtained with its respective BSA control at the hSFA concentration. At hMUFA concentration, the apoptosis level was even lower with linolenic acid than with its BSA control, hence corroborating the anti-apoptotic effect described above. In the presence of insulin however, apoptosis rates were slightly higher. Since PUFA are particularly sensitive to oxidation, they could potentially be oxidized more easily in a hyperinsulinemic condition, thus increasing apoptosis rates. This is although a hypothesis since, to our knowledge, no study has ever been published concerning possible links between insulin and PUFA oxidation levels. For arachidonic acid, it has been demonstrated in turn that its oxidation-derived products have a pro-apoptotic impact on VSMC [39]. As it is only part of the hSFA mix, we were expecting a higher apoptosis rate for this combination than for hMUFA. Nevertheless, in the previously mentioned study, the investigators noticed decreasing cell viability from a minimal concentration of 20 μM for this FFA [39]. Since arachidonic acid concentration in the hSFA combination was 17.1 μM , it was likely too low to create an impact on VSMC apoptosis.

Taken together, the results from this investigation suggest that the hSFA combination was not more harmful for VSMC than the hMUFA combination in a hyperinsulinemic condition. In our previous studies, VSMC apoptosis rates were higher when cells were stimulated with insulin-treated adipocyte supernatants derived from mice fed with

the hSFA diet (AD) rather than with the hMUFA diet (VD). The adipose tissue of mice was conditioned *in vivo* by each high-fat diet for 20 weeks, resulting in metabolic alterations leading to T2D development [27]. Adipocytes were then isolated, stimulated or not with insulin and supernatants were collected to obtain conditioned media for VSMC stimulations. In that case, stimulation media contained components other than FFA, including adipokines, which influenced VSMC functionality and viability. Adiponectin, one of the most important hormones secreted by adipocytes, is associated with an anti-atherogenic impact. It impairs palmitic acid-induced apoptosis of endothelial cells by reducing ROS production. Adipocytes also secrete leptin, which has a pro-atherogenic impact [40] and a mitogenic effect on VSMC [41]. Adipocyte supernatants from hSFA (AD) and hMUFA (VD) groups, used to stimulate VSMC, had lower adiponectin levels but higher leptin levels compared to those from the control diet.

In addition, orally consumed sources of FFA go through a process of absorption and metabolization, which creates an impact on the nature and quantity of FFA released in the blood stream. Circulating FFA are transported and stored in adipocytes. Upon adipocyte isolation, the ratio of FFA released in supernatants could be quite different from the initial proportions found in the diets, due in part to metabolic alterations developed by mice fed on high-fat diets [27]. While some evidences suggest that FFA composition of TAG stored in adipocytes is similar to the FFA composition ingested, conflicting results propose that the ratio of secreted FFA is not always similar to the ratio of FFA into TAG [42–46]. FFA relative release, compared to its percentage into TAG, depends on FFA chain length and unsaturation degree. Accordingly, a higher release is reported for palmitoleic, linolenic and arachidonic acids. This selective mechanism might be altered according to the dysfunction degree in adipocytes, with hypertrophy found to be more extensive in cells from mice fed with the hSFA diet (AD) compared to those from mice fed with the hMUFA diet (VD), a pattern associated to increased lipolysis [47]. Therefore, even if the FFA ratios used in the actual combinations were selected from those found in the mice diets, results on VSMC viability are clearly different. We have observed a difference between: our *in-vitro* study using purified FFA and the *in-vivo* based works, where final FFA concentrations were influenced by the ingestion process and the mouse's metabolic status. Since, *in vivo*, the source of FFA interacting with VSMC does not only originate from the diet, but also in part from *de-novo* synthesis; this factor could have also contributed to this difference in results. Indeed, FFA coming from *de-novo* synthesis, which occurs principally in the liver, are transported throughout the blood flow by very low density lipoproteins (VLDL) and can hence interact with vascular

cells [48]. Of course, in the current in-vitro experimental setting, no adipokines, de-novo synthesis or metabolic alterations, that would have been present in an in-vivo study, were involved. Nevertheless, our in-vitro study allowed us to isolate FFA direct effects from all other components during VSMC stimulations, offering a better-defined environment.

In conclusion, these results demonstrate that complex groups of FFA, representative of what is found in modern diets, may have a negative impact on VSMC viability. They highlight the importance of MUFA in combinations containing high proportions of SFA to attenuate increased VSMC apoptosis rates. They also underline that the relative concentration of a given FFA in a combination is as important as its total concentration on the pro-and anti-apoptotic balance.

Acknowledgments We would like to thank Dr. Christine Des Rosiers's team for their advice on the preparation of fatty acid solutions. This work was supported by a grant from the Montreal Heart Institute Foundation to Dr. Jean-François Tanguay. Corinne St-Denis was supported by a training grant for graduate studies from the Montreal Heart Institute Foundation and by excellence and writing grants from the Medicine and the Postdoctoral and Superior Studies Faculties of Université de Montréal.

Conflict of interest None of the authors has a conflict of interest.

References

- World Health Organization (7th Oct 2011) Causes of death in 2008. http://www.who.int/gho/mortality_burden_disease/causes_death_2008/en/index.html
- Ross R (1999) Atherosclerosis—an inflammatory disease. *N Engl J Med* 340:115–126
- Glass CK, Witztum JL (2001) Atherosclerosis. the road ahead. *Cell* 104:503–516
- Clarke M, Bennett M (2006) The emerging role of vascular smooth muscle cell apoptosis in atherosclerosis and plaque stability. *Am J Nephrol* 26:531–535
- Centers for Disease Control and Prevention (November 7th 2011) National Diabetes Fact Sheet. http://www.cdc.gov/diabetes/pubs/pdf/ndfs_2011.pdf
- Xu J, Zou MH (2009) Molecular insights and therapeutic targets for diabetic endothelial dysfunction. *Circulation* 120:1266–1286
- Absher PM, Schneider DJ, Baldor LC, Russell JC, Sobel BE (1999) The retardation of vasculopathy induced by attenuation of insulin resistance in the corpulent JCR:LA-cp rat is reflected by decreased vascular smooth muscle cell proliferation in vivo. *Atherosclerosis* 143:245–251
- Wang Y, Zhang B, Bai Y, Zeng C, Wang X (2010) Changes in proteomic features induced by insulin on vascular smooth muscle cells from spontaneous hypertensive rats in vitro. *Cell Biochem Biophys* 58:97–106
- Anfossi G, Russo I, Doronzo G, Trovati M (2009) Contribution of insulin resistance to vascular dysfunction. *Arch Physiol Biochem* 115:199–217
- Fung TT, Rimm EB, Spiegelman D, Rifai N, Tofler GH et al (2001) Association between dietary patterns and plasma biomarkers of obesity and cardiovascular disease risk. *Am J Clin Nutr* 73:61–67
- Heidemann C, Schulze MB, Franco OH, van Dam RM, Mantzoros CS et al (2008) Dietary patterns and risk of mortality from cardiovascular disease, cancer, and all causes in a prospective cohort of women. *Circulation* 118:230–237
- Rho MC, Ah Lee K, Mi Kim S, Sik Lee C, Jeong Jang M et al (2007) Sensitization of vascular smooth muscle cell to TNF- α -mediated death in the presence of palmitate. *Toxicol Appl Pharmacol* 220:311–319
- Mattern HM, Hardin CD (2007) Vascular metabolic dysfunction and lipotoxicity. *Physiol Res* 56:149–158
- Artwohl M, Roden M, Waldhausl W, Freudenthaler A, Baumgartner-Parzer SM (2004) Free fatty acids trigger apoptosis and inhibit cell cycle progression in human vascular endothelial cells. *FASEB J* 18:146–148
- Harvey KA, Walker CL, Xu Z, Whitley P, Pavlina TM et al (2010) Oleic acid inhibits stearic acid-induced inhibition of cell growth and pro-inflammatory responses in human aortic endothelial cells. *J Lipid Res* 51:3470–3480
- Akazawa Y, Cazanave S, Mott JL, Elmi N, Bronk SF et al (2010) Palmitoleate attenuates palmitate-induced Bim and PUMA up-regulation and hepatocyte lipoapoptosis. *J Hepatol* 52:586–593
- Eitel K, Staiger H, Brendel MD, Brandhorst D, Bretzel RG et al (2002) Different role of saturated and unsaturated fatty acids in beta-cell apoptosis. *Biochem Biophys Res Commun* 299:853–856
- Maedler K, Oberholzer J, Bucher P, Spinass GA, Donath MY (2003) Monounsaturated fatty acids prevent the deleterious effects of palmitate and high glucose on human pancreatic beta-cell turnover and function. *Diabetes* 52:726–733
- de Vries JE, Vork MM, Roemen TH, de Jong YF, Cleutjens JP et al (1997) Saturated but not mono-unsaturated fatty acids induce apoptotic cell death in neonatal rat ventricular myocytes. *J Lipid Res* 38:1384–1394
- Dyntar D, Eppenberger-Eberhardt M, Maedler K, Pruschy M, Eppenberger HM et al (2001) Glucose and palmitic acid induce degeneration of myofibrils and modulate apoptosis in rat adult cardiomyocytes. *Diabetes* 50:2105–2113
- Hu FB (2003) The Mediterranean diet and mortality—olive oil and beyond. *N Engl J Med* 348:2595–2596
- de Lorgeril M, Salen P, Martin JL, Monjaud I, Delaye J et al (1999) Mediterranean diet, traditional risk factors, and the rate of cardiovascular complications after myocardial infarction: final report of the Lyon Diet Heart Study. *Circulation* 99:779–785
- Espósito K, Marfella R, Ciotola M, Di Palo C, Giugliano F et al (2004) Effect of a Mediterranean-style diet on endothelial dysfunction and markers of vascular inflammation in the metabolic syndrome: a randomized trial. *JAMA* 292:1440–1446
- Renard CB, Askari B, Suzuki LA, Kramer F, Bornfeldt KE (2003) Oleate, not ligands of the receptor for advanced glycation end-products, promotes proliferation of human arterial smooth muscle cells. *Diabetologia* 46:1676–1687
- Yun MR, Lee JY, Park HS, Heo HJ, Park JY et al (2006) Oleic acid enhances vascular smooth muscle cell proliferation via phosphatidylinositol 3-kinase/Akt signaling pathway. *Pharmacol Res* 54:97–102
- Jiang X, Zhang Y, Hou D, Zhu L, Xu W et al (2010) 17 β -estradiol inhibits oleic acid-induced rat VSMC proliferation and migration by restoring PGC-1 α expression. *Mol Cell Endocrinol* 315:74–80
- El Akoum S, Lamontagne V, Cloutier I, Tanguay JF (2011) Nature of Fatty Acids in High Fat Diets Differentially Delineates Obesity-Linked Metabolic Syndrome Components in Male and Female C57BL/6 J Mice. *Diabetol Metab Syndr* 3:34

28. Ray JL, Leach R, Herbert JM, Benson M (2001) Isolation of vascular smooth muscle cells from a single murine aorta. *Methods Cell Sci* 23:185–188
29. Cruzado M, Rislér N, Castro C, Ortiz A, Ruttler ME (1998) Proliferative effect of insulin on cultured smooth muscle cells from rat mesenteric resistance vessels. *Am J Hypertens* 11:54–58
30. Francis GL (2010) Albumin and mammalian cell culture: implications for biotechnology applications. *Cytotechnology* 62:1–16
31. Cnop M, Hannaert JC, Hoorens A, Eizirik DL, Pipeleers DG (2001) Inverse relationship between cytotoxicity of free fatty acids in pancreatic islet cells and cellular triglyceride accumulation. *Diabetes* 50:1771–1777
32. Listenberger LL, Han X, Lewis SE, Cases S, Farese RV Jr et al (2003) Triglyceride accumulation protects against fatty acid-induced lipotoxicity. *Proc Natl Acad Sci U S A* 100:3077–3082
33. Glatz JF, Luiken JJ, Bonen A (2010) Membrane fatty acid transporters as regulators of lipid metabolism: implications for metabolic disease. *Physiol Rev* 90:367–417
34. Baillie AG, Coburn CT, Abumrad NA (1996) Reversible binding of long-chain fatty acids to purified FAT, the adipose CD36 homolog. *J Membr Biol* 153:75–81
35. Luiken JJ, Dyck DJ, Han XX, Tandon NN, Arumugam Y et al (2002) Insulin induces the translocation of the fatty acid transporter FAT/CD36 to the plasma membrane. *Am J Physiol Endocrinol Metab* 282:E491–E495
36. Katsoulis E, Mabley JG, Samai M, Green IC, Chatterjee PK (2009) alpha-Linolenic acid protects renal cells against palmitic acid lipotoxicity via inhibition of endoplasmic reticulum stress. *Eur J Pharmacol* 623:107–112
37. Zhang Y, Dong L, Yang X, Shi H, Zhang L (2011) alpha-Linolenic acid prevents endoplasmic reticulum stress-mediated apoptosis of stearic acid lipotoxicity on primary rat hepatocytes. *Lipids Health Dis* 10:81
38. Zhang Y, Yang X, Shi H, Dong L, Bai J (2011) Effect of alpha-linolenic acid on endoplasmic reticulum stress-mediated apoptosis of palmitic acid lipotoxicity in primary rat hepatocytes. *Lipids Health Dis* 10:122
39. Kalyankrishna S, Parmentier JH, Malik KU (2002) Arachidonic acid-derived oxidation products initiate apoptosis in vascular smooth muscle cells. *Prostaglandins Other Lipid Mediat* 70:13–29
40. Fantuzzi G (2005) Adipose tissue, adipokines, and inflammation. *J Allergy Clin Immunol* 115:911–919 (quiz 920)
41. Beltowski J (2006) Leptin and atherosclerosis. *Atherosclerosis* 189:47–60
42. Conner WE, Lin DS, Colvis C (1996) Differential mobilization of fatty acids from adipose tissue. *J Lipid Res* 37:290–298
43. Halliwell KJ, Fielding BA, Samra JS, Humphreys SM, Frayn KN (1996) Release of individual fatty acids from human adipose tissue in vivo after an overnight fast. *J Lipid Res* 37:1842–1848
44. Raclot T, Groscolas R (1993) Differential mobilization of white adipose tissue fatty acids according to chain length, unsaturation, and positional isomerism. *J Lipid Res* 34:1515–1526
45. Raclot T, Langin D, Lafontan M, Groscolas R (1997) Selective release of human adipocyte fatty acids according to molecular structure. *Biochem J* 324(Pt 3):911–915
46. Raclot T, Mioskowski E, Bach AC, Groscolas R (1995) Selectivity of fatty acid mobilization: a general metabolic feature of adipose tissue. *Am J Physiol* 269:R1060–R1067
47. Guilherme A, Virbasius JV, Puri V, Czech MP (2008) Adipocyte dysfunctions linking obesity to insulin resistance and type 2 diabetes. *Nat Rev Mol Cell Biol* 9:367–377
48. Naik P (2012) Lipid metabolism. *Essentials of biochemistry*, 1st edn. Jaypee Brothers Medical Publishers, New Delhi, pp 190–225

decreases the body fat mass and in parallel increases the lean muscle mass [9]. On the other hand, some publications describe negative effects of CLA. It was shown that CLA may induce non-alcoholic hepatic steatosis in mice as a consequence of delipidation of adipose tissue [10]. In addition, it was proposed that CLA contributes to a decrease in insulin sensitivity in humans [11] and an increase in proinflammatory cytokines in human adipocytes in vitro [12]. However, due to the reported positive effects of CLA on body mass composition and in spite of the observed negative effects, CLA are currently being discussed to be used as food additives in the future. CLA are classified as “novel foods” in Europe and a premarketing risk assessment of CLA is a mandatory part of the novel food approval.

For a reliable risk assessment of CLA it is necessary also to focus on furan fatty acids (furan-FA) which are oxidative products of CLA [13]. Furan-FA are fatty acids characterized by a furan ring flanked by altered alkyl and carboxyl side chains in the α -positions of the furan ring (Fig. 1). The presence of the aromatic furan ring system in furan-FA gives rise to the assumption that these compounds may have toxic potential since furan itself is classified by the International Agency for Research on Cancer (IARC) as group 2B, possibly carcinogenic to humans.

Conjugated linoleic acids preparations may contain significant amounts of furan-FA, and increased intake of CLA, e.g., via food additives might also result in an increased uptake of furan-FA. There are no data available concerning the furan-FA concentrations in CLA supplements or in CLA-containing foodstuffs, however, Yurawecz et al. have

shown that CLA can easily be oxidized in the presence of dioxygen. The authors showed that 3 % of the initial CLA amount of a given sample was converted to furan-FA upon simple stirring of the sample for 46 h at 40 °C [13]. Furan-FA have been poorly characterized so far, and toxicological data are almost not available.

In this study we present data on the toxicological characterization of four different furan-FA isomers by using human cells relevant after oral absorption of the compounds. The human hepatoma cell line HepG2 was chosen as an in-vitro model for the liver as the cells retain many properties of primary liver cells, including metabolic activation [14, 15]. The human colorectal adenocarcinoma cell line Caco-2, on the other hand, is a well-established in-vitro model for human intestinal enterocytes to evaluate nutrient absorption and metabolism. The cells express numerous CYPs including CYP2E1 and have the capacity to detoxify various compounds [16]. By using these cell lines, the four furan-FA isomers were assayed for cytotoxicity and for their effects on cellular proliferation and apoptosis. Moreover, a proteomic approach using two-dimensional gel electrophoresis and mass spectrometry was chosen to identify differentially expressed proteins in Caco-2 cells treated with furan-FA in order to get insights into the cellular effects of furan-FA on the molecular level.

Materials and Methods

Chemicals

All chemicals were purchased from Merck (Darmstadt, Germany) or Sigma Aldrich (Taufkirchen, Germany) in the highest available purity. All reagents and equipment for the two-dimensional gel electrophoresis were purchased from GE Healthcare (Chalfont St. Giles, UK). The furan fatty acid 9,12-epoxy-9,11-octadecadienoic acid (9,11-furan-FA) was obtained from Biotrend (Köln, Germany) and 10,13-epoxy-10,12-octadecadienoic acid (10,12-furan-FA) was obtained from Larodan (Malmö, Sweden). Two additional furan fatty acid isomers, 8,11-epoxy-8,10-octadecadienoic acid (8,10-furan-FA) and 11,14-epoxy-11,13-octadecadienoic acid (11,13-furan-FA), were a kind gift from Prof. Steinhardt (University of Hamburg, Germany). The abbreviations given in brackets are used throughout the manuscript. All fatty acids were dissolved in DMSO to give 0.1 M stock solutions.

Cell Culture

Culture media and supplements were obtained from PAA Laboratories GmbH (Pasching, Austria). The human

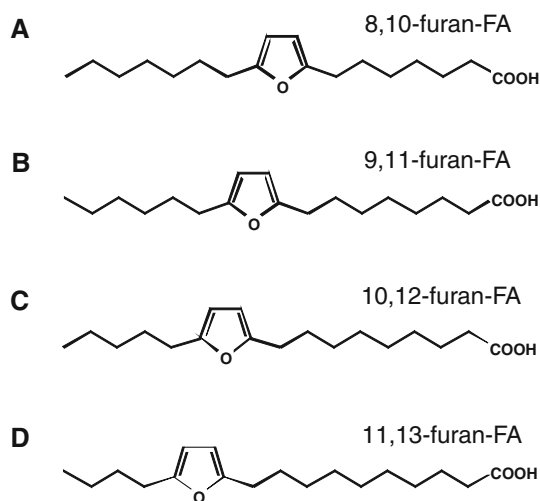


Fig. 1 Structures of furan fatty acids being oxidation products of conjugated linoleic acids [13]: **a** 8,11-epoxy-8,10-octadecadienoic acid (8,10-furan-FA); **b** 9,12-epoxy-9,11-octadecadienoic acid (9,11-furan-FA); **c** 10,13-epoxy-10,12-octadecadienoic acid (10,12-furan-FA); and **d** 11,14-epoxy-11,13-octadecadienoic acid (11,13-furan-FA)

adenocarcinoma cell line Caco-2 (European Collection of Cell Culture, ECACC No. 860 10 202) and V79-cells (ECACC No. 860 41 102) were cultured in Dulbecco's modified Eagle's medium (DMEM) and the human hepatoma cell line HepG2 (ECACC No. 850 11 430) was cultured in Roswell Park Memorial Institute Medium (RPMI), each supplemented with 10 % fetal calf serum, 100 U/mL penicillin and 100 µg/mL streptomycin in a humidified atmosphere of 5 % CO₂ at 37 °C. Cells were passaged every 2–4 days by treatment with 0.1 % trypsin and 0.04 % EDTA and then plated at a density of $1.3\text{--}2 \times 10^4$ cells/cm².

For incubation experiments the cell culture medium was replaced by a serum-free medium supplemented with 1 % insulin–transferrin–selenium (ITS, Invitrogen, Karlsruhe, Germany) and 0.1 mg/mL BSA with various concentrations of the respective fatty acid. Prior to this, furan fatty acids were complexed to fatty acid-free BSA (Sigma-Aldrich, Taufkirchen, Germany), with a molar ratio of fatty acid to BSA of 4:1.

Cytotoxicity Assay

Cells were plated in 96-well plates with 5,000 cells/well for Caco-2 cells and with 10,000 cells/well for HepG2 cells and treated with various concentrations of furan fatty acids for 3 days. Cytotoxicity was estimated by using the neutral red assay. Cells were incubated with 200 µL neutral red dye (0.005 % in DMEM) for 3 h and then washed twice with PBS. After addition of 200 µL of a solution of 50 % ethanol and 1 % acetic acid in water the plates were shaken for 15 min until complete dissolution of the dye. Absorbance at 540 nm was recorded using a Mithras Multimode Reader LB 940 (Berthold Technologies, Vienna, Austria). Values are expressed as percentages of the negative control which were cells exposed to medium containing 0.1 % DMSO. Control values were set as 100 % viable cells.

Cell Proliferation Assay

Caco-2 and HepG2 cells, respectively, were grown and treated with furan-FA as described above. After 48 h of incubation the cell proliferation rate was determined by using the cell proliferation reagent WST-1 (Roche Diagnostics GmbH, Mannheim, Germany) following the protocol described by the manufacturer.

Caspase Activity Assays

To measure the enzymatic activity of caspases as an indicator of apoptosis, Caco-2 cells were treated with furan-FA as described above. The level of apoptosis was determined with the fluorogenic caspase-3 tetrapeptide substrate

Ac-DEVD-AMC (Calbiochem, Darmstadt, Germany) as described by Wenzel et al. [17]. In the case of HepG2 cells, the activity of caspase-3 and caspase-7 was determined using a Caspase-Glo[®]3/7 Assay (Promega, Mannheim, Germany) following the protocol described by the manufacturer.

Ames Test

The bacterial reverse mutation assay (Ames test) was performed according to OECD guideline 471. For detection of the mutagenic potential of 9,11-furan-FA the *Salmonella typhimurium* strains TA98, TA100, TA1535, TA1537 and TA1538 (MoltaxTM) were assayed with various concentrations of the compound in the absence and in the presence of the exogenous metabolic activation system S9, respectively, with the plate incorporation method. The S9 fraction was prepared from livers of rats that had been treated with phenobarbitone and β-naphthoflavone before by a standard procedure according to the OECD guideline. In the absence of the S9 fraction, the following positive controls were used: 3.16 µg/plate 2-nitrofluoren for the strains TA98 and TA1538, 4 µg/plate sodium azide for the strains TA100 and TA1535, and 25 µg/plate 9-aminoacridin for strain TA1537. In the presence of the S9 fraction, 2 µg/plate 2-aminoanthracene was used as a positive control for all strains. The solvent DMSO (50 µL/plate) was used as a negative control. The number of revertants was counted for each plate after 48 h of incubation.

V79 Micronucleus Assay

The in-vitro mammalian cell micronucleus test was performed with V79-cells according to OECD Guideline 487. Cells were cultured on microscope slides and were exposed to 9,11-furan-FA for 3 h and cultured for another 21 h without furan-FA. In a parallel experiment, the S9 fraction was added to the cells during the incubation period of 3 h. Cells were fixed to the microscope slides and nuclei staining was conducted as described in the OECD guideline. Cells containing micronuclei and cells undergoing mitosis were identified via microscopic inspection. 1,000 cells were analysed for each microscope slide, and each experiment was done in duplicate.

Two-Dimensional Polyacrylamide Gel Electrophoresis (2-DE)

The 2-DE methodology is based on the techniques developed by Goerg et al. [18]. For protein extraction, Caco-2 cells were washed threefold with phosphate-buffered saline (PBS) and lysed in 500 µL lysis buffer (7 M urea, 2 M thiourea, 4 % w/v CHAPS, 2 % IPG-buffer (pH 3–10 NL),

1.2 % DeStreak Reagent, 20 mM spermine and 1 % Protease-Inhibitor Cocktail Set III (Merck KGaA, Darmstadt, Germany). After gentle sonication, the samples were centrifuged for 60 min at $100,000\times g$ at 15 °C to remove cellular debris. Protein content of supernatants was determined according to Bradford [19]. The extracts were stored in aliquots at -80 °C.

Protein extracts were separated via 2-DE, in which four technical 2-DE gel replicates were performed for each of the three biological samples. Isoelectric focusing (IEF) was carried out using 24 cm IPG gel strips with a non-linear pH-gradient from pH 3 to pH 10. Rehydration of gel strips was performed in a volume of 450 μ L rehydration buffer [7 M urea, 2 M thiourea, 4 % w/v CHAPS, 0.5 % IPG-buffer (pH3-10 NL) and 1.2 % DeStreak Reagent] containing 200 μ g protein. IEF was performed on the Ettan IPGphor[®] 3 IEF System with a maximum current setting of 50 μ A per strip and the following stepwise conditions: 30 V for 15 h (in-gel rehydration); 200 V for 1.5 h; 500 V for 1 h; gradient from 500 to 1,000 V within 13.5 h; gradient from 1,000 to 8,000 V within 3 h; 8,000 V for 6 h. After IEF separation, the gently washed gel strips were stored at -80 °C until further use. The gel strips were equilibrated for 15 min in equilibration buffer containing 6 M urea, 75 mM Tris (pH 8.8), 30 % v/v glycerol, 2 % w/v SDS and 2 % w/v DTT. Subsequently, the gel strips were equilibrated in the same buffer containing 2.5 % w/v iodoacetamide instead of DTT for another 15 min. The equilibrated strips were then transferred onto the second-dimension SDS-PAGE gels and sealed in place with 0.5 % agarose. SDS-PAGE was performed on lab-made 12.5 % polyacrylamide gels using the ETTAN Dalt twelve[®] separation unit with a constant power of 3 W per gel for 30 min and 15 W per gel for approximately 4.5 h until the dye front reached the bottom of the gels. Gels were fixed in aqueous 10 % acetic acid/30 % ethanol and stained with fluorescent Ruthenium II Tris-complex (10 nM; according to Rabilloud [20]). The fluorescence-stained 2-DE gels were digitally scanned with a ProXPRESS[®] fluorescence imaging workstation (PerkinElmer Lifesciences, Waltham, MA, USA).

Gel Image Analysis

Gel image analysis was carried out using Delta2D software version 3.6 (DECODON, Greifswald, Germany). It includes matching, spot detection, quantification of spots and statistical analysis. Image analysis with Delta2D led to an artificial fusion gel image (union fusion), on which the spot detection was performed automatically (parameters: local background region = 120, average spot size = 15, weak spot sensitivity = 20.0, noise cutoff = 40.0).

The Delta2D software was used to detect and quantify the volume of all protein spots. For the calculation of

Fig. 2 Cytotoxic effect of furan-FA in Caco-2 cells. Cells were treated with **a** 8,10-furan-FA, **b** 9,11-furan-FA, **c** 10,12-furan-FA, and **d** 11,13-furan-FA, respectively, at the indicated concentrations for 72 h. Cell viability was determined by neutral red assay and expressed as percentages of the negative control which was exposed to medium containing 0.1 % DMSO (set as 100 %). Medium containing 0.005 % Triton-X 100 was used as positive control. Data are expressed as the mean \pm SD $n = 3$. * $p < 0.05$ compared with control cells; ** $p < 0.01$ compared with control cells

expression changes, normalized gel images were compared. For statistical analysis, all gels of one concentration were organized in one group which was compared to the group with the gels with the extracts from the untreated control cells. A protein spot was considered as up- or downregulated when the expression ratio changed more than 1.5-fold. Between-group comparisons were performed using the Student's *t* test for independent samples (two tailed), *p* values < 0.05 were considered significant. Spot picking was performed using the InvestigatorTM ProPicTM workstation (Genomic Solutions, Ann Arbor, MI, USA).

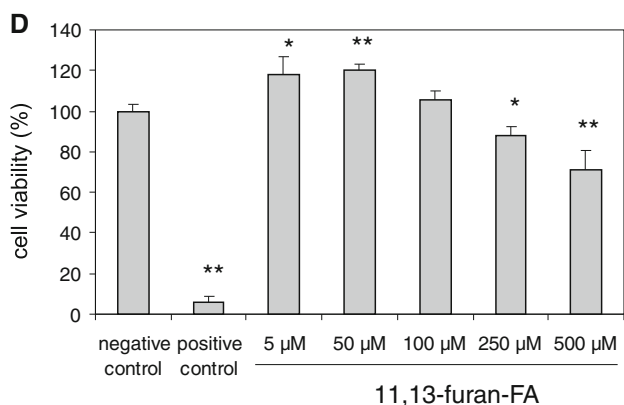
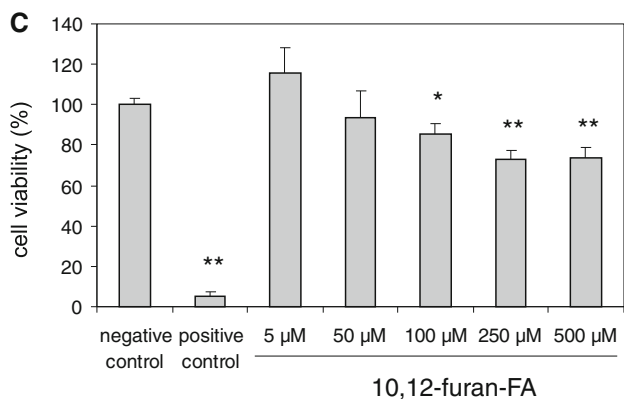
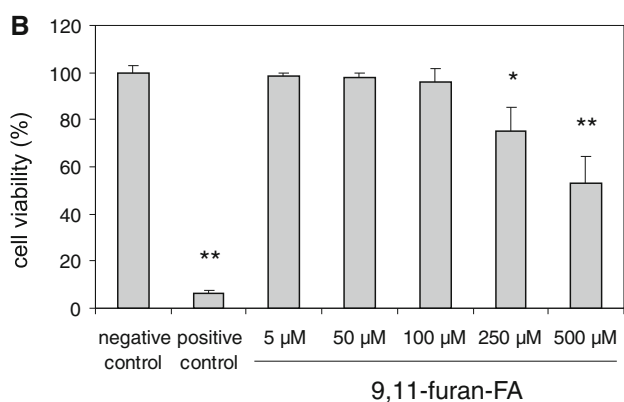
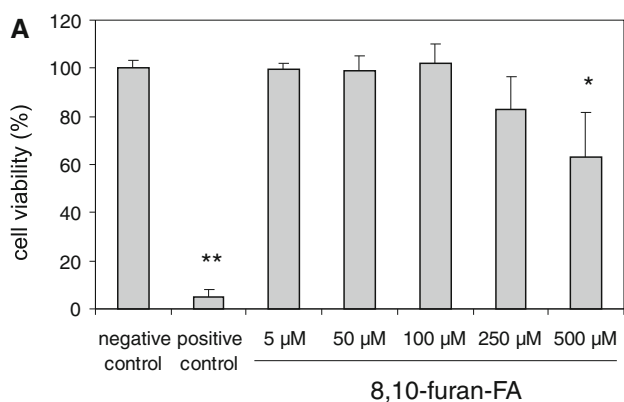
In-Gel Tryptic Digestion, Mass Spectrometry and Database Research

Tryptic in-gel digestion of proteins was carried out according to the protocol of Shevchenko et al. [21]. Extracted peptides were mixed with HCCA matrix, applied to a anchorTM 600 target (Bruker, Bremen, Germany) and subjected to MALDI-TOF analysis using an Ultraflex II mass spectrometer (Bruker, Bremen, Germany). Spectra were recorded in the deflection mode at 30 % laser intensity. Spectra were calibrated externally using a commercial peptide standard (Pepmix Standard 1000-4000; Care, Bremen, Germany). By using the Mascot platform, peptide mass lists were entered into searches against the *Homo sapiens* sequences of the SwissProt database. A maximum of one missed trypsin cleavage, complete modification of cysteine by carboxyamidation, partial methionine oxidation and 100 ppm mass tolerance were specified in the search settings. Results with a *p* value < 0.05 were considered significant.

Results

Cellular Effects of Furan-FA Isomers on Caco-2 Cells

To examine potential effects of furan-FA on cellular viability, cell proliferation and apoptosis rates, Caco-2 cells were treated with four different furan-FA isomers (8,10-furan-FA, 9,11-furan-FA, 10,12-furan-FA, and 11,13-furan-FA) as depicted in Fig. 1. Cellular viability was assayed by taking advantage of the neutral red cytotoxicity assay. No cytotoxic effects were observed for any tested



furan-FA isomer at concentrations lower than 100 μM (Fig. 2). However, 10,12-furan-FA caused a significant cytotoxic effect at a concentration of 100 μM and at higher concentrations. All furan-FA isomers displayed significant cytotoxic effects at a concentration of 500 μM, and except for 8,10-furan-FA also at 250 μM. Taken together, furan-FA displayed weak cytotoxicity in Caco-2 cells that was significant only at very high concentrations.

In a parallel experiment, a cell proliferation assay was conducted to estimate the potential of the furan-FA isomers to affect cellular proliferation. Incubation of the cells with furan-FA did not increase proliferation of the cells. In contrast, high furan-FA concentrations resulted in a decrease of cellular proliferation (data not shown). The results obtained with the WST-1 assay were comparable to those obtained with the neutral red cytotoxicity assay (see above). Thus, the results can not be interpreted as an antiproliferative effect of furan-FA but rather reflects the cytotoxic effects of the compounds at high concentrations.

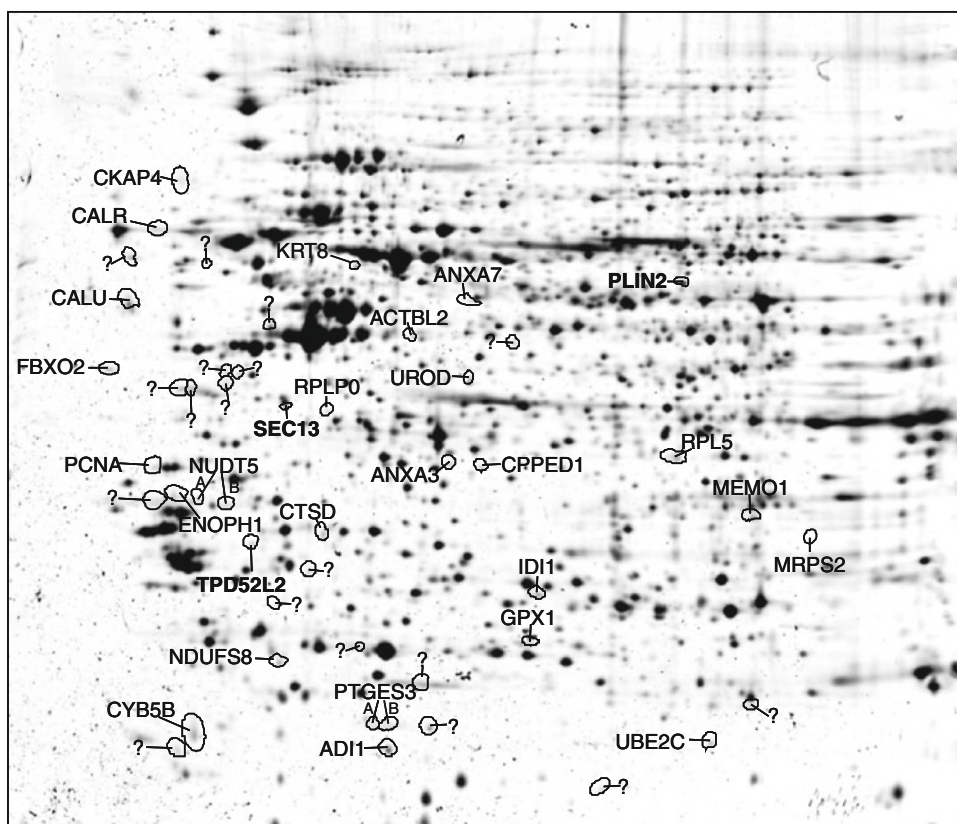
Finally, we investigated the possible effect of furan-FA on the apoptosis rate of Caco-2 cells by using the caspase-3-substrate Ac-DEVD-AMC. In these experiments, camptothecin was used as a positive control and clearly induced apoptosis in Caco-2 cells at a concentration of 25 μM. Nevertheless, no increase of caspase-3-activity was determined in Caco-2 cells upon incubation of the cells with up to 500 μM of the respective furan-FA isomer (data not shown). Hence, furan-FA did not affect apoptosis in this cell line.

In sum, the data indicate, that the furan-FA isomers tested in this study did not affect general cellular parameters such as cytotoxicity, cell proliferation, or apoptosis, of Caco-2 cells up to a concentration of 500 μM.

Identification of Proteins in Caco-2 Cells that were Differentially Regulated upon Exposure to 10,12-Furan-FA

A proteomic approach was chosen to address the question whether furan-FA affect Caco-2 cells on the molecular level. The furan-FA isomer 10,12-furan-FA was chosen for these experiments since this compound is the oxidation product of the most potent CLA isomer t10,c12-CLA. Caco-2 cells were incubated for 48 h with 10, 100, and 1,000 μM of 10,12-furan-FA, respectively. Total protein extracts were separated by two dimensional gel electrophoresis (2-DE). To obtain statistically significant results, three biological replicates were used for analysis and each protein sample was run four times in the 2-DE to get a set of twelve gel images for each 10,12-furan-FA concentration. These gel images were analyzed with Delta2D

Fig. 3 Fusion gel image of the proteome of Caco-2 cells treated with 10,12-furan-FA: The Gene Names were used to designate identified proteins. Upregulated proteins are marked in *bold* letters. Proteins that were not identified are indicated in the figure by a question mark



software as described in the Materials and Methods section. Delta2D analysis resulted in the detection of 1,723 independent protein spots. Image-analysis revealed significant changes (fold change ≥ 1.5 , $p < 0.05$) in the intensities of 48 spots caused upon incubation of the cells with at least one of the tested furan-FA-concentrations. Among these protein spots, 44 were downregulated and only four were upregulated in the furan-FA-incubated cells in comparison to the untreated control cells.

Figure 3 shows the fusion gel image of Caco-2 proteome obtained from all gel images of this project. Regulated spots with a fold change ≥ 1.5 ($p < 0.05$) are indicated by spot shapes, and gene names are given for the proteins of those 30 spots that were identified by MALDI-TOF analysis. Table 1 summarizes the results of the identified proteins. Two proteins, namely NUDT5 (nudix (nucleoside diphosphate linked moiety X)-type motif 5) and PTGES3 (prostaglandin E synthase 3) were each represented by two different spots in the 2-DE gels. They had identical masses but showed slight differences in the pI value. Posttranslational modifications might explain the presence of one and the same protein in more than one spot.

Of the identified proteins, only three proteins were upregulated on incubation of Caco-2 cells with 10,12-furan-FA, and these proteins were associated with lipid droplet biogenesis. Those proteins that were downregulated

were associated with general cellular processes such as transcription, protein biosynthesis and further protein processing (see “Discussion” for details). In sum, there was no indication that any specific signal transduction pathway of toxicological relevance was affected by 10,12-furan-FA in Caco-2 cells.

Cellular Effects of Furan-FA Isomers on HepG2 Cells

Based on the assumption that the furan ring of furan-FA might be activated in the liver by cellular metabolic activity, the human hepatoma cell line HepG2 was included in this study. This cell line was shown to retain many properties of primary liver cells, including metabolic activation [14, 15] and might therefore have the potential to activate the furan ring system of furan-FA. Thus, the cytotoxic potential of the furan-FA isomers as well as the effects of furan-FA on HepG2 proliferation and apoptosis were examined.

The results of the cytotoxicity assay (Fig. 4) are comparable to those obtained with the Caco-2 cell line (Fig. 2). The furan-FA isomers tested in this study displayed cytotoxic effects to HepG2 cells only at high concentrations above 100 μM . Moreover, incubation of HepG2 cells with the furan-FA isomers did not result in any effect on cellular proliferation and on apoptosis (data not shown). Again,

Table 1 MALDI-TOF analysis of proteins that were deregulated upon incubation of Caco-2 cells with 10,12-furan-FA

Gene name	Accession number	Protein name	Mascot score	Sequence coverage (%)	MW/pI (Theory)	Fold change (10/100/1,000 μ M 10,12-furan-FA)		
ACTBL2	Q562R1	Actin, beta-like 2	72	21	42.1/5.29	-1.38	-1.43	-1.5
ADH1	Q9BV57	Acireductone dioxygenase 1	139	59	21.5/5.43	-1.04	-1.42	-1.69
ANXA3	P12429	Annexin A3	179	48	36.5/5.63	-1.1	-1.69	-1.14
ANXA7	P20073	Annexin A7	69	17	53.0/5.52	-1.47	-1.19	-1.62
CALR	P27797	Calreticulin	74	14	48.2/4.29	-1.79	-1.54	-1.36
CALU	O43852	Calumenin	80	14	37.2/4.47	-1.44	-1.34	-1.67
CKAP4	Q07065	Cytoskeleton-associated protein 4	112	20	66.1/5.63	-1.62	-1.81	-1.71
CPPED1	Q9BRF8	Calcineurin-like phosphoesterase domain containing 1	74	28	35.9/5.78	-1.29	-1.52	-1.19
CTSD	P07339	Cathepsin D	86	24	45.0/6.10	-1.28	-1.33	-1.72
CY5B	O43169	Cytochrome b5 type B (outer mitochondrial membrane)	50	36	16.4/4.88	-1.17	-1.55	-1.49
ENOPH1	Q9UHY7	Enolase-phosphatase 1	63	22	29.1/4.66	-1.26	-1.59	-1.41
FBXO2	Q9UK22	F-box protein 2	92	20	33.7/4.29	-1.38	-1.64	-1.38
GPX1	P07203	Glutathione peroxidase 1	96	39	22.2/6.15	-1.42	-1.05	-1.63
IDH1	Q13907	Isopentenyl-diphosphate delta isomerase 1	135	40	26.6/5.93	-1.23	-1.60	-1.35
KRT8	P05787	Keratin 8	211	46	53.7/5.52	-1.87	-1.30	-1.09
MEMO1	Q9Y316	Mediator of cell motility 1	155	42	34.1/6.67	-1.21	-1.26	-1.54
MRPS2	Q9Y399	Mitochondrial ribosomal protein S2	169	30	33.5/5.43	-1.77	-1.43	-1.63
NDUFS8	O00217	NADH dehydrogenase (ubiquinone) Fe-S protein 8, 23 kDa (NADH-coenzyme Q reductase)	70	32	24.2/6.00	-1.22	-1.44	-1.58
NUDT5 (A)	Q9UKK9	Nudix (nucleoside diphosphate linked moiety X)-type motif 5	92	33	24.6/4.87	-1.03	-1.62	-1.33
NUDT5 (B)	Q9UKK9	Nudix (nucleoside diphosphate linked moiety X)-type motif 5	71	22	24.6/4.87	-1.02	-1.20	-1.70
PCNA	P12004	Proliferating cell nuclear antigen	106	26	29.1/4.57	-1.20	-1.60	-1.09
PLIN2	Q99541	Perilipin 2	210	50	48.3/6.34	1.44	2.25	3.51
PTGES3 (A)	Q15185	Prostaglandin E synthase 3 (cytosolic)	67	20	19.0/4.35	-1.26	-1.68	-1.86
PTGES3 (B)	Q15185	Prostaglandin E synthase 3 (cytosolic)	81	26	19.0/4.35	-1.35	-2.16	-1.33
RPLP0	P05388	Ribosomal protein, large, P0	81	32	34.4/5.71	-1.50	1.10	-1.21
RPL5	P46777	Ribosomal protein L5	104	23	34.6/9.73	-1.23	-1.15	-1.88
SEC13	P55735	SEC13 homolog (<i>S. cerevisiae</i>)	87	49	36.0/5.22	1.12	-1.05	1.90
TPD52L2	O43399	Tumor protein D52-like 2	68	36	22.3/5.26	-1.09	1.19	2.19
UBE2C	O00762	Ubiquitin-conjugating enzyme E2C	96	34	19.8/6.82	-1.18	-1.30	-1.74
UROD	P06132	Uroporphyrinogen decarboxylase	164	31	41.1/5.77	-1.21	-1.55	-1.62

these results are in line with those obtained for the Caco-2 cell line. Taken together, there was no indication that HepG2 cells were more sensitive to furan-FA treatment than Caco-2 cells.

The Genotoxic Potential of 9,11-Furan-FA

To further address the question as to whether the furan ring system of furan-FA can be activated enzymatically, the substance was incubated with rat liver homogenate (S9 fraction) that contains numerous enzymes of the CYP

family capable of activating various substances including compounds with aromatic moieties. Two genotoxicity assays, the Ames test and the micronucleus assay, were chosen to examine the effects of metabolic activation of furan-FA in vitro, because positive controls are available for both assays being carried out either with or without S9-mediated metabolic activation. 9,11-furan-FA was chosen for these experiments since we had to focus on one furan-FA isomer for these elaborate assays.

The Ames test was carried out with five different *S. typhimurium* strains according to OECD guideline 471.

These strains harbor either point mutations or frameshift mutations in genes essential for growth under the experimental conditions. Thus, the growth of bacterial colonies is due to the formation of revertants, and the number of revertants increases in the presence of mutagenic compounds. The *S. typhimurium* strains were cultured in the presence of various amounts of 9,11-furan-FA either in the presence or in the absence of the S9 fraction for enzymatic activation. As summarized in Table 2, the respective positive control clearly increased the number of revertants per plate whereas the presence of 9,11-furan-FA did not increase the number of revertants independent of the presence or absence of the S9 fraction. Interestingly, a cytotoxic effect of 9,11-furan-FA on the bacteria was observed. This effect was indicated by an abnormal background growth of the bacteria and by a decrease in the reversion rates in comparison to the negative control (Table 2; values given in brackets). The cytotoxic effect of 9,11-furan-FA was primarily observed when the cells were cultured in the absence of the S9 fraction and was only detected for strain TA1537 for the highest concentration of 9,11-furan-FA in the presence of S9 fraction. Thus, cytotoxic effects induced by the furan-FA isomer seem to be decreased by the S9 fraction.

In the micronucleus assay, the presence of a mutagenic compound results in the formation of micronuclei due to imbalances in cell division and in parallel in a decrease of mitotic activity. The in-vitro micronucleus assay was carried out with V79 cells according to OECD guideline 487. The furan-FA isomer was given to the cells either in the presence or in the absence of the S9 fraction for enzymatic activation. The results of the assay are summarized in Table 3. Again, incubation of the cells with the positive controls clearly increased the number of micronuclei and decreased the number of mitotic events whereas the presence of 9,11-furan-FA had no effect on these two parameters. Incubation of the cells with 9,11-furan-FA in the presence of the S9 fraction yielded similar results (Table 3). Concentrations of 9,11-furan-FA above 100 μM were cytotoxic to V79 cells (data not shown). Thus, 9,11-furan-FA did not display clastogenic potential up to a concentration of 100 μM independent of the presence or absence of the S9 fraction.

Discussion

Due to some properties that are proposed to be beneficial for human health CLA are currently being discussed for use as food additives in the future [22]. CLA preparations might contain significant amounts of furan-FA which are oxidative products of CLA. In particular the presence of a furan ring system in furan-FA raised some concerns on

potential toxic properties of these compounds. Therefore, for a reliable risk assessment of CLA formulas additional data concerning furan-FA toxicity are required. In this study we present first in-vitro data on the toxicological properties of furan-FA on the cellular as well as on the molecular level. By using two cell lines as models for the human intestine (Caco-2) and the human liver (HepG2) general cellular parameters such as cytotoxicity, cell proliferation and apoptosis were examined. Moreover, rat liver homogenate (S9 fraction) was employed for enzymatic activation of the aromatic furan ring in order to generate potential toxic furan-FA derivatives. In case of furan, this compound was shown to be activated by CYP2E1 to form an epoxide which further reacts to the dialdehyde *cis*-2-butene-1,4-dial [23–25]. Epoxides as well as dialdehydes are electrophiles which can covalently bind to proteins, lipids and DNA. Mutations might be induced upon DNA-adduct formation which may be the initial step of cancerogenesis [26, 27]. Indeed, furan has been shown to be cancerogenic in rodents probably due to a genotoxic mechanism (reviewed in Heppner and Schlatter [28]). Several in-vitro genotoxicity assays conducted either with furan or with its metabolite *cis*-2-butene-1,4-dial gave inconsistent results. In some studies, these compounds were shown to be genotoxic in the respective in-vitro assay [26, 29, 30] whereas other studies did not confirm these results [31, 32]. In this study, the Ames test as well as the in-vitro micronucleus assay yielded negative results with 9,11-furan-FA independent of the presence or absence of the S9 fraction for enzymatic activation of the compound. Thus, based on these two in-vitro assays, 9,11-furan-FA seems to have no genotoxic potential. Assuming a similar mechanism of activation one would expect the formation of an epoxide at the furan ring of 9,11-furan-FA as it was observed for furan [23–25]. The high reactivity of epoxides always gives rise for genotoxic potential of an epoxide-containing substance. However, further oxidation of the furan ring system of 9,11-furan-FA would yield a diketone due to the presence of the alkyl and the carboxyl side chain, respectively, at the α position of the furan ring. A diketone is much less reactive than the dialdehyde that is formed upon activation of furan. This might explain that 9,11-furan-FA was negative in the genotoxicity assays also in the presence of S9 fraction for enzymatic activation.

In addition to the direct genotoxic mechanism there are further indirect mechanisms being discussed for cancerogenic activity of furan. As an example, it was shown that furan irreversibly inhibits oxidative phosphorylation in the mitochondria of rat primary hepatocytes [33]. The authors concluded that the resulting lack of ATP might be responsible for inaccurate function of, e.g., DNA-repairing enzymes. In this scenario, furan would not have a direct mutagenic effect on DNA but would more likely prevent

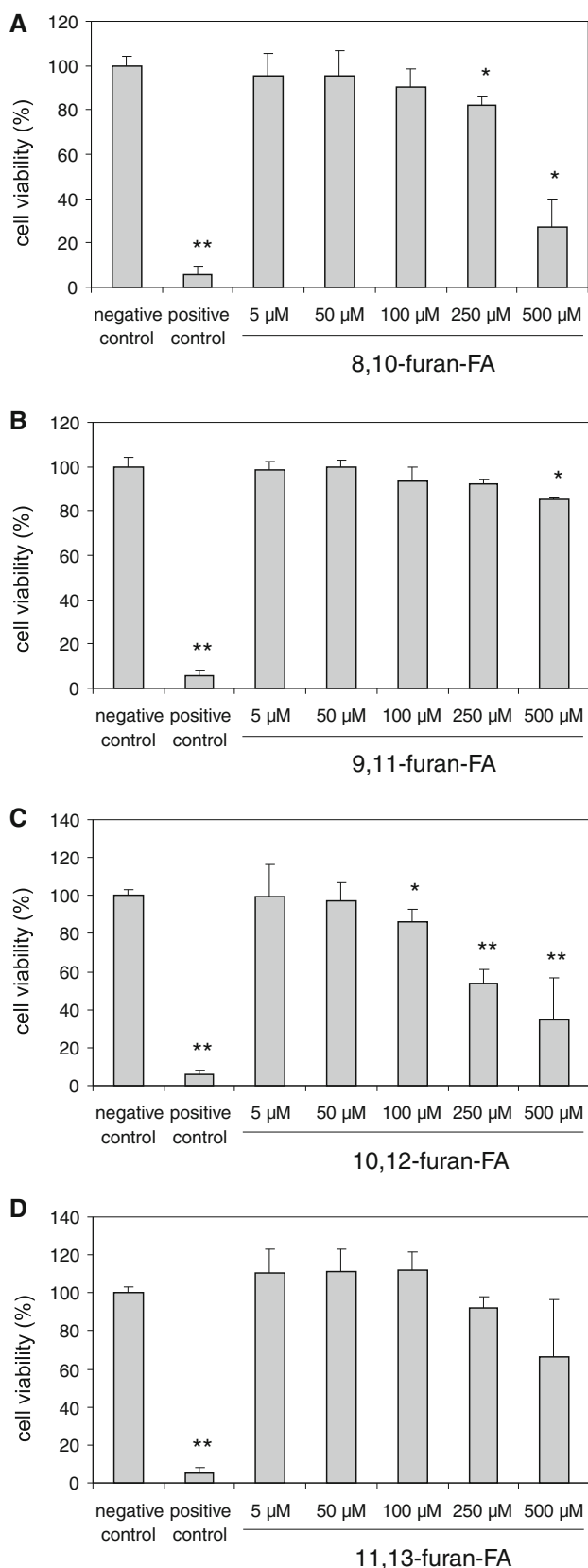


Fig. 4 Cytotoxic effect of furan-FA in HepG2 cells. Cells were treated with **a** 8,10-furan-FA, **b** 9,11-furan-FA, **c** 10,12-furan-FA, and **d** 11,13-furan-FA, respectively, at the indicated concentrations for 72 h. Cell viability was determined by neutral red assay and expressed as percentages of the negative control which was exposed to medium containing 0.1 % DMSO (set as 100 %). Medium containing 0.005 % Triton-X 100 was used as positive control. Data are expressed as means \pm SD $n = 3$. * $p < 0.05$ compared with control cells; ** $p < 0.01$ compared with control cells

efficient DNA repair. In another study it was shown that the strong hepatotoxic effect of furan is partially compensated for by increased proliferation of hepatocytes in mouse livers [34]. Moreover, furan was shown to induce expression of some apoptosis-associated genes in mouse and rat hepatocytes [35, 36]. In general, an imbalance between proliferation and apoptosis plays an important role in cancerogenesis, and furan-induced tumor development might also be due to some indirect mechanism.

In spite of the presence of a furan ring, furan-FA can also simply be regarded as fatty acids. In contrast to furan which is clearly a toxic compound, CLA which are the precursor of furan-FA are being discussed as having properties which might be beneficial for human health. Some studies with a focus on colon cancer indicate that CLA may have anticancerogenic effects. It was shown that the 9,11-furan-FA precursor *cis-9,trans-11-CLA* inhibits proliferation of colon cancer cell lines such as Caco-2 or HT-29 [37]. In addition, CLA was shown to induce apoptosis in HT-29 cells [38] whereas there were only minor effects on apoptosis observed in Caco-2 cells [39]. In vivo, chemically induced colon tumors in rat were inhibited by CLA due to an increased apoptosis rate of the tumor cells [40].

In this study, furan-FA being a chimera with structural characteristics of aromatics and of fatty acids have been examined for their effects on proliferation and apoptosis of two different cell lines. The four furan-FA isomers tested in this study neither induced nor inhibited proliferation in the Caco-2 cell line or in the HepG2 cell line. Moreover, there was no indication that apoptosis was affected by the four furan-FA isomers in these two cell lines. The four compounds displayed only weak cytotoxic effects at concentrations above 100 μ M, however, these high concentrations are not of physiological relevance. Although there are no data available for furan-FA concentrations in human blood serum, total CLA has been determined to be in a range around 20 μ M in human serum [41], and the furan-FA serum concentrations should be clearly below this value. Thus, the in-vitro data of this study do not support the hypothesis that furan-FA might be as toxic as furan or as

Table 2 Ames test

<i>Salmonella</i> strain:	Revertants per plate ^a									
	TA98		TA100		TA1535		TA1537		TA1538	
S9 fraction:	–S9	+S9	–S9	+S9	–S9	+S9	–S9	+S9	–S9	+S9
Negative control (DMSO)	17	18	127	103	11	13	12	11	8	7
Positive controls										
2-Nitrofluoren (3.16 µg/plate)	327								16	
Sodium azide (4 µg/plate)			847		590					
9-Aminoacridin (25 µg/plate)							151			
2-Aminoanthracene (2 µg/plate)	387		408		43		43		41	
9,11-furan-FA										
5 µmol/plate	n.d.	11	n.d.	56	n.d.	5	n.d.	(3)	n.d.	2
1 µmol/plate	(3)	14	(86)	82	(3)	5	(0)	7	(1)	4
0.25 µmol/plate	8	20	115	114	8	10	(0)	8	8	7
0.05 µmol/plate	21	n.d.	147	n.d.	11	n.d.	19	n.d.	8	n.d.

The values given in brackets indicate that cytotoxic effects were observed under the given conditions

n.d. not done

^a The values given are the means of two independent experiments

Table 3 V79 micronucleus assay

S9 fraction:	Micronuclei (%) ^a		Mitosis (%) ^a	
	–S9	+S9	–S9	+S9
Negative control (DMSO)	0.6	1.0	3.0	3.0
Positive control (37.2 ng/mL colcemid)	2.6		0.9	
Positive control (8.33 µg/mL cyclophosphamide)		17.8		1.7
10 µM 9,11-furan-FA	0.4	0.8	3.4	3.6
50 µM 9,11-furan-FA	0.8	0.9	2.3	3.2
100 µM 9,11-furan-FA	0.7	1.4	2.1	3.1

The values given are the means of two independent experiments

^a Percentage of micronuclei in cells and of cells undergoing mitosis, respectively, based on microscopic inspection of 1,000 cells

furan derivatives such as furfural. The general cellular parameters tested in this study gave no evidence for any furan-FA property being of toxicological relevance.

In a previous study it was shown that 9,11-furan-FA was absorbed by Caco-2 cells and incorporated into triglycerides for storage in lipid droplets [42]. Therefore, assuming that furan-FA must have some effect on Caco-2 cells after absorption, a non-targeted proteomic approach was chosen to examine the furan-FA-dependent effects on the molecular level. The 2-DE analysis of furan-FA-treated Caco-2 cells uncovered a set of 48 protein spots with altered expression levels. The proteins of 30 of these spots could be identified by MALDI-TOF analysis (Table 1). Only three of these proteins (PLIN2, TPD52L2 and SEC13) were upregulated upon exposure of the cells to 10,12-furan-FA, and these proteins are associated with lipid droplet biogenesis. PLIN2 is a member of the PAT protein family (perilipin, adipophilin, TIP47) which regulate the coordination of lipid droplet formation and which are associated to the surface of lipid droplets [43]. TPD52L2 is a member of the tumor protein D52 protein family. TPD52, the main member of this family, is a binding partner of

perilipin [44] and of TIP47, which is another lipid droplet-associated protein of the PAT family. Hence, it would be possible, that TPD52L2 is involved in lipid droplet biogenesis via its interaction with members of the PAT-family. SEC13 is the third protein that was found to be upregulated after treatment of Caco-2 with 10,12-furan-FA. In HeLa cells, siRNA knockdown of SEC13 inhibited the transport of PLIN2 to lipid droplets [45]. Thus, the observed increase in SEC13 protein in our study might be associated with the increased PLIN2 requirement for lipid droplet formation.

In summary the three upregulated proteins give some indication on the molecular level for the formation of lipid droplets in Caco-2 cells upon incubation of the cells with 10,12-furan-FA. Lipid droplet biosynthesis is accompanied by reorganization of the cytoskeleton which is indicated by the downregulation of four cytoskeleton-associated proteins (ACTBL, KRT8, CKAP4, MEMO1). Moreover, downregulation of all the other proteins that have been identified in the course of this proteomic study indicate downregulation of general cellular processes such as DNA-replication and transcription (PCNA, UBE2C, NUDT5),

translation and protein biosynthesis (MRPS2, RPLP0, RPL5, ENOPH1 and ADI1) as well as protein processing (CALU, CALR, ANXA3, ANXA7, FBXO2 and CTSD; see Table 1). PCNA acts as a cofactor of DNA polymerase delta and is therefore involved in DNA replication and DNA repair [46]. UBE2C is required for the destruction of mitotic cyclins and for cell cycle progression [47]. Hence, downregulation of UBE2C decreases proliferation of the cells. The protein NUDT5 is a nudix hydrolase which is part of nucleotide metabolism [48] and is able to eliminate toxic nucleotide derivatives from the cells [49] and is also downregulated through treatment with furan-FA.

Regarding protein biosynthesis, three different proteins were identified which are structural constituent of ribosomes (MRPS2, RPLP0, RPL5). ENOPH1 and ADI1 are proteins involved in amino acid metabolism and in particular in the methionine salvage pathway [50, 51]. CALU and CALR are calcium-binding proteins located in the ER which have various functions including chaperone activity, protein folding and trafficking [52]. Furthermore, the proteomic approach identified two different annexins to be downregulated upon furan-FA treatment, ANXA3 and ANXA7. Annexins are proposed to be involved in vesicle trafficking, membrane repair, membrane fusion and ion channel formation [53]. Two of the downregulated proteins, FBXO2 and CTSD, are proteolytic enzymes which are involved in protein degradation [54, 55].

With respect to lipid metabolism and energy expenditure, the proteins identified in this study (PTGES3, IDI1, UROD, CYB5B and NDUFS8) which are involved in these general metabolic processes were also downregulated upon incubation of Caco-2 cells with 10,12-furan-FA. Finally, downregulation of GPX1 which is one of the most important anti-oxidant enzymes in humans [56] indicates that 10,12-furan-FA does not induce oxidative stress in Caco-2 cells.

Taken together, downregulation of the numerous proteins identified in this study indicates that general cellular processes such as DNA replication and transcription, protein biosynthesis, protein processing and transport, lipid and energy metabolism is diminished in Caco-2 cells after exposure to 10,12-furan-FA. This may lead to the interpretation that metabolic activity in general is decreased in the cells which appear to have entered a state of rest. The results of the proteomic study, however, have to be considered as preliminary results and have to be confirmed, e.g., by Western blot experiments in future studies.

The furan-FA isomers examined in this study showed no mutagenic and no cytotoxic effects at concentrations that could be relevant for humans. Moreover, the substances had no effect on cell proliferation and on the apoptosis rate of Caco-2 cells or of HepG2 cells. This suggests that furan-FA have no cancerogenic potential. Furthermore, treatment

of furan-FA with liver enzyme extracts gave similar results indicating that no toxic metabolite was formed from furan-FA by the action of the liver metabolic enzymes. On the molecular level, the proteomic approach gave no indication that any signal transduction pathway of toxicological relevance was affected by 10,12-furan-FA in Caco-2 cells. The proteomic data indicate that the cells store furan-FA in lipid droplets and go into a metabolic state of rest. As neither the cell assays and the genotoxicity tests nor the proteomic study revealed any significant toxic effects after treatment of the cells with furan-FA, our results support the notion that the furan-FA isomers examined in this study have no obvious property of toxicological relevance.

Acknowledgments We thank Linda Brandenburger, Brigitte Finke, Anja Köllner, Christine Meckert, and Marlies Sagmeister for technical assistance. This work was funded by the Deutsche Forschungsgemeinschaft (DFG project LA 1177/5-4).

References

- Kepler CR, Hirons KP, McNeill JJ, Tove SB (1966) Intermediates and products of the biohydrogenation of linoleic acid by *Butyrivibrio fibrisolvens*. J Biol Chem 241:1350–1354
- Kepler CR, Tucker WP, Tove SB (1970) Biohydrogenation of unsaturated fatty acids. IV. Substrate specificity and inhibition of linoleate delta-12-cis, delta-11-trans-isomerase from *Butyrivibrio fibrisolvens*. J Biol Chem 245:3612–3620
- Ha YL, Grimm NK, Pariza MW (1987) Anticarcinogens from fried ground beef: heat-altered derivatives of linoleic acid. Carcinogenesis 8:1881–1887
- Truitt A, McNeill G, Vanderhoek JY (1999) Antiplatelet effects of conjugated linoleic acid isomers. Biochim Biophys Acta 1438:239–246
- Kritchevsky D, Tepper SA, Wright S, Tso P, Czarnecki SK (2000) Influence of conjugated linoleic acid (CLA) on establishment and progression of atherosclerosis in rabbits. J Am Coll Nutr 19:472S–477S
- Lee KN, Kritchevsky D, Pariza MW (1994) Conjugated linoleic acid and atherosclerosis in rabbits. Atherosclerosis 108:19–25
- Nicolosi RJ, Rogers EJ, Kritchevsky D, Scimeca JA, Huth PJ (1997) Dietary conjugated linoleic acid reduces plasma lipoproteins and early aortic atherosclerosis in hypercholesterolemic hamsters. Artery 22:266–277
- O'Shea M, Bassaganya-Riera J, Mohede IC (2004) Immunomodulatory properties of conjugated linoleic acid. Am J Clin Nutr 79:1199S–1206S
- Baddini FA, Fernandes PA, da Ferreira CN, Goncalves RB (2009) Conjugated linoleic acid (CLA): effect modulation of body composition and lipid profile. Nutr Hosp 24:422–428
- Clement L, Poirier H, Niot I, Bocher V, Guerre-Millo M, Krief S, Staels B, Besnard P (2002) Dietary trans-10,cis-12 conjugated linoleic acid induces hyperinsulinemia and fatty liver in the mouse. J Lipid Res 43:1400–1409
- Riserus U, Vessby B, Arnlov J, Basu S (2004) Effects of cis-9,trans-11 conjugated linoleic acid supplementation on insulin sensitivity, lipid peroxidation, and proinflammatory markers in obese men. Am J Clin Nutr 80:279–283
- Chung S, Brown JM, Provo JN, Hopkins R, McIntosh MK (2005) Conjugated linoleic acid promotes human adipocyte insulin

- resistance through NF κ B-dependent cytokine production. *J Biol Chem* 280:38445–38456
13. Yurawecz MP, Hood JK, Mossoba MM, Roach JA, Ku Y (1995) Furan fatty acids determined as oxidation products of conjugated octadecadienoic acid. *Lipids* 30:595–598
 14. Lu SC, Huang HY (1994) Comparison of sulfur amino acid utilization for GSH synthesis between HepG2 cells and cultured rat hepatocytes. *Biochem Pharmacol* 47:859–869
 15. Urani C, Doldi M, Crippa S, Camatini M (1998) Human-derived cell lines to study xenobiotic metabolism. *Chemosphere* 37:2785–2795
 16. Lampen A, Bader A, Bestmann T, Winkler M, Witte L, Borlak JT (1998) Catalytic activities, protein- and mRNA-expression of cytochrome P450 isoenzymes in intestinal cell lines. *Xenobiotica* 28:429–441
 17. Wenzel U, Nickel A, Daniel H (2005) Increased carnitine-dependent fatty acid uptake into mitochondria of human colon cancer cells induces apoptosis. *J Nutr* 135:1510–1514
 18. Gorg A, Obermaier C, Boguth G, Harder A, Scheibe B, Wildgruber R, Weiss W (2000) The current state of two-dimensional electrophoresis with immobilized pH gradients. *Electrophoresis* 21:1037–1053
 19. Bradford MM (1976) A rapid and sensitive method for the quantitation of microgram quantities of protein utilizing the principle of protein-dye binding. *Anal Biochem* 72:248–254
 20. Rabilloud T (2000) Detecting proteins separated by 2-D gel electrophoresis. *Anal Chem* 72:48A–55A
 21. Shevchenko A, Wilm M, Vorm O, Mann M (1996) Mass spectrometric sequencing of proteins silver-stained polyacrylamide gels. *Anal Chem* 68:850–858
 22. EFSA Panel on Dietetic Products NaA (2010) Opinion on the safety of “conjugated linoleic acid (CLA)-rich oil” as a novel food ingredient. *EFSA J* 8:1601–1642
 23. Chen LJ, Hecht SS, Peterson LA (1995) Identification of *cis*-2-butene-1,4-dial as a microsomal metabolite of furan. *Chem Res Toxicol* 8:903–906
 24. Kedderis GL, Carfagna MA, Held SD, Batra R, Murphy JE, Gargas ML (1993) Kinetic analysis of furan biotransformation by F-344 rats in vivo and in vitro. *Toxicol Appl Pharmacol* 123:274–282
 25. Parmar D, Burka LT (1993) Studies on the interaction of furan with hepatic cytochrome P-450. *J Biochem Toxicol* 8:1–9
 26. Byrns MC, Predecki DP, Peterson LA (2002) Characterization of nucleoside adducts of *cis*-2-butene-1,4-dial, a reactive metabolite of furan. *Chem Res Toxicol* 15:373–379
 27. Byrns MC, Vu CC, Neidigh JW, Abad JL, Jones RA, Peterson LA (2006) Detection of DNA adducts derived from the reactive metabolite of furan, *cis*-2-butene-1,4-dial. *Chem Res Toxicol* 19:414–420
 28. Heppner CW, Schlatter JR (2007) Data requirements for risk assessment of furan in food. *Food Addit Contam* 24(Suppl 1): 114–121
 29. Glatt H, Schneider H, Liu Y (2005) V79-hCYP2E1-hSULT1A1, a cell line for the sensitive detection of genotoxic effects induced by carbohydrate pyrolysis products and other food-borne chemicals. *Mutat Res* 580:41–52
 30. Peterson LA, Naruko KC, Predecki DP (2000) A reactive metabolite of furan, *cis*-2-butene-1,4-dial, is mutagenic in the Ames assay. *Chem Res Toxicol* 13:531–534
 31. Durling LJ, Svensson K, Abramsson-Zetterberg L (2007) Furan is not genotoxic in the micronucleus assay in vivo or in vitro. *Toxicol Lett* 169:43–50
 32. Kellert M, Brink A, Richter I, Schlatter J, Lutz WK (2008) Tests for genotoxicity and mutagenicity of furan and its metabolite *cis*-2-butene-1,4-dial in L5178Y tk \pm mouse lymphoma cells. *Mutat Res* 657:127–132
 33. Mugford CA, Carfagna MA, Kedderis GL (1997) Furan-mediated uncoupling of hepatic oxidative phosphorylation in Fischer-344 rats: an early event in cell death. *Toxicol Appl Pharmacol* 144:1–11
 34. Moser GJ, Foley J, Burnett M, Goldsworthy TL, Maronpot R (2009) Furan-induced dose-response relationships for liver cytotoxicity, cell proliferation, and tumorigenicity (furan-induced liver tumorigenicity). *Exp Toxicol Pathol* 61:101–111
 35. Chen T, Mally A, Ozden S, Chipman JK (2010) Low doses of the carcinogen furan alter cell cycle and apoptosis gene expression in rat liver independent of DNA methylation. *Environ Health Perspect* 118:1597–1602
 36. Fransson-Steen R, Goldsworthy TL, Kedderis GL, Maronpot RR (1997) Furan-induced liver cell proliferation and apoptosis in female B6C3F1 mice. *Toxicology* 118:195–204
 37. Lampen A, Leifheit M, Voss J, Nau H (2005) Molecular and cellular effects of *cis*-9, *trans*-11-conjugated linoleic acid in enterocytes: effects on proliferation, differentiation, and gene expression. *Biochim Biophys Acta* 1735:30–40
 38. Cho HJ, Kwon GT, Park JH (2009) *Trans*-10, *cis*-12 Conjugated linoleic acid induces depolarization of mitochondrial membranes in HT-29 human colon cancer cells: a possible mechanism for induction of apoptosis. *J Med Food* 12:952–958
 39. Kim EJ, Holthuizen PE, Park HS, Ha YL, Jung KC, Park JH (2002) *Trans*-10, *cis*-12-conjugated linoleic acid inhibits Caco-2 colon cancer cell growth. *Am J Physiol Gastrointest Liver Physiol* 283:G357–G367
 40. Park HS, Chun CS, Kim S, Ha YL, Park JH (2006) Dietary *trans*-10, *cis*-12 and *cis*-9, *trans*-11 conjugated linoleic acids induce apoptosis in the colonic mucosa of rats treated with 1,2-dimethylhydrazine. *J Med Food* 9:22–27
 41. Mougios V, Matsakas A, Petridou A, Ring S, Sagredos A, Melissopoulou A, Tsigilis N, Nikolaidis M (2001) Effect of supplementation with conjugated linoleic acid on human serum lipids and body fat. *J Nutr Biochem* 12:585–594
 42. Buhke T, Merkel R, Lengler I, Lampen A (2012) Absorption and metabolism of *cis*-9, *trans*-11-CLA and of its oxidation product 9,11-furan fatty acid by Caco-2 cells. *Lipids* 47:435–442
 43. Miura S, Gan JW, Brzostowski J, Parisi MJ, Schultz CJ, Londres C, Oliver B, Kimmel AR (2002) Functional conservation for lipid storage droplet association among Perilipin, ADRP, and TIP47 (PAT)-related proteins in mammals, *Drosophila*, and *Dictyostelium*. *J Biol Chem* 277:32253–32257
 44. Yamaguchi T, Omatsu N, Omukae A, Osumi T (2006) Analysis of interaction partners for perilipin and ADRP on lipid droplets. *Mol Cell Biochem* 284:167–173
 45. Soni KG, Mardones GA, Sougrat R, Smirnova E, Jackson CL, Bonifacino JS (2009) Coatamer-dependent protein delivery to lipid droplets. *J Cell Sci* 122:1834–1841
 46. Hoegge C, Pfander B, Moldovan GL, Pyrowolakis G, Jentsch S (2002) RAD6-dependent DNA repair is linked to modification of PCNA by ubiquitin and SUMO. *Nature* 419:135–141
 47. Arvand A, Bastians H, Welford SM, Thompson AD, Ruderman JV, Denny CT (1998) EWS/FLI1 up regulates mE2-C, a cyclin-selective ubiquitin conjugating enzyme involved in cyclin B destruction. *Oncogene* 17:2039–2045
 48. McLennan AG (2006) The Nudix hydrolase superfamily. *Cell Mol Life Sci* 63:123–143
 49. Kamiya H, Hori M, Arimori T, Sekiguchi M, Yamagata Y, Harashima H (2009) NUDT5 hydrolyzes oxidized deoxyribonucleoside diphosphates with broad substrate specificity. *DNA Repair (Amst)* 8:1250–1254
 50. Myers RW, Wray JW, Fish S, Abeles RH (1993) Purification and characterization of an enzyme involved in oxidative carbon-carbon bond cleavage reactions in the methionine salvage pathway of *Klebsiella pneumoniae*. *J Biol Chem* 268:24785–24791

51. Wray JW, Abeles RH (1995) The methionine salvage pathway in *Klebsiella pneumoniae* and rat liver. Identification and characterization of two novel dioxygenases. *J Biol Chem* 270:3147–3153
52. Coe H, Michalak M (2009) Calcium binding chaperones of the endoplasmic reticulum. *Gen Physiol Biophys* 28 Spec No Focus F96–F103
53. Rojas E, Arispe N, Haigler HT, Burns AL, Pollard HB (1992) Identification of annexins as calcium channels in biological membranes. *Bone Miner* 17:214–218
54. Benes P, Vetvicka V, Fusek M (2008) Cathepsin D-many functions of one aspartic protease. *Crit Rev Oncol Hematol* 68:12–28
55. Ho MS, Tsai PI, Chien CT (2006) F-box proteins: the key to protein degradation. *J Biomed Sci* 13:181–191
56. Steinbrenner H, Sies H (2009) Protection against reactive oxygen species by selenoproteins. *Biochim Biophys Acta* 1790:1478–1485

suitable host can be a potential alternative source of some valuable PUFA besides traditional fermentation techniques. Among them, progress has been made in the accumulation of specific PUFA by using genetic engineering strains of *Saccharomyces cerevisiae* [4] and *Pichia pastoris* [5]. However, its application is also extremely limited due to low and unstable productivity of PUFA. It seems difficult to solve this problem because the regulatory mechanisms of PUFA biosynthesis and the control of desaturase gene expression in these two strains and other organisms are not clearly understood.

In the last few years, more interest has mostly been focused on the regulation of desaturases from different organisms. In *Bacillus subtilis*, two-component prokaryotic modulator-effector pairs DesK/DesR senses a changes in membrane fluidity caused by a temperature downshift or exogenous fatty acids and then regulates the expression of its only desaturase gene ($\Delta 5$, called *des*) [6]. In *S. cerevisiae*, its only desaturase gene ($\Delta 9$, called *OLE1*) is transcriptionally regulated in response to various different environmental stimuli including carbon sources [7, 8], growth temperature [9], fatty acids [10, 11], metal ions [12, 13] and oxygen levels [12, 14]. Two related homologous proteins Spt23p and Mga2p located in endoplasmic reticulum initially can maintain the basal level of transcription after being transported into the nucleus to promote *OLE1* transcription [15, 16]. The Mga2p/Spt23p pathway is also probably involved in the regulation of *OLE1* in response to exogenous unsaturated fatty acids (UFA), low temperature and hypoxic conditions [17–19]. But in these examples, the information about the regulatory mechanism of desaturase genes is still fragmentary, so there have been no complete signaling pathways obtained in the light of our present knowledge and perhaps other new transcription factors, new cellular sensors and new signaling pathways remain to be identified.

Unlike the yeast *S. cerevisiae*, which has only one $\Delta 9$ -desaturase encoded by the *OLE1* gene, *P. pastoris* possesses a relatively complete system of UFA biosynthesis including the formation of two PUFA species linoleic acid (LNA, C18:2n-6) and α -linolenic acid (ALA, C18:3n-3) from the conversion of oleic acid (OLA, C18:1n-9) which requires two other desaturases ($\Delta 12$ and $\Delta 15$) in addition to $\Delta 9$ -desaturase. The methylotrophic yeast *P. pastoris* has also been proved to be an excellent system for high-level expression of heterologous proteins because of many advantages [20, 21]. For the reasons above, *P. pastoris* is a better choice for constructing a transgenic strain for the production of specific fatty acids and a good eukaryotic model organism for studies on the regulation mechanism of fatty acid biosynthesis.

Therefore, in this study, we investigated the effects of different external conditions such as low temperature and exogenous fatty acids on desaturase gene expression, desaturase gene promoter activity and fatty acid production of *P. pastoris* GS115. Moreover, our findings demonstrate

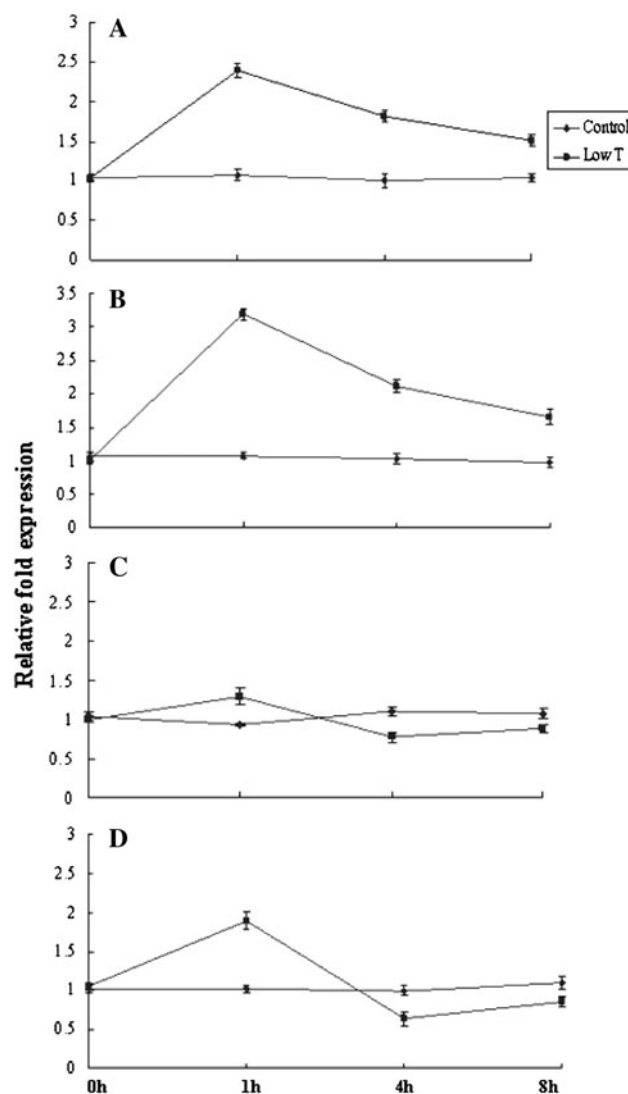


Fig. 1 Time-course expression study of *P. pastoris* GS115 desaturase genes in response to low temperature. The graphs show the relative quantitation results of four desaturase gene expressions (**a** *Fad9A* gene, **b** *Fad9B* gene, **c** *Fad12* gene, **d** *Fad15* gene) by real-time PCR. Relative gene expression measured relative to β -actin and normalized to controls was calculated as $2^{-\Delta\Delta C_T}$. Error bars represent the average SD of three separate experiments with three parallels

that Spt23p plays a role in the regulation of two $\Delta 9$ -desaturase genes and the synthesis of OLA. However, to understand the actual function of Spt23p in the regulation of desaturase gene expression and fatty acid metabolism, further experimental work is needed.

Materials and Methods

Strains and Media

The methylotrophic yeast *P. pastoris* GS115 strain (*his⁻Mut⁺*) commercially available from Invitrogen (San Diego,

Table 1 Primers used in this study

Names	Sequences(5'–3')	Usage
Real-PPD9A-F	GAGACCCCTATAACATCCGA	Cloning partial cDNA of <i>Fad9A</i> for real-time PCR
Real-PPD9A-R	CAGTCCACCATAAACAAGCC	Cloning partial cDNA of <i>Fad9A</i> for real-time PCR
Real-PPD9B-F	CCAAGATACAAGGCAAGAGC	Cloning partial cDNA of <i>Fad9B</i> for real-time PCR
Real-PPD9B-R	CACCGTAGATAAATCCACCC	Cloning partial cDNA of <i>Fad9B</i> for real-time PCR
Real-PPD12-F	CCTACCCCAACACCCCTAAA	Cloning partial cDNA of <i>Fad12</i> for real-time PCR
Real-PPD12-R	CAACTGTGCCAAGATACCCA	Cloning partial cDNA of <i>Fad12</i> for real-time PCR
Real-PPD15-F	TCCTCTCCTGTTTTGATAA	Cloning partial cDNA of <i>Fad15</i> for real-time PCR
Real-PPD15-R	GGACGAGTCTGTGTGTTGTA	Cloning partial cDNA of <i>Fad15</i> for real-time PCR
Real-PPACT-F	GGTCCCCTATTATTTCCAG	Cloning partial cDNA of β -actin gene for real-time PCR
Real-PPACT-R	TCCTTCAGTTTTCCGTCTC	Cloning partial cDNA of β -actin gene for real-time PCR
lacZ-F	<u>GGACTAGT</u> ATGCAAGCTTGCATCCC	Cloning ORF of <i>lacZ</i> gene
lacZ-R	<u>AACTGCAGT</u> TATTTTTGACACCAGAC	Cloning ORF of <i>lacZ</i> gene
PPD15P1000F	<u>CGGGATCC</u> AAACTTTCCACTTCAACT	Cloning promoter region of <i>Fad15</i> gene
PPD15P1000R	<u>GGACTAGT</u> TGAACCCGAAACAGTGACTT	Cloning promoter region of <i>Fad15</i> gene
pIB1-F	ATAGGATTTTTTTTGTTCATT	Verification of homologous recombination for promoter construct
pIB1-R	GAGAAAGGCGGACAGGTATC	Verification of homologous recombination for promoter construct
PPSpt23FA	ATGAACGAAGCATCTTTGGA	Cloning ORF of <i>Spt23</i> and <i>Spt23</i> disruption cassette (<i>Spt23/his</i>)
PPSpt23RA	TCATGGCATTACTGTATTCA	Cloning ORF of <i>Spt23</i> and <i>Spt23</i> disruption cassette (<i>Spt23/his</i>)
PHis4TT-F23	<u>CGGGATCCT</u> CAGAATTGGTTAATTGGTT	Cloning of the <i>His4</i> gene cassette for construction of pMD19T- <i>Spt23/His</i>
PHis4TT-R23	<u>CGGGATCCCCT</u> TAGACATGACTGTTCT	Cloning of the <i>His4</i> gene cassette for construction of pMD19T- <i>Spt23/His</i>

Restriction sites used for cloning purposes are shown by underlining and italics

CA, USA) was used for the whole work. It was grown under normal conditions at 30 °C in a yeast extract–peptone–dextrose (YPD) medium consisting of 1 % yeast extract, 2 % peptone, and 2 % dextrose. Minimal dextrose plates (MD) containing 1.34 % yeast nitrogen base without amino acid, 4×10^{-5} % biotin, 2 % dextrose, 2 % agar were used for the selection of His⁺ transformants. In experiments employing fatty acid supplements, the growth medium was supplemented with 1 % Nonidet P-40 (Sigma, USA) and appropriate fatty acids (Cayman Chemicals, USA) at a concentration of 1 or 2 mM.

Real-Time PCR Analysis of Desaturase Gene Expression

The *P. pastoris* cells were grown until the late exponential growth phase ($OD_{600} = 2.5$) and then shifted quickly to the low-temperature (15 °C), or added high concentration of exogenous fatty acids (at a concentration of 1 mM) to the cultures. Cells were harvested after a further incubation period of 1, 4 and 8 h by centrifugation and washed twice in cold RNase-free water. Total RNA was extracted using TRNzol reagent according to the manufacturer's protocol (TianGen, China). Residual genomic DNA contamination was removed by digestion with 10 units of DNase I (Takara, China) at 37 °C for 30 min followed by inactivation at 80 °C for 10 min. Reverse transcription PCR was

performed using M-MLV reverse transcriptase (Promega, USA) to synthesize the first cDNA. Five pairs of specific primers for real-time PCR (Table 1) were designed according to the previously published gene sequences in the *P. pastoris* GS115 genome database (<http://www.pichiagenome.org/>) [22]. The mRNA levels were measured by the SYBR Green I fluorescence method. Realtime PCR was performed in 96-well optical plates on an iCycler iQ5 multicolor real-time PCR detection system (Bio-Rad). Each reaction was performed according to the manufacturer's protocol (TianGen, China). Relative expression of target gene products was normalized to the housekeeping gene β -actin and calculated using the comparative C_T method, and all the data obtained were treated by the iQ5 optical system software version 2.0.

Fatty Acid Extraction and Analysis

The cultured cells were harvested at different time points by centrifugation and washed three times in distilled water. Subsequently, cellular fatty acids were extracted by incubating 100 mg dry yeast powder in 5 mL 5 % (w/v) KOH/methanol for saponification at 70 °C for 5 h. After the pH was adjusted to 2.0 with HCl, total fatty acids were subjected to methyl esterification with 4 mL 14 % (w/v) boron trifluoride in methanol at 70 °C for 1.5 h. Then, fatty acid methyl esters (FAME) were extracted with *n*-hexane after

addition of saturated sodium chloride solution. The total FAME were analyzed by gas chromatography (GC) using a GC-6890N machine (Agilent, USA) equipped with a flame ionization detector and a HP-INNOWAX capillary column (25.0 m × 0.53 mm × 0.20 μm). The temperatures of the injector and detector were 280 °C, respectively. The oven temperature was programmed starting at 160 °C, and then increased to 210 °C at a rate of 10 °C/min, held for 5 min, and then increased gradually to 240 °C at a rate of 2 °C/min, held for 15 min. Ultra-high purity N₂ was used as the carrier gas at a constant flow rate of 1.0 mL/min. The split ratio was 4:1, and the injection volume was 5 μL. Relevant FAME were identified by comparison of their peaks with those of standards (Cayman Chemicals, USA).

Generation of pFAD15 Promoter–Reporter Gene Construct and β-Galactosidase Assay

The *lacZ* gene was amplified by PCR using YEp356 [23] as the template and then cloned into the promoterless *P. pastoris* integrative pIB1 vector [24] (*SpeI/PstI*) to create pIB1lacZ. The promoter region of *P. pastoris* Δ15-desaturase gene (pFAD15) was obtained from genomic DNA and the PCR product was digested with *Bam*HI and *Spe*I and then inserted into pIB1lacZ which had been digested with the same enzymes. The primers used for the PCR are listed in Table 1. All constructs were sequenced to confirm correct orientation of insertion and no PCR-induced mutations. The *Stu*I-linearized and dephosphorylated promoter–reporter gene construct was directly electrotransformed into strain GS115. The recombinant colonies of His⁺ phenotype were selected on MD plates and evaluated by PCR with primers pIB1-F and pIB1-R (Table 1) and the resulting PCR fragments were subsequently confirmed by DNA sequencing. Positive transformants were grown to late exponential phase in YPD media. After treatments of low temperature and exogenous fatty acids, pFAD15 activities were determined via β-galactosidase assay. β-Galactosidase assay was measured in triplicate with *o*-nitrophenyl-β-D-galactopyranoside (ONPG) as a substrate on permeabilized cells treated with SDS and chloroform according to previously established method [25, 26].

Construction of *P. pastoris* *Spt23*Δ Mutant Strain

The *Spt23* ORF was amplified from genomic DNA by PCR using primer pair PPSpt23FA and PPSpt23RA (Table 1). The amplified fragment was then subcloned into pMD19-T simple vector (TA-cloning vector, Takara, Japan), generating pMD19T-*Spt23*. The *His4* gene cassette was obtained from the plasmid pPIC3.5K (purchased from Invitrogen) by using specific primers containing *Bam*HI flanking restriction sites (Table 1). The resulting fragments were

purified and treated with *Bam*HI, and then ligated into the *Bam*HI site of the plasmid pMD19T-*Spt23* within *Spt23* gene to produce pMD19T-*Spt23*/His. The disruption cassette *Spt23*/His4/*Spt23* was amplified using the corresponding primer pair in Table 1 from pMD19T-*Spt23*/His and transformed into *P. pastoris* GS115 by electroporation. After a double crossover-mediated gene replacement, His⁺ transformants were selected on MD plates lacking histidine at 30 °C. The His⁺ transformants of *Spt23*Δ were further evaluated on genomic DNA by PCR to determine if disruption does occur with primer pair PPSpt23FA and PPSpt23RA, and PHis4TT-F23 and PHis4TT-R23, respectively. All the resulting PCR fragments were subsequently confirmed by DNA sequencing.

Statistical Analysis

Differences in mRNA and β-galactosidase expression between control and other samples, and growth rates between wild type and mutants were evaluated using one-way analysis of variance (SPSS for Windows Version 13.0), which were considered statistically significant when the *P* value was <0.05.

Results

Effects of Low Temperature and Exogenous Fatty Acids on mRNA Expression of Desaturase Genes

Because it has been reported that the desaturase genes are regulated by low temperature and exogenous UFA in *B. subtilis* [6, 27], *S. cerevisiae* [9, 10] and also other fungi [28, 29], the effects of the two factors on expression of desaturase genes in *P. pastoris* were investigated by real-time PCR analysis using the β-actin gene as an internal control. As shown in (Fig. 1), the mRNA expression of four genes reached a maximum at the time point of 1 h, and the increase was followed by a decrease in the mRNA expression at later time-points of 4 and 8 h after the quick shift from 30 to 15 °C. The upregulation of mRNA expression by low temperature was greater for two Δ9-desaturase genes (*Fad9A* and *Fad9B*) compared with the Δ12-desaturase gene (*Fad12*) and Δ15-desaturase gene (*Fad15*) after 1 h incubation at 15 °C and there was little increase in the mRNA level of *Fad12* (1.3-fold) 1 h after the shift. There was almost no change in the gene expression of the control which was cultured at normal growth temperatures during the 8 h period. As shown in Fig. 2, after 1 h of the treatment with 1 mM OLA, mRNA expression of all genes was downregulated rapidly, with *Fad9A* and *Fad9B* being more potent, and no further decrease in the levels of these transcripts was observed at 4

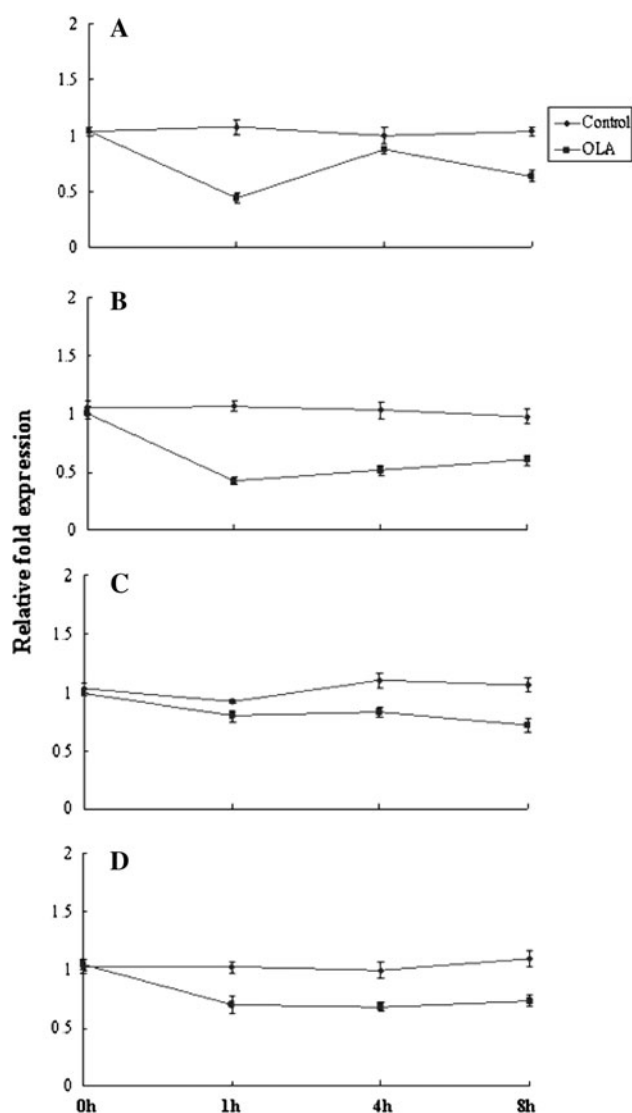


Fig. 2 Time-course expression study of *P. pastoris* GS115 desaturase genes in response to exogenous OLA. The graphs show the relative quantitation results of four desaturase gene expression (a *Fad9A* gene, b *Fad9B* gene, c *Fad12* gene, d *Fad15* gene) by real-time PCR. Relative gene expression measured relative to β -actin and normalized to controls was calculated as $2^{-\Delta\Delta C_T}$. Error bars represent the average SD of three separate experiments with three parallels

and 8 h. However, unlike monounsaturated OLA, saturated STA did not lower mRNA abundance of four genes and even mRNA levels of *Fad9A* and *Fad9B* were slightly increased at 1 h after the addition of STA (Fig. 3).

Changes in Fatty Acid Compositions in Response to Low Temperature and Exogenous Fatty Acids

In order to characterize the relationship between desaturase gene expression and fatty acid production, we measured the relative abundance of the corresponding fatty acid products using GC at the product level. As shown in Table 2, there was

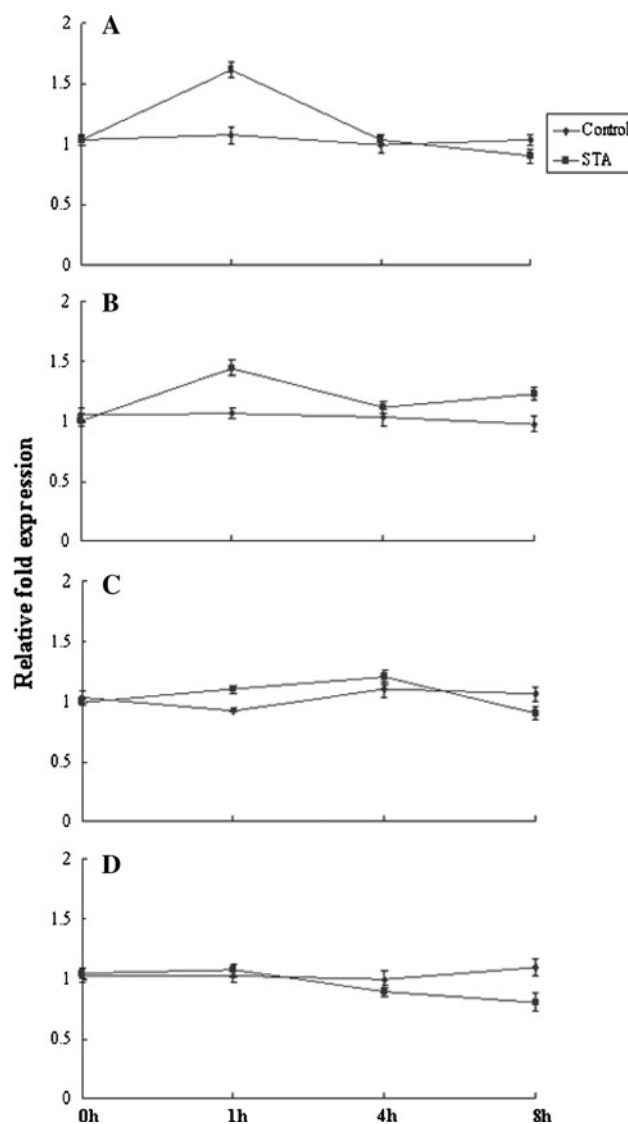


Fig. 3 Time-course expression study of *P. pastoris* GS115 desaturase genes in response to exogenous STA. The graphs show the relative quantitation results of four desaturase gene expression (a *Fad9A* gene, b *Fad9B* gene, c *Fad12* gene, d *Fad15* gene) by real-time PCR. Relative gene expression measured relative to β -actin and normalized to controls was calculated as $2^{-\Delta\Delta C_T}$. Error bars represent the average SD of three separate experiments with three parallels

no obvious increase in the content of corresponding desaturation products OLA + LNA + ALA, LNA + ALA and ALA at the time point of 1 h after the low-temperature shift even though the mRNA expression of $\Delta 9$ -desaturase gene, $\Delta 12$ -desaturase gene and $\Delta 15$ -desaturase gene were all increased at the same time point. Surprisingly, a substantial increase of OLA amount and decrease of ALA content compared with control was observed ($P < 0.05$). As shown in Table 2, the percentage of OLA increased from 60.54 to 69.51 % after 8 h of low temperature treatment, whereas the ALA content decreased from 7.99 % to a minimum value of

Table 2 Changes in relative fatty acid compositions of *P. pastoris* GS115 culture shifted from 30 to 15 °C at different time points

	PAM	STA	OLA	LNA	ALA	Others
Control 0 h	4.46 ± 0.05	1.84 ± 0.06	60.54 ± 1.62	23.79 ± 1.34	7.99 ± 0.86	1.38 ± 0.03
Control 1 h	3.83 ± 0.04	2.91 ± 0.05	60.62 ± 1.53	23.35 ± 1.25	7.64 ± 0.56	1.65 ± 0.03
Control 4 h	3.73 ± 0.06	2.89 ± 0.04	62.65 ± 1.34	22.07 ± 0.98	7.69 ± 0.73	0.97 ± 0.02
Control 8 h	2.34 ± 0.03	2.53 ± 0.04	64.71 ± 1.46	24.82 ± 0.96	4.66 ± 0.48	0.94 ± 0.03
Shift 0 h	4.46 ± 0.05	1.84 ± 0.06	60.54 ± 1.62	23.79 ± 1.34	7.99 ± 0.86	1.38 ± 0.03
Shift 1 h	3.68 ± 0.06	2.31 ± 0.04	62.11 ± 1.78	23.64 ± 1.26	6.34 ± 0.49	1.92 ± 0.05
Shift 4 h	3.43 ± 0.05	2.26 ± 0.06	66.62 ± 1.65	24.09 ± 1.04	2.31 ± 0.03	1.29 ± 0.02
Shift 8 h	3.23 ± 0.03	2.14 ± 0.02	69.51 ± 1.78	19.18 ± 1.08	4.09 ± 0.05	1.85 ± 0.02

All values are the means of three replicates ± SD

Table 3 Changes in relative fatty acid compositions of *P. pastoris* GS115 culture supplemented with 1 mM of different exogenous fatty acids at different time points

	PAM	STA	OLA	LNA	ALA	Others
Control 0 h	4.46 ± 0.05	1.84 ± 0.06	60.54 ± 1.62	23.79 ± 1.34	7.99 ± 0.86	1.38 ± 0.03
Control 1 h	3.83 ± 0.04	2.91 ± 0.05	60.62 ± 1.53	23.35 ± 1.25	7.64 ± 0.56	1.65 ± 0.03
Control 4 h	3.73 ± 0.06	2.89 ± 0.04	62.65 ± 1.34	22.07 ± 0.98	7.69 ± 0.73	0.97 ± 0.02
Control 8 h	2.34 ± 0.03	2.53 ± 0.04	64.71 ± 1.46	24.82 ± 0.96	4.66 ± 0.48	0.94 ± 0.03
STA 0 h	4.46 ± 0.05	1.84 ± 0.06	60.54 ± 1.62	23.79 ± 1.34	7.99 ± 0.86	1.38 ± 0.03
STA 1 h	3.98 ± 0.04	18.99 ± 1.38	50.55 ± 1.33	19.89 ± 1.27	5.54 ± 0.57	1.05 ± 0.03
STA 4 h	3.63 ± 0.05	28.66 ± 1.75	43.74 ± 1.39	17.51 ± 1.14	2.31 ± 0.03	1.29 ± 0.02
STA 8 h	2.23 ± 0.03	31.21 ± 1.68	46.35 ± 1.25	15.47 ± 1.08	4.33 ± 0.52	0.41 ± 0.01
OLA 0 h	4.46 ± 0.05	1.84 ± 0.06	60.54 ± 1.62	23.79 ± 1.34	7.99 ± 0.86	1.38 ± 0.03
OLA 1 h	2.86 ± 0.04	2.05 ± 0.04	57.55 ± 1.28	26.89 ± 1.48	9.54 ± 0.85	1.11 ± 0.02
OLA 4 h	2.51 ± 0.03	1.92 ± 0.04	65.85 ± 1.47	20.52 ± 1.39	7.65 ± 0.54	1.55 ± 0.05
OLA 8 h	1.42 ± 0.02	1.58 ± 0.03	72.38 ± 1.65	21.16 ± 1.25	3.09 ± 0.26	0.37 ± 0.01

All values are the means of three replicates ± SD

2.31 % at 4 h of low temperature treatment, and to 4.09 % after low temperature treatment for 8 h. However, the interesting mechanisms of why low temperature treatment increased the production of OLA but repressed the production of ALA during a short time period remain to be determined at the molecular level in the future. Likewise, changes in desaturase gene expression caused by the addition of STA and OLA did not correspond to the changes observed in fatty acid composition (Table 3). As shown in Table 3, a nearly continuous increase in STA or OLA proportion was observed after feeding STA or OLA. This might be a result of their entering cells and being incorporated into cellular lipids with the passage of time. In contrast, the levels of other fatty acids were reduced on the whole but the LNA and ALA content increased transiently at 1 h after feeding OLA as shown in Table 3. These results indicated that the correlation between changes in mRNA transcript abundance and fatty acid products profiles was varied and there may be post-transcriptional control and other modes of regulation of UFA synthesis in *P. pastoris* when facing different stimuli.

Effects of Low Temperature and Exogenous Fatty Acids on pFAD15 Promoter Activities

There was no direct relationship between mRNA levels of desaturase genes and the relative amount of UFAs. We therefore measured the activity of desaturase gene promoter and we first selected a 1,000-bp 5' flanking fragment of *Fad15* (pFAD15) as the research object and studied the effects of low temperature and exogenous fatty acids on pFAD15 promoter activity. The pFAD15 promoter construct was transformed into GS115 to measure the β -galactosidase activity with wild-type GS115, pIB1 and pIB1lacZ constructs as the control. As shown in Fig. 4, after temperature downshift, β -galactosidase expression was increased approximately 1.2-fold at 1 h, approximately 1.4-fold at 4 h, and increases gradually to a level that is approximately threefold ($P < 0.05$) at 8 h. As shown in Fig. 5, when incubating cells with different fatty acids, neither PAM nor STA had a significant effect on reporter activity, whereas UFA resulted in a continuous, time-

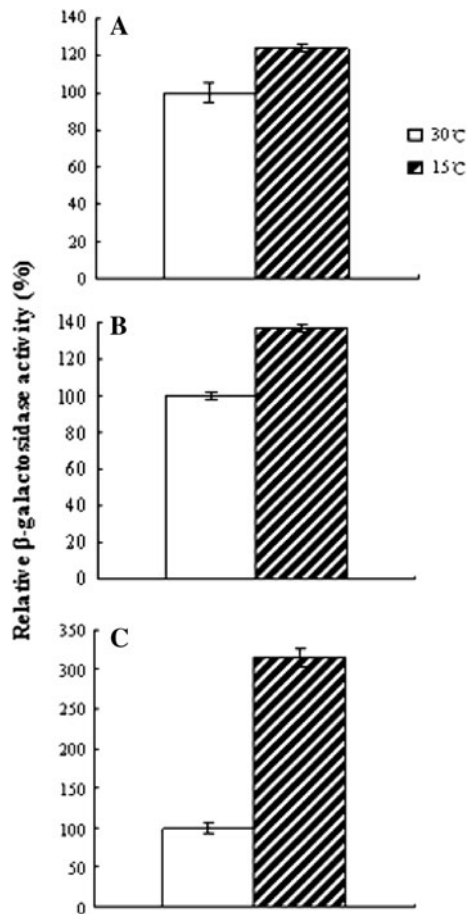


Fig. 4 Analysis of pFAD15 promoter activity under low temperature by β -galactosidase assays. The results were obtained after 1 h (a), 4 h (b), 8 h (c) incubation. All values are mean of three replicates \pm SD

dependent and dose-dependent reduction ($P < 0.05$) in promoter activity, and ALA containing three double bonds appeared to have a more effective inhibition than LNA and OLA. The β -galactosidase activities of control were nearly undetectable.

Possible Function of Spt23p in Transcriptional Regulation of Desaturase Gene Expression

Previous studies have revealed that the transcription of the *S. cerevisiae OLE1* gene appears to be mediated by two homologous proteins Spt23p and Mga2p, and Mga2p was the first identified sensor for low temperature and UFA in the regulation of the *S. cerevisiae OLE1* gene [30]. A homologues of the *S. cerevisiae Spt23/Mga2* genes was found in the published *P. pastoris* GS115 genome using Basic Local Alignment Search Tool (BLAST) searches. To test whether the Spt23p protein of *P. pastoris* GS115 has similar functions in the regulation of its desaturase genes, we constructed the *Spt23* disruption mutant by homologous recombination as described in the “Materials and

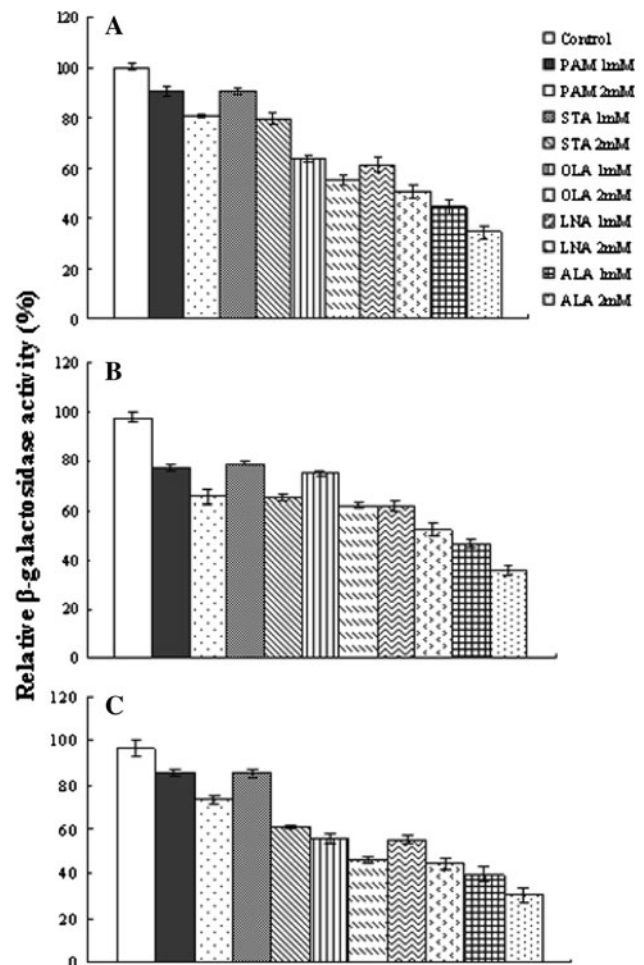


Fig. 5 Effects of different exogenous fatty acids on pFAD15 promoter activity by β -galactosidase assays. The results were obtained after 1 h (a), 4 h (b), 8 h (c) incubation. All values are the means of three replicates \pm SD

Methods” section. After initial selection of *P. pastoris* integrants on MD plates, successful gene disruption was confirmed by PCR amplification using sequence-specific primers and genomic DNA template. The oligonucleotides are shown in Table 1. Wild type GS115 generated a fragment of about 3.3 kb with the primers PPSpt23FA and PPSpt23RA, while *Spt23* Δ generated a fragment of about 7.0 kb because a *His4* gene cassette of about 3.7 kb was inserted into the *Bam*HI site within *Spt23*. Wild type GS115 yielded a 3.7 kb fragment using primers PHis4TT-F23 and PHis4TT-R23, but the wild type could not (Fig. 6). The results confirmed that *Spt23* was deleted via double-crossover homologous recombination. Real-time analysis was performed to determine the effects of disruption of *Spt23* on the transcript levels of desaturase genes. Resulting data showed that the mRNA levels of *Fad9A* and *Fad9B* in the stationary phase cells of Δ *Spt23* mutant were markedly reduced at the levels $<25\%$ of

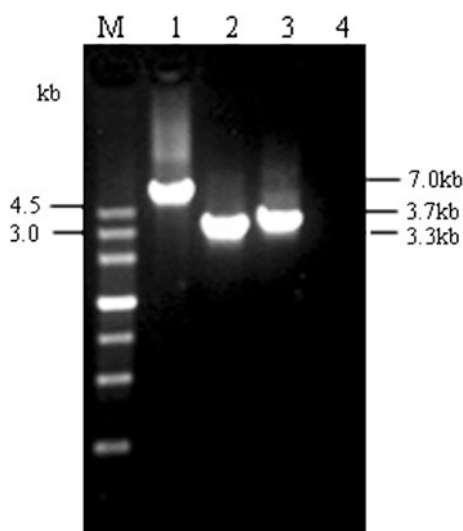


Fig. 6 Identification of *Spt23* mutation by PCR. *M* NI DNA marker III, 1 PCR product with PPSpt23FA and PPSpt23RA (*Spt23* Δ as template), 2 PCR product with PPSpt23FA and PPSpt23RA (wild type as template), 3 PCR product with PHis4TT-F23 and PHis4TT-R23 (*Spt23* Δ as template), 4 PCR product with PHis4TT-F23 and PHis4TT-R23 (wild type as template)

Table 4 Relative expression of desaturase genes in the stationary phase cells of strain *Spt23* Δ

	<i>Spt23</i> Δ	GS115
<i>Fad9A</i>	0.25 \pm 0.03	1 \pm 0.05
<i>Fad9B</i>	0.18 \pm 0.02	1 \pm 0.04
<i>Fad12</i>	0.90 \pm 0.06	1 \pm 0.03
<i>Fad15</i>	1.33 \pm 0.04	1 \pm 0.04

All values are the means of three replicates \pm SD

wild-type ($P < 0.05$). By contrast, the mRNA levels of *Fad12* and *Fad15* changed much less in comparison with the changes in the mRNA levels of *Fad9A* and *Fad9B* (Table 4). We further analyzed the changes in fatty acid composition, a decrease in the relative abundance of OLA and an increase in the relative content of LNA and ALA were observed ($P < 0.05$) (Table 5).

The time-course expression study showed that there were no clear changes in the expression for *Fad9A* and *Fad9B* of *Spt23* Δ strain in response to low temperature and exogenous OLA during the test period which was not

consistent with the results obtained with the wild type strain (Fig. 7). While there were no clear differences in the gene expression profiles of *Fad12* and *Fad15* in response to low temperature and exogenous OLA between the wild-type strain and *Spt23* Δ strains (data not shown). These data indicated that *Spt23p* are probably necessary for the control over the transcription of *Fad9A* and *Fad9B*, but not *Fad12* and *Fad15*. In addition, we also proved that the *Spt23* Δ strain grew much more slowly than wild-type cells under normal growth conditions by monitoring OD₆₀₀ of the cultures at 2-h intervals for 36 h (Fig. 8).

Discussion

In many organisms, multiple types of environmental stress could affect the productivity of PUFA. But a major hindrance preventing thorough investigation into the regulation mechanism of different desaturase when facing external stimuli or internal stimuli has been the lack of an effective way to quantify the amount and activity of desaturase. Thus, one of the aims of this study was to investigate the transcriptional changes of *P. pastoris* desaturase genes in response to various environmental factors such as low temperature and exogenous fatty acids. Both of two conditions can lead to changes in membrane fluidity with resultant subnormal functioning of cellular activities [31]. Our results demonstrate that the transient increase in the mRNA abundance for all desaturase genes occurred in response to low temperature and the repression of desaturase gene transcription by exogenous UFA was also transient which presumably reflects that the transcription of desaturase genes is only regulated by the external signal at the initial stage. It is perhaps noteworthy that expression of *Fad9A* and *Fad9B*, both of which encode $\Delta 9$ -desaturase converting STA into OLA in the first step of *P. pastoris* PUFA synthesis, were strongly regulated compared with the other two desaturase genes. It is also quite interesting for us to investigate the possible reasons in the future.

Further analysis revealed that the fatty acid compositions change irregularly and did not correspond to changes of levels of mRNA expression over a period of hours when cells are shifted to low temperature or exogenous fatty acids. These results demonstrate that UFA synthesis in

Table 5 Fatty acid composition of the stationary phase cells of strain *Spt23* Δ

	PAM	STA	OLA	LNA	ALA	Others
<i>Spt23</i> Δ	31.41 \pm 1.22	4.62 \pm 0.28	19.74 \pm 1.52	26.67 \pm 2.25	11.15 \pm 0.88	6.41 \pm 0.57
GS115	2.84 \pm 0.42	2.63 \pm 0.08	66.4 \pm 2.85	22.5 \pm 1.97	4.76 \pm 0.47	0.77 \pm 0.03

All values are the means of three replicates \pm SD

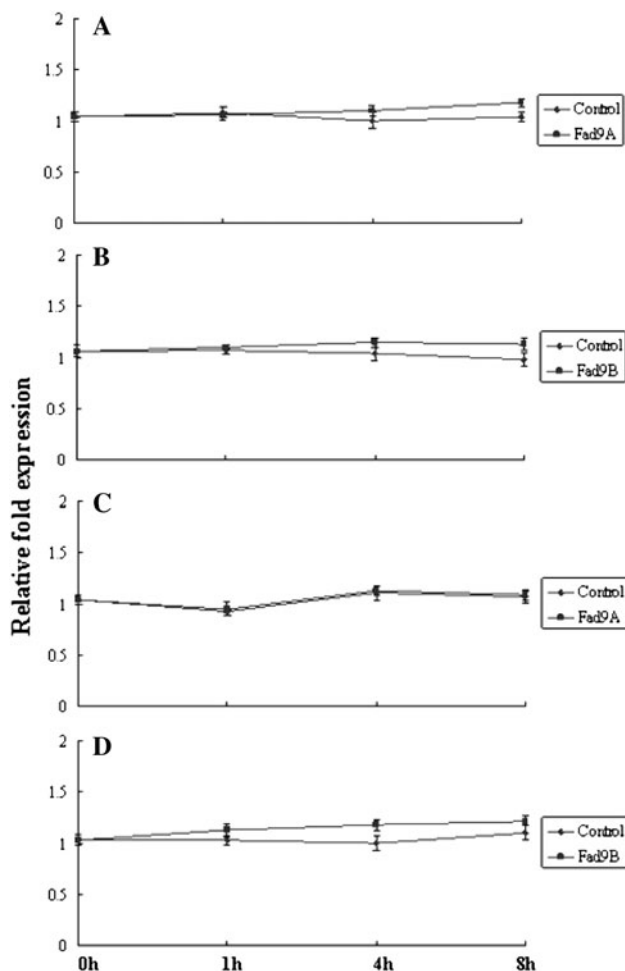


Fig. 7 Time-course expression study of *P. pastoris* *Spt23*Δ strain desaturase genes in response to low temperature and exogenous OLA. The graphs show the relative quantitation results of Δ9-desaturase gene expression (a *Fad9A* gene in response to low temperature, b *Fad9B* gene in response to low temperature, c *Fad9A* gene in response to exogenous OLA, d *Fad9B* gene in response to exogenous OLA) by real-time PCR. Relative gene expression measured relative to β-actin and normalized to controls was calculated as $2^{-\Delta\Delta C_T}$. Error bars represent the average SD of three separate experiments with three parallels

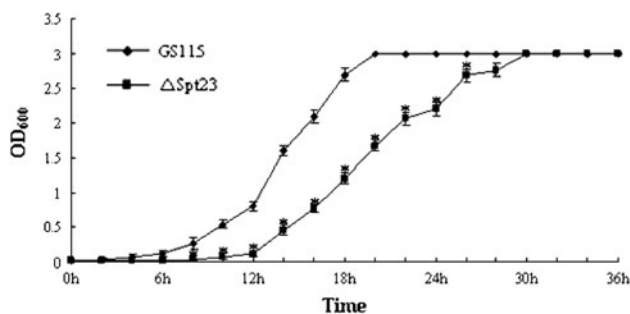


Fig. 8 Growth curves of *P. pastoris* strain GS115 and *Spt23*Δ in YPD liquid medium at 30 °C. The data shown are the mean ± SD of three separate experiments. **P* < 0.05, significantly different

P. pastoris appear to be controlled predominantly by post-transcriptional regulation of desaturase genes. Similar mechanisms were also found in *S. cerevisiae* [10], *Mucor rouxii* [28, 29] and *Synechococcus* sp. [32].

Functional analysis of the pFAD15 promoter indicated that low temperature functions as a transcriptional activator and UFA act as negative regulators of desaturase gene transcription. SFA failed to downregulate the promoter activity. The responses of promoter activities to low temperature and exogenous fatty acids appeared to be different with gene expression profile changes which were basically rapid and transient during the test period. This observation suggested that there may be an unknown end-product (changes in fatty acid compositions) feedback regulation in the transcription of desaturase genes to maintain cellular UFA homeostasis.

P. pastoris Spt23p shared a high degree of sequence identity in the conserved domains with *S. cerevisiae* Spt23p/Mga2p, so we hypothesized that *P. pastoris* Spt23p exerts a similar function with *S. cerevisiae* Spt23p/Mga2p. In this study, we observed that *P. pastoris* Spt23p may control the expression of Δ9-desaturase genes and the production of OLA. Unlike *S. cerevisiae*, in which the simultaneous disruption of Spt23p/Mga2p results in synthetic auxotrophy for UFA due to loss of *OLE1* mRNA [15], in *P. pastoris*, disruption of *Spt23* resulted in substantial inhibition in expression of *Fad9A* and *Fad9B*, production of OLA and strain growth, but these were not completely inhibited as in *S. cerevisiae*. It is not surprising that the regulation of desaturase gene expression in *P. pastoris* is more complex than *S. cerevisiae* and involves multiple signal transduction systems that act at several levels of modulating gene expression.

In conclusion, our study suggests that low temperature and exogenous UFA can regulate the expression of *P. pastoris* desaturase genes at the transcriptional level and the primary function of Spt23p is to serve as a probable transcription regulator of the Δ9-desaturase gene, although perhaps other regulatory proteins and sensing mechanisms remain to be identified in the regulation of Δ9-, Δ12- and Δ15-desaturase genes under a wide range of physiological conditions. Further studies are in progress to address this point which is not clear at the moment.

Acknowledgments This study was supported by the National Natural Science Foundation of China (No. 30771355, 31270096).

References

1. Tapiero H, Nguyen Ba G, Couvreur P, Tew K (2002) Polyunsaturated fatty acids (PUFA) and eicosanoids in human health and pathologies. *Biomed Pharmacother* 56:215–222

2. Calder PC, Yaqoob P (2009) Omega-3 polyunsaturated fatty acids and human health outcomes. *Biofactors* 35:266–272
3. Gill I, Valivety R (1997) Polyunsaturated fatty acids, part 1: occurrence, biological activities and applications. *Trends Biotechnol* 15:401–409
4. Yazawa H, Iwahashi H, Kamisaka Y, Kimura K, Uemura H (2010) Improvement of polyunsaturated fatty acids synthesis by the coexpression of CYB5 with desaturase genes in *Saccharomyces cerevisiae*. *Appl Microbiol Biotechnol* 87:2185–2193
5. Kang DH, Anbu P, Kim WH, Hur BK (2008) Coexpression of Elo-like enzyme and $\Delta 5$, $\Delta 4$ -desaturases derived from *Thraustochytrium aureum* ATCC 34304 and the production of DHA and DPA in *Pichia pastoris*. *Biotechnol Bioprocess Eng* 13:483–490
6. Aguilar PS, Hernandez-Arriaga AM, Cybulski LE, Erazo AC, De Mendoza D (2001) Molecular basis of thermosensing: a two-component signal transduction thermometer in *Bacillus subtilis*. *EMBO J* 20:1681–1691
7. DeRisi JL, Iyer VR, Brown PO (1997) Exploring the metabolic and genetic control of gene expression on a genomic scale. *Science* 278:680–686
8. Smith JJ, Marelli M, Christmas RH, Vizeacoumar FJ, Dilworth DJ et al (2002) Transcriptome profiling to identify genes involved in peroxisome assembly and function. *J Cell Biol* 158:259–271
9. Nakagawa Y, Sakumoto N, Kaneko Y, Harashima S (2002) Mga2p is a putative sensor for low temperature and oxygen to induce *OLE1* transcription in *Saccharomyces cerevisiae*. *Biochem Biophys Res Commun* 291:707–713
10. McDonough V, Stukej J, Martin C (1992) Specificity of unsaturated fatty acid-regulated expression of the *Saccharomyces cerevisiae OLE1* gene. *J Biol Chem* 267:5931–5936
11. Fujiwara D, Yoshimoto H, Sone H, Harashima S, Tamai Y (1998) Transcriptional co-regulation of *Saccharomyces cerevisiae* alcohol acetyltransferase gene, *ATF1* and Δ -9 fatty acid desaturase gene, *OLE1* by unsaturated fatty acids. *Yeast* 14:711–721
12. Kwast KE, Burke PV, Staahl BT, Poyton RO (1999) Oxygen sensing in yeast: evidence for the involvement of the respiratory chain in regulating the transcription of a subset of hypoxic genes. *Proc Natl Acad Sci USA* 96:5446–5451
13. Vasconcelles MJ, Jiang Y, McDaid K, Gilooly L, Wretzel S et al (2001) Identification and characterization of a low oxygen response element involved in the hypoxic induction of a family of *Saccharomyces cerevisiae* genes. *J Biol Chem* 276:14374–14384
14. Ter Linde J, Liang H, Davis R, Steensma H, Van Dijken J et al (1999) Genome-wide transcriptional analysis of aerobic and anaerobic chemostat cultures of *Saccharomyces cerevisiae*. *J Bacteriol* 181:7409–7413
15. Zhang S, Skalsky Y, Garfinkel DJ (1999) *MGA2* or *SPT23* is required for transcription of the $\Delta 9$ fatty acid desaturase gene, *OLE1*, and nuclear membrane integrity in *Saccharomyces cerevisiae*. *Genetics* 151:473–483
16. Zhang S, Burkett TJ, Yamashita I, Garfinkel DJ (1997) Genetic redundancy between *SPT23* and *MGA2*: regulators of Ty-induced mutations and *Ty1* transcription in *Saccharomyces cerevisiae*. *Mol Cell Biol* 17:4718–4729
17. Jiang Y, Vasconcelles MJ, Wretzel S, Light A, Gilooly L et al (2002) Mga2p processing by hypoxia and unsaturated fatty acids in *Saccharomyces cerevisiae*: impact on LORE-dependent gene expression. *Eukaryot Cell* 1:481–490
18. Chellappa R, Kandasamy P, Oh CS, Jiang Y, Vemula M et al (2001) The membrane proteins, Spt23p and Mga2p, play distinct roles in the activation of *Saccharomyces cerevisiae OLE1* gene expression. *J Biol Chem* 276:43548–43556
19. Hoppe T, Matuschewski K, Rape M, Schlenker S, Ulrich HD et al (2000) Activation of a membrane-bound transcription factor by regulated ubiquitin/proteasome-dependent processing. *Cell* 102:577–586
20. Cereghino JL, Cregg JM (2000) Heterologous protein expression in the methylotrophic yeast *Pichia pastoris*. *FEMS Microbiol Rev* 24:45–66
21. Macauley-Patrick S, Fazenda ML, McNeil B, Harvey LM (2005) Heterologous protein production using the *Pichia pastoris* expression system. *Yeast* 22:249–270
22. De Schutter K, Lin YC, Tiels P, Van Hecke A, Glinka S et al (2009) Genome sequence of the recombinant protein production host *Pichia pastoris*. *Nat Biotechnol* 27:561–566
23. Hill JE, Myers AM, Koerner T, Tzagoloff A (1986) Yeast/*E. coli* shuttle vectors with multiple unique restriction sites. *Yeast* 2:163–167
24. Sears IB, O'Connor J, Rossanese OW, Glick BS (1998) A versatile set of vectors for constitutive and regulated gene expression in *Pichia pastoris*. *Yeast* 14:783–790
25. Miller JH (1972) Experiments in molecular genetics. Cold Spring Harbor Laboratory Press, New York
26. Guarente L (1983) Yeast promoters and lacZ fusions designed to study expression of cloned genes in yeast. *Methods Enzymol* 101:181–191
27. Kaan T, Homuth G, Mäder U, Bandow J, Schweder T (2002) Genome-wide transcriptional profiling of the *Bacillus subtilis* cold-shock response. *Microbiology* 148:3441–3455
28. Khoomrung S, Laoteng K, Jitsue S, Cheevadhanarak S (2008) Significance of fatty acid supplementation on profiles of cell growth, fatty acid, and gene expression of three desaturases in *Mucor rouxii*. *Appl Microbiol Biot* 80:499–506
29. Cheawchanlertfa P, Cheevadhanarak S, Tanticharoen M, Maresca B, Laoteng K (2011) Up-regulated expression of desaturase genes of *Mucor rouxii* in response to low temperature associates with pre-existing cellular fatty acid constituents. *Mol Biol Rep* 38:3455–3462
30. Jiang Y, Vasconcelles MJ, Wretzel S, Light A, Martin CE et al (2001) *MGA2* is involved in the low-oxygen response element-dependent hypoxic induction of genes in *Saccharomyces cerevisiae*. *Mol Cell Biol* 21:6161–6169
31. Mansilla MC, Cybulski LE, Albanesi D, De Mendoza D (2004) Control of membrane lipid fluidity by molecular thermosensors. *J Bacteriol* 186:6681–6688
32. Sakamoto T, Higashi S, Wada H, Murata N, Bryant DA (1997) Low-temperature-induced desaturation of fatty acids and expression of desaturase genes in the cyanobacterium *Synechococcus* sp. PCC 7002. *FEMS Microbiol Lett* 152:313–320

biology materials has greatly facilitated the throughput of a fatty acid assay in a simple, rapid, and high throughput way [10–12]. However, the entire procedure for total lipids is time-consuming, requiring 60 min at 100 °C [10] or 2 h at 80 °C [13] with conductive heating for a complete transesterification of fatty acids, and increases the potential for oxidation.

Following the application of microwave irradiation in lipids extraction from foods [14], Lie Ken Jie and Yan-Kit initially applied microwave irradiation to the transformation of fatty acids in 1988 [15], including the esterification of free fatty acids within 5 min using a domestic microwave oven. Ever since, the application of the microwave as an energy source has been further developed in transesterification of phospholipid fatty acids from sheep brain serotonin receptor preparation [15, 16], human blood [17], vegetable and fish oil [18], and glycosphingolipids [19], with a reaction time as short as 20 s [16]. The fatty acid structures of products are identical either from microwave irradiation or the heatblock heating assay [18].

Nevertheless, compared to conductive heating, the transesterification of fatty acids by microwave irradiation using a household microwave oven are incomplete with a recovery of 78 % for total fatty acids in blood [17]. Clearly, the use of a domestic microwave oven in chemical synthesis presents significant safety issues. Thus, the application of microwave radiation in a fatty acid assay has not been further developed or optimally established. Tomas et al. [20] first applied a chemically safe, single-mode microwave oven to quantify meat acylglycerides with methanol and chlorotrimethylsilane. In this study, we sought to optimize the conditions of transesterification in microwave reaction systems for the fatty acids in human serum total lipids using methanol:hexane with acetyl chloride as the catalyst. It proved that the microwave irradiation could significantly reduce the reaction time with complete transesterification of fatty acids under optimal conditions.

Materials and Methods

Chemicals

Methanol was purchased from Burdick & Jackson (Muskegon, MI); hexane from EMD Chemicals Inc (Gibbstown, NJ); acetyl chloride from Sigma–Aldrich (St. Louis, MO); 2,6-Di-*tert*-butyl-4-methylphenol (BHT) from Acros (Geel, Belgium); sodium carbonate (anhydrous powder) from Mallinckrodt Baker, Inc. (Paris, KY). Standard docosatrienoic ethyl ester (22:3n-3) and GC reference standards GLC-462 were purchased from Nu–Chek Prep (Elysian, MN). The latter contains 28 fatty acid methyl esters

(FAME). All chemicals were of analytical grade, commercially purchased, and used without further purification.

Human Serum

All serum samples analyzed in this report were from one research blood donor, with an omnivore diet, in the Clinical Center of the National Institutes of Health. A bulk of blood was collected by venipuncture, and left at room temperature for 1 h prior to being centrifuged at 1,700g for 15 min at 4 °C to collect the serum. The serum was aliquoted, frozen, and stored at –80 °C until analysis.

Instrumentation

Analog Drybath Incubator

An analog heatblock from VWR International, LLC (West Chester, PA) was the conductive heating source as utilized in the reference method for fatty acid determination.

Microwave Reaction Systems

Two microwave reaction systems from CEM Corporation (Matthews, NC) were employed in microwave irradiation fatty acid analysis (microwave assay). Both systems provided constant temperatures at a pre-set number of degrees during transesterification of human serum lipids.

System S is a single-mode microwave reaction system (DISCOVER BenchMate), briefly referred to as Single-mode. Samples were processed one at a time in a pressurized 10-mL Pyrex glass reaction vessel with “snap-on” Teflon cap, which automatically vented when internal pressure reached 300 psi (2,068 pKa). The reaction temperature of 100 or 125 °C was pre-set and directly measured inside the glass vessel with a fiber optic temperature probe. Microwave power was initially set at no greater than 50 or 300 W, and automatically adjusted to maintain the reaction temperature through temperature and pressure feedback in the cavity. The reaction duration was examined at 1–5 min.

System M is a multimode microwave accelerate reaction system (MARS), briefly referred to as Multimode. It can process multiple reactions simultaneously, up to 24 20-mL Pyrex glass vessels or up to 40 10-mL Teflon reaction vessels. The accessory for glass vessels, GlassChem20, included one turntable with a shield containing 24 receptacles. One set of reaction vessels was composed of a glass vessel, a vessel top, a vent plug, and a composite sleeve. Reaction temperatures of 100 or 125 °C was pre-set, measured, and controlled through a single reference vessel using a fiber optic probe inserted into a thermowell that was in direct contact with the sample in the reagent

mixture. For the Teflon vessels, pressurized “snap-on” Teflon caps were employed, and an onboard infrared sensor was used to measure and control the temperature. After having reached the reaction temperature, 100 or 125 °C, the initial microwave power of 400 W ($n \leq 4$) was automatically adjusted to hold the temperature until the end of the reaction. Compressed air was applied to cool down the sample. Reaction duration was examined at a range of 1–10 min.

Gas Chromatography

An Agilent 6890 (Plus LAN) fast gas chromatograph, coupled with a flame ionization detector and a 7683 series injector (Agilent Technologies, Inc., Santa Clara, CA), was employed to acquire the signal of the FAME. A fused-silica, narrow-bore, high-efficiency DB-FFAP capillary column (15 m length \times 0.1 mm ID \times 0.1 μ m film thickness) was used for chromatographic separation of FAME with hydrogen as the carrier gas at a constant pressure of 51.5 psi (355 kPa). The make-up nitrogen gas was set at a constant flow of 10 mL/min. The inlet and detector temperature were set-up at 250 °C. A split ratio of 50:1 was applied. The oven temperature program was initially set at 150 °C with a 0.25 min hold, ramped at 35 °C/min to 200 °C, a further 8 °C/min ramp to 225 °C with a 3.2 min hold, and then 80 °C/min ramp to 245 °C with a 9 min hold to bake off the column. A total of 28 FAME in GLC-462 were eluted in about 8 min with a total run of about 17 min [21]. GC ChemStation Rev. B.01.01 (164) SR1 was employed for data acquisition and peak integration.

Fatty Acid Direct Transesterification Method

The one-step direct transesterification in the Lepage & Roy fatty acid assay [10, 13] was applied as the reference method. Compared to the conventional technique, the quantification of fatty acids in the Lepage & Roy assay was carried out in methanol:hexane (4:1, by vol) with acetyl chloride without prior extraction of lipids. It is rapid and reliable; in particular, capable of maintaining short chain fatty acids, which are essential in dietary studies but easily underestimated in the conventional method during lipid extraction and subsequent evaporation. Briefly, 100 μ L of serum or 0.9 % sodium chloride as the solvent blank was added to a 16 \times 100 mm disposable borosilicate glass test tube placed in ice containing 1.6 mL of methanol, 0.4 mL of hexane, and 200 μ L of acetyl chloride. Standard 22:3n-3 ethyl ester (27.6 nmol per sample) was used as the internal standard (ISTD). The test tubes were then tightly closed under nitrogen with Teflon-lined caps, and heated in an analog heating block at 100 °C for 60 min. Afterwards, the samples were chilled in ice and then neutralized by the

addition of 5 mL of 6 % Na₂CO₃ solution followed by centrifugation at 1,700g for 4 min. The hexane, served as the upper phase containing fatty acid methyl ester, was collected and the volume was reduced to \sim 30 μ L prior to being placed in a GC autosampler tray. In general, 1 μ L of aliquot was injected into GC inlet for data acquisition.

The microwave accelerated fatty acid assay was modified from the above Lepage & Roy procedures with only modification in the heating conditions, including energy source, temperature, duration, and reaction vessels. A set of experiments ($n = 11$) was designed to optimize the reaction duration at 100 or 125 °C with complete transesterification of the fatty acids in the solvent system of methanol, hexane, and acetyl chloride. As presented in Table 1, all procedures across eleven microwave groups (series S and M) were the same except for the varied reaction temperatures (100 or 125 °C), duration (1, 2.5, 5, or 10 min), the initial power of microwave irradiation (50, 300, or 400 W), and materials of reaction vessels (disposal glass, pressurized glass or Teflon). Multispeed magnetic stirring and compressed air cooling were also employed. All of the microwave assays were carried out in triplicate except group M1 (duplicate).

Calculation and Statistics

Data were expressed as means \pm SD in concentrations, μ mol of fatty acid per L serum (μ M), or the proportion of each fatty acid in total amount of the identified fatty acids in each sample (mol%). The concentrations were calculated by comparing the integrated areas of each fatty acid peak in the gas chromatograms with that of the known amount of ISTD added in the sample. Automated data processing through macro programming with Microsoft VBA 6.3 (Microsoft Corp; Seattle, WA) was performed during calculation of fatty acid values. Details were reported in the previous study [13]. Recovery of each fatty acid was defined as the percentage of fatty acid values determined by the microwave assay to those by the reference method. The 20- and 22-carbon fatty acids with three or more carbon-carbon double bonds were categorized as highly unsaturated fatty acids (HUFA), which included 20:3n-6, 20:4n-6, 22:4n-6, and 22:5n-6 in n-6 PUFA; 20:5n-3, 22:5n-3, and 22:6n-3 in n-3 PUFA; and 20:3n-9. The proportion of n-6 or n-3 HUFA, that is n-6 % or n-3 % HUFA, was computed by dividing the sum of n-6 or n-3 HUFA by the total HUFA in each sample and multiplying by 100.

Results of each fatty acid determined by multiple methods were compared by One-way ANOVA followed by a Post Hoc Tamhane's T2 test using SPSS 17.0 (SPSS Inc.; Chicago, IL). Statistic significance for a particular experimental condition was presented in comparison with the reference method at $P < 0.01$.

Table 1 Conditions of transesterification by either conductive heating or microwave irradiation

Groups	Reaction conditions for human serum total lipids					
	Heaters	Temperature (°C)	Duration (min)	Energy sources	Reaction vessels	Abbreviation
Control	Analog heatblock	100	60	conductive	glass 1, 7 mL	C-100x60
S1	Single-mode	100	5	MW ≤ 50 W	glass 2, 10 mL	S1-100x5
S2	Single-mode	100	2.5	↓ ≤ 50 W	↓	S2-100x2.5
S3	Single-mode	100	1	↓ ≤ 50 W	↓	S3-100x1
S4	Single-mode	100	1	300 W	↓	S4-100x1
S5	Single-mode	125	1	300 W	↓	S5-125x1
M1	Multimode	100	1	400 W	glass 2, 20 mL	M1-100x1
M2	Multimode	100	2.5	400 W	↓	M2-100x2.5
M3	Multimode	100	5	400 W	↓	M3-100x5
M4	Multimode	100	10	400 W	↓	M4-100x10
M5	Multimode	125	5	400 W	↓	M5-125x5
M6	Multimode	100	5	↓ 400 W	Teflon, 10 mL	M6-100x5

Groups S4-100×1 and M5-125×5 in **bold** were the optimal conditions examined
S Single-mode microwave reaction system, *M* multimode microwave reaction system, *MW* microwave irradiation, *glass 1* disposable borosilicate glass tube, *glass 2* pressurized borosilicate glass vessel, *Teflon* pressurized Teflon vessel

Results and Discussion

This study focused on microwave irradiation as an alternative energy source for one-step direct transesterification of fatty acid components of total lipids in human serum. The fatty acid concentrations (μmol/L) determined by microwave assays in methanol:hexane:acetyl chloride (4:1:0.2, by vol) were compared in Fig. 1, including total fatty acids (A), low abundance fatty acids (<50 μM; B), intermediate abundance (50–250 μM; C), and high abundance (>250 μM; D). The Lepage & Roy assay was employed as the reference method, which applied the same solvent system but transesterified in a heating block. The corresponding fatty acid profiles (mol%) are presented in Table 2.

Complete Transesterification

It was apparent that the concentrations of various fatty acids in microwave groups S4-100 × 1 and M5-125 × 5 in Fig. 1a–d were consistently close to those in the control group (C-100 × 60). As presented in Table 2, the total amount of fatty acids (μmol/L) was 7,562 (S4-100 × 1) and 7,304 (M5-125 × 5) in microwave groups compared to 7,304 in control group, which represented recoveries of 103 and 100 %, respectively. Similarly, the recoveries of the categorized fatty acids, including saturates, monounsaturates, n-6 PUFA, and n-3 PUFA, were in the ranges of 96–106 % (S4-100 × 1) and 97–102 % (M5-125 × 5). Compared to the control group, it was observed that the recoveries of individual fatty acids ($n = 23$) in both groups were 94 % or greater for all except some minor fatty acids—20:0, 22:0, 24:0, and 24:1n-9, which were lower as 84 %

(range 79–91). These minor ones accounted less than 2.5 % of moles of total fatty acids. In particular, the recoveries of individual PUFA in both groups were in range of 95–105 % except for 18:3n-6 (109 %) and 20:2n-6 (113 %) in S4-100 × 1, and 20:3n-6 (109 %) and 20:5n-3 (109 %) in M5-125 × 5. Marginal greater recoveries for 20:5n-3 could be explained by the reduced potential oxidation in microwave assay, as observed by Khan and William [22]. It was likely similar to 20:3n-6. Furthermore, 100.0 % of ISTD 22:3n-3 ethyl esters added in samples were transmethylated to 22:3n-3 methyl esters in M5-125 × 5, and 99.5 % in S4-100 × 1. Thus, taking the above conditions as optimal, the fatty acids of interest in human serum were completely transesterified for all major ones and most minor ones with microwave irradiation heating at 100 °C for 1 min in Single-mode with an initial power of 300 W (S4-100 × 1) or 125 °C for 5 min in Multimode with 400 W (M5-125 × 5).

Additionally, the recoveries for the categorized fatty acids in group S1-100 × 5, 100 °C for 5 min in Single-mode, were in the range of 96–103 % which indicated a complete transesterification of those in groups S4-100 × 1 and M5-125 × 5. However, upon inspection of panels B and C in Fig. 1, the minor fatty acids—20:0, 22:0, 24:0, and 24:1n-9, reached only 60–69 %. Thus, this was not considered as optimal transesterification.

Given the varied features of the two microwave reaction systems, the difference between the two optimal conditions were expected and could be mainly derived from the different temperature control systems and the varied number of sample processed in each system. The actual temperature in Multimode was measured and controlled by an internal fiber optic probe inserted in the reference vessel,

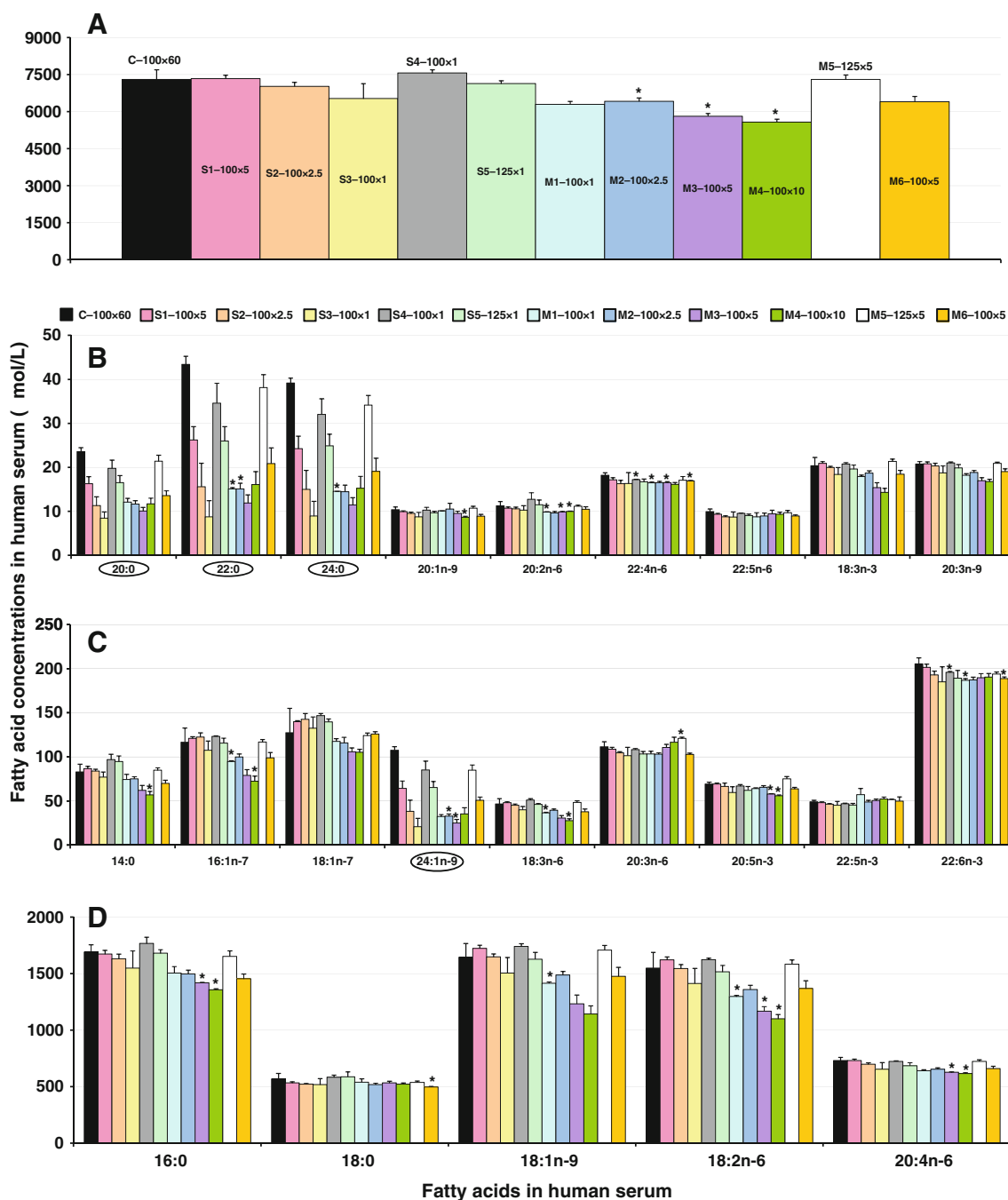


Fig. 1 Comparison of the concentrations of fatty acids ($\mu\text{mol/L}$) in human serum determined by microwave accelerated assay for eleven conditions (S and M series) with those by Lepage & Roy assay, the reference method (control group C-100 \times 60). Values are presented as means \pm SD, $n = 3$ except M1-100 \times 5 ($n = 2$) and C-100 \times 60 ($n = 16$). **a** Total fatty acids; **b** Low abundance fatty acids, $<50 \mu\text{M}$;

c Intermediate abundance fatty acids, $50\text{--}250 \mu\text{M}$; **d** High abundance fatty acids, $>250 \mu\text{M}$. Further details regarding the reaction conditions are presented in Table 1. One-way ANOVA followed by Tamhane's T2 was applied to multiple comparison; asterisks indicate statistically differences in comparison with the control group at $P < 0.01$. Unit conversion: $1 \mu\text{mol/L}$ of fatty acid $\approx 0.36 \mu\text{g/mL}$

but in Single-mode by the cavity outside the reaction vessel. In addition, it would be expected in Multimode that a much higher initial microwave power setting would be needed to maintain the optimal transesterification conditions when the number of samples in each batch increased.

The recent report by Tomas et al. [20] shows similar results ranging between 103 and 117 % for recoveries of 16:0, 18:0, 18:2n-6, and 20:4n-6 in meat acylglycerides using a single-mode microwave reaction system. However, the catalyst (chlorotrimethylsilane) applied in microwave

irradiation to accelerate transesterification is different from that in the reference method (boron trifluoride). This might cause some variation.

Partial Transesterification

In the remaining nine microwave conditions tested, including groups S1–S3, S5, M1–M4, and M6, only

86–99 % of 22:3n-3 ethyl esters were converted to methyl esters. Similarly, the recoveries (%) for total fatty acids, saturates, monounsaturates, and n-6 and n-3 PUFA, were within lower and wider ranges as 76–100, 81–96, 68–103, and 90–99, respectively. It was observable that fatty acids were partially transesterified under these conditions, which were thus considered as sub-optimal. However, after having been calibrated with ISTD, the concentrations of

Table 2 Comparison of fatty acid profiles in human serum total lipids determined by either the Lepage & Roy or microwave irradiation assays

Groups MW (Watt)	C-100 x 60 n/a	S1-100 x 5 50	S2-100 x 2.5 50	S3-100 x 1 50	S4-100 x 1 300	S5-125 x 1 300
Fatty acids	mol% of Total fatty acids					
14:0	1.13 ± 0.1	1.18 ± 0.0	1.20 ± 0.0	1.18 ± 0.0	1.28 ± 0.1	1.33 ± 0.1
16:0	23.2 ± 0.6	22.8 ± 0.0	23.2 ± 0.1	23.8 ± 0.6	23.4 ± 0.4	23.6 ± 0.6
18:0	7.82 ± 0.8	7.27 ± 0.0	7.44 ± 0.1	7.94 ± 0.3	7.72 ± 0.1	8.26 ± 0.7
20:0	0.32 ± 0.0	0.22 ± 0.0	0.16 ± 0.0	0.13 ± 0.0	0.26 ± 0.0	0.23 ± 0.0
22:0	0.60 ± 0.0	0.36 ± 0.0	0.22 ± 0.1	0.14 ± 0.1	0.46 ± 0.1	0.36 ± 0.0
24:0	0.54 ± 0.0	0.33 ± 0.0	0.21 ± 0.1	0.14 ± 0.1	0.42 ± 0.0	0.35 ± 0.0
16:1n-7	1.59 ± 0.1	1.65 ± 0.0	1.74 ± 0.0	1.65 ± 0.1	1.63 ± 0.0	1.62 ± 0.1
18:1n-9	22.5 ± 0.7	23.5 ± 0.1*	23.5 ± 0.2*	23.1 ± 0.2	23.0 ± 0.2	22.8 ± 0.5
18:1n-7	1.73 ± 0.3	1.91 ± 0.0	2.03 ± 0.1	2.03 ± 0.0	1.94 ± 0.1	1.96 ± 0.0
20:1n-9	0.14 ± 0.0	0.14 ± 0.0	0.14 ± 0.0	0.13 ± 0.0	0.14 ± 0.0	0.14 ± 0.0
24:1n-9	1.48 ± 0.1	0.87 ± 0.1	0.54 ± 0.2	0.32 ± 0.1	1.13 ± 0.1	0.91 ± 0.1
18:2n-6	21.2 ± 0.9	22.1 ± 0.0	22.0 ± 0.1	21.7 ± 0.4	21.5 ± 0.3	21.3 ± 0.5
18:3n-6	0.64 ± 0.1	0.65 ± 0.0	0.64 ± 0.0	0.61 ± 0.0	0.67 ± 0.0	0.65 ± 0.0
20:2n-6	0.15 ± 0.0	0.15 ± 0.0	0.15 ± 0.0	0.16 ± 0.0	0.17 ± 0.0	0.16 ± 0.0
20:3n-6	1.53 ± 0.1	1.48 ± 0.0	1.49 ± 0.0	1.55 ± 0.0	1.43 ± 0.0	1.45 ± 0.0
20:4n-6	10.0 ± 0.2	10.0 ± 0.0	9.95 ± 0.1	10.0 ± 0.0	9.58 ± 0.1	9.61 ± 0.3
22:4n-6	0.25 ± 0.0	0.23 ± 0.0	0.23 ± 0.0	0.25 ± 0.0	0.23 ± 0.0	0.23 ± 0.0
22:5n-6	0.14 ± 0.0	0.13 ± 0.0	0.13 ± 0.0	0.13 ± 0.0	0.13 ± 0.0	0.13 ± 0.0
18:3n-3	0.28 ± 0.0	0.29 ± 0.0	0.28 ± 0.0	0.28 ± 0.0	0.27 ± 0.0	0.28 ± 0.0
20:5n-3	0.95 ± 0.0	0.94 ± 0.0	0.95 ± 0.0	0.91 ± 0.0	0.88 ± 0.0	0.87 ± 0.1
22:5n-3	0.67 ± 0.0	0.66 ± 0.0	0.66 ± 0.0	0.69 ± 0.0	0.62 ± 0.0	0.64 ± 0.0
22:6n-3	2.82 ± 0.1	2.74 ± 0.0	2.75 ± 0.0	2.83 ± 0.0	2.59 ± 0.0	2.65 ± 0.1
20:3n-9	0.28 ± 0.0	0.28 ± 0.0	0.29 ± 0.0	0.29 ± 0.0	0.28 ± 0.0	0.28 ± 0.0
Summary	Fatty acid concentrations (μmol/L)					
Σ Fatty acids	7304 ± 388	7340 ± 138	7024 ± 162	6526 ± 605	7562 ± 133	7131 ± 119
Σ Saturates	2450 ± 96	2361 ± 51	2280 ± 59	2172 ± 209	2534 ± 88	2432 ± 86
Σ Mono	2009 ± 164	2067 ± 36	1967 ± 43	1779 ± 162	2126 ± 35	1971 ± 69
Σ n-6 PUFA	2480 ± 169	2552 ± 45	2431 ± 53	2248 ± 212	2550 ± 18	2392 ± 87
Σ n-3 PUFA	344 ± 9	340 ± 6	326 ± 7	308 ± 30	330 ± 3	316 ± 16
Σ n-6 HUFA	873 ± 29	872 ± 16	829 ± 18	783 ± 75	862 ± 7	818 ± 31
Σ n-3 HUFA	323 ± 9	319 ± 6	306 ± 7	290 ± 28	309 ± 3	296 ± 15
Σ HUFA	1217 ± 37	1211 ± 23	1155 ± 23	1092 ± 105	1192 ± 9	1134 ± 47
HUFA	Proportion					
n-6/n-3HUFA	2.70 ± 0.1	2.74 ± 0.0	2.71 ± 0.0	2.70 ± 0.0	2.79 ± 0.0*	2.76 ± 0.0
n-6 % HUFA	71.7 ± 0.4	72.0 ± 0.1	71.8 ± 0.2	71.7 ± 0.1	72.3 ± 0.0*	72.1 ± 0.3
n-3 % HUFA	26.6 ± 0.4	26.3 ± 0.1	26.5 ± 0.2	26.5 ± 0.1	25.9 ± 0.1*	26.1 ± 0.3

Table 2 continued

Groups MW (Watt)	M1-100 x 1 400	M2-100 x 2.5 400	M3-100 x 5 400	M4-100 x 10 400	M5-125 x 5 400	M6-100 x 5 400
Fatty acids	mol% of Total fatty acids					
14:0	1.18 ± 0.1	1.17 ± 0.0	1.07 ± 0.1	1.02 ± 0.1	1.16 ± 0.0	1.09 ± 0.0
16:0	23.9 ± 0.5	23.3 ± 0.2	24.4 ± 0.4	24.4 ± 0.4	22.6 ± 0.1	22.8 ± 0.4
18:0	8.57 ± 0.3	8.09 ± 0.2	9.19 ± 0.4	9.36 ± 0.4	7.37 ± 0.0	7.80 ± 0.3
20:0	0.19 ± 0.0*	0.18 ± 0.0*	0.17 ± 0.0*	0.21 ± 0.0	0.29 ± 0.0	0.21 ± 0.0*
22:0	0.24 ± 0.0*	0.24 ± 0.0*	0.20 ± 0.0*	0.29 ± 0.0	0.52 ± 0.0	0.33 ± 0.0
24:0	0.23 ± 0.0*	0.22 ± 0.0*	0.20 ± 0.0	0.27 ± 0.0	0.47 ± 0.0	0.30 ± 0.0
16:1n-7	1.51 ± 0.0	1.55 ± 0.0	1.36 ± 0.1	1.29 ± 0.1	1.60 ± 0.0	1.54 ± 0.0
18:1n-9	22.5 ± 0.2	23.2 ± 0.2	21.2 ± 0.9	20.5 ± 0.9	23.4 ± 0.0*	23.1 ± 0.5
18:1n-7	1.87 ± 0.1	1.80 ± 0.1	1.82 ± 0.1	1.89 ± 0.0	1.70 ± 0.1	1.97 ± 0.0
20:1n-9	0.16 ± 0.0*	0.16 ± 0.0	0.16 ± 0.0	0.16 ± 0.0	0.15 ± 0.0	0.14 ± 0.0
24:1n-9	0.51 ± 0.0	0.51 ± 0.0*	0.43 ± 0.1*	0.63 ± 0.1	1.16 ± 0.1	0.79 ± 0.0*
18:2n-6	20.6 ± 0.2	21.2 ± 0.3	20.1 ± 0.3	19.7 ± 0.3	21.7 ± 0.0	21.4 ± 0.4
18:3n-6	0.58 ± 0.0	0.62 ± 0.0	0.53 ± 0.0	0.50 ± 0.0	0.66 ± 0.0	0.59 ± 0.0
20:2n-6	0.16 ± 0.0	0.15 ± 0.0	0.17 ± 0.0	0.18 ± 0.0	0.15 ± 0.0	0.16 ± 0.0
20:3n-6	1.64 ± 0.0	1.61 ± 0.0	1.90 ± 0.1	2.09 ± 0.1	1.66 ± 0.0	1.61 ± 0.0
20:4n-6	10.2 ± 0.1	10.2 ± 0.0	10.8 ± 0.3	11.1 ± 0.3	9.91 ± 0.1	10.3 ± 0.0*
22:4n-6	0.26 ± 0.0	0.26 ± 0.0	0.28 ± 0.0*	0.29 ± 0.0	0.23 ± 0.0	0.26 ± 0.0
22:5n-6	0.14 ± 0.0	0.14 ± 0.0	0.16 ± 0.0	0.17 ± 0.0	0.13 ± 0.0	0.14 ± 0.0
18:3n-3	0.28 ± 0.0	0.29 ± 0.0	0.26 ± 0.0	0.26 ± 0.0	0.29 ± 0.0	0.29 ± 0.0
20:5n-3	1.02 ± 0.0*	1.02 ± 0.0*	1.00 ± 0.0	1.00 ± 0.0	1.03 ± 0.0*	1.00 ± 0.0*
22:5n-3	0.91 ± 0.1	0.76 ± 0.0	0.87 ± 0.0	0.94 ± 0.1	0.71 ± 0.0	0.78 ± 0.1
22:6n-3	2.97 ± 0.0	2.92 ± 0.0	3.27 ± 0.1	3.42 ± 0.1	2.66 ± 0.0	2.95 ± 0.1
20:3n-9	0.29 ± 0.0	0.29 ± 0.0	0.29 ± 0.0	0.30 ± 0.0*	0.29 ± 0.0	0.30 ± 0.0
Summary	Fatty acid concentrations (μmol/L)					
Σ Fatty acids	6297 ± 121	6419 ± 140*	5811 ± 111*	5577 ± 122*	7304 ± 181	6396 ± 223
Σ Saturates	2291 ± 232	2133 ± 51	2048 ± 5*	1980 ± 13*	2370 ± 71	2077 ± 52
Σ Mono	1842 ± 290*	1750 ± 43*	1456 ± 82*	1368 ± 88	2053 ± 48	1767 ± 93
Σ n-6 PUFA	2287 ± 296	2197 ± 52*	1976 ± 38*	1900 ± 33*	2518 ± 55	2212 ± 85
Σ n-3 PUFA	337 ± 19	320 ± 6	313 ± 5	313 ± 4*	342 ± 6	321 ± 2*
Σ n-6 HUFA	813 ± 72	787 ± 14	767 ± 7*	762 ± 10*	874 ± 17	794 ± 15
Σ n-3 HUFA	318 ± 17	302 ± 6	298 ± 6	298 ± 5	321 ± 6	302 ± 2*
Σ HUFA	1150 ± 90*	1107 ± 19	1082 ± 12*	1077 ± 14*	1215 ± 23	1116 ± 15*
HUFA	Proportion					
n-6/n-3HUFA	2.56 ± 0.1	2.61 ± 0.0	2.58 ± 0.0	2.55 ± 0.0*	2.73 ± 0.0	2.63 ± 0.1
n-6 % HUFA	70.7 ± 0.8	71.1 ± 0.2	70.9 ± 0.2	70.7 ± 0.0*	71.9 ± 0.1	71.2 ± 0.4
n-3 % HUFA	27.7 ± 0.8	27.2 ± 0.2	27.5 ± 0.3	27.7 ± 0.1*	26.4 ± 0.1	27.1 ± 0.4

^a Values are presented as means ± SD, *n* = 3 except M1-100 × 5 (2) and C-100 × 60 (16); value of “0.0” indicates <0.05

^b One-way ANOVA followed by Tamhane’s T2 test was applied to multiple comparison; asterisks indicate statistically different in comparison with control group at *P* < 0.01

^c Mono-monounsaturates; HUFA: highly unsaturated fatty acids; see footnote to Table 1 for further abbreviations

^d Unit conversion: 1 μmol/L of fatty acid ≈ 0.36 μg/mL

HUFA in these nine groups showed results close to those from the optimal conditions, groups S4-100 × 1 and M5-125 × 5, as summarized in Table 2. The average

concentration of total HUFA in eleven microwave groups was 1,146 ± 53 μmol/L serum with coefficients of variance as low as 4.6 %. It reflected about 94 % (range

89–100 %) of that in the Lepage & Roy control group ($C-100 \times 60$).

In addition, n-6 % HUFA exhibited a very narrow range as 71–72 %, while its counterpart, n-3 % HUFA, as 26–28 %, across the eleven microwave groups presented in Table 2. The ratio of n-6 to n-3 HUFA was 2.6–2.7. Compared to the reference method, their recoveries were 99–101, 98–104, and 95–103 %, respectively. Apparently, these indices were very consistent with those in the control group. A similarity can be observed in Armstrong's study [17] where n-3 % HUFA in human whole blood measured by microwave assay (53.6 %) was close to that by conventional assay (54.4 %) despite low recovery for the concentration of n-3 HUFA (74 %). Thus, if only n-3 % or n-6 % HUFA was of interest in human serum total lipids, transesterification under both optimal and sub-optimal conditions in either single-mode or multimode microwave systems would be sufficient.

Low Efficiency Transesterification

The recoveries of fatty acids 20:0, 22:0, 24:0, and 24:1n-9 in the microwave assay under sub-optimal reaction conditions were significantly lower than under optimal conditions; only 20–70 %, as observable in the bar graph presented in Fig. 1 panels B and C. These low recoveries could not be calibrated by ISTD added prior to chemical analysis. The extension of the reaction time up to 10 min ($M4-100 \times 10$) did not increase the efficiency of transesterification. This is in agreement with a reported study of microwave-assisted extraction of active ingredients of plants [23], in which longer times do not yield higher extraction recovery. It could possibly be explained as some lipids, such as sphingolipids, being more difficult to transesterify than other lipids regarding the microwave irradiation power, duration, and temperature, as suggested by Armstrong et al. [17].

Previously, the low recoveries of transesterification by microwave irradiation using a domestic microwave oven were extensively observed for all fatty acids, such as 78 % for total fatty acids, 61–87 % for PUFA, and 20–30 % for 22:0, 24:0, and 24:1n-9 [17]. In addition to the non-professional microwave irradiation applied, this low efficiency derivatization is probably in part due to a contribution of the applied boron fluoride, which is a better catalyst for methanol methylation of non-esterified fatty acids [24] or transesterification of isolated lipids than the lipid complexes in the biological samples.

Application and Limitation

Compared to the extreme explosive conditions utilized in domestic microwave ovens in previous reports [16, 17],

these innovative microwave reaction systems in this study were designed to be explosion proof for pressurized organic reactions. The transesterification of fatty acids in these systems was not only chemically safe, but also well controlled over the reaction temperature with automated, continuous adjustment of the microwave power. This made it possible to achieve complete transesterification of the fatty acids in human serum total lipids at the conventional reaction temperatures as those in heatblock heating, but greatly reduced the reaction duration. Because of the disparity differences in the capacities, such as pressure control, temperature control, and reaction efficiency, no reaction conditions applied in domestic microwave oven would be examined in these microwave reaction systems.

However, this microwave fatty acid assay was validated only with transesterification of total lipids in one particular solvent system (methanol, hexane, and acetyl chloride) at small sampling size. Further studies are needed to define conditions for fatty acid determination in individual lipid classes or for various tissues. Based on the present work it is expected that such applications could be validated with replacement of the heating block by microwave irradiation and with similar chemical procedures. Future work would also be needed to determine if even faster times are possible.

Summary

Under optimal conditions ($S4-100 \times 1$ and $M5-125 \times 5$) utilizing either a single-mode or a multimode innovative microwave reaction system, microwave irradiation energy could replace the conductive heating to transesterify fatty acids in human serum lipids by methanol, hexane, and acetyl chloride. Microwave irradiation heating provided fatty acid quantifications, which were comparable to the reference method but with greatly reduced reaction duration, from 60 min to 5 min or less. This microwave accelerated fatty acid assay could be useful in small- or large-scale clinical studies and laboratory research as a rapid, reliable, safe, and efficient method.

Acknowledgments The authors wish to acknowledge Drs. Norman Salem Jr., Charlie Serhan, and William E.M. Lands for the valuable advice and encouragement on the method development. Thanks to Ms. Keller Barnhardt for set-up of the microwave reaction systems and to Ms. Cindy Clark from the NIH Library Writing Center for assistance with manuscript editing. This project was funded by the Intramural Research Program of the National Institute on Alcohol Abuse and Alcoholism, National Institutes of Health.

References

1. Mozaffarian D, Wu JH (2011) Omega-3 fatty acids and cardiovascular disease: effects on risk factors, molecular pathways, and clinical events. *J Am Coll Cardiol* 58:2047–2067

2. Calon F, Lim GP, Morihara T, Yang F, Ubeda O, Salem N Jr, Frautschy SA, Cole GM (2005) Dietary n-3 polyunsaturated fatty acid depletion activates caspases and decreases nmda receptors in the brain of a transgenic mouse model of Alzheimer's disease. *Eur J Neurosci* 22:617–626
3. Mahe G, Ronziere T, Laviolle B, Golfier V, Cochery T, De Bray JM, Paillard F (2010) An unfavorable dietary pattern is associated with symptomatic ischemic stroke and carotid atherosclerosis. *J Vasc Surg* 52:62–68
4. Cabre E, Manosa M, Gassull MA (2012) Omega-3 fatty acids and inflammatory bowel diseases: a systematic review. *Br J Nutr* 107(Suppl 2):S240–S252
5. Hibbeln JR, Salem N Jr (1995) Dietary polyunsaturated fatty acids and depression: when cholesterol does not satisfy. *Am J Clin Nutr* 62:1–9
6. Hibbeln JR, Davis JM, Steer C, Emmett P, Rogers I, Williams C, Golding J (2007) Maternal seafood consumption in pregnancy and neurodevelopmental outcomes in childhood (alspac study): an observational cohort study. *Lancet* 369:578–585
7. Liu K-s (1994) Preparation of fatty acid methyl esters for gas-chromatographic analysis of lipids in biological materials. *JA-OCS* 71:1179–1187
8. Stoffel W, Chu F, Ahrens EH (1959) Analysis of long-chain fatty acids by gas-liquid chromatography. *Anal Chem* 31:307–308
9. Morrison WR, Smith LM (1964) Preparation of fatty acid methyl esters and dimethyl acetals from lipids with boron tri-fluoride-methanol. *J Lipid Res* 5:600–608
10. Lepage G, Roy CC (1986) Direct transesterification of all classes of lipids in a one-step reaction. *J Lipid Res* 27:114–120
11. Glaser C, Demmelmair H, Koletzko B (2010) High-throughput analysis of total plasma fatty acid composition with direct in situ transesterification. *PLoS ONE* 5:e12045
12. Glaser C, Demmelmair H, Koletzko B (2010) High-throughput analysis of fatty acid composition of plasma glycerophospholipids. *J Lipid Res* 51:216–221
13. Lin YH, Salem N Jr, Wells EM, Zhou W, Loewke JD, Brown JA, Lands WE, Goldman LR, Hibbeln JR (2012) Automated high-throughput fatty acid analysis of umbilical cord serum and application to an epidemiological study. *Lipids* 47:527–539
14. Carrapiso AI, Garcia C (2000) Development in lipid analysis: some new extraction techniques and in situ transesterification. *Lipids* 35:1167–1177
15. Lie Ken Jie MSF, Cheung YK (1988) The use of a microwave oven in the chemical transformation of long chain fatty acid esters. *Lipids* 23:367–369
16. Banerjee P, Dawson G, Dasgupta A (1992) Enrichment of saturated fatty acid containing phospholipids in sheep brain serotonin receptor preparations: use of microwave irradiation for rapid transesterification of phospholipids. *Biochim Biophys Acta* 1110:65–74
17. Armstrong JM, Metherel AH, Stark KD (2008) Direct microwave transesterification of fingertip prick blood samples for fatty acid determinations. *Lipids* 43:187–196
18. Dasgupta A, Banerjee P, Malik S (1992) Use of microwave irradiation for rapid transesterification of lipids and accelerated synthesis of fatty acyl pyrrolidides for analysis by gas chromatography-mass spectrometry: study of fatty acid profiles of olive oil, evening primrose oil, fish oils and phospholipids from mango pulp. *Chem Phys Lipids* 62:281–291
19. Itonori S, Takahashi M, Kitamura T, Aoki K, Dulaney JT, Sugita M (2004) Microwave-mediated analysis for sugar, fatty acid, and sphingoid compositions of glycosphingolipids. *J Lipid Res* 45:574–581
20. Tomas A, Tor M, Villorbina G, Canela R, Balcells M, Eras J (2009) A rapid and reliable direct method for quantifying meat acylglycerides with monomode microwave irradiation. *J Chromatogr A* 1216:3290–3295
21. Masood A, Stark KD, Salem N Jr (2005) A simplified and efficient method for the analysis of fatty acid methyl esters suitable for large clinical studies. *J Lipid Res* 46:2299–2305
22. Khan MU, Williams JP (1993) Microwave-mediated methanolysis of lipids and activation of thin-layer chromatographic plates. *Lipids* 28:953–955
23. Deng C, Ji J, Li N, Yu Y, Duan G, Zhang X (2006) Fast determination of curcumol, curdione and germacrone in three species of curcuma rhizomes by microwave-assisted extraction followed by headspace solid-phase microextraction and gas chromatography-mass spectrometry. *J Chromatogr A* 1117:115–120
24. Carvalho AP, Malcata FX (2005) Preparation of fatty acid methyl esters for gas-chromatographic analysis of marine lipids: insight studies. *J Agric Food Chem* 53:5049–5059

the American Institute of Nutrition (AIN) [1]. One rationale for developing this diet was to provide researchers with a nutritionally adequate diet that would allow for standardizing studies between laboratories. Not long after this diet was developed several groups reported undesirable physiological effects linked to the diet, such as hemorrhagic deaths [2], nephrocalcinosis [3], and fatty liver [4]. An amended formulation of the diet (AIN-76A) was developed in 1980 with an increased vitamin K content to address the hemorrhagic effect [5]. In 1993 two revised diets were formulated to replace the AIN-76A, a version for growing animals (AIN-93G) and a maintenance formula for mature animals (AIN-93M). These revised diets contained a higher calcium to phosphorus ratio (from 0.75 to 1.3) to prevent the nephrocalcinosis found in female rats consuming the AIN-76A diet [1]. In addition, the carbohydrate composition was changed from 50 % sucrose and 15 % cornstarch in the AIN-76A formula to ~40 % cornstarch, 15 % dextrinized cornstarch, and 10 % sucrose in the AIN-93G diet. This change represents a fivefold decrease in the fructose content of the diet and is not associated with the accumulation of hepatic lipids caused by long-term feeding of the high sucrose levels [6]. Despite the availability of the improved rodent diets, the AIN-76A still remains popular in specific research fields, such as in studies investigating the effects of diet on colon cancer using the aberrant crypt foci model (ACF). In fact, in a database maintained to compare the efficacy of diet modulation on the incidence of ACF, the overwhelming majority of studies have utilized the AIN-76A [7].

The propensity of the AIN-76A diet to result in accumulation of hepatic lipids is potentially of interest to human nutrition, as it is estimated that between 20 and 30 % of adults in Western countries have nonalcoholic fatty liver disease (NAFLD) and this level rises to between 70 and 90 % in obese individuals and those with diabetes [8]. To test the hypothesis that high levels of dietary fructose are responsible for the accumulation of hepatic lipids, Bacon et al. [9] tested the effects of modifying the sucrose content of the AIN-76A diet in a 3-week feeding study in rats. According to the results, diets containing greater than 25 % sucrose resulted in significantly higher hepatic triacylglycerols (TAG) than ones with less than 20 % sucrose or chow.

We recently conducted an ACF study utilizing the AIN-76A diet to investigate the potential chemopreventive effects of a complex milk fat fraction [10]. In the study we used three diets with different fat compositions: (1) corn oil (CO), (2) anhydrous milk fat (AMF), and (3) anhydrous milk fat supplemented with milk fat globule membrane (AMF-MFGM). CO diet is the standard fat source for the AIN-76A diet, and for the AMF diet, the 5 % mass of fat was replaced with AMF. Formulation of the AMF-MFGM

diet was achieved by utilizing an isolate of MFGM (providing 10 % phospholipids of total fat) that was isolated from cream, and which also contained protein, carbohydrate, and minerals in addition to the fat. The details of the diet formulation have been reported previously [10].

MFGM is derived from the apical surface of mammary epithelial cells and surrounds the fat droplets in milk [11]. It is composed primarily of TAG, proteins, and phospholipids (PL) [12]. The composition of the polar lipids of MFGM can vary according to the method of isolation, but the major constituents are phosphatidylcholine (~32 %), phosphatidylethanolamine (32 %), sphingomyelin (~24 %), phosphatidylinositol (~4 %), phosphatidylserine (~3 %), and gangliosides (~3 %) [13]. A large amount of this material is produced in the USA each year as a byproduct of butter production, and is available as a food ingredient. Owing to its unique lipid profile and membrane protein profile, MFGM has been suggested as a potentially bioactive food ingredient with novel nutritional functionalities [14]. Despite this supposition, few studies have been conducted in vivo with either animal models or humans to evaluate the potential of this material as a bioactive ingredient.

The goal of this study was to investigate lipid metabolism in rats fed a diet known to induce hepatic stress. Our approach involved subjecting lipid-metabolizing tissues to two different, yet comprehensive analytical techniques (lipid and gene expression profiling) to understand how the dietary fats affected the lipid metabolism.

Materials and Methods

Animals and Diets

Eleven animals used in this study were among a group of 63 male, weanling Fischer-344 rats (Charles River Laboratories) used in another study [10]. They were randomly assigned to one of three isocaloric dietary treatments that differed only in the fat source [10]. After a 7-day acclimation period on standard chow diets, the rats were individually housed in a room controlled for temperature, humidity, and light cycle and were given free access to experimental diets and deionized water. Food intake and weight were measured weekly. All experimental protocols involving animals were approved by the Utah State University Institutional Animal Care and Use Committee.

Animals were fed experimental diets for 12 weeks. After MRI analysis of body composition (EchoMRI-900TM), rats were killed by cardiac puncture following ketamine/xylazine anesthesia. Liver, adipose, and skeletal muscle tissues and blood samples were collected, flash frozen in liquid nitrogen, and stored at -80 °C for until the time of analysis.

Lipid Extraction

Tissue samples were removed from the freezer and a sample of tissue was cut into small pieces with a razor and placed in a mortar with liquid nitrogen and ground to obtain a fine homogenous powder. About 200 mg of the tissue powder or plasma from each sample was weighed and put into a screw-capped glass tube. Surrogate standards, including sphingomyelin, phosphatidylcholine, phosphatidylserine, phosphatidylethanolamine, diacylglycerol (DG), unesterified fatty acids (FFA), TAG, and cholesteryl esters (CE), were prepared in chloroform. Surrogate standards (100 μ l) for different lipid classes were added to each sample and weights were recorded. Lipids were extracted by the method of Folch et al. [15] with slight modifications. Samples were mixed with 5 ml chloroform/methanol (2:1 with butylated hydroxytoluene, BHT). The whole mixture was sonicated and then agitated for 15–20 min in an orbital shaker at room temperature. The mixture was washed with 0.2 volumes (1 ml for 5 ml solvent mixture) of 0.9 % NaCl solution and vortexed for 20 s. Subsequently, the mixture was centrifuged at 1,500 \times g for 10 min to separate the two phases. The lower (chloroform) phase containing lipids was collected and evaporated under a nitrogen stream and then reconstituted in a small volume of hexane with BHT in a 4-ml amber vial and stored at -80 °C until further analysis.

Separation and Recovery of Different Lipid Classes

Individual lipid classes of the extracted lipid were separated using thin-layer chromatography (TLC). Extracted lipid from each tissue was diluted by hexane with BHT such that 20 μ l of solution contained around 2.5 mg of lipid. Aliquots of 20 μ l were spotted on a 20 \times 20 cm silica gel 60 Å analytical plate (500 μ m layer) (Whatman Inc., Florham Park, NJ). Lipid class standards were also spotted for detecting target bands. Total lipid classes were separated by developing the plate in a solvent system containing hexane, diethyl ether, and formic acid in the ratio of 80:20:2 (v/v/v). The TLC plate was then sprayed with 0.05 % primulin in acetone/water (8:2 v/v). Individual lipid bands on the TLC plate were detected under a hand-held UV lamp and the margins were marked with a pencil. Target lipid classes bands were scraped from the TLC plate using a small razor blade and collected into screw-capped glass tubes. Recovered lipid classes from total lipid TLC plate were PL, DG, FFA, TAG, and CE.

Fatty Acid Methyl Esters

Recovered lipid classes were transesterified into fatty acid methyl esters (FAME) using the method of Curtis et al.

[16] with slight modifications. In each tube, 0.8 ml hexane and 1.2 ml 10 % (v/v) acetyl chloride in methanol were added. Tubes were capped, vortexed for 20 s, and placed in an oven at 100 °C for 40 min. Upon completion of the incubation period, samples were removed and allowed to cool to room temperature. Then 2 ml of a 6 % sodium carbonate solution and 0.4 ml hexane were added into each tube. On subsequent vortexing and centrifuging of tubes two distinct phases were obtained. The top organic layer was removed and transferred to gas chromatography (GC) vials. Solvent was evaporated under a nitrogen stream and FAME were collected in 100 μ l of hexane with BHT and transferred to GC vial inserts. The samples were subsequently analyzed by GC using a GC2010 (Shimadzu Scientific Instruments, Columbia, MD).

GC Data Analysis

For each GC run, standard curves were generated using commercially available FAME standards (Nu-Chek Prep, Elysian, MN). To establish the linearity of the detector response, a three-point calibration was generated with every sample set. The calibration standard, GLC-463, contained 42 fatty acids representing most of the common species found in mammalian tissues and dairy products. Chromatograms of sample FAME were compared with those of FAME standards to identify target fatty acids. The peak area for each fatty acid was then normalized to the peak area and concentration of the corresponding surrogate standard. Next, the molar concentration of the analytes was calculated and then converted to moles of the corresponding lipid classes through molecular weight calculations. The molar concentration of lipid classes was normalized to tissue sample weights to obtain concentrations (μ mol/g tissue) in each tissue. Lastly, the mole percentage of each fatty acid species was calculated.

Gene Expression Analysis

Total RNA was extracted from liver, muscle, and adipose tissue and prepared as previously described [10]. Microarray data were generated by Genome Quebec using the Illumina platform (Illumina, Inc., San Diego, CA). Data were analyzed using FlexArray 1.6, a custom statistical software program developed by Genome Quebec [17]. The expression data were filtered to remove feature ids that have not been detected. Next, a background adjustment and normalization were carried out using the Lumi algorithm (based on lumi Bioconductor package) in FlexArray 1.6. Background correction was carried out by using negative controls. Variance was stabilized by the variance-stabilizing transformation (VST) method and subsequently a robust spline normalization was conducted. Analysis of

variance (ANOVA) was conducted to evaluate significant diet effects on gene expression across treatment groups. The Cyber-T algorithm was employed to identify differentially regulated genes (CT gene lists) among tissues between treatment groups from ANOVA gene lists [18] followed by the Benjamini–Hochberg false discovery rate multiple testing correction [19]. The CT gene lists were then subjected to Kyoto Encyclopedia of Genes and Genomes (KEGG) pathway analysis using ArrayTrack v.3.5.0 (NCTR/FDA) [20].

Real-Time PCR

Total RNA was extracted from liver samples using the RNAeasy Mini-Kit (Qiagen, Valencia, CA). RNA quality was checked and the concentration measured by NanoDrop 1000 (Thermo Fisher, Waltham, MA). RNA (1 µg) was converted to cDNA using high-capacity cDNA reverse transcription kit (Life Technologies, Carlsbad, CA). Validated and predesigned TaqMan primers and probes (Life Technologies) were used to quantify cytochrome P450, family 8, subfamily b, polypeptide 1 (Cyp8b1, ID: Rn00579921_s1), 1-acylglycerol-3-phosphate *O*-acyltransferase 2 (Agpat2, ID: Rn01438505_m1), and angiopoietin-like 4 (Angptl4, ID: Rn01528817_m1). Beta-actin (Actb, ID: ID Rn00667869_m1) was used as an endogenous control. Real-time PCR amplifications were carried out in a DNA Engine Opticon[®] 2 two-color real-time PCR detection system (Biorad, Hercules, CA). PCR results were analyzed with the Opticon Monitor 3 software (Biorad). The comparative C_t method was used to quantify gene expression. ΔC_t was obtained by normalizing to beta-actin. $\Delta\Delta C_t$ was determined by the arithmetic formula described by López-Parra et al. [21]. Symmetrical raw fold change was obtained by comparing $\Delta\Delta C_t$ values of two groups compared.

Liver Fat Analysis by Histology

Cryostat sections in 6 µm thickness were made from liver samples taken out of -80°C freezer. The tissue sections were brought to room temperature on glass slides. The slides were dipped a few times in 60 % triethyl phosphate and then stained in 0.5 % Oil Red O (in 60 % triethyl phosphate) for 15 min. After being rinsed in water for 2 min, the slides were counterstained in Harris modified method hematoxylin stain (Thermo Fisher, Waltham, MA) for 2 min. The slides were placed in saturated lithium carbonate solution for 10 s, rinsed in water for 5 min, and held in water. The slides were mounted with warm glycerin jelly and observed with light microscopy. Color images were captured with a digital camera attached to the microscope. Lipids in randomly sampled areas from each

slide were quantified by ImageJ [22]. The fat content of each sample was expressed by quantification of Oil Red O-stained areas as a percentage of whole area.

Liver Diacylglycerol Acyltransferase (DGAT) Enzyme Assay

The microsomal fraction was obtained by the methods of Ko et al. [23] and Coleman [24]. Rat liver (approximately 1.5 g) was minced and then homogenized in 15 ml of STE buffer (0.25 M sucrose, 10 mM Tris–HCl, pH 7.4, 1.0 mM EDTA) with a Teflon-glass homogenizer at medium speed. The homogenate was centrifuged at $14,000\times g$ for 20 min at 4°C . The supernatant was centrifuged at $100,000\times g$ for 1 h at 4°C to obtain a microsomal pellet. The pellet was suspended in STE buffer without EDTA and centrifuged at $100,000\times g$ for 1 h at 4°C . The final pellet was resuspended in STE buffer without EDTA. Total protein in final solution was quantified by the Bradford assay. The microsomal fractions were stored in aliquots at -80°C .

A fluorescent DGAT assay was carried out as described by McFie and Stone [25]. Briefly, a master mix was prepared in a test tube containing 20 µl of 1 M Tris–HCl (pH 7.6), 4 µl of 1 M MgCl_2 , 10 µl of 4 mM dioleoyl-*sn*-glycerol, 10 µl of 12.5 mg/ml bovine serum albumin, 10 µl of 500 µM NBD-palmitoyl CoA, and 96 µl of water per reaction. Tubes were pre-incubated in a 37°C water bath for 2 min and 50 µl of protein sample was added to start the reaction, which was held at 37°C for 10 min with occasional shaking. The reaction was terminated by addition of 4 ml $\text{CHCl}_3/\text{MeOH}$ (2:1, v/v). Samples were added to 800 µl of water and allowed to sit at room temperature for 1 h. Tubes were centrifuged at $3,000\times g$ for 5 min to separate aqueous and organic phases. The organic phase was removed via pipette and dried under a stream of nitrogen. Lipids were resuspended in 50 µl $\text{CHCl}_3/\text{MeOH}$ (2:1) and spotted on a 20×20 cm TLC plate. TLC plates were developed in the solvent system, hexane/diethyl ether/acetic acid (80:20:1, v/v/v). The plates were air-dried for 1 h and scanned by Typhoon Trio + Laser Imager 7 (GE Healthcare, Waukesha, WI). The following settings were used: excitation, blue (488 nm) LED laser light source; emission, 520 nm BP emission filter. Fluorescence was quantified by ImageJ [22]. The newly synthesized NBD-TAG was quantified as units (fluorescence intensity) of NBD-TAG formed per minute per milligram of protein.

Statistical Analysis

A one-way ANOVA was performed using SAS software version 9.2 (SAS Institute Inc.) to perform comparisons among groups or using FlexArray 1.6 for gene expression among groups and tissues. Group means were compared

using Cyber-T algorithm for gene expression data and Ryan–Einot–Gabriel–Welsch multiple range test for other data. Data were reported as mean \pm standard deviation.

Results

Fatty Acid Profile of Diets

The most abundant fatty acids of the test diets are shown in Fig. 1. Both the milk-fat-based diets have similar fatty acid profiles, and are very different from the CO diet. The milk fat diets both have significant contributions of saturated fatty acids ($\sim 65\%$), whereas in the CO diet the percentage is much lower ($\sim 17.5\%$). All diets have similar levels of monounsaturates, with oleic acid contributing approximately 25%. The other notable difference is in the polyunsaturated fatty acid content (PUFA) content (CO 54%, AMF 4.5%, and AMF-MFGM 6%) and n-6/n-3 ratio (CO 54:1, AMF 6:1, AMF-MFGM 7:1).

Food Intake, Body Weight, Growth Rate, and Body Fat Composition

There were no significant differences in terms of food intake, final body weight, growth rate, or body fat composition (MRI analysis) among groups [10].

Fatty Acids Profile of Red Blood Cells

The red blood cell (RBC) fatty acid profile was measured to compare the CO diet to the milk-fat-based diets, and to determine if the higher polar lipid content of the AMF-MFGM had an effect compared with the AMF diet. RBC fatty acids that were significantly affected by the diets and present at $>1\%$ of total fatty acids are shown in Fig. 2. Not surprisingly,

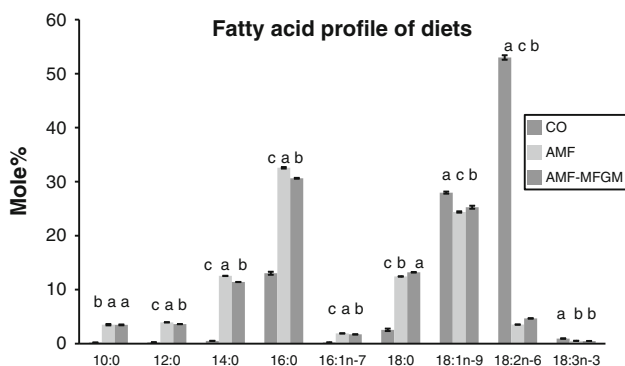


Fig. 1 Fatty acid profile of experimental diets. Only fatty acids significantly different across groups and present at $>1\%$ of total fatty acids are shown. Means in a row with different superscripts are significantly different ($p < 0.05$)

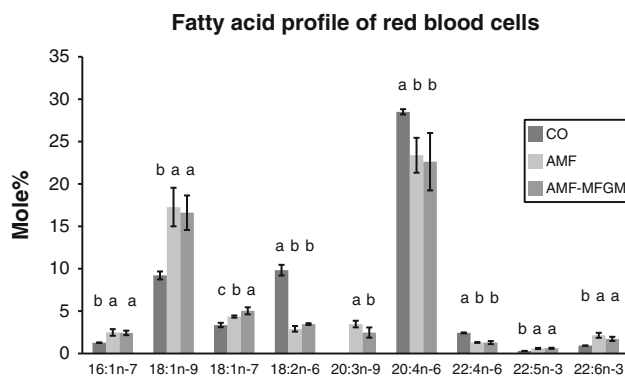


Fig. 2 Red blood cell (RBC) fatty acids from rats fed CO (corn oil), AMF (anhydrous milk fat), and AMF-MFGM (anhydrous milk fat-milk fat globule membrane). Only fatty acids significantly different across diet groups and present at $>1\%$ of total fatty acids are shown. Means in a row with different superscripts are significantly different ($p < 0.05$)

the CO cohort had a higher percentage of 18:2n-6, 20:4n-6, and 22:4n-6, all n-6 fatty acids, presumably because of the high linoleic acid content of the diet. In addition, these animals had lower percentages of 16:1n-7, 18:1n-9, 18:1n-7, 20:3n-9, 20:5n-3, 22:5n-3, and 22:6n-3 compared to the animals fed the milk fat diets. The RBC from animals fed the two milk-fat-based diets had remarkably similar fatty acid profiles with two statistically relevant differences. Namely, the AMF-MFGM-fed animals had a higher percentage of 18:1n-7 and a lower percentage of 20:3n-9.

Fatty Acids Profile of Skeletal Muscle Tissue and Visceral Adipose Tissue

As with the RBC, there were large differences between the fatty acid profile in skeletal muscle and visceral adipose tissue of the rats fed the CO diet versus the milk fat diets which were virtually identical. In skeletal muscle, the CO-fed animals had significantly less 16:1n-7, 18:1n-9, and 20:3n-9, and more 18:2n-6, 20:4n-6, and 22:4n-6 (Fig. 3). Unlike skeletal muscle, the contribution of long chain fatty acids to the adipose lipids was low (Fig. 4). However, among the major fatty acids ($>1\%$ total), the CO animals had less 16:0, 16:1n-7, 18:0, and 18:1n-9 and more 18:2n-6. The only fatty acid that differed among the animals fed the milk fat diets was 20:3n-9, which in both tissues was slightly lower in the AMF-MFGM group.

Fatty Acids Profile of Liver Tissue

Fatty acids in liver tissue which were significantly affected by the CO, AMF, and AMF-MFGM diets and which contribute $>1\%$ of fatty acids in one tissue are presented in Fig. 5. Animals from the CO group had less 16:1n-7, 18:1n-9, 20:3n-9, and 22:6n-3 and more 18:2n-6 and 20:4n-6. Unlike the

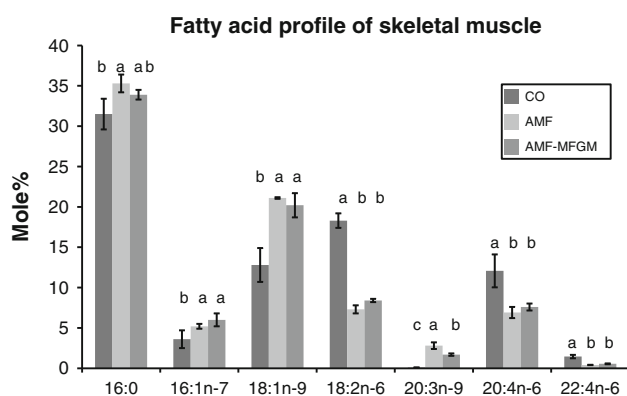


Fig. 3 Fatty acid profile of skeletal muscle from rats fed CO (corn oil), AMF (anhydrous milk fat), and AMF-MFGM (anhydrous milk fat–milk fat globule membrane). Only fatty acids significantly different across diet groups and present at >1 % of total fatty acids are shown. Means in a row with different superscripts are significantly different ($p < 0.05$)

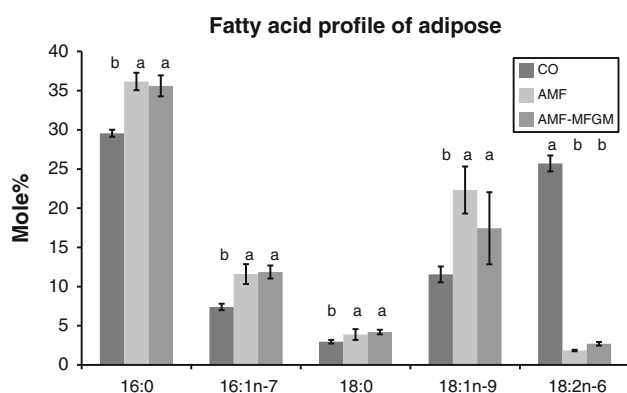


Fig. 4 Fatty acid profile of visceral adipose tissue from rats fed CO (corn oil), AMF (anhydrous milk fat), and AMF-MFGM (anhydrous milk fat–milk fat globule membrane). Only fatty acids significantly different across diet groups and present at >1 % of total fatty acids are shown. Means in a row with different superscripts are significantly different ($p < 0.05$)

RBC, skeletal muscle, and adipose tissues, supplementation of the AMF diet with MFGM results in several differences in the fatty acid profile of the liver. For example, of the six fatty acids which are significantly affected across the diets and present at >1 %, five are significantly different in livers of the animals fed the AMF and AMF-MFGM diets. Thus, the increased polar lipid concentration of the AMF-MFGM diet appears to have significant effects on liver lipid metabolism and partitioning. The largest differences are in 18:1n-9, which is higher in the AMF animals, and 20:4n-6 and 22:6n-3 which are higher in the AMF-MFGM cohort.

Plasma, Visceral Adipose, and Liver Lipid Classes

To better understand the differences in lipid partitioning as affected by the CO, AMF, and AMF-MFGM diets, plasma

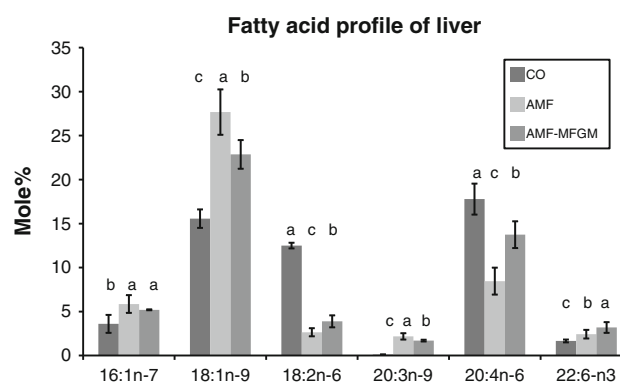


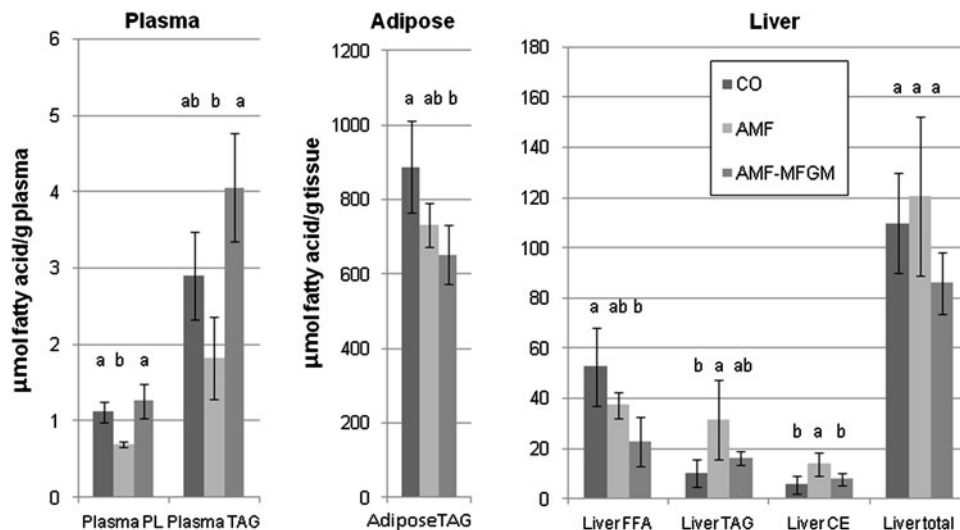
Fig. 5 Fatty acid profile of liver tissue from rats fed CO (corn oil), AMF (anhydrous milk fat), and AMF-MFGM (anhydrous milk fat–milk fat globule membrane). Only fatty acids significantly different across diet groups and present at >1 % of total fatty acids are shown. Means in a row with different superscripts are significantly different ($p < 0.05$)

adipose and liver lipid classes were analyzed and classes with significant differences are shown in Fig. 6. Interestingly, the animals consuming AMF as the fat source had less total PL in plasma than animals fed the CO and AMF-MFGM diets. Additionally, there was less TAG than the animals fed the AMF-MFGM diet. In the visceral adipose, there was more TAG in the animals fed CO than those fed the AMF-MFGM. In the liver, there was more FFA in the animals fed the CO diet than in those fed the AMF-MFGM diet, and a similar trend for the AMF animals, although this was not significant. On the other hand, the CO diet resulted in less accumulated TAG than the AMF diet, with the AMF-MFGM diet in between. Lastly, both the CO and the AMF-MFGM diets resulted in lower hepatic CE than did the AMF diet.

Tissue Gene Expression

In total, 293, 1,124, and 831 genes were found to be differentially expressed respectively in skeletal muscle, adipose, and liver at $p < 0.05$. To identify metabolic pathways that were affected across the three diets all the genes that were differentially regulated according to the ANOVA were analyzed with the program ArrayTrack, a free software tool developed by the National Center for Toxicological Research (NCTR) and the US Food and Drug Administration (FDA). All three diets were compared and the data generated from this analysis are summarized in Table 1. On a diet comparison basis, the fewest number of pathways affected across the three tissues were between the two milk-fat-fed animal groups (22 pathways) and the most pathways were affected between the CO and AMF-MFGM groups (40). In specific tissues, there were 18 pathways differentially affected in skeletal muscle, 31 in adipose, and

Fig. 6 Quantitative analysis of lipid classes from plasma, visceral adipose, and liver. *PL* phospholipids, *TAG* triacylglycerols, *FFA* free fatty acids, *CE* cholesteryl esters. Means in a row with different superscripts are significantly different ($p < 0.05$)



40 in the liver. In specific diet/tissue comparisons, the fewest number of pathways were affected in skeletal muscle between the CO and the AMF diets (2). There were 16 pathways affected between the AMF and CO diets in the liver and 16 pathways between the AMF-MFGM and CO diets in adipose. In the lower half of Table 1 the pathways that were significantly affected across at least two diet combinations are shown. For example, in the muscle tissue, the circadian rhythm pathway (KEGG rno 04710) was significantly affected between all three diets, whereas adipocytokine signaling (rno00020) was only affected in the diet combinations in which AMF was compared. Similar to the fatty acid data of the selected tissues, there were fewer pathways affected in the muscle and adipose tissue compared to the liver. A striking feature of the pathway analysis shown in the bottom half of Table 1 is that only three pathways were different in the liver between the two milk fat diets, whereas >10 were affected when these diets were compared to the CO diet.

Although the two milk fat diets were nearly identical at the fatty acid level, there were several differences in the liver and plasma lipid profiles of the rats fed the AMF and AMF-MFGM diets. Therefore, the expression of several genes of interest was determined using RT-PCR and the results are shown in Table 2. The three genes selected were chosen from the KEGG pathways differentially affected by the milk fat diets in Table 1. The results of the RT-PCR in Table 2 are expressed relative to β -actin, and thus a smaller number indicates a higher expression level. Comparing the two milk fat groups, all three genes are more highly expressed in the livers of the AMF-MFGM rats compared to the AMF group.

Liver Fat Analysis by Histology and DGAT Assay

In general, both the lipid analysis and the gene expression profiling indicated that the diets had the greatest effect on the liver. Although there was not a quantitative difference in the fatty acid content of the livers, there were significant differences in distributions across lipid classes (Fig. 6). For example, there is more triacylglycerol in the livers of rats fed AMF compared to the CO, yet the total fatty acid was not different. Interestingly, expression of diacylglycerol *O*-acyltransferase 2 (DGAT2), was lower in the CO-fed animals than in the other two groups. Consequently, the livers were stained with Oil Red O and DGAT activity was measured via enzymatic assay of the microsomal fraction, and the results are shown in Fig. 7. There was significantly less staining of the hepatic tissue of the CO-fed rat (Fig. 7a), and this corresponded with lower DGAT activity (Fig. 7b).

Discussion

The main focus of this work was to utilize tissue fatty acid profiling and transcriptomics to determine the effects of changing the lipid source of the AIN-76A diet on lipid metabolism. This work was conducted on key tissues involved in lipid metabolism, storage, and processing (skeletal muscle, visceral adipose, and liver) as well as plasma. The fat sources used in formulating the diets (corn oil, anhydrous milk fat, and anhydrous milk fat supplemented with milk fat globule membrane) were originally selected for an ACF study previously reported [10]. In that study, as in most ACF studies, the CO diet was selected as a control, whereas the AMF-MFGM diet was included to

Table 1 Metabolic pathways significantly affected across all three diet combinations

Tissue	Diets			
	Number of pathways affected			
	AMF versus CO	AMF-MFGM versus CO	AMF-MFGM versus AMF	All
Muscle	2	11	5	18
Adipose	9	16	6	31
Liver	16	13	11	40
All	27	40	22	

KEGG pathway	AMF versus CO	AMF-MFGM versus CO	AMF-MFGM versus AMF
Muscle			
Circadian rhythm (rno04710)	✓	✓	✓
PPAR signaling (rno03320)	✓		✓
Adipocytokine signaling (rno04920)		✓	✓
Adipose			
Circadian rhythm (rno04710)	✓	✓	✓
Endocytosis (rno04710)	✓	✓	✓
Butanoate metabolism (rno00650)	✓	✓	✓
Citrate cycle (TCA cycle) (rno00020)	✓	✓	
Liver			
PPAR signaling (rno03320)	✓	✓	✓
C21 steroid hormone metabolism (rno00140)	✓	✓	✓
Biosynthesis of unsaturated fatty acids (rno01040)	✓	✓	
Retinol metabolism (rno00830)	✓	✓	
Starch and sucrose metabolism (rno00500)	✓	✓	
Pyruvate metabolism (rno00620)	✓	✓	
Galactose metabolism (rno00052)	✓	✓	
Insulin signaling pathway (rno04910)	✓	✓	
Maturity onset diabetes of the young (rno04950)	✓	✓	
Androgen and estrogen metabolism (rno00150)	✓	✓	
Glycerophospholipid metabolism (rno00564)		✓	✓

CO corn oil, AMF anhydrous milk fat, AMF-MFGM anhydrous milk fat–milk fat globule membrane

Table 2 Differentially expressed genes by ANOVA in liver from rats fed with diet containing corn oil (control), anhydrous milk fat (AMF), and milk fat globule membrane (AMF-MFGM) (unit: $\Delta\Delta C(t)$)

Genes	CO	AMF	MFGM
Cyp8b1	-0.94 ± 0.75^b	-0.10 ± 0.50^a	-2.49 ± 0.93^c
Agpat2	1.93 ± 2.36^{ab}	2.82 ± 1.14^a	1.14 ± 1.03^b
Angptl4	2.90 ± 2.10^b	4.19 ± 0.99^a	2.34 ± 1.36^b

^{a-c} Means in a row with different superscripts are significantly different ($p < 0.05$)

Table 3 Percentage of 20:3n-9 in highly unsaturated fatty acids (HUFA) in RBC, skeletal muscle, adipose, and liver as a function of diet

%20:3n-9 in HUFA	Corn oil	AMF	AMF-MFGM
RBC	ND ^b	11.05 ± 0.26^a	8.60 ± 2.40^a
Muscle	0.51 ± 0.08^c	20.01 ± 0.45^a	12.44 ± 0.28^b
Adipose	7.92 ± 0.41^c	43.08 ± 2.37^a	31.40 ± 0.37^b
Liver	0.53 ± 0.05^c	15.65 ± 1.67^a	8.64 ± 1.15^b

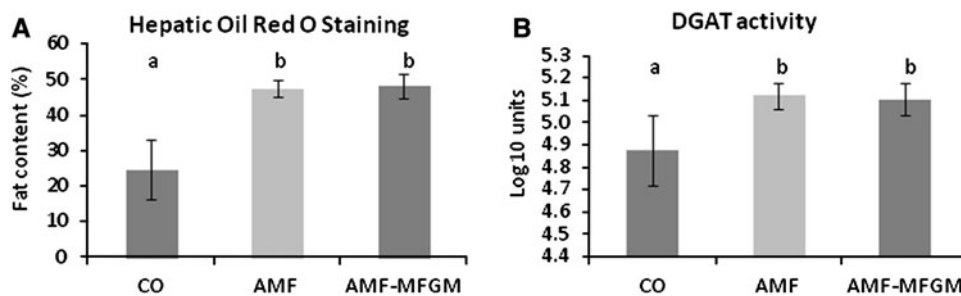
ND not detected

^{a-c} Means in a row with different superscripts are significantly different ($p < 0.05$)

determine potential cancer protective effects of specific lipids associated with this material, such as sphingomyelin and plasmalogens. The AMF diet was included to control

for the potential for other lipids in milk fat to affect the development of ACF, such as butyrate and conjugated linoleic acid.

Fig. 7 Hepatic Oil Red staining (a) and hepatic DGAT activity (b) in liver tissue from rats fed CO (corn oil), AMF (anhydrous milk fat), and AMF-MFGM (anhydrous milk fat–milk fat globule membrane). Means with different superscripts are significantly different ($p < 0.05$)



The membrane composition of RBC reflects dietary fat sources, and several groups have investigated the correlation of RBC fatty acid profiles with disease susceptibility in humans. For example, Harris and Von Schacky [26] showed that the omega-3 index, the combined percentage of EPA (20:5n-3) and DHA (22:6n-3) in RBC, correlates with the risk of coronary heart disease (CHD) in humans with values above 8 % being associated with the most protection and values below 4 % with the least. A similar metric, the percent contribution of omega-6 fatty acids to highly unsaturated fatty acids (% n-6 HUFA), was shown by Lands [27] to correlate with CHD mortality in several human populations with levels below 40 % being protective. The omega-3 indices were 0.9 for the CO diet, 2.5 for the AMF diet, and 2.0 for the AMF-MFGM diet, whereas the % n-6 HUFA levels were 96, 79, and 83 %, respectively. Although these metrics may not be applicable in rodents, it is interesting nonetheless that all three diets result in very low levels of n-3 long chain PUFA in RBC which likely affect many physiological processes.

One interesting fatty acid which is present at significant levels in the RBC, muscle, adipose, and liver of the milk-fat-fed animals, but not those consuming CO, is 20:3n-9. This fatty acid is an elongation product of oleic acid and has been shown to be a sensitive marker of PUFA intake. According to Lands [27], 20:3n-9 correlates with low PUFA intakes and a value of approximately 10 % in the HUFA indicates PUFA insufficiency. To our knowledge, no studies have provided data on the percentage contribution of 20:3n-9 to tissue HUFA for RBC, muscle, adipose, and liver which are shown in Table 3. Animals fed the AMF diet have the highest levels of this fatty acid across all tissues measured, whereas those consuming the AMF-MFGM diets also had high levels. Interestingly, the HUFA percentage of 20:3n-9 in adipose was high for the CO-fed animals, albeit not as high as the other groups. This may be a result of the very low concentration of HUFA in adipose, as the lipids in this tissue are primarily less than 18 carbons in length.

The lipid profiles of the RBC, muscle, adipose, and liver reflect the fat sources of the three diets, and there were few differences between those fed the AMF and AMF-MFGM.

However, there were quantitative differences across lipid classes in both plasma and the liver. Pathway analysis of the gene expression data indicated that the fewest pathways were affected in skeletal muscle and the most in liver. There were no differences in total liver fatty acids between treatments, but there was in the distribution of fatty acid across lipid classes (Fig. 6). One striking feature is the high FFA and low TAG in the livers of the CO-fed rats compared to those fed the AMF-MFGM diet. To further investigate this finding we compared Oil Red O staining in livers across the three treatments, and the results are shown in Fig. 7a. In the rats fed the CO diets there is less Oil Red O staining. According to O'Rourke et al. [28] Oil Red O staining of tissues is well correlated with triglyceride content. The inverse relationship between the hepatic TAG and FFA suggests that the differences may be due to triglyceride synthesis activity. According to the gene expression profiling, DGAT2, the enzyme responsible for the final step in TAG synthesis from diacylglycerols and FFA was 1.25-fold lower in the CO-fed rats compared to those fed AMF and 1.46-fold lower compared to those fed AMF-MFGM. These differences are modest, and it was not clear if their expression would translate into physiological differences. Thus, the triacylglycerol synthetic activity in liver microsomal fractions was measured using a functional assay and the results are shown in Fig. 7b. In agreement with the Oil Red O staining, the DAG activity measure suggests that the differences in FFA, DAG, and TAG levels in the liver may be partially explained by the conversion of FFA and DAG into TAG.

Although excess hepatic TAG storage has typically been viewed as a negative physiological response, it may be protective under some metabolic situations. For example, in a mouse model of nonalcoholic steatohepatitis (NASH), Yamaguchi et al. [29] evaluated the effects of hepatic DGAT2 expression on disease development using an antisense nucleotide treatment. Although reducing expression of DGAT2 did prevent hepatic steatosis, the increase in FFA was associated with markers of lipid peroxidation/oxidant stress and fibrosis. From this study the authors concluded that accumulation of hepatic TAG is actually protective against progressive liver damage in NAFLD. It

is unclear why the CO diet resulted in lower DGAT expression and activity in the CO-fed rats. However, one distinguishing feature of this diet is the PUFA content primarily in the form of linoleic acid. Interestingly, reviewing the fatty acid composition of diets used to study NASH, Romestaing et al. [30] drew the conclusion that dietary PUFA with a high omega-6 to omega-3 ratio may be a causative factor via effects on lipid peroxidation and proinflammatory cytokine production.

There are several differences in the plasma and hepatic lipid profiles of the animals fed the two milk fat diets which is surprising considering the similarity of these diets at the fatty acid level. According to the KEGG pathway analysis conducted on the hepatic gene expression and shown in Table 1, the two milk fat diets affected PPAR signaling (rno03320), C21 steroid hormone metabolism (rno00140), and glycerophospholipid metabolism (rno00564). The affected PPAR signaling in both the liver and skeletal muscle was mediated through PPAR α receptors. The involved genes were associated with lipogenesis, cholesterol metabolism, and fatty acid transport in the liver and with lipogenesis in skeletal muscle. Consequently, the expression of three genes from these pathways was validated using RT-PCR. The genes *Cyp8b1*, *Agpat2*, and *Angptl4* were selected from the differentially expressed genes in the pathways determined by the gene expression profiling. They were chosen owing to their physiological function and potential to affect tissue lipid partitioning, and the results are shown in Table 2. The function of these genes is discussed below including their potential roles in affecting lipid metabolism across the two milk fat groups. Of course these findings are only correlations and positive confirmation of their roles will need to be tested explicitly for confirmation.

Cyp8b1 is a cytochrome P450 enzyme which is a component of the primary bile acid biosynthesis and PPAR α signaling pathways in the liver. *Cyp8b1* is involved in the synthesis of cholic acid [31]. *Cyp8b1* controls the ratio of cholic acid to chenodeoxycholic acid in bile salts, and as cholic acid is less effective in solubilizing cholesterol it may affect its absorption [32]. The AMF-MFGM diet was associated with a lower hepatic cholesteryl ester content (Fig. 6). Milk polar lipids affect both the absorption and fecal excretion of cholesterol when fed both acutely and chronically. For example, Noh and Koo [33] found that infusion of milk sphingomyelin via a duodenal catheter resulted in decreased cholesterol, fat, and vitamin E absorption. In a chronic feeding study, Kamili et al. [34] fed mice high-fat diets for 5 weeks; the diets were supplemented with two different formulations of milk phospholipids at 1.2 % by weight. Both milk polar lipid preparations resulted in significant decreases in liver cholesterol and triglyceride which was accompanied by an

increase in fecal cholesterol excretion. Data from the present study indicate that the decreased cholesterol absorption and increased fecal excretion resulting from luminal milk polar lipids in those previous studies may be mediated, at least in part, by the ratio of bile acids.

Agpat2 is an enzyme responsible for the conversion of lysophosphatidic acid to phosphatidic acid, a step in PL synthesis, and is a component of KEGG pathway glycerophospholipid metabolism. The expression of *Agpat2* was higher in the AMF-MFGM group than the AMF group (Table 2) but there was not a significant difference in hepatic PL. There was, on the other hand, a significant increase in plasma PL in the AMF-MFGM group. The increased plasma PL may result from increased hepatic synthesis and secretion. Previous studies with milk polar lipids have also shown the ability of these constituents to increase both plasma PL and TAG. For example, Wat et al. [35] fed mice both a low-fat, non-purified diet and a high-fat diet formulated with and without a 2.5 % PL-rich milk fat extract. In the mice fed the low-fat, non-purified diet, the milk PL increased the plasma TAG by 20 % and the plasma PL by 5 % compared with values in the control mice fed the low-fat diet. However, in the mice fed the high-fat diets, the PL-rich extract actually reduced both the plasma TAG and PL to levels similar to the low-fat control. The increased plasma lipid concentration in the rats fed the AMF-MFGM diet, compared to those fed the AMF diet, may be a result of either more lipid exported from the liver, or from reduced clearance via peripheral tissues.

Expression of *Angptl4* was also verified by RT-PCR. *Angptl4* is a component of the PPAR α signaling pathway. It is an angiopoietin-like protein which increases plasma TAG via suppression of lipoprotein lipase [36]. Interestingly, there were significant differences in plasma TAG between the two milk-fat-fed groups (Fig. 6). Also known as fasting-induced adipocyte factor (Fiaf), *Angptl4* is highly expressed in the gut epithelium in germ-free mice and prevents accumulation of fat into adipocytes, whereas conventionalization with a microflora suppresses this effect [37]. Although it is not clear if hepatic expression of *Angptl4* in the AMF-MFGM-fed rats contributed to the increase in plasma TAG, this finding indicates a potential mechanism via which this effect was mediated.

Despite the fact that it is still commonly used in ACF studies with rodents [7], the high sucrose content of the AIN-76A diet has been long known to cause fatty liver in animals fed the diet for long periods of time [9]. Therefore, when reviewing the different effects of the fat sources on tissue lipid composition and gene expression it is necessary to keep in mind that these changes are in the context of an overall metabolically stressful diet. From the data presented here, a few hypotheses may be drawn that can be tested in studies designed specifically for their evaluation.

For example, compared to the milk fat diets, the CO diet caused a significant increase in hepatic free fatty acids, a potential trigger for the development of NASH from NAFLD. Conversely, compared to the CO and AMF-MFGM diets, the AMF diet resulted in more hepatic TAG storage which in itself may be undesirable. Supplementing the AMF diet with polar lipids from milk appears to reduce the accumulation of hepatic TAG yet appears to achieve this effect via promotion of lipid export into plasma. The long-term physiological significance of this is unknown. In conclusion, the fat source of the AIN-76A diet affects the tissue profile of key tissues involved in lipid trafficking and storage as well as gene expression networks within these tissues.

Acknowledgments This study was supported by both a seed grant from the Center for Integrated Biosystems at Utah State University and by the Utah Agricultural Experiment Station and was approved as journal paper number 8290. We are grateful to Dallin Snow for preparing RNA samples for Microarray analysis and Dr. Aaron Olsen and Kent Udy for assistance with animal studies.

References

- Reeves PG, Nielsen FH, Fahey GC Jr (1993) AIN-93 purified diets for laboratory rodents: final report of the American Institute of Nutrition ad hoc writing committee on the reformulation of the AIN-76A rodent diet. *J Nutr* 123(11):1939–1951
- Roebuck BD, Wilpone SA, Fifield DS, Yager JD Jr (1979) Hemorrhagic deaths with AIN-76 diet. *J Nutr* 109(5):924–925
- Nguyen HT, Woodard JC (1980) Intranephronic calculosis in rats: an ultrastructural study. *Am J Pathol* 100(1):39–56
- Medinsky MA, Popp JA, Hamm TE, Dent JG (1982) Development of hepatic lesions in male Fischer-344 rats fed AIN-76A purified diet. *Toxicol Appl Pharmacol* 62(1):111–120
- Nutrition A (1980) Second report of the ad hoc committee on standards for nutritional studies. *J Nutr* 110:1726
- Council NR (1995) Nutrient requirements of laboratory animals, vol 4th Revised. National Academy Press, Washington, p 172
- Corpet DE, Tache S (2002) Most effective colon cancer chemopreventive agents in rats: a systematic review of aberrant crypt foci and tumor data, ranked by potency. *Nutr Cancer* 43(1):1–21
- Targher G, Day CP, Bonora E (2010) Risk of cardiovascular disease in patients with nonalcoholic fatty liver disease. *N Engl J Med* 363(14):1341–1350
- Bacon BR, Park CH, Fowell EM, McLaren CE (1984) Hepatic steatosis in rats fed diets with varying concentrations of sucrose. *Fundam Appl Toxicol* 4(5):819–826
- Snow DR, Jimenez-Flores R, Ward RE, Cambell J, Young MJ, Nemere I, Hintze KJ (2010) Dietary milk fat globule membrane reduces the incidence of aberrant crypt foci in Fischer-344 rats. *J Agric Food Chem* 58(4):2157–2163
- Jensen RG (1995) Handbook of milk composition: food science and technology international series. Academic, San Diego, p 919
- Mcpherson AV, Dash MC, Kitchen BJ (1984) Isolation of bovine-milk fat globule-membrane material from cream without prior removal of caseins and whey proteins. *J Dairy Res* 51(1):113–121
- MacGibbon A, Taylor M (2006) Composition and structure of bovine milk lipids. In: Fox PF, McSweeney PLH (eds) *Advanced dairy chemistry*. Springer, New York, pp 1–42
- Spitsberg VL (2005) Invited review: bovine milk fat globule membrane as a potential nutraceutical. *J Dairy Sci* 88:2289–2294
- Folch J, Lees M, Sloane Stanley GH (1957) A simple method for the isolation and purification of total lipides from animal tissues. *J Biol Chem* 226(1):497–509
- Curtis JM, Berrigan N, Dauphinee P (2008) The determination of n-3 fatty acid levels in food products containing microencapsulated fish oil using the one-step extraction method. Part 1: measurement in the raw ingredient and in dry powdered foods. *J Am Oil Chem Soc* 85(4):297–305
- Blazejczyk M, Miron M, Nadon R (2007) FlexArray: a statistical data analysis software for gene expression microarrays. <http://genomequebec.mcgill.ca/FlexArray>. Accessed 8 Oct 2012
- Long AD, Mangalam HJ, Chan BY, Tollerli L, Hatfield GW, Baldi P (2001) Improved statistical inference from DNA microarray data using analysis of variance and a Bayesian statistical framework: analysis of global gene expression in *Escherichia coli* K12. *J Biol Chem* 276(23):19937–19944
- Hochberg Y, Benjamini Y (1990) More powerful procedures for multiple significance testing. *Stat Med* 9(7):811–818
- Tong W, Cao X, Harris S, Sun H, Fang H, Fuscoe J, Harris A, Hong H, Xie Q, Perkins R, Shi L, Casciano D (2003) Array-Track-supporting toxicogenomic research at the US Food and Drug Administration National Center for Toxicological Research. *Environ Health Perspect* 111(15):1819–1826
- Lopez-Parra M, Titos E, Horrillo R, Ferre N, Gonzalez-Periz A, Martinez-Clemente M, Planaguma A, Masferrer J, Arroyo V, Claria J (2008) Regulatory effects of arachidonate 5-lipoxygenase on hepatic microsomal TG transfer protein activity and VLDL-triglyceride and apoB secretion in obese mice. *J Lipid Res* 49(12):2513–2523
- Abramoff MD, Magalhaes PJ, Ram SJ (2004) Image processing with ImageJ. *Biophotonics Int* 11(7):36–42
- Ko JS, Ryu SY, Kim YS, Chung MY, Kang JS, Rho MC, Lee HS, Kim YK (2002) Inhibitory activity of diacylglycerol acyltransferase by tanshinones from the root of *Salvia miltiorrhiza*. *Arch Pharm Res* 25(4):446–448
- Coleman RA (1992) Diacylglycerol acyltransferase and monoacylglycerol acyltransferase from liver and intestine. *Methods Enzymol* 209:98–104
- McFie PJ, Stone SJ (2011) A fluorescent assay to quantitatively measure in vitro acyl CoA:diacylglycerol acyltransferase activity. *J Lipid Res* 52(9):1760–1764
- Harris WS, Von Schacky C (2004) The omega-3 index: a new risk factor for death from coronary heart disease? *Prev Med* 39(1):212–220
- Lands B (2008) A critique of paradoxes in current advice on dietary lipids. *Prog Lipid Res* 47(2):77–106
- O'Rourke EJ, Soukas AA, Carr CE, Ruvkun G (2009) *C. elegans* major fats are stored in vesicles distinct from lysosome-related organelles. *Cell Metab* 10(5):430–435
- Yamaguchi K, Yang L, McCall S, Huang J, Yu XX, Pandey SK, Bhanot S, Monia BP, Li YX, Diehl AM (2007) Inhibiting triglyceride synthesis improves hepatic steatosis but exacerbates liver damage and fibrosis in obese mice with nonalcoholic steatohepatitis. *Hepatology* 45(6):1366–1374
- Romestaing C, Piquet MA, Bedu E, Rouleau V, Dautresme M, Hourmand-Ollivier I, Filippi C, Duchamp C, Sibille B (2007) Long term highly saturated fat diet does not induce NASH in Wistar rats. *Nutr Metab (Lond)* 4:4
- Li-Hawkins J, Gafvels M, Olin M, Lund EG, Andersson U, Schuster G, Bjorkhem I, Russell DW, Eggertsen G (2002) Cholic acid mediates negative feedback regulation of bile acid synthesis in mice. *J Clin Invest* 110(8):1191–1200
- Gafvels M, Olin M, Chowdhary BP, Raudsepp T, Andersson U, Persson B, Jansson M, Bjorkhem I, Eggertsen G (1999) Structure and chromosomal assignment of the sterol 12 α -hydroxylase gene (CYP8B1) in human and mouse: eukaryotic

- cytochrome P-450 gene devoid of introns. *Genomics* 56(2):184–196
33. Noh SK, Koo SI (2004) Milk sphingomyelin is more effective than egg sphingomyelin in inhibiting intestinal absorption of cholesterol and fat in rats. *J Nutr* 134(10):2611–2616
 34. Kamili A, Wat E, Chung RW, Tandy S, Weir JM, Meikle PJ, Cohn JS (2010) Hepatic accumulation of intestinal cholesterol is decreased and fecal cholesterol excretion is increased in mice fed a high-fat diet supplemented with milk phospholipids. *Nutr Metab (Lond)* 7:90
 35. Wat E, Tandy S, Kapera E, Kamili A, Chung RW, Brown A, Rowney M, Cohn JS (2009) Dietary phospholipid-rich dairy milk extract reduces hepatomegaly, hepatic steatosis and hyperlipidemia in mice fed a high-fat diet. *Atherosclerosis* 205(1):144–150
 36. Kersten S (2005) Regulation of lipid metabolism via angiopoietin-like proteins. *Biochem Soc Trans* 33(Pt 5):1059–1062
 37. Backhed F, Ding H, Wang T, Hooper LV, Koh GY, Nagy A, Semenkovich CF, Gordon JI (2004) The gut microbiota as an environmental factor that regulates fat storage. *Proc Natl Acad Sci U S A* 101(44):15718–15723

diseases and cancer. The molecular changes in adipose tissue that promote these disorders are not completely understood. For a long time, fat tissue was perceived as storage of free fatty acids (FFA) in the form of triacylglycerols (TAG). Over the last years, this perception of adipose tissue has been replaced by the notion that adipose tissue has a central role in lipid and glucose metabolism: expressing and secreting factors that play important endocrine functions. These factors include leptin, adiponectin, tumor necrosis factor- α (TNF- α), monocyte chemoattractant protein-1 (MCP-1), interleukin-6 (IL-6) and plasminogen activator inhibitor-1 (PAI-1) [1–3]. Over the years, studies have strengthened the notion that obesity is not a homogeneous condition and that the regional fat distribution is an important indicator for metabolic and cardiovascular alterations [4, 5].

The obesity epidemic has drawn attention to visceral adipose tissue (VAT) as a risk factor for type 2 diabetes and cardiovascular diseases. VAT has been shown to be very important source of circulating FFA. The FFA are much more easily liberated from visceral fat than from subcutaneous fat. Excess of plasma FFA leads to increased FFA uptake by tissues e.g. skeletal muscle and in the result, to intramuscular lipid accumulation. Several lines of evidence suggest that visceral adiposity rather than general adiposity might play an important role in the development of insulin resistance and cardiovascular diseases [6–8]. Epicardial adipose tissue (EAT) is a type of visceral fat that has not been studied as thoroughly as VAT and subcutaneous abdominal adipose tissue (SAT) [9]. EAT as a fat depot might function as a lipid-storing tissue—source of FFA, and as an endocrine organ secreting hormones and other biologically active molecules, which affect glucose homeostasis, energy metabolism, body weight regulation and insulin sensitivity [10–15]. It must be underlined that lipolytic activity in EAT is even higher than in other visceral fat tissues [16]. Data from several studies suggest that accumulation of intramuscular lipids is responsible for induction of insulin resistance in the tissue [17, 18]. Among these lipids are: ceramides (Cer)—central molecules in sphingolipid metabolism, diacylglycerols (DAG) and long chain acyl-CoA (LCACoA). These lipids are probably implicated not only in obesity-associated skeletal muscle but also fat tissue insulin resistance. Recent evidence suggests that adipose tissue inflammation and abnormalities in sphingolipid metabolism may contribute to the metabolic disorders associated with obesity [19]. It has been shown, that ceramide is implicated in the pathogenesis of obesity, insulin resistance [20, 21] and cardiovascular disease [22–24]. Although there is some evidence that ceramide affects insulin stimulated glucose uptake in adipose tissue in the same way as in skeletal muscle, there is very little information about biologically active lipids in SAT. We found only three reports on the ceramide content

in human SAT [25–27]. Ceramide content was higher in SAT of obese men and women compared to lean non-diabetic subjects when the content of Cer was expressed per adipocyte [27]. Moreover, the ceramide level was more highly elevated in the SAT of obese woman with fatty liver than in body mass index (BMI)-matched obese individuals with no hepatic steatosis [25]. However, another report indicated that total adipose tissue ceramide content was lower in the adipose tissue from obese non-diabetic (OND) and obese diabetic (OD) subjects compared to lean non-diabetic (LND) people in spite of greater mRNA levels of SMases, SPT and CDases [26]. Another, *in vitro*, study demonstrated that ceramide plays an important role in the induction of insulin resistance in the adipocytes [28], but the contribution of adipose tissue to the disorder is still unclear. Nothing is known about DAG and LCACoA in adipose tissue and its implication in adipocytes as well as whole body insulin resistance. Recently, it has been found that DAG activates PKC ϵ that results in inhibition of insulin stimulated insulin receptor kinase activity and in the result causes hepatic insulin resistance [29]. However, there is no information about the content of biologically active lipids in visceral fat. Therefore the aim of the present study was to examine the effect of obesity and type 2 diabetes on sphingolipid, DAG, and LCACoA content in human subcutaneous fat and epicardial fat tissue (as visceral fat tissue) and to understand whether relationships exist between the content of these particular lipids and insulin sensitivity.

Materials and Methods

The study included 41 patients undergoing elective coronary bypass graft surgery. The subjects were divided into three groups: (1) lean (BMI \leq 26.0, $n = 14$) without a history of diabetes and with normal fasting blood glucose (\leq 100 mg/dl) and glycated hemoglobin (\leq 6.5 %) level, (2) obese (BMI \geq 30.0) without a history of diabetes and with normal fasting glycemia and glycated hemoglobin level ($n = 12$) and (3) obese with type 2 diabetes ($n = 15$). In the obese diabetic group only patients who were diagnosed as type 2 diabetic of 5–7 years duration were included in the study. All participants according to NYHA (New York Heart Association) were classified to second class that is characterized as mild symptoms and slight limitation during ordinary activity. Six of the volunteers with type 2 diabetes received insulin, two of them received metformin, one received metformin and sulfonylurea, one received insulin together with metformin, and two of the patients were on a diet. All patients were around 60 years old. We used a homeostasis model assessment for calculating insulin resistance (HOMA-IR). Blood samples were taken in a fasting state from the antecubital vein into heparinized

tubes at the day of the surgery. At the beginning of the surgical intervention, a sample of epicardial adipose tissue was taken from the anterior wall of the left ventricle. Subcutaneous adipose tissue was taken from the subcutaneous fat on the sternum. Dissected tissues were promptly frozen in liquid nitrogen and then stored at -80°C until further processing. During the surgery, blood glucose levels were kept within the physiologic range in all patients. The investigation conforms to the principles outlined in the Declaration of Helsinki and was approved by the Ethical Committee for Human Studies of the Medical University of Bialystok. All patients gave their informed consent prior to their inclusion in the study.

Blood Samples

We measured plasma FFA concentration using UPLC/MS according to Persson et al. [30]. Briefly, the concentrations of FFA were measured against a six point standard curve constructed by taking 250 μl of the 400- μM stock solution and making dilutions with 10 mM phosphate buffer to yield 400, 200, 100, 50, 25 and 0 μM standards. Aliquots of 100 μl of plasma were taken for extraction. A quantity of 50 μl of the heptadecanoate internal standard solution was spiked to each concentration standard and each plasma sample. The standards and plasma samples were extracted with freshly prepared Dole solution composed of isopropanol:heptanes:1 M H_2SO_4 (40:10:1; v/v/v). The extracts were allowed to dry under nitrogen. The dried samples were resuspended in 100 μl of buffer A prior to injecting 10 μl onto the LC/MS (Agilent 6460 triple quadrupole) coupled with a Agilent 1290 Infinity UPLC system. Fatty acids were separated on the LC using a reverse-phase Zorbax SB-C18 column 2.1 \times 150 mm, 1.8 μm , using two buffers. Buffer A was 80 % acetonitrile, 0.5 mM ammonium acetate; buffer B was 99 % acetonitrile, 1 % 0.5 mM ammonium acetate. The flow rate was 0.4 ml/min, and the gradient conditions were as follows: 0–3 min isocratic at 55 % B, 3–3.2 min 55–95 % B, 3.2–5 min isocratic at 95 % B, 5–5.5 min 55–95 % B, and 5.5–7 min isocratic at 55 % B.

Moreover, we measured plasma triacylglycerols, total cholesterol, HDL-cholesterol and LDL-cholesterol concentration. The plasma samples were stored at -80°C before analysis. We also measured the fasting plasma insulin and glucose concentration for calculation HOMA-IR (homeostasis model assessment) to estimate insulin resistance.

Adipose Tissue Bioactive Lipids

Sphingolipids

The content of sphingolipids was measured using a UPLC/MS/MS approach according to Blachnio-Zabielska et al.

[31]. Briefly, the adipose tissue samples (40 mg) were homogenized in a solution composed of 0.25 M sucrose, 25 mM KCl, 50 mM Tris and 0.5 mM EDTA, pH 7.4. Immediately afterwards, 50 μl of the internal standard solution (17C-sphingosine and 17C-S1P, and C17-Cer Avanti polar lipids) as well as 1.5 ml of an extraction mixture (isopropanol:water:ethyl acetate, 30:10:60; v:v:v) were added to each homogenate. The mixture was vortexed, sonicated and then centrifuged for 10 min at 4,000 rpm (Sorvall Legend RT). The supernatant was transferred to a new tube and pellet was re-extracted. After centrifugation supernatants were combined and evaporated under nitrogen. The dried sample was reconstituted in 100 μl of LC Solvent A (2 mM ammonium formate, 0.15 % formic acid in methanol) for UPLC/MS/MS analysis. Sphingolipids were analyzed by means of an Agilent 6460 triple quadrupole mass spectrometer using positive ion electrospray ionization (ESI) source with multiple reaction monitoring (MRM). The chromatographic separation was performed using an Agilent 1290 infinity ultra performance liquid chromatography (UPLC). The analytical column was a reverse-phase Zorbax SB-C8 column 2.1 \times 150 mm, 1.8 μm . Chromatographic separation was conducted in binary gradient using 2 mM ammonium formate, 0.15 % formic acid in methanol as solvent A and 1.5 mM ammonium formate, 0.1 % formic acid in water as solvent B at the flow rate of 0.4 ml/min.

Diacylglycerols

Diacylglycerols were extracted together with sphingolipids. A known amounts (50 ng) of internal standard (1,3 dipentadecanoyl-*sn*-glycerol) was added to each sample. Next, samples were extracted as described above. The following DAG were quantified: C18:1/18:2, C16:0/18:2, C16:0/16:0, C16:0/18:1, C18:0/20:0, C18:0/18:1, C18:1/18:1, C18:0/18:2 and C16:0/18:0 using UPLC/MS/MS. The chromatographic separation was performed using an Agilent 1290 infinity ultra performance liquid chromatography (UPLC). The analytical column was a reverse-phase Zorbax SB-C8 column 2.1 \times 150 mm, 1.8 μm . Chromatographic separation was conducted in a binary gradient using 2 mM ammonium formate, 0.15 % formic acid in methanol as solvent A and 1.5 mM ammonium formate, 0.1 % formic acid in water as solvent B at the flow rate of 0.4 ml/min.

Long-Chain AcylCoA

LCACoA was measured according to Blachnio-Zabielska et al. [32]. Briefly, LCACoA was extracted with the use of ACN:2-propanol:methanol (3:1:1; v:v:v). A known amount of heptadecanoyl-CoA was added as an internal standard. The molecules (C14:0-CoA, C16:0-CoA, C16:1-CoA,

Table 1 Anthropometric and clinical parameters in the studied groups

	Control	Obese	Obese + diabetes
<i>n</i>	14	12	15
Sex (M/F)	8/6	9/3	8/7
Age (years)	64.2 ± 8.4	65 ± 8.2	66 ± 6.7
BMI (kg/m ²)	23.7 ± 1.3	32.4 ± 4.8 ^b	36.2 ± 3.8 ^c
Fasting plasma glucose (mg/dl)	85.5 ± 7.7	83.2 ± 5.3	131.5 ± 12.6 ^{c, #}
Fasting plasma insulin (μU/ml)	9.11 ± 3.1	11.3 ± 3.3	14.8 ± 2.9 ^{c, #}
Total cholesterol (mg/dl)	157.4 ± 28.6	181.5 ± 39.7	176.5 ± 29.4
HDL-cholesterol (mg/dl)	47.3 ± 15.1	32.3 ± 7.1	28.3 ± 9.5 ^b
LDL-cholesterol (mg/dl)	83.5 ± 22.1	124.2 ± 30.7 ^a	143.6 ± 38.5 ^c
Triglycerides (mg/dl)	119.4 ± 33	194.3 ± 67 ^b	216.8 ± 69 ^b
HbA1c (%)	5.9 ± 0.8	6.5 ± 0.9	7.6 ± 1.4 ^{b^}
HOMA-IR	1.72 ± 0.6	2.06 ± 0.4	4.5 ± 0.9 ^{c, *}
LVEF (%)	49.4 ± 9.6	37.3 ± 17.1	45.2 ± 15.3
LVEDd (mm)	62.3 ± 4.6	66.4 ± 12.1 ^a	63.7 ± 10.1 ^a
SWT (mm)	13.6 ± 3.9	13.1 ± 2.1	12.2 ± 1.8
LVPWT (mm)	11.7 ± 3.4	12.3 ± 1.9	12.6 ± 2.1
LAD (mm)	43.5 ± 4.7	48.3 ± 6.7 ^a	46.4 ± 4.5

HOMA-IR (mmol/l × μU/ml) = fasting glucose (mmol/l) × fasting insulin (μU/ml)/22.5

Values are expressed as mean ± SD

HbA1c glycated hemoglobin, HOMA-IR homeostasis model assessment, LVEF left ventricular ejection fraction, LVEDd left ventricular end-diastolic diameter, LAD left atrial diameter, SWT septal wall thickness, LVPWT left ventricular posterior wall thickness

^a $p < 0.05$, ^b $p < 0.01$, ^c $p < 0.001$ versus lean non-diabetic, * $p < 0.05$, [^] $p < 0.01$, [#] $p < 0.001$ versus obese non-diabetic

C18:2-CoA, C18:1-CoA, C18:0-CoA, C20:0-CoA) were separated on a reverse-phase Zorbax SB-C18 column 2.1 × 150 mm using a binary gradient with ammonium hydroxide (NH₄OH) in water and NH₄OH in ACN. The LCACoA were quantified using multiple reaction monitoring (MRM) on a Triple quadrupole mass spectrometer in positive electrospray ionization (ESI) mode.

Statistical Analysis

All data are presented as means ± SD. Data were analyzed by one-way analysis of variance (ANOVA), followed by the Newman–Keuls post hoc test. p values <0.05 were taken to indicate statistical significance.

Results

Clinical Characteristics

Clinical characteristics of the studied groups are given in Table 1. In the obese non-diabetic group and in the obese diabetic group the BMI was 37 % ($p < 0.01$) and 53 % ($p < 0.001$) higher as compared to lean non-diabetic participants. The blood glucose concentration in the obese diabetic group was about 54 % ($p < 0.001$) and 58 % ($p < 0.001$) higher compared to the lean non-diabetic and obese non-diabetic subjects respectively. The plasma insulin concentration was 62 % ($p < 0.001$) and 31 % ($p < 0.01$) higher in obese diabetic participants as compared to the lean non-diabetic and obese non-diabetic subjects respectively. There were no significant differences in the content of glucose and insulin concentration between lean non-diabetic and obese non-diabetic subjects. There were also no significant differences in total plasma cholesterol concentration between the three groups. Plasma HDL-cholesterol concentration was almost 40 % ($p < 0.01$) lower in obese diabetic group as compared to the lean individuals. Plasma concentration of the LDL-cholesterol fraction was 49 % ($p < 0.05$) and 72 % ($p < 0.001$) higher in the obese non-diabetic and the obese diabetic groups respectively as compared to the lean group. Plasma triglycerides concentration was 63 % ($p < 0.01$) and 82 % ($p < 0.01$) higher in the obese non-diabetic and obese diabetic groups, respectively compared to the lean participants. The value of glycated hemoglobin (HbA1c) was almost 29 % ($p < 0.01$) higher in the obese diabetic group as compared to the lean control group. HOMA-IR significantly increased only in the obese diabetic group ($p < 0.001$).

Plasma FFA Concentration (Table 2)

All the fatty acid species measured were elevated in the plasma of both obese groups. The greatest increase in both obese groups was observed in palmitate (C16:0) (~2.5 times, for both $p < 0.001$) and in stearic acid (C18:0) concentrations (by 100 %, for both $p < 0.001$) comparing to the lean non-diabetic group. The concentration of oleic acid (C18:1) increased by 63–70 % (for both $p < 0.001$) in the obese non-diabetic and obese diabetic groups respectively. The concentration of arachidonic acid (C20:4) increased by around 30 % in the obese non-diabetic group and by 48 % ($p < 0.001$) in the obese diabetic group.

The linoleic acid (C18:2) concentration increased by around 54–43 % in the obese non-diabetic and obese diabetic groups, respectively (for both $p < 0.01$). The smallest, but still significant changes were noticed in myristic acid (C14:0) and palmitoleic acid (C16:1). The

Table 2 Plasma FFA concentration in lean non-diabetic, obese non-diabetic, and obese diabetic groups

	C14	C16:1	C16	C18:2	C18:1	C18	C20:4	Total
LND	13.3 ± 2.9	23.4 ± 2.9	89.3 ± 6.4	26.8 ± 4.8	154.6 ± 11.4	41.3 ± 2.7	18.7 ± 1.9	372.4 ± 32.5
OND	16.12 ± 3.8 ^a	27.9 ± 4.1 ^a	223.8 ± 36.2 ^c	41.2 ± 5.8 ^b	252.7 ± 37.7 ^c	85.0 ± 11.9 ^c	24.3 ± 2.7 ^c	671.0 ± 94.5 ^c
OD	16.37 ± 2.9 ^a	28.3 ± 3.5 ^a	238.3 ± 37.3 ^c	38.3 ± 6.1 ^b	263.7 ± 47.5 ^c	82.5 ± 8.3 ^c	27.7 ± 3.3 ^c	695.2 ± 102.0 ^c

Values are expressed in nmol/ml (mean ± SD)

LND lean non-diabetic, OND obese non-diabetic, OD obese diabetic

^a $p < 0.05$, ^b $p < 0.01$, ^c $p < 0.001$ versus lean non-diabetic

concentration of the fatty acids increased in both obese groups by around 20 % (for all $p < 0.05$). Total plasma FFA concentration increased by 80–87 % (for both $p < 0.001$) in the obese non-diabetic and obese diabetic groups, respectively as compared to lean non-diabetic participants.

Fat Tissue Sphingolipids Content (Table 3)

Subcutaneous Adipose Tissue

The contents of SPA, S1P, C14-Cer, C16-Cer, C18:1-Cer, C18-Cer and C24:1-Cer in the subcutaneous adipose tissue were greater in obese diabetic subjects as compared to their lean non-diabetic counterparts (for all $p < 0.001$). In the obese non-diabetic group the content of SPA, C14-Cer, C24:1-Cer (for all $p < 0.001$), C18:1-Cer and C24-Cer (for both $p < 0.05$) was greater than in the lean non-diabetic group. Moreover, content of S1P, C16-Cer, C18:1-Cer and C18-Cer was markedly higher in the obese diabetic group compared to the obese non-diabetic group (for both $p < 0.001$).

As expected, total ceramide content was higher in both obese groups as compared to lean non-diabetic subjects ($p < 0.001$). There were also significant differences between total ceramide content in obese non-diabetic and obese diabetic group ($p < 0.001$).

Epicardial Adipose Tissue

In epicardial adipose tissue, the content of Sph, SPA, S1P, C14-Cer, C16-Cer, C18:1-Cer, C18-Cer and C24:1-Cer was higher in the obese diabetic group comparing to the lean non-diabetic counterpart (for all $p < 0.001$). Moreover, the content of Sph, SPA, S1P, C14-Cer, C16-Cer (for all $p < 0.001$) and C18:1-Cer ($p < 0.05$) was greater in the obese non-diabetic group than in the lean non-diabetic group. There were also differences in sphingolipid content between both obese groups. The content of Sph, C14-Cer (for both $p < 0.05$), S1P, C18:1-Cer, C18-Cer and C24:1-Cer (for all $p < 0.001$) was higher in the obese diabetic group as compared to the obese non-diabetic group. Total ceramide content was higher in both obese groups comparing to the lean non-diabetic group (for both $p < 0.001$).

and was significant higher in the obese diabetic group as compare to the obese non-diabetic group ($p < 0.01$).

Fat Tissue DAG Content (Table 4)

Subcutaneous Adipose Tissue

In subcutaneous fat tissue, the content of C18:1/C18:2, C16:0/18:2, C16:0/16:0, C18:0/18:1 (for all $p < 0.001$), C16:0/18:1 ($p < 0.01$) and C18:1/18:1 ($p < 0.05$) increased in the obese diabetic group as compared to lean subjects. The level of C16:0/18:2, C18:1/18:0 (for both $p < 0.001$), C16:0/18:1 ($p < 0.01$) and C18:1/18:1 ($p < 0.05$) was higher in the obese non-diabetic group as compared to the lean non-diabetic group. There were also differences in C16:0/16:0 ($p < 0.001$) and C18:1/18:2 ($p < 0.05$) content between both obese groups. The higher content of the compounds was noticed in the obese diabetic group. As expected, total DAG content increased in both obese groups as compared to the lean control group (for both $p < 0.001$).

Epicardial Adipose Tissue

All measured DAG species increased in the obese diabetic group (for all $p < 0.001$, except C18:0/18:2 where $p < 0.01$) as compared to the lean non-diabetic group. Elevated content of all measured DAG (for all $p < 0.001$ except C16:0/18:2 and C18:0/18:2 where $p < 0.01$) was also noticed in the obese non-diabetic group as compared to the lean control group. Moreover, increased content of C16:0/16:0 ($p < 0.05$) and C18:0/18:1 ($p < 0.01$) was observed in the obese diabetic group comparing to the obese non-diabetic group. As expected, total DAG content in that tissue was also greater in both obese groups as compared to the lean control group (for both $p < 0.001$).

Fat Tissue LCACoA Content (Table 5)

Subcutaneous Adipose Tissue

In both obese groups, the content of C16:1-CoA, C18-CoA (for both $p < 0.05$), C16-CoA and C18:1-CoA (for both $p < 0.01$), was greater as compared to the lean non-diabetic

Table 3 Sphingolipids content in white subcutaneous adipose tissue and epicardial fat tissue in lean non-diabetic, obese non-diabetic, and obese diabetic groups

Sph	SPA	SIP	C14-Cer	C16-Cer	C18:1-Cer	C18-Cer	C20-Cer	C22-Cer	C24:1-Cer	C24-Cer	Total Cer	
SubQ												
LND	0.37 ± 0.08	0.05 ± 0.01	0.028 ± 0.003	0.13 ± 0.02	2.9 ± 0.6	0.17 ± 0.02	0.18 ± 0.07	0.32 ± 0.07	1.2 ± 0.14	1.7 ± 0.3	1.2 ± 0.17	7.8 ± 0.8
OND	0.43 ± 0.08	0.11 ± 0.03 ^c	0.027 ± 0.004	0.23 ± 0.06 ^c	3.2 ± 1.1	0.20 ± 0.05 ^a	0.21 ± 0.06	0.35 ± 0.07	1.3 ± 0.18	2.6 ± 0.3 ^c	1.4 ± 0.15 ^a	9.5 ± 0.9 ^c
OD	0.43 ± 0.09	0.11 ± 0.03 ^c	0.078 ± 0.009 ^{c,#}	0.21 ± 0.04 ^c	5.1 ± 1.3 ^{c,#}	0.32 ± 0.07 ^{c,#}	0.31 ± 0.05 ^{c,#}	0.36 ± 0.11	1.3 ± 0.42	2.4 ± 0.3 ^c	1.4 ± 0.42	11.4 ± 1.2 ^{c,#}
Epicardial												
LND	0.27 ± 0.05	0.06 ± 0.01	0.025 ± 0.002	0.15 ± 0.03	3.7 ± 0.9	0.33 ± 0.08	0.49 ± 0.09	0.32 ± 0.09	0.55 ± 0.09	0.6 ± 0.1	0.5 ± 0.1	6.4 ± 1.1
OND	0.45 ± 0.09 ^c	0.09 ± 0.02 ^c	0.052 ± 0.006 ^c	0.26 ± 0.05 ^c	5.6 ± 0.5 ^c	0.41 ± 0.08 ^a	0.54 ± 0.09	0.33 ± 0.05	0.54 ± 0.08	0.6 ± 0.1	0.6 ± 0.1	8.9 ± 0.4 ^c
OD	0.57 ± 0.11 ^{c,*}	0.11 ± 0.03 ^c	0.080 ± 0.009 ^{c,#}	0.33 ± 0.09 ^{c,*}	5.9 ± 0.8 ^c	0.53 ± 0.08 ^{c,#}	0.70 ± 0.09 ^{c,#}	0.33 ± 0.06	0.60 ± 0.07	0.9 ± 0.1 ^{c,#}	0.6 ± 0.1	9.8 ± 0.8 ^{c,*}

Values are expressed in pmol/mg tissue (means ± SD)

LND lean non-diabetic, OND obese non-diabetic, OD obese diabetic. *SubQ* subcutaneous fat tissue

^a $p < 0.05$, ^b $p < 0.01$, ^c $p < 0.001$ versus lean non-diabetic, * $p < 0.05$, ^ $p < 0.01$, # $p < 0.001$ versus obese non-diabetic

Table 4 Diacylglycerols content in white subcutaneous adipose tissue and epicardial fat tissue in lean non-diabetic, obese non-diabetic, and obese diabetic groups

	C18:1/18:2	C16:0/18:2	C16:0/16:0	C16:0/18:1	C18:0/18:1	C18:1/18:1	C18:0/18:2	C16:0/18:0	Total
SubQ									
LND	13.4 ± 1.06	30.2 ± 4.5	26.9 ± 3.9	62.1 ± 10.4	2.1 ± 0.5	0.09 ± 0.01	1.65 ± 0.35	0.74 ± 0.12	137 ± 12.5
OND	14.6 ± 1.84	77.8 ± 24.4 ^c	27.2 ± 2.7	76.8 ± 10.8 ^b	3.2 ± 0.7 ^c	0.14 ± 0.07 ^a	1.78 ± 0.34	0.72 ± 0.16	202 ± 26.4 ^c
OD	16.8 ± 3.06 ^{c,*}	81.0 ± 24.0 ^c	35.7 ± 5.2 ^{c,#}	74.1 ± 9.2 ^b	3.2 ± 0.6 ^c	0.11 ± 0.03 ^a	1.75 ± 0.30	0.68 ± 0.10	213 ± 28.6 ^c
Epicardial									
LND	0.31 ± 0.05	1.58 ± 0.27	0.40 ± 0.08	2.08 ± 0.39	0.18 ± 0.04	0.03 ± 0.006	0.097 ± 0.013	0.067 ± 0.009	4.73 ± 0.54
OND	0.63 ± 0.11 ^c	2.01 ± 0.35 ^b	0.57 ± 0.09 ^c	3.63 ± 0.74 ^c	0.41 ± 0.07 ^c	0.05 ± 0.007 ^c	0.124 ± 0.031 ^b	0.094 ± 0.019 ^c	7.53 ± 0.90 ^c
OD	0.66 ± 0.12 ^c	2.08 ± 0.36 ^c	0.68 ± 0.11 ^{c,*}	3.61 ± 0.70 ^c	0.52 ± 0.08 ^{c,^}	0.05 ± 0.006 ^c	0.118 ± 0.019 ^b	0.092 ± 0.022 ^c	7.82 ± 0.83 ^c

Values are expressed in pmol/mg tissue (mean ± SD)

LND lean non-diabetic, OND obese non-diabetic, OD obese diabetic. *SubQ* subcutaneous fat tissue

^a $p < 0.05$, ^b $p < 0.01$, ^c $p < 0.001$ versus lean non-diabetic, * $p < 0.05$, ^ $p < 0.01$; # $p < 0.001$ versus obese non-diabetic

Table 5 LCACoA content in white subcutaneous adipose tissue and epicardial fat tissue in lean non-diabetic, obese non-diabetic, and obese diabetic groups

	C14-CoA	C16:1-CoA	C16-CoA	C18:2-COA	C18:1-CoA	C18-CoA	C20-CoA	Total
SubQ								
LND	0.021 ± 0.010	0.035 ± 0.013	0.050 ± 0.01	0.11 ± 0.02	0.30 ± 0.06	0.05 ± 0.02	0.034 ± 0.018	0.60 ± 0.09
OND	0.019 ± 0.005	0.046 ± 0.011 ^a	0.068 ± 0.01 ^b	0.11 ± 0.04	0.39 ± 0.10 ^b	0.07 ± 0.02 ^a	0.035 ± 0.009	0.74 ± 0.07 ^c
OD	0.025 ± 0.020	0.045 ± 0.012 ^a	0.065 ± 0.01 ^b	0.12 ± 0.03	0.37 ± 0.09 ^b	0.07 ± 0.02 ^a	0.042 ± 0.015	0.74 ± 0.08 ^c
Epicardial								
LND	0.021 ± 0.005	0.048 ± 0.01	0.06 ± 0.01	0.13 ± 0.02	0.35 ± 0.07	0.07 ± 0.02	0.046 ± 0.01	0.73 ± 0.07
OND	0.030 ± 0.009 ^b	0.053 ± 0.01	0.09 ± 0.02 ^c	0.13 ± 0.03	0.51 ± 0.10 ^c	0.10 ± 0.03 ^b	0.047 ± 0.01	0.97 ± 0.13 ^c
OD	0.032 ± 0.018 ^a	0.063 ± 0.01 ^a	0.12 ± 0.02 ^{c,*}	0.14 ± 0.03	0.53 ± 0.12 ^c	0.11 ± 0.02 ^c	0.052 ± 0.01	1.06 ± 0.13 ^c

Values are expressed in pmol/mg tissue (means ± SD)

LND lean non-diabetic, OND obese non-diabetic, OD obese diabetic, SubQ subcutaneous fat tissue

^a $p < 0.05$, ^b $p < 0.01$, ^c $p < 0.001$ versus lean non-diabetic, * $p < 0.05$ versus obese non-diabetic

group. The total LCACoA content was also greater in both obese groups ($p < 0.001$) comparing to the lean control group. There were no statistical differences between both obese groups.

Epicardial Adipose Tissue

In the epicardial fat tissue, the content of C14-CoA, C16:1-CoA (for both $p < 0.05$), C16-CoA, C18:1-CoA and C18-CoA (for all $p < 0.001$) was greater in the obese diabetic group comparing to the lean control group. In the obese non-diabetic group, content of C14-CoA, C18-CoA (for both $p < 0.01$), C16-CoA and C18:1-CoA ($p < 0.001$) was higher comparing to the lean non-diabetic group. There was a difference in C16-CoA content between both obese groups. The content of C16-CoA was greater in the obese diabetic group as compared to the obese non-diabetic group ($p < 0.001$). The total LCACoA content was also higher in the both obese groups (for both $p < 0.001$) comparing to the lean non-diabetic group. There were no differences in total LCACoA content between both obese groups.

Associations Between Bioactive Lipids and HOMA-IR (Fig. 1)

We found a strong positive correlation between the total content of ceramide in subcutaneous fat and HOMA-IR ($r = 0.78$, $p < 0.001$). The strongest correlation was noticed with C16-Cer ($r = 0.79$, $p < 0.001$). We did not find such a correlation in epicardial fat tissue. There was also a positive correlation between total DAG content in subcutaneous fat tissue and HOMA-IR ($r = 0.64$, $p < 0.001$) and between HOMA-IR and 16/18:2 DAG ($r = 0.56$, $p < 0.001$). No such associations were detected in epicardial fat tissue. In epicardial fat tissue we found a strong correlation between C16:0-CoA content and HOMA-IR ($r = 0.73$, $p < 0.001$).

Associations Between Bioactive Lipids and Cardiac Structure Alterations

We found highly significant ($p < 0.001$ in all cases) correlations between the content of some lipid species determined in adipose tissue samples and the left ventricular end-diastolic diameter (LVEDd) of the heart. Namely, there was a positive relationship between LVEDd and the level of sphinganine, C18:1-CoA, total acyl-CoA and 18:1/18:1-DAG in the subcutaneous adipose tissue ($r = 0.64$, 0.59, 0.61 and 0.63, respectively). Moreover, a similar correlation was observed for 16:0/18:2-DAG content in the epicardial adipose tissue ($r = 0.59$). These findings suggest the existence of a link between adipose tissue lipid metabolism and alterations in cardiac structure related to the development of cardiomyopathy. However, further studies are required to reveal the nature of this relationship.

Discussion

Obesity is a major global health concern that increases the risk of metabolic and cardiovascular disease. Most of the work in the field of lipid accumulation, obesity and insulin resistance has focused on lipid metabolism in skeletal muscle [20, 33–39]. Although fat tissue is not the main tissue responsible for insulin stimulated glucose uptake, it seems to be the major tissue responsible for induction of the whole body insulin resistance. Our goal was to understand whether adipose tissues lipid content is altered in different fat tissue depots in obese non-diabetic and obese diabetic humans and, if so, whether there was any association between adipose tissue lipids and insulin resistance. In most works about obesity, fat tissue and insulin resistance, only triacylglycerols and adipokines have been taken into consideration. Ours is the first study to provide a comprehensive profile of the distinct molecular species not

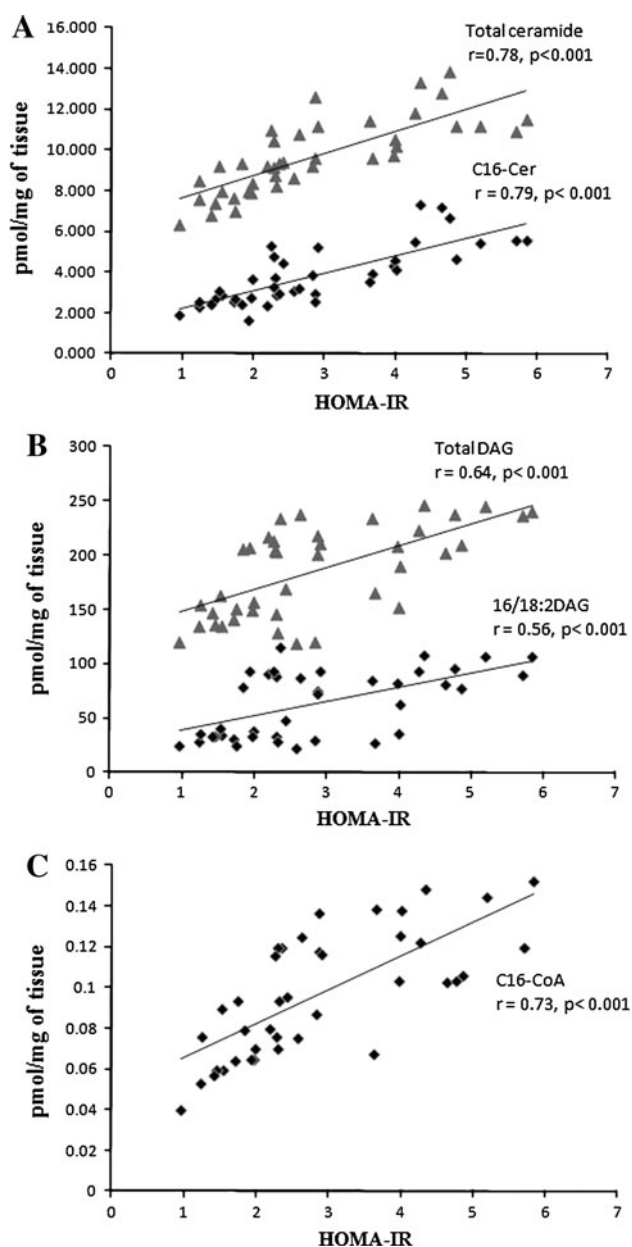


Fig. 1 Relationship between HOMA-IR and lipids content in fat tissue. **a** Filled triangles correlation between total ceramide content in subcutaneous fat tissue and HOMA-IR; diamonds correlation between C16-Cer content in subcutaneous fat tissue and HOMA-IR, **b** Filled triangles correlation between total DAG content in subcutaneous fat tissue and HOMA-IR; diamonds correlation between C16:0/18:2 DAG content in subcutaneous fat tissue and HOMA-IR, **c** Filled triangles correlation between total C16-CoA content in epicardial fat tissue and HOMA-IR

only of ceramides but also of DAG (TIC of DAG in SAT is presented in Fig. 2) and LCACoA within two fat depots (visceral and subcutaneous) of lean non-diabetic, obese non-diabetic and obese diabetic subjects. We have found that the lipid content is elevated in both fat tissue depots. As mentioned above, intramuscular accumulation of the lipids impairs insulin action in skeletal muscle and liver.

In-vitro studies revealed that in 3T3-L1 adipocytes and in brown adipocytes, ceramide impairs insulin stimulated GLUT4 expression and glucose uptake [28]. It has also been shown that ceramide mediates the effect of TNF- α on GLUT4 mRNA content in these cells [40, 41]. Data from brown adipocytes suggest that the de novo ceramide biosynthesis plays a main role in mediating the effect of TNF- α on insulin action in these cells. There are few data from in vitro studies, showing, that pharmacological reduction of glycosphingolipids in cultured adipocytes strikingly improves glycemic control [42]. Such data prove that sphingolipids play an important role not only in regulating skeletal muscle but also adipocyte insulin sensitivity. There is some, but limited information about ceramides in human subcutaneous tissue [27]. Our previous work [26] provided information that ceramide metabolism in human subcutaneous tissue from lean healthy subjects differs from that in both obese non-diabetic and obese diabetic participants. We have demonstrated that total ceramide content decreased in subcutaneous fat tissue in both obese non-diabetic and obese diabetic patients compared to lean non-diabetic subjects. In the present work we have found, that total ceramide content as well as other measured lipids were greater in the both obese groups comparing to the lean non-diabetic group. It should be underlined, that although in both studies we used subcutaneous fat tissue, the tissue was taken from different places. In the previous study [26], the fat was taken from the abdominal region and in the present study the tissue was taken from the subcutaneous fat on the sternum. It appears that the differences in metabolic activity between fat tissues relates not only to subcutaneous and visceral but also to subcutaneous fat tissue from different regions [43, 44]. Obesity is associated with a state of chronic, low-grade inflammation and with increased plasma FFA concentrations which likely contributes to ceramide accumulation. Ceramide synthesis is activated by a variety of mediators, including proinflammatory cytokines, and an increased level of free fatty acids [45, 46]. In our work, we measured plasma FFA concentration and we found, that the concentration of plasma FFA is greater in both obese groups than in the lean group. The highest increase was found in saturated fatty acids concentrations (stearic acid and palmitic acid). There is some data showing that palmitate is responsible for lower adiponectin expression in fat tissue [47]. It is possible, that the mentioned effect of palmitate on adiponectin expression could occur through the increased level of bioactive lipids that contain palmitate.

Another key finding of our study was the positive correlation between total ceramide content in SAT and HOMA-IR ($r = 0.78$) and between C16-Cer content in subcutaneous fat tissue and HOMA-IR ($r = 0.79$) (Fig. 1a). Moreover, other positive correlations were found

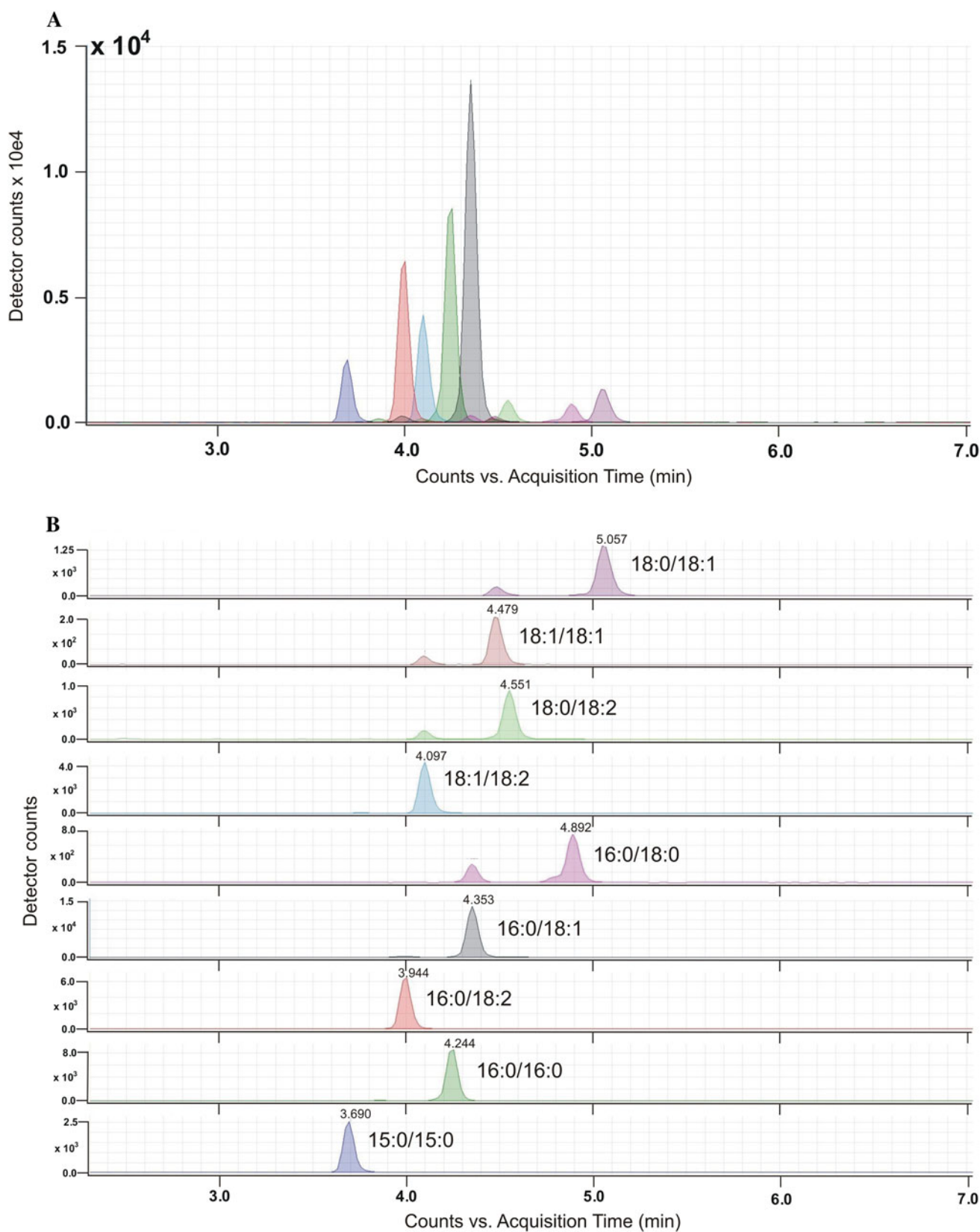


Fig. 2 TIC total ion current of DAG in human subcutaneous adipose tissue (**a**). Peaks of particular DAG species (**b**)

between HOMA-IR and total DAG content in SAT and between HOMA-IR and C16:0/18:2 ($r = 0.56$ and $r = 0.64$, respectively, Fig. 1b). We did not observe such a relation in epicardial fat tissue. However, we found a correlation between C16-CoA content in epicardial fat tissue and HOMA-IR ($r = 0.73$), (Fig. 1c). In the all cases (ceramide, DAG in subcutaneous fat tissue and LCACoA in epicardial fat tissue), the strongest correlation was found with the molecule containing palmitate. A strong positive correlation between hepatic DAG content in lipid droplets and HOMA-IR values had previously been found and that hepatic DAG content in lipid droplets is the best predictor of insulin resistance [48]. Moreover it has been postulated that increases in intracellular diacylglycerol content lead to activation of new protein kinase C (PKC) isoforms that inhibit insulin action in the liver and skeletal muscle [49].

Our data demonstrated that the biologically active lipids increase in fat tissue of obese and obese diabetic patients and correlate with insulin resistance which suggests that they might play some special role in the induction of whole body insulin resistance. However, there is still an open question as to what is the mechanism by which increased lipids content in adipose tissue affects the whole body insulin sensitivity.

In conclusion, this is the first report on bioactive lipid content in human subcutaneous and epicardial adipose tissue of lean non-diabetic, obese non-diabetic, and obese diabetic subjects. The study has shown that in obese and obese diabetic patients, bioactive lipids content is greater in subcutaneous and epicardial fat tissue and the particular lipids content correlates with insulin resistance (HOMA-IR).

Acknowledgments This work was supported by the Polish Ministry of Science and Higher Education (grant no. N N401 531840) and by the Medical University of Białystok (grant numbers 113-18948 and 113-18949).

Conflict of interest There is no conflict of interest for this study

Open Access This article is distributed under the terms of the Creative Commons Attribution License which permits any use, distribution, and reproduction in any medium, provided the original author(s) and the source are credited.

References

- Engeli S, Gorzelniak K, Kreutz R, Runkel N, Distler A, Sharma AM (1999) Co-expression of renin-angiotensin system genes in human adipose tissue. *J Hypertens* 17:555–560
- Scherer PE, Williams S, Fogliano M, Baldini G, Lodish HF (1995) A novel serum protein similar to C1q, produced exclusively in adipocytes. *J Biol Chem* 270:26746–26749
- Winkler G, Kiss S, Keszthelyi L, Sapi Z, Ory I, Salamon F, Kovacs M, Vargha P, Szekeres O, Speer G et al (2003) Expression of tumor necrosis factor (TNF)-alpha protein in the subcutaneous and visceral adipose tissue in correlation with adipocyte cell volume, serum TNF-alpha, soluble serum TNF-receptor-2 concentrations and C-peptide level. *Eur J Endocrinol* 149:129–135
- Kannel WB (1985) Lipids, diabetes, and coronary heart disease: insights from the Framingham Study. *Am Heart J* 110:1100–1107
- Larsson B (1991) Obesity, fat distribution and cardiovascular disease. *Int J Obes* 15(Suppl 2):53–57
- Iacobellis G, Sharma AM (2007) Epicardial adipose tissue as new cardio-metabolic risk marker and potential therapeutic target in the metabolic syndrome. *Curr Pharm Des* 13:2180–2184
- Iacobellis G, Ribaudo MC, Leto G, Zappaterreno A, Vecci E, Di Mario U, Leonetti F (2002) Influence of excess fat on cardiac morphology and function: study in uncomplicated obesity. *Obes Res* 10:767–773
- Iacobellis G, Sharma AM (2007) Obesity and the heart: redefinition of the relationship. *Obes Rev* 8:35–39
- Wajchenberg BL (2000) Subcutaneous and visceral adipose tissue: their relation to the metabolic syndrome. *Endocr Rev* 21:697–738
- Tzanavari T, Giannogonas P, Karalis KP (2010) TNF-alpha and obesity. *Curr Dir Autoimmun* 11:145–156
- Trayhurn P, Wood IS (2004) Adipokines: inflammation and the pleiotropic role of white adipose tissue. *Br J Nutr* 92:347–355
- Prins JB (2002) Adipose tissue as an endocrine organ. *Best Pract Res Clin Endocrinol Metab* 16:639–651
- Owecki M (2009) Fat tissue and adiponectin: new players in critical care? *Crit Care* 13:174
- Gomez S, Demirhan A, Atalar F, Caynak B, Erdim R, Sozer V, Gunay D, Akpınar B, Ozbek U, Buyukdevrim AS (2011) Adipose tissue gene expression of adiponectin, tumor necrosis factor- α and leptin in metabolic syndrome patients with coronary artery disease. *Intern Med* 50:805–810
- Ahima RS (2006) Adipose tissue as an endocrine organ. *Obesity (Silver Spring)* 14(Suppl 5):242S–249S
- Marchington JM, Mattacks CA, Pond CM (1989) Adipose tissue in the mammalian heart and pericardium: structure, foetal development and biochemical properties. *Comp Biochem Physiol B* 94:225–232
- Yu C, Chen Y, Cline GW, Zhang D, Zong H, Wang Y, Bergeron R, Kim JK, Cushman SW, Cooney GJ et al (2002) Mechanism by which fatty acids inhibit insulin activation of insulin receptor substrate-1 (IRS-1)-associated phosphatidylinositol 3-kinase activity in muscle. *J Biol Chem* 277:50230–50236
- Shulman GI (2000) Cellular mechanisms of insulin resistance. *J Clin Invest* 106:171–176
- Shah C, Yang G, Lee I, Bielawski J, Hannun YA, Samad F (2008) Protection from high fat diet-induced increase in ceramide in mice lacking plasminogen activator inhibitor 1. *J Biol Chem* 283:13538–13548
- Summers SA (2006) Ceramides in insulin resistance and lipotoxicity. *Prog Lipid Res* 45:42–72
- Holland WL, Knotts TA, Chavez JA, Wang LP, Hoehn KL, Summers SA (2007) Lipid mediators of insulin resistance. *Nutr Rev* 65:S39–S46
- Auge N, Maupas-Schwalm F, Elbaz M, Thiers JC, Waysbort A, Itohara S, Krell HW, Salvayre R, Negre-Salvayre A (2004) Role for matrix metalloproteinase-2 in oxidized low-density lipoprotein-induced activation of the sphingomyelin/ceramide pathway and smooth muscle cell proliferation. *Circulation* 110:571–578
- Auge N, Negre-Salvayre A, Salvayre R, Levade T (2000) Sphingomyelin metabolites in vascular cell signaling and atherogenesis. *Prog Lipid Res* 39:207–229
- Hojjati MR, Li Z, Zhou H, Tang S, Huan C, Ooi E, Lu S, Jiang XC (2005) Effect of myriocin on plasma sphingolipid metabolism and atherosclerosis in apoE-deficient mice. *J Biol Chem* 280:10284–10289

25. Kolak M, Westerbacka J, Velagapudi VR, Wågsäter D, Yetukuri L, Makkonen J, Rissanen A, Häkkinen AM, Lindell M, Bergholm R et al (2007) Adipose tissue inflammation and increased ceramide content characterize subjects with high liver fat content independent of obesity. *Diabetes* 56:1960–1968
26. Blachnio-Zabielska AU, Pulka M, Baranowski M, Nikolajuk A, Zabielski P, Gorska M, Gorski J (2012) Ceramide metabolism is affected by obesity and diabetes in human adipose tissue. *J Cell Physiol* 227:550–557
27. Blachnio-Zabielska AU, Koutsari C, Tchkonja T, Jensen MD (2012) Sphingolipid content of human adipose tissue: relationship to adiponectin and insulin resistance. *Obesity*. doi:10.1038/oby.2012.126
28. Long SD, Pekala PH (1996) Lipid mediators of insulin resistance: ceramide signalling down-regulates GLUT4 gene transcription in 3T3-L1 adipocytes. *Biochem J* 319(Pt 1):179–184
29. Jornayvaz FR, Shulman GI (2012) Diacylglycerol activation of protein kinase C ϵ and hepatic insulin resistance. *Cell Metab* 15: 574–584
30. Persson XM, Blachnio-Zabielska AU, Jensen MD (2010) Rapid measurement of plasma free fatty acid concentration and isotopic enrichment using LC/MS. *J Lipid Res* 51:2761–2765
31. Blachnio-Zabielska AU, Persson XM, Koutsari C, Zabielski P, Jensen MD (2012) A liquid chromatography/tandem mass spectrometry method for measuring the in vivo incorporation of plasma free fatty acids into intramyocellular ceramides in humans. *Rapid Commun Mass Spectrom* 26:1134–1140
32. Blachnio-Zabielska AU, Koutsari C, Jensen MD (2011) Measuring long-chain acyl-coenzyme A concentrations and enrichment using liquid chromatography/tandem mass spectrometry with selected reaction monitoring. *Rapid Commun Mass Spectrom* 25:2223–2230
33. Straczkowski M, Kowalska I, Baranowski M, Nikolajuk A, Oziomek E, Zabielski P, Adamska A, Blachnio A, Gorski J, Gorska M (2007) Increased skeletal muscle ceramide level in men at risk of developing type 2 diabetes. *Diabetologia* 50: 2366–2373
34. Frangioudakis G, Garrard J, Raddatz K, Nadler JL, Mitchell TW, Schmitz-Peiffer C (2010) Saturated- and n-6 polyunsaturated-fat diets each induce ceramide accumulation in mouse skeletal muscle: reversal and improvement of glucose tolerance by lipid metabolism inhibitors. *Endocrinology* 151:4187–4196
35. Adams JM, Pratipanawatr T, Berria R, Wang E, DeFronzo RA, Sullards MC, Mandarino LJ (2004) Ceramide content is increased in skeletal muscle from obese insulin-resistant humans. *Diabetes* 53:25–31
36. Blachnio-Zabielska A, Baranowski M, Zabielski P, Gorski J (2010) Effect of high fat diet enriched with unsaturated and diet rich in saturated fatty acids on sphingolipid metabolism in rat skeletal muscle. *J Cell Physiol* 225:786–791
37. Blachnio-Zabielska A, Zabielski P, Baranowski M, Gorski J (2011) Aerobic training in rats increases skeletal muscle sphingomyelinase and serine palmitoyltransferase activity. While decreasing ceramidase activity. *Lipids* 46:229–238
38. Blachnio-Zabielska A, Zabielski P, Baranowski M, Gorski J (2010) Effects of streptozotocin-induced diabetes and elevation of plasma FFA on ceramide metabolism in rat skeletal muscle. *Horm Metab Res* 42:1–7
39. Blachnio-Zabielska A, Baranowski M, Zabielski P, Gorski J (2008) Effect of exercise duration on the key pathways of ceramide metabolism in rat skeletal muscles. *J Cell Biochem* 105: 776–784
40. Stephens JM, Pekala PH (1992) Transcriptional repression of the C/EBP-alpha and GLUT4 genes in 3T3-L1 adipocytes by tumor necrosis factor-alpha. Regulations is coordinate and independent of protein synthesis. *J Biol Chem* 267:13580–13584
41. Stephens JM, Pekala PH (1991) Transcriptional repression of the GLUT4 and C/EBP genes in 3T3-L1 adipocytes by tumor necrosis factor-alpha. *J Biol Chem* 266:21839–21845
42. Aerts JM, Ottenhoff R, Powlson AS, Grefhorst A, van Eijk M, Dubbelhuis PF, Aten J, Kuipers F, Serlie MJ, Wennekes T et al (2007) Pharmacological inhibition of glucosylceramide synthase enhances insulin sensitivity. *Diabetes* 56:1341–1349
43. Tchoukalova YD, Koutsari C, Votruba SB, Tchkonja T, Giorgadze N, Thomou T, Kirkland JL, Jensen MD (2010) Sex and depot-dependent differences in adipogenesis in normal-weight humans. *Obesity (Silver Spring)* 18:1875–1880
44. Tchoukalova YD, Votruba SB, Tchkonja T, Giorgadze N, Kirkland JL, Jensen MD (2010) Regional differences in cellular mechanisms of adipose tissue gain with overfeeding. *Proc Natl Acad Sci USA* 107:18226–18231
45. Hannun YA, Obeid LM (2002) The ceramide-centric universe of lipid-mediated cell regulation: stress encounters of the lipid kind. *J Biol Chem* 277:25847–25850
46. Zheng W, Kollmeyer J, Symolon H, Momin A, Munter E, Wang E, Kelly S, Allegood JC, Liu Y, Peng Q et al (2006) Ceramides and other bioactive sphingolipid backbones in health and disease: lipidomic analysis, metabolism and roles in membrane structure, dynamics, signaling and autophagy. *Biochim Biophys Acta* 1758: 1864–1884
47. Xi L, Qian Z, Xu G, Zhou C, Sun S (2007) Crocetin attenuates palmitate-induced insulin insensitivity and disordered tumor necrosis factor-alpha and adiponectin expression in rat adipocytes. *Br J Pharmacol* 151:610–617
48. Kumashiro N, Erion DM, Zhang D, Kahn M, Beddow SA, Chu X, Still CD, Gerhard GS, Han X, Dziura J et al (2011) Cellular mechanism of insulin resistance in nonalcoholic fatty liver disease. *Proc Natl Acad Sci USA* 108:16381–16385
49. Erion DM, Shulman GI (2010) Diacylglycerol-mediated insulin resistance. *Nat Med* 16:400–402

palmitoleic acid is positively correlated with obesity in adults and children [5, 6]. Whether a component of human or livestock diets, palmitoleic acid may act to regulate lipid metabolism.

Previous results from our laboratory showed palmitoleic acid functions to reduce de novo fatty acid synthesis and reduce lipogenic gene expression in cultured bovine adipocytes [7]. Concurrent with 16:1 increasing in palmitoleic acid-treated cells, *cis*-vaccenic (18:1 *cis*-11) and eicosenoic (20:1 *cis*-13) acids also increase. The physiologic consequence, however, of these long-chain MUFA are largely unknown. We hypothesize that 18:1 *cis*-11 and 20:1 *cis*-13 are products of palmitoleic acid elongation that are jointly responsible for the lipogenic effects seen with palmitoleic acid supplementation in bovine adipocytes. Therefore, the objectives of this study were to: (1) confirm elongation products of palmitoleic acid (16:1 *cis*-9) elongation in vitro using stable isotopes and (2) evaluate if exogenous supplementation of palmitoleic acid, elongation products, or both are responsible for decreased desaturation and lipogenesis rates observed with palmitoleic acid supplementation in bovine adipocytes.

Materials and Methods

Cell Culture

Primary bovine stromal vascular cultures were harvested from intermuscular adipose tissue obtained at the lateral edge of longissimus muscle between the longissimus costarum and posterior serratus dorsalis at the 12th rib of two beef carcasses as described by Hirai et al. [8] using slight modifications as described by Pratt et al. [9]. Cells were plated at 1×10^4 cells/cm² and passaged every 2–4 days when 60 % confluent. Cells were incubated at 37 °C under 5 % CO₂ humidified atmosphere with media [Dulbecco's modified Eagles medium (DMEM) containing 10 % fetal calf serum (FCS), and 2× antibiotic/antimycotic (AB/AM; containing 10,000 U/mL penicillin G, 10,000 µg/mL streptomycin, and 25 µg/mL amphotericin B)] replacement every 2 days. After four passages, cell lines were stored in liquid nitrogen at 1×10^6 cells/mL in freezing media (DMEM, 20 % FCS, and 10 % dimethyl sulfoxide) for later use.

Treatments

Individual cultures from two beef carcasses were used in duplicate for each of these two experiments ($n = 4$). Cells were thawed, passaged three times, and seeded in plates at 1×10^5 cells/cm². Cells were allowed to reach confluence, held for 2 days, and differentiated on day 0 with DMEM

containing 5 % FCS, 2× AB/AM, 2.5 µg/mL insulin, 0.5 mM 2-isobutyl-1-methylxanthine (IBMX), 0.25 µM dexamethasone (DEX), 5 µM troglitazone (TRO), and 10 mM acetate [8, 9]. Secondary differentiation media (DMEM, 5 % FCS, 2× AB/AM, 2.5 µg/mL insulin, 5 µM TRO, and 10 mM acetate) was applied for 4 (day 6) along with 0 µM additional fatty acids (control) or 150 µM fatty acids. Fatty acids were bound to fatty acid-free bovine serum albumin (2:1, w/w) as described by Van Harken et al. [10] prior to media addition. Control media contained an equal amount of fatty acid-free bovine serum albumin as used in fatty acid treatment media. According to the objectives of the experiment, cells were either harvested on day 6 for fatty acid composition and lipogenic gene expression or treated with stable isotopes on day 6 for enzymatic activity assays. Previously, our stromal vascular cultures displayed characteristic changes in morphology, lipid-filling, and adipogenic gene expression upon hormonal treatment, consistent with adipocyte differentiation by day 6 [7, 9].

Experiment 1

Previously, our palmitoleic acid-treated cultures showed a dramatic increase in 18:1 *cis*-11 and 20:1 *cis*-13 [7]. It has been proposed that palmitoleic acid can be elongated into 18:1 *cis*-11 and potentially elongated further into a 20C fatty acid [11]. To confirm 18:1 *cis*-11 and 20:1 *cis*-13 as elongation products and to measure elongation in vitro, we added stable isotope labeled palmitoleic acid [150 µM (U-¹³C)16:1] on day 6 for 0, 6, 12, 24, and 36 h to adipocytes cultures. At harvest, cells were washed three times with PBS, removed with trypsin, and placed directly into 2:1 chloroform/methanol (vol/vol) to terminate all enzymatic activity. Cellular fatty acids were extracted using Folch et al. [12] and transmethylated according to Park and Goins [13]. Fatty acid methyl esters (FAME) were analyzed using an Agilent 6890N gas chromatograph (GC; Agilent Technologies, Inc., Santa Clara, CA, USA) equipped with an Agilent 5973 mass spectrometer (MS) using a 100m Varian CP7489 (Varian Instruments Inc., Walnut Creek, CA, USA) capillary column (0.25 mm i.d. and 0.20 µm film thickness). Samples were run in the chemical ionization mode with He as the carrier gas and CH₄ as the reagent gas.

Ions of mass-to-charge ratio (m/z) 268 (m) and 284 ($m + 16$) were selectively measured to calculate the isotopic enrichments of 16:1. Similarly, ion abundance of 298 (m) and 312 ($m + 16$) were measured for 18:1 *cis*-11. We calculated the relative abundance (RA) of labeled ($m + 16$) to unlabeled (m) isotopomers of 16:1 and 18:1 *cis*-11. Fatty acid enrichment was calculated as tracer-to-tracee ratio (TTR), according to Wolfe and Chinkes [14].

$$\text{TTR}_{\text{sample}} = (\text{RA}_{\text{sample}} - \text{RA}_{\text{blank}}).$$

Samples that were not exposed to the labeled isotope served as ‘blanks’. Molar percent excess (MPE) of 16:1 was calculated by $\text{TTR}/(\text{TTR} + 1)$ and fractional synthetic rate (FSR) of elongation was calculated from $\text{TTR}_{18:1 \text{ cis-11}}$ and $\text{MPE}_{16:1}$.

$$\text{FSR}_{\text{elongation}} = \frac{\text{TTR}_{18:1 \text{ cis-11, time1}} - \text{TTR}_{18:1 \text{ cis-11, time0}}}{\text{MPE}_{16:1} \times (\text{time1} - \text{time0})}.$$

Experiment 2

The objective of this experiment was to determine if palmitoleic acid or an elongation product was responsible for changes in lipogenesis. Therefore, we treated adipocytes cultures with 0 μM fatty acids (control) or 150 μM palmitic (16:0), 150 μM palmitoleic, or 150 μM *cis*-vaccenic acids on day 2–6. FAME were prepared from cultures on day 6 as stated above for analysis with an Agilent 6850 GC equipped with an Agilent 7673A automatic sampler. Separations were accomplished using a 100m Supelco SP-2560 (Supelco, Inc., Bellefonte, PA, USA) capillary column (0.25 mm i.d. and 0.20 μm film thickness) according to Duckett et al. [15]. Individual fatty acids were identified by comparison of retention times with standards (Sigma, St. Louis, MO, USA; Matreya, Pleasant Gap, PA, USA). Fatty acids were quantified by incorporating an internal standard, methyl tricosanoic (23:0) acid, into each sample during methylation and expressed as a weight percentage of total fatty acids per well.

Lipogenesis

To measure lipogenesis *in vitro*, we substituted unlabeled acetate in the culture media on day 6 with stable isotope labeled acetate [10 mM ($1\text{-}^{13}\text{C}$)₂] to cultures treated with 0 μM fatty acids (control), 150 μM palmitoleic, or 150 μM *cis*-vaccenic acid for 0, 12, 24, and 36 h. Cells were harvested and FAME prepared as described above. Ions of mass-to-charge ratio (m/z) 270 (m), 271 ($m + 1$), and 272 ($m + 2$) were selectively measured to calculate the isotopic enrichments of 16:0, the primary product of *de novo* lipogenesis.

The formation of a fatty acid polymer, 16:0, from repeating units of acetate is an ideal application of mass isotopomer distribution analysis (MIDA) [14]. Therefore, we used this approach to estimate enrichment in our precursor pool and calculate FSR of lipogenesis. First, we calculated RA of singly ($m + 1$) and doubly ($m + 2$) labeled 16:0 to unlabeled (m) 16:0 isotopomers. To account for background noise and natural abundance of ^{13}C isotope when using a singly-labeled tracer, the enrichment of 16:0 was calculated as $\text{TTR}_{16:0} = (\text{RA}_{\text{sample}} - \text{RA}_{\text{blank}}) \times (1 - A)^N$, where

A was the natural abundance of ^{13}C , $A = 0.011$, and N was the number of C in the fatty acid molecule, $N = 16$ [14]. Samples that were not exposed to labeled isotope served as ‘blanks’. Precursor enrichment in MPE was estimated by:

$$\text{MPE}_{\text{precursor}} = \frac{2 \times (\text{TTR}_{(m+2)}/\text{TTR}_{(m+1)})}{(p - 1) + (2 \times (\text{TTR}_{(m+2)}/\text{TTR}_{(m+1)})}$$

where, p is the number of precursor monomers present in the polymer, $p = 8$. Finally, our estimate of lipogenesis could be derived by calculating FSR [14].

$$\text{FSR}_{\text{lipogenesis}} = \frac{\text{TTR}_{16:0, \text{time1}} - \text{TTR}_{16:0, \text{time0}}}{(p \times \text{MPE}_{\text{precursor}}) (1 - \text{MPE}_{\text{precursor}})^{p-1} (\text{time1} - \text{time0})}.$$

Desaturation

Stearoyl-CoA desaturase 1 (SCD1) is the enzyme responsible for creating a double bond at the Δ^9 position of several fatty-acyl CoA and its preferred substrates are 16:0 and 18:0 [16]. Its transcription and activity can be regulated by certain fatty acids [17], including palmitoleic acid [7]. In order to measure desaturation rates *in vitro*, we added 100 μM [$U\text{-}^{13}\text{C}$]18:0 to cultures treated with 0 μM fatty acid (control) or 150 μM palmitic, palmitoleic, or *cis*-vaccenic acid on day 6 for 0, 12, and 24 h. Samples were prepared and analyzed as described above for analysis with GC–MS. Ions of mass-to-charge ratio (m/z) 298 (m) and 316 ($m + 18$) were selectively measured to calculate the isotopic enrichments of 18:0. Similarly, isotope abundance of 296 (m) and 314 ($m + 18$) was measured for 18:1 *cis*-9. Since tracer enrichment can be measured in this case and the product of the SCD reaction is not a polymer of the tracer, it was not necessary to use MIDA. The FSR was calculated for rate of desaturation using the precursor enrichment, $\text{MPE}_{18:0}$.

$$\text{FSR}_{\text{desaturation}} = \frac{\text{TTR}_{18:1 \text{ cis-9, time1}} - \text{TTR}_{18:1 \text{ cis-9, time0}}}{\text{MPE}_{18:0} \times (\text{time1} - \text{time0})}.$$

Gene Expression

Total cellular RNA was isolated from cells using the *mir*-Vana microRNA Isolation kit (Ambion, Austin, TX, USA) according to the manufacturer’s instructions and RNA quality as described by Duckett et al. [18]. Quality was assessed using a Nanodrop 2000 Spectrophotometer (Thermo Fisher Scientific, Inc., Waltham, MA, USA) and Agilent Bioanalyzer 2100. All tcRNA samples used in real-time PCR had a 260:280 absorbance ratio >1.9 on the Nanodrop and RNA integrity number >9.0 (1.0–10.0 scale) using Agilent RNA 6000 Nano kit. Superscript III reverse transcriptase (Invitrogen Corp., Carlsbad, CA, USA) was used to synthesize first strand cDNA. Real-time PCR was

conducted using an Eppendorf MasterCycler ep realplex (Westbury, NY, USA) with the QuantiTect SYBR Green RT-PCR Two Step Kit (Qiagen, Valencia, CA, USA) according to the manufacturer's directions. Two genes, glyceraldehyde-3-phosphate dehydrogenase (GAPDH) and β -actin, were evaluated as housekeeping genes for data normalization [18]. To determine the appropriate housekeeping gene to be used to normalize the data, the cycle threshold values (C_T) for GAPDH, β -actin, and all target genes per sample were entered into the BESTKEEPER program (<http://www.gene-quantification.info>). The program determines the most stable housekeeping gene to be used for normalization by repeated pair-wise correlation and regression analysis [19]. Both GAPDH and β -actin exhibited a correlation coefficient of 0.99 ($P < 0.001$) in the analysis and were suitable for data normalization. Primers for bovine mRNA were designed using Primer 3 software (<http://www.frodo.wi.mit.edu/primer3/>). Genes of interest for this study were those involved in fatty acid biosynthesis including acetyl-CoA carboxylase (ACC), fatty acid synthase (FASN), fatty acid elongase (ELOVL) -5 and -6, SCD1, sterol regulatory element binding protein-1c (SREBP), and carnitine palmitoyl-transferase 1A (CPT1A). Primer sets were first evaluated according to Duckett et al. [18], with the exceptions of ELOVL5 (forward: 5'-gtcatctggccgtgtacctt-3'; reverse: 5'-gggaagaaaagctgctgatg-3'), ELOVL6 (forward: 5'-ggaagcaacgaagctgac-3'; reverse: 5'-tggtgtgtgtgttctcat-3'), and CPT1A (forward: 5'-gtgatgctgacctgtacgc-3'; reverse: 5'-agcagcacctcagggagta-3').

Statistical Analysis

The data were analyzed using Proc GLM procedure of SAS 9.2 (SAS Institute Inc., Cary, NC, USA) for treatment comparisons over time. For Experiment 1, an analysis of variance (ANOVA) was performed as a completely randomized design with factor time (0, 6, 12, 24, and 36 h). For Experiment 2, a two-way ANOVA was performed as a completely randomized design with factors fatty acid (control, palmitic, palmitoleic, and *cis*-vaccenic), time (0, 12, 24, and 36 h), and two-way interaction. Least squares means were computed and separated statistically using Fisher's protected LSD test. For the analysis of relative gene expression, all C_T values for each sample/primer pair combination and the respective primer efficiency were analyzed using the REST-2009 program (<http://www.gene-quantification.de/rest-2009.html>; [19]) and the data were normalized using GAPDH. This software calculates relative gene expression using Pair-wise Fixed Reallocation Randomization Test and relative expression determined at the 95 % confidence interval.

Results

Experiment 1

Incubating bovine adipocytes with [U - ^{13}C] 16:1 resulted in enrichment ($P < 0.001$) of 16:1 and 18:1 *cis*-11 fatty acids over time. TTR of 16:1 was greater than 0 ($P < 0.01$) 6 h after [U - ^{13}C] 16:1 addition to the media and remained elevated ($P < 0.01$) to 36 h (Fig. 1). Enrichment of 18:1 *cis*-11 as TTR was also greater than 0 ($P < 0.05$) by 6 h and continued to increase ($P < 0.01$) above 6 h levels at 24 and 36 h. The $FSR_{elongation}$ increased ($P < 0.05$) over the 36 h period (Fig. 1).

In addition to label appearing in 16:1 and 18:1 *cis*-11 fatty acids following incubation with [U - ^{13}C] 16:1, enrichment was also seen in 20:1 *cis*-13 and *cis*-9, *cis*-11 CLA after concentrating the samples. These 20:1 *cis*-13 and *cis*-9, *cis*-11 CLA were present at very low levels in our samples ($<1.0/100$ g total fatty acids). Fatty acid peaks contained masses consistent with $m + 16$ enrichment from [U - ^{13}C] 16:1. Enrichment of 20:1 *cis*-13 was present at 24 and 36 h with TTR of 0.15 and 0.20, respectively. Enrichment of *cis*-9, *cis*-11 CLA was present at 24 and 36 h with TTR of 0.42 and 0.55 respectively.

Experiment 2

Comparing fatty acid data between control, palmitic, palmitoleic, and *cis*-vaccenic acid-treated cells, there was a main effect of fatty acid treatment ($P < 0.01$) for total fatty acids (Table 1). Micrograms of total fatty acids were greatest ($P < 0.001$) in palmitoleic and *cis*-vaccenic acid-treated cells at about $2\times$ greater than control cells (Table 1). Palmitic acid-treated cells also had higher ($P < 0.05$) levels of total fatty acids compared with controls, but lower ($P < 0.05$) than palmitoleic and *cis*-vaccenic acid-treated cells, despite being supplemented at the same level.

Palmitic acid-treated cells had increased ($P < 0.05$) levels of 16:0, 18:0, 18:1 *cis*-9, and 18:2n-6 compared with all other treatment groups (Table 1). Palmitoleic acid-treated cells had increased ($P < 0.05$) levels of 16:1 compared with all other treatment groups. In addition, palmitoleic acid cells had increased ($P < 0.05$) levels of 18:1 *cis*-11 and 20:1 *cis*-13 compared with controls, consistent with results from our previous work [7]. *cis*-Vaccenic acid-supplemented cells had slightly elevated ($P < 0.05$) 16:1 compared with controls, but were not different ($P > 0.05$) than palmitic acid-treated cells. Also, *cis*-vaccenic acid-supplemented cells had the greatest ($P < 0.05$) amount of 18:1 *cis*-11 and 20:1 *cis*-13 compared with all other treatment groups. Palmitoleic and *cis*-

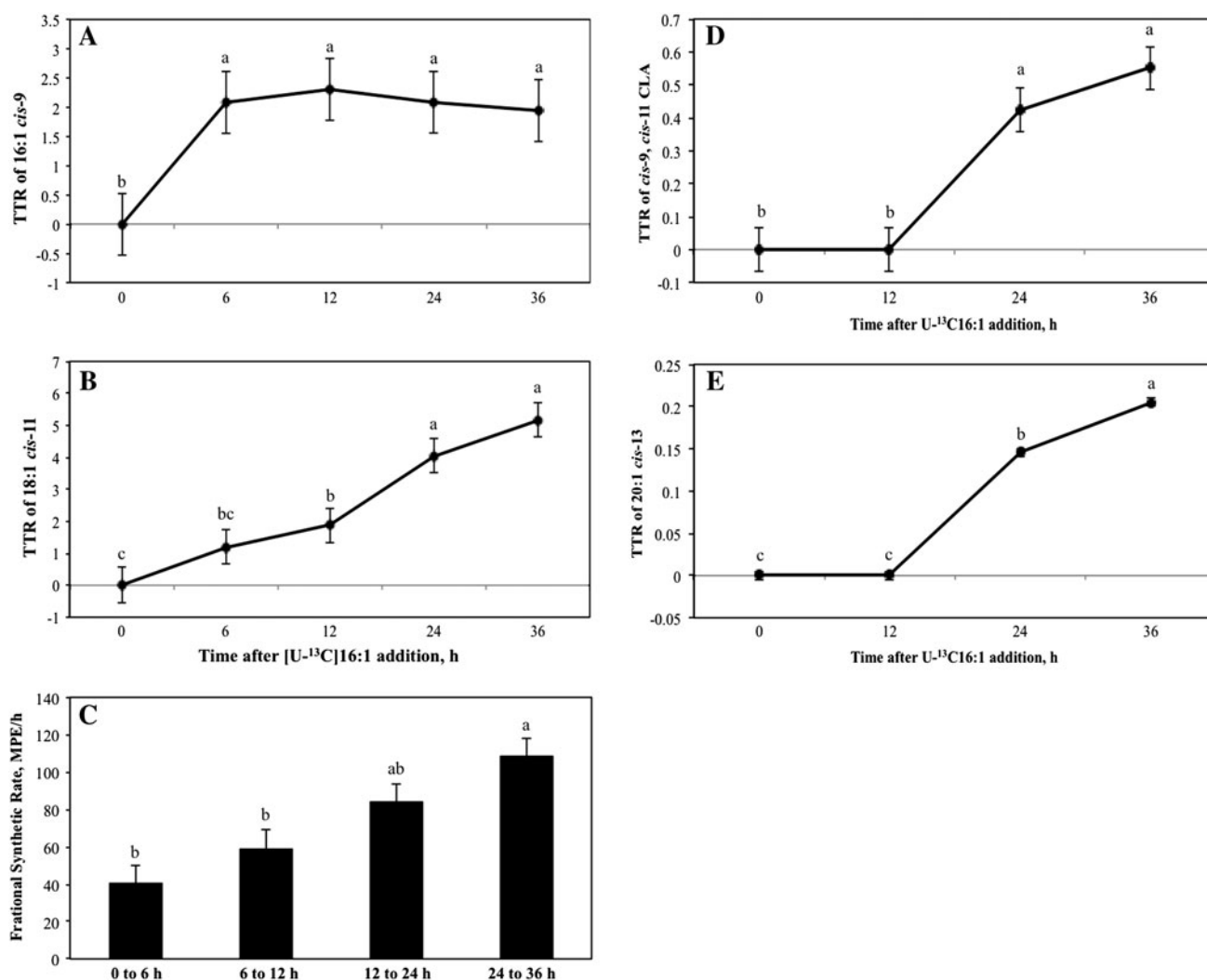


Fig. 1 Elongation of 16:1 to 18:1 *cis*-11 in bovine adipocyte cultures. **a** Main effect of time on tracer-to-tracee ratio (TTR) of 16:1 following 150 μ M [13 C]16:1 addition to the media at 0 h. **b** Enrichment of 18:1 *cis*-11 displayed as TTR over time in cells. **c** Fractional synthetic rate of [13 C]18:1 *cis*-11 from [13 C]16:1 displayed as molar percent excess (MPE) per h and was calculated

over a 36 h period following stable isotope administration. **d** Enrichment of [13 C] 18:2 *cis*-9, *cis*-11 displayed as TTR over time in cells. **e** Enrichment of [13 C] 20:1 *cis*-13 displayed as TTR over time in cells. ($n = 4$, mean \pm SEM). ^{a-c}Time points without a common letter differed ($P < 0.01$)

vaccenic acid-treated cells had the lowest ($P < 0.05$) levels of 18:1 *cis*-9 and 18:2n-6 fatty acids. In addition, C20:4n-6 tended ($P = 0.07$) to be lower in both MUFA-treatment groups compared with controls.

Despite low levels of 18:1 *cis*-9 in both MUFA-treated groups, the desaturation index of 18:1 *cis*-9/18:0 was reduced ($P < 0.05$) in palmitoleic acid treated cells only compared with all other treatment groups (Table 1). The desaturation index of 18:1 *cis*-9/18:0 indicates desaturase activity was only impacted by palmitoleic acid supplementation, not *cis*-vaccenic acid.

Lipogenesis: precursor enrichment, $MPE_{acetate}$, did not change ($P > 0.05$) over time or due to treatment in our cultures using MIDA, nor was there a time by treatment

interaction (Fig. 2), suggesting we had isotopic steady state in our cultures [20]. There was an interaction ($P < 0.01$) between fatty acid treatment and length of [13 C] 2 incubation on 16:0 enrichment. The $TTR_{16:0}$ did not differ ($P > 0.05$) between treatment groups at 0 or 12 h and increased ($P < 0.05$) in all groups over time. At 24 and 36 h time points, $TTR_{16:0}$ was decreased ($P < 0.05$) in palmitic, palmitoleic, and *cis*-vaccenic acid-treated cells compared with controls. The $FSR_{lipogenesis}$, calculated from $MPE_{precursor}$ and $TTR_{16:0}$, also shows a reduction in lipogenesis in palmitic, palmitoleic, and *cis*-vaccenic acid-treated cells. The $FSR_{lipogenesis}$ was decreased ($P < 0.05$) in palmitoleic acid-treated cells between 0 and 12 h and decreased ($P < 0.01$) in all fatty acid-treated cells

Table 1 Fatty acid composition of bovine adipocyte cultures treated with 0 μM fatty acids (control), 150 μM palmitic, palmitoleic, or *cis*-vaccenic acid ($n = 4$)

Fatty acid ($\mu\text{g}/\text{well}$)	Control	150 μM			SEM	<i>P</i> value
		Palmitic	Palmitoleic	<i>cis</i> -vaccenic		
16:0	8.99 ^{cd}	17.6 ^a	10.4 ^{bc}	8.53 ^d	0.49	0.001
16:1 <i>cis</i> -9	0.55 ^c	1.55 ^{bc}	31.9 ^a	2.80 ^b	2.3	<0.0001
18:0	10.2 ^b	12.1 ^a	9.74 ^b	7.24 ^c	0.32	0.002
18:1 <i>cis</i> -9	11.4 ^b	13.2 ^a	8.15 ^c	8.18 ^c	0.35	0.001
18:1 <i>cis</i> -11	3.27 ^c	3.94 ^c	41.6 ^b	70.4 ^a	2.7	0.005
18:2n-6	1.76 ^b	1.93 ^a	1.48 ^c	1.54 ^c	0.04	<0.0001
20:1 <i>cis</i> -13	ND ^c	0.15 ^c	3.29 ^b	3.95 ^a	0.11	<0.0001
20:4n-6	6.42	6.65	6.11	5.84	0.15	0.07
Total fatty acids	67.0 ^c	90.0 ^b	145 ^a	140 ^a	4.6	0.001
16:1/16:0	0.06 ^c	0.09 ^c	3.05 ^a	0.33 ^b	0.06	<0.0001
18:1 <i>cis</i> -9/18:0	1.12 ^a	1.09 ^a	0.84 ^b	1.13 ^a	0.03	0.009

ND fatty acid not detectable

^{a–d} Within a row, means without a common superscript differ ($P < 0.05$)

compared with controls between the 12–24 and 24–36 h time points (Fig. 2).

Desaturation: because the desaturation index of 18:1 *cis*-9/18:0 is not always representative of SCD1 activity [21], we supplemented a labeled substrate of the SCD1 reaction [$U-^{13}\text{C}$]18:0 to our bovine adipocyte cultures to serve as a measurement of desaturase activity. There was a treatment by length of incubation interaction for precursor enrichment, $\text{TTR}_{18:0}$. Enrichment of 18:0 was not different ($P > 0.05$) than 0 at 0 h, but $\text{TTR}_{18:0}$ increased ($P < 0.05$) over time for each sample. However, there was a differential incorporation of labeled [$U-^{13}\text{C}$] 18:0 into the different treatment groups. Cells treated with palmitoleic and *cis*-vaccenic acids had increased ($P < 0.01$) $\text{TTR}_{18:0}$ compared with control and palmitic acid-treated cells (Fig. 3). There was also a treatment by incubation time interaction ($P < 0.01$) for $\text{TTR}_{18:1\text{cis-9}}$. At 0 h, there was no enrichment ($P > 0.05$) of 18:1 *cis*-9 in any treatment group; by 12 h, $\text{TTR}_{18:1\text{cis-9}}$ of palmitoleic acid-treated cells was lower ($P < 0.01$) than all other treatment groups and was not different ($P > 0.05$) than 0. Control, palmitic, and *cis*-vaccenic acid-treated cells did not differ ($P > 0.05$) from each other and were enriched ($P < 0.05$) with 18:1 *cis*-9 at 12 h. By 24 h, all treatment groups had enrichment ($P < 0.05$) of 18:1 *cis*-9 and differed ($P < 0.05$) from each other. Palmitoleic acid-treated cells had reduced ($P < 0.01$) $\text{TTR}_{18:1\text{cis-9}}$ compared to controls, palmitic, and *cis*-vaccenic acid treated cells at 12 and 24 h. Palmitic and *cis*-vaccenic acid-treated cells had higher ($P < 0.05$) $\text{TTR}_{18:1\text{cis-9}}$ at 24 h than controls, which were also higher ($P < 0.05$) than palmitoleic acid-treated cells. Despite increased $\text{TTR}_{18:0}$ in both palmitoleic and *cis*-vaccenic acid-treated cells, only palmitoleic acid-treated cells

showed less ($P < 0.05$) formation of the desaturase product, as $\text{TTR}_{18:1\text{cis-9}}$, than control cells.

The $\text{FSR}_{\text{desaturation}}$ over 0–12 h was decreased ($P < 0.01$) in palmitoleic acid-treated cells compared with all other treatment groups, which did not differ ($P > 0.05$) from each other (Fig. 3). *cis*-Vaccenic acid-treated cells tended ($P = 0.052$) to have a reduced $\text{FSR}_{\text{desaturation}}$ from 0 to 12 h compared with controls. From 12 to 24 h, however, all treatment groups had a different $\text{FSR}_{\text{desaturation}}$. Palmitic acid-treated cells had the highest ($P < 0.01$) rate of desaturation and palmitoleic acid-treated cells had the lowest ($P < 0.01$) $\text{FSR}_{\text{desaturation}}$ from 12 to 24 h (Fig. 3).

Gene expression: palmitic acid supplementation down-regulated ($P < 0.05$) expression of SREBP and up-regulated ($P < 0.05$) CPT-1a mRNA expression (Fig. 4). Palmitoleic acid supplementation down-regulated ($P < 0.05$) FASN, SCD-1, and ELOVL6 mRNA expression and up-regulated ($P < 0.05$) ACC and CPT-1a mRNA expression compared with controls. *cis*-vaccenic acid supplementation up-regulated ($P < 0.05$) ACC and CPT-1a mRNA expression and down-regulated ($P < 0.05$) FASN and ELOVL6 mRNA expression compare to controls.

Discussion

Our previous work with palmitoleic acid supplementation in bovine adipocyte cultures resulted in a large increase in 18:1 *cis*-11 concentration within the cells [7]. Enrichment of 16:1 shortly after [$U-^{13}\text{C}$] 16:1 addition to the media shows that there was rapid incorporation of palmitoleic acid into the adipocytes on day 6. In addition, the enrichment of 18:1 *cis*-11, as shown by $\text{TTR}_{18:1\text{cis-11}}$, confirmed

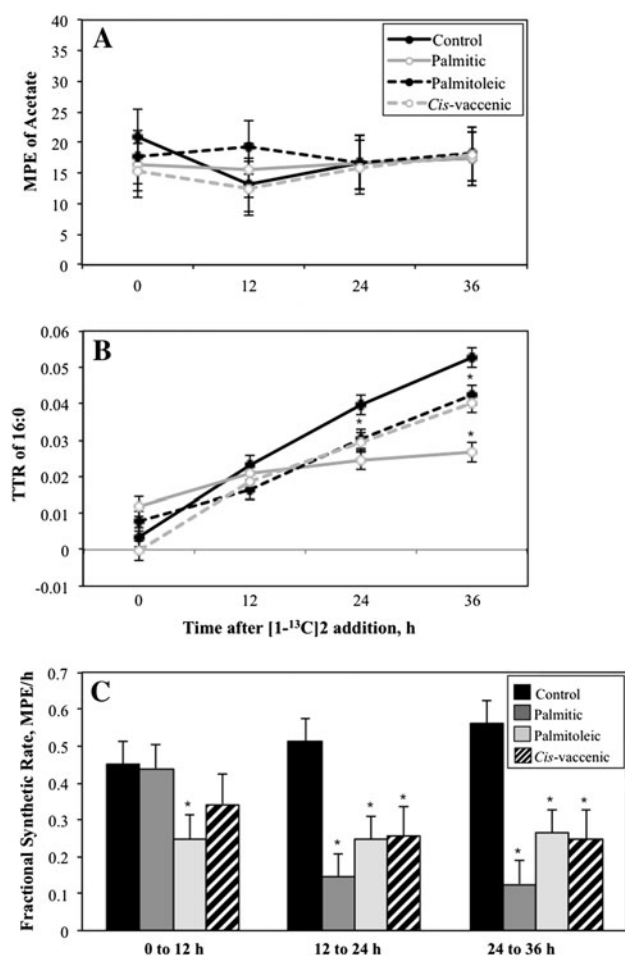


Fig. 2 Lipogenesis in bovine adipocyte cultures treated with 0 μM fatty acid (control), 150 μM palmitoleic, or 150 μM *cis*-vaccenic acid. **a** Estimation of molar percent excess (MPE) of acetate after [^{13}C] 2 addition to the media. **b** Enrichment of 16:0 displayed as tracer-to-tracee ratio of 16:0 over time. **c** Fractional synthetic rate of [^{13}C] 16:0 from [^{13}C] 2 displayed as molar percent excess (MPE) per h calculated over a 36 h period following stable isotope administration. ($n = 4$, mean \pm SEM). Asterisk indicates within a time point, fatty acid-treated cells differed ($P < 0.05$) from controls

18:1 *cis*-11 as a direct elongation product of 16:1. Presence of [^{13}C] tracer in 18:1 *cis*-11 fatty acids definitively shows that palmitoleic acid is taken in by bovine adipocytes and elongated to 18:1 *cis*-11 in vitro. Originally isolated from horse brain [22] and later in intestinal bacteria [23] and a host of mammalian tissues [24], *cis*-vaccenic acid is a MUFA. It can be derived from the diet or biosynthetic pathways, but its role in metabolism is largely unknown. Elongase enzymes generally have chain-length and saturated bond specificity for their fatty acids substrates [25]. The conversion of 16:1 to 18:1 *cis*-11 is generally attributed to the ELOVL6 isoform of the mammalian elongase enzyme, which adds an acetate molecule to the carboxylic acid end of the fatty acyl chain. Mice deficient in ELOVL6 show increased levels of 16:0 and 16:1 *cis*-9 and reduced

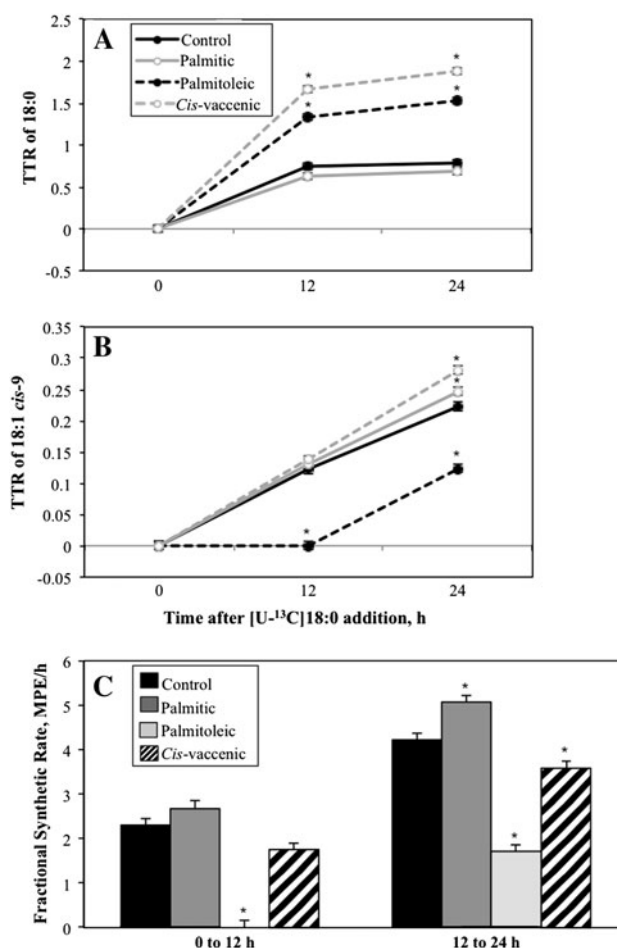


Fig. 3 Desaturation of 18:0 to 18:1 *cis*-9 in bovine adipocyte cultures treated with 0 μM fatty acids (control), 150 μM palmitic, 150 μM palmitoleic, or 150 μM *cis*-vaccenic acid. **a** Tracer-to-tracee ratio (TTR) of 18:0 and **b** 18:1 *cis*-9 displayed over time following 100 μM [^{13}C] 18:0 addition to the media. **c** Fractional synthetic rate of [^{13}C] 18:1 *cis*-9 from [^{13}C] 18:0 displayed as molar percent excess (MPE) per h calculated over a 24 h period following stable isotope administration. ($n = 4$, mean \pm SEM). Asterisk indicates within a time point, fatty acid-treated cells differed ($P < 0.05$) from controls

18:0, 18:1 *cis*-9, 18:1 *cis*-11, and other long chain fatty acids [11]. However, previous work in our lab suggests that ELOVL6 mRNA is down-regulated in response to palmitoleic acid supplementation despite an obvious increase in the ELOVL6 reaction product 18:1 *cis*-11 [7]. This is the first conclusive study in bovine adipocytes that provides proof of 18:1 *cis*-11 elongation from 16:1 *cis*-9. In addition, 18:1 *cis*-11 subsequent elongation to 20:1 *cis*-13 and desaturation to *cis*-9, *cis*-11 CLA have not been reported to date.

We successfully incorporated our fatty acid supplements into bovine adipocyte cultures based on detection of increased levels ($P < 0.01$) of treatment fatty acids in cells after all media had been removed. Reduced total fatty acids in palmitic acid-treated cells compared with MUFA-treated

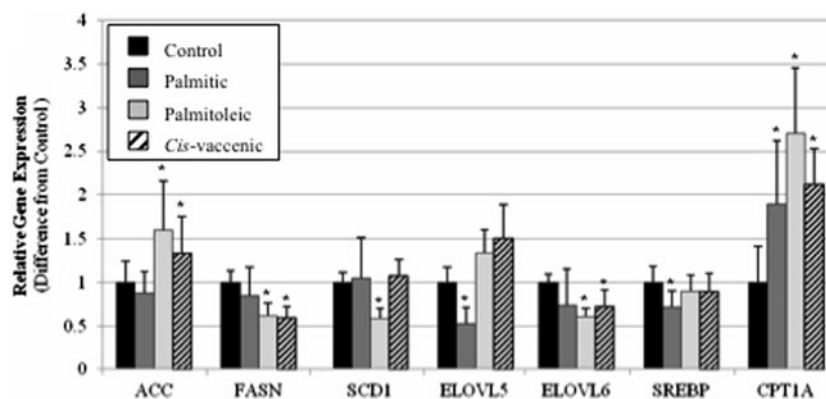


Fig. 4 Relative gene expression of bovine adipocytes supplemented with 0 μ M fatty acids (control), 150 μ M palmitic, 150 μ M palmitoleic or 150 μ M *cis*-vaccenic acid. **a** Expression of sterol response element binding protein-1c (SREBP), fatty acid synthase (FASN), stearoyl-CoA desaturase 1 (SCD1), and **b** Acetyl-CoA carboxylase (ACC), fatty acid elongase (ELOVL) 5 and 6, and carnitine-palmitoyl

transferase 1A (CPT1A), genes associated with fatty acid biosynthesis and metabolism pathways. All C_T values were normalized to glyceraldehyde-3-phosphate dehydrogenase (GAPDH) ($n = 4$). Asterisk indicates gene expression for this treatment differed ($P < 0.05$) from controls

cells may be due to an apoptotic effect of palmitic acid supplementation. In murine adipocytes, palmitic acid induces endoplasmic reticulum stress and apoptosis at 100, 250, and 500 μ M treatment levels [26]. Similarly, we suspected that palmitic acid-supplementation in our bovine adipocyte cultures induced apoptosis, resulting in reduced total lipid accumulation and treatment fatty acid inclusion compared with MUFA-supplemented cells. To test this hypothesis, we treated differentiated adipocytes with palmitic and palmitoleic acid to day 6 and assayed cell viability using the Cell Counting Kit-8 (Dojindo Molecular Technologies, Inc., Rockville, MD, USA) according to manufacturer's instructions. Relative cell viability was greater ($P < 0.05$) for palmitoleic acid-treated cells and controls compared with palmitic acid-treated cells (data not shown). Despite a reduction in cell viability, palmitic acid-treated cells had the greatest levels of 18:0 and 18:1 *cis*-9, which may indicate increased conversion of 16:0 into products with less lipotoxic properties.

Reduced lipogenesis in palmitoleic acid-treated cultures is consistent with our previous results when we supplemented 150 μ M palmitoleic acid, which resulted in approximately 45 % reduction in lipogenesis between 0 and 24 h [7]. In the current study, both MUFA induced a repressive effect on lipogenesis of the same magnitude from 12 to 24 h at approximately 50 %. Therefore, this effect of palmitoleic acid supplementation on lipogenesis cannot be solely attributed to palmitoleic acid as its elongated form, *cis*-vaccenic acid, also displayed anti-lipogenic effects. Palmitic acid-treated cultures also showed a reduction in lipogenesis, but this effect is most likely related to cell viability in palmitic acid-treated cultures discussed previously. The genes that primarily involved in de novo lipogenesis are ACC and FASN. The gene

expression results from these two genes are seemingly contradictory as MUFA treatments increase ACC mRNA and decrease FASN mRNA. However, ACC activity can also be regulated allosterically and through phosphorylation. Regulated by the transcription factor SREBP, FASN gene expression was reduced by approximately 40 % in MUFA treatments, similar to $FSR_{lipogenesis}$ results.

The isotopic measure of SCD1 activity, $FSR_{desaturation}$, showed a more dramatic effect of fatty acid supplementation on desaturase activity than the 18:1 *cis*-9/18:0 desaturation index results. The reduction in desaturase activity due to palmitoleic acid was approximately 100 % from 0 to 12 h and approximately 60 % from 12 to 24 h. By contrast, palmitoleic acid reduced the desaturation index by less than 25 % compared with controls (Table 1). The $FSR_{desaturation}$ also showed a reduction in SCD1 activity by approximately 15 % from 12 to 24 h due to *cis*-vaccenic acid (Fig. 3), whereas the desaturation index for *cis*-vaccenic acid-treated cells was not different from controls. Therefore, the $FSR_{desaturation}$ is a more sensitive measurement of SCD1 activity than the 18:1 *cis*-9/18:0 desaturation index when fatty acids are supplemented to adipocyte cultures.

Transcription of SCD1 mRNA is controlled primarily by SREBP, which binds to the sterol response element in the promoter region of the SCD1 gene [27, 28]. The promoter region of the bovine SCD1 gene contains a fat specific element, PUFA response element, and SREBP-response region [29]. In addition to PUFA, expression of SCD1 is also regulated by its products and not by the availability of its substrates [29]. For instance, the addition of 18:1 *cis*-9 and *cis*-9, *trans*-11 CLA reduced SCD promoter activity, but 18:1 *trans*-11 did not [29]. In this study, palmitoleic acid impacts SCD1 activity based on both the $FSR_{desaturase}$ and desaturase index in addition to

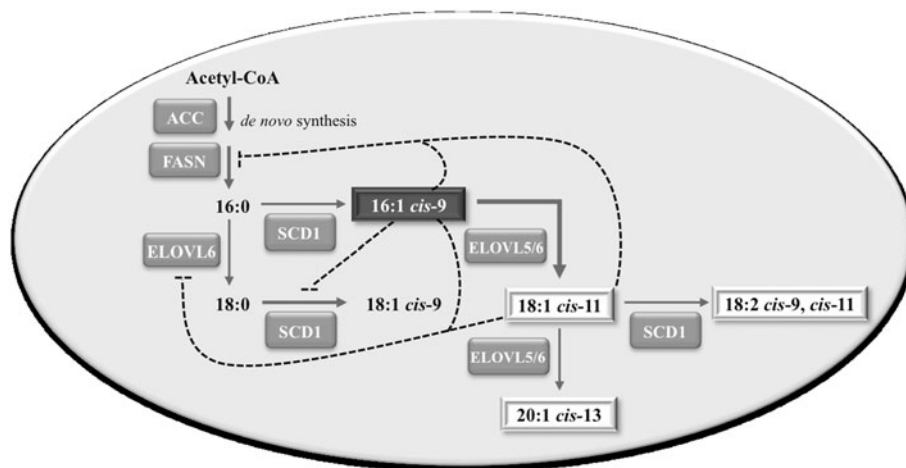
gene expression; whereas, *cis*-vaccenic acid induces a minimal response in rate of desaturation with no effect on the desaturation index or gene expression. In addition, palmitic acid increases the rate of desaturation with no effect on the desaturation index.

Several elongase enzymes are present in mammalian cells and are responsible for adding acetyl-CoA molecules to the carboxylic acid end of a fatty acid hydrocarbon skeleton. Seven elongases have been identified and given the designation of ELOVL for elongation of very long fatty acids (ELOVL 1–7; 30). Elongases can be divided into two groups based on substrate preference: (a) elongation of saturated and monounsaturated fatty acids (ELOVL1, 3, and 6) and (b) elongation of polyunsaturated fatty acids (ELOVL2, 4, 5, and 7; 30, 31). ELOVL1 appears to play a role in elongation of very long chain saturated fatty acids (up to 26C) for sphingolipid formation and maintenance of membrane integrity [30]. ELOVL1 is expressed in lung, brain, kidney and heart but barely detectable in live, brown adipose tissue, and skin [32]. ELOVL2 has been shown to elongate arachidonic acid and long-chain (20C or greater) omega-3 fatty acids in transfected yeast and mammalian cells but no activity was demonstrated for saturated or monounsaturated fatty acids [31]. Expression of ELOVL3 was only detected in skin [32]; however, others have reported strong correlations with ELOVL3 and brown adipose tissues [31]. ELOVL4 is specifically expressed in human retina where it is believed to have a role in elongation of docosahexaenoic (C22:6) acid [31, 32]. ELOVL5 is involved in the elongation of PUFA 18–20C but cannot elongate beyond 22C [31]. ELOVL5 expression is detected all tissues [32]. ELOVL6 is responsible for the elongation of saturated fatty acids 12–16C to 18C and cannot elongate beyond 18C. ELOVL6 is ubiquitously expressed, especially in tissues with high lipid levels like adipose tissue, liver and brain [31, 32]. ELOVL7 exhibits activity for

acyl-CoAs of 16–20C with highest activity for 18:3n-3 and 18:3n-6 [33].

In this study, supplementation of palmitoleic acid to adipocyte cultures resulted in increased levels of 18:1 *cis*-11 and also 20:1 *cis*-13 to a more limited extent. Likewise, supplementation of C18:1 *cis*-11 to adipocyte cultures increased levels of C20:1 *cis*-13. As FASN is not capable of synthesizing fatty acids greater than 16C in length, acetate molecules were most likely added to 16:1 *cis*-9 by an elongase. Others [11] have proposed that 16:1 *cis*-9 can be elongated into 18:1 *cis*-11 and potentially elongated further into a 20C fatty acid, 20:1 *cis*-13, but this study is the first to confirm this pathway through the use of stable isotope technology. Elongation of MUFA is reportedly carried out by ELOVL6 but ELOVL5 has been reported to also have some activity for this reaction as well, especially in the absence of ELOVL6 [34]. Green et al. [34] proposed that ELOVL6 preferentially elongates C16 to C18, which then can be further desaturated to C18:1 *cis*-9, and that ELOVL5 preferentially elongates C16:1 *cis*-9 to C18:1 *cis*-11 based on knockdown and overexpression studies in rat insulinoma cell lines (INS-1). These authors propose a coordinated regulation of the elongases in order to balance the levels of C16:1 *cis*-9, C18:1 *cis*-11 and C18:1 *cis*-9 in the cell. Due to increased fatty acid elongation products (18:1 *cis*-11 and 20:1 *cis*-13) observed in our study, we know elongation occurs in palmitoleic and *cis*-vaccenic acid-treated cultures. However, mRNA expression of ELOVL6 was reduced in both palmitoleic and *cis*-11 vaccenic acid supplemented cells compared to controls; whereas ELOVL5 mRNA expression was not altered with MUFA supplementation. Transcription factors that regulate elongases include SREBP-1c for ELOVL6 [35] and peroxisome proliferator-activated receptor- α (PPAR α) for both ELOVL5 and 6 [36]. Our results would indicate that transcription levels may not be directly related to enzyme

Fig. 5 Proposed fatty acid metabolism and biosynthesis pathways in bovine adipocytes supplemented with palmitoleic acid (16:1 *cis*-9). Dotted lines depict inhibitory effects



activity and that further research is needed to examine regulation of elongases in adipocytes.

Carnitine palmitoyl-transferase 1A is responsible for transporting long chain fatty acids through the outer mitochondrial membrane for the purpose of β -oxidation in the mitochondrial matrix. In ruminants, CPT1A is expressed in numerous tissues including adipose tissue in contrast to a more restricted tissue abundance in monogastrics [37]. Inhibition of CPT1A is primarily attributed to malonyl-CoA, the product of the ACC reaction, in monogastric species [38]. Price et al. [37] found N-terminal sequence differences in ovine CPT1 that alter enzyme kinetics for certain substrates, which differs from that of the rat. All fatty acid treatments in this study resulted in increased CPT1A mRNA, which may lead to increase β -oxidation and ATP production.

In this study, we confirmed 18:1 *cis*-11 and 20:1 *cis*-13 as products of palmitoleic acid elongation in vitro and that *cis*-9, *cis*-11 CLA can also be produced through elongation and desaturation of palmitoleic acid. Supplementation of palmitoleic and *cis*-vaccenic acids reduces lipogenesis and FASN gene expression. However, palmitoleic acid is largely responsible for reducing SCD1 gene expression and desaturation activity with *cis*-vaccenic acid contributing a slight reduction in SCD1 activity. A schematic representation of fatty acid biosynthesis and regulation is depicted in Fig. 5. Overall, palmitoleic acid supplementation is directly responsible for decreased desaturation and jointly responsible, with its elongation products, for reduced lipogenesis. However, more research is still needed to determine the mode of action and potential application of these fatty acids to modulate lipogenesis in vivo.

Acknowledgments Technical contribution No. 6011 of the Clemson University Exp. Stn. This project was funded in part by USDA-NIFA grant award 2010-38942-20745.

References

- McGillis JP (2005) White adipose tissue, inert no more! *Endocrinology* 146(5):2154–2156
- Flier JS (1998) What's in a name? in search of leptin's physiologic role. *J Clin Endocrinol Metab* 83(5):1407–1413
- MacDougald OA, Burant CF (2007) The rapidly expanding family of adipokines. *Cell Metab* 6(3):159–161
- Cao H, Gerhold K, Mayers JR, Wiest MM, Watkins SM, Hotamisligil GS (2008) Identification of a lipokine, a lipid hormone linking adipose tissue to systemic metabolism. *Cell* 134(6):933–944
- Gong J, Campos H, McGarvey S, Wu Z, Goldberg R, Baylin A (2010) Adipose tissue palmitoleic acid and obesity in humans: does it behave as a lipokine? *Am J Clin Nutr* 93(1):186–191
- Okada T, Furuhashi N, Kuromori Y, Miyashita M, Iwata F, Harada K (2005) Plasma palmitoleic acid content and obesity in children. *Am J Clin Nutr* 82(4):747–750
- Burns TA, Duckett SK, Pratt SL, and Jenkins TC (2012) Supplemental palmitoleic (C16:1 *cis*-9) acid reduces lipogenesis and desaturation in bovine adipocyte cultures. *J Anim Sci* (Epub ahead of print)
- Hirai S, Matsumoto H, Hino N, Kawachi H, Matsui T, Yano H (2007) Myostatin inhibits differentiation of bovine preadipocyte. *Domest Anim Endocrinol* 32(1):1–14
- Pratt SL, Burns TA, Curry E, Duckett SK (2010) Expression of microRNA during bovine adipogenesis. *J Nuc Acids Invest* 1(e12):62–70
- Van Harken DR, Dixon CW, Heimberg M (1969) Hepatic lipid metabolism in experimental diabetes. *J Biol Chem* 244(9):2278–2285
- Matsuzaka T, Shimano H (2009) Elovl6: a new player in fatty acid metabolism and insulin sensitivity. *J Mol Med* 87(4):379–384
- Folch J, Lees M, Stanley GHS (1957) A simple method for the isolation and purification of total lipides from animal tissues. *J Biol Chem* 226(1):497–509
- Park PW, Goins RE (1994) In situ preparation of FAME for analysis of fatty acid composition in foods. *J Food Sci* 59:1262–1266
- Wolfe RR, Chinkes DL (2005) Mass isotopomer distribution analysis. In: anonymous isotope tracers in metabolic research: principles and practice of kinetic analysis, Wiley, New York.
- Duckett SK, Andrae JG, Owens FN (2002) Effect of high-oil corn or added corn oil on ruminal biohydrogenation of fatty acids and conjugated linoleic acid formation in beef steers fed finishing diets. *J Anim Sci* 80(12):3353–3360
- Enoch HG, Catalá A, Strittmatter P (1976) Mechanism of rat liver microsomal stearyl-CoA desaturase. Studies of the substrate specificity, enzyme-substrate interactions, and the function of lipid. *J Biol Chem* 251(16):5095–5103
- Ntambi JM (1995) The regulation of stearyl-CoA desaturase (SCD). *Prog Lipid Res* 34(2):139–150
- Duckett SK, Pratt SL, Pavan E (2009) Corn oil or corn grain supplementation to steers grazing endophyte-free tall fescue. II. Effects on subcutaneous fatty acid content and lipogenic gene expression. *J Anim Sci* 87(3):1120–1128
- Pfaffl MW, Horgan GW, Dempfle L (2002) Relative expression software tool (REST[®]) for group-wise comparison and statistical analysis of relative expression results in real-time PCR. *Nucl Acids Res* 30(9):e36
- Martini WZ, Chinkes DL, Barrow RE, Murphey ED, Wolfe RR (1999) Lung surfactant kinetics in conscious pigs. *Am J Physiol Endocrinol Metab* 277(1):E187–E195
- Archibeque SL, Lunt DK, Gilbert CD, Tume RK, Smith SB (2005) Fatty acid indices of stearyl-CoA desaturase do not reflect actual stearyl-CoA desaturase enzyme activities in adipose tissues of beef steers finished with corn-, flaxseed-, or sorghum-based diets. *J Anim Sci* 83(5):1153–1166
- Morton ID, Todd AR (1950) The haemolytic acid present in horse brain; purification and identification as *cis*-octadec-11-enoic acid. *Biochem J* 47(3):327–330
- Hofmann K, Lucas RA, Sax SM (1952) The chemical nature of the fatty acids of *Lactobacillus arabinosus*. *J Biol Chem* 195(2):473–485
- Holloway PW, Wakil SJ (1964) Synthesis of fatty acids in animal tissues. ii. the occurrence and biosynthesis of *cis*-vaccenic acid. *J Biol Chem* 239:2489–2495
- Leonard AE, Pereira SL, Sprecher H, Huang Y (2004) Elongation of long-chain fatty acids. *Prog Lipid Res* 43(1):36–54
- Guo W, Wong S, Xie W, Lei T, Luo Z (2007) Palmitate modulates intracellular signaling, induces endoplasmic reticulum stress, and causes apoptosis in mouse 3T3-L1 and rat primary preadipocytes. *Am J Physiol Endocrinol Metab* 293(2):E576–E586

27. Eberlé D, Hegarty B, Bossard P, Ferré P, Fougère F (2004) SREBP transcription factors: master regulators of lipid homeostasis. *Biochimie* 86(11):839–848
28. Lay SL, Lefrère I, Trautwein C, Dugail I, Krief S (2002) Insulin and sterol-regulatory element-binding protein-1c (SREBP-1C) regulation of gene expression in 3T3-L1 adipocytes. *J Biol Chem* 277(38):35625–35634
29. Keating AF, Kennelly JJ, Zhao F (2006) Characterization and regulation of the bovine stearoyl-CoA desaturase gene promoter. *Biochem Biophys Res Commun* 344(1):233–240
30. Jump DB (2009) Mammalian fatty acid elongases. *Methods Mol Biol* 579:375–389
31. Jakobsson A, Westerberg A, Jackbosson J (2006) Fatty acid elongases in mammals: their regulation and roles in metabolism. *Prog Lipid Res* 45:237–249
32. Wang Y, Botolin D, Christian B, Busik J, Xu J, Jump DB (2005) Tissue-specific, nutritional, and developmental regulation of rat fatty acid elongases. *J Lipid Res* 46:706–715
33. Naganuma T, Yuichiro Y, Takayuki S, Yusuke O, Kihara A (2011) Biochemical characterization of the very long-chain fatty acid elongase ELOVL7. *FEBS Lett* 585:3337–3341
34. Green CD, Ozguden-Akkoc CG, Wang Y, Jump DB, Olson LK (2010) Roles of fatty acid elongases in determination of de novo synthesized monounsaturated fatty acid species. *J Lipid Res* 51:1871–1877
35. Matsuzaka T, Shimano H, Yahagi N, Yoshikawa T, Amemiya-Kudo M, Hasty AH, Okazaki H, Tamura Y, Iizuka Y, Ohashi K, Osuga J, Takahashi A, Yato S, Sone H, Ishibashi S, Yamada N (2002) Cloning and characterization of a mammalian fatty acyl-CoA elongase as a lipogenic enzyme regulated by SREBPs. *J Lipid Res* 43(6):911–920
36. Wang Y, Botolin D, Xu J, Christian B, Mitchell E, Jayaprakasam B, Nair M, Peters JM, Busik J, Olson LK, Jump DB (2006) Regulation of hepatic fatty acid elongase and desaturase expression in diabetes and obesity. *J Lipid Res* 47(9):2028–2041
37. Price NT, Jackson VN, van der Leij FR, Cameron JM, Travers MT, Bartelds B, Huijkman NC, Zammit VA (2003) Cloning and expression of the liver and muscle isoforms of ovine carnitine palmitoyltransferase 1: residues within the N-terminus of the muscle isoform influence the kinetic properties of the enzyme. *Biochem J* 372(3):871–879
38. McGarry JD, Brown NF (1997) The mitochondrial carnitine palmitoyltransferase system: from concept to molecular analysis. *Euro J Biochem* 244(1):1–14

Many studies have shown that conversion of ALA to DHA in vivo is minimal. The conversion of ALA to EPA and DHA in vivo is <2 % [1, 2]. Few studies have, however, shown that ALA can be converted to DHA in reasonable amounts if provided at higher levels in the diet. Ramaprasad et al. [3] have shown that EPA + DHA levels in serum and liver is increased when incremental amounts of ALA are given in the diet. Therefore, innovative approaches are needed to increase long chain omega-3 PUFA levels in serum and tissues, if it has to be derived solely from ALA.

Recent developments in the field of microemulsions are exploited by many investigators for the delivery of biologically important molecules. Studies have shown that EPA levels in the plasma are enhanced tenfold when given in encapsulated form as compared to those given without encapsulation [4]. The bioavailability of EPA and EPA + DHA in rats was enhanced by 45 and 43 %, respectively when provided in a gelled emulsion as compared to those given in the free form [5]. An increase in lipid bioavailability was observed with higher assimilation of DHA when given as liposomes [6]. Liposomes also help in enhancing the bioavailability. A twofold increase in plasma concentration of curcumin was observed in rats when given as a curcumin–phospholipid complex. Curcumin nanoparticles have shown a ninefold increase in bioavailability [7]. Therefore, microemulsions may provide a means of enhancing the bioavailability of lipophilic molecules such as omega-3 fatty acid enriched oils.

The primary objective of this investigation was to explore the possibility of increasing the uptake and conversion of ALA to EPA and DHA using microemulsions. Microemulsions were prepared with different binding materials such as whey protein, gum acacia and lipid. Protein-based emulsifiers such as whey protein increase the viscosity of the interfacial layer and the surrounding water phase, and restrict the penetration and mobility of prooxidants into the oil [8]. Whey protein is a film-forming material with good emulsifying properties. Whey protein is used as hydrogels and a nanoparticulate system for encapsulation and controlled delivery of bioactive compounds [9, 10]. Gum Arabic (gum *Acacia*) is a hydrocolloid produced by the natural exudation of acacia trees and is an effective encapsulation material with high water solubility, low viscosity and acts as an oil-in-water emulsifier [11].

Commercially available phospholipid-based materials are also used as binding materials [12]. Liposomes are used as oral route vectors for delivering fatty acid supplements. Studies have shown that fatty acid absorption including that of omega-3 PUFA is enhanced when given through liposome administration. The high amount of phospholipids in liposomes facilitates the transport of the products to

the unstirred water layer of enterocytes. The bioavailability of omega-3 PUFA is increased when bound to phospholipid (PL) when compared with that delivered through triacylglycerol (TAG) [6, 13, 14]. A study performed on preterm infants showed that the absorption of long chain omega-3 PUFA, especially DHA was greater with formulations of phospholipid as compared to the formulas supplemented with TAG [15]. Studies have also shown that microemulsions protect PUFA from oxidation and they can also be used to increase the uptake of omega-3 PUFA in serum [4, 5].

The aim of the present study was therefore to explore the possibility of delivering omega-3 PUFA-rich oils using different types of microemulsion. The conversion of ALA to long chain omega-3 PUFA when given in microemulsion form was also investigated in this study.

Materials and Methods

Materials

Linseed oil (LSO) was provided by Kamani Flax Omega Industries, Mumbai, India. Sunflower oil (SNO) was purchased from a local market. Lipoid S75-3 (Soy lecithin at 69 % phosphatidylcholine and 10 % phosphatidylethanolamine) was a gift from Lipoid (Ludwigshafen, Germany). Sodium chloride was purchased from Sisco Research Laboratories, Mumbai, India. Whey protein concentrate (WPC) was obtained from Mahaan Foods (Mumbai, India). Gum acacia, maltodextrin, α -tocopherol and sodium azide were procured from Himedia, Mumbai, India. Polyethylene glycol, eicosapentaenoic acid, docosahexaenoic acid and alpha linolenic acid were procured from the Sigma Chemical Company, St. Louis, MO, USA. All the solvents were of analytical grade and distilled before use.

Preparation of LSO/SNO Emulsions

LSO/SNO was encapsulated in microemulsions using one of the three different binding materials. Carbohydrate (gum acacia), protein (whey protein) and phospholipid (lipoid) based materials were used for encapsulating the oil.

1. Carbohydrate based emulsions of LSO/SNO:

The carbohydrate-based emulsion of LSO or SNO was prepared by using gum acacia [16]. The gum acacia (0.5 %) and maltodextrin (20 %) were dissolved in distilled water. The gum acacia solution was heated at 45 °C with constant stirring for 30 min and then allowed to cool. Emulsions with LSO were prepared by adding dropwise and dispersing the oil (10 %) into the aqueous gum acacia solution. Two drops of Tween 80 was added to aid

emulsification. α -Tocopherol (0.065 %) was added as an antioxidant. Sodium azide (0.02 wt%) was added to the emulsions as an antimicrobial agent. The emulsions were homogenized for 5 min at 6,000 rpm using a laboratory mixer (Silverson L4RT, Silverson Machines Ltd., Chesham, Bucks, England). These emulsions were then further homogenized at 800 bar with ten cycles at 4 °C using a high pressure homogenizer (Panda, GEA Niro Soavi, Italy). The emulsions were collected and stored at –20 °C till further use.

2. Protein based emulsions of LSO/SNO:

The protein based emulsions of LSO or SNO were prepared by using Whey protein concentrate (WPC) [17]. The WPC solutions were prepared by dispersing the powder (10 wt%) in buffer solution (5 mM phosphate buffer, pH 7). The pH of WPC solution was adjusted to 7.0. The final concentration of dissolved solid was 30 % (w/w) which comprised 20 wt% maltodextrin and 10 wt% whey protein. Two drops of Tween 80 was added to aid emulsification. α -Tocopherol (0.065 %) and sodium azide (0.02 wt%) were added to the emulsions. The oil-in-water emulsions were prepared in two stages: (a) The core material [LSO or SNO in the ratio of 1:3 (core: wall)] was progressively added to the aqueous phase during pre-emulsion preparation and homogenized for 5 min at 6,000 rpm using a laboratory mixer (Silverson L4RT, Silverson Machines Ltd., Chesham, Bucks., England). (b) These coarse emulsions were then further homogenized at 800 bar with ten cycles at 4 °C using a high pressure homogenizer (Panda, GEA Niro Soavi, Italy). These emulsions were collected and stored at –20 °C till further use.

3. Phospholipid based emulsions of LSO/SNO:

The phospholipid based emulsions of LSO or SNO were prepared using Lipoid S75-3 [12]. The components used to prepare the emulsions were Lipoid (0.075 %), polyethylene glycol (3 %) and NaCl (0.9 %) dissolved in distilled water. LSO or SNO (10 wt%) was added to this lipid solution. The emulsions were homogenized for 5 min at 6,000 rpm using a laboratory mixer (Silverson L4RT, Silverson Machines Ltd., Chesham, Bucks, England). These emulsions were then further homogenized at 800 bar with ten cycles at 4 °C using a high pressure homogenizer (Panda, GEA Niro Soavi, Italy). The emulsions were collected and stored at –20 °C till further use.

Measurement of Encapsulation Efficiency

The encapsulation efficiency of the binding materials was determined as described by Danviriyakul et al. [18]. The total oil in the encapsulated material was extracted in hexane by Soxhlet extraction. The weight of oil extracted

was taken as the amount of oil associated with microcapsules. Adsorbed oil on the surface of microcapsule was extracted by gently shaking the microcapsules in petroleum ether (b.p. 60–80 °C) for 10 min without damaging the microcapsules. The solvent was decanted and the residue was dried in a rotavapor and weighed until constant weight was obtained. Encapsulation efficiency of the binding material calculated as follows.

$$\text{Encapsulation efficiency (\%)} = \frac{[(\text{total oil} - \text{adsorbed oil}) \times 100]}{\text{total oil}} \quad (1)$$

Scanning Electron Microscopy (SEM) of Encapsulated Oil

Scanning electron microscopy was used to study the surface and internal structures of the encapsulated materials as described by Rosenberg et al. [19]. Powder particles were attached to a sample stub with double-sided sticky tape. The specimens were sputter coated with gold using a Polaron sputter coater and examined using a LEO 435 VP (LEO Electron Microscopy Ltd., Cambridge) at an accelerating voltage.

Analysis of Emulsion Particle Size

The particle size distributions of the emulsified lipid droplets were determined using a Mastersizer fitted with small volume sample presentation unit and integration software (Malvern Instruments Ltd., Worcestershire, UK). The particle size distributions were calculated based on a relative particle refractive index of 1.350 [20]. Distilled water was used as the dispersant for the determination of the emulsion lipid globule size distribution. The mean droplet diameter was expressed as the volume mean diameter. Each sample was analyzed in triplicate and the data were reported as averages.

Fatty Acid (FA) Composition

Fatty acid composition of encapsulated oils, dietary lipids, serum, and tissues were analyzed as methyl esters using gas liquid chromatography (Fisons, fitted with a flame ionization detector [FID]) fitted with a fused silica capillary column 25 m \times 0.25 mm (Parma bond FFAP-DF-0.25, Machery-Negal GmbH co., Duren, Germany). The methyl esters of fatty acids were prepared using 14 % BF_3/MeOH as described by Morrison and Smith [21]. The operating conditions of gas liquid chromatography were: column temperature 220 °C, injection temperature 230 °C, and detector temperature 240 °C. Nitrogen was used as the carrier gas. Individual fatty acids were identified by

comparison with the retention times of standards (Nu-Check-Prep, Inc, Elysian MN) and were quantified by an online Shimadzu Chromatopack CR6A integrator. Penta-decanoic acid was used as the internal standard for the quantification of specific fatty acids.

Intestinal Absorption of Encapsulated Oil—Intestinal Everted Sac Model

Male Wistar rats (OUTB-Wistar, IND-cft (2c) weighing 140–150 g were kept for 1 week on standard rodent pellets (Christie Foods, Bangalore, India) with free access to food and water. Rats were sacrificed by anesthetizing with diethyl ether. The abdomen was opened by midline incision. The small intestine was removed by cutting each end. The intestine was washed with 0.9 % saline. After thoroughly cleaning both inside and outside of the small intestine with saline, it was everted and cut into sacs of 8 cm length. Each sac was filled with Krebs–Ringer phosphate buffer containing 10 mM glucose. Absorption of the oil was determined by incubating the everted rat intestinal segments in the Krebs–Ringer phosphate buffer—10 mM glucose medium (10 ml) placed in a series of 25 ml conical flask containing varying concentrations of the oil (1.25–80 mg). The oil was added to this medium containing 0.04 % Tween 20. The flasks were aerated with a 95 % oxygen and 5 % carbon dioxide mixture and maintained at 37 °C in a Julabo shaking water bath for 3 h [22]. The lipids from mucosal medium, serosal fluid and the intestinal tissue were extracted by the Folch procedure (1957) [23].

Absorption of Encapsulated Oil—In Vivo Studies

Male Wistar rats [OUBT-Wistar, IND-cft (2c)] weighing 40 ± 4 g were grouped (six rats in each group) by random distribution and housed in individual cages, under a 12 h light/dark cycle, in an approved animal house facility at the Central Food Technological Research Institute in Mysore, India. The rats were fed standard rodent pellets for 30 days. Growth of the rats was monitored by weighing at regular intervals. The rats had free access to food and water throughout the study. The rats were administered 1 mL of emulsion of SNO or LSO by gavage once a day at 10AM for 30 days. The major fatty acid present in 1 mL of SNO emulsion was 46 mg of LA where as 1 ml of LSO contained 41 mg of ALA. After 30 days of feeding emulsified fats, rats were fasted overnight and sacrificed under ether anesthesia. Blood was drawn by cardiac puncture and serum was separated by centrifugation at 1,100 g for 30 min. The liver was removed, rinsed with ice-cold saline, blotted, weighed and stored at -20 °C until analyzed. The experimental protocol for these studies was approved by the Institutional Animal Ethics Committee recognized by the Government of India.

Statistical Analysis

Fisher's least significant differences (LSD) test was used to differentiate the treatment means and the significant level was reported at $P < 0.05$. Statistical analysis was performed by using Statistica Version 5.5 (Statsoft Inc., OK, USA) software.

Results

Encapsulation Efficiency of Gum Acacia, Whey Protein and Lipoid

Encapsulation efficiency of the binding material indicates the amount of oil that was successfully encapsulated and calculated from total oil in microcapsules and extractable oil from surface. Lipoid showed greater encapsulation efficiency in entrapping oils (83–85 %) followed by Whey protein (74–75 %) and gum acacia (67–68 %). There were no significant differences in the amount of SNO or LSO encapsulated in these binding materials (Table 1).

Particle Size of Microemulsions Containing Oils

The particle size was measured using a particle size analyzer (Malvern Instruments Ltd., Worcestershire, UK). The average particle size of microemulsion containing oil in gum acacia was in the range of 1,092–1,093 nm, whereas the particle size of microemulsions containing oil in whey protein was found to be 700–704 nm. The particle size of microemulsions containing oil in lipoid was found to be 246–249 nm (Table 2). Results showed that high pressure homogenization for ten cycles was optimal for making microencapsulation of selected oils. Beyond ten cycles, no further changes in the particle size were observed. No significant differences in the particle size were observed when LSO or SNO was used as the core material.

Scanning Electron Microscopy of Encapsulated Oils

Scanning electron microscopy (SEM) is an important tool for studying microencapsulation, and helps in the selection

Table 1 Encapsulation efficiency of various binding materials

Oils	Encapsulation efficiency (%)		
	With gum acacia	With whey protein	With lipoid
SNO	67.2 ± 1.1^a	74.2 ± 3.0^b	83.8 ± 1.8^c
LSO	68.4 ± 2.2^a	75.2 ± 2.9^b	84.7 ± 3.1^c

Values are mean \pm SD, $n = 4$; mean in a row with different superscripts differ significantly at $P < 0.05$

SNO sunflower oil, LSO linseed oil

Table 2 Particle size of microencapsulated oils

Groups	Emulsion size (d_{43} , nm)		
	With gum acacia	With whey protein	With lipoid
1 SNO	1,092 ± 4 ^c	704 ± 5 ^b	249 ± 4 ^a
2 LSO	1,093 ± 3 ^c	700 ± 4 ^b	246 ± 3 ^a

Values are mean ± SD, $n = 4$; mean in a row with different superscripts differ significantly at $P < 0.05$

SNO sunflower oil, LSO linseed oil

of wall materials, to view the distribution of core material in microcapsules, and for elucidating the mechanisms of capsule formation. The gum acacia which encapsulated oil showed a rounded external surface with concavities and teeth. The surface had no apparent cracks or porosity. Microcapsules with whey protein showed a spherical shape. No vacuoles were present indicating good microcapsules formation without any breakage. No oil droplets were observed in the outer structure of the capsules. The oil encapsulated with lipoid showed a spheroid shape. The oil was walled and protected by the lipoid and evenly distributed in the capsules (Fig. 1). Thus, differences in the shape of the microcapsules were observed when different binding materials were used.

Fatty Acid Composition of Encapsulated Oils

The fatty acid composition of native and encapsulated oil with different binding materials used in this study is shown in Tables 3 and 4. The major fatty acid of sunflower oil encapsulated with these three binding materials was 58 % linoleic acid, 28 % oleic acid, and 9 % palmitic acid (Table 3). The major fatty acid of linseed oil encapsulated in gum acacia, whey protein and lipoid was 51 % alpha linolenic acid, 21 % oleic acid, and 14 % linoleic acid (Table 4). There was no significant difference in the fatty acid composition of oil encapsulated with three different binding materials as compared to that found in native oil.

Intestinal Absorption of Encapsulated Oils—In Vitro Model Using Intestinal Everted Sacs

The amount of oil absorbed through intestinal everted sacs when given at different concentrations is shown in Tables 5 and 6. Eight-centimeter long intestinal everted sacs were incubated with different amounts (1.25–80 mg) of oil in 10 ml incubation medium. The absorption of oil by the everted intestinal sacs increased proportionately up to 10 mg. No further increase in oil absorption was observed beyond this amount of oil in the incubation medium. No significant difference in the absorption of oil was observed when it was given in encapsulated form in

gum acacia or as non encapsulated form. However, when SNO was given as microemulsions with lipoid there was an increase in the uptake of oil by 50, 33, 28, and 11 % as compared to oil given in native form at 1.25, 2.5, 5 and 10 mg levels. Even though there was no further increase in the absorption of oil given beyond 10 mg levels in the incubation medium, there was a 10 % higher level of absorption of oil given in lipoid at all the concentrations tested (Table 5). Similarly when LSO was given in microemulsions with lipoid, there was an increase in the uptake of oil by 51, 42, 28 and 12 % as compared to those given in native form at 1.25, 2.5, 5 and 10 mg levels, respectively. Thus, at different levels of SNO or LSO, intestinal everted sacs absorbed significantly higher levels of oil in microemulsion form with whey protein or lipoid as compared to oils given in the native form. However, no significant differences in the extent of absorption were observed when SNO or LSO was given at similar concentrations (Table 6).

Effect of Encapsulation on Intestinal Absorption of Omega-6 and Omega-3 Fatty acids—In Vitro Studies

The amount of LA absorbed from the oil is shown in Tables 7, 8. When everted sacs of rat intestine were incubated with SNO containing 5.8 mg LA, 5.1 mg of LA was found in the absorbed lipids. When SNO was encapsulated in whey protein or gum acacia or lipoid and incubated with intestinal everted sacs, the amount of LA observed in oil that was absorbed was 5.1, 5.2 and 5.2 mg, respectively (Table 7). Arachidonic acid was not observed in SNO that was absorbed from the intestinal everted sacs. There was no significant difference in LA content of SNO that was absorbed when given in encapsulated form or when it was given as oil without encapsulation.

When LSO was given without encapsulation or after encapsulation in gum acacia, whey protein or lipoid, the ALA that was present in the oil that was absorbed intestine was found to be 3.6, 3.8, 4.2 and 4.6 mg, respectively (Table 8). The amount of ALA present in LSO used in this study was 5.1 mg. Thus the increase in the amount of ALA found in oil after absorption when given as microemulsions with gum acacia, whey protein and lipoid were 6, 17 and 28 %, respectively as compared to that observed in oil that was absorbed when LSO was provided without encapsulation. Interestingly, when 10 mg of LSO was given as microemulsion with lipoid, 0.48 mg of EPA + DHA was observed in the oil that was absorbed. Thus, a small but a significant amount of ingested ALA was converted to longer chain EPA + DHA when given as microemulsions with lipoid. EPA and DHA were not detected when LSO was given as microemulsions with gum acacia and whey protein.

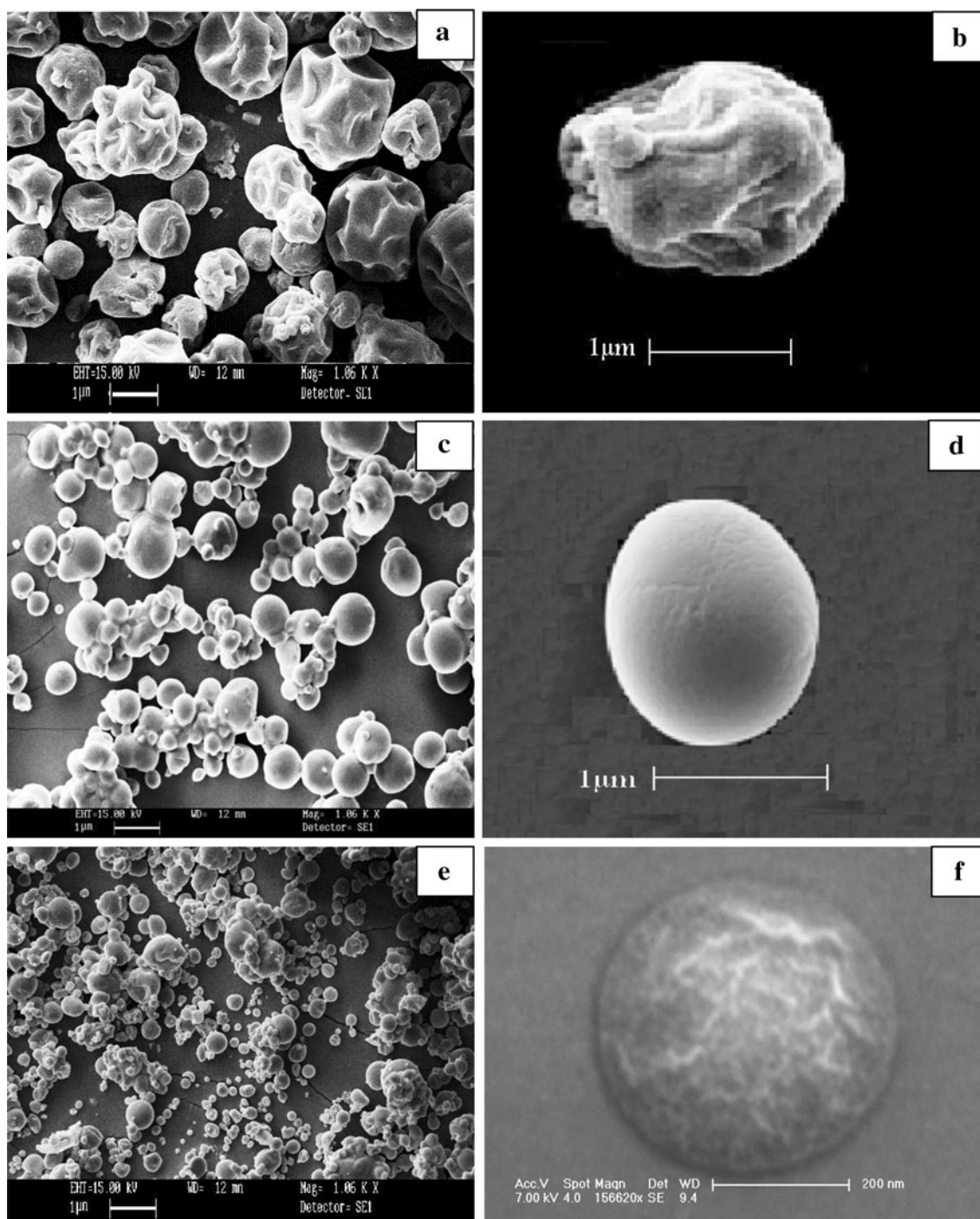


Fig. 1 SEM photograph of **a** oil encapsulated with gum acacia, **b** single particle of gum acacia containing oil, **c** oil encapsulated with whey protein, **d** single particle of whey protein encapsulating oil, **e** oil encapsulated with lipid, **f** single particle of lipid containing oil

Since no advantages in terms of ALA uptake or its conversion to longer chain omega-3 fatty acids were observed when LSO was given as a microemulsion with gum acacia, all further studies were carried out with whey protein and lipid as encapsulating materials.

Serum Fatty Acid Composition of Rat Given Native and Encapsulated Oils

Rats were given native oils or oils after encapsulating in whey protein or lipid daily for a period of 30 days as

Table 3 Fatty acid composition (%) of native oil and microencapsulated oil-SNO

	SNO			
	Without encapsulation	With gum acacia	With whey protein	With lipid
14:0	0.3 ± 0.1 ^a	0.4 ± 0.1 ^a	0.3 ± 0.05 ^a	0.3 ± 0.1 ^a
16:0	9.2 ± 0.3 ^a	9.4 ± 0.2 ^a	9.9 ± 0.4 ^b	9.3 ± 0.3 ^a
18:0	3.7 ± 0.2 ^a	3.8 ± 0.1 ^a	4.2 ± 0.3 ^b	3.7 ± 0.1 ^a
18:1(n-9)	28.5 ± 0.9 ^a	28.1 ± 0.7 ^a	28.2 ± 1.2 ^a	28.2 ± 0.7 ^a
18:2(n-6)	58.3 ± 1.3 ^a	58.3 ± 1.2 ^a	57.4 ± 1.1 ^a	58.5 ± 0.9 ^a

Values are mean ± SD, *nd* not detected, *n* = 6; *SNO* sunflower oil, mean in a row with different superscripts differ significantly at *P* < 0.05

Table 4 Fatty acid composition (%) of native oil and microencapsulated oil-LSO

	LSO			
	Without encapsulation	With gum acacia	With whey protein	With lipid
14:0	0.6 ± 0.2 ^b	0.4 ± 0.1 ^a	0.6 ± 0.05 ^b	0.6 ± 0.1 ^b
16:0	7.8 ± 0.5 ^a	7.6 ± 0.3 ^a	7.2 ± 0.2 ^a	8.3 ± 0.5 ^a
18:0	4.7 ± 0.7 ^a	4.9 ± 0.1 ^a	5.1 ± 0.8 ^a	6.1 ± 0.5 ^b
18:1(n-9)	21.4 ± 0.8 ^a	21.4 ± 0.9 ^a	21.5 ± 0.8 ^a	21.2 ± 0.7 ^a
18:2(n-6)	14.0 ± 1.1 ^a	14.6 ± 1.2 ^a	14.3 ± 1.0 ^a	13.6 ± 1.3 ^a
18:3(n-3)	51.5 ± 2.1 ^a	51.1 ± 2.3 ^a	51.3 ± 2.8 ^a	50.2 ± 2.5 ^a

Values are mean ± SD, *nd* not detected, *n* = 6; *LSO* linseed oil, mean in a row with different superscripts differ significantly at *P* < 0.05

Table 5 Absorption of native oil and microencapsulated oils through intestinal everted sacs—in vitro

Concentration of individual oil provided (mg)	SNO absorbed (mg)			
	Native	With gum acacia	With whey protein	With lipid
1.25	0.8 ± 0.03 ^a	0.88 ± 0.02 ^a	1.09 ± 0.03 ^b	1.20 ± 0.02 ^c
2.5	1.73 ± 0.1 ^a	1.75 ± 0.2 ^a	2.24 ± 0.05 ^b	2.38 ± 0.1 ^c
5	3.73 ± 0.12 ^a	3.83 ± 0.13 ^a	4.58 ± 0.21 ^b	4.77 ± 0.14 ^c
10	8.64 ± 0.13 ^a	8.75 ± 0.1 ^a	9.23 ± 0.2 ^b	9.56 ± 0.2 ^c
20	8.65 ± 0.09 ^a	8.78 ± 0.1 ^a	9.22 ± 0.2 ^b	9.55 ± 0.1 ^c
40	8.61 ± 0.14 ^a	8.71 ± 0.09 ^a	9.23 ± 0.1 ^b	9.54 ± 0.1 ^c
80	8.64 ± 0.10 ^a	8.70 ± 0.08 ^a	9.22 ± 0.1 ^b	9.54 ± 0.1 ^c

Values are mean ± SD, *n* = 6; mean in a row with different superscripts differ significantly at *P* < 0.05

SNO sunflower oil

Table 6 Absorption of native oil and microencapsulated oils through intestinal everted sacs—in vitro

Concentration of individual oil provided (mg)	LSO absorbed (mg)			
	Native	With gum acacia	With whey protein	With lipid
1.25	0.8 ± 0.05 ^a	0.89 ± 0.03 ^a	1.09 ± 0.04 ^b	1.21 ± 0.05 ^c
2.5	1.71 ± 0.2 ^a	1.83 ± 0.1 ^a	2.26 ± 0.1 ^b	2.42 ± 0.1 ^c
5	3.82 ± 0.13 ^a	3.93 ± 0.14 ^a	4.69 ± 0.12 ^b	4.88 ± 0.1 ^c
10	8.63 ± 0.07 ^a	8.89 ± 0.1 ^b	9.28 ± 0.1 ^c	9.65 ± 0.09 ^d
20	8.65 ± 0.2 ^a	8.98 ± 0.1 ^b	9.25 ± 0.1 ^c	9.64 ± 0.1 ^d
40	8.60 ± 0.2 ^a	8.91 ± 0.1 ^b	9.25 ± 0.2 ^c	9.65 ± 0.1 ^d
80	8.63 ± 0.05 ^a	8.90 ± 0.07 ^b	9.24 ± 0.06 ^c	9.60 ± 0.09 ^d

Values are mean ± SD, *n* = 6; mean in a row with different superscripts differ significantly at *P* < 0.05

LSO linseed oil

Table 7 Effect of microemulsified SNO on LA absorption from intestinal everted sacs

	LA absorbed (mg)	ARA present in the oil after absorption (mg)
SNO	5.1 ± 0.09 ^a	nd
SNO in gum acacia	5.1 ± 0.08 ^a	nd
SNO in whey protein	5.2 ± 0.1 ^a	nd
SNO in lipid	5.2 ± 0.1 ^a	nd

The 10 mg of SNO used in the incubation medium contained 5.7 ± 0.09 mg LA, values are mean ± SD, *n* = 6; mean in a column with different superscripts differ significantly at *P* < 0.05

SNO sunflower oil, *nd* not detected

Table 8 Intestinal absorption of ALA from oil encapsulated in various binding materials—in vitro

	ALA absorbed (mg)	EPA + DHA in absorbed lipids (mg)
LSO	3.6 ± 0.03 ^a	nd
LSO in gum acacia	3.8 ± 0.05 ^b	nd
LSO in whey protein	4.2 ± 0.1 ^c	nd
LSO in lipid	4.6 ± 0.1 ^d	0.48 ± 0.03

The 10 mg of LSO used in the incubation medium contained 5.1 ± 0.09 mg ALA, values are mean ± SD, *n* = 6; mean in a column with different superscripts differ significantly at *P* < 0.05

LSO linseed oil, *nd* not detected

described in the Methods section. The serum lipids of rats given SNO, SNO encapsulated in whey protein and SNO encapsulated in lipid contained LA to an extent of 30.4, 31.5 and 30.3 % of the total fatty acids. The arachidonic acid content in the serum lipids of rats given SNO, SNO encapsulated in whey protein and SNO encapsulated in lipid were 13.2, 12.9 and 12.7 % of the total fatty acids. Significant differences were not observed in LA and ARA present in serum lipids of rats given SNO encapsulated in whey protein and SNO encapsulated in lipid as compared to those given SNO without encapsulation (Table 9).

Serum lipids contained omega-3 fatty acids in rats given LSO, LSO encapsulated in whey protein or LSO in lipid. The rats given LSO, LSO encapsulated in whey protein and LSO encapsulated in lipid showed ALA to an extent of 1.8, 2.4 and 3.8 %, respectively of total fatty acids in the serum lipids (Table 10). The EPA content in rats given LSO, LSO encapsulated in whey protein and LSO encapsulated in lipid were found to be 0.6, 0.8 and 4.8 %, respectively. The rats given LSO, LSO encapsulated in whey protein and LSO encapsulated in lipid contained DHA in serum lipids to an extent of 0.4, 0.8 and 3.9 % of total fatty acids (Table 10). This indicated that ALA from LSO, LSO encapsulated in whey protein and LSO encapsulated in lipid were converted to EPA and DHA with a higher degree of conversion being

Table 9 Fatty acid composition (%) of serum lipids in rats given SNO

	SNO		
	Native oil	With Whey protein encapsulation	With lipid encapsulation
16:0	28.4 ± 1.3 ^b	27.8 ± 1.2 ^{ab}	28.5 ± 0.4 ^b
16:1(n-7)	2.3 ± 0.12 ^{ab}	2.5 ± 0.59 ^b	3.3 ± 0.17 ^c
18:0	7.3 ± 0.43 ^b	6.9 ± 0.79 ^{ab}	6.1 ± 0.18 ^a
18:1(n-9)	18.4 ± 0.6 ^a	18.4 ± 1.3 ^a	19.1 ± 0.54 ^a
18:2(n-6)	30.4 ± 1.3 ^a	31.5 ± 1.2 ^b	30.3 ± 0.60 ^{ab}
20:4(n-6)	13.2 ± 0.6 ^a	12.9 ± 0.28 ^a	12.7 ± 0.21 ^a
Total n-6	43.6	44.4	43

Values are mean ± SD, *n* = 6; mean in a row with different superscripts differ significantly at *P* < 0.05

SNO sunflower oil, *nd* not detected

Table 10 Fatty acid composition (%) of serum lipids in rats given LSO

	LSO		
	Native oil	With Whey protein encapsulation	With lipid encapsulation
16:0	27.3 ± 1.4 ^b	26.1 ± 0.94 ^{ab}	25.4 ± 1.6 ^a
16:1(n-7)	2.0 ± 0.38 ^a	1.7 ± 0.27 ^a	1.7 ± 0.23 ^a
18:0	7.6 ± 0.43 ^a	8.4 ± 0.48 ^b	8.5 ± 0.52 ^b
18:1(n-9)	31.1 ± 0.64 ^b	30.6 ± 1.1 ^a	30.5 ± 1.4 ^a
18:2(n-6)	19.3 ± 0.59 ^b	19.7 ± 0.92 ^b	14.0 ± 1.2 ^a
18:3(n-3)	1.8 ± 0.12 ^a	2.4 ± 0.31 ^b	3.8 ± 0.17 ^c
20:4(n-6)	9 ± 0.35 ^b	8.8 ± 0.2 ^b	6.9 ± 0.2 ^a
20:5(n-3)	0.6 ± 0.05 ^a	0.8 ± 0.14 ^b	4.8 ± 0.2 ^c
22:5(n-6)	0.8 ± 0.08 ^c	0.4 ± 0.05 ^b	0.1 ± 0.05 ^a
22:5(n-3)	0.1 ± 0.05 ^a	0.3 ± 0.05 ^b	0.4 ± 0.08 ^c
22:6 (n-3)	0.4 ± 0.05 ^a	0.8 ± 0.05 ^b	3.9 ± 0.21 ^c
Total n-6	29.1	28.9	21.0
Total n-3	2.9	4.3	12.9
n-6/n-3	10.03	6.72	1.62

Values are mean ± SD, *n* = 6; mean in a row with different superscripts differ significantly at *P* < 0.05

LSO linseed oil, *nd* not detected

observed when given as emulsions in lipid. The omega-6 to omega-3 fatty acid ratio in serum lipids given LSO, LSO in whey protein and LSO in lipid were 10.03, 6.72 and 1.62, respectively indicating higher efficacy of microemulsified oils in increasing omega-3 fatty acid levels by replacing omega-6 fatty acids in serum lipids (Table 10).

Liver Fatty Acid Composition of Rat Given Native and Encapsulated Oils

The fatty acid composition of liver lipids in rats given native oil and oils encapsulated with different binding

Table 11 Fatty acid composition (%) of liver lipids in rats given SNO

	SNO		With lipid encapsulation
	Native oil	With whey protein encapsulation	
16:0	26.2 ± 1.6 ^a	26.7 ± 1.4 ^a	26.6 ± 1.3 ^a
16:1(n-7)	2.5 ± 0.3 ^a	2.4 ± 0.3 ^a	2.3 ± 0.2 ^a
18:0	7.8 ± 0.4 ^a	7.8 ± 0.2 ^a	8.1 ± 0.6 ^a
18:1(n-9)	20.1 ± 0.5 ^a	19.4 ± 0.7 ^a	19.2 ± 0.4 ^a
18:2(n-6)	28.8 ± 1.2 ^a	29.6 ± 1.2 ^b	29.4 ± 1.1 ^b
20:4(n-6)	14.6 ± 1.3 ^a	14.1 ± 0.75 ^a	14.4 ± 0.91 ^a
Total n-6 PUFA	43.4	43.7	43.8

Values are mean ± SD, $n = 6$; Mean in a row with different superscripts differ significantly at $P < 0.05$

SNO sunflower oil, *nd* not detected

materials is given in Tables 11, 12. The rats given SNO, SNO encapsulated in whey protein and SNO encapsulated in lipid contained LA to an extent of 28.8, 29.6 and 29.4 % of the total fatty acids in liver. The arachidonic acid content in the liver of rats given SNO, SNO encapsulated in whey protein and SNO encapsulated in lipid were 14.6, 14.1 and 14.4 % of the total fatty acids. Thus, no significant difference in LA or ARA content was observed in rats given SNO, SNO encapsulated in whey protein and SNO encapsulated in lipid as compared to rats given SNO without encapsulation (Table 11).

The ALA levels of liver lipids in rats given LSO, LSO encapsulated in whey protein, and LSO encapsulated in lipid were found to be 2.7, 3.0 and 3.8 %, respectively. The EPA levels in liver lipids of rats given LSO, LSO encapsulated in whey protein and encapsulated in lipid were found to be 1, 2.3 and 6.1 % of the total fatty acids, respectively. The rats given LSO, LSO encapsulated in whey protein and LSO encapsulated in lipid contained DHA to an extent of 0.6, 1 and 4.8 % of total fatty acids in the liver. This indicated that ALA from LSO and LSO encapsulated with whey protein and LSO encapsulated with lipid was converted to EPA and DHA to different extents. The ratio of omega-6 to omega-3 fatty acids in liver lipids of rats given LSO, LSO in whey protein and LSO in lipid were found to be 7.17, 4.56 and 1.51, respectively indicating greater efficiency in conversion of ALA to long chain omega-3 PUFA when LSO was given as a microemulsion in lipid (Table 12).

Discussion

The primary objective of this investigation was to increase the bioavailability of ALA and possibly enhance its conversion

Table 12 Fatty acid composition (%) of liver lipids in rats given LSO

	LSO		
	Native oil	With whey protein encapsulation	With lipid encapsulation
16:0	23.0 ± 1.2 ^{ab}	21.7 ± 0.36 ^a	23.5 ± 0.5 ^b
16:1(n-7)	2.8 ± 0.08 ^b	2.8 ± 0.2 ^b	1.7 ± 0.2 ^a
18:0	10.3 ± 0.2 ^b	11.7 ± 0.4 ^c	8.5 ± 0.7 ^a
18:1(n-9)	27.1 ± 1.0 ^a	27.6 ± 0.5 ^{ab}	28.3 ± 0.6 ^b
18:2(n-6)	20.9 ± 0.9 ^c	18.9 ± 1.0 ^b	13.7 ± 1.1 ^a
18:3(n-3)	2.7 ± 0.3 ^a	3.0 ± 0.2 ^a	3.8 ± 0.1 ^b
20:4(n-6)	10.8 ± 0.9 ^b	10.1 ± 0.58 ^b	8.9 ± 0.1 ^a
20:5(n-3)	1.0 ± 0.1 ^a	2.3 ± 0.1 ^b	6.1 ± 0.2 ^c
22:5(n-6)	0.6 ± 0.03 ^b	0.7 ± 0.08 ^b	0.3 ± 0.05 ^a
22:5(n-3)	0.2 ± 0.01 ^a	0.2 ± 0.05 ^a	0.4 ± 0.02 ^b
22:6(n-3)	0.6 ± 0.08 ^a	1.0 ± 0.1 ^b	4.8 ± 0.1 ^c
Total n-6 PUFA	32.3	29.7	22.9
Total n-3 PUFA	4.5	6.5	15.1
N-6/n-3	7.17	4.56	1.51

Values are mean ± SD, $n = 6$; mean in a row with different superscripts differ significantly at $P < 0.05$

LSO linseed oil, *nd* not detected

to long chain omega-3 PUFA in experimental animals such as rats. ALA is a precursor to DHA which is essential for normal growth and development of infants. Sufficient quantities of DHA need to be provided to pregnant women and to children during the pre- and postnatal period. DHA is a predominant structural fatty acid in the central nervous system and retina, and its availability is crucial for the functioning of the central nervous system. The World Association of Prenatal Medicine, the Early Nutrition Academy, and the Child Health Foundation recommended that pregnant and lactating women should get an average daily intake of least 200 mg of DHA [24]. The majority of the Indian population are vegetarians. They have to obtain DHA by converting ALA present in vegetable oils which they consume from dietary sources. Several studies have shown that conversion of ALA to DHA is very minimal in mammals [25]. However, studies have also shown that when ALA is provided in the diet at higher levels it can drive the system towards formation of DHA [3, 25].

To build enhanced concentration of ALA and its subsequent conversion to DHA innovative approaches are needed. Several studies have shown that the bioavailability of lipophilic molecules can be enhanced significantly when given as microemulsion, nanoemulsion form. Microemulsions have smaller particle size and hence may cross the intestinal barriers more efficiently. Emulsification is an important step in the digestion and absorption of fats. Therefore, emulsification and encapsulation technology can be adopted to enhance bioavailability of lipid and lipid soluble molecules [26, 27].

Our study showed that there was a significant increase in ALA in rats when LSO was given in encapsulated form. When LSO was encapsulated in whey protein or in lipid and incubated with intestinal everted sacs the content of ALA that was absorbed was found to be higher by 17 and 28 % when compared to those given the oil without encapsulation. Interestingly, we also observed a small but significant presence of EPA + DHA in the absorbed lipids when LSO was given after encapsulation with lipid. However, no significant changes were observed in absorption of LA from SNO when it was provided in free or encapsulated form. These observations were made when the intestinal everted sac model was used to study the absorption of oil. The studies were extended *in vivo* by giving rats the encapsulated oils through intubation. The amount of ALA in the serum of rats given without encapsulation of LSO or after encapsulation with whey protein or lipid was found to be 32.1 ± 2.1 , 41.4 ± 5.3 and 48.8 ± 2.2 $\mu\text{g/ml}$ (mean \pm SD), respectively. Thus, the amount of ALA found in serum of rats given LSO encapsulated in whey protein or lipid was higher by 29 and 52 %, respectively as compared to that found in rats given LSO without encapsulation. The amount of EPA in serum was found to be 17 ± 0.9 and 41 ± 1.8 $\mu\text{g/ml}$ (mean \pm SD) in rats given LSO encapsulated in whey protein or lipid, respectively. When the same oil was given without encapsulation, the EPA level in serum was found to be 9.1 ± 1.4 $\mu\text{g/ml}$. Thus, the EPA level in serum was enhanced by 86 and 350 % when LSO was given in the form of encapsulated materials. DHA level in serum lipid was found to be 13 ± 1.9 and 34 ± 2.2 $\mu\text{g/ml}$ when given as emulsions with whey protein and lipid, respectively. The DHA levels in serum were found to be 8.8 ± 1.6 $\mu\text{g/ml}$ when LSO was given without emulsion formation. Thus, the DHA level in serum lipid was increased by 50 and 288 % in rats given LSO emulsion form with whey protein and with lipid, respectively when compared to those given native oil. In liver lipids, the EPA levels was increased by 130 and 510 % in rats given LSO encapsulated with whey protein or with lipid compared to those given native oil. The DHA level in liver was increased by 100 and 875 % in rats given LSO encapsulated in whey protein and in lipid compared to rats given native oil. These studies indicated that ALA was taken up and further metabolized to long chain omega-3 PUFA in a more efficient manner when given in encapsulated form with whey protein or with lipid. However, such a conversion of ALA to EPA or DHA was not observed when LSO encapsulated in gum acacia was given.

The pharmacokinetics of ALA absorption in rats fed flaxseed oil was recently studied by Coudelo et al. [28]. They quantitated the *in-vivo* absorption of ALA in thoracic lymph duct cannulated rats which were fed flaxseed oil in emulsified or non emulsified form. The maximum ALA

concentration in lymph of rats given non emulsified flaxseed oil was found to be 9 mg/ml in 5 h and the area under the curve kinetics was found to be 26 mg/h/ml. However, when flaxseed oil was given after emulsification with lecithin and sodium deoxycholate the maximum ALA concentration in lymph of rats was increased to 14 mg/ml at 3 h and the area under curve kinetics was increased to 48 mg/h/ml. Thus, a 55 % increase in ALA absorption and 85 % increase in ALA in lymph were observed when flaxseed oil was given in emulsion form. Further, the maximum levels of ALA were observed in chylomicrons within 3 h when given in emulsified form as compared to 5 h in control rats given native oil. This indicated a faster and higher rate of ALA absorption from emulsified oil. Earlier studies have also shown that egg phosphatidylcholine and soy phosphatidylcholine significantly enhances the intestinal absorption of triglyceride in rats [29]. Dietary gamma linolenic acid and EPA also showed a significant enhancement in the bioavailability when given as phospholipid emulsions [30, 31]. Marine phospholipids have also been used for making liposomes to deliver triacylglycerols containing EPA and DHA from fish oil. In this system it was observed that the lipid absorption in thoracic lymph duct-cannulated rats was 97 % when given in the liposome form but only 73 % absorption was observed when the oil was given in nonencapsulated form. DHA was assimilated to an extent of 91 % in the liposome group as against 65 % assimilation of DHA in the rats given fish oil without encapsulation [13, 32]. Higher levels of DHA was observed in the plasma TAG when fish oil was given in liposome form as compared to those given fish oil without encapsulation.

Earlier studies focused on the encapsulation of linseed oil to preserve its qualities and prevent oxidation of highly unsaturated ALA. [33, 34]. Recent studies have shown that the bioavailability of EPA and EPA + DHA was enhanced by 45 and 43 % in rats when provided in gelled emulsions (2–5 μm of particle size) as compared to those given without encapsulation [5]. Ammar et al. [4] have shown that the bioavailability of EPA was enhanced tenfold in encapsulated form as compared to those given without encapsulation. Raatz et al. [35] observed that emulsified fish oil had a higher absorption rate and showed enhanced levels of EPA and DHA in the serum of rats as compared to rats given fish oil in capsule form. The ratio of total omega-6 to omega-3 fatty acids in rats given emulsified fish oil was reduced significantly as compared to rats given fish oil in capsule form. Our results are in agreement with these findings where emulsified omega-3 rich oils showed higher bioavailability and resulted in the accumulation of long chain omega-3 fatty acids.

In addition to omega-3 rich oils, the absorption of lipophilic molecules such as curcumin and many drugs are also significantly enhanced when encapsulated in

phospholipid emulsions [36]. The bioavailability of anti-inflammatory compound such as curcumin was enhanced by 69 fold in rats when provided in phospholipid formulation [37, 38]. The antiarthritic drug piroxicam was also absorbed at a faster rate and reached a maximum of 53 $\mu\text{g/ml}$ when given as phospholipid dispersions, but reached a maximum level of 39 $\mu\text{g/ml}$ in plasma when given without phospholipids. The cyclosporin an immunosuppressant drug was absorbed better when given in vesicular lecithin system. Soy lecithin based nanoparticles enhanced the absorption of vinpocetine [39]. The maximum concentration of the drug observed in plasma was 3 $\mu\text{g/ml}$ when given with soy lecithin as compared a value of 0.75 $\mu\text{g/ml}$ when given without lecithin. The microemulsions of lecithin containing lipid as a surfactant enhanced the in-situ permeability of the drug Paclitaxel by threefold through the rat small intestine [40]. Drugs encapsulated in lipid showed higher anti-tumor activity against human breast cancer and multiple myeloma cell lines [41]. The Saquinavir drug loaded in flax seed oil containing lipid emulsion crossed the blood brain barrier [42].

All these studies clearly indicate that phospholipid based liposomes/emulsions could enhance the bioavailability of TAG, omega-3 fatty acids as well as drug molecules which are poorly soluble in aqueous media. We have used lipid to deliver ALA from LSO with greater efficiency. Lipid is made up of soy lecithin and phosphatidylethanolamine which again support the earlier observations that phospholipid based formulation can serve as effective delivery system for lipophilic molecules.

The conversion of linoleic acid however to longer chain ARA was not increased when rats were given SNO in microemulsion form. The rats given SNO, SNO encapsulated in whey protein and SNO encapsulated in lipid contained LA at similar levels in serum (490 ± 17 , 492 ± 18 , and 488 ± 14 $\mu\text{g/ml}$, respectively). The arachidonic acid content in the serum of rats given SNO, SNO encapsulated in whey protein and SNO encapsulated in lipid were also similar (212 ± 17 , 208 ± 11 , and 209 ± 8 $\mu\text{g/ml}$, respectively). Similar trends were observed in liver lipids. Earlier Gariova et al. [30] showed that the pre emulsification of edible oil mixture prior to ingestion increases the absorption of omega-3 fatty acids EPA and DHA but not that of saturated fatty acids and LA. Therefore, though the omega-3 fatty acid pathway appears to be activated when given as microemulsions with lipid, the same trend was not observed with the omega-6 pathway. This may also reflect on the higher levels of omega-6 fatty acids normally found in serum and liver and further requirement for its enhancement may not be warranted. However, since omega-3 fatty acids are limiting this pathway may have been activated. This requires activation of desaturase and elongase enzymes. The phospholipid based emulsions such

as lipid could achieve this as has been observed by increased levels of EPA and DHA in rats given ALA rich oil with lipid. The reason for this needs further investigation.

The ratio of omega-6 to omega-3 fatty acids is often considered to be crucial for the conversion of ALA to long chain omega-3 PUFA as omega-6 fatty acid (LA) can compete with delta-6 desaturase which acts on both omega-6 and omega-3 fatty acids. In our studies, the ratio of total omega-6 to omega-3 fatty acids in serum lipids was reduced by 80 and by 32 % when LSO encapsulated in lipid or with whey protein were given as compared to rats given LSO without emulsification. A similar trend were observed in the liver.

In addition to the nature of the encapsulated material, the particle size may also influence the bioavailability of entrapped materials. The nanoparticles have the ability to cross the gastrointestinal barrier either by passive diffusion or by active processes mediated by membrane-bound carriers or membrane-derived vesicles. Solid lipid nanoparticles (SLN) were used to enhance the bioavailability of γ -tocotrienol by tenfold as compared to the controls which were given as mixed micelles. The pharmacokinetics showed that the plasma concentration of γ -tocotrienol was significantly higher (938 ng/ml) in rats receiving SLN formulation compared to control (212 ng/ml). It is primarily caused by enhanced passive permeability (Abuasal et al.) [43]. The high adhesion of microemulsions to the gastrointestinal tract cause the emulsion droplets to remain closely in contact with intestinal cells for a long period promoting transmembrane transport of encapsulated material. The reduction in particle size increases the surface area of the particles. It has been reported that the delivery of drugs is enhanced when they are emulsified to increase the surface area of the delivery systems. The high dispersibility of emulsions enhances the steady absorption of encapsulated materials.

In conclusion, our study showed that ALA absorption from LSO was enhanced when given in the encapsulated form in lipid. Further ALA was also converted to EPA and DHA when ALA-rich oil such as LSO was given to rats as a microemulsion in lipid. This also caused the omega-6/omega-3 fatty acid ratio in the serum and liver to be lower. Thus, lipid may be a useful phospholipid based emulsifying material for enhancing the uptake of ALA and its conversion to long chain omega-3 fatty acids. However, the exact mechanism in terms of stability, surface area of the emulsion which may influence absorption mechanisms, hydrolysis of TAG in emulsions, chylomicron formation, protecting ALA from β -oxidation pathway to increase its availability to TAG synthesis and influence on desaturase pathway need to be addressed.

Acknowledgments The authors thank the Director of the Central Food Technological Research Institute for his encouragement and

support. D. Sugasini acknowledges the grant of a Senior Research Fellowship by the Indian Council of Medical Research, New Delhi, India. The authors thank A.M. Raichur and S. Anandkumar from the Indian Institute of Science, Bangalore for their help in particle size analysis. The authors also thank C. Radha for help in the operation of the high pressure homogenizer.

Conflict of interest There is no conflict of interest.

References

- Burdge GC, Calder PC (2005) Conversion of α -linolenic acid to longer-chain polyunsaturated fatty acids in human adults. *Reprod Nutr Dev* 45:581–597
- Brenna JT, Salem N, Sinclair AJ, Cunnane SC (2009) α -Linolenic acid supplementation and conversion to n-3 long chain polyunsaturated fatty acids in humans. *Prostag Leukot Essent Fatty Acids* 41:95–99
- Ramaprasad TR, Baskaran V, Sambaiah K, Lokesh BR (2010) Lower efficacy in the utilization of dietary ALA as compared to preformed EPA + DHA on long chain omega-3 PUFA levels in rats. *Lipids* 45:799–808
- Ammar W, Grahame M, Alberto D, Gordo B, Stephen A (2010) Enhanced bioavailability of eicosapentaenoic acid from fish oil after encapsulation within plant spore exines as microcapsules. *Lipids* 45:645–649
- Haug JJ, Sagmo LB, Zeiss D, Olsen IC, Draget IK, Seternes T (2011) Bioavailability of EPA and DHA delivered by gelled emulsions and soft gel capsules. *Eur J Lipid Res* 113:137–145
- Cansell M, Nacka F, Combe N (2003) Marine lipid based liposome increase in vivo FA bioavailability. *Lipids* 38:551–559
- Shaikh J, Ankola DD, Beniwal V, Singh D, Ravikumar NV (2009) Nanoparticle encapsulation improves oral bioavailability of curcumin by at least 9-fold when compared to curcumin administered with piperine as absorption enhancer. *Eur J Pharm Sci* 37:223–230
- Duan J, Zhao Y (2011) Chitosan–whey protein isolate composite films for encapsulation and stabilization of fish oil containing ultra pure omega-3 fatty acids. *J Food Sci* 76:C133–C141
- Gunasekaran S, Ko S, Xiao L (2007) Use of whey proteins for encapsulation and controlled delivery applications. *J Food Eng* 83:31–40
- Subirade M, Remondetto G, Beaulieu L (2003) Whey protein derived biomaterials and their use as bioencapsulation and delivery system. *Chem Ind* 57:617–621
- Minemoto Y, Hakamata K, Adachi S, Matsuno R (2002) Oxidation of linoleic acid encapsulated with gum arabic or maltodextrin by spray-drying. *J Microencaps* 19:181–189
- Zou J, Saulnier P, Perrier T, Zhang Y, Manninen T, Toppila E, Pyykko I (2008) Distribution of lipid nanocapsules in different cochlear cell populations after round window membrane permeation. *J Biomed Mater Res Part B: Appl Biomater* 87B:10–18
- Cansell M, Moussaoui N, Petit AP, Denizot A, Combe N (2006) Feeding rats with liposomes or fish oil differently affects their lipid metabolism. *Eur J Lipid Sci Technol* 108:459–467
- Hossain Z, Kurihara H, Hosokawa M, Takahashi K (2006) Docosahexaenoic acid and eicosapentaenoic acid enriched phosphatidyl choline liposomes enhance the permeability, transportation and uptake of phospholipids in Caco-2 cells. *Mol Cell Biochem* 285:155–163
- Carnielli V, Verlatto G, Pederzini F, Luijendijk I, Boerlage A, Pedrotti D, Sauer P (1998) Intestinal absorption of long chain polyunsaturated fatty acids in preterm infants fed breast milk or formula. *Am J Clin Nutr* 67:97–103
- McNamee BF, O’Riordan ED, O’Sullivan M (1998) Emulsification and microencapsulation properties of gum arabic. *J Agric Food Chem* 46:4551–4555
- Jafari SM, Assadpoor E, Bhandari B, Yinghe HE (2008) Nano-Particle encapsulation of fish oil by spray drying. *Food Res Int* 41:172–183
- Danviriyakul S, McClements DJ, Decker EA, Nawar WW, Chinachoti CP (2002) Physical stability of spray dried milk fat emulsions as affected by emulsifiers and processing conditions. *J Food Sci* 67:2183–2187
- Rosenberg M, Kopelman IJ, Talmon Y (1985) A scanning electron microscopy study of microencapsulation. *J Food Sci* 50:139–144
- Jafari SM, Yinghe HE, Bhandari B (2011) Role of powder particle size on the encapsulation efficiency of oils during spray drying. *Drying Technol* 25:1081–1089
- Morrison WR, Smith LM (1963) Preparation of fatty acid methyl esters and dimethyl acetals with boron trifluoride methanol. *J Lipid Res* 5:600–608
- Suresh D, Srinivasan K (2007) Studies on the in vitro absorption of spice principles—Curcumin, capsaicin and piperine in rat intestines. *Food Chem Toxicol* 45:1437–1442
- Folch J, Lees M, Stanley GHS (1957) A simple method for the isolation and purification of total lipids from animal tissues. *J Biol Chem* 226:497–509
- Kris-Etherton PM, Grieger JA, Etherton TD (2009) Dietary reference intakes for DHA and EPA. *Prostag Leukotr Essentl Fatty Acids* 81:99–104
- Sinclair AJ, Attar-Bashi NM, Li D (2002) What is the role of alpha-linolenic acid for mammals? *Lipids* 37:1113–1123
- Earnest CP, Hammar MK, Munsey M, Mikus CR, David RM, Bralley JA, Church TS (2009) Microencapsulated foods as a functional delivery vehicle for omega-3 fatty acids: a pilot study. *J Int Soc Sports Nutr* 6:12. doi:10.1186/1550-2783-6-12
- Ramaprasad TR, Baskaran V, Sambaiah K, Lokesh BR (2004) Supplementation and delivery of n-3 fatty acids through spray-dried milk reduce serum and liver lipids in rats. *Lipids* 39:627–632
- Couedelo L, Vaysse CB, Fonseca L, Montesinos E, Djoukitch S, Combe N, Cansell M (2011) Lymphatic absorption of α -linolenic acid in rats fed flaxseed oil-based emulsion. *Br J Nutr* 105:1026–1035
- Nishimukai M, Hara H (2007) Soybean phosphatidylcholine-induced enhancement of lymphatic absorption of triglyceride depends on chylomicron formation in rats. *Biosci Biotechnol Biochem* 71:1192–1197
- Garaiova I, Guschina IA, Plummer SF, Tang J, Wang D, Plummer NT (2007) A randomised cross-over trial in healthy adults indicating improved absorption of omega-3 fatty acids by pre-emulsification. *Nutr J* 6:4. doi:10.1186/1475-2891-6-4
- Chilton FH, Surette ME and Koumenis IL (2002) Fatty acid containing emulsion with increased bioavailability. US Patent 2002/0188024A1
- Cansell M (2010) Marine phospholipids as dietary carriers of long chain polyunsaturated fatty acids. *Lipid Technology* 22:223–226
- Jimenez M, Garcia HS, Beristain CI (2004) Spray-drying microencapsulation and oxidative stability of conjugated linoleic acid. *Eur Food Res Technol* 219:588–592
- Partenen R, Raula J, Seppanen R, Buchert J, Kauppinen E, Forsell P (2008) Effect of relative humidity on oxidation of flaxseed oil in spray dried whey protein emulsions. *J Agric Food Chem* 56:5712–5722
- Raatz SK, Redmon JB, Wimmergren N, Donadio JV, Bibus DM (2009) Enhanced absorption of n-3 fatty acids from emulsified

- compared with encapsulated fish oil. *J Am Diet Assoc* 109: 1076–1081
36. Fricker G, Kromp T, Wendel A, Blume A, Zirkel J, Rebmann H, Setzer C, Quinkert RO, Marin F, Goymann CM (2010) Phospholipids and lipid based formulation in oral drug delivery. *Pharm Res* 27:1469–1486
 37. Cuomo J, Appendino G, Dern AS, Schneider E, McKinnon TP, Brown MJ, Togni S, Dixon BM (2011) Comparative absorption of a standardized curcuminoid mixture and its lecithin formulation. *J Nat Prod* 74:664–669
 38. Hu L, Jia Y, Niu F, Jia Z, Yang X, Jiao K (2012) Preparation and enhancement of oral bioavailability of curcumin using microemulsions vehicle. *J Agric Food Chem*. doi:[10.1021/jf204078t](https://doi.org/10.1021/jf204078t)
 39. Luo Y, Chen D, Ren L, Zhao X, Quin J (2006) Solid lipid nanoparticles for enhancing vinpocetine's bioavailability. *J Controlled Release* 114:53–59
 40. Nornoo AO, Zheng H, Lopes LB, Restrepo BJ (2009) Oral microemulsions of paclitaxel: in situ and pharmacokinetic studies. *Eur J Pharm Biopharm* 71:310–317
 41. Maillard S, Ameller T, Gauduchon J, Gougelet A, Gouilleux F, Legrand P, Marsaud V, Fattal E, Sola B, Renoir JM (2005) Innovative drug delivery nanosystems improve the anti-tumor activity in vitro and in vivo of anti-estrogens in human breast cancer and multiple myeloma. *J Steroid Biochem Mol Biol* 94:111–121
 42. Vyas TK, Shahiwala A, Amiji MM (2008) Improved oral bioavailability and brain transport of saquinavir upon administration in novel nanoemulsion formulations. *Int J Pharm* 347:93–101
 43. Abuasal BS, Lucas C, Peyton B, Alayoubi A, Nazzal S, Sylvester PW, Kaddoumi A (2012) Enhancement of intestinal permeability utilizing solid lipid nanoparticles increases γ -tocotrienol oral bioavailability. *Lipids* 47:461–469

that are responsible for off-flavors in fish oils. Thus, it is possible to have oils with very low PV that taste very rancid. Secondary oxidation products are primarily assessed through the use of anisidine value (AV) for which GOED specifies a limit of 20 [1]. AV reflects the level of aldehydes with α - and β -unsaturation. There is very little evidence that AV and sensory properties are correlated; it may be that the sensitivity of this method is not high enough to detect minute changes in aldehyde concentrations that could affect sensory properties [2]. The poor relationship between PV, AV and sensory properties highlights the need for new methods to assess oil quality that correlate well with sensory parameters.

Sensory panels are the most accurate method for assessing fish oil quality as humans are capable of tasting certain compounds at concentrations much lower than chemical techniques are able to detect [2]. Unfortunately, sensory panels can be cost prohibitive due to the expenses associated with their set up and maintenance. An alternative to sensory panels is the use of solid phase microextraction (SPME), coupled with gas chromatography-mass spectrometry (GCMS), which can be used to monitor the presence of volatile secondary oxidation products in the headspace of fish oil. Volatile compounds are responsible for the off flavors and odors caused by oxidation.

The aim of this study is to compare the results of sensory panel assessment of three fish oils with different concentrations of EPA and DHA with PV, AV and proportions of volatile oxidation products. The goal is to create a robust method that can be used to predict sensory quality of fish oil and to identify key oxidative volatiles associated with those sensory properties.

Materials and Methods

Materials

SPME fibers (divinylbenzene/Carboxen/polydimethylsiloxane, 50/30 μm coating), a SPME fiber holder for manual sampling, 22-ml glass vials, polytetrafluoroethylene/silicone rubber septa and screw caps were purchased from Supelco (Oakville, ON). A custom-made heating block designed to accommodate 22-ml glass vials was used to control the temperature. Optima chloroform was obtained from VWR (Mississauga, ON). An Isotemp 100 Series Model 126G oven was used to incubate samples and was obtained from Fisher Scientific (Ottawa, ON) along with all other glassware. Methyl tricosanoate, methyl eicosapentaenoate, methyl docosahexaenoate and 1,2-dipalmitin were purchased from Nu-Chek Prep (Elysian, MN). 1,3-dipalmitin was purchased from Doosan Serdary Research Laboratories (Etobicoke, ON). Tripalmitin was purchased from

Sigma Aldrich (Oakville, ON), along with all other chemicals. Two fish oils containing a blend of mixed natural tocopherols were obtained from Ocean Nutrition Canada Ltd. (Dartmouth, NS) and a third oil was obtained from EPAX (Oslo, Norway). Oil 1 contained approximately 30 % EPA and DHA, while Oil 2 contained roughly 50 %. Oil 3 contained approximately 65 % EPA and DHA. All oils were marketed as triacylglycerols and all were blends of anchovy and sardine oil sourced from Peru.

Experimental Design

Amber bottles (250 ml) were each filled with 200 ml of fish oil and placed, uncapped, in an oven held at 40 °C. Oils were removed from the oven at varying time intervals, ranging from 2 to 15 h, over the course of 10–14 days, with a new bottle being used at each sampling point. From each bottle, aliquots of 14.0 ml were placed in 22-ml glass vials and then capped with phenolic screw caps with PTFE/silicone septa and analyzed with SPME-GCMS. Approximately 15 ml of each sample was used for PV and AV testing, and the remainder of each 200-ml sample was either stored at -80 °C under nitrogen or evaluated by a sensory panel. One sample per 24 h time period underwent PV and AV analysis and was tasted by a sensory panel. All samples were analyzed by SPME-GCMS. The experiment was conducted in triplicate for each of the three oil types.

Measures of Oil Quality

The fatty acid profile of the fish oil was analyzed using the method described by Sullivan Ritter et al. [3]. The PV and AV of each sample was measured in triplicate following American Oil Chemists' Society (AOCS) Official Method Cd 8-53 [4] and AOCS Official Method Cd-18-90 [5], respectively.

Lipid Class Analysis

Lipid classes were analyzed using HPLC. Aliquots of each oil were diluted with $\text{CHCl}_3/\text{MeOH}$ (2:1 by vol) to achieve a final concentration of 0.25 mg/ml. Samples were filtered using 0.45- μm filters and transferred to autosampler vials. Analysis was done in triplicate using a Thermo Finnigan Surveyor HPLC with an autosampler (Thermo Fisher Scientific, Mississauga, ON) coupled to a Sedex 80 low temperature evaporative light scattering detector (Sedere, North York, ON) set to 30 °C with a gain of 8. The injection volume for each sample was 10 μl . The mobile phase was made up of hexane and *tert*-butyl methyl ether (TBME) (Table 1) at a flow rate of 2 ml/min and the total run time was 10 min. Samples were first analyzed on a YMC-Pack PVA-Sil column (5- μm particles,

Table 1 Composition of mobile phase for gradient elution with HPLC analysis

Time (min)	Hexane (%)	TBME (%)
1	98	2
5	100	0
7	100	0
8	98	2
10	98	2

100 × 30 mm I.D.) with matching guard cartridge (2.0 × 20 mm I.D.) to confirm that samples did not contain any monoglycerol (MAG). Because of inconsistent retention times when the YMC-Pack PVA-Sil column was used, a silica column (Waters Spherisorb, 5- μ m particles, 250 mm × 4.6 mm) with matching guard column was used to quantify diacylglycerol (DAG) and triacylglycerol (TAG). The column was held at 20 ± 1 °C. Standard curves were prepared using tripalmitin, 1,2-dipalmitin and 1,3-dipalmitin with concentration ranges between 0.63 and 6.25 mg/ml depending on the standard.

SPME Analysis

The SPME method is described by Sullivan Ritter and Budge [6]. SPME samples were placed in a heating block held at 80 °C and allowed to equilibrate for exactly 15.0 min while the SPME fiber was placed in the injector port of the GC at 250 °C to desorb any volatiles that had accumulated during storage. The SPME fiber was then inserted into the vial at a depth of 2 cm and exposed to the sample headspace for exactly 45.0 min. Extracted volatiles were analyzed by ion trap GCMS in electron ionization mode (200 °C). The fiber was inserted into the injector of the GC to a depth of 5 cm (splitless mode, 250 °C; 1 mm liner) and left for 5 min. Volatile analytes were separated on a free fatty acid phase column (Nitroterephthalic acid modified polyethylene glycol 30 m × 0.25 mm ID × 0.25 μ m film thickness, Agilent, Mississauga, Canada). Helium was used as the carrier gas (1.0 ml/min). The oven temperature was initially held at 40 °C for 5 min and increased at a rate of 10 °C/min to 250 °C and held for 5 min (total run time 29 min). Data were acquired as area counts and converted to area percentages. Retention indexes were calculated by comparing retention times of oxidative volatiles to those of the two closest eluting *n*-alkanes in a C8–C20 retention index (RI) standard. Volatile oxidation products were identified by comparison to pure external standards. When standards were not available, compounds were tentatively identified by matching them with mass spectral data in the NIST/EPA/NIH Mass Spectral Library (National Institute of Standards and Technology), through matching of fragmentation patterns generated by

HighChem Mass Frontier 4.0 (HighChem Ltd., Bratislava, Slovakia) and through comparison to RI and fragmentation patterns available in the literature.

Sensory Assessment of Oil Quality

Between ten and twelve samples from each oil trial were assessed for quality using an untrained, descriptive sensory panel [7]. To assess tasting abilities of potential panelists, volunteers were screened to eliminate those who could not distinguish fishy flavors. This was accomplished by challenging them with a triangle test, consisting of acceptable, fresh fish oil with a low volatile content and fish oil that had been incubated in an open container at 40 °C for 7 days to force the formation of fishy volatiles. Those who could not distinguish between the fishy sample and the fresh sample were removed from the panel. The final panel consisted of 10 volunteers. Each panelist was asked to rank samples on a scale of 1–10, with 10 being “excellent” and 1 being “terrible”, using a fresh vegetable oil sample as a reference. These classifications were then used to assign a scalar value to each tasted sample. Samples with sensory panel scores ≤7 were considered unacceptable, based on the descriptions of the scalar values. Each sample evaluated by the final panel was tasted by a minimum of three people. The design and screening of the sensory panel as well as the score sheets used to evaluate the samples were adapted from guidelines provided by the AOCS [7]. Of the 184 samples analyzed with SPME-GCMS, 93 were evaluated for sensory characteristics, leaving approximately half untasted.

Statistical Analysis

Because SPME-GCMS data was expressed as area percentages, data was transformed using a geometric mean function [8], following Eq. 1.

$$x_n = Ln \frac{a_n}{\sqrt[n]{a_1 a_2 \dots a_n}} \quad (1)$$

where a_n is the amount, in area percent, of each peak quantified in the sample. This was necessary because proportional data are constrained between zero and one, thereby violating the assumption of independence of observations inherent in most statistical techniques [9]. These data were then combined with sensory panel results. The next step in data analysis was to remove outliers, as multivariate techniques are highly influenced by outliers. Mahalanobis distances are commonly employed to identify outliers in multivariate data sets and were used here. This measure takes into account the variance of each variable and the covariance between variables. These were

calculated for all samples as described by Filzmoser and Hron [10] and those with χ^2 statistic greater than the critical value for $p \leq 0.001$ were eliminated. Following this elimination, 10 % of remaining tasted samples were removed from the dataset to be used for method validation.

Because variables were highly correlated with each other, principal component analysis (PCA) was then used to reduce the number of variables in the dataset into a smaller number of uncorrelated variables. The new variables, called principal components (PC), were linear combinations of the original variables and maximized the variability they represented. Each PC had a value, or score, which corresponded to a specific data point (e.g. Fig. 1). Since each PC represented a linear equation of the original variables, loadings were simply the coefficients associated with each original variable in the equation. For instance, if a variable was particularly important in calculating a PC score, its loading might be 10, while a less important variable might have a loading of 0.1. Each replicate of each of the three oils underwent PCA of the covariance matrices. In the present study, the original data set contained 106 volatile oxidation products that were highly correlated and PCA was used to reduce the number of variables into separate PC.

PC scores were then treated as the independent variables in multiple linear regression analysis in order to generate an equation that could be used to predict the sensory quality of fish oil. Multiple linear regression is analogous to simple linear regression, but rather than one explanatory variables, there are multiple ones. This technique also requires that independent variables are uncorrelated. In this case, backwards linear regression was used, which begins by entering all predictor variables, in this case PC, into a regression model. The weakest predictor is then removed and the regression is recalculated. If the removal of a variable significantly weakens the model to the point where it is no longer significant, then that variable is added back

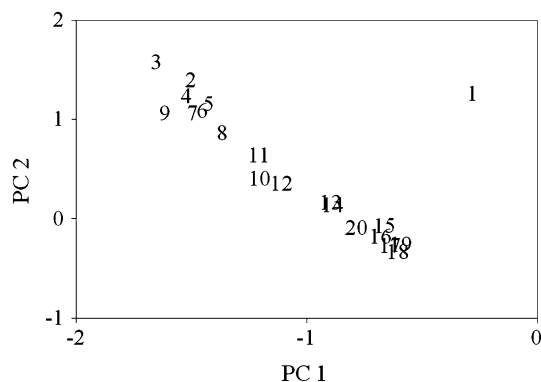


Fig. 1 Scores for principal components for Oil 2 Rep 1. Numbers correspond to the sequence in which samples were taken

in. This is repeated until only significant variables remain in the model. Often, more than one significant model ($p < 0.05$) was generated. In these cases, the model that had the highest R^2 and adjusted R^2 , and lowest standard error of the estimate was selected. To validate the function, a sensory score was calculated for the samples that were tasted but not used to create the regression by calculating the PCA scores for each sample that was not used in the original PCA and regression function and inputting them into the regression equation. The calculated sensory score was then compared to the actual sensory score assigned by the sensory panel. The final step in this analysis was to test in the same way the omitted samples in other trials of the same oil to check for robustness. SPSS 11.0 [11] statistical software was used for all statistical analysis.

Results

Fatty Acid Analysis

All three oils met suppliers' specifications for EPA and DHA (Table 2) and all three had different levels of these fatty acids.

Peroxide and Anisidine Values

As expected, PV and AV increased over time for all three oils. Initial PV was low (2.0 ± 1.3 mequiv/kg) for all samples, indicating that samples were only slightly oxidized at the beginning of the experiment. As the study progressed, the PV increased for all oils, far exceeding the 5 mequiv/kg limit specified by GOED (Fig. 2). Initial AV were also below the GOED limit of 20, with an average starting value of 9.4 ± 1.4 . These values increased over time, but only one sample exceeded this limit at the end of the experiment (Fig. 3). Although the rate of increase of PV and AV differs from oil to oil, the sensory ratings for each oil are consistent within oils of the same type. The average PV at which samples were deemed unacceptable by a sensory panel was 14.9 ± 6.5 mequiv/kg which is almost 3 times the PV limit of 5 mequiv/kg specified by

Table 2 EPA and DHA content ($n = 3$, mean \pm SD) of fish oils

Oil	EPA (mg/g)	DHA (mg/g)	Manufacturers specification (mg/g)
Oil 1	166 ± 1.4	125 ± 0.50	260
Oil 2	312 ± 5.5	225 ± 3.7	500
Oil 3	561 ± 3.3	157 ± 0.45	600

Manufacturer only guarantees an amount for combined EPA + DHA

Fig. 2 Variation in peroxide value (PV; mean \pm SD) in fish oil stored at 40 °C over time. The *dashed line* represents the PV limit set by GOED

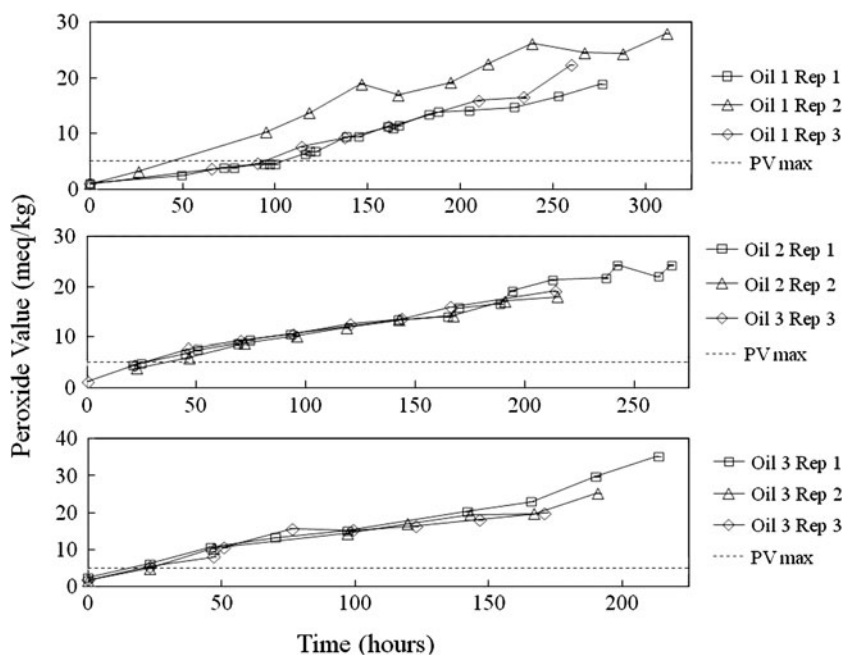
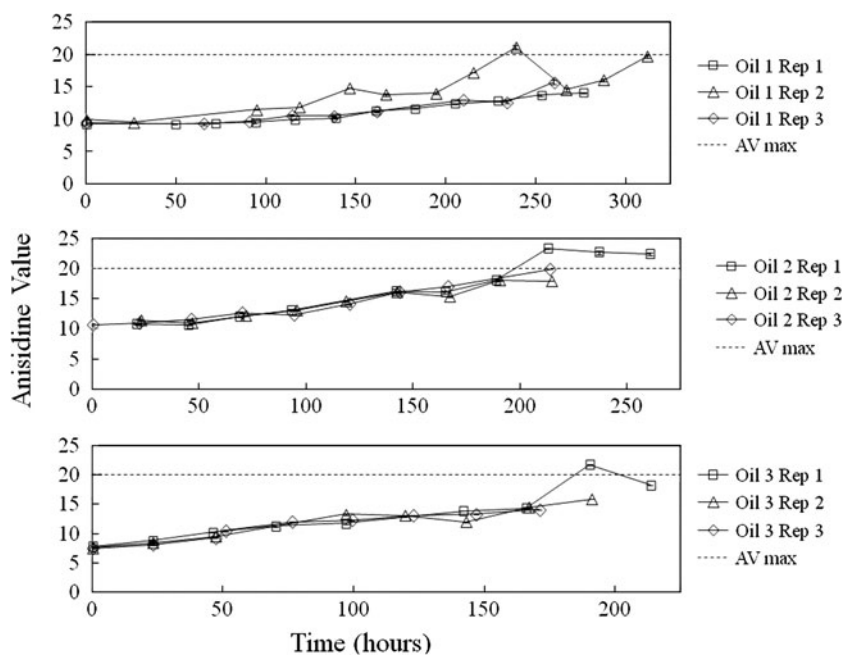


Fig. 3 Variation in anisidine value (AV; mean \pm SD) in fish oil stored at 40 °C over time. The *dashed line* represents the AV limit set by GOED



GOED. The average AV at the sensory rejection point was 14.2 ± 3.7 , almost 6 units below the GOED limit.

Lipid Class Analysis

TAG produced a linear standard curve while polynomial curves were the best fit for 1,2-DAG and 1,3-DAG. Oil 1 had higher TAG and lower DAG levels than specified by the manufacturer (Table 3), but Oil 2 and Oil 3 agreed with the manufacturers' specifications. In the case of Oil 1, the TAG value was likely higher because the oil did not

undergo a concentration step during processing. The FA profile of Oil 1 with EPA and DHA levels of 16.6 and 12.5 %, respectively, was what one would expect to find naturally in a sardine-anchovy oil blend that has not undergone concentration during refining [12].

SPME and Sensory Analysis

A total of 106 oxidation products were detected using SPME-GCMS (Fig. 4). The most common structures were aldehydes and ketones, though alcohols, acids and

hydrocarbons were also detected. Typical compounds associated with oxidation were detected, including 3-hexen-1-ol, heptenal and multiple isomers of 2,4-heptadienal. Sensory scores for the samples ranged from 10 (excellent) to 4 (very poor). The scores of the test samples used to validate the regression models fell within the range of the scores used to build the models. There were no correlations between any of the oxidation products mentioned above and sensory scores.

Statistical Analysis

PCA of SPME-GCMS data generated from five to nine PC for each of the nine oil trials. When these PC were used to develop regression models, from two to five PC were needed to create a significant regression function, depending on the oil type and replicate (Table 4). Although

the percent variance explained by the PC used in the regression models appear low, it was possible to achieve a high R^2 value (e.g. Oil 1 Trial 1). The reverse was also true (e.g. Oil 1 Trial 2). Regression of principal components gave well-fitting, significant ($p < 0.05$) models with for all but one oil replicate for Oil 3 (Table 4). Further statistical analyses on this trial were not carried out.

All samples that had not been used to create the regression functions were assigned sensory ratings using the appropriate regression function (Table 5). The calculated sensory scores for all three replicates of Oil 1 were quite close to the scores given by the sensory panel. All three samples had PV and AV levels below the average rejection values. The regression functions for two of the three replicates of Oil 2 also produced sensory scores that were very close to those given by the sensory panel. The sample with the poor result had a PV of 11.8 ± 0.0 mequiv/kg and an AV of 14.6 ± 0.1 . The AV of the sample was very close to the average AV score at the sensory rejection point, while the PV was approaching the rejection point. The other two replicates of Oil 2 had PV and AV values well below the rejection thresholds. For Oil 3, the regression equation for the first replicate gave scores that were different from those assigned by the sensory panel. This replicate had a PV (23.0 ± 0.0 mequiv/kg) much higher than the average PV at the rejection point. The AV (14.4 ± 0.1) of this sample was also close to the rejection value for AV. In contrast, the regression equations for the second replicate of Oil 3 gave

Table 3 Lipid class composition for fish oil ($n = 3$, mean \pm SD)

Oil	TAG (%)	Suppliers TAG specification	DAG (%)	Suppliers DAG specification
Oil 1	96.7 ± 12.0	70–75	3.35 ± 2.18	20–25
Oil 2	72.3 ± 13.1	70–75	27.7 ± 4.74	20–25
Oil 3	91.5 ± 10.0	90–91	8.55 ± 2.11	8

TAG Triacylglycerol, DAG Diacylglycerol

Fig. 4 Chromatogram of oxidation products for Oil 2 measured after 242 h of heating

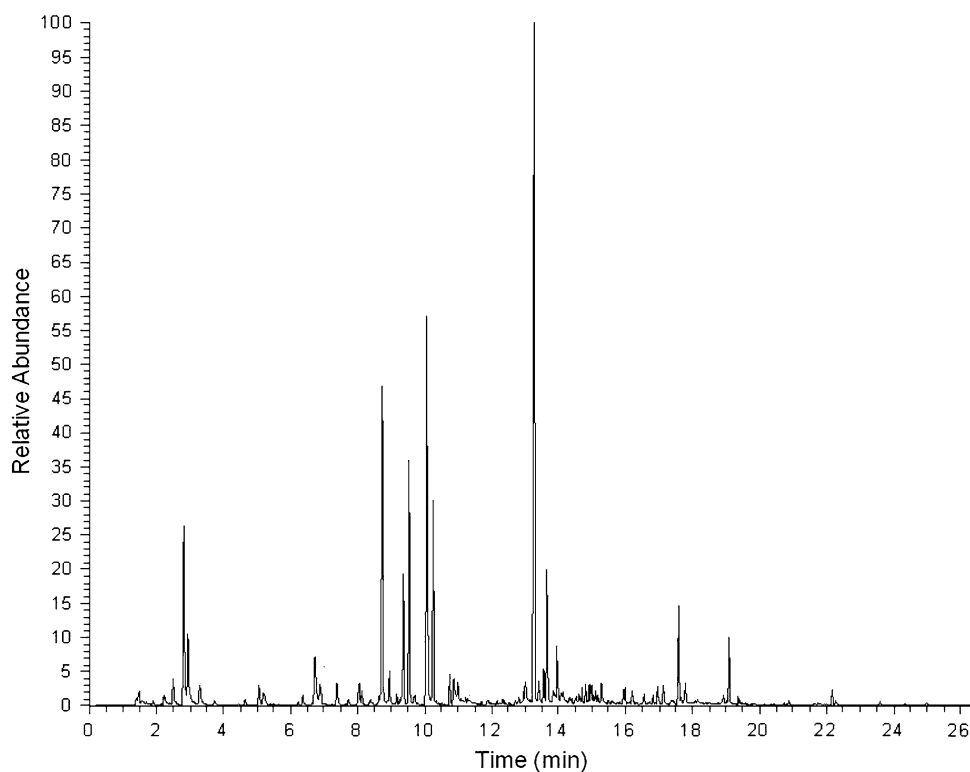


Table 4 Regression models for fish oil samples

Oil	PC in regression model	% Variance explained by PC	<i>p</i>	<i>R</i> ²	Adjusted <i>R</i> ²	Std error of Est.
Oil 1 Trial 1	1, 3	56.2	0.001	1.00	1.00	0.05
Oil 1 Trial 2	1, 4	71.9	0.033	0.68	0.57	1.07
Oil 1 Trial 3	1, 2, 4	78.6	0.026	0.98	0.96	0.41
Oil 2 Trial 1	1, 2, 4, 5	87.7	0.037	0.88	0.77	0.76
Oil 2 Trial 2	1, 2, 3, 6	85.4	0.026	0.95	0.89	0.53
Oil 2 Trial 3	1, 3, 4	62.9	0.036	0.86	0.75	0.90
Oil 3 Trial 1	1, 3, 4, 5, 6	78.4	0.015	0.99	0.98	0.20
Oil 3 Trial 2	1, 2, 3, 5	92.7	0.040	0.98	0.94	0.40

very accurate scores when compared to those given by a sensory panel. This samples had PV (5.0 ± 0.0 mequiv/kg) and AV (8.44 ± 0.1) that were well below the average rejection values. Finally, when regression equations were tested with other replicates of the same oil type, the calculated sensory scores agreed with the actual scores for all but Oil 3 Replicate 2 (Table 5). When the sensory score for the omitted sample from Oil 3 Replicate 2 was calculated using the regression function for Oil 3 Replicate 1 a score of -1 was obtained, a value that is not valid. All other samples were within three sensory units of their taste panel score and most were within one unit.

Discussion

PCA and multiple linear regression were used instead of other multivariate techniques because of the characteristics of the SPME-GCMS data. The high number of volatile oxidation products (>100) resulted in a situation where there were many more variables than tasted samples, which eliminated the use of many common statistical methods such as multivariate analysis of variance (MANOVA). The levels of volatile oxidation products were highly correlated as most compounds were either increasing or decreasing over time making regression on raw data impossible. The

Table 5 Sensory scores given by a taste panel and calculated sensory scores, PV and AV ($n = 3$, mean \pm SD) for select samples

Oil	Sensory panel score	Regression equation used to calculate sensory score	Calculated sensory score	Avg. PV (mequiv/kg)	Avg. AV
Oil 1 Trial 1	6	Oil 1 Trial 1	7	2.5 ± 0.0	9.3 ± 0.0
		Oil 1 Trial 2	4		
		Oil 1 Trial 3	5		
Oil 1 Trial 2	7	Oil 1 Trial 1	7	10.3 ± 0.0	11.5 ± 0.1
		Oil 1 Trial 2	6		
		Oil 1 Trial 3	7		
Oil 1 Trial 3	8	Oil 1 Trial 1	8	4.6 ± 0.0	9.7 ± 0.0
		Oil 1 Trial 2	5		
		Oil 1 Trial 3	7		
Oil 2 Trial 1	9	Oil 2 Trial 1	9	8.66 ± 0.0	12.0 ± 0.1
		Oil 2 Trial 2	9		
		Oil 2 Trial 3	9		
Oil 2 Trial 2	9	Oil 2 Trial 1	9	11.8 ± 0.0	14.6 ± 0.1
		Oil 2 Trial 2	8		
		Oil 2 Trial 3	9		
Oil 2 Trial 3	7	Oil 2 Trial 1	7	10.5 ± 0.0	12.3 ± 0.0
		Oil 2 Trial 2	4		
		Oil 2 Trial 3	5		
Oil 3 Trial 1	8	Oil 3 Trial 1	5	23.0 ± 0.0	14.4 ± 0.1
		Oil 3 Trial 2	8		
Oil 3 Trial 2	8	Oil 3 Trial 1	-1	5.0 ± 0.0	8.44 ± 0.1
		Oil 3 Trial 2	9		

changes in volatile levels occurred gradually so there was no clear divide between acceptable and unacceptable samples, instead there seemed to be an indistinct area where samples were neither good nor bad, making it difficult to obtain valid results using other classification techniques such as discriminant function analysis [6]. This was evident when scores of PC1 versus PC2 were plotted for each oil trial separately; samples showed a clear transition with time, with samples taken early in the time course in one quadrant and late samples in another quadrant (Fig. 3). Samples in the middle of the time course grouped near the center of the plot, emphasizing the lack of a distinct separation between new and old, or acceptable and unacceptable, indicating that the transition from acceptable to unacceptable happened gradually rather than suddenly. This gradual transition made it difficult to pinpoint the exact time when fish oil quality was considered unacceptable.

As an alternative, linear regression was considered. This is a useful technique for characterizing samples, but only if variables are uncorrelated. The volatile oxidation products studied here were highly correlated, so PCA was used to generate uncorrelated variables. PCA also greatly reduced the number of variables to <10. Linear regression of these variables generated a simple equation to assign sensory scores to fish oil samples. One tasted sample, selected at random, was left out of each trial with removal occurring before PCA analysis. Removal at this early point in data analysis allowed the samples to truly serve as a validation of the regression functions. One sample per oil trial corresponded to roughly 10 % of tasted samples being omitted during construction of the regression methods.

The combination of PCA and regression employed in this study allowed all data to be capitalized on as PCA transforms highly correlated variables, in this case volatile oxidation products, into uncorrelated linear combinations of the original variables, while still capturing all variability in the original data set. Initially, SPME-GCMS results of all replicates of all oils were combined and PCA was applied. When PC scores were examined, oils were clearly separated by oil type rather than state of oxidation as was expected due to differences in fatty acid and lipid class profiles between oils. It is well documented that PUFA, including EPA and DHA, oxidize more rapidly than other fatty acids [2, 13] so Oil 2 and Oil 3 which contained higher levels of these fatty acids were expected to oxidize at a different rate than Oil 1, with lower PUFA content. There is some evidence that DAG and MAG oxidize more rapidly than TAG [14, 15], so different levels of these structures in the oils may also be responsible for their clear separation based on volatile secondary oxidation products. Additionally, Oil 1 and Oil 2 were produced by the same manufacturer, while Oil 3 came from another, so slight

differences in oil refining processes could affect the oxidation patterns and stability of the oils. For example, differences in the winterization process may result in oils having higher levels of shorter chain saturated fatty acids, which are more resistant to oxidation. Because PCA results were not useful when applied to all trials of all oils combined in a single group, data were separated by oil type and PCA was applied to Oil 1, 2, and 3 separately. PCA then detected the variance between oil replicates, rather than changes occurring in the same oil due to oxidation, resulting in three distinct groupings of samples according to replicate within a time course. Slight differences between replicates of the same oil were expected, as all trials were done sequentially rather than concurrently. This was done intentionally in order to develop a more robust method but unfortunately prevented all time courses of the same oil from being analyzed as one unit. These results demonstrate the sensitivity of PCA to small changes in volatile composition among replicates of the same oil. Thus, it was necessary to treat each replicate of each oil as an individual experiment.

When regression equations were tested with samples from other replicates of the same oil type, Oils 1 and 2, along with the first replicate of Oil 3 gave results consistent with the sensory panel. The results of the second replicate of Oil 3 were poor, giving an impossible score of -1 . It is unclear what caused this odd result as no inconsistencies in the data were noted. With the exception of Oil 3 Trial 2, the consistency of the calculated scores compared to the sensory panel scores suggests that this classification method is robust and will hold true for oils of the same type, despite the need to develop separate regressions for each time replicate.

When PC and sensory panel scores were used to build regression equations, it became clear that the first PC (PC1) had a large affect on the reliability of the equation as all equations incorporated PC1. This is logical as PC1 is the component that describes the most variability in a given dataset. Because PC are linear combinations of the original variables, each PC is comprised of many oxidation products. For all trials, the compounds that had the highest correlations ($R \geq 0.80$) with each PC used in the regression equations were examined and compared. Since PC1 described such a large proportion of the change that occurred in the dataset and was incorporated into each regression equation, the replicates of the same oil type had many peaks in common, that were also highly correlated with PC1. When all replicates of all three oil types were compared there were eight peaks with high correlations with the PC used in the regression common to all trials (Table 6). These consisted of four aldehydes, one ketone, one benzene derivative and one hydrocarbon all of which had previously been identified in oxidized fish or fish oil. It

is interesting to note that not all of these compounds increased in proportion over time; three actually decreased.

It is well known that aldehydes play a role in the sensory properties of fish oil, and all four aldehydes identified here increase over time. (*E,Z*)-2,4-octadienal has been identified previously as a fish oil oxidation product and is associated with green odors [6, 16]. The second aldehyde, 3,6-nonadienal, is a degradation product of EPA and is associated with a green odor [2]. It has also been identified by MacFarlane et al. [17] as an oxidative volatile associated with sensory properties, and is a key component in the Fatty Acid Smell and Taste (FAST) method of predicting oil quality. The third aldehyde identified was (*E,E*)-2,4-decadienal, a compound with a deep-fried odor that is often identified in oxidized fish oil [17–19]. Jacobsen et al. [18] found that an increase in this oxidation product was correlated with an increase in rancid, fishy flavors in fish oil enriched mayonnaise. The final aldehyde associated with sensory properties of fish oil, (*E,E,Z*)-2,4,7-decatrinal, has been identified in oils and emulsions containing omega-3 fatty acids and is believed to have green, plant-like odors [16, 19, 20].

Only one ketone, 3,5-octadien-2-one, which increased over time, was shown to be strongly related to sensory parameters of all three oil types. The configuration of the double bonds could not be determined. Both the (*E,Z*) and (*E,E*) isomers of this compound have been identified in fish oil-enriched mayonnaise by Jacobsen et al. [18] and Hartvigsen et al. [16], who found that both isomers were strongly correlated with oxidation. Venkateshwarlu et al. [19] identified this ketone in fish oil-enriched milk. The (*E,Z*) isomer has been linked to green, fruity and fatty

odors as well as plastic and synthetic odors, while the (*Z,Z*) isomer is associated with fresh, green and fruity odors [16, 19].

The ether 2-ethylfuran was also identified as being a significant indicator of sensory characteristics, and decreased as oxidation progressed. This is a common oxidation product of omega-3 fatty acids and can be formed from the 12-hydroperoxide of EPA and the 16-hydroperoxide of DHA [21]. Venkateshwarlu et al. [19] identified this compound as having a sweet odor. Since sweet odors are commonly associated with positive sensory properties, a reduction in this compound could mean that positive sensory attributes are being eliminated as oxidation progresses, allowing negative attributes to become more noticeable.

An unknown isomer of decene had a strong relationship to sensory properties of oils and decreased over time. 1-decene can be formed during oxidation of oleic acid which is present in small amounts in fish oil [22]. Chung et al. [23] identified both 1-decene and 3-decene in mackerel although no relationship with sensory properties was mentioned. Although hydrocarbons are generally thought to be flavorless, the importance of this oxidative volatile to predicting sensory quality suggests that it plays a role in the flavor of fish oil.

Benzaldehyde was strongly associated with sensory properties of fish oil and decreased with time. This compound has a sweet odor and has been detected in fish oil-enriched mayonnaise [16], tuna oil [24] and cod liver oil [25]. It is unlikely that benzaldehyde is a direct product of fish oil oxidation, but it could be an oxidation product of a larger benzene derivative that was initially present in the oil. Giogios et al. [26] hypothesized that benzene compounds could be decomposition products of amino acid or sugars, explaining their low levels in fish oils.

PV and AV are convenient ways to monitor the formation of oxidation products in fish oil, but this work supports the well-known issue with these measures: limits, including those specified by GOED do not correlate with sensory properties of the oil. Hydroperoxides are primary oxidation products, which then degrade into volatile secondary oxidation products that are responsible for off-flavors and odors in oils. Frankel [2] has said that sensory panels can detect off-flavors in oils with PV < 1 mequiv/kg. This is supported by results collected by MacFarlane et al. [16] that showed freshly refined fish oil samples with PV of <1 mequiv/kg had strong fishy tastes. In some cases this might be because the hydroperoxides increased to their maximum and had now begun to degrade into secondary oxidation products. In that situation elevated AV would be expected. Conversely, the results of this study suggests that oils with high PV do not necessarily have poor sensory properties, likely because hydroperoxides have not yet

Table 6 Volatile oxidation products correlated with sensory characteristics of all 3 oils

Retention index	Compound	Direction of proportion change	Method of identification
963	2-Ethyl furan	Decrease	b, c
996	Octene	Decrease	b, c, d
1385	3,6-Nonadienal	Increase	b, c
1565	3,5-Octadien-2-one	Increase	b, c
1573	Benzaldehyde	Decrease	a
1608	(<i>E,Z</i>)-2,4-Octadienal	Increase	a
1820	(<i>E,E</i>) 2,4-Decadienal	Increase	a
1879	(<i>E,E,Z</i>) 2,4,7-Decatrinal	Increase	c, d

a: Retention index and MS fragmentation pattern compared with an external standard, b: NIST library match, c: probable ion fragmentation predicted using Mass Frontier 4.0, d: Comparison to retention index and spectral data from literature

degraded to sufficient extent to form detectable levels of secondary oxidation products.

A number of samples in this study had PV >10 mequiv/kg and were classified as acceptable by the sensory panel and the PV at the point of rejection was 14.5 ± 6.5 mequiv/kg, suggesting that the commonly used limit of 5 mequiv/kg is not appropriate. Although there is little evidence that AV is related to sensory properties of fish oils [2], a value of 20 is commonly used as the rejection value when assessing fish oil quality. Because the regression model was created using data produced by monitoring proportions of volatile oxidation products produced over time, these results suggest that AV may be of more importance to sensory quality than was previously thought, with an average AV of 14.2 ± 3.7 at the sensory panel rejection point being lower than the limit of 20 specified by GOED. Interestingly, MacFarlane et al. [17] found that fish oil samples that had poor sensory properties with PV <1 mequiv/kg also had AV <20 indicating that hydroperoxides had likely not yet reached their maximum and begun to degrade. The regression models created from SPME-GCMS data classified samples with AV >14 as unacceptable, with predicted sensory scores ≤ 7 , despite sometimes positive ratings given by the sensory panel. This also suggests that the current limit of 20 is too high. At least one study [27] found that AV was strongly correlated with sensory evaluation and headspace volatiles in partially hydrogenated soybean oil used for frying. The results of this study suggest that PV and AV may both be accurate and reliable methods to assess sensory quality but the limits that are currently used are not ideal, with the PV limit too low and the AV limit too high.

Sensory panels have long been recognized as the best way to monitor fish oil quality; however, the expenses associated with them often prevent them from being implemented. It is costly to train and maintain panels. Often people do not want to participate in a panel that involves tasting foods with poor sensory characteristics, so compensation is essential. A proper sensory panel requires specially designed tasting booths, lighting and air flow systems. Despite the best training, sensory assessment is still highly subjective and even trained panelists can give inaccurate results on occasion. Our results offer support for this. When our regression model was used to assign a sensory score to samples, the majority of the results were within one unit of the score given by the sensory panel. There were three samples that were assigned a high score (8 or 9) by the sensory panel, but when classified using the regression model, received scores of 5 suggesting that the sample was of poor quality. On closer examination, it was found that all three were samples that were taken late in the time course, and all had AV above 14.2, the average AV at the point of sensory panel rejection. Two of the three

samples also had PV >20 mequiv/kg indicating that oxidation had progressed considerably. The combination of these factors suggest that the regression models may actually be more accurate than the sensory panel in predicting the quality of highly oxidized oil samples; however, for the regression model to be accurate the sensory panel must also provide accurate initial assessments as this is the source of the data for the regression equations. Because of the cyclic relationship, it may be more logical to use PV and AV to evaluate the quality of very oxidized samples, or to present the taste panel with more samples to evaluate so that more data is available to build the regression model. This study was very small and limited samples were tasted by the sensory panel. Future research will focus on expanding the sensory panel and the number of oil samples evaluated to improve the robustness of this method.

The method presented here can be used by fish oil refiners and dietary supplement manufacturers to determine if fish oil has acceptable sensory parameters without the need to maintain an expensive sensory panel. Although a panel is required to develop the method, after the initial set up there should be no further need to maintain the sensory panel. Because the PV and AV limits currently used to determine oil quality seem to be of little use in predicting sensory quality, this method will provide more accurate results; however, in a commercial setting it should be possible to determine PV and AV limits that correlate with sensory parameters and then use these as an additional measure of quality. Based on results in this study, a maximum PV limit of 15 mequiv/kg and a maximum AV of 14 would appear to be appropriate for the oils used here.

In conclusion, PCA and linear regression can be used in conjunction with SPME-GCMS of oxidative volatiles to predict the sensory quality of fish oil. The method presented here suggests that the PV and AV values typically used to indicate fish oil quality have little relationship with sensory properties.

References

1. Global Organization for EPA and DHA (2008) Voluntary monograph for omega-3. <http://www.goedomega3.com/>. Accessed May 2008
2. Frankel EN (2005) Lipid oxidation, 2nd edn. The Oily Press, Bridgewater
3. Sullivan Ritter JC, Budge SM, St-Onge M (2009) Determining ethyl esters in fish oil using with solid-phase microextraction and GCMS. *J Am Oil Chem Soc* 86:743–748
4. Firestone D (ed) (1997) Official methods and recommended practices of the American Oil Chemists' Society, 4th edn. Method Cd 8-53, American Oil Chemists' Society, Champaign
5. Firestone D (ed) (1997) Official methods and recommended practices of the American Oil Chemists' Society, 4th edn. Method Cd 18-90, American Oil Chemists' Society, Champaign

6. Sullivan Ritter JC, Budge SM (2012) Fish oil sensory properties can be predicted using key oxidative volatiles. *Eur J Lipid Sci Technol*. doi:10.1002/ejlt.201100330
7. Warner K (1995) Sensory evaluation of oils and fat-containing foods. In: Warner K, Eskin NAM (eds) *Methods to assess quality and stability of oils and fat-containing foods*. AOCS Press, Champaign, pp 49–75
8. Aitchison J (1983) Principal component analysis of compositional data. *Biometrik* 70:57–65
9. Filzmoser P, Hron K, Reimann C (2009) Univariate statistical analysis of environmental (compositional) data: problems and possibilities. *Sci Total Environ* 407:6100–6108
10. Filzmoser P, Hron K (2008) Outlier detection for compositional data using robust methods. *Math Geosci* 40:233–248
11. SPSS Inc. (1999) *SPSS Base 10.0 for Windows User's Guide*. SPSS Inc., Chicago, IL
12. Finley JW, Shahidi F (2001) The chemistry, processing, and health benefits of highly unsaturated fatty acids: an overview. In: Shaidi F, Finley JW (eds) *Omega-3 fatty acids*. American Chemical Society, Washington, pp 2–11
13. Sullivan Ritter JC, Budge SM, St-Onge M (2011) Modeling the primary oxidation in commercial fish oil preparations. *Lipids* 46:87–93
14. Wang T, Jiang Y, Hammond EG (2005) Effect of randomization on the oxidative stability of corn oil. *JAOCS* 82:111–117
15. Kristensen JB, Nielsen NS, Jacobsen C, Mu H (2006) Oxidative stability of diacylglycerol oil and butter blends containing diacylglycerols. *Eur J Lipid Sci Technol* 108:336–350
16. Hartvigsen K, Lund P, Hansen KF, Hølmer G (2000) Dynamic headspace gas chromatography/mass spectrometry characterization of volatiles produced in fish oil-enriched mayonnaise during storage. *J Agric Food Chem* 48:4858–4867
17. Macfarlane N, Salt J, Birkin R (2001) The FAST Index—a fishy scale. *Inform* 12:244–249
18. Jacobsen C, Hartvigsen K, Lund P, Adler-Nissen J, Holmer G, Meyer AS (2000) Oxidation in fish-oil-enriched mayonnaise. *Eur Food Res Technol* 210:242–257
19. Venkateshwarlu G, Let MB, Meyer AS, Jacobsen C (2004) Chemical and olfactometric characterization of volatile flavour compounds in a fish oil-enriched milk emulsion. *J Agric Food Chem* 52:311–317
20. Karahadian C, Lindsay RC (1989) Evaluation of compounds contributing characterizing fishy flavours in fish oils. *J Am Oil Chem Soc* 66:953–960
21. Medina I, Satué-Gracia MT, Frankel EN (1999) Static headspace gas chromatographic analyses to determine oxidation of fish muscle lipids during thermal processing. *J Am Oil Chem Soc* 76:231–236
22. Min DB, Boff JM (2002) Lipid oxidation of edible oils. In: Akoh CC, Min DB (eds) *Food lipids: chemistry, nutrition and biochemistry*, 2nd edn. Marcel Dekker, New York, pp 335–364
23. Chung H, Choi A, Cho IH, Kim YS (2011) Changes in fatty acids and volatile components in mackerel by broiling. *Eur J Lipid Sci Technol* 112:1481–1490
24. Roh HS, Park JY, Park SY, Chun BS (2006) Isolation of off-flavors and odors from tuna fish oil using supercritical carbon dioxide. *Biotechnol Bioprocess Eng* 11:492–496
25. Guillén MD, Carton I, Salmeron J, Casas C (2009) Headspace composition of cod liver oil and its evolution in storage after opening. First evidence of the presence of toxic aldehydes. *Food Chem* 114:1291–1300
26. Giogios I, Grigorakis K, Nengas I, Pappasolomontos S, Papaioannou N, Alexis MN (2009) Fatty acid composition and volatile compounds of selected marine oils and meals. *J Sci Food Agric* 89:88–100
27. Thomkins C, Perkins EG (1999) The evaluation of frying oils with the *p*-anisidine value. *JAOCS* 76:945–947

local topography, wind, cloud cover, aerosols, ozone, green house gases, variable solar radiation fluxes and season [1]. The latest Intergovernmental Panel on Climate Change [2] report predicts, for non-mitigation global warming scenarios, increases in average surface air temperature of between 0.64 and 0.69 °C for 2011–2030 and, depending upon the modeling scenario, increases of as much as 1.8 °C by mid-century (2046–2065). In addition, the IPCC report predicts an increase in the number of extreme heat days for northern temperate ecosystems [2]. Sustained and extreme increases in surface air temperatures have an immediate effect on shallow systems (i.e. streams, ponds) as their water temperatures are directly influenced by air temperatures [3, 4]. Global warming is also contributing to polar stratospheric ozone loss, delaying the recovery of the ozone layer [5] which helps to protect life on the surface of the planet from damaging UVB radiation. Thus, temperature and UVB radiation are inextricably linked to global climate change where they function as key drivers of the proximate physical environment experienced by animals.

Temperature induces strong effects on the physiology of poikilotherms, including fishes. At the cellular level, temperature can be regarded as a stressor to which fish must respond in order to establish a new equilibrium between their environment and the physico-chemical properties of their membranous structures; a phenomena called “homeoviscous adaptation” by Sinensky [6]. Thus, biochemical and physiological adaptations in response to temperature, at the membrane level, provide the most sustained and specific response to fluctuating temperatures experienced by fish. These biochemical responses are principally mediated by changes in the composition and concentrations of individual fatty acids (FA) and sterols in cell membranes [7].

UV radiation also exerts strong effects on the physiology of fishes and other aquatic organisms [8]. In an earlier study, we demonstrated that juvenile Atlantic Salmon (*Salmo salar*, Linnaeus, 1758) exposed to enhanced levels of UVB radiation had higher mass fractions of 18:2n-6 and 18:3n-3, total n-6 FA and saturated fatty acids (SFA) in their tissues compared with fish in reduced UV treatments, suggesting that salmon exposed to UV radiation were more quiescent than fish in the reduced UV treatments resulting in a buildup of catabolic substrates [9]. This finding is broadly consistent with observations of depressed feeding behavior and reduced agonistic interactions in juvenile salmon exposed to UVR in artificial flumes [10]. In addition, exposure to enhanced UVB radiation retarded growth, decreased hematocrit value and plasma protein concentration, in Atlantic Salmon parr [11]. Such effects may, in general, decrease resistance to pathogens in salmonids [12]. Finally, exposure to UVB, regardless of water temperature, had a negative effect on immune function

parameters, growth and physiological condition of Atlantic Salmon parr, although interactive effects between temperature and UVB were also observed [13].

It is important to consider the effects of both UVB and temperature because these two physical forcing variables may act additively or synergistically on specific aspects of fish biochemistry, physiology, and behavior. Thus, we exposed Atlantic Salmon parr to three environmentally realistic [9, 11, 13] spectral treatments differing in the intensity of UVB radiation at two different temperatures (12 and 19 °C). We assayed FA mass fractions in Atlantic Salmon, held in outdoor rearing tanks subjected to different UV and temperature treatments, because lipids are key molecules involved in many cellular and physiological processes and because they are known to be sensitive to stress, including UVR. We tested the null hypotheses that juvenile (parr) Atlantic Salmon exposed to different temperature or UVB regimens demonstrated no direct and/or interactive effects on FA profiles in their dorsal skin, ventral skin, dorsal muscle, or ocular tissue.

Materials and Methods

Experimental Setup

The experiment was conducted at the Institute of Marine Research's (IMR) Austevoll Research Station (60°5'42"N, 5°13'8"E). At the beginning of the experiment 100 juvenile Atlantic Salmon (*Salmo salar*; Norsk LakseAvl strain; mean weight at start = 8.3 g) were placed in tanks (3 m wide × 1 m deep) which were filled with ~4,500 L of sand-filtered freshwater from a nearby lake. Incoming water was routinely aerated, the turnover rate was high, and the fish biomass to water volume ratio was very low, so oxygen was considered to be saturated. The fish were held in nylon net cages (50 × 60 × 60 cm; L × W × H) which were immersed in the water so that the distance from the surface to the bottom of the net cages was 30 cm.

The fish were randomly divided into the cages to achieve an even size distribution, and were fed with a specially prepared salmon feed (see below). The duration of the experiment was 54 days (July 17–September 8, 2003). At the end of the experiment all fish were euthanized using tricaine methanesulfonate (MS-222, Sigma Chemical Co). There were 6 tanks (experimental units) corresponding to the six possible spectral × temperature combinations (see below). Additional details of the experimental setup and conditions can be found elsewhere [9, 11, 13]. Fish were handled, and sacrificed, following standard procedures accepted by the Institutional Animal Care Committee of the Institute of Marine Research, Austevoll Aquaculture Research Station, Storebø, Norway.

Spectral Treatments

The three spectral treatments were: (1) natural sunlight filtered through Rohm Plexiglas® GS-231 (hereafter referred to as -UVR) which has a sharp cutoff below 400 nm (i.e. no UVB or UVA radiation), (2) UVB-depleted solar radiation (hereafter, -UVB) i.e. sunlight screened through polyester plastic film (0.2 mm thick Mylar-D®, DuPont Teijin Films, Delaware, USA, 50 % transmittance at 318 nm), and (3) solar radiation supplemented with UVB radiation (hereafter +UVB) from an overhead fluorescent tube lamp (TL40/12 RS, Philips Lighting, Rosendal, NL, emission maximum at 315 nm) placed 100 cm above the water surface. To remove UVC radiation the lamp was wrapped in cellulose triacetate film (95 mm, Clarifoil Co., UK), and the film was changed every 18 h. The lamp was turned on at noon for 4 h. For the spectral output of the TL40/12 RS lamp, see [14]. For details concerning the average daily irradiances in the +UVB and -UVB treatments see [13] Table 1).

These three spectral treatments were carried out simultaneously at two temperatures; at the normal rearing temperature of salmon in the area of the experimental site (~12 °C) and at ~7 °C above the normal rearing temperature (increased to ~19 °C by a thermostatic heater) to explore potential additive or synergistic effects of different combinations of the two environmental stressors. The temperature of the warm water treatment was consistently higher than the cold water treatment (repeated measures ANOVA on ranks, Tukey multiple comparison p value ≤ 0.0001 ; Fig. 1).

Salmon Diet

The feed was manufactured by Nofima (<http://www.nofima.com/>; formerly SSF, Norway), in spring 2002 and was utilized in another experiment conducted in 2002 [9].

Table 1 Degrees of freedom (d.f.) for three-way and two-way ANOVA tests conducted to assess the effects of temperature and exposure to ultraviolet radiation on fatty acids of Atlantic Salmon parr

Source of variation	Three-way ANOVA d.f.	Two-way ANOVA d.f.
Total	143	35
Temperature	1	1
UV exposure	2	2
Temperature \times UV exposure	2	2
Tissue	3	
Tissue \times temperature	3	
Tissue \times UV exposure	6	
Tissue \times temperature \times UV exposure	6	
Error	120	30

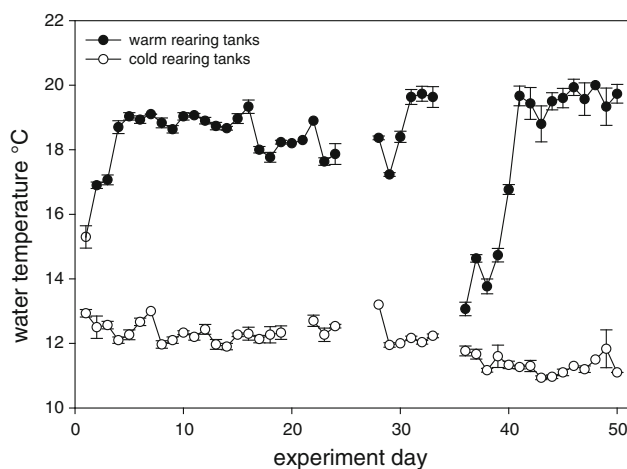


Fig. 1 Mean (\pm SD) water temperature of the experimental tanks used to test for the effects of temperature and UV exposure on juvenile Atlantic Salmon tissues ($n = 3$). The average water temperatures of the warm and cold-rearing tanks were 19 and 12 °C, respectively. Note: the average temperature of the cold rearing tanks was incorrectly reported as 14 °C in Jokinen et al. [13]

Peruvian Anchovy (*Engraulis ringens*) oil was added to the base feed formulation to provide the salmon with key dietary essential n-3 FA. This feed is hereafter referred to as the anchovy feed. The detailed ingredients, gross chemical composition, and energy content of the anchovy feed is provided elsewhere [9]. The feed was processed into 1.0, 1.5 and 2.0 mm diameter pellets so that juvenile salmon could be fed appropriately-sized particles as they grew. The feed was stored in the dark in a -50 °C chest freezer from the time it was manufactured until the end of the 2003 experiment. Salmon were hand-fed ad libitum.

Tissue Collections and Processing

At the end of the experiment, four different tissues were collected from six randomly selected Atlantic Salmon juveniles from each of the spectral and temperature combinations. The tissues sampled included dorsal and ventral skin, dorsal muscle) and ocular tissue. Dorsal skin, adjacent to the dorsal fin, was sampled by gripping it with a pair of surgical pliers and peeling it off the underlying muscle tissue. A surgical razor blade was then used to trim excess fat and/or muscle that remained attached to the skin. Ventral skin was obtained from the region between the pectoral fins and anus. Because we could not efficiently separate the retina from surrounding tissues we here refer to samples consisting of the entire posterior portion of the inner regions of the eye as ocular tissues. Ocular tissue was chosen because dietary supply of docosahexaenoic acid (DHA; 22:6n-3) is known to affect retinal DHA concentrations in fish [17, 18] and visual acuity in vertebrates [19–21]. Finally, UVR negatively affects several aspects of

vision in vertebrates (e.g. major cytoskeletal structures such as microtubules and actin) leading to cataract formation [22, 23]. We chose skinless dorsal muscle (landmarked to either side of the dorsal fin) because it is the largest tissue in these fish and because of its economic importance (i.e. filets). Dorsal skin was chosen because it should be a major target site for UVR damage [15, 16]. Ventral skin is relatively less pigmented (protected) than dorsal skin and, therefore, should be more vulnerable to the effects of UV radiation when/if exposed.

Fatty Acid Analyses

The tissue samples were placed in cryovials, frozen in liquid nitrogen and immediately transferred to a cryogenic freezer (-85°C) where they remained until FA analyses. All tissues were freeze-dried for 48 h prior to analyses. A total of 144 individual tissue samples were analyzed for FA (3 light treatments \times 2 temperatures \times 4 tissues \times 6 fish per treatment cell). Lipids and FAME of the freeze-dried salmon feed and salmon tissues were obtained in a three-step process: extraction [24], derivatization using the boron trifluoride method [25] and quantification on a HP6890 gas chromatograph (as in [26]). Each freeze-dried sample was weighed to the nearest microgram (Sartorius ME5 microbalance), and homogenized to extract the lipids in 2 mL of 2:1 (v/v) chloroform:methanol (modified from Folch et al. [24] in that dry tissues were extracted). This was repeated three times. The resulting supernatants (after centrifugation to remove non-lipid containing material) were combined in a 15-mL centrifuge tube. The lipid extract was then accurately adjusted to 8 mL with 2:1 (v/v) chloroform:methanol, and 1.6 mL of a 0.9 % NaCl in water solution was added. The two phases were then thoroughly mixed and centrifuged (2,000 rpm at 4°C). The upper aqueous layer was removed and discarded. The FA were dissolved in 2 mL hexane prior to derivatization. Two milliliters of BF₃-methanol (10 % w/w) was added and vials were heated (70°C) for 2 h after which 1 mL of water was added. The FAME-containing hexane-layer was carefully removed and put into a 2-mL Kuderna-Danish receiving vial (Sigma #6-4689U). One milliliter of hexane was then added to the original Shimadzu vial to extract the remaining FAME. This step was repeated once more to get the best extraction efficiency (90–95 %). The FAME-hexane solution was evaporated to 2.0 mL using nitrogen gas and transferred to a 2 mL glass GC vial and stored in a -80°C cryogenic freezer prior to GC analysis. FAME were quantified using a Hewlett Packard 6890 GC (splitless injection; column = Supelco SP-2560, 100 m \times 0.25 mm ID \times 0.20 μm thick film) by comparing peak retention times and areas between the samples and standard curves created using a 37-component FAME standard (Supelco

#47885-U). FA results are reported as mass fractions (i.e. μg FAME/mg dry weight tissue).

Statistical Analyses

The effect of water temperature and UV exposure on the FA composition of juvenile Atlantic Salmon tissues was examined using a series of analysis of variance (ANOVA) tests. FA mass fractions were log-transformed prior to analysis to satisfy normality and homogeneity of variance assumptions of parametric analysis. Three-way ANOVAs were used to compare FA composition among the four tissue types (dorsal muscle, dorsal skin, ventral skin and ocular) at two water temperatures (cold and warm) and three UV exposures (+UVB, -UVB and -UVR). Since multiple 3-way ANOVA testing was employed, the false discovery rate correction, which controls the proportion of errors among the rejected hypotheses, was applied to reduce the risk of Type I errors [27]. Two-way ANOVA and Tukey multiple comparison tests were used to compare FA responses to water temperature and UV exposure within each tissue type. Tukey multiple comparison tests control the Type I error rate for multiple pairwise comparisons [28]. Results are presented as untransformed means \pm SD. Differences were considered significant at $p < 0.05$. Statistical analyses were performed using SigmaStat for Windows software (version 3.11; Systat Software Inc., San Jose, CA, USA).

Results

Fatty Acids Profiles of Salmon Tissues

Juvenile Atlantic Salmon tissues had high mass fractions of 22:6n-3, 16:0 and 18:1n-9 (Fig. 2). The mean mass fraction of all other FA was $<5 \mu\text{g}/\text{mg}$ dry tissue. Mass fractions of total FA across all tissue types averaged $43.3 \pm 15.1 \mu\text{g}/\text{mg}$ dry tissue. FA composition differed among tissue type (three-way ANOVA; Tables 1, 2). In general, mass fractions of FA were greater in ocular tissue as compared to dorsal muscle and dorsal and ventral skin (Fig. 2). Differences among tissues were temperature dependent (Table 2). Temperature also interacted with UV exposure although UV exposure main effects were not significant.

Effect of Temperature and UV Exposure on Individual Tissues

The FA composition of dorsal muscle and dorsal and ventral skin tissues were not significantly affected by UV exposure (two-way ANOVA, UV exposure main effect $F_{2,30} \leq 3.1$, p values ≥ 0.06), but were often significantly

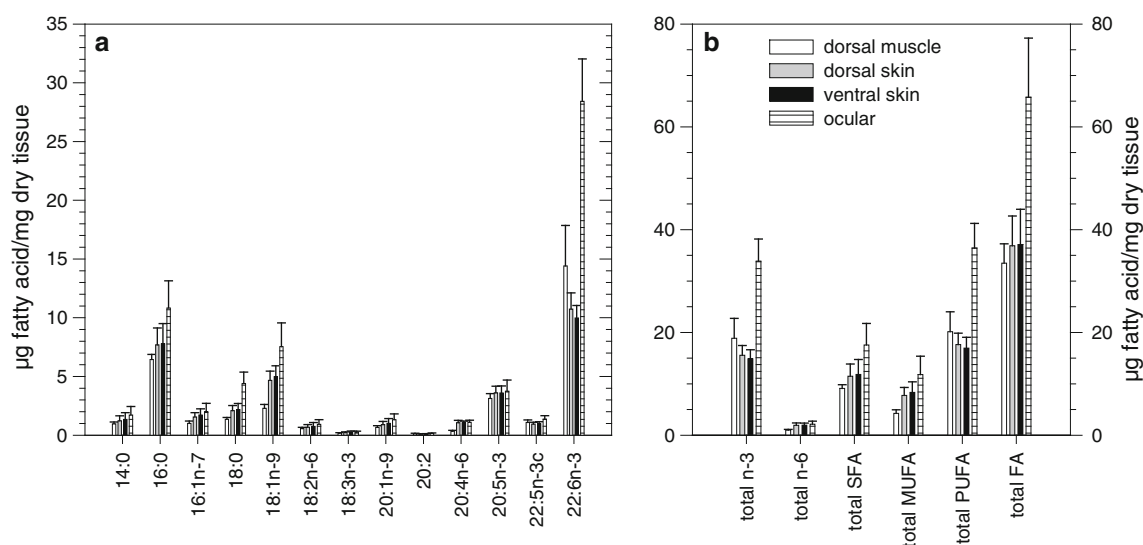


Fig. 2 Mean (\pm SD) mass fractions of individual (a) and summary (b) fatty acids in juvenile Atlantic Salmon tissues ($n = 36$ per tissue)

Table 2 Three-way analysis of variance F values summarizing the response of juvenile Atlantic Salmon tissues to water temperature and UV exposure ($n = 6$ per treatment combination)

Fatty acid	Main effects			Two-way interactions			Three-way interaction
	Tissue	Temperature	UV exposure	Tissue \times temperature	Tissue \times UV exposure	Temperature \times UV exposure	Tissue \times temperature \times UV exposure
14:0	28.71*	164.47*	0.57	15.48*	0.55	3.46 ^a	1.53
16:0	138.90*	214.15*	0.12	17.01*	0.67	7.70*	1.52
16:1n-7	61.11*	73.35*	0.73	10.47*	0.50	3.27 ^a	1.68
18:0	650.60*	271.33*	0.96	10.91*	0.53	8.71*	0.72
18:1n-9	411.96*	79.76*	1.59	14.16*	0.32	3.80 ^a	1.33
18:2n-6	16.91*	109.64*	1.06	16.10*	0.37	2.75	1.67
18:3n-3	11.53*	22.50*	1.40	12.26*	0.57	1.76	1.68
20:1n-9	40.90*	93.35*	1.23	12.63*	0.52	2.60	1.45
20:2	33.04*	18.64*	1.30	55.70*	0.78	3.18 ^a	2.52 ^a
20:4n-6	621.22*	3.15	1.54	25.25*	0.90	6.19*	1.66
20:5n-3	12.43*	95.05*	1.95	14.91*	0.84	3.18 ^a	2.28 ^a
22:5n-3	46.09*	4.08 ^a	0.67	27.72*	1.54	2.95	1.48
22:6n-3	512.22*	19.30*	1.81	19.49*	1.04	9.78*	1.90
Total n-3	357.57*	2.08	1.79	21.32*	1.06	8.30*	2.02
Total n-6	206.97*	91.53*	0.23	24.41*	0.12	4.10*	2.79*
Total SFA	185.27*	239.61*	0.18	17.04*	0.65	7.09*	1.44
Total MUFA	218.93*	96.18*	1.23	13.01*	0.36	3.37 ^a	1.49
Total PUFA	323.64*	0.00	1.71	22.39*	1.00	8.30*	2.16
Total FA	265.73*	52.51*	0.86	25.58*	0.71	8.23*	2.18 ^a

SFA saturated fatty acids, MUFA monounsaturated fatty acids, PUFA polyunsaturated fatty acids, FA fatty acids

* F value was significant at $p < 0.05$

^a F value was not significant after false discovery rate correction for multiple inferences

related to the water temperature at which fish were reared (temperature main effect p values < 0.05). For dorsal muscle tissue, mean mass fractions of the individual FA

16:0 and 18:0, as well as total SFA, were greater in fish raised at the warm water temperature (Table 3). Conversely, 18:3n-3, 20:2, 20:4n-6, 22:5n-3, 22:6n-3, total n-3,

Table 3 Fatty acid mass fractions ($\mu\text{g FA}/\text{mg dry tissue}$) of tissue in juvenile Atlantic Salmon reared at different water temperatures ($n = 18$)

Fatty acid	Dorsal muscle		Dorsal skin		Ventral skin	
	Cold water temperature	Warm water temperature	Cold water temperature	Warm water temperature	Cold water temperature	Warm water temperature
14:0	0.94 \pm 0.13 ^a	1.00 \pm 0.19 ^a	0.91 \pm 0.24 ^a	1.56 \pm 0.29 ^b	0.90 \pm 0.23 ^a	1.80 \pm 0.43 ^b
16:0	6.26 \pm 0.25 ^a	6.63 \pm 0.52 ^b	6.65 \pm 0.74 ^a	8.74 \pm 1.17 ^b	6.26 \pm 0.76 ^a	9.31 \pm 0.78 ^b
16:1n-7	1.02 \pm 0.16 ^a	1.01 \pm 0.22 ^a	1.32 \pm 0.27 ^a	1.80 \pm 0.28 ^b	1.35 \pm 0.28 ^a	2.08 \pm 0.48 ^b
18:0	1.27 \pm 0.09 ^a	1.46 \pm 0.13 ^b	1.77 \pm 0.22 ^a	2.42 \pm 0.32 ^b	1.74 \pm 0.25 ^a	2.64 \pm 0.19 ^b
18:1n-9	2.32 \pm 0.28 ^a	2.27 \pm 0.37 ^a	4.19 \pm 0.52 ^a	5.16 \pm 0.70 ^b	4.29 \pm 0.60 ^a	5.67 \pm 0.64 ^b
18:2n-6	0.57 \pm 0.08 ^a	0.55 \pm 0.13 ^a	0.51 \pm 0.14 ^a	0.85 \pm 0.16 ^b	0.52 \pm 0.14 ^a	0.99 \pm 0.28 ^b
18:3n-3	0.21 \pm 0.02 ^a	0.17 \pm 0.03 ^b	0.19 \pm 0.04 ^a	0.26 \pm 0.05 ^b	0.20 \pm 0.04 ^a	0.31 \pm 0.10 ^b
20:1n-9	0.68 \pm 0.10 ^a	0.67 \pm 0.16 ^a	0.71 \pm 0.18 ^a	1.09 \pm 0.19 ^b	0.71 \pm 0.20 ^a	1.30 \pm 0.35 ^b
20:2	0.17 \pm 0.02 ^a	0.08 \pm 0.01 ^b	0.10 \pm 0.02 ^a	0.11 \pm 0.02 ^b	0.10 \pm 0.01 ^a	0.12 \pm 0.02 ^b
20:4n-6	0.39 \pm 0.03 ^a	0.30 \pm 0.06 ^b	0.99 \pm 0.10 ^a	1.14 \pm 0.24 ^b	0.95 \pm 0.11 ^a	1.15 \pm 0.10 ^b
20:5n-3	3.14 \pm 0.35 ^a	3.12 \pm 0.48 ^a	3.26 \pm 0.27 ^a	3.97 \pm 0.54 ^b	3.13 \pm 0.33 ^a	4.08 \pm 0.36 ^b
22:5n-3	1.26 \pm 0.11 ^a	0.92 \pm 0.12 ^b	0.91 \pm 0.17 ^a	1.00 \pm 0.11 ^b	0.89 \pm 0.14 ^a	1.06 \pm 0.17 ^b
22:6n-3	16.89 \pm 2.61 ^a	11.93 \pm 2.13 ^b	10.98 \pm 1.24 ^{a,B}	10.49 \pm 1.50 ^a	9.57 \pm 1.21 ^a	10.38 \pm 0.74 ^b
Total n-3	21.54 \pm 2.92 ^a	16.19 \pm 2.69 ^b	15.37 \pm 1.66 ^a	15.77 \pm 2.09 ^a	13.82 \pm 1.66 ^a	15.89 \pm 1.17 ^b
Total n-6	1.05 \pm 0.09 ^a	0.94 \pm 0.14 ^b	1.65 \pm 0.15 ^a	2.24 \pm 0.45 ^b	1.61 \pm 0.16 ^a	2.30 \pm 0.24 ^b
Total SFA	8.76 \pm 0.45 ^a	9.45 \pm 0.78 ^b	9.71 \pm 1.22 ^a	13.27 \pm 1.81 ^b	9.28 \pm 1.23 ^a	14.39 \pm 1.42 ^b
Total MUFA	4.24 \pm 0.56 ^a	4.24 \pm 0.82 ^a	6.68 \pm 1.07 ^a	8.80 \pm 1.24 ^b	6.82 \pm 1.14 ^a	9.87 \pm 1.53 ^b
Total PUFA	22.76 \pm 2.96 ^a	17.51 \pm 2.74 ^b	17.12 \pm 1.75 ^a	18.15 \pm 2.55 ^a	15.53 \pm 1.78 ^a	18.34 \pm 1.36 ^b
Total FA	35.77 \pm 3.04 ^{a,A}	31.20 \pm 2.93 ^b	33.51 \pm 3.86 ^a	40.22 \pm 5.49 ^b	31.64 \pm 3.99 ^a	42.59 \pm 4.10 ^b

Values are expressed as means \pm SD. Values in the same row with different letters indicate significant differences between water temperature treatments within each tissue type (two-way analysis of variance temperature effect $p < 0.05$). Interaction terms were not significant ($p \geq 0.05$) with two exceptions

SFA saturated fatty acids, MUFA monounsaturated fatty acids, PUFA polyunsaturated fatty acids, FA fatty acids

^A Total FA was greater in the +UVB treatment as compared to the -UVB treatment at cold water temperature

^B 22:6n-3 was greater at cold water temperature as compared to warm water temperature within the -UVB treatment

total n-6, total polyunsaturated fatty acids (PUFA), and total FA were greater in fish reared at cold water temperature (Table 3). For dorsal and ventral skin tissues, mean mass fractions of the individual FA were greater in fish reared at the warm water temperature with the exception of 22:6n-3 in dorsal skin. The mean mass fractions of the summary FA indices were also greater in fish reared at warm water temperatures although differences in total n-3 and total PUFA were not significant in dorsal skin tissue (Table 3).

For ocular tissue, the mean mass fraction of most FA was greater in fish reared at warm water temperature (two-way ANOVA, temperature main effect p values < 0.05 ; Table 4). The effect of water temperature on FA composition in ocular tissue differed among UV exposure level (interaction effect $F_{2,30} \geq 3.3$, p values < 0.05 ; Table 4). At the colder temperature, juvenile salmon exposed to +UVB had higher mass fractions of 20:2, 20:4n-6, 22:6n-3, total n-3, total n-6, total PUFA and total FA in their ocular tissues

compared to fish exposed to -UVR (Tukey multiple comparisons, p values < 0.05). At warm water temperature, fish exposed to -UVR had higher mass fractions of 14:0, 16:0, 16:1n-7, 20:5n-3, 22:5n-3, total n-3, total n-6, total SFA, total PUFA and total FA in their ocular tissues compared to fish exposed to +UVB (Table 4). At both cold and warm water temperatures, FA mass fractions in ocular tissues of fish exposed to -UVB were intermediate to mass fractions in fish exposed to +UVB and -UVR (Table 4).

Discussion

Water temperatures in native streams and rivers inhabited by Atlantic Salmon can increase in response to the removal of riparian cover and/or because of climate warming. Removal of riparian cover (e.g., due to logging operations) can increase water temperature in streams by as much as 4 to 6 °C [29–31]. Climate model scenarios predict an

Table 4 Fatty acid mass fractions ($\mu\text{g FA}/\text{mg dry tissue}$) of ocular tissue in juvenile Atlantic Salmon reared at different water temperatures and UV exposure levels ($n = 6$)

Fatty acid	Temperature main effect <i>F</i> value	Cold water temperature			Warm water temperature		
		+UVB	–UVB	–UVR	+UVB	–UVB	–UVR
14:0	63.79*	1.37 ± 0.39 ^a	1.10 ± 0.29 ^a	1.03 ± 0.25 ^a	1.91 ± 0.55 ^a	2.25 ± 0.55 ^{ab}	2.65 ± 0.36 ^b
16:0	54.99*	9.91 ± 1.67 ^a	8.91 ± 1.19 ^a	8.57 ± 0.59 ^a	11.52 ± 1.72 ^a	12.22 ± 1.81 ^{ab}	13.84 ± 1.11 ^b
16:1n-7	39.76*	1.79 ± 0.48 ^a	1.44 ± 0.34 ^a	1.35 ± 0.28 ^a	2.09 ± 0.59 ^a	2.53 ± 0.61 ^{ab}	2.87 ± 0.36 ^b
18:0	70.82*	3.86 ± 0.69 ^a	3.65 ± 0.59 ^a	3.37 ± 0.18 ^a	4.84 ± 0.60 ^a	5.10 ± 0.66 ^a	5.58 ± 0.44 ^a
18:1n-9	50.59*	6.59 ± 1.39 ^a	6.06 ± 0.89 ^a	5.53 ± 0.47 ^a	8.03 ± 1.40 ^a	9.43 ± 1.70 ^a	9.60 ± 1.61 ^a
18:2n-6	49.14*	0.77 ± 0.25 ^a	0.59 ± 0.18 ^a	0.54 ± 0.15 ^a	1.01 ± 0.33 ^a	1.25 ± 0.34 ^a	1.40 ± 0.19 ^a
18:3n-3	9.04*	0.28 ± 0.08 ^a	0.21 ± 0.06 ^a	0.19 ± 0.05 ^a	0.25 ± 0.06 ^a	0.29 ± 0.09 ^a	0.34 ± 0.05 ^a
20:1n-9	40.85*	1.16 ± 0.28 ^a	0.95 ± 0.26 ^a	0.85 ± 0.19 ^a	1.40 ± 0.38 ^a	1.69 ± 0.47 ^a	1.91 ± 0.25 ^a
20:2	0.51	0.19 ± 0.05 ^a	0.15 ± 0.04 ^{ab}	0.14 ± 0.03 ^b	0.14 ± 0.02 ^a	0.14 ± 0.03 ^a	0.17 ± 0.02 ^a
20:4n-6	12.72*	1.15 ± 0.14 ^a	0.99 ± 0.15 ^{ab}	0.90 ± 0.05 ^b	1.09 ± 0.13 ^a	1.15 ± 0.16 ^a	1.30 ± 0.19 ^a
20:5n-3	58.61*	3.42 ± 0.59 ^a	2.91 ± 0.41 ^a	2.82 ± 0.26 ^a	4.03 ± 0.78 ^a	4.37 ± 0.76 ^{ab}	4.97 ± 0.41 ^b
22:5n-3	21.28*	1.31 ± 0.18 ^a	1.17 ± 0.16 ^a	1.14 ± 0.13 ^a	1.37 ± 0.26 ^a	1.53 ± 0.32 ^{ab}	1.72 ± 0.18 ^b
22:6n-3	2.35	32.23 ± 3.06 ^a	29.26 ± 3.26 ^{ab}	26.02 ± 0.90 ^b	26.23 ± 3.11 ^a	26.74 ± 4.09 ^a	30.06 ± 2.54 ^a
Total n-3	0.07	37.30 ± 3.59 ^a	33.61 ± 3.84 ^{ab}	30.22 ± 1.12 ^b	31.99 ± 4.04 ^a	33.05 ± 5.08 ^{ab}	37.16 ± 2.98 ^b
Total n-6	52.34*	2.04 ± 0.36 ^a	1.66 ± 0.31 ^{ab}	1.52 ± 0.19 ^b	2.26 ± 0.39 ^a	2.57 ± 0.52 ^{ab}	2.90 ± 0.22 ^b
Total SFA	68.83*	15.58 ± 2.74 ^a	14.03 ± 2.01 ^a	13.35 ± 1.03 ^a	18.98 ± 2.96 ^a	20.40 ± 3.14 ^{ab}	22.99 ± 1.95 ^b
Total MUFA	55.10*	10.20 ± 2.16 ^a	9.01 ± 1.57 ^a	8.23 ± 1.00 ^a	12.59 ± 2.57 ^a	15.04 ± 3.09 ^a	15.72 ± 2.53 ^a
Total PUFA	1.36	39.56 ± 3.90 ^a	35.43 ± 4.18 ^{ab}	31.88 ± 1.28 ^b	34.71 ± 4.55 ^a	36.21 ± 5.67 ^{ab}	40.75 ± 3.25 ^b
Total FA	24.35*	65.34 ± 7.98 ^a	58.46 ± 7.56 ^{ab}	53.46 ± 3.16 ^b	66.28 ± 9.87 ^a	71.65 ± 11.34 ^{ab}	79.46 ± 7.39 ^b

Values are expressed as means ± SD. Values in the same row with different letters indicate significant differences between UV treatments within each water temperature treatment (Tukey multiple comparison test $p < 0.05$)

SFA saturated fatty acids, MUFA monounsaturated fatty acids, PUFA polyunsaturated fatty acids, FA fatty acids

* *F* value was significant at $p < 0.05$

increase in the number of extreme heat days as well as globally-averaged increases in surface air temperatures of between +0.64 and +0.69 °C for 2011–2030 and as much as +1.8 °C by mid-century (2046–2065) [2]. Past climate warming (e.g. the period between 1985 and 2009) has already increased mean night-time surface water temperatures of inland water bodies by an average rate of 0.045 ± 0.011 °C year⁻¹ (and as high as 0.10 ± 0.01 °C year⁻¹) with the greatest warming in the mid- and high latitude ranges of the northern hemisphere [32] inhabited by Atlantic Salmon.

Atlantic Salmon grow optimally at ~16 °C [33]. Here, we demonstrate that increasing the water temperature by ~7 °C (from 12 to 19 °C) had pronounced effects on mass fractions of individual FA and on summary FA measures for all four tissues of Atlantic Salmon (Tables 3, 4). This suggests that anthropogenically-induced (climate change and/or removal of riparian cover) increases in the water temperature of boreal freshwater streams and rivers could affect the nutritional status of juvenile (parr) Atlantic Salmon. This interpretation must be tempered by the reality that Atlantic Salmon will encounter much larger changes in

temperature than the relatively constant conditions to which they were exposed during our experiment. Further, the temperature increase in our experiment should be viewed as a worst-case scenario. Nevertheless, our experimental design isolated the specific effects of temperature on FA profiles, which is difficult to impossible to do in the complex environments of natural streams and rivers. With these caveats in mind, our results can be viewed as indicative of how increasing water temperature in streams and rivers may affect wild juvenile Atlantic Salmon at biochemical and physiological levels during the period prior to and during smoltification. Further, the observed changes in mass fractions of specific FA in dorsal muscle are broadly consistent with what has been observed with respect to membrane adaptations (average membrane lipid order, i.e. fluidity) in response to changing temperature [7]. In agreement with these previous findings we also observed generally higher mass fractions of total and individual SFA (16:0, 18:0) and lower mass fractions of total and individual PUFA (e.g. 18:3n-3, 22:5n-3, 22:6n-3, and 20:4n-6) in dorsal muscle (Table 3) as temperatures increased. Finally, others [34] have commented on the potential of

climate change to affect the health of Atlantic Salmon in native streams/rivers. These authors point out that climate change models for the Maritime Provinces of eastern Canada (where natural reproduction of Atlantic Salmon still occurs) indicate an expected increase in air temperature of between 2 and 6 °C and they highlight how fork lengths (a gross index of fish condition) of Atlantic Salmon are negatively correlated with water temperatures.

Muscle is a good long-term integrator of the effects of changing temperatures and/or diet on a fish's nutritional status [35]. Juvenile salmon remain in freshwater streams and rivers for periods ranging from a year to several years and then transform from parr to smolts during their migration to the ocean. During this period they eat a diet mainly consisting of freshwater invertebrates [36, 37] which contain high levels of C₁₈ PUFA, intermediate levels of C₂₀ PUFA and generally lower levels of C₂₂ PUFA [38–40]. It has been suggested that lipid metabolism in salmon may influence the process of parr-smolt transformation, ultimately affecting successful seawater adaptation [41]. For example, hepatocyte fatty acyl desaturation/elongation activities in juvenile Atlantic Salmon are primarily controlled by environmental factors such as temperature and photoperiod but diet also plays a role [42]. Thus, prior to smoltification the FA composition of parr salmon is influenced by, (1) diet, (2) their ability to modify that dietary FA input via catabolism and by desaturation and elongation pathways and, (3) the influence of water temperature and photoperiod (and possibly also the levels of UV to which they are exposed) on the latter processes. During the period leading up to smoltification, tissue FA composition changes from a typical freshwater pattern, which is relatively low in long-chain polyunsaturated fatty acids (LC-PUFA), to a more typical marine pattern which is relatively rich in LC-PUFA such as 20:5n-3 and 22:6n-3 [42]. Thus, the elevation of n-3 LC-PUFA in salmonids is considered a key pre-adaptive response to seawater entry [43, 44]. Our finding that n-3 LC-PUFA in muscle tissue was reduced at warmer water temperatures—even while diet remained constant—suggests climatic warming and/or removal of riparian cover may affect the physiological competency of Atlantic Salmon with respect to their ability to transition from freshwater to seawater.

The fish feed used in our experiment deviated from the natural, mostly insect-based, food of wild parr salmon in that aquatic insects have relatively higher amounts (both as proportions and mass fractions) of 18:3n-3 and 18:2n-6 and lower amounts of 20:5n-3 and especially 22:6n-3 than the anchovy-based feed. When diets more closely mimic the FA composition of aquatic insects, desaturation of 18:3n-3 and 18:2n-6 to LC-PUFA such as 20:5n-3, 22:6n-3 and 20:4n-6 occurs at a higher rate than when predominantly fish oil diets are fed to Atlantic Salmon parr [41]. Thus,

desaturation rates are expected to be more conservative in our experiment. Nevertheless, we observed significantly lower concentrations of 18:3n-3, 20:4n-6, 22:6n-3, total n-3, total n-6 and PUFA in dorsal muscle of fish raised at the warmer temperature (Table 3). This occurred despite the fact that mass fractions of other FA did not change significantly (e.g. 14:0, 16:1n-7, 18:2n-6, 20:1n-9, 20:5n-3) or else increased (16:0). In our experiments, diet quality (anchovy-based feed) and quantity (all fish were fed ad libitum) was the same in all treatments so any changes in the mass fractions of FA in the four tissues examined here, in response to increasing temperature, are not attributable to differences in the underlying diet. It is also important to note that, in natural situations, the essential FA composition of lower trophic level organisms in aquatic food webs (e.g. algae, seston, zooplankton, and aquatic insects) inhabited by, and ultimately consumed by, higher trophic level consumers like salmon may also be negatively affected by water temperature (e.g. [45, 46]). In addition, all of the salmon used in this experiment came from the same broodstock and were randomly allocated to the different treatments, therefore, it is unlikely that there would have been gross systematic differences among the individual fish (for genetic reasons) with respect to their ability to desaturate and elongate shorter-chain FA. Taken together, these results suggest that desaturase and elongase activities were higher in salmon raised in colder water resulting in generally higher tissue PUFA mass fractions, although we cannot rule out the possibility that dietary PUFA were merely retained at a higher rate in the cold water treatment.

We also observed that mean mass fractions of most of the individual FA in dorsal and ventral skin tissues were greater in fish reared at the warm water temperature with the exception of 22:6n-3 in dorsal skin (Table 3). Although a review of the literature did not reveal previous studies relating water temperature to fish skin FA composition, other researchers have provided evidence that subjecting fish to water temperatures that are substantially different than their optimal growth temperature may increase the risk of parasite infection [47, 48]. For example, sea lice (*Lepeophtheirus salmonis*) infections of cultured Atlantic Salmon are highest in summer and/or in shallow bays when temperatures are warmest [49]. The barrier functions of the skin are primarily a consequence of the lipid composition of the stratum corneum [50], therefore, we suggest that the increases in specific individual FA that we observed as a function of increasing temperature may represent a generalized defense response to the increased risk of parasite infection when salmon are raised in water temperatures that are above their optimal growth temperatures.

UV-induced damage including, for example, sunburn [51, 52] and reduced numbers of mucous secreting goblet cells [15] have been observed in some fish species, whereas

other species appear to benefit from protective substances in their skin [53, 54]. Lipids in the outermost layer of skin (*stratum corneum*) are affected by UV exposure in three ways; (1) β scission (fragmentation of the carbon chain), (2) hydrogenation of the double bond of unsaturated compounds and (3) formation of oxygenated entities from unsaturated lipids [50]. In our experiments, the FA composition of dorsal and ventral skin tissues were largely unaffected by UV exposure. Similarly, Arts et al. [9] did not observe significant changes in mass fractions of individual FA of dorsal skin in Atlantic Salmon exposed to enhanced UVB radiation.

Although the main effects of UV exposure on FA profiles were not significant across tissues in our experiment there were, nonetheless, significant interactive effects between temperature and UV exposure for certain FA and FA summary indices (Table 2). These interactive effects were mostly driven by changes in mass fractions of several FA in ocular tissue (Table 4). Enhanced UVB had different effects on individual FA mass fractions when fish were raised in cold versus warm water conditions. Specifically, ocular tissues of fish raised in cold water demonstrated higher mass fractions of 22:6n-3 and 20:4n-6 in response to enhanced UVB stress, whereas this effect was not observed in ocular tissue of fish raised in warm water. We suggest, for the reasons below, that this may be an adaptive metabolic response of ocular tissues to enhanced UVB stress. We further suggest that future studies examine free radical production, vitamin status and histology in skin and ocular tissues as a function of UV exposure and that fatty acid analyses be conducted on specific phospholipid classes (e.g. phosphatidylcholine, phosphatidylethanolamine) so that the overall response to UV radiation can be better understood.

Compromised vision occurs in fishes exposed to UV radiation under controlled experimental conditions. For example, cataract formation increased in Rainbow Trout (*Onchorynchus mykiss*) that received chronic UV exposure [23] while corneal tissue transmission decreased in UV-exposed Hawaiian Saddleback Wrasse (*Thalassoma duperrey*) [54]. Similarly, damage from ambient solar UVR was concluded to be a contributing factor explaining the formation of anterior lens cataracts in cage-reared Atlantic Halibut (*Hippoglossus hippoglossus*) [55]. Finally, wild Atlantic Salmon postsmolts taken from trawl hauls in the Norwegian Sea demonstrated effects ranging from hazy opacity in the anterior part of their lenses to cataracts affecting the whole lens [56]. These authors concluded that the primary cause of these cataracts was defective osmoregulation but they did not rule out oxidative stress caused by exposure to UV radiation as a contributing factor to osmotic cataract development.

Vertebrate retinal tissue is known to contain high concentrations of 22:6n-3 mostly located in membrane

phospholipids [57] and retinal 22:6n-3 concentration in fish is known to be responsive to dietary 22:6n-3 manipulations [18]. The 22:6n-3 contained in the vertebrate retina plays a crucial role in visual acuity [21], in part by promoting the survival and differentiation of photoreceptors [20]. Thus, 22:6n-3 is critical for both visual acuity (especially at low light intensities, [17]) and schooling behavior in fish [58].

Desaturases and elongases appear to be up-regulated in Atlantic Salmon raised in cold water compared to warm water, as evidenced by significantly higher concentrations of 22:6n-3 in dorsal muscle (Table 3). Up-regulation of enzymatic activity related to the production of higher amounts of n-3 LC-PUFA is consistent with what other researchers have found when teleosts are exposed to colder water temperatures [59]. Although we did not measure cataract formation or lens opacity, the studies summarized above suggest that compromised vision possibly occurred in the Atlantic Salmon parr exposed to enhanced UVB radiation in our experiment. We further suggest that the increased rate of 22:6n-3 synthesis in cold-water-raised salmon likely provided them with a compensatory mechanism to deal with compromised vision as a result of exposure to enhanced UVB radiation. Thus, we hypothesize that, as visual acuity was compromised following exposure to enhanced UVB radiation, salmon in the cold water treatment were able to compensate for reduced light transmission to the retina by increasing the mass fraction of 22:6n-3 (Table 4). We found a similar pattern when comparing the response of ocular tissue FA between two feeds that differed in mass fraction of LC-PUFA [9]. In that study, ocular tissues of fish in the enhanced UVB treatment had higher 22:6n-3 and 20:4n-6 mass fractions when they were fed a LC-PUFA-rich food source as compared to when they were fed a relatively less rich LC-PUFA food source, again suggesting that when higher amounts of LC-PUFA are available (either through diet or through temperature-induced up-regulation of desaturases and elongases) ocular tissues compensate for reduced function (e.g. cataracts, opacity) by increasing 22:6n-3 concentrations.

Conclusions

Raising the water temperature by ~ 7 °C had pronounced effects on FA profiles of dorsal muscle, and dorsal and ventral skin of juvenile (parr) Atlantic Salmon raised in outdoor tanks. We observed higher mass fractions of total and individual SFA (16:0, 18:0) at the higher temperature and lower mass fractions of total and individual PUFA (e.g. 18:3n-3, 22:5n-3, 22:6n-3, and 20:4n-6) in dorsal muscle and higher mean mass fractions of most of the individual FA in dorsal and ventral skin tissues in fish reared at the warmer water temperature. Since biochemically-important

essential FA were negatively affected by temperature, these changes probably forecast a host of ensuing physiological and ecological responses of juvenile Atlantic Salmon to increasing temperatures in native streams and rivers where these salmon mature before smolting and returning to the sea [34, 60]. We further suggest that exposure to enhanced UVB radiation as a result of ozone thinning may add another stress factor to juvenile salmon (with respect to vision) especially when protective riparian cover is removed and/or water temperatures increase.

Changes in nutritional status in early life stages can have unforeseen but significant fitness consequences to animals later in life [61, 62]. Thus, we propose that future studies be designed to assess the effects of temperature and/or exposure to UVR early in life on fitness consequences to later life-history stages of Atlantic Salmon. Finally, we hypothesize that, because some of the LC-PUFA produced in aquatic ecosystems is transferred to adjacent terrestrial systems [63], the reduced nutritional quality (from an essential FA perspective) of juvenile Atlantic Salmon maturing in warmer water may also have long-term health consequences for their mammalian and avian fish predators.

Acknowledgments We thank Penny Kuhn (CONFORTE) for her assistance with the UV measurements and dose estimates. We are grateful to Bjørn Johnson (the Norwegian Radiation Protection Authority), Arne Dahlback (the University of Oslo) and Kåre Edvardsen (the Norwegian Institute for Air Research) for access to the Bergen irradiance data. We also thank Stig Ove Utskot (Institute of Marine Research, Norway) for maintaining tanks and taking care of the fish and Reidun Bjelland for helping with the tissue dissections. Tyler Spencer (Environment Canada) helped with the FA analyses. The project was supported by grants from the Research Council of Norway (140472/130), the Norwegian Institute of Marine Research (Sensory Biology and Behavior Project) and Environment Canada.

References

- McKenzie RL, Aucamp PJ, Bais AF, Björn LO, Ilyas M, Madronich S (2011) Ozone depletion and climate change: impacts on UV radiation. *Photochem Photobiol Sci* 10:182–198. doi:10.1039/C0PP90034F
- IPCC (2007) Climate Change 2007: The physical science basis. In: Solomon S, Qin D, Manning M, Chen Z, Marquis M, Averyt KB, Tignor M, Miller HL (eds) Contribution of working group I to the fourth assessment report of the intergovernmental panel on climate change. Cambridge University Press, Cambridge, UK and New York, p 996
- McKee D, Atkinson D, Collings S, Eaton J, Harvey I, Hatton K, Wilson D, Moss B (2002) Macro-zooplankton responses to simulated climate warming in experimental freshwater microcosms. *Freshw Biol* 47:1557–1570. doi:10.1046/j.1365-2427.2002.00878.x
- Van Doorslaer W, Stoks R, Jeppesen E, De Meester L (2007) Adaptive microevolutionary responses to simulated global warming in *Simocephalus vetulus*: a mesocosm study. *Global Change Biol* 13:848–886. doi:10.1111/j.1365-2486.2007.01317.x
- Rex M, Harris NRP, von der Gathen P, Lehmann R, Braathen GO, Reimer E, Beck A, Chipperfield MP, Alfier R, Allaart M, O'Connor F, Dier H, Dorokhov V, Fast H, Gil M, Kyrö E, Litynska Z, Mikkelsen IS, Molyneux MG, Nakane H, Notholt J, Rummukainen M, Viatte P, Wenger J (1997) Prolonged stratospheric ozone loss in the 1995–96 Arctic winter. *Nature* 389:835–8388. doi:10.1038/39849
- Sinensky H (1974) Homoviscous adaptation—a homeostatic process that regulates the viscosity of membrane lipids in *Escherichia coli*. *Proc Natl Acad Sci USA* 71:522–525
- Arts MT, Kohler CC (2009) Health and condition in fish: the influence of lipids on membrane competency and immune response. In: Arts MT, Kainz M, Brett MT (eds) *Lipids in Aquatic Ecosystems*, Springer, New York, pp 237–255. doi:10.1007/978-0-387-89366-2_10
- Hader DP, Helbling EW, Williamson CE, Worrest RC (2011) Effects of UV radiation on aquatic ecosystems and interactions with climate change. *Photochem Photobiol Sci* 10:242–260. doi:10.1039/C0PP90036B
- Arts MT, Browman HI, Jokinen I, Skiftesvik AB (2010) Effects of UV radiation and diet on polyunsaturated fatty acids in the skin, ocular tissue and dorsal muscle of Atlantic Salmon (*Salmo salar*) held in outdoor rearing tanks. *Photochem Photobiol* 86:909–919. doi:10.1111/j.0031-8655.2010.00733.x
- Holtby LB, Bothwell ML (2008) Effects of solar ultraviolet radiation on the behaviour of juvenile coho salmon (*Oncorhynchus kisutch*): avoidance, feeding, and agonistic interactions. *Can J Fish Aquat Sci* 65:701–711. doi:10.1139/F08-013
- Jokinen IE, Markkula ES, Salo HM, Kuhn P, Nikoskelainen S, Arts MT, Browman HI (2008) Exposure to increased ambient ultraviolet B radiation has negative effects on growth, condition and immune function of juvenile Atlantic Salmon (*Salmo salar*). *Photochem Photobiol* 84:1265–1271. doi:10.1111/j.1751-1097.2008.00358.x
- Markkula SE, Karvonen A, Salo H, Valtonen ET, Jokinen EI (2007) Ultraviolet B irradiation affects resistance of rainbow trout (*Oncorhynchus mykiss*) against bacterium *Yersinia ruckeri* and trematode *Diplostomum spathaceum*. *Photochem Photobiol* 83:1263–1269. doi:10.1111/j.1751-1097.2007.00165.x
- Jokinen IE, Salo HM, Markkula ES, Rikalainen K, Arts MT, Browman HI (2011) Additive effects of enhanced ambient ultraviolet B radiation and increased temperature on immune function, growth and physiological condition of juvenile (parr) Atlantic Salmon, *Salmo salar*. *Fish Shellfish Immun* 30:102–108. doi:10.1016/j.fsi.2010.09.017
- Salo HM, Jokinen EI, Markkula SE, Aaltonen TM, Penttilä HT (2000) Comparative effects of UVA and UVB irradiation on the immune system of fish. *J Photochem Photobiol B* 56:154–162. doi:10.1016/S1011-1344(00)00072-5
- Kaweewat K, Hofer R (1997) Effect of UV-B radiation on goblet cells in the skin of different fish species. *J Photochem Photobiol B Biol* 41:222–226. doi:10.1016/S1011-1344(97)00104-8
- Sharma JG, Masuda R, Tanaka M (2005) Ultrastructural study of skin and eye of UV-B irradiated ayu *Plecoglossus altivelis*. *J Fish Biol* 67:1646–1652. doi:10.1111/j.1095-8649.2005.00871.x
- Bell MV, Batty RS, Dick JR, Fretwell K, Navarro JC, Sargent JR (1995) Dietary deficiency of docosahexaenoic acid impairs vision at low light intensities in juvenile herring (*Clupea harengus* L.). *Lipids* 26:565–573. doi:10.1007/BF02536303
- Bell MV, McEvoy LA, Navarro JC (1996) Deficit of didocosa-hexaenoyl phospholipid in the eyes of larval sea bass fed an essential fatty acid deficient diet. *J Fish Biol* 49:941–952. doi:10.1111/j.1095-8649.1996.tb00091.x
- Jeffrey BG, Weisinger HS, Neuringer M, Mitchell DC (2001) The role of docosahexaenoic acid in retinal function. *Lipids* 36:859–871. doi:10.1007/s11745-001-0796-3
- Politi L, Rotstein N, Carri N (2001) Effects of docosahexaenoic acid on retinal development: cellular and molecular aspects. *Lipids* 36:927–935. doi:10.1007/s11745-001-0803-8

21. Birch EE, Birch DG, Hoffman DR, Uauy R (1992) Dietary essential fatty acid supply and visual acuity development. *Invest Ophthalmol Vis Sci* 33:3242–3253
22. Rafferty NS, Rafferty KA, Zigman S (1997) Comparative response to UV irradiation of cytoskeletal elements in rabbit and skate lens epithelial cells. *Curr Eye Res* 16:310–319
23. Cullen AP, Monteith-McMaster CA, Sivak JG (1994) Lenticular changes in rainbow trout following chronic exposure to UV-radiation. *Curr Eye Res* 13:731–737. doi:10.3109/02713689409047007
24. Folch J, Lees M, Stanley GHS (1957) A simple method for the isolation and purification of total lipides from animal tissues. *J Biol Chem* 226:497–509
25. Morrison WR, Smith LM (1964) Preparation of fatty acid methyl esters and dimethylacetals from lipids with boron fluoridemethanol. *J Lipid Res* 5:600–608
26. Zellmer ID, Arts MT, Abele D, Humbeck K (2004) Evidence of sublethal damage in *Daphnia* (Cladocera) during exposure to solar UV radiation in subarctic ponds. *Arct Antarct Alp Res* 36:370–377. doi:10.1657/1523-0430(2004)036[0370:EOSDID]2.0.CO;2
27. Benjamini Y, Hochberg Y (1995) Controlling the false discovery rate—a practical and powerful approach to multiple testing. *J R Stat Soc Series B Stat Methodol* 57:289–300. doi:0035-9246/95/57289
28. Zar JH (1999) *Biostatistical analysis*, 4th edn. Prentice Hall, Upper Saddle River, New Jersey, pp. 210–214. ISBN 10: 013081542X/0-13-081542-X
29. Gray JRA, Edington JM (1969) Effect of woodland clearance on stream temperature. *J Fish Res Bd Can* 26:399–403. doi:10.1139/f69-038
30. Brown GW, Krygier JT (1970) Effects of clear-cutting on stream temperature. *Water Resour Res* 6:1133–1139. doi:10.1029/WR006i004p01133
31. Macdonald JS, MacIsaac EA, Herunter HE (2003) The effect of variable-retention riparian buffer zones on water temperatures in small headwater streams in sub-boreal forest ecosystems of British Columbia. *Can J For Res* 33:1371–1382. doi:10.1139/X03-015
32. Schneider P, Hook SJ (2010) Space observations of inland water bodies show rapid surface warming since 1985. *Geophys Res Lett* 37, L22405, p 5. doi:10.1029/2010GL045059
33. Elliott JM, Hurley MA (1997) A functional model for maximum growth of Atlantic salmon parr, *Salmo salar*, from two populations in northwest England. *Funct Ecol* 11:592–603. doi:10.1046/j.1365-2435.1997.00130.x
34. Swansburg E, Chaput G, Moore D, Caissie D, El-Jabi N (2002) Size variability of juvenile Atlantic salmon: links to environmental conditions. *J Fish Biol* 61:661–683. doi:10.1006/jfbi.2002.2088
35. Wagner T, Jones ML, Ebener MP, Arts MT, Brenden TO, Honeyfield DC, Wright GM, Faisal M (2010) Spatial and temporal dynamics of lake whitefish (*Coregonus clupeaformis*) health indicators: linking individual-based indicators to a management-relevant endpoint 36:121–134. doi: 10.1016/j.jglr.2009.07.004
36. Thonney JP, Gibson RJ (1989) Feeding strategies of brook trout (*Salvelinus fontinalis*) and juvenile Atlantic salmon (*Salmo salar*) in a Newfoundland river. *Can Field Nat* 103:48–56
37. Descroix A, Desvillettes C, Bec A, Martin P, Bourdier G (2010) Impact of macroinvertebrate diet on growth and fatty acid profiles of restocked 0+ Atlantic salmon (*Salmo salar*) parr from a large European river (the Allier). *Can J Fish Aquat Sci* 67:659–672. doi:10.1139/F10-012
38. Ghioni C, Bell JG, Sargent JR (1996) Polyunsaturated fatty acids in neutral lipids and phospholipids of some freshwater insects. *Comp Biochem Physiol B Biochem Mol Biol* 114:161–170. doi: 10.1016/0305-0491(96)00019-3
39. Sushchik NN, Gladyshev MI, Moskvichova AV, Makhutova ON, Kalachova GS (2003) Comparison of fatty acid composition in major lipid classes of the dominant benthic invertebrates of the Yenisei River. *Comp Biochem Physiol B* 134:111–122. doi: 10.1016/S1096-4959(02)00191-4
40. Torres-Ruiz M, Wehr JD, Perrone AA (2007) Trophic relationships in a stream food web: importance of fatty acids for macroinvertebrate consumers. *J N Am Benthol Soc* 26:509–522. doi: 10.1899/06-070.1
41. Bell JG, Tocher DR, Farndale BM, Cox DI, McKinney RW, Sargent JR (1997) The effect of dietary lipid on polyunsaturated fatty acid metabolism in Atlantic Salmon (*Salmo salar*) undergoing parr-smolt transformation. *Lipids* 32:515–525. doi: 10.1007/s11745-997-0066-4
42. Tocher DR, Bell JG, Dick JR, Henderson RJ, McGhee F, Michell D, Morris PC (2000) Polyunsaturated fatty acid metabolism in Atlantic salmon (*Salmo salar*) undergoing parr-smolt transformation and the effects of dietary linseed and rapeseed oils. *Fish Physiol Biochem* 23:59–73. doi:10.1023/A:1007807201093
43. Sheridan MA, Allen WV, Kerstetter TH (1985) Changes in the fatty acid composition of steelhead trout, *Salmo gairdnerii* Richardson associated with parr-smolt transformation. *Comp Biochem Physiol* 80B:671–676. doi:10.1016/0305-0491(85)90444-4
44. Li H-O, Yamada J (1992) Changes of the fatty acid composition in smolts of masu salmon (*Oncorhynchus masou*), associated with desmoltification and seawater transfer. *Comp Biochem Physiol* 103A:221–226. doi:10.1016/0300-9629(92)90266-S
45. Fuschino JR, Guschina IA, Dobson G, Yan ND, Harwood JL, Arts MT (2011) Rising water temperatures alter lipid dynamics and reduce n-3 essential fatty acid concentrations in *Scenedesmus obliquus* (Chlorophyta). *J Phycol* 47:763–774. doi:10.1111/j.1529-8817.2011.01024.x
46. Gladyshev MI, Sushchik NN, Makhutova ON, Dubovskaya OP, Kravchuk ES, Kalachova GS, Khromechek EB (2010) Correlations between fatty acid composition of seston and zooplankton and effects of environmental parameters in a eutrophic Siberian reservoir. *Limnologia* 40:343–357. doi:10.1016/j.limno.2009.12.004
47. Leibowitz MP, Ariav R, Zilberg D (2005) Environmental and physiological conditions affecting *Tetrahymena* sp. infection in guppies, *Poecilia reticulata* Peters. *J Fish Dis* 28:539–547. doi: 10.1111/j.1365-2761.2005.00658.x
48. Hirazawa N, Takano R, Hagiwara H, Noguchi M, Narita M (2010) The influence of different water temperatures on *Neobenedenia girellae* (Monogenea) infection, parasite growth, egg production and emerging second generation on amberjack *Seriola dumerili* (Carangidae) and the histopathological effect of this parasite on fish skin. *Aquaculture* 299:2–7. doi:10.1016/j.aquaculture.2010.10.029
49. Heuch PA, Revie CW, Gettinby G (2003) A comparison of epidemiological patterns of salmon lice, *Lepeophtheirus salmonis*, infections on farmed Atlantic salmon, *Salmo salar* L., in Norway and Scotland. *J Fish Dis* 26:539–551. doi:10.1046/j.1365-2761.2003.00490.x
50. Merle C, Laugel C, Baillet-Guffroy A (2010) Effect of UVA or UVB irradiation on cutaneous lipids in films or in solution. *Photochem Photobiol* 86:553–562. doi:10.1111/j.1751-1097.2009.00690.x
51. Bullock AM, Roberts RJ, Waddington P (1983) Sunburn lesions in koi carp. *Vet Rec* 112:551
52. Ramos KT, Fries LT, Berkhouse CS, Fries JN (1994) Apparent sunburn of juvenile paddlefish. *Prog Fish Culturist* 56:214–216
53. Blazer VS, Fabacher DL, Little EE, Ewing MS, Kocan KM (1997) Effects of ultraviolet-B radiation on fish: histologic comparison of a UVB-sensitive and a UVB-tolerant species. *J Aquat Animal Health* 9:132–143

54. Zamzow JP (2004) Effects of diet, ultraviolet exposure, and gender on the ultraviolet absorbance of fish mucus and ocular structures. *Mar Biol* 144:1057–1064. doi:[10.1007/s00227-003-1286-2](https://doi.org/10.1007/s00227-003-1286-2)
55. Treasurer JW, Cox DI, Wall T (2007) Epidemiology of blindness and cataracts in cage reared ongrown Atlantic halibut *Hippoglossus hippoglossus*. *Aquaculture* 271:77–84. doi:[10.1016/j.aquaculture.2007.05.008](https://doi.org/10.1016/j.aquaculture.2007.05.008)
56. Bjerås E, Holst JC, Bjerås I, Ringvold A (2003) Osmotic cataract causes reduced vision in wild Atlantic salmon post-smolts. *Dis Aquat Org* 55:151–159. doi:[10.3354/dao055151](https://doi.org/10.3354/dao055151)
57. Fliesler SJ, Anderson RE (1983) Chemistry and metabolism of lipids in the vertebrate retina. In: Holman RT (ed) *Progress in lipid research*, vol 22. Pergamon Press, Oxford, pp 79–131
58. Masuda R, Takeuchi T, Tsukamoto K, Ishizaki Y, Kanematsu M, Imaizumi K (1998) Critical involvement of dietary docosahexaenoic acid in the ontogeny of schooling behaviour in the yellowtail. *J Fish Biol* 53:471–484. doi:[10.1111/j.1095-8649.1998.tb00996.x](https://doi.org/10.1111/j.1095-8649.1998.tb00996.x)
59. Vagner M, Santigosa E (2011) Characterization and modulation of gene expression and enzymatic activity of delta-6 desaturase in teleosts: a review. *Aquaculture* 315:131–143. doi:[10.1016/j.aquaculture.2010.11.031](https://doi.org/10.1016/j.aquaculture.2010.11.031)
60. Jonsson B, Jonsson N (2009) A review of the likely effects of climate change on anadromous Atlantic salmon *Salmo salar* and brown trout *Salmo trutta*, with particular reference to water temperature and flow. *J Fish Biol* 75:2381–2447. doi:[10.1111/j.1095-8649.2009.02380.x](https://doi.org/10.1111/j.1095-8649.2009.02380.x)
61. Metcalfe NB, Monaghan P (2001) Compensation for a bad start: grow now, pay later? *Trends Ecol Evol* 16:254–260. doi:[10.1016/S0169-5347\(01\)02124-3](https://doi.org/10.1016/S0169-5347(01)02124-3)
62. Blas J, Bortolotti GR, Tella JL, Baos R, Marchant TA (2007) Stress response during development predicts fitness in a wild, long lived vertebrate. *Proc Natl Acad Sci USA* 104:8880–8884. doi:[10.1073/pnas.0700232104](https://doi.org/10.1073/pnas.0700232104)
63. Gladyshev M, Arts MT, Sushchik NN (2009) Preliminary estimates of the export of omega-3 highly unsaturated fatty acids (EPA + DHA) from aquatic to terrestrial ecosystems. In: Arts MT, Kainz M, Brett MT (eds) *Lipids in aquatic ecosystems*, Springer, NY, pp 179–209. doi: [10.1007/978-0-387-89366-2_8](https://doi.org/10.1007/978-0-387-89366-2_8)

last 20 years [1–4], especially in relation to eicosapentaenoic acid (EPA; 20:5n-3) and docosahexaenoic acid (DHA; 22:6n-3) [1, 5–7]. The structure of DHA provides this fatty acid with many important functions in fish metabolism [4], and has been demonstrated to be superior to EPA in promoting growth and conferring vitality to larvae [1, 8], being preferentially incorporated into biomembranes [6, 9]. It has been reported that marine fish larvae DHA content rapidly decreases during the first 10 days after hatching, therefore high contents of DHA must be supplied to larvae in order to maintain adequate levels of DHA in growing larvae [1]. Due to their limited capacity to synthesize DHA and EPA from their precursors, fish require diets rich in these fatty acids [10]. Today, live prey substitution by compound diets containing high levels of DHA is crucial for lowering costs and increasing production quality, mainly by reducing the incidence of skeletal deformities and increasing welfare in fingerlings [10]. However, DHA is very susceptible to attack by reactive oxygen species (ROS) due to its high degree of unsaturation [11].

ROS are produced during normal cellular function [12], being beneficial or even indispensable at low concentrations in processes such as defense against microorganisms by contributing to phagocytic bactericidal activity. Fish possess enzyme systems and low-molecular-weight molecules with antioxidant functions capable of neutralizing ROS and protecting against their adverse effects [13]. However, ROS generation can exceed its removal rates and oxidative stress can occur [14] with ROS attacking diverse cellular components. One of the consequences of oxidative stress is the oxidative peroxidation of PUFA. The high unsaturation content of these fatty acids renders them very susceptible to lipid oxidation. Thus, the high requirements of marine fish larvae for long-chain PUFA (LC-PUFA), mainly DHA and EPA, makes them more prone to suffering peroxidative attack than adults [15]. Therefore, the importance of nutrition in the pro-oxidant–anti-oxidant balance process may be highly critical for fish larvae, as their high LC-PUFA contents disposes larval tissues vulnerable to oxidative stress, and an increase in the content of antioxidant nutrients is essential. Among the antioxidant nutrients, vitamin E (tocopherols and tocotrienols) is the major membrane-bound lipid-soluble antioxidant [13], whereas vitamin C (ascorbic acid, vitC) is an important water-soluble antioxidant which protects low density lipoproteins from oxidation and is required for the correct formation of cartilage [16]. The presence of sparing mechanisms between both vitamins was first hypothesized by Tappel [17]. This hypothesis proposes that the oxidized α -tocopherol (α -TOH) is reduced by ascorbate, thereby regenerating α -TOH. In some fish species, the presence of a vitamin C/E sparing mechanism has been suggested [18–22], and reported to influence growth, tissue

composition or immune responses. For instance, supplementation with 100 mg/kg of ascorbyl-2-polyphosphate to an α -TOH-deficient diet in juvenile channel catfish (*Ictalurus punctatus*) decreased vertebral deformities and improved weight gain, feed intake and feed efficiency rate [22]. High supplementation of ascorbate might also spare α -TOH in diets for hybrid tilapia (*Oreochromis niloticus* \times *O. aureus*) as shown by the increased weight gain, feed efficiency and α -TOH concentrations. However, little is known about the effect of both vitamins in preventing oxidative stress in fish larvae, when high levels of LC-PUFA are administered. Similarly, insufficient information exists regarding exact larval requirements for DHA, α -TOH or vitC, with levels ranging from 0.5 to 4 % for DHA [23, 24], 120 to 3,000 mg/kg for α -TOH [25, 26] or 30 to 2,500 mg/kg for vitC [27, 28].

The potentially deleterious effects of ROS are counteracted by a suite of antioxidant enzymes (AOE), including radical-scavenging enzymes such as catalase (CAT; EC 1.15.1.1) and superoxide dismutase (SOD; EC 1.11.1.19) or peroxidases such as glutathione peroxidase (GPX; EC 1.11.1.6). In Manchurian trout larvae (*Brachymystax lenok*), high lipid content microdiets stimulated the activity of AOE, generally accompanied by an increase in thio-barbituric acid reactive substances (TBARS) content [29]. In contrast, Mourente et al. [30] did not find a direct relationship between the activity of AOE and the level of dietary n-3 LC-PUFA in *Dentex dentex* larvae, but decreased α -TOH and increased TBARS contents were found in larvae fed high n-3 LC-PUFA-enriched *Artemia*. Furthermore, it seems that the level of antioxidant enzymes rises with larval development, whereas the level of antioxidant molecules falls [31].

In mammals, ROS can induce changes in gene expression during normal development [32], causing defective embryo development and retardation of embryo growth [33]. Similarly, oxidative stress causes embryonic mortality and developmental arrest in sea urchins (*Paracentrotus lividus* and *Sphaerechinus granularis*) larvae [34]. Oxygen stress during early larval stages of fish may also alter development. Somatic growth in fish is regulated by insulin-like growth factors I and II (IGF-I and IGF-II), two single chain polypeptides that also have a function as myogenic regulatory factors which increase satellite cell proliferation and differentiation [35, 36]. In addition, IGFs stimulate cartilage growth by the incorporation of sulphate into cartilage and also affect cell differentiation, growth and proliferation [37, 38]. Differences in myogenesis regulation, such as myosin isoform expression, have also been observed in the earliest stages and during temperature acclimation [39–41]. However, no information is available about the effect of different dietary components on the regulation of the various components of the IGF signaling

pathways, as well as their role on muscle growth in fish [42].

In previous studies, we have shown the alteration of sea bass (*Dicentrarchus labrax*) larvae oxidative status when they were fed high levels of DHA (5 %), and α -TOH (3,000 mg/kg) having a limited effect in preventing alterations such as muscular dystrophy or hepatic ceroidosis [43, 44]. Therefore, the aim of the present study was to evaluate the combined effect of α -TOH and vitC in preventing oxidative stress in sea bass larvae fed high levels of DHA in relation to larval performance or antioxidant status as well as the incidence of morphological alterations, including the expression of selected related genes.

Materials and Methods

Fish

The experiment was carried out at the Grupo de Investigación en Acuicultura facilities (Telde, Canary Islands, Spain). Sea bass larvae were obtained from a natural spawning from the Instituto de Acuicultura de Torre de la Sal (CSIC, Castellón, Spain). Prior to starting the feeding experiment, larvae were fed enriched yeast-fed rotifers (DHA Protein Selco[®]; INVE, Belgium) until they reached 14 days post-hatching (dph). Then, larvae (total length 8.58 ± 0.64 mm, dry body weight 0.36 ± 0.00 mg) were randomly distributed in experimental tanks ($n = 9$) at a density of 1,000 larvae/tank and were fed one of the experimental diets for 21 days, at a water temperature of 19.5–21.0 °C. All tanks (170 L, light gray color, cylindrical fiberglass tanks) were supplied with filtered sea water (34 ‰ or ppm salinity) at an increasing rate of 1.0–1.5 L/min during the feeding trial. Sea water entered the tank from bottom to top; water quality was tested daily and no deterioration was observed. Water was continuously aerated (125 mL/min), attaining 5–8 g/L dissolved O₂ and 60–80 % saturation.

Diets

Three isonitrogenous and isolipidic experimental microdiets (pellet size <250 μ m) were prepared containing two levels of DHA, vitC and α -TOH (Table 1). The levels of DHA and vitamin E were selected based on previous trial data [43, 44]. In those studies, larvae fed diets containing 1 % DHA and 1,500 mg/kg of α -TOH exhibited low incidence of muscular lesions and TBARS content, whereas larvae fed diets containing 5 % DHA and 3,000 mg/kg of α -TOH showed altered oxidative status with an increase in both parameters. A low oxidation risk diet (1/1,500) contained low DHA (1 % DW) and α -TOH

Table 1 Formulation (in % DW) of experimental diets containing two levels of DHA, vitamin E and ascorbic acid and fed to sea bass (*Dicentrarchus labrax*) larvae for 21 days

Dietary DHA/vitamin E	1/1,500	5/3,000	5/3,000 + vitC
Defatted squid powder ^a	69.00	68.85	68.32
EPA ^b	2.80	1.80	1.80
DHA ^b	0.20	6.70	6.70
Oleic acid ^c	10.00	4.50	4.50
Soy lecithin ^d	2.00	2.00	2.00
Gelatin ^e	3.00	3.00	3.00
Attractants ^f	3.00	3.00	3.00
Taurine ^e	1.50	1.50	1.50
Vitamin premix ^g	6.00	6.00	6.00
Mineral premix ^h	2.50	2.50	2.50
Rovimix stay C 35 ⁱ	–	–	0.53
Vitamin E ^j	–	0.15	0.15

1/1,500 1 % DHA and 1,500 mg/kg vitamin E diet; 5/3,000 5 % DHA and 3,000 mg/kg vitamin E diet; 5/3,000 + vitC 5 % DHA and 3,000 mg/kg vitamin E diet with increased ascorbic acid content

DW dry weight

^a Riber and Son, Bergen, Norway

^b Croda, East Yorkshire, UK

^c Merck, Darmstadt, Germany

^d Acrofarma, Barcelona, Spain

^e Panreac, Barcelona, Spain

^f Attractants premix supplied per 100 g diet: inosine-5-monophosphate 500.0 mg, betaine 660.0 mg, L-serine 170.0 mg, L-phenylalanine 250.0 mg, DL-alanine 500.0 mg, L-sodium aspartate 330.0 mg, L-valine 250.0 mg, glycine 170.0 mg; Sigma-Aldrich, Madrid, Spain

^g Vitamin premix supplied per 100 g diet: Cyanocobalamine 0.030, Astaxanthin 5.00, folic acid 5.44, pyridoxine-HCl 17.28, thiamine 21.77, riboflavin 72.53, Ca-pantothenate 101.59, *p*-aminobenzoic acid 145.00, nicotinic acid 290.16, *myo*-inositol 1450.90, retinol acetate 0.18, ergocalciferol 3.65, menadione 17.28, α -tocopherol acetate 150.00, ascorbyl monophosphate 180.00

^h Mineral premix supplied g per 100 g diet: NaCl 215.133, MgSO₄·7H₂O 677.545, NaH₂PO₄·H₂O 381.453, K₂HPO₄ 758.949, Ca(H₂PO₄)₂·2H₂O 671.610, FeC₆H₅O₇ 146.884, C₃H₅O₃·1/2Ca 1617.210, Al₂(SO₄)₃·6H₂O 0.693, ZnSO₄·7H₂O 14.837, CuSO₄·5H₂O 1.247, MnSO₄·H₂O 2.998, KI 0.742, CoSO₄·7H₂O 10.706

ⁱ Roche, Paris, France

^j DL- α -tocopherol acetate; Sigma-Aldrich

(1,500 mg/kg); a high oxidation risk diet contained the highest DHA (5 % DW) and α -TOH (3,000 mg/kg) levels; and a third diet contained high DHA (5 % DW) and α -TOH (3,000 mg/kg) together with double the quantity of vitamin C than the former two diets (3,600 mg/kg). The protein source used was squid meal defatted 3 consecutive times with a chloroform:squid meal ratio of 3:1 to allow a better control of the fatty acid profile of the microdiet. EPA, DHA, α -TOH, and vitC sources used in the experimental diets were EPA50 and DHA50 (CRODA, East Yorkshire, UK), DL- α -Tocopheryl Acetate (Sigma-Aldrich, Madrid,

Spain) and Rovimix Stay-C 35 (Roche, Paris, France), respectively. Oleic acid (Merck, Darmstadt, Germany) was added to equalize the lipid content in all diets. Microdiets were prepared according to Liu et al. [45] by first mixing the squid powder and water-soluble components, followed by lipid- and fat-soluble vitamins and, finally, warm water-dissolved gelatin. The paste was pelleted and oven-dried at 38 °C for 24 h. Pellets were ground and sieved to obtain particle sizes below 250 µm. Diets were analyzed for proximate and fatty acid composition of dry matter and kept in plastic bags under nitrogen atmosphere at –20 °C until the beginning of the experimental trial. Diets were manually supplied 14 times per day every 45 min from 0900 to 1900 hours. Daily feed supplied was 2, 2.5, and 3 g/tank during the first, second, and third weeks of feeding, respectively. Each diet was tested in triplicate.

Growth and Survival

Final survival was calculated by individually counting live larvae at the beginning and end of the experiment. Growth was determined by measuring dry body weight (105 °C for 24 h) and total length (Profile Projector V-12A; Nikon, Tokyo) of 30 larvae/tank at the beginning, middle, and end of the trial.

Biochemical Analysis

All remaining larvae in each tank were washed with distilled water, sampled, and kept at –80 °C for biochemical composition and TBARS analyses after 12 h of starvation at the end of the trial. Moisture, protein [46], and lipid [47] contents of the larvae and diets were analyzed.

Total Lipid Fatty Acid Analysis

Fatty acid methyl esters (FAMES) were obtained by transmethylation of total lipids as described by Christie [48]. FAMES were separated by GLC, quantified by FID (GC-14A; Shimadzu, Tokyo, Japan) under the conditions described in Izquierdo et al. [49] and identified by comparison with previously characterized standards and GLC–MS.

Determination of α -TOH Content

α -TOH concentrations were determined in diets and larvae samples using high-pressure liquid chromatography (HPLC) with UV detection. Samples were weighed, homogenized in pyrogallol, and saponified as described by McMurray et al. [50] for diets or according to Cowey et al. [51] for larvae. HPLC analysis was performed using a 150 × 4.60 mm, reverse-phase Luna 5 µm C18 column

(Phenomenox, CA, USA). The mobile phase was 98 % methanol pumped at 1.0 mL/min. The effluent from the column was monitored at a wavelength of 293 nm and quantification achieved by comparison with (+)- α -tocopherol (Sigma-Aldrich) as external standard.

Determination of Vitamin C Content

Ascorbil-2-monophosphate concentrations were determined in diets using a HPLC procedure with UV detection. The HPLC system comprised of a 150 × 4.6 mm, 5-µm particle size, Gemini C18 column fitted with a Gemini pre-column of the same material. The mobile phase consisting of phosphate buffer was delivered at a flow rate of 0.8 mL/min. Samples were dissolved with 0.4 M phosphate buffer (pH 3.0) and centrifuged at 1,610g for 5 min at room temperature. The supernatants were kept at 4 °C until assayed. vitC concentrations were determined at a wavelength of 293 nm and quantification achieved by comparison with tris(cyclohexylammonium) ascorbic acid-2-phosphate (Sigma-Aldrich), used as a reference substance.

Measurement of Thiobarbituric Acid Reactive Substances (TBARS)

TBARS were measured in triplicate samples using a method adapted from that used by Burk et al. [52]. Approximately 20–30 mg of larval tissues per sample were homogenized in 1.5 mL of 20 % trichloroacetic acid (w/v) containing 0.05 mL of 1 % BHT in methanol. To this, 2.95 mL of freshly prepared 50 mM thiobarbituric acid solution was added before mixing and heating for 10 min at 100 °C. After cooling, protein precipitates were removed by centrifugation (Sigma 4K15; Osterode am Harz, Germany) at 2,000g, the supernatant was read in a spectrophotometer (Evolution 300; Thermo Scientific, Cheshire, UK) at 532 nm. The absorbance was recorded against a blank at the same wavelength. The concentration of TBA-malondialdehyde (TBARS) expressed as nmol per g of tissue was calculated using the extinction coefficient 0.156 µM⁻¹ cm⁻¹.

Histopathological Sampling

Thirty larvae from each tank were collected every 7th day from the beginning of the feeding trial, and fixed in 10 % buffered formalin for 1 or 2 days, dehydrated through graded alcohols then xylene, and finally embedded in paraffin wax. Six paraffin blocks containing five larvae per tank were sectioned at 3 µm and stained with Hematoxylin and Eosin (H&E) for histopathologic evaluation [53].

Ten larvae per tank were fixed for 24 h at 4 °C in 2.5 % glutaraldehyde in 0.2 M phosphate buffer (pH 7.2).

Samples were then rinsed in phosphate buffer and post-fixed for 1 h in 2 % osmium tetroxide in 0.2 M potassium ferrocyanide. Each larva was then embedded in an Epon/Araldite resin block. Serial transverse and longitudinal larvae thick sections were cut at 1 μm , stained with toluidine blue and examined under light microscopy [54]. Thin sections were cut at 50 nm and stained with lead citrate before observing with a ZEISS EM 910 transmission electron microscope (Germany) at the Electron Microscope Service of University of Las Palmas de Gran Canaria.

In addition, 100 larvae from each tank at 35 dph were fixed in 10 % buffered formalin in order to perform deformity analyses. Prior to staining, larvae were measured under a Profile Projector (PJ 3000; Mitutoyo, Japan), divided into three size classes (<10.0 mm, 10.0–12.0 mm, and >12.0 mm) and stained with Alizarin red [55] to determine bone mineralization. Larvae from the different experimental groups were stained simultaneously in order to prevent any technical variability. Deformities were classified into different groups according to their localization. Firstly, cranial deformities or axial skeleton deformities, which were subdivided into four categories: (1) lordosis, (2) kyphosis, (3) neural process alterations, and (4) others, e.g., vertebral compression or scoliosis. Cranial deformities included those found in the jaws, such as pugheadness or crossbite and opercular deformities. And secondly, axial skeleton deformities included spine curvatures such as lordosis (ventral curvature), kyphosis (dorsal curvature) or scoliosis (lateral curvature); neural processes alterations such as wrong direction or twisting, and vertebral compression that comprises two alterations, the fluttering of vertebral end plates and vertebral fusion. The surface corresponding to bone in whole colored larvae was visualized and quantified using a computerized image analysis package (Image-Pro Plus[®]; Media Cybernetics, MD, USA). By selecting ranges of pixel values in color images the pixels associated with red could be distinguished. The number of selected pixels was then quantified using a particle analysis operation and by counting the area of all bright objects (in pixels). Larval size was estimated by calculating the surface areas (in pixels) covered by whole stained larvae.

RNA Extraction and Quantitative RT-PCR

Molecular biology analyses were carried out at the University of Insubria (Varese, Italy). Total RNA was extracted from sea bass larvae (≈ 200 mg; pool per tank), using PureYield RNA Midiprep System (Promega, Italy). The quantity and purity of RNA was assessed by spectrophotometer. Visualization on 1 % agarose gel stained with ethidium bromide showed that RNA was not degraded. Three micrograms of total RNA was reverse transcribed into complementary DNA (cDNA) in a volume of 12 μl ,

including 1 μl of oligo dT16 primer (50 pmol) and 1 μl of 10 mM deoxynucleotide triphosphates (dNTPS). This mix was heated at 65 °C for 5 min, chilled on ice, and then 4 μl of 5X reverse transcription buffer, 2 μl 0.1 M DTT, 1 μl RNase out and 1 μl of Moloney murine leukemia virus (M-MLVRT) were added. After incubation at 37 °C for 50 min, the reaction was stopped by heating at 75 °C for 15 min.

PCR primers sequences used for the PCR amplification of the cDNAs of target genes were CAT, SOD, GPX, IGF-I, IGF-II, and MyHC. To perform PCR, an aliquot of 4 μl of cDNA was amplified using 25 μl GoTaq Green Master Mix (Promega, Italy) in 50 μl of final volume and 50 pmol of each designed primer.

A total of 31 PCR amplification cycles (eight touch-down) were performed for all primer sets, using an automated Thermal Cycler (MyCycler; BioRad, Italy). An aliquot of each sample was then subject to electrophoresis on a 1 % agarose gel in 1X TAE buffer (Bio-Rad) and bands were detected by ethidium bromide. Samples were run together with a 100 bp \pm 1.5 kb DNA ladder to control molecular weight of the DNA. The negative control (a reaction mixture without cDNA), confirmed the absence of genomic contamination. The PCR products from each primer set amplification were then cloned using pGEM[®]-T easy vector (Promega) and subsequently sequenced in both directions (T7 and SP6).

TaqMan[®] real-time reverse transcription PCR was performed on a StepOne Real-Time PCR System (Applied Biosystems, Italy) using Assays-by-DesignSM PCR primers (Applied Biosystems) and gene-specific fluorogenic probes. Primer sequences and TaqMan[®] probes of target genes were the following:

Target gene: Sea bass CAT.

Forward primer: 5'-ATGGTGTGGGACTTCTGGAG-3'

Reverse primer: 5'-GCTGAACAAGAAAGACACCTGATG-3'

TaqMan[®] probe: 5'-CAGACACTCAGGCCTCA-3'

Target gene: Sea bass SOD.

Forward primer: 5'-TGGAGACCTGGGAGATGTAAC TG-3'

Reverse primer: 5'-TCTTGTCCGTGATGTCGATCTTG-3'

TaqMan[®] probe: 5'-CAGGAGGAGATAACATTG-3'

Target gene: Sea bass GPX.

Forward primer: 5'-AGTTAATCCGGAATTCGTGAG-3'

Reverse primer: 5'-AGCTTAGCTGTCAGGTCGTAAAC-3'

TaqMan[®] probe: 5'-AATGGCTGGAAACGTG-3'

Target gene: Sea bass IGF-I.

Forward primer: 5'-GCAGTTTGTGTGTGGAGAGA
GA-3'
Reverse primer: 5'-GACCGCCGTGCATTGG-3'
TaqMan[®] probe: 5'-CTGTAGGTTTACTGAAATAAA
A-3'

Target gene: Sea bass IGF-II.

Forward primer: 5'-TGCAGAGACGCTGTGTGG-3'
Reverse primer: 5'-GCCTA CTGAAATAGAAGCCTC
TGT-3'
TaqMan[®] probe: 5'-CAAACCTGCAGCGCATCC-3'

Target gene: Sea bass MyHC.

Forward primer: 5'-TGGAGAAGATGTGCCGTACTC
T-3'
Reverse primer: 5'-CGTGTTCATTGATTTGACGGACA
TTT-3'
TaqMan[®] probe: 5'-AACTGAGTGAAGTGAAGACC-3'

Data from TaqMan[®] PCR runs were collected with ABI's Sequence Detector Program. Cycle threshold (Ct) values corresponded to the number of cycles at which the fluorescence emission monitored in real time exceeded the threshold limit. The Ct values were used to create standard curves to serve as a basis for calculating the absolute amounts of mRNA in total RNA. To reduce pipetting errors, master mixes were prepared to set up duplicate reactions (2 × 30 µl) for each sample.

Statistical Analysis

Results are given as mean ± SD. Survival, growth, fatty acid, ossification degree and molecular biology data were tested for normality and homogeneity of variances with Levene's test, not requiring any transformation. Chi-squared test was employed for incidence of muscular lesions, deformities and TBARS content. Survival, growth, fatty acid, ossification degree and molecular biology data were treated by one-way ANOVA. Means were compared by Duncan's test ($P < 0.05$) using SPSS for Windows 14.0 (SPSS, Chicago, IL, USA, 2005). For analysis of one-way ANOVA, the following general linear model was used:

$$Y_{ij} = m + D_i + e_{ij}$$

where Y_{ij} is the mean value of the tank, m is the mean population, D_i is the fixed effect of the diet and e_{ij} is the residual error.

Results

The diet containing about 1 % DHA (diet 1/1,500) showed higher amounts of monoenoic fatty acids than diets containing 5 % DHA (5/3,000 and 5/3,000 + vitC) due to the

higher oleic acid content in the former diet (Table 2). DHA contents in the diets varied from 4.58 % of total fatty acids in the 1/1,500 diet, 24.55 % in the 5/3,000 diet and 27.54 % in the 5/300 + vitC diet. Elevation of dietary DHA (5/3,000 diets or 5/3,000 and 5/3,000 + vitC diets) increased n-3 PUFA and n-3 LC-PUFA fatty acids contents, as well as n-3/n-6 PUFA ratio. α -TOH levels were more than 2 times higher in diets containing 3,000 mg/kg compared to the control diet (1/1,500) (Table 3). vitC contents were also higher in the diet supplemented with vitC than in the others.

All experimental diets were well accepted by larvae. The highest total length was found in the 1/1,500 diet larvae. Increasing DHA from 1 to 5 % in the 5/3,000 diet larvae, significantly reduced larvae total length, despite the α -TOH increase. However, vitC levels in the 5/3,000 + vitC diet enhanced larval total length compared to the 5/3,000 diet larvae ($P = 0.005$). Sea bass larvae survival or dry weight was not significantly different among the treatments (Table 4).

The level of lipid peroxidation-derived aldehydes, as indicated by TBARS content (nmol/g larval tissues) was lowest in larvae fed diet 1/1,500 and was significantly higher in larvae fed the higher DHA content (5/3,000 and 5/3,000 + vitC) diets. However, the inclusion of vitC prevented the formation of hydroperoxides, observed by a decrease in TBARS levels. The lowest α -TOH content was found in larvae fed 5/3,000 diet. However, an increase in dietary vitC contents increased α -TOH levels in larvae fed 5/3,000 + vitC diet. Regarding larval α -TOH contents, the elevation of dietary vitamin E in diet 5/3,000, together with the increase in DHA, in comparison to diet 1/1,500, did not significantly affect the α -TOH contents in the larvae (Table 4).

Fatty acid composition of the larvae (Table 5) generally reflected the fatty acid composition of the diet. Accordingly, a higher content of 18:1n-9 was observed in 1/1,500 larvae. However, its retention rate regarding dietary levels was much lower in 1/1,500 larvae (47.30 %) than in 5/3,000 (67.22 %) or 5/3,000 + vitC larvae (67.82 %), balancing the monoenoic acids content among larvae fed the different dietary treatments. Equally, EPA retention was low in all larvae, especially in those fed 5/3,000 (43.93 %) and 5/3,000 + vitC (43.96 %) diets. The highest content of total n-3 LC-PUFA ($P = 0.006$) was observed in larvae fed the diet supplemented with vitC probably due to a higher dietary content. However, regarding 22:6n-3 content, the highest retention rate was observed in 1/1,500 larvae. Similarly 20:4n-6 was highly retained in larvae fed the 1/1,500 diet, although higher contents were found in larvae fed diets 5/3,000. In contrast to the differences in the n-3/n-6 ratio observed in diets, no differences were observed in larvae among the different treatments.

Histopathological examinations revealed the presence of lesions affecting larvae axial musculature, showing the typical features of necrotic degeneration of muscle.

Table 2 Main fatty acids (% total of fatty acids) of the experimental diets fed to European sea bass for 3 weeks

	Diet		
	1/1,500	5/3,000	5/3,000 + vitC
14:0	1.54	1.26	0.78
14:1n-7	0.15	0.25	0.06
14:1n-5	0.22	0.35	0.09
15:00	0.28	0.43	0.15
15:1n-5	0.02	0.14	ND
16:0ISO	0.14	0.23	0.07
16:0	7.86	5.59	5.08
16:1n-7	3.59	2.26	2.01
16:1n-5	0.19	0.23	0.11
16:2n-6	ND	0.17	0.06
16:2n-4	0.32	0.39	0.26
17:0	1.21	0.82	0.66
16:3n-3	0.08	0.12	0.07
16:4n-3	0.09	0.13	0.10
18:0	1.29	2.29	2.18
18:1n-9 + n-7	55.70	31.12	30.33
18:1n-5	0.72	0.46	0.36
18:2n-9	0.25	0.13	0.02
18:2n-6	7.40	6.99	6.71
18:2n-4	0.46	0.28	0.23
18:3n-6	0.11	0.11	0.10
18:3n-4	0.13	0.10	0.09
18:3n-3	0.72	0.83	0.82
18:3n-1	ND	0.04	0.04
18:4n-3	0.83	0.94	0.98
18:4n-1	0.08	0.08	0.09
20:0	0.10	0.31	0.30
20:1n-9 + n-7	1.10	1.53	1.50
20:1n-5	0.05	0.12	0.11
20:2n-9	0.05	0.04	0.04
20:2n-6	0.09	0.21	0.21
20:3n-6	0.09	0.13	0.14
20:4n-6	0.71	1.57	1.62
20:3n-3	0.07	0.18	0.18
20:4n-3	0.32	0.52	0.54
20:5n-3	8.66	11.04	12.08
22:1n-11	0.17	0.51	0.53
22:1n-9	0.08	0.25	0.24
22:4n-6	0.02	0.19	0.20
22:5n-6	0.19	1.75	1.86
22:5n-3	0.32	1.29	1.42
22:6n-3	4.58	24.55	27.54
SAFA	12.28	10.70	9.16
MUFA	61.99	37.23	35.34
n-3 PUFA	15.68	39.61	43.73
n-6 PUFA	8.61	11.14	10.90

Table 2 continued

	Diet		
	1/1,500	5/3,000	5/3,000 + vitC
n-9 PUFA	57.19	33.10	32.17
n-3 LC-PUFA	13.96	37.58	41.76
n-3/n-6 PUFA	1.82	3.56	4.01
EPA/DHA	1.89	0.45	0.44
ARA/DHA	0.15	0.06	0.06
ARA/EPA	0.08	0.14	0.13

1/1,500 1 % DHA and 1,500 mg/kg vitamin E diet; 5/3,000 5 % DHA and 3,000 mg/kg vitamin E diet; 5/3,000 + vitC 5 % DHA and 3,000 mg/kg vitamin E diet with increased ascorbic acid content

The incidence of muscular lesions increased with DHA dietary content (5/3,000 diet; Table 4). However, inclusion of vitC (5/3,000 + vitC diet) proved to be effective in reducing incidences to less than half of those in 5/3,000 larvae. More detailed features of muscular lesions could be observed on semithin and TEM sections, where muscle degeneration with the presence of hydropic vacuoles and organelles swelling within some of the affected fibers was found in larvae fed the 5/3,000 diet. Some fibers presented disarrangement of the myofilaments just like myelin figures, denoting intracellular lipid oxidation (Fig. 1).

Regarding skeletal morphology, among larvae measuring 10–12 mm, 28.33 ± 1.30 % of the larvae fed the 1/1,500 diet showed skeletal deformities, and similar values were found in those fed the 5/3,000 + vitC diet (29.67 ± 6.51 % of the larvae analyzed). Larvae fed the 5/3,000 diet presented 33.11 ± 5.11 % deformities, but no statistical differences were detected between groups ($P = 0.10$; Table 4). The ossification degree of 35 dph sea bass larvae was determined in terms of surface of mineralized bones per larval surface (Table 4). High dietary levels of DHA decreased the formation of mineralized bone in larvae, whereas increased vitC did not affect mineralization.

Different types of deformities were observed at the end of the experimental period, depending on the level of dietary DHA. All of the experimental groups exhibited a statistically similar percentage of kyphosis, however, no lordosis was observed in larvae fed the 1/1,500 diet (Fig. 2). Skull deformities were especially high in fish fed high DHA levels, although vitC increase reduced the incidence of this deformity ($P = 0.013$).

The general pattern of gene expression, excepting IGF-II, in all groups of sea bass larvae was characterized by a rapid increase between 14 and 26 dph (Figs. 3, 4). CAT gene expression was elevated in larvae fed diets containing a high content of DHA, the highest number of mRNA copies being found in larvae fed diet 5/3,000 + vitC

($P = 0.027$; Fig. 3a). The SOD mRNA expression was also highest in 5/3,000 groups ($P = 0.048$; Fig. 3b). Accordingly, GPX gene expression was quite strong in larvae fed diets containing a high level of DHA compared to larvae fed low levels ($P = 0.039$; Fig. 3c).

The IGF-I gene expression increased from 14 to 26 dph in all treatments, at day 35 showing a decrease in the 1/1,500 and 5/3,000 + vitC fed larvae and a continuous increase in the 5/3,000 fed larvae (Fig. 4a). Regarding IGF-II, gene expression was higher in larvae fed 5/3,000 and 5/3,000 + vitC diets than in those fed diet 1/150 throughout the trial (Fig. 4b).

Table 3 Proximate composition, α -tocopherol and ascorbic acid content (mean \pm SD) in experimental diets fed to sea bass larvae for 3 weeks

	Diets		
	1/1,500	5/3,000	5/3,000 + vitC
Protein (% DW)	74.46 \pm 0.58	76.13 \pm 0.09	72.36 \pm 0.55
Ash (% DW)	5.01 \pm 0.12	5.38 \pm 0.14	5.39 \pm 0.14
Moisture (%)	10.31 \pm 0.46	9.99 \pm 0.28	9.48 \pm 0.11
Lipids (% DW)	14.98 \pm 0.31	15.80 \pm 0.02	15.94 \pm 1.05
α -Tocopherol (mg/kg DW)	1,410.12 \pm 38.77	3,033.01 \pm 43.33	3,179.72 \pm 75.69
Ascorbic acid (mg/kg DW)	1,495.88 \pm 5.54	1,477.44 \pm 3.29	2,998.56 \pm 7.46

1/1,500 1 % DHA and 1,500 mg/kg vitamin E diet; 5/3,000 5 % DHA and 3,000 mg/kg vitamin E diet; 5/3,000 + vitC 5 % DHA and 3,000 mg/kg vitamin E diet with increased ascorbic acid content

DW dry weight

MyHC gene expression was low in larvae fed diet 1/1,500 and significantly increased by the elevation of both α -TOH and DHA in diet 5/3,000 (Fig. 4c). However, the increase in vitC in diet 5/3,000 + vitC significantly reduced MyHC expression to levels similar to those of the 1/1,500 diet.

Discussion

Marine fish larvae are subjected to high levels of oxidative stress when using inert diets due to the high content of LC-PUFA, particularly DHA, and pro-oxidants such as minerals as well as the high surface to volume ratio of these feed particles [56]. Therefore, inclusion of high dietary levels of LC-PUFA to match the high requirements of marine fish larvae may call for increased dietary supplementation with antioxidants such as α -TOH to prevent oxidative damage. For instance, increasing DHA by up to 5 % in diets for sea bass markedly reduced larval survival and growth and increased the incidence of muscular lesions [43]. Even if no differences were observed among treatments in terms of final survival, survival rate ranged from 48 % in larvae fed 5 % DHA diets to 60 % in those fed 1 %. This survival rate may seem low if compared to results obtained from other larval experiments [57], but it is worth mentioning that low larval performance has been related to the use of inert microdiets [58], being improved by cofeeding with rotifers or artemia [58]. Nonetheless, our survival rates were similar to or even higher than those

Table 4 Sea bass larvae performance and levels of lipid peroxidation products (TBARS) and vitamin E (α -tocopherol) content in sea bass larvae at the beginning and after eating the experimental diets with two levels of DHA (1 and 5 %) and α -tocopherol (1,500 or 3,000 mg/kg) and supplemented or not with ascorbic acid (1,800 mg/kg) for 3 weeks

	Diets			
	Initial	1/1,500	5/3,000	5/3,000 + vitC
Results of dietary trial				
Larval total length (mm)	8.58 \pm 0.64	12.60 \pm 0.93a	10.89 \pm 1.24c	11.24 \pm 1.08b
Larval dry weight (mg)	0.36 \pm 0.00	1.33 \pm 0.46	0.94 \pm 0.05	1.01 \pm 0.07
Survival (%)	–	60.51 \pm 9.10	48.42 \pm 4.00	47.43 \pm 10.50
Incidence of muscular lesions (%)	–	17.50 \pm 14.14b	52.63 \pm 15.93a	20.70 \pm 15.62b
Incidence of skeletal malformations (%)	–	28.33 \pm 1.30	33.11 \pm 5.11	29.67 \pm 6.51
Ossification degree rate (%)	–	19.22 \pm 3.60a	15.24 \pm 4.18b	15.07 \pm 4.60b
TBARS				
NMol/g dry mass	62.85 \pm 0.61	166.62 \pm 25.08c	2,402.15 \pm 67.91a	846.87 \pm 94.74b
Vitamin E (α-tocopherol)				
mg/kg dry mass	111.45 \pm 43.26	630.24 \pm 12.39b	542.10 \pm 80.51b	757.12 \pm 44.55a

Data are mean \pm SD. Values within the same row bearing different lowercase letters are significantly different ($P < 0.05$)

1/1,500 1 % DHA and 1,500 mg/kg vitamin E diet; 5/3,000 5 % DHA and 3,000 mg/kg vitamin E diet; 5/3,000 + vitC 5 % DHA and 3,000 mg/kg vitamin E diet with increased ascorbic acid content

DW dry weight

Table 5 Main fatty acid composition of total lipids from sea bass larvae after 3 weeks of feeding the experimental diets (% total fatty acid)

	1/1,500	5/3,000	5/3,000 + vitC
14:0	0.93 ± 0.06	0.76 ± 0.03	0.51 ± 0.28
14:1n-7	0.08 ± 0.01	0.08 ± 0.03	0.34 ± 0.37
14:1n-5	0.07 ± 0.02	0.04 ± 0.01	0.34 ± 0.43
15:0	0.63 ± 0.29	0.98 ± 1.22	0.38 ± 0.26
15:1n-5	0.12 ± 0.10	0.09 ± 0.06	0.79 ± 0.23
16:0ISO	ND	0.11 ± 0.01	0.28 ± 0.25
16:0	17.51 ± 2.44	17.61 ± 0.25	16.32 ± 0.26
16:1n-7	2.02 ± 0.14	1.60 ± 0.06	1.63 ± 0.16
16:1n-5	0.25 ± 0.01	0.25 ± 0.01	0.40 ± 0.18
16:2n-6	0.30 ± 0.00	0.36 ± 0.04	0.46 ± 0.15
16:2n-4	0.93 ± 0.40	0.96 ± 0.15	0.89 ± 0.12
17:0	0.91 ± 0.10	0.80 ± 0.03	0.81 ± 0.08
16:3n-3	0.12 ± 0.01	0.14 ± 0.03	0.09 ± 0.03
16:3n-1	0.10 ± 0.02	0.54 ± 0.10	0.54 ± 0.09
16:4n-3	0.62 ± 0.35	0.44 ± 0.10	0.48 ± 0.01
16:4n-1	ND	0.17 ± 0.01	0.16 ± 0.00
18:0	11.66 ± 3.41	12.29 ± 0.36	11.07 ± 1.04
18:1n-9	26.35 ± 4.87a	20.92 ± 0.51b	20.57 ± 0.13b
18:1n-7	4.85 ± 0.29	4.44 ± 0.39	3.99 ± 0.23
18:1n-5	0.62 ± 0.24	0.49 ± 0.07	0.45 ± 0.12
18:2n-9	ND	0.13 ± 0.11	0.13 ± 0.10
18:2n-6	4.23 ± 0.08	3.90 ± 0.17	3.85 ± 0.14
18:2n-4	0.04 ± 0.05	0.06 ± 0.01	0.07 ± 0.00
18:3n-6	0.43 ± 0.01	0.38 ± 0.04	0.33 ± 0.01
18:3n-4	0.07 ± 0.04	0.06 ± 0.02	0.06 ± 0.02
18:3n-3	0.32 ± 0.05	0.44 ± 0.04	0.46 ± 0.05
18:4n-3	0.29 ± 0.06	0.29 ± 0.13	0.29 ± 0.01
20:0	0.38 ± 0.19	0.47 ± 0.01	0.48 ± 0.04
20:1n-9 + n-7	1.83 ± 0.0	1.77 ± 0.06	1.80 ± 0.02
20:1n-5	0.26 ± 0.15	0.13 ± 0.01	0.13 ± 0.02
20:2n-6	0.50 ± 0.13	0.65 ± 0.08	0.60 ± 0.07
20:3n-6	0.08 ± 0.01	0.08 ± 0.00	0.08 ± 0.01
20:4n-6	2.38 ± 0.04b	3.07 ± 0.22a	3.13 ± 0.24a
20:3n-3	0.12 ± 0.09	0.15 ± 0.04	0.13 ± 0.00
20:4n-3	0.14 ± 0.00	0.16 ± 0.01	0.17 ± 0.01
20:5n-3	5.91 ± 1.18	4.85 ± 0.20	5.31 ± 0.33
22:1n-11	0.46 ± 0.30	0.19 ± 0.08	0.26 ± 0.02
22:1n-9	0.26 ± 0.15	0.26 ± 0.06	0.27 ± 0.05
22:4n-6	ND	0.11 ± 0.02	0.13 ± 0.04
22:5n-6	1.09 ± 0.09	1.26 ± 0.07	1.33 ± 0.05
22:5n-3	0.64 ± 0.26	0.57 ± 0.06	0.64 ± 0.08
22:6n-3	12.79 ± 0.37b	18.04 ± 1.19a	20.26 ± 0.25a
Saturated	32.01 ± 6.29	32.91 ± 1.54	29.56 ± 1.20
Monoenoics	36.73 ± 4.51a	30.20 ± 0.55b	30.56 ± 1.44b
n-3 PUFA	20.94 ± 2.23b	25.11 ± 1.43a	27.83 ± 0.57a
n-6 PUFA	8.45 ± 0.97	9.80 ± 0.47	9.91 ± 0.09
n-9 PUFA	28.44 ± 4.72a	23.08 ± 0.39b	22.76 ± 0.05b

Table 5 continued

	1/1,500	5/3,000	5/3,000 + vitC
n-3 LC-PUFA	12.92 ± 7.45c	23.78 ± 1.42b	26.51 ± 0.67a
n-3/n-6 PUFA	2.51 ± 0.55	2.56 ± 0.05	2.81 ± 0.03
EPA/DHA	0.33 ± 0.07b	1.16 ± 0.10a	1.11 ± 0.17a
ARA/DHA	0.18 ± 0.01b	0.88 ± 0.07a	0.80 ± 0.04a
ARA/EPA	0.54 ± 0.04b	2.56 ± 0.05a	3.00 ± 0.33a

Each value represents mean ± SD. Values within the same row bearing different lowercase letters are significantly different ($P < 0.05$)

1/1,500 1 % DHA and 1,500 mg/kg vitamin E diet; 5/3,000 5 % DHA and 3,000 mg/kg vitamin E diet; 5/3,000 + vitC 5 % DHA and 3,000 mg/kg vitamin E diet with increased ascorbic acid content

ND not detected

obtained in other nutritional experiments in sea bass larvae employing both live prey (3.6 %, [59]) or inert microdiets (41 %, [60]; 33.5 %, [61]), indicating that our results are within normal range. The same applies for growth and deformities rates as around 30 % of marine fish larvae reared in commercial hatcheries exhibit morphological and skeletal deformities [62].

In the present study, high levels of α -TOH (3,000 mg/kg) together with high DHA (5 %) were not able to counteract the adverse effects of lipid oxidation on the incidence of muscular lesions. Accordingly, these larvae showed very high levels of TBARS indicating that their oxidative status is altered when they are fed high DHA levels even at such high dietary α -TOH levels. Moreover, AOE expression was higher in those larvae, denoting a high antioxidant response. A compensatory induction of these endogenous antioxidants is found in animals exposed to dietary oxidative stress [63]. Indeed, α -TOH contents in these larvae were not increased by the elevation of dietary α -TOH levels, suggesting, on the one hand, a prooxidant effect of this vitamin due to the high levels included in the diet or, on the other hand, a depletion of this vitamin to neutralize ROS. Similarly, increased n-3 LC-PUFA did cause depletion of α -TOH contents when this vitamin was supplemented in the diet in previous studies [56, 64, 65].

In contrast, the increase in vitC dietary supplementation from 1,800 to 3,600 mg/kg markedly improved the protection against peroxidation, decreasing TBARS contents to less than one-third, sparing vitamin E that was significantly increased in larval tissues, and effectively reducing the incidence of muscular lesions. vitC supplementation has also been found to reduce TBARS formation in hybrid striped bass (*Morone chrysops* ♀ × *M. saxatilis* ♂) fed diets deficient in α -TOH [26]. The increased α -TOH content found in the present study when larvae were fed high levels of vitC is in agreement with studies in other fish species [19, 21, 56] and denotes the sparing effect of vitC

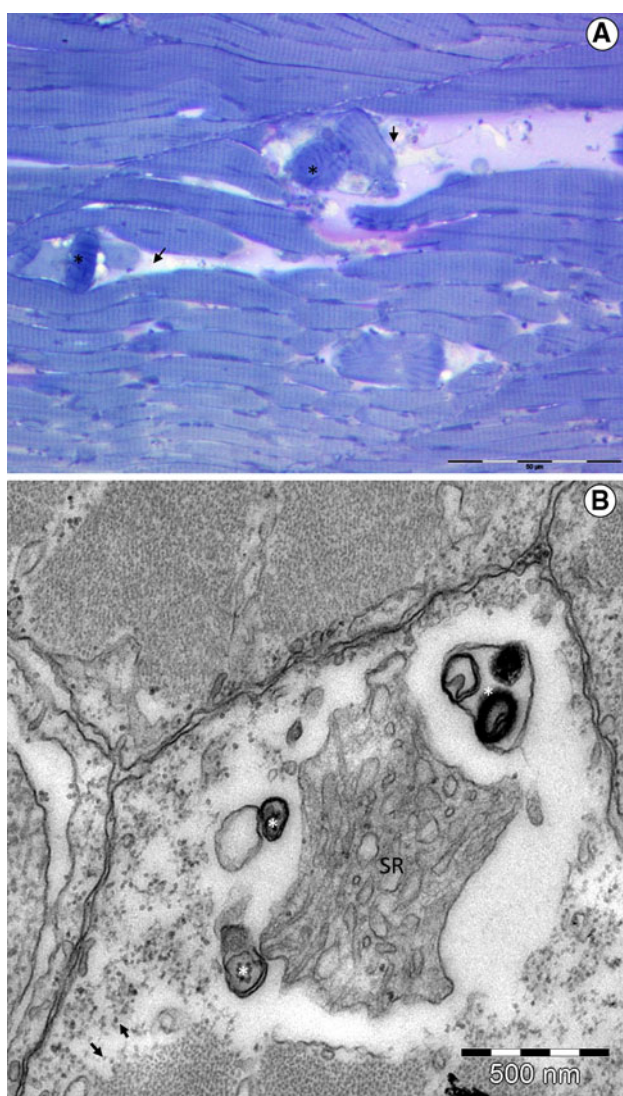


Fig. 1 Longitudinal semithin (a) and transversal electron micrographs (b) of sea bass (*Dicentrarchus labrax*) larvae fed the 5/300 diet. **a** Damaged muscle fibers showing breakage (arrow) as well as darkening due to protein coagulation (asterisk). **b** Affected fiber showing disarrangement of the myofilaments (arrows), swollen sarcoplasmic reticulum (SR) and myelin figures (asterisk)

on α -TOH in sea bass larvae, the first vitamin recycling the second one. Thus, under dietary conditions of high LC-PUFA and α -TOH, vitC dietary contents of 1,800 mg/kg may not be sufficient to recycle α -TOH and prevent the high rate of ROS formation and, therefore, vitC requirements may be higher than under low oxidation risk dietary situations.

vitC is known to be a powerful antioxidant by efficiently trapping peroxy radicals in the aqueous phase before they can initiate lipid peroxidation, thereby protecting the biomembranes [66]. Thus, the decrease in the incidence of muscular lesions observed in the present study, when high levels of vitC were employed, could be due to the

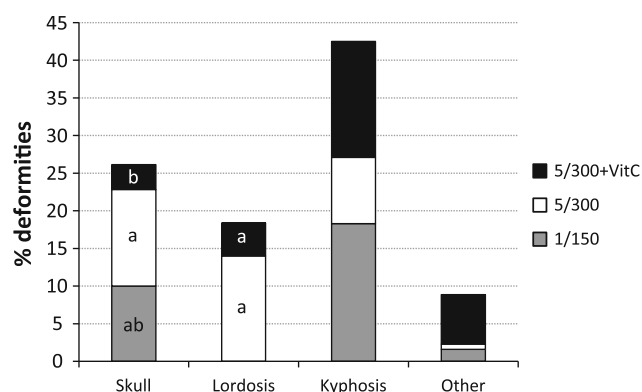


Fig. 2 Skeletal deformities found in 35 dph larvae at the end of the experimental period

protective effect of this antioxidant nutrient, quenching free radicals before they can attack muscular membranes, in addition to recycling α -TOH. Moreover, the species formed after the loss of one electron are relatively stable and fairly unreactive compared to tocopheroxyl radical [67], thus preventing a pro-oxidant action. The reduced incidence of muscular lesions was also accompanied by a decrease in IGF-I expression, the highest IGF mRNA copies occurring in larvae fed the highest DHA and α -TOH levels, which also showed the lowest growth and the highest incidence of muscular lesions. These results are in line with the higher expression of IGF-I found in sea bream larvae fed high DHA levels [68]. In contrast to the present study, in sea bream, high IGF-I expression was correlated with high growth [68], suggesting the negative effect of high DHA contents in sea bass growth in relation to the altered oxidative status. A feasible explanation for the overexpression of IGF-I in larval groups with higher TBARS values could be a compensatory mechanism in fish larvae to try to counteract the adverse effects of ROS, since IGF-I interferes with activation of apoptosis in several cells and organ systems in mammals [69]. For instance, an increase in IGF-I has been found to suppress oxidative stress in atherosclerotic Apo-E-deficient mice [70]. Furthermore, the IGF system can promote muscle growth and differentiation in fish, by activating cell proliferation and DNA synthesis. Thus, the increase in mRNA copies of IGF-I observed in larvae fed 5 % DHA and 3,000 mg/kg α -TOH could also be due to the compensatory regeneration process carried out by satellite cells, and which was not directly reflected on a growth improvement. This is supported by the results of MyHC expression, as a high expression of myosin has been associated with regeneration processes in sea bream after mechanical injury [71]. In addition, in the present study, IGF-I and MyHC expression follows a similar pattern, indicating that their biological functions may be interrelated. In this sense, it is known that

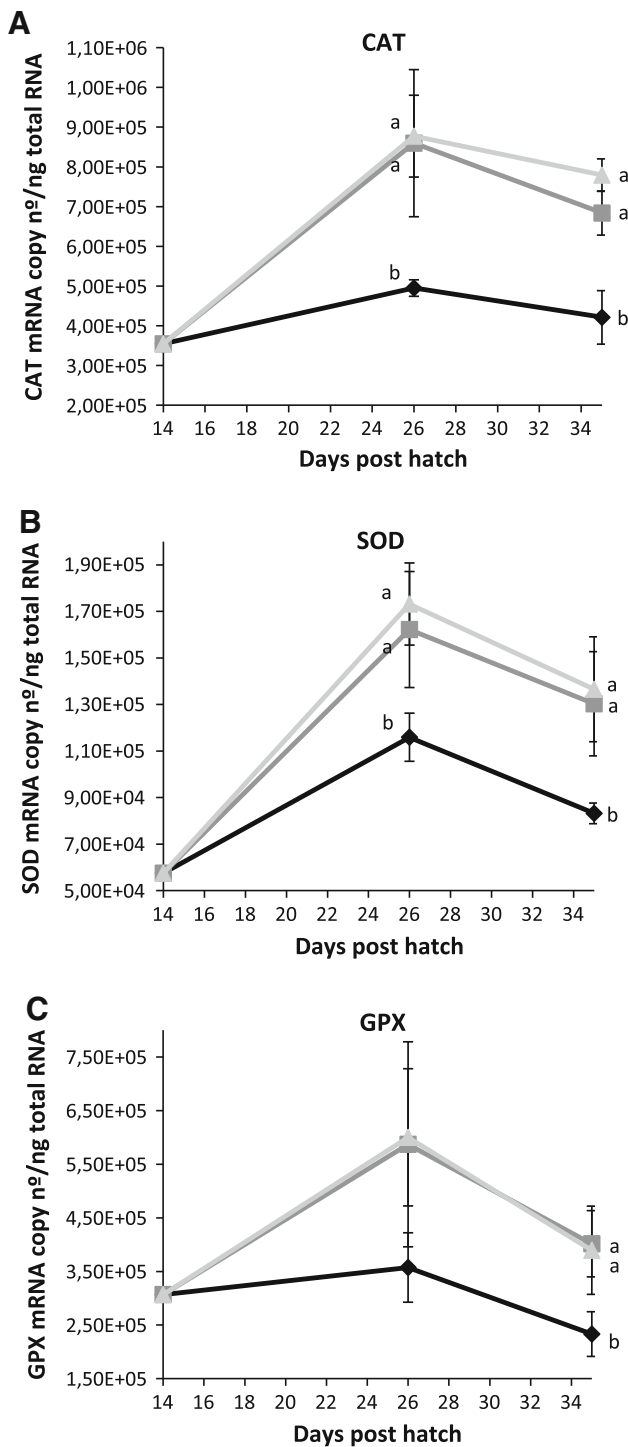


Fig. 3 Catalase (CAT), superoxide dismutase (SOD) and glutathione peroxidase (GPX) expression levels measured by real-time PCR in *Dicentrarchus labrax* larvae fed diets 1/150 (filled diamond), 5/300 (filled square) or 5/300 + vitC (filled triangle). mRNA copy number of each gene was normalized as a ratio to 100 ng total RNA. Values are means, with standard deviations represented by vertical bars. Mean values with different letters were significantly different in gene expression among the treatments at a given sampling points

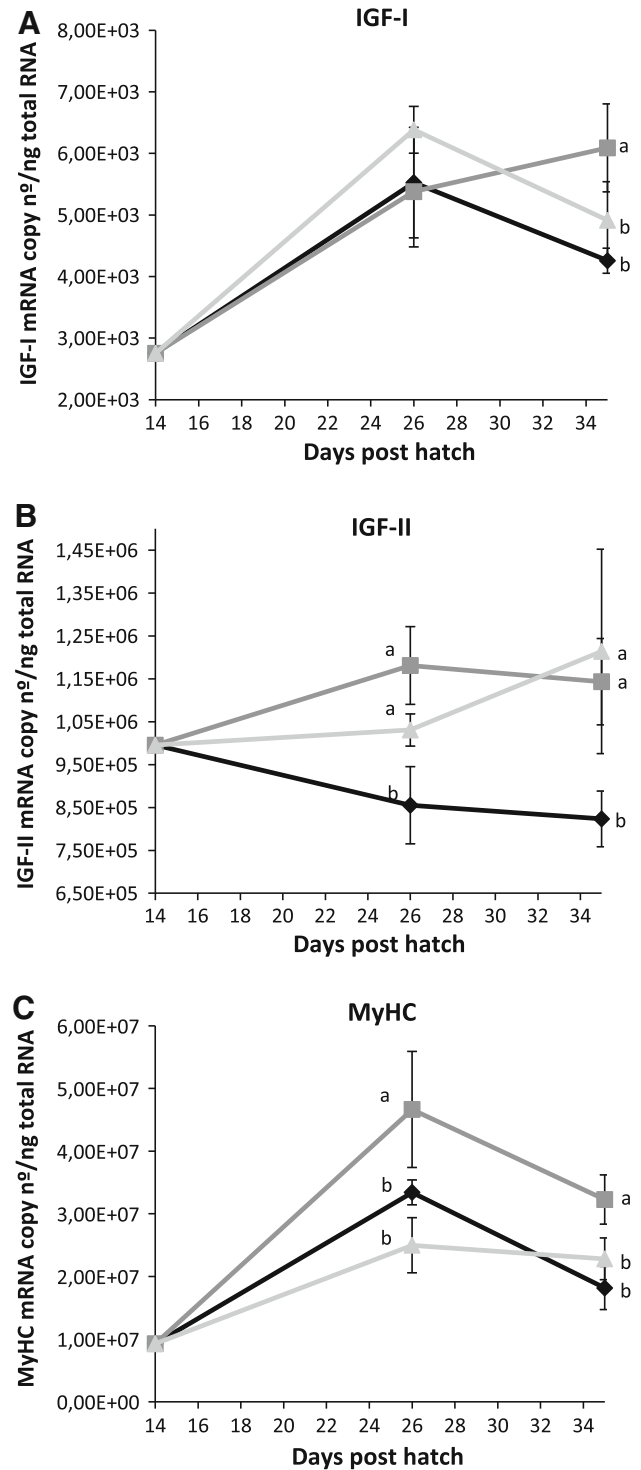


Fig. 4 Insulin-like growth factors I and II (IGF-I and II) and myosin heavy chain (MyHC) expression levels measured by real-time PCR in *Dicentrarchus labrax* larvae fed diets 1/150 (filled diamond), 5/300 (filled square) or 5/300 + AA (filled triangle). mRNA copy number of each gene was normalized as a ratio to 100 ng total RNA. Values are means, with standard deviations represented by vertical bars. Mean values with different letters were significantly different in gene expression among the treatments at a given sampling points

IGF-I overexpression results in greater skeletal muscle mass in fine flounder (*Paralichthys adspersus*, [72]) and in mice, in which IGF-I can activate MyHC as well as other transcriptional factors [73]. Thus, the parallel increase in IGF-I and MyHC expression observed in the present study confirms that, when sea bass larvae are subjected to oxidative stress, a compensatory overexpression of genes related to cell/muscle proliferation occurs.

In the present study, vitC elevation did not reduce the expression of AOE genes, suggesting an antioxidant effect independently of these enzymes, but acting in parallel with them to quench ROS. vitC acts as a cofactor for at least eight enzymes involved in the biosynthesis of collagen and carnitine, conversion of the neurotransmitter dopamine to noradrenaline, metabolism of tyrosine, and amidation of peptide hormones. In this sense, vitC acts with peptidylglycine alpha-amidating monooxygenase (PAM), an enzyme that adds amide groups to peptide hormones, greatly increasing their stability [74, 75]. Thus, the antioxidant role of vitC in fish might not only be reduced to trapping peroxy radicals from the aqueous phase or recycling α -TOH but also to support the formation of molecules with sound antioxidant potential. More studies are required to clarify the interrelationships between the different components of antioxidant defenses in marine fish, as well as to corroborate if the AOE activity really reflects their gene expression.

In terms of skeletal deformities, it can be observed that a DHA increase up to 5 % raised the incidence of alterations in chondroid bone, such as that of the cranium, whereas no differences were found in other deformities attaining intramembranous bone, such as kyphosis. These results match with previous studies on sea bream larvae fed high DHA rotifers (5.2 % DW; [68]), as ROS are known to actively destroy cartilage tissue [76], therefore affecting chondroid bones with characteristics of cartilage rather than directly affecting intramembranous bones. However, in the same study, in contrast to the present one, the incidence of cranial deformities was reduced when high contents of α -TOH were included in the rotifer enrichment media, in relation to the reduced TBARS and AOE expression. In another study from our research group [77], inclusion of organic selenium to diets containing high DHA and α -TOH was enough to decrease the TBARS values, but not to reduce cranial deformities, suggesting that the appearance of these kinds of deformity could not only be related directly to the DHA oxidation but also to the deficit of vitC due to the pro-oxidant environment originated by the high levels of α -TOH and LC-PUFA. Similarly, in the present study, an extra dosage of vitC proved to be efficient in reducing the incidence of cranial deformities when high levels of DHA are included in the diets. Apart from being a potent antioxidant, vitC acts with

three enzymes that participate in collagen hydroxylation by adding hydroxyl groups to the aminoacids proline or lysine in the collagen molecules, greatly increasing stability of the collagen [68]. Thus, the protective effect of vitC on chondroid bones could be due both to its antioxidant activity and to a higher stability in the cartilage formation. Recent work on sea bass larvae also showed a reduction in the incidence of cranial deformities when enhanced levels of vitC were included in the diet (50 mg/kg; [27]). However, in the same study, elevated levels of this nutrient (400 mg/kg) caused a similar percentage of deformities to diets with a deficiency in vitC. In the present work, the levels of vitC employed are much more elevated (1,800 mg/kg), but it also has to be noted that levels of vitC higher than those required for growth are necessary to satisfy the demands of other nutrients, in this case, to counteract the depletion in α -TOH caused by ROS.

The appearance of lordosis in fish fed high DHA and α -TOH content could be related to the high IGF-I expression observed in these larvae caused by an imbalance in the development of the musculoskeletal system, in agreement with previous studies [78]. On the one hand, the high incidence of muscular lesions occurring in these larvae may also contribute to increase the lordosis rate, as a result of the increased muscular tensions created during tissue regeneration. In this sense, Madsen and Dalsgaard [79] showed that the rainbow trout fry syndrome, characterized by muscular dystrophy among other pathologies, was associated with an increased incidence of vertebral deformities. On the other hand, IGF-II expression follows a different tendency within each dietary treatment and also as compared to IGF-I expression. These differences may support the idea that different hormonal signals and mechanisms of gene transcription control the regulation of expression of both IGF forms [80, 81].

In conclusion, an increased dosage of vitC in microdiets for sea bass larvae containing a 5 % of DHA and 3,000 mg/kg of α -TOH was shown to be successful in compensating, to some extent, the effect of lipid oxidation, thereby preventing the appearance of muscular lesions and reducing cranial deformities and TBARS values, a major indicator of oxidative stress. However, no counteracting effect was found on AOE expression, suggesting that other nutrients could be involved in enhancing the antioxidant defenses at such levels. Moreover, a sparing effect between vitC and α -TOH seems to occur in sea bass larvae. The implication of vitC in regulating other antioxidant components requires further investigation.

Acknowledgments Mónica B. Betancor was supported by a grant given by the Cabildo Insular de Gran Canaria. The present study was funded by the Spanish Ministry of Sciences and Education (AGL2009-14661). The experiments were designed according to the Animal Welfare Ethics Committee guidelines of Las Palmas

University. Acknowledgments are due to Instituto de Acuicultura de Torre la Sal that kindly provided the sea bass eggs and to Croda Company that provided DHA and EPA 50.

References

- Watanabe T (1993) Importance of docosahexaenoic acid in marine larval fish. *J World Aquac Soc* 24:152–161
- Watanabe T, Kiron V (1994) Prospects in larval fish dietetics. *Aquaculture* 124:223–253
- Sargent JR, McEvoy L, Estévez A, Bell JG, Bell MV, Henderson RJ, Tocher DR (1999) Lipid nutrition of marine fish during early development: current status and future directions. *Aquaculture* 179:217–229
- Izquierdo MS (2005) Essential fatty acid requirements in Mediterranean fish species. *Cah Opt Med* 63:91–102
- Takeuchi T, Masuda R, Ishizaki Y, Watanabe T, Kanematsu M, Imaizumi K, Tsukamoto K (1996) Determination of the requirement of larval striped jack for eicosapentaenoic acid and docosahexaenoic acid using enriched *Artemia nauplii*. *Fish Sci* 62:760–765
- Copeman L, Parrish C, Brown J, Harel M (2002) Effects of Docosahexaenoic, Eicosapentaenoic and Arachidonic acids on the early growth, survival, lipid composition and pigmentation of yellowtail flounder (*Limanda ferruginea*): a live food enrichment experiment. *Aquaculture* 210:285–304
- Rezek TC, Watanabe WO, Harel M, Seaton PJ (2010) Effects of dietary docosahexaenoic acid (22:6n–3) and arachidonic acid (20:4n–6) on the growth, survival, stress resistance and fatty acid composition in black sea bass *Centropristis striata* (Linnaeus 1758) larvae. *Aquac Res* 41:1302–1314
- Watanabe T, Izquierdo MS, Takeuchi T, Satoh S, Kitajima C (1989) Comparison between eicosapentaenoic and docosahexaenoic acids in terms of essential fatty acid efficacy in larval red seabream. *Nippon Suisan Gakkaishi* 55:1635–1640
- Rodríguez C, Pérez JA, Díaz M, Izquierdo MS, Fernández-Palacios H, Lorenzo A (1997) Influence of the EPA/DHA ratio in rotifers of gilthead seabream *Sparus aurata* larval development. *Aquaculture* 150:77–89
- Koven W, Barr Y, Lutzky S, Ben-Atia I, Weiss R, Harel M, Behrens P, Tandler A (2001) The effects of dietary arachidonic acid (20:4n–6) on growth, survival and resistance to handling stress in gilthead seabream *Sparus aurata* larvae. *Aquaculture* 193:107–122
- Nagaoka S, Okauchi Y, Urano S, Nagashima U, Mukai K (1990) Kinetic and ab initio study of the prooxidant effect of vitamin E: hydrogen abstraction from fatty acid esters and egg yolk lecithin. *JAOAC* 112:8921–8924
- Matés JM (2000) Effects of antioxidant enzymes in the molecular control of reactive oxygen species toxicology. *Toxicology* 153:83–104
- Machlin LJ, Bendich A (1987) Free radical tissue damage, protective role of antioxidant nutrients. *FASEB J* 1:441–445
- Sies H (1985) Oxidative stress: introductory remarks. In: Sies H (ed) *Oxidative stress*. Academic, London, p 18
- Hamre K, Krossøy C, Lock EJ, Moren M (2010) Roles of lipid-soluble vitamins during ontogeny of marine fish larvae. *Aquac Res* 41:745–750
- Levine M (1986) New concepts in the biology and biochemistry of ascorbic acid. *N Eng J Med* 314:892–902
- Tappel AL (1962) Vitamin E as the biological lipid antioxidant. *Vitam Horm* 20:493–510
- Lovell RT, Miyazaki T, Rabegnator S (1984) Requirements for α -tocopherol by channel catfish fed diets low in polyunsaturated triglycerides. *J Nutr* 114:894–901
- Hamre K, Waagbø R, Berge RK, Lie O (1997) Vitamins C and E interact in juvenile Atlantic salmon (*Salmo salar*). *Free Rad Biol Med* 22:137–149
- Sealey WM, Gatlin DM (2002) Dietary vitamin C and vitamin E interact to influence growth and tissue composition of juvenile hybrid striped bass (*Morone chrysops* ♀ × *M. saxatilis* ♂) but have limited effects on immune responses. *J Nutr* 132:748–755
- Shiau SY, Hsu CY (2002) Vitamin E sparing effect by dietary vitamin C in juvenile hybrid tilapia, *Oreochromis niloticus* × *O. aureus*. *Aquaculture* 210:335–342
- Yildirim-Aksoy M, Lim C, Li M, Klesius PH (2008) Interaction between dietary levels of vitamins C and E on growth and immune responses in channel catfish, *Ictalurus punctatus* (Rafinesque). *Aquac Res* 39:1198–1209
- Southgate P, Kavanagh KD (1999) Effects of n-3 fatty-acid composition of enhanced Artemia diet on growth and mortality of *Acartochromis polyacanthus*. *Aquat Living Resour* 12:31–36
- Izquierdo MS (2005) Essential fatty acid requirements in Mediterranean fish species. *Cah Options Med* 63:91–102
- Hamre K, Lie Ø (1995) Minimum requirement of vitamin E for Atlantic salmon (*Salmo salar* L.) at first feeding. *Aquac Res* 26:175–184
- Atalah E, Hernández-Cruz CM, Ganuza E, Benítez-Santana T, Ganga R, Roo J, Fernández-Palacios H, Izquierdo MS (2011) Enhancement of gilthead sea bream (*Sparus aurata*) larval growth by dietary vitamin E in relation to two different levels of essential fatty acids. *Aquac Res*. doi:10.1111/j.1365-2109.2011.02989.x
- Darias MJ, Mazurais D, Koumoundouros G, Le Gall MM, Huelvan C, Desbruyeres E, Quazuguel P, Cahu CL, Zambonino-Infante JL (2011) Imbalanced dietary ascorbic acid alters molecular pathways involved in skeletogenesis of developing European sea bass (*Dicentrarchus labrax*). *Comp Biochem Physiol A* 159:46–55
- Merchie G, Lavens P, Storch V, Ubel U, De Nelis H, Leenheer A, Sorgeloos P (1996) Influence of dietary vitamin C dosage on turbot *Scophthalmus maximus* and European sea bass *Dicentrarchus labrax* nursery stages. *Comp Biochem Physiol A* 114:123–133
- Zhang H, Mu Z, Xu L, Xu G, Liu M, Shan A (2009) Dietary lipid level induced antioxidant response in Manchurian trout, *Brachyrynystax lenok* (Pallas) larvae. *Lipids* 44:643–654
- Mourente G, Tocher DR, Díaz-Salvago E, Grau A, Pastor E (1999) Study of the n-3 highly unsaturated fatty acids requirement and antioxidant status of *Dentex dentex* larvae at the *Artemia* feeding stage. *Aquaculture* 179:291–307
- Rudneva I (1999) Antioxidant system of Black sea animals in early development. *Comp Biochem Physiol C* 122:265–271
- Saal FJ, Roederer M, Herzenberg LA, Herzenberg LA (1990) Intracellular thiols regulate activation of nuclear factor kappa B and transcription of human immunodeficiency virus. *Proc Natl Acad Sci USA* 87:9943–9947
- Agarwal A, Gupta S, Sikka S (2006) The role of the free radicals and antioxidants in reproduction. *Curr Opin Obstet Gynecol* 18:325–332
- Pagano G, de Biase A, Deeva IB, Degan P, Doronin YK, Iaccarino M, Oral R, Trieff NM, Warnau M, Korkina LG (2001) The role of oxidative stress in developmental and reproductive toxicity of tamoxifen. *Life Sci* 68:1735–1749
- Goldspink G, Wilkes D, Ennion S (2001) Myosin expression during ontogeny, post-hatching growth and adaptation. In: Johnston IA (ed) *Muscle development and growth*. Academic, California, pp 43–66
- Bower NI, Li X, Taylor R, Johnston IA (2008) Switching to fast growth: the insulin-like growth factor (IGF) system in skeletal muscle of Atlantic salmon. *J Exp Biol* 211:3859–3870

37. Duan C (1997) The insulin-like growth factor system and its biological actions in fish. *Am Zool* 37:491–503
38. Duan C (1998) Nutritional and developmental regulation of insulin-like growth factors in fish. *J Nutr* 128:306S–314S
39. Watabe S (1999) Myogenic regulatory factors and muscle differentiation during ontogeny in fish. *J Fish Biol* 55:1–18
40. Johnston IA, Hall TE (2004) Mechanisms of muscle development and responses to temperature change in fish larvae. *Am Fish Soc Symp* 40:85–116
41. Silva P, Rowleron AM, Valente LMP, Olmedo M, Monteiro RAF, Rocha E (2008) Muscle differentiation in blackspot seabream (*Pagellus bogavareo*, Brunnich): histochemical and immunohistochemical study of the fibre types. *Tissue Cell* 40:447–458
42. Betancor MB, Caballero MJ, Terova G, Saleh R, Atalah E, Benítez-Santana T, Bell JG, Izquierdo MS (2011) Selenium inclusion decreases oxidative stress indicators and muscle injuries in sea bass larvae fed high DHA microdiets. *Br J Nutr* 13:1–14. doi:10.1017/S0007114512000311
43. Betancor MB, Atalah E, Caballero MJ, Benítez-Santana T, Roo J, Montero D, Izquierdo MS (2011) α -Tocopherol in weaning diets for European sea bass (*Dicentrarchus labrax*) improves survival and reduces tissue damage caused by excess dietary DHA contents. *Aquac Nutr* 17:e112–e122
44. Betancor MB, Caballero MJ, Benítez-Santana T, Saleh R, Roo J, Atalah E, Izquierdo MS (2012) Oxidative status and histological changes in sea bass larvae muscle in response to high dietary content of DHA. *J Fish Dis*. doi:10.1111/j.1365-2761.2012.01447.x
45. Liu J, Caballero MJ, Izquierdo MS, El-Sayed Ali T, Hernández-Cruz CM, Valencia A, Fernández-Palacios H (2002) Necessity of dietary lecithin and eicosapentaenoic acid for growth, survival, stress resistance and lipoprotein formation in gilthead sea bream *Sparus aurata*. *Fish Sci* 68:1165–1172
46. A.O.A.C. (1995) Official methods for analysis, 16th edn. A.O.A.C International, Washington DC
47. Folch J, Lees M, Stanley GHS (1957) A simple method for the isolation and purification of total lipids from animal tissues. *J Biol Chem* 226:497–509
48. Christie WW (1982) Lipid analysis. Pergamon, Oxford
49. Izquierdo MS, Watanabe T, Takeuchi T, Arakawa T, Kitajima C (1990) Optimum EFA levels in artemia to meet the EFA requirements of red seabream (*Pagrus major*). In: Takeda M, Watanabe T (eds) Status of fish nutrition in aquaculture. Proceedings third international symposium on feeding and nutrition in fish. Japan Translation Center, Tokyo, pp 221–232
50. McMurray CH, Blanchflower WJ, Rice DA (1980) Influence of extraction techniques on determination of α -tocopherol in animal feedstuffs. *J AOAC* 63:1258–1261
51. Cowey CB, Adron JW, Walton MJ, Murray J, Youngson A, Knox D (1981) Tissue distribution, uptake and requirement for α -tocopherol of rainbow trout (*Salmo gairdneri*) fed diets with a minimal content of unsaturated fatty acids. *J Nutr* 111:1556–1567
52. Burk RF, Trumble MJ, Lawrence RA (1980) Rat hepatic cytosolic GSH-dependent enzyme protection against lipid peroxidation in the NADPH microsomal lipid peroxidation system. *Biochim Biophys Acta* 618:35–41
53. Martoja R, Martoja-Pearson M (1970) Técnicas de histología animal. Toray-Masson, Barcelona
54. Hoffman EO, Flores TR, Coover J, Garret HB (1983) Polychrome stains for high resolution light microscopy. *Lab Med* 14:779–781
55. Vandewalle P, Gluckmann I, Wagemans F (1998) A critical assessment of the alcian blue/alizarin double staining in fish larvae and fry. *Belg J Zool* 128:93–95
56. Hamre K (2011) Metabolism, interactions, requirements and functions of vitamin E in fish. *Aquac Nutr* 17:98–115
57. Zaki MI, Saad H (2010) Comparative study on growth and survival of larval and juvenile *Dicentrarchus labrax* rearing on rotifer and Artemia enriched with four different microalgal species. *Afr J Biotechnol* 9:3676–3688
58. Lazo JP, Dinis MT, Holt GJ, Faulk C, Arnold CR (2000) Co-feeding microparticulate diets with algae: toward eliminating the need of zooplankton at first feeding in larval red drum (*Sciaenops ocellatus*). *Aquaculture* 188:339–351
59. Süzer C, Firat K, Saka S, Karacaoglan A (2010) Effects of early weaning on growth and digestive enzyme activity in larvae of sea bass (*Dicentrarchus labrax* L.). *Isr J Aquac—Bamidgeh* 59:81–90
60. Villeneuve L, Gisbert E, Le Delliou H, Cahu CL, Zambonino-Infante J (2006) Intake of high levels of vitamin A and polyunsaturated fatty acids during different developmental periods modifies the expression of morphogenesis genes in European sea bass (*Dicentrarchus labrax*). *Br J Nutr* 95:677–687
61. Mazurais D, Darias MJ, Gouillou-Coustans MF, LeGall MM, Huelvan C, Desbruyères E, Quazuguel P, Cahu C, Zambonino-Infante JL (2008) Dietary vitamin mix levels influence the ossification process in European sea bass (*Dicentrarchus labrax*) larvae. *Am J Physiol Regul Integr Comp Physiol* 294:R520–R527
62. Villeneuve L, Gisbert E, Zambonino-Infante J, Quazuguel L, Cahu P (2005) Effect of nature of dietary lipids on European sea bass morphogenesis: implication of 12 retinoid receptors. *Br J Nutr* 94:877–884
63. Blomhoff R (2005) Dietary antioxidants and cardiovascular disease. *Curr Opin Lipidol* 16:47–54
64. Hamre K, Lie Ø (1995) α -tocopherol levels in different organs of Atlantic salmon (*Salmo salar* L.)—effect of smoltification, dietary levels of polyunsaturated fatty acids and vitamin E. *Comp Biochem Physiol* 111A:547–554
65. Kolkovski S, Czesny S, Yackey C, Moreau R, Cihla F, Mahan D, Dabrowsky K (2000) The effect of vitamins C and E in (n-3) highly unsaturated fatty acids-enriched *Artemia nauplii* on growth, survival and stress resistance of fresh water walleye *Stizostedion vitreum* larvae. *Aquac Nutr* 6:199–206
66. Sies H, Stahl W, Sundquist AR (1992) Antioxidant functions of vitamins. Vitamins E and C, beta-carotene and other carotenoids. *Ann NY Acad Sci* 30:7–20
67. Padayatty SJ, Katz A, Wang Y, Eck P, Kwon O, Lee JH, Chen S, Corpe C, Dutta A, Dutta SK, Levine M (2003) Vitamin C as an antioxidant: evaluation of its role in disease prevention. *J Am Coll Nutr* 22:18–35
68. Izquierdo MS, Scolamacchia M, Betancor MB, Roo J, Caballero MJ, Terova G, Witten PE Increased dietary DHA promotes early mineralization in *Sparus aurata* (Linnaeus, 1758) preventing lordosis and kyphosis occurrence, whereas an excess level increases chondroid bones anomalies. Submitted to *Br J Nutr*. doi:10.1017/S0007114512003935
69. Li Q, Li B, Wang X, Leri A, Jana KP, Liu Y, Kajstura J, Baserga R, Anversa P (1997) Overexpression of Insulin-like growth factor-1 in mice protects from myocyte death after infarction, attenuating ventricular dilation, wall stress and cardiac hypertrophy. *J Clin Invest* 100:1991–1999
70. Sukhanov S, Higashi Y, Shai SY, Vaughn C, Mohler J, Li Y, Song YH, Titterton J, Delafontaine P (2007) IGF-1 reduces inflammatory responses, suppresses oxidative stress and decreases atherosclerosis progression in Apo-E deficient mice. *Arterioscler Thromb Vasc Biol* 27:2684–2690
71. Rowleron A, Radaelli G, Mascarello F, Veggetti A (1997) Regeneration of skeletal muscle in two teleost fish: *Sparus aurata* and *Brachydanio rerio*. *Cell Tissue Res* 289:311–322
72. Fuentes EN, Björnsson BT, Valdés JA, Einarsdóttir IE, Lorca B, Alvarez A, Molina A (2011) IGF-I/PI3 K/Akt and IGF-I/MAPK/ERK pathways in vivo in skeletal muscle are regulated by

- nutrition and contribute to somatic growth in the fine flounder. *Am J Physiol Regul Integr Comp Physiol* 300:R1532–R1542
73. Shanely RA, Zwetsloot KA, Childs TE, Lees SJ, Tsika RW, Booth FW (2009) IGF-I activates the mouse type II-b myosin heavy chain gene. *Am J Physiol Cell Physiol* 297:C1019–C1027
74. Eipper BA, Stoffers DA, Mains RE (1992) The biosynthesis of neuropeptides: peptide alpha-amidation. *Annu Rev Neurosci* 15:57–85
75. Eiper BA, Milgram SL, Husten EJ, Yun HY, Mains RE (1993) Peptidylglycine alpha-amidating monooxygenase: a multifunctional protein with catalytic, processing and routing domains. *Protein Sci* 2:489–497
76. Beer AM, Wegener T (2011) Vitamin E for gonarthrosis and coxarthrosis—results of a postmarketing surveillance study. *MMW Fortschr Med* 153:14–20
77. Alves Martins D, Betancor MB, Caballero MJ, Mesa-Rodríguez A, Roo J, Izquierdo MS (2011) Interactions of pro-oxidant and anti-oxidant nutrients in relation to skeleton development in *Dicentrarchus labrax* larvae. II International workshop: interdisciplinary approaches in fish skeletal biology, Tavira, Portugal
78. Fernández I, Hontoria F, Ortíz-Delgado JB, Kotzamanis Y, Estévez A, Zambonino-Infante JL, Gisbert E (2008) Larval performance and skeletal deformities in farmed gilthead sea bream (*Sparus aurata*) fed with graded levels of vitamin A enriched rotifers (*Brachionus plicatilis*). *Aquaculture* 283:102–115
79. Madsen L, Dalsgaard I (1999) Vertebral column deformities in farmed rainbow trout (*Oncorhynchus mykiss*). *Aquaculture* 171:41–48
80. Canalis E, McCarthy TL, Centrella M (1991) Growth factors and cytokines in bone cell metabolism. *Annu Rev Med* 42:17–24
81. Fernández I, Darias M, Andree KB, Mazurais D, Zambonino-Infante JL, Gisbert E (2011) Coordinated gene expression during gilthead sea bream skeletogenesis and its disruption by nutritional hypervitaminosis A. *BMC Dev Biol*. doi:[10.1186/1471-213X-11-7](https://doi.org/10.1186/1471-213X-11-7)

Introduction

Long chain omega-3 (or n-3) fatty acids and alpha-linolenic acid (ALA), are essential for growth and early development, and may play important roles in prevention and treatment of coronary artery disease, hypertension, arthritis, diabetes, and cancer, as well as other inflammatory disorders [1, 2].

Flaxseed (FS) is an oilseed that contains substantial ALA; based on work in our laboratory, as well as that of others, its inclusion in cattle diets increases ALA concentrations in blood plasma, fat and muscle tissues [3–6]. Compared to FS, high oleic acid sunflower seed (SS) contains similar concentrations of linoleic acid (LA), and low concentrations of ALA, but is rich in oleic acid (OA). Consequently, these two oilseed sources may differ in their effects on fatty acid profiles in plasma and subcutaneous fat (SQ) and perhaps growth performance of feedlot cattle. Wheat dried distillers' grains with solubles (DDGS) are a by-product of bioethanol production that can substitute for barley grain and barley silage in feedlot cattle diets [7–9]. Distillers' grains derived from triticale, a cross between wheat and rye, can also be a dietary ingredient for feedlot cattle and may have advantages over wheat as a substrate for ethanol production [10]. In previous studies, replacement of barley grain with wheat DDGS did not alter total *trans* fatty acids, however, it decreased 18:1-*n*-7 and increased vaccenic acid (VA), rumenic acid (RA or CLA-*c*9,*t*11) [11] and ALA in beef fat [12]. Replacement of barley silage with wheat DDGS in the diet of finishing steers also increased ALA concentrations of the pars costalis diaphragmatic muscle [13]. However, little information is available on the effects of a combination of oilseeds and DDGS in feedlot diets on fatty acid profiles in plasma and SQ fat of beef cattle during the finishing period. We hypothesized that inclusion of mixtures of FS or SS with DDGS in finishing feedlot diets, compared to addition of these ingredients alone, will result in more favorable changes in plasma and adipose tissue fatty acid profiles of beef cattle.

Materials and Methods

Animal and Feeding Experiment

The study was conducted at the Lethbridge Research Centre, Agriculture and Agri-Food Canada and was approved by the centre's Animal Care Committee, under the auspices of the Canadian Council of Animal Care [14]. British-continental steers (90) were stratified by body weight and randomly assigned to one of six finishing diets ($n = 15$ per treatment): (1) control (CON) diet, 90 %

barley grain concentrate + 10 % barley silage on a dry matter (DM) basis; and the following diets in which barley grain was substituted with: (2) 30 % DDGS; (3) 10 % FS; (4) 30 % DDGS + 8.5 % FS (FS + DDGS); (5) 10 % SS; and (6) 30 % DDGS + 8.5 % SS (SS + DDGS) (Table 1). Oilseeds in the combination diets were reduced to maintain total dietary lipid levels below 9 % of DM [15] and to determine if favorable changes in the fatty acid profile of adipose tissue could be maintained or enhanced at this reduced level. This approach reduced the likelihood of a fat-mediated reduction in DM digestion while maximizing the likelihood that the addition of oilseeds to the diet would alter the fatty acid profile of fat. With the addition of a vitamin and mineral supplement, all diets fully met or exceeded nutrient requirements of finishing cattle, as recommended by NRC [16] whereas the calculated net energy (NEm, NEg) levels were similar among the diets (Table 1). Steers were housed in individual pens and fed a total-mixed ration ad libitum at 0800 h daily. Orts were collected weekly to estimate daily feed intake of each individual. Barley silage DM was monitored weekly and did not vary sufficiently (<2 %) to merit reformulation of the diet. Steers were weighed at the start of the study and after 6 and 12 weeks to estimate average daily gain and the Gain:Feed ratio over the experimental period. At all three weighings, backfat thickness and rib eye area were estimated with ultrasonography [5], and amounts of trimmable fat and retail product in the carcass estimated [17].

Blood and Subcutaneous Fat Sampling

Blood samples were collected from the jugular vein using evacuated tubes (Becton–Dickinson, Franklin Lakes, NJ, USA) containing Na₂-EDTA at the start of the experiment and after 6 and 12 weeks, as previously described [4, 5]. An initial, subcutaneous fat biopsy (0.2–0.5 g) was recovered 15 cm to the left of the last thoracic vertebrae of each steer as previously outlined [5]. After 6 and 12 weeks, the second and the third biopsies were collected on the same side within the same region but 4 and 8 cm left of the scar from the first biopsy.

Lipid Extraction, Methylation and Gas Chromatograph Determination of Fatty Acids

Lipids in the samples were extracted using published procedures for plasma [4], feed samples and backfat [5]. Unless otherwise designated, all chemicals were purchased from Sigma-Aldrich Inc. (Oakville, ON, Canada). Nonadecanoic acid (C19:0) methyl ester (100 μL, 5.96 mg/mL hexane Nu-Chek Prep, Inc., MN, USA) was added to the lipids as an internal standard. A combined base/acid methylation procedure was used [5, 18]. A gas chromatograph

Table 1 Ingredients, nutrient concentration and fatty acid composition for experimental diets fed to cattle

	Non-OS-diets		FS-diets		SS-diets	
	CON	DDGS	FS	FS + DDGS	SS	SS + DDGS
Ingredient (%DM)						
Barley	85	55	75	46.5	75	46.5
Barley silage	10	10	10	10	10	10
Flaxseed	0	0	10	8.5	0	0
Sunflower seeds (high oleic)	0	0	0	0	10	8.5
Triticale DDGS	0	30	0	30	0	30
Supplements ^a	5	5	5	5	5	5
Nutrients (%DM)						
Dry Matter (%)	73.9	76.2	74.7	76.8	74.5	76.7
Crude protein (%)	12.7	20.1	13.8	21.0	13.5	20.7
Degradable carbohydrate (%)	47.6	30.8	42.0	26.0	42.0	26.0
Ether extract (%)	2.7	3.8	7.1	7.6	8.0	8.3
Calcium (%)	0.6	0.6	0.6	0.7	0.6	0.6
NE _m (Mcal/kg DM)	1.98	2.05	2.00	2.08	2.09	2.15
NE _g (Mcal/kg DM)	1.33	1.40	1.34	1.41	1.44	1.49
Fatty acid (mol%)						
SFA	21.3	17.8	10.5	11.2	10.3	10.4
16:0	19.4	16.0	8.09	8.95	6.94	7.87
18:0	1.58	1.58	2.35	2.20	3.32	3.02
USFA	78.7	82.2	89.5	88.8	89.7	89.6
MUFA	20.3	21.3	16.2	17.4	54.8	49.8
18:1-c9	18.1	19.5	15.1	16.3	53.7	48.1
PUFA	58.3	60.9	73.3	71.4	34.9	39.9
18:3 n-3 (ALA)	7.07	5.88	48.5	39.8	1.51	2.05
18:2 n-6 (LA)	51.3	55.0	24.8	31.6	33.3	37.7

DM dry matter, ADF acid detergent fiber, NDF neutral detergent fiber, FAME fatty acid methyl esters, USFA unsaturated fatty acids, MUFA monounsaturated fatty acids, PUFA polyunsaturated fatty acids

^a The supplement provided 1 kg diet (in DM) with additional: 14.67 mg copper, 58.32 mg zinc, 26.73 mg manganese, 0.66 mg iodine, 0.23 mg cobalt, 0.29 mg selenium, 4825 IU vitamin A, 478 IU vitamin D and 32 IU vitamin E

(Hewlett Packard GC System 6890, Mississauga, ON, Canada), equipped with a flame ionization detector and SP-2560 fused silica capillary column (75 m × 0.18 mm × 0.14 μm, Supelco Inc., Oakville, ON, Canada), was used for separation of fatty acid methyl esters (FAME) [5]. Peaks in chromatograms were identified and quantified using pure methyl ester standards and internal standard obtained from Sigma-Aldrich Inc. when available. Published information on retention time and elution order from previous reports was also used to tentatively identify 18:1-*t*10 and C18:2-*t*11,*c*15 isomers for which no commercial standards were available [19–21].

Statistical Analyses

Data for growth performance, backfat thickness, predicted productivity, and fatty acid composition of plasma and SQ fat were analyzed using the MIXED procedure of SAS [22]. The statistical model included DDGS, OS including FS and SS and the DDGS by OS interaction (DDGS × OS) as fixed effects. The MIXED procedure

with a REPEATED statement was conducted to compare changes of major fatty acids in plasma and backfat within the same treatment over the experimental period or to compare dietary effects within the same period. Turkey's test was used to perform a multiple comparison among treatment means [22].

Results

Dietary Nutrient and Fatty Acid Profiles

Inclusion of DDGS in diets increased dietary crude protein but decreased degradable carbohydrate levels on %DM basis (Table 1). Inclusion of FS or SS raised the dietary crude fat to a level >7 or 8 % respectively, whereas inclusion of DDGS increased dietary total unsaturated fatty acids (USFA) (Table 1). The FS diet had the highest ALA, whereas SS had the highest oleic acid (18:1-*c*9). Inclusion of DDGS in FS- and SS- diets slightly lowered USFA, while increasing LA in diets that contained oilseeds.

Table 2 Body weight change and growth performance of finishing steers during the experimental period (12 weeks)

	Non-OS-diets		FS-diets		SS-diets		SEM	P value			
	CON	DDGS	FS	FS + DDGS	SS	SS + DDGS		DDGS	OS	DDGS × OS	
Body weight (kg)											
Initial	454.1	451.3	456.3	456.9	460.6	451.9	8.2				
6 weeks	528.4	517.1	535.6	515.9	535.3	507.8	9.0	0.01	0.38	0.20	
12 weeks	585.9	573.7	600.4	582.1	601.9	564.0	9.8	0.01	0.31	0.29	
Average daily gain (kg/day)											
6 weeks	1.77	1.57	1.89	1.40	1.78	1.33	0.08	<0.01	0.38	0.20	
12 weeks	1.60	1.46	1.72	1.49	1.68	1.33	0.06	<0.01	0.30	0.28	
Feed intake (kg/day DM)											
6 weeks	8.66	9.50	8.73	9.02	9.31	9.16	0.28	0.08	0.35	0.21	
12 weeks	9.06	10.07	9.37	9.65	9.87	9.79	0.31	0.08	0.56	0.25	
Gain:Feed (kg/kg DM)											
6 weeks	0.20	0.17	0.22	0.16	0.19	0.14	0.01	<0.01	0.02 [#]	0.26	
12 weeks	0.18	0.15	0.18	0.15	0.17	0.14	0.01	<0.01	0.02 [‡]	0.73	

[#] No difference ($P > 0.05$) between Non-OS-diets and FS-diets, and both $>$ SS-diets ($P < 0.05$)

[‡] FS-diets $>$ SS-diets ($P < 0.05$) whereas Non-OS-diets was in between ($P > 0.05$)

Growth Performance

Inclusion of DDGS reduced ($P < 0.01$) body weight although it tended to increase ($P = 0.08$) DM intake after the cattle had been fed diets for 6 and 12 weeks (Table 2). Inclusion of OS in the diet did not affect ($P > 0.05$) final body weight. Inclusion of DDGS in the diets decreased ($P < 0.05$) average daily gain during the first 6 weeks and over the entire 12 weeks experiment. The Gain:Feed ratio was also reduced ($P < 0.01$) as a result of inclusion of DDGS in the diets. Inclusion of SS reduced ($P = 0.02$) the Gain:Feed ratio during the first 6 weeks compared to CON and FS as well as during the overall 12 weeks compared to FS.

Backfat Thickness, Rib Eye Area and Predicted Productivity

After 12 weeks, average backfat thickness and rib eye area approximately doubled from the start of the experiment (Table 3). Inclusion of DDGS reduced ($P = 0.04$) backfat after 12 weeks. There was no significant difference in rib eye area among treatments. Compared to diets that did not contain DDGS, DDGS reduced ($P < 0.02$) trimmable fat and retail product as predicted by body weight, backfat thickness and rib eye area measured after 6 and 12 weeks.

Plasma Fatty Acid Profile

Inclusion of DDGS or OS in the diet increased ($P < 0.05$) plasma total FAME at 12 weeks (Table 4). When comparing mol%, the effect of two main factors (DDGS and

OS) on PUFA and MUFA were different ($P < 0.01$). Inclusion of DDGS increased ($P < 0.05$) PUFA concentrations, but decreased ($P < 0.05$) MUFA. Inclusion of FS resulted in higher ($P < 0.05$) PUFA compared to SS. There was a DDGS by OS interaction ($P < 0.05$) for total n-3 FA, *trans* 18:1, non-conjugated non-methylene interrupted dienes (NCD), *trans* FA, *trans* FA excluding CLA&VA. The FS group had the highest n-3 FA and ALA ($P < 0.05$) among the groups, whereas the FS and DDGS + FS groups were higher ($P < 0.05$) in total n-3 FA and ALA compared to CON and SS groups (Table 4).

Inclusion of DDGS increased ($P < 0.05$) LA which was the most abundant fatty acid in plasma, whereas FS resulted in less ARA ($P < 0.05$) compared to SS- and Non-OS-diets (Table 4). Dietary treatment had no effect on the major CLA e.g., 18:2-*c9,t11* or RA. The plasma lipids contained very small amounts of NCD, including 18:2-*t11,c15* with these concentrations being increased ($P < 0.05$) only in the FS group.

Inclusion of DDGS in CON and FS-diets decreased ($P < 0.05$) total *trans* FA and *trans* FA excluding CLA&VA, whereas SS did not (Table 4). The DDGS, FS and FS + DDGS groups were lower ($P < 0.05$) in total *trans* 18:1 compared to CON. Feeding DDGS decreased ($P = 0.03$) 18:1-*t10* without affecting ($P > 0.05$) 18:1-*t11*. Inclusion of DDGS decreased ($P < 0.01$) plasma concentrations of both palmitic acid (16:0) and palmitoleic acid (16:1). FS-diets resulted in less ($P < 0.05$) 16:0 compared to SS-diets and Non-OS-diets. There was a DDGS by OS interaction ($P < 0.01$) for stearic acid (18:0); the combination of SS and DDGS resulted in the highest ($P < 0.05$)

Table 3 Comparison on ultrasound backfat thickness, rib eye area and estimated trimmable fat and beef retail products

	Non-OS-diets		FS-diets		SS-diets		SEM	P value			
	CON	DDGS	FS	FS + DDGS	SS	SS + DDGS		DDGS	OS	DDGS × OS	
Backfat (mm)											
Initial	6.42	6.42	6.72	6.76	6.93	7.00	0.31				
6 weeks	11.19	10.62	12.26	11.54	12.2	10.68	0.82	0.17	0.48	0.83	
12 weeks	13.84	12.15	14.76	14.35	15.08	12.72	0.85	0.04	0.20	0.52	
Rib eye area (cm ²)											
Initial	40.67	41.24	38.54	39.25	38.39	37.49	1.18				
6 weeks	71.25	67.09	71.07	66.85	67.95	68.81	1.78	0.10	0.91	0.30	
12 weeks	80.56	78.19	81.11	75.46	74.78	79.25	2.57	0.58	0.66	0.15	
Trimmable fat (kg)											
Initial	71.33	72.92	72.88	73.05	74.02	72.25	1.17				
6 weeks	87.50	86.88	91.33	87.14	91.36	84.55	2.01	0.02	0.59	0.32	
12 weeks	99.90	96.64	104.8	100.1	105.2	94.66	2.12	<0.01	0.16	0.22	
Retail product (kg)											
Initial	150.6	153.8	150.0	151.0	151.2	147.3	2.36				
6 weeks	205.0	200.0	209.1	198.6	205.5	198.3	3.37	0.01	0.84	0.72	
12 weeks	231.4	226.1	238.3	224.7	230.7	223.4	4.11	0.01	0.55	0.58	

Trimmable fat—amounts in kg of trimmable fat and retail product—retail product in the carcass which was estimated based on the ultrasound backfat thickness, rib eye area, and bodyweight

levels of plasma 18:0 among groups. Inclusion of DDGS decreased ($P < 0.01$) *cis* 18:1, including *c9* and *c15*. Inclusion of SS increased ($P < 0.05$) 18:1-*c9*, whereas FS increased ($P < 0.05$) 18:1-*c15*.

Temporal Changes in Plasma FA

The effect of oilseed inclusion in combination with DDGS on plasma 18:1-*c9*, CLA&VA, total n-3 FA, NCD and *trans* FA's excluding CLA&VA at 6- and 12-week is shown in Fig. 1. The mol% of plasma 18:1-*c9* was lower ($P < 0.05$) in FS + DDGS after 6 and 12 weeks whereas that in the CON and SS groups was higher ($P < 0.05$) after 12 weeks. Inclusion of DDGS to FS-diet resulted in lower plasma 18:1-*c9* after 6 and 12 weeks compared to levels at the start of the experiment. After 6 and 12 weeks, the mol% of plasma CLA&VA in DDGS, DDGS + FS and SS treatments were lower ($P < 0.05$) than at the start of the experiment. Total n-3 FA concentrations in cattle fed FS increased ($P < 0.05$) over the 12 weeks study, whereas these concentrations decreased ($P < 0.05$) in cattle fed CON, DDGS and SS-diets. Compared to the start of the experiment, plasma NCD did not change ($P > 0.05$) after 6 weeks, with the exception of an increase ($P < 0.05$) in cattle fed FS. However, by 12 weeks, plasma NCD concentrations declined ($P < 0.05$) in all treatments compared to either start or 6 weeks. The plasma total *trans* FA excluding CLA&VA decreased ($P < 0.05$) in cattle fed DDGS, but did not change ($P > 0.05$) in the CON over the experiment. Reductions in

plasma *trans* FA in DDGS, FS + DDGS, SS and SS + DDGS groups were lower ($P < 0.05$) than at the start of the experiment after 12 weeks.

Fatty Acid Profiles of Backfat

The mol% of PUFA in backfat was increased ($P < 0.05$) with inclusion of DDGS. It was also increased with inclusion of FS in the diet as compared to Non-OS or SS-diets, whereas concentrations of total SFA, USFA, MUFA and total CLA + VA were not affected ($P > 0.05$) by treatment (Table 5). Inclusion of FS increased ($P < 0.05$) n-3 FA and ALA with further increases ($P < 0.05$) occurring in these fatty acids as well as in LA when DDGS was included in the diet. Treatments had no effect on the major CLA i.e., 18:2-*c9,t11* or RA. There was a DDGS by OS interaction ($P = 0.03$) for NCD and 18:2-*t11,c15* concentrations in backfat, with FS having the highest ($P < 0.05$) concentrations of NCD and 18:2-*t11,c15* among treatments. Inclusion of DDGS with FS decreased ($P < 0.05$) NCD concentrations they were still higher ($P < 0.05$) than CON, SS and SS + DDGS (Table 5).

Inclusion of FS increased ($P < 0.05$) total *trans* FA and the *trans* FA excluding CLA&VA whereas SS increased ($P < 0.05$) total *trans* 18:1 (Table 5). Inclusion of DDGS decreased ($P < 0.05$) these fatty acids and 18:1-*t10*. Major SFA e.g., 16:0 and 18:0 and major *cis* MUFA e.g., 18:1-*c9* were not affected ($P > 0.05$) by treatments (Table 5; Fig. 2). Inclusion of FS increased ($P < 0.05$) 18:1-*c15* compared to

Table 4 Comparison on fatty acid profile of plasma samples at 12 weeks

	Non-OS-diets		FS-diets		SS-diets		SEM	P value		
	CON	DDGS	FS	FS + DDGS	SS	SS + DDGS		DDGS	OS	DDGS × OS
Total FAME (mmol/L)	3.39	4.90	4.85	6.40	5.29	6.09	0.33	<0.01	<0.01 [†]	0.53
Fatty acid (mol%)										
SFA ^A	37.1	33.0	28.3	27.9	34.5	36.6	1.22	0.44	<0.01	0.06
16:0	11.5	10.7	8.70	8.38	10.9	9.93	0.47	0.01	<0.01 [§]	0.32
18:0	18.8 ^b	17.7 ^{a, b}	16.0 ^a	16.5 ^{a, b}	18.3 ^{a, b}	22.3 ^c	0.93	0.17	<0.01	0.03
USFA ^B	61.5	65.9	70.3	71.2	64.6	62.6	1.24	0.44	<0.01	0.06
MUFA	16.4	8.44	14.2	8.95	18.2	10.3	1.06	<0.01	0.06	0.38
16:1- <i>c</i> 9	2.05	0.72	1.30	0.54	1.84	0.55	0.17	<0.01	0.09	0.30
18:1- <i>c</i> 9	9.41	4.98	8.10	5.53	12.6	6.52	0.72	<0.01	<0.01 [#]	0.08
18:1- <i>c</i> 15	0.32	0.15	1.23	0.58	0.19	0.14	0.09	0.01	<0.01 [*]	0.06
<i>trans</i> 18:1 ^C	1.63 ^c	1.04 ^a	1.11 ^{a, b}	0.93 ^a	1.22 ^{a, b, c}	1.51 ^{b, c}	0.15	0.25	0.08	0.03
18:1- <i>t</i> 10	1.01	0.54	0.61	0.44	0.66	0.66	0.10	0.03	0.10	0.14
18:1- <i>t</i> 11 (VA)	0.32	0.24	0.16	0.25	0.13	0.30	0.05	0.13	0.28	0.06
PUFA	45.1	57.5	56.1	62.2	46.3	52.3	1.81	<0.01	<0.01 [*]	0.16
n-3 FA ^D	4.97 ^b	3.90 ^{a, b}	21.9 ^d	13.0 ^c	3.92 ^{a, b}	3.61 ^a	0.37	<0.01	<0.01	<0.01
18:3n-3 (ALA)	2.59 ^a	2.10 ^a	18.8 ^c	10.8 ^b	2.12 ^a	2.08 ^a	0.27	<0.01	<0.01	<0.01
18:2- <i>c</i> 9, <i>c</i> 12 (LA)	38.3	51.8	33.4	48.4	40.0	46.6	1.87	<0.01	0.10	0.08
20:4n-6 (ARA)	2.82	2.61	1.45	1.55	3.07	2.73	0.16	0.30	<0.01 [‡]	0.44
CLA&VA	0.45	0.39	0.31	0.32	0.29	0.42	0.07	0.60	0.35	0.41
18:2- <i>c</i> 9, <i>t</i> 11 (RA)	0.13	0.15	0.15	0.07	0.16	0.12	0.05	0.44	0.82	0.65
NCD ^E	0.22 ^a	0.12 ^a	0.63 ^b	0.12 ^a	0.14 ^a	0.08 ^a	0.05	<0.01	<0.01	<0.01
18:2- <i>t</i> 11, <i>c</i> 15	0.05 ^a	0.03 ^a	0.29 ^b	0.05 ^a	0.03 ^a	0.02 ^a	0.02	<0.01	<0.01	<0.01
<i>trans</i> FA ^F	1.97 ^{c, d}	1.31 ^{a, b}	1.89 ^c	1.12 ^a	1.51 ^{a, b, c}	1.71 ^{b, c, d}	0.19	0.02	0.79	0.04
<i>trans</i> FA excl.CLA&VA	1.53 ^c	0.92 ^{a, b}	1.58 ^c	0.80 ^a	1.23 ^{a, b, c}	1.29 ^{b, c}	0.15	<0.01	0.93	0.04

^A Sum of: all the listed saturated fatty acids in the table and 14:0, 15:0, 17:0, 22:0

^B Sum of: all the listed unsaturated fatty acids in the table and 14:1-*c*9, 17:1-*c*9, 18:1-*c*11, 18:1-*t*6, 18:1-*t*8, 18:1-*t*9, 18:2-*c*9,*t*13&-*t*8,*c*12, 18:2-*t*10,*c*12, 18:2-*c*9,*t*12&-*t*8,*c*13, 20:1-*c*9

^C Sum of: 18:1-*t*6-*t*8, *t*9, *t*10, and *t*11

^D Sum of: 18:3n-3, 20:5n-3, 22:5n-3, and 22:6n-3

^E Sum of: 18:2-*c*9,*t*13&-*t*8,*c*12, 18:2-*c*9,*t*12&-*t*8,*c*13, and 18:2-*t*11,*c*15

^F Sum of: 18:1-*t*6-*t*8, *t*9, *t*10, *t*11; and 18:2-*c*9,*t*11 + *t*7,*c*9, 18:2-*t*10,*c*12, 18:2-*c*9,*t*13&-*t*8,*c*12, 18:2-*c*9,*t*12&-*t*8,*c*13, and 18:2-*t*11,*c*15

^{a-d} Within a row, means without a common superscript differed ($P < 0.05$)

[†] No difference ($P > 0.05$) between FS-diets and SS-diets, and both $>$ Non-OS-diets ($P < 0.05$)

[§] Non-OS-diets $>$ SS-diets $>$ FS-diets ($P < 0.05$)

[#] No difference ($P > 0.05$) between Non-OS-diets and FS-diets, and both $<$ SS-diets ($P < 0.05$)

^{*} No difference ($P > 0.05$) between Non-OS-diets and SS-diets, and both $<$ FS-diets ($P < 0.05$)

[‡] No difference ($P > 0.05$) between Non-OS-diets and SS-diets, and both $>$ FS-diets ($P < 0.05$)

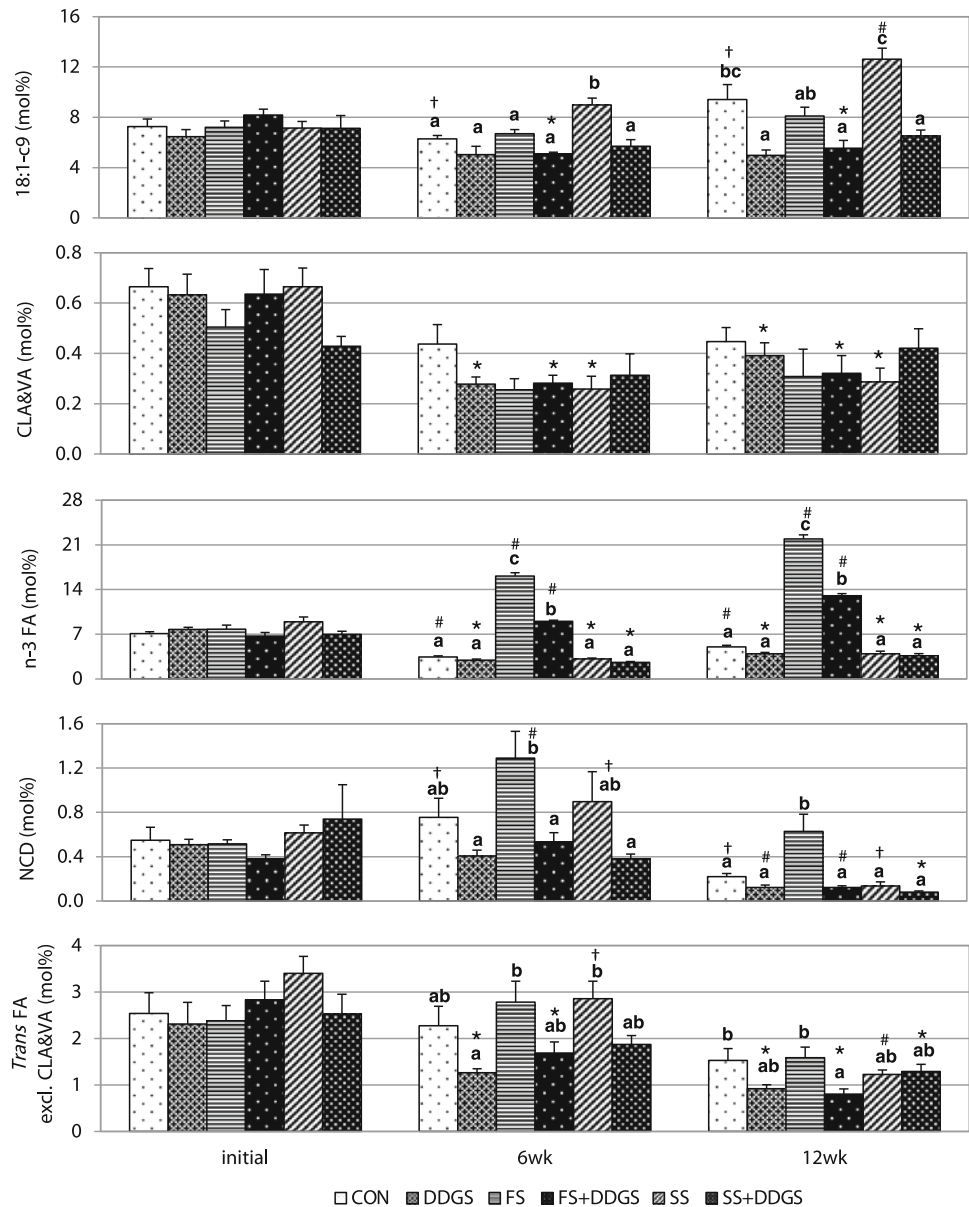
the SS- and Non-OS-diets, whereas inclusion of FS or SS decreased ($P < 0.05$) 16:1-*c*9 compared to Non-OS.

Temporal Changes in Backfat FA

The effect of oilseeds inclusion in combination with DDGS on fat 18:1-*c*9, CLA&VA, total n-3 FA, NCD and *trans* FA excluding CLA&VA at 6- and 12-week is shown in Fig. 2. The mol% of 18:1-*c*9 in backfat increased ($P < 0.05$) over

the 12 weeks period in CON, DDGS and SS + DDGS and exhibited a trend in this direction in all the other treatment groups, whereas total CLA&VA decreased ($P < 0.05$) in CON and exhibited a trend in this direction in all the others. Total n-3 FA in FS and FS + DDGS groups consistently increased ($P < 0.05$) after 6 and 12 weeks, whereas these concentrations decreased ($P < 0.05$) in CON and SS-diets, but did not change ($P < 0.05$) in DDGS or DDGS + SS diets. Levels of n-3 FA were clearly enhanced ($P < 0.05$) in

Fig. 1 Comparison of changes in plasma fatty acid composition over a 12 weeks feeding period. *Within a treatment, means differ from the initial ($P < 0.05$). †Within a treatment, means differ between 6 and 12 weeks ($P < 0.05$) but not from the initial ($P > 0.05$). #Within a treatment, means differ between 6 and 12 weeks and from the initial ($P < 0.05$). a–c Within a period, means without a common letter differ ($P < 0.05$)



the FS-diet by the addition of DDGS. Similar to n-3 FA, NCD in FS group consistently increased after 6 and 12 weeks. Concentrations of NCD also increased ($P < 0.05$) in DDGS + FS group after 6 weeks, but remained fairly constant after 12 weeks. The NCD concentration remained relatively constant in backfat from steers fed the other diets. Compared to initial biopsies the mol% of *trans* FA excluding CLA&VA increased ($P < 0.05$) in all the groups with exception of CON and DDGS groups after 6 weeks and remained relatively constant thereafter.

Discussion

Inclusion of triticale DDGS in the diet tended to increase feed intake, consistent with previous reports in feedlot

cattle [10] but not in lambs [23]. However, this increase in feed intake was not accompanied by an increase in average daily gain and as a consequence, feed efficiency was reduced. Inclusion of DDGS also reduced backfat thickness as well as estimated trimmable fat and retail product at 12 weeks. It is not known why inclusion of 30 % triticale DDGS resulted in a decline in feed efficiency, as a similar response was not observed when wheat DDGS was included in barley grain-based finishing diet at similar levels [8]. The reduction in feed efficiency did not appear to be due to a fat-mediated reduction in fiber digestibility as feed efficiencies were similar among the DDGS and DDGS + oilseed diets. Compared to barley grain, inclusion of DDGS resulted in more protein and crude fat, but less degradable carbohydrate, in the diets which may have reduced feed efficiency in fattening cattle as previously reported [24, 25].

Table 5 Fatty acid profiles in backfat samples taken via biopsy at 12 weeks

	Non-OS-diets		FS-diets		SS-diets		SEM	P value		
	CON	DDGS	FS	FS + DDGS	SS	SS + DDGS		DDGS	OS	DDGS × OS
Fatty acid (mol%)										
SFA ^A	42.7	42.5	41.8	42.4	44.2	41.7	0.88	0.33	0.62	0.22
16:0	29.8	29.2	28.2	29.4	29.3	28.0	0.63	0.62	0.38	0.15
18:0	6.90	7.91	7.51	7.74	8.99	8.64	0.63	0.56	0.06	0.55
USFA ^B	57.3	57.5	58.2	57.6	55.8	58.3	0.89	0.33	0.62	0.22
MUFA	55.5	55.1	54.6	53.8	54.0	55.8	0.97	0.79	0.55	0.40
16:1- <i>c</i> 9	8.06	7.99	7.02	6.76	6.08	6.72	0.51	0.81	0.01 [†]	0.70
18:1- <i>c</i> 9	39.2	40.1	38.6	39.4	40.2	42.1	0.86	0.13	0.08	0.81
18:1- <i>c</i> 15	0.12	0.10	0.98	0.75	0.17	0.13	0.05	0.20	<0.01*	0.45
<i>trans</i> 18:1 ^C	1.30	1.17	1.67	1.28	2.11	1.43	0.17	<0.01	0.02 [#]	0.33
18:1- <i>t</i> 10	0.88	0.66	1.06	0.74	1.23	0.80	0.12	<0.01	0.14	0.70
18:1- <i>t</i> 11 (VA)	0.19	0.23	0.16	0.19	0.19	0.20	0.03	0.36	0.60	0.90
PUFA	1.81	2.40	3.63	3.79	1.75	2.54	0.21	0.01	<0.01*	0.41
n-3 FA ^D	0.12	0.16	0.57	0.69	0.10	0.15	0.03	0.02	<0.01*	0.51
18:3n-3 (ALA)	0.12	0.16	0.57	0.69	0.10	0.15	0.03	0.02	<0.01*	0.51
CLA&VA	0.53	0.52	0.51	0.51	0.53	0.51	0.06	0.84	0.96	0.97
18:2- <i>c</i> 9, <i>t</i> 11 (RA)	0.32	0.28	0.33	0.30	0.32	0.29	0.03	0.19	0.85	0.92
18:2- <i>c</i> 9, <i>c</i> 12 (LA)	1.02	1.64	1.02	1.78	0.98	1.75	0.10	<0.01	0.80	0.78
NCD ^E	0.30 ^a	0.26 ^a	1.66 ^c	0.95 ^b	0.29 ^a	0.27 ^a	0.09	0.03	<0.01	0.03
18:2- <i>t</i> 11, <i>c</i> 15	0.05 ^a	0.04 ^a	0.57 ^c	0.28 ^b	0.05 ^a	0.04 ^a	0.03	0.03	<0.01	0.02
<i>trans</i> FA ^F	1.93	1.72	3.68	2.55	2.74	2.01	0.26	<0.01	<0.01*	0.31
<i>trans</i> FA excl.CLA&VA	1.41	1.20	3.18	2.04	2.20	1.50	0.24	<0.01	<0.01*	0.24

^A Sum of: all the listed saturated fatty acids in the table and 14:0, 15:0, 17:0

^B Sum of: all the listed unsaturated fatty acids in the table and 14:1-*c*9, 17:1-*c*9, 18:1-*c*11, 18:1-*t*6-*t*8, 18:1-*t*9, 18:2-*c*9,*t*13&-*t*8,*c*12, 18:2-*c*9,*t*12&-*t*8,*c*13, 18:2-*t*10,*c*12, 20:1-*c*9, 20:4n-6 (ARA)

^C Sum of: 18:1-*t*6-*t*8, *t*9, *t*10, and *t*11

^D Sum of: 18:3n-3, 20:5n-3, 22:5n-3, and 22:6n-3

^E Sum of: 18:2-*c*9,*t*13&-*t*8,*c*12, 18:2-*c*9,*t*12&-*t*8,*c*13, and 18:2-*t*11,*c*15

^F Sum of: 18:1-*t*6-*t*8, *t*9, *t*10, *t*11; and 18:2-*c*9,*t*11 + *t*7,*c*9, 18:2-*t*10,*c*12, 18:2-*c*9,*t*13&-*t*8,*c*12, 18:2-*c*9,*t*12&-*t*8,*c*13, and 18:2-*t*11,*c*15

^{a-c} Within a row, means without a common superscript differed ($P < 0.05$)

[†] No difference ($P > 0.05$) between FS-diets and SS-diets, and both < Non-OS-diets ($P < 0.05$)

* No difference ($P > 0.05$) between Non-OS-diets and SS-diets, and both < FS-diets ($P < 0.05$)

[#] SS-diets > Non-OS-diets ($P < 0.05$) whereas FS-diets was in between ($P > 0.05$)

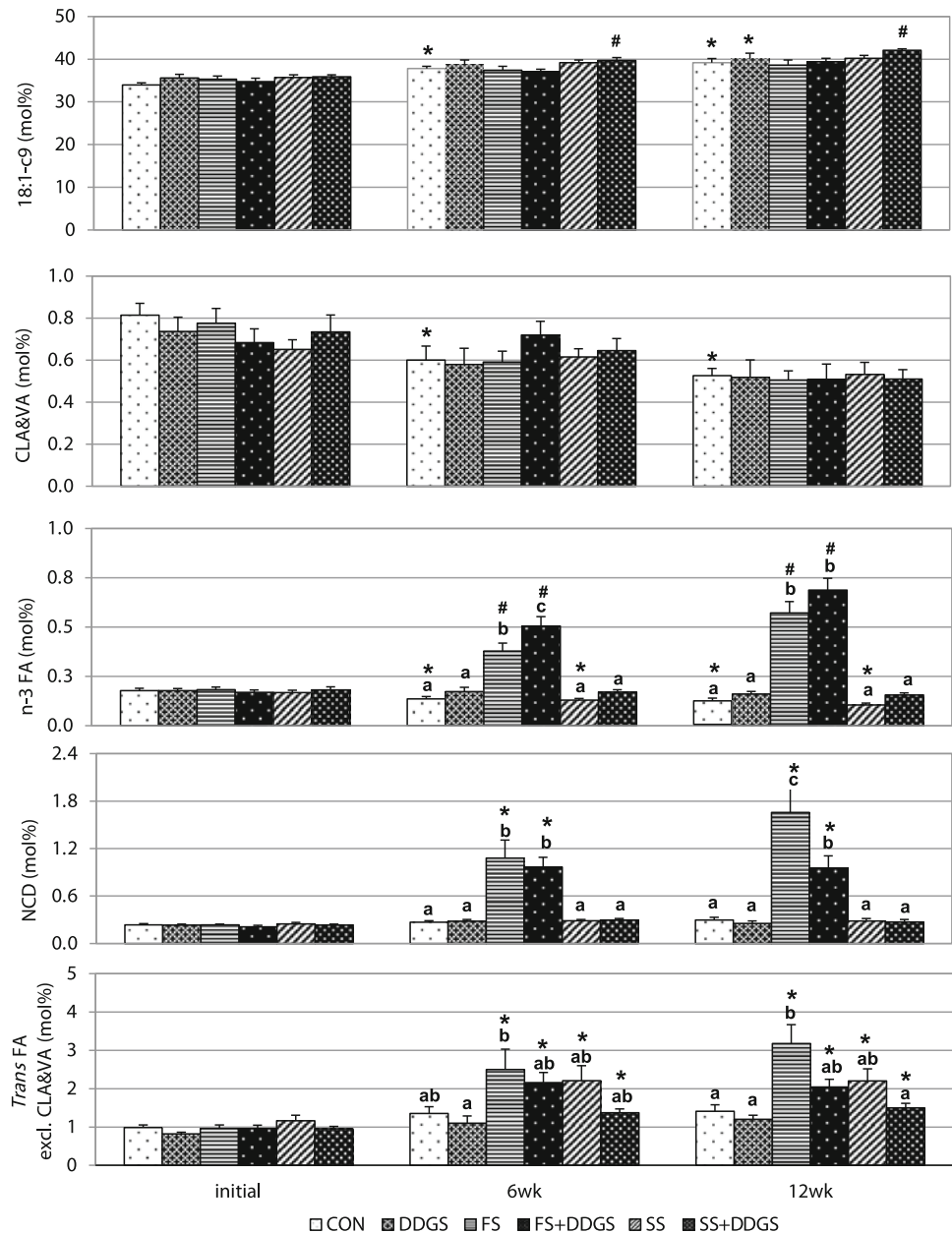
In the present study, inclusion of flaxseed did not affect growth performance during the 12 weeks feeding period, which was generally consistent with a previous study on cull cows when 15 % flaxseed was added to a basal diet composed of 47.5 % barley silage DM [5].

Collection of three biopsy fat samples over the feeding period in the present study clearly documented how the fatty acid composition of adipose was altered by diets containing DDGS, FS and SS (alone or in combination). Inclusion of flaxseed in the diet consistently increased ALA and its biohydrogenation NCD intermediates in backfat, a finding consistent with our studies using cull beef cows fed diets containing 15 % flaxseed and 55 %

silage or hay [5]. Others have also found similar results with flaxseed in terms of an increase in the ALA content of meat from finishing steers [3, 26]. Furthermore, the present study is apparently the first report that inclusion of triticale DDGS along with flaxseed in the finishing diet resulted in an additional increase in ALA levels in backfat without a further increase in NCD. These results support our hypothesis that inclusion of a combination of DDGS and FS in a finishing diet further improves the fatty acid profile of beef through an additional increase in ALA concentrations in adipose tissue.

In several studies, DDGS has been assessed as a replacement for barley grain and silage in diets for feedlot

Fig. 2 Comparison of selected fatty acid composition in backfat over a 12 weeks feeding period. *Within a period, means differ from the initial ($P < 0.05$). #Within a period, means differ between 6 and 12 weeks and from the initial ($P < 0.05$). *a–c* Within a period, means without a common letter differ ($P < 0.05$)



cattle where their inclusion has primarily been from the perspective of as an energy source as opposed to a protein source [7–10]. Although DDGS was not rich in ALA content, it was recently found in our lab that substitution of wheat DDGS for barley and silage in a barley-based finishing diet increased ALA in total FAME by 28 % in the beef pars costalis diaphragmatis [13]. Furthermore, ALA in backfat linearly increased when wheat DDGS replaced barley grain in finishing diets of beef cattle [12]. The mechanism whereby increasing levels of DDGS elevate ALA in adipose tissue remains unclear. Inclusion of DDGS resulted in a 30–40 % increase in the ALA content of DDGS and SS + DDGS diets, a factor that maybe responsible the increased levels of ALA in backfat of steers fed these diets. However, the

inclusion of DDGS in the FS-diet reduced ALA intake by ~10 %, but increased the ALA in backfat of steers fed this diet by almost 20 % as compared to FS alone. The increase of ALA in backfat with inclusion of DDGS in the FS-diet may arise as a result of a number of factors including altered rumen microbial biohydrogenation, or changes in ALA absorption or metabolism in adipocytes [27]. The dienes, including 18:2-*t*11, *c*15, originate from the biohydrogenation of ALA and were found to increase concurrently with ALA in backfat from cull cows fed a 15 % FS-diet [5, 6]. In the present study, inclusion of DDGS with flaxseed resulted in substantial increase in ALA in backfat, but without a corresponding increase in the concentrations of less desirable end products of ALA metabolism such as 18:2-*t*11, *c*15.

The ALA in beef fat is primarily derived from the diet, although compared to monogastric animals, ruminants are far less efficient at incorporating dietary ALA into adipose tissue. Incorporation of ALA into adipose tissue of fattening horses was 10-fold higher than that observed in Japanese Black or Holstein steers fed similar diets [28]. In ruminants, a substantial portion of the dietary ALA in flaxseed is biohydrogenated by rumen bacteria, with concentrations reduced by approximately half after 24 h of rumen exposure [29]. Strategies to reduce the biohydrogenation of alpha-linolenic acid such as inclusion of tannins in the diets of cattle have only been marginally successful [29]. Vitamin E supplementation in beef cattle diets containing flaxseed increased n-3 fatty acids in beef intramuscular fat by approximately 18 % (from 2.0 to 2.4 % of total FAME [30]). Concomitantly, the dienes including 18:2-*t*11, *c*15 were also significantly increased by inclusion of vitamin E in a FS-diet [30], which differs from the observed reduction in dienes observed in the present study as a result of the inclusion of DDGS with FS.

In addition to rumen biohydrogenation, differences between ruminants and monogastric animals in de novo fatty acid synthesis may also affect the fatty acid profile in adipose tissue. Lipogenesis in bovine adipocytes largely depends on synthesis of fatty acids from volatile fatty acids (VFA) arising from rumen fermentation, with acetate and propionate predominating [31]. In a previous study, replacing barley grain and barley silage with triticale DDGS linearly decreased acetate without affecting average daily gain, but increased propionate in rumen of steers [10]. Similar results were also observed in cattle fed diets where wheat DDGS was substituted for these feedstuffs [32]. Such dramatic changes in the amount of acetate and propionate may affect de novo synthesis of SFA and MUFA. Acetate is more extensively used than propionate in fatty acids synthesis in bovine tissues [31] as it is mainly used for gluconeogenesis in the liver [33]. Promotion of high PUFA levels in plasma by inclusion of oilseed or DDGS in the diets may inhibit de novo synthesis of non-essential fatty acids [34], resulting in a proportional increase in ALA concentrations in adipose tissue.

Plasma ALA concentrations have been highly correlated with dietary intake of flaxseed in Holstein cows [4] and beef cows [5]. In the present study, there was a similar elevation in plasma ALA by inclusion of flaxseed in the diet, even though the levels of flaxseed (10 vs. 15 % diet DM) included in the diet were lower than those provided to cull beef cows [4, 5]. After 12 weeks of feeding, plasma ALA was higher in steers fed FS than in those fed DDGS + FS, presumably due to the higher level of flaxseed in the FS-diet compared to DDGS + FS.

Plasma NCD concentrations were reduced with DDGS, suggesting that addition of this by-product might alter ALA

biohydrogenation in the rumen, but the impact of DDGS on the flow of n-3 FA to the duodenum was not examined in this study. It has been suggested that low rumen pH may inhibit ruminal lipolysis and biohydrogenation [27, 35], conditions that are common in cattle fed high grain diets. This relationship was supported by a study where addition of pH neutralizing sodium sesquicarbonate to the rumen of cattle fed a barley grain diet temporarily resulted in a lower 18:1-*t*10/*t*11 ratio in beef [36]. Thus, replacement of barley grain with DDGS lowered starch and increased fiber content of the diet and may have increased ruminal pH. We infer that optimization of omega-3 concentrations in beef depends not only on the nature of the fatty acid profile delivered in the diet, but also on how ruminal biohydrogenation can be manipulated in a manner that favors the flow of omega-3 fatty acids to the lower intestinal tract.

Among the other biohydrogenation intermediates, percentage of CLA plus VA in plasma or adipose tissue was not affected by inclusion of DDGS or oilseeds. However, weight% of C18:1-*t*10 in both plasma and adipose tissue was reduced by inclusion of DDGS. Inclusion of wheat DDGS in a barley grain-based finishing diet increased the ratio of 18:1 *t*11/*t*10 in fat of steers [11, 12], but no similar increase was reported in tail adipose tissue when triticale DDGS was included in a lamb finishing diet [23]. The effect of inclusion of DDGS on major *trans* 18:1 in plasma and fat tissues may also be attributable to alterations in ruminal biohydrogenation.

The high oleic SS that we used in the study contained 63 % OA and 29 % LA, which was opposite to that of high linoleic SS used in previous beef cattle studies with 14–17 % OA and 66–73 % LA [37–39]. However, it was relatively high in LA compared to the high oleic SS used by Gibb et al. [37] with 87 % OA and only 2 % LA. Inclusion of high linoleic SS in beef diets resulted in higher CLA in subcutaneous fat, whereas in the present study inclusion of high oleic SS did not affect CLA plus VA in fat. Furthermore, inclusion of high oleic SS did not affect growth performance, ultrasound backfat thickness or REA, consistent with a previous report [37]. In the present study there was no significant difference in most growth performance parameters, with the exception of the Gain:Feed ratio was lower for high oleic SS than FS.

Trimable fat is a major fat source for ground beef products and increasing the n-3 FA or ALA of this tissue may be the easiest avenue to produce ground beef products that reach the level required for a source omega-3 claim, which is a minimum 130 mg of ALA per 114 g serving in the USA [40] and as high as 300 mg total omega-3 per 100 g serving in Canada [41]. Although inclusion of DDGS in the FS affected performance and reduced predicted trimmable fat and the amount of predicted retail product as compared to FS alone, it did reduce the cost per kg feed and increased ALA

concentration in SQ fat. The total costs for flaxseed, barley and DDGS (average prices were 0.519, 0.211 and \$0.216 per kg respectively [42]) was \$165 per steer for both FS and FS + DDGS treatments (based on 12 weeks feed intake and diet composition) when performance differences were considered. The estimated trimmable fat at 12 weeks in the FS and FS + DDGS treatments could provide 556 and 640 g ALA per steer respectively. With the same feed cost after 12 weeks of feeding, the FS + DDGS treatment could provide 15 % more ALA in trimmable fat compared to FS treatment. In the present study, we were not able to compare complete retail products as the fatty acid compositions were estimated strictly from backfat biopsies. However, there were very close correlations on profiles of major fatty acids including ALA and total n-3 FA between backfat and muscle from beef cows fed with or without inclusion of flaxseed in previous studies [5, 6] and in other studies conducted in our laboratory [43].

In summary, inclusion of 30 % DDGS in a barley grain-based finishing diet with or without FS or high oleic acid SS reduced growth performance of finishing steers. However, inclusion of FS consistently increased ALA in beef cattle during the finishing period. Inclusion of a combination of DDGS and FS further increased ALA accumulation, but lowered levels of *trans* fatty acids and NCD concentrations in backfat. Mixtures of DDGS with FS could reduce the dietary costs associated with promoting favorable changes in the fatty acid profile of beef.

References

1. Simopoulos AP (1991) Omega-3 fatty acids in health and disease and in growth and development. *Am J Clin Nutr* 54:438–463
2. Simopoulos AP (1999) Essential fatty acids in health and chronic disease. *Am J Clin Nutr* 70:560S–569S
3. Kronberg SL, Barceló-Coblijn G, Shin J, Lee K, Murphy EJ (2006) Bovine muscle n-3 fatty acid content is increased with flaxseed feeding. *Lipids* 41:1059–1068
4. He ML, Chung YH, Beauchemin KA, Mir PS, Aalhus JL, Dugan MER, McAllister TA (2011) Inclusion of flaxseed in hay- and barley silage diets increases alpha-linolenic acid in cow plasma independent of forage type. *Lipids* 46:577–585
5. He ML, McAllister TA, Kastelic JP, Mir PS, Aalhus JA, Dugan MER, Aldai N, McKinnon JJ (2011) Feeding flaxseed to beef cows increases concentrations of omega-3 fatty acids and linolenic acid biohydrogenation intermediates in subcutaneous fat. *J Anim Sci* 90:592–604
6. Nassu R, Dugan MER, He ML, McAllister TA, Aalhus JL, Aldai N, Kramer JKG (2011) The effects of feeding flaxseed to beef cows given forage based diets on fatty acids of longissimus thoracis muscle and backfat. *Meat Sci* 89:469–477
7. Walter LJ, Aalhus JL, Robertson WM, McAllister TA, Gibb DJ, Dugan MER, Aldai N, McKinnon JJ (2010) Comparison of wheat or corn dried distillers grains with solubles on performance and carcass characteristics of feedlot steers. *Can J Anim Sci* 90:259–269
8. Gibb DJ, Hao X, McAllister TA (2008) Effect of dried distillers' grains from wheat on diet digestibility and performance of feedlot cattle. *Can J Anim Sci* 88:659–665
9. Yang WZ, Li YL, McAllister TA, McKinnon JJ, Beauchemin KA (2012) Wheat distiller grains in feedlot cattle diets: feeding behavior, growth performance, carcass characteristics, and blood metabolites. *J Anim Sci* 90:1301–1310
10. Wierenga KT, McAllister TA, Gibb DJ, Chaves AV, Okine EK, Beauchemin KA, Oba M (2010) Evaluation of triticale dried distillers grains with solubles as a substitute for barley grain and barley silage in feedlot finishing diets. *J Anim Sci* 88:3018–3029
11. Dugan MER, Aldai N, Kramer JKG, Gibb DJ, Juárez M, McAllister TA (2010) Feeding wheat dried distillers' grains with solubles improves beef trans and conjugated linoleic acid profiles. *J Anim Sci* 88:1842–1847
12. Aldai N, Dugan MER, Aalhus JL, McAllister TA, Walter LJ, McKinnon JJ (2010) Differences in the *trans*-18:1 profile of the backfat of feedlot steers fed wheat or corn based dried distillers' grains. *Anim Feed Sci Technol* 157:168–172
13. He ML, Yang WZ, Dugan MER, Beauchemin KA, McKinnon JJ, McAllister TA (2012) Substitution of wheat dried distillers grains with solubles for barley silage and barley grain in a finishing diet increases polyunsaturated fatty acids including linoleic and alpha-linolenic acids in beef. *Anim Feed Sci Technol* 175:114–120
14. CCAC (1993) Guide to the care and use of experimental animals. Canadian Council of Animal Care, Ottawa
15. NRC (2001) Nutrient requirements of dairy cattle: Seventh revised edition: 2001. National Academy Press, Washington DC
16. NRC (1996) Nutrient requirements of beef cattle: Seventh revised edition: update 2000. National Academy Press, Washington DC
17. Realini CE, Williams RE, Pringle TD, Bertrand JK (2001) Gluteus medius and rump fat depths as additional live animal ultrasound measurements for predicting retail product and trimmable fat in beef carcasses. *J Anim Sci* 79:1378–1385
18. Lock AL, Gamsworthy PC (2002) Independent effects of dietary linoleic and linolenic fatty acids on the conjugated linoleic acid content of cows' milk. *Anim Sci* 74:163–176
19. Kramer JKG, Fellner V, Dugan MER, Sauer FD, Mossob MM, Yurawecz MP (1997) Evaluating acid and base catalysts in the methylation of milk and rumen fatty acids with special emphasis on conjugated dienes and total *trans* fatty acids. *Lipids* 32:1219–1228
20. Ratnayake WMN (2004) Overview of methods for the determination of *trans* fatty acids by gas chromatography, silver-ion thin-layer chromatography, silver-ion liquid chromatography, and gas chromatography/mass spectrometry. *J AOAC Int* 87:523–539
21. Cruz-Hernandez C, Deng Z, Zhou J, Hill AR, Yurawecz MP, Dugan MER, Kramer JKG (2004) Methods for analysis of conjugated linoleic acids and *trans*-18:1 isomers in dairy fats by using a combination of gas chromatography, silver-ion thin-layer chromatography/gas chromatography, and silver-ion liquid chromatography. *J AOAC Int* 87:545–562
22. SAS Institute (2004) SAS 9.1. SAS Inst., Inc., Cary, NC
23. McKeown LE, Chaves AV, Oba M, Dugan MER, Okine E, McAllister TA (2011) Effects of corn-, wheat- or triticale dry distillers' grains with solubles on in vitro fermentation, growth performance and carcass traits of lambs. *Can J Anim Sci* 90:99–108
24. Owens FN, Gill DR, Secrist DS, Coleman SW (1995) Review of some aspects of growth and development of feedlot cattle. *J Anim Sci* 73:3152–3172
25. Gunn PJ, Weaver AD, Lemenager RP, Gerrard DE, Claeys MC, Lake SL (2009) Effect of dietary fat and crude protein on feedlot performance, carcass characteristics, and meat quality in finishing steers fed differing levels of dried distillers grains with solubles. *J Anim Sci* 87:2882–2890

26. Scollan ND, Choi NJ, Kurt E, Fisher AV, Enser M, Wood JD (2001) Manipulating the fatty acids composition of muscle and adipose tissue in beef cattle. *Brit J Nutr* 85:115–124
27. Dugan MER, Aldai N, Aalhus JL, Rolland DC, Kramer JKG (2011) Review: trans-forming beef to provide healthier fatty acid profiles. *Can J Anim Sci* 91:545–556
28. He ML, Ishikawa S, Hidari H (2005) Fatty acid profiles of various muscles and adipose tissues from fattening horses in comparison with beef cattle and pigs. *Asian–Austr J Anim Sci* 18:1655–1661
29. Kronberg SL, Scholljegerdes EJ, Barceló-Coblijn G, Murphy EJ (2007) Flaxseed treatments to reduce biohydrogenation of α -linolenic acid by rumen microbes in cattle. *Lipids* 42:1105–1111
30. Juárez M, Duga MER, Aalhus JL, Aldai N, Basarab JA, Baron VS, McAllister TA (2011) Effect of dietary flax and vitamin E on beef intramuscular fat concentration of biohydrogenation intermediates. *Meat Sci* 88:434–440
31. Hood RL, Thompson EH, Allen CE (1972) The role of acetate, propionate, and glucose as substrates for lipogenesis in bovine tissues. *Int J Biochem* 3:598–606
32. Li YL, McAllister TA, Beauchemin KA, He ML, McKinnon JJ, Yang WZ (2011) Substitution of wheat distillers dried grains with solubles for barley grain or barley silage in feedlot cattle diets: intake, digestibility and ruminal fermentation. *J Anim Sci* 89:2491–2501
33. Vernon RG, Denis RGP, Sorensen A (2001) Signals of adiposity. *Domest Anim Endocrinol* 21:197–214
34. Jump DB, Clarke SD (1999) Regulation of gene expression by dietary fat. *Annu Rev Nutr* 19:63–90
35. Chilliard Y, Glasser F, Ferlay A, Bernard L, Rouel J, Doreau M (2007) Diet, rumen biohydrogenation and nutritional quality of cow and goat milk fat. *Eur J Lipid Sci Technol* 109:828–855
36. Aldai N, Dugan MER, Kramer JKG, Robertson WM, Juárez M, Aalhus JL (2010) *Trans*-18:1 and conjugated linoleic acid profiles after the inclusion of buffer, sodium sesquicarbonate, in the concentrate of finishing steers. *Meat Sci* 84:735–741
37. Gibb DJ, Owens FN, Mir PS, Mir Z, Ivan M, McAllister TA (2004) Value of sunflower seed in finishing diets of feedlot cattle. *J Anim Sci* 82:2679–2692
38. Shah MA, Mir PS, Aalhus JL, Basarab J, Okine EK (2006) Effects of sunflower seeds inclusion in finishing diets for steers on performance, carcass characteristics and muscle and adipose fatty acid composition and meat quality. *Can J Anim Sci* 86:37–48
39. Mir PS, Dugan MER, He ML, Entz T, Yip B (2008) Effects of dietary sunflower seeds and tylosin phosphate on production variables, steers carcass characteristics, fatty acid composition, and liver abscess incidence in crossbred. *J Anim Sci* 86:3125–3136
40. FDA (2007) Federal Register Notice of Proposed Rulemaking (Food Labeling) 72 FR 66103 November 27, 2007: Food labeling: nutrient content claims; alpha-linolenic acid, eicosapentaenoic acid, and docosahexaenoic acid omega-3 fatty acids. vol 72, number 227, pp 66103–66118. <http://www.fda.gov/Food/LabelingNutrition/FoodLabelingGuidanceRegulatoryInformation/RegulationsFederalRegisterDocuments/ucm073457.htm>
41. CFIA (2003) Chapter 7-Nutrient content claims. 7.19 omega-3 and omega-6 polyunsaturated fatty acid claims. Guide to food labeling and advertising retrieved 27th July 2010. <http://www.inspection.gc.ca/english/fssa/labeti/guide/ch7be.shtml>. Accessed 20 April 2012
42. AAFC (2012) Crops market information-weekly price summary. http://www.agr.gc.ca/pol/mad-dam/index_e.php?s1=pubs&s2=pri. Accessed 20 April 2012
43. He ML, Hernandez-Calva LM, McAllister TA, Aalhus JL, Dugan MER, McKinnon JJ (2012) Inclusion of triticale dried distiller grains and flaxseed in feedlot cattle diets increases alpha-linolenic acid in beef without affecting carcass or meat quality traits. *J Anim Sci* 90:600

structurally to three types of analogs: (1) 4-saturated dihydroxy analogs comprising sphinganine (dihydrosphingosine), *trans*-8-sphingenine, and *cis*-8-sphingenine; (2) *trans*-4-unsaturated dihydroxy analogs comprising *trans*-4-sphingenine (sphingosine), *trans*-4,*trans*-8-sphingadienine [d18:2(t4,t8)], and *trans*-4,*cis*-8-sphingadienine [d18:2(t4,c8)]; and (3) 4-hydroxy analogs comprising 4-hydroxysphinganine (phytosphingosine), 4-hydroxy-*trans*-8-sphingenine [t18:1(t8)], and 4-hydroxy-*cis*-8-sphingenine [t18:1(c8)]. Among these analogs, the 8-unsaturated sphingoid bases are exclusively major components in plant glucosylceramides; *trans*-8-sphingenine and *cis*-8-sphingenine are found in limited members of plants such as Brassicaceae and Fabaceae as major components [8, 9]. In contrast, sphinganine, *trans*-4-sphingenine, and 4-hydroxysphinganine are minor or undetectable components in plants.

LC–MS/MS approaches have recently been applied for characterizing glucosylceramide molecular species in plants [10–14]. Despite this, molecular species profiles of the glucosylceramides that differentiate between *cis*-8 and *trans*-8 sphingoid bases are not yet clear in the previous approaches. It is important to develop appropriate techniques for determining the levels of the *cis*-8 and *trans*-8 isomers of sphingoid bases in individual glucosylceramide species, because glucosylceramide species have distinctive physicochemical properties depending on their *cis*-8 and *trans*-8 isomerism [15]. The application of octadecylsilyl (ODS) reversed-phase HPLC to analysis of plant glucosylceramides provides separation of peaks for individual species by acyl chain length and grade of desaturation of the fatty acid moiety. In addition, the peaks for individual species are also separated on the basis of the grade of desaturation and hydroxylation and the *cis*-8 and *trans*-8 isomerism of the sphingoid base moiety [15, 16]. Mobile phases described in the previous reports on LC–MS/MS analysis were rather expensive and complex in preparation [10–13]. We present here the first detailed molecular species analysis by reversed-phase HPLC coupled to ESI–MS/MS with a cost-effective and simple binary gradient for characterizing the *cis*-8 and *trans*-8 isomers of sphingoid bases, and glucosylceramides from rice callus and orchardgrass leaves were analyzed as a typical example of plant samples.

Materials and Methods

Chemicals and Plant Materials

Except where noted, all chemicals were of HPLC grade or highest grade available from Wako Pure Chemical (Osaka, Japan). Glucosylceramides from rice and soybean were purchased from Nagara Science (Gifu, Japan).

The seeds of rice (*Oryza sativa* L. cv. Koshihikari) were dehusked and washed with tap water to remove dust and

other surfactants. These seeds were then surface-sterilized with sodium hypochlorite solution (1 % active chlorine) containing 0.1 % Tween for 20 min, followed by rinsing with 70 % (v/v) ethanol for 30 s. The sterilized seeds were rinsed three times with sterile distilled water. These seeds were cultured for callus induction on modified Murashige and Skoog (MS) medium [17] with the nitrogen components replaced by those of N6 medium [18], supplemented with 30 g/L sucrose, 2 mg/L 2,4-dichlorophenoxyacetic acid, and 8 g/L agar (pH 5.8). The cultures were incubated at 28 °C in the dark. About 100 mg of callus obtained after 30 days of culture was harvested and used for lipid extraction. The seeds of orchardgrass (*Dactylis glomerata* L.) were germinated in a HYPONeX soil mixture (Hyponex Japan, Osaka, Japan) and grown at 28 °C for 3 weeks under a light/dark cycle of 16/8 h. About 1 g of medium-sized and not yet fully expanded leaves was harvested and used for lipid extraction.

Separation and Purification of Glucosylceramides

Total lipids from rice callus and orchardgrass leaves were extracted according to the method of Bligh and Dyer [19]. Then, the total lipids were subjected to mild alkaline hydrolysis with 0.4 M KOH for 2 h at 37 °C. The sample was separated in a Sep-Pak Plus silica cartridge (Waters, Milford, MA, USA) by eluting with chloroform/acetic acid

Table 1 Mass-spectral scan values for MRM detection of glucosylceramide molecular species

Sphingoid base	Fatty acid	[M + H] ⁺ (m/z)	Product ion (m/z)
t18:1	16h:0	732.6	262.3
t18:1	18h:0	760.6	262.3
t18:1	20h:0	788.6	262.3
t18:1	20h:1	786.6	262.3
t18:1	22h:0	816.7	262.3
t18:1	22h:1	814.7	262.3
t18:1	24h:0	844.7	262.3
t18:1	24h:1	842.7	262.3
t18:1	26h:0	872.7	262.3
t18:1	26h:1	870.7	262.3
d18:2	16h:0	714.5	262.3
d18:2	18h:0	742.6	262.3
d18:2	20h:0	770.6	262.3
d18:2	20h:1	768.6	262.3
d18:2	22h:0	798.7	262.3
d18:2	22h:1	796.7	262.3
d18:2	24h:0	826.7	262.3
d18:2	24h:1	824.7	262.3
d18:2	26h:0	854.7	262.3
d18:2	26h:1	852.7	262.3

(100/1, v/v) and chloroform/methanol (2/1, v/v). The chloroform/methanol fraction was applied to liquid chromatography–tandem mass spectrometry (LC–MS/MS). For GC analysis, the chloroform/methanol fraction was separated by silica gel thin-layer chromatography (TLC) (Merck TLC plates, Sigma-Aldrich Japan, Tokyo), using chloroform/methanol/water (65/29/4, by volume) as the solvent system, and the spots of glucosylceramides were scraped off the TLC plates [20].

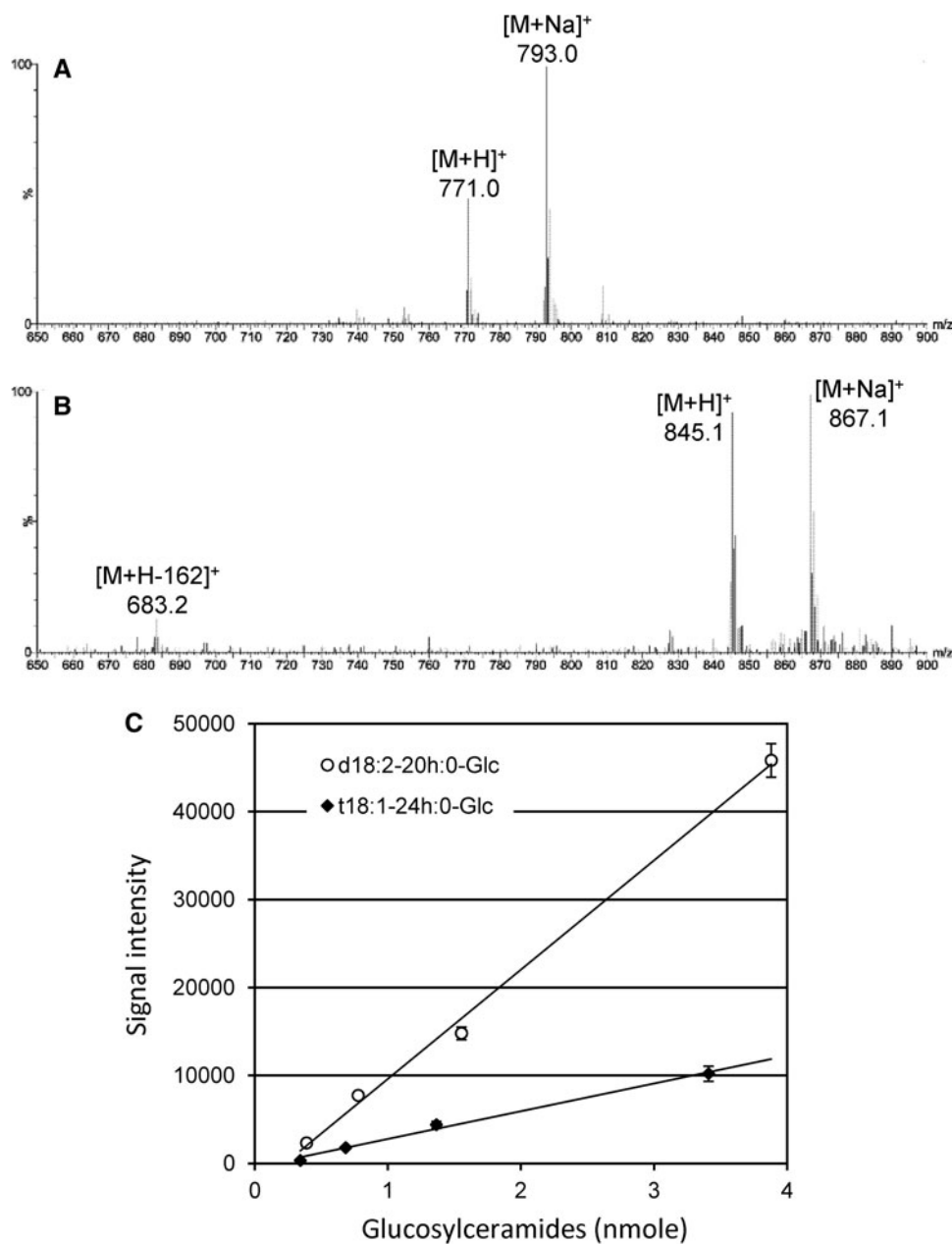
LC–MS/MS Analysis

The LC–MS/MS analysis was performed with NANO-SPACE SI-2 HPLC instruments (Shiseido, Tokyo, Japan)

coupled to an ACQUITY TQD tandem quadrupole mass spectrometer (Waters). Chromatographic separation was performed in two tandemly connected SUPERIOREX ODS columns [(250 × 2.0 mm i.d.) × 2, Shiseido] held at 40 °C. A binary elution gradient consisting of methanol/formic acid (1,000/1, v/v) as solvent A and water/formic acid (1,000/1, v/v) as solvent B was used. The flow rate was 200 μL/min with the following conditions: 95 % solvent A/5 % solvent B initially, then proceed to 100 % solvent B in a linear fashion after 60 min, and then maintained with 100 % solvent B for an additional 30 min. For each run, 1–5 μL of each sample was injected.

The transitions of the precursor ions $[M + H]^+$ to the main product ions of the sphingoid bases were used as

Fig. 1 Measurement of glucosylceramide molecular species containing 4,8-sphingadienine plus 2-hydroxy arachidic acid [d18:2(4,8)-20h:0-Glc] and 4-hydroxy-8-sphingenine plus 2-hydroxy lignoceric acid [t18:1(8)-24h:0-Glc]. MS spectra of d18:2(4,8)-20h:0-Glc (A) and t18:1(8)-24h:0-Glc (B). C Quantitative analysis of d18:2(4,8)-20h:0-Glc and t18:1(8)-24h:0-Glc in mass-spectral signals from ESI–MS/MS. Data represent mean ± SD ($n = 3$)



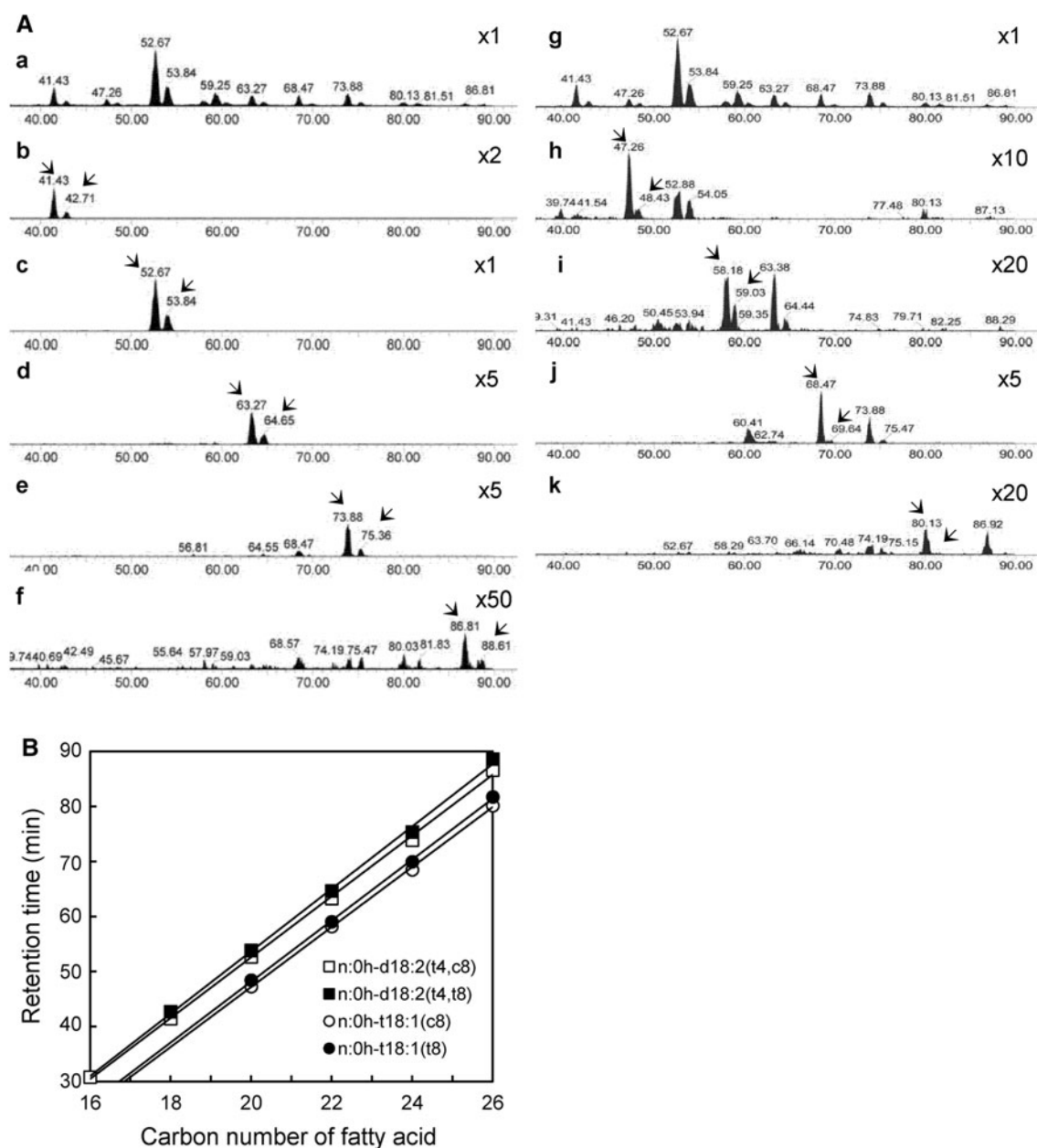


Fig. 2 Separation of glucosylceramide molecular species from callus of rice (*Oryza sativa* L. cv. Koshihikari). **A** Mass chromatograms: *a*, *g* total ion chromatograms of the 30 channels (Table 1 and ref. [14]; *b–f*, *h–k* selected ion chromatograms for the transition of $[M + H]^+$ to 262.3 which were identified as glucosylceramide molecular species containing d18:2-18h:0 (*b*), d18:2-20h:0 (*c*), d18:2-22h:0 (*d*), d18:2-

24h:0 (*e*), d18:2-26h:0 (*f*), t18:1-20h:0 (*h*), t18:1-22h:0 (*i*), t18:1-24h:0 (*j*), and t18:1-26h:0 (*k*). Arrows indicate corresponding molecular species identified. **B** Retention-time plots of HPLC-separated glucosylceramide molecular species. n:0h-, saturated hydroxy fatty acid

precursor/product ion pairs in the positive ionization multiple reaction monitoring (MRM) mode for quantification of the molecular species of the glucosylceramides. For glucosylceramides consisting of 4-hydroxy-8-sphingenine and 4,8-sphingadienine, the transitions of $[M + H]^+$ to 262 and for those with 8-sphingenine, the transitions of $[M + H]^+$ to 264, were used as precursor/product ion pairs; 30 channels of precursor/product ion pairs were selected based on the 2-hydroxy fatty acid composition of

glucosylceramides determined by GC [14]. The following conditions were used: capillary voltage, 3 kV; desolvation gas flow, 600 L/h; nebulizer gas flow, 50 L/h; source temperature, 120 °C; collision gas flow, 0.3 mL/min (4–5 mbar). Molecular species were identified by comparing their retention times with those authentic standards of glucosylceramides from rice, soybean (Nagara Science), and *Rumex obtusifolius* [14] when several peaks were detected.

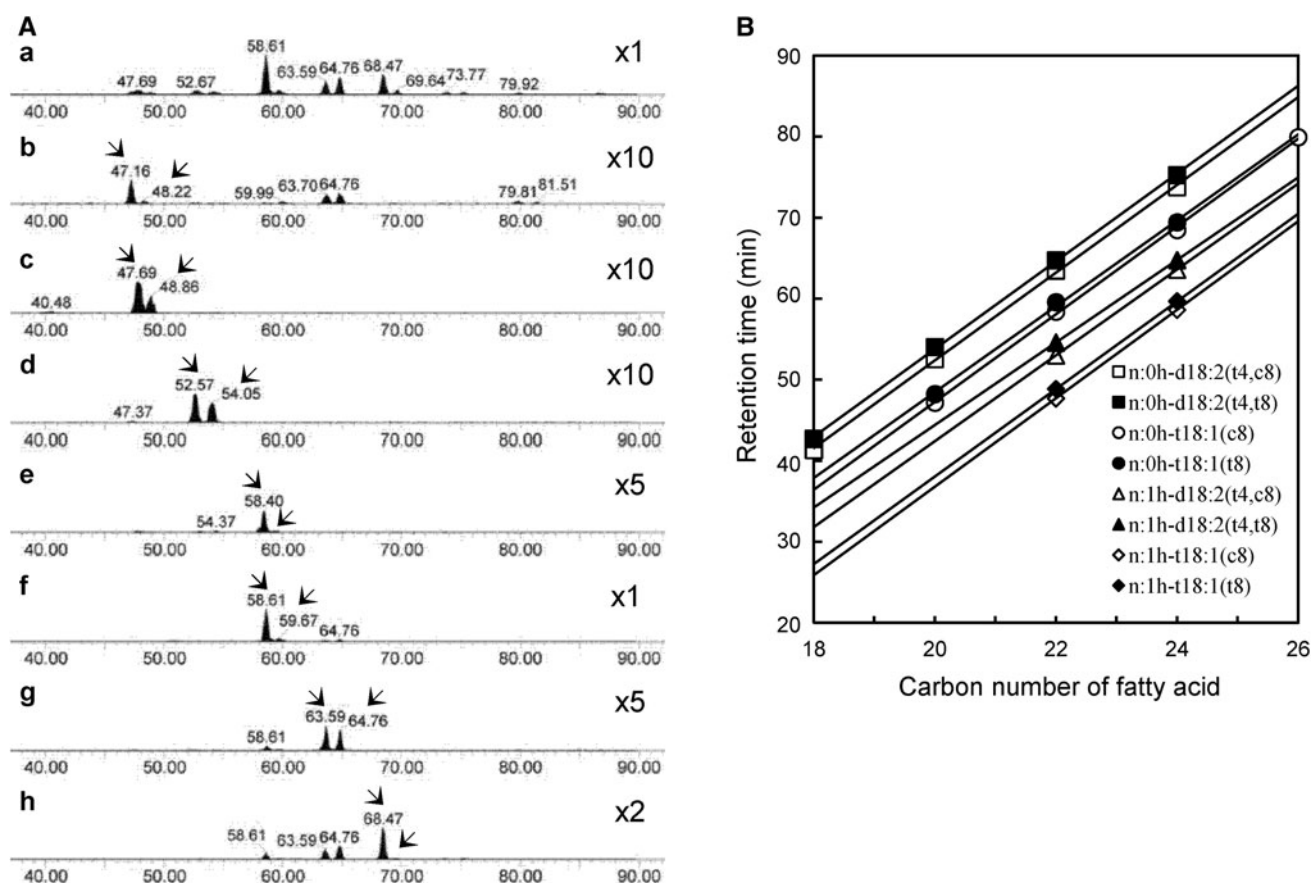


Fig. 3 Separation of glucosylceramides from leaves of orchardgrass (*Dactylis glomerata* L.). **A** Mass chromatograms: (a) total ion chromatogram of the 30 channels (Table 1 and ref. 14); (b–h) selected ion chromatograms for the transition of $[M + H]^+$ to 262.3 which were identified as glucosylceramide species containing t18:1-20h:0

(b), t18:1-22h:1 (c), d18:2-20h:0 (d), t18:1-22h:0 (e), t18:1-24h:1 (f), d18:2-24h:1 (g), and t18:1-24h:0 (h). Arrows indicate corresponding molecular species identified. **B** Retention-time plots of HPLC-separated glucosylceramide molecular species. n:0h-, saturated hydroxy fatty acid; n:1h-, monounsaturated hydroxy fatty acid

HPLC and GC Analyses

Glucosylceramide molecular species with 4,8-sphingadienines and 2-hydroxy arachidic acid [i.e., d18:2(t4,c8)-20h:0-Glc and d18:2(t4,t8)-20h:0-Glc] and their species with 4-hydroxy-8-sphingenines and 2-hydroxytetracosanoic acid [i.e., t18:1(c8)-24h:0-Glc and t18:1(t8)-24h:0-Glc] were fractionated from commercially obtained rice and soybean glucosylceramides (Nagara Science) using an ODS column (SUPERIOREX ODS, 250 × 6.0 mm i.d., Shiseido). The glucosylceramide samples were analyzed with a NANOSPACE SI-2 HPLC system equipped with a 3002 UV-VIS detector (Shiseido). Chromatographic separation was performed in two tandemly connected SUPERIOREX ODS columns [(250 × 2.0 mm i.d.) × 2, Shiseido] held at 40 °C. Elution was carried out at 200 μL/min by isocratic flow with methanol/water (30/1, v/v). Glucosylceramide molecular species were detected by absorbance at 210 nm [15, 16, 21].

The glucosylceramides from rice callus and orchardgrass leaves, which were purified by TLC, were hydrolyzed with 3 % (w/v) HCl (gaseous) in dry methanol at 100 °C for 3 h to analyze the 2-hydroxy fatty acids. After adding water, the resulting fatty acid methyl esters were extracted with *n*-hexane. The 2-hydroxy fatty acid methyl esters were analyzed by a GC-18A gas chromatograph (Shimadzu Scientific) equipped with a TC-1 capillary column coated with dimethyl polysiloxane of 0.25 μm thickness (0.25 mm i.d. × 15 m; GL Science, Tokyo, Japan) and a hydrogen flame ionization detector (FID). The column temperature was programmed from 180 °C to 240 °C at 3 °C/min, and the injector and detector temperatures were maintained at 250 °C. 2-Hydroxy fatty acid methyl esters were identified by comparing their retention times with those of authentic standards that had been prepared from the 2-hydroxy fatty acids of glucosylceramides from rice, soybean (Nagara Science), and *Rumex obtusifolius*.

Four samples of the glucosylceramide molecular species fractionated by HPLC were hydrolyzed with 1 N HCl in

methanol at 80 °C for 18 h to analyze the sphingoid bases. The reaction mixture was washed twice with *n*-hexane and adjusted to pH 9.6 with 6 M KOH. The sphingoid bases were extracted with diethyl ether and converted to fatty aldehydes by the method of NaIO₄ oxidation [7]. The resulting fatty aldehydes were analyzed by GC (GC-18A; Shimadzu Scientific) equipped with a TC-70 capillary column coated with 70 % cyanopropyl polysilphenylene-siloxane of 0.25 μm thickness (0.25 mm i.d. × 60 m; GL Science) and a hydrogen flame ionization detector. The column temperature was maintained at 200 °C. The injector and detector temperature were maintained at 250 °C. Fatty aldehydes were identified by comparing their retention times with those of authentic standards that had been prepared from the sphingoid bases of glucosylceramides from *Lotus japonicus* [9].

Results and Discussion

The transition of precursor ions $[M + H]^+$ to the product ions of sphingoid base moieties was used for identifying and quantifying the glucosylceramide molecular species in plants (Table 1). Because of the variety of individual glucosylceramide species in plant samples, it is difficult to obtain authentic standards with identical chemistry to the glucosylceramides of interest, and commercially available standards are not chemically identical to glucosylceramide species found in plants. Glucosylceramide species such as d18:2(4,8)-20h:0-Glc and t18:1(8)-24h:0-Glc are generally found to be major constituents in plants belonging to the grass family [12, 15, 16, 22]. Thus, to determine the response of the mass-spectral signals, these molecular species purified from commercially obtained rice and soybean glucosylceramides were used as a panel of ideal standards that represent each type of glucosylceramide to be analyzed. In the positive full-scan mode, $[M + H]^+$ and $[M + Na]^+$ were the predominant signals (Fig. 1A, B). In t18:1(8)-24h:0-Glc, the loss of glucose $[M + H - 162]^+$ was detected. The calibration curves were almost linear within the examined range (Fig. 1C), suggesting that the linearity of the mass-spectral responses is good over the range in which the type 2 and 3 analogs are compared. However, the signal intensities were significantly different between d18:2(4,8)-20h:0-Glc and t18:1(8)-24h:0-Glc; d18:2(4,8)-20h:0-Glc showed about 3- to 4-fold greater intensities than did t18:1(8)-24h:0-Glc. From these data, signal intensity/mole factors for the type 2 and 3 analogs could be estimated as 3 and 1, respectively, and these factors were used for the calculation of the relative amount of the glucosylceramide molecular species in this study.

Although ESI-MS/MS approaches have enabled high selectivity and sensitivity for the identification and

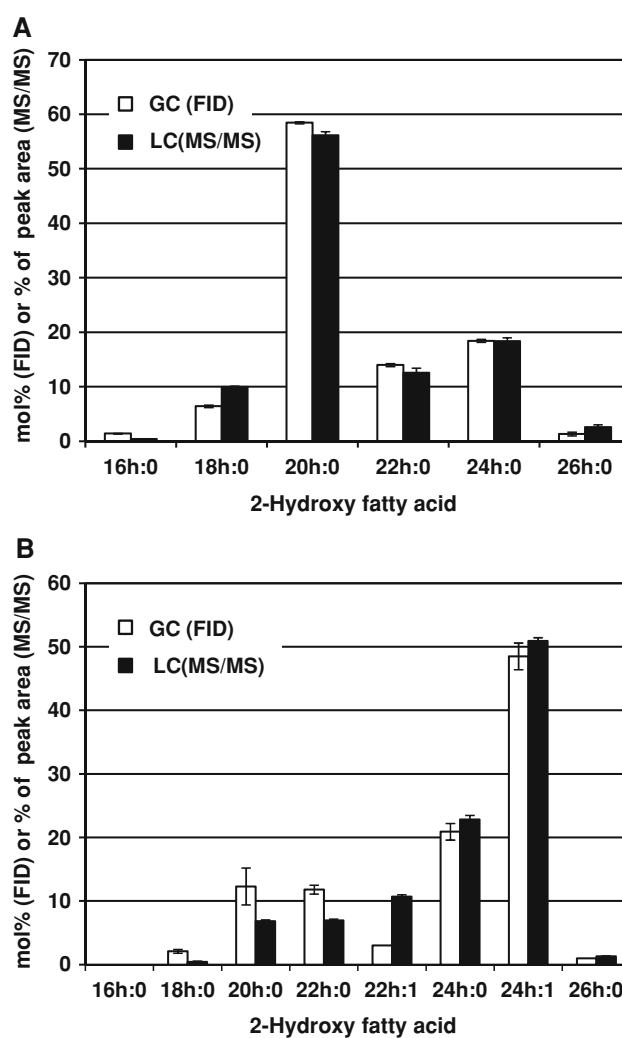


Fig. 4 Comparison of relative peak areas (%) of molecular species containing the corresponding fatty acids as determined by LC-MS/MS and mol % of the major fatty acids determined by GC. In LC-MS/MS data, signal intensity/mole factors for glucosylceramides containing 4,8-sphingadienine [d18:2(4,8)] and 4-hydroxy-8-sphingenine [t18:1(8)] were set as 1 and 3, respectively. Methyl esters of the 2-hydroxy fatty acids formed by the methanolysis of glucosylceramides were analyzed by GC equipped with flame ionization detector. **A** Glucosylceramides from callus of rice; **B** glucosylceramides from leaves of orchardgrass. Data represent mean \pm SD ($n = 3$)

quantification of glucosylceramide molecular species in plants, it is essential to develop applicable methods for differentiation between *cis*-8 and *trans*-8 isomers of sphingoid bases in glucosylceramide species. It has been reported that binary or ternary solvent mixtures containing acetonitrile–water or methanol–tetrahydrofuran–water are applied to LC-MS/MS analysis of plant glucosylceramides as the mobile phase [10–12]. It is clear that the use of acetonitrile reduces instrumental pressure in comparison with methanol. On the other hand, acetonitrile and tetrahydrofuran are currently much more expensive than methanol. In addition, it has recently been required to develop

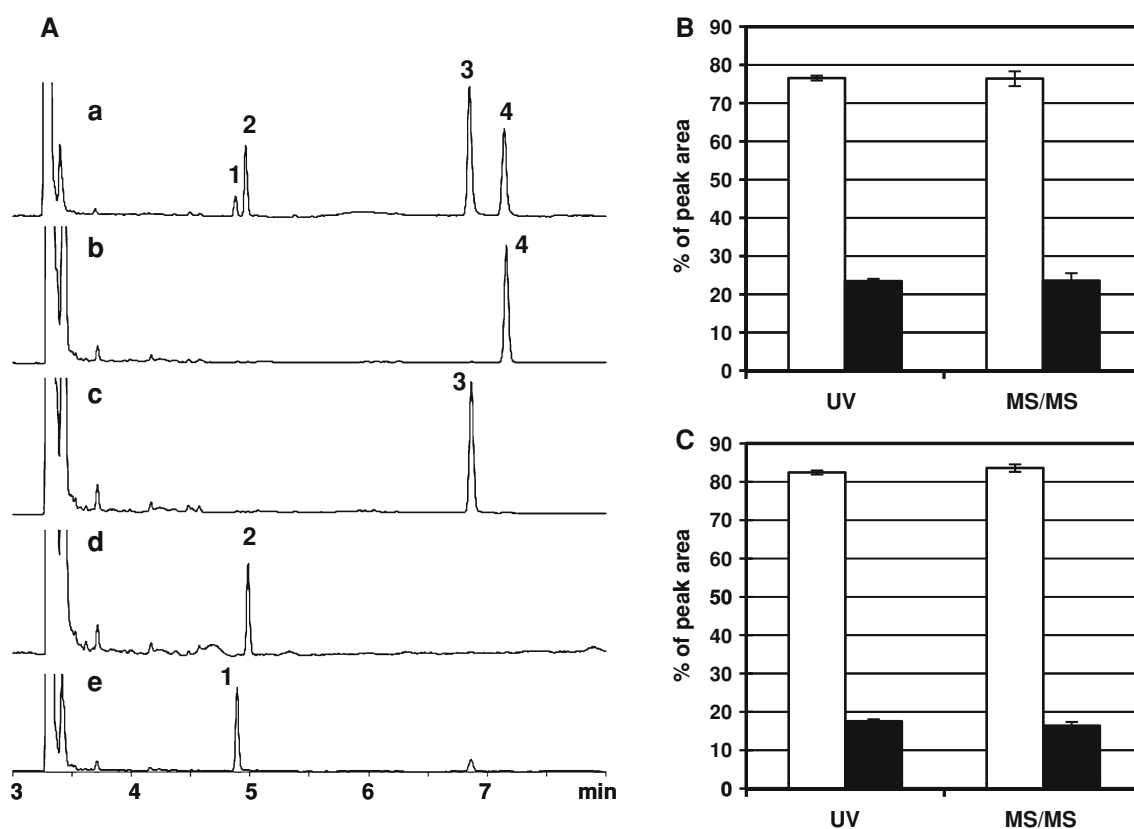


Fig. 5 Analyses of glucosylceramide molecular species having the *cis*-8 and *trans*-8 isomers of sphingoid bases. **A** GC profiles of fatty aldehydes converted from the corresponding component sphingoid bases of glucosylceramide molecular species: *a* an authentic standard prepared from the sphingoid bases of glucosylceramides from *Lotus japonicus* [9], *b* d18:2(t4,c8)-20h:0-Glc, *c* d18:2(t4,t8)-20h:0-Glc, *d* t18:1(c8)-24h:0-Glc, and *e* t18:1(t8)-24h:0-Glc. Peak numbers: 1 t18:1(t8), 2 t18:1(c8), 3 d18:2(t4,t8), and 4 d18:2(t4,c8). **B**, **C** Comparison of the relative peak areas (%) of major glucosylceramide species determined by spectrophotometry and ESI-MS/MS.

Spectrophotometry was performed under absorbance at 210 nm. **B** The level of the *cis*-8 and *trans*-8 isomers of glucosylceramide species containing d18:2(t4,c8)-20h:0 (*open bars*) and d18:2(t4,t8)-20h:0 (*solid bars*). Data represent mean \pm SD ($n = 3$). **C** The level of the *cis*-8 and *trans*-8 isomers of glucosylceramide species containing t18:1(c8)-24h:0 (*open bars*) and t18:1(t8)-24h:0 (*solid bars*). Molecular species containing d18:2(4,8)-20h:0 and t18:1(8)-24h:0 were fractionated from commercially obtained rice and soybean glucosylceramides, respectively. Data represent mean \pm SD ($n = 3$)

alternative methods to reduce or eliminate the use of acetonitrile because acetonitrile prices are unstable and will continue to rise prohibitively. For these reasons, an LC method with a cost-effective and simple binary gradient that enables sufficient separation of individual glucosylceramide species was optimized using methanol–water as a standard system of the mobile phase.

The total ion and selected chromatograms of glucosylceramides from callus of rice are shown in Fig. 2. Using two tandemly connected SUPERIOREX ODS columns, the column backpressure was about 11 MPa in 95 % solvent A/5 % solvent B. Molecular species containing 4,8-sphingadienine attached to 2-hydroxy fatty acids with 18–24 carbon chain length were substantially detected at complete baseline separations with two peaks (Fig. 2A, b–e). In contrast, molecular species containing 4-hydroxy-8-sphingenine attached to 2-hydroxy fatty acids with 20–26 carbon chain length were found in several peaks (Fig. 2A, h–k),

suggesting that the precursor ion selectivity for glucosylceramide species containing 4-hydroxy-8-sphingenine was little specific. For example, peak signals from Fig. 2A–c gave rise to false signal in Fig. 2A–h at 52.88 and 54.04 min. Thus, during the initial stages of this study, the transition of precursor ions $[M + H]^+$ to the product ion of m/z 298.3 was used for the identification and quantification of glucosylceramide molecular species having 4-hydroxy-8-sphingenine [11]; however, the signal intensity of the product ion was very low. For these reasons, the product ion of m/z 262.3 was used for 4-hydroxy-8-sphingenines [10]. Using a glucosylceramide standard purified from soybean glucosylceramides by HPLC, we confirmed that the peaks of t18:1(8)-24h:0-Glc were eluted at 68.47 and 69.64 min. The total ion and selected chromatograms of glucosylceramides from leaves of orchardgrass are shown in Fig. 3A. Molecular species containing monounsaturated 2-hydroxy fatty acids with 22 and 24 carbon chain length were detected. Despite

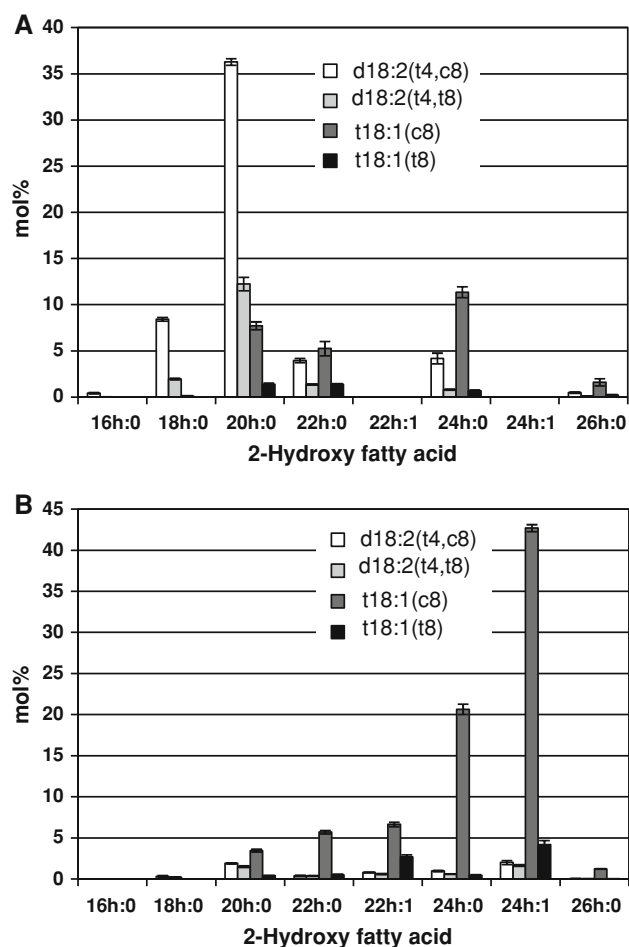


Fig. 6 Composition of the glucosylceramide molecular species from rice and orchardgrass: **A** callus of rice, and **B** leaves of orchardgrass. The alkaline-stable lipid fraction was separated by C_{18} reverse-phase HPLC, and the molecular species of glucosylceramides were analyzed by ESI-MS/MS. Data represent mean \pm SD ($n = 3$)

the retention times of the molecular species containing t18:1(c8)-22h:0 and t18:1(c8)-24h:1 being very close to each other (Fig. 3B, e, f), these species could be differentiated by their product ion spectra in the multiple reaction monitoring mode. Collectively, from these data and the evidence that the former and latter peaks are molecular species having the *cis*-8 and *trans*-8 isomers of sphingoid bases, respectively [15, 16], retention time plots were applied to identify glucosylceramide molecular species (Fig. 2B and 3B). A good fit was found in each of the four types of molecular species containing saturated hydroxy fatty acids, where the coefficients of determination r^2 were >0.998 .

The result of 2-hydroxy fatty acid composition achieved by HPLC-ESI-MS/MS was compared with that achieved by gas chromatography with flame ionization detection (GC-FID) (Fig. 4A), indicating that the two methods yield similar molar compositions. Analysis of glucosylceramides

in orchardgrass leaves by LC-MS/MS and GC-FID showed a tendency of the mass spectrometer to be more sensitive to 22h:1-containing glucosylceramide species than to other 2-hydroxy fatty acid-containing glucosylceramide species, suggesting that this is likely due to the enhancement of the analyte signal in the presence of matrix components. Nevertheless, the 2-hydroxy fatty acid compositions of the orchardgrass glucosylceramides determined by the two methods were similar overall (Fig. 4B).

The *cis*-8 and *trans*-8 configuration of sphingoid bases in four samples of the glucosylceramide molecular species [d18:2(t4,c8)-20h:0-Glc, d18:2(t4,t8)-20h:0-Glc, t18:1(c8)-24h:0-Glc, and t18:1(t8)-24h:0-Glc] fractionated by HPLC were confirmed by GC (Fig. 5A). The relative levels of the *cis*-8 and *trans*-8 isomers of sphingoid bases in these samples were determined by ultraviolet (UV) spectrophotometry and ESI-MS/MS. As shown in Fig. 5B, C, the *cis*-8 and *trans*-8 levels determined by ESI-MS/MS of both species were strikingly similar to those determined by UV spectrophotometry, indicating that both isomers have similar mass-spectral responses.

Molecular species containing d18:2(t4,c8)-20h:0 was the most abundant component, accounting for about 35 % of the total species in glucosylceramide samples from rice callus (Fig. 6A). Among molecular species containing 4-hydroxy-8-sphingene, t18:1(c8)-24h:0-Glc was the predominant species, accounting for about 12 % of the total. In orchardgrass leaves, molecular species containing t18:1(c8) accounted for about 82 % of the total glucosylceramide species; the primary species was t18:1(c8)-24h:1-Glc, which accounted for about 43 % of the total (Fig. 6B).

In the present study, the composition of the glucosylceramide species was determined by LC-MS/MS from the chloroform/methanol fraction of Sep-Pak Plus silica cartridges. This fraction mainly contained glucosylceramides and steryl glucosides as determined by TLC (data not shown). Although we confirmed that glucosylceramide species were sufficiently detected in the current LC-MS/MS system using the crude lipid extract (data not shown), it may be appropriate to perform mild-base hydrolysis of the total lipid extract and subsequent solid-phase extraction, especially for plant samples with green organs to reduce interference with ionization efficiency by other compounds. The current method should be applicable to seeking the active components of glucosylceramide molecular species from vegetative, tuberous or cereal products in response to biological challenges.

Acknowledgments We thank Ayae Wada for technical and experimental assistance. We also thank Dr. Kouhei Yamamoto, Osaka Prefecture University, for his valuable advice. Parts of this work were supported by Special Ordinary Expense Subsidies for Private Universities from the Ministry of Education, Culture, Sports, Science, and Technology (MEXT) of Japan.

References

1. Steponkus PL, Uemura M, Webb MS (1993) A contrast of the cryostability of the plasma membrane of winter rye and spring oat—two species that widely differ in their freezing tolerance and plasma membrane lipid composition. In: Steponkus PL (ed) *Advances in low-temperature biology vol 2*. JAI Press Ltd., London, pp 211–312
2. Minami A, Furumoto A, Uemura M (2010) Dynamic compositional changes of detergent-resistant plasma membrane microdomains during plant cold acclimation. *Plant Signal Behav* 5:115–118
3. Jennemann R, Sandhoff R, Langbein L, Kaden S, Rothermel U, Gallala H, Sandhoff K, Wiegandt H, Gröne HJ (2007) Integrity and barrier function of the epidermis critically depend on glucosylceramide synthesis. *J Biol Chem* 282:3083–3094
4. Tsuji K, Mitsutake S, Ishikawa J, Takagi Y, Akiyama M, Shimizu H, Tomiyama T, Igarashi Y (2006) Dietary glucosylceramide improves skin barrier function in hairless mice. *J Dermatol Sci* 44:101–107
5. Uchiyama T, Nakano Y, Ueda O, Mori H, Nakashima M, Noda A, Ishizaki C, Mizoguchi M (2008) Oral intake of glucosylceramide improves relatively higher level of transepidermal water loss in mice and healthy human subjects. *J Health Sci* 54:559–566
6. Ideta R, Sakuta T, Nakano Y, Uchiyama T (2011) Orally administered glucosylceramide improves the skin barrier function by upregulating genes associated with the tight junction and cornified envelope formation. *Biosci Biotechnol Biochem* 75:151615–151623
7. Ohnishi M, Ito S, Fujino Y (1983) Characterization of sphingolipids in spinach leaves. *Biochim Biophys Acta* 752:416–422
8. Imai H, Morimoro Y, Tamura K (2000) Sphingoid base composition of monoglucosylceramide in Brassicaceae. *J Plant Physiol* 157:453–456
9. Minamioka H, Imai H (2009) Sphingoid long-chain base composition of glucosylceramides in Fabaceae: a phylogenetic interpretation of Fabaceae. *J Plant Res* 22:415–419
10. Bartke N, Fischbeck A, Humpf HU (2006) Analysis of sphingolipids in potatoes (*Solanum tuberosum* L.) and sweet potatoes (*Ipomoea batatas* (L.) Lam.) by reversed phase high-performance liquid chromatography electrospray ionization tandem mass spectrometry (HPLC-ESI-MS/MS). *Mol Nutr Food Res* 50:1201–1211
11. Markham JE, Jaworski JG (2007) Rapid measurement of sphingolipids from *Arabidopsis thaliana* by reversed-phase high performance-liquid chromatography coupled to electrospray ionization tandem mass spectrometry. *Rapid Commun Mass Spectrom* 21:1304–1314
12. Sugawara T, Duan J, Aida K, Tsuduki T, Hirata T (2010) Identification of glucosylceramides containing sphingatrienine in maize and rice using ion trap mass spectrometry. *Lipids* 45:451–455
13. Sugawara T, Aida K, Duan J, Hirata T (2010) Analysis of glucosylceramides from various sources by liquid chromatography-ion trap mass spectrometry. *J Oleo Sci* 59:387–394
14. Watanabe M, Miyagi A, Nagano M, Kawai-Yamada M, Imai H (2011) Characterization of glucosylceramides in the Polygonaceae, *Rumex obtusifolius* L. injurious weed. *Biosci Biotechnol Biochem* 75:877–881
15. Ohnishi M, Imai H, Kojima M, Yoshida S, Murata N, Fujino Y, Ito S (1988) Separation of cerebroside species in plants by reserved-phase HPLC and their phase transition temperature. In: *Proceedings of ISF-JOCS world congress, vol 2*, The Japan Oil Chemists' Society, Tokyo, pp 930–935
16. Cahoon EB, Lynch DV (1991) Analysis of Glucocerebrosides of Rye (*Secale cereale* L. cv Puma) leaf and plasma membrane. *Plant Physiol* 95:58–68
17. Murashige T, Skoog F (1962) A revised medium for rapid growth and bioassays with tobacco tissue cultures. *Physiol Plant* 15:473–497
18. Chu CC, Wang CC, Sun CS, Hsu C, Yin KC, Chu CY, Bi FY (1975) Establishment of an efficient medium for another culture of rice through comparative experiments on the nitrogen sources. *Sci Sin* 18:659–668
19. Bligh EG, Dyer WJ (1959) A rapid method of total lipid extraction and purification. *Can J Biochem Physiol* 37:911–917
20. Imai H, Yamamoto K, Shibahara A, Miyatani S, Nakayama T (2000) Determining double-bond positions in monoenoic 2-hydroxy fatty acids of glucosylceramides by gas chromatography-mass spectrometry. *Lipids* 35:233–236
21. Hirabayashi Y, Hamaoka A, Matsumoto M, Nishimura K (1986) An improved method for the separation of molecular species of cerebrosides. *Lipids* 21:710–714
22. Watanabe M, Imai H (2011) Characterization of glucosylceramides in leaves of the grass family (Poaceae): poeidae has unsaturated hydroxy fatty acids. *Biosci Biotechnol Biochem* 75:1838–1841